

**High serum levels of miRNA 550a-5p and low serum levels of miR-203a are risk factors for incident fractures in older postmenopausal women with Type 2 Diabetes.** Ursula Heilmeyer<sup>\*1</sup>, Matthias Hackl<sup>2</sup>, Sylvia Weilner<sup>2</sup>, Susanna Skalicky<sup>2</sup>, Fabian Schroeder<sup>3</sup>, Iryna Lobach<sup>4</sup>, Soheyla Torabi<sup>1</sup>, Elisabeth Geiger<sup>2</sup>, Klemens Vierlinger<sup>5</sup>, Gudny Eiriksdottir<sup>6</sup>, Elias Gudmundsson<sup>6</sup>, Thor Asplund<sup>7</sup>, Johannes Grillari<sup>8</sup>, Tamara Harris<sup>9</sup>, Thomas M. Link<sup>1</sup>, Vilmundur Gudnason<sup>6</sup>, Ann Schwartz<sup>7</sup>. <sup>1</sup>University of California San Francisco, Department of Radiology & Biomedical Imaging, United states, <sup>2</sup>TamiRNA GmbH, Austria, <sup>3</sup>Austrian Institute of Technology (AIT), Department of Molecular Medicine, Austria, <sup>4</sup>University of California San Francisco, Department of Epidemiology & Biostatistics, United states, <sup>5</sup>Austrian Institute of Technology (AIT), Department of Molecular Medicine, Austria, <sup>6</sup>The Icelandic Heart Association, Iceland, <sup>7</sup>The University of Iceland, Faculty of Medicine, Iceland, <sup>8</sup>University of Natural Resources & Life Sciences, Department of Biotechnology, Austria, <sup>9</sup>National Institute on Aging, Laboratory of Epidemiology & Population Science, United states

Standard DXA or FRAX-scores are limited in assessing fracture risk in Type 2 Diabetes (T2D). Novel, generally applicable biomarkers are thus necessary. MicroRNAs (miRNAs) are secreted into the circulation from cells of various tissues proportional to local disease severity. Serum miRNA classifiers including miR-550a and 203a were recently found to discriminate T2D women with and without prevalent fragility fractures with high specificity and sensitivity (AUC>0.90). However, the role of these miRNAs in predicting incident fragility fractures in T2D and their effects on osteogenic and osteoclast differentiation are unknown.

The AGES-Reykjavik cohort includes 330 T2D postmenopausal women. After excluding those with bone-affecting conditions/medications, 171 remained for analysis. Of those, 71 women suffered an incident fracture during the 10-year follow-up. Baseline serum levels were quantified by qPCR-arrays for 91 miRNAs. Decision tree models -using miRNA expression levels and age or the 10-year FRAX major osteoporotic fracture probability (FRAXmajOF) of ≤20 as decision points- were computed to identify T2D patients at highest risk for developing incident fractures. Kaplan-Meier curves were used to compare fracture incidence. MiR-550a-5p and miR-203a were further assessed by overexpression and knockdown in an in-vitro model of osteogenic and osteoclastic differentiation.

Decision tree models with age and miRNAs identified 3 distinct risk groups for fracture among T2D women: <76 years (y), ≥76 y with low and high serum miR-550a-5p. T2D women ≥76 y with high serum miR-550a-5p (qPCR Ct-value <41) had 61.4% risk of incident fracture over 10 years (Fig.1A). T2D women ≥76 y with low serum miR-550a-5p levels (Ct-values ≥41) had only a 38.5% risk of incident fracture (p=0.044). Women <76 y had 23.3% risk. When performing decision tree models with FRAX and miRNAs the following 3 risk groups were identified (Fig.1B): FRAXmajOF≤20, FRAXmajOF>20 with low and high miR-203a levels. Among T2D women with a FRAXmajOF>20, those with low levels of miR-203a (Ct-value ≥36) had a 67.8% risk of incident fracture, while those with high serum miR-203a levels had only a 34.9% fracture risk. T2D women with a FRAXmajOF≤20 had 17.0% fracture risk. In-vitro results confirmed miR-550a-5p as an inhibitor of osteogenic differentiation.

Overall, these data provide first proof that serum microRNAs can be used to predict fracture risk in T2D women and identify those at high risk of fracture that may benefit most from treatment.

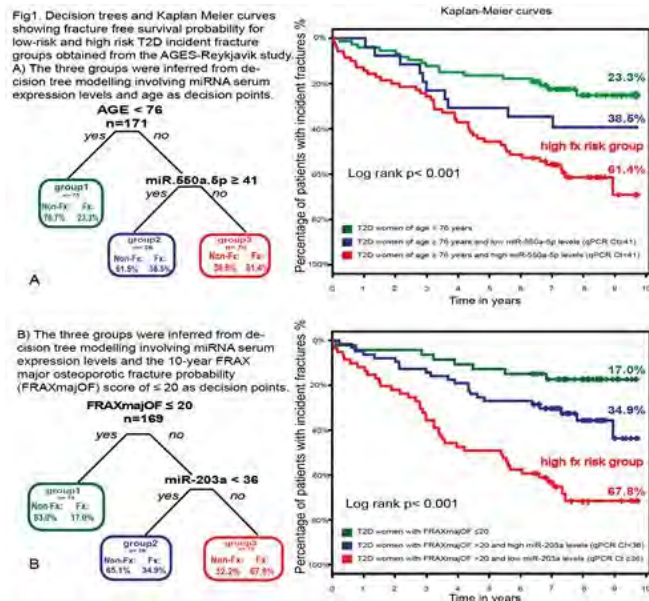


Figure 1  
Disclosures: Ursula Heilmeyer, None.

**Serum Activin A is Increased before iPTH and Associated with Bone Alterations in Chronic Kidney Disease Patients.** Florence Lima<sup>\*</sup>, Marie-Claude Monier-Faugere, Hanna W. Mawad, Hartmut H. Malluche. University of Kentucky, United states

Renal osteodystrophy (ROD) develops in early stages of chronic kidney disease (CKD) and progresses during loss of kidney function. Most recently activin A has been identified as a potential factor playing a role in the early pathogenesis of ROD. Activin A is expressed in bone cells and regulates osteoblastogenesis and osteoclastogenesis. The aims of this study were to 1) test the hypothesis that serum activin A levels increase before intact PTH (iPTH) in CKD, 2) evaluate the histologic changes of bone occurring at various stages of CKD, and 3) establish the relationships between bone abnormalities and serum levels of activin A in patients with various degrees of CKD.

One hundred eighteen subjects with or without CKD stages 2 to 5D underwent anterior iliac crest biopsies after double-tetracycline labeling. Sixteen patients had CKD-2, 29 had CKD-3, 13 had CKD-4 or 5, and 41 had CKD-5D. Nineteen subjects without CKD were included as controls. Serum activin A levels were measured by ELISA and serum iPTH by a radioimmunoassay. Undecalcified bone sections were evaluated by histomorphometry for parameters of bone turnover, mineralization and volume.

Serum activin A and iPTH levels in non-CKD were 393 ± 24 and 35 ± 3 pg/mL. In patients with CKD stages 2, 3 and 4/5, activin levels were 575 ± 50, 590 ± 33 and 678 ± 67 pg/mL, respectively; iPTH levels were 34 ± 3, 47 ± 4 and 106 ± 21 pg/mL, respectively. In patients with CKD-5D, activin A and iPTH were 1205 ± 77 and 556 ± 97 pg/mL. The percent increases in activin A and iPTH levels in CKD stages 2, 3 and 4/5 versus non-CKD are shown in the Figure.

Histomorphometric parameters showed a 2-times higher bone resorption and delayed mineralization in CKD-4 and 5 compared to CKD-2 and 3 (Table). There were significant relationships between serum activin A levels and bone turnover parameters among all CKD patients (BFR/BS, Ob.S/BS, Oc.S/BS and ES/BS, r = 61, 60, 66 and 59, respectively; P<0.01; abbreviations see Table). These correlations were similar to those observed with iPTH.

The data show an increase in serum activin A levels associated with decrease in kidney function as early as CKD stage 2 before elevated levels of iPTH. This is associated with higher bone resorption and delayed mineralization reaching significance at stage 4. The findings suggest that targeting activin A expression early in the course of loss of kidney function may be of interest to protect bone against ROD.

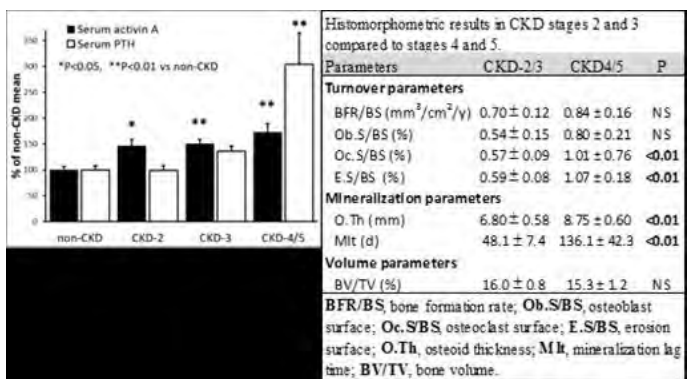


Figure and Table  
Disclosures: Florence Lima, None.

**Autoimmune Hyperphosphatemic Tumoral Calcinosis.** Mary Scott Ramnitz<sup>\*1</sup>, Peter D. Burbelo<sup>2</sup>, Christopher Romero<sup>3</sup>, Shoji Ichikawa<sup>4</sup>, Emily Farrow<sup>5</sup>, Michael Econs<sup>6</sup>, Lori Guthrie<sup>1</sup>, Rachel Gafni<sup>7</sup>, Michael Collins<sup>7</sup>. <sup>1</sup>Skeletal Clinical Studies Section, Craniofacial & Skeletal Diseases Branch (CSDB), National Institute of Dental & Craniofacial Research (NIDCR), National Institutes of Health (NIH), United states, <sup>2</sup>Dental Clinical Research Core, National Institute of Dental & Craniofacial Research (NIDCR), National Institutes of Health (NIH), United states, <sup>3</sup>Division of Pediatric Endocrinology & Diabetes, Icahn School of Medicine at Mount Sinai, United states, <sup>4</sup>Department of Medicine, Indiana University School of Medicine, United states, <sup>5</sup>Center for Pediatric Genomic Medicine, Children's Mercy, United states, <sup>6</sup>Department of Medicine & Department of Medical & Molecular Genetics, Indiana University School of Medicine, United states, <sup>7</sup>Skeletal Clinical Studies Unit, Craniofacial & Skeletal Diseases Branch (CSDB), National Institute of Dental & Craniofacial Research (NIDCR), National Institutes of Health (NIH), United states

Background: Hyperphosphatemic familial tumoral calcinosis (HFTC)/hyperostosis-hyperphosphatemia syndrome (HHS) is an autosomal recessive disorder due to deficiency of or resistance to intact fibroblast growth factor 23 (FGF23). This leads to

hyperphosphatemia, increased renal reabsorption of phosphorus (TRP), and elevated or inappropriately normal 1,25-dihydroxyvitamin D (1,25D). Affected individuals may develop ectopic calcifications and/or diaphyseal hyperostosis. Mutations in *FGF23*, *GALNT3*, or *KLOTHO* have been identified as causative for HFTC/HHS. Here we present the first case of autoimmune hyperphosphatemic tumoral calcinosis. Case: A 6-year old boy presented with right hip pain and development of a firm lesion on the lateral aspect of the hip, confirmed as tumoral calcinosis on biopsy. Biochemical evaluation showed hyperphosphatemia (7.2 mg/dL; nl 3-5.7), increased TRP (98%), and inappropriately normal 1,25D (68 pg/mL; nl 24-86). Intact and C-terminal FGF23 were elevated at 9600 pg/mL (nl 22-63) and 28,500 RU/mL (nl < 230), respectively, findings suggestive of FGF23 resistance due to a *KLOTHO* or possibly an *FGFR1* mutation. However, no causative mutation was identified in *GALNT3*, *FGF23*, *KLOTHO*, or *FGFR1*. The subject was prescribed a low phosphate diet, sevelamer and acetazolamide, with subsequent decrease in blood phosphorus and tumor size. Eight months later, he presented with a 2-week history of polyuria and polydipsia. Blood glucose was 433 mg/dL, insulin 4 mcU/mL, and hemoglobin A1c 10.7%, with positive islet antigen 2 antibodies. Given this new diagnosis of type 1 diabetes, investigation was undertaken to evaluate for possible autoimmune causes of his tumoral calcinosis. Luciferase immunoprecipitation systems (LIPS) were used to evaluate auto-antibodies against FGF23, FGFR1 and several other autoantigen targets. LIPS revealed significantly elevated autoantibodies against FGF23 in the patient that were over 50-fold higher than healthy controls and other subjects with HFTC/HHS. In contrast, there were no detectable autoantibodies against FGFR1. Analysis for *KLOTHO* antibodies as well as functional assays examining whether the anti-FGF23 autoantibodies are neutralizing are currently underway. Conclusion: This is the first reported case of autoimmune hyperphosphatemic tumoral calcinosis with autoantibodies against FGF23. Identification of this novel pathophysiology suggests that immunomodulatory therapy may be an effective treatment.

Disclosures: Mary Scott Ramnitz, None.

## 1004

**Osteopontin Accumulation in the Osteocyte Lacuno-canalicular Network Contributes to the Defective Bone Mineralization of X-linked Hypophosphatemia.** Tchilalo Boukpe<sup>1</sup>, Betty Hoac<sup>2</sup>, Benjamin R Coyac<sup>3</sup>, Michael P Whyte<sup>4</sup>, Francis H Glorieux<sup>2</sup>, Thibaut Leger<sup>5</sup>, Camille Garcia<sup>5</sup>, Philippe Wicart<sup>3</sup>, Agnes Linglar<sup>6</sup>, Catherine Chaussain<sup>3</sup>, Marc D McKee<sup>\*2</sup>. <sup>1</sup>McGill University & University Paris Descartes, France, <sup>2</sup>McGill University, Canada, <sup>3</sup>University Paris Descartes, France, <sup>4</sup>Shriners Hospital for Children, United states, <sup>5</sup>Institut Jacques Monod, University Paris Diderot, CNRS, France, <sup>6</sup>Paris Sud University, France

In X-linked hypophosphatemia (XLH), absence of functional PHEX increases circulating FGF-23 and causes renal phosphate wasting - the primary pathophysiological event responsible for its characteristic rickets/osteomalacia. However, another hallmark of XLH is localized hypomineralization in the perilacunar matrix surrounding osteocytes. These focal defects are commonly referred to as osteocyte "halos" based on their radiolucent appearance in bone-section contact microradiographs, and their lack of mineralization in undecalcified bone histology. Here we explored whether a mineralization inhibitor accumulates locally (in the absence of PHEX enzymatic activity to degrade it) in the pericellular matrix surrounding osteocytes to cause this type of mineralization defect. Given our recent published work demonstrating that the potent, mineralization-inhibiting, bone matrix protein osteopontin (OPN) is a substrate for PHEX, and knowing that PHEX is highly expressed in osteocytes, we examined the distribution of OPN in the osteocyte lacuno-canalicular network of XLH bone. Peri-osteocytic mineralization lesions were confirmed histologically in undecalcified XLH samples, and by correlative backscattered electron imaging detecting differences in mineral density at the microtomed bone/ block surface. Both methods revealed not only the characteristic extensive hypomineralized regions/lesions surrounding osteocytes, but also a mineralization defect in the canalicular network radiating from the osteocytes. To probe these sites for mineralization-inhibiting OPN, light microscopy immunohistochemistry for OPN, as well as ultrastructural assessment by transmission electron microscopy after immunogold labeling for OPN, both showed strikingly high levels of OPN at these mineralization-defect sites. Aligned with our previous work in the Hyp mouse (the murine model of XLH), analysis of noncollagenous proteins obtained by biochemical extraction and then analyzed by SDS-PAGE immunoblotting and mass spectrometry confirmed high levels of OPN and OPN fragments in XLH patient bone extracts. In conclusion, our findings indicate a role for OPN in the defective mineralization of XLH, and provide an explanation for the osteocytic halos that are a hallmark of this disease.

Disclosures: Marc D McKee, None.

## 1005

**Effect of 10 Years of Denosumab Treatment on Bone Histology and Histomorphometry in the FREEDOM Extension Study.** David W Dempster<sup>\*1</sup>, Nadia Daizadeh<sup>2</sup>, Astrid Fahrleitner-Pammer<sup>3</sup>, Jens-Erik Beck Jensen<sup>4</sup>, David Kendler<sup>5</sup>, Ivo Valter<sup>6</sup>, Rachel B Wagman<sup>2</sup>, Susan Yue<sup>2</sup>, Jacques P Brown<sup>7</sup>. <sup>1</sup>Columbia University, United states, <sup>2</sup>Amgen Inc., United states, <sup>3</sup>Medical University Graz, Austria, <sup>4</sup>Hvidovre Hospital, Denmark, <sup>5</sup>University of British Columbia, Canada, <sup>6</sup>Center for Clinical & Basic Research, Estonia, <sup>7</sup>Laval University & CHUL, Canada

Purpose: Denosumab (DMAb) has been associated with low incidence of spine and non-spine, including hip, fractures through 10 years of treatment (Bone ASBMR 2015). Questions about bone safety arose in response to the FREEDOM transiliac crest biopsy findings: low numbers of tetracycline labels were observed with low dynamic parameters of remodeling (Reid JBM 2010). In the FREEDOM Extension, bone biopsies were performed in subjects with 5 years of DMAb treatment and findings were similar to those in subjects with 2 or 3 years of DMAb treatment in FREEDOM (Brown JBM 2012). We now report bone biopsy findings in subjects with 10 years of DMAb treatment.

Methods: A subset of subjects with 10 years of DMAb exposure (3 years FREEDOM + 7 years Extension) participated in a transiliac bone biopsy substudy. Subjects underwent a tetracycline/demeclocycline labeling procedure prior to their bone biopsy visit (6 months after their last DMAb dose); samples were prepared and analyzed according to standard procedures by the Mayo Clinic as previously described (Reid JBM 2010). Continuous and categorical variables were summarized using descriptive statistics.

Results: There were 22 biopsies evaluable for qualitative histology in subjects with 10 years of DMAb exposure; all specimens showed normally mineralized lamellar bone. There was no evidence of pathologic findings, including osteomalacia, woven bone, or marrow fibrosis. There were 21 biopsies evaluable for histomorphometry; these showed that the antiresorptive effects of DMAb were maintained over time. In addition, indicators associated with bone formation and structure (including osteoid surface, osteoid width, and eroded surface) were generally similar to those at years 2/3 and 5 (Table). As part of the analysis of dynamic parameters, the presence of tetracycline labels was reviewed in all biopsies. The percentage of samples with any tetracycline label in trabecular bone has steadily increased over time from 34% in year 2/3, to 43% in year 5, and 77% in year 10; the percentage of samples with any label in cortical bone has remained steady from 57%, to 64%, and 55%, respectively. Double tetracycline labeling of trabecular or cortical bone was found in 7 (32%) subjects at year 10.

Conclusion: Bone histology showed normal bone microarchitecture, and histomorphometry was consistent with DMAb mechanism of action. There was no evidence of progression in the degree of low remodeling with long-term exposure to DMAb.

	FREEDOM		Extension		
	Year 2/3		Year 5		Year 10
	Placebo N = 45	Denosumab N = 47	Cross-over N = 13	Long-term N = 25	Long-term N = 22
Denosumab exposure (years)	0	2-3	2	5	10
Parameter	Median (Q1, Q3)				
Eroded surface/ bone surface (%)	1.0 (0.6, 1.9)	0.2 (0.0, 0.7)	0.2 (0.0, 0.4)	0.1 (0.0, 0.3)	0.3 (0.0, 0.9)
Osteoid surface (%)	6.8 (3.6, 10.1)	0.4 (0.2, 1.2)	0.5 (0.2, 0.7)	0.1 (0.0, 0.8)	0.1 (0.0, 0.2)
Osteoid width (µm)	8.7 (6.4, 11.0)	5.4 (4.4, 7.4)	5.6 (3.3, 6.6)	3.3 (0.0, 7.4)	4.2 (0.0, 7.4)
Mineral apposition rate (µm/d)	0.8 (0.7, 0.8)	0.3 (0.3, 0.5)	0.6 (0.5, 0.7)	0.4 (0.3, 1.1)	0.3 (0.3, 0.3)
Bone formation rate, volume based (%/yr)	14.6 (8.6, 21.8)	0.4 (0.2, 0.8)	1.2 (0.7, 1.3)	2.2 (0.2, 4.7)	0.3 (0.2, 2.8)
Activation frequency (year <sup>-1</sup> )	0.200 (0.120, 0.330)	0.002 (0.001, 0.004)	0.017 (0.011, 0.020)	0.031 (0.001, 0.071)	0.001 (0.001, 0.012)

Table: Bone histomorphometry in FREEDOM and its extension

Disclosures: David W Dempster, Amgen Inc., Eli Lilly & Co., 13; Amgen Inc., Eli Lilly & Co., Radius, Regeneron, Tarsa, 12; Amgen Inc., Eli Lilly & Co., 11  
This study received funding from: Amgen Inc

## 1006

**Alendronate treatment is associated with reduced fracture risk and maintained safety in the oldest old.** Kristian Axelsson<sup>\*1</sup>, Dan Lundh<sup>2</sup>, Mattias Lorentzon<sup>3</sup>. <sup>1</sup>Department of Orthopaedic Surgery, Skaraborg Hospital, Sweden, <sup>2</sup>School of Bioscience, University of Skovde, Sweden, <sup>3</sup>Geriatric Medicine, Department of Internal Medicine & Clinical Nutrition, Institute of Medicine, University of Gothenburg, Sweden

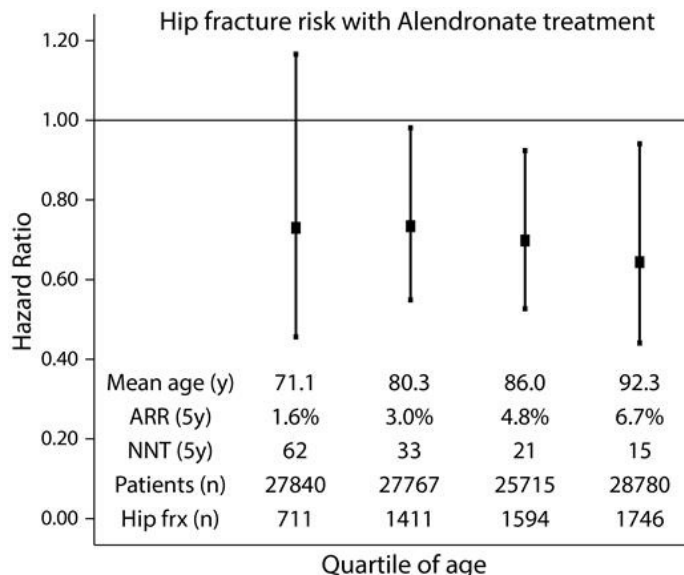
Fracture risk increases with age and peaks above 80 years of age. Yet treatment rates after fracture decline with increasing age in spite of efforts with Fracture Liaison Services, known to increase treatment rates after fracture. In randomized controlled

trials, Alendronate reduced the risk of hip fractures in patients with prior fracture, but a very limited amount of data exists for patients above 80 years of age, causing uncertainty regarding effectiveness and safety. The purpose of this study was to investigate if Alendronate treatment in older patients (>80 years) with prior fracture (secondary prevention) was related to decreased re-fracture rate and sustained safety in a large cohort of older men and women.

A total of 110,190 patients (age 82.4±8.3 years, 65% women) who underwent a fall risk assessment in connection to a visit to a healthcare facility in Sweden (2008-2014) and had a prior fracture were included in the present study. Information concerning prevalent and incident medication, diseases, fractures and deaths, were collected using national registers. Using a Cox proportional hazards model starting at the date of the risk assessment, adjusted for age, sex, weight, height, previous medication (glucocorticoids and calcium/vitamin D), secondary osteoporosis, alcohol usage, rheumatoid arthritis, Charlson comorbidity and exposition time, we investigated the association between use of Alendronate and hip fracture risk. Hip fracture outcome was defined by occurrence of both a hip fracture diagnosis and a code for surgical procedure. The follow-up time was adjusted for death, emigration or end of study period. All analyses were performed for the whole cohort and by quartiles of age.

Alendronate use was associated with a reduced hip fracture risk (Hazard Ratio 0.72, 95%CI 0.61-0.85,  $p < 0.001$ ), which was maintained across all age quartiles. However, the estimated absolute risk reduction at 5 years increased substantially by quartile of age. Adverse events, such as esophagitis, dyspepsia or acid reflux, were not more common in the higher than the lower age quartiles.

We conclude that Alendronate treatment was associated with reduced hip fracture risk in the oldest old and that the number needed to treat in these groups was substantially lower than in the younger age groups. These results suggest that Alendronate treatment in the oldest old is effective and safe, and should be prioritized in order to reduce the high fracture rates in this age group.



Alendronate treatment reduces hip fracture risk in oldest old

*Disclosures: Kristian Axelsson, None.*

## 1007

**The Effect of Bisphosphonates on All-Cause and Post-Fracture Mortality Risk in the Population-based Canadian Multicentre Osteoporosis Study (CaMOS).** Dana Bliuc<sup>\*1</sup>, Thach Tran<sup>1</sup>, Tineke van Geel<sup>2</sup>, John A. Eisman<sup>1</sup>, Tuan V Nguyen<sup>1</sup>, Lisa Langsetmo<sup>3</sup>, Jerilynn C Prior<sup>4</sup>, Robert G Josse<sup>5</sup>, Stephanie M Kaiser<sup>6</sup>, Christopher S Kovacs<sup>7</sup>, Claudie Berger<sup>8</sup>, David Goltzman<sup>9</sup>, David A. Hanley<sup>10</sup>, Jonathan Adachi<sup>11</sup>, Piet Geusens<sup>12</sup>, Joop van den Bergh<sup>2</sup>, Jacqueline R Center<sup>1</sup>. <sup>1</sup>Osteoporosis & Bone Biology, Garvan Institute of Medical Research, Australia, <sup>2</sup>Maastricht University, Netherlands, <sup>3</sup>Department of Medicine, McGill University, Canada, <sup>4</sup>Department of Endocrinology, University of British Columbia, Canada, <sup>5</sup>Department of Medicine, University of Toronto, Canada, <sup>6</sup>Division of Endocrinology & Metabolism at Dalhousie University, Canada, <sup>7</sup>Department of Medicine (Endocrinology & Metabolism) at Memorial University, Canada, <sup>8</sup>McGill University Health Centre, Canada, <sup>9</sup>Departments of Medicine & Physiology of McGill University, Canada, <sup>10</sup>The University of Calgary, Canada, <sup>11</sup>Department of Medicine at McMaster University, Canada, <sup>12</sup>University of Maastricht, Netherlands

Bisphosphonates (BP) may be associated with better survival following fracture. The nitrogen-containing BP (n-BP, e.g. alendronate and risedronate) have a different mechanism of action and higher potency than non-nitrogen BP (e.g. etidronate). However, there is little information on the effect of different BP formulations on mortality risk. The aims of this study were twofold: 1) to determine the overall effect of bisphosphonates (BP) on risk of all-cause mortality; and 2) to determine the effect of n-BP (alendronate, and risedronate) and other BP (etidronate) on mortality risk following fractures of all types.

Fracture and mortality data were collected prospectively over 15 years follow-up (1996-2011), from 5526 women and 2163 men 50+ enrolled in the population-based Canadian Multicentre Osteoporosis Study (CaMos). Co-morbidities, medication and life-style factors were collected yearly. The overall effect of BPs in the total cohort on mortality risk was assessed using a time dependent Cox Model over the whole period of follow-up. The individual effects of alendronate, etidronate and risedronate on mortality were assessed in the fracture cohort using survival analysis from the time of initial osteoporotic fracture until death or end of follow-up.

There were 2202 women and 339 men on BP and 1265 women on hormone therapy (HT), latter used as a treatment comparator. In the multivariable analysis adjusting for all potential confounding, mortality risk was reduced for current BP users [HR 0.58 (0.48-0.71)] and past BP users [HR 0.53 (0.41-0.69)] but not for HT [HR 1.08 (0.87-1.33)]. In men, mortality risk was reduced in current [HR 0.70 (0.49-0.94)] and past BP users [HR 0.49 (0.34-0.70)]. The effect of BP type on post-fracture mortality risk was explored in 1110 women with fractures (alendronate, n=320, etidronate n=212, and risedronate n=160). Mortality risk was reduced for n-BP [multivariable HR: 0.63 (0.47-0.85) for alendronate and 0.48 (0.30-0.76) for risedronate] but not for etidronate [HR: 1.00 (0.75-1.33)]. This decreased mortality effect was not related to a reduction in subsequent fractures [HR 0.90 (95% CI, 0.26-1.22)].

In summary, these data suggest that BP treatment appears to be associated with better survival after adjusting for all confounding factors, in both genders. The effect was only observed for n-BPs and was not related to a decline in subsequent fractures. This observation requires further attention and mechanistic exploration.

*Disclosures: Dana Bliuc, None.*

## 1008

**Calcium plus Vitamin D supplementation, fracture, and cardiovascular outcomes: A Bayesian meta-analysis.** Steven Frost<sup>1</sup>, Kevin Phan<sup>2</sup>, Thach Tran<sup>2</sup>, John Eisman<sup>2</sup>, Tuan Nguyen<sup>\*2</sup>. <sup>1</sup>University of Western Sydney, Australia, <sup>2</sup>Garvan Institute of Medical Research, Australia

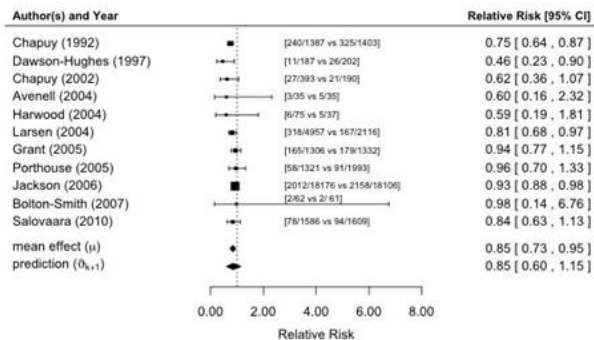
**Aim.** Recent analyses have suggested that calcium plus vitamin D (CaD) supplements were associated with adverse effects on cardiovascular diseases (CVD). However, the effect size is marginal and the association is unclear. In this analysis, we used a Bayesian approach to assess the potential risks and benefits of CaD supplements in terms of fracture prevention and CVD outcomes.

**Methods.** We identified 11 primary randomized controlled trials (RCTs) on the efficacy of CaD on fracture risk which involved 56569 individuals, and 7 post-hoc analyses of RCT on the association between CaD and CVD outcomes which involved 46526 individuals. The data were synthesized by a Bayesian random-effects meta-analysis with non-informative, skeptical and optimistic (for fracture outcome) or "pessimistic" priors (for CVD outcomes). The likelihood of benefit versus risk was analyzed taking into account the utilities associated with fracture and CVD outcomes.

**Results.** CaD supplements reduced the risk of fragility fracture by 15% (RR 0.85; 95%CI 0.73 to 0.95) (Figure). The probability that CaD supplements reduce total fracture risk by 10% or more was 0.85. For hip fracture, the evidence for CaD effect was not clear (RR 0.95; 95%CI, 0.67 - 1.35). Similarly, the association between CaD supplements and myocardial infarction or ischemic heart disease was uncertain as there was a wide confidence interval (RR 1.09; 95%CI, 0.69-1.88). Although CaD supplements were associated with reduced risk of stroke or cerebrovascular disease,

the association was not clear cut (RR 0.89; 95%CI, 0.35-1.94). Overall, after adjusting for the incidence and utilities associated with each outcome, the likelihood of being helped (in fracture prevention) by CaD supplementation is 8.7 times higher than being harmed by myocardial infarction or ischemic heart disease.

Conclusions: We conclude that CaD supplements reduce the risk of fracture, but the effect size is likely modest. The risk for myocardial infarction or ischemic heart disease or stroke in patients taking CaD supplements is uncertain: neither increased nor decreased risk is established. Overall, supplementation of calcium and vitamin D is more likely to help than to harm.



Forest plot of relative risk of fracture for each study and pooled studies.

Disclosures: Tuan Nguyen, None.

## 1009

**Multiorgan Disease in *Cln7G213R* Osteopetrotic Mice.** Antonio Maurizi<sup>1\*</sup>, Mattia Capulli<sup>1</sup>, Juliana Côrtes<sup>2</sup>, Laura Di Rito<sup>1</sup>, Nadia Rucci<sup>1</sup>, Anna Teti<sup>1</sup>. <sup>1</sup>University of L'Aquila, Italy, <sup>2</sup>Associação Fluminense De Educação, Brazil

The *Cln7* gene encodes for the 2C1/1H antiporter type 7 (*CIC7*), indispensable for osteoclast bone resorption. However, *CIC7* is expressed in many organs beyond bone, especially lung and brain, which we hypothesize, could contribute to the morbidity of osteopetrosis. Heterozygous (HT) and homozygous (HO) mice carrying the mouse homologue of the human dominant negative missense *CLCN7G215R* mutation (*Cln7G213R*) presented with lung perivascular fibrosis, more pronounced in HO (HT, 1.5fold; HO, 3.45fold,  $p < 0.001$  vs WT). While HT showed normal bronchoalveolar morphology, HO showed severe atelectasis and airway closure. Immunohistochemistry demonstrated *CIC7* expression in bronchiolar epithelium and alveolar macrophages, suggesting their pathogenic role in *Cln7G213R* mutant lungs. Neurodegeneration is a feature of *Cln7* loss-of-function mutations causing autosomal recessive osteopetrosis, while neural abnormalities are rarely reported in autosomal dominant osteopetrosis (ADO). In our HT mutants, which phenocopy ADO type 2, we observed 1.4fold increased anxiety ( $p < 0.05$ ) and depression ( $p < 0.01$ ) which worsened with age (+1.7fold,  $p < 0.05$ ), with no changes in memory and motor activity. Overt degeneration was observed in cerebellar and cerebral cortices and hippocampus in HO, but not in HT. However, increased  $\beta$ -amyloid accumulation was found in HT amygdala (2.28 fold), hippocampus (3.64fold) and thalamus (4.6fold;  $p < 0.05$ ) suggesting subtle changes and hidden neural phenotype. Furthermore, *Glo1* and *Gad1* enzyme mRNAs, associated with anxiety and depression, were increased in HT brains (1.77fold and 1.23fold, respectively,  $p < 0.05$ ), and the mutant *CIC7* was accumulated in cultured neuron Golgi apparatus (15fold,  $p < 0.05$ ), which appeared 2.5fold enlarged ( $p < 0.02$ ) in hippocampus cryosections. Similar Golgi changes were observed in monocytes and osteoclasts, suggesting a common pathogenic mechanism in cells involved in the multiorgan phenotype of *Cln7G213R* osteopetrosis. *Cln7G213R* cells presented no abnormal *CIC7* accumulation in the upstream ER organelle and no *Bip1* increase, while the downstream lysosomes showed less *CIC7* (-52%,  $p = 0.02$ ) and exhibited reduced acidification (+1.64 pH units,  $p < 0.001$ ). Furthermore, increased LC3 expression suggested altered autophagy. A specific *Cln7G213R* siRNA, proven to cure HT osteopetrosis, rescued Golgi *CIC7* accumulation and lysosomal pH, suggesting that this strategy is suitable to treat the multiorgan disease induced by the *Cln7G213R* mutation.

Disclosures: Antonio Maurizi, None.

## 1010

**Bone with Uncleavable Type I Collagen C-propeptide has Abnormal Development of Multiple Bone Cell Populations and Increased Bone Mineral Density with Age.** Aileen M. Barnes<sup>1\*</sup>, Joseph E. Perosky<sup>2</sup>, Stephane Blouin<sup>3</sup>, M. Helen Rajpar<sup>1</sup>, Basma Khoury<sup>2</sup>, Klaus Klaushofer<sup>4</sup>, Paul Roschger<sup>3</sup>, Nadja Fratzl-Zelman<sup>3</sup>, Kenneth M. Kozloff<sup>2</sup>, Joan C. Marini<sup>1</sup>. <sup>1</sup>NICHD/NIH, United states, <sup>2</sup>University of Michigan, United states, <sup>3</sup>Ludwig Boltzmann Institute of Osteology, Austria, <sup>4</sup>Ludwig Boltzmann Institute of Osteology, 1st Medical Department, Hanusch-Hospital, Austria

Classical osteogenesis imperfecta (OI), or brittle bone disease, is caused by dominant mutations in type I collagen. Mutations in the C-propeptide cleavage site of *COL1A1* or *COL1A2* cause dominant high bone mass (HBM) OI, characterized by bone hypermineralization and normal to increased DXA Z-scores. To elucidate the role of C-propeptide processing in bone formation, we generated heterozygous HBM mice, with both residues of the *COL1A1* cleavage site mutated to prevent cleavage by BMP1. Two-month WT and HBM bones were examined by immunoblotting, TEM, quantitative backscattered electron imaging (qBEI),  $\mu$ CT, and 4-point bending. Six- and 12-month bones were also examined to assess bone mineralization and strength over time.

HBM mice are smaller than WT in weight and length with extremely brittle bones. HBM bone extracts contain pC-collagen and increased monomeric *COL1A1* C-propeptide. Bone collagen fibrils have a "barbed-wire" appearance, consistent with the presence of pC-collagen, while dermal fibrils were smaller and more homogeneous than WT with a loss of large fibrils. qBEI revealed that HBM 2-month cortical femoral bone had increased bone matrix mineralization: CaMean: +5% ( $p = 0.0026$ ), CaPeak: +6% ( $p = 0.0002$ ) vs WT. CaHigh, reflecting the 95<sup>th</sup> percentile, was dramatically increased +470% in HBM vs WT ( $p = 0.0018$ ). Femoral aBMD is decreased at 2 months but is near normal (93%) at 1 year, while vertebral aBMD remains normal. Impaired C-propeptide processing affects bone geometry and biomechanics over time. On  $\mu$ CT, HBM femora have thinner cortices and decreased trabecular bone volume, while cortical and trabecular TMD are normalized at 1 year. Mechanical testing showed decreased femoral stiffness, yield and fracture load, without improvement over time. HBM femora are extremely brittle; post-yield displacement is ~15% of WT ( $p < 0.001$ ). Bone cell differentiation was also affected in HBM. Osteoblast collagen secretion was reduced ~20% in HBM vs WT ( $p = 0.009$ ). Two-month HBM femurs have less dense osteocytes ( $p < 0.0001$ ) but with increased average lacunar area ( $p < 0.001$ ). HBM osteoclast number is normal, but they are smaller in size vs WT ( $p = 0.006$ ).

The HBM mouse recapitulates the increased mineralization seen in patients with high mass bone OI. The changes in multiple bone cell populations support a putative C-propeptide trimer signalling function, influencing collagenous, cellular and mineral properties of bone.

Disclosures: Aileen M. Barnes, None.

## 1011

**A Missense Mutation in the *ZIP14* Gene Results in Abnormal Skull Growth in Patients with Hyperostosis Cranialis Interna.** Gretl Hendrickx<sup>1\*</sup>, Vere M. Borra<sup>1</sup>, Eveline Boudin<sup>1</sup>, Jérôme J. Waterval<sup>2</sup>, Robert J. Cousins<sup>3</sup>, Johannes J. Manni<sup>4</sup>, Wim Van Hul<sup>1</sup>. <sup>1</sup>Centre of Medical Genetics, University & University Hospital of Antwerp, Antwerp, Belgium, <sup>2</sup>Department of Otorhinolaryngology, Radboud University Medical Center, Nijmegen, Netherlands, <sup>3</sup>Food Science & Human Nutrition Department & Center for Nutritional Sciences, College of Agricultural & Life Sciences, University of Florida, Gainesville, Florida, United States of America, <sup>4</sup>Department of Otorhinolaryngology & Head & Neck Surgery, Maastricht University Medical Center, Maastricht, Netherlands, Netherlands

Hyperostosis cranialis interna (HCI) is a rare autosomal dominant skeletal disorder characterized by intracranial hyperostosis and osteosclerosis of the calvaria and skull base, whereas the remainder of the skeleton is not affected. Symptoms are caused by entrapment of cranial nerves due to progressive bone overgrowth. We previously localized the disease causing gene on chromosome 8p21 in a family with HCI. With exome sequencing we now identified a mutation (p.L441R) in the *SLC39A14* (*ZIP14*) gene, which encodes a transmembrane protein that mainly functions as a zinc ( $Zn^{2+}$ ) transporter. Subcellular localization studies indicated that mutant *ZIP14* is no longer present at the membrane and mainly localizes in the cytoplasm. Subsequent  $Zn^{2+}$  uptake and transport experiments with respectively <sup>65</sup>Zn and FluoZin-3AM were performed. Here, the p.L441R mutation impairs the ability of *ZIP14* to transport  $Zn^{2+}$  into the cell, but also causes entrapment of  $Zn^{2+}$  in the cell. Moreover, by performing a cAMP-responsive luciferase reporter assay, we observed a 5-fold increase in activation of cAMP-CREB signaling by mutant *ZIP14*, whereas overexpressing wildtype *ZIP14* slightly decreased cAMP levels. Skull tissue from a HCI patient was obtained and immunohistochemistry experiments were performed with an anti-*ZIP14* antibody. Here, expression of *ZIP14* was detected in skull osteoblasts and not in osteocytes, whereas no osteoclasts could be detected. Moreover, we performed  $\mu$ CT analysis of *Zip14*<sup>-/-</sup> (KO) mice. Compared to wildtype littermates, tibia length of KO mice was significantly reduced, however no difference in the skull phenotype was observed. *In vivo* analysis of the p.L441R mutation was initiated by the development of a *Zip14*<sup>L438R</sup>

flox mouse model and crossing these with different Cre mouse lines. Ubiquitous expression of Zip14<sup>L438R</sup> after crossing with Sox2-Cre mouse resulted in perinatal lethality. Conditional knock-in of Zip14<sup>L438R</sup> in osteoblasts or osteoclasts was achieved by crossing Zip14<sup>lox/lox</sup> mice with either Runx2-Cre or Cathepsin K-Cre mice, respectively. Currently, skeletal phenotyping of osteoblast and osteoclast specific knock-in mice at the age of 6 months is being performed by  $\mu$ CT analysis, dynamic bone histomorphometry and histological stainings of calvaria and long bones.

**Disclosures:** Gretl Hendrickx, None.

## 1012

**Pin1 Inhibitor, Juglone, Could Attenuate Phenotypes of Craniosynostosis Syndrome in FGFR<sup>S252W/+</sup> Mice Through the Reduction of Runx2 Activity.** Hye-Rim SHIN\*, Han-Sol BAE, Rabia Islam, Bong-Su KIM, Young-Dan CHO, Won-Joon YOON, Kyung-Mi WOO, Jeong-Hwa Baek, Hyun-Mo Ryo, Seoul National University, Korea, republic of

In human, missense mutation in FGFRs which induce hyper-activated FGFR signaling can cause various skeletal diseases such as craniosynostosis (CS). CS shows the phenotype of premature fusion of one or more of the craniofacial suture and apert syndrome (AS) is one of the most severe forms of craniosynostosis. We previously identified that Pin1, a cis/trans isomerase, regulates the conformational change of RUNX2, which affects to RUNX2 protein stability and its transcriptional activity in FGF2-induced osteoblast differentiation. Specific aim of this study was to examine whether genetic mutation of FGFR could be overcome by treatment of juglone which is a Pin1 inhibitor. FGFR<sup>S252W/+</sup> and E2A-Cre<sup>+/-</sup> mice were mated and pregnant mice were injected with juglone or vehicle at 14.5d.p.c. Juglone neither caused pregnant mice to die or show toxic effects in them nor did it affect littermate number. Systemic administration of juglone remarkably restored most of the calvaria abnormalities associated with AS which is induced by Ser252Trp mutation of FGFR2; as observed by measurement of skull length, nasal region, skull height and intercanthal distance. With the several in vitro studies, we demonstrated juglone has inhibitory effects on primary osteoblast differentiation and it can also attenuates hyper-activated differentiation pattern of CS mice calvaria cells. In the molecular level, juglone administration in CS mice weakened Runx2 acetylation, thereby recovering hypermorphic expression of active Runx2 through reduced stabilization of the protein. In addition, Runx2 transacting activity in CS mice calvarial osteoblasts and MC3T3-E1 cells was substantially normalized by the juglone treatment. These results illustrate the importance of conformational change of RUNX2 by Pin1 in vivo. Observation in the CS mice model strongly suggest juglone could open a new therapeutic avenue for bone diseases caused by gain-of-function mutation instead of a surgical operation in the human genome.

**Disclosures:** Hye-Rim SHIN, None.

## 1013

**Osteocytic-Specific HIF-1 $\alpha$  Activity Increases Bone Mass through Sirtuin 1-Dependent Decrease of Sclerostin.** Steve Stegen\*<sup>1</sup>, Ingrid Stockmans<sup>1</sup>, Karen Moermans<sup>1</sup>, Peter Carmeliet<sup>2</sup>, Geert Carmeliet<sup>1</sup>. <sup>1</sup>Clinical & Experimental Endocrinology, KU Leuven, Belgium, <sup>2</sup>Angiogenesis & Vascular Metabolism, Vesalius Research Center, KU Leuven/VIB, Belgium

Osteocytes are key regulators of bone remodeling during homeostasis and their cellular fitness is thus important. These cells reside however within a low oxygen microenvironment, suggesting a role of hypoxia signaling for osteocyte function. Osteoprogenitors and osteoblasts have been shown to sense and respond to local changes in oxygen levels, with prolyl hydroxylases (PHDs) acting as the oxygen sensors, and the hypoxia-inducible transcription factor HIF functioning as the effector, but the role of this signaling pathway in osteocytes remains elusive.

To investigate the contribution of PHDs in regulating osteocyte function we generated mice lacking PHD2, the most important isoform, in these cells (*Dmp1-Cre; Phd2<sup>o/c</sup>*), which resulted in stabilization of HIF-1 $\alpha$ . Mutant mice displayed a high bone mass phenotype, caused by increased bone formation and decreased resorption. Osteoblast number and activity was increased, evidenced by serum osteocalcin levels and static and dynamic histological analysis. Bone resorption in *Phd2<sup>o/c</sup>* mice was reduced as shown by a decrease in serum CTX levels and number of osteoclasts, quantified on TRAP-stained histological sections. Mechanistically, stabilization of HIF-1 $\alpha$  in PHD2-deficient osteocytes resulted in a Sirtuin 1 (SIRT1)-dependent decrease in sclerostin and consequently enhanced WNT/ $\beta$ -catenin signaling. As expected from increased HIF signaling, the number and size of blood vessels was increased in the trabecular and cortical bone of *Phd2<sup>o/c</sup>* mice, resulting from elevated *Vegf* transcript levels. Lastly, we show that genetic ablation of *Phd2* was sufficient to protect mice from osteoporotic bone loss. Both hindlimb suspension and ovariectomy resulted in a decrease in trabecular and cortical bone mass in wild-type mice, while *Phd2<sup>o/c</sup>* mice were largely protected from bone loss. Mechanistically, PHD2-deficient osteocytes displayed sustained WNT/ $\beta$ -catenin signaling through SIRT1-dependent downregulation of sclerostin.

Together, HIF-1 $\alpha$  signaling in osteocytes regulates their communication with osteoblasts, osteoclasts and blood vessels during homeostasis and pathology.

**Disclosures:** Steve Stegen, None.

## 1014

**Sclerostin: a Local Rather Than Systemic Regulator of Bone Mass.** Rishikesh N. Kulkarni\*<sup>1</sup>, Aaron Schindeler<sup>2</sup>, Peter I. Croucher<sup>1</sup>, David Little<sup>2</sup>, Paul A. Baldock<sup>1</sup>. <sup>1</sup>Garvan Institute of Medical Research, Australia, <sup>2</sup>The Children's Hospital at Westmead, Australia

Sclerostin is a key inhibitor of WNT signalling in bone and has recently emerged as fundamental to the regulation of bone homeostasis and mechanotransduction. Mechanosensitive osteocytes in bone inhibit the local production sclerostin in response to mechanical loading to increase osteoblast differentiation and bone mass. Sclerostin is normally assumed to travel via the osteocyte canalicular network to act upon local bone-forming osteoblast. However, sclerostin can also be detected in the serum and may have systemic effects. While sclerostin is a secreted protein, it is debatable whether circulating sclerostin acts as a modulator of bone formation. We, therefore, investigated whether circulating sclerostin alters bone mass in an endocrine manner.

To study this, we generated limb-specific sclerostin null mice (*Prrxl1-Cre Sost<sup>fl/fl</sup>*) with sclerostin ablated only in the appendicular skeleton but not in the axial skeleton. These mice were compared to wild type mice with sclerostin intact in the whole skeleton, and to constitutive sclerostin null mice (*Sost<sup>-/-</sup>*) with sclerostin ablated in the whole skeleton. The whole body dual-energy X-ray absorptiometry (DXA) was performed longitudinally to measure bone mineral content (BMC) and bone mineral density (BMD). The mice were culled at 16 wk age to collect blood, femurs, and spine for further analyses.

We found that the serum sclerostin was reduced by 1.7-fold in *Prrxl1-Cre Sost<sup>fl/fl</sup>* compared to control mice, but was undetectable in *Sost<sup>-/-</sup>* mice. The DXA results showed that greater BMD and BMC were present only in the limb but not in the spine of *Prrxl1-CreSost<sup>fl/fl</sup>* mice whereas *Sost<sup>-/-</sup>* mice showed greater BMD and BMC both in the limb and spine. Micro-computed tomography analysis showed greater cortical bone mass in femurs of *Prrxl1-Cre Sost<sup>fl/fl</sup>* and *Sost<sup>-/-</sup>* mice compared to control mice. Importantly, cancellous and cortical bone mass in vertebra did not differ between *Prrxl1-CreSost<sup>fl/fl</sup>* and control mice.

In conclusion, our results show that sclerostin does not alter bone mass in an endocrine manner rather it alters bone mass locally and serum sclerostin might not correctly predict changes in whole body bone mass.

**Disclosures:** Rishikesh N. Kulkarni, None.

## 1015

**Evidence for Autocrine Effects of Sclerostin on Osteocytes: Sclerostin Antibody Treatment Prevents Spaceflight-induced Osteocytic Osteolysis and Skeletal Bone Loss in Mice.** Yoshihito Ishihara\*<sup>1</sup>, Sutada Lotinun<sup>1</sup>, Virginia L. Ferguson<sup>2</sup>, Ted A. Bateman<sup>3</sup>, Louis S. Stodieck<sup>2</sup>, Chris Paszty<sup>4</sup>, Mary L. Bouxsein<sup>5</sup>, Roland Baron<sup>6</sup>. <sup>1</sup>Division of Bone & Mineral Research, Department of Oral Medicine, Infection & Immunity, Harvard School of Dental Medicine, United states, <sup>2</sup>Department of Mechanical Engineering, University of Colorado Boulder, United states, <sup>3</sup>Departments of Biomedical Engineering & Radiation Oncology, University of North Carolina, United states, <sup>4</sup>Department of Metabolic Diseases, Amgen, Inc., United states, <sup>5</sup>Center for Advanced Orthopedic Studies, Beth Israel Deaconess Medical Center & Harvard Medical School, Endocrine Unit, Massachusetts General Hospital, United states, <sup>6</sup>Division of Bone & Mineral Research, Department of Oral Medicine, Infection & Immunity, Harvard School of Dental Medicine & Harvard Medical School, Endocrine Unit, Massachusetts General Hospital, United states

Astronauts lose bone at 10 X the rate of postmenopausal women. This disuse-induced bone loss may be mediated by sclerostin (Sost) since its expression increase during unloading. Sost inhibits WNT signaling, represses bone formation (BFR) and favors bone resorption (BR). Osteocytes (Ocytes), the main source of Sost, are responsible for mechanosensing and key regulators of bone remodeling and homeostasis. Although changes in Sost expression in Ocytes are known to affect BFR and BR, little is known about the potential autocrine effects of Sost on the behavior of Ocytes, and in particular on their ability to regulate the size of their lacunae through osteocytic osteolysis.

To address this question we determined whether Ocyte lacunae were altered during spaceflight and whether a Sost antibody (Scl-Ab) could prevent these changes and improve skeletal homeostasis. 9-week-old female C57Bl/6N mice were exposed to 13 days of microgravity on the Space Shuttle Atlantis (STS-135) or kept on the ground and injected with Scl-Ab (100mg/kg, SC, Amgen) or vehicle 1 day prior to launch. Ground-controls were kept in identical housing as the flight mice.

Backscattered scanning EM revealed that exposure to 13-days unloading during spaceflight enlarged Ocyte lacunar area by 20% (from 31.1 to 37.3 $\mu$ m<sup>2</sup>, p<0.05) with varying degrees of perilacunar demineralization. Pre-flight administration of Scl-Ab prevented these changes (29.6 $\mu$ m<sup>2</sup>, P<0.01). In parallel with the prevention of osteocytic osteolysis, histomorphometry showed that spaceflight decreased trabecular bone due to inhibition of BFR (BV/TV: -23% and BFR/BS: -30%; NS) with a significant decrease in mineral apposition rate (MAR -19%; P<0.05), and an increase in osteoclasts (N.Oc/B.Pm +323%; Oc.S/BS +360%; P<0.05). Scl-Ab also improved these parameters (N.Oc/B.Pm -75%; Oc.S/BS -65% vs flight vehicle; P<0.05) to values similar to ground vehicle control group, resulting in a significant increase in trabecular

bone regardless of loading condition. However, MAR and osteoblastic parameters were still lower in the spaceflight group treated with Scl-Ab than in the ground group treated with Scl-Ab.

Our findings provide direct evidence that spaceflight induces osteocytic osteolysis and that this is modulated by sclerostin in an autocrine manner. Accordingly, Scl-Ab also counteracts the unfavorable effects that spaceflight has on both Ocyte and osteoclast-mediated bone resorption, and osteoblast-mediated bone formation.

**Disclosures:** *Yoshihito Ishihara, None.*

*This study received funding from: NASA (NNJ10GA25A, NNX10AE39G-S1); NSBRI (MA00002, BL01302); Amgen/UCB Pharma; and Bioserve*

## 1016

**The Bone Anabolic Effects of Intermittent Administration of PTH are Independent of Sost/Sclerostin Downregulation.** Jesus Delgado-Calle\*, Rafael Pacheco-Costa, Xiaolin Tu, Kevin McAndrews, Lilian I Plotkin, Teresita Bellido. Department of Anatomy & Cell Biology, Indiana University School of Medicine, United states

Mice lacking the PTH receptor in osteocytes exhibit impaired bone gain in response to intermittent PTH administration (iPTH), and PTH downregulates the expression of the osteocytic Wnt/ $\beta$ -catenin antagonist Sost/Sclerostin (Scl). These findings suggest a critical role of osteocytes in bone anabolism by the hormone through inhibition of Sost/Scl. We examined here whether Sost/Scl downregulation is required for the full bone anabolic response to PTH. Four-month-old Dmp1-8kb-hSOST mice overexpressing a human SOST transgene in osteocytes (TG, n=11-12/group) and control littermates (WT, n=10-11/group) were injected with PTH 1-34 (100 ng/g/day) for 4wks. WT and TG mice express similar levels of murine endogenous Sost mRNA, and human SOST mRNA was only detected in TG mice. Consistent with SOST overexpression, TG mice exhibited a 20% decrease in cancellous bone volume (BV/TV) but no changes in cortical bone area; decreased cancellous mineral apposition rate (MAR), mineralizing surface (MS/BS), and bone formation rate (BFR); and a 65% decrease in serum OCN but no differences in serum CTX or osteoclast number/surface compared to WT mice. iPTH decreased murine Sost expression by 50% in both WT and TG mice; in contrast, human SOST expression in TG mice remained unchanged by the PTH. iPTH increased total and femoral BMD to a similar extent in WT and TG mice (12 and 19% change BMD, respectively), whereas it only increased spinal BMD in WT (9%), but not in TG mice. However, more sensitive measurements by  $\mu$ CT and histomorphometry revealed that iPTH increased spinal cancellous BV/TV by 45%, femoral cortical BA/TA by 8%, and MAR and BFR by 22-24%, similarly in WT and TG mice. However, iPTH did not change serum CTX or osteoclast number/surface regardless of the genotype. In addition, both WT and TG mice receiving iPTH exhibited increased serum OCN (50-70%), and elevated bone mRNA levels of Alpl, Runx2, OCN, and several Wnt target genes, including CyclinD1, Smad6, Wisp2, and Cx43. These results demonstrate that the gain in cancellous and cortical bone, the increase in bone formation and the stimulation of Wnt/ $\beta$ -catenin signaling induced by iPTH occur even in the presence of SOST overexpression, and thus are independent of downregulation of Sost/Scl by the hormone. Taken together with previous evidence, these findings suggest that mechanisms downstream of the PTH receptor other than inhibition of Sost/Scl are responsible for the bone anabolic effects of PTH driven by osteocytes.

**Disclosures:** *Jesus Delgado-Calle, None.*

## 1017

**The effects of aging and sex steroid deficiency on the murine skeleton are independent and mechanistically distinct.** Serra Semahat Ucer\*<sup>1</sup>, Srividhya Iyer<sup>1</sup>, Ha-Neui Kim<sup>1</sup>, Li Han<sup>1</sup>, Jeff Thostenson<sup>2</sup>, Aaron Warren<sup>1</sup>, Julie Crawford<sup>1</sup>, Christine Rutlen<sup>1</sup>, Kelly Allison<sup>1</sup>, Robert Jilka<sup>1</sup>, Charles O'Brien<sup>1</sup>, Maria Almieda<sup>1</sup>, Stavros Manolagas<sup>1</sup>. <sup>1</sup>Center for Osteoporosis & Metabolic Bone Diseases, Univ. Arkansas for Medical Sciences, & Central Arkansas Veterans Healthcare System, United states, <sup>2</sup>Department of Biostatistics, University of Arkansas for Medical Sciences, United states

Old age and sex steroid deficiency are critical factors for the development of osteoporosis. It remains unclear, however, whether and how the molecular and cellular changes caused by the two conditions mechanistically interact. We have sought evidence for the contribution of estrogens to the age-dependent skeletal changes. To do this we ovariectomized (OVX) C57BL/6J mice at 4 or 18 months of age. Six weeks following OVX at either age, the decrease in uterine weight and increase in body weight were indistinguishable between the young and old mice. Nonetheless, femoral cortical thickness and vertebral cancellous bone mass volume did decline and cortical porosity increased in sham-operated mice between 5.5 and 19.5 months of age. Loss of estrogens in the young mice caused a decline in both femoral cortical thickness and cancellous bone volume; albeit, loss of estrogens in the old mice had no effect on femoral cortical thickness, but it still caused a decline in vertebral BV/TV. Loss of estrogens at young or old age had no measurable effect on cortical porosity. Further, we aged mice with a mitochondria-targeted transgene of human catalase – a potent H<sub>2</sub>O<sub>2</sub> inactivating enzyme – in Prx1-Cre or LysM-Cre targeted cells. The decline of cortical thickness, as well as mineralizing surfaces in the endocortical surface, of the femur between 6 and 22 months was partially prevented

by the attenuation of H<sub>2</sub>O<sub>2</sub> generation in mitoCAT;Prx1-Cre mice. On the other hand, the adverse effects of aging on either cortical or cancellous bone was not influenced in mitoCAT;LysM-Cre mice. Nonetheless, the loss of cortical bone was abrogated in both young adult OVX or ORX mitoCAT;LysM-Cre mice and so was the increase in osteoclast numbers in the cortical compartment. These results demonstrate that in mice, the age-dependent decline of cortical thickness and cancellous bone mass as well as cortical porosity are estrogen independent, as they occur in the face of estrogen sufficiency; and that the effects of aging and sex steroid deficiency result from distinct mechanisms. Moreover, the elucidation of distinct pathogenetic mechanisms in the effects of systemic changes (such as aging and sex steroid deficiency) in the cancellous versus the cortical bone compartment supports the fundamental notion that the progenitors responsible for the supply of the executive cells of bone remodeling are greatly influenced by the prevailing microenvironmental niches in each compartment.

**Disclosures:** *Serra Semahat Ucer, None.*

## 1018

**Role of  $\beta$ -catenin Signaling in Osteocytes on Bone and Muscle Properties Across Aging and between Sexes.** Mark Begonia<sup>1</sup>, Julian Vallejo<sup>2</sup>, An-Lin Cheng<sup>3</sup>, Ganesh Thiagarajan<sup>1</sup>, Mark Johnson<sup>4</sup>, Nuria Lara<sup>\*2</sup>. <sup>1</sup>UMKC/School of Computing & Engineer, United states, <sup>2</sup>UMKC/School of Dentistry, United states, <sup>3</sup>UMKC/School of Nursing, United states, <sup>4</sup>UMKC/School of Dentistry, United states

The Wnt/ $\beta$ -catenin signaling pathway is important in bone and muscle development and maintenance. We have recently shown that activation of osteocyte  $\beta$ -catenin signaling is enhanced by factors produced from contracting skeletal muscle and that osteocytes produce a factor(s) that enhances myogenesis and myotube contraction. To determine if altered  $\beta$ -catenin signaling in osteocytes in vivo affects muscle function with aging, we studied male and female mice with deletion of a single allele of  $\beta$ -catenin in osteocytes (HETcKO) at 20 and 72 weeks of age. MicroCT parameters, femur biomechanical data as well as Soleus and EDL muscle weights, lengths and muscle functionality data were analyzed.

Aging had differential effects in males and females. 20 wk old HETcKO females had a decreased trabecular number (25%), increased trabecular spacing (34%), and an increased Young's Modulus (32%) as compared to littermate controls. Cortical thickness and area were reduced by 11% and 2% respectively in males but not in females. Cortical perimeter increased 12% in males and 16% in females. 72 wk old HETcKO female had a 9% decrease in cortical area compared to controls. Trabecular BV/TV decreased by 76% in males and 69% in females; trabecular number decreased by 54% in males and 48% in females. Trabecular spacing was increased by 122% in males and 94% in females. 72 wk old males had a 28% reduction in ultimate load while 72 wk old females had reductions in work to failure (40%) and Young's Modulus (52%) with aging.

Soleus and EDL muscle mass decreased across aging in both males (19%) and females (12%). Although females had a decreased maximal force (22%) with aging, males did not. Compared to littermate controls, soleus muscles in the young female HETcKO group fatigued to a greater extent and had a slower recovery after fatigue.

We observed sex\*age interactions in cortical thickness, bone area, trabecular BV/TV and number, ultimate load and stiffness. There were genotype\*sex interactions in Young's Modulus and sex\*genotype\*age effects on trabecular separation. We observed interaction effects between genotype and age in the EDL and Soleus parameters for both sexes and correlations between bone and muscle properties.

These data demonstrate that loss of a single allele of  $\beta$ -catenin in osteocytes affects not only bone properties, but also influences muscle function in a sex specific manner across aging. These data support our model of bone-muscle crosstalk signaling.

**Disclosures:** *Nuria Lara, None.*

## 1019

**Blocking the Senescence-Associated Secretory Phenotype (SASP) Reduces Osteoclastogenesis and Prevents Age-related Bone Loss.** Ming Xu<sup>\*</sup>, Megan Weivoda, Joshua Farr, Christine Hachfeld, Stephanie Youssef, Glenda Evans, Ming Ruan, David Monroe, Tamar Tchkonja, Sundeeep Khosla, Merry Jo Oursler, James Kirkland. Mayo Clinic, United states

Bone loss occurs with aging; however, the mechanisms for this remain unclear. Senescent cells accumulate during aging and secrete pro-inflammatory cytokines, termed the senescence-associated secretory phenotype (SASP). We hypothesized that the SASP is pro-osteoclastogenic and targeting the SASP could prevent age-related bone loss. To test this hypothesis, we sham-treated or irradiated primary human adipose-derived MSCs to induce senescence and collected both control and senescent conditioned media (CCM and SCM, respectively). We previously demonstrated that inhibition of JAK signaling suppresses the SASP; thus, we treated senescent cells with a JAK inhibitor (JAKi) and collected CM (SCM-J). Freshly isolated mouse bone marrow was cultured overnight in CCM, SCM, SCM-J, or in the presence of M-CSF. Non-adherent cells were plated for osteoclast differentiation; differentiation was assessed by TRAP staining. While cells treated with CCM yielded few osteoclasts, cells treated with SCM prior to differentiation yielded osteoclast numbers comparable to M-CSF treatment. In contrast, SCM-J treated cultures showed significantly decreased osteoclast numbers. JAKi alone did not affect SCM-induced osteoclast differentiation. Using neutralizing antibodies to SASP components, we identified IL-6, IL-8, and PAI-1 as mediators of the pro-osteoclastogenic effect. FACS analysis of

cells treated overnight with CCM or SCM revealed that SCM increased monocyte numbers 2.5-fold compared to CCM. Direct assessment of monocytes showed that SCM significantly reduced monocyte apoptosis and cytotoxicity, indicating a mechanism for the increased osteoclastogenesis. To determine whether inhibiting the SASP would prevent age-related bone loss, we treated 22 month old male mice with JAKi or vehicle for 8 weeks. Femurs and vertebrae from JAKi-treated mice exhibited significantly better trabecular microarchitecture as assessed by mCT. There was no effect on osteoblast-colony forming units (CFUs). In contrast, monocyte-CFUs and osteoclast differentiation were significantly reduced in JAKi mouse bone marrow cultures. Histomorphometry revealed no change in osteoblast but a significant decrease in osteoclast parameters. Importantly, JAKi treatment had little effect on bone parameters in 7-month-old mice, which have markedly fewer senescent cells. These data show that the SASP promotes osteoclastogenesis, and blocking the SASP is an effective strategy to prevent age-related bone loss.

**Disclosures:** Ming Xu, None.

## 1020

**The Longevity-related SirT1 Enzyme Retards Inflamm-aging In Vivo.** Pradeep Kumar Sacitharan<sup>1</sup>, Tonia Vincent<sup>1</sup>, James R Edwards<sup>2</sup>. <sup>1</sup>The Kennedy Institute of Rheumatology, University of Oxford, United Kingdom, <sup>2</sup>The Botnar Research Centre, University of Oxford, United Kingdom

Ageing is accompanied by an increase in inflammatory status. This underlying chronic inflammation may fuel age-related disorders e.g. diabetes, heart disease and arthritis. However, the cause of this inflamm-aging is unknown. We hypothesized that factors linked to ageing and lifespan may also control the normal inflammatory response, where dysregulation with ageing may contribute to an elevated inflammatory state. The class III deacetylase SirT1 is strongly linked to longevity and can extend lifespan in various model systems when over-expressed or stimulated pharmacologically. Our work has shown that SirT1 expression decreases within the ageing skeleton and dysregulates bone remodelling to predispose to age-related bone loss. In addition, loss of SirT1 increases the activity of the common inflammatory mediator NFκB, in vivo.

Using a novel, inducible whole-body SirT1 deletion mouse model (SirT1<sup>fl/fl</sup> x ROSA CreERT2), we examined the inflammatory response within the joint by histomorphometric analysis and profiled inflammatory gene signatures using a low density qPCR array.

SirT1 deficiency increased fibrosis (p<0.05), joint stiffness (p<0.05) and synovitis (p<0.001) score and several inflammatory response genes including IL-1β (p<0.0001), IL-6 (p<0.0001), CCR2 (p<0.001), ADAMTS-4 (p<0.001) and MMP-13 (p<0.01). To assess the accumulative contribution of mechanical joint injury, SirT1-deficient and WT mice underwent joint destabilisation surgery (DMM), an established model of human osteoarthritis (OA). Surprisingly, SirT1-deficient mice (4.462 ± 0.8291) were protected from disease 12 weeks post-DMM compared to control mice (15.58 ± 1.411; p<0.0001). Furthermore, bone marrow chimera experiments showed SirT1-deficient mice receiving WT bone marrow displayed no increase in early synovitis and inflammatory gene expression but had increased long term disease scores (p<0.05), and where the protective nature of SirT1 deficiency post-DMM was lost. The opposite effect was observed in WT mice engrafted with SirT1-deficient bone marrow (p<0.05).

These results suggest that SirT1 has anti-inflammatory effects, and that loss of SirT1 leads to an inflamm-aging phenotype. Interestingly, the increased fibrosis and stiffness of the joint following SirT1 deletion served to stabilise and protect against long term OA.

**Disclosures:** Pradeep Kumar Sacitharan, None.

## 1021

**Patient-specific Musculoskeletal Model of the Spine: Implication for Prediction of Incident Vertebral Fractures.** Hossein Mokhtarzadeh<sup>1</sup>, Katelyn Burkhardt<sup>2</sup>, Brett Allaire<sup>3</sup>, Darlene Lu<sup>4</sup>, Serkalem Demissie<sup>4</sup>, David Kopperdahl<sup>5</sup>, Tony M. Keaveny<sup>6</sup>, Elizabeth J. Samelson<sup>7</sup>, Douglas P. Kiel<sup>8</sup>, Dennis E. Anderson<sup>1</sup>, Mary L. Bouxsein<sup>9</sup>. <sup>1</sup>Department of Orthopedic Surgery, Harvard Medical School, MA, USA; Center for Advanced Orthopaedic Studies, Beth Israel Deaconess Medical Center, MA, USA, United states, <sup>2</sup>Harvard-MIT Division of Health Sciences & Technology, MA, USA; Department of Orthopedic Surgery, Harvard Medical School, MA, USA; Center for Advanced Orthopaedic Studies, Beth Israel Deaconess Medical Center, MA, USA, United states, <sup>3</sup>Center for Advanced Orthopaedic Studies, Beth Israel Deaconess Medical Center, MA, USA, United states, <sup>4</sup>Boston University School of Public Health, MA, USA, United states, <sup>5</sup>O.N. Diagnostics, Berkeley, CA, USA, United states, <sup>6</sup>Departments of Mechanical Engineering & Bioengineering, University of California, Berkeley, CA, USA; O.N. Diagnostics, Berkeley, CA, USA, United states, <sup>7</sup>Institute for Aging Research, Hebrew SeniorLife, Department of Medicine Beth Israel Deaconess Medical Center & Harvard Medical School, Boston, MA, USA., United states, <sup>8</sup>Institute for Aging Research, Hebrew SeniorLife, Department of Medicine Beth Israel Deaconess Medical Center & Harvard Medical School, Boston, MA, USA, United states, <sup>9</sup>Department of Orthopedic Surgery, Harvard Medical School, MA, USA; Center for Advanced Orthopaedic Studies, Beth Israel Deaconess Medical Center, MA, USA; Harvard-MIT Division of Health Sciences & Technology, MA, USA, United states

Vertebral fractures (VFX) are common, affecting 15-35% of the population >50 yrs. Identification of those at highest risk is critical to optimize prevention of VFX. We hypothesized that the risk of a new VFX can be predicted by a biomechanical approach incorporating both spinal loading and vertebral strength. To test this hypothesis we conducted a nested case-control study. We identified new VFX occurring over a mean of 6 years follow-up in the Framingham Heart Study QCT cohort. Cases included those with at least one incident VFX (21 men and 23 women, 50 to 85 yrs). Two controls with no new VFX, matched by age (± 3 yrs) and sex, were selected for each VFX case. We measured spinal curvature and muscle morphology (i.e. cross sectional area and moment arm) at T4-L5 from QCT scans of the trunk, and incorporated these measures, along with subject height and weight, into a validated musculoskeletal model of the thoracolumbar spine (Bruno et al, J Biomech Eng 2015) to predict lumbar vertebral compressive loading for two activities: 1) standing with a 10kg weight in each hand with elbows bent, and 2) 30° of trunk flexion with a 10kg weight in each hand (Figure). We assessed vertebral compressive strength using QCT-based finite element analysis (O.N. Diagnostics, Berkeley, CA), and calculated the factor-of-risk as the ratio between vertebral loading and FEA-estimated strength. Using conditional logistic regression, we found that for both activities, each SD increase in the factor-of-risk significantly increased the risk of incident VFX by about 60% (Table). Adjustment for prevalent VFX did not alter the results. In summary, although limited by a relatively small number of subjects with VFX, this is the first study to demonstrate the feasibility and potential utility of combining vertebral loading estimates derived from sophisticated, subject-specific musculoskeletal models with FEA-derived estimates of vertebral strength to enhance the prediction of VFX risk in older adults.

Table. Association between factor-of-risk and incident VFX for standing and forward flexion with weights.			
	VFX Cases (n=44) (mean ± SD)	Controls (n=88) (mean ± SD)	Odds Ratio (95% CI)*
factor-of-risk – standing with weights	0.31 ± 0.15	0.27 ± 0.10	1.63 (1.05, 2.55), p=0.03
factor-of-risk – flexion with weights	0.30 ± 0.14	0.26 ± 0.08	1.60 (1.04, 2.48), p=0.03

\* per 1 SD increase in factor-of-risk

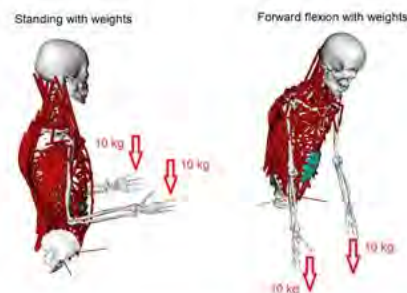


Figure: Two examples of patient-specific musculoskeletal models. Upright standing with 10kg weights in each hand with elbows bent at 90° (left), and 30° of trunk flexion with a 10 kg weight in each hand (right)

Table and Figure

**Disclosures:** Hossein Mokhtarzadeh, None.

## 1022

**Bone Microdamage in Osteoporotic Patients Treated with Bisphosphonates for One to Sixteen Years.** Stefanie Pagano<sup>\*1</sup>, Connie Wood<sup>2</sup>, David Pienkowski<sup>1</sup>, Hartmut Malluche<sup>3</sup>. <sup>1</sup>Department of Biomedical Engineering, University of Kentucky, United states, <sup>2</sup>Department of Statistics, University of Kentucky, United states, <sup>3</sup>Division of Nephrology, Bone & Mineral Metabolism, University of Kentucky, United states

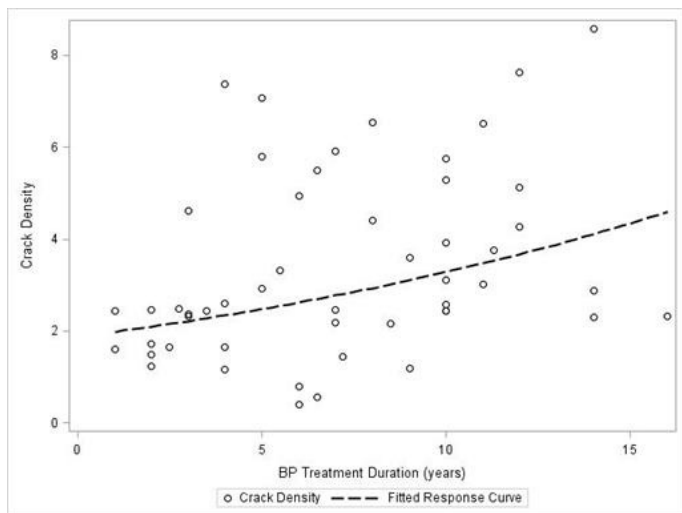
Bone microdamage is a physiologic response to mechanical loading accompanying daily activities. Bone turnover changes alter the rate of microdamage repair, thereby changing the degree of microdamage present. Bisphosphonates (BPs) reduce the rate of bone turnover and thus may affect the degree of microdamage. This study was designed to quantify microdamage in patients with osteoporosis as a function of BP treatment duration.

Anterior iliac crest biopsies were done in 51 Caucasian women (49–87 years) with osteoporosis treated with oral BPs for 1–16 years. Exclusion criteria were: genetic bone diseases, hyperparathyroidism, chronic kidney disease, endocrine diseases, diabetes, history of drug or alcohol abuse, or use of bone metabolism-altering drugs other than oral BPs. Bone samples were sectioned to 100  $\mu$ m, stained with 1% basic fuchsin and examined histomorphometrically by bright field and fluorescent light microscopy. Area of mineralized trabecular bone, crack length and number were measured. Data were analyzed by analysis of covariance. Covariates included bone turnover, age, trabecular bone volume (BV/TV), and trabecular thickness.

Microcrack density, i.e., crack number per mineralized bone area, increased exponentially ( $p=0.019$ ) with the duration of BP treatment (Figure). Microcrack length was not significantly related to the duration of BP treatment. None of the studied covariates were significantly related to microcrack density or length.

This study, with its large sample size and wide range of BP treatment duration in human bone, demonstrates the novel observation of an exponential relationship between microcrack density and BP treatment duration. The present results are in keeping with and expand upon previous results obtained in dogs treated with oral BPs for 1 or 3 years and results obtained in humans comparing bone from untreated osteoporotic patients to group of patients treated with BPs for an average of 5.3 years.

Clinical significance of the present findings awaits additional work relating the degree of microdamage to the load-bearing properties of bone.



Analysis of Bisphosphonate Treatment Duration on Accumulation Microcrack Density

*Disclosures: Stefanie Pagano, None.*

## 1023

**Effects of Type 2 Diabetes on Nanoscale and Whole-Bone Biomechanical Properties.** Claire Acevedo<sup>\*1</sup>, Meghan Sylvia<sup>1</sup>, Eric Schaible<sup>2</sup>, Bernd Gludovatz<sup>2</sup>, Lionel N. Metz<sup>1</sup>, James L. Graham<sup>3</sup>, Robert O. Ritchie<sup>4</sup>, Tamara N. Alliston<sup>1</sup>, Peter J. Havel<sup>3</sup>, Aaron J. Fields<sup>1</sup>. <sup>1</sup>UCSF, United states, <sup>2</sup>LBNL, United states, <sup>3</sup>UC Davis, United states, <sup>4</sup>LBNL, UC Berkeley, United states

Fragility fractures in adults cause significant morbidity and societal expense. Adults with type 2 diabetes (T2D) have a higher fracture risk despite normal or elevated BMD. The fact that diabetic bone is more prone to fracture for a given BMD suggests there are important effects of T2D on bone quality. Here we sought to

determine the effects of T2D on two aspects of bone quality — tissue material properties and bone geometry/microarchitecture — and to assess their relative roles in whole-bone biomechanical behavior.

Ulnae and L4 vertebrae were harvested from 6-month-old lean Sprague Dawley rats and diabetic obese UCD-T2DM rats (diabetic for  $69 \pm 7$  days). Mineralized fibril strain and tissue strain during tensile loading were measured using small-angle X-ray scattering (SAXS) at the Advanced Light Source (LBNL). Collagen cross-linking was determined using a fluorimetric assay. Bone geometry, microarchitecture, and tissue mineralization were characterized with  $\mu$ CT imaging. Bone strength was measured using 3 point-bend tests (ulnae) and compression tests (vertebrae). We explored the role of tissue material properties in whole bone biomechanical behavior using high-resolution finite element modeling.

As shown in the table below, T2D degraded the tensile properties of the mineralized collagen fibrils, reducing collagen fibril strain by 50%. This finding was consistent with increased collagen cross-linking observed in the ulnae of diabetic rats. T2D also caused dramatic deficits in bone geometry and microarchitecture, and small but significant reductions in tissue mineralization. At the whole-bone level, T2D reduced strength per unit bone mass; these reductions were primarily related to the differences in bone geometry and microarchitecture. The findings indicate the T2D compromises nanoscale and whole-bone biomechanical properties. These preliminary studies will allow us to develop diagnostic and therapeutic targets for diabetic bone fragility.

	Lean Sprague Dawley (n = 4-6 rats)	Diabetic obese (n = 4-6 rats)	% change	P value
Ultimate mineralized fibril strain	0.53	0.32	-39.6	0.044
AGEs (ng fluorescence/ $\mu$ g collagen)	$2.08 \pm 0.17$	$2.65 \pm 0.19$	27.4	0.009
Cross-sectional MOI (mm <sup>4</sup> )	$0.255 \pm 0.037$	$0.240 \pm 0.050$	-5.9	0.6496
Vertebral bone mass (mg)	$17.4 \pm 3.5$	$19.1 \pm 2.6$	9.8	0.4105
BV/TV	$0.29 \pm 0.02$	$0.20 \pm 0.03$	-31.0	0.0029
Tb.Th (mm)	$0.083 \pm 0.003$	$0.073 \pm 0.006$	-12.0	< 0.001
Tb.Sp (mm)	$0.271 \pm 0.02$	$0.304 \pm 0.03$	12.2	0.0042
SMI	$-0.05 \pm 0.07$	$0.99 \pm 0.07$	208.0	< 0.001
DA	$1.76 \pm 0.04$	$1.81 \pm 0.041$	2.8	0.04
Cl.TMD (mg HA/cc)	$1293 \pm 23$	$1234 \pm 15$	-4.8	0.001
Tb.TMD (mg HA/cc)	$1216 \pm 16$	$1191 \pm 10$	-2.1	0.016
Vertebral strength/bone mass (N/mg)	$19.25 \pm 1.80$	$13.91 \pm 1.77$	-27.7	0.0004

Table 1

*Disclosures: Claire Acevedo, None.*

## 1024

**Effects of Romosozumab on Remodeling and Bone Strength at the Distal Radius in Ovariectomized Cynomolgus Monkeys.** Michael Ominsky<sup>\*1</sup>, Steven Boyd<sup>2</sup>, Aurore Varela<sup>3</sup>, Jacquelin Jolette<sup>3</sup>, Nancy Doyle<sup>3</sup>, Susan Smith<sup>3</sup>, Kathrin Locher<sup>1</sup>, Sabina Buntich<sup>1</sup>, Rogely Boyce<sup>1</sup>. <sup>1</sup>Amgen Inc., United states, <sup>2</sup>University of Calgary, Canada, <sup>3</sup>Charles River Laboratories Montreal, Canada

Romosozumab (Romo) administration for 12 months was previously shown to improve bone mass and strength at the spine and femur neck in ovariectomized (OVX) cynomolgus monkeys (cynos). Treatment effects at the distal radius were less prominent, with overall increases in bone mineral content (BMC) by pQCT despite transient decreases in cortical BMD that were greatest at month 6. To further characterize the effects at month 6, radial bone strength and histomorphometry were performed in romosozumab-treated OVX cynos. Four months after OVX, 9+ years-old cynos were administered vehicle (Veh, n=12) or 3 mg/kg Romo (n=19) QW SC for 26 weeks. High resolution pQCT (HR-pQCT; Scanco Medical, XtremeCT II) was performed at the right radius metaphysis and diaphysis prior to treatment and at 12 and 25 weeks, with adapted image registration across timepoints to ensure consistent anatomical placement. Strength was assessed at the radial diaphysis (3-point bending) and metaphysis (axial compression) by mechanical testing and finite element (FE) analysis. A series of fluorochrome labels was administered during the study to determine the temporal effects of treatment on intracortical activation at the radial diaphysis by histomorphometry.

By HR-pQCT, cortical tissue BMD was significantly decreased in the radial diaphysis and metaphysis at week 25 with Romo. These changes were consistent with an increase in the activation of intracortical remodeling in the radial diaphysis, without a corresponding increase in cortical porosity by histomorphometry. Romo significantly increased bone area at the radial metaphysis and to a lesser extent at the diaphysis compared to OVX controls (Table). Relative to controls, strength was significantly improved at the radial metaphysis based on yield load by mechanical testing (+13% after accounting for baseline BMC as a covariate) and FE analysis (as % change from baseline at week 25). At the radial diaphysis, Romo did not significantly affect strength by either method. Yield load correlated well between mechanical testing and FE analysis across groups with  $r^2 = 0.63$  and  $0.76$  at the metaphysis and diaphysis, respectively.

These results demonstrate that romosozumab maintained diaphyseal strength and improved metaphyseal strength of the radius of OVX cynomolgus monkeys relative to controls. These effects were associated with increases in cortical bone area that compensated for temporal increases in intracortical remodeling and decreases in cortical BMD.

**Table: %Change in HR-pQCT and FE Strength at the Distal Radius at Week 25**

Scanned Site	Radial Metaphysis		Radial Diaphysis	
	Vehicle	Romosozumab	Vehicle	Romosozumab
Total Area	-1.07 ± 0.54	2.72 ± 1.73	-1.10 ± 0.38	0.71 ± 0.43**
Bone Area	-4.47 ± 1.12	4.77 ± 2.53**	-1.97 ± 0.65	1.66 ± 0.76**
Cortical Tissue BMD	-2.54 ± 0.45	-4.07 ± 0.39*	-3.01 ± 0.49	-4.88 ± 0.56*
Estimated Yield Load	-6.32 ± 2.02	-3.95 ± 2.57**	-1.78 ± 1.63	0.88 ± 1.16

Data: Mean ± SEM as % Change from Baseline at Week 25. \*p<0.05, \*\*p<0.01 vs Vehicle

Table

**Disclosures:** Michael Ominsky, Amgen Inc, 15

This study received funding from: Amgen Inc, UCB Pharma

## 1025

### Regulatory Mechanisms Underlying *Ihh* Transcription in Chondrocytes.

Akira Yamakawa<sup>\*1</sup>, Ung-il Chung<sup>2</sup>, Shinsuke Ohba<sup>2</sup>. <sup>1</sup>Division of Clinical Biotechnology, Center for Disease Biology & Integrative Medicine, Faculty of Medicine, The University of Tokyo, Japan, <sup>2</sup>Department of Bioengineering, School of Engineering, The University of Tokyo, Japan

The gene Indian hedgehog (*Ihh*), expressed in prehypertrophic and hypertrophic chondrocytes, is indispensable for the specification of osteoblast lineages in endochondral ossification. The regulatory mechanisms underlying *Ihh* transcription in chondrocytes are not established. Here we aimed to clarify the regulation of *Ihh* expression in chondrocytes by a genome-wide approach. We first obtained chromatin immunoprecipitation sequencing (ChIP-seq) data for histone modification (H3K36me3 and H3K4me2), Sox9, and Runx2 in mouse P1 rib chondrocytes. H3K36me3 peaks (transcribed regions) were observed in the *Ihh* gene region. We identified five H3K4me2 peaks (putative enhancer regions) upstream of the *Ihh* gene region. They are referred to as A, B, C, D, and E in order from distal to proximal. These peak regions were shared with four Sox9 peaks (A, B, D, and E) and two Runx2 peaks (A, B). We next checked the enhancer activities of the five H3K4me2+ regions by performing *in vitro* reporter assays. We transfected luciferase reporter constructs into which each of the regions was cloned with a mouse *Ihh* promoter (-105 bp to +58 bp) in mouse primary rib chondrocytes, ATDC5 cells, and NIH3T3 cells. At 48 hr after transfection, we analyzed the luciferase activities normalized by Renilla luciferase activity. Regions A and D only showed strong enhancer activities in the mouse primary rib chondrocytes. The endogenous *Ihh* expression levels were correlated with the reporter activity of regions A and D in the three cell types tested. Regions A and D were also responsive to a Sox trio (Sox5, Sox6, and Sox9) and Runx2, but in different manners, which was supported by the presence of Sox9 and Runx2 peaks in our ChIP-seq data. Reporter assays using constructs with various combinations of the five enhancers revealed that region E worked as a suppressor in the enhancer network. Lastly, we assessed the enhancer activity of region A *in vivo* using *lacZ* reporter transgenic mouse lines that had four copies of region A together with the mouse *Ihh* promoter upstream of *lacZ*. Beta-galactosidase activity was observed exclusively in growth plate chondrocytes in forelimbs at embryonic day (E)14.5, suggesting that region A works as a chondrocyte-specific enhancer *in vivo*. *Ihh* expression is thus likely controlled by multiple enhancers, each with distinct regulatory roles. This study is an important first step in identifying the regulatory landscape for *Ihh* expression in the developing skeleton.

**Disclosures:** Akira Yamakawa, None.

## 1026

### Histone Deacetylase 3 Supports Endochondral Bone Formation by Controlling Cytokine Signaling and Matrix Remodeling.

Lomeli Carpio<sup>\*1</sup>, Elizabeth Bradley<sup>1</sup>, Meghan McGee-Lawrence<sup>2</sup>, Megan Weivoda<sup>1</sup>, Daniel Poston<sup>3</sup>, Amel Dudakovic<sup>1</sup>, Ming Xu<sup>1</sup>, Tamar Tchkonina<sup>1</sup>, James Kirkland<sup>1</sup>, Andre van Wijnen<sup>1</sup>, Merry Jo Oursler<sup>1</sup>, Jennifer Westendorf<sup>1</sup>. <sup>1</sup>Mayo Clinic, United states, <sup>2</sup>Augusta University, United states, <sup>3</sup>Creighton University, United states

Histone deacetylase (Hdac) inhibitors are epigenetic therapies for cancer, and are emerging treatments for arthritis, epilepsy and other diseases; however, these drugs inhibit multiple Hdacs and have detrimental effects on the pre- and post-natal skeleton. Several Hdacs contribute to endochondral bone formation. In this study, we defined the cell autonomous role of Hdac3 in chondrocyte maturation by deleting it in type II collagen alpha 1 (Col2a1) expressing chondrocytes. While embryonic deletion of Hdac3 with Col2a1-Cre did not produce viable mice, postnatal deletion of Hdac3 with an inducible Col2a1-Cre model (Hdac3-CKO<sub>Col2ERT</sub>) delayed secondary ossification center formation, altered hypertrophic cartilage maturation in the growth plate and increased

osteoclast activity in the primary spongiosa at 4 weeks-of-age. By 8 weeks, these animals had compromised bone architecture, with significant decreases in trabecular bone and reduced long bone length. Hdac3-depleted immature mouse chondrocyte micromass cultures expressed higher levels of cytokines and matrix degrading genes (e.g. Il-6, Mmp3, Mmp13, Saa3) and lower levels of genes related to extracellular matrix production, bone development, and ossification (e.g. Acan, Col2a1, Ihh, Col10a1). Histone acetylation was increased in and around the genes with elevated expression. NF-κB was also hyperacetylated and activated with Hdac3 deficiency. Increased cytokine signaling led to autocrine activation of Jak/Stat and NF-κB pathways, suppressed chondrocyte maturation, and stimulated paracrine activation of osteoclasts. Blockade of Il-6/Jak/Stat, NF-κB signaling, or the bromodomain extra terminal (BET) family of proteins that recognize acetylated histones and promote transcriptional elongation significantly reduced the inflammatory responses and Mmp expression in Hdac3-deficient chondrocytes as well as secondary osteoclast activation *in vitro*. Finally, treating 6 week old Hdac3-CKO<sub>Col2ERT</sub> mice with the Jak inhibitor, Ruxolitinib, daily for 2 weeks restored trabecular bone volume, femur length, and reduced osteoclast activity in the primary spongiosa. Altogether, these results indicate that Hdac3 controls the temporal and spatial regulation of gene expression and downstream signaling factors in chondrocyte maturation to ensure proper ossification during long bone development.

**Disclosures:** Lomeli Carpio, None.

## 1027

### Analysis of cellular dynamics revealed stem cell niche formation in the postnatal epiphyseal growth plate.

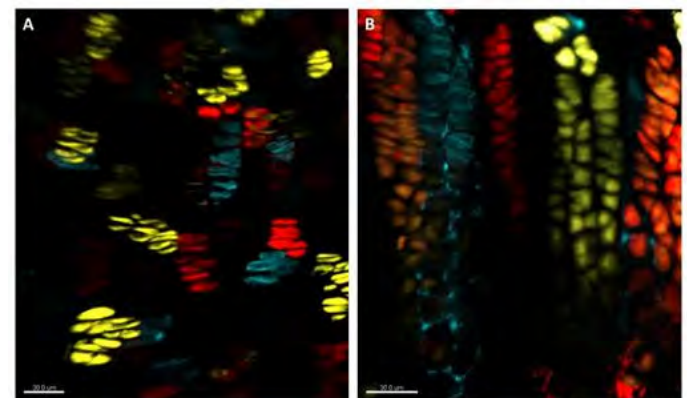
Phillip Newton<sup>\*1</sup>, Simon Suter<sup>2</sup>, Xiaoyan Sun<sup>2</sup>, Lei Li<sup>2</sup>, Meng Xie<sup>2</sup>, Igor Adameyko<sup>2</sup>, Lars Säwendahl<sup>3</sup>, Maria Kasper<sup>2</sup>, Andrei Chagin<sup>2</sup>. <sup>1</sup>Karolinska Institute & Karolinska University Hospital, Sweden, <sup>2</sup>Karolinska Institute, Sweden, <sup>3</sup>Karolinska University Hospital, Sweden

The epiphyseal growth plate can morphologically be separated into three zones, the resting zone with round cells, the proliferative zone with flat columnar chondrocytes, which further differentiate and form the hypertrophic zone with enlarged chondrocytes. It is generally accepted that during longitudinal bone growth flat chondrocytes in the epiphyseal growth plate originate from the resting zone chondrocytes, which are also called stem-like chondrocytes. However, the origin, behaviour and regulation of these resting chondrocytes remain largely unknown.

We employed clonal genetic tracing to gain an insight into the cellular dynamics of the resting cells. Specifically, we crossed the inducible cartilage specific Col2-CreERT strain with Confetti reporter strain, which upon Cre-recombination generates one of four different fluorescent proteins in a stochastic manner. All progeny retain the same colour allowing clonal visualization.

Firstly, this clonal tracing confirmed that flat chondrocytes originate from the resting chondrocytes. However, completely to our surprise, full-growth-plate-thickness large clones (exceeding 20 cells/clone) were formed only at postnatal age, whereas during fetal and early postnatal growth small clones (4-9 cells) were formed. Direct comparison of clonal formation during 10 days chase period started either at P0 or P30 revealed that in young mice only 21.8 % of cells were in clones greater than 10 cells, compared with 74.3% in older mice (p=0.0035). This is in contrast to our expectations as both proliferation and growth rate decrease with age. Detailed analysis of the proliferation rate employing H2B-GFP-retaining mouse strain, and EdU retention, combined with Confetti mice revealed that during fetal and early postnatal growth, round cells are directly recruited into proliferation layer thereby depleting the zone, whereas at later stages, the round cells, which have remained after the formation of the secondary ossification centre, acquire a capacity to renew themselves. This renewal allows generation of large clones, often exceeding 50 cells/clone as visualized by blocking resorption of hypertrophic chondrocytes with a VEGF receptor inhibitor.

Thus, our data suggest that the growth program is changed with age shifting from consumption of the resting cells (fetal program) to their renewal (postnatal program). The development of this self-renewal leads us to conclude that a stem cell niche is formed in postnatal epiphyseal plates.



Clonal tracing of fetal (A) and postnatal (B) growth. Scale bar = 30 μm

Col2-CreERT Confetti tracing in growth plate cartilage

**Disclosures:** Phillip Newton, None.

## 1028

**Conditional Deletion of the *Phd2* Gene in Chondrocytes Produces Defects in Articular Cartilage Development and an Osteoarthritis-like Phenotype in Mice.** Shaohong Cheng\*, Patrick Agahjanian, Sheila Pourteymoor, Catrina Alarcon, Subburaman Mohan. VA Loma Linda Healthcare System, United states

Our recent studies have shown that prolyl hydroxylase domain-containing protein (PHD)2, expressed in chondrocytes, plays a critical role in the regulation of chondrocyte differentiation and endochondral bone formation. Based on this finding and the prevailing idea that hypertrophy and terminal differentiation of chondrocytes contribute to calcification of articular cartilage and ossification that are underlying features of osteoarthritis (OA), we tested the hypothesis that dysregulation of PHD2 in articular chondrocytes contributes to the pathogenesis of OA by influencing chondrocyte differentiation. Immunohistochemistry (IHC) studies revealed high expression of PHD2 in the superficial zone (SZ) while PHD3 expression was seen mainly in the middle and deep zones. PHD1 expression was ubiquitous. Conditional disruption of the *Phd2* gene in floxed mice using Col2 $\alpha$ 1-Cre increased HIF1 $\alpha$  (a target of PHD2) and PHD3 (a target of HIF1 $\alpha$ ) levels in the SZ. In contrast, expression of HIF2 $\alpha$  (a target of PHD3) was decreased in the middle and deep zones. Histological analyses of knee joints revealed that at 4 weeks of age, SZ thickness was reduced by 25% ( $P < 0.001$ ) while the thickness of middle/deep zones containing differentiating chondrocytes was increased by 31% ( $P < 0.001$ ) in the *Phd2* conditional knockout (cKO) mice. At 12 weeks of age, OARSI scores were significantly higher ( $2.0 \pm 0.21$  vs.  $0.54 \pm 0.17$ ,  $P < 0.001$ ) while SZ thickness was 23% lower ( $P < 0.05$ ) in the *Phd2* cKO mice. IHC studies revealed reduced expression of articular cartilage markers (*Prg4*, *Chu*) but increased expression of markers of hypertrophic chondrocytes (*Col10*, *Mmp13*) in the *Phd2* cKO mice. To determine the mechanism for PHD2 regulation of articular chondrocyte differentiation, primary cultures of articular chondrocytes were treated with a PHD2 inhibitor, IOX2, for 72h prior to gene and protein expression measurements. PHD2 inhibition caused significant increases in the expression of markers of chondrocyte differentiation but decreased expression of articular cartilage markers. Western blot analysis revealed increased nuclear levels of HIF1 $\alpha$  but decreased levels of HIF2 $\alpha$  in IOX2-treated cultures. Based on these data, we propose that *Phd2* expression in articular progenitors is essential for maintenance of the articular cartilage phenotype and that disruption of PHD2 signaling results in an OA-like phenotype caused by promotion of differentiation of articular cartilage progenitors.

Disclosures: Shaohong Cheng, None.

## 1029

**Novel Genetic Variants are Associated with Increased Vertebral Volumetric BMD, Reduced Vertebral Fracture Risk, and Increased Expression of *SCLIA3* and *EPHB2*.** Carrie Nielson\*, Ching-Ti Liu<sup>2</sup>, Albert Smith<sup>3</sup>, Cheryl Ackert-Bicknell<sup>4</sup>, Sjur Reppe<sup>5</sup>, Johanna Jakobsdottir<sup>3</sup>, Christina Wassel<sup>6</sup>, Thomas Register<sup>7</sup>, Ling Oei<sup>8</sup>, Nerea Alonso Lopez<sup>9</sup>, Edwin Oei<sup>8</sup>, Neeta Parimi<sup>10</sup>, Elizabeth Samelson<sup>11</sup>, Mike Nalls<sup>12</sup>, Joseph Zmuda<sup>13</sup>, Thomas Lang<sup>14</sup>, Mary Bouxsein<sup>11</sup>, Jeanne Latourelle<sup>15</sup>, Melina Claussnitzer<sup>11</sup>, Kristin Siggeirsdottir<sup>3</sup>, Priya Srikanth<sup>1</sup>, Erik Lorentzen<sup>16</sup>, Liesbeth Vandenput<sup>16</sup>, Carl Langefeld<sup>7</sup>, Laura Raffield<sup>7</sup>, Greg Terry<sup>7</sup>, Amanda Cox<sup>7</sup>, Matthew Allison<sup>17</sup>, Michael Ciriui<sup>17</sup>, Donald Bowden<sup>7</sup>, M. Arfan Ikram<sup>8</sup>, Dan Mellström<sup>16</sup>, Magnus Karlsson<sup>18</sup>, Jeffrey Carr<sup>19</sup>, Matthew Budoff<sup>20</sup>, Caroline Phillips<sup>21</sup>, L. Adrienne Cupples<sup>2</sup>, Wen-Chi Chou<sup>22</sup>, Richard Myers<sup>23</sup>, Stuart Ralston<sup>9</sup>, Kaare Gautvik<sup>5</sup>, Peggy Cawthon<sup>10</sup>, Steve Cummings<sup>10</sup>, David Karasik<sup>11</sup>, Fernando Rivadeneira<sup>8</sup>, Vilmundur Gudnason<sup>3</sup>, Eric Orwoll<sup>1</sup>, Tamara Harris<sup>21</sup>, Claes Ohlsson<sup>16</sup>, Douglas Kiel<sup>11</sup>, Yi-Hsiang Hsu<sup>11</sup>. <sup>1</sup>Oregon Health & Science University, United states, <sup>2</sup>Boston University School of Public Health, United states, <sup>3</sup>Icelandic Heart Association, Iceland, <sup>4</sup>University of Rochester Medical Center, United states, <sup>5</sup>Lovisenberg Diakonale Hospital, Norway, <sup>6</sup>University of Vermont College of Medicine, United states, <sup>7</sup>Wake Forest School of Medicine, United states, <sup>8</sup>Erasmus MC, University Medical Center, Netherlands, <sup>9</sup>University of Edinburgh, United Kingdom, <sup>10</sup>California Pacific Medical Center Research Institute, United states, <sup>11</sup>Harvard Medical School, United states, <sup>12</sup>National Institutes of Health, United states, <sup>13</sup>University of Pittsburgh, United states, <sup>14</sup>University of California, San Francisco, United states, <sup>15</sup>Boston University School of Medicine, United states, <sup>16</sup>University of Gothenburg, Sweden, <sup>17</sup>University of California, San Diego, United states, <sup>18</sup>Lund University, Sweden, <sup>19</sup>Vanderbilt, United states, <sup>20</sup>Los Angeles Biomedical Research Institute, United states, <sup>21</sup>National Institute on Aging, United states, <sup>22</sup>BROAD Institute of MIT & Harvard, United states, <sup>23</sup>Boston University School of Medicine, United states

Genome-wide association studies (GWAS) have revealed numerous loci associated with DXA-measured hip and spine areal bone mineral density (aBMD). We completed the first GWAS meta-analysis (N=15,275) of lumbar spine volumetric BMD (vBMD) measured by quantitative computed tomography (QCT), allowing for the unique examination of the trabecular bone compartment. SNPs that were significantly associated

with vBMD were also examined in two GWAS meta-analyses of cohorts of older adults to determine associations with morphometric vertebral fracture (N=21,701) and clinical vertebral fracture (N=5,893). Expression QTL analyses of human iliac crest biopsies were performed in a sample of 84 postmenopausal women, and the murine osteoblast expression of genes implicated by eQTL or by proximity to vBMD-associated SNPs was examined. We identified significant vBMD associations with five loci, including variants near 3 loci reported in hip and lumbar spine aBMD GWAS (1p36.12, containing *WNT4* and *ZBTB40*; 8q24, containing *TNFRSF11B*; and 13q14, containing *AKAP11* and *TNFRSF11*). Two loci (5p13 and 1p36.12) also contained associations with radiographic and clinical vertebral fracture, respectively. The minor allele of the most significant variant in 5p13 (rs2468531; minor allele frequency [MAF]=3%), which has not previously been linked to BMD or fracture, was associated with higher vBMD ( $\beta = 0.22$ ,  $p = 1.9 \times 10^{-8}$ ) and decreased risk of radiographic vertebral fracture (OR = 0.76; false discovery rate [FDR]  $p = 0.01$ ). The minor allele of the most significant variant in 1p36.12 (rs12742784; MAF=21%) was associated with higher vBMD ( $\beta = 0.09$ ,  $p = 1.2 \times 10^{-10}$ ) and decreased risk of clinical vertebral fracture (OR = 0.79; FDR  $p = 8.6 \times 10^{-4}$ ). Both SNPs are located in the non-coding part of the genome and were associated with increased mRNA expression levels in human bone biopsies: rs2468531 with *SCLIA3* ( $\beta = 0.28$ , FDR  $p = 0.01$ , involved in glutamate signaling and osteogenic response to mechanical loading) and rs12742784 with *EPHB2* ( $\beta = 0.12$ , FDR  $p = 1.7 \times 10^{-3}$ , functions in bone-related ephrin signaling). Both genes are expressed in murine osteoblasts. This is the first study to link *SCLIA3* and *EPHB2* to clinically relevant vertebral osteoporosis phenotypes in older adults. These results may aid in elucidating vertebral bone biology, leading to novel approaches to reducing vertebral fracture incidence.

Disclosures: Carrie Nielson, None.

## 1030

**Menopausal Bone Loss Is Mainly Cortical, not Trabecular, and Does not Attenuate the Heritable Component of Variance in this Microarchitecture: a Prospective Study of Twins.** Åshild Bjørnerem<sup>1</sup>, Xiao-Fang Wang<sup>2</sup>, Minh Bui<sup>3</sup>, Ali Ghasem-Zadeh<sup>2</sup>, Roger Zebaze<sup>2</sup>, John L Hopper<sup>3</sup>, Ego Seeman<sup>\*2</sup>. <sup>1</sup>Department of Health & Care Sciences, UiT – The Arctic University of Norway, Tromsø, Norway, <sup>2</sup>Departments of Endocrinology & Medicine, Austin Health, University of Melbourne, Australia, <sup>3</sup>Centre for Epidemiology & Biostatistics, School of Population & Global Health, University of Melbourne, Australia

Introduction The population variances in trabecular and cortical microstructure are largely heritable. At menopause or shortly before, the rate of remodeling increases, more in trabecular than cortical bone so structural decay proceeds differently in the two compartments. As 80 percent of the skeleton is cortical, we hypothesized that cortical bone loss accounts for most bone loss and the differing rates of loss attenuate the heritability of bone microstructure.

Methods We prospectively quantified distal radial and distal tibial microstructure using high-resolution peripheral quantitative computed tomography (Scanco Medical and StrAx1.0 software) during 3.1 years (range 1.5-4.5) in 199 monozygotic and 125 dizygotic twin pairs aged 25-75 years at baseline in Melbourne, Australia.

Results Heritable factors accounted for ~80% of the variance in microstructure both before and after menopause, but not the variances in the amounts of bone lost during menopause (Tables 1 and 2). During the follow up, the annualized increase in distal tibial total cortical porosity was 0.44% in 180 women remaining premenopausal; 0.80% in 56 women transitioning from pre- to peri-menopause; 1.40% in 34 women transitioning from peri- to postmenopause; 0.83% in 118 women remaining postmenopausal (all  $p < 0.001$ ). Loss of trabecular BV/TV were -0.17%, -0.25% -0.31% and -0.16% in the respective groups (all  $p < 0.001$ ). Of the mean total bone loss of 207 mg from the distal tibia, 74% was cortical and 26% was trabecular. Of this bone loss, 94% occurred during and after menopause and only 6% occurred before menopause. Similar results were found at the distal radius.

Conclusion Over 90 percent of bone lost during advancing age occurs during and after menopause. Of this, most is cortical. Genetic factors account for the diversity in microstructural before and after menopause, but microstructural deterioration during menopause is non heritable.

Table 1. Correlation for MZ and DZ twins, and heritability, at the baseline and follow-up.

	Baseline				Follow-up			
	MZ correlation N = 110 pairs		DZ correlation N = 63 pairs		MZ correlation N = 110 pairs		DZ correlation N = 63 pairs	
	Est	95%CI	Est	95%CI	Est	95%CI	Est	95%CI
Distal Tibia								
Cortical porosity	0.83	(0.53, 0.95)	0.47	(0.22, 0.66)	0.73	± 0.18	0.81	(0.54, 0.93)
Trabecular BV/TV	0.72	(0.48, 0.85)	0.49	(0.24, 0.68)	0.45	± 0.18	0.69	(0.47, 0.83)
							0.43	(0.18, 0.63)
								0.53 ± 0.19

Table 2. Heritability of trait change.

	Genetic correlation		Phenotypic correlation		Change	
	$r_g$	p-value	$r_p$	MZ correlation	DZ correlation	Heritability $h^2 \pm se$
Distal Tibia						
Cortical porosity	0.972 ± 0.025	0.1283	0.924 (0.907, 0.938)	0.26	0.23	0.06 ± 0.28
Trabecular BV/TV	0.981 ± 0.029	0.2449	0.905 (0.884, 0.923)	0.47	0.44	0.06 ± 0.23

Phenotypic correlation is the correlation between the trait at the base line and at the follow-up, adjust for age, weight and height. Genetic correlation ( $r_g$ ) is the correlation due to genetic factors. Under null hypothesis that  $r_g = 1$ , the p-value > 0.05 imply the same set of gene overlap (so call genetic stability, i.e. genetic factors do not affect change), otherwise ( $p < 0.05$ ) imply a genetic factor.

Tables

Disclosures: Ego Seeman, StrAxImages, 15

## 1031

**A Genome-wide Association Study in Adult Caucasians Identifies Novel Loci and Functional Coding Variants Associated with Bone Microarchitecture Assessed by HR-pQCT.** Yi-Hsiang Hsu<sup>1</sup>, Elizabeth J Atkinson<sup>2</sup>, Frederick Kinuya Kamanu<sup>3</sup>, Roby Joehanes<sup>4</sup>, Kerry Broe<sup>3</sup>, L. Adrienne Cupples<sup>5</sup>, Ching-Ti Liu<sup>6</sup>, Serkalem Demissie<sup>5</sup>, David Karasik<sup>3</sup>, Steve K. Boyd<sup>7</sup>, Mary L Bouxsein<sup>8</sup>, Shreyasee Amin<sup>2</sup>, Sundeep Khosla<sup>2</sup>, Douglas P. Kiel<sup>4</sup>.  
<sup>1</sup>Harvard Medical School & HSL Institute for Aging Research, United states, <sup>2</sup>Mayo Clinic, United states, <sup>3</sup>Hebrew SeniorLife Institute for Aging Research, United states, <sup>4</sup>Hebrew SeniorLife Institute for Aging Research & Harvard Medical School, United states, <sup>5</sup>Depart. Biostat., Sch. Public Health, Boston Univ., United states, <sup>6</sup>Depart. Biostat., Sch. Public Health, Boston Univ., United states, <sup>7</sup>University of Calgary, Canada, <sup>8</sup>Beth Israel Deaconess Medical Center & Harvard Medical School, United states

Bone microarchitecture assessed by high resolution peripheral quantitative computed tomography (HR-pQCT) has been reported to be heritable even after adjusting for areal BMD (aBMD), and has been associated with risks of fragility fractures, suggesting that genetic studies of these phenotypes may reveal unique, novel genes that contribute to skeletal integrity, which may not be identified in previous genome-wide association studies (GWAS) of aBMD.

We performed a GWAS (testing both rarer functional variants and common variants) in the Framingham Heart Study (FHS, N=1,365, F=57%) and in a Mayo Clinic Study (MAYO, N=928, F=67%) on HR-pQCT measured trabecular density (TbD,  $\mu\text{g}/\text{cm}^3$ ), trabecular number (TbN,  $\text{mm}^{-1}$ ), cortical volumetric BMD (CtBMD,  $\text{g}/\text{cm}^3$ ), cortical thickness (CtTh,  $\mu\text{m}$ ), and failure load from  $\mu\text{FEA}$  ( $\mu\text{FEA-FL}$ ) at the distal radius and tibia. All measures were obtained from the XTreme CT (Scanco Medical AG). Both studies were genotyped by high-density SNP chips with common and rarer variants across the whole genome as well as functional variants (exome-chip) in coding sequences. Whole genome imputation was performed based on Caucasian haplotype references. Single SNP-phenotype association analyses used a linear regression model in MAYO and a linear mixed-effect regression model for family-based FHS. Additive genetic effect models were adjusted for age, sex, weight and ancestral genetic background. Meta-analysis was done to combine association results from FHS and MAYO. For relatively rare variants (MAF < 1%), we performed gene-based burden tests by the Optimal SKAT test in each study and meta-analyzed results by the seqMeta.

Several genome-wide significant associations ( $p < 5 \times 10^{-8}$ ) were identified in the *CPEDI-WNT16* gene locus (associated with  $\mu\text{FEA-FL}$  and CtBMD at radius and tibia), *PLXNA2* (TbD and  $\mu\text{FEA-FL}$  at distal radius), *ADGRB1* (CtBMD and TbD at distal tibia), *ORS5B3* (CtBMD and  $\mu\text{FEA-FL}$  at distal tibia) as well as 5 additional loci associated with a single measurement. For TbN and CtTh, only suggestive associations ( $p < 5 \times 10^{-6}$ ) were found as were for gene-based burden tests. Other than the *CPEDI-WNT16* locus, our GWAS findings are novel and not previously reported in aBMD GWAS, suggesting that the genetic control of bone microarchitecture may provide additional insights into the pathogenesis of bone fragility not available from aBMD. Meta-analyses in ~6,500 HR-pQCT phenotyped adult Caucasians with replication in additional 3,000 samples is underway.

**Disclosures:** Yi-Hsiang Hsu, None.

## 1032

**Prediction of Fragility Fracture Risk by Genetic Profiling.** Thao P. Ho-Le<sup>1</sup>, Jacqueline R. Center<sup>2</sup>, John A. Eisman<sup>3</sup>, Hung T. Nguyen<sup>4</sup>, Tuan V. Nguyen<sup>5</sup>.  
<sup>1</sup>Centre for Health Technologies, University of Technology, Sydney, Australia, <sup>2</sup>Bone Biology Division, Garvan Institute of Medical Research; St Vincent Clinical School, UNSW Australia, Australia, <sup>3</sup>Bone Biology Division, Garvan Institute of Medical Research; St Vincent Clinical School, UNSW Australia; Notre Dame University School of Medicine, Australia, Australia, <sup>4</sup>Centre for Health Technologies, University of Technology, Australia, <sup>5</sup>Centre for Health Technologies, University of Technology, Sydney; Bone Biology Division, Garvan Institute of Medical Research; School of Public Health & Community Medicine, UNSW Australia, Australia

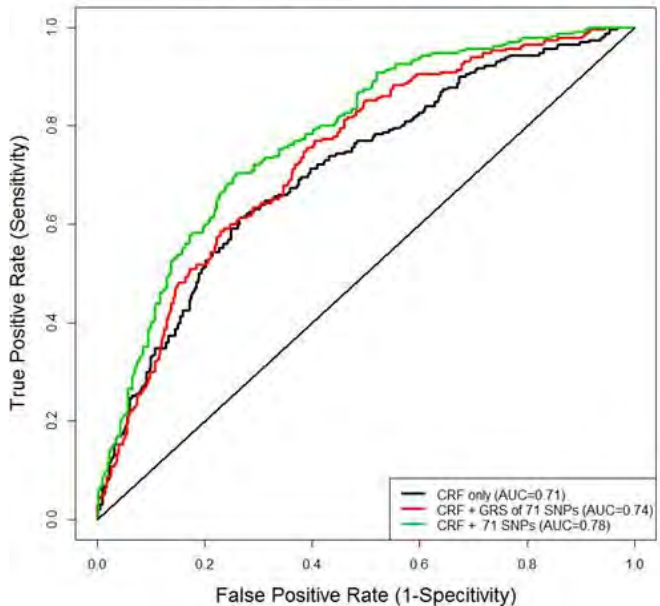
**Aim:** Several common genetic variants associated with bone mineral density (BMD) have been identified by genome-wide association studies. However, the contribution of these variants to fracture prediction remains largely unknown. This study sought to define the predictive value of a genetic profiling in fracture prediction.

**Methods:** Seventy-one BMD-associated genetic variants were genotyped in 556 men and 902 women aged from 60 years who were participants of the Dubbo Osteoporosis Epidemiology Study. A genetic risk score (GRS) was constructed for each individual by summing the weighted number of risk alleles for each SNP, with the weight being log odds ratio. The incidence of fragility fracture was ascertained from X-ray reports between 1990 and 2009. Femoral neck BMD was measured by dual-energy X-ray absorptiometry. The magnitude of association between GRS and fracture risk was assessed by the logistic regression model with and without clinical risk factors. The utility of GRS was assessed in terms of area under the ROC curve (AUC) and integrated reclassification index (NRI).

**Results:** Individuals with a fracture had greater GRS than those without a fracture ( $P < 0.001$ ). The odds of fracture was increased by 47% (odds ratio [OR] 1.47; 95%CI, 1.28-1.69) for each score increase in GRS. After adjusting for age, gender, prior fracture, fall and femoral neck BMD, the association between GRS and fracture risk remained statistically significant (OR 1.44; 95%CI, 1.24-1.67). For hip fracture, increase in GRS was also associated with an elevated risk of fracture (OR 1.66; 95%CI, 1.38-2.0). The AUC for the model with clinical risk factors was 0.71 (95%CI, 0.67 to 0.75); when GRS was added to the model, the AUC value was increased to 0.74 (95%CI, 0.70 to 0.78), and the NRI was improved by 23% at cut-off value of (0, 0.1, 0.2, 1). For hip fracture, the addition of GRS into the clinical risk factors based model resulted in an improvement of AUC from 0.80 (95%CI, 0.74 to 0.86) to 0.87 (95%CI, 0.82 to 0.91), and yielded an NRI gain of 19% in correct reclassification of fracture vs non-fracture.

**Conclusion:** A genetic profiling of BMD-associated genetic variants could improve the accuracy of fracture prediction over and above that of clinical risk factors alone. Given the high prevalence of fracture in the general population, the clinical utility of cumulative genetic risk score can help stratify individuals by fracture status.

Receiver operating characteristic curves for total fracture



Receiver operating characteristic curves for total fracture

**Disclosures:** Thao P. Ho-Le, None.

## 1033

**Hypoxia Signaling-Induced Glycolytic Metabolism in Osteoblasts can Affect Systemic Glucose Homeostasis by Increasing Glucose Utilization by the Skeleton.** Naomi Dirckx<sup>1</sup>, Robert J. Tower<sup>1</sup>, Evi M. Mercken<sup>1</sup>, Tom Breugelmans<sup>1</sup>, Elena Nefvodova<sup>1</sup>, Roman Vangoitsenhoven<sup>2</sup>, Bart Van der Schueren<sup>2</sup>, Chantal Mathieu<sup>2</sup>, Thomas L. Clemens<sup>3</sup>, Christa Maes<sup>1</sup>.  
<sup>1</sup>Laboratory of Skeletal Cell Biology & Physiology (SCEBP), Skeletal Biology & Engineering Research Center (SBE), KU Leuven, Belgium, <sup>2</sup>Clinical & Experimental Endocrinology, KU Leuven, Belgium, <sup>3</sup>Department of Orthopaedic Surgery, Johns Hopkins University School of Medicine, United states

The skeleton has emerged as an important regulator of systemic energy metabolism and glucose homeostasis, with osteocalcin and insulin representing the prime known mediators of these endocrine interactions. As hypoxia is a known regulator of cellular metabolism, we generated conditional knockout (cKO) mice in which Von Hippel Lindau (Vhl), a negative regulator of hypoxia-inducible factor (HIF), was deleted in osteoblast lineage cells by using the *Ox-Cre:GFP* driver. Cultures of Vhl-deficient primary osteoblasts (pOBs) displayed strongly increased glucose uptake and lactate production, associated with a 5-fold overexpression of the hypoxia-regulated glucose transporter 1 (Glut1), and increased expression of the key glycolytic enzymes phosphoglycerate kinase 1 (Pkg1) and pyruvate dehydrogenase kinase 1 (Pdk1) by qRT-PCR. Extracellular flux analysis revealed a decreased oxygen consumption rate and increased extracellular acidification, indicating increased glycolysis at the expense of glucose oxidation. However, ATP levels remained constant, indicating that the low energy production via glycolysis was compensated by the excessive glucose uptake in the mutant cells. Intriguingly, Vhl cKO mice were lean and displayed systemic hypoglycemia with increased glucose tolerance, which could not be explained by alterations in insulin production or sensitivity, nor by increased osteocalcin, as serum osteocalcin was 80% reduced in Vhl cKO mice. Positron

emission tomography (PET) scans and bio-distribution assays using the radioactive tracer  $^{18}\text{F}$ -fluorodeoxyglucose ( $^{18}\text{F}$ -FDG) revealed that the skeleton takes up a considerable portion of injected glucose (13% in control mice) relative to soft tissues (e.g. liver 5%, heart 9.7%, brain 6.5%). Moreover, the uptake of  $^{18}\text{F}$ -FDG was significantly increased in bones of Vhl cKO mice. qRT-PCR analysis of full bones showed significant upregulation of glycolytic markers (Pfkfb3, Pfkfb1) and a 3-fold increased Glut1 expression. To investigate whether the altered systemic glucose homeostasis in Vhl cKO mice could be a direct result of the increased glucose consumption by the mutant osteogenic cells, mice were treated with the Pdk1-inhibitor dichloroacetate (DCA). DCA was able to prevent the development of the metabolic phenotype in postnatal induced Vhl cKO mice. Our findings reveal a novel, potentially direct link between cellular metabolism in bone and whole-body glucose homeostasis, controlled by local hypoxia signaling in the skeleton.

**Disclosures:** Naomi Dirckx, None.

## 1034

**Sclerostin influences body composition by regulating catabolic and anabolic metabolism in adipocytes.** Julie Frey, Soohyun Kim, Zhu Li, Ryan Tomlinson, Mehboob Hussain, Daniel Thorek, Michael Wolfgang, Ryan Riddle\*. Johns Hopkins University, United states

Sclerostin is a well-established regulator of bone acquisition that antagonizes the profound osteo-anabolic capacity of activated Wnt/b-catenin signaling. Intriguingly, clinical data has linked impairments in multiple metabolic indices with increases in serum sclerostin levels. These data, together with the increased production of sclerostin in mouse models of type 2 diabetes, prompted us to investigate extra-skeletal functions of sclerostin and to determine if this Wnt antagonist influences metabolism. Examination of body composition by qNMR and necropsy revealed significant decreases in whole-body fat mass and fat pad weights in *Sost*<sup>-/-</sup> mice relative to control littermates. This phenotype was accompanied by dramatic reductions in adipocyte size, improved glucose tolerance and enhanced insulin sensitivity in white adipose tissue. *Sost*<sup>-/-</sup> mice were also resistant to obesogenic diet-induced disturbances in energy balance as sclerostin deficiency abrogated hepatic steatosis and the development of adipose inflammation. The overproduction of sclerostin as a result of adeno-associated virus gene transfer produced the opposite metabolic phenotype, as mice exhibited an accumulation of adipose tissue with impairments in glucose handling. Mechanistically, sclerostin's effects on body composition appear to be the result of cell non-autonomous enhancements in Wnt signaling in white adipocytes and a shift towards anabolic metabolism in this tissue. White adipose depots isolated from *Sost*<sup>-/-</sup> mice exhibited an enhanced ability to oxidize fatty acids with concomitant increases in the mRNA levels of *Ppargc1a* and *Ucp1* and marked a reduction in *de novo* fatty acid synthesis. Likewise the acquisition of glucose, indexed by the uptake of  $^{18}\text{F}$ -fluorodeoxyglucose, was increased in the inguinal fat pads of *Sost*<sup>-/-</sup> mice relative to controls. Moreover, *in vitro* studies indicate that sclerostin directly regulates adipocyte differentiation and lipid accumulation. Since the levels of under-carboxylated osteocalcin are not affected by sclerostin deficiency, these findings support an unexplored endocrine function for sclerostin that facilitates communication between the skeleton and adipose tissue.

**Disclosures:** Ryan Riddle, None.

## 1035

**Regulation of Appetite by the Skeleton.** Ioanna Mosialou\*, Steven Shikhel, Na Luo, Stavroula Kousteni. Columbia University, United states

Bone has recently emerged as a pleiotropic endocrine organ that secretes at least two hormones, FGF23 and osteocalcin, to regulate kidney function and glucose homeostasis. These findings raised the question as to whether other bone-derived hormones exist and their potential functions. Studies in mice lacking osteoblasts indicated the existence of such hormone(s) that contribute to the endocrine role of the skeleton by regulating a novel function: appetite, a property not affected by osteocalcin. Using genetic and molecular means to search for an appetite-regulating hormone we identified Lipocalin 2 (LCN2), a previously thought adipokine, to be an osteoblast-enriched secreted protein expressed at 10-fold higher levels in osteoblasts as compared to adipocytes. Inactivation of *Lcn2* specifically in osteoblasts (*Lcn2osb*<sup>-/-</sup> mice) increased blood glucose levels, fat mass and body weight, decreased serum insulin and led to glucose intolerance and insulin resistance. These effects resulted mainly from a 23.7% increase in food intake that was first detected at 3 weeks of age and remained elevated thereafter. In contrast, inactivation of *Lcn2* in adipocytes had no effect on any metabolic parameters. To identify the mechanism through which LCN2 suppresses appetite, we examined whether it alters the expression of any peripheral gut or adipose-derived hormone known to affect food intake. *Lcn2osb*<sup>-/-</sup> mice showed lack of any changes in the expression of any of these hormones. This observation led us to examine whether LCN2 acts centrally to regulate food intake. Using *in situ* hybridization analysis we first showed that LCN2 is not expressed in the hypothalamus or brain stem, the two main areas regulating appetite in the brain. Therefore, we tested if LCN2 can cross the blood brain barrier. Peripherally administered recombinant LCN2 accumulated in the brainstem, thalamus and mainly hypothalamus of mice with ubiquitous inactivation of *Lcn2* (*Lcn2*<sup>-/-</sup> mice) at levels equivalent to those observed in wild type. *Lcn2*<sup>-/-</sup> mice also show increase in food intake and have a metabolic phenotype identical to *Lcn2osb*<sup>-/-</sup> mice. To confirm that LCN2 acts directly in the hypothalamus to suppress food intake we delivered LCN2 via intracerebroventricular infusions and

found that a weeklong treatment fully corrected the increased appetite seen in *Lcn2*<sup>-/-</sup> mice. These results identify LCN2 as an osteoblast-derived anorexigenic hormone and the regulation of appetite as an endocrine function of bone.

**Disclosures:** Ioanna Mosialou, None.

This study received funding from: Novo Nordisk

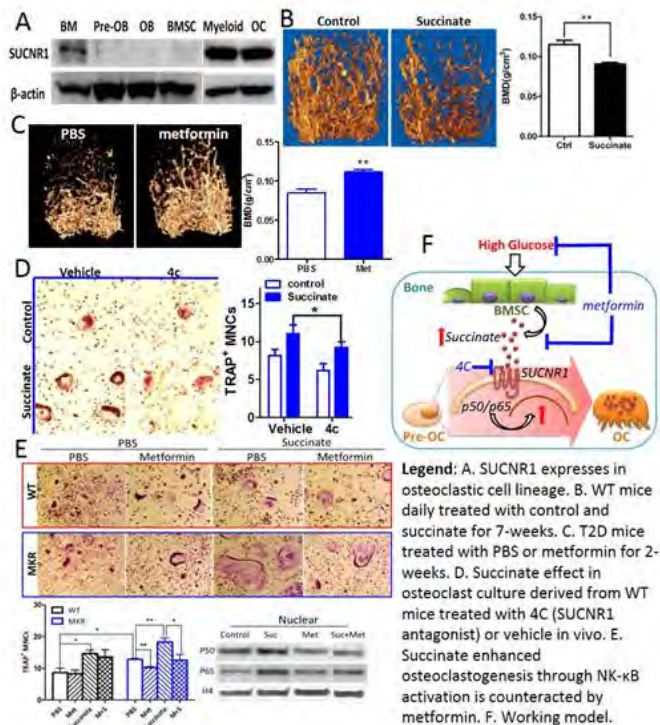
## 1036

**Succinate and its G-Protein-Coupled Receptor Stimulates Osteoclastogenesis and Bone Loss.** Yuqi Guo\*, Tao Yu, Jian Yang, Xin Li. New York University, United states

Bone fragility is a complication of diabetes mellitus, a metabolic disorder characterized by chronic hyperglycaemia with dysregulation in metabolites. The pathophysiological link between diabetes and compromised bone metabolism is not well understood. Recent findings in humans and rodents revealed that impaired osteoblast-mediated bone formation, accelerated osteoclastic-mediated bone resorption, microstructural defect, and poor bone quality are associated with diabetes mellitus. However, regarding the cellular effect, it remains elusive whether there is a direct link between abnormal metabolites resulted from hyperglycemia and the impaired bone cell functions.

We investigate the metabolomics of bone marrow stromal cells (BMSC) derived from hyperglycemic (type-2 diabetes, T2D) and normal (Wildtype, WT) mice using liquid chromatography-mass spectrometry. In comparison to WT BMSCs, 142 metabolites were significantly regulated in T2D BMSCs, in which 126 were upregulated and 16 were downregulated. Succinate, an intermediate metabolite that is catalyzed by fumarate by succinate dehydrogenase (SDH) in Krebs cycle, increased by 30-fold in diabetic BMSCs. It is known that deficient SDH activity leads to succinate accumulation. Indeed, both human and mouse BMSCs cultured with high glucose medium exhibit significantly reduced SDH activity and increased succinate levels. Excessive succinate can act as an extracellular ligand through binding to its specific receptor (SUCNR1), G-protein coupled receptor. Interestingly, SUCNR1 expresses exclusively in osteoclastic but not osteoblastic lineage cells indicating BMSC-derived succinate regulates osteoclasts in a paracrine mode under hyperglycemic condition. Results from succinate colorimetric assay, osteoclast enumeration, bone histomorphometry and micro CT analysis support that an abnormal accumulation of succinate is associated with the enhanced bone loss in T2D mice. Excessive succinate derived from BMSCs or administration of exogenous succinate stimulates osteoclastogenesis *in vitro* and bone loss *in vivo*. Furthermore, we synthesize a SUCNR1 antagonist to block SUCNR1 activation which successfully impedes succinate-enhanced osteoclastogenesis *in vitro* and *in vivo*. We further prove that succinate activates osteoclastogenesis via the canonical NF- $\kappa$ B pathway while administration of metformin, which suppresses succinate accumulation in bone marrow, attenuates succinate-enhanced osteoclastogenesis and bone resorption *in vitro* and *in vivo*.

Our study reveals a novel osteoclastogenesis modulation mechanism mediated by an intermediate metabolite succinate accumulated in bone microenvironment. Thus, targeting succinate signaling could provide a specific and effective treatment for improving bone health in diabetes.



**Legend:** A. SUCNR1 expresses in osteoclastic cell lineage. B. WT mice daily treated with control and succinate for 7-weeks. C. T2D mice treated with PBS or metformin for 2-weeks. D. Succinate effect in osteoclast culture derived from WT mice treated with 4C (SUCNR1 antagonist) or vehicle *in vivo*. E. Succinate enhanced osteoclastogenesis through NK- $\kappa$ B activation is counteracted by metformin. F. Working model.

Succinate stimulates osteoclastogenesis

**Disclosures:** Yuqi Guo, None.

1037

**Osteocalcin Signaling in Myofibers Favors Adaptation to Exercise by Increasing Uptake and Utilization of Nutrients in Adult Mice.** Paula Mera<sup>\*1</sup>, Mathieu Ferron<sup>2</sup>, Cyril Confavreux<sup>3</sup>, Irwin Kurland<sup>4</sup>, Michelle Puchowicz<sup>5</sup>, Gerard Karsenty<sup>1</sup>. <sup>1</sup>Columbia University, United states, <sup>2</sup>Institut de recherches cliniques de Montréal (IRCM), Canada, <sup>3</sup>Université de Lyon, France, <sup>4</sup>Albert Einstein College of Medicine, United states, <sup>5</sup>Case Western Reserve University, United states

The proximity of the two tissues and the fact that bone mass declines at the time muscle mass and functions also decrease have long suggested that a crosstalk between bone and muscle that would modulate the functions of these two tissues, may exist. In the context of this hypothesis the recent identification of bone-derived hormones and their receptors allows determining whether bone influences any aspect of muscle biology. An additional reason to address this question is that the circulating levels of uncarboxylated, i.e., bioactive osteocalcin markedly rise in mice and humans during exercise, i.e., at a time muscle function needs to increase. Here we show through the use of mutant mice lacking either osteocalcin in a cell-specific and inducible manner or its receptor Gprc6a (*Gprc6a<sup>Mck-/-</sup>*), only in myofibers, that osteocalcin signaling in myofibers is necessary for adaptation to exercise in adult mice because it promotes the uptake and catabolism of the two main nutrients of myofibers, glucose and fatty acids. Indeed, metabolic and metabolomics studies performed in *Gprc6a<sup>Mck-/-</sup>* and control littermates before and after exercise, demonstrates that osteocalcin signaling in myofibers during exercise increases glycogen breakdown, glucose uptake, glycolysis and the utilization of glucose in the TCA cycle. Osteocalcin signaling in myofibers also favors in an AMPK-dependent manner fatty acids uptake and oxidation during exercise. These metabolic functions of osteocalcin signaling in myofibers are mediated at least in part by the transcription factor CREB. As a result of this array of metabolic functions, osteocalcin signaling in myofibers favors the production of ATP that is necessary for muscle contraction during exercise. This array of metabolic functions also provides an explanation for why osteocalcin signaling in myofibers is sufficient to increase the exercise capacity of young or older wild type mice. Indeed, acute or chronic delivery of osteocalcin can increase the exercise capacity of young adult mice and restore in 15 month-old mice the exercise capacity of 3 month-old mice. This study demonstrate the existence of an endocrine regulation of muscle function originating from bone and mediated by osteocalcin, that favors adaptation to exercise and can reverse the age-induced decrease in exercise capacity in adult mice.

Disclosures: Paula Mera, None.

1038

**Mechanically-Induced Calcium Oscillations in Osteocytes Facilitate Release of RANKL, OPG, and Sclerostin Through Extracellular Vesicles and Mediate Skeletal Adaptation.** Genevieve Brown<sup>\*</sup>, Andrea Morrell, Samuel Robinson, Rachel Sattler, X. Edward Guo. Columbia University, United states

Calcium ( $\text{Ca}^{2+}$ ) oscillations have been observed in osteocytes in response to mechanical loading *in vitro* and *in situ*, and mechanical loading is known to regulate osteocyte protein expression. Yet, no studies to date have connected  $\text{Ca}^{2+}$ -mediated mechanosensitivity to protein expression changes in osteocytes, and few studies have linked  $\text{Ca}^{2+}$  signaling to long-term adaptive responses. Interestingly,  $\text{Ca}^{2+}$ -dependent contractions, which we have previously reported in osteocytes, facilitate the release of extracellular vesicles (EVs) in other cell types. Though EVs have been identified in osteocytes and shown to contain or co-localize with osteocyte-specific proteins, no studies have explored their role in osteocyte mechanobiology. We mechanically stimulated MLO-Y4 cells and found exposure to fluid flow increased cellular expression of the secretory vesicle marker LAMP1. Treatment of cells with neomycin to inhibit  $\text{Ca}^{2+}$  oscillations diminished this response. Mechanical stimulation of osteocytes induced substantial release of EVs into the culture medium, which was blunted by neomycin. Western blots on EV lysates identified LAMP1, sclerostin, RANKL, and OPG among the proteins contained within these EVs. To investigate the effect of inhibiting  $\text{Ca}^{2+}$  responses on *in vivo* bone mechanical adaptation, we first confirmed the inhibitory effect of neomycin on *ex vivo* osteocyte  $\text{Ca}^{2+}$  dynamics. Neomycin-injected mice showed a decreased number of  $\text{Ca}^{2+}$  peaks observed compared to vehicle-injected controls. Subsequently, we administered neomycin prior to each loading period in an *in vivo* murine tibia loading model for a total of 2 weeks and evaluated bone changes by micro-computed tomography. Neomycin-injected animals saw a significantly reduced difference in cortical thickness and bone volume fraction between loaded and non-loaded limbs compared to vehicle-injected animals. Overall, our data suggests  $\text{Ca}^{2+}$  oscillations regulate osteocyte protein expression and subsequent bone adaptation through the production and release of EVs.

We revealed a novel mechanotransduction pathway by which osteocytes immediately respond to mechanical loading with EV release to transport critical proteins through the bone. Indeed, EVs containing bone-regulatory proteins had a diameter of 175 nm, which is below most reported values for canaliculi; thus transport of these proteins via EVs through the bone is a plausible and intriguing means by which osteocytes may coordinate tissue-level bone adaptation.

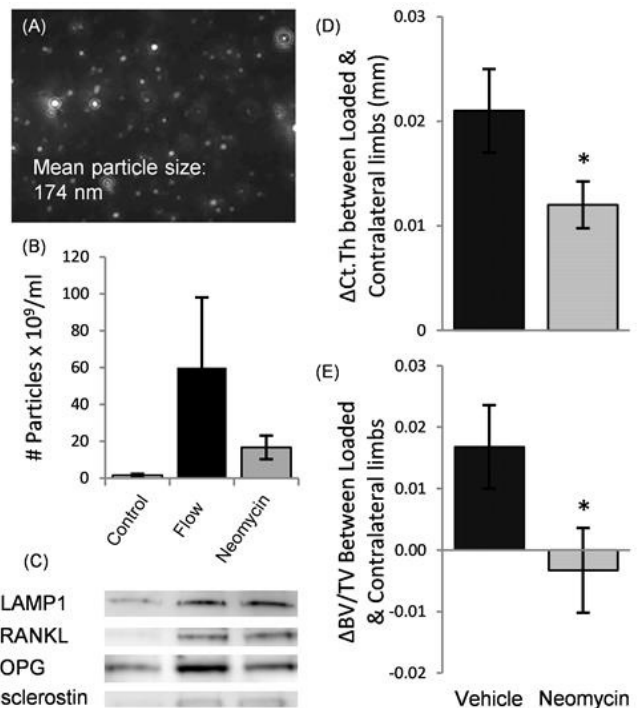


Figure 1. Effect of mechanical loading/neomycin on (A) EV release, (B) particle concentration and (C) protein expression. Effect of neomycin injections on (D) cortical thickness and (E) bone volume fraction in loaded mice.

Figure 1.

Disclosures: Genevieve Brown, None.

1039

**Subchondral bone plate sclerosis during late osteoarthritis is mediated by loading-induced decrease in Sclerostin amount.** Haoruo Jia<sup>\*1</sup>, Xiaoyuan Ma<sup>1</sup>, Zhaochun Yang<sup>2</sup>, Zeyang Sun<sup>3</sup>, Wei Tong<sup>1</sup>, Lin Han<sup>4</sup>, James H-C. Wang<sup>2</sup>, Motomi Enomoto-Iwamoto<sup>5</sup>, Ling Qin<sup>1</sup>. <sup>1</sup>Department of Orthopaedic Surgery, School of Medicine, University of Pennsylvania, United states, <sup>2</sup>Department of Orthopaedic Surgery, University of Pittsburgh School of Medicine, United states, <sup>3</sup>School of Engineering & Applied Science, University of Pennsylvania, United states, <sup>4</sup>School of Biomedical Engineering, Science & Health Systems, Drexel University, United states, <sup>5</sup>Department of Surgery, The Children's Hospital of Philadelphia, United states

Osteoarthritis (OA) is not only a cartilage disease but also a bone disease accompanied by pathological changes in the subchondral bone. We recently generated cartilage-specific EGFR knockout mice (*Col2-Cre Egfr<sup>flox</sup>/Wa5, CKO*) to study the mechanisms of OA pathology. After destabilizing the medial meniscus (DMM), WT (*Egfr<sup>flox/+</sup>*) and *Wa5* (*Egfr<sup>Wa5/+</sup>*, an EGFR dominant negative allele) mice developed mild to moderate OA with no changes in the subchondral bone plate (SBP) at 2-3 months. In contrast, *Egfr<sup>CKO</sup>* mice exhibited many late OA phenotypes, including a complete loss of the cartilage layer and SBP thickening (2-fold) restricted to the medial side only. Underneath the SBP, trabecular bone loss was observed at both medial and lateral sites. Immunohistochemistry revealed a 6.6-fold increase in the number of osteoblasts lining SBP at the medial site. This locally enhanced bone formation was accompanied by an increase in the length of blood vessels aligning SBP surface to support new bone formation. Wnts are potent signals for osteoblastic bone formation. Strikingly, staining for sclerostin, a Wnt antagonist, in osteocytic cell bodies and dendritic processes, was remarkably attenuated in SBP at the medial site of *CKO* DMM joint. The amount of sclerostin at the lateral site was similar to those at sham sites in all three types of mice, as well as those at WT and *Wa5* DMM sites. Mechanical loading is a major regulator of sclerostin in the cortical bone. Using an asymmetric finite element model with effective modulus values obtained from ATF-nanoindentation experiments, we demonstrated that the highest focal stress on SBP in *CKO* joints at late OA stage (without cartilage) drastically increased 14.6-fold compared to that at early OA (with cartilage), indicating that at late OA stage SBP experiences a very high mechanical stress. This loading-induced SBP sclerosis mechanism was not limited to *Egfr<sup>CKO</sup>* mice alone. At 16 weeks post DMMH (DMM and hemisection of meniscus), WT joints developed late OA at the medial site. Similarly, we observed a significant decrease in sclerostin amount only in SBP at the medial site but not at the lateral site. In conclusion, our data demonstrated that drastically elevated mechanical loading on SBP after cartilage depletion attenuates

sclerostin amount in osteocytes and therefore increase SBP thickness. Thus, our study elucidates the mechanism for SBP sclerosis associated with late OA.

**Disclosures:** Haoruo Jia, None.

## 1040

**Mechanical Loading Induces CD31<sup>hi</sup>Emcn<sup>hi</sup> Vessel Formation by Preosteoclast Secretion of PDGF-BB.** Weicheng Xu<sup>\*1</sup>, Hui Xie<sup>1</sup>, Ryan Tomlinson<sup>1</sup>, Zhuqing Xia<sup>1</sup>, Genevieve Brown<sup>2</sup>, Maureen Pickarski<sup>3</sup>, Le Duong<sup>4</sup>, X. Edward Guo<sup>2</sup>, Xu Cao<sup>1</sup>. <sup>1</sup>Department of Orthopaedic Surgery, Johns Hopkins University School of Medicine, United states, <sup>2</sup>Department of Biomedical Engineering, Columbia University, United states, <sup>3</sup>Merck Res. Lab, Bone Biology Group, United states, <sup>4</sup>Merck Res. Labs., Bone Biology Group, United states

Bone is remodeled to adapt to changes in mechanical loading, but the molecular and cellular mechanisms of this process are not well understood. Our previous research has shown that secretion of platelet-derived growth factor-BB (PDGF-BB) from tartrate-resistant acid phosphatase-positive (TRAP<sup>+</sup>) preosteoclasts stimulates the production of a specific blood vessel subtype essential for new bone formation (CD31<sup>hi</sup>Emcn<sup>hi</sup> vessels). As a result, we hypothesized that preosteoclasts may also perform this important function at sites of load-induced bone formation. To test this hypothesis, we subjected adult mice to four weeks of *in vivo* mechanical loading by cyclic hind limb compression. This regimen stimulated the production of new cortical bone at the mid-diaphysis of the tibia and increased the number of TRAP<sup>+</sup> preosteoclasts and CD31<sup>hi</sup>Emcn<sup>hi</sup> blood vessels in the tibial periosteum detected by  $\mu$ CT and immunofluorescence. Importantly, we observed that these periosteal TRAP<sup>+</sup> preosteoclasts expressed PDGF-BB. Therefore, we examined whether secretion of PDGF-BB from TRAP<sup>+</sup> preosteoclasts is required for the production of CD31<sup>hi</sup>Emcn<sup>hi</sup> blood vessels and bone formation following mechanical loading. In mice with the selective deletion of PDGF-BB from the osteoclast lineage (TRAP-Cre), mechanical loading did not stimulate new bone formation or periosteal CD31<sup>hi</sup>Emcn<sup>hi</sup> vessels relative to their WT littermates. These results suggested that secretion of PDGF-BB from TRAP<sup>+</sup> preosteoclasts is required for load-induced bone formation. To further explore the role of preosteoclast-derived PDGF-BB in skeletal adaptation, mice were subjected to hind limb suspension (HLS) with or without administration of the Cathepsin K (CatK) inhibitor L-235 (Merck). As expected, HLS was associated with decreased bone mass and a diminished number of TRAP<sup>+</sup> preosteoclasts and CD31<sup>hi</sup>Emcn<sup>hi</sup> blood vessels in the periosteum, but these effects were reversed by the administration of CatK inhibitor L-235. Taken together, the results from this study illustrate that osteogenic mechanical loading induces the accumulation of periosteal preosteoclasts that secrete PDGF-BB, leading to the formation of CD31<sup>hi</sup>Emcn<sup>hi</sup> vessels to support new bone.

**Disclosures:** Weicheng Xu, None.

## 1041

**Plasma Membrane Disruptions are a Novel Mechanosensation Mechanism in Osteocytes.** Kanglun Yu<sup>1</sup>, Ahmed Elsherbini<sup>1</sup>, David Sellman<sup>2</sup>, Kayce Vanpelt<sup>1</sup>, Oran Kennedy<sup>3</sup>, Anna McNeil<sup>2</sup>, Paul McNeil<sup>2</sup>, Meghan McGee-Lawrence<sup>\*2</sup>. <sup>1</sup>Augusta University, United states, <sup>2</sup>Medical College of Georgia, Augusta University, United states, <sup>3</sup>NYU, United states

Osteocytes are the primary mechanosensory cell in bone, but the ways in which they detect loading remain poorly understood. Plasma membrane disruptions (PMD) develop with mechanical loading under physiological conditions in many cell types (e.g., myocytes, endothelial cells), and act as both a stimulus for tissue adaptation to loading and a source of molecular flux across the cell membrane. However, whether PMD can serve as a mechanosensing mechanism in osteocytes is unknown. The objective of this study was to determine whether PMD occur, and undergo repair, in osteocytes during *in vitro* and *in vivo* physiological loading, and to explore their role in mechanotransduction.

MLO-Y4 cells were tested in fluid flow, laser wounding, and mechanical wounding assays in the presence of membrane impermeant PMD tracers (e.g., fluorescein-dextran, 10 kDa). In fluid flow studies, conducted in the presence of physiological Ca<sup>2+</sup>, PMD events were detected in flow-treated (but not control) cells. PMDs occurred in a dose-responsive fashion to shear stresses (1-3 Pa) and, were most prevalent when loading was applied rapidly (high-impact) instead of gradually (low-impact). In mechanical wounding assays, PMD-affected osteocytes showed evidence of mechanotransduction including nuclear localization of beta-catenin and expression of c-fos. In laser wounding assays, which permit quantification of PMD repair dynamics, osteocytes repaired PMD in the presence of extracellular calcium (1.5 mM), and repaired PMD more rapidly in the presence of Vitamin E (200  $\mu$ M), Vitamin C (1 mM), or poloxamer 188 (2%) supplemented medium, but repair was inhibited following treatment with calpeptin (20  $\mu$ M) or in calcium-free medium, similar to repair processes in other cell types. For *in vivo* studies, female CD1 mice (8 wks) were administered Evans Blue dye, which binds to albumin, as an *in vivo* PMD tracer. Mice were run downhill to exhaustion and bone sections were examined by two-photon microscopy. A baseline level of osteocyte PMD was detected in non-exercised mice, but the number of PMD-labeled osteocytes was increased (+2.8 fold) by a single bout of exercise. Immunostaining revealed that osteocytic expression of beta catenin

was 2.5 fold higher in animals subjected to running, and a majority of the osteocytes expressing beta catenin in the exercised mice had experienced a PMD. These data suggest that PMD may be an upstream signaling event leading to skeletal adaptation to loading.

**Disclosures:** Meghan McGee-Lawrence, None.

## 1042

**Sensory Nerve Signals Mediate Skeletal Adaptation to Mechanical Loads.** Ryan Tomlinson<sup>\*</sup>, Zhi Li, Ryan Riddle, Thomas Clemens. Johns Hopkins University, United states

A critical process required for endochondral bone formation is the invasion of TrkA sensory nerves whose axons are guided to sites of bone formation by retrograde signaling of the neurotrophic factor NGF. As a direct consequence of this developmental process, TrkA sensory nerves densely innervate the periosteal and endosteal surfaces of adult bone, a privileged location for the perception of mechanical signals. Therefore, we hypothesized that NGF-TrkA signaling in sensory nerves is required for skeletal adaptation to the mechanical loads imposed by axial compression of the forelimb. In loaded limbs from NGF-eGFP reporter mice, osteocalcin<sup>+</sup> osteoblasts on the periosteal and endosteal surfaces of bone had robust NGF expression 1 and 3 hours after loading, which returned to baseline by 24 hours. However, NGF expression was not observed in osteocytes at any time point or position in the bone. A similar time course of NGF activation was observed after *in vitro* stretching of primary osteoblasts from NGF-eGFP neonates. To selectively disrupt NGF-TrkA signaling, we used mice harboring TrkA-F592A knockin alleles that render the endogenous TrkA kinase sensitive to inhibition by the membrane-permeable molecule INMPP1. Unlike NGF or TrkA null mice that die perinatally, TrkA-F592A mice live to adulthood and display a normal skeletal phenotype. Following 3 consecutive days of loading, inhibition of TrkA signaling significantly decreased both periosteal and endosteal load-induced bone formation, primarily by decreasing the extent of mineralizing surfaces. To further explore our hypothesis, exogenous NGF was administered to mice 1 hour before loading, which induced thermal hyperalgesia lasting for at least 3 days. Consistent with TrkA inhibition, exogenous NGF significantly increased both periosteal and endosteal load-induced bone formation by increasing the extent of mineralizing surfaces. Finally, TrkA-F592A mice were subjected to an ulnar stress fracture generated by a single bout of fatigue loading. In this setting, inhibition of TrkA signaling decreased both the innervation and vascularization of the woven bone callus, resulting in significantly diminished woven bone formation 7 days after loading. In total, these results show for the first time that osteoblasts on the bone surface release NGF in response to mechanical load to activate TrkA sensory nerves. Moreover, NGF-dependent TrkA signals by sensory nerves are necessary for optimal load-induced bone formation.

**Disclosures:** Ryan Tomlinson, None.

## 1043

**Marrow Adipose Tissue is Distinct from White and Brown Fat and Does Not Beige.** Ryan Berry<sup>1</sup>, Brandon Holtrup<sup>1</sup>, Julie Hens<sup>2</sup>, Gene Ables<sup>2</sup>, Tracy Nelson<sup>1</sup>, Rose Webb<sup>1</sup>, Clifford Rosen<sup>3</sup>, Matthew Rodeheffer<sup>1</sup>, Mark Horowitz<sup>\*1</sup>. <sup>1</sup>Yale School of Medicine, United states, <sup>2</sup>Orentreich Foundation, United states, <sup>3</sup>Maine Medical Center Research Institute, United states

Marrow adipose tissue (MAT) was identified in the bone marrow (BM) more than a century ago and until very recently was thought to be nothing more than filler. Although recent data suggests that MAT has characteristics of brown adipose tissue (BAT) or beige adipocytes, little is known about the origin, development and function of MAT as the identity of the BM adipocyte precursor cell is unknown.

We have performed lineage tracing of BM adipocytes following induction of BM adipogenesis with either rosiglitazone-enriched (rosi) diet or irradiation of double fluorescent *mTmG* reporter mice (which harbor a floxed membrane targeted tdTomato cassette (mT) upstream of a Cre-responsive membrane targeted eGFP cassette (mG)) to determine the ontogeny of BM adipocytes and identity of BM adipocyte progenitor cells. Following either irradiation or rosi diet, all BM adipocytes were eGFP+ and therefore traced by expression of Cre-recombinase in *Adiponectin-Cre:mTmG* and *Osx1-Cre:mTmG* mice. In contrast, adipocytes were not traced (tdTomato+) in *Vav1-Cre:mTmG* or *Myf5-Cre:mTmG* mice.

B6 mice fed a methionine restricted (MR) diet show a pronounced induction of multilocular beige adipocytes in their inguinal depot (IWAT) and a concomitant increase in MAT as compared to mice on control diet. However, unlike the IWAT, none of the marrow adipocytes were multilocular. Using immunohistochemistry, IWAT from the MR mice stained with anti-UCP-1 confirming the presence of beige adipocytes. In contrast, MAT from the same mice was uniformly UCP negative.

We previously demonstrated that all adipocytes in classical white adipose tissue (WAT) depots were traced in *Pdgfr $\alpha$ -Cre:mTmG* mice due to expression of *Pdgfr $\alpha$*  in WAT precursor cells. In contrast, between 50-70% of BM adipocytes were eGFP+ in the same mice. To better understand the relationship between MAT and WAT we examined *Pdgfr $\alpha$ -cre:insulinR<sup>fl/fl</sup>* mice. These mice were found to have a marked increase in MAT and a paucity of WAT, suggesting that the requirement of insulin signaling for adipocyte formation is another distinguisher between MAT and WAT.

Together, the uniform tracing of BM adipocytes by the endosteal cell/osteoblast promoter *Osx1*, the lack of tracing of BM adipocytes by *Myl5* (which traces all brown adipocytes), the absence of multilocular, UCP-1 positive marrow adipocytes and the formation of MAT in the absence of insulin receptor indicate that the MAT depot is distinct from BAT, WAT or beige fat.

**Disclosures:** Mark Horowitz, None.

## 1044

**Phosphate Restriction Promotes the Differentiation of Multipotent Marrow Stromal Cells into Marrow Adipose Tissue.** Frank Ko\*, Marie Demay. Massachusetts General Hospital, United states

Phosphate restriction of growing mice leads to rachitic expansion of the growth plate, decreases trabecular and cortical bone, impairs bone formation, and increases marrow adipose tissue (MAT). Expression of the early osteolineage markers, *Sox9* and *Runx2*, is increased by phosphate restriction, whereas expression of the late markers, *Osterix* and *Osteocalcin*, is decreased, suggesting an arrest in osteoblast differentiation between *Runx2* and *Osterix*. Phosphate restriction also enhances expression of the adipogenic markers, *C/EBP $\alpha$*  and *PPAR $\gamma$* , in bone marrow cells, suggesting that the decreased bone observed in phosphate restricted mice may not only stem from arrested osteoblast differentiation, but also from enhanced differentiation of mesenchymal stem cells (MSCs) into the adipogenic lineage. Thus, lineage tracing analyses were undertaken to address the origin of the pathologic MAT observed in phosphate restricted mice. While ablation of canonical Wnt (cWnt) signaling or *Gsa* in *Osterix*-Cre expressing cells enhances their differentiation into MAT, the pathologic MAT observed in phosphate restricted mice did not originate from these cells.

*LepR*-Cre marks multipotent CXCL12-abundant reticular MSCs (CAR cells) in the bone marrow. To address whether the pathological MAT observed in the phosphate restricted mice originates from these cells, *LepR*-Cre reporter mice were fed a phosphate restricted diet from 28 days to 50 days of age (d28-50). Lineage tracing analyses demonstrated that the increase in LipidTox positive adipocytes observed in the bone marrow of phosphate restricted mice originates from *LepR* expressing CAR cells. Therefore, CAR cells were sorted after one week of phosphate restriction to evaluate mRNA expression. Phosphate restriction led to a marked enhancement in the expression of *PPAR $\gamma$*  and *CEBPA* in sorted CAR cells, associated with a significant decrease in the expression of the cWnt effector *Lef1*, suggesting that impaired cWnt signaling may contribute to the enhanced MAT observed. Consistent with this, activation of cWnt signaling with *LiCl* prevented the increased expression of *PPAR $\gamma$*  and *CEBPA* in bone marrow cells and the block in osteoblast differentiation observed after 1 week of phosphate restriction. These studies suggest that acute dietary phosphate restriction of growing mice enhances marrow adipogenesis by interfering with the cWnt signaling pathway.

**Disclosures:** Frank Ko, None.

## 1045

**Bone Marrow Adiposity is Induced by the Osteocyte Derived Factor Sclerostin.** Michaela Reagan\*, Heather Fairfield, Carolyn Falank, Clifford Rosen. Maine Medical Center Research Institute, United states

Our goal was to explore the regulation of bone marrow adipose tissue (BMAT) by skeletal cells. The bone marrow adipose depot is a dynamic and complex collection of cells regulated by both external signals and cell-autonomous factors. Within the bone marrow (BM), mesenchymal stem cells (MSCs), reside in a multipotent state and are induced to differentiate into one lineage or another based on biochemical and biomechanical cues that can be altered by drugs, mechanical loading, hormones, or pathogenic state. We hypothesized that osteocyte-derived factors may also regulate adipogenic differentiation. In support of this, we observed significantly increased BMAT in *Osteocalcin-Cre/iDTR* (inducible diphtheria toxin (DT) receptor) mice both immediately and 3 weeks after stopping DT treatment, which we hypothesized was due to a spike in osteocyte-derived factors released upon cell death. We found that osteocyte conditioned media (CM) is able to induce adipogenic differentiation of 3T3-L1 cells by >2 fold ( $p < 0.05$ ) *in vitro*. We identified sclerostin (SOST), a Wnt-inhibitor secreted from osteocytes, as a protein able to induce adipogenesis in 3T3-L1 cells (1.5 fold) and BM-MSCs from both mouse (1.5-fold) and human (3-fold). Moreover, SOST induction of BMAT formation *in vitro* was in part due to its antagonistic effects on the adipogenic-inhibitory Wnt1 signaling pathway. To create a more physiologically relevant model of BMAT, we developed the first three-dimensional (3D) model of BMAT from silk scaffolds and human and mouse MSCs differentiated into adipocytes (Fig 1). This model recapitulates bone-fat interactions within the BM niche in a much more realistic manner than possible in 2D. This platform was used to further investigate the relationship of SOST to BM-MSC lineage allocation (osteoblast vs. adipocyte), and to co-culture osteocytes and adipocytes to investigate the relationship between these two cell types. These results demonstrate the feasibility of utilizing a 3D model to investigate the relationship between many cell types in the BM niche, and how those interactions may influence lineage allocation and the delicate equilibrium of the BM. Collectively these data demonstrate that osteocyte-secreted SOST may induce and/or promote adipogenesis in the BM niche through the inhibition of Wnt signaling and contribute to our knowledge of BMAT function and origin in the context of healthy and diseased BM, such as myeloma-packed BM, now being explored in our lab.

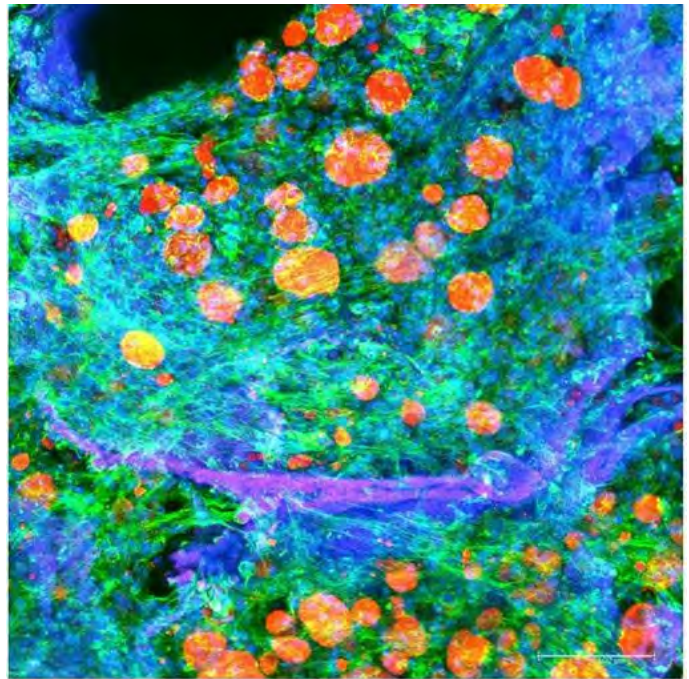


**Figure 2:** Confocal Image of 3D Silk Scaffold BMAT Model. Day 26 of Culture, Day 17 of Adipogenesis, actin (green/phalloidin stain); lipid (red/Oil Red O); scaffold (maroon); nuclei (blue/DAPI). Scale=100 $\mu$ m.

3D Bone Marrow Adipose Model

**Disclosures:** Michaela Reagan, None.

## 1046

**Critical Function Of PTH1R In Regulation Of Mesenchymal Cell Fate And Bone Resorption.** Yi Fan\*<sup>1</sup>, Phuong Le<sup>2</sup>, Jun-ichi Hanai<sup>3</sup>, Ruive Bi<sup>4</sup>, Clifford Rosen<sup>2</sup>, Beate Lanske<sup>1</sup>. <sup>1</sup>Department of Oral Medicine, Infection & Immunity, Harvard School of Dental Medicine, United states, <sup>2</sup>Maine Medical Center Research Institute, United states, <sup>3</sup>Renal Division, Beth Israel Deaconess Medical Center & Harvard Medical School, United states, <sup>4</sup>Endocrine Unit, Massachusetts General Hospital & Harvard Medical School, United states

Age-related osteoporosis is characterized by enhanced skeletal fragility, low bone mass, increased marrow adiposity and high bone resorption. Recent studies have shown that bone marrow pre-adipocytes produce receptor activator of nuclear factor  $\kappa$ B ligand (Rankl) and support differentiation and function of osteoclasts-like cells *in vitro*. PTH1R signaling has been identified in promoting osteoblastogenesis while suppressing adipogenesis in mesenchymal stem cells. The specific actions of PTH1R signaling are complex and still incompletely understood. The aim of this study is to investigate the role of PTH1R signaling in regulating mesenchymal cell fate and coordinating bone resorption. Conditional deletion of the PTH1R using the *Prx1Cre* recombinase led to a substantial increase in marrow adipose tissue (MAT) by 3 weeks of age quantified by osmium tetroxide staining. Isolated MAT from the *Prx1Cre;PTH1R<sup>fl/fl</sup>* mice showed high expression of adipose-related genes, including *Ppar $\gamma$* , *Cebp  $\alpha, \beta, \Delta$* , *Fabp4* and *Adiponectin* compared to their control littermates. Bone marrow stromal cells (BMSCs) under adipogenic culture from the *Prx1Cre;PTH1R<sup>fl/fl</sup>* mice showed enhanced adipogenic differentiation *in vitro*. Moreover, PTH(1-34) significantly inhibited *in vivo* and *in vitro* adipogenesis in control mice and BMSCs but not in mutant mice or cells ablated for PTH1R. Lineage tracing experiments using BMSCs from *Prx1Cre;PTH1R<sup>fl/fl</sup>/Tomato<sup>fl/+</sup>* mice suggested that adiponectin-positive adipocytes derived from Tomato-positive *Prx1* lineage cells. Interestingly, the enhanced adipogenesis in mutant mice was accompanied by increased bone resorption and low bone mass accompanied by high *Rankl* mRNA expression in MAT and bone marrow as well as high RANKL protein levels in serum and supernatant from spun marrow. Furthermore, we noted that *Rankl* mRNA was undetectable in any peripheral adipose tissue suggesting RANKL originates from the MAT. Flow-cytometry analysis of bone marrow cells from mutant mice showed increased pre-adipocytes (Pref-1) number producing RANKL, leading to the associated up-regulation of RANKL. The data indicates that loss of PTH1R from osteoprogenitors (*Prx1Cre*) favors adipogenic differentiation, with marked elevation in RANKL expression and enhanced osteoclastogenesis accompanied by increased bone

resorption. These findings suggest that PTH plays a critical role in determining cell fate in the marrow niche and that marrow adipocytes can mediate bone resorption.

**Disclosures:** Yi Fan, None.

## 1047

**Leptin-induced loss of marrow adipose tissue is mediated by sympathetic and sensory neurotransmission.** Brian S Learman<sup>1</sup>, Tezin Walji<sup>2</sup>, Shaima Khandaker<sup>1</sup>, Kavla Moller<sup>2</sup>, Ben Schell<sup>1</sup>, Clarissa S Craft<sup>2</sup>, Ormond A MacDougald<sup>1</sup>, Erica L Scheller<sup>\*2</sup>. <sup>1</sup>University of Michigan, United states, <sup>2</sup>Washington University, United states

**Background.** Marrow adipose tissue (MAT) has the potential to exert both local and systemic effects on metabolic homeostasis, skeletal remodeling, hematopoiesis, and the development of bone metastases, yet the mechanisms underlying MAT formation and function remain relatively unknown. Cold exposure in rodents promotes thermogenesis, allowing survival at 4°C through elevation of sympathetic tone. Housing mice at 4°C for 21-days leads to 70% loss of regulated marrow adipose tissue (rMAT) in the proximal tibia due to decreases in adipocyte cell size and number; constitutive MAT (cMAT) in the distal tibia remains unchanged. **Objective.** Based on these results, we hypothesized that rMAT is acutely regulated by norepinephrine, released locally by sympathetic neurons, through the β3-adrenergic receptor. Furthermore, differences in sympathetic drive may explain site-specific regulation of rMAT, but not cMAT. **Methods.** To test this hypothesis, we utilized a model of leptin-induced sympathetic drive. Intracerebroventricular (ICV) cannulae were implanted in 13-week-old male C3H/HeJ mice. After 7-days, mice were given 1.5 μg ICV-leptin or vehicle control. Fifteen minutes prior to ICV injection, mice received a subcutaneous dose of saline, β3-adrenergic antagonist, or a combination of sensory neurotransmitter antagonists. This series of injections was performed three times over 24-hours, corresponding to light-dark cycles, at 9 am, 6 pm, and 6 am. The mice were euthanized for analysis starting at 9am on the second day. **Results and Conclusion.** ICV leptin decreased body mass and food intake, confirming its efficacy. Leptin caused a 43% decrease in rMAT volume at the proximal tibial metaphysis while cMAT in the distal tibia and tail remained unchanged. Inguinal and gonadal white adipose tissue mass (iWAT, gWAT) was also decreased, by 28% and 36%, due to a decrease in adipocyte cell size. Pre-treatment with antagonists did not change leptin-mediated decreases in body mass or food intake. However, the β3-adrenergic antagonist completely rescued ICV-leptin induced loss of rMAT volume and iWAT/gWAT cell size. Unexpectedly, inhibition of sensory neurotransmission also blocked loss of rMAT volume, with partial rescue of iWAT and gWAT adipocyte size. These findings provide insight into the site-specific regulation of MAT by the nervous system, including a novel role for sensory neurotransmission, as well as its relationship to nutrient release by peripheral WAT.

**Disclosures:** Erica L Scheller, None.

## 1048

**Marrow adipose tissue expansion coincides with insulin resistance in MAGP1-deficient mice.** Tezin Walji<sup>1</sup>, Sarah Turecamo<sup>1</sup>, Alejandro Coca Sanchez<sup>2</sup>, Bryan Anthony<sup>3</sup>, Grazia Abou Ezzi<sup>3</sup>, Erica Scheller<sup>4</sup>, Daniel Link<sup>4</sup>, Robert Mecham<sup>5</sup>, Clarissa Craft<sup>\*5</sup>. <sup>1</sup>Department of Cell Biology & Physiology, Washington University School of Medicine, United states, <sup>2</sup>Department of Medicine & Medical Specialties, Faculty of Medicine & Health Sciences, University of Alcalá de Henares, Spain, <sup>3</sup>Oncology Division, Department of Medicine, Washington University School of Medicine, United states, <sup>4</sup>Bone & Mineral Diseases Division, Department of Internal Medicine; Washington University School of Medicine, United states, <sup>5</sup>Department of Cell Biology & Physiology, Washington University School of Medicine, St. Louis, United states

Marrow adipose tissue (MAT) is an endocrine organ with the potential to influence skeletal remodeling and hematopoiesis. Pathologic MAT expansion has been studied in the context of severe metabolic challenge; including caloric restriction, high fat diet feeding and leptin-deficiency. The rapid change in peripheral fat and glucose metabolism associated with these models impedes our ability to examine which metabolic parameters precede or coincide with MAT expansion. Microfibril-associated glycoprotein-1 (MAGP1) is a matricellular protein that influences cellular processes by tethering signaling molecules to extracellular matrix structures. MAGP1-deficient (*Mfap2*<sup>-/-</sup>) mice display a progressive excess adiposity phenotype, which precedes insulin resistance, and occurs without changes in caloric intake or ambulation. *Mfap2*<sup>-/-</sup> mice can therefore be used as a model to monitor the physiological consequences of metabolic dysfunction, without the use of modified diet. **Objective:** To correlate parameters of metabolic disease, bone remodeling and hematopoiesis with MAT expansion. **Methods:** WT and *Mfap2*<sup>-/-</sup> mice were analyzed at 2, 6, and 10 months. Metabolic parameters including peripheral adiposity, fasting blood glucose and insulin sensitivity were assessed. Bone mass and osmium-stained marrow adipocytes were quantified by micro-CT. We performed FACS analysis of bone marrow, spleen homogenate and blood samples. **Results:** Marrow adiposity was normal in *Mfap2*<sup>-/-</sup> mice until 6 months of age, however, by 10 months marrow fat

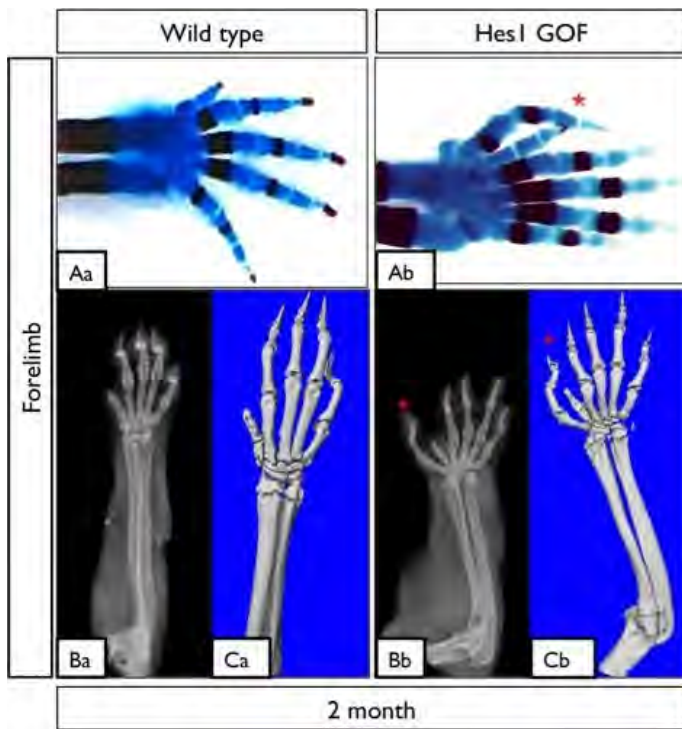
volume had increased 5-fold. MAT expansion was associated with insulin resistance, but not peripheral adiposity or hyperglycemia. Specifically, increased gonadal fat pad mass and hyperglycemia were detectable in *Mfap2*<sup>-/-</sup> mice by 2 months, but peaked by 6 months. *Mfap2*<sup>-/-</sup> mice also had reduced trabecular bone mass by 2 months, but this phenotype did not progress with age or MAT expansion. MAT expansion in the 10 month old *Mfap2*<sup>-/-</sup> mice had relatively minor consequences on hematopoiesis. Bone marrow cellularity was normal, but neutrophil frequency was reduced 13% and macrophage frequency was increased 61%. **Conclusions:** MAT expansion is coincident with insulin resistance, but not excess peripheral adiposity or hyperglycemia in *Mfap2*<sup>-/-</sup> mice. Bone loss is not proportional to the increase in MAT. Furthermore, a five-fold increase in MAT accumulation did not diminish bone marrow cellularity, but did skew the frequency of myeloid progenitor cells.

**Disclosures:** Clarissa Craft, None.

## 1049

**Over-expression of HES1 in skeletogenic mesenchyme results in preaxial polydactyly.** Deepika Sharma<sup>\*1</sup>, Timothy Rutkowski<sup>2</sup>, Anthony Mirando<sup>3</sup>, Matthew Hilton<sup>3</sup>. <sup>1</sup>University of Rochester School of Medicine, Duke University School of Medicine, United states, <sup>2</sup>Emory University, United states, <sup>3</sup>Duke University, United states

Preaxial polydactyly (PPD) is a common congenital birth defect characterized by extra digits in the anterior autopod (hand/foot). Sonic Hedgehog (SHH) signaling is critical in establishing proper digit identity and number, and inappropriate activation has been established as the primary cause for PPD. Mouse models of increased SHH signaling (*Gli3*<sup>xt</sup> mutants) produce a PPD phenotype, although the precise mechanisms are unclear. Interestingly, *Gli3*<sup>xt</sup> mice exhibit increased and expanded *Hes1* expression within the autopod. To determine whether altered *Hes1* expression is relevant to PPD, we generated *Hes1* gain-of-function (GOF) mice that over-expressed *Hes1* within the limb bud mesenchyme (*Prx1Cre;Rosa-Hes1*<sup>fl/fl</sup>)(*Hes1*<sup>GOF</sup>). Skeletal staining and radiographs demonstrate that *Hes1*<sup>GOF</sup> mice develop PPD. To dissect the role of HES1 in PPD and its intersection with SHH, we performed RNAseq, qPCR, and whole mount *in situ* hybridization on E10.5 and E11.5 limb buds, which showed significant decreases in chondrogenic gene expression, altered expression of patterning factors (HOX genes and other transcription factors), enhanced expression of notable SHH and FGF pathway related genes, as well as differential expression of potentially novel regulators of digit development. These data further indicated that HES1 regulates digit number by enhancing mesenchymal cell proliferation and delaying chondrogenesis via at least two mechanisms: 1) reinforcing SHH signaling, and 2) functioning independent or downstream of SHH. The mechanism of HES1 reinforcing SHH signaling was elucidated via altered SHH target gene expression detected by RNAseq and qPCR, decreased GLI3R protein levels assessed via Western blot, and the generation of a *Hes1*<sup>GOF</sup> mutant mouse in the *Gli3*<sup>xt</sup> background (*Prx1Cre;Rosa-Hes1*<sup>fl/fl</sup>;*Gli3*<sup>xt/xt</sup>), which demonstrated a synergistic digit number phenotype greater than either individual mutant phenotype alone. To determine whether HES1 was also capable of regulating digit number by acting independently or downstream of SHH, we generated *Hes1*<sup>GOF</sup> mutant mice in the absence of SHH (*Prx1Cre;Rosa-Hes1*<sup>fl/fl</sup>;*Shh*<sup>fl/fl</sup>). Interestingly, *Hes1* over-expression overcame the constrained digit number phenotype of SHH mutant mice, suggesting that HES1 can function downstream or independent of SHH. Collectively, our data suggest that HES1 regulates digit number by promoting mesenchymal cell proliferation and delaying chondrogenesis via SHH-dependent and -independent or downstream signaling mechanisms.



### Sustained expression of *Hes1* in the developing limb bud skeletogenic mesenchyme leads to a preaxial polydactyly (PPD) phenotype.

(Aa-b) Alcian Blue/Alizarin Red staining of WT and *Prx1Cre;Rosa-Hes1<sup>fl/fl</sup>* (*Hes1* GOF) mutant E18.5 forelimb. The over expression of *Hes1* leads to the development of digits within the anterior compartment.

(Ba-b) X-ray and (Ca-b) MicroCT analysis shows a morphologically normal extra digit (\*). The digit contains all the element of the wild type digits. This phenotype suggests *Hes1* may be a key factor in regulating digit number within the developing limb bud.

*Hes1* gain of function

Disclosures: Deepika Sharma, None.

## 1050

**The Impact and Mechanism of *Tsc1* Deletion in Craniofacial Bone Development.** Xiaoxi Wei<sup>1\*</sup>, Min Hu<sup>2</sup>, Brannon Cavanaugh<sup>3</sup>, Andrea Alford<sup>3</sup>, Rachel Merzel<sup>3</sup>, Mark Banaszak Holl<sup>3</sup>, Fei Liu<sup>4</sup>. <sup>1</sup>Jilin University School & Hospital of Stomatology & University of Michigan School of Dentistry, United states, <sup>2</sup>Jilin University School & Hospital of Stomatology, China, <sup>3</sup>University of Michigan, United states, <sup>4</sup>University of Michigan School of Dentistry, United states

The best known mTOR signaling dysregulation in human disease is called Tuberous Sclerosis (TS). TS is a genetic disorder caused by mutations in either *TSC1* or *TSC2*, which are negative regulators of mTOR signaling. More than 40% of TS patients have sclerotic craniofacial bone lesion with poorly defined mechanisms. Previously we reported a sclerotic craniofacial bone lesion mouse model of TS in which *Tsc1* was deleted in neural crest-derived (NCD) cells by *P0Cre*. Herein, we further determined the impact and mechanism of *Tsc1* deletion on cranial bone development. MicroCT analysis showed an increase in bone parameters (volume, thickness, BV/TV) of frontal bone of *Tsc1<sup>fl/fl</sup>;P0Cre* (CKO) mice. The thickness of CKO frontal bone was 1.5 fold, 2.4 folds, 3.3 folds, and 4.6 folds of control at 1m, 2m, 6m, and 1y respectively (Fig 1). The tissue mineral density (TMD) was increased in 2m (16%), 6m (22%) and 1y (34%) but not 1m group. Bone mass and density increases were also observed in other NCD

intramembranous bones as well as the endochondral bones in the cranial base (pre-, basi-sphenoid bones). Surprisingly, despite the increase in TMD, the mineral/collagen and mineral/protein ratio significantly decreased in CKO bone shown by hydroxyproline assay and Atomic Force Microscope Infrared-spectroscopy measurement, indicating a higher increase in ECM density. To determine the mechanism of increased bone mass, CKO mice were crossed with *Gli1-LacZ* mice and we found a 55% increase of *Gli1-LacZ<sup>+</sup>* cell number in the coronal suture of CKO mice at 6wks, indicating increased cranial mesenchymal stem cells in CKO. However, inducible deletion of *Tsc1* with *Gli1Cre<sup>ER</sup>* led to slightly decreased cranial bone mass. In addition, *Tsc1* deletion with *OsxCre* only caused mild bone mass increase (25% increase in frontal bone thickness, no change in cranial base bones at 1m). Lastly, to determine the extent enhanced mTORC1 signaling was responsible for bone phenotype, the mice were treated with rapamycin, an mTORC1 inhibitor from day 3 to 2m. Rapamycin completely rescued bone mass increase but not TMD increase. In summary, our data suggest that 1) *Tsc1* deletion in NCD cells increases cranial bone mass in both intramembranous and endochondral NCD bones at least partially through expansion of mesenchymal stem cells; 2) *Tsc1* deletion significantly alters bone quality; 3) *Osx<sup>+</sup>* cells are partially responsible for bone mass increase; 4) *Tsc1* regulates bone quantity and quality with different mechanisms.

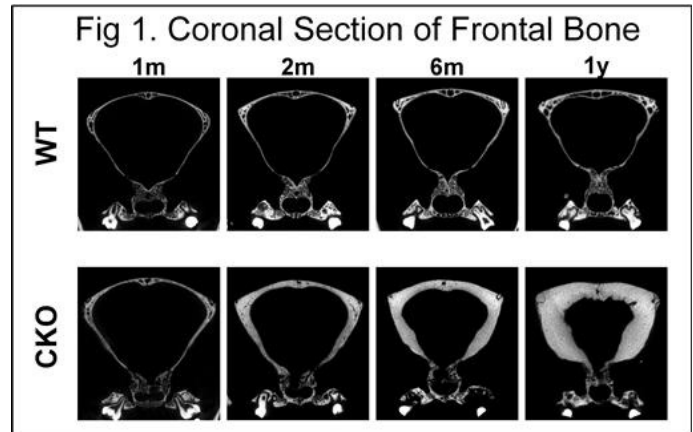


Fig 1

Disclosures: Xiaoxi Wei, None.

## 1051

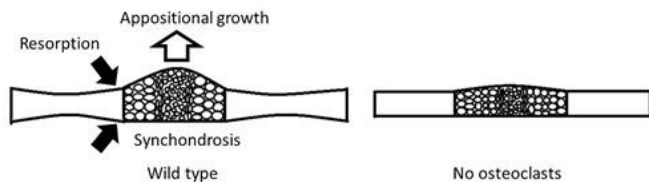
**How do Osteoclasts Shape the Cranial Base Bones During Development?.** Mio Edamoto\*, Yukiko Kuroda, Koichi Matsuo. Keio University School of Medicine, Japan

Cranial base mainly consists of three bones, basioccipital, basisphenoid, and presphenoid bones. The growth of cranial base during endochondral ossification is dependent on the two bipolar growth plates, spheno-occipital and intersphenoid synchondroses. Cranial base bones are responsible for the facial abnormalities seen in patients with Down syndrome, Apert syndrome, Crouzon syndrome, and different craniosynostosis syndromes. In mice, diverse craniofacial phenotypes have been described in gene deletion mutants. However, roles of osteoclasts in cranial base morphogenesis remain unclear. To reveal whether osteoclasts are crucial for growth and re-shaping of cranial base bones, we analyzed normal mice harboring osteoclasts expressing a red fluorescent protein (cathepsin K-cre-tTomato reporter mice), and mice devoid of osteoclasts, namely mice lacking c-Fos or RANKL.

Histological analysis of synchondroses of 3-day-old c-Fos knockout (KO) mice revealed that thickness along the dorsoventral axis in parasagittal sections was smaller than that of control mice. The inner (cambium) layer under the perichondrium contains a few rows of longitudinally oriented cells. In 3-day-old c-Fos KO mice, number of cells in the cambium layer was reduced compared with control mice. These data suggest that cells for appositional growth of cartilage at the perichondrium were reduced in the absence of osteoclasts.

Micro-CT analysis in the mid-sagittal planes showed that, in wild-type mice, the diaphysis of cranial base bones was thinner than the metaphyseal chondro-osseous junction. By contrast, in c-Fos KO mice, the thickness at the chondro-osseous junction remains relatively constant towards diaphysis, suggesting that osteoclasts resorb metaphyseal bone at both endocranial and ectocranial surfaces. Consistently, fluorescence microscopy performed 24 hours after calcein injection into 3-day-old catRANIhepsin K-cre-tTomato reporter mice revealed that calcein-positive areas at the metaphysis correspond to osteoclasts localization on the cranial base bones.

These results suggest that osteoclasts have two distinct roles in morphogenesis of cranial base bones. First, osteoclasts promote appositional growth in thickness at the perichondrium of synchondrosis. Second, osteoclasts chisel at the metaphysis to re-shape and reduce the thickness of cranial base bones.



Cranial base bones

Disclosures: Mio Edamoto, None.

## 1052

**Smpd3 Expression in Both Chondrocytes and Osteoblasts Is Required for Normal Endochondral Bone Development.** Garthiga Manickam<sup>1</sup>, Jingjing Li<sup>1</sup>, Chun-do Oh<sup>2</sup>, Hideyo Yasuda<sup>3</sup>, Pierre Moffatt<sup>1</sup>, Monzur Murshed<sup>1</sup>. <sup>1</sup>McGill University, Canada, <sup>2</sup>Rush University Medical Center, United states, <sup>3</sup>Konkuk University, Korea, democratic people's republic of

Sphingomyelin phosphodiesterase 3 (SMPD3), a lipid-metabolizing enzyme present in bone and cartilage, has been identified as a key regulator of skeletal development. SMPD3-deficient *frolfro* mice, which are homozygous for a loss-of-function mutation (*fragilitas ossium; fro*) in the *Smpd3* gene, show severe congenital skeletal defects hallmarked by poor cartilage and bone mineralization. Here we show that *Smpd3* expression in ATDC5 chondrogenic cells is downregulated by PTHrP through transcription factor SOX9. Furthermore, we show that transgenic expression of *Smpd3* in the chondrocytes of *frolfro* mice corrects the cartilage, but not the bone abnormalities. Additionally, we report the generation of *Smpd3<sup>lox/lox</sup>* mice for the tissue-specific inactivation of *Smpd3* using the Cre-loxP system. We find that the skeletal phenotype in *Smpd3<sup>lox/lox</sup>;Ossx-Cre* mice, in which the *Smpd3* gene is ablated in both late-stage chondrocytes and osteoblasts, closely mimics the phenotype of *frolfro* mice. On the other hand, *Smpd3<sup>lox/lox</sup>;Col2a1-Cre* mice, with *Smpd3* gene knocked out in chondrocytes only, recapitulate the *frolfro* cartilage phenotype. This work demonstrates that SMPD3 has a local role in skeletogenesis and that its expression in both chondrocytes and osteoblasts is required for normal endochondral bone development.

Disclosures: Garthiga Manickam, None.

## 1053

**Compensatory roles of osteoprogenitor YAP and TAZ in skeletal development.** Christopher Kegelman<sup>\*</sup>, James Dawahare, Joel Boerckel. University of Notre Dame, United states

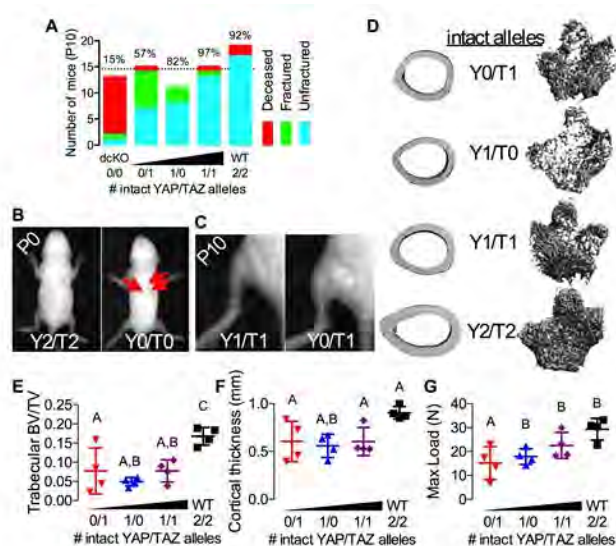
Proper bone development requires coordinated progenitor cell lineage specification and dynamic regulation of bone accrual and maintenance, but the intracellular molecular mediators remain incompletely understood. Recently, the Hippo pathway effector proteins, Yes-associated protein (YAP) and transcriptional co-activator with PDZ-binding motif (TAZ) have emerged as key mediators of cellular mechanotransduction, but exhibit conflicting regulatory functions in osteogenic progenitor differentiation *in vitro*<sup>1,2</sup>. The purpose of this study was to investigate the combinatorial roles of YAP and TAZ in osteoprogenitor cells and their progeny in skeletal development. Since global YAP deletion is embryonic lethal, while TAZ ablation only moderately reduces bone size, cell type-selective dual ablation approaches are necessary to evaluate compensatory functions.

We hypothesized that YAP and TAZ positively and redundantly mediate skeletal growth and development. We generated littermate conditional knockout mice with allele dosage-dependent YAP/TAZ ablation through Cre-recombination under control of the Osterix1 promoter. All animal experiments were approved by the IACUC. Progeny yielded expected Mendelian ratios at birth, but homozygous ablation of both YAP and TAZ (Y0/T0) resulted neonatal lethality by asphyxiation secondary to rib cage malformation (A,B). Double heterozygotes (Y1/T1) and mice featuring a single copy of either YAP (Y1/T0) or TAZ (Y0/T1) lived to maturity, but exhibited allele dosage-dependent decreases in tibial length and body weight, demonstrating compensatory function. Notably, both single-copy conditional mice exhibited spontaneous femoral fractures between P1 and P10, which healed through callus formation (C).

Micro-CT analyses at week 8 revealed defects in trabecular bone quantity and morphology (E) and cortical bone volume and distribution (F), but bone mineral density was not altered. Three-point bend testing of 8 week-old femurs demonstrated YAP/TAZ allele dosage-dependent defects in structural mechanical properties (G). Taken together, these data demonstrate compensatory roles of YAP and TAZ in positive regulation of skeletal development through control of bone structure, maintenance, and resilience. Mechanistic understanding of how these proteins regulate skeletogenesis will guide future therapeutic strategies for targeting skeletal diseases, abnormalities, and healing.

<sup>1</sup>Hong+ Science 2005.309:1074

<sup>2</sup>Seo+ Cell Reports 2013(3):2075



Figure

Disclosures: Christopher Kegelman, None.

## 1054

**Runx2 Activity in Mature Osteoblast is Essential for Postnatal Bone Acquisition and to Prevent Premature Ageing.** Haiyan Chen<sup>\*</sup>, Harunur Rashid<sup>1</sup>, Kayla King<sup>1</sup>, Ying Liu<sup>2</sup>, Jerry Feng<sup>2</sup>, Amjad Javed<sup>1</sup>. <sup>1</sup>Department of Oral & Maxillofacial Surgery, School of Dentistry, University of Alabama at Birmingham, United states, <sup>2</sup>Department of Biomedical Sciences, Baylor College of Dentistry, Texas A&M University, United states

Runx2 transcription factor is essential for commitment and differentiation of osteoblast. Runx2 global null mice fail to develop bone and die at birth. Surprisingly, Runx2 overexpression in osteoblasts leads to osteopenia indicating an inhibitory function of Runx2 in mature osteoblast and postnatal bone synthesis. However, role of endogenous Runx2 gene in mature osteoblast and postnatal skeletogenesis remains unknown. We recently generated Runx2-floxed mice. To study osteoblast function without affecting osteoblast differentiation, we deleted Runx2 gene in mature osteoblast using Osteocalcin-Cre mice. Interestingly, Runx2<sup>OB-/-</sup> mice were born alive and Alizarin red/Alcian blue staining at 1-week showed normal bone development. Thus, Runx2 function in mature osteoblast is not essential for embryonic bone development. Postnatally, Runx2<sup>OB-/-</sup> mice grow poorly and exhibit 35% and 55% less body weight than WT littermates at 1 and 5-months respectively. Growth retardation noted in both genders is unrelated to dental or any issues with feeding and suggest mature osteoblast regulate homeostasis of connective tissue beyond the skeleton. Failed postnatal growth in Runx2<sup>OB-/-</sup> mice was coupled with appearance of hunch back and signs of premature aging, including dull hair, reduced activity, priapism, and sarcopenia. Runx2<sup>OB-/-</sup> mice started to die from 6-weeks of age and none survived beyond 6 months, indicating that Runx2 activity in mature osteoblast is essential for completion of normal life span. Postnatal bones assessed at 5 months showed striking osteoporosis, with a 65% decrease in cortical BV/TV. Surprisingly, significant increase in trabecular BV (42%) and number (30%) was noted in Runx2<sup>OB-/-</sup> mice but trabecular thickness and length were decreased significantly (40%) in mutant bones. Histomorphometry, Calcein double labeling and TRAP staining showed that bone loss was due to reduced bone formation, but not increased bone resorption, suggesting disrupted osteoblast function. Interestingly, mRNA levels of early marker ALP were similar between 5 month old littermates but expression of mature osteoblast/osteocyte markers (BSP, OC, DMP1, SOST) was decreased by 80%. Acid-etch SEM revealed poor mineral quality, abnormal morphology, and pattern of osteocytes distribution in the femur of Runx2<sup>OB-/-</sup> mice. In conclusion, contrary to the popular notion of inhibitory role of Runx2 in mature osteoblast, we demonstrate that Runx2 is required for postnatal bone acquisition.

Disclosures: Haiyan Chen, None.

## 1055

**Osteoclast Precursor Cells That Form Osteoclasts In Vivo Under Homeostatic Conditions Express CX3CR1, Form Osteoclasts Within 5 Days And Rarely Derive From Circulating Cells.** Emilie Roeder\*, Judith Kalinowski, Sandra Jastrzebski, Christian Jacome Galarza, H. Leonardo Aguila, Sun-Kyeong Lee, Ivo Kalajzic, Joseph Lorenzo. UConn Health, United states

Osteoclasts (OC) originate from myeloid cells. However, the nature of the in vivo OC precursor (OCP) is not well defined. We previously identified populations of murine bone marrow (BM) OCP that formed mature OC in vitro with high efficiency. CX3CR1 (the fractalkine receptor) is a well-described myeloid precursor cell marker. Using mice with enhanced green fluorescent protein (EGFP) knocked into the CX3CR1 coding locus and flow cytometry, we found that > 99% of our OCP populations expressed EGFP (i.e. were positive for CX3CR1). However, cultured mature OC did not express EGFP.

We next examined if CX3CR1 is expressed by OCP in vivo. Mice with Cre-ERT2 knocked into the CX3CR1 coding locus were crossed with Ai14 reporter mice, which express tdTomato red fluorescent protein after Cre recombination. Cre-ERT2 recombinase is active only after binding tamoxifen (Tx). 8-wk-old male CX3CR1-Cre-ERT2 x Ai14 mice were injected with Tx (75 mg/Kg) and sacrificed 1 and 5 days later. There was little tdTomato expression in femoral OC at day 1, but strong tdTomato expression at day 5 in many large multinucleated, tartrate-resistant acid phosphatase (TRAP) + OC adjacent to bone in the primary and secondary spongiosa. Control femurs from Ai14 mice treated with Tx or CX3CR1-Cre-ERT2 x Ai14 mice not treated with Tx demonstrated only an occasional fluorescent cell. Since CX3CR1 is not expressed in mature OC, the fluorescent OC must have originated from CX3CR1-expressing OCP.

CX3CR1 marks both BM and circulating myeloid OCP. To define if circulating cells contribute to osteoclastogenesis during homeostasis, we parabiosed TRAP-tdTomato mice (CD45.2) with wild type (WT) mice (CD45.1). TRAP-tdTomato mice use the TRAP (*Acp5*) promoter to drive tdTomato expression in OC. Flow cytometry (CD45.1/2) demonstrated high level mixing of blood cells between the parabiosed mice at 2.5 weeks. At 4.5 weeks we found abundant tdTomato + OC in femurs of the TRAP-tdTomato mice but these were almost undetectable in WT mice. Similarly, cultured BM stimulated to form OC demonstrated fluorescent cells abundantly in cultures from TRAP-tdTomato but not from WT mice. Flow cytometry confirmed low-level engraftment of BM cells after parabiosis.

These results demonstrate that OCP in vivo under homeostatic conditions express CX3CR1, form OC within 5 days and rarely derive from circulating cells. We hypothesize that during normal homeostasis, bone marrow resident cells represent the major OCP source.

*Disclosures: Emilie Roeder, None.*

## 1056

**Synchronized fusion of osteoclast precursors involves syncytin 1, phosphatidylserine and annexins at the surface of the cells.** Santosh Verma\*<sup>1</sup>, Evgenia Leikina<sup>1</sup>, Kamran Melikov<sup>1</sup>, Claudia Gebert<sup>1</sup>, Vardit Kram<sup>2</sup>, Marian Young<sup>2</sup>, Leonid Chernomordik<sup>1</sup>. <sup>1</sup>NICHD, NIH, United states, <sup>2</sup>NIDCR, NIH, United states

Little is known about the cell fusion process that generates osteoclasts, multinucleated cells that resorb bones. One of the key challenges in characterizing developmental fusion events is to uncouple the actual fusion stage from the preceding processes, which prepare macrophages for fusion. Here we separated fusion stage itself from pre- and post- fusion stages. To trigger osteoclastogenesis, we applied M-CSF and RANKL to human monocytes or RANKL to murine macrophage-like RAW cells. We blocked fusion by reversible inhibitor lysophosphatidylcholine, accumulated the ready-to-fuse macrophages and then removed the inhibitor. This approach has allowed us to synchronize most of the cells to fuse within 2 hours. In our search for the proteins that mediate human osteoclast fusion, we first explored whether fusion between monocyte-derived osteoclasts involves syncytin-1 (Syn), an endogenous retroviral protein that fuses human trophoblasts in placentogenesis. A peptide known to specifically block fusogenic restructuring of Syn, inhibited synchronized fusion between human osteoclasts. This finding indicated that Syn plays an important role in fusion between osteoclasts. Since development of fusion competency of osteoclast precursors was not accompanied by any increase in the surface expression of Syn, we focused on mechanisms that might control Syn activity. We found that at the time of fusion, osteoclasts expose at their surface phosphatidylserine (PS), lipid that is normally found only in the inner leaflet of the plasma membrane. Non-apoptotic PS externalization is mediated by TMEM16 scramblases and CaCCinh-A01, an inhibitor of these scramblases, suppressed both PS exposure at the surface of fusion-committed cells and synchronized fusion. Fusion was also suppressed by peptide inhibitors and antibodies to PS-binding proteins annexin A5 (AnxA5) for human monocytes and Anxs A1 and A5 for RAW cells. The importance of Anxs in osteoclast formation was further confirmed by finding that bone marrow cells from mice deficient in both AnxA1 and A5 have a lowered ability to generate osteoclasts. We also found that fusion of human osteoclasts depends on a concerted rather than independent action of AnxA5 and Syn at the surface of the osteoclasts. Our data suggest that, in contrast to dynamin-dependent late stages of osteoclast fusion identified in our recent work, fusion initiation depends on Syn, Anxs and PS at the surface of fusion-committed cells.

*Disclosures: Santosh Verma, None.*

## 1057

**A novel role of c-FMS Intracellular cytoplasmic domain (FICD) as a transcriptional regulator in osteoclastogenesis.** Kyung-Hyun Park-Min, Seyeon Bae, Min Joon Lee, Koichi Murata, Se Hwan Mun\*. Hospital for Special Surgery, United states

M-CSF signaling is critical for osteoclasts and altered M-CSF responses have been linked to exacerbation of diseases such as RA. We have shown that FMS, a receptor for M-CSF, undergoes the shedding process in osteoclast precursor cells (OCPs) upon inflammatory stimulus. Although the FMS-mediated signaling originates from the cell surface and is extensively studied, the precise mechanism of FMS shedding and the role of FMS shedding in osteoclasts remain elusive. Here, we identified novel regulatory pathways that mediate shedding and RIPPING of FMS in osteoclasts, leading to the discovery of a newly identified transcriptional regulator for osteoclastogenesis. TACE is a metalloprotease that is responsible for shedding of FMS and RANK, two essential receptors in osteoclasts and thus we examined if suppressing TACE is beneficial for preventing excessive bone loss. To this end, we generated myeloid-specific TACE-deficient mice (TACE<sup>AM</sup>) and examined bone phenotype of TACE<sup>AM</sup> and their littermate control mice (TACE<sup>con</sup>) by microCT and histomorphometric analysis. Surprisingly, TACE<sup>AM</sup> mice had increased bone mass compared to TACE<sup>con</sup> mice and the osteoclast number and surface in the femur were significantly decreased in TACE<sup>AM</sup> mice. Consistent with in vivo bone phenotype, TACE-deficient OCPs from both human and mice showed the delayed kinetics of OC differentiation compared to control OCPs in vitro. Although the level of FMS on the surface was increased in OCPs from TACE<sup>AM</sup> compared to OCPs of TACE<sup>con</sup>, the expression of RANK, a target of M-CSF signaling, and RANKL-mediated signaling in TACE<sup>AM</sup> OCPs were significantly decreased. We found that defects in osteoclastogenesis of TACE<sup>AM</sup> partially resulted from the loss of a new functional fragment of FMS: FICD (the FMS intercellular domain fragment). FICD is generated by the combination of the conventional RIPPING by TACE and  $\gamma$ -secretase with additional processes that we newly identified. FICD is able to translocate into the nucleus and functions as a novel transcriptional regulator, which directly binds to the RANK promoter and regulates the RANK expression in OCPs. Overexpression of FICD reversed the delayed osteoclastogenesis in TACE<sup>AM</sup>. Therefore, our data suggest that FMS not only transduces signaling as a receptor but is also processed to FICD that traffics into the nucleus, where it functions as an essential transcriptional regulator. Taken together, we propose a novel mechanism and function of FMS processing and FICD in osteoclast differentiation. FMS signaling and FICD independently contribute to the regulation of RANK expression and osteoclastogenesis. A better understanding of the diverse roles of FMS/FICD will advance our understanding of fundamental osteoclast biology, and targeting TACE and the process of FICD generation may serve as novel therapeutic targets for the treatment of pathological bone resorption.

*Disclosures: Se Hwan Mun, None.*

## 1058

**ASXL1 epigenetically suppresses osteoclast formation by methylating NFATc1.** Nidhi Rohatgi\*, Wei Zou, Timothy Hung-Po Chen, Yousef Abu-Amer, Steven Teitelbaum. Washington University in St. Louis, United states

Mammalian ASXL1 is an ETP protein which activates or retards transcription by modifying histone methylation. ASXL1 is a particularly relevant protein as inactivating mutations are commonly associated with myeloid malignancies and are a marker of aggressive disease. The negative impact of mutated ASXL1 on myelodysplasia likely reflects epigenetic transcriptional activation of leukemia-promoting genes in hematopoietic progenitors. Given that ASXL1 is indispensable for myeloid differentiation, we asked if it also regulates the osteoclast. Thus, we mated ASXL1(f/f) mice with those expressing Lysozyme M-Cre to delete ASXL1 in all osteoclast lineage cells. ASXL1-deficient precursors formed significantly more osteoclasts than their littermate controls when exposed to M-CSF and various doses of RANKL (p<0.01). Differentiation markers for osteoclastogenesis, were also increased as much as 10 fold in ASXL1-deficient cells. In keeping with increased osteoclastogenesis, deletion of ASXL1 in myeloid cells results in osteoporosis with decreased BMD and BV/TV in the KO animals (p<0.001) that co-incides with a significant increase in osteoclast number per bone surface (p<.001). Osteoclast differentiation involves of a network of transcription factors, many of which are regulated epigenetically. We therefore asked, if ASXL1 modulates osteoclast differentiation by maintaining a balance between positive and negative epigenetic regulators. In fact, ASXL1 deficiency results in reduction of transcriptional repressor, H3K27me3, which enriches the NFATc1 promoter. Demethylation of H3K27me3 on NFATc1 thereby greatly enhances expression of the osteoclastogenic transcription factor and abundance of the bone resorptive cell. Because the histone demethylase, Jmjd3, promotes osteoclast formation by demethylating NFATc1-associated H3K27, it presented as a reasonable candidate to mediate the osteoclastogenesis of ASXL1<sup>lysM</sup> mice. Supporting this posture, Jmjd3 expression increases 40 fold in ASXL1-deficient osteoclasts. Most importantly, Jmjd3 knockdown in ASXL1<sup>lysM</sup> osteoclast precursors reduces NFATc1 expression and in consequence, arrests osteoclast formation. Thus, in addition to promoting myeloid malignancies, ASXL1 deficiency promotes osteoclastogenesis and osteoporosis, exerting its inhibitory effects by blunting repressive histone methylation of NFATc1.

*Disclosures: Nidhi Rohatgi, None.*

## 1059

**COMMD1 negatively regulates osteoclastogenesis and pathologic bone resorption via pRB-E2F1-CKB pathway and is inactivated by hypoxia.** Koichi Murata\*, Min Joon Lee, Seyeon Bae, Sehwan Mun, Kyung-Hyun Park-Min, Lionel Ivashkiv. Hospital for special surgery, United states

Hypoxia augments osteoclastogenesis and can contribute to bone resorption at hypoxic sites such as bone marrow and the synovium of rheumatoid arthritis (RA) patients. Mechanisms by which hypoxia increases osteoclastogenesis are poorly understood. In this study we used transcriptomic, bioinformatic, and signaling approaches to discover new molecules and pathways that are important for osteoclastogenesis and regulated by hypoxia, and validated the pathophysiological importance of our findings in RA patients and an arthritis model.

We treated human osteoclast precursors (OCPs) with RANKL in either normoxia or hypoxia (2% of O<sub>2</sub>) conditions. RNA sequencing revealed that 152 genes were upregulated by both RANKL and hypoxia. Ingenuity pathway analysis for these genes identified COMMD1 as one of the most significant upstream regulators following Hif1 $\alpha$  and Hif2 $\alpha$ . COMMD1 is copper metabolism MURR1 domain containing 1 that has been implicated in a variety of cellular processes, including copper transport, electrolyte balance and proteosomal degradation. Although COMMD1 mRNA was not changed by RANKL or hypoxia, RANKL induced the accumulation of COMMD1 protein in the nucleus and hypoxia suppressed this accumulation. Knock-down of COMMD1 by siRNAs enhanced human osteoclastogenesis in normoxia and phenocopied hypoxia-mediated enhancement of osteoclastogenesis. We found that COMMD1 expression level was inversely correlated with total sharp scores in RA patients. Consistently, conditional deletion of COMMD1 in myeloid cells resulted in increased bone erosion in the serum-induced arthritis model mice. To identify how inhibition of COMMD1 accelerated osteoclastogenesis, we performed RNA sequencing. Three pathways including cell cycle, NF- $\kappa$ B signaling, and hypoxia pathways were prominently upregulated by RANKL and COMMD1-knockdown, and indeed, E2F1, a key mediator for cell cycle, was a target of COMMD1. E2F1 knockdown inhibited osteoclastogenesis, suggesting that E2F1 is a positive regulator of osteoclastogenesis. E2F1 regulated energy production via glycolysis, and ATP storage via creatine kinase B.

These findings identify COMMD1 as a negative regulator of osteoclastogenesis and pathologic bone resorption. COMMD1 works by suppressing a newly discovered pRB-E2F1-CKB pathway that is important for cell metabolism and osteoclastogenesis. The results also provide insight into mechanisms by which hypoxia promotes osteoclastogenesis by inactivating the negative regulator COMMD1.

**Disclosures:** Koichi Murata, None.

## 1060

**Absence of the VDR in Osteoclasts Results in Increased Bone Resorption and Osteoclast Survival.** Yolandi Starczak\*<sup>1</sup>, Daniel Reinke<sup>2</sup>, Michele V. Clarke<sup>3</sup>, Patricia K. Russell<sup>3</sup>, Katherine R. Barratt<sup>1</sup>, Rachel A. Davey<sup>3</sup>, Howard A. Morris<sup>1</sup>, Gerald J. Atkins<sup>2</sup>, Paul H. Anderson<sup>1</sup>. <sup>1</sup>School of Pharmacy & Medical Sciences, University of South Australia, Australia, <sup>2</sup>Centre for Orthopaedics & Trauma Research, Faculty of Health Sciences, University of Adelaide, Australia, <sup>3</sup>Department of Medicine, Austin Health, University of Melbourne, Australia

Mature osteoclasts express the vitamin D receptor (VDR) and the 1- $\alpha$ -hydroxylase enzyme (CYP27B1) allowing them to respond to vitamin D to regulate the processes of osteoclastogenesis and bone resorption. The *in vivo* demonstration of whether vitamin D activity within osteoclasts is important for regulating osteoclastic bone resorption is required. Osteoclast-specific deletion of the vitamin D receptor (Ctsk<sup>Cre</sup>/Vdr<sup>-/-</sup>) and 1- $\alpha$ -hydroxylase enzyme (Ctsk<sup>Cre</sup>/Cyp27b1<sup>-/-</sup>) were assessed in male and female mice at 6 and 12 weeks of age. In addition, Ctsk<sup>Cre</sup>/Vdr<sup>-/-</sup> and Vdr<sup>fl/fl</sup> mice were assessed under conditions of ovariectomy (OVX) or a low calcium (0.03%), low phosphorous (0.08%) diet (LowCaP). Splenocyte-derived osteoclasts from global Vdr<sup>-/-</sup> and Ctsk<sup>Cre</sup>/Vdr<sup>-/-</sup> mice were assessed in the presence of RANKL + MCSF for TRAP+ cell number, resorptive activity on dentine, and gene-expression profiles. Six week old Ctsk<sup>Cre</sup>/Vdr<sup>-/-</sup> male mice demonstrated a 10% decrease in vertebral bone volume (P<0.05) due to decreased trabecular number (P<0.05) when compared to Vdr<sup>fl/fl</sup> control mice. Consistent with increased bone loss, Ctsk<sup>Cre</sup>/Vdr<sup>-/-</sup> mice demonstrated increased mean osteoclast size (p<0.05) and a strong trend in increased osteoclastogenesis, despite reduced RANKL mRNA levels, when compared to Vdr<sup>fl/fl</sup> animals. When Ctsk<sup>Cre</sup>/Vdr<sup>-/-</sup> mice were fed a LowCaP diet, vertebral bone loss exceeded the bone loss observed in Vdr<sup>fl/fl</sup> mice by a further 22% (P<0.05), suggesting enhanced osteoclastic bone resorption. However, the absence of VDR in mature osteoclasts did not alter the N.Oc/B.Pm or the degree of bone loss due to OVX. No bone or osteoclastic phenotype was observed in Ctsk<sup>Cre</sup>/Cyp27b1<sup>-/-</sup> mice when compared to control mice. Vdr<sup>-/-</sup> splenocyte cultures result in a 50% reduction in the number of TRAP+ osteoclasts. However, Vdr<sup>-/-</sup> osteoclasts that do form appear to be longer lived, as determined by Bax:Bcl2 ratio, and resorption activity on dentine was increased when compared to WT cells. By comparison, Ctsk<sup>Cre</sup>/Vdr<sup>-/-</sup> cultures resulted in an increase in TRAP+ osteoclasts without significant alteration to resorptive activity. These data suggest that the presence of VDR is required for osteoclastogenesis. Furthermore, VDR in mature osteoclasts may also influence survival and resorption activity. Thus, in addition to RANKL-mediated osteoclastogenesis, VDR also directly regulates the generation and activity of osteoclasts *in vitro* and *in vivo*.

**Disclosures:** Yolandi Starczak, None.

## 1061

**First X-linked Form of Osteogenesis Imperfecta, Caused by Mutations in MBTPS2, Demonstrates a Fundamental Role for Regulated Intramembrane Proteolysis in Normal Bone Formation.** Wayne Cabral\*<sup>1</sup>, Uschi Lindert<sup>2</sup>, Surasawadee Ausavarat<sup>3</sup>, Siraprapa Tongkobpetch<sup>4</sup>, Katja Ludin<sup>5</sup>, Aileen Barnes<sup>1</sup>, Patra Yeetong<sup>3</sup>, Maryann Weis<sup>6</sup>, Birgit Krabichler<sup>7</sup>, Chalurnpon Srichomthong<sup>3</sup>, Elena Makareeva<sup>8</sup>, Andreas Janecke<sup>7</sup>, Sergey Leikin<sup>8</sup>, Benno Röthlisberger<sup>5</sup>, Marianne Rohrbach<sup>2</sup>, Ingo Kennerknecht<sup>9</sup>, David Eyre<sup>6</sup>, Kanya Suphapeetiporn<sup>3</sup>, Cecilia Giunta<sup>2</sup>, Vorasuk Shotelersuk<sup>3</sup>, Joan Marini<sup>10</sup>. <sup>1</sup>Section on Heritable Disorders of Bone & Extracellular Matrix, NICHD, National Institutes of Health, United states, <sup>2</sup>Division of Metabolism, Connective Tissue Unit & Children's Research Center, University Children's Hospital Zurich, Switzerland, <sup>3</sup>Center of Excellence for Medical Genetics, Department of Pediatrics, Faculty of Medicine, Chulalongkorn University & Excellence Center for Medical Genetics, King Chulalongkorn Memorial Hospital, the Thai Red Cross Society, Thailand, <sup>4</sup>Center of Excellence for Medical Genetics, Department of Pediatrics, Faculty of Medicine, Chulalongkorn University, & Thai Excellence Center for Medical Genetics, King Chulalongkorn Memorial Hospital, the Thai Red Cross Society, Thailand, <sup>5</sup>Center for Laboratory Medicine, Department of Medical Genetics, Kantonsspital Aarau, Switzerland, <sup>6</sup>Department of Orthopedics & Sports Medicine, University of Washington, United states, <sup>7</sup>Division of Human Genetics, Medical University of Innsbruck, Austria, <sup>8</sup>Section on Physical Biochemistry, National Institute of Child Health & Human Development, National Institutes of Health, United states, <sup>9</sup>Institute of Human Genetics, Westfälische Wilhelms University, Germany, <sup>10</sup>Bone & Extracellular Matrix Branch, National Institute of Child Health & Human Development, National Institutes of Health, United states

Osteogenesis imperfecta (OI) is a heritable bone dysplasia with collagen-related defects. Dominant OI is caused by structural defects in type I collagen or *IFITM5*, while recessive forms are caused by deficiency of proteins that interact with collagen for modification, folding or crosslinking. We have identified the first X-linked form of OI caused by a defect in regulated intramembrane proteolysis (RIP). One type of RIP involves sequential cleavage of substrates by site-1 (S1P) and site-2 protease (S2P), encoded by *MBTPS1* and *MBTPS2*, respectively. S1P and S2P are Golgi membrane proteins that cleave regulatory proteins transported from the ER membrane in response to ER stress or decreased sterol metabolites, thereby releasing N-terminal fragments that activate gene transcription.

In two pedigrees with moderately severe OI, linkage analysis and next generation sequencing identified novel mutations in *MBTPS2*, predicting p.N459S and p.L505F substitutions located in or near the S2P NPDG motif required for metal ion coordination. Neither *MBTPS2* transcripts nor S2P protein were decreased in proband fibroblasts and osteoblasts. However, proband and *Mbtps2*-deficient CHO cells co-transfected with mutant *MBTPS2* and reporter constructs indicate deficient cleavage or activation of RIP substrates OASIS, ATF6 and SREBP. Consistent with diminished OASIS signalling, proband fibroblasts have significantly reduced type I collagen secretion (20-73% of normal control cells). Furthermore, the proportion of collagen with mature crosslinks is decreased in proband fibroblast matrix, suggesting collagen crosslinking may be impaired. Proband bone type I collagen contained less than half the normal level of hydroxylated Lys87, the residue crucial for crosslinking, and is likely caused by decreased Lysyl Hydroxylase 1 (LH1) levels in proband osteoblasts. In addition, proband urinary LP/HP crosslink ratios are increased. These findings suggest abnormal collagen crosslinking undermines bone strength in X-linked OI. Moreover, osteoblasts with mutant S2P exhibit defective differentiation in culture, with reduced expression of genes related to maturation, including *ALPL*. Expression of OASIS and SMAD4, which as a complex upregulate expression of matrix-associated genes such as *MATN1*, were also significantly reduced in proband osteoblasts. These are the first human studies to demonstrate a fundamental role of RIP in bone development, in addition to its function in cholesterol metabolism.

**Disclosures:** Wayne Cabral, None.

## 1062

**Transient Receptor Potential Melastatin 6 (TRPM6) as a Channel-Kinase Regulator of Mineral Metabolism.** Nora Renthal\*, David Clapham. Boston Children's Hospital, United states

Magnesium is involved in most major metabolic processes, working as an enzymatic cofactor and playing a role in the stability of DNA and RNA. Despite this critical function, the mechanisms of magnesium homeostasis remain largely unknown. Much of our continued ignorance stems from the fact that, due to its critical role in the function of the cell and survival of the organism, evolution has ensured the rarity of disorders of magnesium homeostasis. Recently, an opportunity arose for elucidating the mystery of this basic biology in the discovery that patients with a rare defect in magnesium handling, known as Familial Hypomagnesemia with Secondary Hypocalcemia (HSH), were linked to mutations in the ion channel

melastatin-related transient receptor potential 6 (TRPM6). In addition to being one of the few diseases of hypomagnesemia, HSH is one of few diseases linked to mutations in an ion channel. Furthermore, TRPM6 is exceptional among ion channels, as it is one of only two with an intrinsic kinase domain (the other being TRPM7). These unique features raise many questions, both of fundamental channel biology and the physiology of magnesium regulation.

Our studies are the first to methodically scrutinize the dual function of the TRPM6 channel and kinase, investigating the mechanism by which TRPM6 mutations produce the HSH phenotype in patients. Our data suggest TRPM6 produces cleaved kinases (M6CKs), which phosphorylate important downstream effectors of cell cycle regulation. This action is likely to be affected by TRPM6 channel conductance. We propose a mechanism whereby TRPM6 directs epithelial magnesium handling through localized ion signaling, triggering widespread kinase activity. These studies shed light on the signaling advantages of coupling both channel and kinase in the same polypeptide. It is our hope that an improved molecular understanding of TRPM6 will identify new mechanisms maintaining mineral balance in humans and better define the pathophysiology of Familial HSH.

**Disclosures:** Nora Renthal, None.

## 1063

**Vitamin D Deficiency Due to a Recurrent Gain-of-Function Mutation in *CYP3A4* Causes a Novel Form of Vitamin D Dependent Rickets.** Jeffrey Roizen<sup>\*1</sup>, Dong Li<sup>2</sup>, Lauren O'Lear<sup>3</sup>, Muhammad K Javaid<sup>4</sup>, Nicholas Shaw<sup>5</sup>, Peter Ebeling<sup>6</sup>, Hanh Nguyen<sup>7</sup>, Christine Rodda<sup>8</sup>, Kenneth Thummel<sup>9</sup>, Hakon Hakonarson<sup>2</sup>, Michael Levine<sup>3</sup>. <sup>1</sup>Division of Endocrinology & Diabetes The Children's Hospital of Philadelphia, Philadelphia, PA, University of Pennsylvania Perelman School of Medicine, Philadelphia, PA, United States, United states, <sup>2</sup>Center for Applied Genomics, The Children's Hospital of Philadelphia, Philadelphia, PA, University of Pennsylvania Perelman School of Medicine, Philadelphia, PA, United States, United states, <sup>3</sup>Division of Endocrinology & Diabetes, The Children's Hospital of Philadelphia, Philadelphia, PA, University of Pennsylvania Perelman School of Medicine, Philadelphia, PA, United States, United states, <sup>4</sup>National Institute for Health Research (NIHR) Musculoskeletal Biomedical Research Unit, University of Oxford, Oxford, UK, United Kingdom, <sup>5</sup>Birmingham Children's Hospital & University of Birmingham, Birmingham, UK, United Kingdom, <sup>6</sup>Monash University, Monash Medical Centre, Clayton, Victoria, Australia, <sup>7</sup>Monash University, Monash Medical Centre, Clayton, Victoria, Australia, Australia, <sup>8</sup>NorthWest Academic Centre, University of Melbourne, Australia, Australia, <sup>9</sup>Department of Pharmaceutics, University of Washington, Seattle, WA, USA, United states

We evaluated two unrelated and non-consanguineous adolescent females, one originally from Jordan and one from Australia, who had presented with early-onset rickets, reduced serum levels of 25(OH)D and 1,25(OH)<sub>2</sub>D, and deficient responsiveness to vitamin D<sub>2</sub>/D<sub>3</sub>, as well as to activated forms of vitamin D. Targeted analyses of the *CYP2R1*, *CYP27B1* and *CYP24A1* genes revealed normal sequences, thus we analyzed genomic DNA from both patients by whole exome sequencing (WES). We identified an identical heterozygous single nucleotide change in both subjects in exon 10 of the *CYP3A4* gene (c.902T>C) that results in replacement of isoleucine by threonine at codon 301 (p.I301T). This change was not present in other first-degree relatives of the two probands, nor in public databases (1,000 Genomes Project, 6503 exomes from the Exome Sequencing Project (ESP6500SI), and Exome Aggregation Consortium dataset (ExAC v0.3)) and existing data from more than 2,000 WES samples in the CHOP database. *CYP3A4* (EC 1.14.13.97) is a P450 enzyme that metabolizes xenobiotics and many steroid hormones. Because induction of *CYP3A4* by anticonvulsants leads to vitamin D deficiency via generation of the inactive vitamin D metabolites principally 4b,25(OH)<sub>2</sub>D and 1,23R,25(OH)<sub>2</sub>D, we compared the activity of the p.I301T mutant to that of wild type *CYP3A4* and *CYP24A1* (the principle vitamin D degrading enzyme) in HepG2 cells also expressing a 2-hybrid reporter consisting of the ligand-binding domain of the VDR fused to the yeast GAL4 DNA binding domain plus a firefly luciferase reporter gene under the control of nine copies of the yeast Gal4 UAS. The p.I301T mutant showed increased inactivation of calcitriol (Figure 1) relative to wild type *CYP3A4* at multiple calcitriol concentrations (p<0.05 by 2-way ANOVA) and post-hoc multiple-comparison-adjusted analyses confirmed significant differences at 30 ng/mL (p < 0.05), and relative to *CYP24A1* at 30 ng/mL (p<0.01). As measurements are done in whole cells, the kinetic data are apparent values. The apparent catalytic efficiency [Vmax(app)/Km(app)] of the wild type was 0.015, and of the mutant was 0.14. Thus, *CYP3A4* (p.I301T) is nearly 10-fold more active than the wild type enzyme. In summary, we have identified a recurrent missense mutation in *CYP3A4* that results in increased *CYP3A4* activity and enhanced inactivation of vitamin D metabolites. We propose that this gain-of-function mutation of *CYP3A4* causes a novel form of vitamin D dependent rickets.

**Figure 1: CYP3A4 (p.I301T) degrades 1,25(OH)<sub>2</sub>D<sub>3</sub> significantly more than wild type CYP3A4**

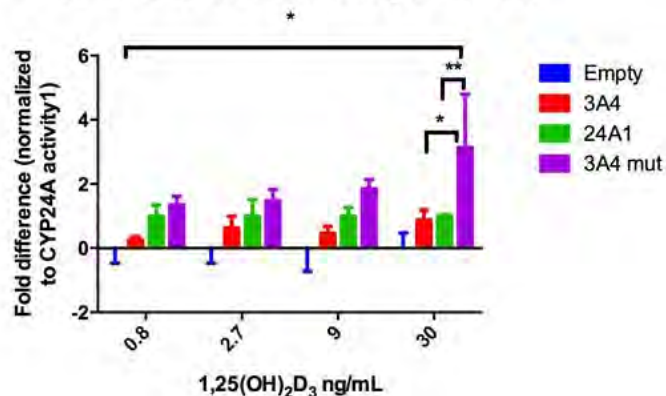


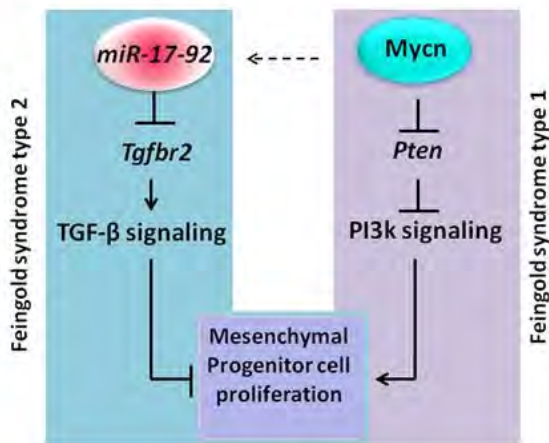
Figure 1: CYP3A4 (p.I301T) degrades 1,25(OH)<sub>2</sub>D<sub>3</sub> significantly more than wild type CYP3A4

**Disclosures:** Jeffrey Roizen, None.

## 1064

**Feingold syndrome skeletal dysplasia, type 1 and 2 are caused by distinct molecular mechanisms.** Fatemeh Mirzamohammadi<sup>\*</sup>, Garyfallia Papaioannou, Elena Paltrinieri, Tatsuya Kobayashi. Endocrine Unit, Massachusetts General Hospital & Harvard Medical School, United states

Feingold syndrome is an autosomal dominant, skeletal dysplasia syndrome characterized by combinations of congenital anomalies including microcephaly, short stature and digital anomalies. In most of the cases, Feingold syndrome is caused by heterozygous loss-of-function mutations of the N-myc gene (*MYCN*; Feingold syndrome type 1). Recently, it has been demonstrated that heterozygous deletion of the *miR-17-92* gene (*MIR17HG*; *Mir17-92*), which encodes a cluster of microRNAs, also causes Feingold syndrome (Feingold syndrome type 2). Since *miR-17-92* expression is regulated by Myc transcription factors, it has been postulated that Myc regulates limb development through *miR-17-92* activation. In this study, we generated mouse models for Feingold syndrome type 1 and 2 by conditionally deleting *Mycn* and *Mir17-92*, respectively, in developing mouse limbs. Both mouse models recapitulated skeletal abnormalities reminiscent of human conditions. In the Feingold syndrome type 2 mouse model, we found that *Mir17-92*-deficiency decreased skeletal mesenchymal cell proliferation via derepression of TGF- $\beta$  receptor II (*Tgfr2*); inhibition of TGF- $\beta$  signaling efficiently rescued the skeletal defects. In the Feingold syndrome type 1 model with conditional *Mycn* deletion, since Myc proteins are a well-known regulator of *Mir17-92*, we hypothesized that the possible upregulation of TGF- $\beta$  signaling due to the reduced *Mir17-92* expression might be responsible for the skeletal defects. Although expression of the *miR-17-92* cluster miRNAs were significantly decreased in *Mycn*-deficient skeletal progenitor cells, we did not find upregulation of TGF- $\beta$  signaling, and unlike in the type 2 model, TGF- $\beta$  signaling suppression in *Mycn*-deficient mice failed to rescue the skeletal abnormalities. However, we found that *Mycn*-deficient mesenchymal cells overexpressed *Pten*, a negative regulator of PI3K signaling that regulates cell proliferation. Upon introducing a floxed *Pten* allele, we found that *Pten* haploinsufficiency significantly rescued the skeletal abnormality caused by *Mycn*-deficiency. These results demonstrate that upregulation of TGF- $\beta$  signaling plays a causal role in the skeletal defect of Feingold syndrome type 2, whereas downregulation of PI3K signaling due to the derepression of *Pten* plays a major role in the pathophysiology of the Feingold syndrome type 1. Thus, despite the phenotypical similarity between Feingold syndrome type 1 and 2, they are caused by distinct molecular mechanisms.



Feingold syndrome skeletal dysplasia, type 1 and 2 are caused by distinct molecular mechanisms

**Disclosures:** Fatemeh Mirzamohammadi, None.

## 1065

**Relationship between parathyroid hormone levels and treatment response in patients with hypophosphatasia treated with asfotase alfa.** Andrew Denker\*, Hui Zhang, Rajendra Pradhan, Alexion Pharmaceuticals, Inc, United states

**Purpose:** Hypophosphatasia (HPP) is a rare, inherited metabolic disease caused by loss-of-function mutation(s) in the gene encoding tissue nonspecific alkaline phosphatase (TNSALP). Lack of TNSALP activity leads to failure to mineralize bone matrix, resulting in rickets/osteomalacia and systemic sequelae. Asfotase alfa is a human recombinant TNSALP that promotes bone mineralization. We sought to characterize changes in serum calcium and parathyroid hormone (PTH) concentrations during initiation of asfotase alfa treatment in patients with HPP.

**Methods:** Patients with HPP  $\leq 5$  years of age enrolled in a Phase II clinical trial (ENB-010-10: NCT01176266) received asfotase alfa (up to 9 mg/kg/week [wk]). Supplementation or restriction of dietary calcium was at the investigator's discretion. Mineralization of bone was assessed by the Radiographic Global Impression of Change (RGI-C) or Rickets Severity Scale (RSS) scores. Serum calcium (Ca) and PTH (intact) levels were summarized using descriptive statistics. Correlations between PTH levels and RGI-C and RSS were assessed using linear regression mixed-effects model methods.

**Results:** 59 patients were enrolled in the study as of the cut-off date (12-Nov-2014). Transient fluctuations were observed in individual PTH levels during the first 24 wks of treatment. Mineralization of bone showed maximal increases during the first 24 wks. At wk 24, median PTH increased by 1.08 pmol/L (N=30, range -3.5 to 45.3) while median Ca decreased by -0.005 mmol/L (N=36, range -1.33 to 0.74). A significant correlation was identified between PTH levels and improvement in RGI-C and RSS over time; the correlation was weak for RGI-C ( $r=-0.0599$ ;  $p < 0.0001$ ) and slightly better for RSS ( $r=0.1712$ ;  $p=0.0001$ ). Asfotase alfa was generally well tolerated, with injection site reactions the most common treatment-emergent adverse events. 3 patients experienced hypocalcemia during the study.

**Conclusions:** Asfotase alfa improved bone mineralization with modulation of serum Ca and PTH. During the first 24 wks, treatment with asfotase alfa was associated with positive changes in serum PTH levels that may or may not be accompanied by negative changes in serum Ca. Supplements of calcium and vitamin D may be required. Measurement of PTH levels could be useful within the first weeks of treatment to demonstrate the pharmacodynamic effect of asfotase alfa.

**Disclosures:** Andrew Denker, Alexion Pharmaceuticals, Inc, 14; Alexion Pharmaceuticals, Inc, 15

This study was supported by Alexion Pharmaceuticals, Inc.

## 1066

**Metabolic Expressivity and Clinical Significance of Genotype-Variations in Hypophosphatasia.** Lothar Seefried\*, Franz Jakob, Franca Genest, Wuerzburg University, Germany

**Purpose:** Hypophosphatasia (HPP) is caused by loss-of-function mutations of the ALPL-gene coding for the tissue nonspecific isoenzyme of alkaline phosphatase (TNAP). Mechanisms for both autosomal recessive as well as dominant inheritance have been described. As yet, more than 300 distinct, predominantly missense mutations have been documented. The work presented here aimed at identifying associations between genotypic constellations or individual mutations with biochemical markers of disease activity.

**Methods:** So far 104 adult patients with clinically established HPP could be enrolled in a cross-sectional trial to assess burden of disease in HPP (ClinicalTrials.gov; NCT 02291497). Genotyping is available for n=95 participants (73 female) by now.

Individual Mutations and genotypic constellations were linked to biochemical markers of the disease (ALP enzymatic activity, Serum-PLP, Serum/Urine-PEA) and global health status as measured by the SF-36.

**Results:** Mean patient age was 47.1 years (range 18-79) with n=76 having adult onset-disease and n=19 eliciting documented infantile/childhood HPP. Most frequent mutations were c.571G>A (n=16), c.526G>A (n=11) and c.1001G>A (n=9). N=67 harbored one, n=28 two mutations, with the latter presenting with sig. lower ALP activity and sig. higher PLP values. A sig. positive correlation was seen between number of incurred fractures and PLP levels ( $p=0.001$ ) but not for residual APL activity or PEA levels. SF-36 physical function and bodily pain subscores revealed greater limitations in participants with more than one mutation.

So far, no correlation pattern could be seen between individual Mutations or affected individual Exons and ALP activity or substrate values. Even in patients with identical mutations including pairs of first-degree relatives metabolic markers were divergent.

**Conclusions:** There was a tendency towards lower ALP, higher PLP and more severe clinical manifestation in patients with two mutation although exceptions were seen in both directions. Considerable discordance of ALP / PLP / PEA and health status is obvious even in patients with identical genotypic constellations. According to these results, it is not possible to infer residual ALP enzyme activity, substrate accumulation or health status from individual ALPL-Mutations and additional factors, including modifier genes, epigenetic and environmental effects as well as para-/endocrine mediators certainly have significant impact on HPP expressivity. Only PLP-level, but not ALP/PEA correlated to fracture incidence implicating that substrate accumulation in general should be further evaluated as a predictive parameter.

**Disclosures:** Lothar Seefried, Alexion Pharmaceuticals, Inc, 11

This study received funding from: Supported by a grant from Alexion Pharmaceuticals, Inc.

## 1067

**IGF-I-Dependent Musculoskeletal Development is Blunted in Adolescents with Insulin Resistance: A 5-Year Prospective Study.** Joseph Kindler\*<sup>1</sup>, Norman Pollock<sup>2</sup>, Emma Laing<sup>2</sup>, Carlos Isaacs<sup>2</sup>, Mark Hamrick<sup>2</sup>, Ke-Hong Ding<sup>2</sup>, Richard Lewis<sup>1</sup>. <sup>1</sup>The University of Georgia, United states, <sup>2</sup>Augusta University, United states

Previous cross-sectional studies have shown that insulin resistance is a negative predictor of pediatric skeletal outcomes. One possible explanation may be related to insulin-like growth factor I (IGF-I), a pivotal hormone involved in muscle and cortical bone development. Our group recently showed that the role of IGF-I in musculoskeletal growth might be compromised in children with insulin resistance. Interpretation of the evidence involving insulin resistance, pediatric muscle/bone growth, and IGF-I, is limited by lack of data on cortical bone and an absence of prospective studies. Therefore, we examined differences in IGF-I-dependent muscle and cortical bone development in adolescents who were insulin resistant vs. insulin sensitive over a period of approximately 2.5-7.5 years. Participants were black and white boys and girls, ranging in age from 8-13 years at baseline and 12-20 years at follow-up. At both visits, tibia pQCT scans (66% site) and fasting blood draws were performed. IGF-I, insulin and glucose were measured in sera. Homeostasis model assessment of insulin resistance (HOMA-IR) was calculated. Adolescents were classified as insulin resistant (n=52; mean HOMA-IR=3.1±1.4) or insulin sensitive (n=53; mean HOMA-IR=1.3±0.4) using a median baseline HOMA-IR cutoff. Race, sex, baseline age, total body fat mass change ( $\Delta$ ), and time between appointments, were statistically controlled in the analyses. Cortical area (Ct.Ar) and muscle cross-sectional area (MCSA) were of primary interest. The insulin resistant individuals had a 14-25% lower  $\Delta$ Ct.Ar,  $\Delta$ total bone area,  $\Delta$ periosteal circumference, and  $\Delta$ polar strength strain index, but a 28% greater  $\Delta$ volumetric bone mineral density, vs. the insulin sensitive group (all  $P \leq .05$ ). Change in MCSA was only 4% lower in the insulin resistant vs. insulin sensitive group ( $P=.54$ ). In the insulin sensitive but not insulin resistant individuals,  $\Delta$ IGF-I was a positive predictor of  $\Delta$ MCSA (insulin sensitive:  $\beta=0.53$ ,  $P<.01$  vs. insulin resistant:  $\beta=0.07$ ,  $P=.55$ ;  $P_{interaction}<.01$ ) and  $\Delta$ Ct.Ar (insulin sensitive:  $\beta=0.37$ ,  $P<.01$  vs. insulin resistant:  $\beta=0.19$ ,  $P=.16$ ;  $P_{interaction}=.13$ ). This is the first study to show differences in cortical bone development prospectively between insulin resistant and insulin sensitive adolescents. Considering that lean body mass is a strong determinant of skeletal growth, cortical bone deficits in adolescents at risk of developing type-2 diabetes may involve blunted IGF-I-dependent muscle development.

**Disclosures:** Joseph Kindler, None.

## 1068

**Are Sex Differences in Fracture Incidence During Adolescence due to Factors Other than Bone Quality? A Longitudinal HR-pQCT Study.** Leigh Gabel\*<sup>1</sup>, Heather M. Macdonald<sup>2</sup>, Heather A. McKay<sup>1</sup>. <sup>1</sup>University of British Columbia & Centre for Hip Health & Mobility, Vancouver Coastal Research Institute, Canada, <sup>2</sup>Centre for Hip Health & Mobility, Vancouver Coastal Health Research Institute, Canada

**Purpose:** Despite greater fracture incidence in boys compared with girls during adolescence, the specifics of bone microstructure and strength accrual during growth

are not well understood. Thus, we aimed to: 1) characterize longitudinal change in growth patterns of bone quality (micro-, macrostructure, density and strength) across adolescence, and 2) compare these growth patterns between boys and girls aligned on biological age.

Methods: We used HR-pQCT to assess bone quality at the distal tibia (8% site) and radius (7% site) in 184 boys and 209 girls (9-20y at baseline). A median of 4 annual measurements at the tibia (n=1240) and 3 at the radius (n=915) were completed from 2008 to 2012. Bone quality outcomes included cortical thickness (Ct.Th), porosity (Ct.Po), area (Ct.Ar) and bone mineral density (Ct.BMD), total area (Tt.Ar) and density (Tt.BMD). We applied finite element analysis to estimate bone strength using ultimate stress (U.Stress) and load-to-strength ratio (radius). We aligned boys and girls on a common maturational landmark (age at peak height velocity; APHV) and fit a mixed effects model.

Results: Groups demonstrated 29-45% more porous cortices compared with girls at the tibia and radius, but rate of Ct.Po accrual did not differ between sexes at APHV. Ct.Th was 7-8% greater in boys at both sites at APHV and rate of Ct.Th accrual was 28-125% greater in boys compared with girls. Boys demonstrated 27-34% greater bone area (Tt.Ar and Ct.Ar) at both sites at APHV, 17-62% greater rate of Ct.Ar accrual and 19-21% lower Tt.Ar accrual at the tibia and radius, respectively, compared with girls. At the tibia, boys demonstrated 2% lower Ct.BMD and 15% lower rate of accrual at APHV, while Ct.BMD and rate of Ct.BMD accrual was similar between sexes at the radius. U.Stress and rate of U.Stress accrual was similar between sexes at the tibia, while boys demonstrated 11% greater U.Stress and 70% greater rate of U.Stress accrual at the radius at APHV. Load-to-strength ratio was 26% lower in boys at APHV, indicating lower risk of distal radius fracture compared with girls.

Conclusion: Contrary to previous HR-pQCT studies that did not align boys and girls at the same biological age, we did not observe sex differences in Ct.BMD at the distal radius. We observed superior bone strength and lower fracture risk at the radius in boys compared with girls, suggesting that sex differences in fracture incidence during adolescence may be due to factors other than bone quality.

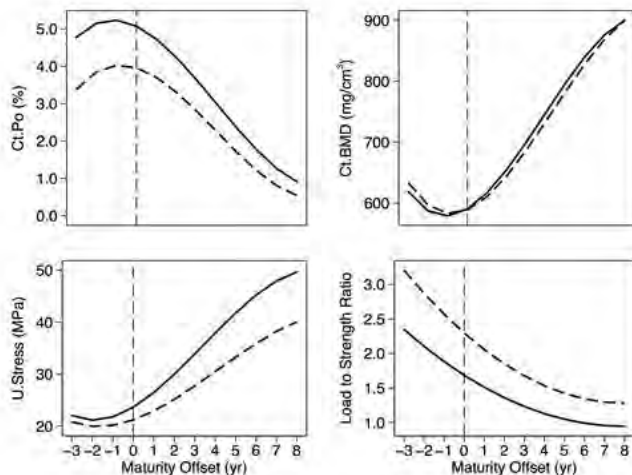


Figure 1. Predicted growth curves at the distal radius for cortical porosity (Ct.Po) and cortical bone mineral density (Ct.BMD), ultimate stress (U.Stress), and load-to-strength ratio, plotted against biological age for boys (solid lines) and girls (dashed lines). The vertical line indicates biological age (years from age at peak height velocity of 0).

Figure 1. Predicted growth curves at the distal radius.

Disclosures: Leigh Gabel, None.

## 1069

**Impaired Cortical and Trabecular Microarchitecture at the Tibia in Adolescents with Anorexia Nervosa.** Vibha Singhal<sup>1</sup>, Shreya Tulsiani<sup>2</sup>, Meghan Slattery<sup>2</sup>, Madhusmita Misra<sup>2</sup>, Anne Klibanski<sup>1</sup>. <sup>1</sup>Massachusetts General Hospital, United states, <sup>2</sup>MGH, United states

Background: Adolescents with anorexia nervosa (AN) have impaired areal bone mineral density (aBMD) and are at increased risk of fractures. However, dual energy x-ray absorptiometry (DXA) measures of aBMD are affected by bone size. In contrast, high resolution peripheral quantitative computed tomography (HRpQCT) allows assessment of volumetric BMD (vBMD) and bone microarchitecture, and microarchitectural changes may precede deficits in aBMD in AN. We have reported that adolescents with AN have impaired cortical and trabecular microarchitecture at the non-weight bearing radius. However, data are lacking regarding the effect of AN on vBMD and bone microarchitecture at the weight bearing tibia. We hypothesized that in adolescents with AN, cortical and trabecular vBMD and microarchitecture would be affected adversely compared to normal weight controls (C).

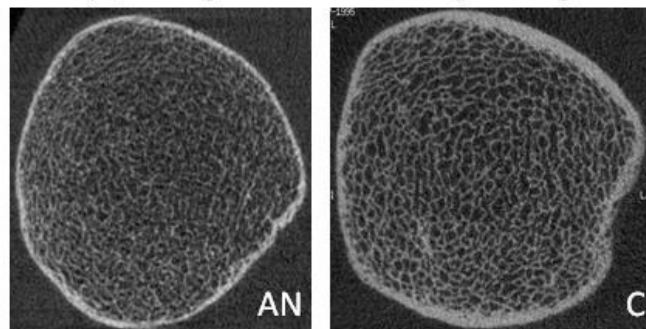
Objective: To compare cortical and trabecular vBMD and bone microarchitecture in adolescent/young women with AN and normal weight controls (C).

Methods: We evaluated 95 subjects, 51 with AN and 44 C 14-22 years old. AN was diagnosed by DSM- IV/5 criteria. We evaluated 1) body composition and aBMD at the spine, hip and whole body (WB) using DXA, and 2) tibial cortical and trabecular vBMD and microarchitecture using HRpQCT.

Results: Groups did not differ for age, bone age, menarchal age, gynecologic age and height. AN subjects had lower weight ( $48.6 \pm 5.7$  vs.  $59.9 \pm 7.2$  kg), BMI ( $17.9 \pm 1.5$  vs.  $22.5 \pm 2.3$  kg/m<sup>2</sup>), fat mass ( $12.0 \pm 3.7$  vs.  $17.9 \pm 4.8$  kg) and lean mass (LM) ( $36.8 \pm 3.4$  vs.  $41.3 \pm 4.7$  kg) than C ( $p < 0.0001$  for all). Among AN girls, mean duration of amenorrhea in the preceding year was  $5.8 \pm 1.2$  months. Areal BMD of the spine, hip and WB was lower in AN than C. At the tibia, AN girls had lower total ( $296.6 \pm 36.5$  vs.  $324.6 \pm 49.4$  mgHA/cm<sup>3</sup>;  $p = 0.004$ ) and cortical vBMD ( $863.5 \pm 31.6$  vs.  $880.5 \pm 36.6$  mgHA/cm<sup>3</sup>;  $p = 0.02$ ), lower cortical area ( $102.4 \pm 17.1$  vs.  $122.6 \pm 21.8$  mm<sup>2</sup>;  $p < 0.0001$ ) and thickness ( $1.1 \pm 0.2$  vs.  $1.2 \pm 0.2$  mm;  $p = 0.0001$ ), lower trabecular number ( $1.8 \pm 0.2$  vs.  $2.0 \pm 0.2$ ;  $p = 0.002$ ) and greater trabecular separation ( $0.5 \pm 0.1$  vs.  $0.4 \pm 0.1$ ;  $p = 0.003$ ). Within the AN group, total and trabecular vBMD correlated positively with hip aBMD and LM; cortical area with hip aBMD, LM and age at AN diagnosis; and cortical thickness with hip aBMD and LM.

Conclusions: Adolescent girls with AN have impaired cortical and trabecular vBMD and microarchitecture at the weight bearing tibia, and cortical parameters correlate with hip aBMD and lean mass.

## HRpQCT Image of Tibia in Two 18 year old girls



Tibia Microarchitecture in Anorexia Nervosa and Control

Disclosures: Vibha Singhal, None.

## 1070

**Dietary Factors during Early Life Program Bone Formation.** Jin-Ran Chen<sup>\*</sup>, Oxana P. Lazarenko, Michael L. Blackburn, Aline Andres, Thomas M. Badger. Arkansas Children's Nutrition Center & the Department of Pediatrics, University of Arkansas for Medical Sciences, United states

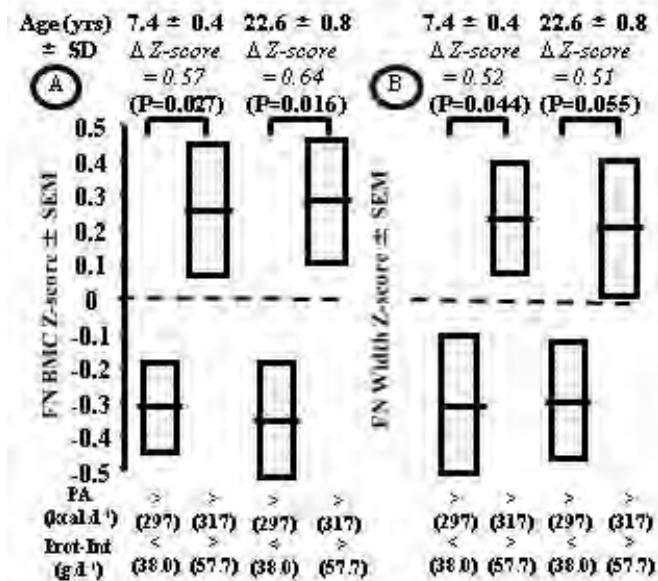
In the first year of life, the choices of foods for most infants are either breast milk (BM), cow's milk formula (MF) or soy infant formula (SF). A substantial number (20-25%) of newborns in the U.S. have been fed soy food in the form of SF. Yet, there has not been a study investigating the effects of SF on full-term infant bone metabolism and structural and functional bone indices in children who were fed SF during infancy. We designed studies both in rodents and humans that investigated whether there are early and persisting effects of SF on bone formation. In our rodent studies, we fed postnatal day (PND) 24 weanling female rats with soy protein isolate (SPI), the sole protein source in SF, for 30 days (PND 55), then switched the SPI diet to a control casein diet until 6 months of age. Using peripheral quantitative CT scanning (pQCT) on tibias, we demonstrated that a short-term early-life SPI diet has modest but persistent effects on bone formation. In our human studies, first, we studied bone turnover markers in urine in 180 healthy 6-month-old infants who were either fed BM (n=60), MF (n=60) or SF (n=60). The bone formation marker osteocalcin, which is only secreted by osteoblasts was measured by a urine ELISA kit developed in our laboratory. Bone resorption marker, collagen crosslink N-terminal telopeptide (NTx), was measured using a kit (from manufacturer). There were no significant differences between MF and SF groups in bone formation and resorption markers, but osteocalcin was substantially increased in MF and SF compared to BM infants ( $p < 0.01$ ). NTx was also significantly increased in both formula infants compared to the BM infants ( $p < 0.05$ ), but to a much lesser degree. Next, children who were originally assessed at 6-month of age were recruited at 5 years for a study to assess their bone strength and quality (radius) using clinical HRpQCT (high resolution of pQCT). As of this time, 48 five-year old children who were exclusively fed BM, MF or SF during their first year of life have been studied (n=8 per each group for both girls and boys). Bone quality, especially bone strength as expressed by the stress-strain index (SSI: a surrogate measure of bone strength determined from a cross-sectional scan by HRpQCT), was significantly higher in SF children compared to children who were fed BM during infancy. Collectively, these rodent and preliminary human results support the idea that increased bone turnover favoring more bone formation is programmed by SF during early life.

Disclosures: Jin-Ran Chen, None.

1071

**Prepubertal Impact of Environmental Factors on Proximal Femur Peak Bone Mass : the Key Role of Protein Intake on the Response to Physical Activity in the Skeletal Development of Healthy Male Subjects.** Thierry Chevalley\*<sup>1</sup>, Jean-Philippe Bonjour<sup>1</sup>, Marie-Claude Audet<sup>1</sup>, Fanny Merminod<sup>1</sup>, Bert van Rietbergen<sup>2</sup>, Rene Rizzoli<sup>1</sup>, Serge Ferrari<sup>1</sup>. <sup>1</sup>Division of Bone Diseases, Switzerland, <sup>2</sup>Eindhoven University of Technology, Netherlands

Bone structure and strength acquired by the end of the growth period is an important determinant of fragility fracture risk in later life. Though genetics appears to be the most important determinant of peak bone mass (PBM) variance, environmental factors such as nutrition and physical activity, which are amenable to modifications, are of special interest for bone health. During growth bone is responsive to changes in nutrition and physical activity, particularly when applied before the onset of pubertal maturation. In prepubertal healthy boys, protein intake (Prot-Int) was shown to enhance the impact of physical activity (PA) on weight-bearing bone structure. We hypothesized that the synergism between Prot-Int and PA on proximal femur as recorded at mean age of 7.4 y would last until reaching PBM. To test this hypothesis, a homogeneous cohort of 124 healthy boys was followed from 7.4 to 22.6 y. At this age, mean T-score ( $\pm$ SD) of DXA-measured femoral neck (FN) was not significantly different ( $0.06 \pm 0.99$ ) from the value used for the clinical diagnosis of osteoporosis, thus indicating PBM attainment. At the age of 7.4 y the 124 subjects were dichotomized according to the median of both PA and Prot-Int. In the two groups with PA above the median (297 and 317 vs 170 and 166 kcal.d<sup>-1</sup>), higher Prot-Int (57.7 vs 38.0 g.d<sup>-1</sup>) was associated with +9.8 % greater FN BMC ( $P < 0.027$ ). At 22.6 y of age, this difference was maintained : FN BMC: + 11.3 % ( $P < 0.016$ ). With PA > median, the differences in Z-scores at Prot-Int above vs below the median, were at 7.4 y +0.57 and at 22.6 y +0.64 for FN, respectively (Fig.A). Further, a larger FN Width was measured at both 7.4 and 22.6 y (Fig.B). Micro-finite element analysis ( $\mu$ FEA) of distal tibia performed at the age of 22.6 y indicates that in the two groups with PA above the median, both stiffness and failure load were greater by +0.40 Z-score with Prot-Int above vs below the median. In conclusion, protein intake increases the impact of physical activity on proximal femur and distal tibia on both structure and mechanical resistance. These effects observed in a cohort of healthy boys at the age of 7.4 y last until the age of 22.6 y. This study demonstrates: 1) the crucial influence of protein intake on the response to enhanced physical activity; 2) the importance of prepubertal years for modifying by environmental factors the trajectory of bone growth and, thereby, for increasing peak bone mass and strength in healthy male subjects.



figure

Disclosures: Thierry Chevalley, None.

1072

**Decreased bone turnover in HIV-infected children on antiretroviral therapy.** Stephen Arpad\*<sup>1</sup>, Stephanie Shiao<sup>1</sup>, Renate Strehlau<sup>2</sup>, Faezah Patel<sup>2</sup>, Ndileka Mbete<sup>2</sup>, Donald McMahon<sup>1</sup>, Louise Kuhn<sup>1</sup>, Ashraf Coovadia<sup>2</sup>, Michael Yin<sup>1</sup>. <sup>1</sup>Columbia University, United states, <sup>2</sup>University of the Witwatersrand, South africa

Introduction: HIV-infected children have decreased bone mineral content (BMC). However, the relationship between chronic inflammation, bone remodeling, and BMC have not been well studied in pediatric HIV.

Methods: 219 HIV-infected and 180 uninfected children enrolled in the CHANGES Bone Study in Johannesburg, South Africa. Whole body (WB) BMC was assessed by dual-energy X-ray absorptiometry. BMC Z-scores adjusted for sex, age, and height were generated. Bone formation and resorption markers, procollagen type 1 N-terminal propeptide (PINP), and C-telopeptide (CTX), were measured as well as soluble CD14 (sCD14), a marker of monocyte activation, proinflammatory cytokines IL-6 and TNF- $\alpha$ , and iPTH and 25(OH)D3.

Results: The 219 HIV-infected children (49% male) were younger than the 180 uninfected children (55% male) (6.36 vs. 7.12 years,  $p < 0.01$ ); 97% were Tanner 1 and mean 25(OH)D3 was 27.7 ng/ml. HIV-infected children were on treatment for a mean of 5.7 years and mean CD4% was 37%; 94% had viral suppression (HIV-1 RNA <400 copies/mL). Mean WB BMC Z-score was lower in HIV-infected than uninfected children (-0.95 vs. -0.79,  $p = 0.05$ ). CTX and PINP concentrations were lower in HIV-infected than uninfected children (Table) and remained lower after adjusting for sex, age, 25(OH)D3, and WB BMC. CTX and PINP were positively correlated to each other ( $r = 0.43$ ,  $p < 0.01$ ). Mean TNF- $\alpha$  was lower in HIV-infected compared to uninfected children (Table), but 98% had TNF- $\alpha$  levels in the normal range. Mean IL-6 was similar in HIV-infected and uninfected children. In contrast, sCD14 was higher in HIV-infected than uninfected children (Table), even after adjustment for sex and age. CTX and PINP correlated poorly with both cytokines ( $r < 0.10$ ) and WB BMC Z-scores ( $r < 0.10$ ).

Conclusions: In a group of HIV-infected children with viral suppression on antiretrovirals with low BMC, pro-inflammatory cytokines known to increase bone resorption, TNF- $\alpha$  and IL-6, were not elevated, but sCD14 was. While formation and resorption do not appear uncoupled, bone turnover markers were decreased in HIV-infected children compared to uninfected children and were not correlated with cytokine levels. These data suggest that in infected children with viral suppression, decreases in bone accrual occur independently of cytokine-mediated bone resorption. A better understanding of mechanisms of bone loss in HIV-infected children is critical to the development of interventions to optimize childhood bone acquisition.

Table

Measurement	HIV+ (N=219)	HIV- (N=180)	P-value
IL-6 (pg/ml), Mean (SD)	1.72 (3.6)	1.73 (3.49)	0.97
sCD14 (ug/ml), Mean (SD)	1453 (550)	1195 (437)	<0.0001
TNF $\alpha$ (pg/ml), Mean (SD)	2.15 (1.35)	2.60 (1.21)	0.0008
CTX (ng/ml), Mean (SD)	1.72 (0.63)	2.05 (0.69)	<0.0001
PINP (ng/ml), Mean (SD)	584 (183)	634 (173)	0.005
iPTH (pg/mL)	31.1 (12.9)	32.1 (15.7)	0.50
25(OH)D3 (ng/ml), Mean (SD)	30.6 (9.8)	24.3 (6.3)	<0.0001

Table

Disclosures: Stephen Arpad, None.

1073

**Hospital based Fracture Liaison Service reduces re-fracture rate and is cost-effective and cost saving.** Charles Inderjeeth\*<sup>1</sup>, Warren Raymond<sup>2</sup>, Elizabeth Geelhoed<sup>3</sup>, Andrew BRIGGS<sup>4</sup>, Kathy Briffa<sup>5</sup>, David Oldham<sup>6</sup>, Jean McQuade<sup>7</sup>, David MOUNTAIN<sup>6</sup>. <sup>1</sup>University of Western Australia & North Metropolitan Health Service, Australia, <sup>2</sup>The University of Western Australia & Sir Charles Gairdner Hospital, Australia, <sup>3</sup>University of Western Australia, Australia, <sup>4</sup>Department of Health, Australia, <sup>5</sup>Curtin University, Australia, <sup>6</sup>Sir Charles Gairdner Hospital, Australia, <sup>7</sup>Arthritis & Osteoporosis WA, Australia

Purpose:

To determine the economic benefits of a FLS in a Western Australian hospital. Osteoporotic fractures impose significant morbidity, mortality and economic burden (1). Research within our hospital confirmed low rates of identification and secondary prevention for patients discharged from Emergency Department (ED) with a fracture (2).

Methods:

Patients over the age of fifty who presented with a fracture to a tertiary Hospital Emergency Department (SCGH) were offered an appointment at the FLS. A retrospective control group from SCGH determined the historical fracture risk without an active FLS intervention. Two other hospital sites acted as prospective control cohorts.

A health economic analysis from the payer's perspective (WA Health Department) examined recurrent fracture rates and quality of life (EQ-5D). Bottom-up costing included medication usage, investigations (e.g. BMD testing), GP visits, hospital presentations & admissions and the cost of fracture determined by the literature or the AR-DRG 2013/14 prices. The mean incremental cost effectiveness ratios/diagrams were derived from 5000 bootstrap iterations. Cost-effectiveness acceptability curves were generated and the willingness-to-pay was \$50,000AUD.

Results:

This FLS program reduced the rate of re-fractures compared to the retrospective cohort and other tertiary hospitals by between 9.2 – 10.2% equating to cost savings of approximately \$750,168 - \$810,400/1,000 patient-years in the first year compared to control cohorts. There was no difference in the QALYs gained across groups in the 12 month follow-up.

The FLS compared to SCGH retrospective cohort had a mean incremental cost of \$6,168 (95CI \$133, \$18,626) per 1% reduction in the 12 month recurrent fracture risk. The FLS compared to other sites had a mean incremental cost of \$6,782 (95CI -\$2,562, \$25,686) per 1% reduction in the 12 month recurrent fracture risk. The FLS compared to SCGH retrospective cohort had a mean incremental cost of \$859 (95CI -\$4,074, \$4,864) per QALY gained at 12 months. The FLS compared to other sites had a mean incremental cost of -\$119 (95CI -\$1,665, \$700) per QALY gained at 12 months. Figure 1 demonstrates that the FLS is cost-effective in delivering a reduction in the fracture rate at 12 months. However, the QALY gained (EQ-5D) and osteoporosis specific QALY gained (ECOS-16) were no different at 12 months between the SCGH FLS and control cohorts.

**Conclusion:**

This FLS demonstrated to be effective in reducing rates of recurrent fracture(s) and resulted in significant cost effectiveness and cost-saving.

**References:**

1. Briggs AM et al.(2015) Hospitalisations, admission costs and re-fracture risk related to osteoporosis in Western Australia: a 10-year review. ANZ J Public Health.
2. Inderjeeth CA et al.(2010) A multimodal intervention to improve fragility fracture management in patients presenting to Emergency Departments. MJA

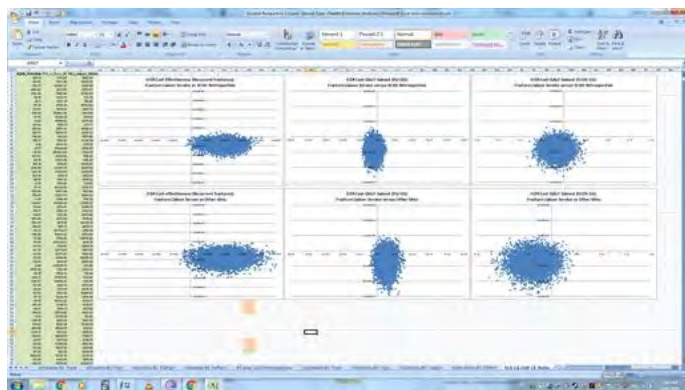


Figure 1: ICER Graphs for Fracture Risk, QALY gained (EQ-5D) and QALY gained (ECOS-16)

**Disclosures:** Charles Inderjeeth, None.

**1074**

**Spine Fracture Prevalence in US Women and Men Aged 40 years and older: NHANES 2013-2014.** Felicia Cosman\*<sup>1</sup>, John Krege<sup>2</sup>, Anne Looker<sup>3</sup>, John Schousboe<sup>4</sup>, Bo Fan<sup>5</sup>, Neda Sarafrazi Isfahani<sup>3</sup>, John Shepherd<sup>5</sup>, Kelly Krohn<sup>2</sup>, Peter Steiger<sup>6</sup>, Kevin Wilson<sup>7</sup>, Harry Genant<sup>5</sup>. <sup>1</sup>Helen Hayes Hospital, United states, <sup>2</sup>Eli Lilly & Company, United states, <sup>3</sup>National Center for Health Statistics, Centers for Disease Control & Prevention, United states, <sup>4</sup>Park Nicollet Clinic & HealthPartners Institute, United states, <sup>5</sup>University of California, United states, <sup>6</sup>Parexel International, United states, <sup>7</sup>Hologic, Inc., United states

**Introduction:** Vertebral fractures have substantial clinical significance but often do not come to medical attention. The primary objective was to determine prevalence of vertebral fractures by Vertebral Fracture Assessment (VFA) in men and women aged ≥40 years. Additional objectives were to determine the characteristics of those with vertebral fractures, compare self-report of vertebral fracture versus VFA evidence of fracture, and assess prevalence in subjects meeting National Osteoporosis Foundation (NOF) criteria for spine imaging.

**Methods:** This was a cross-sectional analysis of 3330 US adults aged ≥40 who participated in the nationally representative National Health and Nutrition Examination Survey (NHANES) during 2013 to 2014 and had evaluable VFA data. Data collected included lateral spine VFA graded by semi-quantitative assessment, bone mineral density (BMD) of lumbar spine and hip, and an osteoporosis questionnaire.

**Results:** The prevalence of vertebral fractures was 5.4% and was similar in men and women. Prevalence increased with age (chi-square P<0.01) from below 5% in those <60 years to 11% of those 70-79 years and 18% of those ≥80 years. Fractures were more common in non-Hispanic whites, in those with a lower body mass index, and in those with lower BMD. Prevalence was higher in subjects who met versus did not meet selected NOF criteria for spine imaging (14% vs. 4.7%, P<0.001). Among subjects with vertebral fractures, 26% had osteoporosis at the lumbar spine or proximal femur by BMD criteria. In those ≥65 years with vertebral fracture, 38% had osteoporosis by at least one site, and 22% had normal BMD at both sites; in subjects ≥65 years without fracture, 14% had osteoporosis by at least one site and 35% had normal BMD at both sites. Only 8% of those with a spine fracture by VFA reported a history of spine fracture by questionnaire, and among those who reported a spine fracture on the questionnaire, only 21% had a fracture by VFA.

**Conclusions:** The results from NHANES 2013-2014 show similar prevalence of vertebral fractures between women and men and increased prevalence with age and lower BMD. Our findings suggest that objective assessments with lateral spine imaging are critical for correctly identifying subjects with vertebral fractures. The study provides support for recommendations from the NOF for targeted lateral spine imaging to identify patients who have undiagnosed vertebral fracture.

**Disclosures:** Felicia Cosman, Eli Lilly and Company, 15

This study received funding from: Eli Lilly and Company

**1075**

**Longer Duration of Diabetes Strongly Impacts Fracture Risk Assessment: The Manitoba BMD Cohort.** William Leslie\*<sup>1</sup>, Suzanne Morin<sup>2</sup>, Sumit Majumdar<sup>3</sup>, Lisa Lix<sup>1</sup>, Helena Johansson<sup>4</sup>, Anders Oden<sup>4</sup>, Eugene McCloskey<sup>4</sup>, John Kanis<sup>4</sup>. <sup>1</sup>University of Manitoba, Canada, <sup>2</sup>McGill University, Canada, <sup>3</sup>University of Alberta, Canada, <sup>4</sup>Centre for Metabolic Bone Diseases, University of Sheffield Medical School, United Kingdom

**Background:** Type 2 diabetes is associated with higher risk for major osteoporotic fracture (MOF) and hip fracture (HF) than predicted from the WHO Fracture Risk Assessment (FRAX) tool. The current analysis examined the potential impact of diabetes duration on fracture risk assessment with FRAX.

**Methods:** Using a clinical DXA registry with all results for Manitoba, Canada, we identified women age >40 y with >10 y of prior health coverage undergoing baseline hip DXA measurements (1996–2013). Diabetes was ascertained using a validated algorithm applied to administrative data, with onset determined from the earliest applicable code. Incident MOF and HF were studied during a mean observation time of 7 y. FRAX input variables came from clinical data collected at the time of DXA testing and linked administrative data. FRAX scores were calculated with femoral neck BMD (Canadian tool). Additional covariates were a general comorbidity score (John's Hopkins aggregated disease groups), falls requiring hospitalization, prior osteoporosis therapy and insulin use. FRAX calibration was assessed from observed vs predicted fracture probability with competing mortality risk included in the calculation.

**Results:** The study population included 49,098 women without diabetes and 8840 women with diabetes; most diagnoses preceded DXA testing (n=2776, 31.4% >10 y; n=1776, 20.1% 5-10 y; n=2098, 23.7% <5 y) with a minority after DXA testing (n=2190, 24.8% within 5 y). Adjusted for FRAX score (Model 1), diabetes duration >10 y was associated with higher risk for MOF (hazard ratio [HR] 1.47, 95% CI 1.30-1.66) which was attenuated but still significant in fully adjusted analyses (HR 1.34, 95% CI 1.17-1.54). No significant effect on MOF was seen for shorter diabetes duration. In contrast, higher risk for HF was seen for all diabetes durations with a gradient of increasing risk with longer duration (HR 1.32, 95% CI 1.03-1.69 for new-onset diabetes, HR 2.10, 95% CI 1.71-2.59 for duration >10 y). There was minimal attenuation when fully adjusted for the additional covariates (Model 2). In those with diabetes duration >10 y FRAX significantly underestimated MOF risk (calibration ratio 1.24, 95% CI 1.08-1.39) and HF risk (1.93, 95% CI 1.50-2.35).

**Summary:** Diabetes is a FRAX-independent risk factor for MOF only in women with long-duration diabetes but diabetes increases HF risk regardless of duration. Those with diabetes >10y are at particularly high risk of fracture.

Duration of diabetes	N	Major Osteoporotic Fractures			Hip Fracture only		
		Model 1 Hazard Ratio (95% CI)	Model 2 Hazard Ratio (95% CI)	Observed to Expected (95% CI)	Model 1 Hazard Ratio (95% CI)	Model 2 Hazard Ratio (95% CI)	Observed to Expected (95% CI)
No diabetes	49098	1.00 (Ref)	1.00 (Ref)	0.98 (0.95-1.01)	1.00 (Ref)	1.00 (Ref)	1.00 (1.01-1.15)
New-onset (0-5 y)	2190	1.02 (0.89-1.17)	0.99 (0.86-1.14)	0.94 (0.80-1.07)	1.32 (1.03-1.69)	1.30 (1.01-1.65)	1.18 (0.95-1.51)
Prev 0-5 y	2098	1.13 (0.98-1.32)	1.07 (0.92-1.25)	1.07 (0.90-1.24)	1.59 (1.23-2.06)	1.54 (1.19-1.99)	1.79 (1.30-2.27)
Prev 5-10 y	1776	1.16 (0.99-1.37)	1.10 (0.93-1.29)	1.13 (0.94-1.33)	1.61 (1.21-2.13)	1.55 (1.17-2.06)	1.46 (0.98-1.96)
Prev >10 y	2776	1.47 (1.30-1.66)	1.34 (1.17-1.54)	1.24 (1.08-1.39)	2.10 (1.71-2.59)	1.94 (1.54-2.44)	1.93 (1.50-2.35)

Table:

**Disclosures:** William Leslie, None.

**1076**

**Measurement of Cortical and Trabecular Deterioration Identifies Postmenopausal Women at Imminent Risk for Fracture: the OFELY Study..** Stephanie Boutroy\*<sup>1</sup>, Roger Zebaze<sup>2</sup>, Elisabeth Sornay-Rendu<sup>1</sup>, Ego Seeman<sup>2</sup>, Roland Chapurlat<sup>1</sup>. <sup>1</sup>INSERM UMR 1033, University of Lyon, France, <sup>2</sup>Austin Health, University of Melbourne, Australia

**Introduction:** Identification of women at risk for imminent fracture (1 to 2 years) may be achieved by quantifying microarchitecture deterioration. We developed the Structural Strength Index (SSI) that combines age, cortical porosity and trabecular density to quantify the probability of fracture. The lower the SSI, the higher the probability of fragility fracture.

**Methods:** We measured distal radius microarchitecture using high resolution peripheral quantitative computed tomography (HRpQCT, Scanco Medical AG, Switzerland) in 589 French postmenopausal women aged 42 to 94 years, of whom 135 sustained incident fractures during 9.4 years. Images were processed blind to fracture status using StrAx1.0 (StraxCorp, Melbourne, Australia) in Melbourne to quantify the SSI. Femoral neck (FN) BMD and FRAX scores (ten-year probability of a major

osteoporotic fracture, without BMD) were measured to compare their ability to identify patients at risk for imminent fracture within the first 2 years of follow-up.

Results: Among the 135 fracture cases (including 33 during the first 2 years of follow-up) compared with the 454 non-fracture controls, the SSI was lower ( $23.9 \pm 9.7$  vs  $28.3 \pm 9.6$ ), the FN T-score was lower ( $-1.6 \pm 0.8$  vs  $-1.3 \pm 0.8$ ) and the FRAX score was higher ( $13.9 \pm 10.8$  vs  $10.0 \pm 9.2$ ) (all  $p < 0.001$ ). For imminent fractures, we used clinical thresholds: SSI  $< 22$ , FN T-Score  $< -2.5$ , and FRAX  $> 20\%$ . FN T-score  $< -2.5$  and FRAX  $> 20\%$  had respectively a sensitivity of 18% and 22% for imminent fracture, 10% and 19% for all fracture and a specificity of 95% and 90%. By comparison, the SSI had a sensitivity of 61% for imminent fracture, 50% for overall fracture prediction and a specificity of 75%. The SSI threshold of 22 was associated with a 4.7 fold increased imminent fracture risk [95%CI: 2.3;9.7]. In a multivariate model, the SSI threshold of 22 predicted imminent and overall fracture independently of the FN T-score  $< -2.5$  and FRAX  $> 20\%$ . In addition, the 3 variables predicted incident fractures during 9.4 years follow-up: HR [95%CI]: 1.7[1.4;2.0] and 1.6[1.3;2.0] for a SD decrease in SSI and FN T-Score respectively and 1.04[1.03;1.05] for an unit increase in FRAX.

Conclusion: This is the first prospective study providing a combined measure of cortical and trabecular microstructural deterioration which identifies women at imminent risk for fracture better than FN BMD and FRAX.

Disclosures: *Stephanie Boutroy, None.*

## 1077

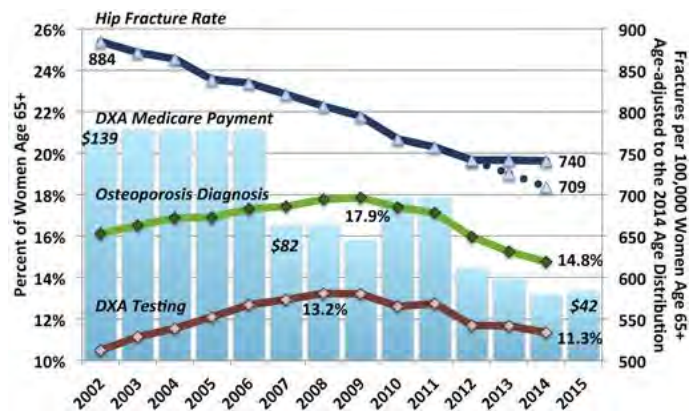
**Hip Fractures and Declining DXA Testing: At a Breaking Point?** E. Michael Lewiecki\*<sup>1</sup>, Robert Adler<sup>2</sup>, Jeffrey Curtis<sup>3</sup>, Robert Gagel<sup>4</sup>, Kenneth Saag<sup>5</sup>, Andrea Singer<sup>6</sup>, Ethel Siris<sup>7</sup>, Nicole C. Wright<sup>8</sup>, Huifeng Yun<sup>9</sup>, Peter M. Steven<sup>10</sup>. <sup>1</sup>UNM Health Sciences Center, United states, <sup>2</sup>VA Medical Center, United states, <sup>3</sup>University of Alabama at Birmingham, Division of Clinical Immunology & Rheumatology, United states, <sup>4</sup>MD Anderson, United states, <sup>5</sup>University of Alabama Birmingham Medical College, United states, <sup>6</sup>MedStar Georgetown University Hospital, United states, <sup>7</sup>New York-Presbyterian Hospital, United states, <sup>8</sup>University of Alabama at Birmingham, United states, <sup>9</sup>University Alabama Birmingham School of Public Health, United states, <sup>10</sup>ISCD, United states

Background. Hip fracture incidence rates have generally decreased over the last 15 years in the U.S. and other developed countries. The dramatic decline has been ascribed to improvements in osteoporosis evaluation and fracture prediction via DXA and the advent of generally safe and effective drugs, starting with oral bisphosphonates in 1995. We sought to examine the latest national trends in hip fracture rates.

Methods. We used health care claims and enrollment data from the 2002-2014 5% sample of Medicare fee-for-service beneficiaries to identify persons with at least one Medicare-paid DXA scan in each year. DXA providers were counted based on the presence of any paid DXA service with technical component for office-based and freestanding providers, and any DXA bill for hospital outpatient departments, during a year. Presence of hip fracture was identified by any ICD-9-CM diagnosis code of 820.0x, 820.2x, or 820.8x on a hospital acute inpatient facility claim, excluding those with mention of trauma. Coding for a diagnosis of osteoporosis (ICD-9-CM 733.0) was assessed.

Results. Age-adjusted hip fracture rates declined linearly (Figure) from 2002 to 2012. In 2013 and 2014, hip fracture rates were greater than predicted trends. DXA testing and diagnosis of osteoporosis started declining in 2009, two years after Medicare decreased office-based DXA reimbursement to levels below the cost of providing the service.

Conclusion. This analysis suggests the trend of decreasing hip fracture rates in the US may be over. Other studies have shown a decrease in osteoporosis prescriptions over this period of time. Although causality cannot be clearly established, there is a plausible chain of events from reduced DXA reimbursement to fewer DXA providers to fewer DXAs performed to fewer women diagnosed to fewer being treated, all leading to an increase in fractures above expected levels. The increase in fracture-related expenses is likely to outweigh the modest savings to Medicare from decreased DXA reimbursement and fewer DXAs performed.



Figure

Disclosures: *E. Michael Lewiecki, Shire, 13; Eli Lilly, Amgen, Merck, Radius Health, 11; Eli Lilly, Amgen, Merck, 11*

## 1078

**Falls Predict Fractures Independently of FRAX Probability: The Osteoporotic Fractures in Men (MrOS) Study.** Nicholas Harvey\*<sup>1</sup>, Anders Odén<sup>2</sup>, Eric Orwoll<sup>3</sup>, Jodi Lapidus<sup>4</sup>, Timothy Kwok<sup>5</sup>, Magnus Karlsson<sup>6</sup>, Björn Rosengren<sup>6</sup>, Östen Ljunggren<sup>7</sup>, Cyrus Cooper<sup>7</sup>, Eugene McCloskey<sup>8</sup>, John Kanis<sup>9</sup>, Claes Ohlsson<sup>2</sup>, Dan Mellström<sup>2</sup>, Helena Johansson<sup>2</sup>. <sup>1</sup>MRC Lifecourse Epidemiology Unit, University of Southampton, United Kingdom, <sup>2</sup>Centre for Bone & Arthritis Research (CBAR), Sahlgrenska Academy, University of Gothenburg, Sweden, <sup>3</sup>Oregon Health & Science University, United states, <sup>4</sup>Department of Public Health & Preventive Medicine, Division of Biostatistics, Oregon Health & Science University, United states, <sup>5</sup>Department of Medicine & Therapeutics & School of Public Health, The Chinese University of Hong Kong, Hong kong, <sup>6</sup>Clinical & Molecular Osteoporosis Research Unit, Department of Clinical Sciences Malmö, Lund University & Department of Orthopedics, Skane University Hospital, Sweden, <sup>7</sup>Department of Medical Sciences, University of Uppsala, Sweden, <sup>8</sup>Centre for Metabolic Bone Diseases, & Centre for Integrated research in Musculoskeletal Ageing (CIMA), Mellenby Centre for Bone Research, University of Sheffield, United Kingdom, <sup>9</sup>Centre for Metabolic Bone Diseases, University of Sheffield, United Kingdom

We have previously demonstrated in the Osteoporotic Fractures in Men (MrOS) Study Sweden cohort that FRAX probability predicts risk of incident falls. Bony fracture is a key consequence of falls, and therefore we investigated, across the 3 MrOS cohorts, whether past falls predicted incident fracture independently of FRAX, and whether these associations varied with age and follow-up time. We studied elderly men recruited from MrOS Sweden, Hong Kong and USA. Baseline data included falls history, clinical risk factors, BMD at femoral neck and calculated FRAX probabilities. An extension of Poisson regression was used to investigate the relationship between falls, FRAX probability and the time-to-event hazard function of fracture. All associations were adjusted for age, time since baseline and cohort in base models; further models were used to investigate interactions with age and follow-up time. Information on falls and FRAX probability was available for: 4365 men in USA (mean age 73.5 years; mean follow-up 10.8 years); 1852 men in Sweden (mean age 75.4 years; mean follow-up 8.7 years); and 1669 men in Hong Kong (mean age 72.4 years; mean follow-up 9.8 years). Rates of past falls were similar at 20%, 16%, and 15% respectively. Across all 3 cohorts, past falls predicted incident fracture at any site [HR: 1.67 (95%CI: 1.49, 1.89)], major osteoporotic fracture (MOF) [HR: 1.56 (95%CI: (1.33, 1.83)] and hip fracture [HR: 1.61 (95%CI: 1.27, 2.04)]. Associations between past falls and incident fracture appeared independent of FRAX probability: adjusted HR (95%CI) any fracture: 1.64 (1.46, 1.85); MOF: 1.53 (1.31, 1.79); and hip: 1.60 (1.26, 2.02). Overall, falls-fracture relationships did not change with time or age (p interaction  $> 0.30$ ) but there was heterogeneity across the 3 cohorts. Thus in Sweden, the HR for falls predicting fracture reduced with follow-up time (p interaction any fracture falls\*time=0.014) and was more marked at younger ages (p interaction=0.0003 for any fracture). In conclusion, past falls predicted incident fracture independently of FRAX probability, confirming the potential value of falls history in fracture risk assessment. Although results from MrOS Sweden suggest the predictive value of past falls for future fracture may vary with age and follow-up time, these results were not apparent in MrOS USA or MrOS Hong Kong.

Disclosures: *Nicholas Harvey, None.*

## 1079

**Intravital Imaging of Osteoblast, Osteocyte and GFP-Collagen Dynamics.** Lora McCormick\*<sup>1</sup>, Michael Grillo<sup>1</sup>, LeAnn Tiede-Lewis<sup>2</sup>, Kun Wang<sup>2</sup>, Hong Zhao<sup>2</sup>, Sarah Dallas<sup>2</sup>. <sup>1</sup>University of Missouri-Kansas City, United states, <sup>2</sup>University of Missouri, Kansas City, United states

Bone formation, remodeling and repair are dynamic processes requiring temporal coordination of cell migration, proliferation, ECM formation and resorption. To better understand these dynamic events, we previously performed live cell imaging in bone explants and primary bone cells from transgenic mice expressing osteoblast and osteocyte lineage reporters and GFP $_{tpz}$ -tagged collagen. Our work showed that osteoblasts are more motile than previously known and that osteocyte differentiation starts when a motile bone surface cell turns on Dmp1-GFP expression, arrests its motility and extends and retracts exploratory dendrites that appear to position the cell for embedding. We also showed that collagen assembly by osteoblasts is highly dynamic and that cell generated forces extend, contract and reshape the fibrils during assembly. To understand in vivo the dynamic properties of bone cells and their ECM interactions, intravital confocal timelapse imaging was performed in parietal bones of 2-3wk old mice. To image osteoblasts and osteocytes, mice expressing Col1a1-DsRed and/or membrane targeted Dmp1-GFP lineage reporters were used. For collagen imaging we used a transgene in which GFP $_{tpz}$  is fused to  $\alpha 2(I)$ collagen. Mice were imaged for up to 8h with or without alizarin red labeling of mineral. Intravital imaging confirmed the motile properties of osteoblasts (velocity  $5.1 \pm 0.7 \mu\text{m/hr}$ ). Motions were random in central areas of the parietals and directional near sutures. A surface motile Dmp1-GFP+ cell population was observed (velocity  $4.5 \pm 0.5 \mu\text{m/hr}$ ). Intravital imaging showed extension and retraction of exploratory dendrites in embedding Dmp1-GFP+ cells, continued dendrite motion in recently embedded cells and shedding of vesicles

from the cell body and dendrites. Near the sutures, osteocytes extended projections and shed vesicles in advance of the mineralization front, which may facilitate mineralization and/or cell-cell communication. Live imaging of GFP-collagen in forming bone suggested that cells physically reshaped collagen fibrils to form holes resembling lacunae. Motions of collagen fibrils in the sutures and cell-mediated fibril rearrangement was also seen. By multiphoton imaging the GFP-collagen transgene allowed imaging of earlier stages of collagen assembly compared with second harmonic imaging. These data confirm *in vivo* the dynamic nature of osteoblasts, osteocytes and the bone ECM assembly process and suggest cells can physically reshape their ECM *in vivo*.

**Disclosures:** Lora McCormick, None.

## 1080

**Induction of the Hajdu Cheney Syndrome Mutation in Osteoblasts Causes Severe Osteopenia.** Stefano Zanotti<sup>1</sup>, Jungeun Yu<sup>1</sup>, Archana Sanjay<sup>1</sup>, Lauren Schilling<sup>1</sup>, Christopher Schoenherr<sup>2</sup>, Aris Economides<sup>2</sup>, Ernesto Canalis<sup>1</sup>. <sup>1</sup>UConn Health, United states, <sup>2</sup>Regeneron Pharmaceuticals, United states

Hajdu Cheney syndrome (HCS) is a rare genetic disorder characterized by severe osteoporosis with fractures. HCS is driven by autosomal-dominant mutations in exon 34 of *NOTCH2* that give rise to deletions of the PEST domain, which is necessary for the degradation of NOTCH2. Therefore, these mutations cause expression of a truncated and presumably stable protein and as a result a NOTCH2 gain-of-function. Recently, we reported that mice harboring a *Notch2* mutation that replicates the one found in an individual with HCS and severe osteoporosis have marked osteopenia secondary to increased bone resorption and osteoclast number. This was attributed to either increased expression of *Rankl* by the osteoblast or an increased osteoclastogenic response to Rankl by osteoclast precursors. To determine the cell lineage responsible for the osteopenic phenotype, a conditional by inversion (COIN) HCS allele of *Notch2* (*Notch2*<sup>COIN(PEST)</sup>) was created. In this model, Cre recombination generates a permanent *Notch2*<sup>ΔPEST</sup> allele expressing a transcript where the sequences coding for the PEST domain and 3'-untranslated region are replaced by a STOP codon and a polyadenylation signal. As such, the *Notch2*<sup>ΔPEST</sup> mouse replicates the mutations found in HCS in a tissue-specific manner. Using a germline-expressed Cre (*Hprt-Cre*) we show that *Notch2*<sup>ΔPEST</sup> mice phenocopy the pronounced osteopenic phenotype of global *Notch2*HCS mutant mice, establishing the validity of the model. To determine the role played by cells of either the osteoclastic or osteoblastic lineage in HCS, we generated *Notch2*<sup>COIN(PEST)/COIN(PEST)</sup> mice hemizygous for either the lyszyme M (*LysM-Cre*) or osteocalcin (*Bglap-Cre*) transgenes. These were crossed with *Notch2*<sup>COIN(PEST)/COIN(PEST)</sup> mice to generate *LysM-Cre;Notch2*<sup>ΔPEST/ΔPEST</sup> and *Bglap-Cre;Notch2*<sup>ΔPEST/ΔPEST</sup> mice that were compared to sex-matched *Notch2*<sup>COIN/COIN</sup> littermates. Whereas *LysM-Cre;Notch2*<sup>ΔPEST/ΔPEST</sup> mice did not exhibit an obvious skeletal phenotype, *Bglap-Cre;Notch2*<sup>ΔPEST/ΔPEST</sup> mice displayed a 50% reduction in cancellous bone volume, decreased connectivity and reduced trabecular number. These observations indicate that the *Notch2*HCS mutation in osteoblasts contributes significantly to the HCS phenotype. In conclusion, the creation of a *Notch2*HCS conditional mutation in osteoblasts causes pronounced osteopenia possibly by regulating Rankl and osteoclastogenesis.

**Disclosures:** Stefano Zanotti, None.

## 1081

**Novel Role for Claudin-11 in the Regulation of Osteoblasts via Modulation of ADAM10-mediated Notch Signaling.** Richard Lindsey<sup>1</sup>, Shaohong Cheng<sup>2</sup>, Weirong Xing<sup>1</sup>, Catrina Alarcon<sup>2</sup>, Sheila Pourteymoor<sup>2</sup>, Alexander Gow<sup>3</sup>, Subburaman Mohan<sup>1</sup>. <sup>1</sup>VA Loma Linda Healthcare System; Loma Linda University, United states, <sup>2</sup>VA Loma Linda Healthcare System, United states, <sup>3</sup>Wayne State University, United states

The claudin (Cldn) family comprises 24 members of 20-34 kDa tetraspan transmembrane proteins of tight junctions. In addition to their established canonical role as barriers that control the flow of molecules in the intracellular space between cells, a distinct non-canonical role for Cldns is now emerging in which they serve as mediators of cell signaling. In our studies on the expression levels of all 24 Cldn family members during osteoblast (OB) differentiation, we determined that Cldn11 showed the largest increase (60-fold) during early stages of OB differentiation. Immunohistochemistry studies revealed that Cldn11 was expressed highly in the lining cells of trabecular (Tb) bone. MicroCT analysis of femurs, tibiae, and vertebrae of mice with targeted disruption of the Cldn11 gene showed that both genders of Cldn11 knockout (KO) mice at 12 weeks of age exhibited a 40% ( $P < 0.01$ ) reduction in Tb bone volume adjusted for tissue volume compared to littermate control mice, and that reduction was caused by significant decreases in Tb number and thickness and a significant increase in Tb separation. Histomorphometry and serum biomarker studies revealed that reduced bone formation and not increased bone resorption is the cause for reduced Tb bone volume in the Cldn11 KO mice. Cldn11 KO OBs had reduced ALP and BSP expression while Cldn11 overexpression in MC3T3-E1 cells increased expression of ALP and BSP. In our studies on the mechanism for Cldn11 effects on OB differentiation, we found that Cldn11 interacted with tetraspanin (Tspan)3 in OBs and that Tspan3 knockdown reduced OB differentiation. Since certain members of the Tspan family (Tspan5 and 10) regulate cell functions via Notch signaling, we evaluated if Cldn11/Tspan3 regulates Notch signaling in OBs. Accordingly, we found that expression of Notch targets Hey1 and Hey2 was significantly upregulated in Cldn11 overexpressing cultures but downregulated in both Cldn11 KO and Tspan3 knockdown OBs. Since ADAM10

has been shown to interact with Tspan family members and regulate Notch signaling, we evaluated if Cldn11 regulates ADAM10 expression and found that Cldn11 overexpressing cells express more mature ADAM10. Furthermore, an ADAM10 inhibitor blocked the Cldn11 effect on OB differentiation. Based on these data, we propose a novel role for Cldn11 in regulating OB functions that acts via interaction with Tspan3 to regulate ADAM10 activity and, thereby, Notch signaling.

**Disclosures:** Richard Lindsey, None.

## 1082

**Double Knockout of Osteopontin and Bone Sialoprotein Genes Results in High Cortical Porosity and Hypomineralization.** Wafa Bouleffour<sup>1</sup>, Laura Juignet<sup>1</sup>, Léa Verdière<sup>1</sup>, Irma Machuca<sup>2</sup>, Mireille Thomas<sup>1</sup>, Norbert Laroche<sup>1</sup>, Arnaud Vanden-Bossche<sup>1</sup>, Jean-Paul Concordet<sup>3</sup>, Denise Aubert<sup>4</sup>, Marie Teixeira<sup>4</sup>, Laurence Vico<sup>1</sup>, Marie-Hélène Lafage-Proust<sup>1</sup>, Luc Malaval<sup>1</sup>. <sup>1</sup>INSERM U1059-SAINBIOSE, Université de Lyon, France, <sup>2</sup>INSERM U1033, Université de Lyon, France, <sup>3</sup>INSERM U565/CNRS UMR7196/Muséum National d'Histoire, France, <sup>4</sup>AniRa PBES, France

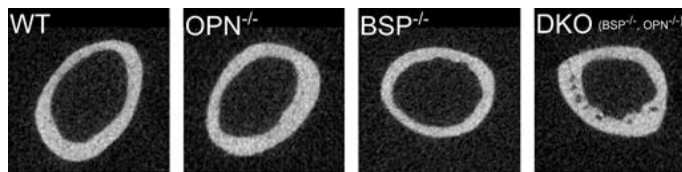
Bone sialoprotein (BSP) and osteopontin (OPN) are two SIBLING (Small Integrin Binding Ligand N-linked Glycoprotein) members, highly expressed in osteoblasts and osteoclasts. Single gene knockout (KO, <sup>-/-</sup>) of BSP or OPN induce specific skeletal and bone cellular phenotypes, suggesting distinct functions. However, we previously showed that functional compensation by OPN exists in BSP<sup>-/-</sup> mice, complicating the understanding of their respective roles. Using site-directed mutagenesis with Transcription Activator-Like Effector Nuclease (TALEN) technology in the homologous-recombination generated BSP<sup>-/-</sup> line, we produced a double gene KO (DKO) of OPN and BSP, along with a simple KO of OPN in the same 129sv/CD1 genetic background.

DKO mice are viable and fertile, but display smaller litter size than wild type (WT;  $5 \pm 1.6$  vs  $9 \pm 0.8$ , N=10 litters,  $p < 0.01$ ). At 2 month (Mo) DKO mice are lighter, with a shorter femur bone and lower trabecular bone volume (BV/TV) than WT (10.2% vs 14.5% in male femur, n=18,  $p < 0.01$ ). Cortices are thinner, less mineralized (-3.5%,  $p < 0.001$ ,  $\mu$ CT) and present with a much higher porosity (+33%,  $p < 0.01$ , cf. Figure). Two Mo old OPN<sup>-/-</sup> femur cortices are thicker than WT. In females, they are significantly more mineralized and BV/TV is higher. At 4 Mo (adults) OPN<sup>-/-</sup> bone parameters tend to normalize, as do BV/TV and cortical thickness in DKO mice, but not their mineralization. Serum phosphate at 4 Mo is higher than WT in DKO males ( $7.9$  vs  $7.0$  mg/dl, n=10,  $p < 0.05$ ) and in OPN<sup>-/-</sup> of both sexes.

Compared to WT calvaria cell cultures, OPN<sup>-/-</sup>, DKO and BSP<sup>-/-</sup> cultures form 50%, 90% and 95% fewer bone nodules than WT, respectively (n=6,  $p < 0.01$  between all groups). In contrast to each single KO, nodule formation by DKO cells is only partially rescued by high density seeding. A lower number of osteoclasts form in DKO bone marrow culture than in WT, as in BSP<sup>-/-</sup> cultures.

Femoral bone marrow ablation (a model of modeling) generates a higher volume of transient medullary bone in DKO and OPN<sup>-/-</sup> than in WT (BV/TV= 39.7 and 31.8%, respectively vs 25.1%, n=6,  $p < 0.05$ ); it is lower in the BSP<sup>-/-</sup>.

The double knockout of BSP and OPN genes thus induces a marked bone phenotype, clearly distinct from those of single KO mice, confirming the part played by the cognate protein in the impact of each individual deletion. Strikingly, the high cortical porosity of DKO mice suggests an active bone remodeling, in the absence of two key regulators of bone cell performance.



$\mu$ CT cortical bone sections of WT and mutant mice

**Disclosures:** Wafa Bouleffour, None.

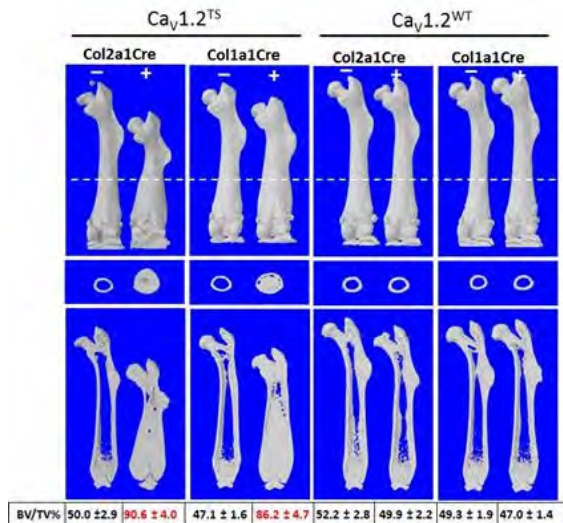
## 1083

**Ca<sup>2+</sup> signaling through the Ca<sub>v</sub>1.2 L-type Ca<sup>2+</sup> channel regulates bone formation.** Chike Cao<sup>1</sup>, Anthony Mirando<sup>2</sup>, Amy McNulty<sup>2</sup>, Farshid Guilak<sup>2</sup>, Matthew Hilton<sup>2</sup>, Geoffrey Pitt<sup>1</sup>. <sup>1</sup>Ion Channel Research Unit; Department of Medicine, Duke University Medical Center, United states, <sup>2</sup>Department of Orthopaedic Surgery, Duke University Medical Center, United states

Timothy Syndrome (TS) is a multi-organ disorder characterized by cardiac arrhythmias and developmental abnormalities. TS patients carry a de novo gain-of-function mutation in the Ca<sub>v</sub>1.2 L-type calcium channel, which has been best characterized in excitable cells such heart, brain, and hormone-secreting cells. The TS mutation reduces channel inactivation and increases Ca<sup>2+</sup> influx into the cell. The myriad phenotypes in TS patients reveals critical but not yet known roles of Ca<sub>v</sub>1.2 in multiple non-excitable tissues.

We previously reported that Ca<sup>2+</sup> influx through Ca<sub>v</sub>1.2 regulates chondrocyte hypertrophy and hyperplasia during mandible development. Here, we investigate the potential role of Ca<sub>v</sub>1.2 in bone formation.

We first found that during skeletogenesis,  $Ca_v1.2$  was highly expressed in perichondrium and/or periosteum by using a  $Ca_v1.2$  *lacZ* reporter mouse. Striking expression of  $Ca_v1.2$  was also observed in the proliferating chondrocytes within the growth plate at P10. Targeted expression of the TS-causing  $Ca_v1.2$  mutant channel ( $Ca_v1.2^{TS}$ ) in the osteoblast lineage cells with *2.3Colla1-Cre*, in the chondrocyte lineage cells with *Col2a1-Cre*, or in both cell types with *Prx1-Cre*, dramatically enhanced bone mass. Histological analysis confirmed that both primary and secondary ossification centers were occupied with excessive bone. In primary bone marrow stromal cell (BMSC) cultures, expression of  $Ca_v1.2^{TS}$  promoted osteoblast differentiation. RNASeq analysis revealed that  $Ca_v1.2^{TS}$  in BSMCs enhanced the expression of extracellular matrix proteins. Gene ablation of  $Ca_v1.2$  in BSMCs inhibited osteogenesis. The L-type calcium channel blocker verapamil (5  $\mu$ M) significantly decreased MC3T3-E1 mineralization, suggesting the role of  $Ca_v1.2$  in bone formation was mediated by  $Ca^{2+}$  signaling. We conclude that  $Ca^{2+}$  influx through  $Ca_v1.2$  is required for bone formation and increased  $Ca^{2+}$  signaling through the TS-causing mutant channel promotes osteoblast differentiation. Our data suggest that increasing  $Ca^{2+}$  signaling through  $Ca_v1.2$  could be an attractive therapeutic strategy for osteoporosis.



$Ca_v1.2$  TS channel but not WT channel enhances bone mass

Disclosures: Chike Cao, None.

## 1084

**Osteoblasts Mediate Immunosuppression During Sepsis by Regulating Lymphopoiesis.** Asuka Terashima<sup>1</sup>, Kazuo Okamoto<sup>1</sup>, Tomoki Nakashima<sup>2</sup>, Koichi Ikuta<sup>3</sup>, Hiroshi Takavanagi<sup>1</sup>. <sup>1</sup>Department of Immunology, Graduate School of Medicine & Faculty of Medicine, The University of Tokyo, Japan, <sup>2</sup>Department of Cell Signaling, Graduate School of Medical & Dental Sciences, Tokyo Medical & Dental University, Japan, <sup>3</sup>Laboratory of Biological Protection, Department of Biological Responses, Institute for Virus Research, Kyoto University, Japan

Adult hematopoietic stem cells (HSCs) are maintained in bone marrow (BM) and give rise to all blood cell types. The maintenance and the differentiation of blood cells including immune cells are essential for host defense. Cells involved in bone homeostasis share microenvironments with HSCs in BM and contribute to hematopoiesis under physiological conditions, but bone cell function in acute immune reactions has been poorly understood. Sepsis is the acute host inflammatory response to severe infection associated with high mortality, which is often caused by the immunosuppression mediated by lymphocyte apoptosis. However, it is unknown how lymphopenia persists after the accelerated lymphocyte apoptosis. Here we show that sepsis rapidly suppressed osteoblastic bone formation and reduced the number of common lymphoid progenitors (CLPs) in the BM as well as the peripheral T and B cell numbers without impairment of osteoclast function, suggesting the role of osteoblasts in the regulation of CLPs. To investigate the precise role of osteoblasts in the regulation of CLPs, we generated osteoblast-ablated mice by mating *Osterix* (*Osx*)-Cre mice with *puAtk* mice. In these mice, Cre-expressing cells can be ablated by ganciclovir (GCV) administration. Similar to sepsis, transient ablation of osteoblasts led to a marked decrease in the CLP number. Interleukin (IL)-7, which is important for maintaining lymphocytes, in BM was decreased during sepsis. Osteoblast-specific IL-7 conditional knock-out (cKO) mice were generated by crossing *Il7<sup>fllox/fllox</sup>* mice with *Osx-Cre* or *Osteocalcin-Cre*. These cKO mice exhibited the lymphopenic phenotype together with a lower CLP number, indicating that osteoblast-derived IL-7 supports CLPs in the BM. Activation of osteoblasts by PTH improves sepsis-induced lymphopenia. In addition, the survival rate for sepsis was decreased in osteoblast-ablated mice. This study demonstrated that IL-7 derived from osteoblasts regulates lymphocyte differentiation in the acute immune reaction, indicating that bone cells serve as a novel therapeutic target of life-threatening process in the immune reactions.

Disclosures: Asuka Terashima, None.

## 1085

**Crispr-Cas9 Engineered Mouse Model for Osteogenesis Imperfecta Type V.** Pierre Moffatt<sup>1</sup>, Janice Penney<sup>1</sup>, Lisa Lamplugh<sup>2</sup>, Yeqing Geng<sup>2</sup>, Marie-Helene Gaumont<sup>2</sup>, Frank Rauch<sup>2</sup>, Yojiro Yamanaka<sup>1</sup>. <sup>1</sup>McGill University, Canada, <sup>2</sup>Shriners Hospitals for Children, Canada

The *IFITM5* gene encodes a small type II transmembrane protein, called BRIL, which is expressed almost exclusively in osteoblasts. The role of BRIL in bone biology is still elusive as the knockout mice do not show any skeletal phenotype. However, a mutation in the 5' UTR of *IFITM5* causes osteogenesis imperfecta (OI) type V in all patients reported so far. OI type V is inherited in an autosomal dominant fashion. The conversion of a -14C into a T creates a novel ATG adding 5 residues (MALEP) in frame with the natural BRIL coding. A previous transgenic approach overexpressing the mutant MALEP-BRIL proposed that it has neomorphic function. Here we used Crispr-Cas9 to engineer an OI type V mouse model harboring a single nucleotide substitution at position -14 in the 5' UTR of *Ifitm5*. Two independent mosaic male founders were obtained and bred to wild type CD1 females. Because no descendants survived past birth, we analyzed embryos at different gestational ages. Heterozygote mutant embryos carrying the -14C to T mutation had severely malformed skeleton. Patterning of whole embryos and skeletal elements appeared normal by E14.5. Despite apparent normal growth plate formation, starting at E15.5, mineralization of all long bones was dramatically reduced as assessed by alizarin red/alcian blue staining. Intramembranous elements like the calvaria and mandibles also were dramatically hypomineralized. The ribs were wavy in shape and radius/ulna were bent to a 90-degree angle at the midshaft where small cartilaginous calluses were often observed, indicative that fracture repair had initiated. Histological analyses revealed the midshaft of long bone was filled with unresorbed COL10-positive cartilage. Gene expression profiling showed impaired/delayed osteoblasts differentiation with downregulation of *Bglap*, *Bsp*, and *Alp*. Furthermore, osteocytes (*Sost*, *Phex*) and osteoclasts (*Trap5*) markers were reduced by up to 10-fold. This was confirmed histologically as long bones of mutant mice lacked a marrow cavity and absence of osteoclasts and osteocytes. Western blotting for BRIL indicated that its production was also significantly reduced at all ages. Although the mechanism at play remains to be established, our results suggest that MALEP-BRIL contributes to auto regulatory negative feedback loop that is detrimental to osteoblast differentiation and function.

Disclosures: Pierre Moffatt, None.

## 1086

**A Loss of Function Mutation in *DDRKG1* Causes Shohat Type SEMD Via Increased *SOX9* Ubiquitination.** Adetutu Egunsola<sup>1</sup>, Yangjin Bae<sup>1</sup>, Ming-Ming Jiang<sup>2</sup>, David Liu<sup>1</sup>, Daniel Cohn<sup>3</sup>, Eric Swindell<sup>4</sup>, Yuqing Chen-Evenson<sup>2</sup>, Terry Bertin<sup>2</sup>, Lisette Nevarez<sup>5</sup>, Richard Gibbs<sup>6</sup>, Philippe Campeau<sup>1</sup>, Mordechai Shohat<sup>7</sup>, Brendan Lee<sup>1</sup>. <sup>1</sup>Molecular & Human Genetics at Baylor College of Medicine, United states, <sup>2</sup>Department of Molecular & Human Genetics at Baylor College of Medicine, United states, <sup>3</sup>Department of Molecular Cell & Developmental Biology; Department of Orthopaedic Surgery International Skeletal Dysplasia Registry University of California, Los Angeles, United states, <sup>4</sup>Department of Pediatrics The University of Texas Medical School at Houston, United states, <sup>5</sup>department of molecular cell developmental biology, University of California Los Angeles, United states, <sup>6</sup>Department of Molecular & Human Genetics; Human Genome Sequencing Center at Baylor College of Medicine, United states, <sup>7</sup>Recanati Institute For Medical Genetics, Rabin & Schneider Medical Centers; Departments of Pediatrics & Medical Genetics, Sackler School of Medicine, Tel Aviv University, Israel

Shohat type spondyloepimetaphyseal dysplasia (SEMD) is a human chondrodysplasia characterized by vertebral, epiphyseal and metaphyseal anomalies. Additional features may include premature osteoarthritis, disproportionate short stature, abdominal distension and hepatosplenomegaly, lordosis, genu varum and joint laxity. Radiographically, affected patients have a delayed bone age, platyspondyly, radiolucency of the femoral metaphyses and fibular overgrowth. The genetic basis of Shohat type SEMD is unknown. By performing whole exome sequencing on affected individuals from three families, we identified a homozygous c.408+1G>A mutation, a donor splice-site mutation, in the *DDRKG1* gene. This mutation causes aberrant splicing leading to a premature stop codon and loss of DDRGK1 protein in patient tissues. To investigate the role of *Ddrkg1* in skeletal development, we used zebrafish and mouse models. *drrgk1* knockdown caused craniofacial defects in zebrafish embryos, while *Ddrkg1* knockout in mice led to embryonic lethality between E11.5-12.5 with delayed mesenchymal condensation in the limb buds. To address a potential target mechanism, we knocked down *Ddrkg1* in ATDC5 cells, and found decreased SOX9 protein and *Col2a1* mRNA. We found similar alterations in E11.5 *Ddrkg1*<sup>-/-</sup> limb buds. To validate *Sox9* as a downstream target of *Ddrkg1*, we rescued the *drrgk1* craniofacial phenotype by overexpressing *sox9a* mRNA in *drrgk1* zebrafish morphants. Since DDRGK1 decreases I $\kappa$ B ubiquitination, we assessed whether DDRGK1 also regulates SOX9 ubiquitination. We found that DDRGK1 and SOX9 interact to form a complex by co-immunoprecipitation. Furthermore, *Ddrkg1* overexpression decreased SOX9 ubiquitination in HEK293T cells. These data support that the *DDRKG1* loss of function mutation causes Shohat Type SEMD in humans. Mechanistically, DDRGK1 directly interacts with SOX9, the master transcription factor of chondrogenesis, and

inhibits its ubiquitination. Hence, loss of DDRGK1 increases SOX9 ubiquitination, its subsequent protein degradation and the loss of target gene expression including *Col2a1*. The importance of these findings were demonstrated as loss of *Ddrgrk1* in mice led to delayed mesenchymal/chondrogenic condensation, partially phenocopying *Sox9* loss of function. Finally, *Sox9* overexpression rescued the chondrogenic and craniofacial phenotype in zebrafish *ddrgrk1* mutants. These data together identify a novel regulatory mechanism for *Sox9* transcriptional regulation of chondrogenesis.

**Disclosures:** *Adetutu Egunsola, None.*

## 1087

**Sclerostin antibody administration converts bone lining cells into active osteoblasts.** Marc Wein<sup>\*1</sup>, Yanhui Lu<sup>1</sup>, Elizabeth Williams<sup>1</sup>, Sang Wan Kim<sup>2</sup>, Tetsuya Enishi<sup>1</sup>, Michael Ominsky<sup>3</sup>, H.Z. Ke<sup>4</sup>, Henry Kronenberg<sup>1</sup>. <sup>1</sup>Massachusetts General Hospital, United states, <sup>2</sup>Seoul National University College of Medicine, Korea, democratic people's republic of, <sup>3</sup>Amgen, United states, <sup>4</sup>UCB, United Kingdom

Sclerostin antibody (Scl-Ab) increases osteoblast activity, in part through increasing modeling-based bone formation on quiescent surfaces. We previously used lineage tracing to show that intermittent parathyroid hormone converts quiescent bone lining cells (BLCs) into active osteoblasts. Here, we used lineage tracing to determine if Scl-Ab promotes the conversion of lining cells into osteoblasts on endocortical, cancellous, and periosteal surfaces.

To label BLCs, tamoxifen-dependent Osteocalcin-Cre/ER mice were intercrossed with a Cre-dependent tdTomato allele. Mice (n=6/group) were treated with tamoxifen at 10 weeks of age to label mature osteoblasts and their progeny. Following a 5 week 'chase' period, one group of mice was sacrificed. The remaining 12 mice were treated with vehicle or Scl-Ab (25 mg/kg) on day 0 and day 3, and all mice were treated with EdU prior to sacrifice on day 7. After sacrifice, tdTomato-positive cells enumerated in the tibia by epifluorescent microscopy. The thickness of all tdTomato-positive cells on bone surfaces was quantified by confocal microscopy, and apoptosis was detected by immunostaining for activated Caspase 3. PINP was measured in serum. Analogous experiments were performed using Dmp1-Cre/ER mice and a b-galactosidase reporter to focus on calvarial and periosteal lining cells in the femur.

In the osteocalcin-Cre/ER mice, Scl-Ab led to a 74% increase in serum PINP (p=0.0032 vs veh). Cell thickness was measured for 89 tdTomato-positive cells on endocortical and trabecular bone surfaces in vehicle-treated mice, and 139 in Scl-Ab-treated mice. At this time point, tdTomato-positive cells with plump osteoblastic morphology were only present with Scl-Ab treatment, consistent with a significant increase in the average thickness of tdTomato-positive cells on bone surfaces (vehicle 4.45 ± 0.79 μm vs Scl-Ab 8.14 ± 0.58 μm (p=0.00364). Across groups, a positive linear correlation was noted comparing serum PINP and average cell thickness (R<sup>2</sup>=0.615, p=0.00012). Scl-Ab did not induce proliferation of tdTomato-labelled cells, as assessed by EdU staining. Scl-Ab did not affect apoptosis of tdTomato-labelled cells. Analogous results were seen with enlargement of bone lining cells after Scl-Ab in the Dmp1-Cre/ER mice (vehicle 1.9 ± 1.2 μm vs Scl-Ab 4.2 ± 1.0 μm, p<0.01).

Lineage tracing demonstrates that the reactivation of quiescent bone lining cells contributes to the acute increase in bone formation following Scl-Ab treatment in mice.

**Disclosures:** *Marc Wein, Amgen, 11*  
*This study received funding from: Amgen*

## 1088

**Dose-response Relationship of Palovarotene in the ALK2 (Q207D) Cre-Inducible Transgenic Mouse Model of HO Under Mild and Severe Injury Conditions.** Isabelle Lemire<sup>\*1</sup>, Dominic Poulin<sup>2</sup>, Philippe Colucci<sup>3</sup>, Michael Harvey<sup>1</sup>. <sup>1</sup>Clementia Pharmaceuticals Inc., Canada, <sup>2</sup>Charles River Montreal ULC, CR-MTL, Canada, <sup>3</sup>Learn & Confirm, Inc., Canada

Fibrodysplasia Ossificans Progressiva (FOP) is a rare, genetic disease of congenital skeletal malformations and progressive heterotopic ossification (HO) that irreversibly restricts movement and physical function, and for which there is no approved treatment. Palovarotene (PVO) is an orally bioavailable retinoic acid receptor gamma (RARγ) selective agonist shown to prevent HO formation in injury-induced and genetic mouse models of FOP. PVO is being investigated in Phase 2 clinical trials as a potential therapy for FOP.

We evaluated the dose-response relationship of orally administered PVO on HO formation (% HO inhibition relative to vehicle-control) in the ALK2 (Q207D) Cre-inducible transgenic mouse model of HO under mild and severe injury conditions. Mice homozygous for the ALK2 (Q207D) transgene were injected intramuscularly into the posterior left femoral muscle region with different concentrations of adenovirus expressing Cre recombinase (Adeno-Cre, to activate the transgene) and cardiotoxin (CTX) to initiate the inflammatory triggering event leading to HO. Daily treatment by oral gavage with various doses of PVO (1 to 15 mg human equivalent dose) or vehicle was initiated on the day of muscle injury (day 19 post partum), and continued for the next 14-15 consecutive days.

MicroCT scans 15 days post-injury revealed the presence of HO in vehicle controls. Mean HO bone volume varied from 10.75 to 80.76 mm<sup>3</sup> depending on the concentrations of Adeno-Cre and CTX: injury conditions resulting in low and highly variable (<40mm<sup>3</sup>, %CV of 118) or high with less variability (≥40 mm<sup>3</sup>, %CV of 40)

HO bone volume were defined as mild or severe, respectively. The degree to which PVO prevented the formation of HO depended on the dose and the experimental conditions. The relationship between PVO doses and % HO inhibition relative to vehicle-control was best characterized using a simple Emax model. The dose-response curve showed a shift to the right when severe HO formation was induced in vehicle-treated animals with greater % HO inhibition in animals administered PVO under mild injury conditions than under severe injury conditions. There was also a clear dose-response relationship in which higher doses of PVO resulted in greater inhibition of HO in this injury-based Q207D mouse model of FOP.

The authors wish to acknowledge Dr. Yuji Mishina and the NIH within the Department of Health and Human Services for contributing the Q207D mouse model of FOP.

**Disclosures:** *Isabelle Lemire, None.*  
*This study received funding from: Clementia Pharmaceuticals Inc.*

## 1089

**The Role of Canonical Wnt Signaling in the Development of Spondyloarthritis.** Wanqing Xie<sup>\*1</sup>, Tianqian Hui<sup>1</sup>, Lifan Liao<sup>2</sup>, Shan Li<sup>2</sup>, Chundo Oh<sup>2</sup>, Qiming Fan<sup>1</sup>, Jeffrey S Kroin<sup>2</sup>, Hee-Jeong Im<sup>2</sup>, Di Chen<sup>2</sup>. <sup>1</sup>Rush University Medical Center, China, <sup>2</sup>Rush University Medical Center, United states

Spondyloarthritis (SpA) is a group of autoimmune disease affecting spine and joint. Up-regulation of canonical Wnt signaling has been reported in patients with SpA. In this study, we determined if activation of β-catenin signaling is the key event leading to the SpA.

To mimic β-catenin activation, three types of transgenic mice, *β-cat(ex3)<sup>Col2ER</sup>*, *β-cat(ex3)<sup>Agcl1ER</sup>*, and *β-cat(ex3)<sup>Gli1ER</sup>*, were generated by breeding *β-catenin(ex3)<sup>fllox</sup>/fllox* mice with *Col2-CreER<sup>T2</sup>*, *Agcl1-CreER<sup>T2</sup>*, and *Gli1-CreER<sup>T2</sup>* transgenic mice. 1) μCT data showed that severe osteophyte formation was found in the disc of entire spine in 3- and 6-month-old *β-cat(ex3)<sup>Col2ER</sup>*, *β-cat(ex3)<sup>Agcl1ER</sup>* mice. 2) Histology and histomorphometry analyses showed that severe destruction of disc tissues, including loss of growth plate (GP), cartilage and disorganized annulus fibrosus (AF) and nucleus pulposus (NP) tissues in 3- and 6-month-old *β-cat(ex3)<sup>Col2ER</sup>* and *β-cat(ex3)<sup>Agcl1ER</sup>* mice. 3) Mineralization of ligaments in the spine was observed in *β-cat(ex3)<sup>Gli1ER</sup>* mice. 4) Severe loss of proteoglycan and defects in cartilage structure were observed in the facet joint of 3- and 6-month-old *β-cat(ex3)<sup>Col2ER</sup>* mice. 5) We have generated immortalized rat AF and NP cell lines. Treatment with BIO (GSK-3β inhibitor), which mimic β-catenin signaling activation, stimulated *Mmp13* (8 and 11 folds), NGF (5 and 2 folds) and *Ccl2* (6 and 11 folds) expression in AF and NP cells. 6) Back pain has been reported in patients with SpA disease and NGF, *Ccl2* are important mediators for pain. We found that *β-cat(ex3)<sup>Col2ER</sup>* mice had significantly increased pain sensitivity with lower von Frey, ambulation and rearing counts. This pain behavior sustained throughout the entire experimental period (4-9 month). 7) To determine if *Mmp13* is a key downstream target of β-catenin signaling, we generated [*β-cat(ex3)/Mmp13*]<sup>Col2ER</sup> double mutant mice and found that deletion of *Mmp13* significantly reversed defects observed in disc tissue of *β-cat(ex3)<sup>Col2ER</sup>* mice, demonstrated by μCT, histology and histomorphometry. Deletion of *Mmp13* also reduced pain sensitivity observed in *β-cat(ex3)<sup>Col2ER</sup>* mice. 8) The increased mineralization of bone tissues were observed in sacroiliac joints of 1-month-old *β-cat(ex3)<sup>Col2ER</sup>* mice, demonstrated by X-ray.

Since all changes observed in *β-catenin* activation mice could be found in patients with SpA, our findings suggest that β-catenin may be a key mediator in SpA development, especially at the bony overgrowth phase.

**Disclosures:** *Wanqing Xie, None.*

## 1090

**Differential effects of the cathepsin K inhibitor, MK-0674, and alendronate on bone mass, remodeling, and strength of cortical bone in cynomolgus monkeys with established osteopenia.** Maureen Pickarski<sup>\*</sup>, Brenda Pennypacker, Le Duong. Merck & Co., Inc, United states

MK-0674 (MK) is a highly orally bioavailable cathepsin K inhibitor with similar potency and selectivity profile as odanacatib, an investigational drug in development for treatment of postmenopausal osteoporosis. The aim of this study was to compare effects of MK to alendronate (ALN) dosed in intervention mode on femoral cortical density, structure, and remodeling/modeling in ovariectomized (OVX) monkeys. Cynomolgus monkeys (10-27 yrs. old) were Sham-operated (N=9) or OVX'd 2 yrs prior to study start. OVX'd animals were randomized into 4 groups (N=14-16/group): untreated control (CON), MK at 0.6 (MK-L) or 2.5 mg/kg (MK-H) (p.o., q.d.), or ALN (30μg/kg; wkly, s.c.) for 24 mo. Prior to drug treatment, osteopenia was confirmed by DXA in OVX'd animals which had significant BMD loss of 8-15% at whole body, lumbar vertebrae and total hip versus Sham. After 24 mo. treatment, whole femur BMD was increased 10% (MK-L, p<0.05) and 15% (MK-H, p<0.01), as compared to a more modest increase of 5% by ALN (NS). Differential treatment effects were shown by pQCT analysis. Central femur (CF) cortical area was 9% (MK-L, NS) and 19% higher (MK-H, p<0.01) compared to CON, and to ALN (p<0.05). Similarly, cortical thickness was 12% (MK-L, NS) and 17% (MK-H, p<0.01) vs. CON, and vs. ALN (p<0.05). Histomorphometric analysis of CF showed similar endocortical bone formation rates (Ec.BFR/BS) at mo. 12 between all treatment

groups. However, by mo. 24, Ec.BFR/BS was significantly reduced by ALN, while MK groups were comparable to CON levels. Moreover, CF periosteal (Ps) BFR/BS was higher by MK-H at mo. 12 (2.2X,  $p<0.05$ ) and mo. 20 (2.6X, NS) whereas ALN had no effect vs. CON. MK dose dependently increased peak load by 11% (MK-L, NS) and 26% (MK-H,  $p<0.05$ ) as compared to ALN (11%, NS) relative to CON levels. Stiffness was increased 12-22% by MK and 10% by ALN treatment. Regression analyses of peak load to pQCT cortical BMC ( $R=0.89$ ,  $p<0.001$ ) and to cortical thickness ( $R=0.60$ ,  $p<0.001$ ) showed highly positive and linear relationships. In osteopenic monkeys, compared to ALN, long-term treatment with MK in intervention mode generally resulted in higher femoral bone mass, cortical thickness and biomechanical properties. ALN treatment slowly decreased femoral Ec.BFR and had no effect on Ps modeling. The differential mechanism of MK-0674, evidenced by the consistent maintenance of Ec remodeling and dose-related increases in Ps modeling, suggests the effects of the CatK inhibitor progressively improved cortical density and structural strength under long-term therapy.

**Disclosures:** *Maureen Pickarski, Merck & Co., Inc, 15*  
*This study received funding from: Merck & Co., Inc*

## 1091

**Genetic Sost Deletion or Pharmacological Inhibition of Sclerostin Prevents Bone Loss and Decreases Osteolytic Lesions in Immunodeficient and Immunocompetent Preclinical Models of Multiple Myeloma.** Jesús Delgado-Calle<sup>\*1</sup>, Judith Anderson<sup>2</sup>, Meloney D Cregor<sup>1</sup>, Dan Zhou<sup>2</sup>, Lilian I Plotkin<sup>1</sup>, Teresita Bellido<sup>1</sup>, G David Roodman<sup>2</sup>. <sup>1</sup>Department of Anatomy & Cell Biology, Indiana University School of Medicine, United states, <sup>2</sup>Department of Medicine, Indiana University School of Medicine, United states

Multiple myeloma (MM) cells induce localized lytic lesions due to increased bone resorption and suppressed bone formation. Osteocytes in mice bearing MM tumors express elevated Sost/Sclerostin (Scl); and serum Scl is increased in MM patients. Based on this evidence, we examined the impact of Sost/Scl on tumor growth and MM-induced bone disease. 6-wk-old SostKO or WT immunodeficient mice (SCID) were injected intratibially with  $10^5$  JJN3 human MM (hMM) cells or saline ( $n=7-10$ /group), and sacrificed after 4wks. KO SCID mice displayed the expected high bone mass phenotype; and hMM-injected KO and WT mice had equivalent tumor engraftment as revealed by serum human kappa light chain levels. hMM-injected WT mice exhibited ~50% decreased tibia cancellous bone volume (BV/TV) and trabecular number (Tb.N), and increased trabecular separation (Tb.Sp). In contrast, hMM-injected KO mice displayed no changes in BV/TV or architecture. Importantly, X-ray analysis revealed that the number and area of osteolytic lesions was reduced in KO (60 and 74%, respectively) compared to WT mice. We next examined the effect of pharmacological inhibition of Scl in an immunocompetent preclinical model of established MM. 6-wk-old C57BLKwRij mice were injected intratibially with  $10^5$  5TGM1 murine MM cells (mMM) or saline. After 4wks mMM-injected mice had a 2-fold increase in the serum tumor engraftment marker IgG2b. Saline or mMM-injected mice were then treated with a Scl neutralizing antibody (Scl-Ab; 15mg/kg/wk) or control antibody (IgG;  $n=6-10$ /group). After 4wks, serum IgG2b was similar in mMM-injected mice receiving Scl-Ab or IgG. mMM-injected mice had ~35% decreased BV/TV, Tb.N, and increased Tb.Sp. In contrast, mMM-injected mice receiving Scl-Ab displayed increased trabecular BV/TV (52%), Tb.N (22%), Tb.Th (33%) and decreased Tb.Sp (14%), results that did not differ from saline-injected mice treated with Scl-Ab. Moreover, the number of osteolytic lesions was reduced by 46% in Scl-Ab treated mice. Further, mMM-injected mice treated with IgG or Scl-Ab showed similar increased serum CTX, whereas mMM-injected mice treated with Scl-Ab had a smaller decrease in serum PINP compared to IgG-treated mice (22 vs 45%). These results demonstrate that increased Scl production by osteocytes inhibits bone formation and contributes to MM-induced bone loss, without affecting tumor growth. These findings provide the rationale for combining Scl-Ab with anti-tumor drugs to treat MM.

**Disclosures:** *Jesús Delgado-Calle, None.*  
*This study received funding from: Eli Lilly Co*

## 1092

**Molecular Mechanisms of Breast Cancer Cellular Dormancy in the Bone Marrow.** Mattia Capulli<sup>\*1</sup>, Dayana Hristova<sup>2</sup>, Ronak Arjan<sup>2</sup>, Alfredo Cappariello<sup>1</sup>, Antonio Maurizi<sup>1</sup>, Argia Ucci<sup>1</sup>, Nadia Rucci<sup>1</sup>, Anna Teti<sup>1</sup>. <sup>1</sup>University of L'Aquila, Italy, <sup>2</sup>University of Manchester, United Kingdom

Breast Cancer Cells (BCC) transit through the bone marrow where they can remain dormant before spreading to other organs. We hypothesized that dormant BCC interact with Spindle-shaped N-cadherin<sup>+</sup> endosteal niche Osteoblasts (SNO) and share mechanisms of quiescence with bone marrow Hematopoietic Stem Cells (HSC). N-Cadherin<sup>+</sup> SNO were sorted and cultured in monolayers on which EGFP<sup>-</sup> (human MDA-MB231) or PKH26-stained (mouse 4T1) BCC were attached for 1 hour, showing an adhesion rate similar to BCC cultured on SNO-depleted osteoblasts (NON-SNO). In contrast, while the number of BCC on SNO was not changed after 24 hours of coculture, their number on NON-SNO doubled ( $p=0.02$ ), forming +3.3fold clones ( $p<0.05$ ). Cultured SNO exhibited about 78% less ALP activity and 58% less Runx2 mRNA expression compared to NON-SNO. Similar to HSC, BCC attached to SNO showed increased expression of Notch2 (2.8fold,  $p=0.013$ ), whose ligand, Jag1, was expressed by SNO. Notch2-specific siRNA increased BCC proliferation on SNO

(1.83fold,  $p=0.04$ ), achieving the proliferation rate of BCC attached to NON-SNO. BCC injected in tibias of immunocompromised mice progressively reached the trabecular endosteal surface ( $p=0.02$ ) and remained non-proliferating for the timeframe of 1 month. They expressed Notch2 and localized near N-Cadherin<sup>+</sup> endosteal cells, whereas cells located far from the endosteal surface (>2 cell distance) were Notch2-negative. Only very rare asymmetric divisions were observed in BCC localized at the endosteal surface, suggesting their stemness, with the farthest daughter cell being Notch2-negative. An *in vivo* competition assay injecting  $10^5$  HSC and increasing ( $10^5-10^6$ ) BCC in busulfan/cyclophosphamide-conditioned immunocompromised mice, showed the engraftment of HSC declining with the increase of administered BCC ( $p=0.037$ ,  $R=0.28$ ), suggesting that BCC and HSC share commonalities for the occupancy of the HSC bone marrow niche. Consistently, Notch2<sup>high</sup>-sorted BCC showed 5.37fold Sca1 ( $p=0.002$ ), 2.6fold Tie2 ( $p=0.0001$ ) and 1.34fold CXCR4 mRNAs higher than Notch2<sup>low</sup>. Interestingly, Sca1 is a biomarker of HSC stemness, and Tie2 and CXCR4 are implicated in the quiescence of HSC attached to SNO. Finally, a single injection of 4.8mg/kg dibenzazepine, a  $\gamma$ -secretase inhibitor dampening the Notch pathway, in mice intratibially injected with BCC after 1 month of presumed dormancy (no overt tumor evident), showed 2 months later an increase of liver metastases (2.5fold,  $p=0.04$ ).

**Disclosures:** *Mattia Capulli, None.*

## 1093

**Targeting TRPV1 on sensory neurons as a potential therapy for breast cancer in bone.** Tatsuo Okui<sup>\*1</sup>, Masahiro Hiasa<sup>1</sup>, Fletcher White<sup>2</sup>, G David Roodman<sup>1</sup>, Toshiyuki Yoneda<sup>1</sup>. <sup>1</sup>Department of Medicine, Hematology Oncology, Indiana University School of Medicine, United states, <sup>2</sup>Department of Anesthesia, Paul & Carole Stark Neurosciences Research Institute, United states

Cancer progression is associated with neurogenesis as well as angiogenesis. Increased neurogenesis in the tumor or cancer invasion around nerves, known as perineural invasion, is correlated with poor outcome in cancer patients. However, the contribution of neurons to cancer progression is unclear. Breast cancer (BC) preferentially spreads to bone and often disseminates to distant organs after a persistent period of dormancy, resulting in secondary metastasis that increases the mortality of BC patients. Bone is densely innervated by sensory neurons (SNs), thus BC cells in bone interact with SNs. We hypothesized that BC progression in bone, subsequent dissemination of BC to visceral organs from bone and bone pain induction are in part regulated by SNs innervating bone. We found that PGP9.5+ peripheral nerve fibers, as well as CD31+ blood vessels, were increased in bone in mice injected intratibially with the 4T1 mouse BC cells (4T1 mice) compared to sham mice. To investigate the contribution of SNs to 4T1 BC progression in bone, we examined the effects of SB366791, a specific antagonist for the transient receptor potential channel-vanilloid subfamily member-1 (TRPV1), which is a pain-mediating acid-sensing ion channel predominantly expressed on SNs. Treatment of 4T1 mice with SB366791 significantly reduced neurogenesis and angiogenesis in bone, 4T1 BC osteolytic colonization of bone and metastasis to lung from bone. In contrast, SB366791 had no effects on 4T1 tumor development and lung metastasis from mammary fat pad. We also found that 5-iodoresiniferatoxin (I-RTX), another selective potent antagonist of TRPV1, inhibited 4T1 BC osteolytic colonization of bone and lung metastasis from bone. Of note, TRPV1 expression was not detected in 4T1 BC cells, and SB366791 and I-RTX did not inhibit 4T1 BC cell growth, suggesting that these antagonists unlikely have direct anti-proliferative effects on 4T1 BC cells. Administration of SB366791 or I-RTX significantly alleviated bone pain in 4T1 mice. Treatment of 4T1 mice with a combination of SB366791 and a suboptimal dose of doxorubicin suppressed 4T1 BC progression in bone, lung metastasis from bone and bone pain to a greater extent than each agent alone. In conclusion, our results uncover the previously-unidentified role of TRPV1 on SNs in BC bone metastasis and secondary metastasis from bone. They suggest that TRPV1 on SNs is a potential and novel therapeutic target for treatment of BC in bone and its sequelae.

**Disclosures:** *Tatsuo Okui, None.*

## 1094

**Myeloid-Derived Suppressor Cells (MDSC) Mediate Prostate Cancer-Bone Interactions.** Serk In Park<sup>\*</sup>, Hye Eun Kim, Hyo Min Jeong, Geurim Son. Korea University College of Medicine, Korea, republic of

The microenvironment of bone metastasis is comprised of diverse stromal cell types that are potentially involved in metastatic progression. Increasing evidence supports that a subset of immature myeloid bone marrow cells, termed Myeloid-Derived Suppressor Cells (MDSC), are frequently increased in cancer patients, contributing to immune evasion, angiogenesis and tumor growth. In contrast, regulation and function of MDSC during the progression of bone metastasis are poorly understood. Recent data from our laboratory highlighted a novel feed-forward mechanism underlying the interactions between prostate cancer cells and MDSC via activation of osteoblasts. Briefly, levels of tumor derived parathyroid hormone-related protein (PTHrP) correlated with MDSC numbers in the tumor tissue, with further evidence for tumor-derived PTHrP potentiates MDSC activity and function within the bone marrow of tumor hosts. More importantly, mechanistic investigations *in vivo* revealed that PTHrP elevated Y418 phosphorylation levels in Src family kinases in MDSC via osteoblast-derived interleukin-6 (IL-6) and VEGF-A, thereby upregulating MMP-9. In the present study, we further discovered that tumor-derived PTHrP rapidly increases MDSC (determined by flow cytometric analyses of CD11b<sup>+</sup>Gr1<sup>+</sup> cells) in the bone marrow and

subsequently in the circulation. We also found that a single injection of recombinant PTHrP rapidly increases C-C chemokine ligand (CCL)-2 as well as VEGF-A and IL-6 in the bone marrow, while administration of PTHrP neutralizing antibodies into PC-3 tumor-bearing mice reduced CCL2, VEGF-A and IL-6 in the bone marrow of tumor hosts. Given our previous data showing CCL2 neutralizing antibody suppressed the development of experimental bone metastases induced by expansion of CD11b<sup>+</sup> immature monocytes, our data collectively showed that osteoblasts orchestrate the prostate tumor progression by expression of cytokines such as CCL2. Our research supports that prostate tumor-bone interactions via PTHrP result in MDSC activation, and warrants more extensive further investigation into the role of osteoblast-derived cytokines, such as CCL2, during the progression of prostate cancer bone metastasis.

**Disclosures:** *Serk In Park, None.*

## 1095

**MicroRNA-30 Family Reduces Skeletal Lesions in Tumor Bearing Mice by Targeting Osteomimicry.** Martine Crosset<sup>1</sup>, Francesco Pantano<sup>2</sup>, Casina Kan<sup>1</sup>, Françoise Descotes<sup>3</sup>, Edith Bonnelye<sup>1</sup>, Saw-See Hong<sup>4</sup>, Philippe Clezardin<sup>\*1</sup>. <sup>1</sup>INSERM, UMR\_S1033, UFR de médecine Lyon-Est, University of Lyon, France, <sup>2</sup>Medical Oncology Dept./Translational Oncology Laboratory, Italy, <sup>3</sup>Service biochimie biologie moléculaire Hospices civils de Lyon, France, <sup>4</sup>Université Claude Bernard Lyon 1 UMR754 INRA-UCBL-EPHE, France

MicroRNAs have key roles in cancer initiation, progression and metastasis. They act as metastasis stimulators or suppressors by regulating a number of genes that are major players in this process. Here, we found that the expression of miR-30 family (miR-30s) was substantially downregulated in primary tumors from breast cancer patients with metastases (n=39) compared to that observed in breast cancer patients with local disease (n=81) [Hazard Ratio (HR) = 0.17; 95% CI = 0.04 – 0.65; P = 0.01]. Mir-30s downregulation was also associated with estrogen receptor (ER) negativity within breast tumors. Compared to human ER positive MCF-7 breast cancer cells, low expression levels of mir-30s were also observed in the human triple negative MDA-MB-231 breast cancer cell line, in its osteotropic cell subpopulation MDA-B02, and in ER negative BC-M1 cells, a cell line derived from disseminated tumor cells isolated from the bone marrow of a patient with breast cancer. We therefore investigated the function(s) of miR-30s using an experimental model of human breast cancer bone metastasis. Restoring miR-30s expression in MDA-B02 (MDA-B02-miR-30) cells prior to tumor cell intra-arterial injection in immunodeficient mice inhibited by 50% the extent of osteolytic lesions and skeletal tumor burden in animals. Additionally, the measurement of tartrate-resistant acid phosphatase (TRAP) staining of bone tissue sections of metastatic legs from mice bearing MDA-B02-miR-30 tumors showed that the active-osteoclast resorption surfaces at the tumor-bone interface were substantially decreased compared with control tumors (77.4% ± 8.1 vs 41.7% ± 16.5 P<0.05). The level of pro-osteoclastic cytokines IL-11 and IL-8 produced in the conditioned medium (CM) from MDA-B02-miR-30 cells was significantly reduced, and was associated with a decreased capability of the CM to promote osteoclastogenesis *in vitro*. Additionally, osteogenic properties of MC3T3-E1 osteoblastic cells were inhibited in the presence of the CM from MDA-B02 cells, whereas miR-30s overexpression repressed this inhibitory effect through a decreased production of the Wnt inhibitor DKK1. Indeed, as opposed to MCF-7 cells, both BC-M1 and MDA-B02 cells produced high levels of osteotropic and osteomimetic proteins (ITGβ3, ITGα5, TWF1, RUNX2, CTGF, CDH-11, Connexin-43, and DKK1) whose expression was repressed by miR-30s. In conclusion, miR-30s interfere with breast cancer bone metastasis formation by inhibiting osteomimicry.

**Disclosures:** *Philippe Clezardin, None.*

## 1096

**Fracture Risk Reduction With Romosozumab: Results of the Phase 3 FRAME Study (FRActure study in postmenopausal woMen with ostEoporosis).** F Cosman<sup>\*1</sup>, DB Crittenden<sup>2</sup>, JD Adachi<sup>3</sup>, N Binkley<sup>4</sup>, E Czerwinski<sup>5</sup>, S Ferrari<sup>6</sup>, LC Hofbauer<sup>7</sup>, E Lau<sup>8</sup>, EM Lewiecki<sup>9</sup>, A Miyauchi<sup>10</sup>, CAF Zerbini<sup>11</sup>, L Chen<sup>2</sup>, J Maddox<sup>2</sup>, PD Meisner<sup>12</sup>, CE Milmont<sup>2</sup>, C Libanati<sup>12</sup>, A Grauer<sup>2</sup>. <sup>1</sup>Helen Hayes Hospital, West Haverstraw, & Columbia University, United states, <sup>2</sup>Amgen Inc., United states, <sup>3</sup>McMaster University, Canada, <sup>4</sup>University of Wisconsin-Madison Osteoporosis Clinical Center & Research Program, United states, <sup>5</sup>Krakow Medical Centre, Poland, <sup>6</sup>Geneva University Hospital, Switzerland, <sup>7</sup>Division of Endocrinology, Diabetes, & Bone Diseases, TU Dresden Medical Center, Germany, <sup>8</sup>Center for Clinical & Basic Research, China, <sup>9</sup>New Mexico Clinical Research & Osteoporosis Center, United states, <sup>10</sup>Miyauchi Medical Center, Japan, <sup>11</sup>Centro Paulista de Investigação Clínica, Brazil, <sup>12</sup>UCB Pharma, Belgium

### Purpose

Romosozumab (Romo) is an investigational bone-forming monoclonal antibody that binds sclerostin and has a dual effect, increasing bone formation and decreasing bone resorption. Here we report results of the FRAME study (NCT01575834).

### Methods

This multicenter, randomized, double-blind, placebo-controlled study enrolled postmenopausal women age 55–90 with osteoporosis (BMD T-score ≤ -2.5 at total hip [TH] or femoral neck). Subjects were randomized 1:1 to placebo (Pbo) or 210mg Romo SC QM for 12 months, followed by 60mg denosumab (DMAB) SC Q6M for 12 months in both groups. The co-primary endpoints were subject incidence of new vertebral fracture through M12 and M24. Secondary endpoints included clinical (nonvertebral [NVT] plus symptomatic vertebral) and NVT fracture, and BMD.

### Results

7180 women (mean age 71, mean TH T-score -2.5) were enrolled. At M12, Romo reduced new vertebral fracture with a relative risk reduction (RRR) of 73% (subject incidence of fracture 1.8% Pbo vs 0.5% Romo; p<0.001). In subjects who received Romo in year 1, vertebral fracture risk reduction persisted through M24 after both groups transitioned to DMAB (2.5% Pbo/DMAB vs 0.6% Romo/DMAB; RRR 75%; p<0.001). Romo reduced clinical fracture risk at M12 (2.5% vs 1.6%; RRR 36%; p=0.008). NVT fracture incidence through M12 was 2.1% for Pbo (lower than expected) vs 1.6% for Romo (RRR 25%; p=0.096), with a similar risk reduction through M24 (Pbo/DMAB vs Romo/DMAB RRR 25%; nominal p=0.029, adjusted p=0.057). A preplanned analysis revealed a significant interaction between treatment and geographic region for NVT fracture at M12 (p=0.042). NVT fracture incidence in Central/Latin America was 1.2% for Pbo vs 1.5% for Romo, whereas a 42% RRR in NVT fracture was observed in rest-of-world (p=0.012). BMD increased with Romo vs Pbo by 12.7% and 5.8% at the lumbar spine and TH, respectively, at M12 (p<0.001). Adverse events were generally balanced between groups, with injection site reactions in 5.2% of Romo and 2.9% of Pbo subjects during year 1. One AFF and 2 ONJ cases were positively adjudicated in the Romo group.

### Conclusion

In postmenopausal women with osteoporosis, Romo 210mg QM was well tolerated and reduced vertebral and clinical fracture risk vs Pbo at M12; vertebral fracture risk reduction persisted in Romo subjects through M24 after both groups transitioned to DMAB. The sequence of Romo followed by DMAB may be a highly effective treatment for postmenopausal women with osteoporosis.

**Disclosures:** *F Cosman, Amgen, Eli Lilly, Merck, Radius, Tarsa, 12; Amgen, Eli Lilly, 13; Amgen, Eli Lilly, 11*

*This study received funding from: Amgen Inc. and UCB Pharma*

## 1097

**Effects of Odanacatib on Transilial Cortical Remodeling/Modeling and Microarchitecture in Postmenopausal Women with Osteoporosis: 5-Year Data from the Extension of the Phase 3 Long-Term Odanacatib Fracture Trial (LOFT).** Robert Recker<sup>\*1</sup>, David Dempster<sup>2</sup>, Bente Langdahl<sup>3</sup>, Graham Ellis<sup>4</sup>, Tobie de Villiers<sup>5</sup>, Dosinda Cohn<sup>6</sup>, Steven Doleckiy<sup>7</sup>, Hilde Giezek<sup>8</sup>, Arthur Santora<sup>6</sup>, Le T Duong<sup>6</sup>. <sup>1</sup>Creighton University, United states, <sup>2</sup>Helen Hayes Hospital, United states, <sup>3</sup>Aarhus University Hospital, Denmark, <sup>4</sup>Synexus Helderberg Clinical Research Centre, South africa, <sup>5</sup>University of Stellenbosch, South africa, <sup>6</sup>Merck & Co., Inc., United states, <sup>7</sup>Formerly Merck & Co., Inc., United states, <sup>8</sup>MSD Europe Inc., Belgium

**Purpose:** Odanacatib (ODN) is a selective oral inhibitor of cathepsin K in development for the treatment of osteoporosis. In this analysis, the effects of ODN on bone remodeling/modeling and microarchitecture were examined in the randomized, double-blind, placebo (PBO)-controlled, event-driven, Phase 3 Fracture Trial (LOFT; NCT00529373) and planned double-blind extension in postmenopausal women with osteoporosis.

**Methods:** A total of 345 transilial bone biopsies, obtained from 258 consenting patients at baseline (BL), 24, 36, and 60 months were assessed by dynamic and static bone histomorphometry. Tetracycline double labeling was administered within ~1 month prior to biopsy.

**Results:** Biopsies at BL, (ODN n=12, PBO n=20), 24 (ODN n=95, PBO n=81), 36 (ODN n=32, PBO n=32), and 60 (ODN n=22, PBO n=12) months were analyzed by histomorphometry. BMD analysis of the patients with biopsies demonstrated that ODN-treated patients responded to therapy. There was no apparent difference in trabecular bone remodeling parameters (including activation frequency, bone formation rate [BFR/BS]) with ODN vs PBO. Over 5 years, endocortical (Ec) bone formation indices (mineralizing surface [MS/BS], mineral apposition rate [MAR] and BFR/BS) and the number of labeled secondary osteons in ODN-treated patient biopsies were similar to PBO. Periosteal (Ps) MS/BS with ODN was generally higher vs PBO, particularly at Month 60 (1.41 vs 0.33%). Ps.MAR and Ps.BFR/BS were generally similar between ODN and PBO; very few scalloped cement lines were observed on the Ps surface. The proportion of patients with double-labeled Ps surface was progressively numerically higher in ODN vs PBO groups over time (Table). Mean [SD] cortical thickness was similar in both groups at Months 24 and 36, and numerically higher with ODN at Month 60 (832.5 [274.8] vs 636.8 [279.9] μm for ODN and PBO, respectively). Mean [SD] cortical porosity was similar in both groups (5.95 [2.98] vs 5.12% [1.76] at Month 60, for ODN and PBO, respectively).

**Conclusion:** ODN treatment for 5 years preserved trabecular, intracortical and Ec remodeling and increased the number of patients with Ps bone formation (modeling), supporting the observed trend for increase in cortical thickness at 60 months compared with PBO. Together with BMD data, these results show that ODN is

effective and appears to have a unique mechanism of action compared to other currently available agents.

Table. Periosteal mineralizing surface with double label

	ODN 50 mg (N=8043) n/m (%)	PBO (N=8028) n/m (%)
Baseline	2/12 (16.7)	6/20 (30.0)
Month 24	38/92 (41.3)	16/73 (21.9)
Month 36	16/30 (53.3)	5/29 (17.2)
Month 60	12/22 (54.5)	1/12 (8.3)

N = total population; n = number of specimens with double labels; m = number of patients with a periosteal mineralizing surface available; ODN = odanacatib; PBO = placebo

Table. Periosteal mineralizing surface with double label

**Disclosures:** Robert Recker, Merck, Lilly, Amgen, 11; Merck, Lilly, 12  
This study was sponsored by Merck & Co. Inc.

## 1098

**Effects of KRN23, an Anti-FGF23 Antibody, in Patients With Tumor Induced Osteomalacia and Epidermal Nevus Syndrome: Results from an Ongoing Phase 2 Study.** [Thomas Carpenter](#)<sup>\*1</sup>, [Paul Miller](#)<sup>2</sup>, [Thomas Weber](#)<sup>3</sup>, [Munro Peacock](#)<sup>4</sup>, [Mary Ruppe](#)<sup>5</sup>, [Karl Insogna](#)<sup>1</sup>, [Suzette Osei](#)<sup>6</sup>, [Diana Luca](#)<sup>6</sup>, [Alison Skrinar](#)<sup>6</sup>, [Javier San Martin](#)<sup>6</sup>, [Suzanne Jan de Beur](#)<sup>7</sup>.  
<sup>1</sup>Yale University School of Medicine, United states, <sup>2</sup>Colorado Center for Bone Research, United states, <sup>3</sup>Duke University, United states, <sup>4</sup>Indiana University School of Medicine, United states, <sup>5</sup>Houston Methodist Hospital, United states, <sup>6</sup>Ultragenyx Pharmaceutical Inc., United states, <sup>7</sup>Johns Hopkins University School of Medicine, United states

Tumor-induced osteomalacia (TIO) and epidermal nevus syndrome (ENS) are rare conditions in which ectopic production of FGF23 can lead to reduced renal phosphate reabsorption, impaired 1,25(OH)<sub>2</sub>D synthesis, and osteomalacia with bone pain and myopathy. KRN23 is an investigational, fully-human monoclonal antibody against FGF23. In an ongoing, open-label study, adults with either ENS or TIO and unresectable or unidentified responsible tumors receive subcutaneous KRN23 (0.3 to 2.0 mg/kg) every 4 weeks (wks). Interim data including baseline characteristics and post-treatment pharmacodynamics are available for 8 subjects and bone imaging and DXA data for 2 subjects who have completed 24 wks of therapy. Eight subjects (7 TIO, 1 ENS) were enrolled. Mean age was 52 y and time since diagnosis ranged from 1-37 y. Baseline serum phosphate ranged from 1.0-3.0 mg/dL (normal 2.5-4.0 mg/dL) and serum intact FGF23 ranged from 94-2569 pg/mL (normal 10-62 pg/mL). Osteomalacia was present in all baseline iliac crest bone biopsies (n=6). Five of 8 subjects had low BMD T-scores in at least one skeletal site. Moderate or severe pain and fatigue were reported in 6 and 7 subjects, respectively. Mean (SE) serum phosphate increased from 1.7 (0.2) mg/dL at baseline to 2.9 (0.56) mg/dL within 1 wk of treatment (Figure) and was accompanied by increased mean TmP/GFR and serum 1,25(OH)<sub>2</sub>D values in all but 1 subject who has metastatic sarcoma. Improvement in skeletal manifestations was evident in the 2 subjects with data up to Wk 24. Subject 1 had a Tc99 bone scan with areas of increased uptake in the ribs/tibia consistent with multiple fractures/pseudofractures. By Wk 24, uptake was normal at the 4 rib sites suggesting healing of fractures, with no new regions of increased uptake. Lumbar spine (LS) and total hip (TH) BMD increased by 2% and 3%, respectively, over 24 wks. Subject 2 had a Tc99 bone scan consistent with fractures/pseudofractures in the clavicle, humerus, and tibia that had not resolved by Wk 24 but with no new regions of increased uptake. LS and TH BMD increased by 21% and 6%, respectively, in this subject over 24 wks. Adverse events (AEs) were observed in 7 of 8 subjects and were frequently musculoskeletal; 2 subjects reported worsening pre-existing restless leg syndrome. No serious AEs were reported. KRN23 treatment increased serum phosphate and 1,25(OH)<sub>2</sub>D in subjects with TIO or ENS. Serial changes in DXA and Tc99 scans suggest an early effect of healing osteomalacia.

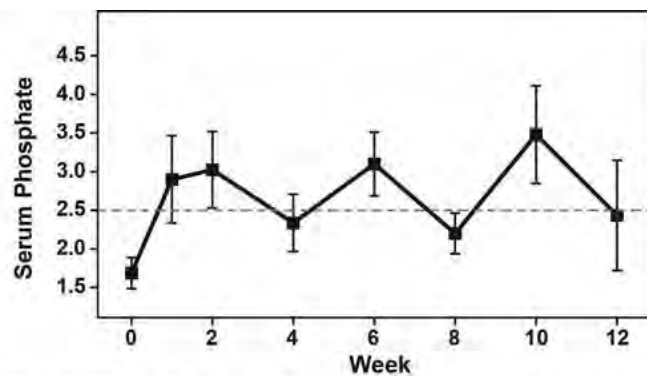


Figure. Mean (SE) Serum Phosphate (mg/dL) in Subjects Treated with KRN23

**Disclosures:** Thomas Carpenter, Ultragenyx, 11; Ultragenyx, 15  
This study received funding from: Ultragenyx Pharmaceutical Inc.

## 1099

**The Long-Term Odanacatib Fracture Trial (LOFT): Cardiovascular Safety Results.** [Michelle O'Donoghue](#)<sup>\*</sup>, [Illaria Cavallari](#), [Marc Bonaca](#), [Stephen Wiviott](#), [Abby Cange](#), [Laura Grip](#), [Naveen Deenadayalu](#), [KyungAh Im](#), [Sabina Murphy](#), [Marc Sabatine](#). Brigham & Women's Hospital, United states

Odanacatib (ODN) is a selective, orally-active inhibitor of cathepsin K that is being developed for the treatment of osteoporosis. The randomized, double-blind, placebo-controlled, Phase III Long-Term Odanacatib Fracture Trial (LOFT; NCT00529373) evaluated the efficacy and safety of ODN 50 mg once weekly to reduce fracture risk in more than 16,000 postmenopausal women with osteoporosis. LOFT was a double-blind, event-driven trial that was followed by a placebo-controlled, double-blind extension period whereby patients were continued on their original treatment assignment for up to 5 years.

Pre-clinical data suggested that inhibition of cathepsin K may reduce atherosclerosis progression and promote plaque stability. After original osteoporosis and adverse event data from the LOFT trial were analyzed, a full, comprehensive and independent adjudication of major adverse cardiovascular events (MACE), atrial fibrillation and flutter events, and all deaths was initiated by the Thrombolysis in Myocardial Infarction (TIMI) Study Group, an academic research group based at Brigham and Women's Hospital using all available data throughout the entire 5-year, double-blind period of LOFT and its extension study.

Overall, the LOFT analysis cohort included 16,071 participants in 40 countries. More than 4300 cardiovascular events (cardiac ischemic events, cerebrovascular events and supraventricular arrhythmias) and deaths have been adjudicated by the independent and blinded TIMI clinical events committee. The TIMI cardiovascular adjudication database will be locked and unblinded, and cardiovascular safety results will be ready for presentation at ASBMR 2016.

**Disclosures:** Michelle O'Donoghue, Merck, 11  
This study received funding from: Merck

## 1100

**Discontinuation of Denosumab and Associated Fracture Incidence: Analysis From FREEDOM and its Extension.** [Jacques P Brown](#)<sup>\*1</sup>, [Serge Ferrari](#)<sup>2</sup>, [Nigel Gilchrist](#)<sup>3</sup>, [Jens-Erik Beck Jensen](#)<sup>4</sup>, [Nico Pannacchiulli](#)<sup>5</sup>, [Chris Recknor](#)<sup>6</sup>, [Christian Roux](#)<sup>7</sup>, [Shawna Smith](#)<sup>5</sup>, [Ove Törring](#)<sup>8</sup>, [Ivo Valter](#)<sup>9</sup>, [Rachel B Wagman](#)<sup>5</sup>, [Andrea T Wang](#)<sup>5</sup>, [Steven R Cummings](#)<sup>10</sup>. <sup>1</sup>Laval University & CHU de Québec (CHUL), Canada, <sup>2</sup>Geneva University Hospital, Switzerland, <sup>3</sup>The Princess Margaret Hospital, New Zealand, <sup>4</sup>Hvidovre University Hospital, Denmark, <sup>5</sup>Amgen Inc., United states, <sup>6</sup>United Osteoporosis Centers, United states, <sup>7</sup>Paris Descartes University, France, <sup>8</sup>Karolinska Institutet, Södersjukhuset, Sweden, <sup>9</sup>Center for Clinical & Basic Research, Estonia, <sup>10</sup>San Francisco Coordinating Center, CPMC Research Institute, United states

Purpose: Denosumab (DMAb) treatment has been shown to decrease fracture (Fx) risk. Unlike bisphosphonates, DMAB is a monoclonal antibody against RANKL. Discontinuation is characterized by reversal of effect, including transient increases in bone turnover markers to above-baseline (BL) levels returning to BL within 2 yr and loss of bone mineral density (BMD) to BL levels. An analysis from FREEDOM showed similar subject incidence of Fx in DMAb and placebo (PBO) groups upon discontinuation. Recent reports describe isolated cases of multiple (≥2) vertebral Fx (Vfx) after DMAb cessation ([Aubrey-Rozier OI 2015](#); [Anastasilakis OI 2015](#); [Popp OI 2016](#)). To better understand Vfx incidence—particularly multiple Vfx—upon

DMAb cessation, we describe VFX risk and possible determinants in subjects who discontinued DMAb during the 3-yr FREEDOM or 7-yr Extension.

Methods: Subjects who received  $\geq 2$  doses of investigational product (IP; DMAb 60 mg Q6M or PBO) and discontinued IP but stayed in study  $\geq 7$  M after the last dose were included in the analysis. Subjects who discontinued DMAb from FREEDOM or Extension were analyzed as one group. A logistic regression model explored covariates related to off-treatment new VFX or multiple new VFX.

Results: Of 1001 subjects who discontinued DMAb during FREEDOM or Extension, 56 (5.6%) sustained new VFX. Upon DMAb discontinuation, new VFX incidence increased relative to the on-treatment period but stayed within the range of those who discontinued PBO, ie, had never been treated (Table). The same pattern was seen in subjects with prior VFX, who had higher on- and off-treatment VFX rates than the overall population. Among subjects with off-treatment new VFX, a greater percentage of those who discontinued DMAb (34/56 [60.7%]) than PBO (10/29 [34.5%]) sustained multiple new VFX. Logistic regression models found prior VFX before or during treatment to be the strongest predictor of off-treatment new VFX, including multiple VFX (odds ratio 2.1-3.4). Off-treatment femoral neck BMD loss was a weak covariate.

Conclusion: Discontinuation of DMAb is associated with an increase in VFX rate to levels comparable to PBO. Among subjects who sustained new VFX after DMAb cessation, there was a greater incidence of multiple new VFX than in PBO. Subjects with prior VFX are at high risk for off-treatment new VFX and should continue osteoporosis therapy. Consequently those who discontinue DMAb should transition to another therapy after the 6-M dosing interval.

	FREEDOM		Extension		
	Year 2/3		Year 5		Year 10
	Placebo N = 45	Denosumab N = 47	Cross-over N = 13	Long-term N = 25	Long-term N = 22
Denosumab exposure (years)	0	2-3	2	5	10
Parameter	Median (Q1, Q3)				
Eroded surface/ bone surface (%)	1.0 (0.6, 1.9)	0.2 (0.0, 0.7)	0.2 (0.0, 0.4)	0.1 (0.0, 0.3)	0.3 (0.0, 0.9)
Osteoid surface (%)	6.8 (3.6, 10.1)	0.4 (0.2, 1.2)	0.5 (0.2, 0.7)	0.1 (0.0, 0.8)	0.1 (0.0, 0.2)
Osteoid width ( $\mu\text{m}$ )	8.7 (6.4, 11.0)	5.4 (4.4, 7.4)	5.6 (3.3, 6.6)	3.3 (0.0, 7.4)	4.2 (0.0, 7.4)
Mineral apposition rate ( $\mu\text{m}/\text{d}$ )	0.8 (0.7, 0.8)	0.3 (0.3, 0.5)	0.6 (0.5, 0.7)	0.4 (0.3, 1.1)	0.3 (0.3, 0.3)
Bone formation rate, volume based (%/yr)	14.6 (8.6, 21.8)	0.4 (0.2, 0.8)	1.2 (0.7, 1.3)	2.2 (0.2, 4.7)	0.3 (0.2, 2.8)
Activation frequency (year <sup>-1</sup> )	0.200 (0.120, 0.330)	0.002 (0.001, 0.004)	0.017 (0.011, 0.020)	0.031 (0.001, 0.071)	0.001 (0.001, 0.012)

Table. Off-treatment VFX incidence in subjects who discontinued IP in FREEDOM or its Extension

Disclosures: Jacques P Brown, Amgen, Eli Lilly, Merck, 12; Amgen, Eli Lilly, 11; Amgen, Eli Lilly, 13

This study received funding from: Amgen Inc.

## 1101

**Blockade of C5aR Impairs Bone Metastases by Decreasing Osteoclastic Activity.** Daniel Ajona<sup>\*1</sup>, Carolina Zanduetta<sup>2</sup>, Leticia Corrales<sup>2</sup>, Maria Jose Pajares<sup>3</sup>, Elena Martinez-Terroba<sup>3</sup>, Fernando De Miguel<sup>1</sup>, Jackeline Agorreta<sup>3</sup>, Naiara Perurena<sup>2</sup>, Luis M Montuenga<sup>3</sup>, Ruben Pio<sup>1</sup>, Fernando Lecanda<sup>2</sup>. <sup>1</sup>Program in Solid Tumors & Biomarkers, Center for Applied Medical Research (CIMA), Pamplona, Spain; Department of Biochemistry & Genetics, School of Sciences, University of Navarra, Pamplona, Spain, <sup>2</sup>Program in Solid Tumors & Biomarkers, Center for Applied Medical Research (CIMA), Pamplona, Spain., Spain, <sup>3</sup>Program in Solid Tumors & Biomarkers, Center for Applied Medical Research (CIMA), Pamplona, Spain; Department of Histology & Pathology, School of Medicine, University of Navarra, Pamplona, Spain., Spain

C5aR is a membrane-associated receptor for C5a, a potent immune mediator generated after complement activation. C5aR expressed in tumor infiltrating immune cells creates a favorable microenvironment for tumor progression. However, the expression of C5aR by cancer cells and its contribution to their malignant phenotype are poorly understood. Inhibition of C5aR activity with a blocking peptide decreased invasiveness and metalloproteolytic activities in A549 lung adenocarcinoma cells. Lentiviral shRNA-mediated C5aR silencing showed unaltered growth kinetics *in vitro* and *in vivo*. Intracardiac inoculation (i.c.) of C5aR-silenced cells led to a dramatic reduction in skeletal metastatic burden ( $p < 0.001$ ), as assessed by bioluminescence imaging, and the presence of osteolytic lesions ( $p < 0.001$ ), evaluated by X-ray and  $\mu\text{CT}$  imaging and histological analysis. A decreased tumor cell growth was detected *in vivo* (Ki-67) ( $p < 0.05$ ). These findings were validated in H460 large-cell lung carcinoma cells using an identical approach. Similarly, pharmacological blockade using a C5a specific inhibitor significantly reduced the osseous metastatic activity of A549 cells after i.c. inoculation. This effect was associated with decreased bone colonization, since intratibial injection of shC5aR cells showed a marked reduction in tumor burden. Interestingly, a reduced TRAP<sup>+</sup> staining was detected in bones derived from shC5aR inoculated animals

( $p < 0.05$ ). These results were correlated *in vitro* with a marked reduction in osteoclastogenic activity (TRAP<sup>+</sup>) induced by conditioned medium derived from shC5aR cells ( $p < 0.001$ ). Transcriptomic analysis identified as a C5aR effector, CXCL16, a potential pro-osteoclastogenic chemokine implicated in tumor progression and metastasis. C5aR silencing markedly reduced the expression levels of CXCL16. In the clinical setting, immunohistochemical analysis revealed that high levels of C5aR in human lung tumors were associated with poor survival ( $p = 0.005$ ) and recurrence-free survival ( $p < 0.001$ ) in a cohort of 76 patients. These data indicate that C5aR disruption abrogates osteoclastogenic activity, critically impairing osseous colonization. We suggest that C5aR could represent a clinically relevant factor in lung cancer prognosis and a potential therapeutic target.

Disclosures: Daniel Ajona, None.

## 1102

**Apoptotic Cell Clearance Drives CXCL5, Accelerates Inflammatory Cell Infiltration, and Supports Prostate Cancer Tumor Growth in Bone.** Hernan Roca<sup>\*</sup>, Marta Purica, Savannah Weidner, Amy Koh, Robert Kuo, Jacques Nör, Lonnie Shea, Laurie McCauley. University of Michigan, United states

Continuous death of cancer cells and their clearance by immune system phagocytes occurs during tumor progression, yet the consequences regarding tumor growth in bone remain largely unknown. The purpose of this study was to determine the role of apoptotic tumor cell clearance (efferocytosis) in tumor growth *in vivo* and the mechanistic underpinnings *in vitro*. Changes in cytokine expression in primary bone marrow derived mouse macrophages interacting with two apoptotic prostate cancer cells (human PC3 and mouse RM1) revealed macrophage production of tumor-promoting inflammatory cytokines including IL-6, CXCL1 and CXCL5 (chemoattractants of monocytes and neutrophils). An *in vivo* syngeneic tumor model was used in which apoptosis-inducible prostate cancer cells (RM1-iCasp9) were co-implanted with vertebral bodies subcutaneously in immune competent mice. Seven days post-surgery, mice were treated with vehicle or the dimerizer drug AP20187 (AP) to induce apoptosis in RM1-iCasp9 cancer cells. Continuous analysis of tumor volume revealed accelerated cancer growth in apoptosis induced mice compared with controls. Single cell analysis of tumors showed a significant increase of tumor-accelerating myeloid inflammatory cells in the mice induced to undergo efferocytosis (AP). These populations included total CD206<sup>+</sup>F4/80<sup>+</sup> (M2 macrophages), Gr-1<sup>+</sup>CD11b<sup>high</sup> (myeloid granulocytes/monocytes associated with suppression of anti-tumoral immunity) and CD68<sup>+</sup>/CD11b<sup>+</sup> (phagocytic) cells. Ly-6B, a marker associated with the activation of inflammatory myeloid cells, was also significantly increased in the AP tumors. Importantly, higher CXCL5 expression was detected in the AP tumors. A similar experiment was conducted with RM1-iCasp9 cells in CXCL5<sup>-/-</sup> and wild type (WT) mice. When both groups were treated with AP, tumor deceleration was observed in the CXCL5<sup>-/-</sup> mice, which correlated with decreased tumor influx of total F4/80<sup>+</sup> macrophages, CD206<sup>+</sup>F4/80<sup>+</sup> (M2), CD68<sup>+</sup>F4/80<sup>+</sup> (phagocytes), myeloid neutrophils (Ly6G<sup>+</sup>/CD11b<sup>+</sup>) and Ly6B<sup>+</sup> cells relative to the WT mice. In contrast, an increase in cells expressing the T-lymphocyte-activating antigen CD86<sup>+</sup> was observed in the tumors of CXCL5<sup>-/-</sup> group. Altogether these findings suggest that CXCL5 accelerates tumor growth and inflammation induced by the myeloid phagocytic clearance of apoptotic cancer cells, a mechanism that may be critical for metastatic bone colonization.

Disclosures: Hernan Roca, None.

## 1103

**Nanoparticle Delivery of Gli Inhibitor Blocks Tumor-Induced Bone Disease.** Kristin Kwakwa<sup>\*1</sup>, Joseph Vanderburgh<sup>2</sup>, Alyssa Merkel<sup>3</sup>, Thomas Werfel<sup>4</sup>, Craig Duvall<sup>4</sup>, Scott Guelcher<sup>5</sup>, Julie Sterling<sup>6</sup>. <sup>1</sup>Department of Cancer Biology, Vanderbilt University; Center for Bone Biology, Vanderbilt University Medical Center, United states, <sup>2</sup>Department of Chemical & Biomolecular Engineering, Vanderbilt University; Center for Bone Biology, Vanderbilt University Medical Center, United states, <sup>3</sup>Department of Veterans Affairs, Tennessee Valley Healthcare System; Center for Bone Biology, Vanderbilt University Medical Center; Division of Clinical Pharmacology, Department of Medicine, Vanderbilt University Medical Center, United states, <sup>4</sup>Department of Biomedical Engineering, Vanderbilt University, United states, <sup>5</sup>Department of Chemical & Biomolecular Engineering, Vanderbilt University; Department of Biomedical Engineering, Vanderbilt University; Center for Bone Biology, Vanderbilt University Medical Center, United states, <sup>6</sup>Department of Veterans Affairs, Tennessee Valley Healthcare System; Center for Bone Biology, Vanderbilt University Medical Center; Division of Clinical Pharmacology, Department of Medicine, VUMC; Department of Cancer Biology, Vanderbilt University, United states

Tumor-induced bone disease is a common comorbidity in patients with advanced cancers of the breast, prostate, and lung. While there are many factors in the bone microenvironment that promote osteolytic bone resorption, we have established that Gli2, a transcriptional activator of Hedgehog (Hh) signaling, is overexpressed in

tumor cells that have metastasized to bone and that this upregulation induces bone destruction. We have also demonstrated that Gli2 expression and function are not always regulated by canonical Hedgehog signaling. Therefore, it is critical to develop therapeutics targeting Gli downstream of the Hh signal transducer smoothened (Smo). Several studies have reported efficacious small-molecule inhibitors of Gli-mediated transcription *in vitro*. Our previous investigations involving the genetic inhibition of Gli2 expression in bony-invasive MDA-MB-231 breast cancer cells using Hh pathway inhibitors (HPIs) are promising; particularly, treatment with HPI-1 (2  $\mu$ M), HPI-3 and HPI-4 (75  $\mu$ M) significantly reduced ( $p < 0.01$ ) mRNA expression of parathyroid hormone-related protein (PTHrP), whose promoter activity is specifically regulated by Gli2. Treatment with the Gli antagonist GANT58 (10  $\mu$ mol) also significantly reduced PTHrP gene expression ( $p < 0.05$ ). Unfortunately, *in vivo* delivery of these drugs to tumors residing in bone has been challenging due to their hydrophobicity. We hypothesized that encapsulating Gli inhibitors within nanoparticles would facilitate delivery of these agents to osteolytic tumors and cause a significant reduction in tumor-induced bone disease. Accordingly, we loaded GANT58 ( $\leq 10$  mg/kg) into reactive oxygen species (ROS)-responsive nanoparticles made from poly(propylene sulfide) and poly(ethylene glycol) (PPS-PEG) block copolymers to inhibit Gli2 expression in bone-tropic MDA-MB-231 cells that were injected into the tibia of athymic nude mice. The GANT58 nanoparticles (GANT58-NPs) were made using an oil-in-water solvent evaporation method and characterized for particle size ( $d=170$  nm), drug loading (13%), and encapsulation efficiency (44%). Our preliminary data shows a preferential localization of GANT58-NPs at the tumor site in bone (~65% increase) compared to non-tumor bone. Furthermore, mice treated intravenously with GANT58-NPs had a 2-fold reduction in tumor lesion area. In summary, nanodelivery of Gli inhibitors is a promising therapy as it allows for targeted inhibition of Gli2 and PTHrP to decrease bone destruction.

**Disclosures:** Kristin Kwakwa, None.

## 1104

**TAK-1 Inhibition Disrupts Pim-2-associated and Pim-2-independent key Signaling Pathways to Effectively Suppress Tumor Growth and Restore Bone Formation in Myeloma.** Jumpei Teramachi<sup>1\*</sup>, Masahiro Hiasa<sup>1</sup>, Asuka Oda<sup>1</sup>, Hirofumi Tenshin<sup>1</sup>, Ryota Amachi<sup>1</sup>, Takeshi Harada<sup>1</sup>, Shingen Nakamura<sup>1</sup>, Kiyoe Kurahashi<sup>1</sup>, Tokeshi Kondo<sup>1</sup>, Hirokazu Miki<sup>1</sup>, Itsuro Endo<sup>1</sup>, Toshio Matsumoto<sup>2</sup>, Masahiro Abe<sup>1</sup>. <sup>1</sup>Tokushima University, Japan, <sup>2</sup>Tokushima University, Guinea

Multiple myeloma (MM) is still incurable with progressive bone loss. Pim-2 is overexpressed in MM cells to mediate their growth and survival signaling, and regarded as an important therapeutic target for MM. Furthermore, Pim-2 is also induced in bone marrow stromal cells (BMSCs) and osteoclasts in bone lesions to enhance osteoclastogenesis and suppress osteoblastogenesis, respectively. We recently found TGF- $\beta$ -activated kinase-1 (TAK-1) as an upstream mediator responsible for Pim-2 up-regulation in MM cells. In the present study, we therefore extended our study to clarify the role of the TAK-1-Pim-2 pathway in tumor growth and bone destruction in MM. TAK-1 was constitutively over-expressed and phosphorylated in MM cells. Although TNF- $\alpha$  and IL-6 further upregulated Pim-2 in MM cells through NF- $\kappa$ B and STAT3 activation, respectively, the TAK-1 inhibitor LLZ1640-2 (LLZ) abolished Pim-2 expression in MM cells even upon stimulation with TNF- $\alpha$  or IL-6, and markedly induced MM cell death. Besides, LLZ suppressed TNF- $\alpha$ -induced p38MAPK and ERK activation, and reduced the transcription factor Sp1 expression and thereby critical pro-survival mediators in MM cells, including IRF-4 and c-Myc, suggesting suppression of the Pim-2-independent survival pathway. Interestingly, TAK-1 was also phosphorylated along with Pim-2 upregulation in MC3T3-E1 preosteoblastic cells by inhibitors of bone formation overproduced in MM, including TNF- $\alpha$ , TGF- $\beta$  and activinA, as well as MM cell conditioned media; however, LLZ restored osteoblastogenesis suppressed by these factors while reducing Pim-2 expression. The TAK-1 inhibition up-regulated in MC3T3-E1 cells Smad1/5 phosphorylation by BMP-2 while suppressing Smad2/3 phosphorylation by TGF- $\beta$ , suggesting potentiation of BMP-2-mediated anabolic signaling. Moreover, RANK ligand upregulated TAK-1 expression and phosphorylation in RAW264.7 preosteoclastic cells; however, LLZ suppressed RANK ligand-induced c-fos and NFATc1 expression in RAW264.7 cells and thereby their osteoclastogenesis. Finally, treatment with LLZ markedly suppressed MM tumor growth and prevented bone destruction in mouse MM models with intra-tibial injection of murine 5TGM1 MM cells. From these results, TAK-1 appears to play a pivotal role in tumor progression and bone destruction in MM. TAK-1 inhibition is suggested to effectively disrupt the Pim-2-associated as well as Pim-2-independent key signaling pathways responsible for tumor progression and bone destruction. Therefore, TAK-1 inhibition may become a unique anti-MM therapeutic option with bone-modifying activity.

**Disclosures:** Jumpei Teramachi, None.

## 1105

**Decreased JMJD3 Expression in Mesenchymal Stem Cells Contributes to Long-term Suppression of Osteoblast Differentiation in Multiple Myeloma.** Wei Zhao<sup>\*1</sup>, Rebecca Silbermann<sup>2</sup>, Juraj Adamik<sup>3</sup>, Deborah Galson<sup>3</sup>, G. David Roodman<sup>4</sup>. <sup>1</sup>Department of Biochemistry & Molecular Biology, Indiana University, United states, <sup>2</sup>Department of Medicine, Hematology Oncology, Indiana University, United states, <sup>3</sup>University of Pittsburgh School of Medicine, United states, <sup>4</sup>Department of Medicine, Hematology Oncology, Indiana University. Department of Medicine, Richard L. Roudebush VA Medical Center, Indianapolis, IN, United states

Multiple myeloma (MM) is the most frequent cancer to involve the skeleton, with over 80% of myeloma patients developing lytic bone disease (MMBD). Importantly, MM-associated bone lesions rarely heal even when patients are in complete remission. Mesenchymal stem cells (MSCs) isolated from MM patients have a distinct genetic profile and an impaired osteoblast (OB) differentiation capacity when compared to healthy donor MSCs. Utilizing an *in vivo* model of MMBD and patient samples, we showed that MSCs from tumor-bearing bones failed to differentiate into OBs weeks after removal of MM cells. Both Runx2 and Osterix, the master transcription factors for OB differentiation, remained suppressed in these MSCs. Currently molecular mechanisms for MM-induced long-term OB suppression are poorly understood. Therefore, we characterized both Runx2 and Osterix promoters in murine pre-osteoblast MC4 cells by ChIP to assess the transcriptional activity. The Runx2 and Osterix transcriptional start sites (TSSs) in untreated MC4 cells were co-occupied by transcriptionally active histone 3 lysine 4 tri-methylation (H3K4me3) and transcriptionally repressive histone 3 lysine 27 tri-methylation (H3K27me3), termed the "bivalent domain". These bivalent domains became transcriptionally silent with increasing H3K27me3 levels when MC4 cells were co-cultured with MM cells or treated with TNF- $\alpha$ , an inflammatory cytokine enriched in MM bone marrow. Furthermore, both MM cells and TNF- $\alpha$  downregulated the H3K27 demethylase JMJD3 and increased global H3K27me3 levels in MC4 cells and murine MSCs. Similarly, knockdown of JMJD3 in MC4 cells inhibited OB differentiation. Consistent with *in vitro* findings, MSCs from MM patients showed markedly decreased JMJD3 expression compared to healthy MSCs. Interestingly, the epigenetic signature at the Runx2 and Osterix TSSs in MC4 cells treated with TNF- $\alpha$  mimicked that of pluripotent MSCs. TNF- $\alpha$  enhanced the expression of MSC marker genes in MC4 cells. Our findings link extracellular stimuli in the MM bone marrow microenvironment to changes of histone modifiers in MSCs. We hypothesize that MM resolves the bivalent domains at the Runx2 and Osterix TSSs to transcriptionally silent domains by decreasing JMJD3 expression, which not only blocks OB differentiation but further reverses this apparent one-way process. Understanding the molecular mechanisms in this pathway should help identify targets to increase bone formation and possibly decrease tumor burden.

**Disclosures:** Wei Zhao, None.

## 1106

**Transforming growth factor beta inhibitor (1D11) combined with Bortezomib improves bone quality in a mouse model of myeloma-induced bone disease..** Alyssa Merkel<sup>\*1</sup>, Sasidhar Uppuganti<sup>2</sup>, Barbara Rowland<sup>3</sup>, Babatunde Oyajobi<sup>4</sup>, Jeffrey Nyman<sup>1</sup>, Julie Sterling<sup>1</sup>. <sup>1</sup>Vanderbilt University Medical Center; Tennessee Valley Healthcare System, Nashville VA, United states, <sup>2</sup>Vanderbilt University Medical Center, United states, <sup>3</sup>Tennessee Valley Healthcare System, Nashville VA, United states, <sup>4</sup>University of Texas Health Science Center San Antonio, United states

Multiple myeloma (MM) patients frequently develop areas of bone destruction as their tumors expand. While therapies exist to treat the bone disease, none fully reverse bone loss or tumor burden. Previous studies in solid tumor models indicate that TGF- $\beta$  inhibition improves bone volume and reduces tumor growth. Since osteoclast-mediated bone resorption can release TGF- $\beta$  from bone, elevated TGF- $\beta$  may contribute to myeloma-related bone loss. Therefore, we hypothesize that inhibition of TGF- $\beta$  signaling will reduce tumor growth, increase bone volume, and improve bone architecture in MM-bearing mice. First, to establish the importance of TGF- $\beta$  signaling in MM, we determined the level of pSmad (a primary mediator of canonical TGF- $\beta$  signaling) by western blot in 5TGM1 myeloma cells and by immunohistochemistry in myeloma-bearing mice. pSmad was detected in the absence of exogenous TGF- $\beta$  treatment, increased 2-fold with the addition of TGF- $\beta$ 1, and was reduced in response to 1D11 treatment, indicating activation of TGF- $\beta$  signaling in our myeloma model. Next, we injected 5TGM1 myeloma cells into immunocompetent KaLwRij and immunocompromised Rag2-/- mice. Following tumor inoculation, mice were treated with 10mg/kg of TGF- $\beta$  inhibitory (1D11) or control (13C4) antibody, with or without the anti-myeloma drug bortezomib (0.5mg/kg). 1D11 monotherapy did not reduce MM tumor burden in either Rag 2-/- or KaLwRij mouse strain, but bortezomib monotherapy and combination therapy with 1D11 + bortezomib significantly decreased spleen weights and serum IgG2bk levels ( $p < 0.01$ ) and reduced tumor burden measured by immunohistochemistry ( $p < 0.05$ ). In both mouse strains, TGF- $\beta$  inhibition increased trabecular bone volume, improved trabecular architecture, and increased tissue mineral density of the trabeculae as assessed by *ex vivo* micro-computed tomography ( $p < 0.05$ , 1D11

vs 13C4). Additionally, 1D11 treatment was associated with significantly greater vertebral body strength in biomechanical compression tests ( $p < 0.01$ ), and increased the number of osteoblasts in myeloma bearing Rag 2-/- ( $p < 0.05$ ) and KaLwRij ( $p < 0.01$ ) mice. These data demonstrate that TGF- $\beta$  inhibition significantly improves bone architectures, but does not improve tumor burden in MM tumor models. However, combination therapy with TGF- $\beta$  (1D11) and proteasome inhibition (bortezomib) may be a promising strategy for reducing patients' risk of bone destruction and pathological fractures, thus improving overall quality of life.

**Disclosures:** Alyssa Merkel, None.

## 1107

**Low Protein Intake Among Older Men is Associated with an Increased Risk of Fracture.** Lisa Langsetmo<sup>\*1</sup>, James Shikany<sup>2</sup>, Peggy Cawthon<sup>3</sup>, John Schousboe<sup>4</sup>, Brent Taylor<sup>5</sup>, Tien Vo<sup>1</sup>, Jane Cauley<sup>6</sup>, Doug Bauer<sup>3</sup>, Eric Orwoll<sup>7</sup>, Kristine Ensrud<sup>5</sup>. <sup>1</sup>University of Minnesota, United states, <sup>2</sup>University of Alabama, Birmingham, United states, <sup>3</sup>University of California, San Francisco, United states, <sup>4</sup>University of Minnesota, Health Partners Institute, United states, <sup>5</sup>University of Minnesota, Veterans Affairs Medical Center, United states, <sup>6</sup>University of Pittsburgh, United states, <sup>7</sup>Oregon Health & Science University, United states

Dietary protein is a potentially modifiable risk factor that may be related to fracture in older men. Our primary objective was to assess the association of protein intake with low-trauma (trauma  $\leq$  fall from standing height) fracture risk among older men. Our secondary objectives were to assess whether the association between protein intake and fracture risk was mediated by: falls, body mass index (BMI), bone mineral density (BMD), appendicular lean mass (ALM), and gait speed (GS). Our hypothesis was that low protein intake vs. moderate protein intake is associated with increased risk of fracture, high protein intake vs. moderate protein intake is not associated with increased risk of fracture, and that the specified risk factors mediate increased fracture risk among those with low protein intake and therefore inclusion of risk factors attenuates the association.

We studied 5888 eligible participants (mean age 73.6 y, range 64-100 y) in the Osteoporotic Fractures in Men Study (MrOS) (2000-02). At baseline protein intake from all sources was assessed as percent of total energy intake (TEI) using the Block food frequency questionnaire. We excluded men with  $\leq 500$  kcal/d TEI or missing  $\geq 10$  items. The median was 15.9% TEI (interquartile range 14.2-17.8%). Low protein intake was defined as the bottom quartile, high protein intake the top quartile, and moderate intake the middle quartiles. Incident fractures were ascertained tri-annually. There were 808 incident low-trauma fractures (excluding those of the head, hands, and feet) over 15 years (63,500 person-y). We used Cox proportional hazards models with age, race, height, center, TEI, physical activity, marital status, osteoporosis, GI surgery, smoking, and use of oral corticosteroids, alcohol, calcium and vitamin D supplements as co-variables to compute hazard ratios (HR) with 95% confidence intervals (CI). Low protein intake was associated with an increased fracture risk (HR=1.28, 95% CI: 1.08-1.51) compared to those with moderate intake. The HR was modestly attenuated after adjusting for total hip BMD (1.21, 95% CI: 1.03-1.44). There was  $< 2\%$  change in the point estimates when adjusted for falls, BMI, ALM, or GS. High protein intake was not associated with fracture risk, HR=1.00 (95% CI: 0.84-1.19). In summary, low protein intake (below 14.2% TEI) was associated with increased risk of fracture in a cohort of older men, suggesting both a potential target population and an appropriate dietary intervention.

**Disclosures:** Lisa Langsetmo, None.

## 1108

**Calcium and/ or Vitamin D Supplementation are not Associated with Ischaemic Heart Disease: Findings from the UK Biobank Cohort.** Nicholas Harvey<sup>\*1</sup>, Stefania D'Angelo<sup>1</sup>, Julien Paccou<sup>2</sup>, Mark Edwards<sup>1</sup>, Steffen Petersen<sup>3</sup>, Cyrus Cooper<sup>1</sup>. <sup>1</sup>MRC Lifecourse Epidemiology Unit, University of Southampton, United Kingdom, <sup>2</sup>Université Lille Nord-de-France, United Kingdom, <sup>3</sup>NIHR Cardiovascular Biomedical Research Unit at Barts, William Harvey Research Institute, Queen Mary University of London, United Kingdom

Several, but not all, meta-analyses have suggested a possible association between calcium (with or without vitamin D) supplementation and an increased risk of myocardial infarction. We aimed to investigate such relationships prospectively in the UK Biobank population-based cohort. UK Biobank comprises 502,664 men and women aged 40-69 years, with detailed assessment at baseline. Supplementation with calcium and/ or vitamin D was self-reported, and we obtained information on incident hospital admission (ICD-10) for ischaemic heart disease (IHD: I20-I25), any cardiovascular event (I63/I64 or I20-I25) and death following these events, through linkage to UK Hospital Episode Statistics with up to 7 years follow-up. We investigated the longitudinal associations between use of calcium and/ or vitamin D supplementation and hospital admission for men and women, using Cox Proportional Hazards models, controlling for age, BMI, smoking, alcohol, educational level, physical activity, and in a

further model, HRT use (in women). All 502,644 participants (median age of 58 years, 54.5% women) had complete data on calcium and vitamin D supplementation. 34,890 of these reported using calcium supplements, with 20,004 using vitamin D supplements and 10,406 both (2.1%). In both crude and adjusted analyses, there were no associations between use of calcium supplements and risk of incident hospital admission with ischaemic heart disease (IHD), any cardiovascular event, or death following either admission category. For example, in the fully adjusted models, the hazard ratio (HR) for IHD admission was 1.06 (95%CI: 0.85, 1.31;  $p=0.62$ ) amongst women taking calcium supplementation. The corresponding HR for men was 1.02 (95%CI: 0.80, 1.30;  $p=0.87$ ). The adjusted HRs for death from IHD were 0.71 (95%CI: 0.32, 1.61;  $p=0.42$ ) in women, and 0.92 (95%CI: 0.52, 1.62;  $p=0.76$ ) in men. In women, further adjustment for HRT use did not alter the associations. Vitamin D and combination supplementation was similarly not associated with any outcome in either sex. In conclusion, use of calcium supplementation was not associated with increased risk of ischaemic or non-ischaemic cardiovascular events leading to hospital admission or death. These findings, from a single very large prospective cohort, support the cardiovascular safety of calcium and vitamin D supplementation, at least within the age range studied. This research has been conducted using the UK Biobank Resource.

**Disclosures:** Nicholas Harvey, None.

## 1109

**Incidence of Hip Fracture after Treatment with B Vitamins (Folic acid, B<sub>12</sub> and B<sub>6</sub>): Extended Follow-up of Two Large Randomized Controlled Trials.** Maria Garcia Lopez<sup>\*1</sup>, Kaare Bonna<sup>2</sup>, Marta Ebbing<sup>3</sup>, Erik F. Eriksen<sup>4</sup>, Clara G. Gjesdal<sup>5</sup>, Ottar K. Nygård<sup>6</sup>, Grete Tell<sup>7</sup>, Haakon E. Mever<sup>8</sup>.

<sup>1</sup>Department of Community Medicine, Institute of Health & Society, University of Oslo, Norway; <sup>2</sup>Department of Clinical Endocrinology, Morbid Obesity & Preventive Medicine, Oslo University Hospital, Norway, Norway, <sup>3</sup>Department of Public Health & General Practice, Norwegian University of Science & Technology, Trondheim; <sup>4</sup>Clinic for Heart Disease, St. Olav's University Hospital, Trondheim; <sup>5</sup>Department of Community Medicine, UiT The Arctic University of Norway, Norway, <sup>6</sup>Norwegian Institute of Public Health, Bergen, Norway, Norway, <sup>7</sup>Department of Clinical Endocrinology, Morbid Obesity & Preventive Medicine, Oslo University Hospital, Norway, Norway, <sup>8</sup>Department of Rheumatology, Haukeland University Hospital, Bergen, Norway, Norway, <sup>9</sup>Department of Clinical Science, University of Bergen, Norway. <sup>10</sup>Department of Heart Disease, Haukeland University Hospital, Bergen, Norway, Norway, <sup>11</sup>Department of Global Public Health & Primary Care, University of Bergen, Bergen, Norway, Norway, <sup>12</sup>Department of Community Medicine, Institute of Health & Society, University of Oslo, Norway; <sup>13</sup>Norwegian Institute of Public Health, Oslo, Norway, Norway

Background. Elevated levels of plasma homocysteine have been associated with increased risk of osteoporotic fractures in observational studies. Treatment with vitamin B<sub>12</sub> and folic acid lowers homocysteine levels in plasma, but it is unsettled if this affects fracture risk.

Objective. To investigate the effect of B-vitamins on the risk of hip fracture utilizing data from two large randomized controlled trials (RCTs) originally set up to study cardiovascular diseases. Due to the factorial design of the trials, we could both study if treatment with folic acid plus vitamin B<sub>12</sub> and treatment with vitamin B<sub>6</sub> influenced on the risk of hipfracture.

Material/methods. Data from two RCTs (NORVIT and WENBIT) were combined (6839 participants). The trials were performed between 1998 and 2005 and had identical design and B-vitamin intervention. Combined analyses of both studies have previously been reported for other endpoints. The interventions, based on a 2x2 factorial design, consisted of a daily capsule with either 1) folic acid (0.8 mg) plus vitamin B<sub>12</sub> (0.4 mg) and vitamin B<sub>6</sub> (40 mg) or 2) folic acid (0.8 mg) plus vitamin B<sub>12</sub> (0.4 mg) or 3) vitamin B<sub>6</sub> alone (40 mg) or 4) placebo. The outcome of the current study was experiencing a hip fracture during the trial or during an extended follow-up (from the trial start for each patient until the end of 2012). Data on hip fractures were retrieved by linkage to NORHip, a database including all hip fractures treated at Norwegian hospitals.

Results. Folic acid plus vitamin B<sub>12</sub> treatment was not associated with the risk of hip fracture, neither during the trial (median 3.3 years; hazard ratio (HR) 0.87; 95% CI 0.48-1.59) nor during the extended follow-up (median 11.1 years; HR 1.08; 95%CI 0.84-1.40). There was no statistically significant association between vitamin B<sub>6</sub> treatment and risk of hip fracture during the trial (HR, 1.43; 95% CI 0.78-2.61). However we found a statistically significant 42% higher risk of experiencing a hip fracture in the group receiving vitamin B<sub>6</sub> compared to the group not receiving vitamin B<sub>6</sub> (HR, 1.42; 95% CI 1.09-1.83) during the extended follow-up.

Conclusion. Treatment with folic acid plus vitamin B<sub>12</sub> was not associated with the risk of hip fracture. Treatment with high dose of vitamin B<sub>6</sub> was associated with a slightly increased risk of experiencing a hip fracture during the extended follow-up.

Trials registration: NCT00671346

**Disclosures:** Maria Garcia Lopez, None.

## 1110

**Long-Term Effects of Vitamin D and Multimodal Exercise on Prevention of Injurious Falls in Older Women. A 2-year follow-up after intervention.** Kirsti Uusi-Rasi<sup>1</sup>, Radhika Patil<sup>1</sup>, Saija Karinkanta<sup>1</sup>, Kari Tokola<sup>1</sup>, Pekka Kannus<sup>1</sup>, Christel Lamberg-Allardt<sup>2</sup>, Harri Sievänen<sup>1</sup>. <sup>1</sup>The UKK Institute for Health Promotion Research, Finland, <sup>2</sup>University of Helsinki, Finland

Previously, a two-year randomized four-arm intervention trial (DEX) assessed the effects of exercise and vitamin D3 on the risk of falls and injurious falls in 409 Finnish women aged 70 to 80 years who were randomly assigned to one of four groups: 1) 20 µg vitamin D3 + exercise (D+Ex+), 2) 20 µg vitamin D3 + no exercise (D+Ex-), 3) placebo + exercise (D-Ex+), and 4) placebo + no exercise (D-Ex-). The trial showed that though the rate of falls did not differ between groups, multimodal supervised exercise training reduced the rate of medically-attended injurious falls. Vitamin D3 had no such effect.

The purpose of this additional two-year follow-up was to assess the long-term effects of the interventions.

In addition to monthly fall diaries, S-25OHD concentrations, DXA-based femoral neck bone mineral density (BMD), and physical functioning (maximal isometric leg extensor strength, 5- times chair stand, walking speed and Timed-Up and Go, TUG) were assessed at 12-month intervals. Negative binomial regression was used to assess incidence rate ratios for falls. Generalized linear mixed models were used to estimate between-group differences in injurious fallers (odds ratio, OR) and physical functioning using age, height, and weight as covariates.

After ceasing the intervention S-25OHD concentrations declined to baseline levels in both supplement groups: mean (SD) S-25OHD being 72.5 (18.5) nmol/L with no between-group differences. Also BMD and physical functioning declined slightly in all groups. No between-group differences remained in BMD, chair-stand time, walking speed or TUG two years after the intervention. However, the maximal isometric leg extensor strength remained 3.4 (0.04 to 6.8) % greater in the former exercise groups. There were no between-group differences in the rate of all falls. However, D+E+ and D-Ex+ had less medically-attended injurious fallers (OR; 95% CI being 0.41; 0.19 to 0.86 and 0.41; 0.19 to 0.90, respectively), when compared with the reference group (D-Ex-), while D+Ex- did not differ significantly from D-Ex- (0.51; 0.23 to 1.13).

No exercise-induced benefits remained in physical functioning two years after cessation of the supervised training, except for a small gain in isometric muscle strength. However, former exercise groups continued to possess reduced risk for medically-attended injurious fallers compared with controls even two years after the intervention period.

*Disclosures: Kirsti Uusi-Rasi, None.*

## 1111

**The Risk of Fracture among Women with Sarcopenia, Low Bone Mass or Both.** Rebekah Harris<sup>1</sup>, Yuefang Chang<sup>1</sup>, Kristen Beavers<sup>2</sup>, Deepika Laddu<sup>3</sup>, Jennifer Bea<sup>4</sup>, Karen Johnson<sup>5</sup>, Meryl LeBoff<sup>6</sup>, Catherine Womack<sup>5</sup>, Robert Wallace<sup>7</sup>, Wenjun Li<sup>8</sup>, Carolyn Crandall<sup>9</sup>, Jane Cauley<sup>1</sup>. <sup>1</sup>University of Pittsburgh, United states, <sup>2</sup>Wake Forest University, United states, <sup>3</sup>Stanford University, United states, <sup>4</sup>University of Arizona Cancer Center, United states, <sup>5</sup>University of Tennessee Health Science Center, United states, <sup>6</sup>Brigham & Women's Hospital, United states, <sup>7</sup>University of Iowa, United states, <sup>8</sup>University of Massachusetts Medical School, United states, <sup>9</sup>University of California Los Angeles David Geffen School of Medicine, United states

In the current study we test the hypothesis that women with both low bone mineral density (BMD) and sarcopenia will have a greater risk of clinical fractures than women with either sarcopenia or low BMD alone and women without either condition. 10,937 women enrolled in the Women's Health Initiative (WHI) Observational and Clinical trials at 3 US Clinical Centers with BMD measurements- Pittsburgh, PA, Birmingham, AL, and Phoenix/Tucson, AZ were included. The baseline mean age of the group was 63.3 years. Appendicular lean mass (ALM) and femoral neck BMD were measured by DXA. The definition of sarcopenia was based on ALM values following the Newman et al approach to adjust for fat mass and height.[1] Linear regression was performed to model the association between ALM on height (meters) and fat mass (kg). The 20<sup>th</sup> percentile of the distribution of residuals was used as the cut point for sarcopenia. Low BMD was defined as a femoral neck T-score < -1.0 based on NHANES III reference database for white women.[2] Participants were classified into 4 mutually exclusive groups based on their BMD and sarcopenia status: normal BMD and no sarcopenia (3,857 women, 35%), normal BMD and sarcopenia (774 women, 7%), low BMD and no sarcopenia (4907 women, 45%), and low BMD and sarcopenia (1399 women, 13%). We followed women for incident fractures over a median follow up of 15.9 years. Cox proportional hazards models were used to estimate the hazard ratio (HR) and 95% confidence interval (CI) for incident fracture. Women with normal BMD and no sarcopenia formed the referent group. Women with low BMD, with or without sarcopenia, respectively, had greater risk of fracture than did women with normal BMD (HR= 1.76, 95% CI= 1.50-2.07 and HR= 1.57, 95% CI=1.38-1.78) that remained statistically significant even with adjustment for important covariates, Table 1. Women with sarcopenia alone had similar hazard ratios to women with normal BMD in both models. The interaction between sarcopenia and low BMD was not statistically significant (p=0.15). Compared to women with normal BMD, women with low BMD irrespective of their sarcopenia status have the highest risk of fracture.

Table: Risk of Fracture by BMD and Body Composition Group

Group	Base <sup>1</sup>	Multi-variable model <sup>2</sup>
No Sarcopenia or low BMD	1.0 (REF)	1.0 (REF)
Sarcopenia	0.92 (.72-1.17)	0.86 (.65-1.14)
Low BMD	1.57(1.38-1.78)	1.58(1.37-1.83)
Low BMD and Sarcopenia	1.76 (1.50-2.07)	1.72 (1.44-2.06)

<sup>1</sup>Base Model adjusted for age, clinic, and race

<sup>2</sup>Multivariate model adjusted for age, race, study assignment, physical function from the RAND score, history of fracture, self-report history of falls in past year, hormone use, self-report physical activity, alcohol consumption, smoking status, corticosteroid use, BMI, dietary calcium intake, dietary vitamin D intake

Table

*Disclosures: Rebekah Harris, None.*

## 1112

**Yogurt consumption is associated with attenuated cortical bone loss independently of total calcium and protein intakes and physical activity in postmenopausal women.** Emmanuel BIVER<sup>\*</sup>, Claire DUROSIER-IZART, Fanny MERMINOD, Thierry CHEVALLEY, Serge FERRARI, René RIZZOLI. Department of Bone Diseases, Geneva University Hospitals & Faculty of Medicine, Switzerland

Purpose: Yogurts provide calcium and proteins together with probiotics with possible effects on gut microbiota, all being potentially beneficial on bone. We investigated the influence of yogurt consumption on bone mineral density (BMD) and microstructure changes in a cohort of healthy postmenopausal women.

Methods: Yogurt consumption (never, <1 and ≥1 serving/day, 125-180 g/d) and total calcium and protein intakes were assessed at baseline with a food frequency questionnaire in 733 postmenopausal women (mean age ± SD 65.0 ± 1.4 years) enrolled in the Geneva Retirees Cohort and followed over 3.0 ± 0.5 years. Cortical (Ct) and trabecular (Tb) bone density and microstructure at the distal radius and tibia were assessed by HR-pQCT (Xtreme CT, Scanco Medical, Bassersdorf, Switzerland), in addition to areal BMD and body composition by DXA, at baseline and at the end of the follow-up.

Results: Yogurt consumption was associated with lower BMI, higher physical activity (PA) and calcium and protein intakes, and similar total energy intakes (3-days estimated food records). Alcohol or tobacco consumption and menopausal hormone therapy use were not different. At baseline, compared with women who never consume yogurts (8.6 %), yogurt consumers (91.4%) had higher lumbar spine BMD (+4.4%, p=0.007), distal 1/3 radius BMD (+3.4%, p=0.021) and tibia Ct area (+5.3%, p=0.041), even after adjustment for BMI, PA and total calcium and protein intakes. Whole body fat mass was lower (-6.4%, p=0.019), independently of total energy intake and PA. The prevalence of low-trauma fractures tended to be lower (19% vs 29%, p=0.058). In the longitudinal analysis, yogurt consumption (≥1 serving/day, 17.6%; <1 serving/day, 73.8% or never, 8.6 %) was associated with attenuated loss of total hip BMD (median annual change -0.1%, -0.4% and -0.6% respectively, p=0.017), of radius Ct area (-0.5%, -1.1% and -1.2%, p=0.004) and thickness (-0.5%, -1.1% and -1.3%, p=0.007), even after adjustment for BMI, PA and total calcium and protein intakes or for dairy protein intake. There was no difference at spine, tibia and Tb compartments.

Conclusion: Radius Ct bone loss is attenuated in yogurt consumers independently of total calcium and protein intakes, total dairy products intakes, or PA, suggesting that yogurt may be more than just a marker of healthy lifestyle. Whether influence on the gut microbiota may contribute to this specific protective effect of fermented dairy product remains to be investigated.

*Disclosures: Emmanuel BIVER, YINI research award supported by Danone Institute International in collaboration with the American Society for Nutrition and the International Osteoporosis Foundation, 11*

*This study received funding from: YINI research award supported by Danone Institute International in collaboration with the American Society for Nutrition and the International Osteoporosis Foundation*

## 1113

**Reproduction-Induced Changes in Maternal Trabecular Bone Microarchitecture Confer Protective Effects against Estrogen Deficiency.** Chantal de Bakker<sup>\*</sup>, Laurel Leavitt, Wei-Ju Tseng, Tiao Lin, Wei Tong, Ling Qin, X. Sherry Liu. University of Pennsylvania, United states

Significant bone loss occurs in the maternal skeleton during pregnancy and lactation. Despite the substantial increase in bone formation after weaning, bone mass

is only partially recovered. However, reproductive history does not increase postmenopausal fracture risk. To explain this paradox, we hypothesized that reproduction-induced skeletal changes may confer protective effects post-menopause.

Rats in the reproductive group underwent 3 cycles of pregnancy, lactation, and weaning. At age 12 mo, virgin (n=4) and reproductive (n=9) rats had ovariectomy (OVX) surgery to induce estrogen deficiency. Trabecular bone loss post-OVX was evaluated at the proximal tibia by *in vivo*  $\mu$ CT.

Prior to OVX, reproductive rats had 43%, 46%, and 73% lower bone volume fraction (BV/TV), trabecular number (Tb.N), and connectivity density (Conn.D), and 19% greater trabecular thickness (Tb.Th) than virgins (Fig A,B;  $p < 0.01$ ). Over 12 wks post-OVX, virgin rats showed 76%, 50%, and 86% reduction in BV/TV, Tb.N, and Conn.D ( $p < 0.01$ ), while reproductive rats had 53% decrease in BV/TV and no change in Tb.N or Conn.D. 12 wks post-OVX, no difference between reproductive and virgin rats in BV/TV, Tb.N, or Conn.D remained, while reproductive rats still had 20% thicker trabeculae than virgins. Furthermore, while our earlier study found that reproduction induced long-term trabecular deterioration at L4, by 12 wks post-OVX, there was no difference between groups at this site.

The disparate baseline trabecular structure between reproductive and virgin rats, combined with their distinctive patterns of post-OVX bone loss, led to the question of whether variations in microarchitecture can impact bone loss rate. Linear regression analysis revealed no correlation between baseline BV/TV and degree of OVX bone loss. However, baseline Conn.D, Tb.N, and Tb.Th were significantly correlated to the % reduction in BV/TV post-OVX ( $r = 0.72, 0.74, 0.80$ , respectively;  $p < 0.05$ ; Fig C), suggesting that a trabecular network of less number and connections, but thicker trabeculae, may be protective against OVX bone loss.

Despite the lower BV/TV, bone loss in response to OVX was remarkably slower in rats with a reproductive history than virgins, resulting in similar bone microstructure 12 wks post-OVX. The unique phenotype of post-reproductive bone microarchitecture exerts a protective effect against estrogen deficiency, which may help to account for low fracture risk in women with a reproductive history.

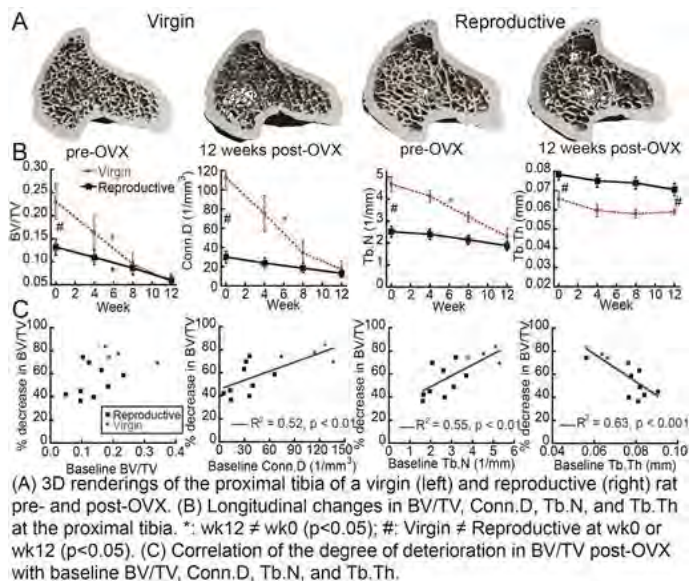


Figure 1

Disclosures: Chantal de Bakker, None.

## 1114

**Pyk2 Deficiency Protects from Glucocorticoid-Induced Bone Resorption and Osteoblast and Osteocyte Apoptosis, but not from the Decrease in Bone Formation.** Amy Sato\*, Meloney Cregor, Keith Condon, Lilian Plotkin, Teresita Bellido. Indiana University School of Medicine, United states

The Pyk2 kinase, a component of osteoclast podosomes, is essential for osteoclast function; and mice lacking Pyk2 (KO) exhibit impaired bone resorption and increased bone mass. In addition, KO mice or wild type (WT) mice treated with a pharmacological inhibitor of Pyk2, display increased bone formation. Further, Pyk2 activity is required for the pro-apoptotic effect of glucocorticoids (GC) on osteocytic cells *in vitro*. We investigated herein the requirement of Pyk2 for the skeletal effects of GC using KO mice. Female 4-month-old KO and WT littermate controls (10/group) were implanted with slow-release pellets containing placebo or prednisolone at 1.4 or 2.1 mg/kg/day, for 4 weeks. KO mice displayed increased BMD (10, 9 and 23% for total, femur and spine), no changes in circulating CTX, P1NP or OCN, and increased TRAP5b. Moreover, although osteoclast number on bone was similar to WT, the number of bone marrow osteoclasts was increased by 3.2-fold in KO mice, explaining the increased serum TRAP5b. GC induced the expected dose-dependent decrease in BMD in WT mice (total: -4 and -7%, femur: -6 and -10%, spine -8 and -14%,  $p < 0.05$ ), but failed to decrease BMD at any site in KO mice. GC at either dose also increased apoptosis of cancellous osteocytes/osteoblasts (11 and 15% and cortical osteocytes (11 and 13%), but did not increase apoptosis in KO mice.

However, both GC doses decreased to the same extent bone formation indexes in WT and KO mice (MS/BS: -18 vs -20%, MAR: -51 vs -52%, and BFR: -60 vs -62%, for WT and KO). GC also reduced the serum bone formation marker P1NP similarly with both doses and in both genotypes (-60 and -38% at 2 and 4 wks). Moreover, dexamethasone equally decreased *ex vivo* matrix mineral production by osteoblasts derived from WT or KO mice, or by WT osteoblasts treated with the Pyk2 inhibitor PF-431396, as quantified by hydroxyapatite and calcium deposition. Further, both doses of GC increased osteoclast number (~50%) and surface (50 and 62%) as well as serum CTX (70 and 90%) and TRAP5b (105 and 118%) in WT mice. In contrast, GC increased osteoclast number in KO mice (40 and 48%), but failed to increase osteoclast surface or serum TRAP5b and CTX, demonstrating that the inherent osteoclast dysfunction conferred by lack of Pyk2 overrides GC-induced resorption. We conclude that Pyk2 deficiency protects from GC-induced bone resorption and osteoblast and osteocyte apoptosis, but it does not prevent GC-induced inhibition of bone formation.

Disclosures: Amy Sato, None.

## 1115

**The Antioxidant Endogenous Response in Bone is Regulated by Nrf2 in a Gender Specific Manner.** Gretel G Pellegrini\*, Meloney Cregor<sup>2</sup>, Cynthya C Morales<sup>2</sup>, Kevin McAndrews<sup>2</sup>, Lilian I Plotkin<sup>1</sup>, David Burr<sup>2</sup>, Connie M Weaver<sup>3</sup>, Teresita Bellido<sup>1</sup>. <sup>1</sup>Indiana University School of Medicine, Roudebush Veterans Administration Medical Center, Indianapolis, United states, <sup>2</sup>Indiana University School of Medicine, United states, <sup>3</sup>Purdue University, United states

Earlier studies showed that the transcription factor Nrf2, which activates antioxidant defense mechanisms, regulates bone accrual by gender specific mechanisms, as it is required in the female skeleton but dispensable, and even detrimental, in the male skeleton. Here, we examined the antioxidant endogenous response and its relationship with bone volume and architecture in female (F) and male (M), young (3 month) and old (15 month) mice expressing (WT) or lacking (KO) Nrf2. Young and old KO mice of either gender exhibited the expected reduction in Nrf2 mRNA expression compared with WT littermates. Nrf2 deletion did not lead to compensatory increase in Nrf1 and Nrf3, other members of this transcription factor family. Loss of Nrf2 decreased Nrf1 expression in F and M bones; it did not alter Nrf3 expression in F bones but decreased it in young M bones. In addition, the expression of Nrf1 and 3 are dependent on Nrf2 in young M bones but only Nrf1 expression depends on Nrf2 in F bones. We next examined in bone the expression of phase II antioxidant enzymes known to be regulated by Nrf2 in other tissues. NAD(P)H quinone dehydrogenase 1 (NQO1), heme oxygenase 1 (HMOX1), ferritin light chain 1 (FTL1) and glutathione S-transferase pi 1 (GSTP) were downregulated in KO, young and old, F mice and young M mice. In addition, WT old M mice exhibited Nrf2 expression as low as KO old M mice and the expression of NQO1, HMOX1, FTL1 and GSTP were also low and not further decreased by Nrf2 deletion. In contrast, the expression of TXNRD1 (thioredoxin reductase 1) and superoxide dismutase 1 (SOD1) was lower in F KO mice but no different in M KO mice of either age compared to the respective littermate WT. Thus, all phase II antioxidant enzymes were dependent on Nrf2 in F, whereas in males TXNRD1 and SOD1 were controlled by alternative mechanisms. Moreover, Nrf2 deficiency affected bone acquisition also depending on the gender. Thus, M KO mice (young and old) exhibited higher bone volume and trabecular thickness compared to WT littermates. In contrast, bone volume was lower in young F KO mice, and trabecular number was also decreased and trabecular spacing was higher in both young and old F KO mice. These findings demonstrate that Nrf2 regulates the antioxidant endogenous response and bone accrual differentially depending on the gender, and suggest that Nrf2-independent mechanisms mediated by TXNRD1 and SOD1 protect the M skeleton against the detrimental effect of oxidative stress.

Disclosures: Gretel G Pellegrini, None.

## 1116

**Abnormalities in pre B cells impair adult bone homeostasis.** Mohamed Khass\*, Harunur Rashid, Peter Burrows, S. Louis Bridges, Amjad Javed, Harry Schroeder. University of Alabama at Birmingham, United states

During their development in the bone marrow, B cells must pass a series of checkpoints that test the integrity and function of their immunoglobulin. The first checkpoint is the formation of the pre B cell receptor (preBCR), which requires successful association of surrogate light chain with nascent  $\mu$  heavy chain (HC) proteins. The close proximity of osteoblasts in bone and developing B cells in bone marrow permits reciprocal cross regulation of these two lineages. However, specific interactions between early B cell subsets and osteoblasts are not well-defined. To gain insight into the interplay between developing B cells and bone formation, we evaluated bone homeostasis in a panel of mutant mice where B cell development is sequentially blocked at different stages including: global  $J_H$  gene null (KO) mice that lack any HCs, the  $\lambda 5$  gene KO lacking the preB cell receptor,  $\mu$ MT mice that lack the membrane bound IgM B cell receptor, and the CD19 KO, in which there are defects in peripheral mature B cells. All KO mice survived until adulthood. We analysed femurs of 6-month old littermates, when postnatal bone development is complete. A significant decrease in trabecular bone volume (40-90%) was observed in  $J_H$ ,  $\lambda 5$  and  $\mu$ MT mutants. The  $\lambda 5$  mutant, with a block at the preBCR stage, had a 90% decrease in trabecular bone. Histological analysis further revealed decreased tubular bone in

$\lambda 5$  and  $\mu$ MT mutants. All mutants had a significant decrease in trabecular number (30-50%) coupled with increased trabecular spacing. Interestingly, cortical bone in all mutants was comparable to wild-type littermates. Double calcine labeling confirmed a significant decrease in active synthesis of both trabecular and cortical bone in the  $\mu$ MT and  $\lambda 5$  mutants. Histomorphometric analysis revealed an increase in both osteoblast and osteoclast numbers, suggesting accelerated bone remodeling. Interestingly, the  $J_H$  and  $\lambda 5$  double KO mice had the most dramatic bone loss and early onset of osteoporosis. These data support a major role for preBCR expression on B cells for maintenance and homeostasis of adult bone. Interestingly, deletion of CD19, which results in defects in the mature B cell compartment, had a minimal effect on bone homeostasis. Taken together, our data show that blocking early development of B cells in the bone marrow affects osteoblast function and postnatal bone synthesis. In conclusion, pre B cells are involved in regulating bone synthesis and maintenance of adult bone mass.

**Disclosures:** Mohamed Khass, None.

This study received funding from: UAB Clinical Immunology and Rheumatology Division

## 1117

**Connexin43 Deficiency Results in a Lean Phenotype in Mice.** Manuela Fortunato\*, Marcus Watkins, Francesca Fontana, Roberto Civitelli, Washington University School of Medicine, United states

Connexin43 (Cx43) is the main gap junction protein expressed in skeletal cells, where it contributes to modulating both arms of the bone remodeling cycle. Osteogenic cells share a common precursor with adipocytes, but few studies exist on Cx43 in fat tissue. In addition to contributing to energy metabolism, the adipose tissue also functions as an endocrine organ to regulate bone homeostasis. Recently, Cx43 and functional gap junctions have been detected in both brown adipose tissue (BAT) and white adipose tissue (WAT), and since Cx43 is involved in such cellular processes as autophagy and mitochondrial homeostasis that can affect cell energy homeostasis, we asked whether deletion of Cx43 would affect metabolism and body composition. While germline ablation of the Cx43 gene (*Gjal*) is perinatally lethal, we have previously demonstrated that heterozygous null *Gjal*<sup>+/-</sup> mice exhibit only modestly delayed ossification after birth, but the skeleton is normal in adult animals. Interestingly, however, using dual energy x-ray absorptiometry (DXA) we find 19-24% reduction in body fat mass in *Gjal*<sup>+/-</sup> mice relative to wild type at age 6 weeks (17.4-18.7 vs. 19.6-24.7, respectively) and 12 weeks (16.8-19.6 vs. 22.4-27.6; p<0.05). Conversely, *Gjal*<sup>+/-</sup> mice have higher lean body mass. We then used *Gjal*<sup>lox/lox</sup> and Tw2-Cre mice to replace *Gjal* with a *LacZ* cassette specifically in the mesenchymal lineage (cKO<sup>Tw2</sup>). Strong  $\beta$ -galactosidase staining is present in BAT, and to a lesser extent in WAT, confirming that Cx43 is expressed in fat, and it is efficiently targeted by Tw2-cre. Intriguingly, body fat mass is significantly lower in cKO<sup>Tw2</sup> than in control mice throughout one year of life (-21-43%, p<0.01), and body weight is 9-15% lower (p<0.01). Accordingly, WAT is reduced relative to control littermates, (1.7-2.2 vs. 2.1-3% WAT/bw), whereas BAT is not different. Serum glucose, triglycerides, free fatty acids, and cholesterol are normal in cKO<sup>Tw2</sup> mice; and oxygen consumption is similar in cKO<sup>Tw2</sup> and control mice (3.67-3.7 vs. 3.77-3.91 mg/g/L, respectively). Absence of systemic alterations of metabolic markers may imply that Cx43 regulates fat tissue via cell autonomous mechanisms. Our data show that Cx43 plays an unexpected role in the regulation of fat homeostasis, favoring accumulation of WAT. Thus, Cx43 may represent a potential new pharmacologic target against obesity.

**Disclosures:** Manuela Fortunato, None.

## 1118

**CD169<sup>+</sup> Osteal Macrophages Promote Osteoblast Maintenance and Bone Healing Independent of Osteoclasts.** Lena Batoon<sup>1</sup>, Martin Wullschlegel<sup>2</sup>, Susan Millard<sup>1</sup>, Corina Preda<sup>3</sup>, Andy Wu<sup>1</sup>, Cameron Sunderland<sup>1</sup>, Simranpreet Kaur<sup>1</sup>, Jean-Pierre Levesque<sup>1</sup>, Liza-Jane Raggatt<sup>1</sup>, Allison Pettit<sup>\*1</sup>. <sup>1</sup>Mater Research Institute - The University of Queensland, Australia, <sup>2</sup>Gold Coast Univeristy Hospital - Griffith University, Australia, <sup>3</sup>Queensland Health, Australia

Evidence regarding the critical contributions of osteal macrophages (osteomacs) to bone homeostasis and repair is mounting. However, previous studies have been confounded by utilization of macrophage depletion models that also target osteoclasts. Distinguishing between the specific roles of macrophages and osteoclasts is an experimental priority given osteoclasts-osteoblasts coupling mechanisms. In order to discover better approaches to delineate between osteomac and osteoclast contributions to bone healing we developed a rapid enzyme free osteomac enrichment protocol that permitted multiplexed phenotyping of minimally manipulated osteomacs via flow cytometry. We demonstrated that osteomacs express the resident macrophage restricted molecule CD169, and based on published literature, we predicted that CD169 would not be expressed by osteoclasts. We confirmed CD169 expression by osteomacs but not by osteoclasts in vivo using the CD169-diphtheria toxin (DT) receptor (DTR) gene knock-in model. DT treatment in naive CD169-DTR mice resulted in a rapid and striking 96.4% reduction in osteomac surface/bone surface (BS) but had no effect on osteoclast surface/BS (p=0.6). The induced loss of osteomacs resulted in a significant 85.3% reduction in osteoblast surface/BS. We next assessed the impact of CD169<sup>+</sup> macrophage depletion in 2 models of bone injury that

heal via either intramembranous (tibial injury) or endochondral (internally-plated femoral full thickness osteotomy model) mechanisms. DT treatment at the time of bone injury in CD169-DTR mice receiving either a tibial injury or femoral osteotomy significantly impaired bone healing by 69.5% and 63.1%, respectively, when assessed in the anabolic phase. Importantly, DT treatment in CD169-DTR mice did not affect osteoclast frequency in either model. In the femoral osteotomy model, the magnitude of callus formation correlated with the number of F4/80<sup>+</sup> macrophages within the callus (r<sup>2</sup>=0.8; p<0.0001). This study exposes the CD169-DTR model as a powerful experimental tool for differentiating functional contributions of osteomacs and osteoclasts in bone biology. Overall these observations provide compelling support that osteomacs, independent of osteoclasts, provide vital pro-anabolic support to osteoblast during both bone growth/homeostasis and bone repair. Therefore osteomacs represent an important target cell when investigating bone regenerative mechanisms.

**Disclosures:** Allison Pettit, None.

## 1119

**Novel Roles of RANK in Osteocytes During Bone Remodeling.** Min Jin<sup>\*1</sup>, Yinshi Ren<sup>2</sup>, Ke Wang<sup>1</sup>, Yuan Hui<sup>3</sup>, Chaoyuan Li<sup>4</sup>, Xiaohua Liu<sup>4</sup>, Haibo Zhao<sup>5</sup>, Lin Chen<sup>6</sup>, Jianquan Feng<sup>4</sup>. <sup>1</sup>Department of Biomedical Sciences, Texas A&M Baylor College of Dentistry, Dallas, United states, <sup>2</sup>Cellular,Developmental & Genome Laboratories, Duke University Musculoskeletal Research center, United states, <sup>3</sup>Department of Orthodontics, Fourth Military Medical University, China, <sup>4</sup>Department of Biomedical Sciences, Texas A&M Baylor College of Dentistry, United states, <sup>5</sup>Center for Metabolic Bone Diseases, University of Arkansas for Medical Sciences, United states, <sup>6</sup>Center of Bone Metabolism & Repair, State Key Laboratory of Trauma, Burns & Combined Injury, Trauma Center, Institute of Surgery Research, China

RANK, which is activated by RANKL released from osteoblasts/osteocytes, plays a key role in osteoclast formation. RANK is also expressed in dog osteoblasts/osteocytes, although it is largely unclear if RANK contributes to bone formation or remodeling. In this study we first demonstrated Rank expressions in both osteoblasts and osteocytes using RT-PCR. Next, we crossed 10kb Dmpl-Cre with Rankl/fl mice to conditionally knockout (cKO) Rank in late osteoblasts and osteocytes. This resulted in a significant deletion of Rank (>60%) in the osteocytes. The Rank cKO mice displayed no apparent change in either bone formation or bone resorption in 1-month-old mice. However, the 4-month-old cKO mice exhibited a sharp reduction in the bone formation rate (6.54 ± 1.09 vs 3.28 ± 0.94 μm/10day) with no significant change in TRAP positive osteoclast number on the bone surface (11.10 ± 5.69 vs 12.84 ± 5.85/mm), leading to a great reduction in cancellous bone volume (7.58 ± 4.06 vs 1.96 ± 0.52%) and a moderate reduction in cortical bone volume. The SEM images revealed a dramatic change in osteocyte morphologies from a spindle shape to round form and laculo-canalicular spaces. There were striking significant increases in the TRAP positive osteocyte numbers (2.72 ± 0.64 vs 28.10 ± 4.72%) in the cKO mice. The real-time RT-PCR data showed a 6-fold increase in Trap (1.36 ± 0.62 vs 8.14 ± 2.63 mm<sup>2</sup>) and an 8-fold increase in cathepsin K (1.22 ± 0.38 vs 9.44 ± 2.92) with no apparent change in Rankl in the cKO bone. Immunohistochemistry stains showed reductions in osterix, BSP and DMP1 in the cKO bone. To further study the potential impact of deleting RANK on the unloading reaction, we used the tail suspension model and compared the cKO and control mice. Our initial studies showed no apparent protective role of deleting Rank associated with the unloading caused bone loss. In other words, the cKO mice continued to lose bone volume in the unloading condition. In summary, deleting Rank in osteocytes has no direct impact on postnatal bone development, but greatly changes bone remodeling: a change in osteocyte morphology, an inhibition in bone mineralization, and an increase in osteolysis with no apparent change in osteoclast formation and function. Our data therefore demonstrate that RANK expression in osteocytes contributes to bone remodeling, which is independent of its mechanosensor role or osteoclast function. This study also provides genetic evidence that RANK plays a dual role in osteocytes during bone remodeling.

( $p < 0.01$ ) vs. only  $27 \pm 13\%$  (NS) in WT mice at 11 weeks of age. The anabolic response to ML was less in the older WT mice but this age-related decline in anabolic response to ML was prevented in cKO mice where an increased Tb.BV/TV was still observed ( $58 \pm 14\%$ ,  $p = 0.057$ ).

We then assessed the role of Ctsk in Ocytes during UL. Mice were subjected to 10 days of normal loading or UL via hindlimb suspension starting at 9 and 13 weeks of age. Ocyte lacunar area did not change with UL. However, 10 days UL of 9 wk old mice revealed a significant decrease in trabecular parameters in both cKO and WT, whereas cortical thickness and cortical bone area decreased only in WT mice. In contrast, cKO prevented trabecular bone loss induced by 10 days UL in 13 wk old mice ( $p < 0.05$  for BV/TV and trabecular thickness), but there were no differences in cortical bone.

Taken together, these results provide direct genetic evidence that cathepsin K is involved in the responses of Ocytes to mechanical loading and in the way these cells influence bone remodeling and homeostasis. Osteocyte-specific deletion of cathepsin K protects against the reduced skeletal mechanosensitivity with aging and partially attenuates the unloading-induced bone loss in mice.

**Disclosures:** Yoshitomo Ishihara, None.

This study received funding from: Merck

## 1121

**MicroRNA miR-23a Cluster Promotes Osteocyte Differentiation by Regulating Prdm16/TGF- $\beta$  Signaling in Osteoblasts.** Huan-Chang Zeng<sup>\*1</sup>, Yangjin Bae<sup>1</sup>, Brian Dawson<sup>1</sup>, Yuqing Chen<sup>1</sup>, Philippe Campeau<sup>2</sup>, Jianning Tao<sup>3</sup>, Brendan Lee<sup>1</sup>. <sup>1</sup>Baylor College of Medicine, United states, <sup>2</sup>Sainte-Justine Hospital, Canada, <sup>3</sup>Sanford School of Medicine of the University of South Dakota, United states

Osteocytes are the terminally differentiated cell type of the osteoblastic lineage. As the most abundant cells in bone (~98%), osteocytes serve important functions in skeletal homeostasis including controlling osteoclastogenesis and biomechanical sensing. Although the transcriptional regulation of osteoblast differentiation has been well-characterized, the factors that regulate differentiation of osteocytes from mature osteoblasts are poorly understood. Here, we show that the microRNA cluster miR-23a~27a~24-2 promotes osteocyte differentiation. Osteoblast-specific gain-of-function (*Coll1-miR23aC*) mice had low bone mass associated with decreased osteoblasts but increased osteocyte numbers. In contrast, loss-of-function transgenic mice overexpressing microRNA decoys for either miR-23a or miR-27a, but not miR24-2, showed the opposite phenotype of decreased osteocyte numbers. RNA-sequencing analysis of bones from the gain-of-function *Coll1-miR23aC* transgenic mice showed altered transforming growth factor  $\beta$  (TGF- $\beta$ ) signaling. Interestingly, Prdm16 transcription factor, a negative regulator of the TGF- $\beta$  pathway, was directly repressed by the miR-23a cluster with concomitant alteration of Sclerostin (*Sost*) expression in osteocytes. Pharmacological inhibition using a TGF- $\beta$  neutralizing antibody, 1D11, rescued the low bone mass and osteocyte phenotypes observed in the gain-of-function *Coll1-miR23aC* transgenic mice. Taken together, the miR-23a cluster regulates osteocyte differentiation by modulating the TGF- $\beta$  signaling pathway through targeting of *Prdm16*.

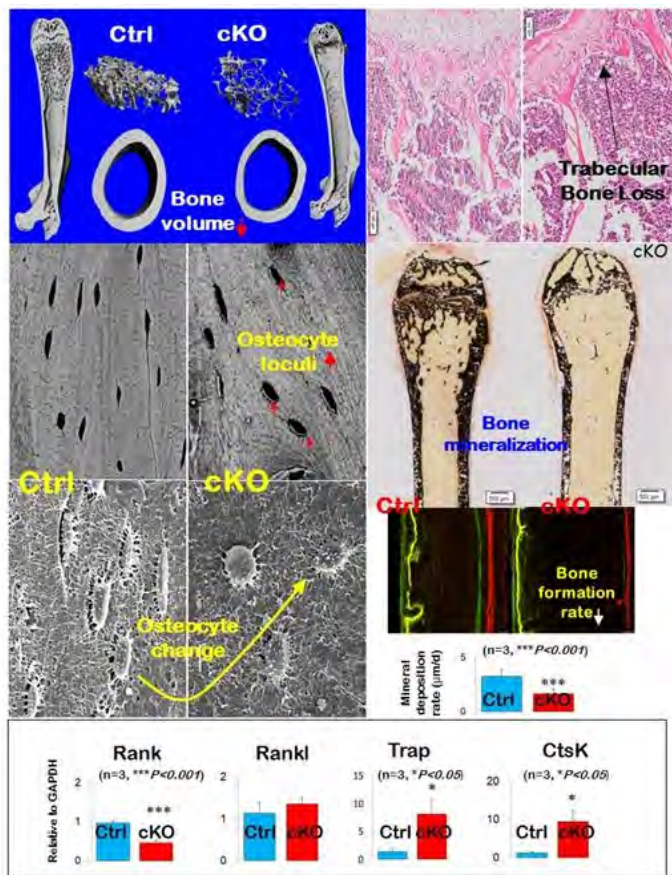
**Disclosures:** Huan-Chang Zeng, None.

## 1122

**Role of FGF9 in Promotion of Early Osteocyte Differentiation and as a Potent Inducer of FGF23 Expression in Osteocytes.** Lora A. McCormick<sup>\*1</sup>, Kun Wang<sup>2</sup>, LeAnn M. Tiede-Lewis<sup>1</sup>, Hong Zhao<sup>2</sup>, Yixia Xie<sup>2</sup>, Samantha Neuburg<sup>3</sup>, Aline Martin<sup>3</sup>, Lynda F. Bonewald<sup>2</sup>, Sarah L. Dallas<sup>2</sup>. <sup>1</sup>University of Missouri-Kansas City, USA, United states, <sup>2</sup>University of Missouri-Kansas City, United states, <sup>3</sup>Northwestern University Feinberg School of Medicine, United states

Since the loss of osteocyte connectivity and dendricity that occurs with aging shares features with age-related neurodegeneration, we hypothesized that there may be common regulatory mechanisms. In a search for neurogenesis-related genes that are enriched in osteocytes, we previously identified the glial cell differentiation factor FGF9 to be highly enriched with osteocyte differentiation in the osteocyte-like cell lines OmGFP66 and IDG-SW3. FGF9 was also shown to downregulate expression of osteoblast markers and upregulate expression of early osteocyte markers while delaying maturation to a late osteocyte phenotype, suggesting that FGF9 may play a role in initiating the osteoblast to osteocyte transition.

To further examine the role of FGF9 in osteocyte differentiation, ex-vivo neonatal mouse calvarial cultures were used as well as the OmGFP66 and IDG-SW3 cell lines, both of which express Dmpl-GFP reporters and are models of osteoblast to osteocyte transition. qPCR analysis showed that treatment of neonatal mouse calvaria with FGF9 strongly downregulated alkaline phosphatase and stimulated expression of early osteocyte markers Dmpl, E11 and PHEX, confirming results with the OmGFP66 cell line. Immunolocalization of FGF9 (LSBio antibody C312611) in 2 and 4wk old mouse femur showed moderate expression in osteoblasts, strong expression in the osteoid osteocyte layer and moderate expression in mature osteocytes, consistent with a role in promoting early osteocyte differentiation. Osteocytes are known to regulate phosphate homeostasis through endocrine secretion of FGF23. Interestingly, FGF9 potentially induced FGF23 mRNA levels in differentiated OmGFP66 cells by as much as 1200-fold within 24h. Dose-response comparisons of FGF9 with 1,25-D3, a known stimulator of FGF23, showed that



Novel Roles of RANK in Osteocytes During Bone Remodeling

**Disclosures:** Min Jin, None.

## 1120

**Cathepsin K is Directly Involved in Osteocyte Lacunae Remodeling and in the Osteocyte-dependent Skeletal Responses to Mechanical Loading and Unloading.** Yoshitomo Ishihara<sup>\*1</sup>, Martin M. Fu<sup>1</sup>, Frank C. Ko<sup>2</sup>, Daniel J. Brooks<sup>3</sup>, Liang Yang<sup>1</sup>, Kenichi Nagano<sup>1</sup>, Riku Kiviranta<sup>4</sup>, Mary L. Bouxsein<sup>5</sup>, Francesca Gori<sup>1</sup>, Roland Baron<sup>6</sup>. <sup>1</sup>Division of Bone & Mineral Research, Department of Oral Medicine, Infection & Immunity, Harvard School of Dental Medicine, United states, <sup>2</sup>Harvard Medical School, Endocrine Unit, Massachusetts General Hospital, United states, <sup>3</sup>Center for Advanced Orthopedic Studies, Beth Israel Deaconess Medical Center, United states, <sup>4</sup>Department of Medical Biochemistry & Molecular Biology, University of Turku, Finland, <sup>5</sup>Center for Advanced Orthopedic Studies, Beth Israel Deaconess Medical Center & Harvard Medical School, Endocrine Unit, Massachusetts General Hospital, United states, <sup>6</sup>Division of Bone & Mineral Research, Department of Oral Medicine, Infection & Immunity, Harvard School of Dental Medicine & Harvard Medical School, Endocrine Unit, Massachusetts General Hospital, United states

We have previously shown that cathepsin K (Ctsk) expression in osteocytes (Ocytes) contributes to the increased remodeling, bone loss and deterioration of mechanical properties observed in mice during lactation. In this study, we hypothesized that Ocyte Ctsk may also play a role in the skeletal responses to mechanical loading (ML) and unloading (UL). To address this hypothesis, DMP1-Cre;Ctsk<sup>fl/fl</sup> mice were used to specifically delete Ctsk in Ocytes (cKO).

For ML studies, female mice left tibiae were loaded at 1200 cycles, 4 Hz, 5 days/week for 2 weeks starting at 9 and 13 weeks of age. The non-loaded right tibiae served as control. Micro-CT and histomorphometric analysis showed that cKO resulted in increased trabecular bone volume (BV/TV:  $20 \pm 4\%$ ,  $p < 0.01$ ) in the control legs of 11 weeks old female mice, but had no effect in older (15 wo) mice.

Backscattered SEM revealed that ML decreased significantly the Ocyte lacunar area in cKO mice but not in their Cre-negative Ctsk<sup>fl/fl</sup> (WT) littermates, suggesting that Ctsk plays an essential role in mechanically-induced Ocyte lacunae remodeling. Importantly, this change in Ocytes was associated with changes in bone remodeling. Histomorphometry showed that ML increased Tb.BV/TV by  $52 \pm 13\%$  in cKO mice

50ng/ml FGF9 was 20-fold more potent than 10nM 1,25-D3 in stimulating FGF23 mRNA expression and 50-fold more potent than FGF2. ELISA measurements confirmed that FGF9 induced FGF23 protein secretion 90-fold to >7000pg/ml in OmGFP66 cells by 24h. 1,25-D3 also increased FGF9 mRNA by 2.5 fold. FGF9 signals mainly through FGF receptor 3 and also 2. OmGFP66 cells were found to express FGFRs 1, 2, and 3 with FGFR2 and 3 downregulated by FGF9 treatment. These data show that differentiating osteocytes express FGF9 and its receptors and suggest FGF9 may act to induce early osteocyte differentiation and may also play a role in phosphate metabolism through regulating expression of FGF23.

**Disclosures:** Lora A. McCormick, None.

## 1123

**Alterations in perilacunar and canalicular remodeling in the Hyp mouse model of XLH.** Janaina deSilva Martins<sup>1</sup>, Marie Demay<sup>2</sup>, Eva Liu<sup>\*3</sup>. <sup>1</sup>Massachusetts General Hospital, United states, <sup>2</sup>Massachusetts General Hospital, Harvard Medical School, United states, <sup>3</sup>Brigham & Women's Hospital, Massachusetts General Hospital, United states

X-linked hypophosphatemia (XLH) results from a mutation in PHEX, leading to elevated serum FGF23 levels, hypophosphatemia and decreased 1,25 dihydroxyvitamin D (1,25D) production. Mice with XLH (Hyp) have osteomalacia, decreased bone strength, and abnormal skeletal microarchitecture. Osteocytes modulate perilacunar/canalicular remodeling, which is important for maintenance of bone quality. We recently showed that Hyp mice have a decreased number of cortical osteocytes and increased osteocyte apoptosis, suggesting that abnormalities in perilacunar remodeling may contribute to the phenotype. The lacunar area normalized to bone area (Lac.Ar/B.Ar) was measured in the mid-diaphysis of Hyp tibiae as a marker of this remodeling process. The lacunar area of d75 Hyp osteocytes was 2.6 fold larger than that of wild type (WT) mice. Osteocytes produce osteoclastic markers, including tartrate resistant acid phosphatase (TRAP) and cathepsin K to regulate perilacunar remodeling. To evaluate periosteocytic resorption, staining for these markers was performed. Compared with WT, Hyp cortical osteocytes have increased TRAP staining and immunoreactivity for cathepsin K. Like perilacunar remodeling, pericanalicular matrix remodeling is also controlled by osteocytes. Thionin staining revealed that Hyp mice have a poorly organized and less extensive canalicular network compared to WT.

To assess whether 1,25D or blocking FGF23 action modulates perilacunar/canalicular remodeling, Hyp mice were treated d2 to 75 with 1,25D (175 pg/g/day) or FGF23 blocking antibody (FGF23Ab, 35 mcg/g 3x/week, Amgen) without phosphate supplementation. Both therapies significantly decreased, but did not normalize, Lac.Ar/B.Ar and partially restored canalicular organization. The similar effects of 1,25D and FGF23Ab on these parameters suggest that extracellular phosphate or 1,25D action may play a role in perilacunar/canalicular remodeling. Therefore, the Lac.Ar/B.Ar and canalicular network was examined in Npt2a KO mice, which have low serum phosphate and high 1,25D levels. These mice have significantly increased Lac.Ar/B.Ar relative to WT. Like those of Hyp mice, the canalicular network of Npt2a KO mice was also disorganized and less extensive.

These results demonstrate altered perilacunar/canalicular remodeling in the Hyp model of XLH. The similar abnormalities in lacunar size and canalicular organization in Hyp and Npt2a KO mice implicate hypophosphatemia in the pathogenesis of this phenotype.

**Disclosures:** Eva Liu, None.

## 1124

**Osteocytes Mediate Bone Pain Through Cell-Cell Communication with Sensory Neurons via Connexin 43.** Masahiro Hiasa<sup>\*1</sup>, Tatsuo Okui<sup>1</sup>, Jesús Delgado-Calle<sup>2</sup>, Teresita Bellido<sup>2</sup>, G David Roodman<sup>1</sup>, Fletcher White<sup>3</sup>, Lilian Plotkin<sup>2</sup>, Toshivuki Yoneda<sup>1</sup>. <sup>1</sup>Department of Medicine, Hematology Oncology, Indiana University School of Medicine, United states, <sup>2</sup>Department Anatomy & Cell Biology, Indiana University School of Medicine, United states, <sup>3</sup>Department of Anesthesia, Paul & Carole Stark Neurosciences Research Institute, United states

Bone is highly innervated by sensory nerves (SNs). Sensitization and excitation of these SNs lead to bone pain. Although the mechanism of bone pain is unclear, interactions between SNs and bone cells in the bone microenvironment are likely involved in the pathophysiology of bone pain. We propose that osteocytes (OCy), which are the most abundant cells in bone and develop cell-cell networks with osteoblasts and osteoclasts to regulate bone remodeling, communicate with SNs and play an important role in bone pain. Immunohistochemistry (IHC) of bone in DMP-1-GFP TG mice revealed that dendritic processes of GFP<sup>+</sup> OCy were in direct physical contact with calcitonin gene related peptide- positive (CGRP<sup>+</sup>) SN fibers. In co-cultures of F11 SN cells and MLO-A5 osteocytic cells, we found that F11 SN cells contacted with dendritic processes of MLO-A5 cells by extending their neurites, and transferred the permeable small dye calcein to MLO-A5 cells. Using Ca<sup>2+</sup> influx imaging assay to evaluate SN excitation, we found that acid (pH 6.5) stimulated SN cell excitation, which was enhanced in co-culture with MLO-A5 cells. Importantly, addition of GAP27, a selective inhibitor of connexin43 (Cx43), or knockdown of Cx43 in MLO-A5 cells abolished the enhanced F11 SN cell excitation in the co-cultures.

Consistent with these data, IHC of bone in DMP-1-GFP TG mice demonstrated that Cx43-positive, GFP<sup>+</sup> osteocytes were in physical contact with CGRP<sup>+</sup> SN fibers by extending their processes. To determine the role of Cx43 in bone pain *in vivo*, we examined the effects of GAP27 in mice injected intratibially with mouse breast cancer E0771 cells by evaluating mechanical allodynia and thermal hyperalgesia. Further, expression of pERK and pCREB, molecular indicators for SN excitation, was also determined in the dorsal root ganglia (DRG) in these mice. We found marked suppression of bone pain and decreased pERK and pCREB expression in DRG in mice treated with GAP27 compared with vehicle-treated mice. More importantly, bone pain was reduced in DMP-1-Cre;Cx43<sup>flx/flx</sup> mice in which Cx43 was selectively deleted in osteocytes compared to control mice. Our data demonstrate that OCy and SN are in intimate physical contact in bone, and that they exchange small molecules via Cx43 to induce SN excitation that results in bone pain. In conclusion, targeting Cx43-mediated OCy-SN communications may provide a new potent approach for treating bone pain associated with bone diseases.

**Disclosures:** Masahiro Hiasa, None.

## 1125

**Screening based on FRAX fracture risk assessment reduces the incidence of hip fractures in older community-dwelling women – results from the SCOOP study in the UK.** EV McCloskey<sup>\*1</sup>, E Lenaghan<sup>2</sup>, S Clarke<sup>3</sup>, C Cooper<sup>4</sup>, R Fordham<sup>2</sup>, N Gittos<sup>5</sup>, I Harvey<sup>2</sup>, R Holland<sup>2</sup>, A Howe<sup>2</sup>, T Marshall<sup>6</sup>, T Peters<sup>7</sup>, JA Kanis<sup>1</sup>, TW O'Neill<sup>8</sup>, D Torgerson<sup>9</sup>, L Shepstone<sup>2</sup>, & the SCOOP Trial Group<sup>10</sup>. <sup>1</sup>University of Sheffield, United Kingdom, <sup>2</sup>University of East Anglia, United Kingdom, <sup>3</sup>University of Bristol, United Kingdom, <sup>4</sup>MRC Lifecourse Epidemiology Unit, University of Southampton, United Kingdom, <sup>5</sup>University Hospitals Birmingham NHS Trust, United Kingdom, <sup>6</sup>Norfolk & Norwich University Hospital, United Kingdom, <sup>7</sup>University of Bristol, United Kingdom, <sup>8</sup>University of Manchester, United Kingdom, <sup>9</sup>University of York, United Kingdom, <sup>10</sup>UK, United Kingdom

### Background

Despite the considerable costs of fragility fractures to society and individuals, the availability of fracture risk tools and effective treatments, community-based screening to prevent fragility fractures is currently not advocated in many countries, including the UK.

### Methods

We conducted a two-arm randomised controlled trial in women aged 70 to 85 years comparing a screening programme based upon the FRAX risk assessment tool with usual management in primary care. In the screening arm, licensed treatment was recommended in woman identified at high risk of hip fracture. The proportion of participants experiencing a fracture was compared over a five year follow-up period.

### Results

A total of 12 483 eligible women, identified in primary care, participated in the trial, with 6 233 randomised to the screening arm. In this arm, treatment was recommended in 898 women (14.4%) identified at high risk. Exposure to osteoporosis medication was higher by the end of the first year in the screening group compared to controls (15.3% vs 4.5%, respectively) with high treatment uptake (78.3% at 6 months) in the high risk subgroup. Despite a non-statistically significant reduction in individuals experiencing any fracture (RRR 7%, -3% to 15%, p=0.199), screening was associated with significant reduction in hip fracture (RRR 27%, 10%-41%, p=0.003). The incidence of major osteoporotic fractures, comprising hip, wrist, humerus and clinical vertebral fractures, was significantly reduced by 12% (2%-21%, p=0.018).

### Conclusions

A systematic, community-based screening programme of fracture risk using the FRAX tool in older women in the UK is feasible and effective in reducing hip fracture risk.

**Disclosures:** EV McCloskey, None.

## 1126

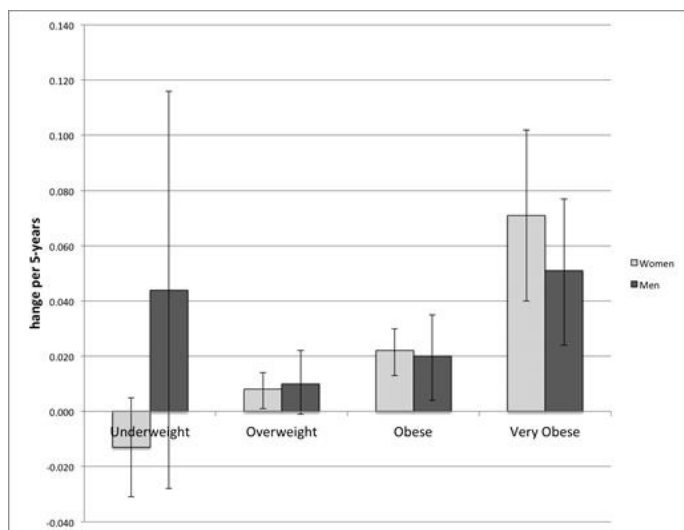
**Baseline Obesity is Predictive of More Rapid Frailty Onset: A 10-year Analysis of the Canadian Multicentre Osteoporosis Study (CaMOS).** Kennedy Courtney<sup>\*1</sup>, Olga Gajic-Veljanoski<sup>1</sup>, George Ioannidis<sup>1</sup>, Jonathan D. Adachi<sup>2</sup>, Claudie Berger<sup>3</sup>, Andy Kin On Wong<sup>4</sup>, Kenneth Rockwood<sup>5</sup>, Susan Kirkland<sup>5</sup>, Parminder Raina<sup>2</sup>, Lehana Thabane<sup>2</sup>, Alexandra Papaioannou<sup>2</sup>. <sup>1</sup>Hamilton Health Sciences – St. Peter's Hospital – GERAS Centre, Canada, <sup>2</sup>McMaster University, Canada, <sup>3</sup>Camos – McGill University, Montreal, Canada, <sup>4</sup>University Health Network, Toronto, Canada, <sup>5</sup>Dalhousie University, Canada

Background: Frailty is often conceived as a wasting disorder, however obese individuals have a high prevalence of chronic diseases and may have impaired strength and function associated with sarcopenic obesity. In cross-sectional studies, a 'U' shaped correlation between body mass index (BMI) and frailty has been demonstrated, suggesting that both under- and over-weight individuals were more likely to be frail. However, whether obesity contributes to frailty onset or progression has not been well examined longitudinally. In the current study, we examined the relationship between baseline BMI and frailty change over 10-years controlling for potential confounding variables.

**Methods:** We examined data from 7753 community-dwelling adults aged 50 years and older participating in the Canadian Multicenter Osteoporosis Study (CaMOS). Using Rockwood's cumulative deficits method, the 30-item CaMOS frailty index was calculated at baseline, years 5 and 10. Baseline BMI scores were divided into: underweight (<18.5), normal weight (18.5 to <25), overweight (25 to <30), obese class I-III (30 to <40) and obese class IV ( $\geq 40$ ). Analyses were adjusted for age, cognitive status, falls, BMD, prevalent/incident fractures and key life style variables including smoking, physical activity, and alcohol. Generalized estimating equations (GEE) were used to determine the rates of change in frailty per 5 years after accounting for correlations due to repeated measurements (year 5 and 10). Multiple imputation was used to explore missing data and selection bias.

**Results:** The cohort included 5566 women (mean age [SD]: 66.8 [9.3] years) and 2187 men (66.3 [9.5] years). The percentages of CaMOS individuals classified as underweight, normal weight, overweight, obese, and obese class IV were 1.7%, 33.6%, 41.4%, 21.9% and 1.4%, respectively. Figure 1 displays the rates of change, and 95% confidence intervals (95% CI), in Frailty Index scores over the 10-year study period for over-and under-weight groups compared to normal weight individuals.

**Conclusion:** In this longitudinal analysis, individuals who were obese at baseline had a faster rate of frailty deficit accumulation over 10-years than normal weight individuals. Individuals who were underweight were not significantly different from normal weight individuals. Very obese individuals, in particular, were at risk for more rapid onset of frailty over time and are a high-risk group who should be considered for tailored frailty interventions.



Change in Frailty Scores (95% CI) Compared to Normal Weight Individuals, By Baseline BMI Category

**Disclosures:** Kennedy Courtney, None.

## 1127

**Low Testosterone, but not Estradiol, Predicts Incident Falls in Older Men - the International MrOS Study.** Liesbeth Vandenput<sup>1</sup>, Dan Mellström<sup>1</sup>, Gail Laughlin<sup>2</sup>, Peggy Cawthon<sup>3</sup>, Jane Cauley<sup>4</sup>, Andrew Hoffman<sup>5</sup>, Magnus Karlsson<sup>6</sup>, Björn Rosengren<sup>6</sup>, Östen Ljunggren<sup>7</sup>, Maria Nethander<sup>1</sup>, Mattias Lorentzon<sup>1</sup>, Jason Leung<sup>8</sup>, Timothy Kwok<sup>8</sup>, Eric Orwoll<sup>9</sup>, Claes Ohlsson<sup>\*1</sup>. <sup>1</sup>University of Gothenburg, Sweden, <sup>2</sup>University of California San Diego, United states, <sup>3</sup>California Pacific Medical Center, United states, <sup>4</sup>University of Pittsburgh, United states, <sup>5</sup>Stanford University, United states, <sup>6</sup>Lund University, Sweden, <sup>7</sup>University of Uppsala, Sweden, <sup>8</sup>Chinese University of Hong Kong, Hong kong, <sup>9</sup>Oregon Health & Science University, United states

Fracture risk is mostly determined by bone strength and fall risk. Many studies have investigated the relationship between serum sex steroids and bone strength in men, revealing the importance of estradiol (E2) for trabecular and cortical bone properties. The predictive value of sex steroids for fall risk has been less well studied. Specifically, the associations between the fall risk and serum testosterone (T) and estradiol (E2), measured by the gold standard mass spectrometry (MS), remain unclear.

Older men (aged  $\geq 65$  yrs) from Sweden (n=2495), the US (n=1933), and Hong Kong (n=1469) participating in the Osteoporotic Fractures in Men Study (MrOS) had baseline E2 and T analyzed by MS and sex hormone-binding globulin (SHBG) by IRMA. Bioavailable (Bio) levels were calculated using mass action equations. Incident falls were ascertained every 4 months during a mean follow-up of 2.7 (Sweden), 11.2 (US) and 3.8 (Hong Kong) years. The association between serum sex steroids and

incident falls was estimated by generalized estimating equations which take into account missing reports.

The incident fall rate was highest in the US and lowest in Hong Kong (Sweden, 0.54; US, 0.82; Hong Kong, 0.15 falls/person/year). In the combined cohort of 5897 men, serum T (OR per SD increase, 95% CI: 0.88, 0.86-0.90) and BioT (0.87, 0.85-0.89) predicted incident falls in models adjusted for age and prevalent falls. However, E2 (0.99, 0.97-1.01), BioE2 (1.00, 0.98-1.02), and SHBG (0.98, 0.96-1.01) were not significantly associated with incident fall risk. The relationship between BioT and fall risk persisted after adjustment for individual physical performance variables (grip strength, timed chair stand, walking speed, narrow walk, and total body lean mass) and was only slightly attenuated after simultaneous adjustment for all performance variables (0.91, 0.89-0.94). Analyses in the respective cohorts showed that in MrOS Sweden and US (high fall rate), both T and BioT predicted incident falls, with BioT being the strongest predictor (Sweden: 0.90, 0.85-0.95; US: 0.87, 0.85-0.89). In MrOS Hong Kong (low fall rate), the association between Bio T and incident falls was not significant (0.99, 0.91-1.07).

In conclusion, low T and BioT levels are associated with an increased fall risk in older men. We propose that low T may influence fracture risk via an increased fall risk whereas low E2, based on previously published data, mainly increases fracture risk through reduced bone strength.

**Disclosures:** Claes Ohlsson, None.

## 1128

**A Single Assessment of BMD Can Strongly Predict Fracture Risk Over 25 years in Post-Menopausal Women: The Study of Osteoporotic Fractures.** Nicola Napoli<sup>\*1</sup>, Jane A. Cauley<sup>2</sup>, Rachel Wagman<sup>3</sup>, Kristine Ensrud<sup>4</sup>, Howard A. Fink<sup>4</sup>, Teresa A. Hillier<sup>5</sup>, Lily Lui<sup>6</sup>, Steve R. Cummings<sup>6</sup>, John T. Schousboe<sup>7</sup>, Dennis M. Black<sup>8</sup>. <sup>1</sup>Washington University School of Medicine, St Louis Mo. Universita' Campus Bio-Medico, Rome, Italy, United states, <sup>2</sup>Department of Epidemiology, University of Pittsburgh, United states, <sup>3</sup>Amgen, United states, <sup>4</sup>VA Medical Center, Minneapolis. University of Minnesota, Minneapolis, United states, <sup>5</sup>Kaiser Permanente Center of Health Research, Portland, United states, <sup>6</sup>California Pacific Medical Center, San Francisco, United states, <sup>7</sup>Park Nicollet Clinic, St. Louis Park, MN. Division of Health Policy & Management, University of Minnesota, Minneapolis, MN, United states, <sup>8</sup>Department of Epidemiology & Biostatistics, University of California San Francisco, United states

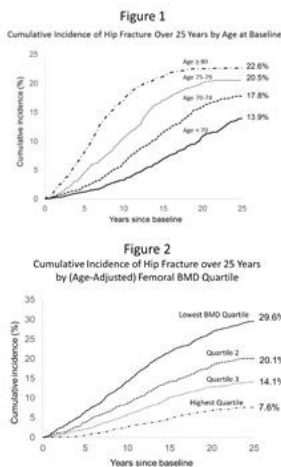
The ability of bone mineral density (BMD) and other risk factors to predict hip and other fracture risk over 5-10 years is well established. However, the value of BMD to predict fracture over the longer term has not been directly studied. The aim of this analysis was to investigate whether a single BMD can directly predict fracture risk over 25 years of follow-up without the need for statistical modeling.

We used data from the Study of Osteoporotic Fractures (SOF) that assessed BMD by dual energy X-ray absorptiometry (DXA) and risk factors in 7959 Caucasian women aged > 67 years in 1988-89. Follow-up for fractures continued for 25 years for hip fracture (HF), and for 20 years for wrist (WF) and any non-vertebral (nVF) fracture. All fractures were centrally adjudicated. Using age-adjusted proportional hazards models, we analyzed the association of femoral neck BMD with subsequent fracture risk for HF, nVF and WF over 20-25 years.

There were 1281 women with HF, 3287 with nVF and 745 with WF. 25 year cumulative incidence of HF was 17.5%; 20 year incidence was 55% for nVF and 13% for WF. For HF, 25 year incidence was highest in those >80 years old (22.6%) compared to 13.9% in women aged <70 years (Figure 1). There was a strong relationship between BMD and 25 year cumulative risk of HF (Figure 2): in the lowest compared to highest BMD quartile, age-adjusted HF risk was 29.6% vs 7.6% [Relative hazard (RH) 4.9 (95% CI: 4.1-6.0)]. Analyzing BMD as a continuous measure, over 25 years, the RH per SD for HF was 2.0 (95% CI: 1.9-2.1) with a similar gradient for WF and nVF. BMD risk prediction diminished only slightly over time: for HF, the RH per SD decreased from 2.6 (95% CI: 2.2-3.0) for 0-5 years to 1.8 (95% CI: 1.4-2.4) for 20-25 years.

We conclude that in older post-menopausal women, a single risk factor assessment, including BMD and age, can strongly predict hip fracture risk for up to 25 years. These results also show directly, without statistical modeling, that long-term risk of hip fracture remains very high in older women, even those over 80 years, supporting the importance of fracture risk assessment and consideration of treatment in these women.

suggesting that remodeling may have created an increased number of smaller trabeculae.



Figures

Disclosures: Nicola Napoli, None.

This study received funding from: Amgen for analysis

## 1129

### Light intensity physical activity measured by accelerometer is associated with favorable bone microarchitecture and strength: The Framingham Study.

Amanda Lorbergs\*<sup>1</sup>, Nicole Spartano<sup>2</sup>, Kerry Broe<sup>3</sup>, Xiaochun Zhang<sup>3</sup>, Robert McLean<sup>1</sup>, Serkalem Demissie<sup>4</sup>, L. Adrienne Cupples<sup>4</sup>, Joanne Murabito<sup>5</sup>, Vasan Ramachandran<sup>6</sup>, Douglas Kiel<sup>7</sup>, Marian Hannan<sup>1</sup>, Steven Boyd<sup>8</sup>, Mary Bouxsein<sup>9</sup>, Elizabeth Samelson<sup>1</sup>. <sup>1</sup>Institute for Aging Research, Hebrew Senior Life & Harvard Medical School, United states, <sup>2</sup>Section of Preventative Medicine & Epidemiology, Boston University School of Medicine, United states, <sup>3</sup>Institute for Aging Research, Hebrew Senior Life, United states, <sup>4</sup>Department of Biostatistics, Boston University School of Public Health, United states, <sup>5</sup>Boston University School of Medicine & Framingham Heart Study, United states, <sup>6</sup>Section of Preventative Medicine & Epidemiology, Medicine, Boston University School of Medicine & Framingham Heart Study, United states, <sup>7</sup>Institute for Aging Research, Hebrew Senior Life, Department of Medicine BIDMC, & Harvard Medical School, United states, <sup>8</sup>McCaig Institute for Bone & Joint Health, University of Calgary, Canada, <sup>9</sup>Center for Advanced Orthopedic Studies, Beth Israel Deaconess Medical Center & Harvard Medical School, United states

Although self-reported physical activity (PA) is recognized to benefit the skeleton, this approach to quantifying PA is limited by individuals' ability to accurately recall past behavior and has led to uncertainty regarding the amount of PA that may benefit the skeleton. Wearable accelerometers permit a direct assessment of PA levels. To better define the magnitude of benefit of PA on cortical and trabecular bone in the adult skeleton, we performed a cross-sectional study to determine the association of accelerometer-measured PA levels and sedentary time, with HR-pQCT bone measures at the weight-bearing tibia.

Using Actical accelerometers and 30-sec epochs, we defined each minute of PA intensity as: sedentary (0-99 counts/epoch), light (100-742 counts/epoch), and moderate to vigorous (>742 counts/epoch). We calculated % of wear time spent sedentary and performing light PA. Due to low % of time spent doing moderate to vigorous PA (MVPA) we present MVPA as min/day. In men and women separately, partial correlations estimated the association between PA and bone measures, adjusted for age (y), height (in), and weight (lb).

Study included 1,097 members of the Framingham Study Offspring cohort (mean age 70y, range 46-95). On average, men and women spent a majority of time as sedentary (83% and 86%, respectively), and 14% and 12% of time in light activities, respectively. Men spent a mean 20min/day and women spent 14min/day in MVPA. Sedentary time was negatively correlated with most bone measures and was significant for TbvBMD, TbTh, TtvBMD, and FEA failure load in men (r=-0.10 to -0.12; TABLE). In women, sedentary time was associated with lower CtTh, TbTh, and FEA failure load (r=-0.09 to -0.10) but associated with increased TbN without an association with TbvBMD. Light PA was associated with higher TtvBMD (r=0.11, p=0.02) in men, higher CtTh and CtTh/TtAr in women (r=0.08 to 0.10, all p<0.05), and FEA failure load (r=0.10, p=0.02). In women, light PA was associated with lower TbN (r=-0.13, p=0.001) and increased TbTh (r=0.09, p=0.03). MVPA was not related to bone measures, except for a positive association with TbTh in men (r=0.11, p=0.02). Our findings provide new evidence that even light intensity activity benefits the adult skeleton. Lack of association of MVPA with bone may be due to low MVPA in our sample. In women, sedentary time results in greater TbN but lower TbTh

Association (partial correlation, r<sup>2</sup>) between time spent in sedentary, light, and moderate-to-vigorous physical activity evaluated by accelerometer and HR-pQCT bone outcomes at the distal tibia in men and women, Framingham Study (N=1,097)

	MEN (N=479)		WOMEN (N=618)			
	SEDENTARY (% of time)	LIGHT (% of time)	MVPA (min/day)	SEDENTARY (% of time)	LIGHT (% of time)	MVPA (min/day)
Cortical vBMD (CtVBMD, mg/cm <sup>3</sup> )	-0.07	0.07	0.02	-0.01	0.01	-0.01
Cortical porosity (CtPo, %)	0.04	-0.04	-0.02	-0.001	-0.004	0.005
Cortical thickness (CtTh, mm)	-0.06	0.08	-0.02	<b>-0.10**</b>	<b>0.10**</b>	0.04
Cortical thickness/total area (CtTh/TtAr, 1/mm)	-0.02	0.05	-0.03	-0.06	0.07	-0.001
Cortical bone area fraction (CtAr/TtAr)	-0.05	0.07	-0.02	-0.08	<b>0.08**</b>	0.01
Trabecular vBMD (TbvBMD, mg/cm <sup>3</sup> )	<b>-0.10**</b>	0.08	0.08	0.04	-0.03	-0.03
Trabecular number (TbN, 1/mm)	0.01	-0.001	-0.02	<b>0.14**</b>	<b>-0.14**</b>	-0.08
Trabecular thickness (TbTh, mm)	<b>-0.12**</b>	0.09	<b>0.11**</b>	<b>-0.09**</b>	<b>0.09**</b>	0.04
Total vBMD (TtvBMD, mg/cm <sup>3</sup> )	<b>-0.11**</b>	<b>0.11**</b>	0.05	0.03	0.04	-0.01
Total cross-sectional area (TtAr, mm <sup>2</sup> )	-0.01	-0.01	0.02	-0.06	0.04	0.08
FEA-estimated failure load (N)	<b>-0.12**</b>	<b>0.11**</b>	0.08	<b>-0.10**</b>	<b>0.10**</b>	0.06

\* Adjusted for age (y), height (in), weight (lb)

\*\* Significant at a p-value < 0.05

\*\*\* Averaged over 5 to 7 days

SEDENTARY = % of accelerometer wear time sedentary

LIGHT = % of accelerometer wear time spent doing light intensity physical activity

MVPA = minutes per day spent doing moderate to vigorous intensity physical activity

vBMD = volumetric bone mineral density

FEA = micro finite element analysis

HRpQCT = high resolution peripheral quantitative computed tomography

Table. Association between PA levels and HR-pQCT bone parameters

Disclosures: Amanda Lorbergs, None.

## 1130

### Functional Performances on Admission Predict Elderly Patients In-hospital Falls.

Marie-Claude Audet<sup>1</sup>, Mélanie Hars<sup>1</sup>, François Herrmann<sup>1</sup>, Alessandro de Sire<sup>1</sup>, Jean-Luc Reny<sup>2</sup>, Gabriel Gold<sup>3</sup>, René Rizzoli<sup>1</sup>, Serge Ferrari<sup>1</sup>, Andrea Trombetti\*<sup>1</sup>. <sup>1</sup>Division of Bone Diseases, Department of Internal Medicine Specialties, Geneva University Hospitals & Faculty of Medicine, Switzerland, <sup>2</sup>Division of Rehabilitation & Internal Medicine, Department of Internal Medicine, Rehabilitation & Geriatrics, Geneva University Hospitals & Faculty of Medicine, Switzerland, <sup>3</sup>Division of Geriatrics, Department of Internal Medicine, Rehabilitation & Geriatrics, Geneva University Hospitals & Faculty of Medicine, Switzerland

Falls are a leading cause of hospital admissions in older adults and a common adverse event during hospitalization. Early identification of inpatients at high risk for falls is a crucial first step toward the implementation of in-hospital proactive prevention strategies. In this prospective study, we aimed to determine the predictive and discriminative ability of various functional tests performed at or close to admission in a geriatric hospital to identify in-hospital fallers.

Patients consecutively admitted to a geriatric hospital were subjected to a battery of functional tests administered by physiotherapists, including: Short Physical Performance Battery (SPPB), Timed Up and Go (TUG), and simplified Tinetti tests (cut-off points: SPPB <6; Tinetti >2; TUG ≥20 sec). Falls during hospital stay were collected using standardized incident report forms. Univariate and multivariate logistic regression models were applied, and the overall discriminative ability of each functional test assessed.

Six hundred and forty seven patients (84.7 ± 6.9 years; 67% female) underwent a functional assessment administered within 4.5 ± 4.7 days of admission. During a mean length of hospital stay of 28 ± 23 days, 230 falls occurred in 134 patients (20.7%). In-hospital fallers displayed significantly poorer functional performances at admission on all tests, as compared to non-fallers (p < .001 for all). In univariate analysis, poorer functional performances had the strongest association with in-hospital falls compared with previous falls or fall as cause of admission. In multivariate analysis including age, sex, previous falls and fall as cause of admission (i.e., variables found to be significant in univariate models), poor performances on the SPPB (adjusted OR, 2.43; 95%CI, 1.04-5.67) and Tinetti (adjusted OR, 4.33; 95%CI, 1.70-11.06) were the only independent predictors of in-hospital falls. Also, poor performances on these tests remained the only significant predictors in stepwise linear regression models. The adjusted AUCs for SPPB and Tinetti performances as predictors of in-hospital falls were 0.71, with a significant incremental predictive value of adding both tests (p < .001).

Our study shows for the first time that poor functional performances, as assessed using the SPPB or the simplified Tinetti test, are significantly and independently associated with incident in-hospital falls in patients admitted to a geriatric hospital.

Disclosures: Andrea Trombetti, None.

## 1131

### A crosstalk between bone and muscle endocrine functions favors adaptation to exercise.

Paula Mera\*, Gerard Karsenty. Columbia University, United states

The bone-derived hormone osteocalcin increases muscle function during exercise in adult mice in part by increasing the uptake and utilization in myofibers of glucose and fatty acids, their main nutrients. To deepen our understanding of the mechanisms of action of osteocalcin on muscle, we performed a transcriptomic analysis after

exercise in muscles of control mice and in muscles of mice lacking osteocalcin signaling in muscle (*Gprc6a<sup>Mck-/-</sup>*). This analysis showed that the expression of a single myokine, interleukin-6 (IL-6), was decreased five fold in muscle of *Gprc6a<sup>Mck-/-</sup>* compared to those of control mice. The same was true albeit to a lesser extent for the expression in muscle of the IL-6 receptor. IL-6, one of the first myokines ever described, sees its circulating levels markedly increased during exercise through unknown mechanisms. IL-6 then favors adaptation to exercise through several means one of them being an increase in the production of glucose and fatty acids, the uptake of which is also enhanced by osteocalcin signaling in myofibers. We could show that the increase in circulating IL-6 levels during exercise does not occur to the same extent in *Osteocalcin-/-* and *Gprc6a<sup>Mck-/-</sup>* as it does in wild type (WT) mice, revealing that osteocalcin is the major regulator of *Il6* expression in muscle and that muscle is the main source of IL-6 found in the general circulation during exercise. Conversely, delivering exogenous osteocalcin to 15 month-old WT mice largely corrects their inability to increase circulating IL-6 levels during exercise. The analyses of osteocalcin signaling in WT and *Il6*-deficient myofibers and the use of a neutralizing antibody against IL-6 in WT mice concur to demonstrate that osteocalcin signaling in myofibers can occur regardless of the presence or absence of IL-6 in muscle or in the general circulation. In contrast, IL-6 favors the generation of undercarboxylated and bioactive osteocalcin in part by increasing the expression of *Rankl* and decreasing the expression of *Osteoprotegerin* in osteoblasts. This feed forward regulation explains why the increase in bone resorption markers and in the circulating levels of bioactive osteocalcin that is seen in WT mice during exercise is not observed in *Il6*-deficient mice. Taken together these data reveal the existence of a positive crosstalk between bone via osteocalcin, and muscle via IL-6, that is necessary and sufficient to allow adaptation to exercise in the mouse.

**Disclosures:** Paula Mera, None.

## 1132

**Intermittent PTH Treatment Induces Bone Anabolism Through Bone Marrow-Resident Regulatory Cells.** Mingcan Yu\*, Abdul Malik Tyagi, Chiara Vaccaro, Jonathan Adams, Emory Hsu, Roberto Pacifici. Emory University, United states

Intermittent PTH (iPTH) administration is the only approved bone anabolic treatment for osteoporosis but its detailed mechanism of action remains unknown. iPTH promotes the production of the osteogenic Wnt ligand Wnt10b by CD8+ cells, and the resulting activation of Wnt signaling in osteoblastic cells, is essential for PTH induced bone anabolism. Here we show that iPTH treatment (80µg/kg/day for 1-4 weeks) increases the differentiation of bone marrow (BM) induced regulatory T cells (iTregs), causing a ~3-fold increase in the number of BM-resident Tregs. To demonstrate relevance, Tregs were depleted in vivo by either treatment of WT mice with anti-CD25 Ab, or by using "depletion of regulatory T cells" (DEREG) mice. In both models in vivo depletion of Tregs prevents the capacity of iPTH to expand BM-resident Tregs, induce Wnt10b production, activate Wnt signaling, stimulate bone formation and increase bone mass. Mechanistically, Tregs block CD28 signaling in BM CD8+ cells by downregulating the costimulatory molecules CD80/86 on antigen presenting cells via their surface receptor CTLA4. Western blots and ChIP assays revealed that by blunting CD28 signaling, Tregs cause the activation of NFAT signaling but block AP-1 generation in BM CD8+ cells. Stimulation of CD8+ cells by iPTH in the presence of low AP-1 activation causes NFAT1/2 to partner with SMAD3, leading to the binding of NFAT1/SMAD3 and NFAT2/SMAD3 complexes to 3 binding sites in the Wnt10b promoter, which cause activation of Wnt10b gene expression. Promoter deletion studies revealed that deletion of the NFAT/SMAD binding site located at ~200 bp proximally to the transcription start site blocks iPTH induced Wnt10b gene expression, demonstrating that this NFAT/SMAD binding site is critical for Wnt10b gene transcription. In summary, these findings demonstrate a novel effect of PTH on the differentiation of Tregs. Expansion of BM-resident Tregs is a critical, previously unknown mechanism by which iPTH exerts its bone anabolic activity. Since biological agents have been developed to induce Treg expansion or inhibition of CD28 signaling, Tregs and CD28 may represent novel therapeutic targets for osteoporosis, or targets to potentiate the bone anabolic activity of PTH.

**Disclosures:** Mingcan Yu, None.

## 1133

**Augmented Fgf23 Secretion in Bone Locally Contributes to Impaired Bone Mineralization in Chronic Kidney Disease in Mice.** Olena Andrukhova\*<sup>1</sup>, Sibel Ada<sup>1</sup>, Sathish Kumar Murali<sup>1</sup>, Jessica Bayer<sup>1</sup>, William G Richards<sup>2</sup>, Reinhold G Erben<sup>1</sup>. <sup>1</sup>Department of Biomedical Sciences University of Veterinary Medicine, Austria, <sup>2</sup>Amgen Inc., United states

Chronic kidney disease-mineral and bone disorder (CKD-MBD) is a systemic disorder of mineral and bone metabolism caused by CKD. Impaired bone mineralization together with increased bony secretion of fibroblast growth factor-23 (FGF23) are typically found in CKD-MBD. We recently showed that FGF23 suppresses the expression of tissue nonspecific alkaline phosphatase (TNAP) in bone cells by a Klotho-independent, FGF receptor-3-mediated signaling axis, leading to the accumulation of the mineralization inhibitor pyrophosphate (PPi). Therefore, we hypothesized that excessive FGF23 secretion may locally impair bone mineralization in CKD-MBD. To elucidate further the pathophysiological role of Fgf23 and its

co-receptor Klotho in CKD-MDB, we used a dual approach, using murine genetic loss-of-function together with pharmacological inhibition models. CKD was induced by 5/6 nephrectomy in 3-mo-old wild-type (WT) mice, vitamin D receptor (VDR) mutant mice, *Fgf23<sup>-/-</sup>/VDR<sup>Δ/Δ</sup>* (Fgf23/VDR), and *Klotho<sup>-/-</sup>/VDR<sup>Δ/Δ</sup>* (Klotho/VDR) compound mutant mice. In addition, Sham-operated and CKD WT, VDR, and Klotho/VDR mice were treated with low dose anti-FGF23 antibody (anti-FGF23Ab, 50 µg per mouse, twice weekly) over 8 weeks post-surgery. This dose of anti-FGF23Ab reduced the elevated levels of circulating Fgf23 in CKD mice to Sham control levels. Treatment of WT, VDR and Klotho/VDR CKD mice with anti-FGF23Ab protected against the CKD-induced decrease in total, trabecular and cortical BMD observed in vehicle-treated CKD mice, 8 weeks post-surgery. TNAP mRNA expression as evidenced by laser capture microdissection in cryosections as well as TNAP enzyme activity measured by histochemistry in plastic sections were suppressed in femoral osteoblasts and osteocytes of WT, VDR, and Klotho/VDR CKD mice, but not Fgf23/VDR CKD mice, relative to Sham controls. Conversely, the bone PPI concentration was increased 3-4-fold in WT, VDR, and Klotho/VDR CKD compared with Sham mice. The suppression of TNAP mRNA abundance and enzyme activity as well as the increase in osteocyte lacunar size were normalized by anti-FGF23Ab treatment in WT, VDR, and Klotho/VDR CKD animals. Collectively, our data suggest that elevated Fgf23 production in bone contributes to the mineralization defect in CKD-MDB by auto-/paracrine suppression of TNAP and subsequent accumulation of PPI in bone. Hence, our study has identified a novel mechanism involved in the pathogenesis of CKD-MBD.

**Disclosures:** Olena Andrukhova, None.

## 1134

**Proximal Tubule-Specific Ablation of  $\alpha$ Klotho Reproduces the Abnormalities of Mineral Metabolism Caused by Systemic  $\alpha$ Klotho KO.** Ai Takeshita\*<sup>1</sup>, Kazuki Kawakami<sup>1</sup>, Jin Nakamura<sup>2</sup>, Kenryo Furushima<sup>1</sup>, Masayasu Miyajima<sup>3</sup>, Motoko Yanagita<sup>2</sup>, Kazushige Sakaguchi<sup>1</sup>. <sup>1</sup>Department of Molecular Cell Biology & Molecular Medicine, Institute of Advanced Medicine, Wakayama Medical University, Japan, <sup>2</sup>Department of Nephrology, Kyoto University Graduate School of Medicine, Japan, <sup>3</sup>Laboratory Animal Center, Wakayama Medical University, Japan

[Background and Aims]  $\alpha$ Klotho is predominantly expressed in renal tubules, parathyroid glands and choroid plexus, and functions as a co-receptor required for FGF receptors to bind to FGF23. The FGF23/ $\alpha$ Klotho/FGFR signal plays important roles in the mineral metabolism. The most prominent roles in the kidney are inhibition of the type 2a and 2c sodium/phosphate cotransporters and suppression of 25-hydroxyvitamin D 1 $\alpha$  hydroxylase (Cyp27b1). These cotransporters and Cyp27b1 are located in the proximal tubules, whereas the expression of  $\alpha$ Klotho is very low in this part of the nephron in contrast to its high expression in the distal tubules. These discrepancies in molecular abundance and localization suggest a possibility that a soluble form of  $\alpha$ Klotho released from the distal tubules might be responsible for the function. To examine whether  $\alpha$ Klotho in the proximal tubules is functionally important for mineral metabolism, we studied the effect of postnatal ablation of  $\alpha$ Klotho specifically from the proximal tubules. [Methods] We generated  $\alpha$ Klotho flox mice by inserting *loxP* sequences surrounding the 2nd exon, and these were mated with mice expressing a transgene for tamoxifen-inducible proximal tubule-specific Cre recombinase, *Ndrp1-CreERT2* ( $\alpha$ Klotho<sup>flox/flox</sup>; *Ndrp1-CreERT2*). We injected tamoxifen intraperitoneally to 6-week-old mice for 5 consecutive days to induce activation of Cre recombinase, and generated mice with  $\alpha$ Klotho conditionally knocked out from the proximal tubules (cKO). As controls, we used mice expressing  $\alpha$ Klotho<sup>flox/flox</sup> alone and heterozygous  $\alpha$ Klotho flox mice coexpressing the Cre transgene ( $\alpha$ Klotho<sup>flox/+</sup>; *Ndrp1-CreERT2*). [Results]  $\alpha$ Klotho cKO induced growth suppression and short life span. In the cKO mice of 9 weeks of age, plasma levels of phosphate, calcium, 1,25(OH)<sub>2</sub>D and FGF23 were significantly up-regulated and PTH level was remarkably down-regulated compared with control groups. Micro-CT analysis revealed reduced femoral bone mineral density and bone mineral content in the cKO mice. We also found calcification of small blood vessels with Von Kossa staining in the kidney. These changes were not observed in the control mice. [Conclusion] Proximal tubule-specific  $\alpha$ Klotho cKO mice show phenotypes resembling the systemic KO mice of  $\alpha$ Klotho or *Fgf23*.  $\alpha$ Klotho in the proximal tubules, although the expression level is low compared with that in the distal tubules, plays a critical role in the renal regulation of mineral metabolism.

**Disclosures:** Ai Takeshita, None.

## 1135

**TGF $\beta$ -Induced Wnt1 Secretion by Osteoclasts Promotes Osteocyte Viability In Vivo.** Megan Weivoda\*<sup>1</sup>, Stephanie Youssef<sup>1</sup>, Ming Ruan<sup>1</sup>, Christine Hachfeld<sup>1</sup>, Glenda Evans<sup>1</sup>, Rachel Davey<sup>2</sup>, Jeffrey Zajac<sup>2</sup>, Brendan Lee<sup>3</sup>, Mark Johnson<sup>4</sup>, Lynda Bonewald<sup>5</sup>, Jennifer Westendorf<sup>1</sup>, Sundeep Khosla<sup>1</sup>, Merry Jo Oursler<sup>1</sup>. <sup>1</sup>Mayo Clinic, United states, <sup>2</sup>University of Melbourne, Australia, <sup>3</sup>Baylor College of Medicine, United states, <sup>4</sup>University of Missouri Kansas City, United states, <sup>5</sup>UMKC, United states

During healthy bone remodeling osteoclast-mediated bone resorption is coupled to bone formation. We previously demonstrated that this coupling is disrupted in mice

with impaired osteoclast TGF $\beta$  signaling (osteoclast specific dominant negative TGF $\beta$  receptor 2, Tgfr2<sup>OelKO</sup>) leading to reduced trabecular bone volume. TGF $\beta$  induces the expression of several candidate coupling factors in osteoclasts; the most highly induced factor is Wnt1, of which depletion has been implicated in osteogenesis imperfecta and early-onset osteoporosis. Therefore, we hypothesized that osteopenia in Tgfr2<sup>OelKO</sup> mice is due to reduced osteoclast-derived Wnt1. To test this hypothesis, we generated osteoclast-specific Wnt1 knockout mice (CtskCre, Wnt1<sup>ff</sup>; Wnt1<sup>OelKO</sup>). Dual-energy X-ray absorptiometry showed significantly reduced BMD at the femur and vertebra in both male and female Wnt1<sup>OelKO</sup> mice at 6 and 12 weeks. Animals were sacrificed at 22 weeks. MicroCT analysis revealed significantly reduced cortical thickness (Ct.Th) and cortical area (Ct.Ar) in male Wnt1<sup>OelKO</sup> femurs, with significant increases in porosity in femurs and vertebrae. Female Wnt1<sup>OelKO</sup> mice exhibited reduced Ct.Th in the vertebrae and decreased Ct.Ar in femurs and vertebrae, with increased porosity in the vertebrae. Female, but not male Wnt1<sup>OelKO</sup> femurs also had a significant reduction in trabecular BV/TV. Dynamic histomorphometry of female Wnt1<sup>OelKO</sup> femur metaphyses revealed a significant reduction in BFR/TV, consistent with the Tgfr2<sup>OelKO</sup> phenotype. Because of the strong cortical phenotype in the Wnt1<sup>OelKO</sup>, we assessed the cortical phenotype in female Tgfr2<sup>OelKO</sup> vertebrae and found a similar reduction in Ct.Th and Ct.Ar. TUNEL staining of female femurs revealed significant increases in apoptotic osteocytes in both Tgfr2<sup>OelKO</sup> and Wnt1<sup>OelKO</sup> mice. To determine whether osteoclast TGF $\beta$  signaling directly affected osteocyte viability, primary osteocytes were pre-treated with conditioned media (CM) from TGF $\beta$  or vehicle treated osteoclasts for 1hr, followed by treatment with 1mM dexamethasone (DEX) for 8hrs. Quantification of apoptotic nuclei revealed that TGF $\beta$  treated osteoclast CM, but not vehicle CM or TGF $\beta$  alone, prevented DEX-induced osteocyte apoptosis. Together, these data show that loss of osteoclast-derived Wnt1 partially phenocopies the Tgfr2<sup>OelKO</sup> bone phenotype. Importantly, these data demonstrate for the first time that osteoclast TGF $\beta$  signaling and subsequent Wnt1 secretion promote osteocyte viability.

**Disclosures:** Megan Weivoda, None.

## 1136

**Sensory Nerve Block Accelerates Bone Loss Induced by Peripheral Nerve Injury.** Allison Dawson<sup>\*1</sup>, Brandon Ausk<sup>1</sup>, Philippe Huber<sup>2</sup>, Edith Gardiner<sup>1</sup>, Leah Worton<sup>1</sup>, Dewayne Threet<sup>1</sup>, Sundar Srinivasan<sup>1</sup>, Ted Gross<sup>1</sup>, Steven Bain<sup>1</sup>. <sup>1</sup>Department of Orthopaedics, University of Washington, United states, <sup>2</sup>Department of Orthopaedics, University of Washington, United states

Peripheral nerve injury (PNI) in mice induces significant ipsi- and contralateral bone loss. Further, contralateral bone loss induced by PNI is attenuated in TRPV1 knockout mice, which have a sensory nerve deficit. As these data and the literature suggest a role for sensory innervation in bone homeostasis, we hypothesized that a sensory nerve block (SNB) would mitigate bone loss following PNI. To test this hypothesis, sixteen-week-old C57/B16 female mice (n=8/group) underwent baseline micro-CT scans of both the right and left proximal tibia and were then randomized to one of 2 groups: 1) PNI of the right sciatic nerve + SNB (PNI-SNB; 0.125% N-methyl amiripryline plus 0.05% capsaicin); 2) PNI of right sciatic nerve + vehicle (PNI-V). MicroCT scans were then performed at 5, 12, and 28 days post PNI to assess bone changes. In addition, mice underwent gait analysis (kinetics and kinematics) to control for effects of PNI-V and/or PNI-SNB on gait-induced loading. As expected, PNI-V induced significant ipsi- and contralateral bone loss within 12 d post-injury (-28.7 and -20.7%, respectively, p<0.05), that progressed to a -35.9% and -29.3% decline by d 28. Surprisingly, and in contrast to our hypothesis, PNI-SNB induced more rapid and profound ipsilateral bone loss compared to PNI-V, reaching -33.4% by d 5 (vs. -12.4% at d 5 in PNI-V; p<0.05) and -49.7 by d 12 (vs. -28.7% in PNI-V; p<0.05). Bone loss in the contralateral limb of PNI-SNB mice was essentially equivalent to PNI-V (less than 2% difference at any time point). Finally, as neither peak ground reaction forces nor gait kinematics were altered in either group, mechanical loading would not appear to be responsible for the observed bone loss. In summary, we now speculate that SNB interacts with PNI to accelerate bone loss via antidromic activation of sensory nerve pathways. In this context, antidromic activation of sensory nerves is known to induce neurogenic inflammation via the release of CGRP and Substance P, two neurotransmitters known to be potent modulators of bone homeostasis. Future studies will therefore seek to use our PNI model to explore the relative influence of CGRP and Substance P signaling on ipsi- and contralateral bone loss following nerve injury or in conditions characterized by sensory nerve deficits.

**Disclosures:** Allison Dawson, None.

## 1137

**Alternative NF- $\kappa$ B Activation in the Mesenchymal Lineage Increases Bone Mass and Drives a Subcutaneous Sarcoma.** Jennifer Davis<sup>\*</sup>, Deborah Novack. Washington University School of Medicine, United states

Bone phenotypes of animals with global deficiencies suggest that alternative NF- $\kappa$ B is a cell-intrinsic negative regulator of osteogenesis, and NIK is the upstream kinase required for its activation. To further explore the role of this pathway in bone, we used NIKD3 (NT3) mice, which bear a constitutively active, lox-Stop-lox allele of NIK placed in the ROSA26 locus crossed with a doxycycline (dox) repressible

Osx-Cre line. Osx-Cre; NT3<sup>+/+</sup> (cACT) mice were generated to activate alt NF- $\kappa$ B signaling in the osteoblast (OB) lineage. Recombination was induced by dox withdrawal at weaning, and controls (CON) were Cre negative littermates.

Consistent with global KO studies, levels of collagen Ia and osteocalcin were severely blunted in cACT OB cultures. However, microCT analysis of 16 week old male and female cACT mice showed a significant increase in both trabecular (e.g. +35% BV/TV in females) and cortical (e.g.+20% Ct.Th in males) parameters compared to CON, a finding opposite to the expected decrease in bone mass. Furthermore, cACT animals showed an enhanced bone formation in response to mechanical anabolic stimulus, with approximately twice Ps.BFR/BS after axial tibial compression for 14 days.

Unexpectedly, both male and female cACT animals developed spontaneous, subcutaneous, soft tissue tumors beginning at 4 months, with all mice (n>100) developing tumors by 7 months of age. Age-matched CON mice never developed tumors, including an aged cohort (n=10) at 1 year. Tumors most often occurred at the neck, but were noted at multiple sites. Recombination of the transgene as well as Osx and Cre expression in the tumor were confirmed by qRT-PCR. Immunohistochemistry revealed robust expression of  $\alpha$ -smooth muscle actin, GFP, and vimentin but low expression of cytokeratin 19, a pattern consistent with a transgene-driven subcutaneous sarcoma.

In summary, although expression of activated NIK in cultured OBs reduced osteogenesis, cACT mice (expressing activated NIK under control of the Osx promoter) showed a surprising increase in basal bone mass as well as enhanced bone formation after *in vivo* loading. Furthermore, activated NIK behaves as an oncogene in subcutaneous mesenchymal cells, driving sarcoma formation. Taken together, these results indicate that the role of alternative NF- $\kappa$ B in the mesenchymal lineage *in vivo* is complex and is not limited to anti-osteogenic effects.

**Disclosures:** Jennifer Davis, None.

## 1138

**HYPOXIA-INDUCIBLE FACTOR 2a IS A NEGATIVE REGULATOR OF OSTEOBLASTOGENESIS.** Kavitha Ranganathan<sup>\*1</sup>, Christophe Merceron<sup>2</sup>, Angela Yao<sup>1</sup>, Laura Mangiavini<sup>3</sup>, Amato Giaccia<sup>4</sup>, Benjamin Levi<sup>5</sup>, Ernestina Schipani<sup>1</sup>. <sup>1</sup>University of Michigan Health Systems, Orthopedic Research Laboratories, United states, <sup>2</sup>University de Nantes France, France, <sup>3</sup>San Raffaele International, Italy, <sup>4</sup>Stanford University, United states, <sup>5</sup>University of Michigan Health Systems, United states

The hypoxia-signaling pathway is a regulator of bone mass. Hypoxia inducible factor-1a (HIF-1a) and HIF-2a are critical components of this pathway. While the role of HIF-1a in bone is actively investigated, the contribution of HIF-2a to the control of bone mass accrual and homeostasis is still poorly understood. We generated mice conditionally overexpressing a mutant HIF-2a protein (HIF-2adPA) that is constitutively stabilized regardless of oxygen tension in mesenchymal progenitors and in their descendants using PRX1Cre mice. Analysis of long bones isolated from PRX1Cre:HIF-2adPA mice revealed a dramatic augmentation in trabecular bone at both 6 and 12 weeks of age and in both sexes in mutants when compared to controls. In agreement with previous findings, bone resorption was impaired in mutants, as shown by the persistence of cartilage remnants within bony trabeculae of adult mutant bones. Strikingly, the numbers of active osteoblasts *in vivo*, bone formation rates, osteogenic differentiation of bone marrow stromal cells *in vitro*, and expression of the master transcription factor of osteoblastogenesis Osterix, were all significantly reduced upon overexpression of HIF-2adPA. Conversely, however, there was an increased number of bone marrow stromal cells within the bone marrow of PRX1Cre:HIF-2adPA mutant bones when compared to controls. Consistent with this latter finding, vascular endothelial growth factor -A (VEGF) was augmented in mutant osteoblastic cells. VEGF is a downstream target of the HIFs, and increased levels of VEGF in cells of the osteoblast lineage have been previously associated with higher bone marrow stromal cell number. Augmenting the number of bone marrow stromal cells, and thus of osteoblast precursors, could in some way counterbalance the HIF-2a inhibitory effect on osteoblast differentiation. In summary, our findings indicate that: 1) overexpression of HIF-2a in cells of the osteoblast lineage results in a net increase of trabecular bone, which is accompanied by an impairment of both formation and resorption; 2) overexpression of HIF-2 expands the pool of osteoblast precursors, but, at the same time, impairs their osteogenic differentiation through direct effect on these cells. These findings establish HIF-2a as a negative regulator of osteoblastogenesis, and represent a paradigm shift as, to this end, activation of the hypoxia signaling pathway has been associated with stimulation, as opposed to inhibition, of bone formation.

**Disclosures:** Kavitha Ranganathan, None.

1139

**Control of skeletal development by the histone methyltransferase Ezh2 in mesenchymal progenitor cells, osteoblasts and chondrocytes.** Amel Dudakovic\*<sup>1</sup>, Emily Camilleri<sup>1</sup>, Meghan McGee-Lawrence<sup>2</sup>, Elizabeth Bradley<sup>1</sup>, Christopher Paradise<sup>1</sup>, Martina Gluscevic<sup>1</sup>, Roman Thaler<sup>1</sup>, Gary Stein<sup>3</sup>, Martin Montecino<sup>4</sup>, Jennifer Westendorf<sup>1</sup>, Andre van Wijnen<sup>1</sup>. <sup>1</sup>Mayo Clinic, United states, <sup>2</sup>Augusta University, United states, <sup>3</sup>University of Vermont College of Medicine, United states, <sup>4</sup>Universidad Andres Bello, Chile

Skeletal development is regulated by epigenetic mechanisms such as microRNAs, DNA methylation, and post-translational modification of histones that control both chondrogenic and osteogenic differentiation. Previous work has demonstrated that enhancer of zeste homolog 2 (Ezh2), a histone 3 lysine 27 (H3K27) methyltransferase, suppresses differentiation of osteogenic progenitors. Inhibition of Ezh2 is bone anabolic in wild type mice and osteo-protective in ovariectomized animals in part because decreased Ezh2 activity enhances osteogenic and impedes adipogenic differentiation of mesenchymal stem cells. Here, we compare conditional deletion of functional Ezh2 (cKO) to wild type (WT) in mice in three mesenchymal compartments: uncommitted mesenchymal cells (Ezh2-cKO<sup>trix1</sup>), osteoblasts (Ezh2-cKO<sup>osb</sup>) and chondrocytes (Ezh2-cKO<sup>col2a1</sup>). The conditional allele of Ezh2 spans exons 16-19 (SET domain, methyltransferase activity) and recombination of this allele renders Ezh2 inactive. We demonstrate that loss of Ezh2 protein reduces H3K27 trimethylation in vitro and in vivo. While conditional genetic loss of Ezh2 in uncommitted mesenchymal cells results in multiple skeletal patterning and bone defects, including shortened forelimbs, craniosynostosis and clinodactyly, these phenotypic abnormalities are not evident when Ezh2 is deleted in the osteoblast or cartilage-lineage. Histological analysis and mRNA-seq profiling suggests that effects of Ezh2 loss in mesenchymal cells are attributable to growth plate abnormalities and premature cranial suture closure due to precocious maturation of osteoblasts. However, deletion of functional Ezh2 in the osteoblast lineage generates a low bone mass phenotype (33.3% reduction in BV/TV, tibias) at weaning (3 weeks) that is less prominent in early adulthood (8 weeks) and fully resolved when mice are skeletally mature (12 weeks). Anatomical and radiographic analysis of cartilage-specific deletion of Ezh2 reveals no skeletal abnormalities (at 4 or 8 weeks), but  $\mu$ CT analysis of tibias (4 weeks) from cKO mice revealed a 42.8% reduction in trabecular bone volume (BV/TV) that resolved by adulthood (8 and 24 weeks), similar to osteoblast inactivation. Thus, Ezh2 inactivation in mesenchymal compartment affects early cartilage and bone development, while osteoblast and cartilage deletion of this epigenetic regulator alters bone quality in young animals.

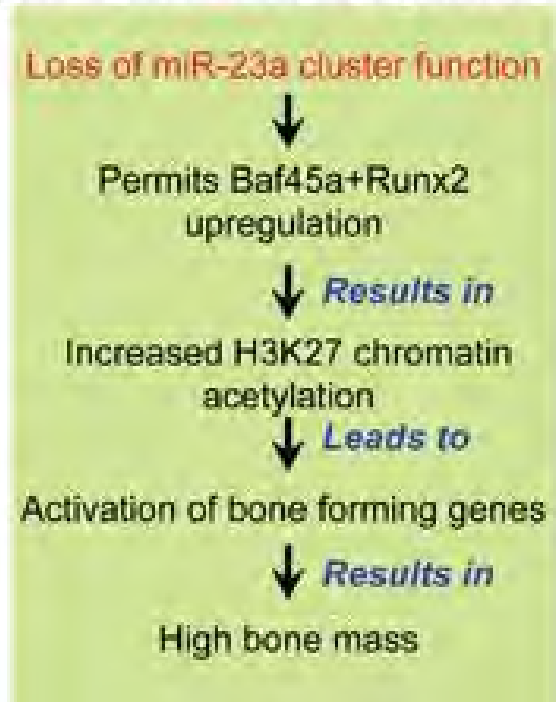
**Disclosures:** Amel Dudakovic, None.

1140

**MiR-23a-cluster Regulates BAF45a to Control a Tissue-specific Epigenetic Mechanism for Bone Formation.** Mohammad Hassan\*, Tanner Godfrey, Harunur Rashid, Amjad Javed. School of Dentistry, University of Alabama, United states

As over 53 million adults in the United States have low bone mass due to arthritis and osteoporosis, novel therapeutic strategies that protect from progressive and chronic bone loss are clearly warranted. The purpose of the proposed research is to refine our central hypothesis that the miR-23a cluster controls bone synthesis and homeostasis by regulating osteoblast-specific transcription factor Runx2 and chromatin remodeling factor BAF45a/PHF10 expression. Current studies do not have any insight on how epigenetic activation by histone acetylation of bone-specific chromatin is maintaining bone mass in vivo. Understanding of this gap is pivotal for further studies to identify specific targets for future therapies, which protect against bone loss. Gene regulation by microRNAs (miRNAs or miRs) is a key regulatory event in many biologic processes including skeletogenesis. Recently, we found that miR-23a cluster represses Runx2 expression, inhibits osteoblast-specific genes, and finally blocks osteoblast differentiation in vitro. However, the inhibitory role of miR-23a cluster during the development and remodeling of bone and the chromatin repression mechanism, leading to this inhibition of essential genes required for bone formation, is unrevealed. To study the role of miR-23a cluster in bone synthesis, we created an inducible miR-23a cluster knockdown mouse model (miR-23aC<sup>ZIP</sup>). Interestingly, our knockdown mice developed high cortical and trabecular bone. RNA sequencing from these mice significantly increased the expression of Runx2, and BAF45a/PHF10. Furthermore, we observed that BAF45a interacted with RUNX2, and together promote osteoblastogenesis. Osteoblast-specific BAF45a knockdown mice (BAF45a<sup>fl</sup>, osteocalcin<sup>cre</sup>) significantly reduced bone development. Knockdown of BAF45a in miR-23a cluster-depleted osteoblasts re-established miR-23a cluster-mediated inhibition, established a direct regulatory link to govern osteogenesis. ChIP assays with bone essential promoters using differentiated miR-23aC<sup>ZIP</sup> calvarial cells revealed higher BAF45a/PHF10 binding and H3K27 acetylation when compared with H3K27 methylation. Together, our findings strongly suggest that H3K27 acetylation of the bone-specific open chromatin is a key chromatin modification event for enhanced osteogenesis.

## Epigenetic mechanism for high bone mass



Baf45a ASBMR Poster.png

**Disclosures:** Mohammad Hassan, None.

1141

**RCOR2/LSD1 Regulatory Node in the Epigenetic Control of Osteoblast Differentiation.** Kati Tarkkonen\*<sup>1</sup>, Rana Al Majidi<sup>1</sup>, Cristina Valensisi<sup>2</sup>, Petri Rummukainen<sup>1</sup>, Lauri Saastamoinen<sup>1</sup>, David Hawkins<sup>3</sup>, Riku Kiviranta<sup>4</sup>. <sup>1</sup>Department of Medical Biochemistry & Genetics, University of Turku, Turku, Finland, Finland, <sup>2</sup>Division of Medical Genetics, Department of Medicine, Department of Genome Sciences, Institute for Stem Cell & Regenerative Medicine, University of Washington School of Medicine, Seattle, USA, United states, <sup>3</sup>Division of Medical Genetics, Department of Medicine, Department of Genome Sciences, Institute for Stem Cell & Regenerative Medicine, University of Washington School of Medicine, Seattle, USA & Turku Centre for Biotechnology, Turku, Finland, United states, <sup>4</sup>Department of Medical Biochemistry & Genetics, University of Turku, Turku, Finland & Division of Endocrinology, Turku University Hospital, Turku, Finland, Finland

Epigenetic mechanisms regulating osteoblast differentiation are still poorly known. In a global transcriptional profiling of MC3T3-E1 osteoblastic cells, we identified RCOR2 as a significantly upregulated gene during differentiation from proliferative to mature osteoblasts. Similar expression profile of RCOR2 was found in mouse primary osteoblasts. RCOR2 belongs to the CoREST/RCOR family of proteins that regulate the action of lysine-specific histone demethylase 1 (LSD1). LSD1 controls gene expression e.g. by demethylating histone H3K4me1/2, leading generally to gene repression. shRNA-mediated silencing of RCOR2 expression in MC3T3-E1 or primary calvarial osteoblasts led to impaired osteoblastic differentiation shown by decreased ALP staining and number of mineralized bone nodules, and reduced the expression of osteoblastic genes including ALP, OSX and OCN. To identify genes and pathways associated with RCOR2 action, we performed RNA-seq analysis of MC3T3-E1-shRCOR2 cells. GO pathway analysis showed upregulation of genes related to cellular metabolism and embryonic morphogenesis in shRCOR2 cells, suggesting RCOR2 to repress these pathways at the onset of differentiation.

LSD1 is abundantly expressed in MC3T3-E1 cells and we showed that RCOR2 and LSD1 co-immunoprecipitated in HEK293T cells. Inhibition of LSD1 activity with small molecular inhibitors S2101 and RN-1 suppressed MC3T3-E1 and primary calvarial cell differentiation, similarly to silencing of RCOR2. The interplay of LSD1 and RCOR2 was further supported by showing that in MC3T3-E1 cells LSD1 regulates expression of a set of genes differentially expressed in shRCOR2 cells. Silencing of RCOR2 did not lead to changes in global H3K4me1/2 levels suggesting that RCOR2/LSD1 complex targets specific promoters. Using our genome-wide H3K4me1 ChIP-seq map of MC3T3-E1 cells, we identified putative enhancer regions in a panel of shRCOR2 affected genes and tested them for H3K4me1 occupancy in shRCOR2 and control cells by ChIP. We observed alterations in H3K4me1 levels

relative to total histone H3 occupancy in RCOR2 knockdown cells, indeed suggesting changes in LSD1 activity at specific genomic sites.

In conclusion, we have identified RCOR2 as a novel regulator of osteoblast differentiation. Moreover, our data strongly suggest RCOR2/LSD1 complex to have important role in controlling osteoblastic phenotype, adding to the growing evidence of histone demethylases being crucial players in osteogenesis.

**Disclosures:** Kati Tarkkonen, None.

## 1142

**Gpmb/Osteoactivin Plays a Novel Role in Autophagy-Mediated Osteoblast Differentiation and Function.** Fatima Jaber<sup>1</sup>, Gregory Sondag<sup>2</sup>, Mohammad Ansari<sup>2</sup>, Fouad Moussa<sup>2</sup>, Asaad Al-Adlaan<sup>1</sup>, Fayez Safadi<sup>2</sup>.

<sup>1</sup>Kent State University, United states, <sup>2</sup>Northeast Ohio Medical University, United states

Autophagy plays an important role in bone homeostasis where it regulates both osteoblast and osteoclast differentiation and function. Glycoprotein nmb (Gpmb), also called osteoactivin (OA) is a novel protein discovered in our lab that positively regulates osteoblast and negatively regulates osteoclast differentiation and function. Recent evidence has shown that Gpmb/OA binds to microtubule-associated protein light chain 3 (LC-3), a marker indicative of autophagic activity and stimulates the recruitment and formation of autophagosomes. In this study, we investigated whether Gpmb/OA regulates osteoblast differentiation and function by mediating the autophagy pathway. First, we examined the expression of Gpmb/OA in osteoblast following induction of autophagy. MC3T3-E1 and primary osteoblasts were treated with Trehalose (TH), an mTOR-independent autophagy enhancer. TH treatment induces mRNA and protein expression of autophagy markers including *ATG5*, *ATG7*, *LC3* and *Beclin-1* as well as Gpmb/OA in a dose- and time-dependent manner. Next, we assessed the effect of TH treatment on autophagosome formation using transmission electron microscopy (TEM) analysis and found that TH treatment causes induction of autophagosome formation associated with the formation of double membrane autophagic vesicles compared to untreated control cells. To determine whether Gpmb/OA binds LC3 in osteoblasts, MC3T3-E1 and primary osteoblast cells were transfected with either GFP-LC3 or control empty vector (GFP-EV) followed by TH treatment. Immunofluorescent analysis revealed that osteoblasts treated with TH display a punctate distribution of LC3 that co-localized with Gpmb/OA compared to untreated cells, suggesting a role of Gpmb/OA in autophagy in osteoblasts. Next, we examined the expression of autophagy markers in bones and osteoblast derived from Gpmb/OA mutant (D2J) mice and found that *ATG5*, *ATG7*, *LC3* expression were downregulated in mutant compared to WT mice. These markers were correlated with a significant reduction of markers of osteoblast differentiation and matrix mineralization. Next, we examined the ability of osteoblast-derived from Gpmb/OA mutant mice to induce autophagy in response to TH treatment. Gpmb/OA mutant osteoblasts showed significant reduction in the expression of autophagy markers associated with *LC3*, *ATG5*, *ATG7* and *Beclin-1* in response to TH treatment when compared to WT TH-treated osteoblasts. Furthermore, ultrastructure analysis showed defective autophagosome formation in Gpmb/OA mutant compared to WT osteoblasts, while overexpression of Gpmb/OA in mutant osteoblasts rescued autophagy pathway and autophagosome formation. These data suggest that Gpmb/OA regulates osteoblast differentiation and function, at least in part, through the autophagy pathway. This study is the first to report a role of Gpmb/OA in autophagy in bone.

**Disclosures:** Fatima Jaber, None.

## 1143

**Blockade of the Activity of the Osteocytic PTH Receptor Target Gene MMP14: a Therapeutic Tool to Prevent Bone Loss and Potentiate Bone Gain Induced by PTH.** Jesus Delgado-Calle<sup>\*</sup>, Benjamin Hancock, Kevin McAndrews, Lilian I Plotkin, Teresita Bellido. Department of Anatomy & Cell Biology, Indiana University School of Medicine, United states

PTH increases bone turnover leading to either bone gain or bone loss depending on the mode and duration of its elevation. Matrix metalloproteinase 14 (MMP14) is a novel target of PTH, and earlier work demonstrated that inhibition of its activity with the highly specific KD014 neutralizing antibody decreases bone resorption and remodeling in mice with constitutive activation of the PTH receptor in osteocytes (caPTHr1). We examined here whether KD014 alters bone catabolism or anabolism induced by PTH. KD014 (30 mg/kg, sc 3xwk, n=10) or saline was administered to 4-month-old mice either 1) fed normal (0.4%) or low (0.01%) Ca diet to increase endogenous PTH for 2wks; or 2) receiving daily injections of PTH (iPTH, 100 ng/g/day) or vehicle for 4wks. The increase in endogenous PTH induced by the low Ca diet (~50%) was not affected by KD014. However, KD014 prevented by 50% the decrease in spinal BMD and blocked completely the increase in circulating CTX and PINP induced by low Ca. Further, iPTH increased spinal and femoral BMD (16, 15, and 20% change vs vehicle), and co-administration of KD014 potentiated the increase in BMD in the spine (25% vs vehicle) but not in the femur. Moreover, combined administration of iPTH and KD014 increased cancellous (L4 and distal femur) bone volume (BV/TV) over iPTH alone (49 vs 37%), but did not alter the increase in femoral cortical bone area (BA/TA; %) induced by iPTH. iPTH alone did not alter

serum CTX or the number/surface of osteoclasts in cancellous bone; in contrast, co-administration of KD014 reduced serum CTX (-40%) and decreased osteoclast number/surface (-21%) below the values exhibited by mice treated with iPTH alone. Importantly, the increase in circulating PINP (37%), mineral apposition (20%) and bone formation (19%) rates induced by iPTH in cancellous bone remained unchanged by co-administration of KD014. Moreover, KD014 administered to vehicle-treated mice increased spinal BMD (4%) but not femoral BMD, increased cancellous BV/TV but not cortical BA/TA, and decreased CTX (-25%). In addition, sRANKL and CTX were increased in culture media from ex vivo organ cultures established from caPTHr1 mice bones, and KD014 decreased sRANKL to WT levels and reduced CTX by 23%. We conclude that pharmacological inhibition of MMP-14 activity prevents the catabolic and potentiates the anabolic skeletal actions of PTH by decreasing sRANKL production and inhibiting bone resorption.

**Disclosures:** Jesus Delgado-Calle, None.

## 1144

**Rorβ Deletion Stimulates Bone Formation and Inhibits Bone Resorption in Aged Mice by Activating Wnt Signaling and Increasing Opg Expression.**

Joshua Farr<sup>\*1</sup>, Kristy Nicks<sup>1</sup>, Megan Weivoda<sup>1</sup>, Elizabeth Atkinson<sup>2</sup>, Sundeep Khosla<sup>1</sup>, David Monroe<sup>1</sup>. <sup>1</sup>Division of Endocrinology, Mayo Clinic College of Medicine, United states, <sup>2</sup>Division of Biomedical Statistics & Informatics, Mayo Clinic College of Medicine, United states

Identifying novel approaches to treat skeletal disorders requires understanding how critical factors regulate osteoblast differentiation and bone remodeling throughout the lifespan. We have previously shown that retinoic acid receptor-related orphan receptor β (Rorβ) negatively regulates osteoblast differentiation and is highly elevated in bone marrow-derived mesenchymal stromal cells (BMMSCs) with aging in both mice and humans. To further elucidate the role of Rorβ in osteoblasts, we used the CRISPR/Cas9 system to delete Rorβ in MC3T3 preosteoblastic cells (ΔRorβ). Comparisons between differentiated ΔRorβ and control cells using whole transcriptome RNAseq and pathway analyses revealed that loss of Rorβ dramatically increased the expression of several osteoblast lineage genes and enhanced the Wnt pathway (i.e. increased expression of *Lef1*, *Tcf7* and *Opg*). These results were further supported by transcription factor binding site analyses, which demonstrated that the promoters of genes regulated in the ΔRorβ cells were highly enriched for *Lef1* binding sites. We then used transfection analysis in combination with Wnt-reporters to show that Rorβ inhibited both β-catenin- and *Lef1*-dependent activation of Wnt signaling, and used Rorβ siRNAs to show inhibition of *Opg* expression. Collectively, these data suggest that Rorβ plays an inhibitory role in osteoblastic differentiation by modulating the Wnt pathway. We next extended on these *in vitro* findings as well as our observation that Rorβ expression increases *in vivo* in BMMSCs with aging by examining the effects of *in vivo* global deletion of Rorβ (Rorβ<sup>-/-</sup>) on the murine skeleton in the setting of chronological aging. Compared to age-matched (12-month) littermate controls, global deletion of Rorβ significantly enhanced trabecular bone microarchitecture at both the femoral metaphysis and lumbar spine (Fig 1), but had no apparent effect on cortical bone. Histological analyses demonstrated that Rorβ<sup>-/-</sup> mice had markedly increased osteoblast numbers and bone formation rates, with concomitant decreases in osteoclast numbers and bone eroded surface. These data demonstrate that loss of Rorβ both *in vitro* and *in vivo* has beneficial effects on the skeleton by increasing bone formation and decreasing bone resorption, perhaps through activation of the Wnt pathway. Our findings suggest that inhibition of Rorβ either directly or by modulating Wnt signaling may represent a novel approach to prevent or treat age-related bone loss.

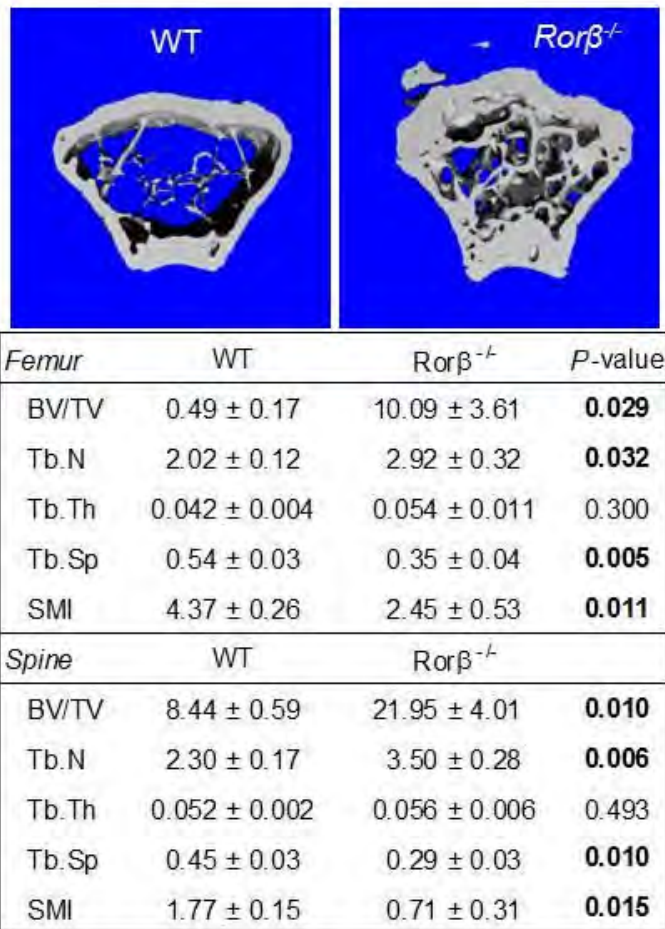


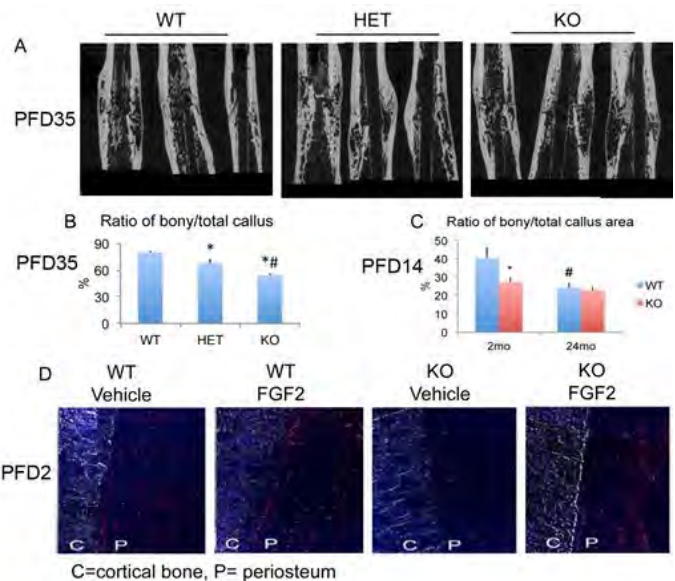
Fig 1

Disclosures: Joshua Farr, None.

## 1145

**Impaired Fracture Healing in Fgf2 Heterozygous and Homozygous Knockout Mice.** Marja Hurley\*, Kimberly Pontoja, Liping Xiao. UConn Health, United states

FGF2 enhances fracture (FX) repair in young animals and a clinical trial of FGF2 in Japan demonstrated its efficacy in enhancing FX healing in young human subjects. However there are no studies on its efficacy in FX repair in old animals or humans. We published that there was a significant decrease in FGF2 in old human mesenchymal progenitor cells (HMDPCs) compared with young, a significant reduction in FGF2 in bones of aged WT mice, and accelerated fracture healing in young 18kDaFGF2Tg mice. We posit that in aged and Fgf2Het mice with low endogenous FGF2 or Fgf2KO mice, FX healing would be impaired. Femur FX healing was determined in 4 month-old WT, Fgf2Het and Fgf2KO male mice. At 21 days post FX (PFD21), x-ray showed calluses were less mineralized in Fgf2het and Fgf2KO compared with WT. MicroCT at PFD35 still showed less mineralization in Fgf2Het and Fgf2KO (Fig. 1A). At PFD35 while callus remodeling was almost complete in WT, there was still ongoing callus remodeling in Fgf2Het and Fgf2KO and the ratio of bony/total callus area was decreased in Fgf2Het compared with WT and further decreased in Fgf2KO (Fig. 1B). Femur FX healing in young (2-months) and aged (24-months) WT and Fgf2KO mice was determined. At PFD14 x-rays showed less mineralized calluses in aged WT and in young and aged Fgf2KO mice. Bony/total callus area was decreased in aged WT compared with young WT mice but was similar to that observed in young and aged Fgf2KO (Fig.1C). To assess whether impaired healing in Fgf2KO was associated with decreased periosteal cell proliferation, femur FX was performed on 6-month-old female WT and Fgf2KO mice. Immediately after FX, mice were sc injected with 100ug/kg FGF2 or vehicle and sacrificed on PFD2. Twenty-four hours prior to sacrifice mice were injected intraperitoneal with EdU (5-ethynyl-2'-deoxyuridine) to assess proliferation. Femurs were harvested and frozen sections stained for EdU, then counterstained with 4'-diamidino-2-phenylindole(DAPI) to identify nuclei. Compared with WT decreased EdU labeled periosteal cells were noted in vehicle treated Fgf2KO femurs that were partially rescued by FGF2 (Fig.1D). In summary, FX healing is impaired in young Fgf2Het, young Fgf2KO mice, aged WT and aged Fgf2KO mice. FGF2 treatment increased periosteal cell proliferation in the early post fracture period in femurs of WT and Fgf2KO mice. Impaired periosteal cell proliferation due to reduced FGF2 expression could contribute to the impaired FX healing.



Figure

Disclosures: Marja Hurley, None.

## 1146

**Bortezomib rescues radiation-induced osteoporosis by promoting DNA repair and cell survival in osteoblasts.** Abhishek Chandra\*, Tiffany Young, Ling Qin. University of Pennsylvania, United states

The maximum benefit of clinical radiotherapy is limited by its damage to tumor neighboring tissues. Bone atrophy and its related fragility fractures are frequent late side effects of radiotherapy in cancer survivors and have detrimental impact on their quality of life. We previously showed that PTH1-34 anabolic injections has the ability to block radiation-induced bone damage by accelerating DNA repair in osteoblasts after radiation. DNA damage responses are tightly regulated by the ubiquitin proteasome pathway. In this study, we examined whether proteasome inhibitors (PSI) have the similar bone protective effects against radiation damage. In vitro, MG132 treatment greatly attenuated apoptosis in irradiated primary osteoprogenitors, osteoblastic UMR106 cells, and osteoblasts in calvarial cultures. This survival effect of MG132 was accompanied by decreases in the number of DNA double-stranded breaks and overall DNA damage, as revealed by  $\gamma$ H2AX foci and comet assays, respectively, and up-regulation of amounts of Ku70 and DNA-PKc, two essential DNA repair proteins in the non-homologous end joining pathway. In vivo, we tested the efficacy of Bortezomib (Bzb), the first PSI approved for cancer treatment, in restoring bone quality after radiation. Two-month-old mice were focally irradiated at the distal metaphyseal region of right femurs by a unique SARRP irradiator that replicates clinical focal radiotherapy with a clinically relevant dosage (8Gy at day 1 and 3). Mice were administered twice weekly with saline or Bzb (1mg/kg) for 4weeks. MicroCT scans revealed a significant 63.7% decrease in trabecular bone volume fraction (BV/TV) in irradiated tibiae compared to the contralateral tibiae in the vehicle group. Strikingly, Bzb completely reversed the effects of radiation on bone ablation with a 4.6-fold increase in BV/TV together with an 86.7% increase in trabecular number and a 52% decrease in trabecular separation compared to vehicle-treated irradiated femurs. Histomorphometry demonstrated that Bzb significantly increased osteoblast number (34.5%) and activity (11.5-fold in MS and 13-fold in BFR) and meanwhile suppressed osteoclasts number (67%). In addition, Bzb treatment drastically reduced the percentage of TUNEL+ osteoblast cells and bone marrow adiposity. Taken together, our data demonstrate a novel role of proteasome inhibitors in attenuating radiation-induced osteoblast apoptosis and identify Bzb as a potential therapy for radiotherapy-related osteoporosis.

Disclosures: Abhishek Chandra, None.

## 1147

**Natural Antibodies Against Oxidized LDL Cause Bone Anabolism.** Elena Ambrogini\*<sup>1</sup>, Xuchu Que<sup>2</sup>, Shuling Wang<sup>2</sup>, Fumihiko Yamaguchi<sup>2</sup>, Annick Deloose<sup>1</sup>, Michela Palmieri<sup>1</sup>, Stuart B Berryhill<sup>1</sup>, Robert S Weinstein<sup>1</sup>, Sotirios Tsimikas<sup>2</sup>, Stavros C Manolagas<sup>1</sup>, Joseph L Witztum<sup>2</sup>, Robert L Jilka<sup>1</sup>. <sup>1</sup>University of Arkansas for Medical Sciences, United states, <sup>2</sup>University of California, San Diego, United states

Atherosclerosis and osteoporosis are epidemiologically linked, suggesting common underlying pathogenic mechanisms. Oxidation of LDL is a fundamental mechanism

of atherogenesis. Oxidized LDL (oxLDL) contains oxidation specific epitopes (OSEs) that are recognized by pattern recognition receptors (PRR) such as toll-like receptors (TLRs) and scavenger receptors (SRs) on endothelial cells and macrophages. Activation of TLRs and SRs stimulates the production of inflammatory cytokines and affects intracellular signaling pathways, leading to vascular calcification. Natural antibodies (nAbs) produced by B1 cells of the innate immune system are also PRR. E06 natural IgM recognizes the phosphocholine moiety of oxidized phospholipids, and the human IK17 nAb recognizes the malondialdehyde epitope in oxLDL. Both nAbs are atheroprotective in the murine LDL receptor knock out (LDLR-KO) model of atherosclerosis. Since these mice also exhibit bone loss, we investigated the effect of nAbs on skeletal homeostasis. Male C57BL/6J mice overexpressing the antigen-binding domain of E06 (WT;E06 mice) exhibited increased vertebral and femoral cancellous, but not cortical, bone mass at 5 months of age, compared to WT controls. To determine the skeletal impact of E06 in the setting of atherosclerosis, male LDLR-KO mice and LDLR-KO;E06 mice were fed a HFD from 2 to 7.5 mo of age. As controls, LDLR-KO mice were maintained on a normal diet. LDLR-KO;E06 mice exhibited an increase in femoral cancellous bone mass compared to the other two groups, confirming the anabolic effect of E06. HFD decreased femoral cortical thickness by decreasing periosteal apposition, and by decreasing endosteal osteoblast number and bone formation rate. LDLR-KO;E06 mice were protected from HFD-induced cortical bone loss by increasing endosteal osteoblast number and bone formation rate. Interestingly, overexpression of the antigen-binding domain of IK17 increased femoral and vertebral cancellous bone, as well as femoral cortical thickness, in HFD-fed 6 mo old male LDLR-KO mice. Finally, E06 IgM prevented the negative effects of oxLDL on the proliferation, differentiation and survival of murine bone marrow-derived osteoblast progenitors. In summary, nAbs against OSEs increase bone mass irrespective of diet, and they attenuate HFD-induced cortical bone loss; most likely by protecting against the anti-osteogenic signals generated by OSE activation of TLRs and SRs on macrophages and osteoblasts.

*Disclosures: Elena Ambrogini, None.*

## 1148

### Short-term Antibiotic-induced Bone loss is preventable by microbial transfer.

Jonathan Schepper\*, Fraser Collins, Regina Irwin, Nara Parameswaran, Laura McCabe. Michigan State University, United states

Antibiotic treatment is common in the US with more than 800 prescriptions per 1000 people. Although effective at treating infections, oral antibiotics can have adverse consequences on the intestinal microbiome. Past studies demonstrate an important role for the microbiome and probiotics in bone health. Therefore, we investigated the role of antibiotic treatment on bone health with or without the supplementation of probiotic or fecal transfer. BLAB/c male (12-week-old) mice were treated for 2 weeks with oral antibiotics (1g/L ampicillin 0.5g/L neomycin) and bone parameters were analyzed 4 weeks after cessation of antibiotic treatment. During the 4-week period, we administered the probiotic lactobacillus reuteri (*L. reuteri*) or performed fecal transplants from healthy mice. Antibiotic treatment without any microbial supplementation significantly decreased in trabecular bone volume fraction (~30%) in the distal femur metaphysis as determined by micro-computed tomography. No reduction in bone volume fraction was observed in mice treated with *L. reuteri*, or that underwent fecal transfer. Analysis of serum bone remodeling parameters indicated significantly lower serum osteocalcin levels (~50% of control levels) in antibiotic treated mice, whereas no reduction was seen in microbial transfer mice. In contrast, Osteoclast (TRAP-5b) serum markers were significantly increased in the antibiotic treated mice compared to the other treatment groups. Together, these data suggest that short-term antibiotic treatment has a long-term detrimental effect on bone, which can be prevented with probiotic supplementation or a normal microbiome fecal transplant.

*Disclosures: Jonathan Schepper, None. This study received funding from: N/A*

## 1149

**Identification and localization of a key skeletal stem cell population with high regenerative potential in the periosteum of growing and adult bones.** Oriane Duchamp de Lageneste\*, Anais Julien, Rana Abou-Khalil, Caroline Carvalho, Giulia Frangi, Céline Colnot. INSERM UMR1163, Imagine Institute, Paris Descartes University, France

Bone regeneration relies on the activation of skeletal stem cells (SSCs) that still remain poorly characterized. Numerous studies have concentrated on bone marrow stromal cells (BMSCs) as the central SSC population within bone for endogenous bone regeneration and cell-based therapy. However, bone marrow contributes marginally to endogenous bone repair, while periosteum is a major source of cells for bone regeneration. In this study, we characterize in detail periosteum-derived skeletal stem cells (PSSCs) in mice. We show that PSSCs, similar to BMSCs, are negative for hematopoietic markers, positive for mesenchymal stem cell (MSC) markers (including Scf, CD29, CD105) and can differentiate into the three mesenchymal lineages (osteogenic, adipogenic, chondrogenic) in vitro. We show that although PSSCs and BMSCs have common embryonic origins, PSSCs exhibit superior bone regenerative potential in mature bones. PSSCs display higher CFU-F activity and cell growth in vitro compared to BMSCs. By transplanting GFP-labelled PSSCs and BMSCs at sites of bone injury in wild type mice, we show that PSSCs can

better integrate in the center of the callus, which was correlated with their enhanced migration capacity in vitro. Transplanted PSSCs exhibit higher contribution to cartilage and bone, and long-term integration into the callus. Microarray analyses of PSSCs and BMSCs isolated from intact and injured tibia 3 days post fracture show an enhanced molecular response to injury of PSSCs. *Periostin* (*Postn*) was one of the up-regulated genes in activated PSSCs and the matricellular protein *Postn* was detected in the stem cell layer of activated periosteum after injury. Bone regeneration was impaired in *Postn* KO mice with decreased callus, cartilage and bone formation leading to fibrosis and non-union. *Postn* inactivation specifically impaired PSSCs in vivo. Transplanted PSSCs strongly expressed *Postn* during their migration into the fracture site and *Postn* was essential for the contribution of PSSCs to cartilage and bone in the callus. In conclusion, this work identifies SSCs from periosteum as a central SSC population with high regenerative potential for endogenous bone repair. We show that Periostin is a key component of the periosteal stem cell niche regulating their ability to respond to injury and directly participate in skeletal repair after transplantation. SSCs within periosteum are therefore a better target to augment bone regeneration clinically.

*Disclosures: Oriane Duchamp de Lageneste, None.*

## 1150

**Bone lining cells are an alternative to MSCs as a source of osteoblasts in adult bone.** Brya G Matthews\*<sup>1</sup>, Igor Matic<sup>1</sup>, Xi Wang<sup>1</sup>, Nathaniel A Dymant<sup>1</sup>, Danka Grcevic<sup>2</sup>, Ivo Kalajzic<sup>1</sup>. <sup>1</sup>UCConn Health, United states, <sup>2</sup>University of Zagreb, Croatia

Mesenchymal stem cells are thought to provide a continuous supply of mature osteoblasts during bone remodeling. However, under certain conditions, bone lining cells (BLCs) can activate into matrix-producing osteoblasts. The ability to identify BLCs and understand their role in bone physiology has been very limited.

We use tamoxifen-treated 10kb-Dmp1CreERT2/Ai9 (iDMP-Ai9) mice (Cre directed Tomato expression) to label osteoblasts, BLCs and osteocytes. Our previous studies show that some osteoblasts remain on the bone surface 6 months after labeling, so we used an osteoblast ablation approach to selectively identify BLCs. We crossed the Col2.3ATK suicide gene into iDMP-Ai9 mice. Following ganciclovir treatment, cuboidal osteoblasts were absent, while flat BLCs were labeled. After 21 days of recovery, new osteoblasts form, and new areas of active bone surface are covered by iDMP-Ai9 expressing osteoblasts indicating activation of BLCs, while proliferation of BLC-derived cells was demonstrated by EdU incorporation. Isolated BLCs can also participate in healing of a calvarial defect and differentiate into osteoblasts and osteocytes. In contrast, when  $\alpha$ SMACreERT2 or Gremlin1CreERT2-labeled mesenchymal progenitors were tracked following Col2.3ATK osteoblast ablation, they showed minimal contribution to osteoblasts.

We utilized the iDMP-Ai9-TK model to characterize the physical and molecular characteristics of BLCs compared to osteoblasts. FACS analysis showed that a large proportion of BLCs express mesenchymal stem cell markers while osteoblasts do not (Sca-1 – 38% vs <2% in Col2.3GFP+ cells, CD51 – 70% vs 20%, LepR – 27% vs 3%). Single cell gene expression analysis indicated significantly higher expression of osteoclast regulators M-CSF and RANKL in BLCs compared to osteoblasts, as well as high expression of Mmp13, and cell cycle checkpoint gene Cdkn1a. We also evaluated the cell shape characteristics of BLCs compared to osteoblasts and osteocytes using two photon microscopy. The median volume of BLCs was more than double that of osteoblasts, and their sphericity was lower, indicating a flatter more disc-like shape.

Our results define the bone lining cells as a source of proliferating and mature osteoblasts during adult bone remodeling. These cells show a number of differences from osteoblasts which suggest they may play as yet undetermined roles in regulation of bone homeostasis.

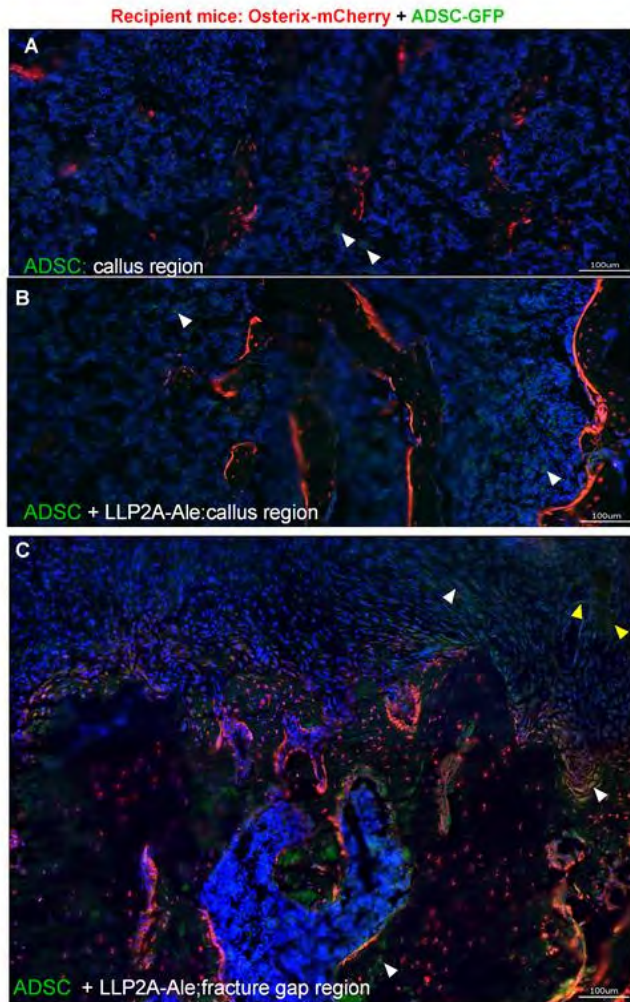
*Disclosures: Brya G Matthews, None.*

## 1151

**Improved Mobilization of Exogenous Mesenchymal Stem Cells to Bone for Fracture Healing.** Wei Yao\*, Evan Lay, Alexander Kot, Hongliang Zhang, Nancy Lane. UC Davis Medical Center, United states

Mesenchymal stem cells (MSCs) transplantation has been tested in both animal and clinical fracture studies. We have developed a bone-seeking compound, LLP2A-Alendronate (LLP2A-Ale) that selectively targets the integrin  $\alpha$ 5 $\beta$ 1 on the cell surface of MSCs and previous studies found that LLP2A-Ale has high affinity for MSCs, stimulates MSC differentiation into osteoblasts in vitro, and increased exogenous MSC homing to bone and reversed bone loss in mouse models of aging and estrogen-deficiency. The primary aim of this study was to evaluate the effect LLP2A-Ale on bone-targeted delivery of MSCs for fracture healing. In addition, we evaluated if there were sex differences in the rate fracture healing and if the treatment efficacy with MSCs, LLP2A-Ale or the combination would differ by sex. A right mid-femur fracture was induced in two-month-old osterix-mCherry (*Osx-mCherry*) male and female reporter mice. At day 1, all mice with fractures (males and females) were randomized to the following treatment groups placebo (phosphate buffered saline, PBS), LLP2A-Ale (500  $\mu$ g/kg, IV at day 1), adipose-derived MSCs (ADSCs) obtained from WT mice transduced to express green-fluorescence protein-vector (GFP) (ADSC-GFP, 3 x10<sup>5</sup>, IV in the tail vein at day 1) with or without LLP2A-Ale. Mice were euthanized on days 14, 21 or 42 post-fracture (PFx) to measure bone engraftment and

retention of the transplanted MSC, callus volume and mineralization, maximum load and work-to-failure, biochemical and surface based bone turnover. Nonparametric Kruskal-Wallis and post-hoc tests were used to determine differences between treatment and placebo groups within the same sex. Two factor ANOVA was used to evaluate treatment and sex effect and their interactions for each individual parameter within a same treatment. At days 42 PFx in the PBS group, females had higher systemic (osteocalcin) and surface-based bone formation rate than males. However, males formed a larger callus and bone strength than females ( $p < 0.05$ ). At day 7-14 PFx, ADSC engraftment in groups treated with "bone-targeting" agent LLP2A-Ale, were initially observed around the dead bone fragments, within fracture gaps, and participated in formation of callus bridges through in endochondral bone formation. By days 42 PFx, ADSC+ LLP2A-Ale treatment resulted in higher mineralization of the callus (20% for females; 25% for males;  $p < 0.05$  vs. PBS) and higher bone strength (work-to-failure, 9% for females; 18% for males,  $p < 0.05$  vs. PBS). We observed a sex-difference in the rate of fracture healing. The combined treatment with ADSCs + LLP2A-Ale was superior to monotherapy on callus formation, which was independent of sex. Increased mobilization of exogenous MSCs by LLP2A-le to fracture sites appeared to accelerate endochondral bone formation and enhance bone tissue regeneration.



day14-homing

Disclosures: Wei Yao, None.

## 1152

**FAK Promotes Osteoprogenitor Cell Proliferation and Differentiation by Enhancing Wnt Signaling.** Chunhui Sun<sup>\*1</sup>, Hebao Yuan<sup>2</sup>, Xiaoxi Wei<sup>3</sup>, Li Wang<sup>3</sup>, Linford Williams<sup>2</sup>, Paul Krebsbach<sup>3</sup>, Jun-Lin Guan<sup>4</sup>, Fei Liu<sup>3</sup>.  
<sup>1</sup>School of Life Science, Jiangsu Normal University, China, <sup>2</sup>University of Michigan, United states, <sup>3</sup>University of Michigan School of Dentistry, United states, <sup>4</sup>University of Cincinnati College of Medicine, United states

Decreased bone formation is often associated with increased bone marrow adiposity. The underlying mechanisms of this negative correlation are incompletely understood. Focal adhesion kinase (FAK) plays important roles in proliferation and differentiation in many cell types. However, the roles of FAK in osteoblast lineage cells are largely unclear. Herein we generated FAK conditional knockout mice with

Osx-Cre. MicroCT analysis revealed an osteopenic phenotype in FAK<sup>F/F</sup>;Osx-Cre (CKO) mice. Two months old male CKO mice had 32% decrease in trabecular BV/TV, 21% decrease in TbN, and 13% decrease in TbTh of femur compared to FAK<sup>F/F</sup> (CTR) mice. There was no significant difference in these parameters between CTR and FAK<sup>F/+</sup>;Osx-Cre (CHet) mice. CKO femur had a 24% decrease in cortical area. In addition, CKO had decrease in frontal and parietal bone volume (30% and 18% respectively) and CHet had decrease only in frontal bone volume (26%). Histomorphometry showed a decrease in osteoblast number but no change in osteoclast number in CKO femur. There was >9 folds increase in bone marrow adipocytes in CKO mice. In in vitro culture, FAK deletion led to decreased bone marrow stromal cell (BMSC) proliferation (cell counting and Ki67 staining) and compromised osteoblast differentiation (ALP staining, AR staining and marker gene expression). Furthermore, BMSCs from CKO mice had significantly increased adipogenesis demonstrated by much more Oil Red O positively stained cells and increased expression of adipogenic differentiation marker genes and transcription factors. Mechanistically, FAK deficiency led to decreased Wnt/ $\beta$ -catenin signaling evidenced by decreased  $\beta$ -catenin protein level, decreased Wnt target gene expression. The decrease in phosphor-GSK3 $\beta$  (S9) level in FAK deficient BMSCs suggested that increased degradation activity of GSK3 complex is responsible for the increased  $\beta$ -catenin degradation. In addition, we found a decrease in the expression of Wnt1, Wnt3a, and Wnt 10b, which are the canonical Wnt ligands known to be expressed in Osx<sup>+</sup> cells. In contrast to BMSCs, FAK deficiency did not compromise the proliferation and differentiation,  $\beta$ -catenin level and mRNA expression of Wnt target genes of primary calvarial osteoblasts. Altogether, our data suggest that FAK promotes Wnt signaling in osteoprogenitor cells, thereby increasing proliferation, decreasing adipogenic differentiation, and enhancing osteogenic differentiation, and thus ultimately increases bone mass.

Disclosures: Chunhui Sun, None.

## 1153

**N-cadherin Modulation of Bone Mass Acquisition is Osteolineage Stage- and Age-Specific.** Francesca Fontana<sup>\*</sup>, Cynthia Brecks, Leila Revollo, Grazia Abu-Ezzi, Manuela Fortunato, Yael Alippe, Gabriel Mbalaviele, Roberto Civitelli. Washington University School of Medicine, United states

We and others have shown that either ablation of the N-cadherin (Ncad) gene (*Cdh2*) in osteolineage cells, or transgenic overexpression of *Cdh2* in osteoblasts leads to low bone mass. We hypothesize that Ncad, a cell adhesion molecule involved in Wnt signaling, has stage-specific actions: it supports mesenchymal stem and progenitor cells (MSPC), but restrains mature osteoblast activity. *Cdh2* ablation using *Osx-cre* (cKO<sup>Osx</sup>) results in reduced bone mineral density (BMD) and trabecular bone volume/tissue volume (BV/TV, by  $\mu$ CT), associated with reduced numbers of bone marrow MSPC (Lin- PDGFR+ Sca1+ cells) and colony forming units (CFU-F). Young cKO<sup>Osx</sup> mice are also smaller, with reduced body weight (-25-30% vs. control at P10), nose-to-tail length (-13-16%,  $p < 0.05$ ) and tibial length (-9-17%,  $p < 0.05$ ). Ablation of *Cdh2* in osteo-chondroprogenitors using *Tw2-cre* also produces short-lived, severely runted pups; whereas *Cdh2* deletion using the limb-restricted *Prx1-cre* results in viable mice of normal size but with low BV/TV (-20-25%,  $p < 0.05$ ) and reduced CFU-F ( $p < 0.05$ ). To further determine whether the growth defect and osteopenia in *Cdh2*-deficient mice are related to Ncad action on MSPC, we administered doxycycline (doxy) to cKO<sup>Osx</sup> pregnant and lactating females to suppress Tet-sensitive *Osx-cre* and *Cdh2* ablation until P28, when *Osx* no longer marks MSPC but only committed osteoblasts (cKO<sup>Osx-OB</sup>). Using the Td-Tomato (TdT) Ai9 mouse reporter, we confirmed 6- to 10-fold reduction of TdT+ cells in the bone marrow and calvaria of *Osx-cre*;Ai9 doxy-treated pups, and efficient recombination (TdT+) after doxy removal in adults. At 2 months, cKO<sup>Osx-OB</sup> mice have normal body weight, length, and long bone morphology, while cKO<sup>Osx</sup> mice remain significantly smaller (-15-20%,  $p < 0.01$ ) than control littermates. Intriguingly, diaphysis trabecularization (by  $\mu$ CT) and total body BMD (by DXA) are actually higher in adult cKO<sup>Osx-OB</sup> than in control mice, consistent with a negative action of Ncad in adult osteogenic cells. Supporting the hypothesis that Ncad loss in adult osteoblasts enhances Wnt sensitivity, introduction of one *Dkk1*-resistant *Lrp5* allele (*Lrp5*<sup>A214V</sup>; associated with high bone mass) in cKO<sup>Osx</sup> does not affect the early growth defect, but completely rescues the low bone mass phenotype. Thus, interference with Ncad in adult animals may enhance the bone anabolic effect of Wnt signaling activation, without a negative effect on MSPC maintenance and skeletal growth.

Disclosures: Francesca Fontana, None.

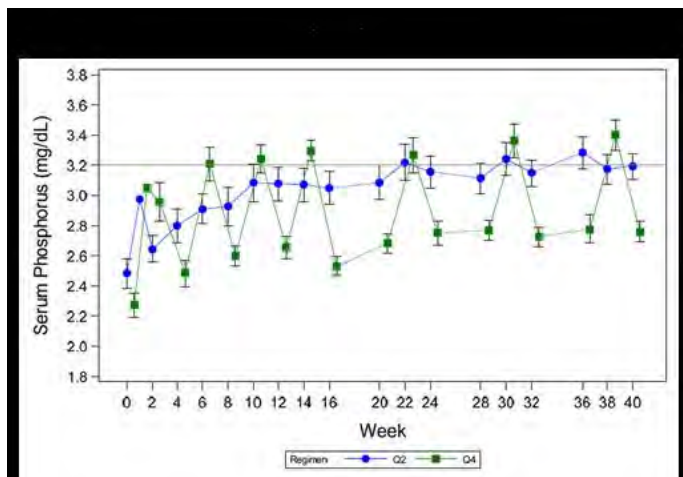
**A Randomized, Open-label Phase 2 Study of KRN23, a Fully Human Anti-FGF23 Monoclonal Antibody, in 52 Children with X-linked Hypophosphatemia (XLH): 40-Week Results.** Thomas Carpenter<sup>1</sup>, Erik Imel<sup>2</sup>, Annemieke Boot<sup>3</sup>, Wolfgang Högl<sup>4</sup>, Agnès Linglart<sup>5</sup>, Raja Padidela<sup>6</sup>, William van't Hoff<sup>7</sup>, Michael Whyte<sup>8</sup>, Chao-Yin Chen<sup>9</sup>, Alison Skrinar<sup>9</sup>, Sunil Agarwal<sup>9</sup>, Emil Kakkis<sup>9</sup>, Javier San Martin<sup>9</sup>, Anthony Portale<sup>10</sup>.  
<sup>1</sup>Yale University School of Medicine, United states, <sup>2</sup>Indiana University School of Medicine, United states, <sup>3</sup>University of Groningen, Netherlands, <sup>4</sup>Birmingham Children's Hospital, United Kingdom, <sup>5</sup>Hôpital Bicêtre, France, <sup>6</sup>Royal Manchester Children's Hospital, United Kingdom, <sup>7</sup>Great Ormond Street Hospital, United Kingdom, <sup>8</sup>Shriners Hospital for Children, United states, <sup>9</sup>Ultragenyx Pharmaceutical Inc., United states, <sup>10</sup>University of California, United states

In XLH, FGF23-mediated hypophosphatemia leads to defective bone mineralization and rickets. KRN23, an investigational product, binds and inhibits FGF23 activity.

In a Phase 2 study, 52 children with XLH (ages 5-12 years,  $\leq$ Tanner 2) were randomized to receive KRN23 biweekly (Q2W) or monthly (Q4W) by subcutaneous injection. KRN23 dose was titrated (maximum 2mg/kg) to target age-appropriate serum phosphate (Pi) concentrations, which were measured Q2W. Radiographs of wrists and knees were assessed by the Thacher Rickets Severity Score (RSS) and the Radiographic Global Impression of Change (RGI-C; -3=worsening; +2 = substantial healing; +3=complete healing).

Results of 40 weeks of KRN23 treatment for all 52 subjects will be presented. For the first 36 subjects, rachitic changes were evident at baseline (mean RSS 1.4) despite prior treatment with oral phosphate/active vitamin D for a mean of 6.6 years before enrollment in 35/36 subjects. KRN23 treatment for 40 weeks significantly improved serum Pi and rickets. Serum Pi increased from baseline in all subjects to near normal levels (mean increase 0.94 mg/dL at Week 38;  $p<0.001$ ) and was more stable with Q2W dosing (Figure). Hyperphosphatemia did not occur in any subject. Serum alkaline phosphatase decreased at Week 40 by a mean of 46 U/L ( $p=0.003$ ). At Week 40, mean RSS improved by 44% ( $p=0.013$ ) in the Q2W group, 14% ( $p=0.3$ ) in the Q4W group, and 30% ( $p=0.008$ ) across both groups. In subjects with higher-severity rickets (baseline RSS  $\geq 1.5$ ), mean RSS improved by 59% ( $p<0.0001$ ) in the Q2W group, 33% ( $p=0.008$ ) in the Q4W group, and 47% ( $p<0.0001$ ) across both groups. Rickets improved at Week 40 by a mean (SE) RGI-C score of +1.6 (0.2) in the Q2W group, +1.2 (0.2) in the Q4W group, and +1.4 (0.1) for both groups ( $p<0.0001$  for all groups). In the subset with higher-severity rickets, substantial healing of rickets (mean RGI-C +2.0 [0.1]) was observed in the Q2W group; mean RGI-C scores were +1.7 (0.2) in the Q4W group, and +1.9 (0.1) for both groups ( $p<0.0001$  for all groups). Most treatment-related adverse events (AEs) were mild; transient injection site reactions (39%) were the most common. One child experienced a serious AE, was hospitalized for fever/muscle pain that resolved, and continues in the trial. No clinically meaningful changes occurred in serum or urine calcium, serum iPTH, or renal ultrasounds.

KRN23 improved serum phosphorus and rickets in children with XLH and was generally safe and well tolerated.



Figure

**Disclosures:** Thomas Carpenter, *Ultragenyx Pharmaceuticals Inc.*, 15; *Ultragenyx Pharmaceuticals Inc.*, 11  
 This study received funding from: *Ultragenyx Pharmaceuticals Inc.* and *Kyowa Hakko Kirin Co., Ltd*

**Odanacatib Efficacy and Safety in Postmenopausal Women with Osteoporosis: 5-Year Data from the Extension of the Phase 3 Long-Term Odanacatib Fracture Trial (LOFT).** Michael R. McClung<sup>1</sup>, Bente Langdahl<sup>2</sup>, Socrates Papapoulos<sup>3</sup>, Kenneth G. Saag<sup>4</sup>, Henry Bone<sup>5</sup>, Douglas P. Kiel<sup>6</sup>, Kurt Lippuner<sup>7</sup>, Toshitaka Nakamura<sup>8</sup>, Ian Reid<sup>9</sup>, Norman Heyden<sup>10</sup>, Carolyn DaSilva<sup>10</sup>, Boyd B. Scott<sup>10</sup>, Rachid Massaad<sup>11</sup>, Keith D. Kaufman<sup>10</sup>, S. Aubrey Stoch<sup>10</sup>, Arthur Santora<sup>10</sup>, Antonio Lombardi<sup>10</sup>.  
<sup>1</sup>Oregon Osteoporosis Center, United states, <sup>2</sup>Aarhus University Hospital, Denmark, <sup>3</sup>Leiden University Medical Center, Netherlands, <sup>4</sup>University of Alabama at Birmingham, United states, <sup>5</sup>Michigan Bone & Mineral Clinic & The Osteoporosis Center at St. Luke's Hospital, United states, <sup>6</sup>Institute for Aging Research, Hebrew Senior Life, Harvard Medical School, United states, <sup>7</sup>Bern University Hospital, Switzerland, <sup>8</sup>University of Occupational & Environmental Health, Japan, <sup>9</sup>University of Auckland, New Zealand, <sup>10</sup>Merck & Co., Inc., United states, <sup>11</sup>MSD Europe Inc., Belgium

Purpose: Odanacatib (ODN), a selective oral inhibitor of cathepsin K, is in development for the treatment of osteoporosis. The randomized, double-blind, placebo (PBO)-controlled, event-driven, Phase 3 Fracture Trial (LOFT; NCT00529373) evaluated efficacy and safety of ODN in postmenopausal women with osteoporosis. In a planned double-blind extension to LOFT, eligible patients continued on their originally assigned treatment for up to 5 years. We present efficacy and safety data for the entire 5-year double-blind period.

Methods: Women  $\geq 65$  years of age with BMD T-score  $\leq -2.5$  at total hip (TH) or femoral neck (FN), or with radiographic vertebral fracture (VFX) and T-score  $\leq -1.5$  at TH or FN, were randomized (1:1) to ODN 50 mg/week or PBO. All received vitamin D<sub>3</sub> (5600 IU/week) and calcium as required. Endpoints included morphometric VFX, hip fracture, non-VFX, clinical VFX, and safety and tolerability.

Results: Of 16,071 patients (8043 ODN, 8028 PBO) in LOFT, 12,290 (6092 ODN, 6198 PBO) completed the study. Among those completing LOFT, 8,257 (4297 ODN, 3960 PBO) who were eligible and consented entered the extension and 6,047 (3432 ODN, 2615 PBO) completed it. Mean (SD) age at randomization was 72.8 (5.3) years, 46.5% had prior VFX, and mean BMD T-scores were lumbar spine (LS) -2.7, TH -2.4, and FN -2.7. Mean (SD) follow-up was approximately 44 (18) months. Compared to PBO, ODN treatment over 5 years resulted in relative risk reductions of 52% for morphometric VFX, 48% for hip fracture, 26% for non-VFX, and 67% for clinical VFX (all  $p<0.001$ ). Compared to PBO, ODN treatment led to progressive mean increases (95% CI) in BMD of 10.9% (10.5, 11.2) at LS and 10.3% (10.0, 10.6) at TH (both  $p<0.001$ ) at 5 years. Incidences of adverse events (AEs) and serious AEs overall were balanced for ODN vs PBO (88.3 vs 88.2% and 30.3 vs 30.4%, respectively). Deaths reported in patients being followed on study were 378 (4.7%) vs 327 (4.1%), ODN vs PBO, respectively (HR 1.12 [95% CI: 0.97, 1.30]); more complete ITT analysis of deaths among all patients, including those who discontinued from study, showed 682 (8.5%) vs 660 (8.2%), respectively (HR 1.04 [95% CI: 0.93, 1.16]). Results of other AEs of interest, including independent adjudication of cardiovascular events, will be presented separately.

Conclusion: Consistent with the results of LOFT, treatment with ODN for up to 5 years reduced the risk of hip, vertebral and non-vertebral fractures and was generally well tolerated.

**Disclosures:** Michael R. McClung, *Amgen*, *Merck*, 12  
 This study was sponsored by *Merck & Co., Inc.*

**Safety of Odanacatib in Postmenopausal Women with Osteoporosis: 5-Year Data from the Extension of the Phase 3 Long-Term Odanacatib Fracture Trial (LOFT).** Socrates Papapoulos<sup>1</sup>, Michael R. McClung<sup>2</sup>, Bente Langdahl<sup>3</sup>, Kenneth G. Saag<sup>4</sup>, Henry Bone<sup>5</sup>, Douglas P. Kiel<sup>6</sup>, Kurt Lippuner<sup>7</sup>, Toshitaka Nakamura<sup>8</sup>, Ian Reid<sup>9</sup>, Norman Heyden<sup>10</sup>, Carolyn DaSilva<sup>10</sup>, Boyd B. Scott<sup>10</sup>, Rachid Massaad<sup>11</sup>, Corinne Jamoul<sup>12</sup>, Keith D. Kaufman<sup>10</sup>, S. Aubrey Stoch<sup>10</sup>, Arthur Santora<sup>10</sup>, Antonio Lombardi<sup>10</sup>, Deborah Gurner<sup>10</sup>.  
<sup>1</sup>Leiden University Medical Center, Netherlands, <sup>2</sup>Oregon Osteoporosis Center, United states, <sup>3</sup>Aarhus University Hospital, Denmark, <sup>4</sup>University of Alabama at Birmingham, United states, <sup>5</sup>Michigan Bone & Mineral Clinic & The Osteoporosis Center at St. Luke's Hospital, United states, <sup>6</sup>Institute for Aging Research, Hebrew Senior Life, Harvard Medical School, United states, <sup>7</sup>Bern University Hospital, Switzerland, <sup>8</sup>University of Occupational & Environmental Health, Japan, <sup>9</sup>University of Auckland, New Zealand, <sup>10</sup>Merck & Co., Inc., United states, <sup>11</sup>MSD Europe Inc., Belgium, <sup>12</sup>Formerly MSD Europe Inc., Belgium

Purpose: Odanacatib (ODN) is a selective oral inhibitor of cathepsin K in development for treatment of osteoporosis (OP). The double-blind (DB), placebo (PBO)-controlled Phase 3 Fracture Trial (LOFT; NCT00529373) examined safety and efficacy of ODN in postmenopausal women with OP. In a planned DB extension to LOFT, eligible patients continued on their originally assigned treatment for up to 5 years. We present safety data for the entire 5-year DB period.

Methods: Women  $\geq 65$  years with BMD T-score  $\leq -2.5$  at total hip (TH) or femoral neck (FN), or with radiographic vertebral fracture and T-score  $\leq -1.5$  at TH or FN, were randomized (1:1) to ODN 50 mg/week or PBO. All received vitamin D<sub>3</sub> (5600 IU/week) and calcium as required. Adjudicated adverse events (AEs) included delayed fracture union, atypical femoral shaft fractures (AFFs), osteonecrosis of the jaw (ONJ), morphea-like skin lesions, systemic sclerosis, serious respiratory infections, and cardiovascular (CV) events.

Results: Of 16,071 patients (8043 ODN, 8028 PBO) in LOFT, 12,290 (6092 ODN, 6198 PBO) completed the study. Among those completing LOFT, 8,257 (4297 ODN, 3960 PBO) who were eligible and consented entered the extension and 6,047 (3432 ODN, 2615 PBO) completed it. Incidences of AEs and serious AEs overall were balanced for ODN vs PBO (88.3 vs 88.2% and 30.3 vs 30.4%, respectively). Deaths reported in patients being followed on study were 378 (4.7%) vs 327 (4.1%), ODN vs PBO, respectively (HR 1.12 [95% CI: 0.97, 1.30]); more complete ITT analysis of deaths among all patients, including those who discontinued from study, showed 682 (8.5%) vs 660 (8.2%), respectively (HR 1.04 [95% CI: 0.93, 1.16]). Delayed fracture union occurred in 18 patients in each group. Femoral shaft fractures occurred more often with ODN (26 patients [0.3%] vs 7 [0.1%]), of which 10 (0.1%) on ODN and none on PBO met criteria for AFF. No cases of ONJ were confirmed. Morphea-like skin lesions occurred more often with ODN (13 [0.2%] vs 3 [ $<0.1\%$ ]), most with onset within 2 years and 15 of 16 improved or fully recovered. Systemic sclerosis occurred in 2 ( $<0.1\%$ ) vs 1 ( $<0.1\%$ ). Serious respiratory infections were balanced (1.6 vs 1.8%). Independent adjudication of CV events is ongoing and will be presented separately.

Conclusion: ODN treatment was generally well tolerated for up to 5 years. Femoral shaft fractures, including AFFs, and morphea-like skin lesions were uncommon but more frequent with ODN. There were no confirmed cases of ONJ.

**Disclosures:** Socrates Papapoulos, Amgen, Axsome, Merck, Mereo Biopharma, Novartis, UCB, 12

This study was sponsored by Merck & Co. Inc.

## 1157

### Longitudinal Changes in Modeling- and Remodeling-Based Bone Formation with an Anabolic vs. an Antiresorptive Agent in the AVA Osteoporosis Study.

David Dempster<sup>1</sup>, Hua Zhou<sup>2</sup>, Robert Recker<sup>3</sup>, Jacques Brown<sup>4</sup>, Christopher Recknor<sup>5</sup>, E. Michael Lewiecki<sup>6</sup>, Paul Miller<sup>7</sup>, Sudhaker Rao<sup>8</sup>, David Kendler<sup>9</sup>, Robert Lindsay<sup>10</sup>, Kregg John<sup>11</sup>, Jahangir Alam<sup>12</sup>, Kathleen Taylor<sup>13</sup>, Valerie Ruff<sup>13</sup>. <sup>1</sup>Regional Bone Center, Helen Hayes Hospital, W Haverstraw, & Department of Pathology & Cell Biology, College of Physicians & Surgeons of Columbia University, NY, United states, <sup>2</sup>Regional Bone Center, Helen Hayes Hospital, United states, <sup>3</sup>Department of Medicine, Division of Endocrinology, School of Medicine, Creighton University, United states, <sup>4</sup>Rheumatology & Bone Diseases Research Group, CHU de Quebec (CHUL) Research Centre & Department of Medicine, Laval University, Canada, <sup>5</sup>United Osteoporosis Centers, United states, <sup>6</sup>New Mexico Clinical Research & Osteoporosis Center, United states, <sup>7</sup>Department of Medicine, CO Center for Bone Research, United states, <sup>8</sup>Bone & Mineral Research Laboratory, Henry Ford Hospital, United states, <sup>9</sup>Department of Medicine (Endocrinology), University of British Columbia, Canada, <sup>10</sup>Regional Bone Center, Helen Hayes Hospital, W Haverstraw, & Department of Medicine, College of Physicians & Surgeons of Columbia University, NY, United states, <sup>11</sup>Eli Lilly & Company, United states, <sup>12</sup>Lilly Research Laboratories, Eli Lilly & Company, United states, <sup>13</sup>Musculoskeletal & Men's Health, Lilly USA, LLC, United states

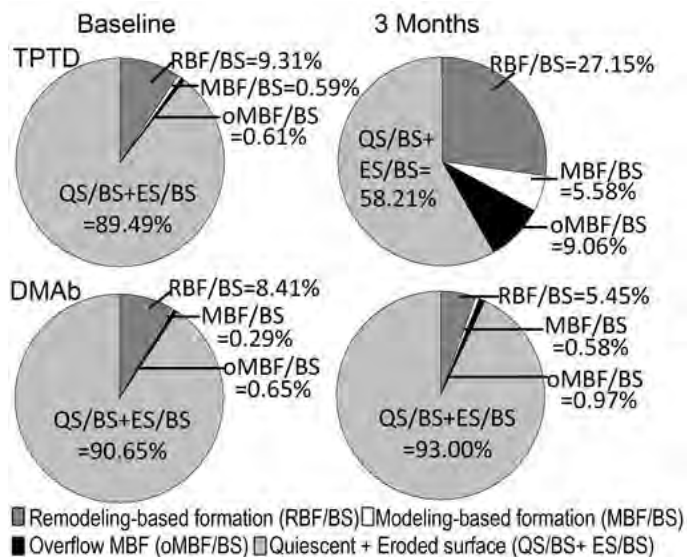
Recently, interest has renewed in modeling-based formation (MBF) as a target for osteoporosis (OP) therapies. Previously, we reported opposite effects in the AVA study of an established anabolic (teriparatide: TPTD) vs. a prototypical antiresorptive (denosumab: DMAB) agent on endogenous PTH and bone formation indices at 3 months in 3 bone envelopes using quadruple fluorochrome labeling (JCEM 2016; 101(4):1353-1363). Here we compare early effects of these agents on remodeling-based formation (RBF) vs. MBF in human transiliac bone biopsies.

Postmenopausal women with OP were randomized to TPTD (20 mcg/day) or DMAB (60 mg once) for 6 months (open-label). Patients underwent double fluorochrome labeling at baseline (BL) and during treatment prior to biopsy at month 3 (a time when any effects of a transient rise in endogenous PTH on bone may be observed). Sites of bone formation in blinded samples were identified by fluorochrome labels and designated as MBF if the underlying cement line was smooth and RBF if scalloped. Formation over smooth cement lines adjacent to scalloped reversal lines was considered overflow MBF (oMBF). The referent for all indices was bone surface (BS). Mean changes from BL between treatment groups were compared using ANCOVA and within treatment group differences were tested by paired T-tests.

In 3 bone envelopes (cancellous, endocortical, periosteal) at BL, mean RBF/BS, MBF/BS, and oMBF/BS were similar between TPTD and DMAB groups. All types of formation in the 3 envelopes significantly increased from BL with TPTD (range: 3- to 21-fold), except RBF and oMBF in periosteal envelope, which were unchanged. Response to TPTD was especially robust in endocortical envelope (Figure). Of note, MBF significantly increased at month 3 in the TPTD group in periosteal envelope

( $p=0.0002$ ). In contrast, all types of formation were decreased or unchanged with DMAB, except MBF/BS, which increased 2-fold in cancellous envelope ( $p=0.0475$ ).

The use of quadruple fluorochrome labeling allowed comparison of longitudinal changes in bone formation from BL to month 3 between TPTD and DMAB. The results indicate that a short course of TPTD significantly increases RBF, MBF, and oMBF in 3 bone envelopes, whereas these indices were generally reduced or unchanged with DMAB, reflecting the marked difference in mechanism of action between the 2 drugs. Further, this study provides the clearest evidence to date that TPTD stimulates bone formation on the periosteal surface.



Proportion of RBF, MBF, and oMBF in Endocortical Envelope

**Disclosures:** David Dempster, Merck, 12; Amgen, 13; Eli Lilly and Company, 13; Amgen, 12; Eli Lilly and Company, 12

This study received funding from: Eli Lilly and Company

## 1158

### Bisphosphonate-related Changes in Bone Turnover are Associated with Vertebral, but not Non-vertebral, Fracture Risk Reduction: A Meta-Regression.

Douglas Bauer<sup>1</sup>, Richard Eastell<sup>2</sup>, Mary Bouxsein<sup>3</sup>, Jane Cauley<sup>4</sup>, Steven Cummings<sup>5</sup>, Anne dePapp<sup>6</sup>, Victor Dishy<sup>7</sup>, Sanya Fanous-Whitaker<sup>8</sup>, Sundeep Khosla<sup>9</sup>, Charles McCulloch<sup>1</sup>, Dennis Black<sup>1</sup>. <sup>1</sup>University of California, San Francisco, United states, <sup>2</sup>University of Sheffield, United Kingdom, <sup>3</sup>Harvard Medical School, United states, <sup>4</sup>University of Pittsburgh, United states, <sup>5</sup>San Francisco Coordinating Center, California Pacific Medical Center, United states, <sup>6</sup>Merck & Co., Inc., Kenilworth, NJ, USA, United states, <sup>7</sup>Daichi Sankyo, Inc., United states, <sup>8</sup>Foundation for the National Institutes of Health, United states, <sup>9</sup>Mayo Clinic College of Medicine, United states

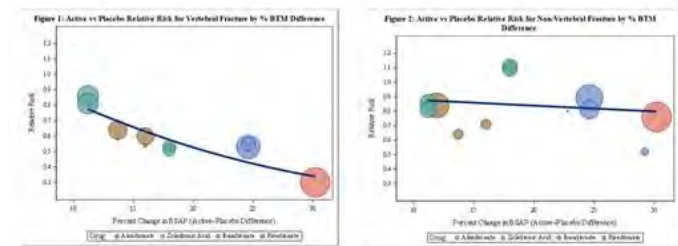
Few pooled analyses of bisphosphonate (BP) trials are available that relate short-term changes in bone turnover markers (BTMs) to fracture reduction. Such information, would be useful to assess new BPs or novel dosing regimens before initiating large fracture trials. A 2002 meta-regression of anti-resorptives found that a 50% reduction in bone formation markers (vs. placebo) predicted a 40% risk reduction in non-vertebral fracture (NVFx) over 2-5 years, but vertebral fractures (VFX) were not assessed and the specific BTMs and analytic approach varied. Since 2002 additional large trials with other BPs (Zoledronic acid, Ibandronate) have been published.

In the FNIH Bone Quality project, we identified published placebo-controlled fracture endpoint trials of osteoporosis treatments, and are collecting individual data from over 120,000 participants including serial BTMs if measured, DXA, and fracture outcomes. This analysis includes the data we received from 11 BP trials that included bone specific alkaline phosphatase (BSAP), the most commonly measured BTM. Using the individual-level BSAP data and the published study-specific relative risks for each fracture outcome, we performed a meta-regression relating the mean net effect of treatment on change in BSAP (active minus placebo percent difference after 3-12 mo.) to the log of overall fracture risk reduction, and used linear regression to plot the best fitting line (larger circles represent larger studies). Separate analyses were performed for VFX and NVFX.

This analysis includes over 28,000 randomized participants from 11 BP trials; change in BSAP was available for 12,000 participants. Fracture follow-up for incident VFX (N=1744) and NVFX (N=3216) ranged from 1-4 years. For VFX (Figure 1), the results showed a strong relationship between treatment-related BSAP change and VFX risk reduction. For example, for 2 hypothetical BPs with 10% vs. 30% reductions in BSAP, the model predicted a 19% vs. 66% reduction in VFX ( $r^2=0.84$ ,  $p=0.001$ ). For

NVFX fracture, the relationship was weaker and not significant (Figure 2); comparable risk reductions were 12% vs 21% ( $r^2=0.06$ ,  $p=0.27$ ).

We conclude that short-term treatment-related changes in BSAP can strongly predict reductions in VFX, but not NVFX, treatment efficacy. Further analyses using our large Bone Quality dataset are under way to examine other BTMs, DXA and QCT-finite element imaging, and to compare them as potential fracture surrogates alone and in combination.



Figure

Disclosures: Douglas Bauer, None.

## LB-1159

**Mutations in Geranylgeranyl Diphosphate Synthase (GGPS1) Identified by Whole-Exome Sequencing in Three Sisters who Sustained Atypical Femoral Fractures during Treatment with Bisphosphonates.** [Neus Roca-Ayats](#)<sup>\*1</sup>, [Natalia Garcia-Giralt](#)<sup>2</sup>, [Maite Falcó](#)<sup>3</sup>, [Nuria Martínez-Gil](#)<sup>3</sup>, [Josep Francesc Abril](#)<sup>4</sup>, [Roser Urreiziti](#)<sup>5</sup>, [Joaquín Dopazo](#)<sup>6</sup>, [José Manuel Quesada Gómez](#)<sup>7</sup>, [Xavier Nogues](#)<sup>2</sup>, [Leonardo Mellibovsky](#)<sup>2</sup>, [Daniel Prieto-Alhambra](#)<sup>8</sup>, [Muhammad K Javaid](#)<sup>8</sup>, [James E Dunford](#)<sup>8</sup>, [R Graham Russell](#)<sup>8</sup>, [Daniel Grinberg](#)<sup>3</sup>, [Susana Balcells](#)<sup>3</sup>, [Adolfo Díez-Pérez](#)<sup>2</sup>. <sup>1</sup>Department of Genetics, Microbiology & Statistics, Centro de Investigación Biomédica en Red de Enfermedades Raras (CIBERER), ISCIII, Universitat de Barcelona, IBUB, Spain, <sup>2</sup>Musculoskeletal Research Group, IMIM (Hospital del Mar Medical Research Institute), Red Temática de Investigación Cooperativa en Envejecimiento y Fragilidad (RETICEF), ISCIII, Spain, <sup>3</sup>Department of Genetics, Microbiology & Statistics, Centro de Investigación Biomédica en Red de Enfermedades Raras (CIBERER), ISCIII, Universitat de Barcelona, IBUB, Spain, <sup>4</sup>Department of Genetics, Microbiology & Statistics, Facultat de Biologia, Universitat de Barcelona, IBUB, Spain, <sup>5</sup>Department of Genetics, Microbiology & Statistics, Centro de Investigación Biomédica en Red de Enfermedades Raras (CIBERER), ISCIII, Spain, <sup>6</sup>Department of Computational Genomics, Centro Investigación Príncipe Felipe, BIER, CIBERER, Spain, <sup>7</sup>Mineral Metabolism Unit, Instituto Maimónides de Investigación Biomédica de Córdoba (IMIBIC), Hospital Universitario Reina Sofía. RETICEF, ISCIII, Spain, <sup>8</sup>NIHR Musculoskeletal BRU & Botnar Research Centre, Nuffield Department of Orthopaedics, Rheumatology & Musculoskeletal Sciences, University of Oxford, United Kingdom

Millions of patients take bisphosphonates (BPs) to reduce fracture risk and improve bone health for osteoporosis or cancer bone disease. Atypical femoral fractures (AFF) are a rare but potentially devastating event, often linked to BP therapy. This has raised significant concerns about BP use and has led to many patients either declining or being denied therapy. However, at present there are no tests that would assist clinical decision making by identifying those at high risk of AFF. Given the low absolute incidence of AFF, there may be underlying rare genetic causes that might interact with BPs to trigger the occurrence of these fractures. The present study explored the genetic background of three sisters with AFF and three additional unrelated AFF cases using exome sequencing, which detected 37 rare mutations (in 34 genes) shared by the three sisters. We found a p.Asp188Tyr mutation in all three sisters in the enzyme geranylgeranyl pyrophosphate synthase (GGPPS) which is critical to osteoclast function, and can also be inhibited by BPs. This mutation in GGPPS is predicted to impair its function, so it may interfere with osteoclast function, with or without any additional interaction with BPs. In addition, the *CYP11A1* gene, involved in steroid metabolism, was mutated in all three sisters and in one unrelated patient, suggesting it could be another potential susceptibility gene for AFF. Pathway analysis among the mutated genes showed enrichment of the isoprenoid biosynthetic pathway (GO:0008299), containing *GGPS1*, *CYP11A1* and *MVD* (p-value 0.0006). Other identified variants may also be involved to some extent in susceptibility to AFF. These include, among others, missense changes in fibronectin (*FNI*) and in *SYDE2* and *NGEF*, two regulators of small GTPases. Our data were

compatible with a model in which an accumulation of susceptibility variants (including some in relevant genes, such as *GGPS1*) constitutes a genetic component of AFF pathogenesis, and may lead to novel risk assessment tools to improve patient decision-making. To this end a gene/protein interaction network was constructed, which should constitute a useful resource for the interpretation of future genetic findings in AFF. In conclusion, a possible genetic background for AFF has been identified.

Disclosures: Neus Roca-Ayats, None.

## LB-1160

**Genome-wide association study of bone mineral density in the UK Biobank Study identifies over 376 loci associated with osteoporosis.** [John P. Kemp](#)<sup>\*1</sup>, [John A. Morris](#)<sup>2</sup>, [Carolina Medina-Gómez](#)<sup>3</sup>, [Celia L. Gregson](#)<sup>4</sup>, [Vincenzo Forgetta](#)<sup>2</sup>, [Katerina Trajanoska](#)<sup>3</sup>, [Nicole M. Warrington](#)<sup>5</sup>, [Jie Zheng](#)<sup>6</sup>, [Celia M.T. Greenwood](#)<sup>7</sup>, [Stephen K. Kaptoge](#)<sup>8</sup>, [Fernando Rivadeneira](#)<sup>3</sup>, [Jonathan H. Tobias](#)<sup>4</sup>, [Cheryl L. Ackert-Bicknell](#)<sup>9</sup>, [J. Brent Richards](#)<sup>10</sup>, [David M. Evans](#)<sup>1</sup>. <sup>1</sup>University of Queensland Diamantina Institute, Translational Research Institute, Brisbane, Queensland, Australia & MRC Integrative Epidemiology Unit, University of Bristol, Bristol, UK., United Kingdom, <sup>2</sup>Departments of Medicine, Human Genetics, Epidemiology & Biostatistics, Lady Davis Institute, McGill University, Montréal, Canada, Canada, <sup>3</sup>Department of Epidemiology, Erasmus Medical Center Rotterdam, Rotterdam, The Netherlands, Netherlands, <sup>4</sup>School of Clinical Sciences, University of Bristol, Bristol, UK, United Kingdom, <sup>5</sup>University of Queensland Diamantina Institute, Translational Research Institute, Brisbane, Queensland, Australia, Australia, <sup>6</sup>MRC Integrative Epidemiology Unit, University of Bristol, Bristol, UK., United Kingdom, <sup>7</sup>Lady Davis Institute for Medical Research, Jewish General Hospital, Montreal, QC, Canada, <sup>8</sup>Department of Public Health & Primary Care, University of Cambridge, Cambridge, UK, United Kingdom, <sup>9</sup>Center for Musculoskeletal Research, University of Rochester, Rochester, New York, USA., United states, <sup>10</sup>Departments of Medicine, Human Genetics, Epidemiology & Biostatistics, Lady Davis Institute, McGill University, Montréal, Canada & Department of Twin Research, King's College London, London, UK., United Kingdom

Aim: Calcaneal quantitative ultrasound (QUS) is a non-invasive method that estimates bone mineral density (eBMD) and predicts fracture risk. Previous genome-wide association studies (GWAS) of dual-energy x-ray absorptiometry (DXA) and QUS derived BMD (n ~ 35,000) have identified up to 68 loci that explain < 5% of the trait heritability. Using the largest genome-wide genotyped cohort in the world (UK Biobank), we first tested whether the genetic determinants of eBMD were similar to DXA-derived BMD. Next we identified individual genetic determinants of BMD by performing a large-scale GWAS of calcaneal eBMD. Methods: 140,623 individuals of white European descent (53% female) with imputed genotype and valid QUS measures were analysed. Pairwise genetic correlations involving eBMD, fracture and DXA-BMD were estimated separately. We next tested the association of genetic variants with eBMD. In-silico fine-mapping was implemented by constructing credible sets with a Bayesian method, followed by coding and non-coding SNP annotation using VEP, deltaSVM, and CATO. Results: Moderate positive genetic correlations between calcaneal eBMD and DXA BMD of the hip were observed ( $r_G = 0.57$ ,  $P = 1 \times 10^{-35}$ ) in addition to a negative genetic correlation with fracture ( $r_G = -0.57$ ,  $P = 4 \times 10^{-15}$ ); confirming the validity of the eBMD measure. GWAS identified 403 independent SNPs from 376 loci (defined as  $r^2 < 0.05$  and  $>500$  MB) attaining genome-wide significance ( $P < 5 \times 10^{-8}$ ), which jointly explained 13% of the variation in calcaneal eBMD. Fifty-one loci, previously associated with DXA-BMD, were replicated and a further 308 novel loci were identified, many of which contained genes that have not been previously implicated in bone physiology. Fine-mapping analyses implicated novel and known genes and predicted causal SNPs. We identified rare genetic variants (MAF < 0.5%) with large effect sizes on eBMD, with supportive evidence from our fine-mapping pipeline that these variants target the novel gene *TTC28*. Preliminary functional studies support a clear loss of bone mineral content in *Ttc28* KO mice. Further preliminary studies showed increased expression of a novel gene *Zhx3* in maturing calvarial osteoblasts and that *Zhx3* KO mice had increased whole-body BMD compared to wild type mice. Conclusion: Using UK Biobank, we increased the number of BMD loci 5-fold, identified etiologic pathways associated with osteoporosis, and implicated novel proteins which serve as potential drug targets in osteoporosis.

Disclosures: John P. Kemp, None.

**LB-1161**

**Histone methyltransferases EZH1 and 2 promote skeletal growth by repressing inhibitors of chondrocyte proliferation and hypertrophy.** Julian Lui\*<sup>1</sup>, Presley Garrison<sup>1</sup>, Quang Nguyen<sup>1</sup>, Michal Ad<sup>1</sup>, Ola Nilsson<sup>2</sup>, Kevin Barnes<sup>1</sup>, Jeffrey Baron<sup>1</sup>. <sup>1</sup>Section on Growth & Development, NICHD, United states, <sup>2</sup>Department of Women's & Children's Health, Karolinska Institute, Sweden

Histone methyltransferases EZH1 and EZH2 catalyze the trimethylation of histone H3 at lysine 27 (H3K27), which serves as an epigenetic signal for chromatin condensation and transcriptional repression. In humans, heterozygous mutations in EZH2 cause Weaver syndrome, which includes marked skeletal overgrowth. In addition, the EZH2 gene lies in a locus associated with human height variation, providing further evidence that EZH2 plays an important role in regulating skeletal growth. Because longitudinal bone growth results from chondrogenesis at the growth plate, we explored the role of Ezh1 and 2 in this process. In mice, neither cartilage-specific knockout of Ezh2 (Col2a1-cre Ezh2 f/f) nor generalized knockout of Ezh1 (Ezh1 -/-) affected skeletal growth, but the combined losses of both histone methyltransferases in cartilage (Col2a1-cre Ezh1 -/- Ezh2 f/f) diminished H3K27 trimethylation and severely impaired skeletal growth. Both of the principal processes underlying growth plate chondrogenesis, chondrocyte proliferation and hypertrophy, were compromised. We found evidence that the decrease in chondrocyte proliferation is due in part to derepression of cyclin-dependent kinase inhibitors Cdkn2a and 2b. In the combined Ezh1/2 knockout mice, Cdkn2a/b expression was elevated in the proliferative zone (assessed by qPCR of laser capture microdissected growth plate tissue), and in monolayer culture of primary mouse chondrocytes, treatment of Ezh1/2 inhibitors led to increased Cdkn2a/b expression and decreased proliferation, which were partially rescued by transfection with Cdkn2a/b-targeting siRNA. In the hypertrophic zone, we found evidence that the ineffective chondrocyte hypertrophy is due to derepression of IGF binding proteins (Igfbps), which led to suppression of IGF signaling. We showed that Igfbp3 and 5 expression was elevated in the hypertrophic zone of the combined Ezh1/2 knockout mice. We then demonstrated in a fetal metatarsal bone culture system that Ezh1/2 inhibitors increased Igfbp3 and 5 expression and suppressed chondrocyte hypertrophy and that addition of exogenous Igf1 completely reversed this suppression. Taken together, our findings reveal a critical role for H3K27 methylation in the regulation of chondrocyte proliferation and hypertrophy in the growth plate, which are the central determinants of skeletal growth.

**Disclosures:** Julian Lui, None.

**LB-1162**

**Clinical Development of an Optimized Abaloparotide Transdermal Patch.** Jamal Saeh\*<sup>1</sup>, David Pais<sup>1</sup>, Ehab Hamad<sup>1</sup>, Joan Moseman<sup>2</sup>, David Wirtanen<sup>2</sup>, Ken Brown<sup>2</sup>, Lisa Dick<sup>2</sup>, Gary Hattersley<sup>1</sup>. <sup>1</sup>Radius Health, United states, <sup>2</sup>3M Drug Delivery Systems, United states

Abaloparotide (ABL) is a novel peptide activator of the PTH1 receptor signaling pathway being developed for the treatment of postmenopausal osteoporosis. Transdermal (TD) delivery provides a promising alternative to subcutaneous (SC) injection and has the potential to improve patient convenience and compliance. We are currently evaluating a novel transdermal technology (sMTS; 3M) to deliver ABL. A proof of concept Phase 2 clinical study was conducted to assess the safety, tolerability, and efficacy of a daily short wear time first generation ABL-TD patch for 6 months. In this study ~36,000 patch applications were performed and an encouraging safety and dermal tolerability profile was observed. Significant BMD gains were seen, however, these gains were lower than observed with ABL-SC. The difference in the pharmacokinetic (PK) profile between ABL-TD and ABL-SC may account for the reduced efficacy, where the first generation patch achieved a more pulsatile PK profile, characterized by a lower AUC. Comparison of the relative variability in BMD and PK between ABL-SC and ABL-TD demonstrated that the patch consistently delivered ABL, with variability similar to SC. A PK/PD relationship analysis ( $C_{max}$  and AUC vs BMD) reveals a dose dependent linear relationship with AUC, suggesting that AUC rather than  $C_{max}$  is a key driver of efficacy. Therefore, to enhance efficacy with ABL-TD, a PK profile equivalent to ABL-SC is needed. Monkey PK studies have been conducted to enable selection of optimized ABL-TD patch formulations. These studies demonstrated the ability to achieve a PK profile comparable to ABL-SC. A Phase 1 clinical study was initiated to enable evaluation of the safety, tolerability, and PK of the optimized ABL-TD patches. This study is a single dose, 4 period crossover study conducted at a single US clinical site. A preliminary analysis suggests that ABL-TD had a comparable safety and tolerability profile to ABL-SC, together with favorable dermal tolerability. Significantly, interim PK data from this ongoing study demonstrated the ability of the formulation excipients to modify the PK of ABL-TD. In addition, user experience surveys and US prescriber research suggest that both physicians and patients prefer the TD patch target profile by nearly 3:1. Together, these data represent the first demonstration of the ability of formulation excipients to optimize the PK profile of ABL-TD and support the continuing clinical development of the ABL-TD patch.

**Disclosures:** Jamal Saeh, Radius Health, 15  
This study received funding from: Radius Health

**LB-1163**

**Effects of Up to 10 Years of Denosumab Treatment on Bone Matrix Mineralization: Results From the FREEDOM Extension.** DW Dempster\*<sup>1</sup>, JP Brown<sup>2</sup>, S Yue<sup>3</sup>, S Rizzo<sup>4</sup>, D Farlay<sup>4</sup>, RB Wagman<sup>3</sup>, A Wang<sup>3</sup>, X Yin<sup>3</sup>, G Boivin<sup>4</sup>. <sup>1</sup>Columbia University, United states, <sup>2</sup>Laval University & CHU de Quebec-(CHUL) Research Centre, Canada, <sup>3</sup>Amgen Inc., United states, <sup>4</sup>INSERM, UMR 1033, Univ Lyon, Université Claude Bernard Lyon 1, France

**Purpose:** In postmenopausal women with osteoporosis, denosumab therapy through 10 years is associated with continued BMD gains and low fracture incidence (Bone ASBMR 2015). To understand the contribution of mineralization to these clinical outcomes, we examined bone matrix mineralization indices at years 2 and 7 of the FREEDOM Extension, representing 5 and 10 years of denosumab treatment, respectively.

**Methods:** FREEDOM was a 3-year, double-blind, placebo-controlled study in postmenopausal women randomized to receive placebo or 60 mg denosumab subcutaneous Q6M (Cummings *NEJM* 2009), that was extended with open-label denosumab for 7 years to eligible participants (Papapoulos *JBMR* 2012). A subset of women underwent transiliac bone biopsies in FREEDOM (years 2 or 3 [Reid *JBMR* 2010]) and the Extension (years 2 [Brown *JBMR* 2014] and 7 [Dempster *ASBMR* 2016]). Bone matrix mineralization was assessed by digitized quantitative micro-radiography in a blinded fashion and analyzed using a code from Matlab program (Montagner *J X-Ray Sci Technol* 2015). The mean degree of mineralization of bone (DMB) and the heterogeneity index (HI) of the distribution of DMB were calculated for cancellous and cortical bone, the endocortical and periosteal cortical sub-compartments, and total bone (cancellous plus cortical).

**Results:** Bone biopsy samples from 72 women in FREEDOM (30 placebo, 42 denosumab at 2 or 3 years) and 28 and 21 women in the Extension who had received denosumab for a total of 5 and 10 years, respectively, were evaluated. Demographics for women in the bone matrix mineralization substudy and FREEDOM were comparable. Through 10 years, denosumab treatment resulted in significant increases in mean DMB and a significantly lower HI in total bone compared with placebo ( $p < 0.05$ ) (Fig.); however, there were no significant differences in mean DMB or HI between 5 and 10 years of denosumab treatment. DMB and HI plateaued between 5 and 10 years of treatment. Similar results were observed in all bone compartments assessed.

**Conclusion:** These findings suggest that mean DMB reaches a maximum by year 5. We propose that clinical outcomes with denosumab through 5 years, as judged through gains in BMD and low fracture incidence, likely reflect closing of the remodeling space and increases in secondary mineralization of bone matrix. We hypothesize that additional mechanisms may contribute to long-term clinical outcomes, including reductions in cortical porosity and modeling-based bone formation.

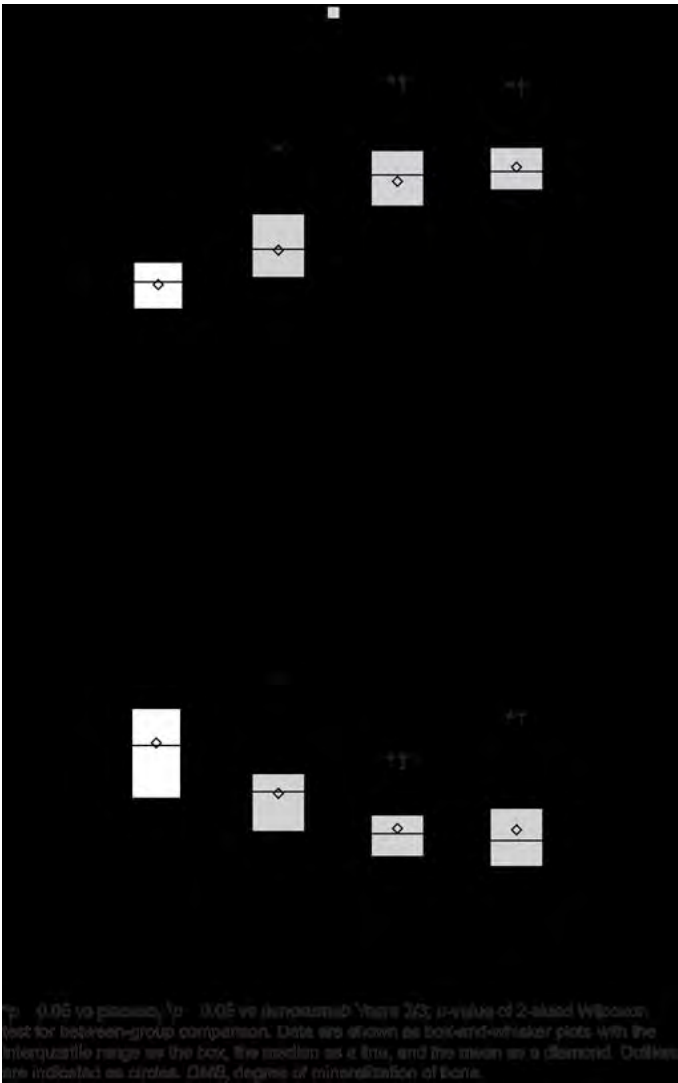


Figure FREEDOM Extension Bone Matrix Mineralization

**Disclosures:** *DW Dempster, Amgen Inc., Eli Lilly & Co., Radius, Regeneron, and Tarsis, 12; Amgen Inc. and Eli Lilly & Co., 13; Amgen Inc. and Eli Lilly & Co., 11*  
 This study received funding from: Amgen Inc.

## FR0001

**Serum 25-Hydroxyvitamin D Values and Risk of All-Cause Mortality: A Population-Based, Retrospective, Cohort Study.** Daniel Dudenkov\*, Kristin Mara, Tanya Petterson, Julie Maxson, Tom Thacher. Mayo Clinic, United states

Background: Levels of serum 25-hydroxyvitamin D [25(OH)D] below 20 ng/mL and above 50 ng/mL have been associated with chronic adverse events including mortality. Our objective was to conduct the first ever comprehensive population-based study in the United States of the relationship of low and high serum vitamin D levels with all-cause mortality.

Methods: We identified all serum 25(OH)D measurements in persons age 18 years and older residing in Olmsted County, MN from 2005 to 2011, using the resources of the Rochester Epidemiology Project. Time zero was thirty days after first documented 25(OH)D measurement. Patients were followed until last clinical visit as an Olmsted County resident, December 31, 2014, or death. Vitamin D was examined as a categorical variable using predetermined ranges of interest: 25(OH)D values <12, 12-19, 20-50 (reference range), and >50 ng/mL. The effect of 25(OH)D on all-cause mortality was assessed using Kaplan-Meier estimates and Cox proportional hazards regression. Multivariate analysis adjusted for age, gender, race, month of 25(OH)D measurement, and Charlson comorbidity index at time of 25(OH)D measurement.

Results: A total of 11,022 unique persons had a 25(OH)D measurement between 2005 and 2011, with a mean 25(OH)D value of 30.0 (SD=12.9) and a mean age of 54.3 (SD=17.2). The study population was mostly female (77.1%) and white (87.6%). The 25(OH)D values <12, 12-20, and >50 ng/mL had hazard ratios of 2.57 (95%CI: 2.05, 3.23), 1.28 (95%CI: 1.04, 1.56) and 1.03 (95%CI: 0.82, 1.48), respectively, compared to 25(OH)D values 20-50 ng/mL. Adjusting for listed covariates, 25(OH)D values <12, 12-20 and >50 ng/mL had hazard ratios of 2.37 (95%CI: 1.87, 3.00), 1.31 (95%CI: 1.06, 1.61) and 1.08 (95%CI: 0.75, 1.56), respectively, compared to the reference range. Kaplan-Meier estimated curves for the four categories are shown in Figure 1.

Conclusion: We observed higher all-cause mortality among patients with 25(OH)D values <20 ng/mL compared to those with 25(OH)D values 20-50 ng/mL. In contrast to previous studies, 25(OH)D values >50 ng/mL were not associated with an increased risk of death compared to 25(OH)D values 20-50 ng/mL.

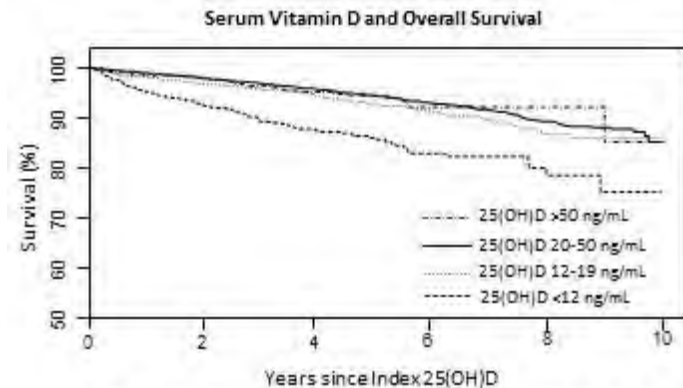


Figure 1. Kaplan-Meier curves for the 25(OH)D categories >50, 20-50, 12-19, and <12 ng/mL. Time zero is thirty days after initial 25(OH)D measurement.

Serum Vitamin D and Overall Survival

Disclosures: Daniel Dudenkov, None.

## FR0006

**Measles Virus Nucleocapsid Protein Expressing Osteoclasts Increase Expression of SPHK1/SIP/S1PR3 to Enhance Osteoblast Differentiation in Paget's Disease.** Yuki Nagata\*, Yasuhisa Ohata, Jolene Windle, David Roodman, Noriyoshi Kurihara. <sup>1</sup>Medicine / Hematology-Oncology, Indiana University, United states, <sup>2</sup>Human & Molecular Genetics, Virginia Commonwealth University, United states, <sup>3</sup>Medicine / Hematology-Oncology, Indiana University; Roudebush VA Medical Center, United states

Paget's Disease (PD) is the most exaggerated example of coupled bone remodeling with increased osteoclast (OCL) formation and increased osteoblast (OB) differentiation. Blocking OCL formation in PD decreases bone formation, demonstrating that the enhanced OB differentiation in PD is driven by OCLs. However, the OCL-derived factors increasing OB differentiation in PD are just being identified. We reported that OCLs from PD patients express measles virus nucleocapsid protein (MVNP), which increases IL-6, IGF1 and ephrinB2 expression in OCLs and ephB4 on OBs to increase OB differentiation. However, these factors do not totally account for the increased OB differentiation in PD. Since we previously showed that MVNP-expressing OCLs (MVNP-OCLs) express high levels of sphingosine-1-phosphate (S1P), and S1P was reported to increase OB differentiation via S1P receptor 3 (S1PR3) (JCI 2013), we examined the roles of S1P and S1PR3 in OB differentiation in PD. We found that

mature MVNP-OCLs produce high levels of Sphk1 and S1P compared to WT OCL. Further, S1P production was dependent on IL-6 since Shpk1 expression was decreased in OCLs from MVNP/IL-6 KO mice. We then assessed S1PR1 and R2 expression on MVNP-OCLs, since we found that S1P binding S1PR1 inhibits immature OCL precursor (pre-OCL) proliferation, while S1P binding S1PR2 inhibits pre-OCL motility and fusion. MVNP expressing pre-OCL expressed high levels of S1PR1 during proliferation, while S1PR2 increased with pre-OCL differentiation. We then tested if S1P (10  $\mu$ M) blocks OCL formation by highly purified MVNP and WT pre-OCL. S1P blocked OCL formation by both MVNP and WT pre-OCL, suppressing both pre-OCL proliferation and fusion, and decreasing levels of DC-STAMP, NFATc-1 and ADAM8. We then determined if MVNP-OCLs induced S1PR3 on OBs in co-cultures of MVNP-OCLs and OBs. MVNP-OCLs increased S1PR3 expression on OBs and enhanced OB differentiation to a greater extent than WT-OCL. To confirm that S1PR3 mediated the enhanced OB differentiation, we treated OCL/OB co-cultures from MVNP and WT mice with an S1PR3 antagonist (VPC23019) or S1PR3 agonist (VPC24191). VPC23019 blocked OB differentiation in MVNP-OCL/OB co-cultures while VPC24191 enhanced SP7 and Col-1 levels in OBs to greater extent in MVNP-OCL/MVNP-OB co-cultures compared to WT-OCL/WT-OB. These results suggest that S1P produced by PD-OCL acts as a coupling factor to block OCL formation, enhance S1PR3 expression in OB, to increase bone formation in PD.

Disclosures: Yuki Nagata, None.

## FR0007

**MVNP Modulation of NFAM1 Signaling Enhances Osteoclast Formation and Bone Resorption Activity in Paget's Disease of Bone.** Yuvaraj Sambandam\*, Kumaran Sundaram, Takamitsu Saigusa, Sudhaker Rao, William Ries, Sakamuri Reddy. <sup>1</sup>Darby Children's Research Institute, Medical University of South Carolina, United states, <sup>2</sup>Division of Nephrology, Medical University of South Carolina, United states, <sup>3</sup>Henry Ford Hospital, United states, <sup>4</sup>College of Dental Medicine, Medical University of South Carolina, United states

Paget's disease of bone (PDB) is a chronic focal skeletal disorder that affects 2-3% of the population over the age 55. The disease is marked by abnormal osteoclasts with excess bone resorption activity and abundant new bone formation of poor quality. We previously detected measles virus nucleocapsid protein (MVNP) transcripts in osteoclasts from patients with PDB. Also, MVNP stimulates pagetic osteoclast formation in vitro and in vivo. We identified that microarray analysis of human bone marrow derived preosteoclast cells transduced with MVNP increased (7-fold) NFAT activating protein with ITAM motif 1 (NFAM1) expression. Therefore, we hypothesize that MVNP modulation of NFAM1 controls pagetic osteoclast differentiation and bone resorption activity. We demonstrate that MVNP expression in normal human peripheral blood monocytes (PBMC) significantly increased (30-fold) NFAM1 mRNA expression without RANKL treatment. Western blot analysis further confirmed that MVNP increased (4.8-fold) NFAM1 expression in these cells. Also, bone marrow cells derived from patients with Paget's disease demonstrated elevated levels of NFAM1 mRNA expression. NFAM1 has been shown to induce ITAM phosphorylation and Syk recruitment. We showed that MVNP transduction into preosteoclast cells increased ITAM phosphotyrosine activation (4.0-fold) and p-Syk (5.5-fold) levels without RANKL stimulation. p-Syk has been implicated in calcium mobilization through activation of PLC $\gamma$ . We demonstrated that shRNA against NFAM1 inhibits MVNP stimulated PLC $\gamma$  expression in preosteoclast cells. Furthermore, MVNP expression upregulates calcineurin, a calcium-dependent serine-threonine phosphatase (8-fold) and NFATc1 (5-fold) transcription factor expression. We then measured intracellular Ca<sup>2+</sup> concentrations in fura-2/AM loaded preosteoclast cells with dual-excitation wavelength fluorescence microscopy. MVNP transduced cells stimulated with RANKL showed elevated Ca<sup>2+</sup> oscillations and intracellular levels. Interestingly, shRNA knock-down of NFAM1 expression significantly decreased MVNP induced calcineurin, p-Syk, NFATc1 expression and intracellular Ca<sup>2+</sup> levels in preosteoclast cells. Furthermore, suppression of NFAM1 inhibits MVNP induced osteoclast differentiation and bone resorption activity in mouse bone marrow cultures. Thus, our results suggest that MVNP modulation of the NFAM1 signaling axis plays a critical role in pagetic osteoclast formation and bone resorption activity.

Disclosures: Yuvaraj Sambandam, None.

## FR0011

**Long-Term rhPTH(1-84) Administration Persistently Affects Bone Remodeling Dynamics and Structure in Hypoparathyroidism.** Mishaela Rubin\*, Natalie Cusano, Hua Zhou, Wen-Wei Fan, Diane Cozadd, Aline Costa, David Dempster, John Bilezikian. Columbia University, United states

rhPTH(1-84) was recently approved in the USA for the treatment of hypoparathyroidism (HYP). We reported that 6 years of rhPTH(1-84) treatment in HYP are associated with an increase in lumbar spine and total hip bone mineral density (BMD) by DXA, with no change at the femoral neck and a decrease at the distal 1/3 radius. The mechanistic bases for these changes are unclear. We therefore investigated histomorphometric changes during 6 years of rhPTH(1-84) treatment in HYP patients (n=6) in comparison to euparathyroid controls (Ct; n=45). HYP (age 43.2  $\pm$  6 [SE] yrs; 4 female; duration 14  $\pm$  6 yrs) underwent tetracycline-labeled transiliac crest bone biopsies before (HYP0) and after 6 years (HYP6) of rhPTH(1-84) treatment. Mineralizing surface was

higher by 7-fold (HYP0:  $0.30 \pm 0.11$  to HYP6:  $7.36 \pm 2.86\%$ ,  $p=0.06$ ), tending to surpass Ct levels (Ct:  $4.33 \pm 0.48\%$ ,  $p=0.07$  vs HYP6). Bone formation rate also tended to be higher (HYP0:  $0.0013 \pm 0.001$  to HYP6:  $0.0417 \pm 0.0049 \text{ um}^2/\text{um}/\text{d}$ ,  $p=0.06$ ) but did not differ from Ct (Ct:  $0.033 \pm 0.004$ ,  $p=0.47$  vs HYP6). Cancellous bone volume was greater (HYP0:  $20.2 \pm 0.88$  to HYP6:  $30.8 \pm 1.2\%$ ,  $p<0.001$ ), exceeding Ct (Ct:  $19.8 \pm 0.66\%$ ,  $p<0.001$  vs HYP6). Trabecular number also was greater (HYP0:  $1.88 \pm 0.13$  to HYP6:  $2.50 \pm 0.14 \text{ #}/\text{mm}$ ,  $p=0.004$ ), surpassing Ct (Ct:  $1.74 \pm 0.05 \text{ #}/\text{mm}$ ,  $p<0.001$  vs HYP6), while trabecular separation was lower (HYP0:  $437.3 \pm 35.9$  to HYP6:  $280.7 \pm 15.8 \text{ um}$ ,  $p=0.005$ ), becoming lower than in Ct (Ct:  $484.7 \pm 19.6 \text{ um}$ ,  $p<0.001$  vs HYP6). Trabecular width tended to be greater (HYP0:  $109.9 \pm 7.9$  to HYP6:  $124.7 \pm 7.6$ ,  $p=0.06$ ) but did not differ from Ct (Ct:  $114.8 \pm 3$ ,  $p=0.26$  vs HYP6). These changes in trabecular architecture were accompanied by intra-trabecular tunneling. Cortical porosity increased (HYP0:  $4.81 \pm 0.57$  to HYP6:  $7.43 \pm 0.90 \text{ #}/\text{mm}^2$ ,  $p=0.001$ ), exceeding Ct values (Ct:  $4.77 \pm 0.36$ ,  $p=0.013$  vs HYP6). These data suggest that long-term rhPTH(1-84) has persistent effects to stimulate the skeleton in HYP. Dynamic indices at 6 years approximate or exceed eparathyroid measures. Structural parameters indicate more numerous and thicker trabeculae, consistent with persistent anabolic changes in the cancellous compartment. In the cortical compartment, long-term catabolic changes persist. Closer surrogate measures of bone strength (e.g. finite element analysis) and larger controlled studies with actual fracture data will be important to determine the long-term effects of rhPTH(1-84) on bone properties in HYP.

**Disclosures:** Mishaela Rubin, Shire Pharma, 11

This study received funding from: Shire Pharmaceuticals

## FR0012

**PTH(1-34) for the primary prevention of post-surgical hypocalcemia: an interventional prospective randomized trial (THYPOS trial).** Andrea Palermo<sup>\*1</sup>, Nicola Napoli<sup>1</sup>, Gaia Tabacco<sup>2</sup>, Giuseppe Mangiameli<sup>3</sup>, Filippo Longo<sup>3</sup>, Daria Maggi<sup>2</sup>, Silvia Briganti<sup>2</sup>, Angelo Lauria Pantano<sup>2</sup>, Anda Naciu<sup>2</sup>, Silvia Angeletti<sup>4</sup>, Fabio Vescini<sup>5</sup>, Paolo Pozzilli<sup>2</sup>, Pier Filippo Crucitti<sup>3</sup>, Silvia Manfrini<sup>2</sup>. <sup>1</sup>University Campus Bio-Medico, Italy, <sup>2</sup>Department of endocrinology, University Campus Bio-Medico, Italy, <sup>3</sup>Department of Surgery, university Campus Bio-Medico, Italy, <sup>4</sup>laboratory, University Campus Bio-Medico, Italy, <sup>5</sup>Department of Endocrinology, Ospedaliero-Universitaria Santa Maria della Misericordia di Udine, Italy

**Context:** Transient hypoparathyroidism after neck surgery is quite common. Therefore, subjects underwent thyroidectomy can experience severe hypocalcemia and often require extended hospitalizations leading to increased healthcare costs. Up to now, there are no studies evaluating the use of teriparatide for prevention of postoperative hypocalcemia. **Objective:** to evaluate if teriparatide is able to prevent post-surgical hypocalcemia in subjects with high risk of hypocalcemia after thyroid surgery. **Design:** Prospective Phase II Randomized Open Label Trial. **Setting:** Surgical ward, University Campus Bio-Medico, Rome. **Patients:** 23 subjects (5 males, 18 females, mean age 53.4, SD 16.9) with iPTH levels at 4 hours after thyroidectomy < 10 pg/ml. **Intervention:** Subjects will be randomized (1:1) to receive subcutaneous administration of 20 mcg of teriparatide every 12 hours until the discharge (treatment group) or to follow the standard clinical care (control group). **Main Outcome Measure:** adjusted serum calcium. **Duration of hospitalization.** **Results:** The groups were well-matched according to the factors that may negatively affect the calcium balance after thyroidectomy. Overall, the incidence of hypocalcemia was 2 in treatment group (both at day 2) and 10 (2 at day 1) in control group (relative risk: 0.218, 95% CI: 0.061 – 0.784). In treatment group, mean serum adjusted calcium concentration on post-operative day 1 and 2 was 8.9 mg/dl and 8.3 mg/dl, respectively; in the control group, mean serum adjusted calcium levels were 8.2 mg/dl (day 1,  $P < 0.001$  vs. treatment group) and 7.64 g/dl (day 2,  $P < 0.001$  vs. treatment group). No subject belonging to treatment group experienced symptoms of hypocalcemia or required calcium/vitamin D administrations. 11/12 belonging to control group experienced minor symptoms such as perioral tingling with positive Chvostek's sign. In only 3 subjects, Trousseau's sign and carpal/跗 spasm were both positive. All these subjects (11/12) required oral calcium and calcitriol administration with fully symptoms resolution. No subjects required intravenous calcium administration. The median duration of hospitalization was 3 days (IQR: 1.25) in control subject and 2 days (IQR: 0.5) in treated subjects ( $P = 0.139$ ). **Conclusions:** our findings suggest that Teriparatide may prevent post-surgical hypocalcemia in high risk subjects after thyroid surgery. This treatment might be also a valuable tool to reduce the duration of hospitalization.

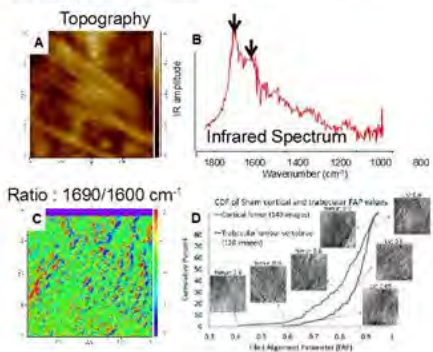
**Disclosures:** Andrea Palermo, None.

## FR0014

**AFM & AFM-IR Studies of Collagen Microstructure and Chemical Composition for Estrogen Depleted and Drug Treated Cortical Bone and Lumbar Vertebrae.** Mark M Banaszak Holl<sup>\*1</sup>, Megan Cauble<sup>2</sup>, Matthew Muckle<sup>3</sup>, Taeyong Ahn<sup>4</sup>, Sriram Vaidyanathan<sup>5</sup>, Rachel Merzel<sup>6</sup>, Jeffrey A. Fessler<sup>3</sup>, Bradford G. Orr<sup>6</sup>, Le T. Duong<sup>7</sup>. <sup>1</sup>Macromolecular Science & Engineering, <sup>2</sup>Chemistry, <sup>3</sup>Biomedical Engineering, University of Michigan, United states, <sup>4</sup>Chemistry, Univ of Michigan, United states, <sup>5</sup>Electrical Engineering, Univ of Michigan, United states, <sup>6</sup>Macromolecular Science & Engineering, Univ of Michigan, United states, <sup>7</sup>Biomedical Engineering, Univ of Michigan, United states, <sup>8</sup>Univ of Michigan, United states, <sup>9</sup>Merck & Co., United states

The nanomorphology and microstructure of type I Collagen has been demonstrated to be altered by estrogen depletion. Although treatments with conventional antiresorptives preserve these structural properties in preclinical models of osteoporosis, the chemical and structural origin of these changes remains poorly understood. In studies of sham operated, ovariectomized (OVX), and OVX/drug treated rabbits, we have employed atomic force microscopy (AFM), as well as AFM-detected infrared (IR) spectroscopy (AFM-IR), to explore the changes in type I collagen fibril nanomorphology, the microstructure of fibril organization, and the spectroscopic signatures associated with the structural change. 9-month-old New Zealand white female rabbits were dosed: sham-operated (n=11), OVX (n=12), OVX + alendronate (ALN, 600 µg/kg/wk, s.c.) (n=12), and OVX + the cathepsin-K inhibitor L-235 (CatKI, 10 mg/kg, daily, p.o.) in prevention mode for 27 weeks (n=13). Samples from the cortical femur and lumbar vertebral were polished, demineralized and imaged using AFM. Auto-correlation of image patches was used to generate a vector field for each image that mathematically approximated the collagen fibril alignment. This vector field was used to automatically compute an information theoretic entropy that was employed as a quantitative fibril alignment parameter (FAP) to allow image-to-image and sample-to-sample comparison. OVX samples contained a tail of lower FAP values representing regions of greater fibril alignment. OVX/ALN treatment resulted in a FAP distribution indicating greater alignment for cortical femur and less alignment for lumbar trabeculae. OVX/CatKI treatment gave a shift in distribution of FAP values indicating less alignment for cortical bone and no change for lumbar trabecular bone. Fibril alignment was also evaluated by considering when a fibril was part of discrete bundles or sheets (classified as *parallel*) or not (classified as *oblique*). For this analysis, a decrease in the proportion of *parallel* fibrils in cortical femur was observed for OVX but no change was observed for the lumbar vertebrae. For cortical femur, OVX/ALN treatment partially prevented the proportion of *parallel* fibrils from increasing and OVX/CatKI treatment completely prevented a change. In trabecular lumbar vertebrae, both OVX/ALN treatment and OVX/CatKI treatment increased the proportion of *parallel* fibrils.

Figure. AFM-IR characterization of surface demineralized sham rabbit cortical bone ( $1 \times 1 \text{ um}$ ) and Fibril Alignment Parameter (FAP): A) topography B) ratio 1690/1600  $\text{cm}^{-1}$  C) IR spectra in region from Amide I band to mineral band D) Cumulative density function (CDF) of cortical and trabecular bone FAP values



Figure

**Disclosures:** Mark M Banaszak Holl, None.

This study received funding from: Merck & Co.

## FR0015

**Age and Gender Differences in Loading Induced Strain and Biomechanical Properties of C57Bl/6 Mice.** Mark T. Begonia, Hammad Mumtaz, Mark Dallas, An-Lin Cheng, Ganesh Thiagarajan<sup>\*</sup>, Mark L. Johnson. University of Missouri-Kansas City, United states

Aging is associated with a diminished ability to form new bone in response to mechanical loads that at younger ages are anabolic. We sought to determine whether aging results in changes in the strains experienced by osteocytes as a possible

explanation for the lack of new bone formation in response to loading. The ulnae of female and male C57Bl/6 mice at ages of 6, 12, and 22 months were subjected to strain gaging and digital image correlation (DIC) experiments to obtain load-strain relationships and validate finite element (FE) models of the strain experienced by osteocytes in the forearm. DIC was used as an alternative since strain gage attachment likely stiffens the bone due to the adhesive and foil. 3-point bending and microCT were also used to obtain the biomechanical properties of each ulna.

Load-strain relationships showed that DIC strains were comparable or significantly higher than strain gage readings, thus highlighting DIC as a viable alternative to strain gaging. Two-way ANOVA confirmed a significant age\*gender interaction ( $p=0.006$ ) and significant changes in DIC strain due to age ( $p<0.0001$ ) and gender ( $p=0.017$ ). From 6 to 22 months, females exhibited a 33% lower DIC strain while males had a 16% decline. Similar analysis of strain gage readings confirmed a significant age\*gender interaction ( $p=0.031$ ) and significant changes based on age ( $p=0.038$ ) but not gender. From 6 to 22 months, females displayed 18% decrease in strain gage values whereas males experienced a 12% increase in strain. This finding shows that aging leads to a higher degree of stiffening in female ulnae compared to males. Biomechanical analysis revealed that the ultimate load and Young's modulus did not significantly change due to age or gender. However, 22 month old females displayed a significantly lower work to failure (38%) compared to the 6 month group. This decline in work to failure shows that aging leads to a lower threshold of energy absorption in female ulnae prior to fracture. Furthermore, this decreased work to failure coincides with the previous observation that female ulnae became stiffer with age since an increased stiffness would likely produce a higher rate of fracture. Overall, this study demonstrated the effects that both age and gender have on the strain response in mouse ulnae. FE models designed to analyze the effects of age and gender on strains at the osteocyte level are currently being validated using these biological strain and biomechanical data.

**Disclosures:** Ganesh Thiagarajan, None.

## FR0016

**Alendronate treatment improves vertebral structural properties and maintains vertebral trabecular bone material properties in hound dogs.** Daniel J Brooks<sup>1</sup>, Julia N Moulton<sup>1</sup>, Caroline DiNapoli<sup>2</sup>, Tessabella Magliochetti<sup>2</sup>, Stephanie McCarthy<sup>3</sup>, Robert M Urban<sup>3</sup>, Deborah J Hall<sup>3</sup>, Thomas M Turner<sup>3</sup>, Mary L Bouxsein<sup>4</sup>. <sup>1</sup>Center for Advanced Orthopaedic Studies, Beth Israel Deaconess Medical Center, United states, <sup>2</sup>Center for Advanced Orthopedic Studies, Beth Israel Deaconess Medical Center, United states, <sup>3</sup>Rush University Medical Center, United states, <sup>4</sup>Center for Advanced Orthopedic Studies, Beth Israel Deaconess Medical Center & Department of Orthopedic Surgery, Harvard Medical School, United states

Although the mechanisms underlying atypical femoral fractures (AFF) are unknown, clinicians and patients are concerned about long-term use of bisphosphonates and their possible association with AFF. A prior study in beagle dogs found that high, but not low, dose alendronate (ALN) treatment reduced whole vertebral toughness (Mashiba et al, 2001). To confirm and extend these findings, we tested the effect of 12 or 18 months ALN treatment on vertebral bone microarchitecture and mechanical properties in large dogs. Skeletally-mature male hound dogs (29.7 ± 3.3 kg, range: 24 to 36 kg) were assigned (n=10 /gr) to: 1) Control, 12 mo; 2) Control, 18 mo, 3) ALN, 12 mo, or 4) ALN, 18 mo. Dogs received daily ALN-filled gelatin capsules at a clinically relevant dose (0.2mg/kg/day) or identical capsules filled with lactose. Dogs received fluorochrome labels for histologic assessment of bone formation rate. At study end, the lumbar vertebrae were collected for bone microstructure (by microCT) and mechanical analyses, including compression testing on the intact L2 vertebral body and of a trabecular bone core from L5. Group differences were assessed by ANOVA and unpaired t-tests. Results: There were no differences by duration of treatment, thus results are presented for both timepoints combined. Confirming an anti-remodeling effect, ALN-treated dogs had lower mineral apposition rate than CON (-18%,  $p<0.05$ ) and had significantly higher BMD, Tb.BV/TV, Tb.Th, tissue mineral density and lower Tb. separation (Table). For the intact L2 vertebral body, ALN dogs had significantly higher work to maximum load and apparent toughness compared to CON. Compression testing of vertebral trabecular bone cores revealed significantly greater stiffness and work to failure in ALN-treated specimens, but no differences in compressive modulus or toughness. In conclusion, we found that ALN treatment in adult male hound dogs led to improved trabecular bone microstructure. Consistent with prior studies, whole vertebral failure load tended to be higher with ALN treatment. Yet, in contrast to prior reports, ALN led to higher work-to-failure and apparent toughness of the whole vertebrae. Further, ALN had no detrimental effects on intrinsic compressive mechanical properties of vertebral trabecular bone. Altogether, these data confirm positive or neutral effects of ALN treatment at clinically relevant doses on mechanical properties of whole vertebrae and of vertebral trabecular bone specimens in dogs.

Table 1. Effect of ALN treatment on vertebral trabecular bone microstructure and mechanical properties in hound dogs (mean ± SD)				
	ALN (n=19)	CON (n=20)	Difference (%)	p-value
<b>Trabecular bone microarchitecture</b>				
BV/TV (%)	25.9 ± 5.5	19.6 ± 2.8	+32%	0.0001
Conn.D. (1/mm <sup>3</sup> )	56.4 ± 25.1	31.3 ± 13.7	+80%	0.0004
Tb.N (1/mm)	2.23 ± 0.35	1.83 ± 0.23	+22%	0.0001
Tb.Th (µm)	124 ± 15	107 ± 9	+16%	0.0001
Tb.Sp (µm)	478 ± 70	566 ± 67	-16%	0.0002
vBMD (mgHA/ccm)	296 ± 55	228 ± 34	+30%	<0.0001
TMD (mgHA/ccm)	859 ± 13	816 ± 16	+5%	<0.0001
<b>Vertebral trabecular bone core mechanical properties</b>				
$\sigma_{ult}$ (MPa)	47.9 ± 10.8	42.5 ± 8.2	+13%	0.0962
Work to $F_{max}$ (mJ)	46.7 ± 33.1	29.9 ± 14.3	+56%	0.0513
Stiffness (N/mm)	1453 ± 492	1035 ± 388	+40%	0.0069
App. $E_{comp}$ (MPa)	2637 ± 842	2390 ± 950	+10%	0.4083
Yield stress (MPa)	42.5 ± 9.4	36.8 ± 7.7	+15%	0.0508
U (mJ/mm <sup>3</sup> )	0.87 ± 0.43	0.77 ± 0.29	+14%	0.3718
<b>Whole vertebral mechanical properties</b>				
$\sigma_{ult}$ (MPa)	46.8 ± 6.2	43.5 ± 6.2	+8%	0.1093
$F_{max}$ (N)	8256 ± 1060	7335 ± 1405	+10%	0.0857
Work to $F_{max}$ (J)	17.8 ± 3.7	14.0 ± 5.2	+27%	0.0140
Stiffness (N/mm)	3728 ± 1237	4318 ± 698	-14%	0.0852
U (mJ/mm <sup>3</sup> )	4.4 ± 0.8	3.4 ± 1.1	+29%	0.0037

Abbreviations: Bone volume fraction (BV/TV), connectivity density (ConnD), trabecular number (Tb.N), trabecular thickness (Tb.Th), trabecular separation (Tb.Sp), bone density (vBMD), tissue mineral density (TMD), ultimate force ( $F_{max}$ ), Ultimate stress ( $\sigma_{ult}$ ), Apparent compressive modulus (App.  $E_{comp}$ ), Toughness (U).

Table 1

**Disclosures:** Mary L Bouxsein, Merck, 11; Eli Lilly, 12; Merck, 12; AgNovos Healthcare, 12; Amgen, 11

This study received funding from: Merck

## FR0017

**Feasibility of Quantitative *In Vivo* Assessment of Mineral and Matrix Properties by Solid-State Phosphorus-31 and Proton Magnetic Resonance.** Xia Zhao<sup>\*1</sup>, Hee Kwon Song<sup>1</sup>, Cheng Li<sup>1</sup>, Alan C Seifert<sup>2</sup>, Felix W Wehrli<sup>1</sup>. <sup>1</sup>University of Pennsylvania, United states, <sup>2</sup>Icahn School of Medicine at Mount Sinai, United states

Magnetic Resonance Imaging (MRI) is potentially suited for providing quantitative insight into the chemistry of bone. Next to collagen making up the bulk of the organic matrix, water accounts for 20-30% of the unmineralized osteoid, occurring in the form of collagen-bound water (BW, ~60-80%) and pore-resident water (PW, 20-40%). Phosphorus-31 (<sup>31</sup>P) has spin 1/2 (like the proton in H<sub>2</sub>O), and occurs in bone predominantly in the form of the orthophosphate anion (PO<sub>4</sub><sup>3-</sup>), permitting direct measurement of mineral constituents. However, until very recently, technological hurdles precluded detection of these nuclei in solid bone due to the extremely short lifetime of the resulting MRI signals (T<sub>2</sub>~100-300µs). The emergence of solid-state imaging techniques and their integration into clinical MRI scanners now allows for direct detection and quantification of matrix and mineral constituents *in vivo*. Here we report the detection and quantification of BW (a surrogate for matrix density) and <sup>31</sup>P in a single integrated imaging procedure in tibial cortical bone.

Mineral <sup>31</sup>P (T<sub>1</sub> ~26s, T<sub>2</sub> ~190µs) was imaged with a zero echo-time (ZTE) MRI sequence optimized for its relaxation properties (<sup>31</sup>P ZTE, ~20min). ZTE MRI is a solid-state imaging technique with effective 'echo times' of microseconds, allowing capture of the rapidly decaying signal from these sources. BW (T<sub>2</sub>~300µs) was imaged by long-T<sub>2</sub>H suppression with T<sub>2</sub>-selective inversion preceding ZTE acquisition (~7min). BW and <sup>31</sup>P concentrations were subsequently derived with the aid of co-imaged reference samples.

The new method has been tested on a clinical MRI system (Siemens 3T) with a custom-designed <sup>1</sup>H/<sup>31</sup>P dual-tuned RF coil on six subjects. Derived BW and <sup>31</sup>P concentrations are summarized in Table 1. Both quantities are in good agreement with previously published results obtained *ex vivo* (Seifert et al, JBMR, 2015). Figure 1 displays <sup>31</sup>P images of the tibia and fibula, along with four reference samples of hydroxyapatite.

This work is the first to demonstrate the feasibility of quantifying bone matrix and mineral density (from which degree of mineralization of bone can be determined) in a single integrated protocol *in vivo*.

## FR0019

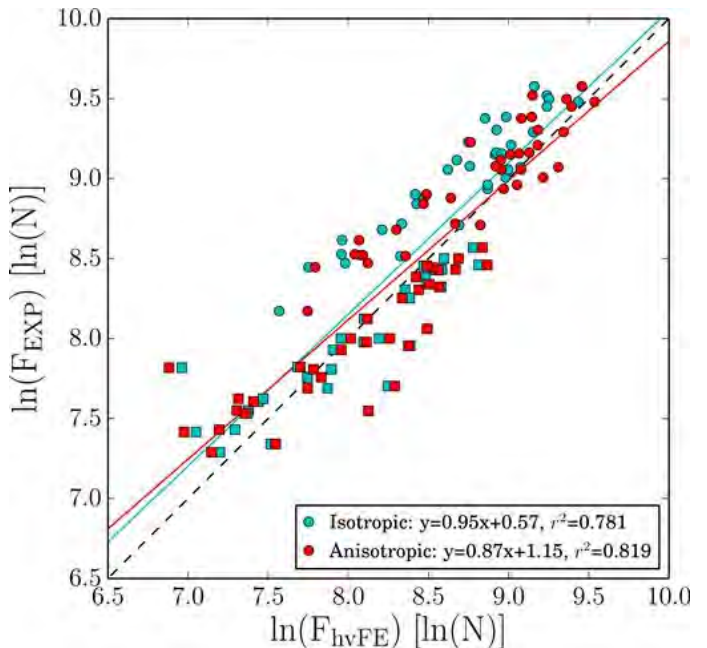
**Mapping of Trabecular Anisotropy Improves QCT-based Finite Element Estimation of Hip Strength in Pooled Stance and Side-Fall Load Configurations.** Jarunan Panyasantisuk<sup>\*1</sup>, Enrico Dall'Ara<sup>2</sup>, Dieter Pahr<sup>3</sup>, Philippe Zysset<sup>1</sup>. <sup>1</sup>Institute for Surgical Technology & Biomechanics, University of Bern, Switzerland, <sup>2</sup>Department of oncology & metabolism & INSIGNEO Institute for in silico medicine, University of Sheffield, United Kingdom, <sup>3</sup>Institute of Lightweight Design & Structural Biomechanics, Vienna University of Technology, Austria

**Introduction:** Finite element analysis (FEA) is becoming a standard to estimate bone strength when CT scans are available. In general, FE models of the hip from *in vivo* CT scans assume isotropic material properties and are validated in a single load configuration. However, the proximal femur exhibits an important trabecular anisotropy and multiple load cases are believed to improve fracture risk prediction. The aim of this study is to compare the *ex vivo* bone strength predictions of isotropic and anisotropic QCT-based non-linear FE models of human proximal femora in both stance and side-fall configurations.

**Materials and methods:** Sixty-nine human proximal femora (37 females, 32 males, age  $77 \pm 11$  years, range 46-96) were scanned with HR-pQCT (0.082mm), clinical QCT (0.3mm) and tested to failure in either stance or side-fall configuration. FE models of the proximal femora were created by converting the QCT image voxels to hexahedral elements (3mm) and by reproducing the two experimental loading scenarios. The anisotropy of trabecular bone was registered from the HR-pQCT images and bone elastic and yield properties were assigned from a previous damage and plasticity model. The isotropic and anisotropic non-linear FE models were loaded to failure and the computed ultimate forces were compared with the biomechanical testing results for both load cases.

**Results:** Ultimate forces computed by isotropic and anisotropic FE models show similar correlations with ultimate force *ex vivo* for individual load configurations (isotropic:  $R^2=0.86$  for stance and  $R^2=0.77$  for side-fall, anisotropic:  $R^2=0.84$  for stance and  $R^2=0.76$  for side-fall), but anisotropic FE models demonstrate slightly but significantly higher correlations (isotropic:  $R^2=0.78$ , anisotropic:  $R^2=0.82$ ) for the pooled stance and side-fall data ( $p<0.05$ ).

**Discussions:** The results suggests that the inclusion of anisotropy in these FE models is not able to improve the prediction of experimental variations within a single load case, but becomes interesting for proper comparison between distinct load cases. Refined FE models of the human proximal femur are expected to improve the accuracy of bone strength predictions and eventually the assessment of fracture risk.



Subject age/years (gender)	Bound Water Concentration (mol/L)	$^{31}\text{P}$ Concentration (mol/L)
29 (M)	9.78	7.23
32 (M)	9.34	7.21
32 (M)	9.41	6.73
43 (M)	9.68	8.16
48 (M)	9.39	6.95
65 (F)	7.95	5.03

**Figure 1.** (a) Average signal intensity vs.  $^{31}\text{P}$  for the four hydroxyapatite (HA) reference samples.  $^{31}\text{P}$  concentration maps superimposed on proton anatomical images for (b) 32-year-old male and (c) 65-year-old female. Note, reduced  $^{31}\text{P}$  concentration in subject of panel (c) along with lower BW density (Table).

Figure

Disclosures: Xia Zhao, None.

## FR0018

**Glycated Osteocalcin Contributes to Loss of Bone Toughness.** Stacyann Morgan<sup>\*1</sup>, Caren Gundberg<sup>2</sup>, Gerard Karsenty<sup>3</sup>, Deepak Vashishth<sup>1</sup>. <sup>1</sup>Rensselaer Polytechnic Institute, United states, <sup>2</sup>Yale University, United states, <sup>3</sup>Columbia University, United states

Non-enzymatic glycation (NEG) of bone matrix proteins produces crosslinks known as advanced glycation end-products (AGEs) which have been shown to be detrimental to bone quality and fracture<sup>1</sup>. Osteocalcin (OC) a major non-collagenous protein in bone undergoes modification by NEG<sup>2</sup> and plays a key role in its biological and mechanical function<sup>3</sup>. Thus, glycated OC may affect bone quality and fracture in diseases such as osteoporosis and diabetes mellitus<sup>2</sup>. However, unlike type I collagen, the effect of glycated OC on bone quality and fracture remains unknown. Using a unique combination of *in vivo* and *in vitro* approach, we have isolated and determined the effects of glycated OC on bone fracture.

Six month old male wild type (WT) and OC knockout ( $n=5/\text{group}$ ) mice femora were used. The femoral head and condyles were removed and a notch created in the mid-shaft of all samples using a slow speed diamond blade saw. The bones were subsequently scanned using microCT (Scanco uCT 40) for measurement of notch angle, cortical thickness and internal and external diameters. One limb was randomly selected from each animal for *in vitro* glycation with ribose sugar while the contralateral limb served as a control. Following glycation, the samples were loaded in 3-pt bending until failure at a loading rate of 0.001mm/s (Elf Enduratec 3200). Paired samples t-test was used to determine differences in propagation toughness between the groups (WT-glycated vs. WT-non-glycated; OC-/- glyated; vs. OC-/- non-glycated). Because NEG modifies the organic matrix including type I collagen and OC, we compared the change in propagation toughness caused by glycation of the organic matrix with (WT-glycated *minus* WT-non-glycated) and without osteocalcin (OC-/- glyated *minus* OC-/- non-glycated) by independent samples t-test.

NEG resulted in a significant decrease in propagation toughness between the WT-glycated and WT-non-glycated groups ( $p=0.009$ ) and similar result was observed for the OC-/- group ( $p=0.012$ ). More importantly, the change in propagation toughness was 20% greater in WT than OC-/- ( $p=0.03$ ). This results indicates for the first time that glycation of osteocalcin contributes to bone toughness and provides new insight into the role of post-translational modification on bone matrix other than type I collagen on bone fracture.

Ref: [1]Vashishth et al. *Bone* 28.2 (2001): 195-201. [2] Poundarik et al. *PNAS* 109.47 (2012): 19178-19183. [3] Gundberg et al. *JBC* 261.31 (1986): 14557-14561.

Disclosures: Stacyann Morgan, None.

Linear regressions between FE and experimental ultimate forces in log space for the combined results

Disclosures: Jarunan Panyasantisuk, None.

**FR0020**

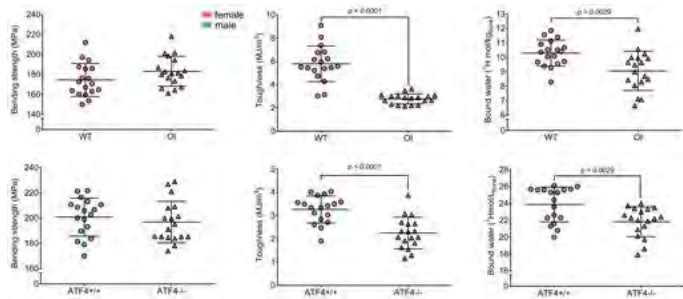
**Matrix-bound water concentration is lower in mice with brittle bones caused by osteogenesis imperfecta and separately ATF4 deficiency.** Mathilde Granke<sup>\*1</sup>, Sasidhar Uppuganti<sup>1</sup>, Amy Creevy<sup>1</sup>, Julie Schnur<sup>2</sup>, Ben Greene<sup>3</sup>, Mark Does<sup>2</sup>, Jeffrey Nyman<sup>1</sup>. <sup>1</sup>Vanderbilt university Medical Center, United states, <sup>2</sup>Vanderbilt University, United states, <sup>3</sup>Genzyme, United states

In human bone, matrix hydration decreases with age causing the organic matrix to become brittle and lowering overall fracture resistance. However, the determinants of collagen-bound water have yet to be identified. Potential candidates encompass matrix-related factors responsible for a disruption in normal mineralization and collagen organization. Using two genetic mouse models exhibiting a brittleness phenotype caused by osteogenesis imperfecta (OI) and the loss of activating transcription factor 4 (ATF4), which is critical to osteoblast maturation, we hypothesize that concentration of matrix-bound water (BW) is significantly lower in fragile bones relative to their controls.

We harvested bones from female heterozygous (*G610C/+*) OI mice and wild-type (+/+) littermates as well as from female and male *Atf4+/+* and *Atf4-/-* littermates at 16 wks of age (n = 18/genotype). Femoral mid-shafts were i) scanned with  $\mu$ CT to obtain tissue mineral density (TMD); ii) analyzed with <sup>1</sup>H NMR to determine BW; iii) subjected to 3pt bending to estimate material strength and toughness; and iv) analyzed with HPLC to quantify enzymatic (pyridinoline (PYD) and deoxypyridinoline (DPD)) and non-enzymatic collagen crosslinks (pentosidine, PE).

Mechanical testing confirmed that OI and ATF4-deficient bones were not weaker but more brittle relative to their controls. The reduced toughness was associated with lower BW in both OI (-12%) and *Atf4-/-* (-9%) bones compared to their controls (Fig). TMD was higher in the OI bones (+4%, p<0.0001) but increased marginally with the loss of ATF4 (p=0.27). DPD was lower (p<0.0001) in OI bones while PYD and PE did not vary among genotypes. In *Atf4-/-* bones, PE concentration in tissue was lower (p = 0.019) while PYD and DPD did not differ from the controls. Multilinear regressions indicated that an increase in TMD and decrease in PE explain 23% of the decrease in BW with the loss of ATF4, while in OI bones, the decrease in BW only correlated with a lower DPD content (R<sup>2</sup>=23%).

For two different genetic mutations, each leading to a brittle bone phenotype, a decrease in matrix-bound water was a common underlying trait across the murine models confirming the relevance of bound water as potential biomarker of brittleness. Since differences in mineralization and in collagen crosslinks do not systematically explain the difference in bound water content, other matrix-related factors (e.g., non-collagenous proteins, collagen structure) may be determinants.



Fig

Disclosures: Mathilde Granke, None.

**FR0021**

**Role of Advanced Glycation End-Products and Cortical Porosity in Type 2 Diabetes.** Lamya Karim<sup>\*1</sup>, Miranda Van Vliet<sup>2</sup>, Kelsey Velie<sup>2</sup>, Ayesha Abdeen<sup>1</sup>, Douglas Ayres<sup>1</sup>, Mary Bouxsein<sup>1</sup>. <sup>1</sup>Harvard Medical School, United states, <sup>2</sup>Beth Israel Deaconess Medical Center, United states

Patients with type 2 diabetes (T2D) have 2-3x increased fracture risk compared to non-diabetics, but the mechanisms underlying this increased risk are poorly understood. Because T2D patients typically have normal or high bone mass, it has been proposed that the high fracture risk results from having poor bone quality due to an accumulation of advanced glycation end-products (AGEs) that are harmful for bone strength and/or increased cortical porosity. Thus, our goal was to investigate if AGEs, cortical porosity, and bone biomechanical properties were altered in adult human T2D bone compared to non-T2D controls.

Femoral neck bone specimens from age- and gender-matched T2D (n=7, 60.0 ± 5.3 yrs) and control (n=7, 60.1 ± 6.1 yrs) Caucasian men and women (age 50 to 68 yrs) undergoing total hip replacement surgery were collected. Specimens were imaged by microcomputed tomography to assess cortical porosity, mechanically tested by reference point indentation, and quantified for bone AGEs by a fluorometric assay.

T2D subjects had greater HbA<sub>1c</sub> than non-diabetic controls (p=0.09). Femoral neck cortical porosity tended to be greater in T2D than in controls (+29%, p=0.15). Indentation distances were greater (+12% to 73%) while unloading and loading slopes (-9% to -10%) were lower in T2D than in controls (Table 1). Cortical and trabecular bone AGEs were 7% and 15% higher in T2D, respectively, but did not

reach statistical significance. Pooling T2D and non-diabetic groups together, we found that bone AGEs quantified at the site of indentation (cortical bone) was positively associated with indentation distances (r=0.56 to 0.81, p≤0.05) and negatively associated with unloading (r=-0.45, p=0.11) and loading (r=-0.60, p≤0.05) slopes (Figure 1).

In summary, femoral neck specimens from individuals with T2D had increased cortical porosity, a trend for increased AGEs, and compromised biomechanical properties. Specifically, probes indented deeper into T2D bone, which had deteriorated stiffness as illustrated by lower unloading and loading slopes. Although we did not detect the expected difference in AGEs between groups, specimens containing higher AGEs had more deteriorated biomechanical properties. These results demonstrate compromised cortical bone biomechanical properties at the femoral neck in T2D, including higher cortical porosity and worse indentation properties. Further work on subjects who have more severe and/or poorly controlled T2D is needed.

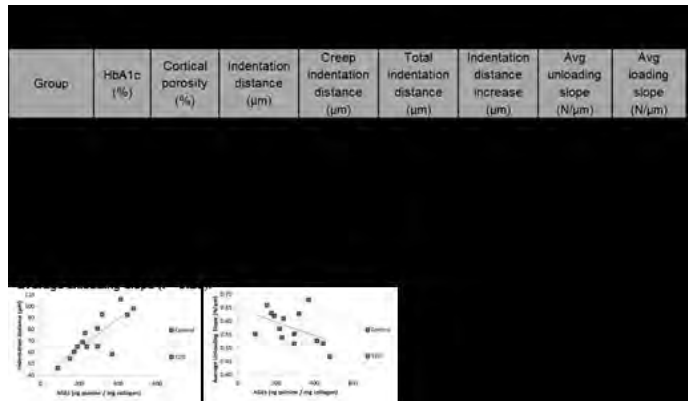


Table 1 and Figure 1

Disclosures: Lamya Karim, None.

**FR0022**

**The Relationship Between Femoral Neck aBMD and the Underlying Morphological and Compositional Traits that are Coordinately Regulated to Establish Mechanical Homeostasis.** Andrew Kozminski<sup>1</sup>, Erin Bigelow<sup>1</sup>, Stephen Schlecht<sup>1</sup>, Robert Goulet<sup>1</sup>, Sioban Harlow<sup>1</sup>, Carrie Karvonen-Gutierrez<sup>1</sup>, Jane Cauley<sup>2</sup>, Karl Jepsen<sup>\*1</sup>. <sup>1</sup>University of Michigan, United states, <sup>2</sup>University of Pittsburgh, United states

The manner in which the skeletal system coordinately regulates multiple traits to establish mechanical homeostasis has been studied primarily for diaphyses but to a lesser extent for metaphyseal regions. How the natural variation in neck width and the accompanying set of traits affect aBMD has not been systematically evaluated. The relationship between clinical computed tomography (CT) and DXA images was analyzed for 213 women (69 black, 144 white; 53-64 years of age) enrolled in the Pittsburgh site of the Study of Women's Health Across the Nation. All studies were conducted with informed consent approved by the site's IRB. The CT analysis site coincided with the region used to measure hip aBMD from the DXA images. Linear regression analyses confirmed a significant positive association between cortical area (CtAr) and total area (TtAr) (R<sup>2</sup>=0.60, p<0.0001), and significant negative associations between TtAr and relative cortical area (RCA=CtAr/TtAr) (R<sup>2</sup>=0.29, p<0.0001) and cortical tissue mineral density (CtTMD) (R<sup>2</sup>=0.18, p<0.0001) and between trabecular vBMD and DXA-bone area (R<sup>2</sup>=0.15, p<0.0001). Thus, women with narrow femoral necks had lower absolute CtAr but higher RCA combined with higher CtTMD and trabecular vBMD compared to women with wide femoral necks (Fig 1). A linear regression analysis between aBMD and each of the cortical and trabecular traits revealed that aBMD was not correlated with TtAr (R<sup>2</sup>=0.0003, p<0.8), correlated weakly with CtAr (R<sup>2</sup>=0.05, p<0.003) but more strongly with CtTMD (R<sup>2</sup>=0.27, p<0.0001). aBMD correlated most strongly with trabecular vBMD (R<sup>2</sup>=0.60, p<0.0001). A multivariate analysis showed that the combination of cortical and trabecular traits, along with body weight, age, and ethnicity, explained 69.4% of the variation in aBMD. Significant independent predictors included body weight, ethnicity, CtTMD, and trabecular vBMD. This study confirmed that women build bones in unique ways relative to the natural variation in external bone size, and that establishing mechanical homeostasis results in significant covariation among CT-attenuating traits at the population level (Fig 1). The lack of a relationship between aBMD and TtAr means that the underlying traits are coordinately adjusted in such a way that the ratio of BMC to bone area is nearly constant across the population. Given that women construct bones differently, the next challenge will be to test whether age-related changes in bone structure also differ among women.

## FR0031

**Novel Associations Between Reduced Serum Sclerostin and Adaptive Bone Changes Following Exercise Training.** *Melissa Ramcharan*<sup>1\*</sup>, *Rachel Izard*<sup>2</sup>, *Bonnie Nolan*<sup>1</sup>, *Lauren Smith*<sup>1</sup>, *Stephen Schlecht*<sup>1</sup>, *William Fraser*<sup>3</sup>, *Julie Greeves*<sup>4</sup>, *Karl Jepsen*<sup>1</sup>. <sup>1</sup>University of Michigan, United states, <sup>2</sup>HQ Army & Training Division, United Kingdom, <sup>3</sup>Norwich Medical School, University of East Anglia, United Kingdom, <sup>4</sup>HQ Army Recruiting & Training Division, United Kingdom

The adaptive response of bone to mechanical loading depends in part on the downregulation of local sclerostin expression. How bone adapts relative to serum sclerostin (sScl) is not well understood. We tested the hypothesis that the bone adaptive response to exercise would depend on reductions in sScl. Associations between changes in sScl levels and lower limb morphology were examined for British male military recruits during 10 weeks of basic training ( $20 \pm 2$  years of age;  $N=108$ ;  $n=76$  with repeat serum measures) as well as for male A/J (AJ) and C57BL/6J (B6) inbred mouse strains during 4 weeks of voluntary cage wheel running from 4 to 8 weeks of age ( $n=14$ /strain/group). Baseline and final sScl levels following exercise were analyzed using species-specific ELISA kits. Morphology of the 38% site of human tibiae was assessed at baseline and after 10 weeks of training using pQCT (Stratec XCT2000L). Mouse femoral midshaft endpoint morphology between exercise and control cohorts was quantified using nanoCT.

Baseline sScl levels were highly variable, ranging from 6 to 92 pM, for humans and 13 to 77 pM for inbred mouse strains (Fig. 1). Among humans, the change in sScl following basic training correlated negatively with baseline sScl ( $R^2 = 0.41$ ,  $p < 0.001$ , Fig. 1A). The change in total cross-sectional area and cortical area correlated negatively with the change in sScl levels ( $R^2 = 0.11-0.14$ ,  $p < 0.02$ ), indicating that adaptive bone changes were greater for men showing large reductions in sScl levels. Finally, significant negative correlations between the change in sScl levels and baseline sScl were seen for exercise and control cohorts in both AJ (Fig. 1B) and B6 (Fig. 1C) mouse strains. However with exercise, AJ mice showed significantly lower sScl levels (ANCOVA,  $p=0.002$ ), and no change in external bone size, but a small increase in cortical area (GLM  $p=0.09$ ). In contrast, B6 mice showed no change in sScl levels, but a decrease in bone size and cortical area (GLM,  $p < 0.05$ ). Our analysis of human and mouse data provided novel information about the association between sScl and adaptive bone changes where the wide inter-individual variation in sScl is clinically meaningful. Our data showed that 1) the baseline sScl is highly predictive of the change in sScl over time and following exercise; 2) humans with high baseline sScl show greater adaptive bone changes following basic training; and 3) the change in sScl following exercise varies with genetic background in mice.

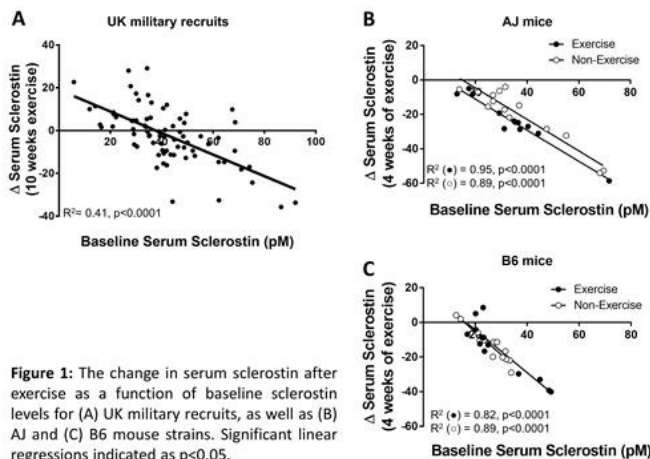


Figure 1. The change in serum sclerostin after exercise in humans and mice

**Disclosures:** *Melissa Ramcharan, None.*

## FR0032

**Associations of Behavioral Characteristics of Young Adults and Bone Health: Iowa Bone Development Study (IBDS).** *Elena Letuchy*, *Julie Eichenberger*<sup>\*</sup>, *Linda Snetselaar*, *Kathleen Janz*, *Trudy Burns*, *Punam Saha*, *James Torner*, *Steven Levy*. University of Iowa, United states

**Purpose:** To characterize behavioral characteristics (physical activity, diet, sleeping patterns, smoking and drinking status) of healthy young adults and describe associations between their cluster membership and bone quality.

**Methods:** DXA scans of whole body, hip and spine (Hologic 4500/Discovery) and pQCT scans of tibia (XCT-2000/3000) at 4% (trabecular) and 66% (cortical) sites were obtained for 303 (166 female) young adults (mean 19.9 years) participating in the

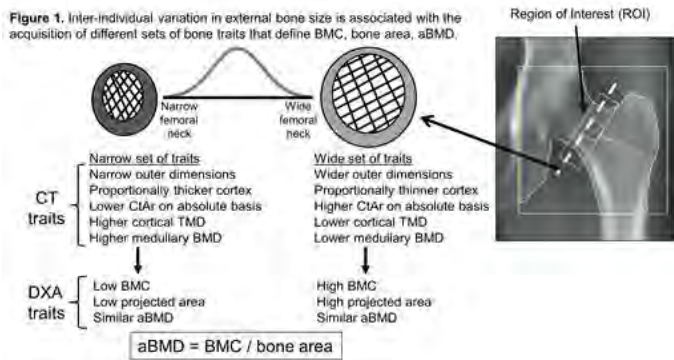


Figure 1

**Disclosures:** *Karl Jepsen, None.*

## FR0023

**Bisphosphonate Pre-Treatments Enhance Trabecular Bone Architecture during Unloading and Reambulation Despite Lower Resorption and Formation.** *Jeremy Black*<sup>\*</sup>, *Jessica Brezicha*<sup>2</sup>, *Corinne Metzger*<sup>3</sup>, *Scott Lenfest*<sup>1</sup>, *Jennifer Kosniowski*<sup>1</sup>, *Susan Bloomfield*<sup>3</sup>, *Matt Allen*<sup>4</sup>, *Harry Hogan*<sup>5</sup>. <sup>1</sup>TAMU Department of Mechanical Engineering, United states, <sup>2</sup>TAMU Department of Biomedical Engineering, United states, <sup>3</sup>TAMU Department of Health & Kinesiology, United states, <sup>4</sup>Department of Anatomy & Cell Biology, Indiana University School of Medicine, United states, <sup>5</sup>TAMU Department of Mechanical Engineering/ Department of Biomedical Engineering, United states

Bisphosphonates (BPs) have been shown to be effective in mitigating negative effects of unloading on bone in animal, bedrest, and space-flight studies. BPs were given in these studies throughout the unloading period, with the majority initiating treatment at the onset of unloading. The goal of the current study, however, was to test the efficacy of BPs when given as a pre-treatment prior to unloading only. We used the adult hindlimb unloaded (HU) rat model to compare alendronate (ALN) and risedronate (RIS) administered as pre-treatments before entering HU. Since ALN has a higher binding affinity than RIS, we hypothesized that ALN would protect better than RIS in this pre-treatment scenario.

Adult male Sprague-Dawley rats (6 mo) were assigned by body weight and total proximal tibia vBMD to 1 of 4 groups: AC (aging control), HU, ALN, and RIS. ALN (2.4  $\mu\text{g}/\text{kg}$ ) and RIS (1.2  $\mu\text{g}/\text{kg}$ ) were given 3x/wk for 4 wks prior to 4 wks of HU. Animals returned to normal ambulation after HU (R0) and recovered for 8 wks (R8). Tibias were collected at R0 and R8. *Ex vivo*  $\mu\text{CT}$  scans were made of the left proximal tibia metaphysis (PTM). The right PTM was analyzed by standard histomorphometry.

HU gave rise to higher osteoclast surface (Oc.S/BS +114%) and lower bone formation rate (BFR -75%) vs AC at R0. Neither BP affected BFR positively compared to HU, but both significantly reduced Oc.S/BS below AC. Even though BFR was lower than HU at R0 for both BPs, measures of trabecular architecture were improved. BV/TV was significantly higher for RIS (+59% vs HU) but not for ALN (+35% vs HU, but n.s.). Similarly, Tb.N was significantly higher for RIS (+48% vs HU) and higher for ALN (+28% vs HU, but n.s.). After 8 wks of recovery (R8), trabecular bone BV/TV remained higher for BP pre-treated animals vs HU but was only significant for RIS (+52% for RIS; +20% for ALN, but n.s.). Additionally, Tb.N was significantly higher vs HU for both BPs at R8 (+58% for RIS; +34% for ALN).

BP pre-treatment clearly prevented bone losses during HU, particularly in the trabecular bone of the PTM, and the benefits persisted through 8 wks of reambulation. While cellular measures varied little between ALN and RIS (BFR, Oc.S/BS),  $\mu\text{CT}$  showed that, contrary to our hypothesis, the trabecular architecture for the RIS treated animals was more robust than for ALN. This suggests that depth of penetration into the bone (which is greater with RIS) may be more important than binding affinity in this scenario.

**Disclosures:** *Jeremy Black, None.*

## FR0025

Withdrawn

longitudinal IBDS since early childhood. DXA-derived bone outcomes included bone mineral content (BMC) and areal density (aBMD). Bone strength measures from pQCT included bone strength index (BSI, compression strength at 4% site), and cortical thickness and polar section modulus (torsion strength at 66% site). Behavioral characteristics of interest were derived from: the Healthy Eating Index (HEI) - compliance with recommended intake; accelerometry (ActiGraph) - minutes of daily moderate/vigorous physical activity (MVPA); and the IBDS lifestyle questionnaire - sleeping, drinking, and smoking status. Latent class analysis (LCA) using Latent GOLD software was applied to investigate clustering of behaviors. Bone quality was estimated for latent classes identified by LCA using sex-specific regression analysis adjusted for participants' height and weight. Least squares mean bone quality measures for identified classes were estimated and compared.

Results: LCA identified 3 groups: healthy behavior (HB, high levels of HEI and MVPA, more sleep and no smoking), unhealthy behavior (UNB, all characteristics opposite of HB), and intermediate behavior (IB). HEI and MVPA were most important for class membership, while drinking habits (binge drinking) was least important and dropped from the final LCA solution. The HB group showed better bone quality across all measured bone outcomes for both sexes, while a small group of participants with consistently unhealthy behaviors had the worst bone quality. Mean BSI for males and females, respectively, was 156.7 and 106.2  $\text{mg}^2/\text{mm}^4$  in the HB group compared to 138.4 and 85.4  $\text{mg}^2/\text{mm}^4$  in the UNB group ( $p < 0.01$ ). Mean hip region aBMD for males was 1.21 vs. 1.10  $\text{g}/\text{cm}^2$ , and for females was 1.04 vs. 0.97  $\text{g}/\text{cm}^2$  ( $p < 0.05$  for all pairwise comparisons), respectively.

Conclusion: Clustering of healthy behaviors in young adults appears to be associated with better bone quality. Healthy eating and high levels of physical activity impact bone positively, while lack of sleep and smoking have moderate negative effects.

**Disclosures:** Julie Eichenberger, None.

## FR0034

**Poor Glycemic Control is Associated with Greater Urinary Calcium Excretion in Adolescents with Type 1 Diabetes.** David Weber<sup>\*1</sup>, Kimberly O'Brien<sup>2</sup>, Mary Leonard<sup>3</sup>, Nova Rackovsky<sup>4</sup>, George Schwartz<sup>4</sup>. <sup>1</sup>University of Rochester, United states, <sup>2</sup>Cornell University, United states, <sup>3</sup>Stanford University, United states, <sup>4</sup>University of Rochester, United states

Background: Type 1 diabetes (T1D) is associated with increased fracture risk and deficits in bone density and structure; yet the etiology is unclear. The goals of this study were to evaluate gastrointestinal calcium absorption, urinary calcium excretion, and estimated calcium retention in T1D adolescents compared to existing normative data, and to identify risk factors for urinary calcium loss in T1D.

Methods: 24 hour urine collections, blood samples, and diet recalls were obtained in 19 T1D subjects (11 F) aged 10-18 yrs. Individuals with celiac disease, renal insufficiency, corticosteroid use, or obesity were excluded. An established dual stable isotope method was used to assess calcium absorption in 8 female subjects with T1D of  $\geq 3$  yrs duration. Subjects received oral (<sup>42</sup>Ca) and IV (<sup>44</sup>Ca) isotope tracers. Fractional calcium absorption was determined as the relative recovery of oral vs IV tracer in a 24-h urine measured by thermal ionization mass spectrometry. Total calcium absorption was calculated as fractional calcium absorption\*calcium intake. Calcium retention was estimated as total calcium absorption - (urine calcium + estimated fecal calcium). Results were compared to existing data in healthy adolescent girls. Means  $\pm$  SD were compared using t-tests; correlations were assessed by Pearson's r and linear regression.

Results: Subjects had T1D duration of  $5.9 \pm 3$  yrs, A1c of  $9.4 \pm 1.4\%$ , and 25OHD of  $24.4 \pm 9.6$  ng/mL. Compared to healthy girls, T1D subjects had similar fractional calcium absorption ( $27.4 \pm 9.4\%$  vs.  $24.5 \pm 8.2\%$ ,  $p=0.44$ ) and a trend toward greater urinary calcium excretion ( $126 \pm 67\text{mg}/\text{d}$  vs.  $94 \pm 44\text{mg}/\text{d}$ ,  $p=0.2$ ). 25% (2/8) of T1D subjects had negative calcium retention. On univariate analysis, 24-h urine calcium excretion was correlated with hemoglobin A1c ( $r=0.75$ ,  $p < 0.01$ ) and urine glucose ( $r=0.56$ ,  $p=0.01$ ) in the entire sample and the subset completing the isotope study ( $r=0.74$ ,  $p=0.03$  for A1c) and ( $r=0.73$ ,  $p=0.04$  for urine glucose). A1c remained associated with urine calcium after adjustment for age, sex, puberty, calcium intake, urine sodium, and bone turnover markers.

Conclusions: Poor glycemic control was associated with greater urinary calcium excretion in adolescents with T1D. Analyses accounting for calcium intake and bone resorption suggest impaired renal calcium reabsorption as the mechanism underlying this relationship. Insufficient calcium availability for bone mineralization during adolescence may have lifelong consequences on bone health.

**Disclosures:** David Weber, None.

## FR0038

**The Muscle-Dependent Link Between IGF-I and Cortical Bone is Suppressed in Children with Insulin Resistance.** Joseph Kindler<sup>\*1</sup>, Norman Pollock<sup>2</sup>, Emma Laing<sup>1</sup>, Carlos Isales<sup>2</sup>, Mark Hamrick<sup>2</sup>, Ke-Hong Ding<sup>2</sup>, Dorothy Hausman<sup>1</sup>, George McCabe<sup>3</sup>, Berdine Martin<sup>3</sup>, Kathleen Hill Gallant<sup>3</sup>, Stuart Warden<sup>4</sup>, Connie Weaver<sup>3</sup>, Munro Peacock<sup>4</sup>, Richard Lewis<sup>1</sup>. <sup>1</sup>The University of Georgia, United states, <sup>2</sup>Augusta University, United states, <sup>3</sup>Purdue University, United states, <sup>4</sup>Indiana University, United states

Insulin-like growth factor I (IGF-I) plays a pivotal role in pediatric cortical bone development, acting through both direct and indirect (i.e., muscle-dependent) means.

Whereas IGF-I-dependent total body muscle mass, and subsequently bone mass accrual, may be compromised in insulin resistant children, cortical bone has yet to be considered in studies examining the IGF-I-muscle-bone relationship in the context of insulin resistance. Therefore, we examined differences in the muscle-dependent relationships between IGF-I and cortical bone in insulin resistant vs. insulin sensitive children.

Participants were early pubertal black and white boys and girls (ages 8-13 years). Tibia cortical bone (66% site) was assessed via pQCT. Total body fat-free soft tissue mass (FFST) was measured via DXA. IGF-I, insulin and glucose were measured in sera, and homeostasis model assessment of insulin resistance (HOMA-IR) was calculated. A HOMA-IR median cutoff was used to classify children as insulin resistant ( $n=159$ ) or insulin sensitive ( $n=156$ ). Race, sex and age were statistically controlled for in our analyses. Our primary outcome was cortical area (Ct.Ar) given the well-characterized role of IGF-I in promoting cortical bone areal expansion. The insulin resistant (HOMA-IR= $5.9 \pm 2.5$ ) vs. insulin sensitive (HOMA-IR= $2.9 \pm 0.8$ ) children had greater IGF-I and FFST, but lower cortical bone mineral content, Ct.Ar, and polar strength strain index (all  $P < 0.05$ ). IGF-I positively predicted FFST (insulin resistant:  $\beta=0.33$ ,  $P < .01$  vs. insulin sensitive:  $\beta=0.47$ ,  $P < .01$ ) and Ct.Ar (insulin resistant:  $\beta=0.24$ ,  $P < .01$  vs. insulin sensitive:  $\beta=0.39$ ,  $P < .01$ ), though these relationships were suppressed in the insulin resistant children (both  $P_{\text{interaction}} < .05$ ). FFST predicted Ct.Ar in both groups (both  $P < .01$ ). Path analyses showed that IGF-I was a positive predictor of Ct.Ar via FFST, though this relationship was attenuated in the insulin resistant ( $\beta_{\text{mediation}}=0.22$ ,  $P < .01$ ) vs. insulin sensitive ( $\beta_{\text{mediation}}=0.34$ ,  $P < .01$ ) children (Fig. 1). Subsequently, explained variability of FFST and Ct.Ar was nearly 10% lower in the insulin resistant vs. insulin sensitive group. Our data are the first to implicate a suppression of IGF-I-dependent muscle mass accretion as a contributor to the smaller cortical bone in children with impaired glucose metabolism. As such, deficits in cortical bone size and subsequent bending strength may help explain the greater propensity for skeletal fracture in obese youth.

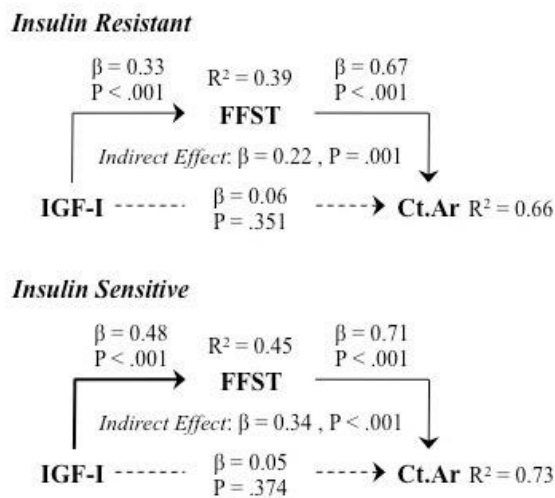


Fig. 1. The muscle-dependent relationship between IGF-I and Ct.Ar is attenuated in the insulin resistant vs. insulin sensitive participants. Broken lines represent nonsignificant relationships and thicker lines represent stronger relationships. IGF-I, insulin-like growth factor I; FFST, fat-free soft tissue mass; Ct.Ar, cortical area.

table

**Disclosures:** Joseph Kindler, None.

## FR0039

**Intestinal microbiome present in Crohn disease impairs the skeletal health and linear growth..** Anu Maharjan<sup>\*</sup>, Young Huh, Maureen Bower, Hong Yuan, Young Truong, Ian Carroll, Francisco Sylvester. University of North Carolina, United states

Background: Crohn disease (CD) is a chronic inflammatory disorder of the gastrointestinal tract. In children CD is frequently associated with significant bone mass deficits and sarcopenia present from diagnosis and persisting even when CD is in clinical remission. Aim: We hypothesized that a dysbiotic enteric microbiota in pediatric CD inhibits skeletal and muscle growth. Methods: We performed fecal microbiota transplant (FMT) from 2 children with newly diagnosed, untreated CD and 2 unaffected age-matched healthy controls (HC) into 15 germ-free (GF) wild type 129S6/SvFv (7 male and 8 female, 6 week old) mice. We measured bone mineral density (BMD), fat mass, and fat-free mass using dual X-ray absorptiometry (DXA) 8 days post-FMT (Lunar Piximus). We tracked daily weight and obtained colon length and histology post-sacrifice. Results: Male mice that received FMT from CD developed

colitis and lost significant percentage of weight from baseline compared to mice that received HC FMT (HC  $5.23 \pm 2.62$  %; CD  $-29.41 \pm 3.54$  %;  $p = 0.0007$  on day 7). However, BMD in male mice did not decrease irrespective of whether they received CD or HC FMT. On the other hand, female mice that received CD FMT had lower BMD ( $\text{g/cm}^2$ ) than HC in the presence of colitis relative to baseline (% change HC  $0.41 \pm 1.45$ ; CD  $-5.57 \pm 1.26$ ;  $p = 0.036$ ). Male mice that received CD FMT with colitis had significant loss in fat-free mass (g) (HC  $3.4 \pm 0.8$ ; CD  $-24.2 \pm 5.7$ ;  $p = 0.009$ ) and in fat mass (g) (HC  $35.4 \pm 13.7$ ; CD  $-32.4 \pm 4.8$ ;  $p = 0.003$ ), but not in female mice. Conclusion: In this model, a CD dysbiotic intestinal microbiome impairs both bone and muscle health but effects depend on sex. This suggests gender influence on colitis susceptibility and the effects of colitis on BMD and body composition.

**Disclosures:** Anu Maharjan, None.

This study received funding from: University of North Carolina TTSA grant

## FR0040

**Aging bone marrow microenvironments impart age-associated changes to hematopoietic stem and progenitor cells.** Corey Hoffman, Frank Akwa, Rachel Rubinova, John Ashton, Mark LaMere, Brandon Zaffuto, Michael Becker, Benjamin Frisch\*, Laura Calvi. University of Rochester School of Medicine & Dentistry, United states

The aging hematopoietic system has decreased immune response, increased risk of leukemia and marrow failure, and decreased function of hematopoietic stem cells (HSCs). To determine if aging alters the ability of the niche to support HSCs, we examined the bone marrow cavity intravitaly in young (8-12 weeks) and aged (>20 months) male mice, where we found a significant loss in bone volume, increased vascular volume, with remodeling of sinusoids and arterioles. These changes were confirmed histologically and quantified by flow cytometry of endothelial populations. We next quantified bone and marrow mesenchymal (MSC) and osteoblastic (OBC) populations previously implicated in HSC regulation. Within bone associated cells (BACs) from bone fragments, phenotypic OBCs and MSCs were significantly reduced in aged mice, as were functional MSCs. These age-dependent decreases in osteoprogenitors were also found in human, spicule-associated cell populations. To determine if these aged microenvironments can impart changes on HSCs, we cocultured aged BACs or marrow cells with young HSCs, and found a significant increase in CD41+ HSCs (a population known to expand with age) in young HSCs exposed to aged marrow microenvironments. Finally, since HSC changes interfering with their ability to interact with the niche could also contribute to HSC dysfunction, we performed transcriptional single cell profiling of HSCs from young vs aged mice. These data identified age-dependent decreased expression of CXCR4, the receptor for the chemokine CXCL12, which is critical for homing to the niche. Since Parathyroid hormone (PTH) can activate the HSC niche, we treated 12 month old mice with PTH and found that the characteristic shifts in HSC pools caused by aging (increased long-term and short-term HSCs, while lymphoid primed MPPs are reduced) were mitigated by PTH, and that the functional PTH-dependent increase in HSCs was preserved. Together these data support a critical role of niche aging in HSC dysfunction by multiple mechanisms, including loss or dysfunction of critical niche populations, redistribution of endothelial populations, induction by aged niche cells of HSC abnormalities, and changes in aged HSC which impair their ability to home to the niche. However, we demonstrate that activation of the niche by PTH remains effective in aging, and therefore may represent a pharmacologic tool to achieve rejuvenation of the hematopoietic system by targeting the niche.

**Disclosures:** Benjamin Frisch, None.

## FR0041

**Erythropoietin signaling regulates bone homeostasis.** Luis Fernandez De Castro Diaz<sup>1</sup>, Soumyadeep Dev<sup>2</sup>, Pamela Robey<sup>1</sup>, Constance Noguchi<sup>2</sup>, Sukanya Suresh<sup>\*2</sup>. <sup>1</sup>Skeletal Biology Section, Craniofacial & Skeletal Diseases Branch, National Institute of Dental & Craniofacial Research, NIH, United states, <sup>2</sup>Molecular Medicine Branch, National Institute of Diabetes & Digestive & Kidney Diseases, United states

Erythropoietin (EPO), a hormone made in kidneys, is essential for erythroid progenitor cell survival, proliferation and differentiation into red blood cells. Although EPO receptor (EPOR) expression extends beyond erythroid cells, studies addressing EPO's effect in non-erythroid tissue are limited. Because bone marrow is the primary site of EPO's action, we hypothesized that EPO also influences bone-forming osteoblasts and bone-resorbing osteoclasts.

We found that TgEPOR transgenic mice with EPOR expression restricted to erythroid cells, had a 40% reduction in trabecular bone mineral density (BMD) ( $n=4$ ,  $p<0.05$ ), as determined by micro-CT scans of femurs. There was no increase in the number of osteoclasts evident in bone sections *in situ*, but increased numbers of giant multinucleated osteoclasts formed in bone marrow cultures *ex vivo*. Compared with WT, cultured isolated TgEPOR calvarial osteoprogenitors had decreased differentiation and mineralization ability, as evaluated by alkaline phosphatase and alizarin staining respectively. Bone histology showed increased numbers of bone marrow adipocytes in young TgEPOR mice compared with WT control mice, suggesting that loss of EPO signaling beyond erythropoiesis promotes bone loss and bone marrow adipogenesis.

Treatment of osteoprogenitors with recombinant EPO increased the proliferation of WT cells ( $n=3$ ,  $p<0.05$ ), but had no effect on TgEPOR cells that do not express EPOR. These data suggest that EPO contributes to bone homeostasis. Interestingly, EPO treatment (1200 U/kg for 10 days) caused a 30% trabecular loss in WT, but not in TgEPOR mice, despite similar increases in hematocrit ( $n=5$ ,  $p<0.05$ ). WT mice treated with EPO had reduced BMP2 and BMP6 levels in the whole bone marrow, but not TgEPOR mice. However, EPO treatment did not induce osteoclastogenesis in the bones of WT or TgEPOR mice, contrary to previous reports of osteoclast induction seen with EPO treatment in WT mice, and suggesting that EPO-associated bone loss with EPO administration in WT mice is not due to increases in osteoclast number.

We suggest that endogenous EPO signaling contributes to bone maintenance and that lack of EPO signaling in non-erythroid cells, particularly bone-resorbing and bone-forming cells, alters their differentiation. Furthermore, exogenous EPO treatment in mice also unbalances bone turnover, and both, disruption of endogenous EPO signaling as well as EPO administration results in bone loss.

**Disclosures:** Sukanya Suresh, None.

## FR0042

**Macrophage Progenitor RIP140 Knockdown Regulates Osteoclast Differentiation and Results in Osteopenia.** Bomi Lee<sup>\*1</sup>, Urszula T. Iwaniec<sup>2</sup>, Russell T. Turner<sup>2</sup>, Li-Na Wei<sup>1</sup>, Anne Gingery<sup>3</sup>. <sup>1</sup>University of Minnesota, United states, <sup>2</sup>Oregon State University, United states, <sup>3</sup>Mayo Clinic, United states

Disruption of skeletal homeostasis through increased resorption or decreased formation results in low bone mass and increased risk of bone fracture. We have previously reported that RIP140 (receptor interacting protein 140, nrip1) acts as a regulatory switch in macrophage M1/M2 polarization using a macrophage progenitor specific RIP140 knockdown (mΦRIP140KD) animal model. Given that osteoclasts are derived from monocyte/macrophage lineage cells, we hypothesized that macrophage progenitor RIP140 activity contributes to the regulation of osteoclast differentiation. To test our hypothesis, we assessed (1) the role of RIP140 in osteoclast differentiation *in vitro*, using RAW cells and primary cultures, as well as (2) the effects of mΦRIP140KD on bone in mice. RAW cells treated with RANKL to induce osteoclast differentiation showed significant reductions in RIP140 protein. Inhibition of Syk, a non-receptor tyrosine kinase known to phosphorylate RIP140 and target it for degradation, and transfection with a non-degradable mutant RIP140 (Y3F) blocked the decrease in RIP140 protein and decreased the expression of NFATc1, CTSK and TRAP, markers of osteoclast differentiation, suggesting that RIP140 suppresses differentiation and maturation of osteoclasts. *In vivo*, mΦRIP140KD mice were sacrificed at 9 weeks of age and femurs and vertebrae were evaluated using microCT and histomorphometry. Additionally, bone marrow was obtained to assess osteoclast differentiation. Osteoclasts derived from mΦRIP140KD mice showed significantly increased expression of NFATc1, CtsK, and TRAP compared to WT, as well as significantly increased TRAP activity. MicroCT analysis revealed osteopenia in mΦRIP140KD male mice with significant reduction in BV/TV at both the distal femur metaphysis (37%) and the vertebra (15%). Histomorphometry of the femurs showed significant reductions in mineralizing perimeter (46%), osteoblast perimeter (57%) and bone formation rate (54%), with no change in MAR and a significant increase in osteoclast perimeter of nearly 2 fold. Treatment of primary WT osteoblast and MC-3T3 cultures with conditioned media isolated from mΦRIP140KD osteoclast cultures resulted in decreased osteoblast markers RUNX2, and alkaline phosphatase as compared to WT conditioned media. These data indicate the uncoupling of osteoblasts from osteoclast differentiation and activity may be occurring in mΦRIP140KD mice.

**Disclosures:** Bomi Lee, None.

## FR0043

**Fat, Inflammation, and Aging.** Raysa Rosario\*, Hongfang Yu, Mark Hamrick, Carlos Isales, Babak Baban, Xing-Ming Shi. Georgia Regents University, United states

Aging is a state of low grade inflammation (inflammaging) and is tightly associated with many age-related diseases including osteoporosis. Emerging evidence showed that with aging the immune cell population shifts from a predominant lymphoid phase towards a predominant myeloid phase (skewing). This transition leads to the entire spectrum of immunological dysfunction, including heightened autoreactivity and excessive inflammation, as well as diminished protective immune responses. Adipose tissue is an endocrine organ and produces, among others, large amounts of inflammatory cytokine. Peroxisome proliferator-activated receptor-gamma (PPAR $\gamma$ ) is a key factor regulating fat and bone cell formation. PPAR $\gamma$  insufficiency increases bone mass and reduces body fat. However, it is not entirely clear how PPAR $\gamma$  insufficiency increases bone because deletion of PPAR $\gamma$  gene in fat tissue also increased bone mass. We hypothesized that bone-specific PPAR $\gamma$  inactivation, which blocks only bone marrow fat formation, may reduce or eliminate marrow fat-generated inflammatory responses, including inflammatory cytokines and inflammatory cells, increases the availability and activity of osteoblasts, and improves immune function, thereby reducing the pace of bone loss in aging. To test this hypothesis we generated PPAR conditional knockout mice and investigated the role of PPAR $\gamma$  (fat and fat-generated cytokines) in immune cell skewing. Our preliminary data show that deficiency of PPAR $\gamma$  reduced the mRNA expression levels of inflammatory cytokines

including TNF- $\alpha$ , IL-1 $\beta$  and IL-6 in the bone marrow stromal cells and prevented/reduced the immune cell skewing, and increased the immunoregulatory indices such as CD4+Foxp3+ Tregs, plasmacytoid dendritic cells, and lowered the production of inflammatory cytokines. These data establish a critical role of PPAR $\gamma$  in the establishment of aged-associated myeloid skewing phenotype, which may contribute to age-associated immune dysfunction.

**Disclosures:** *Raysa Rosario, None.*

## FR0044

**HDL is essential for normal bone formation in mice.** Harry Blair<sup>\*1</sup>, Elena Kalyvioti<sup>2</sup>, Nicholaos Papachristou<sup>2</sup>, Irina Tourkova<sup>3</sup>, Spyros Syggelos<sup>4</sup>, K.E. Kypteos<sup>5</sup>, Dionysios Papachristou<sup>2</sup>. <sup>1</sup>Veteran's Affairs Medical Center & Departments of Pathology & Cell Biology, University of Pittsburgh, United states, <sup>2</sup>Department of Anatomy-Histology-Embryology, & the Unit of Bone & Soft Tissue Studies, University of Patras Medical School, Greece, <sup>3</sup>Pittsburgh VA Medical Center, & Departments of Pathology & Cell Biology, University of Pittsburgh, United states, <sup>4</sup>Dept. Of Pharmacology, School of Medicine, University of Patras, Greece, <sup>5</sup>Dept. Of Pharmacology, School of Medicine, University of Patras., Greece

To explore the hypothesis that fatty acids from HDL are a major source of energy for bone formation, we studied high density lipoprotein (HDL) receptors and bone formation in ApoA1 deficient mice. These animals do not express the major component of HDL, apolipoprotein A-I, which comprises over 80% of the HDL particle and without which only defective giant HDL particles exist. In these animals, the well characterized HDL receptor Scarb1 (SR-B1) is more than two fold increased, while the more strongly expressed Alcam (CD166) candidate receptor is 30% decreased, both of these differences being highly significant. Absence of SR-B1 causes dense bone mediated by increases in ACTH, but in the ApoA1 knockout animal both ACTH and cortisol were unchanged relative to wild type. Bone mass in the ApoA1 is reduced by 40% and highly significantly. Static and dynamic histomorphometry showed that this reflects decreased bone formation, with reduced bone mass. In depth analysis showed that mesenchymal stem cells (MSC) isolated from femoral marrow from these apoA1 knockout mice had reduced osteoblasts and increased adipocytes relative to wild type, even when studied in medium with normal serum (that is, containing normal HDL). The shift in MSC subtypes toward adipocyte precursors in apoA1 knockout MSC isolates was highly consistent. In contrast, osteoclast differentiation was identical in wild type and KO mice. In mRNA or protein isolates from femora of living animals, the peroxisome proliferator-activated receptor gamma (PPAR $\gamma$ ) central to adipocyte development was greatly increased in the ApoA1 knockout, consistent with increased adipocytes and precursors. Further, chemokine pathway proteins including the ligand CXCL12 were decreased while the chemokine receptor CXCR4 was increased. This is consistent with reduced signaling in a pathway that supports MSC homing and osteoblast generation. Additional studies consistent with this hypothesis, in apoA1 knockout animals, showed that expression of the osteoblast-related proteins RunX2, osterix, and Col1a1 were significantly decreased. Additional findings included increased CCAAT/Enhancer Binding Protein CEPBa, which modulates genes involved in cell cycle regulation and central metabolic homeostasis, on which further investigation including the HDL receptor Scarb1 knockout mouse MSC studies are ongoing. In conclusion, apoA-1 deficient mice have reduced bone cell precursor populations and increased adipoblasts.

**Disclosures:** *Harry Blair, None.*

## FR0045

**Bioactive PTHrP(12-48) modulates the bone marrow microenvironment independent of PTH1 receptor, is internalized into cells, and suppresses osteoclast differentiation and lifespan.** Charity Washam<sup>\*</sup>, Diarra Williams, Archana Kamalakar, Nisreen Akel, Frances Swain, Dana Gaddy, Larry Suva. Texas A&M University, United states

Bone metastasis is a common complication of breast cancer that significantly compromises patient survival, partially due to the advanced stage of disease at time of detection. However, despite intense investigation in both the metastatic and adjuvant breast cancer settings, there are currently no high performance biomarkers that can identify or predict the development of bone metastasis. We recently identified a unique PTHrP fragment, PTHrP(12-48), as a serum biomarker in breast cancer patients that correlates with and predicts bone metastasis. In this study, we investigated the signaling pathways and the resultant biologic function of PTHrP(12-48). PTHrP(12-48) structure-function was investigated in silico using sequence- and structure-based bioinformatics techniques. Cleavage site analysis identified lysine-specific monobasic and post-prolyl endoproteases as likely candidates involved in PTHrP(12-48) processing, suggesting that PTHrP(12-48) is actively secreted by breast cancer cells. Structural modeling predicted PTHrP(12-48) forms an alpha helical core followed by an unstructured region after residue 40 or 42. Structure alignment and molecular docking simulations revealed a lack of PTHrP(12-48) interactions with the PTH1 receptor (PTH1R). This observation was confirmed by the lack of PTHrP(12-48)-stimulated cAMP accumulation in PTH receptor expressing

human SaOS2 cells. Using a specific human PTHrP(12-48) antibody that we developed, PTHrP(12-48) was immunolocalized in primary and bone metastatic human breast cancer cells, as well as is within osteoclasts (OCL) in tumor bone biopsies, but had little or no localization in other resident bone cells. In vitro experiments demonstrated that PTHrP(12-48) internalization was observed in SaOS2 cells and in primary human OCL and their precursors within 60 minutes. Interestingly, PTHrP(12-48) suppressed osteoclastogenesis, as well as induced apoptosis of both OCL precursors and mature OCL (as measured by the activation of cleaved caspase 3). Collectively, these data suggest that PTHrP(12-48) is a bioactive breast cancer-derived peptide that plays an important, but as yet completely undefined role in the regulation of the tumor-bone marrow microenvironment. This suggests further interrogation of the role of PTHrP(12-48) in tumor biology is warranted.

**Disclosures:** *Charity Washam, None.*

## FR0046

**Leukemia inhibitory factor receptor (LIFR) signals via Stat3 to mediate tumor dormancy in bone.** Rachelle Johnson<sup>\*</sup>, Rebecca Miao, Amato Giaccia. Stanford University, United states

Breast cancer cells frequently disseminate to the bone marrow, where they may remain dormant and undetected for years. While the microenvironmental factors and cell intrinsic properties that enable tumor cells to exit dormancy remain largely unresolved, we previously demonstrated that loss of the leukemia inhibitor factor (LIF) receptor (LIFR), driven by low oxygen tensions within the bone marrow, enables dormant breast cancer cells to colonize the bone by down-regulating a number of dormancy-associated genes (TSP1, TPM1, TGF $\beta$ 2, P4HA1, miR-190, Selenbp1). The LIFR can elicit downstream signals via STAT3/SOCS3, PI3K/AKT/mTOR, or ERK1/2 signaling. Since genome analyses revealed that down-regulation of LIFR/STAT3/SOCS3 ( $p < 0.01$ ) and LIFR/ERK1/2 ( $p < 0.05$ ), but not LIFR/PI3K/AKT/mTOR signaling resulted in significantly reduced overall survival in patients with invasive breast carcinoma (TCGA database), we hypothesized that these two signaling pathways may be major effectors of LIFR-mediated dormancy in bone. We report here that pharmacological inhibition of ERK1/2 (0.1-10 $\mu$ M AZD6244) or PI3K/AKT/mTOR signaling (10-1000nM BEZ235) in MCF7 breast cancer cells resulted in minimal inhibition of dormancy-associated genes (p27, TSP1, TPM1 mRNA by 20-40%,  $p < 0.05$ ), suggesting that mTOR and ERK1/2 signaling downstream of the LIFR do not elicit the primary signals associated with tumor dormancy. In contrast, blockade of Stat3 signaling in MCF7 cells via a small molecule inhibitor (ML116) significantly reduced mRNA levels of 5 out of 6 of the dormancy-associated genes associated with loss of LIFR (by 31-80%,  $p < 0.01-0.0001$ ), and down-regulated an additional 5 out of 6 dormancy-associated genes regulated independent of the LIFR (by 50-93%,  $p < 0.05-0.001$ ), suggesting that loss of LIFR signaling is primarily mediated via STAT3 signaling. This was supported by reduced basal STAT3 phosphorylation in MCF7shLIFR cells by immunofluorescence *in vitro*. Intracardiac inoculation of MCF7shSTAT3 cells resulted in significantly greater lesion area (clone1: 1.63-fold, clone2: 1.64-fold  $p < 0.05$ ) and lesion number (clone1: 1.67-fold,  $p < 0.01$ , clone2: 1.61-fold,  $p < 0.05$ ) *in vivo* compared to MCF7 non-silencing control tumors, revealing that loss of STAT3 induces osteolysis similar to loss of LIFR *in vivo*. These data indicate that LIFR maintains tumor cell dormancy in bone primarily via STAT3 signaling, and loss of LIFR/STAT3 signaling may be a mechanism by which tumor cells exit a dormant state.

**Disclosures:** *Rachelle Johnson, None.*

## FR0047

**Oncogenic and Osteolytic Function of Histone Demethylase NO66 in Prostate Cancer induced Bone Metastasis.** Krishna Sinha<sup>\*1</sup>, Rozita Bagheri-Yarmand<sup>2</sup>, Nora Navone<sup>2</sup>, Xinhai Wan<sup>2</sup>, Christopher Logothetis<sup>2</sup>, Robert Gagel<sup>2</sup>, Johnny Huard<sup>1</sup>. <sup>1</sup>UT Health Science Center at Houston, United states, <sup>2</sup>MD Anderson Cancer Center, United states

Metastatic cancers that characteristically localize to bone, including those of the prostate, breast, and lung, are often associated with significant osteolysis and periosteal reactions which can predispose patients to pathologic fractures. With specific regard to metastatic prostate cancer (PCa), the genetic and epigenetic factors that affect the interactions between bone cells and PCa cells have not been clearly defined. Epigenetic control of gene expression by histone demethylases plays a pivotal role during tumorigenesis. We previously found that the jumoni C domain-containing NO66 is a histone demethylase that negatively regulates osteoblast differentiation and bone formation; however its roles in PCa and osteolysis are still unclear. By analyzing a multi-cancer tissue microarray, we observed that NO66 is overexpressed in a variety of cancers, including those of the prostate. Further immunohistochemical analyses using tumor xenografts derived from human patients demonstrated high levels of NO66 in advanced-stage PCa. The purpose of this study was to examine the roles of NO66 in the pathogenesis of osteolysis as a result of metastatic PCa. Our data indicate that knockdown of NO66 in PCa cells (specifically, PC3 and DU145 cells) significantly decreased their proliferation and invasion; overexpression of NO66 promoted their proliferation and invasion. These findings suggest that NO66 expression in PCa cells increases their susceptibility to oncogenesis. Strikingly, implantation of NO66-overexpressing PC3 cells into the femora of SCID mice caused massive osteolysis after 3 weeks, similar to that which is observed in clinical medicine. Bone shaft volume and bone mineral density were decreased and the expression levels

of *Dkk1*, *NFκB*, and *Cathepsin K (CtsK)* were increased in xenografts with NO66 overexpression. Furthermore, CHIP sequencing with NO66 and H3K9AC antibodies in PC3(+NO66) cells showed that interaction sites of NO66 colocalize with that of H3K9AC (marker for active gene) in majority of the oncogenes including chemokines, cytokines, which regulates the interactions between PCa and bone cells and induces osteoclastic lesions. Our data suggest that NO66 expression plays an important role in PCa cell proliferation, invasion, and osteolytic potential.

**Disclosures:** Krishna Sinha, None.

## FR0048

**PKC-Zeta downregulation associates with metabolic plasticity in breast cancer cells during bone metastasis.** Manish Tandon\*, Jitesh Pratap. Rush University Medical Center, United states

Bone is one of the most common target sites of distant metastasis of breast cancer, resulting in cancer-related deaths and pathological fractures. The invasive cancer cells display metabolic re-programming to maintain survival during metastases. The bone microenvironment-induced stresses which include low pH, low glucose, and hypoxia facilitate metabolic reprogramming of cancer cells. However, the regulatory mechanisms of metabolic reprogramming of tumor cells in the bone microenvironment are not clear. We hypothesized that the metastatic breast cancer cells utilize alternate source of energy to survive and promote growth in the bone microenvironment. We performed intracardiac injections of firefly luciferase and GFP labeled breast cancer MDA-MB-231 cells, in immunocompromised (SCID) mice. We harvested the tumor tissues from bones followed by sorting for GFP signal to obtain pure population of bone-derived MDA-MB-231 cells. To delineate molecular mechanisms of metabolic adaptation during bone metastasis, we compared gene expression profiles of parental and bone-derived MDA-MB-231 cells. Interestingly, our results show more than six-fold downregulation of protein kinase C- zeta (PKC-ζ) gene expression in bone-derived cells compared to parental cells. We validated this decline in PKC-ζ gene expression and corroborated to downregulated PKC-ζ protein levels. PKC-ζ is one of the two members of the atypical PKC family of isoenzymes (aPKCs) whose genetic inactivation in mice leads to enhanced tumorigenesis. Our data show that bone-derived cancer cells have reduced glycolysis compared to parental cells. Since PKC-ζ deficient cells reprogram their metabolism, these results suggested that bone metastatic cells efficiently utilize glutamine instead of glucose. Therefore, we examined glutamine metabolism associated genes. Our results show that expression of phosphoserine phosphatase, a gene required for serine biosynthetic cascade and glutamine utilization is increased in PKC-ζ deficient bone-derived cells. The bone-derived cancer cells displayed increased dependence on glutamine to preserve survival during glucose-deprivation induced stress. Importantly, the ectopic expression of PKC-ζ induced metabolic stress in bone-derived cells compared to parental cells as examined by autophagy markers. Taken together, our results identified the PKCζ pathway as a novel therapeutic target for survival of metastatic breast cancer cells in the bone microenvironment.

**Disclosures:** Manish Tandon, None.

## FR0051

**Novel ERα positive breast cancer model with estrogen independent growth in the bone microenvironment.** Biancamaria Ricci\*<sup>1</sup>, Aude-Hélène Capietto<sup>2</sup>, Szeman Ruby Chan<sup>3</sup>, Debora V Novak<sup>4</sup>, Robert D Schreiber<sup>3</sup>, Roberta Faccio<sup>2</sup>. <sup>1</sup>Department of Orthopaedic Surgery - Washington University School of Medicine, United states, <sup>2</sup>Department of Orthopaedic Surgery - Washington University School of Medicine, United states, <sup>3</sup>Department of Pathology & Immunology - Washington University School of Medicine, United states, <sup>4</sup>Department of Pathology & Immunology- Washington University School of Medicine, United states

Bone metastasis occur in about 70% of patients with metastatic breast cancer, and two third of these patients are estrogen receptor-alpha positive (ERα+). Despite successful therapeutic options, resistance to endocrine therapy frequently occurs leading to recurrence. Unfortunately, the mechanisms involved in tumor resistance remain to be established, in part due to lack of ERα+ animal models in immune competent mice.

By using two murine ERα+ spontaneous STAT1-/- mammary luminal epithelial tumor cell lines (SSM2 and SSM3) that can grow in 129-WT mice, we established that the bone microenvironment offers growth advantage over primary site or lung in the absence of estrogen.

SSM2 and SSM3 cells grow in the mammary gland of WT mice in an estrogen-dependent manner.

To study the estrogen dependency of the tumor growth in bone, we intratibially injected SSM2 or SSM3 cells into ovariectomized (OVX) or SHAM mice. Interestingly, SSM2 but not SSM3 selectively grew in bones of OVX mice still maintaining ERα expression and JAK2/STAT3 activation.

Next, we asked whether also the lungs could support SSM2 growth in absence of ovarian hormones. Strikingly, SSM2 cells intravenously injected into male mice, which have estrogen levels comparable to OVX mice, did not metastasize to the lungs.

To assess whether SSM2 cells induce unique changes in the bone that would allow estrogen-independent growth of SSM3, we co-injected SSM2 and Luciferase-SSM3 cells in bones of OVX mice. Bioluminescence imaging confirmed the inability of SSM3 cells to grow in the absence of estrogen, suggesting that intrinsic differences between SSM2 and SSM3 cells confer peculiar ability to grow in the bone in a hormone-independent manner.

To further assess if the different sensitivity to estrogen deprivation is dependent on changes to bone residing cells, we counted osteoclast numbers in SSM2 or SSM3 tumor bearing mice and found no significant differences. These results were also confirmed *in vitro*, where we observed similar effects of SSM2 and SSM3 conditioned medium on osteoblast differentiation or osteoclast activation.

All together these data identify a new breast cancer cell line (SSM2) that can be used to understand mechanism of ERα+ tumor resistance to endocrine therapies. Furthermore, our results demonstrate that the bone microenvironment is a unique site for acquisition of tumor-estrogen independency.

**Disclosures:** Biancamaria Ricci, None.

## FR0052

**Effects of cabozantinib alone and in combination with bortezomib in the 5TGM1 murine multiple myeloma model.** Mari I Suominen\*<sup>1</sup>, Katja M Fagerlund<sup>1</sup>, Esa Alhoniemi<sup>2</sup>, Jukka P Rissanen<sup>1</sup>, Jussi M Halleen<sup>1</sup>, Dana T Aftab<sup>3</sup>. <sup>1</sup>Pharmatest Services Ltd., Finland, <sup>2</sup>Avoltus Oy, Finland, <sup>3</sup>Exelixis Inc., United states

Cabozantinib (cabo) inhibits tyrosine kinases including MET, VEGF receptors, and AXL, and has clinical activity in patients with advanced renal cell cancer and other solid tumors with bone metastases. Multiple myeloma (MM) is a plasma cell neoplasia with presence of multiple osteolytic lesions. Circulating levels of HGF and VEGF are upregulated in MM patients, and regulation of plasma cell-osteoblast communication by the HGF-MET signaling pathway has been implicated in the development of lytic bone disease in these patients. We studied the efficacy of cabo in the 5TGM1 murine multiple MM alone and in combination with bortezomib (brtz).

Two daily doses of cabo, 10 and 30 mg/kg, were tested in a 35-day study, and the 10 mg/kg dose was chosen to a 70-day survival study including a combination treatment group with brtz. Lenalidomide showed no effects in the model and could not be used as combination treatment instead of brtz. Serum IgG2b, PINP and TRACP 5b were measured before and 2, 3 and 5 weeks after the inoculation and in the survival study also at sacrifice. Development of osteolytic lesions was detected by X-ray at day 35 and in the survival study also at sacrifice. In the survival study, mice were sacrificed individually when they became paraplegic, lost over 20% of body weight, or had severe breathing problems.

In both studies, by study day 35 the osteolytic lesions were not affected by brtz, were reduced by cabo alone, and further reduced by the combination treatment. Brtz had inhibited the rise in serum IgG2b levels, but cabo and the combination treatment had not. Despite the effects on serum IgG2b, brtz did not significantly increase survival, whereas cabo and the combination treatment did. Increased survival with the combination was significant when compared to brtz monotherapy, but not when compared to cabo monotherapy. Histology of the 35-day study showed that cabo dose-dependently increased the necrotic tumor area in bone. We hypothesized that the rise in IgG2b was due to lysis of plasma cells and not tumor growth. Consistent with this hypothesis, the IgG2b levels of cabo treated mice decreased from day 35 onwards in the survival study.

In summary, cabo increased survival and exhibited bone-protective and anti-tumor effects in this murine model of MM. Combination with brtz showed additive effects on survival. Based on these results, further investigation of cabo in combination with other therapies in multiple myeloma is warranted.

**Disclosures:** Mari I Suominen, Pharmatest Services Ltd, 15  
This study received funding from: Exelixis Inc.

## FR0053

**A Novel Protective Role of GPNMB/Osteoactivin in Post-traumatic Osteoarthritis.** Asaad Al Adlaan\*<sup>1</sup>, Nazar Hussein<sup>1</sup>, Fatima Jaber<sup>1</sup>, Tariq Haqiqi<sup>2</sup>, Fayez Safadi<sup>2</sup>. <sup>1</sup>Kent State University, United states, <sup>2</sup>Northeast Ohio Medical University, United states

Osteoarthritis (OA) is a chronic joint disease causes irreversible damage to the articular cartilage resulting in loss of joint function and subchondral bone remodeling. There is no cure for OA and currently the available treatment like pain management, and joint replacement surgery is used to treat this disease. GPNMB/Osteoactivin is a type-I transmembrane protein plays a vital role in osteogenesis and bone remodeling. However, the function of GPNMB/Osteoactivin in chondrogenesis and cartilage repair is unknown. We first examined the expression GPNMB/Osteoactivin in normal cartilage and found that GPNMB/Osteoactivin mRNA and protein levels are expressed in growth plate chondrocytes and articular cartilage. Next, we assessed the effects of recombinant GPNMB/Osteoactivin using primary mouse chondrocytes on proliferation/viability and extracellular matrix markers. Our results showed that GPNMB/Osteoactivin treatment did not have any effect on cell proliferation/viability, however, there was a significant increase in collagen Type II and aggrecan expression in a dose- and time-dependent manner. These data suggest that GPNMB/Osteoactivin

plays a role in cartilage maintenance. Next, we determined whether GPNMB/Osteoactivin contributes to the OA disease progression. Human osteoarthritic damaged and undamaged cartilage harvested following knee replacement were used to examine GPNMB/Osteoactivin expression, and found that GPNMB/Osteoactivin mRNA was 6-7-fold increased in damaged compared to undamaged cartilage. Similar results were obtained from mouse primary chondrocytes treated with IL-1 $\beta$  and showed a significant increase (4-fold) in GPNMB/Osteoactivin mRNA compared to untreated control. Furthermore, treatment with recombinant GPNMB/Osteoactivin protein showed reduced expression of IL-6 and MMP3 induced by IL-1 $\beta$ . Next, we evaluated the effects of GPNMB/Osteoactivin deficiency on the OA progression using the DMM model. GPNMB/Osteoactivin mutant (DBA/2J) mice showed significantly increased in OARSI scores compared to WT mice. To determine whether epigenetic modifiers (miRNAs) regulating GPNMB/Osteoactivin expression can modulate the cartilage protective effects of GPNMB/Osteoactivin, we found that miRNA 150 targets GPNMB/Osteoactivin in chondrocytes. Next, we examined the effects of miRNA 150 deficiency on the OA progression *in vivo* and found that miRNA 150 KO are more protected against post-traumatic OA compared to WT mice. Furthermore, we assessed the expression of GPNMB/Osteoactivin in miRNA 150 KO chondrocytes and showed a significant increase compared to WT cells. These data suggest that GPNMB/Osteoactivin is a protective factor of OA progression, at least in part, by miRNA 150 regulation. Taken together, these data are the first to report a role for GPNMB/Osteoactivin in cartilage maintenance and protection against the progression of OA.

**Disclosures:** Asaad Al Adlaan, None.

## FR0054

**Articular Cartilage Preservation in Mice Lacking Cathepsin K.** Fabiana Soki<sup>\*1</sup>, Rvu Yoshida<sup>1</sup>, David N. Paglia<sup>1</sup>, Maureen Pickarski<sup>2</sup>, Marc Hansen<sup>1</sup>, Le Duong<sup>2</sup>, Hicham Drissi<sup>1</sup>. <sup>1</sup>Uconn Health Center, United states, <sup>2</sup>Merck & Co., Inc., United states

Osteoarthritis (OA) is a degenerative disease and a major cause of chronic disability in aging individuals. It is postulated that cathepsin K (CatK) expression is upregulated in synovial fibroblasts, chondrocytes and osteoclasts during OA progression. Inhibition of CatK has been shown to delay OA progression but its protective effects are not well delineated. Understanding molecular pathways that regulate subchondral bone and calcified cartilage remodeling during OA progression is a critical step in assessing CatK as a potential drug target. Here we examined the role of CatK in subchondral bone and calcified cartilage remodeling during progression in surgically induced OA in CatK<sup>+/+</sup> and CatK<sup>-/-</sup> mice. Destabilization of the medial meniscus surgery was performed in knee joints of adult CatK<sup>+/+</sup> (WT) and CatK<sup>-/-</sup> (KO) mice. Hind limbs were collected at 1, 2, 4, 8 and 16 weeks post-surgery and Kellgren and Lawrence system (K-L grading) used to score X-ray images to evaluate progression of the disease. A significant difference in disease progression was noticed, with lower K-L scoring in KO mice at 8 and 16 weeks post-surgery. Paraffin embedded sections were stained with Safranin-O/Fast Green and OARSI cartilage OA histopathology grading system was used to determine OA severity in knee joints at 16 weeks for WT and KO mice. WT mice presented more severe OA scoring compared to KO mice indicating a protective role of CatK inhibition in OA progression. TRAP<sup>+</sup> osteoclasts were increased in tibial and femur physis and subchondral bone at 1 and 2 weeks in KO mice. A high frequency of chondroclasts were seen in growth plates of KO mice but much fewer adjacent to subchondral bone. Histomorphometric analyses of subchondral bones from the surgical limbs showed significantly higher bone volume and lower trabecular spacing at 16 weeks in KO mice compared to WT. KO mice presented higher osteoclast number per bone perimeter and osteoclasts surface per bone surface. MicroCT analyses confirmed higher subchondral BV/TV in KO mice as compared to WT in the OA joints; however, this parameter was not different in contralateral KO vs. WT joints. Finally, qPCR arrays comparing osteoclasts to osteoclasts and chondroclasts to chondroclasts from WT and KO mice showed differential gene expression in Gpr68, Syk, Crcl1, Ca2, Itgb3, and Nfatc1. Together, the data support a protective role of CatK inhibition against OA progression through decreased subchondral bone remodeling and a potential role of osteoclasts in earlier stages of disease progression.

**Disclosures:** Fabiana Soki, None.

This study received funding from: Merck & Co., Inc.

## FR0055

**IKK $\beta$  Activation in Postnatal Chondrocytes Results in a Chronic Inflammatory Environment within the Knee Joint and Recapitulates an Age-Associated Osteoarthritis Phenotype.** Sarah Catheline\*, Martin Chang, Michael Zuscik, Jennifer Jonason, University of Rochester, United states

Osteoarthritis (OA) is a degenerative joint disease that causes degradation and eventual loss of cartilage within the synovial joints. Aging is an important contributing factor to the development of OA, and age-related increases in low-grade inflammation are thought to be detrimental to cartilage health. Pro-inflammatory cytokines are believed to disrupt the homeostasis between anabolism and catabolism of the cartilage extracellular matrix (ECM), which results in cartilage degeneration without regeneration. NF- $\kappa$ B has been implicated in regulation of collagenase (i.e., *Mmp13*) and aggrecanase (i.e., *Adamts5*) gene expression, key molecules responsible for the breakdown of cartilage ECM. Here, we present data demonstrating that

canonical NF- $\kappa$ B signaling is active in the cartilage of aged (27-month-old) wild type C57BL/6J mice with osteoarthritic knee joints. Thus, we hypothesize that activation of canonical NF- $\kappa$ B signaling in postnatal chondrocytes will be sufficient to drive the onset of OA. To test this hypothesis, we use the chondrocyte-specific *Acan-CreER<sup>T2</sup>* knock-in allele in combination with the *ROSA-Ikk2ca* allele to generate mice that overexpress a constitutively active form of IKK $\beta$  in chondrocytes. *Acan-Cre<sup>+/+</sup>ER<sup>T2</sup>; ROSA-Ikk2ca<sup>fl/fl</sup>* and *Acan-Cre<sup>+/+</sup>ER<sup>T2</sup>; ROSA-Ikk2ca<sup>fl/fl</sup>* mice are generated and administered tamoxifen at 2 months of age to induce Cre-mediated recombination in postnatal chondrocytes. At 8 months of age, histological analysis reveals that the knee joints of these genetically altered mice remarkably phenocopy those of the aged wild type mice. Specifically, we observe proteoglycan staining loss in the articular cartilage, synovial hyperplasia, and an enlarged meniscus within the knee joints of both groups of mice. Further characterization of the IKK mutant mice reveals decreased staining for PRG4 within the articular cartilage, meniscus and synovium, as well as a decrease in ACAN in the articular cartilage. MMP13-positive cells and increased Alizarin red staining are also found within the enlarged meniscus of these mice, suggesting that the native ECM of the meniscus is undergoing degradation and mineralization. Finally, the IKK mutant mice show an increase in COX-2 positive cells within the articular cartilage and meniscus, further supporting a local inflammatory environment existing within the joints of these mice. Based on the observed phenotypes, this IKK $\beta$  activation model represents a novel murine model of aging-induced osteoarthritis.

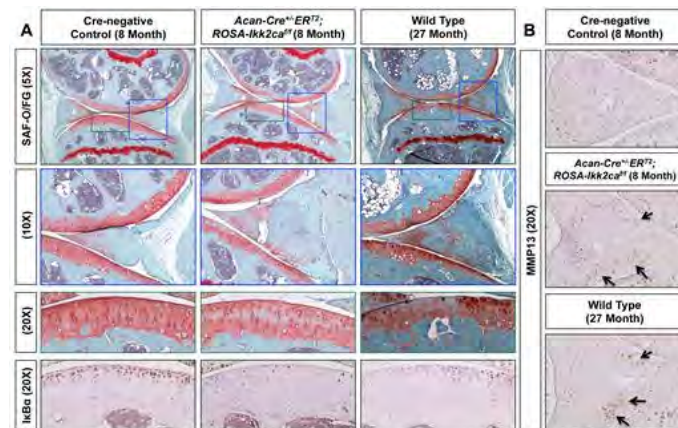


**Figure 1.** *Acan-Cre<sup>+/+</sup>ER<sup>T2</sup>; ROSA-Ikk2ca<sup>fl/fl</sup>* mice at 8 months of age phenocopy aged wild-type mice at 27 months of age, and both show NF- $\kappa$ B activation as well as enhanced MMP13 expression. (A) Safranin-O/Fast Green staining in Cre-negative control and *Acan-Cre<sup>+/+</sup>ER<sup>T2</sup>; ROSA-Ikk2ca<sup>fl/fl</sup>* mice 8 months following tamoxifen administration (100 mg/kg body weight, IP daily for 5 days) at P80, or wild-type mice at 27 months of age (top panel, 5X, second panel, 10X, and third panel, 20X are enlarged images of boxed region in 5X). The bottom panel shows I $\kappa$ B $\alpha$  expression at 20X using immunohistochemistry. (B) MMP13 immunohistochemistry in control, genetically altered, and aged mice (10X). Arrows indicate MMP13 positive cells.

**Figure 1**

**Disclosures:** Sarah Catheline, None.

## FR0056

**Repair of Focal Cartilage Defects in the Rat using Human Embryonic Stem Cell-Derived Articular Cartilage Tissues.** April Craft<sup>\*1</sup>, Subhash Juneja<sup>2</sup>, Heather Whetstone<sup>3</sup>, Christian Veillette<sup>2</sup>, Gordon Keller<sup>4</sup>. <sup>1</sup>Boston Children's Hospital, Harvard Medical School, United states, <sup>2</sup>Arthritis Program, Toronto Western Hospital, Canada, <sup>3</sup>Hospital for Sick Children, Canada, <sup>4</sup>McEwen Centre for Regenerative Medicine, University Health Network, Canada

Osteoarthritis (OA) is a prevalent medical condition that affects the articular cartilage lining our joints. Once damaged, articular cartilage will progressively deteriorate, causing pain and interfering with daily living activities. One of the main challenges associated with articular cartilage repair is that it forms prenatally and regeneration does not normally occur after birth. We hypothesize that human pluripotent stem cells (hPSCs), including both human embryonic stem cells (hESCs) as well as induced pluripotent stem cells (iPSCs), are a potential novel source of articular cartilage for developing new cell or tissue-based therapeutics to repair damaged cartilage because they represent an early embryonic stage of development. To test this, we established a developmental biology-based approach for the efficient and reproducible generation of articular cartilage tissues from hPSCs. The derivative tissues are rich in proteoglycans and express important proteins that function to support compressive loads and lubricate joint surfaces. Importantly, this hPSC-derived articular cartilage resisted ossification and remained stable *in vivo* for extended periods of time when transplanted subcutaneously into mice. Prior to their use in the clinic, however, these tissues must be tested in preclinical animal models of joint trauma or disease. We thus developed and utilized a small animal model of focal cartilage defect repair in which hPSC-derived articular cartilage was implanted into osteochondral defects in the rat knee. Defects implanted with hPSC-derived articular cartilage showed significant regions of stable proteoglycan- and type II collagen-rich cartilage tissue after 2, 6 and 12 weeks. In many cases, engrafted human cartilage was found to be congruent and laterally integrated with the rat articular cartilage. As expected, defects that did not receive implants generated fibrocartilage, which lacks significant amounts of cartilage-specific proteoglycans. These data indicate that hPSC-derived articular cartilage engrafts and remains stable when implanted into an orthotopic and clinically relevant site. This success in the small animal model paves the way for evaluating the potential of hPSC-derived articular cartilage to repair

damaged cartilage in a large animal model, as a prelude to applying this technology to human patients.

**Disclosures:** April Craft, None.

## FR0062

**Inhibition of Epigenetic Factor Dnmt3b within Articular Chondrocytes Coordinates Cellular Metabolic Response during the Development of Osteoarthritis.** Jie Shen<sup>\*1</sup>, Cuicui Wang<sup>1</sup>, Daofeng Li<sup>2</sup>, Jason Myers<sup>3</sup>, John Ashton<sup>3</sup>, Audrey McAlinden<sup>1</sup>, Ting Wang<sup>2</sup>, Regis O'Keefe<sup>1</sup>.  
<sup>1</sup>Department of Orthopaedic Surgery, School of Medicine, Washington University in St. Louis, United states, <sup>2</sup>Department of Genetics, School of Medicine, Washington University in St. Louis, United states, <sup>3</sup>University of Rochester Medical Center, United states

Osteoarthritis (OA) is the most common form of arthritis, is a leading cause of impaired mobility, and is the single most costly condition in the Medicare population. Recent GWAS studies have implicated a distinct DNA methylation signature in OA patients, indicating DNA methyltransferases (*Dnmt*) may play a role in regulating cartilage homeostasis. We observed a marked decrease in *Dnmt3b* expression in murine cartilage with aging and following meniscal ligament injury (MLI) as well as in human OA cartilages.

***Dnmt3b* LOF leads to a progressive OA-like pathology:** To investigate the role of *Dnmt3b* during OA development, we generated *Dnmt3b* loss-of-function (LOF) mice (*Dnmt3b*<sup>Agc1ER</sup>) and showed that ablation of *Dnmt3b* in articular chondrocytes led to a progressive OA-like phenotype in adult mice, including cartilage degradation and subchondral bone sclerosis.

**Metabolic pathways are altered in *Dnmt3b* LOF chondrocytes:** Changes in gene expression and methylation profiles were investigated by integrative analysis of RNA-Seq and Methyl-Seq data. We revealed 44 genes with altered expression and methylation profiles in LOF cells. Gene ontology analysis revealed an enrichment in cellular metabolism. We indeed found higher mitochondrial respiration correlated to an increase in catabolic genes in *Dnmt3b* LOF cells. HPLC-MS further validated that TCA metabolites (e.g. succinate) were increased in *Dnmt3b* LOF cells.

**Increased mitochondrial respiration induces chondrocyte hypertrophy:** To determine if there is a correlation between mitochondrial respiration and chondrocyte hypertrophy, we treated WT chondrocytes with succinate and found an increase in hypertrophic chondrocyte markers. We then treated WT chondrocytes with antimycin A and rotenone following with BMP2 treatment to inhibit mitochondrial respiration. We found that addition of the inhibitors could attenuate the effect of BMP2 as shown by a decrease in mitochondrial OCR and decreases in hypertrophic marker expression.

***Dnmt3b* GOF attenuates OA progression:** MLI surgeries were performed on 10 wk male control and *Dnmt3b* gain-of-function (GOF) mice. *Dnmt3b* GOF mice were protected against cartilage breakdown and subchondral bone sclerosis induced by MLI surgery and *Dnmt3b* GOF chondrocytes displayed lower mitochondrial OCR under BMP2 treatment.

**Conclusion:** *Dnmt3b* plays a critical role in regulating cartilage homeostasis. Cellular metabolism regulated by *Dnmt3b* may provide novel targets for therapeutic approaches to treat OA.

**Disclosures:** Jie Shen, None.

## FR0063

**Bone-Derived Lipocalin 2 is an Anorexigenic Hormone.** Steven Shikhel\*, Stavroula Kousteni, Columbia University, United states

Bone-derived Lipocalin 2 is an anorexigenic hormone

Mice lacking FoxO1 (*FoxO1osb*<sup>-/-</sup>) in osteoblasts have improved energy metabolism, in part due increased osteocalcin bioactivity, but also decreased appetite, a function not regulated by osteocalcin. These observations triggered a search for osteoblast-secreted molecules regulating energy homeostasis downstream of FOXO1. Microarray analysis identified lipocalin2 (LCN2), a 25kDa secreted glycoprotein, upregulated in osteoblasts from *FoxO1osb*<sup>-/-</sup> mice. We show that LCN2, a previously thought adipokine, is an osteoblast-enriched protein regulating energy intake. Mice lacking *Lcn2* specifically in osteoblasts (*Lcn2osb*<sup>-/-</sup>) have a 23.7% increase in food intake which precedes increases in glucose levels and body weight and compromised glucose metabolism. In contrast, inactivation of *Lcn2* in adipocytes has no effect on any metabolic parameters. Indicating a physiological role for LCN2 in the regulation of feeding, serum LCN2 levels increased by 3-fold within an hour of refeeding due to an increase in *Lcn2* expression specifically by osteoblasts. These observations led us to examine whether LCN2 can exert an acute or chronic anorexigenic effect. Intraperitoneal administration of recombinant LCN2 to fasted *Lcn2osb*<sup>-/-</sup> mice immediately after refeeding suppressed food intake within 1 hour and decreased body weight gain within 2 hours as efficiently as in wild type mice. The effects of chronic administration of exogenous LCN2 in lean and obese mice were examined. Daily intraperitoneal administration of LCN2 to wild type mice decreased food intake by 18%, improved glucose tolerance and insulin sensitivity and secretion, increased islet number and  $\beta$ -cell area, decreased body weight and fat mass, and increased energy expenditure and activity. Similarly, administration of rLCN2 improved the metabolic abnormalities of obese diabetic mice with an inactivating mutation in the leptin receptor (*Leprdb/db* mice) as it suppressed food intake by 16.5% and improved

glucose tolerance and insulin sensitivity. In addition, body weight and gonadal fat were decreased and energy expenditure was increased in LCN2-treated *Leprdb/db* mice. These results indicate that LCN2 exerts both an acute and chronic anorexigenic function. Acute suppression of food intake may consist a physiological satiety signal during meals, whereas the sustained effect on appetite may be of biomedical importance since a main problem with anti-obesity treatments, is the quick loss of an effect with repeated administration.

**Disclosures:** Steven Shikhel, None.

This study received funding from: Novo Nordisk

## FR0064

**Osteoblastic Hdac3 Expression Regulates Systemic Energy Metabolism.** Jessica Pierce<sup>\*1</sup>, Kanglun Yu<sup>1</sup>, Ahmed Elsherbini<sup>1</sup>, Elizabeth Bradley<sup>2</sup>, Jennifer Westendorf<sup>2</sup>, Meghan McGee-Lawrence<sup>3</sup>. <sup>1</sup>Augusta University, United states, <sup>2</sup>Mayo Clinic, United states, <sup>3</sup>Medical College of Georgia, Augusta University, United states

Obesity is a leading cause of preventable diseases including type 2 diabetes, and one of the earliest identifiable abnormalities in prediabetes is development of hepatic insulin resistance. Recent studies suggest that bone-derived factors that reduce Rankl/NF- $\kappa$ B signaling may improve hepatic insulin sensitivity and prevent type 2 diabetes in mice and in humans. We recently showed that conditional knockout of the epigenetic regulator, Hdac3, in osteoblast progenitor cells with Osterix-Cre (*Hdac3* CKO) reduced fasting glucose levels, enhanced insulin sensitivity, and prevented high fat diet (HFD)-induced insulin resistance and hepatic steatosis. Neither total nor uncarboxylated osteocalcin levels were increased in the *Hdac3* CKO mice, suggesting that alteration of systemic metabolism did not occur through osteocalcin-dependent mechanisms. Serum levels and skeletal gene expression of Osteoprotegerin (*Opg*), a natural inhibitor of Rankl/NF- $\kappa$ B signaling, were elevated in these mice despite their osteopenic phenotype. We hypothesized that *Hdac3*-depletion in osteoblasts alters the epigenome to increase expression of *Opg*, reducing hepatic NF- $\kappa$ B activation and preserving insulin sensitivity. To test this, we investigated the effects of *Hdac3* on *Opg* promoter activity in vitro and in vivo. *Hdac3* dose-dependently repressed *Opg* transcription, and *Hdac3* inhibition increased H4 acetylation of the osteoblastic *Opg* promoter in ChIP-seq studies, suggesting direct regulation of *Opg* transcription by *Hdac3*. To test the role of *Opg* in the metabolic phenotype of *Hdac3* CKO mice, we crossed *Hdac3* CKO animals with *Opg*<sup>+/-</sup> animals, generating double mutant *Opg*<sup>+/-</sup>:*Hdac3* CKO mice, single mutants, and controls. Animals were placed on a HFD at 4 weeks of age, and insulin tolerance was assessed at 8 weeks of age. Consistent with our previous studies, *Hdac3* CKO single mutant animals demonstrated greater insulin sensitivity after 4 weeks on a HFD than either Cre- or Cre+ control groups. Insulin sensitivity of *Opg*<sup>+/-</sup> single mutants was comparable to control groups, but double mutant *Opg*<sup>+/-</sup>:*Hdac3* CKO animals showed a striking loss of the high insulin sensitivity of *Hdac3* CKO mice. Our data suggest that *Hdac3* CKO mice remain sensitive to insulin on a HFD because enhanced production of *Opg* by osteoblasts influences other metabolic organs including the liver.

**Disclosures:** Jessica Pierce, None.

## FR0067

**FSH Regulates Body Fat and Whole Body Metabolism.** Yaoting Ji<sup>1</sup>, Peng Liu<sup>1</sup>, Elizabeth Rendina-Ruedy<sup>2</sup>, Victoria DeMambro<sup>2</sup>, Tony Yuen<sup>\*1</sup>, Ping Lu<sup>1</sup>, Bin Zhou<sup>3</sup>, Ling-Ling Zhu<sup>1</sup>, Samuel Robinson<sup>3</sup>, Eric Yu<sup>3</sup>, Christoph Buettner<sup>1</sup>, Maria New<sup>1</sup>, Marc Feldmann<sup>4</sup>, Bian Zhuan<sup>5</sup>, Jay Cao<sup>6</sup>, Edward Guo<sup>3</sup>, Jameel Iqbal<sup>1</sup>, Li Sun<sup>1</sup>, Clifford Rosen<sup>2</sup>, Mone Zaidi<sup>1</sup>. <sup>1</sup>Icahn School of Medicine, United states, <sup>2</sup>Maine Medical Center Research Institute, United states, <sup>3</sup>Columbia University, United states, <sup>4</sup>Kennedy Institute of Rheumatology, United Kingdom, <sup>5</sup>Wuhan University, China, <sup>6</sup>USDA Department of Agriculture, United states, <sup>7</sup>Greater Los Angeles VA Medical Center, United states

Menopause is associated with high follicle stimulating hormone (FSH), modest increases in body fat and bone loss. We previously showed that Fsh has skeletal actions. For example, a highly specific polyclonal antibody (Fsh pAb) raised to a 13 aa sequence of Fsh $\beta$ , which blocks Fsh $\beta$ -Fshr binding, was found to inhibit bone resorption, stimulate bone formation, and prevent ovariectomy (OVX)-induced bone loss in mice. Fsh receptors have been identified on mesenchymal stem cells (MSCs) in mice and humans, which raises the question whether the Fsh pAb could reduce total fat mass. Here, we report full length *Fshr* cDNA sequences and detect Fshr protein on murine MSCs and 3T3L1 cells. Fsh increased and Fsh pAb attenuated adipocyte differentiation (Oil Red-O) *in vitro* and expression of adipocytic genes. Moreover, cells from the stromal vascular fraction of white adipose tissue (WAT) in *Fshr*<sup>-/-</sup> mice displayed reductions in Oil Red-O-staining. Fsh also inhibited and Fsh pAb stimulated white-to-beige transition of adipocytes, measured by *Ucp1* promoter-driven *Luc* activity in 'Thermo' cells. *In vivo*, Fsh pAb was administered i.p. (10 mg/kg/day) to pair-fed, OVX or sham operated B6 mice for up to 8 weeks. qNMR showed reduced total fat mass in Fsh pAb-treated mice. Decrements in total, visceral and subcutaneous fat ( $\mu$ CT), as well as in bone marrow fat by osmium  $\mu$ CT were also observed in pAb-treated OVX and sham mice. When B6 mice were fed a high fat diet

(HFD) for 8 wks, increases in total, subcutaneous and visceral fat ( $\mu$ CT and/or qNMR) were noted with control Ab, but these increases were blunted significantly with Fsh pAb, and were not seen in HFD-fed *Fshr*<sup>-/-</sup> mice. Finally, we noted significant reductions in adipocyte size and upregulation of *Ucp1* (immunostaining and qPCR) in inguinal WAT. Fsh pAb also up-regulated *Ucp1* expression in interscapular brown adipose tissue (BAT), and increased *Luc* activity in 'Thermo' mice fed a HFD, as well as *in vitro*, in 'Thermo' cells. Metabolic cage data with OVX or HFD-fed mice treated with Fsh pAb showed increased energy expenditure and decreased respiratory quotient. Taken together our data point to a potent, physiologically relevant, action of Fsh on whole body metabolism. Whether these adipogenic changes also impact the skeleton requires further studies. Fsh Abs show promise for treating both bone loss and obesity in the postmenopausal state.

**Disclosures:** Tony Yuen, None.

## FR0071

**Adipocyte- and Osteoblast-Specific Function of Protein Phosphatase 5 (PP5) in Modulation of PPAR $\gamma$  and Runx2 Activities and Regulation of Bone Mass and Energy Metabolism.** Lance A. Stechschulte<sup>\*1</sup>, Piotr J. Czernik<sup>2</sup>, Edwin R. Sanchez<sup>1</sup>, Renny Franceschi<sup>3</sup>, Beata Lecka-Czernik<sup>1</sup>. <sup>1</sup>University of Toledo Health Science Campus, United states, <sup>2</sup>MicroTomografix Ltd, United states, <sup>3</sup>Periodontics & Oral Medicine University of Michigan School of Dentistry, United states

Two transcription factors, PPAR $\gamma$  and Runx2, are key regulators of mesenchymal stem cell (MSC) differentiation toward adipocytes (AD) and osteoblasts (OB), respectively. Both factors are subjected to posttranslational modifications, which determine their activities. Dephosphorylation of PPAR $\gamma$  at S112 and S273 is required for activation of pro-AD and insulin sensitizing activities, whereas phosphorylation of Runx2 at S319 is required for pro-OB activity. Upon treatment with PPAR $\gamma$  full agonist rosiglitazone that promotes MSCs commitment toward AD and away from the OB lineage, both PPAR $\gamma$  and Runx2 undergo dephosphorylation which increases PPAR $\gamma$  and suppresses Runx2 activity. We have identified the Protein Phosphatase 5 (PP5) as an enzyme activated by rosiglitazone and inversely regulating PPAR $\gamma$  and Runx2 activities associated with phosphorylation. We have also demonstrated that PP5 global deficiency increases bone mass, renders skeleton refractive to the negative effect of rosiglitazone, and induces beige adipocytes with bone anabolic activities. To assess tissue-specific contributions to increased bone mass we knocked-down (KD) PP5 specifically in either adipocyte (AdipoCrePP5fl/fl) or osteoblast (PrxCrePP5fl/fl) lineage. Adipocyte-specific PP5 KD results in increased energy expenditure reflected in increased heat production and locomotor activity and associated with induction of beige adipocytes, decreased body weight by 10%, and reduction in body fat by 30%. Most importantly, AdipoCrePP5fl/fl mice have increased bone mass reflected in increased global BMD (8%) and associated with increased number of trabeculae (13%) in the proximal tibia. In contrast, PrxCrePP5fl/fl mice have the same body weight and fat content as WT mice, but decreased energy expenditure reflected in decreased heat production and locomotor activity. However, PrxCrePP5fl/fl mice have high bone mass with increased global BMD (10%), increased cortical thickness (6%), and increased thickness of trabeculae (24%). In conclusion, both metabolic status of fat tissue determined by PPAR $\gamma$  activity and PPAR $\gamma$ /Runx2 interplay in the regulation of MSCs differentiation contribute simultaneously to the control of bone mass and energy metabolism. These findings underscore complexity of shared mechanisms regulating bone and energy metabolism and implicate that pharmacological treatment of pathological alterations of one process requires attention to the other process.

**Disclosures:** Lance A. Stechschulte, None.

## FR0073

**Cyclophilin D Knock-out Mice Show Enhanced Resistance to Osteoporosis and to Metabolic Changes Observed in Aging Bone.** Laura Shum<sup>\*</sup>, Roman Eliseev. University of Rochester, United states

Purpose: Oxidative stress and hormone depletion are pathogenic factors associated with aging that converge on mitochondria and impair function via opening of the mitochondrial permeability transition pore (MPTP), a large non-selective pore regulated by cyclophilin D (CypD). When the MPTP is opened, integrity of the mitochondrial membrane is disrupted, which impairs mitochondrial function. As bone has high energy demands for matrix production, it is expected to be highly sensitive to mitochondrial dysfunction. Despite this, the role of mitochondria and the MPTP in aging has not been elucidated. Our goal was to determine whether mitochondria are impaired in aging bone, and to see if protecting mitochondria from MPTP opening via CypD deletion protects against bone loss.

Methods: C57BL/6J and CypDKO male mice were used for all experiments. Bones were imaged via micro computed tomography (microCT), and subjected to biomechanical testing, histomorphometry analysis, bone formation analysis using fluorescent labeling, metabolomic studies, and electron microscopy. Bone marrow stem (a.k.a. stromal) cells (BMSCs) were isolated and mitochondrial membrane potential analyzed via staining with CMXRos and flow cytometry.

Results: We found that bone mass, bone strength, bone formation, and BMSC osteogenic function progressively decline with age in C57BL/6J mice. We also determined that oxidative metabolism is impaired in aging bone leading to a glycolytic shift. Mitochondria in osteocytes appear swollen, which is a major marker of MPTP opening. BMSC mitochondrial membrane potential is decreased

in aged mice. However, in the CypDKO mice, bone mass, bone strength, bone formation, and BMSC function do not decline, nor do they show the glycolytic shift, swollen mitochondria or depolarization of BMSC mitochondria seen in the C57BL/6J mice.

Conclusion: CypD deletion protects against bone loss in aging mice, in addition to preventing decline in bone formation and the mitochondrial changes observed in wild type C57BL/6J mice. Together, these data demonstrate that mitochondria are impaired in aging bone, and that CypD deletion protects against this impairment to prevent bone loss. This implicates CypD-regulated MPTP and mitochondrial dysfunction in the impairment of bone cells and in aging-related bone loss. Our findings suggest mitochondrial metabolism as a new target for bone therapeutics, and inhibition of CypD as a novel strategy against bone loss.

**Disclosures:** Laura Shum, None.

## FR0075

**Fkbp10 is essential for normal bone quality and joint homeostasis in postnatal mice.** Joohyun Lim<sup>\*1</sup>, Caressa Lietman<sup>1</sup>, Hamilton Wang<sup>1</sup>, Ingo Grafe<sup>1</sup>, Elda Munivez<sup>1</sup>, Merry Ruan<sup>1</sup>, Keren Machol<sup>1</sup>, Brian Dawson<sup>1</sup>, Terry Bertin<sup>1</sup>, Yuqing Chen<sup>1</sup>, Hao Ding<sup>2</sup>, Dongsu Park<sup>1</sup>, Xiahong Bi<sup>2</sup>, Catherine Ambrose<sup>3</sup>, Nadia Fratzi-Zelman<sup>4</sup>, Paul Roschger<sup>4</sup>, Klaus Klaushofer<sup>4</sup>, Ingo Schmidt<sup>5</sup>, Peter Fratzi<sup>5</sup>, Jyoti Rai<sup>6</sup>, MaryAnn Weis<sup>6</sup>, David Eyre<sup>6</sup>, Deborah Krakow<sup>7</sup>, Brendan Lee<sup>1</sup>. <sup>1</sup>Department of Molecular & Human Genetics, Baylor College of Medicine, United states, <sup>2</sup>Department of Nanomedicine & Biomedical Engineering, University of Texas Health Science Center at Houston, United states, <sup>3</sup>Department of Orthopaedic Surgery, University of Texas Health Science Center at Houston, United states, <sup>4</sup>Ludwig Boltzmann Institute of Osteology, Hanusch Hospital of WGKK & AUVVA Trauma Centre Meidling 1st Med. Dept. Hanusch Hospital, Austria, <sup>5</sup>Department of Biomaterials, Max Planck Institute of Colloids & Interfaces, Research Campus Golm, Germany, <sup>6</sup>Department of Orthopaedics & Sports Medicine, University of Washington, United states, <sup>7</sup>Department of Orthopaedic Surgery, David Geffen School of Medicine at UCLA, United states

Osteogenesis imperfecta (OI) is a genetic disorder that is characterized by low bone mass, increased susceptibility to fracture and progressive bone deformities. Recently, we and others identified loss-of-function mutations in FK506 binding protein 10, 65 kDa (*FKBP10*) that cause progressively deforming OI, with a subset of patients exhibiting joint contractures also known as Bruck syndrome. That joint deformities occur in conjunction with bone fragility suggests novel mechanisms may govern *FKBP10*-related bone and connective tissue disease. However, the role of *FKBP10* in bone formation and joint homeostasis is not completely understood. To fill this knowledge gap, we conditionally deleted *Fkbp10* in osteoblasts with the rat 2.3kb *Colla1-Cre* and in tendon cells with *Scx-Cre*, *in vivo*. Using micro-computed tomography and quantitative backscattered electron imaging, we found only minimal alterations in bone mass and matrix mineralization in bone-specific *Fkbp10* conditional knockout mice. However, mass spectroscopy of bone collagen revealed a significant decrease in mature hydroxylysine-aldehyde crosslinking. Furthermore, mutant mice displayed altered collagen and matrix components as well as reduced mineral crystal size by Raman spectroscopy and small angle X-ray scattering, respectively, which was accompanied by a marked reduction in biomechanical strength. Thus, *Fkbp10* is essential for normal bone quality but may be dispensable for bone mass. In tendons, conditional removal of *Fkbp10* resulted in mice with joint contractures. Histological analyses showed that tendon-specific *Fkbp10* conditional knockout mice exhibit synovial inflammation and severe osteoarthritis. Moreover, live-confocal imaging of wild type and mutant mice harboring the *Scx-gfp* reporter revealed that tendon-specific deletion of *Fkbp10* increases cell number and cellularity, which are hallmarks of tendinopathy. Taken together, these results suggest that *Fkbp10* is required for normal bone quality and joint homeostasis. Importantly, bone- and tendon-specific *Fkbp10* conditional knockout mice recapitulates key features of the human disease and, thus, may provide animal models that are necessary to identify critical therapeutic targets for the treatment of OI and Bruck syndrome, respectively.

**Disclosures:** Joohyun Lim, None.

## FR0076

**Anti-Notch2 Antibodies Reverse the Severe Osteopenia of Hajdu Cheney Syndrome Mutants.** Ernesto Canalis<sup>\*</sup>, Archana Sanjay, Jungeun Yu, David Bridgewater, Stefano Zanotti. UConn Health, United states

Notch receptors play a critical role in skeletal development and bone homeostasis. Hajdu Cheney Syndrome (HCS) is a devastating disease associated with a gain-of-*NOTCH2* function mutation and characterized by acro-osteolysis, severe osteoporosis with fractures and sudden death. We created a mouse model harboring a *Notch2* allele reproducing the mutation found in HCS. The 6955C>T mutation, verified by DNA sequencing of the mouse line, creates a STOP codon in exon 34 upstream the PEST domain leading to the formation of a truncated stable protein product (*Notch2*<sup>Q2319X</sup>) with increased Notch2 activity. Heterozygous *Notch2*<sup>Q2319X</sup> mutant mice had pronounced osteopenia, and exhibited 50-55% decrease in cancellous and 20-40% decrease in cortical bone compared to sex-matched littermate controls. The mechanism

responsible was enhanced osteoclastogenesis causing an increase in osteoclast number and eroded surface in cancellous bone and endocortical surfaces. In an attempt to correct the osteopenia, antibodies to the negative regulatory region (NRR) of Notch2 (10 mg/Kg) were administered to prevent the activation of Notch2. Antibodies or control anti-ragweed antibodies were given twice a week x 8 to 1 month old male *Notch2<sup>Q2319X</sup>* mutant or control littermate mice and sacrificed 4 weeks later. The profound decreases in cancellous bone volume, connectivity, trabecular number and cortical osteopenia of *Notch2<sup>Q2319X</sup>* mutant mice were reversed by the anti-Notch2 NRR antibody so that these parameters were no longer different between *Notch2<sup>Q2319X</sup>* mutant and control littermate sex-matched mice. Histomorphometric analysis revealed normalization of osteoclast number and eroded surface in *Notch2<sup>Q2319X</sup>* mutants treated with anti-Notch2 NRR. Moreover, the increased capacity of bone marrow-derived macrophages from *Notch2<sup>Q2319X</sup>* mutants to form multinucleated osteoclasts in response to Rankl, was suppressed by anti-Notch2 NRR antibodies at 10µg/ml. In conclusion, the severe cancellous and cortical bone osteopenia exhibited by a mouse model harboring the HCS mutation is reversed by preventing the activation of Notch2 with antibodies to the Notch2 NRR. The mechanism involves the reversal of the effect of the *Notch2<sup>Q2319X</sup>* mutation on osteoclastogenesis.

**Disclosures:** Ernesto Canalis, None.

## FR0077

**CRISPR/Cas9-generated Mouse Model of Autosomal-dominant Hypocalcemia Harboring the Activating G Protein Alpha 11 Mutation Arg60Cys and Use of Calcilytics and a Gα1/Gα11-specific Inhibitor.** Kelly Lauter Roszko<sup>\*1</sup>, Ruiye Bi<sup>1</sup>, Sarah Howles<sup>2</sup>, Hans Brauner-Osborne<sup>3</sup>, Xiaofeng Xiong<sup>3</sup>, Fadil Hannan<sup>4</sup>, M Andrew Nesbit<sup>5</sup>, Rajesh Thakker<sup>6</sup>, Kristian Stromgaard<sup>3</sup>, Thomas Gardella<sup>1</sup>, Michael Mannstadt<sup>1</sup>. <sup>1</sup>Endocrine Unit, Massachusetts General Hospital, United states, <sup>2</sup>University of Oxford, United Kingdom, <sup>3</sup>Department of Drug Design & Pharmacology, University of Copenhagen, Denmark, <sup>4</sup>University of Liverpool, United Kingdom, <sup>5</sup>Ulster University, United Kingdom, <sup>6</sup>Nuffield Department of Clinical Medicine, University of Oxford, United Kingdom

Parathyroid hormone (PTH) acts to maintain extracellular calcium in a tightly regulated range. Inadequate PTH levels result in hypocalcemia and hyperphosphatemia. Activating mutations in *GN11*, encoding Gα11, have recently been implicated in autosomal dominant hypocalcemia type 2 (ADH2) and are thought to activate the CASR pathway. One such mutation, uncovered in a family with ADH2, is the heterozygous missense mutation c.178C→T leading to the replacement of arginine 60 with cysteine in helix α1 of the GTPase domain.

We expressed wildtype (WT) Arg60 and mutant Cys60 Gα11 in HEK293 cells stably expressing the CASR and measured the intracellular calcium response to changes in extracellular calcium concentrations. This showed a leftward shift of the concentration-response curve in the cells expressing mutant Gα11, consistent with an increased sensitivity to calcium.

We used CRISPR/Cas9 to create a mouse model of the Arg60Cys mutation. Compared to littermates WT for Gα11, 9-week-old mice heterozygous and homozygous for R60C were hypocalcemic (iCa<sup>2+</sup>=1.26±0.03, 1.20±0.04, and 1.12±0.05 mmol/L). Compared to WT animals, PTH was inappropriate in heterozygous and homozygous animals (PTH=123±60, 124±17, and 62±18 pg/mL). We explored the effect of calcilytics on these mice by injecting 30 mg/kg of NPS2143 i.p.; 4 hours after injection, serum calcium was increased in mice WT, heterozygous and homozygous for R60C (1.38±0.12; 1.29±0.04; and 1.25±0.09 mmol/L). Serum PTH increased in all animal groups.

We tested the effects of the specific Gα11/Gαq inhibitor YM-254890. A single dose of YM-254890 given i.p. at 0.15mg/kg led to an increase in calcium in WT mice, and in mice heterozygous for R60C (calcium increased from 1.22±0.03 to 1.27±0.02; and 1.19±0.03 to 1.23±0.03). Published crystallography studies predict that YM-254890 inhibits WT Gα11, but not Gα11 R60C. Further studies are needed to test whether the observed effects of YM-254890 are due to the effect on WT Gα11. In summary, we have used CRISPR/Cas9 to create a mouse with the p.Arg60Cys mutation found in humans with ADH2. Our mouse model mimics the biochemical findings of the human disease, namely hypocalcemia and inadequate PTH. We have used the mouse model to show efficacy of treatment with a calcilytic. A Gα11/Gαq inhibitor increased serum calcium in WT animals, and in mice heterozygous for R60C and is therefore an important new tool to explore pathways affected by mutations in Gα11 and a potential treatment.

**Disclosures:** Kelly Lauter Roszko, None.

## FR0078

**Generation and Phenotypic Characterization of a *Lrp4* R1170Q Knock-In Mouse Model.** Eveline Boudin<sup>\*1</sup>, Igor Fijalkowski<sup>1</sup>, Stephan Sonntag<sup>2</sup>, Gretl Hendrickx<sup>1</sup>, Timur A Yorgan<sup>3</sup>, Thorsten Schinke<sup>3</sup>, Geert Mortier<sup>1</sup>, Wim Van Hul<sup>1</sup>. <sup>1</sup>Centre of Medical Genetics, University & University Hospital of Antwerp, Belgium, Belgium, <sup>2</sup>PolyGene AG, Rümlang, Switzerland, Switzerland, <sup>3</sup>Department of Osteology & Biomechanics, University Medical Center Hamburg, Germany, Germany

Throughout the years, it became clear that proteins deficient in rare monogenic sclerosing bone disorders such as sclerostin or cathepsin K are important regulators of bone remodeling and promising targets for the development of therapeutic agents for osteoporosis. We were recently able to show that mutations in the *low density lipoprotein receptor related protein 4 (LRP4)* gene are the cause of some cases of sclerosteosis, a rare monogenic bone disorder marked by syndactyly and hyperostosis of the skull and tubular bones among other symptoms. LRP4 is shown to regulate bone formation by facilitating the inhibitory actions of sclerostin on the Wnt/β-catenin signaling pathway. So far, three patients with sclerosteosis causing mutations in LRP4 have been described. Furthermore, we recently demonstrated that the mutation W1186S causing mutation in LRP4 results in highly increased sclerostin levels in the sclerosteosis patient (z-score +7), indicating that LRP4 has a role in sequestering sclerostin at the bone surface. As LRP4 clearly is an important regulator of bone formation and an interesting therapeutic target for treatment of osteoporosis, increased knowledge on the mechanism of action of LRP4 is required.

In order to further elucidate the mechanism whereby LRP4 facilitates the inhibitory actions of sclerostin, we generated in collaboration with Polygene (Rümlang, Switzerland), a *Lrp4* R1170Q knock-in (KI) mouse model. R1170Q is the most recently identified sclerosteosis causing *LRP4* mutation and the arginine at position 1170 seems to have an important role in the binding of sclerostin since this amino acid is mutated in two different sclerosteosis patients. The mutation is located at the inside of the third β-propeller domain which is shown to be important for the binding of sclerostin. Previous studies demonstrated that complete loss of *lrp4* in mice results in perinatal lethality. Here, we show that homozygous R1170Q KI mice are born at the expected frequencies and that they are viable and fertile. Furthermore, preliminary µCT analysis results of the skull and femur of 4 month old mice clearly demonstrate an increased bone mass at the tubular bones and at the skull in the presence of either one or two copies of the mutant allele compared to wild type mice. More detailed phenotyping is ongoing and results will be presented. However our preliminary data indicate that the *Lrp4* R1170Q knock-in mouse is a good model to study the role of *Lrp4* in the regulation on bone remodeling.

**Disclosures:** Eveline Boudin, None.

## FR0080

**Increased Trabecular Bone, Altered Glucose Homeostasis and Improved Biomechanics in an Osteocalcin Null Rat Model Created by CRISPR/Cas9 Technology.** Laura Lambert<sup>\*1</sup>, Anil Challa<sup>1</sup>, Aidi Niu<sup>1</sup>, Lihua Zhou<sup>1</sup>, Janusz Tucholski<sup>1</sup>, Maria Johnson<sup>1</sup>, Tim Nagy<sup>1</sup>, Alan Eberhardt<sup>1</sup>, Patrick Estep<sup>1</sup>, Robert Kesterson<sup>1</sup>, Jayleen Grams<sup>2</sup>. <sup>1</sup>UAB, United states, <sup>2</sup>UAB/Birmingham VA Medical Center, United states

Osteocalcin (bglap) is expressed by osteoblasts and is commonly used as a marker of bone turnover. A mouse model of osteocalcin deficiency implicated osteocalcin as a mediator of changes to the skeleton, endocrine system, reproductive organs, and central nervous system. Differences between mouse and human osteocalcin at both the genome and protein levels caution against extrapolating findings from the mouse model to humans. To further examine the role of osteocalcin in disease, we created a Sprague Dawley rat model with complete loss of osteocalcin using CRISPR/Cas9 since the rat shares greater synteny with humans in having a single gene. Animals with mutant bglap alleles were bred to homozygosity and compound heterozygosity and analyzed via dual-energy X-ray absorptiometry, glucose and insulin tolerance testing, micro computed tomography, and a three-point break biomechanical assay at five months of age. Complete loss of osteocalcin resulted in significantly increased trabecular thickness (p=0.002), density (p=0.001), and volume (p=0.002). Cortical bone volume (p=0.138) and density (p=0.192) were not increased in null animals; however, periosteal (13.37±0.11 mm null and 12.76±0.16 mm WT, p=0.007) and endosteal (7.63±0.04 mm null and 7.18±0.14 mm WT, p=0.003) measurements were significantly increased over wild type indicating increased overall bone size. Improved functional quality was shown by an increase in failure load (251.1±12.3 N null vs 159.7±7.6 N WT; p=0.005) during the biomechanical assay. There was no significant difference between groups in fasting glucose (p=0.21); however, 75 minutes after insulin injection the groups diverged, indicating increased insulin sensitivity in null animals (10.04±0.70 mg·dl<sup>-1</sup> null and 13.00±0.73 mg·dl<sup>-1</sup> WT; p=0.034). Osteocalcin null animals exhibited lower blood glucose levels at 30 minutes post glucose injection (16.62±0.73 mg·dl<sup>-1</sup> null and 18.34±1.38 mg·dl<sup>-1</sup> WT; p=0.028). Total body weight (p=0.548), percent fat mass (p=0.172), percent lean mass (p=0.331), bone mineral density (p=0.964), and bone mineral content (p=0.192) were not significantly different. There was no significant difference between groups in gonadal fat pad (p=0.273) or testes (p=0.090) weights. This rat model of complete loss of osteocalcin provides a platform for further understanding the role of osteocalcin in disease and serves as

a novel model of increased bone formation with potential utility in osteoporosis and osteoarthritis research.

**Disclosures:** Laura Lambert, None.

## FR0081

**Multi-Trait Mapping Reveals Novel Loci Controlling Relationships between Calcium Absorption, Bone Density, and Serum 1,25 Dihydroxyvitamin D in BXD Mice.** James Fleet\*, Kritikan Chanpaisaeng, Perla Reyes-Fernandez, Rebecca Replogle. Department of Nutrition Science, Purdue University, United states

We previously used single trait mapping to identify genetic loci controlling phenotypes for bone and calcium (Ca) metabolism as well as their response to low dietary Ca intake. Mice from 51 BXD recombinant inbred lines were fed either adequate (0.5%) or low (0.25%) Ca diets from 4 to 12 weeks of age ( $n=8/\text{diet}/\text{line}$ ). Ca absorption (CaAbs), bone mass (BMC and BMD), serum 1,25 dihydroxyvitamin D (1,25 D), and FGF-23 were measured in both diet groups and the response to dietary Ca restriction (RCR) was calculated for each phenotype in each line. Linear regression analysis revealed expected and novel correlations among our phenotypes that suggest the existence of genetic loci that coordinately regulate multiple traits. To test this hypothesis we used principle components analysis (PCA) to group traits based on their correlations and we used the resulting principle components (PC) for genetic mapping using composite interval mapping. Candidate genes underlying loci were identified with PROVEAN analysis (protein coding effects) or eQTL analysis in WebQTL (mRNA level effects). A PC for the positive correlation between CaAbs and 1,25 D mapped to a QTL on Chr 9 (LOD = 12); in addition, a PC for the negative relationship between BMD/BMC RCR and serum 1,25 D mapped to this locus (LOD = 8.4). We previously showed that the Chr 9 QTL controls serum 1,25 D levels through a cis eQTL controlling renal *Ets-1* mRNA levels. Two PC's were identified that condensed either BMD RCR and BMC RCR or CaAbs on the adequate or low Ca diet. These PC's mapped to a locus on Chr4 (LOD=3.8) that we previously showed influences many bone and mineral metabolism phenotypes. *Tecan2* mRNA was identified as cis eQTL in this region; its bone and kidney mRNA levels correlate positively to BMD ( $r = 0.4$ ) and negatively to BMC RCR ( $r = -0.39$ ) and CaAbs ( $r = -0.57$ ). Novel QTL were identified by mapping a PC for the positive relationship between CaAbs, BMD RCR, and BMC RCR: Chr11 (LOD=3.8), Chr13 (LOD=5.5), Chr15 (LOD=7.7), Chr19 (LOD=8.5). *Dennd3* (Chr15) was a cis eQTL expressed in kidney; this protein influences endocytic recycling of proteins. *Slc22A29* (Chr19) has a non-synonymous coding variant that could affect cation transport in the kidney. Our study demonstrates that multi-trait mapping can capture novel loci not identified in single trait mapping. Using this approach, we have identified several interesting candidate genes that influence multiple bone and Ca metabolism phenotypes.

**Disclosures:** James Fleet, None.

## FR0083

**The Effects of Soluble Activin Receptor Type IIB (ActRIIB-mFc) Treatment on Muscle and Bone Properties of Two Distinct Osteogenesis Imperfecta Mouse Models.** Youngjae Jeong<sup>1</sup>, Marybeth Brown<sup>2</sup>, Ferris Pfeiffer<sup>3</sup>, Mark Dallas<sup>4</sup>, Yixia Xie<sup>5</sup>, R. Scott Pearsall<sup>6</sup>, Sarah Dallas<sup>4</sup>, Charlotte Phillips<sup>7</sup>. <sup>1</sup>Department of Biochemistry, University of Missouri, United states, <sup>2</sup>Department of Biomedical Sciences & Physical Therapy Program, University of Missouri, United states, <sup>3</sup>Department of Bioengineering, University of Missouri, United states, <sup>4</sup>Department of Oral & Craniofacial Biology, University of Missouri at Kansas City, United states, <sup>5</sup>Department of Oral & Craniofacial Sciences, University of Missouri at Kansas City, United states, <sup>6</sup>Accelaron Pharma Inc., United states, <sup>7</sup>Departments of Biochemistry & Child Health, University of Missouri, United states

Bone is inherently mechanosensitive and the largest physiological loads bone experiences are due to muscle mass and force, with a positive correlation between bone and muscle mass. Myostatin, a TGF- $\beta$  family member, signals through activin receptor type II to negatively regulate muscle. Recent studies have demonstrated inhibition of myostatin with soluble activin receptor type IIB [ActRIIB-mFc, Accelaron Pharma] led to improved muscle and bone properties in mature rodents. Osteogenesis imperfecta (OI) is a heritable connective tissue disorder that exhibits compromised biomechanical integrity in type I collagen containing tissues, such as bone, due to mutations in the type I collagen genes. In the following study, we investigated the effects of ActRIIB-mFc on bone and muscle properties in two distinct OI mouse models [heterozygote *+G610C* and homozygous *oim/oim*]. At 2 months of age, bi-weekly treatments of either vehicle (Tris-Buffered Saline) or ActRIIB-mFc (10mg/kg) were given for 8 weeks to wildtype (WT), *+G610C* and *oim/oim* mice. At 4 months, mice were anesthetized and skeletal muscle force was measured by *in-situ* muscle contractile testing prior to sacrifice. All groups of ActRIIB-mFc treated mice exhibited increased body weight and hindlimb skeletal muscle wet weights as compared to their vehicle treated controls. ActRIIB-mFc treated *oim/oim* mice also exhibited increased peak tetanic force in soleus, gastrocnemius and tibialis anterior muscles as compared to vehicle treated controls.

These parameters were also increased in ActRIIB-mFc treated WT and *+G610C* mice but did not reach significance. By  $\mu$ CT analyses, femoral cortical bone thickness (CBT) and polar moment of area were increased with ActRIIB-mFc treatment in WT and *+G610C* mice, whereas in *oim/oim* mice CBT only reached significance. By torsional loading to failure analyses, WT and *+G610C* femora exhibited increases in torsional ultimate strength with ActRIIB-mFc treatment, as well as increases in energy to failure in WT with treatment. Our findings suggest that systemic administration of ActRIIB-mFc induced increased muscle mass in WT, *+G610C* and *oim/oim* and increased contractile force in *oim/oim* mice. The cortical bone geometries were increased with ActRIIB-mFc treatment in all genotypes, while the bone biomechanical integrity was improved in WT and *+G610C* mice. Our results suggest that soluble ActRIIB-mFc may provide a new therapeutic option to improve muscle and bone properties in OI.

**Disclosures:** Youngjae Jeong, None.

## FR0084

**Osteoprotegerin is Critical for the Formation of Heterotopic Ossification.** Song Xue<sup>1</sup>, Roberto Fajardo<sup>2</sup>, Kevin McHugh<sup>1</sup>. <sup>1</sup>University of Florida, United states, <sup>2</sup>University of Texas Health Science Center San Antonio, United states

**Introduction:** Heterotopic ossification (HO) is the formation of bone in non-osseous tissues and occurs subsequent to trauma. There are currently no effective treatments for HO other than surgical excision of the ossified tissue which is an extremely difficult procedure. There is therefore a significant unmet need for effective and non-invasive treatment of HO.

Bone metabolism is regulated by the local expression and ratio of the osteoclast inducer Receptor Activator of Nuclear Factor  $\kappa$ B Ligand (RANKL) to the native osteoclast inhibitor osteoprotegerin (OPG). Osteoblasts express high ratios of RANKL/OPG early in their differentiation, thus driving resorption, while mature, mineralizing, osteoblasts express low RANKL/OPG ratios. We hypothesize that ossifying HO cells express high OPG, blocking osteoclast formation and favoring maintenance of heterotopic bone. In previous studies, we employed a constitutively-active BMP receptor-mediated model of ectopic bone formation (caALK2) and show that administration of OPG blocking antibody increased markers of resorption, improved motion and decreased HO formation. In the current studies we test the role of OPG expression in the formation of ectopic bone in the OPG deleted (OPG<sup>-/-</sup>) mouse background.

**Methods:** With the caALK2 mouse model (an inducible Q207D mutant of the BMP receptor ALK2), expression of the caALK2 transgene was induced by intramuscular (IM) injection of Cre-recombinase delivered by an adenoviral vector (Ad-Cre). HO production was quantified over time by a "range-of-motion" (ROM) assay. The caALK2:OPG<sup>-/-</sup> mouse strain was generated by breeding caALK2 into OPG knockout mouse background. The resorption inhibitor alendronate was administered via IP injection. Micro-CT was used to quantify HO formation. Histology was used to characterize the HO formed and to identify TRAP positive osteoclasts. Immunohistochemistry was used to identify OPG producing cells.

**Results:** We found that in contrast to caALK2 mouse, which makes robust and reproducible HO bone, caALK2:OPG<sup>-/-</sup> mice make very little ectopic bone. The bone volume was statistically significantly reduced in OPG KO mouse compared to caALK2 mouse (Fig 1A). The ROM was statistically improved in OPG KO mice. HO bone formation was rescued in the OPG mouse with alendronate treatment with a statistically significant increase in ROM (Fig 1B).

**Discussion:** Our studies strongly suggest that OPG is critical for ectopic bone formation or for its maintenance. The data support our novel hypothesis that osteoclastic resorption is inhibited, at least in part, by OPG in HO and that removing such inhibition will allow osteoclastic resorption of HO bone. Fracture healing is unaffected or accelerated in the OPG KO mouse and therefore pro-resorptive treatment approaches to HO will not affect bone healing.

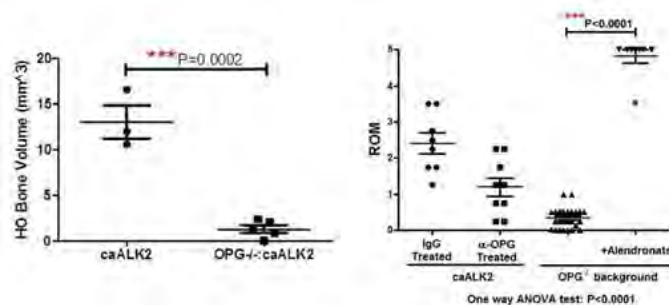


Fig 1

**Disclosures:** Song Xue, None.

**FR0085**

**Epigenomic Signature of Bisphosphonate use.** Roby Joehanes\*, Yi-Hsiang Hsu, David Karasik, Douglas Kiel. Institutes for Aging Research; Hebrew SeniorLife; Harvard Medical School, United states

Bisphosphonates (BP) have been the first line drug for treating osteoporosis. However, their use has been reported to be associated with several rare side effects, such as osteonecrosis of the jaw and atypical femur fracture. The incidence of such side effects has been reported to correlate with the duration of BP use, raising the possibility that exposure to BP could affect DNA methylation, which could play a role in the risk for these side effects. We hypothesized that BP use induces alteration of DNA methylation signatures that eventually contribute toward such side effects.

We investigated the DNA methylation in whole blood of 2,648 Framingham Osteoporosis Study participants (1,210M/1,348F) using the Illumina HumanMethylation BeadChip 450K over 485,512 cytosine-phosphate-guanine (CpG) sites. Of these samples, 293 (27M/266F) were BP users (210 alendronate, 72 risedronate, and 11 ibandronate). We used linear mixed effects models with methylation proportion (beta) as the outcome, BP use as the variable of interest, adjusting for sex, age, smoking status, menopause status, blood cell count, family correlation structure, and applicable technical covariates, such as batch and lab effects. We adjusted for multiple testing using Benjamini and Hochberg's False Discovery Rate (FDR).

At a significance level of FDR<0.05, 15 CpG sites were significantly associated with BP use (TABLE). Gene-set enrichment pathway analyses revealed genes *ACVR1*, *ABCG1*, *LRRCL1*, *SLC9A1*, *CASK*, and *CLIC1*, which are involved in estradiol downregulation response.

In conclusion, our results suggest that BP may have induced DNA methylation patterns that lower estradiol response, which is consistent with recent findings (PMID: 26358930) that estradiol levels differ between BP responders and non-responders.

Probe ID	Chr.	Location	Gene Symbol	Coef.	SE	P	FDR
cg17501210	6	166,970,252	<i>RPS6KA2</i>	0.0187	0.0030	3.0E-10	0.0001
cg14622782	X	41,782,111	<i>CASK</i>	0.0161	0.0028	1.4E-08	0.0033
cg08863422	2	232,290,901		0.0171	0.0031	4.9E-08	0.0079
cg18909389	6	31,701,110	<i>CLIC1</i>	-0.0112	0.0021	2.0E-07	0.0210
cg00712762	1	36,351,470	<i>EIF2C1</i>	-0.0073	0.0014	2.2E-07	0.0210
cg15614653	2	129,104,464		0.0119	0.0023	2.8E-07	0.0223
cg06500161	21	43,656,587	<i>ABCG1</i>	-0.0101	0.0020	3.6E-07	0.0251
cg01298945	14	73,259,435	<i>DPP3</i>	0.0063	0.0013	4.5E-07	0.0272
cg25130381	1	27,440,721	<i>SLC9A1</i>	-0.0085	0.0017	7.8E-07	0.0368
cg22321559	X	16,738,200	<i>SYAP1</i>	0.0035	0.0007	8.1E-07	0.0368
cg23663298	11	61,912,356	<i>INCENP</i>	-0.0070	0.0014	9.2E-07	0.0368
cg26403843	5	158,634,085	<i>RNF145</i>	-0.0158	0.0032	9.5E-07	0.0368
cg00495036	2	158,733,490	<i>ACVR1</i>	-0.0035	0.0007	1.1E-06	0.0368
cg23370548	1	6,471,486		0.0111	0.0023	1.1E-06	0.0368
cg11475305	6	53,663,860	<i>LRRCL1</i>	0.0039	0.0008	1.1E-06	0.0368

Table. Fifteen CpG sites associated with bisphosphonate use at FDR<0.05.

**Disclosures:** Roby Joehanes, None.

**FR0086**

**Comprehensive genome characterization of alcohol-induced osteonecrosis of femoral head.** Dewei Zhao\*, Yan Ding. The Affiliated Zhongshan Hospital of Dalian University, China

Excessive alcohol consumption is widely recognized as a major risk factor for osteonecrosis of femoral head (ONFH). However, the pathogenesis of alcohol-induced ONFH still remains unclear. Here we performed deep sequencing of RNA isolated from paired necrosis (15) and normal (n=15) tissue samples collected from patients diagnosed as alcohol-induced ONFH. Genome-wide transcriptome analysis identified a total of 484 genes are differentially expressed in ONFH samples, with 46 down- and 428 -up regulated genes when compared to controls (FDR-adjusted p < 0.05). Gene ontology and pathway analysis by GSEA reveal significant dysregulation of genes involved in alcohol metabolic process, extracellular matrix organization and collagen formation, hemoistasis, metabolism of lipids and lipoproteins, GPCR signaling, complement and coagulation cascade, and TGF- $\alpha$  signaling (PITX2-, COMP, DCN, INHBA, THBS4), suggesting alcohol induces bone remodeling by osteoblasts. We identified polymorphism of Arg48His (rs1229984) for ADH1B and novel mutations at the 3'UTR region of ADH1B from the ONFH samples. Dysregulation of the differentially expressed genes were validated by real-time quantitative PCR and genotypes of the ADH1B were confirmed by DNA-PCR followed by Sanger sequencing. We further found that ADH1B was over-expressed in osteocytes by Immunohistochemistry (IHC). Genetics linkage analysis between alcohol-induced ONFH patients and non-ONFH alcoholics (n=30) show likelihood of developing ONFH for individuals with concurrent SNP Arg48His and 3'UTR mutation in ADH1B. Take together, for the first time, we identified novel mutations in ADH1B gene and its overexpression in osteocytes, and link ADH1B gene dysregulation in the osteocytes to the alcohol-induced osteonecrosis of femoral head.

**Disclosures:** Dewei Zhao, None.

**FR0090**

**Several novel susceptibility loci identified in trans-ethnic genome-wide association for trabecular volumetric bone mineral density.** Xiaoying Fu\*, Hong-Wen Deng. Center for Bioinformatics & Genomics, Tulane University, New Orleans, LA, USA Department of Biostatistics & Bioinformatics, School of Public Health & Tropical Medicine, Tulane University, New Orleans, LA, United states

Currently, genome-wide association studies (GWAS) have identified a number of loci for osteoporosis. However, most studies focused on Caucasians and areal bone mineral density (aBMD) which missing the geometric features of bone. Volumetric bone mineral density (vBMD) measured by quantitative computed tomography (QCT) provides the chance to investigate the microstructure of bone in 3D manner. QCT is able to separate cortical and trabecular bone. In particular, trabecular bone density which mainly depends on number and size of trabeculae, is the most sensitive parameter for bone metabolism and more accurate in diagnosis of osteoporosis and fracture prediction.

To discover novel genetic factors for trabecular vBMD, we performed a trans-ethnic meta-analysis (n=1,817), with replication (n=3,117) for trabecular vBMD in lumbar spine. A Bayesian framework was used in trans-ethnic meta-analysis. 3 loci reached genome-wide significant level with Bayes factor (BF) larger than 6 (FMN2, rs1414660, BF=7.17; ADAM11, rs880295, BF=6.23; and SLC30A8, rs60124396, BF=6.14). FMN2 (rs9287237) is the locus identified in previous trabecular vBMD GWAS study. Interestingly, rs9287237 and rs1414660 are in the same linkage disequilibrium (LD) block in Caucasians, but different LD blocks in Africans. For African Americans in our study, rs1414660 did show independent significant signal. This may hint the information of fine-mapping for causal variants using populations with different LD structure. The locus in ADAM11 is validated as a cis-eQTL site in monocytes (potential precursors for osteoclasts) and a DNase I hypersensitive site specified in osteoblast cells, which suggesting that this locus is likely to have effect in bone metabolism. In gender specified analysis, 6 loci showed significant signal in male (IPO9-AS1, rs71635556, BF=6.17; LOC105373275, rs5015668, BF=6.32; 4p16.1, BF=6.91; TMEM246-AS1, rs5899447, BF=6.578; CRB2, rs10760279, BF=6.55; and TMEM132C, rs7978608, BF=6.26) and 2 in female (SLC35F1, rs17079881, BF=6.22 and 12q24.13, BF=6.39). Among which, SLC35F1 has been reported in association with aBMD.

In this study, we identified several novel genes and confirmed a previously reported gene in associated with trabecular vBMD. Our findings extend the insight into genetic architecture and pathogenesis of bone disease beyond Caucasians and aBMD. Furthermore, these findings suggest the potential advantages of using diverse populations in novel loci discovery and fine-mapping.

**Disclosures:** Xiaoying Fu, None.

**FR0092**

**Genetic Ablation of *Fgf23* Does not Modulate Experimental Heart Hypertrophy Induced by Pressure Overload.** Svetlana Slavic\*, Kristopher Ford, Ute Zeitz, Reinhold Erben, Olena Andrukhova. University of Veterinary Medicine, Vienna, Austria

Increased levels of FGF23 have been associated with cardiac hypertrophy in chronic kidney disease patients. Using transverse aortic constriction (TAC) as model, we examined whether *Fgf23* is involved in the development of heart hypertrophy during pressure overload. TAC or sham surgeries were performed in 3-month-old, male wild-type (WT), *VDR<sup>Δ/Δ</sup>* or *Fgf23<sup>-/-</sup>/VDR<sup>Δ/Δ</sup>* compound mutant mice. *Fgf23<sup>-/-</sup>* mice were crossed with mice expressing a nonfunctioning vitamin D receptor (*VDR<sup>Δ/Δ</sup>*) to overcome the deleterious effects of elevated vitamin D hormone production in these mice. All animals were kept life-long on a rescue diet enriched with calcium, phosphate, and lactose. TAC was performed by ligating the aortic arch around a 27-gauge needle, followed by rapid removal of the needle. Animals were killed 4 weeks postsurgery. Serum intact *Fgf23* levels as well as the ratio between intact and c-terminal *Fgf23* profoundly increased as early as 24 h after TAC, and serum intact *Fgf23* remained highly elevated (15-fold vs. sham) until 4 weeks after surgery. Cardiac, but not bone *Fgf23* mRNA levels increased significantly after TAC. Interestingly, TAC strongly induced cardiac transcription of the *Fgf23* glycosylating enzyme *GalNAc-transferase 3*, suggesting reduced cleavage of *Fgf23* locally produced in the heart. Cardiac transcription of other *Fgf23* processing enzymes such as *Fam20c* and *Furin* was not altered by TAC. In response to TAC, mice developed cardiac hypertrophy as evidenced by increased heart weight, increased left ventricular (LV) wall thickness, and increased LV cardiac mass assessed by echocardiography. However, there were no differences in LV hypertrophy parameters or the degree of LV functional impairment between *Fgf23<sup>-/-</sup>/VDR<sup>Δ/Δ</sup>* mice and WT or *VDR<sup>Δ/Δ</sup>* mice after TAC. Moreover, absence of *Fgf23* did not reduce myocardial expression of hypertrophy-associated genes such as atrial natriuretic peptide and alpha smooth muscle actin in *Fgf23<sup>-/-</sup>/VDR<sup>Δ/Δ</sup>* compared to WT and *VDR<sup>Δ/Δ</sup>* mice. In conclusion, increased myocardial *Fgf23* production, reduced cleavage, may contribute to the significant rise in serum intact *Fgf23* during pressure overload. However, because genetic deletion of *Fgf23* did not influence the development of heart hypertrophy in the TAC model, the pathophysiological role of high circulating intact *Fgf23* in TAC remains elusive.

**Disclosures:** Svetlana Slavic, None.

**FR0094**

**TNF $\alpha$  triggers renal FGF23 expression and elevates systemic FGF23 levels in mouse models of chronic kidney disease.** Daniela Egli-Spichtig<sup>\*1</sup>, Pedro Imenez Silva<sup>2</sup>, Bob Glaudemans<sup>3</sup>, Gehring Nicole<sup>2</sup>, Carla Bettoni<sup>4</sup>, Martin Zhang<sup>5</sup>, Desiree Schoenenberger<sup>2</sup>, Michal Rajski<sup>2</sup>, David Hoogewijs<sup>2</sup>, Felix Knauf<sup>6</sup>, Isabelle Frey-Wagner<sup>7</sup>, Gerhard Rogler<sup>7</sup>, Farzana Perwad<sup>5</sup>, Foeller Michael<sup>8</sup>, Florian Lang<sup>9</sup>, Roland H. Wenger<sup>2</sup>, Ian Frew<sup>2</sup>, Carsten A. Wagner<sup>2</sup>. <sup>1</sup>Institute of Physiology, University of Zurich; Division of Pediatric Nephrology, University of California San Francisco, United states, <sup>2</sup>Institute of Physiology, University of Zurich, Switzerland, <sup>3</sup>University of Zurich, Switzerland, <sup>4</sup>Institute of Physiology, University of Zurich, Switzerland, <sup>5</sup>Division of Pediatric Nephrology, University of California San Francisco, United states, <sup>6</sup>Universitätsklinikum Erlangen, Nephrologie und Hypertensiologie, Germany, <sup>7</sup>Division of Gastroenterology & Hepatology, University Hospital Zurich, Switzerland, <sup>8</sup>Ernährungsphysiologie, Martin-Luther-University Halle-Wittenberg, Germany, <sup>9</sup>Institute of Physiology, University of Tuebingen, Germany

Fibroblast growth factor 23 (FGF23) regulates phosphate homeostasis and is directly linked to all-cause mortality in chronic kidney disease (CKD). In polycystic kidney disease (PKD) animal models plasma FGF23 rises, however, *Fgf23* expression in bone is unchanged and the kidney becomes a site of FGF23 production. Since local hypoxia and inflammation develop in polycystic kidneys, we examined whether hypoxia or inflammation affects FGF23 expression in bone and kidney of CKD animal models. We investigated two CKD mouse models, the *Pkd1* conditional KO mouse and the oxalate induced nephropathy mouse model (0.63% oxalate in calcium-free diet).

Both CKD mouse models showed de novo renal *Fgf23* expression and elevated plasma FGF23 levels whereas *Fgf23* expression in bone was unchanged. Kidneys of CKD animals were affected by inflammation showing increased *Tnf $\alpha$*  and *Tgfb $\beta$*  mRNA expression. Furthermore, kidneys of PKD mice had increased phosphorylation of the Nf $\kappa$ B subunit p65. TNF $\alpha$ /Nf $\kappa$ B signaling increases *Nurr1* expression, an orphan nuclear receptor involved in the PTH dependent regulation of *Fgf23* expression in bone. In PKD kidneys, *Nurr1* expression was upregulated and NURR1 protein was predominantly localized in the cell nucleus and partially overlapped with FGF23 protein expression in cyst lining epithelial cells. TNF $\alpha$  but not hypoxia stimulated *Fgf23* mRNA expression in primary mouse osteocytes which was paralleled by upregulation of *Nurr1* expression. Antibody-mediated neutralization of TNF $\alpha$  in CKD animals reduced renal TNF $\alpha$  expression and decreased plasma FGF23 levels. To further investigate whether TNF $\alpha$  is commonly involved in FGF23 regulation, we examined mice with unilateral ureteral obstruction (UUO) a model of nephritis as well as the *IL-10* KO mouse, a model of inflammatory bowel disease. In UUO mice, we detected increased *Tnf $\alpha$*  and *Nurr1* expression which was paralleled by renal *Fgf23* mRNA expression. In *IL-10* KO mice suffering from acute inflammatory bowel disease anti-TNF $\alpha$  treatment normalized elevated plasma FGF23 levels.

In conclusion, the inflammatory cytokine TNF $\alpha$  triggers ectopic renal *Fgf23* expression in CKD animal models and contributes to elevated systemic FGF23 levels. The TNF $\alpha$ -dependent upregulation of FGF23 might be triggered by Nf $\kappa$ B-NURR1 signaling and TNF $\alpha$  blockade normalizes plasma FGF23 levels. Changes in FGF23 expression pattern in UUO and *IL-10* KO mice indicate that TNF $\alpha$  may stimulate FGF23 expression independent of renal function.

**Disclosures:** Daniela Egli-Spichtig, None.

**FR0097**

**Lrp6 is a Novel Target of the PTH-activated aNAC Transcriptional Coregulator.** Martin Pellicelli<sup>\*</sup>, Hadla Hariri, Julie Miller, René St-Arnaud. Shriners Hospitals for Children - Canada, Canada

In the nucleus of differentiated osteoblasts, the alpha chain of Nascent polypeptide associated complex (aNAC) associates with transcription factors, components of the basic transcriptional machinery, and other partners to regulate the expression of target genes such as *Bglap* (Osteocalcin). The subcellular localization and activity of aNAC are tightly regulated by phosphorylation of key amino acid residues.

PTH mediates phosphorylation of aNAC at residue serine 99 through a Gas-PKA-dependent pathway. In order to identify additional target genes affected by PTH-mediated aNAC phosphorylation, we performed ChIPSeq analysis against aNAC in MC3T3-E1 cells treated with vehicle or PTH(1-34). RNASeq was performed in parallel. Candidate genes that showed increased aNAC binding to their promoter and increased expression following PTH(1-34) treatment were selected for further analysis. This strategy identified the *Low-density lipoprotein-related receptor 6 (Lrp6)* gene as a potential new aNAC target. LRP6 acts as a co-receptor for Frizzled and the PTHR1 to allow optimal activation of Wnt and PTH signaling pathways in osteoblasts and osteocytes.

ChIPSeq results were validated using conventional quantitative ChIP. PTH(1-34) treatment of MC3T3-E1 cells led to an 8-fold enrichment of the S99-phosphorylated aNAC at the *Lrp6* promoter. Knockdown of aNAC decreased basal expression of *Lrp6* by 35% and blocked the stimulation of *Lrp6* expression by PTH(1-34).

To identify the sequence bound by aNAC to regulate *Lrp6* gene expression, we cloned the mouse *Lrp6* promoter (-2523 bp/+120 bp) upstream from the firefly luciferase reporter. Deletions and point mutations experiments confirmed that the

aNAC regulation of *Lrp6* transcription requires an element covering from -343bp to -331bp. Expression of the reporter is reduced by more than 50% when this element is deleted or mutated. The ability of aNAC to bind this response element was validated by a supershift of the protein complex using anti-aNAC antibody in Electrophoretic Mobility Shift Assays.

This study identified a new aNAC target gene induced by the PTH signaling pathway. It is also the first study that characterizes transcriptional regulation of *Lrp6* gene expression. This discovery will further our understanding of how the PTH-Gas-aNAC cascade contributes to optimal bone development.

**Disclosures:** Martin Pellicelli, None.

**FR0099**

**The Deacetylase, Sirtuin 1, is Necessary for Parathyroid Hormone's Actions on Murine Bone.** Nicola Partridge<sup>\*1</sup>, Teruyo Nakatani<sup>1</sup>, Jennifer Westendorf<sup>2</sup>, David Sinclair<sup>3</sup>, Yurong Fei<sup>4</sup>. <sup>1</sup>New York University, United states, <sup>2</sup>Mayo Clinic, United states, <sup>3</sup>Harvard Medical School, United states, <sup>4</sup>North Shore LIJ Health System, United states

Parathyroid hormone (PTH) is essential for bone physiology. Sirtuin 1 (SIRT1) is a Class III histone deacetylase and has been associated with bone acquisition. In this project, we aimed to investigate the function of SIRT1 in the actions of PTH on bone. *Sirt1* osteoblast-specific knockout (*Sirt1*<sup>Ob-/-</sup>) and control *Sirt1*<sup>lox/lox</sup> (*Sirt1*<sup>fl/fl</sup>) mice were offspring from breeding units of *Sirt1*<sup>fl/fl</sup> (female) and *Colla1* 2.3kb-Cre (male) transgenic mice. All mice were on C57BL/6J genetic background. Two-month-old *Sirt1*<sup>Ob-/-</sup> and control female mice were infused continuously with PTH (8 ug/100g/day) or vehicle released from osmotic pumps for 14 days. Femur BMD and cortical thickness were significantly decreased in *Sirt1*<sup>Ob-/-</sup> mice compared with controls. PTH treatment significantly reduced cortical bone volume/total volume (BV/TV) and increased cortical porosity while significantly increasing trabecular number, BMD, and BV/TV in controls; however, these changes were not observed in *Sirt1*<sup>Ob-/-</sup> mice. At the basal level, *Sirt1*<sup>Ob-/-</sup> mice showed increased mRNA expression of bone formation markers, *bone sialoprotein (BSP)*, *Colla1*, *Osterix*; and bone degradation/resorption markers, *matrix metalloproteinase 13 (Mmp13)*, *cathepsin K*, and *tartrate-resistant acid phosphatase (Trap)*. Continuous PTH treatment increased these markers with smaller fold changes in *Sirt1*<sup>Ob-/-</sup> mice. These mice displayed reduced basal mRNA expression of receptor activator of nuclear factor-kappaB ligand (*Rankl*) and osteoprotegerin (*OPG*). PTH suppressed both markers and *Sirt1* deficiency attenuated these changes. Further, SIRT1 inhibition with EX527 in osteoclastic RAW 264.7 cells *in vitro* significantly increased *Trap* and *Cathepsin K* mRNA expression, while decreasing the size of TRAP-staining multinucleated cells. SIRT1 inhibition at the late stage of osteoclast differentiation significantly suppressed *Trap*, *Cathepsin K* and *Carbonic anhydrase* mRNAs, while significantly increasing *Nfat2* mRNA compared with controls. Overall, PTH reduced cortical bone but increased trabecular bone in controls, while *Sirt1* deficiency attenuated the bone response to PTH. Thus, SIRT1 is necessary for normal bone accrual and for PTH's actions on bone.

**Disclosures:** Nicola Partridge, None.

**FR0100**

**A role for TIEG and estrogen-regulated miRNAs in mediating SOST expression in bone..** Malayannan Subramaniam<sup>\*</sup>, Kevin Pitel, Elizabeth Bruinsma, John Hawse. Mayo Clinic, United states

TIEG knockout (KO) mice exhibit a female-specific osteopenic phenotype and altered expression of TIEG in humans is associated with osteoporosis. Gene expression profiling of long bones isolated from TIEG KO mice revealed a 12-fold increase in SOST expression relative to WT littermates. This was accompanied by a 2-fold increase in circulating serum sclerostin (Scl) levels in KO animals suggesting that TIEG regulates SOST expression. Analysis of the SOST promoter revealed a number of putative TIEG regulatory elements and transfection of TIEG into U2OS cells resulted in 90% suppression of a SOST promoter reporter construct. 5'-deletion analysis of the SOST promoter indicated that the region between -2.0 and -1.8 kb upstream of the transcriptional start site is necessary for suppression by TIEG. ChIP assays revealed that TIEG associates with the -2.0 kb SOST promoter, but not the -1.8 kb fragment, confirming that TIEG's regulatory elements lie within this 200 bp region. CRISPR mediated deletion of TIEG in SW3 osteocyte cells resulted in significant increases in SOST expression mimicking the results obtained from TIEG KO long bones. TIEG deletion in SW3 cells also resulted in delayed mineralization and decreased expression of osteocyte marker genes. We next performed ovariectomy (OVX) and estrogen replacement therapy (ERT) studies in WT and TIEG KO mice followed by miRNA and mRNA seq analysis of cortical and trabecular compartments of femurs. SOST expression was 24-fold higher in cortical bone compared to trabecular bone of WT mice. In cortical bone, SOST expression was increased following OVX only in WT mice and was suppressed following ERT in both genotypes. In contrast, SOST expression in trabecular bone was decreased following OVX and significantly increased following ERT in both genotypes. Of the expressed miRs in bone, 3 were predicted to target SOST (miR-542-5p, -676-5p and -211-5p). Each of these miRs exhibited decreased expression following OVX and increased expression following ERT in cortical bone with opposite patterns in trabecular bone of both genotypes suggesting a role for these miRs in mediating estrogen regulation of

SOST expression. Circulating serum Scl protein increased following OVX and decreased in response to ERT in WT mice. Conversely, Scl protein was elevated in KO mice but did not respond to OVX and ERT. These data implicate important roles for TIEG and estrogen-regulated miRs in modulating SOST expression in bone.

**Disclosures:** Malayannan Subramaniam, None.

## FR0110

### Mechanoresponsive miR-138-5p targets MACF1 to inhibit bone formation.

Airong Qian<sup>1\*</sup>, Zhihao Chen<sup>1</sup>, Fan Zhao<sup>1</sup>, Chao Liang<sup>2</sup>, Lifang Hu<sup>1</sup>, Chong Yin<sup>1</sup>, Peng Shang<sup>1</sup>, Ge Zhang<sup>3</sup>. <sup>1</sup>Key Laboratory for Space Biosciences & Biotechnology, Institute of Special Environmental Biophysics, School of Life Sciences, Northwestern Polytechnical University, China, <sup>2</sup>Institute for Advancing Translational Medicine in Bone & Joint Diseases, School of Chinese Medicine, Hong Kong Baptist University, China, <sup>3</sup> Institute for Advancing Translational Medicine in Bone & Joint Diseases, School of Chinese Medicine, Hong Kong Baptist University, China

MicroRNAs (miRNAs) play important roles in the regulation of target gene expression to coordinate broad spectrum of biological processes. Recent studies have discovered that miR-214, miR-103a and miR-103, were sensitive to mechanical stimulation to regulate osteoblast differentiation or proliferation. However, functional roles of miRNAs in mechanotransduction in bone formation and further mechanism have not been well characterized.

This study aimed to identify specific miRNAs and their regulatory roles in the process of bone loss induced by mechanical unloading condition. We assessed the expression of miRNAs involved in bone formation in bone specimens from 70 osteoporotic individuals with bedridden states in clinical settings. The expression of miR-138-5p altered with bedridden time and was negatively correlated with the expression of the bone formation marker genes ALP and in bedridden women and men. Moreover, consistent results were found in bone tissue and ALP positive cells in hind limb unloading (HLU) and 20-month aging mice. In addition, we further explored the relationship between miR-138-5p expression and mechanical unloading condition in MC3T3-E1 cells under Random Position Machine (RPM) condition. We consistently found that high miR-138-5p expression increased gradually and ALP activity decreased in osteoblasts after RPM treatment for 12h, 24h, 48 h, respectively.

Target prediction analysis tools and luciferase activity were used to confirm microtubule actin crosslinking factor 1 (MACF1) as a direct target of miR-138-5p, and miR-138-5p inhibited MACF1 expression and osteoblast differentiation in vitro. To investigate loss-of-function of miR-138-5p on osteoblast differentiation under RPM condition in vitro, we treated mouse preosteoblast MC3T3-E1 cells with antagomir-138-5p and cultured cells under RPM condition. The results indicated that miR-138-5p functions as a mechanical unloading sensitive miRNA and plays a negative role in RPM-induced osteoblast differentiation reduction. Predominantly, we found an inhibitory role of miR-138-5p in regulating the bone formation in HLU mice and aging mice and in vivo pretreatment with antagomir-138-5p, partly recovered the bone loss caused by mechanical stimulation reduction.

Taken together, these results suggest that in vivo inhibition of miR-138-5p by anti-miR-138-5p could represent a potential therapeutic strategy for ameliorating bone loss.

**Disclosures:** Airong Qian, None.

## FR0111

### Osteoblast-Derived Paracrine Factors Regulate Angiogenesis in Response to Mechanical Stimulation. Chao Liu<sup>\*</sup>, Xin Cui, Thomas Ackermann, Vittoria Flamini, Weiqiang Chen, Alesha Castillo. New York University, United states

Angiogenesis, the process by which new vessels emerge from existing vessels, is critical for normal skeletal development, homeostasis, and repair. There is close proximity between cells of the osteogenic lineage and endothelial cells (ECs) participating in angiogenesis in bone, suggesting reciprocal regulation via paracrine signaling and cell-cell contact. As bone is a mechanically sensitive organ, we hypothesized that mechanical stimulation regulates "osteo-angio" communication. The purpose of this study was to examine the influence of mechanical stimulation on osteoblasts' ability to regulate EC behavior. ECs (C166-GFP, ATCC) were treated with conditioned media (CM) from: (1) preosteoblasts (MC3T3-E1 subclone 4, ATCC) held under static culture (static CM); (2) preosteoblasts stimulated with pulsatile fluid shear stress (0.8 Pa, 3 Hz) (loaded CM); (3) unconditioned growth media (-ve control); and (4) VEGF (+ve control), and EC proliferation, migration, and tubule formation were quantified. In addition, EC sprouting in response to CM or cultured osteoblasts was quantified using a dual-channel collagen gel-based microfluidic device, which mimicked vessel geometry (Fig 1). Lastly, soluble angiogenic factors released by osteoblasts were measured using an antibody array (R&D Systems). Differences between treatment groups were assessed by a one-way ANOVA with a Tukey's post-hoc analysis for multiple comparisons. We found that loaded CM significantly enhanced EC proliferation (50% increase) and migration (>200% increase) relative to static CM. Tubule length and junction density were promoted in all treatments groups relative to the -ve control, which exhibited virtually

no tubule formation. Static CM enhanced sprouting frequency (50% increase) relative to the -ve control, whereas loaded CM significantly enhanced both sprouting frequency (80% increase) and length (30% increase). In addition, sprouting frequency (~50% increase) and length (~50% increase) were significantly increased in response to mechanically-stimulated osteoblasts cultured directly in an adjacent collagen channel. Osteoblasts released angiogenic factors, of which osteopontin, PDGF-AA, IGBP-2, MCP-1, and Pentraxin-3 were upregulated in response to mechanical loading. Our data show that CM from mechanically-stimulated osteoblasts promote EC proliferation, migration, and sprouting, which suggests that mechanical forces may regulate angiogenesis in bone by modulating "osteo-angio" crosstalk.

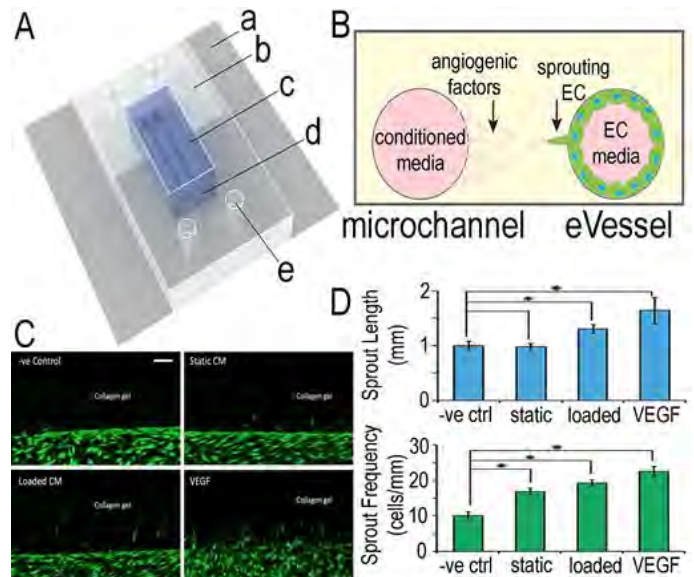


Figure 1. Microfluidic device with endothelial cells sprouting in response to soluble factors in adjacent channel. (A) Schematic of the device that consisted of a. glass cover slip, b. PDMS outer structure, c. collagen I gel with d. cylindrical channels that are connected to e. ports for fluid perfusion. (B) Theoretical model of endothelial sprouting in response to angiogenic factors in osteoblast conditioned media (CM). (C) Longitudinal view of endothelial cell layer inside the channel. The cells penetrated into the collagen gel toward the adjacent channel (above, out of view), which is filled with osteoblast and control CM. (D) Quantification of endothelial sprouting length and frequency in response to osteoblast CM and control CM in adjacent channel. Scale bar = 100  $\mu$ m.

Figure 1

**Disclosures:** Chao Liu, None.

## FR0113

### Osteocyte distribution does not influence locations of mechanically induced bone formation in cancellous bone. Erin Cresswell<sup>\*</sup>, Thu Nguyen<sup>1</sup>, Michael Horsfield<sup>1</sup>, Thomas Metzger<sup>2</sup>, Glen Niebur<sup>2</sup>, Christopher Hernandez<sup>1</sup>.

<sup>1</sup>Cornell University, United states, <sup>2</sup>University of Notre Dame, United states

Mechanical adaptation in bone is attributed to the response of osteocytes to local tissue stress/strain leading to bone formation. Recent studies in live animals found mechanically induced bone formation in cancellous bone to be spatially associated with local tissue strain energy density (SED), however, at best SED explained only 32-47% of the locations of new bone formation [1,2]. Here we determine how accounting for osteocyte distribution influences the ability to predict locations of bone formation in cancellous bone. Under IACUC approval, the caudal 8<sup>th</sup> vertebrae of six month old female Sprague Dawley rats (n=7) were subject to cyclic compressive loading (between 25N and 75N for 300 cycles at 0.5Hz) once per day (days 0, 1, 2). Bone formation labels were administered on day 5 and 10 and animals were euthanized on day 14. Loaded vertebra were submitted to three different imaging modalities to: 1) determine the distribution of tissue stress/strain using micro-CT based finite element models (11  $\mu$ m voxel size), 2) identify new bone formation using three-dimensional dynamic bone histomorphometry (0.7x0.7x5.0  $\mu$ m voxel size), and 3) determine the distribution of osteocyte lacunae using high resolution micro-CT (1.5  $\mu$ m voxel size). The ability to predict the locations of mechanically induced bone formation was compared among three different assays: 1) SED at the bone surface, 2) SED multiplied by osteocyte density at the bone surface, and 3) the "osteoblast recruitment stimulus" (first proposed by Huiskes [3]), which represents a sum of the mechanical stimulus experienced by each osteocyte in the bone tissue. As in prior work, the probability of observing bone formation was increased at regions experiencing greater strain energy density ( $R^2=0.79$ ,  $p<0.0001$ ). Including osteocyte density reduced the strength of the correlation ( $R^2=0.26$ ,  $p=0.03$ ) and the "osteoblast recruitment stimulus" showed no correlation ( $p=0.25$ ). These findings suggest that the osteocyte lacunar density in a region of cancellous bone has little effect on the locations of new bone formation, suggesting that the mechanisms of transmitting bone forming signals within

cancellous bone is complicated and may require examination of fluid flow in the marrow and within osteocyte lacunae.

[1] Schulte, FA et al., PlosOne 2013. [2] Cresswell, EN et al., JBiomech 2016. [3] Huiskes, R et al., Nature 2000.

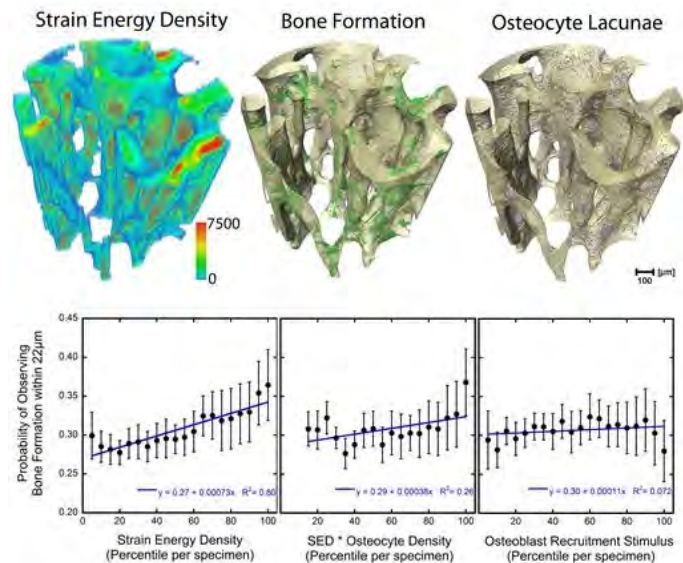


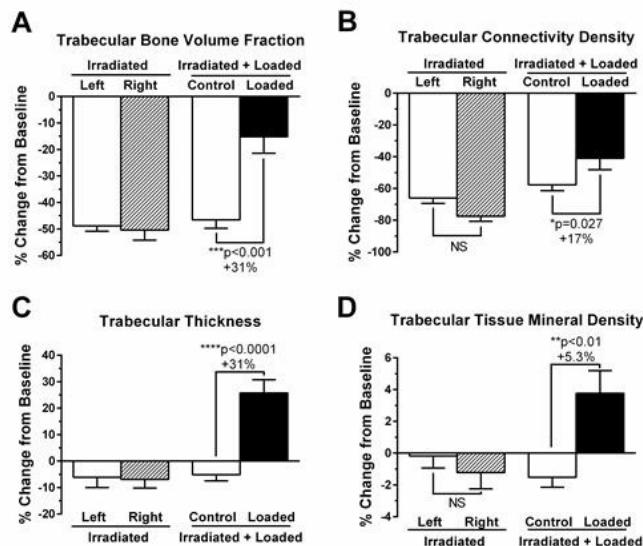
Figure 1

Disclosures: Erin Cresswell, None.

## FR0114

**Radiation-induced bone loss is attenuated by mechanical loading.** Peter Govey<sup>1</sup>, Yue Zhang<sup>2</sup>, Henry Donahue<sup>\*2</sup>. <sup>1</sup>Penn State, United states, <sup>2</sup>Virginia Commonwealth University, United states

Incidental exposure of bone to ionizing radiation, as occurs during radiotherapy for some localized malignancies and blood or bone marrow cancers, as well as during space travel, incites dose-dependent bone morbidity and increased fracture risk. Rapid trabecular and endosteal bone loss reflects acutely increased osteoclastic resorption as well as decreased bone formation due to depletion of osteoprogenitors. Because of this dysregulation of bone turnover, bone's capacity to respond to a mechanical loading stimulus in the aftermath of irradiation is unknown. We employed a mouse model of total body irradiation and bone marrow transplantation simulating treatment of hematologic cancers, hypothesizing that compression loading would attenuate bone loss. Furthermore, we hypothesized that loading would upregulate donor cell presence in loaded tibias due to increased engraftment and proliferation. We lethally irradiated 16 female C57Bl/6J mice at 16 wks with 10.75 Gy, then IV-injected 20 million GFP(+) total bone marrow cells (IACUC #42521). That same day, we initiated 3 wks compression loading (1200 cycles 5x/wk, 10 N) in the right tibia of 10 of these mice while 6 mice were sham controls. As anticipated, before-and-after microCT scans demonstrated loss of trabecular bone (-48.2% Tb.BV/TV) and cortical thickness (-8.3%) following irradiation and bone marrow transplantation. However, loaded bones lost 31% less Tb.BV/TV and 8% less cortical thickness (both  $p < 0.001$ ). Loaded bones also had significant increases in trabecular thickness and tissue mineral densities from baseline. Analysis of donor cell presence in loaded vs. non-loaded tibias revealed no significant increase in total marrow cell proportion or donor DNA in cortical bone, though there was an apparent trend of increased donor DNA in loaded bones. However, we did find that mechanical loading attenuated radiation-induced bone loss. Importantly, these results demonstrate that both cortical and trabecular bone exposed to high-dose therapeutic radiation remain capable of an anabolic response to mechanical loading. These findings inform our management of bone health in cases of incidental radiation exposure.



Trabecular microstructure parameters significantly regulated by loading, as indicated by microCT. n=10 for 'Irradiated+Loaded' mice and n=6 for 'Irradiated' mice.  $p < 0.05$  considered significant by paired two-tailed t-test. Percent changes indicate effect of loading relative to contralateral controls.

Donahue HJ

Disclosures: Henry Donahue, None.

## FR0115

**A Metabolite of Contracted Muscle,  $\beta$ -aminoisobutyric Acid, BAIBA, Inhibits Trabecular Bone Loss by Hindlimb Unloading Potentially through Maintenance of Osteocyte Viability.** Yukiko Kitase<sup>\*1</sup>, Jianxun Yi<sup>1</sup>, Julian Vallejo<sup>1</sup>, Harika Vemula<sup>2</sup>, William Gutheil<sup>2</sup>, Marco Brotto<sup>3</sup>, Lynda Bonewald<sup>1</sup>. <sup>1</sup>University of Missouri-Kansas City, Department of Oral & Craniofacial Sciences, School of Dentistry, United states, <sup>2</sup>University of Missouri-Kansas City, School of Pharmacy, United states, <sup>3</sup>University of Texas at Arlington, United states

Exercise clearly has beneficial effects on neural, metabolic and musculoskeletal systems but many of the cellular and molecular mechanisms responsible are not known.  $\beta$ -aminoisobutyric acid, BAIBA, is a small molecule produced by skeletal muscle during exercise that induces the browning of white fat. To determine whether BAIBA may play a role in muscle to bone crosstalk, the effects of BAIBA on bone were examined. L-BAIBA, but not D-BAIBA, preserves MLO-Y4 osteocyte-like cell viability under oxidative stress, reduces reactive oxygen species and induces expression of anti-oxidative enzymes. L-BAIBA is more potent than N-acetylcysteine but works by a different mechanism as western blot analysis showed an increase in anti-oxidant enzymes such as catalase (1.8 fold) by L-BAIBA, but not by N-acetylcysteine. Ex vivo, L-BAIBA, but not D-BAIBA is elevated with 90 Hz contraction of Soleus (young:  $5.7 \pm 0.9 \mu\text{M}$ , old:  $9.4 \pm 0.9 \mu\text{M}$ ) and extensor digitorum longus, EDL, (young:  $4.6 \pm 0.9 \mu\text{M}$ , old:  $7.3 \pm 0.7 \mu\text{M}$ ) muscles compared to static muscle ( $0.9 \pm 0.1 \mu\text{M}$ ) from both young (5 mo) and old (22 mo) C57Bl/6 mice. Preincubation of enriched primary osteocytes for 24 hrs with 0.1-10  $\mu\text{M}$  BAIBA prevented H<sub>2</sub>O<sub>2</sub> (0.3 mM) induced cell death in cells from young (5 mo) but not old (22 mo) mice. As BAIBA was reported to bind Mas-related G-protein coupled receptor, type D (MRGPRD), an antagonist to this receptor, MU6840, was tested and found to block the protective effects of L-BAIBA. MRGPRD mRNA was highly expressed in young, but not old primary osteocytes, which may be the reason L-BAIBA does not protect old osteocytes from H<sub>2</sub>O<sub>2</sub> induced cell death. In vivo hindlimb unloading using 5 mo male mice was conducted for 2 wks with and without the addition of L-BAIBA (100mg/kg/day) in drinking water (n=6). EDL and soleus muscles from both hindlimbs were tested for ex vivo contractility and right tibia for  $\mu\text{CT}$  analysis. Ingestion of L-BAIBA prevented the reduction of contractile force output in soleus, but not EDL. Animals receiving L-BAIBA showed 25% higher BV/TV and 38.5% higher trabecular bone connectivity compared to controls. This study suggests that L-BAIBA is one of the molecular mechanisms mediating the beneficial effect of exercise in the maintenance of bone homeostasis. L-BAIBA or its analogues have the potential to be used as a novel therapeutic intervention against disuse-induced deterioration of the musculoskeletal system.

Disclosures: Yukiko Kitase, None.

## FR0116

**Osteocytic gene expression is not rapidly altered following muscle paralysis.** Dylan Mogk, Leah Worton, Dewayne Threet, Brandon Ausk, Edith Gardiner, Steven Bain, Ted Gross\*. University of Washington, United states

Although transient calf paralysis induces relatively mild gait dysfunction, the neuromuscular dysfunction induces osteoclast resorption within just 3 d that results in profound tibia trabecular and cortical bone loss that is complete in less than 2 wk. Recent studies have indicated that calf paralysis alters tibia bone marrow gene expression prior to and coincident with the onset of osteoclastic activation. Given the essential role of osteocytes in modulating both osteoblast and osteoclast function and their interaction with muscle in a variety of contexts, this study assessed whether osteocyte enriched bone samples demonstrated altered gene expression following muscle paralysis. In this study, transient calf paralysis was induced in C57 female mice (16 wk; n=10) via a single injection of Botulinum Toxin A (BTxA; 2U/100g). Mice were sacrificed 1 d (n=5), or 3 d (n=5) post-paralysis. Additionally, 5 mice served as naïve controls. The right tibia of each mouse was removed, a 5 mm section of the proximal tibia was isolated and the marrow flushed. All samples were processed for qRT-PCR. A panel of genes was assessed that included genes found to be upregulated in bone marrow within 3 d of paralysis [RANKL, TNF $\alpha$ , Tac1 (encoding for Substance P) and CGRP] and genes associated with osteocyte function (OPG, SOST, Casp3). Gene expression was normalized to HPRT. Tac1, CGRP and TNF $\alpha$  expression was negligible. RANKL expression was not elevated in the bone samples following calf paralysis (1 d: -2.8%; 3 d: -43.8% vs naïve). OPG expression was also reduced at 1 d (-27.2%) and 3 d (-65.6%) vs naïve samples. SOST expression was not altered at 1 d (-13.3%) and was elevated at 3 d vs naïve controls (+117.6%). Finally, Casp3 expression was diminished at 1 d (-40.8%) and 3 d (-45.1%) vs naïve bones. Limitations of this study include the size of the gene panel and metaphyseal bone samples that did not include bone marrow but retained non-osteocytic surface cell populations. However, these data suggest that the pro-inflammatory bone marrow environment rapidly induced by muscle paralysis is not primarily mediated by direct osteocyte gene expression. Further, it does not appear that osteocyte apoptosis, which has been implicated as a mediator of micro-crack damage repair, is acutely induced by transient muscle paralysis.

**Disclosures:** Ted Gross, None.

## FR0117

**Transgenic Expression of FNDC5 Impacts Skeletal Turnover by Targeting Osteoblasts, Osteoclasts and Adipocytes.** clifford rosen\*<sup>1</sup>, christiane wrann<sup>2</sup>, bruce spiegelman<sup>2</sup>, mary bouxein<sup>3</sup>, roland baron<sup>4</sup>, kneichi nagano<sup>4</sup>, phuong le<sup>1</sup>, michaela reagan<sup>1</sup>, lynda bonewald<sup>5</sup>. <sup>1</sup>maine medical center research institute, United states, <sup>2</sup>dana farber cancer institute, United states, <sup>3</sup>Harvard Medical School, United states, <sup>4</sup>harvard dental school, United states, <sup>5</sup>university of missouri kansas city, United states

Results from cross-sectional and longitudinal exercise studies are conflicted relative to BMD changes, ranging from modest increases to mild bone loss. Fibronectin type III domain-containing protein 5 (FNDC5), the precursor of irisin, is a transmembrane protein expressed in muscle and cleaved during exercise. Irisin is highly conserved in mammals and can induce a thermogenic program in white adipose tissue. We hypothesized that expression of the parent protein FNDC5, in muscle would recapitulate a chronic exercise program and impact bone turnover. To test this, we utilized the MCK promoter to express Fndc5 in muscle of C57BL6 mice (Fndc5Tg). We measured bone mass by  $\mu$ CT, bone turnover markers and histomorphometry in male Fndc5Tg and B6 littermates (WT) at 8, 16, 56 weeks. We did primary bone marrow (BM) cultures to test the pace of osteoblast, osteoclast and adipocyte differentiation from those mice. There were no differences in body weight or femur length of mice by genotype at any age. However, by  $\mu$ CT femur trabecular BV/TV in Fndc5Tg was markedly reduced at 8 & 16 wks vs WT ( $p < 1.0 \times 10^{-4}$ ), but similar to WT at 56 wks (Fig.1A). Cortical thickness was reduced at 8 & 16 weeks vs WT ( $p < 1.0 \times 10^{-4}$ ). Tibial histomorphometry at 8 wks showed reduced BV/TV, BFR and MAR in the Fndc5Tg vs WT ( $p < 0.001$ ); at 56 wks there were no genotypic differences. Consistent with these data, serum PINP and Ocn were also lower in the 4 week Fndc5Tg vs WT ( $p < 0.05$ ,  $p < 0.01$  respectively) while CTX did not differ. Primary BM cells were cultured in osteogenic, or adipogenic media, or with RANKL+mCSF. CFU-Fs, Alp+ and Von Kossa+ colonies were greater in the Fndc5Tg vs WT ( $p < 0.05$ ) and Ocn mRNA was 2.5 fold greater in the Tg vs WT cells ( $p = 0.001$ ). TRAP+ osteoclast colony numbers after mCSF and RANKL were also increased vs WT ( $p < 0.01$ ) as was Oil Red O adipocyte staining ( $p < 0.01$ ) (Fig1B). Ucp1, Cidea, Prdm16, Fndc5 and adipoQ were increased in Fndc5Tg adipocytes ( $p < 0.001$  vs WT). Bone +marrow gene expression showed increased Sost, Nfkb, Glut1, Pdk4 and Fndc5 mRNA in the Fndc5Tg ( $p < 0.05$  vs WT). In sum, we found that expression of Fndc5 in several tissues (muscle, bone, fat) resulted in impaired bone acquisition but enhanced osteoblast, osteoclast and adipogenic differentiation in vitro. Sustained increases in Fndc5 illustrate that bone is a potential target of FNDC5/irisin, and the complex interaction of this myokine with cells in the marrow niche may provide new insights into bone development.

Fig1A. Differences femoral BV/TV and conn density at 3 ages in Fndc5Tg and WT ( $p < 1.0 \times 10^{-4}$ )

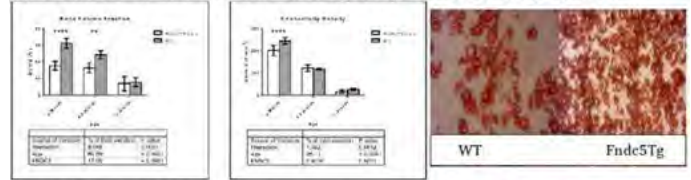


Figure 1B. Number of Oil Red O cells in marrow stromal cultures were statistically greater in the Fndc5Tg (right) vs WT (left).

1A.Changes in Trabecular BV/TV and 1B BMSC adipogenic cultures

**Disclosures:** clifford rosen, None.

## FR0118

**Hindlimb Immobilisation, but Not Castration, Induces Reduction of Undercarboxylated Osteocalcin Associated with Muscle Atrophy in Rats.** Xuzhu Lin\*<sup>1</sup>, Erik Hanson<sup>1</sup>, Andrew Betik<sup>1</sup>, Tara Brennan-Speranza<sup>2</sup>, Alan Hayes<sup>1</sup>, Itamar Levinger<sup>3</sup>. <sup>1</sup>Institute of Sport, Exercise & Active Living (ISEAL), Victoria University, Australia, <sup>2</sup>Department of Physiology & Bosch Institute for Medical Research, University of Sydney, Australia, <sup>3</sup>Exercise & Active Living (ISEAL), Victoria University, Australia

Background: Undercarboxylated osteocalcin (ucOC) has been reported to be involved in the regulation of glucose metabolism and male fertility. It is also implicated in cell growth and strength in skeletal muscle. However, whether muscle loss, during atrophic conditions, is related to a reduction in ucOC remains unclear. We tested the hypothesis that in rats, both hindlimb immobilisation and testosterone depletion (via castration), leads to a reduction in serum ucOC and this reduction is associated with the degree of muscle atrophy as well as changes in atrophy signaling pathways.

Methods: Rats were subject to a 10-day hindlimb immobilisation 7 days after castration or sham surgery. We measured ucOC, testosterone, and insulin levels as well as mass and strength of EDL and soleus muscles in rats with or without the intervention. We examined the expression and activity of the putative ucOC-sensitive receptor in muscle and its two possible downstream kinases, GPRC6A, ERK and AMPK, as well as the expression and activity of proteins in the muscle atrophy signaling network.

Results: Hindlimb immobilization, but not castration, resulted in lower ucOC levels (70%,  $p < 0.05$ ) compared with non-immobilised rats. Lower ucOC correlated with lower muscle mass and muscle strength in both EDL (mass:  $r = 0.53$ ,  $p < 0.01$ ; strength:  $r = 0.56$ ,  $p < 0.01$ ) and soleus (mass:  $r = 0.37$ ,  $p < 0.05$ ; strength:  $r = 0.46$ ,  $p < 0.05$ ) in all animals. Although testosterone levels were significantly reduced post castration (by 90%,  $p < 0.001$ ), only small reductions in serum ucOC and muscle mass were observed ( $p > 0.05$ ). For the EDL muscle, ucOC levels were associated with p-ERK and p-AMPK, and lower phosphorylated ERK or AMPK correlated with lower phosphorylated mTOR, P70S6K, and pro-autophagy kinase ULK1. In the much more severely atrophic soleus, both ucOC level and GPRC6A expression were associated with phosphorylated AMPK, and lower phosphorylated AMPK was correlated with lower phosphorylated FOXO1 and ULK1 but higher ubiquitin E3 ligase Fbx32 expression and higher insulin levels.

Conclusion: Our data indicate that reduced ucOC level, decreased muscular GPRC6A expression, and attenuated muscular ERK and AMPK activities in atrophic condition is related to muscle loss in a muscle-type specific manner.

**Disclosures:** Xuzhu Lin, None.

## FR0123

**Treatment of Aged Mice With PDGF-bb and Bortezomib (a Proteasome Inhibitor) Enhances Fracture Repair.** Hengwei Zhang\*, Mengmeng Wang, Brendan Boyce, Lianping Xing. University of Rochester, United states

Protein ubiquitination and proteasome degradation regulate differentiation of mesenchymal stem cells (MSCs) to osteoblasts (OB). We found that inhibition of protein degradation by the proteasome inhibitor, Bortezomib (Btz), enhanced fracture repair in aged mice partially by promoting MSC proliferation, but the molecular mechanisms involved is unknown. Here, we performed ubiquitin proteomics in Btz-treated MSCs and OBs and identified increased ubiquitinated (Ub) platelet-derived growth factor receptor beta (PDGFRb) in OBs, which was confirmed by Ub assays. PDGFRb is the receptor for PDGF-bb, which regulates cell proliferation. PDGF-bb is FDA-approved to enhance diabetic wound healing and promote periodontal bone regeneration, but its effects on bone repair are controversial. We hypothesize that the aging process triggers Ub and proteasomal degradation of PDGFRb in MSCs, reducing PDGF-bb-mediated proliferation of fracture callus cells, which can be prevented by Btz. We used 3-m-old young and 19-m-old aged male mice. Western blot analysis demonstrated decreased PDGFRb levels in bone marrow, cortical bone and fracture callus from aged mice. PDGF-bb promoted proliferation of callus-derived MSCs from young, but not from aged mice ( $\text{mm}^2/\text{well}$ : 37+ 7 in young+PDGF-bb vs. 2+1 in aged+PDGF-bb, and 11+1 in young+PBS vs. 2+0.5 in aged+PBS). Addition

of Btz to aged cells along with PDGF-bb increased proliferation ( $\text{mm}^2/\text{well}:90+10\text{-young vs. }70+15\text{-aged}$ ). To examine if the combination of PDGF-bb+Btz promotes fracture repair, we performed open-tibial surgery in aged mice and treated them with vehicle, PDGF-bb, Btz, PDGF-bb+Btz, or PDGF-bb+Btz+su16f (a PDGF-bb inhibitor) on days 1, 3, and 5 post-fracture and assessed callus volume on day 14 via microCT. PDGF-bb had no effect, while Btz moderately increased callus volume. PDGF-bb+Btz further enhanced callus volume, which was blocked by su16f ( $\text{mm}^3: 2.1+0.4$  in vehicle,  $2.4+0.5$  in PDGF-bb,  $3+0.7$  in Btz,  $3.9+0.6$  in PDGF-bb+Btz, and  $1.8+0.2$  in PDGF-bb+Btz+su16f). Furthermore, treatment of MSCs with TNF or TGF- $\beta$  (expression of both of which increases with aging) led to PDGFRb Ub and degradation. Thus, accelerated ubiquitination and degradation of PDGFRb with aging might explain the low efficacy of PDGF-bb in elderly patients. Btz or other proteasome inhibitors in combination with PDGF-bb may be useful in the treatment of fracture and bone/soft tissue defects in patients with decreased PDGFRb signaling (e.g. aged and diabetic).

**Disclosures:** Hengwei Zhang, None.

## FR0125

**Patterns of estrogen use and kyphosis in older women 15 years later.** Gina Woods\*<sup>1</sup>, Mei-Hua Huang<sup>2</sup>, Howard Fink<sup>3</sup>, Corinne McDaniels-Davidson<sup>1</sup>, Peggy Cawthon<sup>4</sup>, Deborah Kado<sup>1</sup>. <sup>1</sup>University of California, San Diego, United states, <sup>2</sup>University of California, Los Angeles, United states, <sup>3</sup>VA Healthcare System, United states, <sup>4</sup>California Pacific Medical Center Research Institute, United states

Age-related hyperkyphosis (HK) is caused in part by vertebral fractures and low BMD, both of which commonly occur in older postmenopausal women. We previously reported in cross-sectional analyses that compared to never users, self-reported estrogen use was not associated with kyphosis, but did find that these women (mean age 69, SD = 4 at the time estrogen use was assessed) experienced less kyphosis progression over time. Given these initial findings, we have further examined patterns of estrogen use over 15 years and its subsequent effects on kyphosis in women in their mid-80's.

Using data from the Study of Osteoporotic Fractures that included 1063 women in whom detailed information was available on self-reported estrogen use over 7 clinic visits spanning an average of 15 years and Cobb angle of kyphosis at year 15, we performed multivariable linear regression analyses. We classified estrogen users as continuous users (reported taking estrogen >86% of visits), intermittent users (reported taking estrogen between 14-71% of visits), past users (reported having taken estrogen at the baseline, but no subsequent visits), and never users (reported never taking estrogen at any visit). Cobb angle (T4-T12) of kyphosis was measured from lateral spine x-rays.

Women were a mean age of 83.7 years (SD = 3.3) and had a mean Cobb angle of 51.3° (SD = 14.6). Mean total hip BMD was 0.724 g/cm<sup>2</sup>, BMI 26.5 kg/m<sup>2</sup>, and body weight 65.3 kg. In age and clinic adjusted models, women reporting continuous or even past estrogen use had less kyphosis compared to never users (Table). Adjustment for number of prevalent vertebral fractures, family history of HK, history of DDD, hip or spine BMD, and body weight modulated but did not significantly alter these findings.

Postmenopausal estrogen use prevents bone loss, but these beneficial effects are rapidly reversed with cessation of therapy. The present analysis demonstrates that not only continuous estrogen use, but past use (reported use before the baseline visit) was associated with less kyphosis 15 years later, even after adjustment for BMD. Beyond effects on bone density, estrogen may exert effects on paraspinal musculature or trunk lean mass, both of which influence kyphosis. How estrogen may exert protective effects many years after cessation of therapy is unclear. As others have proposed, perhaps there is a window of time in which postmenopausal estrogen replacement is most beneficial.

**Table: Patterns of estrogen use and its effects on kyphosis 15 years later**

Duration of estrogen use over 15 years	Age/Clinic Adjusted Model		Fully Adjusted Model <sup>1</sup>	
	$\beta$ -estimate (Cobb angle degrees)*	p-value	$\beta$ -estimate (Cobb angle degrees)*	p-value
Continuous (n = 147)	-3.9	0.008	-2.9	0.04
Intermittent (n = 217)	-1.3	0.31	-1.5	0.23
Past (n = 335)	-3.0	0.01	-2.6	0.02

\* Comparison group is never users (n = 729).

<sup>1</sup>Adjusted for age, clinic, number of prevalent vertebral fractures, family history of hyperkyphosis, history of DDD, BMD, and body weight

Table 1

**Disclosures:** Gina Woods, None.

## FR0126

**No effect of vitamin D on Physical Performance and balance in Elderly Women.** J Christopher Gallagher\*<sup>1</sup>, Shervin Yousefian<sup>1</sup>, Lynette Smith<sup>2</sup>. <sup>1</sup>Creighton University Medical School, United states, <sup>2</sup>University Nebraska Medical Center, United states

Introduction: The effect of vitamin D supplementation on physical performance is controversial. Few studies show an improvement in physical performance on daily

vitamin D 1,000 IU, others show no effect. We analyzed physical performance tests in our vitamin D dose ranging study.

Design: 163 independent living women entered a 1-year double blind randomized dose ranging study of daily vitamin D 400,800,1600,2400,3200,4000,4800 IU or placebo together with calcium ~580mg/d (total intake ~1200mg). Diet vitamin D was 114 IU. The main inclusion criteria were serum 25OHD  $\leq 20\text{ng/ml}$ ; no known disease or drugs affecting calcium or bone metabolism.

Standard physical performance tests included Timed up and Go, Timed walk-slow and fast Chair Rising test both 3 and 5 times, Grip strength (Jamar) and Balance measured by the Biodex instrument. This was a secondary analysis using Intent to treat and statistical analysis used Chi square and ANOVA.

Results: Age range 57-87 years, mean age 66.2 years (SD 7.3), mean BMI 30.3 kg/m<sup>2</sup> (SD 5.9). Compliance, measured every 3 months, was 94% for vitamin D and 91% calcium. 147 women completed study. There was a non-significant decline in all physical performance tests Timed up and Go, Timed walk, Chair Rising test, Grip strength at the end of 12 months. There was no effect on balance on vitamin D in any dose group.

Conclusions: In this clinical trial no dose of vitamin D ranging from 400 to 4800 IU daily had any effect on physical performance falls compared to other dose groups or placebo.

**Disclosures:** J Christopher Gallagher, None.

## FR0129

**Intranuclear Actin Polymerization Controls MSC Differentiation.** Buer Sen<sup>1</sup>, Gunes Uzer<sup>1</sup>, Zhihui Xie<sup>1</sup>, Cody McGrath<sup>1</sup>, Amel Dudakovi<sup>2</sup>, Maya Styner<sup>1</sup>, Andre Van Wijnen<sup>2</sup>, Janet Rubin\*<sup>1</sup>. <sup>1</sup>UNC School of Medicine, United states, <sup>2</sup>Mayo Clinic, United states

Cytoskeletal actin structure modulates MSC differentiation: an enhanced cytoplasmic actin cytoskeleton is thought to promote osteogenesis and decrease adipogenesis. While a functional role for actin dynamics within the nucleus is unknown, the presence of intranuclear actin is critical for gene transcription. We recently showed that cofilin-mediated nuclear influx of G-actin strongly promotes bone marrow derived MSC differentiation; G-actin transport into the nucleus after cytochalasin D (CytoD) cytoplasmic actin depolymerization caused a rapid and robust Runx2 dependent osteogenesis, and to a lesser degree, PPARG dependent adipogenesis, both in vitro and within murine tibiae. Interestingly, confocal images revealed CytoD-treated MSC display intranuclear actin rod-like structures, which increase nuclear size. This led to our hypothesis that formin-driven changes in the polymerization state of intra-nuclear actin are critical to the MSC differentiation program: we here asked whether intranuclear actin structure contributes to a specific MSC phenotype. We first showed that CytoD remains extranuclear, and as such CytoD does not directly regulate gene expression, and does not prevent nuclear actin polymerization. Next we demonstrated intranuclear actin polymerization using an actin stain that is specific for nuclear F-actin (LifAct-GFP-NLS). We found that the formin mDia1, responsible for end-to-end actin polymerization, was largely localized to the MSC cytoplasm, while mDia2 was entirely intranuclear. CytoD induced mDia1 nuclear entry. siRNA silencing of mDia1, but not mDia2, prevented both osteogenesis and adipogenesis. In contrast, treatment with CK666, an inhibitor of Apr2/3 complex induced actin branching, inhibited CytoD induced osteogenesis, but enhanced CytoD induced adipogenesis. These results indicate intranuclear actin polymerization is necessary for MSC differentiation. But while end-on-end actin fiber growth supports both osteogenesis and adipogenesis, branching of actin polymers is critical for osteogenic differentiation only. This suggests that Runx2 and PPARG access to respective genomic targets is dependent on intranuclear actin polymerization and branching, altering nuclear architecture to unmask transcription factors gene targets or alter heterochromatinization. In sum, our work shows that gene expression leading to MSC osteogenesis and adipogenesis is modulated by nuclear structure, which is itself subject to biochemical and mechanical inputs.

**Disclosures:** Janet Rubin, None.

This study received funding from: NIH

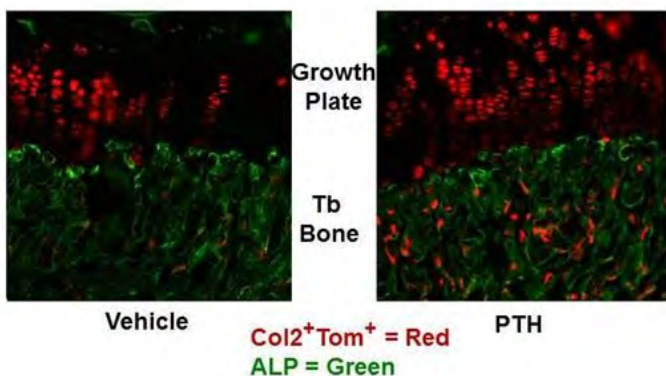
## FR0130

**Chondrocyte (CC) to Osteoblast (OB) Transdifferentiation Represents a Major Mechanism for Promotion of Trabecular (Tb) Bone Formation (BF) in Mice.** Patrick Aghajanian\*, Shaohong Cheng, Chandrasekhar Kesavan, Weirong Xing, Jon Wergedal, Subburaman Mohan. VA Loma Linda Healthcare System, United states

Recent studies demonstrated that the prepubertal rise in thyroid hormone (TH) levels is necessary for the initiation and progression of BF at the epiphysis in mice. To determine the mechanisms for TH-induced BF, Rosa-td tomato<sup>Col2-Cre-ERT2</sup> (Tom<sup>+</sup>) mice were injected with a single dose of 100  $\mu\text{g}$  tamoxifen (Tam) at postnatal day (P)3 to mark the CCs. At P6, 7, 8, 9, & 10, mice were euthanized, and frozen sections were used for IHC to trace the lineage of Col2-expressing Tom<sup>+</sup> CCs. At P6, much of the epiphysis was covered with immature Tom<sup>+</sup> CCs expressing Sox9. At P8, Tom<sup>+</sup> CCs at the middle of epiphysis began to express MMP13, a marker of hypertrophic CCs.

At P9, Tom<sup>+</sup> cells expressed high levels of DMP1 & ALP, markers of OBs, while high MMP13 expression is seen in Tom<sup>+</sup> cells surrounding the ossification center. At P10, Tom<sup>+</sup> cells expressed high levels of DMP1 & ALP in the newly forming bone areas while MMP13 expression preceded DMP1 & ALP expression. No Sox9 expression was detected in DMP1- and ALP-expressing Tom<sup>+</sup> cells. Methimazole-treated hypothyroid mice failed to express OB markers in Tom<sup>+</sup> cells at P14. To further examine the role of TH in CC-to-OB transdifferentiation, tibial epiphyses from TH-deficient Tsh<sup>hy<sup>+</sup>/hy<sup>-</sup></sup> and euthyroid Tsh<sup>hy<sup>+</sup>/+</sup> mice at P5, 6, 7, 8, 9, & 10 were examined with IHC using markers of MSCs, immature and mature CCs, OBs, endothelial cells, proliferation, and apoptosis. Temporal expression patterns of these markers were consistent with transdifferentiation of CCs to OBs and not with the existing paradigm involving resorption of cartilage and BF by cells brought in through invading vasculature. We next determined if CC-OB transdifferentiation contributes to BF in adult mice. Twelve-week-old Tom<sup>+</sup> mice were given 1 mg Tam daily for two consecutive days and treated daily with vehicle or PTH (160 µg/kg) for two weeks. µCT analysis revealed that Tb BV/TV increased by 60% (*P* < 0.01) in PTH-treated mice. IHC revealed marked increases in Tom<sup>+</sup> cells expressing OB markers in Tb bone of PTH-treated mice (Fig. 1). *In vitro* studies with serum-free ATDC5 CCs showed that PTH treatment increased expression of hypertrophic CC markers. Conclusions: 1) "Hypertrophic CCs" is a misnomer; they are in fact OBs, 2) Transdifferentiation of CCs into OBs is a significant mechanism for new BF that occurs during growth and in response to PTH, and 3) CCs as a source of OBs should be considered in strategies to develop BF therapies for osteoporosis.

Figure 1



abstract figure 1

Disclosures: Patrick Aghajanian, None.

### FR0133

**Mature Chondrocytes Are Able to Develop into Bone Marrow Osteo/Mesenchymal Progenitor Cells and Canonical Wnt Signaling Is Required for These Progenitor Cells to Commit to Osteogenic Fate in Endochondral Bones.** Xin Zhou<sup>\*1</sup>, Ailing Hunag<sup>1</sup>, Klaus von der Mark<sup>2</sup>, Benoit de Crombrughe<sup>1</sup>. <sup>1</sup>UT MD Anderson Cancer Center, United states, <sup>2</sup>University Erlangen-Nuremberg, Germany

Our lineage tracing studies together with those of other groups, used cre/reporter mouse models to identify mature chondrocytes as a major source of osteoblasts in endochondral bone formation. A similar process is also involved in endochondral bone fracture repair.

Two possible hypotheses could account for the chondrocyte to osteoblast transition. One is that hypertrophic chondrocytes directly transdifferentiate into osteoblasts. Another is that hypertrophic chondrocytes first dedifferentiate into osteo/mesenchymal progenitors, which later differentiate into osteoblasts. Our recent data revealed that in bone marrow a population of skeletal mesenchymal progenitors are derived from mature chondrocytes, potentially favoring the second hypothesis.

Inactivation of β-catenin in hypertrophic chondrocytes led to marked decrease in trabecular formation (Golovchenko et al, Bone 2013). To evaluate our hypothesis and to test whether canonical Wnt signaling plays a role in "chondrocyte to osteoblast" transition, we genetically either inactivated or activated β-catenin in mature chondrocytes in cre/reporter mouse models. Our data showed that deletion of β-catenin in mature chondrocytes led to a 2 fold increase in the number of chondrocyte-derived osteo/mesenchymal progenitors in bone marrow mesenchymal cell culture, a phenotype was associated with a reduced bone volume. In day 14 Col10a1-Cre/β-Catenin<sup>-/-</sup>TdTomato mice, only tomatom<sup>+</sup> bone marrow cells, no tomatom<sup>+</sup> osteocytes were observed on trabecular and endosteal surfaces, and no tomatom<sup>+</sup> osteocytes within the cortex. Unlike the wild-type mature chondrocyte-derived osteo/mesenchymal progenitors, which exhibited osteogenesis capacity, the Col10a1-Cre/β-Catenin<sup>-/-</sup> chondrocyte-derived osteo/mesenchymal progenitors completely failed to differentiate into mature osteoblasts in the *in vitro* osteogenesis assay. However, the Col10a1-Cre/β-Catenin<sup>-/-</sup> osteo/mesenchymal progenitors displayed enhanced adipogenesis capacity. In contrast, constitutive activation of β-catenin in mature chondrocytes led to an absence of chondrocyte-derived bone marrow osteo/

mesenchymal progenitors, increased numbers of chondrocyte-derived mature osteoblasts, and was associated with an increased bone volume phenotype.

These results support our "two steps" hypothesis. Wnt/β-catenin signaling is essential for step 2: mature chondrocyte-derived osteo/mesenchymal progenitor to mature osteoblast differentiation.

Disclosures: Xin Zhou, None.

### FR0134

**Notch Activation Enhances Mesenchymal Stem Cell Sheet Osteogenic Potential by Inhibition of Cellular Senescence.** Bo Tian<sup>\*</sup>, Sheila Rogers, Dollie Smith, Todd Jaeblon, Massimo Max Morandi, John Marymont, Yufeng Dong. LSU Health Sciences Center, United states

Our previous studies confirmed the therapeutic effects of short-term (1-day) cultured mesenchymal stem cell (MSC) sheet transplantation on allograft repair. A limiting factor in their application is the loss of MSC Multipotency as a result of high density cell sheet culture-induced senescence. In the study reported in this article, we first tested whether Notch activation could be used to prevent or delay sheet-culture-induced cell aging using *in vitro* experiments. Second, a mouse femur critical sized bone defect model was used to determine the functionality of transplanted MSC sheets. Our results showed that, during *in vitro* long-term (3-day) cell sheet culture, MSCs progressively lose their progenitor characteristics by showing decreased CD105 subpopulations and increased cellular senescence. In contrast, Notch activation by Jagged1 in MSC sheet culture showed a reduced cellular senescence and a decreased cell cycle arrest compared with control MSCs without Notch activation. Importantly, knockdown of Notch target gene Hes1 totally blocked the inhibition effect of Jagged1 on cellular senescence and cell cycle inhibitor p16 expression (Fig. 1). Finally, the *in vivo* allograft transplantation data showed a significant enhanced callus formation and biomechanical properties in Notch activation cultured long-term sheet groups when compared with long-term cultured sheet without Notch activation (Fig. 2). Our results suggest that Notch activation by Jagged1 could be used to overcome the stem cell aging caused by high density cell sheet culture, thereby increasing the therapeutic potential of MSC sheets for tissue regeneration.

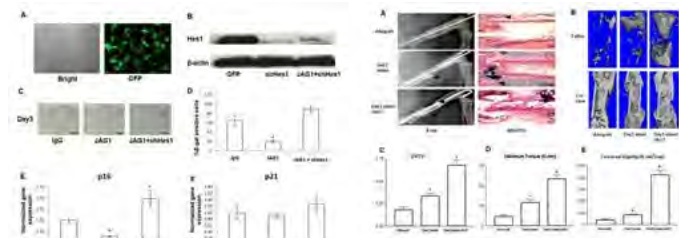


Figure 1: Hes1 is required for Jagged1-induced inhibition of MSC aging. (A) Bright field image showed a high transfection efficiency in lentiviral GFP control MSCs after 24 hours of culture. Scale bar represents 50 µm. (B) Western blot analysis confirmed the knockdown of Hes1 in MSCs. (C) SA-β-gal staining was performed to determine the extent of senescence in short-term cultured MSCs at day 3 in cell sheet culture with Jagged1 treatment. Scale bar represents 100 µm. (D) Quantitative reverse transcription polymerase chain reaction (qRT-PCR) data showed the decreased expression of p16 by Jagged1. (E) qRT-PCR data on changes were observed in p21 expression in 3-day sheet cultures. Results are mean ± s.d. All experiments were performed in triplicate. \*P<0.05 vs GFP control cells.

Figures

Disclosures: Bo Tian, None.

### FR0135

**Transcriptional Control of CaSR by P300 in MSCs is mediated by HIF-1α.** Fengjie Zhang<sup>1</sup>, Wing Pui Tsang<sup>1</sup>, Qiling He<sup>2</sup>, Chao Wan<sup>\*1</sup>. <sup>1</sup>School of Biomedical Sciences, The Chinese University of Hong Kong, Hong Kong, <sup>2</sup>Department of Microbiology, University of Alabama at Birmingham, United states

Calcium sensing receptor (CaSR) plays critical roles in the maintenance of constant blood Ca<sup>2+</sup> concentration and bone mass through regulating the bioavailability of parathyroid hormone. Bone cell-specific activation or deletion of CaSR *in vivo* revealed its essential direct function in regulating skeletal development and homeostasis in a hormone-independent manner. However, how the CaSR expression is regulated in bone lineage cells is largely unknown. In a study to define the impact of conditional deletion of HIF-1α with Dermo1-Cre mouse in the developing mesenchyme, we observed smaller and under-mineralized skeletons in the mutants with decreased CaSR protein expression in cranial bones. We confirmed CaSR down-regulation by Adenovirus (Ad)-Cre mediated deletion of HIF-1α in mesenchymal stem cells (MSCs) isolated from the bone marrow of HIF-1α<sup>lox/lox</sup> mice. We next searched promoter region of CaSR for putative binding sites of transcriptional factors and found that there was a binding site for p300 at the transcription initiation start site -564. CHIP assay confirmed the occupancy of the CaSR promoter region by p300 and the relative abundance of the p300-CaSR promoter region bound complexes decreased by 75 percent in HIF-1α deleted MSCs. We then sub-cloned the mouse CaSR gene promoter region containing p300 binding site into a promoter-less luciferase reporter vector and transfected the plasmid into the HIF-1α<sup>lox/lox</sup> MSCs. Notably, CaSR promoter luciferase activity was significantly decreased following

either Ad-Cre mediated deletion of HIF-1 $\alpha$  or siRNA knockdown of p300. We further detected the CaSR, p300 and HIF-1 $\alpha$  mRNA/protein levels in the MSCs with individual or double deletion of HIF-1 $\alpha$  and p300 followed by exposure of cells to normoxia or hypoxia. Accumulation of HIF-1 $\alpha$  markedly increased while deletion of HIF-1 $\alpha$  significantly reduced CaSR mRNA/protein levels, which was more prominent under hypoxia than that of normoxia. Interestingly, HIF-1 $\alpha$  and p300 regulate each other's expression and deletion of p300 had equivalent effects on CaSR as HIF-1 $\alpha$ . Double deletion did not further decrease CaSR mRNA/protein levels as compared with the single deletion. Knockdown of CaSR showed similar phenotype of impaired osteogenic differentiation of MSCs as that of HIF-1 $\alpha$  deletion. Our data suggest the transcriptional control of CaSR by p300 in MSCs mediated by HIF-1 $\alpha$ , and HIF-1 $\alpha$  might regulate osteoblast differentiation through CaSR in a cell autonomous fashion.

**Disclosures:** *Chao Wan, None.*

*This study received funding from: NSFC/RGC Joint Research Scheme (N\_CUHK4451/10), Hong Kong RGC GRF (14121815)*

## FR0137

**Alterations in hip Shape may Explain the Increased Risk of hip Osteoarthritis in Individuals with High Bone Mass.** Celia Gregson<sup>1</sup>, Anjali Patel<sup>1</sup>, Denis Baird<sup>1</sup>, Sarah Hardcastle<sup>1</sup>, Ben Faber<sup>1</sup>, George Davey Smith<sup>2</sup>, Jenny Gregory<sup>3</sup>, Richard Aspden<sup>3</sup>, Jon Tobias<sup>1</sup>. <sup>1</sup>Musculoskeletal Research Unit, School of Clinical Sciences, University of Bristol, Bristol, UK, United Kingdom, <sup>2</sup>MRC Integrative Epidemiology Unit, University of Bristol, Bristol, UK, United Kingdom, <sup>3</sup>Arthritis & Musculoskeletal Medicine, Institute of Medical Sciences, University of Aberdeen, UK, United Kingdom

Alterations in hip shape such as cam-type deformities are known risk factors for hip osteoarthritis (OA). People with High Bone Mass (HBM) are susceptible to a 'bone-forming' OA phenotype. We aimed to determine whether hip shape varies in HBM, and its contribution to hip osteophytosis.

HBM cases, recruited by screening DXA databases across 15 UK centres, had total hip or L1 BMD Z-score  $\geq +3.2$ ; controls constituted unaffected relatives. AP pelvic X-rays were graded for OA features and analysed by statistical shape modelling (SHAPE Aberdeen); 58 points mark the proximal femur and acetabular eyebrow. Procrustes analysis adjusts for differences in hip size/location/rotation, before principal component (PC) analysis generates ten PCs (hip shape modes [HSM]); each describes and quantifies a linearly independent variation of hip shape. All HSMs were compared between HBM cases and controls, adjusting *a priori* for age, gender, height, & weight using linear regression (standardised coefficients are presented).

257 HBM cases (mean[SD] age 63.1[11.5] years, 75.9% female) & 131 controls (60.2[12.8] years, 48.1% female) were analysed. HSM3, HSM1, HSM2 & HSM5 were most markedly different between HBM cases and controls; mean differences ( $\beta$  0.27 [95%CI 0.48,0.06],  $p=0.012$ ), (0.25 [0.04,0.47],  $p=0.020$ ), (0.22 [0.02,0.42],  $p=0.033$ ), and (0.21 [0.00,0.42],  $p=0.052$ ) respectively. Together these 4 modes explained 65.5% of hip shape variation. In HBM, HSM3 represents larger femoral head size with reduced sphericity (cam-type deformity), HSM1 a larger greater trochanter, reduced femoral head sphericity and wider femoral shaft, HSM2 reduced acetabular coverage and HSM5 a larger greater trochanter.

Hip osteophytes (grade  $\geq 2$ ) were more common amongst HBM cases than controls (21.2% vs. 12.0%; OR 1.98 [1.04,3.77],  $p=0.03$ ). Whilst HSM3, HSM1 & HSM5 were independent of osteophytes, a 1SD reduction in acetabular coverage (HSM2) was associated with OR 1.28 [1.02,1.61],  $p=0.03$  of acetabular and medial femoral osteophytes.

HBM individuals have different hip shapes compared with controls, with greater cam-type deformity, larger trochanters and wider femoral shafts. Reduced acetabular coverage is associated with osteophytosis in HBM, suggesting hip shape changes contribute to hip OA in HBM. Assuming biomechanical factors underlie these relationships, our findings support reduced acetabular coverage, as seen in acetabular dysplasia, as a potential risk factor for hip OA in the wider population.

**Disclosures:** *Celia Gregson, None.*

## FR0138

**Genome-wide association study of knee bone marrow lesions and association with previously reported bone mineral density loci.** Michelle S. Yau<sup>1</sup>, Braxton D. Mitchell<sup>2</sup>, Rebecca D. Jackson<sup>3</sup>, Marc C. Hochberg<sup>2</sup>, Douglas P. Kiel<sup>1</sup>, David T. Felson<sup>4</sup>. <sup>1</sup>Hebrew SeniorLife, BIDMC/Harvard, United states, <sup>2</sup>University of Maryland School of Medicine, United states, <sup>3</sup>The Ohio State University, United states, <sup>4</sup>Boston University School of Medicine, United states

Bone marrow lesions (BMLs) are areas of damage in the subchondral bone that may be an early sign of knee osteoarthritis (OA). BMLs have been associated with clinically relevant outcomes, such as pain and OA progression, and are associated with local BMD, suggesting that underlying bone pathology may be involved. We therefore conducted a genome-wide association study of BMLs in the Osteoarthritis Initiative (OAI) and the Framingham Osteoarthritis Study, and determined whether BMD genetic loci were also associated with BMLs.

We included 1,027 Caucasians from OAI (57% women, age 65 $\pm$ 9 yrs), a longitudinal study of individuals with or at high risk for knee OA and 304 Caucasians from Framingham (62% women, age 66 $\pm$ 9 yrs), a community-based study of prevalent knee OA. Participants were genotyped with the Illumina Omni-Quad 2.5M array or Affymetrix 500K Dual GeneChip+50K gene-centered MIP set for OAI and Framingham studies, respectively. Both cohorts were imputed to 1000G. A BML summary index was derived using MRI-based semi-quantitative BML severity scores across 15 sub-regions of the knee (0-45). We conducted linear regression, adjusting for age, sex, and study-specific principal components, then combined results using an inverse variance fixed-effects meta-analysis.

About 48% of OAI and 30% of Framingham participants had radiographic knee OA (KL $\geq 2$ ), and 77% of OAI and 79% of Framingham had a BML summary index  $> 1$ . In both cohorts, mean BML summary index was higher in those with knee OA (5 vs 2). We identified 22 loci that met suggestive significance ( $p < 1 \times 10^{-6}$ ), of which 3 met genome wide significance ( $p < 5 \times 10^{-8}$ ): 1) rs6070523 (maf=3%,  $\beta = -2.0$ ,  $se = 0.4$ ,  $p = 1.1 \times 10^{-8}$ ), 2) rs117994469 (maf=3%,  $\beta = -3.0$ ,  $se = 0.5$ ,  $p = 2.8 \times 10^{-8}$ ), 3) rs188681806 (maf=1%,  $\beta = -4.5$ ,  $se = 0.8$ ,  $p = 2.8 \times 10^{-8}$ ). Of 62 previously reported loci for BMD, we identified 3 nominally significant loci ( $p < 0.05$ ) associated with BMLs: 1) FOXL1 (rs10048146, maf=20%,  $\beta = -0.5$ ,  $se = 0.2$ ,  $p = 0.01$ ), 2) TXNDC3, rs10226308, maf=20%,  $\beta = -0.4$ ,  $se = 0.2$ ,  $p = 0.02$ ), 3) DCDC5 (rs163879, maf=31%,  $\beta = 0.29$ ,  $se = 0.13$ ,  $p = 0.03$ ). For FOXL1 and TXNDC3, the high BMD allele was protective for BMLs.

In conclusion, we identified 3 novel genome-wide significant loci and 3 previously reported BMD loci that were associated with BMLs, suggesting that there may be unique processes associated with BML development. Further work to understand the biology underlying these findings may reveal novel therapeutic targets for knee OA.

**Disclosures:** *Michelle S. Yau, None.*

## FR0139

**Odanacatib Prevents Cartilage Damage and Osteophyte Development in the Anterior Cruciate Ligament Transection Rabbit Model of Osteoarthritis.** Ya Zhuo<sup>1</sup>, Maureen Pickarski<sup>2</sup>, Gregg Wesolowski<sup>3</sup>, Jacques Yves Gauthier<sup>4</sup>, Le Duong<sup>2</sup>. <sup>1</sup>Merck & Co. Inc, United states, <sup>2</sup>Merck & Co. Inc., United states, <sup>3</sup>Formerly Merck & Co., Inc., United states, <sup>4</sup>Formerly Merck & Co., Inc., Canada

Osteoarthritis (OA) is a chronic degenerative joint disease and the main cause of age-related disability. Cathepsin K (CatK) degrades key cartilage components including type II collagen and aggrecan and has been implicated as a potential therapeutic target for the treatment of OA. The CatK inhibitor odanacatib (ODN, MK-0822) is currently being developed for the treatment of osteoporosis. A prodrug of ODN was designed to improve plasma concentration of ODN in rabbits. Here, we investigated the disease modifying effects of ODN in the anterior cruciate ligament transection (ACLT) rabbit model of OA. Seven-month old rabbits underwent Sham (N=9) or ACLT-surgery. The ACLT animals were randomized (N=7-9/group) and treated 4-5 days post-surgery with either vehicle (VEH) or prodrug of ODN at 0.6, 2 or 6 mg/kg/day p.o. for 8 weeks. Changes in cartilage damage, subchondral bone volume and osteophyte area were determined by histology and biomarkers. Urinary collagen type I helical peptide (HP-I), a bone resorption marker, and urinary collagen type II C-telopeptide (CTX-II), a cartilage degradation marker, were measured at wk 6 and 8. It was observed that 8 wks of ODN prodrug treatment (2 and 6 mg/kg/day) resulted in convincing chondroprotective effects with significant reduction in the Mankin score by 16 and 21% ( $p < 0.05$ ), and decreases in CTX-II by 80 and 88% ( $p < 0.01$ ), respectively, compared to VEH. While subchondral bone volume (BV/TV) in VEH group was significantly lower than that in Sham ( $p < 0.05$ ), ODN treatment at 0.6, 2 or 6 mg/kg/day group prevented the ACLT-induced subchondral bone loss. Additionally, HP-I was reduced by 58-67% ( $p < 0.001$ ) in all ODN groups vs. VEH group. Finally, image analysis of osteophyte area revealed that ODN prevented osteophyte growth by 20% ( $p < 0.01$ ) as compared to VEH. In summary, we demonstrated that inhibition of CatK by ODN provided great benefits in ACLT rabbit OA model, protecting against 1) cartilage degradation, 2) subchondral bone loss, and 3) osteophytosis. The preclinical results support that CatK inhibition may be a potential approach for the development of disease-modifying therapeutics for osteoarthritis.

**Disclosures:** *Ya Zhuo, Merck. Co. Inc., 15*

*This study received funding from: Merck & Co. Inc.*

## FR0140

**Proteasome Inhibition Is a Potential Treatment for Osteoarthritis by Attenuating Inflammation and Improving Lymphatic Function.** Xi Lin<sup>\*</sup>, Wensheng Wang, Wen Sun, Michael Zuscik, Lianping Xing. University of Rochester Medical Center, United states

Osteoarthritis (OA) is a whole joint disease associated with chronic inflammation in synovium and surrounding soft tissues. Various cell types participate in OA pathogenesis by producing catabolic factors that are accumulated in the joint space to accelerate tissue damage. We have reported that the synovial lymphatic system (SLS) removes catabolic factors and inflammatory cells from arthritic joints, associated with reduced lymphatic draining function in OA. However, how inflammation affects the

SLS, the cellular and molecular mechanisms involved, and if its inhibition could be a benefit in OA have not been studied. We hypothesize that OA is associated with inflammatory M1 macrophage (M1)-mediated SLS dysfunction due to elevated protein ubiquitination and degradation, which can be attenuated by Bortezomib (Btz), a clinically used proteasome inhibitor. To test this hypothesis, we used Meniscal-ligamentous injury-induced mouse model of OA in WT C57BL/6 mice. First, we performed RNAseq and pathway analysis in purified lymphatic endothelial cells (LECs) isolated from OA synovium and found highly activated inflammatory pathways. Flow analysis indicated significantly increased percentage of M1s, but not M2s, in OA vs. sham synovium (F4/80+CD86+ M1s:  $1.89 \pm 0.35$  vs.  $0.80 \pm 0.19\%$ ; F4/80+CD36+ M2s:  $1.35 \pm 0.29$  vs.  $1.52 \pm 0.15\%$ ). IHC confirmed increased M1s, but not M2s, in OA and some of M1s are localized adjacent to lymphatic vessels. Secondly, we co-cultured M1s or M2s with LECs and demonstrated that M1s induced expression of TNF (8-fold), IL-1 (10-fold), iNOS (40-fold) in LECs. Next, we examined ubiquitinated (Ub) proteins by Western blot and found that OA synovium and M1s had markedly increased total Ub proteins (1.5-fold, and 3.2-fold, respectively). Finally, we treated M1s and OA mice with Btz and found that Btz inhibited M1-induced TNF, IL-1 and iNOS expression in LECs. More importantly, intra-articular injection of Btz significantly reduced changes in synovial volume by ultrasound ( $3.61 \pm 0.41$  vs.  $4.64 \pm 0.65$  mm<sup>3</sup> with DMSO) and OA tissue damage by histology (OARSI score:  $1.7 \pm 1$  vs.  $3.5 \pm 2$  with DMSO), and increased synovial lymphatic clearance by near-infrared lymphatic imaging ( $65.2 \pm 6.1$  vs.  $48.2 \pm 9.3\%$  with DMSO). In conclusion, OA-associated M1s affect SLS, which can be attenuated by Btz. Proteasome inhibition may represent a new therapy for OA by controlling inflammation and improving SLS function.

**Disclosures:** Xi Lin, None.

## FR0142

**Superficial cells disappear during early stages of osteoarthritis via accelerated differentiation into chondrocytes.** Lei Li<sup>1\*</sup>, Thibault Boudierlique<sup>2</sup>, Phillip Newton<sup>2</sup>, Elena Kozhemyakina<sup>3</sup>, Andrew Lassar<sup>3</sup>, Matthew Warman<sup>4</sup>, Björn Barenius<sup>5</sup>, Igor Adamevko<sup>2</sup>, Andrei Chagin<sup>2</sup>. <sup>1</sup>Department of Physiology & Pharmacology, Karolinska Institutet, Sweden, <sup>2</sup>Department of Physiology & Pharmacology, Karolinska Institute, Sweden, <sup>3</sup>Harvard Medical School, Boston, Massachusetts, United states, <sup>4</sup>Orthopaedic Research Labs, Boston Children's Hospital, Boston, Massachusetts, United states, <sup>5</sup>Södersjukhuset, Stockholm, Sweden

It is believed that articular cartilage does not renew itself. However, the presence of articular chondrocyte progenitor cells in the superficial zone has been suggested from lineage tracing experiments in mice (Kozhemyakina E et al., Arthritis and Rheumatism, 2015, 67:1261), and these cells may have the capacity to participate in cartilage renewal/repair.

We confirmed that superficial zone of articular cartilage contains progenitors for other articular chondrocytes during mouse development utilizing clonal genetic tracing in mice with Prg4CreERT2 and ROSA26Confetti alleles. We then explored the behavior of superficial zone cells during development of post-traumatic osteoarthritis (OA). It is known that the first steps of OA are associated with substantial loss of the superficial cells. The main believe is that the cells are worn out or died out. We visualized individual superficial zone cells by injecting tamoxifen at 45 days of age. We then performed medial meniscus tearing (MMT) surgery at 60 days of age to induce OA and analyzed the location of the Cre-recombined superficial zone cells one month later. It turned out that traced cells were observed deeper in the tissue during early stages of surgery-induced OA. Careful analysis of cell death, combined with confocal visualization of confetti-traced cells revealed that neither superficial cells nor their progeny are dying despite slight increase in the number of TUNEL-positive cell was found deep in the tissue (increased from  $0.4 \pm 0.05\%$  to  $0.7 \pm 0.2\%$  of TUNEL positive cells, n=3). Interestingly, cell proliferation in the middle zone of operated legs was higher than that in sham ones. Thus, the loss of the superficial cells can be either due to their accelerated differentiation into chondrocytes or migration inside the tissue. Immunohistochemistry staining combined with confetti cell visualization revealed that some traced cells are positive for Sox9 and Mef2C suggesting that accelerated differentiation of the Prg4-labeled cells into chondrocytes may occur at early steps of OA. However, this increase is not statistically significant (n=3) and, alternative scenario with accelerated migration of these cells into the tissue cannot be excluded. Additional characterization is currently ongoing and will be presented at the meeting.

To conclude, our data suggest that during early stages of post-traumatic OA superficial cells do not self-renew, but instead directly differentiate into deeper zone chondrocytes.

**Disclosures:** Lei Li, None.

## FR0143

**Changes in Membrane Potential Regulates RANKL Intracellular Transport via Voltage-gated Calcium Channels in Osteoblasts.** Takuya Notomi<sup>1\*</sup>, Miyuki Kuno<sup>2</sup>, Akiko Hiyama<sup>1</sup>, Yoichi Ezura<sup>3</sup>, Kiyoshi Ohura<sup>1</sup>, Masaki Noda<sup>3</sup>. <sup>1</sup>Osaka Dental University, Japan, <sup>2</sup>Osaka City University, Japan, <sup>3</sup>Tokyo Medical & Dental University, Japan

Parathyroid hormone (PTH) and 1 $\alpha$ ,25-dihydroxyvitamin D<sub>3</sub> (VD<sub>3</sub>) are important factors in Ca<sup>2+</sup> homeostasis, and promote osteoclastogenesis by modulating receptor

activator of nuclear factor kappa-B ligand (RANKL) mRNA expression. However, their contribution to RANKL intracellular transport, including the trigger for RANKL lysosomal vesicle fusion to the cell membrane, is unclear. In neurons, depolarization of membrane potential increases the intracellular Ca<sup>2+</sup> level and promotes neurotransmitter release via fusion of the synaptic vesicles to the cell membrane. To determine whether changes in membrane potential regulates cellular processes such as RANKL intracellular transport in MC3T3-E1 osteoblasts (OBs), we generated a light-sensitive OB cell line and developed a system for altering their membrane potential via delivery of a blue light stimulus. In the membrane fraction of RANKL-overexpressing OBs, PTH and VD<sub>3</sub> increased the membrane-bound RANKL level at 10 min after application without affecting the mRNA expression level, and depolarized the cell membrane while transiently increasing the intracellular Ca<sup>2+</sup> level. To investigate the contribution of the different subtypes of voltage-gated Ca<sup>2+</sup> channels, the expression of all known  $\alpha$  subunits was examined. L-type (Cav1.2) and T-type (Cav 3.1 and Cav3.2) subunits were highly expressed in OBs. In our novel OB line stably expressing the channelrhodopsin-wide receiver, blue light-induced depolarization increased the membrane-bound RANKL level, which was reversed by treatment of blockers for L-type voltage-gated Ca<sup>2+</sup> channels and Ca<sup>2+</sup> release from the endoplasmic reticulum but not T-type voltage-gated Ca<sup>2+</sup> channels. In co-cultures of osteoclast precursor-like RAW264.7 cells and light-sensitive OBs overexpressing RANKL, light stimulation induced an increase in tartrate-resistant acid phosphatase activity and promoted osteoclast differentiation. These results indicate that depolarization of the cell membrane is a trigger for RANKL lysosomal vesicle fusion to the membrane and that membrane potential contributes to the function of OBs. In addition, the non-genomic action of VD<sub>3</sub>-induced RANKL lysosomal vesicle fusion included the membrane-bound VD<sub>3</sub> receptor (1,25D<sub>3</sub>-MARRS receptor). Elucidating the mechanism of RANKL intracellular transport regulation by PTH and VD<sub>3</sub> will be useful for the development of drugs to prevent bone loss in osteoporosis and other bone diseases.

**Disclosures:** Takuya Notomi, None.

## FR0144

**Osteoblasts Inhibit Osteoclast Formation by Targeting Prdm1 via the Mechanism Underlying Matrix Vesicle-Mediated Transfer of miR-125b.** Yasumasa Irie<sup>1\*</sup>, Tomoko Minamizaki<sup>2</sup>, Faisal Ahmed<sup>2</sup>, Yuko Nakao<sup>3</sup>, Hirotaka Yoshioka<sup>2</sup>, Kotaro Tanimoto<sup>2</sup>, Katsuyuki Kozai<sup>5</sup>, Yuji Yoshiko<sup>2</sup>. <sup>1</sup>Department of Calcified Tissue Biology, Department of Pediatric dentistry, Hiroshima University Institute of Biomedical & Health Sciences, Hiroshima, JAPAN., Japan, <sup>2</sup>Department of Calcified Tissue Biology, Hiroshima University Institute of Biomedical & Health Sciences, Hiroshima, JAPAN., Japan, <sup>3</sup>Department of Calcified Tissue Biology & Department of Orthodontics & Craniofacial Developmental Biology, Hiroshima University Institute of Biomedical & Health Sciences, Hiroshima, JAPAN., Japan, <sup>4</sup>Orthodontics & Craniofacial Developmental Biology, Hiroshima University Institute of Biomedical & Health Sciences, Hiroshima, JAPAN., Japan, <sup>5</sup>Pediatric dentistry, Hiroshima University Institute of Biomedical & Health Sciences, Hiroshima, JAPAN., Japan

Matrix Vesicles (MVs) secreted from osteoblasts and chondrocytes serve as initial mineralization sites in the osteoid. Recent evidence indicates that MVs share common hallmarks with exosomes, suggesting MVs as vesicular lipid transporters involved in cell-cell communications. Current trends with the roles of exosomal miRNAs raise the question whether MVs include miRNAs that play a fundamental role in bone. Our global analysis of miRNAs identified 172 miRNAs in MVs isolated from mouse osteoblast cultures. We reported that not only MVs but also miR-125b inhibits osteoclast formation in mouse bone marrow macrophage (BMM) cultures. A positive correlation between miR-125b levels in MVs and antiosteoclast activity *in vitro* and miR125b accumulation in the bone matrix led us to uncover the role of MV-miR-125b in bone *in vivo*. We generated transgenic (Tg) mice overexpressing miR-125b under the control of the human osteocalcin promoter. Tg mice were grossly normal and born in Mendelian ratios. Micro-CT analysis revealed that Tg mice had increased bone volume systemically. This structural change mostly arose in trabecular bones that occupied marrow cavities. Without significant effects on the number of osteoblasts, decreased number of osteoclasts was observed in Tg mice. Calvaria cells and BMMs from Tg mice differentiate into osteoblasts and osteoclasts, respectively, in a similar manner to those from the wild type (WT). To clarify the molecular mechanism underlying impaired osteoclastic bone resorption in Tg mice, we searched miR-125b target genes in BMMs. Of predicted targets of miR-125b, Prdm1, a transcription repressor, was downregulated in BMMs treated with MVs. miR-125b also decreased Prdm1 levels in the mouse RAW264.7 macrophage cell line, with resultant increases in the Irf-8 and Mafk antiosteoclast factor genes. miR-125b decreased 3' UTR luciferase activity of the Prdm1 gene. Inhibition of the binding between the 3'UTR of Prdm1 and miR-125b rescued impairment of osteoclast formation in RAW264.7 cells treated with either MVs or MiR-125b. Thus, our findings reveal that osteoblasts inhibit osteoclast formation by targeting Prdm1 via the mechanism underlying MV-mediated transfer of miR-125b. This may provide a novel therapeutic target for osteolytic bone diseases.

**Disclosures:** Yasumasa Irie, None.

## FR0145

**Truncation of the Cx43 C-terminal domain disrupts multiple signaling pathways and recapitulates the skeletal phenotype of full length Cx43 conditional deletion in the osteoblast lineage.** Megan C. Moorer\*<sup>1</sup>, Carla Hebert<sup>2</sup>, Ryan E. Tomlinson<sup>3</sup>, Shuo Liu<sup>2</sup>, Max Chason<sup>4</sup>, Joseph P. Stains<sup>2</sup>.  
<sup>1</sup>University of Maryland, Baltimore, Graduate School, United states, <sup>2</sup>University of Maryland, Baltimore, United states, <sup>3</sup>Johns Hopkins University, United states, <sup>4</sup>University of Maryland, United states

Intercellular communication through connexin43 (Cx43)-containing gap junctions contributes to peak bone mass and bone quality. Although it is clear that Cx43 plays a role in osteoblast-lineage cells, the molecular mechanisms underlying Cx43's action in bone are not fully defined. While gap junctions are often thought of as passive conduits for diffusion of small molecules, we hypothesize that Cx43 is an active participant in signaling, where the Cx43 C-terminus (CT) is a docking platform for signaling effectors and is required for efficient downstream signaling and osteoblast function. To test this hypothesis, we characterized the skeletal phenotype of 6 week old male Cx43 -/K258stop mice, which have a truncation mutation at K258 that removes much of the Cx43 CT. Consistent with our hypothesis, these mice closely mimic the skeletal phenotype of the osteoblast-specific deletion of full length Cx43. The Cx43 -/K258stop mice have increased femoral diaphyseal marrow cavity area, with increases in both endosteal ( $4.15 \pm 0.2$  vs  $5.26 \pm 0.38$  mm) and periosteal ( $5.0 \pm 0.26$  vs  $5.72 \pm 0.34$  mm) perimeters due to enhanced periosteal apposition and endosteal resorption, increased cortical porosity ( $0.31 \pm 0.18$  vs  $1.12 \pm 0.27$ ), and cortical thinning relative to Cx43+/− controls. In male mice, no changes in trabecular parameters were observed. The same pattern was also observed in 12 week old male mice. Consistent with a recent report, a trabecular phenotype (decreased BV/TV) was seen in female Cx43 -/K258stop, suggesting sexual dimorphism. qPCR of RNA extracts from cortical bone (tibial diaphysis) revealed that truncation of Cx43 reduced the mRNA levels of genes involved in both osteoblast differentiation and collagen processing. Tissue extracts from cortical bone showed that Cx43 truncation resulted in reduced levels of pPKC $\delta$ , pERK, and active  $\beta$ -catenin, signaling effectors that bind to the Cx43 CT and play a role in osteoblast differentiation and function. In total, these data suggest that the Cx43 CT is required for optimal osteoblast signaling and gene expression, and that absence of the Cx43 CT in male mice results in a skeletal phenotype analogous to deletion of the entire Cx43 gene in osteoblasts. These data also imply that Cx43 gap junctions not only exchange signals, but also must recruit the appropriate effector molecules to the Cx43 CT in order to optimally affect cell function and bone acquisition.

**Disclosures:** Megan C. Moorer, None.

## FR0147

**CRISPR/Cas9 Editing of IFITM5 Introduces BRIL p.Ser40Leu Substitution, Connecting Types V and VI OI, and Suppresses PEDF-mediated Induction of PPAR $\gamma$ .** Heeseog Kang\*<sup>1</sup>, Joan C. Marini<sup>1</sup>, Susan Crawford<sup>2</sup>.  
<sup>1</sup>NIH, United states, <sup>2</sup>Northwestern University, United states

Osteogenesis imperfecta (OI) type VI is caused by recessive null mutations in *SERPINF1*, encoding pigment epithelium-derived factor (PEDF), an anti-angiogenic secretory glycoprotein. We previously reported findings in *IFITM5*, encoding BRIL (Bone Restricted Ifitm-Like), a transmembrane protein upregulated in osteoblasts during mineralization, that connect BRIL and PEDF expression in osteoblasts from OI patients. The osteoblasts of patients with type V OI, with a 5'-end mutation in BRIL (c.14C>T), display increased *SERPINF1* expression and PEDF secretion. In contrast, a p.Ser40Leu substitution in BRIL impairs BRIL trafficking to the plasma membrane and causes clinical findings of atypical type VI OI with extremely severe bone dysplasia and histological features of type VI OI bone, but without clinical findings of type V OI. Patient osteoblasts with BRIL p.Ser40Leu display decreased *SERPINF1* expression and PEDF secretion. Little is known about the mechanism by which BRIL mutations impact *SERPINF1* expression and thereby matrix mineralization. To investigate this mechanism, we generated CRISPR/Cas9 clones containing the *IFITM5* (c.119C>T, p.Ser40Leu) mutation. In CRISPR/Cas9-edited clones, *SERPINF1* expression was decreased and PEDF secretion was reduced to 21% of a wild-type BRIL control clone, recapitulating our previous observation with cells from the atypical OI type VI proband. Surprisingly, we found that the p.Ser40Leu clones also had a 3-fold increase in *IFITM5* transcripts, increasing the BRIL protein level vs a wild-type control clone. We confirmed a similar increase in *IFITM5* transcripts in osteoblasts from the BRIL p.Ser40Leu proband, which may represent an abortive attempt to generate BRIL protein capable of insertion in the plasma membrane. Consistent with this interpretation, *serpinf1*<sup>-/-</sup> murine and type VI OI *SERPINF1*-null osteoblasts do not have increased *IFITM5* transcripts. Moreover, clones with BRIL p.Ser40Leu had decreased expression of PPAR $\gamma$ . PEDF has been shown to induce PPAR $\gamma$  in non-bone cells including macrophages and vascular endothelial cells. PPAR $\gamma$  expression was also decreased in osteoblasts from the OI patient with BRIL p.Ser40Leu substitution and from *serpinf1*-null mice. These results demonstrate that BRIL-mediated induction of PEDF activates PPAR $\gamma$ -mediated cellular pathways in bone forming cells. This study also demonstrates that CRISPR/Cas9-mediated gene editing is a useful tool to study molecular mechanisms of OI-causing mutations.

**Disclosures:** Heeseog Kang, None.

## FR0148

**Deletion of Axin1 in Osteoblast Progenitor Cells Leads to Delayed Endochondral Bone Formation through Inhibition of Osteoclast Formation.** Bing Shu\*<sup>1</sup>, Yongjian Zhao<sup>1</sup>, Chunchun Xue<sup>1</sup>, Rong Xie<sup>2</sup>, Yongjun Wang<sup>3</sup>, Di Chen<sup>2</sup>.  
<sup>1</sup>Longhua Hospital, Shanghai University of Traditional Chinese Medicine; Spine Research Institute, Shanghai University of Traditional Chinese Medicine, China, <sup>2</sup>Rush University Medical Center, United states, <sup>3</sup>School of Rehabilitation Science, Shanghai University of Traditional Chinese Medicine; Spine Research Institute, Shanghai University of Traditional Chinese Medicine, China

Axin1 is a key regulator in canonical Wnt/ $\beta$ -catenin signaling pathway and its role in endochondral bone formation is currently unknown. We have recently generated *Axin1* conditional knockout (cKO) mice (*Axin1*<sup>fllox/fllox</sup>) by breeding *Axin1*<sup>fllox/fllox</sup> mice with *Osx-Cre* mice.

The phenotypes of bone development and postnatal bone formation were analyzed in new born and 1-, 2-, and 4-week-old *Axin1*<sup>Osx</sup> mice. The result of immunohistochemistry (IHC) showed that expression of  $\beta$ -catenin was increased on the surface of trabecular bone and on the endosteal surface of the cortical bone in *Axin1*<sup>Osx</sup> mice. Alizarin red/Alcian blue staining of whole skeletal preparation showed no significant difference in the overall skeletal pattern formation in new born *Axin1*<sup>Osx</sup> mice. The hypertrophic zone of tibia growth plate of new born and 1-week-old *Axin1*<sup>Osx</sup> mice was significantly expanded in *Axin1*<sup>Osx</sup> mice. Large numbers of chondrocytes and unresorbed cartilage matrix were found in the middle of the bone marrow cavity in new born and 1-week-old *Axin1*<sup>Osx</sup> mice and in the secondary ossification center of 2- and 4-week-old *Axin1*<sup>Osx</sup> mice. Chondrocyte apoptosis in the bone marrow cavity of tibia was reduced and osteoclast formation in metaphyseal and subchondral bone areas of tibia was significantly decreased in *Axin1*<sup>Osx</sup> mice, demonstrated by decreases in tartrate-resistant acid phosphatase (TRAP), matrix metalloproteinase 9 (MMP9) and Cathpsin K staining. IHC results also showed increased osteoprotegerin (OPG) expression in tibiae of *Axin1*<sup>Osx</sup> mice. The results of real-time PCR showed that ratio of *Opg* receptor activator for nuclear factor- $\kappa$ B ligand (*Rankl*) was much higher in primary calvarial cells of *Axin1*<sup>Osx</sup> mice. Osteoclast formation in bone marrow cells (BMCs) cultured with the conditioned media (CM) collected from primary calvarial cells derived from *Axin1*<sup>Osx</sup> mice was significantly decreased compare to the BMCs cultured with the CM derived from Cre-negative calvarial cells. The results of IHC staining also detected decreased expression of nuclear factor of activated T-cells cytoplasmic 1 (NFATc1) and c-fos in *Axin1*<sup>Osx</sup> mice. In conclusion, deletion of *Axin1* in osteoblast progenitor cells caused reduction of osteoclast formation, which in turns leads to the inhibition of chondrocyte apoptosis, cartilage matrix resorption and endochondral bone formation in *Axin1*<sup>Osx</sup> mice.

**Disclosures:** Bing Shu, None.

## FR0149

**Engineering a hyper-anabolic, super-secreting osteoblast.** Sara Young, Yu Shao, Paul Childress, Ronald Wek, Joseph Bidwell\*. Indiana University School of Medicine, United states

Mice lacking the transcription factor *Nmp4* make more bone in response to anabolic PTH than their wild type (WT) littermates. In vitro, *Nmp4*<sup>-/-</sup> mesenchymal stem/progenitor cells (MSPCs) exhibit enhanced mineralization and elevated mRNA expression for bone matrix proteins and secreted pro-osteogenic factors *Igf1* and *Bmp2*. These cells also manifest an attenuated expression of the anti-osteogenic factor *Igf1*. This study addresses how loss of *Nmp4* generates a hyper-anabolic, super-secreting osteoblast. Differentiating professional secretory cells appropriate ribosome biogenesis, mRNA translation, and the unfolded protein response (UPR). c-Myc is a master driver of ribosome biogenesis and mRNA translation. The UPR mediates endoplasmic reticulum (ER) expansion necessary for managing the resultant increase in protein client loads. Upon UPR activation the sensor PERK phosphorylates eIF2 $\alpha$  (eIF2 $\alpha$ -P), which represses translation initiation and reduces influx of proteins into the overloaded ER. However, eIF2 $\alpha$ -P also induces a feedback mechanism through enhanced expression of Gadd34, which drives dephosphorylation of eIF2 $\alpha$ -P to restore protein synthesis. Thus the Gadd34 pathway is likely key to accommodating elevated professional secretory activity. For the present studies, cultures of expanded uncommitted and osteogenic differentiating MSPCs were established from WT and *Nmp4*<sup>-/-</sup> mice. RNA-seq, ChIP-seq, immunoblot analysis, luciferase assays, and polysome profiling were used to evaluate cell phenotypes. Key findings showed that *Nmp4* associates with the promoters of both *c-Myc* and *Gadd34*. *Nmp4*<sup>-/-</sup> MSPCs exhibited increased expression of these proteins, attenuated expression of eIF2 $\alpha$ -P, elevated levels of total cellular RNA, and a dramatic increase in ribosome number and heavy polysomes, indicative of much higher levels of protein synthesis. The expression of genes regulating the UPR, e.g. *Atf4*, *Atf6*, *Bip*, and *Chop* were significantly enhanced in the *Nmp4*<sup>-/-</sup> MSPCs. The transcriptome of the null cells showed elevated expression of genes driving osteogenesis e.g. *Wnt4* +12.5-fold, *Wnt7b* +45-fold vs WT but downregulation of genes that suppress osteogenesis, e.g. *Wif1* -26-fold, *Sfrp1*, -5.9-fold vs WT. Genome-wide ChIP-seq profiling identified direct *Nmp4* gene targets. These data support our hypothesis that *Nmp4* suppresses the anabolic profile of the osteoblast secretome and UPR and translational machinery that delivers it.

**Disclosures:** Joseph Bidwell, Eli Lilly, 11  
 This study received funding from: Eli Lilly & Co

**FR0150**

**Glutaminase acts in osteoblasts to regulate bone formation.** Yilin Yu<sup>1</sup>, Everett Knudsen<sup>1</sup>, Fanxin Long<sup>2</sup>, Courtney Karner\*<sup>1</sup>. <sup>1</sup>Duke University School of Medicine, United states, <sup>2</sup>Washington University School of Medicine, United states

Wnt signaling has emerged as a critical regulator of osteoblast differentiation and bone formation. A defining feature of osteoblasts is their capacity to produce large amounts of extracellular matrix proteins. Wnt signaling stimulates bone formation by increasing both the number of osteoblasts and their protein-synthesis activity. Increased protein synthesis is very demanding, both energetically and synthetically. How osteoblasts meet these increased energetic and biosynthetic demands is not well understood. We have recently discovered that glutamine metabolism is a critical mediator for Wnt to stimulate osteoblast differentiation and activity. Glutamine is a conditionally essential amino acid that can be metabolized into alpha-ketoglutarate to replenish the TCA (tricarboxylic acid) cycle metabolites, a process termed glutamine anaplerosis. The enzyme glutaminase (GLS) catalyzes the deamination of glutamine to form glutamate, the rate-limiting step in glutamine anaplerosis. During osteoblast differentiation, Wnt stimulates GLS activity and glutamine anaplerosis through the TCA cycle in order to meet the energetic requirements of protein synthesis. Here we show GLS is required for physiological bone formation both *in vitro* and *in vivo*. Using Crispr/Cas9 technology we show GLS protein expression is required for osteoblast differentiation and mineralization in ST2 cells. Likewise, genetic deletion of a floxed GLS allele in Sp7 positive osteoblast precursors reduces bone formation *in vivo*. Decreased bone formation in Sp7Cre;Gls<sup>fl/m</sup> mice is due primarily to decreased osteoblast activity in this model. Finally, in a mouse model for human osteosclerosis caused by hyperactive Wnt signaling, pharmacological inhibition of GLS activity suppresses excessive bone formation. Thus, the manipulation of GLS activity may provide a valuable therapeutic approach for normalizing deranged protein anabolism associated with human bone diseases.

**Disclosures:** Courtney Karner, None.

**FR0151**

**Kindlin-2 Plays A Pivotal Role in Skeletal Development and Homeostasis through Its Expression in Osteoblastic Cells and Osteocytes.** Huiling Cao\*, Guozhi Xiao. Department of Biology & Shenzhen Key Laboratory of Cell Microenvironment, Southern University of Science & Technology, China

The signals that control bone mass in mammals are incompletely understood. Here we show that Kindlin-2, a key factor that activates integrin and regulates cell adhesion and migration, plays a critical role in controlling bone mass in mice. Newborn mice lacking Kindlin-2 expression in osterix (Ox) expressing cells (Kindlin-2<sup>Ox</sup>) display a marked delay in calcification of calvarial bones without showing defects in the development of limbs and digits. However, after birth, the Kindlin-2<sup>Ox</sup> mice rapidly develop a severe growth retardation with significantly shortened limbs and reduced body size when compared with their wild-type control littermates. At two months of age, Kindlin-2<sup>Ox</sup> mice exhibited a severe osteoporotic phenotype. Loss of Kindlin-2 dramatically reduces the number of osteoprogenitors/osteoblasts and impairs osteoblast differentiation *in vitro* and *in vivo*. Interestingly, deleting Kindlin-2 expression in osteocytes also causes a severe osteoporosis and impairs the intermittent PTH induction of bone formation in adult mice. Ablation of Kindlin-2 expression in osteocytes markedly up-regulates the expression of Mef2C and its downstream target Sost, a potent inhibitor of the Wnt/ $\beta$ -catenin signaling, at both protein and mRNA levels. Thus, Kindlin-2 plays a critical role in control of bone mass through its expression in osteoprogenitors as well as in osteocytes.

**Disclosures:** Huiling Cao, None.

**FR0152**

**Legumain is a Novel Regulator of Bone Formation and Deregulated in Postmenopausal Osteoporosis.** Abbas Jafari\*<sup>1</sup>, Diyaqo Qanic<sup>2</sup>, Thomas L. Andersen<sup>3</sup>, Li Chen<sup>2</sup>, Nicholas Ditzel<sup>4</sup>, Sundeep Khosla<sup>5</sup>, Harald T. Johansen<sup>6</sup>, Per Kjærsgaard-Andersen<sup>7</sup>, Jean-Marie Delaisse<sup>8</sup>, Basem M. Abdallah<sup>9</sup>, Daniel Hesselton<sup>10</sup>, Rigmor Solberg<sup>6</sup>, Moustapha Kassem<sup>2</sup>. <sup>1</sup>Department of Cellular & Molecular Medicine, University of Copenhagen, Denmark, <sup>2</sup>Endocrine Research Laboratory (KMEB), Odense University Hospital & University of Southern Denmark, Denmark, <sup>3</sup>Department of Clinical Cell Biology (KCB) Institute of Regional Health Science University of Southern Denmark, Denmark, <sup>4</sup>Endocrine Research Laboratory (KMEB), Odense University Hospital & University of Southern Denmark, Denmark, <sup>5</sup>Endocrine Research Unit, Mayo Clinic College of Medicine, United states, <sup>6</sup>Department of Pharmaceutical Biosciences, School of Pharmacy, University of Oslo, Norway, <sup>7</sup>Department of Orthopaedic Surgery, Vejle/Lillebaelt Hospital, Denmark, <sup>8</sup>Department of Clinical Cell Biology, Vejle/ Lillebaelt Hospital, Institute of Regional Health Research, University of Southern Denmark, Denmark, <sup>9</sup>Department of Endocrinology & Metabolism, Endocrine Research Laboratory (KMEB), Odense University Hospital & University of Southern Denmark, Denmark, <sup>10</sup>St Vincent's Clinical School, UNSW, Australia

It is increasingly recognized that secreted factors have an important role in mediating the functions of human skeletal (stromal, mesenchymal) stem cells (hMSC). We have determined the secretome of human MSC at the baseline and during osteoblast (OB) differentiation using stable isotope labeling by amino acids in cell culture (SILAC) and identified several novel regulators of hMSC differentiation. In the present study, we show that legumain (also known as asparaginyl endopeptidase) is a novel regulator of bone formation and its expression level and cellular localization are abnormal in the bone microenvironment of postmenopausal osteoporotic patients. Legumain expression and activity were down-regulated during *in vitro* and *in vivo* OB differentiation of hMSC. Silencing of legumain expression or pharmacological inhibition of its activity in *ex vivo* hMSC cultures, enhanced OB differentiation, and *in vivo* heterotopic bone formation, and reduced adipocyte (AD) differentiation. Ectopic expression of legumain in hMSC reduced *ex vivo* OB differentiation and enhanced AD differentiation. We found that the inhibitory effects of legumain on OB differentiation are mediated through degradation of the bone matrix protein fibronectin. At the organismal level, legumain-deficient zebrafish show precocious OB differentiation accompanied by increased vertebral mineralization. A similar phenotype was obtained by post-embryonic pharmacological inhibition of legumain activity. Legumain serum levels in women decrease by ageing, but these levels do not depend on estrogen or osteoporosis status. However, histological analysis of legumain in the bone microenvironment patients with postmenopausal osteoporosis revealed localized ectopic expression of legumain in bone marrow adipocytes and reduced adjacent trabecular bone volume. Our data demonstrate a novel role of legumain in regulation of hMSC lineage fate and bone formation and suggest that altered proteolytic activity in the bone microenvironment may contribute to development of osteoporosis.

**Disclosures:** Abbas Jafari, None.

**FR0153**

**TUT7/ZCCHC6 is a novel regulator of matrix mineralization and osterix activity in osteoblasts.** Gregory Sondag\*<sup>1</sup>, Mohammad Khan<sup>1</sup>, Mohammad Ansari<sup>2</sup>, Nazar Hussein<sup>3</sup>, Sara Haynie<sup>1</sup>, Fayez Safadi<sup>1</sup>, Tariq Haqqi<sup>1</sup>. <sup>1</sup>Northeast Ohio Medical University, United states, <sup>2</sup>Northeast Ohio Medical, United states, <sup>3</sup>Kent State University, United states

Mechanisms associated with intrinsic mRNA regulation are important players in development and disease processes. The terminal uridylyl transferases (TUT) are a family of enzymes involved in the regulation of mRNA turnover and apoptosis-mediated global mRNA decay. However, their role in skeletal homeostasis has not yet been explored. In this study, we investigated the role of TUT7/ZCCHC6 in osteogenesis and bone homeostasis in mice. We first examined the expression of TUT7 in osseous tissues and discovered a differential pattern of TUT7 expression, being high in calvaria and long bones in young mice and decreased in aged mice. TUT7 was also highly expressed during early stages of osteoblast (OB) differentiation. Next, we generated TUT7KO mice by gene targeting and characterized their skeletal phenotype. Deletion of TUT7 was not lethal and neonatal TUT7KO mice developed normally similar to wildtype (WT) littermates as shown by skeletal prep. However, at 4 and 8 weeks of age TUT7KO mice have significantly increased bone mass compared to WT as shown by DXA, microCT, and histomorphometric analyses. TUT7KO mice also had higher levels of osteocalcin in plasma as determined by ELISA suggesting an increase in bone formation. *Ex vivo* analysis of bone marrow derived osteoprogenitor cells, primary calvarial and adult OB from TUT7KO mice demonstrated an increase in matrix mineralization as determined by von Kossa staining. These data suggest that TUT7 plays an important role in OB function. Interestingly, osteoclasts derived from TUT7KO mice showed no significant difference in differentiation and function as determined by TRAP staining and osteoclast activity. Using total RNA from bone and OB of WT and

TUT7KO mice, we analyzed the expression of genes known to be important in osteogenesis. Our results showed that constitutive expression of master transcription factor *osx* was significantly upregulated in OB derived from TUT7KO mice compared to WT. Importantly genes known to be regulated by *Osx* were also expressed at significantly higher levels in OB. Regulation of *Osx* activity by TUT7 was demonstrated using an *Osx* reporter activity assay and its inhibition by overexpression of TUT7 in OB. Overall, our data demonstrate that TUT7 is a negative regulator of bone formation through suppression of *Osx* in OB. Taken together, this study is the first to demonstrate the role of TUT7 in bone formation and identifies a potential target for therapeutic development.

**Disclosures:** Gregory Sondag, None.

## FR0154

**Pyk2-Deletion Potentiates Osteoblast Differentiation and Mineralization By Estrogen and Raloxifene..** Sumana Posritong<sup>\*1</sup>, Pierre P. Eleniste<sup>1</sup>, Evan R. Himes<sup>2</sup>, Melissa A. Kacena<sup>2</sup>, Angela Bruzzaniti<sup>1</sup>. <sup>1</sup>Indiana University School of Dentistry, United states, <sup>2</sup>Indiana University School of Medicine, United States

The hormonal and cellular mechanisms that control bone formation and bone mass are not completely understood. The proline-rich tyrosine kinase 2 (Pyk2) is important for osteoblast (OB) activity and bone formation. However, while female Pyk2-deficient (Pyk2-KO) mice exhibit elevated bone volume/total volume (BV/TV), Pyk2-KO male mice exhibit a bone phenotype similar to wild-type (WT) mice. Further, we found that 17 $\beta$ -estradiol (E2) supplementation of ovariectomized (OVX) female mice results in a greater increase in BV/TV in Pyk2-KO OVX mice than in WT OVX mice. Therefore, we examined if Pyk2 might regulate bone mass in part by modulating the estrogen signaling response in OBs. Calvarial OBs were isolated from Pyk2-KO and WT neonatal mice and cultured in osteogenic media for 4-28 days, in the presence or absence of E2 or raloxifene, a selective ER modulator. In Pyk2-KO OBs cultured for 4 days, we found reduced ER $\alpha$  protein levels compared to WT OBs. In contrast, ER $\beta$  protein levels and ER $\alpha$ /ER $\beta$  mRNA expression in Pyk2-KO OBs were similar to WT OBs. Consistent with a role in early OB proliferation, Pyk2-KO OBs cultured for 4 days showed significant increases in *c-fos* mRNA expression and metabolic activity (MTS assay) compared to WT OBs. Pyk2-KO OBs also exhibited significantly increased *collagen type 1* mRNA expression, which was further enhanced when Pyk2-KO OBs were cultured with E2, whereas E2 had no effect on WT OBs. We next examined Pyk2-KO OBs differentiated for 14-28 days with or without E2 or raloxifene. Pyk2-KO OBs showed higher levels of alkaline phosphatase (ALP) activity and calcium deposition than WT OBs. In the presence of E2 or raloxifene, ALP activity and calcium deposition were further augmented in the Pyk2-KO OB cultures, but not in WT OBs. Taken together, our results suggest that Pyk2 is integrated into the estrogen and ER $\alpha$ /ER $\beta$  signaling cascade to inhibit early OB proliferation via ER $\alpha$  and that Pyk2-deletion promotes bone formation and potentiates the effects of estrogen and raloxifene on OB differentiation and mineralization.

**Disclosures:** Sumana Posritong, None.

## FR0155

**A novel Osteoblast Differentiation inhibiting lncRNA, AK138929.** Chong Yin<sup>\*1</sup>, Yan Zhang<sup>1</sup>, Kun Yan<sup>1</sup>, Zhihao Chen<sup>1</sup>, Dijie Li<sup>1</sup>, Fan Zhao<sup>1</sup>, Lifang Hu<sup>1</sup>, Yonghua Wang<sup>2</sup>, Ge Zhang<sup>3</sup>, Peng Shang<sup>1</sup>, Airong Qian<sup>1</sup>. <sup>1</sup>School of Life Sciences, Northwestern Polytechnical University, China, <sup>2</sup>School of Life Sciences, Northwest A&F University, China, <sup>3</sup>School of Chinese Medicine, Hong Kong Baptist University, Hong Kong

Long noncoding RNAs (lncRNAs) are a class of transcripts longer than 200 nucleotides. Recently lncRNAs have been focused as important novel regulators for development, carcinogenesis, and bone formation. In cellular level, lncRNAs regulate almost all cell processes such as proliferation, differentiation, and senescence. MACF1 is a cytoskeletal protein that promotes osteoblast differentiation and bone formation. Our previous studies have found that MACF1 regulates nuclear translocation of  $\beta$ -catenin, which implies MACF1 may function as a regulator to osteogenic non-coding RNAs. For the purpose of discovering lncRNAs involved in osteogenesis, we initiated characterization of lncRNAs in pre-osteoblast by gene expression profiling analysis.

We performed mRNA-array, miRNA-array, and lncRNA-array on MACF1 low expression MC3T3-E1 cell line and negative control. Array data were analyzed by Gene Coexpression Networks to obtain the gene expression pattern changed by MACF1. Functional lncRNAs were further screened by LncTar and miranda database.

We have assessed the expression of lncRNAs in femur tissues from 6, 12, and 18month aging C57BL6 mice. The expression of AK138929, altered with aging process. Besides, the expression of AK138929 decreased during osteoblastic differentiation processes. We further explored that down-regulation of AK138929 in MC3T3-E1 cell line increased osteogenic gene *ALP* and *RUNX2* expression, ALP activity and calcium nodules.

We have found 12 binding sites of mir-489-3p in the sequence of AK138929 through prediction by LncTar and RNA22. Moreover, in MC3T3-E1 cell line, AK138929 siRNA enhanced mir-489-3p level. We consistently found that agomir-489-3p increased

*ALP* and *RUNX2* expression as well as ALP activity and calcium nodules. For further investigating the mechanism of mir-489-3p, we have predicted its target gene PTPN6 by Gene Coexpression Networks and miranda. Besides, protein level of PTPN6 was proved negatively regulated by mir-489-3p. We have also found the down-regulation of PTPN6 enhanced *ALP* expression, ALP activity and calcium nodules.

In conclusion, we have discovered AK138929 as a novel osteogenic regulator. AK138929 inhibits osteoblast differentiation through AK138929 - mir-489-3p - PTPN6 pathway. The finding has revealed a new mechanism of osteoblast differentiation.

**Disclosures:** Chong Yin, None.

## FR0157

**Epigenetic Regulation of Osteoblast Differentiation by Vitamin C Involving Prolyl Hydroxylase Domain-containing Protein 2 (PHD2).** Richard Lindsey<sup>\*1</sup>, Shaohong Cheng<sup>2</sup>, Sheila Pourteymoor<sup>2</sup>, Catrina Alarcon<sup>2</sup>, Subburaman Mohan<sup>1</sup>. <sup>1</sup>VA Loma Linda Healthcare System; Loma Linda University, United states, <sup>2</sup>VA Loma Linda Healthcare System, United States

The importance of vitamin C in regulating osteoblast (OB) differentiation is well established. Our recent studies have provided direct evidence for the involvement of PHD2 in mediating vitamin C effects on osteogenic cells. Because of the recent finding that AA promoted demethylation of many gene promoters via activation of ten eleven translocases (TETs) in embryonic stem cells and because PHDs, like TETs, belong to a family of 2-oxoglutarate-dependent dioxygenases that depend on AA for their activities, we hypothesized that the biological effects of vitamin C on OBs are in part due to PHD2-mediated conversion of 5-methylcytosine (5-mC) to 5-hydroxymethylcytosine (5-hmC) in the promoter regions of target genes involved in the OB differentiation program. Treatment of MC3T3-E1 and primary OBs with AA significantly increased the amount of 5-hmC as measured by dot-blot assays using polyclonal anti-5-hmC antibody (1.9- and 1.7-fold, respectively,  $P < 0.01$ ) as well as by 5-hmC specific ELISA (3.5- and 2.8-fold,  $P < 0.05$ ). The effect of AA on the 5-hmC increase was time and dose-dependent, with the greatest effect observed at 72 hr of treatment. In order to determine if AA-induced DNA demethylation is caused by PHD2, we evaluated if PHD2 is localized in the nucleus. We found that PHD2 but not PHD1 is localized in the nucleus as determined by western immunoblot analysis and immunohistochemistry staining. Furthermore, AA treatment increased nuclear uptake of PHD2. Inhibition of PHD2 activity by a chemical inhibitor, IOX2, or knockdown of PHD2 expression blocked AA effects on hydroxylation of 5-mC. We next evaluated if AA induced demethylation of CpG sites in the promoter region of AA target genes involved in OB differentiation. We found that AA treatment of primary cultures of mouse calvarial osteoblasts for 72 hr increased 5-hmC levels in the transcription start site region containing CpG islands of known AA target genes *Osx*, *Alp*, and *Ihh* by 182%, 141%, and 64%, respectively (all  $P < 0.05$ ). Furthermore, IOX2 treatment blocked the AA effect on demethylation of the *Osx* gene, thus suggesting involvement of PHD2 in this process. Based on our findings, we conclude that vitamin C promotes transcription of target genes in part by epigenetic modification of DNA involving demethylation by a PHD2-mediated mechanism in OBs and that this mechanism should be exploited towards development of anabolic therapies for osteoporosis treatment.

**Disclosures:** Richard Lindsey, None.

## FR0158

**miR-1254 inhibits expression of sclerostin in human osteoblastic cell lines.** Osman M Azuraidi<sup>\*</sup>, Peter Wilson, Kasia Goljanek-Whysall, Jane P Dillon, Nick Rhodes, James A Gallagher. University of Liverpool, United Kingdom

Sclerostin is an osteocyte-derived glycoprotein coded by the *SOST* gene that functions as a negative physiological regulator of bone formation. Hence there is considerable interest in sclerostin as a potential target for therapy of osteoporosis. MicroRNAs (miRNAs) are small, non-coding RNAs that regulate gene expression by promoting the degradation of specific mRNAs. We aimed to identify miRNAs that regulate sclerostin in human bone. We used RT-PCR to investigate expression of the *SOST* gene in human osteosarcoma cell lines representing different stages of osteoblast differentiation. *SOST* transcripts were undetectable in MG63 cells the least differentiated cell type but were present in TE85 cells, which are intermediate in differentiation, and most highly expressed in Saos-2 cells, which represents a mature stage of the osteoblast / osteocyte lineage. Next we undertook an analysis of the miRNA transcriptome of the three cell lines using an Affymetrix array. We identified more than 500 miRNAs which were differentially expressed between the three cell lines but we focussed on those which had the highest expression in MG-63, intermediate in TE-85 and lowest in Saos-2. Using on-line algorithms including miRWalk, miRanda, RNA2 and Targetscan, one of these miRNAs, miR-1254, was predicted to be a potential regulator of *SOST* expression. Therefore we transfected TE85 and Saos-2 cells with miR-1254 mimic, miR-1254 antagonist and scrambled miRNA (-ve control) using Lipofectamine 2000 in serum free media. After 6 hours of incubation, serum free media was replaced with media containing 10% bovine calf serum. Non-transfected cells were also used as control. In cells that were transfected with miR-1254 mimic, real-time PCR results showed a robust increase in miR-1254

expression in both cell lines indicating that transfection was efficient. In Saos-2 cells transfection with miR-1254 mimic inhibited expression of SOST by over 60% ( $p < 0.05$ ) and in TE85 cells by over 80% ( $p < 0.05$ ). miR-1254 antagonist elevated SOST expression in both cell types whereas the scrambled miRNA had no significant effect. The effects on SOST expression also translated into an effect on secretion of sclerostin into conditioned medium as determined by ELISA. miR-1254 mimic inhibited secretion of sclerostin by TE85 cells by over 60% whereas miR-1254 antagonist elevated secretion by 20%. These results suggest that miR-1254 could be used to develop a new class of therapeutic agents to prevent bone loss.

**Disclosures:** Osman M Azuraidi, None.

## FR0159

**Modulation of the histone H3K27 methyltransferase EZH2 stimulates WNT, PTH and BMP2-related paracrine signaling to promote osteogenesis.** Christopher Paradise\*, Amel Dudakovic, Martina Glusevic, Farah Ahmed, Eric Lewallen, Roman Thaler, Andre van Wijnen, Mayo Clinic, United states

Bone stimulatory therapeutics that promote bone formation include bone morphogenetic proteins (i.e. BMP2) and intermittent treatment with parathyroid hormone (PTH) or PTH related protein, as well as antibody-suppression of WNT inhibitors (e.g., SOST). Furthermore, inactivation of EZH2, an epigenetic regulator with histone 3 lysine 27 (H3K27) methyltransferase activity, using a pharmacological inhibitor (GSK126) is bone anabolic in skeletally mature mice and osteo-protective in estrogen-depleted (ovariectomized) mice. These biological effects are directly related to the ability of EZH2 inhibition to promote osteogenic differentiation and inhibit adipogenic differentiation of mesenchymal stem cells. In this report, we assessed the molecular mechanisms by which EZH2 inhibition promotes osteogenic differentiation. Results from mRNA-seq and ChIP-seq analyses suggest that EZH2 inhibition is anti-proliferative and generates a quiescent cellular state by upregulating the CDK inhibitory protein CDKN2A/p16 and down-regulating expression of genes required for mitosis. This quiescent state is conducive for expression of bone-related extracellular matrix proteins (e.g., collagens) that support matrix mineralization. More excitingly, we find that EZH2 inhibition modulates WNT, PTH and BMP signaling. Several Wnt ligands (e.g., Wnt10b, Wnt10a, and Wnt6) are robustly expressed in differentiating MC3T3 cells. Interestingly, the pro-osteogenic Wnt10b is greatly up-regulated by EZH2 inhibition. Similarly, the PTH receptor (Pthr1h) is also enhanced by GSK126 in pre-osteoblasts. Western blotting analysis demonstrates that EZH2 inhibition enhances Smad1/5 phosphorylation, a well-established biomarker for the activation of BMP2 signaling, in MC3T3 cells. Furthermore, EZH2 inhibition stimulates the expression of BMP2-responsive genes, including several genes involved in osteoblast differentiation (e.g., PTH1R, DLX5, SP7, and IBSP). These data suggest a mechanism by which EZH2 controls paracrine signaling in osteoblasts involving the WNT, PTH and BMP2 pathways to stimulate osteogenic differentiation. The exciting ramification is that inhibitors of EZH2, which include well-tolerated and orally available drugs, may be effective in stimulating bone acquisition by supporting the endogenous local activation of natural bone stimulatory ligands at physiological doses in bone.

**Disclosures:** Christopher Paradise, None.

## FR0160

**Protein Kinase D1 Plays an Important Role in Osteogenesis.** Wendy Bollag\*, Vivek Choudhary<sup>1</sup>, Qing Zhong<sup>1</sup>, Kehong Ding<sup>1</sup>, Jianrui Xu<sup>1</sup>, Lakiea Bailey<sup>1</sup>, Maribeth Johnson<sup>1</sup>, Yun Su<sup>1</sup>, Mohammed Elsalanty<sup>2</sup>, Meghan McGee-Lawrence<sup>1</sup>, Xingming Shi<sup>1</sup>, Carlos Isaales<sup>1</sup>. <sup>1</sup>Medical College of Georgia at Augusta University, United states, <sup>2</sup>Augusta University, United states

The serine-threonine protein kinase D1 (PKD1) has been reported to play a role in a number of cellular functions, including proliferation and differentiation, cell survival, autophagy, Golgi trafficking and migration. Heterozygous transgenic mice expressing a knocked in dominant-negative PKD1 mutant allele show reduced pubertal bone mass. The dominant-negative mutant used for these studies inhibits both PKD2 and PKD1; in addition, the mutant PKD1 exerts effects in several bone cell types, making identification of the exact mechanism of the low bone mass difficult. Our data indicate that PKD1 is expressed in bone marrow-derived mesenchymal stem cells (BMMSC), and we hypothesized that PKD1 is involved in osteogenesis *in vitro* and *in vivo*. Using BMMSCs isolated from floxed PKD1 mice, we found that PKD1 ablation with adenovirus-mediated expression of Cre recombinase inhibits BMMSC differentiation (in terms of alizarin red and alkaline phosphatase staining) in osteogenic medium *in vitro*. This effect is particularly prominent when osteogenic differentiation is enhanced by co-treating cells with bone morphogenetic protein-2 (BMP2) upon initiation of the differentiation process with osteogenic medium. Conditional knockout mice in which PKD1 is ablated in osteoprogenitor cells by osterix promoter-driven Cre recombinase were generated. Digimus analysis of bone mineralization in these mice indicated that 3-month-old (3mo) conditional knockout (cKO) mice exhibit a significantly reduced ( $p < 0.05$ ) bone mineral content (BMC) and bone mineral density (BMD), with a 7% lower BMD (mean  $\pm$  SD) of  $0.0840 \pm 0.0069$  g/cm<sup>2</sup> ( $n=7$ ) in comparison with a value of  $0.0907 \pm 0.0051$  for floxed littermate controls ( $n=10$ ) and a 17% reduction in BMC. By microCT analysis of the femoral head, 3mo cKO mice also show a decreased BMD ( $1.2267 \pm 0.107$  versus  $1.3722 \pm 0.086$ ;  $p < 0.05$ ) although no other parameters are

significantly altered. 6mo cKO mice ( $n=10-11$ ) also exhibit a similar approximate 17% reduction in BMC and 7% decrease in BMD; in these 6mo cKO mice trabecular thickness is significantly decreased and trabecular number increased by microCT analysis. Taken together, both our *in vitro* and *in vivo* results suggest a potentially important role for PKD1 in bone formation through modulation of stem cell/osteoprogenitor cell function.

**Disclosures:** Wendy Bollag, None.

## FR0165

**ICOS-Ligand Triggering Impairs Osteoclast Differentiation and Function.** CASIMIRO L GIGLIOTTI<sup>1</sup>, ELENA BOGGIO<sup>1</sup>, NAUSICAA CLEMENTE<sup>1</sup>, Chiara Dianzani<sup>2</sup>, Annalisa Chiochetti<sup>1</sup>, Renzo Boldorini<sup>1</sup>, Michela Bosetti<sup>3</sup>, Giancarlo Isaia<sup>4</sup>, Patrizia D'Amelio\*<sup>4</sup>, Umberto Dianzani<sup>1</sup>. <sup>1</sup>Interdisciplinary Research Center of Autoimmune Diseases (IRCAD) & Department of Health Sciences, University of Piemonte Orientale (UPO), Italy, <sup>2</sup>Department of Drug Science & Technology, University of Torino, Italy, <sup>3</sup>Departamento de Medicina Celular y Molecular, Centro de Investigaciones Biológicas, Consejo Superior de Investigaciones Científicas, Spain, <sup>4</sup>Dept of Medical Science University of Torino, Italy

**Background.**

B7h (CD275, also known as ICOSL, B7H2, B7-RP1, GL50) belongs to the B7 family of surface receptors and binds ICOS (CD278), which belongs to the CD28 family. The main known function of B7h is the triggering of ICOS, which acts as a costimulatory molecule for activated T cells by modulating their cytokine secretion. Since recent reports have shown that, in endothelial cells, dendritic cells and tumour cells, B7h triggering modulates several activities, we analysed the effect of B7h triggering by recombinant ICOS-Fc on osteoclasts (OCs) differentiation and function both *in vitro* and *in vivo*.

**Methods**

OCs were obtained by stimulating human monocytes obtained from healthy donors and cultured in a differentiation medium. At different times, cells were treated with 1 mg/ml of either ICOS-Fc (a fusion protein of the extracellular portion of the human ICOS fused to the human IgG1 Fc portion) or ICOS-msFc composed of the human ICOS fused to the mouse IgG1 Fc. Controls were performed using F119S-ICOS-Fc, carrying the F119S substitution in the human ICOS amino acid sequence. Cell viability, differentiation and function were evaluated.

*In vivo* effect of ICOS-Fc was evaluated by treating with 100 mg ICOS-msFc, or F119S-ICOS-Fc two models of osteoporosis: mice treated with soluble RANKL or ovariectomized. Mice were sacrificed and organs and bones were collected for analysis.

**Results**

Our results showed that OCs precursors and mature OCs express B7h. The triggering of B7h with ICOS-Fc inhibits RANKL-mediated differentiation of human monocytes to OCs by inhibiting the acquirement of the OCs morphology, the CD14 Cathepsin K<sup>+</sup> phenotype, and the expression of tartrate resistant acid phosphatase, OSCAR, NFATc1, and DC-STAMP. Moreover, ICOS-Fc induces a reversible decrease in the sizes of cells and nuclei and Cathepsin K expression in mature OCs. Finally, ICOS-Fc inhibits the osteolytic activities of OCs *in vitro*, and the development of bone loss in mouse osteoporosis induced by either soluble RANKL or ovariectomy *in vivo* (Fig.1).

**Conclusion.**

B7h plays a role in OCs differentiation and function and its triggering by ICOS-Fc inhibits osteoclastogenesis and bone resorption.

These data open a novel field in the pharmacological use of agonists and antagonists of the ICOS/B7h system.

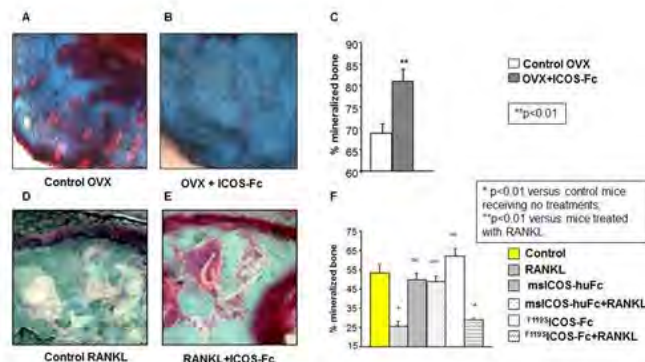


**Figure 1.** Effects of treatment with ICOS-Fc in a mouse osteoporosis induced by OVX or by treatment with RANKL. Representative images of cortical bone from OVX mice treated with PBS (A) or ICOS-Fc (B) and from RANKL injected mice treated with PBS (D) or ICOS-Fc (E). Bar graphs show the following: (C) proportion of calcified bone evaluated in 6 sections from each OVX mouse (3 sections/leg) and (F) proportion of calcified bone evaluated in 6 sections from each RANKL treated mouse (3 sections/leg). Data are means $\pm$ SEM.

Figure 1

**Disclosures:** Patrizia D'Amelio, None.

## FR0166

**Osteoclast Vitamin D Receptor Increases Bone Resorption and Regulates Osteoblast Activity in vivo.** Na-Rae Park<sup>\*1</sup>, Da-In Yeo<sup>2</sup>, Gyeong-Hwa Kim<sup>2</sup>, Xiangguo Che<sup>1</sup>, Yu-ra Choi<sup>2</sup>, Clara Yongjoo Park<sup>2</sup>, Shigeaki Kato<sup>3</sup>, Je-Yong Choi<sup>2</sup>. <sup>1</sup>Department of Biochemistry & Cell Biology, Kyungpook National University School of Medicine, Daegu, South Korea, Korea, republic of, <sup>2</sup>Department of Biochemistry & Cell Biology, BK21 PLUS KNU Biomedical Convergence Program, Kyungpook National University, School of Medicine, Daegu, South Korea, Korea, republic of, <sup>3</sup>Soma Central Hospital, Fukushima, Japan, Japan

The vitamin D receptor (VDR) plays important roles in maintaining skeletal health. The active vitamin D metabolite, 1,25-dihydroxy vitamin D, induces the receptor activator of nuclear factor  $\kappa$ B ligand (RANKL) in osteoblasts that stimulates osteoclast differentiation and bone resorption. Despite *in vitro* evidence of the VDR in osteoclasts, its presence and role *in vivo* is controversial. We investigated the function of VDR in mature osteoclasts *in vivo* by deleting exon3 of the *Vdr* (*Vdr*<sup>ΔOclAOc</sup>) in male mice. These mice were developed by crossing *Cathepsin K*<sup>Cre</sup> mice with floxed *Vdr* (*Vdr*<sup>fl/fl</sup>) mice. Bone shape did not differ between male wild type (WT) and *Vdr*<sup>ΔOclAOc</sup> mice at 4, 8, or 16 weeks. Femoral trabecular thickness (Tb.Th) was greater at 4, 8, and 16 weeks, while bone volume to tissue volume ratio (BV/TV) was greater at 8 and 16 weeks in *Vdr*<sup>ΔOclAOc</sup> mice compared to WT assessed by microcomputed tomography ( $\mu$ CT). No difference was found in tibial osteoclast surface (Oc.S/BS) or osteoclast number (N.Oc) at any time point between genotypes assessed by tartrate resistant acid phosphatase (TRAP) staining. Dynamic histomorphometric analysis of vertebra resulted in greater trabecular mineralizing surface (MS/BS) and cortical mineral apposition rate (MAR) in *Vdr*<sup>ΔOclAOc</sup> mice compared to WT mice. Through bone marrow monocyte culture, we found that *Vdr*<sup>ΔOclAOc</sup> osteoclasts tend to differentiate more rapidly, but resorption activity is lower than WT osteoclasts. Collectively, these results indicate that the VDR in mature osteoclasts regulates bone mass homeostasis by enhancing their resorption activity and decreasing osteoblast activity.

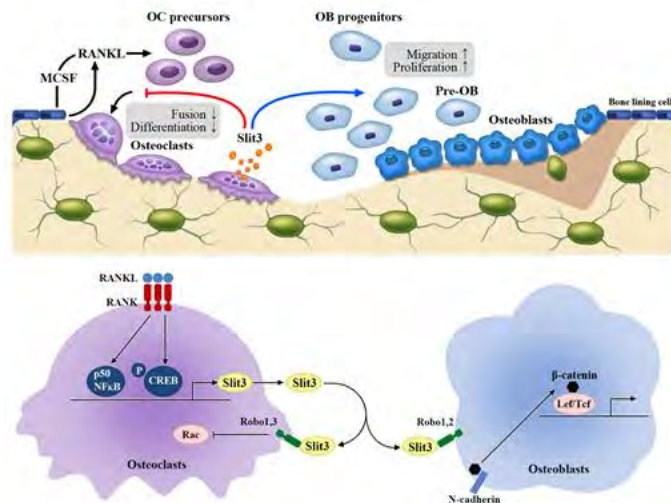
**Disclosures:** Na-Rae Park, None.

This study received funding from: National Research Foundation of Korea grant

## FR0167

**Osteoclast-Secreted Slit3 as a Novel Regulator Linking Bone Resorption and Formation.** Beom-Jun Kim<sup>\*1</sup>, Young-Sun Lee<sup>2</sup>, Sun-Young Lee<sup>2</sup>, Seung Hun Lee<sup>1</sup>, Jung-Eun Kim<sup>3</sup>, Eun-Ju Chang<sup>4</sup>, Seung-Wan Kim<sup>5</sup>, Sung Ho Ryu<sup>6</sup>, Sun-Kyeong Lee<sup>7</sup>, Joseph A Lorenzo<sup>8</sup>, Seong Hee Ahn<sup>9</sup>, Hyeonmok Kim<sup>1</sup>, Jung-Min Koh<sup>1</sup>. <sup>1</sup>Division of Endocrinology & Metabolism, Asan Medical Center, University of Ulsan College of Medicine, Korea, republic of, <sup>2</sup>Asan Institute for Life Sciences, Korea, republic of, <sup>3</sup>Department of Molecular Medicine, Cell & Matrix Research Institute, Kyungpook National University School of Medicine, Korea, republic of, <sup>4</sup>Department of Anatomy & Cell Biology, Cellular Dysfunction Research Center & BMIT, University of Ulsan College of Medicine, Korea, republic of, <sup>5</sup>Department of Pharmacology, University of Ulsan College of Medicine, Korea, republic of, <sup>6</sup>Department of Life Science & Division of Molecular & Life Sciences, Pohang University of Science & Technology, Korea, republic of, <sup>7</sup>UConn Center on Aging, University of Connecticut Health Center, United states, <sup>8</sup>Division of Endocrinology, Department of Medicine, University of Connecticut Health Center, United states, <sup>9</sup>Department of Internal Medicine, Inha University School of Medicine, Korea, republic of

To understand how osteoclasts talk to osteoblasts, we recently established an experimental model of the coupling phenomenon, finding that the conditioned media from mature osteoclasts stimulated the migration of osteoblast lineages. By using a fractionated secretomic approach, the axon-guidance molecule Slit3 was identified as a novel chemokine that stimulates osteoblast migration and proliferation by activating beta-catenin and inhibits bone resorption by suppressing pre-osteoclast fusion in an autocrine manner. Mice deficient in *Slit3* or its receptor *Robo1* exhibit osteopenic phenotypes due to lower bone formation and higher bone resorption. Interestingly, mice lacking *Slit3* in osteoclasts (*Slit3*<sup>ctsk<sup>-/-</sup></sup>) had low bone mass, whereas neuron-specific *Slit3*-deficient mice (*Slit3*<sup>nestin<sup>-/-</sup></sup>) had normal bone mass, supporting the importance of Slit3 as a local determinant of bone metabolism. In postmenopausal women, higher circulating Slit3 levels were associated with higher bone mass. When seven *SLIT/ROBO*-related genes were tested in 4,877 postmenopausal women, only a genetic variant of *SLIT3* was significantly associated with bone parameters. Notably, injection of a truncated recombinant Slit3 markedly rescued bone loss after ovariectomy. These results indicate that Slit3 plays an osteoprotective role by synchronously stimulating bone formation and inhibiting bone resorption and is thus a novel therapeutic target for metabolic bone diseases.



Graphical Abstract

**Disclosures:** Beom-Jun Kim, None.

## FR0170

**Osteoclasts as an intracellular growth niche for *Staphylococcus aureus*.** Jennifer Krauss<sup>\*1</sup>, Emily Goering<sup>2</sup>, Deborah Novack<sup>1</sup>. <sup>1</sup>Washington University School of Medicine, United states, <sup>2</sup>Washington University, United states

Osteomyelitis (OM) is an infection-driven inflammatory disease of bone elicited by a complex interaction between microorganisms and host cells that culminates in pathological bone loss. Accumulating evidence indicates that *Staphylococcus aureus*, the primary causative agent of OM, can invade osteoblasts resulting in inflammatory responses and RANKL expression; thus, leading to robust osteoclast (OC) recruitment at sites of bone infection. In contrast to osteoblasts, which restrict intracellular bacterial growth, we present the novel finding that *S. aureus* can exploit and proliferate to high numbers within OCs and their lineage-committed precursors. We hypothesize that OCs serve as a privileged intracellular replicative niche during *S. aureus*-mediated OM. In support of this notion, we observe that levels of intracellular *S. aureus* dramatically increase between 1.5 and 18 hours post-infection in OCs and their mononuclear TRAP+ precursors. In contrast, we observe a 10-fold decrease in viable bacteria counts over the same time course in bone-marrow macrophage (BMM) controls, as these innate immune cells promote killing. Furthermore, we observe that RANKL treatment of BMMs uniquely promotes intracellular replication of *S. aureus*, while IFN-gamma enhances killing and IL-4 allows persistence. We find that at least 48 hours of RANKL stimulation prior to infection is required to permit intracellular replication, suggesting that RANKL-mediated transcriptional programs that drive OC lineage commitment are required to subvert killing and promote replication. Moreover, we find that *S. aureus* is unable to replicate in NFATc1-deficient cells under osteoclastogenic conditions, whereas overexpression of NFATc1 enhances replication in WT controls. However, ectopic expression of NFATc1 in BMMs, in the absence of RANKL signaling, fails to support replication, indicating that RANKL-induced signaling pathways that synergize with NFATc1 are also important. In this regard, we find that genetic ablation of key alternative NF- $\kappa$ B pathway components NIK or RelB severely reduce the ability of *S. aureus* to replicate in RANKL-stimulated OC precursors, consistent with the impaired capacity of these cells to generate OCs. Collectively, our findings expand the biological importance of osteoclasts beyond bone resorption and demonstrate that OCs are an intracellular growth niche for *S. aureus*; thus contributing to the clinical problems of antibiotic efficacy, chronicity, and recurrence of OM.

**Disclosures:** Jennifer Krauss, None.

## FR0172

**The Lipid Phosphatase Inpp4b Modulates Bone Homeostasis Through the PKC $\beta$ /GSK-3 $\beta$  Signaling Pathway.** Lina Saad<sup>\*</sup>, Monica Pata, Jean Vacher. IRCM, Canada

Bone is a dynamic organ that constantly undergoes remodeling. During these remodeling processes, bone resorption is under the control of osteoclasts. Mature osteoclasts are multinucleated cells that derive from the hematopoietic monocyte/macrophage lineage and loss of osteoclast activity leads to malignant osteopetrosis. The most severe form of the disease in mice and humans is associated with mutations affecting the *Ostm1* gene responsible for the osteopetrotic grey-lethal (*gl*) phenotype in mice. By comparing gene expression, we have identified the mouse homologue of the human and rat inositol polyphosphate 4-phosphatase b (Inpp4b) to be consistently

down regulated in *g/g* osteoclasts. To gain insight into the direct role of *Inpp4b* in bone homeostasis regulation, we produced a null allele of *Inpp4b*. The systemic *Inpp4b* ablation resulted in an osteoporotic phenotype and defined *Inpp4b* as a negative regulator of osteoclastogenesis via the *Nfatc1* signaling pathway. However, the molecular mechanism through which *Inpp4b* can regulate osteoclast differentiation remains elusive. Among several osteoclast-specific signaling cascades analyzed upon RANKL stimulation and upstream of *Nfatc1*, only the PKC $\beta$  pathway was modulated in absence of *Inpp4b*. We found that *Inpp4b* depletion induces the activation of the kinase PKC $\beta$ , as revealed by the significant increase in the phosphorylation level of the protein with time. Interestingly, we also demonstrated that the GSK-3 $\beta$  protein, a downstream effector of PKC $\beta$ , was inactivated by phosphorylation in the same cells. Since it is known that PKC $\beta$  positively regulates RANKL-induced osteoclastogenesis by inactivating GSK-3 $\beta$  and stimulating *Nfatc1* transcriptional activity, these data are consistent with our characterization of enhanced osteoclastogenesis and osteoporosis in *Inpp4b*-deficient mice. Taken together, our results provide strong evidence for a role of *Inpp4b* in osteoclastogenesis and bone homeostasis through the PKC $\beta$ /GSK-3 $\beta$  signaling pathway. Further studies will determine if PKC $\beta$  inhibition could provide a protective effect on bone loss in *Inpp4b*-deficient mice, and in osteoporosis in general.

**Disclosures:** Lina Saad, None.

## FR0173

**Towards a gene regulatory network in the feedback inhibition of osteoclasts by CD8 T cells.** Elena Shashkova\*<sup>1</sup>, Anna Cline-Smith<sup>1</sup>, Jahnvi Trivedi<sup>1</sup>, Chloe Ferris<sup>1</sup>, Zachary Buchwald<sup>2</sup>, Jesse Gibbs<sup>3</sup>, Deborah Novack<sup>3</sup>, Rajeev Aurora<sup>1</sup>. <sup>1</sup>Saint Louis University, United states, <sup>2</sup>Emory University School of Medicine, United states, <sup>3</sup>Washington University School of Medicine, United states

Osteoimmunology arose from the recognition of the crosstalk between the skeletal and immune systems. We discovered that osteoclasts act as antigen-presenting cells to CD8 T cells. Cross-presentation of antigens to CD8 T cells by osteoclasts leads to expression of CD25 and FoxP3, markers of regulatory T cells. Osteoclast-induced FoxP3+ CD8 T cells (T<sub>REG</sub>) are immunosuppressive and also suppress bone resorption by osteoclasts forming a negative feedback loop. Here we show that Notch signaling is required for the induction of FoxP3 in T<sub>REG</sub>. Inhibition of Notch receptor cleavage by  $\gamma$ -secretase inhibitor reduced expression of FoxP3. Priming by osteoclasts resulted in cleavage of Notch-1 and Notch-4 receptors on CD8 T cells and subsequent translocation of Notch intracellular domains (ICDs) to the nucleus. Cleavage of Notch-4 was induced by Delta like ligand 4 (Dll4), a Notch ligand that is expressed by mature osteoclasts. In contrast, Notch-1 cleavage is ligand-independent and induced by T cell receptor stimulation. We show that RBPJ-dependent expression of a reporter gene is activated in T<sub>REG</sub>. Notch-1 and Notch-4 ICDs bind to RBPJ-binding sites in the regulatory regions of FoxP3 gene as demonstrated by ChIP-qPCR. These results show that Notch activation induced by osteoclasts provides a differentiation signal to CD8 T cells to become T<sub>REG</sub>. Additionally, we found that osteoclasts induce T-bet and Eomesodermin (Eomes) dependent expression of IFN- $\gamma$  in T<sub>REG</sub>. Pharmacological inhibition of I $\kappa$ B kinase complex completely blocked IFN- $\gamma$ , and significantly reduced T-bet and Eomes production by T<sub>REG</sub>. Inhibition of Notch signaling did not affect the induction of either of these proteins. We demonstrate that IFN- $\gamma$  produced by T<sub>REG</sub> is required for suppression of osteoclastogenesis and for degradation of tumor necrosis factor receptor-associated factor 6 (TRAF6) in osteoclast precursors. TRAF6 prevents signaling through receptor activator of NF $\kappa$ B (RANK) needed for osteoclastogenesis. Knockout of IFN- $\gamma$  rendered T<sub>REG</sub> inefficient in preventing actin ring formation in osteoclasts, a process required for bone resorption. *In vivo* generated IFN- $\gamma$ <sup>-/-</sup> T<sub>REG</sub> had impaired ability to protect mice from bone resorption and bone loss in response to high-dose RANKL. Together, our results show that NF $\kappa$ B, Notch, T-bet and Eomes form a gene regulatory network that induces FoxP3 and IFN- $\gamma$  in T<sub>REG</sub>, which then mediates protection from bone loss.

**Disclosures:** Elena Shashkova, None.

## FR0174

**Novel critical role for EZH2-increased H3K27 trimethylation and C/EBP $\beta$ -LAP to LIP switch at the MafB promoter during the early phase of osteoclastogenesis.** Juraj Adamik\*, Peng Zhang, Quanhong Sun, Deborah L. Galson. University of Pittsburgh, United states

In response to RANK activation, BMM differentiation into osteoclasts (OCL) is guided by epigenetic regulatory mechanisms such as histone methylation and acetylation. Key OCL regulatory gene promoters in BMM harbor bivalent histone modifications that combine activating H3K4me3 and repressive H3K27me3 marks, which upon RANKL stimulation resolve into repressive or activating architecture. EZH2 is the histone methyltransferase component of the PRC2 complex, which catalyzes H3K27me3 modifications. We found that EZH2 activity and total cellular H3K27me3 levels are upregulated during the initial 24h of RANKL-induced osteoclastogenesis. Targeting the EZH2 SET domain with the selective inhibitor GSK126 during RANKL treatment decreased total H3K27me3 levels and the expression of c-Fos, NFATc1, RANK, Cathepsin K, OSCAR, and DC-STAMP, and blocked formation of TRAP-positive multi-nuclear OCL. GSK126 addition during

the first 24h of RANKL treatment was necessary and sufficient to inhibit formation of mature OCL, whereas treatment of primary BMM during the 3-day M-CSF expansion phase did not alter subsequent OCL formation. The GSK126 dose used did not exhibit cytotoxic effects. We found that EZH2 inhibition upregulated expression of the OCL inhibitory factor MafB. Chromatin IP confirmed that GSK126 treatment prevented RANKL-induced H3K27 trimethylation of the MafB promoter in BMM during the first 24h. We observed that GSK126 reduced the pAKT-pmTOR-pS6RP signaling axis resulting in translational changes that increased the C/EBP $\beta$ -LAP:LIP isoform ratio. We demonstrate the direct involvement of endogenous C/EBP $\beta$ -LAP/LIP isoform switching at the MafB promoter through ChIP analyses with antibodies directed towards either the N (LAP) or the C-terminus (LAP+LIP) of C/EBP $\beta$ . We show that GSK126 inhibits the recruitment of RANKL-induced inhibitory LIP while increasing the binding of the LAP isoform to result in increased MafB expression. In summary, EZH2 is a novel regulator of osteoclastogenesis, playing an early critical role by inhibiting MafB expression. In addition to direct chromatin repression, EZH2 enhances activation of the mTOR pathway, which increases translation of the C/EBP $\beta$ -LIP isoform. This results in enrichment of repressive C/EBP $\beta$ -LIP isoform at the MafB promoter. The results indicate that EZH2 activity is essential during the early phase of RANKL activation to establish the repressive chromatin architecture required for proper progression of OCL differentiation.

**Disclosures:** Juraj Adamik, None.

## FR0175

**Comparative roles of c-Fos and C/EBP $\alpha$  in osteoclast differentiation through regulation by the RANK cytoplasmic IVVY538-538 motif in a RBP-J downregulation manner.** Joel Jules\*, Wei Chen, Yi-Ping Li. University of Alabama at Birmingham, United states

Binding of the receptor activator of nuclear factor  $\kappa$ B (RANK) ligand (RANKL) to its receptor RANK on osteoclast (OC) precursors can strongly upregulate FBI osteosarcoma oncogene (c-Fos) and CCAAT/enhancer binding protein- $\alpha$  (C/EBP $\alpha$ ), two critical OC transcription factors. However, the influence of c-Fos and C/EBP $\alpha$  on osteoclastogenesis has not yet been compared. Here we showed that overexpression of c-Fos or C/EBP $\alpha$  in mouse bone marrow (MBM) cells, primary OC precursors, could upregulate OC genes and thereby initiated osteoclastogenesis in a similar fashion without RANKL stimulation. However, while C/EBP $\alpha$  overexpression could upregulate c-Fos in MBM cells independently of RANKL, c-Fos overexpression was unable to upregulate C/EBP $\alpha$ . Consistently, C/EBP $\alpha$  overexpression exhibited a stronger ability in promoting OC differentiation than c-Fos overexpression. RANK has a cytoplasmic IVVY535-538 (IVVY) motif that is essential for OC differentiation. Hence, we investigated the role of this motif in regulating the expressions of C/EBP $\alpha$  and c-Fos during OC differentiation. We showed that mutational inactivation of IVVY motif blocked OC differentiation by in part inhibiting C/EBP $\alpha$ , but not c-Fos, expression. We thus hypothesized that C/EBP $\alpha$  overexpression might rescue OC differentiation in cells expressing mutated IVVY motif. However, we found that overexpression of C/EBP $\alpha$  or c-Fos could only mediate OC differentiation in cells expressing normal, but not mutated, IVVY motif. Notably, our data showed that inactivation of IVVY motif significantly abrogated the expression of OC genes as compared with vector control and normal IVVY motif, suggesting that inactivation of IVVY motif might also trigger upregulation of OC inhibitors in blocking OC differentiation. Consistently, we showed that inactivation of IVVY motif lead to a drastic upregulation of RBP-J, a potent inhibitor of OC differentiation. Mechanistically, overexpression of C/EBP $\alpha$  or c-Fos in the mutated-IVVY-motif expressers failed to regulate the deregulated RBP-J expression, leading to abrogation of OC genes. Accordingly, RBP-J silencing in RAW264.7 cells expressing mutated IVVY motif partially rescued osteoclastogenesis with C/EBP $\alpha$  or c-Fos overexpression, but C/EBP $\alpha$  exhibited stronger osteoclastogenic ability than c-Fos. Collectively, the results indicate that C/EBP $\alpha$  is a stronger inducer of OC differentiation than c-Fos via in part regulation by RANK IVVY535-538 motif which involves downregulation of RBP-J.

**Disclosures:** Joel Jules, None.

## FR0176

**Notch2 Expression is Required for Spleen B Cell Allocation and Osteoclastogenesis.** Archana Sanjay\*, Bhavita Walia, Jungeun Yu, Stefano Zanotti, Ernesto Canalis. UConn Health, United states

The immune and skeletal systems are closely related and B and T cells regulate bone remodeling. B cells can influence osteoclast differentiation through the synthesis of receptor activator of nuclear factor kappa-B ligand (RANKL) and osteoprotegerin. The Notch2 receptor is a determinant of skeletal and B cell function, and gain of *NOTCH2* function mutations are associated with Hajdu Cheney Syndrome (HCS), a devastating disease characterized by osteoporosis and an inflammatory reaction that leads to acro-osteolysis. We created a mouse model reproducing the HCS mutation (*Notch2*<sup>O2319X</sup>) and heterozygous global mutant mice displayed gain of Notch2 function, profound osteopenia, increased osteoclast formation and bone resorption. Culture of splenocytes from heterozygous *Notch2*<sup>O2319X</sup> in the presence of M-CSF resulted in increased TRAP<sup>+</sup> multinucleated osteoclasts compared to controls. Heterozygous *Notch2*<sup>O2319X</sup> mice exhibited splenomegaly and altered splenic architecture. In the mutant spleen, the characteristic perifollicular rim marking the

marginal zone, which is the interface between the non-lymphoid red pulp and the lymphoid white-pulp, merged with components of the white pulp. As a consequence, the marginal zone of *Notch2<sup>Q2319X</sup>* mice occupied most of the splenic structure. To explore mechanisms involved, lymphocyte populations from the bone marrow, spleen, thymus and peripheral blood harvested from heterozygous *Notch2<sup>Q2319X</sup>* mice and littermate sex-matched controls were analyzed by flow cytometry analysis. The number of CD3<sup>+</sup> T cells and immature and mature B220<sup>+</sup> B cells were not different between the two genotypes. In contrast, *Notch2<sup>Q2319X</sup>* mice had 4-5 fold-increase in the CD21<sup>+</sup>/CD23<sup>low</sup> splenic marginal zone B cells and a proportional decrease in splenic follicular B cells (CD21<sup>low</sup>/CD23<sup>+</sup>). This cell allocation was specific to the spleen and in the bone marrow compartment these two cell populations were comparable between the two genotypes. RT-PCR analysis of FACS sorted splenic marginal zone and follicular B cells demonstrated the expression of *Notch2<sup>Q2319X</sup>* mutant transcripts only in mutant mice. Neither RT-PCR nor immunohistochemistry of spleen sections revealed a difference in RANKL expression between genotypes. In conclusion, these studies demonstrate that Notch2 determines splenic cell allocation and as a consequence may influence osteoclastogenesis, bone resorption and possibly explain the inflammatory reaction and acro-osteolysis of HCS.

**Disclosures:** Archana Sanjay, None.

## FR0177

**Similarities between IL8 and RANKL Stimulation of Osteoclast Formation Suggests a Highly Conserved Signaling Cascade that Facilitates Bone Resorption in Breast Cancer.** Diarra Williams<sup>\*1</sup>, Archana Kamalakar Kamalakar<sup>1</sup>, Nisreen Akel<sup>1</sup>, Frances Swain<sup>2</sup>, Dana Gaddy<sup>1</sup>, Larry Suva<sup>1</sup>. <sup>1</sup>Texas A&M University, United states, <sup>2</sup>Texas A&M University, United Kingdom

Bone metastasis is a frequent occurrence in breast cancer patients that leads to osteolysis and severe skeletal effects such as hypercalcemia and, intractable bone pain as well as pathological fractures that results in a significant decline in patient quality of life and survival. Although breast cancer metastasis to bone is multifactorial, the deleterious osteolytic effects on the skeleton are predominately mediated by tumor-secreted factors such as Interleukin 8 (IL8) that directly or indirectly stimulate osteoclast differentiation and activity at the metastatic site. We have previously shown that in breast cancer patients bone resorption is significantly correlated with IL8 levels, and that the modulation of IL8 expression directly regulates osteoclast differentiation similar to RANK ligand (RANKL). In this study, the IL8 signaling pathways that lead to the upregulation of osteoclastogenesis and the ability of IL8 to induce these pro-osteoclastogenic effects were investigated. To elucidate the specific signaling pathways, human peripheral blood mononuclear cells (PBMCs) were plated in 24 well tissue culture plates and treated with mCSF alone, mCSF+RANKL or mCSF+IL8. Cells were allowed to differentiate for 4 days (osteoclast precursors) or 10 days (mature osteoclasts) prior to RNA isolation and RNA-seq analysis. Pathway analysis revealed the significant upregulation of NFB, ERK, P38, and AKT pathways by both IL8 and RANKL at days 4 and 10. IL8 also induced the phosphorylation of ERK, P38, and AKT, which was not suppressed by an inhibitor of RANKL, RANK-Fc, demonstrating the effects were not mediated by the induction of RANKL expression. In addition, a transgenic mouse model containing a human bacterial artificial chromosome encoding human IL8 (hIL8tg/BAC) and expressing low circulating IL8 levels (15-20 pg/ml) has a low bone mass phenotype by  $\mu$ CT and histomorphometric analysis. The low bone mass was characterized by increased bone resorption and decreased osteoblast numbers. This effect was recapitulated in *ex vivo* bone marrow cultures demonstrating a decrease in osteoblast recruitment and differentiation, as well as an increase in osteoclastogenesis. In conclusion, the convergence of RANKL and IL8-induced signaling pathways demonstrates the essential nature of the regulators of osteoclastogenesis, yet supports the idea that multiple tumor-derived factors facilitate bone metastasis by stimulating osteoclastogenesis and bone resorption.

**Disclosures:** Diarra Williams, None.

## FR0178

**Deletion of Mitofusin-2 in Osteocytes Causes a Profound Skeletal Phenotype Characterized by Reduced Bone Turnover.** Meiling Zhu<sup>\*</sup>, Ben-hua Sun, Christine Simpson, Steven Tommasini, Karl Insogna. Yale University School of Medicine, United states

Mitofusin 2 (MFN2) is a multifunctional outer membrane mitochondrial GTPase whose role extends beyond its best-described activity: regulating the shape and fusion of this organelle. It has been implicated in mediating cellular responses to oxidative stress, and has a role in autophagy and mitophagy in particular. Osteocytes are long-lived cells that are thought to be sensitive to the oxidative and metabolic stresses that occur with aging and autophagy is posited to be one adaptive mechanism employed by osteocytes in response to these challenges. To determine if MFN2 plays a role in osteocyte metabolism, we deleted MFN2 in osteocytes by crossing mice bearing a floxed MFN2 allele with animals expressing cre under the control of an 8-kb DMP1 promoter (kindly provided by Dr. Charles O'Brien, U. of Arkansas). These animals evidenced no skeletal phenotype at 10 wks of age, but serial measurements in the same cohort of animals demonstrated that by 15 weeks of age, the knockout animals had developed significant osteopenia both by DXA and uCT, which worsened at 20 and 25

wks. Thus femur BMD was 22% lower than littermate controls at 15 wk, 28% lower at 20 wks and 38% lower at 25 wks. Similar changes were evident in the spine. MicroCT analyses at 25 weeks showed markedly reduced BV/TV in both femoral (by 82%) and spinal (by 45%) trabecular bone, as well as femoral cortical bone mass (by 2.2%). Biomechanical testing at 25 weeks showed significantly reduced stiffness ( $p=0.003$ ), maximum load ( $p=0.002$ ) and total work ( $p=0.04$ ). Serum CTx and PINP were both significantly lower in the knock out mice suggesting a lower rate of skeletal remodeling (CTx:  $12.9 \pm 1.2$  vs  $22.7 \pm 2.5$ ,  $p=0.01$ ; PINP:  $22.2 \pm 3.1$  vs  $30.1 \pm 8.2$ ). Static histomorphometry showed reduced BV/TV ( $1.7 \pm 0.5$  vs.  $12.8 \pm 1.3$ ,  $p<0.001$ ) with reduced numbers of osteoblasts per bone perimeter ( $5.0 \pm 1.9$  vs.  $17.3 \pm 5.8$ ), but normal NOc/BPm although total Oc number was reduced. Dynamic histomorphometry showed a reduced BFR/BS ( $186 \pm 73$  vs  $311 \pm 27$ ). These data identify MFN2 as having a key role in osteocyte metabolism. Given the rapidity with which this skeletal phenotype develops and its severity, MFN2 is likely to be important to osteocyte function throughout the lifespan.

**Disclosures:** Meiling Zhu, None.

## FR0179

**Deletion of YAP and TAZ in Osteoblasts and Osteocytes Suppresses Bone Formation and Reduces Bone Mass.** Jinhui Xiong<sup>\*</sup>, Marilina Piemontese, Yu Liu, Yuko Fujiwara, Priscilla Baltz, Charles O'Brien. University of Arkansas for Medical Sciences, United states

Mechanical stimulus plays an important role in maintaining bone homeostasis. Osteocytes have been proposed as important mechanosensing cells in bone. However, the mechanism by which osteocytes sense and respond to mechanical signals is unclear. Recently the activity of YAP (Yes associated protein) and TAZ (transcriptional co-activator with PDZ-binding motif), two related transcription cofactors that control organ size in a redundant manner, have been shown to be regulated by mechanical signals such as extracellular matrix stiffness and fluid shear stress. Thus, it is possible that YAP and TAZ may play a role in mechanosensation in bone. To elucidate the role of YAP and TAZ in late stages of the osteoblast lineage, we deleted the genes encoding YAP and TAZ using Dmp1-Cre transgenic mice which cause Cre-mediated recombination in mature osteoblasts and osteocytes. Mice lacking both the YAP and TAZ genes in Dmp1-Cre-targeted cells, hereafter referred to as Dmp1-Cre;YAP<sup>fl/fl</sup>;TAZ<sup>fl/fl</sup> mice, were born at the expected rate and had normal body weights. The deletion of YAP and TAZ genes was confirmed by a more than 70% reduction of loxP-flanked DNA in genomic DNA isolated from osteocyte-enriched cortical bone. Male and female Dmp1-Cre;YAP<sup>fl/fl</sup>;TAZ<sup>fl/fl</sup> mice exhibited decreased bone mineral density at 4 and 12 weeks of age as measured by DXA. Consistent with this, cancellous bone volume in the femur measured by  $\mu$ CT at 12 weeks of age was also decreased in Dmp1-Cre;YAP<sup>fl/fl</sup>;TAZ<sup>fl/fl</sup> mice of both sexes. This change was associated with decreased trabecular number, increased trabecular separation, as well as decreased cortical thickness. Similar changes in vertebral cancellous bone were also noted in both genders. Histomorphometric analysis of the vertebra from 12 week old female Dmp1-Cre;YAP<sup>fl/fl</sup>;TAZ<sup>fl/fl</sup> mice revealed that osteoblast number and perimeter were significantly decreased. Consistent with this, the bone formation rate was reduced due to both decreased mineralizing surface and mineral appositional rate. The mRNA for the bone formation marker osteocalcin was also decreased in the 5<sup>th</sup> lumbar vertebra. Together, these results demonstrate that YAP and TAZ in mature osteoblasts and osteocytes play an important role in maintaining bone homeostasis by promoting bone formation via effects on osteoblast number.

**Disclosures:** Jinhui Xiong, None.

## FR0180

**HDAC5 is required for loading-induced sclerostin down-regulation.** Marc Wein<sup>\*1</sup>, Elizabeth Williams<sup>1</sup>, Maureen O'Meara<sup>1</sup>, Belinda Beqo<sup>1</sup>, Leah Worton<sup>2</sup>, Edith Gardiner<sup>2</sup>, Paola Divieti-Pajevic<sup>3</sup>, Ted Gross<sup>2</sup>, Henry Kronenberg<sup>1</sup>. <sup>1</sup>Massachusetts General Hospital, United states, <sup>2</sup>University of Washington, United states, <sup>3</sup>Boston University, United states

Purpose: Loading increases bone formation, in part through down-regulating sclerostin (encoded by the gene SOST) production by osteocytes. However, the mechanisms responsible are largely unknown. We previously showed that the class IIa histone deacetylase HDAC5 is a negative SOST regulator in osteocytes. Class IIa HDACs can act as signaling molecules by dynamic phosphorylation-dependent shuttling between the cytoplasm and the nucleus. Here, we sought to determine the role for HDAC5 in osteocytic responses to mechanical forces.

Methods: Ocy454 cells were subjected to fluid flow shear stress (FFSS) to mimic mechanical loading. Gene expression was measured by RT-qPCR, and HDAC5 phosphorylation and nuclear localization were assessed using phospho-specific antibodies and subcellular fractionation. HDAC5-deficient Ocy454 cells were generated using CRISPR/Cas9-mediated gene deletion. Wild type and HDAC5-deficient female mice (n=8/group) were subjected to *in vivo* cantilever bending of the right tibia. Loading was performed once daily for 3 consecutive days (100 cycles/d, 2500  $\mu$ -epsilon peak normal strain), and mice were sacrificed 24 hours after the last loading episode. Cortical bone RNA was analyzed by RT-qPCR comparing the loaded and contralateral tibia. Immunohistochemistry was performed for sclerostin and activated beta-catenin.

Results: In Ocy454 cells, 2 hour exposure to FFSS (~8 dynes/cm<sup>2</sup>) leads to DMP1 up-regulation, and down-regulation of SOST mRNA. FFSS promotes dephosphorylation of HDAC5 at serines 259/279, and HDAC5 nuclear translocation. HDAC5-deficient Ocy454 cells show reduced SOST down-regulation in response to FFSS (37% down-regulation in HDAC5 KO cells vs 81% down-regulation in WT cells,  $p=0.046$ ). In contrast, HDAC5-deficient cells show normal up-regulation of DMP1. *In vivo*, WT mice show expected-loading-induced SOST mRNA down-regulation (38% down-regulation compared to contralateral limb,  $p=0.027$ ), while HDAC5<sup>-/-</sup> mice fail to alter SOST expression in response to loading. These results were confirmed at the protein level by sclerostin immunohistochemistry. Finally, while WT mice show increased periosteal beta-catenin positive osteoblasts in response to loading, which did not occur in the absence of HDAC5.

Conclusions: In osteocytes, HDAC5 responds to mechanical stimuli by translocating from the cytoplasm to the nucleus. HDAC5 is required for loading-induced SOST down-regulation *in vitro* and *in vivo*.

Disclosures: Marc Wein, None.

## FR0181

**Increased Wnt/ $\beta$ -catenin Signaling and Decreased Osteoclastogenic Potential of Osteocytic Cells Lacking Cx37.** Rafael Pacheco-Costa\*, Iraj Hassan, Lilian Plotkin. Indiana University School of Medicine, United states

Connexin (Cx) 37 is a gap junction protein expressed in osteoblasts, osteocytes and osteoclasts. We have previously shown that global deletion of Cx37 results in increased bone mass due to defective osteoclast formation. Thus, Cx37 is required for osteoclast differentiation and fusion and its absence leads to arrested osteoclast maturation and high bone mass in mice. We now show that, in addition, deletion of Cx37 from osteocytic MLO-Y4 cells using shRNA results in decreased RANKL and increased OPG expression, resulting in a 5-fold decrease in RANKL/OPG ratio. Furthermore, luciferase activity in osteocytic cells expressing an OPG reporter construct is increased in the absence of Cx37, and it is further increased by treatment with the activator of the Wnt/ signaling LiCl, consistent with the fact that OPG is a recognized Wnt/ $\beta$ -catenin target gene. Moreover, protein and mRNA levels for  $\beta$ -catenin were also increased in Cx37-silenced cells, as were other canonical Wnt target genes Axin2, Smad6, Wisp2 and CyclinD1. As found *in vitro*,  $\beta$ -catenin protein expression was increased in lumbar vertebrae from Cx37-deficient mice. Furthermore, mRNA levels for the Wnt/ $\beta$ -catenin target genes Axin2, CyclinD1, and Smad6 were increased in lumbar vertebrae preparations. We next examined the contribution of Cx37 expressed in osteocytes. For this, mice lacking Cx37 were crossed with DMP1-GFP mice, which express green fluorescent protein in osteocytes, allowing for isolation of these cells using fluorescence activated cell sorting (FACS). As in whole vertebra, Cx37-deficient osteocytes expressed higher levels of Axin2, CyclinD1 and Smad6, compared to wild type controls. We conclude that, in addition to its direct role on osteoclast differentiation, Cx37 deficiency decreases osteoclast formation by reducing RANKL/OPG ratio in osteoblastic cells, potentially due to increase Wnt/ $\beta$ -catenin signaling. This effect contrast with that of Cx43-deletion, which results in increased osteoclast recruitment and formation, likely secondary to increased osteocyte apoptosis. These findings add to the role of Cx37 in bone homeostasis that is not compensated for by Cx43 *in vivo*.

Disclosures: Rafael Pacheco-Costa, None.

## FR0182

**Osteocyte-Driven Perilacunar Remodeling is Impaired in Glucocorticoid Induced Osteonecrosis.** Tristan Fowler\*<sup>1</sup>, Claire Acevedo<sup>1</sup>, Courtney Mazur<sup>1</sup>, Faith Hall-Glenn<sup>1</sup>, Aaron Fields<sup>1</sup>, Hrishkesh Bale<sup>2</sup>, Robert Ritchie<sup>2</sup>, Jeffrey Lotz<sup>1</sup>, Thomas Vail<sup>1</sup>, Tamara Alliston<sup>1</sup>. <sup>1</sup>University of California San Francisco, United states, <sup>2</sup>Lawrence Berkeley National Laboratory, United states

Despite the therapeutic value of glucocorticoids (GCs), bone fragility and osteonecrosis (ON) are serious known side effects. The effect of GCs on bone mass are well known, however the cellular mechanisms by which GCs compromise bone quality remain unclear. Osteocytes (OCYs) maintain bone quality through the process of perilacunar remodeling (PLR), though the effect of GCs on this process remains unknown. Here we test the hypothesis that GCs deregulate PLR through dynamic repression of PLR enzyme expression, disruption of the lacuno-canalicular network (LCN), and reduction of bone matrix integrity. To test this hypothesis, we evaluated the temporal effect of GCs on PLR enzyme expression, LCN connectivity, and bone matrix composition and organization. Two-month-old male FVB mice were implanted with pellets containing placebo or prednisolone (2.8 mg/kg/d) and sacrificed at 7 and 21 days (n=8/group). As expected,  $\mu$ CT revealed significant decreases in bone mass following 21, but not 7, days of GC treatment. qRT-PCR of RNA from marrow-flushed humeri was used to determine the effect of GCs on PLR. Within 7 days, GCs significantly repressed several genes implicated in PLR, including MMP2, MMP13, MMP14, CA-II, CatK, and TRAP (n $\geq$ 6,  $p\leq$ 0.05). Immunohistochemistry revealed that GCs repress MMP13, MMP14 and CatK expression in OCYs, prior to detectable changes in bone mass. To determine if repression of PLR factors by GCs corresponds to functional defects, we evaluated lacunar size and matrix mineralization using high-resolution X-ray tomographic microscopy (XTM). XTM analysis exposed

dramatic GC-dependent decreases in lacunar size and increased bone matrix mineralization at 7 days, results that are consistent with histologic findings of reduced LCN area and collagen organization (n $\geq$ 3,  $p\leq$ 0.05). GC-dependent disruption of the LCN and bone matrix composition and organization correspond to observations in human ON. We used *in vitro* and *in vivo* approaches to determine if GC directly impacts PLR as a result of OCY apoptosis. GC-dependent changes in PLR gene and protein expression are apoptosis independent and PLR outcomes are affected prior to detectable GC-induced apoptosis in cortical bone. This suggests that the deregulation of PLR by GC plays a causal role in loss of matrix integrity in ON and bone fragility. Therefore, this study implicates GCs in the dynamic regulation of PLR enzyme expression, OCY connectivity, and maintenance of bone quality.

Disclosures: Tristan Fowler, None.

## FR0183

**Osteocytes Utilize Lacunar Acidification to Remove Calcium from Their Perilacunar Matrix During Lactation.** Katharina Jähn\*<sup>1</sup>, Shilpa Kelkar<sup>2</sup>, Hong Zhao<sup>2</sup>, Yixia Xie<sup>2</sup>, LeAnn M Tiede-Lewis<sup>2</sup>, Vladimír Dusevich<sup>2</sup>, Sarah L Dallas<sup>2</sup>, Lynda F Bonewald<sup>2</sup>. <sup>1</sup>University Medical Center Hamburg-Eppendorf, Germany, <sup>2</sup>University of Missouri-Kansas City, United states

Osteoclasts are essential for bone remodeling, shaping and repairing bone matrix, while also mobilizing calcium. However, osteocytes appear to be responsible for the rapid blood calcium spike that occurs within minutes in response to PTH. With the surface area of the osteocyte lacunocanalicular network estimated at >400 times the area of the bone surface, osteocytes could be responsible for rapid mobilization of calcium from bone. We have shown that osteocytes express 'osteoclast-specific' genes during lactation and that PTHrP, which is highly elevated during lactation, is responsible for osteocyte perilacunar remodeling through PTHrP-signaling. We hypothesized that to remove calcium, osteocytes must acidify their microenvironment in response to PTHrP. To test this hypothesis, *in vitro* and *in vivo* experiments were performed using primary osteocytes and cell lines and using virgin and lactating Col-GFP mice and normal CD1 mice. Genes associated with osteoclast resorption but not osteoclast differentiation were increased with osteocyte differentiation of IDG-SW3 cells. Addition of PTHrP to these cells induced proton generation, which was more pronounced at the osteocyte stage compared to the osteoblast stage. Bafilomycin, which blocks acidification by inhibiting vacuolar ATPase, blocked PTHrP-induced proton generation. Based on proton generation and bone fluid volumes, a theoretical *in vivo* pH of ~6.2 in response to PTHrP was calculated. Unlike osteoclasts that form a sealing zone to contain protons, osteocytes may be immersed in mild acid, suggesting they may be adapted to tolerate lower pH. We found that osteocytes, but not osteoblasts nor fibroblasts, remain viable for two days at acidic pH *in vitro*. A novel transgenic mouse line in which a GFP $\beta$  tag is placed in the N-terminus of the  $\alpha$ 2(I)-collagen chain was used to examine perilacunar remodeling. Surprisingly, GFP-fluorescence was reduced not only around lacunae but throughout the matrix of lactating Col-GFP mice compared to virgin controls. As GFP fluorescence is quenched at low pH, this is most likely due to decreased pH throughout the bone. To further examine osteocyte acidification *in vivo*, virgin and lactating CD1 mice were injected with a pH indicator, acridine orange. Confocal microscopy showed osteocyte-induced acidification and quantitation of fluorescence using ImageJ showed a significant reduction in pH. In lactating animals on a low calcium diet, bone loss was more dramatic in the endosteal compared to the periosteal cortical bone compartment suggesting the endosteal bone is preferentially targeted for removal during lactation. This study shows that osteocytes acidify their microenvironment and that osteocyte-induced acidification plays a role in bone resorption during lactation - another addition to the list of functions for osteocytes.

Disclosures: Katharina Jähn, None.

## FR0185

**Acute *in vivo* osteocyte responses to mechanical load in mice bearing a genetic intracellular calcium sensor: recruitment of responding cells depends on both strain magnitude and loading frequency.** Karl J Lewis\*<sup>1</sup>, Joyce Louie<sup>1</sup>, Samuel Stephen<sup>1</sup>, Zeynep Seref-Ferlengez<sup>2</sup>, David C Spray<sup>2</sup>, Mia M Thi<sup>2</sup>, Robert J Majeksa<sup>1</sup>, Sheldon Weinbaum<sup>1</sup>, Mitchell B Schaffler<sup>1</sup>. <sup>1</sup>Dept. of Biomedical Engineering, City College of New York, United states, <sup>2</sup>Dept. of Neuroscience, Albert Einstein College of Medicine, United states

Osteocytes are considered the principal mechanosensory cells of bone, but how osteocytes encode mechanical information *in vivo* is not well understood. Using mice that express a genetically encoded Ca<sup>2+</sup> indicator in osteocytes and a novel *in vivo* loading and imaging system, we measured changes in osteocyte Ca<sup>2+</sup> levels during *in vivo* loading of bone at defined strain levels and loading frequencies. Osteocyte-targeted expression of the fluorescent Ca<sup>2+</sup> sensor GCaMP3<sup>1,2</sup> was achieved by crossing Ai38 mice (bearing the GCaMP3 gene construct behind a Lox-STOP-Lox codon<sup>3</sup>) with DMP1-Cre mice (from Dr. L. Bonewald<sup>4</sup>). Following IACUC-approved procedures, anesthetized mice were placed in a custom device to permit 3-point bending of their 3rd metatarsals (MT-3) on the stage of a multiphoton microscope (MPM, Bruker Instruments). Bones were loaded cyclically (haversine waveform under displacement control) to calibrated tensile strains of 250, 500, 1000,

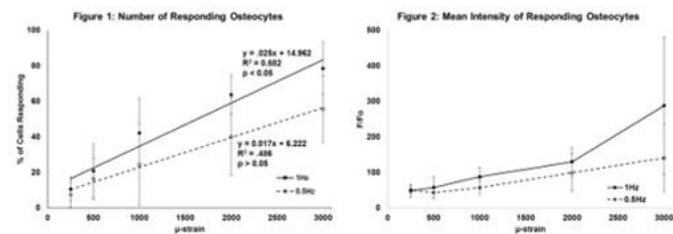
2000 and 3000  $\mu$ -strain at either 0.5 or 1Hz. GCaMP3 signal visualization during loading under a 40X water immersion objective (LUMPLFLN 40XW, Olympus) used 920nm excitation and 490-560nm band pass detection. Time series images were acquired between  $\pm 100\mu$ m of the midshaft to avoid strain gradient effects. For each osteocyte,  $Ca^{2+}$  signal pixel intensity values were collected in each frame before and during loading (ImageJ, NIH). Statistical analyses were performed using SPSS (IBM).

As applied strain increased, the number of responding osteocytes increased in a strongly linear fashion at 1Hz ( $p < 0.05$ , regression analyses) but not at 0.5Hz (Fig 1). Further, the slopes of the regression lines (i.e. recruitment rate of responding cells) differed significantly (Fig 1,  $p < 0.01$  ANCOVA), indicating a frequency dependence as well. In contrast, the magnitude of  $Ca^{2+}$  responses in individual cells was not dependent on strain magnitude (Fig 2).

Our findings indicate that the osteocyte network *in vivo* encodes loading information in a physiologically relevant range by altering cell recruitment, while  $Ca^{2+}$  signaling of individual cells is effectively binary. These responses further support the concept that osteocytes *in vivo* "listen better" to loading frequencies associated with normal gait than to those associated with lower intensity motions.

References: 1)Nakai J+ Nature Biotech 2001. 2)Tian L+ Nat Meth, 2009. 3)Zariwala + J. Neurosci. 2012. 4)Lu Y+ J Dent Res 2007.

Acknowledgements: Grants AR041210, AR057139, DK091466 & DK081435



Figures

Disclosures: Karl J Lewis, None.

### FR0187

**Vitamin D regulates perilacunar remodeling and osteocyte survival in human and murine bone.** Tim Rolvien<sup>\*1</sup>, Björn Busse<sup>2</sup>, Klaus Püschel<sup>3</sup>, Matthias Krause<sup>4</sup>, Marie B. Demay<sup>5</sup>, Michael Amling<sup>2</sup>. <sup>1</sup>Department of Osteology & Biomechanics, University Medical Center Hamburg-Eppendorf, Hamburg, Germany, Germany, <sup>2</sup>Department of Osteology & Biomechanics, University Medical Center Hamburg-Eppendorf, Germany, <sup>3</sup>Department of Legal Medicine, University Medical Center Hamburg-Eppendorf, Hamburg, Germany, Germany, <sup>4</sup>Department of Trauma & Reconstructive Surgery, Asklepios Clinic St. Georg, Hamburg, Germany, Germany, <sup>5</sup>Endocrine Unit, Massachusetts General Hospital, Harvard Medical School, Boston, Massachusetts 02114, United states

Osteocytes are the most abundant bone cells and react precisely to external stimuli. Vitamin D and osteocytes cooperatively regulate bone remodeling as well as phosphate and calcium homeostasis. However it has been unclear how vitamin D affects osteocyte quantity, connectivity and size in the context of enhanced or diminished bone formation and mineralization.

60 iliac crest biopsies of patients with variable vitamin D levels were analyzed for osteocyte parameters, i.e. number of osteocytes per bone area (N.Ot/B.Ar), number of empty lacunae per bone area (N.Empt.Lc/B.Ar), lacunar area (Lc.Ar) or number of osteocyte canaliculi per osteocyte lacuna (N.Ot.Ca/Ot.Lc). The same parameters were also quantified in mice lacking the vitamin D receptor (*Vdr*<sup>-/-</sup>) compared to wildtype littermates (n=20). Methods included histology, histomorphometry, quantitative backscattered electron imaging (*qBEI*), acid etching and high-resolution  $\mu$ -CT.

Cortical and cancellous bone of patients with vitamin D deficiency exhibited a decreased number of viable osteocytes, whereas the number of empty lacunae was increased compared to non-deficient patients. Moreover, an impaired connectivity of osteocytes via canaliculi was detected in patients with vitamin D deficiency. Finally, increased osteoid indices in vitamin D deficient human bone correlate with increased osteocyte apoptosis, which could be due to premature aging inside the osteoid frame. In *Vdr*-deficient mice, osteocyte number was decreased compared to wildtype controls, and their osteocyte lacunae were enlarged. While a high calcium diet normalized the osteocyte lacunar area in *Vdr*-deficient mice, the number of osteocytes was still lower than in wildtype littermates.

The decreased osteocyte number in *Vdr*-deficient mice on both, a normal and a high calcium diet, suggests a mechanism that is directly dependent on the *Vdr* since, vitamin D may promote the transition from osteoblasts to osteocytes. Increased lacunar areas in *Vdr*-deficient mice support the osteocytic osteolysis theory, which explains their correction by the high calcium diet. Our study demonstrates that the diminished bone quality in vitamin D deficiency is associated with osteocyte deficiency and enhanced perilacunar remodeling.

Disclosures: Tim Rolvien, None.

### FR0196

**Trabecular bone score (TBS) reference values from all combination of lumbar vertebrae in dual-energy absorptiometry (DXA) from NHANES 2005-2008 multiethnic Survey.** Bo Fan<sup>\*</sup>, John Shepherd. University of California San Francisco, United states

TBS is tool to assess bone microarchitecture status from lumbar spine DXA scans. For any tool useful in the clinical practice, it is crucial to have normal reference data compare to for diagnosis diseases and monitoring the treatment progress. To date, US reference data for TBS have been limited to convenience and/or community-based samples. The construction of reference ranges that accurately represent the population at large is essential for the correct identification of fracture risk from TBS. Nationally representative reference data for TBS are lacking. The aims of the study were to develop sex-, race/Hispanic origin- and age-specific reference data for TBS with all the combination of vertebrae using NHANES population based data from 2005-2008. TBS data for 8388 participants age 20 years and older from NHANES 2005-2008 were downloaded from NHANES data website. The TBS scores were derived from re-analyzing Spine DXA scans using TBS iNsite<sup>®</sup> version 2.1 software (Med-Imaps, Pessac, France). LMS method was used to generate gender-, race/Hispanic origin - and age specific normative curves. General linear regression was used to test gender and race/Hispanic origin differences. 6766 (3586 male) participants with BMI value within 15-37 kg/m<sup>2</sup> and valid TBS scores for four lumbar vertebrae were included in the analysis. Table 1 shows the race/Hispanic origin distribution. Figure 1 shows the 50th (median) and 3rd centiles of race/Hispanic origin by age. The median as well as 3rd centiles of TBS decreased with age from 20 to 80+ in all groups. Figure 2 shows Non-Hispanic white female of all the vertebrae combination reference. There was no statistically significant difference in TBS between genders over all. Differences between race/Hispanic origin groups were modest, and varied with gender and these differences varied with age for male as well. Non-Hispanic White females had higher value than non-Hispanic black and Mexican American females and differences were fairly constant with age; larger differences were observed between blacks and whites of both sexes and the differences were more variable with age for male. All the combination of vertebrae references tracks well, however varied with combinations. The reference data presented here may be useful in assessing individual's fracture risk arising from a wide variety of conditions and chronic diseases. The race/Hispanic origin difference varies by age in males and needs further investigate.

Table 1: Race/Hispanic origin distribution by sex of the sample

Race/Hispanic Origin	Gender		Total
	Male	Female	
Mexican American	755	674	1429
Non-Hispanic White	2005	3775	5780
Non-Hispanic Black	826	731	1557
Total	3586	5180	8766

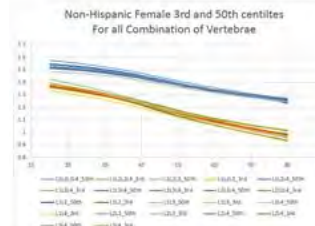


Figure 2: 3rd and 50th (Median) reference values of all combination of vertebrae for Non-Hispanic Female population

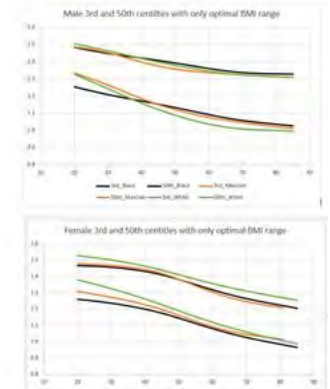


Figure 3: 3rd and 50th (Median) reference values of Black, Mexican and White for Male and Female population

Table and Figures

Disclosures: Bo Fan, None.

This study received funding from: The study was partially funded by Medimaps

### FR0204

**Accuracy of MRI-Based Measures of Bone Strength Compared to Direct Mechanical Testing.** Elizabeth A. Kobe<sup>\*</sup>, Olivia M. Teter, Michelle Slinger, Karyll Davis, Abigail Hong, Chamith S. Rajapakse, Felix W. Wehrli. University of Pennsylvania Perelman School of Medicine (Radiology), United states

It is now possible to non-invasively estimate bone strength at distal skeletal extremities in human subjects using MRI- or HR-pQCT-based finite element (FE) modeling. Although resolutions achievable by in-vivo bone imaging modalities are on the order of trabecular bone thickness, mechanical parameters estimated using MRI and HR-pQCT have been previously shown to correlate with those derived from high-resolution micro-CT images of cadaveric bone. The objective of this study was to validate MRI-based measures of bone strength by comparing to direct mechanical testing of bone specimens.

Human cadaver tibia specimens were sectioned into 20-mm thick segments 15mm proximal to the distal end plate from 13 male and 5 female donors aged 33-88 years. This segment, which corresponded to the in-vivo MRI scan region, was imaged on a clinical 3-Tesla scanner (Siemens Tim Trio, Erlangen, Germany) using a 3D fast large-angle spin echo (FLASE) pulse sequence with the same parameters used for patient

imaging (flip angle 140°, TR/TE 80/10.5 ms, and voxel size 0.137x0.137x0.410 mm<sup>3</sup>). After imaging the specimens were stored at -20°C until mechanical testing.

The acquired MR images were processed to generate a FE model. Simulated compression was applied to mimic loading conditions for standing. Using the simulated force-displacement curve, stiffness was calculated as the initial tangent, yield point was defined as the point at which plastic deformation occurs and was found using the 0.2% offset rule, and ultimate point was defined as the point of maximum force.

Specimens then underwent uniaxial compression tests at a displacement rate of 1mm/min using a servo-hydraulic material testing machine (MTS810, MTS, Minneapolis, MN). Stiffness, yield strength, and ultimate strength were calculated analogously to the approach described for the finite-element simulation above (Figure 1).

Correlation between the computationally-predicted stiffness and experimentally measured values was assessed. The analysis revealed a strong positive correlation between the experimental and computational stiffness values (R<sup>2</sup>=0.84; p < 0.0001) and a moderately strong positive correlation between the experimental and computational yield (R<sup>2</sup>=0.49; p=0.0006) and ultimate strengths (R<sup>2</sup>=0.52; p=0.0004), respectively.

The findings from this study support the use of MRI-based FE analysis to reliably predict the mechanical competence of distal extremities in human subjects in clinical settings.

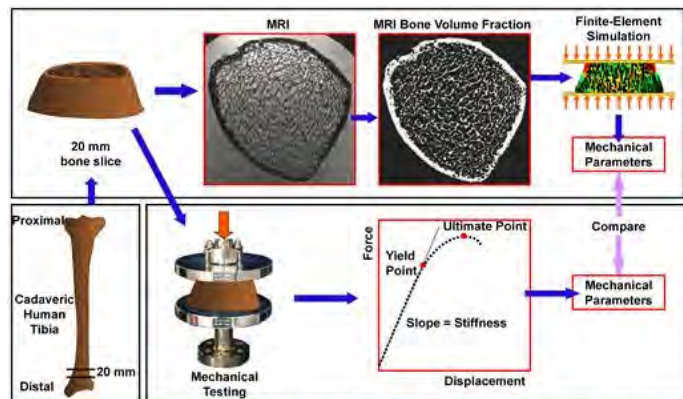


Figure 1: Schematic flowchart illustrating the ex-vivo validation of MRI-based assessment of mechanical parameters, including specimen preparation, MR imaging, finite element modeling, and mechanical testing.

Figure 1

Disclosures: Elizabeth A. Kobe, None.

FR0205

**Assessment of bone strength and cortical porosity in a group of premenopausal women with celiac disease after 3-years on gluten-free diet.** María Belen Zanchetta<sup>1</sup>, Vanessa Carla Longobardi<sup>\*1</sup>, Fernando Silveira<sup>2</sup>, Florencia Costa<sup>1</sup>, Cesar Bogado<sup>3</sup>, Julio Cesar Bai<sup>1</sup>, Jose R Zanchetta<sup>1</sup>. <sup>1</sup>MD, Argentina, <sup>2</sup>PH, Argentina, <sup>3</sup>PHD, Argentina

Previously we identified a significant deterioration of trabecular and cortical microarchitecture in peripheral bones of premenopausal women with recently diagnosed celiac disease (CD) using High Resolution peripheral Compute Tomography (HR-pQCT), where trabecular bone was the most impaired.

**Aim:** To assess bone strength and cortical porosity measured by HR-pQCT in CD women after 3-years on gluten-free diet (GFD) and to compare the results with a group of healthy women of similar age and BMI.

**Methods:** This study is part of a prospective design evaluating CD patients at diagnosis and yearly after GFD. In the 3<sup>rd</sup> year-visit, 24 premenopausal women were evaluated to assess bone strength and cortical porosity by HR-pQCT in addition to the standard test to assess bone health (DXA scans, lab test and clinical evaluation). We assessed cortical porosity, calculated as the percentage of void space in the cortex, and bone strength by microstructural finite element analysis (F.E.A) to calculate whole-bone stiffness and failure load (Scanco softwares). Results were compared with a control group of 18 healthy women of similar age and BMI who underwent the same procedures. Comparisons between groups were performed using unpaired T test or Wilcoxon Rank Sum according to data distribution.

**Results:** CD patients and healthy controls were comparable in terms of age, height, weight and BMI (p=NS). Results are shown in the table. The cortical compartment (density, thickness and porosity), did not reach statistical significance between groups. CD patients had lower stiffness and failure load at the radius (-14 %; p<0.01) and at the tibia an 8% lower although not statistically significant.

**Conclusions:** In this group of premenopausal women with celiac disease, despite 3 years on a gluten-free diet, bone strength in the radius is significantly lower compared to a control group of similar age and BMI. Prospective follow-up would enable us to assess the total extent of the recovery with treatment. -language:EN-US>CD patients and healthy controls were comparable in terms of age, height, weight and BMI (p=NS). Results are shown in the table. The cortical compartment (density, thickness and porosity), did not reach statistical significance between groups. CD patients had lower stiffness and failure load at the radius (-14 %; p<0.01) and at the tibia an 8% lower although not statistically significant.

**Conclusions:** In this group of premenopausal women with celiac disease, despite 3 years on a gluten-free diet, bone strength in the radius is significantly lower compared to a control group of similar age and BMI. Prospective follow-up would enable us to assess the total extent of the recovery with treatment.

**Assessment of Bone strength and Cortical Porosity in a group of premenopausal women with celiac disease after 3-years on gluten-free diet**  
Table. Comparison between women with celiac disease after 3-years on GFD and healthy controls (mean ± SD)

	Healthy control (n=18)	CD after 3-years GFD (n=24)	P
Age (years)	30.4 ± 5.6	33.7 ± 8.5	0.12
Height (m)	1.61 ± 0.07	1.59 ± 0.05	0.17
Weight (kg)	58.7 ± 7.7	61.9 ± 17	0.94
BMI (kg/m <sup>2</sup> )	22.6 ± 2.3	24.7 ± 6.8	0.58
<b>HR-pQCT Distal Radius</b>			
Stiffness (N/mm)	72549 ± 9052	62003 ± 9258 (-14.5%)	<0.01
Failure load (N)	3670 ± 482	3143 ± 464 (-14.3%)	<0.01
Cortical pore volume (%)	1.23 ± 5.66	1.01 ± 0.40	0.12
<b>HR-pQCT Distal tibia</b>			
Stiffness (N/mm)	186487 ± 25396	171802 ± 27378 (-8 %)	0.09
Failure load (N)	9466 ± 1262	8700 ± 1353 (-8%)	0.07
Cortical pore volume (%)	3.13 ± 1.41	2.97 ± 1.11	0.68

Table. Comparison between women with celiac disease after 3-years on GFD and healthy controls

Disclosures: Vanessa Carla Longobardi, None.

FR0216

**Weight Change in Men in Late Life and Bone Microarchitecture at the Distal Tibia.** Kristine Ensrud<sup>\*1</sup>, Tien Vo<sup>2</sup>, Lisa Langsetmo<sup>2</sup>, Andrew Burghardt<sup>3</sup>, John Schousboe<sup>2</sup>, Jane Cauley<sup>4</sup>, Sharmila Majumdar<sup>3</sup>, Brent Taylor<sup>1</sup>, Andrew Hoffman<sup>5</sup>, Eric Orwoll<sup>6</sup>. <sup>1</sup>University of Minnesota / VA Health Care System, United states, <sup>2</sup>University of Minnesota, United states, <sup>3</sup>University of California, United states, <sup>4</sup>University of Pittsburgh, United states, <sup>5</sup>Stanford University, United states, <sup>6</sup>Oregon Health & Science University, United states

Findings from previous studies suggest that older adults who experience weight loss have higher rates of bone loss and an increased risk of fracture at the hip. However, effects of weight loss in late life on compartment-specific bone mineral density (BMD) and bone microarchitecture are uncertain. To examine associations of weight change with compartmental BMD and microarchitecture at a weight-bearing site, we used data from 1507 men who attended the Year 14 exam of the MrOS study and had high resolution peripheral quantitative computed tomography (HRpQCT) scans of the distal tibia. Weight change from Year 7 to Year 14 exams (mean 7.2 years between exams) was classified as moderate weight loss (loss ≥10%), mild weight loss (loss 5% to <10%), stable weight (<5% change) or weight gain (gain ≥5%). Mean HRpQCT parameters (95%CI) were calculated by category of weight change using linear regression models. Base models were adjusted for age, race and site; multivariable models were further adjusted for health status, body mass index and physical activity level.

Mean age was 84.3 years; 211 men (14%) had moderate weight loss, 365 (24%) had mild weight loss, 813 (54%) had stable weight and 118 (8%) gained weight. In base and multivariable models (see Table), cortical BMD and thickness at the distal tibia were lower in a graded manner across weight change categories (p-trend <0.001 for both measures) with a 5% lower BMD and a 10% lower thickness among men with moderate weight loss compared to those with weight gain. In addition, cortical porosity was higher in a graded manner across weight change categories (p-trend 0.02) with an 11% higher porosity among men with moderate weight loss compared to those with weight gain. There were no differences in trabecular BMD and other trabecular parameters (trabecular bone volume fraction, trabecular number, trabecular thickness) across weight change categories. Estimated failure load was lower across weight change categories (p-trend <0.001) with a 6% lower estimated failure load among men with moderate weight loss compared to those with stable weight.

In conclusion, weight loss in men in late life is associated with detrimental effects on cortical (but not trabecular) BMD and microarchitecture at the distal tibia. These findings suggest that weight loss may be associated with an increased risk of fractures at weight-bearing sites due in part to lower cortical thickness and greater cortical porosity among men with weight loss.

Table. Mean Compartmental BMD and Bone Microarchitecture Parameters (95% CI) at Distal Tibia According to Weight Change Category

	Moderate Weight Loss (Loss ≥10%) (n=211)	Mild Weight Loss (Loss 5% to <10%) (n=365)	Stable Weight (Loss or Gain <5%) (n=813)	Weight Gain (Gain ≥5%) (n=118)	P for trend
Cortical BMD, mg/cm <sup>3</sup>	753.0 (742.9-763.1)	763.9 (756.3-771.5)	780.0 (774.9-785.1)	793.2 (780.0-806.5)	<0.001
Trabecular BMD, mg/cm <sup>3</sup>	182.5 (177.4-187.7)	182.1 (178.3-186.0)	183.2 (180.7-185.8)	178.1 (171.4-184.8)	0.71
Cortical Thickness, mm	1.39 (1.34-1.45)	1.46 (1.42-1.50)	1.51 (1.48-1.54)	1.53 (1.46-1.60)	<0.001
Cortical Porosity, %	4.5 (4.3-4.7)	4.3 (4.2-4.5)	4.3 (4.2-4.4)	4.0 (3.7-4.3)	0.02
FEA Estimated failure load, N	13044 (12654-13434)	13412 (13120-13704)	13890 (13634-14026)	13520 (13007-14033)	<0.001

\*Model adjusted for age, race, site, health status, body mass index and physical activity level

Table

Disclosures: Kristine Ensrud, None.

## FR0218

**Accelerated Bone Loss at the Hip: Association with Increased Risk of Subsequent Mortality in Older Men.** Peggy Cawthon<sup>1</sup>, Eric Orwoll<sup>\*2</sup>, Sheena Patel<sup>1</sup>, Susan Ewing<sup>3</sup>, Kristine Ensrud<sup>4</sup>, Jane Cauley<sup>5</sup>, Jennifer Lyons<sup>6</sup>, Lisa Fredman<sup>6</sup>, Deborah Kado<sup>7</sup>, Andrew Hoffman<sup>8</sup>. <sup>1</sup>California Pacific Medical Center Research Institute, United states, <sup>2</sup>Bone & Mineral Unit, Oregon Health & Science University, United states, <sup>3</sup>University of California San Francisco, United states, <sup>4</sup>University of Minnesota & Minneapolis VA Health Care System, United states, <sup>5</sup>University of Pittsburgh, United states, <sup>6</sup>Boston University School of Public Health, United states, <sup>7</sup>University of California San Diego, United states, <sup>8</sup>Stanford University & VA Palo Alto Health Care System, United states

Low bone mineral density (BMD) is associated with an increased risk of mortality in older adults. It also may lead to fractures, which in turn, increases the risk of mortality. While rapid bone loss is a risk factor for increased mortality in older women, few studies have been conducted in men. We hypothesized that a higher rate of bone loss is a marker for overall health decline and thus related to increased risk of mortality in older men.

Change in femoral neck BMD was assessed in 4,400 MrOS participants who had 2-3 repeat dual x-ray absorptiometry scans over an average of  $4.6 \pm 0.4$  SD years between the baseline and final BMD measure. Change in BMD was estimated using mixed effects models, and analyzed as a continuous variable. Men were also grouped into three categories of BMD change: *maintenance* [ $n=1087$ ; change  $\geq 0$  g/cm<sup>2</sup>]; *expected loss* [ $n=2768$ ; change between  $0$  g/cm<sup>2</sup> and  $>-1$  SD below mean change ( $>-0.034$  g/cm<sup>2</sup>)]; and *accelerated loss* [ $n=545$ ; change  $-1$  SD below mean change or worse ( $-0.034$  g/cm<sup>2</sup>)]. Multivariate proportional hazards models were used to estimate the risk of all-cause mortality over the  $8.1 \pm 2.8$  SD years that followed assessment of BMD change (see table footnote for adjustments). Mortality was centrally adjudicated by physician review of death certificates.

At baseline, the mean age of participants was 72.9 years (SD  $\pm 5.5$  yrs). The average BMD loss was  $-0.013 \pm 0.022$  SD g/cm<sup>2</sup> over 4.6 years. Men who maintained BMD were less likely to die during the subsequent follow-up period (33.7%) than men who had accelerated BMD loss (60.6%) ( $p < .001$ ). Compared to men who had maintained BMD, those who had accelerated BMD loss had a 1.44-fold increased risk of mortality in multivariate-adjusted models. (Table) When compared to men who had expected BMD loss, men with accelerated loss had an increased risk of mortality (multivariate HR: 1.43, 95%CI: 1.26-1.63). There was no significant difference in mortality risk between men who maintained BMD (33.7%) compared to men with expected loss of BMD (36.9%) (multivariate HR=1.00). Each 1 SD decrease in BMD change was associated with a subsequent 1.36-fold increased risk of mortality. Adjustment for baseline BMD or the final BMD level did not substantially alter results.

In conclusion, accelerated loss of femoral neck BMD is a risk factor for mortality in men that is not explained by concurrent change in weight or physical activity.

Table. Hazard ratios (95% confidence intervals) for mortality by change in femoral neck BMD among 4400 MrOS participants

BMD change category	Risk of all-cause mortality		
	Multivariate model	Multivariate model + baseline BMD	Multivariate model + final BMD
Maintenance	1.00 (reference)	1.00 (reference)	1.00 (reference)
Expected loss	1.00 (0.89, 1.13)	1.00 (0.88, 1.12)	0.96 (0.85, 1.09)
Accelerated loss	1.44 (1.23, 1.68)	1.44 (1.23, 1.68)	1.35 (1.15, 1.59)
Per SD decrease	1.36 (1.23, 1.51)	1.37 (1.23, 1.53)	1.33 (1.19, 1.48)

Multivariate models are adjusted for baseline age, clinic site, weight, physical activity, self-reported health, presence of at least one comorbid condition, smoking status, chair stands performance, concurrent change in weight, and concurrent change in self-reported physical activity.

Table\_ASBMRAbstract\_Cawthon

Disclosures: Eric Orwoll, None.

## FR0220

**Genome-Wide Association Study of DNA Methylation Identifies a Novel Locus Associated with Bone Mineral Density.** John Morris<sup>\*1</sup>, Pei-Chien Tsai<sup>2</sup>, Yi-Hsiang Hsu<sup>3</sup>, Roby Joehanes<sup>3</sup>, Jie Zheng<sup>4</sup>, Katerina Trajanoska<sup>5</sup>, Mette Soerensen<sup>6</sup>, Vincenzo Forgetta<sup>7</sup>, Kaare Christensen<sup>6</sup>, Lene Christiansen<sup>6</sup>, Tim Spector<sup>2</sup>, Fernando Rivadeneira<sup>5</sup>, Jonathan Tobias<sup>4</sup>, David Evans<sup>4</sup>, Douglas Kiel<sup>3</sup>, Brent Richards<sup>1</sup>, Jordana Bell<sup>2</sup>. <sup>1</sup>Department of Human Genetics, McGill University, Canada, <sup>2</sup>Department of Twin Research & Genetic Epidemiology, King's College London, United Kingdom, <sup>3</sup>Department of Medicine, Institute for Aging Research, Hebrew SeniorLife, BIDMC, & Harvard Medical School, United states, <sup>4</sup>MRC Integrative Epidemiology Unit, University of Bristol, United Kingdom, <sup>5</sup>Department of Epidemiology, Erasmus Medical Center, Netherlands, <sup>6</sup>The Danish Twin Registry, Epidemiology, Institute of Public Health, University of Southern Denmark, Denmark, <sup>7</sup>Centre for Clinical Epidemiology, Lady Davis Institute, Jewish General Hospital, McGill University, Canada

## Purpose

Genetic and environmental determinants of osteoporosis risk may converge through the epigenome, providing a tool to better understand the pathophysiology of osteoporosis. Since the epigenetics of bone mineral density (BMD) has been largely unexplored in humans, we undertook a comprehensive genome-wide assessment of the influence of epigenetic changes on BMD.

## Methods

We undertook an international, large-scale epigenome-wide association study of BMD using the Illumina Infinium HumanMethylation450 array to measure site-specific DNA methylation across four cohorts in up to 4,559 samples of European descent. Using these data, we aimed to identify differentially methylated probes (DMPs) associated with femoral neck and lumbar spine BMD. We used whole-blood since epigenetic changes are partially stable across tissues, immune cells may influence BMD, and some bone cells arise from monocyte-macrophage precursors. We performed sex-pooled and stratified analyses, controlling for age, weight, smoking status, sex (for pooled analyses), estimated white blood cell proportions, and random effects for relatedness and batch effects. We defined statistical significance of DMPs as being associated with BMD at a 1% false-discovery rate (FDR).

## Results

We identified one DMP significantly associated ( $P = 2.92 \times 10^{-10}$ ) with femoral neck BMD in females ( $N = 3,312$ ). The DMP maps to the liver carboxylesterase 1 (*CES1*) gene 5' UTR. The DMP is within a novel locus for bone biology as there are no previously identified genetic associations with BMD and *CES1*. Ongoing analyses aim to explore the tissue specificity of the signal across blood and additional tissues, and assess whether corresponding gene expression changes are observed. Further follow-up experiments to assess genetic interaction with the DMP, understand the sex-specificity of the association, and the function of DNA methylation and *CES1* with respect to BMD are underway. Results for sex-pooled and male-only analyses were not statistically significant.

## Conclusion

Undertaking the most comprehensive genome-wide analysis to-date for the role of whole-blood methylation in BMD, we identified a novel epigenetic locus for bone biology mapping to *CES1*. Interrogation of the function of this region will help to understand how environmental and genetic effects converge upon the epigenome to regulate BMD.

Disclosures: John Morris, None.

## FR0223

**Biochemical Markers of Inflammation Associated with Increased Mortality in Hip Fracture Patients.** Debbie Norring-Agerskov<sup>\*1</sup>, Lise Bathum<sup>1</sup>, Ole Vesteraager Pedersen<sup>2</sup>, Jes Bruun Lauritzen<sup>3</sup>, Henrik Jørgensen<sup>4</sup>, Niklas Rye Jørgensen<sup>5</sup>. <sup>1</sup>Department of Clinical Biochemistry, Hvidovre Hospital, University of Copenhagen, Denmark, <sup>2</sup>Department of Clinical Immunology, Næstved Sygehus, Denmark, <sup>3</sup>Department of Orthopaedic Surgery, Bispebjerg Hospital, University of Copenhagen, Denmark, <sup>4</sup>Department of Clinical Biochemistry, Bispebjerg Hospital, University of Copenhagen, Denmark, <sup>5</sup>Department of Clinical Biochemistry, Rigshospitalet Glostrup, University of Copenhagen, Denmark

Purpose: Hip fractures constitute a worldwide health problem and several studies have shown that hip fracture patients have an excess morbidity as well as mortality. Inflammatory blood markers could be of importance in predicting the outcome following a hip fracture and we therefore examined the relation of such markers taken at admission with mortality in these patients.

Methods: Since 2008, every hip fracture patient admitted to Bispebjerg Hospital, Denmark, has been registered in a Hip Fracture Database containing a variety of variables such as ID number, admission date, date of surgery etc. Furthermore,

biological material in the form of whole blood, serum and plasma has been collected on 749 patients at admission, constituting the biobank used in this study. Subsequently we analyzed serum levels of suPAR and plasma levels of transferrin, ferritin and iron. Plasma CRP was, however, measured at admission as part of the routine blood tests and was used as a reference from previous studies. Information about risk factors such as demographics, medication use and prior diseases was collected from Statistics Denmark.

The primary outcome was 30-days mortality. The association between the blood markers and mortality was examined using cox proportional hazards models. Hazard ratios (HR) were expressed per quartile increase.

Results: Data on plasma CRP at admission was only available for 398 patients due to later introduction of CRP to the set of routine blood tests. From the biobank, data was complete in 710 patients. Of these, 72 patients (10.2%) died within 1 month after sustaining a hip fracture (table 1). Serum SuPAR had the highest HR per quartile increase with an unadjusted HR of 1.9 (1.5 – 2.4) and a HR of 1.7 (1.4 – 2.2) after adjustment for age, sex and comorbidities. Plasma CRP and ferritin also showed increased risk with adjusted HRs of 1.5 (1.1 – 1.9) and 1.6 (1.3 – 2.0) respectively. The reverse applied for plasma transferrin: risk of death decreased as quartiles increased, adjusted HR 0.8 (0.6 – 0.9). There was no difference in mortality between the quartiles of plasma iron.

Conclusion: This study shows that 30-days mortality after a hip fracture is associated with the investigated inflammatory markers. Increase in SuPAR, CRP and ferritin and decrease in transferrin were related to 30-days mortality in hip fracture patients. Thus, the high mortality following a hip fracture might be related to an excessive inflammatory response.

Table 1. Baseline characteristics

	Hip fracture patients		p value
	Survived at 30 days	Died within 30 days	
N (%)	638 (89.8)	72 (10.2)	NA
Sex female, n (%)	455 (71.3)	45 (62.5)	0.1
Age (years), mean (SD)	80.0 (11.9)	85.3 (8.8)	<0.0001
CCI, median (range)	1 (0.0 12.0)	2 (0.0 9.0)	0.002
SuPAR, median (range)	2.6 (0.5 16.0)	3.8 (1.4 16.0)	<0.0001
CRP, median (range)	10.0 (3.0 230.0)	32.0 (10.0 294.0)	0.0002
Transferrin, median (range)	22.3 (8.8 40.5)	19.7 (8.5 36.8)	0.002
Ferritin, median (range)	220.5 (2.0 2000.0)	344.0 (27.0 2000.0)	<0.0001
Iron, median (range)	5.0 (1.0 47.0)	5.0 (2.0 25.0)	0.4

NA: Not applicable.

Table 1: Basic Characteristics

Disclosures: *Debbie Norring-Agerskov, None.*

## FR0224

**Fracture Risk After Bariatric Surgery: Roux-en-Y Gastric Bypass Versus Adjustable Gastric Banding.** Elaine Yu<sup>\*1</sup>, Moa Park<sup>2</sup>, Joan Landon<sup>2</sup>, Seoyoung Kim<sup>2</sup>. <sup>1</sup>Endocrine Unit, Massachusetts General Hospital, United states, <sup>2</sup>Division of Pharmacoepidemiology & Pharmacoeconomics, Brigham & Women's Hospital, United states

Purpose: The long-term consequences of bariatric (weight loss) surgeries on clinical fracture risk are unclear. Roux-en-Y gastric bypass is known to cause rapid post-surgical bone loss, whereas studies suggest that adjustable gastric banding has a relatively minimal effect on bone. We sought to compare fracture risk in adults after gastric bypass and gastric banding procedures.

Methods: Utilizing data from a U.S. commercial health plan from 2005-2013, we conducted a cohort study to examine the incidence rates (IRs) and risk of non-vertebral fracture (i.e. hip, humerus, forearm, and pelvis) among morbidly obese adults who underwent gastric bypass compared with gastric banding. Morbid obesity, bariatric surgery type, and fracture outcomes were based on a combination of diagnosis and procedure codes. To balance differences between the groups, we used 1:1 propensity score matching adjusting for demographics, index year, health care utilization intensity, comorbidities (e.g. diabetes, COPD, heart disease, fatty liver, hyperlipidemia, etc) and medications (e.g. oral glucocorticoids, SSRIs, PPIs, beta blockers, etc). A Cox proportional hazards model evaluated the risk of non-vertebral fractures in the gastric bypass group versus gastric banding.

Results: The matched cohort (n=15,168) was predominantly female (79%) with a mean ± SD age of 44 ± 11 years. During a mean follow-up time of 2.3 ± 1.9 years, a total of 296 non-vertebral fractures occurred. The estimated IR of nonvertebral fractures per 1000 person-years was 10.1 [95% confidence interval (CI) 8.7–11.7] among the gastric bypass patients and 7.1 (95% CI 6.0–8.5) among gastric banding patients. Gastric bypass patients had an increased risk of any nonvertebral fracture [hazard ratio (HR) = 1.4, 95% CI 1.1–1.8] and humerus fracture [HR = 1.8, 95% CI 1.1–3.1] compared with gastric banding patients. There was a trend for an increased risk of wrist fracture (Table). There did not appear to be an increased risk of hip fracture in gastric bypass patients as compared with gastric banding.

Conclusion: Gastric bypass is associated with a 42% increased risk of non-vertebral fracture compared with gastric banding. Fracture risk should be considered

in risk:benefit discussions of bariatric surgery, particularly among patients with high baseline risk of osteoporosis who are deciding between gastric bypass and gastric banding procedures.

Table. Cox Proportional Hazard Ratios of Non-vertebral Fracture by Fracture Site and Bariatric Surgery Procedure

Outcome	Group	Events	Hazard Ratio	95% Confidence Interval
Any Non-vertebral Fracture	Gastric Bypass	171	1.42	1.11 - 1.81
	Gastric Banding	125	reference	reference
Humerus Fracture	Gastric Bypass	41	1.83	1.07 - 3.13
	Gastric Banding	26	reference	reference
Wrist Fracture	Gastric Bypass	79	1.41	0.98 - 2.03
	Gastric Banding	56	reference	reference
Hip Fracture	Gastric Bypass	51	1.18	0.78 - 1.80
	Gastric Banding	43	reference	reference
Pelvic Fracture	Gastric Bypass	13	2.08	0.78 - 5.54
	Gastric Banding	7	reference	reference

Table

Disclosures: *Elaine Yu, None.*

## FR0225

**Fracture Risk Assessment In Long term care: FRAIL.** Sarah Berry<sup>\*1</sup>, Yoojin Lee<sup>2</sup>, Andrew Zullo<sup>2</sup>, Vincent Mor<sup>2</sup>, Kevin McConeghy<sup>2</sup>, Geetanjoli Banerjee<sup>2</sup>, Ralph D'Agostino<sup>3</sup>, Douglas Kiel<sup>1</sup>. <sup>1</sup>Hebrew SeniorLife & BIDMC, United states, <sup>2</sup>Brown University, United states, <sup>3</sup>Boston University, United states

Purpose: Nearly 10% of hip fractures (fx) in the U.S. occur among nursing home (NH) residents. Existing screening models are unlikely to perform well in the NH because risk factors differ in this setting. Having an appropriate screening model for NH residents is important to inform treatment decisions. We developed a model to predict 2-year risk of hip fx using readily available clinical information in a large sample of long-stay NH residents.

Methods: Medicare claims data was linked with the Minimum Data Set (MDS), a federally mandated assessment performed quarterly on all U.S. NH residents. We identified 1,418,943 residents with ≥ 100 days in the same facility between 5/2007 and 4/2008. The sample included residents aged ≥ 65 years without advanced dementia, and not prescribed an osteoporosis drug (n=719,567). A 2/3 random sample was selected to develop our model. Hip fx was defined using Medicare inpatient diagnostic codes. Information on 80 characteristics from 8 domains was obtained using the baseline MDS or prior Medicare claims. Residents were followed until the first event of hip fx, death, or censoring after 2-years. Competing risk regression was used. Characteristics associated with hip fx (p≤0.05) in bivariate models were entered into 8 domain models, with significant characteristics included in a composite model. We considered clinically plausible interactions. To assess model discrimination and generalizability, we calculated the C-index in men and women across all U.S. census divisions.

Results: In the derivation sample (n=419,668), mean age was 84 years and 71% were female. During followup, 3.5% experienced a hip fx, whereas 42.0% died without hip fx. In the composite model, 18 characteristics remained significant (Table). Falls and wandering were strong predictors of hip fx. Requiring total assistance with transfers was protective. No interactions were significant. The C-index was consistent in men and women across census divisions (mean=0.70, range 0.68-0.73). Model performance was similar in the remaining 1/3 validation sample (mean=0.71, range 0.68-0.75).

Conclusion: The FRAIL model is the first hip fx prediction model developed for the NH. It identifies a different pattern of risk factors compared with community models. This 2-year risk model offers good discrimination in men and women across regions. It is a practical tool that can identify NH residents at high risk of fracture who could potentially benefit from treatment.

Domain	Characteristic	Composite model HR (95%CI)
Demographics	Age (per 5 yrs)	1.03 (1.02, 1.04)
	Female	1.24 (1.19, 1.29)
	Race/ethnicity	
	White	REF
	Black	0.56 (0.53, 0.60)
	Hispanic	0.96 (0.85, 1.10)
Cognitive/Functional	Asian	0.63 (0.52, 0.78)
	Native American	1.20 (0.96, 1.51)
	Cognitive Performance Scale (per point increase)	1.03 (1.02, 1.04)
	ADL hierarchical scale	
	Independent or Mild Dependence	REF
	Moderate Dependence	1.01 (0.96, 1.06)
	Extensive Dependence	0.86 (0.81, 0.92)
	Total Dependence	0.74 (0.69, 0.81)
	Locomotion in Room	
	Independent	REF
	Limited Assistance	0.80 (0.76, 0.85)
	Extensive Assistance	0.69 (0.63, 0.75)
Falls and fracture	Total Assistance	0.48 (0.45, 0.52)
	Urinary continence	
	Continent or Mostly Continent	REF
	Mostly Incontinent	0.85 (0.81, 0.89)
	Always Incontinent	0.75 (0.71, 0.80)
	History of fall	1.29 (1.24, 1.33)
	Transfers	
	Independent	REF
	Limited Assistance	0.96 (0.90, 1.01)
	Extensive Assistance	0.76 (0.70, 0.82)
Neuropsychiatric	Total Assistance	0.60 (0.53, 0.67)
	Easily distracted	1.08 (1.03, 1.13)
Pain	Wandering	1.32 (1.26, 1.39)
	Arthritis	0.96 (0.93, 1.00)
Nutrition	BMI (per kg/m <sup>2</sup> )	0.95 (0.94, 0.95)
Co-morbidities	Diabetes mellitus	1.09 (1.05, 1.13)
	Medications	
Medications	Acetylcholinesterase inhibitors	1.10 (1.05, 1.14)
	Alpha blockers	0.90 (0.93, 0.97)
	Antianxiety/sedatives	1.11 (1.07, 1.14)
	SSRI antidepressants	1.10 (1.06, 1.14)

Abbreviations: HR-Hazard Ratio; CI-Confidence Intervals; ADL-Activities of Daily Living; BMI-Body Mass Index; SSRI-Selective Serotonin Reuptake Inhibitor

Table

Disclosures: Sarah Berry, Amgen, 11

### FR0227

**Vertebral Fractures have Similar Impact as hip Fractures on the Progression of Frailty.** Olga Gajic-Veljanoski<sup>1</sup>, Jonathan D. Adachi<sup>2</sup>, Courtney Kennedy<sup>3</sup>, George Ioannidis<sup>4</sup>, Claude Berger<sup>5</sup>, Andy Kin On Wong<sup>6</sup>, Kenneth Rockwood<sup>7</sup>, Susan Kirkland<sup>7</sup>, Parminder Raina<sup>8</sup>, Lehana Thabane<sup>8</sup>, Alexandra Papaioannou<sup>1</sup>, The CaMos Research Group<sup>5</sup>. <sup>1</sup>McMaster University & Hamilton Health Sciences/St. Peter's Hospital – GERAS Centre, Canada, <sup>2</sup>McMaster University & St. Joseph's Healthcare Hamilton, Canada, <sup>3</sup>Hamilton McMaster University & Health Sciences/St. Peter's Hospital - GERAS Centre, Canada, <sup>4</sup>McMaster University & Hamilton Health Sciences/St. Peter's Hospital – GERAS Centre, Canada, <sup>5</sup>Camos – McGill University, Canada, <sup>6</sup>University Health Network, Canada, <sup>7</sup>Dalhousie University, Canada, <sup>8</sup>McMaster University, Canada

Purpose: Clinical vertebral fractures (VF) significantly affect the risk of repeat fractures and mortality, but their impact on frailty is unknown. We explored the effects of incident vertebral, hip and other osteoporotic fractures on the progression of frailty.

Methods: Our cohort included participants of the Canadian Multicentre Osteoporosis Study (CaMos) aged 50 years and older, followed for 10 years (1996-2006). Frailty was assessed 3 times using the 30-item CaMos Frailty Index (CFI); an increase of 0.03 was considered clinically important. Incident low-trauma fractures were categorized by fracture site (hip, VF, nonhip-nonVF) or by fracture number. We developed 3 models (Model 1: whole sample; Model 2: participants without prior fracture; Model 3: those with prior fracture, Table) using generalized estimating equations and examined rates of change in frailty per 5 years after accounting for correlations between repeated measurements. The analyses were stratified by sex (when appropriate) and adjusted for age, prior fracture, body mass index (BMI), weight loss, physical activity, BMD (bone mineral density), antiresorptive therapy, and other risk factors for frailty or fractures. Multiple imputation and worst/best case scenarios addressed bias due to missing data and attrition.

Results: The cohort included 5566 women (mean age ± standard deviation: 66.8 ± 9.3 years) and 2187 men (66.3 ± 9.5 years) with 1206 and 368 prevalent low-trauma fractures, and mean baseline CFI scores of 0.15 ± 0.11 and 0.12 ± 0.10, respectively. Over 10 years, 893 new fractures occurred in women and 151 in men (% with hip fracture: 17.8 [women]/ 26.6 [men]; % with VF: 4.8 /10.9). The progression of frailty was affected by fracture site and was different between the sexes (Table). After an incident hip fracture versus no fracture, the adjusted CFI score significantly

increased by 0.07 in women (95% confidence interval [CI]: 0.03-0.11) and by 0.12 in men (95% CI: 0.08-0.16). An incident VF similarly increased the mean CFI by 0.05 in women (95% CI: 0.02-0.08) but not in men (0.01; 95% CI: -0.07-0.09). The rates of change remained stable in our sensitivity analyses.

Conclusions: Incident clinical vertebral fractures, in addition to hip fracture, significantly accelerate the progression of frailty, after adjusting for prior fractures. Preventing vertebral and hip fractures in women and men will alleviate the burden of frailty and will have long-term benefits on patient outcomes.

Table. Effects of incident low-trauma fractures\* by fracture skeletal site on the rate of change in frailty over 10 years in CaMos participants aged 50 years and older

Model Parameter	Model 1 <sup>a</sup> : CaMos participants with or without prior fracture (N=7753)		Model 2 <sup>a</sup> : CaMos participants without prior fracture (N=6162)		Model 3 <sup>a</sup> : With prior fracture (N=1574)
	Women	Men	Women	Men	Both Sexes
	Estimate <sup>b</sup> (95% CI)	Estimate <sup>b</sup> (95% CI)	Estimate <sup>b</sup> (95% CI)	Estimate <sup>b</sup> (95% CI)	Estimate <sup>b</sup> (95% CI)
Prevalent Fracture					
Non-hip-nonVF	0.003 (-0.01-0.01)	0.004 (-0.01-0.02)			0.01 (0.00-0.03) <sup>c</sup>
Clinical VF	-0.01 (-0.03-0.12)	0.04 (0.01-0.08) <sup>c</sup>			0.01 (-0.02-0.04)
Hip	0.03 (0.00-0.06) <sup>c</sup>	0.03 (-0.01-0.07)	NA	NA	0.04 (0.01-0.07) <sup>c</sup>
None	0.00 [reference]	0.00			0.00
Incident Fracture					
Non-hip-nonVF	0.01 (-0.00-0.03)	0.03 (-0.01-0.07)	0.02 (0.00-0.04) <sup>c</sup>	0.05 (0.00-0.10) <sup>c</sup>	0.002 (-0.03-0.03)
Clinical VF	0.05 (0.02-0.08) <sup>c</sup>	0.01 (-0.07-0.09)	0.06 (0.02-0.10) <sup>c</sup>	-0.02 (-0.05-0.01)	0.04 (-0.01-0.10)
Hip	0.07 (0.03-0.11) <sup>c</sup>	0.12 (0.08-0.16) <sup>c</sup>	0.07 (0.01-0.13) <sup>c</sup>	0.11 (0.06-0.16) <sup>c</sup>	0.07 (0.01-0.12) <sup>c</sup>
None	0.00 [reference]	0.00	0.00	0.00	0.00

\*Exclude head, finger and toe fractures. <sup>a</sup>Multivariable adjustments were made for: age, time (i.e., time point of the CaMos Frailty Index [CFI] measurement: baseline, 5 and 10 years), age\*time interaction, sex (Model 3 only), ethnicity, BMI, physical activity, sedentary lifestyle, total calcium and vitamin D intakes, MMSE score, SF-36 scores, education, smoking, alcohol consumption, employment history, living alone, BMD T score (femoral neck), antiresorptive treatment, history of falls, bed rest, and excessive weight loss (> 10 pounds in the last month). <sup>b</sup>Estimate denotes the mean change in the CFI score per 5 years; CI denotes confidence interval; VF denotes vertebral fracture. <sup>c</sup>p < 0.05.

Table

Disclosures: Olga Gajic-Veljanoski, None.

### FR0228

**Estrogen-Containing Contraceptives are Associated with Reduced Risk of Stress Fracture in Female Soldiers.** Kristin L. Popp<sup>1</sup>, Julie M. Hughes<sup>2</sup>, Craig J. McKinnon<sup>2</sup>, Kathryn E. Ackerman<sup>3</sup>, Joseph R. Kardouni<sup>2</sup>, Katelyn I. Guerriere<sup>2</sup>, Ronald W. Matheny, Jr.<sup>2</sup>, Mary L. Bouxsein<sup>4</sup>. <sup>1</sup>Endocrine Unit, Massachusetts General Hospital & Harvard Medical School, United states, <sup>2</sup>Military Performance Division, United States Army Research Institute of Environmental Medicine, United states, <sup>3</sup>Divisions of Sports Medicine & Endocrinology, Boston Children's Hospital, Endocrine Unit, Massachusetts General Hospital, & Harvard Medical School, United states, <sup>4</sup>Endocrine Unit, Massachusetts General Hospital, Harvard Medical School & Center for Advanced Orthopedic Studies, Beth Israel Deaconess Medical Center, Department of Orthopaedic Surgery, United states

Over 9,000 Soldiers are diagnosed with a stress fracture annually in the U.S. Armed Forces, costing the Department of Defense an estimated \$100 million. Female Soldiers have a 3- to 4-fold greater risk for stress fracture than their male counterparts. Due to positive effects of estrogen on bone metabolism in energy deficient and hypogonadal athletes, it has been suggested that hormonal contraceptives may reduce the risk of stress fracture (SF) in women. However, benefits of hormonal contraceptives on bone health remain controversial. Objective: We determined the association between hormonal contraceptive prescriptions and SF risk in U.S. Army Soldiers. Methods: We conducted a nested case control study using data from the Total Army Injury and Health Outcomes Database from 2002 to 2011. We identified female Soldiers who had SF at the lower extremity and pelvis (n=9,778; mean age 23.3 ± 5.6 yrs). Each Soldier with a SF was density matched by length of time in the military and race, with 4 controls (n=39,112; age 22.5 ± 5.3 yrs). We recorded contraceptive prescriptions within 6 months prior to SF diagnosis, and used conditional logistic regression to calculate rate ratios (RR) and 95% confidence intervals for SF with adjustment for age, ethnicity and education level. Results: Risk of SF was determined for Soldiers prescribed oral combination (estrogen and progestin, n=5,940), non-oral combination (estrogen and progestin, n=1,249), and progestin-only contraceptives (n=1,001). SF risk was 39% lower in those prescribed oral (RR=0.61, 95% CI [0.56, 0.066]) and 27% lower in those prescribed non-oral (RR=0.73, 95% CI [0.62, 0.85]) combination contraceptives. In contrast, for those prescribed progestin-only contraceptives, there was no statistically significant effect on SF risk (RR=0.89, 95% CI [0.75, 1.06]). A race-stratified analysis in Caucasian, Black and Asian Soldiers confirmed that the protective effect of estrogen-containing contraceptives is consistent across racial groups. Conclusion: This large study, with nearly 50,000 women, indicates that estrogen-containing contraceptives may reduce the risk of SF in female Soldiers. Prospective studies are needed to confirm these results and identify the mechanisms underlying this protective effect.

The views expressed in this abstract are those of the authors and do not reflect the official policy of the Department of Army, Department of Defense, or the U.S. Government.

Disclosures: Kristin L. Popp, None.

**FR0229**

**Pubertal timing predicts adult non-vertebral fracture risk in men – the BEST cohort.** Claes Ohlsson\*<sup>1</sup>, Maria Bygdell<sup>1</sup>, Liesbeth Vandenput<sup>1</sup>, Dan Mellström<sup>1</sup>, Arvid Sonden<sup>2</sup>, Jenny Kindblom<sup>1</sup>. <sup>1</sup>Center for Bone & Arthritis Research, Institute of Medicine, the Sahlgrenska Academy at Gothenburg University, Sweden, <sup>2</sup>Bioinformatics Core Facility, Sahlgrenska Academy at University of Gothenburg, Sweden

**Introduction:** Sex steroids are major regulators of bone mass acquisition during sexual maturation and late puberty results in low cortical volumetric BMD in young adult men. However, the role of variations within the normal range in pubertal timing for adult fractures risk is unknown in men. Age at Peak Height Velocity (PHV;  $\geq 2$  years after onset of puberty in boys) is an established method to objectively determine pubertal timing. We, herein, evaluated the association between age at PHV and adult non-vertebral fracture risk after 20 years of age in men.

**Methods:** Detailed growth data (height and weight) from centrally archived school health care records and mandatory military conscription tests were collected for all children born 1945 or later in Gothenburg (= the BMI Epidemiology Study, BEST; n=400,000). Age at PHV was calculated using the Infancy-Childhood-Puberty model. In the present study, all men born 1945-1961, with sufficient information on height for calculation of age at PHV and available personal identity number for linkage with high quality Swedish national disease registers, were included (31,567 out of 50,020 men fulfilled these criteria). Subjects were followed in the registers until December 2013. In total 3,924 men (12.4%) sustained at least one non-vertebral fracture after 20 years of age. The average follow-up time after 20 years of age was 35.5 years (In total 1,120,273 person-years follow-up). There was no loss in follow-up.

**Results:** Mean age at PHV was  $14.05 \pm 1.11$  years. Cox proportional hazard regression models adjusted for birth year revealed that age at PHV was directly associated with adult fracture risk ( $p < 0.001$ ). Inclusion of a quadratic term for age at PHV in the model revealed a non-linear association between age at PHV and adult fracture risk. Subjects with age at PHV in the highest quartile ( $> 14.8$  years) had a robustly increased risk of adult non-vertebral fractures compared with the subjects in the three other quartiles (Hazard Ratio, HR, 1.16, 95% CI 1.08-1.24; Q4 vs Q1-3). This association remained unchanged after further adjustment for birthweight, BMI at eight years of age, country of birth and adult educational level (HR 1.16, 95% CI 1.08-1.25 Q4 vs Q1-3).

**Conclusions:** Using the unique BEST cohort including men born as early as in 1945 and followed until December 2013, we provide compelling statistical evidence that late puberty is an independent predictor of increased adult non-vertebral fracture risk in men.

**Disclosures:** *Claes Ohlsson, None.*

**FR0230**

**The Effects of Cross-sex Hormonal Treatment in Transgender Persons on their Bone Mineral Density: a 1 year Prospective Observational Study.** Chantal Wiepjes\*, Mariska Vlot, Maartje Klaver, Paul Lips, Renate de Jongh, Annemieke Heijboer, Martin den Heijer. VU Medisch Centrum, Netherlands

**Introduction:** Estrogen has positive effects bone mineral density (BMD), in particular by inhibiting bone resorption. Testosterone increases bone size, but the effect on BMD is less clear. Cross-sex hormonal treatment (CHT) in transgender persons can affect BMD. Therefore, we aimed to investigate the first-year effects of CHT on BMD in male-to-female (MtFs) and female-to-male (FtMs) transgender persons.

**Methods:** This is a prospective observational study and part of the European Network for Investigation of Gender Incongruence. In 89 MtFs and 99 FtMs who completed one year CHT a dual-energy X-ray absorptiometry was performed to measure lumbar spine (LS) and total hip (TH) BMD before and after one year CHT. MtFs were treated with cyproterone acetate and oral or transdermal estradiol, FtMs received transdermal or intramuscular testosterone. Analyses were adjusted for change in tobacco use, alcohol use, and body weight, in order to investigate possible mediating factors, were stratified for age ( $< 50$  vs.  $\geq 50$  years), and reported as percentage mean increase (95%CI).

**Results:** In MtFs the mean LS and TH BMD increased with 3.71% (2.85, 4.59) and 1.52% (0.90, 2.14), respectively. Adjustments for change in tobacco or alcohol use did not alter the results. Only the TH BMD change attenuated to 1.18% (0.52, 1.83) after adjusting for change in body weight. The increase in LS and TH BMD did not differ between age groups (LS 3.72 vs. 3.67%, TH 1.51 vs. 1.61%).

In FtMs the mean LS BMD increased with 0.81% (0.07, 1.54). However, this increase was explained by an increase in BMD in persons  $\geq 50$  years (4.51% (1.53, 7.49), vs. 0.53% (-0.21, 1.26) in persons  $< 50$  years). The TH BMD increased with 0.91% (0.29, 1.53) and did not differ between age groups. The overall LS and TH BMD change increased after adjustment for tobacco and alcohol use (LS 1.13% (0.33, 1.94), TH 1.21% (0.55, 1.87)) and attenuated after adjustment for change in body weight (LS 0.45% (-0.34, 1.25), TH 0.57% (-0.09, 1.23)).

**Conclusion:** After one year CHT BMD increases in MtFs. In FtMs, the LS BMD increases only in postmenopausal biological women, indicating that the increase in BMD is mainly a result of the aromatization of testosterone to estradiol. The attenuation of BMD increase after adjustment for change in body weight might indicate that the increase in BMD is partially mediated by a positive effect of increase in body weight caused by CHT.

**Disclosures:** *Chantal Wiepjes, None.*

**FR0231**

**CHANGE IN BONE STRUCTURE WITH AGE AS ASSESSED BY PERIPHERAL QUANTITATIVE COMPUTED TOMOGRAPHY AND RELATIONSHIPS WITH MUSCLE IN OLDER MEN AND WOMEN.** Elaine Dennison\*, Kate Ward, Karen Jameson, Mark Edwards, Cyrus Cooper. MRC Lifecourse Epidemiology Unit, United Kingdom

**Objective:** Cross-sectional analyses have shown strong associations between muscle size and both bone geometry and strength. There is little data on the effect of muscle size on changes in bone structure over time. We investigated this using a well phenotyped cohort of older men and women.

**Methods and Methods:** We studied 194 men and 178 women from the Hertfordshire Cohort Study each of which underwent peripheral quantitative computed tomography (pQCT) of the radius (66%) and tibia (14%) in 2004-5 and then again in 2011-12. Percentage change per year was calculated for muscle cross-sectional area (CSA) and diaphyseal bone parameters (total area (Tt.Ar), cortical area (Ct.Ar), cortical density (Ct.BMD), and polar stress strain index (SSIP)).

**Results:** The mean(SD) age of men and women at baseline was 68.9 and 69.3 years respectively. Mean(SD) follow up time was 7.17(0.39)years. Tt.Ar increased with age and at a greater rate in men than women in the radius (median: men 1.53%/year, women 0.94%/year,  $p < 0.001$ ). In both the radius and tibia, Ct.Ar reduced more rapidly in women than men (radius median: men 0.17%/year, women 0.49%/year,  $p < 0.001$ ). Rates of muscle loss were similar in men and women (forearm: men 0.75%/year, women 0.71%/year  $p = 0.424$ ). In men, rate of loss of Ct.Ar was positively associated with rate of loss of muscle CSA ( $\beta$ (95%CI): radius 0.31(0.17,0.45)  $p < 0.001$ ; tibia 0.18(0.03,0.33),  $p < 0.05$ ). A similar trend was shown in women but did not reach significance. Baseline muscle CSA was not associated with the rate of change in Ct.Ar.

**Conclusion:** Changes in diaphyseal bone structure with age differ in men and women. In men, the rate of loss of Ct.Ar is associated with rate of loss of muscle CSA and not its baseline level. This suggests that interventions to maintain muscle mass may help to ameliorate the age-related deterioration in bone health.

**Disclosures:** *Elaine Dennison, None.*

**FR0232**

**Gender differences in proximal femur shape: findings from a population based study in adolescents.** Monika Frysz\*<sup>1</sup>, Denis Baird<sup>2</sup>, Jennifer S Gregory<sup>3</sup>, Rebecca J Bar<sup>3</sup>, Richard M Aspden<sup>3</sup>, Lavinia Paternoster<sup>1</sup>, Jon H Tobias<sup>2</sup>. <sup>1</sup>School of Social & Community Medicine, University of Bristol, UK; MRC Integrative Epidemiology Unit at the University of Bristol, UK, United Kingdom, <sup>2</sup>Musculoskeletal Research Unit, School of Clinical Sciences, University of Bristol, UK, United Kingdom, <sup>3</sup>Arthritis & Musculoskeletal Medicine, Institute of Medical Sciences, University of Aberdeen, UK, United Kingdom

**Aims**

Hip shape contributes to the risk of both hip osteoarthritis and hip fracture. Both disorders are commoner in women, but the contribution of gender differences in hip shape is unknown. To examine this question, we aimed to characterize gender differences in hip shape using Statistical Shape Modelling (SSM) in a large cohort of late adolescents, and determine whether differences which are present can be explained by those in body size and/or hip geometry.

**Methods**

Hip DXA scans were obtained in offspring from the Avon Longitudinal Study of Parents and Children, from which minimum femoral neck width (FNW) was derived using automated hip analysis software. To quantify hip morphology, the images were analyzed using Shape software (Aberdeen, UK) based on a 58-point SSM describing proximal femur shape including the acetabular eyebrow and lesser trochanter. Procrustes analysis was used to standardize scans in terms of size and rotation. Principal component analysis was used to generate independent modes of variation (hip shape mode (HSM) scores) for each image. We used linear regression to examine gender differences for the top ten HSMs, adjusting in turn for weight, height and FNW. Results are expressed as partial correlation coefficients with 95% confidence intervals.

**Results**

Data were available from 1937 males and 2459 females. Mean (SD) participant age was 17.8 (0.4) years. Despite size adjustment, overall hip shape showed males to have wider femoral neck compared with females. The first five hip shape modes, which together explained 68% variability, each showed strong evidence for gender differences ( $p < 0.001$ ). Three modes, HSM2, HSM3 and HSM5, were related to differences in body size and were attenuated towards the null following weight and height adjustment. The gender difference in HSM1 attenuated by 50% after further adjustment for FNW, though a strong association persisted [0.313 (0.222, 0.404)  $p < 0.001$ ]. HSM4 was independent of FNW and showed the strongest evidence of gender differences in our fully adjusted model [-0.704 (-0.796, -0.611)  $p < 0.001$ ].

**Conclusion**

Several components of hip shape show major gender differences. Whereas these are partly explained by differences in height, weight and FNW, certain differences are also present which are independent of gender differences in body size and hip geometry. These could play an as yet unrecognized role in predisposing to hip fracture and hip osteoarthritis in later life.

**Disclosures:** *Monika Frysz, None.*

**FR0233**

**High Risk of Second Fracture within 1, 2, 5 years after Prior Fracture among Women 65 years or Older.** Akhila Balasubramanian<sup>1</sup>, Jie Zhang<sup>2</sup>, Lang Chen<sup>2</sup>, Deborah Wenkert<sup>1</sup>, Shanette G Daigle<sup>2</sup>, Andreas Grauer<sup>1</sup>, Jeffrey R Curtis<sup>1,2</sup>.

<sup>1</sup>Amgen, United states, <sup>2</sup>University of Alabama at Birmingham, United states

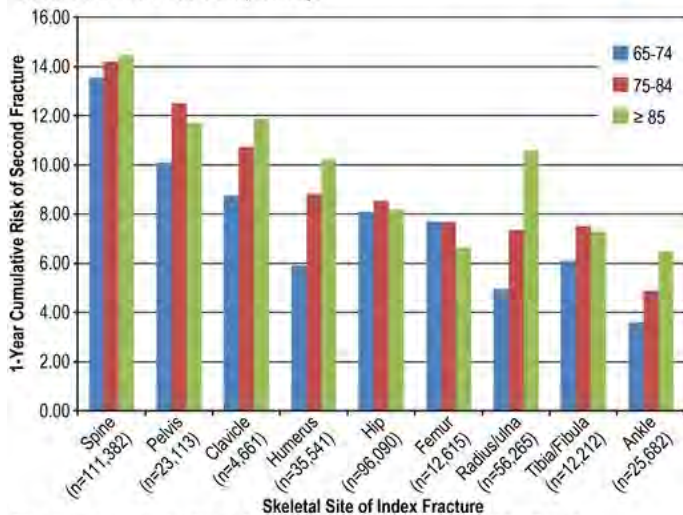
**Purpose:** Although prior fracture is an established risk factor for subsequent fracture, post-fracture treatment rates are low. Quantifying the 1, 2 and 5 year (yr) risk of a second fracture among older women may clarify the urgency of initiating intervention after a fracture.

**Methods:** This retrospective cohort study used claims data from Medicare, a public health plan that covers > 90% of US residents age ≥ 65 (100% sample from 2010-2012; 5% sample from 2006-2009). Eligible women were age ≥ 65 who sustained a fracture (index date) and were continuously enrolled for 1 year pre-index and ≥ 1 year (≥ 2 or ≥ 5 years for longer-term outcomes) post-index. Women with baseline claims for hospice care, cancer, or Page's disease; and those who died or had hospice claims within 30 days post-index were excluded. Eligible index and second fractures included closed fractures at any site other than face/skull/finger/toe. We calculated the cumulative incidence of another incident fracture from 30 days post-index to 1, 2, and 5 years post-index. Death was considered a competing risk.

**Results:** A total of 377561, 210621, and 10969 women with index fractures were assessed for risk of a second fracture at 1, 2, and 5 years post-index, respectively. Patient baseline characteristics were similar in these cohorts; mean age was approximately 81 yrs and approximately 88% were white. The cumulative risk of a second fracture was 9.8%, 17.9% and 30.9% at 1, 2, and 5 years post-index, respectively. Among patients age ≥ 75, 7-14% fractured again within 1 year following any type of initial fracture except ankle; the risk rose to 15-20% within 2 years following most types of index fractures and up to 25% following a vertebral fracture. For patients age 65-74, the risk of second fracture was 7-14% in the year following a fracture of the spine, hip, pelvis, femur, or clavicle; 5-6% following other index fractures except ankle. Corresponding 2-yr risk estimates were 15-25% and 10-12%, respectively.

**Conclusions:** This study, which included the vast majority of older women with fracture in the US for recent years, demonstrated that the risk of suffering a second fracture in the near-term (1-2 yrs) is high. Women with index fractures of the spine, hip, pelvis, femur or clavicle, and all women age ≥ 75 yrs were at particularly high risk despite a competing mortality risk, up to 25% at 2 years post-index fracture. Our findings highlight the need for timely post-fracture care among older women.

Risk of second fracture\* within 1 year following prior fracture in women age ≥ 65 years, by skeletal site of index fracture and patient age



\*The outcome is a composite of closed fractures at any skeletal site other than skull/face/fingers/toes

Figure

**Disclosures:** Jeffrey R Curtis, Janssen, 11; Amgen, 12; Crescendo, 11; Janssen, 12; Pfizer, 12; BMS, 12; Corrona, 11; BMS, 11; Rochel/Genentech, 12; Corrona, 12; Crescendo, 12; Pfizer, 11; Rochel/Genentech, 11; AbbVie, 11; Amgen, 11; UCB, 11; AbbVie, 12; UCB, 12  
This study received funding from: Amgen

**FR0234**

**Imminent Risk of Clinical Vertebral Fracture After Fracture (Reykjavik Study).**

Helena Johansson<sup>1</sup>, Kristin Siggeirsdóttir<sup>2</sup>, Nicholas C Harvey<sup>3</sup>, Anders Odén<sup>1</sup>, Vilmundur Gudnason<sup>2</sup>, Eugene McCloskey<sup>1</sup>, Gunnar Sigurdsson<sup>2</sup>, John Kanis<sup>1</sup>. <sup>1</sup>Centre for Metabolic Bone Diseases, University of Sheffield, United Kingdom, <sup>2</sup>Icelandic Heart Association, Kopavogur, Iceland, <sup>3</sup>MRC Lifecourse Epidemiology Unit, University of Southampton, United Kingdom

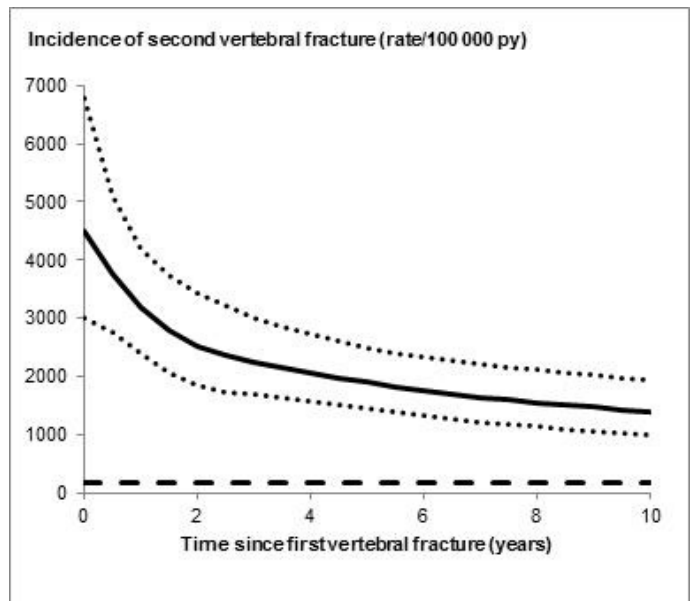
**Objectives** We aimed to determine whether the predictive value of a past clinical vertebral fracture for future vertebral fracture changed with time, hypothesizing that the predictive value would be greater for immediate compared with more distant events.

**Material and methods** We studied a population-based cohort of 18,872 men and women born between 1907 and 1935 who attended the Reykjavik Study during 1967–1991. Data on all fractures were extracted from participant entry into the study up to December 31, 2012. Where reports contained records of more than one fracture at the same site within 30 days, only the first fracture was included. 1365 patients experienced one or more clinical vertebral fracture and were included in the analysis of a second vertebral fracture. An extension of Poisson regression was used to investigate the relationship between the first and second fracture. All associations were adjusted for age and time since baseline.

**Results** 289 patients experienced a second clinical vertebral fracture. The risk of a second vertebral fracture after a first increased by 12% for each year of age (95% CI: 1.06-1.19) in the age span between 50 and 70 years and was 38% higher for women than men (95% CI: 1.03-1.86). The risk of a second vertebral fracture was greatest immediately after the first fracture and thereafter decreased with time though remained higher than the population risk throughout follow up (Figure). For example, 1 year after the first clinical vertebral fracture the risk of a second fracture was 16.8 (95% CI: 12.5-22.8) higher than the population risk. After 10 year this risk ratio was 7.4 (95% CI: 5.2-10.6).

**Conclusions** The risk of a clinical vertebral fracture after a first vertebral fracture was greatest immediately following the index event, with a declining, but still increased, risk in subsequent years. These results suggest that pharmacological approaches to secondary fracture prevention may be most usefully targeted during the period immediately following a first fracture.

Figure: Risk of a clinical vertebral fracture after a first vertebral fracture per 100 000 (95% CI). The dashed line is the risk of first vertebral fracture in the total population. The risk of vertebral fracture in the figure is for a woman 60 years of age.



Figure

**Disclosures:** Helena Johansson, None.

**FR0235**

**Kidney Function and Fracture Risk among Older Male Veterans.**

Rasheeda Hall<sup>1</sup>, Rick Sloane<sup>1</sup>, Robert Adler<sup>2</sup>, Kenneth Lyles<sup>1</sup>, Joanne LaFleur<sup>2</sup>, Cathleen Colon-Emeric<sup>1</sup>. <sup>1</sup>Duke University, United states, <sup>2</sup>Richmond VAMC, United states, <sup>3</sup>University of Utah, United states

**Background**

Older adults develop age-related decline in kidney function. We do not know if mild reductions in estimated glomerular filtration rate (eGFR) increases fracture risk, or the impact of competing mortality on CKD-related fracture risk in older adults.

**Methods**

Longitudinal national cohort using linked Veteran Affairs (VA) and Medicare administrative data including all males aged 65 and over with eGFR < 60 ml/min/1.73m<sup>2</sup> and an equal random sample of controls with normal renal function (n=712,917). eGFR was estimated with the Modification of Diet in Renal Disease equation using baseline creatinine values. Subjects were followed up to 10 years for clinical fracture and mortality. Association of baseline eGFR with fracture risk was evaluated with a Cox Proportional Hazards model and a competing risk model controlling for known fracture risk factors (race, body mass index, tobacco use, alcohol dependence, chronic steroid use, androgen deprivation therapy, rheumatoid arthritis, hyperthyroidism, diabetes, obstructive lung disease, chronic liver disease, and malabsorption). To account for time at risk for fracture prior to cohort entry, age was included in the model as a time scale.

**Results**

In this cohort, 356,459 Veterans had eGFR < 60 ml/min/1.73m<sup>2</sup>, of which 95.1% were classified as stage 3 CKD (eGFR 30-59), 4.3% stage 4 (15-29), and 0.6% stage 5 (<15). During follow-up, 12.0% experienced at least one fracture. Compared to Veterans with eGFR > 60 ml/min/1.73m<sup>2</sup>, unadjusted hazard ratios (95% CI) for fractures were 0.99 (0.98, 1.03), 1.41 (1.36, 1.47), and 2.10 (1.90, 2.31) for Veterans with

stage 3, 4, and 5 CKD respectively. The estimates for stage 4 and 5 were attenuated but remained significant and clinically important when competing mortality risk was considered. The eGFR impact was similar across all decades of age except for increased hazard of fracture in younger patients with CKD 5. Adjusting for known fracture risk factors slightly attenuated the HRs but did not alter the overall findings.

**Conclusion**

Among older male Veterans, eGFR < 30 increases fracture risk beyond known fracture risk factors, even accounting for differential mortality. Older Veterans with mild reductions in eGFR (30-59) may not experience an increase in fracture risk due to CKD.

**Disclosures:** Cathleen Colon-Emeric, None.

**FR0236**

**Lower TBS Score is a Risk Factor for Atypical Femur Fractures but not Independent of Duration of Antiresorptive Therapy.** Andy Kin On Wong<sup>\*1</sup>, K. Shawn Davison<sup>2</sup>, William D. Leslie<sup>3</sup>, Jonathan D. Adachi<sup>4</sup>, Jacques P. Brown<sup>5</sup>, Robert G. Josse<sup>6</sup>, Aliya Khan<sup>4</sup>, Angela M. Cheung<sup>1</sup>. <sup>1</sup>University Health Network, Canada, <sup>2</sup>University of Victoria, Canada, <sup>3</sup>University of Manitoba, Canada, <sup>4</sup>McMaster University, Canada, <sup>5</sup>Laval University, Canada, <sup>6</sup>St. Michael's Hospital, Canada

**Objectives:** To determine whether trabecular bone score (TBS) is associated with atypical femur fractures (AFFs). **Methods:** A cross-sectional analysis compared women with AFFs from the Ontario AFF Cohort Study with controls from two clinical studies. AFFs were ascertained by ASBMR task force criteria. Lumbar spine DXA scans were used to compute TBS across L1 to L4. Fractured vertebrae were excluded. 10-year fracture risk categories were determined by 2010 Osteoporosis Canada Guidelines. **Covariates:** age, height, weight, history of fragility fractures, parental hip fractures, glucocorticoids use, and duration of antiresorptive therapy were obtained. **Data analysis:** General linear models determined differences in TBS between different fracture risk groups and the AFF cohort, adjusting for covariates. Logistic regression provided odds ratios for AFFs per standard deviation (SD) decrease in TBS, adjusting for the same covariates. **Results:** Among 2906 women examined (69.3±10.4y old), those with AFFs (N=141) used antiresorptives for longer (10.4±6.1y vs. 1.7±3.0y) and 44.7% were Asian (1.7% for non-AFFs). TBS in the AFF group (least square mean: 1.269±0.011) was significantly lower compared to the low fracture risk group (1.307±0.003, p<0.001) but not to moderate (1.271±0.004) or high (1.250±0.007) fracture risk groups (Figure 1). Odds for AFFs were 1.24-fold higher (95% confidence interval: 1.01, 1.53) for every SD (0.108) decrease in TBS, and remained significant after accounting for age, height, weight and use of glucocorticoids. Further adjustment for duration of antiresorptive therapy attenuated this relationship (1.08(0.84, 1.38)), but was partly recovered if additionally accounting for lumbar spine BMD (1.18(0.89, 1.56)). Area under the ROC for the corresponding significant adjusted model was 0.559(0.513, 0.604). Among Asians, these associations were absent (N=109). Ethnicity played a significant role in TBS differences but DXA manufacturer did not contribute to models. **Conclusions:** Lower TBS is associated with AFFs, but this relationship is not independent of duration of antiresorptive therapy. Our previous investigation showing that larger trabecular separation at the distal tibia, as measured by high-resolution peripheral quantitative computed tomography, was associated with AFFs. The large degree of overlap in TBS distribution between AFFs and controls suggests that TBS cannot be used to screen for those at risk for AFFs.

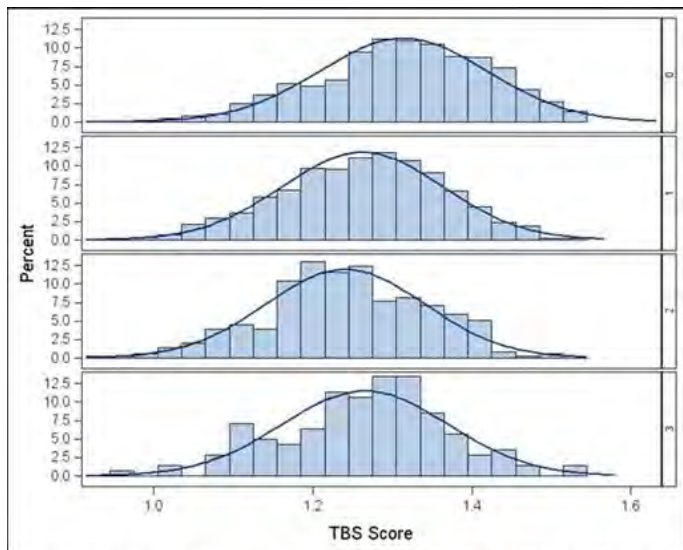


**Figure 1.** Distribution of TBS score in the AFF group as compared to low, moderate, and high fracture risk categories as defined by the 2010 Osteoporosis Clinical Guidelines (CAROC). Distributions were not adjusted for covariates.

Figure 1

**Disclosures:** Andy Kin On Wong, None.

**FR0237**

**Prediction of two-year risk of fracture among older US women.** Annette Adams<sup>\*1</sup>, Eric Johnson<sup>2</sup>, Hui Zhou<sup>1</sup>, Robert Platt<sup>3</sup>, Deborah Wenkert<sup>4</sup>, Steven Jacobsen<sup>1</sup>, Akhila Balasubramanian<sup>4</sup>. <sup>1</sup>Kaiser Permanente Southern California, United states, <sup>2</sup>The Center for Health Research, United states, <sup>3</sup>McGill University Health Center Research Institute, Canada, <sup>4</sup>Amgen Inc, United states

**Purpose:** Current algorithms for identifying patients at high risk of fracture focus on long-term risk. Physicians and their patients could benefit from a pragmatic prediction model to identify patients at imminent (12-24 months) risk of fracture to deliver timely care.

**Methods:** This retrospective cohort study included women ≥50 years who were members of Kaiser Permanente Southern California, a racially diverse, integrated healthcare delivery system in the United States. Using a randomly selected outpatient visit between 2008 and 2012 as the index date, we followed women for up to two years for the occurrence of closed fracture at any site other than skull/face/fingers/toes. After identifying candidate predictor characteristics recorded in the electronic healthcare databases, we developed a pragmatic model to predict 2-year fracture risk using Cox regression.

**Results:** Our cohort included 332,598 women with mean±sd age 62.6±10.56 years; 6,343 women had fractures for a two-year cumulative incidence of 1.9%. Our full prediction model evaluated 27 candidate predictors; the strongest predictors (hazard ratios ≥2.0) were age, history of fracture in 12 months prior to baseline ("recent fracture"), and bone mineral density (BMD) T-score. After applying a step-down selection method, the final model included 10 predictors: age, race/ethnicity, body mass index, BMD T-score, recent fracture, fall risk, alcoholism, chronic obstructive pulmonary disease, gastrointestinal disorder, and use of antidepressant medications. This model explained 97% of the variance explained by the full model, and discriminated risk effectively (c-statistic = 0.78). Patients in the top decile of predicted risk suffered a higher risk of fracture (8.6%) than patients in the bottom decile (0.3%). The observed risks of fracture agreed closely with the predicted risks across all deciles. Patients in the top decile had a mean predicted risk ≥9.6% and accounted for 44.9% of all fractures. They had mean age 82.0±7.19 years, mean BMD T-score -2.98±0.95, and 7.8% had a recent fracture; in the bottom decile these estimates were 52.8±3.66 years, -0.65±0.90, and 0%, respectively.

**Conclusion:** Our data suggest that 10 predictors routinely collected in an electronic health record can estimate the imminent risk of fracture in a diverse cohort of women. Patient age, recent fracture history and BMD were the strongest of these predictors. Future work will evaluate its external validity and clinical utility.

**Table:** Hazard Ratios Estimating Effect on 2-year Fracture Risk of Predictors in Final Reduced Model

Predictor	N	HR (95% CI)
Age		**
Race/Ethnicity		
White	187,469	1.00
Asian	25,675	0.52 (0.46, 0.60)
Black	24,474	0.49 (0.43, 0.57)
Hispanic	73,461	0.79 (0.74, 0.85)
Other	21,519	0.57 (0.49, 0.68)
BMD Status <sup>1</sup>		
Normal	11,489	1.00
Low bone mass	32,834	1.98 (1.59, 2.46)
Osteoporosis	24,266	2.86 (2.31, 3.54)
History of fracture within 12 months pre-index		
No	326,966	1.00
Yes	5,632	3.06 (2.78, 3.38)
Fall Risk Assessment Tool (FRAT) score		
0	171,666	1.00
1	130,982	1.38 (1.30, 1.47)
≥2	29,950	1.79 (1.66, 1.94)
Alcoholism <sup>2</sup>		
No	326,982	1.00
Yes	5,616	1.83 (1.60, 2.10)
Chronic obstructive pulmonary disease		
No	326,966	1.00
Yes	5,632	1.30 (1.22, 1.38)
Gastrointestinal disorder <sup>3</sup>		
No	321,513	1.00
Yes	11,085	1.44 (1.32, 1.58)
Antidepressant use		
No	270,826	1.00
Yes	61,772	1.28 (1.21, 1.36)
BMI		**

\*\*Age and BMI were modeled using restricted cubic splines. Age had 5 knots at the following percentiles: 5, 27.5, 50, 72.5, and 95. BMI had 3 knots at the 10th, 50th, and 90th percentiles. This method does not give a summary hazard ratio and CI per unit increase.

<sup>1</sup>BMD status was unknown for 264,009 (79%) patients

<sup>2</sup>Alcoholism – ICD-9 codes 291.x, 303.x, 305.x, V11.3.

<sup>3</sup>Gastrointestinal disorder – ICD-9 codes for: ulcerative colitis (556.x), celiac disease (579.0), inflammatory bowel disease (555.x, 556.x), gastric bypass/gastroectomy (V45.86), Crohn's disease (555.x), malnutrition (260, 261, 262, 263.0, 263.1, 263.8, 263.9, 579.3, 648.9x, 995.84), intestinal malabsorption (579.0, 579.1, 579.3, 579.4, 579.8, 579.9), anorexia (307.1, 783.0), and cachexia (799.4).

Table 1

**Disclosures:** Annette Adams, Amgen Inc, 11; Otsuka, 11; Merck, 11  
This study received funding from: Amgen Inc.

**FR0240**

**Impact of Frailty on Health Care Services Use among Non-institutionalized Quebec Seniors with Non-hip Fracture: a Population-based Study using Administrative Databases.** Vanessa Fillion<sup>1</sup>, Marie-Josée Sirois<sup>1</sup>, Suzanne N Morin<sup>2</sup>, Philippe Gamache<sup>3</sup>, Sonia Jean<sup>\*3</sup>. <sup>1</sup>Laval University, Canada, <sup>2</sup>McGill University, Canada, <sup>3</sup>INSPQ, Canada

**Purpose:** The number of frail elderly is likely to increase as the population ageing accelerates. Since frail elders are at risk of falls, hospitalization and disabilities, they

are likely to require more health care and services. The aim of this study consists to examine the impact of frailty on the use of emergency department (ED) visits and visits to a general practitioner (GP) among non-institutionalized seniors who sustained a non-hip fracture.

Methods: A retrospective population-based cohort study was performed with the use of linked healthcare administrative databases from the province of Quebec, Canada. All non-institutionalized seniors (≥65 years) who sustained a non-hip fracture between January 1, 1997 and December 31, 2012 were identified with a validated algorithm based on physicians' claims databases (sensitivity >80%). Their frailty status was measured using the Elderly Risk Assessment index (ERA index). Univariate Poisson regression analyses were used to describe the use of ED visits and visits to a GP one year post-fracture according to frailty status. Multivariate analysis were performed to adjust for confounding variables (age, sex, site of fracture, level of healthcare service consumption before the fracture, number of comorbidities, material and social deprivation index).

Results: The study cohort includes 179,734 seniors ≥ 65 years old (mean age 76.3 years, 74% women), non-institutionalized in the year before the fracture. According to the ERA index, the proportions of seniors in the cohort considered as frail (frailty score >16) and non-frail (frailty score -7 to -1) were, respectively, 13% and 4.7%. In the year following the fracture, the mean number of ED visits and the mean number of visits to a GP increased rapidly with the frailty score (Table 1). Our regression analyses show that, in the year following the fracture, the number of ED visits and the number of visits to a GP were significantly higher in frail elderly comparatively to non-frail seniors [adjusted relative risk of 2.95 (95% CI: 2.83-3.08) for ED visits and 1.24 (95% CI: 1.21-1.28) for visits to a GP].

Conclusions: This study suggests that frail seniors with a minor fracture require more healthcare services after their incident fracture than non-frail seniors. Furthermore, using a frailty assessment index in healthcare administrative databases can help identify seniors that are at high risk of needing more health services and, therefore, improve their care.

	Number of emergency department visits <sup>1</sup>			Number of visits to a general practitioner <sup>2</sup>		
	Mean (Median; Q1-Q3)	Non-adjusted Relative risk (95% CI)	Adjusted <sup>2</sup> Relative risk (95% CI)	Mean (Median; Q1-Q3)	Non-adjusted Relative risk (95% CI)	Adjusted <sup>2</sup> Relative risk (95% CI)
All	7.47 (3; 9-9)	NA	NA	17.4 (12; 5-22)	NA	NA
Frailty score:						
-7 to -1 (non-frail)	3.1 (0; 0-4)	1.00	1.00	10.4 (7; 3-13)	1.00	1.00
0 to 3	4.0 (1; 0-5)	1.19 (1.15-1.23)	1.12 (1.08-1.16)	14.0 (10; 4-18)	1.27 (1.24-1.29)	1.17 (1.15-1.20)
4 to 8	6.6 (3; 0-8)	1.81 (1.75-1.87)	1.50 (1.44-1.55)	19.1 (13; 6-24)	1.57 (1.54-1.61)	1.32 (1.29-1.35)
9 to 15	10.3 (6; 1-13)	2.79 (2.70-2.89)	2.20 (2.12-2.29)	20.1 (14; 6-26)	1.63 (1.59-1.66)	1.29 (1.26-1.32)
16+ (frail)	16.2 (10; 4-20)	4.25 (4.10-4.41)	2.95 (2.83-3.08)	22.0 (15; 6-29)	1.74 (1.69-1.78)	1.24 (1.21-1.28)

<sup>1</sup> Visits during hospitalization were excluded.  
<sup>2</sup> Adjusted age, sex, site of fracture, level of healthcare service consumption before the fracture, number of comorbidities, material and social deprivation index.

Table

Disclosures: *Sonia Jean, None.*

## FR0245

**The Activating Patients at Risk for Osteoporosis (APROPOS) Study: a Randomized Trial within the GLOW Cohort.** Maria Danila<sup>1\*</sup>, Ryan Outman<sup>1</sup>, Elizabeth Rahn<sup>1</sup>, Amy Mudano<sup>1</sup>, David Redden<sup>1</sup>, Peng Li<sup>1</sup>, Fred Anderson<sup>2</sup>, Jeffrey Curtis<sup>1</sup>, Susan Greenspan<sup>3</sup>, Andrea LaCroix<sup>4</sup>, Michael Miller<sup>5</sup>, Jeri Nieves<sup>6</sup>, Stuart Silverman<sup>7</sup>, Amy Warriner<sup>1</sup>, Nelson Watts<sup>8</sup>, Nicole Wright<sup>1</sup>, Kenneth Saag<sup>1</sup>. <sup>1</sup>The University of Alabama at Birmingham, United states, <sup>2</sup>University of Massachusetts Medical School, United states, <sup>3</sup>University of Pittsburgh, United states, <sup>4</sup>University of California San Diego, United states, <sup>5</sup>University of Oklahoma, United states, <sup>6</sup>Helen Hayes Hospital, United states, <sup>7</sup>Cedars Sinai Hospital, United states, <sup>8</sup>Merck Health, United states

Purpose: To improve the rate of osteoporosis medication use in women with a prior fracture we developed and implemented a tailored, educational, direct-to-patient video intervention to provide information about reducing fracture risk with osteoporosis medications.

Methods: We conducted a controlled, randomized clinical trial of our novel intervention among US women in the GLOW cohort with self-reported fracture history who were not currently using osteoporosis therapy. The primary outcome at 6 months follow-up was self-report of osteoporosis medication use. Secondary outcomes included self-reported use of calcium and vitamin D supplementation and bone density testing. Missing data were treated with multiple imputation and the outcomes (proportions) were compared by chi square test using intent-to-treat analysis.

Results: We randomized 2684 women to receive the intervention materials or usual care. Study participants were 92.6% Caucasian, with a mean (SD) age 74.9 (8.0) years, had some college education (76.7%), in good health (84.6%), and a self-reported lower than average risk for osteoporosis (40.0%). In the 12 months prior to randomization, 1390 women reported talking with their doctor regarding osteoporosis, 7.4% reported a fracture, vitamin D or calcium supplementation were reported as 83.5% and 68.6%, respectively. We observed no differences in sociodemographic characteristics and no significant differences in the primary (11.7% vs 11.4%) and secondary (calcium, 31.8% vs 32.6%; vitamin D, 41.3% vs 41.9%; bone density, 61.8% vs 57.1%) end points

between the intervention and usual care groups. Exploratory post-hoc analyses demonstrated that women in the intervention arm had more favorable views towards osteoporosis medications compared with the usual care arm and a lower proportion were in the unaware and uninvolved stages of behavior change regarding osteoporosis medications (64.1% vs. 68.8%, raw p=0.028). We found that barriers to treatment were higher in the intervention, as compared to usual care arm at 6 months: concerns regarding osteonecrosis of the jaw (28.9% vs 24.6%, raw p=0.031) and difficulty in taking/remembering to take osteoporosis medications (22.0% vs 18.1%, raw p=0.03).

Conclusion: This randomized study testing a novel, personalized educational intervention, did not increase the use of osteoporosis therapy at 6 months. The intervention appeared to have influenced participants' readiness for behavior change.

Disclosures: *Maria Danila, None.*

## FR0247

**Calcium and Vitamin D Supplementation Leads to Greater Improvements in Trabecular Bone Microarchitecture in Young Adults undergoing Initial Military Training.** Erin Gaffney-Stomberg<sup>1\*</sup>, Katelyn Guerriere<sup>1</sup>, Sonya Cable<sup>2</sup>, Mary Bouxsein<sup>3</sup>, Julie Hughes<sup>1</sup>, James McClung<sup>1</sup>. <sup>1</sup>USARIEM, United states, <sup>2</sup>WAMC, United states, <sup>3</sup>Harvard Medical School, United states

There is a high incidence of stress fracture during initial military training (IMT). Previous studies demonstrated that daily supplemental Ca (2000 mg/d) and vitamin D (vit D; 800-1000 IU/d) throughout IMT reduced stress fracture incidence, maintained PTH, and increased distal tibia vBMD compared to placebo. In this study, we determined the effects of a lower dose of Ca (1000 mg) along with vit D (1000 IU) on changes in bone metabolism and microarchitecture during IMT. Volunteers (n=50 male, n=50 female) were block randomized by race and sex to receive a Ca and vit D fortified or placebo snack bar (135 kcal) daily throughout 9 wk of IMT. Serum bone turnover markers, 25OHD, dietary intake, and HR-pQCT scans of the tibia (61µm<sup>3</sup> voxel size, XtremeCT2, Scanco Medical) were collected at the start and end of IMT. Data were analyzed using linear mixed modeling with time and treatment as the fixed factors and subject IDs as random effects (SPSS, v21). Race and sex were only included if the model fit improved based on Akaike's Information Criterion. Mean compliance was >98% in both groups. There were no group differences in baseline dietary Ca and vit D; however total Ca (1965 ± 438 vs. 1066 ± 478 mg/d, p<0.001) and vit D intakes (1151 ± 129 vs. 199 ± 143 IU/d, p<0.001) during IMT were higher in the treatment group compared to placebo. CTX (p<0.05) and iCa (p<0.01) increased, whereas PTH decreased (p<0.05), irrespective of treatment. A time-by-group interaction (p=0.01) was observed for 25OHD only when race was included in the model; 25OHD increased significantly more in the Ca and vit D group (10.5 ng/ml, p<0.001) compared to placebo (5.5 ng/ml, p<0.001). Total vBMD (1.68 ± 2.63%, p<0.001), trabecular (Tb) vBMD (1.89 ± 3.20%, p<0.001) and cortical vBMD (0.95 ± 1.71, p<0.001) increased, while Tb separation decreased (-1.16 ± 3.01%, p<0.001) similarly in both groups. However, both TbBV/TV (3.93 ± 4.32% vs. 2.33 ± 3.38) and Tb thickness (8.52 ± 4.73% vs. 4.83 ± 4.91%) increased significantly more (time-by-group, p<0.01) in the Ca and vit D group compared to placebo (p<0.001 all such). Taken together, these data support intakes of Ca and vit D above the dietary reference intakes (1000 mg and 600 IU, respectively) to optimize bone adaptation to IMT and possibly reduce stress fracture risk.

The views expressed in this abstract are those of the authors and do not reflect the official policy of the Department of Army, Department of Defense, or the U.S. Government.

	% Change (mean ± SD)		Statistical Effects (p-value)	
	Placebo	Ca and Vit D	Time	Time*Group
Total vBMD	1.71 ± 2.34	1.65 ± 2.94	<0.001	0.99
Tb. vBMD	1.88 ± 2.96	1.91 ± 3.48	<0.001	0.73
Tb.BV/TV	2.33 ± 3.38	3.93 ± 4.32	<0.001	0.01
Tb. Number	0.76 ± 3.57	0.65 ± 4.54	0.15	0.83
Tb. Thickness	4.83 ± 4.91	8.52 ± 4.73	<0.001	<0.001
Tb. Separation	-1.00 ± 2.55	-1.31 ± 3.46	<0.001	0.55
Cortical vBMD	1.02 ± 1.59	0.88 ± 1.84	<0.001	0.12

table

Disclosures: *Erin Gaffney-Stomberg, None.*

## FR0250

**Effects of Low-fat Dairy Foods on Bone and Body Composition, Lipid Profile and Pro-inflammatory Markers in Overweight/Obese Women During the Weight Loss Regimen.** Ashley Carter<sup>1\*</sup>, Pei-Yang Liu<sup>2</sup>, HyeHyung Shin<sup>3</sup>, Youjin Kim<sup>4</sup>, Jasminka Ilich<sup>1</sup>. <sup>1</sup>Florida State University, United states, <sup>2</sup>University of Akron, United states, <sup>3</sup>Samsung Life Insurance, Korea, democratic people's republic of, <sup>4</sup>The State University of New Jersey, United states

Recent research shows that adiposity could have a damaging effect on bone and metabolic profile, depending on the amount and distribution of fat in body. Weight-loss regimens are being employed with various success rates. Our objective was to investigate whether weight loss could be achieved easier and with better outcomes, using calcium (Ca) supplements or low-fat dairy products, each as a complement to

the underlying hypocaloric diet. We investigated changes in: a) bone and body composition; b) visceral fat in android/gynoid regions and; c) lipid profile and pro-inflammatory markers in blood.

A total of n=97 overweight/obese Caucasian early postmenopausal women completed the 6 months follow-up and had complete data-sets. They were divided in 3 groups: 1) Supplement (630 mg Ca+400 IU vitamin D/day); 2) Dairy (low-fat dairy consumption, 4-5 servings/day); and 3) Control (placebo). Each included moderate energy restriction (~85% of energy needs). Bone and body composition of total body and android/gynoid regions was measured by Lunar iDXA. Serum glucose, insulin, lipids (cholesterol, triglycerides, LDL, HDL), as well as Apo A1, Apo B, and CRP were analyzed in fasting blood samples by commercially available ELISA kits.

Overall, the participants lost 4.0% of body weight and 3.5% of body fat. The difference among the groups was significant, with the highest decrease in weight, BMI, android/gynoid and total body fat in Dairy group, compared to Supplement and Control group. The loss of android and total body lean mass was significantly lower in Dairy group compared to other two. There was no change in total body BMD. There was improvement in each measured blood parameter, probably due to weight loss, except in glucose, HDL and Apo A which remained the same. Dairy group showed the highest decrease in total cholesterol and LDL (6.1% and 7.7%), respectively, compared to Supplement (3.2% and 3.4%) and Control (3.8% and 1.7%) groups. Apo B decreased in Dairy group only.

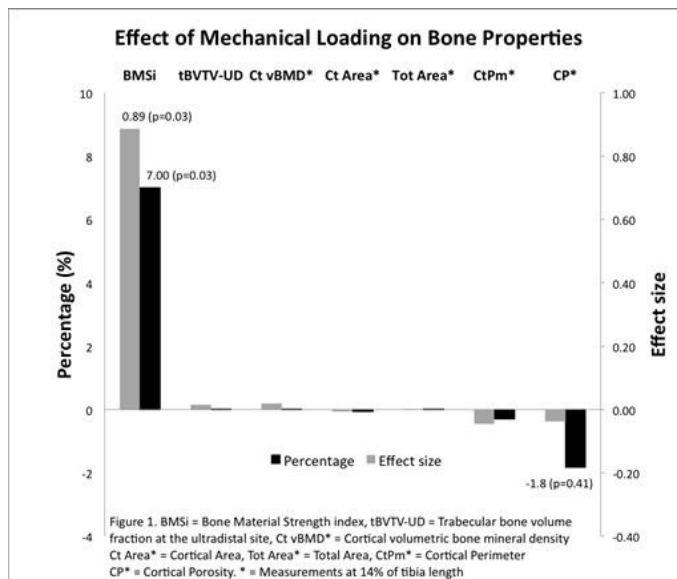
In conclusion, the hypocaloric treatments with increased Ca intake either via low-fat dairy foods or via Ca supplements was associated with greater weight reduction toward a healthier body composition and better lipid profile, with the best outcomes in a low-fat Dairy group. Increasing low-fat dairy foods to 4-5 servings per day may be beneficial for weight loss/maintenance and lead to more favorable body composition and metabolic profile in postmenopausal women.

**Disclosures:** Ashley Carter, None.

## FR0251

**High Impact Mechanical Loading Increases Bone Material Strength – Results from a 3-Month Intervention Study.** Daniel Sundh\*, Mattias Lorentzon, Martin Nilsson, Michail Zoulakis, Martin Hellgren. Geriatric Medicine, Department of Internal Medicine & Clinical Nutrition, Institute of Medicine, University of Gothenburg, Gothenburg, Sweden, Sweden

Bone has several ways of adapting to loading, including redistributing bone mass, altered geometry and microarchitecture, but these effects usually require interventions with longer duration, typically over at least 6 months. Due to previous methodological limitations it is not known how bone material properties are affected by loading in humans. The aim of the present study was to investigate the effect of 3-month unilateral high impact exercise program on bone material properties and bone microarchitecture in healthy postmenopausal women. A total of 20 healthy and physically inactive, postmenopausal women ( $55.6 \pm 2.3$  years (mean  $\pm$  standard deviation (SD))) were included and asked to perform an exercise program of daily one-legged jumps (with incremental number, from 3x10 to 4x20 jumps/day) during three months. All participants were asked to register their performed jumps in a structured diary. The participants were instructed to jump and land on the back of the foot without mitigating the shock in order to increase the impact and loading on the leg. The included women chose one leg as intervention leg and the other leg was used as control. The operators were blinded to participant's choice of leg for intervention. The predefined primary outcome was change in bone material strength index (BMSi), measured with a handheld reference probe indentation instrument (Osteoprobe®, Active Life Scientific) at the mid tibia. Bone microarchitecture was measured with high-resolution peripheral quantitative computed tomography (XtremeCT, Scanco Medical) at the ultradistal and at 14% of the bone length (distal). Differences were analyzed by paired samples t-test. The overall compliance to the jumping program was 93.6%. Relative to the control leg, BMSi of the intervention leg increased 7% or 0.89 SD ( $p=0.03$ ) during the study. No difference was seen for cortical porosity ( $-0.04\%$ ;  $p=0.41$ ) or any other XtremeCT assessed bone parameters at the distal or ultradistal tibia (Figure 1). In conclusion, unilateral high impact loading increased bone material strength in postmenopausal women without affecting any XtremeCT obtained bone parameters, indicating that intense mechanical loading has the ability to rapidly improve bone material properties which strengthens the bone prior to any increases in bone mass.



Effect of Mechanical Loading on Bone Properties

**Disclosures:** Daniel Sundh, None.

## FR0252

**High Intensity Progressive Resistance Training for Postmenopausal Women with Low to Very Low Bone Mass: The LIFTMOR Trial.** Steven Watson\*<sup>1</sup>, Benjamin Weeks<sup>1</sup>, Lisa Weis<sup>2</sup>, Amy Harding<sup>1</sup>, Sean Horan<sup>1</sup>, Belinda Beck<sup>1</sup>. <sup>1</sup>School of Allied Health Sciences & Menzies Health Institute Queensland, Griffith University, Gold Coast, Australia, Australia, <sup>2</sup>The Bone Clinic, Brisbane, Australia, Australia

**Introduction:** The ability of bone to respond to a mechanical stimulus is highly dependent on the nature of the applied load. Few load cycles inducing high-magnitude strains at high rates is the most osteogenic protocol. In fact, fewer than 6 repetitions of >85% 1 repetition maximum is required to improve bone mass. This protocol has not traditionally been recommended for individuals with osteoporosis owing to a perceived increased risk of fracture. The purpose of the LIFTMOR trial is to determine the safety and efficacy of brief but high intensity progressive resistance training (HiPRT) to reduce risk of osteoporotic fracture in postmenopausal women with low bone mass.

**Methods:** Postmenopausal women with low bone mass (T-score <-1.0, screened for conditions and medications that influence bone and physical function) were recruited. Participants were randomized to either 8 months of twice-weekly, 30-minute, supervised HiPRT or a home-based, low intensity exercise (CON) program. Functional performance related to risk of fracture (timed up-and-go, functional reach, 5-times-sit-to-stand, back extensor strength and leg extensor strength), physical activity enjoyment (PACES), as well as whole body, lumbar spine and proximal femur BMD, muscle and fat mass (DXA) were measured. Compliance and adverse events were monitored. Treatment effects were examined with repeated measures ANOVA, using an intention-to-treat approach.

**Results:** Seventy-five women ( $67 \pm 6$  years,  $161.7 \pm 6.0$  cm,  $63.0 \pm 10.5$  kg, T-score  $-2.1 \pm 0.8$ ) were enrolled. HiPRT (n=37) improved LS BMD ( $+2.7 \pm 3.2\%$  vs  $-1.3 \pm 2.5\%$ ,  $p<0.001$ ), FN BMD ( $-0.24 \pm 2.3\%$  vs  $-1.5 \pm 2.5\%$ ,  $p=0.028$ ), height ( $+0.2 \pm 0.6$  cm vs  $-0.2 \pm 0.5$  cm,  $p=0.002$ ) and physical activity enjoyment ( $+3.4 \pm 5.7$  vs  $-1.1 \pm 6.5$ ,  $p=0.002$ ) compared to CON (n=38). HiPRT improved all functional performance measures compared to CON ( $p<0.05$ ). No between-group effect was observed for weight, lean or fat mass, although both groups lost fat (HiPRT,  $-2.0 \pm 0.8$  kg,  $p=0.015$ ; CON,  $-1.9 \pm 0.8$  kg,  $p=0.021$ ). Compliance was high (HiPRT,  $89 \pm 11\%$ ; CON,  $84 \pm 27\%$ ) and no adverse events were observed in either group.

**Discussion:** Findings indicate that brief, supervised HiPRT provides a more positive stimulus to bone and functional indices of fracture risk than low intensity exercise. Despite perceived risks, HiPRT is a safe, efficient and enjoyable therapeutic option for postmenopausal women with low bone mass.

**Disclosures:** Steven Watson, None.

## FR0258

**LGG and VSL#3 Probiotics Prevent Ovariectomy Induced Bone Loss and Induce Bone Anabolism in Normal Mice by Decreasing Gut Permeability and Inducing Wnt10b Production.** Jau-Yi Li<sup>1</sup>, Abdul Malik Tyagi<sup>1</sup>, Emory Hsu<sup>1</sup>, Marcelo Steiner<sup>1</sup>, Jonathan Adams<sup>1</sup>, Rheinallt Jones<sup>2</sup>, Roberto Pacifici<sup>1</sup>. <sup>1</sup>Emory University, School of Medicine, United states, <sup>2</sup>Department of Pediatrics, Emory University, United states

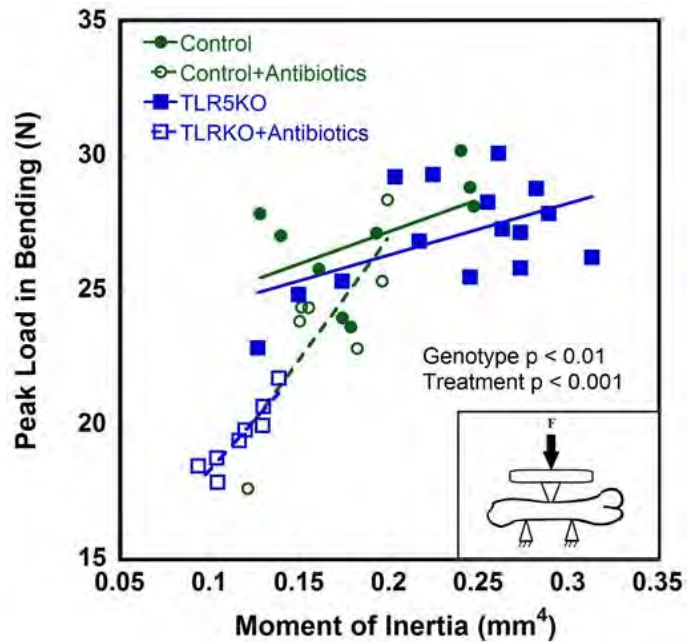
Probiotics, which are defined as viable microorganisms that confer a health benefit, prevent ovariectomy (ovx) induced bone loss, but their mechanism of action remains unknown. To investigate this matter, 10-week-old mice were ovx or sham operated and treated for 4 weeks with vehicle or the probiotics *L. rhamnosus* GG (LGG) and VSL#3 (1 X 10<sup>9</sup> total bacteria twice weekly). Control treatments included vehicle, a strain of *E. coli* not exerting a probiotic effect, and LGG pili mutant (LGGM), a strain lacking epithelial adhesion. In a second experiment, LGG and VSL#3 were administered to intact 16 week old mice for 8 weeks. In vivo and in vitro  $\mu$ CT measurements revealed that LGG or VSL#3 completely prevented the increase in bone resorption and the loss of spinal and femoral bone volume (BV/TV) induced by ovx. LGGM was only partially effective and *E. Coli* did not prevent bone loss. Moreover, LGG or VSL#3 induced a significant increase in bone formation and BV/TV when fed to intact mice, while *E. Coli* and LGGM did not. These effects required the adherence of probiotics to the intestinal wall. We also found that ovx increases gut permeability by decreasing the gut epithelial tight junction proteins Claudin 2, 3, 15, and of the junction adhesion molecule Jam3. Increased gut permeability causes enhanced production of the inflammatory/osteoclastogenic factors RANKL, TNF and IL-17 in the intestine and the bone marrow. Treatment with LGG and VSL#3 (but not *E. Coli* and LGGM) normalized epithelial tight junction proteins thus preventing the detrimental effects of ovx on gut permeability and cytokine production in the gut and the bone marrow. Mechanistic studies of the bone anabolic activity of probiotics in intact mice revealed that LGG and VSL#3 increase stromal cell commitment to the osteoblastic lineage and osteoblast differentiation by activating Wnt signaling. This effect was secondary to increased production of the osteogenic Wnt ligand Wnt10b. In summary, administration of probiotics capable of adhering to the intestinal wall prevents the increase in gut permeability induced by estrogen deficiency, thereby dampening the ensuing osteoclastogenic immune cell response. In addition, in estrogen replete mice LGG and VSL#3 increase bone formation and bone mass by stimulating osteoblastogenesis via the Wnt10b/Wnt signaling pathway. Probiotics supplementation may thus represent an effective therapeutic strategy for the prevention and treatment of postmenopausal bone loss.

Disclosures: Jau-Yi Li, None.

## FR0259

**The Gut Microbiome Influences Bone Strength and Regulates Differences in Bone Biomechanical Phenotype Among Inbred Mouse Strains.** Jason Guss<sup>1</sup>, Michael Horsfield<sup>1</sup>, Fernanda Fontenele<sup>1</sup>, Taylor Sandoval<sup>1</sup>, Marysol Luna<sup>1</sup>, Fnu Apoorva<sup>1</sup>, Svetlana Lima<sup>1</sup>, Rodrigo Bicalho<sup>1</sup>, Marjolein van der Meulen<sup>1</sup>, Ankur Singh<sup>1</sup>, Ruth Ley<sup>1</sup>, Steven Goldring<sup>2</sup>, Christopher Hernandez<sup>1</sup>. <sup>1</sup>Cornell University, United states, <sup>2</sup>Hospital for Special Surgery, United states

The gut microbiome influence a number of conditions that alter bone structure and strength including obesity, diabetes, and inflammatory bowel disease. There are conflicting data regarding the effect of the microbiome on bone. Some studies suggest the absence of the microbiome increases bone mass [1] while others suggest that it decreases bone mass [2,3]. Here we test the idea that alterations in the gut microbiome modify bone mechanical properties by comparing the skeletal phenotype in wild type C57BL/6J mice and C57BL/6J mice deficient in toll-like receptor 5 (TLR5KO). TLR5 is an innate immune receptor for flagellin, and TLR5KO mice show an altered gut microbiome [4]. The effect of disruption of the microbiome on bone phenotype in each strain was determined by comparing animals treated with antibiotics from 4-16 weeks of age (1 g/L ampicillin, 0.5 g/L neomycin in drinking water) to untreated animals (n = 7-15/group, 39 animals total). Treatment shifted the gut microbiota composition from one dominated by the phylum Bacteroidetes to one dominated by Proteobacteria. Treatment was associated with reduced femoral bone strength in bending (Fig. 1). Reductions in strength caused by treatment could not be explained by alterations in bone morphology (differences between solid and dashed regression lines,  $p < 0.001$ ), suggesting that treatment impaired bone tissue material properties. In untreated mice, there were small differences in strength between the WT and TLR5KO that could not be explained by bone morphology (solid regression lines differ,  $p < 0.01$ ). Differences between mouse strains were eliminated by treatment (dashed lines similar). Femoral geometry did not differ among groups after accounting for body mass. Changes in bone biomechanical phenotype were correlated with alterations in splenic immune cell populations; TLR5KO mice had depleted B cell populations ( $p < 0.001$ ), and antibiotic treated mice had reductions in both B and T cell populations ( $p < 0.001$ ), suggesting that alterations in bone biomechanical phenotype may reflect modulation of the immune system by the gut flora. We conclude that changes in the gut microbiome can change bone mechanical properties by altering tissue material properties. Additionally, differences in bone biomechanical phenotype among mouse strains can depend on the presence and content of the gut microbiome. [1]Sjogren, K+, JBMR 2012 [2]Schepper, J+, ASBMR 2015 [3]Schwarzer, M+, Science 2016 [4]Vijay-Kumar, M+, Science 2010



Moment of Inertia vs. Peak Load in Bending

Disclosures: Jason Guss, None.

## FR0260

**Delayed bone healing in type 1 diabetic rats is ameliorated by insulin treatment.** Ariane Zamarioli<sup>1</sup>, Francisco de Paula<sup>1</sup>, Maysa Campos<sup>1</sup>, Raquel Silva<sup>2</sup>, José Volpon<sup>1</sup>. <sup>1</sup>School of Medicine of Ribeirão Preto, Brazil, <sup>2</sup>School of Dentistry of Ribeirão Preto, Brazil

We assessed the effect of metabolic control on microstructural changes during fracture healing in diabetic rats. Thirty-eight female Wistar rats weighing approximately 200g were divided into three groups: (1) CON: weight-matched control rats, n=11; (2) DM: type 1 diabetic rats, n=13 and; (3) DM+INS: diabetic rats treated with insulin, n=14. DM and DM+INS rats received a single intravenous injection with streptozotocin to induce diabetes. Control rats were injected with citrate buffer alone. Diabetes was diagnosed based on blood glucose concentrations ( $\geq 250$  mg/dL on two consecutive days). Rats from group DM+INS received daily insulin treatment to control blood glucose concentration below 200 mg/dL. Thirty days after diabetes induction (or buffer injection), the animals were anesthetized, and a closed bone fracture was produced in the right mid-femur. Then a surgical procedure with a 1-mm-diameter Kirschner wire was conducted for bone fragments stabilization. The status of the fracture was radiographically confirmed immediately after surgery and then followed-up weekly. Twelve rats either died or were excluded from the study (CON: 2 died during anaesthesia; DM: 2 were not diagnosed with diabetes and, 2 were excluded due to highly comminuted fracture; DM+INS: 2 were not diagnosed with diabetes, 2 were not successfully treated with insulin and, 2 died during anaesthesia). On day 14 post-surgery, twenty-six rats were killed, blood was collected for serum bone markers analysis and, the femurs were harvested in preparation for DXA assessment,  $\mu$ CT, and histological analysis. Bone callus was analyzed by calculating BMD and callus volume and by histological images. Poorly controlled glucose (DM rats without treatment) leads to dramatic changes in bone healing; with a deficit of 60% in callus volume and 40% in mineralization. Circulating level of IGF-1 was significantly reduced in these animals (-70%). On the other hand, the administration of insulin mitigates the deleterious effects of diabetes by accelerating bone callus formation not only in volume but also in bone density and ossification, which may be explained by an increase of 107% in circulating IGF-1 associated with a 47% reduction in circulating RANK-L. We concluded that poor diabetes control has detrimental effects on bone healing. However, insulin treatment not only improves the metabolic control, it restores the serum levels of IGF-I and RANK-L, creating condition for adequate fracture repair.

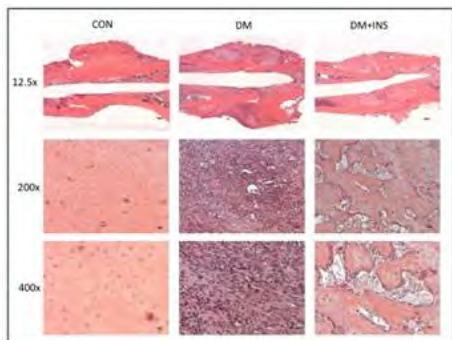


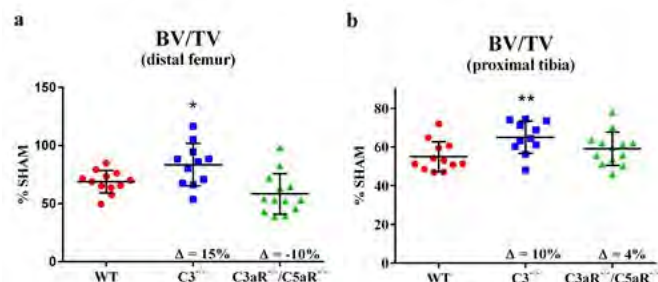
Figure 1. Histological assessment of bone healing.

Disclosures: Ariane Zamarioli, None.

## FR0261

**Different Effects of Absence of Complement Component 3 and Anaphylatoxin Receptors on Tissue-Level Properties of Bone.** Danielle MacKay<sup>1</sup>, Thomas Kean<sup>1</sup>, Kristina Bernardi<sup>2</sup>, Heather Haeberle<sup>3</sup>, Catherine Ambrose<sup>4</sup>, Feng Lin<sup>5</sup>, James Dennis<sup>1</sup>. <sup>1</sup>Baylor College of Medicine, United states, <sup>2</sup>Seattle Children's Hospital, United states, <sup>3</sup>University of Texas, United states, <sup>4</sup>University of Texas Health Science Center at Houston, United states, <sup>5</sup>Cleveland Clinic Lerner Research Institute, United states

The past two decades have brought a major shift in our concept of the interactions between bone and the immune system. Substantial *in vitro* data show that the complement cascade of innate immunity, widely recognized for its pathogen-lysing capacity, also plays a significant role in bone biology. To our knowledge, we are one of only two groups that has reported on the *in vivo* role of complement component 3 (C3) in bone homeostasis within a model of postmenopausal osteoporosis. We have shown improved mechanical properties at the femoral neck of ovariectomized C3<sup>-/-</sup> mice (C3<sup>-/-</sup> OVX) in association with a reduction in tissue-level bone loss at both the distal femur and the proximal tibia. Here, we investigate the mechanism behind these results with corresponding analyses in mice lacking the receptors for the C3- and C5-derived anaphylatoxins, C3aR and C5aR (C3aR<sup>-/-</sup>/C5aR<sup>-/-</sup>) after OVX. Data were generated using micro-CT, histomorphometry, and mechanical testing. Mice were bred and housed in accordance with the guidelines of the ACUC of Benaroya Research Institute. At 6 weeks of age, OVX or sham surgeries were performed under isoflurane anesthesia. At 12 weeks, animals were euthanized for tissue harvest. Data are presented as a percentage of the mean sham-operated value  $\pm$  S.D. Significance versus WT control was calculated by unpaired Student's t-test. Micro-CT at the distal femur and proximal tibia showed that C3aR<sup>-/-</sup>/C5aR<sup>-/-</sup> OVX does not recapitulate the diminished tissue-level bone loss seen in C3<sup>-/-</sup> OVX (a,b). Interestingly, osteoblast activity in both C3<sup>-/-</sup> OVX and C3aR<sup>-/-</sup>/C5aR<sup>-/-</sup> OVX is increased over that of WT. These findings suggest that anaphylatoxin signaling through cognate receptors is not the singular mechanism by which C3 contributes to bone loss at ovariectomy.



Trabecular bone loss at the distal femur and proximal tibia is greater in WT and C3aR<sup>-/-</sup>/C5aR<sup>-/-</sup>.

Disclosures: Danielle MacKay, None.

## FR0263

**S-Allylmercapto-N-Acetylcysteine Modulates Stromal Bone Marrow Cells and Bone Structure in Adult Healthy and Diabetic Mice.** Naphtali Savion<sup>\*</sup>, Reem Abu-Kheit, Shlomo Kotev-Emeth, Yankel Gabet. Sackler Faculty of Medicine, Tel Aviv University, Israel

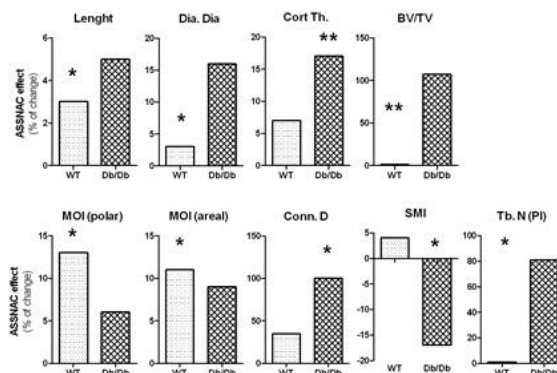
Oxidative stress is suggested to play a major role in reduced bone quality and strength in both adult healthy and diabetic mice. The aim of the study was to test the ability of S-allylmercapto-N-acetylcysteine (ASSNAC), an activator of nuclear factor-erythroid 2-related factor-2 (Nrf2), to increase the protection of bone marrow (BM)

cells from diabetes-associated glycated albumin-induced oxidative stress and to improve bone microarchitecture, quality and strength in adult healthy and diabetic mice.

The protective effect of ASSNAC from glycated albumin cytotoxicity was studied in cultured rat stromal BM cells (SBMC). The *in vivo* effect of ASSNAC (50 mg/kg/day) was tested in healthy and diabetic (C57BLKS/J Leprdb<sup>+/+</sup>) female mice by daily i.p. injection at the age of 12 to 20 weeks. The following parameters were studied: (1) the number of adherent SBMC; (2) the populations of BM cells using fluorescently labeled antibodies to CD45 and CD73, measured by fluorescence activated cell sorting (FACS); (3) the level of glutathione in BM cells; (4) morphometric parameters of the femur bone by the Micro-Computed Tomography ( $\mu$ CT).

Cultured SBMC treated with ASSNAC demonstrated an increased glutathione level (up to 2-fold) and significant resistance to cytotoxic levels of glycated albumin. Adult healthy female mice treated with ASSNAC demonstrated significant increase in SBMC: cell number (160%), percentage of bone-forming stromal cells (CD73+/CD45<sup>-</sup>; 234%) and glutathione level (210%); and increase in the femur bone: length (3%), diameter (3%) and moment of inertia [13% (polar), 11% (areal)]. Treatment of diabetic mice demonstrated significant increase in: bone length (5%), cortical thickness (17%), trabecular number (81%), connectivity of the structure (100%) and in the quantity of trabecular plate-like structures.

In conclusions: *In vitro* studies demonstrate that ASSNAC protects SBMC from oxidative stress. *In vivo* studies demonstrate that ASSNAC protects the femur from oxidative stress as well as enhances the number of SBMC and the percentage of bone-forming SBMC in the BM. Furthermore, it improves the microarchitecture of the femur of adult healthy female mice and to higher extent of diabetic female mice. These findings suggest the potential of ASSNAC to protect bones from oxidative stress associated osteoporosis and to improve bone quality and mechanical strength [based on the improved structural moment of inertia] in adult healthy and diabetic mice.



The percent of change induced by ASSNAC on femur bone parameters measured by  $\mu$ CT in adult healthy (WT) and diabetic (Db/Db) mice; significant effects of ASSNAC are marked: \* p<0.05 and \*\*p<0.01.

Savion et al - ASSNAC improves femur microarchitecture

Disclosures: Naphtali Savion, None.

## FR0265

**Bone Loss After Roux-en-Y Gastric Bypass in Mice is Independent of Weight Loss.** Elaine Yu<sup>1</sup>, Joseph Brancale<sup>2</sup>, Matthew Scott<sup>1</sup>, Daniel Brooks<sup>1</sup>, Scott Lajoie<sup>2</sup>, Lee Kaplan<sup>2</sup>, Mary Bouxsein<sup>1</sup>. <sup>1</sup>Endocrine Unit, Massachusetts General Hospital, United states, <sup>2</sup>Obesity, Metabolism & Nutrition Institute, Massachusetts General Hospital, United states

Purpose: We recently showed that Roux-en-Y gastric bypass (RYGB) surgery in diet-induced obese mice leads to cortical and trabecular deterioration in a manner similar to that seen in human studies of RYGB. We used this animal model to examine whether bone loss after RYGB is dependent on weight loss.

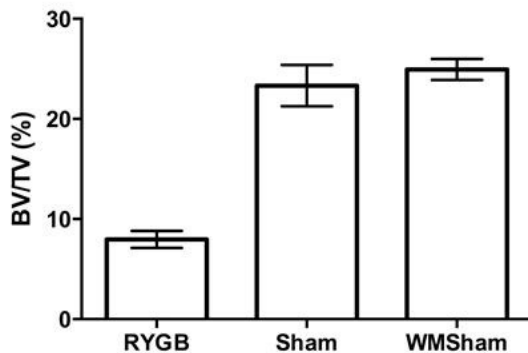
Methods: We compared adult male C57BL/6 mice that underwent RYGB (n=6) with sham-operated mice (Sham; n=5) and sham-operated mice that were food-restricted to match the weights of the RYGB-treated group (Weight-matched sham, WMSHAM; n=7). Operations were performed at 19-21 weeks of age, and mice sacrificed ~8 weeks later. We characterized bone microarchitecture with micro-computed tomography ( $\mu$ CT) at the lumbar vertebrae (L5) and femur. We used osmium tetroxide staining and mCT to assess bone marrow adipose tissue (MAT) at the tibia. Differences between groups were assessed by ANOVA with Tukey's adjustment for multiple comparisons.

Results: Final weights were similar in the RYGB (31  $\pm$  2 g) and WMSHAM (33  $\pm$  2 g) groups, both significantly lower than the weights of the Sham group (49  $\pm$  4 g, p<0.001). Trabecular bone volume fractions in the lumbar spine and femur were 60 to 68% lower in RYGB mice than either Sham or WMSHAM groups (Figure; p<0.001 for all). This deficit in trabecular bone was accompanied by a significantly lower trabecular number (by 30% to 38%) and thickness (by 10% to 38%), and increased trabecular spacing (by 48% to 158%) at these sites (p<0.005 for all). RYGB was also associated with decreased cortical thickness, cortical tissue mineral density, and polar moment of inertia, and higher cortical porosity at the femur as compared to Sham and

WMSHAM groups ( $p \leq 0.008$  for all). RYGB-treated mice had 80% lower MAT than the WMSHAM group ( $4 \pm 6\%$  vs.  $22 \pm 9\%$ ;  $p=0.028$ ).

Conclusion: In adult mice, RYGB leads to significant worsening of cortical and trabecular microarchitecture in a manner that is independent of weight loss. Further, despite lower bone density and similar weight loss as WMSHAM animals, RYGB-treated mice are protected from the increase in MAT that is a hallmark of calorie restriction. These intriguing results suggest that this surgical manipulation exerts a specific effect on bone density and marrow fat that is independent of weight loss. Mechanistic understanding of this effect may yield new targets for effective treatment of metabolic bone disorders.

### Vertebral Bone Volume Fraction



Tukey's multiple comparisons test	Adjusted P Value
RYGB vs. Sham	< 0.0001
RYGB vs. WMSHAM	< 0.0001
Sham vs. WMSHAM	0.1361

Figure - Trabecular Bone Volume Fraction at L5 Vertebra

Disclosures: Elaine Yu, None.

This study received funding from: Johnson & Johnson

## FR0266

**Irreversible Deterioration of Cortical and Trabecular Microstructure Associated with Breastfeeding.** Ashild Bjornerem<sup>1</sup>, Ali Ghasem-Zadeh<sup>2</sup>, Xiaofang Wang<sup>2</sup>, Minh Bui<sup>2</sup>, Susan P Walker<sup>2</sup>, Roger Zebaze<sup>2</sup>, Ego Seeman<sup>2</sup>. <sup>1</sup>UiT The Arctic University of Norway, Australia, <sup>2</sup>University of Melbourne, Australia

Estrogen deficiency associated with menopause is accompanied by an increase in the rate of bone remodelling and the appearance of a remodelling imbalance; each of the greater number of remodelling transactions deposits less bone than was resorbed resulting in microstructural deterioration. The newly deposited bone is also less completely mineralized than the bone resorbed. We examined whether breastfeeding, an estrogen deficient state, compromises bone microstructure and matrix mineral density.

Distal tibial and distal radial microarchitecture were quantified using high-resolution peripheral quantitative computed tomography in 58 women prior, during and after breastfeeding, and in 48 controls during one to five years follow-up.

Five months of exclusive breastfeeding increased cortical porosity by 0.6% (95% confidence interval [CI], 0.3 to 0.9), reduced matrix mineralization density by 0.26% (95% CI, 0.12 to 0.41), (all  $P < 0.01$ ), reduced trabecular number by 0.22 per mm (95% CI, 0.15 to 0.28), and increased trabecular separation by 0.07 mm (95% CI, 0.05 to 0.08) at the distal tibia, (all  $P < 0.001$ ).

Relative to pre-breastfeeding, at a median of 2.6 years (range 1 to 4.8) after cessation of breastfeeding, cortical porosity remained 0.58 SD (95% CI, 0.48 to 0.68) higher, matrix mineralization density remained 1.28 SD (95% CI, 1.07 to 1.49) lower, trabeculae were 1.33 SD (95% CI, 1.15 to 1.50) fewer and 1.06 SD (95% CI, 0.91 to 1.22) more greatly separated at the distal tibia (all  $P < 0.001$ ). All deficits were greater than in controls. The results were similar at the distal radius.

Bone microstructure may be irreversibly deteriorated following cessation of breastfeeding.

Disclosures: Ashild Bjornerem, None.

## FR0268

**A unique peptide containing the heparin binding domain of IGFBP-2 increases bone mass in ovariectomized (OVX) rats.** Gang Xi<sup>1</sup>, Christine Wai<sup>1</sup>, Thierry Abrisat<sup>2</sup>, Thomas Delale<sup>2</sup>, Victoria DeMambro<sup>3</sup>, Clifford Rosen<sup>3</sup>, David Clemmons<sup>1</sup>. <sup>1</sup>University of North Carolina at Chapel Hill, United states, <sup>2</sup>Alize Pharma III, France, <sup>3</sup>Maine Medical Center Research Institute, United states

Our previous studies showed that IGFBP-2 is required for osteoblast differentiation and that it stimulated bone formation in *Igfbp2*<sup>-/-</sup> mice. A pegylated 13 amino acid peptide that contains a unique heparin binding domain (HBDpeg) of IGFBP-2 replicated its effects on bone mass acquisition in *Igfbp2*<sup>-/-</sup> mice. Therefore, we determined if human HBDpeg could increase bone mass in wild type (WT), OVX rats. All animals were scanned using DEXA to obtain basal femoral areal bone mineral density (aBMD) and 6 sham and 6 OVX rats were sacrificed for basal femoral micro CT analysis. Sham or OVX (N=10/group) rats were randomized to receive control peptide or HBDpeg (6mg/kg) every 80 hrs S.C. for 8 weeks. Three additional groups (N=10 OVX/group) were treated with either, 0.7mg/kg HBDpeg, 2mg/kg HBDpeg, or PTH (50 ug/kg/day). Two months post-surgery, and prior to treatment, DEXA showed OVX femoral and tibial BMD were reduced  $15.4 \pm 2.5\%$  ( $p < 0.001$ ) and  $10.7 \pm 2.6\%$  ( $p < 0.01$ ), respectively, compared to sham. MicroCT showed BV/TV, connectivity and trabecular number in femoral trabecular bone were reduced  $28.5 \pm 6.1\%$  ( $p < 0.05$ ),  $83.2 \pm 5.7\%$  ( $p < 0.01$ ) and  $48.7 \pm 6.5\%$  ( $p < 0.001$ ), respectively, whereas, trabecular spacing increased  $148 \pm 50\%$  ( $p < 0.001$ ).

In control peptide treated OVX rats, DEXA scanning data showed  $16.0 \pm 7.4\%$  ( $p < 0.001$ ) and  $11.4 \pm 7.8\%$  ( $p < 0.01$ ) decreases in femoral and tibial BMD, respectively, compared to Sham rats. After 8 weeks of treatment, PTH and 6 mg/kg of HBDpeg increased femoral BMD  $5.6 \pm 3.0\%$  ( $p > 0.05$ ) and  $6.2 \pm 2.4\%$  ( $p < 0.05$ ) compared to control peptide treatment. MicroCT showed OVX control peptide rats had 41.0%, 81.0% and 64.3% decreases in femoral trabecular BV/TV, connectivity and trabecular number, respectively, and 441% increase in trabecular spacing, compared to Sham rats. In OVX rats treatment with 6 mg/kg HBDpeg increased femoral BV/TV, connectivity and trabecular number  $22.7 \pm 2.5\%$  ( $p < 0.001$ ),  $12.8\%$ ,  $3.0\%$ , respectively, whereas the increase in BV/TV with PTH was significantly lower vs control peptide:  $9.2 \pm 4.0\%$ . The 0.7 mg/kg and 2 mg/kg HBDpeg doses increased femoral trabecular BV/TV  $16.7 \pm 3.2\%$  ( $p < 0.001$ ) and  $18.2 \pm 2.4\%$  ( $p < 0.001$ ), respectively, compared to control peptide and significantly greater than the PTH treatment. Our results clearly demonstrate that HBDpeg increased bone mass in the OVX rats and was more potent than PTH at the doses tested. The findings suggest that it may be an excellent candidate for developing an anabolic strategy to treat osteoporosis.

Disclosures: Gang Xi, Alize Pharma III, 11

This study received funding from: Alize Pharma III

## FR0272

**Biopsy-based bone remodeling characteristics of premenopausal women with idiopathic osteoporosis on selective serotonin reuptake inhibitors (SSRIs).** Adi Cohen<sup>1</sup>, Mafo Kamanda-Kosseh<sup>1</sup>, Donald McMahon<sup>1</sup>, David Dempster<sup>2</sup>, Hua Zhou<sup>2</sup>, Joan Lappe<sup>3</sup>, Robert Recker<sup>3</sup>, Julie Stubby<sup>3</sup>, Mariana Bucovsky<sup>1</sup>, Elizabeth Shane<sup>1</sup>. <sup>1</sup>Columbia University, United states, <sup>2</sup>Helen Hayes Hospital, United states, <sup>3</sup>Creighton University, United states

Serotonin, a neurotransmitter found primarily in the gut and CNS, may also affect bone metabolism at the cellular level. Elevated levels of circulating serotonin and use of selective serotonin reuptake inhibitors (SSRIs), commonly prescribed for depression or anxiety, have been associated with low BMD and increased fracture risk. Skeletal mechanisms are under investigation; some studies suggest negative effects of gut serotonin on bone formation and differential effects of CNS serotonin. No consistent effects of SSRIs on circulating bone turnover markers have been documented.

Among 94 premenopausal women with idiopathic osteoporosis (IOP) recruited for both characterization and treatment studies, 15% reported SSRI use, a substantially larger proportion compared to premenopausal controls with normal BMD and no low trauma fractures (n=40; 3% on SSRIs).

To investigate mechanisms of SSRI effects on skeletal health, we compared tissue-level bone remodeling in transiliac bone biopsies performed in women with IOP reporting current SSRI use (IOP+SSRI; n=14), to women with IOP not using SSRIs (IOP-SSRI; n=80) and healthy controls not using SSRIs (C; n=39).

Dynamic indices of bone turnover were calculated using standard tetracycline double label techniques in 64 IOP and 39 C women, and were based on the first set of labels (pretreatment) in 30 IOP women who underwent quadruple labeling prior to bone biopsy as part of an ongoing treatment study.

IOP+SSRI and IOP-SSRI were similar in terms of age, BMI, body fat, number of fractures and BMD by DXA (Table). As previously reported, IOPs had significantly lower BMD and BMI compared to C. IOP+SSRI and IOP-SSRI did not differ in terms of biopsy-based remodeling characteristics at any bone surface. There was no evidence of low bone turnover among IOP+SSRI. At the endocortical surface, remodeling indices tended to be higher in IOP+SSRI.

These tissue-level data from bone biopsies performed in premenopausal women with IOP on SSRIs do not support the hypothesis that SSRIs are associated with low bone formation.

	IOP-SSRI N=80	IOP+SSRI N=14	p: IOP-SSRI vs. IOP+SSRI	Controls (-SSRI) N=39	p: Controls vs. IOP-SSRI	p: Controls vs. IOP+SSRI
Age (yrs)	38 ± 7	37 ± 7	0.7	37 ± 8	0.6	1
BMI (kg/m <sup>2</sup> )	22.3 ± 4.0	23.6 ± 5.3	0.3	25.9 ± 4.7	<0.001	0.1
DXA body fat (%)	33.5 ± 7.4	34.2 ± 7.1	0.8	35.6 ± 7.2	0.1	0.5
DXA Z scores						
Lumbar spine	-1.7 ± 1.2	-1.5 ± 0.8	0.5	0.7 ± 0.9	<0.001	<0.001
Total hip	-1.3 ± 0.9	-0.9 ± 1.0	0.1	0.5 ± 0.6	<0.001	<0.001
Femoral neck	-1.6 ± 0.9	-1.1 ± 1.3	0.09	0.4 ± 0.7	<0.001	<0.001
# of fractures	2.3 ± 2.7	1.8 ± 1.7	0.5	NA		
<b>Bone Remodeling: Cancellous Surface</b>						
MdPm (%)	4.3 ± 3.3	4.9 ± 3.6	0.5	3.2 ± 2.6	0.07	0.07
MAR (µm/d)	0.59 ± 0.10	0.62 ± 0.10	0.4	0.64 ± 0.09	0.007	0.3
BFR/BS (mm <sup>3</sup> /mm <sup>2</sup> /yr)	0.010 ± 0.008	0.011 ± 0.007	0.6	0.008 ± 0.007	0.3	0.2
<b>Bone Remodeling: Endocortical Surface</b>						
MdPm (%)	8.9 ± 6.9	11.7 ± 8.3	0.2	7.1 ± 5.2	0.2	0.07
MAR (µm/d)	0.51 ± 0.17	0.56 ± 0.18	0.3	0.56 ± 0.22	0.2	0.9
BFR/BS (mm <sup>3</sup> /mm <sup>2</sup> /yr)	0.019 ± 0.016	0.026 ± 0.017	0.1	0.017 ± 0.015	0.6	0.08
<b>Bone Remodeling: Intracortical Surface</b>						
MdPm (%)	9.2 ± 7.9	8.3 ± 8.2	0.7	8.4 ± 8.3	0.6	1
MAR (µm/d)	0.67 ± 0.20	0.71 ± 0.23	0.5	0.72 ± 0.18	0.2	0.8
BFR/BS (mm <sup>3</sup> /mm <sup>2</sup> /yr)	0.025 ± 0.022	0.024 ± 0.023	0.9	0.023 ± 0.023	0.7	0.9

SSRITable

Disclosures: *Adi Cohen, None.*

### FR0275

**Bone Loss Countermeasures for Long Duration Spaceflight.** Elisabeth Spector<sup>\*1</sup>, Toshio Matsumoto<sup>2</sup>, Jeffrey Jones<sup>3</sup>, Jay Shapiro<sup>4</sup>, Thomas Lang<sup>5</sup>, Linda Shackelford<sup>6</sup>, Scott M. Smith<sup>6</sup>, Harlan Evans<sup>1</sup>, Robert Ploutz-Snyder<sup>7</sup>, Jean Sibonga<sup>6</sup>, Joyce Keyak<sup>8</sup>, Toshi Nakamura<sup>9</sup>, Kenjiro Kohri<sup>10</sup>, Hiroshi Ohshima<sup>11</sup>, Gilbert Moralez<sup>12</sup>, Adrian LeBlanc<sup>13</sup>. <sup>1</sup>Wyle Science, Technology & Engineering Group, United states, <sup>2</sup>U of Tokushima Graduate School of Medicine, Japan, <sup>3</sup>Baylor College of Medicine, United states, <sup>4</sup>Kennedy Krieger Institute, United states, <sup>5</sup>UCSF, United states, <sup>6</sup>NASA Johnson Space Center, United states, <sup>7</sup>Universities Space Research Association, United states, <sup>8</sup>U of California at Irvine, United states, <sup>9</sup>U of Occupational & Environmental Health, Japan, <sup>10</sup>Nagoya City U, Japan, <sup>11</sup>JAXA, Japan, <sup>12</sup>U of N Texas Health Science Center, United states, <sup>13</sup>Baylor College of Medicine & Universities Space Research Association, United states

Bone loss during weightlessness has been known since early spaceflight. Assuming that the decrease in musculoskeletal forces encountered in space is the primary source for this bone atrophy, exercise has been implemented essentially on all long duration missions with varying success. More recently resistive exercise prescriptions using new devices (IRED, ARED) have been implemented with some success. However during a long mission, e.g., Mars, where equipment failure or other conditions could preclude adequate musculoskeletal loading, blocking the spaceflight-induced elevated bone remodeling might be a useful adjunct with the added benefit of reducing elevated urinary Ca. Methods: In this study, measurements of bone mass and metabolism included DXA, QCT, pQCT, urinary and blood biomarkers. We have completed analysis of pre and post-flight (~R+1 wk) data from 7 crewmembers treated with 70 mg/wk oral alendronate during flight (mean flight duration 164 ± 15 days) and in 8-9 of 10 controls using ARED exercise alone (flight duration 158 ± 21 days). DXA results: Control group BMD results (%change vs. preflight, mean ± SD) were: lumbar spine -2.6 ± 1.9; total hip -3.5 ± 2.2; trochanter -4.1 ± 2.7; femur neck -1.9 ± 4.1, while changes in the Treated group were: lumbar spine +2.8 ± 4.0; total hip -0.2 ± 1.5; trochanter +0.02 ± 2.3; femur neck -0.7 ± 1.2. Statistical analyses revealed significant group by time effects for all regions except the femur neck, indicating a positive treatment effect of bisphosphonates. QCT results: Changes in BMD and Finite Element-calculated strength are shown in the table below. While the group by time interactions were significant only for the femur neck, Controls showed mean losses in most parameters while the Treated group means were essentially unchanged. Bone marker results: Relative to the Treated group, the Control group showed significantly greater changes in excretion (in-flight vs. pre-flight) of the resorption marker NTX as well as of Urinary Ca, indicating a positive treatment effect of bisphosphonates. Conclusions to date: Our data show that exercise plus an antiresorptive will be effective in reducing bone loss, preventing the elevation of bone resorption and decreasing excretion of urinary Ca. Calculated bone strength is preserved. Targeted high resistive exercise alone can significantly attenuate bone loss and maintain bone strength but not necessarily completely.

Table 1. QCT vBMD and FE Strength Changes after Flight

	ARED Control (n=9) % Change	Alendronate + ARED (n=7) % Change
<b>QCT BMD (g/cm<sup>3</sup>)</b>		
<b>Total Hip</b>		
Trabecular	-7.4 ± 5.6	-1.1 ± 9.8
Cortical	-2.4 ± 1.7	-0.6 ± 4.7
<b>Trochanter</b>		
Trabecular	-6.8 ± 6.2	-1.9 ± 9.9
Cortical	-3.2 ± 2.5	-0.5 ± 5.0
<b>Femur Neck</b>		
Trabecular	-12.9 ± 12.8	6.5 ± 14.8 <sup>1</sup>
Cortical	-1.6 ± 2.6	-1.0 ± 4.8
<b>Finite Element Strength (N)</b>		
Non-Linear Stance	-5.6 ± 3.0	0.8 ± 10.1
Non-Linear Fall	-3.1 ± 5.8	-0.1 ± 7.6

<sup>1</sup>Time x Group interaction, p<0.05

Table 1

Disclosures: *Elisabeth Spector, None.*

### FR0284

**Effect of Teriparatide or Risedronate in BMD and Fracture Recovery in Elderly Patients with a Recent Pertrochanteric Hip Fracture: Final Results of a 78-week Randomized Clinical Trial.** Jorge Malouf<sup>\*1</sup>, Umberto Tarantino<sup>2</sup>, Per Aspenberg<sup>3</sup>, Søren Overgaard<sup>4</sup>, Costantino Corradini<sup>5</sup>, Jan Stepan<sup>6</sup>, Lars Borris<sup>7</sup>, Pedro García-Hernández<sup>8</sup>, Eric Lespessailles<sup>9</sup>, Frede Frihagen<sup>10</sup>, Kyriakos Papavasiliou<sup>11</sup>, Helmut Petto<sup>12</sup>, José Ramón Caeiro<sup>13</sup>, Fernando Marin<sup>14</sup>. <sup>1</sup>Internal Medicine; Hospital San Pablo, Spain, <sup>2</sup>Orthopaedic Surgery; University Tor Vergata, Italy, <sup>3</sup>Department of Clinical & Experimental Medicine, Linköping University, Sweden, <sup>4</sup>Orthopaedic Surgery, University of Southern Denmark, Denmark, <sup>5</sup>Orthopaedic Institute Gaetano Pini, Italy, <sup>6</sup>Institute of Rheumatology, Charles University, Czech republic, <sup>7</sup>Orthopaedic Surgery, University Hospital, Denmark, <sup>8</sup>Osteoporosis Center, University Hospital, Mexico, <sup>9</sup>IPROS Unit, Hôpital Porte Madeleine, France, <sup>10</sup>Orthopaedic Surgery, University Hospital, Norway, <sup>11</sup>Orthopaedic Surgery, Aristotle University, Greece, <sup>12</sup>Eli Lilly Austria GmbH, Austria, <sup>13</sup>Orthopaedic Surgery, University Hospital, Spain, <sup>14</sup>Eli Lilly Research Centre Ltd, Erl Wood Manor, United Kingdom

Purpose: To present final results of a clinical trial comparing teriparatide (TPTD) 20 µg QD with risedronate (RIS) 35 mg QW started within 2 wks after surgical repair of a pertrochanteric hip fracture.

Methods: Main inclusion criteria: BMD T-score ≤ -2.0SD and a low-trauma hip fracture (AO/OTA 31-A1 or A2) treated with osteosynthesis. During the first 26-wks, patients received double-dummy study drug with oral/injectable placebo and Ca+vitD<sub>3</sub>, followed by open-label therapy for up to 78-wks with the same drug they were randomized to. Primary endpoint was change from baseline in lumbar spine (LS) BMD at 78-wks. Secondary and exploratory endpoints were proximal femur BMD, function, hip pain, quality of life (QoL), radiology outcomes, and safety. Mixed models for repeated measures (MMRM) or logistic regression were used for the analyses.

Results: 224 patients were randomized; 171 (TPTD:86, RIS:85) contributed to the efficacy analyses. Mean (SD) age: 77 (8) yrs; 77% women; 26% with prior history of low-trauma fracture after age 50 yrs. Mean (SD) baseline LS and femoral neck (FN) T-scores were -2.16 (1.36) and -2.63 (0.59). At 78 wks, TPTD arm showed significantly greater increase in LS BMD (+11.10% vs +6.45%; p<0.0001, full-adjusted MMRM, Figure), and FN BMD (+1.96% vs -1.19%; p=0.0033). There was no significant between-group difference for changes in total hip BMD. Time to complete the timed up-and-go (TUG) test was significantly shorter with TPTD at 6, 12, 18 and 26 wks (range: -3.2 to -5.9 seconds; p<0.05 full-adjusted MMRM). Hip pain during the TUG test by 100 mm Visual Analog Scale was significantly lower with TPTD at 18 wks (adjusted absolute difference: -11.3 mm; p<0.05, and -10.0 and -9.3 mm at 12 and 26 wks; p<0.1 full-adjusted MMRM). No significant between-group differences in QoL by SF-36, Charnley's hip pain scores, ability to walk or the use of walking aids during follow-up. Frequencies of radiographic fracture healing, implant failure (TPTD:7, RIS:9), loss of reduction (TPTD:2, RIS:4) and non-union (0 cases) were similar. There were 2 and 7 new hip fractures

with TPTD and RIS, respectively (p=0.17). Hypercalcemia and hyperuricemia were more frequent with TPTD.

Conclusions: Patients treated for pertrochanteric fracture had a higher increase in LS and FN BMD after 78 wks' treatment with TPTD compared to RIS. TPTD-treated subjects reported a shorter time to complete the TUG test. Other fracture-healing outcomes were similar with both treatments.

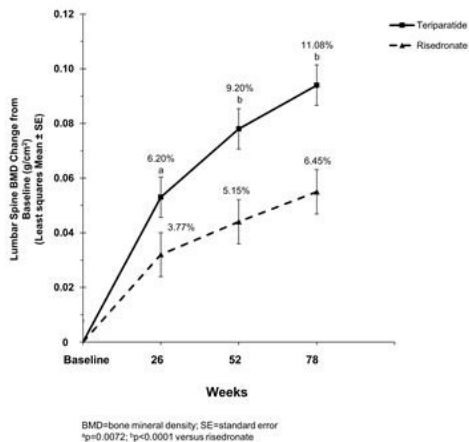


Figure. Change in lumbar spine BMD after 78 weeks' treatment with teriparatide or risedronate

Disclosures: Jorge Malouf, None. This study received funding from: Eli Lilly and Company

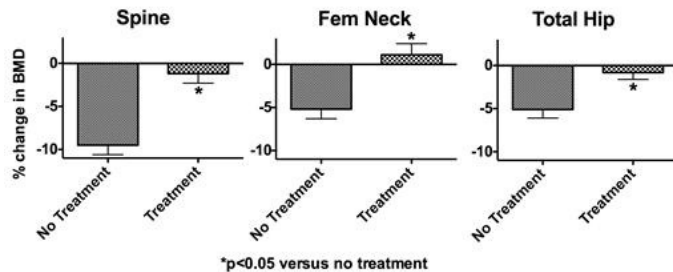
### FR0286

**Relative Efficacy of Prompt Follow-up Therapy in Postmenopausal Women Completing the Denosumab and Teriparatide Administration (DATA) Study.** Benjamin Leder\*, Linda Jiang, Joy Tsai. Massachusetts General Hospital, United states

Patients who discontinue denosumab (DMAB) and teriparatide (TPTD) experience rapid bone loss. The relative efficacy of antiresorptive agents to prevent this bone loss is not established. In the DATA and DATA-Switch studies, postmenopausal women were randomized to 2-yr of TPTD, DMAB, or both (COMBO). Then, women originally assigned to TPTD were switched to 2-yr of DMAB (Group A), women assigned to DMAB were switched to TPTD (Group B), and women assigned to COMBO were switched to DMAB alone (Group C). Women completing DATA/DATA-Switch were counseled to follow-up with their physicians promptly and strongly consider re-initiation of osteoporosis therapy. A letter was also sent to the subject's physician describing the potential for rapid bone-loss. We then asked women who completed DATA-Switch to return for a f/u spine, femoral neck (FN) and total hip (TH) DXA at least 12 months and no more than 22 months after their last study visit.

Of the 69 women who completed DATA-Switch, 42 returned for imaging and provided information about their post-study course. The mean age at follow-up was 70.1 ± 5.6. Twenty women did not receive osteoporosis medications whereas 22 did (7 alendronate, 2 ibandronate, 6 IV zoledronic acid, 7 DMAB). The mean time between the conclusion of DATA-Switch and the f/u visit was 15.4 ± 3.6 months. In those treated, the mean gap between the conclusion of DATA-Switch and re-initiating therapy was 3.4 ± 2.9 months. In those re-initiating therapy, BMD at all sites remained stable whereas in untreated women BMD decreased by -9.5 ± 1.1, 5.2 ± 1.1, and 5.1- ± 1.0 at the spine, TH, and FN, respectively (fig). Among treated women, those receiving DMAB gained more FN BMD (3.7 ± 2.6%) than those receiving bisphosphonates (-1.3 ± 3.2%, p=0.001) (other sites did not differ). Additionally, FN BMD decreased more in untreated women discontinuing DMAB (Groups A and C, -7.4 ± 4.4%) than those discontinuing TPTD (Group B, -1.1 ± 3.6%) (p<0.05). A similar pattern was observed at the TH but not the spine where BMD decreased by -9.6 ± 1.0% in groups A+C and -9.3 ± 3.1% in Group B.

In this uncontrolled, non-randomized, extension to DATA-Switch, spine and hip BMD did not decrease in osteoporotic women who received prompt antiresorptive therapy but did in women left untreated. Bone loss was greatest in untreated women discontinuing DMAB. These results should be considered when contemplating "drug holidays" in women receiving DMAB and TPTD.



figure

Disclosures: Benjamin Leder, Amgen, 11; Amgen, 12; Lilly, 11; Merck, 12; Lilly, 12 This study received funding from: Amgen, Lilly

### FR0288

**The Risk of Subsequent Osteoporotic Fractures Is Decreased in Patients Experiencing Fracture While on Denosumab: Results From the FREEDOM and FREEDOM Extension Studies.** DL Kendler\*, A Chines<sup>2</sup>, ML Brandi<sup>3</sup>, S Papapoulos<sup>4</sup>, EM Lewiecki<sup>5</sup>, J-Y Reginster<sup>6</sup>, C Roux<sup>7</sup>, M Munoz Torres<sup>8</sup>, A Wang<sup>2</sup>, HG Bone<sup>9</sup>. <sup>1</sup>University of British Columbia, Canada, <sup>2</sup>Amgen Inc., United states, <sup>3</sup>University of Florence, Italy, <sup>4</sup>Leiden University Medical Center, Netherlands, <sup>5</sup>New Mexico Clinical Research & Osteoporosis Center, United states, <sup>6</sup>University of Liège, Belgium, <sup>7</sup>Paris Descartes University, France, <sup>8</sup>Hospital Universitario San Cecilio, Spain, <sup>9</sup>Michigan Bone & Mineral Clinic, United states

Purpose: Osteoporosis is a common, progressive condition leading to increased bone fragility and susceptibility to fracture. Although osteoporosis therapy decreases fracture risk, fractures while on any current treatment can occur and do not necessarily represent treatment failure. It is therefore of interest to assess whether patients who fracture on denosumab (DMAB; FREEDOM and FREEDOM Extension [Ext]) experience a lower risk of subsequent fracture continuing on therapy than those on placebo (pbo) who have fractured.

Methods: During FREEDOM, postmenopausal women with osteoporosis were randomized to pbo or DMAB for 3 yrs. During the 7-yr Ext, all participants were allocated to receive DMAB. In this analysis, we report subsequent osteoporotic fractures (new vertebral or nonvertebral) in subjects who received ≥2 doses of DMAB during FREEDOM or the Ext, had an osteoporotic fracture while on treatment, and continued treatment post-fracture, compared with subsequent fractures in FREEDOM pbo subjects. These subsequent fractures were analyzed as recurrent events using the stratified Cox model with the robust variance estimation adjusting for prior fracture.

Results: During FREEDOM, 438 pbo and 272 DMAB subjects had an osteoporotic fracture (mean age at first on-study fracture: 74.1 and 74.5 yrs, respectively). Of these, there were 54 (12.3%) and 24 (8.8%) subjects who had ≥1 subsequent fractures in the pbo and DMAB groups, respectively. Adjusted subject incidence per 100 patient-yrs was lower for DMAB (6.7) vs pbo (10.1). Combining all subjects on DMAB from FREEDOM and the Ext for up to 10 yrs, 794 (13.7%) subjects had an osteoporotic fracture while on DMAB (mean age at first on-study fracture: 76.5 yrs). Of these, one or more subsequent fractures occurred in 144 (18.1%) subjects, with an adjusted subject incidence of 5.8 per 100 patient-yrs, similar to FREEDOM DMAB (6.7 per 100 patient-yrs). Among subjects with ≥1 subsequent fracture, 90% had only 1, and spine fracture was most frequent. The risk of having subsequent on-study osteoporotic fractures was lower in all DMAB subjects compared with pbo subjects (HR 0.60 [95% CI: 0.43-0.81]; p=0.0012; Figure).

Conclusions: The risk of a second fracture with continued DMAB treatment remains lower than pbo, thus suggesting that a fracture sustained while on DMAB is not necessarily indicative of a treatment failure, and continuation of treatment should be considered.

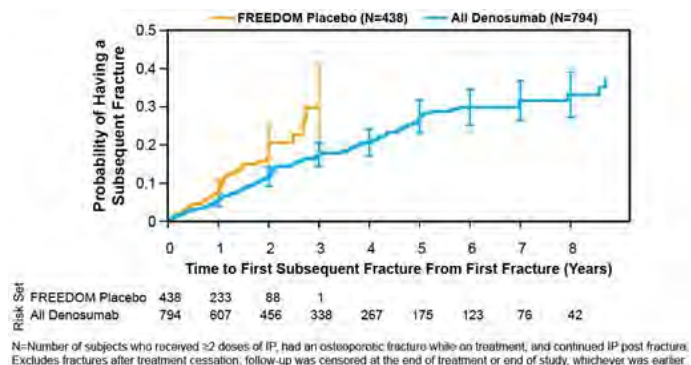


Figure: Time to First Subsequent Osteoporotic Fracture Among Placebo and All Denosumab Subjects Who

Disclosures: DL Kendler, Amgen, Eli Lilly, Astra Zeneca, Astalis, 11; Amgen, Eli Lilly, 13; Amgen, Eli Lilly, 12 This study received funding from: Amgen Inc.

**FR0289**

**Denosumab Treatment for 10 Years in Postmenopausal Women with Osteoporosis was Associated with Substantially Lower Fracture Incidence Relative to Their Baseline FRAX-predicted Probability.** E Siris<sup>\*1</sup>, N Pannacciulli<sup>2</sup>, PD Miller<sup>3</sup>, EM Lewiecki<sup>4</sup>, R Chapurlat<sup>5</sup>, E Jódar Gimeno<sup>6</sup>, NS Daizadeh<sup>2</sup>, RB Wagman<sup>2</sup>, JA Kanis<sup>7</sup>. <sup>1</sup>Columbia University Medical Center, United states, <sup>2</sup>Amgen Inc., United states, <sup>3</sup>Colorado Center for Bone Research, United states, <sup>4</sup>New Mexico Clinical Research & Osteoporosis Center, United states, <sup>5</sup>Hôpital Edouard Herriot, France, <sup>6</sup>Hospital Universitario Quirónsalud Madrid, Spain, <sup>7</sup>University of Sheffield, United Kingdom

Purpose: Denosumab (DMAB) is approved for treating postmenopausal women with osteoporosis (OP) at high risk for fracture. The placebo (pbo)-controlled FREEDOM trial and its active-treatment Extension (Ext) investigated the efficacy and safety of DMAB for up to 10 yrs. The lack of a long-term control group in the Ext, however, limits the ability to evaluate long-term efficacy. We used two approaches to put DMAB's 10-yr anti-fracture efficacy into perspective. First, we compared the 10-yr observed cumulative incidence of major osteoporotic (MOP; hip, clinical spine, forearm, or humerus) and hip fracture in subjects who completed the Ext with the 10-yr fracture probability predicted at baseline by FRAX (a computer-based algorithm assessing fracture probability from clinical risk factors).<sup>1</sup> The 10-yr MOP fracture rate was also compared with that estimated for a hypothetical cohort of 10-yr pbo controls (virtual twins).

Methods: Subjects in this analysis received 10 yrs of DMAB (3 yrs FREEDOM; 7 yrs Ext; 60 mg Q6M), completed the 10-yr visit, and missed ≤1 dose in FREEDOM and ≤1 dose in the Ext (n=1,278). Kaplan-Meier estimates of cumulative 10-yr incidence of MOP and hip fracture were determined. Ten-yr probability of fracture predicted by FRAX (with FN BMD) at FREEDOM baseline was also calculated. Rate of MOP fracture in a hypothetical cohort of 10-yr pbo controls (virtual twins) was estimated using a previously described simulation method and baseline characteristics identical to the 10-yr DMAB completers.<sup>2,3</sup>

Results: The observed cumulative 10-yr fracture incidence (95% CI) was lower than the 10-yr mean (SD) fracture probability predicted by FRAX for both MOP (10.75% [9.05%–12.46%] vs 16.42% [9.06%]; Figure) and hip (1.17% [0.58%–1.76%] vs 6.14% [6.52%]) fracture. The observed cumulative 10-yr MOP fracture incidence was also significantly lower than the estimated virtual twins fracture rate (10.75% [9.05%–12.46%] vs 23.13% [17.76%–28.87%]; RR=0.49 [0.36–0.64]).

Conclusions: Fracture incidence with 10 yrs of DMAB treatment in postmenopausal women with OP was lower than the 10-yr probability predicted by FRAX for both MOP and hip fracture. It was also lower than the fracture rate estimated in a hypothetical cohort of 10-yr pbo controls for MOP fracture. These data support the long-term efficacy of DMAB in reducing MOP and hip fractures.

References: <sup>1</sup>https://www.shef.ac.uk/FRAX/index.aspx; <sup>2</sup>Vittinghoff *Stat Med* 2010; <sup>3</sup>Papapoulos *Osteoporos Int* 2015

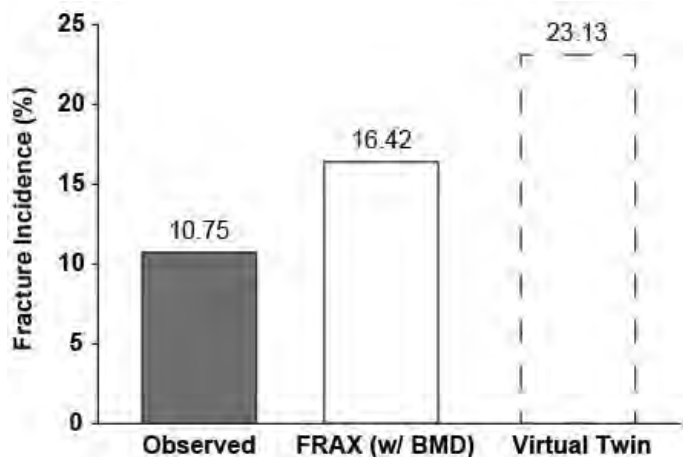


Figure. Ten-year Observed, FRAX-predicted, and Virtual Twin-estimated MOP Fracture Incidence

Disclosures: E Siris, Amgen, Merck, Radius, 12  
This study received funding from: Amgen Inc.

**FR0291**

**Effect of Risedronate on Bone Loss due to Anastrozole Given to Prevent Breast Cancer: 5-year Results from the IBIS-II Prevention Trial.** Ivana Sestak<sup>\*1</sup>, Jack Cuzick<sup>1</sup>, Glen Blake<sup>2</sup>, Raj Patel<sup>3</sup>, Robert Coleman<sup>4</sup>, Richard Eastell<sup>5</sup>. <sup>1</sup>Centre for Cancer Prevention, Queen Mary University, United Kingdom, <sup>2</sup>Division of Imaging Sciences, King's College London, United Kingdom, <sup>3</sup>Charing Cross Hospital, United Kingdom, <sup>4</sup>Yorkshire Cancer Research Professor of Medical Oncology, Department of Oncology & Metabolism, Weston Park Hospital, University of Sheffield, United Kingdom, <sup>5</sup>Metabolic Bone Centre, Northern General Hospital, United Kingdom

Background: Anastrozole (A) has been shown to prevent breast cancer in postmenopausal women at high risk of the disease, but has been associated with substantial accelerated bone mineral density loss and increased fractures. Here, we investigate the effect of risedronate (R) on bone mineral density (BMD) after 5 years of follow-up in the IBIS-II prevention trial.

Methods: In the IBIS-II trial, a randomised, placebo-controlled trial of A in postmenopausal women at increased risk of breast cancer, 1410 women were enrolled in the bone sub-study and stratified into three strata according to their baseline T-score at spine or femoral neck (stratum I (N=760): T-score>-1.0; stratum II (N=500): -1.0<T-score>-2.5; stratum III (N=150): -2.5<T-score>-4.0 or/and two fragility fractures). The primary objective was to compare the effect of R versus placebo (P) in osteopenic women who were randomised to A in the main study. Secondary objectives included the effect of A on BMD in the other two strata and the association of BMD loss according to age and body mass index (BMI). All results are presented as mean % BMD changes (95% CI) between baseline and 5 years of follow-up.

Results: Baseline and 5-year BMD data was available for a total of 765 women. 5-year mean % BMD change at the spine for women randomised to A and receiving R was -0.4% compared to -4.5% for those not on R (P<0.0001; Table 1). Mean % BMD change at the total hip was not significantly different between R users and non-users at 5 years of follow-up (P=0.23; Table 1). Women in stratum I not receiving R had a significant BMD decrease at the spine and total hip (P<0.0001). In osteoporotic women, who all received R, a significant increase was observed after 5 years of follow-up in BMD at the spine, but not at the total hip (Table 1). Women aged 60 years or younger had a larger BMD decrease at the spine but not total hip than older women in stratum I and II. No significant increase in fractures was observed with A compared to P (Table 1).

Conclusions: Our results show that women with osteopenia on A and receiving R for 5 years showed a highly significant difference in BMD change at the spine, but not at the total hip, compared to those not receiving R. Women with healthy bone randomised to A showed a large BMD decrease when compared to P, with large differences between age groups. Overall, our results suggest that BMD loss at the spine but not the total hip due to A can be controlled with risedronate treatment.

Table 1: 5-year mean % BMD changes (95% CI) and fractures according to strata and treatment allocation.

	Stratum I		Stratum II				Stratum III	
	A (N=205)	P (N=213)	A/R (N=59)	A/R (N=67)	P/P (N=73)	P/R (N=57)	A/R (N=50)	P/R (N=43)
Spine	-5.3 (-6.0 to -4.6)	-1.8 (-2.5 to -1.1)	-4.5 (-5.7 to -3.4)	-0.4 (-1.6 to 0.9)	-0.04 (-1.2 to 1.2)	4.0 (2.3 to 5.7)	0.3 (-1.4 to 2.0)	8.9 (2.3 to 5.4)
Total hip	-5.3 (-5.9 to -4.7)	-3.0 (-3.6 to -2.5)	-3.6 (-5.1 to -2.2)	-2.5 (-3.6 to -1.4)	-2.8 (-3.6 to -2.1)	1.0 (-0.2 to 2.2)	-0.7 (-1.9 to 0.5)	0.2 (-0.9 to 1.4)
Fractures	52	37	50	20	29	18	9	20

A=Anastrozole, P=Placebo, R=Risedronate, Grey shaded area=Primary comparison

Table 1

Disclosures: Ivana Sestak, None.  
This study received funding from: Sanofi-Aventis, AstraZeneca

**FR0294**

**Fracture risk after discontinuation of denosumab.** Akeem Yusuf<sup>\*1</sup>, Haifeng Guo<sup>1</sup>, Akhila Balasubramanian<sup>2</sup>, Nicola Pannacciulli<sup>2</sup>, Rachel Wagman<sup>2</sup>, J. Michael Sprafka<sup>2</sup>. <sup>1</sup>Chronic Disease Research Group, United states, <sup>2</sup>Amgen Inc., United states

Denosumab (DMAB) treatment has been shown to decrease fracture (Fx) risk. Unlike bisphosphonates, DMAB is a soluble inhibitor of RANKL, and discontinuation is characterized by reversal of effect. There is a need to better understand Fx risk associated with DMAB discontinuation.

Using Medicare administrative claims data, we identified female beneficiaries aged ≥65 years who initiated DMAB between 10/1/2010 and 06/30/2012 and were continuously enrolled for ≥12 months prior to the treatment index date. Treatment discontinuation was defined as the absence of a DMAB claim within 6 months + 8 weeks following a previous claim. We evaluated Fx risk among discontinuers who remained off therapy without reinitiating or switching treatment. Endpoints of interest included (i) vertebral Fx and (ii) a composite endpoint of Fx at any skeletal site other than skull/face/finger/toe ('any Fx'). We compared Fx incidence rates between 3 periods using incidence rate ratios (IRR): early (first 90 days of treatment), on-treatment (day 91 to discontinuation), and off-treatment (discontinuation to end of follow-up) periods.

We identified 7,855 eligible denosumab-treated patients who subsequently discontinued and remained off treatment. The study cohort had mean  $\pm$  SD age  $79.4 \pm 7.5$  years; 88.5% were white. Approximately one-fourth (1,988 patients) had prior exposure to other osteoporosis medications and 10.9% (857 patients) had a previous Fx during baseline. The mean  $\pm$  SD duration of the on-treatment and off-treatment periods was  $6.94 \pm 3.78$  months and  $6.28 \pm 4.18$  months, respectively. Compared to the early treatment period, incidence rates of vertebral Fx and any Fx decreased during the on-treatment period by 52.8% and 32.6%, respectively. Fx incidence rates increased during the off-treatment period; however, they remained below the baseline rates observed during the early treatment period [IRR (95% CI): vertebral Fx, 0.70 (0.54-0.93); any Fx, 0.90 (0.77-1.05)]. Results for patients with and without prior fracture history were consistent with that of the main analysis.

Consistent with the reversibility of DMAB effect, this large, population-based study of older women showed reductions in Fx rates during the on-treatment period, followed by an increase in Fx rates during the off-treatment period. Importantly, Fx rates during the approximately 6-12 month off-treatment period remained lower than the observed baseline rates in this population.

Table 1. Fracture incidence rates in patients treated with denosumab who later discontinued and remained off treatment

Fracture incidence rates/100 patient-years	Vertebral fractures	Any fracture*
Early period	4.39	12.62
On-treatment	2.07	8.51
Off-treatment	3.09	11.40
Fracture incidence rate ratios (95% CI)		
On-treatment vs. early period	0.47 (0.35-0.63)	0.67 (0.57-0.79)
On-treatment vs. off-treatment	0.67 (0.51-0.87)	0.75 (0.65-0.85)
Off-treatment vs. early period	0.70 (0.54-0.93)	0.90 (0.77-1.05)

\*Any fracture\* was a composite endpoint of fracture at any skeletal site other than skull/face/finger/toe

Table 1

Disclosures: Akeem Yusuf, None.

This study received funding from: Amgen Inc.

## FR0296

**Pathogenesis of Atypical Femur Fractures: Analysis at Midpoint of Recruitment.** Pooja Kulkarni<sup>1</sup>, Mahalakshmi Honasoge<sup>1</sup>, Elizabeth Warner<sup>1</sup>, Arti Bhan<sup>1</sup>, Shirri Levy<sup>1</sup>, Heather Remtema<sup>1</sup>, George Divine<sup>2</sup>, Sudhaker Rao<sup>1</sup>. <sup>1</sup>Henry Ford Division of Endocrinology, Diabetes & Bone & Mineral Disorders, United states, <sup>2</sup>Henry Ford Public Health Services, United states

Background: Atypical femur fractures (AFF) are an established complication of long-term bisphosphonate (BP) therapy. While considered rare based on retrospective database analyses, the true prevalence of AFF remains unknown. We designed and initiated a prospective study to determine the frequency and pathogenesis of AFF and report our results at the mid-point of the study.

Methods: From June 14, 2014 to March 29, 2016, we recruited 525 patients: 255 BP-unexposed and 270 BP-exposed (at least  $\geq 2$  years) with a mean age of  $67 \pm 8.5y$ . AFFs are diagnosed using Hologic software designed to detect AFF or by digital x-rays of both femurs in AP projection. Incomplete AFFs were confirmed by bone scan and/or tomosynthesis.

Results: BP-exposed patients were 4y older ( $69.1 \pm 8.9y$  vs.  $65.5 \pm 8.1y$ ;  $p < 0.001$ ) than non-exposed patients. The mean duration of BP-exposure was  $6.4 \pm 4.3y$  (range 2-20y) and ethnic composition was similar in both groups. Most patients were on one of the three approved oral BPs, with the exception of 15 on Denosumab and 10 on Zoledronate. BP-exposed patients who sustained AFFs were 2y older than those who did not ( $71 \pm 7.7y$  vs  $69 \pm 8.9y$ ;  $p=ns$ ), and were exposed to BPs 2y longer than those without AFF ( $8.3 \pm 4y$  vs.  $6.2 \pm 4y$ ). Although there was trend for longer duration of BP exposure, it did not reach statistical significance ( $p < 0.089$ ).

The frequency of AFF was 4.1% (11/270), much higher than suggested by the retrospective database analyses, lower than our preliminary estimate (12%), and about the same as our predicted estimate (5%) at the beginning of the study. The 11 AFF patients in our study had 14 femur AFFs: Four patients had bilateral AFF; one had AFF in one femur and multiple incomplete AFFs in the other (hitherto unreported), two patients had complete AFF in each femur and one patient had incomplete AFF in both femurs.

Despite several barriers (fear of bone biopsy even when sustained AFF, needles, transportation arrangements, busy schedule, perception that participation would not benefit them), we exceeded the expected number of enrolled subjects since June 2014. In the next 20 months, we expect to enroll 475 more patients to The frequency of AFF may be higher than estimated and appears to be related to the duration of BP therapy.

Conclusion: Continued surveillance and research are required to determine the true prevalence and pathogenesis of AFF since such fractures are life-changing events in the individual patient.

Disclosures: Pooja Kulkarni, None.

## FR0297

**Surgically Treated Osteonecrosis and Osteomyelitis of the jaw and Oral Cavity in Patients Highly Adherent to Alendronate Treatment. User-only National Cohort Study.** Bo Abrahamsen<sup>1</sup>, Pia A Eiken<sup>2</sup>, Daniel Prieto-Alhambra<sup>3</sup>, Richard Eastell<sup>4</sup>. <sup>1</sup>Holbæk Hospital & University of Southern Denmark, Denmark, <sup>2</sup>Hillerød Hospital, Denmark, <sup>3</sup>NIHR Musculoskeletal Biomedical Research Unit, University of Oxford, United Kingdom, <sup>4</sup>Metabolic Bone Centre, Northern General Hospital, United Kingdom

Background: Osteonecrosis of the jaw (ONJ) is regarded as a rare event in users of oral bisphosphonates whereas it is a common adverse event in an oncology setting where dose intensity is higher and the route is intravenous. Despite this, there is no clear indication that the risk of ONJ increases with increasing treatment time for oral bisphosphonates.

Methods: We used national health registers to track in- and outpatient events until 31/DEC/2013 in 61,990 men and women aged 50 to 94 who began alendronate treatment between 1/JAN/1996 and 31/DEC/2007. For the purpose of the analysis Surgically treated probable ONJ was defined by surgery to the oral cavity or the jaws for conditions coded by ICD-10 as osteonecrosis or osteomyelitis, excluding osteoradionecrosis. The study period was truncated at death, end of study or failing refill adherence ( $< 80\%$  MPR). Risk factors for ONJ were identified by Cox proportional hazards analysis.

Results: The strongest predictors of surgically treated ONJ in highly adherent users were rheumatic disorders (OR 1.75, 95% CI 1.14-2.69), chronic lung diseases (OR 1.78, 1.14-2.77), diabetes (OR 2.32, 1.21-4.43), prednisolone use (OR 1.72, 1.11-2.66) and ulcer disease (OR 1.85, 1.02-3.36). PPI use was not a significant risk factor when models were adjusted for ulcer disease. Using MPR as a continuous time dependent covariate rather than as a truncation threshold demonstrated a significant relationship between refill compliance and the ONJ outcome (OR 1.62, 1.05-2.48).

Discussion: The rate of surgically treated osteomyelitis and osteonecrosis of the jaw or oral is low, even in long term adherent users despite a nominally significant influence of treatment duration and refill adherence on the risk of this adverse outcome. The results also suggest that the risk is higher in patients with conditions likely to directly or indirectly affect the oral mucosa.

Duration of highly adherent alendronate exposure, years	Persons with events	Patient years at risk	Rate per 10,000 patient years
Before start (last 12mo)	7	61,990	1.13 (0.45-2.33)
0-5	77	194,445	3.96 (3.13-4.95)
5 to 10	27	56,269	4.80 (3.16-6.98)
10+	3	5,292	5.67 (1.17-16.57)

Results

Disclosures: Bo Abrahamsen, Novartis, 11; UCB, 11

## FR0299

**Differential Effects of Odanacatib Therapy on Markers of Bone Resorption and Formation in Postmenopausal Women with Osteoporosis: A Subgroup Study of the 5-Year Data from the Extension of the Phase 3 Long-Term Odanacatib Fracture Trial (LOFT).** Le T. Duong<sup>1</sup>, Maureen Pickarski<sup>1</sup>, Seth Clark<sup>1</sup>, Hilde Giezek<sup>2</sup>, Dosinda Cohn<sup>1</sup>, Rachid Massaad<sup>2</sup>, S. Aubrey Stoch<sup>1</sup>. <sup>1</sup>Merck & Co., Inc., United states, <sup>2</sup>MSD Europe Inc., Belgium

Purpose: Odanacatib (ODN) is a selective oral inhibitor of cathepsin K (CatK) in development for osteoporosis treatment. To further inform the mechanism of action of ODN on the inhibition of collagen processing, a subset of patients who completed 60 months of therapy in the randomized, double-blind, placebo (PBO)-controlled, event-driven, Phase 3 Fracture Trial (LOFT; NCT00529373) and planned double-blind extension (n=112) was evaluated.

Methods: Patients from LOFT with archived serum (s) and urine (u) samples collected at baseline (BL), month (M) 6, 12, 24, 36, 48, and 60 were assayed in a "batch-manner" for markers of bone resorption (sCTX, u $\alpha$ -CTX/Cr, u $\beta$ -CTX/Cr, and uNTx/Cr), target engagement (s1-CTP), osteoclast number (sTrap-5b), and bone formation (sPINP and sBSAP). Results were expressed as time-dependent geometric mean (% change) vs BL and compared ODN vs PBO. Cross-selectivity of the CrossLaps CTx assay, which selectively recognizes only the  $\beta$ -CTX epitope, but also detects larger molecular weight CTx species including 1-CTP, was evaluated and a best-fit model developed to explain sCTX response in ODN-treated patients.

Results: ODN treatment rapidly reduced and maintained the levels of bone resorption markers uNTx/Cr, u $\alpha$ -CTX/Cr, and u $\beta$ -CTX/Cr until M60 vs PBO (Table). However, ODN reduced sCTX in the first 2 years which then slowly returned to BL by M48, maintaining a difference vs PBO. ODN increased 1-CTP at M6 to M60 vs PBO (Table), indicative of CatK inhibition. In ODN-treated patients, sTrap-5b levels were similar to BL up to M12, subsequently increasing by 17-30% from M24 to M60 vs BL. The sCTX best-fit model, accounting for u $\beta$ -CTX/Cr reduction, larger CTx species (e.g. 1-CTP) accumulation and osteoclast number increases in the ODN group, was identified within 0.0% (BL) to 4.4% (M6) of the observed sCTX returning to BL in ODN-treated patients by M48. By M6, ODN

treatment reduced PINP and BSAP vs PBO although levels returned to near-BL and were comparable to PBO levels by M48 and M60.

Conclusion: The consistent and significant reductions of uNTX,  $\alpha$ - and  $\beta$ -CTX over 5 years of treatment support ODN's persistent efficacy to inhibit bone resorption. The increases in larger CTx species and Trap-5b explain the return of sCTX to BL. Transient reductions observed in PINP and BSAP, as well as the time-dependent increases in 1-CTP and Trap-5b in the ODN group underscore the unique mechanism mediating collagen processing and bone turnover by ODN.

Table. Changes in bone turnover markers – geometric least squares mean percent changes from baseline

Markers	ODN 50 mg once weekly (%)		Placebo (%)	
	M6	M60	M6	M60
uNTx/Cr	-59.4	-36.7	-4.0	13.0
u $\alpha$ -CTX/Cr	-96.5	-91.7	7.1	26.5
u $\beta$ -CTX/Cr	-94.8	-85.5	-0.6	22.5
sCTX	-53.5	-6.4	7.1	29.6
s1-CTP	120.3	266.3	2.9	26.7
sTrap-5b	-5.6	26.5	-3.9	-0.9
sPINP	-41.6	8.5	-16.0	6.7
sBSAP	-29.7	-4.9	-12.1	-5.4

NTx = N-telopeptides of type 1 collagen; Cr = creatinine; CTx = C-telopeptides of type 1 collagen; 1-CTP = pyridinoline cross-linked carboxyterminal telopeptide of type 1 collagen; Trap-5b = tartrate-resistant acid phosphatase-5b; PINP = N-terminal propeptides of type 1 collagen; BSAP = bone-specific alkaline phosphatase.

Table. Changes in bone turnover markers

Disclosures: **Le T. Duong**, Merck & Co (employment), 15  
This study was sponsored by Merck & Co. Inc.

## FR0304

**Soluble Interleukin-6 receptor released by osteocytes promotes bone formation and maintains trabecular bone mass by *trans*-signaling.** Melissa Murat, Emma C Walker, Patricia Ho, Brett Tonkin, Narelle McGregor, T J Martin, Natalie A Sims\*. St. Vincent's Institute of Medical Research, Australia

Interleukin 6 (IL-6) is a major therapeutic target for inflammatory bone disease, but its effect is mediated by two receptor-mediated pathways. In cells that express the membrane bound IL-6 receptor (IL-6R) it acts through *cis*-signaling. In addition IL-6 utilizes a soluble form of the receptor (sIL-6R) by *trans*-signaling; this can occur in any cell, including IL-6R negative cells. The role of IL-6 in bone and the relative importance of these two pathways is controversial, since osteoblasts express low IL-6R levels, but their support of osteoclast formation requires sIL-6R.

To determine the role of *trans*-signaling *in vivo*, we assessed PEPCK-sgp130 mice in which sIL-6R action is specifically blocked by circulating sgp130-Fc, a stable gp130 co-receptor homodimer. At 12 weeks of age, both male and female PEPCK-sgp130 mice ( $n > 9$ /group) demonstrated lower trabecular bone volume (22% and 38% less, respectively,  $p = 0.02$ ), and lower trabecular number (17% and 33% less, respectively,  $p = 0.03$ ,  $p = 0.008$ ) than controls, indicating that IL-6 *trans*-signaling is required for normal trabecular bone mass.

Treatment of C57BL/6 mice ( $N = 6-8$ /group) for 5 days with calvarial injections of either IL-6+sIL-6R (200ng+100ng) or 200ng hyper-IL-6 (synthetic IL-6 covalently linked to sIL-6R, capable only of *trans*-signaling) stimulated bone formation, increasing calvarial thickness by  $17 \pm 6 \mu\text{m}$  (13%) and  $24 \pm 6 \mu\text{m}$  (18%) respectively ( $p < 0.05$ ). In contrast, treatment with 200ng IL-6 alone was ineffective. In addition, IL-6+sIL-6R treatment (but not IL-6 alone) suppressed sclerostin mRNA levels in OCY454 osteocytes and differentiated Kusa 4b10 cells. This indicates that even though osteoblasts respond to IL-6 *cis*-signaling with increased STAT3 phosphorylation, IL-6 promotes bone formation only through *trans*-signaling, and this may be mediated by inhibition of sclerostin expression.

Finally we observed that, as OCY454 cells and Kusa 4b10 stromal cells differentiated into osteocytes, mRNA levels and sIL-6R protein release progressively increased, reaching levels as high as 150pg/ml, parallel with their increase in sclerostin expression. This indicates that osteocytes are a local paracrine source of sIL-6R. Thus IL-6, through *trans*-signaling, reduces sclerostin expression, stimulates bone formation, and is required for normal trabecular bone mass. This raises the possibility that therapeutic inhibition of IL-6, as in current clinical practice, could directly suppress bone formation.

Disclosures: **Natalie A Sims**, None.

## FR0306

**1,25(OH)<sub>2</sub>D<sub>3</sub> Prevents Bone Aging by Inhibiting Oxidative Stress And Inactivating p16-Rb And p53-p21 Signaling.** Renlei Yang\*<sup>1</sup>, Lulu Chen<sup>1</sup>, Wei Zhang<sup>1</sup>, David Goltzman<sup>2</sup>, Dengshun Miao<sup>1</sup>. <sup>1</sup>Nanjing Medical University, China, <sup>2</sup>McGill University, Canada

We compared the bone phenotypes of 10-week-old  $1\alpha(\text{OH})\text{ase}^{-/-}$  mice fed a high calcium/phosphate (rescue) diet after weaning with age- and diet-matched wild-type mice. We found that serum 1,25(OH)<sub>2</sub>D<sub>3</sub> was undetectable and serum calcium, phosphorus and PTH were normalized, however, BMD, bone volume, osteoblast number, ALP-positive and type I collagen-positive areas were decreased significantly and the percentage of  $\beta$ -galactosidase-positive osteocytes was significantly increased. ROS levels of bone marrow cells were markedly increased, and the expression levels of p16, p53 and p21 and senescence-associated secretion phenotype (SASP) molecules including IL-1 $\alpha$ , TNF $\alpha$ , MMP3 and MMP13 were dramatically up-regulated in bone tissue of  $1\alpha(\text{OH})\text{ase}^{-/-}$  mice. These results support the concept that 1,25(OH)<sub>2</sub>D<sub>3</sub> deficiency induced aging in bone. Next we asked whether 1,25(OH)<sub>2</sub>D<sub>3</sub> can prevent bone aging by inhibiting oxidative stress and inactivating p16-Rb and p53-p21 signaling. To answer this question,  $1\alpha(\text{OH})\text{ase}^{-/-}$  mice and their wild-type littermates after weaning were injected subcutaneous with vehicle or 1,25(OH)<sub>2</sub>D<sub>3</sub> (1  $\mu\text{g}/\text{kg}$ ) thrice weekly or were fed a rescue diet with or without supplementation with the antioxidant NAC (N-acetyl-L-cysteine, 1mg/ml). In addition compound mutant mice with homozygous deletion of both p16 and  $1\alpha(\text{OH})\text{ase}$  [ $1\alpha(\text{OH})\text{ase}^{-/-}$ p16<sup>-/-</sup>] or compound mutant mice homozygous for  $1\alpha(\text{OH})\text{ase}$  deletion and heterozygous for p53 deletion [ $1\alpha(\text{OH})\text{ase}^{-/-}$ p53<sup>+/-</sup>] were generated and fed the rescue diet. Bone phenotypes of all models were analyzed at 10 weeks of age. Exogenous 1,25(OH)<sub>2</sub>D<sub>3</sub> supplementation rescued the bone aging phenotype induced by 1,25(OH)<sub>2</sub>D<sub>3</sub> deficiency. Thus, osteoblastic bone formation parameters were significantly increased, senescent osteocytes was clearly decreased, the ROS levels of bone marrow cells were markedly decreased, and the expression levels of p16-Rb and p53-p21 signaling molecules and SASP molecules were dramatically down-regulated. NAC supplementation of the rescue diet produced similar effects to 1,25(OH)<sub>2</sub>D<sub>3</sub> treatment on bone aging induced by 1,25(OH)<sub>2</sub>D<sub>3</sub> deficiency. Deletion of p16 or p53 in  $1\alpha(\text{OH})\text{ase}^{-/-}$  mice also largely rescued the bone aging phenotypes induced by 1,25(OH)<sub>2</sub>D<sub>3</sub> deficiency. The results of this study therefore indicate that in addition to regulating calcium/phosphate homeostasis, 1,25(OH)<sub>2</sub>D<sub>3</sub> can prevent bone aging by inhibiting oxidative stress and inactivating p16-Rb and p53-p21 signaling.

Disclosures: **Renlei Yang**, None.

## FR0307

**A Maternal Low Protein Diet During Pregnancy and Weaning Negatively Impacts Offspring Bone Mineral Density.** Ke-Hong Ding\*<sup>1</sup>, Kunlun Yu<sup>1</sup>, Qing Zhong<sup>1</sup>, William Hill<sup>1</sup>, Xingming Shi<sup>1</sup>, Jianrui Xu<sup>1</sup>, Wendy Bollag<sup>1</sup>, Monte Hunter<sup>1</sup>, Meghan McGee-Lawrence<sup>1</sup>, Mona El Refaey<sup>2</sup>, Maribeth Johnson<sup>1</sup>, Mohammed Elsalanty<sup>1</sup>, Ying Han<sup>3</sup>, Mark Hamrick<sup>1</sup>, Carlos Isaacs<sup>1</sup>. <sup>1</sup>Medical College of Georgia, United states, <sup>2</sup>Ohio University, United states, <sup>3</sup>Stomatology Hospital of Xi'an Jiaotong University, China

Epidemiologic data from studies such as the "The Dutch Famine Birth Cohort Study" demonstrate an association between insufficient maternal diet during pregnancy and detrimental long-term health conditions in the offspring including high blood pressure, obesity and diabetes. However, few studies have evaluated the impact of maternal diet composition on the skeletal health of offspring. Standard dietary protein content in a purified mouse diet is 18%. In studies approved by the Institutional Animal Care and Use Committee, twenty 3-month old C57BL/6 female mice were maintained on a standard 18% protein diet but when they became pregnant half of the pregnant females were switched to an isocaloric low-protein (8%) diet and half were maintained on the standard 18% protein diet for the duration of the pregnancy and during the weaning period (about 6 weeks). Upon weaning both male and female offspring were then maintained on a standard 18% protein purified diet and sacrificed at 3 months of age. Bone mineral density was evaluated by Digimul (Kubtec), bone turnover was measured by bone histomorphometry and biochemical markers of bone turnover by ELISA (PYD). There was no significant difference in body weight between the offspring at 3 months [Female:  $19.1 \pm 0.44$  (18% protein;  $n = 5$ ) vs.  $18.5 \pm 0.38$  gm+SD (8% protein;  $n = 6$ ); Male:  $24.6 \pm 1$  (18% protein;  $n = 8$ ) vs.  $24.3 \pm 0.6$  gm+SD (8% protein;  $n = 3$ );  $p = \text{ns}$ ]. However, BMD was significantly lower in the female offspring of those mothers maintained on a low-protein diet during pregnancy [Female:  $0.076 \pm 0.005$  (18% protein;  $n = 5$ ) vs.  $0.070 \pm 0.002$  gm/cm<sup>2</sup>+SD (8% protein;  $n = 6$ ); Male:  $0.077 \pm 0.004$  (18% protein;  $n = 8$ ) vs.  $0.076 \pm 0.003$  g/cm<sup>2</sup>+SD (8% protein;  $n = 3$ );  $p < 0.01$  for females 18 vs. 8% dietary protein]. PYD, a marker of bone breakdown, was significantly lower in the offspring of those mothers maintained on a low protein diet [Female:  $3.12 \pm 0.32$  (18% protein;  $n = 5$ ) vs.  $2.71 \pm 0.8$  nmol/L+SD (8% protein;  $n = 6$ );  $p < 0.001$ ]. Similarly, by histomorphometry, the mineral apposition rate was lower in the female offspring of the mothers maintained on the low protein (8%) diet [Female:  $0.64 \pm 0.05$  (18% protein;  $n = 5$ ) vs.  $0.53 \pm 0.13$  um/day+SD (8% protein;  $n = 6$ )]. These data are consistent with low bone turnover (both formation and breakdown) in the offspring of mothers maintained on a low protein diet. Further, these data suggest that maternal diet composition, in addition to caloric content, can have a significant effect on skeletal health in the offspring.

Disclosures: **Ke-Hong Ding**, None.

## FR0308

**Free Fatty Acid Receptor 4 (GPR120) Stimulates Bone Formation and Suppresses Bone Resorption in the Presence of Elevated *n*-3 Fatty Acid Levels.** Seong Hee Ahn<sup>\*1</sup>, Sook-Young Park<sup>2</sup>, Ji-Eun Baek<sup>2</sup>, Su-Youn Lee<sup>2</sup>, Wook-Young Baek<sup>2</sup>, Sun-Young Lee<sup>2</sup>, Young-Sun Lee<sup>2</sup>, Hyun Ju Yoo<sup>3</sup>, Hyeonmok Kim<sup>4</sup>, Seung Hun Lee<sup>4</sup>, Dong-Soon Im<sup>5</sup>, Sun-Kyeong Lee<sup>6</sup>, Beom-Jun Kim<sup>4</sup>, Jung-Min Koh<sup>4</sup>. <sup>1</sup>Department of Endocrinology & Metabolism, Inha University Hospital, Inha University School of Medicine, Korea, republic of, <sup>2</sup>Asan Institute for Life Sciences, Korea, republic of, <sup>3</sup>Biomedical Research Center, Asan Medical Center, University of Ulsan College of Medicine, Korea, republic of, <sup>4</sup>Division of Endocrinology & Metabolism, Asan Medical Center, University of Ulsan College of Medicine, Korea, republic of, <sup>5</sup>Molecular Inflammation Research Center for Aging Intervention (MRCA) & College of Pharmacy, Pusan National University, Korea, republic of, <sup>6</sup>UConn Center on Aging, University of Connecticut Health Center, Korea, republic of

Free fatty acid receptor 4 (FFA4; also known as GPR120) has been reported to be a receptor for *n*-3 fatty acids (FAs). Although *n*-3 FAs are beneficial for bone health, a role of FFA4 in bone metabolism has been rarely investigated. We noted that FFA4 was more abundantly expressed in both mature osteoclasts and osteoblasts than their respective precursors, and that it was activated by docosahexaenoic acid (DHA). FFA4 knockout (*Ffar4*<sup>-/-</sup>) and wild-type mice exhibited similar bone masses when fed on a normal diet. Since *fat-1* transgenic (*fat-1*<sup>Tg+</sup>) mice endogenously converting *n*-6 to *n*-3 FAs contain high *n*-3 FA levels, we crossed *Ffar4*<sup>-/-</sup> and *fat-1*<sup>Tg+</sup> mice over 2 generations to generate 4 genotypes of mice littermates: *Ffar4*<sup>+/+</sup>;*fat-1*<sup>Tg+</sup>, *Ffar4*<sup>+/+</sup>;*fat-1*<sup>Tg-</sup>, *Ffar4*<sup>-/-</sup>;*fat-1*<sup>Tg+</sup>, and *Ffar4*<sup>-/-</sup>;*fat-1*<sup>Tg-</sup>. Female and male littermates were included in ovariectomy- and high-fat diet (HFD)-induced bone loss models, respectively. Female *fat-1*<sup>Tg+</sup> mice decreased bone loss after ovariectomy both by promoting osteoblastic bone formation and inhibiting osteoclastic bone resorption than their wild-type littermates, only when they had the *Ffar4*<sup>+/+</sup> background, but not the *Ffar4*<sup>-/-</sup> background. In a HFD-fed model, male *fat-1*<sup>Tg+</sup> mice had higher bone mass resulting from stimulated bone formation and reduced bone resorption than their wild-type littermates, only when they had the *Ffar4*<sup>+/+</sup> background, but not the *Ffar4*<sup>-/-</sup> background. In vitro studies supported the role of FFA4 as *n*-3 FA receptor in bone metabolism. In conclusion, FFA4 is a dual-acting factor that increases osteoblastic bone formation and decreases osteoclastic bone resorption, suggesting that it may be an ideal target for modulating metabolic bone diseases.

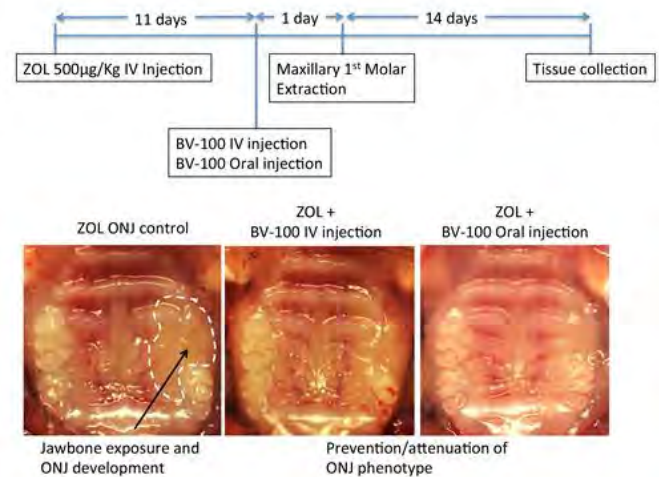
**Disclosures:** Seong Hee Ahn, None.

## FR0310

**Competitive equilibrium-based displacement of bisphosphonates for the prevention of BRONJ.** Akishige Hokugo<sup>\*1</sup>, Shuting Sun<sup>2</sup>, Mark Lundy<sup>2</sup>, Charles E. McKenna<sup>3</sup>, Frank H. Ebetino<sup>2</sup>, Ichiro Nishimura<sup>4</sup>. <sup>1</sup>Regenerative Bioengineering & Repair (REBAR) Lab, Division of Plastic & Reconstructive Surgery Department of Surgery, David Geffen School of Medicine at UCLA, United states, <sup>2</sup>BioVinc LLC, United states, <sup>3</sup>Department of Chemistry, USC Dornsife College of Letters, Arts & Sciences, United states, <sup>4</sup>Weintraub Center for Reconstructive Biotechnology, UCLA School of Dentistry, United states

Osteonecrosis of the jaw (ONJ) has been reported as a severe oral complication typically described in intravenously treated cancer patients or, less often, in osteoporosis patients treated by oral administration with nitrogen-containing bisphosphonates (BPs). We previously reported that an equilibrium-dependent BP-bone mineral interaction allowing a previously adsorbed fluorescent labeled BP to be displaced from HAP by another BP could be demonstrated in vitro. Here we examine whether pre-adsorbed BP can be displaced by a competing BP administered by local injection in vivo, and whether antiresorptive inactive BPs can be used to reduce ONJ in our model by displacing zoledronate from jawbones. Fluorescent labels were linked to zoledronate (5-FAM-ZOL and AF647-ZOL). Male C57Bl/6 mice (25-week old) were intravenously (iv) injected with 100  $\mu$ L of 50  $\mu$ M AF647-ZOL. After two days, 10  $\mu$ L of 5-FAM-ZOL at 0, 1, 10 and 50  $\mu$ M was locally injected at the subperiosteal space of cranial bone and palatal gingiva. Mice were euthanized after 2 hours and cranial and maxilla bones were harvested and subjected to high resolution CCD camera-based bio-fluorescence analysis, then processed for non-decalcified cryosections for confocal laser scanning microscopy. After AF647-ZOL was adsorbed on cranial and maxilla bone, subsequent 5-FAM-ZOL application displaced a significant amount of the AF647-ZOL at the bone surface. The 5-FAM-ZOL labeling was limited to the external surface of cranial bone, suggesting that the local injection did not give rise to systemic 5-FAM-ZOL circulation. To evaluate the ONJ preventive effect of the displacement approach, male mice were iv injected with 500  $\mu$ g/kg of ZOL. After one day, an antiresorptive inactive BP, BV-100, was iv or orally injected. The left maxillary

first molar was extracted and the wound healing observed 2 weeks later. Wound healing was nearly completed in the control mice, whereas ZOL injected mice showed delayed healing with gingival swelling, consistent with an ONJ-like lesion. In contrast, the challenge with BV-100 resulted in an ONJ lesion area with a much attenuated phenotype, suggesting that BV-100 had substantially displaced ZOL from jawbone to block the induced ONJ. Our data strongly suggest that "competitive equilibrium"-based displacement of legacy BPs, accumulated at the jawbone from routine antiresorptive therapy (eg bone metastases, osteoporosis), may provide the basis for developing a novel preventive modality of ONJ.



**Fig**

**Disclosures:** Akishige Hokugo, None.

## FR0311

**Maxillary Periodontitis and Osteonecrosis of the Jaw-Like Lesions in Rice Rats (*Oryzomys palustris*) Fed a Standard Diet and Treated with Zoledronic Acid.** J. Ignacio Aguirre<sup>\*1</sup>, Jonathan Messer<sup>1</sup>, Jessica Jiron<sup>1</sup>, Hung-Yuan Chen<sup>1</sup>, Evelyn Castillo<sup>1</sup>, Jorge Mendieta Calle<sup>1</sup>, Catherine Van Poznak<sup>2</sup>, Donald Kimmel<sup>1</sup>. <sup>1</sup>Department of Physiological Sciences, University of Florida, United states, <sup>2</sup>Internal Medicine Oncology, University of Michigan, United states

Osteonecrosis of the jaw (ONJ) is an adverse event seen in patients given powerful anti-resorptives (pARs). We hypothesize that when infection related to severe periodontitis (PD) kills bone tissue and pARs slow the resorption of this necrotic bone, an ONJ lesion with its characteristic dead bone, is created. To investigate the roles of dose/duration of zoledronic acid (ZOL), a pAR, on the prevalence of both PD and ONJ-like lesions, we performed two parallel experiments with variation in diet. We present here data from rice rats fed a standard diet. 224 healthy female rice rats were weaned. At age 4 wks, 12 rats were necropsied. The rest were weight-randomized into five groups. Each group received one of five ZOL treatment regimens: 0, 8, 20, 50, or 125  $\mu$ g/kg ZOL IV monthly. At 12, 18, 24, and 30 wks, groups (N=8-13) were necropsied. At necropsy all rats underwent oral exams. High resolution photos of the four jaw quadrants were obtained and examined by three independent observers who provided PD scoring and located/diagnosed ONJ-like lesions using a 0-5 scale<sup>1</sup>. Maxillary (Mx) PD lesions ranged from locally-inflamed gingiva between molars 2-3 (M2M3) to exposed, necrotic bone involving M1M3 and the hard palate. ONJ-like lesions were identified grossly as exposed bone and are being formally confirmed histopathologically. Two-factor ANOVA (ZOL dose/time) of PD Score and ONJ-like lesion prevalence was completed. Fisher's PLSD test was used to compare groups as appropriate. 15% (N=25) of ZOL-exposed rats developed ONJ like Mx lesions, while none showed gross PD or ONJ-like mandibular (Mn) lesions. PD prevalence was 300% higher in the Mx than the Mn. We found: 1) no PD or ONJ-like lesions were present in age 4wks rats; 2) all 0  $\mu$ g/kg ZOL groups had significant, focal PD lesions of similar severity, with no ONJ; 3) all groups given  $\geq 20$  $\mu$ g/kg ZOL, regardless of duration, had more severe PD lesions than 0 or 8 $\mu$ g/kg ZOL groups; 4) most ONJ occurred at  $\geq 18$ wks and  $\geq 20$  $\mu$ g/kg; and 5) prevalence of PD and ONJ-like lesions increased significantly with longer duration and higher dose, with an interaction of ZOL dose/duration (all P<.0001). This is the first experiment to demonstrate a positive relationship of relevant ZOL dose and duration to prevalence of Mx PD and ONJ-like lesions in rice rats fed standard rat chow. It also shows that rice rats simply fed a standard diet develop focal, self-limited Mx PD by age 16wks. <sup>1</sup>Aguirre JI et al. J Bone Min Res 27:2130-2143(2012).

**Disclosures:** J. Ignacio Aguirre, None.

**FR0312**

**Bone-Targeted Bortezomib Prevents OVX- and Myeloma-Induced Bone Loss with Less Systemic Adverse Effects more Effectively than Bortezomib.** Hua Wang<sup>\*</sup>, L. Xiao<sup>1</sup>, Hengwei Zhang<sup>1</sup>, Wen Sun<sup>1</sup>, Frank Hal Ebetino<sup>1</sup>, Robert K. Boeckman, Jr.<sup>1</sup>, Babatunde Oyajobi<sup>2</sup>, Brendan Boyce<sup>1</sup>, Lianping Xing<sup>1</sup>. <sup>1</sup>University of Rochester Medical Center, United states, <sup>2</sup>University of Texas Health Science Center at San Antonio, United states

Bortezomib (Btz) is a proteasome inhibitor approved by FDA to treat multiple myeloma (MM) patients. It also increases bone volume by inhibiting osteoclasts (OCs) and stimulating osteoblasts (OBs) in mice. However, Btz has severe systemic adverse effects, limiting its use as a bone anabolic agent. Here, we designed and synthesized a bone-targeted (BT) Btz by conjugating Btz to a non-bioactive bisphosphonate via a carbamate linker. BT-Btz inhibited OC formation and bone resorption and stimulated OB differentiation in vitro to a similar degree as Btz. In vivo, BT-Btz was more effective than Btz in 3 mouse models. 1) BT-Btz treatment of 7-wk-old WT mice increased OB differentiation and trabecular bone volume more than Btz (CFU-ALP#:  $46 \pm 7$  vs.  $34 \pm 7$ ; BV/TV:  $20 \pm 1\%$  vs.  $17 \pm 0.6$ ). 2) BT-Btz treatment of OVX-mice increased OB differentiation, bone volume and strength more than Btz (CFU-ALP#:  $58 \pm 8$  vs.  $34 \pm 10$ ; BV/TV:  $14 \pm 3\%$  vs.  $9 \pm 1$ ; energy to yield:  $0.9 \pm 0.1 \text{N} \cdot \text{mm}$  vs.  $0.6 \pm 0.1$ ). 3) BT-Btz treatment of MM mice induced by 5TGM1-GFP myeloma cells decreased tumor burden, lower limb disability, and bone loss more than Btz (GFP intensity:  $2.2 \pm 1.8 \times 10^8$  vs.  $0.7 \pm 1.6$ , disability: 80% vs. 16%; BV/TV:  $11.8 \pm 3.1\%$  vs.  $7.4 \pm 2.1$ ). Lastly, we compared the systemic toxicities of Btz and BT-Btz to vehicle-treated mice. In the thymus, Btz, but not BT-Btz, decreased weight ( $66 \pm 11$  mg vs.  $31 \pm 5$  vs.  $60 \pm 6$ ), total cell # ( $155 \pm 13 \times 10^6$  vs.  $14 \pm 4$  vs.  $143 \pm 17$ ), CD3+ T cell # ( $20 \pm 2 \times 10^6$  vs.  $4 \pm 1$  vs.  $21 \pm 8$ ) and B220 B+ cell # ( $2.9 \pm 0.5 \times 10^6$  vs.  $0.7 \pm 0.2$  vs.  $2.8 \pm 1$ ). In bone marrow, neither Btz or BT-Btz affected total cell #, but BT-Btz induced a greater reduction in CD19+ B cells ( $22 \pm 0.8\%$  vs.  $14 \pm 2$  vs.  $10 \pm 2$ ). In the peripheral blood, compared to vehicle, Btz, but not BT-Btz, reduced platelet # ( $426 \pm 95$  vs.  $125 \pm 17 \times 10^3/\text{ml}$  vs.  $231 \pm 67$ ), red blood cell # ( $6.6 \pm 1 \times 10^6/\text{ml}$  vs.  $5 \pm 1$  vs.  $7 \pm 1$ ) and white blood cell # ( $4.5 \pm 1.4 \times 10^3/\text{ml}$  vs.  $1.3 \pm 0.3$  vs.  $5.2 \pm 1.9$ ), and Btz, but not BT-Btz, reduced sympathetic nerve myelin thickness ( $3.6 \pm 0.7$  vs.  $2.4 \pm 0.6$  vs.  $3.8 \pm 0.9$ ) and myelinated axon diameter ( $2.1 \pm 0.6$  vs.  $1.3 \pm 0.2$  vs.  $2.4 \pm 0.7$ ). In summary, BT-Btz more potently increased bone volume and reduced MM-induced bone destruction with less systemic adverse effects than Btz. We conclude that BT-Btz represents a novel therapeutic approach to prevent pathologic bone degradation and stimulate new bone formation in inflammatory bone and joint disorders, osteoporosis, cancer-related bone loss, and other common skeletal diseases.

**Disclosures:** Hua Wang, None.

**FR0313**

**Co-deletion of Lrp5 and Lrp6 in bone severely diminishes bone gain from sclerostin antibody administration.** Kyung-Eun Lim<sup>\*</sup>, Bart Williams<sup>2</sup>, Chris Paszty<sup>3</sup>, Matthew Warman<sup>4</sup>, Alexander Robling<sup>1</sup>. <sup>1</sup>Indiana University School of Medicine, United states, <sup>2</sup>Van Andel Research Institute, United states, <sup>3</sup>Amgen, Inc., United states, <sup>4</sup>Boston Children's Hospital, United states

Sclerostin antibody is a potent osteogenic agent that acts via the Wnt signaling pathway. Based on low osteoblastic activity in *Lrp5*<sup>-/-</sup> mice, and enhanced osteoblastic activity in *Lrp5*-HBM mice (*Lrp5*-G171V or A214V), we surmised in previous work that the osteogenic effects of sclerostin inhibition occurred mainly through increased *Lrp5*-mediated Wnt signaling. Contrary to our expectations, in both genetic and pharmacologic studies, *Sost*/sclerostin suppression significantly increased osteogenesis regardless of *Lrp5* status, suggesting that osteogenic action can occur through *Lrp6*, or through other yet undiscovered mechanisms independent of *Lrp5/6*. To distinguish between these two possibilities we generated mice with compound deletion (*lox*/*Dmp1*-Cre approach) of *Lrp5* and *Lrp6* in bone and treated them with Scl-Ab. All mice were compound *lox* for *Lrp5* and *Lrp6* (*Lrp5*<sup>fl/fl</sup>; *Lrp6*<sup>fl/fl</sup>). *Dmp1*-Cre positive (transgenic, TG) and negative (nontransgenic, NTG) mice (*n*=7-9 per geno/sex) were injected with Scl-Ab from 4.5-14 wks of age. For all data reported we found similar effects for male and female mice. Prior to initiation of treatment, TG mice exhibited significantly less DEXA-derived whole body bone mineral content (BMC) than sex-matched NTG littermates, indicating that *Lrp5/6* deletions were effective. By 14 wks, Scl-Ab-treated NTG males had 216mg more BMC than vehicle-treated NTG littermates ( $407 \pm 20$ mg for vehicle vs  $623 \pm 20$ mg for Scl-Ab-treated, a 53% increase, *p*<0.01), whereas Scl-Ab-treated TG males had only 62mg more BMC than vehicle-treated TG littermates ( $194 \pm 23$ mg for vehicle vs  $256 \pm 38$ mg for Scl-Ab-treated, a 32% increase, *p*<0.01). In other words, there was a 3.5-fold greater absolute BMC gain ( $216$  vs  $62$ mg) in the NTG males compared to the TG males, thus highlighting the importance of both *LRP5* and *LRP6* for sclerostin function. The fact that the TG mice did gain some BMC (62mg) with Scl-Ab could be due to incomplete recombination of one or more of the four floxed *Lrp5/6* alleles in each targeted cell, or to antibody-induced promotion of Wnt signaling in cell types earlier in the mesenchymal/osteoblast differentiation pathway than the *Dmp1*-expressing stage. In conclusion, unlike with the deletion of *Lrp5* alone, the bone-selective late-stage co-deletion of *Lrp5* and *Lrp6* significantly impairs the osteogenic action of Scl-Ab, and highlights a major role for both *Lrp5* and *Lrp6* in the mechanism of action for the bone-building effects of sclerostin antibody.

**Disclosures:** Kyung-Eun Lim, None.

**FR0314**

**Forces Associated with SpaceX Launch do not Impact Bone Healing but Unloading Inhibits Bone Regeneration.** Paul Childress<sup>\*</sup>, Cynthia-May S. Gong<sup>2</sup>, Evan Himes<sup>1</sup>, Sungshin Choi<sup>2</sup>, Yasaman Shirazi-Fard<sup>2</sup>, Todd McKinley<sup>1</sup>, Tien-min Chu<sup>3</sup>, Nabarun Chakraborty<sup>4</sup>, Rasha Hammamieh<sup>4</sup>, Melissa Kacena<sup>1</sup>. <sup>1</sup>Department of Orthopaedic Surgery, Indiana University School of Medicine, United states, <sup>2</sup>WYLE Labs, United states, <sup>3</sup>Department of Biomedical & Applied Sciences, Indiana University School of Dentistry, United states, <sup>4</sup>US Army Center for Environmental Health Research, United states

Segmental bone defects (SBDs) secondary to trauma invariably result in a prolonged recovery with an extended period of limited weight bearing on the affected limb. Soldiers sustaining blast injuries and civilians sustaining high energy trauma typify such a clinical scenario. These patients frequently sustain composite injuries with SBDs in concert with extensive soft tissue damage. For soft tissue injury resolution and skeletal reconstruction a patient may experience limited weight bearing for upwards of 6 months.

Many small animal investigations have evaluated interventions for SBDs. While providing foundational information regarding treatment of bone defects, these models do not simulate limited weight bearing conditions after injury. As an example, mice ambulate immediately following anesthetic recovery and in most cases are normally ambulating within 1-3 days post-surgery. Thus, to better test novel bone healing strategies there is a need to develop new models that combine disuse with bone healing. To this end we will be working in the ultimate disuse environment, microgravity ( $\mu\text{G}$ ), on SpaceX-10. In preparation for this mission we conducted launch simulation and hindlimb unloading (HLU) studies on mice which underwent a SBD surgery. In brief, a 2 mm defect was created in the femur of 10 week-old C57BL/6 male mice (*n*=9/10/group). To mimic our upcoming spaceflight, 3 days after surgery, mice were: a) subjected to launch simulation (vibration and gravitational forces), b) served as launch negative controls, c) immediately after launch simulation were subjected to HLU to simulate unloading in spaceflight, or d) served as HLU negative controls. Mice were euthanized after 28 days and bone healing was examined via  $\mu\text{CT}$ . These studies demonstrated that our surgical procedure can withstand the forces and vibrations associated with launch. Additionally, forces and vibrations associated with launch did not impact bone healing (*p*=0.3). However, HLU resulted in a 52.5% reduction in total callus volume (*p*=0.0003). Taken together, these findings suggest that mice having a femoral SBD surgery can withstand the conditions associated with launch and that launch itself does not impact bone healing, but that the lack of weight-bearing associated with HLU, does impair bone healing. Based on these findings we will proceed with testing the bone healing efficacy of current and novel therapies using the unique spaceflight environment as an unloading model.

**Disclosures:** Paul Childress, None.

**FR0315**

**Single Bisphosphonate Dosing Enhances Effects of Sclerostin Antibody On Stiffness of the Vertebral Body During Growth in an Osteogenesis Imperfecta Mouse Model.** Diana Olvera<sup>\*</sup>, Basma Khoury<sup>1</sup>, Joan C. Marini<sup>2</sup>, Michelle S. Caird<sup>1</sup>, Kenneth M. Kozloff<sup>1</sup>. <sup>1</sup>Orthopaedic Research Laboratories, Department of Orthopaedic Surgery, University of Michigan, United states, <sup>2</sup>Bone & Extracellular Matrix Branch, National Institute of Child Health & Human Development, NIH, United states

Osteogenesis imperfecta (OI) is a genetic disorder caused by collagen-related mutations which leads to increased bone fragility and low bone mass. Brittle bones are the hallmark of OI and the annual fracture rate is most prominent during childhood. Clinically, antiresorptive bisphosphonates (BP) are used in an attempt to increase bone mass and reduce fracture risk. We have recently shown a significant anabolic response to sclerostin antibody (SclAb) in bones from young mice harboring an OI-causing defect. Therefore, the purpose of this study is to evaluate whether the concurrent use of BP and SclAb confers structural and functional gains in vertebral bone mass through independent means between the two interventions. To model the effects of BP and SclAb in OI, we used *Brtl*<sup>+/+</sup> mice, with a G349C mutation on *coll1a1* and WT controls. At 21 days of age, male mice received a single injection of BP at either 0.3mg/kg or 0.625mg/kg of pamidronate (PAM) or saline control. After a three day latency period, mice were randomly assigned to SclAb treatment or saline groups and injected subcutaneously twice a week for two weeks, at 25mg/kg. Mice were euthanized at day 37. MicroCT of lumbar vertebrae (Fig.1A) revealed that treatment with PAM alone induced a dose dependent preservation of trabecular number at 0.3 mg/kg (*Brtl*<sup>+/+</sup> 6%; WT 7%) and 0.625 mg/kg (*Brtl*<sup>+/+</sup> 10%; WT 12%) vs. untreated control. SclAb led to an average increase in trabecular thickening of 12% for *Brtl*<sup>+/+</sup> and 23% for WT across the range of PAM dosing, and increased trabecular number independent of PAM in WT. Together, these effects led to a maximum increase in bone volume fraction of 33% for *Brtl*<sup>+/+</sup> and 43% for WT over untreated controls. While PAM had no effect on lumbar vertebral cortical thickness, SclAb induced average cortical thickening gains of 9% in *Brtl*<sup>+/+</sup> and 6% in WT. Functionally, dosing with PAM alone induced a dose dependent increase in stiffness at 0.3 mg/kg (*Brtl*<sup>+/+</sup> 60%; WT 28%) and 0.625 mg/kg (*Brtl*<sup>+/+</sup> 90%; WT 73%) vs. untreated control, but did not improve maximum load (Fig. 1B). SclAb led to further stiffening of the bone on top of PAM effects, but unlike PAM alone, increased maximum load by up to 49% in *Brtl*<sup>+/+</sup> and up to 56% in WT. Although SclAb alone can significantly improve

maximum load, minimal BP dosing may help amplify the effects of SclAb to further improve vertebral rigidity, a beneficial outcome for children with OI.

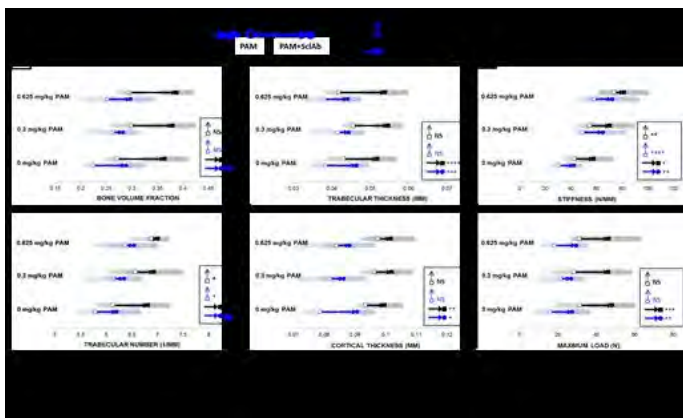


Figure 1

Disclosures: Diana Olvera, None.

### FR0316

#### Alleviating Osteonecrosis of the Femoral Head by Suppressing the ER Stress.

Daquan Liu<sup>1</sup>, Xinle Li<sup>1</sup>, Jie Li<sup>1</sup>, Shuang Yang<sup>1</sup>, Hiroki Yokota<sup>2</sup>, Ping Zhang\*<sup>2</sup>. <sup>1</sup>Department of Anatomy & Histology, School of Basic Medical Sciences, Tianjin Medical University, China, <sup>2</sup>Department of Biomedical Engineering, Indiana University-Purdue University, United states

Osteonecrosis of the femoral head (ONFH) is a serious orthopedic problem in the hip joint. Salubrinal is a synthetic compound that inhibits de-phosphorylation of eukaryotic translation initiation factor 2 alpha (eIF2 $\alpha$ ), and at a proper dose it reduces cell death from the endoplasmic reticulum (ER) stress. Little is known whether ONFH-driven ischemia triggers the ER stress, and whether salubrinal administration mitigates symptoms associated with the ER stress. Using a rat model, we examined a hypothesis that salubrinal suppresses the ER stress and enhances angiogenesis and bone remodeling.

Twenty seven male SD rats (~12 wks) were randomly divided into 3 groups: sham control group, osteonecrosis group, and salubrinal-treated osteonecrosis group (n=9). Osteonecrosis was induced by transecting the ligamentum teres followed by a tight ligature around the femoral neck. A dosage of 0.1 mg/kg salubrinal was administered subcutaneously every day for 4 weeks to the salubrinal-treated group. We evaluated salubrinal's effect on angiogenesis and bone remodeling, as well as the development of endothelial cells, osteoclasts, and osteoblasts.

A PERK-ATF4 axis of the ER stress was activated in the ONFH model, and we observed ONFH-induced bone loss and reduction in vessel perfusion in the femoral head ( $p < 0.01$ ). Salubrinal significantly restored bone mass and vessel perfusion of the femoral head by suppressing the ER stress ( $p < 0.05$ ). Salubrinal also inhibited osteoclastogenesis and stimulated osteoblast development ( $p < 0.05$ ). Furthermore, it promoted the proliferation, migration, and angiogenesis of endothelial cells through elevating the levels of phosphorylated eIF2 $\alpha$ , as well as ATF4 and VEGF ( $p < 0.05$ ).

Collectively, this study demonstrates that the ER stress is induced in the surgery-induced ONFH model, and salubrinal improves ONFH symptoms by suppressing the ER stress and enhancing angiogenesis and bone remodeling.

Disclosures: Ping Zhang, None.

### FR0319

#### In Vivo Hypobaric Hypoxia, Hypodynamia and Bone Healing in Mice.

Marjorie DURAND\*, Xavier Holy, Institut de Recherche Biomédicale des Armées, France

Although several techniques are used to manage bone defect, post-traumatic bone reconstruction represents an ongoing challenge for the orthopaedic community. Angiogenesis is essential during bone regeneration and is triggered by hypoxic stimuli. Hypoxia is also believed to induce both mesenchymal (MSC) and hematopoietic stem/progenitor cell mobilization - a process involved in bone healing mechanism. Herein, we addressed the effects of a hypoxic challenge applied to mice during the repair of a femoral bone defect. Additionally, to mimic conditions of non weight-bearing limb immobilization in patients suffering from bone trauma, our hypoxic mouse model was subjected to hindlimb unloading.

A drill-hole was performed in the right femur of adult male C57/BL6J mice. Four days after surgery, mice were subjected to hindlimb unloading for one week. Seven days after surgery, mice were either housed for 4 days into a hypobaric room (FiO<sub>2</sub> = 10%) or kept under normoxic conditions. Unloaded control mice were either housed in hypobaric or normoxic conditions. Animals (n=10/group) were sacrificed on post-surgery day 11 to allow for collection of both contralateral and lesioned femurs, blood and spleen.

As hypothesized, hypobaric hypoxia applied during the repair process was found to enhance bone healing efficiency by increasing the closing of the cortical defect and the newly synthesized bone volume in the cavity by +55% and +35%, respectively.

Interestingly, this effect was not related to an extended mobilization of MSC-derived osteoprogenitors from the contralateral femur to the lesioned femur. Proteomic data and histomorphometric analysis rather suggested that bone repair improvement likely resulted from the acceleration of natural bone healing process by hypoxia. Moreover, the hypoxia-driven enhanced bone healing was not impacted by hindlimb unloading. Similarly, unloading did not influence bone healing efficiency in normoxic mice in spite of a drop in the bone marrow number of MSCs. Alternatively to the hypoxic challenge, we further investigated the healing effect of erythropoietin (EPO), identified as a downstream target of the hypoxic response pathway, and showed that a ten day systemic treatment of EPO enhanced bone healing.

In conclusion, our results indicated that hypobaric hypoxia applied in the course of bone repair accelerated the healing process. The effect of hypoxia was likely to be correlated with the EPO production pathway. Thus, EPO may serve as a therapeutic agent to facilitate bone regeneration.

Disclosures: Marjorie DURAND, None.

### FR0320

#### Role of matrix-bound Bisphosphonates in the development of osteonecrosis of the jaw.

Ranya Elsayed<sup>1</sup>, R. Nicole Howie<sup>2</sup>, Sudha Ananth<sup>1</sup>, Pheba Abraham<sup>1</sup>, Mohamed Awad<sup>1</sup>, Zachary Patterson<sup>1</sup>, Mohammed Elsalanty\*<sup>3</sup>. <sup>1</sup>Augusta University, United states, <sup>2</sup>Medical University of South Carolina, United states, <sup>3</sup>Dental College of Georgia, Augusta University, United states

Bisphosphonates deposit in the bone matrix in human patients for many years. Previous studies investigating bisphosphonate complications focused mostly on their systemic effects. We hypothesize that matrix-bound bisphosphonate molecules are biologically active and contribute to the pathogenesis of bisphosphonate-related osteonecrosis of the jaw (BRONJ). In this study, we examined the distribution and accessibility to chelation of matrix-bound bisphosphonates *in vivo*, *ex vivo*, and *in vitro*, using Far-red fluorescent pamidronate (FRFP) tracing as well as mass spectrometry. We tested the effect of matrix-bound bisphosphonates on osteoclast differentiation *in vitro* using TRAP staining and osteoclast resorption assay. We also tested the effect of zoledronate chelation on the healing of post-extraction defect in the jaw in rats. Our results confirmed that bisphosphonates deposited preferentially to certain bone sites *in vivo*, including the alveolar bone, proximal and distal ends of the long bones, and bodies of the vertebrae. Bisphosphonates also bound to dentin matrix *in vitro* in a dose-dependent manner. Matrix-bound bisphosphonates impaired the differentiation of osteoclasts, evidenced by TRAP activity and resorption assay. Chelation with EDTA significantly reduced bisphosphonate content in the matrix of dentin discs. The application of EDTA to extraction sockets in bisphosphonate-treated rats reduced the bisphosphonate content on the surface of dental socket. Bisphosphonate-treated rats that underwent bilateral dental extraction with unilateral EDTA treatment showed significant improvement in alveolar healing scores on the chelated sites, evidenced by mucosal healing and micro-CT analysis ( $p = 0.0087$ ). The results suggest that matrix-bound bisphosphonates are biologically accessible and could contribute to the pathogenesis of BRONJ. The use of chelating agent is a promising strategy for the prevention of BRONJ following dental procedures in bisphosphonate-treated patients.

Disclosures: Mohammed Elsalanty, None.

### FR0323

#### Dental Findings from the National Institutes of Health Fibrous Dysplasia/McCune-Albright Syndrome Cohort.

Andrea Burke\*, Alison Boyce, Michael Collins. NIDCR, United states

Purpose: Fibrous Dysplasia/McCune-Albright syndrome (FD/MAS) is a rare disease which is caused by somatic activating mutations in G-protein coupled receptor/cAMP-regulating protein, Gs-alpha, which is coded for by the GNAS gene (Weinstein, 1991). Fibrous Dysplasia occurs when osteogenic precursors proliferate and replace normal bone with fibrous tissue/woven bone. The craniofacial bones are the most frequently affected in patients with FD (Collins, 2005). While previous reports have described some of the craniofacial and dental findings in FD/MAS (Akintoye, 2013), including an increased number of craniofacial surgeries and an increased prevalence of osteonecrosis of the jaws (Boyce, 2015; Metwally, 2015), a definitive description of the cohort is lacking. The aim here is to better define the specific dental problems in this population.

Methods: Retrospective data from the NIH FD/MAS cohort was reviewed: 207 subjects with FD/MAS were evaluated, including radiographic studies and medical/dental clinical records.

Results: Of the 207 subjects, 110/207 had FD of the maxilla or mandible (53%) and 95/207 (45%) were evaluated for dental findings as part of the natural history protocol. Dental findings included malocclusion, including crowding and rotation of teeth, with 50/95 (53%) of subjects reporting a significant malocclusion. Orthodontic therapy was reported in 35/95 (37%) of the screened subjects. Eight subjects (8%) reported having root canal therapy. Twelve subjects (13%) were noted to have gingivitis or periodontal disease at the time of evaluation. Twenty-two (23%) subjects were documented as having significant dental caries, and eight subjects (8%) were noted to have enamel hypomineralization. Five subjects were diagnosed with osteonecrosis of the jaws (5%), associated with bisphosphonate treatment. Other characteristic findings included temporomandibular joint dysfunction and short labial/lingual frenum.

Conclusion: FD/MAS subjects with craniofacial disease have unique dental needs, making it important that they be evaluated by a specialist. Findings included an

elevated incidence of malocclusion, and subsequent need for orthodontic treatment. There is also an increased prevalence of ONJ and enamel hypomineralization. This data will help guide treatment, and provide long-term study into the dental effects of fibrous dysplasia in the craniofacial bones.

**Disclosures:** Andrea Burke, None.

## FR0324

**Increased Risk of Breast Cancer in Polyostotic Fibrous Dysplasia and McCune-Albright Syndrome.** Bas Majoor\*, Olaf Dekkers, Sander Dijkstra, Judith Bovee, Vincent Smit, Neveen Hamdy, Natasha Appelman-Dijkstra. Leiden University Medical Center, Netherlands

Introduction Fibrous dysplasia (FD) is caused by mutations of the GNAS-gene, which have also been identified in associated tumours, eg myxomas (Mazabraud syndrome) and in McCune-Albright Syndrome (MAS) in intraductal pancreatic mucinous cysts and thyroid cancers. Breast cancer has been reported in MAS but has been linked to hormonal dysregulation. To explore the relationship between breast cancer and FD we studied the incidence of breast cancer in our FD cohort and used data from the Dutch Pathology Registry (PALGA), a nationwide database of histology reports, to validate our findings.

Methods Data were retrieved from 131 female FD patients (94 monostotic, 26 polyostotic and 11 MAS) followed-up in our centre between 1990-2015. Data were collected on age of onset and localisation of FD, and on occurrence, age at diagnosis, type of carcinoma and known risk factors for breast cancer. Standardized morbidity ratios (SMR) were estimated using data from the Dutch National Cancer Registry and the prevalence of breast cancer in FD patients was validated using histology reports obtained from the PALGA database for with a report of breast cancer between 1992-2015.

Results Nine patients (6.8%, 6 polyostotic FD, 3 MAS) developed breast cancer at a median age of 46yrs (37-54) vs a national median age of 61yrs. Eight patients had FD localisations at the thorax, including ribs, sternum and thoracic spine, and 7 patients had FD lesions of the midline or ipsilateral to the breast cancer. The SMR was 6.1 (95%CI: 2.7-10.8) for all FD patients (n=131) and 21.1 (95%CI: 8.8-38.7) for FD patients with thorax lesions (n=42). Within the FD group the odds ratio was 44 (95%CI: 5-374) for FD with thorax lesions. The PALGA data confirmed an increased prevalence of breast cancer in FD. Mean age at time of histology of FD was 34yrs ( $\pm 17.4$ SD) and similar to findings from our cohort, 6.51% of all female FD patients from the PALGA database developed breast cancer at a low median age at time of histology of breast cancer of 51yrs (27-75).

Conclusion We found that patients with polyostotic FD and MAS have an increased risk of breast cancer, especially in patients with thorax lesions and this occurs at a younger age. The exact mechanism remains to be elucidated but may be linked to the recently identified GNAS mutations in breast cancer. Although perhaps premature, these findings do suggest that screening for breast cancer may be considered in FD patients, particularly those with thorax lesions.

**Disclosures:** Bas Majoor, None.

This study received funding from: Leiden University Bontius Foundation Grant for research into fibrous dysplasia.

## FR0325

**Inhibition of Activin A Stops the Regrowth of Surgically Resected Heterotopic Bone in a Mouse Model of Fibrodysplasia Ossificans Progressiva and Indicates a New Potential Path to Therapy.** Lily Huang, Liqin Xie, Nanditha Das, Xialing Wen, Lili Wang, Andrew Murphy, Vincent Idone, Aris Economides, Sarah Hatsell\*. Regeneron Pharmaceuticals, United states

Fibrodysplasia ossificans progressiva (FOP) is a rare genetic disorder characterized by episodic yet cumulative heterotopic ossification (HO), which develops connections to the normal skeleton, resulting in progressive immobility. The heterotopic bone cannot be resected because such procedures result in regrowth of the resected lesions and induction or exacerbation of additional HO. FOP is caused by mutations in ACVR1, with the most common mutation altering arginine 206 to histidine (ACVR1<sup>R206H</sup>). Using a genetically accurate mouse model of FOP - *Acvr1*<sup>[R206H]Flox<sup>+/+</sup></sup> *Gt(ROSA26)* *Sor*<sup>CerERT2/+</sup> - we have demonstrated that unlike wild type ACVR1, ACVR1<sup>R206H</sup> perceives Activin A as an agonistic ligand, and that it is this new property of ACVR1<sup>R206H</sup> that drives HO. Furthermore, using neutralizing anti-Activin A antibodies we have shown that there is an absolute requirement for Activin A to initiate HO (Hatsell, Idone et al; PMID 26333933). Here we extend our findings and demonstrate that inhibition of Activin A in a surgery setting (where an HO lesion is resected while the mice are administered antibody) provides 'therapeutic' benefit. In this setting, inhibition of Activin A stops further growth of existing or partially resected HO lesions. Importantly, whereas surgery (in the absence of anti-Activin A) induces 'explosive' growth of the resected lesion as well as nearby lesions, this effect is greatly inhibited in the presence of the antibody. Given that the majority of FOP patients already present with ongoing or existing HO at the time of diagnosis (and also the number of patients with developed disease), our results not only demonstrate that Activin A remains a key HO-promoting factor even after initiation of HO but also indicate a new potential path to therapy where surgical intervention may be incorporated.

**Disclosures:** Sarah Hatsell, None.

This study received funding from: Regeneron Pharmaceuticals

## FR0326

**Ambulatory Performance in Adolescents and Adults with Hypophosphatasia Treated with Asfotase Alfa: Data from a Phase II, Randomized, Dose-ranging, Open-label, Multi-center Study.** Priya S. Kishnani\*<sup>1</sup>, Cheryl Rockman-Greenberg<sup>2</sup>, Katherine L. Madson<sup>3</sup>, Marisa Gavron<sup>4</sup>, Uchenna Iloeje<sup>4</sup>, Michael P. Whyte<sup>5</sup>. <sup>1</sup>Duke University Medical Center, United states, <sup>2</sup>University of Manitoba, Canada, <sup>3</sup>Shriners Hospital for Children, United states, <sup>4</sup>Alexion Pharmaceuticals, United states, <sup>5</sup>Shriners Hospital for Children & Washington University School of Medicine, United states

Purpose: Hypophosphatasia (HPP) is the rare metabolic disease due to loss-of-function mutation(s) in the gene encoding tissue nonspecific alkaline phosphatase (TNSALP). Affected adolescents/adults may experience fractures, arthropathies, pain, and muscle weakness, impairing mobility and quality of life. We examined if the effects of asfotase alfa, a TNSALP replacement, on ambulation in such patients (pts; Kishnani, ENDO2016, OR26-3) were influenced by baseline (BL) ambulatory status.

Methods. *Post hoc* analysis of a Phase II study of asfotase alfa for adolescents/adults with HPP (NCT01163149). Pts aged 13-65 years (y) were randomized to untreated control (n=6) or treatment (tx) either with 0.3 (n=7) or 0.5 mg/kg/day (n=6) asfotase alfa for 6 months (mo). All then received 0.5 mg/kg/day, increased 6-12 mo later to 1 mg/kg 6x/week by protocol amendment. Analysis was performed relative to tx start with dose group data combined. Performance changes on the 6-Minute Walk Test (6MWT), including use of assistive devices, were examined for both pts with normal performance (NP,  $\geq 84\%$  of distance predicted for age, height, and gender; Henricson, 2012; Geiger, 2007) and low performance (LP;  $< 84\%$  predicted) at BL. Data are reported as mean (95% confidence interval).

Results. 19 pts enrolled (age  $< 18$ y, n=6; age  $\geq 18$ y, n=13). 17 pts had  $\geq 3$ y and 10 had  $\geq 4$ y tx (3 pts withdrew: 2 injection site lipodystrophy at 2 y and 3.5y, 1 poor compliance at 2.5y). Median age at HPP symptom onset was 2y (min, max: 0, 36; n=18). At BL, the LP group (n=9) walked 347m (278, 417; 62.3% [53.4, 71.3] predicted), the NP group (n=6) walked 540m (462, 617; 92.3% [84.9, 99.8] predicted), 2 pts were unable to complete the 6MWT, and 1 was excluded (cognitive impairment). The LP group improved by +57m (17, 97; +11.2% [2.8, 19.5] predicted,  $p < 0.01$ ) at 6 mo and +66m (7, 125; +13.4% [2.1, 24.8] predicted,  $p < 0.05$ ) by last assessment (LA). The NP group improved by +37.5m (7, 68; +7.6% [1.0, 14.2],  $p < 0.05$ ) at 6 mo, and +57m (0, 135, n=5; +12.8% [0.6, 24.9] predicted,  $p < 0.05$ ) by LA. Both pts who at BL could not complete the 6MWT improved distance walked during tx (variable; up to 204m and 160m, respectively). At BL, 5 pts needed an assistive device during the 6MWT: at 2y, 2 reduced and 3 eliminated this need for devices on the 6MWT.

Conclusions. Adolescents/adults with HPP experienced clinically important improvements in their ambulatory performance during asfotase alfa tx regardless of BL ambulatory status.

**Disclosures:** Priya S. Kishnani, Alexion Pharmaceuticals, Inc, 15; Alexion Pharmaceuticals, Inc, 11

This study was supported by Alexion Pharmaceuticals, Inc.

## FR0327

**Skeletal, growth, and functional improvements in infants and young children with life-threatening hypophosphatasia treated with asfotase alfa for 5 years.** Jill H. Simmons\*<sup>1</sup>, Nick Bishop<sup>2</sup>, Richard Lutz<sup>3</sup>, Hui Zhang<sup>4</sup>, Kenji P. Fujita<sup>4</sup>, Michael P. Whyte<sup>5</sup>. <sup>1</sup>Vanderbilt University School of Medicine, United states, <sup>2</sup>University of Sheffield, United Kingdom, <sup>3</sup>University of Nebraska Medical Center, United states, <sup>4</sup>Alexion Pharmaceuticals, Inc, United states, <sup>5</sup>Shriners Hospital for Children & Washington University School of Medicine, United states

Hypophosphatasia (HPP) in infants features poor bone mineralization leading to rickets and is sometimes complicated by seizures, respiratory compromise, poor growth, and/or delayed gross motor function (MF). Asfotase alfa is a first-in-class enzyme-replacement therapy approved for pediatric-onset HPP<sup>1</sup>. We have reported improved survival, skeletal manifestations, respiratory function, growth, and MF in infants and young children with life-threatening HPP treated with asfotase alfa (ENB-003-08/NCT01205152) for up to 3 years (yrs)<sup>1,2</sup>. Here, we report the 5-yr experience.

Change in HPP-related skeletal disease was assessed with the Radiographic Global Impression of Change (RGI-C) scale (-3=severe worsening; +3=near-complete healing). Length/height assessments used a stadiometer and Z-scores were calculated from population-appropriate growth standards (Centers for Disease Control charts, 2000). MF was determined by the Bayley Scales of Infant Development III (BSID-III) scaled score for patients (pts) aged  $\leq 42$  months (mo), and the Locomotion Subtest of the Peabody Developmental Motor Scales 2<sup>nd</sup> edition (PDMS-2) standard score for pts aged  $\geq 43$  mo to  $\leq 71$  mo. Score increases reflect greater skill acquisition.

At baseline (BL), pts (n=11) were median (min, max) 13.6 (0.7, 36.4) mo of age. 1/pt withdrew consent; 1 died (sepsis unrelated to treatment)<sup>1</sup>. 9/11 pts received 5 yrs treatment in this Phase II, multicenter, open-label study (generally 6 mg/kg/week subcutaneously, dose adjustments permitted). RGI-C scores documented significant skeletal improvement by 6 mo sustained through 5 yrs (Table). Length/height and weight Z-scores from BL to Yr 5 reflected catch-up growth (Table). BSID-III scaled scores at BL/first assessment indicated functional delay in all pts (Table); scores

improved by Yr 1, with the fine MF median score attaining the normal range<sup>1</sup>. 5 pts transitioned to PDMS-2 by Yr 5, scoring near the normal range. The most common adverse events (AEs) were mild-to-moderate injection site reactions; 3 serious AEs were considered possibly drug-related (chronic hepatitis in 1 pt, resolved; craniosynostosis and conductive deafness in 1 pt, dose unchanged).

In these infants and young children with HPP treated with asfotase alfa, substantial improvements in skeletal manifestations and motor function were sustained through 5 yrs of treatment, along with catch-up growth in most pts. Asfotase alfa was well-tolerated, with most AEs considered mild or moderate.

	BL (N=11)	Year 1 (n=9)	Year 2 (n=9)	Year 5 (n=9)
<b>RGI-C</b>	—	+2.7 (+1.3, +3.0)	+2.0 (+2.0, +3.0)	+2.0 (+2.0, +3.0)
<b>Growth assessment</b>				
<b>Length/height Z-score</b>	-3.7 (-9.2, -0.7)	-2.9 (-9.2, -1.2)	-2.7 (-8.4, -1)	-2.7 (-9.0, 0.1)
<b>Weight Z-score</b>	-3.8 (-5.4, -0.5)	-3.3 (-6.3, -1.7)	-2.4 (-4.8, -0.9)	-1.2 (-5.0, 0.2)
<b>Functional assessment</b>				
	BL/FA			
<b>BSID-III*</b>				
<b>n</b>	11	7	6	—
<b>GMF scaled score</b>	1 (1, 9)	2 (1, 5)	5 (1, 7)	—
<b>FMF scaled score</b>	5 (1, 13)	7 (6, 10)	9.5 (7, 11)	—
<b>PDMS-2*</b>				
<b>n</b>	—	—	1	5
<b>Locomotion standard score</b>	—	—	5 (5, 5)	7 (4, 13)

Data reported as median (minimum, maximum). No hypothesis testing was performed.  
n, patients for whom data were available/who could accomplish the test.  
\*Mean (standard deviation) for healthy age-matched peers is 10 (3).  
BL, baseline; BSID-III, Bayley Scales of Infant Development III; FA, first assessment; FMF, fine motor function; GMF, gross motor function; PDMS-2, Peabody Developmental Motor Scales; RGI-C, Radiographic Global Impression of Change

1. Whyte MP, et al. *N Engl J Med* 2012;366:904-13  
2. Bishop N, et al. *Horm Res Paediatr* 2014;82[Suppl. 1]:1-105

Table

**Disclosures:** Jill H. Simmons, Alexion Pharmaceuticals, Inc, 13  
This study was supported by Alexion Pharmaceuticals, Inc.

## FR0328

**Subtrochanteric, diaphyseal femoral fractures in Hypophosphatasia.** Franca Genest\*, Lothar Seefried, Wuerzburg University, Germany

**Introduction:** Published evidence of several case reports suggests that Hypophosphatasia (HPP) is associated with increased risk for subtrochanteric femoral (pseudo)-fractures. In patients on long-term antiresorptive treatment subtrochanteric, so-called atypical femoral fractures (AFF) were supposed to be associated with suppressed bone remodeling and limb geometry. However, the commonalities and disparities between AFFs and lower limb stress fractures in HPP are still unclear.

**Methods:** Monocentric, retrospective analysis of medical records and radiographs of 140 adult HPP patients to evaluate frequency and characteristic features of subtrochanteric, diaphyseal femoral fractures. Date acquisition included fracture morphology, course of occurrence, diagnosis and treatment, limb/bone geometry, genotype, previous medical treatment (particularly antiresorptives), ALP activity, PLP level, Vitamin D and Bone Mineral Density (DXA).

**Results:** By now, 21 subtrochanteric femoral fractures were identified in 12 patients (11 female). None was caused by an adequate trauma. Based on available radiographs, all fractures initiated from the lateral cortex. Prodromal symptoms were documented in n=4 patients. In total 20/21 fractures were treated surgically with some form of intramedullary rodding (n=19) or plating (n=1). Delayed fracture healing was reported by 8 of these 12 patients. Revision surgery was required in 4/12 patients due to implant failure or recurrent fracture. Mean age at the time of fracture was 43.6 (range 20-59 years). Genotype was available for 9 patients with 8 of them harboring two mutations. Available PLP and PEA levels in n=10 patients were considerably elevated in all of them, ranging from 159-1959ng/ml (Reference 7-30ng/ml) and from 19.3-180mmol/molKrea (Reference 2.3-11.3mmol/molKrea) for PLP and PEA in urine, respectively. Lumbar spine BMD, available for 10 patients was elevated with positive T-Scores in 8/10 (T-Score range -0.6 to + 7; mean T-Score +2.33). Previous treatment with bisphosphonates could be revealed in 6 patients with a cumulative exposure times ranging from 1 to 10 years (mean 5 years).

**Discussion:** The risk of subtrochanteric/diaphyseal femoral fractures appears to be considerably elevated in HPP (nearly 10% of patient in this cohort), particularly in case of additional exposure to bisphosphonates and in those eliciting elevated lumbar spine BMD. Clinical and radiographic findings of subtrochanteric fractures in HPP are similar to what is known for AFF in the setting of long-term antiresorptive treatment, suggesting a common pathophysiological background. Consequently, patients experiencing AFFs should be screened for low ALP values/HPP and HPP should be ruled out before starting antiresorptive treatment. Results for PEA/PLP suggest elevated substrate levels to be a potential indicator for this kind of fracture.

**Disclosures:** Franca Genest, None.

## FR0329

**Utilization of an algorithm to identify individuals at risk for hypophosphatasia (HPP) within an electronic health record (EHR) database.** Joseph Biskupiak\*<sup>1</sup>, Amy Sainski<sup>1</sup>, Minkyung Yoo<sup>1</sup>, Diana Brixner<sup>1</sup>, Uchenna Iloeje<sup>2</sup>. <sup>1</sup>Pharmacotherapy Outcomes Research Center, Department of Pharmacotherapy, University of Utah, United states, <sup>2</sup>Alexion Pharmaceuticals, Inc., United states

**Objectives:** HPP is a rare, metabolic disease caused by loss-of-function mutation(s) in the *ALPL* gene resulting in low tissue-nonspecific alkaline phosphatase (TNSALP) activity and defective bone/teeth mineralization. It is multi-systemic, ranging from still birth in the most severe form to developmental delays, failure to thrive, poor bone health with deficient mineralization, multiple fractures, severe pain, impaired mobility and disability later in life. HPP is often misdiagnosed because of low awareness and absence of age and gender specific ALP reference ranges. We present an algorithm for identifying probable HPP patients in an EHR database.

**Methods:** The University of Utah Healthcare system EHR database representing 1.6 million individuals from Jan. 1990 thru Dec. 2014 was queried for patients with a disorder of phosphorous metabolism (ICD9 275.3) or a low ALP (CPT code 84705). Of these patients, patients with persistently low ALP ( $\geq 2$  measurements, low age-gender specific levels, never normal, no bisphosphonates,) were screened for clinical, biochemical and radiographic evidence of HPP: seizures/respiratory failure in children <5 years old; elevated serum PLP or PPI; elevated urine PEA; HPP family history; radiographic evidence of hypomineralization/osteomalacia; history or treatment of non-traumatic fractures/premature tooth loss/craniosynostosis/multiple fractures/rickets. Patients with  $\geq 1$  of these additional manifestations were considered as probable HPP patients. Protocol was approved by the University of Utah IRB.

**Results:** Of 5262 patients coded with a disorder of phosphorus metabolism or low ALP, 42 were identified as probable HPP patients by persistently low ALP and relevant symptomatology. The mean (SD) number of serum ALP tests in the 42 patients was 16.5 (21.9) with a median of 5 tests. Age distribution was 0-6 months: n = 3; 7 months -<18 years: n = 9; 18+ years: n = 30. Of all individuals identified as probable HPP, only 3 had a known diagnosis of HPP.

**Conclusions:** Utilizing this algorithm, we were able to identify 42 patients in a hospital setting with a probable diagnosis of HPP; only 3 carried the HPP diagnosis. A chart abstraction study is underway to evaluate each of the identified patients to better understand the likelihood of a diagnosis of HPP and the severity of disease burden.

**Disclosures:** Joseph Biskupiak, None.

This study was supported by Alexion Pharmaceuticals, Inc.

## FR0330

**SLC34A1/NPT2a Mutations cause Hereditary Hypophosphatemic Rickets with Hypercalciuria.** Alyssa Chen\*<sup>1</sup>, Avram Traum<sup>2</sup>, Amita Sharma<sup>2</sup>, Henry Fehrenbach<sup>3</sup>, Anne Schafer<sup>4</sup>, Dolores Shoback<sup>4</sup>, Magged Hussein<sup>5</sup>, Bernd Hoppe<sup>6</sup>, Harald Jüppner<sup>2</sup>, Clemens Bergwitz<sup>1</sup>. <sup>1</sup>Yale School of Medicine, United states, <sup>2</sup>Massachusetts General Hospital, United states, <sup>3</sup>Klinikum Memmingen, Germany, <sup>4</sup>University of California San Francisco, United states, <sup>5</sup>King Faisal Specialist Hospital & Research Center, Saudi arabia, <sup>6</sup>Universität Bonn, Germany

We previously reported inactivating mutations on both parental alleles of the solute carrier family 34, member 3 (*SLC34A3*), the gene encoding the sodium-dependent phosphate cotransporter 2c (*NPT2c*), as cause of hereditary hypophosphatemic rickets with hypercalciuria (HHRH), an autosomal recessive renal phosphate-wasting disorder. Individuals affected by HHRH show increased urinary phosphate excretion leading to hypophosphatemic rickets, bowing, and short stature as well as appropriately elevated 1,25(OH)<sub>2</sub>D levels. Elevated 1,25(OH)<sub>2</sub>D levels, in turn, result in hypercalciuria because of enhanced intestinal calcium absorption and reduced parathyroid hormone (PTH)-dependent calcium reabsorption in the distal renal tubules. As recently shown, heterozygous *SLC34A3/NPT2c* mutations are frequently associated with idiopathic hypercalciuria (IH), which may cause nephrocalcinosis and kidney stones. To determine the genetic basis in 15 thus far unclassified individuals with HHRH or IH, in whom *SLC34A3/NPT2c* was normal, we performed whole-exome sequencing. Two individuals were found to carry biallelic, while four individuals were heterozygous for sequence variants in *SLC34A1*, predicted to change the amino acid sequence of the sodium-dependent co-transporter 2a (*NPT2a*) encoded by this gene. Two of these variants (*c.271\_291del:p.91\_97del, c.644+1G>A*) were recently reported in children affected by idiopathic infantile hypercalcemia (IIH), while *c.G284A:p.R95H, c.389-5C>T, c.T774C:p.H258H, c.C1702T:p.H568Y* were not previously reported in HHRH, IH, or IIH. One individual was found to carry the previously reported heterozygous mutation in *FGF23 c.G536A:p.R179Q* that is diagnostic for autosomal dominant hypophosphatemic rickets (ADHR). Evaluation of additional 53 genes known to cause nephrolithiasis or hypophosphatemic disorders revealed rare (minor allele frequency of less than 1%) non-synonymous heterozygous nucleotide sequence variants in *FAM20C* (four individuals), *SLC34A2, SLC12A1, SLC3A1* (two individuals each) and *ADCY10, XDH, CLCNKB, GRHRP, TRPM6* (one individual each). Segregation analysis and correlation with clinical symptoms is necessary to determine the significance of these sequence variants.

**Disclosures:** Alyssa Chen, None.

## FR0331

**Evaluating the Effects of KRN23, a Fully Human Anti-FGF23 Monoclonal Antibody, on Functional Outcomes in Children with X-linked Hypophosphatemia (XLH): 40-week Interim Results from a Randomized, Open-label Phase 2 Study.** Erik Imel<sup>1</sup>, Thomas Carpenter<sup>2</sup>, Agnès Linglart<sup>3</sup>, Annemieke Boot<sup>4</sup>, Wolfgang Högl<sup>5</sup>, Raja Padidela<sup>6</sup>, William van't Hoff<sup>7</sup>, Anthony Portale<sup>8</sup>, Sunil Agarwal<sup>9</sup>, Chao-Yin Chen<sup>9</sup>, Alison Skrinar<sup>9</sup>, Javier San Martin<sup>9</sup>, Michael Whyte<sup>10</sup>. <sup>1</sup>Indiana University School of Medicine, United states, <sup>2</sup>Yale University School of Medicine, United states, <sup>3</sup>Hôpital Bicêtre, France, <sup>4</sup>University of Groningen, Netherlands, <sup>5</sup>Birmingham Children's Hospital, United Kingdom, <sup>6</sup>Royal Manchester Children's Hospital, United Kingdom, <sup>7</sup>Great Ormond Street Hospital, United Kingdom, <sup>8</sup>University of California, United states, <sup>9</sup>Ultragenyx Pharmaceutical Inc., United states, <sup>10</sup>Shriners Hospital for Children, United states

XLH is a hypophosphatemic disorder mediated by high circulating FGF23. The resulting skeletal abnormalities, including rickets and bowing of the legs, can significantly impair gross motor function and quality of life in childhood or adulthood. Current treatment with oral phosphate/active vitamin D is suboptimal in many patients.

In a Phase 2 study, 52 XLH children (ages 5-12 years) received KRN23 subcutaneously biweekly or monthly. At study entry, 35 of the first 36 subjects enrolled had received oral phosphate/active vitamin D for a mean of 6.6 years. Interim 40-week data from these 36 subjects showed KRN23 significantly improved serum phosphorus and rickets. Walking ability (six-minute walk test [6MWT]) and patient-reported pain and functional disability (Pediatric Outcomes Data Collection Instrument [PODCI]) were assessed for these 36 subjects at Week 40. Analysis included the full cohort and a pre-specified subset with more severe baseline (BL) rickets (Rickets Severity Score [RSS]  $\geq 1.5$ ).

At BL, 14/36 (39%) subjects had walking impairment defined as 6MWT distance  $< 80\%$  predicted for age; 10/14 had RSS  $\geq 1.5$  and 4/14 had RSS  $< 1.5$ . Those with walking impairment (BL mean distance 412 meters, mean 70% predicted) improved by a Least Squares (LS) mean of 79 meters (m) ( $p < 0.0001$ ), a 19% increase. Subjects with RSS  $\geq 1.5$  improved by a LS mean of 94 m ( $p < 0.0001$ ), a 22% increase, and patients with RSS  $< 1.5$  improved by a LS mean of 79 m ( $p < 0.0001$ ), a 21% increase at Week 40.

At BL, 15/36 (42%) subjects had substantial functional impairment (PODCI Global Functioning score  $< 40$ ) with a BL mean of 24.5 ( $> 2$  SD below the normal mean of 50, 1 SD=10); 10/15 had RSS  $\geq 1.5$  and 5/15 had RSS  $< 1.5$ . Subjects' scores showed particular functional impairments in the Sports/Physical Function (PF) and Pain/Comfort domains (BL means of 17.5 and 24.8 respectively). After 40 weeks of KRN23 treatment, mean score increases were +15.1, +18.3, and +12.5 for overall Global Functioning, the Sports/PF domain, and the Pain/Comfort domain, respectively (Figure). For those with impairments, subjects with RSS  $\geq 1.5$  had mean increases of +17.9, +22.0, and +16.6, while subjects with RSS  $< 1.5$  had mean increases of +9.6, +11.0, and +4.4 for Global Functioning, the Sports/PF domain, and the Pain/Comfort domains, respectively.

Walking ability, pain, and function are impaired in some children with XLH despite current treatment. These data suggest KRN23 may substantially improve these key functional outcome measures.

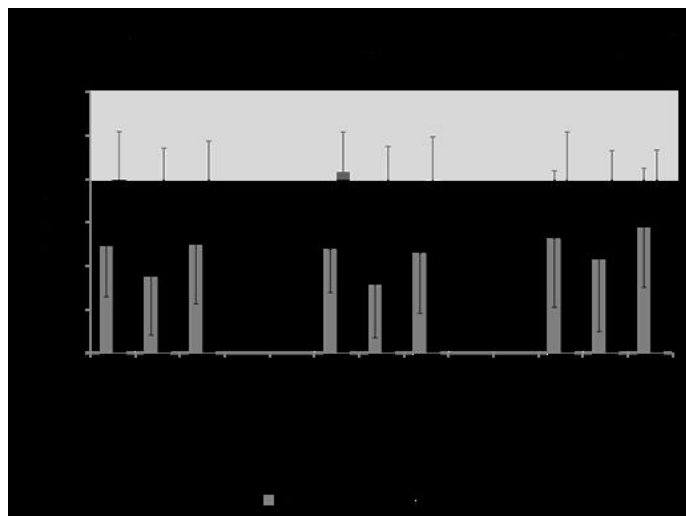


Figure.

**Disclosures:** Erik Imel, Ultragenyx Pharmaceuticals Inc., 11; Ultragenyx Pharmaceuticals Inc., 15  
This study received funding from: Ultragenyx Pharmaceutical Inc. and Kyowa Hakko Kirin Co., Ltd.

## FR0332

**Factors Associated with Serum Intact FGF23 Levels in Patients with X-linked Hypophosphatemic Rickets.** Keiko Yamamoto\*, Takuo Kubota, Kei Miyata, Shinji Takevari, Kenichi Yamamoto, Hirofumi Nakayama, Makoto Fujiwara, Taichi Kitaoka, Satoshi Takakuwa, Keiichi Ozono. Department of Pediatrics, Osaka University Graduate School of Medicine, Japan

Fibroblast growth factor 23 (FGF23) decreases renal phosphate reabsorption and serum 1,25-dihydroxyvitamin D [ $1,25(\text{OH})_2\text{D}$ ] levels. X-linked hypophosphatemic rickets (XLH) is caused by mutations in the *PHEX* gene and accompanied by decreased serum inorganic phosphate (IP) and elevated serum FGF23 levels. Patients with XLH are generally treated with oral active vitamin D and phosphate, but some previous reports indicated that serum FGF23 levels increased with this treatment. However, factors related to serum FGF23 levels during the treatment in XLH patients remain unclear. Objective and hypotheses: We analyzed factors related to serum intact FGF23 levels in treated XLH patients to obtain better outcomes. Methods: Sixteen patients (male 12, female 4) with XLH and normal kidney function were included. The mean age at the first visit was 8 months, and the mean observation period was 5.6 years. We used all the data measured or obtained during the observation period as follows. We examined the association of serum intact FGF23 levels with age, doses of active vitamin D (alfacalcidol) and phosphate, serum calcium (Ca), IP, alkaline phosphatase (ALP), intact parathyroid hormone (PTH),  $1,25(\text{OH})_2\text{D}$ , and creatinine (Cr) levels in the XLH patients before and during the treatment using linear mixed-effects models in SPSS ver.23 software as statistic analysis. Results: Values associated with serum intact FGF23 levels in the XLH patients were age [negative association (neg),  $p=0.000$ ], serum Ca [positive association (pos),  $p=0.000$ ], IP (pos,  $p=0.000$ ), ALP (neg,  $p=0.007$ ),  $1,25(\text{OH})_2\text{D}$  (pos,  $p=0.001$ ), and Cr (pos,  $p=0.001$ ). Conclusion: Serum intact FGF23 levels were positively associated with serum Ca, IP,  $1,25(\text{OH})_2\text{D}$  and Cr levels and negatively with age and serum ALP levels, raising the possibility that Ca might induce FGF23 production as well as IP and  $1,25(\text{OH})_2\text{D}$ . We might be careful not to overcorrect serum Ca, IP,  $1,25(\text{OH})_2\text{D}$  levels during the treatment of XLH patients because increased FGF23 could exacerbate bone phenotypes and biochemical parameters. Considering the association of intact FGF23 with age and serum Cr levels in XLH patients, age and serum Cr levels could be involved in serum FGF23 levels, although their mechanisms are unclear.

**Disclosures:** Keiko Yamamoto, None.

## FR0333

**Non-lethal Type VIII Osteogenesis Imperfecta has Elevated Bone Matrix Mineralization.** Nadja Fratzi-Zelman<sup>1</sup>, Aileen M. Barnes<sup>2</sup>, MaryAnn Weis<sup>3</sup>, Erin Carter<sup>4</sup>, Theresa E. Hefferan<sup>5</sup>, Giorgio Perino<sup>4</sup>, Weizhong Chang<sup>6</sup>, Peter A. Smith<sup>6</sup>, Paul Roschger<sup>1</sup>, Klaus Klaushofer<sup>1</sup>, Francis H. Glorieux<sup>7</sup>, David R. Eyre<sup>3</sup>, Cathleen Raggio<sup>8</sup>, Frank Rauch<sup>7</sup>, Joan C. Marini<sup>2</sup>. <sup>1</sup>Ludwig Boltzmann Institute of Osteology at Hanusch Hospital of WGKK & AUVA Trauma Centre Meidling, 1st Med. Dept. Hanusch Hospital, Vienna, Austria, <sup>2</sup>Section on Heritable Disorders of Bone, NICHD, NIH, Bethesda, United states, <sup>3</sup>The Orthopaedic Research Laboratories, University of Washington, Seattle, United states, <sup>4</sup>Hospital for Special Surgery, New York, United states, <sup>5</sup>Department of Orthopedics, Mayo Clinic College of Medicine, Rochester, United states, <sup>6</sup>Shriners' Hospital for Children, Chicago, United states, <sup>7</sup>Shriners' Hospital for Children & McGill University, Montreal, Canada, <sup>8</sup>Department of Orthopedics, Mayo Clinic College of Medicine, Seattle, United states

**Purpose:** Type VIII Osteogenesis Imperfecta (OMIM #601915) is a recessive form of lethal or severe OI caused by null mutations in *P3H1*, which encodes prolyl 3-hydroxylase 1 (P3H1). P3H1 3-hydroxylates select prolyl residues of types I, II and V collagen. We present here the first complete clinical and bone material description of type VIII OI from 5 non-lethal cases, including two children homozygous for the West African *P3H1* allele treated with pamidronate from infancy throughout childhood.

**Methods:** Clinical examinations, including aBMD, radiographs, serum and urinary metabolites. Collagen biochemistry examined by mass spectrometry, collagen fibrils examined by TEM. Bone biopsy samples from non-treated patients were analyzed for histomorphometry; bone mineralization density distribution (BMDD) was assessed in all cases by quantitative backscattered electron imaging (qBEI) and compared with references from healthy, type VII and OI children with collagen-gene mutations.

**Results:** Type VIII OI patients have extreme growth deficiency, L1-L4 aBMD Z-score: -5 to -6, and normal bone formation markers. Collagen from bone and skin tissue, and cultured osteoblasts and fibroblasts has near absent 3-hydroxylation (1-4%). Moreover, collagen fibrils showed abnormal diameters and irregular borders. Bone histomorphometry revealed decreased cortical width, very thin trabeculae with patches of increased osteoid, although overall osteoid surface was within normal range. qBEI showed elevated bone matrix mineralization in cancellous and cortical bone: the most frequent calcium concentration, CaPeak was increased by +8.8% and +11.5% respectively (both  $p < 0.001$ ) and the fraction of highly mineralized bone, CaHigh, was increased by 12-fold and 25-fold respectively (both  $p < 0.001$ ) compared to healthy controls but not versus OI types I and VII. Interestingly, the fraction of

lowly mineralized bone (CaLow) was significantly elevated in OI type VIII versus healthy controls, OI type I and VII mirroring the foci of increased osteoid formation observed in bone histomorphometry. The increase of bone matrix mineralization was similar in treated and untreated patients.

Conclusions: P3H1 is the unique enzyme responsible for collagen 3-hydroxylation in skin and bone. Bone from non-lethal type VIII OI children is similar to type VII, especially bone matrix hypermineralization, but has distinctive features including osteoid accumulation and an increased proportion of lowly mineralized bone.

**Disclosures:** Nadja Fratzl-Zelman, None.

## FR0335

**Intra-Tibial Injection of Lymphatic Endothelial Cells Leads to Aggressive Osteolysis, a Mouse Model of Gorham-Stout Disease.** Hua Wang\*, Wensheng Wang, Xing Li, Wen Sun, Brendan Boyce, Lianping Xing. University of Rochester Medical Center, United states

Gorham-Stout disease (GSD) is a rare bone disorder, characterized by aggressive osteolysis associated with localized proliferation of lymphatic vessels within bone marrow cavities. The etiology of GSD is poorly understood and there is no effective therapy or animal model of the disease. Here, we studied the effects of lymphatic endothelial cells (LECs) on osteoclasts (OCs) or osteoblasts (OBs) and if they could cause a GSD osteolytic phenotype in mice. We first examined the effect of a mouse LEC line on OC and OB differentiation in co-cultures. LECs significantly increased RANKL-mediated OC formation (#/well:  $250 \pm 10$  vs.  $0 \pm 0$  in PBS) and bone resorption (pits area/slice:  $0.78 \pm 0.05$  mm<sup>2</sup> vs.  $0 \pm 0$  in PBS), but had no clear effect on OBs. LECs expressed high levels of M-CSF, an essential survival and activating factor for OCs and monocytes, but not of other osteoclastogenic factors, including RANKL, IL-6 and TNF. LEC-mediated OC formation and bone resorption were blocked by an M-CSF neutralizing antibody or by Ki20227, an inhibitor of the M-CSF receptor, c-Fms. We next injected LECs into the tibiae of WT C57BL/6 mice and 2 weeks later observed massive osteolysis on X-ray and micro-CT scanning. Histology showed that LEC-injected tibia had significant trabecular and cortical bone loss (BV/TV:  $14.5 \pm 3.9\%$  vs.  $1.1 \pm 0.7$ ) and increased OC numbers ( $14.8 \pm 5.5$ /mm vs.  $4.8 \pm 2.2$  in PBS-injected). M-CSF protein levels were significantly higher in serum and bone marrow plasma of mice given intra-tibial LEC injections (serum:  $1.8 \pm 0.3$  vs.  $1.3 \pm 0.15$  ng/ml in PBS-injected; bone marrow:  $59 \pm 6$  vs.  $22 \pm 4$  pg/ml in PBS-injected). Immunofluorescence staining of tibial sections showed extensive replacement of bone and marrow by podoplanin+ LECs that also stained strongly positively for M-CSF. Treatment of LEC-injected mice with Ki20227 significantly decreased tibial bone destruction (BV/TV:  $6.1 \pm 2.0\%$  vs.  $3.4 \pm 2.2$  in vehicle). In addition, lymphatic vessels in bone samples from GSD patients also stained positively for M-CSF. Thus, LECs cause bone destruction in vivo in mice by secreting M-CSF, which promotes OC formation and activation. Blocking M-CSF signaling may represent a new therapeutic approach for treatment of patients with GSD. Furthermore, tibial injection of LECs represents a useful mouse model to study GSD.

**Disclosures:** Hua Wang, None.

This study received funding from: The Lymphatic Malformation Institute

## FR0336

**Meckel's and condylar cartilages anomalies in achondroplasia result in defective development and growth of the mandible.** Martin Bioso Duplan<sup>1</sup>, Davide Komla-Ebri<sup>2</sup>, Yann Heuzé<sup>3</sup>, Valentin Estivals<sup>2</sup>, Emilie Gaudas<sup>2</sup>, Nabil Kaci<sup>2</sup>, Catherine Benoist-Lasselain<sup>2</sup>, Michel Zerah<sup>4</sup>, Ina Kramer<sup>5</sup>, Michaela Kneissel<sup>6</sup>, Diana Graus Porta<sup>6</sup>, Federico Di Rocco<sup>7</sup>, Laurence Legeai-Mallet<sup>\*2</sup>. <sup>1</sup>Institut Imagine, France, <sup>2</sup>Institut Imagine-INSERM U1163, France, <sup>3</sup>UMR5199 PACEA, Université de Bordeaux, France, <sup>4</sup>Hôpital Necker, France, <sup>5</sup>Novartis, Switzerland, <sup>6</sup>Novartis, France, <sup>7</sup>Neurochirurgie Pédiatrique, Hôpital Femme Mère Enfant CHU de Lyon, France

Activating FGFR3 mutations in human result in achondroplasia (ACH), the most frequent form of dwarfism, where cartilages are severely disturbed causing long bones, cranial base and vertebrae defects. Since mandibular development and growth rely on cartilages that guide or directly participate to the ossification process, we investigated the impact of FGFR3 mutations on mandibular shape, size and position. By using CT-scan imaging of ACH children and by analyzing Fgfr3Y367C/+ mice, a model of ACH, we show that FGFR3 gain-of-function mutations lead to structural anomalies of primary (Meckel's) and secondary (condylar) cartilages of the mandible, resulting in mandibular hypoplasia and dysmorphogenesis. These defects are likely related to a defective chondrocyte proliferation and differentiation and pan-FGFR tyrosine kinase inhibitor NVP-BGJ398 corrects Meckel's and condylar cartilages defects *ex vivo*. Moreover, we show that low dose of NVP-BGJ398 improves *in vivo* condyle growth and corrects dysmorphologies in Fgfr3Y367C/+ mice, suggesting that postnatal treatment with NVP-BGJ398 mice might offer a new therapeutic strategy to improve mandible anomalies in ACH and others FGFR3-related disorders.

**Disclosures:** Laurence Legeai-Mallet, None.

## FR0338

**Rescue of Short-lived Progressive Ankylosis Protein in Craniometaphyseal Dysplasia.** Jitendra Kanaujiya\*, Edward Bastow, Zhifang Hao, Ernst J Reichenberger, I-Ping Chen. University of Connecticut Health, United states

Mutations in the progressive ankylosis protein (ANKH, mouse ortholog ANK) are responsible for craniometaphyseal dysplasia (CMD), characterized by progressive thickening of craniofacial bones and widened metaphyses in long bones. Pathogenesis of CMD remains unknown and treatment for CMD is limited to risky and repetitive surgeries to relieve cranial nerve compression for preventing loss of vision, hearing, facial palsy and severe headache. We have reported a knock-in mouse model (*Ank*<sup>K1/K1</sup>) fully replicating features of human CMD. Interestingly, ablation of ANK (*Ank*<sup>KO/KO</sup> mice) also leads to some CMD-like phenotypes. The mechanism leading to shared phenotypes between *Ank*<sup>K1/K1</sup> and *Ank*<sup>KO/KO</sup> mice has not been investigated. We studied dominant negative effects of mutant ANK/ANKH to better understand CMD.

First we examined the expression and localization of ANK/ANKH by immunoblots and confocal immunocytochemistry and subsequently studied the degradation rate of wt and mutant ANK by [<sup>35</sup>S]-methionine pulse-chase assays. We investigated the involvement of proteasome and lysosomal degradation pathways in rapid turnover of CMD mutant ANK. Mutant ANK/ANKH protein levels were noticeably lower than wt ANK/ANKH expression levels in several model systems including rat osteosarcoma-derived (ROS) cells overexpressing wt or CMD mutant ANK, osteoclasts from *Ank*<sup>+/+</sup>, *Ank*<sup>+/K1</sup> and *Ank*<sup>K1/K1</sup> mice, as well as differentiated osteoblasts from CMD patients and healthy control subjects. While wt ANK was mostly associated with ER, Golgi and lysosomes, CMD mutant ANK was mislocalized within cells. CMD mutant ANK protein was significantly less stable in comparison to wt ANK. Half-lives of wt and CMD mutant ANK were approximately 8 and 2 hours, respectively. Interestingly, inhibitors of proteasomal degradation (MG-132, Bortezomib, and Epoxomicin), but not lysosomal degradation pathways rescued exogenous CMD mutant ANK expression in ROS cells in a dose-dependent manner as shown by immunoblots and by immunocytochemistry.

In summary, ANK/ANKH proteins with CMD mutations are short-lived and mislocalized. The unique phenotype in *Ank*<sup>K1/K1</sup> mice compared to *Ank*<sup>KO/KO</sup> mice includes massive jaw bones and club-shaped femurs and therefore suggests that CMD is not merely caused by a loss-of-function. However, we believe that our findings will direct future studies to investigate possible therapeutic strategies to partially ameliorate or delay phenotypes in CMD by increasing levels of functional ANKH.

**Disclosures:** Jitendra Kanaujiya, None.

## FR0339

**Small molecule Alk inhibitors with improved selectivity and pharmacokinetics inhibit heterotopic ossification without toxicity in a mouse model of fibrodysplasia ossificans progressiva.** Daniel Perrien\*, Corey Hopkins, Craig Lindsley, Audrey Frist, Heather Durai, Nicole Fleming, Sabrina Booton, Charles Hong. Vanderbilt University Medical Center, United states

Fibrodysplasia ossificans progressiva (FOP) is a disease characterized by episodic heterotopic ossification of skeletal muscle and connective tissues for which there is currently no treatment. The discovery that FOP is caused by a point mutation in the Type 1 BMP receptor, Alk2, creates the opportunity for development of small molecule inhibitors that target the precise cause of the disease. However, first generation Alk inhibitors targeting the ATP binding pocket of Alks, such as LDN and DMH1, showed little selectivity among Type 1 receptors and possessed poor solubility and pharmacokinetic (PK) properties. In order to develop a better compound, this group has used traditional medicinal chemistry approaches to modify the DMH1 backbone in search of molecules with improved selectivity, solubility, and PK properties sufficient for potential clinical development. Iterative modifications to the DMH1 backbone revealed that addition of heterocyclic ring structures improved PK and solubility without substantial effects on selectivity. Further addition of fluorine(s) to the heterocyclic ring groups improved selectivity with the IC<sub>50</sub> for Alk2 being as much as 50-10,000 fold lower than for all other Type 1 receptors. Adding a piperazine group to the opposite end of the molecule appears to improve solubility and protein binding, with serum free fractions up to 4%. To test *in vivo* efficacy and toxicity of select Alk inhibitors, 4-week old Alk2<sup>Q207D</sup> mice received i.m. injections of Ad-cre followed by cardiotoxin (CTX) in the gastrocnemius. Mice received i.p. injections of vehicle, or 10 mg/kg DMH1, VU2733, or VU2735 once- or twice-daily starting on the day of CTX injection until sacrifice. The formation of HO was measured by weekly *in vivo* radiographs and *ex vivo* microCT. DMH1 and VU2735 significantly inhibited HO compared to Veh. Complete blood counts, serum ALT, AST, and total iron were not significantly affected by any of the compounds. Histopathological analyses of numerous soft tissues did not reveal any drug-related alterations. These data demonstrate that the current generation of DMH1-derived Alk inhibitors may be acceptable for future clinical development to treat FOP.

**Disclosures:** Daniel Perrien, La Jolla Pharmaceutical Company, 11

This study received funding from: La Jolla Pharmaceutical Company

## FR0344

**Thoracic muscle density and size are associated with kyphosis severity: Framingham Study.** Amanda Lorbergs<sup>1</sup>, Dennis Anderson<sup>2</sup>, Brett Allaire<sup>2</sup>, Douglas Kiel<sup>3</sup>, Michelle Yau<sup>1</sup>, Mary Bouxsein<sup>4</sup>, L. Adrienne Cupples<sup>5</sup>, Tom Travison<sup>1</sup>, Elizabeth Samelson<sup>1</sup>. <sup>1</sup>Institute for Aging Research, Hebrew Senior Life & Harvard Medical School, United states, <sup>2</sup>Center for Advanced Orthopedic Studies, Beth Israel Deaconess Medical Center, United states, <sup>3</sup>Institute for Aging Research, Department of Medicine BIDMC, & Hebrew Senior Life & Harvard Medical School, United states, <sup>4</sup>Center for Advanced Orthopedic Studies, Beth Israel Deaconess Medical Center & Harvard Medical School, United states, <sup>5</sup>Department of Biostatistics, Boston University School of Public Health & Framingham Heart Study, United states

Studies suggest that back extensor muscle weakness is associated with more severe thoracic kyphosis. Lumbar paraspinal muscle density, reflecting greater intramuscular fat content, has also been shown to be associated with more severe kyphosis. Muscle properties of the thoracic spine, where most kyphosis angulation is observed, have not been investigated, but represent a potentially important and modifiable determinant of a hunched posture. We conducted a cross-sectional study to determine the association between thoracic and lumbar spinal muscle size and density and kyphosis severity.

Participants included 793 members (424 women, 369 men) of the Framingham Offspring and Third Generation cohorts who underwent quantitative computed tomography (QCT) scans. We evaluated trunk muscle cross-sectional area (CSA, mm<sup>2</sup>) and density (Hounsfield units, HU) in the thoracic (T8) and lumbar (L3) regions. In the thoracic region, we measured paraspinal (erector spinae (ES), transversospinalis (TS)) and posterior (ES, TS, and trapezius) muscles. In the lumbar region, we measured extensor (ES, TS) and paraspinal (ES, TS, psoas, and quadratus lumborum) muscles. We processed lateral QCT scout films with SpineAnalyzer software (Optasia Medical Ltd.) to evaluate kyphosis (T4-T12 Cobb angle, degrees). We used linear regression to estimate the association between muscle CSA (mm<sup>2</sup>) and density (HU) and kyphosis (degrees), adjusted for sex, age, height, and weight. Results did not differ between women and men, and adjustment for potential confounders (smoking, physical activity, bone density, vertebral fracture) did not affect findings. Therefore, we performed the analysis in the total sample and used a parsimonious model.

Mean age was 60y and ranged from 50 to 85y. Mean kyphosis angle was 32.9° (SD=9.1). Greater muscle CSA and density at the thoracic spine were associated with a less severe kyphosis;  $r = -0.21$  to  $-0.30$ , all  $p < 0.01$  (TABLE). In contrast, there was no association between muscle CSA and density at the lumbar spine and kyphosis severity;  $r = -0.002$  to  $-0.06$ , all  $p > 0.05$ .

Our study showed that larger and higher density thoracic, but not lumbar, trunk muscles are associated with a more upright posture in older women and men. Thus, we conclude that maintaining or improving upper back muscle strength may prevent or reduce age-related kyphosis. Rehabilitation interventions should target thoracic spinal muscles to understand their contribution to postural changes over time.

Association (partial correlation, r)* between thoracic and lumbar trunk muscle cross-sectional area (CSA) and density (HU) and kyphosis angle (degrees) in women and men, Framingham Study (N=793)		
	r*	p-value
<b>Thoracic (T7-T8)</b>		
Posterior		
CSA (mm <sup>2</sup> )	-0.30	<0.01
Density (HU)	-0.21	<0.01
Paraspinal		
CSA (mm <sup>2</sup> )	-0.29	<0.01
Density (HU)	-0.21	<0.01
<b>Lumbar (L3-L4)</b>		
Extensor		
CSA (mm <sup>2</sup> )	-0.05	0.18
Density (HU)	-0.002	0.95
Paraspinal		
CSA (mm <sup>2</sup> )	-0.06	0.08
Density (HU)	-0.04	0.27

\*Adjusted for sex, age (y), height (in), weight (lb)

Table. Association between trunk muscle density and CSA and angle kyphosis angle

Disclosures: *Amanda Lorbergs, None.*

## FR0345

**Targeted Spine Strengthening Exercise Program to Reduce Hyperkyphosis in Older Adults: Preliminary Results from the SHEAF Study.** Wendy B. Katzman<sup>1</sup>, Deborah M. Kado<sup>2</sup>, Eric Vittinghoff<sup>1</sup>, Anne Schafer<sup>1</sup>, Roger K. Long<sup>1</sup>, Shirley Wong<sup>1</sup>, Amy Gladin<sup>3</sup>, Nancy E. Lane<sup>4</sup>, Feng Lin<sup>1</sup>. <sup>1</sup>UCSF, United states, <sup>2</sup>UCSD, United states, <sup>3</sup>Kaiser Permanente Northern CA, United states, <sup>4</sup>UCDavis, United states

Presence of hyperkyphosis in older adults is associated with reduced physical mobility, quality of life and health status, and there is no standard intervention to reduce age-related kyphosis progression. Preliminary studies suggest that targeted spine strengthening exercises are safe and may improve kyphosis, but randomized controlled trial (RCT) data are lacking. We performed a single-site RCT, the Study of Hyperkyphosis, Exercise and Function (SHEAF), to investigate the efficacy of a targeted spine strengthening exercise program, compared with no exercise intervention, among community-dwelling older men and women on the primary outcome Cobb angle of kyphosis and secondary clinical measures of kyphosis, physical function and health-related quality of life (HRQoL).

Ninety-nine men and women aged  $\geq 60$  years with thoracic kyphosis  $\geq 40^\circ$  were randomized in parallel-group design, with 1:1 randomization to exercise or attentional control groups. Study performance sites included one academic medical center and one local community medical center. The intervention included exercise and postural training, delivered by a physical therapist in groups of 10, consisting of 1-hour classes, 3 times a week for 6 months. Controls received monthly health education meetings in groups of 10 participants with monthly calls from the study coordinator to monitor physical activity and adverse events. The primary outcome was change in Cobb angle of kyphosis measured from standing lateral spine radiographs at baseline and 6-months. Secondary outcomes include change in clinical measures of kyphosis (Debrunner kyphometer), physical function and HRQoL. ANCOVA was used to assess effects of the intervention on change from baseline to 6 months in primary and secondary endpoints.

Participants were  $70.6 \pm 0.6$  years old with Debrunner kyphosis  $54.1 \pm 8.6$  degrees. Groups were no different at baseline. Preliminary findings are  $-3.8 \pm 6.6$  degrees ( $p < 0.001$ ) with-in group change in Debrunner kyphosis over 6-months in the active group and  $-0.9 \pm 6.9$  degrees ( $p = 0.37$ ) in the control group. There is a significant  $-2.9$  degree 95% CI  $(-5.6, -0.1)$  difference in change between groups,  $p = 0.04$ . A targeted spine strengthening exercise program reduced the clinical Debrunner measure of kyphosis and prevented kyphosis progression compared to the control. Preliminary results suggest that targeted spine strengthening exercise and postural training is an effective treatment option for older adults with hyperkyphosis.

Disclosures: *Wendy B. Katzman, None.*

## FR0348

**A Sumo peptidase, SENP6, promotes KAP1-mediated p53 suppression to maintain osteochondroprogenitor dynamics.** Jianshuang Li<sup>1\*</sup>, Di Lu<sup>1</sup>, Hong Dou<sup>2</sup>, Huadie Liu<sup>1</sup>, Kevin Weaver<sup>1</sup>, Wenjun Wang<sup>3</sup>, Jiada Li<sup>4</sup>, Edward Yeh<sup>2</sup>, Bart Williams<sup>1</sup>, Ling Zheng<sup>3</sup>, Tao Yang<sup>1</sup>. <sup>1</sup>Van Andel institute, United states, <sup>2</sup>MD Anderson Cancer Center, United states, <sup>3</sup>College of Life Sciences, Wuhan University, China, <sup>4</sup>State Key Laboratory of Medical Genetics & School of Life Sciences, Central South University, China

The development, growth, and renewal of skeletal tissues rely on the proper dynamics of osteochondroprogenitors (OCPs). The sumoylation/desumoylation process has emerged as a pivotal mechanism for stem cell/progenitor homeostasis, and excessive sumoylation has been associated with cell senescence and tissue aging. To date, the connection between the sumoylation/desumoylation pathway in OCP dynamics and in skeletal development or homeostasis is unclear. SUMO1/Sentrin Specific Peptidase 6 (SENP6) is a desumoylase that has been reported to regulate genome stability, cell division, autoimmune responses, and hematopoietic stem cell renewal. Recently, SNPs near the *Senp6* locus had been associated with osteoarthritis, and osteoarthritic tissues show decreased *Senp6* expression. Here we show that postnatal loss of SENP6 leads to premature aging phenotypes, including skin pigmentation and kyphosis. Moreover, OCP-specific SENP6 knockout mice (*Prx1-Cre, Senp6<sup>fl/fl</sup>* and *Derm1-Cre, Senp6<sup>fl/fl</sup>*) had smaller skeletons, with elevated apoptosis and cell senescence in the OCPs and chondrocytes. In *Senp6<sup>-/-</sup>* cells, the p53 and the senescence-associated secreted phenotypes (SASP) pathways are the two most significantly elevated, and the loss of *Trp53* partially rescued the skeletal and cellular phenotypes caused by OCP-specific *Senp6* loss. Furthermore, we show that SENP6 interacts with and desumoylates KREB-associated protein 1 (KAP1, also called Trim28 or Tif1 $\beta$ ), which is a negative regulator of p53 stability and activity. In the *Senp6* KO cells, KAP1 is destabilized, leading to excessive p53 signaling. Our data reveal a crucial role for the SENP6-KAP1-p53 axis in regulating OCP and chondrocyte survival and homeostasis, skeletal development, and aging.

Disclosures: *Jianshuang Li, None.*

**FR0349**

**Ablation of IGF-1R Signaling in Osteochondroprogenitor Cells Induces a Substantial and Persistent Attenuation of Skeletal Development.** Alessandra Esposito\*, Joseph Temple, Tieshi Li, Lai Wang, Anna Spagnoli. Rush University Medical Center, United states

The type 1 insulin-like growth factor ligand and receptor (IGF-1/IGF-1R) both have key anabolic roles in postnatal skeletal development. However, their associated signaling network remains poorly understood because IGF-1/IGF-1R knockouts (KO) mice die prenatally for systemic complications. Recent reports have suggested a key role for periosteal cells in skeletal development, and as such, periosteally-localized IGF-1/IGF-1R KO mice present a viable means to investigate this pathway without systemic complications. As we have previously identified and traced a population of periosteally-localized Prx1+ progenitor cells, we generated a new line of mutant mice in which the entire Prx1+ cell lineage was IGF-1R deficient (IGF1KO). To test the hypothesis that IGF-1R signaling in osteochondroprogenitors (OCP) is essential for normal bone development and homeostasis, we characterized the skeletal ontogenesis of IGF1KO mice. Specifically, we generated IGF1KO mutant mice by crossing Prx1-Cre+ mice with *igf1r*-floxed gene and characterized their hind-limbs from postnatal day 1 (P1) to 12 weeks (W). *In vivo*, we first evaluated skeletal growth by longitudinally measuring the tibial length of IGF1KO mice and their control littermates. From P1 to P10, IGF1KO tibiae were shorter than controls (30%,  $p=0.05$ ). This relative deficiency was reduced to 15% at 12W. Next, we evaluated skeletal growth by labeling the developing bone front with injections of calcein (day 2) and alizarin red (day 7). As measured by post-mortem bone histomorphometry analysis, IGF1KO mice had decreased mineral apposition rate (28%) and bone formation rate/bone volume (50%) compared to controls. For post-mortem studies, tibiae from P1 to 12W mice were harvested and fixed in 4% PFA. For histology, samples were decalcified, embedded in paraffin, sectioned, and stained for H&E. At all times, IGF1KO mice had a thicker, hypercellular periosteum and porous cortical bone compared to controls. For structural measurements, fixed tibiae were evaluated by  $\mu$ CT at 8W and 12W. At both times, IGF1KO mice were skeletally deficient compared to controls: they had a reduced bone volume fraction (17%,  $p=0.059$ ) in the trabecular bone region and a reduced cortical thickness (20%,  $p=0.05$ ) in the diaphysis. Together, our results suggest that IGF-1R signaling derived from periosteally-localized OCP cells is essential for normal skeletal development. Studies are in progress to further characterize the nature of such mechanisms.

*Disclosures:* Alessandra Esposito, None.

**FR0350**

**Actin Filament Associated Protein 1 (AFAP1) is a Novel Regulator of Bone Formation.** Holly Corkill\*<sup>1</sup>, Albena Gesheva<sup>2</sup>, Kier Blevins<sup>1</sup>, Broc Wenrich<sup>1</sup>, Evan Frigoletto<sup>1</sup>, Jess Cunnick<sup>1</sup>, John Arnott<sup>1</sup>, Youngjin Cho<sup>1</sup>. <sup>1</sup>The Commonwealth Medical College, United states, <sup>2</sup>University of Scranton, United states

Actin Filament Associated Protein 1 (AFAP1) is an actin filament crosslinking protein and an adaptor protein that can integrate signal inputs to specific cellular compartments or regulate actin cytoskeletal integrity. Although the knowledge on normal developmental role for AFAP1 and upstream and downstream signaling components/target genes involved in AFAP1 signaling has been limited, we recently began to investigate AFAP1 as a novel regulator of bone growth. We made the novel finding that AFAP1 is expressed in differentiating osteoblasts, is induced by TGF- $\beta$ 1 and regulates expression of CCN2, an anabolic matricellular protein that regulates osteoblast differentiation and function. Using AFAP1 null mice (AFAP<sup>-/-</sup>) we demonstrated that these mice have low body weight, shortened limbs, reduced bone mineralization and impaired osteoblast growth, differentiation and function. Here, we report the micro CT analysis of AFAP1 null mice displaying a significant reduction in trabecular bone volume (BV/TV) in distal femurs of 4 week and 8-week-old female AFAP1<sup>-/-</sup> mice and a significant reduction in trabecular bone volume in lumbar vertebrae (L5) compared to wild type and heterozygote. Similarly, osteoblast specific null AFAP1 mice (Conditional knock-out; CKO) display shortened limbs and reduction in body weight and skeletal preparation of newborn CKO mice show defects in both intramembranous and endochondral ossification; hypo-mineralization in the frontal, parietal and occipital bones, widened fontanel and reduced ossification in several other bones including the mandible. Micro-CT analysis CKO mice show delayed mineralization in calvarias with the presence of irregularly shaped gaps in calvarial sutures. Micro-CT analysis of 5 weeks old tibia shows a reduction in trabecular bone volume and architecture in CKO mice compared to controls while the cortical thickness was relatively unaffected. Taken together, these results demonstrate that AFAP1 is important for normal skeletogenesis probably through control of osteoblast differentiation and function.

*Disclosures:* Holly Corkill, None.

**FR0351**

**Dysregulated murine bone osteogenesis and adipogenesis upon loss of chemokine Cxcl12/Sdf1 in the osteoprogenitor cells.** Yi-Shiuan Tzeng\*<sup>1</sup>, Ni-Chun Chung<sup>2</sup>, Hsiang-Ru Huang<sup>2</sup>, Yu-Ren Chen<sup>1</sup>, Dar-Ming Lai<sup>2</sup>.

<sup>1</sup>Graduate Institute of Oncology, National Taiwan University College of Medicine, Taiwan, province of china, <sup>2</sup>Department of Surgery, National Taiwan University Hospital, Taiwan, province of china

Bone marrow mesenchymal stem/progenitor cells give rise to osteo-lineage cells as well as adipocytes. It is intriguing how the fate decision is made during the development. In our previous work we established the chemokine Cxcl12/Sdf-1 conditional knockout mice and demonstrated an altered hematopoiesis in adult mice upon the Cxcl12 deficiency and it is not a cell-autonomous phenotype for the hematopoietic stem cells. Here we analyzed the possible alteration of the mesenchymal compartment upon Cxcl12-deficiency. To address this topic, we created the tissue specific Cxcl12 target deletion using various Cre strains including Prx1, Osterix, Collagen1a1, Tie2 and the beta-actin Cre. We found that mice deficient of Cxcl12 in Prx1- and Osterix-, but not Collagen1a1- or Tie-2-expressing cells developed the significant change of trabecular bone structure and loss of mineral density which was accompanied with increased marrow adiposity. Bone mRNA expression profile also reflected the shift from osteogenesis to adipogenesis. *In vitro* isolated primary bone mesenchymal stem/progenitor cells also revealed the reduced osteogenesis and increased adipogenesis upon Cxcl12 deficiency. Interestingly, adult stage deletion of Cxcl12, either using the tamoxifen-triggered beta-actin-CreER or doxycycline-controlled Osterix-Cre mice, did not develop such phenotype. Our results revealed that the chemokine Cxcl12 participates in the early bone mesenchymal stem/progenitor cell fate decision during the developmental stage.

*Disclosures:* Yi-Shiuan Tzeng, None.

**FR0352**

**GATA4 Regulates RUNX2 expression in osteoblasts.** Susan Miranda, Aysha Khalid\*, Gustavo Miranda-Carboni. University of Tennessee, United states

GATA4 is a zinc-finger transcription factor that is essential in various tissues, such as heart, kidneys and intestine, and more recent studies showed that it also has a role in bone mineralization. Previously we have shown that *in vivo* deletion of *Gata4*, driven by Cre-recombinase under the control of the *Col1a1* 2.3 kb promoter, results in incomplete perinatal lethality, decreased trabecular bone properties, and abnormal bone development in P0 mice. Analysis of the trabecular bone of 14 week old males and females by Micro-CT showed significantly reduced values for BV/TV and trabecular (Tb) number, while Tb separation was greater in the femur and tibia of knockout mice. However, deleting *Gata4* did not have any effect on cortical bone properties. Histological analysis of the tibia and femur showed that knockouts not only had reduced Tb number and increased Tb separation, but also had reduced osteoblast surface/bone surface (Obs/BS), osteoblast perimeter and osteoclast perimeter. Analysis of the cDNA of bone marrow mesenchymal stem cells from wild type control (WT) and cKO mice differentiated for 14 days in osteogenic media demonstrated a significant reduction in *Runx2* gene expression and alizarin red staining in osteoblasts from cKO mice as compared to controls. Gene expression levels determined by qPCR for *Runx2* were also reduced in primary calvarial cells infected with lentivirus expressing shRNA directed to *Gata4* (shGATA4), as compared to GFP (shGFP). To determine if *Runx2* is a direct target of GATA4, ChIP was performed, and indeed GATA4 is recruited to the *Runx2* promoter. Furthermore, when *Gata4* is knocked down, the chromatin at the *Runx2* promoter is not open, as detected by ChIP with antibodies to the open chromatin mark H3K4me2 (histone 3 lysine 4 dimethylation). Together the data suggest that GATA4 binds near *Runx2* promoter, helps open the chromatin to regulate *Runx2* expression and subsequent bone mineralization.

*Disclosures:* Aysha Khalid, None.

**FR0353**

**Gut Microbiota Induce IGF-1 and Promote Bone Formation and Growth.** Jing Yan\*<sup>1</sup>, Jeremy Herzog<sup>2</sup>, Kelly Tsang<sup>1</sup>, Maureen Bower<sup>2</sup>, Balfour Sartor<sup>2</sup>, Antonios Aliprantis<sup>2</sup>, Julia Charles<sup>1</sup>. <sup>1</sup>Brigham & Women's Hospital & Harvard Medical School, United states, <sup>2</sup>University of North Carolina at Chapel Hill, United states

Appreciation of the role of the gut microbiome in regulating vertebrate metabolism has exploded recently. However, the effects of gut microbiota on skeletal growth and homeostasis have only recently been explored. To understand the effects of short-term and long-term colonization of microbiota on bone, we colonized sexually mature germ-free (GF) mice with conventional gut microbiota. We found that colonization increased both bone formation and resorption, with the net effect of colonization varying with the duration of colonization. After one month of colonization, reduced bone mass was observed, reflecting increases in bone resorption. However, bone formation was significantly increased. Increased bone formation was demonstrated by both elevated bone formation rate measured by dynamic histomorphometry and increases in serum

PINP, a marker of bone formation. In addition, short-term colonized mice displayed a wider growth plate, suggesting that microbiota promotes longitudinal bone growth. In mice colonized for 8 months, increased bone formation and growth plate activity predominate, resulting in equalization of bone mass and increased longitudinal and radial bone growth. Serum levels of insulin like growth factor 1 (IGF-1), a hormone with known actions on skeletal growth, were substantially increased in response to colonization, with significant increases in liver and adipose tissue IGF-1 production. Antibiotic treatment of conventional mice, in contrast, decreased serum IGF-1 and inhibited bone formation, suggesting that skeletal effects of microbiota are mediated by IGF-1. Treatment with vancomycin, a non-absorbable antibiotic that only targets gram positive bacteria, was sufficient to decrease serum IGF-1 and inhibit bone formation, indicating that gram positive commensals are sufficient for the regulation of bone formation by microbiota. In conclusion, our study demonstrates that long term colonization with microbiota provide a net anabolic stimulus to the skeleton, which is likely regulated by IGF-1. Manipulation of the microbiome may afford opportunities to optimize bone health and growth.

**Disclosures:** *Jing Yan, None.*

## FR0354

**Impact of Maternal Myostatin and the Uterine Environment on Offspring Bone Strength in Wildtype and Osteogenesis Imperfecta Model (oim) Mice.** Arin Oestreich<sup>\*1</sup>, William Kamp<sup>2</sup>, Marcus McCray<sup>2</sup>, Stephanie Carleton<sup>2</sup>, Natalia Karasova<sup>3</sup>, Kristin Lenz<sup>2</sup>, Youngjae Jeong<sup>2</sup>, Salah Daghlas<sup>2</sup>, Xiaomei Yao<sup>4</sup>, Yong Wang<sup>5</sup>, Ferris Pfeiffer<sup>6</sup>, Laura Schulz<sup>1</sup>, Charlotte Phillips<sup>7</sup>. <sup>1</sup>Department of Ob, Gyn & Women's Health, University of Missouri School of Medicine, United states, <sup>2</sup>Department of Biochemistry, University of Missouri, United states, <sup>3</sup>Transgenic Research Core, University of Missouri, United states, <sup>4</sup>Department of Restorative Clinical Sciences, University of Missouri-Kansas City, United states, <sup>5</sup>Department of Oral & Craniofacial Sciences, University of Missouri - Kansas City, United states, <sup>6</sup>Department of Orthopaedic Surgery, University of Missouri, United states, <sup>7</sup>Departments of Biochemistry & Child Health, University of Missouri School of Medicine, United states

Osteogenesis imperfecta (OI) is a heritable connective tissue disorder resulting in bone deformity and fragility for which there is no cure and treatment strategies remain limited. During fetal development, the prenatal environment plays a primary role in lifelong bone health, and may provide a novel developmental window for treatment of OI. When maternal myostatin, a TGF- $\beta$  family member and circulating negative regulator of muscle growth, is deficient in the maternal environment, offspring have larger muscle mass, suggesting maternal myostatin developmentally programs offspring muscle size. Here, by three independent studies, we demonstrate that decreased myostatin in the maternal environment programs offspring bone to have increased strength and integrity. First we examined offspring from Wt or *+mstn* murine dams and sires and found by torsional loading to failure that maternal myostatin deficiency improved femoral biomechanical strength of wildtype (Wt) male offspring at 4 months of age, the age of peak bone mass ( $p \leq 0.05$ , Fisher's Protected LSD), independent of sire genotype. We then investigated whether maternal myostatin deficiency could improve bone strength and integrity in the adult osteogenesis imperfecta murine (*oim*) model. Femora of male *+oim* offspring from natural mating of *+mstn* dams to *+oim* sires had a 14.7% and 23.6% increase in the whole bone mechanical properties torsional ultimate strength and energy to failure, respectively, and a 28.6% increase in bone material property, tensile strength, when compared to age, sex, and genotype matched offspring from natural matings of *+oim* dams and sires. In a third study, we tested whether the beneficial effect of maternal myostatin deficiency is conferred pre- or post-implantation, by transferring embryos from *+oim* donor dams mated to *+oim* sires into either *+oim* or *+mstn* recipient dams at gestation d3.5. Myostatin deficiency in the recipient dam increased femoral torsional strength of *+oim* male offspring, demonstrating that reduction of myostatin in the post-implantation environment programmed increased bone strength in male *+oim* mice. Our results indicate that maternal myostatin deficiency influences bone biomechanical properties in adult offspring, which persist throughout adulthood, and that the OI bone is able to respond to effects of maternal myostatin. Thus, targeting the gestational environment *in utero* provides a potential therapeutic window and novel approach for treating OI.

**Disclosures:** *Arin Oestreich, None.*

## FR0355

**The RhoGAP Myo9b is Essential for Normal Bone Growth and Osteoblast Responsiveness to IGF-1.** Brooke McMichael<sup>1</sup>, Yong-Hoon Jeong<sup>2</sup>, Justin Auerbach<sup>1</sup>, Cheol-Min Han<sup>2</sup>, Ryan Sedlar<sup>2</sup>, Martin Baehler<sup>3</sup>, Sudha Agarwal<sup>2</sup>, Do-Gyoon Kim<sup>2</sup>, Beth Lee<sup>\*1</sup>. <sup>1</sup>The Ohio State University College of Medicine, United states, <sup>2</sup>The Ohio State University College of Dentistry, United states, <sup>3</sup>Institut für Molekulare Zellbiologie, Universität Muenster, Germany

**Purpose:** Rho GTPases regulate the actin machinery of cells and therefore play critical roles in cell adhesion, shape, polarity, and migration. Although at least 20 Rho GTPases are expressed in humans, this number is dwarfed by that of their regulator proteins, the RhoGEFs and RhoGAPs, which tightly regulate Rho GTPase activity in space and time. The goal of this study was to define the role of a RhoA-specific RhoGAP, Myo9b, in skeletal growth and osteoblast function.

**Methods:** The growth and skeletal health of *Myo9b*<sup>+/+</sup>, *Myo9b*<sup>+/-</sup>, and *Myo9b*<sup>-/-</sup> mice were assessed using standard techniques (body mass, microCT, histomorphometry, 3-point bending). Osteoblastic cells deficient in Myo9b, either by knockout or siRNA-mediated knockdown, were examined for Myo9b expression and distribution, morphology, spreading and migration, and responses to IGF-1.

**Results:** *Myo9b*<sup>-/-</sup> mice, and to a lesser extent, *Myo9b*<sup>+/-</sup> mice, demonstrated markedly suppressed growth during early puberty. At 4 weeks of age, femurs from female *Myo9b*<sup>-/-</sup> mice showed strongly decreased trabecular and cortical bone and diminished bone strength, while femurs from male mice were mostly unaffected. By 12 weeks of age, femurs from male *Myo9b*<sup>-/-</sup> mice also were affected, though females had a more severe phenotype. The timing and sex-specific defects caused by Myo9b deficiency suggested the possibility of aberrant IGF-1 signaling. Immunocytochemistry revealed that Myo9b is expressed in the focal adhesions of osteoblastic cells. The complete absence of Myo9b caused severe defects in cellular adhesion and spreading, resulting in an inability to culture mesenchymal stem cells or osteoblasts from *Myo9b*<sup>-/-</sup> mice long-term. Therefore, *in vitro* studies were performed by knocking down Myo9b expression in the murine pre-osteoblast line MC3T3-E1. Seventy percent knockdown of Myo9b resulted in cells with diminished numbers of focal adhesions and a poor ability to spread on fibronectin-coated surfaces. Cells deficient in Myo9b also were unable to undergo IGF-1-induced spreading, stress fiber formation, and migration.

**Conclusions:** These data demonstrate a previously unknown role for Myo9b in regulating skeletal growth and health. This was confirmed by *in vitro* studies, which demonstrated that osteoblastic cells deficient in Myo9b had defects in cellular adhesion and responsiveness to IGF-1. These findings also indicate that Rho activity lies at an intersection between mechanical and IGF-1-mediated signaling.

**Disclosures:** *Beth Lee, None.*

**SA0001**

See Friday Plenary Number FR0001.

**SA0002**

**The Association of Gender, Antiepileptic Drug Use and Hypovitaminosis D among Patients with Epilepsy.** Poranee Ganokroj, Natnicha Houngngam, Lalita Wattanachanya\*. Chulalongkorn University & King Chulalongkorn Memorial Hospital, Thailand

Vitamin D plays roles in calcium homeostasis, bone metabolism and several noncalcemic effects. Low vitamin D levels have been reported in patients with epilepsy, with consequently reduced bone mineral density (BMD) and increased fracture risk. However, data from the Asians are scarce. We aimed to determine the prevalence of and risk factors for hypovitaminosis D among Thai patients with epilepsy. This was a cross-sectional study to determine serum 25-hydroxyvitamin D (25(OH)D) levels in Thai patients with epilepsy who attended the epilepsy clinic at Kingchulalongkorn Memorial Hospital, Bangkok, Thailand from July 2015 to September 2015. Hypovitaminosis D was defined as vitamin D insufficiency, vitamin D deficiency and severe vitamin D deficiency (25(OH)D 20–29.9 ng/mL, 10–19.9 ng/mL, and <10 ng/mL respectively). Hypovitaminosis D prevalence was calculated and risk factors were determined using multivariate logistic regression. A total of 210 patients with epilepsy were included. The mean age was 38.6 ± 10.9 years and 58% were females. The mean body mass index was 23.02 ± 3.5 kg/m<sup>2</sup>. The median time from the diagnosis of epilepsy was 20.6 years (range, 1–59) years. All were on antiepileptic drugs (AEDs) with sixty percent were using enzyme-inducing AEDs. Overall, the mean 25(OH)D level was 17.61 ± 3.54 ng/mL with 96.2% of the patients had 25(OH)D levels of lesser than 30 ng/mL. The prevalence of vitamin D insufficiency, vitamin D deficiency, and severe vitamin D deficiency were 28.6%, 57.6% and 10%, respectively. In multivariate analysis, female gender (odds ratio: 2.4, p = 0.05) and enzyme-inducing AEDs use (odds ratio: 2.8, p = 0.01) were independent predictors of hypovitaminosis D. In conclusion, hypovitaminosis D is highly prevalent in AEDs-treated epileptic patients. Treatment of low vitamin D in these patients should be considered especially in the high risk groups to prevent reduction in BMD and other hypovitaminosis D-related conditions.

Keywords: Epilepsy, antiepileptic drugs, vitamin D deficiency, Asian

**Disclosures:** Lalita Wattanachanya, None.

**SA0003**

**Vitamin D in Older People (VDOP): A Does Ranging Intervention Trail to Prevent Bone Loss.** Terry J Aspray\*<sup>1</sup>, Roger M Francis<sup>1</sup>, Elaine McColl<sup>2</sup>, Thomas J Chadwick<sup>2</sup>, Elaine Stamp<sup>2</sup>, Ann Prentice<sup>3</sup>, Inez Schoenmakers<sup>3</sup>.  
<sup>1</sup>Institute for Cellular Medicine, Newcastle University, United Kingdom,  
<sup>2</sup>Institute for Health & Society, Newcastle University, United Kingdom,  
<sup>3</sup>MRC Human Nutrition Research, United Kingdom

**Introduction**

Vitamin D insufficiency is common in older people in the UK and can lead to secondary hyperparathyroidism and bone loss. However, previous trials have yielded conflicting evidence, with vitamin D supplementation preventing bone loss in subjects at risk of vitamin D deficiency, but the optimal plasma concentrations of 25 hydroxy vitamin D (25OHD) and parathyroid hormone (PTH) remains unclear.

**Methods**

This randomised, double blind intervention trial tested the effect of a monthly dose of oral vitamin D<sub>3</sub> on change in total hip (TH) and femoral neck (FN) Bone Mineral Density (ΔBMD, Lunar iDXA), plasma 25(OH)D (Δ25(OH)D: LC-MS/MS), parathyroid hormone (ΔPTH; Immulite) and safety markers. Community dwelling men and women aged over 70 years (n=376) were randomly allocated to 12 months' treatment with either 12kIU [reference], 24kIU or 48kIU/month. Treatment started between November and May and 329 (88%) completed 12 months' treatment.

**Results**

There were no differences in baseline characteristics. However, at 12 months there were significant group differences and a dose response for Δ25(OH)D but not ΔTH-BMD or ΔFN-BMD, while PTH decreased with 48kIU but not 24kIU/month compared with the reference (12kIU) dose (see table).

Baseline PTH, 25(OH)D, fat mass, height, estimated GFR and gender did not influence ΔTH-BMD, although the oldest quartile showed a negative (aged 77+ years, p=0.01) and body weight a positive (p=0.03) effect on TH-BMD, adjusted for dose of supplement. Baseline FN-BMD, female gender and PTH were associated with a decrease in FN-BMD. At baseline, PTH was associated with older age, weight and low 25OHD. Higher bCTX and PTH at 12 months but no other biomarkers were associated with a decrease in TH-BMD. There were no significant gender differences in these relationships and no group differences in number of falls or adverse events, with no cases of renal stones or hypercalcaemia.

**Conclusion**

We conclude that supplementation with 12kIU, 24kIU or 48kIU/month vitamin D is safe and associated with improvements in vitamin D status, with a decrease in PTH (particularly at the highest dose) in this population at risk of vitamin D deficiency. No

significant decrease in BMD at total hip or femoral neck occurred, despite an anticipated decrease in TH-BMD of ~0.6% in this age/geographical group. However, no dose effect of supplement on ΔBMD was seen.

Table	Time		12kIU		24kIU		48kIU		ANOVA		ANCOVA	
	month	mean	SD	mean	SD	mean	SD	12kIU/24kIU	12kIU/48kIU			
Number	0	113		114		116		-				
Male %	0	53.3		52.4		49.2		-				
Weight (kg)	0	73.9	11.93	77.2	14.53	76.1	14.23	0.149				
Height (cm)	0	167.2	8.07	167.1	9.86	167.4	10.01	0.967				
BMI (kg/m <sup>2</sup> )	0	26.4	3.66	27.6	4.12	27.1	3.97	0.068				
25(OH)D (nmol/L)	0	43.0	2.8	42.4	2.8	41.3	2.9	0.795				
Change 25(OH)D (nmol/L)	0-12	12.6	2.5	24.1	2.6	39.0	2.6	<0.001	<0.001	<0.001		
PTH (pg/ml)	0	43.9	3.3	41.4	3.3	44.0	3.3	0.607				
Change PTH (pg/ml)	0-12	-2.3	2.6	-1.4	2.6	-9.1	2.7	<0.001	0.777	0.003		
Change TH-BMD (g/cm <sup>2</sup> )	0-12	0.0007	0.0256	-0.0011	0.0260	-0.0031	0.0265	0.227	0.385	0.076		
Change FN-BMD (g/cm <sup>2</sup> )	0-12	0.0047	0.0351	0.0020	0.0348	0.0036	0.0366	0.420	0.381	0.724		

VDOP table of results

**Disclosures:** Terry J Aspray, None.

This study received funding from: *Arthritis Research UK*

**SA0004**

**Clinical Characteristics, Causes and Survival in 115 Cancer Patients with PTHrP-mediated Hypercalcaemia.** Dong Jin Chung\*, Joon Jin, Jin Ook Chung, Dong Hyeok Cho, Min Young Chung. Chonnam National University Medical School, Korea, republic of

The aim of this study is to determine the proportion of cancers presenting with PTHrP-mediated hypercalcaemia, examine the clinical and biochemical characteristics, and identify predictive factors for survival. Cancer patients with PTHrP-mediated hypercalcaemia who were treated at Chonnam National University Hospital in Korea from January 2005 to January 2015 were retrospectively reviewed. Of all 115 patients, solid organ malignancies were the most common etiology (98 cases, 85.2%), with squamous cell carcinoma (50 cases, 43.4%), adenocarcinoma (27 cases, 23.4%). Interestingly, hepatocellular carcinoma (18 cases, 15.7%) and cholangiocarcinoma (11 cases, 9.6%) were much more common causes than other previous reports. Hematologic malignancy was less common (17 cases, 14.8%), with multiple myeloma (9 cases, 7.8%) and non-Hodgkin's lymphoma (5 cases, 4.3%). Albumin-corrected serum total calcium were 14.0 ± 1.7 mg/dL. Severe hypercalcaemia as determined by albumin-corrected serum calcium level of >14 mg/dL was observed in 59 cases (51.3%). Serum PTH levels were 6.6 ± 9.9 pg/mL. Ninety-two cases (80%) had suppressed PTH levels of less than the lower normal limit of 9 pg/mL. Plasma PTHrP level was 9.4 ± 12.3 pmol/L. Pearson correlation analysis showed that albumin-corrected serum calcium correlated to plasma PTHrP in solid organ malignancy (r=0.41, p=0.000). There were significant differences in gender (male 83.6 vs. 58.8%), serum phosphorus (3.1 ± 1.1 vs. 4.6 ± 1.4 mg/dL), serum creatinine (1.3 ± 0.7 vs. 2.7 ± 1.8 mg/dL), serum PTH (5.6 ± 7.9 vs. 12.2 ± 16.5 pg/mL), and plasma PTHrP (10.6 ± 12.9 vs. 2.4 ± 1.3 pg/mL) between patients with solid organ and hematologic malignancy. In accordance with previous other reports, PTHrP-mediated hypercalcaemia was most frequently caused by solid organ malignancy. However, hepatocellular carcinoma and cholangiocarcinoma were important causes of PTHrP-mediated hypercalcaemia in this study may be due to geographic differences in cancer incidence. Median survival was only 37 days (interquartile range, 19–93 days). There was significant difference in median survival between two groups (35 days [interquartile range, 18–78 days] for solid organ malignancy, and 72 days [interquartile range, 19–318 days] for hematologic malignancy; p=0.015). Cox regression analysis identified age, the type of malignancy and the time interval of developing hypercalcaemia after cancer diagnosis as independent predictive factors for survival time.

**Disclosures:** Dong Jin Chung, None.

**SA0005**

**Relationship between biochemical and imaging biomarkers of vascular calcification in normal weight, overweight and obese individuals.** Antoine Bouquegneau\*<sup>1</sup>, Jennifer Walsh<sup>2</sup>, Amy Evans<sup>2</sup>, Fatma Gossiel<sup>2</sup>, Margaret Paggiosi<sup>2</sup>, Richard Eastell<sup>2</sup>. <sup>1</sup>Department of Nephrology - Dialysis - Transplantation CHU Sart-Tilman, Liège, Belgium, <sup>2</sup>Mellanby Centre for Bone Research, Department of Oncology & Metabolism, The University of Sheffield, Sheffield, United Kingdom, United Kingdom

Background: Vascular calcification (VC) predicts the development of vascular diseases in the obese population. VC development results from an imbalance between inhibitors and promoters of mineralization in the arterial wall. The main aim of this study was to evaluate the relationships between biomarkers and the amount of VC in an obese population with normal renal function.

**Methods:** We recruited 148 men and women, aged 55 to 75 years, with normal kidney function, and divided them into three categories based on body mass index (BMI); normal weight (BMI 18.5-25 kg/m<sup>2</sup> n=58), overweight (25-30 kg/m<sup>2</sup> n=30) and obese (>30 kg/m<sup>2</sup> n=60). We measured biomarkers including matrix Gla protein (MGP), fibroblast growth factor 23 (FGF-23), klotho, osteoprotegerin (OPG), sclerostin and fetuin A and compared the results with measurements of calcification by non-invasive imaging techniques. VC at the distal radius and tibia was determined from high-resolution peripheral quantitative computed tomography (HR-pQCT) images using the approach of Patsch et al. (2014). Abdominal aortic calcification (AAC) was assessed from quantitative computed tomography images of the lumbar spine (L1-L3) using a modified 8-point scale.

**Results:** In our population, the level of VC was higher in men (HR-pQCT p=0.01) and in older patients (HR-pQCT tibia and AAC, p<0.05). BMI and the level of VC were poorly correlated (p>0.05). The inactive form of MGP (dephosphorylated and uncarboxylated MGP) was correlated with BMI but not with the level of VC; the intact form of FGF-23 and OPG were correlated with AAC; sclerostin was associated with tibia VC; fetuin A was significantly correlated with VC (Table).

**Conclusion:** Establishing new surrogate markers for the detection of VC are important for prognosis and for drug development. In our obese population with normal renal function, higher fetuin A was associated with lower levels of VC at all sites. In contrast, higher OPG and sclerostin were associated with higher levels of VC.

	Intact FGF-23	MGP inactive	Fetuin A	Klotho	OPG	Sclerostin
HRpQCT VC radius site	Rho -0.111 p=0.201	Rho 0.069 p=0.430	Rho -0.209 p=0.016	Rho 0.06 p=0.448	Rho 0.049 p=0.557	Rho 0.06 p=0.471
HRpQCT VC tibia site	Rho -0.129 p=0.137	Rho 0.089 p=0.311	Rho -0.192 p=0.026	Rho 0.042 p=0.631	Rho 0.1 p=0.228	Rho 0.230 p=0.005
AAC-QCT	Rho -0.226 p=0.011	Rho 0.032 p=0.730	Rho -0.222 p=0.013	Rho -0.039 p=0.664	Rho 0.328 p=0.0001	Rho -0.015 p=0.864
BMI	Rho 0.05 p=0.565	Rho 0.413 p=0.0001	Rho 0.025 p=0.777	Rho -0.100 p=0.248	Rho -0.120 p=0.149	Rho 0.205 p=0.013

Table

**Disclosures:** Antoine Bouquegneau, None.

This study received funding from: Immunodiagnostic Systems

## SA0006

See Friday Plenary Number FR0006.

## SA0007

See Friday Plenary Number FR0007.

## SA0008

**An overview of the etiology, clinical manifestations, management strategies and complications of hypoparathyroidism: An update from the Canadian National Hypoparathyroidism Registry.** Aliya Khan\*, Reema Shah, Hamid Syed, Tayyab Khan, J.E.M. Young. McMaster University, Canada

Hypoparathyroidism is characterized by absent or inappropriately low levels of Parathyroid hormone (PTH), with low serum calcium and elevated phosphate levels, and presents unique therapeutic challenges. Data regarding disease manifestations in the Canadian population are lacking.

We established a Canadian registry of patients with hypoparathyroidism and reviewed baseline and follow-up data with respect to etiology, presenting symptoms, current treatment and complications of this condition. The study was approved by the Research Ethics Board at McMaster University and all patients provided informed consent.

Most patients (58/80; 72.5%) had postsurgical hypoparathyroidism, followed by idiopathic/autoimmune disease (16/80; 20.0%), pseudohypoparathyroidism (4/80; 5.0%) and congenital hypoparathyroidism (2/80; 2.5%). The mean age of onset was 43 years (Range: 10 days – 92 years). Paresthesias in the upper and lower extremities were the most common presenting symptom and experienced by approximately 54% of patients. Approximately 16% of patients reported tetany and 14% had seizures. 40% of patients required hospitalization at the time of presentation, and patients with idiopathic or autoimmune disease were twice as likely to be hospitalized compared to those with postsurgical disease. Current treatment options were reviewed, and 72.% of patients were receiving more than 4 medications to maintain calcium levels. Almost all patients were receiving calcium supplements (93.8%) with calcitriol being used by 86.3%; 29 patients (36.3%) were on hydrochlorothiazide and 4 patients (5%) were receiving parathyroid hormone. Complications were reviewed and 10 patients had brain imaging completed with 8 having evidence of basal ganglia calcification. 13 of 36 (36.1%) patients who received an abdominal ultrasound showed evidence of nephrolithiasis or nephrocalcinosis. Of note, all patients with nephrolithiasis or basal ganglia calcification had a calcium phosphate product of <4.4 mmol<sup>2</sup>/L<sup>2</sup>. Renal impairment was present in 67.6% who had chronic kidney disease Stage II or higher.

Our findings provide valuable insights into the etiology, symptomatology, treatment strategies and complications of hypoparathyroidism in a Canadian population. Renal complications of nephrocalcinosis and nephrolithiasis were present in over one third of treated patients despite maintenance of a calcium phosphate product in the desired range. The ideal calcium phosphate product needs to be reconsidered. Skeletal health does require further evaluation and assessment of bone strength would be of value in this patient population.

**Disclosures:** Aliya Khan, None.

This study received funding from: Calcium Disorders Clinic, McMaster University

## SA0009

**Determinants of Bone Mineral Density Changes Post-Parathyroidectomy in Patients with Primary Hyperparathyroidism.** Shilpa Shetty\*, Li Hao Richie Xu, Beverly Huet, John Poindexter, Jennifer Rabaglia, Naim Maalouf. UT Southwestern Medical Center, United states

**Background:** Primary hyperparathyroidism (PHPT) is a relatively common condition associated with increased osteoclastic activity, resulting in decreased bone mineral density (BMD) and increased fracture risk. Parathyroidectomy is the only definitive cure, but is associated with variable degree of BMD improvement. Determinants of BMD improvement post-parathyroidectomy have not been well established, but may help identify patients who benefit from anti-osteoporosis therapy post-parathyroidectomy.

**Objectives:** To determine predictors of BMD improvement in patients who have undergone parathyroidectomy for primary hyperparathyroidism.

**Methods:** Retrospective review of patients with a diagnosis of primary hyperparathyroidism who have undergone parathyroidectomy, with available BMD measurement pre- and >9 months post-parathyroidectomy.

**Results:** 37 patients were included in this analysis. 89% were female, 46% were Hispanic and 27% were African American. Mean age was 60 years, and mean BMI 32 Kg/m<sup>2</sup>. Mean baseline serum calcium was 11.1 mg/dl, PTH 132 pg/ml, serum creatinine 0.83 mg/dl and serum 25-OH-vitamin D 22.3 ng/ml. Mean femoral neck and lumbar spine T-scores were -1.1 and -1.2 respectively. After a median follow-up of 1.7 years, the mean change from baseline in lumbar spine BMD was +1.9% and at the femoral neck was +2.6%. In univariate analysis, significant predictors of greater increase in femoral neck BMD younger age (p=0.01), higher pre-operative serum PTH (p=0.05), with a trend for higher BMI (p=0.07). In multivariable analysis, higher BMI, younger age and non-African American race remained major predictors of femoral neck BMD improvement, explaining 32% of the variance in change in femoral neck BMD.

**Conclusions:** Parathyroidectomy results in a significant but variable improvement in lumbar spine and femoral neck BMD in PHPT patients. Demographic parameters explain some of the variability in BMD improvement. Post-parathyroidectomy, closer BMD monitoring may be warranted in older, African American and/or leaner PHPT patients.

**Disclosures:** Shilpa Shetty, None.

## SA0010

**Expression profile of microRNAs in multiple endocrine neoplasia type 1.** gurjeet kaur\*<sup>1</sup>, Sanjay Bhadada<sup>2</sup>. <sup>1</sup>PhD student, India, <sup>2</sup>Additional Professor, India

**Introduction:** Multiple Endocrine Neoplasia type 1 syndrome is autosomal-dominant disorder in which there is a germ line mutation in chromosome 11q13. The classical clinical manifestation of MEN1 is the triad of parathyroid adenoma, pancreatic neuroendocrine tumors and pituitary, most commonly parathyroid adenoma and pancreatic neuroendocrine tumors. The clinical symptoms of these tumors are Renal & gallstones, severe bone pains & fractures and psychiatric moans. The exact mechanism of tissue selective tumorigenesis in case of parathyroid adenoma formation is not fully elucidated. In this regard to tissue selective regulations, microRNAs are interesting candidates for further evaluations. MicroRNAs are group of universally present small non coding, 18 - 22 nucleotide long RNAs that are the central players of gene expression regulations. These molecules can negatively regulate protein expression by promotion of mRNA degradation or inhibition of mRNA translation. mir-24 and mir-135b have been in silico selected and quantified in multiple endocrine neoplasia type 1 patients.

**Objective:** In present study, we investigated the expression profile of mi-24 and mir-135b in MEN1 cases of parathyroid adenoma. We hypothesized that mir-24 and mir-135b are differentially expressed in these cases and can be predicted as diagnostic markers in parathyroid adenoma patients.

**Disclosures:** gurjeet kaur, None.

This study received funding from: PGIMER Intramural funding

## SA0011

See Friday Plenary Number FR0011.

**SA0012**

See Friday Plenary Number FR0012.

**SA0013**

**Site Specific Difference Of Bone Geometry Indices In Hypoparathyroid Patients.** HyeSun Park\*, Sung kil Lim, Yumie Rhee, Da Hea Seo, Dongdong Zhang, Division of Endocrinology & Metabolism, Department of Internal Medicine, Yonsei University College of Medicine, Korea, republic of

Higher bone mineral density (BMD) compared with general population is often observed in hypoparathyroid patients. However, the increased BMD does not necessarily mean solid bone microstructure. The objective of this study was to evaluate the bone microstructure of hypoparathyroid patients by using hip structure analysis (HSA).

Hypoparathyroid patients over 20 years old with at least 1 year of disease duration were recruited to see the effect of PTH insufficiency on bone metabolism. Among 95 hypoparathyroid patients, data available from 31 patients were included for analyzing bone geometry parameters by HSA. The control data was obtained from the previous study which assessed bone geometric parameters of 3,580 Korean people who participated in the Fourth Korean National Health and Nutrition Examination Survey (KNHANES IV). Sex-, age-, and BMI-matched 3 control subjects to each patient were extracted. We compared bone geometric parameters of hypoparathyroid patients with those of control subjects at each age group. The BMD data were reviewed retrospectively and the bone geometry parameters of the patients were analyzed by HSA program.

Mean Z scores of hypoparathyroid patients at lumbar spine, femoral neck and total hip were  $0.64 \pm 1.04$ ,  $0.59 \pm 1.09$  and  $0.58 \pm 0.89$ , respectively. Of interest, their bone geometric parameters differed site specifically. Compared to controls, cross section area (CSA) and cortical thickness (C.th) were high and buckling ratio (BR) was low at femoral neck and intertrochanter. However, inverse trends were shown at femoral shaft, that is, CSA and C.th were low and BR was high.

Our study shows the site specifically different effects of hypoparathyroidism on microstructure of bone. Different bone components, marrow composition or site specific modeling based bone formation can be suspected to be the contributing factors for this site specific difference. However, further studies will be needed to investigate exact mechanism, and its relation to fracture risk.

*Disclosures: HyeSun Park, None.*

**SA0014**

See Friday Plenary Number FR0014.

**SA0015**

See Friday Plenary Number FR0015.

**SA0016**

See Friday Plenary Number FR0016.

**SA0017**

See Friday Plenary Number FR0017.

**SA0018**

See Friday Plenary Number FR0018.

**SA0019**

See Friday Plenary Number FR0019.

**SA0020**

See Friday Plenary Number FR0020.

**SA0021**

See Friday Plenary Number FR0021.

**SA0022**

See Friday Plenary Number FR0022.

**SA0023**

See Friday Plenary Number FR0023.

**SA0024**

**Collagen nanoelasticity is tunable via osmotic pressure.** Orestis Andriotis, Sylvia Desissaire, Philipp Thurner\*, Vienna University of Technology, Austria

Proteoglycans bear high negative charge, are usually found in the vicinity of collagen fibrils, and exert osmotic pressure by retracting intrafibrillar ions from them. Ion retraction results in lower hydration levels of fibrils, hence we hypothesized that both structure and mechanics of collagen fibrils will be influenced. Here, we present results of structural and mechanical changes of individual collagen fibrils with increasing osmotic pressure, assessed by atomic force microscopy (AFM) imaging, cantilever-based nanoindentation and tensile tests of individual collagen fibrils.

Collagen fibrils from tail-tendon of wild type mice (2 months) were deposited onto poly-L-lysine-coated glass slides, washed with distilled water and air-dried. Individual collagen fibrils were imaged with AFM in air, in phosphate buffered saline (PBS) solution (pH7.4) containing polyethylene glycol (PEG; 200 gr/mol) at concentrations of 0M–3.5M. AFM height-image data was used to determine average collagen fibril diameter. Shrinking was defined taking fibril height at fully hydrated state in PBS as 100%. AFM indentation force-displacement curves from collagen fibrils were analyzed using a Hertzian model assuming quadratic contact area. Tensile experiments were performed gluing one fibril end on the AFM cantilever and the other onto the glass slide.

Hydration with PBS caused a ( $1.54 \pm 0.09$ ) fold increase in fibril diameter vs. air-dried state. Dehydration with increasing PEG concentration resulted in 14% to 22% shrinking (figure 1a). This caused the indentation modulus to increase, from ( $9 \pm 1$ ) MPa in 0.1M of PEG to ( $364 \pm 18$ ) MPa (~42-fold) in 3.5M of PEG (figure 1b). Tensile force-displacement (fig. 1c) behaviour and tensile modulus (fig.1d) change with increasing PEG concentration. In PBS a larger toe region and a steady increase from 1.02 stretch was observed, while in 3.5M PEG the toe region was substantially shorter followed by an almost 6-fold increase in the tensile modulus at 1.015 stretch.

Removal of ions and dehydration causes fibril diameter reduction. As a result, collagen molecules are more densely packed and interact more strongly with each other. The increase in indentation modulus is mostly related to increase of the fibril density. Increase in tensile modulus stems from lower lateral spacing and increasing inter-molecular density of non-covalent interactions. This renders collagen fibrils to be tunable nonlinear springs, with tunability depending on hydration.

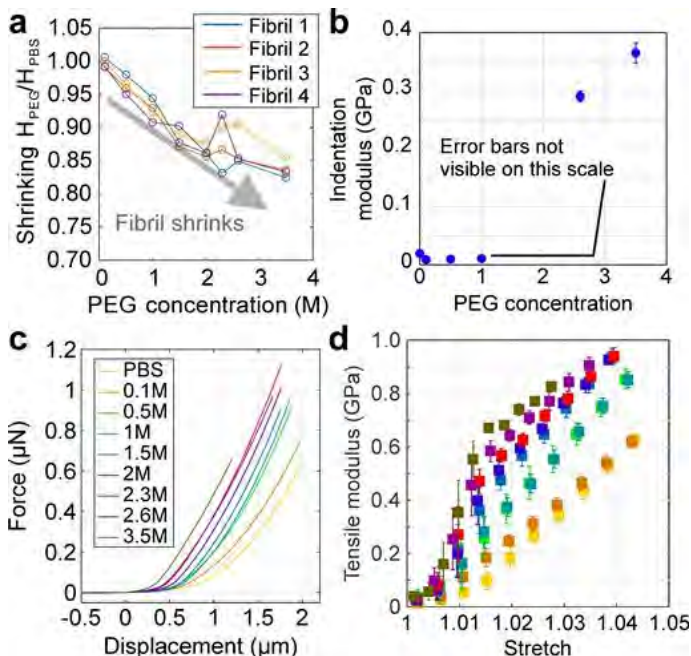


Figure 1

*Disclosures: Philipp Thurner, None.*

**SA0025**

Withdrawn

**SA0026**

**Identification of the Damping Matrix for a Dynamic Finite Element Model of the rat Forelimb.** Wubin Cheng\*, Kim Harrison, Majid Nazemi, David Cooper, James Johnston. University of Saskatchewan, Canada

Purpose: Whole-body vibration (WBV) is a promising non-pharmacological therapy to treat osteoporosis for patients. The exact mechanisms of how WBV promote bone formation are largely unknown, but are thought to be related to vibration frequency and magnitude or vibration transmissibility through bone. A dynamic subject-specific finite element (FE) model would help investigate bone formation in response to vibrational frequency and magnitude. However, no dynamic FE models have been incorporated with damping factors of bone.

Methods: We applied computational analyses and mechanical testing to determine the damping matrix for a dynamic FE model for a rat forelimb. The first 2 resonance (natural) frequencies and damping ratios of the ulna were obtained by vibration testing. Modal parameters in higher order were obtained by an FE analysis, with bone modeled as having an elastic modulus of 17 GPa, Poisson's ratio of 0.3 and density of 1.6 g/cm<sup>3</sup>. The damping matrix of the ulna was modeled as a linear combination of the mass matrix and stiffness matrix of the ulna. A linear interpolation method was used to derive two damping coefficients for the model.

Results: Experimental testing indicated bone's first resonance frequency was 433 Hz, with a damping ratio was 3.62%, and the second resonance frequency was 770 Hz, with a damping ratio of 4.47%. FE modal analyses indicated a first natural frequency of 426 Hz and a second natural frequency of 702 Hz. We identified a damping coefficient "alpha" of 2.357 and "beta" of 2.76e-5.

Conclusion: This result suggests that noticeable damping exists in the rat ulna, which is important for dynamic FE modeling of bone. This damping could be due to viscous damping resulting from interstitial fluid flow in bone. A dynamic FE model incorporated with damping factors could advance our understanding of bone formation mechanism behind bone's response to WBV.

*Disclosures: Wubin Cheng, None.*

**SA0027**

**Long-term Administration of Oncology Doses of Zoledronic Acid does not Compromise Femoral Biomechanical Properties in Rice Rats (*Oryzomys palustris*).** Jonathan Messer\*, Hung-Yuan Chen, Jessica Jiron, Evelyn Castillo, Jorge Mendieta Calle, Donald Kimmel, J. Ignacio Aguirre. University of Florida, United states

Long-term use of powerful anti-resorptives (pAR) for treatment of osteoporosis and skeletal-related events of bone metastases is associated with atypical femoral fractures (AFF). AFFs occur most often in the lateral, subtrochanteric cortex of the proximal femur, perhaps suggesting that pARs have deleterious effects on cortical bone mechanical properties. However, little is known about the extent to which chronic administration of pARs in a full range of therapeutic doses affects cortical bone mechanical properties. We examined the effects of a pAR, zoledronic acid (ZOL), on the biomechanical properties of rice rat (*Oryzomys palustris*) femora. We hypothesize that ZOL acts in a dose and time-dependent fashion to improve bone strength without changing bone material properties. Rats aged 4 weeks (n=5-12) were fed standard rat chow and given IV injections of 0, 8, 20, 50, or 125 µg ZOL/kg body weight every 4 weeks for 12 or 30 weeks. At necropsy, left femora were cleaned, wrapped in saline-soaked gauze, and frozen at -20°C. After thawing, peripheral quantitative computed tomography (pQCT) was used to determine bone mineral content (cortical, Ct.BMC and trabecular, Tb.BMC), cortical area (Ct.Ar), and cortical thickness (Ct.Th). Three-point bending tests of the central femur (Bose Electroforce 5500 test instrument) were used to generate load-displacement curves that were then used to derive ultimate load (ULD), ultimate stress (ULS), stiffness (STF), work to fracture (WTF), and Young's modulus (YM). Two-way ANOVA (time and dose) was completed. There was a strong positive effect of time on Tb.BMC, Ct.BMC, Ct.Th, Ct.Ar, ULD, ULS, STF, WTF, and YM. There was also a positive effect of ZOL dose on Tb.BMC, Ct.BMC, and Ct.Ar at 30 weeks. However, ZOL had no dose-dependent effects on bone strength and material properties of the femoral midshaft. These data suggest that cortical bone strength and biomechanical properties improve between four and eight months of age in rice rats. They further indicate that six months of ZOL at either osteoporosis or higher oncology doses, causes no deleterious effects on these basic endpoints that reflect cortical bone strength and material properties. These findings may suggest that longer ZOL treatment duration, or other mechanisms, such as those related to pAR effects on bone turnover or healing, may underlie any pAR association with AFF.

*Disclosures: Jonathan Messer, None.*

**SA0028**

**Nanoparticulate Mineralized Collagen Scaffolds Induce in Vivo Bone Regeneration Independent of Progenitor Cell Loading or Exogenous Growth Factor Stimulation.** Xiaoyan Ren\*<sup>1</sup>, Victor Tu<sup>1</sup>, David Bischoff<sup>2</sup>, Daniel Weisgerber<sup>3</sup>, Michael Lewis<sup>4</sup>, Dean Yamaguchi<sup>5</sup>, Timothy Miller<sup>6</sup>, Brendan Harley<sup>3</sup>, Justine Lee<sup>6</sup>. <sup>1</sup>UCLA & VA Great Los Angeles Healthcare System, United states, <sup>2</sup>VA Great Los Angeles Healthcare System, United states, <sup>3</sup>University of Illinois at Urbana-Champaign, United states, <sup>4</sup>VA Great Los Angeles System, United states, <sup>5</sup>VA Great Los Angeles Healthcare System, United states, <sup>6</sup>UCLA & VA Great Los Angeles Healthcare System, United states

Current strategies for skeletal regeneration often require co-delivery of scaffold technologies, growth factors, and cellular material. However, isolation and expansion of stem cells can be time consuming, costly, and requires an additional procedure for harvest. Further, the introduction of supraphysiologic doses of growth factors may result in untoward clinical side effects, warranting pursuit of alternative methods for stimulating osteogenesis. In this work, we describe a nanoparticulate mineralized collagen glycosaminoglycan scaffold that induces healing of critical-sized rabbit cranial defects without addition of expanded stem cells or exogenous growth factors. We demonstrate that the mechanism of osteogenic induction corresponds to an increase in canonical BMP receptor signalling secondary to autogenous production of BMP-2 and -9 early and BMP-4 later during differentiation. Thus, nanoparticulate mineralized collagen glycosaminoglycan scaffolds may provide a novel growth factor-free and ex vivo progenitor cell culture-free implantable method for bone regeneration.

*Disclosures: Xiaoyan Ren, None.*

**SA0029**

**Sensitivity of Proximal Femur Regions to Mechanical Loading in Young Adults.** Fátima Baptista\*, Edgar Lopes, Vera Zymbal. Exercise & Health Laboratory, Faculty of Human Kinetics, University of Lisbon, Portugal

OBJECTIVE: Since the regions of the proximal femur (PF) with increased risk of structural failure during a fall are those with less adaptive protection by mechanical loading from daily physical activity (PA) the purpose of this study was to compare the bone mineral density (BMD) of different regions of interest of the PF in young adults with different impact loads.

METHODS: Participants were 134 young adults 20 to 30 yrs old divided into 2 groups according to the impact of PA performed in the last 12 months: high impact PA (HPA), (44 men and 25 women) and low impact PA (LPA), (34 men and 31 women). Each group was subdivided into two subgroups according to gender. BMD of PF was assessed by DXA (QDR Explorer, Hologic, Waltham, MA, USA) in manufacturer's regions of interest and included integral femoral neck (FN), inter-trochanter (IT) and trochanter (TR) and in regions suggested by Li et al. (2009) that included femoral head (FH), superolateral femoral neck (SFN), and intertrochanteric region (ITR). The Bone-Specific Physical Activity Questionnaire (BPAQ, Weeks et al., 2008) was used to estimate the impact load.

RESULTS: Comparisons between groups by ANCOVA adjusted for body height revealed differences in BMD between HPA and LPA at all PF regions. HPA groups reveal BMD values 9-29% higher than LPA groups, except at FH region (p<0.01). Men with HPA showed higher BMD values than women at all regions, except at FH region (p<0.01). There were no BMD differences between genders in LPA groups. When comparisons of BMD according to group and gender were additionally adjusted for lean body mass, the magnitude of differences between PA groups was maintained or decreased (10-24%) but became non-significant at FN and at SFN between HPA and LPA women; BMD differences between men and women with HPA also disappeared, except at TR, while BMD differences at FH between men and women with LPA became significant.

CONCLUSION: The effects of mechanical loading on BMD is most pronounced in men than in women and ITR and SFN regions of PF identified by Li et al. (2009) appear to be more sensitive to mechanical load variations than manufacturer's regions, especially in women.

*Disclosures: Fátima Baptista, None.*

**SA0030**

**Why Do Spine Fusions Fail?.** J Edward Puzas\*. University of Rochester School of Medicine & Dentistry, United states

Over 400,000 Americans undergo spine fusion procedures each year. The number of procedures has increased by 137% in the ten-year period ending in 2008. The cost per operation is approximately \$90,000 totaling over \$35B/year. Yet radiographically about 15% of the procedures fail and only 66% of patients report a satisfactory outcome. Why does a solid fusion mass fail to form in every case and what is the biological reason for preventing adequate bone formation after placement of the autologous or commercially obtained bone graft material? Our hypothesis is that there is a toxic substance in some bone grafts that inhibits osteoblastic bone formation.

That toxic substance is lead (Pb). Pb levels in autologous or commercial grafts are never measured prior to their use in patients.

We sampled over 50 autologous and commercially-obtained bone graft specimens that would normally be discarded after surgery. We found lead levels ranging from undetectable to 5.0 micrograms Pb/g bone. 5.0 micrograms Pb/g bone is high enough to create millimolar concentrations of Pb around the graft during its remodeling.

Our basic science experiments have shown that Pb at between 5 and 10 micromolar can strongly inhibit collagen synthesis, alkaline phosphatase levels, osteocalcin expression and proliferation in osteoblasts. Pb appears to have this effect by markedly up-regulating the expression of the SOST gene and inducing high levels of the bone formation inhibitor, sclerostin. mRNA and protein levels for sclerostin are elevated by 5-10 fold in cultures of osteoblasts in vitro when exposed to Pb. Moreover, when mice are exposed to lead in their drinking water to achieve a bone Pb level of 5 micrograms Pb/g bone, histochemical analyses show high levels of sclerostin protein in osteocytes and osteoblasts.

How can a heavy metal ion such as Pb induce expression of a specific gene product? Our preliminary data indicate that this occurs through inhibition of Smad3 phosphorylation by the type I TGFbeta receptor. Normally, p-Smad3 is a repressor of SOST expression and thus, when phosphorylation of this transcription factor is inhibited (by Pb) there is a de-repression of SOST induction and an elevation of sclerostin protein.

Our conclusion is that the Pb content of autologous and/or commercially purchased bone graft material is a new risk factor for the clinical failure of spine fusions. Further human studies are underway to document this in a patient population.

Disclosures: J Edward Puzas, None.

SA0031

See Friday Plenary Number FR0031.

SA0032

See Friday Plenary Number FR0032.

SA0033

Lean and fat mass indices: An alternative to BMI for assessing growth outcomes in young children. Neil R. Brett\*, Kristina E. Parsons, Catherine Vanstone, Hope A. Weiler, McGill University, Canada

Data on lean mass index and body composition in healthy preschool age children is limited. Such data is fundamental to the evaluation of growth outcomes. The objective was to explore lean and fat mass across age and between sexes in healthy young Canadian children. Secondary data was derived from three studies of healthy children 2-5 y (n=201) from the Greater Montreal area. Children underwent standardized anthropometry measurements as well as having whole body bone mineral content (BMC), whole body and regional lean mass and fat mass measured using dual-energy x-ray absorptiometry (Hologic Discovery 4500A, APEX software version 13.3). Ethnic background and demographics were surveyed. A mixed model ANOVA with Bonferroni post-hoc testing was used to test for differences between sexes and over age. Children were 53% (107/201) male, age 2.0-5.9 y, 81% (163/201) white and 59% (118/201) from families with incomes  $\geq$  \$75,000 Canadian. All body composition outcomes were not different between white versus non-white children (between all children and within sexes) ( $p > 0.05$ ). Height, weight and BMI z score, height-for-age and weight-for age z scores did not differ by age or sex ( $p > 0.05$ ). As shown in Table 1, increments in age, but not sex, significantly increased BMC ( $p < 0.05$ ) and being male significantly increased lean mass index (LMI). The overall effect of being male and increasing age significantly decreased fat mass index (FMI) and significantly increased fat free mass ( $p < 0.05$ ). Fat free mass index (FFMI) and appendicular FFMI, along with android:gnoid fat mass ratio (mean  $\pm$  SD,  $0.25 \pm 0.05$ ) were not affected by age or sex ( $p > 0.05$ ). These data in healthy young Canadian children suggest that sex differences in body composition may be seen in early childhood whilst differences in BMC may not. In addition, FMI might offer an important alternative to BMI in assessing adiposity or quality of growth in the preschool years.

Table 1. Bone mineral content and indices of fat and lean mass in 2-8 y old boys and girls.

Age	Sex, n	BMC (g)	Fat mass (kg)	Fat free mass (kg) <sup>1</sup>	FMI <sup>2</sup> (kg/m <sup>2</sup> )	LMI <sup>3</sup> (kg/m <sup>2</sup> )	FFMI <sup>4</sup> (kg/m <sup>2</sup> )	Appendicular FFMI <sup>5</sup> (kg/m <sup>2</sup> )
2.0-2.9	F, 15	556.0 $\pm$ 54.0 <sup>a</sup>	4.3 $\pm$ 1.1	8.8 $\pm$ 1.2 <sup>a</sup>	5.1 $\pm$ 1.1 <sup>ab</sup>	10.4 $\pm$ 0.8 <sup>a</sup>	11.2 $\pm$ 0.7	11.3 $\pm$ 0.7
	M, 15	348.0 $\pm$ 78.2 <sup>a</sup>	4.4 $\pm$ 0.8	9.7 $\pm$ 1.3 <sup>a</sup>	5.1 $\pm$ 0.9 <sup>ab</sup>	11.2 $\pm$ 0.7 <sup>ab</sup>	11.8 $\pm$ 0.7	11.8 $\pm$ 0.7
3.0-3.9	F, 47	603.6 $\pm$ 55.7 <sup>a</sup>	4.9 $\pm$ 1.0	9.7 $\pm$ 1.3 <sup>a</sup>	5.3 $\pm$ 0.9 <sup>a</sup>	10.4 $\pm$ 1.0 <sup>a</sup>	11.1 $\pm$ 1.0	11.0 $\pm$ 1.0
	M, 34	605.5 $\pm$ 53.6 <sup>a</sup>	4.3 $\pm$ 0.9	10.5 $\pm$ 1.3 <sup>a</sup>	4.6 $\pm$ 0.9 <sup>a</sup>	11.1 $\pm$ 0.9 <sup>ab</sup>	11.8 $\pm$ 0.8	11.8 $\pm$ 0.8
4.0-4.9	F, 72	713.5 $\pm$ 83.0 <sup>a</sup>	5.0 $\pm$ 1.2	12.5 $\pm$ 1.3 <sup>b</sup>	4.2 $\pm$ 0.6 <sup>a</sup>	11.0 $\pm$ 1.0 <sup>ab</sup>	11.6 $\pm$ 1.0	11.7 $\pm$ 1.0
	M, 20	710.7 $\pm$ 68.7 <sup>a</sup>	4.6 $\pm$ 1.1	13.4 $\pm$ 1.5 <sup>b</sup>	3.8 $\pm$ 0.9 <sup>a</sup>	11.5 $\pm$ 0.9 <sup>ab</sup>	12.2 $\pm$ 0.9	12.2 $\pm$ 0.9
5.0-5.9	F, 10	747.3 $\pm$ 73.2 <sup>a</sup>	5.2 $\pm$ 1.1	13.5 $\pm$ 1.7 <sup>b</sup>	4.2 $\pm$ 0.8 <sup>ab</sup>	10.8 $\pm$ 0.7 <sup>ab</sup>	11.2 $\pm$ 0.7	11.2 $\pm$ 0.7
	M, 20	818.6 $\pm$ 96.1 <sup>a</sup>	4.4 $\pm$ 0.9	14.4 $\pm$ 1.7 <sup>b</sup>	3.3 $\pm$ 0.6 <sup>a</sup>	11.4 $\pm$ 0.7 <sup>ab</sup>	12.1 $\pm$ 0.7	12.1 $\pm$ 0.7

Data are mean  $\pm$  SD. <sup>1</sup> Fat free mass not including BMC. <sup>2</sup> FMI = total fat mass/height<sup>2</sup>. <sup>3</sup> LMI = fat free mass/height<sup>2</sup>. <sup>4</sup> FFMI = (fat free mass - BMC)/height<sup>2</sup>. <sup>5</sup> Appendicular FFMI = (fat free mass - BMC of the appendicular skeleton)/height<sup>2</sup>. <sup>a</sup><sup>b</sup><sup>ab</sup> superscripts denote significant differences for that variable between ages and/or sexes ( $p < 0.05$ ) using a mixed model ANOVA adjusting for energy intake, macronutrient intake, ethnicity and family income.

Table 1

Disclosures: Neil R. Brett, None.

SA0034

See Friday Plenary Number FR0034.

SA0035

Precision of pQCT Measurements of Total, Trabecular and Cortical Bone Area, Content, Density, and Strength in Children. Whitney Duff<sup>1</sup>, Kelsey Björkman<sup>2</sup>, Chantal Kawalilak<sup>3</sup>, Sheldon Wiebe<sup>4</sup>, Saija Kontulainen<sup>2</sup>.

<sup>1</sup>Department of Gastroenterology, College of Medicine, University of Saskatchewan, Canada, <sup>2</sup>College of Kinesiology, University of Saskatchewan, Canada, <sup>3</sup>Department of Mechanical Engineering, College of Engineering, University of Saskatchewan, Canada, <sup>4</sup>Department of Radiology, College of Medicine, University of Saskatchewan, Canada

Peripheral quantitative computed tomography [pQCT] imaging has been increasingly used in pediatric research to monitor skeletal development. However, it is unknown how precise bone measurements with pQCT are in children. The objectives of this study were to characterize pQCT precision errors in bone area, volumetric density, and estimated strength measurements at the distal and shaft sites of the radius and tibia in children as well as to determine whether scan quality influenced precision. We recruited 34 (14 boys, 20 girls) children (mean age:  $10.5 \pm 1.7$  yrs) for duplicate measurements of the distal radius, radial shaft, distal tibia, and tibial shaft using pQCT (Stratec XCT2000). Scans were performed a minimum of 24 hours apart. Images were analysed using manufacturer software (Stratec Medical, version 6). Scan quality were classified as: 1) Good scan, or 2) Scan with inconsistent reference line, broken cortex, or  $>5$  rating (Blew et al., 2014). Outcomes for the distal sites included: Total area (ToA; mm<sup>2</sup>), content (ToC; mg/mm), and density (ToD; mg/cm<sup>3</sup>); trabecular area (TrA; mm<sup>2</sup>), content (TrC; mg/mm), and density (TrD; mg/cm<sup>3</sup>); and bone strength indices during compressions (BSIC; mg<sup>2</sup>/mm<sup>4</sup>). Outcomes for shaft sites included: Total area (ToA; mm<sup>2</sup>); cortical area (CoA; mm<sup>2</sup>), content (CoC; mg/mm), density (CoD; mg/cm<sup>3</sup>), and thickness (CoTHK; mm); and strength-strain indices in torsion (SSIP; mm<sup>3</sup>). Precision was assessed by calculating root-mean-squared coefficient of variation (CV%) for each outcome and limits of agreement. Distal radius precision errors were: ToA (10.6%), ToC (8.4%), ToD (4.3%), TrA (15.3%), TrC (19.4%), TrD (5.0%), and BSIC (8.1%). Radial shaft precision errors were: ToA (6.7%), CoA (5.1%), CoC (4.4%), CoD (4.5%), CoTHK (7.6%), and SSIP (6.2%). Distal tibia precision errors were: ToA (9.0%), ToC (8.2%), ToD (2.2%), TrA (11.5), TrC (14.6%), TrD (3.6%), and BSIC (7.9%). Tibial shaft precision errors were: ToA (5.9%), CoA (2.0%), CoC (1.7%), CoD (2.5%), CoTHK (4.2) and SSIP (6.3%). Majority of precision errors for all scans, including scans with inconsistent reference lines and broken cortices, were within the 95% limits of agreement (Figure 1 bone strength example). Results suggest that bone properties in children can be imaged with precision errors comparable to those reported for adults in our lab. Reported precision errors will assist in selection and interpretation of pQCT outcomes in studies monitoring bone development in children.

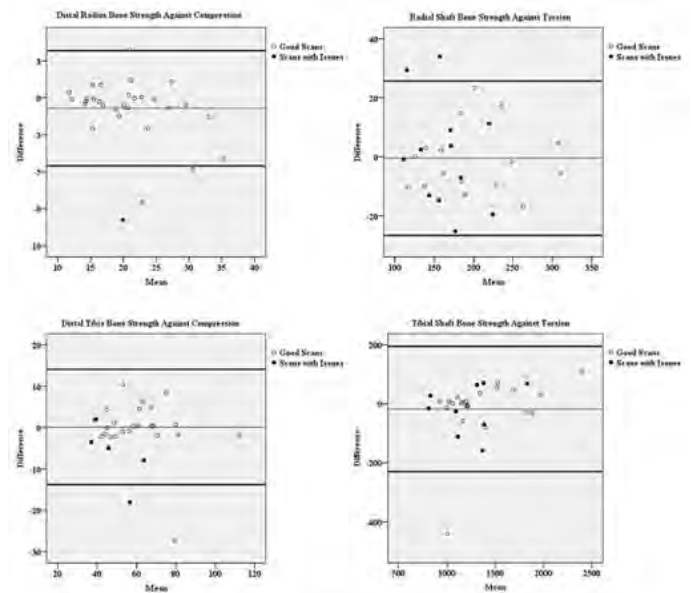


Figure 1. Bland-Altman plots of all scans. Thick lines represent 95% limits of agreement of scans with consistent reference lines and intact cortices. Thin lines represent mean difference. Open circles identify good scans (i.e. scans with no issues). Closed circles identify scans with issues, defined as inconsistent reference line placement, broken cortex, or rating of  $>5$  (Blew et al., 2014).

Image

Disclosures: Whitney Duff, None.

## SA0036

**Prickle1 is required for neural crest development.** Yong Wan\*, Brandi Gillian, Brian Cusack, Heather Szabo-Rogers, university of pittsburgh, United states

*Beetlejuice (Bj)* mice are named after the 1980s movies character for their microcephalic skull. The *Bj* mice have a point mutation in the *Prickle1* protein (C161F). The *Bj* mice mutants develop defects in neural crest derived structures in the skull vault, face, and cranial base. The *Bj* mice have defects in bones that undergo both intramembraneous and endochondral ossification. We observe smaller frontal bones in the skull vault, and disorganized endochondral bones of cranial base including the basiphenoid bone. Intriguingly, the mesodermally-derived parietal bone and basioccipital are not significantly affected. These data suggest that *Prickle1* is required for neural crest development. We characterized the rate of proliferation and differentiation in both the skull vault and cranial base. We found no difference in proliferation in the frontal bone, while proliferation is decreased in the basiphenoid bone. We tested the progression of ossification in both locations and found that differentiation in the frontal bone is accelerated, while osteoblast differentiation is inhibited in basiphenoid bone. We also found that cell migration is also partly blocked in the frontal and maxillary bone of the *Bj* mutant. We are currently determining if loss of *Prickle1* function may be altering both canonical Wnt/beta-catenin signaling and hedgehog signaling. We conclude that *Prickle1* function is required in the neural crest derived craniofacial regions.

**Disclosures:** *Yong Wan, None.*

## SA0037

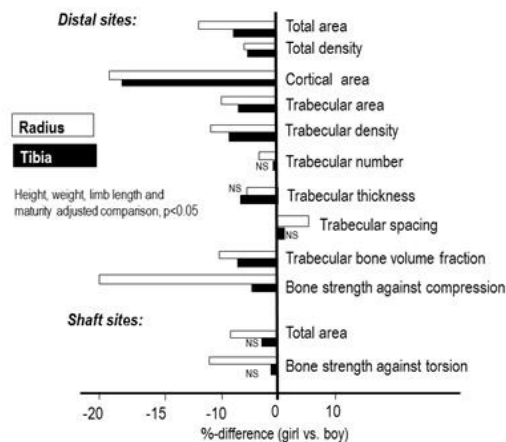
**Sexual Dimorphism in the Distal Radius and Tibia Bone Size, Density, Micro-architecture and Strength is Manifested in Favor of Boys Already in Childhood.** Saija Kontulainen\*<sup>1</sup>, Kelsey Bjorkman<sup>1</sup>, Chantal Kawalilak<sup>1</sup>, Whitney Duff<sup>2</sup>, Hassanali Vatanparast<sup>1</sup>, J.D. Johnston<sup>1</sup>.  
<sup>1</sup>University of Saskatchewan, Canada, <sup>2</sup> University of Saskatchewan, Canada

Sex-differences in bone strength manifest at late puberty likely due to sex-specific hormonal stimulus to bone development. Comparisons of bone structural properties between sexes in years preceding the pubertal growth are lacking. Our objective was to assess sex-differences in bone strength, size, density and micro-architecture in childhood.

We scanned distal and shaft sites of the radius and tibia from 85 girls and 75 boys (mean age 10.8, SD 1.8 yrs) using peripheral quantitative computed tomography (pQCT) and high resolution pQCT. We defined biological age by calculating age from the estimated age at peak height velocity (aPHV). We included participants with a biological age of 0 to -4 years from aPHV and excluded post-menarcheal girls. We measured and compared (t-tests) anthropometrics, physical activity levels and dietary intakes of protein, calcium and vitamin D between sexes to identify covariates (for bone outcomes) that differed between sexes. We used MANCOVA (covariates: biological age, limb length, height and weight) to compare total, cortical and trabecular bone areas and densities, trabecular micro-architecture (thickness and number) and bone volume fraction, and estimated bone strength against compression at distal sites between girls and boys. We also compared total and cortical areas, cortical density and bone strength against torsion at the shaft sites of the radius and tibia.

At the distal radius, girls had 10-19% smaller total, cortical and trabecular area, 7-10% lower total and trabecular density, 4% fewer trabeculae and 20% lower estimated bone strength against compression (Fig. 1). We observed similar sex-differences at the distal tibia (Fig. 1). At the radius shaft, girls had 20% smaller total area and 12% lower bone strength against torsion. We did not observe any sex-differences at the tibia shaft (Fig. 1).

Results suggest that boys have favorable bone size, density, micro-architecture and strength particularly at the distal radius and radius shaft already in childhood. These findings indicate that, in addition to systemic factors (e.g. hormones), local factors (e.g. mechanical loading) may contribute to sex-specific bone development in childhood. A better understanding of sex-specific development in bone structure, micro-architecture and strength, along with information of modifiable factors, will guide investigations and strategies aiming to optimize primary prevention of osteoporosis and bone fragility, particularly in females.



Sex-differences (%) in bone outcomes at the radius (white bars) and tibia (black) in children.

**Disclosures:** *Saija Kontulainen, None.*

## SA0038

See Friday Plenary Number FR0038.

## SA0039

See Friday Plenary Number FR0039.

## SA0040

See Friday Plenary Number FR0040.

## SA0041

See Friday Plenary Number FR0041.

## SA0042

See Friday Plenary Number FR0042.

## SA0043

See Friday Plenary Number FR0043.

## SA0044

See Friday Plenary Number FR0044.

## SA0045

See Friday Plenary Number FR0045.

## SA0046

See Friday Plenary Number FR0046.

## SA0047

See Friday Plenary Number FR0047.

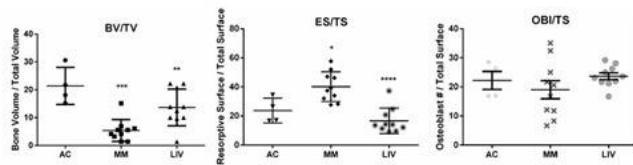
## SA0048

See Friday Plenary Number FR0048.

## SA0049

**The Effects of Low Magnitude Mechanical Signals on Myeloma-induced Osteolysis are Both Anti-resorptive and Systemic.** Gabriel M. Pagnotti\*<sup>1</sup>, Kimberly DeCarr<sup>1</sup>, Janet Rubin<sup>2</sup>, Steven D. Bain<sup>3</sup>, Clinton T. Rubin<sup>1</sup>.  
<sup>1</sup>Stony Brook University, United states, <sup>2</sup>University of North Carolina: Chapel Hill, United states, <sup>3</sup>University of Washington, United states

Multiple myeloma(MM), characterized by uncoupled formation and resorption during bone remodeling, renders patients susceptible to acute osteolysis and fracture of critical, load-bearing bone. While exercise and other modes of mechanical signals are non-pharmacological and can improve musculoskeletal health, compromised bone resulting from MM may not withstand the extreme mechanical loads incurred during exercise without increasing risk-of-fracture. Low intensity vibrations(LIV), a form of mechanical signal demonstrated as anabolic to bone, was explored as a potential means of preserving bone in 34 skeletally-mature mice randomized into age-matched control(AC:n=8), MM(n=12) and LIV(n=13), where both MM and LIV harbored myeloma engraftment in the bone marrow. LIV received mechanical signals at 90Hz(0.3g for 15min/day, 5day/w) while MM and AC received SHAM-treatment over 8w. Histomorphometric analyses of distal femora in MM revealed no primary spongiosa, yet they were partially protected by LIV. Tb.BV/TV in MM was 75%(p<0.001) lower than AC, while LIV was 36%(p<0.05) below AC, resulting in 60%(p<0.01) greater BV/TV than MM. Eroded surface per trabecular surface(ES/TS) in MM was 70%(p<0.05) greater than AC, while LIV was 58%(p<0.0001) below MM. Osteoblast number per trabecular surface(OBI/TS) was 14%(NSD) lower in MM as compared to AC, whereas LIV was 24%(NSD) greater than MM. Investigating whether these results extended into the spine, high-resolution  $\mu$ CT(10 $\mu$ m) was performed on L5 vertebrae, where 0.377mm<sup>3</sup> of trabecular bone through the vertebral body(d=0.98mm; h=0.5mm) was evaluated. Bone volume fraction(BV/TV) decreased 35%(p<0.05) in MM versus AC, having increased by 27%(p<0.05) in LIV relative to MM. Trabecular connectivity-density decreased by 35%(p<0.05) in MM as compared to AC but increased 46%(p<0.05) in LIV from MM. Trabecular number(Tb.N) decreased 16%(p<0.05) in MM from AC and increased 13%(NSD) in LIV versus MM. Trabecular structure model index(SMI) increased 38%(p<0.05) in MM from AC and decreased 5%(NSD) in LIV versus MM. The anti-resorptive effects measured in LIV outperform pro-formative ones, suggesting an influence on factors regulating osteoclast activity, highlighting the role mechanical signals might play in preserving bone quantity and quality in lytic cancers; perhaps ultimately achieved by recoupling the bone remodeling process. Therefore, LIV may serve to systemically protect weight-bearing bones from fracture in cancer patients.



Histomorphometry

**Disclosures:** Gabriel M. Pagnotti, None.  
This study received funding from: NIH

## SA0050

**The Role of the COP9 Signalosome in the Pathogenesis of Osteosarcoma.** William Samsa\*. Guang Zhou. Case Western Reserve University, United states

The COP9 Signalosome (CSN) is a highly conserved complex involved in diverse cellular processes including cell cycle progression, apoptosis, and the regulation of DNA damage repair through controlling gene transcription, protein subcellular localization, and protein stability. Jun activation domain binding protein 1 (JAB1), also known as COPS5 and CSN5, is the fifth component of the CSN and harbors its catalytic activity to deneddylate the E3-cullin RING ubiquitin ligases. JAB1 is recognized as a potential oncogene, as it is overexpressed in many cancers and negatively regulates the tumor suppressor p53. Indeed, the loss of Jab1 in mice results in decreased levels of DNA repair protein RAD51 through p53-dependent mechanisms, and sensitizes osteosarcoma cells to  $\gamma$ -radiation-induced apoptosis. In the United States, osteosarcoma is the most common type of primary bone malignancy. Osteosarcoma has a high incidence of metastases to the lung, with a clinical outcome of fewer than 30% of these patients surviving 5 years after the initial diagnosis. Therefore, a better understanding of the pathogenesis of osteosarcoma is important for diagnosis and treatment. Osteosarcoma occurs predominantly in adolescents and selectively in the growth plates of rapidly growing bones. However, the role of JAB1 in osteosarcoma pathogenesis remains to be further elucidated. We recently showed that JAB1 plays an essential role in embryonic limb development and early osteoblast differentiation by generating a *Jab1*<sup>flx/flx</sup>; *Prx1*-cre mutant mouse model to delete *Jab1* specifically in osteochondral progenitor cells. These mutants exhibited reduced primary ossification center sizes and reduced mineralization. We also deleted *Jab1* in osteoblast precursor cells by generating *Jab1*<sup>flx/flx</sup>; *Osx*-Cre mutant mice, and found that that these mutant mice had dwarfism at weaning age and reduced trabecular bone formation. Interestingly, osteosarcoma patient tissue samples

exhibited strong immunostaining for JAB1, which correlated with mortality, and short hairpin knockdown of JAB1 in the aggressive human osteosarcoma cell line 143B resulted in significantly decreased oncogenic properties. Lastly, the overexpression of *Jab1* in mice on a p53<sup>+/+</sup> background increased the osteosarcoma incidence by 11 months of age. Therefore, JAB1 plays a stage-specific role in skeletal homeostasis and can be a potential therapeutic target for cancer treatment.

**Disclosures:** William Samsa, None.

## SA0051

See Friday Plenary Number FR0051.

## SA0052

See Friday Plenary Number FR0052.

## SA0053

See Friday Plenary Number FR0053.

## SA0054

See Friday Plenary Number FR0054.

## SA0055

See Friday Plenary Number FR0055.

## SA0056

See Friday Plenary Number FR0056.

## SA0057

**Saturated Fatty Acids Differently Alter Osteoarthritis Development in Diet Induced Obese Rats.** Indira Prasadam\*, Sunderajhan Sekar, Yin Xiao, Ross Crawford. Institute of Health & Biomedical Innovation & Queensland University of Technology, Australia

Osteoarthritis (OA) is the most common joint disease across worldwide. For many years, epidemiological studies continued to suggest that high fat diets are linked to an increased incidence of OA. However, so far we do not have a clear understanding of what fat types that should be avoided and how much of each type alters OA risk. The predominant saturated fatty acids (SFA) in human diets are lauric acid (LA, C12:0), myristic acid (MA, C14:0), palmitic acid (PA, C16:0) and stearic acid (SA, C18:0). The aim of this study was to determine whether diets containing these SFA together with excess simple carbohydrates induce both osteoarthritis (OA)-like changes in knee joints as well as signs of metabolic syndrome in rats. Wistar rats were fed either a corn starch diet or a diet composed of simple sugars together with 20% LA, MA, PA, SA or beef tallow as a high-carbohydrate, high-fat diet for 16 weeks. Energy consumption, metabolic parameters, systolic blood pressure, heart and liver structure and function, and plasma biochemistry including serum inflammatory cytokines were measured. The knee-joints were assessed for changes to articular cartilage and subchondral bone. *In vitro* phenotypic changes were assessed in SFA-treated human chondrocytes and bovine cartilage explant cultures. Our results indicate that diets containing beef tallow, SA, MA or PA induced both signs of metabolic syndrome and cartilage degradation similar to OA, suggesting that increased metabolic risk increases OA risk. In contrast, LA-fed rats showed minimal signs of metabolic syndrome with minimal changes in cartilage structure. Further, MA, PA and SA but not LA increased release of matrix sulfated proteoglycans from bovine cartilage explants and human chondrocytes. These results together suggests SFA that induce metabolic syndrome in rats also increase OA risk. Thus, replacing dietary MA, PA and SA with LA may decrease development of both metabolic syndrome and OA. In conclusion, our study indicates that effect of saturated fats on OA risk depends on the kind of fatty acids in the food. Thus, reducing or modulating certain types of saturated fatty acids in the diet may help in preventing or slowing the progression of OA.

**Disclosures:** Indira Prasadam, None.

## SA0058

**Modulation of Hypoxia Signaling, but not Angiogenesis Alone, Improves Regenerative Outcome During Endochondral Bone Tissue Engineering.** Pieter-Jan Stiers\*, Nick van Gestel, Steve Stegen, Riet Van Looveren, Sophie Torrekens, Geert Carmeliet. Clinical & Experimental Endocrinology, KU Leuven, Belgium

The success of bone tissue-engineered implants largely depends on how well implanted cells adapt and survive in the hostile environment they will encounter. As cartilage is naturally avascular, cells in an implant that induces endochondral ossification via a

cartilage template may survive better in poorly vascularized bone defects. However, the question remains whether this hypothesis holds true for constructs of clinically relevant size, as angiogenesis is an inherently slow process and chondrocytes in the center of large constructs may not survive indefinitely without oxygen or nutrients. To study this, we have looked at the effect of VEGF and hypoxia signaling in an endochondral bone tissue-engineered implant to determine whether these strategies can be combined to improve regeneration.

Fibroblast growth factor 2-pretreated murine periosteum-derived cells (mPDC) were suspended in collagen and injected ectopically. These cells initially undergo chondrogenesis, but display poor survival and cartilage formation in the center of large constructs at later time points. In an attempt to alleviate this via enhanced angiogenesis, mPDC were transduced with adenovirus expressing VEGF or GFP before implantation, and VEGF-transduced cells showed a 4-fold increase of VEGF mRNA. No changes in proliferation or chondrogenesis were observed 3 and 7 days after implantation. At day 7, blood vessel ingrowth was increased in constructs overexpressing VEGF and a higher number of mPDC expressed type I collagen, leading to a modest increase in mineralized tissue analyzed by  $\mu$ CT (110–140% of control). However, at day 14 most non-mineralized tissue in VEGF constructs was fibrotic, whereas control samples contained less mineralized tissue but more cartilage was still present. As VEGF alone had negative effects on the centrally localized cells, hypoxia signaling was enhanced via knockdown of prolyl hydroxylase domain-containing protein 2. These constructs developed less fibrosis and hypoxia at later time points, suggesting a protective effect of hypoxia signaling on chondrogenesis during endochondral bone tissue engineering.

Together these results show that VEGF can be used to increase angiogenesis and osteogenesis but can also cause adverse effects unless dosed and timed carefully, whereas modulation of hypoxia signaling may present a better therapeutic strategy to improve regeneration in large tissue-engineered constructs.

**Disclosures:** Pieter-Jan Stiers, None.

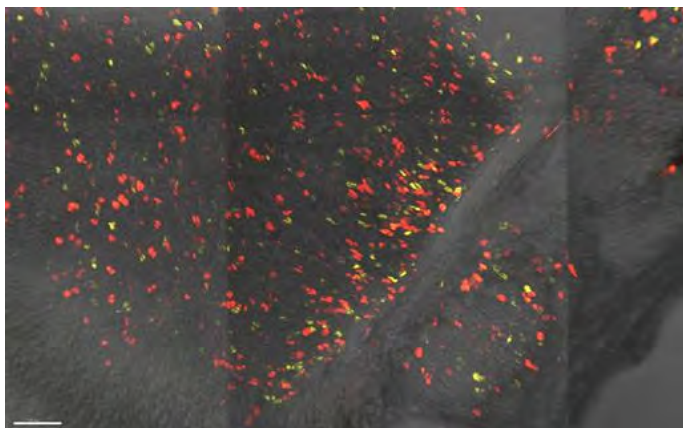
## SA0059

**mTORC1 Modulates Craniofacial Cartilage Development in Zebrafish and Mice.** Meng Xie<sup>\*1</sup>, Lei Li<sup>1</sup>, Phillip Newton<sup>1</sup>, Evgeny Ivashkin<sup>1</sup>, Vyacheslav Dyachuk<sup>2</sup>, Olov Andersson<sup>3</sup>, Hong Qian<sup>4</sup>, Igor Adamevko<sup>1</sup>, Andrei Chagin<sup>1</sup>. <sup>1</sup>Department of Physiology & Pharmacology, Karolinska Institutet, Stockholm SE-171 77, Sweden., Sweden, <sup>2</sup>Neuroscience Dep., Karolinska Institutet, Sweden, <sup>3</sup>Department of Cell & Molecular Biology (CMB), C5, Karolinska Institutet, Sweden, <sup>4</sup>Department of Medicine, Huddinge (MedH), H7, Karolinska Institutet, Sweden

Vertebrate craniofacial development is mainly accomplished by neural crest cell migration, condensation and differentiation, which contribute to most of the cartilage, bone and connective tissue of the head skeleton. Cartilage provides a template for bone development and aberrant cartilage development often leads to craniofacial abnormalities and permanent alterations. Mechanistic target of rapamycin complex I (mTORC1) has been long known as a key intracellular protein complex with kinase activity, which integrates multiple extracellular signals into metabolic cell response.

In the present study, we showed that CRISPR/Cas9 knockout of mTORC1 components as well as pharmacological disruption during early zebrafish development led to formation of smaller and structurally altered facial cartilages due to inhibition of chondrocyte proliferation and hypertrophy. In addition, pharmacological inhibition of mTORC1 activity specifically during neural crest cell migration period resulted in formation of a thinner and elongated craniofacial structures. Similar facial alterations were observed in E17.5 mouse embryos, if exposed to rapamycin at E10.5, time point of neural crest cell migration. Genetic manipulation of mTORC1 activity in cartilage during development is ongoing.

Taken together, our data revealed a significant role of mTORC1 in regulating craniofacial skeleton development in both fish and mammal that may shed light on understanding of mechanisms underlying craniofacial abnormalities.



Genetic cell tracing in mouse embryonic frontal bone

**Disclosures:** Meng Xie, None.

## SA0060

**Raf Kinases are Essential for Phosphate Induction of Erk1/2 Phosphorylation in Hypertrophic Chondrocytes and Normal Endochondral Bone Development.**

Garyfallia Papaioannou<sup>\*1</sup>, Elizabeth T. Petit<sup>2</sup>, Eva S. Liu<sup>3</sup>, Manuela Baccarini<sup>4</sup>, Catrin Pritchard<sup>5</sup>, Marie B. Demay<sup>1</sup>. <sup>1</sup>Endocrine Unit, Massachusetts General Hospital & Harvard Medical School, United states, <sup>2</sup>Endocrine Unit, Massachusetts General Hospital, United states, <sup>3</sup>Endocrine Unit, Massachusetts General Hospital, Harvard Medical School & Brigham & Women's Hospital, United states, <sup>4</sup>Department of Microbiology, Immunology & Genetics, Center of Molecular Biology, Max F. Perutz Laboratories, University of Vienna, Austria, <sup>5</sup>Department of Molecular Cell Biology, University of Leicester, UK, United Kingdom

During endochondral ossification chondrocytes form an organized structure which, following vascular invasion, is progressively replaced by bone. The growth plate is comprised of resting, proliferating and hypertrophic chondrocyte zones which undergo coordinated proliferation, differentiation and apoptosis. Hypophosphatemia causes rickets by impairing hypertrophic chondrocyte apoptosis. Phosphate induction of Erk1/2 phosphorylation in hypertrophic chondrocytes is required for phosphate-mediated apoptosis and normal growth plate maturation. Erk1/2 is phosphorylated directly by MEK1/2 which is activated by a number of different signaling molecules including Raf isoforms. Expression of A- and B-Raf in the growth plate was reported to be localized to proliferative chondrocytes and ablation of these two isoforms in chondrocytes does not alter skeletal development or maturation. Ablation of C-Raf, which is expressed predominantly in hypertrophic chondrocytes, results in expansion of the hypertrophic chondrocyte layer, decreased hypertrophic chondrocyte apoptosis and impaired vascularization of the growth plate. However, ablation of C-Raf does not impair phosphate-induced Erk1/2 phosphorylation in cultured hypertrophic chondrocytes, but rather leads to rickets by decreasing VEGF protein stability.

To determine if Raf isoforms are required for phosphate-induced hypertrophic chondrocyte apoptosis, mice lacking all three Raf isoforms in chondrocytes were generated (Global ablation of A-Raf; Col II-Cre ablation in B-Raf *fff* and C-Raf *fff* mice). Deletion of all three Raf Kinases, or the presence of only one Raf allele, led to neonatal death and a significant increase of the size of the hypertrophic chondrocyte layer. This was accompanied by decreased pERK1/2 immunoreactivity in the hypertrophic chondrocyte layer and a decrease in vascular invasion, as shown by endomucin staining. Phosphate induced Erk1/2 phosphorylation in cultured chondrocytes was ablated in primary chondrocytes lacking all three Raf isoforms. These data demonstrate that Raf Kinases exert essential but partially redundant roles in growth plate maturation and are required for phosphate-induced Erk1/2 phosphorylation.

**Disclosures:** Garyfallia Papaioannou, None.

## SA0061

**Role of Discoidin Receptor 2 in Intervertebral Disc Development and Degeneration.** chunxi Ge<sup>\*1</sup>, Ernestina Schipani<sup>2</sup>, Renny Franceschi<sup>1</sup>, Hanshi Sun<sup>1</sup>.

<sup>1</sup>University of Michigan School of Dentistry, United states, <sup>2</sup>University of Michigan School of Medicine, United states

Intervertebral disc (IVD) degeneration is the major cause of lower back pain, a condition that affects 85 percent of the population at some point in their lives and incurs a healthcare cost in the United States of \$100 billion/year. Current treatments focus on pain management, physiotherapy or, in more advanced cases, surgery (spinal fusion, disc arthroplasty). No current treatments are totally satisfactory. An ideal therapeutic strategy would be to prevent IVD degeneration before it becomes a major source of pain and disability. To accomplish this, we need a detailed understanding of mechanisms controlling IVD formation and age-dependent degeneration so that targeted therapies can be developed. We recently made the novel discovery that disruption of discoidin receptor 2 (Ddr2) causes major changes in IVD development first seen at P0 that persist as mice grow and mature in the absence of changes in hyaline cartilage joints such as the knee. At P0, mutant IVDs have a reduced number of cells separating the NP from future endplate regions, but normal NP morphology. By 3 months, mutant IVDs have a grossly altered morphology of both annulus fibrosus (AF) and nucleus pulposus (NP). The AF of mutants is more cellular and contains disorganized concentric lamellae while end plates are thinner and less organized. The NP phenotype is of particular interest since the normal reduction in NP size and infiltration with cartilage that normally occurs as mice mature is apparently blocked or at least delayed. Significantly, age-dependent NP degeneration and loss of hydration are responsible for the inability of IVDs to absorb compressive loads, which leads to further degeneration and loss of function. As will be shown, Ddr2 is present in select AF and NP regions that become restricted with age. The significance of these findings are as follows: i) The observation that Ddr2 loss affects both the AF and NP implies either that it functions in both compartments or is involved in processes whereby one compartment affects the other (e.g. migration of cells between compartments, communication between compartments). In either case, understanding Ddr2 function in the IVD would elucidate fundamental processes

governing the formation and maintenance of this important structure. ii) If DDR2 is involved in age-dependent loss/degeneration of the NP, it may be a potential target for reversing some aspects of IVD degeneration. Significantly, as a collagen-activated receptor tyrosine kinase, DDR2 is a druggable target that can be inhibited by known tyrosine kinase inhibitors.

**Disclosures:** *chunxi Ge, None.*

## SA0062

See Friday Plenary Number FR0062.

## SA0063

See Friday Plenary Number FR0063.

## SA0064

See Friday Plenary Number FR0064.

## SA0065

**Bone Marrow Adipose Changes After Gastric Bypass Surgery-Induced Weight Loss Are Influenced by Diabetes Improvement and Total Body Fat Loss.** Tiffany Kim<sup>\*1</sup>, Ann Schwartz<sup>2</sup>, Xiaojuan Li<sup>2</sup>, Kaipin Xu<sup>2</sup>, Dennis Black<sup>2</sup>, Dimitry Petrenko<sup>3</sup>, Lygia Stewart<sup>1</sup>, Stanley Rogers<sup>2</sup>, Andrew Posselt<sup>2</sup>, Jonathan Carter<sup>2</sup>, Dolores Shoback<sup>1</sup>, Anne Schafer<sup>1</sup>.

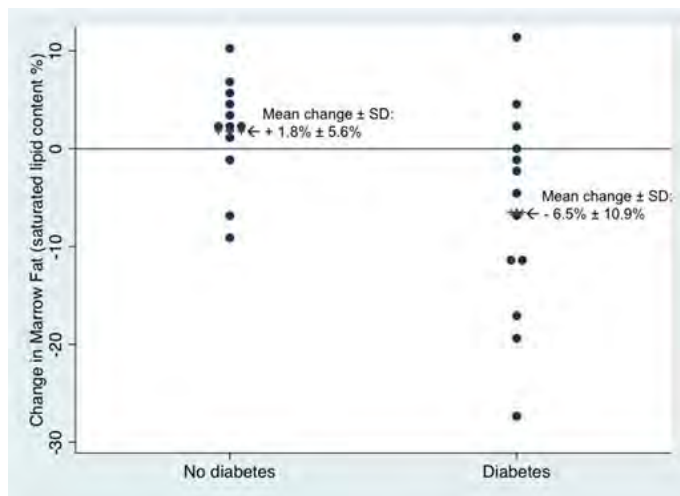
<sup>1</sup>University of California, San Francisco & the San Francisco VA Medical Center, United states, <sup>2</sup>University of California, San Francisco, United states, <sup>3</sup>Alabama College of Osteopathic Medicine, United states

Roux-en-Y gastric bypass (RYGB) is a powerful tool for the treatment of obesity and diabetes. However, RYGB increases bone turnover and decreases bone mineral density (BMD). Growing evidence indicates that marrow adipose tissue (MAT) is implicated in the interaction between bone, fat and glucose metabolism. We hypothesized that weight loss and glucose metabolism both regulate MAT, and the longitudinal effect of RYGB-induced weight loss on MAT varies depending on diabetes status.

We enrolled 30 morbidly obese women (14 diabetic, 16 non-diabetic) and measured vertebral MAT before and 6 months after RYGB with 3T magnetic resonance spectroscopy. We calculated saturated lipid content (%) as fat/(fat+water) x 100. Other measures included BMD and body composition by dual-energy X-ray absorptiometry and quantitative computed tomography.

Mean pre-op body mass index (BMI) for diabetic women (42 kg/m<sup>2</sup>) was lower than nondiabetic women (46 kg/m<sup>2</sup>), likely reflecting a lower threshold for gastric bypass referral in diabetes. Other baseline characteristics were similar, including mean MAT (49% in diabetic and 50% in nondiabetic women) and age (48 years in both groups). At baseline, lower BMI correlated with higher MAT ( $r=-0.37$ ,  $p=0.04$ ), but there was a trend towards a correlation between higher visceral fat and higher MAT ( $r=0.33$ ,  $p=0.07$ ). Women with higher MAT had lower spinal volumetric BMD ( $r=-0.72$ ,  $p<0.01$ ) and femoral neck areal BMD ( $r=-0.65$ ,  $p<0.01$ ). Six months post RYGB, women lost a mean 27 kg and 35% of total body fat. BMD significantly declined at the spine and hip. In diabetic women, mean A1c decreased from 7.6% to 5.7%. Mean MAT in diabetic women decreased 6.5% ( $p=0.05$ ) and conversely, in nondiabetic women, was maintained (+1.8%,  $p=0.29$ ;  $p=0.03$  for difference between groups). Overall, greater A1c declines correlated with declines in MAT ( $r=0.50$ ,  $p=0.01$ ). Among diabetic women, declines in visceral fat correlated with declines in MAT ( $r=0.59$ ,  $p=0.04$ ). However, among nondiabetic women, those with greater decreases in total body fat mass were more likely to have increases in MAT ( $r=-0.69$ ,  $p=0.01$ ).

In conclusion, MAT changes after RYGB correlated with metabolic and fat improvements, and depended on diabetes status. By understanding MAT in rapid weight loss and diabetes, we may better understand the role of MAT in the diminished bone structure and strength observed in these metabolic conditions.



Changes in vertebral marrow fat 6 months after gastric bypass surgery, stratified by diabetes status

**Disclosures:** *Tiffany Kim, None.*

## SA0066

**Exercise Shrinks Marrow Adipocytes by Burning Fat.** Maya Styner<sup>\*1</sup>, Gabriel Pagnotti<sup>2</sup>, Xin Wu<sup>1</sup>, Cody McGrath<sup>1</sup>, Buer Sen<sup>1</sup>, Gunes Uzer<sup>1</sup>, Zhihui Xie<sup>3</sup>, Xiaopeng Zong<sup>4</sup>, Martin Styner<sup>5</sup>, Clinton Rubin<sup>2</sup>, Janet Rubin<sup>1</sup>. <sup>1</sup>Department of Medicine, Division of Endocrinology, University of North Carolina, Chapel Hill, NC, United states, <sup>2</sup>Department of Biomedical Engineering, State University of New York, Stony Brook, NY, United states, <sup>3</sup>Department of Medicine, Division of Endocrinology, University of North Carolina, Chapel Hill, NC, United states, <sup>4</sup>Biomedical Research Imaging Center, University of North Carolina, Chapel Hill, NC, United states, <sup>5</sup>Departments of Psychiatry & Computer Science, University of North Carolina, Chapel Hill, NC, United states

A dogma which requires revision has been that marrow adipose tissue (MAT) and bone quantity are inversely proportional: this arose with the recognition that MAT is high in post-menopausal osteoporotic patients, paraplegics and the elderly, states which correlate with low bone density and fractures. Whether this holds true for the increase in bone fat accompanying obesity in humans and rodents is unclear. In this study, we tested the response of MAT to running exercise in the setting of diet-induced obesity (DIO). Four week old, female C57BL/6 mice were provided low fat diet (LFD) or high fat diet. After 12 weeks, mice were further divided into control (LFD, DIO) or exercise groups (LFD-E, DIO-E) given access to voluntary running wheels (4 groups,  $n=7$ /group). DIO and LFD mice ran similar distances. Total body fat mass in DIO ( $4.8 \pm 0.9g$ ) decreased with exercise, DIO-E ( $2.1 \pm 0.6g$ ,  $p<0.01$ ). Lean mass was higher in DIO relative to LFD ( $p<0.01$ ) but was not altered by exercise. Weights after 6 weeks of running were  $22.8 \pm 1.6g$  (LFD),  $22.8 \pm 1.2g$  (LFD-E),  $27.2 \pm 2.0g$  (DIO), and  $25 \pm 2.6g$  (DIO-E) ( $p<0.001$  DIO vs. LFD). Histology of the femur was utilized to determine marrow adipocyte size ( $\mu m^2$ ): LFD  $375.4 \pm 16.32$ , LFD-E  $251.0 \pm 4.611$ , DIO  $560.3 \pm 21.71$ , DIO-E  $340.9 \pm 13.46 \mu m^2$ . Adipocyte area was increased by obesity (LFD vs DIO  $p<0.0001$ ) and reduced by exercise (LFD vs LFD-E; DIO vs DIO-E  $p<0.0001$ , Figure 1). Exercise reduced MAT volume ( $p < 0.05$ ) as measured by osmium- $\mu$ CT. Femoral MAT was also assessed by 9.4T MRI with fat image intensity by normalization and correction for T1 and T2 effects, with volumetric images normalized to total bone volume (Figure 1). MRI volumetric fat quantification correlated with the osmium  $\mu$ CT ( $r = 0.645$ ;  $p < 0.01$ ). Tibial mRNA demonstrated increased *perilipin 3* (*PLIN3*) with exercise, consistent with increased lipid beta oxidation; thus, the decrease in adipocyte size is likely due to marrow fat utilization as a local energy store.  $\mu$ CT derived trabecular BV/TV in the tibia was not decreased by DIO and was increased by exercise (LFD  $9.691 \pm 1.143$ , LFD-E  $11.53 \pm 0.712$ , DIO  $9.783 \pm 0.515$ ,  $11.60 \pm 1.424$ ; exercise effect  $p < 0.001$ ). The exercise-associated lower marrow lipid content and adipocyte size - via histology, osmium- $\mu$ CT, and MRI - thus appears to be due to utilization of local MAT lipids potentially for skeletal anabolism.

SA0069

**Osteocyte-specific ablation of Pparγ (Ocy-Pparγ) improves energy metabolism and prevents fat accumulation and steatosis in response to a high fat diet.** Julia brun<sup>\*1</sup>, flavien Berthou<sup>2</sup>, Mirko Trajkovski<sup>2</sup>, Michelangelo Foti<sup>2</sup>, Pierre Maechler<sup>2</sup>, serge ferrari<sup>1</sup>, Nicolas Bonnet<sup>1</sup>. <sup>1</sup>Service des Maladies Osseuses, Switzerland, <sup>2</sup>laboratoires des Maladies métaboliques, Switzerland

Pparγ is a transcriptional regulator of energy metabolism. We demonstrated that Dmp1-Cre/Pparγ Lox-mice (KO) have increased bone mass and energy metabolism. Here we investigated the role of Ocy-Pparγ deletion on glucose and bone metabolism during a high fat diet (HF).

Wildtype (WT) and KO male mice aged of 16 weeks received a HF or chow diet (60% vs CD 10% of fat) for 12 weeks. Lean & fat, bone structure, metabolic rate and tissue temperature were evaluated by echoMRI, microCT, labmaster and infrared camera. In order to identify potential osteokines mediating Ocy metabolic functions, we performed primary osteoblasts (OB) cultures from long bones. Conditioned medium (CM) was added on primary hepatocytes. Co-culture of OBKO was also performed with primary pancreatic islet extracted from WT, insulin were quantified by ELISA.

Vertebral BV/TV was higher in KO (+39% vs WT, p<0.01) but was similarly decreased by HF in KO and WT (-12% vs CD, Pinter =0.3). Under HF, movement, VO2 and heat were higher in KO (+41%, +13%, +13% vs WT, p<0.05). HF induced fat mass increase was prevented in KO (+17% vs CD and +44% vs CD in WT, p<0.05) whereas increased in lean mass was greater (+14.2% vs CD and +9.6% vs CD in WT). Body temperature was also higher, particularly in the BAT-neck region (+1.5% vs WT, p<0.01). UCP1&3 and PPARβ&γ expression in BAT was higher in KO (84%, 139%, 125% and 167% vs WT, p<0.01). UCP1 expression and staining indicate a browning of the WAT. As a result, glucose and insulin tolerance test were improved in the KO (AUC -22% and -9% vs WT, p<0.05).

In vitro, lipid droplets were decreased in hepatocytes exposed to KO vs WTCM. CD36 fatty acid transporter expression was lower with KO CM (-51% vs no OB CM and -52% vs WT CM, all p<0.001) and Pparα expression higher (+48% vs no OB CM and +22% vs WT CM, all p<0.05). These results were confirmed by western blot. Co-culture with OBKO increased insulin production by pancreatic islets (+130% vs no OB and +83% vs OBWT, both p<0.01). Finally, two osteokines were particularly secreted by KO, undercarboxylated osteocalcin and BMP7, respectively +23.7% and +8.4% vs WT, p<0.05.

In conclusion, ablation of Pparγ by Dmp1-Cre improves bone mass but does not prevent the effects of HF on bone. In contrast, it improves BAT activity and insulin sensitivity, preventing fat accumulation, steatosis and improving glucose homeostasis. The contribution of osteocalcin and BMP7 on glucose homeostasis and steatosis remains to be determined.

**Disclosures:** Julia brun, None.

SA0070

**Serum Phosphate is Related to Fat Mass in Healthy Adults.** Emma Billington<sup>\*1</sup>, Greg Gamble<sup>2</sup>, Ian Reid<sup>2</sup>. <sup>1</sup>University of Calgary, Canada, <sup>2</sup>University of Auckland, New Zealand

**Background:** Inorganic phosphate is an important component of bone mineral, and plays a crucial role in cellular energy metabolism. We recently identified an inverse relationship between serum phosphate concentration and fat mass in a cohort of healthy men. The aim of the present study was to determine whether this association is present in other populations, and to assess whether parathyroid hormone (PTH), a phosphaturic hormone and also a correlate of fat mass, influences this relationship.

**Methods:** Individuals from three independent cohorts were studied. One cohort consisted of healthy adult males (Male Cohort, n=323), and two consisted of healthy postmenopausal women (Female Cohort 1, n=185; and Female Cohort 2, n=1471). Associations between serum phosphate and weight, body mass index (BMI) and fat mass were assessed.

**Results:** Serum phosphate was inversely correlated with weight, BMI and fat mass in each of the three cohorts (r = -0.13 to -0.32, p-value <0.0001 to 0.02). Associations between phosphate and fat mass in each cohort are shown in Figure 1. PTH concentrations were assessed in both the Male Cohort and in Female Cohort 1, and PTH was positively correlated with fat mass in both of these cohorts (Male Cohort: r = 0.23, p = 0.005; Female Cohort 1: r = 0.22, p=0.003). Following adjustment for PTH, relationships between serum phosphate and fat mass remained significant in both the Male Cohort (r = -0.20, p = 0.01) and Female Cohort 1 (r = -0.26, p = 0.0004). After an additional adjustment for age and glomerular filtration rate, the association between phosphate and fat mass remained significant in Female Cohort 1 (p=0.0005) but was marginal in the Male Cohort (p = 0.06)

**Conclusions:** Serum phosphate is inversely associated with measures of adiposity in both women and men, independent of PTH. The mechanisms and biological significance of this finding remain to be determined, though fibroblast growth factor 23 (FGF23) is a likely mediator.

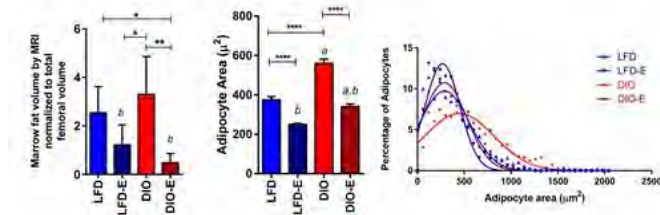


Figure 1

**Disclosures:** Maya Styner, None.

SA0067

See Friday Plenary Number FR0067.

SA0068

**Osteocalcin levels in adult women with different body mass index having normal glucose and hemoglobin A1c levels.** Susana Zeni<sup>\*1</sup>, Liliana Zago<sup>2</sup>, Carlos Lugones<sup>3</sup>, Graciela Brito<sup>3</sup>, Carlos A Gonzalez Infantino<sup>4</sup>. <sup>1</sup>INIGEM, Argentina, <sup>2</sup>Dep. Nutrition. School of Pharmacy & Biochemistry.UBA, Argentina, <sup>3</sup>INIGEM. Hospital de Clinicas.UBA/ CONICET, Argentina, <sup>4</sup>Dep. Nutrition. Hospital de Clinicas. School of Medicine., Argentina

Osteocalcin (OC) plays crucial roles in glucose homeostasis. OC level in the circulation appears to be associated with glucose and fat metabolism- Although still it remains controversial if it are the levels of total OC and/or undercarboxylated OC (ucOC) which present such association. The present study evaluated the levels of ucOC, total OC, leptin and insulin, in 226 overweight or obese (degree I and II) adult non-diabetic women, having levels of glucose (80 to 110 mg/dL) and hemoglobin A1c (HbA1c <5.7 %) within normal range. Women, aged 20 to 86 years were divided in 4 groups according to their menopausal status: premenopause (PreM) (<45 ys); perimenopause (periM) (45 and <50), early menopause (EM) (50 to 65 ys) and late menopause (LM) (>65 ys). Body weight and height were used to calculate BMI score for determining overweight and the degree of obesity. Calcium intake (CaI) was estimated by a semi-quantitative food frequency questionnaire. Serum levels of glucose, cholesterol, triglycerides, HbA1c were carried out automatically using standard laboratory methods. Enzyme immunoassays were used for serum ucOC (ng/mL), OC (ng/mL), leptin (ng/mL), insulin (uIU/L) levels determination. Levels of 25hydroxyvitamin D (25OHD) (ng/mL) were assayed by a competitive protein-binding method. Some results (mean±SD) are shown in the table: (\*) p<0.05 vs. overweight and \*\* p<0.05 vs degree I of obesity.

Respectively of the mean age, the levels of ucOC, insulin and leptin increased as the BMI increased while OC levels decrease in degree II obese women.

For a same BMI, ucOC showed a tendency to increase while OC did not change with increasing age.

**Conclusions:** Although further studies are needed, the present study showed that the levels of ucOC and not the levels of total OC are BMI-dependent in normoglycemic non-diabetic women. Grants: PROINCE E-006 (UNLaM 2015-2016) and CONICET

Menopausal status	ucOC	OC	Insulin	Leptin
<b>Overweight:</b>				
preM	1.96±1.08	29.9±2.7	9.2±3.9	11.1±3.3
periM	2.75±1.22	31.3±7.3	5.8±1.1	9.7±1.7
EM	2.20±1.34	35.1±5.3	6.1±1.7	9.7±1.1
LM	3.81±1.89	29.1±4.6	5.2±1.4	7.3±2.5
<b>Degree I obesity</b>				
preM	2.21±0.98*	30.0±2.21	11.7±1.9*	17.8±4.3*
periM	2.93±0.78*	31.6±5.9	11.8±2.4*	18.2±2.4*
EM	3.41±0.96*	37.1±9.5	9.8±1.5*	20.9±5.2*
LM	3.81±0.96	24.9±4.5	11.8±3.2*	17.7±6.3*
<b>Degree II obesity</b>				
preM	4.08±0.41**,**	19.9±8.6**,**	16.0±6.4**,**	43.7±8.8**,**
periM	4.50±0.22**,**	21.6±11.3**,**	12.5±2.5**,**	25.3±6.14**,**
EM	4.11±0.6**,**	21.7±4.7**,**	10.3±1.7*	27.1±4.4**,**
LM	5.52±1.7**,**	26.9±5.2	12.8±1.8**,**	31.0±8.2**,**

Table

**Disclosures:** Susana Zeni, None.

cells to use OxPhos or in media containing antimycin A (AntA) to inhibit OxPhos. Mitochondrial function and glycolysis were assessed using the Seahorse apparatus. Luciferase reporters were used to detect changes in signaling pathways. Alkaline phosphatase (ALP) was detected via specific staining. Real time RT-PCR was used to assay changes in gene expression.

Results: Incubation of cells in glucose-free galactose/pyruvate media led to an increase in OxPhos. AntA inhibited OxPhos leading to compensatory upregulation of glycolysis (Fig. 1A). Of various luciferase reporters tested (e.g. BMP, TGFb, Runx2, and Wnt/b-catenin) only Wnt/b-catenin TopFlash reporter showed significant responses to manipulation of cell energy metabolism. Induction of OxPhos using galactose/pyruvate media led to an increase in TopFlash activity while inhibition of OxPhos with AntA led to its decrease (Fig. 1B). Similar responses were observed in expression of Wnt/b-catenin target genes and in ALP staining. Wnt/b-catenin is known to be regulated via acetylation. Activation of OxPhos increases AcCoA, a substrate for acetylation reactions. Mitochondrial AcCoA is converted to citrate which is transported into the cytosol and converted back into AcCoA by ATP citrate lyase (ACLY). To find out whether OxPhos regulates Wnt/b-catenin via acetylation, we used ACLY inhibitor, SB20140. SB20140 prevented OxPhos-mediated activation of Wnt/b-catenin (Fig. 1C) and expression of its target genes, and decreased ALP staining.

Conclusions: While further studies on delineating the cross-talk between OxPhos and osteogenic signaling are ongoing, our results to date suggest that OxPhos promotes Wnt/b-catenin signaling via the mechanism involving acetylation (Fig. 1D). Our data also suggest that by manipulating cell bioenergetics we can affect MSC fate decisions.

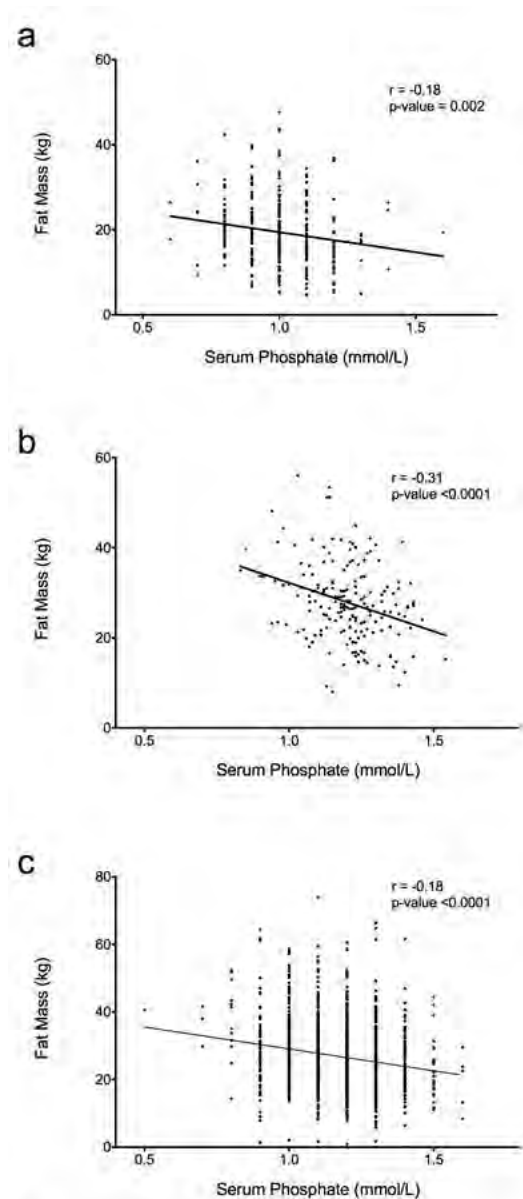


**Figure 1** Relationship between serum phosphate and fat mass in three independent cohorts, (a) Male Cohort (n=323), (b) Female Cohort 1 (n=185), and (c) Female Cohort 2 (n=1471).

Figure 1

Disclosures: Emma Billington, None.

### SA0071

See Friday Plenary Number FR0071.

### SA0072

**Cross-talk between oxidative metabolism and osteogenic signaling.** Roman Eliseev\*, Melanie Busch, Noelle White. University of Rochester, United states

Introduction: Bone marrow mesenchymal stem (a.k.a. stromal) cells (MSCs), precursors of osteoblasts and other lineages, are key elements of bone maintenance and repair. Undifferentiated MSCs produce ATP primarily via glycolysis. During osteogenic differentiation, mitochondrial oxidative phosphorylation (OxPhos) is activated. Our goal was to determine whether oxidative metabolism regulates osteogenic differentiation of MSCs and delineate signaling mechanisms involved in such a regulation.

Methods: Energy metabolism was manipulated in C3H10T1/2 cells by either incubation in media where glucose was replaced with galactose and pyruvate to force

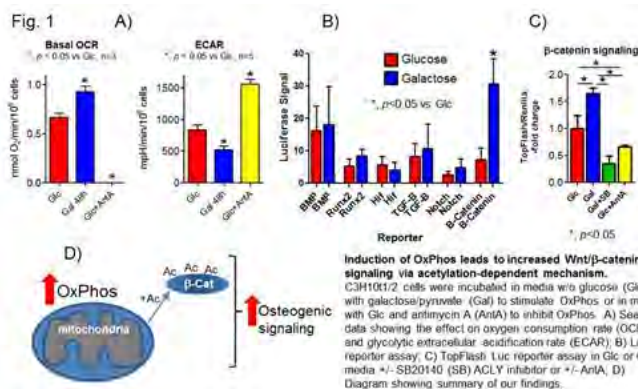


Figure 1

Disclosures: Roman Eliseev, None.

### SA0073

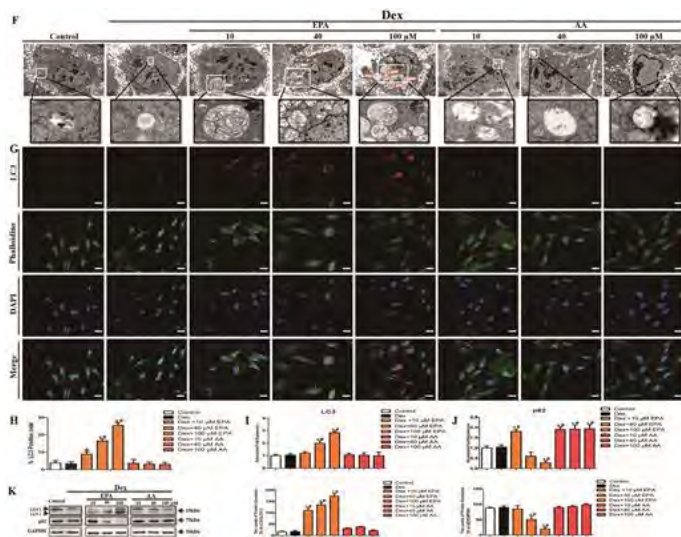
See Friday Plenary Number FR0073.

### SA0074

**Eicosapentaenoic acid attenuates Dexamethasone-induced apoptosis by inducing adaptive autophagy via GPR120 in murine Bone Marrow-Derived Mesenchymal Stem Cells.** Bo Gao\*<sup>1</sup>, Liu Yang<sup>2</sup>, Zhuo-Jing Luo<sup>2</sup>. <sup>1</sup>Xijing Hospital, Fourth Military Medical University, United states, <sup>2</sup>Xijing Hospital, Fourth Military Medical University, China

Long-term use of glucocorticoids is a widespread clinical problem, which currently has no effective solution other than discontinuing the use. Eicosapentaenoic acid(EPA), an omega-3 long chain polyunsaturated fatty acid(n-3 PUFA), which is largely contained in fish or fish oil, has been reported to promote cell viability and improve bone metabolism. However, little is known about the effects of EPA on dexamethasone(Dex)-induced cell apoptosis and whether EPA is an essential remedy for clinical use for attenuating the side-effects of Dex is largely unknown. In this study, we showed that EPA induced autophagy of murine bone marrow-derived mesenchymal stem cells(mBMMSCs). Meanwhile, EPA, but not arachidonic acid (AA), markedly inhibited Dex-induced apoptosis and promoted the viability of mBMMSCs. We also observed that EPA-induced adaptive autophagy was modulated by GPR120, but not GPR40. Further experiments showed that the mechanism of EPA-induced autophagy associated with GPR120 modulation involved an increase in the active form of AMP-activated protein kinase and a decrease in the activity of mammalian target of rapamycin. The protective effect of EPA on Dex-induced apoptosis via GPR120-mediated induction of adaptive autophagy was supported by in vivo experiments. In summary, our findings may have important implications in developing future strategies to use EPA in the prevention and therapy of the side effects induced by long-term Dex-abuse

healing is genetically determined is critical for design and interpretation of studies aimed at finding genes that modulate the healing process.



EPA-induced adaptive autophagy attenuated Dex-induced apoptotic cell death

**Disclosures:** Bo Gao, None.

This study received funding from: This work was supported by the National Natural Science Foundation of China (81472043 and 81572192), and the Program for Changjiang Scholars and Innovative Research Team in University (No. IRT13051).r

## SA0075

See Friday Plenary Number FR0075.

## SA0076

See Friday Plenary Number FR0076.

## SA0077

See Friday Plenary Number FR0077.

## SA0078

See Friday Plenary Number FR0078.

## SA0079

**Genetic Variation Affects the Rate of Tibial Fracture Healing.** Jun Zhang\*, Dana A. Godfrey, Robert D Maynard, Michael J Zuscik, Cheryl L. Ackert-Bicknell. Center for Musculoskeletal Research, University of Rochester Medical Center, United states

Examinations of fracture healing in inbred strains of mice have suggested that many aspects of this process are controlled by genetics. However, these initial studies could not capture the phenotypic range of variation of normal healing. This study was designed to establish degree of healing achieved by 3 weeks post fracture in 8 inbred strains: 129S1/SvImJ, A/J, C57BL/6J (B6), CAST/EiJ, NOD/ShiLJ, NZO/HILJ, PWK/PhJ and WSB/EiJ. These strains capture a substantial proportion of the known genetic variation in mice and should equally encapsulate the breadth of phenotypic variation in bone healing. Ten male mice of each strain were used. At 16 weeks of age, open osteotomies of left tibiae and intermedially fixations with a pin were performed. Both the fractured and contralateral tibiae were harvested 21 days post fracture for  $\mu$ CT imaging to examine the callus, and torsional testing was conducted to assess the degree of return to mechanical integrity. We observed clear differences in fracture healing between the 8 strains and using these data, we estimated broad-sense heritability using the interclass correlation coefficient. Qualitatively, we observed that the B6, NOD/LtJ and NZO/HILJ formed larger calluses than the other strains based on examination of the radiographic images. Further,  $\mu$ CT of fractured tibiae demonstrated statistically significant differences in mineralized callus volume. (Largest: B6:  $7.02 \pm 1.83 \text{ mm}^3$  vs. Smallest: WSB/EiJ:  $0.90 \pm 0.012 \text{ mm}^3$ ). From this, we estimate proportion of the variance attributed to strain (i.e. heritability) of the callus volume to be 68.2%. After normalizing fractured tibiae to the non-fractured controls, torsional testing also demonstrated significant differences in relative maximal torque and torsional rigidity (one-way ANOVA,  $p < 0.001$ , Fig. 1), with a heritability estimate of 36.7% for maximum torque. The B6 mice had the highest percentage of return to mechanical stability relative to the unfractured tibia (Fig. 1) however, for relative torsional rigidity, 129S1/SvImJ ( $126.19 \pm 19.12\%$ ) has the highest value (Fig. 1). Our study suggests genetic variation is an important contributor to fracture healing. This is the first study to estimate heritability of key benchmarks of fracture healing early in the healing process. Understanding the degree to which

**Figure 1**

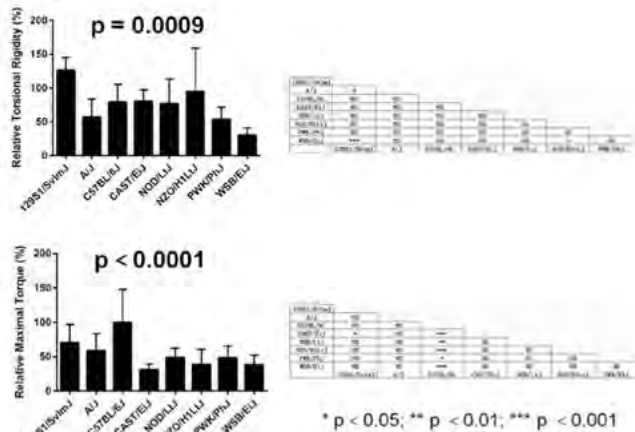


Figure 1

**Disclosures:** Jun Zhang, None.

## SA0080

See Friday Plenary Number FR0080.

## SA0081

See Friday Plenary Number FR0081.

## SA0082

**Spectrum of bone architectural abnormalities detected by  $\mu$ CT screening of mouse gene knockout lines.** Cheryl Ackert-Bicknell<sup>\*1</sup>, Douglas Adams<sup>2</sup>, Renata Rydzik<sup>2</sup>, LI Chen<sup>2</sup>, Zhihua Wu<sup>2</sup>, Seung-Hyun Hong<sup>2</sup>, Gaven Garland<sup>3</sup>, Pujan Joshi<sup>2</sup>, Caibin Zhang<sup>2</sup>, John Sundberg<sup>3</sup>, Dong-Guk Shin<sup>2</sup>, David Rowe<sup>2</sup>. <sup>1</sup>University of Rochester, United states, <sup>2</sup>University of Connecticut, United states, <sup>3</sup>The Jackson Laboratory, United states

The International Mouse Phenotyping Consortium (IMPC) is a multi-site program that is examining mice with defined inactivating mutations (KO) of protein-encoding genes. We have developed a computer-controlled, observer-independent and digital workflow to assess the bone phenotype from one IMPC site (The Jackson Laboratory). No pre-selection of the KO lines was imposed other than requiring that homozygous KO mice be viable up to 12 weeks of age. A frequency distribution plot for  $\mu$ CT assessment of BV/TV in femur and vertebra of monthly control groups and all KO lines was generated. Lines that fell at the extremes of the curve were classified as having a strong phenotype (9/61=15%, 5 with high trabecular bone volume [HTBV] and 4 with low trabecular bone volume [LTBV]), while those at the margins of the curve were considered to have a moderate phenotype (13/61=21%, 6 with HTBV and 7 with LTBV). There was a remarkable dimorphic difference between sexes. We identified lines with a phenotype only in females (4 with LTBV, 4 with HTBV) or in males (4 with LTBV, 2 with HTBV) and lines where both sexes were affected (3 with LTBV and 5 with HTBV). Dimorphism of skeletal site was also found: femur only (5 with LTBV and 3 with HTBV), vertebra only (1 with LTBV, 7 with HTBV) and both sites (5 with LTBV and 1 with HTBV). Of the lines with a strong phenotype, 3 with HTBV were unanticipated (*Bzw2*, *IL24* and *Ccdc120*) while 2 would have been expected (*Osm* and *Oestamp*) based the literature. KO lines with an unanticipated LTBV were *Cp*, *Dnajb3* and *Hr1d*, while *Irf8* was expected. The IMPC uses whole body DXA to identify lines with an abnormality in skeletal mass. It was successful in identifying 2 with HTBV (*Bzw2* and *Ccdc120*) due to high cortical bone area, but missed the remaining 3 lines with a large HTBV phenotype and all 4 lines with a large LTBV. Only 1 of the 13 lines with a moderate phenotype was identified by DXA. Our screen could not confirm 6 genes that are reported in the literature to have either a skeletal phenotype or strong in vitro evidence for an anticipated in vivo phenotype (*Gpnmb*, *Ghsr*, *Adora1b*, *CD33*, *Cers5* and *Il6st*) and this may reflect difference in genetic background. The details of these lines can be found at [www.bonebase.org](http://www.bonebase.org). It appears that genes that can control major alterations in bone architecture are relatively common but their detection requires a comprehensive  $\mu$ CT based study of male and female mice that includes axial and appendicular bone.

**Disclosures:** Cheryl Ackert-Bicknell, None.

**SA0083**

See Friday Plenary Number FR0083.

**SA0084**

See Friday Plenary Number FR0084.

**SA0085**

See Friday Plenary Number FR0085.

**SA0086**

See Friday Plenary Number FR0086.

**SA0087**

**TRAC, a novel time and cost saving gene expression analysis technology with improved efficacy.** Jani Salmivaara<sup>1</sup>, Oona Kivelä\*<sup>1</sup>, Jussi Halleen<sup>2</sup>, Jari Rautio<sup>3</sup>. <sup>1</sup>ValiRx Finland Ltd, Finland, <sup>2</sup>Pharmatest Services Ltd, Finland, <sup>3</sup>Biotech Start-Up Management, Finland

Gene expression analysis in the oncology space is largely performed with the classic and widely accepted methods real-time RT-PCR, microarray and next generation sequencing. These technologies are, however, too time consuming and expensive to be used in large scale screens with high sample numbers. TRAC (Transcription analysis with the aid of Affinity Capture) technology provides a solution for focused gene expression screening with unique combination of multiplex analysis, high-throughput sample processing, high precision and flexibility. Lysates of cells or tissues are directly applicable as sample material in TRAC assay without RNA extraction or cDNA conversion. The assay enables detection of up to 30 targets per sample and 96 samples per assay with 3-4h run time. In TRAC assay, each target mRNA of interest is recognized by a specific labeled ssDNA probe. Probes with different lengths and labels can be used for high-level of multiplexing. Hybridization of probes and targets takes place in solution, after which the probe-transcript complexes are captured by streptavidin coated magnetic beads. Unbound material is washed off and the probes are eluted for detection. The probes are then detected and quantified by capillary electrophoresis, which resolves the probes according to both size and fluorescence. The aim of this study was to apply TRAC assay to analyze the expression fingerprints of 16 gene markers related to angiogenesis, cell adhesion, protease activity and plasminogen activation, in cultured cells treated with different drug candidates. The expression of the target genes was analyzed from four different colon cancer cell lines (COLO, HT-29, CaCo2, DLD) to study culture age dependent effects and responses to drug candidates. By comparison of expression fingerprints between non-treated cell line cultures, altogether four genes were identified as being expressed at higher level in one or two of the cell lines compared to the others. These genes were trypsinogen (PRSS1-3) in COLO, Serine protease inhibitor (SPINK) in HT-29, Protease Cathepsin B (CTSB) in COLO and cyclin D1 (CCND1) in DLD and CaCo2 cell lines. The data showed good correlation with real-time RT-PCR results and reproducibility (CV <12%) and functioned as proof-of-concept for suitability of TRAC for screening purposes. Multiplex detection with TRAC from lysates offered high efficiency and significant cost and time savings compared to single-plex qPCR assay in large scale evaluation of drug candidates.

*Disclosures: Oona Kivelä, ValiRx Finland Ltd, 11*

**SA0088**

**Increased Detection of Genetic Loci Associated With Risk Predictors of Osteoporosis Using a Pleiotropic cFDR Method.** Jonathan Greenbaum\*, Kehao Wu, Lan Zhang, Hui Shen, Jigang Zhang, Hong-Wen Deng. Tulane University Department of Biostatistics & Bioinformatics, United states

Although GWAS have been successful in identifying some osteoporosis associated loci, the findings explain only a small fraction of the total genetic variance. In this study we use a recently developed novel pleiotropic conditional false discovery rate (cFDR) method to identify novel genetic loci associated with two risk traits for osteoporosis (especially for the risk of osteoporotic fractures), Height (HT) and Femoral Neck (FNK) BMD. The cFDR method allows us to improve the detection of associated variants by incorporating any potentially shared genetic mechanisms between the two associated traits. We analyzed the summary statistics from two independent GWAS meta-analyses for single nucleotide polymorphisms (SNPs) that are associated with HT and FNK BMD. Using the cFDR method, we show enrichment in the identification of SNPs associated with each trait conditioned on their strength of association with the second trait. The findings revealed 18 SNPs that are associated with both HT and FNK BMD, 6 of which had not previously been reported to play a role in bone health. The novel SNPs located at *KIF1B* and the intergenic region between *FERD3L* and *TWISTNB* are noteworthy as these genes may be associated with processes that are functionally important in bone metabolism. By leveraging GWAS results from related phenotypes, it is possible to explain a greater proportion of trait heritability and to gain a better understanding of the shared genetic influence between associated traits.

*Disclosures: Jonathan Greenbaum, None.*

**SA0089**

**Individual Variants and Genetic Risk Score for Puberty Timing Associate with Pediatric Bone Mineral Density.** Diana Cousminer\*<sup>1</sup>, Jonathan Mitchell<sup>1</sup>, Alessandra Chesi<sup>1</sup>, Sani Roy<sup>1</sup>, Heidi Kalkwarf<sup>2</sup>, Joan Lappe<sup>3</sup>, Vincente Gilsanz<sup>4</sup>, Benjamin Voight<sup>5</sup>, Sharon Oberfield<sup>6</sup>, John Shepherd<sup>1</sup>, Andrea Kelly<sup>1</sup>, Shana McCormack<sup>1</sup>, Struan Grant<sup>1</sup>, Babette Zemel<sup>1</sup>. <sup>1</sup>Children's Hospital of Philadelphia, United states, <sup>2</sup>Cincinnati Children's Hospital Medical Center, United states, <sup>3</sup>Creighton University, United states, <sup>4</sup>Children's Hospital of Los Angeles, United states, <sup>5</sup>University of Pennsylvania, United states, <sup>6</sup>Columbia University Medical Center, United states, <sup>7</sup>University of California San Francisco, United states

Background: Later puberty is associated with lower areal bone mineral density (aBMD) in adulthood, especially in females. Genome-wide association studies (GWAS) have reported 130 puberty-associated variants, but the impact of this variation on pediatric aBMD during skeletal development is unknown. Methods: In the European-ancestry subset of the multicenter, longitudinal Bone Mineral Density in Childhood Study (BMDCS) of healthy children ages 5 to 20 years, aBMD of the spine, total hip, femoral neck, and distal radius, and bone mineral content (BMC) of the total body less head (TBLH) were measured (n=1450). Using sex-stratified linear mixed models in STATA, we tested 126 of the 130 known puberty-associated alleles for association with age- and sex-specific aBMD (or BMC) Z-scores (aBMDz), adjusted for height z-score, study center, age, physical activity, dietary calcium, and body mass index z-score. The Bonferroni-adjusted significance threshold was  $P=3.9 \times 10^{-4}$ . Additionally, we constructed combined-allele genetic risk scores (GRS) weighted on menarche-delaying (female GRS) or age at voice break-delaying (male GRS) effect estimates and tested these scores for associations as described above. We also tested whether the GRS had consistent associations with bone outcomes across age and pubertal (Tanner) stage (ie statistical interactions). Results: Three puberty-delaying alleles were negatively associated with aBMDz in girls (rs2600959 at the radius, and rs9475752 and rs1400974 at TBLH). The female GRS was associated with 0.2 yr later menarche ( $P=8.2 \times 10^{-5}$ ), but associations with aBMDz scores were inconsistent in girls. The male GRS was strongly negatively associated with aBMDz scores at all skeletal sites (all sites,  $P<0.04$ ). In boys, the puberty-delaying allele at rs113388806 associated with lower total hip and spine aBMD, and at rs2063730 with lower femoral neck aBMD, in older, but not younger boys (GRS x age interactions,  $P=9.7 \times 10^{-6}$ ,  $3 \times 10^{-4}$ , and  $4.9 \times 10^{-4}$ , respectively). We also observed significant negative GRS x age and GRS x Tanner stage interactions with aBMD at many of the skeletal sites in both sexes. Conclusions: Concordant with epidemiological observations, puberty-delaying loci associate with lower aBMD during skeletal growth, although individual associations are sex-specific and vary across age and Tanner stage. These studies highlight the utility of genetic studies to investigate the complex relationship between pubertal development and bone health.

*Disclosures: Diana Cousminer, None.*

**SA0090**

See Friday Plenary Number FR0090.

**SA0091**

**Elevations in FGF23 precede abrogation of either phosphate or iron homeostasis in the Ebf1-KO model of renal insufficiency.** Jackie Fretz\*, Tracy Nelson, Li Li. Yale School of Medicine-Orthopaedics, United states

Phosphate and iron metabolism are linked intimately through the phosphatonin FGF23. Iron status is inversely correlated to the level of circulating FGF23, and improvement in iron status within individual patients correlates with a decrease in FGF23. Development of anemia during CKD is a multifactorial process, but the exact mechanisms are still not completely understood. To better understand the events regulating the early dysfunction of iron bioavailability, phosphate balance and FGF23 we employed targeted deletion of the transcription factor Early B cell Factor 1 (Ebf1) from the kidney stromal progenitors (using Foxd1-cre). This results in a developmental abrogation of outer cortex development, and animals present with glomerulonephritis, phosphate wasting, moderate elevations in FGF23, and anemia. The cells where Ebf1 has been deleted are the same cells that produce the majority of erythropoietin (Epo) to regulate the production of new red blood cells. Also, elevated FGF23 has been shown to negatively regulate erythropoiesis. In this study we profiled the sequential presentation of indicators of renal dysfunction (NGAL, albuminuria, hematuria, TGFB), phosphate imbalance (PTH, 1,25(OH)<sub>2</sub>D<sub>3</sub>, serum phosphate, phosphaturia), and regulators of iron bioavailability and transport (hepcidin, transferrin, erythrocyte counts, Epo, and splenic erythropoiesis) to better understand the events that initiate and drive abrogation of the phosphate, iron, FGF23 regulatory axis. We report here that elevations in circulating FGF23 coincide with the earliest indicators of renal dysfunction, well in advance of albuminuria, and precede changes in urinary phosphate wasting or changes in iron homeostasis. Histological abnormalities are apparent at postnatal day 14, but proteinuria is not apparent until day 24, with splenomegaly at day 28. Serum Epo was normal until disease was well established, at 1 month, but was preceded by transferrin loss in the urine. Neither 1,25(OH)<sub>2</sub>D<sub>3</sub> nor serum PTH were changed. This is comparable to observations from the global Ebf1-KO mouse whose pathology indicates a primary FGF23 elevation (hypophosphatemia, inappropriately normal

1,25(OH)<sub>2</sub>D<sub>3</sub> status, barely elevated PTH, three-fold increase in circulating FGF23). We conclude that it is primary elevations in FGF23 that drive the subsequent perturbations of phosphate and iron homeostasis in this model, and not a primary Epo-insufficiency generated by the actions of Ebf1 in the renal stroma.

**Disclosures:** Jackie Fretz, None.

## SA0092

See Friday Plenary Number FR0092.

## SA0093

**The roles of *ENPP1* in osteocytes under phosphate overload condition..** Ryuichi Watanabe\*, Takeshi Miyamoto, Morio Matsumoto, Masaya Nakamura. Department of Orthopaedic Surgery, Keio University School of Medicine, Japan

**Background:**

*ttw* (tip-tow walking) mice with a homozygous missense mutation of *ENPP1* gene exhibit the postnatal development of progressive ankylosing intervertebral and peripheral joint hyperostosis such as spinal ligamentous ossification and ectopic calcification on the Achilles tendons and articular cartilage. *ENPP1* regulates the production of pyrophosphate (PPi), a well-known inhibitor of hydroxyapatite crystallization, and disruption of *ENPP1* function promotes ectopic calcification on the joints and ligaments. We have previously shown that high phosphate diet exacerbated, growth retardation, the spinal ligamentous ossification and reduced bone density in *ttw* mice at the last meeting. But the precise mechanism underlying regulation in *ENPP1* gene expression is unclear. Thus, the objective of this study is to determine the responsible tissues of *ENPP1* gene expression on phosphate overload response.

**Methods and Results:**

To determine which tissues are responsible for *ENPP1* mRNA expression under phosphate overload condition, wild-type mice were fed with high phosphate diet for 8 weeks and *ENPP1* mRNA expression in several tissues was analyzed by RT-PCR. Among the tissues tested, we found that the highest *ENPP1* mRNA expression in long bones harvested from the mice fed with high phosphate diet. *ENPP1* mRNA expression was upregulated in MC3T3E1 cells with phosphate treatment concomitantly with elevated *FGF23* expression, which is upregulated upon osteocytes differentiation from osteoblasts, in both time-dependent and dose-dependent manners. Based on these results, we newly established *Enpp1* flox mice, and we generated *Enpp1* global knockout mice by crossing *Enpp1* flox mice with CAG-Cre mice to yield CAG-Cre/*Enpp1* cKO mice. Those mice fed with high phosphate diet from 8 weeks of age and exhibited ectopic calcification of spinal ligament, reduced growth, and vascular calcification in the kidney and aorta, phenotypes resembled to those of *ttw*<sup>-/-</sup> mice placed on high phosphate diet. Thus, *Enpp1* flox mice was considered to be successfully established. Then, in order to analyze the roles of *ENPP1* in osteocytes, we generated osteocyte specific *Enpp1* conditional knockout mice in which *Enpp1* flox mice were crossed with osteocyte specific DMP1-Cre mice. We are currently analyzing the phenotype of DMP1-Cre/*Enpp1*<sup>lox/lox</sup> mice and discuss whether osteocytes could regulate the *ENPP1* expression under phosphate overload condition.

**Summary:**

The increased *ENPP1* expression levels in long bones with dietary phosphate overload *in vivo* and in osteocyte-like cells treated with phosphate *in vitro* suggest that *ENPP1* plays a role of phosphate metabolism regulator in osteocytes.

**Disclosures:** Ryuichi Watanabe, None.

## SA0094

See Friday Plenary Number FR0094.

## SA0095

**NLRP3 Inflammasome Promotes Bone resorption In Non-inflammatory Conditions Of Accelerated Bone Turnover.** Yael Allipe\*, Chun Wang, Biancamaria Ricci, Rong Zeng, Chao Qu, Roberto Civitelli, Deborah Novack, Yousef Abu-Amer, Gabriel Mbalaviele. Washington University School of Medicine, United states

Mutations that activate NLRP3 inflammasome, which is responsible for IL-1 $\beta$  and IL-18 maturation cause inflammatory bone loss in humans and mice, but the role of this inflammasome in bone in non-inflammatory conditions remains unknown. We performed flow cytometry analysis of freshly isolated wild-type (WT) mouse bone marrow cells. We found that around 10% of monocytes were labeled with a fluorescent probe (FLICA), which binds only to active NLRP3 complex, suggesting that this inflammasome is activated in homeostatic bone conditions. Analysis of FLICA<sup>+</sup> cells by fluorescence microscope revealed the presence of activated inflammasome in nearly 40% of osteoclasts (OC) developing from bone marrow macrophages in the presence of M-CSF/RANKL, indicating that NLRP3 assembles an active inflammasome during osteoclastogenesis in the absence of inflammatory signals. To assess the influence of NLRP3 on bone remodeling, we evaluated the

impact of *Nlrp3* knockout (KO) on bone using two clinically relevant models characterized by high bone resorption: hyperparathyroidism (achieved via ALZET osmotic pump-mediated infusion of PTH for 2 weeks), and estrogen deficiency (bone indices measured 4 and 8 weeks post-OVX). While baseline bone mass indices were comparable between WT and mutant mice (e.g., 0.21  $\pm$  0.01 vs 0.18  $\pm$  0.01) ablation of *Nlrp3* reduced metabolic disease-induced osteopenia in both models. Specifically, bone mass loss in OVX over sham operation was about 32% in WT vs 12% in KO mice; in PTH- over vehicle-treated group was 18% in WT vs 2% in KO mice). Since NLRP3 senses signals triggered by crystalline particulates or degradation products of extracellular matrix as danger associated molecular patterns (DAMPs), we tested whether bone particles (BP) prepared from bovine cortical bones or synthetic hydroxyapatite crystals (HA) activate NLRP3 in the OC lineage *in vitro*. Exposure of LPS-stimulated macrophages to 500  $\mu$ M HA or 2.5 mg/ml BP increased dramatically IL-1 $\beta$  secretion by 170-fold and 1000-fold over LPS alone, respectively, in NLRP3-dependent manner as IL-1 $\beta$  production was blunted in *Nlrp3* KO cells. Importantly, bone DAMPs enhanced osteoclastogenesis induced by M-CSF/RANKL in WT by 1.5-fold, a response that was reduced in *Nlrp3* KO cells. Thus, signals originating from the bone matrix activate the NLRP3 inflammasome in the OC lineage, and may represent a positive feedback that amplifies bone resorption in pathologic conditions of accelerated bone turnover.

**Disclosures:** Yael Allipe, None.

## SA0096

**From Conditional ER $\alpha$  Deletion Mouse Models to Novel Gene Targets of the Anti-Resorptive Effects of Estrogens.** Srividhya Iyer\*<sup>1</sup>, Ha-Neui Kim<sup>1</sup>, Serra Semahat Ucer<sup>1</sup>, Li Han<sup>1</sup>, Aaron Warren<sup>1</sup>, Julie Crawford<sup>1</sup>, Rafael DeCabo<sup>2</sup>, Haibo Zhao<sup>1</sup>, Maria Almieda<sup>1</sup>, Stavros Manolagas<sup>1</sup>. <sup>1</sup>Center for Osteoporosis & Metabolic Bone Diseases, Univ. Arkansas for Medical Sciences, & Central Arkansas Veterans Healthcare System, United states, <sup>2</sup>Laboratory of Experimental Gerontology, National Institute on Aging, National Institutes of Health, United states

Studies of mice with conditional deletion of the ER $\alpha$  have elucidated that the anti-resorptive effects of estrogens on cancellous and cortical bone result from ER $\alpha$  signaling on cells of the myeloid lineage (targeted by LysM-Cre) and mesenchymal cells (targeted by Prx1-Cre or Osx1-Cre), respectively. However, the gene targets of these effects remain elusive. We have isolated ER $\alpha$  deleted cells from these mice and performed microarray analysis. The expression of Fas ligand, a purported target gene of estrogens in osteoclasts, was not altered in ER $\alpha$  deleted macrophages or mature osteoclasts; and in contrast to published findings by others, FasL<sup>gld/gld</sup> mice which lack functional FasL lost cortical and cancellous bone following OVX indistinguishably from FasL-intact controls. Instead, we found that the highest up-regulated mRNAs in macrophages from ER $\alpha$ <sup>fl/fl</sup>;LysM-Cre mice, as compared to ER $\alpha$ <sup>fl/fl</sup> controls, encode the heterodimeric calcium binding proteins S100A8 and S100A9, which stimulate osteoclast formation via the Toll-like receptor 4 and activation of NF-kB. The highest up-regulated gene in sorted GFP<sup>+</sup> calvaria-derived osteoblasts from ER $\alpha$ <sup>fl/fl</sup>;GFP;Osx1-Cre mice was matrix metalloproteinase 13, recently shown to mediate osteoclast fusion independent of its enzymatic activity. In the same ER $\alpha$  deleted cells, the expression of the stromal cell-derived factor1 (SDF1) a.k.a CXCL12—a chemotactic cytokine that is abundantly expressed in Prx1-Cre targeted cells and promotes osteoclast generation, was increased by 3-fold. Similarly, the mRNA and secreted protein levels of SDF1 were 5- and 100- fold higher in bone marrow cell cultures from ER $\alpha$ <sup>fl/fl</sup>;Prx1-Cre mice as compared to controls. Furthermore, the number of osteoclasts was 2-fold higher in co-cultures of ER $\alpha$ <sup>-/-</sup> bone marrow stromal cells with ER $\alpha$ <sup>+/+</sup> macrophages and this difference was abrogated by a neutralizing SDF1 antibody. More strikingly, ovariectomy or orchidectomy increased SDF1 levels in the bone marrow plasma of wild type C57BL/6 mice. These results suggest that the effects of estrogens on cancellous versus cortical bone are not only mediated by distinct cell types but also different target genes. Moreover, the fact that the highest up-regulated genes in both myeloid and mesenchymal lineage cells lacking ER $\alpha$  promote the generation, fusion, and lifespan of osteoclasts, provides compelling evidence that they are the elusive targets of the direct and indirect anti-resorptive effects of estrogens, respectively.

**Disclosures:** Srividhya Iyer, None.

## SA0097

See Friday Plenary Number FR0097.

## SA0098

**Anabolic Effects of Parathyroid Hormone is MKP1 Independent in Male Mice Bone.** Nabanita Datta\*, Sonali Sharma, Chandrika Mahalingam. Wayne State University School of Medicine, United states

Parathyroid hormone (PTH) has long been known to act as a bone anabolic agent when administered intermittently, although the exact underlying mechanisms remain largely unknown. MAPK phosphatase1 (MKP1), a negative regulator of Mitogen Activated Protein Kinases (MAPKs), has been identified to be a PTH target gene *in vitro* and *in vivo*. Using global MKP1 knockout mice we previously observed

osteopenia in female knockout animals with attenuated anabolic action of PTH. Here we explored the role of MKP1 in mediating the bone anabolic effects of PTH in male mice. Male MKP1 knockout mice, characterized by micro-CT analysis at the proximal tibiae, showed osteopetrosis with an increase in bone mineral density, bone volume, trabecular thickness and a decrease in trabecular spacing at 16-17 and 26-27 weeks of age, relative to wildtype controls. To examine the bone anabolic effects of PTH in the absence of MKP1 in males, we injected 16-17 week-old knockout males and wildtype control littermates with 50 µg/kg PTH or vehicle 5 times per week over 4 weeks. Intermittent PTH treatment of MKP1 knockout male mice led to increase in bone mass (BV/TV) comparable to those observed in wildtype controls. MKP1 deficiency did not compromise the ability of PTH to increase osteoblast number. In conclusion, our data suggest that in contrast to females the bone anabolic effects of PTH is independent of MKP1 in male mice.

**Disclosures:** Nabanita Datta, None.

## SA0099

See Friday Plenary Number FR0099.

## SA0100

See Friday Plenary Number FR0100.

## SA0101

**Androgen Receptor SUMOylation Regulates Bone Mass in Male Mice.** Jianyao Wu<sup>\*1</sup>, Sofia Movérare-Skrtic<sup>1</sup>, Fu-Ping Zhang<sup>2</sup>, Matti Poutanen<sup>3</sup>, Claes Ohlsson<sup>1</sup>. <sup>1</sup>Center for Bone & Arthritis Research, Institute of Medicine, Sahlgrenska Academy, University of Gothenburg, Sweden, <sup>2</sup>Department of Physiology, & Turku Center for Disease Modeling, Institute of Biomedicine, University of Turku, Finland, <sup>3</sup>Center for Bone & Arthritis Research, Institute of Medicine, Sahlgrenska Academy, University of Gothenburg, Sweden; Department of Physiology, & Turku Center for Disease Modeling, Institute of Biomedicine, University of Turku, Finland, Finland

The crucial effects of androgens on the male skeleton is at least partly mediated via the androgen receptor (AR), supported by that male AR knockout mice have reduced trabecular and cortical bone mass. Furthermore, extensive studies using mouse models with cell-specific inactivation of AR revealed that AR in osteoblasts is required for the regulation of trabecular bone mass in male mice. In addition to hormone binding, the AR activity is regulated by post-translational modifications, including SUMOylation. SUMOylation is a reversible modification in which Small Ubiquitin-related Modifier proteins (SUMOs) are attached to the AR, and thereby regulate the activity of the AR and change its interactions with other proteins.

There are two distinct SUMOylation sites in the N-terminal region of the AR but the physiological role of these *in vivo* is unknown. To elucidate the importance of SUMOylation of AR for male bone metabolism, we generated a mouse model devoid of two of the AR SUMOylation sites (AR<sup>SUM-</sup> mice) by introducing two point mutations, K381R and K500R. AR<sup>SUM-</sup> mice displayed normal body weight, were apparently healthy and had normal serum testosterone levels. In addition, the weights of two well-established androgen responsive tissues, seminal vesicles and muscle levator ani, were not significantly altered. The skeleton of 6-month-old male AR<sup>SUM-</sup> mice was evaluated using µCT as well as static and dynamic histomorphometry.

Male AR<sup>SUM-</sup> mice displayed significantly reduced trabecular bone volume fraction in the distal metaphyseal region of femur compared with WT mice (BV/TV,  $-19 \pm 4.9\%$ ,  $p < 0.05$ ). The number of osteoblasts per bone perimeter was substantially reduced ( $-60.5 \pm 7.2\%$ ,  $p < 0.001$ ), while no significant effect was observed on the number of osteoclasts in the trabecular bone of male AR<sup>SUM-</sup> mice compared with WT mice. The bone formation rate was reduced ( $-32.6 \pm 7.4\%$ ,  $p < 0.05$ ) as a result of reduced mineralizing surface per bone surface in AR<sup>SUM-</sup> mice compared with WT mice ( $-24.3 \pm 3.6\%$ ,  $p < 0.001$ ). Finally, there was a moderate reduction in the cortical bone thickness in the diaphyseal region of femur in male AR<sup>SUM-</sup> mice compared with WT mice ( $-7.1 \pm 1.7\%$ ,  $p < 0.05$ ).

In conclusion, mice devoid of AR SUMOylation at K381 and K500 have reduced trabecular bone mass as a result of reduced bone formation. We propose that methods modulating AR SUMOylation might result in a rather bone-specific anabolic effect.

**Disclosures:** Jianyao Wu, None.

## SA0102

**Glucocorticoid Signaling Is important For Exercise-induced Bone Formation.** Robert MacDonell<sup>1</sup>, Jianrui Xu<sup>\*1</sup>, KeHong Ding<sup>1</sup>, Qing Zhong<sup>1</sup>, William Hill<sup>1</sup>, Wendy Bollag<sup>1</sup>, Monte Hunter<sup>1</sup>, Meghan McGee-Lawrence<sup>1</sup>, Mona El Refaey<sup>2</sup>, Maribeth Johnson<sup>1</sup>, Christopher Treager<sup>3</sup>, Ying Han<sup>4</sup>, Mohammed Elsalanty<sup>1</sup>, Mark Hamrick<sup>1</sup>, Xingming Shi<sup>1</sup>, Carlos Isaacs<sup>1</sup>. <sup>1</sup>Medical College of Georgia, United states, <sup>2</sup>Ohio State University, United states, <sup>3</sup>Medical College of Georgia, United states, <sup>4</sup>School & Hospital of Stomatology Xi'an Jiaotong University, China

Glucocorticoids (GCs) are beneficial in the treatment of inflammatory and autoimmune diseases although long-term GCs at pharmacologic doses are associated with osteoporosis and fractures predominantly affecting trabecular bone (spine). However, GCs role in normal bone physiology is less clear. Inflammatory cytokines are important for initiation of bone formation as for example after a fracture or induced by exercise. Nevertheless, unchecked inflammation can also lead to bone loss (e.g. rheumatoid arthritis), and physiologically the body responds by increasing endogenous anti-inflammatory hormones such as GCs. We were thus interested in evaluating the impact of unchecked inflammation induced by exercise in a mouse model in which the glucocorticoid receptor (GR) had been selectively knocked out in bone cells (mesenchymal stem cells). Our group has previously shown that trabecular bone mineral density (BMD) increases in wild type mice by 20-35% after 4-weeks of treadmill exercise. The experimental mice were separated into 3 groups: (1) Exercised Cre-Col3.6 GR-KO mice (N=10); (2) Exercised Cre littermate control mice (N=8); and (3) Sedentary Cre littermate control mice (N=8) and subjected to treadmill exercise of 30/min day for 4 weeks (no incline). The mice were sacrificed at the end of the four weeks, and tibia, femur, and spine samples were collected. Analysis of mineralization in the spine (Kubtec, Digimus) revealed that bone mineral content (BMC) and density (BMD) in the exercised GR-KO mice were lower compared to littermate exercised controls. Further, µCT analysis of the spine (L3) revealed that the GR-KO mice had greater trabecular separation ( $n=0.0035$ ) and lower trabecular connectivity density than exercised littermate controls ( $n=0.0037$ ). These results indicate that a lack of functional GR in mesenchymal stem cells leads to an impaired response to normally pro-osteogenic interventions such as exercise possibly through disruption of the normal compensatory response to inflammation.

**Disclosures:** Jianrui Xu, None.

## SA0103

**Influence of Progesterone Nuclear Receptor Signaling in Osteoprogenitor Cells on Sexual Dimorphism of Trabecular Bone Mass.** Alexander Kot<sup>\*</sup>, Zengdong zhong, Hongliang Zhang, Evan Lay, Nancy Lane, Wei Yao, UC Davis Medical Center, United states

Progesterone is a sex steroid mostly known for its reproductive system effects. Its functions are largely mediated through the progesterone nuclear receptor (PR), a ligand-regulated transcription factor. The PR is present in osteoblasts and osteoclasts; however, its effect on bone remains unclear. We determined that compared to 1-12 month old wild type (WT) littermates, global PR knockout (PRKO) mice had increased bone mass – female PRKO mice had increased bone formation and male PRKO mice had decreased bone resorption. We hypothesized that the PR in osteoprogenitors may be a key regulator of sexual dimorphism in bone mass acquisition.

We crossed PR-flox and Prx1-cre mice to obtain mice with the PR deleted in osteoprogenitors (Prx1:PRcKO) and WT littermates of both sexes. Bone mass acquisition, bone turnover and bone mechanical properties were evaluated in 2 and 6 month old mice by µCT, histomorphometry and 3-point bending tests respectively. To elucidate a mechanism by which the lack of osteoprogenitor PR signaling influences bone mass, we cultured MSCs from bone for RNA-seq. Two factor ANOVA was used to evaluate genotype and sex effects and their interaction for bone outcome variables. For RNA-Seq, differentially expressed genes were identified using EdgeR with FDR  $< 0.01$  after Benjamin-Hochberg correction for multiple testing. Kyoto Encyclopedia of Genes and Genomes (KEGG) pathway and gene ontology analyses were used to define functional groups of genes.

Compared to WT littermates, Prx1:PRcKO males and females had increased distal femur BV/TV and trabecular surface bone formation at 2 and 6 months of age ( $p < 0.05$ ), with greater effects in males ( $p < 0.05$ ). No significant change was observed for the cortical bone, bone strength, bone size and femur length. Preliminary results from the whole MSC transcriptome revealed that PR ablation had a sex specific effect on gene expression with more transcriptional changes observed in males (Figure). Pathways significantly overrepresented ( $p < 0.01$ ) in differentially expressed genes between the male Prx1:PRcKO and male WT groups included: osteoclast differentiation, NF-kappa B signaling, immune and inflammatory response.

These results suggest that PR signaling in osteoprogenitors is a critical regulator of bone mass acquisition and may explain sex differences. Further studies of PR signaling may provide strategies to augment bone mass.

## SA0106

**Epigenetic Signals Modulate 1,25(OH)<sub>2</sub>D<sub>3</sub> Regulation of Innate Immune Responses in Lung Epithelial Cells.** [Ran Wei](#)<sup>1\*</sup>, [Ki-Yoon Kim](#)<sup>2</sup>, [Puneet Dhawan](#)<sup>3</sup>, [Gill Diamond](#)<sup>4</sup>, [Sylvia Christakos](#)<sup>3</sup>. <sup>1</sup>Department of Microbiology, Biochemistry & Molecular Genetics, Rutgers- New Jersey Medical School, United states, <sup>2</sup>Department of Microbiology, Biochemistry & Molecular Genetics, Rutgers-New Jersey Medical School, United states, <sup>3</sup>Department of Microbiology, Biochemistry & Molecular Genetics, Rutgers-New Jersey Medical School, United states, <sup>4</sup>Department of Oral Biology, University of Florida, United states

A principal defense mechanism protecting the lungs against infection is the production of antimicrobial peptides. We earlier reported that cathelicidin (LL-37) and CD14 (a TLR4 co-receptor that aids antimicrobial peptide production) are induced by 1,25(OH)<sub>2</sub>D<sub>3</sub> in human airway epithelial cells with a resultant increase in antimicrobial activity. Currently very little is known concerning molecular level changes that control the expression of LL-37 and CD14 in lung epithelial cells. We found that butyrate or trichostatin A (histone deacetylase inhibitors; HDACi) significantly enhance 1,25(OH)<sub>2</sub>D<sub>3</sub> induction of LL-37 and CD14 mRNA and transcription in lung epithelial cells (2 – 6 fold). Dominant negative (DN) BRG1 (BRG1 is a component of the SWI/SNF chromatin remodeling complex) inhibits the stimulatory effect of 1,25(OH)<sub>2</sub>D<sub>3</sub>, indicating that the SWI/SNF complex is involved in mediating 1,25(OH)<sub>2</sub>D<sub>3</sub> regulation of innate immune responses. Treatment with HDACi relieved the inhibition by BRG1-DN. ChIP/re-ChIP assays showed direct protein-protein interaction between C/EBP $\alpha$  and BRG1 as well as recruitment of BRG1 and C/EBP $\alpha$  to C/EBP sites in the LL-37 and CD14 promoters in response to 1,25(OH)<sub>2</sub>D<sub>3</sub>. ChIP/re-ChIP analysis also indicated an increase in acetylated histone 4 in association with BRG-1 in response to 1,25(OH)<sub>2</sub>D<sub>3</sub> at the C/EBP sites. Thus our findings suggest that one mechanism of enhancement of 1,25(OH)<sub>2</sub>D<sub>3</sub> induction of LL-37 and CD14 by HDACi is enhanced cooperation between acetylation and chromatin remodeling (through BRG1) allowing for efficient initiation of transcription. BRG1 can be an activator or a repressor depending on differential cooperation with and recruitment of BRG1 associated factors. We found that protein arginine methyltransferase 5 (PRMT5), a type II methyltransferase, interacts with BRG1 and represses LL-37 and CD14 mRNA and transcription. Our findings indicate the requirement of the C/EBP site for the inhibitory effect of PRMT5. This mechanism of negative regulation may be important for times when induction of LL-37 or CD14 by 1,25(OH)<sub>2</sub>D<sub>3</sub> is not needed or the repression may be involved in the cyclical transcriptional process that requires both activating and repressive epigenetic mechanisms. Our findings define novel mechanisms and key mediators involved in the regulation by 1,25(OH)<sub>2</sub>D<sub>3</sub> of innate immune responses in lung epithelial cells.

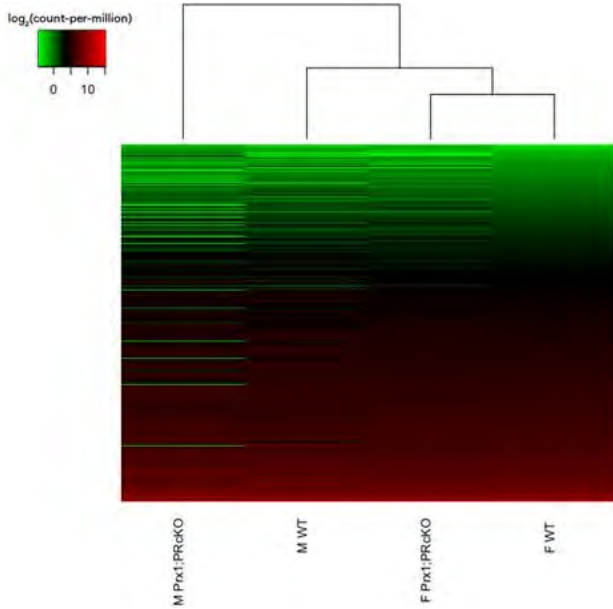
*Disclosures:* Ran Wei, None.

## SA0107

**Vitamin D metabolism in human mesenchymal stem cells: Effects of body composition and leptin.** [Jing Li](#)<sup>\*</sup>, [Julie Glowacki](#), [Meryl LeBoff](#), [Shuanhu Zhou](#). Brigham & Women's Hospital, United states

There is growing interest in the regulation and function of extrarenal vitamin D hydroxylases. We reported that human mesenchymal stem cells (hMSCs) express D-relevant genes and synthesize 1 $\alpha$ ,25(OH)<sub>2</sub>D. CYP27B1 expression decreases with age and is influenced by serum 25-hydroxyvitamin D [s25(OH)D]. Thus, clinical characteristics of subjects from whom hMSCs are obtained influence D-relevant gene expression. Obesity is associated with low s25(OH)D and high bone mineral density (BMD). In this study, we tested the hypotheses that body composition influences expression of D-hydroxylase genes in hMSCs, that *in vitro* leptin treatment of hMSCs has direct effects on D-hydroxylases, and that D-metabolism in hMSCs may regulate osteoblastogenesis in possible autocrine/paracrine manner. For 49 enrolled subjects (age 41-83 yr), body mass index (BMI) was calculated, s25(OH)D was measured with an isotopic assay, and Fat Mass Index (FMI) and BMD were measured by DXA. Thresholds for obesity were set at BMI  $\geq$  30 kg/m<sup>2</sup> or FMI  $\geq$  13 kg/m<sup>2</sup> for women and  $\geq$  9 kg/m<sup>2</sup> for men. hMSCs were isolated from tissues discarded during arthroplasty, for gene expression by PCR. There were inverse correlations for s25(OH)D with BMI (p=0.033) and with FMI (p=0.003). There was a positive correlation for CYP27B1 expression in hMSCs with FMI; and CYP27B1 was higher in FMI-obese subjects than non-obese (p=0.001). There were no significant associations for CYP27B1 and CYP24A1 with either BMI or FMI. Spine BMD was inversely correlated with constitutive expression of CYP24A1 (p=0.032) but not with other D-hydroxylases. Those correlations raised the question of how obesity could influence vitamin D metabolism in, and osteoblast differentiation of hMSCs. Treating hMSCs for 6 hrs with 10 or 100 ng/mL of leptin *in vitro* downregulated CYP24A1 (p<0.05) and upregulated CYP27B1 (p<0.05). In addition, leptin significantly stimulated BMP-7 gene expression and ALP activity in hMSCs. That spine BMD was inversely correlated with expression of CYP24A1 suggested that D-metabolism in hMSCs may play a role in bone formation. That was supported by direct treatment of hMSCs with leptin, which inhibited CYP24A1 expression and stimulated CYP27B1, BMP-7, and osteoblastogenesis. Leptin effects on D-metabolism in hMSCs may protect the bone from low s25(OH)D in obese subjects. This research demonstrates links between obesity and low s25(OH)D level, high BMD, and vitamin D metabolism and osteoblastogenesis in hMSCs.

*Disclosures:* Ran Wei, None.



Overall-genomic changes

*Disclosures:* Alexander Kot, None.

## SA0104

Withdrawn

## SA0105

**25(OH)D<sub>3</sub> HALF-LIFE IS LONGER IN OLDER THAN YOUNGER ADULTS.** [Inez Schoenmakers](#)<sup>1\*</sup>, [Shima Assar](#)<sup>1</sup>, [Terry Aspray](#)<sup>2</sup>, [Ann Prentice](#)<sup>1</sup>, [Kerry Jones](#)<sup>1</sup>. <sup>1</sup>MRC Human Nutrition Research, United Kingdom, <sup>2</sup>Newcastle University, Institute for Cellular Medicine, United Kingdom

#### Background

Ageing may be associated with an increase in plasma PTH and 1,25(OH)<sub>2</sub>D and a decline in kidney function. This may affect 25(OH)D expenditure.

#### Methods

We investigated 25(OH)D<sub>3</sub> half-life (*t*<sub>1/2</sub>) and its determinants in 47 older (70+; mean (SE): 75.5(0.7) years) and 50 younger (25-40; 30.2(0.7) years) men and women in the UK during winter when there is no cutaneous vitamin D synthesis. Each participant received 40 nmol stable isotope of 25(OH)D<sub>3</sub> orally as a tracer and 25(OH)D<sub>3</sub> *t*<sub>1/2</sub> was calculated from plasma tracer concentrations over the following 6-30 days.

#### Results

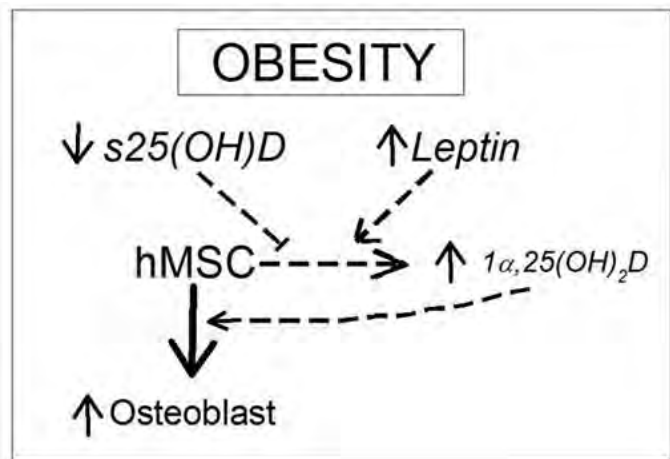
Data are given in (mean (SE) or mean (lnmean (lnSE)). Plasma 25(OH)D<sub>3</sub> *t*<sub>1/2</sub> was significantly longer (20.3 (0.5) and 17.2(0.6) days, respectively) in older than younger adults ( $P < 0.0001$ ). Body Mass Index (BMI) (26.9 (3.29; 0.02) vs. 21.9 (3.09; 0.01) kg/m<sup>2</sup>;  $P < 0.001$ ) and vitamin D intake (3.62 (1.29; 0.1) vs. 2.50 (0.92; 0.08)  $\mu$ g/day;  $P = 0.005$ ) were significantly higher in older than in younger adults. Plasma PTH (47.2 (3.9; 0.06) vs. 38 (3.7; 0.06) pg/ml;  $P = 0.02$ ), c-FGF23 (96.4 (4.57; 0.01) vs. 65.0 (4.17; 0.06) RU/ml  $P = 0.01$ ), 25(OH)D<sub>3</sub> (43.5 (3.7; 0.08) vs. 28.6 (3.4; 0.06) nmol/l;  $P < 0.0001$ ) and ionised Ca [pH 7.4]; (ciCa) (1.19 (0.01) vs 1.16 (0.01) mmol/l;  $P = 0.003$ ) were significantly higher in older compared to younger adults. Creatinine clearance (cCrCl) was significantly lower in older than in younger adults (114 (4.74; 0.06) vs 88 (4.47; 0.09) l/min/1.73m<sup>2</sup>;  $P = 0.02$ ). Plasma 1,25(OH)<sub>2</sub>D (128.7(5.7) vs 116.4(3.6) pmol/l;  $P = 0.07$ ) did not differ between groups.

In older adults, 25(OH)D<sub>3</sub> *t*<sub>1/2</sub> was positively associated with cCrCl (slope (coefficient (SE)) 1.87 (0.75) days per l/min/1.73m<sup>2</sup>;  $P = 0.01$ ) and negatively with vitamin D intake (slope -1.81 (0.66) days per  $\mu$ g/day;  $P = 0.01$ ). In younger adults, 25(OH)D<sub>3</sub> *t*<sub>1/2</sub> was positively associated with plasma 25(OH)D (slope 3.8 (1.21) days per lnmol/l;  $P = 0.09$ ) and ciCa (slope 31 (12) days per mmol/l;  $P = 0.01$ ). The age-group interaction term of the regression analyses of these variables on 25(OH)D<sub>3</sub> *t*<sub>1/2</sub> was significant, indicating differences in the relationships with 25(OH)D<sub>3</sub> *t*<sub>1/2</sub> between age-groups. BMI, PTH, c-FGF23 and 1,25(OH)<sub>2</sub>D did not significantly predict 25(OH)D<sub>3</sub> *t*<sub>1/2</sub>.

#### Conclusions

Plasma 25(OH)D<sub>3</sub> *t*<sub>1/2</sub> was longer in older than younger adults. The predictors of 25(OH)D<sub>3</sub> *t*<sub>1/2</sub> differed between age-groups.

*Disclosures:* Inez Schoenmakers, None.



Obesity-Vitamin D-Leptin-hMSCs

Disclosures: Jing Li, None.

## SA0108

**Disruption of Aldehyde Dehydrogenase 2 (Aldh2) Gene Results in Suppression of Increase in Trabecular Bone Mass After Climbing Exercise in Growing Mice.** Kayoko Furukawa<sup>1</sup>, Kunitaka Menuki<sup>2</sup>, Manabu Tsukamoto<sup>2</sup>, Takafumi Tajima<sup>1</sup>, Hokuto Fukuda<sup>1</sup>, Toshiharu Mori<sup>2</sup>, Akinori Sakai<sup>2</sup>. <sup>1</sup>MD, Japan, <sup>2</sup>MD, Ph.D, Japan

Purpose: Aldehyde dehydrogenase2 (ALDH2) degrades acetaldehyde produced by the metabolism of alcohol. The inactive ALDH2 phenotype is prevalent in East Asians, and an association between this ALDH2 polymorphism and osteoporosis has been reported. In our previous study, we found that alcohol consumption resulted in decreased trabecular bone volume in *aldh2* knockout (*Aldh2*<sup>-/-</sup>) mice compared with that in wild-type (*Aldh2*<sup>+/+</sup>) mice. We previously developed a mouse voluntary climbing exercise model as a physiological mechanical loading model and reported that climbing exercise increased bone formation in wild-type (*Aldh2*<sup>+/+</sup>) mice. However, the effect of *aldh2* gene on the skeletal phenotype in climbing exercise remains unknown. The aim of this study was to clarify the effect of climbing exercise on trabecular bone structure and dynamics in *aldh2*-disrupted mice in absence of alcohol consumption.

Method: 4-week-old male *Aldh2* knockout mice (*Aldh2*<sup>-/-</sup>) and wild-type (*Aldh2*<sup>+/+</sup>) mice were divided into ground control (GC) group and climbing exercise (EX) group in each genotype for 4 weeks. At the age of 8 weeks, bone histomorphometry was performed at the secondary spongiosa of the tibias. Bone marrow cells from the lateral femur and tibia were used for mRNA expression analysis.

Result: Histomorphometrical study revealed that trabecular bone volume (BV/TV) in the *Aldh2*<sup>+/+</sup>/EX group was significantly increased compared with that in the *Aldh2*<sup>+/+</sup>/GC group. Bone formation rate (BFR/BS) in *Aldh2*<sup>+/+</sup>/EX group was significantly increased compared with that in the *Aldh2*<sup>+/+</sup>/GC group. There were no significant differences in BV/TV and BFR/BS between *Aldh2*<sup>-/-</sup>/GC and *Aldh2*<sup>-/-</sup>/EX. Quantitative RT-PCR revealed significant decrease in p21 mRNA expression in *Aldh2*<sup>+/+</sup>/EX group compared with that in the *Aldh2*<sup>+/+</sup>/GC group. These differences were not observed in the respective knockout groups.

Conclusion: Disruption of aldehyde dehydrogenase 2 (*Aldh2*) gene results in suppression of increase in trabecular bone mass after climbing exercise in growing mice.

Disclosures: Kayoko Furukawa, None.

## SA0109

**Mechanically-Induced Osteocyte-Th17 Cell Signaling and Osteoclastogenesis.** Travis McCumber<sup>\*</sup>, Michael Turturro, Kristen Drescher, Diane Cullen. Creighton University, United states

Repetitive mechanical loading of bone can result in microcracks within the mineralized matrix. Microdamage is repaired through a process known as targeted bone remodeling. Osteocyte apoptosis has been associated with the localized recruitment of osteoclasts to the damaged area; however, the extracellular signals initiating the process are still unknown. We have previously reported an increase in T cell stimulatory cytokines in association with increased RANKL and osteoclasts within fatigue loaded rat ulna compared to non-loaded controls. These findings were suggestive of a relationship between bone fatigue and the recruitment of both T cells and osteoclasts. We hypothesized that repetitive fluid shear stress (FSS) would induce osteocyte production of cytokines (TGF- $\beta$ 1 and IL-6) known to stimulate Th17 cells

secretion of osteoclastogenic cytokines (IL-17 and RANKL) and subsequently induce osteoclastogenesis.

MLO-Y4 osteocyte-like cells were exposed to FSS ( $7 \pm 3$  or  $10 \pm 3$  dynes, 1Hz) or Static control. MLO-Y4 cells and culture medium were collected after 15, 30, 60, or 180 minutes of FSS exposure or Static control conditions. ELISA analysis of MLO-Y4 medium revealed greater TGF- $\beta$ 1 and IL-6 in FSS versus Static medium,  $P < 0.01$ . Murine spleen cells were then cultured in T cell supportive conditions and treated with 25% FSS or Static MLO-Y4 medium. T cells and culture medium were collected 72 hours post plating. ELISA analysis of T cell culture medium revealed greater IL-17 in T cell cultures treated with FSS MLO-Y4 medium versus Static MLO-Y4 medium,  $P < 0.03$ . MLO-Y4 cells were then co-cultured with murine spleen cells in osteoclast supportive conditions and treated with 25% T cell medium (MLO-Y4 FSS or Static conditioned). Osteoclasts and culture medium were collected 10 days post plating. TRAP staining and ELISA analysis of osteoclast cultures revealed greater osteoclasts and RANKL in cultures treated with T cell medium (MLO-Y4 FSS conditioned) versus T cell medium (MLO-Y4 Static conditioned),  $P < 0.01$ .

These results demonstrate an *in vitro* signaling mechanism where mechanically-induced osteocytes potentiate the secretion of osteoclastogenic cytokines from Th17 cells, and the subsequent formation of osteoclasts. Future *in vivo* loading studies examining the osteoclast response in relation to the described osteocyte-Th17 cell signaling mechanism would provide a new paradigm for the study and understanding of targeted bone remodeling in response to mechanical stress.

Disclosures: Travis McCumber, None.

## SA0110

See Friday Plenary Number FR0110.

## SA0111

See Friday Plenary Number FR0111.

## SA0112

**Mechanical LINC between nucleus and cytoskeleton regulates  $\beta$ catenin nuclear access.** Gunes Uzer<sup>\*</sup>, Guniz Bas, Melis Olcum, Buer Sen, Zhihui Xie, Cody McGrath, Maya Styner, Janet Rubin. University of North Carolina, United states

Mechanical signals generated during functional loading promote osteoblastogenesis at load bearing sites.  $\beta$ catenin ( $\beta$ cat) signaling supports osteoblast and inhibits adipocyte recruitment from mesenchymal stem cells (MSC).  $\beta$ cat control of gene expression relies on non-classical nuclear shuttling involving  $\beta$ cat's direct interaction with nuclear pore complexes (NPCs). MSC mechanosensitivity is in-part regulated at the nuclear surface via LINC complexes (Linker of Nucleoskeleton and Cytoskeleton) that integrate the nucleus into the cytoskeleton. As LINC directly binds cytoskeletal actin filaments, NPCs and  $\beta$ cat, it may also have a role in  $\beta$ cat nuclear delivery. Here we hypothesized that LINC complexes regulate nuclear  $\beta$ cat availability in response to mechanical challenge. To understand the mechanically-induced interaction of  $\beta$ cat with the nuclear envelope, we applied high magnitude strain (HMS, 2%, 0.17Hz) or low intensity vibration (LIV, 0.7g, 90Hz) to murine MSCs and isolated NPC-rich nucleoskeletal (NSk) fractions to probe for  $\beta$ cat. On average, HMS and LIV increased the  $\beta$ cat-NSk association by 2-fold ( $p < .01$ ). We next asked if LINC connectivity was critical for mechanically-induced  $\beta$ cat-NSk association: un-anchoring the  $\beta$ cat-binding element of LINC, Nesprin-2, via *Sun1/2* deletion decreased both basal NSk-bound  $\beta$ cat (50%,  $p < .001$ ) and mechanically induced  $\beta$ cat-NSk association ( $p < .001$ ). Further, immunostaining showed that in LINC deficient MSCs where Nesprin-2 was displaced from nuclear envelope,  $\beta$ cat was less tightly localized to nucleus increasing its cytoplasmic staining (1.4-fold,  $p < .001$ ). This suggests that LINC positions  $\beta$ cat at the nuclear envelope, thus providing access to NPC for inward transfer. We tested this possibility by measuring fluorescence recovery of GFP- $\beta$ cat in the nucleus to quantify the rate of  $\beta$ cat nuclear entry: LINC deficient MSCs showed a 51% recovery delay ( $p < .01$ ), indicating a LINC-dependence of  $\beta$ cat nuclear entry. We next considered if strengthening LINC-mediated connectivity would improve  $\beta$ cat-NSk association. Daily application of LIV x5d increased Nesprin-2 expression by 69% ( $p < 0.05$ ), resulting in 49% increase in HMS-induced  $\beta$ cat-NSk association compared to non-LIV group. In summary, our data indicates that LINC-mediated connectivity enables  $\beta$ cat nuclear transfer. As such, mechanically induced adaptations of LINC complexes may represent a novel avenue for increasing  $\beta$ cat signaling and improving MSC fate decisions.

Disclosures: Gunes Uzer, None.

## SA0113

See Friday Plenary Number FR0113.

## SA0114

See Friday Plenary Number FR0114.

**SA0115**

See Friday Plenary Number FR0115.

**SA0116**

See Friday Plenary Number FR0116.

**SA0117**

See Friday Plenary Number FR0117.

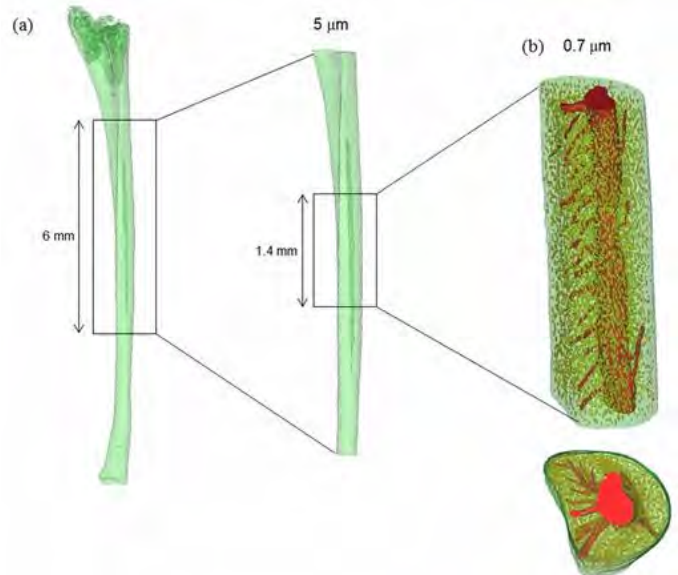
**SA0118**

See Friday Plenary Number FR0118.

**SA0119**

**Age-related Changes in the 3D Microstructural Mouse Cortical Bone Using High Resolution Desktop Micro-CT System.** Haniyeh Hemmatian<sup>\*1</sup>, Michaël R Laurent<sup>2</sup>, Frank Claessens<sup>3</sup>, Dirk Vanderschueren<sup>4</sup>, Harry van Lenthe<sup>1</sup>. <sup>1</sup>Biomechanics Section, Department of Mechanical Engineering, KU Leuven, Belgium, <sup>2</sup>Laboratory of Molecular Endocrinology, Department of Cellular & Molecular Medicine, KU Leuven, <sup>2</sup>-Gerontology & Geriatrics, Department of Clinical & Experimental Medicine, KU Leuven, Belgium, <sup>3</sup>Laboratory of Molecular Endocrinology, Department of Cellular & Molecular Medicine, KU Leuven, Belgium, <sup>4</sup>Clinical & Experimental Endocrinology, Department of Clinical & Experimental Medicine, KU Leuven, Belgium

Osteoporosis is an age-related disease that affects millions of people. It is characterized by a systemic impairment of bone mass and deterioration in bone microarchitecture resulting in fragility fractures. It has been postulated that bone's microporosity plays key biological and mechanical roles. Considering that mechanosensitivity is changing with aging we hypothesized that bone microarchitecture at old age would differ from that at young age. To test this hypothesis we used desktop micro-computed tomography ( $\mu$ CT) for 3D visualization and morphometric analysis of mouse cortical bone porosity at different hierarchical levels as a function of age. The fibular midshaft of 6 young-adult (5-months) and 6 old (23-months) female C57BL/6 mice were imaged nondestructively using  $\mu$ CT (SkyScan 1172, Bruker) at nominal resolutions of 5 and 0.7 micrometer to quantitatively determine the 3D morphology of cortical bone microstructure at macro and micro levels, respectively. Figure 1 shows 3D renderings of representative volumes of interest for analyses at the macro-level (a) and micro-level (b). At the macro-level, 5-months bones exhibited significant differences ( $p < 0.05$ ) in total tissue volume, cortical bone volume density, mean periosteal and endosteal perimeter compared with 23-months bones. At the micro-level, we concluded that aging results in significantly decreasing canal number density ( $p < 0.001$ ) and canal volume density ( $p < 0.01$ ) with no significant variations in the mean canal length and diameter. The mean canal number density at 23 months of age ( $90 \text{ mm}^{-3}$ ) was significantly lower than that at 5 months of age ( $242 \text{ mm}^{-3}$ ). No significant differences were found in lacuna number density and lacuna volume density. In old bones, mean lacuna volume ( $243 \mu\text{m}^3$ ) was significantly ( $p < 0.05$ ) smaller than in young bones ( $279 \mu\text{m}^3$ ). Furthermore, the shape of the lacunae changed from flat in young age to more round at old age. Our hypothesis was confirmed: in mice, bone microarchitecture at old age differs from that at young age. The biological implications will be subject of further study. Furthermore, microCT-based 3D visualization and quantification of cortical bone microstructure can enhance our understanding of the role these features play in bone modeling and remodeling during aging.



3D renderings of representative volumes of interest at the macro-level (a) and micro-level (b)

**Disclosures:** *Haniyeh Hemmatian, None.*

*This study received funding from: The research is funded by the European Commission through MOVE-AGE, an Erasmus Mundus Joint Doctorate programme (2011-0015)*

**SA0120**

**Bmi1 Plays A Critical Role in Protecting Bone Against Premature Aging by Inactivating p16 and p53 Signaling And Inhibiting Oxidative Stress.** Xianhui Lyu<sup>\*</sup>, Qian Wang, Jianliang Jin, Dengshun Miao. Nanjing Medical University, China

Our previously study has demonstrated that *Bmi1* deficiency resulted in an osteoporotic phenotypes with significantly upregulating p16 and p53 expression levels in bony tissue. In this study, we also found that ROS levels were increased dramatically in bone marrow cells and bone marrow mesenchymal stem cells (BM-MSCs) and senescent BM-MSCs induced by  $\text{H}_2\text{O}_2$  were increased markedly in *Bmi1* deficient mice. To investigate whether the osteoporotic phenotypes caused by *Bmi1* deficiency were resulted from bone premature aging through inactivating p16 and p53 signaling and inhibiting oxidative stress, we generated the compound mutant mice with homozygous deletion of both p16 and *Bmi1* [*Bmi1*<sup>-/-</sup>p16<sup>-/-</sup>] or the compound mutant mice with homozygous deletion of both p53 and *Bmi1* [*Bmi1*<sup>-/-</sup>p53<sup>-/-</sup>], or *Bmi1*<sup>-/-</sup> mice after weaning were supplemented with the antioxidant N-acetylcysteine (NAC, 1mg/ml) in their drinking water, and compared them with the untreated *Bmi1*<sup>-/-</sup> and their wild-type littermates at 5 weeks of age. Results showed that skeletal size, cortical and trabecular bone volume, osteoblast number, ALP-, type I collagen- and osteocalcin-positive areas, the mRNA expression levels of Runx2, ALP, type I collagen and osteocalcin, total CFU-f and ALP-positive CFU-f and proliferation of BM-MSCs were all significantly decreased, whereas TRAP positive osteoclast surface and RANKL gene expression levels were increased significantly in *Bmi1*<sup>-/-</sup> mice. Deletion of p16 in *Bmi1*<sup>-/-</sup> mice were largely rescued all alterations observed in *Bmi1*<sup>-/-</sup> mice. In addition, the  $\text{H}_2\text{O}_2$ -induced senescent BM-MSCs derived from *Bmi1* deficient mice were markedly decreased by deletion of p16. Deletion of p53 in *Bmi1*<sup>-/-</sup> mice produced similar effects to deletion of p16 on the osteoporotic phenotypes caused by *Bmi1* deficiency. NAC supplementation was not only decreased ROS levels dramatically in bony tissue and in BM-MSCs, but also largely rescued the osteoporotic phenotypes caused by *Bmi1* deficiency with markedly decreased senescent osteocytes. The results of this study therefore indicate that *Bmi1* plays a critical role in protecting bone against premature aging by inactivating p16 and p53 signaling and inhibiting oxidative stress.

**Disclosures:** *Xianhui Lyu, None.*

**SA0121**

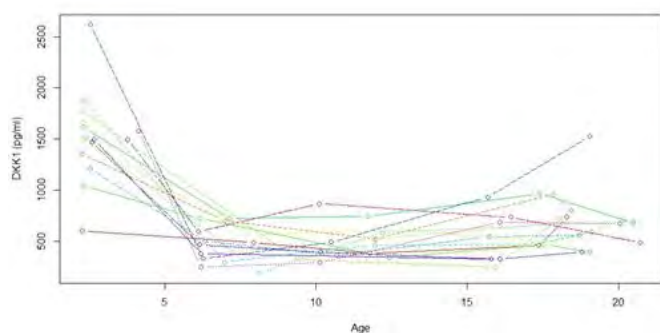
**Change in Circulating Serum Dickkopf-related protein 1 Levels over Lifetime Predicts End of Life Hip Shape and BMD Distribution.** Ellen E. Quillen<sup>\*1</sup>, Todd L. Bredbenner<sup>2</sup>, Donald E. Moravits<sup>2</sup>, Arthur E. Nicholls<sup>2</sup>, Yicki Mattern<sup>1</sup>, Anne Sheldrake<sup>1</sup>, Jaydee Foster<sup>1</sup>, Lorena M. Havill<sup>1</sup>, Daniel P. Nicoletta<sup>2</sup>. <sup>1</sup>Nature Biomedical Research Institute, United states, <sup>2</sup>Southwest Research Institute, United states

The overarching goal of this study is to understand the complex interactions between material, structural, and biochemical contributors to bone fragility. Here we describe the relationship between a known regulator of the Wnt-signaling pathway and bone shape and density in elderly baboons as a model for human osteoporosis.

For each animal, the Milliplex Human Bone Magnetic Bead Panel was run with two internal quality controls on the Luminex analyzer to assess serum concentrations of Dickkopf-1 (DKK-1) across retrospective samples. Osteopontin (OPN), parathyroid hormone (PTH), and osteoprotegerin (OPG) were also measured, but no relationships were identified. DKK-1 is an inhibitor most active during development with decreasing expression with age (see figure). Serum was selected from banked samples drawn at five time points across the lifespan of 15 baboons (7 female, 8 male). Note that animals were chosen that lived at least 20 years, the equivalent of approximately 60 human years. No animals were sacrificed for this study; all died of natural causes or were euthanized for other reasons. The slope of longitudinal DKK-1 concentrations as a function of time was determined for each animal and related to composite traits describing combinations of shape and density of the left proximal femur.

Isolated femurs collected at necropsy with minimal freeze/thaw cycling were micro-CTed and three-dimensional imaging data was digitally reconstructed. Independent shape and density vectors were identified that describe the shape and BMD distribution for each femur and PCA was used to determine composite traits that describe inherent combinations of shape and density distribution traits within the set of femurs. The relationship between the first 10 factors – those that cumulatively describe 69.4% of the total sample variation – and the slope of DKK1 concentration were examined using Spearman's rank coefficient.

Sharper declines in DKK-1 across the lifespan are associated with smaller values of wf2 ( $R^2 = 0.39$ ;  $p = 0.009$ ). Wf2 is broadly associated with overall shape variability of the proximal femur after adjusting for scaling to femur size in wf1 as well as variation in bone mineral density. There is no effect of DKK-1 serum concentration on the bone shape trait when only the serum sample drawn at necropsy is considered, providing support for a cumulative effect of Wnt-signaling on bone shape across the lifetime.



Serum DKK-1 by age in study sample

**Disclosures:** Ellen E. Quillen, None.

## SA0122

**DNA damage and senescence in osteoprogenitors expressing *Osx1* may cause their decline in number with age.** [Ha-Neui Kim](#)<sup>\*1</sup>, [Jianhui Chang](#)<sup>2</sup>, [Lijian Shao](#)<sup>2</sup>, [Li Han](#)<sup>1</sup>, [Srividhya Iyer](#)<sup>1</sup>, [Aaron Warren](#)<sup>1</sup>, [Stavros Manolagas](#)<sup>1</sup>, [Robert Jilka](#)<sup>1</sup>, [Charles O'Brien](#)<sup>1</sup>, [Daohong Zhou](#)<sup>2</sup>, [Maria Almeida](#)<sup>1</sup>. <sup>1</sup>Central Arkansas Veterans Healthcare System, University of Arkansas for Medical Sciences, United states, <sup>2</sup>University of Arkansas for Medical Sciences, United states

Cellular senescence is a process in which cells stop dividing and initiate a gene expression pattern known as the senescence associated secretory phenotype (SASP). DNA damage and cellular senescence increase with aging and contribute to age-related pathologies, at least in part, via decreasing the number of stem/progenitor cells. The DNA damage response (DDR) is a major cause of senescence. Up-regulation of the cell cycle inhibitors p16<sup>INK4A</sup> or p21 in response to p53 activation is one important component of the DDR. Accumulation of the transcription factor GATA4, another component of the DDR, stimulates NFκB and the SASP. Importantly, removal of senescent cells via genetic or pharmacologic means attenuates the age-dependent degeneration of several tissues. Age related bone loss in mice results from a decrease in bone formation and an increase in endocortical and endosteal bone resorption. However, the mechanisms responsible for these effects remain unclear. Here, we examined whether osteoblast progenitors are altered with aging. To this end, we generated *Osx1-Cre*;TdrFP mice, in which osteoprogenitors, and any cells derived from osteoprogenitors, will express the tdrFP fluorescent protein. Accordingly, all osteoblast and osteocytes in the bone of these mice were TdrFP+, up to 24 months of age. FACS analysis of the TdrFP-*Osx1* cells present in the bone marrow revealed that the number of these cells declines by approximately 50% between 6 and 24 months of age in female and male mice. Moreover, TdrFP-*Osx1* cells from old mice exhibited elevated DNA damage and senescence, as indicated by increased γH2AX foci in the nucleus, up-regulation of phospho-p53 and p21 levels, and G1 cell cycle arrest. These osteoprogenitors also exhibit increased protein levels of GATA4 and NFκB, the latter determined by the phosphorylation of p65 and IκB. Bone marrow stromal cells from old TdrFP-*Osx1* mice cultured in osteogenic medium for 10 days also exhibited elevated levels of p21, GATA4, and p-p65; as well as increased expression of SASP genes, including the pro-osteoclastogenic factors TNFα, IL1α, RANKL, and MMP13. Together, our findings indicate that the decrease in bone formation and increase in bone resorption with aging could be accounted for by intrinsic defects in osteoblast progenitors that lead to a decrease

in their numbers and increased support of osteoclast formation. Removal of such senescent cells may represent a therapeutic approach for age-associated osteoporosis.

**Disclosures:** Ha-Neui Kim, None.

## SA0123

See Friday Plenary Number FR0123.

## SA0124

**May Satellite Cells CD44+ Drive Muscle Regeneration in Osteoarthritis Patients?.** [Umberto Tarantino](#)<sup>1</sup>, [Jacopo Baldi](#)<sup>\*1</sup>, [Manuel Scimeca](#)<sup>2</sup>, [Eleonora Piccirilli](#)<sup>1</sup>, [Gasbarra Elena](#)<sup>1</sup>, [Elena Bonanno](#)<sup>2</sup>. <sup>1</sup>Department of Orthopaedics & Traumatology, Università degli Studi di Roma "Tor Vergata", Italy, <sup>2</sup>Department of Biomedicine & Prevention, Anatomic Pathology Section, Università degli Studi di Roma "Tor Vergata", Italy

### Introduction

Osteoarthritis and osteoporosis are strongly associated with specific muscle fiber atrophy characterized by an important imbalance between synthesis and deterioration of muscle proteins and cells. The potential mechanisms involved in the reduction of skeletal muscle mass converge on satellite cells, contributing to their failure in repairing damaged muscle fibers.

### Materials and Methods

We obtained muscle biopsies from 20 female patients underwent total hip arthroplasty for osteoarthritis (OA) (mean age  $71.6 \pm 10.3$ ) and 20 age matched female patients with osteoporotic fragility fracture of the femoral neck (OP). Our goal was to show that the osteophyte formation and the regenerative capacity of stem cells of skeletal muscle are determined by the same factors. In particular, thanks to the morphometric analysis, immunohistochemistry, transmission electron microscopy and immuno-gold labeling we investigated the role of BMP-2, BMP-4 and CD44+ in the activity of stem cells of skeletal muscle.

### Results

In OA patients muscle loss rate was replaced by adipose tissue (18.32%), in OP muscle atrophic fibers were substituted by adipose (8.27%) and connective tissue (6.68%). The morphometric analysis in OA patients showed 38.00% of atrophic fibers (17.90% typeI and 20.10% typeII). In OP group, we observed more than 50.00% of atrophic fibers with prevalence of typeII fibers (21.10% typeI and 39.20% typeII). Moreover we found that OA muscle biopsies there were a significantly higher number of BMP-2-positive fibers ( $62.79 \pm 6.205$ ) as compared with muscle of OP patients ( $13.92 \pm 3.343$ ). Finally results showed a significantly different rate of CD44+ cells in OA as compared with OP.

### Discussion

The expression of CD44, involved in the migration and fusion of satellite cells, suggests that BMPs can induce muscle regeneration by activating satellite cells. A significant expression of BMP-2 and BMP-4 in muscle tissue of OA patients could explain a lower level of muscle atrophy compared with OP patients.

### Conclusion

The finding that both the activity of satellite muscle stem cells and bone remodelling are related to the same factors could explain the molecular mechanism of more relevant bone-muscle related diseases of the elderly, such as sarcopenia, osteoarthritis, and osteoporosis. We think that the control of physiological BMP-2 balance between bone and muscle tissue may be considered as a new pharmacological target.

**Disclosures:** Jacopo Baldi, None.

## SA0125

See Friday Plenary Number FR0125.

## SA0126

See Friday Plenary Number FR0126.

## SA0127

**Bmp2 Gene is required for In Vivo Differentiation of αSMA+ Periodontal Stem-like cells and In Vitro for Differentiation Associated changes in mRNA and Candidate Genomic Level Enhancer Function.** [Stephen E Harris](#)<sup>\*1</sup>, [Audrey Rakian](#)<sup>1</sup>, [Rebecca Neitzke](#)<sup>1</sup>, [Michael Rediske](#)<sup>1</sup>, [Marie A Harris](#)<sup>1</sup>, [Ivo Kalajzic](#)<sup>2</sup>, [Jian Q Feng](#)<sup>3</sup>, [Jelica Gluhak-Heinrich](#)<sup>1</sup>, [Yong Cui](#)<sup>1</sup>. <sup>1</sup>UTHSCSA, United states, <sup>2</sup>U. of Connecticut Health Center, United states, <sup>3</sup>Baylor College of Dentistry, United states

The *Bmp2* gene is conditionally removed from αSMA+ periodontal progenitors (PP) with αSMA-CreERt2 at P2-P4 which normally differentiates to alveolar bone, cementums, and PDL. These tissues show major phenotypic alterations and the most pronounced reduction in surrounding alveolar bone is around the teeth and reduced cellular and acellular cementum. Using Col12 immunocytochemistry, we found these defects in the PDL attachment to cementum and bone. Using the Rosa-loxP-stop-loxP-Tomato lineage tracing system, we demonstrate, in a quantitative manner, reduction of 50 to 80% in

the progression of  $\alpha$ SMA+ PP to alveolar bone, PDL, and cellular cementum, using overlays of Osterix, Scleraxis and Dmp1 confocal immunocytochemistry. We expanded  $\alpha$ SMA+ PP from mandibles of *Bmp2<sup>flx/flx</sup>* mice, using ECM from StemBioSystems. Using Adenovirus-CMV-Cre and control, we deleted the endogenous *Bmp2* gene in vitro and carried out differentiation assays and RNA-seq analysis of mRNA coding transcripts and long-noncoding RNAs (lncRNAs). Deletion of the *Bmp2* gene disrupts differentiation capacity of the PPs that can be partially rescued with 200ng/ml of recombinant BMP2. We demonstrate major reduction of PDL Scleraxis marker, cementocytes DMP1 marker, and various osteoblast markers by the in vitro deletion of *Bmp2* gene. Several relevant networks of genes associated with bone and cementum and PDL are also modulated in the absence of the *Bmp2* gene. A network of lncRNAs was identified that overlay with H3K27ac enhancer marks and RNAPol2, by Chip-seq, in  $\alpha$ SMA+ bone marrow stromal cells, and represent a set of enhancer RNAs regulated during differentiation of  $\alpha$ SMA+ PP and depend on the endogenous *Bmp2* gene. We focused on the enhancer-lncRNA domains in the *Bmp2* gene and the Osterix gene, both highly induced during differentiation. The *Bmp2* gene transcription unit lies in a gene desert of over 1.6 Mbases. In the 3' region, 300 to 800kb 3' of the transcription start site, we identified 3 super-enhancer regions 5-20kb and associated lncRNAs induced over 50 fold upon differentiation of the  $\alpha$ SMA+ PP cells. These same *Bmp2* eRNAs are also induced during differentiation of bone marrow MSC to osteoblasts and osteocytes. The Osterix gene is activated within 24hr of rBMP2 treatment and we demonstrate several enhancer-lncRNA activation domains, at 24hrs after rBMP2 treatment and in the fully differentiated state by day 26.

**Disclosures:** Stephen E Harris, None.

## SA0128

**High-content *in vivo* imaging of zebrafish bone regeneration reveals dynamic NADH events during osteoblast dedifferentiation.** Claire Watson\*, Edith Gardiner, Werner Kaminsky, Ronald Kwon, University of Washington, United states

Cellular reprogramming is the process by which adult somatic cells are artificially dedifferentiated into a progenitor state. While natural bone cell dedifferentiation is infrequent in mammals, other vertebrates possess the ability to regenerate amputated bony appendages through epimorphic regeneration, a process characterized by the formation of a proliferative mass of dedifferentiated cells called the blastema. The molecular events driving dedifferentiation and the constraints that dictate its segregation across species are unknown. Here, we show an association between osteoblast dedifferentiation and metabolic status during zebrafish tail fin regeneration. Previously, we described a custom multi-modal high-content imaging system that enables simultaneous evaluation of osteoblast differentiation status (via an *osterix/Sp7:EGFP* transgene), cell metabolism (via NADH autofluorescence), and mineral accrual (via Rotopol acquired birefringence). Using this system, we subjected adult *Tg(Sp7:EGFP)* zebrafish to caudal fin amputation and monitored these signaling dynamics for 14 days post amputation (dpa). A custom mapping approach was developed to register images from different time points (Fig. 1A), generating virtual time-lapse sequences that revealed dynamic signaling events at every tissue location. As previously reported [1], during blastema formation, we observed a transient decrease in *Sp7*<sup>+</sup> cells proximal to the amputation stump indicative of osteoblast dedifferentiation. Analysis of NADH in the same location revealed a transient NADH spike coincident with decreased *Sp7* signal. In newly forming bone segments, no NADH spikes were observed. In contrast, at 14dpa, a time point in which bone growth and mineralization had largely plateaued, we observed a distinct, high-magnitude NADH spike in many distal bone segments. This NADH event was also coincident with a transient decrease in *Sp7*<sup>+</sup> cells, and preceded the resorption of bony segments at the end of several rays, retraction of the distal-most fin tissue, and subsequent bony growth. Collectively, our studies suggest that regenerating bone may recover from stationary growth through secondary regeneration events. Further, they implicate a novel association between osteoblast dedifferentiation and metabolic status by revealing a high-magnitude, dynamic NADH signal coincident with both primary and secondary dedifferentiation events.

[1] Knopf, F. et al. *Dev Cell* 2011; 20:713-24.

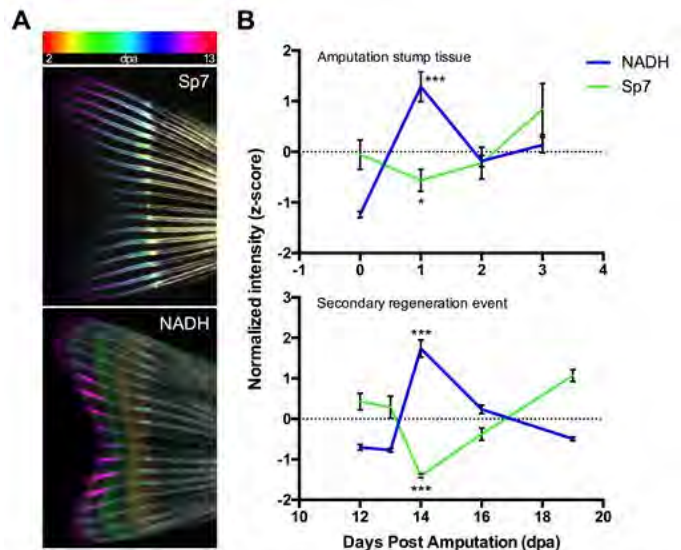


Figure 1. Registered time-lapse images of caudal fin regeneration reveal a relationship between NADH and *Sp7* during osteoblast dedifferentiation. (A) Mapped fins of 6 images depicting *Sp7* and NADH signal taken approximately every other day between 2-13 dpa. (B) Coincident changes in NADH and *Sp7* seen in both the amputation stump (top) and the distal regenerate (bottom). Significance values indicate a difference from the previous day in a Tukey's post-hoc test following a one-way ANOVA of each signal. \* $P < 0.05$ , \*\*\* $P < 0.001$ .

Figure 1

**Disclosures:** Claire Watson, None.

## SA0129

See Friday Plenary Number FR0129.

## SA0130

See Friday Plenary Number FR0130.

## SA0131

**Commitment and differentiation of mesenchymal stromal cells is controlled by novel regulatory regions and transcription factor programs.** Jonathan Gordon\*, Hai Wu, Coralee Tye, Joseph Boyd, Janet Stein, Gary Stein, Jane Lian, University of Vermont College of Medicine, United states

Adult bone formation requires a highly regulated program of differentiation from a mesenchymal-derived osteoprogenitor to a mature osteocyte. Epigenetic mechanisms control mesenchymal stromal cell (MSC) commitment to a mature osteoblast through facilitating of binding of transcriptional regulators to promoter regions of genes, however less well understood are inter- and intra-genic regulatory regions that control cell-type-specific gene expression programs. These regulatory elements called cis-regulator modules, are bound by transcription factors (TFs) and specific post-translationally modified histones, and play key roles in the control of tissue morphogenesis. To define novel regulatory regions during osteogenesis, pluripotent *CD45<sup>-</sup>/Ter119<sup>-</sup>/SCA1<sup>+</sup>/CD29<sup>+</sup>/Nestin<sup>+</sup>/CD146<sup>+</sup>/aSMA<sup>+</sup>* MSCs and analogous human MSC populations, were isolated by FACS to obtain a homogenous population of cells that were differentiated to mature osteoblasts. We then used ChIP-seq to develop genome-wide enrichment profiles of intergenic genomic regions of occupied by TFs, cofactors, chromatin regulators, and transcription apparatus occupying osteogenic enhancers in MSCs. Supervised pattern discovery was performed using ChromHMM to segment genomic regions into active, quiescent, TF-bound, transcribed and super-enhancer regions. From this analysis, we identified novel enhancers near genes involved in osteogenesis and novel enhancers for bone formation were predicted in intragenic regions of several osteoblast-related genes. Several novel enhancers were identified near canonical bone-related genes (e.g. *Runx2*, *Sp7*, *Fgfr1*) and several regions near coding and noncoding genes (i.e. lncRNA, miRNA) with yet unknown functions in osteogenesis. In addition, by evaluating transcription factor binding profiles and by using gene set enrichment analysis (GSEA) and regulatory module predictions we defined novel transcription factor and epigenetic modifier programs that control osteoblast-related gene expression and osteogenic differentiation.

In conclusion, we have defined novel regulatory regions, denoted by histone modifications and transcription factor binding sites that function as enhancers critical for osteogenic differentiation. This comprehensive epigenetic signature of lineage

commitment and osteoblast differentiation is clinically relevant to pathogenic conditions involving bone loss and repair.

**Disclosures:** Jonathan Gordon, None.

## SA0132

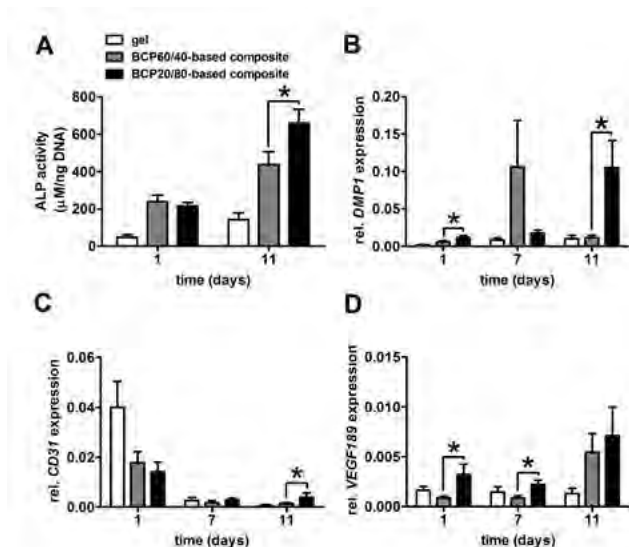
**Enhanced Osteogenic and Vasculogenic Differentiation Potential of Human Adipose Stem Cells on Biphasic Calcium Phosphate Scaffolds in Fibrin Gels.** Fransisca van Esterik<sup>\*1</sup>, Behrouz Zandieh-Doulabi<sup>1</sup>, Cees Kleverlaan<sup>2</sup>, Jenneke Klein-Nulend<sup>3</sup>. <sup>1</sup>Department of Oral Cell Biology, Academic Centre for Dentistry Amsterdam (ACTA), University of Amsterdam & Vrije Universiteit Amsterdam, MOVE Research Institute Amsterdam, Netherlands, <sup>2</sup>Department of Dental Materials Science, Academic Centre for Dentistry (ACTA), University of Amsterdam & Vrije Universiteit Amsterdam, MOVE Research Institute Amsterdam, Netherlands, <sup>3</sup>Department of Oral Cell Biology, Academic Centre for Dentistry (ACTA), University of Amsterdam & Vrije Universiteit Amsterdam, MOVE Research Institute Amsterdam, Netherlands

**Introduction:** For bone tissue engineering synthetic biphasic calcium phosphate (BCP) with a hydroxyapatite/ $\beta$ -tricalcium phosphate (HA/ $\beta$ -TCP) ratio of 60/40 (BCP60/40) is successfully clinically applied in e.g. bone augmentation procedures, but the high percentage of HA may hamper efficient scaffold remodeling. Whether BCP with a lower HA/ $\beta$ -TCP ratio (BCP20/80) is more desirable is still unclear. Vascular development is needed before osteogenesis can occur. We aimed to test the osteogenic and/or vasculogenic differentiation potential as well as degradation of composites consisting of human adipose stem cells (hASCs) seeded on BCP60/40 or BCP20/80 incorporated in fibrin gels that trigger neovascularization for bone regeneration.

**Methods:** hASCs were seeded on BCP60/40 or BCP20/80 and incorporated in fibrin gels, or directly incorporated in fibrin gels, and cultured up to 11 days. Cell attachment to both BCPs was determined after 30 min, and cell proliferation (DNA content), osteogenic differentiation potential (alkaline phosphatase activity, *RUNX2*, *osteonectin*, *DMP1*, *COL1*, *COL3* gene expression) and vasculogenic differentiation potential (*CD31*, *VEGF165*, *VEGF189*, *EDN1*, *COL1*, *COL3* gene expression), and fibrin degradation products (ELISA) were assessed after culture.

**Results:** hASC attachment to BCP60/40 and BCP20/80 within 30 min was similar (>93%). After 11 days of culture, BCP20/80-based composites showed increased alkaline phosphatase activity (5.0-fold) and *DMP1* gene expression (day 1: 2.1-fold; day 11: 9.2-fold; Fig. 1A,B), but not *RUNX2* and osteonectin expression, compared to BCP60/40-based composites. BCP20/80-based composites also showed enhanced expression of the vasculogenic markers *CD31* (day 11: 2.8-fold) and *VEGF189* (day 1: 3.6-fold; day 7: 2.6-fold; Fig. 1C,D), but not *VEGF165* and endothelin-1. *COL1* and *COL3* expression were similar in both composites. Fibrin degradation products were increased by 1.7-fold in BCP20/80-based composites at day 7, but reached similar levels at day 11.

**Conclusion:** BCP20/80-based composites showed increased alkaline phosphatase activity as well as *DMP1*, *CD31*, and *VEGF189* gene expression, and increased fibrin degradation compared to BCP60/40-based composites. Thus BCP20/80-based composites showed enhanced osteogenic and vasculogenic differentiation potential compared to BCP60/40-based composites *in vitro*, suggesting that these composites might be more promising for *in vivo* bone augmentation.



Enhanced ALP activity, and gene expression of DMP1, CD31, and VEGF189 in BCP20/80-based composites

**Disclosures:** Fransisca van Esterik, None.

## SA0133

See Friday Plenary Number FR0133.

## SA0134

See Friday Plenary Number FR0134.

## SA0135

See Friday Plenary Number FR0135.

## SA0136

**A novel combination of bone micro architecture descriptors and selected ROIs for the identification of osteoarthritis.** Richard Ljuhar<sup>\*1</sup>, Stefan Nehrer<sup>2</sup>, Benjamin Norman<sup>1</sup>, Davul Ljuhar<sup>1</sup>, Tobias Haftner<sup>1</sup>, Jiri Hladuvka<sup>3</sup>, Marianne Bui Thi Mai<sup>3</sup>, Helena Canhão<sup>4</sup>, Jaime Branco<sup>5</sup>, Ana Maria Rodrigues<sup>4</sup>, Nelia Gouveia<sup>5</sup>, Astrid Fahrleitner-Pammer<sup>6</sup>, Hans-Peter Dimai<sup>6</sup>. <sup>1</sup>Braincon Technologies, Austria, <sup>2</sup>Center for Regenerative Medicine & Orthopedics, Danube University, Austria, <sup>3</sup>VRVis Research Competence Center, Austria, <sup>4</sup>Faculdade de Medicina da Universidade de Lisboa, Portugal, <sup>5</sup>NOVA Medical School Faculdade de Ciências Médicas Universidade Nova de Lisboa, Portugal, <sup>6</sup>Department of Internal Medicine, Division of Endocrinology & Metabolism, Medical University of Graz, Austria

**OBJECTIVE:** The relationship between knee osteoarthritis (OA) progression and changes in subchondral tibial bone structure has recently been recognized and various texture descriptors have been proposed to detect early stages of OA. However the application of such algorithms is largely dependent on the region of interest (ROI) selected within the subchondral bone area. Therefore, the appropriate selection of ROIs plays a crucial role for the significance of the analysis. Based on our previous work<sup>1</sup>, the present study aims to a) investigate the potential of a combined bone micro architecture algorithm (BMA) as an efficient alternative to established OA descriptors, and b) to define the most significant ROIs for OA discrimination.

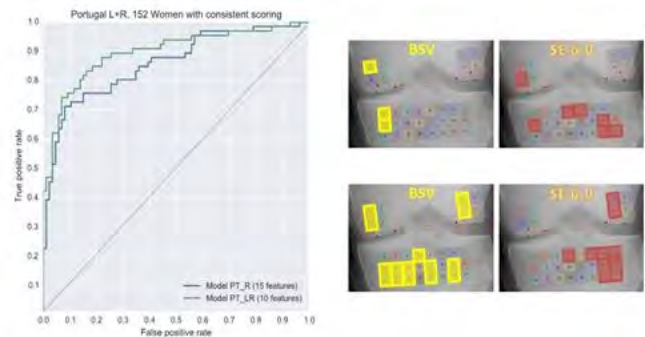
**METHODS:** 89 left and 64 right knee joint radiographs of Caucasian females were available, 66 cases and 86 controls. In contrast to our prior work which was limited to proximal tibia, the additional (and novel) effort is to investigate two regions in both condyles of the distal femur. The selected area of the proximal tibia involved a matrix of 3x8 ROIs, whereas a 2x2 matrix was defined for each condyle of the distal femur. Bone Structure Value (BSV) and Shannon Entropy (SE) were calculated for each of the 32 ROIs, respectively. Based on these 64 variables, combinations of ROIs, both individually and in the context of other features and their descriptors, were systematically investigated using statistical and machine learning methods to identify the best performance for discrimination between case and controls.

**RESULTS:** In addition to the tibial changes, our results indicate that OA is also affecting the subchondral bone structure in femur condyles. By combining the BSV and SE, the odds ratio increased significantly from 3.08 (95% CI: 1.78-5.30) to 14.82 (95% CI: 6.69-32.83) when using 15 features, and to 39.75 (95% CI: 15.41-102.51) based on 10 features. By using the selected 10 features the accuracy was found to be 0.86, reflecting a significant improvement compared to the accuracy achieved when calculating a single mean value for the 3x8 ROIs of the proximal tibia alone (0.62 vs. 0.86).

**CONCLUSIONS:** The combination of subchondral ROIs of both femur condyles and the proximal tibia clearly improve the discrimination between OA cases and controls. The model can further be improved by incorporating shape descriptors and a full automation, exploiting recent advances in segmentation and/or landmarking.

<sup>1</sup> See Abstract [1009], ASBMR 2015

## Feature selection based on BMA analysis results



Descriptor selection for OA discrimination

**Disclosures:** Richard Ljuhar, None.

**SA0137**

See Friday Plenary Number FR0137.

**SA0138**

See Friday Plenary Number FR0138.

**SA0139**

See Friday Plenary Number FR0139.

**SA0140**

See Friday Plenary Number FR0140.

**SA0141**

**Osteoclast microRNA Profiling in Erosive Rheumatoid Arthritis.** Hugues Allard-Chamard<sup>\*1</sup>, Gilles Boire<sup>1</sup>, Artur De Brum-Fernandes<sup>1</sup>, Michelle Scott<sup>2</sup>, Luigi Bouchard<sup>2</sup>, Sophie Roux<sup>1</sup>. <sup>1</sup>Rheumatology, Faculty of Medicine, Sherbrooke University, Canada, <sup>2</sup>Biochemistry, Faculty of Medicine, Sherbrooke University, Canada

**Introduction.** Rheumatoid arthritis (RA) is a common systemic disease with a potential for periarticular bone destruction, yet a fraction of patients remain non-erosive. The clinical and structural phenotypic outcomes of RA result from the integration of a series of epigenetic changes including microRNAs (miRs) as part of the interplay between predisposing genetics and environmental factors. miR expression profiles have been found to be altered in RA synovium and peripheral blood mononuclear cells (PBMCs), but their relationships with synovitis-associated bone destruction in RA is unknown. Because bone-resorbing osteoclasts (OCs) are the cells responsible for erosions adjacent to RA synovitis, we studied miR profiles in OCs from patients with RA.

**Methods.** Using a deep sequencing study (HiSeq Illumina system; Genome Quebec), we compared genome-wide miR expression in PBMC-derived OCs from rapidly erosive (n=8) and long-term non-erosive (n=8) seropositive RA (all RA expressed both RF and anti-CCP2) and age- and sex- matched healthy controls (n=11). miRs found to be differentially expressed using deep sequencing analysis were validated with quantitative PCR (qPCR). Correlation analysis with their serum expression was performed.

**Results.** Using RNAs extracted from mature OCs, 80 miRs were found to be differentially expressed between OCs from erosive or non-erosive RA and controls in the deep sequencing analysis. To date, 8 of these 80 were validated using qPCR in 4 matched trios (erosive, non-erosive and controls), including miR 103a-3p, 103b-5p, 21-5p, 31-3p/5p, 423 3p/5p, 93-5p. Only miR 31-3p showed both higher expression in erosive RA ( $p < 0.01$ , ANOVA multiple comparisons) and correlation with serum levels ( $p < 0.05$ , Pearson's  $r = 0.971$ ). In an *in-vitro* model of OC differentiated from human cord blood monocytes (n=2), we showed that miR 31-3p inhibitors and mimics transfection respectively decreased and increased bone resorption.

**Conclusion.** Identifying miR signature in OCs of patients with RA who have rapidly erosive lesions may help to determine biomarkers for erosion. Our results also suggest that as previously reported in murine models, miR-31 is involved in the regulation of bone resorption in human OCs.

**Disclosures:** Hugues Allard-Chamard, None.

**SA0142**

See Friday Plenary Number FR0142.

**SA0143**

See Friday Plenary Number FR0143.

**SA0144**

See Friday Plenary Number FR0144.

**SA0145**

See Friday Plenary Number FR0145.

**SA0146**

**Conditional Knockout of the MicroRNA 17-92 Cluster in Type-I Collagen Expressing Cells Decreases Alveolar Bone Size and Incisor Teeth Mechanical Properties.** Subburaman Mohan<sup>1</sup>, Micheal Ibrahim<sup>2</sup>, Chandrasekhar Kesavan<sup>\*2</sup>. <sup>1</sup>VA Loma Linda Healthcare System, United states, <sup>2</sup>VA Loma Linda Healthcare System, United states

MicroRNA (miR)s play essential roles in regulating a variety of cellular processes by modulating the mRNA and/or protein levels of their targets. We recently reported that

conditional disruption of the miR17-92 cluster in type-I collagen expressing osteogenic lineage cells resulted in decreased periosteal bone formation and mineral apposition rates in long bones suggesting that the miR17-92 cluster is essential for osteoblast differentiation/function. Consistent with these findings, a study showed that the expression levels of miR17-92 cluster miRs are increased during odontogenesis. Since similar regulatory pathways are predicted to control osteogenesis and odontogenesis, we hypothesized that the miR17-92 cluster was also essential for dental bone development and maintenance. To test this hypothesis, we evaluated the incisor tooth phenotype by micro-CT of 5 and 12 weeks old conditional knockout (CKO) mice deficient in the miR17-92 cluster in type-I collagen expressing cells and bone strength by finite element analysis. A scout view of the lower jaw using micro-CT analysis revealed an overall reduction in the size of lower jaw in the CKO mice compared to WT mice. The incisor teeth size of 5 and 12 weeks old CKO mice revealed a 23-30% reduction in tissue volume (TV) and bone volume (BV), respectively with no change in bone volume/tissue volume (BV/TV). Accordingly, the stiffness and failure load of incisor teeth assessed by finite element analysis revealed an 18-40% decrease in the CKO compared to WT mice. A positive correlation between bone parameters and strength data suggests that the decreased mechanical properties of incisor teeth are due to decreased TV and BV. Furthermore, our study also found that the molar length was reduced by 16-18% in the 5 and 12 week old CKO compared to WT mice. These data suggest that miR17-92 cluster is at least in part involved in regulating the tooth size and to some extent the longitudinal tooth growth. Subsequently, we also found that the width of alveolar bone was reduced by 25% with a 16% increase in periodontal ligament space, suggesting that these mice are susceptible to tooth movement. By histology, we found that the height of ameloblasts was reduced by 16% in the incisor of CKO mice leading us to speculate that miRs in miR17-92 cluster primarily affect ameloblast activity. In conclusion, our data provides the first experimental evidence that the miR17-92 cluster plays a key role in regulating tooth development by influencing its length and size, and, thereby its strength.

**Disclosures:** Chandrasekhar Kesavan, None.

**SA0147**

See Friday Plenary Number FR0147.

**SA0148**

See Friday Plenary Number FR0148.

**SA0149**

See Friday Plenary Number FR0149.

**SA0150**

See Friday Plenary Number FR0150.

**SA0151**

See Friday Plenary Number FR0151.

**SA0152**

See Friday Plenary Number FR0152.

**SA0153**

See Friday Plenary Number FR0153.

**SA0154**

See Friday Plenary Number FR0154.

**SA0155**

See Friday Plenary Number FR0155.

**SA0156**

**Autophagy suppresses proliferation of bone marrow-derived osteoblast progenitor cells (BMOPCs) by targeting Cyclin D1.** Li Wang<sup>\*1</sup>, Paul Krebsbach<sup>1</sup>, Jun-Lin Guan<sup>2</sup>, Fei Liu<sup>1</sup>. <sup>1</sup>University of Michigan School of Dentistry, United states, <sup>2</sup>University of Cincinnati College of Medicine, United states

BMOPCs play pivotal roles in bone growth and remodeling. Autophagy, a conserved catabolic process, has numerous connections to human physiology and disease. Increasing evidence showed the important roles of autophagy in the development and differentiation of progenitor cells but its role in BMOPCs is unknown. In this study, we aimed to determine the function of autophagy in BMOPCs. Using BMOPCs obtained from long bone of 6-8 wks GFP-LC3 transgenic mice, autophagic vesicle (GFP-LC3 puncta) was examined to

monitor autophagy. Immunofluorescence with anti-Osterix antibody and ALP staining were performed to monitor osteoblast differentiation. Our data showed that the percentage of Osterix+ cells increased from 12% at day 3 to 97% at day 7 but only 1% of them are ALP+, confirming that these cells were osteoblast progenitor cells. Interestingly, 89% of BMOPCs has autophagic vesicle at day 4 while only 36% at day 7. Within Osterix+ cell population, percentage of autophagy active cells decreased from 95% at day 3 to 38% at day 7. The high autophagy activity at early culture was confirmed by both LC3II conversion assay (Western blot) and transmission electronic microscopy. To determine the role of autophagy in BMOPCs, FIP200 or Atg5, two autophagy essential genes were deleted in Osterix+ cells with *Osx-Cre* transgenic mice and we found increased colony forming units (CFU-F) and ALP+ colonies (CFU-ALP) in autophagy deficient BMOPCs (either FIP200 or Atg5 deletion). As a first step to elucidate the mechanism of CFU increase in CKO cells, the effect of autophagy deficiency on proliferation was determined by examining the expression of proliferation marker Ki67. Autophagy deficient BMOPCs had increased percentage of Ki67+ cells compared to CTR cells (49% vs. 28%, n=3, p<0.05), suggesting autophagy function inhibits BMOPC proliferation. In addition, the percentage of Ki67+ cells of BMOPCs without autophagic vesicle was much higher than the cells with autophagic vesicles (25% vs 4%, n=3, p<0.05). To determine the underlying mechanism by which autophagy regulates BMOPC proliferation, the expression level of Cyclins was examined. Preliminary data showed that the level of Cyclin D1 but not Cyclin B1, Cyclin D2 or Cyclin E was significantly up-regulated in autophagy deficient BMOPCs. In summary, our data showed that 1) BMOPCs have transient autophagy activation in *in vitro* culture; 2) autophagy inhibits BMOPC proliferation likely through promoting Cyclin D1 degradation.

**Disclosures:** Li Wang, None.

## SA0157

See Friday Plenary Number FR0157.

## SA0158

See Friday Plenary Number FR0158.

## SA0159

See Friday Plenary Number FR0159.

## SA0160

See Friday Plenary Number FR0160.

## SA0161

**Control of bone resorption by the rate of osteoprogenitor recruitment during bone remodeling.** Nicolai E Lassen<sup>1</sup>, Thomas L Andersen<sup>1</sup>, Kent Soe<sup>1</sup>, Ellen M Hauge<sup>2</sup>, Soren Harving<sup>3</sup>, Gete ET Eschen<sup>2</sup>, Jean-Marie Delaisse<sup>\*1</sup>.  
<sup>1</sup>Vejle/Lillebælt Hospital, University of Southern Denmark, Denmark, <sup>2</sup>Aarhus hospital, Denmark, <sup>3</sup>Aalborg Hospital, Denmark

No answers have been given to basic questions such as what controls the progress of bone resorption in a remodeling unit once it has been initiated, or what are the dynamics of the osteoclast and osteoprogenitor cell populations meeting on the bone surface. These questions cannot be investigated by common bone histomorphometry. Here, we took benefit of longitudinal sections through Haversian remodeling units, because they allow to examine the successive steps of the remodeling cycle in their natural order. A total of 13 bone remodeling sites were analyzed in either femurs collected during corrective surgery for coxa valga patients, or fibula collected from patients who underwent reconstructive surgery. Serial sections were immunostained for osteoclast and osteoblast lineage markers. The investigated Haversian remodeling units consisted of a typical cutting cone (cc) of variable length showing a clear eroded surface/cement line, and at least the first part of a closing cone showing osteoid deposition over the cement line. We identified (i) osteoclasts packed at the tip of the cc initiating resorption and elongating the cc, and (ii) osteoclasts on the cc wall, sparsely distributed amongst reversal cells. The resorptive activity of the latter osteoclasts was shown by the widening of the cc until bone formation was initiated. Accordingly, widening was commensurate with the cc length, and represented 55 to 95% of the overall amount of bone removed in the cc. Virtually all reversal cells lining the cc were positive for osteoblast lineage markers and proved to be osteoprogenitors. We found that the density of the latter cells progressively grew, showing 14 cells/mm in the first quarter of the cc, and reaching always at least 40 upon initiation of bone formation. This value of 40 was independent of the length of the cc. This suggests that bone formation is initiated only above a threshold cell density, and that the rate of osteoprogenitor recruitment differs in different canals. Thus the slower this recruitment, the longer the exposure of the cc to secondary resorption steps and the wider the cc becomes, in line with our observations. In conclusion, we show that secondary resorption steps occur during the whole period of osteoprogenitor recruitment on the eroded surface; that bone formation starts only above a critical osteoprogenitor cell density; and thus that the extent of secondary resorption is controlled by the rate of osteoprogenitor recruitment.

**Disclosures:** Jean-Marie Delaisse, None.

## SA0162

**Cross Talk Between CD36 and CD47/Tsp1 in Osteoclastogenesis.** Joanne Walker\*, Srinivas Koduru, Ben-hua Sun, Meiling Zhu, Christine Simpson, Madhav Dhodapkar, Karl Insogna. Yale University School of Medicine, United states

It has been previously reported that antibody-mediated blockade of CD47-thrombospondin 1 (TSP-1) interactions blocks osteoclast formation from human osteoclast precursors *in vitro* and attenuates PTH-induced hypercalcemia *in vivo* in mice (Blood 114:3413). There are two cell-associated binding partners for TSP1, CD47 and CD36. Osteoclast formation was attenuated but not absent when pre-osteoclasts isolated from CD47<sup>-/-</sup> mice were co-cultured with wild-type osteoblasts. Similarly, suppressing CD47 in human osteoclast progenitors using siRNA technology attenuated but did not abrogate osteoclastogenesis. Suppressing CD36 using the same approach also attenuated osteoclast formation. A selective agonist for CD36, p907, partially rescued the effect of a neutralizing antibody to TSP-1 in control cells but not when CD36 expression was suppressed using siRNA. Consistent with the *in vivo* PTH infusion studies just mentioned, female mice in which both CD47 and CD36 were genetically absent had a blunted response to a hypercalcemic infusion of PTH (20.0±1.3 vs. 15.1±1.3, n=9 per genotype, p=0.01). TSP-1 suppresses nitric oxide (NO) production in part by inhibiting cyclic GMP generation. Suppressing NO is known to stimulate osteoclastogenesis. Inhibiting TSP-1 increased cyclic GMP and NO production in osteoclasts consistent with its anti-osteoclastogenic action (p=<0.01, n=3). L-NAME, a NO synthase inhibitor, completely restored murine osteoclastogenesis in the presence of the anti-TSP-1 antibody, supporting the conclusion that NO is in the downstream effector pathway of TSP-1. The CD36 agonist, p907 partially suppressed NO production in antibody-treated cultures. We conclude that both CD47 and CD36 play roles in mediating TSP-1-dependent osteoclast formation.

**Disclosures:** Joanne Walker, None.

This study received funding from: NIH

## SA0163

**Fluoride regulates osteoclastogenesis in a strain-specific manner.** Flávia Amadeu de Oliveira<sup>\*1</sup>, Amanda Amaral Pereira<sup>1</sup>, Talita da Silva Ventura<sup>1</sup>, Marília Buzalaf<sup>1</sup>, Rodrigo Cardoso de Oliveira<sup>1</sup>, Camila Peres-Buzalaf<sup>2</sup>.  
<sup>1</sup>University of Sao Paulo, Brazil, <sup>2</sup>Universidade do Sagrado Coração, Brazil

Altered osteoclastogenesis may result in either osteoporotic or osteopetrotic bone phenotype. Increased osteoclastogenesis presents a central role in several inflammatory diseases that are associated to severe bone loss. Besides the anticariogenic role of fluoride (F), it is widely consumed in the drinking water allowing its accumulation in the bone. Recently F has been shown to modulate *in vivo* bone formation in a strain-specific dependent manner. It enhances bone formation in 129P3/J but not in A/J mice. However, its effect on osteoclastogenesis and the strain dependency remains uncertain. The objective was to evaluate the effect of F on formation and function of bone marrow macrophage-derived osteoclasts from A/J and 129P3/J mice, knowing as susceptible and resistant phenotype mice to F responses. Thus, bone marrow macrophage cells from both strains were cultivated in  $\alpha$ -MEM medium containing M-CSF and RANKL in presence or absence of 10<sup>-3</sup> or 10<sup>-5</sup> M of F, for 7 days. The number of osteoclasts was evaluated by tartrate-resistant acid phosphatase (TRAP) staining and their functional responses were evaluated by TRAP, and bone resorptive activities. In A/J-derived cells, F at 10<sup>-3</sup> and 10<sup>-5</sup> M significantly increased TRAP activity compared to untreated cells (p< 0.05). However, no significant alteration was observed in F-treated 129P3/J cells compared to untreated cells. Moreover, control A/J and 129P3/J present similar TRAP activity, suggesting that the strain-specific response was associated to F effect. While the percentage of resorptive areas in 129P3/J-derived osteoclast was slightly altered upon F treatment, it significantly enhanced A/J-osteoclast mineral resorptive activity. Therefore, F enhances osteoclast formation and function in A/J cells but not in 129P3/J-derived cells. These results provide a novel knowledge about the contribution of F in enhancing osteoclastogenesis in a strain specific manner.

**Disclosures:** Flávia Amadeu de Oliveira, None.

## SA0164

**Function of novel splicing variant of NF- $\kappa$ B receptor activator (vRANK).** Riko Kitazawa<sup>\*1</sup>, Ryuma Haraguchi<sup>2</sup>, Yosuke Mizuno<sup>1</sup>, Yasuhiro Kobayashi<sup>3</sup>, Sohei Kitazawa<sup>2</sup>.  
<sup>1</sup>Department of Diagnostic Pathology, Ehime University Hospital, Japan, <sup>2</sup>Department of Molecular Pathology, Ehime University Graduate School of Medicine, Japan, <sup>3</sup>Institute of Oral Science, Matsumoto Dental University, Japan

Receptor activator of NF- $\kappa$ B (RANK) is a member of the tumor necrosis factor receptor (TNFR) family expressed in osteoclast precursors, and RANK-RANK ligand (RANKL) signaling plays a central role in differentiation, activation and survival of osteoclasts. We have identified a novel alternative splicing variant of mouse and human RANK gene (vRANK) that contains an intervening exon between exons 1 and 2 of full-length RANK (fRANK) mRNA. Since this novel exon contains a stop codon, vRANK

encodes short truncated amino acids that have a portion of the signal peptide of vRANK and additional amino acids that show no homology to previously reported domains. By transient transfection of RAW264.7 cells with vRANK-GFP and -Flag expressing constructs, vRANK was found localized mostly in the cytoplasm and partly in the cell membrane, but was not secreted into the culture supernatant. In the HL60 human myelomonocytic leukemic cell line, vRANK expression was induced by PMA or TGF- $\beta$  in the presence of Vitamin D3 in an ERK-dependent manner through the Sam68 system. When overexpressed *in vitro*, vRANK in mouse pre-osteoclastic RAW264.7 cells decreased the formation of TRACP-positive multinucleated giant cells and negated the anti-apoptotic effect of sRANKL. When systemically overexpressed *in vivo*, the CAGcre+vRANK mouse showed high fatality before weaning; a 13-week survivor displayed severe cardiac dilatation with cardiomyopathy and bronchopneumonia. When selectively overexpressed among the monocyte-macrophage lineage *in vivo*, the LysMcre+vRANK mouse showed decreased osteoclastogenesis in *ex vivo* culture of spleen cells, but did not show increased bone mass measured by micro CT analyses. Taken together, these results suggest that vRANK is a novel bioactive peptide that not only reduces the number of RANKL-induced mature osteoclasts, but also exhibits profound systemic effects on bone metabolism. We are now creating CTSKcre+vRANK mice to analyze the effects of vRANK on mature osteoclasts.

**Disclosures:** Riko Kitazawa, None.

## SA0165

See Friday Plenary Number FR0165.

## SA0166

See Friday Plenary Number FR0166.

## SA0167

See Friday Plenary Number FR0167.

## SA0168

**Smad4 In Osteoclasts Reduce Bone Mass by Inhibiting Osteoclast Differentiation.** Mayu Morita<sup>\*1</sup>, Ryotaro Iwasaki<sup>2</sup>, Hiromasa Kawana<sup>2</sup>, Shigevuki Yoshida<sup>2</sup>, Taneaki Nakagawa<sup>2</sup>, Takeshi Miyamoto<sup>3</sup>. <sup>1</sup>DDS, Japan, <sup>2</sup>DDS, Ph.D, Japan, <sup>3</sup>MD, Ph.D, Japan

**Background:** Bone is constantly resorbed and formed throughout life by coordinated actions of osteoclasts and osteoblasts. There are many factors that balance between bone formation and bone resorption, and TGF $\beta$  and BMP2, which is categorized in TGF $\beta$  super family, are also cytokine of those factors. Smad4 is a transcriptional factor and downstream of TGF $\beta$  and BMP pathway. Smad4 was reportedly played pivotal roles for mesenchymal stem cell migration and bone formation, however, roles of Smad4 on osteoclasts remain largely unknown. Thus, objects of our study are to clarify the roles of Smad4 on osteoclasts differentiation.

**Methods:** For *in vitro* analysis, bone marrow cells isolated from wild-type mice were cultured for 72 h with M-CSF. Then, adherent cells were collected and cultured in 96-well plates with M-CSF and RANKL with or without TGF $\beta$ 1. Osteoclastogenesis was evaluated by TRAP staining, and TRAP-positive multi-nuclear cells containing more than three nuclei were scored as osteoclasts. Total RNAs were isolated from bone marrow cultures, and quantitative PCR was performed.

Osteoclast specific Smad4 conditional knockout mice (*Ctskerel+Smad4<sup>fl/fl</sup>*) were generated, and *Ctskerel+Smad4<sup>fl/fl</sup>* and control littermates were analyzed. 8 wk old mice were necropsied, and their hind limbs were removed, fixed with 70% ethanol, and subjected to DEXA analysis to measure bone mineral density and to bone histomorphometric analysis.

**Results:** TGF $\beta$ 1 inhibits osteoclastogenesis *in vitro*. Expression of the osteoclast differentiation markers *Ctsk* and *NFATc1* was significantly inhibited, and *Bcl6* and *Irf8* mRNA expression was upregulated following stimulation of wild-type osteoclasts with TGF $\beta$ 1. *Bcl6* and *Irf8* upregulation was significantly blocked in Smad4 cKO cells. *Bcl6*-deficient and *Irf8*-deficient cells were resistant to inhibition of osteoclastogenesis and suppression of osteoclastic gene expression by TGF $\beta$ 1. We found that Smad4 cKO mice exhibited significantly reduced bone mass compared with controls.

Our data demonstrate that Smad4 in osteoclasts is required to inhibit osteoclastogenesis through upregulating *Bcl6* and *Irf8*. Smad4 is required for maintaining bone mass *in vivo*.

**Disclosures:** Mayu Morita, None.

## SA0169

**Functional Role of Endothelin in Inflammatory Bone Loss.** Inik Chang<sup>\*</sup>, Sue Young Oh, Dong Min Shin. Yonsei University College of Dentistry, Korea, republic of

Chronic inflammation close to bone leads to loss of bone in inflammatory diseases. Periodontitis is a very common oral inflammatory disease and results in the destruction of supporting connective and osseous tissues of tooth. Although the etiology is still unclear, Gram-negative bacteria, especially *Porphyromonas gingivalis* in subgingival

pockets has been thought as one of the major etiologic agent. Endothelin (ET) is a family of three 21 amino acid peptides, ET-1, -2 and -3 that activate G-protein coupled receptors (ETRs), ET<sub>A</sub> and ET<sub>B</sub>. Expression of ET-1 and ETRs is detected in the periodontal tissues and the ET-1 levels in gingival crevicular fluid are increased in the periodontitis patients. Although it has been reported that ET regulates bone formation and osteoblastic bone metastases of certain solid tumors, little is known about its role in bone destruction. Therefore, in this study, we explored the function of ET as a critical regulator of inflammatory bone loss during periodontitis.

ET-1 and ET<sub>A</sub>, but not ET<sub>B</sub> were abundantly expressed in both human gingival epithelial cells (HGECs) and gingival fibroblasts (HGFs). Stimulation of HGECs with *P. gingivalis* increased the expression of ET-1 and ET<sub>A</sub> suggesting the activation of ET signaling pathway. Production of pro-inflammatory cytokines, IL-1 $\beta$ , IL-6, IL-8, and TNF $\alpha$  was significantly enhanced by the activation of ET-1/ET<sub>A</sub> in both HGECs and HGFs. Inhibition of the ET-mediated secretion of pro-inflammatory cytokines reduced the formation of osteoclasts suggesting the indirect involvement of ET in osteoclastogenesis via inflammatory cytokines. In addition, activation of ET-1/ET<sub>B</sub> signaling pathway augmented the number of multinucleated osteoclasts implicating its function as a direct stimulator of osteoclast differentiation.

Together, our study showed that *P. gingivalis*-mediated overproduction of ET-1 accelerates alveolar bone loss directly via the ET<sub>B</sub>-mediated acceleration of osteoclastogenesis and indirectly through the ET<sub>A</sub>-mediated production of pro-inflammatory cytokines. Currently, we are investigating the underlying molecular mechanisms of ET-mediated osteoclastogenesis. We are also examining the therapeutic effect of ETR inhibitors on the animal model of periodontitis.

**Disclosures:** Inik Chang, None.

## SA0170

See Friday Plenary Number FR0170.

## SA0171

**Selective Serotonin Reuptake Inhibitors (SSRIs) inhibit Ca<sup>2+</sup>-calmodulin/CREB/NFATc1 signaling in osteoclasts in a 5HTT-independent manner.** Maria Jose Ortuno<sup>\*</sup>, Subramanyam Venkata, Henry M. Colecraft, Patricia Ducy. Columbia University, United states

While long-term use of SSRIs is associated with bone loss and/or an increased risk of fracture, several clinical studies have reported that shorter treatments decrease bone resorption parameters. To better understand this latter effect mice were treated with fluoxetine for 3 weeks and analyzed by histomorphometry, microCT and gene expression assays. This short treatment caused an increase in bone mass associated with decreased osteoclasts number and function although the *Opg/Rankl* ratio was not changed. Yet, fluoxetine decreased the expression of genes encoding proteins controlling several key aspects of osteoclasts differentiation and function. This effect of fluoxetine on bone resorption was independent of 5HTT, the serotonin transporter mediating SSRIs canonical mode of action, as *5HTT<sup>-/-</sup>* mice responded to this drug as wild-type mice did. Instead, *in vitro* studies showed that fluoxetine directly inhibit multiple aspects of osteoclast biology by interfering with the Ca<sup>2+</sup>-calmodulin/CREB/NFATc1 pathway. Indeed, Fura-2 calcium imaging experiments showed that fluoxetine decreases intracellular Ca<sup>2+</sup> levels in multinucleated osteoclasts. Moreover, treatment with W5, a selective antagonist of Ca<sup>2+</sup>-calmodulin signaling or reducing *Creb* expression through gene inactivation reproduced and abolished the effect of fluoxetine on the expression of osteoclast differentiation markers as well as on their resorptive ability.

A similar inhibition of Ca<sup>2+</sup> signaling by fluoxetine was previously reported in Jurkat T lymphocytes. Accordingly, expression of *Creb* and *NFAT* but also of *ROR $\gamma$ 1*, the gene encoding the master regulator of lymphocyte Th17 differentiation and a key component of the osteoimmune crosstalk, was reduced in the spleen of fluoxetine-treated mice. Thus, our study uncovered a direct inhibitory effect of fluoxetine on Ca<sup>2+</sup>/NFATc1 signaling in osteoclasts that could also affect Th17 lymphocyte activation and may explain the beneficial effect of SSRIs on osteoarthritis.

**Disclosures:** Maria Jose Ortuno, None.

## SA0172

See Friday Plenary Number FR0172.

## SA0173

See Friday Plenary Number FR0173.

## SA0174

See Friday Plenary Number FR0174.

## SA0175

See Friday Plenary Number FR0175.

## SA0176

See Friday Plenary Number FR0176.

**SA0177**

See Friday Plenary Number FR0177.

**SA0178**

See Friday Plenary Number FR0178.

**SA0179**

See Friday Plenary Number FR0179.

**SA0180**

See Friday Plenary Number FR0180.

**SA0181**

See Friday Plenary Number FR0181.

**SA0182**

See Friday Plenary Number FR0182.

**SA0183**

See Friday Plenary Number FR0183.

**SA0184**

**Occurrence of apoptosis in cementocytes.** Katharina Oliveira\*, Raquel Silva, Marcio Beloti, Alberto Consolaro, Lea Silva. University of São Paulo, Brazil

Background: The cementoblast is a cell type that lines the apical portion of the root surface of the tooth, playing an important role in protecting the root resorption. In turn, cementocytes are cells very similar to the osteocytes, and represent imprisoned cementoblasts at the cementum matrix during its formation. It has been shown in the literature that Thiazolidinediones (TZD), a class of medication for diabetes control, leads to increased apoptosis in osteocytes. Aim: The aim of this study was to demonstrate, in vivo, the occurrence of apoptosis on cementocytes after a TZD (Rosiglitazone) administration compared to wild type mice. Methods: Briefly, twenty four male C57BL/6 mice were divided into three groups: 1 control, which received only the vehicle administration via oral for 1 week (PBS + DMSO 10%) and other two groups, which received 10 mg/kg of Rosiglitazone + PBS + DMSO 10% for 1 or 2 weeks, respectively. Upon completion of the time courses, mice were killed by CO<sub>2</sub>, and the mandibles were dissected and subjected to routine histotechnical processing. The sections were analyzed through transferase-mediated dUTP nick-end labeling (TUNEL) and 4',6-diamidino-2-phenylindole (DAPI) staining of nuclear morphology ( $\alpha=0.05$ ). Results: The control group showed significantly lower apoptotic cells/total cells ratio, when compared to the experimental groups, in TUNEL and DAPI techniques ( $p = 0.01$  and  $p = 0.004$ , respectively). Conclusion: Despite the significant difference between the control and experimental groups, this is the first study that demonstrates the apoptosis in cementocytes, induced by the TZD and also as a physiological phenomenon. This fact may help to clarify other relationships between this cell type and other bone cells that remains unknown.

*Disclosures: Katharina Oliveira, None.*

**SA0185**

See Friday Plenary Number FR0185.

**SA0186**

**Cinacalcet hydrochloride increases bone strength in patients with renal hyperparathyroidism.** Aiji Yajima\*<sup>1</sup>, Ken Tsuchiya<sup>1</sup>, Yasuo Imanishi<sup>2</sup>, Masaaki Inaba<sup>2</sup>, Yoshihiro Tominaga<sup>3</sup>, Tatsuhiko Tanizawa<sup>4</sup>, Akemi Ito<sup>5</sup>, Kosaku Nitta<sup>1</sup>. <sup>1</sup>Kidney Center, Medicine, Tokyo Women's Medical University, Japan, <sup>2</sup>Department of Metabolism, Endocrinology & Molecular Medicine, Osaka City University Graduate School of Medicine, Japan, <sup>3</sup>Department Endocrine Surgery, Nagoya Second Red Cross Hospital, Japan, <sup>4</sup>Tanizawa Clinic, Orthopedic Surgery, Japan, <sup>5</sup>Ito Bone Histomorphometry Institute, Japan

Background: Reduction in osteocyte density leads to accumulation of microcracks, resulting in increased bone fragility in both human (Qiu S. J Bone Miner Res 2005) and mouse (Ikeda K. Geriatr Gerontol Int 2008). And osteocyte lacunae after osteocyte death became filled by mineralized matrix, resulting in increased micropetrosis area if serum parathyroid hormone (PTH) levels were maintained low (Yajima A. J Bone Miner Res 2010, Frost HM. J Bone Joint Surg Am 1960). Microcracks appear to

progress in micropetrosis area, increasing the fracture rate (Qiu S. Bone 2005). Osteocyte number in micropetrosis area and in the other area was measured before and after total parathyroidectomy with immediate autotransplantation (parathyroidectomy) and treatment with cinacalcet hydrochloride (HCL) in patients with renal hyperparathyroidism.

Methods: Eighteen dialysis (HD) patients received parathyroidectomy and transiliac bone biopsies before and at 2-9 weeks after parathyroidectomy (Group I). And eight HD patients with renal hyperparathyroidism were treated by cinacalcet HCL and received bone biopsies before and at 1 year after the treatment (Group II). Osteocyte number in micropetrosis area (N.Ot/Mp.V;N/mm<sup>2</sup>) and in the other area (N.Ot/(BV-Mp.V);N/mm<sup>2</sup>) were measured before and after the treatment.

Results: Serum intact PTH (i-PTH) levels decreased from 1331.6 ± 623.2 to 17.1 ± 19.8 pg/ml after parathyroidectomy. N.Ot/Mp.V was decreased from 162.8 ± 73.4 to 108.3 ± 83.8 N/mm<sup>2</sup> ( $P<0.001$ ), and N.Ot/(BV-Mp.V) was not changed from 245.1 ± 68.2 to 265.1 ± 74.5 N/mm<sup>2</sup> after parathyroidectomy (Group I). Serum i-PTH levels decreased from 903.6 ± 503.0 to 212.7 ± 98.1 pg/ml after the treatment with cinacalcet HCL. N.Ot was not changed in both micropetrosis area (100.1 ± 68.2 to 99.6 ± 76.1 N/mm<sup>2</sup>) and in the other area (240.1 ± 56.3 to 279.6 ± 88.6 N/mm<sup>2</sup>) after the treatment (Group II).

Conclusion: Cinacalcet HCL did not reduce osteocyte number in both micropetrosis area and in the other area, suggesting that this agent improves bone strength by maintaining osteocytic perilacunar/canalicular system. Osteocyte number decreased after parathyroidectomy for renal hyperparathyroidism in HD patients (Yajima A. J Bone Miner Res 2010). Parathyroidectomy reduces osteocyte number in only the micropetrosis area.

*Disclosures: Aiji Yajima, None.*

**SA0187**

See Friday Plenary Number FR0187.

**SA0188**

**Establishing reference intervals of serum 24,25-dihydroxyvitamin D and 25-hydroxyvitamin D-to-24,25-dihydroxyvitamin D ratio by LC-MS/MS.** Jonathan Tang\*<sup>1</sup>, Holly Nicholls<sup>1</sup>, Isabelle Picc<sup>1</sup>, Christopher Washbourne<sup>1</sup>, John Dutton<sup>1</sup>, Sarah Jackson<sup>2</sup>, Julie Greeves<sup>2</sup>, William Fraser<sup>1</sup>. <sup>1</sup>University of East Anglia, United Kingdom, <sup>2</sup>HQ Army Recruiting & Training Division, United Kingdom

Background: 24,25-dihydroxyvitamin D (24,25-d(OH)D) is converted from 25-hydroxyvitamin D (25(OH)D) by 24-hydroxylase. Recent studies suggest the production of 1,25-dihydroxyvitamin D (1,25-d(OH)D) from 25(OH)D is driven by the catabolism of 24,25-d(OH)D. Genetic mutations resulting in loss-of-function of the CYP24A1 gene are associated with hypercalcaemic conditions. We developed a liquid chromatography tandem mass spectrometry (LC-MS/MS) assay to measure simultaneously 24,25-d(OH)D and 25(OH)D to investigate vitamin D status and metabolism.

Objective: Using a LC-MS/MS method, we aim to establish from a large cohort healthy individuals: 1) the reference interval of serum 24,25-(OH)<sub>2</sub>D; 2) the expected ratio of serum 25(OH)D to 24,25-(OH)<sub>2</sub>D; 3) 24,25-(OH)<sub>2</sub>D cut-off value for 24,25-(OH)<sub>2</sub>D at the clinically significant change between inadequate and sufficient 25(OH)D status.

Method: Prior to LC-MS/MS analysis 100µL of sample was extracted using [<sup>2</sup>H<sub>6</sub>]-24,25-dihydroxyvitamin D<sub>3</sub> as internal standard, the method involved a derivatisation step to enhance ionisation efficiency. The reference intervals of serum 24,25-d(OH)D was determined in samples obtained from 1996 healthy individuals, (mean (±SD) age 25(±2) yr, BMD T-score 1.2(±0.1), mean serum [25(OH)D] 63.7(±29.4) nmol/L, parathyroid hormone (PTH) 1.6-6.9 pmol/L, adjusted calcium 2.2-2.6 mmol/L).

Results: The LC-MS/MS assay achieved adequate sensitivity, precision, and demonstrable reproducible recovery to satisfy industry method validation criteria. We found concentrations of 24,25(OH)<sub>2</sub>D<sub>3</sub> exhibited a positive, concentration-dependent relationship which correlated with serum 25(OH)D<sub>3</sub>: [24,25(OH)<sub>2</sub>D<sub>3</sub>] = 0.1 x [25(OH)D<sub>3</sub>] - 0.64;  $r^2 = 0.754$ . In contrast, the 25(OH)D<sub>3</sub>:24,25(OH)<sub>2</sub>D<sub>3</sub> ratio showed an indirect relationship with 25(OH)D<sub>3</sub> that was significantly elevated ( $p<0.001$ ) at 25(OH)D concentration <50 nmol/L. We established reference intervals of normal 25(OH)D<sub>3</sub>:24,25(OH)<sub>2</sub>D<sub>3</sub> ratio is 7-20. Serum 24,25(OH)<sub>2</sub>D concentration of >4.2 nmol/L was identified as diagnostic cut-off for 25(OH)D replete.

Conclusion: The reference intervals we established for 25(OH)D:24,25-(OH)<sub>2</sub>D ratio and 24,25-(OH)<sub>2</sub>D cut-off value for 25(OH)D replete provide guidance to clinicians in the diagnosis of patients with an altered state vitamin D catabolism, thus facilitate investigations into the underlying causes and possibly help decide on the best course of treatment.

*Disclosures: Jonathan Tang, None.*

**SA0189**

**Relationship Between Serum Levels of Fibroblast Growth factor 23 (FGF23) and Osteoporotic Fracture Risk in Postmenopausal Women with Chronic Kidney Disease Stage G2.** Mika Yamauchi\*<sup>1</sup>, Kiyoko Nawata<sup>2</sup>, Masahiro Yamamoto<sup>1</sup>, Toshitsugu Sugimoto<sup>1</sup>. <sup>1</sup>Internal Medicine 1, Shimane University Faculty of Medicine, Japan, <sup>2</sup>Health & Nutrition, The University of Shimane, Japan

Objective: Fibroblast growth factor 23 (FGF23) is secreted by osteocytes and is involved in phosphate (P) metabolism. Increases in this factor are known to occur

with decreased renal function. Moreover, it has been reported that the presence of high levels of fibroblast growth factor 23 (FGF23) is a risk factor for osteoporotic fracture in elderly men. The aim of the present study was to elucidate the association between FGF23 and osteoporotic fracture in postmenopausal women.

**Material and Methods:** We enrolled 190 postmenopausal women who were undergoing examination for osteoporosis. Serum levels of Ca, P, Cr, PTH, 25-hydroxy vitamin D [25(OH)D], FGF23, PINP, CTX and sclerostin were measured. The BMD of the lumbar spine (L2-4) and femoral neck (FN) was measured using dual-energy X-ray absorptiometry, the presence or absence of morphological vertebral fracture was determined, and the presence or absence of existing non-vertebral fracture was determined through physician interviews.

**Results:** Mean values of age were  $63.2 \pm 7.5$  years, and their BMI was  $22.9 \pm 3.1$  kg/m<sup>2</sup>. The mean values of measured variables were: Ca  $9.1 \pm 0.3$  mg/dL, P  $3.5 \pm 0.4$  mg/dL, Cr  $0.58 \pm 0.10$  mg/dL, 25(OH)D  $16.0 \pm 4.2$  ng/mL, FGF23  $33.9 \pm 9.1$  pg/mL, PINP  $54.0 \pm 16.6$  ng/mL, CTX  $0.401 \pm 0.150$  ng/mL and sclerostin  $1.30 \pm 0.46$  ng/mL. Mean BMD value were  $0.839 \pm 0.149$  g/cm<sup>2</sup> (T score  $-1.6 \pm 1.3$ ) at L2-4, and  $0.621 \pm 0.090$  ( $-1.5 \pm 0.8$ ) at FN. FGF23 levels showed significantly positive correlations with BMI, serum levels of P, Cr and L2-4 BMD and negative correlation with PINP. FGF23 was not significantly different between subjects with and without vertebral fractures and between subjects with and without nonvertebral fractures. Since FGF23 is linked to renal function, further analysis was conducted by the patients' chronic kidney disease (CKD) stage. In group of subjects with CKD Stage G2 (eGFR: 60-89 mL/min/1.73 m<sup>2</sup>), FGF23 was significantly elevated in subjects with nonvertebral fractures ( $p < 0.05$ ), but not in those with vertebral fractures. Logistic regression analysis identified FGF23 as a significant risk factor for nonvertebral fracture, even after adjusted for age, BMI, Ca, P, Cr, PTH, 25(OH)D, CTX, sclerostin and BMD [odds ratio: 1.89(95%CI:1.07-3.34),  $p < 0.05$ ].

**Conclusion:** This study showed that increased levels of FGF23 is a risk factor for nonvertebral fracture in postmenopausal women with early stage of CKD.

**Disclosures:** Mika Yamauchi, None.

## SA0190

**Serum osteoprotegerin is a marker of both fracture and cardiovascular risk in older men – the prospective STRAMBO study.** Pawel Szulc\*<sup>1</sup>, Lorenz C Hofbauer<sup>2</sup>, Roland Chapurlat<sup>1</sup>. <sup>1</sup>INSERM UMR 1033, University of Lyon, Hospices Civils de Lyon, France, <sup>2</sup>Universitätsklinikum Carl Gustav Carus, Technische Universität Dresden, Germany

Fragility fractures and major adverse cardiac and cerebrovascular events (MACCE) often occur in one person. However, data on shared biological markers are scarce. We assessed the utility of serum OPG to predict fragility fracture and MACCE in men. In a cohort of 817 men aged 60-87, serum OPG was measured at baseline (ELISA Biomedica). Bone mineral density (BMD) and trabecular bone score (TBS) were assessed by DXA. BMD- and TBS-adjusted FRAX for major osteoporotic fracture (MOPFx) was calculated on the FRAX website. Over 8 yrs of prospective follow-up, 101 men had incident fragility fracture (vertebral fracture in 47, non-vertebral fracture in 61, MOPFx in 62) and 87 men had incident MACCE (acute coronary syndrome, stroke, sudden death).

After adjustment for FRAX, higher OPG levels were associated with higher risk of fragility fracture (HR= 1.34 per SD, 95%CI: 1.11-1.61,  $p < 0.005$ ). Fracture incidence was higher in the fourth OPG quartile compared to three lower quartiles (Q1- 11%, Q2- 12%, Q3- 12%, Q4- 18%). After adjustment for FRAX, fracture risk was twofold higher in the highest OPG quartile vs. three lower quartiles combined (HR= 1.98, 95%CI: 1.31-2.99,  $p < 0.005$ ). A similar pattern was found for vertebral fracture, MOPFx and non-vertebral fracture analyzed separately, e.g., non-vertebral fracture risk was higher in the highest OPG quartile vs. the three lower quartiles combined (HR= 2.38, 95%CI: 1.43-3.96,  $p < 0.005$ ). In the analysis limited to the men with FRAX for MOPFx of less than 15%, higher OPG levels were associated both with higher risk of all fragility fractures (HR= 1.29 per SD, 95%CI: 1.06-1.58,  $p < 0.05$ ) and of various fracture subgroups (e.g., vertebral fracture: HR= 1.49 per SD, 95%CI: 1.10-2.02,  $p < 0.01$ ).

After adjustment for age, weight, lifestyle and cardiovascular risk factors, higher OPG levels were associated with higher risk of MACCE (HR= 1.39 per SD, 95%CI: 1.09-1.77,  $p < 0.01$ ). The incidence of MACCE increased across the OPG quartiles (Q1- 5%, Q2- 8%, Q3- 9%, Q4- 16%). After adjustment for confounders, the risk of MACCE was higher in the highest OPG quartile vs. the lowest one (HR= 2.73, 95%CI: 1.06-7.03,  $p < 0.05$ ).

Thus, the older men with higher OPG levels are at increased risk of both fragility fracture and MACCE after adjustment for relevant confounders. Our data corroborate the role of OPG as a risk factor for bone and vascular health. OPG measurement may improve identification of older men at increased cardiovascular and fracture risk.

**Disclosures:** Pawel Szulc, None.

## SA0191

**25-Hydroxyvitamin-D Concentration and Bone Mineral Density as Predictors of Fragility Fracture in a Bone Health Clinic.** Matthew McCarley\*, Gordon Klein, Kelsey L. Wise, Ronald W. Lindsey. University of Texas Medical Branch, United states

**Purpose.** The literature is conflicting regarding whether 25-hydroxyvitamin-D (25(OH)D) serum concentration and dual-energy x-ray absorptiometry (DEXA) T-score can predict fragility fracture. We hypothesized that each would be lower in patients who had sustained a fragility fracture prior to initial presentation vs those who had not.

**Methods.** We reviewed the charts of 102 patients who presented to our institution's bone health clinic from 11/2013 through 02/2016 and who had initial-visit 25(OH)D results. Other initial-visit data recorded were DEXA T-score (n=92); history of fragility fracture (yes 64, no 38); sex (11M, 91F); age (range 50-92 yr); race; body mass index (BMI); smoking history; corticosteroid use; presence of rheumatoid arthritis (RA); and presence of diabetes mellitus (DM). We compared the fracture group patients with regard to 25(OH)D concentration and DEXA T-score based on number of fractures sustained and whether they had sustained a hip fracture prior to initial presentation. Discrete data were compared using t-test or Chi-square tests; continuous data were compared using Pearson correlation.

**Results.** The mean 25(OH)D values were similar in the fracture and non-fracture groups ( $37.12 \pm 17.02$  vs  $38.55 \pm 16.42$  ng/mL;  $p = 0.676$ ), as were the mean DEXA T-scores ( $-2.28 \pm 1.33$  vs  $-1.82 \pm 1.1$ ;  $p = 0.075$ ). The groups did not statistically differ with regard to demographic variables or risk factors. Patients with RA (n=7) had a lower mean 25(OH)D value (mean  $22.57 \pm 8.46$  vs  $38.77 \pm 16.67$ ;  $p = 0.001$ ). BMI inversely correlated with 25(OH)D concentration (Pearson correlation coefficient (R)=-0.211,  $p = 0.033$ ). Age inversely correlated with T-score (R=-0.269,  $p = 0.009$ ), whereas BMI directly correlated with T-score (R=0.259,  $p = 0.013$ ). The other demographic variables and risk factors studied were not significantly associated with either 25(OH)D or T-score. Within the fracture group, the mean T-score was lower for patients who had sustained a hip fracture (n=15) compared with those who had sustained a fragility fracture elsewhere ( $-3.12 \pm 1.02$  vs  $-2.03 \pm 1.32$ ;  $p = 0.004$ ), but their mean 25(OH)D values did not differ ( $34.33 \pm 25.49$  vs  $37.98 \pm 13.69$ ;  $p = 0.602$ ). There was no significant difference in 25(OH)D concentration ( $39.23 \pm 19.87$  vs  $36.59 \pm 16.39$ ;  $p = 0.664$ ) or T-score ( $-1.94 \pm 1.48$  vs  $-2.37 \pm 1.29$ ;  $p = 0.375$ ) between those patients who had sustained multiple fragility fractures compared with those who had sustained only one.

**Conclusions.** In this cohort of patients referred to a bone health clinic, serum 25(OH)D concentration and DEXA T-score did not distinguish those who had sustained a fragility fracture from those who had not. Patients with RA and those with higher BMI had a lower serum 25(OH)D concentration. Among patients with a prior fragility fracture, those with a prior hip fracture had lower bone density. Obesity may confound the reliability of 25(OH)D as a predictor of fragility fracture.

**Disclosures:** Matthew McCarley, None.

## SA0192

Withdrawn

## SA0193

**Evaluation of Trabecular Bone Score in Patients with a Distal Radius Fracture.** Hyun Sik Gong\*. Department of Orthopedic Surgery, Seoul National University College of Medicine, Korea, republic of

**Background:** The trabecular bone score (TBS) is associated with vertebral and non-vertebral fractures in postmenopausal women and may have value for assessing microarchitectural deterioration other than low bone mass. Limited TBS data are available on patients with a distal radius fracture (DRF), which often occurs in the osteopenic or normal bone mineral density (BMD) ranges. We aimed to determine whether TBS has additive value for predicting DRF independent of BMD.

**Methods:** We compared BMD and TBS in 269 women with a DRF with age- and BMI-matched control patients who had no history of osteoporotic fracture. BMD was measured at the lumbar spine and femur using DEXA scans, TBS was calculated on the same spine image, and the differences in BMD and TBS were assessed between the groups. A multivariate logistic regression analysis was used to analyze the odds ratio (OR) for the occurrence of DRF using age, BMI, lumbar spine BMD, total femoral BMD, and TBS.

**Results:** Patients with a DRF had significantly lower femoral BMD (neck, trochanter, and total) than that of control patients ( $p = 0.004$ , 0.001, and 0.010, respectively). However, lumbar spine BMD and TBS were not significantly different between the groups ( $p = 0.367$  and 0.708, respectively). The multivariate analysis indicated that only total femoral BMD was significantly associated with the occurrence of DRF (OR, 1.102; 95% confidence interval, 0.018–0.569;  $p = 0.009$ ).

**Conclusion:** TBS was not different between women with a DRF and those without a history of osteoporotic fracture, suggesting that TBS measured at the lumbar spine does not reflect early microarchitectural changes of the distal radius. Femoral BMD is a reliable indicator of bone fragility in patients with a DRF.

**Disclosures:** Hyun Sik Gong, None.

## SA0194

**Patients with Klinefelter syndrome have severe bone microarchitecture impairment: the KLINOS study.** Cyrille CONFAVREUX<sup>\*1</sup>, Anne PIOT<sup>2</sup>, Pawel SZULC<sup>3</sup>, Justine BACCHETTA<sup>2</sup>, Sylviane AILLOUD<sup>4</sup>, Hervé LEJEUNE<sup>5</sup>, Roland CHAPURLAT<sup>2</sup>, Stéphanie BOUTROY<sup>3</sup>, Ingrid PLOTTON<sup>6</sup>. <sup>1</sup>INSERM UMR1033 – LYOS - Université de Lyon - Hospices Civils de Lyon, France, <sup>2</sup>INSERM UMR1033 – LYOS - Université de Lyon, Hospices Civils de Lyon, France, <sup>3</sup>INSERM UMR1033 – LYOS - Université de Lyon, France, <sup>4</sup>Hospices Civils de Lyon, France, <sup>5</sup>Reproductive Medicine Department, Hospices Civils de Lyon, France, <sup>6</sup>INSERM UMRS1208 INRA- StemGame - Université de Lyon - Department of Molecular Hormonology & Endocrinology, Hospices Civils de Lyon, France

Klinefelter syndrome (KS) is a frequent disease due to the karyotype disorder XXY (1/660 male births). Patients with KS have an increased incidence of hip fracture and a prevalence of osteoporosis of about 40%. Data on bone microarchitecture are scarce in KS patients and we aimed to analyze it in vivo by high resolution peripheral quantitative tomography (HRpQCT). Non-mosaic KS patients included in the French Research Fertility Program were included before introduction of androgen therapy. They underwent assessment of areal BMD at lumbar spine and hip as well as whole body composition by DXA (DiscoveryA, Hologic®) and bone microarchitecture at distal tibia and distal radius by HR-pQCT (XtremeCT, Scanco Medical AG®). Each patient was age-matched with three healthy men from the STRAMBO cohort. Statistical analyses were adjusted for height and body weight. Twenty-two patients with KS and 66 healthy controls were included in this analysis. Mean ( $\pm$ SD) age and body mass index of KS patients were  $29 \pm 7$  years and  $23.2 \pm 4.4$  kg/m<sup>2</sup>. None of the subjects had fracture history. 36% of KS patients had low serum total testosterone (<10nmol/L). Relative appendicular lean mass was lower in KS than controls ( $7.5 \pm 1.3$  vs  $8.9 \pm 1.0$  kg/m<sup>2</sup>;  $p < 0.001$ ). Lumbar spine and total hip areal BMD were significantly lower in KS patients than controls:  $0.94 \pm 0.16$  vs  $1.08 \pm 0.14$  g/cm<sup>2</sup> and  $0.83 \pm 0.16$  vs  $0.98 \pm 0.14$  g/cm<sup>2</sup> respectively ( $p < 0.01$ ). At the tibia (figure 1), trabecular bone was impaired as reflected by a lower volumetric density:  $193 \pm 39$  vs  $225 \pm 34$  mg/cm<sup>3</sup> ( $p < 0.001$ ) and trabecular number:  $1.86 \pm 0.25$  vs  $2.03 \pm 0.29$  ( $p < 0.05$ ). KS patients also had a 24% thinner cortex at the tibia compared to healthy controls (cortical thickness:  $1.13 \pm 0.30$  vs  $1.48 \pm 0.27$   $\mu$ m;  $p < 0.001$ ). By contrast, distal radius microarchitecture was not significantly different between KS patients and controls. In young KS patients, naïve of androgen therapy, we observed lower areal and volumetric BMD and severely impaired trabecular and cortical bone microarchitecture at the weight-bearing distal tibia. This study will allow for the analysis of bone microarchitecture impairment according to testosterone serum levels in KS patients.

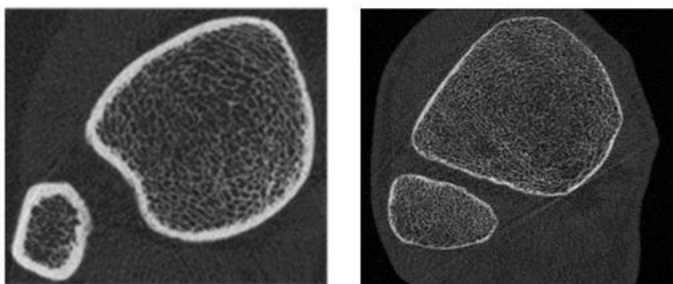


Figure 1: illustrative sections of distal tibia microarchitecture by HR-pQCT in a healthy subject (left) and a Klinefelter syndrome patient (right)

Figure 1

**Disclosures:** Cyrille CONFAVREUX, None.

This study received funding from: Research Grant from Roche Chugai

## SA0195

**The trabecular bone score reflects bone microarchitecture at the peripheral skeleton in kidney transplant recipients.** Matthew Luckman<sup>\*1</sup>, Didier Hans<sup>2</sup>, Natalia Cortez<sup>3</sup>, Kyle Nishiyama<sup>3</sup>, Sanchita Agarwal<sup>4</sup>, Lucas Nikkel<sup>5</sup>, Sapna Iyer<sup>6</sup>, Chengchen Zhang<sup>3</sup>, Edward Guo<sup>3</sup>, Donald McMahon<sup>3</sup>, Elizabeth Shane<sup>3</sup>, Tom Nickolas<sup>3</sup>. <sup>1</sup>Department of Human Nutrition, Columbia University, United states, <sup>2</sup>Lausanne University, Switzerland, <sup>3</sup>Columbia University, United states, <sup>4</sup>Columbia University, United states, <sup>5</sup>University of Rochester, United states, <sup>6</sup>Kaiser Health Center, United states

Fractures, particularly at the peripheral skeleton, are 4-fold more common after kidney transplantation than in the general population. We previously used high-resolution peripheral quantitative computed tomography (HRpQCT) to demonstrate that progressive abnormalities in trabecular (Tb) and cortical (Ct) microarchitecture and strength occur over the first year of kidney transplantation. However, HRpQCT is a research tool lacking wide availability. In contrast, the trabecular bone score (TBS) is a novel and widely available tool that uses gray-scale variograms of the

lumbar spine (LS) image from dual energy X-ray absorptiometry (DXA) to assess Tb quality. No studies have investigated whether TBS characterizes bone quality in kidney transplant recipients. We hypothesized that LS TBS would be related to measures of Tb quality measured at the ultradistal radius and tibia by HRpQCT, and that during the first year of transplantation changes in TBS would reflect the evolution of Tb and Ct microarchitecture and strength. In 47 patients (33 men, age  $51 \pm 14$  years) we measured LS TBS, bone mineral density (BMD) by DXA at the LS, total hip (TH) and forearm, and bone geometry, mass, microarchitecture and strength at the radius and tibia by HRpQCT with finite element analysis pre- and 3-, 6- and 12-months post-transplantation. Spearman correlations determined relationships between TBS, DXA and HRpQCT. Mixed models determined how percent changes in TBS and in LS and TH BMD predicted percent changes in HRpQCT parameters. At baseline, TBS correlated with: LS, TH and ultradistal radius BMD; Ct area, density and thickness, Tb density, thickness, separation and heterogeneity, and stiffness and failure load at the radius; and Ct area, density and porosity at the tibia (Table 1). Over the first year of transplantation, each percent decrease in TBS was associated with decreases in Tb area ( $-0.04 \pm 0.02\%$ ) and number ( $-0.35 \pm 1.4\%$ ), and increases in Tb thickness ( $0.45 \pm 0.15\%$ ), separation ( $0.40 \pm 0.15\%$ ) and network heterogeneity ( $0.48 \pm 0.20\%$ ) at the radius, and decreases in Tb area ( $-0.02 \pm 0.01\%$ ) and failure load ( $-0.22 \pm 0.09\%$ ) at the tibia (all  $p < 0.05$ ). Changes in LS and TH BMD did not predict changes in HRpQCT. In conclusion, TBS was a marker of Tb and Ct bone quality and strength and changes in TBS reflected changes in Tb bone quality at the peripheral skeleton. TBS may be a useful tool to assess and monitor both bone quality and strength and fracture risk after kidney transplantation.

	Lumbar Spine	Total Hip	Forearm	Radius	Tibia	LS BMD	TH BMD	Forearm BMD	Radius BMD	Tibia BMD	Tb Area	Tb Density	Tb Number	Tb Thickness	Tb Separation	Tb Heterogeneity	Stiffness	Failure
TBS	0.60	0.58	0.10	0.10	0.30	0.40	-0.01	0.20	0.40	-0.01	0.37	0.20	0.40	-0.37	0.30	0.40	0.40	0.40
Stiffness	0.60	0.58	0.10	0.10	0.30	0.40	0.01	0.20	0.40	0.01	0.37	0.20	0.40	-0.37	0.30	0.40	0.40	0.40
Failure	0.60	0.58	0.10	0.10	0.30	0.40	0.01	0.20	0.40	0.01	0.37	0.20	0.40	-0.37	0.30	0.40	0.40	0.40

Table 1

**Disclosures:** Matthew Luckman, None.

## SA0196

See Friday Plenary Number FR0196.

## SA0197

**Validation study of a new ultrasonic device targeting cortical bone by HR-pQCT.** Ko Chiba<sup>\*1</sup>, Ryoichi Suetoshi<sup>2</sup>, Narihiro Okazaki<sup>3</sup>, Avako Kurogi<sup>3</sup>, Tatsuo Arai<sup>2</sup>, Takeshi Kawajiri<sup>2</sup>, Shuntaro Sato<sup>4</sup>, Makoto Osaki<sup>3</sup>. <sup>1</sup>Department of Orthopaedic Surgery, Nagasaki University Hospital, Japan, <sup>2</sup>Technology Development & Researching Laboratory, Furuno Electric Co., Ltd, Japan, <sup>3</sup>Department of Orthopaedic Surgery, Nagasaki University Hospital, Japan, <sup>4</sup>Clinical Research Center, Nagasaki University Hospital, Japan

**Introduction:**

Quantitative ultrasound (QUS) is a simple, non-invasive bone densitometer without radiation exposure. QUS mainly evaluates cancellous bones of the calcaneus, although cortical bone is now thought to be more important to determine bone fragility. We developed a new ultrasonic device using high frequency (3MHz) targeting cortical bones measuring the cortical speed of sound (cSOS) at the diaphysis of the tibia and radius.

The purpose of this study is to investigate what type of structural and material properties of cortical bone the cSOS reflects by using high-resolution peripheral quantitative CT (HR-pQCT).

**Methods:**

In 19 volunteers (aged 33-73, 2 males and 17 females), cortical speed of sound (cSOS) at the mid-tibia and radius was measured by the new ultrasonic device (Furuno Electric Co., Ltd, Japan). Cortical bone parameters (Ct.Th, Ct.Po, Ct.BMD) at the same site were analyzed by HR-pQCT (XtremeCT II, Scanco, Switzerland). Areal bone mineral density (aBMD) at the lumbar spine and proximal femurs were measured by DXA. Finally, the correlations with each parameter were analyzed.

**Results:**

cSOS had a strong correlation with Ct.BMD measured by HR-pQCT ( $R = 0.826$ ,  $P < 0.001$ ). There were no correlations between cSOS and DXA parameters.

**Conclusions:**

cSOS measured by the new ultrasonic device may evaluate bone qualities of cortical bones since Ct.BMD is a parameter depending on the mineralization of cortical bones and cortical porosities.

## SA0199

**Analyzing the cortical and trabecular bone of type 1 diabetes patients using 3D-DXA – a longitudinal study.** Ludovic Humbert<sup>1</sup>, Martin Keil<sup>2</sup>, Gabriele Lehmann<sup>3</sup>, Alexander Sämam<sup>2</sup>, Roger Fonolla<sup>1</sup>, Thomas Neumann<sup>2</sup>. <sup>1</sup>Galgo Medical, Spain, <sup>2</sup>Department of Internal Medicine III, Jena University Hospital, Germany, <sup>3</sup>Institute of Medical Statistics, Computer Sciences & Documentation, Jena University Hospital, Germany

This study aims to analyze the changes in cortical and trabecular bone in patients with type 1 diabetes after a 7-years follow-up.

85 patients (43 men and 42 women, age at study entry  $44.0 \pm 8.8$  years) with type 1 diabetes (duration  $21.8 \pm 10.4$  years) were included in this study. DXA scans (Lunar Prodigy scanner, GE Healthcare, Madison, WI) were acquired at baseline and after at 7-years follow-up. Left and right femur DXA scans were acquired for most of the patients, resulting in a total of 168 scans at baseline and 168 scans at follow-up. The 3D-DXA software (Galgo Medical, Barcelona, Spain) was used to analyze the changes in cortical and trabecular bone between baseline and follow-up. 3D-DXA registers a 3D appearance model of the femoral shape and density onto the DXA projection to obtain a 3D subject-specific model of the femur of the patient and quantify the volumetric BMD (vBMD), volume (for trabecular and cortical regions) and cortical thickness distribution. The 3D-DXA measurements at baseline and 7-years follow-up were compared using paired samples Student's t-test.

A statistically significant increase of the weight of the patients was found after the 7-years follow-up ( $81.8 \pm 17.8$  kg) in comparison with baseline ( $78.5 \pm 16.0$  kg,  $p < 0.001$ ). A statistically significant decrease of the integral vBMD ( $-5.7$  mg/cm<sup>3</sup>,  $-1.7\%$ ,  $p < 0.001$ ) and trabecular vBMD ( $-5.8$  mg/cm<sup>3</sup>,  $-3.6\%$ ,  $p < 0.001$ ) was observed at the total femur region of interest. Regarding the cortical layer, neither the vBMD of the cortex nor the cortical thickness showed statistically significant change between baseline and follow-up. A statistically significant increase of the volume of the proximal femur was found ( $+2.3$ cm<sup>3</sup>,  $+2.7\%$ ,  $p < 0.001$ ), corresponding to an outward displacement of the cortical surface.

The 3D-DXA analysis of the 85 with type 1 diabetes included in this study showed a statistically significant decrease of the vBMD of the trabecular bone, together with an outward cortical displacement, with no statistically significant change in terms of cortical thickness and density.

**Disclosures:** Ludovic Humbert, None.

## SA0200

**Bone structural components and lean mass assessed by 3D-DXA in Hip Fracture Patients.** Luis Del Rio<sup>1</sup>, Silvana Di Gregorio<sup>1</sup>, Patricia Sanchez<sup>2</sup>. <sup>1</sup>MD, Spain, <sup>2</sup>CTD, Spain

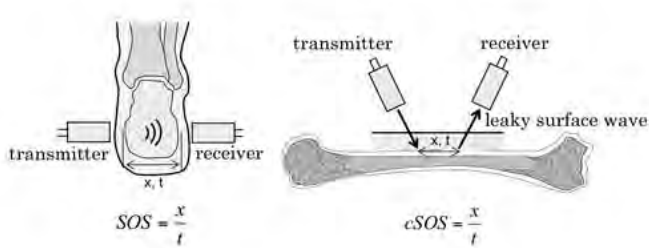
Bone mass, macrostructure and lean mass are being identified as main contributors of strength of upper femur. The purpose of this study has been to assess the role of the cortical and trabecular bone as well as muscle mass in the hip fracture production. We used a new DXA application which allow 3D bone volume reconstruction from standard 2D DXA scans, providing a three dimensional approach of the femoral shape and bone density spatial distribution and measurement cortical thickness. The purpose of this study was to analyze these measurements in a cohort of elderly patients suffering a recent hip fracture.

Methods: A prospective study was carried out to collect scans from 96 patients of both sexes, older of 75 years, who have suffered a hip fracture indoor in a shorter interval of 2 weeks. None of the patients had osteoporotic fracture history at baseline. 3D-DXA technology in an early version (Galgo Medical S.L; Barcelona, Spain) was used to obtain patient-specific models from the 2D-DXA scans performed in the opposite femur (iDXA model GE Healthcare). The 3D-DXA algorithm made the registration of a 3D appearance model incorporating statistical information about the femoral shape and density onto the 2D DXA image. From the resulting patient-specific models the volumetric BMD can be automatically quantified as well as the volume (for trabecular and cortical regions) and cortical thickness distribution. Also, a total body scan was performed in these patients for body composition analysis purpose. The parameters were compared with reference values obtained on age and sex matched healthy volunteers and also on young people of same sex.

Results: A 47.1% of these patients were classified as osteoporotic using the WHO criteria. The femur of the patients suffering hip fracture show a significant less vBMD and BMC in cortical and trabecular bone ( $p > 0.001$ ). The average cortical thickness was also lower for fracture group (1.49 mm) than for sex and age-matched references (1.63 mm,  $p < 0.001$ ). This difference was bigger (26%) at the antero-superior radiant of femoral neck. The limb lean mass had a good correlation with all the bone parameters ( $r:0.218-0.375$ ). Trabecular bone parameters (vBMD, BMC) were the most deviated from reference values.

Conclusion: Both trabecular as well as cortical bone assessed by 3D-DXA are decreased in patients suffering hip fracture.

**Disclosures:** Luis Del Rio, None.



image

**Disclosures:** Ko Chiba, None.

This study received funding from: Furuno Electric Co., Ltd.

## SA0198

**Analyzing the cortical and trabecular bone of tenofovir-treated HIV patients using 3D-DXA.** Robert Güerri-Fernández<sup>1</sup>, Ludovic Humbert<sup>2</sup>, Judit Villar-García<sup>3</sup>, Roger Fonolla<sup>4</sup>, Lucia Moro<sup>5</sup>, Leo Mellibovsky<sup>6</sup>, Xavier Nogues<sup>7</sup>, Marta Trenchs-Rodríguez<sup>8</sup>, Hernando Knobel<sup>3</sup>, Adolfo Díez-Pérez<sup>6</sup>.

<sup>1</sup>Infectious Diseases Hospital del Mar Medical Research Institute, Spain, <sup>2</sup>Galgo Medical, Barcelona, Medical, Spain, <sup>3</sup>Infectious Diseases, Hospital del Mar., Spain, <sup>4</sup>GALGO Medical, Barcelona, Spain, Spain, <sup>5</sup>Internal Medicine, Hospital del Mar Medical Research Institute, Spain, <sup>6</sup>Internal Medicine, Hospital del Mar., Spain, <sup>7</sup>Internal Medicine, Hospital del Mar, Barcelona, Spain, <sup>8</sup>Catalan Institute of Health, ICS, Barcelona, Spain, Spain

The purpose of this study was to analyze the changes in cortical and trabecular bone in HIV patients after one year of treatment with tenofovir using 3D-DXA.

34 HIV patients (27 men and 7 women) were included in this study. DXA scans (QDR 4500 SL, Hologic, Waltham, MA, USA) were acquired at baseline and after a 1-year treatment with tenofovir. The 3D-DXA software (Galgo Medical, Barcelona, Spain) was used to analyze the changes in cortical and trabecular bone after 1-year of treatment. 3D-DXA registers a 3D appearance model of the femoral shape and density onto the DXA projection to obtain a 3D subject-specific model of the femur of the patient and quantify the volumetric BMD (vBMD), volume (for trabecular and cortical regions) and cortical thickness distribution. The 3D-DXA measurements at baseline and after treatment were compared using paired samples Student's t-test.

Mean age at baseline was  $36.5 \pm 7.5$  years. A statistically significant decrease of the integral vBMD ( $-11.9$  mg/cm<sup>3</sup>,  $-3.0\%$ ,  $p = 0.001$ ) and cortical vBMD ( $-4.0$  mg/cm<sup>3</sup>,  $-0.4\%$ ,  $p = 0.004$ ) was observed at the neck. The cortex at the neck was also significantly thinner after 1-year of treatment ( $-0.05$  mm,  $-3.2\%$ ,  $p = 0.006$ ). No significantly significant difference was observed for the trabecular vBMD at the neck.

The 3D-DXA analysis of the 34 HIV patients included in this study showed that treatment with tenofovir induces significantly significant changes at the cortex (thickness and density).

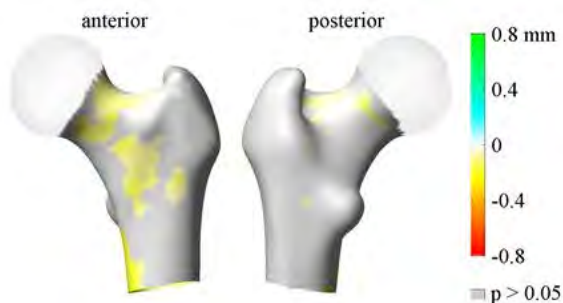


Figure: Color map showing statistically differences in cortical thickness baseline-follow up

**Disclosures:** Robert Güerri-Fernández, None.

## SA0201

**Chronic Joint Pain is Associated with Spinal Osteoporosis in Midlife Asian Women.** Yue Luna Wang<sup>1</sup>, Susan Jane Sinclair Logan<sup>2</sup>, Lay Wai Khin<sup>3</sup>, Saw Myat Sabai<sup>1</sup>, Pa Pa Thu Win<sup>1</sup>, Yean Ling Mayvien Teo<sup>1</sup>, Stephen Fearn<sup>4</sup>, Smagula<sup>4</sup>, Jane A. Cauley<sup>5</sup>, Eu-Leong Yong<sup>1</sup>. <sup>1</sup>Department of Obstetrics & Gynaecology, National University of Singapore (NUS), Singapore, Singapore, <sup>2</sup>Department of Obstetrics & Gynaecology, National University Hospital (NUH), Singapore, Singapore, <sup>3</sup>Singapore Institute for Clinical Sciences - A\*STAR, Singapore, Singapore, <sup>4</sup>Department of Psychiatry, Western Psychiatric Institute & Clinic, University of Pittsburgh Medical Center (Pennsylvania), United States of America, United states, <sup>5</sup>Department of Epidemiology, University of Pittsburgh (Pennsylvania) Graduate School of Public Health (GSPH), United States of America, United states

**Purpose:** Menopause leads to a myriad of symptoms & diseases including osteoporosis (OP). Vasomotor symptoms (VMS) are associated with OP in Caucasian women but are uncommon in Asians. Bone loss in the spine may precede the hip in women. Our aims were to identify symptoms most commonly associated with menopause in Singaporean women, to explore these symptoms' relationship with spinal (Sp) bone mineral density & propose an alternative OP screening tool in this population.

**Methods:** Women aged 45-69 attending gynecology clinics for "well woman" checks were recruited from 2014-2015. Menopausal symptomatology and other risk factors for OP were collected using validated questionnaires. Physical performance including grip strength was measured using the Short Physical Performance Battery. Sp T-scores were defined as normal, osteopenia & OP as per WHO criteria. Univariate and multivariable stepwise multinomial logistic regressions were performed to generate an area under the curve (AUC), sensitivity & specificity using STATA version 14.

**Results:** 512 women with mean age of 57.0 (SD  $\pm$  6.3) were recruited. Spinal OP was diagnosed in 6.8%. Common menopausal complaints were joint/muscular discomfort (38%), sleep problems (32%), vaginal dryness (25%), VMS (24%), exhaustion (23%), sexual problems (20%), bladder problems (17%), depressed mood (15%) and irritability (14%). Chronic joint pain, not related to injury, was a significant predictor of SpOP [RRR=2.30, (95%CI: 1.01-5.25), p=0.047]. Other self-reported pain symptoms (chronic back pain, chronic knee pain, acute joint stiffness and acute pain while walking) & menopausal symptoms were not significantly associated with SpOP. Using chronic joint pain, age, weight, menopausal status and right handgrip strength, we developed a screening tool that outperformed Osteoporosis Self-Assessment Tool for Asians (OSTA) - AUC values for our model and OSTA were 84% (2.94% sensitivity, 99.6% specificity) and 79% (2.86% sensitivity, 99.5% specificity), respectively (p=0.023).

**Conclusion:** Unlike in Caucasian populations, VMS were neither a common menopausal symptom nor predictive of SpOP in midlife Singaporean women. The most common menopausal symptom was joint/muscular pain; with chronic joint pain, unrelated to injury, as a significant predictor of SpOP. The combination of chronic joint pain, age, weight, menopausal status and right handgrip strength may be a better screening tool than OSTA in predicting SpOP in midlife Asian women.

**Disclosures:** Yue Luna Wang, None.

## SA0202

**Feasibility study of a Quality Control methodology for TBS.** Renaud Winzenrieth<sup>1</sup>, Jessy Libber<sup>2</sup>, Diane Krueger<sup>2</sup>, Franck Michelet<sup>1</sup>, Neil Binkley<sup>2</sup>. <sup>1</sup>R&D department, Med-Imaps SASU, France, <sup>2</sup>University of Wisconsin Osteoporosis Clinical Research Program, United states

**Objective:** It is essential that stability of instruments producing quantitative measurements be documented. In DXA this is achieved by routine spine phantom scanning. At this time, there is no a method to validate Trabecular Bone Score (TBS) stability over time. As such, the aim of this study is to develop Quality Control (QC) methodology for TBS using a new TBS phantom.

**Materials & Methods:** A TBS phantom has been developed that is comprised: a soft tissue (14 cm tissue equivalent, 100% fat content) and a TBS component that generates 4 different TBS values. TBS mean value of the phantom is for the QC. Using this phantom, data has been acquired on two GE-Lunar devices (iDXA and Prodigy) during 33 non-consecutive days. Each day, two sets of 5 acquisitions of the phantom were done, with complete repositioning between the two sets. We arbitrary selected the 10 first days (n = 100 scans) to create TBS reference values for each densitometers QC. Phantom precision was computed for both densitometers. To develop a TBS QC, we followed the methodology proposed by Lu et al. (JBMR,1996); i.e. using Shewart 2 and Tabular CuSum techniques. TBS standard deviation for the QC was not derived from the phantom precision but from a performance target similar to the one on BMD method: TBSsd = in-vivo L1-L4 TBSsd / 2.5. TBSsd = 0.008; i.e. a ratio of 2.5 exists between in-vivo BMD precision and the BMD phantom precision.

**Results:** Phantom precision is lower than the target TBSsd for both devices (0.005 vs 0.008 and 0.002 vs 0.008 for Prodigy and iDXA respectively). Shewart and CUSUM graphs for Prodigy related to the mean TBS values of the phantom are presented in Fig. 1. Neither Shewart nor CuSum techniques reported measurement instability for either DXA devices during the follow-up.

**Conclusion:** This first study demonstrates the possibility to develop a QC approach for TBS. The two densitometers exhibited stable TBS values during 23 days of follow-up. Phantom precision is sufficient to provide a daily QC value. Day number needed to create a stable reference value has to be determined and optimized. Further studies are needed to assess the sensitivity of this method to identify densitometer TBS performance changes.

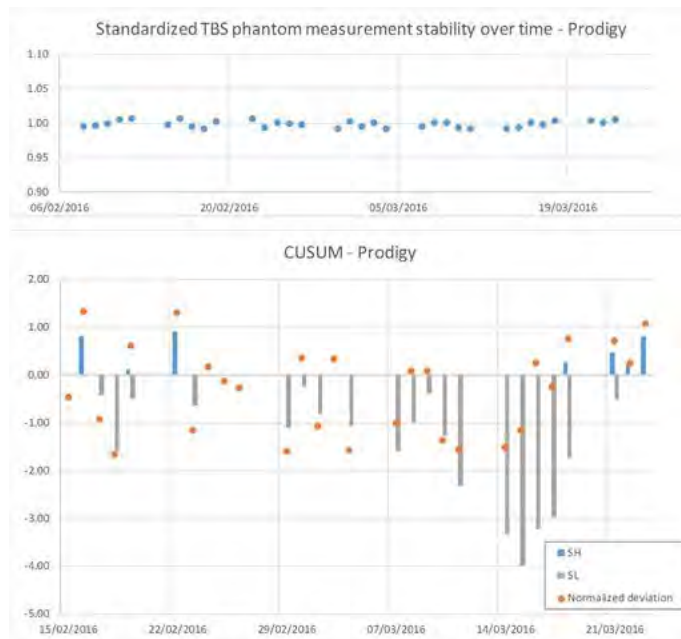


Figure 1: Shewart and CuSum parameter values during the follow-up for Prodigy DXA device.

Figure 1

**Disclosures:** Renaud Winzenrieth, Mes-Imaps, 15

## SA0203

**Performance of FRAX in Clinical Practice According to WHO and NOF Definitions of Osteoporosis in Canadian Women and Men: The Manitoba BMD Cohort.** William Leslie<sup>1</sup>, Sumit Majumdar<sup>2</sup>, Suzanne Morin<sup>3</sup>, Lisa Lix<sup>1</sup>, John Schousboe<sup>4</sup>, Kris Ensrud<sup>4</sup>, Helena Johansson<sup>5</sup>, Anders Oden<sup>5</sup>, Eugene McCloskey<sup>5</sup>, John Kanis<sup>5</sup>. <sup>1</sup>University of Manitoba, Canada, <sup>2</sup>University of Alberta, Canada, <sup>3</sup>McGill University, Canada, <sup>4</sup>University of Minnesota, United states, <sup>5</sup>Centre for Metabolic Bone Diseases, University of Sheffield Medical School, United Kingdom

**Aim:** FRAX is used to select individuals at high fracture risk for osteoporosis treatment. In older US men from MrOS, observed 10-year fracture probability exceeded FRAX-predicted probability when osteoporosis was defined by WHO criteria (female femoral neck T-score <-2.5) or National Osteoporosis Foundation (NOF) criteria (minimum spine or hip sex-matched T-score <-2.5). We examined the performance of FRAX in four distinct subgroups based on osteoporosis definition (WHO vs NOF) and FRAX score (high vs low).

**Methods:** Using the Manitoba (Canada) clinical DXA registry, we studied women and men age >40 y with baseline hip and spine DXA scans (1996-2013). FRAX probability including BMD (Canadian tool) was computed. Subjects were classified into four non-overlapping subgroups: osteoporosis by WHO criteria; osteoporosis by NOF (but not WHO) criteria; high fracture risk by FRAX (major osteoporotic fracture [MOF] >20% or hip fracture [HF] >3%, without osteoporosis by either criteria); and low fracture risk (MOF <20% and HF <3% without osteoporosis). Incident MOF and HF were ascertained using validated algorithms. We evaluated fracture stratification (hazard ratios [HR]) and calibration ratios (observed vs predicted 10-year fracture probability with competing mortality).

**Results:** The population included 62,275 women (5,345 MOF and 1471 HF) and 6455 men (405 MOF and 108 HF). FRAX scores were strongly predictive of MOF (HR per SD: women 2.12, 95% CI 2.06-2.18; men 1.89, 95% CI 1.73-2.08; p sex-interaction=1.0) and HF (women 4.78, 95% CI 4.44-5.14; men 4.20, 95% CI 3.22-5.49; p sex-interaction=0.7). Similar HRs were seen among the 7577 (12%) women and 540 (8%) men with osteoporosis by WHO criteria, and 7941 (13%) women and 981 (15%) of men with osteoporosis by NOF (non-WHO) criteria. In those with WHO osteoporosis, FRAX was well-calibrated for both MOF and HF (observed vs predicted probability ratio ~1). In those with NOF (non-WHO) osteoporosis, observed MOF probability slightly exceeded predicted probability in women (15.0% vs 13.1%; ratio 1.14, 95% CI 1.07-1.22) and men (14.0% vs 10.3%; ratio 1.36, 95% CI 1.09-1.64) but no miscalibration was detected for HF in women (3.3% vs 3.2%; ratio 1.05, 95% CI 0.89-1.21) or men (4.5% vs 3.9%; ratio 1.15, 95% CI 0.69-1.61).

Summary: FRAX was a strong predictor of MOF and HF in both women and men. FRAX performed well in those with osteoporosis defined by both WHO and NOF criteria.

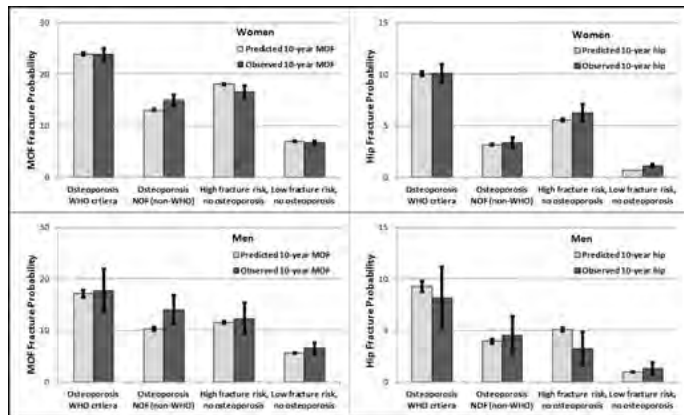


Figure: Predicted vs observed fracture probability by osteoporosis and risk subgroup (95% CI bars).

Disclosures: William Leslie, None.

**SA0204**

See Friday Plenary Number FR0204.

**SA0205**

See Friday Plenary Number FR0205.

**SA0206**

**Body Mass Index is Negatively Correlated with Lumbar Spine Trabecular Bone Score on Hologic but not GE-Lunar Densitometers.** Gillian Mazzetti<sup>1</sup>\*, Claudie Berger<sup>1</sup>, William Leslie<sup>2</sup>, Didier Hans<sup>3</sup>, Lisa Langsetmo<sup>1</sup>, David Hanley<sup>4</sup>, Christopher Kovacs<sup>5</sup>, Jerilynn Prior<sup>6</sup>, Stephanie Kaiser<sup>7</sup>, K. Shawn Davison<sup>8</sup>, Robert Josse<sup>9</sup>, Alexandra Papaioannou<sup>10</sup>, Rick Adachi<sup>10</sup>, David Goltzman<sup>1</sup>, Suzanne Morin<sup>1</sup>. <sup>1</sup>McGill University, Canada, <sup>2</sup>University of Manitoba, Canada, <sup>3</sup>University of Lausanne, Switzerland, <sup>4</sup>University of Calgary, Canada, <sup>5</sup>Memorial University, Canada, <sup>6</sup>University of British Columbia, Canada, <sup>7</sup>Dalhousie University, Canada, <sup>8</sup>Saskatoon Osteoporosis & CaMos Centre, Canada, <sup>9</sup>University of Toronto, Canada, <sup>10</sup>McMaster University, Canada

Objective: Trabecular bone score (TBS) is a grey-level texture measure derived from lumbar spine dual energy X-ray absorptiometry (DXA) images that predicts fractures in men and women, independently of bone mineral density (BMD). Increased amounts of abdominal soft tissue, such as adiposity in individuals with elevated body mass index (BMI), will absorb more X-rays during image acquisition and must be accommodated by the TBS algorithm, as for BMD. We aimed to determine if the relationship between BMI and TBS varied between two major manufacturers' densitometers.

Methods: We identified 1919 women and 811 men, participants of the Canadian Multicentre Osteoporosis study, aged ≥ 40 years with a valid lumbar spine BMD measured on GE-Lunar (4 centres) or Hologic (3 centres) densitometers at Year 10 of follow up. TBS was blindly calculated for L1-L4 (TBS iNsite<sup>®</sup> software version 2.1; Medimaps, Merignac, France). Bivariate Pearson correlation coefficients for BMI versus TBS and BMI versus BMD stratified by manufacturer were calculated to determine the strength of the relationships between these variables. Age-adjusted linear regression models, with TBS as dependent variable, were used to investigate the interaction of BMI by manufacturer.

Results: A significant negative correlation between TBS and BMI was observed when TBS measurements were performed on Hologic densitometers in men ( $r = -0.36$ ,  $p < 0.001$ ) and women ( $r = -0.33$ ,  $p < 0.001$ ); this was not seen when TBS was measured on GE-Lunar densitometers (Table). The linear regression models showed significant interactions between BMI and densitometer manufacturer for men and for women ( $p < 0.05$ ). Similar positive correlations were observed between BMD and BMI when BMD measurements were performed on both Hologic and GE-Lunar densitometers in both men and women.

Conclusion: BMI significantly affects TBS values in men and women when measured on Hologic but not on GE-Lunar densitometers. This has implications for clinical and research applications of TBS, especially when TBS is measured sequentially on DXA densitometers from different manufacturers or when results from different machines are pooled for analysis.

Table Pearson correlation coefficients of body mass index (BMI) with lumbar spine trabecular bone score (TBS) and bone mineral density (BMD)

	Densitometer manufacturer			
	Hologic†		GE-Lunar†	
	BMI, Men N = 331	BMI, Women N = 827	BMI, Men N = 480	BMI, Women N = 1092
Lumbar spine TBS	-0.36*	-0.33*	-0.01	-0.02
Lumbar spine BMD	0.26*	0.25*	0.24*	0.25*

\* $P < 0.05$ ; † QDR 4500, Discovery or Delphi; ‡ Prodigy

Table - Pearson correlation coefficients of body mass index (BMI) with lumbar spine trabecular bone

Disclosures: Gillian Mazzetti, None.

**SA0207**

**Finite Element Analysis Based in pQCT Imaging To Improve Assessment of Fracture Risk.** Dale Robinson<sup>1</sup>, Qichun Song<sup>2</sup>, Hongyuan Jiang<sup>1</sup>, Peter Vee Sin Lee<sup>1</sup>, John Wark<sup>3</sup>. <sup>1</sup>University of Melbourne, Australia, <sup>2</sup>2nd Affiliated Hospital, Xi'an Jiaotong University, China, <sup>3</sup>University of Melbourne & Royal Melbourne Hospital, Australia

Bone mineral density (BMD) using dual-energy X-ray absorptiometry (DXA) is the 'gold standard' for osteoporotic fracture risk assessment. However, many individuals who are not diagnosed as osteoporotic by DXA experience fracture; more accurate methods are needed for clinical prediction of bone strength. Peripheral quantitative computed tomography (pQCT) obtains 3D BMD measurements which can be combined with finite element (FE) analysis to model the effect of spatial BMD distribution on bone's mechanical properties. These models may offer an improved evaluation of bone strength that better reflects fracture risk.

Tibial pQCT of two cohorts was examined: (1) fracture group: 29 women (age  $63.2 \pm 9.3$  years) who had experienced a low-trauma fracture, and (2) control group: 28 healthy women (age  $22.9 \pm 2.2$  years) with no history of fracture. A Stratec XCT-3000 pQCT scanner was used to acquire axial cross-sections of the tibia at 4% and 66% of the bone length, measured from the distal end. Image slices were 2 mm thick with an in-plane resolution of  $0.4 \times 0.4$  mm. Images were segmented and used to create FE models. Each voxel was converted to Young's modulus based on its BMD. Three loading conditions were considered: compression, torsion and bending about an in-plane axis that was rotated in  $1^\circ$  increments from  $0^\circ$  to  $359^\circ$ . The applied load for each case was increased until the global maximum or minimum principal strain exceeded the tensile or compressive yield strain of the tibia ( $0.0065\epsilon$  and  $0.0073\epsilon$ , respectively). These data were compared with average density, total area and stress strain indices (SSIx, SSly and SSIp<sub>ol</sub>) calculated for each image by the Stratec operating software.

At the 4% site, the variable with the largest normalized difference between the fracture and control groups was the compressive strength ( $34.7 \pm 3.9\%$ ; Table 1). At the 66% site, the variables predicted from the FE model had larger normalized differences than each Stratec variable: minimum bending strength had the largest normalized differences between the fracture and control groups ( $16.7 \pm 3.3\%$ ).

Estimates of bone strength derived from FE models of a single 2 mm thick imaging slice differed between groups to a greater extent than standard pQCT imaging variables. Therefore, these FE models provide a potential improvement in fracture risk prediction and, given their simplicity, present a feasible method to be implemented with clinical pQCT imaging.

	Difference at 4% site (% of maximum)	Difference at 66% site (% of maximum)
<b>Stratec software variables</b>		
Average density	$23.6 \pm 2.6^*$	$5.0 \pm 3.3$
Total area	$-11.5 \pm 2.9^*$	$3.6 \pm 1.7$
SSIx	$28.2 \pm 4.4^*$	$13.2 \pm 3.5^*$
SSly	$33.5 \pm 4.7^*$	$14.3 \pm 3.2^*$
SSIp <sub>ol</sub>	$31.6 \pm 4.4^*$	$13.6 \pm 3.2^*$
<b>FE model variables</b>		
Compressive strength	$34.7 \pm 3.9^*$	$16.6 \pm 3.7^*$
Torsional Strength	$30.9 \pm 4.0^*$	$15.3 \pm 3.2^*$
Minimum bending strength	$22.3 \pm 3.3^*$	$16.7 \pm 3.3^*$

\*Variable was significantly different ( $p < 0.05$ ) between the groups

Table 1. Differences between fracture and control groups for each variable (mean ± 1SD)

Disclosures: John Wark, None.

## SA0208

**Fracture Discrimination Using a Novel Pulse-Echo Ultrasound Device.** John Schousboe<sup>1</sup>, Ossi Riekkinen<sup>2</sup>, Janne Karjalainen\*<sup>2</sup>. <sup>1</sup>Park Nicollet Institute, United states, <sup>2</sup>Bone Index Finland, Finland

While dual energy x-ray absorptiometry (DXA) remains the primary method of diagnosing osteoporosis, it has the disadvantages of being non-portable and exposing those having the test to some ionizing radiation. Although the cost of DXA is modest, this is still sufficient to limit access. The aim of this study was to estimate whether or not pulse-echo ultrasonometry (US) can discriminate those who had from those who did not have fractures.

In total 555 Caucasian female subjects were enrolled between ages 50 and 89 stratified by age decade. Subjects were examined using US measurements of cortical bone thickness (radius and tibia) and Density Index (DI)<sup>1</sup> and DXA measurement of bone mineral density (BMD) of the femoral neck and total hip. Fractures within the prior five years before the study date were confirmed by review of all radiology reports by the author (JTS). Logistic regression models were run to estimate the associations of multi-site and single-site DI, cortical thickness each with confirmed clinical fractures.

Ninety-five individuals (17.0%) had 102 fractures within the five years prior to the study date. The majority of these were in the distal radius/wrist, lumbar spine, or thoracic spine. One standard deviation decrease in femoral neck BMD was associated with fractures with an odds ratio of 1.47 (95% C.I. 1.11 to 1.95). Decreases of multi-site and single-site DI and cortical thickness at the proximal and distal tibia were similarly modestly associated with a higher age-adjusted odds ratio of a fracture (table 1).

Measures of cortical thickness of the tibia were as strongly associated with radiographically confirmed fractures as was femoral neck BMD, and our results compare favorably to the discrimination of prior fractures that have been shown with other ultrasound and peripheral bone mass measurement devices. Pulse-echo US shows promise as a tool for fracture risk assessment, and future prospective studies on prediction of incident fractures are warranted.

## References

[1] Karjalainen, Osteoporos Int., 2015

Table 1: Associations\* of Bone Ultrasound Parameters with Clinical Fracture (Confirmed on Clinical Radiographs) within the Prior 5 Years

Parameter	Odds Ratio per SD decrease (95% C.I.)		
	Ultrasound Parameter, Age-adjusted only	Ultrasound Parameter Adjusted for Age & Femoral Neck BMD	Femoral Neck BMD (Adjusted for Age and Ultrasound Parameter)
Multi-Site Density Index	<b>1.36</b> (1.05 to 1.76)	1.18 (0.88 to 1.58)	<b>1.37</b> (1.01 to 1.86)
Single-Site Density Index	<b>1.37</b> (1.04 to 1.82)	1.20 (0.89 to 1.61)	<b>1.38</b> (1.03 to 1.85)
Proximal Tibia Thickness	<b>1.56</b> (1.18 to 2.06)	<b>1.43</b> (1.08 to 1.91)	<b>1.34</b> (1.01 to 1.78)
Distal Tibia Thickness	<b>1.38</b> (1.09 to 1.76)	<b>1.29</b> (1.00 to 1.65)	<b>1.38</b> (1.05 to 1.82)
Distal Radius Thickness	1.09 (0.83 to 1.43)	0.98 (0.74 to 1.29)	<b>1.47</b> (1.11 to 1.95)

\*Associations with p-value&lt;0.05 shown in bold italics

Table 1.

Disclosures: Janne Karjalainen, Bone Index Finland, 14  
This study received funding from: Bone Index Finland

## SA0209

**Reliable quantification of marrow fat unsaturation level using in vivo MR spectroscopy.** Xiaojuan Li\*<sup>1</sup>, Kaipin Xu<sup>1</sup>, Sigurdur Sigurdsson<sup>2</sup>, Trisha Hue<sup>1</sup>, Ann Schwartz<sup>1</sup>. <sup>1</sup>University of California, San Francisco, United states, <sup>2</sup>Icelandic Heart Association, Iceland

More evidences have demonstrated that bone marrow fat, both contents and composition (such as unsaturation level), plays an active role affecting bone quantity and quality. MR spectroscopy (MRS) has been applied for non-invasive quantitative evaluation of marrow fat. However, quantifying unsaturated lipids using in vivo MRS is challenging due to its overlapping to water resonance. The goal of this study was to develop a reliable method for marrow fat unsaturation level quantification using in vivo MRS.

Single voxel MRS (1.5 Tesla) were collected from L1-L4 in 23 subjects from the Age Gene/Environment Susceptibility-Reykjavik (AGES-Reykjavik) cohort in Iceland. Among them, 3 subjects were rescanned for evaluating reproducibility. A fully automated time-domain based spectral fitting algorithm using Voigt models was developed. Four lipid peaks (Fig 1) and water resonance were quantified. Fat content (FC) and unsaturation level (UL) were calculated as FC=total lipids/(total lipids+water) and UL=unsat lipids/total lipids. A grading system was developed for evaluating the resolution of unsaturated lipids: 0: well resolved; 1: partially resolved; 2: not resolved, Fig 1.

In spectra with well or partially resolved unsaturated lipids (grade 0 and 1), the average scan/rescan CV was 1.1% and 6.3% for FC and UL respectively. Among the total 92 spectra for 23 subjects, 18, 65 and 9 spectra were graded as 0, 1 and 2, respectively. Spectra with grading 2 were removed from data analysis. In 15 subjects who had all four levels with unsaturated lipids well or partially resolved, L4 had significantly higher FC compared to other levels, consistent with previous reports; however, no significant differences were found in UL between levels. UL was significantly correlated to FC (R=-0.87, P < 0.05). Significant higher FC and lower UL were found in women compared to men (FC: 64.7 ± 6.7% vs 57.7 ± 4.3%, P=0.037; UL: 3.4 ± 0.8% vs 4.2 ± 0.4%, P=0.033; age 84.7 ± 5.4yrs vs 84.8 ± 2.8yrs, P=0.99).

Inclusion, we have developed a novel spectral fitting method that can reliably quantify marrow fat unsaturation level even for partially resolved unsaturated lipids with excellent in vivo reproducibility. The CVs for both FC and UL from this study were superior to previously reported results. We will apply the algorithm to the large-scale data collected in the AGES-Reykjavik cohort for exploring the relationship between marrow composition, bone and body composition.

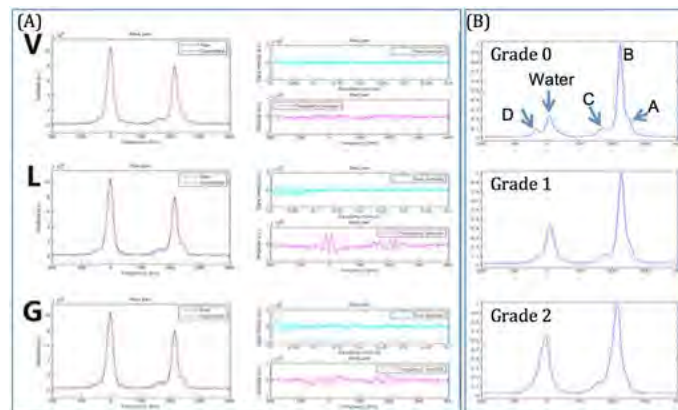


**Figure 1** (A) Numerical simulations (data not shown) and experimental data showed the new algorithm using Voigt model (V), which is a linear combination of Lorentzian and Gaussian decays, had improved the spectral fitting significantly as compared to using pure Lorentzian (L) or Gaussian (G) models. The left column illustrates the fitting while corresponding time- and frequency-domain fitting residuals are plotted in the right column. The new algorithm reduced 46% and 27% fitting errors compared to using pure Lorentzian or Gaussian models respectively. (B) The grading of the resolution of unsaturated lipids: 0: well resolved; 1: partially resolved; 2: not resolved. Five peaks including lipids A at 0.9 ppm, B at 1.3 ppm, C at 2.1 ppm, D at 5.3 ppm, and water resonance at 4.7 ppm were quantified.

Figure 1

Disclosures: Xiaojuan Li, None.

## SA0210

**Risk factors including age, gender, osteoporosis in spine or hip, and local osteoporosis for more severe pattern of fracture in proximal humerus fracture.** Kyoung Hwan Koh, Jin Hwan Kim\*. Inje University Ilsan Paik Hospital, Korea, republic of

## Purpose

Reduced bone mineral density (BMD) has been shown as one of the significant risk factors for proximal humerus fracture and can be correlated to the severity of fracture. Purpose of this study is to evaluate the correlation of local BMD assessed by plain radiographs with the severity of fracture in proximal humerus fractures.

## Methods

Fracture of proximal humerus which treated by open reduction and internal fixation with locking plate were consecutively included between 2014 and 2015. Deltoid tuberosity index and cortical bone thickness average (CBTAVG) were measured for evaluation of local BMD. Plain radiographs and additional CT scans of the fracture were evaluated for fracture severity (from 0 to 3; 3 is most severe fracture). It was scored by experienced orthopaedic surgeons according to the radiographic parameters such as metaphyseal comminution, angulation, and medial hinge disruption.

Risk factors for fracture severity including demographics, medical comorbidities, BMD of hip and spine, CBTAVG, and deltoid tuberosity index were analyzed using univariate analysis. Multivariate analysis was performed to identify the independent factors affecting the fracture severity.

## Results

42 patients were taken surgery for proximal humerus fracture. After exclusion of 5 patients (one patient under the age of 18, 3 arthroscopic reduction and suture fixation, 1 case of delayed union after conservative treatment), a total of 37 were analyzed. There were 6 male and 31 female patients with a mean age of 69.6 years (± 16). Mean BMI was 24.4 (± 16.0) Mean T-score in BMD was -2.4 in spine and -2.0 in hip joint at the time of injury (18 osteoporosis, 10 osteopenia, and 9 normal). Ten patients had a prior fragility fracture either in hip, spine, or wrist. 27 patients had medical comorbidities and 34 fractures injured by minor trauma were regarded as fragility

fracture. There were twenty 2-part, fourteen 3-part, and three 4-part fractures by Neer classification.

Univariate analysis showed age, gender, medical morbidity, CBTAvg less than 6mm was related to the severity of fracture. In multivariate analysis, age ( $P=0.002$ ) and CBTAvg ( $P=0.01$ ) were the independent risk factors for fracture severity.

#### Conclusion

Age and local osteoporosis were the independent risk factors for more severe pattern of fracture in proximal humerus fracture. BMD in spine or hip, gender, and other medical morbidities were not independent risk factors for severe form of fracture.

**Disclosures:** Jin Hwan Kim, None.

## SA0211

**Subject-Specific Finite Element Modeling Based on HR-pQCT at the Distal Tibia Predicts Bone Strength at Hip and Spine.** Andres Kroker\*, Ryan Plett, Britta Jorgenson, Kyle Nishiyama, Steven Boyd. 1. McCaig Institute for Bone & Joint Health, 2. Department of Radiology, Cumming School of Medicine, University of Calgary, Calgary, AB, Canada, Canada

High-resolution peripheral quantitative computed tomography (HR-pQCT) is a novel imaging modality that allows the assessment of bone microarchitecture at peripheral skeletal sites such as the radius and tibia in humans *in vivo*. More importantly, these images can be used to perform patient specific finite element analysis (FEA) to estimate bone strength; however, it is not well understood how these bone strength estimates relate to true bone strength at axial skeletal sites such as the hip and spine.

The goal of this study is to determine if bone strength at axial skeletal sites can be predicted by HR-pQCT estimates of bone strength at the peripheral skeleton and if those predictions are superior to DXA measurements at the axial sites themselves. Left and right distal tibia and radius of ten cadavers were imaged with HR-pQCT using a standard *in vivo* imaging protocol (9.02 mm segment, 82  $\mu$ m isotropic voxel size). The proximal femurs and L4 spines of the same cadavers were imaged using DXA. Following imaging, all L4 vertebral bodies and femurs were mechanically tested to failure to provide a ground-truth bone strength at these sites.

Measures of DXA areal bone mineral density (aBMD) significantly correlated with mechanically determined failure load (femur  $r=0.74-0.84$ ; L4  $r=0.77$ ). HR-pQCT derived volumetric bone mineral density (vBMD) of the radius significantly correlated with L4 failure load ( $r=0.82-0.85$ ), while tibia vBMD correlated significantly with both femur ( $r=0.71-0.75$ ) and L4 ( $r=0.96$ ) failure load. All correlations were significant to  $p<0.05$ . Patient-specific FEA at the radius did not significantly correlate with femoral failure load, whereas it correlated moderately with L4 FL ( $r=0.65-0.75$ ). FEA of the tibia correlated strongly with both femoral ( $r=0.80-0.83$ ) and especially L4 FL ( $r=0.90-0.91$ ).

Our findings show that measures at the tibia correlate better with the femoral and L4 strength than the radius. A possible explanation is that the tibia is a weight-bearing skeletal site, and is a good indicator of axial weight-bearing sites of the hip and spine. Notably, the correlations between tibial measurements and the ground-truth strength at the hip and spine were as good or stronger than the DXA-based aBMD measures, even though DXA is measured at the actual skeletal site. Our sample of complete cadaveric skeletons was small ( $N=10$ ); however, the strong correlations suggest HR-pQCT at the tibia is a good predictor of axial skeleton bone strength.

**Disclosures:** Andres Kroker, None.

## SA0212

**The Canadian Multicentre Osteoporosis Study (CaMos) and Vertebral Fractures.** Brian Lentle\*<sup>1</sup>, Claudie Berger<sup>2</sup>, Jacques Brown<sup>3</sup>, Lisa Langsetmo<sup>4</sup>, Doneal Thomas<sup>2</sup>, Benjamin Fine<sup>5</sup>, Kevin Lian<sup>1</sup>, Arvind Shergill<sup>5</sup>, J Jacques Trollip<sup>1</sup>, Linda Probyn<sup>6</sup>, William D Leslie<sup>7</sup>, Stephanie M Kaiser<sup>8</sup>, Jonathan D Adachi<sup>9</sup>, Tanveer Towheed<sup>10</sup>, David A Hanley<sup>11</sup>, K Shawn Davison<sup>12</sup>, Jerilynn Prior<sup>1</sup>, David Goltzman<sup>13</sup>. <sup>1</sup>UBC, Canada, <sup>2</sup>CaMos, RI-MUHC, McGill University, Canada, <sup>3</sup>Centre Hospitalier de l'Université Laval, Canada, <sup>4</sup>University of Minnesota, Canada, <sup>5</sup>University of Toronto, Canada, <sup>6</sup>Sunnybrook Health Sciences Centre, Canada, <sup>7</sup>University of Manitoba, Canada, <sup>8</sup>Dalhousie University, Canada, <sup>9</sup>McMaster University, Canada, <sup>10</sup>Queen's University, Canada, <sup>11</sup>University of Calgary, Canada, <sup>12</sup>University of Victoria, Canada, <sup>13</sup>McGill University, Canada

Using data from 4 centres (3149 participants and 6927 serial X-rays), we compared the Genant Semi-Quantitative (GSQ) and modified Algorithm-based Qualitative (mABQ) methods for diagnosing prevalent and incident vertebral fractures (VF). The ABQ tool was modified (mABQ) to include cortical buckling/breaks.

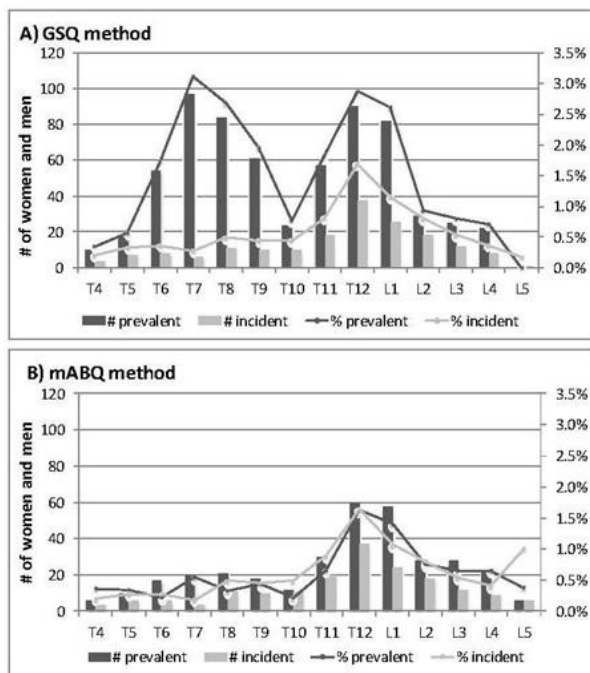
Spine images (T4-L4) of CaMos men and women > 50 years old at baseline (1995-97) and at Year 5, 10 and 16 follow-ups were included. Two trained technologists triaged participants into those with GSQ VF (any grade) and those without. A single

radiologist (BL) reviewed serial X-rays for participants with any triaged GSQ VF and a random sample of those without GSQ VF for presence and grade of VF using GSQ, with or without mABQ signs. Sex stratified linear and logistic regressions, adjusted for age, body mass index and height, tested the association of prevalent VF with femoral neck (FN) BMD and incident VF.

Using GSQ, the prevalence of VF was 13.6% (95%CI: 12.1; 15.1) in women and 15.5% (13.0; 18.0) in men; using mABQ it was 6.7% (5.6; 7.8) in women and 4.7% (3.3; 6.2) in men. Incident VF rates (per 1000 person-years) were 5.8 (4.7; 7.2) in women and 4.9 (3.3; 7.2) in men using GSQ, and 5.7 (4.6; 7.2) in women and 4.7 (3.2; 7.0) in men using mABQ. Incident and prevalent VF show different distributions when plotted by vertebral segment (Fig 1). For GSQ-defined VF, the adjusted FN BMD was 0.042g/cm<sup>2</sup> (0.029; 0.056) lower in women and 0.036 g/cm<sup>2</sup> (0.013; 0.058) in men. For mABQ-defined VF, adjusted FN-BMD was 0.061g/cm<sup>2</sup> (0.042; 0.080) lower in women and 0.075g/cm<sup>2</sup> (0.034; 0.116) in men. Since all prevalent mABQ VF were also GSQ VF, we divided the GSQ VF group into mABQ VF and GSQ alone. Compared with participants with GSQ VF alone, women and men with prevalent mABQ VF had lower FN BMD by 0.037g/cm<sup>2</sup> (0.012; 0.065) and 0.075g/cm<sup>2</sup> (0.025; 0.125). Participants with prevalent GSQ VF were 5.1 (3.3; 7.8) times more likely than normals to have incident GSQ VF; those with prevalent mABQ VF were 9.9 (6.0; 16.4) times more likely to have incident mABQ VF than normals.

Our 16-year VF data demonstrate reductions in FN BMD in those with VF by both mABQ and GSQ methods; more conservative estimates of VF prevalence with mABQ, especially in the thoracic spine; equivalent estimates of VF incidence with both methods; but a higher likelihood for future VF with the mABQ method.

**Fig 1: Numbers and percentage of prevalent and incident vertebral fractures in 4 centres of the CaMos cohort of women and men ages 50 and older by vertebral segment from thoracic (T) to lumbar (L) by the Genant Semi-Quantitative (A) and the modified Algorithm Based Qualitative (B) methods.**



GSQ= Genant Semi-Quantitative  
mABQ= modified Algorithm-based Qualitative to include cortical buckling

Table 1

**Disclosures:** Brian Lentle, None.

## SA0213

**The Impact of QCT Reconstruction Kernel on Bone Mineral Density and Finite Element Estimated Bone Strength.** Andrew Michalski\*<sup>1</sup>, W. Brent Edwards<sup>2</sup>, Steven Boyd<sup>1</sup>. <sup>1</sup>Department of Radiology, Cumming School of Medicine, University of Calgary, Canada, <sup>2</sup>Faculty of Kinesiology, University of Calgary, Canada

Computed tomography (CT) is emerging as an opportunistic imaging modality to assess osteoporosis. Quantitative CT (QCT) is well suited in bone imaging for the quantification of volumetric bone mineral density (vBMD), bone mineral content (BMC), and total bone volume (BV). Finite element (FE) analysis is commonly used to estimate bone stiffness and strength in osteoporosis. In QCT-FE, a key step is the conversion of density-calibrated Hounsfield Units (HU) to voxel-specific elastic moduli through exponential relationships. It is known that HU are influenced by QCT

acquisition and reconstruction parameters. CT projection data are reconstructed using convolution kernels – a standard clinical kernel smooths data and suppresses noise, and a bone-specific kernel sharpens the image to enhance edges, resulting in increased noise. The effect of the reconstruction kernel on quantified measures of bone quality is key, and important for accurate non-invasive assessment of bone strength. The purpose of this study was to determine the effects of QCT reconstruction kernels on the assessment of bone quality through measures of vBMD, BMC, BV, and FE predicted bone strength and stiffness. Clinical QCT scans (Sensation 64 Cardiac, Siemens Medical Systems, Forchheim, Germany) of the proximal femur were reconstructed using two convolution kernels, a bone-specific kernel (B70) and a standard clinical kernel (B30). Scans were calibrated to density values using a density calibration phantom (QRM, Moehrendorf, Germany) with known calcium hydroxyapatite concentrations. The proximal femur was segmented based on a density threshold of 0.15 g/cm<sup>3</sup> and manual corrections were applied to account for areas of lower density. Quantitative analyses were performed on density calibrated whole segmented bone, combining cortical and trabecular regions during investigation. QCT-FE analysis was performed using a standard side-ways fall loading configuration. Output measures of vBMD, BMC, BV, and FE estimated bone strength and stiffness were compared for each reconstruction kernel. Significant differences were found in the measures of vBMD (Average % Difference: -2.2%, p<0.001), BMC (Average % Difference: 0.8%, p<0.01), and BV (Average % Difference: 3.0%, p<0.001) between the two reconstruction kernels. These data demonstrate how the reconstruction convolution kernel plays a major role in assessing bone quality, and appropriate corrections are essential for the goal of standardizing QCT.

**Disclosures:** Andrew Michalski, None.

## SA0214

**Trabecular Bone Score (TBS) and its association with Cobb angle kyphosis in older men.** Erin Deiotte<sup>1</sup>, Jian Shen<sup>1</sup>, Jaclyn Bergstrom<sup>1</sup>, Jeanne Nichols<sup>1</sup>, John Schousboe<sup>2</sup>, David Wing<sup>1</sup>, Gina Woods<sup>1</sup>, Nancy Lane<sup>3</sup>, Wendy Katzman<sup>4</sup>, Deborah Kado<sup>\*1</sup>. <sup>1</sup>University of California, San Diego, United states, <sup>2</sup>Park Nicollet Institute & University of Minnesota, United states, <sup>3</sup>University of California, Davis, United states, <sup>4</sup>University of California, San Francisco, United states

While vertebral fractures and lower areal BMD are risk factors for kyphosis progression in older persons, it is unknown whether trabecular bone score (TBS) might capture other aspects of bone microarchitecture that could play an important role in the development of age-related hyperkyphosis (HK). Beyond areal BMD, TBS may provide information on bone quality and vertebral mechanical behavior.

Using data in 2,344 men aged >65 and older from MrOS who had both baseline TBS and Cobb angle kyphosis measured, we hypothesized that degraded TBS score would be associated with worse kyphosis. After excluding men taking osteoporotic medications (n = 253) and men with BMI <15 or ≥35 kg/m<sup>2</sup> (n = 99), 1997 men, mean age 73.6 (SD = 5.9), comprised the study sample. Linear and logistic multivariable regression analyses were done controlling for age, clinic, race, BMI, hip or spine BMD and prevalent vertebral fracture.

Men had a mean kyphosis angle of 38.7° ± 11.5. 295 (15%) were classified as hyperkyphotic (>50°), and 416 (21%) had degraded TBS (≤1.2). In linear regression analysis adjusted for age, clinic, race and BMI, lower TBS score was associated with worse kyphosis (p = 0.0003). After further adjustment for either hip BMD (p = 0.04), prevalent vertebral fracture (p = 0.06), or spine BMD (p = 0.32), the association was substantially weakened, indicating the areal BMD explained away most of the effects of TBS on kyphosis. However, compared with men with TBS>1.2, kyphosis was significantly worse in those with degraded TBS, with these men being at 1.47 times higher odds of having HK (95% CI: 1.06-2.06, p = 0.02) after adjusting for age, clinic, race, BMI, hip BMD and prevalent vertebral fracture. If spine instead of hip BMD was included in the model, the odds decreased to 1.35 (95% CI: 0.97-1.89, p = 0.08).

Older men with degraded TBS are more likely to have HK that is not explained by underlying prevalent vertebral fractures. Although areal spine BMD is considered problematic due to DJD changes and surrounding age-related calcification, it does appear to correlate strongly with age-related kyphosis in older men.

**Disclosures:** Deborah Kado, None.

## SA0215

**Ultrashort Echo Time Magnetization Transfer (UTE-MT) Imaging and Modeling of Cortical Bone.** Yajun Ma<sup>\*1</sup>, Eric Chang<sup>2</sup>, Jiang Du<sup>1</sup>. <sup>1</sup>Department of Radiology, University of California, San Diego, United states, <sup>2</sup>VA San Diego Healthcare System, San Diego; Department of Radiology, University of California, San Diego, United states

**Purpose:** To evaluate the collagen proton fraction and proton exchange rate between water proton and collagen protons in human cortical bone using ultrashort TE magnetization transfer (UTE-MT) imaging and signal modeling.

**Methods:** Data were acquired with a 2D UTE-MT sequence on a clinical 3T Signa TwinSpeed scanner (GE Healthcare Technologies, Milwaukee, WI) with a maximum gradient strength of 40 mT/m and a maximum slew rate of 150 mT/m/ms. An eight-channel T/R knee coil was employed for imaging. The MT preparation consisted of a Fermi shaped RF pulse (duration = 8 ms) followed by a gradient crusher. UTE-MT imaging parameters were: TR = 100 ms, TE = 8 μs, flip angle = 10°, FOV = 21x21cm<sup>2</sup>,

matrix = 128x128, bandwidth = 250 kHz, slice thickness = 6 mm; four MT powers (600°, 900°, 1200° and 1500°) and five MT frequency offsets (2, 5, 10, 20 and 50 kHz) with a total scan time of 14.3 min. A multi-TR UTE protocol was employed for T1 measurement, with sequence parameters the same as the UTE-MT protocol except for no MT preparation, a higher flip angle of 60°, and five TRs of 16, 60, 100, 200 and 400 ms. Two-pool UTE-MT modeling (water and collagen protons) was performed on the datasets with a continuous wave power equivalent (CWPE) approximation (Henkelman et al. MRM 1994, Ramani et al. MRI 2002). The CWPE approximation treats the MT pulse as a rectangular continuous wave pulse with the same mean saturating power in each repetition time. UTE-MT modeling was applied to cadaveric bovine bone samples (n=5) and healthy human volunteers (n=2) to quantify bound water and collagen protons in cortical bone in vitro and in vivo.

**Results:** Excellent UTE-MT modeling was achieved in both bovine bone and the volunteers. The results of MT modeling for bovine bone samples were as follows: collagen proton fraction 62.1±4.7 %, proton exchange rate from water to collagen 27.1±6.2 s<sup>-1</sup>, T2 values of water and collagen proton were 0.18±0.11 ms and 14.1±1.2 us respectively. Figure 1 shows the acquired UTE-MT images and the fitting curves from the volunteer. For human tibia, the results were as follows: collagen proton fraction 51.5 %, proton exchange rate from water to collagen was 10.2 s<sup>-1</sup>, T2 values of water and collagen proton were 0.63 ms and 14.6 us respectively. Future work will focus on three-pool UTE-MT modeling to evaluate bound and pore water as well as collagen protons.

**Conclusion:** The results show that UTE-MT modeling can be used to quantitative evaluate collagen and water protons in cortical bone in vitro and in vivo. The new information on bone water and organic matrix may provide novel biomarkers for bone quality and quantity.

### Clinical Relevance

UTE-MT modeling can quantify the collagen proton fraction and exchange rate in cortical bone. This technique may have applications in diffuse bone disease including osteoporosis, renal osteodystrophy, Paget disease, and osteomalacia.

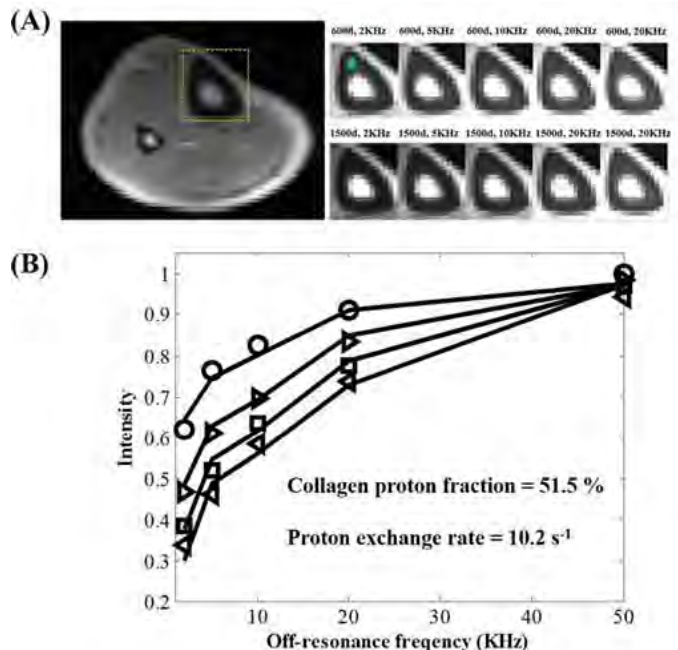


**Figure:** UTE-MT imaging and signal modeling of the tibia midshaft of a 43 year old volunteer: (A) shows UTE-MT images acquired with two sets of MT powers (i.e. 600° and 1500°) for MT modeling. Mean signal intensities within the green ROIs were used for MT modeling. (B) shows UTE-MT modeling fitting results. Experimental data were acquired with five off-resonance frequencies (i.e. 2, 5, 10, 20, 50 kHz) and four different pulse powers (i.e. 600° (circles), 900° (right-pointing triangles), 1200° (squares) and 1500° (left-pointing triangles)). The corresponding fitting results were expressed by lines. The collagen proton fraction was 51.5% and the proton exchange rate from water to collagen was 10.2 s<sup>-1</sup>.

Figure 1

**Disclosures:** Yajun Ma, None.

**SA0216**

See Friday Plenary Number FR0216.

**SA0217**

**A Mathematical Model to Quantify Links Between Bone Mineral Density, Patient Factors and Therapeutic Interventions on Fracture Risk in Patients with Osteoporosis.** Rena Eudy\*, William Gillespie, Matthew Riggs, Marc Gastonguay. Metrum Research Group LLC, United states

**Objective:** To develop a predictive model that describes the probability of fracture in patients with osteoporosis having different individual characteristics and subject to various classes of treatments.

**Methods:** The analysis dataset, including individual-level (NHANES, 2005-2008) and summary-level data, was aggregated from a comprehensive, systematic literature search of published clinical studies (1995-2015), recording fracture rate and bone mineral density (BMD) associated with various treatments. The final metadataset was comprised of 21 studies investigating the effects of bisphosphonates, teriparatide, denosumab, and raloxifene in 65254 patients over a cumulative 56.75 years on study. A Bayesian approach (OpenBUGS v3.2.2A) was used to construct a time-to-event hazard model including available covariate effects; model evaluations included deviance criteria and posterior predictive check (PPC).

**Results:** Covariates included lumbar spine BMD, BMI, years post-menopause (YPM), fracture measure method (clinical or radiological) and type (vertebral and/or nonvertebral fractures), and a drug effect that included interaction with BMD. The mean baseline hazard estimate was 0.0433/year, 95%CI: 0.0296, 0.0616) at a reference BMI 27.1 and YPM 20. Coefficients for BMI and YPM effects were -0.0174 (-0.0507, 0.0157) m<sup>2</sup>/kg and 0.045 (0.0299, 0.0608)/year, respectively. Results also quantified drug effects on fracture risk that were often independent of the BMD increase elicited by the therapy. PPCs showed that this hazard model predicted both the individual and population level data (Figure 1).

**Conclusion:** In addition to further supporting evidence that therapy effects on bone composition and strength are not fully represented by BMD measurements alone, model development quantitatively links patient characteristics and response to therapy to fracture reduction. Model-generated predictions help to determine the extent to which the variability in these factors contribute to fracture risk.

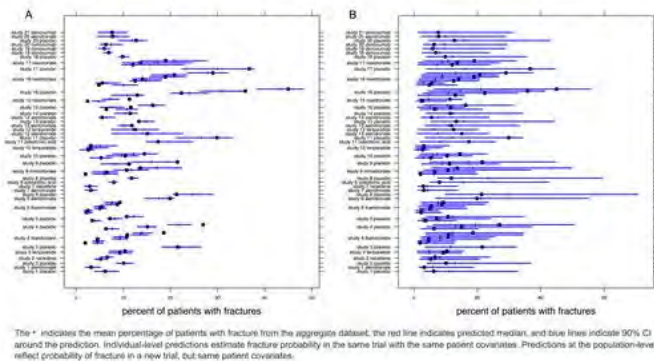


Figure 1: Individual (A) and population (B) -level PPCs grouped by study arm

**Disclosures:** Rena Eudy, None.

This study received funding from: Metrum Institute

**SA0218**

See Friday Plenary Number FR0218.

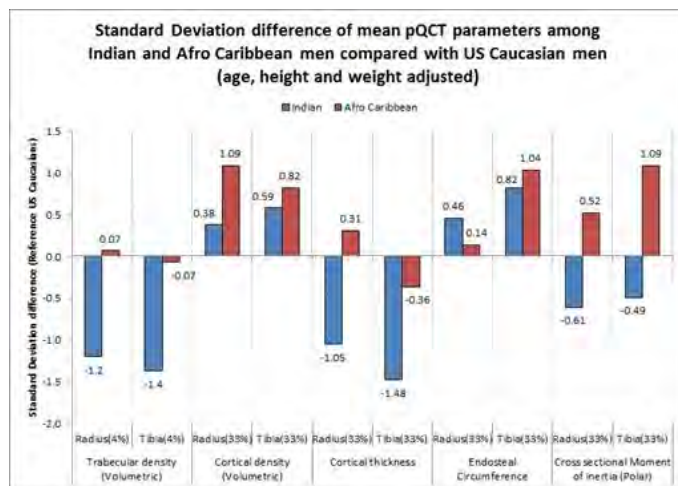
**SA0219**

**Comparison of Volumetric Bone Mineral Density and Macro-architecture among Indian, United States Caucasians and Afro Caribbean Older Men.** Guru Rajesh Jammy\*<sup>1</sup>, Robert M. Boudreau<sup>1</sup>, Tushar Singh<sup>1</sup>, Pawan Sharma<sup>2</sup>, Kristine E Ensrud<sup>3</sup>, Joseph M. Zmuda<sup>1</sup>, P S Reddy<sup>2</sup>, Anne B Newman<sup>1</sup>, Jane A Cauley<sup>1</sup>. <sup>1</sup>Department of Epidemiology, University of Pittsburgh, United states, <sup>2</sup>SHARE INDIA - Medciti Institute of Medical Sciences, India, <sup>3</sup>Division of Epidemiology & Community Health, University of Minnesota; Department of Medicine, University of Minnesota; Center for Chronic Disease Outcomes Research, VA Health Care System, Minneapolis., United states

Accelerated population aging has placed more individuals at risk for osteoporosis and hip fractures, especially in the developing world. The future

bulk of hip fractures are anticipated to occur in China and India. Hip fracture rates have been shown to differ globally by 200%. The factors that underlie geographical differences in hip fracture rates are unknown. Bone Mineral Density (BMD) by Dual energy X ray absorptiometry (DXA) among Indian women was 27% lower compared to the US women. Peripheral quantitative computerized tomography (pQCT) measures of volumetric BMD (vBMD) and bone macro-architecture among Indian population have not been described. We compared pQCT parameters among Indian, United States Caucasians and Afro Caribbean men aged 60 years and older. We studied men enrolled in the Mobility and Independent Living among Elders Study (MILES) in rural India (N=245); Osteoporotic Fractures in Men Study (MrOS) in the US (N=1147) and the Tobago Bone Health Study on the Island of Tobago, Trinidad and Tobago (N=896). pQCT across the studies was calibrated using European forearm phantom. We compared the trabecular vBMD (radius 4% & tibia 4%); cortical vBMD, cortical thickness, endosteal circumference and cross sectional moment of inertia at radius 33% & tibia 33%.

Indian men were significantly younger [Mean (SD) = 68 (6.6)] compared to the Caucasian men [77 (5.1)] but were similar in age compared to the Afro Caribbean men [69 (6.7)]. The BMI (kg/m<sup>2</sup>) of Indian men [21.5 (3.9)] was significantly lower compared to the US Caucasians [27.9 (3.9)] and Afro Caribbean men [26.9 (4.5)]. Indian men were also shorter and lighter. Age, height and weight adjusted mean pQCT parameters among Indian and Afro Caribbean men compared with US Caucasian men as reference group are shown (Figure 1). After adjusting for age, height and weight, Indian men had lower Trabecular vBMD [1.05 to 1.48 SD], cortical thickness [1 to 1.5 SD] and cross sectional moment of inertia [0.49 to 0.61 SD] compared to Caucasians; cortical vBMD [0.38 to 1.09 SD] and endosteal circumference [0.46 to 1.04 SD] of Indian and Afro Caribbean men were higher than the Caucasians; all the differences were statistically significant for Indian men compared to the Caucasian and Afro Caribbean men. These findings indicate overall reduced bone strength and suggest underlying higher risk for osteoporotic fractures among rural Indians and points towards a greater future burden.



pQCT parameters among Indian and Afro Caribbean men compared with US Caucasians

**Disclosures:** Guru Rajesh Jammy, None.

**SA0220**

See Friday Plenary Number FR0220.

**SA0221**

**Regional Variations in Rates of Osteopenia, Osteoporosis, Fractures, and Bone Mineral Density Screening in Male US Veterans.** Joanne LaFleur\*<sup>1</sup>, Yan Cheng<sup>1</sup>, Jacob Crook<sup>2</sup>, Robert Adler<sup>3</sup>, Kenneth Lyles<sup>4</sup>, Cathleen Colon-Emeric<sup>4</sup>. <sup>1</sup>University of Utah College of Pharmacy Department of Pharmacotherapy, United states, <sup>2</sup>University of Utah Division of Epidemiology, United states, <sup>3</sup>Richmond VA Medical Center, United states, <sup>4</sup>Duke University Department of Geriatrics, United states

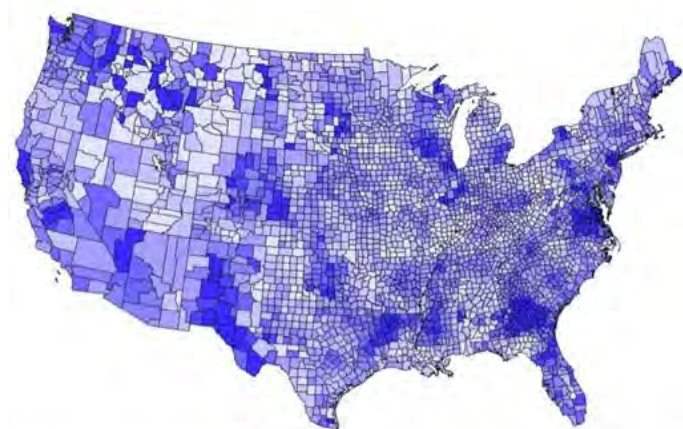
**Background:** Regional variation in fracture rates has been cited in numerous studies. It is not known whether regional variation is driven by regional differences in rates of identification and treatment, whether it is due to differences in disease patterns, or both. We examined regional variations in rates of osteopenia, osteoporosis fractures, and bone mineral density screening using dual-energy x-ray absorptiometry (DXA) in Veterans.

**Methods:** All male United States (US) Veterans ages 50+ with primary care encounters in the Veterans Affairs Health Care System (VAHCS) from 1999-2009 were included. DXA scans were identified using Current Procedural Terminology (CPT) codes from VAHCS datasets and Medicare data as well as by natural

language processing (NLP) of VAHCS radiology reports and clinical notes. DXA results were identified using NLP from radiology reports and clinical notes. Osteoporosis diagnoses and osteoporotic fractures were identified using codes from the 9th Revision of the International Classification of Diseases (ICD-9). Incidence rates for DXA scans, osteopenia, osteoporosis, and osteoporotic fractures were calculated overall and by geographic region, age, race/ethnicity, and body mass index (BMI).

Results: A total of 4.9 million veterans received care in the 11-year observation period. The mean (SD) age of the cohort was 65.3 (10.4). A total of 389,425 Veterans had at least 1 DXA scan after age 50. The figure shows the geographic variation in incidence of DXA screening events across the continental US. The incidence of screening scans ranged from 0.696 (95% CI 0.648, 0.744) to 1.08 (95% CI 1.03, 1.14) scans per 100 PY for the midwestern to the western census regions, respectively. Urban settings tended to have the highest incidence of DXA screening scans (1.20, 95% CI 1.20, 1.21) and isolated small rural towns had the lowest (0.98, 95% CI 0.97, 1.00). Rates of osteoporosis and osteopenia also showed highly variable rate distributions according to geographic regions.

Conclusions: High variability was observed in rates of DXA screening scans, osteopenia, osteoporosis, and fractures. Variability appeared to be associated with variations in both rates of screening as well as in rates of bone disease across the US.



Key: Incidence per 100 PY

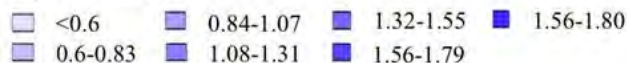


Figure. Variation in rates of DXA screening scans across the continental US

Disclosures: Joanne LaFleur, None.

## SA0222

**Relationship Between Serum Vitamin B6 and Bone Mineral Density in the Middle-aged and Elderly People in Shanghai, China.** Lin Chen<sup>\*1</sup>, Jing Wang<sup>2</sup>, Chenguang Li<sup>1</sup>, Liang Qiao<sup>1</sup>, Xiaofeng Qi<sup>1</sup>, Qiang Wang<sup>1</sup>, Xuejun Cui<sup>3</sup>, Bing Shu<sup>1</sup>, Yongjun Wang<sup>4</sup>. <sup>1</sup>Longhua Hospital, Shanghai University of Traditional Chinese Medicine; Spine Research Institute, Shanghai University of Traditional Chinese Medicine, China, <sup>2</sup>Longhua Hospital, Shanghai University of Traditional Chinese Medicine; Shanghai Geriatric institute of Chinese Medicine, China, <sup>3</sup>Longhua Hospital, Shanghai University of Traditional Chinese Medicine, China, <sup>4</sup>Longhua Hospital, Shanghai University of Traditional Chinese Medicine; School of Rehabilitation Science, Shanghai University of Traditional Chinese Medicine; Spine Research Institute, Shanghai University of Traditional Chinese Medicine, China

Background: Lower vitamin B6 (Pyridoxine) concentration was found to be a novel and potentially modifiable factor for osteoporosis, but the relationship between vitamin B6 concentration and bone mineral density (BMD) is inconsistent. The objective of this study was to determine the association between serum vitamin B6 concentration and BMD in the middle-aged and elderly people in Shanghai, China.

Methods: A total of 726 respondents (men aged from 50 to 79 and women aged from 45 to 79) in Shanghai were included in this study. Serum vitamin B6 was detected and lumbar spine BMD was measured by dual energy X-ray absorptiometry (DXA).

Results: Serum vitamin B6 was positively associated with gender ( $r=0.138$ ,  $P<0.001$ ). No statistical significant relationship was found between vitamin B6 and age (female,  $r=-0.05$ ,  $P=0.23$ ; male,  $r=-0.02$ ,  $P=0.83$ ). There was also no significant relationship between vitamin B6 and T value of BMD (female,  $r=0.00$ ,  $P=0.95$ ; male,  $r=0.00$ ,  $P=0.96$ ).

Conclusions: Serum vitamin B6 concentration was association with gender, but not age or lumbar spine BMD.

Disclosures: Lin Chen, None.

## SA0223

See Friday Plenary Number FR0223.

## SA0224

See Friday Plenary Number FR0224.

## SA0225

See Friday Plenary Number FR0225.

## SA0226

**Osteoporosis and Functional Outcome after a Distal Radius Fracture in Men – A prospective study of the first post-fracture year.** Lisa Egund<sup>\*</sup>, Fiona McGuigan, Kristina Akesson. Clinical & Molecular Osteoporosis Research Unit, Department of Clinical Science Malmö, Lund University & Department of Orthopedics, Skåne University Hospital Malmö, Sweden, Sweden

Osteoporosis is associated with increased fracture severity and a higher incidence of fracture instability in general, but whether bone density influences functional outcome is still unclear; in men this knowledge is non-existent. The purpose of this prospective study was to evaluate the role of osteoporosis on functional outcome in men with distal radius fracture at 1 year after injury.

### Methods

Adult men presenting with a distal radius fracture were recruited consecutively during 2003-07 and followed for 1 year post-fracture; 101 men completed the study (mean 55y; range 22-88y). Treatment methods were cast  $\pm$  prior reduction or surgery according to the local treatment protocol. Data included medical history, injury mechanism, hand dominance and complications. DXA was measured at hip and spine; osteoporosis was defined as T-score below  $-2.5$ . Charlson Comorbidity Index (CCI) was estimated. Fractures were classified according to AO and radiographic parameters were measured. Main outcome was DASH (Disability of the Arm, Shoulder and Hand) score at 1 year post-fracture; a score  $>25$  being indicative of poor outcome.

### Results

Fractures were classified as type A (26), B (10), C (65). Method of treatment was cast (49), closed reduction and cast (23) and surgery (29, most external fixation). Three patients experienced minor complications (pin infection) and 8 major complications (tendon/ligament rupture, malunion requiring surgery). Osteoporosis was evident in 21 men; 80 were non-osteoporotic. Only age differed between the osteoporotic and non-osteoporotic group; 65y vs 53 y,  $p=0.003$ . Prior fracture was more common in osteoporotic men; 4/21 vs 3/80,  $p=0.014$ .

Men with osteoporosis had a mean DASH score of  $16 \pm 25$  SD compared to  $9 \pm 15$  SD in the non-osteoporotic, although not significant ( $p=0.24$ ). Poor outcome was proportionally more common (4/21 vs 10/80), but not significantly predicted by osteoporosis (OR 1.75, 95% CI: 0.47-6.30).

Increasing age and the occurrence of complications were predictors of a worse functional outcome (DASH unit: 0.4 (0.15-0.61;  $p=0.002$ ); 12.0 (1.3-22.6; 0.03). Neither univariate linear or multivariate regression analysis with covariates age, AO class, treatment, complications, radiography or CCI showed significant correlation between BMD and functional outcome.

### Conclusion

In this prospective study, to our knowledge the first on men with distal radius fracture, BMD was of lesser importance for functional outcome at 1 year after injury.

Disclosures: Lisa Egund, None.

## SA0227

See Friday Plenary Number FR0227.

## SA0228

See Friday Plenary Number FR0228.

## SA0229

See Friday Plenary Number FR0229.

**SA0230**

See Friday Plenary Number FR0230.

**SA0231**

See Friday Plenary Number FR0231.

**SA0232**

See Friday Plenary Number FR0232.

**SA0233**

See Friday Plenary Number FR0233.

**SA0234**

See Friday Plenary Number FR0234.

**SA0235**

See Friday Plenary Number FR0235.

**SA0236**

See Friday Plenary Number FR0236.

**SA0237**

See Friday Plenary Number FR0237.

**SA0238**

**A One Year Post Hip Fracture Survey: Why Are Older Adults Not Receiving Osteoporosis Treatment.** Mia Barnett<sup>1</sup>, Judy Beizer<sup>2</sup>, Stuart Weirnerman<sup>1</sup>, Liron Sinvani<sup>1</sup>, Gisele Wolf-Klein<sup>1</sup>, Andrei Kozikowski<sup>1</sup>. <sup>1</sup>Northwell Health, United states, <sup>2</sup>St. John's University College of Pharmacy & Health Sciences, United states

The National Osteoporosis Foundation estimates that by 2030, 11.9 million US adults will be diagnosed with osteoporosis, and 250,000 patients sustain a hip fracture each year. Yet, the estimated treatment rate for osteoporosis post-hip fracture ranges from 2-25%. Our objective was to explore post-hip fracture patient knowledge, perceptions, barriers and decision process regarding osteoporosis management.

We conducted a prospective cross-sectional telephone survey combined with a retrospective chart review of all hip fracture patients age 65 and over, discharged from two tertiary care hospitals in 2014. Chart data included demographics, insurance status, medical history, and medications. The follow-up one-year telephone survey assessed diagnosis and management information, recent falls and family history.

Of the 482 hip fracture patients, the first 100 subjects were invited to participate in the follow-up survey, and 42 were consented; 86% were female and 69% white, with a mean age of 86. Only 12% of patients reported having a family history of osteoporosis. Most resided at home (88%), assisted living (7%) or in a skilled nursing facility (5%). The majority (71%) reported having not been told that they had osteoporosis. Further, 57% reported that their hospital physicians had not suggested osteoporosis medication and 36% had not received a prescription for osteoporosis. Post-hospitalization, 38% sustained a fall; of those, 44% had an additional fracture. Most (95%) had seen their doctor within the last six months. Over half (52%) reported having a DEXA scan. Of the 64% who were prescribed treatment (most commonly calcium and vitamin D), 85% reported compliance. When asked if they would now accept osteoporosis medication, 50% were not sure, with 25% agreeing and 25% rejecting. Finally, 36% felt that the best time for osteoporosis education would be during a follow-up with their primary care doctor, while 26% preferred education prior to hospital discharge, and 19% during rehabilitation.

Our data highlights an urgent need for osteoporosis education and management following hip fracture, and identifies the importance of individualizing osteoporosis education across the multiple settings of the continuum of care.

**Disclosures:** Mia Barnett, None.

**SA0239**

**Factors Associated with the Online Uptake of a Multi-modal Educational Intervention for the Activating Patients at Risk for Osteoporosis (APROPOS) Study: a Randomized Trial within the GLOW Cohort.** Maria Danila<sup>1</sup>, Elizabeth Rahn<sup>\*1</sup>, Ryan Outman<sup>1</sup>, Amy Mudano<sup>1</sup>, Tammi Thomas<sup>1</sup>, Jeroan Allison<sup>2</sup>, Fred Anderson<sup>2</sup>, Julia Anderson<sup>3</sup>, Peter Cram<sup>4</sup>, Jeffrey Curtis<sup>1</sup>, Liana Fraenkel<sup>5</sup>, Susan Greenspan<sup>6</sup>, Andrea LaCroix<sup>7</sup>, Sumit Majumdar<sup>8</sup>, Michael Miller<sup>9</sup>, Jeri Nieves<sup>10</sup>, David Redden<sup>1</sup>, Monika Safford<sup>11</sup>, Stuart Silverman<sup>12</sup>, Ethel Siris<sup>13</sup>, Daniel Solomon<sup>14</sup>, Amy Warriner<sup>1</sup>, Nelson Watts<sup>15</sup>, Robert Yood<sup>16</sup>, Kenneth Saag<sup>1</sup>. <sup>1</sup>The University of Alabama at Birmingham, United states, <sup>2</sup>University of Massachusetts Medical School, United states, <sup>3</sup>Group Health Cooperative, United states, <sup>4</sup>University of Toronto, Canada, <sup>5</sup>Yale University, United states, <sup>6</sup>University of Pittsburgh, United states, <sup>7</sup>University of California - San Diego, United states, <sup>8</sup>University of Alberta, Canada, <sup>9</sup>The University of Oklahoma, United states, <sup>10</sup>Helen Hayes Hospital, United states, <sup>11</sup>Weill Cornell Medical Center, United states, <sup>12</sup>Cedars-Sinai Medical Center, United states, <sup>13</sup>Columbia University Medical Center, United states, <sup>14</sup>Brigham & Women's Hospital, United states, <sup>15</sup>Mercy Health Osteoporosis & Bone Health Services, United states, <sup>16</sup>Reliant Medical Group, United states

**Purpose:** An urgent need exists for effective educational interventions aimed at increasing osteoporosis therapy initiation. We developed an innovative and tailored educational intervention to inform women about the need for osteoporosis treatment and to determine factors associated with intervention uptake.

**Methods:** US women in the Global Longitudinal Study of Osteoporosis (GLOW) with past self-reported fractures and not currently using osteoporosis therapy were eligible to participate in APROPOS. We delivered the intervention through a website that included educational videos tailored by participants' race/ethnicity, barriers to treatment, readiness for behavior change, and treatment history. To encourage participant engagement, we contacted participants via phone calls and an interactive voice response system. We examined intervention uptake by assessing participants' successful website login within 60 days of initial contact attempt. Bivariate tests and stepwise multivariable logistic regression evaluated differences in intervention uptake by sociodemographic characteristics, type of contact, health literacy, self-reported history of depression, readiness for behavior change, and whether participants expressed concerns about osteoporosis.

**Results:** A total of 1342 women were mailed an introductory letter and intervention materials via standard mail and/or email. Participants assigned to receive intervention materials were 92.9% Caucasian, with a mean (SD) age 74.9 (8.0) years and the majority (77.7%) had some college education. Overall, 28.1% (n=377) of participants accessed the intervention within 60 days after initial contact. Compared to the women who did not logon to view the intervention, women who logged on to their personalized website were more likely to have provided an email address (adjusted OR=6.07, 95% CI 4.53-8.14), and less likely to self-report depression (adjusted OR 0.72, 95% CI 0.51-0.996). In addition, there was approximately 20% lower odds of accessing the videos for every ten years of advancing age (adjusted OR=0.82, 95% CI 0.66-0.95).

**Conclusion:** We developed and implemented a novel, tailored, multi-modal intervention to improve initiation of osteoporosis therapy. Having provided an email address was the most important factor independently associated with accessing the intervention online. The design and uptake of this online intervention may have implications for future studies aimed at improving osteoporosis treatment uptake.

**Disclosures:** Elizabeth Rahn, None.

**SA0240**

See Friday Plenary Number FR0240.

**SA0241**

**Impact of Gastrointestinal Events on Patient-Reported Outcomes in Asia-Pacific Women with Osteoporosis: Baseline Results of the MUSIC OS-AP Study.** Ankita Modi<sup>1</sup>, Peter Ebeling<sup>2</sup>, Mel Lee<sup>3</sup>, Yong-Ki Min<sup>4</sup>, Ambrish Mithal<sup>5</sup>, Xiaoqin Yang<sup>\*1</sup>, Santwona Baidya<sup>6</sup>, Shuvayu Sen<sup>1</sup>, Shiva Sajjan<sup>1</sup>. <sup>1</sup>Merck & Co., Inc., United states, <sup>2</sup>Monash University, Australia, <sup>3</sup>Chang Gung Memorial Hospital, Taiwan, province of china, <sup>4</sup>Sungkyunkwan University, Korea, republic of, <sup>5</sup>Medanta the Medicity, India, <sup>6</sup>Optum, Australia

**Purpose:** The Medication Use Patterns, Treatment Satisfaction, and Inadequate Control of Osteoporosis Study in the Asia-Pacific Region (MUSIC OS-AP) was designed to estimate the impact of gastrointestinal (GI) events on patient-reported outcomes in women with postmenopausal osteoporosis.

**Methods:** MUSIC OS-AP included an observational cohort study of women  $\geq 50$  years of age with physician-confirmed osteoporosis. We report the results from the baseline assessment of patients treated with oral anti-osteoporosis therapies. Patients with baseline GI events were defined as those with GI events in the 6 months before the start of observation and included a variety of mild to moderate clinical symptoms.

Adherence was measured by the Adherence Evaluation of Osteoporosis Treatment (ADEOS) questionnaire and defined as a score of  $\geq 20$  out of 22, and treatment satisfaction was measured by the Osteoporosis Patient Satisfaction Questionnaire (OPSAT; scale 0-100). General health-related quality of life was measured by the European Quality of Life-5 Dimensions (EQ-5D) questionnaire (visual analog scale [VAS] 0-100 and utility score -0.59 to 1.0) and osteoporosis-specific quality of life by the Osteoporosis Assessment Questionnaire (OPAQ; scale 0-100). The association of GI events with each of these outcomes was determined by covariate-adjusted regression analysis of differences in the least squares mean scores of patients with and without GI events. Health care resource use was measured as the number of osteoporosis-related primary care and specialist physician visits over the past 3 months, and multivariate regression analysis was used to assess the association of GI events with the likelihood of each type of visit.

Results: GI events were reported by 59.9% of the 3,286 patients. The rate of adherence was 38%. Differences (95% CI) in the least squares mean scores between patients with and without baseline GI events were -0.348 (-0.591, -0.104;  $P=0.005$ ) for the adherence score, -6.940 (-8.007, -5.874;  $P<0.001$ ) for the OPSAT score, -0.092 (-0.109, -0.074;  $P<0.001$ ) for the EQ-5D utility score, -4.614 (-5.795, -3.433;  $P<0.001$ ) for the EQ-5D VAS score, and -3.663 (-4.763, -2.563;  $P<0.001$ ) for the OPAQ physical function score. GI events had no association with primary care or specialist visits.

Conclusions: The results indicate that GI events at baseline were associated with lower adherence score, treatment satisfaction, and quality of life in women treated for osteoporosis.

**Disclosures:** Xiaojin Yang, Merck & Co., Inc., 15  
This study received funding from: Merck & Co., Inc.

## SA0242

**Over 48,000 Ontario seniors have started denosumab: patient characteristics, regional variation in use and persistence with therapy.** Suzanne M. Cadarette\*, Giulia P. Consiglio, B. Boyd Hao, Joann K. Ban, M. Amine Amiche. University of Toronto, Canada

Background: Denosumab was added to the Ontario public drug formulary in February 2012 to treat severe osteoporosis. Seniors contraindicated for oral bisphosphonates or having experienced a decline in bone mineral density (BMD) after 1-year of continuous oral osteoporosis therapy are eligible for denosumab coverage, provided they also meet at least two of the following three criteria: 1) age  $> 75$  years, 2) BMD t-score  $\leq -2.5$  SD, or 3) prior fragility fracture.

Objectives: To describe denosumab use among seniors in Ontario since its addition to the provincial formulary.

Methods: We identified patients aged 66 or more years starting denosumab from 2012/02 to 2015/03, and followed them through to 2016/01 (last date at time of analysis). Patient characteristics were summarized based on medical and pharmacy claims within the year prior to denosumab initiation, and stratified by residence in the community or long term care (LTC). The rate of new denosumab use per 1000 was calculated and compared between regions after direct standardization to the 2014 Ontario population age and sex. We calculated persistence with denosumab therapy using a 60-day permissible gap, censoring on death or end of follow-up. We summarized persistence as a continuous variable and the proportion persisting with therapy for each year of observation.

Results: We identified 48,535 new users of denosumab (97% women, 89% in community, 79% in urban areas), at a rate of  $\sim 1\%$  of female seniors annually. Denosumab users residing in the community were younger (mean age=78.2, SD=7.5 vs. 86.6 years, SD=6.6), had a higher prevalence of BMD testing (61% vs. 4%) and prior oral bisphosphonate use (9% vs. 3%), yet lower prevalence of fracture (12% vs. 20%) compared to LTC patients. Regional differences in the rate of denosumab use were noted with highest rates in urban Mississauga (54/1000) and Hamilton (50/1000), and lowest rates in rural South East (16/1000) and North West (17/1000) regions. The mean length of persistence with therapy was 1.6 years (SD=1, median=1.4). Seventy-two percent persisted  $\geq 1$  year (71% community, 76% LTC), 55%  $\geq 2$  years (54% community, 56% LTC), and 43%  $\geq 3$  years (43% community, 36% LTC).

Conclusion: New exposure to denosumab is increasing at a rate of about 1% of female seniors annually, and regional differences were identified. On average, patients persisted with denosumab therapy for at least 1.5 years, and over 40% persisted for more than 3 years.

**Disclosures:** Suzanne M. Cadarette, None.

## SA0243

**Patient- and Hospital-Level Factors associated with Receipt of Bone Densitometry (DXA) in Male Veterans Hospitalized for Hip Fracture.** Samantha Solimeo\*, Gary Rosenthal, Mary Vaughan Sarrazin, CADRE, Iowa City VA HCS & Department of Internal Medicine, University of Iowa, United states

Purpose: To identify patient and hospital factors associated with osteoporosis (OP) evaluation, as measured by receipt of dual-energy X-ray absorptiometry (DXA), among male veterans ages 50 and older treated for hip fracture in Department of Veterans Affairs (VA) inpatient settings.

Methods: Male patients ages 50 and older treated for hip or pelvis fracture were identified from VA inpatient claims (CY 2009-2012). Exclusions were made for patients with hospice or palliative care at the time of the encounter (n=188); Paget's or

osteomalacia (n=71); spinal cord injury (n=143), or history of prior DXA (n=467), OP diagnosis (n=957), or pharmacotherapy (n=561). Receipt of post-fracture DXA up to 2 years after the fracture were identified in VA and CMS encounter data for the remaining sample (n=4713). We used Cox proportional hazards model with random effects for the facility to evaluate associations between patient and hospital complexity and DXA screening. Patient-level factors include demographic (age, race, VHA eligibility category, income, and rural residence) and comorbid conditions. A single hospital characteristic reflected the complexity of services available at the patient's hospital, using the VA complexity classification that reflects hospital volume, case mix, clinical services and available specialties, residency programs, and research funding.

Results: Overall, 11% of patients received a DXA within two years of fracture. Increasing patient age was significantly associated with a lower likelihood of DXA receipt. No other demographic characteristics were related to DXA receipt. Several comorbid conditions were identified as significantly associated with likelihood of DXA, including history of lymphoma, non-metastatic cancer, arthritis, coagulation disorders, fluid or electrolyte imbalance, and drug abuse. Increasing hospital complexity was associated with higher likelihood of DXA.

Conclusion: We found that a minority of men were evaluated with DXA within the two years following VA inpatient treatment for hip fracture. Patient's dual eligibility for VA and CMS services, race, rural residence, and income level were not associated with likelihood of testing, and few clinical characteristics appeared significant. The complexity of the patients' assigned healthcare facility was significantly associated with likelihood of DXA. These findings confirm the importance of healthcare delivery systems in managing OP care after sentinel events.

**Table 1: Patient Characteristics and Frequency of Post Fracture DXA**

	Number, % of total	Number of patients who Received DXA, %
Overall	4713 100	531 11.3%
<b>Demographic Characteristics</b>		
Age at time of fracture (mean, SD)	76.65 11.12	73.5 10.3
VA-CMS dual eligible	3085 65.4	361 11.8
<b>Race and ethnicity</b>		
White	3626 76.9	415 11.4
Black	500 10.6	55 11.0
All other	345 7.3	39 11.3
Missing	242 5.1	22 9.1
<b>Rural residence (RUCA)</b>		
Isolated	222 4.7	22 9.9
Small rural	292 6.2	36 12.3
Large rural	394 8.4	35 8.9
Urban	2801 59.4	336 12.0
Missing	1004 21.3	102 10.2
<b>VA means category</b>		
Service connected	1569 33.3	178 11.3
Low income	1795 38.1	206 11.5
All other	1349 28.6	147 11.0
<b>Clinical Characteristics</b>		
Congestive heart failure	847 18.0	72 8.5
Arrhythmia	1217 25.8	105 19.8
Valvular disorder	309 6.6	30 9.7
Pulmonary circulatory disorder	127 2.7	13 10.2
Peripheral vascular disease	708 15.0	82 11.6
Uncomplicated hypertension	2874 61.0	319 11.1
Complicated hypertension	355 7.5	33 9.3
Paralysis	76 1.6	7 9.2
Neurological disorder	613 13.0	49 8.0
Chronic obstructive pulmonary disease	1286 27.3	134 10.4
Uncomplicated diabetes	1466 31.1	153 10.4
Complicated diabetes	663 14.1	70 10.6
Hypothyroid	254 5.4	24 9.5
Renal failure	619 13.1	53 8.6
Liver disease	394 8.4	25 12.9
AIDS	31 0.6	7 22.6
Peptic ulcer	71 1.5	8 11.2
Lymphoma	57 1.2	9 15.8
Metastatic cancer	89 1.9	8 9.0
Nonmetastatic cancer	837 17.8	108 13.0
Arthritis	90 2.0	16 17.8
Coagulation Disorder	163 3.4	26 16.0
Obesity	121 2.6	23 19.0
Weight loss	305 6.5	36 11.9
Fluid or electrolyte disorder	699 14.8	60 8.6
Blood loss anemia	37 0.8	3 8.1
Deficiency anemia	314 6.6	22 7.0
Alcohol abuse	429 9.1	66 15.4
Drug abuse	194 4.1	19 9.8
Psychosis	517 11.0	52 10.0
Depression	1170 24.8	141 12.0
Ulcer no bleeding	55 1.1	8 14.5
Parkinson's disease	368 7.8	32 8.7

\* $p<0.05$ , Fisher's Exact or Chi square where appropriate

Table 1

**Disclosures:** Samantha Solimeo, None.

## SA0244

**Rush Fracture Liaison Service for Capturing "missed opportunities" to Treat Osteoporosis..** MILLI JAIN\*<sup>1</sup>, SHUCHI SHAH<sup>2</sup>, SANFORD BAIM<sup>1</sup>.  
<sup>1</sup>RUSH university, United states, <sup>2</sup>Graduate College, Rush University, United states

Fragility fractures occur in almost one in two older women and one in three older men (1). A fragility fracture is highly predictive of future fractures (1), increases morbidity, mortality, emotional and financial burden to the patient and their families, and healthcare costs to society. A Fracture Liaison Service (FLS) has been described as one of most effective interventions for secondary fracture prevention (1). We initiated such a service by instituting an automated alert in the electronic medical record system that is triggered by a historical and/or an acute fracture in patients aged 50 years or older, seen in the emergency department or admitted to the inpatient

services. We report the results of the first 100 patients evaluated by the FLS. Traumatic fractures and malignancy related pathological fractures were not included.

Results: 59% were females, 55% were Caucasians, 33% African Americans, 6% Hispanic, 5% Asians and 1% native Americans. Acute and/or historical fracture was seen in 98%, while 2% were seen for osteoporosis without a fracture. Of all patients with fractures, 95% had fragility fractures while 3% had high trauma fractures but orthopedic surgeon suspected osteoporosis during internal fixation. Out of 95 fragility fractures, 32 presented with a first-time fracture, 31 had only a history of fracture(s), and 37 had both a historical and acute fracture(s). 16% of all patients had been previously diagnosed with osteoporosis of which 3 presented with a first-time fracture, 1 had a historical fracture, 10 had both historical and acute fracture(s), and 2 had a DXA diagnosis of osteoporosis without a prevalent fracture. 30% patients had DXA prior to FLS consult. 20% were ever prescribed anti-osteoporosis medications and 4% were actively taking them when seen. 83% patients did not have a diagnosis of osteoporosis documented prior to FLS consult. 50% (41/82 patients tested) had secondary hyperparathyroidism, 39% (34/87 patients tested) had vitamin D deficiency including 20.6% (18/87) with an undetectable 25 hydroxy vitamin D.

Conclusions: This study supports previous published fracture data and the American Society of Bone Mineral Research Task Force findings that osteoporotic fractures are grossly undiagnosed and untreated. Among secondary factors, vitamin D deficiency was common. The high number of repeat fracture(s) shows the importance of a FLS in secondary prevention.

#### Reference

(1) Eisman JA et al. *J Bone Miner Res.* 2012 Oct;27(10):2039-46.

**Disclosures:** MILLI JAIN, None.

## SA0245

See Friday Plenary Number FR0245.

## SA0246

**Clinical Utility of Spinal Imaging in Patients Deemed at Moderate Fracture Risk in an Orthopaedic Post Fracture Intervention Program for Osteoporosis Care.** Earl Bogoch, Victoria Elliot-Gibson\*, Erin Norris, Robert Josse, Joanna Sale. St. Michael's Hospital, Canada

Purpose: To describe the impact of spinal imaging on fracture risk stratification for treatment-naïve fragility fracture (FF) patients in a Canadian Fracture Liaison Service (FLS).

Methods: A FLS was implemented to increase the intervention rates in females and males  $\geq 50$  years presenting with a FF of the wrist, shoulder, vertebrae and hip. This program provides education, fracture risk assessment in accordance with Osteoporosis Canada's 2010 Guidelines, and referral for further assessment and treatment, as indicated. Data were collected through an audit of electronic health records. This report focuses on a cohort of wrist and shoulder FF patients, seen by a metabolic bone specialist, who completed bone densitometry (BMD) with a femoral neck T-score available, and either a vertebral fracture assessment (VFA) or thoracic and lumbar spinal x-rays.

Results: Between August, 2011 and November, 2015, 127 patients with wrist (n = 78) or shoulder (n = 49) FF met entry criteria. There were 37 males, mean age 69.7 (SD 11.5) and 90 females mean age 66.7 (SD 10.2). Eighty-nine patients completed VFA, 37 completed thoracic/lumbar spinal x-rays, and one completed both. Ninety-eight (77%) patients did not have a documented vertebral fracture on VFA or x-ray. Sixty-four (50%) patients were deemed to be at high risk for future fracture using the Canadian Association of Radiologists and Osteoporosis Canada (CAROC, 2010) risk assessment tool, and of these 19 (30%) were found to have a new vertebral fracture. However, this new vertebral fracture did not change the risk categorization as they were already high risk. Fifty-five (86%) of the 64 high risk FF patients received a prescription for pharmacotherapy, five (8%) of 64 declined pharmacotherapy, 2 (3%) of 64 had a delay in initiating pharmacotherapy and two (3%) received a recommendation of vitamin D and calcium. Sixty-three patients (50%) were deemed to be at moderate risk of future fracture using CAROC 2010 and 10 (16%) had a previously unknown vertebral fracture which increased their risk category to high, prompting a prescription of pharmacotherapy for all 10, in which one patient declined. Of the fifty-three FF patients remaining at moderate risk, 49 (92%) received guideline recommendations for vitamin D and calcium, and four (8%) received an additional recommendation of specific anti-osteoporosis pharmacotherapy.

Conclusion: In 30% of high risk FF patients, mean age 72, we found a previously unknown vertebral fracture, which did not change treatment recommendations. In 16% of FF patients deemed to be at moderate risk, mean age 63, a vertebral fracture was identified which did change treatment recommendations. In selected cases, specifically FF patients at moderate risk of future fracture, a VFA or spinal x-rays may help to inform the need for specific anti-osteoporosis pharmacotherapy.

**Disclosures:** Victoria Elliot-Gibson, Novartis Canada Ltd, 11; Mr. and Mrs. W. Saunderson, 11; Amgen Canada Inc, 11; Warner Chilcott, 11; Helen McCrea Peacock Foundation, 11; Merck Frosst Canada Inc, 11; Martin Family Foundation, 11; Mr. Clifford Martin, 11; Procter and Gamble Pharmaceuticals Inc, 11; Alliance for Better Bone Health, 11

## SA0247

See Friday Plenary Number FR0247.

## SA0248

**Cardiovascular disease and calcium supplementation: a cross-sectional study primary care in South Brazil.** Ronaldo Godinho, Pietra Zorzo, Thales Ilha, Adhan de Vieira, Felipe Langer, Leo Dal Osto, Rafaela Copes, Fabio Comim, Melissa Premaor\*. Federal University of Santa Maria, Brazil

There is no consensus about calcium supplementation in postmenopausal women and its effects in the cardiovascular risk. Studies carried out in different populations have shown different results. Despite the fact that the Brazilian population has low calcium intake and a mixed background the cardiovascular risk in subjects taking calcium is not known. The aim of this study was to evaluate the association between calcium supplementation and cardiovascular disease in postmenopausal women attending the primary care in Brazil. We conducted a cross-sectional study in the municipality of Santa at Santa Maria (parallel 29o South), Brazil from 1 March to 31 August 2013. Postmenopausal women aged 55 years or older who had at list one appointment at their GP practice in the two years prior the study were recruited from March 1st to August 31st, 2013. Women with cognitive impairment were excluded. The subjects were questioned about the calcium supplement, comorbidities, and CVD. Generalized linear regression models were performed to evaluate the association and adjust for potential confounders. From the 1301 women invited to participate in the study, 1057 completed the questionnaire. Their mean [mean (SD)] age was 67.2(7.6) years. The frequency of calcium supplementation was 18.6%. There was no association between heart failure, stroke, and ischemic heart disease and calcium supplementation [RR (95% CI) - 0.3 (-0.9, 0.4), -0.2 (-0.8, 0.4); - 0.5 (-1.0, 0.02); respectively]. In conclusion, we found no increased risk of CVD in women using calcium supplementation at the primary care in South Brazil.

**Disclosures:** Melissa Premaor, None.

## SA0249

**Dietary Calcium Intake and Vascular Markers in Healthy Postmenopausal Women.** Angel Ong\*<sup>1</sup>, Shubhbrata Das<sup>2</sup>, Hope Weiler<sup>1</sup>, Michelle Wall<sup>3</sup>, Angela Cheung<sup>4</sup>, Elham Rahme<sup>5</sup>, Susan Whiting<sup>6</sup>, Stella Daskalopoulou<sup>7</sup>, David Goltzman<sup>7</sup>, Suzanne Morin<sup>7</sup>. <sup>1</sup>School of Dietetics & Human Nutrition, McGill University, Canada, <sup>2</sup>Division of Experimental Medicine, Department of Medicine, McGill University, Canada, <sup>3</sup>McGill University Health Centre Research Institute, Canada, <sup>4</sup>Department of Medicine, University of Toronto, Canada, <sup>5</sup>Division of Clinical Epidemiology, McGill University Health Centre Research Institute, Canada, <sup>6</sup>College of Pharmacy & Nutrition, University of Saskatchewan, Canada, <sup>7</sup>Department of Medicine, McGill University Health Centre Research Institute, Canada

Purpose: Meta-analyses suggest an association between calcium (Ca) supplements and increased rates of cardiovascular events. Whether dietary Ca intake has similar effects on vascular health is unknown. The objective of this cross-sectional analysis was to examine the association between dietary Ca intake and vascular parameters including carotid intima-media thickness (cIMT) and carotid-femoral pulse wave velocity (cfPWV) in healthy postmenopausal women.

Methods: Baseline data of 36 postmenopausal women were analyzed. All were non-users of Ca or vitamin D supplements and participants of a randomized controlled trial (RCT) that aims to evaluate the effect of dietary Ca as compared to supplemental Ca intake on vascular health (ClinicalTrials.gov NCT0173140). Usual dietary Ca intake (in previous month) was categorized into 3 levels (<600, 600-1000, and >1000 mg/d). Blood pressure (BP), body composition, physical activity level (PAL), serum lipid profile and high-sensitivity C-reactive protein (hsCRP) were assessed. cIMT and cfPWV were measured by B-mode ultrasound and applanation tonometry. Differences in vascular markers across levels of Ca intake were analyzed using one-way ANOVA. We created multivariable linear regression models to examine the association between dietary Ca intake and cIMT and cfPWV.

Results: Participants, mean  $\pm$  SD age 59  $\pm$  6 y, had a systolic BP (SBP) of 115  $\pm$  11 mmHg, body mass index (BMI) of 25.7  $\pm$  3.4 kg/m<sup>2</sup>, and waist circumference (WC) of 90.3  $\pm$  8.6 cm. Eighty-two percent were never smokers, and 52% reported a high PAL (median 60 [IQR 35-100] MET-hour/week). There were no significant differences in BMI, WC, total and LDL-cholesterol, or hsCRP across groups of Ca intake. SBP was observed to be higher in the highest Ca intake group compared to the moderate intake group (122  $\pm$  7 mmHg vs 111  $\pm$  12 mmHg, p=0.02). There was no difference in cIMT nor cfPWV across groups. After adjusting for age, SBP and WC, there was no significant association between Ca intake and cIMT nor cfPWV in linear regression models (Table).

Conclusion: In this cross-sectional analysis of a small sample of healthy postmenopausal women, dietary Ca intake was not associated with vascular parameters. Our RCT will provide longitudinal data necessary to evaluate the association between Ca intake (supplements and diet) on vascular health.

Table. Multiple linear regression results for cIMT and cfPWV

Vascular Markers	Model	Parameter Estimate	Standard Error	95% Confidence Interval	P Value
cIMT <sup>a</sup>	Intercept	0.284	0.260	(-0.247, 0.184)	0.28
	Dietary calcium intake 1 (<600 mg/d) <sup>c</sup>	-0.001	0.042	(-0.086, 0.084)	0.99
	Dietary calcium intake 3 (>1000 mg/d) <sup>c</sup>	0.020	0.014	(-0.009, 0.048)	0.18
	Age (y)	0.007	0.003	(0.001, 0.014)	0.03
	Systolic BP (mmHg)	-0.001	0.002	(-0.005, 0.003)	0.47
	Waist circumference (cm)	0.001	0.002	(-0.004, 0.005)	0.74
cfPWV <sup>b</sup>	Intercept	0.710	3.447	(-6.330, 7.749)	0.84
	Dietary calcium intake 1 (<600 mg/d) <sup>c</sup>	-0.091	0.553	(-1.22, 1.037)	0.87
	Dietary calcium intake 3 (>1000 mg/d) <sup>c</sup>	0.102	0.187	(-0.280, 0.485)	0.59
	Age (y)	0.099	0.042	(0.012, 0.185)	0.03
	Systolic BP (mmHg)	0.027	0.026	(-0.026, 0.079)	0.30
	Waist circumference (cm)	-0.025	0.028	(-0.082, 0.032)	0.38

<sup>a</sup> Model summary:  $F_{(5,30)} = 2.450$ ,  $p = 0.056$ ,  $R^2 = 0.290$ , Adjusted  $R^2 = 0.172$ .

<sup>b</sup> Model summary:  $F_{(5,30)} = 2.930$ ,  $p = 0.029$ ,  $R^2 = 0.328$ , Adjusted  $R^2 = 0.216$ .

<sup>c</sup> Dietary calcium intake = Total calcium intake

cIMT, carotid intima-media thickness; cfPWV, carotid-femoral pulse wave velocity.

Table - Multiple linear regression results for cIMT and cfPWV

Disclosures: Angel Ong, None.

## SA0250

See Friday Plenary Number FR0250.

## SA0251

See Friday Plenary Number FR0251.

## SA0252

See Friday Plenary Number FR0252.

## SA0253

**Moderate-to-vigorous Physical Activity but not Sedentary Time is Associated with Musculoskeletal Health Outcomes in a Cohort of Australian Middle-aged Women.** Feitong Wu<sup>\*1</sup>, Karen Wills<sup>1</sup>, Laura Laslett<sup>1</sup>, Brian Oldenburg<sup>2</sup>, Graeme Jones<sup>1</sup>, Tania Winzenberg<sup>1</sup>. <sup>1</sup>Menzies Institute for Medical Research, University of Tasmania, Australia, <sup>2</sup>School of Population & Global Health, University of Melbourne, Australia

Few studies have described associations between physical activity and sedentary behaviour and musculoskeletal outcomes in younger adults. Therefore, this study aimed to describe associations between objectively-measured physical activity and sedentary time and musculoskeletal health outcomes in middle-aged women.

A population-based sample of 309 women (aged 36-57 years) had total physical activity (accelerometer counts/minute of wear time), and time spent sedentary, in light and moderate-to-vigorous physical activities (MVPA) (by Actigraph GT1M accelerometer), lumbar spine (LS) and femoral neck (FN) bone mineral density (BMD) (by dual-energy X-ray absorptiometry), lower limb muscle strength (LMS) and dynamic and static balance tests (timed up and go test (TUG), functional reach test (FRT), lateral reach test (LRT) and step test (ST)) measured. Cross-sectional associations between BMD and balance were assessed using linear regression.

Total physical activity was beneficially associated with FN BMD ( $\beta$  (95% confidence interval) = 0.011 g/cm<sup>2</sup>, 0.003 to 0.019), LMS (2.13 kg, 0.21 to 4.06) and TUG (-0.080 seconds, -0.129 to -0.030), after adjustment for confounders. MVPA was also beneficially associated with FN BMD (0.0050 g/cm<sup>2</sup>, 0.0007 to 0.0094), LMS (1.48 kg, 0.45 to 2.52), ST (0.12 steps, 0.02 to 0.23) and TUG (-0.043 seconds, -0.070 to -0.016). Associations between MVPA and LMS, TUG and ST persisted after further adjustment for sedentary time. Only TUG was associated with sedentary time, with a detrimental effect (0.075 seconds, 0.013 to 0.137) and this did not persist after further adjustment for MVPA. Light physical activity was not associated with any outcome.

MVPA appears more important than light or sedentary activity for many musculoskeletal outcomes in younger women. This needs to be considered when developing interventions to improve habitual physical activity that aim to improve musculoskeletal health.

Disclosures: Feitong Wu, None.

## SA0254

**Yoga-Associated Vertebral Compression Fractures: Experience from a Tertiary Referral Care Center.** Jad Sfeir<sup>\*</sup>, Vikram Sonawane, Mehrsheed Sinaki, Matthew Drake. Mayo Clinic, United states

Background: There is increasing awareness in the general population and among healthcare providers as to the importance of exercise for maintenance of bone health.

Despite this, the safety of prescribed or recreational exercise in at-risk populations remains under-reported and under-publicized. Yoga has gained widespread popularity due to its physical and psychological benefits. When practiced in a population at increased fracture risk, however, yoga may exceed the biomechanical competence of the spine. Thus rather than increasing bone density as noted in recent news reports, some yoga poses may instead induce vertebral compression fractures (VCF).

Objectives: To increase awareness regarding the safety of yoga in relation to yoga-associated VCF.

Methods: Nine patients who sustained VCF while practicing yoga were identified from the Mayo Clinic medical records. We reviewed the records of these patients including biochemical parameters, bone mineral density, fracture location, and documented yoga poses to determine risk factors for yoga-associated VCF.

Results: Eight women and 1 man with a median age of 66 years (range 53-87) developed VCF 1 month to 6 years after initiating yoga-associated spinal flexion exercises (SFE). VCF presented with back pain and occurred in the T-spine (n=6), L-spine (n=4) and C-spine (n=1). Four patients had osteoporosis by BMD criteria prior to VCF and 2 had osteopenia (median T-score -2.35; range -3.3 to +2.0). Interestingly, all patients had their lowest T-scores at the spine. Three patients had a history of fragility fracture prior to the index VCF. While one patient had primary hyperparathyroidism and another was treated with high dose prednisone, no other risk factors for bone loss including medications or secondary osteoporosis causes were identified in the other patients.

Conclusion: This study identified patients in whom increased torque pressure and compressive mechanical loading occurring during yoga SFE resulted in de novo VCF. Despite the need for selectivity in yoga poses in populations at increased fracture risk, scientific and media reports continue to advertising yoga as a bone protective activity. Accordingly, yoga is misconceived as a 'one-size-fits-all' prescription. Instead, the appropriate selection of patients likely to benefit from yoga must be a cornerstone of fracture prevention.

Disclosures: Jad Sfeir, None.

## SA0255

**Comparison of Lifestyle Factor, Nutritional Status and Bone Mineral Density in Korean Women.** Hee-Sook Lim<sup>1</sup>, Tae-Hee Kim<sup>2</sup>, Dong-Won Byun<sup>\*3</sup>, Hae-Hyeog Lee<sup>2</sup>, Yoo-Jin Park<sup>2</sup>. <sup>1</sup>Department of Nutrition, Soonchunhyang University Bucheon Hospital, Korea, republic of, <sup>2</sup>Department of Obstetrics & Gynecology, Soonchunhyang University College of Medicine, Korea, republic of, <sup>3</sup>Division of Endocrinology & Metabolism, Department of Internal Medicine, Soonchunhyang University College of Medicine, Korea, republic of

Background and Purpose: Osteoporosis has been suggested as a problem in correlation with aging phenomenon caused by life extension. The risk of bone-related disease is higher in females than in males. Genetic and environmental factors are known to play a key role in bone metabolism and diet is considered as one of the most important environmental factors. The purpose of this study was to assess the status of BMD and to compare the dietary intakes and life behaviors in Korean women.

Method: A total of 160 subjects participated in this study. Subjects were surveyed via self-administered questionnaire regarding their general characteristics, dietary behaviors, and physical activities. Nutrient intakes of the subjects were assessed by semi-quantitative food frequency questionnaire. The BMDs of the lumbar spine and femoral neck were measured by dual energy X-ray absorptiometry (DEXA). The subjects were divided into two groups on their BMD.

Result: Average age, height, and weight were 56.3 yrs, 155.8 cm, and 56.6 kg, respectively, with no significant differences. Classification according to T-score of the subjects were 68.2% and 31.8%, in normal and osteoporosis groups, respectively. A Alcohol consumption and regular exercise frequency was not significant differences but frequency of osteoporosis group was higher than normal group. The intake of calcium, vitamin A, vitamin C, and zinc were significantly lower in osteoporosis group while protein, potassium and sodium intake were higher.

Conclusion: These findings indicate that further studies targeting nutritional interventions should be performed to reduce osteoporosis in Korean women.

Disclosures: Dong-Won Byun, None.

## SA0256

**Does Magnesium Status Influence Bone Mineral Density?.** Michael Johnson<sup>1</sup>, R. Erin Johnson<sup>2</sup>, Karen Hansen<sup>\*1</sup>. <sup>1</sup>University of Wisconsin School of Medicine & Public Health, United states, <sup>2</sup>Saint Luke's Health System, United states

The relationship between magnesium status and osteoporosis is uncertain. A recent meta-analysis (Osteoporos Int 2016; 27:1389-1399) found a weakly positive correlation between dietary magnesium intake and femoral neck (0.14, 95% CI 0.001, 0.280), hip (0.16, 95% CI 0.001, 0.320) and forearm (0.29, 95% CI 0.020, 0.530) bone mineral density (BMD). However, data from the Women's Health Initiative indicated a higher risk of wrist fracture in women with higher magnesium intake (Am J Clin Nutr 2014;99:926-33). We performed a post-hoc analysis of data from a clinical trial (JAMA-Intern Med 2015 Oct 1:175(10): 1612-21) to evaluate the relationship between magnesium and BMD. We hypothesized that higher magnesium intake and serum magnesium levels would correspond to higher BMD.

230 postmenopausal women ages  $61 \pm 6$  years old with 25(OH)D 14-27 ng/mL were randomized to one year of placebo, low or high-dose vitamin D. Subjects completed 4-7 day food diaries, serum magnesium and BMD at 0 and 12 months. We measured C-telopeptide (CTX) and bone-specific alkaline phosphatase (BSAP) in a subset of women who came to all six study visits fasting, with phlebotomy before 10 am (n=149). We used Spearman correlation coefficients to evaluate relationships between dietary and serum magnesium, measures of BMD and bone turnover.

Dietary magnesium positively correlated with baseline femoral neck ( $\rho$  0.153, 95% CI 0.021, 0.281) but not spine, hip or total body BMD. By contrast, serum magnesium levels were inversely associated with baseline femoral neck, hip and total body BMD (Table). Moreover, serum magnesium levels were inversely associated with the one-year change in total body BMD (Table). Serum magnesium levels were inversely correlated with BSAP at 0 ( $\rho$  -0.153, 95% CI -0.311 to 0.012) and 12 months ( $\rho$  -0.172, 95% CI -0.328 to -0.007). Serum magnesium levels were inversely correlated with CTX at 12 months ( $\rho$  -0.168, 95% CI -0.324 to -0.003) but not at baseline.

In this post-hoc analysis, higher serum magnesium levels correlated inversely with baseline BMD, one-year changes in total body BMD, and bone formation. Our data, coupled with data linking higher magnesium intake to higher fracture risk, suggest that more magnesium intake is not necessarily better for bone health. Further carefully designed studies are needed, to evaluate the relationship between dietary magnesium intake, serum magnesium levels and skeletal health.

Spearman Correlations between Serum Magnesium and Bone Mineral Density (BMD)				
BMD at Skeletal Site	Baseline		Annualized Change	
	$\rho$ (95% Confidence Interval)	p-value	$\rho$ (95% Confidence Interval)	p-value
Spine	-0.128 (-0.257 to 0.005)	$p = 0.053$	0.018 (-0.118 to 0.153)	$p = 0.790$
Trabecular Bone Score	0.033 (-0.101 to 0.166)	$p = 0.616$	0.112 (-0.024 to 0.245)	$p = 0.097$
Femoral Neck	-0.239 (-0.360 to -0.109)	$p < 0.001$	0.003 (-0.132 to 0.139)	$p = 0.960$
Total Hip	-0.212 (-0.336 to -0.081)	$p = 0.001$	-0.061 (-0.195 to 0.076)	$p = 0.372$
Total Body	-0.187 (-0.313 to -0.055)	$p = 0.004$	-0.160 (-0.290 to -0.024)	$p = 0.018$

Table

Disclosures: Karen Hansen, None.

## SA0257

**Increased Milk Protein Isolate Consumption during Diet-Induced Energy Restriction Does Not Influence Changes in Bone Quantity in Overweight and Obese Older Adults.** Christian Wright\*, Jing Zhou, Wayne Campbell, Purdue University, Department of Nutrition Science, United States

The pervasiveness of obesity is an ever prevalent reality amongst US adults and diet-induced weight loss is an effective strategy to decrease adiposity and improve overall metabolic health. High protein weight loss diets are commonly adopted for weight loss due to their preferential decrease of fat mass over fat-free mass. However, diet-induced weight loss is shown to decrease bone quantity over time and the effect of increased protein intake during energy restriction on bone quantity is still unclear. The purpose of this study was to assess the effect of dietary protein on bone quantity (bone mineral density (BMD) & content (BMC)) during diet-induced energy restriction in overweight/obese adults (randomized, double-blind, parallel, and controlled diet design). Forty-three participants (11M:32F, aged  $53 \pm 1$  y, BMI  $30.6 \pm 0.5$  kg/m<sup>2</sup>, Mean  $\pm$  SE) consumed an energy-balanced diet with 0.8 g protein/kg baseline body mass<sup>-1</sup>·d<sup>-1</sup> for 3 wk (baseline control) before being randomized into either a normal protein (NP, control, n=23) or high protein (HP, n=20) (0.8 vs. 1.5 g·kg<sup>-1</sup>·d<sup>-1</sup>) energy-restricted diet (750 kcal/d deficit) for 16 wk. The HP group consumed their 0.7 g·kg<sup>-1</sup>·d<sup>-1</sup> of additional protein from milk protein isolate. Baseline (wk 4) and post (wk 20) BMD and BMC (total body, lumbar spine (L1-L4), femoral neck, and total hip) were measured (Lunar iDXA and enCORE version 11.2; GE Healthcare). Over the 16-wk intervention, regardless of group distinction, participants lost weight ( $-8.2 \pm 0.4$  kg) through decreases in fat mass ( $-7.0 \pm 0.4$  kg) and lean mass ( $-1.2 \pm 0.2$  kg). Anticipated age and gender differences in indices of bone quantity were observed as older women displayed lower values than younger men. Protein intake did not influence changes in bone quantity during the 16-wk energy-restricted diet. Hip BMD ( $p=0.0346$ ,  $-0.004 \pm 0.002$  g/cm<sup>2</sup>) and BMC ( $p=0.0413$ ,  $-0.17 \pm 0.08$  g) decreased over time with no changes in other skeletal sites. Higher protein intake achieved through increased milk protein isolate consumption does not influence weight loss-induced bone loss in overweight and obese older adults.

Disclosures: Christian Wright, None.

This study received funding from: National Dairy Council

## SA0258

See Friday Plenary Number FR0258.

## SA0259

See Friday Plenary Number FR0259.

## SA0260

See Friday Plenary Number FR0260.

## SA0261

See Friday Plenary Number FR0261.

## SA0262

**Upregulation of SOST before arthritis onset in arthritis model could partly explain paradoxical effect of sclerostin inhibition in arthritis.** Guillaume Courbon\*, Raphaëlle Lamarque, Marie-Thérèse Linossier, Norbert Laroche, Thierry Thomas, Laurence Vico, Hubert Marotte, INSERM 1059, University of Lyon, France

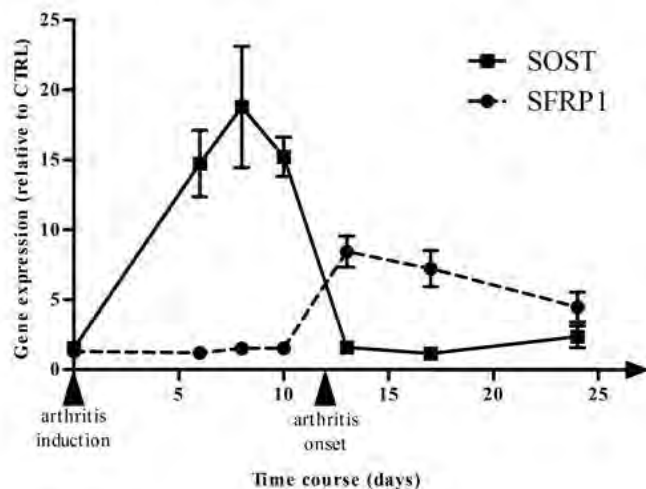
Purpose. Periarticular bone loss in rheumatoid arthritis is considered to be mainly related to synovial inflammation leading to uncoupling between decreased bone formation and increased bone resorption. However, it has been recently demonstrated a paradoxical exacerbation of joint damage when blocking sclerostin in various arthritis models. Phase specific changes in Wnt pathway activity over the course of the disease could participate in the underlying mechanisms of these results. Thus, we proposed to determine kinetic expressions of Wnt inhibitors in a classic rodent model of arthritis, the rat adjuvant induced arthritis (AIA).

Methods. Arthritis was induced (AIA, n=35) or not (CTRL, n=35) at baseline. Inflammation and loss of articular function were monitored. Periarticular bone loss and joint damage were evaluated before, during and after arthritis onset in a 7 time-point follow-up, using micro-computed tomography ( $\mu$ -CT) and histomorphometry. Gene expressions were assessed by quantitative RT-PCRs at each time point.

Results. AIA onset occurred at day 12 post-induction ( $p < 0.001$ ). Surprisingly, histomorphometry and  $\mu$ -CT showed bone alterations as early as day 8. Indeed, cortical porosity increased and trabecular network was significantly impaired ( $p < 0.01$ ). Moreover, these early bone alterations before arthritis onset predicted arthritis severity outcome. As expected, gene expression confirmed an early upregulation of bone resorption markers like RANKL from day 8 to day 24 ( $p < 0.01$ ). More interestingly, expression of bone formation inhibitors followed a specific pattern with SOST upregulation only before arthritis onset ( $p < 0.01$ ) and return to normal expression afterwards while frizzled related protein 1 (SFRP1) expression only increased after arthritis onset ( $p < 0.01$ ).

Conclusions. Bone alterations before arthritis onset supports the hypothesis of an early involvement of bone compartment in arthritis. The specific pattern of sclerostin expression suggested that sclerostin might play dual effects depending on arthritis phases. In addition, SFRP1 later increased expression could play a strong role in bone formation alteration related to arthritis. We infer from our results that better deciphering Wnt pathway changes during arthritis is required before using biologics targeting this pathway for preventing periarticular bone loss.

Figure: Gene expression pattern of SOST and SFRP1 in the course of arthritis



Figure

Disclosures: Guillaume Courbon, None.

## SA0263

See Friday Plenary Number FR0263.

## SA0264

**Association between bone turnover markers and level of cognition in older community dwelling individuals with memory concerns.** Ryan Ross\*, Raj Shah, Rick Sumner. Rush University Medical Center, United states

Osteoporosis and Alzheimer's disease (AD) are chronic diseases of aging resulting in significant morbidity and mortality. While it would seem that osteoporosis and AD are unrelated but co-occurring conditions affecting different organ systems, recent animal and human studies have found potential links. For instance, the bone derived hormone, osteocalcin, improves anxiety and learning deficiencies in mice [1]. Additionally, persons with mild cognitive impairment and mild AD have increased markers of bone resorption and formation [2]. Thus, the two common diseases may share similar or interacting early mechanisms. To further understand the association between osteoporosis and AD, we investigated circulating bone biomarkers from community-dwelling patients without clinical dementia, and correlated these levels with global cognition scores.

Plasma samples were obtained from a previously performed six-month, randomized trial. Plasma at baseline was used to measure circulating biomarker concentrations and the global cognition (z-score), calculated by converting raw scores from 19 cognitive function tests. Bone biomarkers included osteocalcin (total, undercarboxylated, and carboxylated), procollagen type I N-terminal propeptide (PINP), C-terminal telopeptide (CTX-1), Dickkopf-related protein 1 (DKK1), osteoprotegerin (OPG), osteopontin (OPN), parathyroid hormone (PTH), and sclerostin. Bone biomarkers and the previously measured concentrations of amyloid beta (A $\beta$ ) 40 and 42 were correlated with global cognition scores in at least 94 subjects ( $80 \pm 7.7$  years of age, 83% female).

Concentrations of A $\beta$ 40 and 42, components of amyloid plaques formed in AD, were negatively correlated with global cognition ( $r=-0.29$ ,  $p=0.003$  and  $r=-0.22$ ,  $p=0.027$ , respectively). Of the bone biomarkers tested, only OPG and sclerostin were correlated with global cognition ( $r=-0.33$ ,  $p=0.001$  and  $r=-0.25$ ,  $p=0.015$ , respectively). OPG levels were not correlated with the circulating concentrations of A $\beta$ 40 or A $\beta$ 42, while sclerostin levels were significantly correlated with A $\beta$ 42 levels ( $r=0.21$ ,  $p=0.038$ ), but not to A $\beta$ 40.

OPG is a circulating hormone known to control the differentiation of osteoclasts, while sclerostin is an osteocyte-derived protein that limits bone formation. The goodness of fit of the two bone derived biomarkers were similar to the amyloid proteins, furthering the possible link between bone and brain health.

[1]. Oury et al. Cell 2013.

[2]. Luckhaus et al. J Neural Transm 2009.

Disclosures: Ryan Ross, None.

## SA0265

See Friday Plenary Number FR0265.

## SA0266

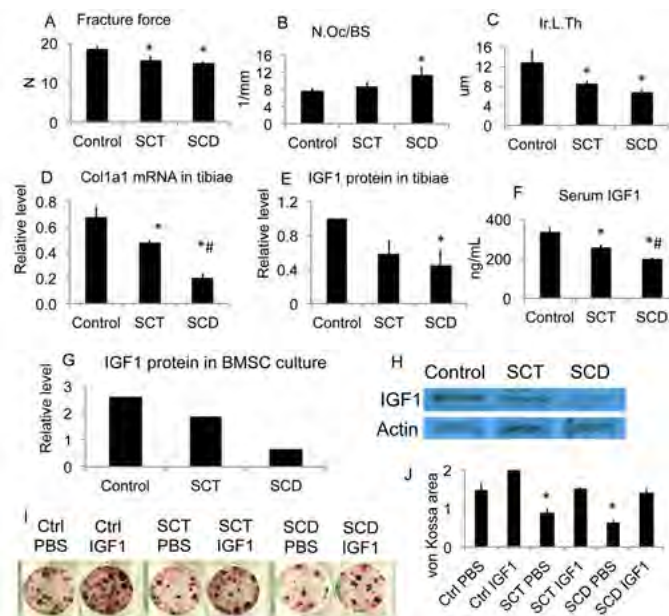
See Friday Plenary Number FR0266.

## SA0267

**Loss of Bone in Sickle Cell Trait and Sickle Cell Disease Female Mice Is Associated with Reduced IGF-1 in Bone and Serum.** Liping Xiao\*<sup>1</sup>, Biree Andemariam<sup>1</sup>, Pam Taxel<sup>1</sup>, Douglas J Adams<sup>1</sup>, William T Zempsky<sup>2</sup>, Marja M Hurley<sup>1</sup>. <sup>1</sup>UConn Health, United states, <sup>2</sup>Connecticut Children's Hospital, United states

Sickle cell disease (SCD) is associated with increased bone loss. However, the molecular mechanisms of bone loss in SCD have not been fully investigated. Sickle cell trait (SCT) is clinically silent but very common in African American (AA). There are no data on the effect of SCT on bone metabolism or fracture. Although the incidence of hip fracture in AA women is about half of white women, the etiology and risk factors of fracture in AA women are not clearly defined. We hypothesized that SCT is a state of reduced bone mineralization and may contribute to racially disparate outcomes among AAs with bone fracture. We used murine models of SCD and SCT to define the molecular mechanism of bone loss. Characterization of the bone phenotype of 24-week old female transgenic SCD and SCT mice revealed significant reductions in bone mineral density (BMD) and bone mineral content (BMC) relative to control with a further significant decrease in SCD compared with SCT. By microCT, femur mid-diaphyseal cortical area was significantly reduced in SCT and SCD. Cortical thickness was significantly decreased in SCD versus control. Diaphysis structural stiffness and strength were significantly reduced in SCT and SCD (Fig.1A). Histomorphometry showed a significant increase in osteoclast perimeter in SCD and significantly decreased bone formation in SCD and SCT compared with control with a further significant decrease in SCD compared with SCT (Fig.1B&C). Collagen-I mRNA (Fig.1D) was significantly decreased in tibiae from SCT and SCD and Osterix, runx2, osteocalcin and dmp1 mRNA were

significantly decreased in tibiae of SCD compared with control. Serum osteocalcin was significantly decreased and ferritin was significantly increased in SCD compared with control. Insulin like growth factor-1 (Igf-1) mRNA and protein (Fig.1E) in tibiae and serum Igf-1 (Fig.1F) were significantly decreased in SCD and SCT. Igf-1 protein was decreased in bone marrow stromal cells from SCT and SCD cultured in osteogenic media (Fig.1G&H). Crystal violet staining revealed fewer cells and significantly reduced alkaline phosphatase positive mineralized nodules in SCT and SCD that was rescued by Igf-1 treatment (Fig.1I&J). We conclude that reduced bone mass in SCD and SCT mice carries architectural consequences that are detrimental to the mechanical integrity of femoral diaphysis. Furthermore reduced Igf-1 and osteoblast terminal differentiation contributed to reduced bone formation in SCT and SCD mice.



Figure

Disclosures: Liping Xiao, None.

## SA0268

See Friday Plenary Number FR0268.

## SA0269

**Effects of Obesity and Diabetes on the Rate of Bone Density Loss in Women: The Manitoba BMD Cohort.** William Leslie\*<sup>1</sup>, Suzanne Morin<sup>2</sup>, Sumit Majumdar<sup>3</sup>, Lisa Lix<sup>1</sup>. <sup>1</sup>University of Manitoba, Canada, <sup>2</sup>McGill University, Canada, <sup>3</sup>University of Alberta, Canada

Objective: Type 2 diabetes (T2D) is a risk factor for osteoporotic fracture independent of FRAX probability despite higher bone mineral density (BMD). Obesity, also associated with higher BMD, may be less protective against fracture than previously assumed. Mechanisms responsible for these observations are unclear. We examined rate of BMD loss in women with diabetes and/or obesity as a possible mediating factor.

Methods: Using the Manitoba (Canada) clinical DXA registry, we identified women  $\geq 40$  years undergoing baseline and follow up BMD assessments (1996 – 2013). We excluded women with significant exposure to osteoporosis medications, systemic estrogen, glucocorticoids or aromatase inhibitors, or with measured weight change of  $>10\%$ . Rate of BMD change ( $g/cm^2/y$ ) for the lumbar spine (L1-L4), total hip and femoral neck was studied in relation to previously diagnosed diabetes (using a validated algorithm) and WHO body mass index (BMI) categories in age-adjusted generalized additive models.

Results: The study population included 4,960 women (mean age 62.1 years, mean BMD testing interval 4.3 years). Baseline age-adjusted BMD was greater at all sites for women with diabetes and for increasing BMI category ( $P<0.001$ ). In women with diabetes ( $N=359$ ) vs without diabetes ( $N=4,815$ ) unadjusted BMD loss was less at the lumbar spine ( $-0.0020$  vs  $-0.0047$   $g/cm^2/y$ ,  $P=.007$ ), similar at the total hip ( $-0.0083$  vs  $-0.0066$   $g/cm^2/y$ ,  $P=0.386$ ) and slightly greater at the femoral neck ( $-0.0069$  vs  $-0.0054$   $g/cm^2/y$ ,  $P=.034$ ). When adjusted for age and BMI, diabetes was still associated with slightly greater femoral neck BMD loss ( $-0.0018$   $g/cm^2/y$ ,  $P=0.012$ ) but no significant effect of diabetes was seen on the lumbar spine or total hip (Table). However, this rate of BMD loss would need to be sustained for over 20 years before femoral neck BMD would become average for age. Compared with normal BMI, overweight and obesity were associated with reduced BMD loss at the lumbar spine. BMI category did not affect BMD loss at the total hip or femoral neck. When modeled as a continuous variable with cubic splines, there was a strong

linear effect of increasing BMI on attenuated BMI loss at the lumbar spine with negligible effects on hip BMD.

Summary: Diabetes was associated with slightly greater BMD loss at the femoral neck but not at other measurement sites. BMD loss at the lumbar spine was reduced in overweight and obese women, but BMI did not significantly affect hip BMD loss.

BMI category	N	Lumbar spine BMD change		Total hip BMD change		Femoral neck BMD change	
		g/cm <sup>2</sup> /y (95% CI)	P	g/cm <sup>2</sup> /y (95% CI)	P	g/cm <sup>2</sup> /y (95% CI)	P
Underweight (<18.5 kg/m <sup>2</sup> )	84	-0.007 (-0.044; 0.0030)	0.704	0.0018 (-0.0100; 0.0067)	0.699	-0.0029 (-0.0058; 0.0000)	0.052
Normal (18-25 kg/m <sup>2</sup> )	2060	REFERENT	N/A	REFERENT	N/A	REFERENT	N/A
Overweight (25-30 kg/m <sup>2</sup> )	1816	0.0019 (0.0008; 0.0030)	<0.001	0.0004 (-0.002; 0.0028)	0.781	0.0006 (-0.0002; 0.0014)	0.163
Obese 1 (30-35 kg/m <sup>2</sup> )	844	0.0028 (0.0019; 0.0038)	<0.001	-0.0023 (-0.0053; 0.0007)	0.138	0.0009 (-0.0008; 0.0013)	0.511
Obese 2 (>35 kg/m <sup>2</sup> )	370	0.0063 (0.0044; 0.0083)	<0.001	-0.0006 (-0.0048; 0.0035)	0.775	-0.0012 (-0.0026; 0.0003)	0.107
Diabetes	359	-0.0033 (-0.0032; 0.0007)	0.203	-0.0015 (-0.0056; 0.0026)	0.470	-0.0018 (-0.0032; -0.0004)	0.012

Boldface indicates significant effect.

Table

Disclosures: William Leslie, None.

## SA0270

**Insulin Sensitivity is Positively Associated with Appendicular Bone Density.** Se-Min Kim\*<sup>1</sup>, Xiuqing Guo<sup>2</sup>, Yii-Der I. Chen<sup>2</sup>, Willa A. Hsueh<sup>3</sup>, Jerome L. Rotter<sup>2</sup>, Mark O. Goodarzi<sup>1</sup>. <sup>1</sup>Cedars-Sinai Medical Center, United states, <sup>2</sup>Harbor-UCLA Medical Center, United states, <sup>3</sup>The Ohio State University, United states

Introduction: The links between type 2 diabetes (T2DM) and osteoporosis are complex, and predicting skeletal health in T2DM using vertebral and femoral neck BMD is challenging. The purpose of this study is to examine how glucose homeostasis relates to bone mass phenotypes to understand the pathophysiological link between DM and osteoporosis.

Methods: Metabolic (via oral glucose tolerance test (OGTT) and euglycemic-hyperinsulinemic clamp) and bone density phenotypes (via DEXA) were assessed in the UCLA/Cedars-Sinai Mexican-American Coronary Artery Disease (MACAD) cohort. Insulinogenic index (IGI30 = (insulin at 30 minutes - fasting insulin)/(glucose at 30 minutes - fasting glucose) reflecting acute insulin secretion, glucose infusion rate required to maintain euglycemia at steady state of the clamp (M value, units mg/kg/min) reflecting insulin sensitivity, and metabolic clearance of insulin (MCI, units mL/m<sup>2</sup>/min) were measured. We computed univariate correlation coefficients between total, pelvic, lumbar spine (LS), arm and leg BMD and glucose homeostasis indices and body composition variables. Multiple regression analyses were performed to identify the variables independently associated with each regional BMD.

Results: 778 subjects (mean age, 34.5±9.0) without history of diabetes were analyzed. Insulin sensitivity (M value) was positively associated with arm (0.134, p=0.0003) and leg BMD (0.076, p=0.043), but not with LS BMD (0.010, p=0.78). Pelvic BMD showed, however, negative correlation with M value (-0.165, p<0.0001). 2-hour OGTT glucose levels showed negative correlation with arm (-0.176, p<0.0001), and leg BMD (-0.148, p<0.0001). In multivariate analyses, M value showed significant association with arm (0.053, p=0.029) and leg BMD (0.064, p=0.017) after adjustment for age, sex and BMI. LS and pelvic BMD were not associated with any of the glucose homeostasis indices after adjustment.

Conclusion: This study is the first to use euglycemic-hyperinsulinemic clamps to correlate BMD phenotypes with glucose homeostasis. We found insulin sensitivity is independently positively associated with appendicular BMD, but not with vertebral or pelvic BMD. This finding implies that measuring appendicular BMD might be a better predictor of skeletal health in T2DM. The different reaction to glucose homeostasis in appendicular bone versus vertebral and pelvic bone might be related to their cortical-bone dominant microarchitecture and yellow fat-rich bone marrow.

Disclosures: Se-Min Kim, None.

## SA0271

**Type 2 Diabetes Mellitus Is Associated with Enhanced Bone Microarchitecture but Lower Bone Material Strength and Poorer Physical Function in Elderly Women.** Anna G. Nilsson\*<sup>1</sup>, Daniel Sundh<sup>2</sup>, Martin Nilsson<sup>2</sup>, Robert Rudang<sup>2</sup>, Anna Darelid<sup>2</sup>, Michail Zoulikis<sup>2</sup>, Dan Mellström<sup>2</sup>, Mattias Lorentzon<sup>2</sup>. <sup>1</sup>Institute of Medicine, Sahlgrenska Academy, Gothenburg University, Sweden, <sup>2</sup>Geriatric Medicine, Centre for Bone & Arthritis Research, The Sahlgrenska Academy, University of Gothenburg, Sweden

Type 2 diabetes mellitus (T2DM) is associated with an increased risk of fractures according to several recent studies. The underlying mechanisms remain unclear, and previous small case-control studies on bone microarchitecture have shown conflicting results.

We have studied a population-based sample of 1057 women aged 75-80 in Gothenburg, randomly invited from the population registry. Physical function tests, bone densitometry by DXA and HR-pQCT (XtremeCT, Scanco Medical) were performed and a subgroup of 477 women also underwent bone microindentation (Osteoprobe®, Active Life Scientific) at the tibia. Women treated with bone-specific medication were excluded from the analysis (n=62).

A total of 99 women had T2DM. Women with T2DM had highly similar age (77.7±1.5 vs. 77.7±1.5 years, ns) and height (161.5±5.3 vs 162.1±5.8 cm, ns) as the

women without diabetes but had significantly higher body weight (76.3±12.5 vs. 68.0±11.5 kg, p<0.001) and BMI (28.4±7.0 vs. 25.2±6.0 kg/m<sup>2</sup>, p<0.001). Bone mineral density by DXA was significantly higher in women with T2DM in total hip (+7.6%), spine (+7.5%), and total body (+2.9%) (p<0.001 for all). Higher values were also seen for ultradistal tibial and radial trabecular bone volume fraction and for distal cortical volumetric BMD, cortical thickness and cortical area (Table 1), whereas radial cortical porosity was lower (1.5±1.1 vs 2.0±1.7 %, p=0.001) in T2DM. Adjustment for body weight eliminated the differences in BMD by DXA except in total hip, and attenuated that in cortical porosity whereas the other variables measured by HR-pQCT remained significantly higher in T2DM. However, bone material strength measured by microindentation (BMSi) was significantly lower in T2DM (74.9±7.6 vs 78.0±7.3, p<0.01), and remained so after adjustment for body weight. Furthermore, there was a clear impairment in different measures of physical function (one leg standing: -22%, 30 s chair-stand test: -8%, timed up and go: +10%, walk time 10 m: +8.1%; p<0.05-0.01) in women with T2DM (Table 1).

In conclusion, we observed enhanced bone microarchitecture in a relatively large sample of elderly women with T2DM in the population compared to non-diabetics. Reduced BMSi and impaired physical function may explain an increased fracture risk in T2DM.

Table 1. Bone and function variables in a population-based sample of women.

	T2DM (n=99)	Non-diabetics (n=890)
HR-pQCT of the non-dominant radius		
tBV/TV (%)	11.4±3.4 <sup>a</sup>	10.0±3.4
Cortical bone area (mm <sup>2</sup> )	62.0±8.6 <sup>a</sup>	57.0±9.6
Cortical vBMD (mg/cm <sup>3</sup> )	1028.3±34.4 <sup>a</sup>	1011.2±43.0
Cortical thickness (mm)	1.72±0.25 <sup>a</sup>	1.56±0.30
Cortical porosity (%)	1.5±1.1 <sup>a</sup>	2.0±1.7
BMSi	74.9±7.6 <sup>b</sup>	78.0±7.3
Function tests		
One leg standing (s)	9.6±7.7 <sup>b</sup>	12.3±8.6
Timed up and go (s)	9.5±3.2 <sup>a</sup>	8.6±3.0

Results are presented as mean ± SD. tBV/TV=trabecular bone volume fraction. a=p<0.001, b=p<0.01 for statistical difference between the groups

Table 1. T2DM and bone in elderly women by AG Nilsson

Disclosures: Anna G. Nilsson, None.

## SA0272

See Friday Plenary Number FR0272.

## SA0273

**Effects of Alendronate and Low-intensity Pulsed Ultrasound Therapies on Bone Mineral Density in Cancellous Osteotomy Sites in the Proximal Tibias of Rats with Glucocorticoid-induced Osteoporosis.** Tetsuya Kawano\*, Naohisa Miyakoshi, Yuji Kasukawa, Chie Sato, Masashi Fujii, Masazumi Suzuki, Norimitsu Masutani, Manabu Akagawa, Yuichi Ono, Yoichi Shimada. Department of Orthopedic Surgery, Akita University Graduate School of Medicine, Japan

Purpose: Glucocorticoid-induced osteoporosis (GIO) causes fragility fractures, and can prolong bone healing. We have previously reported that alendronate (ALN) increases the bone mineral density (BMD) in cancellous bone osteotomy sites and that low-intensity pulsed ultrasound (LIPUS) improves cancellous bone healing after osteotomy in aged rats. However, the effects of ALN and/or LIPUS on BMD and bone healing at the osteotomy sites in a GIO model are unclear. Thus, we aimed to evaluate the effects of ALN and/or LIPUS on BMD and rate of bone union in cancellous osteotomy sites in GIO rats.

Methods: We administered prednisolone (10 µg/kg/day) subcutaneously 5 days per week for 4 weeks to 9-month-old female Sprague-Dawley rats, then performed osteotomies on their right proximal tibial metaphyses. We then created the following five groups of rats: 1) Control (n=4), normal aged rats treated with vehicle of prednisolone and ALN and sham LIPUS; 2) GIO-control (n=5), treated with ALN vehicle and sham LIPUS; 3) GIO-ALN (n=5), treated with ALN (1 µg/kg/day) and sham LIPUS; 4) GIO-LIPUS (n=6), treated with vehicle of ALN and LIPUS (SEFHS; Teijin, Osaka, Japan) exposure (20 min/day); and 5) GIO-combined (n=6), treated with ALN and LIPUS exposure. We assessed BMD by dual-energy x-ray absorptiometry (Hologic QDR-4500; Hologic, Marlborough, MA, USA) and evaluated bone histomorphometric variables (bone volume [BV/TV], osteoid surface [OS/BS], eroded surface [ES/BS]), and the rate of cancellous bone union in the osteotomy sites 2 weeks after these treatments.

Results: BMD was significantly higher in the GIO-ALN than the control group (P=0.0171). Combined therapy with ALN and LIUPS increased the BV/TV (P<0.05) significantly and tended to increase the rate of bone union (P=0.05) compared with the GIO-control group. OS/BS was significantly lower in the GIO-Control group than the Control group (P<0.05). ES/BS did not differ significantly between treatment groups.

Conclusion: Combined therapy with ALN and LIPUS increases bone volume and enhances bone union in GIO rats.

Disclosures: Tetsuya Kawano, None.

## SA0274

**Bone Metabolism Dysfunction Mediated by the Increase of Proinflammatory Cytokines in Chronic HIV Infection.** Erika Grasiela Marques de Menezes\*<sup>1</sup>, Alcyone Artioli Machado<sup>2</sup>, Fernando Barbosa Jr<sup>2</sup>, Francisco Jose Albuquerque de Paula<sup>2</sup>, Anderson Marliere Navarro<sup>2</sup>. <sup>1</sup>Sao Paulo State University, Brazil, <sup>2</sup>University of Sao Paulo, Brazil

Despite the efficacy of antiretroviral therapy (ART) on the control of viral replication, the current challenge is to decrease the chronic inflammatory status and toxicity of the antiretroviral drugs that contribute to increase the risk of metabolic complications. Objective: To verify the influence of proinflammatory cytokines on bone metabolism mediated by chronic HIV infection. Materials and Methods: A cross-sectional study was conducted with 50 HIV-infected adult men treated or not with ART. Dual energy x-ray absorptiometry (DXA) was performed to assess bone mineral density. Biochemical analysis were performed of IL-6, TNF- $\alpha$ , osteocalcin, PTH, 25-OH-D, total calcium, albumin, 24h urinary calcium and urinary deoxypyridinoline. Results: The participants not treated with ART exhibited higher values of IL-6 and TNF- $\alpha$  than the participants treated with ART for more than 2 years. The TNF- $\alpha$  values was higher in the participants treated with ART for less than 2 years than in participants treated with ART for more than 2 years ( $p < 0.05$ ). The increased values of urinary deoxypyridinoline indicated a high reabsorptive activity of bone tissue in all groups, with a significant difference between the participants not treated with ART and the participants treated with ART for less than 2 years. Through the DXA we found a bone mass reduction in all bone sites in each group. Conclusion: The increase production of proinflammatory cytokines, most notably in the viremic group have demonstrated to stimulate osteoclast activity affecting bone mass and the reduction of bone mineral density was observed in all bone sites principally for the groups in treatment with antiretroviral.

**Disclosures:** Erika Grasiela Marques de Menezes, None.

## SA0275

See Friday Plenary Number FR0275.

## SA0276

**Bone Quantity and Quality Impairments Contribute to the Fragility of Rib in End-Stage Cystic Fibrosis Patients.** Louis-Georges Ste-Marie\*<sup>1</sup>, Natalie Dion<sup>1</sup>, Delphine Farlay<sup>2</sup>, Safietou Sankhe<sup>3</sup>, Sébastien Rizzo<sup>2</sup>, Valérie Jomphe<sup>1</sup>, Nathalie J Bureau<sup>1</sup>, Georges Boivin<sup>2</sup>, Larry C Lands<sup>4</sup>, Pasquale Ferraro<sup>1</sup>, Geneviève Mailhot<sup>3</sup>. <sup>1</sup>CHUM-Centre hospitalier de l'université de Montréal, Canada, <sup>2</sup>INSERM, UMR 1033, Université de Lyon, Université Claude Bernard Lyon 1, France, <sup>3</sup>Research Centre, CHU Sainte-Justine, Canada, <sup>4</sup>MUHC-McGill University, Canada

Advancements in care have considerably extended the life expectancy of cystic fibrosis (CF) patients. As these latter get older come co-morbidities such as CF-related bone disease (CFBD), which progresses with disease severity and puts patients at high risk for fractures, particularly of the ribs and the vertebrae. Evidence that CF patients with vertebral fractures had higher bone mineral density (BMD) than the no fracture group led us to postulate that bone quality contributes to skeletal fragility in these patients. We therefore examined rib specimens resected at the time of lung transplant in CF patients to measure variables of bone quantity and quality. In this exploratory study, we analysed 19 end-stage CF and 13 control rib specimens resected from otherwise healthy lung donors. BMD, bone microarchitecture, static variables of bone formation and resorption and microcrack density of rib specimens were quantified by imaging, histomorphometric and histological methods. To further evaluate the contribution of bone mineralization on bone fragility, the technique of digitized microradiography (Montagner et al. 2015, J X-Ray Sci Technol 23:201-11) was used to assess the degree of mineralization of bone (DMB) and the heterogeneity index of the mineralization (HI). Compared to controls, CF ribs exhibited lower areal and volumetric trabecular BMD, decreased trabecular thickness and osteoid parameters, and a marked increase in microcrack density. Trabecular volume, structure model index, cortical thickness, cortical porosity and static parameters of bone resorption were similar in both groups. DMB of total bone (cortical + trabecular), but not HI, was slightly increased in CF specimens, probably due to an augmented proportion of interstitial bone. The combination of reduced bone mass, altered microarchitecture, uncoupled bone remodeling (normal bone resorption but decreased formation), increased microdamage and increased DMB, may lead to decreased bone strength and provide an explanation for the increased incidence of rib fractures previously reported in this population. This exploratory study also showed that rib specimen is a valuable tool for the assessment of bone quantity and quality. Ultimately, these findings will help to treat and prevent CFBD in end-stage CF patients.

Controls	Cystic fibrosis	p value

Table 1

**Disclosures:** Louis-Georges Ste-Marie, None.

## SA0277

**Denosumab Versus Bisphosphonate Treatment for Secondary Osteoporosis Caused by Rheumatoid Arthritis.** Havato Kinoshita\*<sup>1</sup>, Naohisa Miyakoshi<sup>2</sup>, Takeshi Kashiwagura<sup>3</sup>, Hidekazu Abe<sup>1</sup>, Yusuke Sugimura<sup>4</sup>, Yoichi Shimada<sup>2</sup>. <sup>1</sup>Ugo municipal hospital, department of orthopedic surgery, Japan, <sup>2</sup>Akita University graduate school of medicine, Department of orthopedic surgery, Japan, <sup>3</sup>Akita city hospital, department of orthopedic surgery, Japan, <sup>4</sup>Nakadori general hospital, department of orthopedic surgery, Japan

Background: Rheumatoid arthritis (RA) is caused by upregulation of proinflammatory cytokines. A key feature of RA is overexpression of receptor activator of nuclear factor kappa-B ligand (RANKL) in the synovial membrane, which promotes osteoclast differentiation and increases bone resorption. The anti-RANKL antibody, denosumab, prevents RANKL/RANK interactions and inhibits osteoclast-mediated bone resorption.

Objectives: The aim of this study was to compare the effects of denosumab with bisphosphonates, which directly prevent osteoclast-mediated bone resorption, on inflammation and secondary osteoporosis caused by excessive bone resorption in RA patients.

Methods: RA patients were enrolled from the Akita Orthopedic Group on Rheumatoid Arthritis (AORA) registry. Among these, 58 patients were newly treated with denosumab and 49 patients were treated with bisphosphonates. For RA, the Steinbrocker classification was measured at pretreatment. Use of glucocorticoids, methotrexate and biological agents, the disease activity score (DAS)28-erythrocyte sedimentation rate (ESR), the simplified disease activity index (SDAI), ESR, and matrix metalloproteinase 3 were measured at pretreatment, and 6 and 12 months after treatment. For bone metabolism, bone-specific alkaline phosphatase (BAP) and tartrate-resistant acid phosphatase 5b (TRACP-5b), reflecting bone formation and resorption, respectively, and bone mineral density (BMD) of the lumbar and femoral neck were measured at pretreatment, and 6 and 12 months after treatment. Data were analyzed using the chi-square test or one-way analysis of variance, and multiple comparisons using Scheffe's and Dunn's *post hoc* tests, as appropriate.

Results: In the denosumab group, the Steinbrocker class and stage were higher ( $p < 0.0001$  and  $p = 0.0062$ , respectively), and the use of biological agents was higher at pretreatment, and 6 and 12 months after treatment ( $p = 0.0002$ ,  $p = 0.004$  and  $p = 0.0028$ , respectively) compared with the bisphosphonates group. There were no significant differences in DAS28-ESR or SDAI. Denosumab reduced BAP at 6 and 12 months compared with pretreatment ( $p = 0.006$  and  $p = 0.0132$ , respectively). Although there was no significant difference in BMD of the lumbar and femoral neck, a trend towards an increase with denosumab and a decrease with bisphosphonates was revealed.

Conclusions: Neither denosumab nor bisphosphonates suppressed RA activity; however, denosumab inhibited bone turnover more effectively than bisphosphonates.

**Disclosures:** Havato Kinoshita, None.

## SA0278

**Dipeptidyl Peptidase-4 Activity and Osteoporosis. Findings from the Cardiovascular Health Study.** monique bethel\*<sup>1</sup>, Petra Buzkova<sup>2</sup>, Laura Carbone<sup>1</sup>, Howard Fink<sup>3</sup>, John Robbins<sup>4</sup>, Carlos Isales<sup>1</sup>, William Hill<sup>5</sup>. <sup>1</sup>Medical College of Georgia, United states, <sup>2</sup>University of Washington, United states, <sup>3</sup>University of Minnesota, United states, <sup>4</sup>University of California, United states, <sup>5</sup>Augusta University, United states

Purpose: Dipeptidyl Peptidase IV (DPP4) inactivates hormones that stimulate postprandial insulin secretion, and several DPP-4 inhibitors are approved diabetes medications. Though DPP-4 also is known to modulate bone resorption, the relationship between DPP-4 levels and bone mass is uncertain. The purpose of the present study was to examine possible associations between plasma DPP-4 activity in elderly subjects enrolled in the Cardiovascular Health Study (CHS) and BMD, body composition measurements, and incident hip fractures.

Methods: All 1536 male and female CHS participants who had evaluable DXA scans and plasma for DPP-4 activity were included in the analyses. BMD of the lumbar spine, total hip, femoral neck and total body, and body composition measurements (total and % lean, total and % fat, and total body mass) were determined using Hologic QDR-2000 densitometers (Hologic, Inc., Waltham, MA) done during the 1994-1995 CHS study visit. Incident hip fractures following DPP-4

measurements were analyzed until a hip fracture event, death, loss to follow-up, or June 30, 2013. Hip fractures caused by motor vehicle accidents or severe injury were excluded.

Results: Mean levels of DPP-4 activity were significantly higher in Blacks (227+ 78) compared with non-Blacks (216+ 89) ( $p=0.04$ ). There was no significant association of DPP-4 activity with age or gender ( $p>0.14$  for both). In multivariable adjusted models including age, race, clinic site, gender, smoking, alcohol use, BMI, change in BMI over two years, frailty status, physical activity, diabetes status, and medication use, there was no significant association of plasma DPP-4 activity with lumbar spine, total hip, femoral neck, or total body BMD in overall models ( $p> 0.55$  for all) or gender stratified analyses ( $p >0.23$  for both). DPP-4 activity was not significantly associated with any body composition measurement, including total lean, % lean, total fat, % fat or total body mass ( $p> 0.31$  for all), or with incident hip fractures (HR 1.12 (95% CI 0.93-1.36)) (per increases of 100 DPP-4 Absorbance Units).

Conclusions: Endogenous levels of DPP-4 were not associated with BMD, body composition or incident hip fractures in this cohort of elderly community dwelling black and white men or women. These findings suggest that clinical use of DPP-4 inhibitors for treatment of Diabetes Mellitus may not affect skeletal health or body composition.

**Disclosures:** *monique bethel, None.*

## SA0279

**Evidence for the prevention of bone loss in postmenopausal breast cancer patients treated with aromatase inhibitors.** Peter Schwarz<sup>\*1</sup>, Bo Abrahamsen<sup>2</sup>. <sup>1</sup>Dept. Endocrinology, Rigshospitalet, Copenhagen University, Denmark, <sup>2</sup>University of Southern Denmark & Holbæk Hospital, Denmark

Breast cancer (BC) is the most common cancer in women. In postmenopausal women with estrogen receptor (ER) dependent BC, anti-hormone therapy is an option with aromatase inhibition (AI), resulting in decreased estrogen production. Available therapeutic options for management of bone loss in patients receiving AI are zoledronic acid (ZA), risedronate (Ris), alendronate (Aln) and denosumab (Dmab).

Aim: To investigate the evidence of bone loss prevention in AI treated BC patients.

Methods: In PubMed and Embase 373 studies were identified on AI treatment and BMD or fracture. In total 31 RCT studies was found during the evaluation; ZA 18, Ris 9, Aln 2 and Dmab 2.

Results: Evaluation of ZA treatment showed 18 RCT studies on BMD or fracture. However in several cases the cohorts were reported on more than once. We found in total 7 cohorts evaluated after 12 to 61 months. In all cohorts the treatment was ZA acid 8 mg/year vs placebo ( $n= 1,551$  vs. 1,550). The absolute difference in mean lumbar spine and total hip BMD's between patients in treatment or placebo was 8.9% and 5.9%, respectively. None of the studies reported severe side effects. The evaluation of Ris treatment showed 8 RCT studies on BMD or fracture. However, 1 study reported only on bone markers. Of the remaining 7 studies 2 studies were excluded. The 2 studies excluded were 1 study on a mix of Aln and Ris and 1 study of 6 month length and 2.5 mg Ris per day. The remaining 5 studies reported were 24 month RCT's. In all 5 studies the treatment was Ri 35 mg/week vs. placebo ( $n= 429$  vs. 291). The absolute difference in mean lumbar spine and total hip BMD's between patients in treatment or placebo was 4.5% and 3.1%, respectively. Two RCT's are published on Aln of whom only one study had a long time follow-up (36 months). None of the studies on bisphosphonate reported severe side-effects. Evaluation of Dmab treatment showed 9 RCT papers where two papers reported on BMD and fracture. These papers were on the same cohort and they reported on 24 mo of Dmab 60 mg every 6 mo vs. placebo ( $n= 123$  vs. 122) an absolute mean lumbar difference in spine BMD of 7.6% and no severe side-effects.

Conclusion: Among anti-resorptives, ZA currently has the highest evidence for prevention of AI associated bone loss in postmenopausal women with early BC. Data on fracture prevention is sparse.

**Disclosures:** *Peter Schwarz, Novartis, 11*

## SA0280

**Osteoporosis with Multiple Spontaneous Vertebral Fractures in a Young Male Carrying Triple Polymorphism in COL1A, VDR and LRP5 Genes.** Panagoullia Kollia<sup>1</sup>, Eleni Vafeiadou<sup>2</sup>, John Yovos<sup>\*2</sup>, Maria Yavropoulou<sup>2</sup>. <sup>1</sup>Department of Genetics & Biotechnology, Faculty of Biology, School of Physical Sciences, University of Athens, Athens, Greece., Greece, <sup>2</sup>Laboratory of Clinical & Molecular Endocrinology, AHEPA University hospital, Aristotle University of Thessaloniki, Greece

Background: Osteoporosis is a common disease with a strong genetic component. Several studies have reported vitamin D receptor gene (VDR), estrogen receptor alpha (ESR $\alpha$ ), interleukin -6 (IL-6), collagen type I (COL1A1), and LDL receptor-related protein 5 (LRP5) as the most potential candidates. However, most of the studies have been carried out in postmenopausal women and older men, showing inconsistent results.

Case presentation: We report a case of a 26 year old male presented with severe back pain of acute onset, without reference to any kind of trauma, and diffuse myalgia. X-rays of the lumbar and the thoracic spine revealed 2 Grade 3, according to Genant's semiquantitative method, vertebral fractures in Th10 and Th11 and multiple Grade 1 fractures from Th8 to L2. Measurement of bone mineral density (BMD) by dual-energy X-ray absorptiometry (DXA) (Lunar prodigy) showed severe osteoporosis of the lumbar spine (T-score=-3.0, BMD= 0,866 gr/cm2). A complete laboratory and biochemical work up was performed to exclude secondary causes of osteoporosis. Total genomic DNA was extracted from peripheral blood and was used as template for genotype analysis.

Genotype analysis was performed using a novel Real-Time PCR assay based on SimpleProbe<sup>®</sup> melting curve analysis for the mutations of p.V667M and p.A1330V of LRP5 gene and the polymorphisms g.63980 G→A and g.6252 G→T of VDR and COL1A1 genes, respectively. The patient was heterozygous for the p.V667M mutation of LRP5 gene and for the BsmI [g.63980 G→A, rs1544410] and SpI polymorphisms [g.6252 G→T, rs1800012] of VDR and COL1A1 genes, respectively. Genotype analysis further excluded all types of osteogenesis imperfecta.

The patient was treated with daily s.c injections of recombinant teriparatide for 24 months followed by one i.v injection of zoledronate 5 mg with significant gains in the bone mass of the lumbar spine (Tscore=-2.0, BMD=0.970 gr/cm2). One year later the patient demonstrated no further changes in bone mass and did not sustain a new vertebral or non-vertebral fracture.

Conclusion: Polymorphic SpI binding site in the COL1A1 gene, BsmI restriction enzyme polymorphism of the VDR and V667M mutation of the LRP5 gene have been independently associated with osteoporosis. We show here that the co-existence of these 3 polymorphic sites in a young male adult caused severe osteoporosis with multiple fractures, suggesting a combining effect and/or interaction among the 3 haplotypes

**Disclosures:** *John Yovos, None.*

## SA0281

**TBS VARIATION IN BREAST CANCER WOMEN COMPLETING AI-THERAPY: A PROSPECTIVE STUDY OF THE B-ABLE COHORT.** MARIA RODRIGUEZ-SANZ<sup>1</sup>, MARTA PINEDA-MONCUSI<sup>1</sup>, NATALIA GARCIA-GIRALT<sup>1</sup>, SONIA SERVITJA<sup>2</sup>, TAMARA MARTOS<sup>2</sup>, JOSEP BLANCH-RUBIÓ<sup>3</sup>, IGNASI TUSQUETS<sup>2</sup>, MARIA MARTINEZ<sup>2</sup>, JAIME RODRIGUEZ-MORERA<sup>4</sup>, ADOLFO DíEZ-PÉREZ<sup>4</sup>, JOAN ALBANELL<sup>2</sup>, XAVIER NOGUES-SOLAN<sup>\*4</sup>. <sup>1</sup>IMIM (Hospital del Mar Research Institute), Red Temática de Investigación Cooperativa en Envejecimiento y Fragilidad (RETICEF), Barcelona, Spain, <sup>2</sup>Cancer Research Program, IMIM (Hospital del Mar Research Institute), Medical Oncology Department, Hospital del Mar, Autonomous University of Barcelona, Barcelona, Spain., Spain, <sup>3</sup>Medical Reumatology Department, Hospital del Mar, Barcelona, Spain., Spain, <sup>4</sup>Internal Medicine Department, Hospital del Mar, Universitat Autònoma de Barcelona, Barcelona, Spain

PURPOSE: The trabecular bone score (TBS) is a new additional texture parameter postulated to reflect bone microarchitecture, being able to capture roughly one third of fractures misclassified using BMD alone. The purpose of the study is to characterize TBS variation at the end of aromatase inhibitor (AI) therapy in postmenopausal women with breast cancer. METHODS: B-ABLE is a prospective cohort of 735 women treated with AIs according to the American Society of Clinical Oncology recommendations: 5 years of AI starting within 6 weeks postsurgery or 1 month after the last cycle of chemotherapy (5y-AI group) or alternatively switching to an AI after taking tamoxifen for 2 to 3 years (pTMX-AI group). TBS and BMD changes and their correlation at the end of AI-therapy were evaluated. RESULTS: AI treatment completion was achieved by 277 women. Of these, 70 (25.3%) were allocated to BP therapy. Significant TBS decreases were observed in BP-non-treated patients at the end of AI-therapy, both in pTMX-AI (-2.94%) and 5y-AI (-2.93%) groups. An inter-group comparison did not reveal significant differences in TBS decreases between pTMX-AI and 5y-AI patients. As regards BMD, significant decreases were also detected in both pTMX-AI (-4.14%) and 5y-AI (-2.28%) patients. In this case, pTMX-AI patients experienced significantly greater BMD decline when compared to 5y-AI patients. Regarding BP-treated patients, the TBS remained stable in both pTMX-AI and 5y-AI groups at the end of treatment. Compared to baseline, there was a significant increase in BMD at the end of treatment in both groups, reaching +2.30% in pTMX-AI and +5.33% in 5y-AI patients (Fig.1). There were not statistically significant differences between both groups. During AI-therapy a large number of BP-non-treated patients (approximately 30%) decreased by one TBS category. No significant differences were detected in the frequency distribution throughout TBS categories in BP-treated patients. Only moderate ( $r=0.4$ ;  $P<0.001$ ) and weakly ( $r=0.1$ ;  $P<0.01$ ) correlations were detected between BMD and TBS values and between their variations, respectively. CONCLUSIONS: AI-therapy induces significant decreases in TBS, comparable to those in BMD. On the other hand, maintenance, rather than major improvements in TBS was observed in BP-treated patients. AI treatment leads to bone microarchitecture deterioration, which seems to be partially dimmed by BPs.

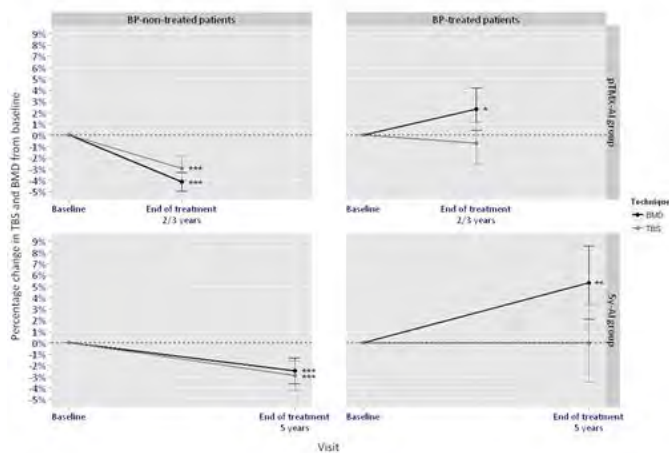


Figure 1

Disclosures: XAVIER NOGUES-SOLAN, None.

## SA0282

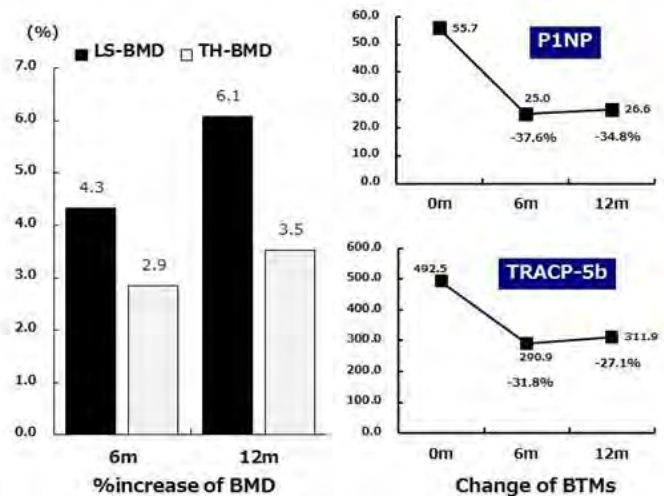
**The Predictors for Twelve Months Efficacy of Denosumab, an Anti-RANKL Antibody, on Osteoporosis in Rheumatoid Arthritis Patients from Japanese Multicenter Study (TBCR-BONE).** Yuji Hirano<sup>1</sup>, Yasuhide Kanayama<sup>2</sup>, Masaaki Isono<sup>3</sup>, Nobunori Takahashi<sup>4</sup>, Naoki Ishiguro<sup>4</sup>, Toshihisa Kojima<sup>5</sup>. <sup>1</sup>Rheumatology, Toyohashi Municipal Hospital, Japan, <sup>2</sup>Orthopaedic Surgery & Rheumatology, Toyota Kosei Hospital, Japan, <sup>3</sup>Rheumatology, Toyohashi Municipal Hospital, Japan, <sup>4</sup>Orthopaedic Surgery, Nagoya University Graduate School of Medicine, Japan, <sup>5</sup>Orthopaedic Surgery, Nagoya University Graduate School of Medicine, Japan

**Purpose:** Although medication of rheumatoid arthritis (RA) has been improved, treatment of concomitant disease in RA patients, such as osteoporosis (OP), will be more important. Although denosumab (DMB), an anti-RANKL antibody, was approved for treatment of OP in Japan in 2013, clinical data is lacking in RA-OP. The objectives of this study is to investigate the 12 months efficacy of DMB on RA-OP and predictors of efficacy from multicenter registry study in Japan (TBCR-BONE).

**Methods:** 79 female RA-OP treated with DMB were included. Bone mineral density of lumbar spine (LSBMD) and total hip (THBMD) and bone turnover markers (BTM) were measured at baseline and every 6 months to 12 months.

**Results:** Mean age was 70 years old. Mean RA duration was 16 years. Mean DAS28-CRP was 2.7. 44% of cases had the past history of fracture. Mean FRAX was 27%. Daily teriparatide (dTPTD) was used in 13 cases before DMB treatment. LSBMD and THBMD at 6m and 12m were significantly increased compared with baseline (Figures). Mean %decrease in P1NP were 37.6% at 6m and 34.8% at 12m (Figures). Mean %decrease in TRACP-5b were 31.8% at 6m and 27.1% at 12m (Figures). Next, all cases were divided into two group, good outcome group (GO) and non-good outcome group (non-GO), by median %increase of LSBMD and THBMD at 12 months. Mean %increase of LS-BMD at 12m in LS-GO (n=35) was significantly larger than that in LS-non-GO (n=38) (10.8% vs. 1.7%). Rate of patients treated with dTPTD just prior to DMB in LS-GO was significantly lower compared with that in LS-non-GO. %increase at 6m in LSBMD of LS-GO was significantly high compared with that in LS-non-GO (7.9% vs. 1.0%). Mean %increase of THBMD at 12m in TH-GO (N=35) was significantly larger than that in TH-non-GO (n=37) (6.4% vs. 0.8%). Body weight and body mass index were significantly low in TH-GO compared with that in TH-non-GO. Baseline CRP (mg/dl) in TH-GO was significantly low compared with that in TH-non-GO (0.56 vs. 0.89). Both baseline P1NP and TRACP-5b in TH-GO were higher than that in TH-non-GO. %increase at 6m in THBMD of TH-GO was significantly high compared with that in TH-non-GO (4.9% vs. 1.0%).

**Conclusions:** DMB was effective in RA-OP. Early response of BMD increase and baseline BTM level were suggested to be one of the predictors of the efficacy of DMB in RA-OP. Efficacy of DMB, especially in THBMD, may be influenced by inflammation status via excess of RANKL.



Table

Disclosures: Yuji Hirano, None.

## SA0283

**Short-term smoking cessation improved bone formation in male smokers.** Reiko Watanabe<sup>\*</sup>, Nobuyuki Tai, Junko Hirano, Daisuke Inoue, Ryo Okazaki. Teikyo University Chiba Medical Center, Japan

**Background & Aim:** Smoking increases fracture risk and contributes to COPD-associated osteoporosis. However, its impact on bone metabolism is largely unknown. We thus aimed to determine the effect of smoking cessation on bone metabolism.

**Subject & Method:** In this prospective study, we recruited 29 Japanese male healthy volunteers with smoking habit (37.7 ± 8.2 years old, 16.9 ± 11.3 pack years). Pulmonary function test was done before smoking cessation, and various bone and calcium metabolic markers, inflammatory markers and plasma cotinine levels were examined at 0, 1, 4, and 12 weeks.

**Result:** Mean FEV1.0/FVC, FEV1.0%predicted was 81.9% and 101.7%, respectively. Cotinine concentration was 149 ± 119 pg/ml at baseline. We confirmed that cotinine levels clearly decreased after smoking cessation except for one subject who failed, and the remaining 28 subjects were analysed. Smoking cessation caused increases in osteocalcin (OC) at 1, 4 and 12 weeks (0w; 15.0 ± 5.0ng/ml, 1w; 18.0 ± 4.2ng/ml, +26.4%, 4w; 17.8 ± 4.8ng/ml, +23.3%, 12w; 18.2 ± 5.5ng/ml, +27.8%, p<0.001), and in P1NP at 1,12 weeks(0w; 44.0 ± 15.5ng/ml, 1w; +10.0%, p=0.011, 12w; +14.2%, p=0.002). On the other hand, Tracp-5b significantly decreased at 12 weeks (0w; 323 ± 111mU/dl, 12w; 248 ± 83.6mU/dl, -21.8%, p<0.001). Interestingly, PTH showed no correlation with 25-hydroxyvitamin D at baseline, and both were significantly increased after smoking cessation. Percent changes in P1NP positively correlated with %changes in intact PTH (r=0.556, p=0.002 at 4w). Also, mean TNF-α levels were 1.36 ± 0.37 pg/ml at baseline, and significantly decreased by 17.3% at 12 weeks. When subjects were divided in two groups by baseline TNF-α, higher TNF-α group tended to be lower in baseline OC, P1NP and Tracp-5b. Before smoking cessation, IL-6 was detected in 18 subjects, and only 4 subjects remained detectable 4 weeks after smoking cessation. Subjects with detectable levels of IL-6 (IL-6g) at baseline showed significantly higher white blood cell count and hsCRP, and tending to be lower in OC. Compared to non-IL-6 detecting group, %changes in OC after smoking cessation was significantly higher in IL-6g (0w; 13.9 ± 5.2 vs. 16.8 ± 4.5 ng/ml, 4w; 34.8% vs. 3.7%, 12w; 40.3% vs. 4.3%, p<0.001).

**Conclusion:** The results suggest that bone formation is suppressed by smoking and recovers after cessation. Inflammatory cytokines and disturbed PTH-D axis may be involved in smoking-associated bone metabolic abnormalities in a partially reversible manner.

Disclosures: Reiko Watanabe, None.

## SA0284

See Friday Plenary Number FR0284.

## SA0286

See Friday Plenary Number FR0286.

## SA0287

**Response to teriparatide treatment differs by anatomical site and bone compartment.** Margaret Paggiosi<sup>1</sup>, Lang Yang<sup>1</sup>, Daniel Blackwell<sup>1</sup>, Jennifer Walsh<sup>1</sup>, Nicola Peel<sup>2</sup>, Eugene McCloskey<sup>1</sup>, Richard Eastell\*<sup>1</sup>. <sup>1</sup>Mellanby Centre for Bone Research, Department of Oncology & Metabolism, The University of Sheffield, United Kingdom, <sup>2</sup>Mellanby Centre for Bone Research, Sheffield Teaching Hospitals NHS Foundation Trust, United Kingdom

Teriparatide, the only currently licensed anabolic treatment for severe osteoporosis, stimulates both bone formation and bone resorption and therefore has the potential to exert distinct effects on different bone compartments. Large increases in spine bone mineral density (BMD) occur during treatment with teriparatide, but the concomitant effects on the peripheral skeleton are not well described. We characterised the central and peripheral skeleton using imaging techniques to better understand the mechanism of action of teriparatide.

Women (n = 20, ages 65.4 ± 5.5 years) with postmenopausal osteoporosis, defined as a BMD T-score ≤ -2.5 at the total hip or lumbar spine by dual energy x-ray absorptiometry (DXA), were recruited to an open label study of subcutaneous teriparatide at the licensed dose (Forsteo 20 mcg daily) for 104 weeks. Total body and regional BMC were measured by DXA (Hologic Discovery A). Radius and tibia volumetric BMD (vBMD) and microstructural properties were assessed by high resolution peripheral quantitative computed tomography (Scanco XtremeCT) using standard and extended cortical bone analyses. Trabecular bone structure of vertebra T12 was studied using high-resolution quantitative computed tomography (GE Lightspeed).

Overall, by week 104, no significant change in total body or sub-total body BMC was detected. Lumbar spine (p=0.0001) and pelvis (p=0.0005) BMC had increased (Fig 1.) but, in contrast, there was a decrease in the skull (p=0.008) and arms (p<0.01) BMC. Peripheral changes included a significant decrease in cortical vBMD (radius mean change = -3.6%, p=0.02; tibia mean change = -3.4%, p=0.002) and cortical tissue mineral density (TMD) (radius mean change = -3.7%, p=0.006, tibia mean change = -3.9%, p=0.0006). Cortical porosity increased at both the radius (mean change = +18.8%, p=0.007) and tibia (mean change = +10.3%, p=0.05) but cortical pore diameter remained unchanged. There were no statistically significant changes in all radius and tibia trabecular bone parameters. Within the vertebra there was an increase in trabecular number and thickness (mean change = +32.0% and +24.0% respectively, p<0.05).

In conclusion, we have shown the mechanism of action of teriparatide to increase BMC within the central skeleton is through an increase in trabecular number and thickness. In contrast, within the peripheral skeleton teriparatide decreases BMD through a reduction in cortical TMD and an increase in cortical porosity.

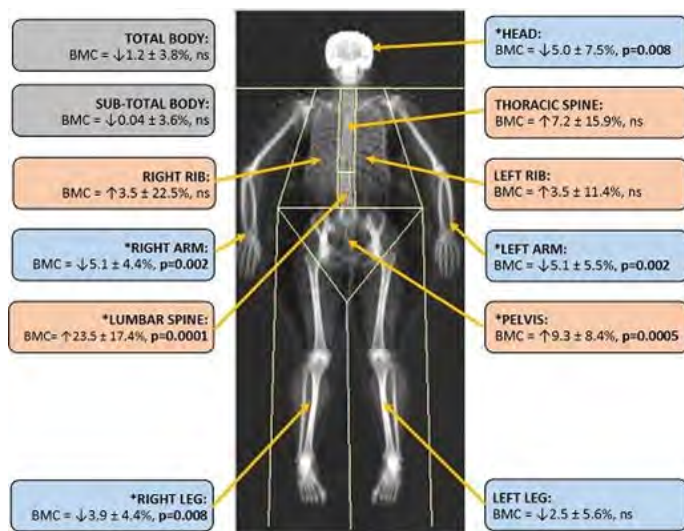


Fig 1. Percent changes (mean ± SD) in bone mineral content after 2 years of teriparatide treatment

**Disclosures:** Richard Eastell, Eli Lilly and Company Limited, Hampshire, UK, 11; Eli Lilly and Company Limited, Hampshire, UK, 12  
This study received funding from: Eli Lilly and Company Limited, Hampshire, UK

## SA0288

See Friday Plenary Number FR0288.

## SA0289

See Friday Plenary Number FR0289.

## SA0290

**Effect of Long-term Denosumab Treatment on Bone Mineral Density in Women with Osteoporosis and Contraindications to Oral Bisphosphonates - Observational Study.** Andrzej Sawicki\*. Medical Centre Synexux, Poland

**Objectives:** In clinical trials denosumab treatment was well-tolerated, significantly increased BMD and decreased risk fractures. The goal of this study is to evaluate whether osteoporotic women with contraindication or intolerance or resistance, to oral bisphosphonates treatment (e.g. GERD) presents positive effect on bone mass after denosumab treatment. We report observational Bone Mineral Densitometry (BMD) results up to 5 years of treatment in open study in out-patients clinic.

**Materials/Method:** The study was performed in 238 women with osteoporosis aged 29 to 93 with contraindication or intolerance or resistance to oral bisphosphonates treatment.

**Treatment:** standard dose of 60 mg denosumab treatment every six months sc. and individualized supplementation 400-800 mg of elemental calcium plus 400-1500 IU vitamin D3 or 0.25-1.0 mg 1-alpha OHD3 daily. BMD was assessed by Hologic 4500 every six months and we presents results before and after 12, 24, 36, 48, 60 months.

**Results:** Table 1 Percentage change in BMD from baseline and after 6, 12, 18, 24 months denosumab. Denosumab treatment was well accepted and tolerated, none adverse events related to denosumab treatment were observed.

**Conclusions:** Our data indicate that denosumab treatment up to 5 years in patients with contraindication or intolerance or resistance to oral bisphosphonates treatment is associated with continued gains in BMD

Table 1 Percentage change in BMD from baseline and after 6, 12, 18, 24 months denosumab

Months	12 m	24m	36 m	48 m	60 m
Region					
AP Spine	+7,6	+11,2	+13,6	+17,0	+18,7
F Neck	+5,2	+7,4	+8,5	+11,2	+12,1
Total Hip	+4,9	+6,5	+8,9	+9,2	+9,3

Note: number of patients in 12, 24, 36, 48, 60 months groups is not the same.

Table 1

**Disclosures:** Andrzej Sawicki, None.

## SA0291

See Friday Plenary Number FR0291.

## SA0292

**Efficacy and Safety of Denosumab in Chinese Postmenopausal Women with Osteoporosis at Increased Risk of Fracture: Results From a 12-Month, Randomized, Double-blind, Placebo-controlled Phase III Study.** Han Min Zhu<sup>1</sup>, Hai Tang<sup>2</sup>, Qun Cheng<sup>1</sup>, Liang He<sup>3</sup>, Peng Qiu Li<sup>4</sup>, Qing Yun Xue<sup>5</sup>, De Cai Chen<sup>6</sup>, Xiao Lan Jin<sup>7</sup>, Wen Jing Zhu<sup>8</sup>, Hong Xin Zhao<sup>8</sup>, Antonio Nino<sup>9</sup>, Zhen Lin Zhang<sup>10</sup>. <sup>1</sup>Huadong Hospital Affiliated to Fudan University, China, <sup>2</sup>Beijing Friendship Hospital, Capital Medical University, China, <sup>3</sup>Beijing Jishuitan Hospital, China, <sup>4</sup>Sichuan Provincial People's Hospital, China, <sup>5</sup>Beijing Hospital, China, <sup>6</sup>West China Hospital, Sichuan University, China, <sup>7</sup>Chinese People's Liberation Army General Hospital of Chengdu, China, <sup>8</sup>GlaxoSmithKline (China) R&D Company Limited, China, <sup>9</sup>Metabolic Pathways & Cardiovascular Therapeutic Area Unit, GlaxoSmithKline, Collegeville, Pennsylvania, USA, United states, <sup>10</sup>The Sixth People's Hospital affiliated to Shanghai Jiaotong University, China

**Introduction:** Osteoporosis affects more than 54.1 million (30.8%) Chinese women over age 50. The incidence of osteoporotic fracture has risen in China over the past decade. Denosumab (DMAB) reduces bone resorption by targeting the receptor activator of nuclear factor-κB ligand.

**Objectives:** This study evaluated the efficacy and safety of DMAB in Chinese postmenopausal women with osteoporosis.

**Methods:** 12-month, randomized, double-blind, placebo-controlled study in Chinese postmenopausal women aged 60 to 90 years with osteoporosis (-4.0 < BMD T-score < -2.5 at either the lumbar spine or total hip) and at least one risk factor for fracture. Patients were randomized 3:1 to DMAB 60 mg or placebo (PBO), administered as a single subcutaneous injection at baseline and Month 6 (M6). The primary efficacy endpoint was percent change from baseline in lumbar spine BMD (Month 12). Safety and tolerability were assessed including collecting all adverse events (AEs) and performing vital signs measurement and a standard panel of laboratory tests.

**Results:** A total of 485 subjects were randomized, 484 subjects received study medication and 452 subjects completed the study. Baseline demographics were similar between groups. The mean age was 68.9 years in DMAB group and 69.6 years in PBO group. In Intent-to-Treat (ITT) population, the mean difference of percent increase in BMD at lumbar spine at M6 and M12 was 3.2% and 4.4%, respectively, vs. placebo (P<0.0001). Similarly, DMAB significantly increased

BMD at total hip, femoral neck and trochanter at M6 by 2.3%, 1.6% and 3.4%, and M12 by 3.3%, 2.6% and 4.7%, vs. PBO ( $P < 0.0001$ ). The median reduction relative to PBO in serum CTX and PINP at M12 were 52.6% and 51.2%, respectively, ( $P < 0.0001$ ). AEs and serious non-fatal AEs between DMAb group and PBO group were similar (47% vs. 54% and 2% vs. 3%). Most common AEs were arthralgia and blood cholesterol increased; most increases were investigator-judged as treatment related. Two subjects (<1%) in the DMAb group experienced a fatal AE (oesophageal carcinoma, sudden cardiac death.) Neither was judged by the investigator as related to study medication.

Conclusions: The results of this study are consistent with results from globally conducted studies. DMAb was effective in increasing BMD and decreasing bone turnover markers over a 12-month period in Chinese postmenopausal women. AEs were similar between groups, no new safety concerns were identified with DMAb.

**Disclosures:** Antonio Nino, GlaxoSmithKline, 15  
This study was sponsored by GlaxoSmithKline.

## SA0293

**Exploratory Pooled Analysis on the Effect of Ibandronate in the MOVER and MOVEST Studies by Propensity Score Matching.** Seitaro Yoshida<sup>\*1</sup>, Masato Tobinai<sup>1</sup>, Koichi Endo<sup>1</sup>, Shingo Katakura<sup>1</sup>, Junko Hashimoto<sup>1</sup>, Rumiko Matsumoto<sup>2</sup>, Hiroshi Hagino<sup>3</sup>, Masko Ito<sup>4</sup>, Tetsuo Nakano<sup>5</sup>, Hideki Mizunuma<sup>6</sup>, Toshitaka Nakamura<sup>7</sup>. <sup>1</sup>Chugai Pharmaceutical Co. Ltd., Japan, <sup>2</sup>Taisho Pharmaceutical Co. Ltd., Japan, <sup>3</sup>Tottori University, Japan, <sup>4</sup>Nagasaki University, Japan, <sup>5</sup>Tamana Central Hospital, Japan, <sup>6</sup>Hirosaki University, Japan, <sup>7</sup>National Center for Global Health & Medicine, Japan

Purpose: Monthly intravenous (IV) ibandronate (IBN) 1mg demonstrated non-inferiority to daily oral risedronate (RIS) in reducing the incidence of vertebral fractures over 3 years in the MOVER study (Nakamura T, et al. Calcif Tissue Int 2013). Monthly oral IBN 100mg showed non-inferiority to monthly IV IBN 1mg in lumbar spine (LS; L2–L4) bone mineral density (BMD) gains at 1 year in the MOVEST study (Nakamura T, et al. Osteoporos Int 2015). We conducted an exploratory, pooled data analysis to compare LS BMD gains at 1 year between the two studies.

Methods: To take into account differences in eligibility criteria between these two studies, we defined a modified per-protocol-set (mPPS) that included patients with vertebral fractures (excluding LS fractures) and LS BMD changes from baseline  $\leq 30\%$  after 1 year of treatment in the MOVER study. We then constructed a pooled data set based on the mPPS in the MOVER study and the PPS in the MOVEST study. To estimate gains in LS BMD from baseline to 1 year in the two studies, in addition to the standard pooled data analysis, we conducted a 3-arm matching data analysis using propensity score matching (PSM) to improve comparability between treatment groups from independent studies.

Results: In the pooled data analysis, LS BMD gains at 1 year with IV IBN, oral IBN and RIS were 5.46%, 5.54% and 4.98%, respectively. The number of patients matched by 3-arm PSM was 49, which corresponds to a caliper value of 0.5 of pooled standard deviations of the logit of the propensity score, considering the stability of estimated results. In the matched data analysis, LS BMD gains at 1 year were 4.91%, 5.70% and 4.73% with IV IBN, oral IBN and RIS, respectively.

Conclusion: This exploratory, pooled data analysis showed that BMD gains with IV IBN and oral IBN were comparable with results of the MOVEST study, and that the IV IBN group showed greater BMD gains than the RIS group, which was similar to the results of the MOVER study. Thus, the efficacy of IV IBN and oral IBN appears to be similar. From the PSM data analysis, due to the lower stability of estimated results, we had difficulty in interpreting results with caliper values  $< 0.5$ . With caliper values  $\geq 0.5$ , we observed similar results to those of the pooled data analysis. Although the current analysis is limited by the number of patients, PSM made it easier to compare LS BMD gains among patients receiving different treatment regimens.

**Disclosures:** Seitaro Yoshida, Chugai Pharmaceutical Co. Ltd., 15  
This study received funding from: Chugai Pharmaceutical Co. Ltd

## SA0294

See Friday Plenary Number FR0294.

## SA0295

**Improving Feasibility for The Effectiveness of DiscontinuiG bisphosphonates (EDGE) Trial: A Pilot Study.** Nicole Wright<sup>\*1</sup>, P. Jeffrey Foster<sup>2</sup>, Amy Mudano<sup>2</sup>, E. Michael Lewiecki<sup>3</sup>, William Shergy<sup>4</sup>, Jeffrey Curtis<sup>2</sup>, Gary Cutter<sup>5</sup>, Maria Danila<sup>2</sup>, Meredith Kilgore<sup>6</sup>, Cora Lewis<sup>7</sup>, Sarah Morgan<sup>2</sup>, David Redden<sup>5</sup>, Amy Warriner<sup>8</sup>, Kenneth Saag<sup>9</sup>. <sup>1</sup>Department of Epidemiology, University of Alabama at Birmingham, United states, <sup>2</sup>Division of Clinical Immunology & Rheumatology, University of Alabama at Birmingham, United states, <sup>3</sup>University of New Mexico, United states, <sup>4</sup>Rheumatology Associates of North Alabama, United states, <sup>5</sup>Department of Biostatistics, University of Alabama at Birmingham, United states, <sup>6</sup>Department of Health Care Organization & Policy, University of Alabama at Birmingham, United states, <sup>7</sup>Division of Preventive Medicine, University of Alabama at Birmingham, United states, <sup>8</sup>Division of Endocrinology, Diabetes & Metabolism, University of Alabama at Birmingham, United states, <sup>9</sup>Division of Clinical Immunology & Rheumatology, United states

Purpose: The optimal duration of bisphosphonate therapy is a key question for patients and providers. Data from clinical trial extensions and observational studies have significant limitations. The Effectiveness of DiscontinuiG bisphosphonates (EDGE) study is a planned large, simple, pragmatic clinical trial to determine effectiveness of randomizing alendronate (ALN) users to continue or discontinue ALN after at least 3 years of therapy. We conducted a 6-month pilot study to determine feasibility and work flow in busy medical practices to recruit patients to the ensuing EDGE trial.

Methods: The EDGE pilot trial focused on: 1) evaluating administrative aspects of trial conduct (e.g. time to contract, IRB approval), 2) assessing site and patient recruitment rates, and 3) evaluating post-randomization adherence and outcome data collection. We sought to randomize 36 current ALN users (women aged  $\geq 65$ ). We surveyed participants at 1 and 6 months after randomization to assess adherence and adverse events.

Results: Nine sites participated, including 7 community physicians, and 2 academic medical centers. On average it took 3.4 months (*min* 0.9, *max* 7.7) to execute contracts and 13.9 days (*min* 6.0, *max* 20.0) for IRB approval. The UAB IRB served as the central IRB of record for 8 of the 9 sites. Sites recruited 27 patients (13 to continue ALN, and 14 to discontinue ALN); 2 sites were unable to recruit any patients. The mean (SD) time to first enrolled patient was 5.5 (2.9) months. Patients were on average 74.5 (6.1) years old, used ALN for 5.0 (2.4) years, and 24% were non-Caucasian. Over follow-up, 15% of patients did not adhere to their randomized treatment arm: 22% stopped using ALN in the continuation arm and 9.1% restarted ALN in the discontinuation arm. To date, no fractures or other adverse events have been reported.

Conclusions: The administrative procedures of the EDGE study were generally feasible, with minimal disruption to clinic flow. In this convenience sample, participant recruitment was suboptimal across most practice sites. A moderate proportion of patients crossed-over from their randomization assignment. We have updated cross-over assumptions and will use a more comprehensive/multi-faceted approach to readily identify and target our recruitment efforts with supplementation from administrative databases and patients from large health maintenance organizations to effectively achieve the scientific goals of the full EDGE study.

**Disclosures:** Nicole Wright, Amgen, 11

## SA0296

See Friday Plenary Number FR0296.

## SA0297

See Friday Plenary Number FR0297.

## SA0298

**Comparison of Osteoporosis Pharmacotherapy Fracture Rates: Analysis of a MarketScan® Claims Database Cohort.** Alan Reynolds<sup>\*1</sup>, Paul Kocis<sup>2</sup>, Guodong Liu<sup>3</sup>, Ed Fox<sup>4</sup>. <sup>1</sup>Penn State College of Medicine, United states, <sup>2</sup>Penn State Hershey Medical Center, United states, <sup>3</sup>Penn State Public Health Sciences, United states, <sup>4</sup>Penn State Hershey Bone & Joint Institute, United states

This study retrospectively used a large claims database to quantify real-world fracture rates among patients on each osteoporosis medication. The Truven Health Analytics MarketScan® Databases from 2008-2012 was used. All patients who started a new osteoporosis medication were identified. Patients who had a 12-month period of taking no osteoporosis medication leading up to starting the new medication were included in the study. This cohort was then divided into subgroups by each medication, and the number of patients who sustained a fracture at least 12 months after starting a new osteoporosis medication was recorded, as well as demographic and risk factor information. A logistical regression was used to isolate contributions

of risk factors, and to compare drugs head to head. All drugs were compared to alendronate directly since it was the most widely used drug in the study.

Absolute fracture rates, demographic information and risk factor prevalence can be seen in Table 1. In addition, logistical regression revealed a statistically significant difference between alendronate and teriparatide, with alendronate being superior at preventing fractures. No other head-to-head drug comparisons were statistically significant in the regression analysis despite some variance in their fracture rates. Regression analysis also showed a statistically significant increased risk of fracture for most risk factors. In descending order of magnitude of risk, having a prior fall was followed by diabetes, osteoarthritis, alcohol abuse, being a smoker, inflammatory bowel disease, use of an oral glucocorticoid, asthma and COPD. Risk factors found not to have a correlation included rheumatoid arthritis and celiac disease.

Overall, medications that are most frequently administered orally had the lowest absolute fracture rates, and more recently approved and parenteral medications with lower numbers of treated patients had higher rates of fracture while on treatment. These results, including the overall fracture rate of 1.55 fractures per 100 person years of treatment, underline the effectiveness of all osteoporosis medications and confirm findings of prior studies that have failed to find a significant difference between the efficacy of different agents.

Medication	Alendronate	Calcitonin	Denosumab	Teriparatide	Risedronate	Zoledronic acid	Total
Total number of patients	25,399	4,076	9,753	4,813	524	132	51,558
Number male patients (%)	2615 (7.2)	139 (13.0)	0 (0)	138 (14.4)	9 (1.7)	50 (1.7)	34 (14.3)
Average age	56.8	59.1	55.7	56.6	56.7	56.5	56.8
Smoking	1759 (6.7)	78 (7.3)	0 (0)	305 (5.9)	181 (3.9)	46 (8.8)	6 (8.8)
Alcohol abuse	177 (0.67)	8 (0.74)	0 (0)	47 (0.62)	17 (0.35)	38 (0.40)	4 (1.15)
Osteoarthritis	1207 (4.9)	77 (7.2)	0 (0)	435 (8.4)	159 (3.4)	268 (5.3)	49 (8.8)
Celiac disease	103 (0.4)	13 (1.3)	0 (0)	54 (0.54)	23 (0.48)	64 (0.73)	1 (0.76)
Inflammatory bowel disease	1562 (6.1)	96 (8.9)	0 (0)	626 (6.3)	282 (5.9)	577 (6.6)	41 (7.8)
Diabetes type 1	623 (2.4)	34 (3.2)	0 (0)	181 (1.8)	77 (1.6)	202 (2.37)	10 (1.5)
Use of oral glucocorticoid drug	4867 (19.2)	709 (66.0)	5 (15.6)	5947 (59.7)	2666 (56.8)	1174 (13.7)	325 (62.0)
Asthma, COPD, chronic bronchitis, emphysema	5433 (20.6)	309 (28.0)	1 (22.2)	2028 (20.4)	891 (18.0)	1808 (20.5)	151 (28.0)
Fall in past 12 months	427 (1.6)	21 (2.0)	0 (0)	159 (1.6)	49 (1.0)	118 (1.3)	14 (2.7)
Osteoarthritis or degenerative joint disease	7992 (25.9)	362 (33.7)	1 (11.1)	2796 (28.1)	1269 (26.7)	2329 (26.6)	198 (37.8)
Fractures	854	37	1	325	319	280	40
Patients with fracture(s) (%)	3.35	8.45	11.1	3.26	2.50	3.18	7.33
Average follow-up (days)	724	717	430	741	735	751	714
Fracture rate, 100 person years	1.54	1.75	9.24	1.61	1.24	1.54	3.9

Table 1

Disclosures: Alan Reynolds, None.

SA0299

See Friday Plenary Number FR0299.

SA0300

**Effects of a therapy with anti-RANKL antibody denosumab on bone metabolism markers and QOL in patients with osteoporosis.** Toshihisa Maeda\*<sup>1</sup>, Shinya Havashi<sup>1</sup>, Yasushi Miura<sup>2</sup>, Yoshitada Sakai<sup>3</sup>, Rvosuke Kuroda<sup>1</sup>, Masahiro Kurosaka<sup>1</sup>. <sup>1</sup>Department of Orthopaedic Surgery, Kobe University Graduate School of Medicine, Japan, <sup>2</sup>Division of Orthopedic Science, Department of Rehabilitation Science, Kobe University Graduate School of Health Sciences, Japan, <sup>3</sup>Division of Rehabilitation Medicine, Kobe University Graduate School of Medicine, Japan

Objectives: This study aimed to investigate the effects of denosumab, a human monoclonal antibody against receptor activator of nuclear factor kappa B ligand (RANKL), on bone metabolism markers and health-related quality of life (QOL) obtained from a questionnaire survey in patients with osteoporosis in a prospective study.

Material and Methods: The study included 400 patients with osteoporosis who treated with denosumab (age 80.4 ± 7.7 y.o.; including 82 patients switched from the other medications). The following clinical evaluations were performed before the first administration of denosumab and after 6 and 12 months of the treatment: bone mineral assay in the distal end of the radius using dual X-ray absorptiometry (DXA); serum levels of P1NP and TRACP-5b. A questionnaire survey employing 100 mm visual analogue scale (VAS) scores for low back pain and the MOS Short-Form 36-Item Health Survey (SF-36) for QOL was also carried out.

Results: The bone density relative to the young adult mean (YAM) ratio was significantly increased both 6 and 12 months after the treatment with denosumab as compared to that determined before the first administration (51.6 ± 10.6 % pre-treatment, 52.1 ± 10.8 % [P<0.05] after 6 months, and 52.6 ± 10.8 % [P<0.001] after 12 months). The serum levels of P1NP and TRACP-5b were significantly decreased (P1NP: 55.9 ± 30.1 µg/L, 24.5 ± 17.4 µg/L [P<0.001] and 26.1 ± 15.0 µg/L [P<0.001]; TRACP-5b: 545 ± 246 mU/dL, 290 ± 145 mU/dL [P<0.001] and 288 ± 159 mU/dL [P<0.001], respectively). The VAS scores for low back pain showed significant improvement (41.4 ± 30.0 mm, 26.8 ± 27.2 mm [P<0.05] and 23.1 ± 21.8 mm [P<0.001], respectively). The SF-36 scores 6 months after the treatment with denosumab, as compared to those before the first administration, improved in three categories including physical functioning (77.9 points pre-treatment, 82.7 points [P<0.05] after 6 months), role physical (78.7 points, 82.5 points [P<0.05], respectively) and bodily pain (68.0 points, 75.6 points [P<0.05], respectively).

Conclusions: This study demonstrated that denosumab significantly suppressed bone turnover, increased bone strength in patients with osteoporosis, and improved the patients' QOL in the physical dimension categories including physical functioning,

role physical and bodily pain. It is suggested that denosumab potentially contributes to the improvement of QOL as well as the increase of bone strength.

Disclosures: Toshihisa Maeda, None.

SA0301

**PDGF-BB inhibits BMP2-Smad signaling during osteogenic differentiation of periosteal progenitor cells.** Xi Wang\*, Bryna Matthews, Ivo Kalajic. UConn Health, United states

Increasing evidence has demonstrated a critical role of the periosteum during fracture healing, but the factors that influence the differentiation of periosteal progenitor cells (PPC) are not well defined. Platelet derived growth factor (PDGF) is well known as a mitogenic and chemotactic molecule, but its osteogenic effects and underlying mechanisms of action need further investigation. Our preliminary data indicated that PDGF blocked BMP2-induced osteogenic differentiation, leading to our hypothesis that PDGF is a negative regulator of BMP2 signaling. We aimed to investigate the crosstalk between PDGF and BMP2 signaling in PPCs.

In order to culture PPCs, periosteum is harvested from mouse femurs and tibias, followed by enzymatic digestion and in vitro expansion. Osteogenic differentiation assays were performed in primary cells and evaluated based on mineralization, Col2.3GFP activity and expression of bone sialoprotein and osteocalcin.

PDGF-BB (10ng/ml) prevented mineralized nodule formation and dramatically reduced osteogenic gene expression in PPCs. In addition, while BMP2 (100ng/ml) significantly promoted the differentiation of PPCs, this effect was blocked by PDGF-BB treatment. PDGF did not alter expression of BMP signaling pathway components Bmp2, Bmpr1a, Bmpr2 and Noggin following 24h treatment. We then further determined the effects of PDGF-BB on BMP2-induced downstream signaling in PPCs. Western blot results showed that BMP2 clearly induced the phosphorylation of Smad1/5/8 in PPCs after 20 minutes, which was inhibited by the addition of PDGF-BB.

PDGF receptors are receptor tyrosine kinases that can activate several downstream cascades including the ERK and PI3K/Akt pathway. To determine if these pathways mediate the effects of PDGF on the BMP2 pathway, PPCs were treated with BMP2, PDGF-BB and inhibitors during osteogenesis. While combinatory treatment of PDGF and BMP2 prevented osteogenic differentiation of PPCs, addition of either ERK inhibitor (U0126) or Akt inhibitor (LY294002) blocked this effects and significantly promoted the expression of BSP and osteocalcin.

In conclusion, our data show that PDGF-BB blocks BMP2-induced osteogenic differentiation of periosteal progenitors in vitro. Our data indicates a PDGF-mediated inhibition of BMP2-Smad signaling pathway as the likely mechanism. ERK and PI3K/Akt signaling are involved in the negative regulation of BMP2 by PDGF-BB, presenting potential molecular targets.

Disclosures: Xi Wang, None.

SA0302

**Thrombospondin status affects matrix-level control of endogenous TGF-beta bioavailability via tissue specific mechanisms.** Dylan Shearer\*, Nolan Bick, Anita Reddy, Andrea Alford. University of Michigan, United states

Thrombospondins (TSP) 1 and 2 are implicated in extracellular matrix (ECM) control of TGF-beta signaling. Here, we studied the impact of TSP1 and TSP2 status on smad2/3 phosphorylation in femoral diaphyses and distal femora of 6-week old female wild-type (WT; n=11), TSP1-/- (n=4) and TSP2-/- (n=6) mice. Mice were euthanized using IACUC approved methods. Femora were dissected, soft tissue was removed and proximal ends were cut at the greater trochanter. Diaphyses and distal ends were separated and proteins extracted in detergent-based lysis buffer. Soluble proteins were subjected to phospho-smad2/3 (Cell Signaling) Western blot and stripped and re-probed for total smad2/3 (Santa Cruz Biotechnology). In TSP2-/- diaphyses, smad2/3 phosphorylation was reduced to 30% of WT (p<0.01 Tukey post-hoc test). Specifically, phospho-smad2/3 intensity normalized to that of total smad2/3 was 2.04 ± 0.4, 2.81 ± 0.8, 0.64 ± 0.1 in diaphyses of WT, TSP1-/- and TSP2-/- mice, respectively; ANOVA p<0.001. In distal femora, TSP2 status did not affect smad2/3 phosphorylation. Instead, in TSP1-/- distal femora phospho-smad2/3 was almost 7-fold higher than WT (Tukey post-hoc p<0.0001). Specifically, phospho-smad2/3 intensity normalized to that of total smad2/3 was 1.14 ± 0.6, 7.85 ± 1.8 and 0.66 ± 0.4 in distal ends of WT, TSP1-/- and TSP2-/- mice, respectively (ANOVA p<0.0001). Next, we addressed the possibility that differences in TGF-beta signaling are due to known effects of TSPs on collagen fibrillogenesis. Detergent insoluble pellets obtained above were dried, acid hydrolyzed and hydroxyproline content measured. In diaphyses, insoluble hydroxyproline content was reduced compared to WT in both TSP1-/- and TSP2-/- samples (ug hydroxyproline/mg pellet wet weight: 1.69 ± 0.5, 0.98 ± 0.4, 0.96 ± 0.5 in WT, TSP1-/- and TSP2-/- diaphyses, respectively; ANOVA p<0.05). In distal femora, TSP1 status impacted levels of insoluble collagen more significantly than TSP2 status (ug hydroxyproline/mg pellet wet weight: 1.32 ± 0.6, 0.44 ± 0.2 and 0.98 ± 0.3 in WT, TSP1-/- and TSP2-/- distal femurs, respectively (ANOVA p<0.05; Tukey post-hoc p<0.05 TSP1-/- vs. WT). Together, our results suggest that TSP1 limits TGF-beta signaling in the ECM of the distal femur, while TSP2 facilitates TGF-beta signaling in the ECM of the diaphysis. Our TGF-beta

data do not correlate with insoluble collagen content, suggesting that TSPs affect collagen fibrillogenesis and TGF-beta bioavailability by independent, contextual pathways.

**Disclosures:** Dylan Shearer, None.

## SA0303

**Smoothed Agonist (SAG) Induced Mouse Calvarial Defect Healing.** Soonchul Lee\*, Hsin Chuan Pan, Alan Nguyen, Jia Shen, Swati Shrestha, Greg Asatrian, Nicholas Bernthal, Kang Ting, Chia Soo, Aaron James. UCLA, United states

Hedgehog (Hh) signaling positively regulates both endochondral and intramembranous ossification. Previously, stromal cell mediated calvarial defect healing has been shown to be dependent on intact Hh signaling (Levi and James et al., Stem Cells Dev 2011). Here, we examined whether use of an acellular scaffold treated with the small molecule Smoothed agonist (SAG) could aid in critical size mouse calvarial defect repair.

A 3 mm non-healing defect was created in the mid-parietal bone of CD1 mice. Treatment groups consisted of scaffold alone (custom fabricated hydroxyapatite coated PLGA scaffold, 3 mm dm x 0.5 mm thickness with DMSO carrier control), or scaffold with SAG (0.5-1.0 mM). N=8-10 mice per treatment group. Evaluation was performed at 4 and 8 weeks postoperative, by a combination of high resolution micro computed tomography (microCT), histology (H&E, Massons Trichrome), histomorphometry, and immunohistochemistry (BSP, OCN, CD31, VEGF).

Results showed that SAG induced significant and dose-dependent calvarial bone healing by all radiographic parameters (microCT imaging, microCT time lapse reconstructions, and microCT based quantification) (Fig. 1). Histologic analysis showed that most SAG-induced new bone formation was at the leading edge of the parietal bone defect, rather than in a peri-dural location. As expected from a critical size defect, minimal bone healing was found under control-treated conditions. Histomorphometric analysis showed an increase in parameters of bone formation (Bone Area, fractional Bone Area), but also an increase in the number of blood vessels (increased blood vessel number, blood vessel area). Additionally, a significant reduction in chronic inflammatory cells was observed with SAG treatment (including a reduction in persistent multinucleated giant cells).

In summary, local Smoothed Agonist (SAG) application induces dose-dependent calvarial defect healing in a mouse model. Nevertheless, complete defect healing was not observed with SAG treatment in any sample. SAG has other beneficial attributes, including a potential reduction in chronic inflammation and increase in defect site vascularization. Collectively, these attributes suggest that SAG could be used in combination with other growth and differentiation factors for improved bone defect repair.

Col.II expressing chondrocytes (KO) (floxed EFNB2 X Col.II promoter driven Cre-recombinase). A unilateral closed tibia fracture was made in the KO and their control littermates (control). At day 10,  $\mu$ CT showed that BV/TV (43%) and Tb.Th (20%) were significantly decreased in the KO callus compared with the control callus. Histologic analysis identified less newly formed bone but more cartilage with more immature chondrocytes in the KO callus than in the control callus. Compared to the controls, in the KOs, the cambium layer of the periosteum close to or surrounding the callus (C/S periosteum) was thinner and contained fewer progenitor cells. Fewer cells and vessels migrated into the callus from the periosteum (invasion front) in the KOs. Immunohistochemistry revealed fewer Sox2 expressing stem cells in the C/S periosteum and invasion front, with reduced cell proliferation (PCNA) and VEGF production in the KO callus compared to the control callus. In contrast, more apoptotic cells were observed in the C/S periosteum and the invasion front by TUNEL assay in the KOs than in the controls. Compared to the control callus, the number of osteocalcin expressing osteoblasts was decreased in the bone surface while osteocalcin expressing hypertrophic chondrocytes were increased in cartilage in the KO callus. Our data indicate that during the fracture repair, ephrin B2 in chondrocytes stimulates fracture healing by promoting periosteal stem cell activation, proliferation, survival and differentiation into osteoblast and/or chondrocytes, facilitating cartilage to bone conversion.

**Disclosures:** Yongmei Wang, None.

## SA0306

See Friday Plenary Number FR0306.

## SA0307

See Friday Plenary Number FR0307.

## SA0308

See Friday Plenary Number FR0308.

## SA0309

**High fat diets rich in monounsaturated or saturated fatty acids differentially alter vitamin D hydroxylase and bone in older female mice..** Yang Wang\*, Joshua Miller, Patricia Buckendahl, Sue Shapses. Rutgers University, United states

Obesity induced by high fat diets (HFD) is inversely associated with vitamin D status and bone health. Yet these associations and the direct effect of excessive fat intake on both hepatic and renal vitamin D metabolism have not been addressed. In this study, we examined if excess energy intake from fat, or the type of fat [monounsaturated fatty acids (MUFA) vs. saturated fatty acids (SFA)], affects circulating 25-hydroxycholecalciferol [25(OH)D] concentration, and whether this is due to an impairment of enzymes involved in vitamin D metabolic pathways in an adult murine model. The second objective was to determine the effects of dietary fatty acids on bone mass and quality. We examined 21 eight-month-old female C57BL/6J mice that were fed *ad libitum* with one of the three diets: normal fat diet (NFD) (10% fat as energy) or HFD (45% fat as energy) enriched either with MUFA or SFA. After 10wk, mice were analyzed for serum 25(OH)D (ELISA), protein (western blotting) and gene expression (real-time PCR) of vitamin D hydroxylases, body composition (magnetic resonance imaging), bone mineral density (dual-energy x-ray absorptiometry), and microstructure (micro-computed tomography). We found the HFD enriched with SFA, not MUFA, resulted in greater energy intake, weight gain, total body fat, and liver fat compared with the NFD ( $P<0.05$ ). Serum 25(OH)D showed a trend to be lower due to HFD compared with NFD ( $P=0.07$ ). Furthermore, high SFA resulted in a lower renal Cyp24a1 and higher hepatic Cyp2r1 mRNA expression than the NFD group ( $P<0.01$ ; Figure). In addition, while the BMD did not differ among groups, the BMD/ body weight (Figure) and trabecular (Tb) bone volume fraction (BV/TV) were lowest with SFA ( $P<0.05$ ) when compared with NFD. In conclusion, dietary SFA and MUFA differentially affect hepatic hydroxylase gene expression. In addition, Tb bone quality is compromised by SFA diet, yet the mechanism whereby different fatty acids regulate bone remains unclear.

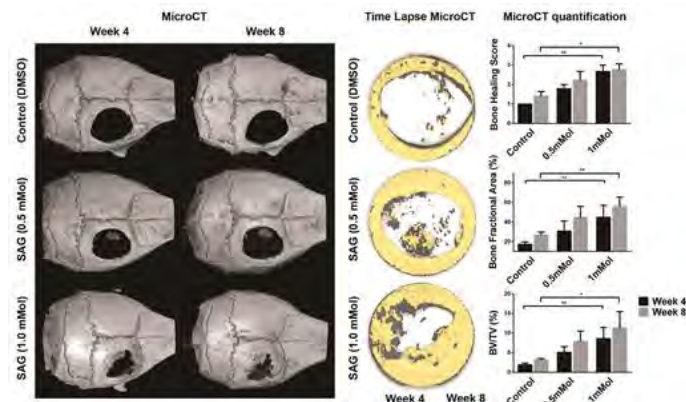


Figure 1

**Disclosures:** Soonchul Lee, None.

## SA0304

See Friday Plenary Number FR0304.

## SA0305

**Ablation of Ephrin B2 in Chondrocytes Leads to Impaired Osteoprogenitor Stem Cell Activation and Delayed Fracture Repair.** Yongmei Wang\*, Lin Ling, Nicholas Heiniger, Wasima Wayer, Thai Nguyen, Carly Matsukuma, Daniel Bikle. Endocrine Unit, University of California, San Francisco/San Francisco VA Medical Center, United states

Fracture repair is a complex process, recapitulating endochondral bone development in a number of ways, but the mechanism of progenitor differentiation remains unclear. Previous studies demonstrated that ephrin B2 and its receptor EphB4 are critical for endochondral bone development, in this study, we investigate the role of ephrin B2 on fracture repair by deleting ephrin B2 in

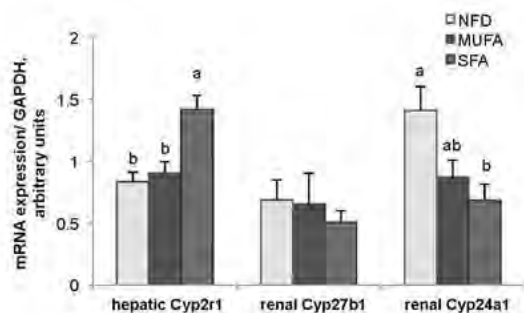


Figure 1. Vitamin D hydroxylases gene expression in mice.

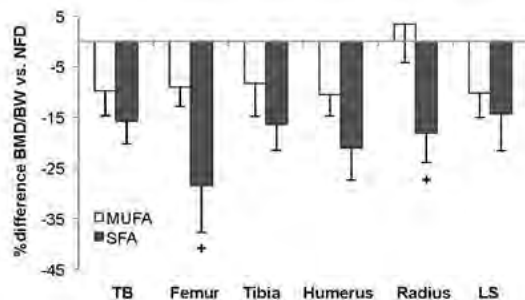


Figure 2 Difference for BMD values adjusted for body weight (BW) in high fat diet mice compared with their weight-matched normal fat diet controls. + Trend to differ from MUFA.

Table

Disclosures: Yang Wang, None.

## SA0310

See Friday Plenary Number FR0310.

## SA0311

See Friday Plenary Number FR0311.

## SA0312

See Friday Plenary Number FR0312.

## SA0313

See Friday Plenary Number FR0313.

## SA0314

See Friday Plenary Number FR0314.

## SA0315

See Friday Plenary Number FR0315.

## SA0316

See Friday Plenary Number FR0316.

## SA0317

**Bisphosphonate-Modified PEG-NELL, a Novel Bone-Targeted Molecule, as a Systemic Therapeutic for Osteoporosis.** Yulong Zhang<sup>1\*</sup>, Justine Tanjaya<sup>2</sup>, Jin Hee Kwak<sup>2</sup>, Mengliu Yu<sup>3</sup>, Soonchul Lee<sup>4</sup>, Jiayu Shi<sup>5</sup>, Rui Dong<sup>6</sup>, Jia Shen<sup>5</sup>, Eric Chen<sup>5</sup>, Xinli Zhang<sup>5</sup>, Chia Soo<sup>7</sup>, Benjamin Wu<sup>8</sup>, Kang Ting<sup>7</sup>. <sup>1</sup>Department of Bioengineering, UCLA, Los Angeles & Division of Advanced Prosthodontics, School of Dentistry, UCLA, Los Angeles, United states, <sup>2</sup>Division of Growth & Development, Section of Orthodontics, School of Dentistry, UCLA, Los Angeles & Department of Craniofacial Research Institute, School of Dentistry, UCLA, Los Angeles, United states, <sup>3</sup>Department of Craniofacial Research Institute, School of Dentistry, UCLA, Los Angeles, CA 90095, United states, <sup>4</sup>Orthopaedic Hospital Department of Orthopaedic Surgery & the Orthopaedic Hospital Research Center, UCLA, Los Angeles, United states, <sup>5</sup>Division of Growth & Development, Section of Orthodontics, School of Dentistry, UCLA, Los Angeles, United states, <sup>6</sup>Department of Bioengineering, UCLA, Los Angeles, United states, <sup>7</sup>Orthopaedic Hospital Department of Orthopaedic Surgery & the Orthopaedic Hospital Research Center, UCLA, Los Angeles & Division of Plastic & Reconstructive Surgery, Department of Surgery, David Geffen School of Medicine, UCLA, Los Angeles, United states, <sup>8</sup>Department of Bioengineering, UCLA, Los Angeles & Division of Advanced Prosthodontics, School of Dentistry, UCLA, Los Angeles & Weintraub Center for Reconstructive Biotechnology, School of Dentistry, UCLA, Los Angeles, United states

NEL-like molecule-1 (NELL-1), a potent pro-osteogenic secretory molecule, has demonstrated the promising effect of reversing osteoporosis. This study was conducted to enhance the binding affinity of NELL-1 into the bone tissues and to reduce the off-target effect by modifying its structure. To improve its circulation time and stability, NELL-1 was first PEGylated and then conjugated with bisphosphonate (BP), which can guide the protein to bind with hydroxyapatite (HA) on bone tissues due to its high bone-binding affinity. To measure the modification degree of BP-PEG-NELL, a modified NELL-1 was determined using HA powder. Next, the *in vitro* bioactivity of BP-PEG-NELL was determined by ALP staining (day 6, 12) and Alizarin red staining (day 21). Finally, to examine the biodistribution of BP-PEG-NELL, four CD-1 adult mice were injected via the tail vein with the protein labeled with VivoTag 680XL. Organs were harvested at 48 h post-injection and imaged via the IVIS Lumina II imaging system. The results of the fluorometric assay showed that three BP molecules were conjugated with one PEG-NELL molecule. The bone-binding affinity of BP-PEG-NELL was significantly greater than that of PEG-NELL, and the protein absorption rate was significantly increased from 20.1% to 83.6%. The thermal shift assay also showed that the denaturation temperature increased from 49.8 °C to 54.5 °C, suggesting that BP-PEG-NELL has a higher thermal stability compared to unmodified NELL-1. BP-PEG-NELL demonstrated a mainly preserved bioactivity after modification. The biodistribution study exhibited a greater amount of protein retention on the targeted bone tissues (calvaria, femur, tibia, and vertebrae) of the BP-PEG-NELL group when compared to the PEG-NELL groups (increased up to 30-80%). Moreover, the protein distribution into the vital organs such as the liver and spleen were significantly decreased after BP modification. Overall, these data suggest that BP modification not of PEG-NELL not only significantly increased protein binding on the targeted bone tissues *in vivo* by altering its biodistribution pattern, but also reduced the off-target effect on the vital organs while preserving its bioactivity *in vitro*. The current findings provide strong rationale that BP-modified PEG-NELL is an effective approach that can be further developed into a novel systemic therapeutic for the treatment of osteoporosis.

Disclosures: Yulong Zhang, None.

This study received funding from: KT, CS, XZ, and BMW are co-founders of Bone Biologics Inc. which licensed Nell-1 from UCLA

## SA0318

**Changes of Articular Cartilage and Subchondral Bone in Rat Osteoarthritis Model Induced by Surgical MMT and MCLT Operation.** ZhiQi Peng<sup>\*</sup>, Jukka Vääräniemi, Katja M Fagerlund, Jukka P Rissanen, Jenni Bernoulli, Jussi M Halleen, Jukka Morko. Pharmatest Services Ltd, Finland

Osteoarthritis (OA) is the most common form of joint disorders and manifested by gradually increasing damage in articular cartilage and subchondral bone. Articular cartilage and subchondral bone are different tissue types. Alterations of either tissue type modulate the properties and functions of other parts of osteochondral junction. For OA studies, we have set up several experimental models in rat knee including medial meniscal tear combined with medial collateral ligament transection (MMT+MCLT) and anterior cruciate ligament transection alone and combined with partial medial meniscectomy. Although all these rat OA models exhibit obvious damage in articular cartilage, there are differences in subchondral bone changes between the models. In order to understand subchondral bone changes in osteoarthritic rat knee, we analyzed medial tibial epiphysis in the rat MMT+MCLT model in more detailed by bone histomorphometry. Eighteen or twenty-five days after

the MMT+MCLT operation, articular cartilage was obviously damaged in the medial tibial plateau of operated right knee. Bone volume (BV/TV) was significantly increased in the medial tibial epiphysis of MMT+MCLT knee when compared with contralateral left knee. Double labeling parameters showed that bone formation rate was dramatically increased in the medial tibial epiphysis of MMT+MCLT knee as well. However, when comparing the total amount of bone (TBV) in medial tibial epiphysis, there was no difference between MMT+MCLT knee and contralateral knee. Rather, the total area of medial tibial epiphysis was markedly decreased in MMT+MCLT knee. This was associated with significantly decreased thickness of medial tibial epiphysis or epiphyseal marrow cavity. These results indicated that medial tibial epiphysis went through a compression deformation after the surgical MMT+MCLT operation in rats. Furthermore, fluorescence labeling demonstrated a growth rate in the medial tibial epiphysis of contralateral knee indicating endochondral ossification and the formation of new subchondral bone. This growth activity disappeared in the medial tibial epiphysis of MMT+MCLT knee within seven days after the operation. This study demonstrated that a composite surgery is capable of inducing serious damages in articular cartilage and epiphyseal bone in rats. These damages should be taken into account when selecting animal models for studying the preclinical efficacy of disease modifying OA drug candidates.

**Disclosures:** *ZhiQi Peng, None.*

### SA0319

See Friday Plenary Number FR0319.

### SA0320

See Friday Plenary Number FR0320.

### SA0321

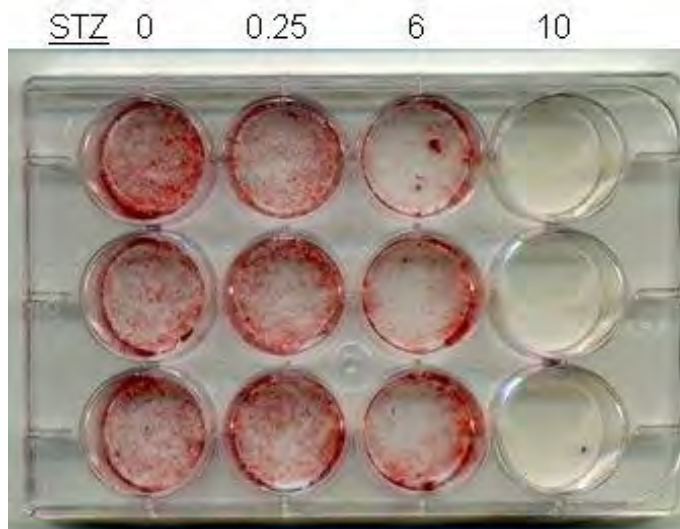
**The Effects of Streptozotocin on Osteoblast to Osteocyte Differentiation *In Vitro*.** Amanda Sutherland<sup>1</sup>, Tammy Brown<sup>2</sup>, Donna Pacicca<sup>2</sup>.  
<sup>1</sup>University of Kansas School of Medicine, United states, <sup>2</sup>Children's Mercy Hospital, United states

Streptozotocin (STZ) induced diabetes mellitus (DM) is a common method used to study DM *in vivo*, however, the inherent effects STZ has on osteoblasts, osteocytes, and the differentiation of osteoblasts to osteocytes has not been well studied. STZ is generally thought to enter the cell via glucose transporter 2, which is not highly expressed in bone. We used the IDG-SW3 cell line to mimic the osteoblast to osteocyte differentiation pathway in order to study the effects of STZ on osteoblasts, osteocytes, and differentiation *in vitro*.

Differing STZ concentrations (based around a typical rodent dose of 70 mg/kg used to induce diabetes) were applied in solution at either time 0 for 24 hours, or 24 hours pre-harvest, followed by culture for 7 and 28 days. Media glucose was measured at baseline and at each harvest using a glucometer. Alizarin Red S assay was used to quantify mineralization at 7 and 28 days. qPCR was performed for genes b-actin (control gene), E11, keratocan, SOST, Col1, GLUT1, and GLUT2. Total DNA content per well was used to approximate cell number. LDH assay was used to assess viability.

Following the day 0 STZ exposure, mineralization was decreased in the 0.25, 6, and 10 mM exposure groups at day 28 ( $p < 0.01$ ). Keratocan expression was significantly decreased at 6 and 10 mM following a time 0 STZ exposure on both days 7 and 28 ( $p < 0.01$ ). However, SOST and Col1 expression were not significantly affected on day 28. GLUT2 expression was only observed on day 7 after a time 0 STZ exposure, not after pre-harvest exposure. STZ exposure did not have a significant effect on cell viability at any time point, as demonstrated by lack of significant differences in glucose utilization and LDH.

Although osteoblast and osteocytes do not significantly express GLUT2, we showed STZ exposure at 6 mM (which corresponds to the Vd of 70 mg/kg) has an effect on these cells *in vitro*. STZ had the greatest effect on the osteoblast-like cells at day 7 by causing decreased expression of keratocan. The effect on osteoblasts is further evidenced by the decreased mineralization at day 28 following increasing doses of STZ. Although the mechanism by which STZ enters osteoblasts and osteocytes remains unclear because of their low levels of GLUT2 expression, STZ exposure causes functional effects on osteoblastic cells without causing cell death.



Day 28 IDG-SW3 cells, STZ day 0

Mineralization at day 28

**Disclosures:** *Amanda Sutherland, None.*

### SA0322

**The Effects of Switching From Teriparatide to Anti-Rankl Antibody on Bone Metabolism.** Toshinobu Omiya<sup>1</sup>, Jun Hirose<sup>2</sup>, Yuhō Kadono<sup>3</sup>, Yasunori Omata<sup>4</sup>, Naohiro Izawa<sup>5</sup>, Takeshi Miyamoto<sup>6</sup>, Sakae Tanaka<sup>7</sup>.  
<sup>1</sup>oomiya9ort@yahoo.co.jp, Japan, <sup>2</sup>j.hirose513@gmail.com, Japan, <sup>3</sup>ykadono-ky@umin.net, Japan, <sup>4</sup>grandbleu\_1024@yahoo.co.jp, Japan, <sup>5</sup>izawa.naohiro@gmail.com, Japan, <sup>6</sup>miyamoto@z5.keio.jp, Japan, <sup>7</sup>tanakas-ort@h.u-tokyo.ac.jp, Japan

**Purpose:** There is accumulating clinical evidence that both teriparatide (PTH) and anti-RANKL (receptor activator of nuclear factor  $\kappa$ B ligand) antibody effectively increase bone mineral density (BMD) and reduce fragile fractures in patients with osteoporosis. However, differences in detailed histological appearance of bones after administration of PTH, anti-RANKL or switching from PTH to anti-RANKL antibody have not been clarified. The objective of this study was to analyze these differences in structural and histological appearance using ovariectomized (OVX) mice.

**Materials and Methods:** Twelve-week-old female C57BL/6 mice were either ovariectomized or sham operated (SHAM group). Four weeks after the surgeries, the OVX mice were subjected to one of the following four treatment options: phosphate-buffered saline (PBS) for 8 weeks (OVX group), PTH (80  $\mu$ g/kg/day, 3 days a week) for 4 weeks followed by PBS for 4 weeks (PTH4W group), PTH for 8 weeks (PTH8W group) and PTH 4 weeks followed by anti-RANKL antibody (RANKL-MCA, single injection of 5 mg/kg) (SWITCH group). All mice were sacrificed 12 weeks after the surgeries. BMD was measured at the proximal tibia, femur and lumbar spine. Hind limbs and lumbar spines were subjected to micro CT and histomorphometric analysis.

**Results:** A comparable increase in BMD was observed in PTH8W group and SWITCH group, while BMD in the PTH4W group significantly decreased after discontinuation of PTH treatment. In the cancellous bone, histomorphometric analysis demonstrated that both bone formation and resorption parameters significantly increased in PTH8W group and decreased in SWITCH group. In contrast, in the cortical bone, bone formation parameters increased on the periosteal surface in both PTH8W and SWITCH groups, while those on the endosteal surface increased in PTH8W group and markedly suppressed in SWITCH group. Bone resorption significantly decreased on the periosteal and endosteal surfaces in SWITCH group.

**Conclusion:** Our results suggest that switching from PTH to anti-RANKL antibody had distinct effects on cancellous and cortical bones as compared to treatment with PTH alone.

**Disclosures:** *Toshinobu Omiya, None.*

### SA0323

See Friday Plenary Number FR0323.

### SA0324

See Friday Plenary Number FR0324.

**SA0325**

See Friday Plenary Number FR0325.

**SA0326**

See Friday Plenary Number FR0326.

**SA0327**

See Friday Plenary Number FR0327.

**SA0328**

See Friday Plenary Number FR0328.

**SA0329**

See Friday Plenary Number FR0329.

**SA0330**

See Friday Plenary Number FR0330.

**SA0331**

See Friday Plenary Number FR0331.

**SA0332**

See Friday Plenary Number FR0332.

**SA0333**

See Friday Plenary Number FR0333.

**SA0334**

**Characteristics of Vertebral Deformity in Gaucher Disease: the Gaucherite Study UK.** Fjola Johannesdottir\*, Timothy M. Cox, Patrick Deegan, Simona D'Amore, Kenneth E. Poole. Department of Medicine, University of Cambridge, United Kingdom

**Objective:** Type 1 (non-neuronopathic) Gaucher disease (GD1) is a recessively inherited lysosomal disorder characterized by accumulation of  $\beta$ -glucosylceramides in pathological macrophages occurring especially in spleen, liver and bone marrow. Kyphoscoliosis is an established feature in the more severe neuronopathic Type 3 GD. The skeletal manifestations of GD1 are not well understood but are among the most disabling. We sought to establish whether there was vertebral deformity in adults with GD1 and determine its association with enzyme replacement therapy (ERT) and splenectomy.

**Methods:** Thirty-six individuals (mean age at scan 56 yrs. (SD: 12); 22 women; 14 men) from the ongoing Gaucherite study (UK) with type 1 GD who had available MR imaging and clinical data were analysed. The midsagittal MRIs of the lumbosacral region, L1-L4, were evaluated morphometrically and vertebral deformity defined by adapting the Genant semi-quantitative method. Bone marrow involvement was estimated as the ratio of the average T1-weighted gray value of vertebral body and healthy intervertebral disc (Ratio VD).

**Results:** Although only 7 patients had DXA defined osteoporosis, 19 (53%) had a deformed vertebra (4 had 2 vertebrae deformed). Most of the deformed vertebrae were classified as biconcave (19/23). Sixty-one per cent of the vertebrae were graded as mild and 39% as moderate. Thirty-four patients were receiving enzyme therapy and most (32/34) had had this treatment for at least 10 years. Those with deformity were significantly older when they started ERT and had received it for fewer years (Table 1). Twenty-six per cent of those with deformity had had splenectomy as opposed to 59% of those without deformity, but the significance of this difference was only at the 9% confidence level ( $p=0.09$ ).

**Conclusion:** These preliminary findings, in a relatively small group, showed that mild-to-moderate lumbar vertebral deformity was frequent in adults with type 1 Gaucher disease; the most common vertebral body shape was biconcave. This suggests that the underlying mechanism for vertebral deformity among Gaucher patients is different from that in osteoporotic disease where wedge deformity is the most common.

Table 1

	With Deformity	Without Deformity	p-value
Number (N)	19	17	0.74
Lumbar lordosis angle (degree)*	52 (18)	52 (8)	0.86
Ratio VD**	1.53 (0.17)	1.62 (0.26)	0.25
Age at scan (yrs)*	59 (12)	52 (11)	0.08
Age started treatment (yrs)*	45 (15)	34 (11)	0.02
Years on treatment (yrs)*	14 (6)	18 (4)	0.03
Splenectomy (N (%))	5 (26%)	10 (59%)	0.09

\*The ratio of the average T1-weighted gray value of vertebral body and healthy intervertebral disc. 29 individuals had measurements; 13 with deformity, 16 without deformity. \*\*Data presented as mean (SD)

GD patient  
biconcave vertebrae

Table 1

**Disclosures:** *Fjola Johannesdottir, None.***SA0335**

See Friday Plenary Number FR0335.

**SA0336**

See Friday Plenary Number FR0336.

**SA0337**

**Observation of Recurrent Bone Marrow Oedemas in HIV Patients on Antiviral Therapy.** Sebastian Radmer<sup>1</sup>, Ilko Kastirr<sup>\*2</sup>, Reimer Andresen<sup>2</sup>. <sup>1</sup>Centre for Orthopaedics, Berlin, Germany, <sup>2</sup>Institute of Diagnostic & Interventional Radiology/Neuroradiology, Westkuestenlinikum Heide, Academic Teaching Hospital of the Universities of Kiel, Luebeck & Hamburg, Heide, Germany

**Introduction:** Severe pain and functional impairment can point to the presence of a bone marrow oedema. Typical localisations are the periarticular bone segments of the lower limbs and the vertebral bodies. Mechanical, metabolic, ischaemic and reactive/degenerative causes are under discussion. The diagnosis is rendered on the basis of MRI findings, which show a diffuse signal attenuation in the T1-weighted and a diffuse signal increase in the strongly T2-weighted fat-suppressed sequences. We report on the recurrent incidence of multiple bone-marrow oedemas in 5 HIV patients receiving antiviral therapy.

**Material and method:** In 5 HIV-positive male patients (average age 51.1 (38-63) years) exercise-related pain occurred in different joint regions (3 patients foot/ankle, 1 patient knee, 1 patient hip). All patients were receiving antiviral treatment with Atripla® (active constituents: efavirenz, emtricitabine, tenofovir). Major findings of the clinical examination were a doughy swelling of the affected area and a marked tenderness to pressure. Both a conventional radiograph and an MRI scan of the affected region were performed in all patients. With regard to therapy, the affected joint was mobilised without weight-bearing, while analgesic/anti-inflammatory medication as well as physiotherapy and lymph drainage were used as supportive measures. Vitamin-D levels were additionally determined in all patients.

**Results:** In all 5 patients, a fracture could be ruled out in the conventional X-ray, but a bone marrow oedema could be clearly visualised with the aid of MRI. A marked improvement in symptoms occurred in all patients under therapy, but a recurrence of bone-marrow oedemas was seen over the further course in 4/5 patients, both at the point of first manifestation and in other joint regions. Vitamin-D levels were in the normal range in all patients.

**Discussion:** The possible presence of a bone-marrow oedema should be considered in HIV patients with joint complaints of unclear origin. The aetiology of the bone-marrow oedema remains unclear, with a conceivable explanation in the present cases being that tenofovir impairs the function of the tubule cell in the proximal tubule and increases the secretion of phosphate. In such cases, a switch of antiviral therapy can be considered after consultation with the treating virologist/ internist.

**Disclosures:** *Ilko Kastirr, None.***SA0338**

See Friday Plenary Number FR0338.

**SA0339**

See Friday Plenary Number FR0339.

## SA0340

**Anxiety Disorders and Falls among Older Adults.** Kara Holloway<sup>1</sup>, Lana Williams<sup>1</sup>, Sharon Brennan-Olsen<sup>1</sup>, Amelia Morse<sup>1</sup>, Mark Kotowicz<sup>1</sup>, Geoff Nicholson<sup>2</sup>, Julie Pasco<sup>\*1</sup>. <sup>1</sup>Deakin University, Geelong, VIC Australia, Australia, <sup>2</sup>Melbourne Medical School, Western Campus, The University of Melbourne, VIC, Australia, Australia

**Purpose:** Falls are common among older adults and can lead to serious injuries, including fractures. Depression has previously been shown to be associated with increased falls risk; however the association with anxiety disorders, another common psychiatric disorder, is relatively unknown. Thus, we aimed to determine associations between anxiety disorders and falls in older adults.

**Methods:** Participants were 487 men and 376 women aged  $\geq 60$  years enrolled in the Geelong Osteoporosis Study, Australia. Lifetime history of any anxiety disorder was diagnosed using the Structured Clinical Interview for Diagnostic and Statistical Manual of Mental Disorders, Fourth Edition, Non-patient edition (SCID-I/NP). Falls were determined by self-report. Individuals were considered fallers if they had one or more falls over the past 12 months. In men, a falls-risk score (Elderly Falls Screening Test (EFST)) was also calculated. Binary logistic regression was used to determine the association between anxiety and falls. Multivariable models included age, sex, weight, height, lean mass, mean arterial pressure, mood disorders, psychotropic medication use, cardiovascular medication use, narcotic analgesic use, mobility, socioeconomic status, average glasses of alcohol per day and highest number of glasses of alcohol per day as potential confounders.

**Results:** Among fallers, 24 of 299 (8.0%) had a lifetime history of anxiety disorder compared to 36 of 634 (5.7%) non-fallers ( $p=0.014$ ). Examination of the association between anxiety and falls suggested differential relationships for men and women. In men, following adjustment for age, psychotropic medications, mobility and blood pressure, lifetime anxiety disorder was associated with falling (OR 2.96; 95%CI 1.07-8.21) and with EFST score (OR 3.46; 95%CI 1.13-10.6). In women, an association between lifetime anxiety disorder and falls was explained by age, psychotropic medication use, poor mobility and socioeconomic status.

**Conclusion:** Although anxiety disorders were independently associated with a 3-fold increase in likelihood of reported falls and high falls risk among men, an independent association was not detected among women. These results may aid in prevention of falls through specific interventions aimed at reducing anxiety, particularly in men.

**Disclosures:** Julie Pasco, None.

## SA0341

**Distal Radius Fracture Patients Show Reduced Ability of Dynamic Body Balancing.** Hidetoshi Kaburagi<sup>\*1</sup>, Koji Fujita<sup>1</sup>, Akimoto Nimura<sup>2</sup>, Takashi Miyamoto<sup>1</sup>, Ryuichi Kato<sup>3</sup>, Atsushi Okawa<sup>1</sup>. <sup>1</sup>Dept. of Orthopedic Surgery, Tokyo Medical & Dental University, Japan, <sup>2</sup>Dept. of Clinical Anatomy, Tokyo Medical & Dental University, Japan, <sup>3</sup>JA Kyosai Research Institute, Japan

**Background:** Fragility fractures of the distal radius are associated with an increased risk of future hip and spine fracture so the importance of body balancing ability and bone quality in fall and secondary fracture prevention is well recognized. We assessed body balancing ability, grip strength and bone quality of patients with distal radius fractures who underwent surgery.

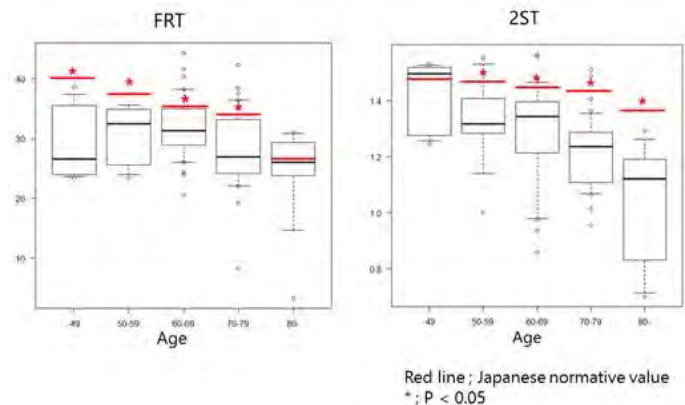
**Methods:** A prospective multicenter study, approved by IRA, of 94 women (age $>45$  years) with their first fragility fracture of the distal radius who underwent surgery in registered hospitals from January to December in 2015 was conducted. Two weeks after surgery, their body balancing ability was measured by four methods: Functional Reach Test (FRT), Timed Up and Go test (TUG), 2 Step test (2ST) and Timed Unipedal Stance test with eyes open (TUS). 2S is the score obtained by dividing height by the maximum length of the double stride. Grip strength on the non-fracture side (GS) and bone density (T-score) were also measured at the same time point. Statistical analysis was performed using the Student's t test to compare the results with Japanese normative values and  $p<0.05$  was considered significant.

**Results:** FRT was 29.6 cm in women in their 40s ( $p=0.03$ ), 31.1 cm in women in their 50s ( $p=0.002$ ), 32.5 cm in women in their 60s ( $p<0.001$ ) and 28.2 cm in women in their 70s ( $p<0.001$ ). TUG was 7.7 s in women in their 50s ( $p<0.001$ ), 7.1 s in women in their 60s ( $p=0.002$ ) and 8.1 s in women in their 70s ( $p=0.004$ ). 2ST was 1.40 in women in their 40s, 1.32 in women in their 50s ( $p=0.003$ ), 1.29 in women in their 60s ( $p<0.001$ ), 1.21 in women in their 70s ( $p<0.001$ ) and 1.02 in women in their 80s ( $p=0.01$ ). TUS was 55 s in women in their 60s ( $p<0.001$ ). GS was 20.9 kg in women in their 50s, 19.3 kg in women in their 60s and 18.2 kg in women in their 80s. Only 25% of subjects showed a lower T-score than  $-2.5$ .

**Summary:** Patients with distal radius fractures in their 50s, 60s and 70s showed significantly lower body balancing ability, especially during dynamic motion like FRT, TUG and 2ST. GS was also significantly lower in women in their 50s, 60s and 80s.

Three-quarters of patients did not show osteoporosis. This is compatible with the fact that distal radius fractures tend to be primary fragility fracture and patients were relatively younger.

Patients with distal radius fractures should be identified as those at "high risk" of falls and secondary fractures. Intensive training could be effective for fall prevention.



Results of FRT and 2ST

**Disclosures:** Hidetoshi Kaburagi, None.

## SA0342

**Age-related Changes and Sex-related Differences in Spinal Kyphosis Angles and Spinal Mobility in an Elderly Japanese Population.** Yuji Kasukawa<sup>\*</sup>, Naohisa Miyakoshi, Michio Hongo, Yoshinori Ishikawa, Daisuke Kudo, Masazumi Suzuki, Tetsuya Kawano, Norimitsu Masutani, Manabu Akagawa, Yuichi Ono, Yoichi Shimada. Department of Orthopedic Surgery, Akita University Graduate School of Medicine, Japan

Kyphosis and decreased mobility of the lumbar spine have been shown to increase the risk of falls and to impair both quality of life and the ability to perform activities of daily living in elderly Japanese people. However, age-related changes and sex-related differences in individuals with adequate kyphotic or lordotic angles of the thoracic or lumbar spine are still unclear. The aim of this study was to evaluate age-related changes in spinal kyphosis of 572 subjects (252 men, 320 women) aged  $\geq 50$  years. The subjects were divided into four groups based on age: 50 to 59 years ( $n=22$  men,  $n=35$  women), 60 to 69 years ( $n=79$ men,  $n=126$  women), 70 to 79 years ( $n=106$ men,  $n=125$  women), and 80 to 89 years ( $n=45$ men,  $n=34$  women). We assessed the thoracic kyphosis (TK) angle, lumbar kyphosis (LK) angle, and spinal inclination (SI) in a neutral standing position. The range of motion of the thoracic and lumbar spine and the SI were measured with the SpinalMouse® (Idiag, Volketswil, Switzerland). The height of both men and women decreased significantly with aging ( $P<0.0001$  and  $P<0.0001$ , respectively). The body mass index did not change significantly with aging in either sex. In men, significant increases with aging were seen in the TK angle ( $P=0.0403$ ) and SI ( $P=0.0020$ ), but not in the LK angle. In women, significant increases with aging were seen in the LK angle ( $P<0.0001$ ) and SI ( $P<0.0001$ ), but not in the TK angle. In men, significant decreases with aging were seen in the mobility of the thoracic spine ( $P=0.0444$ ), mobility of the lumbar spine ( $P=0.0006$ ), and mobility of spinal inclination ( $P=0.0005$ ). In women, significant decreases with aging were seen in the mobility of the lumbar spine ( $P<0.0001$ ) and mobility of spinal inclination ( $P=0.0288$ ). A previous study reported that the shape of the sagittal spinal curvature in comparably aged women with osteoporosis differed between Japan and the United States. In addition, these age-related changes and sex-related differences in spinal alignment or mobility should be considered when treating spinal deformity in elderly patients.

**Disclosures:** Yuji Kasukawa, None.

## SA0343

**Prevalence of Sarcopenia in Korean Patients After Hip Fracture: A Case-Control Study.** Yong-Chan Ha<sup>\*1</sup>, Ho-Yeon Chung<sup>2</sup>, Hyoung-Moo Park<sup>1</sup>. <sup>1</sup>Chung-Ang University College of Medicine, Korea, republic of, <sup>2</sup>Kyung Hee University, Korea, republic of

**Purpose:** Sarcopenia-related falls and fractures are increasing worldwide due to the aging population. This study evaluated anthropometric characteristics related to hip fracture in Korean patients, 2) investigated sarcopenia prevalence in hip fracture (HF) and non-hip fracture (NF) groups, and 3) investigated the correlation between sarcopenia and osteoporosis.

**Methods:** This case-control study examined 359 HF and 1,614 NF patients using Korea National Health and Nutrition Examination Survey data. We performed whole-body dual energy X-ray absorptiometry to analyze body composition using the

skeletal muscle mass index (SMI: lean mass/height<sup>2</sup>) and bone mineral density (BMD). We used stepwise logistic regression analysis to determine risk factors associated with hip fracture.

Results: Lower appendicular SMI (P < 0.001), leg muscle mass (P < 0.001), and higher prevalence of sarcopenia (P < 0.001) were observed in the HF group after adjustment for age and gender. In multivariate analysis, sarcopenia, older age, and lower BMD were associated with the occurrence of a hip fracture (odds ratio [OR] 1.875, P < 0.001; OR 1.154, P < 0.001; OR 6.52, P < 0.001, respectively). There was a positive correlation between appendicular SMI and whole-body BMD in the NF group (R = 0.13, P < 0.001; R = 0.12, P < 0.001, respectively). However, there was no significant correlation between appendicular SMI and whole-body BMD in the HF group.

Conclusions: This study showed a higher prevalence of sarcopenia and osteoporosis in patients with hip fractures compared with a normal population, and higher prevalence of sarcopenia in men.

Disclosures: *Yong-Chan Ha, None.*

**SA0344**

See Friday Plenary Number FR0344.

**SA0345**

See Friday Plenary Number FR0345.

**SA0346**

**Postmenopausal Women with Sarcopenia have Higher Prevalence of Fragility Fractures.** María Belen Zanchetta<sup>1</sup>, ruben abdala<sup>1</sup>, vanesa carla longobardi<sup>2</sup>, fabio massari<sup>1</sup>, Fernando silveira<sup>3</sup>, Rodolfo spivacow<sup>1</sup>, Paula rey<sup>1</sup>, Cesar Bogado<sup>4</sup>, jose r. zanchetta<sup>1</sup>. <sup>1</sup>md, Argentina, <sup>2</sup>mb, Argentina, <sup>3</sup>b, Argentina, <sup>4</sup>PHD, Argentina

Recent scientific evidences had highlighted the importance of evaluating sarcopenia, a significant aged decline in muscle mass and function, in women with osteoporosis and high fracture risk. Objectives: describe the prevalence of sarcopenia in a cohort of postmenopausal ambulatory women older than 60 years who consulted in an Osteoporosis clinic. Secondary, describe the association between sarcopenia and prevalent fractures, falls, physical activity and vitamin D status.

Methods: We used the diagnostic criteria proposed by the European Working Group on Sarcopenia in Older People (EWGSOP). All patients underwent DXA scans (lumbar spine, hip and total body) to measure muscle mass and hand grip dynamometry, chair stand test and 4 mts walk gait speed to measure muscle strength and performance. All clinical factors related to bone health were consigned by a specialized physician.

Results: Between January 2015 and March 2016, 250 ambulatory women were evaluated. Cohort median age was 70.4 ± 7.7 years (media ± DS), 47 (18.8%) patients fulfilled EWGSOP criteria and 203 did not (non sarcopenia group). Women with sarcopenia have significant lower weight (56.4 ± 8.8 vs. 63 ± 11 kg, p<0.01), BMI (22.6 ± 3.3 vs. 25.6 ± 4.4, p<0.01), FN BMD (0.714 ± 0.093 vs. 0.763 ± 0.095 g/cm<sup>2</sup>, p<0.01) and TH BMD (0.734 ± 0.094 vs. 0.805 ± 0.107 g/cm<sup>2</sup>, p<0.01). Nineteen (40.4%) sarcopenic women had positive fragility fracture history (wrist, vertebra or hip) compared to 32 (15.9%) of no sarcopenic women (p<0.01). Twenty-three sarcopenic patients (48.9%) referred having had a fall in the last year vs. 74 (36.5%) in the non sarcopenic group (p=0.11). There were no significant differences between the groups regarding age, height, vitamin D values, total body fat, LS BMD, osteoporosis in any DXA region or referred physical activity (see table). Conclusion: In this group of ambulatory women older than 60 years old who consulted in an Institution specialized in osteoporosis, 18.8% met EWGSOP criteria for diagnosis of sarcopenia. Sarcopenic women had significantly higher osteoporotic fractures prevalence and a tendency of higher fall history in the last year. According to our preliminary results, identifying patients with sarcopenia could be an useful tool to identify patients at higher risk of fall and fracture.

Table 1

	Sarcopenia (n=47)	Non sarcopenia (n=203)	p
Total body fat (%)	38 ± 7.5 (n=46)	38.6 ± 7.6 (n=199)	0.61
Vitamin D (ng/ml)	31.7 ± 11.3 (n=35)	31.4 ± 10.6 (n=110)	0.88
At least one fall in the last year	48.9% (n=23)	36.5% (n=74)	0.11*
Physical activity	36.2% (n=17)	36.0% (n=73)	0.9*
Fragility fracture	40.4% (n=19)	15.9% (n=32 de 201)	<0.01**
Osteoporosis in any DXA region	55.6% (n=25 de 45)	44.3% (n=86 de 194)	0.17*

The P value corresponds to Student's t-test.  
\*Logical variance.  
\*\*Two-Sample Proportion Test

Table

Disclosures: *María Belen Zanchetta, None.*

**SA0347**

**The difference in association of vitamin D with body composition between men and women.** Woong Hwan Choi<sup>\*</sup>. Division of Endocrinology, Department of Internal Medicine, College of Medicine, Hanyang University, Korea, republic of

Sarcopenia is believed to associate with metabolic syndrome and insulin resistance. We compared two sarcopenia definitions regarding their relationship with metabolic syndrome and insulin resistance.

The data from Korea National Health and Nutrition Examination Survey (2008-2010, 3,176 subjects aged over 65 years old), were analyzed. To define sarcopenia, we used appendicular lean mass (ALM)/(height (ht))<sup>2</sup> and ALM/trunk lean mass (TLM) at a value more than 1 SD or 2 SD below the mean of a young reference group. Metabolic syndrome was defined using National Cholesterol Education Program (NCEP) criteria and insulin resistance was assessed with the homeostasis model of insulin resistance.

The prevalence of sarcopenia (below 1 SD) in men and women as determined by ASM/ht<sup>2</sup> was 43.6% and 8.5%, respectively, and by ASM/TLM was 57.4% and 40.8%, respectively. When adjusted by age, exercise, smoking, and alcohol, sarcopenia (below 2 SD) by ALM/TLM increased the risk of metabolic syndrome (men; OR=2.441, 95% CI = 1.773-3.359, women; OR=2.906, 95% CI = 1.950-4.331), but sarcopenia by ALM/ht<sup>2</sup> (men; OR=0.019, 95% CI = 0.004-0.085, women; OR=0.056, 95% CI= 0.006-0.506) decreased. Insulin resistance was positively correlated with ALM/ht<sup>2</sup> (men: B = 0.102; p < 0.001 and women: B = 0.104; p < 0.001) but negatively with ALM/TLM (men: B = -0.148; p < 0.001 and women: B = -0.094; p < 0.001).

The correlations between ALM/TLM and metabolic changes associated with sarcopenia and Sarcopenic obesity were stronger than with ALM/ht<sup>2</sup>.

Disclosures: *Woong Hwan Choi, None.*

**SA0348**

See Friday Plenary Number FR0348.

**SA0349**

See Friday Plenary Number FR0349.

**SA0350**

See Friday Plenary Number FR0350.

**SA0351**

See Friday Plenary Number FR0351.

**SA0352**

See Friday Plenary Number FR0352.

**SA0353**

See Friday Plenary Number FR0353.

**SA0354**

See Friday Plenary Number FR0354.

**SA0355**

See Friday Plenary Number FR0355.

**LB-SA0356**

**Case report of hypercalciuria and markedly elevated 1,25-dihydroxyvitamin D in a patient with Diamond Blackfan Anemia: Could 24 hydroxylase enzyme deficiency be the cause?** Caitlin White\*<sup>1</sup>, Farzana Savani<sup>2</sup>, Ravinder J Singh<sup>3</sup>, Dawn Milliner<sup>4</sup>, Alan Wasserstein<sup>5</sup>, Mona Al Mukaddam<sup>1</sup>.

<sup>1</sup>University of Pennsylvania, Division of Endocrinology, United states, <sup>2</sup>University of Pennsylvania, Division of Hematology, United states, <sup>3</sup>Mayo Clinic, Department of Lab Medicine, United states, <sup>4</sup>Mayo Clinic, Division of Nephrology, United states, <sup>5</sup>University of Pennsylvania, Division of Nephrology, United states

Diamond Blackfan anemia (DBA) is a rare inherited disorder with pure red blood cell aplasia. Treatment generally involves a corticosteroid trial, chronic red blood cell transfusion and concomitant use of iron chelators to prevent transfusional iron overload. Iron overload is known to be associated with multiple endocrinopathies including primary hypogonadism, hypothyroidism, hypoparathyroidism, diabetes mellitus, hypopituitarism and osteoporosis. In addition, iron chelators may lead to hypercalciuria and nephrolithiasis. Here we present a case of a patient with transfusion dependent DBA who presented with osteoporosis, hypercalciuria and markedly elevated 1,25-dihydroxyvitamin D levels. A 33 year old man with transfusion-dependent DBA (due to inherited RPS19 mutation) early trial with prednisone was not successful getting transfused 3 units of packed red blood cells every 3 weeks on deferasirox 24 mg/kg (Jadenu) daily for iron chelation presented for evaluation of osteoporosis. He had been treated for growth hormone deficiency from age 11-15. At age 24, he was diagnosed with primary hypogonadism necessitating testosterone replacement. A subsequent screening DXA scan demonstrated lowest Z-score of -3.3 at the left hip, and by age 31 he had developed multiple asymptomatic mid-thoracic vertebral fractures. Initial laboratory evaluation included: ferritin 963 ng/mL (nl 30-400), calcium 9.8 mg/dL (nl 8.9-10.3), albumin 4.7 g/dL (nl 3.5-5.1), PTH 1.9 pmol/L (nl 1.3-6.8), 25 hydroxyvitamin D 25 ng/mL (nl 20-57), and CFX 938 pg/mL (nl 93-630). Phosphorus and renal function was normal. A 24-hour urinary calcium was 562 mg (nl <250). Testosterone was 589 ng/dL (nl 239-836) on androgen replacement. 1,25-dihydroxyvitamin D was 174 pg/mL (19.9-79.3). Due to the markedly elevated 1,25-dihydroxyvitamin D with a low-normal 25 hydroxyvitamin D in the absence of hyperparathyroidism, lymphoma or granulomatous disease, blood was sent to Mayo Clinic for 24,25 dihydroxyvitamin D level measurement, which was 0.2 ng/mL, with a concomitant 25 hydroxyvitamin D of 25 ng/mL, resulting in a 25 hydroxyvitamin D:24,25 dihydroxyvitamin D ratio of 125. A ratio greater than 80 is suggestive of homozygous deficiency of the 24 hydroxylase enzyme. 1,25-dihydroxyvitamin D is deactivated by 24 hydroxylase (encoded by CYP24A1 gene) and there have been several reports of mutations in CYP24A1 resulting in elevated 1,25-dihydroxyvitamin D and causing hypercalciuria, nephrolithiasis and bone disease. As far as we are aware, this is the first case report of a patient with DBA with hypercalciuria and osteoporosis with markedly elevated 1,25-dihydroxyvitamin D and low 24,25 dihydroxyvitamin D suggestive of 24 hydroxylase deficiency. This case raises questions regarding the appropriate evaluation of patients on chronic blood transfusions with osteoporosis and hypercalciuria, and the safest treatment options.

*Disclosures: Caitlin White, None.*

**LB-SA0357**

**BORON SUPPLEMENTATION IMPROVES BONE HEALTH OF NON-OBESE DIABETIC MICE.** Renata Dessordi\*<sup>1</sup>, Adriano Levi Spirlandeli<sup>2</sup>, Ariane Zamarioli<sup>3</sup>, José Batista Volpon<sup>3</sup>, Anderson Marliere Navarro<sup>2</sup>. <sup>1</sup>Department of Food & Nutrition, Faculty of Pharmaceutical Sciences, State University of São Paulo - UNESP, Brazil, <sup>2</sup>Department of Clinical Medicine, Ribeirão Preto Medical School, University of São Paulo - FMRP/USP, Brazil, <sup>3</sup>Biomechanics, Medicine & Rehabilitation, School of Medicine of Ribeirão Preto, University of São Paulo, Brazil

Diabetes Mellitus is a condition that predisposes a higher risk for the development of osteoporosis. This illness deregulates the activity of osteoblasts and osteoclasts. The objective of this study was to investigate the influence of boron supplementation on bone microstructure and strength in control and non-obese diabetic mice for 30 days. The animals were supplemented with 40 µg/0.5 ml of boron solution and controls received 0.5 ml of distilled water daily. We evaluated the biochemical parameters: total calcium, phosphorus, magnesium and boron; bone analysis: bone computed microtomography, and biomechanical assay with a three point test on the femur. This study consisted of 28 animals divided into four groups: Group water control - Ctrl (n=10), Group boron control - Ctrl ± B (n=8), Group diabetic water - Diab (n=5) and Group diabetic boron - Diab ± B (n=5). The results showed that cortical bone volume and the trabecular bone volume fraction was higher for Diab ± B and Ctrl ± B compared with the Diab and Ctrl groups (p≤0.05). The trabecular specific bone surface was greater for the Diab ± B group, and the trabecular thickness and structure model index had the worst values for the Diab group. The boron serum dosages were higher for the Diab ± B group compared with non-supplemented groups. The magnesium concentration was lower for Diab and Diab ± B compared with controls. The biomechanical test on the femur revealed maintenance of parameters of the bone strength in animals Diab ± B compared with the Diab group and controls. The results

suggest that boron supplementation improves parameters related to bone strength and microstructure of cortical and trabecular bone in diabetic animals and controls that were supplemented.

*Disclosures: Renata Dessordi, None.*

**LB-SA0358**

**The Effects of Experimental Periodontitis on Alveolar Bone Mass and Mineralization.** Mandee Yang\*<sup>1</sup>, Grace Eun Nam<sup>1</sup>, Michael Baldwin<sup>2</sup>, Atriya Salamati<sup>2</sup>, Zi-Jun Liu<sup>1</sup>. <sup>1</sup>Dept of Orthodontics, School of Dentistry, University of Washington, Seattle, United states, <sup>2</sup>Dept of Oral Health Sciences, School of Dentistry, University of Washington, Seattle, United states

Alveolar bone loss is a hallmark of periodontal disease. However, it is not clear how this bone loss is related to the disturbed process of bone remodeling through regional mineralization. The current study is to quantify the alveolar bone loss and to examine its regional mineral apposition rate (MAR) in an experimental periodontitis pig model. Seven three-month-old pigs were periodically inoculated with 4 types of periodontal bacteria, along with a ligature around the last maxillary deciduous premolar for 8 weeks to induce periodontitis (PG). Eight same-aged pigs served as the control (CG). For quantification of bone loss, two sets of cone-beam CT (CBCT) were taken for PG before and after the induction of the disease while one set was taken for CG. A custom-made seat was placed on the CBCT chair for scanning while the pig was intubated with 3% isoflurane. CBCT images were used to create 3D models using ITK-Snap and Invivo5. Volumetric measurements of the total alveolar bone and 2.5mm-height alveolar ridges surrounding the target tooth were taken and compared within PG before and after the induction and with CG. For MAR measurements, bone labeling dyes, calcein and alizarin, were administered through IV 7 and 2 days respectively before euthanasia. The harvested blocks were embedded in micro-bed resin and successive sections were taken at 30µm thickness coronally. Three sections that contained the most intact buccal and palatal roots of the target molar were selected and examined under epifluorescence. The inter-label distance between the two vital markers at the surfaces of the alveolar ridges and underneath the root furcation were measured, and the MARs were calculated. The results indicate that a significant 28-30% loss of total alveolar bone mass was seen in PG in which the loss of alveolar ridge took up a major component. In CG, the MAR was significantly higher at the furcation than those at both the buccal and palatal ridges. Compared with CG, PG animals showed more interrupted labeled bands with lower MARs at the furcation and buccal ridge, but the MARs at the palatal ridge were close between the two groups. The examination of associations between quantified bone loss and regional mineralization is underway. These results suggest that in young growing pigs, experimental periodontitis not only leads to alveolar bone loss but inhibits mineral apposition for new bone formation, thus impairing the capacity of alveolar bone remodeling and coupling.

*Disclosures: Mandee Yang, None.*

**LB-SA0359**

**Prevention of Breast Cancer Skeletal Metastases with Parathyroid Hormone.** Srilatha Swami\*<sup>1</sup>, Joshua Johnson<sup>1</sup>, Lance Bettinson<sup>1</sup>, Megan Albertelli<sup>2</sup>, Joy Wu<sup>1</sup>. <sup>1</sup>Division of Endocrinology, Department of Medicine, Stanford University School of Medicine, United states, <sup>2</sup>Department of Comparative Medicine, Stanford University School of Medicine, United states

Breast cancer frequently metastasizes to the skeleton, in response to many of the same growth factors and cytokines in bone marrow that support normal hematopoiesis. Breast cancer patients are also at risk for accelerated bone loss due to chemotherapy, premature menopause, and aromatase inhibition. Recombinant parathyroid hormone (PTH [1-34], teriparatide) is the only anabolic agent approved for treatment of osteoporosis. Signaling through the PTH receptor PTH1R in the osteoblast lineage regulates the bone marrow hematopoietic niche in mice and humans. However, the effects of PTH on the skeletal metastatic niche in breast cancer are unknown. Using orthotopic models of murine 4T1-LuBiG (4T1), mouse mammary tumor cells that stably express the luciferase gene and GFP protein, we demonstrate for the first time that PTH significantly reduced the incidence of spontaneous skeletal metastases, without affecting metastases to other internal organs. Although PTH treatment did not affect the growth of either the primary tumor or cultured 4T1 cells, PTH decreased expression of several pro-metastatic genes in the primary tumor. PTH treatment also attenuated tumor engraftment rate and volume when murine 4T1 or human MDA-MB-231-Fluc (MDA) cells were injected directly into the tibial bone marrow cavity. In transwell migration assays, PTH inhibited the migration of both 4T1 and MDA cells towards MC3T3-E1 murine pre-osteoblastic cells. We have previously reported that expression of VCAM-1 is increased in the bone marrow of mice lacking PTH1R in osteoblast progenitors. Conversely, we report here that PTH treatment of MC3T3-E1 cells significantly decreased mRNA levels of *Vcam1* as well as several other genes (*Mmp10*, *Mmp11*, *Mmp13*, *Cxcl12*, *Tgfb*, *Rankl*, and *Vegfr1*) implicated in the metastatic niche. Overexpression of VCAM-1 in MC3T3-E1 cells increased 4T1 migration, which was attenuated by PTH. In summary, PTH treatment decreased breast cancer skeletal metastases, preserved bone microarchitecture, and prolonged survival in a murine model of metastatic breast cancer. In cultured osteoblasts, PTH inhibited the migratory potential of the cancer cells. Together these data demonstrate

that PTH renders the skeletal niche less favorable to the recruitment and engraftment of breast cancer cells. Anabolic PTH is an approved FDA drug and a useful therapeutic option that warrants further evaluation.

Total Count (2405 characters – Limit 2500 characters)

Disclosures: *Srilatha Swami, None.*

## LB-SA0360

**Crucial role of Elov6 in chondrocyte growth and differentiation during growth plate development in mice.** Masako Shimada<sup>1</sup>, Manami Kikuchi<sup>2</sup>, Takashi Matsuzaka<sup>2</sup>, Yoshimi Nakagawa<sup>2</sup>, Hitoshi Shimano<sup>2</sup>. <sup>1</sup>Graduate School of Nutritional Science, Sagami Women's University, Japan, <sup>2</sup>Department of Internal Medicine, Faculty of Medicine, University of Tsukuba, Japan

ELOVL family member 6, elongation of very long chain fatty acids (Elov6) is a microsomal enzyme, which regulates the elongation of C12-16 saturated and monounsaturated fatty acids. Elov6 has been shown to be associated with various pathophysiologies including insulin resistance, atherosclerosis, and non-alcoholic steatohepatitis. To investigate a potential role of Elov6 during bone development, we here examined a skeletal phenotype of *Elov6* knockout (*Elov6*<sup>-/-</sup>) mice. The *Elov6*<sup>-/-</sup> skeleton was smaller than that of controls, but exhibited no obvious patterning defects. Histological analysis revealed a reduced length of proliferating and an elongated length of hypertrophic chondrocyte layer, and decreased trabecular bone in *Elov6*<sup>-/-</sup> mice compared with controls. These results were presumably due to a modest decrease in chondrocyte proliferation and accelerated differentiation of cells of the chondrocyte lineage. Consistent with the increased length of the hypertrophic chondrocyte layer in *Elov6*<sup>-/-</sup> mice, *Collagen10a1* was identified as one of the most affected genes by ablation of *Elov6* in chondrocytes. Furthermore, this elevated expression of *Collagen10a1* of *Elov6*-null chondrocytes was likely associated with increased levels of *Foxa2/ta3* and *Mef2c* mRNA expression. Relative increases in protein levels of nuclear *Foxa2* and cytoplasmic histone deacetylase *4/5/7* were also observed in *Elov6* knockdown cells of the chondrocyte lineage. Collectively, our data suggest that Elov6 plays a critical role for proper development of embryonic growth plate.

Disclosures: *Masako Shimada, None.*

## LB-SA0361

**Cold stress in mice requires Nerve Growth Factor activity in brown fat and increases Osteocalcin expression in bone.** Claudia Camerino<sup>\*</sup>, Elena Conte, Adriano Fonzino, Kejla Musaraj, Roberta Caloiero, Domenico Tricarico. University of Bari, Italy

Brown adipose tissue (BAT) is controlled by the sympathetic nervous system (SNS) and has the ability to dissipate energy through uncoupling protein-1 (UCP-1), influencing energy expenditure. Besides BAT, the SNS influences bone, and recent studies have demonstrated a positive correlation between BAT activity and bone. Nerve Growth Factor (NGF) genes are expressed in brain, white adipose tissue (WAT), BAT and bone where it coordinates brain and body reactions to challenges. Similarly Osteocalcin besides its role in bone metabolism acts as an hormone regulating glucose metabolism and brain. We previously showed that NGF and its receptor p75NTR genes are highly expressed in BAT versus brain in mice, suggesting that NGF may act as a regulator of energy. To further investigate the role of NGF and osteocalcin in bone and energy regulation we analyzed NGF and its receptor p75NTR and Osteocalcin mRNA from 3 months old mice after cold exposure. UCP-1 was used as positive control. Mice were divided into three groups: room temperature (RT), cold stress for 6h and 5 days (n = 5 for each group). Mice as control group were all placed at RT (23 °C) for 5 days, while the cold groups were placed at 4 °C for the abovementioned times. The mice were subsequently sacrificed and the interscapular BAT, bone and brain were analyzed for mRNA extraction. The exposure of 6 h to cold stress enhanced mRNA levels of UCP-1 and NGF genes by 3 and 2.5 fold vs controls, respectively, reducing mRNA of p75NTR by 19 fold. The UCP-1 gene was still up-regulated after 5 days of cold stress, the NGF gene was not affected and mRNA of the p75NTR gene was reduced by 7 fold vs controls. The mRNA NGF/NGFR genes were not affected in bone or brain following cold stress. The mRNA levels of osteocalcin in bone were upregulated following 6h and 5 days cold exposure vs controls. Osteocalcin gene in brain was downregulated following cold stress. Our study shows that NGF mRNA expression significantly increases after 6 hours of cold stress however with minor extent with respect to UCP-1. The enhanced mRNA level of NGF is observed in parallel with the decrease of NGF receptor gene expression. We found no change in NGF and p75NTR expression in brain or bone, but osteocalcin genes were upregulated in bone following cold stress. These results suggest that during cold stress when BAT-dependent thermogenesis is required, NGF activity is required, and osteocalcin may exert a local protective effect on bone mass.

Disclosures: *Claudia Camerino, None.*

## LB-SA0362

**Genetic Risk of Hip Fracture Due to Bone Quality Deficit.** Daniel Evans<sup>1</sup>, Tamara Alliston<sup>2</sup>, Bin Zhang<sup>3</sup>, Jack Youngren<sup>2</sup>, Robert Recker<sup>4</sup>, Joan Lappe<sup>4</sup>, Sjur Reppe<sup>5</sup>, Thomas Lang<sup>\*2</sup>. <sup>1</sup>California Pacific Medical Center, United states, <sup>2</sup>University of California, San Francisco, United states, <sup>3</sup>Mount Sinai School of Medicine, United states, <sup>4</sup>Creighton University, United states, <sup>5</sup>Oslo University Hospital, Norway

Osteoporotic fractures often occur in people without low BMD, highlighting the potential importance of poor bone tissue quality (BTQ). However, little is known about the genetic and molecular regulators of BTQ and their relation to fracture risk.

To address this, we analyzed publically available gene expression data obtained from iliac crest biopsies from 27 female fracture cases (OP, defined by T<-2.5 and a prevalent low trauma fracture) and 39 non-fractured control females of similar age (Jemtland et al., Bone, 2011). Jemtland et al. reported 609 transcripts that were differentially expressed between OP and controls. From the same data, we identified 24 candidate BTQ-related transcripts that were differentially expressed between OP and controls independent of age, BMI and both hip and spine BMD (Figure 1). Genetic predictors of expression of each of the 24 candidate BTQ genes were identified as cis-expression single nucleotide polymorphisms (eSNPs) within 250 kb of sequence flanking each candidate BTQ gene from an archived expression quantitative trait locus study in human osteoblasts (Grundberg, Genome Res 2009). Significant eSNPs (P≤0.05) were identified for 63% of the 24 candidate BTQ genes. The LASSO machine learning algorithm with 10-fold cross-validation identified seven eSNPs associated with decreased risk of incident hip fractures and four with increased risk. The number of fracture risk increasing and decreasing eSNP alleles were separately summed to create person-specific unweighted eSNP risk scores. Risk scores were evaluated in women in the Study of Osteoporotic Fractures (SOF). SOF participants were elderly (age mean ± SD = 71.8 ± 5.5 years), fractures were validated by X-ray, and mean follow-up time was 12.7 years. Cox Proportional Hazard models tested eSNP risk score associations with incident fracture. To interpret hazard ratios, eSNP risk scores were converted to Z-score units (SD units from the mean).

In SOF, higher values of the protective (P) risk score conferred lower risk of fracture (HR=0.86, p=0.002) and higher values of the risk increasing (RI) score conferred higher risk (HR=1.14, p=0.007). Both associations were significant (p=0.002 and p=0.015 for P and RI respectively) even after adjustment for femoral neck BMD.

Thus, our approach has yielded allelic scores associated with incident fracture independently of aBMD. This method thus shows promise to develop a serum-based assay for genetic risk of fracture due to poor BTQ.

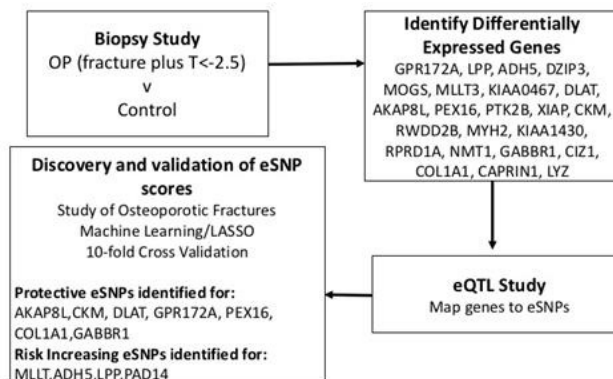


Figure 1

Disclosures: *Thomas Lang, None.*

## LB-SA0363

**Effect of iron deficient diet on Fetuin A, calciprotein particle and FGF23 levels in an adriamycin-induced early CKD model mouse.** Masanori Takaiwa<sup>\*1</sup>, Kosei Hasegawa<sup>2</sup>, Takayuki Miyai<sup>2</sup>, Hirokazu Tsukahara<sup>2</sup>.

<sup>1</sup>Department of Pediatrics, Matsuyama Red Cross Hospital, Japan, <sup>2</sup>Department of Pediatrics, Okayama University Graduate School of Medicine, Dentistry & Pharmaceutical Sciences, Japan

FGF23 is involved in the pathogenesis of CKD-MBD and cardiovascular disease in CKD. Deficiency of Fetuin A (Fet-A) is associated with increased arterial calcification and mortality in CKD. Calciprotein particle (CPP), a fetuin-mineral complex, is increased in CKD and reflects extraosseous calcification stress. Previously, we produced an early CKD model mouse by adriamycin (ADR) treatment. Using this model, we observed that Fe deficiency enhanced the FGF23 elevation. In this study we examined the effect of Fe deprivation on FGF23, Fet-A and CPP in this model.

Upon making six experimental groups (2%-Fe and 2%-Fe-CKD groups - fed a 2% Fe diet; 0.6%-Fe and 0.6%-Fe-CKD groups - fed a 0.6% Fe diet; 0.02%-Fe and 0.02%-Fe-CKD groups - fed a 0.02% Fe diet), 10-week-old male C57BL/6J mice were administered either ADR (2%-Fe-CKD, 0.6%-Fe-CKD and 0.02%-Fe-CKD groups)

or serine every 7 days, 4 times in total. On day 28 of the experiment, 7 days after the last injection, the animals were sacrificed. Data were expressed as the mean  $\pm$  SEM. A value of  $p < 0.05$  was considered significant (Tukey's test).

The kidneys of ADR treated animals were smaller in size ( $p < 0.01$ ). There was no difference in Ca, Pi and PTH among all groups. In the 0.02%-Fe-CKD group, intact FGF23 ( $670.7 \pm 134.4$  pg/ml), and a ratio between the intact FGF23 and C-terminal FGF23 (Int/C-FGF23 ratio) were higher than in the other groups ( $p < 0.01$ ). Serum Fet-A was lower in the 0.02%-Fe-CKD group ( $55.0 \pm 2.0$  ng/ml) than the 0.6%-Fe group ( $125.1 \pm 18.8$  ng/ml) and all other groups ( $p < 0.05$ ). Simultaneously, relative Fet-A mRNA of the 0.02%-Fe-CKD group was suppressed compared with the other ADR treated groups ( $p < 0.05$ ). By contrast, the abundance of CPP-composing Fet-A level, expressed as a percentage of Fet-A separated in sediment after high-speed centrifugation (reduction ratio) was higher in the 0.02%-Fe-AN group ( $0.578 \pm 0.051$ ) than the 0.6%-Fe group ( $0.274 \pm 0.093$ ) and all other groups ( $p < 0.05$ ).

In this study, the increased intact FGF23 and Int/C-FGF23 ratio of the 0.02%-Fe-CKD group suggested that the FGF23 elevation was enhanced by the Fe deficiency. Significantly, the 0.02%-Fe-CKD group showed decreased Fet-A expression associated with relatively increased CPP. Hence, it is suggested that Fe deprivation during early CKD might accelerate CKD-MBD progression, and strengthen the ectopic mineralization stress, by inducing aberrant FGF23 proteolysis and Fet-A deficiency.

**Disclosures:** Masanori Takaiwa, None.

## LB-SA0364

**The Calcium-Sensing Receptor Supports the Growth and Survival of Breast Cancer Cells By Stimulating Parathyroid Hormone-related Protein Production.** Wonnam Kim\*, Miralireza Takyar, Jaekwang Jeong, Pamela Dann, John Wysolmerski. Yale School of Medicine, United states

One of the most common sites of metastases for breast cancer is the skeleton. In order for breast cancer cells to grow in the bone microenvironment, they must adapt to high levels of extracellular calcium. Cells respond to extracellular calcium by activating the calcium-sensing receptor (CaSR), a G protein-coupled receptor that binds and signals in response to calcium and other cations. CaSR is expressed in many breast cancer cell lines and its expression has been shown to be higher in bone metastases than in primary tumors in patients. Therefore, we studied the role of CaSR in breast cancer cell behavior. We report that activation of CaSR with high extracellular calcium promotes the proliferation of human breast cancer cells and tumor cells cultured from MMTV-PyMT mice. CaSR knock down or treatment with CaSR antagonist, NPS2143 decreased the proliferation of breast cancer cells. Activation of CaSR also increased the production of parathyroid hormone-related protein (PTHrP). Since PTHrP has been reported to increase proliferation in some breast cancer cells, we knocked down PTHrP in BT474 and MDA-MB-231.1833 cells, which reduced their proliferation. Knocking down CaSR or PTHrP, and NPS2143 treatment also dramatically induced apoptosis in high extracellular calcium concentrations. The effects of CaSR on tumor cell growth appear to be mediated by nuclear actions of PTHrP that decrease p27 levels, increase CDK2 activity, and that prevent nuclear accumulation of apoptosis-inducing factor (AIF). PTHrP knock down did not reproduce the effects of either CaSR or PTHrP knock downs. Effects of transfecting wt-PTHrP could not be replicated by adding PTHrP to the culture media or by transfecting mutant DNLS-PTHrP unable to enter the nucleus. In order to determine whether these findings were relevant *in vivo*, we knocked out CaSR in breast tumors in MMTV-PyMT transgenic mice. These mice showed decreased tumor PTHrP expression, slower tumor growth and prolonged survival. CaSR knockout tumors had reduced BrdU incorporation and increased p27 levels. At normal calcium levels, rates of apoptosis were negligible in both knockout and control tumors but CaSR-knockout tumor cells underwent apoptosis when grown at high calcium *ex vivo*. Our data demonstrate that the CaSR promotes the survival and proliferation of breast cancer cells, in part, by activating a nuclear PTHrP signaling pathway.

**Disclosures:** Wonnam Kim, None.

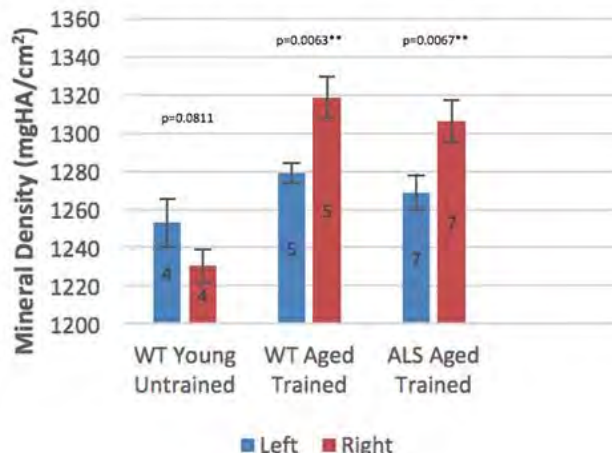
## LB-SA0365

**Isometric Force Training Enhances Bone Density in Aged and ALS Rat Forelimbs.** Ajay K. Patel\*<sup>1</sup>, Mark Dallas<sup>2</sup>, Yixia Xie<sup>2</sup>, Kimberly G. Stanford<sup>3</sup>, John A. Stanford<sup>3</sup>, Lynda Bonewald<sup>2</sup>. <sup>1</sup>University of Missouri-Kansas City School of Medicine, United states, <sup>2</sup>University of Missouri-Kansas City School of Dentistry, United states, <sup>3</sup>University of Kansas Medical Center, United states

Aging and amyotrophic lateral sclerosis (ALS) are associated with loss of bone mass. Exercise and loading of the skeleton increases bone mass. It is assumed that the loading of the skeleton by muscle is responsible for the majority of increase in bone mass. We used isometric force training to determine whether we could increase bone mass and density in rat models of aging and ALS. Rats were trained to use their right paw to press an isometric force-sensing disc for water reinforcement. The left limb was used as a within-animal untrained control. The effects of this loading system on bone was evaluated in aged (22 month) Sprague Dawley, wildtype, WT, rats (n=5) and the SOD1-G93A rat model of ALS (n=7). After learning the task under a 20 gram force requirement, a 30 gram force requirement was implemented for 15 days followed by a 40 gram force requirement for another 15 days. Rats trained on average 4 days per

week, with 8-minute training sessions per day. Forelimbs were harvested for micro CT analyses of the humerus of both proximal trabecular and cortical data from the midshaft and 4mm distal regions from the midshaft for bone mineral density, BV/TV, trabecular spacing, and thickness. Comparisons using paired t-test and one way ANOVA revealed that of all the bone parameters tested, only bone mineral density (mmHA/ccm) in the midshaft was affected by resistance training. In the wild type aged rats, the mean left, untrained humerus cortical bone midshaft density was 1279.3, while the mean trained right humerus was 1318.9 ( $P=0.0063$ ). For the SOD1-G93A rats the corresponding values were 1268.7 and 1306.3 ( $P=0.0067$ ). In the young control rats (6 mo) with no training, the values were 1253.2 and 1230.3 ( $P=N.S.$ ). Despite a decrease in body weight from a peak of 402  $\pm$  12g to 364  $\pm$  16g on the final day, ALS rats exhibited a significant training-related increase in bone density. Our results show that changes in bone density can occur in the absence of anabolic bone formation.

## Cortical Bone Midshaft Density



Cortical Bone Midshaft Density

**Disclosures:** Ajay K. Patel, None.

## LB-SA0366

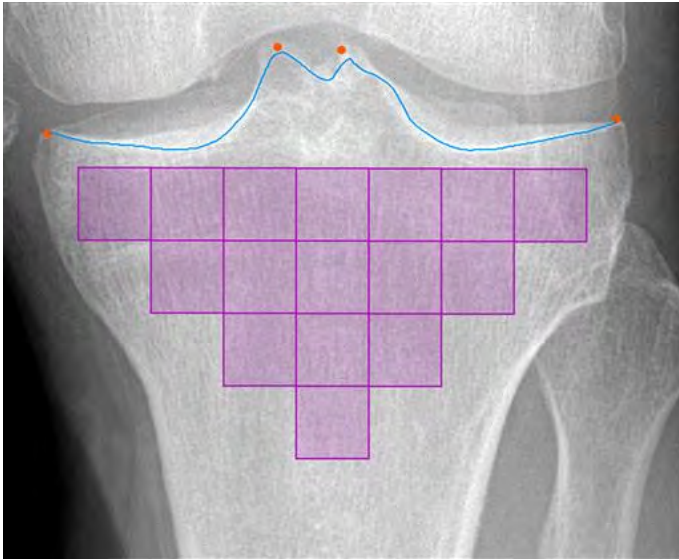
**Subchondral Tibial Bone Texture Predicts Incident Radiographic Knee Osteoarthritis: Data From The Osteoarthritis Initiative.** Thomas Janvier\*<sup>1</sup>, Rachid Jennane<sup>1</sup>, Hechmi Toumi<sup>1</sup>, Eric Lespessailles<sup>2</sup>. <sup>1</sup>Univ. Orléans, I3MTO - EA 4708, France, <sup>2</sup>CHR Orléans, Service de Rhumatologie, France

**Purpose:** Examine whether trabecular bone texture (TBT) parameters assessed on computed radiographs could predict incident knee osteoarthritis (OA) and the early joint space narrowing (JSN).

**Methods:** Data were obtained from the OAI public use data set. We studied subjects without radiographic knee OA at baseline — Kellgren-Lawrence (KL) grade 0. All patients had bilateral fixed flexion computed radiographs acquired 48 months apart among 4 different radiographic centers. From the 4796 subjects at baseline, 344 knees — 319 subjects were considered eligible for the study. Every radiograph was semi-automatically segmented into a patchwork of 16-squared Region of Interest (ROI) described in Figure. On each ROI, one-dimensional fractal descriptors were computed along the vertical and horizontal axis for two observation scales. The obtained TBT parameters were combined with patients age, gender, body mass index (BMI) and the center of acquisition in logistic regression models. These models were evaluated using the area under the receiver operating characteristic curves (AUC) and the diagnostic odds ratio (DOR). Incident knee OA status over the 48 months was investigated in two different ways, (a) the KL scale — grade 0 to a grade  $\geq 2$ , (b) the tibiofemoral JSN worsening — grade 0 to a grade  $\geq 1$ .

**Results:** From the 344 knees, 63 (18%) developed incident OA after 48 months. Among these knees 44 (13%) worsen their JSN grade. Neither age, gender and BMI, even combined did predict incident radiographic OA (AUC 0.56) nor JSN worsening (AUC 0.59). The combination of all the TBT parameters increased significantly the prediction of both incident radiographic OA (AUC 0.64) and JSN worsening (AUC 0.72). For the two models (KL grade or JSN worsening), including only the clinical covariates, the DOR were always  $< 1$  indicating a poor efficiency for knee OA prediction. However, DOR results confirmed the added value of TBT for the incident radiographic OA (DOR 4.97) and JSN worsening (DOR 5.16) prediction.

**Conclusions:** These results showed that TBT parameters on baseline radiographs predicted radiographic incident knee OA defined as KL  $\geq 2$  or JSN worsening  $\geq 1$  at 48 months whereas clinical covariates did not.



Knee trabecular bone mapping using a semi-automatic algorithm for ROIs selection.

*Disclosures:* Thomas Janvier, None.

## LB-SA0367

**miR-9-5p targets LRP5 to inhibit beta-catenin mediated osteogenesis.** Tianhao Sun<sup>\*1</sup>, Frankie Leung<sup>1</sup>, Songlin Peng<sup>2</sup>, William W. Lu<sup>1</sup>. <sup>1</sup>University of Hong Kong, Hong Kong, <sup>2</sup>Department of Spine Surgery, Shenzhen People's Hospital, Jinan University Second College of Medicine, China

miR-9-5p and low-density lipoprotein receptor-related protein 5 (LRP5) play vital roles in multiple biological processes. However, their relationships and roles in osteogenesis remain to be defined. In the present study, we investigate the roles of miR-9-5p and LRP5 in osteogenesis. Quantitative real-time PCR (qPCR), cell proliferation assay, molecular cloning, luciferase reporter assay, Western Blot, cell apoptosis assay and other methods were used. Firstly, we found elevated expression levels of miR-9-5p in bone tissues from osteoporotic patients with vertebral compression fractures. Secondly, we revealed that miR-9-5p targeted LRP5. Additionally, we revealed that loss of function of LRP5 resulted in decreased  $\beta$ -catenin levels and osteogenesis *in vitro* and *in vivo*. Finally, we revealed that loss of function of LRP5 induced skeletal cell apoptosis through hairy and enhancer of split-1 (Hes1). In conclusion, our findings reveal miR-9-5p inhibits  $\beta$ -catenin mediated osteogenesis by targeting LRP5.

*Disclosures:* Tianhao Sun, None.

## LB-SA0368

**NUMBL Negatively Regulates NF- $\kappa$ B Signaling via Interaction with TAK1/TRAF6 During Osteoclastogenesis.** Gaurav Swarnkar<sup>\*</sup>, Kannan Karuppaiah, Gabriel Mbalaviele, Yousef Abu-Amer. Washington University School of Medicine, United states

The transcription factor NF- $\kappa$ B is a family of proteins involved in signaling essential for normal osteoclast differentiation and function. Many studies have established various signaling molecules as regulators of NF- $\kappa$ B signaling in various cell types. Recently, we have shown that TGF- $\beta$  Activated Kinase-1 (TAK1) deficiency is associated with an increase in NUMB-like (NUMBL) and simultaneous decrease in TAK1-Associated Adapter Protein (TAB2) expression. NUMBL is an evolutionary conserved protein that has been shown to play a role in cell fate determination during development. We have shown that increased NUMBL expression, owing to TAK1 deficiency, regulates osteoclast differentiation via Notch Intracellular Domain (NICD)/Recombination Signal Binding Protein for Immunoglobulin Kappa J Region (RBPJ) axis. However, the interaction of NUMBL with TAK1/NF- $\kappa$ B signaling during osteoclast differentiation has not been fully elucidated. In this study, we found that whereas NUMBL overexpression causes a decrease in osteoclastogenesis, knockdown of NUMBL using a dominant negative phosphotyrosine-binding (PTB) domain of NUMBL does not inhibit osteoclast differentiation. Interestingly, we observed that during osteoclast differentiation, NUMBL expression is regulated transcriptionally and post-translationally. On one hand, NUMBL mRNA expression decreases upon RANKL stimulation in WT bone marrow macrophages (BMM) but not in TAK1-null BMMs. On the other hand, NUMBL is degraded via K48-poly-ubiquitination as evident by hypo-K48-polyubiquitination of NUMBL in TAK1-deficient cells when compared with WT cells. This indicates that TAK1/TAB2 may mediate poly-ubiquitination of NUMBL for proteasomal degradation. Mechanistically, in

TAK1-null cells, the increase in NUMBL expression was associated with a concomitant decrease in Tumor Necrosis Factor Receptor Associated Factor 6 (TRAF6) and NF- $\kappa$ B Essential Modulator (NEMO) expression that results in the inactivation of NF- $\kappa$ B signaling. Based on our findings and other reports, we speculate that NUMBL directly interacts with TRAF6 and TAB2 and leads to their degradation via the proteasome. Collectively, our data suggest that NUMBL acts as a negative regulator of NF- $\kappa$ B signaling via the NICD/RBPJ axis and also via interaction with TRAF6/TAB2/TAK1 complex. Additional studies investigating the transcriptional control of NUMBL during osteoclastogenesis will provide insights into the role of NUMBL in regulating bone homeostasis.

*Disclosures:* Gaurav Swarnkar, None.

## LB-SA0369

**RBP-J-Regulated miR-182 Promotes TNF- $\alpha$ -Induced Osteoclastogenesis and bone resorption.** Kazuki Inoue<sup>\*1</sup>, Christine Miller<sup>1</sup>, Mahmoud Elguindy<sup>1</sup>, Xiaoyu Hu<sup>2</sup>, Lionel Ivashkiv<sup>3</sup>, Baohong Zhao<sup>4</sup>. <sup>1</sup>Arthritis & Tissue Degeneration Program, David Z. Rosensweig Genomics Research Center, Hospital for Special Surgery, United states, <sup>2</sup>Institute for Immunology & School of Medicine, Tsinghua University, China, <sup>3</sup>Arthritis & Tissue Degeneration Program, David Z. Rosensweig Genomics Research Center, Hospital for Special Surgery & Weill Cornell Graduate School of Medical Sciences, United states, <sup>4</sup>Arthritis & Tissue Degeneration Program, David Z. Rosensweig Genomics Research Center, Hospital for Special Surgery & Department of Medicine, Weill Cornell Medical College, United states

TNF- $\alpha$  plays a major role in driving pathologic bone resorption in inflammatory diseases, such as rheumatoid arthritis (RA), but little is known about mechanisms that restrain TNF- $\alpha$ -induced inflammatory osteoclastogenesis. Our findings and human genetic evidence of the association of *RBPJ* allelic polymorphisms with RA identified RBP-J as a key negative regulator that restrains TNF-induced osteoclastogenesis and inflammatory bone resorption. Yet the mechanisms by which RBP-J inhibits TNF signaling are not fully understood. Recently, we applied next-generation sequencing and profiled the miRNAs specifically involved in TNF- $\alpha$ -induced osteoclast differentiation, and identified the most abundant miRNA, miR-182, induced by TNF- $\alpha$  and whose expression is repressed by RBP-J. Downregulation of miR-182 dramatically suppressed the enhanced osteoclastogenesis induced by TNF- $\alpha$  in RBP-J-deficient cells. Complementary loss and gain of function approaches showed that miR-182 is a strong positive regulator of the osteoclastogenic transcription factors NFATc1 and Blimp1. Moreover, we identified that Foxo3 and Maml1, direct targets of miR-182, play important inhibitory roles in TNF- $\alpha$  mediated osteoclastogenesis. RBP-J-regulated miR-182 promotes TNF- $\alpha$  induced osteoclastogenesis via inhibition of Foxo3 and Maml1. Most recently, we generated myeloid lineage/osteoclast precursor conditional *Mir182* transgenic (Tg) mice by crossing LSL-miR-182 mice with *LysMcre* mice (*Mir182<sup>ctg</sup>*). TNF- $\alpha$  induced osteoclast differentiation and osteoclast marker gene expression, including *Acp5*, *CtsK*, *Igfb3* and *Calcr*, as well as the expression levels of the key osteoclastogenic regulators NFATc1 and Blimp1 were dramatically enhanced in the *Mir182<sup>ctg</sup>* cell cultures. Interestingly, these changes were not observed in RANKL-induced osteoclastogenesis, and *Mir182<sup>ctg</sup>* mice do not exhibit a significant bone phenotype under physiological conditions. In contrast, administration of TNF- $\alpha$  to the calvarial periosteum resulted in markedly enhanced osteoclast formation and resorptive pits on the calvarial bones of the *Mir182<sup>ctg</sup>* mice compared with the controls. These data collectively indicate an important predominant role for miR-182 in the regulation of inflammatory osteoclastogenesis and bone resorption both *in vitro* and *in vivo*. Targeting of the newly discovered RBP-J-miR-182-Foxo3/Maml1 axis may represent a novel therapeutic approach to suppress inflammatory osteoclastogenesis and pathological bone resorption.

*Disclosures:* Kazuki Inoue, None.

## LB-SA0370

**Office-based prescreening of cortical bone thickness in female hip arthroplasty patients.** Sanaz Nazari-Farsani<sup>1</sup>, Kari Peura<sup>1</sup>, Mia Vuopio<sup>2</sup>, Jessica Alm<sup>2</sup>, Hannu Aro<sup>\*2</sup>. <sup>1</sup>University of Turku, Finland, <sup>2</sup>Turku University Hospital, Finland

### Objectives

Female hip arthroplasty patients over 65 years of age are at highest risk for periprosthetic fractures of uncemented stems probably because of poor bone quality. Dual-energy X-ray absorptiometry (DXA) screening for low bone mineral density (BMD) of the proximal femur may help in risk assessment of this complication. We asked if office-based measurement of cortical bone thickness could be useful for prescreening of female arthroplasty patients.

### Methods

Sixty-one postmenopausal women with primary hip osteoarthritis and without diseases or drugs affecting bone metabolism underwent preoperative measurement of apparent multi-site (tibia and radius) cortical bone thickness using a mobile pulse-echo ultrasound device. The cortical bone thickness index obtained from the measurements takes into account the patient's age and body characteristics (weight and height). An index below 0.876 g/cm<sup>2</sup> was applied according to the previously

defined 90% sensitivity threshold as indication for DXA screening. The normalized cortical bone index was validated against local BMDs measured by standard DXA.

**Results**

The normalized cortical bone index was below the threshold value in 23 women (38%), who were considered to require DXA screening. The index correlated significantly ( $r=0.558$ ,  $p<0.001$ ) with the BMD of the femoral neck. The approach showed 68% sensitivity, 80% specificity, 65% positive predictive value and 82% negative predictive value in the identification of patients with osteoporotic or osteopenic BMD of the index hip. Applying T-score  $< -2.0$  of the femoral neck as the discriminator, the index showed 100% sensitivity and 84% specificity.

**Conclusion**

The normalized cortical bone index reduced the need of preoperative DXA in women scheduled for hip arthroplasty for identifying patients at risk for low periprosthetic bone mass.

**Disclosures:** Hannu Aro, None.  
This study received funding from: Amgen Inc

**LB-SA0371**

**Health literacy and the agreement between osteoporosis defined by self-report versus bone mineral density results in older women.** Sarah M Hosking\*<sup>1</sup>, Rachel Buchbinder<sup>2</sup>, Amanda L Stuart<sup>1</sup>, Julie A Pasco<sup>1</sup>, Natalie K Hyde<sup>1</sup>, Lana J Williams<sup>1</sup>, Sharon L Brennan-Olsen<sup>1</sup>. <sup>1</sup>School of Medicine, Deakin University, Australia, <sup>2</sup>Department of Epidemiology & Preventive Medicine, Monash University, Australia

Health literacy plays a role in the way individuals find, understand and use health information, however, associations between health literacy and understanding of osteoporosis status are unknown. Previous research has reported poor agreement between self-reported osteoporosis and BMD results with or without fracture; health literacy is likely to influence this association.

We aimed to explore associations between health literacy and agreement between self-report and confirmed osteoporosis based upon BMD and/or combined BMD and fracture criteria in older women.

Data were collected for participants aged  $\geq 50$ yr at the most recent follow-up of women enrolled in the Geelong Osteoporosis Study, a population-based cohort located in south-eastern Australia. BMD was measured by DXA (Lunar DPX-L). We defined osteoporosis as BMD T-score less than -2.5 at the hip and/or spine, or the combination of BMD in the osteopenic range (T-score -1 to -2.5) and any adult (aged  $\geq 20$ yr) fracture. Health literacy was ascertained using the Health Literacy Questionnaire (HLQ), a multi-dimensional tool that generates scores that range from 1 to 4 or 5 across nine domains of health literacy. In this sample, 426 participants had DXA results, self-reported diagnoses, fracture history, and HLQ scores. Effect sizes (ES) [95%CI] were calculated for differences in mean HLQ domain scores between participants who correctly vs. incorrectly self-reported osteoporosis.

Of the 426 participants (median age: 65.95 (IQR 58.5-74.1)), 114 (26.8%) incorrectly self-reported (105 had study defined osteoporosis but did not self-report, nine self-reported osteoporosis but did not meet study criteria for osteoporosis). Compared to participants who self-reported correctly, those who self-reported incorrectly had lower mean scores for two HLQ domains: 'Ability to find good health information' (ES -0.08 [-0.15, -0.01]  $p=0.029$ ), and 'Understanding health information' (ES -0.08 [-0.17, 0.00]  $p=0.047$ ). No differences in mean scores were seen for remaining domains (see table).

These data suggest that individuals who incorrectly self-report osteoporosis status may have difficulty finding and also understanding health information.

**Table: HLQ scores by self-report of osteoporosis status**

HLQ Domains	Correct	Incorrect	Effect size (95%CI)
	Mean (SD)		
Healthcare provider support	3.22 (0.50) n=311	3.22 (0.57) n=114	-0.00 (-0.08, 0.08)
Having sufficient information	3.06 (0.37) n=311	3.11 (0.50) n=114	0.07 (-0.04, 0.17)
Actively managing health	2.96 (0.46) n=311	3.06 (0.53) n=112	0.08 (-0.01, 0.17)
Social support for health	3.09 (0.46) n=311	3.07 (0.56) n=113	-0.01 (-0.10, 0.08)
Appraisal of health information	2.79 (0.47) n=311	2.80 (0.56) n=113	0.01 (-0.08, 0.09)
Actively engaging with healthcare providers	4.21 (0.51) n=310	4.13 (0.62) n=111	-0.05 (-0.13, 0.03)
Navigating the healthcare system	4.15 (0.51) n=310	4.06 (0.63) n=110	-0.06 (-0.14, 0.02)
Finding health information	4.12 (0.51) n=310	3.98 (0.73) n=110	-0.08 (-0.15, -0.01)*
Understanding health information	4.31 (0.47) n=310	4.20 (0.62) n=111	-0.08 (-0.17, -0.00)*

\* Results with p-value  $< 0.05$

Table: HLQ scores by self-report of osteoporosis status

**Disclosures:** Sarah M Hosking, None.

**LB-SA0372**

**Association of Musculoskeletal Health Score with Fracture Risk in the MrOS cohort.** Bjoern Buehring\*<sup>1</sup>, Brian Lewis<sup>1</sup>, Karen Hansen<sup>2</sup>, Steven Cummings<sup>3</sup>, Nancy Lane<sup>4</sup>, Neil Binkley<sup>1</sup>, Kristine Ensrud<sup>5</sup>, Peggy Cawthon<sup>6</sup>. <sup>1</sup>Osteoporosis Clinical Research Program, University of Wisconsin-Madison, United states, <sup>2</sup>Department of Medicine, UW-Madison, United states, <sup>3</sup>California Pacific Medical Center Research Institute, United states, <sup>4</sup>University of California Davis, United states, <sup>5</sup>Department of Medicine, University of Minnesota, United states, <sup>6</sup>California Pacific Medical Center, United states

**Introduction:** Osteoporosis, obesity and sarcopenia are risk factors for fractures and their combination has a negative effect on musculoskeletal health (MSKH). We proposed a score-based approach to define this combination as "dysmobility syndrome (DS)" or decreased MSKH ( $\downarrow$ MSKH). DS increases mortality in the NHANES cohort but no data exist on fracture risk. The most widely used fracture risk calculator, the WHO FRAX tool, does not include several measures of MSKH such as physical function, muscle mass or falls. In this analysis of the Osteoporotic Fractures in Men (MrOS) cohort, we examine whether individuals with  $\downarrow$ MSKH/DS have a higher incidence of fragility fractures and whether this composite score confers additional risk for fracture, beyond risk estimates provided by FRAX.

**Methods:** The score-based approach to define  $\downarrow$ MSKH/DS includes six factors which assigned one point to each: appendicular lean mass/height<sup>2</sup>  $< 7.26$  kg/m<sup>2</sup>, body fat  $> 30\%$ , T-score  $\leq -2.5$ , grip strength  $< 30$  kg, gait speed  $< 1.0$  m/s, and falls in last 12 months. A score  $\geq 3$  indicated  $\downarrow$ MSKH/DS. We used multivariate logistic regression models to examine the association of  $\downarrow$ MSKH/DS with risk of hip and major osteoporotic fractures (MOF). We generated odds ratios (OR) for hip fractures and MOF using quartiles of FRAX 10 year risk of hip fractures / MOF and the presence of  $\downarrow$ MSKH/DS.

**Results:** 5827 men ages  $74 \pm 6$  years with a mean BMI of  $27.4 \pm 3.8$  kg/m<sup>2</sup> had complete data necessary for this analysis. 391 males (6.7%) met criteria for  $\downarrow$ MSKH/DS. 571 (10%) experienced a MOF including 245 (4%) hip fractures. In multivariate analyses, quartiles of FRAX MOF risk and the presence of  $\downarrow$ MSKH/DS independently increased odds of MOF. Only quartiles FRAX hip fracture risk increased odds of hip fracture, although the lower confidence interval for  $\downarrow$ MSKH/DS was close to 1 (see Table 1).

**Conclusion:**  $\downarrow$ MSKH/DS was associated with increased MOF fracture incidence even after adjusting for quartiles of FRAX risk in this cohort of older men. Our study suggests that using a composite assessment of MSKH in addition to already available tools such as FRAX may improve identification of individuals at high fracture risk. Additional analyses are necessary to examine whether this approach can better distinguish between those who will fracture and who will not and whether the results

can be reproduced in women.

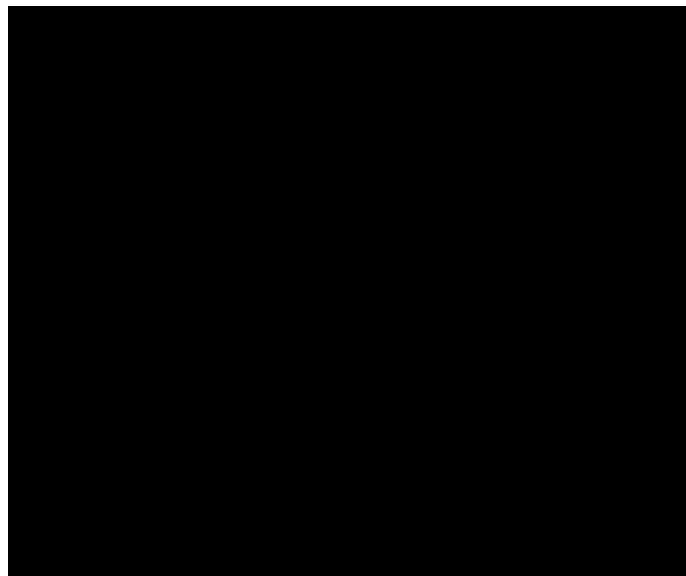


Figure 1 - Odds Ratios

Disclosures: Bjoern Buehring, None.

## LB-SA0373

**Dietary Calcium Intake and Cardiovascular Health: Is there any relationship?** Shubhabrata Das<sup>\*1</sup>, David Goltzman<sup>2</sup>, Angel M. Ong<sup>3</sup>, Jessica Gorgui<sup>4</sup>, Michelle Wall<sup>5</sup>, Suzanne N. Morin<sup>6</sup>, Stella S. Daskalopoulou<sup>7</sup>.

<sup>1</sup>Division of Experimental Medicine, Department of Medicine, McGill University, Montreal, Canada; McGill University Health Centre Research Institute, Montreal, Canada, Canada, <sup>2</sup>Departments of Medicine & Physiology, McGill University, Montreal, Canada, Canada, <sup>3</sup>School of Dietetics & Human Nutrition, McGill University, Sainte-Anne-de-Bellevue, Canada; McGill University Health Centre Research Institute, Montreal, Canada, Canada, <sup>4</sup>Department of Pharmaceutical Science, Faculty of Pharmacy, Université de Montréal, Montreal, Canada, Canada, <sup>5</sup>McGill University Health Centre Research Institute, Montreal, Canada, Canada, <sup>6</sup>Division of Internal Medicine, Department of Medicine, McGill University, Montreal, Canada; McGill University Health Centre Research Institute, Montreal, Canada, Canada, <sup>7</sup>Divisions of Internal & Experimental Medicine, Department of Medicine, McGill University, Montreal, Canada; McGill University Health Centre Research Institute, Montreal, Canada, Canada

**Introduction:** Calcium intake, recommended for osteoporosis prevention has been reported to be associated with cardiovascular (CV) outcomes. We examined the association of dietary calcium intake (dCa) with surrogate CV markers, including carotid intima-media thickness (cIMT), arterial stiffness and hemodynamics in healthy postmenopausal women.

**Methods:** Healthy postmenopausal women without any CV risk factors, participating in a randomized controlled trial studying the effect of calcium supplementation vs. dietary calcium on vascular health, were recruited. Cross-sectional analyses of baseline data of the participants are presented. Peripheral systolic and diastolic blood pressures (pSBP, pDBP) were measured by BpTRU device. cIMT of both common-carotid arteries was measured by B-mode ultrasonography (Philips-iU22). Arterial stiffness (carotid-to-femoral pulse wave velocity [cFPWV] and carotid-to-radial pulse wave velocity), central SBP and DBP (cSBP, cDBP), mean arterial pressure (MAP), and hemodynamic parameters (pulse pressure, augmentation pressure, augmentation index corrected for 75 bpm) were obtained non-invasively by applanation tonometry (SphygmoCor). Usual dCa intake of the previous month was estimated using a validated food frequency questionnaire. Measurements were compared across groups of <600, 600-1000 and >1000 mg/day of dCa by one-way analysis of variance (ANOVA) and covariance (ANCOVA).

**Results:** We evaluated 83 postmenopausal women (mean age 60.4 ± 6.3 years; body mass index 25.6 ± 3.8 kg/m<sup>2</sup>). Mean dCa was 857 ± 333 mg/day. Although within normal range, vascular parameters had a non-significant, U-shaped relationship with dCa, i.e., the middle group of dCa (600-1000 mg/d) had lower values than the extreme 2 groups (<600 mg/d and >1000 mg/d). In unadjusted analyses, women with dCa >1000 mg/day had significantly higher cFPWV, pSBP, cSBP, and MAP compared to those with 600-1000 mg/day; however, significance was lost for all other parameters except for MAP after adjustment for pertinent covariates (Table).

**Conclusion:** In healthy postmenopausal women, a non-significant, U-shaped relationship of vascular parameters across the 3 dCa groups was noted; dietary

calcium may have favourable effect on MAP for those consuming 600-1000 mg/day compared to >1000 mg/day intake. Of note, our population had optimal/normal BP. Our ongoing study including a larger sample-size will determine the relationship between dCa and surrogate CV markers.

Table: Adjusted mean (95% confidence interval) of cIMT, arterial stiffness, and hemodynamic parameters across dietary calcium groups

	Dietary calcium (mg/d)		
	<600 (n=19)	600-1000 (n=40)	>1000 (n=24)
dCa (mean±SD, mg/d)	452±94	803±123	1269±212
cIMT (mm) <sup>a</sup>	0.63 (0.59, 0.67)	0.63 (0.60, 0.66)	0.65 (0.62, 0.69)
cFPWV (m/s) <sup>a</sup>	7.6 (6.9, 8.3)	7.4 (7.0, 7.9)	7.8 (7.2, 8.5)
pSBP (mmHg) <sup>a</sup>	116 (111, 121)	111 (108, 115)	118 (113, 122)
pDBP (mmHg) <sup>a</sup>	73 (70, 76)	71 (69, 73)	74 (72, 77)
cSBP (mmHg) <sup>a</sup>	105 (99, 111)	103 (99, 107)	111 (106, 116)
cDBP (mmHg) <sup>a</sup>	66 (63, 70)	66 (63, 68)	69 (66, 72)
MAP (mmHg) <sup>a</sup>	83 (79, 87)	81 (78, 84) <sup>*</sup>	87 (83, 91)

Table: <sup>a</sup> adjusted for age, BMI, physical activity, smoking and MAP; <sup>b</sup> adjusted for age, BMI, physical activity and smoking. \* P<0.05, significantly different from >1000 mg/d dietary calcium intake

cDBP: central diastolic blood pressure; cFPWV: carotid-to-femoral pulse wave velocity; cIMT: carotid intima-media thickness; cSBP: central systolic blood pressure; dCa: dietary calcium intake; MAP: mean arterial blood pressure; pDBP: peripheral DBP; pSBP: peripheral SBP

Table: Adjusted mean (95% confidence interval) of cIMT, arterial stiffness, & hemodynamic parameters

Disclosures: Shubhabrata Das, None.

## LB-SA0374

**Is sitting time (sedentary behaviour) associated with Bone Mineral density? Results from the CaMos population-based cohort.** Jerilynn C. Prior<sup>\*1</sup>, Bradley Drayton<sup>2</sup>, Zeljko Pedisic<sup>3</sup>, Claudie Berger<sup>4</sup>, David Goltzman<sup>5</sup>,

Adrian Bauman<sup>2</sup>. <sup>1</sup>UBC, Canada, <sup>2</sup>Sydney University, Australia, <sup>3</sup>Victoria University, Australia, <sup>4</sup>CaMos, RI-MUHC, McGill University, Canada, <sup>5</sup>McGill University, Canada

Physical activity levels are consistently associated with bone mineral density (BMD) in both cross-sectional and longitudinal analysis. Recent research interest has explored the relationships between sedentary behaviour and health outcomes, and whether these are independent of physical activity levels. In this context, the research question of interest is whether sedentary behaviour (sitting time) is associated with BMD in population studies, as such an association could have implications for falls and fracture prevention.

This study examined the relationship between sitting time and BMD in the Canadian Multicentre Osteoporosis Study (CaMos). Baseline relationships were sought in the 8319 adult Canadian men and women assessed in 1995-1997 with available BMD at the spine (L1-L4), femoral neck or total hip. BMD was measured using DXA methods in nine centres across Canada and was converted into Hologic equivalent measures. Total physical activity was assessed in a validated instrument of vigorous activities and walking (with moderate activities excluded). Sitting time was measured in two ways, first summing sitting watching television and sitting during travel (Car, bus) in reported hours per week, and secondly reported sitting at work (hrs/week). Linear regressions were used with total physical activity and both sitting measures expressed in quartiles, and BMD as the dependent variable. Models were unadjusted, adjusted for age and sex, and adjusted for the age\*sex interaction.

Mean BMD values (mean, sd) were for the lumbar spine 0.97g/cm<sup>2</sup> (0.18), femoral neck 0.74g/cm<sup>2</sup> (0.14) and hip 0.90g/cm<sup>2</sup> (0.16). Median (interquartile range) weekly physical activity was 5.0 hours (3-10), median time sitting watching TV or in travel 21 hrs/week (14-28), and sitting at work 24.5hrs/week (3.5-38.5). For sitting watching TV/travel, there were no significant associations with spine BMD in any model, a weak non-linear association with femoral neck BMD only for quartile 2 sitting versus quartile 1 (estimate of 0.007g/cm<sup>2</sup>), and a weak but nonsignificant association when a quadratic model was fitted. Similar nonsignificant results were observed for total hip BMD. For the sitting at work variable no overall significant relationships were seen for spinal, femoral neck or total hip BMD.

Overall in these data, the relationship between sitting time and BMD was usually nonsignificant, and was nowhere near as consistently strong as the relationship between physical activity and BMD.

Disclosures: Jerilynn C. Prior, None.

## LB-SA0375

**Oxidative stress impairs the expression levels of *Lgr4* in osteoblastic cells.** Chantida Pawaputanon Na Maharakham<sup>\*1</sup>, Yoichi Ezura<sup>1</sup>, Yayoi Izu<sup>2</sup>, Katsuhiko Nishimori<sup>3</sup>, Yuichi Izumi<sup>4</sup>, Masaki Nada<sup>5</sup>. <sup>1</sup>Department of Molecular Pharmacology, Medical Research Institute, Tokyo Medical & Dental University, Japan, <sup>2</sup>Department of Animal Risk Management, Chiba Institute of Science, Japan, <sup>3</sup>Laboratory of Molecular Biology, Department of Molecular & Cell Biology, Graduate School of Agricultural Science, Tohoku University, Japan, <sup>4</sup>Department of Periodontology, Graduate School of Medical & Dental Sciences, Tokyo Medical & Dental University, Japan, <sup>5</sup>Yokohama City Minato Red Cross Hospital, Japan

Osteoblasts are main target cells of oxidative stress in the progression of osteoporosis. The excessive of ROS including superoxide anion, hydroxyl radical, and hydrogen peroxide, increases the oxidative stress leading to cellular dysfunction, apoptosis and cell death. A nonsense mutation of LGR4 in elderly humans has been reported that is strongly associated with low BMD and high risk osteoporotic fracture, similar to the phenotypes of *Lgr4* mutant mice. Most recently, *Lgr4* has been identified as a new receptor for bone remodeling. However, the role of LGR4 in the pathogenic condition at adult stage such as osteoporosis remains poorly understood. To understand the possible roles of *Lgr4* in the oxidative stress-induced dysfunction of osteoblast, H<sub>2</sub>O<sub>2</sub> was herein utilized to generate ROS in osteoblastic MC3T3-E1 cells. Our in vitro experiments, we found that H<sub>2</sub>O<sub>2</sub> (1mM) suppressed *Lgr4* mRNA expression in MC3T3-E1 cells within 12 hours. This was associated with the decline function of osteoblastic cell including the reduction in mRNA levels of osteogenic marker genes including *Runx2*, *Osx*, *Coll1a1*, *Alp*, *Bsp* and *Opg* in MC3T3-E1 cells. The suppression of *Lgr4* required new protein synthesis. As functional aspects, *Lgr4* was up-regulated by BMP(100ng/ml) and required for BMP effects on osteoblastic differentiation. However, BMP-induced *Lgr4* expression was abolished by 1mM H<sub>2</sub>O<sub>2</sub>. When *Lgr4* was knocked down, H<sub>2</sub>O<sub>2</sub>-induced downregulation of *Osx* and *Alp* mRNA expression was no longer observed. Our study revealed that TGF- $\beta$  (10ng/ml) suppressed *Lgr4* expression in MC3T3-E1 cells. In the present of TGF- $\beta$ , H<sub>2</sub>O<sub>2</sub> no longer suppressed *Lgr4* mRNA expression. In conclusion, we discovered that oxidative stress reduces *Lgr4* mRNA expression.

**Disclosures:** Chantida Pawaputanon Na Maharakham, None.

## LB-SA0376

**POTENTIAL RISK FACTORS FOR VERTEBRAL FRACTURES IN SURVIVORS OF CHILDHOOD ACUTE LYMPHOBLASTIC LEUKEMIA.** Melissa Fisceletti<sup>\*1</sup>, Josée Dubois<sup>1</sup>, Marie-Claude Miron<sup>1</sup>, Mariia Samoilenko<sup>2</sup>, Geneviève Lefebvre<sup>3</sup>, Renaud Winzenrieth<sup>4</sup>, Maja Krajinovic<sup>1</sup>, Caroline Laverdière<sup>1</sup>, Daniel Sinnett<sup>1</sup>, Nathalie Alos<sup>1</sup>. <sup>1</sup>Sainte Justine University Health Center, Canada, <sup>2</sup>Université de Montréal, Canada, <sup>3</sup>Université de Québec à Montréal, Canada, <sup>4</sup>Medimaps Group, France

**BACKGROUND and OBJECTIVES:** Pediatric acute lymphoblastic leukemia (ALL) cure rates have neared 90%. Vertebral fractures (VF) and low bone mineral density (BMD) are known to occur at the time of ALL diagnosis and during treatment, but it is still unclear if they recover or persist long after remission. The purpose of the PÉTALE study was to better define the prevalence of VF and the clinical and biological characteristics associated with VF among childhood ALL survivors. We drew our sample of participants (n=250) from a pool of 350 French-Canadian survivors of pediatric ALL.

**METHODS and RESULTS:** Our cohort included 51% females; mean age at diagnosis of 6y (range 1-18y); mean age at recruitment of 22y (range 7-41); median time since diagnosis was 16y (range 6-28y); 55% of patients were classified as high risk at diagnosis. All patients underwent a lateral thoraco-lumbar spine radiograph to detect VF according to the Genant method and a DXA scan to evaluate lumbar spine BMD (LS BMD). The prevalence of VF was 22% with 88% of the VFs being classified as grade 1 fractures. In Poisson regression models used to predict VF, potential protective factors included BMD Z-score (RR=0.71, 95%CI 0.55-0.91, p =0.008) and TBS (RR=0.70, 95%CI 0.54-0.90, p = 0.006). Potential risk factors identified were male sex (RR = 2.08, 95%CI 1.13-3.81, p = 0.019); effective corticosteroid cumulative dose (RR=2.16, 95%CI 1.17-3.98, p = 0.013) and change in body mass index (BMI) during treatment (RR = 1.13, 95%CI 1.003-1.270, p = 0.045). Age at diagnosis did not have a significant predictive impact on VF (RR=1.045, 95%CI 0.96-1.13, p = 0.28).

**CONCLUSIONS:** Our results show a high prevalence VF in survivors of pediatric ALL with a high proportion of grade 1 VF. Low BMD Z-scores, low TBS, male sex, greater increase in BMI during treatment and higher effective corticosteroid cumulative dose are possible risk factors for persistent VF in survivors. The cross-sectional nature of the study does not allow us to differentiate these vertebral deformities between incompletely reshaped fractures and late occurring fractures. However, this is the first study that reports the prevalence of persistent or late occurring VF in both female and male survivors. VF in this population may impact clinical guidelines for careful follow-up of osteoporosis risk factors in ALL survivors.

The PÉTALE project is funded by a CIHR team grant.

**Disclosures:** Melissa Fisceletti, None.

## LB-SA0377

**Are the cracks starting to appear in bisphosphonate therapy?.** Shaocheng Ma, Andi Jin, Justin Cobb, Rajarshi Bhattacharya, Ulrich Hansen, Richard Abel\*. Imperial College, United Kingdom

Bisphosphonates (BP) are the first line therapy for preventing fragility fractures. However, concern regarding the efficacy is growing because BP use is associated with over-suppression of remodeling. Animal studies have reported that BP therapy is associated with accumulation of micro-cracks and a reduction in bone mechanical properties, but the effect on humans has not been investigated. Our aim was to quantify the mechanical strength of bone treated with BP, and correlate this with the microarchitecture and density of micro-damage in comparison with untreated fractured and non-fractured controls.

Trabecular cores from patients treated with BP were compared with patients who had not received any treatment for bone metabolic disease. Non-fractured cadaveric femora from individuals with no history of bone metabolic disease were used as controls. Cores were imaged in high resolution (~1.3 $\mu$ m) using Synchrotron X-ray tomography (Diamond Light Source). Scans were used for structural and material analysis, then cores were mechanically tested in compression. Micro-damage was classified as: micro-cracks (Fig 1A), diffuse damage and perforations. Synchrotron micro-CT stacks were visualised and analysed using ImageJ, Avizo and VGStudio MAX.

Patients treated with BP (17.2 MPa) had significantly lower tissue strength than untreated fracture (24.0 MPa) and non-fracture controls (28.0 MPa). Yet treated and untreated hip-fracture patient's exhibited comparable bone microarchitecture, volume fraction and apparent density. The data also reveal that the BP group had the highest micro-damage density across all groups. The BP group (7.7/mm<sup>3</sup>) also exhibited significantly greater micro-crack density than the fracture (4.3/mm<sup>3</sup>) and non-fracture (4.1/mm<sup>3</sup>) controls. Furthermore, the BP group (1.9/mm<sup>3</sup>) demonstrated increased diffuse damage when compared to the fracture (0.3/mm<sup>3</sup>) and non-fracture (0.8/mm<sup>3</sup>) controls. In contrast, the BP group (1.9/mm<sup>3</sup>) had fewer perforations than fracture (3.0/mm<sup>3</sup>) and non-fracture controls (3.9/mm<sup>3</sup>).

Despite having comparable microarchitecture, apparent and material density, patients taking BP exhibited weaker tissue strength than untreated hip-fracture patients. This weakness is likely to be the result of the greater density of accumulated micro-damage found in BP treated bone. BP inhibits bone remodelling, potentially reducing the number of perforated trabeculae, but perhaps over-suppression leads to the accumulation of micro-cracks (Fig 1B) and diffuse damage which reduce strength.

In a subgroup of hip-fracture patients BP appeared to offer no mechanical advantage in resisting femoral fractures. BP accumulated micro-damage may have weakened the trabecular bone in the femoral head and neck thereby increasing the risk of a fracture during a trip or fall.



Figure 1

**Disclosures:** Richard Abel, None.

## LB-SA0378

**Pain, quality of life and safety outcomes of kyphoplasty for vertebral compression fractures.** Alexander Rodriguez\*<sup>1</sup>, Howard Fink<sup>2</sup>, Lynn Mirigian<sup>3</sup>, Nuria Guanabens<sup>4</sup>, Richard Eastall<sup>5</sup>, Kristina Akesson<sup>6</sup>, Robert Wermers<sup>7</sup>, Douglas Bauer<sup>8</sup>, Peter Ebeling<sup>1</sup>. <sup>1</sup>Monash University, Australia, <sup>2</sup>Minneapolis VA Health Care System, United states, <sup>3</sup>American Society for Bone & Mineral Research, United states, <sup>4</sup>University of Barcelona, Spain, <sup>5</sup>University of Sheffield, United states, <sup>6</sup>Lunds University, Sweden, <sup>7</sup>Mayo Clinic, United states, <sup>8</sup>University of California San Francisco, United states

Balloon kyphoplasty (BK) is used to treat vertebral compression fractures (VCF) and may improve quality of life and reduce pain. We conducted a systematic review to evaluate outcomes of BK versus other treatments for VCF.

We searched multiple electronic databases to May 2016 for randomised controlled trials (RCT) and quasi-randomised trials (CCT) comparing BK with control treatment in adults >40 years with VCF; outcomes were pain, back disability, quality of life, new VCF and adverse events (AE). One reviewer extracted data, a second checked accuracy, and 2 reviewers independently rated risk of bias. Mean differences and 95% confidence intervals were calculated for continuous data using inverse-variance models. Risk ratio (RR) of new VCF and AE were calculated using Mantel-Haenszel models.

Nine unique RCTs and 1 CCT met eligibility criteria (n=1,837 participants). Mean age ranged: 61-76 yr. 74% of participants were female. Follow-up duration ranged: 1 day-60 months (mo). Versus non-surgical management (NSM), BK was associated with statistically significantly reduced pain (VAS) through 24 mo; less back disability (RMDQ) through 12 mo, and better quality of life through 6 (SF36-PCS) or 24 mo (EQ5D) (k=1 RCT, n=300 participants) [Table]. Magnitude of benefits for all self-reported outcomes appeared to lessen over time and most were less than minimally clinically important differences. Risk of new clinical VCF was non-significantly increased at 1 mo (RR, 1.59 [95%CI, 0.63-4.00]) and no different at 12 mo (1.00 [0.66-1.51]; k=2, n=220). Risk of any AE was higher at 1 mo (1.73 [1.35-2.21]) but not 12 mo (1.08 [0.98-1.19]). Versus vertebroplasty (VP), BK was not associated with reductions in pain (VAS), back disability (ODI) or quality of life (SF36-PCS and EQ5D) [Table], and risks for new clinical VCF were similar at 1 mo (0.89 [0.60, 1.33]; k=2, n=549) and 12 mo (0.94 [0.75, 1.18]; k=6, n=760). Versus VP, BK was associated with reduced risk of any AE (0.65 [0.48, 0.90]; k=2, n=451) at 1 mo. Studies were limited in that participants were not masked to treatment.

BK was associated with statistically significantly improved clinical outcomes versus NSM of uncertain clinical significance. Outcomes after BK versus VP appeared similar. Further data are needed to determine the long-term efficacy and safety of the procedure over existing management options.

Table. Kyphoplasty vs. Other Treatments, Mean difference in change in self-reported outcomes from baseline\* (95%CI or p-value)

BK vs. NSM (total: k=1, n=300)	VAS	RMDQ	SF36-PCS	EQ5D
1 mo	-2.2 (-1.6, -2.8)	-4.0 (-5.5, -2.6)	5.2 (2.9, 7.4)	0.18 (0.08, 0.28)
3 mo	-1.8 (<0.01)	-3.8 (<0.01)	4.5 (<0.01)	0.10 (<0.01)
6 mo	-1.6 (<0.01)	-3.1 (<0.01)	3.2 (0.9, 5.6)	0.13 (<0.01)
12 mo	-0.9 (-1.5, -0.3)	-2.6 (-4.1, -1.0)	1.5 (-0.8, 3.9)	0.10 (<0.01)
24 mo	-0.8 (-1.4, -0.2)	-1.4 (0.08)	1.7 (-0.6, 4.0)	0.08 (0.04)
BK vs. vertebroplasty (total: k=4, n=685)	VAS	ODI	SF36-PCS	EQ5D
1 mo	-0.28 [-0.43, -0.13] (k=1, n=107)	No data	No data	No data
3 mo	-0.11 [-0.28, 0.06] (k=2, n=419)	-0.86 [-2.37, 0.64] (k=2, n=399)	-0.30 [-2.68, 2.06] (k=1, n=291)	-0.03 [-0.08, 0.03] (k=1, n=292)
6 mo	-0.10 [-0.18, -0.02] (k=1, n=100)	No data	No data	No data
12 mo	-0.16 [-0.28, -0.04] (k=2, n=378)	-0.91 [-2.37, 0.54] (k=2, n=347)	-1.50 [-4.05, 1.05] (k=1, n=256)	-0.01 [-0.08, 0.07] (k=1, n=258)
24 mo	0.00 [-1.26, 1.26] (k=1, n=220)	-1.00 [-6.91, 4.91] (k=1, n=201)	0.01 [-3.05, 3.25] (k=1, n=200)	-0.03 [-0.11, 0.05] (k=2, n=202)

k = number of RCTs; n = number of participants; NSM = non-surgical management; VAS = pain visual analogue scale; RMDQ = Roland Morris Disability Questionnaire; SF36-PCS = Short form 36 Physical Component Summary scale; EQ5D = EuroQol 5 Dimensions; ODI = Oswestry Disability Index; n/a = not applicable; VCF = new vertebral compression fracture; AE = adverse event; mo = months

\*For VAS, RMDQ and ODI, negative values indicate more improvement from baseline for kyphoplasty versus nonsurgical management; for SF36-PCS and EQ5D, positive values indicate more improvement from baseline for kyphoplasty versus nonsurgical management.

Rodriguez Kyphoplasty table

Disclosures: Alexander Rodriguez, None.

## LB-SA0379

**Blackberry, blueberry, and strawberry polyphenol-rich extracts attenuate osteoclast differentiation in LPS-stimulated RAW264.7 macrophages.** Rafaela Feresin\*<sup>1</sup>, Yitong Zhao<sup>2</sup>, Marcus Elam<sup>3</sup>, Bahram Arjmandi<sup>4</sup>. <sup>1</sup>Department of Dietetics & Nutrition, University of Arkansas for Medical Sciences, United states, <sup>2</sup>Department of Nutrition, Food & Exercise Sciences, Florida State University, United states, <sup>3</sup>Department of Human Nutrition & Food Science, California State Polytechnic University, United states, <sup>4</sup>Department of Nutrition, Food & Exercise Sciences & Center for Advancing Exercise & Nutrition Research on Aging, Florida State University, United states

Osteoporosis is a chronic disease characterized by low bone mass and deterioration of bone microstructure which results in increased bone fragility and propensity to fracture. Inflammation has been shown to play a role in the progression and development of osteoporosis. Increased levels of pro-inflammatory cytokines disrupt normal bone remodeling by increasing the rate of bone resorption resulting in a net bone loss. Although several treatment options exist, a considerable number of people prefer alternative and/or complementary therapies such as functional foods and dietary supplements. Epidemiological studies demonstrate that consumption of fruits and vegetables is associated with decreased incidence of chronic diseases including osteoporosis. This fact has been primarily attributed to high polyphenolic content of fruits and vegetables. Berries are rich in polyphenols and have been shown to have high antioxidant and anti-inflammatory capacity. Thus, the aim of this study was to examine the ability of blackberry (BL), blueberry (BB), and strawberry (SB) polyphenol-rich extracts to modulate osteoclast differentiation in lipopolysaccharide (LPS)-stimulated RAW264.7 macrophages. Cells were cultured in the presence of RANKL (30 ng/ml) for four days and subsequently treated with different doses of berry polyphenol-rich extracts (0, 50, 250, 500 µg/ml) 2 hours prior to stimulation with 100 ng/ml LPS for 24 hours. LPS increased the number of TRAP-positive cells by 35% compared to control ( $P = 0.09$ ). Pre-treatment with BB polyphenol-rich extract at doses of 250 and 500 µg/ml decreased osteoclast differentiation by 60% and 75%, respectively, compared to LPS ( $P \leq 0.001$ ). In addition, BL polyphenol-rich extract was only able to suppress osteoclast differentiation at a dose of 500 µg/ml by 53% ( $P \leq 0.05$ ). Finally, the number of TRAP-positive cells were also attenuated by pre-treatment with SB polyphenol-rich extract at doses of 50, 250 and 500 µg/ml by 47%, 50% and 74%, respectively, compared to LPS ( $P \leq 0.05$ ). No cytotoxicity was observed for any of the doses tested in our study. Our findings demonstrate a role for BL, BB and SB polyphenol-rich extracts on osteoclast differentiation. Thus, further research is needed to examine the mechanisms underlying these effects.

Disclosures: Rafaela Feresin, None.

## LB-SA0380

**TGF-β Signaling in a Mouse Model of Severe Osteogenesis Imperfecta.** Josephine Tauer\*<sup>1</sup>, Sami Abdullah, Frank Rauch. Shriners Hospital for Children & McGill University, Canada

Osteogenesis imperfecta (OI) is caused by either mutations of type I collagen (dominant OI) or of its post-translational modification machinery (recessive OI); leading to characteristic brittle bones, fractures and extraskeletal manifestations. In mouse models of recessive (*Crtp-/-*) and dominant OI (*Col1a2tm1.1Mcbr*) bone phenotype could be corrected by targeting the excessive TGF-β signaling in both mouse models by a specific TGF-β antibody (Grafe I et al, Nat Med 2014;20(6):670-5). As now TGF-β seems to be a possible pathomechanism of OI and promising treatment target, we investigated TGF-β signaling in bone and muscle tissue and the effect of anti-TGF-β treatment on bone in a new mouse model of OI that mimics human OI type IV very closely, *Colla1<sup>fl/+</sup>* (Chen F et al, J Bone Miner Res 2014;29:1412-23). Compared to wild type (WT), cavial bone of young *Colla1<sup>fl/+</sup>* mice showed a higher activation of the TGF-β signaling, evaluated by immunoblots of the intracellular TGF-β pathway. Examination of the TGF-β signaling in muscle tissue of adult *Colla1<sup>fl/+</sup>* mice revealed that quadriceps, gastrocnemius and tibialis anterior of WT as well as *Colla1<sup>fl/+</sup>* mice have a reduced until no activation of the intracellular TGF-β pathway, whereas a diminished TGF-β signaling could be detected in soleus and extensor digitorum longus of the *Colla1<sup>fl/+</sup>* mice compared to WT. However, we treated 8 week-old male *Colla1<sup>fl/+</sup>* mice with a TGF-β neutralizing antibody at a dose of 10 mg/ body weight once or three times a week over a period of 8 weeks. Compared to controls that received either non-specific control antibody at the same dose or saline once a week, anti-TGF-β treatment improved the femoral length of *Colla1<sup>fl/+</sup>* mice only. Anti-TGF-β treatment had no significant effect on overall body composition of *Colla1<sup>fl/+</sup>* mice, examined by body weight, and had no significant effect on BV/TV, trabecular structure as well as the mechanical properties of the femora, evaluated by µCT and 3-point bending test. These results indicate that anti-TGF-β treatment might be useful for mild and moderate OI but not for severe forms of OI such as OI type IV. Nevertheless, further investigations are needed to verify these observations.

Disclosures: Josephine Tauer, None.

**LB-SA0381**

**Two-Year, School-Based Resistance Band Exercise Increases Bone Acquisition in Adolescent Girls.** Deena Weiss\*<sup>1</sup>, Jodi Douthwaite<sup>2</sup>, Jill Thein-Nissenbaum<sup>1</sup>, Tamara Scerpella<sup>1</sup>. <sup>1</sup>University of Wisconsin, United states, <sup>2</sup>SUNY Upstate Medical University, United states

**Introduction:** Exercise may enhance bone growth, benefiting lifelong skeletal health. An effective, generalizable exercise program has not been identified. We previously evaluated a school-based, resistance-band, exercise intervention in adolescent girls, identifying femoral neck (FN) and lumbar spine (LS) benefits over 1 school year (Y1). The current analysis evaluates cumulative benefits after the 2<sup>nd</sup> school year (Y2).

**Methods:** Girls entering 6<sup>th</sup> grade were enrolled and block-randomized by school site. At site 1, girls had standard gym classes, 2-3 days/week, 45 minutes (min)/session (CON). At site 2, gym classes included 8-12 min of resistance band training/session (INT). Y1 effort was recorded to calculate effort-min (sum of daily min x effort score [lo=1, med=2, hi=3], e\*m), yielding 2 groups: LO = 774 e\*m, HI = 1561 e\*m. Y2 spot-checks confirmed group consistency.

At baseline (BL), 1<sup>st</sup> follow-up (FU1: Y1 end) and 2<sup>nd</sup> follow-up (FU2: Y2 end) we measured height, weight and non-dominant grip strength. Calcium and vitamin D intakes were assessed via food frequency questionnaire. Inter-scan organized activity dose (h/wk) was calculated from calendar-based questionnaires. Menarche date was recorded and maturity groups were assigned: 1) PRE= pre-menarche at BL and FU2; 2) PERI= pre-menarche at BL, post-menarche at FU2; 3) POST= post-menarche at BL and FU2. Dual-energy X-ray absorptiometry scans (DXA, Lunar Prodigy) measured bone mineral content (BMC) and areal bone mineral density (BMD) for whole body (WB), sum of legs (LEGS), sum of arms (ARMS), lumbar spine (L1-L4), femoral neck (FN), ultradistal radius (radUD) and 1/3 radius (rad1/3). WB scans assessed non-bone lean mass, fat mass and % body fat. Multiple linear regression evaluated INT as a factor in bone outcomes, accounting for BL height, height change, inter-scan interval, organized activity, calcium and vitamin D.

**Results:** 62/68 subjects provided FU2 data. There was no significant bias in maturity status by INT group (chi-square analysis). At FU2 there were no significant differences in INT vs CON for age, height, weight, BMI, % body fat, inter-scan organized activity, calcium or vitamin D. There were INT advantages in FNBMD, LSBMC, LSBMD, SUBBMC and LEGSBMC, regardless of effort ( $p < 0.05$ ), with INT explaining up to 1% of variance; for FN & LS outcomes this effect was similar to variance explained by height change (1-3%). Comparing HI vs LO/CON, INT explained 1.5-3% of variance for FN & LS, benefits were greater for all bone outcomes, and HI FNBMC advantage was also significant ( $p < 0.001$  to  $p < 0.05$ ).

**Conclusion:** Only 8-12 minutes of resistance band training, 2-3 times/week over two school years was associated with benefits in regional and whole body bone development in adolescent girls. Further work, evaluating persistence of benefits beyond intervention cessation, is warranted to evaluate the potential for public health recommendations.

**Disclosures:** Deena Weiss, None.

**SU0001**

**Chronic Kidney Disease and Aging Diminish Bone Quality in C57Bl/6 Mice.** Chelsea Heveran<sup>\*1</sup>, Eric Livingston<sup>2</sup>, Sarah Whetstone<sup>1</sup>, Moshe Levi<sup>3</sup>, Ted Bateman<sup>2</sup>, Karen King<sup>3</sup>, Virginia Ferguson<sup>1</sup>. <sup>1</sup>University of Colorado at Boulder, United states, <sup>2</sup>University of North Carolina at Chapel Hill, United states, <sup>3</sup>University of Colorado School of Medicine, United states

Chronic Kidney Disease (CKD) increases the prevalence of bone fracture, especially among the elderly (Coresh, Lancet, 2012). Deleterious changes in bone quality occur with CKD in adolescent mice (Heveran, Bone, 2016); however, the combined effects of CKD and aging have not been elucidated. To our knowledge, this study is the first to investigate how CKD and aging together diminish bone quality.

Male C57Bl/6 mice at three ages (Young = 3 mo, Middle-Age = 15 mo, Old = 21 mo) underwent 5/6<sup>th</sup> nephrectomy to establish CKD or Sham surgeries (N = 48, n = 6-10 per age/treatment). Mice were euthanized three months post-procedure. MicroCT evaluated microarchitecture of cortical femur and trabecular tibia bone. Femurs were broken *via* three-point bending and then dehydrated, embedded, and polished. A co-located nanoindentation-Raman system (5  $\mu$ m spherical tip; 785 nm laser) evaluated microscale modulus and chemistry in arrays extending through the cortical thickness (spacing = 10  $\mu$ m, n = 6 bones/group). Nanoindentation and Raman required repeated-measures ANCOVA, otherwise two-factor ANOVA was used.

CKD was confirmed with increased serum BUN (age: p>0.05, CKD: p<0.001). Age and CKD both diminished cortical thickness (age: p<0.001, CKD: p<0.001) and cortical porosity (age: p<0.01, CKD: p<0.001). Age and CKD also reduced trabecular thickness (age: p<0.05, CKD: p<0.001), number (age: p<0.001, CKD: p<0.05) and spacing (age: p<0.001, CKD: p<0.05). Age and CKD lowered stiffness (age: p<0.01, CKD: p<0.001) and max load (age: p<0.001, CKD: p<0.001) from three-point bending.

Nanoindentation modulus and chemistry worsened with age and CKD. Modulus lowered with age (p<0.001) and possibly with CKD (p=0.098). Modulus tended to decrease in Young and Middle-Age mice with CKD compared to Sham (Young: -3.80%, p=0.071; Middle-Age: -4.30%, p=0.073). Mineral:matrix (v<sub>i</sub> phosphate:amide III) increased with age (p<0.001) and CKD (p<0.001); this ratio increased with CKD compared with Sham for Young (+12.8%, p=0.027) and Middle-Age mice (+17.9%, p<0.001). Carbonate:phosphate was lower in Old mice with CKD compared with Sham (-5.83%, p=0.016).

In summary, aging and CKD both reduced the cortical and trabecular bone microstructure and mechanical performance of bone, and also altered tissue-scale chemistry. Bone quality is thus reduced with CKD in addition to aging, which may help explain the clinically-observed bone fragility with kidney disease.

Acknowledgements: NIH T32AG000279, UL1TR001082.

*Disclosures: Chelsea Heveran, None.*

**SU0002**

**FRAX with and without DXA result in prediction of the risk of bone fractures in patients with end-stage renal disease undergoing dialysis - 4-year observational study.** Jerzy Przedlacki<sup>\*1</sup>, Paweł Żebrowski<sup>1</sup>, Ewa Wojtaszek<sup>2</sup>, Mariusz Mieczkowski<sup>2</sup>, Agnieszka Grzeiszczak<sup>2</sup>, Monika Staszów<sup>2</sup>, Michał Pyrża<sup>2</sup>, Małgorzata Kościelska<sup>2</sup>, Małgorzata Kepska<sup>2</sup>, Joanna Matuszkiewicz-Rowińska<sup>2</sup>. <sup>1</sup>Chair & Department of Nephrology, Dialysis & Internal Diseases, Medical University of Warsaw, Poland, <sup>2</sup>Chair & Department of Nephrology, Dialysis & Internal Medicine, Medical University of Warsaw, Poland

Despite overall increased risk of bone fractures in patients with end-stage renal disease (ESRD) undergoing dialysis the optimal prediction method of particularly high risk in selected patients was not established. There were only some, mostly retrospective data showing the significance of FRAX in prediction of fracture risk in dialysis patients. The purpose of the study was to assess the usefulness of FRAX with and without DXA result in prediction of major and any bone fracture risk in 4-year observational study in patients with ESRD undergoing dialysis. Seventy-six patients (37 men and 39 women) aged 60.2 ± 14.0 years and dialyzed for 0.1-29 years (51 hemodialysis, 25 peritoneal dialysis) from 1 dialysis center were observed for 4 years between 2007 and 2015. They were treated with calcium carbonate, alfacalcidol to keep PTH serum level in optimal range based on KDIGO recommendation. No one was receiving antiresorptive or anabolic drugs used in osteoporosis. Major and separately all non-traumatic bone fractures were noted. FRAX results were calculated with its polish version, once with DXA result (T-score of femoral neck, Discovery A machine, Hologic) and once without. The area under the curve (AUC) was calculated for both FRAX results and separately for every particular parameter of FRAX calculator for major and any fracture. Thirteen major bone fractures in 10 patients (clinically overt spine - 3, hip - 6, radial bone - 3, humeral bone - 1) and twenty-seven of any bone fractures in 16 patients (except major fractures, ribs - 4, clavicle - 3, pelvis - 1, other - 6) were recognized. AUC of FRAX with DXA results of major bone fractures was 0.69 (95% CI, 0.49-0.89) and of any fracture 0.57 (95% CI, 0.40-0.74) and without DXA results 0.51 (95% CI, 0.33-0.69) and 0.51 (95% CI, 0.37-0.65) respectively. AUC of particular parameters of FRAX of major fractures was between: 0.36 (95% CI, 0.18-0.54) for age and 0.65 (95% CI, 0.48-0.81) for previous fractures, and for any fracture between 0.32 (95% CI, 0.18-0.46) for age and 0.61 (95% CI, 0.48-0.73) for previous fractures and 0.61 (95% CI, 0.43-0.79) for lower BMI. We conclude that, on the basis of AUC calculation, FRAX with DXA result better predicts the risk

of major bone fractures than without DXA results, but the difference was not large enough to be considered statistically significant. When any bone fracture risk was analyzed this difference was less pronounced.

*Disclosures: Jerzy Przedlacki, None.*

**SU0003**

**Effect of Bisphosphonates on Cytokine/Chemokine-mediated Angiogenesis in Alveolar Bone.** Mohamed Awad<sup>\*</sup>, Sudha Ananth, Ranya Elsayed, Amany Tawfik, Mohammed Elsalanty. Augusta University, United states

Spontaneous occurrence of bisphosphonate-related osteonecrosis of jaw suggests a multifactorial pathogenesis. We hypothesize that zoledronate impairs the early angiogenic response in the bone microenvironment. We tested the effects of zoledronate on endothelial cell expression of angiogenic cytokine receptors [PDGFRb & VEGFR], chemokine receptors [CXCR4], angiogenic factors [TNF- $\alpha$ , HIF-1 $\alpha$  & E-Nos], angiostatic cytokine [IFN- $\beta$ ] and their receptor [CXCR5]. HUVEC cells were treated with increasing doses of Zoledronate. We assessed gene expression through qRT-PCR, protein expression using immunoprecipitation and western blotting, and immunofluorescence flow cytometry for receptors distributions. We also tested the vascular perfusion of alveolar bone in zoledronate-treated animals after dental extraction, using microCT-angiography. Results showed significant downregulation in PDGFR-b, VEGFR and CXCR4 [p=0.017, 0.004 and 0.035, respectively], and angiogenic factors TNF- $\alpha$ , HIF-1 $\alpha$  & E-Nos [p value = 0.1481, 0.0001 and 0.0032 respectively]. There was an upregulation in angiostatic cytokine [IFN- $\beta$ ; p value=0.1786] and receptor [CXCR5; p value=0.4296]. Initial micro-CT results suggest an inhibition in vascular perfusion of alveolar bone in zoledronate-treated animals. We concluded that zoledronate inhibits the early angiogenic response in the alveolar bone, which could predispose to the osteonecrosis.

*Disclosures: Mohamed Awad, None.*

**SU0004**

**Serum Osteocalcin Concentration is an Independent Risk for Incident Type 2 Diabetes Mellitus in Japanese Postmenopausal Women.** Tomohiko Urano<sup>\*1</sup>, Masataka Shiraki<sup>2</sup>, Tatsuhiko Kuroda<sup>3</sup>, Shiro Tanaka<sup>4</sup>, Fumihiko Urano<sup>5</sup>, Kazuhiro Uenishi<sup>6</sup>, Satoshi Inoue<sup>7</sup>. <sup>1</sup>The University of Tokyo, Japan, <sup>2</sup>Research Institute & Practice for Involutional Diseases, Japan, <sup>3</sup>Public Health Research Foundation, Japan, <sup>4</sup>Kyoto University, Japan, <sup>5</sup>Washington University School of Medicine, United states, <sup>6</sup>Kagawa Nutrition University, Japan, <sup>7</sup>Tokyo Metropolitan Institute of Gerontology, Japan

Context: Osteocalcin, is produced by osteoblasts, has recently been demonstrated to have an unexpected role in glucose metabolism. Osteocalcin knock-out mice showed decreased pancreatic beta-cell proliferation and increased in insulin resistance. These pathophysiological features are similar to those of diabetes mellitus and metabolic syndrome. Increasing evidences suggest that osteocalcin might be involved in the regulation of glucose homeostasis. Recently, several clinical studies have also shown that an association between glucose metabolism and osteocalcin exists in humans. However, direct relationship between serum osteocalcin levels and risk of incident type 2 diabetes mellitus is not clear in humans.

Objective: The objective of the study was to investigate whether levels of osteocalcin are the risk of incident type 2 diabetes mellitus or not. Methods: This study included 1691 Japanese postmenopausal women, 61 incident diabetes cases and 1630 non-diabetic control participants in the observation period. Baseline concentrations of intact osteocalcin, HbA1c, bone-specific alkaline phosphatase, triglycerides, adiponectin, leptin, urinary N-telopeptides were assessed.

Results: Osteocalcin concentration was significantly lower in the cases with incident diabetes cases than in non-diabetic control participants. Serum osteocalcin levels were also significantly correlated with HbA1c among 1691 Japanese postmenopausal women (R = -0.12, P < 0.0001). In receiver operating characteristic curve analysis, the optimal cut-off level for serum osteocalcin levels to predict the development of type 2 diabetes mellitus was 6.1 ng/mL. The group with baseline osteocalcin level < 6.1 ng/mL showed a significantly higher risk for developing diabetes than the group with baseline osteocalcin level > 6.1 ng/mL (log-rank test, P < 0.0001) during the mean observation period (7.6 ± 6.1 years; mean ± SD). After adjusting for potential confounders, the multivariate Cox proportional hazards models retained age, triglycerides, adiponectin/leptin ratio, which is known as a parameter of insulin resistance, and osteocalcin as independent risk factors for a development type 2 diabetes mellitus.

Conclusions: Our results indicate that decreased levels of serum osteocalcin predict risk for future development of type 2 diabetes mellitus in Japanese postmenopausal women. Further prospective studies are needed to verify the optimal cut-off value of osteocalcin for predicting incident type 2 diabetes mellitus in males and females.

*Disclosures: Tomohiko Urano, None.*

**SU0005**

**The majority of adults with persistent hypophosphatasemia harbor mutations in the *ALPL* gene.** Indira Rai\*<sup>1</sup>, Juan Dong<sup>2</sup>, Richard Berg<sup>3</sup>, Erica Scotty<sup>3</sup>, Fergus McKiernan<sup>4</sup>. <sup>1</sup>Marshfield Clinic, United states, <sup>2</sup>Prevention Genetics, United states, <sup>3</sup>Center for Biomedical Informatics, Marshfield Medical Research Foundation, United states, <sup>4</sup>Marshfield Medical Research Foundation, United states

**Introduction:** We have previously shown that adults with persistently low serum values of alkaline phosphatase (ALP; persistent hypophosphatasemia) share phenotypic features with the adult form of hypophosphatasia (HPP), a rare inherited condition of impaired mineralization of bones and teeth.<sup>1</sup> Low serum ALP activity in HPP results from mutations in the *ALPL* gene located on chromosome 1p36.1-p34 and is the cardinal biochemical feature of all forms of HPP. The purpose of this study is to determine the proportion of adults with persistent hypophosphatasemia who harbor mutations in the *ALPL* gene.

**Methods:** This study was approved by Marshfield Clinic IRB. Of 260 adults with persistent hypophosphatasemia previously described (ALP almost always  $\leq 30$ U/L; normal 40-120), approximately 100 were found to be alive, living within the Marshfield Clinic catchment area and had a postal mailing address on file through which contact was initially made. Genomic DNA was extracted from peripheral blood of consenting subjects and *ALPL* gene mutational analysis performed using PCR and Sanger sequencing methods. Variants found in this study are classified into 5 categories (pathogenic, likely pathogenic, variants of unknown significance (VUS), likely benign, and benign) based on the ACMG sequence variants interpretation guidelines.

**Results:** Thus far, of 32 enrolled subjects, 28 have completed mutational analyses. 21 of these 28 individuals (75%) are heterozygous for a pathogenic or likely pathogenic *ALPL* variant, 2 are heterozygous for a VUS (1 of these is novel) and 5 are negative for an *ALPL* gene variants as sequenced. The recurrent variants are c.571G>A (n=5), c.211C>T (n=2), c.1276G>A (n=2) and c.984\_986delCTT (n=2).

**Conclusion:** The majority of 28 adult subjects with persistent hypophosphatasemia are heterozygous for pathogenic or likely pathogenic variants of the *ALPL* gene. Since race and family history of these individuals are unknown we cannot state whether individuals who carry the same recurrent *ALPL* variants are biologically or ethnically related. Large deletions or duplications in the *ALPL* gene cannot be detected by our analysis technique, although such variants are observed in only 5 of 315 mutations registered in an *ALPL* gene specific variant database.

Further genetic, clinical and imaging evaluation is warranted to elucidate the correlations between genotype and phenotype in adults with persistent hypophosphatasemia and *ALPL* mutations.

McKiernan FE, JBMR 2014;29:1651-70.

**Disclosures:** Indira Rai, None.

This study received funding from: Alexion Pharmaceuticals, Inc

**SU0006**

**Vitamin D Levels in Patients with Diabetes Mellitus Type 1 and 2.** Vaclav Vyskocil\*, Anna Planickova. Charles University Hospital Metabolic Bone Disease Centre, Czech republic

The authors examined a group of 1998 diabetes patients which included 1278 females and 720 males. Only 109 patients suffered from diabetes mellitus type I (DMT1) and 1889 patients diabetes mellitus type II (DMT2).

Patients were divided into six age categories: 18-25,26-39,40-54,55-65,66-80,81 and more. Vitamin D level was measured in all patients. Age categories were selected according to the age groups in the control group of 2900 patients without diabetes where DXA measurement was previously performed. DMT1 group of 109 patients (75 women and 34 men) had average vitamin D level 55.6 nmol/l (median 48.6 nmol/l), DMT2 group of 1889 patients (1203 women and 686 men) had average vitamin D level 53.8 nmol/l, (median 51.5 nmol/l). All patients from the control group had repeatedly checked level of vitamin D and basic parameters (weight, height, BMI and supplementation with calcium and vitamin D). The results were compared with a set of newly measured patients without diagnosis of E10 and E11. DM patients had significantly lower vitamin D level than the control group. The group was divided into 2 groups. One received supplementation with calcium and vitamin D and second group without supplementation, and according to the season of blood samples examination - summer and winter. Level of vitamin D was related not only to the age group, but also to the time of blood sample tests, supplementation and BMI.

The authors tried to determine the change in the level, respectively the difference (trend) between the group supplemented and nonsupplemented.

**Disclosures:** Vaclav Vyskocil, None.

**SU0007**

**Effect of a Rare Genetic Variant of *TM7SF4* Gene on Osteoclast Phenotype in Paget's Disease of Bone.** Emilie Laurier\*<sup>1</sup>, Nathalie Amiable<sup>2</sup>, Edith Gagnon<sup>2</sup>, Jacques P. Brown<sup>3</sup>, Laetitia Michou<sup>4</sup>. <sup>1</sup>CHU de Québec research centre, Canada, <sup>2</sup>CHU de Quebec research centre, Canada, <sup>3</sup>CHU de Quebec research centre & departement of medicine, division of rheumatology, CHU de Québec-Université Laval, Canada, <sup>4</sup>CHU de Quebec research centre & departement of medicine, division of rheumatology, CHU de Quebec-Université Laval, Canada

**Background:** Dendritic Cell-Specific Transmembrane Protein (DC-STAMP) is a transmembrane protein involved in osteoclastogenesis playing a key role in the fusion of mononuclear osteoclasts. We previously reported a rare genetic variant (rs62620995) in the *TM7SF4* gene coding for the DC-STAMP protein, present in 2.8% of pagetic patients and 1.4% of healthy controls in the French-Canadian population. This variant leads to the change of a leucine, a highly conserved amino acid through evolution, into a phenylalanine at position 397, which may be damaging according to *in silico* predictions.

**Purpose:** This study aimed at determining the functional effects of this rare variant on the osteoclast phenotype in Paget's disease.

**Methods:** 50 ml of peripheral blood were collected in four pagetic patients carrier of this variant, four pagetic patients non carrier of this variant and four healthy controls. Monocytes were collected after Ficoll gradient and cultured in a medium containing RANKL (40 ng/ml) and hMCSF (25 ng/ml). At the end of the differentiation period, we assessed the osteoclast phenotype by estimating the percentage of multinucleated cells (three nuclei and more), the mean number of nuclei per multinucleated cell and the mean area of resorbed bone. From cell lysates, we quantified gene expression of *SQSTM1*, *DC-STAMP*, *OS9*, *CREB3*, *LAMP1*, *OC-STAMP*, and *NFATC1* genes. Proteins encoded by these genes were further investigated by Western Blot. Statistical analyses relied on ANOVA followed by a Tukey post-test.

**Results:** The percentage of multinucleated cells was higher in patients non carrier of the variant (80.9  $\pm$  12.8%) and in mutated patients (76.6  $\pm$  26.8%), than in healthy controls (59.7  $\pm$  23.8%). The mean number of nuclei per multinucleated cell was significantly higher in mutated patients (7.2  $\pm$  4.3) than in controls (4.9  $\pm$  2.0),  $p=0.05$ , but not significantly different from patients non carrier of the variant (6.1  $\pm$  2.9). The mean area of resorbed bone did not differ significantly between the three groups. Gene expression analysis did not reveal any differences. DC-STAMP protein was more expressed in mutated patients and controls than in patients non carrier.

**Conclusion:** These preliminary results suggest that this genetic variant of *TM7SF4* gene encoding the DC-STAMP protein tend to increase the mean number of nuclei per osteoclast. Further analyses will help at better understanding the role of this variant on mononuclear osteoclasts fusion.

**Disclosures:** Emilie Laurier, None.

**SU0008**

**Comparison of cinacalcet and subtotal parathyroidectomy for treating hypercalcemia in tertiary hyperparathyroidism.** Namki Hong\*<sup>1</sup>, Hyemin Jo<sup>1</sup>, Da Hea Seo<sup>1</sup>, Jong Ju Jeong<sup>2</sup>, Yumie Rhee<sup>1</sup>. <sup>1</sup>Department of Internal Medicine, Severance Hospital, Endocrine Research Institute, Yonsei University College of Medicine, 120-752, Korea, republic of, <sup>2</sup>Thyroid Cancer Clinic, Yonsei University College of Medicine, Seodaemun-gu, Korea, republic of

**Purpose:** Hypercalcemia after kidney transplant is commonly attributed to tertiary hyperparathyroidism. We aimed to compare the clinical outcomes after subtotal parathyroidectomy or cinacalcet for treatment of tertiary hyperparathyroidism.

**Methods:** Data of subjects with diagnosis of tertiary hyperparathyroidism from January 2011 to December 2015 were retrieved from electronic registry of Severance hospital, Korea. Subjects were excluded if they had an estimated glomerular filtration rate (eGFR) < 30 mL/min/1.73m<sup>2</sup>, received a transplant within 3 months, or used cinacalcet with parathyroidectomy. Index date was defined as first subtotal parathyroidectomy or cinacalcet prescription date. Study outcomes were normalization of calcium, intact PTH (iPTH), renal function, and change of femur neck bone mineral density (FNBM) during 12 months after index date.

**Results:** Among subtotal parathyroidectomy (N=22) and cinacalcet group (N=9), proportion of male sex (58.1%), median age (50.5 years), serum iPTH, calcium, and eGFR at baseline did not differ significantly. At 12 months, median calcium level was normalized in both groups (11.3 to 9.0 mg/dL in parathyroidectomy,  $P<0.001$ ; 11.8 to 10.3 mg/dL in cinacalcet,  $P=0.043$ ) although iPTH reduction was greater in parathyroidectomy (223.5 to 54.2 pg/mL,  $P<0.001$ ) compared to cinacalcet group (248.5 to 184.8 pg/mL,  $P=0.043$ ). Compared to parathyroidectomy, cinacalcet was associated with slight decrease of FNBM (%) but the association lost statistical significance after adjustment for potential confounders including age, body mass index, bisphosphonate, calcium, and cholecalciferol supplements use ( $\beta=-5.04$ ,  $P=0.097$ ).

**Conclusion:** Our study suggests that cinacalcet therapy may provide useful alternative strategy for subtotal parathyroidectomy in treating tertiary hyperparathyroidism in real-world setting.

**Disclosures:** Namki Hong, None.

## SU0009

### Estimated Prevalence of Chronic Hypoparathyroidism Through the Analysis of a Regional Dataset. Luisella Cianferotti\*<sup>1</sup>, Simone Parri<sup>1</sup>, Giorgio Gronchi<sup>1</sup>, Carla Rizzuti<sup>2</sup>, Gemma Marcucci<sup>1</sup>, Maria Luisa Brandi<sup>1</sup>.

<sup>1</sup>Metabolic Bone Diseases Unit, Department of Surgery & Translational Medicine, University of Florence, Italy, <sup>2</sup>Region of Tuscany, Italy

Chronic hypoparathyroidism is an endocrine condition characterized by insufficient PTH secretion of action, lasting for at least 6 months. It comprises rare, mostly genetically determined conditions and more frequent forms such as surgical hypoparathyroidism. To date, very few studies have addressed the prevalence and incidence of hypoparathyroidism. The aim of this study has been to estimate the prevalence of this disorder through the analysis of a regional database in a mediterranean country (Region of Tuscany, Italy). This database includes records pertaining to pharmaceutical prescriptions both from hospital physicians and general practitioners in the whole population of Tuscany (3,709,673) in a 5 year period (2009-2013). Data from four different flows (pharmaceutical distribution dataset for drugs reimbursed by public health system, hospital discharge and exemption codes, general data flow) has been used. Each subject was anonymously identified with an univocal number. Duplicated records were removed. Since hypoparathyroidism requires chronic therapy with active vitamin D analogs (AVDA, i.e. calcitriol, alfa-calcidol, dihydrotachysterol), data from 62,786 subjects taking one or more of these drugs (at least one prescription) have been retrieved. The mostly prescribed drug was calcitriol, accounting for 97% of total prescriptions. Within this group, 6882 subjects received therapy with AVDA for at least 6 months (further referred to as chronic therapy), and a subgroup of 1,278 individuals were on the medication until the end of the study period. An exemption code for hypoparathyroidism was assigned to 488 subjects. Within this group, 55 individuals were on chronic therapy with AVDA. 337 had been discharged from regional hospitals for hypoparathyroidism, tetany, or hypocalcemia. Among these individuals, 17 subjects were on chronic therapy with AVDA. In parallel, 264 subjects on chronic AVDA within the group of patients having undergone neck surgery (thyroidectomy/parathyroidectomy/laryngectomy) were identified. In order to analyze the incidence of surgical hypoparathyroidism, in this latter cluster of patients, a sample of 176 individuals starting therapy with AVDA within one month since surgical procedure was detected. In conclusion, period prevalence of chronic hypoparathyroidism in a 5-year period in a subset of the Italian population is 0.034% (34/100,000). Estimated prevalence of surgical hypoparathyroidism is 2%.

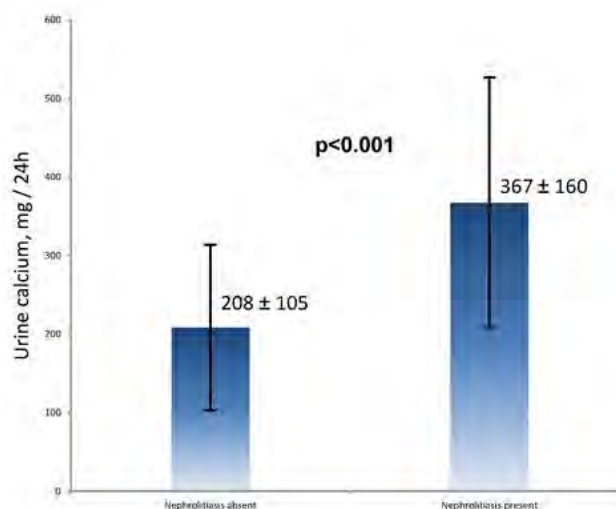
**Disclosures:** Luisella Cianferotti, None.

## SU0010

### Occult Nephrolithiasis in Primary Hyperparathyroidism is Associated with Higher Activated Vitamin D Levels and Urinary Calcium Excretion. Leonardo Bandeira\*<sup>1</sup>, Diane Cozadd<sup>1</sup>, Mariana Bucovsky<sup>1</sup>, Donald McMahon<sup>1</sup>, James Lee<sup>2</sup>, Shonni Silverberg<sup>1</sup>, Marcella Walker<sup>1</sup>.

<sup>1</sup>Metabolic Bone disease unit, College of Physicians & Surgeons, Columbia University Medical Center, United states, <sup>2</sup>Department of Surgery, Columbia University Medical Center, United states

While symptomatic nephrolithiasis occurs in approximately 17% of patients with primary hyperparathyroidism (PHPT), the incidence of occult stones is unknown. The 2014 guidelines for the management of asymptomatic PHPT suggest renal imaging for all patients and referral for parathyroidectomy (PTX) when an occult stone is present. This study was designed to investigate the prevalence of and risk factors for occult renal stones in PHPT. PHPT patients at our institution now routinely undergo renal imaging (ultrasound, x-ray, CT or MRI) as part of their clinical evaluation. We are prospectively collecting data on patients without a clinical history of nephrolithiasis, including demographic data, medical history, biochemistries (serum 25-hydroxyvitamin D (25OHD), 1,25-dihydroxyvitamin D (1,25(OH)<sub>2</sub>D), phosphorus, estimated glomerular filtration rate (eGFR), calcium, albumin, parathyroid hormone and urinary calcium) and radiology results. To date, 54 patients (83% female, 70% white, mean age 64±11 yrs) with mild PHPT (mean calcium 10.5±0.4 mg/dl, PTH 92±48 pg/ml, 25OHD 28±11 ng/ml) have been enrolled. 63% met calcium, osteoporosis, eGFR or age criteria for PTX. Occult kidney stones were identified by imaging in 10 patients (18.5%, 95%CI: 8-35.6%). Those with vs. without nephrolithiasis had greater urine calcium excretion (367±160 vs 208±105 mg/24h, p<0.001; 315±116 vs 188±74 mg/g creatinine, p=0.002) and a trend toward higher serum 1,25(OH)<sub>2</sub>D (100±21 vs 68±23 pg/ml, p=0.056). There were no between-group differences in age (66±7 vs 64±12 yrs, p=0.56), mean daily vitamin D supplement intake (1080±1120 vs 804±882 IU/day, p=0.40), weight (167±35 vs 162±45 lbs, p=0.95), race (80% vs 68% white, p=0.29), serum calcium (10.6±0.3 vs 10.5±0.5 mg/dl, p=0.44), PTH (111±57 vs 89±46 pg/ml, p=0.50), 25OHD (30±11 vs 28±12 ng/ml, p=0.63), phosphate (3.3±0.5 vs 3.2±0.4 mg/dl, p=0.69), eGFR (76±11 vs 81±20 ml/min, p=0.27), BMD by DXA at any site or rates of osteoporosis (56% vs. 42%, p=0.49). Occult nephrolithiasis is not uncommon among asymptomatic PHPT patients. It was associated with greater urinary calcium excretion and trend to higher serum 1,25(OH)<sub>2</sub>D levels. These preliminary data support the indication for renal imaging in asymptomatic PHPT patients and suggest that higher activated vitamin D levels may lead to greater urinary calcium excretion and occult nephrolithiasis in PHPT.



Urine calcium

**Disclosures:** Leonardo Bandeira, None.

This study received funding from: Joseph Weintraub Family Foundation

## SU0011

### Preliminary Biopsy Findings Indicate Opposing Effects of Vitamin D and PTH on Bone Remodeling in PHPT. Marcella Walker\*<sup>1</sup>, Hua Zhou<sup>2</sup>, Mariana Bucovsky<sup>1</sup>, David Dempster<sup>1</sup>, Shonni Silverberg<sup>1</sup>. <sup>1</sup>Columbia University, United states, <sup>2</sup>Helen Hayes Hospital, United states

Data regarding the skeletal effects of vitamin D (25OHD) deficiency in primary hyperparathyroidism (PHPT) are limited. We have shown that lower 25OHD in PHPT is associated with higher PTH levels. Using dual x-ray absorptiometry (DXA), TBS, high resolution peripheral quantitative computed tomography (HRpQCT) and central QCT, we have shown that lower 25OHD and higher PTH is associated with modestly lower bone mineral density (BMD) by DXA at the cortical 1/3 radius and greater cortical porosity at the tibia by HRpQCT; in contrast trabecular BMD and microarchitecture is not adversely affected. In this study, we assessed the effect of 25OHD on bone microarchitecture and turnover with tetracycline-labeled percutaneous iliac crest bone biopsy. Five individuals (Mean age±SD 55±3 yrs, 60% women) with PHPT (serum calcium 10.7±0.5mg/dl, PTH 83±31pg/ml, 25OHD 30ng/ml) have had a biopsy. Biopsy results are stratified by sex due to normal range differences. In men (N=2), cancellous bone volume (BV/TV), trabecular width (Tb.Wi) and number (Tb.No) and eroded surface (ES/BS) were increased, while cortical width (Ct.Wi), mineralizing surface (MS/BS), mineral apposition rate (MAR), bone formation rate (BFR) and osteoid surface (OS/BS) were normal (Table). In women, indices tended to be normal. In the cancellous compartment, only Tb.No and Act.F were associated with calcitropic factors: Tb.No with 25OHD (r=0.90, p=0.04) and PTH with Act.F (r=0.89, p=0.04); in the cortex, 25OHD was negatively associated with endocortical adjusted apposition rate (Aj.AR; r=-0.92, p=0.03) and endo- and intracortical activation frequency (Act.F; r=-0.88 and -0.89, p<0.05 for both). PTH was positively associated with Ct. porosity (r=0.93, p=0.02) and OS/BS (r=0.87, p=0.06) while calcium was negatively associated with Ct.Wi (r=-0.87, p=0.06). In summary, trabecular indices in PHPT are preserved or increased, as expected. In the cancellous compartment, higher 25OHD was associated with trabecular structural advantages while higher PTH was associated with increased remodeling. In the cortex, higher 25OHD was associated with reduced remodeling; in contrast, higher PTH and calcium were associated with deleterious cortical effects, including greater extent of osteoid, increased porosity and thinning. Bone remodeling in PHPT is complex and may be driven by different, competing calcitropic factors that have opposing effects with different structural outcomes depending on the skeletal compartment.

	Normal Range Men Age 50-59	Men	Normal range Women Age 55-64	Women
<b>Bone Structure</b>				
BV/TV (%)	7.4-20.4	22.7±0.1	13.7-28.4	20.9±6.1
Tb.WI (µm)	70.7-128.1	136.3±2.1	76-169	123.6±36.1
Tb.No (#/mm)	1.0-1.6	1.7±0.02	1.4-2.4	1.7±0.02
Tb.Sp (µm)	500-887	587±5	310-566	579±7
Ct.WI (µm)	403-978	533±23	475-1431	608±247
<b>Cancellous Bone Remodeling</b>				
MS/BS (%)	2.7-14.8	9.4±1.3	2.3-19.5	5.8±1.6
MAR (µm/day)	0.52-0.82	0.573±0.006	0.49-1.06	0.554±0.067
BFR (µm <sup>3</sup> /µm <sup>2</sup> /day)	0.017-0.083	0.054±0.008	0.012-0.152	0.032±0.006
OS/BS (%)	3.4-15.9	14.2±7.7	7.8-31.6	10.4±0.8
ES/BS (%)	2.1-3.8	6.8±2.6	1.8-8.7	7.5±4.5

Table

Disclosures: Marcella Walker, None.

### SU0012

**The Prevalence of Normocalcemic Primary Hyperparathyroidism among Blood Donors Volunteers.** Salvatore MINISOLA<sup>\*1</sup>, Vittoria DANESE<sup>1</sup>, Federica FERRONE<sup>1</sup>, Valeria FASSINO<sup>1</sup>, Giancarlo FERRAZZA<sup>2</sup>, Enrico PANZINI<sup>2</sup>, Veronica CECCHETTI<sup>1</sup>, Jessica PEPE<sup>1</sup>, Frank BLOCKI<sup>3</sup>, Cristiana CIPRIANI<sup>1</sup>. <sup>1</sup>Department of Internal Medicine & Medical Disciplines, University of Rome “Sapienza”, Policlinico Umberto I, Viale del Policlinico 155, 00161 Rome, Italy, <sup>2</sup>Department of Immunohematology & Transfusion Medicine, University of Rome “Sapienza” Policlinico Umberto I, Viale del Policlinico 155, 00161 Rome, Italy, <sup>3</sup>DiaSorin, 1951 Northwestern Avenue, Stillwater, MN, USA., United states

Normocalcemic primary hyperparathyroidism (NPHPT) is defined by consistently elevated serum PTH values with normal total and ionized (Ca<sup>++</sup>) serum calcium concentration, in the absence of identifiable causes for elevated PTH concentrations. Here we report the final results of a study aimed at evaluating the prevalence of NPHPT in a large cohort of blood donors volunteers.

**MATERIAL AND METHODS.** We enrolled 2355 healthy blood donors (1732 males and 625 females; mean age ± SD = 40 + 12 years ). After informed consent was obtained, a blood sample was taken for measuring serum Ca<sup>++</sup> (Nova 8; Nova Biochemical, Waltham, MA), 25(OH)vitamin D and immunoreactive, 1-84, PTH (DiaSorin, LIAISON).

**RESULTS.** There were 216 subjects (9.2 %) with serum PTH levels above normal range, 20 of them also had elevated Ca<sup>++</sup> levels. Among the remaining 196 subjects, 114 volunteered to be studied again after vitamin D supplementation (50,000 UI cholecalciferol weekly for 4 weeks), for the determination of serum ionized and total calcium, phosphorus, 25(OH)vitamin D, 1-84 PTH, anti-transglutaminase antibodies, 24-hour urine calcium and creatinine clearance. In 83 subjects (including two with positive anti-transglutaminase antibodies) PTH normalized after vitamin D supplementation. In 8 of the remaining subjects, hypercalciuria was the only biochemical abnormality found. No other biochemical abnormalities were found in the remaining 23 subjects.

**CONCLUSIONS.** This study demonstrates that in healthy blood donors hypovitaminosis D is the most frequent condition underlying raised serum PTH levels. We showed a 0.97 % prevalence of increased PTH levels (in the setting of normocalcemia) not related to identifiable causes. It is not known at present if NPHPT subjects represent the tail of the Gaussian distribution, if they have an altered set point for PTH and calcium or if they will develop the classical biochemical PHPT.

Disclosures: Salvatore MINISOLA, Dia Sorin, 11  
This study received funding from: DiaSorin

### SU0013

**Bisphosphonates do not affect collagen-bound water in a rat model of estrogen withdrawal.** Mathilde Granke<sup>\*1</sup>, Sasidhar Uppuganti<sup>1</sup>, Julie Schnur<sup>2</sup>, Daniel Perrien<sup>1</sup>, Mark Does<sup>2</sup>, Jeffry Nyman<sup>1</sup>. <sup>1</sup>Vanderbilt University Medical Center, United states, <sup>2</sup>Vanderbilt University, United states

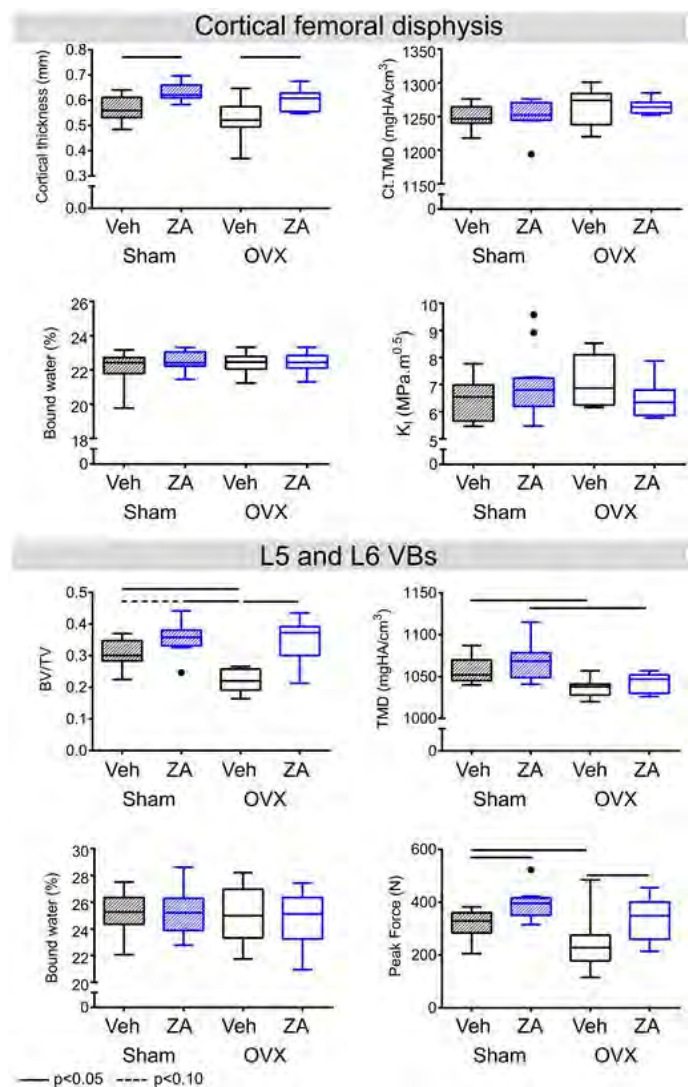
Conferring ductility to the skeletal matrix, collagen-bound water (BW) is a potential clinical surrogate of bone’s ability to resist fracture. BW results from hydrogen bonds between H<sub>2</sub>O and hydroxyl groups (OH) within proteins as well as from electrostatic attraction to surface charges on mineral crystals (Ca<sup>2+</sup>). Since bisphosphonates are hydrophilic molecules with high binding affinity to bone mineral and since estradiol contains OH, we hypothesized that Zoledronic Acid (ZA)

treatment prevents an ovariectomy-related decrease in BW, thereby rescuing impaired mechanical properties of both cortical and trabecular compartments.

Retired Sprague-Dawley breeders underwent ovariectomy (n=22) or sham surgery (n=24) at 6 months of age (Charles River). Four weeks post-surgery, half the rats within each surgery group received a one-time intravenous injection of ZA (0.1 mg/kg body weight) with the other half receiving vehicle saline. Rats were euthanized 16 weeks post injection. Femoral mid-shafts, L5 and L6 VBs were scanned with µCT to obtain tissue mineral density (TMD), cortical structure and trabecular bone volume fraction (BV/TV). Notched femurs and L6 VBs underwent three-point bending and compression testing to determine fracture toughness and strength, respectively. For each rat, a 5-mm segment of the femoral mid-shaft and the L5 VB were analyzed with <sup>1</sup>H NMR to assess BW by characterizing of T2 spectrum obtained from Carr-Purcell-Meiboom-Gill measurements.

As expected, ZA-treatment increased BV/TV (L6), regardless of surgery type, causing the lumbar VBs to sustain a higher peak force during compression (Fig). It did not however rescue the OVX-related decrease in trabecular TMD (Fig). ZA-treatment also increased cortical thickness and normalized the OVX-related increase in porosity of the femur mid-shaft, but it did not affect cortical TMD or fracture toughness for either sham or OVX rats (Fig). For both VB and femur mid-shaft, BW did not change with either OVX surgery or bisphosphonate treatment.

For rats, which experience lower osteonal remodeling than do human bones, neither ovariectomy nor ZA-treatment affected the fracture toughness and bound water of cortical bone. This suggests that estradiol and ZA is not present within extracellular matrix with enough concentration to promote bound water. Being an anti-resorptive, ZA-treatment did rescue the OVX-induced reduction in VB strength by maintaining BV/TV, not by promoting bound water per bone volume.



Fig

Disclosures: Mathilde Granke, None.

## SU0014

**Characterization of High and Low Turnover Bone Disease Associated with Chronic Kidney Disease.** Tepei Ito<sup>\*1</sup>, Megumi Asai<sup>1</sup>, Yuva Kanehira<sup>1</sup>, Mitsuru Yashiro<sup>2</sup>, Tomohiro Sonou<sup>3</sup>, Takashi Shigematsu<sup>3</sup>, Hiroimi Kimura-Suda<sup>1</sup>. <sup>1</sup>Graduate School of Photonics Science, Chitose Institute of Science & Technology, Japan, <sup>2</sup>Division of Nephrology, Department of Internal Medicine, Wakayama Medical University, Japan, <sup>3</sup>Division of Nephrology, Department of Internal Medicine, Wakayama Medical University, Japan

Bone mineral metabolism disorders associated with chronic kidney disease (CKD) can be classified into high and low turnover bone disease. We previously showed that the femur in high turnover disease was characterized by a decrease in the number of trabeculae, mineral-to-matrix ratio, carbonate-to-phosphate ratio, and collagen fiber orientation. However, an increase in hydroxyapatite crystallite orientation has been reported to cause a decrease in bone strength under multiple stresses. In this work, rat femurs in both high and low turnover disease associated with CKD were examined using FTIR and IR dichroism imaging to characterize and compare bone quality between high and low turnover disease. Seven-week-old Sprague-Dawley (SD) rats were randomly divided into 3 groups; a sham operation was performed in one group (Sham), and 5/6 subtotal nephrectomy was performed in the other two groups (H-CKD, L-CKD), with parathyroidectomy also performed in one of the two groups (L-CKD). All rats were fed special diet with controlled P and Ca content. After 18 weeks, rats were sacrificed, and each femur was removed, embedded in PMMA and sectioned (3  $\mu$ m) by microtome along the long axis. The following bone quality indicators were assessed by FTIR imaging and IR dichroism imaging: mineral-to-matrix ratio, carbonate-to-phosphate ratio, mineral crystallinity, mineral maturity, and collagen fiber orientation. H-CKD and L-CKD rats were confirmed to show high and low turnover bone disease, respectively, by biochemical tests. No differences were observed in mineral-to-matrix ratio or mineral crystallinity between the H-CKD and L-CKD rats; however, the carbonate-to-phosphate ratio and mineral maturity in H-CKD rats were significantly decreased compared to those in L-CKD rats. These results indicated that the hydroxyapatite crystals in H-CKD rats were immature. Collagen fibers in the cortical bone in the H-CKD and L-CKD rats were aligned longitudinally, and the degree of collagen fiber orientation was lower in the metaphysis than in the diaphysis. The immature hydroxyapatite crystals were also aligned longitudinally, and the degree of immature hydroxyapatite crystals was lower in the metaphysis than in the diaphysis. However, a reduction in immature hydroxyapatite crystal orientation was particularly apparent in the metaphysis of H-CKD rats; i.e., immature hydroxyapatite crystal orientation in H-CKD rats was less affected by collagen fiber orientation than that in L-CKD rats.

**Disclosures:** Tepei Ito, None.

## SU0015

**Effect of Once-Weekly hPTH(1-34) on Collagen Fiber Orientation in Lumbar Vertebrae of Ovariectomized Monkeys.** Hiroimi Kimura-Suda<sup>\*1</sup>, Tepei Ito<sup>1</sup>, Yuva Kanehira<sup>1</sup>, Megumi Asai<sup>1</sup>, Aya Takakura<sup>2</sup>, Ryoko Takao-Kawabata<sup>2</sup>, Yukihiro Isogai<sup>2</sup>. <sup>1</sup>Chitose Institute of Science & Technology, Japan, <sup>2</sup>Pharmaceutical Research Center, Asahi Kasei Pharma Corporation, Japan

Bone strength arises from both bone mineral density (BMD) and bone quality. The following factors are generally accepted to influence bone quality: rate of turnover, architecture and geometry, mineral and collagen matrix properties, and microdamage accumulation. We demonstrated that the use of human PTH(hPTH) (1-34) as a bone formation agent improved BMD, bone geometry and architecture, and collagen cross-links. We also showed that collagen fiber orientation had a strong influence on bone strength. In this work, we characterized bone quality using Fourier transform infrared (FTIR) imaging with a polarizer to assess the effect of hPTH(1-34) on collagen fiber orientation in the lumbar vertebrae of ovariectomized monkeys administered once-weekly hPTH(1-34). Female cynomolgus monkeys aged 12.0  $\pm$  1.5 years were divided into four groups: one group underwent a sham operation (Sham), and three groups had both ovaries surgically removed 1 week before starting treatment (OVX). Two OVX groups were subcutaneously administered once-weekly hPTH(1-34) for 18 months at 1.2  $\mu$ g/kg (L-PTH) or 6.0  $\mu$ g/kg body weight (H-PTH). The Sham and OVX control groups received subcutaneous injections of 0.1% saline containing bovine serum albumin as a vehicle. The seventh lumbar vertebra was removed after sacrifice, embedded in PMMA, and sagittal sections (3  $\mu$ m) were prepared for FTIR imaging. The mineral/collagen ratio, carbonate/phosphate ratio, and crystallinity were determined using the FTIR images, and collagen fiber orientation was assessed using IR images. The mineral/collagen ratio was reduced in both the trabecular and cortical bone in the OVX control group and L-PTH group, but was improved in the H-PTH group. The L-PTH group showed less calcification than the OVX control group. The carbonate/phosphate ratio in the trabecular bone was slightly increased in the OVX control group and was improved in the H-PTH group. However, there was no difference in crystallinity between the groups. Dorsal-ventral collagen orientation in the trabecular bone was reduced in the OVX control group, but was increased in both PTH groups. These results indicate that collagen fiber orientation in both PTH groups

was improved during bone formation. Bone strength in the PTH groups was improved. In conclusion, improvement in collagen fiber orientation contributes to increased bone strength in the lumbar vertebrae of OVX monkeys administered once-weekly hPTH(1-34).

**Disclosures:** Hiroimi Kimura-Suda, Asahi Kasei Pharma Corporation, 11  
This study received funding from: Asahi Kasei Pharma Corporation

## SU0016

**Effects of BMU and Lamellar Thickness on Single Osteonal-Unit Fatigue Life.** George Pellegrino<sup>\*1</sup>, Max Roman<sup>2</sup>, J. Christopher Fritton<sup>1</sup>. <sup>1</sup>Rutgers University / NJ Medical School / Orthopaedics, United states, <sup>2</sup>NJ Institute of Technology / BME, United states

A remodeling cycle sets the size of the osteon and associated lamellae in the bone multi-cellular unit (BMU). Treatments that affect bone quality act directly on these micro-structural features through the bone cells [1]. Yet, little is known about how micro-structure affects bone's response to dynamic loading. We previously found that fatigue life for canine rib tissue treated 3 years with a high-dose bisphosphonate was decreased and associated with smaller osteon wall thickness [2]. There was no effect on osteon density or porosity. To better understand the possible roles of osteon size, lamellar thickness and number on fatigue life, three finite element models were examined with the eventual goal of simulating the previous experiment: 1) a single osteon with heterogeneous lamellae and inter-lamellae regions, 2) the osteon with cement line, set within interstitial tissue (Figure 1), and 3) a control, homogenous, interstitial-only tissue. Osteon size was incrementally decreased for each model, and variations in lamellar number and relative thickness were explored. In all variations the smaller osteons failed faster for model 1, and the osteon complexes in 2 well outlived the homogenous control. This suggests that as the volume of interstitium increases, the fatigue life of the whole tissue decreases. However, for model 2, fatigue life was dependent on the lamellar features and smaller osteons (and in some cases the whole complex) outlived the larger ones. Thinning of lamellae and thickening of the interlamellar regions provided an increase in fatigue life of the osteon. For the smallest osteons, decreasing lamella / interlamella pair numbers provided the greatest increase in osteon fatigue life. Variations in lamellar and inter-lamellar thickness, and number appear to play a large role in fatigue life and perhaps more so when overall BMU size is limited. Further expansion of this model will allow exploration of the effects of osteon and lamellar structure on whole-bone tissue fatigue, of importance toward understanding the long-term effects of treatments on bone quality and useful life. References: 1) Geissler et al., J Biomech, 2015 2) Bajaj et al., Bone, 2014.

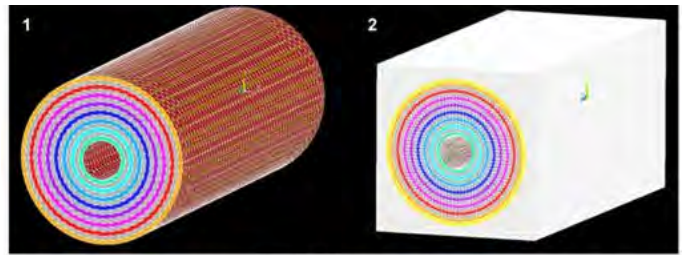


**Figure 1.** Osteon models, 1). Osteon with heterogeneous layers 2). Osteon, with cement line, set in interstitial surround.

Figure 1

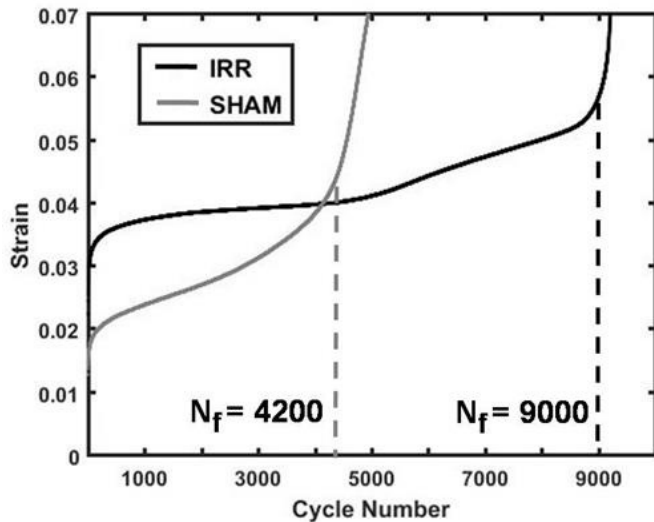
**Disclosures:** George Pellegrino, None.

## SU0017

**Effects of Ionizing Radiation on Ex-Vivo Fatigue Mechanics of Mouse Vertebra.** Megan Pendleton<sup>\*1</sup>, Joshua Alwood<sup>2</sup>, Grace O'Connell<sup>1</sup>, Tony Keaveny<sup>1</sup>. <sup>1</sup>University of California Berkeley, United states, <sup>2</sup>NASA Ames Research Center, United states

Human-occupied expeditions to Mars can only be undertaken if the associated health risks to the astronauts are deemed acceptable. One such risk is exposure to high levels of ionizing radiation. While high levels of ionizing radiation as part of radiotherapy have been shown to increase risk of hip fractures, the underlying mechanisms of possible radiation-induced bone-weakening are not well understood. Our first step in addressing this was to look for changes in the mechanics of the bone. We conducted radiation-exposure pilot experiments to determine if ionizing radiation, delivered at space-relevant doses, can alter the mechanical properties of mouse vertebrae, for repetitive loading *ex-vivo*. We hypothesized that radiation-induced changes to the organic matrix would decrease energy dissipation mechanisms intrinsic to bone and manifest in decreased cycles to failure. After appropriate institutional approval, 17-week old male mice were randomly assigned to be exposed to either <sup>137</sup>Cs  $\gamma$  radiation (2 Gy acute dose) or a sham procedure (n=6 per group). Animals were euthanized 11-days post-irradiation. After euthanasia, the L5 vertebrae were extracted, the endplates planed off, and the resulting specimens were subjected to

uniform compression loading at room temperature in a saline-water bath. Specimens were cyclically loaded with a 2 Hz sinusoidal waveform in force control to approximately 50% of the estimated ultimate load. The tests were stopped at failure identified by a rapid increase in strain per cycle. We found that all specimens exhibited the classical tertiary shape for cyclic loading (Figure). For this pilot study, the trends suggest that irradiation increased the number of cycles to failure (mean  $\pm$  SD: IRR=11,865  $\pm$  8268, SHAM=2,720  $\pm$  3750;  $p=0.07$ ) and decreased the rate of deformation per cycle (IRR=0.013  $\pm$  0.014, SHAM=2.59  $\pm$  3.73;  $p=0.12$ ). However, these are preliminary results and will be used primarily to improve on the original power analysis conducted. The observed trends suggest that irradiation may actually increase the resistance to bone failure under cyclic loading. One possible mechanism includes chain scission of the collagen, which might enable energy to be dissipated in a less detrimental manner than by generating cracks (fatigue) or causing inter-lamellar slip (creep). Ongoing work will increase the number of specimens to confirm these trends and investigate underlying mechanisms.



Irradiated vs. Sham - Strain per Cycle

Disclosures: Megan Pendleton, None.

## SU0018

**Ribitation of Human Cortical Bone decreases Bound water, alters the Secondary structure of Collagen, but does not affect Tissue resistance to Cyclic microindentation.** Sasidhar Uppuganti<sup>1</sup>, Mathilde Granke<sup>1</sup>, Amy Creecy<sup>1</sup>, Shoshana Hodes<sup>2</sup>, Deanna Bradley<sup>1</sup>, Mark Does<sup>1</sup>, Jeffrey Nyman<sup>3</sup>. <sup>1</sup>Vanderbilt University, United states, <sup>2</sup>Lafayette College, United states, <sup>3</sup>Vanderbilt University, VA Tennessee Valley Healthcare System, United states

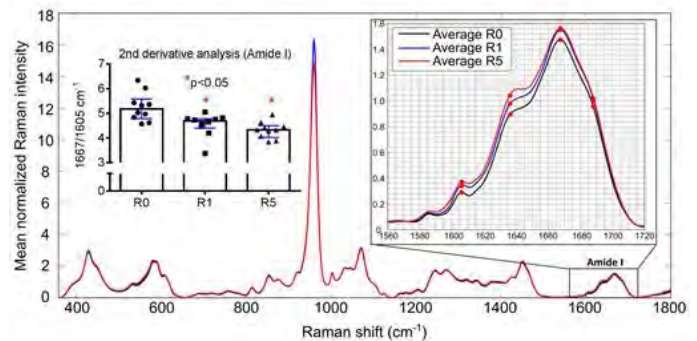
As one reason why fragility fractures occur in non-osteoporotic patients (T-scores  $>$  -1.5), age-related increases in glycation-mediated, non-enzymatic collagen cross-links reduce bone quality through stiffening of the collagen. DXA is insensitive to these advanced glycation end-products (AGEs) within the skeletal matrix. Clinically viable, matrix-sensitive tools such as Raman spectroscopy (RS), magnetic resonance imaging (MRI), and cyclic-reference point microindentation (cRPI) could be sensitive to AGE accumulation and thus provide alternate fracture risk predictors. We hypothesized that the formation of AGEs in collagen would alter the RS spectra of the bone matrix, reduce matrix-bound water fraction (BW), and reduce the resistance of the matrix to microindentation.

Cortical beams were cut from the femoral mid-diaphysis of human cadavers (5F/5M, age=55  $\pm$  4 yr) and machined into 3 samples (~5mmx5mmx2.5 mm) per donor. Paired bone segments were polished and randomly assigned to one of three ribitation groups at 37°C for 4 weeks at neutral pH: phosphate buffered saline (R0), 100 mM (R1), or 500 mM (R5) ribose buffered solution (each with 0.02% Sodium azide to prevent protein degradation). Each sample was then successively analyzed with i) <sup>1</sup>H NMR to determine changes in BW, ii) RS to assess tissue composition, and iii) cRPI to determine tissue-level mechanical properties. High performance liquid chromatography (HPLC) assay was used to quantify pentosidine (PE), an AGE marker.

As designed, ribitation increased PE (R0-R1:  $p=0.041$ ; R0-R5:  $p<0.0001$ ). Accompanying this AGE accumulation was a decrease in BW (R0-R5:  $p=0.011$ ; R1-R5:  $p=0.005$ ). Ribitation did not demineralize the bone nor affect the mineral phase as there were no differences in  $u_2PO_4^{3-}$ /Amide III ( $p=0.135$ ), carbonate substitution ( $p=0.148$ ), or crystallinity ( $p=0.056$ ) among the groups. Using 2<sup>nd</sup> derivative analysis of the Amide I band, we found that 2 shoulders at 1605  $cm^{-1}$  and 1636  $cm^{-1}$  differed between control and ribose incubation (Fig). Intensity ratios of 1667/1605, 1667/1640  $cm^{-1}$  were lower in R5 than in R0 ( $p=0.0004$  and 0.0001, respectively). There were no differences in any cRPI parameters among the 3 groups ( $p=0.076$  for CID R1-R5).

Proton NMR, which underpins clinical MRI, and RS are sensitive to AGE accumulation in human bone. As such, they potentially could be developed to

improve fracture risk assessment through clinical measurements of bound water and the secondary structure of collagen (Amide I).



Ribitation\_Human Cortical Bone\_ASBMR\_Fig.1

Disclosures: Sasidhar Uppuganti, None.

## SU0019

**Differential Response of Trabecular Bone to Unloading in Two Substrains of C57BL/6 Mice.** Jeyantt Srinivas Sankaran<sup>1</sup>, Manasvi Varshney<sup>1</sup>, Alyssa Tuthill<sup>1</sup>, Leah Rae Donahue<sup>2</sup>, Stefan Judex<sup>1</sup>. <sup>1</sup>Stony Brook University, United states, <sup>2</sup>The Jackson Laboratory, United states

Two substrains of C57BL/6 mice, C57BL/6J:B6J and C57BL/6N:B6N, are commonly used as genetic background for knockout (KO) mice to investigate the role of specific genes in modulating musculoskeletal phenotype and response to external stimuli. These two substrains differ by only a small array of subtle allelic differences. To elucidate the role of these small genomic differences, 9 wk old female B6J and B6N mice ( $n=34$ ) were assigned to baseline control (BC), age matched control (AC), and hindlimb unloaded (HLU) groups. Following a 2 wk HLU protocol, trabecular microarchitecture and cellular activity in the femoral metaphysis was measured by microcomputed tomography ( $\mu$ CT), histomorphometry, and histology. At baseline, B6N mice had 21% lower bone volume fraction (BV/TV), 6% lower trabecular number (Tb.N) and 6% trabecular thickness (Tb.Th) when compared to B6J substrain (all  $P<0.05$ ). In spite of less tissue present, mineralizing surface (MS/BS), bone formation rate (BFR/BS), osteoblast surface (Ob.S/BS) and osteoblast number (Ob.N/BS) were 62%, 46%, 35% and 23% greater in B6N than B6J mice (all  $P<0.05$ ). At 11 wks, trabecular micro-architectural differences between B6N and B6J mice persisted but the differences in cellular activity had ceased. The response of the trabecular compartment to unloading was not different between the B6N and B6J substrains when comparing HLU to AC mice. However, compared to BC, HLU B6N had 26% greater trabecular separation (Tb.Sp) whereas HLU B6J mice experienced only 14% greater Tb.Sp (Gene\*HLU,  $P<0.05$ ). Similarly, when compared to BC mice, HLU significantly suppressed trabecular MS/BS (29%), BFR/BS (22%), Ob.N/BS (52%), Ob.S/BS (60%) in B6N mice while there were no significant differences in MS/BS, BFR/BS and Ob.N/BS (and 26% lower Ob.S/BS) between HLU and BC in B6J mice (Gene\*HLU, all  $P<0.05$ ). No differences were observed between substrains when comparing HLU to AC mice. These results demonstrate that the differential response of B6N and B6J substrains to HLU is only apparent longitudinally but not between age-matched controls and HLU mice. This may suggest that the underlying mechanism is based on differences in bone morphology and cellular activity between B6J and B6N mice. Together, this data highlights that even very subtle genomic differences can significantly alter skeletal morphology and adaptation to unloading and that these two substrains cannot be used interchangeably for KO experiments.

Disclosures: Jeyantt Srinivas Sankaran, None.

## SU0020

**The Effects of Botox-induced Muscle Paralysis on Bone Microporosities in Skeletally Mature Rats.** Vittorio Gatti<sup>\*</sup>, Bishoy Ghobryal, Michelle Gelbs, Michael Gerber, Luis Cardoso, Susannah Fritton. City College of New York, United states

It is known that skeletal unloading impairs bone mass balance, increasing bone fragility and potentially leading to osteoporosis. However, the effect of disuse on bone microporosities is still poorly understood. In this work we used an osteopenia model where a transient muscle paralysis was induced by injection of botulinum toxin to investigate the effect of skeletal unloading on bone's microporosities. Sixteen 20-week-old female Sprague-Dawley rats were injected in the right lower-limb muscles with either Botox (Allergan) (BTX,  $n=8$ ) (1 unit in the upper and lower quadriceps, calf, and biceps femoris)

or saline solution (CTRL, n=8) using an IACUC-approved procedure. After injection, gait ability was monitored for 28 days. Four weeks post-injection, quadriceps and calf muscles were excised and weighed to assess muscle atrophy. Right and left tibiae were scanned at 2.1- $\mu$ m resolution using a high-resolution micro-CT system (Skyscan). Trabecular bone microarchitecture (BV/TV, Tb.Th, Tb.N and Tb.Sp) and vascular canal architecture (Ca.Dm, Ca.Sp and Ca.V/TV) were quantified from the proximal tibial metaphysis. In addition, the metaphyseal cortical bone structure (Ct.Th, Ct.Ar and Ct.Ar/B.Ar) was analyzed. BTX injection induced a significant gait disability that was maximal 14 days post-injection, and showed a small but significant improvement 26 days post-injection. The right calf and quadriceps muscle mass showed a ~60% decrease in the BTX-injected rats compared to CTRL. Trabecular bone volume fraction, trabecular thickness and trabecular number were significantly lower in the right tibiae (BTX-injected) compared to the contralateral, uninjected tibiae. However, no significant differences in trabecular bone microarchitecture parameters were observed between the BTX-injected and saline-injected CTRL in the proximal tibia metaphysis. Vascular canal separation was significantly reduced in the BTX-injected rats compared to CTRL, while no significant changes were observed for other vascular porosity parameters. Finally, the metaphysis cortical thickness, cortical area and cortical area fraction were significantly lower in BTX compared to CTRL. These results demonstrate that Botox-induced muscle paralysis affects the cortex structure and spacing of cortical vascular canals in the rat proximal tibia four weeks post-injection. Future studies will investigate earlier time points to further assess the effects of disuse and muscle atrophy on bone's microporosities.

**Disclosures:** Vittorio Gatti, None.

## SU0021

**Computational Model Development of Spaceflight Bone Physiology.** James Pennline\*<sup>1</sup>, Christopher Werner<sup>2</sup>, Beth Lewandowski<sup>1</sup>, Angelo Licata<sup>3</sup>. <sup>1</sup>NASA Glenn Research Center, United states, <sup>2</sup>ZIN Technologies, Inc., United states, <sup>3</sup>Cleveland Clinic, United states

**Purpose:** Current spaceflight exercise countermeasures don't completely eliminate bone loss and thereby places astronauts at greater risk of fracture later in life. To address this concern, we are working with NASA's bone discipline to develop a validated computational model to understand and estimate changes in volumetric bone mineral density (vBMD) in response to spaceflight unloading and in-flight and post flight exercise countermeasures.

**Methods:** The model is constructed by a mathematical formulation of the rate of formation minus the rate of resorption at the bone remodeling unit level in the femoral neck. It includes the removal and replacement of structural units in both cortical and trabecular bone and the cellular dynamics of the RANK, RANKL and OPG pathway. Frost's mechanostat theory is used to model the effect of strain stimulus from skeletal loading. A sensing level is defined proportional to the expression of NO and PGE<sub>2</sub> that weights the level of cellular response to mechanical stimulus to determine if it is sufficient for maintaining mass or bone health. For calculation of stresses and strains from mechanical loading a finite element model of the proximal femur is integrated with the model.

**Results:** A preliminary test of the validity of the model was conducted using the fact that the mature healthy adult takes between 5000 to 10000 steps at an average walking speed of 5km/h and has a body weight between 565 and 791 N. Results showed that the model predicts little to no change from initial vBMD after one year of loading from 5000 and 10000 steps for lowest and highest weight individuals. Additional validation testing was done using bed rest data and post flight astronaut data. QCT data from 16 control subjects of a 90 day bed rest study and DXA data from 15 control subjects of a 120 day bed rest study were used. The model prediction results of the average BMD loss of the control subjects are close to or within the standard deviation of the experimental data, but not always within the standard error of the experimental data. The model's predictive ability was also tested with post flight data from 16 crew members who had been on a 4 to 6 month spaceflight. Literature data was used that suggests that astronauts, being highly active, engage in activity equivalent to 12,500 to 18000 steps. A simulation of average vBMD change during one year of post flight with a daily load equivalent of 12,500 steps per day of a 1g walking load or a daily load equivalent of 18,000 steps, resulted in predictions of BMD recovery that were within the standard error of the experimental change in vBMD.

**Conclusions:** Results of the testing suggest that the model forms a good basis for predicting averaged individual changes in vBMD based on bed rest and flight data. It may be used as a tool for testing the benefit of an exercise prescription given future enhancements and development to the full proximal femur.

**Disclosures:** James Pennline, None.

## SU0022

**Contribution of mineral characteristics to the tissue level material properties in Lrp5 mutant mouse models.** Sabah Nobakhti\*<sup>1</sup>, Sandra Shefelbine<sup>2</sup>, Sandip Basu<sup>3</sup>. <sup>1</sup>Department of Mechanical & Industrial Engineering, Northeastern University, United states, <sup>2</sup>Department of Mechanical & Industrial Engineering, Department of Bioengineering, Northeastern University, United states, <sup>3</sup>Brucker Nano Surfaces Division, United states

**Introduction:** Lrp5 plays a critical role in Wnt signaling in bone by affecting bone mass. It has been shown that Lrp5 knock-out homozygous and heterozygous mutations have decreased bone mass [1]. Also, heterozygous point mutation in Lrp5

gene at amino acid 214 (a214v) containing a neomycin-resistance cassette (neo) has comparable bone mass to their control group while the point mutation without the cassette has increased bone mass [2].

In this study, we examine the effects of Lrp5 mutations (knock-out  $-/-$ , heterozygous  $+/-$ , and heterozygous point mutation  $214v/+$  neo) on the mineral density, mineral size, mineral/matrix composition, and tissue material properties. We hypothesize that Lrp5 mutations not only affect the bone mass, but also alter the bone tissue properties.

**Method:** Lrp5  $-/-$ , Lrp5  $+/-$  and Lrp5  $214v/+$  neo (8w age, M and F) mutations bred on a mixed C57BL/6 background were studied and compared to a C57BL/6 (10w age, F) control.

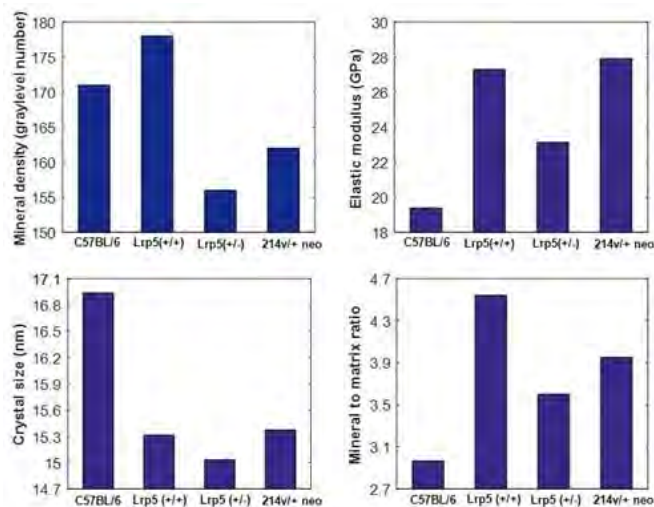
To measure tissue modulus, nanoindentation was performed in a constant strain-rate dynamic mode with 75-100 distinct indentations points on each tibia sample (Berkovich tip, grid spacing 10 micron, NanoForce, Bruker, US). Tibiae were then carbon coated and used for qBSE imaging (Evo, Ziess, Germany) calibrated by standards [3]. Humeri of the same animals were used for X-ray diffraction (Rigaku RAPID II, Rigaku Americas Corp, US) performed in a transmission mode with  $\lambda = 1.5418\text{\AA}$  and thermal gravimetric analysis (Q50, TA Instruments, US) conducted at 10°C/min under air flow from ~ 25°C to 900°C.

**Results and Discussion:** Our results demonstrate that Lrp5 mutations affect the bone tissue properties. Previous studies showed that Lrp5  $-/-$  and Lrp5  $+/-$  both had lower bone mass compared to control [1]. However, we show at the tissue level mineral density was higher in Lrp5  $-/-$  than in controls and lower in Lrp5  $+/-$  than controls (Fig. 1). The Lrp5  $214v/+$  neo showed no differences in bone mass [2], but the mineral density was lower compared to controls. Interestingly, regardless of changes in the overall bone mass and mineral density, Lrp5 mutations had decreased crystal size, increased tissue elastic modulus and increased mineral to matrix ratio in all the phenotypes. As a result, characterizing tissue level changes in bone is critical for understanding the full effects of mutations affecting bone mass.

[1] Holmen, S., et al., JBMR, 2004.

[2] Cui, Y., et al., Nature medicine, 2011.

[3] Roschger, P., et al., Bone, 1998.



Bone tissue properties measured for Lrp5 mutations and C57BL/6 control.

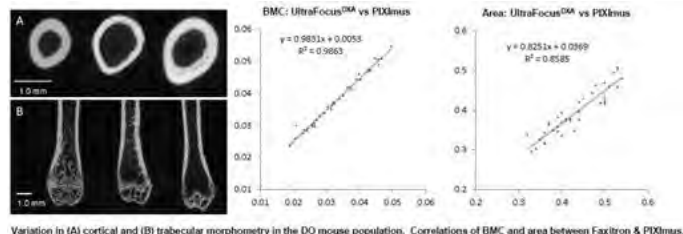
**Disclosures:** Sabah Nobakhti, None.

## SU0023

**Correlation of DXA Measured on Isolated Femurs by Faxitron and PIXImus Densitometry versus Ashing and MicroCT.** Douglas Adams\*<sup>1</sup>, Jeffrey Nyman<sup>2</sup>, Dana Godfrey<sup>3</sup>, Renata Rydzik<sup>1</sup>, Svetlana Lublinsky<sup>1</sup>, David Rowe<sup>1</sup>, Cheryl Ackert-Bicknell<sup>3</sup>. <sup>1</sup>University of Connecticut Health, United states, <sup>2</sup>Vanderbilt University Medical Center, United states, <sup>3</sup>University of Rochester, United states

Dual-energy X-ray absorptiometry (DXA) provides a valuable noninvasive tool in clinical care for diagnosis and monitoring of osteoporosis and skeletal health. Bone mineral density (BMD) as measured by DXA is a two-dimensional quantitative measurement of bone mass, defined by quantifying total bone mineral content (BMC) via calibrated X-ray attenuation and dividing BMC by the projected skeletal silhouette area. Pre-clinical studies in rodents have long used a DXA system affording ~180  $\mu$ m spatial resolution (PIXImus II, GE Lunar). This system is no longer manufactured, prompting suppliers of rodent digital X-ray imaging systems to develop and offer DXA capability. These new systems have higher spatial resolution (~50  $\mu$ m) and potential improvement in accuracy and precision. This study compared DXA measurements by the PIXImus II to the UltraFocus<sup>DXA</sup> (Faxitron Bioptics). Isolated femurs from 435 Diversity Outcross (DO) mice were imaged by 3D microCT (Scanco  $\mu$ CT40) and DXA (PIXImus II). These DO mice demonstrated a tremendous breadth of femoral morphometry and tissue mineral density via  $\mu$ CT, as well as BMD by DXA (Figure). Using these data, 40 femurs were selected spanning the range of BMD. After blind

coding and a 2<sup>nd</sup> DXA scan by PIXImus, two independent DXA scans were performed using the UltraFocus<sup>DXA</sup>. A 3<sup>rd</sup> PIXImus scan was performed and each femur was ashed at 600°C. BMC obtained by Faxitron (F) or PIXImus (P) correlated to each other and to ash (A) weight (Figure: F vs P R<sup>2</sup> = 0.986; F vs A R<sup>2</sup> = 0.990; P vs A R<sup>2</sup> = 0.989). Areal BMD (R<sup>2</sup> = 0.83, slope = 1.006) and projected area (R<sup>2</sup> = 0.86, slope = 0.825) also correlated between the two DXA instruments. Repeated measurements using Faxitron demonstrated highest precision in BMC (R<sup>2</sup> = 0.995) followed by area (R<sup>2</sup> = 0.967) and BMD (R<sup>2</sup> = 0.910). PIXImus reproducibility was similar. Volumetric BMD (ash weight divided by μCT femur volume) did not correlate with areal BMD (R<sup>2</sup> = 0.05), despite reasonable correlation of volume to projected area (R<sup>2</sup> = 0.65). Further improvements in rodent DXA imaging systems afforded by higher resolution detectors may provide increased fidelity in BMD via refinement in accuracy of projected area, in particular, as well as in BMC. It will be important to test each system offering DXA capability against established benchmarks to assure accuracy and precision of BMD and body composition (not measured here) prior to embarking on large pre-clinical studies.



(A) cortical and (B) trabecular morphometry in DO femora. Correlation of DXA measurements.

Disclosures: Douglas Adams, None.

SU0024

**Determination of Osteocyte Lacunar Strains using Confocal Microscopy and Finite Element Modeling.** Pravraj Kola, Mark T. Begonia, Leann Tiede-Lewis, Sarah Dallas, Mark L. Johnson, Ganesh Thiagarajan\*. University of Missouri Kansas City, United states

The mechanism by which osteocytes convert mechanical load into biological signals is not fully understood. We have shown that osteocytes in the mouse ulna subjected to axial loading show heterogeneous activation of β-catenin signaling. To determine if this variable activation corresponds to a minimum local strain threshold required to initiate osteocyte responses we have developed 2-D and 3-D finite element (FE) models to examine the strain distributions in/around osteocyte lacunae. We analyzed how variations in perilacunar and bone matrix modulus as well as osteocyte position and orientation within the bone relative to the direction of applied load affected strains around osteocytes.

The 2-D model was created in FEBio Software Suite based on idealized structures, while the 3-D model was developed by importing confocal image stacks of cortical osteocytes from transverse sections of a 5mo female mouse femur into Mimics® Innovation Suite. The 3-D model contained 17 osteocytes of various sizes. Strains were analyzed in the three subregions - cell body, bone fluid space, and perilacunar region. Strain ratios were calculated to compare the maximum strains in the subregions to the global strain in the surrounding bone. Variations in elastic modulus between bone, the lacunar fluid and cell body were also tested.

In the 2-D model, the strain ratios decreased by ~15% as the perilacunar modulus increased from 5 GPa to 20 GPa. Lacunae oriented horizontally and diagonally with respect to the load experienced a strain magnification of ~10x to ~6x respectively - while lacunae oriented vertically had a strain magnification of only ~2x. The maximum strains in all three subregions increased with their proximity to the applied load. Lacunar strains in the 3-D model (in which most of the lacunae were oriented almost vertically) had a strain magnification of 2-3x and were 28-57% lower in the osteocytes positioned farthest from the applied loading compared to those near the load. Our 3-D model, based on empirical data, is a more realistic representation of the osteocyte structure and arrangement in bone, and therefore produces a better FE prediction of the strains experienced by the osteocyte. Together these findings indicate that the strain response not only depends on the alignment of the osteocyte, but also the osteocyte location. Our findings also suggest that lacunar orientation with respect to the load may contribute to the heterogeneity in the biological response.

Disclosures: Ganesh Thiagarajan, None.

SU0025

**Global Phosphorylation of Human Osteopontin.** Grazyna Sroga\*, Deepak Vashishth. Rensselaer Polytechnic Institute, United states

Current studies of protein phosphorylation focus primarily on the importance of specific phosphoproteins and the landscapes of their phosphorylation in regulation of different cellular functions. Mass spectrometry (MS) has become the technique of choice to identify phosphorylated residues within such proteins. However, global changes in protein phosphorylation measured “in bulk” are equally important. For example, correct global phosphorylation of different bone matrix proteins is critical to healthy tissue

biomineralization. Osteopontin, bone sialoprotein, and bone acidic glycoprotein-75 are the key acidic phosphoproteins present in the mineralized phase of bone matrix and are generally restricted in their distribution to calcified tissues [1]. The goal of our current research is to determine to what degree the levels of global phosphorylation of osteopontin (OPN) contribute to the measured global phosphorylation of all bone matrix proteins.

Tibias from 31 healthy donors (17 females and 14 males) served as the source of cortical bone. Extracellular bone matrix proteins were isolated as described by Sroga et al [2]. Measurement of total phosphorylation of extracellular bone matrix proteins was performed according to Sroga and Vashishth [3]. Levels of OPN were determined using enzyme-linked immunosorbent assay (ELISA).

We established that the level of global protein phosphorylation in human posterior cortex bone was inversely related to the age (p<0.001, R<sup>2</sup> = 0.46) and was on average about 1.5-fold lower in the tenth than in the third decade of human life. The amount of OPN in bone matrix did not show a pronounced change over a human life-time. However, the levels of global bone matrix phosphorylation determined “in bulk” appeared to be influenced by the phosphorylation and the content of OPN in bone.

To our knowledge, this is the first study on the relationship between the levels of global bone matrix phosphorylation and phosphorylation of OPN in humans.

[1] Gorski, Calcif Tissue Int. (1992) 50(5), 391-396  
 [2] Sroga et al, PLoS One (2015) 10(1): e0117046.doi:10.1371/journal.pone.0117046  
 [3] Sroga and Vashishth, Analytical Biochemistry (2016) 499, 85-89

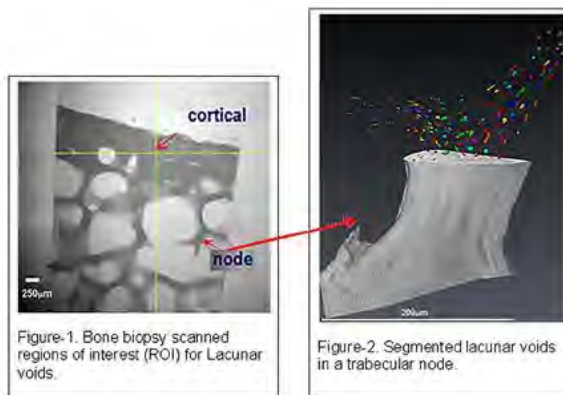
Acknowledgement: NIH grants R01AR49635 and NSF 1363526 (Vashishth).

Disclosures: Grazyna Sroga, None.

SU0026

**Lacunar Void Properties in Bone Tissue from Women Treated With Alendronate.** Mohammed Akhter\*, Brad Hugenroth, Robert Recker. Creighton University, United states

Osteoporotic (low-trauma) fractures are a significant public health problem. For women, up to 50% of those over 50 yrs of age are at high risk of osteoporotic fracture. Along with other measures of bone quality, osteocyte lacunar properties may also influence bone strength. Measurements of lacunar properties would benefit from the use of a 3D imaging technique that evaluates them in situ in bone biopsy specimens. Using this technology, we used previously prepared human transiliac bone specimens to examine the relationship between alendronate treatment and osteocyte lacunar properties (volume (μm<sup>3</sup>), surface area (μm<sup>2</sup>)). This project used the MicroXCT-200 (Carl Zeiss) system to quantify osteocyte lacunar properties in transiliac bone biopsy specimens from post-menopausal women who were treated with alendronate (10mg daily for 2yrs; n=8; age 66 ± 4yrs) and separate non-treated (control) postmenopausal women (n=8; age 67 ± 3 yrs) to understand the treatment-related effects on osteocyte lacunar void properties. Each specimen was prepared with a maximum thickness of 0.5mm for optimal image quality. Two cortical [Cort] and trabecular [Trab] sites (2 nodal regions) were selected for 0.6mm pixel resolution (PR) scanning (Figure-1). The field of view (FOV) was 0.6mmx0.6mm (1000x1000 pixels). Avizo (FEI) software was used to segment the lacunar voids. Using the one-way ANOVA (SPSS), the treatment and site (cortical vs trabecular) related differences were analyzed. Greater than 4000 segmented lacunar voids were analyzed within each group of biopsies (Figure-2). The lacunar void volume and surface area were either smaller (Cort) or showed declining trends (Trab) in the alendronate treated group (Table 1). Furthermore, lacunar volume was significantly lower in trabecular (nodes) than in cortical bone tissue independent of treatment (Table 1). Additional work is needed to confirm if variation in lacunar void size and other properties have any influence on bone quality/strength of bone tissue.



	Cort-Vol (μm <sup>3</sup> )	Cort-Surf-Area (μm <sup>2</sup> )	Trab-Vol (μm <sup>3</sup> )	Trab-Surf-Area (μm <sup>2</sup> )
Post-menopausal (control)	230 ± 11 <sup>ns</sup>	258 ± 6	184 ± 6 <sup>c</sup>	278 ± 6 <sup>b</sup>
Alendronate	213 ± 7 <sup>c</sup>	245 ± 5	166 ± 6	258 ± 7

Means ± Sem, Vol-Volume, Surf-Surface, \* P<0.05 due to treatment, <sup>b</sup> P<0.1 due to treatment, <sup>c</sup> P<0.05 due to site (Cort vs. Trab)

Figures 1, 2, and Table

Disclosures: Mohammed Akhter, None.

## SU0027

**Relationship Between Oxidative Stress And Trabecular Bone Microstructure In Osteoporotic Patients.** Mercè Giner<sup>\*1</sup>, Cristina Miranda<sup>2</sup>, M Jose Montoya<sup>3</sup>, Sergio Portal<sup>4</sup>, M Angeles Vazquez<sup>3</sup>, M Jose Miranda<sup>2</sup>, Pedro Esbrit<sup>4</sup>, Ramon Perez-Cano<sup>1</sup>. <sup>1</sup>HUV Macarena/ University of Seville, Spain, <sup>2</sup>HUV Macarena, Spain, <sup>3</sup>University of Seville, Spain, <sup>4</sup>IVSF Jimenez Diaz, Spain

Experimental studies have suggested that oxidative stress is an important factor in the regulation of bone remodeling. Thus, low antioxidant levels are associated with a reduced bone mineral density and increased risk of osteoporotic fracture. Whether oxidative stress is related to fracture risk is poorly understood

M&M: Cross-sectional study in 21 subjects divided into 3 groups: 7 osteoporotic hip fracture (age: 75 ± 5) (OP); 8 osteoarthritis, undergoing hip replacement, (71 ± 4) (OA) and 6 OA ≤ 55 years old.

We carried out total hip and femoral neck BMD (DXA-Hologic Discovery), microstructural and biomechanical characteristics of trabecular bone from femoral head (Micro-CT-Scan Sky 1172). In macerated trabecular bone, we quantified gene expression of catalase, GADD45 (oxidative stress genes), Runx2 and osteoprotegerin (OPG) by qPCR.

The results are statistically analyzed with the Kruskal-Wallis and Dunn's post-hoc and correlations by Pearson coefficient (SPSS 22.0), p ≤ 0.05.

RESULTS: Osteoporotic subjects have an increased expression of catalase and GADD45, suggesting increased oxidative stress in osteoporotic trabecular bone regardless of age and sex.

We also observed a significant increase in the expression of Runx2 and OPG in OP group.

As expected, BMD values are lower in OP subjects and they have a worse biomechanical and microstructure trabecular bone.

CONCLUSION: These results suggest that osteoporotic patients have an increase of the oxidative stress and bone activity with alterations in the osteogenic genes.

Disclosures: Mercè Giner, None.

## SU0028

**Sex-specific Cellular Differences in Mouse Bone with Moderate Iron Elevations Leads to Differences in Mechanical Properties.** Rihana Bokhari<sup>\*1</sup>, Corinne Metzger<sup>1</sup>, Matthew Allen<sup>2</sup>, Scott Lenfest<sup>1</sup>, Jennifer Kosniowski<sup>1</sup>, Derek Seidel<sup>1</sup>, Harry Hogan<sup>1</sup>, Nancy Turner<sup>1</sup>, Sara Zwart<sup>1</sup>, Susan Bloomfield<sup>1</sup>. <sup>1</sup>Texas A&M University, United states, <sup>2</sup>Indiana University, United states

Moderate elevations in iron stores accelerate loss of BMD in middle-aged men and women over 3 years, but are associated with elevated vertebral fracture incidence in women only (Kim *et al.* JBMR, 2012). To further explore potential sex differences in the response to elevated iron stores and test directly for mechanical properties to follow up the aforementioned study's findings, we tested whether increasing iron stores would lead to bone loss. Male and female C57BL/6 mice (n=21 male and n=25 female; age 16 wks) were fed AIN93-G purified diet with normal (45 mg FE/kg, CC) or high (650 mg FE/kg, FE) iron content. After 8 wks on the diet, liver iron in the FE mice was approximately 28% higher than in CC. Males and females receiving the FE diet had 38% and 33% respectively greater distal femur cancellous BV/TV than control mice (p < 0.001; by SkyScan µ-CT). Males but not females had greater trabecular number, and trabecular thickness (p < 0.001). Bone mineral density was 7% and 4% higher in male and female FE groups, respectively, compared to CC (In vivo PIXImus, GE Lunar Prodigy). Ultimate load and stiffness at mid-femur (by 3-point bending) were 17% and 25% higher, respectively, in male FE mice, but no changes were observed in female mice on the high iron diet (p < 0.01). Ultimate load at the femoral neck (axial loading at the femoral head) was 34% higher in male FE mice, but no changes were observed for female mice on FE diet, nor for stiffness in either sex (p < 0.05). Cortical bone formation rate did not differ between males and females with elevated iron. Serum measures of C-terminal telopeptides (CTX) of type 1 collagen was 10% greater in FE females (p < 0.05) with no change in FE males, while N-terminal propeptide of type 1 procollagen (PINP) was 15% greater in FE males (p < 0.05) but not females. These data indicate that, although bone volume and density were higher in both sexes following iron treatment, systemic changes in resorption/formation are different. This suggests sex-specific differences exist at the cellular level in response to elevated dietary iron, which may contribute to enhancement of structural mechanical properties only in males.

Support from NASA via Space Biology Grant NNX13AL25G is gratefully acknowledged.

Disclosures: Rihana Bokhari, None.

## SU0029

**Spinal Loading Estimates from a Detailed Musculoskeletal Model of the Thoracolumbar Spine Explains the High Incidence of Vertebral Fractures at the Thoracolumbar Region.** Katelyn Burkhart<sup>\*1</sup>, Alexander Bruno<sup>1</sup>, Brett Allaire<sup>2</sup>, Hossein Mokhtarzadeh<sup>3</sup>, Dennis Anderson<sup>3</sup>, Mary Bouxsein<sup>4</sup>. <sup>1</sup>Harvard-MIT Division of Health Sciences & Technology; Center for Advanced Orthopaedic Studies, Beth Israel Deaconess Medical Center, United states, <sup>2</sup>Center for Advanced Orthopaedic Studies, Beth Israel Deaconess Medical Center, United states, <sup>3</sup>Center for Advanced Orthopaedic Studies, Beth Israel Deaconess Medical Center; Department of Orthopedic Surgery, Harvard Medical School, United states, <sup>4</sup>Harvard-MIT Division of Health Sciences & Technology; Center for Advanced Orthopaedic Studies, Beth Israel Deaconess Medical Center; Department of Orthopedic Surgery, Harvard Medical School, United states

Vertebral fractures (VFX) are the most common osteoporosis-related fracture and represent half of the 1.5 million fractures that occur in the US each year. VFX occur most frequently in the mid-thoracic and thoracolumbar spine regions, but the reasons for this site-specific occurrence of fracture are not understood. We hypothesize that increased spinal loading in these regions leads to VFX. Until recently no methods existed to estimate loading at all regions of the spine, and thus no prior studies have explored how thoracic and lumbar spine loading vary with everyday activities or with spinal curvature. Thus, our study's objective was to describe how vertebral compressive loads and factor-of-risk (FOR) vary along the spine for different activities and varying thoracic kyphosis. To accomplish this, we used a validated musculoskeletal model of the thoracolumbar spine to estimate vertebral loading. We created this model, including 552 muscle fascicles, individual thoracic and lumbar vertebrae, sacrum, pelvis, individual ribs and sternum, a lumped head and neck, and upper extremities using OpenSim software (Bruno *et al.* 2015). Muscle morphology and body size were adjusted to that of older women using previously published data (Anderson *et al.* 2012). To determine the influence of spinal curvature on loading, thoracic kyphosis was varied (26°, 50°, and 74°). We simulated different activities, including standing, opening a window, axial twist with weights, and pushing a shopping cart. Average compressive strength for vertebrae between T6 and L5 was estimated using integral volumetric BMD and vertebral cross-sectional area measured from quantitative computed tomography (QCT) scans in 276 women (aged 40 to 80) from the Framingham Heart Study QCT cohort. FOR at each spinal level was defined as vertebral load/strength, with higher values indicating increased risk of VFX. We found that activities showed a local peak in vertebral compressive loading between T11 and L1, but did not show a peak in the mid-thoracic spine (Fig 1a). Larger thoracic kyphosis further increased the T11-L1 loading peak. FOR was highest between T11 and L1 (Fig 1b), indicating the highest risk of fracture in this region. In sum, vertebral loading estimates from this realistic thoracolumbar spine model explain, for the first time, the high incidence of VFX at the thoracolumbar region. Further, our model shows that greater thoracic kyphosis leads to slightly increased spinal loads and risk of VFX.

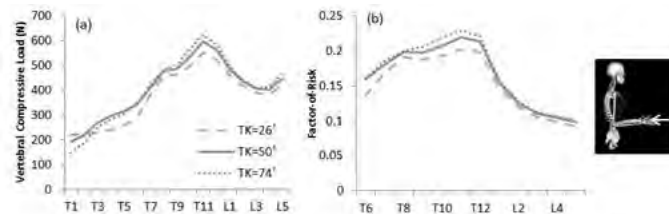


Figure 1. Vertebral compressive loading on T1 through L5 (a) and factor-of-risk for vertebral fracture (b) for pushing a shopping cart (standing with elbows flexed 90°, resisting 5 kg of force in each hand) with varying thoracic kyphosis (TK).

Figure 1

Disclosures: Katelyn Burkhart, None.

## SU0030

**Exogenous Hedgehog Signal Inhibition Impairs Fracture Healing.** Clayton Maschhoff<sup>\*1</sup>, Xiaochen Liu<sup>1</sup>, Jennifer McKenzie<sup>1</sup>, Matthew Silva<sup>1</sup>, Michael Gardner<sup>2</sup>. <sup>1</sup>Washington University in St. Louis School of Medicine, United states, <sup>2</sup>Stanford University Medical Center, United states

Hh signaling is activated during bone healing and recent studies indicate it may be crucial to this process. Attenuation of Hh signaling using transgenic mice reduces bone matrix deposition during fracture healing. However, it is not known if pharmacological modulation of the Hh pathway can affect fracture healing. We hypothesized that Hh pathway inhibition using the Hh antagonist GDC-0449 reduces Hh signaling and delays fracture healing in young mice. We used three-point bending to create a mid-diaphyseal femur fracture in 10-wk old female C57Bl/6 WT mice and in transgenic Hh reporter mice (Gli1-Cre-Ert2;Ai14). Mice were administered either GDC-0449 (50 mg/kg) or vehicle, orally, 2x/day. At designated time points ranging

from 3-21 days, the fractured femurs were harvested and processed for gene expression, microCT, histology, or torsion testing. This study was approved by our institutional animal care committee. Fluorescent histology from Gli1 reporter mice demonstrated reduced Gli1 signaling with GDC-0449 treatment (n=1/grp). Similarly, preliminary gene expression results showed that Hh signaling in bone was downregulated in the GDC-0449 treated group when compared to the vehicle group. Gli1 and Pth1 were reduced 97 and 86%, respectively, at day 7, while the bone formation marker Ibsp was reduced 90% at days 7 and 10 after GDC-0449 treatment (n=1-4/grp). Radiographs showed a delay in early callus formation with GDC-0449 treatment (Fig 1, n=8-15/grp). MicroCT analysis showed that GDC-0449 treatment reduced callus bone mineral density (BMD) at day 14 (-18%; p<0.05) but increased callus BMD at day 21 (+31%; p<0.01) (n=12-14/grp). Callus volume did not differ with treatment at either timepoint. Histology images showed delayed callus formation and healing with GDC-0449 treatment (n=2-6/grp). Torsion testing at day 14 revealed that GDC-0449 treated mice tended to twist without fracture, indicating non-union. On the other hand, by day 21 peak torque of the GDC-0449 treated mice was marginally higher than in the vehicle group (n=2-8/grp). These results support our hypothesis that pharmacologic manipulation of the Hh pathway can diminish Hh signaling and delay fracture healing. Reductions in Hh signaling have the strongest effect on early callus mineralization, but may lead to a "rebound" effect with enhanced bone formation after day 14. This study furthers our understanding of when (and where) Hh signaling is critical during the healing process.

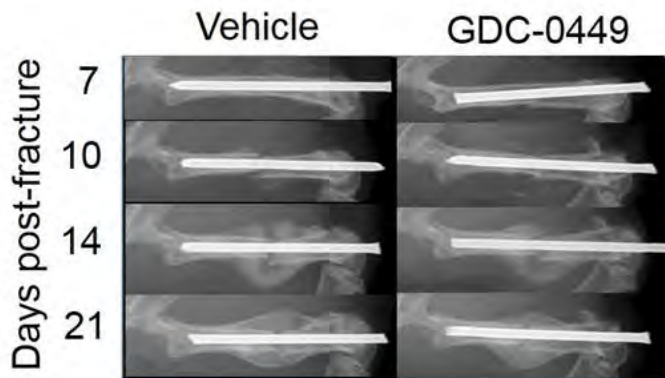


Figure 1. Hh inhibition with GDC-0449 impairs callus healing

**Disclosures:** Clayton Maschhoff, None.  
This study received funding from: OREF

## SU0031

**Childhood Cancer Survivors (CCS) are at High Risk of Reduced Bone Mass during Bone Mass Accrual.** NATASCIA DI IORGI<sup>1</sup>, VERA MORSELLINO<sup>2</sup>, ANNALISA GALLIZIA<sup>1</sup>, FEDERICA CERONI<sup>3</sup>, ANGELA PISTORIO<sup>4</sup>, RICCARDO HAUPT<sup>4</sup>, MOHAMAD MAGHNI<sup>1</sup>. <sup>1</sup>University of Genova, Department of Clinical & Experimental Endocrinology, Giannina Gaslini Hospital, Italy, <sup>2</sup>Department of Hematology, Oncology & Bone Marrow Transplantation, Giannina Gaslini Hospital, Italy, <sup>3</sup>Great Ormond Street Hospital, Pediatric & Neonatal Surgery Department, London, United Kingdom, <sup>4</sup>Epidemiology, Biostatistics & Committees Unit, Giannina Gaslini Institute, Italy

**Purpose:** Childhood cancer survivors (CCS) are at risk for low bone mineral density (BMD). Aim of our study was to evaluate the prevalence of low BMD and its determinants in a single-center cohort of CCS.

**Methods:** One-hundred-eighty-seven CCS (103M, 84F) diagnosed with liquid-LT- (n=48), solid-ST- (n=88) and brain tumor-BT- (n=51) at the age of 5.3±3.2 yrs underwent height, BMI (SDS), Tanner staging and DXA scan for total body-TB and spine-L1-L4 BMD (gr/cm<sup>2</sup>, Z-score), BMC (gr) and for TB fat mass (FM, Kg) and free fat mass (FFM, Kg). The more representative diagnosis were ALL (n=34), NB/GNB (n=24), Wilms-T (n=16), NHL (n=12), HL (n=12), RMS (n=10), Ewing-T (n=6), embryonal-T (n=20), germinal-T (n=9), tumors of the sellar region (n=6) and astrocytic-T (n=6). Endocrine defects were found in n=9 LT, n=16 ST and n=50 BT; 48/51BT underwent CRT (mean total dose 5397.5±1426.1 cGy).

**Results:** Patients were evaluated 6.8±3.3 yrs after off-therapy at the age of 13.0±2.0 yrs. LT were significantly younger than BT (12.9±1.8 vs 13.7±1.7 yrs, P<0.05) and BT shorter than ST (-0.60±1.26 vs 0.24±1.37 SDS, P<0.001); the 3 categories did not differ for Tanner stage nor for BMI SDS (range 1.34-LT to 1.57-BT). BT presented a lower TBBMD (-0.61±0.89) and L1-L4BMD Z-scores (-0.74±1.14) compared to ST and LT (P's<0.01). A TBBMD Z-score <-2 and between -2 and -1 was found in 4.8% (7.8%-BT, 6.5%-LT and 2.2%-ST) and 14% (23.5%-BT, 6.2%- LT and 12.6%- ST) of CCS, respectively; a L1-L4BMD Z-score <-2 and between -2 and -1 in 7% (13.7%-BT, 6.5%-LT and 3.4%-ST) and 15.6% (19.6%- BT, 16.7%-LT and 12.6%-ST), respectively. TBBMD Z-score was directly associated to FFM in all groups (r's=0.51, P's<0.05) to FM in ST and LT (r=0.44 and 0.30, respectively, P's<0.05) and inversely to RT dose in BT (r=-0.30, P=0.037); hormone

defects were inversely related to L1-L4 and TBBMDZ-scores in LT and ST, but not in BT. Multiple regression analyses showed that L1-L4BMD Z-score was independently and inversely predicted by age at evaluation and hormone defects and directly by FFM and FM after correction for Tanner stage and height SDS (R<sup>2</sup>0.33, P<0.0001), while TBBMDZ-score by all the previous parameters, except for Tanner stage (R<sup>2</sup>0.50, P<0.0001).

**Conclusion:** Up to 14% of BT CCS and 6.5% of LT CCS present a low bone mass at the age of 13 yrs, 7 yrs after off-therapy. Older age, hormone defects and CRT are negative predictors of low BMD.

**Disclosures:** NATASCIA DI IORGI, None.

## SU0032

**Tmem178 deficiency aggravates macrophage activation syndrome by promoting M1 macrophage polarization.** Sahil Mahajan<sup>1</sup>, Corinne Decker<sup>1</sup>, Elizabeth Mellins<sup>2</sup>, Roberta Faccio<sup>1</sup>. <sup>1</sup>Department of Orthopaedic Surgery, Washington University, United states, <sup>2</sup>Department of Pediatrics, Stanford University, United states

Dysregulation of innate immune cells occurs in systemic Juvenile Idiopathic Arthritis (sJIA). In addition, excessive inflammatory cytokine production and accumulation of hemophagocytic macrophages is observed in a severe, potentially lethal, complication of sJIA, termed macrophage activation syndrome (MAS). Currently there are no biomarkers to identify sJIA patients at high risk of developing MAS and the exact role of macrophages in the disease pathophysiology remains to be determined.

Tmem178 is a novel integral membrane protein, which we find to be down-regulated in human CD14<sup>+</sup> monocytes from sJIA patients compared with healthy donors. To determine whether downregulation of Tmem178 may play a role in sJIA and MAS, we employed a MAS model consisting of repeated injections of CpG (TLR9 ligand) in WT and Tmem178-/- mice. A significant increase in splenomegaly and decreased platelet and RBC counts were observed in Tmem178-/- mice compared with WT animals. This result correlated with increased serum levels of pro-inflammatory cytokines and decreased IL-10 in the null mice. Histological analysis revealed excessive fibrin thrombi and inflammatory infiltrates in livers of Tmem178-/- mice compared with WT. *In vitro*, loss of Tmem178 increased IL-1, IL-6 and TNF levels in macrophages, while reducing the levels of IL-10. Consistent with this observation, we found an increase in M1 marker genes, including iNOS and CCL5, and increased phosphorylation of STAT1 and STAT3, in Tmem178-/- macrophages compared with WT.

To further understand the importance of macrophages in MAS, we used another MAS animal model that involves LCMV infection in perforin deficient (Prf-/-) mice, which leads to death by day 21 due to a cytokine storm. Macrophages were depleted by clodronate-loaded liposomes administered during the initial phases of disease development or after disease onset. Interestingly, we found that earlier depletion of macrophages imparted protection while the later depletion increased the susceptibility to LCMV infection. This finding suggests that two different macrophage subsets might be involved in MAS, with M1 pro-inflammatory macrophages regulating disease initiation and M2 anti-inflammatory macrophages contributing to disease resolution. Most importantly, we show that Tmem178 deficiency induces M1 macrophage polarization and aggravates MAS, suggesting that Tmem178 might be a novel regulator and potential biomarker of MAS in sJIA patients.

**Disclosures:** Sahil Mahajan, None.

## SU0033

**X-Linked Hypophosphatemic Rickets due to a 112kb deletion of the PHEX gene and Mosaic Turner Syndrome (45,X/46,XX).** Alaina P Vidmar<sup>1</sup>, Pedro A Sanchez-Lara<sup>2</sup>, Brian Miyazaki<sup>3</sup>, Pisit Pitukcheewanont<sup>4</sup>. <sup>1</sup>Center for Endocrinology, Diabetes & Metabolism Children's Hospital of Los Angeles & Keck School of Medicine of University of Southern California, Los Angeles, California, United States, <sup>2</sup>Center for Personalized Medicine, Department of Pathology & Pediatrics Children's Hospital Los Angeles & Keck School of Medicine of University of Southern California, Los Angeles, California, United States., United states, <sup>3</sup>Center for Endocrinology, Diabetes & Metabolism. Children's Hospital Los Angeles & Keck School of Medicine of University of Southern California, Los Angeles, California, United States., United states, <sup>4</sup>Center for Endocrinology, Diabetes & Metabolism Children's Hospital Los Angeles & Keck School of Medicine of University of Southern California, Los Angeles, California, United States., United states

Turner syndrome (TS) is defined by one of several mechanisms of partial or complete monosomy X including 45,X (60%), 45,X/46,XX mosaicism (30%), or other structural abnormality of X chromosome (10%). Affected females have variable expressivity. X-Linked Hypophosphatemic Rickets (XLHR) is an inherited disorder characterized by renal phosphate wasting, aberrant vitamin D metabolism, and abnormal bone mineralization. Loss-of-function mutations in the PHEX gene (found at Xp22.11) cause XLHR. There are currently no published cases in the medical literature that report concomitant TS with XLHR.

We report a 3-year-old female with congenital heart defect, microcephaly (-3.23SD), developmental delay, dysmorphic features, short stature (-4.13 SD) and poor weight gain (-2.75 SD) found to have XLHR secondary to multiple chromosome anomalies including a small microdeletion of part of the PHEX gene, mosaic TS (45,X/46,XX). She was also found to have a 9.98Mb terminal deletion of chromosome 2 (2q37.1q37.3) which explains her associated clinical findings mentioned above.

At 23 months of age, she was admitted to the hospital for poor weight gain and was found to have rachitic changes on imaging associated with mild hypocalcemia and hypophosphatemia. Her initial work up revealed: phosphate: 2.3 mg/dL (4.5-6), calcium: 7.9 mg/dL (8-10.2), PTH: 401 pg/mL, alkaline phosphatase: 530 U/L (80-270), 25-hydroxy vitamin D: 22 µg/L (>30), urine phosphate: 270 mg/dL, tubular reabsorption of phosphate (TRP) of 40%, fibroblast growth factor-23: 494 RU/ML (<230). Skeletal survey revealed prominent beading/knobs of bone at the chostochondral joint, osteopenia, fraying of bilateral humeri and femurs evidence for rickets. Review of the chromosomal microarray analysis revealed multiple abnormalities including a small interstitial deletion encompassing only part of the PHEX gene (OMIM # 307800) which confirmed the diagnosis of XLHR. The terminal deletion of chromosome 2 (2q37.1q37.3) explained her associated clinical findings. She was started on supplementation with phosphate, calcitriol and cholecalciferol and her lab values improved to calcium: 9.7 mg/dL, phosphate: 3.6 mg/dL, PTH of 64 pg/mL.

This is the first case report of a XLHR patient secondary to an interstitial constitutional PHEX gene deletion and Mosaic Turner Syndrome (45,X/46 XX).

**Disclosures:** *Alaina P Vidmar, None.*

## SU0034

**An Exploratory Analysis of Modeled Bone Stresses at the Radial Metaphysis in the Context of Circum-menarcheal Gymnastic Loading.** *Karen Troy*<sup>1</sup>, *Tamara Scerpella*<sup>2</sup>, *Jodi Dowthwaite*<sup>3</sup>. <sup>1</sup>Worcester Polytechnic Institute, United states, <sup>2</sup>University of Wisconsin - Madison, United states, <sup>3</sup>SUNY Upstate Medical University, United states

**PURPOSE:** We used paired pQCT scans to yield bone strength indices and estimate stresses experienced during gymnastic loading, across growth from pre-menarche (PRE) to post-menarche (POST).

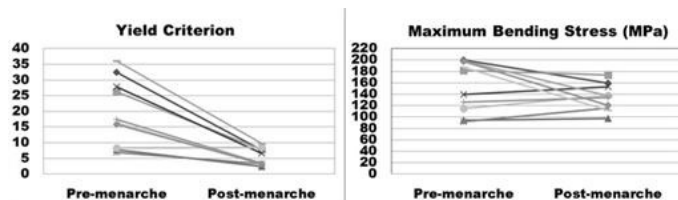
**METHODS:** Gymnasts were selected from a longitudinal study, featuring annual 4% distal radius pQCT scans (Stratec XCT 2000). Inclusion criteria were: inter-scan gymnastic exposure  $\geq 6$ h/wk and appropriately timed, high quality 4% distal radius pQCT scans (1 to 3 years PRE-menarche and POST-menarche; 3 to 4.5 yr inter-scan interval). Images were used to generate 2D finite element models with subject-specific geometry and inhomogeneous material properties [1]. A forward handspring vault was simulated [2], with boundary conditions based on anthropometric data. Peak bending stress ( $\sigma_b$ ) and ellipsoidal yield criterion (YC) were calculated as follows:  $YC = (\sigma_b/\sigma_y)^2 + ((\tau/\tau_y)^2)^2$ ,  $\sigma_y = 68\rho^2$  and  $\tau_y = 21.6\rho^{1.65}$ . Integral, cortical (cort) and trabecular (trab) bone volume, mineral content, density, cort/trab area ratio, compressive and bending strength indices, and principal moments of inertia were calculated using a periosteal threshold of  $\geq 250$ mg/cm<sup>3</sup> and cort/trab threshold  $\geq 650$ mg/cm<sup>3</sup> [3]. Paired t-tests evaluated PRE-POST differences; Pearson r assessed paired scan correlations.

**RESULTS:** Mean (sd) subject ages were: PRE= 11.3yrs (0.9); POST= 14.9yrs (1.5); gynecological ages were: PRE= -1.8yrs (0.5); POST= +2.1yrs (0.6). Inter-scan interval ranged from 3.0 to 4.3yrs (mean 3.8yrs (0.6)). Significant PRE-POST differences were detected for YC (decrease,  $p=0.001$ ) and various bone indices (increase,  $p \leq 0.001$ : integral volume, BMC, density, cross-sectional area; cort/trab area ratio; compressive and bending strength indices; all moments of inertia). We detected no significant PRE-POST difference for  $\sigma_b$  ( $p>0.15$ ) or for trabecular volume, BMC or density ( $p>0.22$ ). Despite medium ( $r>0.39$ ) to large ( $0.39 < r < 0.62$ ) effect sizes, few paired scan correlations were significant (YC, bending strength index, cort/trab area ratio:  $r > 0.65$ ,  $p < 0.05$ ).

**CONCLUSION:** In the context of circum-menarcheal gymnastic loading, most integral bone geometry, density and strength indices increased. Based on finite element analysis, these changes appear to be accompanied by a significant reduction in YC, whereas Maximum Bending Stress is more stable.

**References:**

- [1] Kourtis et al, Comput. Methods Biomech. Biomed. Engin. 2008.
- [2] Penitente and Sands, J Hum. Kinet. 2015.
- [3] Edwards et al, Osteoporos. Int. 2013.



Picture

**Disclosures:** *Karen Troy, None.*

## SU0035

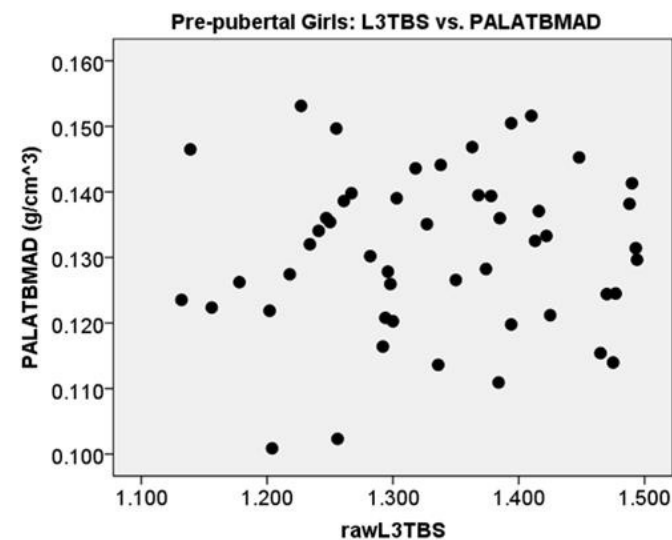
**DXA Trabecular Bone Score Correlates Poorly with Posteroanterior-Lateral Bone Mineral Apparent Density, Exercise Exposure and Key Diet Variables in Pre-pubertal Girls.** *Jodi Dowthwaite*<sup>1</sup>, *Renaud Winzenrieth*<sup>2</sup>, *Dongliang Wang*<sup>1</sup>, *Paula Rosenbaum*<sup>1</sup>, *Tamara Scerpella*<sup>3</sup>. <sup>1</sup>SUNY Upstate Medical University, United states, <sup>2</sup>Med-Imaps SASU, France, <sup>3</sup>University of Wisconsin - Madison, United states

**PURPOSE:** In adults, trabecular bone score (TBS) correlates positively with fracture risk. There are limited data on TBS associations in children. We hypothesized that TBS would correlate positively with bone mineral apparent density (BMAD) and other bone strength indices calculated from paired posteroanterior and supine lateral DXA scans (PALAT).

**METHODS:** DXA scans were performed in 50 pre-pubertal girls, including non-gymnasts (n=30) and gymnasts (prior year exposure  $\geq 6$ hr/wk, n=19): paired PALAT lumbar, PA proximal femur, PA whole body. For vertebra L3, raw TBS was calculated from PA scans; 3D geometry, density and strength indices were calculated from PALAT data. Whole body and proximal femur scans yielded body composition and femoral neck BMD. Annual mean hours per week of non-aquatic organized activity were calculated for the year prior to DXA (calendar-based questionnaire). The Harvard youth adolescent questionnaire (YAQ) assessed protein, calcium and vitamin D intakes. Basic anthropometry was performed. Pearson correlations evaluated associations among variables. Independent t-tests evaluated raw between-group differences.

**RESULTS:** Subject age ranged from 7.8 to 12.8 years; gynecological age ranged from  $\geq -5.7$  years to  $-2.1$  years (known menarche date, n= 31/50). L3TBS ranged from 1.13 to 1.49. We detected no significant correlations between L3TBS and age, height, sitting height, weight, body mass index, whole body non-bone lean mass, percent body fat, waist girth, hip girth, non-aquatic organized exercise exposure, protein, calcium or vitamin D. We did not detect a correlation between L3TBS and PALAT L3BMAD ( $\rho=0.06$ ,  $p>0.67$ ). L3TBS correlated positively with L3 PABMD, PABMC, and many vertebral body-specific indices (LATBMC, PALAT cross-sectional area, PA width, LAT depth) and FNBMAD ( $\rho=0.32$  to  $0.43$ ,  $p<0.03$ ). In the sub-sample with known menarche date, we did not detect a linear correlation between L3TBS and gynecological age or age at menarche. Without adjustment for age or body size, we did not detect gymnastic group differences for any lumbar bone variables other than ln PALAT fracture risk index ( $p<0.05$ ), but gymnasts had higher FNBMAD and lower percent body fat than non-gymnasts ( $p<0.03$ ).

**CONCLUSION:** Despite substantial sample variance, we did not detect a correlation between TBS and 3D vertebral body-specific density (PALAT BMAD) in pre-pubertal girls; instead, L3TBS correlated primarily with 3D geometric indices, PABMD, PABMC and LATBMC.



Pre-pubertal Girls TBS

**Disclosures:** *Jodi Dowthwaite, None.*

## SU0036

**Insights from Murine Carpal Bone Development into the Pathogenesis of Human Carpal-Tarsal Osteolysis Syndromes: Is Osteolysis Really the Cause?** *Emma Duncan*<sup>1</sup>, *Syndia Lazarus*<sup>2</sup>, *Hsu-Wen Tseng*<sup>2</sup>, *Felicity Lawrence*<sup>3</sup>, *Mia Woodruff*<sup>3</sup>, *Allison Pettit*<sup>4</sup>. <sup>1</sup>Royal Brisbane & Women's Hospital, The University of Queensland & Queensland University of Technology., Australia, <sup>2</sup>The University of Queensland Diamantina Institute, Australia, <sup>3</sup>Queensland University of Technology, Australia, <sup>4</sup>Mater Research Institute - The University of Queensland, Australia

**Purpose:** Multicentric carpal-tarsal osteolysis (MCTO); multicentric osteolysis, nodulosis and arthropathy (MONA); and Winchester syndromes are three distinct

skeletal dysplasias characterised by carpal/tarsal and epiphyseal abnormalities. They are caused by mutations in v-maf musculoaponeurotic fibrosarcoma oncogene ortholog B (MAFB), matrix metalloproteinase 2 (MMP2) and matrix metalloproteinase 14 (MMP14), respectively; however, the underlying pathophysiology is unclear. Osteoclast-mediated osteolysis has been regarded as the main mechanism, but does not explain the site-specific skeletal distribution. We hypothesized that MAFB, MMP2 and MMP14 have integral roles in carpal/tarsal and epiphyseal bone development.

Methods: Neonatal mouse forepaws were imaged by micro-computed tomography. Both undecalcified and decalcified sections were histologically examined. Tartrate resistant acid phosphatase (TRAP) staining was performed to identify osteoclasts. Immunohistochemistry was used to assess MAFB, MMP2 and MMP14 expression.

Results: Murine forepaw ossification occurred sequentially, similar to ossification of the human carpus. Sub-articular regions of endochondral ossification showed morphological and calcification patterns that were distinct from archetypical physal endochondral ossification, both in terms of timing and cell organisational structure. This suggests that two different forms of endochondral ossification occur that are regulated in distinct ways. The skeletal sites exhibiting the greatest abnormality in the carpal-tarsal osteolysis syndromes are regions of sub-articular ossification. Thus, abnormal bone formation in areas of sub-articular ossification may explain the site-specific distribution of the carpal-tarsal osteolysis phenotype. MafB, Mmp2 and Mmp14 were widely expressed, and TRAP staining notably absent, in the sub-articular regions of the cartilage anlagen at a time point comparable to the age at onset of the osteolysis syndromes in humans. Enthesal expression of all three proteins was also evident, with particularly prominent expression of Mmp2.

Conclusions: Abnormal peri-articular skeletal development and modelling rather than excessive bone resorption, may be the underlying pathophysiology of these skeletal syndromes, which would have implications for therapeutic choices in affected individuals.

Disclosures: Emma Duncan, None.

## SU0037

**The Role and Interactions of 25-OHD, Parathyroid Hormone, and Serum Calcium in Pediatric Patients with Fractures Compared with Healthy Controls.** Rocio Crabb<sup>1</sup>, Selina Poon<sup>2</sup>, Ashley Olson<sup>3</sup>, Sara Merwin<sup>4</sup>, Rachel Gecelter<sup>2</sup>, Stephen Wendolowski<sup>2</sup>, Jare Philip<sup>2</sup>, Joanna Fishbein<sup>5</sup>, Jahn Avarello<sup>2</sup>. <sup>1</sup>Hofstra Medical School, United states, <sup>2</sup>Cohen Children's Medical Center, United states, <sup>3</sup>Cohen Children's Medical Center, United states, <sup>4</sup>Montefiore Medical Center, United states, <sup>5</sup>Feinstein Institute for Medical Research, United states

Purpose: High rates of Vitamin D (25-OHD) deficiency (DEF) are reported worldwide in healthy children. The relationship of 25-OHD & parathyroid hormone (PTH) in bone health has not been well studied in the pediatric population. We investigated if children with fracture are more likely to have lower serum 25-OHD than those without fracture, and evaluated relationships between 25-OHD to serum PTH & calcium (Ca).

Methods: This is a cross-sectional study in the Northeastern US. Pediatric patients of diverse ethnicity & race ages 1-17 presenting to a tertiary care children's emergency department requiring IV access as part of standard care were enrolled from January 2014. Exclusions: steroids >30 days in past year, IBD, malabsorption, bone dysplasia, malignancy, hypothyroidism, & prior study enrollment. Cases were fracture patients and controls were healthy patients without fracture. After informed consent, 25-OHD, PTH & Ca were drawn. Demographic, injury location, mechanism & previous fracture data were collected. We defined 25-OHD  $\geq 30$ ng/ml sufficient (SUFF), 20.0-29.9ng/ml insufficient (INSUFF) & <20ng/ml DEF. Families received results with advice to follow-up with PCP. Enrollment continues to the 350 sample size.

Results: 197 subjects are enrolled (114 controls, 83 cases). Mean 25-OHD was 23.7  $\pm$  8.6: 23.5  $\pm$  9.2 in controls, 23.9  $\pm$  7.7 in cases. 23.5% of controls were 25-OHD SUFF, 30.9% DEF, 45.7% INSUFF. 25.2% of cases were SUFF, 37.4% DEF, 37.4% INSUFF. 25-OHD in White subjects was 26.81  $\pm$  8.91, 19.92  $\pm$  6.50 in Black/African American, 19.85  $\pm$  7.76 in Asian, 22.18  $\pm$  7.73 in Hispanic, 26.28  $\pm$  9.24 in Other, 21.64  $\pm$  7.12 in Indian (p<0.001). Hyperparathyroidism was present in 10.3% of fracture subjects & 1.2% of controls – all were either INSUFF or DEF for 25-OHD. Mean serum Ca was 9.9  $\pm$  0.5, hypocalcemia was present in 1.4% overall: 10.0  $\pm$  0.4 in controls, 9.7  $\pm$  0.6 in cases. Mean PTH was 30.8  $\pm$  15.5: 26.6  $\pm$  12.1 in controls, 36.3  $\pm$  18.2 in cases (p<0.001).

Conclusion: A majority of our sample was found to be 25-OHD INSUFF or DEF with lowest levels in Blacks, Asians and Hispanics compared with Whites. 25-OHD was not significantly different between fracture & non-fracture groups & therefore may not be a predictor of fracture risks. Hypocalcemia was rare. Further investigation is warranted of the higher PTH in the fracture group, suggesting up regulation of PTH following bone disruption, similar to results from a previous study.

	Total = 197		Mean		
	N	%	25-OHD	PTH	Calcium
Fracture	83	42.1	23.8	36.3	9.8
Controls	114	57.9	23.6	26.6	10
White	81	41.1	26.8	31.2	9.8
Asian	23	11.7	19.8	34.3	9.9
Indian	13	6.6	21.6	31	10
Black or African American	41	20.8	23.8	31.7	9.9
Hispanic	20	10.2	22.2	27.5	9.9
Other	19	9.6	26.3	26.3	10

Patient Demographic and Lab Values

Disclosures: Rocio Crabb, None.

## SU0038

**Criteria defining low body weight: Which are the most relevant for predicting low bone mineral density in adolescent females with anorexia nervosa?.** Nurgun Kandemir<sup>\*</sup>, Kendra Becker, Vibha Singhal, Shreya Tulsiani, Ryan Woolley, Meghan Slattery, Kamryn Eddy, Madhusmita Misra, Anne Klibanski. Massachusetts General Hospital, United states

Adolescents with anorexia nervosa (AN) are at increased risk for low bone mineral density (BMD) and fractures compared to healthy adolescents. Diagnostic criteria for AN (specifically weight and menstrual status) are less rigid in DSM-5 than DSM-IV. This may impact on fracture risk in AN diagnosed using the new criteria. However, data are lacking regarding the impact of weight cut-offs to predict bone outcomes.

We therefore evaluated the relationship between BMD and parameters used to define low body weight in adolescents with AN. We also determined whether a specific cut-off for weight parameters may better predict those at risk for low BMD, and the impact of amenorrhea.

We included 353 females, 262 with a diagnosis of AN and 91 controls (C) 12-21 years old (17.2  $\pm$  2.1 years). Lumbar spine and whole body less head areal BMD was determined by dual-energy X-ray absorptiometry (DXA) (Hologic 4500A). Height adjusted BMD Z-scores were calculated using data from the Bone Mineral Density in Childhood Study. Percentage of expected body weight (%EBW) was calculated based on the subject's weight relative to (i) weight corresponding to the 50<sup>th</sup> percentile of BMI for age (%EBW-BMI), and (ii) weight corresponding to the subject's height percentile (%EBW-Ht). BMI percentiles were obtained from age and sex specific reference tables. We further characterized the AN group according to %EBW-BMI and %EBW-Ht  $\leq$  or > 85% and  $\leq$  or > 90%, BMI percentile  $\leq$  or > 5<sup>th</sup> and  $\leq$  or > 10<sup>th</sup>, and BMI  $\leq$  or > 17.5 or  $\leq$  or > 18.5.

AN were older than C, but did not differ for height Z-scores, bone age or maturity. Using cut-offs for %EBW-Ht, AN at >85 or >90% EBW-Ht did not differ from C for BMD Z-scores at either site, but differed significantly from AN at  $\leq 85$  or  $\leq 90\%$  EBW-Ht. For other measures, regardless of the cut-off used to define low weight (85 or 90% EBW-BMI, 5<sup>th</sup> or 10<sup>th</sup> percentile for BMI, BMI of 17.5 or 18.5), AN had lower BMD Z-scores than C, and AN above the respective weight cut-off had BMD Z-scores intermediate between those below the weight cut-off and C. Within AN, BMD Z-scores did not differ based on amenorrhea status. However, amenorrheic AN >85% EBW-Ht had lower spine BMD Z-scores compared to controls.

A diagnosis of AN is thus highly predictive of low BMD Z-scores, with lower weight defined by various measures correlating with lower BMD. However, AN girls at >85% EBW-Ht do not appear to be at increased risk for low BMD compared with controls except at the spine when amenorrheic.

Disclosures: Nurgun Kandemir, None.

## SU0039

**Osteocytes regulate myelopoiesis via secreted factors.** Ehab Azab<sup>\*</sup><sup>1</sup>, Yuhei Uda<sup>2</sup>, Chao Shi<sup>2</sup>, Christopher Dedic<sup>2</sup>, Forest Lai<sup>2</sup>, Ningyuan Sun<sup>2</sup>, Majed Alshehri<sup>2</sup>, Maureen O'Meara<sup>3</sup>, Marc Wein<sup>3</sup>, keertik Fulzele<sup>2</sup>, Paola Divieti Pajevic<sup>1</sup>. <sup>1</sup>Boston University- Department of Molecular & Cell Biology, United states, <sup>2</sup>Boston University, United states, <sup>3</sup>Massachusetts General Hospital, United states

Post-natally bone marrow is the site of hematopoiesis which begins with a small population of life-long self-renewing long-term hematopoietic stem cells (HSCs) giving rise to short-term HSCs, which gradually lose lineage differentiation potential and become multipotent progenitors. Further lineage restriction gives rise to either common lymphoid progenitors (CLP) or common myeloid progenitors (CMP). Previous studies showed that osteocytes are in contact with bone marrow cells through their dendritic processes. Osteocytes also express several receptors including G protein-coupled receptors (GPCR) capable of regulating hematopoiesis. Mice lacking Gs $\alpha$  expression in osteocytes display hematopoietic abnormalities, including a dramatic expansion of myeloid cells. To investigate the molecular mechanisms by which osteocytes control myelopoiesis, we established an osteocytic cell line lacking Gs $\alpha$  expression and asked

whether osteocytes regulate myeloid cell proliferation and maturation by cell-to-cell contact or by secreted factors. We used a conditionally immortalized cells line, namely Ocy454, to knock-down (KD) or knock-out (KO) Gsz using either lentiviral shRNA or CRISPR/Cas9 gene editing. Ocy-GszKD and Ocy-GszKO cells were allowed to proliferate and differentiate for 5-6 days in regular medium prior to be cultured for additional 24hr in low serum medium (0.1% FBS). Condition media (CM) was collected and used in an in-vitro methylcellulose colony assay. Briefly, for myeloid colony assay formation, bone marrow cells were isolated from long bones of 6-8 weeks WT mice and cultured in methylcellulose containing CM from Ocy-GszKD and Ocy-GszKO cells of controls. Myeloid colonies were evaluated after 5 days in culture. Treatment with CM from Ocy-GszKD and Ocy-GszKO cells significantly increased the number of myeloid colonies compared to CM from controls or from non-treated cells. Since both Ocy-GszKD and Ocy-GszKO cells express and secrete high level of sclerostin, we next investigate whether the myeloproliferative effect was sclerostin-dependent. Indeed, sclerostin-depleted CM was still capable of supporting myelopoiesis, indicating that other factors must be affecting BM cells proliferation and differentiation. Initial size fractionation of the CM indicates that the biological activity resides in molecules smaller than 10 KD. In conclusion we demonstrated that osteocyte secrete factors capable of regulating myelopoiesis through Gsa mediated mechanism.

**Disclosures:** Ehab Azab, None.

## SU0040

**Conditioned-medium of amniotic fluid-derived stromal cells ameliorate bone mass and bone marrow angiogenesis.** Sun Wook Cho<sup>\*1</sup>, Hyun Jin Sun<sup>1</sup>, JoonHo Lee<sup>2</sup>, Eun Sil Koh<sup>3</sup>, Chan Soo Shin<sup>1</sup>. <sup>1</sup>Seoul National University Hospital, Korea, republic of, <sup>2</sup>Yonsei University College of Medicine, Korea, republic of, <sup>3</sup>National Medical Center, Korea, republic of

Bone contains a blood-rich marrow which supports tissue remodeling and repair process. Epidemiologic studies demonstrated that systemic disease of vascular insufficiency is related to fracture risk. The aim of this study was to investigate the effects of conditioned medium of human amniotic fluid-derived stromal cell (AFSC-CM) on bone mass and marrow vasculature. AFSCs were collected from mid-trimester (16-19 weeks) amniotic fluid, and conditioned media were harvested from passages 1-3 AFSCs (AFSC-CM). C57BL/6 mice (female, 16-week-old) were treated with AFSC-CM or PBS by intraperitoneal injections for 6 weeks. After 6 weeks, microCT analyses showed that fractional trabecular bone volume and cortical thickness were significantly increased by 40% and 4%, respectively, in AFSC-CM than PBS group. Serum P1NP showed a significant increase in AFSC-CM than PBS group, while TRAB5b showed no significant difference between groups. Collectively, AFSC-CM showed anabolic actions on bone. Furthermore, immunohistochemical staining demonstrated that Von Willebrand factor-positive endothelial cells were increased in AFSC-CM than PBS group. Flow cytometric analysis of flushed whole marrow cells showed that CD31+ or CD34+ endothelial progenitor cells were increased in AFSC-CM than PBS group, suggesting that AFSC-CM also enhanced marrow angiogenesis. Treatment of AFSC-CM increased ALP activity in calvarial osteoblasts or human mesenchymal stem cells in vitro, while it had no effects on RANKL-dependent osteoclastogenesis in primary cultured bone marrow-derived monocyte/macrophages. In primary cultured human microvascular endothelial cells, AFSC-CM treatment enhanced cell migration and tube formation potentials. Finally, to explore the mechanism of AFSC-CM effects on bone, cytokine array analyses were performed and showed that several angiogenic factors such as insulin-like growth factor-binding protein (IGFBP)-1, IGFBP-2, leptin, and monocyte chemoattractant protein-1 were highly increased in AFSC-CM. In conclusion, AFSC-CM had dual actions on bone anabolisms and marrow angiogenesis, and might have a therapeutic potentials in osteoporosis especially related to vascular insufficiency.

**Disclosures:** Sun Wook Cho, None.

## SU0041

**Ossified Bone Marrow Blood Vessel Volume and Short-Term Intermittent PTH (1-34) Administration in Mature and Middle-Aged C57BL/6 Mice.** Seungyong Lee<sup>\*</sup>, Rhonda Prisby. University of Delaware, United states

Intermittent parathyroid hormone (PTH) administration augments bone volume and is a common treatment for osteoporosis. We previously reported progressive bone marrow blood vessel (BMBV) ossification (i.e., the conversion of bone marrow blood vessels into bone) with advancing age in rats. We theorized that such pathology may exacerbate age-related declines in bone blood flow. Since intermittent PTH administration augments bone, it may also serve to increase BMBV ossification. We assessed the influence of 10 days of intermittent PTH 1-34 administration on trabecular and cortical bone and BMBV ossification in mature (6-8mon; n=20) and middle-aged (10-12mon; n=20) male and female C57BL/6 mice. Mice were equally divided by gender into CON and PTH groups and given PTH 1-34 (43 µg/kg/d) or PBS (50 µl) for 10 consecutive days. Left femora were collected at sacrifice to assess trabecular bone microarchitecture (BV/TV [%], Tb.Th [µm], Tb.N [1/mm<sup>2</sup>], and Tb.Sp [µm]) in the distal femoral metaphysis. Cortical bone parameters (BV/TV [%], cortical thickness [µm], and cross sectional moment of inertia [CSMI, mm<sup>4</sup>]) were assessed at the femoral mid-shaft. BMBV ossification (ossified vessel volume [OsVV, %] and ossified vessel thickness [OsV.Th, µm]) was assessed in the

medullary cavity of the femoral shaft. All parameters were assessed by µCT (Scanco Medical). No gender-related differences were observed, so female and male data were pooled and analyzed according to group. Trabecular bone parameters were similar among groups. Cortical BV/TV tended (p=0.06) to be higher in mature-PTH (32.1 ± 0.8%) vs. middle-aged-CON (28.8 ± 0.7%), while cortical thickness and CSMI did not differ among groups. Strikingly, OsVV (Figure 1) was augmented (p<0.05) in middle-aged-PTH (0.22 ± 0.06%) vs. mature-CON (0.07 ± 0.03%) and tended (p<0.10) to be higher than mature-PTH (0.09 ± 0.03%) and middle-aged-CON (0.10 ± 0.04%). Ossified vessels were thicker (p<0.05) in middle-aged-PTH (23.3 ± 2.5µm) vs. mature-CON (10.1 ± 2.3µm), mature-PTH (13.0 ± 2.4µm) and middle-aged-CON (14.9 ± 2.5µm). In conclusion, this is the first report of bone marrow blood vessel ossification in mice. Intermittent PTH administration elicited bone growth on ossified bone marrow blood vessels by 10 days; i.e., at a time point when trabecular and cortical bone mass were unaffected. Although used as treatment for osteoporosis, intermittent PTH administration may impact the patency of bone marrow blood vessels.

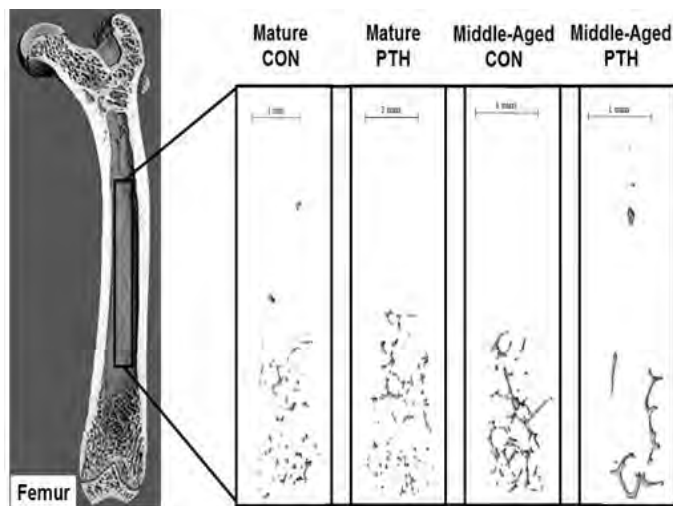


**Figure 1.** Bone marrow blood vessel (BMBV) ossification in mature and middle-aged CON and PTH-treated mice.

Figure 1

**Disclosures:** Seungyong Lee, None.

## SU0042

**Evidence to Support Causality of White Blood Cell Counts on Bone Mineral Density.** John Morris<sup>\*1</sup>, Stephanie Ross<sup>2</sup>, William Astle<sup>3</sup>, Heather Elding<sup>4</sup>, Tao Jian<sup>5</sup>, Dace Ruklisa<sup>3</sup>, John Danesh<sup>4</sup>, David Roberts<sup>6</sup>, Willem Ouwehand<sup>3</sup>, Adam Butterworth<sup>5</sup>, Nicole Soranzo<sup>3</sup>, Brent Richards<sup>1</sup>.

<sup>1</sup>Department of Human Genetics, McGill University, Canada, <sup>2</sup>Department of Epidemiology, Biostatistics & Occupational Health, McGill University, Canada, <sup>3</sup>Department of Haematology, University of Cambridge, Cambridge Biomedical Campus, United Kingdom, <sup>4</sup>Department of Human Genetics, The Wellcome Trust Sanger Institute, Wellcome Trust Genome Campus, Hinxton, United Kingdom, <sup>5</sup>Department of Public Health & Primary Care, University of Cambridge, Strangeways Research Laboratory, United Kingdom, <sup>6</sup>Blood Research Group, NHS Blood & Transplant, John Radcliffe Hospital, Headley Way, Headington, United Kingdom

**Purpose:** Although observational studies have demonstrated an association between immune system cell counts and bone mineral density (BMD), these estimates may be confounded by inflammation, reverse causation, or unmeasured confounders. We applied Mendelian randomization (MR) methods to estimate the effect of white blood cell (WBC) counts on BMD using the largest genome-wide association studies (GWAS) at our disposal.

**Methods:** We identified 538 genome-wide significant SNPs ( $P < 5 \times 10^{-8}$ ) associated with 11 respective measurements of myeloid, lymphoid, and total WBC counts (median 125 SNPs per trait) from a GWAS of up to 172,435 European individuals (*unpublished*). We then obtained the corresponding SNP BMD effect estimates from GEFOS-seq, a GWAS of 32,735 and 28,498 European individuals for femoral neck and lumbar spine BMD, respectively. MR effects were estimated from the pooled effects of these 538 SNPs on BMD, weighted by their effect sizes on WBC counts, providing 22 MR estimates (11 WBC counts  $\times$  2 BMD measures). We applied a conservative Bonferroni-adjusted P-value threshold of  $2.3 \times 10^{-3}$  ( $P = 0.05/22$ ) to account for multiple testing. MR Egger regression sensitivity analyses were conducted to assess pleiotropy.

**Results:** Overall, we observed six of 11 WBC counts had significant MR effects ( $P < 2.3 \times 10^{-3}$ ) for both BMD measures. These were for myeloid WBC counts (myeloid

WBCs, granulocytes, sum of basophils and neutrophils, sum of neutrophils and eosinophils, and neutrophils) and total WBC count. Effect directions were negative, with the most significant MR effects estimated for the effect of granulocyte counts on lumbar spine (effect = -0.110,  $P = 2.35 \times 10^{-5}$ ) and femoral neck BMD (effect = -0.092,  $P = 3.97 \times 10^{-5}$ ). We determined that increases in myeloid WBC counts will decrease BMD. We discounted pleiotropic effects for significant MR analyses based on non-significant MR Egger regression results ( $P > 0.05$ ).

Conclusion: In a large-scale multi-cohort MR study, we found a strong negative relationship between several myeloid WBC counts and BMD, suggesting a clear role for the innate immune system in bone biology and osteoporosis etiology. These results provide rationale to identify the mechanism whereby myeloid WBCs decrease BMD in humans. Further work will partition the SNPs used to estimate the effect of each WBC count independently and interrogate if specific cytokines can be identified with significant effects on BMD.

Disclosures: John Morris, None.

## SU0043

**MFG-E8 Mutant Mice Exhibit Reduced Bone Mass and Enhanced Anabolic Response to Parathyroid Hormone.** Megan Michalski\*, Benjamin Sinder, Amy Koh, Hernan Roca, Laurie McCauley. University of Michigan, United states

Parathyroid hormone (PTH 1-34) administered intermittently (iPTH) causes an anabolic response in bone, yet exact mechanisms remain elusive. PTH modulates osteoblast apoptosis and macrophages phagocytose apoptotic cells in a process called efferocytosis. Milk fat globule-EGF factor 8 (MFG-E8) functions as a bridge between phagocytes and apoptotic cells. MFG-E8 mutant mice (KO) are deficient in efferocytosis, accumulate apoptotic cells, and exhibit low bone mass. MFG-E8KO mice were used to investigate the functional role of MFG-E8 in bone turnover and PTH anabolism. MFG-E8KO mice (8wk) were analyzed for skeletal phenotypes compared to WT controls via  $\mu$ CT. Skeletally mature (16wk) MFG-E8 KO and WT mice were administered iPTH (50 $\mu$ g/kg/d) or vehicle (veh) for 6wks. Skeletal phenotypes were assessed via  $\mu$ CT, serum P1NP, TRAcP5b, and CTX-I analyzed, static and dynamic bone histomorphometry performed, and flow cytometric analysis of bone marrow populations and CBC of peripheral blood completed. MFG-E8KO (8wk) mice exhibited reduced trabecular and cortical bone compared to WT controls. Skeletally mature MFG-E8KO mice also displayed reduced bone parameters (-32% trabecular BV/TV) vs. WT. MFG-E8KO treated with iPTH showed a robust anabolic response in trabecular BV/TV (+122%), exceeding the anabolic response in iPTH-tx WT mice (+48%). Serum P1NP, TRAcP5b and CTX-I were significantly increased in iPTH-tx KO and WT mice. KO mice exhibited a larger increase in P1NP (+529%) than WT (+351%). Serum TRAcP5b was lower in veh-tx KO mice compared to veh-tx WT. KO mice had increased Ocs/BS compared to WT, and iPTH decreased Ocs/BS in KO but not in WT mice. CD11b<sup>hi</sup>, GR-1<sup>+</sup> and CD11b<sup>hi</sup>, Ly6G<sup>+</sup> cells in the bone marrow were higher in KO compared to WT, and iPTH decreased CD68<sup>hi</sup> cells in the marrow of both WT and KO mice. Given that MFG-E8 is a regulator of an important efferocytic pathway and KO mice have decreased bone, these data suggest that apoptotic cell clearance plays an important role in steady state bone turnover. The stronger anabolic response in iPTH-tx KO vs. WT suggests that MFG-E8 may restrict anabolic actions of PTH in bone and alter how the bone forming unit responds to PTH. Alternatively, PTH may differentially regulate other efferocytic pathways which compensate for the loss of MFG-E8-mediated efferocytosis. Together, these data give us insight into the role of MFG-E8-mediated efferocytosis in bone turnover and expand our knowledge of its influence on PTH anabolism.

Disclosures: Megan Michalski, None.

## SU0044

**IL-32 is produced by myeloma cells in response to hypoxia: potential role for exosomal IL-32 in multiple myeloma bone disease.** Muhammad Zahoor\*<sup>1</sup>, Siv Moen<sup>2</sup>, Marita Westhrin<sup>3</sup>, Katarzyna Maria Psonka-Antonczyk<sup>4</sup>, Anders Waage<sup>3</sup>, Glenn Buene<sup>3</sup>, Anne-Marit Sponaas<sup>3</sup>, Therese Standaal<sup>5</sup>. <sup>1</sup>Centre of Molecular Inflammation Research, Norwegian University of Science & Technology, Trondheim, Norway & Department of Cancer Research & Molecular Medicine, Norwegian University of Science & Technology, Norway, <sup>2</sup>Centre of Molecular Inflammation Research, Norwegian University of Science & Technology, Trondheim, Norway & Department of Cancer Research & Molecular Medicine, Norwegian University of Science & Technology, Norway, <sup>3</sup>Department of Cancer Research & Molecular Medicine, Norwegian University of Science & Technology, Norway, <sup>4</sup>Biophysics & Medical Technology, Department of Physics, Norwegian University of Science & Technology, Trondheim, Norway, Norway, <sup>5</sup>Centre of Molecular Inflammation Research, Norwegian University of Science & Technology, Trondheim, Norway, 2 Department of Cancer Research & Molecular Medicine, Norwegian University of Science & Technology, Norway

Multiple myeloma is a hematological cancer characterized by expansion of malignant plasma cells in the bone marrow. Most patients develop a severe osteolytic bone disease. The loss of bone is due to increased bone degradation combined with lack of bone repair. In the myelomatous bone marrow there is a persistent low-grade

inflammation that increases as the disease progresses. In this study we aimed to identify inflammatory factors produced by myeloma cells and to address whether they influence the function or differentiation of bone cells. For this purpose we assessed the mRNA expression of inflammatory related genes in freshly obtained myeloma cells by Nanostring analyses. We found that interleukin-32 (IL-32) was one of the most highly expressed genes (n=8, median =11529 mRNA copies, range 6283-169732). Strikingly, the expression of IL-32 in myeloma cell lines was significantly lower (n=12, median = 241 mRNA copies, range 36- 1010, Mann-Whitney U test,  $p < 0.001$ ). The bone marrow microenvironment is hypoxic. Hence we investigated if the big difference in IL-32 levels between primary cells and cell lines could be due to hypoxia. Indeed, when primary cells and cell lines were cultured in low oxygen (2% O<sub>2</sub>) for 24 hours, IL-32 mRNA and protein increased. Further, we found that IL-32 was secreted from myeloma cells both as a free protein and on extracellular vesicles (EV) of approximately 160 nm as determined by Nanosight analyses. Recombinant IL-32 and EV isolated from an IL-32 expressing myeloma cell line promoted osteoclast differentiation in vitro. Similarly, TRAP positive bone surface was increased when recombinant IL-32 and EV containing IL-32 were injected on top of the calvaria of 8-week old male RAG2/GC KO mice. In summary, our data support that IL-32 is expressed by myeloma cells in response to hypoxia, that it is secreted on extracellular vesicles and promotes osteoclast differentiation. Hence targeting IL-32 might be beneficial in the treatment of myeloma bone disease.

Disclosures: Muhammad Zahoor, None.

## SU0045

**Involvement of the p62/Gfi1 axis in Multiple Myeloma Bone Disease.** Daniela Petrusca\*<sup>1</sup>, Cheolkyu Park<sup>1</sup>, Rebecca Silbermann<sup>1</sup>, Dan Zhou<sup>1</sup>, Noriyoshi Kurihara<sup>1</sup>, Yasuhisa Ohata<sup>1</sup>, Judith Anderson<sup>1</sup>, G. David Roodman<sup>2</sup>. <sup>1</sup>Indiana University, Department of Medicine/Hematology-Oncology, United states, <sup>2</sup>Indiana University, Department of Medicine/Hematology-Oncology; Rodebush VA, United states

Multiple myeloma bone disease (MMBD) is characterized by severe osteolytic bone destruction accompanied by profoundly suppressed or absent bone formation which negatively impacts patient survival. We and others showed that adhesive interactions between bone marrow stromal cells (BMSC) and MM cells play a key role in MMBD because they activate multiple signaling pathways and induce potent mediators that regulate osteoclast and osteoblast (OB) activity and promote tumor growth. We previously identified Sequestosome-1 (p62) as a potential target for MMBD treatment because it serves as a platform for formation of multiple signaling complexes that are involved in MMBD and are induced in BMSC by adhesive interactions with MM cells. Recently, we found that these adhesive interactions increased expression of the transcriptional repressor Gfi1 (growth factor independence1) in both MM exposed BMSC (MM-BMSC) and MM cells, and that Gfi1 suppressed OB differentiation in BMSC. However, Gfi1's role in MM cells is unclear. Therefore, we assessed the role of the p62 /Gfi1 axis in MM growth using CD138<sup>+</sup> cells and BMSCs from MM patients and healthy donors and murine BMSC from p62 WT and KO mice. Gfi1 was highly expressed (mRNA and protein levels) in patient MM cells compared to healthy donor cells, and Gfi1 mRNA expression and protein levels were further increased in MM cells treated with IL-6, TNF $\alpha$ , sphingosine-1-phosphate (S1P) and in 3D MM cell/mouse calvaria co-culture assays. Lentiviral knockdown (KD) of Gfi1 in MM cells using Gfi1shRNA inhibited MM cell growth and induced apoptosis, as measured by increased mRNA levels of *Bax*, *PUMA*, *Noxa*, and cleaved caspase 3 protein levels, and decreased Mcl-1 and c-Myc compared to MM cells infected with a non-mammalian shRNA. Adhesive interactions with normal and MM patient-derived BMSC enhanced *Gfi1*, *IL6* (3 fold) and the pro-survival marker *SphK1* (2.5 fold) mRNA and protein in MM cells. Importantly, *Gfi1* KD profoundly downregulated *SphK1* mRNA levels in MM cells and reduced expression of phospho-SphK1. The negative effects of Gfi1 KD in MM cells were partially restored by either IL-6 treatment or direct co-culture with MM-BMSC. However, co-culture of MM cells with p62KO BMSC blocked the upregulation of *Gfi1* and *IL6* mRNA levels in MM cells. These results suggest that the p62/Gfi1 axis plays a key role MM cell survival and that Gfi1 may mediate the anti-apoptotic effects of IL-6 by increasing SphK1 expression and activity.

Disclosures: Daniela Petrusca, None.

## SU0046

**Analysis of osteogenic and adipogenic differentiation potential of osteosarcoma cells transformed by Notch1 oncogene.** Kirby Rickel\*, Fang Fang, Jianning Tao. Sanford Research & University of South Dakota, United states

Osteosarcoma (OS) is the most common type of solid bone tumor, mainly affecting children and young adults with a 70% five-year survival rate. The primary treatment for OS is a combination of surgery and chemotherapy but once metastasis occurs, OS becomes resistant to chemotherapy and survival is greatly reduced. Therefore, it is important to develop second-line therapies to treat OS. Our previous studies generated a Notch1 gain of function mouse model of OS and from this model, generated a tumor cell line. We hypothesize this tumor cell line has characteristics similar to mesenchymal stem cells (MSCs), which may contribute to

its chemoresistance. In this study, we examined differences in osteogenic and adipogenic differentiation potential among our OS tumor cell line, an osteoblast cell line, and a MSC line. When grown in osteogenic differentiation media, our OS tumor cell line differentiated into an osteoblast lineage. In adipogenic differentiation media, our OS tumor cell line differentiated into adipocytes, suggesting MSC characteristics. Quantitative real-time PCR confirmed these results, revealing upregulation of genes involved in adipogenesis. However, our OS tumor cell line had a significantly decreased differentiation capacity compared to the MSC line when dexamethasone alone was used. Moreover, western blot analysis revealed dysregulation of Wnt and mTOR signaling in our OS tumor cell line. Together, these results suggest that OS tumor cells transformed by Notch1 oncogene have stem cell characteristics, which may be maintained by signaling pathways such as Wnt and mTOR. In the future, we may target these signaling pathways to revert the stem cell-like characteristics of osteosarcoma, making it more vulnerable to chemotherapy treatments.

**Disclosures:** Kirby Rickel, None.

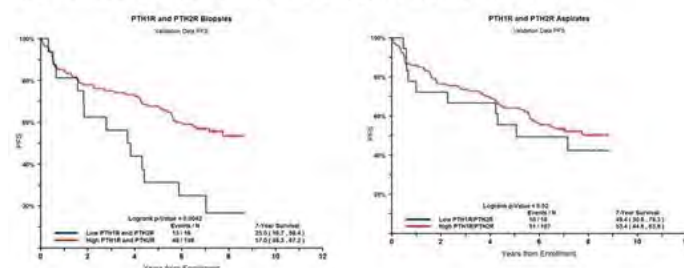
This study received funding from: Sanford Research

## SU0047

**The Expression of PTH1 and PTH2 Receptors in Bone Marrow is Associated with the Progression of Newly Diagnosed Myeloma Patients.** Maurizio Zangari<sup>1</sup>, Amy Buros<sup>1</sup>, Donghoon Yoon<sup>1</sup>, Antonio Branca<sup>1</sup>, Carolina Schinke<sup>1</sup>, Sharmilan Thanendrarajan<sup>1</sup>, Larry Suva<sup>2</sup>, Meera Mohan<sup>1</sup>, Faith Davies<sup>1</sup>, Frits van Rhee<sup>1</sup>, Gareth Morgan<sup>1</sup>. <sup>1</sup>University of Arkansas for Medical Sciences, United states, <sup>2</sup>Texas A&M University, United states

Total Therapies (TT) Trials enrolled newly diagnosed multiple myeloma (NDMM) patients. These protocols included sequential cycles of chemotherapy: induction, melphalan-based autologous stem cell transplantation, and consolidation followed by 3 years of maintenance. We have demonstrated that baseline biopsy gene expression levels of PTH receptors type 1 and type 2 (PTH1R and 2R) are positively associated with overall survival in patients enrolled in TT3a protocol (logrank p-value+5.71e-05). In this study, the correlation of PTH1R and PTH2R expression from baseline bone biopsies with progression free survival (PFS) in a larger, independent set of patients enrolled in TT trials was examined and compared to the effect on PFS of PTH1R and PTH2R expression by purified plasma cells. Affymetrix U133 gene expression profiling (GEP) was performed on bone biopsies obtained from 166 TT3a patients. A running log rank test analysis determined the optimal threshold for probe-association with PFS in MM from both the bone biopsy and marrow aspirates. The identified cut-off expression levels were then applied to an independent data set of an additional 125 patients (56% male; median age at enrollment 58 years; 22% were high risk disease based on 70 GEP model) enrolled in other TT trials. To confirm expression of PTH1R and 2R in bone marrow, real-time PCR using Taqman probes (PTH1R: Assay ID Hs00174895\_m1 and PTH2R: Assay ID Hs00175044\_m1) was performed. The expression levels of either PTH1R or PTH2R in bone marrow biopsies was not significantly associated with patient outcome. However, subjects (n=16) with low biopsy expression of both PTH1R and PTH2R genes experienced significantly inferior PFS (p=0.0042). Interestingly, eighteen patients with low PTH1R and PTH2R expression in purified plasma cells did not experience altered disease progression (Figure 1). In addition, the robust effect of bone biopsy PTH1R and 2R expression on PFS was confirmed in additional multivariate analyses. Real-time PCR demonstrated high levels of PTH1R and PTH2R transcripts at the bone marrow level. These findings demonstrate that the baseline expression of PTH1R and PTH2R in bone marrow biopsy and not purified plasma cells correlates with PFS in NDMM. These data implicate the PTH signaling pathway within the bone marrow microenvironment and not by plasma cells, as a major regulator of MM and suggest a close interaction between the PTH axis in bone and disease progression.

Figure 1: PFS for PTH1R and PTH2R in bone marrow biopsies and bone marrow aspirates



table

**Disclosures:** Maurizio Zangari, None.

## SU0048

**Abrogation of prostaglandin E and its receptor EP4 signaling in osteoblasts prevents the bone destruction induced by human prostate cancer.** Kenta Watanabe<sup>1</sup>, Michiko Hirata<sup>1</sup>, Tsukasa Tominari<sup>1</sup>, Takayuki Maruyama<sup>2</sup>, Masaki Inada<sup>\*1</sup>, Chisato Miyaura<sup>1</sup>. <sup>1</sup>Tokyo University of Agriculture & Technology, Japan, <sup>2</sup>Ono Pharmaceutical Co., Ltd., Japan

We have reported that the metastasis of malignant melanoma to bone was promoted by prostaglandin E2 (PGE2) produced by the tumor host stromal tissue (*J. Biol. Chem.* 2015). Although bone metastases frequently occur in prostate cancer patients, the significance of PGE2 in stromal responses to the tumor is not known. Patients with advanced prostate cancer show sclerotic bone metastases, which cause chronic pain and pathologic fractures, however, the invasion of prostate cancer cells into bone tissues firstly induces bone destruction by increased osteoclast-mediated bone resorption. In this study, we investigate the roles of PGE2 and its receptor EP4 play a pivotal role in bone destruction and metastasis in an experimental metastasis model of human prostate cancer. Using PC-3 prostate cancer cells that are stably transfected with luciferase, we showed that the development of bone metastasis was accompanied by increased osteoclastic bone resorption in the bone metastasis microenvironment, and could be abrogated by an EP4 receptor antagonist. The growth of PC-3 cells in vitro was not influenced by PGE2 or by the EP4 antagonist treatment, however, cell-cell interactions between fixed PC-3 cells and host osteoblasts induced PGE2 production and RANKL expression in the osteoblasts. Addition of an EP4 antagonist suppressed both PGE2 and RANKL expression induced by the PC-3-osteoblast interaction, which would have consequent effects on osteoclast activation and osteolysis. In conclusion, the present study clearly showed that bone metastasis of human prostate cancer PC-3 was detected in vivo by the luminescence signals in the experimental metastasis model of nude mice, and the bone metastasis with increased osteoclastic bone resorption was abrogated by treatment of EP4 antagonist in vivo. The cell-to-cell interactions between PC-3 cells and host osteoblasts induced RANKL expression and PGE2 production by the osteoblasts, and adding EP4 antagonist suppressed the RANKL expression. Our data further define the mechanism by which the blockade of PGE-EP4 signaling inhibits bone metastasis of prostate cancer. This strengthens the concept that EP4 antagonists could be useful as therapeutic agents in advanced prostate cancer.

**Disclosures:** Masaki Inada, None.

## SU0049

**Effects Of P2X7R Activation On Receptor And Cell Functions In Human Myeloma Cell Lines.** Ankita Agrawal<sup>\*1</sup>, Lars Kruse<sup>1</sup>, Annette Vangsted<sup>2</sup>, Alison Gartland<sup>3</sup>, Niklas Jørgensen<sup>1</sup>. <sup>1</sup>The Research Centre for Ageing & Osteoporosis, Department of Clinical Biochemistry, Rigshospitalet, Glostrup, Denmark., Denmark, <sup>2</sup>Department of Haematology, Rigshospitalet, Copenhagen, Denmark, Denmark, <sup>3</sup>The Mellanby Centre for Bone Research, Department on Human Metabolism, The University of Sheffield, Sheffield, UK, United Kingdom

Purpose: Myeloma is a malignancy of plasma cells in the bone marrow. Even with the widespread use of novel agents, myeloma remains incurable and new treatment strategies are needed. Expression and function of P2X7R is implicated in leukemia and osteosarcoma and a high number of loss of function alleles in P2X7R gene are associated with a greater risk of myeloma than individuals not carrying these variant alleles. Therefore, the purpose of the study was to characterize P2X7R function in human myeloma cell lines (hMCL).

Methods: hMCL RPMI8226, U266 and NCIH929 were stimulated with 500  $\mu$ M or 300  $\mu$ M BzATP to assess YO-PRO-1 uptake or change in FLUO-4 fluorescence respectively with or without pre-treatment with P2X7R antagonists on NOVOstar. Treatment with 300  $\mu$ M BzATP followed by combined DAPI/ BrdU staining for quantitation of cell cycle phases by flow cytometry after 1 and 3 days, proliferation by colorimetric tetrazolium based assay and apoptosis by Annexin V/ PI assay after 2 days were analyzed.

Results: BzATP caused significant YO-PRO-1 uptake in all 3 hMCL compared to non-stimulated cells. Dye uptake was blocked in the presence of P2X7R antagonists at concentrations greater than 1  $\mu$ M in RPMI8226 and U266 but not in NCIH929. Significant increase in intracellular calcium concentrations due to BzATP was inhibited in the presence of P2X7R antagonists only in RPMI8226 hMCL. RPMI8226 showed a marked increase in percentage of cells in S phase of the cell cycle, with a concomitant reduction in the cells in G2/M and G1 phase after 1 day of BzATP treatment which was not seen after 3 days nor in the other hMCL. BzATP caused a significant reduction in proliferation with RPMI8226 more sensitive than the U266 and NCIH929. This inhibition of proliferation was accompanied by induction of cell apoptosis as assessed by flow cytometry. The increase in percentage of apoptotic cells was variable between the experiments but consistently more than the untreated controls and comparable to that induced by an antineoplastic agent bortezomib in RPMI8226, U266, less so in NCIH929.

Conclusions: P2X7R activation alters cell cycle progression in hMCL RPMI8226 whilst inhibiting cell proliferation and induction of apoptosis. Effects in U266 and NCIH929 are less pronounced and could be mediated by other P2 receptors. The data demonstrates the potency of P2X7R activation in controlling myeloma cell growth and highlights the potential of P2 receptors as targets in myeloma.

**Disclosures:** Ankita Agrawal, None.

**SU0050**

**Secreted microRNAs from Prostate Cancer Cells: Novel Therapeutic Targets.** Nicholas Farina<sup>\*1</sup>, Cody Callahan<sup>1</sup>, Coralee Tye<sup>1</sup>, Joseph Boyd<sup>1</sup>, Gary Stein<sup>2</sup>, Janet Stein<sup>3</sup>, Jane Lian<sup>4</sup>. <sup>1</sup>University of Vermont, United states, <sup>2</sup>University of Vermont Medical School, United states, <sup>3</sup>University of Vermont, United states, <sup>4</sup>University of Vermont, United states

**Introduction:** More than 80% of men with aggressive prostate cancer (PCa) develop metastatic disease and skeletal complications. Secreted microRNAs (miRNA) are emerging as biomarkers for monitoring disease progression and as therapeutic targets for PCa. Here we tested the hypothesis that miRNAs secreted from prostate cancer cells in the primary tumor function to alter the normal tissue environment and promote PCa. **Methods:** Use global miRNA (Affymetrix miRNA v4.0 arrays, miRBase v20) and gene expression (by stranded RNA-seq analysis) to 1) define cohorts of miRNAs secreted from prostate cancer cells representing different disease stages, 2) identify expression levels of their target mRNAs. RNA was isolated from normal prostate epithelial, early stage AR+ LNCaP, and metastatic PC-3 cells and from their conditioned media. Global expression of both secreted and extracellular miRNAs were interrogated with RNA-Seq profiles to identify differential expression (DE) of miRNA targets predicted from reciprocal miRNA – mRNA expression changes. **Results:** Secreted miRNAs candidates for promoting PCa progression were identified by comparing DE miRNAs between the 3 prostatic cell lines and their conditioned media. Numerous miRNAs are found to be both secreted and expressed robustly in the cell layer, while unique subsets of miRNAs in each cell line are either preferentially secreted or retained within the cell. Putative mRNA targets of these miRNAs were identified in our gene expression data from the reciprocal mRNA-miRNA relationships. The miRNAs were found to be associated with pathways known to play a role in PCa and metastatic bone disease including ErbB, Wnt, TGF- $\beta$ , and MAPK signaling, as well as biological processes unassociated with PCa. Functional *in vitro* studies were performed for miRNAs that were overexpressed or inhibited in highly metastatic PC-3 cell lines, by assaying, invasion, migration, and proliferation. For example, inhibition of miR-30a-5p, a known tumor suppressor, increases migration rate of RWPE-1 and PC-3 cells to heal a cell layer scratch, while overexpression prevents wound closure in RWPE-1 cells. **Conclusion:** Our combined data identify, for the first time, miRNAs secreted from prostate tumor cells that promote metastatic events of prostate cancer. Several of these miRNAs have been reported to be elevated in PCa patient serum and can provide diagnostic/prognostic biomarkers of tumor development, response to treatment, and recurrence.

**Disclosures:** Nicholas Farina, None.

**SU0051**

**The histone methyltransferase EZH2 is a novel therapeutic target in multiple myeloma bone disease.** Juraj Adamik<sup>\*1</sup>, Peng Zhang<sup>1</sup>, Quanhong Sun<sup>1</sup>, Rebecca Silbermann<sup>2</sup>, G. David Roodman<sup>3</sup>, Deborah L. Galson<sup>1</sup>. <sup>1</sup>University of Pittsburgh, United states, <sup>2</sup>Indiana University, United states, <sup>3</sup>University of Indiana, Veterans Administration Medical center, United states

Multiple myeloma (MM) is the most frequent cancer to involve the skeleton, with over 80% of patients developing osteolytic bone lesions due to hyperactivation of osteoclasts (OCL) that can result in severe bone pain and frequent pathological fractures and enhanced mortality. These bone lesions rarely heal even after therapeutic remission due to MM-induced suppression of bone marrow stromal cells (BMSC) differentiation into functional osteoblasts (OB), enhancing their support of MM growth, survival, and drug-resistance. We reported that MM cells induce increased recruitment of EZH2, the histone methyltransferase component of the Polycomb repressive complex 2 (PRC2), to the *Runx2* gene in the murine pre-OB cell line MC4 resulting in H3K27me3-mediated repression of *Runx2*, thereby causing repression of OB differentiation. In the present study, we show that H3K27me3 levels are elevated on the *Runx2* promoter in MM patient derived BMSC. Importantly, we found that the selective EZH2 inhibitor GSK126 enhances the active architecture at the *Runx2* promoter in both BMSC from MM patients and MM-treated MC4 cells, and rescues the osteogenic potential and mineralization capability. Therefore, we investigated the effects of GSK126 on MM cells. GSK126 inhibition of EZH2 induced dose-dependent, caspase 3-mediated, apoptosis of 5 human MM cell lines (U266, RPMI, MM1.S, H929 and JLN3) and the murine 5TGM1 MM cell line. In addition, GSK126 showed synergistic MM cell cytotoxic effects when used in combination with a suboptimal dose of the proteasome inhibitor bortezomib. Lastly, we analyzed the effects of GSK126 on pro-inflammatory, myeloma-amplified osteoclastogenesis. We reported that expansion of bone marrow monocytes (BMM) in the presence of MM1.S conditioned media significantly enhanced formation of TRAP-positive multinucleated OCL. We found that GSK126 significantly blocked the upregulation of OCL marker genes NFATc1, RANK, Cathepsin K, OSCAR, and DC-STAMP resulting in suppression of myeloma-enhanced, RANKL-induced osteoclastogenesis. Our study demonstrates that selective inhibition of the epigenetic modifier EZH2 using GSK126 *in vitro* decreases MM cell survival and positively regulates the bone microenvironment by suppressing OCL formation and improving the osteogenic potential of BMSC. These data suggest that targeting EZH2 activity may prove a valuable therapeutic strategy to improve bone health and limit disease progression in MM patients.

**Disclosures:** Juraj Adamik, None.

**SU0052**

**Coculture with Adipose Derived Stem Cells Inhibits Inflammation and Improves Differentiation of ATDC5 Chondrogenic Progenitor Cells.** Zhibo Sun<sup>\*</sup>, Xiaoyan Tang, Lakshmi Nair, Cato Laurencin. UConn Health Center, United states

Osteoarthritis (OA) is regarded as a complex multifactorial disease that may eventually affect the structure of all joint tissues, including cartilage, subchondral bone and synovium. Clinically, OA patients have different extent of synovitis, as shown by the increased level of interleukin-1  $\beta$  (IL-1  $\beta$ ), tumor necrosis factor  $\alpha$ , and complement factors. Adipose derived stem cells (ADSCs) have received increased attention in regenerative medicine. In order to better understand the effect of ADSCs on the prevention of OA progression, an *in vitro* model of OA was established.

To isolate ADSCs, we collected fat pad from the inguinal region of 6-8 week old mice and enzymatically digested for 2 hours. The study has four groups. Group 1: ATDC5 treated with 10 ng/ml IL-1  $\beta$ ; Group 2: ATDC5 without treatment; Group 3: ATDC5 treated with 10 ng/ml IL-1  $\beta$  for 24 h, and then cocultured with ADSCs for another 24 h; Group 4: ATDC5 were cocultured with ADSCs for 24 h. And then ATDC5 were induced to chondrogenic differentiation for 21 d. ADSCs identification was made by flow cytometry. MTS assay was used to evaluate the effects of IL-1  $\beta$  on the proliferation of ATDC5. Gene expression and chondrogenic differentiation was evaluated by expression of COX2, MMP3, MMP9, MMP13, TIMP1, type II collagen, type X collagen, aggrecan and alcian blue staining.

Flow cytometric analysis showed that 96.4% are CD90+, 99.4% are CD29 and 98.4% express CD105. Only 1.6% cells express CD45. The result of MTS showed that there were no significant differences by the treatment of IL-1  $\beta$  ( $P > 0.05$ ). The PCR results showed that ADSCs enhanced the expression of TIMP1 and inhibited the increase of COX2, MMP3, MMP9 and MMP13 levels in IL-1 $\beta$ -treated ATDC5 ( $P < 0.001$ ). The expression of COX2, MMP3, MMP9 and MMP13 was downregulated in Group 4 when compared with Group 2 ( $P < 0.01$ ). The expression of the chondrogenic differentiation markers was obviously enhanced in Group 4 when compared to other groups ( $P < 0.01$ ). Coculture with ADSCs can also effectively enhance the expression of type II collagen and aggrecan in Group 3 compared to Group 1 and 2 ( $P < 0.01$ ). Group 3 and 4 had the stronger alcian blue staining than the other two groups.

In conclusion, our data show that ADSCs can effectively relieve inflammation and improve chondrogenesis of ATDC5 cells, suggesting therapeutic potential for OA. We are currently evaluating the related mechanism.

**Disclosures:** Zhibo Sun, None.

**SU0053**

**Inhibition of Osteoclast-secreted Sphingosine 1 Phosphate reduces chondrocyte catabolism and prevents osteoarthritis in mice.** Chahrazad CHERIFI<sup>\*1</sup>, Augustin LATOURTE<sup>1</sup>, Pascal RICHETTE<sup>2</sup>, Eric HAY<sup>3</sup>, Martine COHEN-SOLAL<sup>2</sup>. <sup>1</sup>INSERM U1322, UNIVERSITY PARIS 7, France, <sup>2</sup>INSERMU1132, University Paris7, Hopital Lariboisiere, France, <sup>3</sup>INSERMU1132, University Paris7, France

**Purpose:** High osteoclastogenesis accompanies early stages of osteoarthritis (OA). Cartilage loss is reduced when osteoclast activity is inhibited in OA mice with bone hyperresorption. Although osteoclast-produced molecules affects chondrocyte metabolism, the mechanism by which inhibition of osteoclasts protects from cartilage damage is unclear. Our purpose was to investigate the role of Sphingosine 1 Phosphate (S1P) secreted by osteoclasts (Oc) in chondrocyte in OA.

**Methods:** The expression of S1P kinase (SPHK1) in human and murine OA joints was assessed by immunohistochemistry. S1P release from Oc was confirmed by SPHK1 activity. Primary murine chondrocytes and cartilage explants were cultured with osteoclast conditioned media (Oc-CM) to quantify matrix protein expression and proteoglycan content (RT-qPCR, WB, safranin O). S1P receptors antagonists (JTE-013 for S1PR2 and VPC 23019 for S1PR 1 and 3) as well as siRNA strategies were used to block S1P signaling. The contribution of S1P signaling in OA development was investigated in DMM receiving JTE-013.

**Results:** SPHK1 expression and activity increased with osteoclast differentiation and was expressed in human OA cartilage. Primary murine chondrocytes and femoral head explants cultured in the presence of Oc-CM induced a lower proteoglycan release and a higher metalloprotease expression (MMP3, MMP13, ADAMTS-4, ADAMTS-5) compared to controls. Oc-CM promoted the expression of S1P receptors 1-3 in chondrocytes, as well as the activation of the MAPK signaling pathway. However, Oc-CM enhanced MMP-3 and -13 by receptor S1PR2 only, but not by S1PR1-R3. This effect was confirmed in femoral head explants. Moreover, administration of JTE-013 in DMM mice reduced OA score ( $6.25 \pm 0.63$  vs  $4.14 \pm 0.26$ ,  $p < 0.05$ ) and MMP-13 expression compared to controls.

**Conclusion:** Activation of S1P signaling by osteoclasts promotes chondrocyte catabolism by the activation S1PR2. The inhibition of S1P was able to prevent OA in mice. Therefore, subchondral bone manipulations may affect chondrocyte function and OA.

**Disclosures:** Chahrazad CHERIFI, None.

**SU0054**

**Secreted factors from synovial fibroblasts immediately regulate gene expression in articular chondrocytes.** Anke Jeschke\*, Martin Bonitz, Stephanie Peters, Michael Amling, Thorsten Schinke. Department of Osteology & Biomechanics, University Medical Center Hamburg Eppendorf, Germany

Although articular cartilage degeneration represents a major public health problem, the underlying molecular mechanisms are poorly characterized and the treatment options for osteoarthritis are still limited. We have previously applied genome-wide expression analyses with porcine samples to identify specific markers of either growth plate or articular cartilage. Since the molecular differences observed in the native tissues were also found in cultured chondrocytes derived from both sites, we utilized primary porcine articular chondrocytes (PPACs) for the present study. More specifically, we treated PPACs by administration of conditioned medium from porcine synovial fibroblasts (SF-CM) and then assessed their molecular behavior. While we did not observe effects of SF-CM on proliferation or metabolic activity, a 24-hour administration of SF-CM to PPACs significantly increased apoptotic indices. The deduced negative influence of SF-CM on PPACs was further confirmed at the transcriptional level. More specifically, we found that 6-hour administration of SF-CM to PPACs significantly reduced expression of chondrocytic markers (*ACAN*, *THBS4*), while it strongly induced expression of *SDC4*, encoding a positive regulator of articular cartilage breakdown. Using *SDC4* expression as a read-out we additionally found that i) conditioned medium from human synovial fibroblasts has the same effect, that ii) addition of serum abolishes this effect, and that iii) the *SDC4*-inducing activity is found in a fraction of approximately 40 kDa after separating the SF-CM by gel filtration. To identify additional SF-CM-responsive genes in PPACs we further applied genome-wide expression analysis and subsequent qRT-PCR. We thereby observed that SF-CM strongly induces *MMP13* expression in PPACs, even after 2 hours of incubation, and that this effect was not observed in primary porcine growth plate chondrocytes. Taken together, our data strongly suggest that synovial fibroblasts secrete one or more molecule(s) that induce specific signaling events in articular chondrocytes.

**Disclosures:** *Anke Jeschke, None.*

**SU0055**

**The role of camk in degenerative cartilage of rats mandibular condylar induced by unilateral anterior crossbite.** Xianghong Wan<sup>1</sup>, Mian Zhang<sup>1</sup>, Jing Zhang<sup>1</sup>, Lei Lu<sup>1</sup>, Hongyun Zhang<sup>2</sup>, Hongxu Yang<sup>1</sup>, Meiqing Wang<sup>\*1</sup>. <sup>1</sup>College of Stomatology, Fourth Military Medical University, China, <sup>2</sup>College of Stomatology, Forth Military Medical University, China

**Purpose:** The Ca<sup>2+</sup>/calmodulin-dependent protein kinase II (CaMKII) is the CaMK isoform which is widely expressed including in articular cartilage. It promotes chondrocytes to differentiate via Indian hedgehog (Ihh) pathway. Whether it involves in osteoarthritis remains obscure. Temporomandibular joint (TMJ) is frequently suffered from OA most often due to dental biomechanical effects. Currently, we used a rat OA model developed in our lab to investigate the role of CaMKII in development of TMJ OA. **Materials and methods:** Sprague-Dawley female rats were treated by installing metal prosthesis onto the right side maxillary and mandibular incisors to create a relation of unilateral anterior crossbite (UAC) as we reported. KN93, the competitive inhibitor of CaMK was injected to TMJ of UAC rats at 4- and 8-weeks. Animals were sacrificed at 8- and 12-weeks, respectively. Hematoxylin-eosin (HE) and safranin O (SO) staining were carried out for studying the morphological changes of the condylar cartilage. Immunohistochemical (IHC) staining and Western blot was used to observe CaMK? and Ihh expression. Real-time PCR analysis was adopted to detect the expression of differentiation and proliferation related genes. **Results:** Cartilage degeneration progressed with time was observed in UAC cartilage, showing as reduction in cartilage thicknesses and SO positive staining area compared with the age matched controls. There was increased number of CaMKII positive cells and Ihh positive cells. The mRNA expression levels of differentiation related genes, such as *Mmp13*, *Adamts5*, *Alp* were up-regulated but the proliferation and matrix related genes like *Pcna*, *Col2a1* and *Aggrecan* were down-regulated. The expression of phosphorylation CaMK? protein as well as Ihh protein from UAC condyle cartilage were both increased. Injection of KN93 revised these molecular changes and rescues the cartilage phenotype. **Conclusion:** In the UAC induced TMJ OA cartilage there was enhanced chondrocytes differentiation mediated by CaMK?-Ihh signaling. Inhibition of this pathway improved the degenerative changes, yet worth a further study using genetically modified animals.

**Disclosures:** *Meiqing Wang, None.*

*This study received funding from: NSFC No.81530033*

**SU0056**

**Changes in the phosphorylation of guanylyl cyclase-B (GC-B) regulates bone growth in a mouse model.** Jerid Robinson\*<sup>1</sup>, Leia Shuhaibar<sup>2</sup>, Siu-Pok Yee<sup>2</sup>, Laurinda Jaffe<sup>2</sup>, Lincoln Potter<sup>1</sup>. <sup>1</sup>University of Minnesota, United states, <sup>2</sup>University of Connecticut Health Centers, United states

Guanylyl cyclase-B (GC-B), also known as natriuretic peptide receptor 2 (Npr2), is a membrane bound receptor that converts GTP to the second messenger cGMP in response to the extracellular binding of its ligand, C-type natriuretic peptide (CNP). To transmit the extracellular binding signal to stimulate maximum GTP catalysis, GC-B must be phosphorylated on multiple serine and threonine residues, and dephosphorylation inactivates GC-B. In fact, GC-B dephosphorylation is a regulatory element in the resumption of meiosis in ovarian follicles. In this study, we investigated the physiologic effects of a constitutively phosphorylated form of GC-B using a knockin mouse expressing a mutant form of GC-B where all known phosphorylation sites were mutated to the phospho-mimetic glutamate (GC-B<sup>7E/7E</sup>). In this way, we can study the role of GC-B dephosphorylation in regulating chondrogenesis in a mouse model. We observed that the GC-B<sup>7E/7E</sup> mice have longer naso-anal, femoral, and tibial length at 4, 8, and 16 weeks compared to GC-B<sup>WT/WT</sup> mice. At 4 weeks, GC-B<sup>7E/7E</sup> mice were 7% longer than GC-B<sup>WT/WT</sup> littermates, at all indices. By 8 weeks, GC-B<sup>7E/7E</sup> mice were 12% longer than GC-B<sup>WT/WT</sup> mice, and this effect was sustained at 16 weeks. GC-B<sup>7E/7E</sup> mice also had longer CA5 vertebrae and tails, which grow by a mix of endochondral and membranous ossification, compared to GC-B<sup>WT/WT</sup> mice. Importantly, there were no differences in cranial width between GC-B<sup>WT/WT</sup> and GC-B<sup>7E/7E</sup> mice, consistent with GC-B only being involved in endochondral and not membranous ossification. Together, these data indicate that changes in GC-B phosphorylation regulate endochondral bone growth in mice. By blocking or reducing GC-B dephosphorylation, it may be possible to develop novel therapeutic strategies for disproportionate chondrodysplasias.

**Disclosures:** *Jerid Robinson, None.*

**SU0057**

**Dwarfism in Agcl1-Cre Mice is Associated With Decreased Expression of Aggrecan in Chondrocytes.** Harunur Rashid\*, Haiyan Chen, Mohammad Hassan, Amjad Javed. Department of Oral & Maxillofacial Surgery, School of Dentistry, University of Alabama at Birmingham, United states

The Cre-loxP recombination system is a powerful tool for spatio-temporal inactivation of genes but its success depends on efficiency of the Cre driver-lines. Cre-transgenics mostly created by random integration are fraught with leaky and poor Cre expression due to copy-number and site of integration effect. To circumvent these issues Cre lines are developed by homologous recombination. In Aggrecan-Cre (Agcl<sup>Cre</sup>) model, 3.8kb fragment comprising Cre recombinase fused with estrogen receptor is inserted in the 3'UTR of the Aggrecan gene locus. The objective of this study was to determine efficient dosage of Cre recombinase in Agcl<sup>Cre</sup> mouse. At birth wild-type (WT) and Agcl<sup>Cre</sup> mice were similar in size and weight. However, homozygous Agcl<sup>Cre/Cre</sup> (HM) mice exhibited growth retardation in post-natal life. Compared to WT, the HM mice showed 22% reduced body weight at 3 weeks and 32% at 3 months. In addition, by 3 month of age, total body and limb lengths in HM mice were shorter by 22% and 35% respectively. Body weight and size of heterozygous Agcl<sup>+Cre</sup> (HT) mice were comparable to WT littermates. Aggrecan is a major chondroitin sulfate proteoglycan expressed by the proliferative chondrocytes of growth plate and the articular cartilage. Histologic analysis of femurs revealed 20% reduction in the length of proliferative zone and 40% reduction of proteoglycan within cartilage. These changes were not limited to growth plate, as thickness of articular cartilage was also decreased by 30% in HM mice. Consistent with the impaired cartilage matrix, early chondrocytes markers Sox9 and Col2 showed 50% reduced expression. Deficiency in the cartilage matrix of Agcl<sup>Cre</sup> HM mice is similar to phenotype of global Agcl<sup>+/-</sup> heterozygous mice. For a molecular understanding of dwarfism, we performed RNA and protein analysis. We found 40% decrease in Aggrecan mRNA and 45% decrease in levels of Aggrecan protein in HM mice. Aggrecan mRNA was decreased by 18% in HT mice but levels of Aggrecan protein were comparable to WT littermate. These data indicate presence of Cre-transgene in the 3'UTR of Aggrecan allele likely caused mRNA instability leading to a decrease in Aggrecan protein and dwarfism. Finally we confirmed Cre activity in Agcl<sup>Cre</sup> HT mice by using td-Tomato reporter line. We find single copy of Cre-transgene is sufficient for efficient gene deletion in chondrocyte. Thus heterozygous Agcl<sup>Cre/+</sup> mice that exhibit no phenotype should be used to delete target gene in cartilage tissue.

**Disclosures:** *Harunur Rashid, None.*

## SU0058

**Novel Intracellular Function of CCN2 -Role of Interaction Between CCN2 and Rab14 in Vesicle Trafficking in Chondrocytes-** Mitsuhiro Hoshijima\*<sup>1</sup>, Takako Hattori<sup>2</sup>, Eriko Aoyama<sup>3</sup>, Takashi Nishida<sup>2</sup>, Satoshi Kubota<sup>2</sup>, Hiroshi Kamioka<sup>4</sup>, Masaharu Takigawa<sup>3</sup>. <sup>1</sup>Department of Orthodontics Okayama University Graduate School of Medicine, Dentistry & Pharmaceutical Sciences, Advanced Research Center for Oral & Craniofacial Sciences, Japan, <sup>2</sup>Department of Biochemistry & Molecular Dentistry Okayama University Graduate School of Medicine, Dentistry & Pharmaceutical Sciences, Japan, <sup>3</sup>Advanced Research Center for Oral & Craniofacial Sciences Okayama University Graduate School of Medicine, Dentistry & Pharmaceutical Sciences, Japan, <sup>4</sup>Department of Orthodontics Okayama University Graduate School of Medicine, Dentistry & Pharmaceutical Sciences, Japan

CCN family 2 / connective tissue growth factor (CCN2 / *ctgf*) is strongly expressed in cartilage and modulates chondrocyte differentiation and proliferation by binding various molecules. The objective of this study is to identify a CCN2-interactive protein and to investigate physiological significance of its interaction in chondrocytes. We carried out a yeast two-hybrid screening using CCN2 as a bait and a cDNA library from the human chondrocytic cell line, HCS-2/8, and identified Rab14 GTPase (Rab14) as a CCN2-interactive peptide. Rab14 is known to be involved in vesicle trafficking between the golgi complex and endosomes. For analysis of the CCN2 domain binding to full-length Rab14, we carried out growth tests of yeast transformants in selection media. CCN2 bound to Rab14 through its IGFBP domain among the four domains in CCN2. To detect the colocalization between CCN2 and Rab14 in the cells, GFP tagged CCN2 (GFP-CCN2), Halo tagged Rab14 (Rab14 WT), a constitutive active form (Rab14 CA), and a dominant negative form (Rab14 DN) of Rab14 were overexpressed in COS7 cells. Ectopically overexpressed Rab14 showed diffused cytosolic distribution in COS7 cells, however, when Rab14 WT or Rab14 CA overexpressed with GFP-CCN2, Rab14 distribution changed as dotted spot every distributed within cytosol and Rab14 and GFP-CCN2 showed good colocalization. Coexpression of Rab14 DN and GFP-CCN2 also showed dotted codistribution, but more concentrated in perinuclear area. In addition, HCS-2/8 chondrocytic cells were transfected with *rab14* or *ccn2* siRNA, and gene expression of *bip*, *chop* and *aggrexin* mRNA was monitored by real-time PCR. Decrease in *rab14* or *ccn2* mRNA by siRNA enhanced the expression of *chop* and *bip* mRNA significantly. Furthermore, to study the effect of interaction between CCN2 and its interactive proteins on proteoglycan synthesis, HCS-2/8 cells were transfected with Rab14 WT or Rab14 CA or Rab14 DN, and the proteoglycan accumulation was monitored by Toluidine Blue or Alcian Blue staining. Rab14 DN-overexpressed in HCS-2/8 cells decreased proteoglycan accumulation to less than 75% as compared to Rab14 WT-overexpressed in the cells. Our results suggest that intracellular CCN2 is associated with Rab14 on proteoglycan-containing vesicles during their transport from golgi to endosomes in chondrocytes and that the association play some role in proteoglycan synthesis by chondrocyte.

**Disclosures:** Mitsuhiro Hoshijima, None.  
This study received funding from: JSPS

## SU0059

**Targeting Developmental Phases of Heterotopic Ossification with BMP Receptor Inhibitors Allows for Delayed, Short-term Treatment.** Shailesh Agarwal\*<sup>1</sup>, Shawn Loder<sup>1</sup>, John Li<sup>1</sup>, Christopher Breuler<sup>1</sup>, James Drake<sup>1</sup>, Cameron Brownley<sup>1</sup>, Jonathan Peterson<sup>1</sup>, Kavitha Ranganathan<sup>1</sup>, Oluwatobi Eboda<sup>1</sup>, Hsiao Hsin Sung<sup>1</sup>, Shuli Li<sup>1</sup>, Nabuhiko Kamiva<sup>2</sup>, Yuji Mishina<sup>1</sup>, Benjamin Levi<sup>1</sup>. <sup>1</sup>University of Michigan, United states, <sup>2</sup>University of Texas - Southwestern, United states

**PURPOSE:** Trauma-induced heterotopic ossification (tHO) is the aberrant growth of bone in soft tissue, which develops in patients with severe musculoskeletal trauma. Morbidity associated with excision, recurrence, and the inability to reverse chronic deformity make tHO prevention critically important. Although long-term treatment with non-specific Bmp receptor inhibitors reduces tHO, this approach is not clinically feasible due to adverse effects associated with systemic non-specific inhibition. We utilize three therapeutic approaches to reduce tHO when administered during different histologic phases and demonstrate the effect of targeting the type I Bmp receptor Acvr1.

**METHODS:** Wild-type mice underwent 30% total body surface area partial thickness burn with a 60C metal block for 18 seconds. The Achilles tendon was transected immediately afterwards. Mice underwent daily injection of LDN19 (6mg/kg), LDN21 (6 mg/kg), or Alk3fc (2mg/kg) during weeks 0-2 (inflammatory), 2-4 (chondrogenesis), 4-6 (osteogenesis), or 0-6 (long-term) after burn/tenotomy. Mice with genetic knockout of Acvr1 (*Ub.creER/Acvr1<sup>fl/fl</sup>*) were treated with tamoxifen to induce post-natal loss followed by injury. HO was quantified by microCT 9 weeks after injury, and cartilage formation was followed using pentachrome staining.

**RESULTS:** Daily long-term treatment with LDN19, LDN21, or Alk3-fc all significantly reduced tHO (LDN19: 2.66 mm<sup>3</sup>, LDN21: 2.34 mm<sup>3</sup>, Alk3-fc: 2.95

mm<sup>3</sup>, Control: 6.51 mm<sup>3</sup>, p<0.05 for pairwise comparisons with control). LDN19 during weeks 0-2 after injury significantly reduced tHO (2.91 mm<sup>3</sup>, p<0.05) while LDN21 during weeks 2-4 was most effective (2.89 mm<sup>3</sup>, p<0.05) (Fig 1). Treatment from weeks 0-2 coincided with significant reduction in neutrophil, macrophage, and mesenchymal cell infiltration on histology (p<0.05). Treatment from weeks 2-4 coincided with reduction in ectopic chondrogenesis by Alcian blue staining. Finally, Acvr1 knockout significantly reduced tHO (1.00 mm<sup>3</sup> v. 4.36 mm<sup>3</sup>, p<0.05).

**CONCLUSIONS:** Bmp receptors can be inhibited for short periods of time after injury to prevent tHO. Bmp inhibitors administered immediately following injury may act through their effects on the inflammatory response rather than differentiation, but these drugs also have effects on differentiation when inflammation is allowed to proceed normally. Finally, targeting Acvr1 may allow for effective therapy with improved specificity.

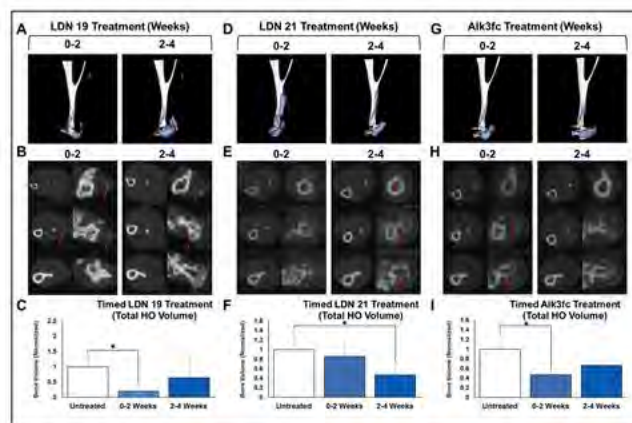


Figure 1

**Disclosures:** Shailesh Agarwal, None.

## SU0060

**Epigenetic Regulator, Uhrf1, Controls not Only Cell Proliferation but Also Chondrocyte Differentiation During Limb Development.** Michiko Yamashita\*<sup>1</sup>, Kazuki Inoue<sup>1</sup>, Iori Sakakibara<sup>1</sup>, Yuuki Imai<sup>1</sup>. Division of Integrative Pathophysiology, Proteo-Science Center, Ehime University, Japan

Ubiquitin-like with PHD and ring finger domains 1 (Uhrf1) plays a significant role in both physiological and pathological condition such as various types of cancers. Uhrf1 can recognize H3K9me2/3 and ubiquitinates H3K23 residue and governs Dnmt1 activity mediated maintenance DNA methylation, which is well-known molecular mechanism during cell proliferation. However, the function of *Uhrf1* is completely unknown in musculoskeletal tissues or cells, especially during cell differentiation. Here, we analyzed physiological function of *Uhrf1* in skeletal tissue using limb-specific *Uhrf1* knockout mice.

Limb mesenchymal cell specific *Uhrf1* KO mice (cKO) have been generated by crossing *Prx1-Cre* mice with *Uhrf1* flox mice. Appearance of cKO mice displayed remarkably shortened limbs when compared with control mice. Bone mineral density (BMD) of cKO male femur at 6 weeks of age was about 20% lower than that of control group. Long bone length was 30-40% lower than that of control group, calculated from soft X-ray. Furthermore,  $\mu$ CT revealed angular and rotational deformities in cKO femur (Figure 1). H&E staining of proximal humerus at postnatal day 7 showed that columnar structures of chondrocytes in growth plate of cKO mice were disturbed and the area of growth plate cartilage was significantly decreased in cKO mice (n=3-6).

In addition, we examined function of Uhrf1 in chondrocyte differentiation using primary cultured chondrocytes obtained from knee cartilages of cKO mice and control mice. Alcian Blue Staining after treatment with 100 ng/ml rhBMP-2 for 7 days displayed that cartilage matrix synthesis by primary cultured chondrocytes obtained from cKO was decreased compared to that from control. Moreover, expression levels of early marker genes were decreased, on the other hand, late marker genes' expression was increased in cKO group. Especially, an expression level of *Mmp13* was significantly elevated in cKO group. These results suggested that Uhrf1 might be a positive regulator in chondrocyte differentiation and maintenance DNA methylation might have important role not only in cell proliferation but also cell differentiation. To unveil the molecular function of *Uhrf1* in chondrocyte differentiation, genome-wide integrated analyses with RNA-seq and methylated DNA immunoprecipitation and high throughput sequencing (MeDIP-seq) provides Uhrf1 mediated target genes during chondrocyte differentiation and limb development.



Figure 1

Disclosures: Michiko Yamashita, None.

### SU0061

**Exercise or Caloric Restriction Treatments Beneficially Affect Trabecular Microarchitecture, while Cortical Bone Strength is only Improved with Exercise in Obese, T2D rats.** Laura Ortinau\*, Matthew Richard, Rebecca Dirkes, Melissa Linden, R. Scott Rector, Pamela Hinton. University of Missouri, United states

Individuals with type 2 diabetes (T2D) have greater fracture risk, despite normal bone mineral density (BMD). Here we tested the hypothesis that treatment of hyperphagic, T2D Otsuka Long-Evans Tokushima Fatty (OLETF) rats with treadmill running exercise (EX) or caloric restriction (CR) would improve bone outcomes. Eight-wk old, male OLETF rats were fed a high-fat, high-sucrose diet with cholesterol (HFSC: 45% kcal fat; 17% kcal sucrose; 1% w/w cholesterol) and maintained in a sedentary cage condition until onset of hyperglycemia (20 wks of age). At 20 wks, OLETF rats were randomly assigned to three groups: ad libitum fed, sedentary (O-SED); ad libitum fed, treadmill running (O-EX); or, sedentary, 30% CR relative to O-SED (O-CR). Sedentary Long-Evans Tokushima Otsuka rats served as non-hyperphagic, lean controls (L-SED). At 32 wks of age, total body BMD was measured by DXA prior to sacrifice and then blood and tibiae collected. Serum bone turnover markers were assessed using ELISA. Cortical morphometry and trabecular microarchitecture was determined by  $\mu$ CT and bone strength was assessed using torsional loading to failure. A one-way ANCOVA was used to test for group differences ( $p < 0.05$ ), using body weight at 20 wks of age and the change in body weight from 20 to 32 wks of age as covariates. Fasting glucose was greater in O-SED vs. L-SED; EX or CR attenuated this increase. Total body BMD was similar between L-SED and O-SED; EX or CR increased BMD vs. O-SED. CR, but not EX, reversed the reduction in P1NP observed in O-SED ( $p < 0.01$ ). EX, but not CR, reversed the increase in CTx seen in O-SED. Serum sclerostin was elevated in O-SED, O-EX, and O-CR vs L-SED. Compared to L-SED, O-SED had reduced trabecular number (TbN;  $p = 0.06$ ), and increased structural model index (SMI;  $p < 0.01$ ). EX or CR increased bone volume and TbN and reduced trabecular separation; CR, but not EX, reduced SMI. Tibia cortical thickness (CtTh) and relative cortical area (CtAr/TtAr) were similar between L-SED and O-SED; EX increased CtTh and CtAr/TtAr vs all treatments. Relative to L-SED, O-SED had reduced whole-bone strength (Tmax;  $p = 0.06$ ) and stiffness (Ks;  $p < 0.01$ ). EX, but not CR, normalized Tmax and Ks. Tissue-level stiffness (Su) was not different between L-SED, O-SED, and O-CR. EX increased Su vs O-SED and O-CR ( $p < 0.05$ ). Overall, T2D negatively affected bone outcomes, and EX or CR treatment positively affected tibial trabecular microarchitecture; however, only EX increased tibial strength.

Disclosures: Laura Ortinau, None.

This study received funding from: Department of Nutrition & Exercise Physiology; Margaret Mangel Faculty Research Catalyst Fund.

### SU0062

**Role of Panx1-P2X7R Signaling in Anabolic Bone Response of Type 1 Diabetic Mice.** Zeynep Seref-Ferlengez\*<sup>1</sup>, Aylin E. Uyar<sup>1</sup>, Marcia Urban-Maldonado<sup>1</sup>, Mitchell B. Schaffler<sup>2</sup>, Hui B. Sun<sup>1</sup>, Sylvia O. Suadican<sup>1</sup>, Mia M. Thi<sup>1</sup>. <sup>1</sup>Albert Einstein College of Medicine, United states, <sup>2</sup>City College of New York, United states

Type 1 diabetes (T1D) manifests at early adolescence and leads to significant skeletal complications and increases risk of osteoporosis and fractures. Our previous

studies demonstrated that high glucose levels, a hallmark of T1D, alter the osteocytes, key mechanosensing cells, response to mechanical stimulation. We also showed that the Panx1-P2X7R signaling complex plays essential roles in osteocyte ATP and  $Ca^{2+}$  mechanosignaling. Given that maintenance of skeletal integrity in response to daily physical activity relies on ability of bone cells to perceive and respond to mechanical loading, and that P2X7R plays essential roles in bone mechanotransduction, we investigated whether impaired anabolic response to mechanical loading in T1D is associated with altered Panx1-P2X7R signaling. In this study we used the Akita (C57BL/6J-Ins2<sup>Akita</sup>) mouse model of T1D and Panx1-KO mice. Akita, Panx1-KO and age-matched wildtype (WT) mice (8 wk old, male,  $n = 7$ /group) were submitted to mechanical loading by treadmill running (2 or 4 weeks; 5 days/wk, 300 m/day) or to normal cage control activity. All animals were euthanized immediately after the last running bout. Right hindlimbs were used for histomorphometry, and lefts were used to study the expression of Panx1 and P2X7R by Western blotting (pulverized osteocytes enriched bones). All experiments were performed under IACUC approval. Histomorphometry studies showed that 4-wk loading caused radial expansion in femur ( $p < 0.05$ ; Fig. 1) in WT mice compared to cage controls. In contrast, Akita and Panx1-KO mice did not show anabolic response with loading. Basal Panx1 and P2X7R expression levels in Akita bones were significantly lower compared to age-matched WT controls. Panx1 and P2X7R were markedly upregulated in WT loaded bone following 2-wk treadmill-loading when compared to non-loaded controls (Fig. 2). Nonetheless, levels of both Panx1 and P2X7R in 4-wk loaded WT bone were comparable to non-loaded controls. This adaptive response was not lost in diabetic bone, but was dysregulated particularly in regard to Panx1 expression (red traces), which indicates that diabetic mice are unable to properly adapt to mechanical loading. Our current findings demonstrate that load-induced bone anabolic response is impaired in T1D similar to Panx1-KO mice and is likely related to T1D-induced dysregulation of Panx1-P2X7R, which is essential for proper response to mechanical loading and maintenance of bone health.

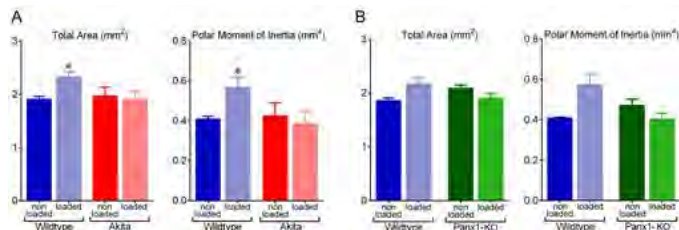


Figure 1. Load-induced anabolic response is impaired in (A) Akita T1D mice and in (B) Panx1-null mice compared to age-matched wildtype. Histological studies showing load-induced changes in Total Bone Area and Polar Moment of Inertia (J) in 12-week Akita, Panx1-KO and age-matched wildtype mice. Mechanical loading (treadmill running, 300 meter/day for 5 consecutive days with 2 resting days) was imposed for 4 weeks while the age-matched controls (cage activity),  $n = 7$ /group for (A) and  $n = 4$  for (B). Data are presented as the means  $\pm$  SEM.

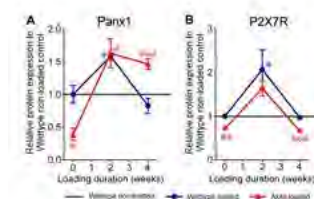


Figure 2. Mechanosignaling complex Panx1 and P2X7R responds differently to mechanical loading in wildtype and Akita mice. Expression of Panx1 (A) and P2X7R (B) Akita mice compared to their age-matched wildtype after 2 or 4 weeks of loading (treadmill running). \* $P < 0.05$ , \*\*\* $P < 0.001$ , wildtype vs. respective Akita,  $n = 4$  (each group in 2-week loading);  $n = 7-9$  (each group in 4-week loading). Data are presented as the means  $\pm$  SEM.

Figures

Disclosures: Zeynep Seref-Ferlengez, None.

### SU0063

**Association of Increased Serum Leptin with Ameliorated Anemia and Body Mass Index in Stage 5 Chronic Kidney Disease Patients after Parathyroidectomy.** Yao Jiang<sup>1</sup>, Jingjing Zhang<sup>1</sup>, Yanggang Yuan<sup>1</sup>, Xiaoming Zha<sup>1</sup>, Changying Xing<sup>1</sup>, Chong Shen<sup>2</sup>, Zhixiang Shen<sup>3</sup>, Chao Qin<sup>1</sup>, Ming Zeng<sup>1</sup>, Guang Yang<sup>1</sup>, Huijuan Mao<sup>1</sup>, Bo Zhang<sup>1</sup>, Xiangbao Yu<sup>1</sup>, Bin Sun<sup>1</sup>, Chun Ouyang<sup>1</sup>, Xueqiang Xu<sup>1</sup>, Yifei Ge<sup>1</sup>, Jing Wang<sup>1</sup>, Lina Zhang<sup>1</sup>, Chen Cheng<sup>1</sup>, Caixia Yin<sup>1</sup>, Jing Zhang<sup>1</sup>, Huimin Chen<sup>1</sup>, Haoyang Ma<sup>1</sup>, Ningning Wang<sup>\*</sup>. <sup>1</sup>The First Affiliated Hospital with Nanjing Medical University, China, <sup>2</sup>Nanjing Medical University, China, <sup>3</sup>Jiangsu Province Geriatric Hospital, China

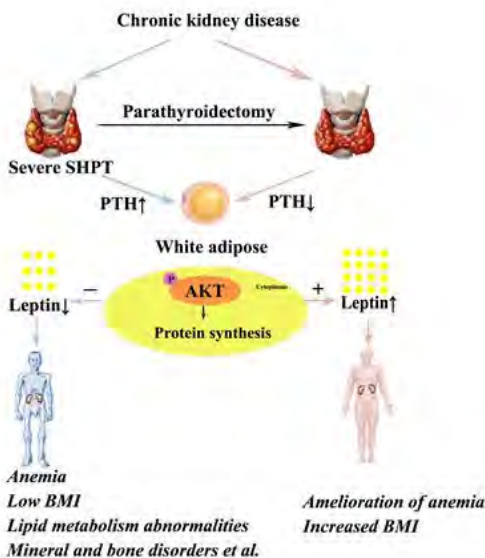
Background: Leptin is an adipokine that has a wide spectrum of biological activities such as hematopoiesis, energy homeostasis and bone metabolism, but its association with secondary hyperparathyroidism (SHPT), a complication of chronic kidney disease-mineral bone disorder (CKD-MBD), remains obscure. Parathyroidectomy (PTX) is recommended to severe SHPT patients. Here we investigated the associations of circulating leptin levels and clinical characteristics in CKD patients and their changes after PTX, effects of PTX on leptin production were analyzed both *in vivo* and *in vitro*.

Methods: This cross-section study enrolled 100 controls and 209 stage 5 CKD patients [median serum intact parathyroid hormone (iPTH): 404.9pg/ml], with a longitudinal observation on 40 PTX patients (baseline median serum iPTH: 1970.8pg/

ml, median follow-up time: 5.7 months). Serum Leptin was determined by ELISA and adjusted by body mass index (BMI). 3T3-L1 adipocytes were stimulated with 10% human serum or different concentrations of P, Ca, and PTH. The serum stimulated groups included healthy controls, No-PTX CKD patients, preoperative and postoperative PTX patients. Leptin in the medium were measured by ELISA. Leptin, phosphate-Akt and Akt protein in cytoplasm were detected by Western.

Results: Serum leptin levels increased in parallel to BMI both in controls and CKD patients. Owing to a larger proportion of CKD patients with BMI < 23 (a marker of malnutrition), approximate Inleptin/BMI between controls and patients were proved. Serum Inleptin/BMI was positively correlated with hemoglobin and serum albumin levels in CKD group. Higher lnPTH was associated with lower Inleptin/BMI in PTX patients. Retrieved preoperative anemia and low BMI were related with postoperative increased Inleptin/BMI. Severe SHPT inhibited uremia-enhanced leptin production in adipocytes, which could be attenuated after PTX. High PTH, not calcium or phosphorus, reduced Akt phosphorylation and leptin production. Up-regulated Akt signaling mediated postoperative increased leptin production *in vitro*.

Conclusions: Serum Inleptin/BMI related with anemia, albumin, and bone metabolism disorder in CKD patients. Successful PTX improved anemia and BMI in severe SHPT patients, which correlated with increased circulating leptin levels via up-regulated Akt pathway in adipocytes. Our findings indicated the therapeutic potential of leptin and related target pathway to improve the quality of life and survival in CKD.



Leptin in CKD: A Link between Anemia, BMI and SHPT.

Disclosures: Ningning Wang, None.

## SU0064

**Does the Adipokine, Adiponectin, play a role in the Coupling between Fat and Bone?.** Jillian Cornish\*, David Musson, Dorit Naot, University of Auckland, New Zealand

Objectives: Clinical studies found that the circulating levels of adiponectin, a peptide hormone secreted from adipocytes, are inversely related to visceral fat mass and to bone mineral density (BMD) and it has been suggested that adiponectin plays a role in the coupling between fat and bone. Laboratory investigations of adiponectin activity in bone produced inconsistent results. The aim of our study was to elucidate the role of adiponectin in skeletal physiology through a comprehensive analysis of the bone phenotype of adiponectin-knockout (APN-KO) mice.

Methods: Ten wild-type C57Bl/6J (WT) and 10 APN-KO (C57Bl/6J background) female mice were culled at 8, 14, 21 and 28 weeks and groups of 12 mice at 37 weeks. BMD and body composition were determined longitudinally in the last two groups by DXA. Micro-architecture of femora was analysed by micro CT (SkyScan 1172). Bone material properties were determined by nano-indentation and bone strength by three-point bending.

Results: The main differences between the groups were the lower cortical bone fraction in APN-KO at all the time points ( $P < 0.001$ ) and lower cortical thickness from week 14 onwards ( $P < 0.01$ ). Trabecular bone fraction was lower only in young animals ( $P < 0.05$ ). The longitudinal study found lower BMD in APN-KO mice ( $P = 0.04$ ) and a substantial reduction in percentage fat ( $P < 0.0001$ ). Bone material properties and strength were similar in the two groups. We found that adiponectin deficiency affects bone geometry and BMD negatively, but the differences in bone properties are fairly moderate and do not compromise bone strength.

Conclusion: Our study of the bone properties of adiponectin-knockout mice found negative effects of adiponectin-deficiency on bone geometry and density, suggesting a positive activity of adiponectin in bone. Assuming adiponectin has similar effects in humans, the low circulating levels of adiponectin associated with increased fat mass

are therefore unlikely to directly contribute to the parallel increase in bone mass, and our results do not support a direct role for adiponectin in the coupling between fat and bone tissue.

Disclosures: Jillian Cornish, None.

## SU0065

**High Fat Diet-Induced Maternal Obesity Programs Skeletal Development in Mice.** Jin-Ran Chen\*, Oxana P. Lazarenko, Michael L. Blackburn, Kartik Shankar, Arkansas Children's Nutrition Center & the Department of Pediatrics, University of Arkansas for Medical Sciences, United States

Nutritional status during intrauterine and/or early postnatal life has substantial influences on adult offspring health, mostly linked with permanent metabolic changes. However, evidence on the impact of high fat diet (HFD)-induced maternal obesity on regulation of adult offspring bone formation is sparse. Thus, we investigated the effects of maternal obesity in mice on both fetal skeletal development and adult offspring bone metabolism. Female C57BL/6J mice were fed either a low-fat AIN-93G control diet or a HFD (45% fat calories) for 12 wks starting at postnatal day 21 (PND21). After 12 wks of these diets, lean (from control diet) and obese (from HFD) female mice were time-impregnated ( $n = 6$  per group) by control diet male mice. At gestational day 17.5 (E17.5), all fetuses were taken and embryonic osteogenic calvarial cells (EOCCs) were isolated. Consistent with Alizarin red bone mineralization staining results, 3D (three dimensional) micro-CT on embryos showed decreased bone volumes of fetuses from obese dams compared to those from control dams. Impaired skeletal development of fetuses from obese dams was associated with increased senescence signaling in EOCCs, as reflected by increased senescence-associated  $\beta$ -galactosidase (SA $\beta$ G) activity, the Senescence-Associated Secretory Phenotype (SASP) and increased PPAR $\gamma$  expression. Bone marrow osteoblastic cells from osteoblast conditional PPAR $\gamma$  knockout mice (PPAR $\gamma^{fl/fl}$ :Col3.6-Cre) showed decreased cellular senescence. On the other hand, over-expression of PPAR $\gamma$  in osteoblastic cells accelerated cellular senescence. In a second set of studies, we utilized offspring from the same HFD-driven maternal obesity model in C57BL/6J mice. Offspring were weaned onto either control or HFD diets creating four groups, control-control (both dams and offspring with control diet), control-HFD (control diet in dams and HFD in offspring), HFD-control (HFD in dams and control diet in offspring) and HFD-HFD (both dams and offspring with HFD). At 20 wks of age, micro-CT and *ex vivo* bone formation analyses showed significant negative effects of both maternal HFD per se and the combination of maternal and offspring HFD on trabecular bone formation, especially in male offspring. Consistent with our hypotheses, both PPAR $\gamma$  and senescence signaling were increased in the offspring bone due to maternal HFD. These findings indicate maternal obesity-associated increasing of fetal pre-osteoblastic cell senescence signaling is under control through PPAR $\gamma$  expression.

Disclosures: Jin-Ran Chen, None.

## SU0066

**The Relationship between Insulin Resistance and Lipids Overflow with Marrow Adipose Tissue (MAT) and Bone Mineral Density (BMD).** Iana de Araujo\*, Carlos Salmon, Marcello Nogueira Barbosa, Jorge Elias Jr, Francisco de Paula, Ribeirao Preto Medical School, University of São Paulo, Brazil

Introduction: Excessive storage of fat as well the overflow of lipids to other tissues generates functional (i.e insulin resistance) and structural (i.e. NASH) disorders. It is still unknown the effects of insulin resistance and the spill over of lipids to MAT and BMD, the aim of the present study was to evaluate the relationship of insulin resistance, visceral adipose tissue (VAT) and intrahepatic lipids (IHL) with MAT and BMD.

Material and Methods: The study comprised two groups; control (C) and obese (O) (C: 7M/13F vs O: 6M/12F, age (C: 55 $\pm$ 7 vs O: 51 $\pm$ 12 years), weight (C: 67 $\pm$ 8 vs O: 84 $\pm$ 19 Kg  $p < 0.05$ ) height (C=1.67 $\pm$ 0.09 vs O=1.63 $\pm$ 0.12m) and BMI (C: 24.1 $\pm$ 1.6 vs O: 31.3 $\pm$ 4.4 Kg/m $^2$   $p < 0.05$ ). Blood samples were collected for measurements of HbA1C, as well as glucose and insulin for HOMA-IR calculation. BMD was assessed in lumbar spine and total hip by DXA. 1-H magnetic resonance spectroscopy (1.5T) was used to evaluate MAT in the lumbar spine (L3).

Results: The groups were matched by age, sex and height. The O group had weight and BMI higher than C. The serum levels of insulin (C=7.98 $\pm$ 3.05 vs O=14.83 $\pm$ 9.02 $\mu$ IU/mL) and HOMA-IR (C=1.81 $\pm$ 0.72 vs O=3.25 $\pm$ 2.14) were higher in O than in C,  $p < 0.05$ . BMD was non-significantly higher in obese group: L1-L4 (C=0.943 $\pm$ 0.115 vs O=0.977 $\pm$ 0.170) and total hip (C=0.899 $\pm$ 0.114 vs O=0.936 $\pm$ 0.134 g/cm $^2$ ). VAT (C= 7,832 $\pm$ 4,826 vs O=10,619 $\pm$ 4,909 mm $^3$ ), and IHL (C=3.2 $\pm$ 3.7 vs O=7.4 $\pm$ 7.2%) were higher in O than in C,  $p < 0.05$ . Curiously, MAT was non-significantly lower in O group (C=35.5 $\pm$ 9.3 vs O=31.8 $\pm$ 6.2%). Weight correlated positively with IHL in O group ( $r = 0.53$ ,  $p < 0.05$ ). There was no correlation between HOMA-IR and MAT in both groups. There was a positive correlation between HOMA-IR with IHL in the C group ( $r = 0.50$ ,  $p < 0.05$ ). Additionally, VAT was positively correlated with IHL in O group ( $r = 0.62$ ,  $p < 0.05$ ). Conversely, neither VAT nor IHL was correlated with MAT in either group. Moreover, there was no relationship between MAT with serum levels of insulin and HOMAR-IR.

Conclusion: The present results indicate that MAT has a unique relationship with body weight, other fat depots, insulin sensitivity and lipids overflow. Differently from the classical association between VAT and IHL and the positive relationship between VAT and IHL with serum levels of insulin and HOMA-IR, the present data did not show any association between MAT with VAT, IHL, serum levels of insulin and HOMA-IR. Also, BMD has no relationship with insulin resistance.

Disclosures: *Iana de Araujo, None.*

## SU0067

**Glucose intolerance induced by persistent activation of calcium-sensing receptor.** Kiyoe Kurahashi<sup>1</sup>, Itsuro Endo<sup>1</sup>, Mayuko Nakamura<sup>1</sup>, Yukiyo Ohnishi<sup>1</sup>, Takeshi Kondo<sup>1</sup>, Shinichi Aizawa<sup>2</sup>, Toshio Matsumoto<sup>3</sup>, Seiji Fukumoto<sup>3</sup>, Masahiro Abe<sup>1</sup>. <sup>1</sup>Department of Medicine & Bioregulatory Sciences, University of Tokushima Graduate School of Medical Sciences, Japan, <sup>2</sup>Genetic Engineering Team, RIKEN Center for Life Science Technologies, Japan, <sup>3</sup>Fujii Memorial Institute of Medical Sciences, Tokushima University, Japan

Background: Calcium-sensing receptor (CaSR) is expressed in several tissues including parathyroid gland, kidney, bone, and intestines to regulate Ca homeostasis. Activating mutations of CaSR cause autosomal dominant hypocalcemia type 1 (ADH1). Patients with ADH1 show hypocalcemia, hyperphosphatemia, and relative hypercalciuria. Previously, we have created knock-in mice of human activating mutant CaSR (KI mice) as model mice for ADH1. KI mice mimicked almost all the biochemical features of ADH1. In addition, we have shown that a calcilytic compound, an antagonist of CaSR, improved those biochemical features of KI mice. On the other hand, CaSR is also expressed in beta cells of pancreas islets. Transient activation of CaSR in islets interacts with voltage-dependent calcium channel to stimulate insulin secretion. However, it is unknown if persistent activation of CaSR alters glucose metabolism especially *in vivo*.

Methods: We performed glucose tolerance test and histological analysis of pancreas islets including immunostaining for insulin and glucagon in wild-type and KI mice. Insulin protein quantification and insulin secretion test using isolated pancreas islets were also performed. Finally, the effect of a calcilytic was evaluated by glucose tolerance test.

Results: KI mice showed significantly higher plasma glucose with decreased basal and glucose-stimulated insulin levels compared with wild-type littermates by both oral glucose tolerance test (OGTT) and intra-peritoneal glucose tolerance test (PGTT). No differences were observed in islets volume, islets structure and protein amount of both insulin and glucagon in islets between KI and wild-type littermate. Isolated islets cells from KI mouse exhibited lower insulin secretion stimulated by glucose. Old KI mice also exhibited glucose intolerance with the same pancreatic islets number and volume compare to those of younger mice. A calcilytic ameliorated glucose intolerance of KI mice. Furthermore, decreased plasma glucose with increased insulin levels were observed in wild-type littermates treated with the calcilytic by OGTT.

Conclusion: These observations demonstrate that persistent activation of CaSR causes glucose intolerance. Furthermore, it is possible that CaSR is a therapeutic target for disordered glucose metabolism.

Disclosures: *Kiyoe Kurahashi, None.*

## SU0068

**No Association Between the Bone Turnover Markers CTX and P1NP and Insulin Sensitivity or Beta-cell Function in Healthy men.** Morten Frost<sup>\*</sup>, Kurt Højlund, Jens-Jacob Lauterlein, Henning Beck-Nielsen. Department of Endocrinology, Denmark

Insulin resistance could impair cellular glucose uptake, reducing bone turnover. We explored the relationship between bone turnover and insulin secretion and sensitivity.

Methods: Healthy men were identified among RISC study participants. Baseline insulin sensitivity (M/I-value) based on hyperinsulinaemic-euglycaemic clamp (HEC), and baseline and 3-year follow-up beta-cell glucose sensitivity and rate sensitivity based on 2h-oral glucose tolerance tests (OGTT) were used. Fasting and insulin-stimulated (120 min) markers of bone formation (PINP) and resorption (CTX) were measured. Association between insulin sensitivity or indices of beta-cell function and bone turnover markers (BTMs) were assessed using regression analyses with/without adjustment for age and BMI.

Results: Data on HEC and OGTT were available in 584 men, and 508 had normal glucose tolerance (NGT). Age and BMI of the participants were 42 years (IQR 36-49) and 26.1 ± 3.4 kg/m<sup>2</sup>. Insulin sensitivity was 115.4 (85.0-155.8) mmol·min<sup>-1</sup>·[kg<sup>0.75</sup>·F<sup>-1</sup>·[mmol/l]<sup>-1</sup>. Fasting PINP and CTX were 49.1 µg/L(17.0) and 0.47 ng/L(0.17) and decreased after insulin stimulation by 5.0% and 8.1% (both p<0.001). BTMs were inversely associated with fasting p-glucose and 2-h p-glucose at baseline in unadjusted but not adjusted analyses. Baseline PINP was associated with fasting p-glucose after 3 years follow-up after adjustments. Neither of the BTMs was associated with measures of insulin sensitivity or beta-cell function. Baseline BTMs were not associated with changes in HOMA-IR. BTMs were reduced in response to insulin during the clamp, not favouring anabolic effects of insulin on bone remodelling. This study does not support an association between insulin sensitivity or beta-cell function and bone metabolism.

Disclosures: *Morten Frost, None.*

## SU0069

**Regulation of Mitochondrial Uniporter Expression by 1,25-Dihydroxyvitamin D<sub>3</sub> in Human Muscle Cells.** Zachary Ryan, Xuewei Wang, Rajiv Kumar<sup>\*</sup>. Mayo Clinic, United states

1,25-Dihydroxyvitamin D<sub>3</sub> (1,25(OH)<sub>2</sub>D<sub>3</sub>) increases muscle cell oxygen consumption rate (OCR) and reduces the rate of apoptosis in muscle cells. The increases in OCR are dependent on the expression of the vitamin D receptor (VDR). Low amounts of mitochondrial Ca<sup>2+</sup> can boost ATP synthesis, but excessive amounts trigger mitochondrial failure and cell death. Excess Ca<sup>2+</sup> entry in mitochondria has been associated with apoptosis and necrosis in many pathological states.

To gain insights into the mechanism by which 1,25(OH)<sub>2</sub>D<sub>3</sub> alters OCR and apoptosis, we assessed the expression of the major mitochondrial Ca<sup>2+</sup> transporter, the MCU uniporter and its associated components (MICU1, MICU2 and EMRE). Primary cultures of human muscle cells were treated with 1,25(OH)<sub>2</sub>D<sub>3</sub> (10<sup>-8</sup>M) or vehicle (ethanol) for 48 hours. Cell protein was isolated and western blots were performed using specific antibodies against MCU, MICU1, MICU2 and EMRE. Specific bands were imaged and quantitated and density was corrected for the expression of porin. In addition, we examined the expression of specific modulators of apoptosis. Table 1 shows that the expression of MCU and MICU1 and 2 was decreased. EMRE was unchanged following 1,25(OH)<sub>2</sub>D<sub>3</sub> treatment. The expression of mRNAs for the pro-apoptotic factors, caspase 3 and BAX were decreased (p less than 0.003 and 0.0006, respectively). The mRNA for the anti-apoptotic factor MCL1 was increased (p = 2.9E-34).

The results show a decrease in expression of MCU, MICU1 and MICU2, but no change in the expression of EMRE. The expression of the pro-apoptotic protein mRNAs, BCL2-associated X protein and caspase 3 decreased. At the same time, the expression of the anti-apoptotic protein myeloid cell leukemia 1 (MCL1) increased.

We conclude that 1,25(OH)<sub>2</sub>D<sub>3</sub> decreases expression of components of the Ca<sup>2+</sup> uniporter, MCU that are associated with decreases in the expression of pro-apoptotic factors suggesting that changes in mitochondrial Ca<sup>2+</sup> uptake mediated by 1,25(OH)<sub>2</sub>D<sub>3</sub> modulate the rate of apoptosis in muscle cells.

	Vehicle		1,25(OH) <sub>2</sub> D <sub>3</sub> Treated		P value
	Ave	SE	Ave	SE	
MCU/PORIN	2.01	0.36	1.28	0.08	0.05
MICU1/PORIN	0.70	0.16	0.34	0.09	0.06
MICU2/PORIN	0.11	0.01	0.07	0.01	0.005
EMRE/PORIN	1.29	0.18	1.04	0.12	0.25

Table 1

Disclosures: *Rajiv Kumar, None.*

## SU0070

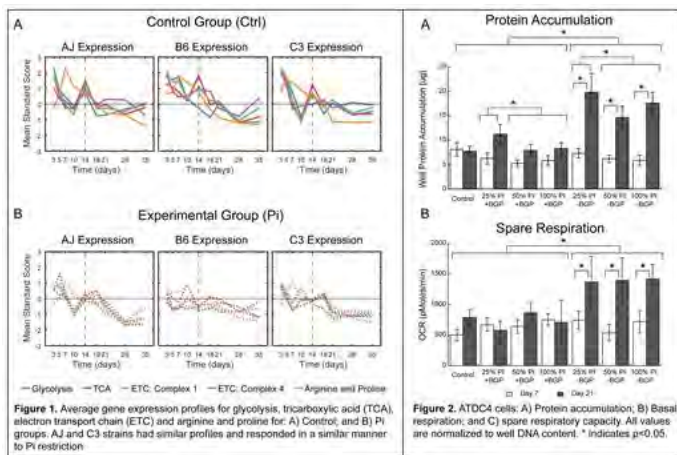
**Role of Phosphate in the Central Ox/Phos Metabolic Processes and Its Linkage to Collagen Production.** Amira Hussein<sup>\*</sup>, Kevin Blank, Deven Carroll, Kyle Lybrand, Margaret Cooke, Heather Matheny, Brenna Hogue, Serkalem Demissie, Louis Gerstenfeld. Boston University, United states

Introduction: Prior studies of mice given a phosphate (Pi) deficient diet during fracture healing showed diminished skeletal progenitor commitment, delayed chondrocyte maturation and callus mineralization. Transcriptomic analysis of callus gene expression showed mitochondrial oxidative phosphorylation (ox/phos) genes were significantly down regulated (p=3.16x10<sup>-23</sup>). The goal of this study was to determine how Pi restriction effect on ox/phos is interrelated to intermediate metabolism gene expression and functionally related to phenotype.

Methods: Femora fractures were generated in three strains of male mice. Pi deficiency was initiated 2 days prior to fracture and maintained for 14 days after which mice were returned to normal diet. Controls were fed a normal diet. Microarray analysis of total callus RNAs was carried out over 35-days of healing. Gene expression values were compared between the groups using analyses of covariance with strain and time points as covariates to examine diet effect (FDR q-value≤0.05). Cluster analysis of ox/phos and intermediate metabolism genes was performed to identify gene groups showing common temporal responses. Functional Pi restriction studies were performed using ATDC5 chondroprogenitors cells. Growth, differentiation, protein and collagen accumulation, matrix mineralization and oxidative function were assessed.

Results: Comparison of the temporal clustering patterns identified how strain specific profiles for specific ox/phos, tricarboxylic acid cycle, and arginine and proline metabolism genes were co-regulated and coordinated with, pyruvate dehydrogenase, and two subunits of prolyl 4-hydroxylase in response to Pi conditions. In vitro studies showed that chondrocyte differentiation was associated with 2X increase in oxidative respiration. In the absence of BGP normal differentiation proceeded with 1.5X greater accumulation in total protein in the absence of mineralization. In these cultures oxidative respiration was an additional 2X higher. When differentiation was not induced with ascorbic acid and BGP oxidative respiration showed no increase and was comparable to levels seen with 25% of normal Pi levels.

Discussion: Since complex IV genes of the electron transport, arginine and proline metabolism, and prolyl 4-hydroxylase are all commonly regulated by HIF1- $\alpha$ , this suggests a central means by which metabolic regulation is coordinated with collagen production which would balance bone and blood vessel formation.



Figures

Disclosures: Amira Hussein, None.

## SU0071

**Treatment with soluble activin type IIB receptor rescues ovariectomy-induced bone loss and fat gain in mice.** Tero Puolakkainen<sup>1</sup>, Petri Rummukainen<sup>1</sup>, Olli Ritvos<sup>2</sup>, Eriika Savontaus<sup>1</sup>, Riku Kiviranta<sup>1</sup>. <sup>1</sup>University of Turku, Finland, <sup>2</sup>University of Helsinki, Finland

In postmenopausal osteoporosis hormonal changes lead to increased bone turnover and bone loss. This results in impaired bone microstructure and increased risk for fracture. The decline in sex hormones is also associated with accumulation of adipose tissue especially in waist and abdomen, which may have negative metabolic effects such as increased insulin resistance. Activin type IIB receptors bind several cytokines of the TGF- $\beta$  superfamily including myostatin and activin A. We have previously shown that a soluble activin type IIB receptor (ActRIIB-Fc) increases bone and muscle mass in mdx mouse model of Duchenne muscular dystrophy and enhances fracture healing in closed tibial fracture model. As ActRIIB-Fc does increase muscle and bone mass, we hypothesized that ActRIIB-Fc treatment could improve bone and muscle mass, inhibit fat accumulation and restore metabolic parameters in an ovariectomy (OVX) model of post-menopausal osteoporosis.

Female C57Bl/6 mice were subjected to SHAM or OVX procedures and received intraperitoneal injections of either PBS or ActRIIB-Fc (5mg/kg) once a week for 7 weeks. Mice were imaged with Echo MRI at 1, 5 and 8 weeks to measure amount of fat and lean masses. Glucose tolerance test (GTT) was performed at 7 weeks. Samples were collected 8 weeks after OVX. Fat tissues from different depots were weighed. Femurs were imaged with micro-computed tomography ( $\mu$ CT).

As expected bone mass decreased in OVX-PBS mice compared to the SHAM-PBS group but treatment with ActRIIB-Fc rescued these changes as Bv/Tv increased by 110%  $p < 0.05$  and 220%  $p < 0.05$ , Tr.N by 88%  $p < 0.05$  and 180%  $p < 0.05$  and cortical bone area by 15%  $p < 0.05$  and 16%  $p < 0.05$  in SHAM and OVX groups respectively, compared to their PBS treated controls. Echo MRI showed that OVX-PBS mice accumulated more fat compared to SHAM-PBS group during the experiment. Treatment with ActRIIB-Fc was able to counteract this as fat mass decreased by 23%  $p < 0.05$  in OVX-Act compared to OVX-PBS group. ActRIIB-Fc also decreased gonadal WAT weight by 42%  $p < 0.05$  and mesenteric WAT by 25%  $p < 0.05$  in OVX-Act mice. OVX itself did not affect glucose levels in GTT but surprisingly ActRIIB-Fc treatment resulted in impaired glucose clearance in both SHAM and OVX groups.

ActRIIB-Fc is a potent bone-enhancing agent that also increases muscle and reduces fat masses. Despite these positive changes we observed that surprisingly ActRIIB-Fc does impair glucose tolerance, the mechanism of which is under investigation.

Disclosures: Tero Puolakkainen, None.

## SU0072

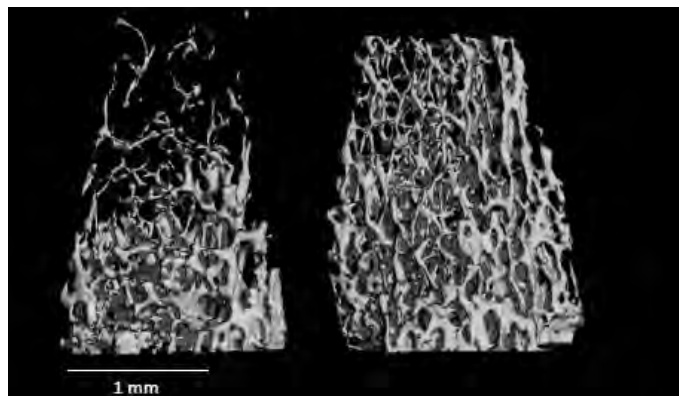
**Rhbd2 knock-out mice display distinct bone phenotypes: a genetic association study with Collaborative Cross mice.** Roei Levy<sup>1</sup>, Clemence Levet<sup>2</sup>, Keren Cohen<sup>1</sup>, Mathew Freeman<sup>2</sup>, Richard Mott<sup>3</sup>, Fuad Iraqi<sup>1</sup>, Yankel Gabet<sup>1</sup>. <sup>1</sup>Tel Aviv University, Israel, <sup>2</sup>Dunn School of Pathology, United Kingdom, <sup>3</sup>UCL Genetics Institute, United Kingdom

Bone microarchitecture evaluated at high resolution in 3D space is an important determinant of bone strength. Despite ongoing efforts in utilizing genomic data to fully map the genes responsible for bone microstructure, the complex genetic

interactions that govern it remain only partially resolved. We thus opted for a Genome-Wide Association Study in Collaborative Cross (CC) mice, which offer high allelic diversity, to bioinformatically analyze bone microarchitecture traits obtained via micro-computed tomography ( $\mu$ CT). We performed a detailed haplotype mapping across 70K SNPs in 34 CC lines of both genders on cortical and trabecular traits of femurs, morphometrically analyzed at a resolution of 10  $\mu$ m; these included cortical thickness (Ct.Th), trabecular bone volume fraction (BV/TV), number (Tb.N), thickness (Tb.Th), connectivity density (Conn.D), separation (Tb.Sp), and structural morphometric index (SMI) in the distal femur, as well as volumetric bone mineral density (vBMD) in the entire femur volume.

Heritability of all traits exceeded 55%. We found 5 marked loci in 4 of the traits. For these loci we gathered information mined from existing databases and ancestral imputation analyses, to shortlist potential candidate genes. Aside from genes whose role in bone biology is already established, our data pointed to new genes with yet unknown bone-related functions. In particular, *Rhbd2* stood out as a meaningful candidate gene associated with BV/TV and Tb.N. To validate this, we inspected *Rhbd2*<sup>-/-</sup> mice using  $\mu$ CT. Our results confirmed that *Rhbd2* tightly regulates femoral bone microarchitecture: *Rhbd2*<sup>-/-</sup> male mice had higher trabecular BV/TV, Tb.N and SMI, and lower Conn.D and Tb.Sp, compared with wild type mice. Although Tb.Th and vBMD remained unaffected, at the midshaft, Ct.Th was significantly higher in the *Rhbd2*<sup>-/-</sup> mice.

The robust teaming of high-resolution bone microarchitecture imaging with the diversity of the CC population enabled a further decryption of the genetic influence on bone microarchitecture. Here, *Rhbd2*, known for its role in esophageal cancer and involvement in secretion of TNF $\alpha$ , transpires as playing a major role in reducing the number and volume of the femoral trabeculae as well as the cortical thickness. Further studies are needed to decipher the exact mechanisms by which *Rhbd2* affects bone remodeling and test whether its activity may be manipulated pharmaceutically towards the treatment of skeletal disorders.



Difference in Femoral Trabecular Bone Between KO and WT Rhbd2 Mice

Disclosures: Roei Levy, None.

## SU0073

**Calcium Metabolism of 6 and 17 Month-old Vitamin D Receptor Knockout Mice: A Pilot Study.** Yu-ra Choi<sup>1</sup>, Clara Yongjoo Park<sup>1</sup>, Xiangguo Che<sup>1</sup>, Na-Rae Park<sup>1</sup>, Da-In Yeo<sup>1</sup>, Shigeaki Kato<sup>2</sup>, Je-Yong Choi<sup>1</sup>. <sup>1</sup>Kyungpook National University, Korea, republic of, <sup>2</sup>Soma Central Hospital, Japan

Previously reported vitamin D receptor knock-out (*Vdr* KO) mice are infertile and rarely survive beyond 15 weeks unless fed a rescue diet (2.0% Ca, 20% lactose, 1.25% P). However, our *Vdr* KO mice (*Vdr*<sup>L-L</sup>, Yamamoto 2013), which were systemically deleted of *Vdr* by crossing *CMV-cre* mice with *floxed Vdr* mice, were fertile and survived over 16 months despite intake of standard chow (1.2% Ca, 1% P, 1400 IU/kg Vitamin D<sub>3</sub>) and deionized water. In order to understand the calcium metabolism in these mice, we compared wild type (WT) and *Vdr*<sup>L-L</sup> mice at 6 and 17 months ( $n=1-7$ /group). *Vdr*<sup>L-L</sup> mice displayed alopecia and weighed less than WT mice. *Vdr*<sup>L-L</sup> mice had lower serum Calcium than WT at both time points. Serum Phosphate was also lower in male *Vdr*<sup>L-L</sup> mice, but was higher in female *Vdr*<sup>L-L</sup> mice at 6 months when compared to WT mice. Renal *Cyp27b1* and *Cyp24a1* mRNA were consistently higher and lower, respectively, in *Vdr*<sup>L-L</sup> compared to WT mice. Vertebral trabecular bone volume, bone surface, and trabecular number were lower, whereas trabecular thickness was higher at 6 months but lower at 17 months in both male and female *Vdr*<sup>L-L</sup> mice compared to WT mice. Especially at 17 months, more osteoid was visible in *Vdr*<sup>L-L</sup> vertebrae. Expression of *Vdr* mRNA in duodenum and kidney increased with age in WT mice, but was expectedly low in *Vdr*<sup>L-L</sup> mice regardless of age. Duodenal *Cabp9k* and *Trpv6* and renal *Cabp9k*, *Npt2a*, *Npt2c* and *Pth1r* mRNA expression was higher at 6 months, but lower at 17 months in *Vdr*<sup>L-L</sup> mice compared to WT. These genes markedly increased with age in WT but not in *Vdr*<sup>L-L</sup> mice. On the other hand, duodenal *Npt2b* mRNA decreased with age in WT mice, but was constantly low in *Vdr*<sup>L-L</sup> mice. Renal *Trpv5* mRNA expression was higher in *Vdr*<sup>L-L</sup> mice and dramatically increased at 17 months. The high expression of genes that induce intestinal absorption and renal reabsorption of Calcium and Phosphate despite the lack of *Vdr* may explain the longevity of our *Vdr*<sup>L-L</sup> mice.

Disclosures: Yu-ra Choi, None.

## SU0074

**Characterization of a Mouse Model with a cMET Mutation-Causing Osteofibrous Dysplasia.** Ralph Zirngibl<sup>1\*</sup>, Andrew Wang<sup>1</sup>, Simon Kelley<sup>2</sup>, Raymond Poon<sup>2</sup>, Benjamin Alman<sup>3</sup>, Peter Kannu<sup>2</sup>, Irina Voronov<sup>1</sup>. <sup>1</sup>University of Toronto, Canada, <sup>2</sup>Hospital for Sick Children, Canada, <sup>3</sup>Duke University, United states

Osteofibrous Dysplasia (OFD) in humans is characterized by the bowing/fracture involving mostly the tibia and fibula by the age of 10, with characteristic fibrous lesions in the affected bones. We have identified a mutation in cMET, the hepatocyte growth factor (HGF) receptor, resulting in skipping of exon 14, as a common feature in four families with the OFD. To elucidate the role of cMET in OFD, using the CRISPR/Cas9 system, we have generated a mouse model mimicking human point mutation (exon 15 deletion in mouse).

Heterozygous cMet<sup>ΔE15</sup> (cMet<sup>ΔE15</sup>) mice are indistinguishable from wild type (WT) in gross appearance. Interbreeding of heterozygous animals failed to generate homozygous animals at weaning, suggesting embryonic lethality. Gene expression analysis of bones from cMet<sup>ΔE15</sup> mice showed reduced expression of early osteoblast markers *Runx2* and *Sp7* (Osterix), as well as late markers (*Ibsp*, *Ssp1*, *Sost*). Osteoblastic differentiation of mouse bone marrow mesenchymal stem cells (BMSCs) *in vitro* revealed a reduced capacity of cMet<sup>ΔE15</sup> BMSCs to form CFU-ALP and CFU-O; however, this defect could be partially rescued by higher cell density. Expression of *Runx2* and *Sp7* was also decreased in the cMet<sup>ΔE15</sup> BMSCs, while the more mature gene markers were not, suggesting a progenitor and/or niche defect. *In vitro* cMet<sup>ΔE15</sup> osteoclast (OC) formation was decreased; however, the resorptive ability of a bone-like substrate was increased in cMet<sup>ΔE15</sup> OCs compared to the WT cells. Gene expression of OC markers tartrate resistant alkaline phosphatase (TRAP) and the  $\alpha 3$  subunit of the V-ATPase was also increased in cMet<sup>ΔE15</sup> cells, supporting increased activity results. Furthermore, the expression of cMet in cMet<sup>ΔE15</sup> OC was decreased at both the RNA and protein levels. These results suggest that cMET lacking exon 15 plays a negative role in both osteoblast and OC formation with the net result leading to reduced bone strength observed in OFD.

**Disclosures:** Ralph Zirngibl, None.

## SU0075

**Differential Roles of Runx2 Deficiency in Chondrocytes and Osteoblasts for Cleidocranial Dysplasia.** Kayla King<sup>1\*</sup>, Harunur Rashid<sup>1</sup>, Mitra Adhami<sup>1</sup>, Haiyan Chen<sup>1</sup>, Yang Yang<sup>2</sup>, Amjad Javed<sup>1</sup>. <sup>1</sup>Department of Oral & Maxillofacial Surgery, School of Dentistry, University of Alabama at Birmingham, United states, <sup>2</sup>Department of Pathology, School of Dentistry, University of Alabama at Birmingham, United states

The Runx2 transcription factor is essential for differentiation of mesenchymal cells to functional chondrocytes and osteoblasts. In humans, haploinsufficiency of Runx2 is associated with cleidocranial dysplasia (CCD), characterized by short stature, hypoplastic clavicles and open sutures/fontanels in the skull. These skeletal elements are formed by intramembranous and/or endochondral ossification but the cell type specific roles of Runx2 in CCD defects remain unknown. Here, we identified the contribution of Runx2 deficiency and haploinsufficiency to the CCD phenotype by deleting Runx2 in chondrocytes and committed osteoblasts using Col2a-Cre and Col1a-Cre mice. Runx2 deficiency in chondrocytes leads to short stature, stunted craniofacial growth, and perinatal lethality due to failed endochondral ossification. Skull plates were poorly developed with wide-open anterior and posterior fontanels and sutures in the homozygous mice. Expression analysis revealed near absence of the mature chondrocyte marker, ColX, in sutures. This is consistent with the fact that suture closure occurs through endochondral ossification. Mice with haploinsufficiency of the Runx2 gene in chondrocytes showed dose dependent effects of the CCD phenotype. Surprisingly, clavicle development was comparable among the three genotypes. Mice with Runx2 deficiency in committed osteoblasts exhibited normal endochondral ossification. However, intramembranous ossification was impaired, with a decrease in mineralization of the frontal, parietal and occipital bones. Poor skull development was coupled with open sutures and fontanels in homozygous mice. To understand if Runx2 deficiency in osteoblasts is associated with delayed or failed closure of fontanels and sutures, we evaluated littermates until adulthood. To our surprise, impaired skull development persisted throughout postnatal life. By 1-month, fontanels and sutures were nearly closed in wildtype and heterozygous mice. However, anterior and posterior fontanels along with sutures remained open in homozygous mice. Furthermore, the lamboid suture, posterior fontanel and the occipital bone displayed abnormal angulation and positioning. Skull bone volume was decreased by 47% at 1-month and 61% at 3-months of age. Clavicles were developed but exhibited a range of hypoplasticity in the homozygous mice. In conclusion CCD phenotypes of open fontanels, sutures and hypoplastic clavicles are caused by cell specific function and dosages of Runx2 gene.

**Disclosures:** Kayla King, None.

## SU0076

**P2X7 receptor inhibition reduces bone resorption in vivo.** Solveig Petersen<sup>1\*</sup>, Maria Ellegaard<sup>1</sup>, Susanne Syberg<sup>1</sup>, Peter Schwarz<sup>2</sup>, Michael Boes<sup>3</sup>, Niklas Rye Jørgensen<sup>4</sup>. <sup>1</sup>Copenhagen University Hospital Rigshospitalet, Denmark, <sup>2</sup>Copenhagen University Hospital Rigshospitalet & Faculty of Health & Medical Sciences, University of Copenhagen, Denmark, <sup>3</sup>Affectis Pharmaceuticals AG, Martinsried, Germany, <sup>4</sup>Copenhagen University Hospital Rigshospitalet & University of Southern Denmark, Denmark

**Purpose:** The aim of the project was to investigate the potential of the purinergic P2X7 receptor antagonist AFC-5278 (AFC) in treating osteoporosis in an animal model of estrogen-depletion-induced bone loss.

**Methods:** For this purpose we used an experimental animal model where six-months old female nullipara rats were ovariectomized and left for three months to develop estrogen-withdrawal-induced bone loss. At the age of eight months animals were allocated to one of the following treatment groups: a) PTH(1-34) (PTH) 40 µg/kg body weight i.p.; b) Alendronate (ALN) 28 µg/kg body weight by oral gavage; c) AFC 50 mg/kg body weight oral gavage; d) AFC 150 mg/kg body weight oral gavage; e) AFC 300 mg/kg body weight oral gavage; f) Vehicle oral gavage (VEH). Animals were dosed five times per week and after six weeks of treatment animals were euthanized and the following examinations were done: DXA (bone mineral density (BMD) and -content (BMC), bone strength, µCT, serum bone turnover markers (CTX-I and PINP). Data was analyzed using analysis of variance with post hoc correction for multiple testing. N=15 for all treatment groups.

**Results:** Compared to VEH (mean±SEM) (0.428 g ±0.009) both ALN (mean: 0.465 ± SEM: 0.032 g;  $p < 0.01$ ) and PTH (0.488 ± 0.009 g;  $p < 0.001$ ) increased whole body BMC while AFC treatment did not significantly increase BMC in the animals. The same was seen for BMC and BMD at the femoral head. Decreased cortical porosity (µCT) was seen with AFC 300 mg/kg (0.019±0.001;  $p < 0.05$ ), PTH(1-34) (0.018±0.001;  $p < 0.05$ ), and ALN (0.019±0.001;  $p < 0.05$ ) when compared to VEH (0.022±0.001). For the remaining cortical parameters no significant effects of AFC were detected. Trabecular spacing was also decreased for AFC 300 mg/kg (0.195±0.008 mm;  $p < 0.05$ ), PTH (0.177±0.015 mm;  $p < 0.05$ ), and ALN (0.157±0.002 mm;  $p < 0.05$ ) compared to VEH (0.227±0.010 mm). Again, AFC did not affect any other trabecular parameters. AFC did not affect bone strength (max load) neither at the mid-femur nor the femoral neck. Finally, the two highest doses of AFC reduced bone resorption significantly as determined by serum-CTX-I (AFC 150 mg/kg: 13.1±0.8 ng/ml;  $p < 0.01$ . AFC 300 mg/kg: 15.6±1.2 ng/ml;  $p < 0.05$ ) when compared to VEH (22.3±2.9 ng/ml). No effects of AFC were seen on bone formation as determined by PINP.

**Conclusion:** The study has demonstrated that P2X7R inhibition by AFC reduces bone resorption in vivo. However, the resulting effects on bone structure are minor.

**Disclosures:** Solveig Petersen, None.

## SU0077

**Phenotypic Severity of Autosomal Dominant Osteopetrosis Type II (ADO2) Mice on Different Genetic Backgrounds Recapitulates the Features of Human Disease.** Imranul Alam<sup>\*</sup>, Dana Oakes, Amie McQueen, Dena Acton, Austin Reilly, Rita Gerard-O'Riley, Michael Econs, Indiana University School of Medicine, United states

Autosomal dominant osteopetrosis type II (ADO2) is a heritable osteosclerotic bone disorder due to dysfunctional osteoclast activity. ADO2 is caused by missense mutations in the chloride channel 7 (*CLCN7*) gene characterized by osteosclerosis with multiple fractures. ADO2 can result in osteomyelitis, visual loss and bone marrow failure. Currently, there is no cure for ADO2, and until recently no appropriate animal model of ADO2 existed to understand better the pathogenesis of this disease and to test new therapies. Therefore, we created ADO2 knock-in mouse model with a G213R (human homolog of G215R) missense mutation in the *Cln7* gene on 129S1 background, and demonstrated that this mouse model phenocopies human ADO2. As ADO2 gives rise to incomplete penetrance (66%) in human and marked phenotypic variability is observed among patients with the same mutation, we hypothesized that the severity and penetrance of ADO2 will also vary in mouse models on different genetic backgrounds. To test this, we created ADO2 mouse models in DBA/D2, C57BL/6J/B6 and Balb/c strains, and compared bone phenotypes and performed serum biochemical analysis between strain- and age-matched wild-type (WT) and ADO2 mice. At 12 weeks of age, whole body aBMD was higher (4-7% in male; 1-5% in female) in the ADO2 mice compared to their wild-type littermates. In addition, trabecular BV/TV at distal femur was significantly higher (33-106% in male; 36-76% in female) in the ADO2 mice compared to the strain-matched WT counterparts (Figure 1). Serum Ca, P, alkaline phosphatase and PINP levels were similar in the WT and ADO2 mice on all genetic backgrounds but TRAP was higher (40-81% in male; 33-95% in female) and CTX/TRAP ratio was lower (39-53% in male and 3-41% in female) in the ADO2 mice compared to their strain-matched wild-type littermates. We also found that young (12 weeks) ADO2 mice on 129S1 background exhibited 2-fold higher trabecular BV/TV whereas old (18 months) ADO2 mice displayed 4-7 fold higher BV/TV compared to their age-matched wild-type controls. In summary, phenotypic severity in ADO2 mice varied markedly on different genetic backgrounds and became more pronounced with age, which resembles the wide variations in phenotype observed in ADO2 patients. These mouse models will help us

to identify genes/factors that influence severity and penetrance of ADO2, and test innovative therapies to treat this incurable disease.

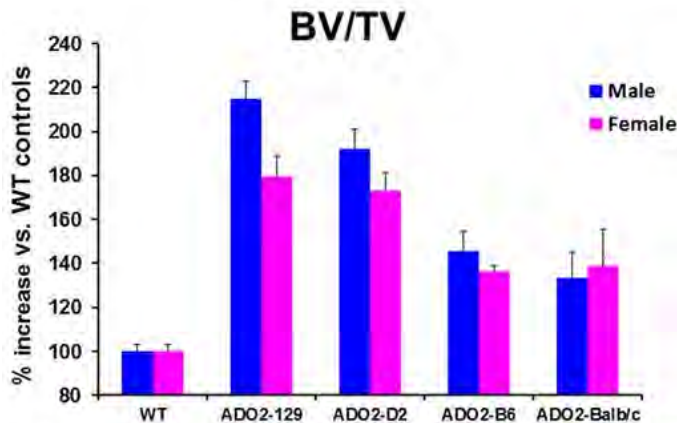


**Figure 1: Percent increase of BV/TV in 12-week-old ADO2 mice on different genetic backgrounds**

Figure 1

Disclosures: Inranul Alam, None.

## SU0078

**Spatiotemporal Regulation of Osteogenesis and Angiogenesis in Autograft and Allograft Repair.** Tao Wang, Xiping Zhang\*. University of Rochester Medical Center, United states

Vascularization is a key determinant in bone graft healing and repair. Autografts are vastly superior to allografts and synthetic grafts largely due to the fact that autografts can be rapidly revascularized and form new bone whereas allografts cannot. With a goal to gain a deeper understanding of the mechanisms of bone graft revascularization and repair, we performed bone graft transplantation in a cranial defect window chamber model that permits high resolution, four-dimensional analyses of osteogenesis and angiogenesis via multiphoton laser scanning microscopy. Using an *Osx-RFP<sup>cherry</sup>* transgenic mouse model that labels osteoblastic lineage cells, we showed that autograft repair initiated from donor periosteum, which led to a massive induction of *OSX-RFP+* cells on top of bone autografts. These *OSX-RFP+* cells were closely associated with small vessel angiogenesis, which peaked at 2-3 weeks post-surgery. At week 5, angiogenesis was reduced and small vessels regressed, coincided with graft-host bony union. Compared with autografts, allograft repair displayed a delay in angiogenesis at week 1. Isolated colonies of *OSX-RFP+* cells appeared at week 2 on graft surface and along edges of the grafts. While abundant blood vessels were found in the transcalvarial tunnels and surrounding allografts, most vessels were not associated with *RFP+* osteoblasts. At week 5, a large amount of blood vessels were found persisted at graft-host interface, disrupting bony union. Quantitative analyses showed a similar amount of total vessel formation at the repair site in autografts and allografts, yet a 10-fold reduction of *OSX-RFP+* cell-associated blood vessels in allografts at week 2. Histology analyses demonstrated thick new bone formation on top of autografts at week 5, consistent with a 2.3-fold increase in graft volume as measured by MicroCT. In comparison, allograft only showed a thin layer of bone on its surface with no significant change in graft volume over 5 week period. In summary, our study demonstrates a novel approach that allows high spatio-temporal resolution analyses of graft repair and revascularization. Our data further show a critical role of the spatiotemporal regulation of angiogenesis in osseointegration and bone graft revascularization. A deeper understanding of bone graft repair and revascularization will aid in development of novel tissue engineering constructs that can effectively replace autograft for repair and reconstruction of large bone defects.

Disclosures: Xiping Zhang, None.

## SU0079

**Transcriptomic Analysis of Osteoclasts from Autosomal Dominant Osteopetrosis type2 (ADO2) Mice harboring the G213R Mutation of the Chloride-Proton Antiporter type 7 (CIC7).** Antonio Maurizi\*<sup>1</sup>, Nadia Rucci<sup>1</sup>, Tina Schleicher<sup>2</sup>, Yadhu Kumar<sup>2</sup>, Anna Teti<sup>1</sup>, Mattia Capulli<sup>1</sup>. <sup>1</sup>Dept. of Biotechnological & Applied Clinical Sciences, University of L'Aquila, Italy, <sup>2</sup>GATC Biotech AG, Germany

Heterozygous mutations of *CIC7* induce ADO2, impairing osteoclast resorption lacuna acidification. We observed that this mutation also increases lysosomal pH

(+1.64 pH units,  $p < 0.001$ ) and induces Golgi enlargement (+1.8fold,  $p = 0.008$ ), thus suggesting that the osteoclast function can be impaired at various levels. To verify this hypothesis, primary osteoclasts were obtained from WT and ADO2 mice carrying the *CIC7* G213R mutant and subjected to RNA deep sequencing by Illumina Hi Seq 2500 technology. We found 387 over- and 63 under-expressed transcripts in ADO2 vs WT osteoclasts ( $p < 0.05$ ). The highest expressed genes were grouped by the Gene Ontology terms. Statistically significant enrichment was observed for genes involved in the biological processes of cell adhesion ( $p < 0.0001$ ), integrin signaling ( $p < 0.001$ ) and regulation of apoptosis ( $p = 0.05$ ). Grouping these genes for their molecular functions, revealed an enrichment of the metal and ion binding function ( $p < 0.05$ ), peptidase activity ( $p = 0.008$ ) and integrin binding function ( $p = 0.01$ ). The analysis of the cellular components revealed an enrichment of transcripts for proteins localized in endoplasmic reticulum ( $p < 0.001$ ) and basement membrane ( $p < 0.001$ ). Conversely, biological processes such as immune response ( $p = 0.04$ ), chemotaxis ( $p < 0.0001$ ), cell proliferation ( $p < 0.001$ ) and regulation of endocytosis ( $p = 0.05$ ) were enriched in the group of under-expressed transcripts of ADO2 vs WT osteoclasts. Interestingly, further investigations using the KEGG pathway analysis revealed higher expression in ADO2 of genes involved in osteoclast differentiation ( $p < 0.05$ ). Accordingly, in vitro osteoclastogenesis was faster and more prominent in ADO2 bone marrow cultures vs WT (1.7fold,  $p < 0.01$ ), probably triggered by increased circulating PTH levels (1.98fold,  $p = 0.045$ ) and consequent increased number of osteoclast precursors in the ADO2 bone marrow (1.4fold,  $p = 0.05$ ). Of note, other pathways more active in ADO2 osteoclasts were cytokines-cytokine receptors ( $p < 0.001$ ), Jak/Stat signal ( $p = 0.001$ ), extracellular matrix-receptor ( $p < 0.001$ ) and focal adhesion ( $p < 0.001$ ). All together, these results suggest that the heterozygous impairment of *CIC7* function in ADO2 osteoclasts does not cause only a defective bone resorption, but also an impairment of pathways essential for multiple osteoclast functions. We expect this research to pave the way for the identification of druggable targets that could improve the osteoclast function in ADO2.

Disclosures: Antonio Maurizi, None.

## SU0080

**CNP/NPRB Signaling Expands the Hypertrophic Zone in the Growth Plate Cartilage by Modulating Cell Cycle.** Keiko Yamamoto\*<sup>1</sup>, Masanobu Kawai<sup>1</sup>, Miwa Yamazaki<sup>2</sup>, Kanako Tachikawa<sup>1</sup>, Wei Wang<sup>3</sup>, Takuo Kubota<sup>3</sup>, Keiichi Ozono<sup>3</sup>, Toshimi Michigami<sup>1</sup>. <sup>1</sup>Osaka Medical Center & Research Institute for Maternal & Child Health, Japan, <sup>2</sup>Osaka Medical Center & Research Institute for Maternal Child Health, Japan, <sup>3</sup>Osaka University Graduate School of Medicine, Japan

Natriuretic peptide receptor B (NPRB) is a guanylyl cyclase and produces cyclic GMP when bound by C-type natriuretic peptide (CNP). Inactivating mutations in NPRB lead to severe dwarfism called acromesomelic dysplasia. On the other hand, activating mutations in NPRB cause skeletal overgrowth disorder, which is now established as a disease entity named epiphyseal chondrodysplasia, Miura type (ECDM). Although these diseases indicate the critical role for CNP/NPRB pathway in skeletal growth, the underlying mechanism still remains unclear. We here aimed to determine how CNP/NPRB signal expands the growth plate using a transgenic mouse model for ECDM and a chondrocytic cell line. The mouse model for ECDM harbors the activating mutation in NPRB (p.V883M) identified in the firstly reported family, which is expressed specifically in chondrocytes under the control of *Col11a2* promoter/enhancer (NPRB[p.V883M]-Tg). NPRB [p.V883M]-Tg shows an increased production of cGMP in the cartilage and skeletal overgrowth similar to in ECDM patients. Detailed histological analyses of the growth plate in femurs of 4-week-old mice revealed the longitudinal expansion of hypertrophic zone in NPRB [p.V883M]-Tg compared with controls ( $258.5 \pm 44.2 \mu\text{m}$  vs.  $165.9 \pm 46.9 \mu\text{m}$ ;  $p < 0.05$ ), while the width of proliferating zone was comparable. Then, the size (area) of the chondrocytes in the hypertrophic zone was measured using an image analyzing software. Interestingly, the population of smaller cells (area  $< 200 \mu\text{m}^2$ ) was increased in NPRB [p.V883M]-Tg compared with controls ( $8.7 \pm 2.9\%$  vs.  $1.5 \pm 1.7\%$  of total;  $p < 0.05$ ), although the mean of the cell area was similar. We next examined the effects of NPRB activation in a chondrogenic cell line ATDC5. The cells were treated with CNP (1  $\mu\text{M}$ ) or vehicle for 48 hours at 0, 2, 4, 6, 8 weeks of chondrogenic induction, and the gene expression was analyzed. We found the expression pattern of *cyclin D1*, a gene related to cell cycle, was altered by CNP treatment. In untreated ATDC5 cells, the expression of *cyclin D1* was peaked at 4 weeks and was declined thereafter. Addition of CNP at 6 and 8 weeks up-regulated *cyclin D1* to the similar level as at 4 weeks. Moreover, phosphorylation of CREB, a transcription factor regulating *cyclin D1*, was increased by 30-min treatment with CNP when added at 6 weeks. These findings suggest that CNP/NPRB signal expands hypertrophic zone rather than proliferating zone, which may involve the modulation of cell cycle.

Disclosures: Keiko Yamamoto, None.

## SU0081

**Femoral Geometry Parameters Correlate to Bone Bone Expression Levels and Differ Between Osteoporotic and Healthy Postmenopausal Women.** Sjur Reppe\*<sup>1</sup>, Yi-Hsiang Hsu<sup>2</sup>, Thomas Beck<sup>3</sup>, Ole K. Olstad<sup>1</sup>, Vigdis T. Gautvik<sup>4</sup>, David Karasik<sup>5</sup>, Kaare M. Gautvik<sup>6</sup>. <sup>1</sup>Oslo University Hospital, Norway, <sup>2</sup>Harvard Medical School, Institute of Aging research, United states, <sup>3</sup>Beck Radiological Innovations, United states, <sup>4</sup>University of Oslo, Institute of Basic Medical Sciences, Norway, <sup>5</sup>Bar-Ilan University, Faculty of Medicine, Israel, <sup>6</sup>University of Oslo, Norway

Bone geometry is a heritable trait known to contribute to fracture risk, founded on the genetic makeup which determines gene expression levels affecting the bone phenotype. We have performed global expression profiling of postmenopausal trans-iliac bone biopsies and correlated gene expression levels to hip geometry. The bone biopsies were obtained from Norwegian women (50–86 years), with varying bone mineral density (BMD; assigned as osteoporotic (OP) with fracture, and healthy). All were free of primary diseases and medications known to affect the skeleton. Bone total RNA was subjected to global transcript profiling using HG-U133 plus 2.0 microarrays (Affymetrix). DXA scans from the bone donors were subjected to hip structural analysis (HSA). Filtered transcript levels from 80 bone donors were correlated with hip bone geometry data; adjusted for multiple testing using FDR. Neck Length, Narrow Neck Width (NN\_Width) and Neck Shaft Angle (NSA) were not different between OP and healthy. In contrast, Students t-test identified markedly and highly significant differences between OP and healthy for NN\_Z, NN\_AvgBR, S\_AvgBR, S\_Width and S\_Z (see table). Various hip geometry parameters were correlated with transcript signal values across donors. Numbers of correlated transcripts at various adjusted p-values are shown in the table. Functional annotation clustering using Ingenuity Pathway Analysis on all transcripts at adj. p<0.15 identified “Protein Ubiquitination Pathway” (p=9.42E-06), “Calcium Signaling” (p=7.79E-05) and “Integrin Signaling” (p=1.11E-04) as top-most affected canonical pathways. In “Physiological System Development and Function” category, “Skeletal and Muscular System Development and Function” (p=5.58E-03 - 1.27E-11), “Cardiovascular System Development and Function” (p=5.58E-03 - 3.70E-10) and “Embryonic Development” (p=6.72E-03 - 3.70E-10) came out on top. When all transcripts at 15% FDR were pooled, more than 95% showed different distribution between OP and healthy (T-test p-value<0.05). Also, 5 of our hip structure GWAS SNPs were associated with 18 of the topmost hip structure correlated transcripts. We have for the first time identified bone transcript levels strongly associated with femoral structure, especially for section modulus and buckling ratio. Most of the structure parameters were different between OP and healthy and this difference was reflected by the number of transcripts correlated to the different geometry parameters.

	Differences in hip geometry between osteoporotic and healthy	Number of transcripts correlating with hip geometry parameters (adjusted p-values)		
	Students t-test p-values	p<0.05	p<0.10	p<0.15
NeckLength	7.01E-1	-	-	3
NN_Width	8.67E-2	-	-	10
NSA	6.42E-1	-	-	-
NN_Z	2.16E-19	8	51	179
NN_AvgBR	7.13E-26	36	163	439
S_AvgBR	2.31E-16	6	29	93
S_Width	6.04E-4	-	2	19
S_Z	5.09E-12	2	17	64

NeckLength: Distance from center of femoral head to intersection of neck and shaft; NN\_Width: Outer diameter of the bone at narrow neck region (NN); NSA: neck shaft angle; Z: section modulus (index of bending strength in the image plane); BR: buckling ratio (an estimate of cortical stability in buckling); S: shaft region

Table

Disclosures: Sjur Reppe, None.

## SU0082

**Unique transcriptomic signatures in the mouse skull vault.** Yong Wan, Matthew Rogers, Brian Cusack, Heather Szabo-Rogers\*. University of Pittsburgh, United states

Craniosynostosis (CS) results from the premature fusion of the skull bones, resulting in constrained growth and altered morphology of the skull. By understanding and elucidating the regional differences in the developing skull we will be able to identify and develop better treatments for CS. Postnatal osteoblasts derived from the frontal bones have superior proliferation, differentiation and migration ability than those derived from the parietal bone. An RNASeq analysis of the neural crest-derived frontal bones and the mesodermally-derived parietal bones identified over 700 uniquely expressed transcripts between the two compartments. We found that members of the Wnt, BMP, FGF, and TGF-beta signaling pathway are differentially expressed in these compartments. We found that chemical inhibition of ALK5 (with ALK5 inhibitor) and ROCK (with Y-26732) enhance mineralization of the embryonic frontal bone-derived osteoblasts compared to the parietal bone osteoblasts. We confirmed differential

expression of *Crispld1*, *Wif1*, *Cytl1*, *Casq2* and *Moxd1* by real-time PCR and in situ hybridization. We are currently testing the function of these proteins in the development of the embryonic frontal and parietal bones.

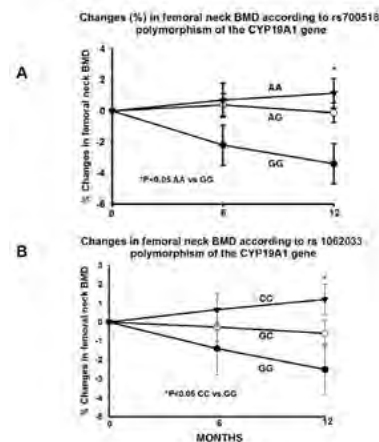
Disclosures: Heather Szabo-Rogers, None.

## SU0083

**A haplotype in the CYP19A1 gene is associated with variable musculoskeletal response to testosterone therapy in men with hypogonadism.** Georgia Colleluori\*<sup>1</sup>, Lina Aguirre<sup>2</sup>, Richard Dorins<sup>2</sup>, David Robbins<sup>2</sup>, Clifford Qualls<sup>3</sup>, Dean Blevins<sup>1</sup>, Dean Blevins<sup>1</sup>, Dennis Villareal<sup>4</sup>, Reina Villareal<sup>4</sup>. <sup>1</sup>Baylor College of Medicine, United states, <sup>2</sup>New Mexico VA Health Care System, United states, <sup>3</sup>University of New Mexico School of Medicine, United states, <sup>4</sup>Michael E. DeBakey VA Medical Center, United states

Background: A haplotype in the CYP19A1 gene (which encodes aromatase) is associated with estrogen levels, bone mineral density (BMD) and fracture prevalence and this is mostly due to the single nucleotide polymorphisms (SNPs) rs700518 and rs1062033. These SNPs are in linkage disequilibrium (LD) and show in-vitro differences in allelic expression and activity. The effect of these linked SNPs on the response and susceptibility to side effects from testosterone (T) therapy in men with hypogonadism is unknown. Our objective is to evaluate the effect of the rs1062033 and rs700518 SNPs on 1) the musculoskeletal response and 2) changes in hematocrit (HCT) and prostate specific antigen (PSA) with T therapy in men with hypogonadism. Methods: Single arm clinical trial involving 105 men, 40-74 yo, average morning T (2 samples) <300 ng/dL, given T cypionate 200 mg every 2 weeks IM. Areal BMD and body composition by DXA; C-telopeptide (CTX) by ELISA; genotyping by Taqman SNP allelic discrimination assay. Results: Figure 1 shows that those with GG genotype for the rs700518 (Fig.1A) and GG genotype for the rs1062033 (Fig. 1B) experienced bone loss at the femoral neck despite T therapy at 6 mo which became significant at 12 mo compared to AA for rs700518 and CC for rs1062033 who had increases in BMD, while GA and GC had intermediate changes. CTX increased among patients with the GG compared to those with GA+AA genotypes at 6 mo (24.7 ± 18.9vs.-20.5 ± 10.2%, p0.04) and 12 mo (171.9 ± 61.1vs.9.2 ± 28.4%, p0.01) for the rs700518. There were no differences in HCT and PSA changes at 6 and 12 mo. All decreases total and trunk fat mass at 12 mo but it was greater in AA than GA+GG for total and trunk (-13.2 ± 2.50vs. -6.9 ± 1.4%, p0.04) fat in rs700518 and in CC than the GC+GG for total and trunk (-10.7 ± 6.7vs.-6.3 ± 6.8%, p0.02) fat in rs1062033. All had increases in lean mass at 12 mo but the AA genotype had greater increase than the GA+GG (6.46 ± 1.04vs.3.96 ± 0.60%, p0.04) in rs700518 and CC than GC+GG (5.9 ± 4.9vs.3.5 ± 3.3%, p0.03) in rs1062033. The 2 SNPs are in partial LD (r<sup>2</sup>=0.22) in our sample. Conclusion: Subjects with the GG genotype in both SNPs respond the least to T treatment (decrease BMD; attenuated decrease in body fat and increase in lean mass). AA genotype of rs700518 and CC genotype of rs1062033 are the best responders: stable BMD and marked improvement in body composition. GA and GC genotypes showed intermediate responses. So far no genotype is predisposed to increased side effects.

Figure 1



Femoral Neck BMD Changes according to rs700518 and rs1062033 polymorphisms of the CYP19A1 gene

Disclosures: Georgia Colleluori, None.

## SU0084

**Comparative Gene-based Analysis for Consecutive Studies of GEFOS.** Wei Zhu\*<sup>1</sup>, Hong-wen Deng<sup>1</sup>, Kehao Wu<sup>2</sup>, Hao He<sup>1</sup>, Lan Zhang<sup>1</sup>, Yong Zeng<sup>1</sup>. <sup>1</sup>Tulane University, United states, <sup>2</sup>Tulane, United states

Osteoporosis is a complex human skeletal disease characterized by bone fragility. Bone mineral density (BMD) is a major risk factor used for the clinical diagnoses of

osteoporosis. As the largest effort to date, the consecutive studies of Genetic Factors for Osteoporosis projects (GEFOS2 and GEFOS-SEQ) used meta-analysis of GWAS with high density SNPs to identify risk genetic variants for osteoporosis. The original GEFOS2 and GEFOS-SEQ studies individually reported 62 and 21 BMD-related loci reaching genome-wide significant level, and 12 loci (17.1%) were common in the two studies. By using Knowledge-based mining system for Genome-wide Genetic studies (KGG), we performed a gene-based analysis to identify BMD-associated genes harboring multiple associated SNPs from the two GEFOS studies. In total, 66 and 56 BMD-associated genes were respectively identified in GEFOS2 and GEFOS-SEQ projects with significant P-value ( $P < 2 \times 10^{-6}$ ) after Bonferroni correction. The analysis in GEFOS-SEQ study confirmed 44 identified genes (56.4%) from GEFOS2 study and exclusively detected 12 novel genes (15.4%). Among the 12 genes, 5 genes (*NAGS*, *TMEM101*, *PYY*, *MPP3*, and *C17orf105*) are for femoral neck BMD, 4 genes (*HOXC9*, *RBBP8NL*, *MFSN5* and *SFRP4*) for lumbar spine BMD and *C11orf58* for both BMD traits, which have not been reported in previous GWAS studies. Compared with original studies, the gene-based analysis replicated 23 BMD-related loci (37.1%) reaching genome-wide significant level from GEFOS2 study and 16 loci (76.2%) from GEFOS-SEQ study. This study complementarily enhanced the detecting efficiency for traditional GWAS in identifying disease susceptibility genes and obtaining replicable BMD-related genes.

**Disclosures:** Wei Zhu, None.

## SU0085

**The Human P2X7 Receptor Single-Nucleotide Polymorphism 853G>A Is Associated With Fracture Prevalence.** Lars Kruse<sup>\*1</sup>, Maria Ellegaard<sup>1</sup>, Magnus Karlsson<sup>2</sup>, Björn Rosengren<sup>2</sup>, Mattias Lorentzon<sup>3</sup>, Claes Ohlsson<sup>3</sup>, Dan Mellström<sup>3</sup>, Peter Schwarz<sup>4</sup>, Niklas Rye Jørgensen<sup>5</sup>.

<sup>1</sup>Research Centre of Ageing & Osteoporosis, Departments of Biochemistry & Endocrinology, Rigshospitalet, Copenhagen, Denmark, Denmark, <sup>2</sup>Clinical & Molecular Osteoporosis Research Unit, Department of Clinical Sciences & Orthopaedics, Skåne University Hospital, Lund University, Malmö, Sweden, <sup>3</sup>Center for Bone & Arthritis Research, Sahlgrenska Academy, University of Gothenburg, Gothenburg, Sweden, <sup>4</sup>Research Centre of Ageing & Osteoporosis, Departments of Biochemistry & Endocrinology, Rigshospitalet, Copenhagen, Denmark & Faculty of Health & Medical Sciences, University of Copenhagen, Denmark, Denmark, <sup>5</sup>Research Centre of Ageing & Osteoporosis, Departments of Biochemistry & Endocrinology, Rigshospitalet, Copenhagen, Denmark & Institute of Clinical Research, University of Southern Denmark, Odense, Denmark, Denmark

**Background:** The P2X7 receptor is an ATP-gated cation channel. It has been shown to be involved in regulation of osteoblast and osteoclast activity. Single-nucleotide polymorphisms (SNP) in the human P2X7 receptor gene have been associated with changes in bone phenotype: Loss-of-function SNP's with increased loss of bone mineral density (BMD) after menopause and gain-of-function SNP's with decreased fracture risk.

**Aim:** The aim of the study was to investigate whether P2X7 receptor SNP's are associated with BMD and vertebral fracture (VF) prevalence in old men.

**Methods:** A total of 2,015 men aged 70-81 years participating in the MrOS Sweden study were genotyped for 12 functional P2X7 receptor variants. The allele frequencies of the 12 SNP's analysed in the MrOS Sweden Cohort were comparable to prior published data from the Danish Osteoporosis Prevention Study (1). Genotyping was performed using the Sequenom MassARRAY and Illumina HumanOmni1\_Quad\_v1-0 B array. Spine and hip BMD was measured using DXA at baseline. Prevalent VF's were analysed by lateral thoracic and lumbar spine radiographs (Th4 to L5) in 1,586 of the participants either at baseline or at the 3- or 5-year follow-up. Differences in BMD and fracture prevalence according to genotype were analysed by ANOVA and Chi Square test, respectively. Data are presented as mean  $\pm$  SD and considered significant at  $p \leq 0.05$ .

**Results:** The study population was at baseline  $75.4 \pm 3.2$  years of age, had a BMI of  $26.4 \pm 3.6$  kg/m<sup>2</sup> and a spine BMD of  $1.127 \pm 196$  mg/cm<sup>2</sup>. Three hundred and twelve (19.7 %) of the x-rayed participants had at least one VF. There was an association of P2X7 receptor SNP 853G>A and the prevalence of VF, (40.0% of heterozygous carriers had VF vs 20.4% of homozygous WT carriers;  $p = 0.01$ ). We found no significant difference in BMD of the spine, total hip and femoral neck between wildtype and variant allele carriers of the P2X7 receptor gene.

**Conclusion:** Our data suggests that the P2X7 receptor SNP 853G>A is associated with VF prevalence but not BMD in old Swedish men. However, whether P2X7 receptor polymorphisms are associated with rate of bone loss cannot be excluded. Moreover, risk stratification of haplotypes according to gain- or loss-of-function might reveal additional associations to BMD or fracture prevalence.

(1) Jørgensen NR et al. European Journal of Human Genetics (2012) 20, 675-681

**Disclosures:** Lars Kruse, None.

## SU0086

**Network Based Subcellular Proteomics in Monocyte Membrane Revealed Novel Candidate Genes Involved in Osteoporosis.** Yong Zeng<sup>\*1</sup>, Lan Zhang<sup>2</sup>, Wei Zhu<sup>2</sup>, Hui Sheng<sup>2</sup>, Hao He<sup>2</sup>, Yu Zhou<sup>2</sup>, Qing Tian<sup>2</sup>, Fei-Yan Deng<sup>3</sup>, Li-Shu Zhang<sup>1</sup>, Hong-Gang Hu<sup>1</sup>, Hong-Wen Deng<sup>2</sup>. <sup>1</sup>Beijing Jiaotong University, China, <sup>2</sup>Tulane University, United states, <sup>3</sup>Soochow University, China

Osteoporosis is a metabolic bone disease which was mainly characterized by low bone mineral density (BMD). As the precursors of osteoclasts, peripheral blood monocytes (PBMs) are supported to be important candidates for identifying genes related to osteoporosis. Membrane proteins play multiple roles in different biological processes. In this study, to investigate the associations between monocyte membrane proteins and osteoporosis, based on high throughput LC-MS system, we performed subcellular proteomics in 59 male subjects with discordant BMD levels, with 30 high vs. 29 low BMD subjects. Here, a total of 1,070 membrane proteins were identified and quantified. By comparing the proteins' expression level using student t test, 39 proteins were differentially expressed between high and low BMD groups. Protein localization prediction supported that the differentially expressed proteins: P4HB ( $p=0.0021$ ), ATP2A3 ( $P=0.0008$ ), ITGB1 ( $P=0.0385$ ), ERAP1 ( $P=0.0036$ ) are significant membrane proteins. Subsequently, integrated gene enrichment analysis, functional annotation, pathway and network analysis based on multiple bioinformatics tools highlighted that P4HB, ATP2A3, ITGB1, ERAP1 are enriched in osteoporosis related pathways and terms including "Monocyte and its Surface Molecules", "calcium ion binding", "Reduction of cytosolic calcium levels" respectively. Gene-disease association study also indicated that these four genes are all involved in osteoporosis. Results from genome wide association study provided additional evidences to this study. All together, our study strongly supported the contribution of the genes P4HB, ATP2A3, ITGB1, ERAP1 to osteoporosis risk.

**Disclosures:** Yong Zeng, None.

## SU0087

**FGF23 Neutralizing Antibody Ameliorates Hypophosphatemia and Impaired FGF Receptor Signaling in Kidneys of FGF2 High Molecular Weight Isoform Transgenic Mice.** erxia du<sup>\*</sup>, Liping Xiao, Marja Hurley. Uconn Health, United states

Transgenic mice overexpressing the high molecular weight Fibroblast Growth Factor-2 isoforms in osteoblast lineage cells (HMWFGF2Tg) phenocopy the Hyp mouse, homolog of human X-linked hypophosphatemic rickets with, phosphate wasting and abnormal fibroblast growth factor (FGF23), fibroblast growth factor receptor (FGFR), Klotho and mitogen activated protein kinases (MAPK) signaling in kidney. Since HMWFGF2Tg mice have increased expression of FGF23 in bone and serum, we assessed whether FGF23 neutralizing antibody could rescue hypophosphatemia and impaired FGFR signaling in kidneys of HMWFGF2Tg male mice. Base line bone mineral density and bone mineral content in 1 month-old HMWFGF2Tg mice were significantly reduced compared with Vector/Control. Serum FGF23 was significantly increased in HMWFGF2Tg. Vector and HMWFGF2Tg mice were intra-peritoneally injected with FGF23 neutralizing antibody (FGF23Ab) or control IgG and were euthanized 24h post treatment. Serum phosphate was significantly reduced in HMWFGF2Tg and was rescued by FGF23Ab. Serum PTH was significantly increased in HMWFGF2Tg but was not reduced by FGF23Ab. Serum 1,25(OH)<sub>2</sub> Vitamin D was inappropriately normal in HMWFGF2Tg and was significantly increased in both Vector and HMWFGF2Tg by FGF23Ab. Analysis of HMWFGF2Tg kidneys revealed significantly increased mRNA expression of the FGF23 co-receptor Klotho, early growth response-1 transcription factor (Egr-1) mRNA, an indicator of FGF23 signaling as well as the mRNA for the transcription factor c-Fos that were all significantly decreased by FGF23Ab. A significant reduction in the phosphate transporter Npt2a mRNA was also observed in HMWFGF2Tg kidneys. FGF23Ab reduced p-FGFR1, KLOTHO, p-ERK1/2, EGR1, C-FOS and increased NPT2A protein in HMWFGF2Tg kidneys. We conclude that FGF23 blockade rescued hypophosphatemia by regulating FGF23/FGFR downstream signaling in HMWFGF2Tg kidneys. We further conclude that HMWFGF2 isoforms regulate PTH expression independent of FGF23/FGFR signaling.

## SU0089

**Regulation of FGF23 Production by Extra-Long Gs $\alpha$  Variant XL $\alpha$ s in Acute Kidney Injury.** Qing He<sup>\*1</sup>, Marc Wein<sup>1</sup>, Jordan Spatz<sup>1</sup>, Antonius Plagge<sup>2</sup>, Paola Divieti Pajevic<sup>3</sup>, Harald Jüppner<sup>1</sup>, Murat Bastepe<sup>1</sup>. <sup>1</sup>Endocrine Unit, Department of Medicine, Massachusetts General Hospital & Harvard Medical School, Boston, MA, USA, United states, <sup>2</sup>Department of Cellular & Molecular Physiology, Institute of Translational Medicine University of Liverpool, Liverpool, United Kingdom, United Kingdom, <sup>3</sup>Department of Molecular & Cell Biology, Goldman School of Dental Medicine, Boston University, Boston, MA, USA, United states

FGF23 is a bone-derived endocrine hormone regulating the renal excretion of phosphate and the synthesis of 1,25-dihydroxyvitamin D (1,25(OH)<sub>2</sub>D). FGF23 levels are significantly elevated in chronic kidney disease and directly related to mortality in this condition. FGF23 levels are also elevated in acute kidney injury and correlate with increased risk of death or need for dialysis. Mechanisms underlying the kidney injury-induced FGF23 production are poorly defined.

The *GNAS* locus encodes the  $\alpha$ -subunit of the stimulatory G protein (Gs $\alpha$ ) and its extra-long variant XL $\alpha$ s. Gs $\alpha$  stimulates cAMP generation and plays important roles in skeletal development and mineral ion homeostasis. XL $\alpha$ s is expressed in bone and can also stimulate cAMP generation when overexpressed. In addition, evidence from certain patients with *GNAS* mutations and mouse models indicates that XL $\alpha$ s is involved in the actions of calciotropic hormones and bone metabolism.

We have now found that at postnatal day 10 (P10) XL $\alpha$ s knockout (XLKO) mice exhibit hyperphosphatemia (11.4 $\pm$ 0.43 vs. 10.2 $\pm$ 0.21 mg/dl in WT), increased serum 1,25(OH)<sub>2</sub>D (224.8 $\pm$ 3.49 vs. 142.5 $\pm$ 4.02 pmol/L in WT), and reduced serum FGF23 (204.4 $\pm$ 10.50 vs. 398.7 $\pm$ 10.14 pg/mL in WT). FGF23 mRNA levels in XLKO femurs were also significantly reduced (57.7 $\pm$ 3.26% of WT levels). CRISPR/Cas9-mediated knockout of XL $\alpha$ s in a murine osteocytic cell line (Ocy454) significantly decreased FGF23 mRNA (14.8 $\pm$ 2.11% of control levels), indicating that XL $\alpha$ s regulates FGF23 expression in a cell-autonomous manner. FGF23 levels in adult XLKO mice were also decreased (389.0 $\pm$ 10.09 vs. 501.5 $\pm$ 12.90 pg/mL in WT); however, the difference was not statistically significant (p=0.079). We then tested whether XL $\alpha$ s is required for increased FGF23 production in response to acute kidney injury by injecting high dose folic acid into XLKO and WT littermates. Folic acid led to the expected deleterious effects in renal tubules of both XLKO and WT mice, as determined by histological analyses, and resulted in comparable increases in serum phosphate and blood urea nitrogen (BUN) levels. In contrast, the elevation of serum FGF23 was significantly lower in XLKO mice than WT littermates (1389.4 $\pm$ 158.11 vs. 3474.8 $\pm$ 199.32 pg/mL in WT at 24 hours after folic acid injection, p<0.01).

These results suggest that FGF23 expression is regulated directly by the action of XL $\alpha$ s in bone cells, and that XL $\alpha$ s plays an important role in kidney-injury induced FGF23 production.

**Disclosures:** Qing He, None.

## SU0090

**The Regulatory Mechanisms of FGF23 Activity via GALNT3 by Phosphate.** Yuichi Takashi<sup>\*1</sup>, Yuka Kinoshita<sup>2</sup>, Nobuaki Ito<sup>2</sup>, Maria Tsoumpra<sup>1</sup>, Shun Sawatsubashi<sup>1</sup>, Toshio Matsumoto<sup>1</sup>, Seiji Fukumoto<sup>1</sup>. <sup>1</sup>Tokushima University, Japan, <sup>2</sup>The University of Tokyo Hospital, Japan

**Purpose:** Fibroblast growth factor 23 (FGF23) is a phosphaturic hormone produced by bone, especially by osteocyte. A part of FGF23 protein is cleaved into inactive fragments before or during the process of secretion. We have previously shown that O-glycosylation of FGF23 protein by GalNac-T3, a gene product of *GALNT3*, inhibits this cleavage. On the other hand, it was reported that phosphorylation of FGF23 protein by FAM20C enhances this cleavage. Therefore, FGF23 action seems to be regulated not only by its production but also by this post-translational modification of FGF23 protein. However, the precise regulatory mechanisms of FGF23 activity by phosphate are unknown. **Methods:** We first examined the effect of high (1.2%) or low (0.3%) phosphate diet in 4-week-old male ICR mice. Mice were fed with each diet for 2 weeks. We measured serum full-length Fgf23 by ELISA and analyzed gene expressions in femur by quantitative PCR. In addition, we investigated whether phosphate regulates the post-translational processing in *in vitro* experiments. Human *FGF23* was overexpressed in UMR106 cells with various concentrations of extracellular phosphate and the processing of FGF23 protein was analyzed by western blotting of conditioned media using an antibody recognizing C-terminal portion of FGF23 protein. **Results:** While there were no differences in serum UN, Cre, Ca and FE<sub>Ca</sub>, serum phosphate and FE<sub>Pi</sub> were significantly higher in high phosphate diet group. A high phosphate diet increased serum full-length Fgf23 concentration. The diet also enhanced *Galnt3* and *Fam20c* expression without changing *Fgf23* expression in the femur. These results indicate that the post-translational modification of FGF23 protein is more sensitive to changes in dietary phosphate than *Fgf23* expression. In *in vitro* experiments, higher extracellular phosphate increased full-length / C-terminal fragment ratio of FGF23 protein indicating that phosphate prevented the processing of FGF23 protein. Increase of extracellular phosphate also enhanced *Galnt3* and *Fam20c* expression. Furthermore, the overexpression of *GALNT3* together with *FGF23* increased full-length / C-terminal fragment ratio of FGF23 protein in the

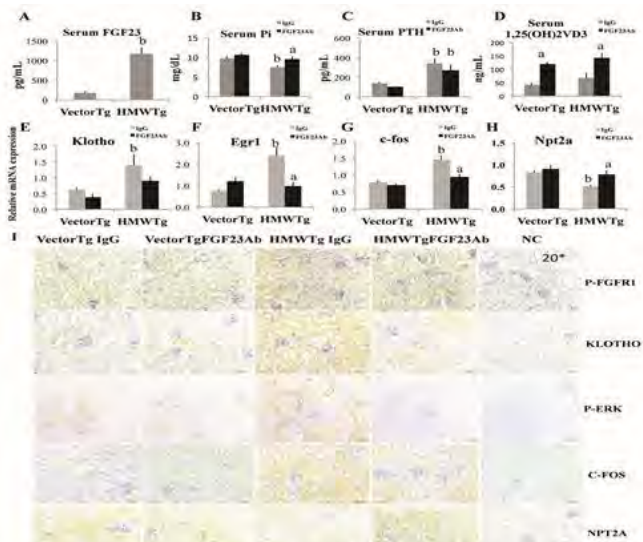


**Figure 1. FGF23 neutralizing antibody ameliorates hypophosphatemia and impaired FGF23/FGFR signaling in kidneys of HMWtg mice.** (A) Serum FGF23 was increased in HMWtg mice. FGF23 neutralizing antibody reduced decreased serum Pi (B) in HMWtg mice, did not effect PTH (C) and further increased 1,25(OH)<sub>2</sub>VD3(D) both in serum of Vector and HMWtg mice. n=6/group. To further examine signaling pathways involved in Pi regulation in kidneys of HMWtg mice, qPCR and IHC staining were performed. mRNA of klotho(E), Egr1 (F), c-Fos(G) and Npt2a (H). FGF23Ab rescued increased klotho, Egr1, c-Fos and decreased Npt2a mRNA in HMWtg mice. (I) FGF23Ab, decreased p-FGFR1, KLOTHO, p-ERK C-FOS and increased NPT2A protein. Values are mean $\pm$ SE, n=3/group. a, significant effect of FGF23Ab; b, Significant effect of HMWFGF2, p<0.05.

Figure 1

**Disclosures:** erxia du, None.

## SU0088

**Klotho Lacks a Fgf23 Independent Role in Mineral Homeostasis.** Olena Andrukhova<sup>\*1</sup>, Jessica Bayer<sup>2</sup>, Ute Zeitz<sup>2</sup>, Sathish Kumar Murali<sup>2</sup>, Reinhold Gottfried Erben<sup>2</sup>. <sup>1</sup>Department of Biomedical Sciences University of Veterinary Medicine, Austria, <sup>2</sup>Department of Biomedical Sciences University of Veterinary Medicine, Austria

Fibroblast growth factor-23 (FGF23) is a bone-derived hormone regulating vitamin D hormone production and renal handling of minerals by signaling through a FGF receptor/ $\alpha$ Klotho (Klotho) receptor complex. Whether Klotho has FGF23-independent effects on mineral homeostasis is a controversial issue. Here, we aimed to shed more light on this controversy by comparing male and female triple knockout mice with simultaneous deficiency in *Fgf23* and *Klotho* and a nonfunctioning vitamin D receptor (VDR) (*Fgf23/Klotho/VDR*) with double (*Fgf23/VDR* and *Klotho/VDR*) and single *Fgf23*, *Klotho* and VDR mutants. All genotypes were generated by breeding triple heterozygous mice. Ablation of vitamin D signaling is known to rescue the severe phenotype of *Fgf23* and *Klotho* single mutants. To correct the intestinal calcium and phosphate absorption defect in VDR mutants, all mice were kept lifelong on a rescue diet enriched with calcium, phosphate, and lactose. As expected, 4-wk-old *Fgf23* and *Klotho* knockout mice were hypercalcemic and hyperphosphatemic, whereas VDR, *Fgf23/VDR* and *Klotho/VDR* mice on rescue diet were normocalcemic and normophosphatemic. Serum levels of calcium, phosphate, and sodium did not differ between 4-wk-old triple *Fgf23/Klotho/VDR* and double *Fgf23/VDR* or *Klotho/VDR* knockout mice. Three-mo-old male and female *Fgf23/VDR* and *Klotho/VDR* compound mutants were characterized by hyperphosphatemia, hypocalcemia, increased serum PTH as well as renal calcium and sodium wasting. Notably, 3-mo-old *Fgf23/Klotho/VDR* triple knockout mice were indistinguishable from double *Fgf23/VDR* and *Klotho/VDR* compound mutants in terms of body weight, serum calcium, serum phosphate, serum sodium, serum PTH as well as urinary calcium and sodium excretion. Protein expression analysis revealed increased membrane abundance of sodium-phosphate co-transporter 2a (NaPi-2a), and decreased expression of sodium-chloride co-transporter (NCC) and transient receptor potential cation channel subfamily V member 5 (TRPV5) in *Fgf23/Klotho/VDR*, *Fgf23/VDR*, and *Klotho/VDR* mice, relative to WT and VDR mice, but no differences between triple and double knockouts. Similarly, tibial and vertebral total, cortical and trabecular BMD measured by pQCT were unchanged in 4-wk-old and 3-mo-old *Fgf23/Klotho/VDR* mice compared with *Fgf23/VDR* and *Klotho/VDR* mice. In conclusion, our data suggest that the main physiological function of Klotho for mineral homeostasis *in vivo* is its role as co-receptor mediating Fgf23 action.

**Disclosures:** Olena Andrukhova, None.

conditioned media compared to cells overexpressing *FGF23* alone. On the other hand, the overexpression of *FAM20C* together with *FGF23* decreased full-length / C-terminal fragment ratio of FGF23 protein. These results indicate that the effect of phosphate on *Galnt3* was dominant over that of *Fam20c* in the regulation of FGF23 processing. Conclusions: Phosphate regulates FGF23 activity at least in part by enhancing *GALNT3* expression and preventing the processing of FGF23 protein.

**Disclosures:** Yuichi Takashi, None.

This study received funding from: Chugai Pharmaceutical Co. Ltd.

## SU0091

**Does the lactation/low Ca model of induced bone remodeling affect circulating mineral metabolism markers?** Ryan Ross\*, Brittany Wilson, Rick Sumner. Rush University Medical Center, United states

Feeding lactating rats a low calcium diet induces bone remodeling [1,2], providing a model to study matrix mineralization after weaning when the dams are returned to a normal calcium diet [3]. Our recent study of the dams showed that many aspects of matrix mineralization are normal [3]. However, it is unclear whether the matrix maturation process occurs in the presence of a normal mineral metabolism environment.

This study used 50 10-week old Sprague-Dawley timed-pregnancy rats. At parturition, litters were normalized to 11 pups and the dams were split into two groups: rats fed a normal calcium diet during lactation (lact/norm Ca) or a low Ca diet (lact/low Ca). 25 age-matched virgin rats fed a normal Ca diet (virgin/norm Ca) served as controls. At weaning, rats in the lact/low Ca group were switched to a normal Ca diet. 5 rats per group were sacrificed at weaning, 1, 2, 7, and 14 days post-weaning. Serum levels of Ca, phosphate, PTH, PTHrP, calcitonin, and FGF23 were assessed and analyzed with non-parametric statistics.

Most of the between-group differences involved FGF23. Compared to virgin/norm Ca, lact/norm Ca rats had elevated FGF23 at days 2, 7 and 14, while levels in lact/low Ca were depressed at weaning and elevated at days 1, 2 and 14. Compared to lact/norm Ca, lact/low Ca FGF23 levels were depressed at weaning and day 7. Compared to virgin/norm Ca, phosphate levels were higher in lact/norm Ca and lact/low Ca rats at weaning and day 1. Ca levels were higher in lact/low Ca compared to virgin/norm Ca rats at day 1. Calcitonin was depressed in lact/norm Ca rats compared to virgin/norm Ca rats at day 7.

The combination of lactation with a low Ca diet leads to extensive bone resorption followed by formation after weaning, thereby generating large regions of mineralizing matrix. Most of the changes in mineral metabolism markers were transient and early (either no changes or return to control values by day 2). It is likely that the elevated FGF23 in both lactation groups was due to the early transient elevated phosphate levels. In the lact/low Ca group, FGF23 levels returned to control values by day 7, but were slightly elevated at 14 days. These findings suggest that post-weaning bone matrix maturation in the lact/low Ca model occurs in a largely normal mineral metabolism environment.

[1] Ruth Am J Anat 1953, [2] de Winter et al. Calcif Tissue Int 1975, [3] Ross et al. ORS 2016

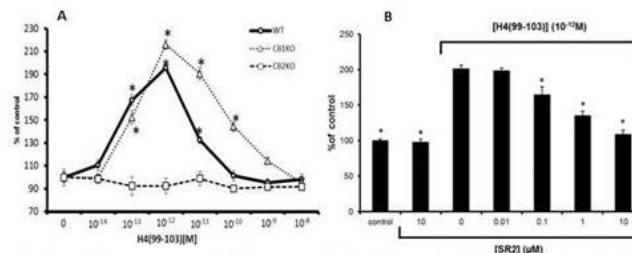
**Disclosures:** Ryan Ross, None.

## SU0092

**H4(99-103) is an Endogenous Peptide that Signals via the CB2 Cannabinoid Receptor.** Bitya Raphael\*, Natalya Kogan<sup>2</sup>, Malka Attar-Namdar<sup>2</sup>, mukesh Chourasia<sup>3</sup>, Avital Shurki<sup>3</sup>, Roger G. Pertwee<sup>4</sup>, Maria G. Cascio<sup>5</sup>, Andreas Zimmer<sup>6</sup>, Itai Bab<sup>2</sup>, Yanke Gabet<sup>1</sup>. <sup>1</sup>Department of Anatomy & Anthropology, Sackler Faculty of Medicine, Tel Aviv University, Tel Aviv, Israel, <sup>2</sup>Bone Laboratory, Institute of Dental Sciences, Faculty of Dental Medicine, Hebrew University of Jerusalem, Jerusalem, Israel, <sup>3</sup>Institute for Drug Research, Faculty of Medicine, Hebrew University of Jerusalem, Jerusalem, Israel, <sup>4</sup>Institute of Medical Sciences, University of Aberdeen, Aberdeen, Scotland, United Kingdom, <sup>5</sup>Institute of Medical Sciences, University of Aberdeen, Aberdeen, Scotland, United Kingdom, <sup>6</sup>Institute of Molecular Psychiatry, University of Bonn, Bonn, Germany, Germany

The endocannabinoid (EC) system consists of the arachidonic acid derived ECs anandamide and 2-arachidonoylglycerol, their metabolizing enzymes, and CB1 and CB2 cannabinoid receptors. Studies of the skeletal EC system in mice and humans suggest the occurrence of a CB2 tone, which protects the skeleton against age-related bone loss. It is unlikely that fatty acid derived ECs generate such a tone, as they are short-lived neurotransmitter-like compounds synthesized 'on demand'. Although the existence of endogenous peptides that regulate the EC system has never been reported, we hypothesized that the CB2 tone is maintained by circulating peptide agonists. One such peptide candidate is H4(99-103), which is present in the circulation at significant concentrations. Studies on the skeletal EC system, showed a striking similarity between the biological activities of H4(99-103) and that of potent CB2 agonists, which target the same mitogenic signaling pathway and have similar anti-inflammatory and skeletal effects. The activity of H4(99-103) was tested *in vitro* and *in vivo* on wild type and CB2-deficient cells and

mouse models, respectively, and in human derived osteoblasts. Our results indicate that like a selective CB2 agonist, H4(99-103) triggers *ex vivo* a proliferative dose-dependent response in osteoblasts, inhibitable by genetic or pharmacological ablation of CB2. Characteristic of CB2 agonists, H4(99-103) restrains *ex vivo* osteoclastogenesis and induces osteoclast apoptosis dose-dependently in WT but not in CB2-deficient cells. A hallmark of CB2 activation is the attenuation of inflammation. Indeed, *in vivo*, H4(99-103) markedly decreases acute inflammation measured manually and histologically as ear swelling following topical application of xylene. This effect is completely absent in CB2 knockout mice. *In vitro*, a similar CB2-dependent inhibition of macrophage inflammatory response (RNA expression of TNF $\alpha$ , IL1 $\beta$  and IL6) was observed with either a CB2 agonist or H4(99-103). Our results demonstrate that H4(99-103) signals in bone and inflammatory cells via CB2. Docking simulation suggests that H4(99-103) binds to CB2 at an allosteric site. These findings are the first demonstration of an endogenous peptide that signals via CB2 in health and disease. Studies are in progress to further characterize the binding determinants of H4(99-103) to CB2 and assess the role of H4(99-103) in maintaining the CB2 tone in the skeletal system and attenuating age-related bone loss.



**A. Mitogenic dose-response activity in mouse osteoblasts.** H4 (99-103) stimulates number of WT and CB2<sup>-/-</sup>, but not CB2<sup>-/-</sup> mouse calvarial osteoblasts. \*p<0.05 vs. untreated. **B. CB2 agonistic activity of H4(99-103) in human osteoblasts.** SR144528 (SR2), a CB2 selective antagonist inhibits dose-dependently H4(99-103) mitogenic activity. \*p<0.05 vs. H4(99-103)-treated (no SR2) cultures. Means±SE, n=3.

Mitogenic dose-response activity in mouse and human osteoblasts

**Disclosures:** Bitya Raphael, None.

## SU0093

**Calcium fluxes at the bone-plasma interface: effects of parathyroid hormone.** Christopher Dedic\*<sup>1</sup>, Jacky T. Hung<sup>2</sup>, Alan M. Shipley<sup>3</sup>, Andrew L. Miller<sup>2</sup>, Joseph G. Kunkel<sup>4</sup>, Paola Divieti Pajevic<sup>1</sup>, Alessandro Rubinacci<sup>5</sup>. <sup>1</sup>Goldman School of Dental Medicine, Boston University, United states, <sup>2</sup>HKUST, Division of Life Science, China, <sup>3</sup>Applicable Electronics LLC, United states, <sup>4</sup>Marine Science Center, University of New England, United states, <sup>5</sup>Bone Metabolism Unit, Scientific Institute San Raffaele, Italy

In land-living vertebrates including humans, the calcium ion concentration of the extracellular fluid, ECF-[Ca]<sup>2+</sup> is set at a genetically predetermined set point which combines the operational level of the kidney and bone-plasma interfaces. ECF-[Ca]<sup>2+</sup> is maintained within a narrow oscillation range by the regulatory action of endocrine loops established by Parathyroid Hormone, Calcitonin and 1,25(OH)<sub>2</sub>D. This model of "reactive homeostasis" implies two correction mechanisms, i.e. tubular Ca reabsorption and osteoclast Ca resorption. Although their alterations have an effect on ECF-[Ca]<sup>2+</sup> maintenance, they cannot fully account for rapid correction of the continuing perturbations of plasma calcium, which occur daily in life. We therefore hypothesized that the cellular system able to fulfill the homeostatic demand by sustaining a steady release of calcium into the ECF without activating remodeling might be an osteocyte-bone lining cell syncytium (OBLCS). OBLCS is a network of stellate cells buried within the bone matrix, the osteocytes, having an asymmetrical arborization of dendrites polarized toward the bone surfaces, which comes into contact with the bone lining cells covering quiescent bone surfaces. To explore the hypothesis that the cell system responsible for Ca<sup>2+</sup> fluxes at the bone-ECF interface is regulated by PTH and its effect on osteocytes, we have performed direct real-time measurements of Ca<sup>2+</sup> fluxes at the bone plasma interface in *ex-vivo* metatarsal bones maintained in physiological conditions and exposed to PTH. To further characterize whether the PTH receptor on osteocytes is a critical component of the minute-to-minute calcium plasma calcium regulation, metatarsal bones from mice lacking the PTH receptor in these cells were tested for rapid calcium exchange. Direct real-time measurements of Ca<sup>2+</sup> fluxes and concentration gradients at the bone-plasma calcium interface in isolated bone using SIET offered the unique opportunity to investigate how calcium gets into and out of bone almost instantaneously and what regulates its movement. Our data demonstrated that calcium fluxes at the bone-plasma interface are independent of PTH and its signaling through its receptor. Indeed acute PTH addition was unable to affect Ca<sup>2+</sup> fluxes, indicating that the minute-to-minute calcium homeostasis is independent of PTH actions on osteocytes

**Disclosures:** Christopher Dedic, None.

## SU0094

**Novel BAT precursor-derived cell lines with normal *Gnas* methylation maintain predominantly maternal *Gsz* expression: new tools for studying paternal *Gsz* regulation.** Olta Tafaj<sup>1</sup>, Harald Jüppner<sup>1</sup>, Steven Hann<sup>2</sup>, Matthew Warman<sup>2</sup>, Lee S. Weinstein<sup>3</sup>. <sup>1</sup>MGH, United states, <sup>2</sup>Boston Children's Hospital, United states, <sup>3</sup>National Institutes of Health, United states

Pseudohypoparathyroidism type Ia (PHP1A) is caused by heterozygous, inactivating mutations affecting exons 1-13 of the maternal *GNAS* allele that encode the  $\alpha$ -subunit of the stimulatory G protein (*Gsz*). These mutations cause resistance to parathyroid hormone (PTH) and frequently other hormones mediating their actions through *Gsz*-coupled receptors. No hormonal resistance is observed when the same or similar *GNAS* mutations occur on the paternal allele. Observations similar to those in PHP1A patients had been observed in mice lacking *Gnas* exon 1 or 2, thus leading to the hypothesis that the paternal exon 1 promoter undergoes tissue-specific silencing through as-of-yet undefined mechanisms. Cells with predominantly maternal *Gsz* expression are present in proximal renal tubules (PRT) and in subpopulations within thyroid, pituitary and central nervous system. Taking advantage of a SNP in *Gnas* exon 11 (rs13460569; C in 129Sv; G in C57/BL6), we recently showed that predominantly maternal *Gsz* expression is maintained throughout life in brown adipose tissue (BAT). To further understand the mechanism underlying silencing of the paternal *Gnas* allele in BAT, we isolated primary mature brown adipocytes from newborn wild-type (WT) mice and showed that predominantly maternal *Gsz* expression is maintained in these cells. Because mature adipocytes are post-mitotic, we isolated adipocyte precursor cells (APC) from neonatal mice derived from matings between floxed *Gnas* exon 1 (E1fl/fl) females and WT males that were homozygous SNP rs13460569 (C or G, respectively). After immortalization, clonal APC lines (n=19) were generated and parent-specific *Gsz* expression was investigated. Individual E1fl/WT cell lines showed normal allele-specific *Gnas* methylation, yet revealed considerable differences in the maternal contribution to total *Gsz* mRNA expression; namely 72±0.34% (n=5), 55±1.9% (n=12), or 25±4.8% (n=2). The relative contribution of each parental allele to *Gnas* mRNA expression was maintained for more than 30 passages. These novel cell lines can now be used to investigate the epigenetic and non-epigenetic mechanisms that contribute to the differential regulation of the *Gnas* allele inherited from mother versus father.

**Disclosures:** Olta Tafaj, None.

## SU0095

**Comparison of Frequency of Glucocorticoid-induced Osteoporosis and Osteonecrosis in Three Different Mice Strains.** Geetha Mohan<sup>1</sup>, Kie Shidara<sup>1</sup>, Evan Lay<sup>1</sup>, Alexander Kot<sup>1</sup>, Hongliang Zhang<sup>1</sup>, Tara Rogers<sup>1</sup>, Karl Jepsen<sup>2</sup>, Wei Yao<sup>1</sup>, Nancy Lane<sup>1</sup>. <sup>1</sup>UC Davis Medical Center, United states, <sup>2</sup>University of Michigan, United states

Glucocorticoids (GC) are frequently used to treat diverse inflammatory diseases. While they are effective, complications of GC use includes osteoporosis (OP) and atraumatic osteonecrosis (ON). Presently, there is no effective medical treatment for GC-induced ON so there is a need to develop an animal model to study both the pathology and novel treatment strategies. The aim of our study was to establish GC-induced OP and ON in three different mice strains (BALB/c, C57BL/6, and Swiss-Webster (SW)).

Seven-week-old male BALB/c, C57BL/6, and SW mice were randomized into placebo and GC groups. BALB/c and C57BL/6 mice were treated with oral dexamethasone (4mg/L) in drinking water for 90 days. SW mice were treated with 5mg slow release prednisolone pellet for 90 days. Study outcome measures included trabecular bone volume fraction (BV/TV; distal femur and vertebral body), distal femoral cortical bone volume (Ct. BV) measured by ex-vivo micro-CT; tibial bone strength by 3-point bending test, vertebral body bone strength by compression testing, biochemical measures of bone turnover by serum PINP, and evidence of ON by histology (Yang et al, J Orthop Res. 2009). Non-parametric Kruskal-Wallis test was used to determine the differences between the groups.

GC treatment reduced trabecular BV/TV (distal femur and lumbar vertebral body) and femoral Ct. BV of BALB/c mice but not the C57BL/6 compared to placebo (p<0.05) (Table 1). GC treated SW mice had lower trabecular BV/TV (vertebral body) and lower femoral Ct. BV compared to placebo (p<0.05). GC treatment reduced tibial bone strength compared to placebo in all three strains of mice (p<0.05). GC treatment also reduced the bone formation marker PINP in all GC treatment groups compared to placebo (p<0.05). GC-induced ON lesions were observed in the distal femur of BALB/c (95%), C57BL/6 (62%) and SW (18%) mice.

Mouse strain-specific differences were found in the development of GC-induced OP and ON and BALB/c mice were more susceptible to developing GC-induced osteonecrosis and osteoporosis.

Table 1 Effect of GC on trabecular BV/TV and cortical bone volume of BALB/c, C57BL/6 and Swiss Webster mice

BV/TV	Distal femur	
	Placebo Mean ± SD	GC Mean ± SD
BALB/c	0.150 ± 0.022	0.120 ± 0.015**
C57BL/6	0.143 ± 0.026	0.146 ± 0.046
SW	0.167 ± 0.033	0.083 ± 0.026
BV/TV	Vertebral body	
	Placebo Mean ± SD	GC Mean ± SD
BALB/c	0.200 ± 0.018	0.155 ± 0.017****
C57BL/6	0.200 ± 0.021	0.193 ± 0.043
SW	0.316 ± 0.051	0.170 ± 0.072*
Ct.BV (mm <sup>3</sup> )	Cortical bone volume	
	Placebo Mean ± SD	GC Mean ± SD
BALB/c	0.032 ± 0.003	0.026 ± 0.001**
C57BL/6	0.037 ± 0.004	0.033 ± 0.005
SW	0.513 ± 0.127	0.297 ± 0.056****

GCON-table

**Disclosures:** Geetha Mohan, None.

## SU0096

**Opposing Actions of SHH and IHH Control Transition of Proliferating Immature Chondrocytes into Mature Hypertrophic Chondrocytes during Secondary Center Ossification.** Patrick Aghajanian<sup>\*</sup>, Weirong Xing, Shaohong Cheng, Sheila Pourteymoor, Subburaman Mohan. VA Loma Linda Healthcare System, United states

We have recently shown that the rapid increase in thyroid hormone (TH) levels that occurs during the prepubertal growth period in mice is obligatory for initiation and progression of secondary ossification centers (SOC) in the epiphysis. While TH promotion of chondrocyte hypertrophy during SOC formation is predicted to involve activation of Indian hedgehog (IHH) signaling, nothing is known on the role of sonic hedgehog (SHH) signaling in this process. In this study, we used real time RT-PCR to measure gene expression in epiphyses of TH-deficient *Tshr*<sup>-/-</sup> mice compared to euthyroid control mice at postnatal day 7 and found that, while *Ihh* expression decreased 7-fold, *Shh* expression increased 15.8-fold ( $P < 0.001$ ). Immunohistochemistry revealed that SHH was mainly expressed in proliferating immature chondrocytes (CCs) while IHH expression was seen in maturing hypertrophic CCs. Based on our finding that TRβ1 expression increases in epiphyseal CCs during the prepubertal growth period and contributes to increased *Ihh* expression, we evaluated the role of TRβ1 in regulating *Shh* expression. We found that knockdown of TRβ1 using lentiviral shRNA increased *Shh* expression (3.5-fold,  $P < 0.01$ ), thus suggesting that TRβ negatively regulates *Shh* expression although it positively regulates *Ihh* expression. To address the role of SHH, we overexpressed *Shh* or *GFP* control in epiphyseal CCs using adenoviral vectors and found cell proliferation as measured by CyQuant assay was increased by 80% ( $P < 0.01$ ) in *Shh*-overexpressing CCs versus *GFP* control. *Shh* overexpression increased expression of immature CC markers (*Sox9* by 62%, *Col2* by 260%, and *Acan* by 300%, all  $P < 0.01$ ) but decreased expression of mature hypertrophic CC markers (*Mmp13* by 42% and *RankL* by 64%). Expression levels of *Ptch1* and *Gli1* but not *Gli2* and *Gli3* were increased by *Shh* overexpression, thus suggesting that the SHH effect on target gene expression is mediated via *Gli1*. Knockdown of *Ihh* using lentiviral vectors significantly modulated expression of hypertrophic CC markers, an effect mediated by changes in *Gli2* expression. Based on these data and other published data, we propose a model in which the increase in TH levels during the prepubertal growth period positively regulates TRβ1 expression to fine tune levels of SHH and IHH and, thereby, control the transition of proliferating immature CCs into mature hypertrophic CCs in the epiphyses during secondary center ossification.

**Disclosures:** Patrick Aghajanian, None.

## SU0097

**Glucocorticoids suppress OPG expression in vivo and negatively affect cortical bone by acting directly on osteoblast-lineage cells.** Marilina Piemontese<sup>\*</sup>, Yu Liu, Jinhu Xiong, Yuko Fujiwara, Priscilla Baltz, Charles OBrien. University of Arkansas for Medical Sciences, United states

Therapeutic use of glucocorticoids is a major cause of bone loss and fractures. Studies in mice have produced conflicting results regarding the mechanisms by which

this occurs. Specifically, some studies suggest that glucocorticoids cause bone loss by acting on osteoblast-lineage cells, but others suggest that they do so by acting on osteoclasts. To clarify the cellular targets and the mechanisms of action of glucocorticoids on bone, we examined adult mice with loss of glucocorticoid receptor (GR) function in specific cell types. Loss of GR function in osteoclasts was achieved by crossing GR-*fl/fl* mice with LysM-Cre mice. Skeletal development and growth were normal in these mice, as was osteoclast formation *in vitro*. Moreover, administration of exogenous glucocorticoids resulted in similar vertebral and femoral cortical bone loss and development of porosity in both genotypes, as measured by microCT. The changes in femoral cortical bone were associated with an increase in osteoclast number at the endocortical surface. Cancellous bone volume was not affected by glucocorticoid administration in either genotype. These results demonstrate that excess glucocorticoids do not act directly on osteoclasts to cause cortical bone loss. We next examined mice with deletion of the GR in osteoblast-lineage cells using the osteocalcin-Cre transgene. Under basal conditions, these mice showed a profound reduction in cancellous bone volume but increased cortical thickness; the latter was due to a reduction in medullary area. These changes were associated with elevated OPG mRNA in cortical bone preparations. These results demonstrate that endogenous glucocorticoids act directly on osteoblasts to promote cancellous bone accrual but at the same time reduce the accrual of cortical bone. Glucocorticoid administration caused loss of vertebral and femoral cortical bone, development of cortical porosity, and increased osteoclast-specific gene expression in the control mice; however deletion of the GR from the osteoblast lineage completely protected mice from these changes. Consistent with this, glucocorticoids suppressed OPG mRNA abundance in the cortical bone of control mice but this did not occur in mice lacking GR in osteoblasts. Collectively, these studies demonstrate that the negative impact of glucocorticoids, whether endogenous or exogenous, on cortical bone is mediated exclusively by direct action on osteoblast-lineage cells, possibly via suppression of OPG.

**Disclosures:** *Marilina Piemontese, None.*

## SU0098

**Optimal dose of tamoxifen for inducible Cre recombinase technology in male mouse bone.** Ferran Jordi<sup>1\*</sup>, Michael Laurent<sup>1</sup>, Vanessa Dubois<sup>2</sup>, Rougin Khalil<sup>1</sup>, Ludo Deboel<sup>1</sup>, Brigitte Decallone<sup>1</sup>, Geert Carmeliet<sup>1</sup>, Ludo Van den Bosch<sup>3</sup>, Frank Claessens<sup>1</sup>, Dirk Vanderschueren<sup>1</sup>. <sup>1</sup>KU Leuven, Belgium, <sup>2</sup>Institut Pasteur de Lille, France, <sup>3</sup>VIB, Belgium

**Introduction:** Tamoxifen (TAM)-inducible Cre recombinases (CreER) represent a powerful tool for testing gene function in bone physiology and disease. However, selective estrogen receptor modulators also influence trabecular and cortical bone development in mice. Thus, the bone phenotype observed in CreER-induced gene knockout mice could be confounded by TAM effects, generating erroneous conclusions. Here, our aim was to describe an optimized TAM regime that induced an efficient CreER-driven gene-knockout with minimal bone affection. **Methods:** we assessed by microCT and serum osteocalcin the effect of repeated once-daily doses for 2, 4 and 10 days of TAM (130 mg/kg) on the femur of 6-week-old male WT C57BL/6J mice. The same experimental design was used to compare the efficiency of the different regimes in knocking out the androgen receptor (AR) in the nervous system of AR floxed mice expressing a CreER under the control of the neuronal promoter Thy1. **Results:** TAM produced a dose-dependent enhancement of trabecular bone volume and trabecular number, reaching  $P < 0.05$  by ANOVA in 4 and 10 doses groups (47 and 185%,  $P < 0.01$  and  $0.0001$  vs. vehicle, respectively). Femur length was significantly increased in a dose-related fashion in all TAM-treated groups. In cortical bone, 10 doses reduced both cross-sectional area and medullary area ( $P < 0.01$  vs. vehicle), while cortical thickness remained unaltered. Similarly, only the highest dosage regime showed an increase in osteocalcin serum levels (180% vs. vehicle,  $P < 0.0001$ ). Since the anabolic action of TAM on bone was so dramatic after 10 days, the group was excluded in subsequent studies. Administration of TAM in AR<sup>flox</sup>-Thy1CreER+ mice induced a drop in AR mRNA levels restricted to the nervous system. Both mice treated with 2 and 4 doses showed a similar reduction in AR mRNA in brain (~70%,  $P < 0.0001$  vs. AR<sup>flox</sup>-Thy1CreER-), but not levator ani muscle. In both regimes, the reduction in mRNA levels was more pronounced in Thy1-CreER-positive regions (cerebral cortex:~80%; hippocampus:~90%; brainstem:~75%). **Conclusion:** We describe an optimized TAM regime of two doses that successfully induces CreER-driven gene inactivation while marginally affecting bone length and not significantly affecting cortical and trabecular microstructure. However, our results highlight the importance of good control groups when working with TAM-inducible CreER recombinase technology to study bone phenotypes.

**Disclosures:** *Ferran Jordi, None.*

## SU0099

**Phosphorylation of S122 in ER $\alpha$  is Important for the Skeletal Response to Estrogen Treatment.** Karin Gustafsson<sup>1</sup>, Sofia Movérare-Skrtic<sup>1\*</sup>, Vikte Lionikaite<sup>1</sup>, Helen Farman<sup>1</sup>, Jianyao Wu<sup>1</sup>, Petra Henning<sup>1</sup>, Annica Andersson<sup>1</sup>, Ulrika Islander<sup>1</sup>, Angelina Bernardi<sup>1</sup>, Sara Windahl<sup>1</sup>, Klara Sjögren<sup>1</sup>, Antti Koskela<sup>2</sup>, Juhu Tuukkanen<sup>2</sup>, Andree Krust<sup>3</sup>, Pierre Chambon<sup>3</sup>, Claes Ohlsson<sup>1</sup>, Marie Lagerquist<sup>1</sup>. <sup>1</sup>Centre for Bone & Arthritis Research, Sahlgrenska Academy at University of Gothenburg, Sweden, <sup>2</sup>Department of Anatomy & Cell Biology, University of Oulu, Finland, <sup>3</sup>Institut de Génétique et de Biologie Moléculaire et Cellulaire (CNRS, INSERM, ULP, Collège de France), France

It is well established that estrogen, mainly via estrogen receptor alpha (ER $\alpha$ ), has positive effects on bone, but estrogen is not considered as a treatment option against osteoporosis due to negative side-effects in other tissues. ER $\alpha$  is widely subjected to posttranslational modifications (PTMs), which can affect cellular responses to estrogen in a tissue specific manner by influencing the function of ER $\alpha$  and its interactions with other proteins. The *in vivo* role of PTMs of ER $\alpha$  for the skeleton is unknown but the PTM site S122 in ER $\alpha$  is known to modulate ER $\alpha$  transcriptional activity *in vitro*. Our aim was to investigate if phosphorylation of the PTM site S122 in ER $\alpha$  is involved in ER $\alpha$ -mediated bone effects *in vivo*. To this end, we used mice with a point mutation in S122 (S122A) and compared them to wild-type (WT) littermates. Twelve-week-old mice were ovariectomized and treated with estradiol (E2, 160 ng/day/mouse) or vehicle for four weeks. Tibiae were analyzed using  $\mu$ CT and humeri were exposed to a three-point bending test. E2 treatment increased cortical thickness in both WT and S122A females, however, the cortical thickness in E2-treated S122A mice was significantly decreased compared to E2-treated WT mice (-6%,  $p < 0.05$ ). Importantly, the functional three-point bending test demonstrated that E2 treatment increased maximal load at failure (Fmax) in WT mice (+25%,  $p < 0.001$ ) while no significant effect of E2 treatment was observed in S122A mice, demonstrating that phosphorylation of S122 is crucial for the E2 effect on mechanical strength of cortical bone. In conclusion, our results show that the S122 phosphorylation site is involved in the skeletal response to estrogen treatment and this finding is the first *in vivo* proof of a physiological role of phosphorylation in ER $\alpha$ .

**Disclosures:** *Sofia Movérare-Skrtic, None.*

## SU0100

**Sex Differences in the Regulation of Circadian Genes by Glucocorticoid Treatment.** Tara Rogers<sup>\*</sup>, Sidhartha Hazari, Evan Lay, Geetha Mohan, Aris Alexandrou, Wei Yao, Nancy Lane. UC Davis Medical Center, United states

Circadian rhythm is regulated in the hypothalamus using input from the light/dark cycle and synchronizing circadian oscillators in the brain with peripheral tissues. Clock-controlled genes encode proteins that regulate body processes; dysregulation of circadian rhythm is associated with metabolic conditions. Glucocorticoids (GC) induce bone loss, primarily in females, and suppress the HPA axis, altering circadian rhythm. We hypothesized that GCs induce changes in the circadian rhythm of bone cells and this may be related to GC-induced bone loss. We performed a pilot study to evaluate the effects of short-term GC treatment and withdrawal on circadian gene expression using a murine model, and to determine if these changes are sex-dependent. Swiss-Webster female (n=6) and male (n=6) mice 4 weeks of age, were treated with methylprednisolone (2.5mg/21 day slow release pellet) for 7 days. Control mice (n=3 females, 3 males) were treated with placebo pellets for 7 days. Treated mice (n=3 females, 3 males) and controls were sacrificed after 7 days of treatment; remaining mice (n=3 females, 3 males) were observed for 7 days of recovery and then sacrificed. Whole tibia bone and osteocyte extracts of mRNA were collected. An RT-PCR array of circadian gene expression was performed; fold changes were calculated. Western blots were performed to confirm select gene expression from PCR array, GC significantly up-regulated expression of Mtnr1b and Opn4 compared to controls in the tibias of females; up-regulation was sustained during recovery. Recovery also significantly up-regulated Crx, Mtnr1a, Ppara, Rorb, and Pax4 in females. A trend toward down-regulation for these genes was seen in males (Table). GC significantly up-regulated expression of Creb1, Csnk1a1, FbxI3, Per1 and Per2 in the tibias of males but not females. Western blots indicated that GC decreased expression of CLOCK-1 and beta actin in osteocytes of females; expression was restored in recovery. GC treatment changed circadian related gene expression in bone, with sex differences during treatment and recovery. Circadian genes may be important in regulating bone cell metabolism in the presence of GC; further investigation is warranted.

mRNA fold changes from whole tibia bone of GC-treated mice compared to controls

Mice	Circadian Genes						
	Crx	Mtnr1b	Mtnr1a	Ppara	Rorb	Pax4	Opn4
GC female	5.0	3.0*	1.1	1.1	2.9	3.4	3.9*
GC female + recovery	5.6*	3.1*	2.7*	2.4*	2.8*	4.5*	2.0*
GC male	-2.3	-5.4	-1.4	-3.9	-5.2	-1.3	-2.4
GC male + recovery	-13.6	-12.1	-4.6	-1.9	-8.5	-3.6	-5.2

\*P-value  $\leq 0.05$

GC-Circadian-Gene-table

Disclosures: Tara Rogers, None.

## SU0101

**1,25-dihydroxyvitamin D treatment leads to FGF23 resistance in the Hyp mouse model of XLH.** Janaína Da Silva Martins\*, Eva Liu, Marie Demay. Massachusetts General Hospital, United states

Hyp mice exhibit increased circulating levels of FGF23, renal phosphate wasting and impaired activation of vitamin D. Daily treatment of Hyp mice with 1,25-dihydroxyvitamin D (1,25D, 175 pg/g/day) from d2-d75 normalizes body weight and vertebral height, and improves bone histomorphometric and biomechanical parameters. Daily 1,25D also normalizes PTH, increases serum phosphate levels and decreases renal phosphate wasting in Hyp mice, despite a 15.7 fold increase in bone FGF23 mRNA levels in 1,25D treated Hyp mice vs Hyp control mice and a 108.6 fold increase vs WT controls. This suggests that 1,25D impairs the biological activity of FGF23 or cause resistance to FGF23 signaling.

Expression of GALNT3, which glycosylates FGF23 increasing its stability, was decreased in the bones of 1,25D treated Hyp mice compared to WT, but did not differ from that of untreated Hyp controls. However, expression of FAM20C, which phosphorylates FGF23 preventing its glycosylation, thereby decreasing its stability, was increased in the bones of 1,25D treated Hyp mice compared to WT and untreated Hyp controls. This suggests 1,25D may increase FGF23 cleavage in Hyp mice, altering the ratio between intact biologically active FGF23 and inactive C-terminal fragments.

Intact and cleaved FGF23 protein levels were evaluated in the bones of 1,25D treated, control Hyp and WT mice. FGF23 was immunoprecipitated from lysates of d35 humeral diaphyses and immunoprecipitated proteins were subjected to Western analyses. The expression of intact FGF23 was increased in the bones of untreated Hyp mice vs those of WT mice. Consistent with the increase in FGF23 mRNA expression in the bones of 1,25D treated Hyp mice, 1,25D treatment of Hyp mice increased intact FGF23 protein levels vs that seen in WT and Hyp controls. However, the levels of C-terminal FGF23 fragments were not increased in 1,25D treated Hyp mice vs those observed in Hyp control mice, demonstrating that 1,25D does not increase FGF23 cleavage in Hyp mice. Serum intact FGF23 levels were increased 16 fold in Hyp and 29 fold in 1,25D treated Hyp vs WT mice. However, neither 1,25D nor the Hyp mutation altered the ratio of intact vs C-terminal FGF23 in the circulation. Thus, 1,25D treatment of Hyp mice markedly increases bone and serum intact FGF23 levels. Based on the improvement in mineral ion homeostasis in 1,25D treated Hyp mice, this finding suggests that 1,25D causes resistance to the biological effects of FGF23.

Disclosures: Janaína Da Silva Martins, None.

## SU0102

**Automated ELISA For Direct Measurement of Free 25OH Vitamin-D.** Ernst Lindhout\*<sup>1</sup>, Leon Swinkels<sup>1</sup>, Marloes Geurts<sup>1</sup>, Mike Martens<sup>1</sup>, Nicolas Heurreux<sup>2</sup>. <sup>1</sup>Future Diagnostics, Netherlands, <sup>2</sup>DIAsource Immunoassays, Belgium

Recent studies suggest that the concentration and genotype of Vitamin D binding protein (DBP) are important factors that determine the bioavailability of 25OH Vit D in blood. There is accumulating data that for instance in pregnant women, chronic kidney disease, liver failure, bladder cancer and pancreatic cancer, or in hemodialysis patients the measurement of free-25OH Vit D in serum provides more relevant diagnostic information than total 25OH Vit D.

To measure Free 25OH Vit D in blood Future Diagnostics developed a direct ELISA method<sup>1</sup>.

The Free 25OH Vit-D assay that reproducibly determines the level of free 25OH Vit D in serum was implemented and validated on an open ELISA platform. After adaptation of the assay protocol on the instrument, manual and automated results

were compared in terms of dose response curve, accuracy, precision, sensitivity and drift. The data shows that the performance of the Free 25OH Vit D assay on the open ELISA platform (Dyngex DS2) with hands-on time of <30min is comparable with the manual performed assay. Control precision: CTRL1 manual 1.5% CV, Automatic 0.8%CV. CTRL2 Manual 4.3% CV, Automated 0.2% CV. Sample correlation;  $r = 0.986$ , Automated = 1.09 \* Manual - 0.62.

The (automated) Free-25OHD ELISA can be used as a valuable tool in studies to establish the clinical relevance of free 25OH Vit D.

<sup>1</sup>ASBMR Annual meeting 2015 Abstract MO0133 Optimization of an Elisa for the Direct Measurement of Free 25OH Vitamin D

Disclosures: Ernst Lindhout, None.

This study received funding from: Future Diagnostics

## SU0103

**Vitamin D deficiency disrupts male gonadal function through extensive changes in both reproductive and hormone producing cells.** Jiarong Li\*<sup>1</sup>, Xiuying Bai<sup>2</sup>, Andrew Karaplis<sup>2</sup>, Richard Kremer<sup>1</sup>. <sup>1</sup>MUHC, Canada, <sup>2</sup>Lady Davis Institute, Canada

Vitamin D (VD) has multiple functions in addition to its effects on bone and mineral homeostasis. A recently recognized target of VD, from studies in the vitamin D receptor (VDR) knock out model, is the male reproductive system. These studies showed that the VD metabolizing enzyme (activating and inactivating) expression in the testes, mature spermatozoa, and ejaculatory tract structure were affected suggesting that both systemic and local VD metabolism may influence male reproductive function. However, it is not yet known which cell(s) is(are) the main VD target in the testis and to what extent VD is important for sex hormone production and spermatozoa function. Vitamin D deficiency has also been shown to affect male fertility but the impact of vitamin D deficiency itself on the male reproductive and gonadal hormonal systems has not yet been investigated. Here we investigated the role of vitamin D on both reproductive and hormone producing cells and its impact on signaling pathways. First, we observed histologically that Leydig cells and Sertoli cells as well as seminiferous tubules were decreased in number in VDR knockout animals. TUNEL assay revealed enhanced apoptosis in these cellular structures. The abundance of spermatids and sperm were dramatically reduced in the VDR knockout group. Next, using gene expression microarray, we analyzed whole testes gene expression in VDR knockout and their normal controls and confirmed selected genes signaling involved in spermatogenesis and sperm immobilizing activities by real-time RT-PCR. The results show that Apod, Trhde, Speer, Astx, Bsp2 and Ceacam involved spermatogenesis and/or sperm immobilizing activities are significantly decreased in VDR knockout testes. In another set of experiments we bred wild type FVB mice under UV free conditions. Three weeks after birth, the male pups were weaned and fed *ad libitum* either a 25 IU/Kg vitamin D deficient diet (n=13) or a 1000 IU/Kg normal vitamin D diet (n=11) and maintained on these diets for 4 months and sacrificed. Histological analysis revealed a similar pattern as the one observed with the VDR knockout animals with disruption of the normal reproductive and hormonal producing cells as well as a reduction in sperm production. In summary our data demonstrate that Vitamin D has a direct effect on male fertility in mice through specific testes developmental abnormalities and signaling pathways involved in spermatogenesis and sperm immobilizing activities.

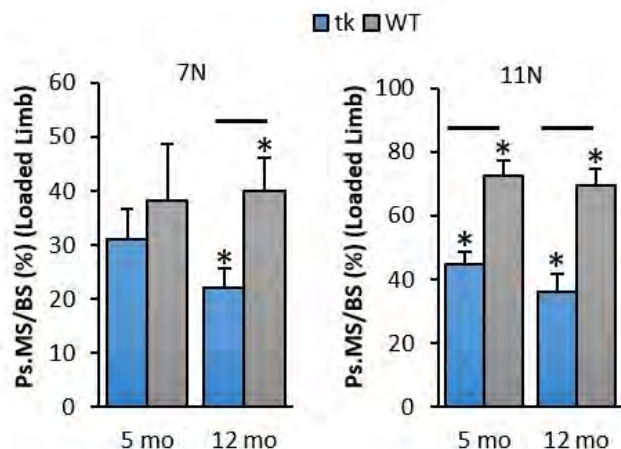
Disclosures: Jiarong Li, None.

## SU0104

**Ablation of proliferating osteoblasts reduces loading-induced bone formation.** Heather Zannit\*, Michael Brodt, Matthew Silva. Washington University in St. Louis, United states

Mechanical loading is a potent stimulus for new bone formation. To make bone, either existing osteoblasts on the bone surface are activated or new osteoblasts are recruited through differentiation or proliferation. The relative contribution of these different mechanisms to loading-induced bone formation is not known. Preliminary studies revealed a large proliferative response on the periosteum after tibial compression in mice at high force (woven bone inducing) but less so after loading at lower force (lamellar bone inducing). We hypothesize that proliferation of osteoblast-lineage cells is critical to woven bone formation but not critical to lamellar bone formation. To investigate the importance of osteoblast proliferation on loading-induced bone formation, we utilized mice that allow inducible ablation of replicating osteoblasts and pre-osteoblasts (3.6Coll1a1-tk mice). Ganciclovir (GCV) is given to interact with the thymidine kinase (tk) transgene, causing dividing tk+ cells to die. Control animals were wildtype littermates also dosed with GCV. Two ages were investigated: young-adult (5 mo) and middle-aged (12 mo). The right tibias were cyclically loaded for 5 consecutive days at a peak force of 7 or 11 N to induce lamellar or woven bone formation, respectively. Mice were administered dual fluorochromes for dynamic histomorphometry analysis. In 5 mo mice loaded to 11 N, experimental (tk) mice had less periosteal mineralizing surface (Ps.MS/BS) and double labeled surface (Ps.dLS/BS) than bones from control (WT) mice. Woven bone incidence was lower as well (1/6 tk vs. 4/5 WT). However, these parameters did not reach statistical significance between tk vs. WT when 5 mo mice were loaded to 7 N. In 12 mo mice loaded to 7 and 11 N, the tk mice had less Ps.MS/BS and Ps.dLS/BS than bones from WT mice (p<0.05). Strikingly, we found the 12 mo tk animals loaded to 11 N did not have any woven bone (0/9 tk vs. 8/12 WT), but all had double labeled (lamellar)

surface. Our findings show that when loading induced proliferation of osteoblast lineage cells is blocked, woven bone formation is prevented in 12 mo mice and greatly diminished in 5 mo mice. Similarly, loading-induced lamellar bone formation is significantly reduced in 12 mo mice, and partially reduced in 5 mo mice. Taken together, we conclude that osteoblast proliferation induced by loading is a critical source of bone forming osteoblasts in both woven and lamellar bone.



Ablation of proliferating osteoblasts reduced periosteal mineralizing surface

Disclosures: Heather Zannit, None.

### SU0105

**IL-17R and RANKL Expression Following In Vivo Fatigue Loading.** Michael Turturro<sup>1</sup>, Travis McCumber<sup>1</sup>, John Billheimer<sup>2</sup>, Mohammed Akhter<sup>2</sup>, Diane Cullen<sup>1</sup>. <sup>1</sup>Creighton University School of Medicine, United states, <sup>2</sup>Creighton University, United states

Microdamage in bone following fatigue loading is repaired through targeted remodeling where osteoclasts remove damaged bone tissue. The mechanism for targeted osteoclast recruitment currently is associated with osteocyte apoptosis. We have previously shown elevated IL-2 at 24 and 48 hrs after fatigue damage suggesting that osteoclast recruitment may involve an inflammatory pathway. TH17 cells secrete the IL-17 cytokine which binds to IL-17R on osteocytes and stimulates RANKL. Mechanical loading of osteocytes releases IL-6 and TGFβ, factors in TH17 cell activation. We hypothesize that 48 hrs after in vivo fatigue loading, both IL-17R and RANKL levels will increase on osteocyte cell surfaces, suggestive of TH17 involvement.

Right ulnas of Sprague Dawley Rats (female, 6 months, n=8) were fatigue loaded to 40% loss of modulus, left ulna were the control. Ulnae were collected 48 hrs post load, and were stained for RANKL or IL-17R and DAPI. Three images from the medial ulna cortex were blind coded and semi-automatically quantified for osteocytes positive for RANKL or IL-17R antibody as a percent of total osteocytes. Differences between ulnas were compared by General Linear Model for repeat measures at P<0.05. Extensive microcrack damage was seen in loaded versus nonloaded ulna with no difference in osteocyte density due to load at 48 hrs. The percent osteocytes positive for RANKL was greater in the loaded ulnas than control (46.4% vs 33.6%, P<0.02). IL-17 expression was seen in all sections, with no difference between the loaded and contralateral ulnae (29.5% vs 27.2%).

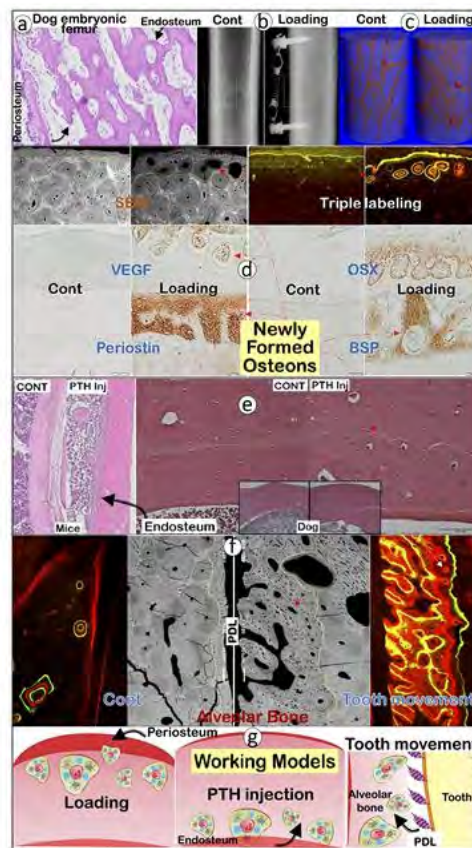
High RANKL expression in loaded legs corresponds with increased intracortical osteoclast number previously reported at 48hr. Our results show that IL-17R is detectable on osteocytes from ulna in fatigue loaded animals. Similar IL-17R staining in both loaded and nonloaded legs could be the result of systemic circulation of IL-17, as seen for IL-2 protein levels. The same study showed IL-2 was greatest in loaded ulna at 24 hours, however similarly elevated in both loaded and unloaded ulnae at 48 hours. If IL-17R follows a similar pattern, then time points before the current 48 hrs and unloaded control animals are needed to differentiate a local versus systemic responses. A better and broader understanding of the bone remodeling associated with fatigue damage will lead to better treatment/prevention of fatigue damaged bone for diseases such as osteoporosis.

Disclosures: Michael Turturro, None.

### SU0106

**Unique Osteon Patterns Form in Response to Loading and Intermittent PTH Injections.** Ke Wang<sup>1</sup>, Yuan Hui<sup>2</sup>, Yinshi Ren<sup>3</sup>, Ying Liu<sup>4</sup>, Xianglong Han<sup>5</sup>, Jianquan Feng<sup>4</sup>. <sup>1</sup>Department of Biomedical Science, Texas A&M Health Science Center, Baylor College of Dentistry, United states, <sup>2</sup>Department of Orthodontics, Fourth Military Medical of University, China, <sup>3</sup>Cellular, Developmental, & Genome Laboratories, Musculoskeletal Research Center, Duke University, United states, <sup>4</sup>Department of Biomedical Science, Texas A&M Health Science Center, Baylor College of Dentistry, Dallas, United states, <sup>5</sup>State Key Laboratory of Oral Diseases, West China Hospital of Stomatology, Sichuan University, China

Most, if not all, bone studies focus on rodents, which do not have an osteon structure, the basic unit of bone formation and remodeling found in large mammals. Recent studies showed an astonishing defect in the Haversian-canal-osteon structures in human patients with osteoporosis. Currently, we know very little about how osteons are formed, as that type of study has fallen out of favor since the beginning of molecular biology era. In this study, we first demonstrated that primary osteons in the embryonic dog femur originated proportionally from both the periosteum and endosteum layers (Fig a). Next, we examined whether constant forces generated for 5 weeks using open-coil springs anchored on miniscrew implants in the tibia with a force 0, 100 g (left), and 200 g (right) separately (Fig b) to study the impact of loading on osteon formation. In the loading groups (6 adult dogs), there were sharp increases in Haversian canals shown using uCT (Fig c). The images of backscattered SEM and triple labeling (taken 10 days apart) displayed many newly formed osteons, which were mainly derived from the periosteum layer. These osteons expressed high levels of endothelial and bone markers, including VEGF, OSX, periostin and BSP (Fig d). This asymmetric contribution of the osteon formation from the periosteum prompted us to initiate a different set of experiments, in which we tested the impact of intermittent injections of PTH on WT mice and 4 young adult dogs (10 ug/kg per day for four weeks). Interestingly, the increased bone volume was associated with the expanded endosteum layer in mice (Fig e, left). Similarly, the bone volume expanded in the PTH- treated dogs, in which the lamellar structure on the endosteum side was replaced by the newly formed osteons (Fig e, right). We then asked whether similar events would occur in intramembranous bone in response to mechanical loading. Using a tooth movement model, we observed numerous osteons using backscattered SEM and triple labelled images (Fig f). This newly formed bone originated from the periodontal ligaments (PDL). For the first time, these data collectively revealed how mechanical loading initiates osteon formation from either the periosteum or PDL, which is different from the PTH-induced osteon formation occurring mainly on the endosteum side (Fig g).



Unique Osteon Patterns Form in Response to Loading and Intermittent PTH Injections

Disclosures: Ke Wang, None.

**SU0107**

**Myosin Motors Direct mTORC2 Recruitment to the Cell Membrane to Regulate MSC Lineage Fate.** William Thompson\*<sup>1</sup>, Yong Li<sup>1</sup>, Gunes Uzer<sup>2</sup>, Janet Rubin<sup>2</sup>. <sup>1</sup>Indiana University, United states, <sup>2</sup>University of North Carolina, United states

Bone quality and quantity is inversely proportional to adipogenic commitment of marrow derived mesenchymal stem cells (mdMSCs), where increased adipogenesis depletes the progenitor pool for osteogenesis. Mechanical strain suppresses adipogenesis by activating a cascade involving Fyn, mTORC2, and Akt, which culminate in both enhanced Beta catenin nuclear entry and cytoskeletal reinforcement. Knockdown of Fyn, Akt, or the mTORC2 subunit Rictor restricts mechanical suppression of adipogenesis, resulting in increased adipogenic commitment of mdMSCs. Previous work has demonstrated that this signaling cascade initiates at focal adhesion (FA) platforms, where mechanical strain recruits both Fyn and mTORC2 to further amplify downstream responses; however, the mechanisms responsible for recruiting these signals to FAs is unclear. A 10 minute bout of mechanical strain is sufficient to induce actin cytoskeletal stress fibers. Disruption of this cytoskeletal structure prevents activation of the Fyn/mTORC2/Akt cascade. Furthermore, visualization of Akt, using immunostaining, after mechanical strain, reveals Akt aligned in a pattern similar to actin cytoskeletal struts. These observations led us to hypothesize that recruitment of these upstream kinases to FA platforms requires movement along the actin cytoskeleton in response to strain. Myosins are molecular motors that carry "cargo" to various intracellular locations in a variety of cell types. Myosins also regulate cytoskeletal reorganization in pre-adipocytes, suggesting a role in adipogenic commitment. Mass spec analysis, following immunoprecipitation of Rictor, revealed a strong association with both myosin 1C and myosin 9. Co-immunoprecipitation studies confirmed that both myosin 1C and myosin 9 associate with Rictor. Importantly, mechanical strain enhanced the binding of myosin 1C with Rictor, while the affinity of myosin 9 with Rictor was not affected. These data suggest that myosin 1C is a critical component of strain-induced recruitment of signaling effectors to the plasma membrane, where signal amplification results in an anti-adipogenic response. In summary, activation of signaling cascades that direct mdMSC lineage allocation are both temporally and spatially regulated. Mechanical force is necessary for spatial partitioning of Fyn/mTORC2/Akt and myosin motors are necessary for carrying this "signaling cargo" to sites of focal attachments, where force is transmitted, and subsequent signal activation occurs.

**Disclosures:** William Thompson, None.

**SU0108**

**Taxol-induced stabilization of the microtubule network blunts the osteoblast/osteocyte response to fluid flow shear stress.** James Lyons\*<sup>1</sup>, Jaclyn Kerr, Christopher Ward, Joseph Stains. University of Maryland Baltimore, United states

The underlying molecular mechanisms by which bone cells sense and respond to mechanical strain are incompletely understood. In many tissues, the microtubule (MT) network is a critical element for mechanotransduction by altering the stiffness of the cytoskeleton. We hypothesized that the MT network modulates bone mechanotransduction by dynamically regulating cytoskeletal stiffness. Using real time, live cell imaging of Ca<sup>2+</sup> with Fluo-4, we observed that the MT stabilizing agent Taxol (1  $\mu$ M, 2 h) significantly blunts the magnitude and duration of fluid flow shear stress (FFSS, 4 dynes/cm<sup>2</sup>)-induced intracellular Ca<sup>2+</sup> relative to vehicle treated controls in UMR106 osteoblast-like cells and OCY454 osteocyte-like cells *in vitro*. Using a Mn<sup>2+</sup> quench assay in UMR106 cells, we confirmed that Taxol inhibited FFSS-induced Ca<sup>2+</sup> influx ( $\approx$  5-fold). A preliminary qRT-PCR screen of Ca<sup>2+</sup> channel expression in OCY454 cells revealed abundant expression of the well-studied mechanically gated Piezo1/2 cation channels, among others already implicated in FFSS-induced Ca<sup>2+</sup> influx. Additionally, modulation of the MT network with Taxol blunted the FFSS-induced activation of ERK signaling in UMR106 cells. Stabilization of the MT network with Taxol reduced the FFSS-induced down regulation of sclerostin in OCY454 cells. Furthermore, treatment with Taxol increased SOST gene expression basally in both UMR106 (2.4-fold) cells and OCY454 (2.4-fold) cells, consistent with decreased mechanotransduction. Atomic force microscopy revealed that OCY454 cells treated with taxol have increased cytoskeletal stiffness indicated by an increased resistance ( $\approx$ 3.5 fold) to mechanical indentation. Preliminary analysis of 8-week old C57BL/6 mice (N=3/group) treated with taxol (2 mg/kg *i.p.* - at d1, d3, d5 and d7, then euthanized at d30) revealed decreased cortical bone volume (0.51 v 0.43 mm<sup>3</sup>), decreased cortical cross sectional area (0.86 vs 0.73 mm<sup>2</sup>), and decreased mean polar moment of inertia (0.49 vs 0.36 mm<sup>4</sup>) relative to vehicle treated mice. While the actions of taxol in this context are complex, this observation is at least consistent with the possibility of the involvement of the MT network in mechanotransduction. These *in vitro* and preliminary *in vivo* studies suggest a role of the MT network in osteocyte mechanotransduction.

**Disclosures:** James Lyons, None.

**SU0109**

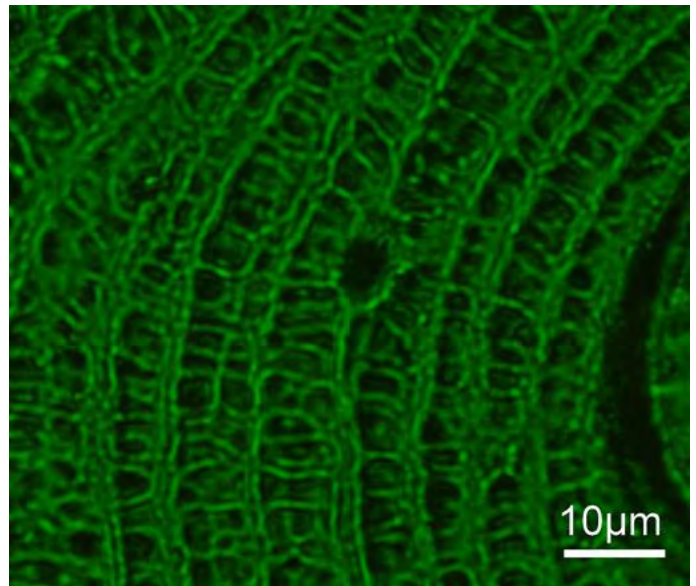
**Collagen Fibers in Human Osteons are Visible by Green Polarization Interference Color Staining.** Santiago Gomez\*. Departamento de Anatomía Patológica, University of Cadiz, Spain

The appearance of lamellar bone can be easily observed under polarization microscopy. In human osteons, an example of a lamellar bone type, bright and dark lamellae alternate in circular layers everywhere. However, the significance of these bright or dark polarization images is still debated, especially in regards to the predominant orientation of collagen fibers (more transverse or more longitudinal) or the matrix compositional differences in bone lamella (dense or loose collagen layers). This is because in polarization microscopy of bone, the sections examined are rather thick and the collagen fibers within a lamella are not individually resolved.

This problem can be solved with a novel polarization microscopy method. Such method is based on (i) the use of a 505nm dichroic interference filter, (ii) a no Koehler illumination source and (iii) the examination of thinner bone sections than those prepared for ordinary polarization microscopy (i.e., on a decrease in the optical path length difference).

The new microscope consists of a conventional finite optical microscope equipped with a white light, nonfocused (afocal) illumination system, crossed polars, a 505nm dichroic interference filter tilted at 45°, a 520nm barrier filter and a CCD digital camera for recording purposes. Afocal illumination is essential to eliminate stray light from the image. The dichroic interference filter is situated in front of the analyzer and it contributes to the generation of green polarization interference color by both cutting off and ( $\frac{1}{4} \lambda$ ) retarding the waves of the ordinary and extraordinary rays. In this microscopy, since nondiffracted light is absent from the image, birefringent objects look green against a dark field.

Any mineral contribution to the images was eliminated in this study. Thus, the poly-methyl methacrylate embedded mineralized sections from human femur were (i) ground plane-parallel to 15- $\mu$ m in thickness and (ii) decalcified with a 2.5% phosphomolybdic-phosphotungstic acid treatment. Consequently, high-resolution, sharp images of green color stained silhouettes of collagen fibers (0.6-1.2  $\mu$ m diameter) for human osteons were obtained from transverse (figure), longitudinal and oblique bone sections. Even though the arrangement of collagen fibers in osteons was strongly dependent on the plane of the section, fibers were frequently seen interlacing each other, changing in direction or forming a 3D-"crochet" fabric.



Collagen fibers seen in a cross-section

**Disclosures:** Santiago Gomez, None.

**SU0110**

**Prostaglandin E2 signaling through EP4 receptor interacts with Keap1/Nrf-2 pathway in myogenesis and aging.** Chenglin Mo\*<sup>1</sup>, Lynda Bonewald<sup>2</sup>, Marco Brotto<sup>1</sup>. <sup>1</sup>University of Texas-Arlington, United states, <sup>2</sup>University of Missouri-Kansas City, United states

In our previous studies, we have identified PGE2 as one of the potential factors for biochemical signaling from bone to muscle. PGE2 signaling through EP4 receptor has been shown to be important for proper maintenance of intracellular ROS levels during proliferation in primary mouse myoblasts. Since Keap1/Nrf-2 signaling pathway plays a critical role in antioxidant response, but the role of this pathway remains unclear in skeletal muscle, we considered whether EP4-mediated regulation of intracellular ROS levels is associated with the activity of Keap1/Nrf-2 pathway in proliferation and differentiation of myoblasts. After effectively knocking down EP4 gene using siRNA ( $\approx$ 90% knockdown), the number of mouse primary myoblasts reduced by 23.4  $\pm$  4.3%

( $p < 0.05$ ), which is accompanied by  $24.1 \pm 4.6\%$  ( $p < 0.05$ ) reduction in Cyclin E expression, and  $323.7 \pm 25.7\%$  ( $p < 0.05$ ) and  $204.2 \pm 17.2\%$  ( $p < 0.05$ ) increase in myostatin and p27 expression, respectively. At the same time, mRNA levels of target genes of Keap1/Nrf-2 pathway (Gclc, Gclm, Hmox1 and Nqo1) reduced to 65.3%, 45.3%, 28.1%, and 36.9%, respectively. When myogenic differentiation starts, knocking down EP4 using siRNA significantly inhibited myogenesis in both mouse primary myoblasts and the C2C12 cell line, but this effect was myogenin-independent, because EP4 knockdown did not alter the expression of myogenin at the RNA and protein levels. Similar to proliferation, after 24 hours of differentiation, transfection with 50nM EP4 siRNA significantly downregulated mRNA levels of Gclc, Gclm, Hmox1 and Nqo1 to  $72.1 \pm 1.8\%$ ,  $79.4 \pm 7.1\%$ ,  $60.2 \pm 6.4\%$ , and  $44.9 \pm 4.2\%$  ( $p < 0.05$  for all genes). Since ROS plays an important role during aging, and is likely to be a major contributor to bone to muscle signaling, we also determined EP4 receptor gene expression in SOL and EDL muscles in young (5 months) and older (19 month) mice. Interestingly, EDL and SOL muscles from old mice have an average of 4-fold higher EP4 receptor gene expression than muscles from young mice. Our data suggest that EP4 signaling could interact with other pathways, such as Keap1/Nrf-2, to regulate myogenesis in skeletal muscle. These findings could have important implications for bone to muscle signaling during aging.

**Disclosures:** Chenglin Mo, None.

## SU0111

**Differential Effects of the Muscle Factors, Irisin and BAIBA on Osteoblasts and Osteocytes.** Tsutomu Matsumoto<sup>\*1</sup>, Yukiko Kitase<sup>1</sup>, Bruce Spiegelman<sup>2</sup>, Lynda Bonewald<sup>1</sup>, Christiane Wrann<sup>2</sup>. <sup>1</sup>university of missouri-kansas city school of dentistry, department of oral & craniofacial science, United states, <sup>2</sup>Dana-Farber Cancer Institute, and Department of Cell Biology Harvard Medical School, United states

Muscle has been shown to secrete a plethora of cytokines and metabolites, especially in response to contraction. Some of these have overlapping functions such as the cleaved protein fragment, irisin, (12kDa) and the small molecular weight metabolite,  $\beta$ -aminoisobutyric acid, BAIBA that play a role in the browning of white fat and in insulin metabolism.

As we hypothesized that muscle communicates with bone independent of loading through secreted factors, the effects of irisin and BAIBA were compared to contracted 90Hz EDL and soleus muscle conditioned media (CM). Both BAIBA (0.1-10 mM) and irisin (1-500 ng/ml) are protective at preventing H<sub>2</sub>O<sub>2</sub> (0.3 mM) induced oxidative cell death in MLO-Y4 osteocyte like cells, showing similar functions and consistent with our previous results with muscle CM. BAIBA, similar to muscle CM, had no effect on osteoblast proliferation or differentiation, but did induce a significant increase in prostaglandin E<sub>2</sub> and a decrease in sost/sclerostin expression in osteocytes. Therefore, we hypothesized that muscle targets osteoblasts indirectly through osteocytes. When irisin was compared to BAIBA by testing on IDG-SW3 cells, distinctly different effects between the two factors were observed particularly at the late osteocyte stage.

IDG-SW3 cells at days 3, 14, and 28 were treated for 24hrs with BAIBA (1-100 $\mu$ M) and irisin (10- 500ng/ml). IDG-SW3 cells differentiate from the late osteoblast (Day 3: high alkaline phosphatase and collagen expression) to early osteocyte (Day 14; Dmp1) to late osteocytes (Day 28; Sclerostin).

Neither factor had any effect on alkaline phosphatase at days 3 and 14. Neither factor had any effect on Dmp1 at day 3 but both inhibited Dmp1 at day 14 (BAIBA 27%; irisin 30%). While BAIBA increased collagen 1 $\alpha$  expression at day 3 (47%) and decreased at day 14 (36%), irisin had no effect. However, at day 28, BAIBA significantly decreased (62%) while irisin significantly increased sost expression (72%).

These results show that BAIBA more consistently recapitulates findings with contracted muscle conditioned media with regards to sost expression whereas irisin does not suggesting that irisin is not present in sufficient concentration or that factor neutralization occurs. It also suggests that muscle factors with similar functions with regards to fat and liver metabolism can have different effects on bone. But regardless of effect, the osteocyte is a major target.

**Disclosures:** Tsutomu Matsumoto, None.

## SU0112

**Therapeutic Effect of Alendronate on Skeletal Muscle Atrophy *in vitro* and *in vivo*.** Shing-Hwa Liu<sup>\*</sup>, Rong-Sen Yang, Chen-Yuan Chiu, National Taiwan University, Taiwan, province of china

**Introduction:** Alendronate is widely used for the treatment of osteoporosis in the elderly and postmenopausal women. Osteopenic menopausal women with 6 months of alendronate therapy have been observed to improve not only lumbar bone mineral density but also handgrip strength. The effect and mechanism of alendronate on muscle strength still remain unclear. Here, we investigated the therapeutic potential of alendronate on skeletal muscle atrophy *in vitro* and *in vivo*.

**Methods:** Mouse skeletal muscle C2C12 myoblasts were cultured for the myotube formation and atrophy with or without dexamethasone treatment (muscle atrophy inducer). Moreover, adult male ICR mice were treated with alendronate (0.015-1 mg/kg/day) for 1 month, while denervation-induced muscle atrophy was obtained and evaluated 7 days later. The protein expressions were determined by Western blotting or immunohistochemistry. Muscle fatigue responses were examined by the rotarod performance test.

**Results:** Alendronate (1  $\mu$ M) significantly promoted the myotube formation (about 50.77% increase,  $P < 0.01$ ) and hypertrophy (about 2.17-fold increase in over 10 nuclei myotube,  $P = 0.003$ ) in C2C12 myoblasts under differentiation medium. The SIRT-3 protein was down-regulated and myogenic differentiation-related proteins (myogenin and myosin heavy chain (MHC)) were up-regulated in alendronate-treated C2C12 myoblasts ( $P < 0.01$ ). Besides, alendronate (1  $\mu$ M) inhibited dexamethasone-induced skeletal muscle atrophy (about 1.47-fold increase in 20  $\mu$ m diameter myotube,  $P < 0.001$ ) and Atrogin-1 protein expression and reversed dexamethasone-inhibited FoxO3a phosphorylation ( $P < 0.01$ ), indicating an involvement of SIRT-3/FoxO3a-related signaling pathway. Moreover, alendronate administration protected from denervation-induced muscle atrophy in mice by enhancing skeletal muscle mass and muscular endurance, accompanying with a decline of Atrogin-1 and SIRT-3 protein expressions ( $P < 0.01$ ).

**Conclusion:** Sirtuin-3 (SIRT-3), a sirtuin family member of NAD<sup>+</sup>-dependent deacetylase, has been shown to negatively regulate skeletal muscle mass. In this study, we found that alendronate promoted the myotube formation and inhibited muscle atrophy via SIRT-3 down-regulation *in vitro* and *in vivo*. We also postulated that the reversibility of alendronate in muscle atrophy might be linked to the stimulation of hypertrophic myotube formation. These findings suggest a novel use for alendronate in skeletal muscle atrophy or sarcopenia treatment.

**Disclosures:** Shing-Hwa Liu, None.

## SU0113

**The Role of a Novel Gene, Fam210a (family with sequence similarity 210, member a) in Bone and Muscle.** Ken-ichiro Tanaka<sup>\*1</sup>, Yingben Xue<sup>1</sup>, J Brent Richards<sup>2</sup>, David Goltzman<sup>1</sup>. <sup>1</sup>Calcium Research Laboratory, McGill University Health Centre, & Division of Endocrinology, Department of Medicine, McGill University, Montreal, Quebec, Canada, Canada, <sup>2</sup>Departments of Medicine, Human Genetics, Epidemiology & Biostatistics, McGill University, Montreal, Quebec, Canada, Canada

**Background:** Osteoporosis and sarcopenia are known to be aging-related diseases associated with the deterioration of bone and muscle strength, and they often coexist among elderly people. Recently, an interaction between muscle and bone has been noted. Genome-Wide Association Studies (GWAS) have identified SNPs intronic to FAM210A, which are strongly associated with the risk of fracture, but less so with bone mineral density (BMD) reduction [Nat Genet 2012]. Although FAM210A protein is expressed in a variety of tissues such as bone and muscle, the skeletal function of FAM210A remains unknown.

**Aims:** We investigated the effect of Fam210a on bone and muscle using 2-month-old mice with targeted deletion of Fam210a (Fam210a<sup>-/-</sup>). We examined tissue expression of Fam210a protein by Lac Z staining, and evaluated their phenotypes by examining serum and urine biochemistry, BMD, biomechanical tests, parameters of trabecular and cortical bone micro-architecture using micro computed tomography ( $\mu$ CT), and average quadriceps muscle cross-sectional area.

**Results:** Fam210a<sup>-/-</sup> mice died *in utero* after embryonic day 9.5. We therefore examined the phenotypes of Fam210a<sup>+/-</sup> mice. By Lac Z staining, Fam210a was expressed in a variety of tissues including bone, muscle, heart and brain. There was no difference in the levels of serum and urine calcium as well as phosphate between wild-type (WT) and Fam210a<sup>+/-</sup> mice. BMD and bone mineral content (BMC) of Fam210a<sup>+/-</sup> mice tended to be lower than those of WT, but these differences were not significant (female:  $p = 0.085$  and  $p = 0.077$ , respectively; male:  $p = 0.079$  and  $p = 0.075$ , respectively). Three point bending tests showed that the maximal load and stiffness of Fam210a<sup>+/-</sup> mouse bones were significantly lower than those of WT mice (female:  $p = 0.003$  and  $p = 0.037$ , respectively; male:  $p = 0.014$  and  $p = 0.016$ , respectively). In addition, by  $\mu$ CT, cortical bone volume and cortical thickness of Fam210a<sup>+/-</sup> mice were significantly lower than those of WT mice ( $p = 0.010$  and  $p = 0.024$ , respectively). In contrast, there was no difference in trabecular microarchitecture between WT and Fam210a<sup>+/-</sup> mouse bones. Of interest, the average muscle fiber cross-sectional area of Fam210a<sup>+/-</sup> mice was significantly lower than that of WT mice ( $p = 0.004$ ).

**Conclusions:** Our findings indicate that Fam210a has a crucial role in modulating bone strength via effects on cortical bone and muscle tissues. Fam210a might be an important factor in the interaction between muscle and bone.

**Disclosures:** Ken-ichiro Tanaka, None.

*This study received funding from: Canadian Institutes of Health Research; Richard and Edith Strauss Postdoctoral Fellowship in Medicine; Abroad Research Fellowship from Banyu Life Science Foundation International*

## SU0114

**Age Affects Bone Regeneration in the Murine Rib Resection Model.** Katelyn Malchester<sup>\*1</sup>, Peter Fung<sup>1</sup>, Cindy Choi<sup>1</sup>, Payal Verma<sup>1</sup>, Denise Liberton<sup>1</sup>, Murat Sincan<sup>1</sup>, Danielle Donahue<sup>1</sup>, Brenda Klaunberg<sup>1</sup>, Tina Kilts<sup>1</sup>, Marian Young<sup>1</sup>, Stephanie Kuwahara<sup>2</sup>, Francesca Mariani<sup>2</sup>, Janice Lee<sup>1</sup>. <sup>1</sup>NIDCR, United states, <sup>2</sup>USC, United states

The mechanism by which bone regeneration occurs in skeletal defects is poorly understood, especially in the context of aging. From previous human rib resection data, we demonstrated that there was a statistically significant difference in rib regeneration based on age. Young patients (<20 years old) fully regenerated their rib

within 3 months, while older patients (>20 years old) regrew 50% after 6 months in skeletal defects averaging 6 cm in size, as determined by quantitative computed tomography. The aim of this pilot experiment was to create a murine rib resection model that recapitulates these findings, to determine if young mice have a greater capacity to regenerate bone than old mice. Rib resection was performed under sterile surgical conditions on female C57BL/6 mice that were skeletally immature or "young" (2 months old, n=5) and skeletally mature or "old" (16 months old, n=6). Rib 7 or 8 from the right flank was excised in an average resection length of 7.75mm. Periosteum was left intact, and muscle and skin layers were closed. Animals were imaged roughly every 5 days via micro-computed tomography (uCT) (35 micron resolution) to view spontaneous bone regeneration. After 40 days, on average, the young and old mice regenerated 133.5% and 3.21% bone volume, respectively. The effect size was 264% ( $P=0.0152$ , T-Test, Satterthwaite Unequal). The young mice also started regenerated within the first 5-10 days post-resection. Based off of our data, we can conclude that this is a viable murine model to use when attempting to define the youthful microenvironment's role on spontaneous bone regeneration. Our future plans include performing RNA sequencing, histology, cytokine and cellular profile analysis of the regenerated bone, and to compare differentially expressed genes within the two populations as compared to the human data.

**Disclosures:** *Katelyn Malchester, None.*

## SU0115

**Association of Magnesium with Blood and Urinary Bone Biomarkers in Osteopenic Postmenopausal Women.** Kelli George\*, Neda Akhavan, Shirin Pourafshar, Negin Navaei, Elizabeth Foley, Elizabeth Clark, Bahram Arjmandi. Florida State University, United states

Osteoporotic fractures are highly prevalent in postmenopausal women due to a decrease in estrogen production and structurally smaller bones when compared to men which leads to increased morbidity and mortality. Osteoporosis affects over 200 million women worldwide, with an estimated 1 in 3 women over age 50 experiencing osteoporotic fractures. The role of magnesium in bone health is often overlooked when compared to other biomarkers; however, it has been shown that magnesium contributes to the structure of bone, stimulates the thyroid to produce calcitonin, and regulates parathyroid hormone. The purpose of this cross-sectional study was to examine the relationship between magnesium and blood and urinary markers of bone metabolism in postmenopausal women. For this purpose, blood and urine parameters related to bone metabolism from 57 osteopenic women under age 65 (mean age of  $54.26 \pm 5.8$ ) who were not on hormone replacement therapy were evaluated. The results from this study showed that serum magnesium levels had a significant positive association with osteocalcin ( $P = 0.028$ ), a marker of bone formation, and a significant negative association with tartrate-resistant acid phosphatase ( $P = 0.035$ ), a marker of bone resorption. Additionally, urinary magnesium levels were negatively correlated with age ( $P < 0.001$ ). The results of this study possibly suggest that higher levels of magnesium are associated with a lower bone resorption rate. Additionally, our data suggests that aging may be a contributing factor to a decrease in urinary magnesium levels. However, the exact relationship between magnesium status and markers of bone turnover is not well understood and further studies are required to examine such a relationship mechanistically.

**Disclosures:** *Kelli George, None.*

## SU0116

**Blood flow regulates function of endothelium in the skeletal system.** Saravana Ramasamy\*<sup>1</sup>, Anjali Kusumbe<sup>2</sup>, Ralf Adams<sup>1</sup>. <sup>1</sup>Max Planck Institute for Molecular Biomedicine, Germany, <sup>2</sup>Max Planck Institute for Molecular Biomedicine, India

Blood flow has been linked to bone repair and maintenance, however fundamental aspects of hemodynamics in bone endothelial cell function and osteogenesis remain little understood. Here we show that the bone vasculature generates a peculiar blood flow pattern, which critically regulates skeletal angiogenesis. Intravital imaging of bone vasculature reveals that vessel growth in murine bone involves the extension and anastomotic fusion of endothelial buds. Impaired blood flow leads to defective endothelial buds, thus reduced angiogenesis and osteogenesis, and downregulation of Notch signaling in endothelial cells. In aged mice, skeletal blood flow and endothelial Notch activity were also reduced leading to decreased angiogenesis and osteogenesis, which was reverted by genetic reactivation of Notch in the endothelium. Administration of Alendronate also led to enhanced blood flow and angiogenesis in aged mice. We propose that blood flow and endothelial Notch signaling are key factors controlling ageing processes in the skeletal system.

**Disclosures:** *Saravana Ramasamy, None.*

*This study received funding from: Max Planck Institute for Molecular Biomedicine*

## SU0117

**Is Age-Related Bone Loss Microbiota Dependent?.** Jing Yan\*<sup>1</sup>, Jeremy Herzog<sup>2</sup>, Kelly Tsang<sup>1</sup>, Maureen Bower<sup>2</sup>, Balfour Sartor<sup>2</sup>, Antonios Aliprantis<sup>1</sup>, Julia Charles<sup>1</sup>. <sup>1</sup>Brigham & Women's Hospital, United states, <sup>2</sup>University of North Carolina at Chapel Hill, United states

**Introduction:** Age-related osteoporosis is associated with increased bone resorption by osteoclasts (OC), cells derived from osteoclast progenitors (OCP) under the influence of receptor activator of NF- $\kappa$ B ligand (RANKL). The mechanisms underlying increased bone resorption during aging remain unclear. Colonization of germ-free (GF) mice with microbiota increases bone resorption, while aging has been linked to intestinal dysbiosis in humans. We therefore hypothesized that gut microbiota might drive age-related bone loss via effects on osteoclast progenitor frequency and/or differentiation potential.

**Methods:** We analyzed conventionally housed mice at 3- and 24-month-old and GF mice at 3, 10, and 24 months. The effect of colonization was examined in 3-month-old GF and colonized littermates one month after colonization. Femurs were analyzed by microCT. Bone marrow OCPs and CD4 T cells were quantified by flow cytometry. The differentiation potential of sorted OCP was assessed by ex vivo culture. Expression of RANKL and OPG in BM mesenchymal stem cell (BMSC) culture and bone was analyzed by qPCR.

**Results:** Femoral bone mass (BV/TV) decreased with age in both conventional and GF mice. Neither aging nor colonization changed the capacity of purified OCP to differentiate into OC in response to RANKL in vitro. Aging but not colonization increased OCP numbers. We next analyzed BM environmental factors that could affect OCP differentiation in vivo. Mesenchymal stem cells isolated from aged bone had an increased RANKL:OPG mRNA ratio compared to young mice. Similar trends were seen after colonization of GF mice. We also found that the frequency of TNF $\alpha$ -producing CD4 T cells increased in the BM with both age and colonization.

**Conclusion:** Both aging and colonization of GF mice results in a pro-osteoclastogenic BM environment. However, GF mice are not protected from age-related bone loss indicating that microbiota-independent mechanisms contribute to bone loss during aging.

**Disclosures:** *Jing Yan, None.*

## SU0118

**Loss of the Longevity Gene SirT1 Dysregulates Chondrocytes and Leads to an Arthritic Phenotype In Vivo, Via Impaired Autophagy.** Pradeep Kumar Sacitharan\*<sup>1</sup>, Tonia Vincent<sup>1</sup>, James R Edwards<sup>2</sup>. <sup>1</sup>Kennedy Institute of Rheumatology, University of Oxford, United Kingdom, <sup>2</sup>The Botnar Research Centre, University of Oxford, United Kingdom

Ageing is universally linked to skeletal deterioration. Common mechanisms may control both processes, where dysregulation may predispose to bone loss and osteoarthritis (OA). The epigenetic deacetylase SirT1 controls lifespan and decreases with age. However, the role of SirT1 in joint disease is unclear. Human samples, novel genetically modified mice, a surgical disease model and a new therapeutic approach were employed alongside advanced cellular and molecular studies to explore the hypothesis that SirT1 is dysregulated in OA human cartilage, disrupting normal lifespan-protecting mechanisms such as autophagy, which can be targeted to reduce OA.

Autophagy degrades unwanted proteins, and is defective in ageing. Inhibition of SirT1 in HTB94 chondrocytes decreased chondrogenic (COL2A1, ACAN, SOX-9,  $p < 0.01$ ) and autophagy markers (BECN1, ULK-1, LC3,  $p < 0.01$ ). LC3 protein conversion, essential for autophagosome formation, was positively regulated with SirT1 activity in chondrocytes (western blot, FACS ( $p < 0.001$ )) and cartilage explants from LC3-GFP reporter mice ( $p < 0.0001$ ), demonstrating changes in SirT1 alters autophagic flux. Immunoprecipitation analysis showed direct SirT1 binding with ATG5, -7, beclin1, and LC3 and dysregulated acetylation in line with pharmacological activation (SRT1720;500nM) or inhibition of SirT1 (EX-527;100nM).

Human OA cartilage showed decreased SirT1 compared to healthy cartilage ( $p < 0.05$ ). A previously undescribed inducible, articular cartilage-specific SirT1 deletion murine model (SirT1<sup>fl/fl</sup>/Aggrecan CreERT2 mice (SirT1<sup>Agg</sup>)), showed greater cartilage degradation, increased OA disease score and epiphyseal volume (vs WT,  $p < 0.001$ ) on histomorphometric and uCT analysis at 2, 6, 12 mths. SirT1<sup>Agg</sup> mice showed decreased ACAN, COL2A1 ( $p < 0.001$ ) and autophagy markers BECN1, ULK-1, LC3, ATG5, ATG7, ATG13 ( $p < 0.01$ ), decreased LC3 protein in hip explants ( $p < 0.01$ ), and decreased autophagosome number (SEM,  $p < 0.05$ ). Induction of experimental OA (destabilisation of the medial meniscus (DMM) surgery) exacerbated cartilage degradation in SirT1<sup>Agg</sup> mice vs WT and decreased LC3 staining. However, activation of autophagy using Spermidine (5mM) protected against DMM-induced joint destruction in WT ( $p < 0.001$ ) but not in SirT1<sup>Agg</sup> mice.

These studies suggest that declining SirT1 in ageing human cartilage, or SirT1 deletion in murine chondrocytes, results in OA due to dysregulated autophagy, and which may be rescued by increasing autophagic flux.

**Disclosures:** *Pradeep Kumar Sacitharan, None.*

## SU0119

**The intracortical accumulation of enlarged lacunae is a key contributor to the increased cortical porosity and trabecularization during aging.** Christina Møller Andreassen<sup>1</sup>, Jean-Marie Delaïsse<sup>2</sup>, Bram C. J. van der Eerden<sup>3</sup>, Dorie Birkenhäger-Frenkel<sup>3</sup>, Johannes P. T. M. van Leeuwen<sup>3</sup>, Ming Ding<sup>1</sup>, Thomas Levin Andersen<sup>2</sup>. <sup>1</sup>Orthopaedic Research Laboratory, Department of Orthopaedic Surgery & Traumatology, Odense University Hospital, Institute of Clinical Research, University of Southern Denmark, Denmark, <sup>2</sup>Department of Clinical Cell Biology, Vejle Hospital/Lillebaelt Hospital, Institute of Regional Health Research, University of Southern Denmark, Denmark, <sup>3</sup>Laboratory for Calcium & Bone Metabolism, Department of Internal Medicine, Erasmus MC, Netherlands

The present study investigates the histological characteristics of the intracortical pores contributing to the increased cortical porosity and trabecularization during aging, in order to improve our understanding of the responsible intracortical bone remodeling events.

A detailed histomorphometric analysis of the intracortical pores was performed on sections from transiliac bone specimens from 35 women (age 16-78 years) undergoing forensic examination due to a sudden unexpected death.

Overall the investigated transiliac bone specimens had a statistically significant age-dependent increase in the cortical porosity ( $p < 0.05$ ) and the mean pore diameter (All:  $p = 0.055$ ; Age > 20 years:  $p < 0.01$ ), and a reduction in the cortical thickness ( $p < 0.01$ ). However, the overall pore density did not increase with the age.

The detailed analysis of the intracortical pores contributing to the porosity included collectively 3969 pores, which were subdivided into five subtypes according their morphology: 68.3% of these pores were refilled osteons with a quiescent surface, 8.8% of the pores were asymmetrically refilled osteons with both a quiescent and eroded surface, 6.5% of the pores had only eroded surfaces and no formative osteoid surfaces, 7.0% of the pores had formative osteoid surfaces, while 5.9% of the pores were refilled osteons with extensive erosions widening the previously quiescent pores. In 34.8% of the latter pores the widening resulted in the merge of two or more previously quiescent pores, forming enlarged irregular shaped lacunae. Although the widened previously quiescent pores and the formed lacunae only account for 5.9% and 2.1% of the pores, they on average contribute to 44.4 ± 22.1% and 30.3 ± 23.3% of the cortical porosity. Interestingly, these two types of pores showed a statistically significant age-dependent increase in their contribution to the cortical porosity ( $p < 0.001$ ) and pore density (number/mm<sup>2</sup>) ( $p < 0.01$ ), while the pores with formative osteoid surfaces showed an age-dependent decrease in their contribution to the cortical porosity ( $p < 0.01$ ).

Collectively, this study supports that the accumulation of widened previously quiescent pores and lacunae contributes to the increased cortical porosity during aging. The fact that the lacunae were often marrow infiltrated and located proximate to the endosteum surface further supports that the formation of lacunae may also contribute to the trabecularization of the cortical bone, leading to reduced cortical thickness.

**Disclosures:** Christina Møller Andreassen, None.

## SU0120

**Body Composition Phenotype of Osteosarcopenia, Osteoporosis and Sarcopenia: SARCOS Study.** Alberto Frisoli Jr\*, Fabiola Martin, Sheila Ingham, Antonio Carlos Carvalho. Universidade Federal de São Paulo, Brazil

**Introduction:** In clinical practice, substantial heterogeneity is observed among sarcopenic and osteoporotic patients; however, until now, the concomitant occurrence of these two syndromes has not been evaluated in terms of lean and fat mass, muscle strength and bone mineral density (BMD) in men and women. The goal of this study was to examine the differences of body composition and muscle strength profile between older men and women with osteoporosis, sarcopenia by EWGSOP and Osteosarcopenia.

**Methods:** Cross-sectional analysis of data from SARCOS study, an observational study of the epidemiology of Sarcopenia and Osteoporosis in regard to mortality and disability in older outpatients from a Cardiology Division in a School of Medicine. All subjects underwent DEXA evaluation of total body (n=215, 99 men and 116 women). Sarcopenia was defined by EWGSOP (weakness or low gait speed plus low appendicular muscle mass). Osteoporosis was defined as BMD t-score ≤ - 2.5 SD (lumbar spine or proximal femur). Osteosarcopenia phenotype was defined as the presence of Osteoporosis at any bone site plus Sarcopenia by EWGSOP. Osteoporosis and Sarcopenia were analyzed in an isolated way.

**Results:** Osteosarcopenia occurred in 20.2% of men and 14.8% of women (p=0.037), sarcopenia in 13.1% of men and 4.9% of women (p=0.017), osteoporosis was found in 9.1% of men and 39.3% of women (p<0.001). Men with Osteosarcopenia were older, and presented a tendency of lower BMD compared to men with osteoporosis only, and a tendency of lower appendicular muscle mass compared to Sarcopenia only; however, the BMI, muscle strength and fat index were significantly lower compared to subjects with osteoporosis and sarcopenia only. In women, subjects with osteosarcopenia were older, with a significantly lower BMD at all bone sites except for the distal forearm; appendicular muscle mass and other body parameters were significantly lower compared to women with osteoporosis and sarcopenia only, as demonstrated in table 1.

**Conclusion:** The osteosarcopenia phenotype was more prevalent in men than in women. Osteosarcopenia, in both genders, was characterized by very low body composition parameters and grip strength.

**Implications:** The screening for osteosarcopenia may help to identify older adults with higher risk for disability and fractures.

	Age, years (SD)	Fat index Kg/m <sup>2</sup> (SD)	% total body fat (SD)	BMI, Kg/m <sup>2</sup> (SD)	Grip strength, Kg (SD)	AMM/Height <sup>2</sup> , Kg/m <sup>2</sup> (SD)	BMD Hip total, g/cm <sup>2</sup> (SD)	BMD Neck, g/cm <sup>2</sup> (SD)	BMD distal forearm, mg/cm <sup>2</sup> (SD)	BMD Spine, g/cm <sup>2</sup> (SD)
<b>Men</b>										
Osteosarcopenia	81.5 (8.14)	2.45 (0.99)	29.43 (9.0)	22.92 (3.5)	21.53 (5.36)	6.37 (0.4)	0.777 (0.11)	0.752 (0.06)	0.687 (0.11)	1.027 (0.15)
Sarcopenia	80.5 (4.84)	3.20 (0.91)	35.90 (6.1)	25.63 (3.1)	23.23 (5.76)	6.60 (0.4)	0.914 (0.08)	0.872 (0.05)	0.741 (0.06)	1.278 (0.16)
Osteoporosis	78.2 (4.71)	2.98 (0.91)	32.13 (5.5)	26.39 (3.7)	28.00 (6.14)	7.51 (0.4)	0.795 (0.10)	0.731 (0.07)	0.696 (0.08)	1.014 (0.15)
None	76.5 (6.31)	3.56 (1.3)	34.35 (7.3)	27.89 (3.6)	29.53 (5.38)	7.77 (0.6)	1.031 (0.15)	0.971 (0.15)	0.824 (0.11)	1.277 (0.21)
p	<.001	0.004	0.048	<.001	<.001	<.001	<.001	<.001	<.001	<.001
<b>Women</b>										
Osteosarcopenia	83.0 (7.0)	3.63 (1.4)	39.63 (1.4)	22.81 (3.8)	13.05 (4.06)	5.22 (0.5)	0.701 (0.10)	0.673 (0.10)	0.522 (0.14)	0.838 (0.12)
Sarcopenia	76.7 (4.0)	3.81 (1.2)	39.76 (10.1)	22.00 (2.0)	12.00 (5.51)	4.81 (0.3)	0.832 (0.07)	0.796 (0.05)	0.626 (0.05)	1.152 (0.25)
Osteoporosis	80.5 (7.4)	5.13 (1.9)	42.70 (8.4)	27.66 (3.9)	15.34 (5.70)	6.33 (0.7)	0.764 (0.11)	0.747 (0.11)	0.527 (0.10)	0.938 (0.17)
None	79.1 (6.8)	5.61 (2.0)	45.15 (7.5)	28.41 (4.8)	17.36 (4.75)	6.33 (0.8)	0.932 (0.10)	0.882 (0.10)	0.667 (0.08)	1.168 (0.15)
p	<.001	0.003	0.059	<.001	0.008	<.001	<.001	<.001	<.001	<.001

Table 1—Body composition and muscle strength of older men and women with osteosarcopenia (SARCOS), sarcopenia, osteoporosis and none

Table 1—Body composition and muscle strength of older men and women with osteosarcopenia (SARCOS), s

**Disclosures:** Alberto Frisoli Jr, None.

## SU0121

**HISTORY OF FALLS, SUBJECTIVE WELL-BEING, HEALTH BEHAVIOR AND OTHER HEALTH FACTORS AS PREDICTORS OF FALLS IN POSTMENOPAUSAL WOMEN.** Risto Honkanen<sup>1</sup>, Nadia Afrin<sup>1</sup>, Pyry Lykkala<sup>1</sup>, Päivi Rauma<sup>1</sup>, Heikki Kröger<sup>2</sup>, Toni Rikonen<sup>1</sup>, Lana Williams<sup>3</sup>, Heli Koivumaa-Honkanen<sup>4</sup>. <sup>1</sup>University of Eastern Finland, Finland, <sup>2</sup>University of Eastern Finland, Department of Surgery, Finland, <sup>3</sup>Impact Research Centre, Deakin University, Australia, Australia, <sup>4</sup>Department of Psychiatry, Kuopio University Hospital, 5Lapland Hospital District, Rovaniemi, Finland, Finland

**Introduction:** Knowledge of predictors of falls in women before old age is scanty. The purpose was to find these predictors. **Methods:** Kuopio Osteoporosis Risk Factor and Prevention (OSTPRE) study cohort, Finland was used: 8656 women aged 57-66 responded to health questions in 1999 and to fall questions in 2004. We compared women with frequent falls (2+ within 12 m)(n=2016) to women with no falls (n=5259) and excluded occasional (one fall) fallers (n=1381) resulting in study population of 7275 women. Subjective well-being (SWB) was measured with four questions: feelings of interest in life, ease of living, happiness and loneliness. Number of reported chronic health disorders diagnosed by a physician was a measure of morbidity. Logistic regression was the statistical method. **Results:** Fall history was the strongest predictor of fall (OR 3.16 (95% CI 2.8-3.6)), followed by morbidity (OR=1.14 (1.1-1.2)) for one unit increase, SWB (OR 1.06 (1.04-1.1)), BMI (OR 1.04 (1.02-1.04)), smoking (OR 0.71 (0.6-0.9)), use of antidepressants (OR 1.62 (1.3-2.1)), leisure physical activity (PA)(OR 0.89 (0.8-1.001)). The adjusted final model included: fall history (extremely strong), morbidity (strong), SWB (strong), mobility (moderate), smoking (weak protection!), alcohol (weak), PA (weak). R<sup>2</sup> of the model was 5-8%. **Conclusions:** The strong effect of fall history suggests a genetic trait. Health status and SWB are also considerably related to fall risk, health behaviour to some degree but partly controversially. Further study aims to reveal interactions of predictors and potential causal pathways including if residual confounding explains the seemingly positive effect of smoking.

**Disclosures:** Nadia Afrin, None.

## SU0122

**Poor Physical Fitness is associated with Low Bone Material Strength in Older Adults with Type 2 Diabetes.** Yoann Barnouin<sup>\*</sup>, Sanjay Mediwal, Alessandra Celli, John Wade, Georgia Colleluori, Dean Blevins, Reina Villareal, Dennis Villareal. Baylor College of Medicine/Center for Translational Research on Inflammatory Diseases at MEDVAMC, United states

**Background:** Several risk factors specific to type 2 diabetes (T2D) (e.g., poor glycemic control, T2D duration, diabetic complications) may exacerbate the gradual decline in physical function and increase in fracture risk with aging. The novel technique of bone microindentation allows for measurement of bone material strength, a property which could be one of the key determinants of higher fracture risk in T2D. Interestingly, it has been suggested that functional impairments mediate

associations between fracture risk and T2D. However, no current studies have investigated the association between aerobic fitness and bone material strength in older patients with T2D.

**Objective:** The present study aimed to determine the relationship between aerobic fitness and bone material strength in older adults with T2D.

**Methods:** Twenty-seven subjects (age 65-85 yrs) with T2D were recruited from an ongoing randomized controlled trial designed to examine the effects of a lifestyle intervention strategy (behavioral diet therapy for weight loss and exercise training). Peak aerobic capacity ( $VO_{2peak}$ ) was assessed during a graded treadmill test using indirect calorimetry.  $VO_{2peak}$  was normalized for body weight, fat-free mass (FFM), and appendicular lean mass (ALM) as determined by dual-energy X-ray absorptiometry. Microindentation testing was performed using the OsteoProbe RUO Reference Point Indenter to assess bone material strength index (BMSi) at the mid-tibia.

**Results:** Average BMSi was  $70.5 \pm 6.5$  while average  $VO_{2peak}$  was  $17.1 \pm 4.1$  ml/kg/min (RER:  $1.1 \pm 0.1$ ). Cross-sectional data analysis from baseline testing showed no significant association between BMSi and  $VO_{2peak}$  relative to body weight ( $p = .118$ ).  $VO_{2peak}$  relative to FFM or ALM is a measure of the ability of muscle to maximally consume oxygen. We found a significant positive correlation between BMSi and  $VO_{2peak}$  relative to FFM ( $r = .40$ ;  $p = .037$ ), and a trend for positive correlation between BMSi and  $VO_{2peak}$  relative to ALM ( $r = .34$ ;  $p = .086$ ).

**Conclusion:** These preliminary findings suggest that bone material strength, one of the key determinants of bone quality, is correlated with aerobic fitness in older adults with T2D. Recent findings suggest that advanced glycation endproducts (AGEs) could explain this association. Since caloric restriction and physical activity significantly reduce AGEs, an intensive lifestyle intervention should confer beneficial effects on bone quality and physical fitness in older adults with T2D.

**Disclosures:** Yoann Barnouin, None.

## SU0123

**Silk fibroin nanoparticle enhances stability and sustained release of bone morphogenetic protein-2.** Bong-soo Kim\*, Woo-jin Kim, Won-jun Yoon, Hyun-mo Ryoo, Jung-hwa Baek, Kyung-mi Woo. Seoul National University, Korea, republic of

Bone morphogenetic protein 2 (BMP-2) is a strong osteoinductive growth factor. Conventional delivery of BMP-2 soaked in absorbable collagen sponge generated many complications such as swelling and ectopic bone formation around applied area. These unwanted problems came from inappropriately high dosage of BMP-2 because of short half-life and abrupt release from the carrier.

In this study, we designed BMP-2/silk fibroin nanoparticle (BMP-2/SF) as a carrier for the BMP-2 to improve its release profile and stability in biological fluid. Sonication of mixture solution of silk fibroin, polyvinyl alcohol (PVA) and BMP-2 achieved successfully encapsulated of BMP-2 in the particle. Scanning electron microscope (SEM) analysis of self-assembled BMP-2/SF showed smooth surfaced spherical particles. The zeta-sizer analysis indicated that the particles have average diameter 500-700nm and zeta-potential -20mV. Loading capacity of BMP-2 in the particle is around 80%. Releasing profile was sustained about 30 days and reached plateau until 40% release. The stability and bioactivity of encapsulated BMP-2 was strongly enhanced even in 10% fetal bovine serum in the media compared with naïve BMP-2 protein. Particle itself does not show cytotoxicity. Bioactivities of encapsulated BMP-2 assessed by alkaline phosphatase activity *in vitro* and osteogenic potential in intramuscular ectopic bone formation and calvarial critical-size defect model *in vivo* indicated BMP-2/SF successfully stimulated ALP activity *in vitro*, and osteogenic potentials *in vivo*. These results imply the clinical potential of silk fibroin nanoparticle and BMP-2 because of its long-lasting release pattern and enhancement of protein stability.

**Disclosures:** Bong-soo Kim, None.

## SU0124

**Adipose derived mesenchymal stem cells seeded on TiO<sub>2</sub> granules increases osteoblast numbers *in vivo*.** Morten Dahl\*. PhD student, DDS, Denmark

**Purpose:** Tissue engineering involves the *in vitro* seeding of cells onto scaffolds supporting cell adhesion, migration, proliferation and differentiation, and defines the 3D-shape of the tissue to be engineered. Adipose derived mesenchymal stem cells (ADMSCs) express osteoblastic lineage genes and stain strongly for alkaline phosphatase. Besides their osteogenic potential, they may generate neoangiogenesis and mineralization. Adipose tissue is an easily accessible rich resource of osteogenic ADMSCs with fewer complications. Porous titanium granules are a suitable carrier. The purpose of the current study was to evaluate the early effect of ADMSCs seeded on porous titanium granules implanted subcutaneously in mice.

**Materials and methods:** First ADMSCs were cultivated in osteoblast medium. Hereafter seeded either on Ti or TiO<sub>2</sub> granules or without titanium granules. In 24 Balb/cJ mice randomly divided in two groups with Ti or TiO<sub>2</sub> granules, respectively, four subcutaneous created pockets were filled randomly. After two weeks of observation all mice were euthanized, the four pockets with surrounding musculature of each animal were dissected free, fixated in 70% ethanol and prepared for non-decalcified specimens. All sections were stained with toluidine blue and basic fuchsin for quantitative histology.

**Results:** A statistically significantly higher fractional surface ratio was found between TiO<sub>2</sub> compared to Ti granules with cells of osteoblasts (OB) ( $Md_{Ti+}=0.000$ ,

$Md_{TiO_2+}=0.0028$ ,  $p=0.002$ ) and of osteoclasts (OC) ( $Md_{Ti+}=0.079$ ,  $Md_{TiO_2+}=0.090$ ,  $p=0.036$ ). Likewise a statistically significantly higher fractional surface ratio was found between TiO<sub>2</sub> compared to Ti granules without cells of OB ( $Md_{Ti-}=0.000$ ,  $Md_{TiO_2-}=0.0021$ ,  $p=0.002$ ) and of OC ( $Md_{Ti-}=0.071$ ,  $Md_{TiO_2-}=0.124$ ,  $p=0.003$ ). At the same time a statistically significant difference in amount of OB per granule material was found between TiO<sub>2</sub> and Ti granules with cells ( $Md_{Ti+}=0.000$ ,  $Md_{TiO_2+}=1040.36$ ,  $p=0.001$ ) and without cells ( $Md_{Ti-}=0.000$ ,  $Md_{TiO_2-}=673.70$ ,  $p=0.002$ ).

**Conclusion:** A higher appearance of osteoblasts and osteoclasts on TiO<sub>2</sub> compared to Ti granules suggests a more osteoinductive scaffold in TiO<sub>2</sub>. Osteogenic ADMSCs seeded on TiO<sub>2</sub> granules may be used as carriers for bone reconstruction.

**Disclosures:** Morten Dahl, None.

## SU0125

**Functional Engraftment of Murine Pre-Osteoblastic Cells in a Zebrafish Model of Epimorphic Bone Regeneration.** Barrie Sugarman\*, Brandon Douglass, Claire Watson, Christopher Allan, Ronald Kwon. University of Washington, United states

Urodeles such as newts and salamanders have the capacity to regenerate limbs following amputation through epimorphic regeneration, a process characterized by the formation of a proliferative mass of partially dedifferentiated cells called the blastema. Epimorphic regeneration has not been observed in mammals. Xenograft models capable of directing mammalian cells into this process may reveal new factors to enhance cellular reprogramming, stimulate proliferation, and/or differentiate cells into an osteoblastic state. However, such models have yet to be developed due to incompatibilities in amphibian and mammalian biology (e.g., differences in body temperature). To address this challenge, our goal was to develop a xenograft model of epimorphic regeneration by introducing mammalian osteoblastic cells into the regenerating zebrafish tail fin (a tractable model of epimorphic bone regeneration that molecularly resembles amphibian limb regeneration). Adult zebrafish were subjected to caudal fin amputation and housed in ~33°C water, a temperature which we found was permissive to both fish and cell survival. Three days post amputation (dpa), zebrafish were injected with CM-Dil-labeled MC3T3-E1 murine pre-osteoblastic cells in the proximal blastema, and subjected to daily *in vivo* imaging. Injected cells exhibited clear engraftment and stability for up to 48 hours post injection; decreased fluorescence was observed at 2-3 days post injection potentially due to fish immune system activity. Image analysis revealed a ~50% increase in cell number by 24 hours post injection ( $n=3$ ). In addition, average migration distance was ~4x higher in the anterior-posterior direction compared to the dorsal-ventral axis ( $n=3$ ). Cells injected into Wnt:GFP transgenic reporter fish proximal to the Wnt+ blastema population revealed co-localization with Wnt+ cells 24h post injection (Fig 1A), whereas cells injected distal to the Wnt+ blastema cell population remained localized to the distal epidermis in a manner that was boundary-restricted by the Wnt+ population (Fig 1B). Collectively, our studies suggest that the regenerating zebrafish tail fin may serve as a viable system for xenograft models of epimorphic bone regeneration. Provided the correct conditions, mammalian osteoblastic cells may be capable of engrafting and proliferating in an epimorphic bone regeneration process.

\*BSS and BGD contributed equally to this work.

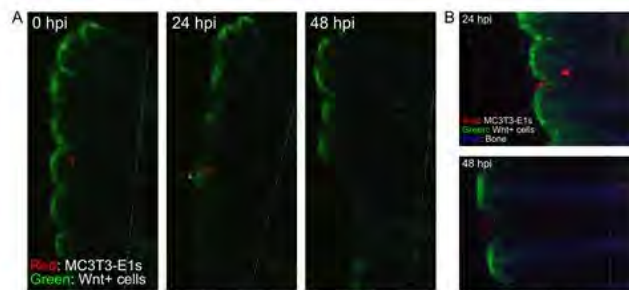


Fig 1: Engraftment of MC3T3-E1 pre-osteoblastic cells in the regenerating tail fin of Wnt:GFP transgenic zebrafish. (A) MC3T3-E1 cells injected proximal to Wnt+ blastemal cells exhibit co-localization with the Wnt+ population 24 hours post injection (hpi), and engraftment into newly regenerated tissue by 48 hpi. (B) MC3T3-E1 cells injected distal to the Wnt+ blastema cell population remained localized to the distal epidermis. The amputation plane is demarcated by the dotted line in all images.

Figure 1

**Disclosures:** Barrie Sugarman, None.

## SU0126

**Lin-/Lepr+ Cells are an Important Source of Osteoprogenitors in Adult Life.** Joshua Farr\*<sup>1</sup>, Megan Weivoda<sup>1</sup>, Elizabeth Atkinson<sup>2</sup>, Sundeep Khosla<sup>1</sup>, David Monroe<sup>1</sup>. <sup>1</sup>Division of Endocrinology; Mayo Clinic College of Medicine, United states, <sup>2</sup>Division of Biomedical Statistics & Informatics; Mayo Clinic College of Medicine, United states

Mesenchymal stromal cells (MSCs) are multipotent cells capable of differentiation to adipogenic, chondrogenic and osteogenic lineages. Recently, *in vivo* fate mapping

has demonstrated that Leptin receptor+ (Lepr+)-expressing MSCs arise postnatally and are the main source of adipocytes and osteoblasts in adult bone marrow (Cell Stem Cell 15:154-68, 2014). Thus, Lepr may be a marker for highly enriched adult bone marrow MSCs. Although much is known about the niche and developmental potential of Lepr+ MSCs, both characterization and knowledge of the physiological functions of these cells has been lacking. To address these important gaps, we isolated hematopoietic lineage negative (Lin-) cells by MACS from the bone marrow of adult (6-month-old) wild-type mice. These cells were then labeled with a Lepr antibody and magnetic activated cell sorting (MACS) was used to rapidly isolate the Lin-/Lepr+ population, which we compared to the Lin-/Lepr- population using whole transcriptome RNA sequencing (RNAseq) and pathway analyses. In addition to expected higher expression of *Lepr* (7.5-fold), RNAseq showed that expression levels of several MSC markers (i.e., *Acta2*, *Alcam*, *Cxcl12*, *Grem1*, *Kitl*, *Thy1* and *Vcam1*), adipogenic markers (i.e., *Adipoq*, *Adipsin*, *C/EBPa*, *C/EBPd*, *Cebpb*, *Fabp4*, *Irs1*, *Spl* and *Pparg*) and osteoblast lineage markers (i.e., *Alpl*, *Ibsp*, *Runx2*, *Sparc* and *Spp1*) were significantly higher in Lin-/Lepr+ cells. Interestingly, RNAseq also revealed that multiple Notch and Wnt signaling targets were significantly higher in Lin-/Lepr+ cells. Ingenuity pathway analysis confirmed that multiple pathways with important known functions in bone were significantly activated in Lin-/Lepr+ cells, including NF- $\kappa$ B Signaling, Mouse Embryonic Stem Cell Signaling and Wnt/ $\beta$ -catenin Signaling. Finally, when cultured in the presence of osteogenic media for seven days, Lin-/Lepr+ cells exhibited robust mineralization as evidence by Alizarin Red staining, whereas Lin-/Lepr- cells had not yet mineralized (Figure). Collectively, our data demonstrate that Lin-/Lepr+ cells represent a highly enriched bone marrow MSC population that expresses high levels of both adipogenic and osteogenic markers, and that several important bone pathways are activated in Lin-/Lepr+ cells. These findings strongly support that Lin-/Lepr+ cells are an important source of osteoprogenitors in adult life. Therefore, rapid isolation of these cells will be useful to study defects in bone formation with age.

## SU0127

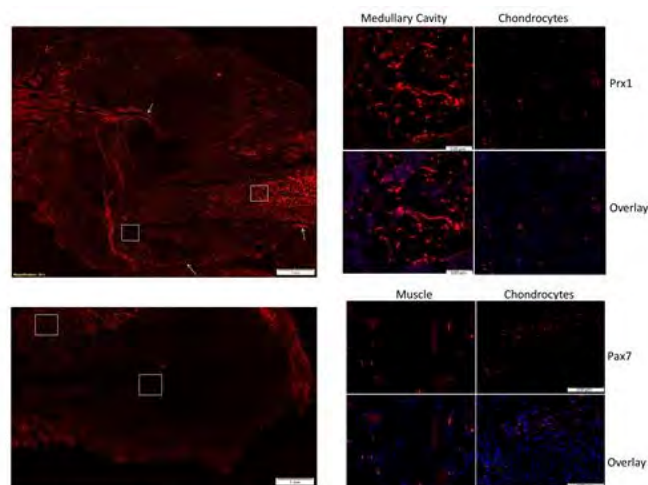
**Multiple Populations of Progenitor Cells Contributes to Post-natal Bone Formation.** Beth Bragdon\*, Kyle Lybrand, Louis Gerstenfeld. Boston University School of Medicine, United states

During fracture repair muscle satellite and periosteal cells defined by their expression of Pax7 and Prx1 transcription factors (TF) respectively, contribute to callus tissue formation. Other TFs associated with embryonic stem cells are also expressed. Little is known about the progenitor cell populations that contribute to ectopic bone formation. The objective of this study was to characterize the stem cell TFs and progenitor cell populations that contribute to post-natal bone formation.

Methods: Fractures were generated in the right femora of male C57BL/6J mice. Tissue was harvested at 1, 2, 3, and 5 days post-fracture. Ectopic bone was induced by implanting 50mg of human demineralized bone matrix (Medtronic Inc with an MTA) onto the femoral surface of male B6.129S7-Rag1<sup>tm1Mom</sup>/J mice and harvested at 2, 4, and 8 days post-surgery. Expression of *Sox2*, *Nanog*, *Oct4* (ES), *Pax7* (satellite cells), and *Prx1* (periosteal osteochondral progenitor cells) were evaluated by RT-qPCR. Inducible Prx1 Cre ERT and Pax7 Cre ERT transgenic mouse models were crossed with the B6.Cg-Gt(ROSA)26sor<tm14 (CAG-tdTomato)Hze>/J mouse (Ai14) to create transgenic reporter mouse models, Prx1/Ai14 and Pax7/Ai14. Animals were injected with tamoxifen 3 days prior to fracture and continued three times per week until euthanasia. Tissue was collected over 14 days.

Results: Ectopic bone induction and fracture showed increased ES cell markers, *Sox2* and *Nanog*, induction of greater than 100X and 10X respectively between 0-4 days. *Prx1* and *Pax7* were also induced but showed more prolonged expression through day 5 and day 8 in fracture callus and ectopic bone respectively. Prx1 lineage tagged osteoblasts were observed throughout the medullary space, in a small number of chondrocytes and throughout the periosteum while Pax7 cell lineage tagged cells contributed to much lesser degree and were only seen in callus chondrocytes (figure1). Interestingly both Prx1 and Pax7 tagged cells were identified in the surrounding soft tissue.

Discussion: The expression of Prx1 and Pax7, thought to be separately associated with stem cells in the periosteum and muscle, are found to be up regulated in both fracture and ectopic bone formation. This suggests that these factors are not exclusively tissue restricted to but may be more generally functional in axial skeletal stem cells. However the cell distribution of these factors does show some exclusivity between anatomical differing populations of cells.



Top. Prx1 tagged cells in fracture callus at day 10. Prior to fracture the Prx1 driven dTomato was induced with tamoxifen. White arrows point to periosteal surface. Bottom panel. Tamoxifen was given prior to fracture. Pax7 tagged cells (red) in fracture callus at day 7. Nuclei were stained with dapi (blue).

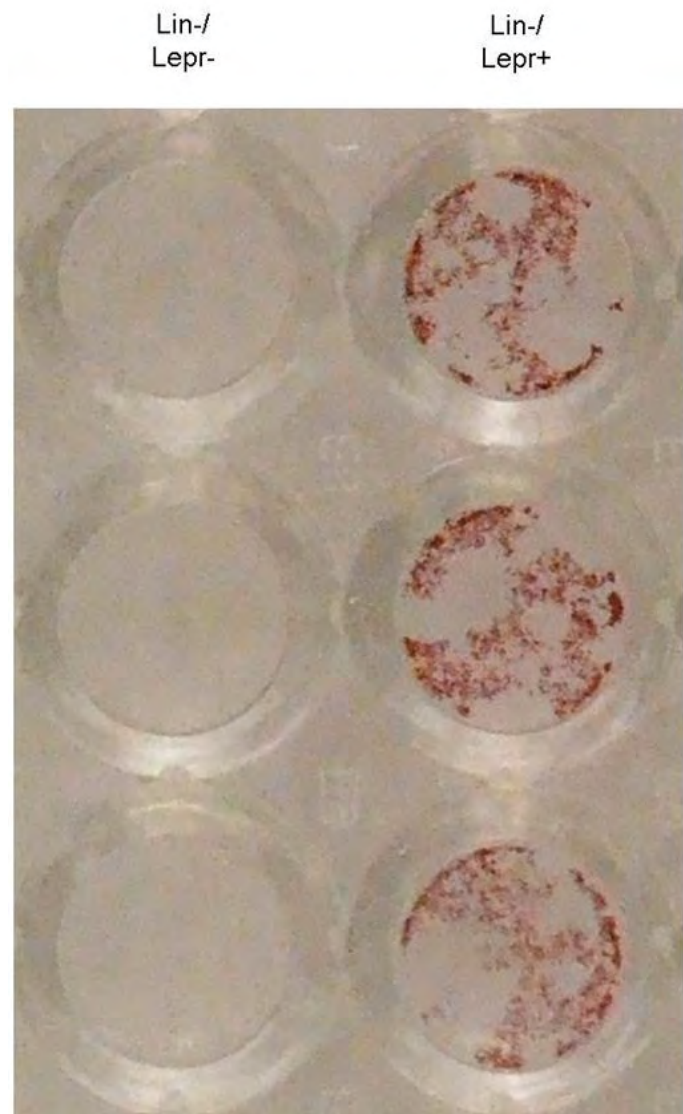
figure 1

Disclosures: Beth Bragdon, None.

## SU0128

**Prx1 Ablation Results in Impaired Long Bone Fracture Healing.** Lai Wang\*<sup>1</sup>, Alessandra Esposito<sup>1</sup>, Ping Ye<sup>2</sup>, Tieshi Li<sup>1</sup>, Joseph Temple<sup>1</sup>, Anna Spagnoli<sup>1</sup>. <sup>1</sup>Rush University Medical Center, United states, <sup>2</sup>The University of North Carolina at Chapel Hill, United states

The use of mesenchymal stromal cells (MSC) in fracture repair has been receiving special attention due to their potential role in tissue regeneration. One family of transcriptional factors implicated with regulation of MSC fate is the paired-related homeobox protein family. Prx1 is required for early events of skeletogenesis in multiple lineages. Deficiency of Prx1 leads to skeletal defects in limbs. Our preliminary data in *Prx1CreER;ROSA26* reporter mice demonstrated Prx1 expression in periosteum of postnatal tibias, as well as rapid accumulation of chondrocytes, osteoblasts, and perivascular cells derived from Prx1-expressing cells into the callus of fractured tibias. The purpose of this study is to verify whether multipotent



Figure

Disclosures: Joshua Farr, None.

Prx1-expressing cells are essential in fracture healing. The role of Prx1 was evaluated in vivo by analyzing tibial fracture-healing model in *Prx1CreER;R26DTA<sup>fl/fl</sup>* male mice, in which Prx1 expression was ablated when tamoxifen was administered. The mutant mice and their littermate controls were subjected to tibia fracture at age of postnatal 12-14 weeks. 4-OH-tamoxifen was injected intraperitoneal 0.5mg/mouse/day for 6 days started two days before fracture. Mice were euthanized and the tibias were dissected 7 days after fracture. Micro-computed tomography (micro-CT) analysis revealed that the volume of callus, soft tissue and new bone was significantly decreased in *Prx1CreER;R26DTA<sup>fl/fl</sup>* mice compared to their control littermates. Tibia fracture callus samples were fixed and decalcified, and subjected to frozen sections. Histology analysis of these frozen sections showed that, at day 7 after fracture, the fracture gap was filled with cartilage and newly-formed woven bone. Safranin O/Fast-green staining indicated that cartilage formation was reduced in *Prx1CreER;R26DTA<sup>fl/fl</sup>* mice. Immunofluorescence studies were performed to characterize the phenotype of the cells involved in the formation of fracture callus. Sox9, an important transcription factor in the chondrogenic commitment of the progenitors during fracture healing, was less expressed in the soft callus of Prx1 mutant mice. In conclusion, these findings provided evidence that Prx1-expressing cells play a crucial role in promoting fracture healing by serving as multipotent progenitors.

**Disclosures:** Lai Wang, None.

## SU0129

**Combining TGF- $\beta$  Type II Receptor (Tgfr2)-expressing Joint Progenitors and Degradable Scaffolds from PLLA Fibers for Tendon-Bone Junction Tissue-Engineering.** Tieshi Li<sup>1\*</sup>, Harshini Ramakrishna<sup>2</sup>, Ting He<sup>2</sup>, Joseph Temple<sup>1</sup>, Martin King<sup>2</sup>, Anna Spagnoli<sup>1</sup>. <sup>1</sup>Rush University Medical Center, United states, <sup>2</sup>North Carolina State University, United states

With the objective of repairing torn tendon-bone junctions and treating cartilage degeneration, we have reported the identification and characterization of joint Tgfr2-expressing cells as slow-proliferating joint progenitors within specific joint niches including tendon-to-bone insertion sites. These progenitor cells have bidirectional effects (chondrogenic or fibrogenic) through different signaling pathways. This study aimed to develop a combined system of a degradable scaffold and Tgfr2-expressing progenitors for tendon-bone junction regeneration. We applied novel textile technology to develop 3D tubular scaffolds to mimic the structural, mechanical and immunochemical properties of natural mouse tendons. The double-layer scaffold created a hierarchical pore distribution from outside to inside the scaffold. Two types of poly-L-lactide (PLLA) fibers were used to create different surface textures: the round fiber had a smooth surface while the 4DG<sup>TM</sup> fibers had microgrooves. Four types of double-layer scaffolds were developed: Scaffold1: braided both layers using round fibers; Scaffold2: braided both layers using 4DG<sup>TM</sup> fibers; Scaffold3: weft knitted inner layer and braided outer layer, both using round fibers; Scaffold4: weft knitted inner layer using round fibers and braided outer layer using 4DG<sup>TM</sup> fibers. Tgfr2-expressing joint progenitor cells (GFP as a reporter of Tgfr2 gene), isolated from E14.5 embryonic limbs of Tgfr2-Bac mice were seeded onto the four scaffolds coated with fibronectin and cultured with or without TGF $\beta$ 1 treatment for 14 days. Micromass cultured and seeded cells on Scaffold3 without fibronectin coating were used as the control. At Day7 and Day14, an AlamarBlue assay was used to quantify cell proliferation, and laser scanning confocal microscopy (LSCM) was used to observe cell attachment and migration through the layers of the scaffold. RT-PCR was performed with extracted mRNA to validate cell differentiation. We found that the fibronectin coating promoted cell attachment and proliferation on the scaffolds. The outer layer, which has bigger pores, provided sufficient fiber surface area for cell attachment and also allowed internal cell penetration. The inner layer with smaller pores helped cell interaction. Cell proliferation increased from Day 7 to Day 14 on Scaffolds 1, 3 and 4 but not on Scaffold2. Whereas, early cell differentiation was found on Scaffold2, which was associated with significantly higher expression of Collagen 1 (fibrogenic marker), Collagen 2 (chondrogenic marker) and Tenascin C. TGF $\beta$ 1 treatment induced cell proliferation on Scaffolds 1 and 4 at Day 7. It also induced up-regulated Collagen 2 but not Collagen 1 in Scaffold3. Our preliminary data showed improved control over proliferation and differentiation of Tgfr2-expressing progenitors by tuning the scaffold design and adding TGF $\beta$ 1 treatment.

**Disclosures:** Tieshi Li, None.

## SU0130

**An In Vivo Histomorphometric Approach to Monitor Bone Apposition and Differentiation of Skeletal Progenitor Cells into Osteoblasts and Osteocytes.** Shu-Chi A. Yeh<sup>1\*</sup>, Katarzyna Wilk<sup>1</sup>, Charles P. Lin<sup>2</sup>, Giuseppe Intini<sup>3</sup>. <sup>1</sup>Department of Oral Medicine, Infection, & Immunity, Harvard School of Dental Medicine, United states, <sup>2</sup>Advanced Microscopy Program, Center for Systems Biology & Wellman Center for Photomedicine, Massachusetts General Hospital, Harvard Medical School, United states, <sup>3</sup>Department of Oral Medicine, Infection, & Immunity, Harvard School of Dental Medicine., United states

Background: Ex vivo histomorphometry is commonly used to quantitatively assess bone formation (Dempster et al., J Bone Miner Res. 2013). While providing good

resolution, this approach typically involves time-consuming histological preparation and lacks 3D information.  $\mu$ CT (Waarsing et al., Bone. 2004) is a good alternative to provide 3D bone structure in vivo. However,  $\mu$ CT provides only morphological information and conventional immunohistochemistry is still required to probe other cellular events. Intravital fluorescence microscopy (IVM) (Lo Celso et al., Nature. 2009) may represent an attractive option to obtain bone measurements while performing longitudinal monitoring of dynamic biological processes in vivo. In this work we hypothesized that IVM, in combination with fluorescence lineage tracing analysis, can be used to study bone formation and skeletal stem cell differentiation at the osteogenic fronts of the coronal suture. Methods: Lineage tracing was performed using Prx1-creER-eGFP mice crossed with Rosa-tdTomato mice. Upon tamoxifen induction (1 mg/day, 3 days, IP), animals were treated with calvarial subcutaneous injections of either human recombinant WNT3a (in PBS, 44ng/day) or just PBS for 2 weeks. Calcein blue (100 mg/Kg, IP) was used to label the existing bone fronts on day 1, and tetracycline (45 mg/Kg, IP) was administered 4 hours before imaging to stain the new bone fronts on day 28. Then, IVM was employed to visualize the bone fronts and the TdTomato+ osteoblasts and osteocytes descendant from the Prx1+ cells. Quantification was performed by counting tdTomato+ cells in the newly formed bone and by measuring the bone growth rates using reconstructed z-stacks of 40  $\mu$ m in thickness. Results: Fig. 1 demonstrates the bone structure (gray), the newly formed bone between Calcein Blue and Tetracycline staining (see blue and white dashed lines, respectively), the Prx1 expressing cells in the suture (yellow, since co-expressing EGFP and tdTomato, see yellow arrows) and their progeny as mature osteoblasts or osteocytes in the new bone (red, see red arrows). Greater bone growth rate ( $p < 0.01$ ), and more Prx1 descendants ( $p < 0.01$ ) in the newly formed bone were observed in WNT3a treated animals, suggesting that Prx1+ progenitors differentiate upon hrWNT3a treatment. Conclusion: Our results demonstrated that IVM, in combination with fluorescence lineage tracing, may represent a promising tool to perform in vivo histomorphometric analysis.

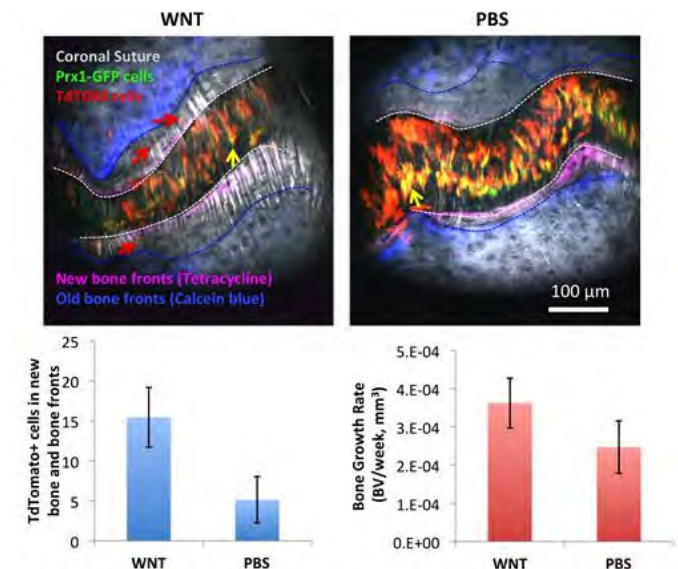


Fig. 1

**Disclosures:** Shu-Chi A. Yeh, None.

## SU0131

**Differentiation of hiPSCs into Osteoblasts by Using Small Molecule Inducers Under Fully Defined Xeno-free Conditions.** Denise C. Zujur<sup>1\*</sup>, Kosuke Kanke<sup>2</sup>, Ung-il Chung<sup>1</sup>, Shinsuke Ohba<sup>1</sup>. <sup>1</sup>The University of Tokyo, Department of Bioengineering, Japan, <sup>2</sup>The University of Tokyo, Japan

Induced pluripotent stem cells (iPSCs) have emerged as a promising option for studies of tissue development, drug screening, and cell-based therapies. From the clinical perspective, it is prerequisite to develop efficient methods to direct iPSCs into specific lineages. Production of mixed cell population, persistence of undifferentiated cells, and the use of animal-derived components are common limitations of current methods. Here, we developed a strategy to efficiently differentiate hiPSCs into osteoblasts under fully defined, xeno-free conditions. The osteogenic induction of two independent hiPSC lines was successfully achieved by small molecule-mediated manipulation of signaling pathways that had been identified as key players in osteoblast development. CHIR99021 was used to activate canonical Wnt signaling. Smoothed agonist (SAG) and cyclopamine (Cyc) were used to activate and repress hedgehog (Hh) signaling, respectively. BMP-dependent osteogenic molecule (TH) that we previously identified (Ohba S. et al., Biochem Biophys Res Commun, 2007), was also used. hiPSC differentiation was examined by gene expression analyses with RT-qPCR, protein expression analyses with immunostaining, and calcification analyses with von Kossa staining. The initial 3-day treatment with CHIR and Cyc strongly induced mesodermal differentiation of hiPSCs as indicated by the suppression of pluripotency markers (REX1, NANOG, POU5F1, and SOX2) and the specific upregulation of mesoderm markers (T and MIXL1). Osteoblast specification was then

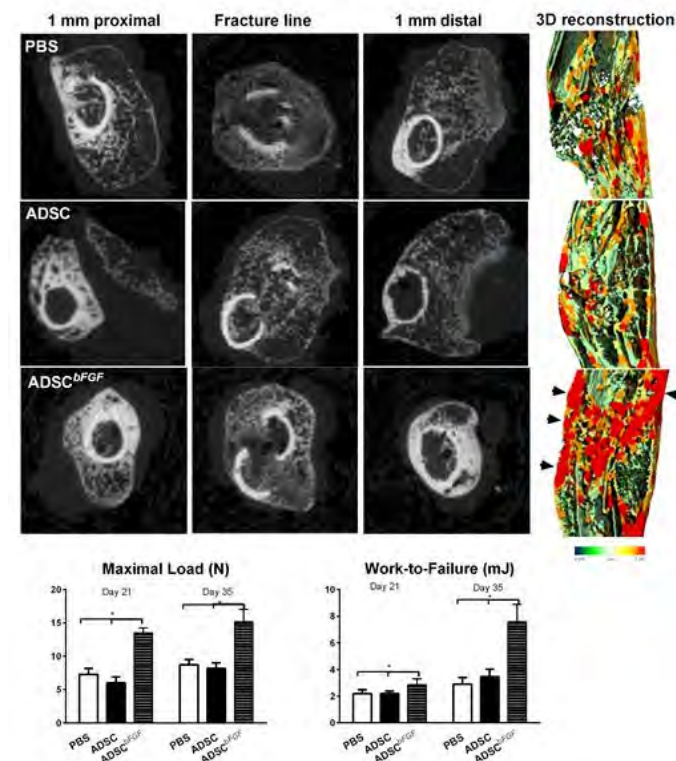
induced by a 7-day treatment with SAG and TH, with cells strongly expressing RUNX2 and COL1A1. Osteoblast maturation was subsequently achieved by the stage-specific manipulation of Hh signaling and the activation of canonical Wnt signaling, as evidenced by the expression of mature osteoblast markers (SP7, IBSP, and BGLAP) as well as by matrix calcification on day 21. Thus, we generated a robust system to differentiate hiPSCs into osteoblasts by properly manipulating signaling pathways involved in osteoblast commitment and maturation. The xeno-free condition, the short period of treatment, and the stability of the inducers in the developed protocol will facilitate its application to the clinical context for skeletal regenerative therapies.

Disclosures: Denise C. Zujur, None.

### SU0132

**Engineering MSC to Overexpress bFGF to Accelerate Fracture Healing.** Hongliang Zhang, Evan Lay, Alexander Kot, Nancy Lane, Wei Yao\*. UC Davis Medical Center, United states

Traumatic fractures during one's lifetime often require hospitalization, surgery, frequent physician visits, and lost time from work. Delayed union or nonunion of bone fragments occurs in about 5%–10% of patients with bone fracture. Thus, there is still an unmet medical need for the healing of fractures and shortening of the time to union. In-depth studies of cellular and molecular mechanisms of bone healing are required for further improvement of procedures aimed at stimulating bone regeneration. In this study, we engineer MSC to over-express bFGF and evaluated its effects on fracture healing. Adipose-derived mouse MSC was transduced to express bFGF and green fluorescence protein (ADSC<sup>bFGF</sup>-GFP). Closed-femoral fractures were performed at the osterix-mCherry reporter mice of both sexes. These mice were then received  $3 \times 10^5$  ADSC transfected with control vector or bFGF via intramuscular injection approximate to the fracture sites. Mice were euthanized at days 7, 14, and 35 to monitor MSC engraftment, osteogenic differentiation, callus formation and bone strength. Compared to MSC culture alone, MSC<sup>bFGF</sup> had increased bFGF expression and higher levels of bFGF and VEGF in the culture supernatant for up to 14 days. ADSC<sup>bFGF</sup> treatment increased GFP-labeled MSCs at the fracture gaps and GFP-MSCs were incorporated into the newly formed callus. qRT-PCR on the callus revealed a 2- to 12-fold increase in gene or protein expressions associated with nervous system regeneration, angiogenesis and matrix formation. VEGF expression was higher at the periosteum region of the callus in mice received MSC<sup>bFGF</sup>. MSC<sup>bFGF</sup> treatment significantly increased remodeling of the collagen into mineralized callus and bone strength (Figure). MSCs engineered to express bFGF expedited fracture healing by increasing directly MSC engraftment to fracture gaps and also via a paracrine mechanism through releasing growth factors such as bFGF and VEGF that supported injury repair. This novel treatment may reduce time for fracture healing. Additional studies are undergoing to further the mechanistic studies and prepare MSC<sup>bFGF</sup> for future clinical applications.



MSC-bFGF-FX

Disclosures: Wei Yao, None.

### SU0133

**Osthole promotes osteoporotic fracture repair by augmenting the recruitment, proliferation and differentiation of muscle-derived stem cells.** Dezhi Tang\*, Weiwei Da, Yongjian Zhao, Lin Chen, Hao Xu, Bing Shu, Qi Shi, Yongjun Wang. Spine Research Institute, Shanghai University of Traditional Chinese Medicine, Shanghai 200032, China, China

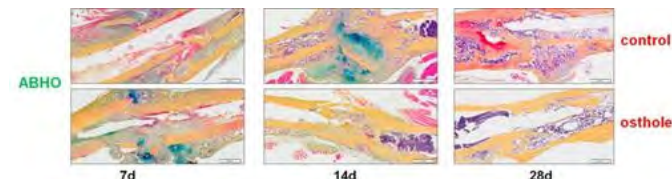
Osthole promotes osteoporotic fracture repair by augmenting the recruitment, proliferation and differentiation of muscle-derived stem cells. De-Zhi Tang<sup>1,2\*</sup>, Wei-Wei Da<sup>1,2</sup>, Yong-Jian Zhao<sup>1,2</sup>, Lin Chen<sup>1,2</sup>, Hao Xu<sup>1,2</sup>, Bing Shu<sup>1,2</sup>, Qi Shi<sup>1,2</sup>, Yong-Jun Wang<sup>1,2,3</sup>

<sup>1</sup> Spine Research Institute, Shanghai University of Traditional Chinese Medicine, Shanghai 200032, China

<sup>2</sup> Longhua Hospital, Shanghai University of Traditional Chinese Medicine, Shanghai 200032, China

<sup>3</sup> Rehabilitation Medical School, Shanghai University of Traditional Chinese Medicine, Shanghai 200032, China

With an aging population, osteoporotic fractures are increasing in incidence. There is currently an urgent unmet need for inducing bone formation as well as improving implant fixation in situations such as hip joint replacement. It has been reported that muscle-derived stromal cells (MDSCs) play an important role in stimulating the fracture repair. In our previous study, we have shown that Osthole could significantly stimulate bone formation and reverse ovariectomized-induced bone loss. Here, using a murine tibial fracture model of 12-month-old wild-type mice, we found that Osthole at the concentration of 5 mg/kg/d accelerated the fracture healing by the ABH/OG staining and enhanced the union strength by the biomechanical analysis. We also found that Osthole increased bone mass of union by the  $\mu$ CT analysis and simulated Runx2 expression in the fracture sites to promote bone formation by the immunostaining. Moreover, we show that Osthole promoted the proliferation and differentiation of MDSCs from the adjacent fracture muscles by the fluorescent immunostaining. We also performed the fluorescent immunostaining and found that Osthole augmented the recruitment of MDSCs to the fracture sites. In addition, we also used MDSCs of human patients with osteoporotic fracture and found that Osthole promoted osteogenic differentiation of MDSCs, demonstrated by increasing the expression of ALP, Runx2 and Osteocalcin in human MDSCs after the treatment of Osthole at low concentrations. These data indicate that Osthole promotes osteoporotic fracture repair by augmenting the recruitment, proliferation and differentiation of MDSCs. Since our findings are based on a combination of an in vivo murine model and human specimens, it may translate to clinical application. Acknowledgement: This work was supported in part by the National Basic Research Program of China (973 Program, 2010CB8530400), the Development Program of Innovation Team of Ministry of Education (IRT1270), the Program of Natural Science Foundation of China (81473701), Outstanding Young Training Plan in Shanghai Health System (XYQ2013085), Shanghai Rising-Star Program (14QA1403500), Scientific Research Innovation Project of Shanghai Education Committee (14YZ051), TCM key projects of science and technology commission of Shanghai(15401917100).



ABH/OG Staining

Disclosures: Dezhi Tang, None.

### SU0134

**Articular cartilage calcification of the hip and knee is independent of age but associated with histological osteoarthritis: evidence for a systemic disorder.** Thelonius Hawellek<sup>1</sup>, Jan Hubert<sup>1</sup>, Sandra Hischke<sup>1</sup>, Jessica Bertrand<sup>2</sup>, Thomas Pap<sup>2</sup>, Matthias Krause<sup>1</sup>, Klaus Püschel<sup>1</sup>, Wolfgang Ruether<sup>1</sup>, Andreas Niemeier<sup>\*1</sup>. <sup>1</sup>University Medical Center Hamburg-Eppendorf, Germany, <sup>2</sup>University Hospital Münster, Germany

**Objectives:** Based on the concept of a systemic predisposition for articular cartilage calcification (CC), the aim of this study was to determine the prevalence and amount of bilateral CC of hip and knee joints in an unselected sample cohort by high-resolution digital contact radiography (DCR) and to analyze the association of CC with histological OA.

**Methods:** Both hip and knee joints of 87 donors (48 m and 39 f; mean age 62) were analyzed by DCR in this post-mortem study of an unselected cohort of donors. Histological OA (OARSI) of the main load bearing area of femoral heads and medial femoral condyles was determined.

**Results:** The prevalence of CC of the femoral head was 96.6%, of the knee 94.3%. Bilateral calcification was detected in 79.3% of hips and 86.2% of knees. Concomitant CC of all four joints was detected in 69.0% of donors. There was no difference between the amount of CC of hips and knees (p=0.47). The amount of CC of any

given hip or knee correlated with that of the contralateral hip ( $r_s=0.54$ ,  $p<0.001$ ) or knee ( $r_s=0.50$ ,  $p<0.001$ ). There was a correlation between the amount of CC and histological OA (hips  $r_s=0.48$ ,  $p<0.001$ , knees  $r_s=0.30$ ,  $p=0.004$ ), but not between CC and age (hips  $r_s=0.09$ ,  $p=0.42$ ; knees  $r_s=0.10$ ,  $p=0.34$ ).

**Conclusions:** These data support the concept that articular CC occurs as the result of a systemic disorder. CC appears to be an early element of hip and knee OA pathogenesis independent of age, suggesting a causal relationship between CC and OA.

**Disclosures:** *Andreas Niemeier, None.*

## SU0135

**NBQX, an AMPA-kainate glutamate receptor antagonist, alleviates degeneration, bone remodelling and inflammation in a model of post-traumatic osteoarthritis.** Cleo Bonnet<sup>1</sup>, Sophie Gilbert<sup>1</sup>, Anwen Williams<sup>2</sup>, Emma Blain<sup>1</sup>, Deborah Mason<sup>\*1</sup>. <sup>1</sup>Arthritis Research UK Biomechanics & Bioengineering Centre, Pathophysiology & Repair Division, School of Biosciences, Cardiff University, United Kingdom, <sup>2</sup>Institute of Infection & Immunity, School of Medicine, Cardiff University., United Kingdom

**Objectives:** Synovial fluid glutamate concentrations increase in arthritis. We have shown that kainate (KA) and AMPA glutamate receptor (GluRs) activation increases interleukin-6 release, that these GluRs localise to osteoarthritic bone and their antagonist (NBQX) reduced bone remodelling in rat inflammatory arthritis. Here, we determined whether NBQX influenced joint degradation and inflammation in anterior-cruciate ligament (ACL) rupture-induced osteoarthritis (OA). We also investigated whether high glutamate concentrations influenced osteocyte-derived mediators of inflammation or remodelling.

**Methods:** For ACL rupture, mouse right knees were loaded and the ACL ruptured (12N). NBQX (20mM) or vehicle was injected (intra-articular) into the loaded knee immediately following ACL rupture (n=5). Knee swelling was measured on days 0, 1, 2, 3, 7, 16, 21. On day 21, mice were culled and knees taken for histology (OARSI score). For cell culture, MLO-Y4 cells ( $1.5 \times 10^6$  cells/ml) were incorporated into acid-soluble rat tail tendon type I collagen (2 mg/ml in MEM, pH7.4) gels with/without MC3T3-E1 ( $1.5 \times 10^5$  cells/well) layered on top and cultured at 37 °C (DMEM 5% dialysed FBS) for 1 week. After glutamate (5, 250 or 500µM) incubation Trizol was added (10, 30, 60 mins; 1,3,24 hrs) for RNA extraction. mRNA expression of cathepsin-K, RANKL, osteoprotegerin, type-1 collagen and IL6 was determined by RT-qPCR of RNA extracted separately from surface osteoblasts and encased osteocytes.

**Results:** After ACL rupture, knee swelling was significantly reduced after NBQX treatment on days 1 ( $P<0.01$ ) and 2 ( $P<0.05$ ) and after day 1 showed no difference to day 0 values. Day 21 joint degradation was reduced following NBQX treatment ( $P<0.001$ ) with the greatest reduction seen in bone remodelling (50% reduction,  $P<0.01$ ). Cathepsin K expression was 100 times greater in MLO-Y4 cells in mono-culture compared to those in co-culture and 10 times greater than MC3T3 expression. The RANKL:OPG ratio was also 100 times greater in mono-culture MLO-Y4 cells compared to MLO-Y4 and MC3T3 cells in co-culture. Glutamate concentration dose dependently reduced mean IL-6 expression and increased RANKL:OPG mRNA expression in MLO-Y4 monocultures.

**Conclusion:** This study provides new evidence that NBQX treatment is effective at relieving inflammation and joint degradation, by influencing bone remodelling in OA. High glutamate concentrations released in OA joints may act on osteocytes to increase RANKL mediated bone remodelling. NBQX shows promise as a new disease-modifying drug that targets bone remodelling in injury-induced osteoarthritis.

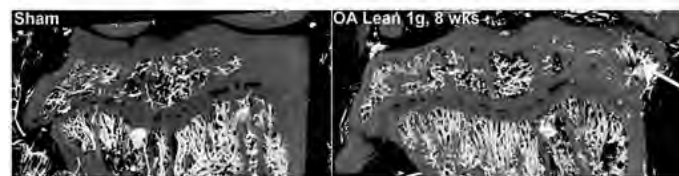
**Disclosures:** *Deborah Mason, None.*

## SU0136

**Obesity and Overweight Exert Specific Effects on Subchondral Bone Structure and Vascularisation in a mouse model of Surgically-Induced Knee Osteoarthritis: Comparing High Fat Diet to Hypergravity.** Damien Cleret<sup>\*1</sup>, Benoit Dechaumet<sup>1</sup>, Bernard Roche<sup>1</sup>, Arnaud Vanden Bossche<sup>1</sup>, Norbert Laroche<sup>1</sup>, Laurence Vico<sup>1</sup>, Xavier Houard<sup>2</sup>, Marie-Hélène Lafage-Proust<sup>1</sup>. <sup>1</sup>INSERMU1059-Université de Lyon, France, <sup>2</sup>INSERM UMR5938, France

Subchondral bone angiogenesis is involved in osteoarthritis (OA) pathophysiology and may respond differently to OA-promoting factors. Obesity is a major risk factor for OA. Our aim was to discriminate the respective role of load increase due to overweight and of metabolic disorders related to fat accumulation in joint deterioration and OA-associated angiogenesis. C57BL/6j male mice were divided into 4 groups (20/group). At 2 months (Mo), one group was fed with high fat diet (HFD 60% fat) to induce insulin-resistance and obesity (Ob) while the 3 others had standard chow (Lean) until the end of the experiment. At 4 Mo, 60 mice (including Ob) underwent surgical destabilization of the medial meniscus (DMM) to induce right knee OA and 20 Lean mice had sham surgery (Sham-Lean). 20 OA-Lean mice were

then submitted to 2g hypergravity (OA-Lean-2g) in a centrifuge (1.4m radius with swinging gondolas, CNES France) to mimic overweight. All other mice were kept at 1g. All groups were killed at 4 or 8 weeks (wks) post DMM. After barium infusion the knee bone and vascular network microstructure was imaged by high resolution µCT (NanoCT, GE, @3µm, Fig Top), and quantified after thresholding (ImageJ software). After resin embedding followed by safraninO/FastGreen staining, quantitative histology was performed. Thus, we compared the respective effects of isolated mechanical load induced by hypergravity (body weight X 2) to those of load combined to metabolic disorders (HFD) on OA severity (cartilage and subchondral bone thickness, Th), epiphysis subchondral bone mass /microstructure and angiogenesis (V Nb /mm<sup>2</sup>) at the medial tibia compartment. Joint cartilage thinning significantly worsened with time with no difference between OA groups at 8 wks (Fig Bottom Table). Hypergravity did not aggravate OA-induced cartilage thinning and prevented OA-related subchondral bone alterations while Ob led to epiphysis trabecular bone loss. OA induced epiphysis bone marrow angiogenesis as early as 4 wks post DMM in both OA-Lean 1g and 2g groups, but not in the Ob group. Obesity and 2g had opposite effects on vessel size. Hypervascularized osteophytes were observed in most of the OA mice at 8 wks (Fig Top Arrow). During post-traumatic OA, obesity and overweight exert specific effects on the subchondral bone plate and the epiphysis bone marrow vascular network. These results should be taken into account when testing molecules targeting bone angiogenesis in order to treat or prevent OA lesions



Data ± SD at 8 weeks	Sham			
	1g	Lean	2g	Ob
Body mass (g)	33±3	33±3	32±2	37±3*
Cartilage Th, µm	40.3 ± 5.3	22.8 ± 6.2***	27.0 ± 4.6***	24.1 ± 3.5***
Subchondral plate Th., µm	56.6 ± 11.0	78.1 ± 12.3*	52.5 ± 17.6†	71.6 ± 14.8*
Epiphysis BV/TV, %	32.1 ± 4.1	29.9 ± 4.3	27.4 ± 5.1	18.7 ± 4.1****
Tb N, /mm	5.73 ± 0.55	5.12 ± 0.66	5.72 ± 0.95 <sup>ns</sup>	3.77 ± 0.69**
Vessel Nb /mm <sup>2</sup>	113.0 ± 27.6	162.3 ± 33.9*	159.8 ± 32.8 <sup>ns</sup>	104.0 ± 23.2†
Vessel Th, µm <sup>2</sup>	18.0 ± 2.7	16.7 ± 2.1	14.4 ± 1.0 <sup>ns</sup>	22.1 ± 3.1**

\*p < .05, \*\*p < .01, \*\*\*p < .001. Vs Sham, \*p < .05, †p < .01, ‡p < .001 vs OA Lean 1g. <sup>ns</sup>p > .05, <sup>ns</sup>p > .001 vs OA Ob.

Top: Fig, Bottom: Table

**Disclosures:** *Damien Cleret, None.*

*This study received funding from: SERVIER*

## SU0137

**Osteonecrosis of the femoral head is associated with low bone mass: a controlled prospective study.** Muhammad Soyfoo<sup>1</sup>, Valérie Gangji<sup>\*1</sup>, Audrey Heuschling<sup>1</sup>, Céline Gillet<sup>2</sup>, Joanne Rasschaert<sup>2</sup>, Rodrigo Moreno-Reyes<sup>1</sup>, Jean-Philippe Hauzeur<sup>3</sup>. <sup>1</sup>Hôpital Erasme, Université Libre de Bruxelles, Belgium, <sup>2</sup>Faculty of Medicine, Université Libre de Bruxelles, Belgium, <sup>3</sup>CHU Sart Tilman, Belgium

Osteonecrosis of the femoral head (ONFH) is characterized by epiphyseal necrosis that can lead to subchondral fracture, femoral head collapse and hip replacement. In Caucasians, the most common risk factors for ONFH are glucocorticoids (GC) use and alcohol abuse. Osteoporosis (OP) and ONFH share common features such as the occurrence of fracture, risks factors (GC and alcohol) and altered bone cells functions.

**Objectives:** This study was undertaken to study BMD in patients with prefractural (stage 1 and 2) and fractural stages (stage 3 and 4) of ONFH and to determine whether ONFH at a fractural stage was associated with an increased prevalence of OP.

**Methods:** We included 243 patients with ONFH and 399 age and sex-matched healthy controls in this prospective controlled trial. Data was gathered including demography, risk factors, ARCO staging of ONFH and bone mineral density (BMD). Patients were stratified according to the staging (prefractal and fractural stages) of ONFH at diagnosis and BMD.

**Results:** Overall, BMD (defined by the T-score) was significantly lower in the ONFH group at both the femoral head ( $-0.96 \pm 1.11$  (SD)) and the lumbar spine ( $-1.22 \pm 1.47$ ) compared to the control group ( $-0.55 \pm 0.97$  and  $-0.73 \pm 1.31$ ) ( $p<0.01$ ). The ONFH group depicted a significantly higher proportion of osteopenia (50.39% vs 40.87%,  $p=0.027$ ) and of OP (18.78% vs 7.33%,  $p<0.001$ ) relative to the control group. Furthermore, we observed that stage 1-2 ONFH patients (53.86%) (but not stages 3-4) were at a higher risk of osteopenia than the control group (40.88%,  $p=0.0203$ ) with an odds ratio of 1.27 (95% CI: [0.78; 2.06]). Moreover, stage 3 and 4 ONFH patients (25.31%) were at a higher risk of osteoporosis (with an odds ratio of 4.89 (95% CI: [2.77; 8.76]) than patients in the stage 1 and 2 group (7.24%,  $p<0.001$ ) and compared to the control group (with an odds ratio of 4.89 7.33%,  $p<0.001$ ).

Multivariate logistic regression showed that the GC use was the only independent factor associated with a higher risk of OP in stage 3-4 ONFH.

Conclusions: This study showed that fractural stages ONFH were associated with a 5-fold risk of osteoporosis. Therefore, the assessment of bone mass appear to be clinically relevant.

Disclosures: Valérie Gangji, None.

## SU0138

**Swedish Farmers Have Higher Risk for Knee and Hip Replacement than Other Occupations.** Helena Johansson<sup>\*1</sup>, Cecilie Hongslo Vala<sup>2</sup>, Anders Odén<sup>3</sup>, Mattias Lorentzon<sup>2</sup>, Eugene McCloskey<sup>3</sup>, John Kanis<sup>3</sup>, Nicholas C Harvey<sup>4</sup>, Stefan Lohmander<sup>5</sup>, Johan Kärrholm<sup>6</sup>, Dan Mellström<sup>2</sup>. <sup>1</sup>Centre for Bone & Arthritis Research (CBAR), Sahlgrenska Academy, University of Gothenburg, Sweden, <sup>2</sup>Centre for Bone & Arthritis Research (CBAR), Sahlgrenska Academy, University of Gothenburg, Sweden, <sup>3</sup>Centre for Metabolic Bone Diseases, University of Sheffield, United Kingdom, <sup>4</sup>IMRC Lifecourse Epidemiology Unit, University of Southampton, United Kingdom, <sup>5</sup>Department of Orthopedics, Clinical Sciences Lund, Lund University, Sweden, <sup>6</sup>Department of Orthopedics, Clinical Sciences, University of Gothenburg, Sweden

**Purpose** Total hip and knee replacement is dependent on economic status, education, urban status and latitude of residence which in Sweden is possible to investigate from national registers. The risk of replacement could also be dependent on physical activity which is a variable that is not available in the registers. Since occupation is available and an occupation that represents high physical activity is farming, the aim of this study was to investigate the risk of hip and knee replacement in farmers in Sweden.

**Material and methods** We studied the risk of hip and knee replacement due to primary osteoarthritis in all men and women aged 40 years or more in Sweden between 1987 and 2002. The population with a documented occupation comprised 3.5 million individuals, of whom 123,300 were farmers. The effects on hip and knee replacement of age, sex, income, education, location of residence and occupation were examined by a modification of Poisson regression.

**Results** 2,703 farmers and 32,676 individuals with other occupations had a knee replacement (5,349 and 63,473 for hip replacement). The risk of knee replacement rose with age, low income, low education, south latitude and rural area for men and women. Farmers are older, have lower income, lower education and live more south and rural than the general population. For women, being a farmer was associated with an increased risk of knee replacement, hazard ratio (HR) 1.83 (95% CI: 1.71, 1.96) age adjusted. For men the risk of knee replacement was doubled compared to other occupations, adjusted for age (HR: 2.01, 95% CI: 1.91, 2.11). For hip replacement the HR was 1.44 (95% CI: 1.35, 1.53) and 2.04 (95% CI: 1.97, 2.11), for men and women respectively. When also adjusted for rural status, income, education and latitude the effect was similar for knee replacement with a HR of 1.56 (95% CI: 1.46, 1.68) for women and 2.02 (95% CI: 1.91, 2.13) for men. For hip replacement the HR was 1.40 (95% CI: 1.31, 1.49) and 2.05 (95% CI: 1.98, 2.13), for men and women respectively. The higher risk for replacement with a farming profession was age-dependent, with higher HR for younger farmers.

**Conclusions** Our results indicate that farming, representing an occupation with high physical activity in men, is associated with a higher risk of hip and knee replacement.

Disclosures: Helena Johansson, None.

## SU0139

**Trabecular Rod and Plate Deficiencies are Distinctly Different in Subchondral Bone in Human Osteoarthritic Knees.** Xingjian Zhang<sup>\*1</sup>, Yan Chen<sup>2</sup>, Yizhong Hu<sup>1</sup>, Y. Eric Yu<sup>1</sup>, Ting Wang<sup>2</sup>, Frankie K. L. Leung<sup>2</sup>, Xu Cao<sup>3</sup>, William X. Lu<sup>2</sup>, X. Edward Guo<sup>1</sup>. <sup>1</sup>Columbia University, United states, <sup>2</sup>The University of Hong Kong, Hong kong, <sup>3</sup>Johns Hopkins University School of Medicine, United states

Osteoarthritis (OA) is a prevalent joint disease, yet the pathogenesis of OA is currently unclear. Recent biologic studies suggest a critical role of the subchondral bone in OA. For instance, uncoupled resorption in subchondral bone induces cartilage degradation and OA in the knee, and blocking this resorption attenuates cartilage damage. Furthermore, our prior work identified the loss of trabecular rods as a consistent microstructural marker in OA development. To further investigate the pathological progression of OA at this level, we examined changes in trabecular plate and rod microstructure between OA and normal knees.

OA (n=78) and healthy control (n=11) tibial plateaus were collected from total knee replacement patients and cadavers with no history of metabolic bone disease or fracture. Samples were scanned by  $\mu$ CT at a voxel size of 17 $\mu$ m. Cubic subregions was selected from subchondral trabecular bone under intact and severely damaged cartilage in OA samples and compared to corresponding anatomic regions in controls. Individual trabecular segmentation was used to analyze trabecular morphology.

We discovered a deficiency in trabecular rods under intact cartilage in OA samples compared to control, which persists in the subchondral bone under severely damaged

regions. Orientation analysis revealed that rod deficiency was uniform in all directions. Conversely, we observed no change in plate bone volume fraction under intact cartilage, but an increase in this parameter under severely damaged cartilage. We also discovered that plates under intact region were preferentially lost in the transverse direction. Furthermore, plate and rod trabecular thickening was observed both under intact and damaged cartilage.

Our observations provide important insights into OA pathogenesis, suggesting that deficiencies in trabecular plates and rods in are distinctly different. In mild OA regions, rod deficiency likely occurs because rods are more vulnerable to resorption, as they have higher surface-to-volume ratio compared to plates. The deficiency of transverse plates is likely a result of unloading in this direction, while the overall higher load placed on the fewer remaining trabeculae initiates thickening. These microstructural changes disrupt the original supporting bed of subchondral bone and create unfavorable mechanical conditions, such as local stress concentration in the cartilage, which could provide a biomechanical basis for the progressive development of OA.

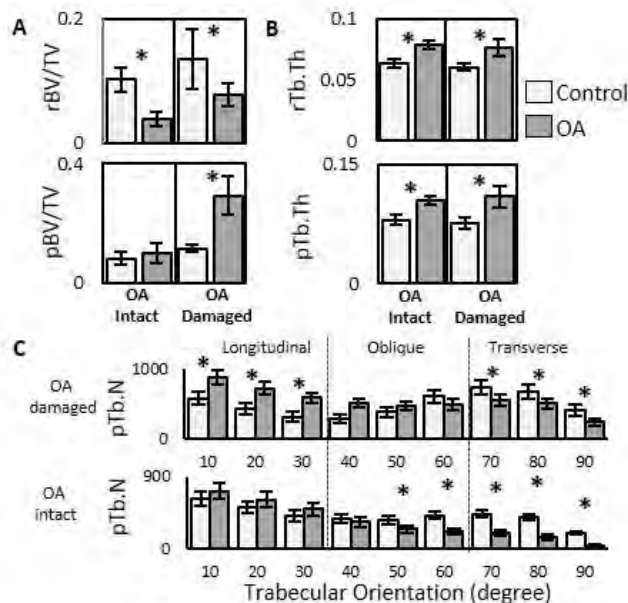


**Figure 1.** (A) rBV/TV and pBV/TV, (B) trabecular thickness of rods (rTb.Th) and plates (pTb.Th), and (C) orientation distribution of the number of trabecular plates (pTb.N) of subchondral trabecular bone under intact cartilage and severely damaged cartilage in terminal OA knees compared to healthy control.

ASBMR abstract figure

Disclosures: Xingjian Zhang, None.

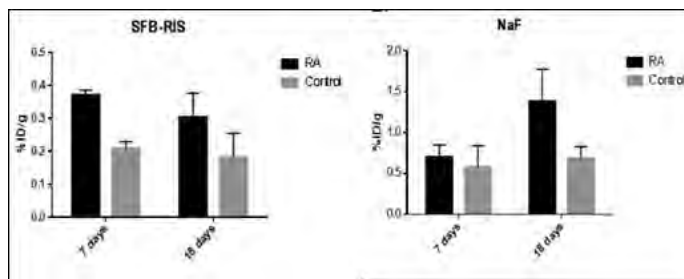
## SU0140

**A Novel Bisphosphonate <sup>18</sup>F-PET Probe for Early Detection of Rheumatoid Arthritis.** Shuting Sun<sup>\*1</sup>, Zibo Li<sup>2</sup>, Eric Richard<sup>1</sup>, Mark Lundy<sup>1</sup>, Mengzhe Wang<sup>2</sup>, Hui Wang<sup>2</sup>, Charles McKenna<sup>3</sup>, Frank Ebetino<sup>1</sup>. <sup>1</sup>BioVinc LLC, United states, <sup>2</sup>Department of Radiology & Biomedical Research Imaging Center, University of North Carolina, Chapel Hill, United states, <sup>3</sup>Department of Chemistry, USC Dornsife College of Letters, Arts & Sciences, United states

Rheumatoid arthritis (RA) is a chronic disease affecting around 1% of the adult population in developed countries. Uncontrolled RA will result in severe joint damage leading to disability, reduced quality of life, and additional sequelae. RA is currently regarded as an incurable disease, and the goal of current therapies is remission of the disease; thus diagnosis at the earliest stage of disease is becoming very important. The workhorse of RA monitoring has been physician assessment of joints assisted by classic radiographical (x-ray) imaging, however, conventional radiography cannot easily detect the earliest disease stages where inflammation is occurring in the soft tissue of the joint and poorly predicts disease progression in these patients. As a result there is a significant clinical need for an imaging method that will reliably show disease activity early in RA. We have developed the first novel bisphosphonate (BP)-based <sup>18</sup>F PET agent capable of detecting early bone destructive activity in animal models of RA.

Specifically, we have developed a pyridinium analog of risedronate, <sup>18</sup>F-RIS-SFB, as a PET imaging probe. In the rat (Lewis rats, 6-12 weeks of age) model of rheumatoid arthritis caused by subcutaneous injection of heat killed *Mycobacterium tuberculosis* (strain H37Ra), we found that the rats displayed clinically visible signs of inflammation in the ankle and paw that became measurable significantly at day 12. The swelling was easily identifiable by day 16, but undetectable in the rats on day 7.

Rats were given a total of 500  $\mu\text{Ci}$  (approximately 0.5 nmole) of freshly prepared  $^{18}\text{F}$ -RIS-SFB by IV injection and imaged on a GE eXplore Vista small animal PET system. Significant ( $P = 0.0002$ ) differences in the bone uptake in these rats were readily detected at day 7 when administered with  $^{18}\text{F}$ -RIS-SFB. In contrast, no bone changes were clearly identified with the control rats administered  $\text{Na}^{18}\text{F}$  until day 18. This first BP  $^{18}\text{F}$ -PET imaging probe successfully detects the presence of early bone involvement, even before visible signs of inflammation in this model. We believe it is identifying erosive activity on bone since  $\text{Na}^{18}\text{F}$ , a marker of bone formation, failed to detect these early signs of bone involvement. We hope such early diagnosis of bone involvement in RA may alter treatment strategies and allow more comprehensive therapy for these patients in the long term.



PET imaging comparison of  $^{18}\text{F}$ -SFB-RIS and  $\text{Na}^{18}\text{F}$  at day 7 and 18

**Disclosures:** Shuting Sun, BioVinc, 14

This study received funding from: BioVinc LLC

## SU0141

**Mechanisms of human mesenchymal stromal cells during bone regeneration are impacted by the associated biomaterial.** Miryam Mebarki<sup>1</sup>, Laura Coquelin<sup>1</sup>, Marine Tossou<sup>2</sup>, Julie Leotot<sup>3</sup>, Philippe Hernigou<sup>4</sup>, Hélène Rouard<sup>1</sup>, Nathalie Chevallier<sup>\*1</sup>. <sup>1</sup>IMRB U955-E10, INSERM, Creteil, France, France, <sup>2</sup>Faculty of Medicine, Paris Est University, Creteil, France, France, <sup>3</sup>Engineering & cellular therapy unit, French Blood Service, Creteil, France, France, <sup>4</sup>Orthopaedic Surgery Department, Henri-Mondor AP-HP Hospital, Creteil, France, France

Despite bone capacity to regenerate after injury, incomplete consolidation concerns 1 million persons per year. Cell engineering involving human bone marrow mesenchymal stromal cells (hBM-MSCs) associated with biomaterials emerge as a new strategy to repair this defect. hBM-MSCs are used for their ability to induce new bone formation. Nevertheless, their mechanisms of action stay poorly known and heterogeneities are observed as a function of the donor but also of the associated scaffold. In our study, we assessed the impact of biomaterials on hBM-MSCs mechanisms during bone regeneration. Two biomaterials commonly used in clinic were studied. The synthetic hydroxyapatite/beta-tricalcium-phosphate scaffold (HA/ $\beta$ TCP) and the biologic gamma-irradiated-processed bone allograft (Tutoplast<sup>®</sup> process Bone [TPB]). To this aim, a 6 weeks time course of biomaterial implanted subcutaneously in SCID mice associated to hBM-MSCs from 3 donors was performed.

Histological analysis showed a significant higher bone and bone marrow formation *in vivo* when hBM-MSCs were combined with TPB. This was associated to a better cell attachment on this biomaterial which can be explained by a larger directly accessible surface area. One day post-graft almost all hBM-MSCs were present on TPB, whereas only half of them were found on HA/ $\beta$ TCP. Cell loss on HA/ $\beta$ TCP does not appear to be due to a higher apoptosis or inflammation. In fact, non-adherent cells migrate to adjacent muscle and skin and disappear after 72 hours while adherent cells survive up to 6 weeks on biomaterials. We then assessed their function *in vivo* and found that hBM-MSCs are able to chemoattract and induce osteogenic differentiation of mouse cells independently of the type of biomaterial. Interestingly, human osteoblastic genes (hRunx2, hBSP and hOC) are significantly more expressed when hBM-MSCs are combined with TPB. In contrast, a higher gene expression of hRANKL associated to a higher osteoclastic activity is observed when cells are grafted on HA/ $\beta$ TCP.

We showed that biomaterials have an impact on grafted cell fate and consequently on the balance between direct osteoblastic differentiation and paracrine osteoclastic activity. This mechanism associated to a better cell survival due to a larger directly accessible surface area, favor bone and bone marrow formation.

In conclusion, the clinical choice of associated scaffold is critical for good bone repair by preserving grafted cells and their osteogenic potential.

**Disclosures:** Nathalie Chevallier, None.

## SU0142

**The Mineral Component of Bone Controls Gene Expression in Migrating Osteoblasts.** Johannes Wischmann<sup>\*</sup>, Philipp Mayer-Kuckuk. Technical University Munich, Germany

Bone formation, for example during bone remodeling or fracture repair, requires mature osteoblasts to deposit bone with remarkable spatial precision. As osteoblast

precursors derive either from circulation or resident stem cell pools, they and their progeny are required to migrate within the three-dimensional bone space and to navigate to their destination, i.e. the site of bone formation. In addition to chemotactic cues, osteoblasts sense other classes of signals and utilize them as landmarks for navigation. The composition of the osseous surface guides adhesion and hence migration efficiency and can also provide steering through haptotaxis. For this study, we hypothesized that the mineral component of the osseous surface provides important signals for migrating osteoblasts. To begin to identify such signals, we decided to screen for changes in global gene expression using gene arrays. Osteoblast migration was assessed on either porcine or human bone seeded with human osteoblast-like cells or primary human osteoblasts. In a first set of experiments, we compared randomly migrating human osteoblasts on native or demineralized bone and identified a unique set of genes with differential expression and a suggested function in cell migration. In a second set of experiments, we compared the first gene expression patterns to cells undergoing migration in chemotactic gradients of TGF- $\beta$ 1, PDGF-BB or VEGF. This enabled us to differentiate between the inherent gene sets necessary for proper osteoblast migration dependent of the mineralization status of the surface and gene sets that function additionally in response to osteoblast chemotaxis. Our findings offer entirely new insights into the role of the mineral components as signal in osteoblast navigation and may have direct clinical relevance in pathologies characterized by altered bone mineral, including osteoporosis.

**Disclosures:** Johannes Wischmann, None.

## SU0143

**Dispensability of Stabilin-1 to the Bone Development and Bone Cell Function.** Seong-Hwan Kim<sup>\*1</sup>, Soon-Young Kim<sup>1</sup>, Eun-Hye Lee<sup>1</sup>, Suk-Hee Lee<sup>1</sup>, Yeon-Ju Lee<sup>1</sup>, Yeo Hyang Kim<sup>2</sup>, Seung-Yoon Park<sup>3</sup>, Jung-Eun Kim<sup>1</sup>. <sup>1</sup>Department of Molecular Medicine, CMRI, BK21 Plus KNU Biomedical Convergence Program, Kyungpook National University School of Medicine, Korea, republic of, <sup>2</sup>Department of Pediatrics, Kyungpook National University Hospital, Korea, republic of, <sup>3</sup>Department of Biochemistry, School of Medicine, Dongguk University, Korea, republic of

Stabilin-1, a transmembrane receptor, regulates molecule recycling and cell homeostasis by controlling intracellular trafficking pathway. In addition, it participates in cell-cell adhesion and transmigration. Stabilin-1 is widely expressed in various organs, including the bone. Stabilin-1 has been detected in the synovial tissue of patients with rheumatoid arthritis and osteoarthritis and in bone marrow macrophages. However, effects of stabilin-1 on the bone have not been studied to date. In this study, the function of stabilin-1 was investigated in the bone by using a Stab1 knockout (Stab1 KO) mouse model. Stabilin-1 was expressed in osteoblasts and osteoclasts. Stabilin-1 expression was almost maintained during osteoblast differentiation but was significantly decreased after osteoclast differentiation. Analysis of the bone phenotype by performing microcomputed tomography showed negligible difference between wild-type (WT) mice and Stab1 KO mice. Bone volume and trabecular thickness and number were almost identical in both groups. Moreover, histological analysis showed no differences in the morphology and arrangement of bone cells between the two groups. To determine whether stabilin-1 affected osteoblast and osteoclast function, the assessment of dynamic histomorphometric indices and the establishment of *in vitro* primary cell cultures were performed. No functional defects in bone formation by osteoblasts and bone resorption by osteoclasts were observed between WT and Stab1 KO mice. Together, these results indicated that although stabilin-1 was highly expressed in the bone cells of mice, its deletion did not affect bone phenotype and bone cell function.

**Disclosures:** Seong-Hwan Kim, None.

## SU0144

**Involvement of the Aryl hydrocarbon receptor in cigarette smoke-induced inhibition of bone regeneration.** Chawon Yun, Michael Schallmo, Ryan Freshman, Andrew George, Joseph Weiner, Danielle Chun, Ralph Cook, Jonghwa Yun, Anjan Ghosh, Erin Hsu<sup>\*</sup>, Wellington Hsu. Department of Orthopaedic Surgery, Northwestern University Feinberg School of Medicine, United states

Cigarette smoking significantly impairs bone regeneration and is associated with higher rates of pseudarthrosis after spine fusion procedures. However, the molecular mechanisms underlying these effects are unclear. Numerous toxic ligands for the Aryl hydrocarbon receptor (Ahr) are present in cigarette smoke, and recent work has implicated the Ahr in mediating the inhibition of osteogenic differentiation. Our previous work with dioxin, a minor constituent of cigarette smoke and high-affinity prototypical ligand of the Ahr, has shown that dioxin-induced Ahr activation inhibits bone regeneration and spine fusion *in vivo*. The purpose of this study was to elucidate the downstream mechanisms underlying the adverse effects of particulate phase extract ("tar"/"PPE") from cigarette smoke on bone regeneration. Bone marrow stromal cells (BMSC) were harvested from Long-Evans rats, and cultured under standard or osteogenic conditions. PPE was prepared by drawing smoke from reference cigarettes through a 0.1  $\mu\text{m}$  PTFE filter and washing the filter in DMSO overnight, yielding a final concentration of 40 mg/mL. Factors critical to osteogenesis

were then evaluated after BMSC were exposed to DMSO vehicle control, 10 nM dioxin (positive control), 0-100 µg/mL PPE, or co-treatment of PPE with one of three Ahr antagonists (4 µM Resveratrol, 2 µM  $\alpha$ -Naphthoflavone, or 10 µM 3'-Diindolylmethane). Endpoints included MTS, ALP activity, mineralization, and osteogenesis-related gene and protein expression. PPE reduced MTS and ALP activities, as well as inhibited mineral deposition compared with vehicle control. PPE treatment led to reduced expression of the pro-osteogenic proteins CXCL12 and RUNX2, as well as increased expression of PARP, a marker of apoptosis. Exposure to PPE also reduced expression of the pro-osteogenic genes *Alp*, *Ocn*, *Runx2*, *Cxcl12*, *Phex*, and *Opn*, as well as increased expression of *Cyp1b1*, a marker of Ahr activation. Co-treatment with each of the three Ahr antagonists generally mitigated these effects. Our results suggest that Ahr activation may play a critical role in the adverse effects of cigarette smoke on bone healing, but that these effects may be reduced with Ahr antagonist co-treatment. Dietary supplementation with Ahr antagonists should be investigated as a therapeutic option to block these inhibitory effects.

**Disclosures:** Erin Hsu, None.

## SU0145

**Jun N-terminal Kinases (JNKs) Act in Osteoblasts to Control Adolescent Bone Formation.** Ren Xu<sup>\*1</sup>, Yeon Suk Yang<sup>2</sup>, Sarfaraz Lalani<sup>2</sup>, Na Li<sup>3</sup>, Roger Davis<sup>4</sup>, Jae-Hyuck Shim<sup>3</sup>, Matthew Greenblatt<sup>3</sup>. <sup>1</sup>Dept of Medicine & Dept of Pathology, Weill Cornell Medical College, Cornell University, United states, <sup>2</sup>Department of Medicine, Weill Cornell Medical College, Cornell University, United states, <sup>3</sup>Department of Pathology & Laboratory Medicine, Weill Cornell Medical College, Cornell University, United states, <sup>4</sup>Program in Molecular Medicine, University of Massachusetts Medical School, United states

The c-Jun N-terminal kinases (JNKs) are members of the mitogen activated protein kinases (MAPKs) and are ancient and evolutionarily conserved regulators of proliferation, differentiation and cell death responses. Currently, *in vitro* studies using chemical inhibitors suggest that JNKs play an important role in osteoblast differentiation but offer conflicting data about whether the JNK pathway augments or represses osteoblast differentiation, and the contribution of JNK to regulation of bone mass *in vivo* remains unclear.

Here we show that *Jnk1*<sup>-/-</sup> but not *Jnk2*<sup>-/-</sup> mice display osteopenia that is most severe during adolescent bone modeling at 3-4 weeks of age. Accompanying this, *Jnk1*<sup>-/-</sup> mice display an occipital-predominant impairment in calvarial mineralization. In order to both confirm that these effects were osteoblast intrinsic and assess whether redundancy with JNK1 masks a potential contribution of JNK2, mice with a conditional deletion of *Jnk1* and *Jnk2* floxed conditional alleles in osteoblasts (*Jnk1*<sup>osx</sup>*Jnk2*<sup>osx</sup>) were bred. These mice displayed a similar degree of osteopenia as *Jnk1*<sup>-/-</sup> mice, suggesting that JNK1 is the major mediator of JNK signaling in osteoblasts *in vivo*.

Consistent with these *in vivo* findings, *Jnk1*<sup>-/-</sup> osteoblasts display a selective defect in the late stages of osteoblast differentiation *in vitro*, with impaired mineralization activity but intact upregulation of alkaline phosphatase. Downstream of JNK1, phosphorylation of JUN and *Fra-1* mRNA levels are impaired in *Jnk1*<sup>-/-</sup> osteoblasts. In order to identify the transcriptional targets of JNK1-regulation, RNA sequencing analysis of *Jnk1*<sup>-/-</sup> osteoblasts was performed, identifying that JNK1 is required for upregulation of several osteoblast-derived proangiogenic factors such as FGF2 and VEGF. Taken together, this study establishes that JNK1 plays a critical role in promoting osteoblast activity both *in vivo* and *in vitro*, displaying a robust contribution to postnatal modeling in both intramembranous craniofacial and endochondral bones.

**Disclosures:** Ren Xu, None.

## SU0146

**Pathologic Minerals of Human Penile Tissues Resemble Alveolar Bone.** Lynn Yang<sup>\*1</sup>, Ling Chen<sup>1</sup>, Feifei Yang<sup>1</sup>, Amanda Reed-Maldonado<sup>2</sup>, Ryan Hsi<sup>2</sup>, Marshall Stoller<sup>2</sup>, Tom Lue<sup>2</sup>, Sunita Ho<sup>1</sup>. <sup>1</sup>Division of Biomaterials & Bioengineering, Department of Preventive & Restorative Dental Sciences, School of Dentistry, United states, <sup>2</sup>Department of Urology, School of Medicine, United states

Peyronie's disease (PD) involves the development of inelastic Peyronie's plaque (PP) in chronically inflamed circumferential layers (tunica albuginea). 3-9% of adult men are affected with PD. PD involves distortion in normal contours of the tissue causing penile deformity during erection. The exact cause of PP is unknown, although minor penile injuries are reported by 1/3 of patients. The etiology of PD and mechanistic link to mineralization from the perspective of regaining function are poorly understood.

Histological and histomorphometric analyses, and mineral density (MD) of volumes of plate-like PP taken from patients (n=7) using conventional stains and high resolution micro-computed tomography were performed. Lower and higher MD values from 926-1257 mg/cc similar to MD of human alveolar bone (570-1415mg/cc) were observed. Morphological features with lower (1.1%) and higher (3.2%) pore densities revealed from X-ray tomography, conventional histology, and electron

microscopy suggested hierarchical and ordered circumferential arrangement of mineralized collagenous matrix – a characteristic measure due to osteon-like features, capillaries, and lacunae within PP. Histological staining with tartrate-resistant acid phosphatase (TRAP), alkaline phosphatase (ALP), picosirius red (PSR), and von Kossa stain of the cryosections confirmed mineralizing osteonal structures similar to that seen in alveolar bone. Energy-dispersive X-ray (EDX) maps of calcium (Ca) and phosphorus (P) at tissue- and fibrillar-levels was suggestive of apatite-based minerals (Figure). The distinct features of large open pores with capillaries in the mineralized PP resemble osteons in alveolar bone. Cells with osteocyte-like configuration were observed in the mineralized structure, and at the interface between fibrous and mineralizing zones of PP.

Based on structural, biochemical, and elemental similarities between PP and alveolar bone, additional studies are needed to understand ossification of the tunica albuginea. Specifically, what are the causes and sources of osteogenic lineage found in PP? Pathological mineralization in other tissues including vasculature and kidney appear to be associated with a re-differentiation of local cells into osteoblasts through shifts in biophysical cues. We hypothesize that function-induced shifts in cyclic loads are the ideal stimuli for intramembranous ossification through differentiation of locally occurring precursors to osteoblastic lineage.

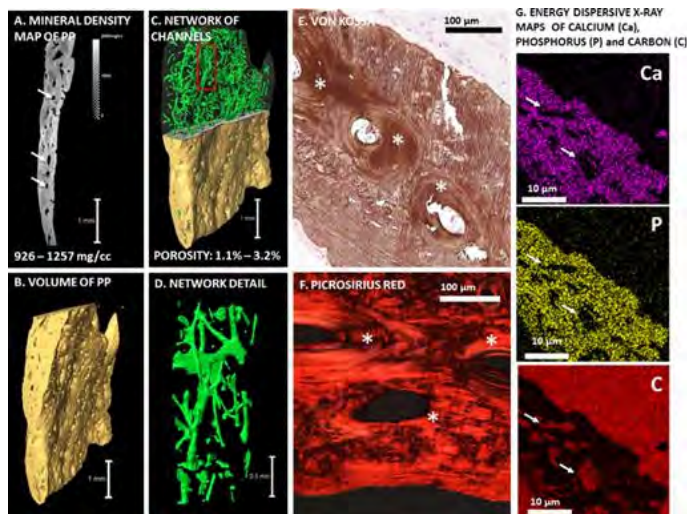


Plate-like Peyronie's plaque (PP) resembles alveolar bone

**Disclosures:** Lynn Yang, None.

## SU0147

**Phosphate-Induced Formation of Mineralization-Competent Matrix Vesicles Is Enhanced by Ca<sup>2+</sup> and cAMP in *in vitro* Models of Osteogenic and Vascular Mineralization.** Sandeep Chaudhary<sup>\*1</sup>, Maria Kuzynski<sup>1</sup>, Elia Benias<sup>2</sup>, Massimo Bottini<sup>3</sup>, Callie Mobley<sup>1</sup>, Jose-Luis Millan<sup>4</sup>, Dobrawa Napierala<sup>1</sup>. <sup>1</sup>Oral & Maxillofacial Surgery, Institute of Oral Health Research, School of Dentistry, University of Alabama at Birmingham, Birmingham, AL, USA, United states, <sup>2</sup>Department of Oral Biology, University of Pittsburgh, Pittsburgh, PA, USA, United states, <sup>3</sup>Department of Experimental Medicine & Surgery, University of Rome Tor Vergata, Rome, Italy, & Inflammatory & Infectious Disease Center, Sanford Burnham Prebys Medical Discovery Institute, La Jolla, CA, USA, United states, <sup>4</sup>Sanford Children's Health Research Center, Sanford Burnham Prebys Medical Discovery Institute, La Jolla, CA, USA, United states

A specific sub-population of extracellular vesicles, matrix vesicles (MV), facilitates mineralization of skeletal and dental tissues. Extracellular vesicles have also been suggested to contribute to ectopic mineralization of blood vessels. MV enriched in tissue-nonspecific alkaline phosphatase (TNAP/ALPL), PHOSPHO1 phosphatase, and PO<sub>4</sub><sup>3-</sup> and Ca<sup>2+</sup> transporters support the formation of hydroxyapatite and thus mineralization. However, the molecular mechanisms regulating MV formation are not well known. Recently, we have demonstrated that phosphate is sufficient to induce MV secretion from the osteogenic 17IIA11 cell line through a mechanism involving activation of Erk1/2. Here, we compared molecular mechanisms of phosphate-induced formation of mineralization-competent MV in the context of physiological and pathological mineralization *in vitro*. Mineralization and formation of mineralization-competent MV were analyzed in osteogenic cell lines (17IIA11, ST2, and MC3T3-E1), vascular aortic smooth muscle cell line (MOVAS), and primary aortic smooth muscle cells. Phosphate signaling was induced by Na-Pi buffer (10mM, pH7.4). MV were isolated from the extracellular matrix by collagenase treatment and characterized by nanoparticle tracking analyses and Western blot. Mineral inside MV was detected using transmission electron microscopy with electron diffraction and atomic force microscopy with phase analyses. Phosphate treatment significantly enhanced the production of MV in all osteogenic and vascular smooth muscle cells.

MV secreted in response to phosphate were 80-200nm in size, which is smaller than apoptotic bodies. Comparison of cleaved caspase-3 in cells grown under standard conditions and treated with phosphate showed no differences, suggesting that phosphate does not induce apoptosis. All analyzed cell types activated Erk1/2 in response to phosphate. Inhibition of Erk1/2 activation resulted in the secretion of fewer MV in 17IIA11 cells. Activation of cAMP-PKA signaling with forskolin and Ca<sup>2+</sup> signaling with CaCl<sub>2</sub> enhanced phosphate-induced MV formation. This was reduced by treatment with PKA inhibitor and Ca<sup>2+</sup> chelators, respectively. However, these inhibitors had no effect on stimulation of MV secretion by phosphate alone. In addition, we demonstrated that MV produced by 17IIA11 cells contained mineral and were positive for TNAP, PHOSPHO1, and annexins, and thus are mineralization competent. Altogether, our results suggest that secretion of MV during the initiation of mineralization is a common process in physiologic and ectopic mineralization and involves similar molecular mechanisms.

*Disclosures: Sandeep Chaudhary, None.*

## SU0148

**Transdifferentiation of MSC-derived osteoblasts following co-culture with MSC-derived adipocytes.** Aline Clabaut\*. PMOI lab, France

In osteoporosis, bone loss is accompanied by an increase of adiposity in bone marrow. A dialogue between adipocytes and osteoblasts is one of the ways occurring in the competition between Mesenchymal Stem Cells (MSCs) lineage commitments, supporting adipocyte differentiation at the expense of osteoblast differentiation. Using an *in vitro* coculture model based on human primary MSCs, we previously shown that MSC-derived adipocytes induce MSC-derived osteoblasts to differentiate towards an adipocyte-like phenotype. Indeed, upon coculture, MSC-derived osteoblasts showed appearance of adipocyte and decrease of late osteogenic mRNA markers. To confirm the co-localization of adipogenic and osteoblastic proteins on a single cell level, we performed double immunofluorescence microscopic analyses. These results clearly showed that at less 10% of the osteoblastic cells expressed the adipogenic marker PPAR $\gamma$ 2, when osteoblasts cells are incubated during 48h with adipocyte conditioned medium. On molecular level, such conversion was confirmed by upregulated expression of reprogramming gene (OCT4). Moreover, whole genome methylation analyses showed that levels of 5-methylcytosine (5-mc) was strongly decreased in osteoblastic cells after co-culture accompanied by changes in the expression profile of enzymes implicated in methylation (TET1 and EZH2). These results confirm transdifferentiation of osteoblastic cells in our co-culture model and suggest that this phenotypic commitment could be controlled by epigenetic mechanisms. This knowledge could help to develop a new and appealing therapeutic strategy for osteoporosis treatment.

*Disclosures: Aline Clabaut, None.*

## SU0149

**A gram positive bacteria membrane component derived lipoteichoic acid induces PGE<sub>2</sub>-mediated inflammatory periodontal bone resorption.** Tsukasa Tominari\*, Kenta Watanabe, Michiko Hirata, Chisato Miyaura, Masaki Inada. Tokyo university of agriculture & technology, Japan

Toll-like receptors (TLRs) are the mold receptors play a critical role in innate immunity and various ligands for TLRs regulate the host defense against the pathogens. We have reported that lipopolysaccharide (LPS), an outer membrane component of gram-negative bacteria, is a potent toxin for inflammatory bone resorption such as periodontitis through TLR4 signaling. The other TLRs, TLR1/2 heterodimer recognizes triacylated lipopeptides from gram-negative bacteria, whereas TLR2/6 heterodimer recognizes diacylated lipopeptides from gram-positive bacteria. We have reported roles of TLR1/2 induced prostaglandin (PG) E<sub>2</sub>-mediated and receptor activator of NF $\kappa$ B ligand (RANKL)-mediated osteoclast differentiation, and that TLR2 heterodimer signaling induced mouse experimental periodontitis *in vivo*. In this study, we examined the influence of lipoteichoic acid (LTA) from gram-positive bacteria, a natural ligand for TLR2/6 heterodimer, on inflammatory bone resorption. In cocultures of mouse primary osteoblast (POB) and bone marrow cell, LTA significantly induced osteoclast differentiation. Further treatment of LTA to osteoclast, LTA directly enhanced its life span. In osteoblasts, LTA increased PGE<sub>2</sub> production in conditioned medium and up-regulated the mRNA expression of membrane bound PGE synthase (mPGES)-1, cyclooxygenase (COX)-2 and RANKL. Indomethacin inhibited LTA-induced RANKL mRNA expression. To compare the LTA induced NF $\kappa$ B activity, the degradation of I $\kappa$ B was measured. LTA promoted degradation of I $\kappa$ B, suggesting RANKL production was increased by NF $\kappa$ B nuclear translocation in osteoblasts. In *ex vivo*, LTA was induced bone resorbing activity in mouse calvarial organ cultures, treatment of COX-2 inhibitor was suppressed its bone resorbing activity. LTA also induced bone resorption in organ cultures of mouse alveolar bone, COX-2 inhibitor was suppressed its bone resorbing activity. In conclusion, LTA induced inflammatory bone resorption through TLR2/6 signaling promoted RANKL expression via mPGES-1- and COX-2- mediated PGE<sub>2</sub> production. LTA may contribute to PGE<sub>2</sub>-mediated inflammatory bone resorption in gram positive bacteria related periodontitis.

*Disclosures: Tsukasa Tominari, None.*

## SU0150

**Inhibition of Neuropeptide Y Y1 Receptor Induces Osteoblastic Differentiation in MC3T3-E1 Cells.** Motoki Yahara\*<sup>1</sup>, Mari Sato<sup>2</sup>, Kiyomi Tsuji-Tamura<sup>2</sup>, Kanchu Tei<sup>1</sup>, Masato Tamura<sup>2</sup>. <sup>1</sup>Oral & Maxillofacial Surgery, Grad. Sch. Dent. Med., Hokkaido University, Japan, <sup>2</sup>Biochemistry & Molecular Biology, Grad. Sch. Dent. Med., Hokkaido University, Japan

The neuropeptide Y (NPY) has known as one of the major neural signaling molecule. In addition, the NPY, produced by peripheral tissues including osteoblasts, binds to its Y1 receptor which belongs to the G-protein coupled receptor family. Osteoblasts-specific Y1 receptor knockout mice revealed a high bone mass that similar the bone phenotype of germline Y1 receptor knockout mice, indicating a role for the NPY-Y1 receptor axis as a regulator of bone homeostasis. We have previously shown that expression of Y1 receptor was induced by bone morphogenetic protein (BMP) 2 signaling during osteoblast differentiation in C2C12 cells. In bone microenvironment, both peripheral nerve fiber and osteoblasts releases NPY. However, the autocrine effects of NPY-Y1 receptor axis on osteoblasts remain unexplored. In the present study, we used an RNA interference approach targeted to Y1 receptor to determine whether NPY-Y1 receptor axis acts as an autocrine for controlling osteoblasts. We found that knockdown of Y1 receptor by siRNA results in induction of ALP activities and mineralization in MC3T3-E1 cells. The mRNA expression level of ALP, osteocalcin, alpha(I) collagen was also increased by inhibition of Y1 receptor via NPY signaling pathway. Although following transfection with Y1 receptor siRNA, Runx2 and osterix gene expression was increased, cell proliferation and caspase3/7 activity did not alter in MC3T3-E1 cells. In the presence of ascorbic acid and  $\beta$ -glycerophosphate, Y1 receptor siRNA dramatically up-regulated ALP activity and mineralization. Moreover, inhibition of Y1 receptor modulated PTH-induced BMP2 gene expression. These results show that Y1 receptor inhibition up-regulates osteoblastic differentiation, suggesting a role for the NPY-Y1 receptor axis as an autocrine mechanism in osteoblasts and of regulator for osteoblastic differentiation.

*Disclosures: Motoki Yahara, None.*

## SU0151

**Neuropeptide Y Induces Hematopoietic Stem/Progenitor Cell Mobilization by Regulating Matrix Metalloproteinase-9 Activity Through Y1 Receptor in Osteoblasts.** Woo-Kie Min\*<sup>1</sup>, Jae-sung Bae<sup>2</sup>. <sup>1</sup>Department of Orthopaedic Surgery, Kyungpook National University Hospital, Korea, republic of, <sup>2</sup>Department of Physiology, Cell & Matrix Research Institute, School of Medicine, Kyungpook National University, Korea, republic of

Hematopoietic stem/progenitor cell (HSPC) mobilization is an essential homeostatic process regulated by the interaction of cellular and molecular components in bone marrow niches. It has been shown by others that neurotransmitters released from the sympathetic nervous system regulate HSPC egress from bone marrow to peripheral blood. In this study we investigate the functional role of neuropeptide Y (NPY) on this process. NPY deficient mice had significantly impaired HSPC mobilization due to increased expression of HSPC maintenance factors by reduction of matrix metalloproteinase-9 (MMP-9) activity in bone marrow. Pharmacological or endogenous elevation of NPY led to decrease of HSPC maintenance factors expression by activating MMP-9 in osteoblasts, resulting in HSPC mobilization. Mice in which the Y1 receptor was deleted in osteoblasts did not exhibit HSPC mobilization by NPY. Furthermore, NPY treatment in ovariectomized mice caused reduction of bone loss due to HSPC mobilization. These results suggest a new role of NPY on HSPC mobilization, as well as the potential therapeutic application of this neuropeptide for stem cell-based therapy.

*Disclosures: Woo-Kie Min, None.*

## SU0152

**PTH-Stimulated Osteogenesis in Human Bone Marrow Stromal Cells Is Inhibited by SAA1 and SAA2 Secreted by Preosteoclasts in a Prostaglandin-Dependent Manner.** Shilpa Choudhary\*, Elizabeth Santone, Mary Beth McCarthy, Michael Francke, Augustus Mazzocca, Carol Pilbeam. UConn Musculoskeletal Institute, UConn Health, United states

In mice, continuous PTH suppresses its own osteogenic effects by stimulating the expression of cyclooxygenase 2 (Cox2) and Rankl in osteoblasts (OBs). The combination of Cox2-produced prostaglandin E<sub>2</sub> (PGE<sub>2</sub>) and Rankl induces preosteoclasts to secrete serum amyloid A3 (Saa3), which then blocks PTH-stimulated cAMP production and OB differentiation. In humans, *SAA3* is a pseudogene, while SAA1 and SAA2, like murine Saa3, are acute phase proteins. This study determined if SAA1 and SAA2 inhibited the osteogenic effects of PTH in human bone marrow stromal cells (hBMSCs). De-identified bone marrow samples were collected from proximal humeri of consenting patients undergoing rotator cuff surgery. Marrow was centrifuged and nucleated cells were cultured in OB differentiation medium with vehicle or PTH (10 nM) for up to 21 days. Cells were treated with NS398, an inhibitor of COX2 activity, or OPG, an inhibitor of RANKL action, from the beginning of culture. Markers of OB differentiation, alkaline phosphatase and osteocalcin, were measured by qPCR, and mineralization, by alizarin red staining. PGE<sub>2</sub> was not

detectable in the medium of vehicle- or NS398-treated cultures. PTH induced *RANKL* expression and formation of osteoclastlike cells in hBMSCs. As seen in murine BMSCs, PTH stimulated OB differentiation only in NS398- or OPG-treated hBMSCs. Genes reported to mediate the anabolic effects of PTH—*IGF1*, *BMP2*, *RUNX2* and *WNT10B*—were elevated by PTH only in OPG- or NS398-treated cultures. The WNT antagonist *DKK1* was inhibited by PTH only in OPG- or NS398-treated cultures. To assess secretion of SAA from preosteoclasts, marrow was expanded with hM-CSF to make bone marrow macrophages (hBMMs), which were treated with RANKL to stimulate osteoclastogenesis. RANKL increased the secretion of SAA1 and SAA2 on days 4-5 of culture prior to the appearance of TRAP+ multinucleated osteoclastlike cells on day 7. RANKL did not increase *SAA1* and *SAA2* expression in NS398-treated cultures. Conditioned medium from RANKL treated hBMMs, but not from RANKL+NS398 treated hBMMs, added to hBMSCs prevented PTH-stimulated OB differentiation. Addition of recombinant SAA1 and SAA2 to hBMSCs in the presence of OPG inhibited PTH-stimulated OB differentiation. We conclude that SAA is a novel means by which preosteoclasts can inhibit PTH-stimulated OB differentiation in hBMSCs. Because SAA proteins can be elevated to high levels during inflammation, they may mediate bone loss associated with inflammation.

**Disclosures:** *Shilpa Choudhary, None.*

## SU0153

**Beneficial Effects of Low Doses of the Phytoestrogen Quercetin on Osteoblastic Cells.** Virginia Lezcano<sup>\*1</sup>, Lilian I Plotkin<sup>2</sup>, Susana Morelli<sup>3</sup>. <sup>1</sup>INBIOSUR UNS, Argentina, <sup>2</sup>Department of Anatomy & Cell Biology, Indiana University School of Medicine, Indianapolis, IN, Roudebush Veterans Administration Medical Center, Indianapolis, IN., United states, <sup>3</sup>INBIOSUR (UNS-CONICET) Departamento de Biol., Bioq. y Fcia., Universidad Nacional del Sur, Bahía Blanca, Argentina., Argentina

Currently, there is a global trend to use natural bioactive compounds such as phytoestrogens (PEs), present in a wide variety of foods, for their beneficial biological effects demonstrated *in vitro* and *in vivo* including antioxidant, anti-inflammatory, anticancer, and antidiabetic activities. PEs are plant-derived non-steroidal compounds that bind to estrogen receptors and have estrogen-like activity. Given that the increase in life expectancy of the population has led to bone health becoming a major concern, in this work we investigated the effects of the PE quercetin (QUE) on the estrogen receptor-positive murine osteoblastic cell line MC3T3-E1. A dose dependent effect of QUE was observed on cell viability after 48 h of exposure, determined by MTS assay; with inhibition of cell viability at 20-100  $\mu$ M concentrations and no change at lower concentrations. In parallel, by trypan blue assay a significant increase in cell number was obtained at 1  $\mu$ M QUE. The wound healing assay show that low doses of QUE stimulate osteoblastic cell migration, with a significant closure at 12h, which further increases after 24h of treatment. Cell migration and proliferation are specific cell functions that require cell attachment and spreading. Using a cell adhesion assay we found a 60% increase in cellular adhesion when cells were treated with 1  $\mu$ M of QUE, and no changes were observed with higher concentrations. QUE is generally considered to have strong antioxidant potency and provides protection against oxidative injury in cultured cells. We found that the pretreatment with 1 or 10  $\mu$ M of QUE for 48h protects against H<sub>2</sub>O<sub>2</sub>-induced toxicity in MC3T3-E1 cells. Altogether, these results indicate that the beneficial effects of QUE on bone formation cells are observed at low doses while high doses of QUE have shown to be deleterious for MC3T3-E1 cells. Furthermore, QUE at high doses increases Erk1/2 and decreases Akt activation, with the consequent increase in the levels of active pro-apoptotic protein BAD, as assessed by Western blot analysis; and blockade of Erk1/2 activity with PD98059 decreases cell death induced by QUE. Based on these findings, we conclude that QUE has positive effects on migration, proliferation, adhesion and antioxidation of osteoblastic cells when it is used at doses lower than 20  $\mu$ M; and may be consider a potential natural therapeutic alternative for bone healing repair in osteopathologies.

**Disclosures:** *Virginia Lezcano, None.*

## SU0154

**Decreased bone density and osteoblast activity in Rad-null mice.** Catherine Withers<sup>\*</sup>, Jonathan Satin, Douglas Andres. University of Kentucky, United states

Rad GTPase, a member of the RGK (Rem, Rad, Gem/Kir) subfamily of Ras-related small G-proteins, has primarily been studied as a potent negative regulator of L-type calcium channel current in the heart, but the role of Rad in bone has not been evaluated. Rad-null mice are smaller in size than wildtype littermates from birth through adulthood, and Rad loss has no effect on gross skeletal development. Microcomputed tomography analysis indicates that Rad depletion leads to a significant reduction in both cortical and trabecular bone density. The total cross-sectional area and the medullary area of Rad-null femurs are larger than wildtype, while the cortical bone area and cortical thickness are significantly reduced and the cortical porosity is significantly higher in Rad-null femurs. Trabecular bone density is also significantly reduced, with Rad-null femurs exhibiting a decrease in trabecular bone volume fraction, a decrease in trabecular number, and an increase in trabecular spacing. Dynamic histomorphometric analysis of Rad-null femurs indicates that the periosteal bone formation rate is slower and the periosteal mineralizing surface is smaller in the absence of Rad. Tartrate-resistant acid phosphatase staining of

osteoclasts is not different in wildtype and Rad-null femur sections, suggesting that the deficits in bone density in Rad-null mice are not due to increased bone resorption. Conversely, expression of osteoblast marker genes is lower in the absence of Rad, suggesting that the bone deficits observed in Rad-null mice may instead be due to depressed bone formation by osteoblasts. In this vein, primary osteoblasts isolated from Rad-null mice exhibit reduced calcium deposition compared to wildtype osteoblasts by alizarin red staining. Together, these data suggest that Rad GTPase is a novel signaling protein involved in osteoblast differentiation and activity.

**Disclosures:** *Catherine Withers, None.*

## SU0155

**Identification of a chemical compound that stimulates osteoblast differentiation and inhibits osteoclast differentiation.** Ju Ang Kim<sup>\*</sup>, Young-Ae Choi, Yong Chul Bae, Hong-In Shin, Eui Kyun Park. Kyungpook National University School of Dentistry, Korea, republic of

Through screening to isolate small molecule that controls bone formation and bone resorption, we found that some compounds strongly stimulated osteoblast differentiation and mineral deposition in human bone marrow mesenchymal stem cells (BMSCs), and inhibited osteoclast differentiation of mouse bone marrow cells. Of some positive compounds, KR-34A induced mineral deposition in a dose dependent manner, and expression of osteoblast marker genes such as *ALP*, *COL1*, *ON*, *OPN*, and *OC*. Analysis of transcription factors that control osteoblast differentiation showed that expression of *RUNX2* and *SP7* were induced by KR-34A. KR-34A also induced transcriptional activation and nuclear translocation of Runx2. In addition, KR-34A induced phosphorylation of p38MAP kinase and ERK, and KR-34A-induced mineral deposition was dramatically inhibited by MEK inhibitors, PD98059 and U0126. U0126 also inhibited expression of RUNX2. Thus, KR-34A stimulation of osteoblast differentiation is mediated through expression, nuclear translocation and transcriptional activation of Runx2 by ERK signaling pathway. On the other hand, KR-34A dose-dependently inhibited osteoclast differentiation as assessed by TRAP staining and activity. Expression of osteoclast marker genes was also significantly inhibited by KR-34A in a dose dependent manner.

Taken together, our data demonstrate that KR-34A stimulates osteoblast differentiation through RUNX2, and inhibit osteoclast differentiation. The data presented in this study strongly suggest that KR-34A has both anabolic and antiresorptive activities, and thus potential candidate molecule for intervention of skeletal disease including osteoporosis, arthritis and osteolysis.

**Disclosures:** *Ju Ang Kim, None.*

## SU0156

**Igfbp2, Inhhb and Sema4f are Wnt3a-inducible in Osteoblasts, Independent of Lrp5/6 receptors.** Aimy Sebastian<sup>\*1</sup>, Nicholas R. Hum<sup>2</sup>, Deepa K. Muruges<sup>2</sup>, Sarah Hatsell<sup>3</sup>, Aris N. Economides<sup>3</sup>, Gabriela G. Loots<sup>2</sup>. <sup>1</sup>UC Merced, School of Natural Sciences, United states, <sup>2</sup>Lawrence Livermore National Laboratories, Physical & Life Sciences Directorate, United states, <sup>3</sup>Regeneron Pharmaceuticals, United states

Wnt signaling is a major regulator of bone metabolism yet, very little is known about the target genes regulated by LRP5/6 mediated Wnt signaling in osteoblasts. To identify genes regulated by canonical Wnt signaling, neonatal calvarial osteoblasts (OB) isolated from *C57Bl6* (*WT*), *Lrp5* knockout (*Lrp5*<sup>KO</sup>) and *Lrp5/6* double knockouts (*Lrp5/6*<sup>KO</sup>) were treated with Wnt3a for 24 hrs and gene expression changes were quantified by RNA-Seq. *Lrp5/6* deficient OBs were generated by treating *Lrp5*<sup>fllox/fllox</sup>, *Lrp6*<sup>fllox/fllox</sup>, *UBC-CreERT2* OBs with tamoxifen *in vitro*; *Lrp5/6* expression was 30% of *WT* levels, in these OBs. In *WT* OB we identified 257 genes including several Wnt pathway members such as *Porcen*, *Fzd1*, *Lef1*, *Tcf7* and *Axin2* as up-regulated and 359 genes including master regulator of chondrogenesis *Sox9* and adipogenesis regulator *Pparg* as down-regulated in response to Wnt3a treatment. Comparison of Wnt3a targets with gene expression data from different stages of osteoblast differentiation suggested that majority of the genes up-regulated by Wnt3a are highly expressed during early stages of osteogenic differentiation and possibly involved in the regulation of osteoblast proliferation/differentiation. Consistent with this, MC3T3 pre-osteoblastic cells treated with Wnt3a displayed a significant increase in proliferation. By comparing *Lrp5*<sup>KO</sup> to *WT* OB we identified 146 genes up and 498 genes down-regulated in *Lrp5*<sup>KO</sup> OB. Only 15 genes identified as Wnt3a targets in *WT* OB showed >1.5 fold up or down-regulation in *Lrp5*<sup>KO</sup> OB relative to *WT* OB. Next, we compared Wnt3a treated *Lrp5*<sup>KO</sup> OBs to sham treated *WT* OBs and found that 76% (469/616) of the Wnt3a targets were >1.5 fold up or down-regulated in *Lrp5*<sup>KO</sup> OBs in response to Wnt3a treatment, suggesting that Wnt3a mediated signaling is largely unaffected by the loss of *Lrp5* in osteoblasts. We identified 162 genes differentially regulated between *Lrp5/6*<sup>KO</sup> OB and *WT* controls. These genes include 33 Wnt3a targets including *Porcen*, *Tcf7* and *Axin2*. Only 34 genes were found to be >1.5 fold up or down-regulated between Wnt3a treated and sham treated *Lrp5/6*<sup>KO</sup> OBs. Interestingly, Wnt3a treatment differentially regulated 15 Wnt3a targets including *Igfbp2*, *Inhhb*, and *Sema4f* in *Lrp5/6*<sup>KO</sup> OB possibly through an *Lrp5/6* independent mechanism, which requires further validation. Altogether, this study has identified several novel Wnt target genes and provides some new insights into *Lrp5/6* dependent Wnt signaling in osteoblasts.

**Disclosures:** *Aimy Sebastian, None.*

## SU0157

**Sexual Dimorphism in the Endothelin Signaling Axis in Bone.** Michael Johnson\*<sup>1</sup>, Luisa Meyer<sup>1</sup>, Heidi-lynn Ploeg<sup>1</sup>, Everett Smith<sup>2</sup>, Karen Hansen<sup>1</sup>, Robert Blank<sup>3</sup>. <sup>1</sup>University of Wisconsin-Madison, United states, <sup>2</sup>University of Wisconsin, United states, <sup>3</sup>Medical College of Wisconsin, United states

Endothelin (ET) signaling is sexually dimorphic. In humans, testosterone increases and estradiol decreases ET1 expression. SNPs in *ECE1*, encoding ET converting enzyme 1, are associated with hypertension in women but not men. We previously showed in congenic mice that a ~3 Mb chromosome segment including *Ece1* displays a sex x genotype interaction for the cross-sectional area (CSA) of the femoral diaphysis. To test the hypothesis that endothelin signaling affects bone differentially in males and females, we performed a 2x3 factorial study of mineralization in cultured TMOB cells. Cells were allowed to mineralize +/- BQ-123, an inhibitor of the EDNRA type receptor, in the presence of dihydrotestosterone (DHT), estradiol (E2), or no added sex steroid. In the absence of BQ-123, sex steroid had no effect on mineralization. In the presence of BQ-123, E2 decreased ( $p < 0.01$ ) and DHT increased ( $p = 0.017$ ) mineralization. BQ-123 and E2 led to an increase of DKK1 secretion, which was not observed with BQ-123 + DHT. In a 2x2 factorial experiment, we exposed femoral head trabecular bone cores from a man and a woman to +/- 15 microns of compressive (3000 micro strain) loading at 2Hz and 120 cycles and +/- BQ-123. There was no significant difference in average change in bone stiffness between male and female cores. In female cores, inhibition of ET1 signaling decreased % change in stiffness in the unloaded blocked group relative to control ( $p=0.025$ ) and the difference between the load only and load blocked groups approached significance ( $p=0.07$ ). In contrast, in male cores, the blockade of ET1 signaling made no difference in bone stiffness over the course of the experiment. Female cores showed a sustained, significant increase of DKK1 secretion in the presence of BQ-123 that was not seen in male cores. Mice in which *Ece1* was ablated globally after birth, or in the osteoblast lineage using an SP7-driven Cre, both displayed decreased femoral BMD in experimental females ( $p=0.028$  and  $0.018$  respectively) but not males. Our data support the existence of differential sensitivity of male and female bone to ET signaling. This difference may contribute to the sexual dimorphism of bone size and fracture susceptibility.

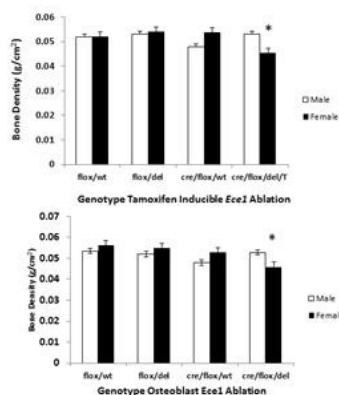


Fig 1. Panel A) Bone densities of mice globally ablated in *Ece1*. Panel B) Bone Densities of mice *Ece1* ablated in the osteoblast lineage.

Abstract Figure

Disclosures: Michael Johnson, None.

## SU0158

**The plant-derived metabolite sulforaphane promotes osteoblastic differentiation by epigenetically reprogramming the phenotypic memory of human mesenchymal stromal cells.** Roman Thaler\*<sup>1</sup>, Farzaneh Khani<sup>1</sup>, Xianhu Zhou<sup>1</sup>, Markus Schreiner<sup>1</sup>, Amel Dudakovic<sup>1</sup>, Allan B. Dietz<sup>2</sup>, Andre J. van Wijnen<sup>3</sup>. <sup>1</sup>Department of Orthopedic Surgery, Mayo Clinic, United states, <sup>2</sup>Department of Laboratory Medicine & Pathology, Mayo Clinic, United states, <sup>3</sup>Departments of Orthopedic Surgery, Biochemistry & Molecular Biology, Mayo Clinic, United states

Skeletal issues that arise from age-related degeneration or injuries require effective repair strategies. Adipose-derived mesenchymal stem/stromal cells (AMSCs) have gained significance, because they can easily be obtained in abundant quantity and are capable of differentiating into osteoblastic cells at low efficiency. Because cell differentiation is largely controlled by modifications in chromatin organization, we examined epigenetic mechanisms that control osteogenic lineage commitment. We have previously shown that the natural compound Sulforaphane (SFN) induces bone anabolic effects in mice by epigenetic mechanisms that mediate active DNA

demethylation. Here, we investigated the translational question whether SFN has potential utility in skeletal tissue regeneration by modulating the differentiation potential of human AMSCs. We find that SFN stimulates expression of osteogenic markers like BGLAP2, RUNX2, COL1A1 and LOX, as well as increases mineralization of the extra cellular matrix after 24 days upon osteogenic induction. Yet, SFN decreases fat droplet formation and expression of the adipose tissue related genes PPARG, PLIN1 or CEBPA. Thus, our results show that SFN significantly shifts the differentiation potential of AMSCs by promoting osteoblastic lineage commitment, while inhibiting adipogenic differentiation. Mechanistically, SFN induces extensive epigenetic reprogramming of the chromatin within 4 to 12 hours after treatment by significant modulation of the expression of 79 epigenetic regulators. Furthermore, the temporal window in which SFN drives AMSCs into a more osteogenic phenotype is limited to the first 12-24 hours after induction of differentiation. SFN establishes a pro-osteogenic and anti-adipogenic memory on the chromatin of these cells, because the phenotypic shift induced by 24 hours SFN treatment endures in control media over multiple cell divisions (i.e., 3 to 4 passages). Collectively, our study shows that the natural compound SFN epigenetically reprograms AMSCs, which retains osteoblastic phenotypic commitment during osteogenic lineage progression, but suppresses the adipogenic phenotype. Therefore, we propose that SFN may be an effective stimulator of bone cell differentiation of mesenchymal stem cells in skeletal regenerative therapies.

Disclosures: Roman Thaler, None.

## SU0159

**A Small Molecular Inhibitor of Lrrk1 Identified by Homology Modeling and Virtual Screening Suppresses Osteoclast Activity but Not Osteoclast Formation.** Helen Goodluck\*<sup>1</sup>, Canjun Zeng, Subburaman Mohan, weirong xing. Musculoskeletal Disease Center, Jerry L. Pettis Memorial VA Medical Center, United states

Targeted knockout (KO) of the *Lrrk1* gene in mice causes severe osteopetrosis due to dysfunction of osteoclasts (OCs), and a human mutation of *Lrrk1* leads to osteosclerotic metaphyseal dysplasia in long and short tubular bones. While bone resorption (BR) was reduced dramatically, bone formation (BF) was not affected in the *Lrrk1* KO mice. *Lrrk1* KO mice responded normally to PTH anabolic treatments but were resistant to ovariectomy-induced bone loss. These observations make *Lrrk1* an attractive antiresorptive drug target because *Lrrk1* KO mice have normal membranous bone and inhibiting *Lrrk1* may not interfere with OC-coupled BF in the maxilla and mandible or cause osteonecrosis of the jaw. In this study, we used TGF $\beta$  activation kinase 1 as a template to build a 3D structure of the *Lrrk1* kinase domain (KD) using the ESyPred3D homology modeling program and identified an active pocket in the KD with Molsoft 3.7. A total of 16,000 compounds from the Chembridge database were screened by docking to the active pocket. Four inhibitors that docked into the pocket with high scores were chosen for evaluation of biological effects on OCs *in vitro*. Treatment of OC precursors with 5  $\mu$ M IN01 and IN02 but not IN03 or IN04 significantly inhibited OC formation. In a BR pit assay, IN04 at 1-10  $\mu$ M caused a dose-dependent inhibition of pit area with a maximum of 75% inhibition ( $P < 0.01$ ) at 10  $\mu$ M vs vehicle controls. To examine the mechanism for IN04's effect, OCs were stained with Alexa Fluor 488-phalloidin after IN04 or vehicle treatment for visualization of actin ring formation and sealing zones by confocal microscopy. Vehicle-treated OCs displayed a typical appearance with clear actin ring formation. Cross sections of OCs revealed that clustered F-actin forms a peripheral sealing zone from both views. In contrast, IN04-treated OCs showed diffused F-actin in the cytoplasm that failed to form peripheral sealing zone on bone slices. The phenotypic features of mature OCs treated with IN04 are very similar to the dysfunctional OCs derived from *Lrrk1* KO mice, suggesting the inhibitor may suppress OC activity via inactivating *Lrrk1* function. Accordingly, IN04 at 16 nM completely blocked ATP binding to *Lrrk1* KD and inhibited *Lrrk1* kinase activity as determined by ATP binding and kinase assays *in vitro*. We conclude that IN04, a small molecular inhibitor identified by homology modeling of *Lrrk1* KD, is a potent inhibitor of *Lrrk1* kinase and thereby suppresses osteoclastic BR *in vitro*.

Disclosures: Helen Goodluck, None.

## SU0160

**Alveolar Bone Loss is Significantly Diminished in the SH3BP2 Loss-of-function Mouse Model of Periodontitis.** Mizuho Kittaka\*<sup>1</sup>, Collin Schlosser, Kotoe Mayahara, Yasuyoshi Ueki. University of Missouri-Kansas City, School of Dentistry, United states

Gain-of-function mutations in the SH3-domain binding protein 2 (SH3BP2), a signaling adapter protein widely expressed in myeloid cells, are responsible for a craniofacial genetic disorder, Cherubism (OMIM#118400). Our previous study showed that loss-of-function of SH3BP2 protects against inflammatory bone loss in collagen-induced and TNF- $\alpha$  overexpression mouse models of inflammatory arthritis. Since periodontitis is a chronic inflammatory disease that causes tooth loss by mechanisms that reduce alveolar bone volume, we hypothesized that the lack of SH3BP2 would protect against bone loss in a mouse periodontitis model.

Periodontitis was experimentally induced in *Sh3bp2*<sup>-/-</sup> and wild-type control (*Sh3bp2*<sup>+/+</sup>) mice by tying a 5-0 silk suture around the maxillary left second molar. Maxillae were collected and subjected to micro-CT scanning at 5 days after suture

placement. Alveolar bone volume underneath the second molar was quantified and the ratio of alveolar bone volume on the ligated side compared to the contralateral unligated side was calculated to assess bone loss. Histomorphometric analysis was performed to quantify osteoclast numbers on alveolar bone surface (N.Oc/BS). mRNA expression of inflammatory cytokines including TNF- $\alpha$ , IL-1 $\beta$ , and IL-6 as well as cytokines that regulate osteoclast formation such as RANKL and OPG were analyzed by qPCR using RNA samples isolated from gingival tissues.

Micro-CT analysis showed that lack of SH3BP2 reduced the rate of alveolar bone loss compared to the unligated side in *Sh3bp2*<sup>-/-</sup> mice (female: 17.3  $\pm$  5.8%, n=5; male: 10.2  $\pm$  10.8%, n=4) compared to *Sh3bp2*<sup>+/+</sup> mice (female: 29.5  $\pm$  2.7%, n=3; male: 28.8  $\pm$  0.71%, n=3). Osteoclast numbers showed no significant difference (9.0  $\pm$  2.1/mm in *Sh3bp2*<sup>-/-</sup>, n=8 vs. 9.6  $\pm$  3.0/mm in *Sh3bp2*<sup>+/+</sup>, n=6). qPCR analysis showed equivalent expression levels of *Tnf* and *Il1b* or even higher levels of *Il6* and *Rankl*/*Opg* ratio in *Sh3bp2*<sup>-/-</sup> mice compared to *Sh3bp2*<sup>+/+</sup> mice.

Sensitivity to the alveolar bone loss induced by periodontitis was diminished in *Sh3bp2*<sup>-/-</sup> mice, while mRNA expression of inflammatory cytokines was not suppressed. Furthermore, expression of osteoclastogenesis-related genes and osteoclast numbers were comparable to *Sh3bp2*<sup>+/+</sup> mice. These data suggest that SH3BP2 plays a role in alveolar bone loss by suppressing osteoclast activation and identify SH3BP2 as a novel regulator of pathological alveolar bone resorption in periodontitis and a potential target for therapeutics.

**Disclosures:** Mizuho Kittaka, None.

## SU0161

**Bone-Targeted Chloroquine Inhibits Osteoclastogenesis and Bone Resorption More Effectively Than Chloroquine.** Zhenqiang Yao<sup>\*1</sup>, Xiaodong Hou<sup>2</sup>, Wei Lei<sup>2</sup>, Lifeng Xiao<sup>3</sup>, Frank H. Ebetino<sup>4</sup>, Robert K. Boeckman<sup>3</sup>, Brendan Boyce<sup>1</sup>. <sup>1</sup>University of Rochester Medical Center, United states, <sup>2</sup>Henan University First Affiliated Hospital, China, <sup>3</sup>University of Rochester, United states, <sup>4</sup>BioVinc LLC, United states

Chloroquine (CQ), a widely used anti-malarial drug, is still used for treatment of rheumatoid arthritis in some parts of the world. We recently reported that CQ inhibits osteoclast (OC) formation by preventing TRAF3 degradation. A concern with long-term treatment of patients with CQ is its adverse effects including retinal toxicity and blindness. A strategy is to administer CQ in a form that targets it to bone, thus allowing it to be given to patients at reduced doses with a lower risk of adverse effects, while delivering effective concentration preferentially to bone. We synthesized a novel bone-targeted CQ (BTCQ) by linking CQ to a bisphosphonate (BP) with a high affinity for bone but no anti-OC activity. We found that 1  $\mu$ M BTCQ inhibited OC and resorption pit formation as effectively as 3  $\mu$ M CQ. To study if BTCQ binds to bone to exert its antiresorptive effects, we incubated bone slices overnight with 0, 10, 30 and 100  $\mu$ M BTCQ or CQ. The bone slices were transferred to wells in new plates to culture OCs from mouse bone marrow cells. We found that bone slices incubated with 10, 30 and 100  $\mu$ M BTCQ had a dose-dependent, significantly reduced resorption pit area (0.22  $\pm$  0.01, 0.20  $\pm$  0.01, and 0.05  $\pm$  0.01 mm<sup>2</sup>/bone slice, respectively) compared to those incubated with similar doses of CQ (0.24  $\pm$  0.01, 0.22  $\pm$  0.01, and 0.23  $\pm$  0.01 mm<sup>2</sup>, respectively) versus 0.25  $\pm$  0.01 mm<sup>2</sup> in vehicle-treated slices. A form of BTCQ designed such that the linker was not cleavable had no significant effect on resorption pit formation. Furthermore, BTCQ inhibited RANKL-induced TRAF3 degradation more effectively than CQ. Finally, we treated WT mice with BTCQ or CQ (2, 15 or 50 mg/kg) for 10 days and gave PTH injections (10 $\mu$ g, 3x/day) during the last 3 days. PTH increased OC formation in tibial sections (361 $\pm$ 74/mm<sup>2</sup> vs. 97 $\pm$ 26/mm<sup>2</sup> in vehicle-treated controls). Only high dose (50 mg/kg; not 15 and 2 mg/kg) CQ inhibited PTH-induced OC formation (189 $\pm$ 55, 312 $\pm$ 84 and 367 $\pm$ 75 OCs/mm<sup>2</sup>, respectively), while BTCQ (as low as 2 mg/kg) effectively prevented PTH-induced OC formation (125 $\pm$ 52/mm<sup>2</sup>). In summary, BTCQ can efficiently bind to bone matrix and release sufficient CQ to inhibit OC formation and bone resorption both in vitro and in vivo by preventing TRAF3 degradation more effectively than CQ. Thus, BTCQ is a novel and potentially safer bone selective anti-resorptive agent for the prevention of bone loss in diseases characterized by increased OC formation.

**Disclosures:** Zhenqiang Yao, None.

## SU0162

**Osteoclasts from L-plastin Null Mice are Defective in Sealing Ring Formation and Bone Resorption.** Meenakshi Chellaiah<sup>\*1</sup>, Tao Ma<sup>1</sup>, Celeste Morley<sup>2</sup>, Sunipa Majumdar<sup>3</sup>. <sup>1</sup>University of Maryland, Dental School, United states, <sup>2</sup>Washington University School of Medicine, Pediatric Research, United states, <sup>3</sup>University of Maryland Dental School, United states

Background: Bundling and stability of actin filaments comprise a fundamental step in sealing ring formation in osteoclasts (OCs). An actin bundling protein L-plastin (LPL) was shown to have a role in the cross linking of actin filaments into tight bundles. This increase their stability by protecting them against depolymerization. We have identified the role of LPL in the formation of actin aggregates [indicated as Nascent Sealing Zones (NSZs)] during the early phase of sealing ring formation by OCs on bone surface. LPL phosphorylation on serine residues (S5 and

S7) by TNF- $\alpha$  signaling regulates this assembly. Here, we used LPL knock-out (LPL<sup>-/-</sup>) mice model to show the key role of LPL in the assembly of NSZs.

Methods: OCs derived from bone marrow cells of wild type (WT) and LPL<sup>-/-</sup> mice (C57/BL6 strain) were used. Short term time-lapse video recordings at 3-4 h and 8-12 h and actin staining/ confocal microscopy analyses were used to demonstrate the formation of NSZs and mature sealing rings in OCs cultured on dentine slices. Bone resorption assay in vitro was also performed.

Results: LPL deficiency did not affect OC differentiation, podosome assembly/ disassembly and migration in vitro. NSZs and mature sealing rings were observed at 3-4 h and 8-12h, respectively in WT OCs cultured on dentine slices in the presence of TNF- $\alpha$ . LPL deficiency produces OC dysfunction due to a defect in the formation of NSZs. As a result, these OCs are hyporesorptive in nature and hence made superficial resorption pits in vitro. Transduction of TAT-fused full-length LPL (FL-LPL) peptide into LPL<sup>-/-</sup> OCs rescued the formation of NSZs and sealing rings in a time-dependent manner. This response was not observed with a control peptide. Localization of integrin  $\alpha$ v $\beta$ 3 and cortactin was observed in the NSZs of WT OCs in a time-dependent manner. An inhibitor to integrin  $\alpha$ v or a siRNA to cortactin did not affect the formation of NSZs; however, affected the formation of mature sealing rings.

Conclusions: Podosome formation is LPL-independent. The formation of NSZs and mature sealing rings appears to be podosome-independent. However, NSZs formation is LPL-dependent. NSZs function as a platform from which maturation of sealing ring occurs. Localization of integrin  $\alpha$ v $\beta$ 3 in NSZs and activation of integrin-mediated signaling regulates the maturation of NSZs to sealing rings. LPL plays a novel role at the early phase of sealing formation and is a new/novel target for anti-osteoporosis therapy. [Supported by R01-NIH-NIAMS 5R01AR066044]

**Disclosures:** Meenakshi Chellaiah, None.

## SU0163

**Slow and Fast Bone Resorption Modes of Human Osteoclasts Revealed by Time-lapse Recording.** Kent Soe<sup>\*</sup>, Jean-Marie Delaisse, Vejle Hospital/ University of Southern Denmark, Denmark

The mechanism responsible for the formation of resorption lacunae by osteoclasts (OCs) is commonly ascribed to a "resorption cycle", which consists of successive resorption and migration episodes. In this model the OC is stationary during resorption and displays a firmly attached actin ring making round resorption pits. However, OCs also make long and deep cavities appearing as trenches that are difficult to conciliate with this model. Here we follow the generation of both types of cavities in real-time and found that trenches reflect a "super-resorption" mode compared to pits. OCs generated from male blood donors were seeded on rhodamine-labeled cortical bone slices and incubated with SiR-Actin allowing visualization of F-actin of live cells. Time-lapse recordings were made with a confocal microscope on four OC preparations, taking pictures at 20 min intervals for 40 to 72h. A total of 219 resorbing OCs were monitored. About 39% did not move on the bone surface while resorbing, thus generating a pit, and of those 2/3 made only a single pit while 1/3 made multiple pits, in line with the classical resorption model. The other 61% of the OCs glided over the bone surface while continuously resorbing, thus generating trenches. However, 80% of these trench-forming OCs started by making a pit and subsequently switched to horizontal resorption extending the trench from one side of the pit. Importantly, once trench formation was initiated, it only rarely stopped (11%), whereas pit formation stopped after 14.5h on average. Even more important, the erosion rate of a trench-forming OC was on average 2.3 times faster, compared with pit-forming OCs. Accordingly, an OC making a trench eroded a four times larger surface than an OC making a pit in our experiments. Considering the recent report showing that trenches are deeper than pits it can be estimated that the trench-mode removes bone volume at a 3.2 times faster rate than the pit-mode. In conclusion, these data demonstrate the existence of a much more aggressive OC resorption mode compared with the well-known resorption model generating pits: it is characterized by trench-forming OCs, which resorb at a higher rate, without interruption and over larger areas. Interestingly, OCs can switch from pit- to trench-mode but apparently not back again. These results highlight the need of categorizing the OCs according to their resorption mode when evaluating their resorptive power and the impact of various drugs and conditions.

**Disclosures:** Kent Soe, None.

## SU0164

**TGF- $\beta$ 1 Liberated through Osteoclast-mediated Bone Resorption Regulates Odontoblast Differentiation and Tooth Root Formation.** Jue Wang<sup>\*1</sup>, Li Cao<sup>2</sup>, Wei Chen<sup>2</sup>, Hongbing Jiang<sup>2</sup>, Zheng Zhu<sup>2</sup>, Zhihe Zhao<sup>3</sup>, Yi-Ping Li<sup>2</sup>. <sup>1</sup>Department of Pathology, University of Alabama at Birmingham; State Key Laboratory of Oral Diseases, Department of Orthodontics, West China Hospital of Stomatology, Sichuan University, United states, <sup>2</sup>Department of Pathology, University of Alabama at Birmingham, United states, <sup>3</sup>State Key Laboratory of Oral Diseases, Department of Orthodontics, West China Hospital of Stomatology, Sichuan University, China

Tooth root is essential for normal physiological function of the tooth, and a healthy root provides reliable foundation for restoration as required clinically. The mechanism underlying how tooth root formation is regulated remains unclear. We

hypothesized that the growth factor(s) liberated from osteoclast (OC)-mediated bone resorption regulate tooth root formation. To test this hypothesis, we used our previously generated *Atp6i* deficient (*Atp6i*<sup>-/-</sup>) mice as a human osteopetrosis disease model. *Atp6i*<sup>-/-</sup> mice showed defective osteoclast function and no root formation and eruption as seen in human osteopetrosis with *ATP6i* mutation. Our result showed that *Atp6i* deficiency largely impaired the proliferation and differentiation of root odontogenic cells. Expressions of nuclear factor I-C (NFIC), osterix and dentin sialoprotein, markers for root-odontoblast differentiation, were all largely decreased in odontoblasts of tooth root formation lesions in *Atp6i* deficient mice. Notably, the activation of Smad2/3 (pSmad2/3) signaling pathway was significantly abrogated, indicating that transforming growth factor- $\beta$  (TGF- $\beta$ ) signaling was attenuated in *Atp6i*-deficient odontoblasts. Our result showed that active TGF- $\beta$ 1 level was barely detectable in *Atp6i*<sup>-/-</sup> OC bone resorption-conditioned medium (BRCM) but was high in WT OC BRCM. To test whether TGF- $\beta$ 1 liberated from OC-mediated bone resorption regulates odontoblast differentiation, we cultured pre-odontoblasts cells with the conditioned medium from *Atp6i*<sup>-/-</sup> or WT OCs and found that odontoblast differentiation and Smad2/3 activation were drastically abrogated in *Atp6i*<sup>-/-</sup> conditioned medium as compared with that in conditioned medium from WT OCs. Consistently, TGF- $\beta$ 1 depletion using anti-TGF- $\beta$ 1 antibody neutralization in WT OC BRCM completely compromised the ability of WT OC BRCM to induce odontoblast differentiation. Collectively, our data indicate that TGF- $\beta$ 1 liberated from OC-mediated bone resorption is essential for tooth root formation, and poor tooth eruption and root development in human osteopetrosis patients may result from failure of liberating TGF- $\beta$ 1 from alveolar bone matrix due to dysregulated OC function and impaired bone resorption, bone formation and dentin formation triple coupling. These findings provide important insights into the cellular and molecular mechanisms of tooth root development and formation in both physical and pathological condition, and may also provide effective therapeutic strategies.

**Disclosures:** Jue Wang, None.

## SU0165

**4-phenylbutyric Acid Decreases Osteoclastogenesis via Modulating Autophagy.** HS CHOI\*. University of Ulsan, Korea, republic of

Osteoclasts contribute mainly to bone resorption in inflammatory joint diseases. Destruction of bone has been frequently accompanied by infection and chronic inflammation. LPS stimulates inflammatory bone loss via recruitment of inflammatory cells, generation and activation of proinflammatory cytokines. 4-phenylbutyric acid (4-PBA) approved by FDA has been known to act as an ammonia scavenger, histone deacetylase inhibitor and ER stress inhibitor. 4-PBA inhibited the formation of large osteoclasts (>20 nuclei) induced by LPS in RANKL-pretreated preosteoclast, although it did not affect total number of TRAP-positive multinuclear osteoclasts (MNCs). 4-PBA significantly decreased secreted level of cathepsin K, resulting in reduced bone resorption, compared with LPS only. Interestingly, 4-PBA inhibited autophagy flux activity, the lipidation of microtubule-associated protein light chain 3 (LC3) (conversion of LC3I to LC3II) and ATG4B that were induced upon LPS stimulation in osteoclast. Our findings suggest that 4-PBA inhibits LPS-induced OC formation via modulating autophagy. This work was supported by the Basic Science Research Program (2015R1A2A2A01002417; 2014R1A6A1030318) and the Bio & Medical Technology Development Program of the NRF (2012M3A9C3048683) funded by the Korean government.

**Disclosures:** HS CHOI, None.

## SU0166

**Follistatin-like 1 promotes osteoclast formation via RANKL-mediated NF- $\kappa$ B activation and M-CSF-induced precursor proliferation.** Hyun-Ju Kim\*<sup>1</sup>, Woo Youl Kang<sup>1</sup>, Sook Jin Seong<sup>1</sup>, Shin-Yoon Kim<sup>2</sup>, Young-Ran Yoon<sup>1</sup>. <sup>1</sup>Department of Biomedical Science, Cell & Matrix Research Institute, BK21 Plus KNU Biomedical Convergence Program, Clinical Trial Center, School of Medicine, Kyungpook National University & Hospital, Korea, republic of, <sup>2</sup>Skeletal Diseases Genome Research Center, School of Medicine, Kyungpook National University, Korea, republic of

Follistatin-like 1 (FSTL1) functions as a pivotal modulator of inflammation and is implicated in many inflammatory diseases such as rheumatoid arthritis. Here, we report that FSTL1 is strongly upregulated and secreted during osteoclast differentiation of bone marrow-derived macrophages (BMMs) and that FSTL1 positively regulates osteoclast formation induced by RANKL and M-CSF. The overexpression of FSTL1 or treatment with recombinant FSTL1 (rFSTL1) in BMMs enhances the formation of multinuclear osteoclasts and the induction of c-Fos and NFATc1, transcription factors important for osteoclastogenesis. Conversely, knockdown of FSTL1 using a small hairpin RNA suppresses osteoclast formation and the expression of these transcription factors. While FSTL1 does not affect RANKL-stimulated activation of p38 MAPK, phosphorylation of I $\kappa$ B $\alpha$ , JNK, and ERK were increased by overexpression or addition of rFSTL1. Furthermore, rFSTL1 increased RANKL-induced NF- $\kappa$ B transcriptional activity in a dose-dependent manner. In addition to its role in osteoclastogenesis, FSTL1 promotes proliferation of osteoclast precursors by increasing M-CSF-induced ERK activation, which in turn leads to accelerated osteoclast formation. Together, our findings demonstrate that FSTL1 is a secreted

osteoclastogenic factor that plays a critical role in osteoclast formation via the NF- $\kappa$ B and MAPKs signaling pathways.

**Disclosures:** Hyun-Ju Kim, None.

## SU0167

**Functional Role of Hedgehog Signaling in Osteoclast Lineage.** Ryuma Haraguchi\*<sup>1</sup>, Riko Kitazawa<sup>2</sup>, Yuuki Imai<sup>3</sup>, Sohei Kitazawa<sup>1</sup>. <sup>1</sup>Ehime University Graduate School of Medicine, Japan, <sup>2</sup>Ehime University Hospital, Japan, <sup>3</sup>Ehime University Proto-Science Center, Japan

**Background:** *The osteolytic bone lesion* is one of the representative histopathological features in paraneoplastic syndromes. Cancer-derived secretory factors in the bone microenvironment directly or indirectly induce activation of osteoclasts and lead to disturbance in the balance between bone formation and bone resorption. Previous studies have shown that Hedgehog (Hh) ligands, signaling molecules essential for various organogenesis and physiological homeostasis, secreted by tumor cells induce osteoclast differentiation and enhance the activity of mature osteoclasts. The paracrine Hh signal from cancer cells regulates a RANK-RANKL signaling axis through the directional activation of transcriptional factor Runx2, which consequently and indirectly augments osteoclastic activity with the up-regulation of bone resorption markers, MMPs, TRACP and cathepsin K, on the osteoclastic lineage. The direct influence of Hh signaling on osteoclasts is, however, still unknown. To investigate the functional significance of the hedgehog signaling pathway in osteoclasts, we generated the osteoclast lineage-specific deletion mutant of Smoothened (Smo), a cell surface Hh signal downstream effector, with the use of a knock-in Cre mouse line to the *LysM* gene locus (*LysMcre*; *Smo* flox/flox mouse).

**Finding:**  $\mu$ CT analysis of long bones revealed that the trabecular bone volume fraction (BV/TV) and thickness (Tb.Th) in *LysMcre*; *Smo* flox/flox mice increased compared with those in control mice. These bone phenotypes became evident in 6-week-old, and then the most remarkable phenotypes were observed by 35-week-old. Immunohistological analysis of mutant trabecular bones confirmed the reduced number of cathepsin K-positive osteoclasts. On the other hand, no difference was observed in the number of Osterix-positive osteoprogenitor cells between control and mutant trabecular bones.

**Conclusion:** Inactivation of the *Smo* gene in osteoclastic lineages resulted in increased trabecular bone mass with decreased bone resorption attributed to reduced osteoclastogenesis. These findings raise the possibility that the Hh signal acts as a positive regulator of osteoclastogenesis through direct influence on the monocytic-macrophage lineage. We are currently conducting an in-vitro culture analysis with the use of spleen-derived osteoclasts for understanding the regulatory mechanism of osteoclastic differentiation under the influence of the Hh signaling pathway.

**Disclosures:** Ryuma Haraguchi, None.

## SU0168

**Integrin  $\alpha$ v $\beta$ 3 Signaling is not Required for TNF- $\alpha$  Mediated L-plastin Phosphorylation and Nascent Sealing Zones Formation in Osteoclasts.** Sunipa Majumdar\*, Meenakshi Chellaiah. University of Maryland, Dental School, United states

**Background:** While many of the proteins that compose the sealing ring have been identified, their function is still poorly understood in osteoclasts (OCs). We have previously shown the unique role of an actin binding protein named L-plastin (LPL) in the assembly of a precursor sealing zone which we named "nascent sealing zones (NSZs)". Although, TNF- $\alpha$  was shown to stimulate resorptive activity of OCs independently of  $\alpha$ v $\beta$ 3, little is known about its role in LPL phosphorylation and sealing ring formation. Therefore, our goal is to identify the essential function of LPL phosphorylation on serine residues by TNF- $\alpha$  signaling in actin bundling, a process required for NSZs formation and bone resorption. Methods: OCs produced from the bone marrow cells of WT mice (C57/BL6 strain) and RAW cells were used. Matured OCs were incubated with native mouse bone particles (BPs) in the presence of TNF- $\alpha$  for 3 to 4h for immunoblotting analyses with an antibody to p-serine and LPL. Also, some cultures were incubated with inhibitors (Src, Rho kinase, PKC, PKA, PI3-K, or TRAF6) or blocking antibodies (TNF- $\alpha$  or TNF-R1) to attenuate LPL phosphorylation. Cells plated on dentine slices were analyzed for F-actin content, NSZs/sealing ring formation and bone resorption activity.

**Results:** Actin bundling and NSZs formation are dependent on LPL phosphorylation mediated by TNF- $\alpha$  signaling which involves TRAF6, Src, Rho kinase and PI3-K. Inhibitors to these signaling proteins diminished the formation of NSZs at 3-4h or mature sealing rings at 8-14h. Furthermore, a significant decrease in NSZs, F-actin content, and mature sealing ring was observed in OCs treated with an antibody to TNF- $\alpha$  or TNF-R1. Neither LPL phosphorylation nor NSZs formation was affected by an inhibitor to integrin  $\alpha$ v $\beta$ 3 or SiRNA to  $\beta$ 3.

**Conclusions:** LPL phosphorylation by TNF- $\alpha$  signaling is critical during the early stages of sealing ring formation. Our observations suggest a sequential processes in the sealing ring formation i.e. OCs adhesion to the bone surface  $\rightarrow$  formation of NSZs by TNF- $\alpha$  signaling  $\rightarrow$  Maturation to sealing ring by  $\alpha$ v $\beta$ 3 signaling  $\rightarrow$  Bone resorption. Manipulation of LPL phosphorylation may provide a novel approach to regulating OC sealing ring formation and bone resorption [Supported by R01-NIH-NIAMS 5R01AR066044].

**Disclosures:** Sunipa Majumdar, None.

**SU0169**

**Role of CrkII Signaling in RANKL-Induced Osteoclast Differentiation and Function.** Byung Chul Jeong<sup>\*1</sup>, Inyoung Kim<sup>2</sup>, Jung Ha Kim<sup>2</sup>, Kabsun Kim<sup>2</sup>, Semun Seong<sup>3</sup>, Nacksung Kim<sup>1</sup>. <sup>1</sup>Department of Pharmacology, Medical Research Center for Gene Regulation & BK21plus, Chonnam National University Medical School, Korea, republic of, <sup>2</sup>Department of Pharmacology, Medical Research Center for Gene Regulation, Chonnam National University Medical School, Korea, republic of, <sup>3</sup>Department of Biomedical Sciences, Chonnam National University Medical School, Korea, republic of

Rac1, a member of small GTPases, is a key regulator of osteoclast differentiation and function. The Crk family adaptor proteins, consisting of Src homology (SH) 2 and SH3 protein-binding domains, regulate cell proliferation, migration, and invasion through Rac1 activation. In this study, we examined the role of CrkII in osteoclast differentiation and function. Retroviral overexpression of CrkII in osteoclast precursors enhanced osteoclast differentiation and resorptive function through Rac1 activation. The knockdown of CrkII in osteoclast precursors using small interfering RNA inhibited osteoclast differentiation and its resorption activity. Unlike wild-type CrkII, overexpression of the three SH domains in mutant forms of CrkII did not enhance either osteoclast differentiation or function. Phosphorylation of p130 Crk-associated substrate (p130Cas) by osteoclastogenic cytokines in preosteoclasts increased the interaction between p130Cas and CrkII, which is known to be involved in Rac1 activation. Furthermore, transgenic mice over-expressing CrkII under control of a tartrate-resistant acid phosphatase promoter exhibited a low bone mass phenotype, associated with increased resorptive function of osteoclasts in vivo. Taken together, our data suggest that the p130Cas/CrkII/Rac1 signaling pathway plays an important role in osteoclast differentiation and function, both in vitro and in vivo.

**Disclosures:** Byung Chul Jeong, None.

**SU0170**

**The Role of the V-ATPases and Lysosomal Positioning in mTORC1 Signaling in Osteoclasts.** Andrew Wang<sup>1</sup>, Danielle Johnson<sup>2</sup>, Luciene Lacroix<sup>1</sup>, Celeste Owen<sup>3</sup>, Bowen Gao<sup>4</sup>, Paul Corey<sup>5</sup>, John Brumell<sup>2</sup>, Irina Voronov<sup>\*1</sup>. <sup>1</sup>Faculty of Dentistry, University of Toronto, Canada, <sup>2</sup>Cell Biology Program, Hospital for Sick Children, Canada, <sup>3</sup>Mount Sinai Hospital, Canada, <sup>4</sup>University of Toronto, Canada, <sup>5</sup>Dalla Lana School of Public Health, University of Toronto, Canada

Mammalian target of rapamycin (mTOR) is a serine/threonine kinase responsible for cellular responses to growth factors and nutrient availability. In cells, it exists as part of two complexes, complex 1 (mTORC1) and complex 2 (mTORC2). mTORC1 is activated by numerous stimuli, including amino acids, promoting cell proliferation, differentiation, and growth. mTORC1 regulation is tightly linked to lysosomes and to the vacuolar H<sup>+</sup>-ATPases (V-ATPases), the ubiquitous multi-subunit proton pumps responsible for acidification of the intracellular and extracellular compartments; however, the role of the V-ATPases in mTORC1 signaling is not clear.

mTOR is important for osteoclastogenesis: inhibition of mTORC1 results in decreased osteoclast formation; however, the precise mechanism of mTORC1 signaling in osteoclasts is not known. To elucidate the role of the V-ATPases in mTORC1 signaling in osteoclasts, we used a mouse model with a dominant negative point mutation (R740S) in the V-ATPase  $\alpha 3$  subunit. The V-ATPases containing  $\alpha 3$  subunit are localized to the lysosomes in non-resorbing osteoclasts. As a result, the osteoclasts with R740S mutation have an increased lysosomal pH (pH 6.3, 5.7, and 4.5, in R740S/R740S, +/R740S and +/+ cells, respectively).

mTORC1 is activated by the amino acids and is not active upon amino acid withdrawal, therefore, to characterize mTORC1 activity we performed starvation (HBSS, 60 min) and recovery (supplemented media, 30 min) experiments. mTORC1 was inactivated by starvation in all three genotypes; however, basal mTORC1 activity, as measured by the phosphorylation levels of mTORC1 substrate p-p70S6K, was higher in +/R740S and R740S/R740S cells compared to +/+ controls, suggesting that lysosomal pH plays a role in mTORC1 signaling. To assess mTOR/lysosome colocalization (since active mTOR resides on the lysosome), we examined the cells using confocal microscopy. The cells were subjected to starvation/recovery conditions, and stained for mTOR and lysosomal marker LAMP2. mTOR co-localization with LAMP2 was not significantly affected in all three genotypes, and starvation did not have an effect on this co-localization, even though the lysosomal positioning did change. These results contradict current mTOR/lysosome localization studies, suggesting that the mechanism of mTORC1 signaling is different in osteoclasts compared to the other cells. Future experiments will assess whether osteoclasts have unique mTOR organelle distribution patterns.

**Disclosures:** Irina Voronov, None.

**SU0171**

**Functional analysis of Cadm1 gene, involved in epigenetic regulation during osteoclastogenesis.** Shinya Nakamura<sup>\*1</sup>, Naohiro Izawa<sup>1</sup>, Hiroyuki Aburatani<sup>2</sup>, Takeshi Miyamoto<sup>1</sup>, Sakae Tanaka<sup>1</sup>. <sup>1</sup>Orthopaedic Surgery & Spinal Surgery, The University of Tokyo, Tokyo, Japan, Japan, <sup>2</sup>Genome Science Division, Research Center for Advanced Science & Technology, The University of Tokyo, Tokyo, Japan, Japan

<Backgrounds and Purposes> Recently, epigenetic regulation mechanisms during cell differentiation, especially ES cell differentiation, have been elucidated with the progress of big data analysis. However epigenetic regulation mechanisms during osteoclastogenesis have not been fully elucidated yet. Recent studies have shown that specific histone modifications, such as H3K4me3 around the transcription start sites (TSS) of genes, regulate gene transcription. This means that the histone modifications around the TSS of key lineage-specific genes tend to change from bivalent H3K4me3/H3K27me3 to monovalent H3K4me3 during the course of differentiation. In this study, we identified candidate genes which were regulated by such epigenetic control during osteoclastogenesis and studied its functional roles.

<Materials and Methods> Bone marrow derived-macrophages (BMMs), which were cultured from male mice bone marrow cells with M-CSF, and osteoclasts (OCs), which were cultured from BMMs with M-CSF and RANKL, were used. H3K4me3, H3K27me3 and binding of Nfatc1, which is known as master regulator of osteoclastogenesis, were evaluated using ChIP-seq. We also evaluated gene expression changes by RNA-seq. From these data, we identified candidate genes important in osteoclastogenesis.

<Results and Discussions> During the course of differentiation from BMMs to OCs, we extracted the genes which change from bivalent H3K4me3/H3K27me3 to monovalent H3K4me3 around the TSS (within 5kbp). We narrowed down the gene lists whose expressions were above a certain level and 49 genes were left. Among them, 33 genes, to which Nfatc1 was bound, were chosen as candidates genes important in osteoclastogenesis. From these candidate genes we focused on Cadm1 (cell adhesion molecule 1), belonging to the immunoglobulin superfamily cell adhesion molecule group. Cadm1 is involved in the morphogenesis and the regulation of the invasion and metastasis of cancer cells via an adhesion between neighboring cells. We have revealed that Cadm1-knockout mouse exhibited osteoporosis with high bone turnover, though there was no difference in the osteoclastogenesis cultured from bone marrow cells with M-CSF and RANKL. It was thought that the osteoporosis came from osteoblast function abnormalities or the collapse of the coupling mechanism between osteoclasts and osteoblasts.

**Disclosures:** Shinya Nakamura, None.

**SU0172**

**Osteoclasts are Deficient in the Expression of Osteogenic Coupling Factors Following Ischemic Osteonecrosis Of The Femoral Head.** Naga Suresh Adapala<sup>\*1</sup>, Harry K.W. Kim<sup>1</sup>, Ryosuke Yamaguchi<sup>1</sup>, Hicham Drissi<sup>2</sup>. <sup>1</sup>Texas Scottish Rite Hospital for Children, United states, <sup>2</sup>University of Connecticut Health Center, United states

Purpose: Legg-Calvé-Perthes disease is a childhood ischemic osteonecrosis of the femoral head (ONFH) that leads to bone loss and femoral head deformity. The mechanisms of decreased bone formation following ONFH are unknown. During normal bone remodeling, osteoclasts (OC) produce osteogenic coupling factors that can support osteoblast (OB) formation. Following ONFH, excessive bone resorption is uncoupled from OB formation. We hypothesized that OCs in ONFH are deficient in the expression of coupling factors, and in supporting OB formation. The purpose of this study was to determine (1) in vivo gene expression of coupling factors in OCs following ONFH (2) effect of NBF (necrotic bone fluid, saline flush of necrotic femoral head) on coupling factor expression (3) effect of NBF-primed OCs on OB differentiation.

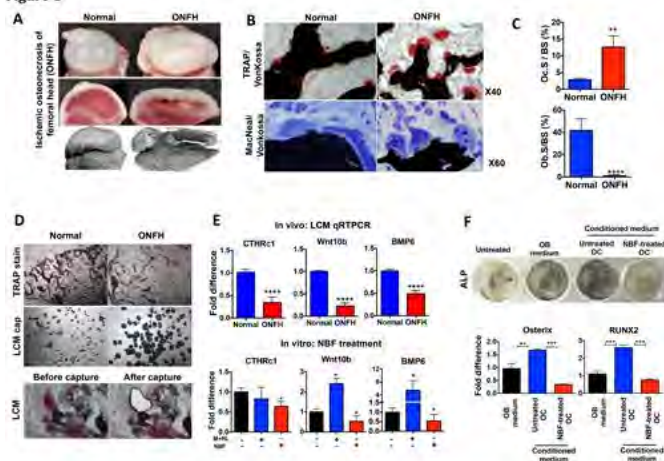
Methods: ONFH was induced in right femoral heads of 6-wk old piglets (n=12) by femoral neck ligation; the left femoral head served as normal control. At 8-wks after surgery, numbers of OCs and OBs were quantified by Bioquant analysis. OCs were captured from frozen sections by laser capture microdissection (LCM), and the gene expression was analyzed by qRT-PCR. In vitro, OCs were treated with NBF for 6h prior to RNA isolation. For OC-conditioned medium, OCs on pig dentine discs were primed with NBF for 12h, then cultured for 48h in fresh OC medium. The OB differentiation was assessed by osterix and RUNX2 mRNA levels, alkaline phosphatase (ALP) and alizarin red staining. NBF was analyzed by ELISA and western blotting.

Results: Bioquant analysis revealed a significant increase in OC numbers in ONFH compared to normal (>4-fold, P<0.01) but OB numbers were significantly decreased (38-fold, P<0.0001). qRT-PCR analysis of OCs obtained by LCM showed that, among the coupling factors tested, the gene expression of CTHRC1, Wnt10b and BMP6 was significantly lower (P<0.0001 for each) in ONFH compared to normal. In vitro, treatment of OCs cultured on pig dentine with NBF inhibited CTHRC1, Wnt10b and BMP6 expression. Furthermore, conditioned medium from NBF-primed OCs inhibited OB differentiation, as evidenced by decreased osterix and RUNX2 gene expression in bone marrow stromal cells, ALP and alizarin red staining. NBF contained several alarmins (damaged cell and matrix factors e.g. HMGB1) and pro-inflammatory cytokines (e.g. IL-6) compared to normal.

Conclusion: OCs are deficient in the expression of osteogenic coupling factors following ONFH and in supporting OB formation.

address this issue, we generated mutant mice in which ATM is specifically disrupted in osteoclasts (*Atm<sup>Ctsk</sup>* mice).

Figure 1



(A) Bone loss and femoral head deformity in ONFH in piglets (B and C) Increased number of osteoclasts and decreased number of osteoblasts in repair tissue (D, E top panel) Laser capture microdissection method and qRT-PCR analysis (E bottom panel) In vitro effect of NBF on OC gene expression (F) Osteoclast conditioned medium from NBF-primed OCs does not support osteoblast differentiation. P value  $<0.05$ ,  $* <0.01$ ,  $** <0.001$ ,  $*** <0.0001$ .

Osteoclasts are deficient in the expression of osteogenic coupling factors following ONFH

Disclosures: Naga Suresh Adapala, None.

### SU0173

Supportive Role of CD44-ICD in RUNX2- Mediated Transcriptional Regulations in Prostate Cancer Cells. Linda Senbanjo\*, Meenakshi Chellaiah. University of Maryland Baltimore, United states

Background: Previous studies from our laboratory provided compelling evidence of a significant increase in the expression of CD44 in prostate cancer cells (PCa) cells derived from human bone metastases (PC3). However, CD44 expression is very negligible or not observed in LNCaP cells which are derived from lymph node metastases. CD44 promotes migration and invasion of PC3 cells. Runx2, a bone-specific transcriptional regulator for an osteoclast differentiation protein called RANKL, is highly expressed in PC3 cells. CD44 signalling regulates the phosphorylation and hence localization of RUNX2 in nucleus. Recent studies by others have shown that Intracellular domain of CD44 (CD44-ICD) functions as a co-transcriptional factor for RUNX2 in the regulation of expression of genes involved in migration/invasion (MMP9 etc.) in other cancer cells. Therefore, the present study aims to determine the regulatory role of CD44-ICD in PCa cells.

Methodology/Principle finding: We used knock down and over expression strategy to determine the roles of CD44 and RUNX2, respectively in PC3 cells. Immunoblotting analyses and osteoclastogenesis in vitro were done. Our findings revealed the following: a) CD44 signaling is essential for RUNX2- mediated RANKL expression, osteoclastogenesis, and hence bone resorption in vitro; b) CD44-ICD was observed in the highly metastatic PC3 cells and not in LNCaP; c) Upon cleavage, localization of CD44-ICD in the nucleus is greater than cytoplasm of PC3 cells; d) CD44 regulates Runx2 phosphorylation; Runx2 knock-down (KD) reduces RANKL and osteoclastogenesis in vitro; e) RANKL expression is CD44 and RUNX2-dependent as knocking down of either CD44 or the RUNX2 strongly affected RANKL expression; f) RUNX2 over expression increases CD44-ICD/ RUNX2 interaction in the nuclei.

Conclusions: Increased localization of CD44-ICD in the nucleus of RUNX2 over-expressing cells not only suggest the interaction of CD44-ICD with RUNX2 but also a supportive role as a transcriptional co-factor for RUNX2 in the regulation of expression metastasis related genes [Supported by R01-NIH-NIAMS 5R01AR066044].

Disclosures: Linda Senbanjo, None.

### SU0174

Conditional Abrogation of *Atm* in Osteoclasts Leads to Reduced Bone Mass and Extended Osteoclast Lifespan. Toru Hirozane\*, Takahide Tohmonda, Masaki Yoda, Masayuki Shimoda, Yae Kanai, Morio Matsumoto, Hideo Morioka, Masaya Nakamura, Keisuke Horiuchi. Keio University School of Medicine, Japan

#### Introduction

Ataxia-telangiectasia mutated (ATM) plays a major role in the DNA damage response. We previously found that ATM is activated during osteoclastogenesis; however, the potential function of ATM in bone metabolism is poorly understood. To

#### Methods

*Atm* floxed mice were crossed with Cathepsin K-Cre recombinase transgenic mice to specifically inactivate ATM in osteoclasts. Bone morphometric analysis and  $\mu$ CT analysis were done using the femur collected from 3-week-old and 9-week-old male *Atm<sup>Ctsk</sup>* mice and their littermate control mice. In vitro osteoclast formation assay was performed using bone marrow cells harvested from adult male *Atm<sup>Ctsk</sup>* and control mice. The expression levels of osteoclast-related transcripts and proteins were evaluated by quantitative PCR and western blotting, respectively. To evaluate the ratio of apoptotic osteoclasts in vivo, tibial sections were dually stained for TUNEL and TRAcP. Pit formation assay was performed by incubating bone marrow macrophages with M-CSF and RANKL for 5 and 10 days.

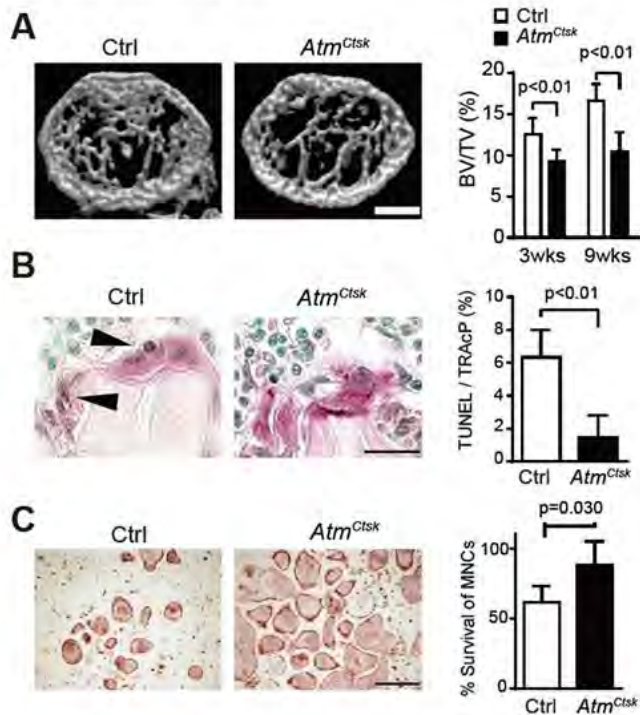
#### Results and Discussion

Bone morphometric analysis and  $\mu$ CT analysis showed that *Atm<sup>Ctsk</sup>* mice have reduced bone mass compared to control mice, potentially due to increased bone resorption (A). Although lack of ATM in osteoclast precursors did not result in any remarked impact on their differentiation, we found that osteoclasts lacking ATM are less prone to apoptosis both in vivo and in vitro, indicating that ATM negatively regulates osteoclast longevity (B and C). As a result of the extended lifespan osteoclasts lacking ATM showed an overall increase in the amount of bone resorption compared to control cells. Furthermore, we found that NF- $\kappa$ B, a signaling molecule critically involved in the regulation of osteoclast survival, is highly activated in osteoclasts lacking ATM compared to control mice. Taken together, these observations indicate that ATM is involved in the regulation of osteoclast survival via modulating NF- $\kappa$ B activity.

#### Conclusion

Our data show that *Atm<sup>Ctsk</sup>* mice exhibit reduced bone mass due to increased bone resorption, and that abrogation of ATM in osteoclasts renders these cells less prone to apoptosis and extends their lifespan.

### Conditional abrogation of *Atm* in osteoclasts leads to reduced bone mass and extended osteoclast lifespan



(A)  $\mu$ CT analysis of the distal femur.

(B) Tibial sections dually stained for TRAcP and TUNEL. Arrowheads indicate TUNEL-positive nuclei in TRAcP-positive multinucleated cells.

(C) The ratio of surviving osteoclasts in growth factor-deprived conditions. p-value was calculated from Student's t test.

Hirozane T

Disclosures: Toru Hirozane, None.

## SU0175

**Changes in Wnt Receptor Expression Accompany Altered Canonical Wnt Signaling in Osteoclast Progenitors with Aging or Ovariectomy.** Stephanie Youssef\*, Ming Ruan, Christine Hachfeld, Glenda Evans, Joshua Farr, David Monroe, Sundeep Khosla, Jennifer Westendorf, Merry Jo Oursler, Megan Weivoda. Mayo Clinic, United states

Canonical and non-canonical Wnt signaling pathways are both crucial for skeletal development and homeostasis. Activation of canonical versus non-canonical signaling is determined by the presence of Wnt ligands and Wnt receptor (Lrp4/5/6, Fzd1-10, Ror2, Ryk) complexes. Importantly, changes in Wnt receptor complex composition affect the responses to specific Wnt ligands. While both canonical and non-canonical Wnt pathways promote osteoblastogenesis, they have differential effects on osteoclastogenesis, with canonical signaling reducing and non-canonical signaling increasing differentiation of early osteoclast progenitors (pOCs). Because pOC numbers increase and contribute to bone loss with aging and estrogen deficiency, we hypothesized that early pOCs exhibit changes in Wnt receptor expression with aging and ovariectomy (OVX) leading to reduced canonical Wnt signaling and increased osteoclastogenic potential. To test our hypothesis, we used magnetic activated cell sorting to rapidly isolate pOCs (Rank+ monocytes) from the bone marrow of young, adult, and old (1, 4, and 24 months) female mice. Additionally, pOCs were isolated from adult female mice one week following sham or OVX. The RNA was immediately isolated to obtain a "snap-shot" of the *in vivo* expression of canonical and non-canonical Wnt receptors and canonical Wnt target genes using qPCR. Compared to young pOCs, adult pOCs showed significantly increased expression of Fzd-1, -3 and -8, whereas the opposite was found for Fzd10. Adult pOCs also showed significantly increased levels of Axin2 and a trend for increased levels of Lef1 (canonical Wnt target genes) compared to young pOCs. Expression levels of Fzd3, -6, -7, and -10 and Lrp4 were significantly decreased in old pOCs versus adult pOCs; this correlated with significantly reduced levels of the canonical Wnt target genes Axin2 and c-Myc. Following OVX, expression levels of Fzd9 and 10, which are both associated with non-canonical Wnt signaling, were significantly upregulated while Lrp4 and the canonical targets Lef1 and Axin2 were decreased. Overall, our data show that both aging and estrogen deficiency alter pOC Wnt receptor expression *in vivo*. Indeed, canonical Wnt target gene expression was significantly reduced, consistent with the increased pOC numbers observed in these conditions. These data suggest that restoring canonical Wnt signaling may be an effective strategy to reduce pOC numbers in patients at risk for accelerated bone loss.

**Disclosures:** *Stephanie Youssef, None.*

## SU0176

**TMEM178 is a novel negative regulator of store operated calcium entry in osteoclasts.** Zhengfeng Yang\*, Corrine Decker, Roberta Faccio. Department of Orthopaedic Surgery, Musculoskeletal Research Center, Washington University School of Medicine, United states

Cytoplasmic calcium oscillations are necessary for NFATc1 activation, the master transcriptional regulator of osteoclastogenesis. Calcium oscillations are dependent on extracellular calcium influxes through store operated calcium entry (SOCE) and calcium re-uptake into the endoplasmic reticulum (ER). Intriguingly, calcium oscillations mainly occur during the early stages of osteoclast (OC) differentiation, while diminishing in mature cells. Evidences indicate that SOCE gradually decreases during OC differentiation, but the exact mechanisms by which calcium levels are reduced in mature OCs remain to be established.

We recently identified transmembrane protein (TMEM)-178, an ER localized protein which is upregulated during osteoclastogenesis, as a novel negative regulator of RANKL-induced calcium fluxes, NFATc1 activation and osteoclastogenesis. In systemic Juvenile Idiopathic Arthritis patients, TMEM178 levels are reduced and its downregulation correlates with the extent of erosive disease. To investigate whether TMEM178 negatively regulates calcium oscillations by affecting calcium fluxes via SOCE, we performed calcium imaging in WT and *Tmem178*<sup>-/-</sup> preOCs. We found that *Tmem178* deficiency increases transient ER calcium release in response to ATP, and enhances SOCE-mediated calcium entry compared with WT cells. Both the frequency and amplitude of calcium oscillations are increased in *Tmem178*<sup>-/-</sup> preOCs after SOCE activation. By contrast, ectopic expression of TMEM178 significantly suppresses SOCE and limits OC differentiation.

To evaluate how TMEM178 affects SOCE, we analyzed the interaction of TMEM178 with STIM1 and ORAI1, two integral components of SOCE. TMEM178 specifically associates with STIM1 but not ORAI1. Structure/function analysis revealed that neither the C-terminal nor the N-terminal domain of TMEM178 is required for TMEM178/STIM1 interaction. To evaluate the role of the 3 transmembrane (TM) domains, we replaced the second transmembrane domain (TM2) either with TM1 or TM3, or we generated a construct where both TM1 and TM2 were replaced by TM3. We found that TM1 and TM2 but not TM3 are important for STIM1 association, SOCE activation and osteoclastogenesis.

Taken together, these findings demonstrate a novel mechanism for downregulation of calcium fluxes during OC differentiation via upregulation of TMEM178 and suppression of SOCE. Moreover, TMEM178 transmembrane region is responsible for STIM1 binding and regulation of SOCE.

**Disclosures:** *Zhengfeng Yang, None.*

## SU0177

**24-Hour Profile of Serum Sclerostin and Its Association With Bone Biomarkers in Men.** Christine Swanson\*<sup>1</sup>, Orfeu Buxton<sup>2</sup>, Steven Shea<sup>3</sup>, Sheila Markwardt<sup>3</sup>, Eric Orwoll<sup>3</sup>. <sup>1</sup>University of Colorado, United states, <sup>2</sup>Pennsylvania State University, United states, <sup>3</sup>Oregon Health & Science University, United states

Osteoclasts and osteoblasts appear to display endogenous circadian rhythms. Bone resorption markers, and to a lesser degree, bone formation markers, increase overnight with peaks in the early morning and nadirs in late afternoon. These rhythms are influenced by food, but are largely independent of posture, sex, normal light/dark cycles, PTH, GH, and cortisol. The osteocyte exerts important effects on bone remodeling. The study purpose was to evaluate 24-h profiles of osteocyte markers and their relationship to bone turnover markers.

Markers of bone formation (PINP), bone resorption (CTX) and osteocyte function (sclerostin, FGF-23) were measured q2 hours in serum obtained over a 24-h period (n = 10 healthy men aged 20-65 years). To establish rhythmicity, individual profiles were smoothed using a locally weighted nonlinear regression procedure (8 h window) and 24-h amplitude of fitted values evaluated relative to the intra-assay CV. Mean amplitude  $\pm$  SD were calculated for metabolites with confirmed rhythmicity. To assess temporal relationships between pairs of significantly rhythmic metabolites, lags between nadirs were estimated for each individual. Mixed effects regression analyses also assessed age effects on marker patterns; from these models the mean 24-h level and 95% CI for each age group was estimated (age groups: 20-27years n = 6; 55-65years n = 4).

CTX rhythmicity was confirmed, with peak levels at 4 AM. No discernible 24-h rhythm was identified for PINP. Sclerostin demonstrated 24-h rhythmicity in 7/10 men, but phase was variable. FGF-23 levels were rhythmic in all but with inconsistent phase. The sclerostin nadir preceded the CTX nadir by 0.8 h  $\pm$  9.1 h, but there was a large range (-10 to +12 h; negative indicates CTX nadir preceded sclerostin nadir) and the FGF-23 nadir preceded that of sclerostin by 0.2 h (range -10 to +11h), suggesting no clear relationships (Figure 1). FGF-23 did not vary with age. Mean 24-h CTX level was 0.431 ng/mL in older men, 0.884 ng/mL in younger men (p = 0.02). Mean CTX amplitude was larger in younger than older men (0.365 vs. 0.156 ng/mL p < 0.001). The 24-hr profiles of sclerostin and FGF-23 suggest that osteocyte function is rhythmic but timing varies between individuals. These findings in relation to the consistent CTX rhythm and lack of PINP rhythm, suggest that the osteocyte does not direct the 24-h rhythmicity of other bone turnover markers in healthy adult men, at least via sclerostin or FGF-23-mediated mechanisms.

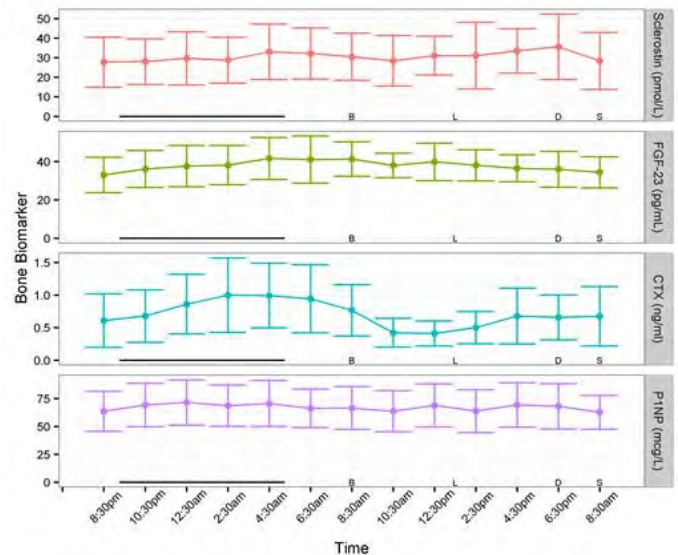


Figure 1

**Disclosures:** *Christine Swanson, None.*

## SU0178

**Activation of AMP-activated Protein Kinase Decreases RANKL Expression and Increases Sclerostin Expression by Inhibiting the Mevalonate Pathway in Osteocytic MLO-Y4 Cells.** Ippei Kanazawa\*, Maki Yokomoto-Umakoshi, Ayumu Takeno, Ken-ichiro Tanaka, Masakazu Notsu, Toshitsugu Sugimoto. Shimane University Faculty of Medicine, Japan

Background: Increasing evidence indicates that osteoporosis is a disorder of energy metabolism. Recent studies have shown that AMP-activated protein kinase (AMPK), which is a crucial regulator of energy and metabolic homeostasis at the cellular and whole-organism levels, plays pivotal roles in bone physiology. We previously reported that AMPK is expressed in an osteocytic cell line, MLO-Y4 cell, and that AMPK

activation exerted protective effects against homocysteine-induced apoptosis of the cells. However, the effects of AMPK activation on RANKL and sclerostin expression in osteocytes are unclear.

**Aim:** This study aimed to investigate whether or not AMPK regulates RANKL and sclerostin expression in osteocytes.

**Methods:** MLO-Y4 cells were cultured on collagen-coated plates in  $\alpha$ -minimum essential medium supplemented with 10% fetal bovine serum and 1% penicillin-streptomycin in 5% CO<sub>2</sub> at 37°C. To examine the expressions of RANKL and sclerostin, quantitative real-time PCR and Western blot were performed.

**Results:** Real-time PCR showed that AMPK activation by 5-aminoimidazole-4-carboxamide ribonucleotide (AICAR) significantly decreased the expression of *Rankl* in a dose- and time-dependent manner and significantly increased the expression of *Sost*, the gene encoding sclerostin, in MLO-Y4 cells. Western blotting confirmed that AICAR decreased RANKL protein levels and increased sclerostin levels. In addition, suppression of AMPK1 by siRNA significantly increased the expression of *Rankl* on 4 days after the transfection of siRNA, while *Sost* expression was not changed. Simvastatin, an inhibitor of HMG-CoA reductase, significantly decreased *Rankl* expression and increased *Sost* expression in MLO-Y4 cells. Supplementation with mevalonate or geranylgeranyl pyrophosphate, which are downstream metabolites of HMG-CoA reductase, significantly reversed the effects of AICAR.

**Conclusion:** These findings indicated that AMPK activation decreased RANKL expression and increased sclerostin expression by inhibiting the mevalonate pathway in osteocytic MLO-Y4 cells.

**Disclosures:** *Ipppei Kanazawa, None.*

## SU0179

### Alternation in Gap-junctional Intercellular Communication Capacity During the Ex Vivo Transformation of Osteocytes in the Embryonic Chick Calvaria.

Ziyi Wang, Naoya Odagaki, Tomoyo Tanaka, Mana Hashimoto, Hiroshi Kamioka\*. Okayama University Graduate School of Medicine, Dentistry & Pharmaceutical Sciences, Department of Orthodontics, Japan

**Aim:** Gap junctional intercellular communication (GJIC) is thought to play an important role in the integration and synchronization of bone remodeling. In this study we analyzed the difference in the GJIC capacity of younger and developmentally mature osteocytes. **Methods:** We first established an embryonic chick calvaria growth model to show the growth of the calvaria in embryos at 13 to 21 days of age. We then applied a fluorescence recovery after photobleaching (FRAP) technique to compare the difference in the GJIC capacity of younger osteocytes with that of more mature osteocytes. Finally, we quantified the dye (Calcein-AM) diffusion from the FRAP data using a mathematic model of simple diffusion which was also used to identify simple diffusion GJIC pattern cells (fitted model) and accelerated diffusion GJIC pattern cells (non-fitted model). **Results:** The relationship between the longest medial-lateral length of the calvaria (frontal bone) and the embryonic age fit a logarithmic growth model:  $length = 5.144 \times \ln(day) - 11.340$ . The morphometric data during osteocyte differentiation showed that the cellular body becomes more spindle-shaped and that the cell body volume decreased by approximately 22% with an increase in the length of the processes between the cells. However, there were no significant differences in the cellular body surface area or in the distance between the mass centres of the cells. The dye-displacement rate in younger osteocytes was significantly higher than that in developmentally mature osteocytes: dye displacement only occurred in 26.88% of the developmentally mature osteocytes, while it occurred in 64.38% of the young osteocytes. Additionally, in all recovered osteocytes, 36% of the developmentally mature osteocytes were the non-fitted model cells while 53.19% of the young osteocytes were the non-fitted model, which indicates the active transduction of dye molecules. However, there were no statistically significant differences between the young and developmentally mature osteocytes with regard to the diffusion coefficient, permeability coefficient, or permeance of the osteocyte processes, which were  $3.93 + 3.77 (\times 10^{-8} \text{cm}^2/\text{s})$ ,  $5.12 + 4.56 (\times 10^{-7} \text{cm}^2/\text{s})$  and  $2.99 + 2.47 (\times 10^{-13} \text{cm}^2/\text{s})$  (mean + SD) respectively. **Conclusions:** These experiments comprehensively quantified the GJIC capacity in the embryonic chick calvaria and indicated that the cell-cell communication capacity of the osteocytes in the embryonic chick calvaria was related to their age.

**Disclosures:** *Hiroshi Kamioka, None.*

## SU0180

**Analysis of Intracellular Ca<sup>2+</sup> Mobilization by 3D Time-lapse Imaging in Bone.** Tomoyo Tanaka\*<sup>1</sup>, Mitsuhiro Hoshijima<sup>2</sup>, Junko Sunaga<sup>3</sup>, Takashi Nishida<sup>2</sup>, Taiji Adachi<sup>3</sup>, Hiroshi Kamioka<sup>1</sup>. <sup>1</sup>Department of Orthodontics, Graduate School of Medicine, Dentistry & Pharmaceutical Sciences, Okayama University, Japan, <sup>2</sup>Advanced Research Center for Oral & Craniofacial Sciences, Dental School, Okayama University, Japan, <sup>3</sup>Department of Biomechanics, Institute for Frontier Medical Sciences, Kyoto University, Japan

Osteocytes and osteoblasts form a three-dimensional (3D) cellular network in bone. Cellular network of osteocytes has important roles in mechanosensation and mechanotransduction related to bone homeostasis. Previous studies indicated that fluid shear stress was specifically delivered to bone surface and enhanced the

activation of the autonomous intracellular Ca<sup>2+</sup> ([Ca<sup>2+</sup>]<sub>i</sub>) oscillations in osteoblasts and osteocytes embedded within a bone matrix via gap junction-mediated cell-cell communication. However the molecular mechanisms by which osteocytes regulate bone formation and remodeling in the 3D environment poorly understood. Here we observed 3D time-lapse autonomous and flow induced Ca<sup>2+</sup> signaling in osteocytes and analyzed [Ca<sup>2+</sup>]<sub>i</sub> mobilization of osteoid-osteocytes and mature osteocytes in chick calvaria. Embedded osteocytes in the bone were visualized at 20 μm depth with a FLUOVIEW FV1200 MPE microscopy system (Olympus, Tokyo Japan). [Ca<sup>2+</sup>]<sub>i</sub> was monitored using a calcium indicator probe, Fluo-8 No Wash Calcium Assay Kit (AAT Bioquest, Inc.) and analyzed in real time. In response to the flow, [Ca<sup>2+</sup>]<sub>i</sub> significantly increased in mature osteocytes in comparison with osteoid-osteocytes. Furthermore, to investigate the differences in response between mature osteocytes and osteoid-osteocytes in detail, we used osteocyte-like cell line, MLO-Y4 which were cultured within type I collagen gels as a 3D. To study the changes over time in the mRNA expression of osteocyte marker genes, the *Sost* and *Dmpl* during differentiation of MLO-Y4 cells were studied *in vitro*, mRNA samples were collected on 7 days and 15 days and evaluated for the gene expression. On day 15, *Sost* mRNA level was increased in comparison with day 7, whereas *Dmpl* mRNA expression was remarkably decreased. These results indicated that MLO-Y4 cells differentiated into mature osteocyte-like cells by long term culture. To assess the functional changes with the osteocyte differentiation, the expression of osteocyte related genes were examined. As a result, the *Cx43*, *c-Fos* and *Colla1* mRNA expression were significantly increased on day 15 in comparison with day 7. These findings collectively indicate that [Ca<sup>2+</sup>]<sub>i</sub> mobilization is increased by the formation of gap junctional intracellular communication with the differentiation of osteocytes. These effects regulate mineralization-related genes in the osteocyte lineage.

**Disclosures:** *Tomoyo Tanaka, None.*

*This study received funding from: Grant-in-Aid for Scientific Research (no. 16H05549) from the Ministry of Education, Culture, Sports, Science and Technology (MEXT), Japan.*

## SU0181

### Elevated Bone Resorption and Pro-Inflammatory Cytokines are Mitigated by a Soy Protein Diet in a Rodent Model of Inflammatory Bowel Disease.

Corinne Metzger\*<sup>1</sup>, Anand Narayanan<sup>2</sup>, David Zawieja<sup>2</sup>, Susan Bloomfield<sup>1</sup>. <sup>1</sup>Texas A&M University, United states, <sup>2</sup>Texas A&M Health Science Center, United states

Inflammatory bowel disease (IBD) causes bone loss and 40% greater fracture incidence. Using a rodent IBD model, we previously discovered altered osteocyte protein responses concurrent with increased bone resorption and decreased bone formation. In a rodent IBD model, a soy protein diet lowered tumor necrosis factor- $\alpha$  (TNF- $\alpha$ ) gene expression in the gut and mitigated disease symptoms (Jiang, J Nutr; 2011). In this current study, we examined the impact of a moderately high soy protein diet (PRO) on osteocyte protein prevalence of TNF- $\alpha$ , interleukin-6 (IL-6), and sclerostin and on bone turnover. We hypothesized that PRO in IBD would decrease bone resorption and increase bone formation by decreasing TNF- $\alpha$  and IL-6, both proposed stimulators of resorption, and sclerostin, a formation inhibitor. Male SD rats (2 months, n=24) were divided into three groups: IBD (rectal TNBS instillations for 4 weeks + diet with 20% of kcal from casein), vehicle controls (VEH; vehicle instillations for 4 weeks + 20% casein diet), and IBD+PRO (TNBS instillations + diet with 35% of kcal from soy protein). Immunohistochemical staining of the distal femur cancellous compartment demonstrated 72% higher osteoclast surface in IBD vs. VEH identified by cathepsin K (CatK) and 50% lower osteoblast surface in IBD vs. VEH identified by osterix (Sp7). Higher osteoclast surface and lower bone formation rate (BFR) was also observed IBD vs. VEH via histomorphometry of the proximal tibia. IBD+PRO CatK surface was 62% lower than IBD and 34% lower than VEH, but Sp7 surface was not different than IBD. Histomorphometric changes were similar, with lower osteoclast surface in IBD+PRO vs. IBD, but BFR was the same between IBD and IBD+PRO. %TNF- $\alpha$ + osteocytes were 165% higher in IBD compared to VEH, while IBD+PRO was equal to VEH. Regression analysis showed %TNF- $\alpha$ + significantly predicted CatK surface across all groups (R<sup>2</sup>=0.229, p=0.018). Similar to %TNF- $\alpha$ +, %sclerostin+ osteocytes were 42% elevated in IBD compared to VEH, with IBD+PRO no different than VEH. The decline in %sclerostin+ in IBD+PRO did not correlate with the lower Sp7 surface in IBD+PRO. These data demonstrate that the moderately high soy protein diet significantly reduced TNF- $\alpha$  prevalence in osteocytes and reduced osteoclast surface. Interestingly, reducing the pro-inflammatory state of bone via this soy protein diet was unable to rescue the declines in osteoblast surface seen in IBD.

**Disclosures:** *Corinne Metzger, None.*

## SU0182

**How the European eel (*Anguilla anguilla*) loses its skeletal framework across lifetime.** [Tim Rolvien](#)<sup>\*1</sup>, [Florian Nagel](#)<sup>2</sup>, [Petar Milovanovic](#)<sup>3</sup>, [Sven Wuertz](#)<sup>4</sup>, [Robert Percy Marshall](#)<sup>1</sup>, [Felix N. Schmidt](#)<sup>1</sup>, [Michael Hahn](#)<sup>1</sup>, [Paul Eckhard Witten](#)<sup>5</sup>, [Michael Amling](#)<sup>1</sup>, [Bjoern Busse](#)<sup>1</sup>. <sup>1</sup>Department of Osteology & Biomechanics, University Medical Center Hamburg-Eppendorf, Germany, <sup>2</sup>Gesellschaft für Marine Aquakultur mbh, Germany, <sup>3</sup>Laboratory for Anthropology, Institute of Anatomy, School of Medicine, University of Belgrade, Serbia, <sup>4</sup>Leibniz Institute Freshwater Ecology & Inland Fisheries, Germany, <sup>5</sup>Department of Biology, Research Group Evolutionary Developmental Biology, Ghent University, Germany

In European eels (*Anguilla anguilla*), most bone is lost prior to the start of the animals' spawning to the Sargasso Sea. We studied this phenomenon in order to unravel mechanisms and consequences of bone loss.

Three groups were investigated: juvenile, mid-aged, and mature (induced by hormone injection). Calcium, phosphorus and cortisol levels were measured in the blood. Body morphometry, micro-computed tomography, histologic assessment of structural and cellular characteristics as well as compositional analyses by back-scattered electron microscopy (qBEI) and Fourier Transform Infrared Spectroscopy (FTIR) were performed on eels' vertebral and cranial bones to assess the mechanisms of bone resorption. Here, two types of mineralized tissue were found in the endoskeleton of European eels. While notochord extracellular sheaths with high mineral content were specifically found in the inner zones of the vertebrae, cellular (osteocytic) bone was present in the outer zones of the vertebrae and in skulls signifying the predominant site of cranial and vertebral bone loss. Of note, bone resorption occurred exclusively where cellular bone was present and did not encompass demineralization or osteocytic osteolysis. Clearly, the main cause for the tremendous bone loss in maturing eels was attributed to osteoclastic resorption by multinucleated osteoclasts associated with the prominent presence of eroded bone surfaces.

Preserving mechanical stability and releasing minerals for energy metabolism are two mutually exclusive functions of the skeleton. These functions are possibly orchestrated through the presence of two spatially separated hard tissues: first, cellular bone that is subject to mineral release following resorption and second acellular notochord sheath that is inaccessible for resorption to ensure a minimum of mechanical stability throughout life. Clearly, eel bone is structurally optimized to meet the metabolic challenge of fasting during a 5000 km journey to the spawning areas while the function of the vertebral column is maintained to achieve this goal.

**Disclosures:** [Tim Rolvien](#), None.

## SU0183

**Mineral matrix carbonate ion substitution returns to baseline levels in both HYP and wild-type mice one month after lactation.** [Kunal Agarwal](#)<sup>\*1</sup>, [Carolyn Macica](#)<sup>2</sup>, [Steven Tommasini](#)<sup>1</sup>. <sup>1</sup>Yale University, United states, <sup>2</sup>Frank H. Netter, M.D., School of Medicine at Quinnipiac University, United States

X-linked hypophosphatemia (XLH) is a metabolic disease characterized by an impaired mineral metabolism. As a result, questions regarding the body's ability to meet the increased demands for phosphate during pregnancy and lactation have been raised. Using HYP mice, a murine model of XLH, we have shown that carbonate substitutes for phosphate in the skeleton matrix as a way to provide phosphate to the fetus while overall maternal bone mass is maintained. However, it is unknown if this phenomenon continues after lactation has ceased. We hypothesized that osteocyte modulation of carbonate substitution decreases once the increased mineral demands of reproduction were over. Using Raman Spectroscopy, we analyzed the mineral matrix immediately surrounding osteocyte lacunae for the carbonate to phosphate ratio. We examined wild-type (WT) and HYP mice before pregnancy, at the end of pregnancy (E18.5), at the end of a 21-day lactation period, and 1 month post-weaning. We scanned 16 points, each 10µm apart, in a grid pattern within the cortical bone of the femoral diaphysis. We found that intracortical carbonate content significantly decreased ( $p < 0.05$ ) returning to baseline levels after 1 month recovery compared to at the end of lactation in both WT and HYP. The carbonate content fell 21% between the end of lactation and the 1 month recovery period in HYP as compared to a 9% drop in WT (Fig. 1). As expected, HYP mice had a significantly increased amount of carbonate ion substitution, with the levels being almost 40% greater immediately after lactation and 20% greater after recovery compared to WT ( $p < 0.05$ ). These results show that the amount of carbonate ion substitution within the bone matrix decreases as the demand for phosphate decreases. This change is very crucial in HYP mice as it suggests there is no cumulative effect and multiple pregnancies in XLH are not deleterious to skeletal integrity. Despite showing significant recovery, HYP mice continue to have elevated carbonate levels compared to WT mice. Previous work revealed that osteocyte expression of MMP13 correlated with the increase in carbonate ion substitution during reproduction. Thus, we expect a decrease in MMP13 expression 1 month post-weaning. Ongoing immunohistochemistry staining for MMP13, tartrate-resistant acid phosphatase (TRAP), alkaline phosphatase, and receptor activator of nuclear factor kappa-B ligand (RANKL) will provide further insight into the mechanism of the observed recovery.

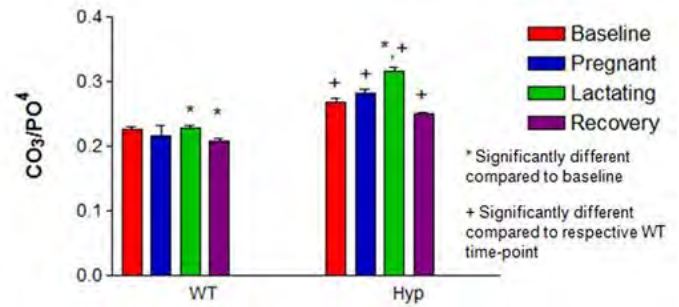


Figure 1

**Disclosures:** [Kunal Agarwal](#), None.

## SU0184

**RNA Sequencing Reveals Common Gene Expression Patterns in Osteocyte-Enriched Bone of Two Osteogenesis Imperfecta Mouse Models.** [Sarah Zimmerman](#)<sup>\*</sup>, [Melissa Heard](#), [Milena Dimori](#), [Roy Morello](#). University of Arkansas for Medical Sciences, United states

Osteogenesis imperfecta (OI) is the most common inherited connective tissue disorder and is characterized by osteopenia and bone fragility. The osteoblast has been the most thoroughly studied cell type in OI since it produces large amounts of type I collagen, and the majority of OI cases are caused by mutations in type I collagen. However, observations in OI patients and animal models often reveal high numbers of osteoclasts as well as osteoblasts, accompanied by high bone turnover. Thus, the pathology of OI likely arises from multiple factors and involves all the cells of the bone. The osteocyte can regulate many processes of bone homeostasis, indeed, it has been proposed to be a key regulator of bone remodeling. Of particular importance to these studies, the osteocyte is located in a prime position to respond to bone material quality. We hypothesize that the abnormal bone matrix in OI causes dysregulation in osteocytes of key signaling pathways controlling bone turnover, including Tgf-beta signaling. To test this hypothesis, we performed RNA sequencing (RNASeq) on osteocyte-enriched bone from wild type (WT) mice and two OI mouse models: the osteogenesis imperfecta murine (*oim*) mouse is a model for "classical" OI caused by a *Colla2* mutation, and the *Crtap*- mouse is a model of recessive OI type VII which is caused by mutations in cartilage-associated protein (CRTAP). RNASeq detected 544 and 855 transcripts that were differentially expressed (DE, at least 2-fold change) in *oim* and *Crtap*-, respectively, compared to WT controls. There was substantial overlap of DE transcripts in the OI models; 281 transcripts appeared in both DE lists (52% of the total *oim* list and 33% of the total *Crtap*- list). Conversely, a DE analysis comparing *oim* to *Crtap*- generated a list of only 49 transcripts. This suggests that osteocyte gene expression is similar between the two OI models but quite different from WT. Additionally, the RNASeq results indicated an increase in Tgf-beta signaling, seen as an increase in expression of multiple Tgf-beta target genes. Functional annotation enrichment analysis showed that both OI models have an up-regulation of genes related to extracellular matrix production and organization as well as a down-regulation of cytokine/chemokine signaling. While the analysis of the complete set of the RNASeq data is ongoing, overall these studies are providing a new insight into the molecular changes underlying the pathology of OI.

**Disclosures:** [Sarah Zimmerman](#), None.

## SU0185

**The Osteocyte Network Formation is Influenced by the Thick Collagen Bundle Formation during Bone Modeling.** [Mana Hashimoto](#)<sup>\*1</sup>, [Noriyuki Nagaoka](#)<sup>2</sup>, [Tadahiro Imura](#)<sup>3</sup>, [Toru Hara](#)<sup>4</sup>, [Hirosaki Kamioka](#)<sup>1</sup>. <sup>1</sup>Okayama University Graduate School of Medicine, Dentistry & Pharmaceutical Sciences, Department of Orthodontics, Japan, <sup>2</sup>Okayama University Dental School, Advanced Research Center for Oral & Craniofacial Sciences, Japan, <sup>3</sup>Proteo-Science Center, Ehime University, Japan, <sup>4</sup>National Institute for Materials Science, Japan

AIM: Osteocytes form the cellular network by their long processes and act as mechanosensory cells in bone. However, it is unknown how this cellular network is formed and what kind of factors influence the network formation. Focused ion beam-scanning electron microscopy (FIB-SEM) has increasingly found use in biological research. The main application is in the acquisition of three-dimensional data by tomography. We therefore reconstructed three-dimensional images of the osteocyte network as well as the collagen fibrils during bone modeling. Based on the positional relationships of osteocytes and collagen fibrils, we analyzed the influence of the collagen bundle formation on the osteocyte network formation. METHODS: The 17-day-old embryonic chick calvaria were fixed and prepared for FIB-SEM observation with en bloc electrical staining. The samples were milled by FIB at 25 nm in thickness, and their images were captured by SEM. Approximately 1000 images were obtained and reconstructed into three-dimensional images using the Amira software program. To inhibit the collagen cross-linkage,  $\beta$ -Aminopropionitrile (BAPN) was administered to

the embryonic chick, and then calvaria were dissected after three days and observed using a second harmonic generation (SHG) microscope to confirm the effect of BAPN on collagen bundling. The samples same as the sample which we observed using a SHG microscope were stained using fluorescent-labeled phalloidin to visualize the osteocyte network formation with a confocal laser microscope. A morphometric analysis was performed to analyze the relationship between the osteocyte network formation and collagen bundle formation. RESULTS: Three-dimensionally reorganized images obtained using FIB-SEM revealed that osteocyte processes elongate into the bone matrix while avoiding the thick collagen bundles with a diameter exceeding several micrometers due to cross-linkage. In our BAPN experiments, we observed significant differences in the osteocyte network formation of the calvaria administered BAPN versus the control calvaria with respect to loss of regularity. In addition, the SHG microscopic images confirmed low regularity in collagen bundle organization in the calvaria administered BAPN. CONCLUSION: Our findings suggested that the osteocyte network formation was influenced by the thick collagen-bundle formation. We have considered the possibility of matrix-oriented osteocyte network formation.

**Disclosures:** Mana Hashimoto, None.

## SU0186

**Induced Sclerostin Expression in Human Dermal Fibroblasts is Positively Regulated by Prostaglandin E2 via EP1 Receptor..** Makoto Fujiwara<sup>\*1</sup>, Shinji Takeyari<sup>1</sup>, Mohammad Saiful Islam<sup>1</sup>, Chiho Nakano<sup>2</sup>, Kenichi Yamamoto<sup>1</sup>, Hirofumi Nakayama<sup>1</sup>, Satoshi Takakuwa<sup>1</sup>, Taichi Kitaoka<sup>1</sup>, Takuo Kubota<sup>1</sup>, Keiichi Ozono<sup>1</sup>. <sup>1</sup>Department of Pediatrics, Osaka University Graduate School of Medicine, Japan, <sup>2</sup>The First Department of Oral & Maxillofacial Surgery, Osaka University Graduate School of Dentistry, Japan

**Background:** Sclerostin, encoded by *SOST*, is a secretory protein expressed specifically in osteocytes and suppresses osteogenesis by the inhibition of the WNT signaling. Regulatory mechanism of *SOST* expression remains unclear mainly due to difficulty in using osteocytes in vitro. By transducing 4 transcription factors, we have succeeded in inducing sclerostin in human dermal fibroblasts as a substitute for osteocytes (Fujiwara M et al. BONE 2016). In osteocytes, prostaglandin E2 (PGE2) is known to suppress *SOST* expression with its enhanced expression rapidly following mechanical loading. In this study, we aim to assess the regulation of PGE2 on the induced *SOST* expression in dermal fibroblasts.

**Methods:** We introduced ATF3, KLF4, PAX4 and SP7 genes into human dermal fibroblasts using retrovirus, then analyzed expression levels of *PTGER1-4* coding PGE2 receptor EP1-4 as well as *SOST* by real time PCR after 1 week culture. Subsequently, we analyzed the expression of the induced *SOST* with 5 nM PGE2 or indomethacin in last 24 hours. Furthermore, the effect of ONO-8713, an antagonist of EP1, on the induced *SOST* expression with PGE2 was assessed.

**Results:** Combination of ATF3, KLF4, PAX4 and SP7 induced *SOST* expression 182 times compared to mock in human dermal fibroblasts at 1 week after transduction. As for PGE2 receptors, the expression of *PTGER1* significantly increased after 4 TFs transduction (10.2 times compared to mock), while that of *PTGER2-4* decreased or did not change. As for the induced *SOST* expression, adding PGE2 showed further increase (3.6 times compared to vehicle), though indomethacin treatment indicated little change. On the other hand, the addition of ONO-8713 with PGE2 following 4 TFs transduction increased the induced *SOST* expression only 1.4 times compared to vehicle, and decreased it by 52 % compared to that of PGE2 alone.

**Conclusion and discussion:** In osteocytes, PGE2 was reported to effect on *SOST* expression negatively via EP2 or EP4. Our study indicates the possibility that the induced *SOST* expression is positively regulated by exogenous PGE2 via EP1 in dermal fibroblasts. Although there has been no report about the association between *SOST* regulation and EP1, this finding might imply the relationship between *SOST* regulation and some PGE2-EP1-mediated physiological reaction including response to pain or stress. Further study is required to elucidate the general mechanism of the regulation of PGE2 on *SOST* expression.

**Disclosures:** Makoto Fujiwara, None.

## SU0187

**Association of Circulating Dipeptidyl-peptidase 4 Levels with Osteoporotic Fracture in Postmenopausal Women.** Hyeonmok Kim<sup>\*1</sup>, Ki Hyun Baek<sup>2</sup>, Sun-Young Lee<sup>3</sup>, Seong Hee Ahn<sup>4</sup>, Seung Hun Lee<sup>1</sup>, Jung-Min Koh<sup>1</sup>, Yumie Rhee<sup>5</sup>, Chong Hwa Kim<sup>6</sup>, Deog-Yoon Kim<sup>7</sup>, Moo-Il Kang<sup>2</sup>, Beom-Jun Kim<sup>1</sup>, Yong-Ki Min<sup>8</sup>. <sup>1</sup>Asan Medical Center, University of Ulsan College of Medicine, Korea, republic of, <sup>2</sup>Seoul St. Mary's Hospital, The Catholic University of Korea College of Medicine, Korea, republic of, <sup>3</sup>Asan Institute for Life Science, Korea, republic of, <sup>4</sup>Inha University School of Medicine, Korea, republic of, <sup>5</sup>Severance Hospital, Yonsei University College of Medicine, Korea, republic of, <sup>6</sup>Sejong General Hospital, Korea, republic of, <sup>7</sup>Kyunghee University School of Medicine, Korea, republic of, <sup>8</sup>Sungkyunkwan University School of Medicine, Korea, republic of

**Purpose:** Evidence indicates that dipeptidyl-peptidase 4 (DPP4) plays a distinct role in bone metabolism. However, there has been no report on the association, if any,

between circulating DPP4 levels and osteoporosis-related phenotypes. This study aimed to determine if DPP4 predicts osteoporotic fracture (OF) risk in postmenopausal women.

**Methods:** This is a case-control study conducted in multiple centers in Korea. We enrolled 178 cases with OF and 178 age- and body mass index-matched controls. OF was assessed by an interviewer-assisted questionnaire and lateral thoracolumbar radiographs. Bone turnover markers (BTMs), bone mineral density (BMD), and plasma DPP4 levels were obtained in all subjects.

**Results:** After adjustment for potential confounders, subjects with OF had significantly higher plasma DPP4 levels than those without ( $P = 0.021$ ). Higher DPP4 levels were significantly associated with higher levels of all BTMs, but not with BMD at all measured sites. The differences in DPP4 levels according to OF status disappeared after an additional adjustment for each BTM, but not after adjustment for any BMD values. BTMs explained approximately half of the relationship between DPP4 and OF. The risk of OF was 3.80-fold (95% confidence interval = 1.53–9.42) higher in subjects in the highest DPP4 quartile than in those in the lowest quartile after adjustment for potential confounders, including femoral neck BMD.

**Conclusion:** DPP4 may be associated with OF by at least partly mediating the bone turnover rate. Circulating DPP4 levels may be a potential biomarker that could increase the predictive power of current fracture risk assessment models.

**Disclosures:** Hyeonmok Kim, None.

## SU0188

**High Prevalence (64%) of Mutations in the LRP5 and/or COL1A1 Genes in Male & Juvenile Female Patients with Osteoporosis.** Christian Wüster<sup>\*1</sup>, Susanne Thomczyk<sup>2</sup>, Wolfgang Höppner<sup>3</sup>, Klaus Edgar Roth<sup>2</sup>, Philipp Drees<sup>2</sup>. <sup>1</sup>Center for Hormones & Metabolism Prof. Wüster, Germany, <sup>2</sup>Orthopaedics, Orthopaedic & Rheumatoid Surgery, University Mainz, Germany, <sup>3</sup>Bioglobe GmbH Hamburg, Germany

**Introduction:** Several genetic causes of osteoporosis have been identified. Single mutations have been shown in some individual patients or several polymorphisms in population-based studies. The intention of the study was to investigate bone mineral density (BMD), fracture rates, markers of bone turnover (BTMs) and special point mutations (COL1A1 and LRP5) in a larger group of male and juvenile female patients with established osteoporosis in a clinical setting.

**Patient characteristics:** 194 patients [39 males (20%) and 155 females (80%)] with a mean age of 48 years in man and 54 years in women were included into the study. BMD was measured by DXA (Medix DR, MediLink, France), fractures were recorded by history and BTM measured by ELISAs (ids, Frankfurt, Germany). Genetic mutations were analyzed by bioglobe, Hamburg, Germany. We divided patients into 4 groups: patients with no mutations (A), with mutations in COL1A1 (B) or LRP5 (C) and a mutation in both genes (COL1A1 & LRP5) (D).

**Results:** 124 patients (64%) [25 males (m) & 99 females (f)] had at least one mutation. Group A (no mutation) consisted of n=72 (37%) [15 m & 60 f], group B (COL1A1): n=38 (20%) [8 m & 30 f], group C (LRP5): n= 43 (22%) [12 m & 34 f] and group D (COL1A1 & LRP5): n=35 (18%) [ 6 m & 29 f]. There was no significant difference in fracture rates, mean BMD and BTMs between the 4 groups.

**Discussion:** There is a high prevalence of mutations in the COL1A1 and/or LRP5 genes in selected patients with osteoporosis (males and young females). There was no difference in their clinical characteristics versus those patients without a mutation. Further studies have to show whether the presence of a mutation has a significant influence on treatment outcome.

**Conclusions:** Genetic screening should be considered as a routine investigation in patients with osteoporosis.

**Disclosures:** Christian Wüster, None.

## SU0189

**Serum Carboxy-terminal Telopeptide of Type 1 Collagen (1CTP) is the Strongest Predictor of Survival Among Bone Turnover Markers in a Cohort of Japanese Subjects Undergoing Coronary Angiography: CHIBA (Coronary Heart Disease of Ischemia and Bone Association) Study.** Nobuyuki Tai<sup>\*</sup>, Reiko Watanabe, Junko Hirano, Toshihiro Amaki, Fumitaka Nakamura, Ryo Okazaki, Daisuke Inoue. Teikyo University Chiba Medical Center, Japan

**Background:** Some bone turnover markers have been shown to be associated with mortality and cardiovascular (CV) events. However, specific role for each bone turnover marker in mortality and CV events has not been established. We previously reported that an MMP-dependent collagen marker, 1CTP, was strongly correlated with NT-proBNP and LV ejection fraction as well as high bone turnover at baseline and that it was a strong predictor of all-cause mortality in Japanese males undergoing coronary angiography (CAG).

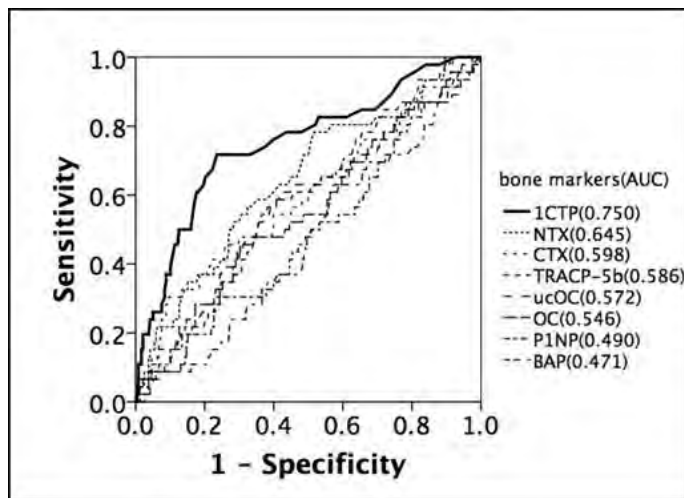
**Aim:** To evaluate the ability of bone turnover markers to predict all-cause mortality in Japanese subjects including both males and females in CHIBA study.

**Methods:** This study is a longitudinal cohort study. Subjects undergoing CAG were recruited in our hospital from Jan 2006 to Dec 2007. Subjects with renal insufficiency

(eGFR < 30), glucocorticoid therapy and drugs affecting bone metabolism were excluded. Bone turnover markers (ICTP, NTX, CTX, TRACP-5b, P1NP, BAP, osteocalcin (OC), undercarboxylated OC (ucOC), 25(OH)D, 1,25(OH)2D, intact PTH) were measured at baseline. The primary endpoint was all-cause mortality and ascertained using mail questionnaires and confirmed using medical records from Dec 2014 to Apr 2015.

Results: 291 subjects (217 males and 74 females) aged  $66.1 \pm 10.9$  y.o. were followed up for  $80.0 \pm 18.8$  months. All-cause death occurred in 47 subjects (16.1%) and causes of death included cancer (n=15), CV event (n=9), congestive heart failure (n=5), infection (n=5), sudden death (n=3), trauma (n=3) and others (n=7). Multivariate cox regression analysis showed that ICTP and age were independent predictors of all-cause mortality after adjustment for sex, eGFR, NT-proBNP, coronary stenosis lesions and causes of death. ROC analysis of bone markers revealed that ICTP showed the highest prognostic efficiency for all-cause mortality (AUC : ICTP 0.750, NTX 0.645, CTX 0.598, TRACP-5b 0.586, ucOC 0.572, OC 0.546, P1NP 0.490, BAP 0.471)(See figure). The best cut off value for ICTP was 3.95ng/ml with 71.7% sensitivity and 75.6% specificity.

Conclusions: Among various bone turnover markers clinically available, ICTP was found to be the strongest predictor of all-cause death in Japanese subjects undergoing CAG. ICTP may thus be a useful prognostic marker in the context of coexistent cardiovascular and bone abnormalities.



ROC curves of bone turnover markers for mortality

Disclosures: Nobuyuki Tai, None.

## SU0190

**Validation of a Novel, Rapid, High Precision Sclerostin Assay Which is Not Confounded by Sclerostin Fragments.** Matthew Drake\*, Sundeep Khosla. Mayo Clinic College of Medicine, United states

Sclerostin is a 190 amino acid protein secreted primarily by osteocytes. It was initially identified due to mutations in the SOST gene associated with high bone mass phenotypes. Much recent work has sought to determine the importance of sclerostin across an array of conditions which affect the human skeleton. However, accurate measurement of sclerostin from serum and plasma sources remains a significant impediment, with currently available commercial assays showing marked differences in measured sclerostin values. Accordingly, sclerostin assay standardization remains an important but unmet need before sclerostin measurements can be used for the clinical management of bone disease. Here we characterize a novel automated chemiluminescent sclerostin assay (LIAISON, DiaSorin) which overcomes many of these limitations. Important assay characteristics include: a wide dynamic range (0-6500 pg/mL); high intra (<2.5%) and inter (<5%) assay precision; matched serum and plasma equivalence (< 10% difference); exquisite specificity for the intact sclerostin molecule (does not detect sclerostin in samples from patients with sclerosteosis; does not detect thrombin digested recombinant sclerostin fragments); and rapid assay results (65 minutes). Serum sclerostin levels measured with the LIAISON assay in a population-based sample of adult men (n=278) and women (n=348) demonstrated that sclerostin levels were significantly higher in men as compared to women and were positively associated with age in both sexes, consistent with previously published work from our group. In postmenopausal women, serum sclerostin levels measured with the LIAISON assay were reduced in response to treatment with either estrogen or teriparatide, again consistent with previous findings. Collectively, the above data demonstrate that the LIAISON sclerostin assay provides a reliable tool for more confident assessment of emergent mechanisms wherein sclerostin may both impact and shape a number of bone related pathologies.

Disclosures: Matthew Drake, None.

This study received funding from: DiaSorin, Inc.

## SU0191

**Assessment of Mineral Micro-Structure Related Cortical Bone Quality - A Clinical Study in Post-Menopausal Women and Dialysis Patients Using Ultrasounds.** Kosei Yoh\*, Ryoichi Suetoshi<sup>2</sup>, Tatsuo Arai<sup>3</sup>, Dorian Cretin<sup>3</sup>, Akira Okayama<sup>4</sup>, Hirovuki Ogura<sup>4</sup>, Shotaro Tsuji<sup>4</sup>. <sup>1</sup>Faculty of Health Science, Aino University, Japan, <sup>2</sup>Furuno Electric Co., Ltd., Japan, <sup>3</sup>Furuno Erectic. Co., Ltd., Japan, <sup>4</sup>Sasayama Medical Center, Hyogo College Of Medicine, Japan

### Introduction

Conventionally, QUS are used to evaluate the bone density, by measuring the Speed of Sound (SOS) at which ultrasounds propagate in the heel. On the other hand, the speed of ultrasounds propagating through the cortical bone (cortical Speed of Sound: cSOS) can be used to assess bone quality. Following this hypothesis, its relationship with calcification and cortical porosity has been shown in a recent investigation using HR-pQCT. In this study, we aim at clarifying the potential use of cSOS clinically, by focusing on bone quality differences in post-menopausal women and dialysis patients.

### Methods

Participants were split into 3 groups: 91 young and healthy subjects aged 22 to 44 years (Male: 47, Female: 44), 64 elderly volunteers aged over 60 years not taking any osteoporosis drugs (M: 30, F: 34) and 64 dialysis patients aged 37 to 75 years (M: 33, F: 31). Their bone quality index cSOS at the mid-shaft tibia using a device in clinical trial (Furuno, Japan), as well as their traditional QUS bone density index SOS were measured. Elderlies had also their DXA BMD and bone turnover markers (BAP, TRACP-5b) measured.

### Results

Concerning males, no difference in cSOS between young and elderly groups were observed. On the other hand, the cSOS of elderly women (Mean  $\pm$  SD,  $3858 \pm 79$  m/s) was significantly lower for the young women ( $3971 \pm 63$  m/s,  $p < 0.001$ ). Also, cSOS in the group of dialysis patients ( $3843 \pm 121$  m/s) were significantly lower than those in the group of young people ( $3956 \pm 63$  m/s), for both males and females ( $p < 0.001$ ). No correlation was observed between cSOS and neither SOS nor BMD, showing cSOS to be independent of bone density. For all post-menopausal women with low-cSOS, bone formation markers (BAP) were normal but markers characteristic of metabolic anomalies in the bone resorption (TRACP-5b) were elevated. In dialysis patients, a negative correlation ( $r = -0.58$  to  $-0.45$ ,  $p < 0.05$ ) between cSOS and both the dialysis time and intact-PTH was found.

### Discussion

The decline in cSOS in post-menopausal women and dialysis patients can be explained by the decrease of mineralization and the increase of porosity due to a bone mineral metabolism abnormality. Since cSOS allows us to capture the cortical bone deteriorations in bone quality, and considering that those cannot be evaluated by conventional apparatuses such as DXA and QUS, we can expect cSOS to be useful in the prevention of bone fractures by bone quality driven early treatment.

Disclosures: Kosei Yoh, None.

This study received funding from: Furuno Electric Co., Ltd.

## SU0192

**Early Cortical, but not Trabecular, Microarchitectural Changes by HRpQCT Identify Postmenopausal Women at Risk for Rapid Bone Loss at the hip or Spine.** Sundeep Khosla\*, Kristy Nicks<sup>1</sup>, Andrew Burghardt<sup>2</sup>, Elizabeth Atkinson<sup>1</sup>, Louise McCready<sup>3</sup>, Matthew Drake<sup>1</sup>, Shrevesee Amin<sup>1</sup>. <sup>1</sup>Mayo Clinic College of Medicine, United states, <sup>2</sup>University of California, San Francisco, United states, <sup>3</sup>Mayo Clinic College of Medicine, United states

There is general agreement that postmenopausal women with osteoporosis by BMD (T score < -2.5) or with a history of osteoporotic fractures should be considered for pharmacological therapy. For women with osteopenia (T-scores -1 to -2.5), current guidelines recommend treatment based on 10-yr fracture risk calculated from FRAX. However, neither BMD at a given time point nor FRAX discriminate slow from rapid bone loss. Thus, we tested the hypothesis that early (over 6-12 months) microstructural changes evident by HRpQCT may identify the subset of women with rapid bone loss by DXA over 3 yrs (defined as  $>3\%/3$  yr at the total hip or spine), thus enabling clinicians to target these women for closer follow-up and/or earlier treatment. We studied 193 early postmenopausal women aged 50-61 yrs who were otherwise in good health and not on medications known to affect bone metabolism. Changes in HRpQCT parameters from baseline to 6 or 12 months were tested for predicting rapid bone loss by DXA, as defined above. The Table below shows the ability of changes in the tibia HRpQCT parameters at 12 months (which were more predictive than the radius HRpQCT parameters or than the 6 month changes) in identifying women undergoing rapid bone loss at the hip or spine (OR [95% CI] per 1%/yr change in HRpQCT parameter). As is evident, 12 month changes in trabecular parameters were not predictive of 3 yr changes in hip or spine DXA; by contrast, changes in cortical porosity, thickness, and vBMD at 12 months were predictive of 3 yr changes in DXA at both the hip and spine, with cortical vBMD having the highest ORs, perhaps because it may integrate both porosity and thickness (the latter through partial volume effects). In a similar analysis, serum bone turnover markers measured at baseline performed relatively poorly at predicting rapid bone loss [e.g., OR for CTX/SD increase, 1.08 (0.80-1.46) and 1.19 (0.89-1.61) for the hip and spine, respectively; OR for PINP/SD increase, 1.00 (0.74-1.35) and 1.15 (0.86-1.55) for the

hip and spine, respectively]. We conclude that 12 month changes in tibial cortical, but not trabecular, parameters by HRpQCT are predictive of rapid bone loss in early postmenopausal women. These findings suggest that early cortical microarchitectural deterioration following the menopause may reflect overall bone loss at distant sites, including the hip and spine, and could be useful in identifying postmenopausal women at risk for rapid bone loss.

	OR [95% CI] for rapid bone loss at the <b>hip</b> by DXA over 3 yrs based on 12 month change in HRpQCT	OR [95% CI] for rapid bone loss at the <b>spine</b> by DXA over 3 yrs based on 12 month change in HRpQCT
<b>Cortical</b>		
↓vBMD	1.62(1.29-2.04)***	1.37 (1.12-1.68)**
↓Thickness	1.26 (1.14-1.39)***	1.19 (1.09-1.31)***
↑Porosity	1.08 (1.04-1.11)***	1.08 (1.03-1.11)***
<b>Trabecular</b>		
↓BV/TV	1.08(0.97-1.21)	1.08 (0.97-1.20)
↓TbN	0.99 (0.95-1.03)	1.02 (0.98-1.06)
↓TbTh	1.03 (0.98-1.07)	0.99 (0.95-1.03)
↑TbSp	0.99 (0.95-1.03)	1.02 (0.98-1.06)

\*P < 0.05; \*\*P < 0.01; \*\*\*P < 0.001

Table 1

Disclosures: *Sundeep Khosla, None.*

### SU0193

**Longitudinal changes of bone microstructure in men with osteopenia and osteoporosis.** Kiyoshi Sada\*<sup>1</sup>, Andrew Burghardt<sup>1</sup>, Anne Schafer<sup>2</sup>, Galatea Kazakia<sup>1</sup>, Ko Chiba<sup>3</sup>, Narihiro Okazaki<sup>3</sup>, Sharmila Majumdar<sup>1</sup>.  
<sup>1</sup>Musculoskeletal Quantitative Imaging Research Group, Department of Radiology & Biomedical Imaging, University of California, San Francisco, United states, <sup>2</sup>Endocrine Research Unit, San Francisco Veterans Affairs Medical Center, San Francisco, United states, <sup>3</sup>Department of Orthopaedic Surgery, Nagasaki University Hospital, Japan

**Introduction:** Though male osteoporosis is not as prevalent as female osteoporosis, the consequences of male osteoporosis are more severe, including higher mortality after hip fracture and a greater decrease in quality of life. This study aims to characterize longitudinal changes of cortical bone microstructure in men with osteopenia and osteoporosis.

**Methods:** This 1-year longitudinal study consisted 65 subjects. Their mean age was 62.9±7.7. They underwent blood examination, HR-pQCT (XtremeCT, Scanco Medical), and dual-energy X-ray absorptiometry (DXA) at lumbar spine, hip, and radius at baseline and 1-year later. We categorized participants into two groups by DXA BMD status: (1) normal and (2) osteopenia/osteoporosis groups. The distal tibia and radius of subjects were scanned using HR-pQCT to exclusively measure cortical bone status: each scan region was 37.5mm (tibia) or 24.5mm (radius) proximal to the standard reference line position.

**Results:** At the tibia, no significant changes in integral BMD were observed after 12-months in either group. However, significant increases in cortical porosity were observed in the normal group alone (5.79±7.98%). In the osteopenia/osteoporosis group, loss of total BMD at the radius (-0.64±1.19%) was driven by a significant decrease in cortical thickness (-1.28±1.41%).

**Conclusion:** In men with healthy bone density profiles, cortical porosity may provide early indications of age-related bone loss. In contrast men with low bone density or osteoporosis are characterized by gross cortical thinning.

Disclosures: *Kiyoshi Sada, None.*

### SU0194

**Peri- and Post- Menopause Bone Microarchitecture: Accelerated Changes are Marked by Increasing Cortical Porosity.** Jennifer Bhatla\*<sup>1</sup>, Lauren Burt<sup>1</sup>, David Hanley<sup>2</sup>, Steven Boyd<sup>1</sup>. <sup>1</sup>McCaig Institute for Bone & Joint Health, Department of Radiology, Cumming School of Medicine, University of Calgary, Calgary, Canada, Canada, <sup>2</sup>McCaig Institute for Bone & Joint Health, Departments of Community Health Sciences & Oncology, Cumming School of Medicine, University of Calgary, Calgary, Canada, Canada

Accelerated bone loss occurs during menopause, presumably accompanied by bone microarchitecture changes. Bone mineral density changes have primarily been characterized by dual x-ray absorptiometry with 2D cross sectional data. Our five-year longitudinal high resolution peripheral quantitative computed tomography (HR-pQCT) study aims to assess 3D bone microarchitecture, which influences strength, to compare rate of change between peri- and post-menopause women.

Participants were selected from the Calgary Canadian Multicentre Osteoporosis Study (CaMos) cohort based on menopause questionnaire data (stage 1-5). Perimenopause women (n=26) were defined as beginning transition to near the end (stage 2-4), when menstrual cycles become irregular. Post-menopause women (n=65) had completed transition (stage 5). HR-pQCT (Scanco Medical, Switzerland) tibia and radius scans, performed at baseline and follow up (mean 5.5yrs), assessed total, cortical and trabecular bone mineral density (Tt.BMD, Ct. BMD, Tb.BMD), total area (Tt.Ar), cortical and trabecular thickness (Ct.Th, Tb.Th) and cortical porosity (Ct.Po). To compare repeat scans, automated 3D image registration was conducted (IPL software). Finite element modeling (FAIM software) estimated failure loads. T-tests compared differences within and between groups.

Both groups experienced reduced bone quality over time. The radius and tibia had significant decreases in Tt.BMD, Ct.BMD, and Ct.Th (-0.3 to -1.1%/yr), and increases in Tb.Ar (0.1 to 0.4%/yr) and Ct.Po (6 to 11%/yr). Tibia Tt.Ar increased (0.06 to 0.13%/yr) and radius Ct.Ar decreased (-0.9 to -1.0%/yr). Radius failure load changed in post-menopause women. The rate of change (RoC) between groups was not different at the radius, but tibia Tt.Ar and Ct.Po RoC differed. Peri- compared to post-menopausal women experienced accelerated Ct.Po RoC (9.0 and 6.3%/yr respectively, p=0.046) and less Tt.Ar RoC (0.06 and 0.13%/yr, p=0.017).

Accelerated Ct.Po RoC during menopause transition is a marker of increased microarchitecture changes, consistent with increased bone remodeling due to estrogen deficiency, and thought to influence cortical bone loss. Both groups experienced decreasing Ct.Th and increasing Ct.Po. Increasing tibia cross-sectional area (Tt.Ar and Tb.Ar) may offset microarchitecture changes as failure load did not decrease. As a marker of accelerated change, Ct.Po may be an early indicator of bone loss, with implications for prevention strategies.

Disclosures: *Jennifer Bhatla, None.*

### SU0195

**Reproducibility of Bone Mineral Density and Microstructural Parameters Measured by Second Generation HR-pQCT.** Ko Chiba\*<sup>1</sup>, Narihiro Okazaki<sup>1</sup>, Ayako Kurogi<sup>1</sup>, Yusaku Isobe<sup>2</sup>, Shuntaro Sato<sup>3</sup>, Kiyoshi Sada<sup>4</sup>, Makoto Osaki<sup>5</sup>. <sup>1</sup>Department of Orthopedic Surgery, Nagasaki University Hospital, Japan, <sup>2</sup>Nagasaki University School of Medicine, Japan, <sup>3</sup>Clinical Research Center, Nagasaki University Hospital, Japan, <sup>4</sup>Department of Radiology & Biomedical Imaging, University of California, San Francisco, Japan, <sup>5</sup> Department of Orthopedic Surgery, Nagasaki University Hospital, Japan

**Introduction:**

High resolution peripheral quantitative CT (HR-pQCT) was developed in 2004 in Switzerland enabling us to analyze patients' bone microstructure non-invasively. It was upgraded in 2014 with a higher resolution and a faster scan time (XtremeCT II, Scanco Medical). The second generation HR-pQCT was installed at Nagasaki University for the first time in Japan in 2015.

The purpose of this study is to investigate the precision of the second generation HR-pQCT by analyzing the reproducibility of each parameter.

**Method:**

Fifteen volunteers (aged 20-74 years; 8 males and 7 females) participated in this study. One tester (an orthopedic surgeon with two years' experience in HR-pQCT study) scanned the 15 subjects 3 times at 0, 1, and 4 weeks to investigate intra-tester reproducibility. Two other testers (orthopedic surgeons with two years and one month of experience, respectively) also scanned the 15 subjects to investigate inter-tester reproducibility.

The coefficient of variance (%CV) of the 3 measured values was calculated, and the reproducibility was evaluated by the root-mean-square of %CV (RMS%CV) of the 15 cases.

**Results:**

The RMS%CV of intra- and inter-testers were 0.56~2.32% and 0.62~2.75% in bone mineral density parameters; 0.75~3.98% and 0.72~2.63% in bone microstructural parameters; and 11.0~13.3% and 12.2~13.1% in cortical porosity, respectively.

**Conclusion:**

Reproducibility of the measured value by second generation HR-pQCT were good in bone mineral density and microstructural parameters, though not excellent in cortical porosity. Inter-tester reproducibility did not show a marked difference from intra-tester reproducibility.

		Radius		Tibia		Ave.
		Intra-tester RMS%CV	Inter-tester RMS%CV	Intra-tester RMS%CV	Inter-tester RMS%CV	
Geometry	Tb.Ar	0.38	0.48	0.61	0.66	0.53
	Ct.Ar	1.27	1.54	2.36	2.48	1.91
	Ct.Pm	0.27	0.32	0.19	0.22	0.25
BMD	Tot.vBMD	1.02	1.12	1.39	1.71	1.31
	Tb.vBMD	1.54	1.47	1.30	1.29	1.40
	Tb.Meta.vBMD	1.84	1.62	1.10	1.15	1.43
	Tb.Inn.vBMD	2.02	2.75	2.32	2.27	2.34
	Ct.vBMD	0.56	0.62	0.68	0.80	0.67
Cancellous bone	Tb.BV/TV	2.14	1.64	1.60	1.40	1.70
	Tb.N	2.04	1.33	2.41	2.32	2.03
	Tb.Th	1.00	0.72	0.75	0.97	0.86
	Tb.Sp	1.63	0.98	1.70	1.53	1.46
	Tb.1/N.SD	3.98	2.63	1.72	1.24	2.39
Cortical bone	Ct.Th	1.17	1.31	1.11	1.16	1.19
	Ct.Po	13.28	13.13	11.03	12.16	12.40
	Ct.Po.Dm	5.38	6.34	4.63	4.28	5.16
	Ave.	2.47	2.38	2.18	2.23	

table

Disclosures: Ko Chiba, None.

## SU0196

**A Population-Based Assessment of the Performance of FRAX in Celiac Disease: The Manitoba BMD Cohort.** William Leslie<sup>1</sup>, Donald Duerksen<sup>1</sup>, Lisa Lix<sup>1</sup>, Suzanne Morin<sup>2</sup>, Sumit Majumdar<sup>3</sup>, Helena Johansson<sup>4</sup>, Anders Oden<sup>4</sup>, Eugene McCloskey<sup>4</sup>, John Kanis<sup>4</sup>. <sup>1</sup>University of Manitoba, Canada, <sup>2</sup>McGill University, Canada, <sup>3</sup>University of Alberta, Canada, <sup>4</sup>Centre for Metabolic Bone Diseases, University of Sheffield Medical School, United Kingdom

**Aim:** FRAX is used for fracture risk assessment in the general population, but its applicability to specific diseases is uncertain. Celiac disease (CD) adversely impacts bone strength, but has not been systematically studied in relation to FRAX.

**Materials:** Using the Manitoba (Canada) clinical DXA registry, we identified women and men age  $\geq 40$  y with baseline DXA (1996–2013). CD status was ascertained from administrative data using a case definition validated against anti-domyosial antibody positivity in a province-wide serological database (sensitivity 84%, specificity 97%, point prevalence 13.6%). FRAX 10-year fracture probability was computed (Canadian tool). Incident major osteoporotic fractures (MOF) were ascertained from diagnoses in linked administrative data. We assessed FRAX stratification (Cox regression) and calibration (observed vs predicted 10-year fracture probability with competing mortality).

**Results:** We identified 693 subjects with CD and 68,037 without CD. CD subjects were younger ( $58 \pm 11$  y vs  $64 \pm 11$  y,  $p < 0.001$ ) and had lower femoral neck Z-score ( $-0.3 \pm 1.1$  vs  $0.0 \pm 0.9$ ,  $p < 0.001$ ). During median 7 years follow up, 58 (8.4%) with CD and 5692 (8.4%) without CD sustained MOFs. FRAX predicted MOF equally well in those with and without CD when computed without BMD (gradient of risk = 1.66 [95% CI 1.28-2.16] vs 1.95 [1.89-2.00], p-interaction $>0.2$ ) and with BMD (gradient of risk = 1.80 [1.43-2.27] vs 2.09 [2.03-2.15], p-interaction $>0.2$ ). CD was associated with increased fracture risk adjusted for age and sex (aHR 1.37, 95% CI 1.05-1.77) and adjusted for FRAX score computed without secondary osteoporosis or BMD (aHR 1.43, 95% CI 1.11-1.86). However, CD was no longer a significant risk factor for MOF when secondary osteoporosis or BMD inputs were included in the FRAX calculation ( $p > 0.1$ ). FRAX was well-calibrated in the non-CD population (predicted probability MOF 11.0% without BMD, 10.6% with BMD; observed probability 10.8% [95% CI 10.5-11.1%]). FRAX underestimated MOF risk when computed without secondary osteoporosis or BMD inputs (predicted probability 7.4%; observed probability 10.8% [95% CI 7.8-13.9%]), but was concordant with outcomes when FRAX included secondary osteoporosis (predicted probability 10.1%) or BMD (probability predicted 8.6%) (Figure). **Conclusions:** CD is independently associated with lower BMD and increased risk for MOF. FRAX appropriately captures this excess risk through the secondary osteoporosis and BMD inputs.

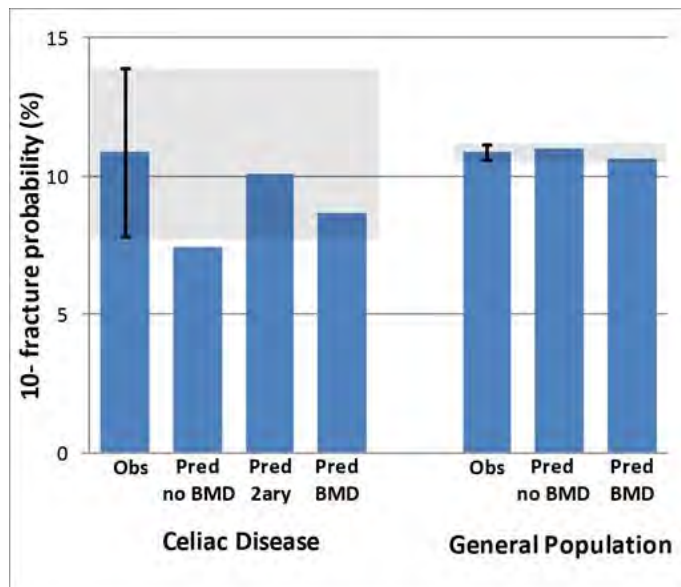


Figure: Observed (shaded 95% CI limits) vs Predicted MOF fracture probability.

Disclosures: William Leslie, None.

## SU0197

**The Effect of White vs Asian Ethnicity on the Performance of FRAX in Canadian Women: The Manitoba BMD Cohort.** William Leslie<sup>1</sup>, Sumit Majumdar<sup>2</sup>, Suzanne Morin<sup>3</sup>, Lisa Lix<sup>1</sup>, Helena Johansson<sup>4</sup>, Anders Oden<sup>4</sup>, Eugene McCloskey<sup>4</sup>, John Kanis<sup>4</sup>. <sup>1</sup>University of Manitoba, Canada, <sup>2</sup>University of Alberta, Canada, <sup>3</sup>McGill University, Canada, <sup>4</sup>Centre for Metabolic Bone Diseases, University of Sheffield Medical School, United Kingdom

**Objective:** The WHO FRAX tool is calibrated to the fracture epidemiology in the target population. The Canadian FRAX tool was calibrated using nationwide mortality and hip fracture hospitalization data, and reflects the dominant European population. Whether this tool performs equally well in other Canadian ethnic populations is uncertain.

**Methods:** Using the Manitoba (Canada) clinical DXA registry, we identified self-identified White and Asian women age 40 years and older undergoing baseline hip DXA assessment (1996–2013). FRAX 10-year fracture probability (Canadian tool) was computed for each woman. We also computed (from DXA) total hip area and hip axis length (HAL), skeletal parameters known to be associated with ethnicity and fracture risk. Incident major osteoporotic fracture (MOF) and hip fracture (HF) were ascertained from linked population-based administrative data using validated algorithms. We assessed Cox regression for fracture prediction (hazard ratios, HR) and FRAX calibration ratios (observed vs predicted 10-year fracture probability with competing mortality).

**Results:** The study population included 58,108 White women and 1182 Asian women. White women had 4,913 incident MOF and 1,369 HF during mean 7 y of follow up while Asian women had 43 incident MOF and 5 HF during mean 6 y of follow up. Age-adjusted BMD, FRAX scores and crude fracture rates were lower in Asian vs White women. Adjusted for FRAX score with BMD, Asian (vs White) ethnicity was a marker of significantly lower risk for MOF (HR 0.57, 95% CI 0.42-0.77) and HF (HR 0.25, 95% CI 0.10-0.61). Effects were attenuated but not eliminated with further adjustment for total hip area, HAL, and osteoporosis treatment (MOF HR 0.67, 95% CI 0.48-0.94 and HF HR 0.45, 95% CI 0.19-1.10). In both groups FRAX with BMD predicted MOF (HR per SD: White 2.11, 95%CI 2.04-2.17 vs Asian 1.86, 95% CI 1.36-2.55; p-interaction=0.46) and HF (HR per SD: White 4.71, 95%CI 4.37-5.00 vs Asian 8.96, 95% CI 2.01-39.9; p-interaction=0.36). Calibration analyses (Figure) showed that the Canadian FRAX tool with or without BMD was reasonably well-calibrated for White women but significantly underestimated fracture risk in Asian women. **Summary:** The Canadian FRAX tool stratifies fracture risk in White and Asian women equally well, but systematically underestimates fracture risk in Asian women. This may have implications for the calibration and use of FRAX in other ethnically-diverse countries.

SU0199

**Genetic Determinant of Trabecular Bone Score (TBS).** Lan T Ho-Pham<sup>\*1</sup>, Didier Hans<sup>2</sup>, Linh D Mai<sup>3</sup>, Minh C Doan<sup>3</sup>, Tuan V Nguyen<sup>4</sup>. <sup>1</sup>Bone & Muscle Research Division, Ton Duc Thang University, Viet nam, <sup>2</sup>Center of Bone disease, Lausanne University Hospital, Switzerland, <sup>3</sup>Department of Internal Medicine, Pham Ngoc Thach University of Medicine, Viet nam, <sup>4</sup>Osteoporosis & Bone Biology Program, Garvan Institute of Medical Research; School of Public Health & Community Medicine, University of New South Wales; Centre for Health Technologies, University of Technology Sydney, Australia

Introduction. Trabecular bone score has emerged as a predictor of fragility fracture, but its etiological determinants have not been well documented. In this study, we sought to determine the genetic contribution to the variation of TBS in the general population.

Methods. This study was designed as a population based family study, which involved 556 women and 189 men from 265 families. The participants were recruited from Ho Chi Minh City (Vietnam). The individuals aged 53 years (SD 11). We measured lumbar spine bone mineral density (BMD; Hologic Horizon) and then derived the TBS from the BMD scan. A biometric model was applied to the data to partition the variance of TBS into two components: one due to additive genetic factors, and one due to environmental factors. The index of heritability was estimated as the ratio of genetic variance to total variance of a trait. Bivariate genetic analysis was conducted to estimate the genetic correlation between lumbar spine BMD and TBS.

Results. TBS was strongly correlated with lumbar spine BMD ( $r = 0.73$ ;  $P < 0.001$ ). TBS was also significantly associated with age and height, and the two factors accounted for 33% variance of TBS. After adjusting for age and height, average TBS in men was higher than women (1.37 [SD 0.09] vs 1.31 [SD 0.11]). Results of genetic analysis showed that the index of heritability of TBS was 0.51 (95% CI, 0.44 - 0.58), which was not much different from that of lumbar spine BMD (0.53; 95% CI, 0.42 - 0.60). Moreover, the genetic correlation between TBS and LSBMD was 0.34 (95% CI, 0.19 - 0.45).

Conclusions. These data, for the first time, suggest that half of the variance in TBS between individuals is under genetic influence, and this effect magnitude is similar to that of lumbar spine BMD. This finding provides a scientific justification for the search for specific genetic variants that may be associated with TBS and fracture risk.

**Disclosures:** Lan T Ho-Pham, None.

This study received funding from: This research is funded by Foundation for Science and Technology Development of Ton Duc Thang University (FOSTECT, <http://fostect.td-t.edu.vn>), Grant number FOSTECT.2014.BR.09

SU0200

**Increased Trabecular Bone Score in Kidney Transplant Recipients.** Murtaza Bharmal<sup>\*1</sup>, Sahithi Jarugula<sup>2</sup>, Renaud Winzenrieth<sup>3</sup>, Edward Leib<sup>1</sup>. <sup>1</sup>University of Vermont College of Medicine, United states, <sup>2</sup>University of Vermont Medical Center, United states, <sup>3</sup>Med-Imaps, France

Background: Renal transplantation is known to increase the overall risk of fracture 3.6-3.8 fold in comparison to healthy individuals. Although areal bone mineral density (aBMD) is commonly used to assess fracture risk in the general population, its utility in kidney transplant recipients (KTR) remains unclear. Trabecular bone score (TBS), a measure of bone texture analysis derived from the DXA spine image, has been shown to capture differences in bone structure that aBMD has not. The aim of this study was to use TBS to evaluate bone microarchitecture in KTR in comparison to controls.

Methods: In this case-control study, subjects were men and women who underwent kidney transplant at a single university medical center and who have had post-transplant bone density testing. Each KTR case was matched for sex, age ( $\pm 4$  years) and BMI ( $\pm 4$  kg/m<sup>2</sup>) with one healthy control, excluding those with historical fragility fractures and any treatment or illnesses that could influence bone metabolism. Independent variables and clinical risk factors for bone disease were examined across the two groups and a least angle regression analysis was performed.

Results: This study included an original 163 kidney transplant recipients, of whom 139 subjects (mean age 57.8  $\pm$  12.7 years, BMI 28.0  $\pm$  4.5 kg/m<sup>2</sup>) were sex-age-BMI matched to 139 controls (mean age 58.3  $\pm$  12.3 years, BMI 27.6  $\pm$  4.3 kg/m<sup>2</sup>). Table 1 identifies the clinical risk factors present in both populations. KTR cases had a significantly higher lumbar TBS ( $p < 0.005$ ), whereas site-matched aBMD did not vary significantly ( $p = 0.17$ ). KTR cases with fractures had no statistically significant difference for TBS ( $p = 0.61$ ) or BMD ( $p = 0.40$ ) relative to those without fractures. Least angle regression analysis revealed that TBS values were significantly influenced by sex, age, AP Spine aBMD, and being a kidney transplant recipient (TBS = 1.347 - 0.071[if Male] - 0.004\*age + 0.143\*AP Spine aBMD + 0.051 [if in KTR group],  $r^2 = 0.26$ ,  $p = 0.001$ ). Variables of six month smoking history, parental hip fracture, anti-seizure medication use, parathyroid disease, thyroid disease, or diabetes minimally influenced TBS values in this population.

Conclusions: The data suggests that being a KTR is associated with an increase in TBS at the lumbar spine whereas a non-significant effect is seen with BMD. This study shows for the first time a positive relationship with axial trabecular bone score and KTR. Further studies are necessary to confirm these results.

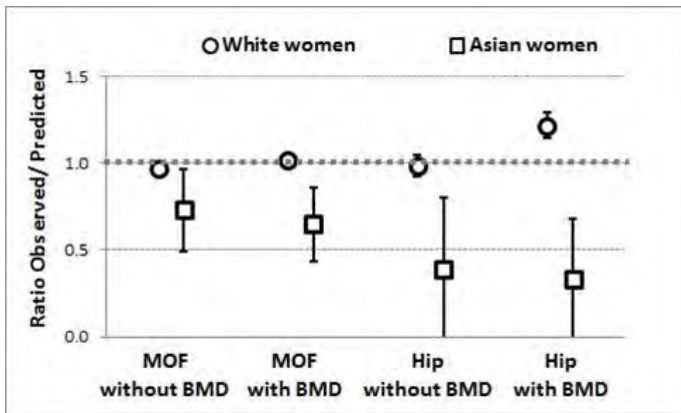


Figure: FRAX calibration ratios (observed vs predicted 10-year fracture probability with 95% CI bars)

**Disclosures:** William Leslie, None.

SU0198

**FRAX and the Confounding Effect of Hip Area in Canadian White Women: The Manitoba BMD Cohort.** William Leslie<sup>\*1</sup>, Sumit Majumdar<sup>2</sup>, Suzanne Morin<sup>3</sup>, Lisa Lix<sup>1</sup>, Helena Johansson<sup>4</sup>, Anders Oden<sup>4</sup>, Eugene McCloskey<sup>4</sup>, John Kanis<sup>4</sup>. <sup>1</sup>University of Manitoba, Canada, <sup>2</sup>University of Alberta, Canada, <sup>3</sup>McGill University, Canada, <sup>4</sup>Centre for Metabolic Bone Diseases, University of Sheffield Medical School, United Kingdom

Aim: DXA provides an areal bone mineral density (BMD) measurement that is confounded by skeletal size. Smaller hip area correlates with younger age and lower fracture risk despite a greater prevalence of osteoporotic BMD. No studies to date have examined whether FRAX is affected by hip area.

Methods: Using the Manitoba (Canada) clinical DXA registry, we identified women aged >40 y self-identified as White with baseline hip DXA (1996–2013). Women were categorized by total hip area quintile (Q1=smallest [referent] to Q5=largest). Total hip area and hip axis length (HAL), a FRAX-independent risk factor for fracture, were obtained from DXA images. FRAX fracture probability (Canadian tool) was computed without and with BMD. Incident major osteoporotic fracture (MOF) and hip fracture (HF) were ascertained using validated algorithms, Cox regression (hazard ratios, HR, for fracture according to hip area) and FRAX calibration ratios (observed vs predicted 10-year fracture probability with competing mortality) were determined.

Results: The cohort included 58,108 women, with 4,913 MOF and 1,369 HF during mean 7 years follow up. Smaller hip area was associated with younger age, lower prevalence of prior fracture, lower age-adjusted femoral neck BMD and lower FRAX scores, while age-adjusted MOF and HF rates were greater in those with larger hip areas ( $p$ -trend for quintiles  $< 0.001$ ). Larger hip area was associated with greater risk for MOF and HF when adjusted for FRAX score, and this effect increased when BMD was included in the FRAX calculation (Table). The largest effect was seen for HF prediction from FRAX with BMD (HR 1.90, 95% CI 1.58-2.27 for largest vs smallest hip area). When additionally adjusted for HAL (available in 48,344 women), hip area was no longer significantly associated with MOF or HF fracture risk. FRAX without BMD was well-calibrated across all hip area quintiles (calibration ratios ~1); FRAX with BMD significantly underestimated MOF risk in the largest hip area quintile (calibration ratio Q5=1.12) and underestimated HF risk in the three largest hip area quintiles (calibration ratios Q3=1.21, Q4=1.30, Q5=1.44).

Summary: Skeletal size affects fracture risk assessment based upon FRAX in Canadian White women, with fracture risk underestimated in those with larger hip area when FRAX includes BMD. Including HAL in the risk assessment compensates for confounding by skeletal size, and provides for more accurate assessment of fracture risk.

TABLE: Adjusted hazard ratios (HR, 95%CI) and calibration ratios (observed/predicted probability) for fracture by total hip area quintile.

Major osteoporotic fracture (MOF)	FRAX without BMD			FRAX with BMD		
	HR, FRAX	HR, FRAX+HAL	Calibration Ratio	HR, FRAX	HR, FRAX+HAL	Calibration Ratio
Q1 (SMALLEST)	1.00 (REF)	1.00 (REF)	0.97 (0.89-1.04)	1.00 (REF)	1.00 (REF)	0.93 (0.86-1.00)
Q2	1.00 (0.91-1.10)	0.99 (0.88-1.10)	0.96 (0.89-1.03)	1.06 (0.96-1.16)	1.01 (0.90-1.13)	0.98 (0.92-1.05)
Q3	0.99 (0.90-1.08)	0.97 (0.86-1.08)	0.91 (0.85-0.98)	1.07 (0.97-1.17)	1.01 (0.90-1.13)	0.96 (0.90-1.03)
Q4	1.08 (0.99-1.15)	1.05 (0.95-1.18)	0.93 (0.82-1.04)	1.19 (1.08-1.30)	1.11 (0.98-1.25)	1.05 (0.99-1.12)
Q5 (LARGEST)	1.12 (1.03-1.23)	0.97 (0.85-1.11)	1.01 (0.95-1.07)	1.27 (1.16-1.39)	1.05 (0.92-1.20)	1.12 (1.05-1.18)
Hip Fracture (HF)	FRAX without BMD			FRAX with BMD		
	HR, FRAX	HR, FRAX+HAL	Calibration Ratio	HR, FRAX	HR, FRAX+HAL	Calibration Ratio
Q1 (SMALLEST)	1.00 (REF)	1.00 (REF)	0.85 (0.70-1.00)	1.00 (REF)	1.00 (REF)	0.88 (0.72-1.04)
Q2	1.14 (0.93-1.39)	1.06 (0.83-1.35)	0.98 (0.83-1.12)	1.36 (1.12-1.66)	1.16 (0.91-1.48)	1.15 (0.98-1.32)
Q3	1.13 (0.93-1.38)	1.04 (0.81-1.32)	0.97 (0.84-1.10)	1.43 (1.18-1.74)	1.20 (0.94-1.53)	1.21 (1.05-1.37)
Q4	1.22 (1.01-1.48)	1.04 (0.81-1.33)	1.01 (0.88-1.14)	1.62 (1.34-1.96)	1.25 (0.99-1.62)	1.30 (1.13-1.48)
Q5 (LARGEST)	1.33 (1.11-1.59)	0.89 (0.68-1.15)	1.06 (0.94-1.17)	1.90 (1.58-2.27)	1.16 (0.88-1.51)	1.44 (1.29-1.60)

Boldface indicates  $p < 0.05$ . HRs are adjusted for FRAX alone or FRAX+HAL (hip axis length). Calibration includes competing mortality.

Table

**Disclosures:** William Leslie, None.

BMI, diabetes still remained association in both men and women. Yearly difference of BMD in spine and femur were not significantly different between diabetic and non-diabetic subjects in both men and women.

Compared to diabetic subjects with BMI < 25, BMD was significantly higher than subjects with BMI ≥ 25 in both sex. There were no difference in the incidence of overall osteoporotic fracture and new osteoporotic fracture in subjects with diabetes compared with normoglycemic subjects in both men and women. Also, yearly difference of BMD in spine and femur were not significantly different between diabetic and non-diabetic subjects in both men and women.

**Conclusion**

Subjects with diabetes have higher BMD but have an increased risk of osteoporotic fracture for given age and BMD. These findings suggested that hyperglycemic status could reflect risk of fracture.

*Disclosures: Ki-Hyun Baek, None.*

**SU0202**

**Preliminary Comparison Between Normative Spine TBS Data for Moroccans Men and Women.** Abdellah El Maghraoui<sup>1</sup>, Doris Tran<sup>2</sup>, Renaud Winzenrieth<sup>\*2</sup>, Aziza Mounach<sup>1</sup>. <sup>1</sup>Rheumatology Department, Military Hospital Mohammed V, Rabat, Morocco, Morocco, <sup>2</sup>R & D Department, Med-Imaps, Bordeaux, France, France

**Introduction**

The Trabecular Bone Score is an index reflecting the bone microarchitecture at spine. Interpretation of this score for clinical use requires to compare TBS value to age-related reference data based on healthy population. The aim of this study was to investigate the age related changes of the spine microarchitecture assessed by TBS in healthy maroccans men and women.

**Methods**

Healthy men and women were recruited. The inclusion criteria were: Age from 30 to 90 y.o., BMI from 15 to 37 kg/m<sup>2</sup> and BMD Z-score at L1-L4 within 2SD. Exclusion criteria were previous low energy fracture at any site, traumatic fracture at spine, at femur, any treatment and/or, any illness that would be expected to impact bony metabolism (excepted HRT, Calcium/Vit D), previous spinal surgery, scoliosis at lumbar spine higher than 20°, more than two non-assessable lumbar vertebrae, early menopause or surgical menopause.

BMD was evaluated at spine (L1-L4) of DXA scans assessed by Prodigy DXA device (GE-LUNAR, Madison). TBS was computed based on the DXA scan with TBS iNsign software (Med-Imaps, France).

Age-related curves for TBS were created using Excel solver and multiple regressions. The generalized reduced gradient approach that was used is a nonlinear optimization algorithm. The end point of the optimization was to minimize the sum of the square errors between data and predicted values.

**Results**

103 men aged from 30 to 79 years and 383 women from 30 to 80 years were included in the study.

TBS and BMD values at L1-L4 were poorly correlated with BMI (respectively r=-0.07 and 0.23 in men and r=0.05 and 0.16 in women). TBS was poorly correlated with weight (r=-0.15 in men and 0.04 in women) and height (-0.19 in men and -0.03 in women) whereas higher correlations were obtained for BMD. BMD vs weight and BMD vs height were respectively r=0.29 and 0.19 for men and r=0.30 and r=0.30 for women). TBS decreased with aging in both men and women. Between 30 and 80 y.o., TBS in men decreased of 14% (-0.9 SD) and 17% (-1.5 SD) in women at L1-L4.

Compared to European data results are consistent but slightly higher since linear declines of 13.5% and 16.7% have been observed between 40 and 90 for men and women respectively.

**Conclusion**

Results were consistent with previous published data for European men and women. A TBS decrease with aging was observed in both men and women. As expected, the decrease was greater for men. These data are the first step to define Moroccan reference data.



TBS decrease related to age in Moroccans men and women

*Disclosures: Renaud Winzenrieth, None.*

**Table 1: Comparison of base line characteristics in KTR cases versus controls**

	Control group n=439	KTR group n=139	p
Male	77 (17%)	77 (55%)	-
Age (years)	58.3 ± 12.3	57.3 ± 12.7	0.76
Weight (kg)	79.1 ± 13.3	79.6 ± 16.3	0.81
Height (cm)	169.9 ± 8.9	168.1 ± 9.6	0.22
BMI (kg/m <sup>2</sup> )	27.6 ± 4.3	28.0 ± 4.3	0.8
BMD - AP5 spine (g/cm <sup>2</sup> )	1.171 ± 0.120	1.204 ± 0.216	0.17
TBS H	1.226 ± 0.160	1.284 ± 0.142	0.009

**Table 2: Clinical Risk Factors**

	Control group n=439	KTR group n=139
Six month smoking history	14 (3%)	22 (16%)
35 Alcoholic beverages per day	0 (0%)	3 (2%)
Eating disorder	0 (0%)	1 (1%)
Family history of fracture	42 (10%)	16 (12%)
Parental hip fracture	16 (4%)	10 (7%)
Steroid use	0 (0%)	163 (100%)
Anticoagulation medication use	0 (0%)	6 (4%)
Endometriosis/Prostate cancer injections	0 (0%)	0 (0%)
Depo provera use	0 (0%)	1 (1%)
Aromatase inhibitor use	0 (0%)	0 (0%)
Thiazolidinone use	0 (0%)	3 (2%)
Parathyroid disease	0 (0%)	32 (23%)
Thyroid disease	0 (0%)	24 (17%)
Malabsorption	0 (0%)	0 (0%)
Rheumatoid Arthritis	0 (0%)	4 (3%)
Diabetes	0 (0%)	73 (52%)
Bariatric surgery/Gastric bypass	0 (0%)	4 (3%)
Fracture after age 40	0 (0%)	29 (21%)
Back surgery	0 (0%)	0 (0%)
Estrogen treatment	16 (4%)	9 (6%)
Breast cancer treatment	0 (0%)	0 (0%)

|| Male, || Female for female subjects only, || Male, || Female for female subjects only, || Male, || Female

Tables for TBS and Kidney Transplantation

*Disclosures: Murtaza Bharmal, None.*

**SU0201**

**Longitudinal Assessment of Bone Mineral Density in Diabetes and Non-diabetes Subjects: The Chungju Metabolic Disease Cohort(CMC) Study.** Kwanhoon Jo<sup>1</sup>, Ki-Hyun Baek<sup>\*2</sup>, Je-ho Han<sup>3</sup>, Mooil Kang<sup>4</sup>. <sup>1</sup>Seoul St. Mary Hospital, Korea, republic of, <sup>2</sup>Yeouido St. Mary Hospital, Korea, republic of, <sup>3</sup>Incheon St. Mary Hospital, Korea, republic of, <sup>4</sup>Seoul St. Mary Hospital, Korea, republic of

**Objectives**

Several factors increase the risk of fragility fracture, including low bone mineral density, diabetes, and low weight. The associations among these factors have been investigated, but there were few data about longitudinal follow up, and few studies are available in men. The aim of this study was to evaluate the associations between diabetes, bone mineral density, fractures in a longitudinal, prospective, population-based cohort of postmenopausal women and elderly men.

**Methods**

We analyzed 2854 subjects of the CMC cohort in Chungju, Korea. : 1403 subjects were men over 50 years old and 1451 were postmenopausal women. Diabetes (ascertained by self-report, the use of medication for diabetes or an elevated fasting glucose level) was reported in 503 individuals. During a mean of 3.98 ± 1.42 years of follow-up, bone mineral density (BMD) at the lumbar spine and hip were evaluated using DXA at least twice during May 2007 to Dec 2015. A enquiry about health disorders, medications, use of HT, gynecological and fracture history was done in every visit. Subjects who received the treatment of osteoporosis were excluded. Subjects were divided into those with or without diabetes, obese or not (categorized according to BMI).

**Results**

Compared with non-diabetic subjects, diabetic subjects were heavier, thicker waist circumference, had a higher BMI, and significantly higher bone mineral density in spine and total hip in all subjects. The incidence of overall osteoporotic fracture and new osteoporotic fracture was higher in subjects with diabetes compared with normoglycemic subjects in both men and women. The correlation between diabetes and osteoporotic fracture was significant. After adjusted for age, weight,

## SU0203

**TBS Measurements May be Less Impacted by Differences in Age, BMI and Body Composition than BMD.** Diane Krueger<sup>1</sup>, Jessie Libber<sup>1</sup>, Renaud Winzenrieth<sup>\*2</sup>, Neil Binkely<sup>1</sup>. <sup>1</sup>University of Wisconsin, United states, <sup>2</sup>Medimaps Group, France

Trabecular Bone Score (TBS), a surrogate for trabecular structure, uses DXA images acquired to assess BMD. DXA measured BMD is confounded by conditions such as osteoarthritis and tissue thickness. TBS may be less affected by these issues, as has been demonstrated with osteoarthritis. Although it is recommended that TBS not be measured in individuals with BMI > 38 kg/m<sup>2</sup>, little data exist on the impact of body composition. The purpose of this study is to investigate if body composition, abdominal visceral adipose tissue (VAT) or BMI confound TBS measurement.

To evaluate this, 868 adult women having whole body and spine DXA scans on a GE Lunar iDXA were studied. Subject mean age and BMI were 61.3 ± 13.9 (range 26.9 – 95.8) years and 20.0 ± 6.3 (range 15.2 – 54.3) kg/m<sup>2</sup>, 201 were age ≤ 50 years. Mean L1-4 BMD and TBS (TBS iNsite v2.2, Med-Imaps, France) were calculated on spine scans. Subjects were categorized based on WHO T-score classification and proposed TBS structure categories with cut points at 1.230 and 1.310 (McCloskey et al. JBMR, 2015). Whole body scans were used to determine BMI and body composition, including VAT. In an effort to normalize for body size, and to concentrate on the lumbar spine area, the android/gynoid (A/G) fat ratio was determined. Additionally, women ≤ age 50 were evaluated to reduce the impact of bone deterioration with advancing age.

In the entire cohort, ANOVA analysis revealed the most degraded TBS group had the highest fat A/G ratio and VAT volume compared to those with better TBS (p < 0.05). Importantly, similar relationships were observed when the cohort was limited to women age ≤ 50 years. Conversely, in the overall cohort, the osteoporotic group had the lowest A/G fat ratio and VAT volume (p < 0.05) compared to those with better BMD. Larger VAT volume was associated with higher BMD in those ≤ 50 (p < 0.05). As could be expected, L1-L4 TBS declined with age while BMD declined until ~65 years, when it plateaued. Finally, BMD was higher in those groups with higher BMI, while TBS was relatively unaffected.

In conclusion, high A/G fat ratio and high VAT volume is associated with better BMD but poorer TBS, consistent with limited reports linking high VAT with poorer bone structure. The BMD plateau at age 65, but ongoing TBS decline, reinforces the concept that TBS is unaffected by osteoarthritis. Finally, these data suggest that BMI may not directly affect TBS.

*Disclosures: Renaud Winzenrieth, None.*

## SU0204

**African American Men and Women have lower TBS than Caucasians.** Rajesh Jain<sup>\*</sup>, Tamara Vokes. University of Chicago Department of Endocrinology, Diabetes, & Metabolism, United states

**Background:** Trabecular bone score (TBS), a textural analysis of the lumbar spine, has been shown to predict fracture risk, but this has been in predominantly Caucasian (CA) populations. Given lower fracture rates in African Americans (AA), we expected that they would have higher TBS. Instead, we found that AA women had, if anything, lower TBS than CA women. However, because these patients were recruited for osteoporosis studies, there may have been a component of selection bias, with AA only being referred if they had higher risk for fragility. The current study aims to expand our sample size and to minimize the ethnicity-based selection bias by examining TBS in all densitometry patients. Further, the inclusion of men decreases the likelihood of selection bias because, regardless of ethnicity, men are referred for densitometry only if they have risk factors for osteoporosis.

**Methods:** This is a retrospective analysis of all bone density scans obtained in AA and CA subjects 40 years and over between 2011 and 2016 in which TBS was available. TBS was standardized (TBSstd) i.e. expressed as the number of standard deviations above or below the mean TBS of the entire sample.

**Results:** Among the total of 4,311 scans, there were 2,152 CA (483 male) and 2,159 AA (233 male). In both genders, the lowest of the femoral neck, total hip, or lumbar spine T-scores (Low T) was higher in AA compared to CA, while the lowest of Z-scores (Low Z) was lower in AA (Table 1). Further, in both genders, TBS was significantly lower in AA than in CA. To control for possible selection bias, TBS was also adjusted for low Z and remained significantly lower in AA compared to CA.

**Discussion/Conclusion:** In a large unselected group of patients referred for densitometry, AA of both genders had significantly lower TBS than CA. We minimized the effect of possible selection bias in two ways. First, the ethnic differences in TBS were present in men who are likely to be referred to densitometry only if they have risk factors for osteoporosis, regardless of ethnicity. Second, when adjusting TBS for low Z-score, the ethnic differences in TBS were only slightly attenuated and remained highly statistically significant. In conclusion, this largest study to date of AA subjects demonstrated lower TBS than in CA even when controlling for selection bias, suggesting likely ethnic differences in TBS, which should be considered when applying this novel tool to a multi-ethnic clinical practice.

Table 1

	Low T			Low Z			TBS <sub>std</sub>			TBS <sub>std</sub> adjusted for low Z-score		
	AA	CA	P-value	AA	CA	P-value	AA	CA	P-value	AA	CA	P-value
<b>Women</b>	-1.4± 1.2	-1.9± 1.0	<.0001	-1.0± 1.1	-0.6± 0.9	<.0001	-0.2± 1.0	0.2± 1.0	<.0001	-0.2± 1.0	0.1± 1.0	<.0001
<b>Men</b>	-1.1± 1.4	-1.5± 1.2	<.0001	-1.4± 1.3	-0.8± 1.2	<.0001	-0.1± 1.0	0.2± 1.0	<.0001	0.0± 1.0	0.2± 1.0	<.0001

\*All TBSstd adjusted for BMI

Table 1

*Disclosures: Rajesh Jain, None.*

## SU0205

**3D-DXA analysis of the changes in cortical and trabecular bone in patients with celiac disease after 1-year on gluten-free diet.** María Belen Zanchetta<sup>\*1</sup>, Ludovic Humbert<sup>2</sup>, Martelli Yves<sup>2</sup>, Vanesa Longobardi<sup>1</sup>, Mariela Sesta<sup>3</sup>, cesar bogado<sup>4</sup>, Jose Zanchetta<sup>1</sup>. <sup>1</sup>MD, Argentina, <sup>2</sup>MD, Spain, <sup>3</sup>PH, Argentina, <sup>4</sup>PHD, Argentina

We have previously found a significant deterioration of trabecular and cortical microarchitecture in peripheral bones of patients with undiagnosed celiac disease (CD) with HR-pQCT. Up to now, there is no data evaluating cortical and trabecular bone at proximal femur, using 3D Dual X-ray Absorptiometry (DXA) in patients with celiac disease.

This study aims to analyze long term effect of gluten-free diet (GFD) in cortical and trabecular bone using 3D-DXA, in CD patients.

**Design:** 25 premenopausal women with CD were included in this study. DXA scans (Lunar Prodigy scanner, GE Healthcare, Madison, WI) were acquired at diagnosis of CD (baseline) and after a 1-year on GFD. The 3D-DXA software (Galgo Medical, Barcelona, Spain) was used to analyze the changes in cortical and trabecular bone between baseline and follow-up. 3D-DXA registers a 3D appearance model of the femoral shape and density onto the DXA projection to obtain a 3D subject-specific model of the femur of the patient and quantify the volumetric BMD (vBMD), volume (for trabecular and cortical regions) and cortical thickness distribution. The 3D-DXA measurements at baseline and after the 1-year on GFD were compared using paired samples Student's t-test.

**Results:** mean age at baseline was 30.4 ± 8.6 years. A statistically significant increase of the integral vBMD (+13.0 mg/cm<sup>3</sup>, +4.0%, p=0.008) and trabecular vBMD (+19.3 mg/cm<sup>3</sup>, +14.8%, p=0.022) was observed at the total femur region of interest. However, no statistically significant changes was observed for the cortical vBMD (p=0.950). Similar findings were found for the bone mass. An increase of +1.0 g (p=0.003) was found at the trabecular compartment whereas no change was observed at the cortex (+0.0 g, p=0.970). No statistically significant change was observed for the cortical thickness (-0.01 mm, p=0.767).

**Conclusion:** The 3D-DXA analysis of the 25 patients with CD included in this study showed that 1-year on gluten-free diet treatment resulted in a statistically significant increase of the trabecular vBMD and BMC, with no statistically significant change in terms of cortical thickness and density.

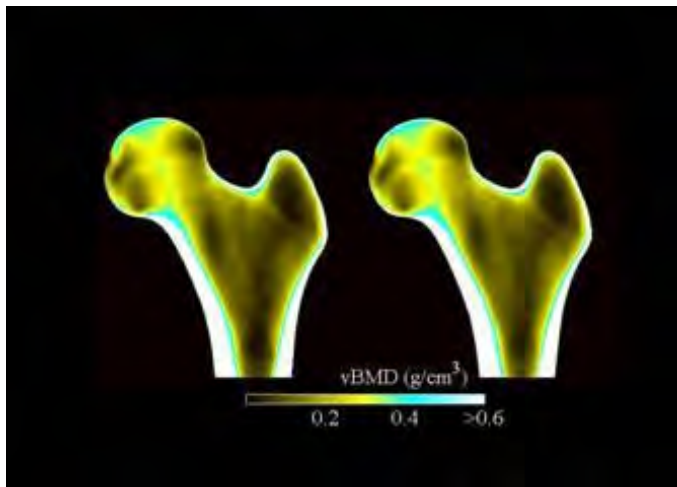


Figure 1: Front slice showing the average vBMD values at baseline (left) and after a 1-year gluten-f

*Disclosures: María Belen Zanchetta, None.*

SU0206

**Analysis of the Change in the Superior and Inferior Cortical Structure of the Female Femoral Neck Between 19 and 97 Years.** Benjamin Khoo\*<sup>1</sup>, Keenan Brown<sup>2</sup>, Richard Prince<sup>3</sup>. <sup>1</sup>Medical Technology & Physics, Sir Charles Gairdner Hospital, Australia, <sup>2</sup>Mindways Software Inc, United states, <sup>3</sup>School of Medicine & Pharmacology, University of Western Australia, Australia

**Introduction:** Previous small studies identify femoral neck (FN) cortical expansion and thinning occurring with increasing age. In this presentation we report structural trends occurring along the FN with age in a larger number of individuals.

**Methods:** Hip QCT performed on 507 participants between the ages of 19 y and 97 y were analysed with BIT Mindways (Mindways Software). Scans were performed using relatively thick slices (>1.5 mm) resulting with relatively low doses. To investigate structural geometrical trends, an eccentricity of 1.4 was selected to represent a consistent identifiable distance along the FN; a section was identified and split along a plane orthogonal to the long axis of the femur into a superior and inferior region which remained constant as the FN cross section increased with age. Total cross sectional, superior and inferior cortical thickness average (a\_Ct) and the displacement between centre-of-mass (CoM) and geometric centre (d) was calculated and plotted against age.

**Results:** From age 19, as a result of periosteal bone apposition, averaged total FN cross sectional area increased at 2.5 mm<sup>2</sup>/y (P=0.001) from 950 mm<sup>2</sup> and d increased in the inferior direction by 0.03 mm/y (P<0.001). The averaged total a\_Ct decreased linearly at a rate of 0.03 mm/y (P<0.001) from 3.5 mm at 19 y. The superior\_Ct decreased at 0.02 mm/y (P<0.001) from 2.3 mm while the inferior region decreased by 0.03 mm/y (P<0.001) from 4.6 mm, age accounted for 20 to 24% of the variance in the reduction in a\_Ct.

**Conclusion:** These data support previous QCT, but not ex vivo, studies demonstrating that the reduction in total FN cortical thickness with age occurs in both the superior and inferior regions. The superior region is thinner than the inferior at age 19 and becomes progressively more so probably resulting in increasingly greater vulnerability to bending stresses and fracture than at the inferior region.

**Disclosures:** Benjamin Khoo, None.

SU0207

**Comparison of the bone geometry, volumetric density, and microstructure between the standard fixed offset and the relative offset method of HR-pQCT.** Narihiro Okazaki\*<sup>1</sup>, Ko Chiba<sup>1</sup>, Ayako Kurogi<sup>1</sup>, Yusaku Isobe<sup>2</sup>, Shuntaro Sato<sup>3</sup>, Kiyoshi Sada<sup>4</sup>, Makoto Osaki<sup>1</sup>. <sup>1</sup>Department of Orthopaedic Surgery, Nagasaki University Hospital, Japan, <sup>2</sup>Nagasaki University School of Medicine, Japan, <sup>3</sup>Clinical Research Center, Nagasaki University Hospital, Japan, <sup>4</sup>Department of Radiology & Biomedical Imaging, University of California, San Francisco, United states

**Objective:**

In the manufacturer's standard scan protocol of high-resolution peripheral quantitative computed tomography (HR-pQCT), scanned sites are determined by the fixed offset from the reference lines at the distal radius and tibia. However, because this protocol does not take into account the length of the forearm or lower leg, the scanned site might be shifted to relatively more proximal when the bone length is short. In studies of children, the scanned sites have been determined by using the relative offset depending on the bone length because of the large differences in their physique. We compared the measurements obtained by the standard fixed offset and the relative offset at the distal radius and tibia in healthy Japanese adult subjects.

**Methods:**

The subjects consisted of 31 healthy Japanese volunteers (11 females, 20 males). The mean age was 45.7 ± 13.6 (range 21-76 years). The distal radius and tibia were scanned using HR-pQCT (XtremeCT II, Scanco Medical) with a voxel size of 61 µm by the standard fixed offset method and the relative offset method. In the relative offset method, the scanned site was 4% of the forearm length proximal to lateral edge of the distal radial joint surface, and 7.3% of the lower leg length proximal to the most distal edge of the tibial joint surface. We measured the bone geometry, volumetric density, and microstructure parameters, and compared the differences of these parameters between the 2 methods.

**Results:**

The mean body height was 166.6 cm (range: 151 - 181cm), the mean length of forearm was 257.3 mm (range: 226 - 281 mm), and the mean length of lower leg was 354.2 mm (320 - 394 mm). The bone geometry, volumetric density, and microstructure parameters at the distal radius and tibia are displayed in Table 1. At the distal radius, trabecular area (Tb.Ar), cortical perimeter (Ct.Pm), and cortical vBMD (Ct.vBMD) were significantly different between the 2 methods (p = 0.0017, 0.0187, 0.0020, respectively). At the distal tibia, there was no difference between the 2 methods.

**Conclusion:**

At the distal radius, Tb.Ar was significantly smaller, Ct.Pm was shorter, and Ct.vBMD was higher in the standard fixed offset method than in the relative offset method. We should be careful of the differences of the scanned site when we compare populations with different physical constitutions.

Table 1

The means of the bone geometry, volumetric density, and microstructure parameters at the distal radius and tibia obtained by the standard fixed offset method and the relative offset method

	Distal Radius			Distal Tibia		
	Standard fixed offset method	Relative offset method	p value	Standard fixed offset method	Relative offset method	p value
	Mean ± SD	Mean ± SD		Mean ± SD	Mean ± SD	
<b>Geometry</b>						
Tb.Ar (mm <sup>2</sup> )	294.1 ± 43.9	322.9 ± 43.6	N.S.	751.8 ± 119.0	782.7 ± 105.9	N.S.
Tb.Ar (mm <sup>2</sup> )	232.6 ± 37.8	265.5 ± 38.8	0.0017**	625.3 ± 114.6	657.3 ± 102.4	N.S.
CL.Ar (mm <sup>2</sup> )	65.3 ± 16.0	61.5 ± 16.0	N.S.	131.0 ± 35.0	131.0 ± 38.4	N.S.
Ct.Pm (mm)	71.8 ± 6.1	75.6 ± 5.6	0.0187*	106.9 ± 8.9	109.1 ± 7.9	N.S.
<b>Volumetric Density</b>						
Tb.vBMD (mg HA/cm <sup>3</sup> )	310.8 ± 71.8	279.7 ± 70.2	N.S.	283.3 ± 75.9	277.6 ± 76.0	N.S.
Ct.vBMD (mg HA/cm <sup>3</sup> )	142.3 ± 46.6	143.6 ± 44.2	N.S.	151.1 ± 48.2	155.3 ± 48.1	N.S.
Cv.vBMD (mg HA/cm <sup>3</sup> )	924.3 ± 51.5	824.6 ± 56.2	0.0020**	999.7 ± 66.1	896.3 ± 65.2	N.S.
<b>Microstructure</b>						
BV/TV (%)	21.1 ± 6.2	21.3 ± 6.0	N.S.	23.0 ± 6.3	23.5 ± 6.3	N.S.
Tb.Sp (mm)	1.27 ± 0.26	1.30 ± 0.23	N.S.	1.20 ± 0.19	1.23 ± 0.20	N.S.
Tb.Th (mm)	0.23 ± 0.02	0.23 ± 0.02	N.S.	0.25 ± 0.03	0.25 ± 0.03	N.S.
Tb.Sp (mm)	0.79 ± 0.32	0.75 ± 0.21	N.S.	0.83 ± 0.16	0.80 ± 0.15	N.S.
Ct.Th (mm)	1.09 ± 0.25	0.97 ± 0.23	N.S.	1.40 ± 0.40	1.40 ± 0.40	N.S.
Ct.Po (µm)	0.62 ± 0.52	0.69 ± 0.53	N.S.	2.12 ± 1.15	2.30 ± 1.14	N.S.
Ct.Po.Dm (mm)	0.17 ± 0.03	0.17 ± 0.03	N.S.	0.22 ± 0.03	0.22 ± 0.03	N.S.

Mean ± SD; N.S. = not significant  
 \*p < 0.05, \*\*p < 0.01, \*\*\*p < 0.001  
 Tb.Ar: total area, CL.Ar: cortical area, Tb.Ar: trabecular area, Ct.Pm: cortical perimeter, Tb.vBMD: total volumetric bone mineral density, Tb.vBMD: trabecular vBMD, Ct.vBMD: cortical vBMD, Cv.vBMD: trabecular bone volume fraction, Tb.Th: trabecular thickness, Tb.Sp: trabecular separation, BV/TV: trabecular bone volume fraction, Ct.Th: cortical thickness, Ct.Po: cortical porosity, and Ct.Po.Dm: cortical pore diameter

Table 1

**Disclosures:** Narihiro Okazaki, None.

SU0208

**Estimation of cortical thickness: the effect of two reconstruction kernels on two different segmentation methods.** Oleg Musevko, Klaus Engelke\*. IMP, University of Erlangen-Nuremberg, Germany

**Purpose:** To investigate dependence of the cortical thickness assessment by two different segmentation algorithms on two CT reconstruction kernels.

**Methods:** QCT datasets of the proximal femur for 10 patients were acquired with a standard and a sharp kernel. A standard local adaptive threshold, aka 50%-method (LAT50, [1]) was used to compute the cortical thickness in femur neck, trochanter, intertrochanter (IT), and total femur. In the same VOIs, the hybrid model-based profile analysis (HMPA, a new method for cortex 'deconvolution' [2]) was applied to compute the cortical thickness more accurately. Discrepancies between the estimated thickness values at the standard and the sharp kernel were calculated for HMPA and LAT50.

**Results:** The relative difference (%) in the cortical thickness for the two kernels is shown in Figure for each VOI, with LAT50 and HMPA-results combined pairwise. Correlation between LAT50 and HMPA thickness was higher at the standard kernel with R<sup>2</sup>=0.69 as compared to R<sup>2</sup>=0.49 for the sharp one. Overestimation of the thickness at the standard kernel by the LAT50 as compared to the HMPA was 37 ± 4% (total femur), it becomes lower if to apply LAT50 to the sharp kernel images but still significant: 21 ± 6% (total femur), 26 ± 2% (neck), 10 ± 5% (IT).

**Conclusions:** The sharp kernel increases contrast of the cortex as compared to the standard kernel but also increases noise. As result, both algorithms produced lower (and more accurate) thickness values at the sharp kernel; expectedly, a more accurate HMPA was less stable with respect to the reconstruction kernel, in particular at the femur neck where the cortex is most thin, but overall LAT50 and HMPA were not significantly different at the relative difference between two kernels. Both algorithms showed largest dependency on the kernel at the trochanter VOI, probably due to its complex geometry. The least influence of the kernel for LAT50 was at the neck, since its thin cortex is greatly overestimated by the method and the role of the kernel/noise is secondary [2]. For HMPA, the least dependence on the kernel was in IT, where cortical thickness is maximal. Importantly, sharp kernel did not allow eliminating the overestimation of the thickness by LAT50, which was largest at neck and lowest at IT.

- [1] Prevrhal, S., Engelke, K., Kalender, W.A., 1999, Phys. Med. Biol. 44, 751-64.
- [2] Musevko, O., Gerner, B., Engelke, K., 2015, MICCAI-CSI2015, pp. 66-75.

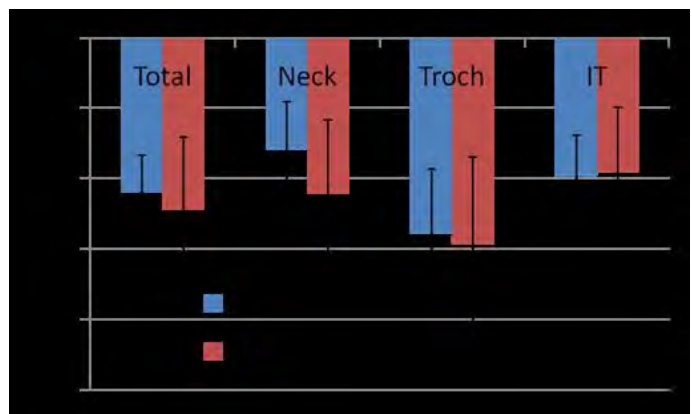


Figure: The relative error (%) in the cortical thickness between two kernels for two algorithms

**Disclosures:** Klaus Engelke, None.

## SU0209

**In Vivo Bone Microstructure Analysis of Fracture Healing by HR-pQCT.**

Kazuaki Yokota\*<sup>1</sup>, Ko Chiba<sup>1</sup>, Narihiro Okazaki<sup>1</sup>, Ayako Kurogi<sup>1</sup>, Makoto Era<sup>2</sup>, Yuichiro Nishino<sup>3</sup>, Takashi Miyamoto<sup>4</sup>, Makoto Osaki<sup>1</sup>.

<sup>1</sup>Department of Orthopedic Surgery, Nagasaki University Hospital, Japan,

<sup>2</sup>Department of Orthopedic Surgery, Mitsubishi Nagasaki Hospital, Japan,

<sup>3</sup>Department of Orthopedic Surgery, Saiseikai Nagasaki Hospital, Japan,

<sup>4</sup>Trauma Center, Nagasaki University Hospital, Japan

**Introduction:**

It has been difficult to study fracture healing in living patients at the micro level. HR-pQCT is a high-resolution clinical CT for human peripheral sites, which enables us to analyze bone microstructure of living humans non-invasively.

In this pilot study, we observed fractured sites of a fracture patient longitudinally using HR-pQCT and investigated changes of bone microstructure in the process of fracture healing.

**Methods:**

A 44-year-old patient with a distal radius fracture was treated with a volar locking plate (VA-LCP Distal Radius Plate, DePuy Synthes) and participate in this study.

The fracture site was scanned by HR-pQCT (XtremeCT II, Scanco Medical) at the interval of one week after the surgery. Bone formation at the fractured gap of cortical bone, bone mineral density (BMD) of cancellous bone, and outer callus formation were analyzed by dedicated software (TRI/3D-BON, Ratoc System Engineering).

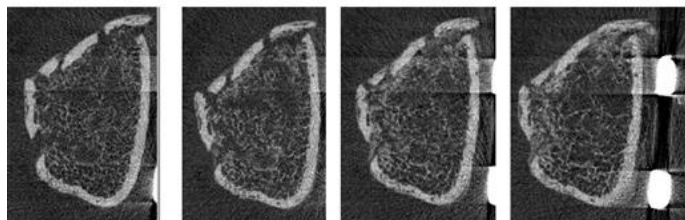
**Results:**

Bone formation was observed at the fractured gap recovering cortical bone connectivity. Before or simultaneously, the BMD of cancellous bones under the fracture sites increased. There was almost no outer callus formation in this case.

**Conclusions:**

Cancellous bones under the cortical bone gap may play an important role in the process of fracture healing at the human epiphyseal fractures.

1 week      4 weeks      8 weeks      12 weeks



image

*Disclosures: Kazuaki Yokota, None.*

## SU0210

**In Vivo Evaluations of MRI Bound and Pore Water Measures of Cortical Bone in Osteoporotic Patients.** Mary Kate Manhard\*, S. Bobo Tanner, Jeffrey Nyman, Mark Does, Vanderbilt University, United states**Purpose**

Osteoporotic fractures are a growing problem, and current DXA methods do not identify all individuals at risk of a fragility fracture. MRI based methods such as bound and pore water concentration mapping in cortical bone offer additional information about fracture risk. Bound water concentration is a measure of water bound to the collagen matrix of cortical bone, and has been shown to report on toughness. Similarly, pore water concentration is a measure of cortical bone porosity. This work compares these MRI measures in patients with DXA-defined osteoporosis to those from healthy controls in order to assess the sensitivity of these measurements in a relevant population.

**Methods**

Subjects beginning a new drug treatment for osteoporosis (mean age 63 years, 9F) and healthy controls (mean age 34 years, 6M/7F) were recruited with IRB approval and written informed consent. MRI scans (3T Philips Achieva) using ultra-short echo time (UTE) methods with relaxation selective pulses were collected to independently acquire maps of bound and pore water concentrations within the cortical bone of the tibia mid-shaft. Both bound and pore water scans were collected in 3D for a total scan time of approx. 30 minutes; mean bound and pore water values were compared between healthy and osteoporotic subjects.

**Results**

Fig 1 (top) shows images and bound and pore water maps from two representative subjects, one with osteoporosis and one healthy control. In the osteoporotic subject, the bound water is much lower and the pore water is higher compared to the healthy

tibia. Fig 1 (bottom) shows differences in mean bound and pore water across healthy and osteoporotic subjects. A significant decrease in bound water and a significant increase in pore water was observed in the osteoporotic subjects compared to the healthy subjects.

**Conclusions**

MRI measures of cortical bone are sensitive enough to detect differences between normal and osteoporotic bone in which subjects with low T-scores have low matrix-bound water and high pore water concentrations. These results support the continued development of MRI based measurements of bound water and pore water maps as potential surrogates of tissue quality and intracortical porosity. Towards that end, the methods are currently being applied using 2D methods to significantly reduce scan time to under 2 minutes. Future studies will investigate osteoporotic patients following drug treatment to assess changes in response to treatment.

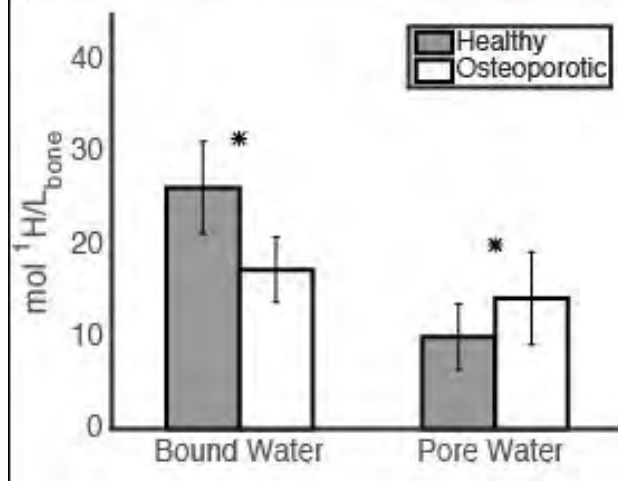
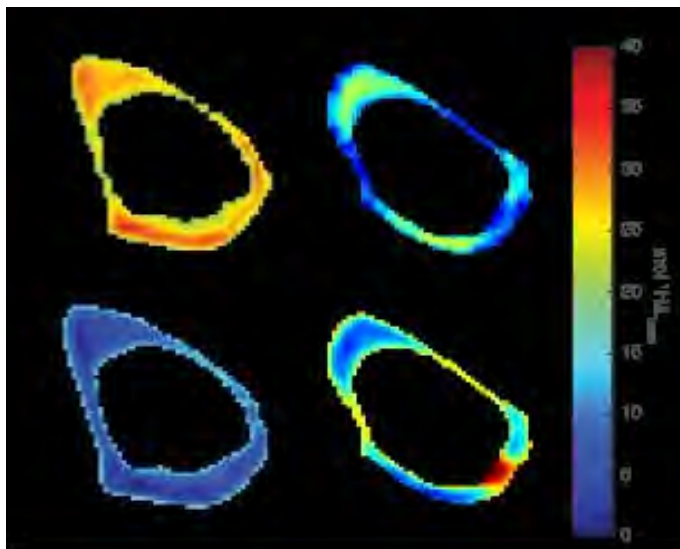


Figure 1: Osteoporotic vs healthy subjects

*Disclosures: Mary Kate Manhard, None.*

## SU0211

**Poor Trabecular Microarchitecture at Distal Radius Predicts Fractures in Older men – the Prospective STRAMBO Study.** Pawel Szule\*, Stéphanie Boutroy, Roland Chapurlat, INSERM UMR 1033, University of Lyon, Hôpital Edouard Herriot, France

In older men areal bone mineral density (aBMD) measured by DXA poorly predicts fractures. Our aim was to evaluate the utility of bone microarchitecture assessed by high resolution peripheral quantitative computed tomography (HR-pQCT) for fracture prediction in men. At baseline 756 men aged 60-87 had aBMD (HOLOGIC Discovery A), trabecular bone score (TBS, MEDIMAPS) and bone microarchitecture (XtremeCT, SCANCO MEDICAL AG) measurements. During a prospective 8-year follow-up, 100 men had incident fragility fractures including 47 men with radiographic vertebral fractures and 61 men with non-vertebral fractures. The models were adjusted for TBS-corrected FRAX for major osteoporotic fractures (FRAX-TBS) calculated on the FRAX website.

Most trabecular parameters at distal radius and cortical parameters at distal tibia predicted fragility fractures (HR=1.29-1.56 per SD change,  $p < 0.005$ ). Distal radius trabecular number (Tb.N) predicted single and multiple fractures (HR= 1.56 and 1.70 per SD,  $p < 0.001$ ) as well as vertebral fractures and non-vertebral fractures analyzed separately. Trabecular volumetric BMD (Tb.vBMD) in the subendocortical compartment predicted all fractures and vertebral fractures. By contrast, Tb.vBMD in the central compartment did not predict fractures. Distal tibia cortical parameters predicted all fragility fractures and non-vertebral fractures (e.g., cortical vBMD: HR=1.44 per SD change, 95%CI: 1.19-1.74,  $p < 0.001$ ), but not vertebral fractures. In the analysis limited to men with FRAX-TBS  $< 15\%$ , distal radius Tb.N was most consistently associated with the risk of various types of fracture. Distal tibia parameters did not predict fractures in this group. Introduction of distal radius Tb.N in the statistical model increased the estimated fracture risk by  $> 2\%$  (vs. FRAX-TBS alone) in 27% of the cohort including 44% of men with incident fractures. In this group fracture incidence was more than twofold higher compared to men who had smaller change in the estimated fracture risk (decrease or increase  $< 2\%$ ). The pattern remained significant after further adjustment for baseline FRAX-TBS (HR= 2.45, 95%CI: 1.63-3.69,  $p < 0.001$ ).

Thus, in older men poor trabecular microarchitecture at distal radius (mainly low Tb.N) was associated with high risk of fragility vertebral and non-vertebral fracture after adjustment for FRAX and TBS. The assessment of distal radius bone microarchitecture may further improve fracture prediction in older men compared with FRAX and TBS.

**Disclosures:** Pawel Szulc, None.

## SU0212

**Sensitivity and specificity of osteoporosis diagnostics at primary healthcare with Bindex.** Janne Karjalainen<sup>1</sup>, Ossi Riekkinen<sup>1</sup>, John Schousboe<sup>2</sup>, Heikki Kröger<sup>3</sup>. <sup>1</sup>Bone Index Finland, Finland, <sup>2</sup>Park Nicollet Institute, United states, <sup>3</sup>Kuopio University Hospital, Finland

An ultrasound based device (Bindex<sup>®</sup>) has been recently introduced to address the challenges in osteoporosis (OP) diagnostics at primary care (1). Bindex measures cortical thickness and determines parameter called density index (DI). Thresholds for DI in osteoporosis assessment have been determined in Finnish Caucasian population ( $n = 448$ ) along the International Society of Clinical Densitometry (ISCD) guidelines (2). In this study, the sensitivity and specificity are assessed in data set combining three independent trials.

A total of 1830 Caucasian females were enrolled for the study (age  $67.2 \pm 8.9$  years) for two clinical trials in Finland and one in the United States. Subjects were measured with dual energy X-ray absorptiometry (DXA) for bone mineral density (BMD) at hip and femoral neck. The DI was determined based on cortical thickness measurements at proximal tibia alone (DI<sub>1</sub>), and with thickness information included from distal tibia and radius (DI<sub>3</sub>). Subjects were diagnosed with OP when T-score at either location was at or below -2.5 (NHANES III). A subgroup of 1344 subjects was formed in which the subjects with T-score between -2.1 and -2.9 were removed due to the precision error based uncertainty of osteoporosis/healthy status (3).

Osteoporosis was diagnosed in 374 subjects (T-Score  $\leq -2.5$ ) and 163 subgroup subjects (T-Score  $\leq -2.9$ ). The sensitivity and specificity of DI<sub>1</sub> and DI<sub>3</sub> in the total population of 1830 ranged from 82% to 87%. Following the guidelines of the ISCD, approximately 70% of the subjects could have been classified as healthy or osteoporotic by ultrasound measurement and 30% would have needed DXA for diagnostic verification. In the subgroup analysis the DI sensitivity ranged from 90 to 93% and specificity was 87%.

The suggested thresholds for the DI were tested in a large population and performance of the technique seems consistent when data from several studies were combined. The ultrasound based Bindex measurement for osteoporosis detection shows good performance for OP detection at primary care level.

- (1) Karjalainen et al. Osteoporos Int, 2016,
- (2) Hans et al., J Clin Densitom., 2008,
- (3) Kiebzak et al., J Clin Densitom., 2007

**Disclosures:** Janne Karjalainen, Bone Index Finland, 14  
This study received funding from: Bone Index Finland

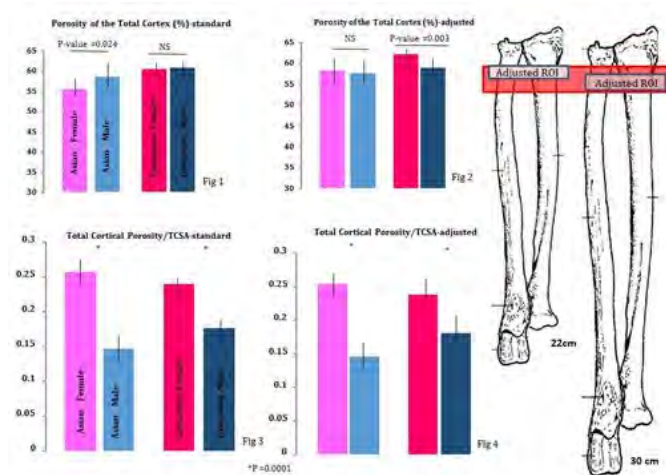
## SU0213

**Sexual and Racial Dimorphism in bone microarchitecture requires adjustment of the region of interest for skeleton dimensions.** Ali Ghasem-Zadeh\*, XiaoFang Wang, Roger Zebaze, Ego Seeman. Austin Health, University of Melbourne, Australia

**Introduction** Bone size, shape, and micro-architecture vary point by point around and along the length of a bone, especially at metaphyses, irregularly designed ends of long bones. Image acquisition using HR-pQCT is achieved by scanning fixed region of interest (ROI) without considering bone length. Given the heterogeneity in structure, sex and racial differences may be a consequence of measuring different regions rather than true differences in bone. To quantify sexual and racial differences in bone microarchitecture we examined effects of placement of the ROI to ensure anatomical identity was maintained by sex and race.

**Methods** In 77 women (40 Asian and 37 Caucasian) and 85 men (37Asian and 48 Caucasian), age range 22-52 years, the distal part of non-dominant radius was scanned using HR-pQCT. Images were analysed slice by slice using StrAx 1.0. Total vBMD and porosity of total and compact cortex were assessed using the standard-fixed method (110 slices) versus a region of 4.3-6.2% of the radius length before and after adjustment for total cross sectional area (TCSA) of the ROIs.

**Results** The standard-fixed method produced either no differences in porosity or higher porosity in males than females (Fig 1). After adjusting for bone length to ensure the same anatomical location, differences in porosity either disappeared or reversed (Fig2). However, when the standard-fixed or adjusted ROI was adjusted by total CSA, the same result was found; females had higher porosity than males in both races and there is no racial differences in men and women (Fig3-4). **Conclusion** Differences in the relative to position of the ROI has biologically significant effects on cortical porosity which may result in erroneous reporting of age, sex and racial differences in this trait. Adjustment for Total CSA is sufficient to correct for anatomical variation in the ROI in persons with differences in radius length.



Site variation-Ali

**Disclosures:** Ali Ghasem-Zadeh, None.

## SU0214

**Spinal Bone Density Assessment on Virtual Non-contrast images.** James Leake, MD<sup>1</sup>, Xinhui Duan<sup>1</sup>, Keenan Brown<sup>2</sup>, Orhan Oz<sup>1</sup>. <sup>1</sup>UT Southwestern Medical Center, United states, <sup>2</sup>Mindways Software, United states

**Purpose**

Iodine-enhanced contrast exams were known to have artificially higher bone mineral density (BMD) estimation due to contrast influence. Virtual non-contrast (VNC) images derived from dual energy CT imaging are designed to remove iodine component from the image. This study evaluates the feasibility of BMD estimation in contrast CT patient exam using VNC images.

**Method**

This study was approved by local IRB. All patients ( $n=10$ ) selected had a multi-phase CT exam scanned on a dual energy CT scanner (Siemens Healthcare FLASH or FORCE). The exam included one non-contrast scan and two contrast scans (arterial and venous or nephrogram delayed phase) of the abdomen. Conventional images were generated for all the scans and VNC images for contrast scans. BMD calibration was performed in an asynchronous manner, i.e., patient and calibration phantom were scanned separately. A proprietary BMD calibration phantom (15 cm long and 5 cm diameter, Mindways Software, Inc. Austin, TX) was scanned using the same scanner as the patient exams. The BMD values were obtained through QCT Pro software (Mindways, spine module) on lumbar spine L1 and L2.

**Result**

The estimated BMDs from non-contrast (reference) scans were  $145.4 \pm 39.3$  (range 96.2-220.0) mg/ml. Linear regression results showed the BMD derived from VNC images had strong correlation with the BMD from reference scans with the slope of 0.64 ( $R^2 = 0.936$ ), 0.61 ( $R^2 = 0.921$ ) and 0.55 ( $R^2 = 0.87$ ) for the arterial, venous and nephrogram+delayed phases, respectively.

**Conclusion**

As expected trabecular BMD was higher on contrast scans, but the VNC images provide a promising way to correct the error and obtain accurate BMD information from contrast exams.

**Clinical Relevance**

Asynchronous BMD assessment is a recently FDA approved procedure. Our study suggests opportunistic BMD from VNC scans maybe useful to identify

patients requiring formal bone mass assessment because of low BMD or occult fractures.

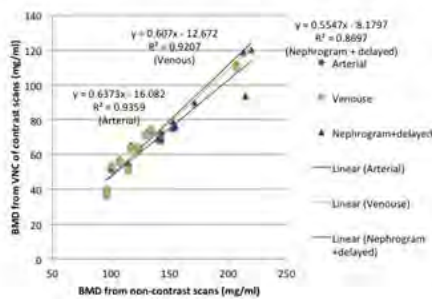


Figure. Linear regression of BMD from non-contrast scans and VNC of contrast scans.

Figure. Linear regression of BMD from non-contrast scans and VNC of contrast scans

Disclosures: James Leake, MD, None.

## SU0215

**Three-dimension Assessment of Spinal and Pelvic Parameters in Patients with Vertebral Fractures and High Risk of Falls.** Marie Fechtenbaum<sup>1</sup>, Jacques Fechtenbaum<sup>2</sup>, Adrien Etcheto<sup>2</sup>, Antoine Feydy<sup>3</sup>, Christian Roux<sup>2</sup>, Karine Briot<sup>2</sup>. <sup>1</sup>Rehabilitation department, Cochin hospital, Paris, France, France, <sup>2</sup>Rheumatology department, Cochin hospital, Paris, France, France, <sup>3</sup>Radiology Department, Cochin Hospital, Paris, France, France

Thoracic kyphosis and other postural parameters related to the sagittal global spinal balance can influence the biomechanical environment of the spine and increase risk of fractures and falls. These parameters can be influenced by vertebral fractures (VFs) in osteoporotic patients. This study aims to evaluate the three-dimension (3D) measurements of spinal and pelvic parameters for identifying patients with VFs, and those at high risk of falls.

Two hundred and sixty patients aged 70.6 ( $\pm$  10.3) years at high risk of fracture, underwent a standardized lateral and antero-posterior full skeleton radiographs by EOS<sup>®</sup> (low dose biplanar imaging system). Spinopelvic parameters were measured from EOS<sup>®</sup> using the 3D modeling of the spine curvature (SterEOS software 1.6). We assessed spinal (thoracic and lumbar Cobb's indices, thoracic tilt and lumbar tilt) and pelvic parameters (pelvic tilt, sacral slope, and pelvic incidence). Sagittal global spinal balance measured by the C7 plumb line and the spinosacral angle (SSA) were measured. Full Balance integrated Index (FBI) (which estimate the amount of correction needed in kyphotic patients) was calculated. VFs were evaluated according to Genant's classification. High risk of falls was defined by a Timed Up and Go test (TUG) > 14 sec. We compared these parameters in patients with and without VF and in patients with high risk or not of falls. Discriminative value of these parameters was assessed using Area Under the Curve (AUC) and multivariate logistic regression.

Ninety-eight patients had at least 1 VF, with a mean SDI of 4.66  $\pm$  4.25. The greater the SDI, the greater were the thoracic Cobb's angle and pelvic tilt and the lesser the lumbar Cobb's angle. Thoracic and lumbar tilts and sacral slope were not affected by SDI increase. The sagittal spinal balance assessed by C7 plumbline (p=0.08) and SSA (p<0.0001) was significantly altered in patients with at least one VF whereas FBI was not. Using AUCs, SSA has a higher discriminative value than C7 plumb line (0.638 and 0.563), respectively. Variables significantly associated with high risk of falls (TUG>14 sec) were low Lumbar Cobb Index (p<0.0001), high C7 plumbline (p=0.083), low SSA (p=0.0003) and high FBI (p=0.015). Using multivariate analysis, age is associated with the risk of falls (OR=1.10, p=0.006) and high lumbar Cobb Index is a protective factor (OR=0.93, p=0.001).

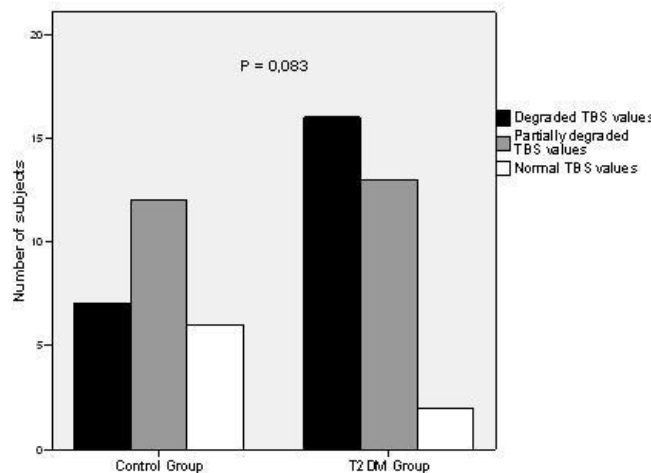
3-D assessment of spinal and pelvic curves is significantly altered in subjects over 50 years patients with at least one VF and is associated with high risk of falls. Lumbar lordosis is a relevant parameter in the assessment of the risk of falls in this population.

Disclosures: Marie Fechtenbaum, None.

## SU0216

**Trabecular Bone Score in Type 2 Diabetes Mellitus: Preliminary Data of Cross-sectional Case-control Study.** Manuel Muñoz Torres<sup>\*1</sup>, Maria Dolores Avilés Perez<sup>2</sup>, Antonia García Martín<sup>2</sup>, Cristina Novo Rodríguez<sup>2</sup>, Rossana Manzanares Córdova<sup>2</sup>, Rafael Nieto Serrano<sup>3</sup>. <sup>1</sup>Bone Metabolic Unit, Endocrinology Division. Complejo Hospitalario Universitario de Granada (ibs.Granada). Spain., Spain, <sup>2</sup>Bone Metabolic Unit, Endocrinology Division. Complejo Hospitalario Universitario de Granada (ibs.Granada). Spain, Spain, <sup>3</sup>Nuclear Medicine Unit. Complejo Hospitalario Universitario de Granada (ibs.Granada). Spain., Spain

Type 2 diabetes mellitus (T2DM) is a risk factor for osteoporotic fractures although bone mineral density is increased. Therefore, there is a need for improved approaches to estimate fracture risk in such patients. Trabecular Bone Score (TBS) is a new technique to determine the trabecular bone microarchitecture. Our aim was to evaluate the usefulness of TBS in T2DM patients. We compared TBS values in T2DM group (n: 31) and control group (n: 25) and we analyzed its relationship with bone mineral density (BMD), history of prior fractures and glycemic control. TBS values were determined using TBS InSight<sup>®</sup> software. In all cases BMD was evaluated by dual-energy X-ray absorptiometry (DXA Hologic Inc; Bedford MA) and 3D DXA (Galgo Medical, Spain). T2DM patients had lower TBS than controls (1.14  $\pm$  0.17 vs 1.25  $\pm$  0.16, P = 0.013). However, we did not find differences between groups in DXA or 3D DXA parameters. In T2DM group, TBS at the lumbar spine showed degraded microarchitecture (TBS  $\leq$  1.2) in 16 patients (51.6%); 13 patients (41.9%) had partially degraded structure (TBS > 1.20 & < 1.35); and only 2 patients (6.5%) had normal TBS values (TBS  $\geq$  1.35). TBS results differed between groups close to statistical significance (Figure 1). We did not find differences in TBS values according densitometric diagnosis of osteoporosis or history of prior fracture in either group. We found a significant correlation of TBS with age, body mass index and lumbar spine BMD both in diabetic patients and controls (P < 0.05). Finally, we did not observe relationship with glycemic control or duration of diabetes in T2DM group. In conclusion, TBS is shown as a promising method in the clinical assessment of trabecular bone microstructure in T2DM



jpeg

Disclosures: Manuel Muñoz Torres, None.

## SU0217

**Complications and Skeletal Health in Long Duration Type 1 Diabetes.** Hillary Keenan<sup>\*1</sup>, Ernesto Maddaloni<sup>2</sup>, Varant Kupelian<sup>3</sup>, Liane Tinsley<sup>1</sup>, Maya Khatri<sup>1</sup>. <sup>1</sup>Joslin Diabetes Center, United states, <sup>2</sup>University Bio-Medica Roma, Italy, <sup>3</sup>Alexion Pharmaceuticals, United states

Bone is a heavily vascularized tissue and is the source of vascular repair cells used throughout the body. As dysregulation of vascular endothelial growth factor through insulin signaling and hyperglycemia has been implicated as the primary factor in several diabetic vascular complications and bone health. We sought to investigate this relationship in individuals with extreme duration type 1 diabetes (T1D). The Joslin 50-Year Medalist study assessed individuals with documentation of 50 or more years of insulin dependent diabetes via physical examination, medical history, and biospecimen collection. Median age, HbA1c, and disease duration in 1007 participants was 65 years, 7.1%, and 53 years, respectively. The prevalence of self reported lifetime fragility fractures was 1.2%. These individuals were also significantly protected from vascular complications with a proliferative diabetic retinopathy (PDR) prevalence of only 46.6%, nephropathy (eGFR  $\leq$  45 ml/min/1.73 m<sup>2</sup>) prevalence of 12.5%, and 65.5% had neuropathy (MNSI  $\geq$  2). Additionally, 45% had cardiovascular disease

(CVD). These complications were not associated with glycemic control or disease duration in this population. To determine if there is a relationship of skeletal health and complications, two convenience samples of Medalists were assessed using DXA (N=65) and HR-pQCT (N=28). These groups were comparable to the overall cohort. Low bone mineral density at the hip was significantly associated with CVD (adjusted OR=7.5, 95%CI: 1.2, 46.8), however, microvascular complications were not (adjusted ORs (95%CI) for: PDR 1.2 (0.4, 4.0), neuropathy 1.0 (0.3, 3.0), nephropathy 5.6 (0.7, 47.1)). However, the HR-pQCT data show PDR was associated with lower trabecular thickness at the tibia ( $0.067 \pm 0.007$  vs.  $0.075 \pm 0.012$  mm,  $p=0.07$ ) and neuropathy was associated with lower cortical vBMD at both the tibia ( $p=0.05$ ) and radius ( $p=0.002$ ). The association of CVD with BMD in this population is not surprising given findings from the Framingham Heart Study and European studies. Association between microvascular complications and differences in bone microarchitecture is novel and suggests different underlying mechanisms than between overall BMD and CVD. Uncovering the reasons for these differences may lead to successful targeting of therapies for skeletal health deterioration.

**Disclosures:** Hillary Keenan, None.

## SU0218

**Estimating the Prevalence of Osteoporosis Among Adults in the United States Using the National Bone Health Alliance Diagnostic Criteria.** Nicole Wright<sup>1</sup>, Kenneth Saag<sup>2</sup>, Bess Dawson-Hughes<sup>3</sup>, Sundeep Khosla<sup>4</sup>, Ethel Siris<sup>5</sup>. <sup>1</sup>Department of Epidemiology, University of Alabama at Birmingham, United states, <sup>2</sup>Division of Clinical Immunology & Rheumatology, University of Alabama at Birmingham, United states, <sup>3</sup>USDA Human Nutrition Research Center at Tufts University, United states, <sup>4</sup>Division of Endocrinology, Metabolism, Diabetes, Nutrition, & Internal Medicine, Mayo Clinic, United states, <sup>5</sup>Division of Endocrinology, Columbia University Medical Center, United states

**Purpose:** The National Bone Health Alliance (NBHA) developed new osteoporosis diagnostic criteria to better identify individuals at high risk for fragility fractures. We sought to estimate the prevalence of osteoporosis in adults  $\geq 50$  years in the United States (US) using these criteria.

**Methods:** Utilizing 2005-2008 National Health and Nutrition Examination Survey (NHANES) data, we identified participants with osteoporosis if they had any one of the following: 1) T-score  $\leq -2.5$ ; 2) qualifying low trauma hip fracture irrespective of BMD, or clinical vertebral, proximal humerus, pelvis, or distal forearm fracture with T-score of  $< -1.0$   $> -2.5$ ; or 3) FRAX score at the National Osteoporosis Foundation (NOF) intervention thresholds ( $\geq 3\%$  for hip fracture risk or  $\geq 20\%$  for major osteoporotic fracture risk). We calculated the proportion of persons meeting each element and estimated the prevalence of osteoporosis according to the NBHA criteria overall, by sex and age.

**Results:** The population included 1,948 (54.3%) men and 1,639 (45.7%) women; 12% were 80+ years and 21% were from racial/ethnic minority groups. The prevalence (SE) of osteoporosis based on BMD at the femoral neck or lumbar spine alone was 4.0% (0.45) in men and 15.5% (0.81) in women. Qualifying fractures alone did not uniquely identify many individuals in both sexes as there was considerable overlap with osteoporosis based on T-score. The prevalence (SE) of osteoporosis based on FRAX alone was 11.6% (0.83) in men and 13.0% (0.97) in women. When combined, we estimated that 16.0% (0.8) of men and 29.9% (1.0) of women 50+ years have osteoporosis according to the NBHA criteria. The prevalence increased with age to 46.3% in men and 77.1% in women 80+ years. The combination of FRAX score and qualifying fractures was the largest contributing factor defining osteoporosis in older men (70-79: 88.1%; 80+: 80.1%); whereas, T-score was the largest contributing factor in older women (70-79: 49.2%; 80+: 43.5%). The differences in contributing factors were statistically significant ( $p < 0.05$ ).

**Conclusions:** In a representative sample of US adults age 50+ years, 16% of men and 29.9% of women 50+ have osteoporosis based on the NBHA diagnostic criteria. Although the expanded definitions increases the prevalence of osteoporosis compared to BMD alone based definitions, this expansion may better identify those at elevated fracture risk in the ongoing public health effort to reduce the burden of fractures in older women and men.

**Disclosures:** Nicole Wright, Amgen, 11

## SU0219

**Prevalence of Osteoporosis and Low Bone Mass among Puerto Rican Adults: Results from the Boston Puerto Rican Osteoporosis Study.** Sabrina E. Noel<sup>1</sup>, John L. Griffith<sup>2</sup>, Nicole C. Wright<sup>3</sup>, Bess Dawson-Hughes<sup>4</sup>, Katherine L. Tucker<sup>1</sup>. <sup>1</sup>University of Massachusetts Lowell, United states, <sup>2</sup>Northeastern University, United states, <sup>3</sup>University of Alabama at Birmingham, United states, <sup>4</sup>Jean Mayer USDA Human Nutrition Research Center on Aging, Tufts University, United states

**Purpose:** Despite recent evidence that indicates Hispanics have a higher prevalence of osteoporosis than non-Hispanic whites, little is known about the skeletal health of Puerto Ricans living on the U.S. mainland. The objective of this study was to examine the prevalence of osteoporosis and low bone mass (LBM) among 930 Puerto Ricans

aged 47 to 77 y from the Boston Puerto Rican Osteoporosis Study (BPROS). Methods: Bone mineral density was measured using dual-energy X-ray absorptiometry. Osteoporosis was defined as T-scores  $\leq -2.5$  SD below peak bone mass and LBM as T-scores between -1.0 and -2.5. Estimates were adjusted to the age and sex distribution of the U.S. Puerto Rican population using 2010 Census data and were calculated for the full sample, as well as by sex and age categories (45-49, 50-59, 60-69 and 70-79 y), to facilitate comparisons with the most recent published National Health and Nutrition Examination Survey (NHANES) data. Results: In BPROS, the age and sex-adjusted prevalence estimates of osteoporosis and LBM were 9.3% and 36.8%, respectively. A greater percentage of women had osteoporosis and LBM than men (11.2% vs. 8.8% and 46.9% vs. 34.4%, respectively); however, differences between men and women were significant for LBM ( $P < 0.001$ ) and not osteoporosis ( $P = 0.28$ ). Surprisingly, the highest prevalence of osteoporosis among men was for those aged 50-59 y (11%) and lowest for those  $> 70$  y (3.7%). Compared with published results from NHANES, a greater percentage of BPROS men at ages 50 to 59 and 60-69 y had osteoporosis, compared with all men in the U.S. (50-59: 11.5% vs. 3.4%, and 60-69: 6.8% vs. 3.3%); however, confidence intervals were wide and overlapped between groups. For women, the prevalence of osteoporosis increased across age categories. A total of 9.7% of Puerto Rican women aged 50-59 had osteoporosis compared with 6.8% of those in NHANES. The prevalence of osteoporosis for women aged 60-69 and 70-79 y was similar in the BPROS and NHANES (10.9% vs. 12.3% and 24.3% vs. 25.7%, respectively); confidence intervals between groups overlapped. Conclusions: Our results indicate that Puerto Rican adults have a high prevalence of osteoporosis; and these were unexpectedly high among men and women in their 50s. There is an urgent need to gain a deeper understanding of the factors related to bone health to inform culturally and linguistically tailored interventions to improve skeletal health in this underserved, understudied population.

**Disclosures:** Sabrina E. Noel, None.

## SU0220

**The Cross-Sectional Survey Study of Osteoporosis in Shanghai Middle-Aged and Elderly People of China.** Jing Wang<sup>1</sup>, Bing Shu<sup>2</sup>, Chen-guang Li<sup>1</sup>, Xiao-feng Qi<sup>2</sup>, Liang Qiao<sup>2</sup>, Lin Chen<sup>2</sup>, Qiang Wang<sup>2</sup>, Xue-jun Cui<sup>2</sup>, Yong-jun Wang<sup>2</sup>. <sup>1</sup>Longhua Hospital, Shanghai University of Traditional Chinese Medicine, China, <sup>2</sup>Spine Research Institute, Shanghai University of Traditional Chinese Medicine, China

**Background:** Osteoporosis (OP) is a growing problem worldwide, with the greatest burden resulting from fractures. Greater awareness of the relationship between comorbidities and osteoporosis may improve prevention and treatment of osteoporosis.

**Methods:** A cross-sectional survey was conducted in 4186 respondents (men aged from 50-79 and women aged from 45-79) from two sub-districts in Shanghai, China. All the respondents were interviewed and completed the questionnaire. Bone mineral density (BMD) of lumbar vertebrae was measured by Dual Energy X-ray Absorptiometry (DXA) in 4066 respondents (97.13%).

**Result:** Overall, according to the BMD, 988 respondents (24.29%) were diagnosed osteoporosis and 1757 respondents (41.95%) were diagnosed osteopenia. Among female respondents, 847 (28.95%) were diagnosed osteoporosis and 1359 respondents (45.16%) were diagnosed osteopenia. Osteoporosis was positively associated with increasing age, body mass index, hypertension, hyperlipemia and osteoarthritis (trend test,  $P < 0.05$ ) in female respondents.

**Conclusions:** The prevalence of osteoporosis in China is substantially higher than that in Western countries, especially in female population. Further population-based studies are needed to investigate the epidemiology of osteoporosis.

**Disclosures:** Bing Shu, None.

## SU0221

**Impact of Body Weight Dynamics Following Intentional Weight Loss on Fracture Risk: Results from The Action for Health in Diabetes Study.** Kristen Beavers<sup>1</sup>, Rebecca Neiberg<sup>2</sup>, Karen Johnson<sup>3</sup>, Ramon Casanova<sup>2</sup>, Ann Schwartz<sup>4</sup>, Carolyn Crandall<sup>5</sup>, Cora Lewis<sup>6</sup>, Xavier Pi-Sunyer<sup>7</sup>, Stephen Kritchevsky<sup>2</sup>. <sup>1</sup>Wake Forest University, United states, <sup>2</sup>Wake Forest School of Medicine, United states, <sup>3</sup>University of Tennessee, United states, <sup>4</sup>UCSF School of Medicine, United states, <sup>5</sup>David Geffen School of Medicine at UCLA, United states, <sup>6</sup>University of Alabama School of Medicine, United states, <sup>7</sup>Columbia University, United states

**Purpose:** To explore the impact of body weight change following intentional weight loss on fracture risk in overweight and obese adults with diabetes.

**Methods:** 1912 individuals with type 2 diabetes (baseline age:  $58.5 \pm 6.7$  years, 58% women, baseline BMI:  $35.7 \pm 6.0$  kg/m<sup>2</sup>) who participated in the Look AHEAD Study and lost weight one year after being randomized to an intensive lifestyle intervention were assessed. Body weight was measured annually and participants were categorized as regainers, cyclers, or continued losers/maintainers, based on a  $\pm 3\%$  annual change in weight from year 1 to year 4. If percent weight change between each year and the previous year or year 1 exceeded a 3% gain or loss, participants were categorized as regainers or continued losers, respectively. Percent weight change between each year and the previous year or year 1 within 3% led to a categorization of maintainer. If a participant had both regainer and loser categories, their final category was cyler.

Adjudicated fracture incidence was captured from years 4 through 13 (mean fracture follow-up duration 11.2 years from baseline) and defined as a composite of lower/upper arm, spine, pelvis, hip, and lower leg fractures. Overall and gender-stratified models of fracture were performed using Cox proportional hazards models, adjusting for gender (when appropriate), age, race/ethnicity, baseline BMI category, and baseline bone-positive and bone-negative medication use.

Results: 57, 22 and 21% of participants were classified as regainers, cyclers, and continued losers/maintainers, respectively, and 219 fractures (men n=63; women n=156) were recorded during the follow-up period. Overall, patterns of weight change were not associated with incident fracture ( $p=0.99$ ) and did not interact with gender ( $p=0.14$ ). Gender-stratified results were also non-significant, although modest, differential signals were noted (see Table 1).

Conclusion: Patterns of weight change following intentional weight loss were not associated with incident fracture in this cohort of overweight and obese adults with diabetes. Gender-stratified analyses may suggest differential associations for men and women, but a formal test of interaction was not significant. Future research in this area is warranted.

**Table 1.** Adjusted\* hazard estimates of fracture for weight pattern categories, overall and by gender.

	Loser or Maintainer	Regainer	Cycler
	HR (95% CI)	HR (95% CI)	HR (95% CI)
Overall (n=1912)	REF	0.98 (0.70, 1.39)	0.99 (0.66, 1.49)
Males (n=804)	REF	0.69 (0.39, 1.23)	0.47 (0.20, 1.09)
Females (n=1108)	REF	1.26 (0.77, 2.05)	1.14 (0.73, 1.78)

\*Model statements are adjusted for age category, gender (when appropriate), race, baseline BMI category, and baseline bone-positive (androgens, antacids, antiestrogen, antiresorptive, calcium, estrogens, macrominerals, microminerals/trace elements, and selective estrogen receptor modulators) and bone-negative (antihypertensives, loop diuretics, selective serotonin reuptake inhibitors, thyroid hormones, tricyclic antidepressants, and thiazolidinediones) medication use.

Table 1

Disclosures: *Kristen Beavers, None.*

## SU0222

**Achieving Freedom from Glucocorticoids Use might Decrease the Risk of Clinical Fractures in Patients with Rheumatoid Arthritis: Five-Year Results of the TOMORROW Study.** [Tatsuya Koike](#)<sup>1</sup>, [Kenji Mamoto](#)<sup>2</sup>, [Yuko Sugioka](#)<sup>3</sup>, [Masahiro Tada](#)<sup>2</sup>, [Tadashi Okano](#)<sup>2</sup>, [Kentaro Inui](#)<sup>4</sup>. <sup>1</sup>Search Institute for Bone & Arthritis Disease (SINBAD), Shirahama Foundation for Health & Welfare, Japan, <sup>2</sup>Department of Orthopedic Surgery, Osaka City University Medical School, Japan, <sup>3</sup>Center for Senile Degenerative Disorders (CSDD), Osaka City University Medical School, Japan, <sup>4</sup>Department of Rheumatology, Osaka City University Medical School, Osaka, Japan

Patients with rheumatoid arthritis (RA) who have muscle weakness and painful joints might be at increased risk of falls and fractures especially under the treatment with glucocorticoid (GC). However, previous studies have provided no answer to reduce the risk of fractures. The present study prospectively investigates correlations between decreasing doses of GC and the incidence of clinical fractures in patients with RA based on the TOMORROW study (UMIN00003876) that started in 2010. We evaluated anthropometric parameters, bone mineral density, disease activity, RA medication, and the incidence of clinical fractures over a period of five years in 202 patients with RA (mean age, 58.6 years; mean disease duration, 14.0 years). We also assessed the effects of GC doses on the incidence of clinical fractures over the same period in patients with RA using multivariate regression analysis. The incidence of clinical fractures in patients with RA was 0.042/person-years (py). There were 87 RA patients (41.8%) treated with GC whose incidence rate and

number of clinical fractures were significantly higher than those without GC treatment (27.4% vs. 11.9%;  $p = 0.008$ ; 0.063 vs. 0.012 py;  $p = 0.012$ , respectively). After adjusting for fracture risk factors including age, sex, smoking, and body mass index, multivariate logistic regression analysis revealed that GC administered within the five-year period was a significant risk factor for clinical fractures (odds ratio [OR], 2.58; 95% confidence interval [CI], 1.22-5.44,  $p = 0.013$ ). A mean GC dose during the 5-year period of  $\geq 2$  mg/day increased risk for fractures in patients with RA (OR 3.48). Although only reducing the GC dose did not decrease the risk of clinical fractures in patients with RA, risk was significantly lowered when the dose was reduced to zero within the five-year period (OR, 0.21). Medication with GC was a significant risk factor for clinical fractures, and low doses are apparently significantly associated with an increased frequency of fractures among patients with RA. However, reducing the GC dose to zero among RA patients within five-years could lower the risk for clinical fractures. We concluded that GC medication should be tapered to zero over a period of five years in patients after RA activity is controlled.

Table: Odds ratios for clinical fractures during five years

	OR	95% CI	p
History of fractures	1.99	0.95-4.16	0.069
Average GC dose ( $\geq 2$ mg/day/5 y)	3.48	1.19-10.21	0.023
Only reducing GC within 5 y	0.61	0.21-1.78	0.362
Reducing GC to zero within 5 y	0.21	0.07-0.65	0.006
Bisphosphonate medication	3.37	1.51-7.54	0.003
Low BMD at thoracic vertebrae ( $< 0.7$ g/cm <sup>2</sup> )	4.44	1.69-11.64	<0.001

BMD, bone mineral density; CI, confidence interval; GC, glucocorticoid; OR, odds ratio; RA, rheumatoid arthritis.

Table 1

Disclosures: *Tatsuya Koike, None.*

## SU0223

**Epidemiological Characteristics of Femoral Fractures in Sergipe, 2010 - 2015, BRAZIL.** [Priscila Soares Pereira](#), [Francisco de Assis Pereira\\*](#), [Carlos Umberto Pereira](#), [Anna Klara Bohland](#), [Patricia Monique Pereira](#), [Larissa Tiziane Pereira](#). Universidade Federal De Sergipe, Brazil

Introduction: The social and economic cost of femoral fractures is high due the morbidity relating to the fracture itself, among other factors. despite the importance of this issue, studies on this topic are still scarce in Brazil.

Methods: The data were obtained from the SUS (*sistema unico de saude*) (system of the Brazilian unified national health) database using software tabwin and analysed with the statistical package for the social sciences (SPSS 10.0).

Results: The sample of 5323 cases. 2358 (44%) men, 2965 (56%) women. 45% presented fractures in the femur's neck region; 49% peritrochanteric and 6% subtrochanteric. the average time of hospitalization was of 8,9 days (1 to 29 days). there was not important spatial correlations or temporal spatial correlations. despite the lack of temporal and spatial correlations, the number of femoral fractures in elderly Brazilians was high, with heavy financial and social costs. 10% of the patients were submitted hospitalization in unit therapy intensive and the intra-hospital mortality rate was 3%. the financial cost with fractures from 2010 to 2014 was 8.804.399,89 reais.

Conclusion: The epidemiological profile is similar found in the literature. preventive measures such as early diagnosis and treatment of osteoporosis and public health policies are urgently needed to control predisposing factors for femoral fractures.

Disclosures: *Francisco de Assis Pereira, None.*

## SU0224

**Incident Fracture is Associated with a Period of Accelerated Loss of Hip BMD: The Study of Osteoporotic Fractures.** [Blaine Christiansen](#)<sup>1</sup>, [Stephanie Litwack Harrison](#)<sup>2</sup>, [Howard Fink](#)<sup>3</sup>, [Nancy Lane](#)<sup>1</sup>. <sup>1</sup>University of California Davis Health System, United States, <sup>2</sup>University of California, San Francisco, United States, <sup>3</sup>University of Minnesota, United States

Introduction: One of the most reliable predictors of future fracture is a prevalent fracture at any skeletal site (Klotzbuecher et al., JGIM, 2000), even after controlling for bone mineral density (BMD). The etiology of this phenomenon remains unclear. Our *in vivo* mouse studies find that bone fracture initiates bone resorption at sites distal from the fracture site, leading to a reduction in trabecular bone volume by 2 weeks post-fracture. However, systemic bone loss following a fracture has not been carefully evaluated in human clinical cohort studies. Based on our preliminary data, we hypothesized that older women who sustained an incident fracture at any skeletal site would exhibit a greater loss of hip BMD than women with no fracture.

Methods: We tested our hypothesis using data from 4,193 Caucasian women aged >65 years who were enrolled in the Study of Osteoporotic Fractures (SOF) and

completed serial measurements of BMD at the spine and hip and adjudication of incident fractures between study visits 4 and 6 (~5 year interval). Women also provided information on potential confounding variables, including tests of strength and function, cognitive exams, use of medication, and health habits. Baseline characteristics at visit 4 were compared across fracture status. Generalized linear models were used to calculate percent change in total hip BMD between visit 4 and visit 6 for each incident fracture type, and for upper and lower extremity fractures combined (Table). Multivariate adjusted models were used to control for (1) age and days from the fracture to visit 6, and (2) age, days from the fracture to visit 6, walking speed, and total hip BMD at visit 4.

Results: Participant characteristics at visit 4 were similar for women without fracture (n = 3,764) and those with one (n = 392) or multiple (n = 37) incident fractures during follow-up with the exception that those with incident fracture(s) tended to be older, have slower walking speed, and have lower total hip BMD. We found that incident fracture was associated with significantly greater loss of total hip BMD during this time period compared to those that did not fracture (Table). Of note, women who sustained a humerus or elbow fracture exhibited a loss of total hip BMD nearly twice that of women without fracture. This greater reduction in BMD was maintained even after controlling for age, walking speed, and baseline hip BMD. No differences were observed in reduction of total hip BMD based on time from incident fracture to follow-up DEXA.

Conclusions: We observed a significantly greater reduction in total hip BMD during the 5 year period in which an extremity fracture occurred in elderly Caucasian women compared to those that did not fracture. This may support identification of incident fractures at any site in elderly women, and may indicate the use of therapies to prevent BMD loss and future fractures.

Table. Percent change in total hip BMD by incident fracture between visit 4 and visit 6

Fracture Type	N	Time from Incident Fracture to Follow-Up DEXA (days) - Mean (Range)	Mean percent change in BMD		
			Unadjusted (SD)	Multivariate-adjusted (95%CI) <sup>1</sup>	Multivariate-adjusted (95%CI) <sup>2</sup>
None	3764		-2.96 (0.10)	-2.93 (0.09)	-2.93 (0.09)
Humerus	53	772 (105-1712)	-5.38 (0.79)**	-6.81 (0.86)**	-6.74 (0.86)**
Elbow	24	982 (54-1762)	-5.16 (1.18)	-6.70 (1.19)**	-6.69 (1.19)**
Wrist	93	872 (32-1861)	-3.93 (0.61)	-5.27 (0.67)**	-5.25 (0.67)**
All Upper Extremity Single Fractures	170	857 (32-1861)	-4.58 (0.45)**	-5.72 (0.53)**	-5.68 (0.53)**
Multiple Fractures - Upper Extremity Only	9	710 (136-1973)	-5.69 (1.84)	-7.17 (1.85)*	-7.10 (1.85)*
Ankle	64	904 (112-1900)	-3.12 (0.71)	-4.65 (0.77)*	-4.70 (0.77)*
Foot	50	870 (86-1914)	-2.95 (0.79)	-4.09 (0.84)	-4.12 (0.84)
Toe	25	832 (46-1502)	-1.64 (1.21)	-3.52 (1.24)	-3.46 (1.24)
Lower leg	14	926 (161-1787)	-3.39 (1.48)	-4.33 (1.48)	-4.26 (1.48)
Hip	69	793 (55-1956)	-6.37 (0.89)**	-7.45 (0.95)**	-7.26 (0.95)**
All Lower Extremity Single Fractures	222	855 (46-1956)	-3.62 (0.41)	-4.60 (0.50)**	-4.58 (0.50)**
Multiple Fractures Including Lower Extremity	37	702 (25-1973)	-5.66 (1.01)**	-7.20 (1.07)**	-7.13 (1.07)**

<sup>1</sup>adjusted for age and days from fracture to visit 6  
<sup>2</sup>adjusted for age, days from fracture to visit 6, walking speed and total hip BMD at visit 4  
 \* <0.05, \*\* <0.01, \*\*\* <0.001

Table: Percent change in total hip BMD by incident fracture between visit 4 and visit 6

Disclosures: Blaine Christiansen, None.

## SU0225

**Metabolic Syndrome and Risk of Incident Fall Injury in Community-Dwelling Older Adults: the Health, Aging, and Body Composition Study.** Naoko Sagawa<sup>\*1</sup>, Brian C. Callaghan<sup>2</sup>, Robert M. Boudreau<sup>1</sup>, Aaron I. Vinik<sup>3</sup>, Ann V. Schwartz<sup>4</sup>, Teresa M. Waters<sup>5</sup>, Jane A. Cauley<sup>1</sup>, Elsa S. Strotmeyer<sup>1</sup>. <sup>1</sup>University of Pittsburgh, United states, <sup>2</sup>University of Michigan, United states, <sup>3</sup>Eastern Virginia Medical School, United states, <sup>4</sup>University of California San Francisco, United states, <sup>5</sup>University of Tennessee, United states

In older adults, fall injuries are an important cause of morbidity and mortality. Metabolic syndrome (MetS) is prevalent, and past studies found inconsistent associations with falls and fractures. We investigated the association of MetS and its components with incident fall injuries in the Health, Aging, and Body Composition Study, a prospective cohort study of community-dwelling Medicare beneficiaries (N=2363; age 74 ± 3, BMI 27 ± 5 kg/m<sup>2</sup>, 52% women, 38% black, 45% MetS, 20% diabetes). Predictors included MetS and its components defined from the updated National Cholesterol Education Program/Adult Treatment Panel III. Fall injuries (1997-98 baseline to 12/31/08) were defined as any unique event from Medicare claims with a fall code (E880-888) plus non-fracture injury or fracture (800-829), or non-vertebral fracture. Initial fall injury (N=678) occurred in 5 ± 3 years, with others censored at death (N=502)/data end date (N=1183; 10 ± 2 years). Stepwise Cox regression models in all participants and stratified by glycemic status were built for outcomes of total fall injuries and separately by fracture (Fx) and non-fracture (non-Fx) fall injuries. Participants with fall injuries were more likely white (62 vs. 58%), women (64 vs. 47%), older age (74 ± 3 vs. 73 ± 3 years), and had fall history (26 vs. 20%), poor vision (55 vs 51%), lower bone mineral density (0.91 ± 0.16 vs. 0.83 ± 0.16 g/cm<sup>2</sup>), lower diastolic blood pressure (BP; 70 ± 12 vs. 72 ± 11 mmHg), and lower BMI (27 ± 5 vs. 28 ± 5 kg/m<sup>2</sup>), all p < 0.05. MetS was not associated with total fall injuries, Fx, or non-Fx fall injuries. Individuals with high waist circumference (67% fall injuries vs. 59% no injuries; p < 0.05) had increased risk of total fall injuries, Fx, and non-Fx fall injuries (Table). In individuals with diabetes (age 74 ± 6, 44% women, 50% black, 81% MetS), MetS increased risk of total fall injuries and Fx, but not non-Fx injuries; and individual MetS components were not related. In individuals with normal

glycemia (age 73 ± 3, 54% women, 35% black, 22% MetS), high waist circumference, but not MetS, increased total fall injuries, Fx, and non-Fx fall injury risk (Table), and high BP (HR=0.58; 95%CI: 0.36-0.93) decreased non-Fx fall injury risk. MetS components of triglycerides and HDL-cholesterol were not associated with fall injuries in any group. MetS in diabetes and high waist circumference in all participants and those with normal glycemia independently predicted risk of incident fall injuries in older adults.

Table: Metabolic syndrome and high waist circumference\* and incident fall injury risk for all participants and stratified by glycemic status<sup>†</sup>

	Total fall injury (N=678)	Fracture (N=518)	Non-fracture fall injury (N=160)
<b>Overall (N=2363)</b>			
Metabolic syndrome	1.09 (0.92-1.29)	1.15 (0.95-1.39)	0.91 (0.64-1.29)
High waist circumference	<b>1.35 (1.09-1.66)§</b>	<b>1.28 (1.01-1.63)§</b>	<b>1.67 (1.08-2.58)§</b>
<b>Diabetes (N=485)</b>			
Metabolic syndrome	<b>1.81 (1.02-3.21)§</b>	<b>2.28 (1.10-4.73)§</b>	1.40 (0.55-3.59)
High waist circumference	1.03 (0.62-1.74)	1.06 (0.57-1.97)	0.93 (0.36-2.39)
<b>Prediabetes (N=696)</b>			
Metabolic syndrome	1.03 (0.76-1.42)	1.02 (0.72-1.46)	1.00 (0.49-2.05)
High waist circumference	1.14 (0.77-1.69)	1.10 (0.71-1.71)	1.36 (0.57-3.23)
<b>Normal glycemia (N=1182)</b>			
Metabolic syndrome	1.02 (0.79-1.33)	1.09 (0.81-1.47)	0.77 (0.42-1.41)
High waist circumference	<b>1.63 (1.23-2.16)§</b>	<b>1.55 (1.13-2.13)§</b>	<b>2.43 (1.34-4.45)§</b>

\*High waist circumference was defined as ≥102 cm in men and ≥88 cm in women.

†Diabetes was defined as fasting glucose ≥126 mg/dL or 2-h glucose ≥200 mg/dL or hypoglycemic medication use. Prediabetes was defined as fasting glucose ≥100 mg/dL or 2-h glucose ≥140 mg/dL.

§All models were adjusted for age, site, race, gender, weight, and height, with adjustment for additional variables if P < 0.1: education, total number of medications, opioid use, 10-g monofilament insensitivity, and bone mineral density.

Table

Disclosures: Naoko Sagawa, None.

## SU0226

**Overall Pediatric Fracture Incidence is Declining and Fracture Etiology is Changing - Trends over Six Decades.** Vasileios Lempesis<sup>\*1</sup>, Björn Rosengren<sup>1</sup>, Jan-Åke Nilsson<sup>1</sup>, Lennart Landin<sup>1</sup>, Carl-Johan Tiderius<sup>1</sup>, Magnus Karlsson<sup>2</sup>. <sup>1</sup>Department of Orthopedics & Clinical Sciences, Skåne University Hospital, Lund University, Sweden, <sup>2</sup>Department och Orthopedics & Clinical Sciences, Skåne University Hospital, Lund University, Sweden

Purpose: A third of all children sustain fractures. It is therefore essential to identify changes in pediatric fracture incidence (to predict future fracture burden) and unravel changes in etiology (to identify new preventive fields).

Methods: Our hospital is the only in an urban region with 276244 inhabitants year 2006 and all hospital records have since a century been saved (including diagnosis registry, charts and radiographs). Through these we identified incident fractures with etiology in children (aged < 17) during six separate periods from 1950 to 2006. We estimated period specific fracture rates and age and gender standardized time trends by use of official annual population data. Rates are reported as number of fractures per 10000 person-years, changes between periods as rate ratios (RR) with 95% CI and etiology as proportion (%) of all fracture trauma.

Results: The overall pediatric fracture rate was in 1950/1955 135 per 10000 person-years (166 in boys and 102 in girls) and in 2005/2006 176 (228 in boys and 122 in girls). The age standardized male/female ratio during these two periods were 1.6 (1.4 to 1.9) and 1.8 (1.6 to 2.1). Fracture incidence increased in all periods until age 14 in boys and 12 in girls where after the incidence declined. The age and gender standardized overall fracture rate increased from 1950/1955 to 1976/1979 with 47% (RR 1.47; 1.33 to 1.62) and decreased from 1976/1979 to 2005/2006 with 13% (RR 0.87; 0.80 to 0.96). Trends differed with fracture type and gender. For example, the age standardized distal forearm fracture rate increased from 1950/55 to 2005/2006 by 43% (RR 1.43; 1.15 to 1.68) while clavicle fracture rate showed a declining trend (RR 0.82; 0.57 to 1.17). The age standardized overall fracture incidence decreased in girls from 1976/1979 to 2005/2006 by 22% (RR 0.78; 0.66 to 0.90) while it was unchanged in boys (RR 0.93; 0.83 to 1.05). Also fracture etiology changed with time. From 1950/1955 to 2005/2006, traffic accidents decreased from 25% to 13% and home injuries from 11% to 2% while in sports increased from 26% to 40%, in playgrounds from 6% to 12% and in fights from 2% to 8%.

Conclusion: Pediatric fracture rate has decreased since 1976/1979. Etiologies have changed since 1950. Our data highlight the importance of new calculations of future resource allocation, show that preventions in traffic and home have been successful, and suggest a shift in prevention on etiologies of growing importance.

Disclosures: Vasileios Lempesis, None.

**SU0227**

**Predictors of imminent fracture risk in Medicare-enrolled men and women.** Akeem Yusuf\*<sup>1</sup>, Yan Hu<sup>1</sup>, David Chandler<sup>2</sup>, Barry Crittenden<sup>2</sup>, Richard Barron<sup>2</sup>. <sup>1</sup>Chronic Disease Research Group, United states, <sup>2</sup>Amgen Inc., United states

Osteoporotic fractures constitute a large health burden for the older population. However, there is limited information on risk factors associated with imminent risk (12-24 months) of fractures. In this study, we sought to identify predictors of imminent risk for fracture in the Medicare population.

This was a large retrospective cohort study using data from the 20% Medicare database. The study population included all Medicare beneficiaries alive and aged ≥ 67 years on January 1, 2011 (index date), continuously enrolled in Medicare Parts A, B and D between January 1, 2009 and March 31, 2011, and non-participation in HMO, no evidence of malignant neoplasm (excluding melanoma) or Paget's disease of bone in the 12-months prior to the index date. Patients were followed for 12 or 24 months after the index date and index osteoporotic fracture was assessed during the follow-up. Multivariate Cox proportional hazards models were used to evaluate potential predictors of imminent fracture including demographic and clinical characteristics, fall and frailty markers, and concomitant medications.

The study included 1,780, 451 patients with mean age 78, 66% women, and 85% white. During 12 and 24 months follow-up, 3.0% and 5.4% had an index fracture respectively. Factors most strongly associated with imminent fractures (within 12 mo. follow-up) included increasing age, female gender, white race, previous fracture history, comorbidities (including osteoporosis, cardiovascular disease, COPD, ankylosing spondylitis, depression, and mood disorders) and previous falls (Table 1). Other factors associated with imminent fracture risk included frailty/physical function markers (use of ambulance/life support, difficulty walking and use of durable medical equipment). The findings were largely consistent for factors associated with imminent risk for fracture within 24 months.

Factors associated with 12-24 month risk for fracture include predictors included in 10-year risk prediction models such as older age, female gender, and white race, and history of fractures.. These findings are consistent with results reported by Weycker D et al. 2015 and Bonafede M et al. ASBMR 2015. Clinician awareness of these predictive factors will facilitate improved identification and treatment of patients at imminent risk for fracture.

Table 1. Factors strongly associated with imminent fracture risk in the 12 and 24 months follow-up periods

	12-month risk		24-month risk	
	HR <sup>1</sup>	95% CI	HR <sup>1</sup>	95% CI
<b>DEMOGRAPHIC</b>				
Age				
67-69	Ref		Ref	
70-74	1.22	1.17-1.26	1.22	1.19-1.26
75-79	1.69	1.63-1.76	1.73	1.68-1.77
80-84	2.29	2.21-2.37	2.38	2.32-2.44
85+	3.12	3.01-3.23	3.27	3.19-3.35
Male gender	0.55	0.54-0.56	0.54	0.53-0.55
Race				
White	Ref		Ref	
Black	0.43	0.41-0.45	0.42	0.41-0.44
Hispanic	0.70	0.66-0.75	0.72	0.69-0.75
Asian	0.66	0.62-0.71	0.66	0.63-0.69
Other Races	0.81	0.75-0.87	0.80	0.76-0.85
Previous fracture	2.46	2.41-2.52	2.21	2.17-2.25
Falls	1.18	1.14-1.21	1.16	1.14-1.19
<b>CLINICAL COMORBIDITY</b>				
Osteoporosis	1.22	1.18-1.25	1.21	1.18-1.24
Cardiovascular disease	1.11	1.09-1.13	1.12	1.10-1.13
COPD <sup>3</sup>	1.16	1.14-1.19	1.17	1.15-1.19
Ankylosing spondylitis	1.52	1.36-1.70	1.41	1.29-1.55
Depression	1.14	1.11-1.17	1.13	1.11-1.16
Mood and anxiety disorders	1.07	1.03-1.11	1.10	1.07-1.13
<b>FRAILITY MARKERS</b>				
Ambulance life support	1.16	1.13-1.19	1.15	1.13-1.17
Difficulty walking	1.15	1.12-1.18	1.14	1.12-1.16
Use of DME <sup>2</sup>	1.12	1.09-1.14	1.11	1.09-1.13
<b>CONCOMITANT MEDICATION FACTORS</b>				
Osteoporosis medications	1.26	1.24-1.29	1.27	1.25-1.29
Glucocorticoids	1.13	1.11-1.15	1.13	1.12-1.15
Heparin	1.21	1.14-1.26	1.16	1.11-1.21
CNS <sup>4</sup> active medications	1.13	1.10-1.16	1.11	1.09-1.13

<sup>1</sup>Hazard ratio; <sup>2</sup>Durable Medical Equipment; <sup>3</sup>Chronic obstructive pulmonary disease; <sup>4</sup>Central nervous system

Table 1

**Disclosures:** *Akeem Yusuf, None. This study received funding from: Amgen Inc.*

**SU0228**

**Rate of Bone Loss Is Not Different Between Females Who Fracture and Those Who Do Not Fracture.** Lauren Burt\*<sup>1</sup>, Sarah Manske<sup>1</sup>, David Hanley<sup>2</sup>, Steven Boyd<sup>1</sup>. <sup>1</sup>McCaig Institute for Bone & Joint Health, Department of Radiology, Cumming School of Medicine, University of Calgary, Canada, <sup>2</sup>McCaig Institute for Bone & Joint Health, Departments of Community Health Sciences & Oncology, Cumming School of Medicine, University of Calgary, Canada

Longitudinal studies using high-resolution peripheral quantitative computed tomography (HR-pQCT) provide volumetric information on changes in bone density and microarchitecture. In our nested case-control study we aimed to explore baseline assessment of bone density and microarchitecture compared with 5-year changes in these parameters, to determine which is more predictive of fracture risk.

Women from the Calgary cohort of the Canadian Multicentre Osteoporosis Study (CaMos) had HR-pQCT scans of their non-dominant radius and tibia at baseline and 5-year follow-up. Total volumetric BMD (Tt.BMD), trabecular BMD (Tb.BMD), trabecular number (Tb.N) and trabecular separation (Tb.Sp) were assessed. Failure load was estimated from finite element analyses. Yearly questionnaires captured fragility fractures. Fragility fractures were defined as a fracture resulting from a fall at standing height or less. HR-pQCT outcomes were compared between those who fractured during the study and age-matched controls. T-tests compared differences between groups and odds ratios (OR) were calculated from binary logistic regression.

The nested cohort consisted of 81 women (age 71 ± 6 years). Over the 5-year study 27 women reported fragility fractures (lower limb: 11; upper limb: 9; torso: 7). The fracture group had lower baseline radial Tt.BMD, Tb.BMD, Tb.N, and failure load with higher Tb.Sp than the non-fracture group at baseline. Specifically, decreases in Tb.N (6.17 OR; 1.39 - 27.49 95% CI) were associated with increased fracture risk. Similarly, increases in Tb.Sp (10.25 OR; 1.03 - 101.64 95% CI) was associated with increased fracture risk. Baseline tibial differences nor tibial rate of change were different between groups.

Rate of bone change was not different between groups suggesting baseline radial levels of bone density, microarchitecture and strength play a larger role in fracture prediction than radial rate of change. These data suggest emphasis should be placed on increasing peak bone mass to help decrease the risk of fragility fracture later in life.

**Disclosures:** *Lauren Burt, Osteoporosis Canada, 11*

**SU0229**

**A Prospective Study of Gout and Risk of Fracture in Women.** Julie M Paik\*<sup>1</sup>, Seoyoung C Kim<sup>1</sup>, Diane Feskanich<sup>1</sup>, Hyon K Choi<sup>2</sup>, Daniel H Solomon<sup>1</sup>, Gary C Curhan<sup>1</sup>. <sup>1</sup>Brigham & Women's Hospital, Harvard Medical School, United states, <sup>2</sup>Massachusetts General Hospital, Harvard Medical School, United states

**Background:** Uric acid may be linked to bone health through its anti-oxidant or pro-oxidant effects, thereby affecting bone resorption and formation, or through inhibition of vitamin D activation which could result in higher parathyroid hormone level. However, prior studies on the relation between serum uric acid level and bone mineral density have demonstrated conflicting results. To date, there have been no prospective studies examining the relation between gout, a disease characterized by hyperuricemia and inflammation, and risk of incident hip or wrist fracture in women.

**Methods:** We conducted a prospective observational study of gout and risk of incident wrist (distal radius) fracture and hip fracture in women participating in the Nurses' Health Study (n=76,571 at analysis baseline with 14 years of follow-up for the wrist fracture analysis and 22 years of follow-up for the hip fracture analysis). Gout history and incident wrist and hip fracture were assessed by biennial questionnaires. Cox proportional-hazards models were used to simultaneously adjust for potential confounders.

**Results:** During the follow-up period, there were 3,529 incident wrist fractures (1990-2004) and 2,094 incident hip fractures (1990-2012), with 98 wrist and 115 hip fractures among participants with gout. After adjusting for potential risk factors, including body mass index, race, physical activity, history of falls, smoking status, alcohol intake, intakes of calcium, protein, vitamin D, and vitamin A, history of hypertension or diabetes, menopausal status, and postmenopausal hormone use, the relative risk of wrist fracture in women with a history of gout compared with women without gout was 1.06 (95% CI 0.87 to 1.30). The multivariable-adjusted relative risk of incident hip fracture in women with a history of gout compared with women without gout was 1.36 (95% CI 1.12 to 1.65).

**Conclusion:** Gout is associated with an increased risk of hip fracture but is not significantly associated with risk of wrist fracture in women. While our study cannot determine a causal link between gout and hip fractures, this association may be valuable when considering the management of patients at risk of hip fractures.

**Disclosures:** *Julie M Paik, None.*

**SU0230**

**Associations of Parity and Breast-feeding with Hip Fracture Incidence in the Women's Health Initiative.** Carolyn Crandall<sup>1\*</sup>, Jane Cauley<sup>2</sup>, Jingmin Liu<sup>3</sup>, Polly Newcomb<sup>3</sup>, Kelli Ryckman<sup>4</sup>, Lisette Jacobson<sup>5</sup>, Marcia Stefanick<sup>6</sup>, Mara Vitolins<sup>7</sup>, JoAnn Manson<sup>8</sup>. <sup>1</sup>University of California, Los Angeles, United states, <sup>2</sup>University of Pittsburgh, United states, <sup>3</sup>Fred Hutchinson Cancer Research Center, United states, <sup>4</sup>The University of Iowa, United states, <sup>5</sup>University of Kansas School of Medicine-Wichita, United states, <sup>6</sup>Stanford University School of Medicine, Stanford University, United states, <sup>7</sup>Wake Forest School of Medicine, United states, <sup>8</sup>Brigham & Women's Hospital, Harvard Medical School, United states

**Background.** During pregnancy and lactation, calcium absorption more than doubles, whereas during lactation, the maternal skeleton resorbs to provide the majority of calcium contained in breast milk. During pregnancy and lactation, levels of parathyroid hormone-related hormone are increased. The associations of pregnancies, live births, and lactation with incident fractures during the postmenopausal period are not well-understood.

**Methods.** We analyzed data from 93,676 postmenopausal women participating in the Women's Health Initiative Observational Study. Using Cox proportional hazards regression analysis, we examined associations of fracture incidence with several aspects of parity (nulliparity, number of pregnancies, age at first term pregnancy, and number of full-term pregnancies) and breastfeeding (number of episodes of breastfeeding for at least one month, number of children breastfed, age when first breastfed, total number of months breastfed for at least 1 month, and total number of months breast fed for any duration).

**Results.** The mean age of participants was 63.6 years (SD=7.4); mean follow-up 7.9 years (SD=1.6). Ten percent of participants were nulliparous. In fully adjusted models, compared with never breastfeeding, a history of breastfeeding for at least one month was associated with a decreased risk of hip fracture (yes vs. no, hazard ratio [HR] 0.79, 95% confidence interval [CI] (0.69 - 0.90)). Compared with never breastfeeding, the HRs [95% CI] for hip fracture for categories of breastfeeding duration were: HR 0.79 [0.67 - 0.93] for 1-6 months, HR 0.73 [0.57 - 0.92] for 7-12 months, HR 0.84 [0.66 - 1.09] for 13-23 months, and HR 0.81 [0.59 - 1.11] for 24+ months, p trend =0.01 (Table). Number of pregnancies, parity, age at first birth, number of children breastfed, age at first breastfeeding, and age at last breastfeeding were not statistically significantly associated with hip fracture incidence.

**Conclusions.** Total breastfeeding duration of 1-12 months was associated with decreased risk of hip fractures. Biological mechanisms underlying these associations warrant elucidation.

The WHI program is funded by the National Heart, Lung, and Blood Institute, National Institutes of Health, U.S. Department of Health and Human Services through contracts HHSN268201100046C, HHSN268201100001C, HHSN268201100002C, HHSN268201100003C, HHSN268201100004C, and HHSN271201100004C.

Table. Associations of lactation patterns with hip fractures\*

Predictor	Univariate model		Model 1		Model 2	
	HR (95% CI)	p	HR (95% CI)	p	HR (95% CI)	p
<b>Lactation Pattern</b>						
Breastfed for at least one month	N=92,045 Ref(1.00)	0.0037	N=37,042 Ref(1.00)	<b>0.0064</b>	N=48,735 Ref(1.00)	<b>0.0007</b>
No	0.96(0.80, 1.01)		0.77(0.64, 0.93)		0.79(0.69, 0.90)	
Yes						
How many children breastfed?	N=91,756 Ref(1.00)	0.4210	N=37,007 Ref(1.00)	0.3506	N=48,669 Ref(1.00)	0.0684
None						
1	0.86(0.73, 1.02)		0.77(0.59, 1.01)		0.77(0.63, 0.95)	
2	0.85(0.71, 1.01)		0.74(0.56, 0.98)		0.77(0.63, 0.95)	
3	0.92(0.75, 1.13)		0.85(0.63, 1.16)		0.80(0.66, 1.05)	
4	0.96(0.73, 1.25)		0.74(0.48, 1.14)		0.76(0.55, 1.04)	
5	1.11(0.77, 1.61)		0.80(0.27, 1.23)		0.81(0.51, 1.29)	
6	1.35(0.80, 2.30)		0.94(0.35, 2.52)		1.23(0.67, 2.23)	
7	0.92(0.38, 2.23)		1.03(0.25, 4.13)		0.42(0.15, 1.09)	
8+	0.76(0.29, 2.04)		0.60(0.08, 4.26)		0.72(0.23, 2.26)	
Number of months breastfed	N=91,756 Ref(1.00)	0.3359	N=36,944 Ref(1.00)	0.0796	N=48,555 Ref(1.00)	<b>0.0131</b>
Never breastfed						
1-6	0.91(0.79, 1.05)		0.77(0.62, 0.97)		0.79(0.67, 0.93)	
7-12	0.84(0.69, 1.03)		0.71(0.52, 0.96)		0.73(0.57, 0.92)	
13-23	0.95(0.77, 1.17)		0.76(0.53, 1.09)		0.84(0.66, 1.09)	
24+	0.81(0.64, 1.11)		0.90(0.59, 1.37)		0.81(0.59, 1.11)	

Model 1: included the following covariates: age, race/ethnicity, income, smoking status, alcohol consumption, hysterectomy, years since menopause, family history of fracture, HRT use status, HRT route of delivery, recency of HRT use, menopausal hormone therapy use at follow-up, use of osteoporosis prescription, aromatase inhibitors, tamoxifen use, antidepressant use, glucocorticosteroid use, corticosteroid use, proton pump inhibitor use, use of anti-epileptics, use of anti-neoplastics, use of thiazolidinediones at baseline; calcium and vitamin D intake, physical activity (total METU/week). Model 2: included all the variables in Model 1 and weight at age 35, maximum adult weight and minimum adult weight; weight at age 35, maximum adult weight and minimum adult weight.

Table

**Disclosures:** Carolyn Crandall, None.

**SU0231**

**Demographic and clinical patterns in primary fracture prevention.** Annette Adams<sup>\*1</sup>, David Yi<sup>1</sup>, Fang Niu<sup>2</sup>, Rita Hui<sup>2</sup>, Joan Lo<sup>3</sup>. <sup>1</sup>Dept of Research & Evaluation, Kaiser Permanente Southern California, United states, <sup>2</sup>Pharmacy Outcomes Research Group, Kaiser Permanente California, United states, <sup>3</sup>Division of Research, Kaiser Permanente Northern California, United states

**Purpose:** To describe bone mineral density (BMD) and fracture history prior to initiation of oral bisphosphonate (BP) therapy, and to identify demographic and clinical characteristics that may distinguish women receiving BP for primary or secondary fracture prevention.

**Methods:** We retrospectively identified women aged ≥50 years from Kaiser Permanente Southern California who initiated oral BP therapy between 2004 and 2012 and had continuous health plan enrollment ≥1 year prior to BP initiation (index). For the period prior to index, we used electronic health record (EHR) data on fractures to classify women as: a) those with fracture prior to index (fracture group); and b) those with no observed fracture diagnosis prior to index (no-fracture group). Information on age, race/ethnicity and BMD was obtained from EHR. The groups were compared with regard to demographic and clinical characteristics.

**Results:** Among 94073 women initiating oral BP, 22825 (24.2%) had a prior fracture, including 11949 (12.7%) with a major osteoporotic fracture and 10876 (11.6%) with other clinical fractures. The remaining 71248 (75.7%) had no known fracture history. Compared to the fracture group, the no-fracture group was more likely to be aged <65 years (36.6% vs 30.4%, p<0.01), of Asian race (15.0% vs 6.2%, p<0.01), and have osteoporosis by BMD criteria (66.6% vs 63.2%, p<0.01). For the 22825 women with prior fracture, 12720 (55.7%) women had fractures diagnosed within 1 year prior to BP initiation, including 8717 (68.5%) with major osteoporotic fracture. Comparing women initiating BP during 2009-2012 vs 2004-2007, a greater proportion were age 65 or older (70.2% vs 60.6%, p<0.01) and initiated BP in the setting of a prior fracture (27.5% vs 23.6%, p<0.01). Among those initiating BP for primary prevention (without prior fracture), fewer women in the latter era were under age 65 years (27.7% vs 43.0% for 2009-2012 vs 2004-2007, p<0.01) and slightly more had osteoporosis by BMD criteria (66.0% vs 62.4%, p<0.01).

**Conclusions:** Age-, race-, and BMD-related differences distinguish women with and without fractures prior to initiating BP. Temporal trends demonstrate a shift towards BP treatment in older women (including primary prevention) and those with prior fracture, likely reflecting the integration of fracture risk assessment in clinical care. Awareness of these patterns may inform ongoing screening and prevention efforts to reduce osteoporotic fractures in postmenopausal women.

**Disclosures:** Annette Adams, Merck, 11; Otsuka, 11; Amgen Inc, 11

**SU0232**

**Effects of Insulin Resistance on Bone Microarchitecture in Non-Diabetic, Older Adults: Framingham HR-pQCT Study.** Elizabeth Samelson<sup>\*1</sup>, L. Adrienne Cupples<sup>2</sup>, Kerry Broe<sup>3</sup>, Robert Mclean<sup>4</sup>, Marian Hannan<sup>5</sup>, Serkalem Demissie<sup>2</sup>, Ching-ti Liu<sup>6</sup>, Douglas Kiel<sup>3</sup>, Mary Bouxsein<sup>7</sup>. <sup>1</sup>Hebrew SeniorLife Harvard Medical School, United states, <sup>2</sup>Boston University, United states, <sup>3</sup>hebrew seniorlife, United states, <sup>4</sup>hebrewseniorlife, United states, <sup>5</sup>hebrew seniorlife, United states, <sup>6</sup>boston univeristy, United states, <sup>7</sup>Beth Israel Deaconess Medical Center, United states

We have shown that older adults with type 2 diabetes (T2D) have greater total and trabecular BMD, but increased cortical porosity and decreased bone size, compared to no-T2D. The natural history T2D is characterized initially by insulin resistance (IR) for many years, prior to development of frank T2D, when insulin levels decline. Thus, increased BMD observed in T2D may be due to anabolic effects of insulin and/or increased loading due to heavier weight. We investigated the association between HOMA-IR and HR-pQCT microarchitecture at the tibia and radius in no-T2D, stratified by obesity (BMI>30 kg/m<sup>2</sup>). Participants included 878 no-T2D (59% women) members of the Framingham Study. Mean age was 64 yr (range, 40-87). 27% were obese. Linear regression was used to estimate associations between bone indices and HOMA-IR, adjusted for age, sex, and weight, in obese and non-obese individuals. In non-obese individuals, we found: 1) HOMA-IR was associated with more favorable bone indices for most cortical and trabecular measures at the tibia and radius (r=0.08 to 0.19, all p<0.01, TABLE); 2) HOMA-IR was inversely associated with tibia and radius cross-sectional area (r=-0.17 to -0.26, p<0.01); 3) there was no association between HOMA-IR and cortical porosity or trabecular number. In contrast, in obese persons: 1) HOMA-IR was associated with more favorable bone indices for most cortical and trabecular measures at the radius (r=0.13 to 0.20, all p<0.05) but not the tibia (except trabecular vBMD (r=0.12, p=0.05); 2) HOMA-IR was inversely associated with radius cross-sectional area (r=-0.15, p=0.02); 3) there was no association between HOMA-IR and cortical porosity or cortical vBMD. Among no-T2D, IR appears to have beneficial effects on total and trabecular bone density and microarchitecture, but detrimental effects on bone size. IR does not seem to favorably impact cortical porosity. This is consistent with our previous findings showing decreased bone size and increased cortical

porosity in T2D compared to no-T2D. The positive association between IR and several indices at the weight-bearing tibia observed in non-obese individuals, but not in obese individuals, suggests that higher BMD in T2D may be due, in part, to anabolic effects of insulin, prior to diagnosis of T2D, rather than increased loading from higher weight. As individuals progress to T2D, other factors, such as accumulation of advanced glycation endproducts, may contribute to increased skeletal fragility.

Association (Correlation, r)* between HOMA-IR and HR-pQCT bone indices at tibia and radius in non-diabetics, according to obesity status: Framingham Study. Significant correlations highlighted in bold.	Non-Obese (N=640)				Obese (N=238)			
	Tibia		Radius		Tibia		Radius	
	r	p	r	p	r	p	r	p
HR-pQCT Measures								
Cortical vBMD (mg/cm <sup>3</sup> )	<b>0.10</b>	<0.01	.06	0.11	0.01	0.87	0.07	0.24
Cortical porosity (%)	-0.06	0.08	-0.01	0.80	-0.03	0.57	-0.11	0.10
Cortical thickness (mm)	<b>0.12</b>	<0.01	0.07	0.06	0.06	0.33	<b>0.16</b>	0.01
Cortical thickness:total area (1/mm)	<b>0.19</b>	<0.01	<b>0.14</b>	<0.01	0.08	0.20	<b>0.18</b>	<0.01
Cortical area fraction	<b>0.17</b>	<0.01	<b>0.13</b>	<0.01	0.07	0.24	<b>0.18</b>	<0.01
Trabecular vBMD (mg/cm <sup>3</sup> )	<b>0.08</b>	0.04	<b>0.08</b>	0.04	0.12	0.05	<b>0.17</b>	<0.01
Trabecular number (1/mm)	<0.01	0.86	0.06	0.12	0.03	0.59	<b>0.13</b>	0.04
Trabecular thickness (mm)	<b>0.11</b>	<0.01	0.05	0.17	0.10	0.10	0.11	0.09
Total vBMD (mg/cm <sup>3</sup> )	<b>0.16</b>	<0.01	<b>0.12</b>	<0.01	0.10	0.10	<b>0.20</b>	<0.01
Cross-sectional area (mm <sup>2</sup> )	<b>-0.26</b>	<0.01	<b>-0.17</b>	<0.01	-0.08	0.19	<b>-0.15</b>	0.02
Failure load (N)	-0.03	0.40	-0.12	0.76	0.04	0.56	0.10	0.14

TABLE

Disclosures: Elizabeth Samelson, None.

### SU0233

#### Fracture Risk Indices from DXA-Based Finite Element Analysis Stratify Hip Fracture Better Than Femoral Neck BMD: A Cross-Sectional Validation Study. Shuman Yang\*, William Leslie, Yunhua Luo, Andrew Goertzen, Sharif Ahmed, Linda Ward, Lisa Lix. University of Manitoba, Canada

Background: Finite element analysis (FEA) is a computational method to quantify the strength of complex materials. We developed a tool that automatically performs FEA on dual energy x-ray absorptiometry (DXA)-based hip scans to generate site-specific fracture risk indices (FRIs). FRIs reflect the likelihood of hip fracture from a sideways fall. This cross-sectional study examined the associations between FRIs and prior hip fracture.

Methods: Using the Manitoba BMD Database, we identified prior hip fracture cases and a random sample of non-fracture controls at about 1:2 ratio (all women age ≥ 65 years, hip T-scores below -1, no osteoporosis treatment). Femoral neck, intertrochanteric and subtrochanteric FRIs were derived from anonymized DXA scans (Prodigy, GE Healthcare) in 324 hip fracture cases and 658 non-fracture controls). Logistic regression was used to estimate odds ratios (ORs) between FRIs (per SD increase) and hip fracture. We compared c-statistics for FRIs vs femoral neck BMD.

Results: Average age, body mass index (BMI) and femoral neck T-scores were 78.3 years, 24.7 kg/m<sup>2</sup>, and -2.7 in fracture cases and 74.7 years, 25.7 kg/m<sup>2</sup> and -2.2 in controls, respectively (all P < 0.01). Pearson correlation coefficients for femoral neck, intertrochanteric and subtrochanteric FRIs and femoral neck BMD were -0.79, -0.60, -0.67, respectively (all P < 0.01). FRIs were significantly associated with hip fracture risk after adjusting for age, BMI and femoral neck BMD, or FRAX score (Table). Intertrochanteric and subtrochanteric FRIs gave significantly higher c-statistics (Table; all P ≤ 0.03) than femoral neck BMD. Subgroup analyses by age (< 75 vs ≥ 75 years), BMI (< 25 vs ≥ 25 kg/m<sup>2</sup>), and BMD (T-score < -2.5 vs ≥ -2.5) found that FRIs were even more strongly associated with hip fracture in women who were younger, had higher BMI or higher BMD (all P for interaction < 0.1). Intertrochanteric and subtrochanteric FRIs were more strongly associated with hip fracture in women with FRAX score < 3% than ≥ 3% (all P for interaction < 0.05).

Summary: Femoral neck, intertrochanteric and subtrochanteric FRIs were associated with prior hip fracture independent of BMD and other FRAX covariates. Intertrochanteric and subtrochanteric FRIs had better performance than femoral neck BMD for stratifying hip fracture risk. Prospective studies are warranted to determine whether FRIs from DXA-based FEA are better than BMD for predicting incident hip fractures.

Variable	c-statistic (95% CI)	OR (95% CI) <sup>a</sup>	OR (95% CI) <sup>b</sup>	OR (95% CI) <sup>c</sup>
Femoral neck FRI	0.73 (0.69, 0.76)	2.11 (1.79, 2.49)	1.35 (1.04, 1.74)	1.36 (1.13, 1.64)
Intertrochanteric FRI	0.78 (0.75, 0.81)	2.55 (2.06, 3.16)	1.75 (1.37, 2.23)	1.81 (1.44, 2.27)
Subtrochanteric FRI	0.77 (0.74, 0.80)	2.75 (2.25, 3.36)	2.10 (1.65, 2.66)	2.09 (1.68, 2.60)
Femoral neck BMD	0.74 (0.71, 0.77)	2.26 (1.91, 2.67)	Not applicable	Not applicable

Adjusted for <sup>a</sup>age, BMI; <sup>b</sup>age, BMI and femoral neck BMD; <sup>c</sup>FRAX score without including prior hip fracture (hip fracture with BMD).

Table. Hip fracture risk stratification: c-statistics, and ORs (per SD change)

Disclosures: Shuman Yang, None.

### SU0234

#### Parathyroid tumors and hypertension-epidemiology of a neuroendocrine link?.

Carmen Gabriela Barbu\*<sup>1</sup>, Suzana Florea<sup>2</sup>, Amalia Arhire<sup>2</sup>, Luminita Cima<sup>1</sup>, Anca Sirbu<sup>1</sup>, T Radu<sup>3</sup>, Alice Albu<sup>1</sup>, Olteea Ionescu<sup>2</sup>, Sorina Martin<sup>1</sup>, Crina Filisan<sup>2</sup>, Simona Fica<sup>1</sup>. <sup>1</sup>Carol Davila University, Elias Hospital Endocrine Department Hospital, Bucharest, Romania, <sup>2</sup>Elias University Hospital, Bucharest, Romania, <sup>3</sup>Elias University Emergency Hospital, Bucharest, Romania

Objective: This study aims to evaluate the prevalence of high blood pressure (hypertension - HTN) in patients with known primary hyperparathyroidism due to parathyroid adenomas (PHP) as a rationale for another neuroendocrine link between parathyroid tumors and HTN.

Subjects: Medical records of 65 patients, 27 women (84.37 %) and 5 men (15.63%) aged between 15 and 88 years with PHP due to parathyroid tumors hospitalized in our department between 01.01 .2011 - 31.12.2013 were evaluated. Of these 33 (32 women and one man) had also hypertension.

Method: A retrospective descriptive study was conducted based on hospital discharge diagnosis codes: E21.0 for primary hyperparathyroidism and respectively, I10 for hypertension in patients hospitalized in our department in the selected period. Data from medical records were collected only from the patients with parathyroid tumors and HTN.

Results: From a total of 3675 inpatients hospitalized in our department during the period 01.01.2011 - 31.12.2013, 65 patients have primary or secondary discharge diagnosis of primary hyperparathyroidism (a PHP prevalence of 17.68/1000 in the study population compared to a prevalence of 3/1000 in the European population) and 1289 had primary or secondary discharge diagnosis of HTN (a HTN prevalence of 35% compared to the prevalence in the Romanian population of 40.1%).

The prevalence of PHP in patients with hypertension was 49.61/1000 compared to 17.41/1000 in the analyzed population and to 3/1000 in the European population. Prevalence of hypertension in patients with PHP was 51% compared to 35.1% in the study population and to 40.1% in the general population.

In age groups of 25-34 years, 35-44 years, 45-54 years, 55-64 years and over 65 years, the prevalence of hypertension in patients with PPH in the group analyzed was 0.2%, 0.3%, 24%, 48% and, respectively 98%. In the general population, for the same age groups the prevalence of hypertension is 7.2%, 12.2%, 20.3%, 24.1% and 34%. It is noted a higher prevalence of hypertension in patients with PHP aged over 45, which represents the age group where primary hyperparathyroidism is most frequent.

Conclusion: The prevalence of hypertension was found in a higher percentage of patients with PHP due to parathyroid tumors compared to the prevalence in the general population (51% vs 40.1%), which might be a background for a neuroendocrine link in clinical practice.

Aknowledgement. This study was done through partial funding from RENET grant PN-II-PT-PCCA-2011-3.2.0623

Disclosures: Carmen Gabriela Barbu, None.

### SU0235

#### Performance of Predictive Tools to Identify Individuals at Risk of Osteoporotic Fractures: a Systematic Review and Meta-analysis.

Claudia Beaudoin\*<sup>1</sup>, Lynne Moore<sup>1</sup>, Mathieu Gagné<sup>2</sup>, Louis Bessette<sup>3</sup>, Louis-Georges Ste-Marie<sup>4</sup>, Jacques P. Brown<sup>3</sup>, Sonia Jean<sup>2</sup>. <sup>1</sup>Université Laval, Canada, <sup>2</sup>Institut national de santé publique du Québec, Canada, <sup>3</sup>CHU de Québec Research Centre, Canada, <sup>4</sup>Université de Montréal, Canada

Introduction: Many tools exist to assess fracture risk, but there is no consensus on which one is the most valid. The objective of this review is to determine which tool has the best predictive accuracy to identify individuals at high risk of osteoporotic fractures.

Methods: Prospective and retrospective studies assessing the accuracy of tools to predict fractures were searched in MEDLINE, EMBASE, Evidence-Based Medicine Reviews and Global Health. Studies were eligible if the predictive accuracy was assessed in a population independent of the derivation cohort. Studies in which a tool was developed in one part of a cohort and validated in another part were excluded. Data from included studies were extracted and meta-analyses on area under the curve (AUC) were conducted.

Results (preliminary): A total of 31 validation studies assessing the accuracy of 11 different tools (FRAX, FRC, Garvan, QFracture, WHI hip fracture risk score, OSIRIS, ORAI, OST, SCORE, FRISC, mSOF index) were found. QFracture had the best accuracy to identify individuals at high risk of hip (AUC (95% CI) = 0.890 (0.888-0.892)) and osteoporotic (AUC [95% CI] = 0.817 (0.815-0.819)) fractures (Table 1). The discriminative ability of the other tools was acceptable (AUC between 0.72 and 0.81) for prediction of hip fractures and low for prediction of osteoporotic fractures (AUC between 0.63 and 0.73). Substantial heterogeneity was present in all meta-analyses.

Conclusions: The results of this systematic review suggest that QFracture is the tool with the highest predictive accuracy for identifying individuals at high risk of hip and osteoporotic fractures. The increased performance of QFracture could be attributable to the integration of a higher number of risk factors, several of which are

comorbidities. Since QFracture has only been validated in individuals from the country where it was derived (United Kingdom), a validation in other populations should be performed.

Tool	Hip		Osteoporotic	
	N	AUC (95% CI)	N	AUC (95% CI)
FRAX without BMD	14	0.77 (0.73-0.81)	17	0.65 (0.63-0.67)
FRAX with BMD	11	0.78 (0.75-0.82)	16	0.68 (0.67-0.70)
FRC without BMD	2	0.77 (0.66-0.89)	1	0.66 (0.63-0.70)
FRC with BMD	2	0.82 (0.77-0.88)	1	0.70 (0.67-0.73)
Garvan without	2	0.72 (0.64-0.80)	4	0.63 (0.58-0.67)
Garvan with BMD	5	0.74 (0.70-0.79)	5	0.66 (0.63-0.70)
QFracture	2	0.89 (0.89-0.89)	2	0.82 (0.82-0.82)
OSIRIS	-	-	1	0.70 (0.66-0.74)
ORAI	-	-	1	0.71 (0.68-0.75)
OST	-	-	2	0.63 (0.49-0.77)
FRISC	-	-	1	0.73 (0.66-0.79)
SCORE	-	-	1	0.71 (0.67-0.75)
mSOF index	-	-	1	0.66 (0.57-0.75)
WHI hip fracture risk score	2	0.81 (0.78-0.84)	-	-

Table 1: Summary AUCs for prediction of hip and osteoporotic fractures

*Disclosures: Claudia Beaudoin, None.*

## SU0236

**Prior Fragility Fracture Predicts Cardiovascular Events in Men: Results from UK Biobank.** Julien Paccou<sup>1</sup>, Stefania D'Angelo<sup>1</sup>, Mark Edwards<sup>1</sup>, Cyrus Cooper<sup>1</sup>, Steffen Petersen<sup>2</sup>, Nick Harvey<sup>1</sup>. <sup>1</sup>MRC Lifecourse Epidemiology Unit, University of Southampton, United Kingdom, <sup>2</sup>NIHR Cardiovascular Biomedical Research Unit at Barts, William Harvey Research Institute, Queen Mary University of London, United Kingdom

**Objective:** We aimed to explore relationships between prior fracture and risk of incident cardiovascular events.

**Methods:** UK Biobank is a large prospective cohort comprising 502,664 men and women aged 40-69 years, with detailed assessment at baseline. History of fracture was self-reported, and we obtained information on incident hospital admission (ICD-10) for ischaemic heart disease (IHD: I20-I25) and for any cardiovascular event (I63/I64 or I20-I25) through linkage to UK Hospital Episode Statistics. We used Cox Proportional Hazards models to investigate the prospective relationships between prior fracture and hospital admission for men and women, controlling for age, BMI, smoking, alcohol, educational level, physical activity, systolic blood pressure, calcium and vitamin D use, HRT (women) and additionally for heel bone ultrasound attenuation (BUA).

**Results:** 482,683 participants (median age of 58 years, 54.6% women) had complete data on past fracture and BUA. 45,596 participants reported a previous fracture (9.5%). Amongst men, a history of any fracture was associated with increased risk of admission for IHD (adjusted HR: 1.18; 95%CI: 1.03, 1.36; p=0.02), but this became non-significant when heel bone ultrasound was also included. The relationship between past fragility fracture (hip, spine, wrist, arm) and admission for IHD was stronger and remained significant with full adjustment (HR: 1.75; 95%CI: 1.23, 2.49). Associations with hospitalisation for any cardiovascular event in men followed a similar pattern [HR for admission after prior fragility fracture: 1.74; 95%CI: 1.24, 2.43]. Although in crude models similarly increased risk of cardiovascular admission with prior fracture was noted in women, these became non-significant after adjustment (p>0.3).

**Conclusions:** Prior fragility fracture is an independent risk factor for incident cardiovascular events. Further work may clarify whether this association is causal or represents shared risk factors, but these findings are likely to be of value in risk assessment of both osteoporosis and cardiovascular disease. This research has been conducted using the UK Biobank Resource.

*Disclosures: Julien Paccou, None.*

## SU0237

**Serum Adiponectin Levels and Bone Strength According to Metabolic Health in Korean Adults: The KoGES- ARIRANG Study.** Jung Soo Lim<sup>\*1</sup>, EunHee Choi<sup>2</sup>, Sang Baek Koh<sup>3</sup>, Song Vogue Ahn<sup>3</sup>. <sup>1</sup>Department of Internal Medicine, Yonsei University Wonju College of Medicine, Korea, republic of, <sup>2</sup>Institute of Lifestyle Medicine, Yonsei University Wonju College of Medicine, Korea, republic of, <sup>3</sup>Department of Preventive Medicine, Yonsei University Wonju College of Medicine, Korea, republic of

Purpose Adiponectin has been thought to influence bone metabolism through enhancing the proliferation and differentiation of osteoblasts. Moreover, adiponectin possesses insulin-sensitizing properties. However, recent studies have shown that serum adiponectin levels are also higher in metabolically healthy obese individuals. The aim of the study was to investigate the association of serum adiponectin levels with bone strength according to metabolic health in Korean adults in a population-based longitudinal study.

**Methods** A total of 9,172 adults (59.4% women, 40.3% obese) aged 40-70 years assessed in the Korean Genomic Rural Cohort Study from 2005 to 2008 were examined. Subjects were classified into four subgroups according to metabolic health as follows: metabolically healthy non-obese (MHNO), metabolically unhealthy non-obese (MUNO), metabolically unhealthy obese (MUO), and metabolically healthy obese (MHO) subjects. Individuals were classified as metabolically healthy if all three diseases (type 2 diabetes mellitus, hypertension, and dyslipidemia) were absent. Also, obesity was defined as BMI of more than or equal to 25 kg/m<sup>2</sup>. The serum concentrations of adiponectin were measured by radioimmunoassay. In addition, bone status was assessed using the calcaneal quantitative ultrasound method.

**Results** The prevalence of each group was as follows: MHNO (10.2%), MUNO (49.3%), MUO (37.5%), and MHO (2.8%) subjects. MUNO group was the most common in both sexes (52.2% in male and 47.6% in females, respectively). In addition, Serum adiponectin levels were increased in the following order: MUO, MUNO, MHO, and MHNO groups. However, both T-score and bone stiffness index (BSI) showed the highest levels in MHO group and the lowest levels in MUNO group. Subgroup analysis showed that there was a significant correlation between serum adiponectin and BSI levels in men aged 55 or older and postmenopausal women who belonged to the MUNO group (r = -0.146, P < 0.001 vs r = -0.095, P < 0.001), but not in young adults.

**Conclusions** Our results suggest that increased adiposity may affect bone strength differently according to metabolic health. Further investigations are needed to clarify the casual relationship.

*Disclosures: Jung Soo Lim, None.*

## SU0238

**Short-Term Subsequent Fracture Risk in Patients with a Recent History of Low-Trauma Non-Vertebral Fracture.** Aude Deloumeau<sup>\*</sup>, Anna Molto, Maxime Dougados, Christian Roux, Karine Briot. Paris Descartes University, Cochin Hospital, Department of Rheumatology, Paris, France, France

Low-trauma fractures tend to cluster in time and subsequent fractures increase morbidity, and mortality in osteoporotic patients. Both bone and fall related risk factors contribute to refracture. The aim of this study was to identify the risk factors of short-term subsequent non vertebral fracture in patients with a recent fracture.

Patients were consecutively included from the Fracture Liaison Service (FLS) which provides routine assessment for osteoporosis subjects over the age of 50 years, hospitalized for a low trauma non vertebral fracture in the Orthopaedics department. Demographic data, location and date of occurrence of previous non-vertebral fractures, risk factors for osteoporosis, history and number of falls in the previous year, use of a walking aid, visual impairment and intake of anti-osteoporotic treatment were assessed. Bone mineral density was measured at the lumbar spine and femoral neck; presence of vertebral fracture was assessed using vertebral fracture (VFA). Using univariate and multivariate analysis, we identified the risk factors associated with the risk of new non-vertebral fracture in patients with a recent fracture, i.e. less than 3 years before inclusion in the FLS.

Seven hundred patients were included (86% women; 75 ± 12 years), with a mean femoral neck T-score of -2.3 ± 1.0. Prevalence of osteoporosis was 50%; 247 patients had at least one vertebral fracture using VFA. Three hundred and forty four (49%) patients were in the FLS because of a hip fracture. Among the 700 patients, 256 had a history of low trauma non vertebral fracture: 99 within the last 3 years preceding the current fracture and 147 more than 3 years before. There was no difference in body mass index or T-scores between patients with or without previous fracture. Using multivariate analysis, the risk of being in the FLS with a previous fracture less than 3 years before was associated with use of a walking aid (OR = 1.85, 1.01-3.44), history of falls in the year before (OR = 2.34, 1.32-4.18) and history of major non-vertebral fracture (OR = 1.94, 1.11-3.40). Low BMD or other bone risk factors, including the presence of vertebral fractures were not associated with an increased risk in these patients.

Risk factors of falls and previous major non-vertebral fractures are the main risk factors of short term recurrent non-vertebral fracture. These factors can help in the selection of patients at high risk of recurrent fracture, at highest priority for a treatment.

*Disclosures: Aude Deloumeau, None.*

## SU0239

**A Demonstration Study of the Fracture Liaison Service (FLS) Model of Care for Patients with Osteoporotic Fractures.** Susan Greenspan<sup>1</sup>, Andrea Singer<sup>\*2</sup>, Robert Recker<sup>3</sup>, David Lee<sup>4</sup>, Simone Karp<sup>5</sup>, Brian Marchand<sup>6</sup>, Debbie Zeldow<sup>4</sup>, Larry Stern<sup>7</sup>. <sup>1</sup>UPMC, United states, <sup>2</sup>MedStar Georgetown University Hospital, United states, <sup>3</sup>Creighton University, United states, <sup>4</sup>NBHA, United states, <sup>5</sup>CECity, United states, <sup>6</sup>CECity, Inc., United states, <sup>7</sup>Merck, United states

**Purpose:** Although half of women and one-quarter of men over 50 sustain an acute osteoporotic fracture, less than a quarter receive appropriate secondary fracture prevention. The goal of this demonstration project was to examine the effectiveness of a cloud-based registry application to support the FLS model of care ("FLS App") for secondary fracture prevention at 3 academic medical centers.

**Methods:** The Bone Health Collaborative (National Bone Health Alliance, National Osteoporosis Foundation and CECity/Premier), developed a web-based registry application to deploy the FLS model of care to coordinate post-fracture care. The pre-post study design examined the number of men and women over age 50 years who received appropriate assessment (bone mineral density [BMD], vitamin D levels) and pharmacologic treatment within 6 months of an acute fragility fracture. A retrospective chart review was used to collect baseline data at each health care facility (N=344 patients). For the post evaluation (N= 148 patients), the FLS coordinator or champion examined these parameters during the 6 months following enrollment and collected pertinent data on the FLS App. Provider and data collection surveys were used to elicit provider satisfaction and barriers to collecting patient information prior to implementation of the project and at the conclusion of the study. Comparisons between pre-post FLS periods were done using chi-square tests.

**Results:** At baseline, tests and treatment data were missing for 20-30% [s1] of patients. The [GS2] FLS App and service model helped manage patients' health information and treatment records. Missing data were minimized after the adoption of the FLS App. The results showed that the demonstration study increased BMD tests among patients with fractures from 21.2% at baseline to 92.9% in the post-implementation period ( $p < 0.001$ , see figure, Proportion  $\pm$  Standard Error,  $*p < 0.001$  Post to Pre FLS). The monitoring of vitamin D level was improved from 22.0% to 84.0% ( $p < 0.001$ ), and pharmacologic prescriptions increased from 19.5% at baseline to 54.1% in the post-implementation period ( $p < 0.001$ ).

**Conclusions:** We observed significant improvements in managing acute fractures in osteoporotic patients and enhancing treatment via utilization of the FLS App. The FLS App and model of care has the potential to provide continuity of care, effectively manage osteoporotic patients, improve outcomes and reduce medical costs.

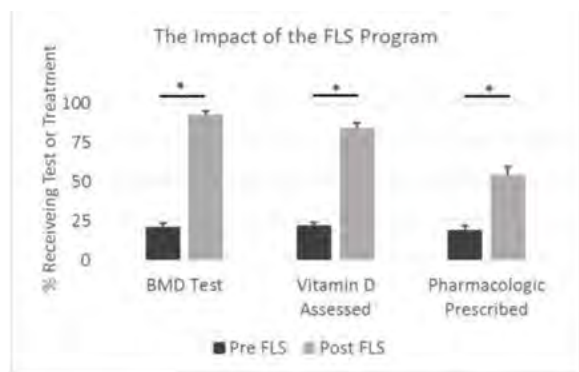


Figure: Proportion  $\pm$  Standard Error,  $*p < 0.001$  comparing Post to Pre FLS

Abstract Image

**Disclosures:** Andrea Singer, Merck, 11  
This study received funding from: Merck

## SU0240

**Bone Health ECHO: An Innovative Strategy of Telementoring to Improve Osteoporosis Care in Underserved Communities.** E. Michael Lewiecki<sup>\*1</sup>, Matthew F. Bouchonville II<sup>2</sup>, David H. Chafey<sup>2</sup>, Sanjeev Arora<sup>2</sup>. <sup>1</sup>New Mexico Clinical Research & Osteoporosis Center, United states, <sup>2</sup>University of New Mexico School of Medicine, United states

**Background.** Project ECHO (Extension for Community Healthcare Outcomes) is a model for telementoring healthcare professionals in underserved areas to achieve advanced levels of knowledge in the care of chronic complex diseases. An ECHO proof-of-concept study with chronic hepatitis C demonstrated treatment outcomes with primary care providers in rural New Mexico similar to those of an academic

specialty clinic. The ECHO model has since been adapted for use in other states and countries for a wide range of diseases.

**Purpose.** To launch and evaluate Bone Health ECHO, a demonstration project for telementoring healthcare professionals on the management of osteoporosis and metabolic bone diseases.

**Methods.** Bone Health ECHO learning partners are tracked by specialty, location, attendance, and level of participation. Outcomes are assessed through weekly continuing medical education (CME) evaluations and twice-yearly self-efficacy questionnaires. This is a report of Bone Health ECHO activity for the first 5 months of activity since its launch on October 6, 2015.

**Results.** A total of 19 Bone Health ECHO clinics were held during the period of observation, with participation of 69 individuals including 44 bone health learners. The learners represented the following areas of discipline: 24 physicians, 14 physician extenders (nurse practitioners, physician assistants), and 6 other or unknown. Physician specialty distribution was 6 primary care (internal medicine, family practice), 8 endocrinology, 2 rheumatology, 4 orthopedics, 2 radiology, 1 resident in internal medicine and 1 unknown. Geographic distribution (Figure) of bone health learners: 20 New Mexico, 18 other US states, 2 other countries (both Chile), and 4 unknown.

**Discussion.** Bone Health ECHO is a novel strategy to provide healthcare professionals in underserved areas with an advanced level of knowledge in the care of patients with skeletal disorders. Lessons learned from this demonstration project will guide the development of additional Bone Health ECHO clinics. Replication of Bone Health ECHO in other states and countries is a force multiplier to demonopolize expertise in osteoporosis care, enhance the effectiveness of fracture liaison services, and reduce the osteoporosis treatment gap.

**Conclusion.** Bone Health ECHO is a novel strategy for improving the care of osteoporosis in underserved communities. More data are needed to assess clinical outcomes and cost-effectiveness.



Distribution of ECHO Learning Partners. The star represents the ECHO hub in Albuquerque, NM.

**Disclosures:** E. Michael Lewiecki, Amgen, 11; Lilly, 11; Merck, 11

## SU0241

**Capture the Fracture by SMS.** Robert Theiler<sup>1</sup>, Gregor Freystaetter<sup>\*1</sup>, Heike Bischoff-Ferrari<sup>1</sup>, Christian Meier<sup>2</sup>, Andreas Platz<sup>3</sup>, Hans-Ulrich Mellinger<sup>4</sup>. <sup>1</sup>University Hospital Zurich, Switzerland, <sup>2</sup>Universität Basel, Switzerland, <sup>3</sup>Triemli Spital, Switzerland, <sup>4</sup>Kantonsspital St. Gallen, Switzerland

**Aim:**

To test if SMS is a useful tool to improve adherence to drug therapy in osteoporosis patients. SMS message with a clear treatment recommendation (based on the FRAX assessment tool and Swiss guidelines) was sent to patients with a recent osteoporotic fracture. Actions taken by the primary care physician (PCP) were evaluated by a standardized questionnaire.

**Methods:**

The study was initiated by the Swiss Society Against Osteoporosis (SVGO). After ethical approval five osteoporosis centres in Switzerland were asked to participate. Triemli Spital Zurich (centre 1) and Kantonsspital St. Gallen (centre 2) agreed to include at least 100 patients over the age of 50 years with a fracture. Six month after fracturing, participants were asked to complete a questionnaire evaluating which osteoporosis related measures had been implemented since hospital discharge. Statistical analysis was done using the StatsDirect statistical software, version 2.8.0.

**Results:**

A total number of 1,323 fracture patients from centre 1 (n=1,175; 88.8%) and from centre 2 (n=148; 11.2%) were invited to participate between January 2013 and January 2015. For both centres, 399 patients (30.2%) agreed to participate. The results are summarized in tables 1 and 2. Patients agreeing to receive treatment recommendations were significantly younger (median age 66 vs 81 years). About one third of participants did not schedule an appointment with their PCP. Two thirds of

patients organized an appointment. PCPs followed treatment recommendations in 50 to 100%.

#### Conclusion:

The SMS tool appears to be an appropriate measure to capture the fracture in patients younger than 70 years. For older seniors a fracture liaison service might be a better procedure to ensure appropriate treatment.

Acknowledgment: This study was supported by an unrestricted research grant by the Qualitouch Foundation, the SVGO and Amgen Switzerland.

## SU0243

**Influence of Gastrointestinal Events on Non-treatment of Asia-Pacific Women with Osteoporosis: Perspectives from Physicians in the MUSIC OS-AP Study.** Ankita Modi<sup>1</sup>, Peter Ebeling<sup>2</sup>, Mel Lee<sup>3</sup>, Yong-Ki Min<sup>4</sup>, Ambrish Mithal<sup>5</sup>, Xiaoqin Yang<sup>\*1</sup>, Santwona Baidya<sup>6</sup>, Shuvayu Sen<sup>1</sup>, Shiva Sajjan<sup>1</sup>. <sup>1</sup>Merck & Co., Inc., United states, <sup>2</sup>Monash University, Australia, <sup>3</sup>Chang Gung Memorial Hospital, Taiwan, province of china, <sup>4</sup>Sungkyunkwan University, Korea, republic of, <sup>5</sup>Medanta the Medicity, India, <sup>6</sup>Optum, Australia

**Purpose:** The objectives of the physician survey component of the Medication Use Patterns, Treatment Satisfaction, and Inadequate Control of Osteoporosis Study in the Asia-Pacific Region (MUSIC OS-AP) were to describe physicians' approaches to treatment of women with postmenopausal osteoporosis and to understand the influence of gastrointestinal (GI) events on treatment in clinical practice.

**Methods:** Physicians were recruited from 5 Asia-Pacific countries: Australia, New Zealand, Taiwan, Korea, and India. Questionnaires collected information about the physician's medical specialty, practice size, and setting; standard practices for diagnosis and treatment of patients with osteoporosis; and perspectives on osteoporosis treatment approaches and medication adherence. Treatment approaches were examined specifically with regard to the management of patients with GI events.

**Results:** A total of 59 physicians completed the survey. The most frequently prescribed or recommended treatments were vitamin D (84.1% of physicians), calcium (81.8%), and oral bisphosphonates (58.6%). When choosing a medication for treatment-naïve patients, GI sensitivity was often or always a consideration for 79% of physicians. Among physicians not prescribing pharmacologic treatment, GI sensitivity was the reason 17.5% of the time. Physicians reported that, before starting pharmacologic treatment, a mean (range) of 20.7% (0-75%) of patients had experienced upper GI events and 10.9% (0-40%) had experienced lower GI events. After starting treatment, 15.4% (1-50%) of patients experienced a new GI event. For patients with pre-existing GI conditions, physicians most frequently ranked the use of non-oral osteoporosis medication as the first treatment strategy (47%), followed by co-prescription with a proton pump inhibitor or other gastroprotective agent (31%) and modification of the frequency or dosing of the drug (17%). For patients developing GI symptoms after starting pharmacologic treatment, the most frequent management strategy was to check if the patient is taking their osteoporosis medication correctly as prescribed (64%), followed by temporary discontinuation of the medication until GI events have resolved (31%) and co-prescription with a proton pump inhibitor or other gastroprotective agent (24%).

**Conclusions:** A history of GI events influences the prescribing practices of physicians in the Asia-Pacific region and sometimes results in the non-treatment of women with osteoporosis.

**Disclosures:** Xiaoqin Yang, Merck & Co., Inc., 15  
This study received funding from: Merck & Co., Inc.

Table 1 Baseline characteristics of fracture patients

Variable	All	Participants	Non-participants	p value
N	1323 (100.0%)	399 (30.2%)	924 (69.8%)	
Center 2 KSSG (%)	148 (11.2%)	109 (27.3%)	39 (4.2%)	<0.0001
Center 1 TriemliSpital (%)	1175 (88.8%)	290 (72.7%)	885 (95.8%)	<0.0001
Men (%)	327 (24.7%)	132 (33.1%)	195 (21.1%)	<0.0001
Age (Median, IQR), Jahre	77.0 (66.0 to 84.0)	66.0 (58.0 to 74.0)	81.0 (72.0 to 86.0)	<0.0001
Fracture VertEx (%)	251 (19.0%)	88 (22.1%)	163 (17.6%)	0.0568
Fracture RadiusEx (%)	155 (11.7%)	67 (16.8%)	88 (9.5%)	0.0002
Fracture HumerusEx (%)	142 (10.7%)	35 (8.8%)	107 (11.6%)	0.1232
Fracture HipEx (%)	270 (20.4%)	55 (13.8%)	215 (23.3%)	<0.0001
Fracture OtherOPEx (%)	384 (29.0%)	129 (32.3%)	255 (27.6%)	0.0755
Fracture NonOPEx (%)	118 (8.9%)	24 (6.0%)	94 (10.2%)	0.0119

\* For information only, as non-normally distributed, median and IQR should be preferred

Table 2 Post-SMS action

Variable	n/N (%)
Post-SMS Action: no GP visit by patient (n/N, %)	132/399 (33.1%)
Post-SMS action: GP appointment (n/N, %)	267/399 (66.9%)
GP action: nothing (n/N, %)	119/267 (44.6%)
GP action: Densitometry (n/N, %)	62/267 (23.2%)
GP action: novel therapy (n/N, %)	50/267 (18.7%)
GP action: change of therapy (n/N, %)	11/267 (4.1%)
GP action: continue therapy (n/N, %)	17/267 (6.4%)
GP action: Patient already on therapy (n/N, %)	8/267 (3.0%)

Baseline characteristics and Post-SMS action

**Disclosures:** Gregor Freystaetter, None.  
This study received funding from: Amgen

## SU0242

**Closing the Treatment Gap: Establishment of a Fracture Liaison Service in Germany.** Markus Rossmann<sup>\*1</sup>, Jonas Pommerening<sup>1</sup>, Wanja Wolters<sup>1</sup>, Georg Dahmen<sup>2</sup>, Andreas Schüsseler<sup>2</sup>, Catharina Bullmann<sup>2</sup>, Wolfgang Lehmann<sup>1</sup>, Johannes Rueger<sup>1</sup>, Eric Hesse<sup>1</sup>. <sup>1</sup>Department of Trauma, Hand & Reconstructive Surgery, University Medical Center Hamburg-Eppendorf, Germany, <sup>2</sup>Osteoporosis-Network Hamburg, Germany

Patients with osteoporotic fractures are frequently treated in trauma surgery. While fracture fixation is at the center of patient care, treatment of the underlying bone disorder is often not considered, thereby increasing the risk for subsequent fractures. Closing this treatment gap is therefore among the greatest challenges in modern trauma surgery. To address this problem, we established a fully structured, multidisciplinary, sector-spanning Fracture Liaison Service (FLS), which is among the first and largest in Germany serving a population of about 2 million people. Residents in trauma surgery of the local University Hospital who are dedicated to the FLS identify inpatients with an incident fragility fracture, focusing on postmenopausal women and men over 60 years of age. Next, patients answer a questionnaire to assess risk factors for fragility fractures and are provided with comprehensive information about the disease and the possibility to be treated within the FLS. All patients are free to choose one of 20 osteoporosis experts participating in the network to be referred to for further diagnosis and treatment. The multidisciplinary FLS consists of specialists in trauma- and orthopedic surgery, endocrinology and internal medicine, all working in private practice. Preliminary results demonstrate that about 20 patients per week can be included in the FLS, an efficacy that reaches more than 90% of patients fulfilling the inclusion criteria. To reach this goal, a highly motivated clinical FLS team is essential. Difficulties were encountered with patients suffering from dementia or other conditions compromising compliance. More clinical and logistic data are currently acquired and evaluated. We conclude that a multidisciplinary FLS is a powerful interface between inpatient surgical care and outpatient osteoporosis treatment. This system may reach the majority of patients with fragility fractures and can subject them to an adequate treatment, which will reduce morbidity, mortality and the socio-economic costs.

**Disclosures:** Markus Rossmann, None.

## SU0244

**Secondary Prevention Gap After a Hip Fracture: the SPARE-HIP Prospective Cohort Anti-Osteoporosis Treatment Rates During Hospital Admission and at 1 and 4 Months Post-Fracture.** Daniel Prieto-Alhambra<sup>\*</sup>, Ignacio Andrés Cano<sup>2</sup>, María Asenjo Cambra<sup>3</sup>, Antonio Balfagon Ferrer<sup>4</sup>, Alejandro Bañuelos Díaz<sup>5</sup>, Fátima Brañas Baztán<sup>6</sup>, Manuel Francisco Bravo Bardají<sup>7</sup>, José Ramón Caeiro Rey<sup>8</sup>, Vicent Climent-Peris<sup>9</sup>, Jose Carlos Diaz Miñarro<sup>10</sup>, Ángel Díez Rodríguez<sup>11</sup>, Emma Escudero Martínez<sup>12</sup>, Maria Teresa Espallargas Doñate<sup>13</sup>, Iñigo Etxebarria-Foronda<sup>14</sup>, Laura Ezquerro Herrando<sup>15</sup>, Jesus Fernandez-Lombardia<sup>16</sup>, Lara Guardado<sup>17</sup>, Miguel Martínez Ros<sup>18</sup>, Damián Mifsut Miedes<sup>19</sup>, Sarah Mills Gañan<sup>20</sup>, José Manuel Olmos Martínez<sup>21</sup>, Pilar Sáez López<sup>22</sup>, Mónica Salomé Domènech<sup>23</sup>, Miguel Sanz Sainz<sup>24</sup>, Jorge Juan Sierra Serrano<sup>25</sup>, Jordi Teixidor Serra<sup>26</sup>, Óscar Tendero Tendero Gómez<sup>27</sup>, Óscar Torregrasa Suau<sup>28</sup>, Antonio Herrera<sup>29</sup>, Adolf Díez-Pérez<sup>30</sup>.

<sup>1</sup>NDORMS, University of Oxford, United Kingdom, <sup>2</sup>Orthopaedic Surgery, Traumatology & Rheumatology Department, Hospital Puerta del Mar, Spain, <sup>3</sup>Geriatric Medicine Department, Hospital Universitario de Getafe, Spain, <sup>4</sup>Orthopaedic Surgery & Traumatology Unit, Hospital Universitario y Politécnico La Fe de Valencia, Spain, <sup>5</sup>Department of Orthopaedic Surgery, Hospital Universitario del Río Hortega, Spain, <sup>6</sup>Geriatric & Internal Medicine Department, Hospital Universitario Infanta Leonor, Spain, <sup>7</sup>Department of Orthopaedic Surgery, Hospital Regional Universitario Carlos Haya, Spain, <sup>8</sup>Department of Orthopaedic Surgery, Complejo Hospitalario Universitario de Santiago de Compostela, Spain, <sup>9</sup>Orthopaedics & Traumatology Department, Hospital Lluís Alcanyis, Spain, <sup>10</sup>Hospital Universitario Reina Sofia, Spain, <sup>11</sup>Orthopaedic Surgery & Traumatology Service, Hospital Virgen del Puerto, Spain, <sup>12</sup>Department of Orthopaedic Surgery, Complejo Hospitalario Universitario de Pontevedra, Spain, <sup>13</sup>Department of Orthopaedic Surgery, Hospital Obispo Polanco, Spain, <sup>14</sup>Department of Orthopaedic Surgery, Alto Deba Hospital, Spain, <sup>15</sup>Orthopaedic Surgery & Traumatology Service, Hospital Clínico Universitario de, Spain, <sup>16</sup>Department of Orthopaedic Surgery, Hospital Universitario San Agustín, Spain, <sup>17</sup>Geriatric Medicine Department, Hospital Universitario San Carlos, Spain, <sup>18</sup>Orthogeriatric Unit, Hospital Virgen de la Arrixaca, Spain, <sup>19</sup>Hospital Clínico de Valencia, Spain, <sup>20</sup>Department of Orthopaedic Surgery, Hospital Universitario La Paz, Spain, <sup>21</sup>Internal Medicine Service, RETICEF, IDIVAL, Universidad de Cantabria, Spain, <sup>22</sup>Geriatric Medicine Department, Hospital Nuestra Señora de Sonsoles, Spain, <sup>23</sup>Orthopaedic Surgery & Traumatology Department, Hospital Universitario Parc Tauli, Spain, <sup>24</sup>Orthopaedic Surgery & Traumatology Service, Hospital Universitario Miguel Servet, Spain, <sup>25</sup>Orthopaedic Surgery & Traumatology Service, Hospital San Pedro, Spain, <sup>26</sup>Trauma Unit, Hospital Vall d'Hebron Barcelona, Universitat Autònoma de Barcelona, Spain, <sup>27</sup>Department of Orthopaedic Surgery, Hospital Universitario Son Espases, Spain, <sup>28</sup>Bone Metabolism Unit, Internal Medicine Service, Hospital General Universitario de Elche, Spain, <sup>29</sup>Department of Surgery, Medicine School, University of Zaragoza, Spain, <sup>30</sup>Department of Internal Medicine, Hospital del Mar-IMIM & Autonomous University of Barcelona, Spain

**Purpose**

There is RCT (HORIZON) and observational evidence that anti-osteoporosis treatment can reduce fracture risk following a hip fracture. We studied the proportion of patients who are or start anti-osteoporosis treatment/s during a hospital admission for a hip fracture, and at 1- and 4-month follow-up. For comparison, we also report on the patients on anti-thrombotic and antibiotic prophylactic therapy at the time of fracture.

**Methods**

The SPARE-HIP (Spanish Registry of Hip and Proximal Femur Fractures) cohort comprises of a consecutive sample of hip/proximal femur fracture patients recruited from a representative 45 hospitals between Jan/15 and Feb/16. Patients were consented and recruited at the time of hip/proximal femur fracture, and then followed after 1 and 4 months.

Local investigators reported on whether patients were on treatment or started anti-osteoporosis, anti-thrombotic and antibiotic therapy during admission, and whether patients were on anti-osteoporosis agents at 1 and 4-month follow-up.

Number and % of patients on the above treatments were reported with 95% confidence intervals assuming a binomial distribution.

**Results**

A total of 852 participants were recruited, with inter-trochanteric (44.7%) and intra-capsular (36.0%) being the most common hip fractures.

Although 329 (38.6%) had a history of previous osteoporotic fracture, only 67 (7.9% [6.1% to 9.7%]) were on anti-osteoporosis therapy. This increased during admission up to 19.8% [17.2% to 22.5%], whilst in 21.1% [20.5% to 23.3%] of cases treatment was considered “unnecessary”, and 2.8% [1.7% to 3.9%] awaited DEXA

scan at discharge. By contrast, uptake of both anti-thrombotic and anti-biotic treatments had almost universal coverage: 95.2% [93.7% to 96.6%] and 96.4% [95.1% to 97.6%] respectively.

Anti-osteoporosis treatment rates improved at 1- and 4-month follow-up: 213/741 (28.7% [25.5% to 32.0%]) and 211/580 (36.4% [32.5% to 40.3%]).

**Conclusions**

There is an unresolved treatment gap in the secondary prevention of fractures, both before and after a hip/proximal femur fracture: only 1 in 5 patients are started on therapy during hospital admission, and only over 1 in 3 are treated (if survived) at 4 months after discharge. Interestingly, anti-thrombotic and anti-biotic prophylaxis has a much higher uptake and close to 100% of patients in the same centres. There is a need for improvement in the delivery of secondary fracture prevention amongst hip fracture patients.

**Disclosures:** Daniel Prieto-Alhambra, Amgen, 12; Servier, 11

This study received funding from: Investigator Initiated Study sponsored by AMGEN

## SU0245

**Treatment gaps in osteoporosis are more prevalent in patients less than 65 years old in a regional general hospital setting in Singapore.** Linsey Gani<sup>\*</sup>, Ravan Alsuwaigh, Thomas King, Joan Khoo. Changi General Hospital, Singapore

**Background:** Singapore has an ageing population, with those over 65 years predicted to triple by 2030. Half of all patients presenting with a hip fracture have a previous history of fracture, and while fracture liaison services are considered the best standard of care globally, such services are not routine in Singapore. We aimed to assess the treatment gaps in patients presenting to a regional hospital system, particularly in patients under 65 years of age.

**Methods:** Retrospective analysis of patients presenting to Changi General Hospital, Singapore with fragility fracture. Data were extracted from all admissions between 1st December 2013 to 1st December 2014. Patient demographics, site of fracture, calcium, vitamin D and antiresorptive treatment initiation status 1-year post admission were recorded. Serum 25-hydroxyvitamin D levels and bone mineral density were documented. Patients were divided into younger than 65, or 65 years and above.

**Results:** There were 94 (18.0%) fragility fractures in patients less than 65 years old and 427 fractures inpatients more than 65 years old. There was a male predominance in the younger population (56% versus 25%). Fracture types were different in the younger versus older population; hip fractures (36.2% versus 57.0%, P<0.001), vertebral fractures (18.7% versus 31.2%, P=0.024), distal wrist (20.9% versus 3.1%, P<0.001) and humerus (11.0% versus 3.1%, P=0.002). BMD measurement in younger patients was significantly less prevalent (35.2% versus 61.0%, P<0.001), as was initiation of antiresorptive treatment (12.1% versus 37.1%, P<0.001). Vitamin D measurement was uncommon (28.6% versus 24.6% in the younger and older population respectively, P=0.52), and median values were low (19.1ug/L and 22.0ug/L in younger and older groups respectively, P=0.27). Vitamin D and calcium supplementation rate were significantly lower in the younger patients (4.4% versus 17.4%, P=0.003).

**Conclusion:** Patients under the age of 65 presenting with fragility fracture had a male predominance and a higher percentage of distal wrist and shoulder fractures compared to patients aged 65 and above. Vitamin D insufficiency was prevalent. Treatment gaps were more prevalent in patients less than 65 years old with significantly lower rates of BMD measurement, calcium and vitamin D supplementation and antiresorptive treatment. This highlights opportunities for fracture liaison services in Singapore regional hospitals to improve care and reduce further fractures.

**Disclosures:** Linsey Gani, None.

## SU0246

**Fracture Risk Specific Treatment Initiation Rates in an Orthopaedic Fracture Liaison Service.** Earl Bogoch, Victoria Elliot-Gibson<sup>\*</sup>, Dorcas Beaton, Robert Josse, Joanna Sale, Erin Norris. St. Michael's Hospital, Canada

**Purpose:** To describe pharmacotherapy initiation rates for treatment naïve fragility fracture (FF) patients seen through a Fracture Liaison Service (FLS) in a manner consistent with recommendations based on national guidelines. Methods: A FLS was implemented to increase the intervention rates in females and males ≥ 50 years presenting with a FF of the the wrist, shoulder, vertebrae and hip. This program provides education, fracture risk assessment in accordance with Osteoporosis Canada's 2010 Guidelines, and referral for further assessment and treatment, as indicated. Data were collected through patient survey, FLS screening form, and/or audit of electronic health records. Results: From December, 2010 to November, 2013, 230 outpatients and 203 inpatients, were identified and underwent fracture risk assessment. There were 133 males, mean age 71.7 (SD 12.7) and 300 females mean age 70.8 (SD 13.1). Fracture locations were: 166 wrist, 64 shoulder, nine vertebral, and 194 hip. All hip and vertebral fractures (n=203) were automatically classified at high risk of future fracture, in addition to 28% (n =47) wrist and 42% (n = 27) shoulder fractures classified as high risk. Ninety-four percent (n = 261) of high risk patients were assessed by a specialist (n = 253) or primary care physician (PCP) (n = 8). Seventy percent of high risk patients (n = 193) were prescribed/recommended pharmacotherapy in addition to vitamin D and calcium; 15% (n = 42) were recommended vitamin D and calcium only due to pharmacotherapy contraindications (e.g., renal impairment); 9% (n = 24) had situational or insuperable barriers that precluded pharmacotherapy initiation (e.g. death (n=12), refusal (n = 1),

lived out of country (n = 1), did not attend assessment (n = 10); and it was the decision of the physician not to initiate pharmacotherapy after assessment (6% (n = 18)). One hundred and nineteen wrist and 37 shoulder fracture patients were classified as moderate risk of future fracture. Sixty-five percent (n = 102) were assessed by a specialist (n = 79) or PCP (n = 23). All moderate risk patients were recommended vitamin D and calcium and 15% (n = 23) were also recommended pharmacotherapy (13% (n=16) wrist, 19% (n=7) shoulder). Conclusions: An evaluation of an orthopaedic initiated FLS reveals risk specific treatment initiation comparable to rates found in efficacy trials. Because intervention thresholds vary in international guidelines, reports of FLS programs should report risk/guideline specific care.

**Disclosures:** Victoria Elliot-Gibson, Procter and Gamble Pharmaceuticals Inc, 11; Martin Family Foundation, 11; Helen McCrear Peacock Foundation, 11; Warner Chilcott, 11; Novartis Canada Ltd, 11; Alliance for Better Bone Health, 11; Mr. and Mrs. W. Saunderson, 11; Mr. Clifford Martin, 11; Merck Frosst Canada Inc, 11; Amgen Canada Inc, 11

## SU0247

**Age-specific thresholds for sufficient 25(OH)-vitamin D serum levels in patients with clinical risk factors for osteoporosis and fractures.** Oliver Bock\*, Susanne Pyttel, Ute Dostmann. MVZ Promedio GmbH - Integrated Medicine, Laboratory Medicine, Germany

**Background:** Despite the large amount of studies published on vitamin D and musculoskeletal health, the threshold for a sufficient serum 25(OH)D concentration is still debated and there has been no clear consensus on assessment and treatment of vitamin D deficiency. International recommendations vary from 50 to 75 nmol/L (20-30 ng/mL). Clinical practice as regards vitamin D supplementation is inconsistent.

**Objective:** To determine thresholds of sufficient 25(OH)D serum concentrations based on complex examinations of laboratory parameters of calcium/phosphate homeostasis and bone turnover in a major German cohort of individuals with defined clinical risk factors (CRF) for osteoporosis and fractures (acc.to German DVO Guidelines 2009, and QFracture Score 2013).

**Results:** In 2014 we examined a total of 7,253 patients (mean age = 62.6 yrs (SD 13.92); f 64.4%, m 35.6%) with CRF for osteoporosis and fractures. The prevalence of 25(OH)D serum levels <75 nmol/L was 87.7%. 25(OH)D serum levels below 50 nmol/L (deficiency) and 25 nmol/L (severe deficiency) were detected in 55.0% and 15.7% of patients, respectively. There was no clear increase in the prevalence of vitamin D deficiency with age when using these fixed thresholds for definition.

Elevated PTH levels (>65 ng/L) were found in 20.9% of 5,119 samples tested - with an inverse correlation to 25(OH)D serum levels (p<0.05) and positive relationship to increased bone turnover markers (B-AP, OC, DPD). The prevalence of secondary hyperparathyroidism (sHPT) was significantly higher in individuals aged >70 yrs.

The serum 25(OH)D threshold associated with certain prevalence of sHPT was gender-unspecific, but increased with age and decreasing renal function. In a model of sHPT prevalence as low as 5%, this threshold was 45 and 48 nmol/L in patients aged 50-60 and 60-70 yrs, 64 nmol/L in patients aged 70-80 yrs, and 77 nmol/L in those > 80 yrs. Otherwise, lower 25(OH)D serum levels seem to be sufficient in younger individuals aged <50 yrs with a calculated threshold of 37 nmol/L in this model.

**Conclusion:** Mean 25(OH)D serum levels did not decrease with age, nor did the prevalence of vitamin D deficiency defined by fixed serum 25(OH) levels increase significantly. In fact, higher 25(OH)D serum levels were needed to realize low prevalence of sHPT and to prevent increased bone turnover in the elderly and in patients with renal insufficiency. This supports the idea of age-specific thresholds for a sufficient serum 25(OH)D concentration.

**Disclosures:** Oliver Bock, None.

## SU0248

**Comparative effects of high-dose vitamin D2 versus vitamin D3 on serum total and free 25-hydroxyvitamin D and markers of calcium homeostasis.** Albert Shieh\*<sup>1</sup>, Rene Chun<sup>1</sup>, Christina Ma<sup>1</sup>, Martin Hewison<sup>2</sup>, John Adams<sup>1</sup>. <sup>1</sup>UCLA, United states, <sup>2</sup>The University of Birmingham, United Kingdom

**Context:** Controversy persists over: 1) how to best restore low serum 25-hydroxyvitamin D (25D) levels [vitamin D2 (D2) vs. vitamin D3 (D3)]; 2) how to best define vitamin D status [total (protein-bound + free) vs. free 25D]; and 3) how best to assess the bioactivity of free 25D.

**Objective:** To assess: 1) the effects of D2 vs. D3 on serum total and free 25D; and 2) whether change in intact parathyroid hormone (iPTH) is more strongly associated with change in total vs. free 25D.

**Design:** Participants previously enrolled in a D2 versus D3 trial were matched for age, body mass index and race/ethnicity. Participants received 50,000 IU of D2 or D3 twice weekly for 5 weeks, followed by a 5-week equilibration period. Biochemical assessment was performed at baseline and at 10 weeks.

**Setting and Participants:** 38 adults (19 - D2; 19 - D3) >18 years with baseline 25D levels <30 ng/ml recruited from an academic ambulatory osteoporosis clinic.

**Outcome Measures:** Serum measures: total 25D; free 25D (directly measured); 1,25-dihydroxyvitamin D (1,25D); calcium; iPTH. Urine measures: fasting calcium:creatinine ratio.

**Results:** Baseline total (22.2 + 3.3 vs. 23.3 + 7.2 ng/ml, p=0.5) and free (5.4 + 0.8 vs. 5.3 + 1.7 pg/ml, p=0.8) 25D levels were similar between D2 and D3 groups. Increases in total (+27.6 ng/ml versus 12.2 ng/ml, p=0.001) and free (+3.6 pg/ml versus +6.2 pg/ml,

p=0.02) 25D levels were greater with D3 vs. D2. Percent change in iPTH was more strongly associated with change in free (but not total) 25D, without and with adjustment for supplementation regimen, change in 1,25D and change in calcium.

**Conclusions:** D3 increased total and free 25D levels to a greater extent than D2. Free 25D may be superior to total 25D as a marker of vitamin D bioactivity.

**Disclosures:** Albert Shieh, None.

## SU0249

**Musculoskeletal form and function in Chinese postmenopausal women are influenced by both calcium intake and vitamin D status.** Feitong Wu\*<sup>1</sup>, Laura Laslett<sup>1</sup>, Qian Zhang<sup>2</sup>, Xiaoqi Hu<sup>2</sup>, Hui Pan<sup>2</sup>, Feng Pan<sup>1</sup>, Jing Tian<sup>1</sup>, Gongbu Pan<sup>1</sup>, Kun Zhu<sup>3</sup>, Richard Prince<sup>3</sup>. <sup>1</sup>Menzies Institute for Medical Research, University of Tasmania, Australia, <sup>2</sup>National Institute for Nutrition & Health, Chinese Centre for Disease Control & Prevention, China, China, <sup>3</sup>Department of Endocrinology & Diabetes, Sir Charles Gairdner Hospital, Perth, Australia, Australia

The interaction of calcium intake and vitamin D status on fracture propensity remains controversial however some studies have identified a role for both in improving bone structure and muscle strength and balance, important factors for falls. This cross-sectional study of a population with lower calcium intake and vitamin D status than that now encountered in many Western studies aimed to examine firstly whether thresholds exist for the association of 25(OH)D with these bone and neuromuscular outcomes and secondly examine potential interactions between serum 25-hydroxyvitamin D (25(OH)D) and calcium intake on these variables.

Study participants were 441 community-dwelling Chinese women aged 60-88 years. Bone structure was examined by DXA BMD of total body, lumbar spine (LS), total hip and femoral neck (FN). Neuromuscular functions examined were handgrip and lower limb muscle strength, one-leg standing time with eyes closed and time completing the Timed Up and Go test (TUG). The data was examined by linear and by locally weighted smoothing (LOWESS) plots and piecewise regressions for 25(OH)D and calcium intake separately and together before and after adjustment for age, season and body weight. To evaluate the size of the effects tertiles of calcium intake (127-695, 695-982, 87-2436 mg/d) and tertiles of 25(OH)D (<29, 29-42, and 42+ nmol/L) were examined in a cross tabulation analysis.

Mean age was 68.2 (5.6) yrs, mean 25(OH)D was 38.9 (17.4 nmol/L) and mean calcium intake was 861 (352) mg/day. In regression analysis before and after adjustment serum 25(OH)D was significantly associated with BMD at all sites and one leg standing times (p<0.05) but there were no thresholds i.e. relations were linear across the range. Higher calcium intake was significantly associated with higher LS and FN BMD, TUG, and both muscle strength tests (p<0.05). Crosstabs identified benefit of a high calcium intake in participants in the lowest tertile of serum 25(OH)D for hip and FN BMD. High calcium intake also speeded TUG in all tertiles of 25(OH)D. High calcium intake improved handgrip strength only in the highest tertile of serum 25(OH)D (p for trend=0.040) and LMS only in the middle tertile (p for trend=0.005). No other additive effects were identified in these analyses.

Chinese postmenopausal women living in Beijing may benefit from increases in calcium intake and vitamin D to improve factors known to reduce fracture risk in other populations. These hypotheses are now being studied in an RCT.

**Disclosures:** Feitong Wu, None.

## SU0250

**Predictors of Maternal Response to Gestational Vitamin D Supplementation: Findings from the MAVIDOS Trial.** Rebecca Moon<sup>1</sup>, M Kassim Javaid<sup>2</sup>, Stefania D'Angelo<sup>1</sup>, Sarah Crozier<sup>1</sup>, Inez Schoenmakers<sup>3</sup>, Nicholas Bishop<sup>4</sup>, Stephen Kennedy<sup>5</sup>, Aris Papageorgiou<sup>5</sup>, Robert Fraser<sup>6</sup>, Saurabh Gandhi<sup>6</sup>, Ann Prentice<sup>3</sup>, Cyrus Cooper<sup>1</sup>, Nicholas Harvey\*<sup>1</sup>, MAVIDOS Trial Group<sup>1</sup>. <sup>1</sup>MRC Lifecourse Epidemiology Unit, University of Southampton, United Kingdom, <sup>2</sup>NIHR Oxford Musculoskeletal Biomedical Research Unit, University of Oxford, United Kingdom, <sup>3</sup>MRC Human Nutrition Research, United Kingdom, <sup>4</sup>Academic Unit of Child Health, Sheffield Children's Hospital, University of Sheffield, United Kingdom, <sup>5</sup>Nuffield Department of Obstetrics & Gynaecology, John Radcliffe Hospital, University of Oxford, United Kingdom, <sup>6</sup>Sheffield Hospitals NHS Trust (University of Sheffield), United Kingdom

We investigated which maternal and environmental characteristics were associated with 25-hydroxyvitamin D [25(OH)D] status following vitamin D supplementation during pregnancy, using data from the MAVIDOS randomised double-blind placebo-controlled trial. Women with a baseline 25(OH)D between 25 and 100nmol/l were randomised to 1000 IU/day cholecalciferol or matched placebo from 14 weeks gestation until delivery of the baby. At 14 and 34 weeks gestation, maternal anthropometry (height, weight, skinfold thickness), health and lifestyle were assessed and 25(OH)D measured (Diasorin Liaison, all samples in a single batch). Compliance with study medication was determined at delivery by pill count. We used linear regression to investigate the associations between maternal characteristics and 25(OH)D at 34 weeks gestation for each group separately. The analysis included 829 women

(422 placebo, 407 cholecalciferol). Supplementation was associated with a higher maternal plasma 25(OH)D concentration at 34 weeks gestation [mean 67.7nmol/l (SD 21.3nmol/l)] vs [43.1nmol/l (SD 22.5nmol/l)],  $p < 0.0001$  for the supplemented and placebo group, respectively]. Amongst women randomised to cholecalciferol, pregnancy weight gain (kg) from 14 to 34 weeks gestation ( $\beta = -0.78$ ; 95%CI: -1.37, -0.20); compliance (%) with study medication ( $\beta = 0.33$ , 95%CI: 0.12, 0.55); 25(OH)D at 14 weeks gestation ( $\beta = 0.28$ , 95%CI: 0.16, 0.39) and season of delivery (summer vs winter:  $\beta = 10.4$ ; 95%CI: 6.3, 14.5) were independently associated with 25(OH)D at 34 weeks gestation (all  $p \leq 0.004$ ). Our results suggest that women who have lower 25(OH)D in early pregnancy, deliver in winter and gain more weight during pregnancy have a reduced 25(OH)D response to supplementation with 1000 IU/day cholecalciferol. These findings will inform future studies aimed at establishing optimal dose regimens for vitamin D repletion in pregnancy stratified by individual characteristics.

MAVIDOS Trial Group: Nigel K Arden, Andrew Carr, Elaine M Dennison, Richard Eastell, Keith M Godfrey, Hazel M Inskip, M Zulf Mughal, David M Reid, Sian M Robinson

RJM & MKJ are joint first author; CC and NCH are joint senior author

Disclosures: Nicholas Harvey, None.

## SU0251

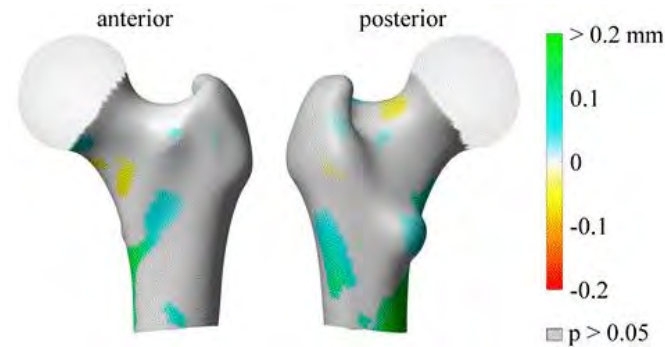
**3D-DXA analysis showed that moderate to high-magnitude whole body vibration training over one year increased femoral cortical thickness in low-active postmenopausal women.** Marion Pasqualini<sup>1</sup>, Ludovic Humbert<sup>\*2</sup>, Hervé Locrelle<sup>1</sup>, Hubert Marotte<sup>1</sup>, Marie-Hélène Lafage-Proust<sup>1</sup>, Thierry Thomas<sup>1</sup>, Laurence Vico<sup>1</sup>. <sup>1</sup>INSERM 1059, University of Lyon, France, <sup>2</sup>GALGO Medical, Spain

Whole body vibration (WBV) modulates bone structural balance. However no effect of WBV with low-magnitude acceleration ( $< 1g$ ) has been demonstrated on bone structure and density in clinical trials conducted in postmenopausal women. Our working hypothesis was that these results were related to a combination of insufficient magnitude WBV and subject's physical activity too high for identifying additional effects of WBV on bone. In addition, WBV effects may be limited to the cortical envelope and 3D-DXA might be more appropriate to analyse such changes. Therefore, we conducted a study evaluating proximal femur changes by 3D-DXA after one year of  $> 1g$  WBV in low-active ( $< 2$  hours physical activity/week) postmenopausal women with moderate risk of fracture (FRAX score between 3 and 10% including DXA measures). WBV training included sessions of 20 min., 3 times a week for 12 months while performing passive and light active squat exercises always with bent knees [plate acceleration 1 to 7g; frequency 35 to 45Hz; amplitude 0.2 – 0.8 mm]. Ninety four women were included in this analysis. DXA scans were acquired using Lunar iDXA scanner (GE Healthcare, Madison, WI) at baseline and after a 1-year of WBV. The 3D-DXA software (Galgo Medical, Barcelona, Spain) was used to analyze the changes in cortical and trabecular bone after 1-year of WBV. 3D-DXA registers a 3D appearance model of the femoral shape and density onto the DXA projection to obtain a 3D subject-specific model of the femur of the patient and quantify the volumetric BMD (vBMD), volume (for trabecular and cortical regions) and cortical (neck, inter-trochanter, shaft and total) thickness distribution. The 3D-DXA measurements at baseline and after training were compared using paired samples Student's t-test.

Mean age at baseline was  $63.7 \pm 4.8$  years. A non-significant increase in integral vBMD (+2.8 mg/cm<sup>3</sup>, +0.9%,  $p = 0.158$ ), cortical vBMD (+2.3 mg/cm<sup>3</sup>, +0.1%,  $p = 0.098$ ) and trabecular vBMD (+2.3 mg/cm<sup>3</sup>, +1.9%,  $p = 0.221$ ) was observed at the total femur region of interest. At the cortical level, no change was seen at the neck and inter-trochanter levels while a significant increase in total cortical thickness and shaft cortical thickness was revealed by 3D-DXA technique after 1-year of treatment (+0.02 mm, +0.9%,  $p = 0.045$ , and +0.04 mm, +1.6%,  $p = 0.021$ , respectively).

In conclusion, moderate to high-magnitude WBV over one year significantly increased femoral cortical thickness at specific sites in sedentary postmenopausal women as measured by 3D-DXA.

Figure: Map showing statistically significant differences in color ( $p < 0.05$ , paired samples t-test) in cortical thickness between baseline and follow-up



figure

Disclosures: Ludovic Humbert, None.

## SU0252

**Influence of Physical Activity on Proximal Femoral Bone Density Distribution, Structural Patterns and Estimated Strength: A Within-Subject Controlled Study.** Stuart Warden<sup>\*1</sup>, Julio Carballido-Gamio<sup>2</sup>, Joyce Kevak<sup>3</sup>, Alyssa Weatherholt<sup>1</sup>, Mariana Kersh<sup>4</sup>, Divya Shah<sup>3</sup>, Thomas Lang<sup>2</sup>, Robyn Fuchs<sup>1</sup>. <sup>1</sup>Indiana University, United states, <sup>2</sup>University of California San Francisco, United states, <sup>3</sup>University of California Irvine, United states, <sup>4</sup>University of Illinois Urbana-Champaign, United states

Projectional radiography studies have shown bone mass benefits of physical activity (PA) on the proximal femur; however, projectional techniques average data over large tissue volumes which may obscure important spatially heterogeneous adaptations to PA. The current study used quantitative computed tomography, computational anatomy approaches and subject-specific finite element modeling (FEM) to assess PA effects on the proximal femur. PA effects were examined within-subject by assessing dominant-to-nondominant (D-to-ND) leg differences in proximal femur properties in baseball pitchers ( $n=16$ ; pitchers) and high/long jump athletes ( $n=12$ ; jumpers). Pitchers and jumpers unilaterally expose one leg (stride and jump leg, respectively) to heightened physical activity enabling the contralateral side to serve as an internal control site. D-to-ND leg differences in pitchers and jumpers were compared to those in controls ( $n=12$ ) to correct for normal limb dominance. Pitchers had 4.1% (95%CI, 1.6 to 6.5%) and 3.3% (95%CI, 0.9 to 5.7%) greater D-to-ND leg differences in total hip volumetric bone mineral density (vBMD) than controls and jumpers, respectively (all  $P < 0.01$ ). No differences were observed between controls and jumpers (all  $P = 0.14-0.87$ ). The greater total vBMD in pitchers resulted from D-to-ND leg differences in the femoral neck and trochanteric regions, as well as in the cortical and trabecular bone compartments within these regions. Voxel-based morphometry analyses in pitchers revealed D-to-ND leg differences in vBMD distribution within the primary compressive trabeculae, inferior femoral neck and throughout the greater trochanter region (Figure 1A). Cortical thickness mapping showed thickening in the regions of the inferior femoral neck, greater trochanter and gluteal tubercle (Figure 1B). FEM revealed pitchers had 5.4% (95%CI, 0.2 to 10.6%) greater D-to-ND leg differences in fracture load during single-leg stance than controls ( $P = 0.04$ ). There were no D-to-ND leg differences in fracture load during a sideways fall between groups ( $P = 0.75$ ). These data reveal the spatially heterogeneous adaptation of the proximal femur to repetitive PA, with adaptation primarily being in regions associated with weight bearing and muscle related forces (i.e. inferior femoral neck and greater trochanter, respectively). The data also suggest baseball pitchers, but not jumping athletes, provide an internally controlled model for exploring the benefits of PA on the proximal femur.

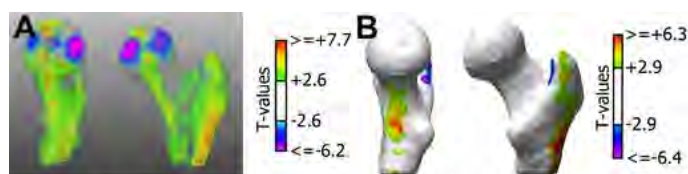


**Figure 1.** Medial (left image) and anterior (right image) views of A) voxel-based morphometry and B) cortical mapping analyses in pitchers. Regions where dominant hips had greater vBMD and cortical thickness than contralateral nondominant hips are represented by positive T-values. Negative T-values represent regions where dominant hips had lower vBMD and cortical thickness than nondominant hips. Non-significant regions are rendered transparent and white in A) and B), respectively.

Figure 1

Disclosures: Stuart Warden, None.

## SU0253

**Integrated Care Management Programs for Osteoporosis, Sarcopenia, Fall Prevention, Frailty Indices and Quality of Sleep with Multiple Interventions for High Risk Elderly Population in Taiwan.** Rong-Sen Yang<sup>\*</sup>. Department of Orthopedics, National Taiwan University Hospital, Taiwan, province of china

Background/Purpose: To examine the effects of 4 independent but integrated programs on multiple outcomes among community-dwelling older adults with high osteoporotic fracture risks in Taiwan.

Methods: Our entire study included 4 programs with 7 subprograms. Core assessments include demographics, bone mineral density (BMD), fall numbers, sarcopenia, frailty and quality of sleep. Interventions include health promotion

educations to improve awareness, screening and referral, exercise programs, nutrition evaluation and consultation, and post-fracture care. Major outcomes included muscle mass, grip strength, walking speed, lower leg extension power, frailty indicators by Fried's criteria and quality of sleep by Pittsburgh Sleep Quality Index (PSQI).

Results: In total 1,913 subjects were enrolled. *Program #1* used sensors built-in smart wristband to dynamic measure sleep quality and walking step numbers. We found that decreasing body fat was significantly associated with number of steps ( $p < 0.05$ ). Also, the use of smart wristband improved appendicular muscle mass (+5.0%). *Program #2* found that after 12 weeks of 3 different exercise interventions, walking speed ( $1.3 \pm 0.3$  m/s vs.  $1.4 \pm 0.3$  m/s,  $p < 0.05$ ), leg extension power ( $23.2 \pm 5.0$  kg vs.  $27.5 \pm 5.4$  kg,  $p < 0.001$ ), chair-stand test ( $12.8 \pm 4.1$  times/30 sec vs.  $14.8 \pm 4.6$  times/30 sec,  $p < 0.001$ ), timed up-and-go test ( $9.6 \pm 2.9$  sec vs.  $8.0 \pm 2.4$  sec,  $p < 0.001$ ) were significantly improved. One of the 5 frailty indicators, percentage of low energy expenditure, changed from 7.2% to 0.7% ( $p < 0.05$ ). Differential improvements for several indices were also noted among 3 groups. *Program #3* found that 58% of psychiatric patients had low BMD. Health promotion improved medication adherence rate to >80%. The core muscle exercise training improved grip muscle strength on average 3.6 kg. *Program #4* found that good quality of sleep could improve BMD, which should be assessed and incorporated into decisions of treatments.

Conclusion: This integrated study showed significant improvements on osteoporosis awareness, sarcopenia, frailty, and sleep quality and decrease falling episodes.

**Disclosures:** Rong-Sen Yang, None.

This study received funding from: Wang Jhan-Yang Charitable Trust Fund

## SU0254

**Using behaviour change theory and user perspectives to design patient education materials to enhance uptake of Too Fit To Fracture recommendations.** Christina Ziebart<sup>1</sup>, Caitlin McArthur<sup>1</sup>, Alexandra Papaioannou<sup>2</sup>, Angela Cheung<sup>3</sup>, Judi Laprade<sup>4</sup>, Ravi Jain<sup>5</sup>, Linda Lee<sup>6</sup>, Jeffrey Templeton<sup>1</sup>, Lora Giangregorio<sup>\*1</sup>. <sup>1</sup>University of Waterloo, Canada, <sup>2</sup>McMaster University & Geriatric Education & Research in Aging Sciences Centre, Canada, <sup>3</sup>University Health Network & University of Toronto, Canada, <sup>4</sup>University of Toronto, Canada, <sup>5</sup>Osteoporosis Canada, Canada, <sup>6</sup>McMaster University & Centre for Family Medicine, Canada

Purpose: Evidence-based exercise and physical activity recommendations have been developed for older adults with osteoporosis. We report on how we identified patients' perceived barriers to implementing exercise recommendations, and used behaviour change theory to tailor a knowledge translation (KT) intervention.

Methods: Focus groups, interviews and interactive discussions, using a semi-structured guide, were conducted to exchange knowledge with older adults across Ontario, Osteoporosis Canada, stratified by gender and urban/rural location. Interactions were transcribed verbatim and two researchers performed coding of data and identified emerging themes. Using Behaviour Change Wheel (BCW), themes were categorized into capability, opportunity and motivation; how they informed the development of an example KT tool, and an estimate of its reach is described.

Results: There were 243 participants, mean age  $72 \pm 8.3$ . Barriers were as follows: Capability - co-morbidities, lack of exercise knowledge and low exercise self-efficacy; Opportunity - exercise support and resources, exercise social engagement and time; Motivation - fear, trust in exercise professionals, lack of incentive and receptiveness. A 13-part video series was created using the following BCW intervention functions: modeling, persuasion, training, incentivisation, education and enablement. Videos featured four different cases addressing common barriers, patient questions or case presentations, with variable age and gender. Since their release in November 2015, the videos have collectively had >18,000 YouTube views and >100 tweets/retweets (excluding ours) as of April 2016, and were featured in communications by the Canadian Society for Exercise Physiology, Osteoporosis Canada, ASBMR and IOF, among other organizations.

Conclusions: We provide an example of how behaviour change theory and knowledge user perspectives can be used to guide the development of novel educational tools for patients.

**Disclosures:** Lora Giangregorio, None.

## SU0255

**Anti-Inflammatory and Possible Bone-Protective Effects of Dried Plum Polyphenols In Vitro.** Neda Akhavan<sup>\*1</sup>, Lili Kamkar<sup>1</sup>, Shirin Hooshmand<sup>2</sup>, Sarah Johnson<sup>3</sup>, Bahram Arjmandi<sup>1</sup>. <sup>1</sup>Florida State University, United states, <sup>2</sup>San Deigo State University, United states, <sup>3</sup>Colorado State University, United states

Osteoporosis is a degenerative disease associated with aging and menopause and is characterized by decreased bone mass, increased bone fragility, and increased structural corrosion of bone tissue. Chronic inflammation may play a role in the perturbed bone remodeling process in turn contributing to osteoporosis. Previous findings from our lab, and that of others, indicate that dried plums are

highly effective in preventing and reversing ovarian hormone-deficiency-associated bone loss in a rat model of osteoporosis, as well as in preventing bone loss in postmenopausal women, perhaps through increasing bone formation relative to bone resorption. Polyphenol-rich diets have been linked to decreases in inflammation, and the bone-protective effects of dried plums may be largely due to its polyphenol content. The purpose of this study was to investigate the anti-inflammatory and possible bone-protective properties of polyphenols extracted from dried plum in vitro using MC3T3-E1 osteoblastic cells and RAW264.7 macrophage cells. MC3T3-E1 cells were dose-dependently treated with dried plum polyphenol extracts (0, 0.5, 1, 10, 100, 1000 µg/ml) where supernatants were analyzed for cell viability assessed via resazurin assay and mineralized nodule formation via Alizarin red staining. LPS-induced RAW264.7 cells were similarly dose-dependently treated with dried plum polyphenol extracts where nitric oxide (NO) was measured using Griess reagent, cyclooxygenase-2 (COX-2) was assessed via western blot, and cell viability was evaluated via resazurin assay. Results from this study showed that dried plum polyphenols dose-dependently increased nodule mineralization without affecting cell viability as shown by the resazurin assay. At a dose of 1000 µg/mL, dried plum polyphenols had an anti-inflammatory effect, as evidenced by a significant decrease in NO levels and COX-2 expression, without compromising cell viability. Findings from this study suggest that the bone-protective effects of dried plum may be to the anti-inflammatory properties of its polyphenols. Further studies are needed to understand the direct effects of dried plum polyphenols and their metabolites on bone remodeling.

**Disclosures:** Neda Akhavan, None.

This study received funding from: Professorship

## SU0256

**Melatonin-micronutrients Osteopenia Treatment Study (MOTS).** Sifat Maria<sup>\*1</sup>, Dr. Paula Witt-enderby<sup>1</sup>, Dr. Mark Swanson<sup>2</sup>, Dr. Frank D'Amico<sup>3</sup>, Larry Enderby<sup>4</sup>, Brianna Enderby<sup>5</sup>, Dr. Holly Lassila<sup>1</sup>. <sup>1</sup>Duquesne University, United states, <sup>2</sup>Naturopath, Heart Preventics, LLC, United states, <sup>3</sup>Duquesne University, United states, <sup>4</sup>Enderby Healthcare/Legal Consulting, LLC, United states, <sup>5</sup>Pharm. D, Duquesne University, United states

Menopausal transition is often associated with bone loss. The debilitating consequences of bone deterioration i.e. osteopenia, osteoporosis and related fractures, as well as high treatment costs and low compliance with the current therapies greatly influence their overall health related quality of life. A one year double-blind RCT was designed to assess the effects of combination natural bone tropic agents: melatonin, strontium citrate, vitamin D<sub>3</sub> (cholecalciferol) and vitamin K<sub>2</sub> (MK-7) (MSDK) on bone health and quality of life in post-menopausal osteopenic women. A total of 22 women (ages 49-75) were randomized to receive either MSDK (n = 11) or placebo (n = 11) p.o. nightly for 12 months. Bone mineral density (BMD) was measured by dual-energy X-ray absorptiometry. Participant's serum bone turnover markers P1NP, OC and CTx and serum vitamin D<sub>3</sub> and CRP were measured at months 0, 6, and 12. Nocturnal urinary melatonin level was measured at month 12. Quality of life questionnaires measuring menopausal symptoms (MENQOL), anxiety (STAI), stress (PSS) and depression (CES-D) were administered at months 0, 6, and 12. Participants kept daily diaries recording information about pill intake, sleep duration, exercise, other supplements, and general well-being. Compared to placebo, one year of MSDK treatment showed significant increase in lumbar spine BMD (4.3%), left femoral neck BMD (2.2%), with an upward trend for total left hip BMD (5.03% vs. 2.2% in placebo;  $p = 0.069$ ). MSDK reduces bone turnover ratio (CTx:P1NP) by increasing serum P1NP level (vs. placebo;  $p = 0.023$  and  $p = 0.004$  at months 6 and 12, respectively). Serum OC level remained steady with MSDK throughout the study. Serum CRP level showed a downward trend, suggesting the possible anti-inflammatory effect of MSDK in favor of bone health. The MENQOL vasomotor, physical, psychosocial, and sexual domains, STAI, PSS and CES-D scores did not differ between groups. However, diary analysis revealed a positive impact of MSDK on general well being, particularly with respect to sleep quality, but not sleep duration. Possible confounding factors such as use of multivitamins/herbal supplements/OTC products, exercise intensity etc. were assessed and did not differ between groups. Study subjects were 92.4% complaint with the MSDK therapy compared to 90.03% in placebo, with no reported side effects.

## SU0258

**Effects of glycemic control on bone turnover in older Mexican Americans with type 2 diabetes: data from the Cameron County Hispanic Cohort in Texas.** Nahid Rianon<sup>\*1</sup>, Scott M Smith<sup>2</sup>, MinJae Lee<sup>1</sup>, Paul Musgrave<sup>1</sup>, Gordon P Watt<sup>3</sup>, Shahla Nader<sup>1</sup>, Sundeep Khosla<sup>4</sup>, Catherine G Ambrose<sup>1</sup>, Joseph B McCormick<sup>5</sup>, Fisher-Hoch Susan<sup>5</sup>. <sup>1</sup>University of Texas Medical School at Houston, United states, <sup>2</sup>NASA JSC, United states, <sup>3</sup>Brownsville Campus of UT School of Public Health, United states, <sup>4</sup>Mayo Clinic College of Medicine, United states, <sup>5</sup>Brownsville Campus of the UT School of Public Health, United states

High bone turnover, evidenced by high serum osteocalcin (OC) concentration, is indicated as risk of fracture in old age. However, low bone turnover has been reported in patients with type 2 diabetes (T2D) who also have high fracture risk. Poor glycemic control indicated by higher glycated hemoglobin levels (HbA1c) has been associated with lower serum OC in older Caucasian and Asian patients with T2D. There remains a gap in knowledge about effects of T2D on bone turnover status in Hispanic populations. We report bone turnover in association with glycemic control in 72 older Mexican American ( $\geq 50$  years) men (N=21) and women (N=51) with type 2 diabetes from the Cameron County Hispanic Cohort (CCHC) in Texas. Prevalence of T2D is about 30% in this cohort who live in health disparity due to poor access to health care.

Separate multivariable linear regression models were conducted to determine association between high/diabetic levels of HbA1c ( $< 6.5$  normal vs.  $\geq 6.5$  high) and serum OC after controlling for age, body mass index (BMI,  $\geq 30$  obese vs.  $< 30$  non-obese), visceral fat, femoral neck BMD and serum concentrations of creatinine, calcium, and vitamin D for men and women. Interaction effects were assessed while developing final multivariable model to identify factors that modify the association between HbA1c and OC.

Participants' ages were  $66 \pm 9$  (mean  $\pm$  SD) years for men and  $67 \pm 8$  years for women. HbA1c was  $8.0 \pm 2.0$  for men and  $7.8 \pm 2.0$  for women. There were no significant differences for BMI, femoral neck BMD, serum calcium or 25-hydroxyvitamin D concentrations between men and women. High HbA1c was significantly associated with lower OC levels in men in both age groups (mean difference in OC between high vs. low HbA1c [95% confidence interval] for older group ( $\geq 65$  years) was  $-9.51$  ( $-16.36$  to  $-2.65$ ) and for younger group ( $< 65$  years) was  $-25.54$  ( $-38.02$  to  $-13.05$ )). There was no significant associations between HbA1c and OC in women.

Altered metabolic state due to poor glycemic control may be responsible for the low turnover indicating underlying structural changes leading to fracture risk. A more active younger bone with higher turnover may be counteracting the deleterious effects on OC compared to the older less active bones with longer effects of metabolic changes. Understanding impact of disease duration on bone metabolism resulting from abnormal glycemic control over time is recommended to demystify effects of HbA1c on diabetic bones.

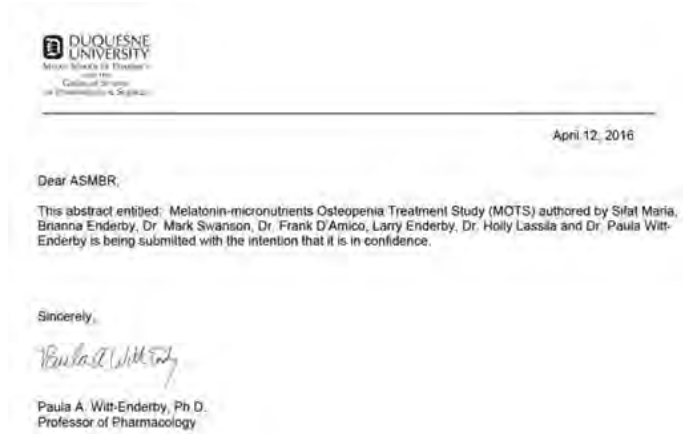
**Disclosures:** Nahid Rianon, None.

*This study received funding from: Center for Clinical and Translational Science, UT Medical School at Houston; and Herzstein Foundation*

## SU0259

**GATA-3 Participates in Bone Healing Through Transcriptionally Upregulating *bcl-xL* Gene Expression.** Mei-Hsiu Liao<sup>\*</sup>, Pei-I Lin, Ruei-Ming Chen. Graduate Institute of Medical Sciences, College of Medicine, Taipei Medical University, Taiwan, province of china

Our previous study has shown that GATA-DNA-binding protein (GATA)-3, a transcription factor, can transduce survival signals in osteoblasts through regulation of antiapoptotic *bcl-xL* gene expression (J Bone Min Res 2010; 25:2193-2204). This study was further aimed to evaluate the roles of GATA-3 in bone healing and the possible mechanisms. ICR mice were operated with metaphyseal bone defects in the left femurs for 1, 3, 5, and 7 days. Analysis of micro-computed topography ( $\mu$ CT) showed that the bone healing was time-dependently taken place in the bone defect sites. In parallel, the trabecular bone numbers and mineral calluses augmented. Scanning coronal sections of the femurs using confocal microscopy showed specific upregulation of GATA-3 in the wounded site. Interestingly, both GATA-3 and alkaline phosphatase (ALP), a biomarker of osteoblasts, were highly expressed and colocalized in the bone defect area (Fig. 1). In addition, GATA-3 and Runx2 mRNA and protein expressions were significantly induced. Analyses of confocal microscopy and co-immunoprecipitation further showed the association of nuclear GATA-3 and Runx2. Sequentially, levels of Bcl-X<sub>L</sub> mRNA were triggered in bone healing. Bioinformatic search indicates the existence of the GATA-3-specific DNA-binding element in the promoter region of *bcl-xL* gene. The results by the chromatin immunoprecipitation assay demonstrated the binding of GATA-3 to its specific binding element in *bcl-xL* gene. Therefore, this study shows that GATA-3 participates in bone healing via regulation of *bcl-xL* gene expression. Furthermore, GATA-3 can function as a biomarker signature for diagnosis and prognosis of bone-related diseases such as bone fracture or osteoporosis.



Letter of confidentiality

**Disclosures:** Sifat Maria, None.

## SU0257

**Mandibular Periodontitis and Osteonecrosis of the Jaw-Like Lesions in Rice Rats (*Oryzomys palustris*) fed a High Sucrose-Casein Diet and treated with Zoledronic Acid.** Donald Kimmel<sup>\*1</sup>, Jonathan Messer<sup>1</sup>, Hung-Yuan Chen<sup>1</sup>, Jessica Jiron<sup>1</sup>, Jorge Mendieta Calle<sup>1</sup>, Evelyn Castillo<sup>1</sup>, Cathy van Poznak<sup>2</sup>, Jose Aguirre<sup>1</sup>. <sup>1</sup>University of Florida, United states, <sup>2</sup>University of Michigan, United states

Osteonecrosis of the jaw (ONJ) is an adverse event seen in patients given powerful anti-resorptives (pARs). We hypothesize that when infection related to severe periodontitis (PD) kills bone tissue and pARs slow the resorption of this necrotic bone, an ONJ lesion with its characteristic dead bone, can be created. To investigate the relationship of dose/duration of zoledronic acid (ZOL), a pAR, to the prevalence of both PD and ONJ-like lesions, we did two parallel experiments with variation in diet. We present here data from the traditional high sucrose-casein (HSC) diet rice rat/PD model. 218 healthy female rice rats were weaned. At age 4 wks, 12 rats were necropsied. The rest were weight-randomized into five groups. Each group received one of five ZOL treatment regimens: 0, 8, 20, 50, or 125  $\mu$ g/kg ZOL IV monthly. At 12, 18, 24, and 30 wks, groups (N=8-13) were necropsied. At necropsy, all rats underwent oral exams. High resolution photos of all four jaw quadrants were obtained and examined by three independent observers who provided PD scoring and located/diagnosed ONJ-like lesions using a 0-5 scale<sup>1</sup>. Mandibular (Mn) PD lesions ranged from locally-inflamed gingiva with recession on the mesiolingual aspect of molar 1 (M1) to exposed, necrotic bone completely involving M1M3 and the lingual plate. ONJ-like lesions were identified grossly as exposed bone and are being confirmed histologically. Two-factor ANOVA (ZOL dose/time) of PD Score and ONJ-like lesion prevalence was completed. Fisher's PLSD test was used to compare groups as appropriate. 15% (N=22) of ZOL-exposed rats had ONJ like lesions. Three had ONJ-like lesions in both the maxilla (Mx) and Mn, while 19 had only Mn lesions. Mn PD prevalence was 120% great than that in the Mx. We found: 1) no PD or ONJ-like lesions were present in age 4wks rats; 2) no significant PD/ONJ-like lesions occurred with 0 $\mu$ g/kg ZOL; 3) ONJ-like lesions occurred at  $\geq 12$ wks, but only with  $\geq 20\mu$ g/kg ZOL; 4) groups given  $\geq 20\mu$ g/kg ZOL had more severe PD lesions than 0 or 8 $\mu$ g/kg ZOL groups; and 5) prevalence of PD and ONJ-like lesions increased significantly with greater dose and longer duration, with an interaction of ZOL dose/duration (all  $P < .0001$ ). This is the first statistically significant experimental demonstration of a positive relationship of relevant ZOL dose and duration to prevalence of mandibular PD and ONJ-like lesions in the traditional HSC diet rice rat model.

<sup>1</sup>Aguirre JI et al. *J Bone Min Res* 27:2130-2143 (2012).

**Disclosures:** Donald Kimmel, None.

*This study received funding from: NIDCR*

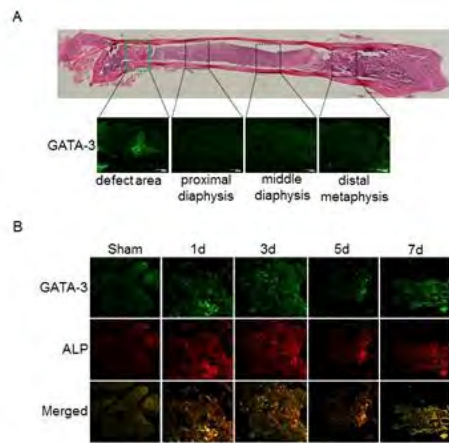


Fig. 1

Fig. 1. Specific expression of GATA-3 in the bone defect area and its colocalization with ALP

**Disclosures:** Mei-Hsiu Liao, None.

## SU0260

**The Effect of Bariatric Surgery on Serum 25-OH Vitamin D Levels: A Systematic Review and Meta-Analysis.** Herman Bami\*, Aashish Kalani, Jonathan Adachi, Arthur Lau, McMaster University, Canada

**Background and Purpose:** Currently, bariatric surgery has been shown to be effective in enhancing weight loss. However, concerns have emerged including a reduction in vitamin D levels, which can further lead to complications such as osteoporosis, frailty and fractures. The purpose of this review was to determine whether there is a significant decline in serum 25-OH vitamin D (25-OH-D) levels in patients undergoing gastric bypass surgery for weight loss compared to surgical candidates who did not undergo the procedure.

**Methods:** An electronic search was conducted in MEDLINE, Pubmed, EMBASE and Cochrane databases to 6 January 2015. Eligible trials included randomized controlled trials (RCT) or controlled observational studies of patients who have undergone laparoscopic gastric bypass surgery. The following data was extracted: study design, participants, demographic information, types of intervention, types of comparison, outcome measures, and results. Statistical analysis was carried out using the Cochrane Collaboration Review Manager (RevMan 5.0) and a random effects model was implemented. Outcomes were expressed as weighted mean difference (WMD). The primary outcome examined was change in 25-OH-D levels at 12 months post surgery and secondary outcomes included change in bone mineral density (BMD) measurements at 12 months post surgery at the lumbar spine (LS) and total hip (TH).

**Results:** We included 3 studies (134 patients) for our primary outcome and 2 studies (84 patients) for our secondary outcomes. There was a trend towards increased 25-OH-D levels in the surgical group (WMD, 13.69%, 95% CI=0.18 to 27.20,  $p=0.05$ ,  $I^2=1\%$ ). A significant BMD reduction was however shown at the TH (WMD, -7.33%, 95% CI=-8.70 to -5.97,  $p<.001$ ,  $I^2=0\%$ ) and a trend towards decline was observed at the LS (WMD, -1.74%, 95% CI=-3.55 to 0.08,  $p=0.06$ ,  $I^2=0\%$ ).

**Conclusion:** Although there does seem to be a potential effect of bariatric surgery on vitamin D levels, it was not shown to be statistically significant due to the small number of studies. There was however a statistically significant reduction in BMD at the TH and a trend towards decline at the LS, despite the small sample size. Further research needs to be conducted on the differences in bone mineral health between surgery recipients and those eligible for surgery. Additionally, the above study will be further updated to include studies conducted within the past year and other recorded outcomes.

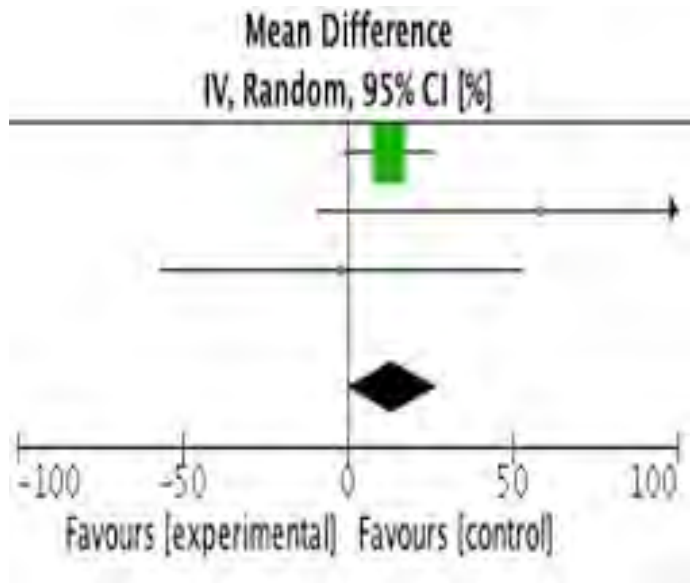


Figure 1 - Forest plot of vitamin D levels at 12 months post bariatric surgery

**Disclosures:** Herman Bami, None.

## SU0261

**Analgesic Effects of Minodronate in a Rat Model of Chronic Pain.** Masazumi Suzuki\*, Naohisa Miyakoshi, Yuji Kasukawa, Koji Nozaka, Hiroyuki Tsuchie, Masashi Fujii, Chie Sato, Norimitsu Masutani, Tetuya Kawano, Yoichi Shimada, Department of Orthopedic Surgery, Japan

The superior analgesic effects of minodronate compared with other bisphosphonates has been previously reported. However, to our knowledge, there are no studies analyzing the analgesic effects of bisphosphonates on chronic pain. The purpose of the present study was to evaluate the analgesic effects of minodronate (MIN), alendronate (ALN), and pregabalin (PRG) on chronic pain caused by chronic constriction injury (CCI) of the sciatic nerve. Four-week-old female Wistar rats underwent ovariectomy. At 8 weeks old, the left sciatic nerve was ligated to induce the chronic pain model (CCI side), and sham surgery was performed on the right posterior limb as a CCI control (control side). The rats were divided into the following four groups: 1) MIN group, administered with minodronate (0.15 mg/kg/week) (n = 10); 2) ALN group, administered with alendronate (0.15 mg/kg/week) (n = 10); 3) PRG group, administered with pregabalin (10 mg/kg) (n = 9); and 4) Control group, administered with vehicle (n = 10). Treatments were administered subcutaneously every week for 2 weeks immediately after CCI. To quantify the sensitivity to a tactile stimulus, paw withdrawal in response to a tactile stimulus was measured using von Frey filaments at 0, 1, and 2 weeks after CCI. Von Frey filaments were applied to the plantar surface of the hindpaws for 3 s, and this was repeated three times. Paw withdrawal in response to the stimulus was evaluated by scoring as follows: 0, no response; 1, a slow and/ or slight response to the stimulus; 2, a quick withdrawal response; 3, an intense withdrawal response away from the stimulus. The mean value of the score was adopted as the pain score. After evaluating the response, bilateral femurs were harvested for bone mineral density (BMD) measurements. The pain score of the CCI side was significantly higher than that of the sham side in all groups ( $p < 0.05$ ) at each time point. The pain score for the MIN group, but not the ALN group, of the CCI side was significantly lower ( $p = 0.05$ ) at 0 and 1 week after CCI. Total femoral BMD of the CCI side was significantly lower in the PRG and Control groups than those of the MIN and ALN groups ( $p < 0.05$ ). No significant difference was identified for BMD between the MIN and ALN groups. In conclusion, minodronate showed a significant analgesic effect on chronic pain and suppressed osteoporotic changes caused by CCI.

**Disclosures:** Masazumi Suzuki, None.

## SU0262

**Establishment of autoinflammatory disease model in mice.** Takatsugu Oike\*, Takeshi Miyamoto, Hiroya Kanagawa, Yasuo Niki, Morio Matsumoto, Masaya Nakamura, Department of Orthopaedic Surgery, Keio University School of Medicine, Japan

**BACKGROUND.** Recently, IL-1 is implicated in the pathogenesis of auto-inflammatory syndrome, which is characterized by poly-arthritis in large joints, rash, fever and elevated white blood cells. IL-1 is also noticed as a therapeutic target of adult onset "IL-1 diseases", including adult onset Still's disease. To date, several animal rheumatoid arthritis models such as Collagen-Induced Arthritis/Adjuvant-Induced

Arthritis (CIA/AIA) were established, however, no animal models for IL-1 diseases were reported.

**METHODS.** We newly generated conditional transgenic mice of human IL-1 (IL-1 cTg), in which human IL-1 $\alpha$  was driven under a Cre/loxP system, in a C57/BL6 background. We crossed the IL-1 cTg mice with inducible Cre mice, Mx Cre mice, to yield Mx Cre/IL-1 cTg mice. PolyIpolyC was administered to eight-week old Mx Cre/IL-1 cTg mice, and the phenotypes such as arthritis and peripheral blood counts were observed. Mx Cre/IL-1 cTg mice were also crossed with IL-6 knockout (IL-6 KO) mice to yield Mx Cre/IL-1 cTg/IL-6 KO.

**RESULTS.** Arthritis development in large joints was seen in all Mx Cre/IL-1 cTg mice one week after polyIpolyC administration. Elevated white blood cell counts, dermatitis, and splenomegaly were detected in these mice. Micro CT analysis demonstrated the joint destructions in large joints in Mx Cre/IL-1 cTg mice. Interestingly, these phenotypes were rescued in Mx Cre/IL-1 cTg/IL-6 KO.

**CONCLUSION.** We successfully generated a new IL-1 disease model, and show that IL-6 may represent a therapeutic target to this disease.

**Disclosures:** Takatsugu Oike, None.

## SU0263

**Negative Effects of Repetitive Mild Traumatic Brain Injury (TBI) on Trabecular BMD, Microarchitecture, and Mechanical Properties.** Chandrasekhar Kesavan\*, Heather Watt, Subburaman Mohan, VA Loma Linda Healthcare System, United states

Central nervous system control of skeletal development and homeostasis via neuroendocrine circuits involving pituitary and direct neuronal pathways are increasingly being recognized. It is, therefore, likely that an acute impact on the brain will adversely affect skeletal metabolism by disrupting normal neural regulation of the skeleton. Because mild TBI is the most common degree of head injury, we evaluated in this study the consequence of repetitive mild TBI on bone. To induce mild TBI, a weight drop model was adopted in which a fixed weight (72 g) was dropped on top of the skull of 5 week old anesthetized C57BL/6J mice, once per day for 4 days from varying heights (0.5, 1.0 and 1.5 meters). There were no significant differences in body weight between impacted and control anesthetized mice at 2 or 4 weeks post-impact, thus suggesting no adverse effects of the chosen impact on somatic growth. *In vivo* micro-CT analysis of tibial metaphysis at 2 weeks post-impact revealed 14%, 9%, and 15% reduction in trabecular BV/TV at 0.5, 1.0, and 1.5 meter drop heights, respectively. Trabecular number and thickness were reduced while separation was increased in the impacted mice compared to control mice. Accordingly, apparent modulus, a mechanical property of trabecular bone which reflects bone strength, was reduced by 22% ( $P < 0.05$ ) in the 1.5 meter weight drop height group. Serum levels of osteocalcin were decreased by 22%, 15%, and 19% in the 0.5, 1.0 and 1.5 meter drop heights, respectively. Since TBI has been shown to induce growth hormone deficiency in clinical studies, we measured serum IGF-1 levels and found 18-32% reductions in TBI mice. Serum osteocalcin and IGF-1 levels correlated with trabecular BV/TV ( $r = 0.37$  and  $0.40$ ,  $P < 0.05$ ). Eight weeks after TBI impact, the deficit in trabecular BV/TV was still significant (18% reduction,  $P < 0.05$ ) at 1.5 meter drop height. In order to determine if TBI-induced skeletal changes were caused by impaired mobility, we measured grip strength, which reflects motor function, and found no significant differences between control and 1.5 meter weight drop post impact, thus suggesting that skeletal changes in TBI mice are not caused by immobility. Based on our data, we conclude that repetitive mild TBI exerts significant negative effects on trabecular bone mass and mechanical properties by influencing osteoblast function via reduced endocrine IGF-1 action.

**Disclosures:** Chandrasekhar Kesavan, None.

## SU0264

**Progesterone and Women's Bone Formation—this is a Causal Relationship.** Jerilynn C. Prior\*. University of British Columbia—CeMCOR, Canada

Progesterone (P4) was postulated to be bone-anabolic in 1990<sup>1</sup>. P4 *causally* increases bone formation meeting Hill's criteria<sup>2</sup>. Basic science: Osteoblast (OB) P4 receptor (PR) was sex<sup>3</sup>/steroid-specific<sup>4</sup>. P4 *in vitro* increased hOB differentiation/alkaline phosphatase (ALP)<sup>5</sup>. P4 did not alter OPG<sup>6</sup>. Clinical: *Cyclic* medroxyprogesterone (MPA) in RCT in women 20-42 y with hypothalamic amenorrhea/silent ovulatory disturbances (SOD, with regular cycles), increased bone mineral density (aBMD) ( $P = 0.0001$ )<sup>7</sup>. 20% of 1-y vBMD change in 66 reg. cycling women related to mean luteal length (@P4 exposure)<sup>8</sup>. Menstrual estradiol downswings produced early cycle higher bone resorption<sup>9</sup>; formation is needed to prevent BMD loss. Over a third of regular cycles were anovulatory (by P4) in ~4000 women 20-49 y in a random population<sup>10</sup>. A meta-analysis of 6 prospective studies showed a WMD in BMD of -0.86%/y in women with more vs fewer SOD<sup>11</sup> (Figure).

Women post-ovariectomy in a 1-y RCT of OB-PR-acting MPA vs CEE-MPA had no effect on high resorption/did not prevent BMD loss despite increased ALP<sup>12</sup>. However, a meta-analysis of RCTs in menopausal women randomized directly to CEE+MPA vs CEE alone showed a +0.5%/y greater BMD gain on CEE+MPA vs CEE ( $p = 0.004$ ; 95% CI 0.179, 0.827%)<sup>13</sup>.

We currently lack data on P4 treatment related to bone histomorphometry, strength and fracture risk. But evidence-based data showed *cyclic* MPA was bone-anabolic in premenopausal women with abnormal cycles/SOD<sup>7</sup> and MPA increased formation in menopause on CEE<sup>14</sup>. P4 is effective for symptomatic perimenopause<sup>15</sup>, treats menopausal hot flashes<sup>16</sup> and had cardiovascular safety<sup>17</sup>; progesterone is a useful bone therapy across women's lifespan.

Women at increased fracture risk on >5 y n-bisphos. have low formation and need therapy. Could P4-antiresorptive co-therapy potentially prevent fractures?

Ref: 1.Prior *Endocr Rev* 1990;11:386; 2. Hill *A J R Soc Med* 2015;108:32; 3. Ishida *Bone* 1997;20:17; 4. Ishida *Endocrinology* 1999;140:3210; 5. Schmidmayr *Geburtsh Frauenheilk* 2008;68:1; 6. Liao *J Endocr Invest* 2002;25:785; 7. Prior *Am J Med* 1994;96:521; 8. Prior *N Engl J Med* 1990;323:1221; 9. Kalyan *Eukaryot Gene Expr* 2010;20:213; 10. Prior *PLOS One* 2015;10:e0134473; 11. Li *Epidemiol Rev* 2014;36:147; 12. Prior *J Bone Min Res* 1997;12:1851; 13. Prior *J Bone Min Res* 2013;28[S1]; 14. Seifert-Klauss *J Osteop* 2010;20:10:845180; 15. Prior *FVVObstGyn* 2011;3:109; 16. Hitchcock *Menopause* 2012;19:886; 17. Prior *PLOS One* 2014;9:e84698

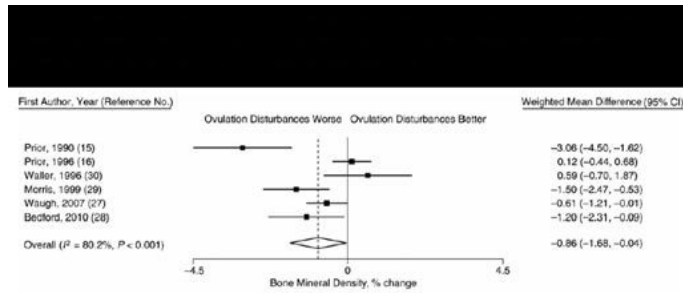


Figure: A random-effects meta-analysis of six prospective studies of menstrual cycles and ovulation

**Disclosures:** Jerilynn C. Prior, None.

## SU0265

**The Control of Regulatory T cells Influx by CCL22 is a Critical Determinant of Resident and Inflammatory Cells Pro-Reparative Phenotype in Chronic Inflammatory Osteolytic Lesions.** Andreia Espindola Vieira<sup>1</sup>, Priscila Colavite<sup>1</sup>, Angelica Fonseca<sup>1</sup>, Carolina Favaro Francisoni<sup>1</sup>, Ana Paula Trombone<sup>2</sup>, Charles S Sfeir<sup>3</sup>, Steven R Little<sup>3</sup>, Gustavo Garlet<sup>4\*</sup>. <sup>1</sup>FOB/USP, Brazil, <sup>2</sup>USC, Brazil, <sup>3</sup>University of Pittsburgh, United states, <sup>4</sup>Sao Paulo University, Brazil

Previous studies demonstrate that regulatory T cells (Tregs) arrest chronic inflammatory osteolytic lesions by attenuating inflammation and catabolic pathways that drive soft and mineralized tissue destruction. Since Tregs comprise a very small fraction of inflammatory infiltrate which is unproportional to its marked effects, Tregs are supposed to mediate the conversion of a tissue-destructive milieu into a pro-regenerative one in collaboration with other cells types. In the present study we investigated the potential modulation of macrophages and mesenchymal stem cells fate and function by Tregs in experimental periapical lesions (ePL) induced in C57Bl/6 mice.

In the presence of functional Tregs the levels of MSCs makers (CD29, CD44, CD73, CD90, CD105, CD106, CD166, NANOG, Stro-1 and CXCR4) mRNA (qPCR) were significantly increased, as well the M2 markers (Fizz-1 and Arg), being associated with reduced inflammation and bone loss. Conversely, Tregs inhibition (anti-GITR treatment) decreases the levels of MSCs markers and the M2/M1 rate, leading to increased lesions severity. From the therapeutic viewpoint, the induction of Tregs migration by CCL22-releasing PLGA formulation replicate outcome of the spontaneous Tregs migration, but result in an early attenuation of bone loss and inflammatory cell influx, and early conversion of macrophages into an M2 phenotype, as well early increase in MSCs and regeneration markers expression. Accordingly, Ms and MSCs extracted from periapical lesions (sorted with different markers sets by FlowCytometry) in the presence of active Tregs present higher levels healing markers expression as well increased immunosuppressive properties *in vitro* when compared to MSCs from tissues without Tregs.

The results demonstrated that active Tregs chemoattraction redirects of Ms and MSCs towards a pro-reparative phenotype, and that its chemoattraction by CCL22-releasing formulation can be used to manage inflammatory bone loss.

Supported by scholarships/grants from FAPESP and NIH R01DE02105801A.

**Disclosures:** Gustavo Garlet, None.

**SU0266**

**Temporal Sequence of Molecular, Cellular, Vascular and Anatomical Changes Leading to Glucocorticoid-induced Osteonecrosis of the Femoral Head in Mice.** Robert S Weinstein\*<sup>1</sup>, Erin A Hogan<sup>1</sup>, Marilina Piemontese<sup>1</sup>, Michael J Borrelli<sup>2</sup>, Serguei Liachenko<sup>3</sup>, Charles A O'Brien<sup>1</sup>, Stavros C Manolagas<sup>1</sup>. <sup>1</sup>Center for Osteoporosis & Metabolic Bone Diseases, Division of Endocrinology & Metabolism, Central Arkansas Veterans Healthcare System & the University of Arkansas for Medical Sciences, United states, <sup>2</sup>Department of Radiology, Central Arkansas Veterans Healthcare System & the University of Arkansas for Medical Sciences, United states, <sup>3</sup>National Center for Toxicological Research/Food & Drug Administration, United states

Osteonecrosis of the hip develops in up to 40% of patients receiving long-term systemic therapy with glucocorticoids and may occur without widespread osteoporosis. However, the pathological changes responsible remain obscure. We have examined the consecutive molecular, cellular, vascular and anatomical changes that occur during the development of glucocorticoid-induced osteonecrosis. To do this, we administered pulsed doses of glucocorticoids, a regimen associated with a greater risk of osteonecrosis than steady-state treatment. Prednisolone pellets (2.1 mg/kg/d) were implanted in 7-month-old mice on day 0, 14 and 28 and necropsies were performed on day 14, 28 and 42, respectively. We found that fourteen days after the first pellet was implanted, the femoral head expression of osteocalcin, OPG, RANKL, and VEGF was decreased. Similarly, femoral head strength and bone formation rate decreased prior to any detectable changes in femoral head density or microarchitecture as determined by  $\mu$ CT; and prior to any changes in distal femoral or vertebral bone. By day 42, femoral head density and trabecular thickness as well as vertebral compression strength decreased but there were no changes in vertebral mineral density, distal femoral  $\mu$ CT, or femoral 3-point bending. The loss of femoral head density and cancellous architecture was accompanied by a 2.5-fold and 6.3-fold increase in extraordinarily large, intensely TRAP stained cancellous and endocortical osteoclasts at day 14 lasting until day 28, after which the osteoclast numbers returned to control values by day 42. Unexpectedly, this pronounced osteoclastosis was accompanied by a decrease in RANKL, and particularly in OPG. Lastly, we imaged the femoral head vascularity using  $\mu$ CT of decalcified bone after perfusion with lead chromate. Glucocorticoids converted the normal dendritic vasculature to pools and lakes. These changes were accompanied by a striking increase in femoral head edema as detected by magnetic resonance imaging (MRI) - robust diagnostic evidence of osteonecrosis. Collectively, these findings reveal a pathophysiological sequence during which an initial decrease in femoral head OPG, RANKL, and VEGF by glucocorticoids caused increased osteoclastogenesis and reduced vascularity and mechanical strength well before the loss of bone mass and microarchitectural deterioration occurred; thus rendering the femoral head vulnerable to the development of osteonecrosis.

*Disclosures:* Robert S Weinstein, None.

**SU0267**

**RTC - The Effect of Metformin on Bone Assessed by Bone Mineral Density and Trabecular Bone Score.** Azra Karahasanovic\*<sup>1</sup>, Thomas Peter Almdal<sup>2</sup>, Peter Vestergaard<sup>3</sup>, Louise Lundby Christensen<sup>4</sup>, CIMT Trial group (coordinating member: Thomas Peter Almdal)<sup>2</sup>, Pia Eiken<sup>5</sup>. <sup>1</sup>Department of Cardiology, Nephrology & Endocrinology, Nordsjællands Hospital, Hillerød & Faculty of Health & Medical Sciences, University of Copenhagen, Copenhagen, Denmark, <sup>2</sup>Department of Endocrinology, Rigshospitalet, Copenhagen, Denmark, <sup>3</sup>Departments of Clinical Medicine & Endocrinology, Aalborg University Hospital, Aalborg, Denmark, <sup>4</sup>Department of Paediatrics & Adolescent Medicine, Nordsjællands Hospital, Hillerød, Denmark, <sup>5</sup>Department of Cardiology, Nephrology & Endocrinology, Nordsjællands Hospital, Hillerød & Faculty of Health & Medical Sciences, University of Copenhagen, Copenhagen, Denmark, Denmark

**Background**

Osteoporosis and type 2 diabetes mellitus (T2DM) are common diseases. Recent evidence indicates that the two diseases could be linked. Currently used tests are not sufficient in assessing fracture risk, as patients with T2DM have increased fracture risk despite normal or even increased bone mineral density (BMD). This could indicate that the increased fracture risk is caused by changes in cortical bone porosity and destruction of trabecular bone microarchitecture, rather than caused by diminished bone mineral density. Trabecular bone score (TBS) evaluates the pixel gray-level variations in lumbar spine dual-energy X-ray absorptiometry (DXA) images and has been suggested to be a good indicator of bone microarchitecture and bone health in T2DM. Glucoselowering drugs may affect bone quality and several in vitro, ex vivo and in vivo and clinical studies suggest that metformin might have an anabolic effect on bone. However, no (long-term) placebo controlled randomized trials (RCTs) evaluating the effect of metformin on bone quality have previously been performed.

**Aim**

The aim of this substudy of the Copenhagen Insulin Metformin Therapy (CIMT) trial is to examine the effect of 18 months treatment with metformin compared with placebo on changes in BMD and TBS in patients with T2DM.

**Methods**

Multicentre, randomized, 18 months placebo-controlled trial assessing blindly metformin versus placebo in combination with insulin. Inclusion criteria were T2DM, HbA1c  $\geq$  7.5%, BMI > 25 kg/m<sup>2</sup>. Main outcome measures in this study are mean changes in BMD and TBS.

**Results**

Out of 412 randomized patients, 48 did not complete the DXA scans at 18 months. The metformin+insulin group gained less in BMI and had a greater reduction in HbA1c than the placebo+insulin groups ( $P < 0.05$ ). Changes in BMD (spine, total hip, hip-neck) and TBS did not differ between the groups after 18 months of intervention ( $P > 0.05$ ).

**Conclusion**

We did not detect a differentiated effect of 18 months treatment with metformin compared with placebo on BMD or TBS in patients with T2DM.

*Disclosures:* Azra Karahasanovic, None.

**SU0268**

**The Association Between Type 2 Diabetes Mellitus and Bone Quality as Measured with HR-pQCT – The Maastricht Study.** Ellis AC de Waard\*<sup>1</sup>, Joost JA de Jong<sup>1</sup>, Hans HCM Savelberg<sup>2</sup>, Tineke A van Geel<sup>3</sup>, Boy JHM Houben<sup>4</sup>, Ronald MA Henry<sup>4</sup>, Miranda T Schram<sup>4</sup>, Pieter C Dagnelie<sup>5</sup>, Carla J van der Kallen<sup>4</sup>, Simone JS Sep<sup>4</sup>, Coen DA Stehouwer<sup>4</sup>, Nicolaas C Schaper<sup>6</sup>, Tos TJM Berendschot<sup>7</sup>, Jan SAG Schouten<sup>7</sup>, Piet PMM Geusens<sup>8</sup>, Annemarie Koster<sup>9</sup>, Joop PW van den Bergh<sup>10</sup>. <sup>1</sup>Maastricht University, Department of Internal Medicine, Subdivision of Rheumatology, Maastricht, the Netherlands & NUTRIM School for Nutrition & Translational Research in Metabolism, Maastricht University, Maastricht, the Netherlands, <sup>2</sup>Maastricht University, Department of Human Movement Science, Maastricht, the Netherlands & NUTRIM School for Nutrition & Translational Research in Metabolism, Maastricht University, Maastricht, the Netherlands, <sup>3</sup>Maastricht University, Department of Family Medicine, Maastricht, the Netherlands & NUTRIM/CAPHRI, Maastricht University, Maastricht, the Netherlands, <sup>4</sup>Maastricht University Medical Center, Department of Internal Medicine, Maastricht, the Netherlands & CARIM School for Cardiovascular diseases, Maastricht University, Maastricht, the Netherlands, <sup>5</sup>Maastricht University, Department of Epidemiology, Maastricht, the Netherlands & CAPHRI/CARIM, Maastricht University, Maastricht, the Netherlands, <sup>6</sup>Maastricht University Medical Center, Department of Internal Medicine, Maastricht, the Netherlands & CAPHRI/CARIM, Maastricht University, Maastricht, the Netherlands, <sup>7</sup>University Eye Clinic Maastricht, Maastricht, The Netherlands, <sup>8</sup>Maastricht University Medical Centre/CAPHRI, Department of Internal Medicine, Subdivision of Rheumatology, Maastricht, the Netherlands & University of Hasselt, Biomedical Research Institute, Hasselt, Belgium, <sup>9</sup>Maastricht University, Department of Social Medicine, Maastricht, the Netherlands & CAPHRI School for Public Health & Primary Care, Maastricht University, Maastricht, the Netherlands, <sup>10</sup>Maastricht University Medical Centre/NUTRIM, Department of Internal Medicine, Subdivision of Rheumatology, Maastricht, the Netherlands & VieCuri Medical Center, Department of Internal Medicine, Subdivision of Endocrinology, Venlo, the Netherlands, Netherlands

**Purpose:** To compare volumetric bone mineral density (vBMD), bone microarchitecture and bone strength in participants with and without type 2 diabetes using high-resolution peripheral quantitative computed tomography (HR-pQCT).

**Methods:** Cross-sectional data of a subset of 375 participants from The Maastricht Study. At baseline, participants underwent an oral glucose tolerance test and medication interview to stratify them into normal glucose metabolism (NGM) or type 2 diabetes mellitus (T2DM). Participants with impaired glucose metabolism (N=59) were excluded. 24-61 months after baseline, the non-dominant distal radius of participants was scanned on a clinical HR-pQCT scanner (XtremeCT; Scanco Medical AG, Switzerland) by use of the standard in vivo protocol. Scans with quality grade 1-4 were used for subsequent image analysis (standard analysis, micro finite element analysis and extended cortical bone analysis, N=306). Bone parameters between the groups were compared using linear regression analysis.

**Results:** 246 participants had NGM and 60 T2DM. T2DM individuals were somewhat older, had a higher BMI and were less often female (age: NGM 56.7 $\pm$ 8.2, T2DM 62.3 $\pm$ 7.6 years,  $p < 0.001$ ; BMI: NGM 25.8 $\pm$ 3.7, T2DM 30.7 $\pm$ 5.4 kg/m<sup>2</sup>,  $p < 0.001$ ; women: NGM 52.4%, T2DM 43.3%,  $p = 0.21$ ). The median (IQR) HbA1c of the T2DM group was 50.5 (12.0) mmol/mol (6.8 (1.1) %) and the median (IQR) diabetes duration was 51.0 (15.5) months. Unadjusted analyses showed that cortical porosity and cortical pore volume were significantly higher in the T2DM group compared to the NGM group (Table 1). After adjustment for age, sex and BMI, the

association between T2DM and cortical porosity or cortical pore volume were no longer statistically significant (log cortical porosity: B 0.03, 95%CI -0.11-0.16, log cortical pore volume: B -0.001, 95%CI -0.14-0.14). vBMD, all other bone micro-architectural parameters and bone strength were not significantly different between both groups in both unadjusted and adjusted analyses.

Conclusions: Cortical porosity and cortical pore volume at the distal radius were significantly higher in participants with T2DM compared to participants with NGM. However, micro-architectural parameters and bone strength were not significantly different compared to the NGM group after adjustment for age, sex and BMI, indicating that in this group of relatively well-regulated subjects with a median diabetes duration of 51 months bone micro-architectural properties may not be compromised.

Table 1. HR-pQCT parameters according to diabetes status.

	NGM (N=246)	T2DM (N=60)	P- value*	P- value#
<b>Volumetric bone mineral density</b>				
- Total vBMD (mgHA/cm <sup>3</sup> )	302.0 (61.5)	310.1 (78.4)	0.39	0.68
- Cortical vBMD (mgHA/cm <sup>3</sup> )	852.5 (72.9)	836.5 (92.0)	0.15	0.69
- Trabecular vBMD (mgHA/cm <sup>3</sup> )	165.0 (39.5)	168.1 (44.0)	0.60	0.56
<b>Micro-architectural parameters</b>				
- Trabecular number (1/mm)	1.94 (0.32)	2.00 (0.36)	0.24	0.90
- Trabecular thickness (mm)	0.071 (0.01)	0.070 (0.01)	0.63	0.45
- Trabecular separation (mm), median (IQR)	0.44 (0.10)	0.43 (0.09)	0.39	0.70
- Cortical thickness (mm)	0.75 (0.21)	0.78 (0.27)	0.36	0.82
- Cortical pore volume (mm <sup>3</sup> ), median (IQR)	12.98 (8.22)	17.10 (9.33)	<0.01	0.99
- Cortical porosity (%), median (IQR)	2.55 (1.57)	2.92 (1.96)	<0.01	0.71
- Cortical pore diameter (mm), median (IQR)	0.16 (0.02)	0.17 (0.02)	0.25	0.40
<b>Bone strength</b>				
- Stiffness (kN/mm)	95.4 (27.7)	95.7 (28.2)	0.93	0.14
- Failure load (N)	4552.2 (1305.2)	4586.3 (1322.8)	0.86	0.15

Mean and standard deviation are reported unless stated otherwise. \*Unadjusted P-value.  
#P-value adjusted for age, sex and BMI.

Table 1. HR-pQCT parameters according to diabetes status.

Disclosures: *Ellis AC de Waard, None.*

## SU0269

**Annual change in fracture load of vertebra estimated by CT-based 3-dimensional finite element modeling in breast cancer patients with aromatase inhibitor therapy..** *Koshi Kishimoto*<sup>\*1</sup>, *Eiji Itoi*<sup>2</sup>. <sup>1</sup>Tohoku Kosai Hospital, Japan, <sup>2</sup>Department of Orthopaedic Surgery, Tohoku University, Japan

Adjuvant aromatase inhibitor (AI) therapy reduces recurrence of post-menopausal endocrine-responsive breast cancers and improve survival rate. However, depletion of estrogen level by AI therapy causes high bone turnover and accelerates bone loss. Previous clinical studies reported that AI therapy decreased bone mineral density (BMD) measured using dual X-ray absorptiometry (DXA) by approximately 2% per year in lumbar spine and hip. Recently developed CT based 3-dimensional finite element modeling (CT/FEM) can provide another aspect of bone strength assessment. In this study, the annual change in estimated fracture load of vertebra as well as BMD and bone turnover markers were analyzed in the patient receiving AI therapy. This study was conducted after approval from ethical committee of authors' institute. Seventeen patients who underwent surgical treatment for breast cancer and planned to start AI therapy were screened by X-ray and DXA. Six patients who diagnosed as having normal BMD without osteoporotic fracture enrolled in this study with written informed consent. CT image from thorax to pelvis, bone specific alkaline phosphatase (BAP), TRACP-5b, X-ray and DXA (Hologic) data were acquired at baseline and 1-year after the start of AI therapy. CT data were transferred into personal computer. Finite element models were constructed on MECHANICAL FINDER v6.1 software (RCCM, Tokyo, Japan). Nonlinear FE analysis of L1 vertebra was performed based on previous report. Trabecular bone was simulated using 2-mm linear tetrahedral elements and outer surface of the cortical shell was modeled using 0.4-mm-thick 2-mm triangular plates. Mechanical properties of each element were computed from the Hounsfield unit value. A uniaxial compressive load was applied on the upper surface and the lower surface was restrained. Fracture load was defined as being when at least one element failed. Fracture load of L1 vertebra estimated by CT/FEM was 3268 ± 752 N (average ± SD n=6) at the time of enrollment. After 1-year observation, fracture load of L1 vertebra decreased by 4.3 ± 22.6% from baseline on average. Elevated serum BAP and TRACP-5b levels were seen after 6-month AI therapy. Vertebral fracture was not recognized during study period. Lumbar spine BMD decreased by 2.4 ± 2.7% from baseline after 1-year AI therapy. Our results indicate that estimated fracture load might show larger variation than DXA after AI therapy. CT/FEM might provide fracture prediction for breast cancer patients who receive AI therapy.

Disclosures: *Koshi Kishimoto, None.*

## SU0270

**Sad bones: Serotonin Reuptake Inhibitors and Bone Health in an Irish Population.** *James Mahon*<sup>\*</sup>, *Richard M Duffy*, *Clodagh Power*, *Nessa Fallon*, *Georgina Steen*, *Joseph Browne*, *MC Casey*, *JB Walsh*, *Kevin McCarroll*. St James's Hospital, Ireland

### Background

Depression and antidepressant medications (ADTs) have a negative effect on bone health. However, there is little evidence on relative impact of different ADTs, nor has the effect of ADTs been studied in an Irish population. We aimed to establish the effect of ADTs on bone health and to identify the impact of different ADTs in patients attending a tertiary referral centre for osteoporosis in Ireland.

### Method

We retrospectively identified all patients attending our clinic whose prescription included the following ADTs: Venlafaxine, citalopram, escitalopram, fluoxetine, sertraline and paroxetine. We compared these with a randomly selected control group not prescribed ADTs. We examined DXA T-scores and BMD, history of fracture of hip, spine, vertebra and other sites, and biochemical markers of bone turnover.

### Results

649 individuals: 203 on ADT; 446 control. Mean age of entire cohort 66.74 years (SD 14.92); 80.8% female; mean BMD total hip 0.791g/cm<sup>3</sup> (SD 0.106); mean BMD spine 0.898g/cm<sup>3</sup> (SD 0.182). Patients on ADTs had significantly lower BMD than controls: BMD hip was 0.079g/cm<sup>3</sup> lower in patients on ADTs (SE 0.017, 95%CI 0.049-0.109, p<0.001). BMD spine did not differ significantly between the two groups (p=0.672). Those on ADTs were significantly more likely to have had a hip fracture: OR 4.08 (95% CI 2.70-6.17, p=0.001). And BMD hip was significantly lower in patients on ADTs who had never had a hip fracture: BMD mean difference 0.064g/cm<sup>3</sup> (SE 0.017, 95%CI 0.029-0.098, p<0.001). A chi squared test showed significant variation in prevalence of hip osteoporosis between different ADTs, p=0.014. Highest rates were observed in citalopram, 56.7% (n=60), and lowest rates in fluoxetine (n=16). The OR for hip osteoporosis comparing citalopram to fluoxetine is 9.15 (95% CI 1.91-43.87 Pearson's Chi squared test p=0.002). For biochemical markers of bone turnover, fluoxetine was the only SSRI with statistically significant lower levels of CTX, mean reduction 0.148ng/ml (95%CI 0.070-0.226, p=0.001).

### Conclusion

Our study confirmed in an Irish population that ADTs have a negative impact on BMD of hip in particular and are associated with higher risk of hip fracture. SSRI medications have a role in mediating this reduced BMD. While no single drug was identified as clearly causing a greater reduction in BMD or increased fracture, some evidence indicates that fluoxetine may be safer and that this may be mediated through a modest effect of lesser bone resorption.

Disclosures: *James Mahon, None.*

## SU0271

**Bone density and microarchitecture in Hepatitis C and HIV coinfected postmenopausal minority women.** *Michael Yin*<sup>\*1</sup>, *Zhang Chengchen*<sup>1</sup>, *Kyle Nishiyama*<sup>1</sup>, *Jayesh Shah*<sup>1</sup>, *Susan Olender*<sup>1</sup>, *David Ferris*<sup>2</sup>, *Mariana Bucovsky*<sup>1</sup>, *Ivelisse Colon*<sup>1</sup>, *Donald McMahon*<sup>1</sup>, *Cosmina Zeana*<sup>2</sup>, *Elizabeth Shane*<sup>1</sup>. <sup>1</sup>Columbia University Medical Center, United states, <sup>2</sup>Bronx Lebanon Hospital Center, United states

Introduction: Fracture incidence is higher and areal bone mineral density (aBMD) by DXA are lower in HIV-infected persons with HIV/HCV-co-infection (HIV+/HCV+) than those with HIV infection alone (HIV+). However HIV+/HCV+ patients tend to have lower body mass index (BMI) and truncal fat raising a concern that differences by DXA are overestimated.

Methods: We measured areal BMD (aBMD) by DXA at the spine (LS), femoral neck (FN), total hip (TH), and radius (1/3R, UDR), volumetric BMD (vBMD) and microarchitecture at the spine (L1 L2) and hip by central quantitative CT (cQCT) and radius and tibia by high resolution peripheral QCT (HRpQCT), respectively, in 181 (40 HIV+/HCV+ and 141 HIV+) postmenopausal women. Data are presented as Mean ± SD. T test was used to assess the between-group difference on bone and body composition variables. ANOVA was used to compare between-group difference adjusted for other covariates.

Results: HIV+/HCV+ women were similar to HIV+ women in age (57±5 vs 57±5 years, p=0.88) and race/ethnicity (55% African American) but lower in BMI (28±5 vs 31±6 kg/m<sup>2</sup>, p=0.016) and truncal fat (13±6 vs 16±6kg, p=0.012). HIV+/HCV+ women had lower DXA T scores at the LS, TH, UDR (p<0.05) even after adjusting for BMI or truncal fat. DXA aBMD and cQCT vBMD were well correlated at the spine and hip (r= 0.71 to 0.79, p<0.001). There was a trend for lower vBMD of the lumbar spine and total hip in HIV+/HCV+ compared to HIV+ (Table), but trabecular parameters did not differ. In contrast, HRpQCT-derived vBMD at the tibia, and other trabecular and cortical parameters were 7-18% lower in HIV+/HCV+ than HIV+; radial parameters did not differ (Table).

Conclusion: Spine and hip aBMD differences between HIV+/HCV+ and HIV+ postmenopausal women may be overestimated by DXA, as vBMD differences are smaller and not significant. At the tibia, vBMD and microarchitectural parameters are significantly worse in HIV+/HCV+ co-infected women. These data suggest that the higher fracture rates observed in HIV+/HCV+ than HIV+ individuals are due in part to true deficits in BMD and microarchitecture.

Table	HIV-mono-infected (N=141)	HIV/HCV co-infected (N=40)	P value
<b>DXA</b>			
LS T score	-1.03±1.36	-1.82±1.20	0.001
FN T score	-1.00±1.04	-1.26±0.95	0.144
TH T score	-0.53±0.98	-1.01±0.81	0.005
R13 T score	-0.34±1.43	-0.72±1.36	0.128
UDR T score	-0.36±1.18	-0.97±1.07	0.004
<b>cQCT</b>			
LS total vBMD (g/cm <sup>3</sup> )	0.23±0.04	0.22±0.03	0.075
Total hip vBMD (g/cm <sup>3</sup> )	0.28±0.05	0.26±0.03	0.074
<b>Tibia HRpQCT</b>			
Total vBMD (mg HA/cm <sup>2</sup> )	261.0±56.31	232.9±50.93	0.006
Cortical thickness (µm)	1.10±0.22	1.01±0.25	0.035
Trabecular vBMD (mg HA/cm <sup>2</sup> )	136.1±42.22	113.8±36.35	0.003
Trabecular thickness (µm)	0.07±0.02	0.06±0.01	0.004

table

Disclosures: Michael Yin, None.

## SU0272

**Testosterone Plus Finasteride Prevents Bone Loss and Inhibits Androgen-Mediated Prostate Enlargement in a Rodent Spinal Cord Injury Model.** Ean Phillips\*, Joshua Yarrow, Christine Conover, Andrea Vasconez, Jonathan Alerte, Taylor Bassett, Stephen Borst, Fan Ye. North Florida/South Georgia Veterans Health System, United states

We have reported that testosterone-enanthate (TE) prevents sublesional cancellous bone loss acutely after spinal cord injury (SCI). Our purpose was to analyze whether TE prevents the chronic cancellous/cortical bone deficits that develop in a rodent SCI model that exhibits low testosterone and whether Finasteride (FIN; type II 5 $\alpha$ -reductase inhibitor) prevents TE-induced prostate growth without inhibiting the beneficial skeletal responses. Forty 16-week old male Sprague-Dawley rats received: 1) SHAM surgery (T9 laminectomy), 2) severe (250 kdynes) contusion SCI, 3) SCI+TE (7.0mg/week, i.m.), or 4) SCI+TE+FIN (5mg/kg, s.c. daily). Mass of the highly androgen-sensitive levator ani/bulbocavernosus muscle was 12% lower in SCI vs SHAM ( $p < 0.05$ ) and 18-19% higher in SCI+TE and SCI+TE+FIN vs SCI ( $p < 0.05$ ), mimicking changes in serum testosterone.  $\mu$ CT analysis at the distal femur showed that cancellous bone mineral density (cBMD) was 38% lower in SCI vs SHAM, characterized by a 43% lower cancellous bone volume (BV/TV, %), a 49% lower trabecular number (Tb.N, #/mm), a 52% higher trabecular separation (Tb.Sp, mm), and an unexpected 10% higher trabecular thickness (Tb.Th, mm) after SCI ( $p \leq 0.01$  for all). In contrast, SCI+TE and SCI+TE+FIN displayed a 46-54% higher cBMD ( $p < 0.01$ ), 63-65% higher BV/TV ( $p < 0.05$ ), 73-95% higher Tb.N (SCI+TE  $p < 0.05$ ; SCI+TE+FIN  $p < 0.01$ ), and a 47-54% lower Tb.Sp ( $p < 0.001$ ) vs SCI, values not different than SHAM. Tb.Th was also 8-11% higher in SCI+TE vs SHAM ( $p < 0.01$ ) and SCI+TE+FIN ( $p < 0.05$ ). Cortical bone area (Ct.Ar, mm<sup>2</sup>) and cortical area fraction (Ct.Ar/Tt.Ar, %) at the distal femur were 14% lower ( $p < 0.01$ ) and 12% lower ( $p < 0.05$ ) in SCI vs SHAM, respectively. TE did not prevent the cortical bone loss, with SCI+TE and SCI+TE+FIN displaying 10% lower bone area (Tt.Ar, mm<sup>2</sup>) ( $p < 0.05$  SCI+TE only), 20-21% lower Ct.Ar ( $p < 0.01$  for both), 10-20% lower Ct.Ar/Tt.Ar (SCI+TE trend,  $p = 0.051$ ; SCI+TE+FIN  $p \leq 0.001$ ), and 9% lower cortical thickness (Ct.Th, mm) ( $p \leq 0.05$ , SCI+TE+FIN only) vs SHAM. In addition, SCI+TE prostate mass was 75-115% higher vs SHAM/SCI. FIN prevented prostate enlargement with prostate mass being 35% lower in SCI+TE+FIN vs SCI+TE ( $p \leq 0.001$ ) and not different than SHAM/SCI. Our findings indicate that TE prevented the chronic cancellous bone loss after SCI and that FIN did not block this skeletal benefit, but completely prevented TE-induced prostate enlargement. In contrast, TE did not prevent the cortical bone deficits after SCI.

Disclosures: Ean Phillips, None.

## SU0273

**Adenine Dose Study Modeling Chronic Kidney Disease for One Month in Older Male and Female BALB/c Mice.** Kelly Crane\*, William Schroeder, Ryan Clark, Karen King. University of Colorado School of Medicine, United states

Purpose: Chronic kidney disease (CKD) alters mineral metabolism (mineral loss in bone but gain in cardiovascular and renal tissues) and may cause early death. Our target patient population is the mature adult; therefore, we desire a method suitable for modeling CKD in older mice. Bone changes occur slowly; therefore, we desire a model in which animal survival is robust despite renal damage. Adenine added to the mouse diet precipitates in the kidney which induces damage. This method has been successfully used to model CKD in younger mice. However, it has never been applied to older mice. This preliminary study tests different doses of adenine in the diet, given over a one-month period, in older male and female mice.

Methods: Male and female BALB/c mice were obtained from the NIH/NIA aged rodent colony at 24 weeks of age (analogous to ~30 year-old humans). All animals

received the base casein diet for the first seven days. Then, four different doses of adenine (in the casein diet) were administered in a 7-day induction phase followed by a 21-day maintenance phase. The four doses were 0.30% induction / 0.20% maintenance; 0.30% / 0.15%; 0.20% / 0.15%; and 0.20% / 0.10%. Control was the base casein diet. Mice were individually housed (N = 10 total, 1 mouse/sex/diet). Body masses were measured three times per week until death or euthanasia due to low body mass. Kidneys were sectioned at 5  $\mu$ m and analyzed via H&E, PAS, and von Kossa staining.

Results: All adenine treated mice lost body mass (>30%) and most died before the study ended at 35 days. Females died faster than the dose-matched males. Even the lowest dose of adenine led to abnormal kidney histology (Figure 1). Alterations included dilated tubules and Bowman's spaces, peritubular leukocytes, thickening and atrophy of tubular basement membranes, and mineralization of tubular structures. Control mice did not lose body mass and had normal appearing kidney histology.

Conclusions: Adenine can be used to create a model of CKD - induced through tubulointerstitial nephropathy - in older mice; however, a low dose of adenine should be used. A low dose of 0.2% adenine for seven days followed by 0.1% adenine for 21 days is sufficient to model CKD but may result in early death.

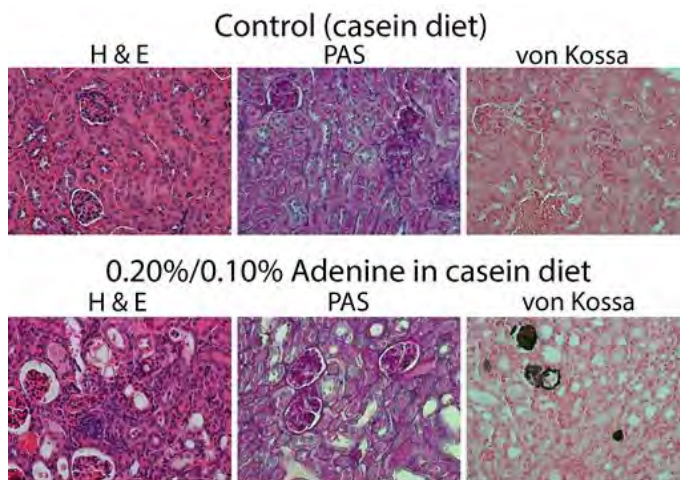


Figure 1: Kidney histology of two 28 week-old female BALB/c mice after one month of adenine (upper) or control (lower) diet. 40X magnification.

Figure

Disclosures: Kelly Crane, None.

## SU0274

**Anemia is Associated with Fractures Independent of BMD in Elderly Men.** Rodrigo Valderrabano<sup>\*1</sup>, Jennifer Lee<sup>2</sup>, Li-Yung Lui<sup>3</sup>, Andrew R Hoffman<sup>2</sup>, Steven R. Cummings<sup>3</sup>, Eric Orwoll<sup>4</sup>, Joy Y Wu<sup>1</sup>. <sup>1</sup>Division of Endocrinology, Stanford University School of Medicine, United states, <sup>2</sup>Division of Endocrinology, Stanford University School of Medicine / Palo Alto Veterans Affairs Health Care System, United states, <sup>3</sup>San Francisco Coordinating Center, California Pacific Medical Center, United states, <sup>4</sup>Department of Medicine, Bone & Mineral Unit, Oregon Health & Science University, United states

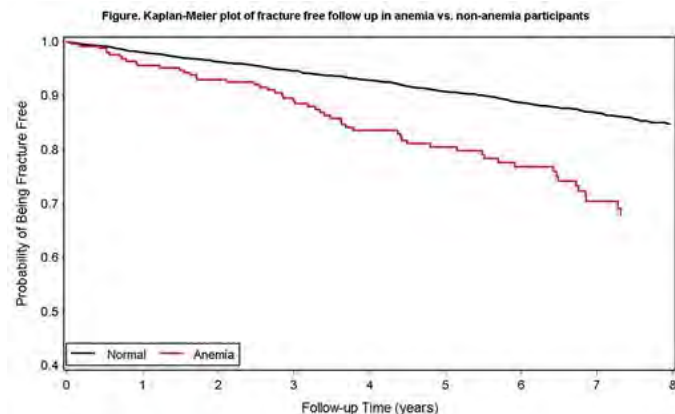
Purpose: Anemia is an important health problem worldwide. Preclinical studies in mice have revealed that osteoblasts can impact erythrocyte numbers, and we have found that bone loss in the hip is associated with anemia in older men. Associations exist between hemoglobin and bone mineral density (BMD) in both sexes and there is a 38% increased risk of hip fracture in women with anemia. We sought to determine whether anemia was associated with fractures in men and whether BMD or change in BMD would attenuate this association.

Methods: The Osteoporotic Fractures in Men (MrOS) study is a community-dwelling prospective cohort of men aged 65 years or older, who underwent DXA scans at baseline and at the 3<sup>rd</sup> visit (7 years after baseline), complete blood counts (CBC) at the 3<sup>rd</sup> visit and longitudinal adjudicated fracture reporting. 3,631 men with CBC data were analyzed. The outcomes of interest were: any, non-spine and spine incident fractures following visit 3. Multivariable-adjusted (MVA) Cox models were used to estimate the hazard ratios (HR) and 95% confidence intervals (CI) of each outcome (median 7.2 years follow up): 1) without BMD, 2) with BMD (visit 3), 3) with annualized percent change in BMD (baseline to visit 3) at the total hip (TH).

Results: Age, BMI, history of fracture prior to visit 3, bone medication use, and self-reported health were associated with fractures or anemia (Hgb < 12g/dL) and were included into MVA models. Anemia was associated with increased risk of any (HR 1.72; 95% CI 1.31-2.28) and non-spine (HR 1.78; 95% CI 1.32-2.39) fractures. Including change in BMD in the model slightly attenuated the association with any (HR 1.61; 95% CI 1.21-2.14) and non-spine (HR 1.61; 95% CI 1.18-2.18) fractures. Including absolute BMD did not significantly alter the anemia-fracture association.

Men with anemia had a lower probability of being fracture free during follow up (Figure). Anemia was not observed to be associated with spine fracture.

Conclusions: In a cohort of community dwelling older men, anemia was associated with an increased risk of non-spine fracture independent of BMD. We have previously found change in BMD to be associated with anemia, but in this analysis it did not appear to explain the relationship of anemia and risk of fracture. A hemoglobin measure may be useful in bone health assessments. Further studies are needed to assess whether anemia could be a modifiable risk factor for fracture.



Kaplan-Meier Plot of fx free follow up anemia vs non-anemia

Disclosures: **Rodrigo Valderrabano**, None.

## SU0275

**Cortical Thinning in Patients with Primary Sclerosing Cholangitis.** Tobias Schmidt\*<sup>1</sup>, Thorsten Schinke<sup>1</sup>, Michael Amling<sup>2</sup>. <sup>1</sup>Department of Osteology & Biomechanics, University Medical Center Hamburg Eppendorf, Germany., Germany, <sup>2</sup>Department of Osteology & Biomechanics, University Medical Center Hamburg Eppendorf, Germany, Germany

### Objective

Metabolic bone disease frequently occurs in patients with chronic liver disease and is associated with increased risk of fractures. While bone disease in patients with progressive liver disease has been studied extensively, less is known about bone disease in patients with Primary Sclerosing Cholangitis (PSC). The objective of this study was to assess the bone microstructure by HR-pQCT in patients with PSC.

### Methods

Bone microstructure of 50 patients diagnosed with PSC were analysed by high-resolution peripheral quantitative computed tomography (XtremeCT, SCANCO Medical, Brüttsellen, Switzerland) at the tibia. The manufacturer's standard protocol was used to analyze the bone microstructure, including trabecular bone volume to total bone volume (BV/TV), trabecular number (Tb.N), trabecular thickness (Tb.Th), and cortical thickness (C.Th). HR-pQCT values were normalized to reference values of gender 20-29 years as previously described (1). BMD of lumbar spine and left femoral neck were measured using dual-energy X-ray densitometry (DXA). Additionally, osteology laboratory data were determined.

### Results

Interestingly, analyses of bone microstructure at the tibia by HR-pQCT revealed that bone disease in PSC patients mainly affects the cortical bone. Mean values were calculated for BV/TV (88.95% ± 19.62), Tb.N (104.69% ± 15.39), Tb.Th (83.85% ± 14.77) and C.Th (59.86% ± 13.94), showing strong reduction in cortical thickness. No correlation was observed with age, disease severity and disease duration. T-Score of lumbar spine and femoral neck significantly correlated with BV/TV, Tb.N, Tb.Th and C.Th. However, no significant correlations were found regarding osteology laboratory data.

### Conclusion

In this study, we demonstrate that PSC patients show reduced cortical thickness. While a strong correlation of BV/TV, Tb.N, Tb.Th and C.Th with the T-Score of lumbar spine and femoral neck can be observed, no correlation with clinical or laboratory data could be identified. This suggests that cortical bone loss seems to start early in PSC and occurs independently of age, disease duration and disease severity. Further translational studies are necessary to clarify the mechanism of PSC mediated cortical bone loss.

1. Macdonald HM, Nishiyama KK, Kang J, Hanley DA, Boyd SK. Age-related patterns of trabecular and cortical bone loss differ between sexes and skeletal sites: a population-based HR-pQCT study. *J Bone Miner Res.* 2011;26(1):50-62.

Disclosures: **Tobias Schmidt**, None.

## SU0276

**Disrupted Trabecular Microarchitecture at Both Distal Radius and Tibia in Patients with Monoclonal Gammopathy of Undetermined Significance.** Emily Stein\*, Mariana Bucovsky, Jennifer Mosby, Jing Fu, Chengchen Zhang, Kyle Nishiyama, X Guo, Suzanne Lentzsch, Elizabeth Shane. Columbia University, United states

Fracture risk is elevated in patients with monoclonal gammopathy of undetermined significance (MGUS). However, the pathogenesis of bone disease in these patients is poorly understood. Prior work using high resolution peripheral computed tomography (HRpQCT) has demonstrated abnormal microarchitecture at the distal radius, with predominantly cortical (Ct) abnormalities reported. At the tibia, volumetric BMD (vBMD) and microarchitecture have not been evaluated. We hypothesized that patients with MGUS would have abnormal microarchitecture at both radius and tibia compared to controls, reflecting global skeletal effects of the disease. We enrolled 33 subjects: patients with MGUS were matched 1:2 by sex, age and race/ethnicity to controls (C). All had aBMD of lumbar spine (LS), total hip (TH), femoral neck (FN), 1/3 (1/3R) and ultradistal radius (UDR) by DXA. Trabecular (Tb) and Ct vBMD and Tb microarchitecture were measured by HRpQCT (voxel size ~82 μm) of the distal radius and tibia. Mean age of enrolled subjects was 70 ± 9 yrs, 75% were female, and 58% were Caucasian. BMI was similar between groups. Mean Z-scores in MGUS (LS -0.3, TH -0.3, FN -0.6, 1/3R 0.0, UDR -0.5) were lower than those in C at the LS, FN and UDR (p<0.05), and tended to be lower at the 1/3R (p=0.07). By HRpQCT, total cross-sectional area was similar between groups at both sites. There were substantial microarchitectural differences between MGUS and C (Table). At the radius, MGUS subjects had lower total, Ct and Tb vBMD, lower Ct thickness and Tb thickness. They tended to have lower Tb number and greater Tb separation. At the tibia, MGUS subjects had lower total and Tb vBMD. They tended to have thinner Tb, greater Tb separation and heterogeneity. There were no differences in markers of bone turnover, P1NP or CTX, between the groups. Interleukin-6 was numerically greater but not statistically different (MGUS: 2.9 ± 5.4 vs. C: 1.4 ± 0.7 pg/ml; p=0.3). There was no difference in level of macrophage inflammatory protein-1 alpha. In summary, patients with MGUS had had lower vBMD and worse microarchitecture than matched controls at both the radius and tibia. At the radius, Ct and Tb abnormalities were observed, while at the tibia, Tb abnormalities predominated. Our results suggest that in addition to previously described Ct deficits, deterioration of Tb bone may be an important factor contributing to generalized skeletal fragility in patients with MGUS.

### Microarchitecture in MGUS compared to C (% difference)

	RADIUS	p-value	TIBIA	p-value
Total Density (mgHA/cm <sup>3</sup> )	-29	<0.02	-20	<0.04
Ct Density (mgHA/cm <sup>3</sup> )	-7	<0.03	-4	0.28
Ct Thickness (mm)	-30	<0.002	-9	0.48
Tb Density (mgHA/cm <sup>3</sup> )	-29	<0.03	-26	<0.01
Tb Number (1/mm)	-18	0.07	-12	0.22
Tb Thickness (mm)	-16	<0.02	-14	0.051
Tb Separation (mm)	+34	0.16	+30	0.10
Heterogeneity (mm)	+59	0.23	+97	0.08

Table. Microarchitectural Differences in MGUS and Control Subjects

Disclosures: **Emily Stein**, None.

## SU0277

**Effects of Roux-En-Y Gastric Bypass and Sleeve Gastrectomy on Bone Mineral Density and Marrow Adipose Tissue.** Miriam Bredella<sup>1</sup>, Logan Greenblatt<sup>2</sup>, Alireza Eajazi<sup>1</sup>, Martin Torriani<sup>1</sup>, Elaine Yu\*<sup>2</sup>. <sup>1</sup>Musculoskeletal Radiology, Massachusetts General Hospital, United states, <sup>2</sup>Endocrine Unit, Massachusetts General Hospital, United states

Purpose: Bariatric surgery is associated with bone loss but skeletal consequences may differ between Roux-en-Y gastric bypass (RYGB) and sleeve gastrectomy (SG), the two most commonly performed bariatric procedures. Furthermore, severe weight loss is associated with high marrow adipose tissue (MAT), which may contribute to impaired skeletal health after bariatric surgery. The purpose of our study was to determine the effects of RYGB and SG on BMD and MAT. We hypothesized that both bariatric procedures would lead to a decrease in BMD and an increase in MAT.

Methods: We studied 21 adults (18 F, 3 M; mean age 49 ± 9 [SD] yrs) with morbid obesity (mean BMI 44.1 ± 5.1 kg/m<sup>2</sup>) prior to and 1 year after RYGB (n=11) and SG (n=10). Subjects underwent DXA of the lumbar spine, hip, and subtotal body to assess areal BMD (aBMD; Discovery A, Hologic) and QCT of the L1-2 vertebrae and hips to assess volumetric BMD (vBMD; QCTPro, Mindways). MAT was assessed by

1H-MR spectroscopy (3T, Siemens Trio) of the L1-2 vertebrae, proximal femoral metaphysis and mid-femoral diaphysis using a single-voxel PRESS sequence without water suppression. Groups were compared by ANOVA and 1-year changes within groups were assessed using paired t-tests.

Results: Baseline characteristics were similar between groups. Mean weight loss was  $-36 \pm 10$  kg in the RYGB and  $-28 \pm 11$  kg in the SG group ( $p=0.23$ ). Mean serum calcium, 25(OH)-vitamin D, and PTH were unchanged after surgery and within the normal range in both groups. aBMD by DXA declined to a greater extent in the RYGB than the SG group at the total hip ( $-10.5 \pm 3.1$  vs  $-6.8 \pm 4.0\%$ ,  $p=0.04$ ) and subtotal body ( $-3.9 \pm 3.4\%$  vs  $1.3 \pm 3.1\%$ ,  $p<0.01$ ). There were similar patterns of decline in hip vBMD by QCT although differences between RYGB and SG groups were not significant ( $-6.9 \pm 6.0$  vs  $-3.2 \pm 5.9\%$ ,  $p=0.20$ ). Spine aBMD and vBMD declined from baseline within both the RYGB and SG groups, but the bone loss was not different between groups (aBMD  $-4.9 \pm 5.3$  vs  $-2.8 \pm 3.8\%$ ,  $p=0.33$ ; vBMD  $-7.1 \pm 4.3$  vs  $-3.9 \pm 3.9\%$ ,  $p=0.12$ ). MAT content of the lumbar spine did not change from baseline in the RYGB group but increased by  $20 \pm 27\%$  after SG ( $p=0.04$ ). There were no significant changes in femoral MAT content between and within groups.

Conclusion: RYGB may be associated with greater bone loss at the total hip than SG. Contrary to our hypothesis, vertebral MAT increased only after SG but not RYGB, despite marked declines in body weight in both groups.

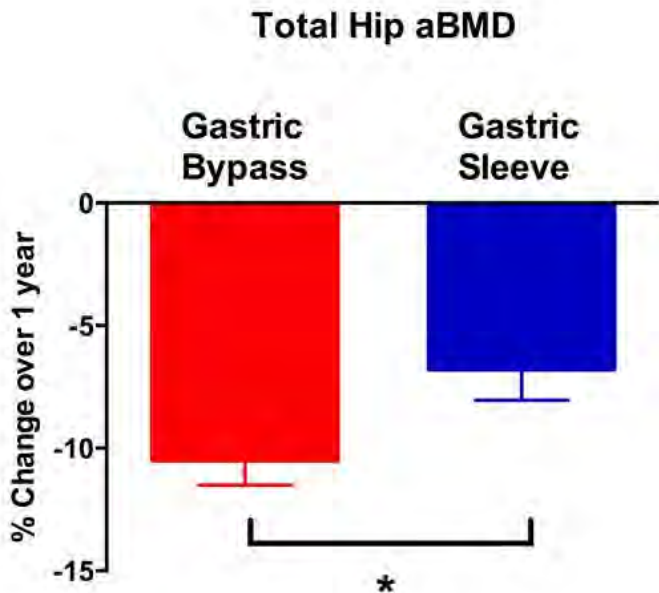


Figure: Change in total hip bone density after gastric bypass and gastric sleeve

Disclosures: Elaine Yu, None.

## SU0278

**Endocrine Manifestations of Systemic Mastocytosis in Bone.** Kamyar Asadipooya\*. Fellow in Endocrinology & Metabolism, NYU School of Medicine, United states

Endocrine Manifestations of Systemic Mastocytosis in Bone  
Kamyar Asadipooya, MD1, Patricia Freitas Corradi, MD, Loren Wissner Greene, MD, MA

1Kamyar Asadipooya MD, Fellow in Endocrinology and Metabolism, NYU Langone Medical Center, NYU School of Medicine

### Disease Overview:

Clonal, neoplastic proliferation of abnormal mast cells (MC) results in Systemic Mastocytosis (SM) when mast cells are found in one or more organ systems other than skin. Presence of multifocal clusters of abnormal mast cells is major criteria for diagnosis. Elevated serum tryptase, abnormal MC expression of CD25 and/or CD2, and presence of KIT D816V mutation are minor criteria for diagnosis.

### Manifestation and Diagnosis:

SM manifestations are attributed to the degree of mast cell proliferation, activation and degranulation. SM has a variable prognosis and presentation, from indolent to "smoldering" to life-threatening disease.

### Bone manifestations of SM include:

osteopenia with or without lytic lesion, osteoporosis with or without atraumatic fracture, osteosclerosis, and isolated lytic lesion.

Male sex, older age, higher bone resorption marker, lower DKK1, lower BMD, absence of urticaria pigmentosa, and alcohol intake are associated with fracture.

Table 1. Studies reporting fracture rate and risk factors in patients with mastocytosis in order of the year of publication

### Treatment:

Treatment of SM is generally palliative. Most therapy is symptom-directed; and, infrequently, chemotherapy for refractory symptoms is indicated. Antihistamines may alleviate some of the direct bone effects of histamine. Bisphosphonates including alendronate, clodronate, pamidronate and zoledronic acid are recommended as a first line treatment of SM and osteoporosis. Interferon  $\alpha$  may act synergistically with bisphosphonates.

Since elevations of RANKL and OPG have been reported in SM, denosumab might be effective for bone manifestations of SM.

Table 2. Reported treatment of osteoporosis in the patients with mastocytosis in order of the years of publication

Disclosures: Kamyar Asadipooya, None.

## SU0279

**Gene Expression Profiling of Osteoblastic Cells Cultured with Lithocholic Acid or Bilirubin. Implications in the Pathogenesis of Osteoporosis in Liver Diseases.** Silvia Ruiz-Gaspà\*<sup>1</sup>, Albert Parés<sup>2</sup>, Marta Dubreuil<sup>1</sup>, Andrés Combalia<sup>1</sup>, Pilar Peris<sup>1</sup>, Ana Monegal<sup>1</sup>, Nuria Gunañens<sup>1</sup>. <sup>1</sup>Metabolic Bone Diseases Unit, Department of Rheumatology, Hospital Clinic, University of Barcelona, IDIBAPS, CIBERehd, Barcelona, Spain, Spain, <sup>2</sup>Liver Unit, Hospital Clínic, University of Barcelona, IDIBAPS, CIBERehd, Barcelona, Spain., Spain

Low bone formation is considered to be the main feature in osteoporosis associated with cholestatic and end-stage liver diseases. Previous studies have demonstrated the deleterious consequences of retained substances such as lithocholic acid (LCA) and bilirubin (Bil) on osteoblastic cells. These effects are neutralized by ursodeoxycholic acid (UDCA). To gain new insights into cholestatic-induced osteoporosis, we have assessed the differential gene expression of osteoblastic cells under varied culture conditions.

The experiments were performed in human osteosarcoma cells (Saos-2), cultured with LCA (10 microM), Bil (50 microM) or UDCA (10/100 microM) at 2 and 24 hours. Expression of several signalling pathways and related bone genes were assessed by TaqMan microfluidic cards. The 88 genes covered a broad range of functional activities including apoptosis, osteoclast and osteoblast differentiation and mineralization and expression of genes involved in collagen synthesis and degradation, growth factors and vascularisation.

LCA up-regulated several genes, most of them involved in apoptosis (BAX, BCL10, BCL2L13, BCL2L14) but also MGP, BGLAP, SPP1 and CYP24A1, and down-regulated BMP3, BMP4 and DKK1. Parallel effects were observed by Bil, which up-regulated apoptotic genes and CSF2, and down-regulated antiapoptotic genes BCL2 and BCL2L1. Moreover, Bil down-regulated BMP3, BMP4, DPP1 and SMAD6. UDCA has specific consequences since differential expression was observed particularly at 100 microM up-regulating BMP2, BMP4, BMP7, CALCR, SPOCK3, SPP1 and DMP1, and down-regulating antiapoptotic genes and RANKL. UDCA down-regulated collagen genes with no changes in metalloproteinases. Furthermore, most of the differential expression changes induced by LCA and Bil were partially or completely neutralized by UDCA. No differential expression effects of LCA and Bil were observed regarding metalloproteinases, MAPKs, growth factors, vascularisation and oncogenes.

These observations reveal novel target genes, whose regulation by retained substances of cholestasis may provide new approaches for understanding the pathogenesis of osteoporosis in cholestatic and end-stage liver diseases.

Disclosures: Silvia Ruiz-Gaspà, None.

## SU0280

**Increase in Bone Mineral Density and Trabecular Bone Score in Graves' Disease After Anti-thyroid Medical Therapy.** So Young Ock<sup>1</sup>, Yong Jun Choi<sup>2</sup>, Yoon-Sok Chung\*<sup>2</sup>. <sup>1</sup>Kosin University, Korea, republic of, <sup>2</sup>Ajou University, Korea, republic of

### OBJECTIVES

The purpose of this study was to evaluate changes in bone quantity based on bone mineral density (BMD) and bone quality based on trabecular bone score (TBS) in Graves' disease patients after anti-thyroid medical therapy.

### RESEARCH DESIGN AND METHODS

This retrospective study included premenopausal female and male patients with Graves' disease who received BMD measurement more than two times during treatment. BMD and thyroid function tests with serum free T4, TSH (thyroid stimulating hormone) and TSH receptor antibody were collected two times as follow-up. TBS was calculated using TBS insight® software with DXA images.

### RESULTS

A total of 30 Graves' disease patients (17 males (56%) and 13 premenopausal females (44%)) with a mean age of  $35.3 \pm 9.9$  years were included. The mean follow-up period of subjects was  $20.7 \pm 8.5$  months. Levels of free T4, TSH and TSH receptor antibody improved at follow up ( $2.94 \pm 1.09$  ng/dL to  $1.33 \pm 0.28$  ng/dL,

0.03 ± 0.02 uIU/mL to 1.06 ± 0.96 uIU/mL, 31.77 ± 38.13 IU/L to 7.69 ± 6.39 IU/L,  $P < 0.001$ , respectively). Mean BMD (lumbar spine) values also improved from 1.110 ± 0.120 g/cm<sup>2</sup> to 1.149 ± 0.121 g/cm<sup>2</sup> ( $P = 0.001$ ) at follow-up. TBS increased from 1.364 ± 0.078 to 1.371 ± 0.092 after treatment as well ( $P = 0.001$ ).

#### CONCLUSION

Both bone density and quality improved after anti-thyroid treatment in premenopausal female and male Graves' disease patients.

**Disclosures:** Yoon-Sok Chung, None.

## SU0281

**Trabecular Bone score (TBS) and Bone Mineral Density in Recent Kidney Transplantation Patients.** Shogo Nakayama<sup>1</sup>, Eisuke Tomatsu<sup>1</sup>, Yasumasa Yoshino<sup>1</sup>, Izumi Hiratsuka<sup>1</sup>, Sahoko Sekiguchi-Ueda<sup>1</sup>, Megumi Shibata<sup>1</sup>, Taihei Itoh<sup>2</sup>, Hitomi Sasaki<sup>3</sup>, Midori Hasegawa<sup>4</sup>, Mamoru Kusaka<sup>3</sup>, Ryoichi Shiraki<sup>3</sup>, Takashi Kenmochi<sup>2</sup>, Yukio Yuzawa<sup>4</sup>, Kiyotaka Hoshinaga<sup>3</sup>, Atsushi Suzuki<sup>1</sup>. <sup>1</sup>Division of Endocrinology & Metabolism, Fujita Health University, Japan, <sup>2</sup>Department of Organ Transplant Surgery, Fujita Health University, Japan, <sup>3</sup>Department of Urology, Fujita Health University, Japan, <sup>4</sup>Division of Nephrology, Fujita Health University, Japan

**Background:** In kidney transplantation (KTx) recipients, pre-existing chronic kidney disease-mineral and bone disease (CKD-MBD) and other clinical risk factors such as hyperparathyroidism and glucocorticoid therapy would make osteoporosis as a serious problem. With progress of transplantation procedure and its safety, the number of preemptive KTx from living-donor has been increasing in Japan. In order to improve bone health after KTx, more precise assessment of CKD-MBD at KTx under current situation should be needed. However, extraskeletal calcification and bone deformity could interfere with precise assessment of bone mineral density (BMD) in the patients with CKD-MBD. In the present study, we estimated bone-related markers and bone mineral density (BMD) in short-term after KTx.

**Subjects and Methods:** This observational study was done in Fujita Health University Hospital, and post-KTx recipients in 2014 and 2015 were recruited (n=37, M/F=23/14, age 51 ± 14 years old). Serum samples were collected and lumbar and femoral neck BMD was measured before initial discharge after KTx (mean duration 22 ± 12 days). Single KTx was done in 26 cases, while other 11 cases with type 1 diabetes were performed simultaneous pancreas-kidney transplantation. Maintenance dialysis before KTx was done in 23 cases, whose median hemodialysis duration was 35 months (10-84, interquartile range). Their mean serum creatinine level after KTx was 1.31 ± 0.45 mg/dL.

**Result:** Median intact parathyroid hormone (iPTH), bone-specific alkaline phosphatase, tartrate-resistant acid phosphatase form 5b (TRACP 5b) were 100 pg/mL, 12.4 µg/L, 336 mU/dL, respectively. Mean BMD of lumbar spine evaluated by DXA was 0.94 ± 0.16 g/cm<sup>2</sup>, and their mean femoral neck BMD was 0.63 ± 0.12 g/cm<sup>2</sup>. TBS evaluated on lumbar spine (L1-L4) was 1.32 ± 0.08. Lumbar TBS score was significantly associated with lumbar BMD ( $p = 0.04$ ) but not with femoral neck BMD ( $P = 0.08$ ). When we compare each lumbar body TBS and its BMD, L1 TBS was related to L1 BMD, but other lumbar body TBS was not associated with each lumbar body BMD. On the other hand, both total and each lumbar body BMD were strongly associated with femoral neck BMD. **Conclusion:** We found that lumbar TBS was related to lumbar BMD, but its association with femoral neck BMD was not strong as lumbar BMD with femoral neck BMD in recent KTx patients.

**Disclosures:** Shogo Nakayama, None.

## SU0282

**Abaloparatide-SC has Minimal Effects in Subjects with Mild or Moderate Renal Impairment: Results from the ACTIVE Trial.** John P Bilezikian<sup>1</sup>, Gary Hattersley<sup>2</sup>, Gregory Williams<sup>2</sup>, Ming-Yi Hu<sup>2</sup>, Lorraine A Fitzpatrick<sup>2</sup>, Socrates Papapoulos<sup>3</sup>. <sup>1</sup>Columbia University College of Physicians & Surgeons, United states, <sup>2</sup>Radius Health, Inc., United states, <sup>3</sup>Leiden University Medical Center, Netherlands

**BACKGROUND:** ACTIVE was an 18-month, double-blind, active comparator trial in which 2463 postmenopausal women with osteoporosis were randomized to abaloparatide-SC, placebo or open-label teriparatide. Abaloparatide-SC significantly increased BMD and reduced fracture risk in vertebral, nonvertebral, clinical and major osteoporotic fractures compared to placebo.

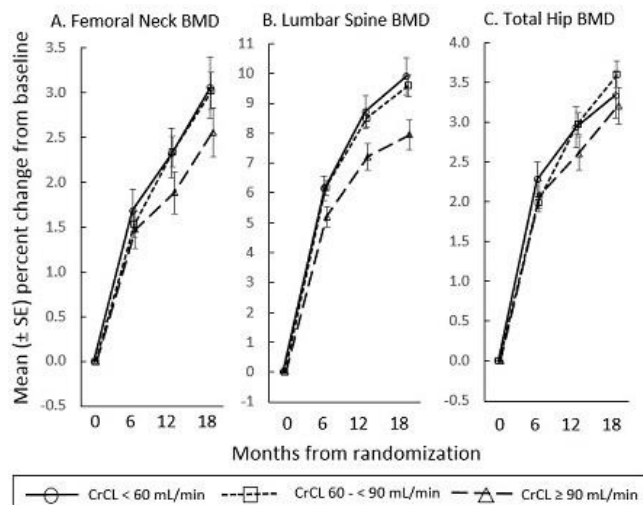
**METHODS:** Patients with significantly impaired renal function (creatinine >2.0 mg/dL or creatinine clearance (CrCl) by Cockcroft-Gault calculation <37 mL/min) were excluded. A post-hoc analysis evaluated the effect of renal function on safety and efficacy endpoints. There were 527 subjects with baseline CrCl <60 mL/min, 1276 with CrCl 60 to 90 mL/min, and 660 with CrCl of ≥90 mL/min.

**RESULTS:** Population PK analysis demonstrated increased exposure to abaloparatide-SC with increasing renal impairment. Despite the estimated increased exposure to abaloparatide-SC, there were no increases in adverse events or decreases in efficacy. Overall there were no meaningful differences in the percentage change from baseline in BMD among patients with differing baseline renal function; the mean percentage change in BMD in patients with a baseline CrCl ≥90 mL/min was slightly

less at the femoral neck and lumbar spine versus patients with baseline CrCl of 60 to 90 mL/min and 90 mL/min (Figure 1). This difference was less apparent for total hip BMD. Similarly, the incidence of treatment-emergent adverse events (TEAEs), serious TEAEs, related TEAEs, severe TEAEs, adverse events (AEs) leading to death or to study drug discontinuation were comparable among the different renal impairment groups. With the possible exception of anemia, nausea and hypercalcemia, there was no discernible pattern of increased incidence of TEAEs with worsening renal impairment. The incidences of hypercalcemia (either reported as an AE or defined as albumin-adjusted serum calcium level ≥10.7 mg/dL) generally increased with decreasing renal function in the abaloparatide-SC and teriparatide treatment groups. The incidence of hypercalcemia was lower for abaloparatide-SC than teriparatide overall ( $p = 0.006$ ) and within each renal function category. The higher incidence of hypercalcemia in the teriparatide group was significant compared to abaloparatide-SC in patients with CrCl <60 mL/min (10.9% vs 3.6%, respectively,  $p = 0.008$ ). A subset of patients underwent renal CT scans to assess kidney calcification. There was no evidence of increased calculi or soft tissue calcification in the abaloparatide-SC or teriparatide patients compared to placebo. Evaluation of AEs potentially associated with renal impairment in the entire study population showed no evidence of drug-induced renal impairment.

**CONCLUSIONS:** These results potentially support the use of abaloparatide-SC in patients with mild and moderate renal impairment.

Figure 1. BMD Changes by Renal Function (ITT Population in Abaloparatide-SC Treatment Group)



Renal CrCl and BMD with Abaloparatide-SC Treatment

**Disclosures:** John P Bilezikian, Merck, 12; Shire, 12; Radius Health, Inc, 12; Amgen, 12; Shire, 11

This study received funding from: Radius Health

## SU0283

**Effect of Recent Fracture on the PINP Response to Teriparatide in Postmenopausal Osteoporosis.** Richard Eastell<sup>1</sup>, John Kreege<sup>2</sup>, Damon Disch<sup>2</sup>, Fernando Marin<sup>2</sup>. <sup>1</sup>University of Sheffield, England, United Kingdom, <sup>2</sup>Eli Lilly & Company, United states

**Introduction & Objectives:** The response to teriparatide treatment may be assessed by serial measurements of the bone formation marker, procollagen I N-propeptide of type I collagen (PINP), where an increase of >10 µg/L is the least significant change. An uncertainty about PINP monitoring is whether increases in PINP during fracture healing might obscure a treatment response.

**Materials & Methods:** To test the hypothesis that PINP would increase in response to teriparatide in women with a recent fracture, data were used from the EUROFOR trial. The population was women (aged ≥55 years) with postmenopausal osteoporosis who had at least 1 documented vertebral or nonvertebral fragility fracture in the past 3 years. The women (N=752) were treated with teriparatide 20 µg/day (TPTD) by subcutaneous injection. Most had taken antiresorptive therapy in the past (n=574) although some were treatment naïve (n=178). Fracture frequency (FR) was defined as recent for a fracture within the last 6 months (n=331), not-so-recent for a fracture in the last 7 months to 12 months (n=148), and not recent as no fracture in the past 12 months (n=273). Total serum PINP (Roche Diagnostics) was measured at baseline, 1 month, and 6 months, and a response was defined as an increase from baseline >10 µg/L. The effects of prior antiresorptive therapy (AR), FR, time, and the interactions of these variables on PINP concentration and on response rate were analyzed by mixed model repeated measure.

**Results:** PINP increased consistently during TPTD treatment over time regardless of FR (interaction  $p > .2$ , Table). Statistically significant effects on PINP concentration were observed for AR (lower than naïve), time (higher after 1 month and even higher after 6 months of teriparatide), and FR (higher after recent fracture) (all  $p < .05$ ). An interaction between AR and time was observed, such that the baseline

PINP was lower and the incremental increase greater by 6 months after antiresorptive treatment (p<.05). At 6 months, the response rate was between 84% and 95% regardless of FR (Table). There were more responders at 6 months than 1 month (p=.002) regardless of FR (interaction p=.33). Response rates were not significantly affected by AR or FR (p>.2).

Conclusion: A PINP response to teriparatide can be identified even in patients with a recent fracture.

Table: Procollagen Type I N Propeptide (µg/L)

	Baseline		1 Month		6 Month	
	N	LS Mean* (SE)	N	LS Mean* (SE)	N	LS Mean* (SE)
<b>Previous antiresorptive</b>						
<b>Recent fracture</b>	232	39 (1.8)	224	79 (3.3)	183	172 (8.3)
<b>Not so recent fracture</b>	109	38 (2.6)	106	76 (4.7)	86	160 (11.9)
<b>No recent fracture</b>	233	28 (1.8)	225	66 (3.2)	193	159 (8.3)
<b>Naïve</b>						
<b>Recent fracture</b>	99	62 (2.7)	97	102 (5.0)	81	178 (12.7)
<b>Not so recent fracture</b>	39	54 (4.3)	39	92 (7.9)	29	171 (19.9)
<b>No recent fracture</b>	40	45 (4.3)	39	91 (7.8)	35	126 (19.8)

Abbreviations: Response Rate=PINP increase from baseline >10 µg/L. Recent fracture=fracture within the last 6 months; Not so recent fracture=fracture within past 6 to 12 months; No recent fracture=fracture from 12 to 36 months.

\*Least square mean from an MMRM analysis that included antiresorptive (AR) status, fracture recency status (FR), time, and all interactions in a repeated measures model. The AR by time interaction was significant (p=.026); the rest were not (p>.2). Time, AR, and FR status were significant (p<.001, .026, and p=.003, respectively).

Table

Disclosures: Richard Eastell, Eli Lilly & Company, 11  
This study received funding from: Eli Lilly & Company

### SU0284

**Fracture Incidence and Changes in Back Pain and Quality of Life in Patients with Osteoporosis Treated with Teriparatide: Results from the European Extended Forsteo® Observational Study (ExFOS).** Bente Langdahl<sup>1</sup>, Östen Ljunggren<sup>2</sup>, Eric Lespessailles<sup>3</sup>, George Kapetanios<sup>4</sup>, Tomaz Kocjan<sup>5</sup>, Nicola Napoli<sup>6</sup>, Tatjana Nikolic<sup>7</sup>, Pia Eiken<sup>8</sup>, Helmut Petto<sup>9</sup>, Thomas Moll<sup>10</sup>, Erik Lindh<sup>11</sup>, Fernando Marin<sup>12</sup>. <sup>1</sup>University Hospital, Aarhus, Denmark, <sup>2</sup>University Hospital, Uppsala, Sweden, <sup>3</sup>Orléans Hospital, France, <sup>4</sup>Papageorgiou General Hospital, Thessaloniki, Greece, <sup>5</sup>University Medical Centre, Ljubljana, Slovenia, <sup>6</sup>University Campus Bio-Medico, Rome, Italy, <sup>7</sup>University Hospital, Zagreb, Croatia, <sup>8</sup>University of Copenhagen, Denmark, <sup>9</sup>Eli Lilly, Europe, Austria, <sup>10</sup>Eli Lilly, Europe, Switzerland, <sup>11</sup>Eli Lilly, Europe, Sweden, <sup>12</sup>Eli Lilly, Europe, Spain

Background: The initial approved maximum treatment duration of teriparatide (TPTD) for postmenopausal osteoporosis (OP) in the EU was 18 months (mo). More recently, treatment duration was extended to 24 mo and new indications (male and corticoid-induced OP) were approved.

Objectives: To describe clinical fractures (Fx), back pain (BP) and quality of life (QoL) in patients with OP treated with TPTD for up to 24 mo and followed-up after TPTD was stopped.

Methods: Prospective, observational study in 8 EU countries. Clinical Fx data were summarized in 6-mo intervals and analyzed using logistic regression with repeated measures (RM). Contrasts were made between the odds of Fx in the first 6 mo of TPTD and each subsequent 6-mo period. Changes from baseline in QoL (EQ-5D<sup>TM</sup>) and BP 100-mm VAS were analysed using an RM model.

Results: There were 1531 patients (90.7% female) with post-baseline data (TOTAL), 1455 of them received ≥1 dose of TPTD (TREAT). At baseline, mean (SD) age was 70.3 (9.8) yrs, 85.4% of patients had previous OP Fx (54.6% with ≥2 spine Fx). Only 11.4% were OP-treatment naïve. During the TPTD treatment phase 103/1455 (7.1%) patients had ≥1 Fx in the TREAT cohort. Odds of Fx was highest in the first 6 mo (0.031) and was reduced in all subsequent 6-mo intervals; thus, a 52% decrease in Fx risk was observed in the >18- to 24-mo period (odds of Fx: 0.015) compared with the first 6-mo period (p=0.013). During the combined TPTD treatment period and the follow-up period (up to 111 mo), 179/1531 (11.7%) patients sustained ≥1 Fx in the TOTAL cohort. Most patients (98.9%) received anti-OP drugs, mainly bisphosphonates (51.4%) or denosumab (22.3%) at some point after stopping TPTD. Odds of Fx continued to numerically decrease up to 60 mo of follow-up compared with the first 6 mo of TPTD treatment. In the TOTAL cohort, BP VAS was reduced at each 3-mo interval from baseline (least squares [LS] means: -9.9 and -20.9 mm at 3 and 48 mo respectively, p<0.001). Mean EQ-5D VAS increased (LS means:

+5.1 and +12.1 mm at 3 and 48 mo, p<0.001). Both improvements were sustained after stopping TPTD.

Conclusion: In a real-life clinical setting in patients with severe OP, the risk of clinical Fx decreased significantly during 24 mo of TPTD treatment. This was associated with a reduction in BP and improvements in QoL, and these changes were maintained for up to 24 mo after TPTD termination. Results should be interpreted in the context of a non-controlled observational study.

Disclosures: Bente Langdahl, Eli Lilly, Merck, Amgen and UCB, 13; Eli Lilly, Novo Nordisk, and Orkla Health, 11  
This study received funding from: Eli Lilly and Company

### SU0285

**Bone Microarchitecture After Discontinuation of Denosumab in Postmenopausal Women with Low Bone Mass.** E Seeman<sup>1</sup>, R Zebaze<sup>1</sup>, JR Zanchetta<sup>2</sup>, DA Hanley<sup>3</sup>, A Wang<sup>4</sup>, C Libanati<sup>5</sup>, RB Wagman<sup>4</sup>. <sup>1</sup>Austin Health, University of Melbourne, Australia, <sup>2</sup>Instituto de Investigaciones Metabólicas, Argentina, <sup>3</sup>University of Calgary, Health Sciences Centre, Canada, <sup>4</sup>Amgen Inc., United states, <sup>5</sup>UCB Pharma, Belgium

Introduction: Cessation of denosumab (DMAB) results in increased remodeling and bone loss. Fracture rates are no higher than placebo (PBO) after stopping DMAB (Brown *JBM* 2013) but ~35% of the women received antiresorptives. Case reports of vertebral fractures raise concerns that release from RANKL inhibition after stopping DMAB results in rapid microstructural deterioration (Aubry-Rozier; Popp; Anastasilakis; *Osteoporos Int* 2015). The aim of this study was to quantify any microarchitecture changes following cessation of DMAB. Methods: Women completing a 12-month PBO controlled study of the effects of DMAB on microarchitecture (NCT00293813) for whom ≥12 months had elapsed since the end-of-study visit were eligible for this new study (NCT00890981) provided they remained untreated. They had a single follow-up measurement of distal radius and distal tibia microstructure using HR-pQCT and forearm BMD using DXA. The primary endpoint was the percent change in distal radius cortical thickness relative to the baseline of the parent study. Secondary endpoints were trabecular morphology, BMD, and CTx and PINP levels. Analysis of covariance included age, baseline values, effects of treatment in the parent study, time since last dose of DMAB or PBO. Results: Forty and 39 subjects had received DMAB or PBO 6 monthly, respectively. Mean (SD) age was 63.7 (6.1) years; mean (SD) time since the last DMAB or PBO dose (scheduled at 6 months) was 32.1 (2.6) months. After stopping DMAB, the increases in cortical thickness at the radius were lost but cortical thickness remained above the previous PBO group (p=0.077, table). The gain in cortical vBMD achieved with DMAB in the parent study was also attenuated; however, cortical vBMD remained higher than the former PBO group (p=0.023, table). Trabecular vBMD increased similarly in both groups. Results at the tibia were similar. Radial BMD (by DXA) also decreased but remained higher in former DMAB than former PBO groups: 2.1% at the 1/3 distal radius (p=0.018), 2.1% at the total radius (p=0.004), and 1.6% at the ultradistal radius (p=0.091). Conclusion: Discontinuation of DMAB reverses the benefits achieved in microstructure and BMD. The increase in trabecular vBMD is probably an artifact produced by intracortical remodeling trabecularising the cortex. Several traits remain higher than had no treatment been given. If benefits of DMAB are to be retained treatment needs to be continued or followed by an alternative antiresorptive.

Percent Change From Baseline of the Parent Study in HR-pQCT Parameters at the Distal Radius at 32 Months After the Last Dose in the Parent Study

HR-pQCT Measurement	% Change From Baseline LS Mean (95% CI)	% Difference Relative to Placebo LS Mean (95% CI)	P-value*
<b>Cortical thickness</b>			
Placebo (n=39)	-5.5 (-6.3, -2.8)	3.7 (-0.4, 7.8)	0.077
Denosumab (n=37)	-1.8 (-4.8, 1.2)		
<b>Cortical vBMD</b>			
Placebo (n=39)	-1.0 (-1.7, -0.3)	0.9 (0.1, 1.7)	0.023
Denosumab (n=37)	-0.03 (-0.8, 0.8)		
<b>Trabecular vBMD</b>			
Placebo (n=39)	5.1 (2.3, 8.0)	0.7 (-2.5, 4.0)	0.656
Denosumab (n=37)	5.9 (2.8, 9.0)		
<b>Total vBMD</b>			
Placebo (n=39)	-1.2 (-2.6, 0.2)	1.5 (-0.6, 3.5)	0.165
Denosumab (n=37)	0.3 (-1.2, 1.7)		

\*Not adjusted for multiplicity

Table

Disclosures: E Seeman, Amgen, Allergan, Asahi, Merck Sharp & Dohme, Sanofi, and StraxCorp, 15; Amgen, Asahi, Genzyme, and Warner-Chilcott, 11  
This study received funding from: Amgen Inc.

## SU0286

**Denosumab (DMAb) and Total Lean body Mass: Exploratory Analyses from the FREEDOM Study.** Yves Rolland<sup>1</sup>, Philippe de Souto Baretto<sup>1</sup>, Matteo Cesari<sup>1</sup>, Lisa Hamilton<sup>2</sup>, Michel Réglade<sup>3</sup>, Nico Panacciuoli<sup>4</sup>, Lama Kalouche-Khalil<sup>5</sup>. <sup>1</sup>Gérontopôle, Centre Hospitalier Universitaire de Toulouse (Pr Bruno Vellas), France, <sup>2</sup>Amgen Ltd., United Kingdom, <sup>3</sup>Amgen France, France, <sup>4</sup>Amgen Inc, United states, <sup>5</sup>Amgen (Europe) GmbH, Switzerland

## Purpose

DMAb is approved for use in postmenopausal women with osteoporosis at increased or high risk of fracture. In the placebo (PBO)-controlled FREEDOM study DMAB was nominally associated with a reduction in falls (6.4% of DMAB patients reported at least one fall vs 5.3% of PBO patients,  $p=0.023$  [data on file]; when excluding falls associated with fracture: 5.7% vs 4.5%,  $p=0.02$  [Cummings, 2009]). Non-clinical evidence indicates that inhibition of the RANK pathway may have a positive effect on skeletal muscle function (Dumont, 2014; Wang, 2014). Using data from FREEDOM and the dual-energy x-ray absorptiometry (DXA) substudy (Cummings, 2009; Bolognese, 2013), we tested the hypothesis that RANKL inhibition by DMAB contributed to the reduction in falls observed in FREEDOM via improved muscle mass and strength.

## Methods

Total body (without head) lean mass, a surrogate for muscle mass (Cesari, 2015), was measured from DXA scans performed annually. Eight items from the Osteoporosis Assessment Questionnaire-Short Version (OPAQ-SV), completed in the FREEDOM study at baseline and every 6 months for 36 months, which focus on the number of days (no, few, some, most or all) patients are able to perform tasks requiring muscle strength were also used as surrogates for muscle function.

## Results

In total, 441 women participated in the DXA substudy (232 DMAB, 209 PBO). Patient demographics were balanced across treatment groups (mean [SD] age 73 [5] years in both groups; mean (SD) BMI: DMAB, 25.4 [4.4] kg/m<sup>2</sup>, PBO, 25.2 [4.2]) and similar to those of the overall FREEDOM study (Bolognese, 2013). Mean (SD) baseline total body lean mass was similar across treatment groups; at months 12, 24 and 36, the least-squares estimate (SE) of the percent change from baseline did not differ between the two groups (Table). There was no difference between treatment groups in strength-related OPAQ-SV responses (data not shown).

## Conclusions

Our data do not support the hypothesis that RANKL inhibition by DMAB contributed to the reduction in falls observed in FREEDOM via improved muscle mass and strength. Further research regarding the possible effect of RANKL inhibition on skeletal muscle function may be warranted.

## Acknowledgements

FREEDOM was funded by Amgen; Claire Desborough of Amgen (Europe) GmbH provided writing assistance for this abstract.

	DMAB	PBO	DMAB-PBO
Baseline total body lean mass, g			
N	176	160	
Mean (SD)	35156 (4526.7)	34842 (4485.1)	
Percent change from baseline at Month 12			
N	164	146	
LS Mean (SE/95% CI)*	-0.5 (0.3)	-0.1 (0.3)	-0.4 (-1.1, 0.4)
Percent change from baseline at Month 24			
N	155	135	
LS Mean (SE)	-0.5 (0.3)	-0.4 (0.3)	-0.2 (-1.0, 0.7)
Percent change from baseline at Month 36			
N	136	122	
LS Mean (SE)	-0.5 (0.3)	-0.4 (0.4)	-0.2 (-1.3, 0.6)

\*SE presented for DMAB and PBO, 95% CI presented for DMAB-PBO; "-" not calculated.

LS, least squares; n, number of patients with data at the relevant time point; SE, standard error.

Table. Total body lean mass

**Disclosures:** Yves Rolland, Amgen, Pfizer, 15; Lactalis, Nestlé, Nutricia, Lilly, 11 This study was funded by Amgen.

## SU0287

**Influence of glucocorticoids on effect of denosumab on osteoporosis in patients with Japanese rheumatoid arthritis; 12 months of follow-up ~a Multicenter Registry Study~.** Yasuhide Kanayama<sup>1</sup>, Yuji Hirano<sup>2</sup>, Nobunori Takahashi<sup>3</sup>, Shuji Asai<sup>3</sup>, Naoki Ishiguro<sup>3</sup>, Toshihisa Kojima<sup>3</sup>. <sup>1</sup>Toyota Kosei Hospital, Japan, <sup>2</sup>Toyoashi Municipal Hospital, Japan, <sup>3</sup>Nagoya University Hospital, Japan

## [Objectives]

To investigate the efficacy of DMB for 12 months on glucocorticoid-induced OP in Japanese RA patients.

## [Methods]

Patients with a diagnosis of RA according to the 2010 ACR/EULAR criteria who had been prescribed DMB from Tsurumi Biologics Communication Registry

(TBCR)-BONE between October 2013 and April 2015 were enrolled. The final study cohort of 81 patients received continuous DMB therapy more than 12 months. The DMB dose was 60mg at once every 6 months. In all cases native or activated vitamin D has been used.

We reviewed the results for 6 and 12 months about the increase and decrease of bone mineral density(BMD) of lumbar spine(LS) and total hip(TH) by DEXA and bone turnover markers, intact n-terminal propeptide type I procollagen(PINP) and tartrate-resistant acid phosphatase form 5b(TRACP-5b).

## [Results]

In the patients receiving oral prednisolone group(n=29, R-PSL) and not receiving group(n=52, N-PSL), the number of female was each 27(93%) and 50(96%) cases( $p=0.544$ ). The mean age was 68.8 ± 7.9 and 71.0 ± 7.3 years old ( $p=0.317$ ); disease duration was 15.2 ± 10.0 and 16.2 ± 13.4 years ( $p=0.894$ ); the body mass index was 20.2 ± 3.6 and 19.8 ± 2.8 ( $p=0.832$ ) and the FRAX was 33.4 ± 18.3 and 22.3 ± 13.2 ( $p=0.006$ ). Clinical findings related to RA and OP at baseline were as follows; CRP 1.1 ± 1.3 and 0.5 ± 1.0 mg/dl( $p=0.022$ ); DAS-CRP 3.17 ± 1.15 and 2.45 ± 1.16( $p=0.004$ ); m-HAQ 1.17 ± 0.90 and 0.79 ± 0.79( $p=0.059$ ); PINP 61.0 ± 35.1 and 53.8 ± 31.6 µg/l( $p=0.855$ ); TRACP-5b 503 ± 237 and 492 ± 213 mU/dL ( $p=0.855$ ); LS-BMD 0.85 ± 0.18 and 0.82 ± 0.16 g/cm<sup>2</sup>( $p=0.310$ ) and TH-BMD 0.60 ± 0.10 and 0.60 ± 0.08 g/cm<sup>2</sup> ( $p=0.944$ ). The rate of decreased PINP from baseline to 6 and 12 months were each -33.4% vs -38.4% ( $p=0.694$ ) at 6 month and -17.9% vs -40.5% ( $p=0.234$ ) at 12 month and TRAC-5b were -31.9% vs -33.4% ( $p=0.581$ ) at 6 month and -24.1% vs -29.8% ( $p=0.645$ ) at 12 month in the R-PSL group vs N-PSL group.

The rate of increased LS-BMD from baseline to 6 and 12 months were each 3.6% vs 4.5% ( $p=0.317$ ) at 6 month and 4.7% vs 6.8% ( $p=0.163$ ) at 12 month and TH-BMD were 3.3% vs 2.7% ( $p=0.551$ ) at 6 month and 3.9% vs 3.3% ( $p=0.784$ ) at 12 month in the R-PSL group vs N-PSL group (Fig.1).

The rate of patients who did not increase LS-BMD and TH-BMD for 12 months were each 10.7% vs 8.0% ( $p=0.687$ ) and 15.4% vs 8.0% ( $p=0.320$ ) in the R-PSL group vs N-PSL group.

## [Conclusion]

DMB was effective in OP of RA patients. Glucocorticoids use did not influence the efficacy of DMB in the short period of 6 and 12 months.

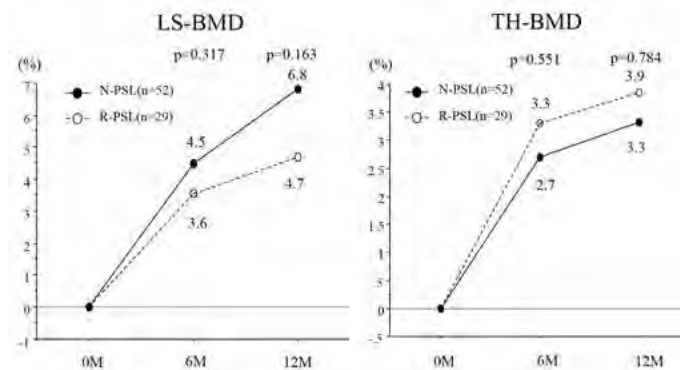


Figure 1: The rate of increased LS-BMD and TH-BMD from baseline to 6 and 12 month

Figure1

**Disclosures:** Yasuhide Kanayama, None.

## SU0288

**Monthly Oral Ibandronate 100mg Is as Effective as Monthly Intravenous Ibandronate 1mg in Patient Subgroups of the MOVEST Study.** Masako Ito<sup>1</sup>, Toshitaka Nakamura<sup>2</sup>, Hiroshi Hagino<sup>3</sup>, Junko Hashimoto<sup>4</sup>, Yoshihiro Asao<sup>4</sup>, Masao Yamamoto<sup>4</sup>, Koichi Endo<sup>4</sup>, Kyoko Katsumata<sup>4</sup>, Rumiko Matsumoto<sup>5</sup>, Tetsuo Nakano<sup>6</sup>, Hideki Mizunuma<sup>7</sup>. <sup>1</sup>Nagasaki University, Japan, <sup>2</sup>National Center for Global Health & Medicine, Japan, <sup>3</sup>Tottori University Faculty of Medicine, Japan, <sup>4</sup>Chugai Pharmaceutical Co. Ltd., Japan, <sup>5</sup>Taisho Pharmaceutical Co. Ltd., Japan, <sup>6</sup>Tamana Central Hospital, Japan, <sup>7</sup>Hirosaki University, Japan

**Purpose:** The phase III MOVEST study evaluated the efficacy and safety of monthly oral ibandronate (IBN) 100mg in comparison with monthly intravenous (IV) IBN 1mg for Japanese patients (pts) with primary osteoporosis. Mean relative changes from baseline in lumbar spine (LS; L2-L4) bone mineral density (BMD) at 12 months showed non-inferiority of oral to IV IBN. BMD gains at the total hip and femoral neck were also confirmed (Nakamura T, et al. Osteoporos Int 2015). Here we present subgroup analyses of the study.

**Methods:** 422 Japanese pts, aged ≥55 years, with primary osteoporosis were randomized to receive monthly oral IBN 100mg plus monthly IV placebo, or monthly IV IBN 1mg plus monthly oral placebo. We assessed LS BMD gains in the following subgroups: LS BMD T-score at screening (≥ -3.0 or < -3.0), prevalent vertebral fracture (yes or no), age (<75 or ≥75 years), baseline vitamin D (25OHD) levels (<20 or ≥20ng/mL), bisphosphonate (BP) treatment history (yes or no), and prior osteoporosis drug treatment other than BP (yes or no).

Results: The per-protocol set comprised 372 pts, 183 pts receiving oral IBN and 189 pts receiving IV IBN. In pts with LS BMD T-score  $\geq -3.0$  or  $< -3.0$  at screening, BMD gains were 4.42% and 5.79%, respectively, with oral IBN and 4.60% and 5.83%, respectively, with IV IBN. In pts with or without prevalent vertebral fractures, BMD gains were 5.21% and 5.23%, respectively, with oral IBN and 5.01% and 5.49%, respectively, with IV IBN. In pts aged  $<75$  or  $\geq 75$  years, BMD gains were 5.46% and 4.51%, respectively, with oral IBN and 5.25% and 5.77%, respectively, with IV IBN. In pts with baseline 25OHD levels  $<20$  or  $\geq 20$ ng/mL, BMD gains were 4.76% and 5.35%, respectively, with oral IBN and 6.57% and 5.05%, respectively, with IV IBN. In pts with or without prior BP treatment, and pts receiving osteoporosis drug treatment other than BP, BMD gains were similar to the above-mentioned results. There were no apparent differences in the safety profiles of the two treatment groups.

Conclusion: We showed that monthly oral IBN 100mg could be as effective as monthly IV IBN 1mg by subgroup analysis. Monthly oral IBN 100mg demonstrated comparable BMD gains as IV IBN 1mg in pt subgroups defined by baseline BMD, vertebral fracture, age, 25OHD levels, and prior osteoporosis treatment. These data suggest that oral IBN shows high utility in the lifestyle and disease conditions associated with osteoporosis in Japanese pts.

**Disclosures:** Masako Ito, Chugai Pharmaceutical Co. Ltd., 12; Daiichi Sankyo Inc., 12; Chugai Pharmaceutical Co. Ltd, 12; Asahi Kasei Pharma Corp., 12; Astellas Pharma Inc., 12; Ono Pharmaceutical Co. Ltd, 12  
This study received funding from: Chugai Pharmaceutical Co. Ltd

**SU0289**

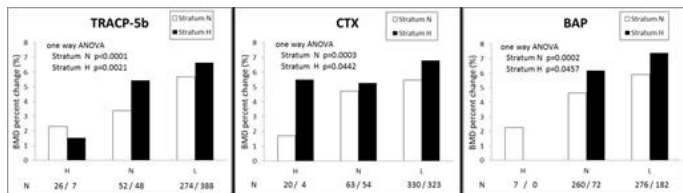
**Relationship Between Suppression of Bone Turnover Markers and Future Increase in Bone Mineral Density in Risedronate Treatment.** Taro Mawatari<sup>1</sup>, Ryoichi Muraoka<sup>2</sup>, Yukihide Iwamoto<sup>3</sup>. <sup>1</sup>Hanamomachi Hospital, Japan, <sup>2</sup>EA Pharma Co., Ltd., Japan, <sup>3</sup>Department of Orthopaedic Surgery, Kyushu University, Japan

Purpose: While bone turnover markers (BTMs) are useful to monitor response and adherence to osteoporosis treatment, the relationship between risedronate-related suppression of BTMs and future increase in bone mineral density (BMD) has not been fully established yet. This relationship was examined in detail by the sub-analysis for the data from the risedronate 75 mg once monthly Japanese phase III trial.

Methods: This Study included 788 postmenopausal women with osteoporosis who had measurements of vertebral BMD, BTMs (serum TRACP-5b (tartrate-resistant acid phosphatase 5b), urinary CTX (C-terminal cross-linking telopeptide of type I collagen), and serum BAP (bone alkaline phosphatase)). The subjects were stratified into two strata, depending on whether the BTMs at baseline were higher than upper limit of normal (ULN) [Stratum H] or not [Stratum N]. Furthermore, the subjects were divided into three subgroups according to the change in BTMs at 3 months: Group L (reduction more than minimal significant change (MSC)), Group N (change within MSC), and Group H (elevation more than MSC). The ULN and MSC of BTMs was defined as 420 mU/dL and 12.4% for TRACP-5b, 301.4µg/mmolCr and 23.5% for CTX and 29.0 U/L and 23.1% for BAP. Percent change in BMD at 12 months was compared among subgroups and strata mentioned above.

Results: BMD increased in both strata and in all groups, while the average BMD gain in Group L was significantly greater than that in the other two groups in both strata. BMD in Stratum H and in Group L increased more than that in Stratum N and in Group L on all BTMs. The difference between two strata's BMD gain in Group L on TRACP-5b, CTX and BAP was 0.95%, 1.33% and 1.49%, respectively.

Conclusions: BMD in Group L increased significantly compared with that in the other Groups by risedronate treatment for 12 months regardless of initial bone turnover, while the BMD gain was the greatest when BTMs are more than ULN at baseline. These results suggest that monitoring BTMs at baseline and at 3 months after initiation of risedronate treatment may be useful in predicting future BMD gain.



Figure

**Disclosures:** Taro Mawatari, None.

**SU0290**

**Safety, Pharmacokinetics, and Changes in Bone Metabolism Associated with Zoledronic Acid Treatment in Japanese Patients with Primary Osteoporosis.** Satoshi Tanaka<sup>1</sup>, Masataka Shiraki<sup>2</sup>, Hiroaki Suzuki<sup>1</sup>, Satoko Ueda<sup>1</sup>, Toshitaka Nakamura<sup>3</sup>. <sup>1</sup>Asahi Kasei Pharma corporation, Japan, <sup>2</sup>Research Institute & Practice for Involutional Diseases, Japan, <sup>3</sup>Gotanda Rehabilitation Hospital, Japan

Zoledronic acid (ZOL) is used as yearly intravenous infusion in many countries. ZOL is anticipated to be approved for clinical use in Japan in near future. In order to

investigate the pharmacokinetics of ZOL and assess the safety of and changes in bone metabolism associated with ZOL treatment in Japanese patients, this single-administration study was conducted.

This one-year, single-blinded, parallel-group study included 24 female Japanese patients (45-79 years) who had been diagnosed with primary osteoporosis. The patients were randomly allocated to either a 4- or 5-mg group, with baseline CrCl levels balanced between the groups. All the patients were also given daily oral calcium (460 mg) and vitamin D (10.0 µg). The following bone turnover markers were measured: i-OC, BAP, PINP, TRACP-5b, s-NTx, DPD, and serum sclerostin. ECG parameters (heart rate, RR, QRS, QT, and QTc) and body temperature were measured and included in the safety assessments.

As the result, mean plasma concentrations of zoledronic acid peaked in both groups immediately after administration, and decreased to  $\leq 1\%$  of peak levels after 24 h. Non-compartmental analysis revealed that  $C_{max}$  increased in proportion to the dose ( $370 \pm 78.5$  and  $471 \pm 76.1$  ng/mL in the 4- and 5-mg groups, respectively). In both groups, bone resorption markers (TRACP-5b, s-NTx, DPD) decreased from Day 15 after administration, and bone formation markers (i-OC, BAP, PINP, ucOC) decreased from 3 months after administration. Most of the bone markers could maintain the levels at 12 month lower than pre-treatment levels. Drug-related adverse events occurred in seven and 10 subjects in the 4- and 5-mg groups, respectively. The most frequent drug-related adverse event was pyrexia, occurred in 4 and 5 subjects in the 4- and 5-mg groups, respectively. Most of the adverse events occurred 1 to 3 days after administration, and resolved within 7 days of onset. Body temperature increased by  $0.88 \pm 0.74^\circ\text{C}$  in the 4-mg group 24 h after administration, and by  $1.00 \pm 0.79^\circ\text{C}$  in the 5-mg group, then returned to baseline levels by Day 4. No major variations were evident in ECG parameters. No serious adverse events were reported.

In conclusion, this study demonstrated acceptable pharmacokinetics and changes in bone metabolism associated with zoledronic acid treatment in Japanese osteoporosis patients. Both 4- and 5-mg doses demonstrated acceptable safety and sustained antiresorptive effects for the duration of the study.

**Disclosures:** Satoko Ueda, Asahi Kasei Pharma Corporation, 15  
This study received funding from: Asahi Kasei Pharma Corporation

**SU0291**

**The Incidence and Predictors of Acute Phase Response to Zoledronic Acid in Asian compared to Non-Asian Women in the HORIZON Pivotal Fracture Trial..** Dennis M. Black<sup>1</sup>, Anne Schafer<sup>2</sup>, Tiffany Kim<sup>3</sup>, Jane A. Cauley<sup>4</sup>, Satoko Ueda<sup>5</sup>, Ian R. Reid<sup>6</sup>. <sup>1</sup>Department of Epidemiology & Biostatistics, University of California San Francisco, United states, <sup>2</sup>University of California, San Francisco & the San Francisco VA Medical Center, United states, <sup>3</sup>VA Medical Center San Francisco, United states, <sup>4</sup>Department of Epidemiology, University of Pittsburgh, United states, <sup>5</sup>Asahi-Kasei, Japan, <sup>6</sup>Department of Medicine, University of Auckland, New Zealand, New Zealand

Zoledronic acid (ZOL) is a bisphosphonate used as an annual infusion internationally to treat osteoporosis. The HORIZON-PFT study was a randomized, double-blind, placebo-controlled study in 7765 osteoporotic women who received either ZOL 5 mg or placebo (PBO) for 3 years and showed ZOL reduced vertebral, hip, and non-vertebral fractures. The study also confirmed that women on ZOL developed acute phase response (APR), including pyrexia and myalgia, within 3 days of ZOL administration about 3 times more commonly than on PBO. Subsequent analyses suggested that APR was more common in Asian women. In anticipation of ZOL approval in Japan in 2016, this analysis aimed to explore the incidence and predictors of APR in 1089 women from 19 Asian sites (in China, Hong Kong, Korea, Taiwan and Thailand) compared to women at 216 other study sites outside Asia.

APR was defined as any MedDRA preferred term occurring  $<3$  days after the first infusion which differed significantly by treatment group. We compared APR incidence in Asians to non-Asians within ZOL and placebo (PBO) groups and compared relative risks (ZOL vs. PBO) in the two subgroups. We then studied baseline APR predictors in Asians and non-Asians separately within ZOL and PBO using logistic regression. Baseline predictors analyzed included age, hip BMD, fracture history, weight, BMI, activity, medication use and medical conditions.

APR was more frequent in Asian vs. non-Asian women on ZOL (62% vs 39%). However, APR was also more frequent in Asian vs. non-Asian women on PBO (22% vs. 10%). The relative risks (RR) for APR for ZOL vs. PBO were similar in Asian (RR=2.8,  $p<.001$ ) compared to non-Asian women (RR=3.8,  $p<.001$ ).

Among Asian women, significant predictors of lower APR incidence on ZOL included older age, prevalent vertebral fracture (VFX), prior bisphosphonate (BP) use, calcitonin use and smoking. Among non-Asian women, predictors of lower APR in women on ZOL included older age, VFX, prior BP, current calcitonin use, lower activity, hypertension and lower creatinine clearance. Weight, BMI and BMD were not predictive for either group.

In summary, the incidence of APR symptoms among Asians is higher in both the placebo and ZOL groups compared to non-Asians, suggesting some cultural differences in APR symptom reporting. However, the relative risks for ZOL vs. PBO are similar in Asians vs. non-Asians suggesting that APR with ZOL is actually similar in the two populations.

**Disclosures:** Dennis M. Black, Asahi-Kasei, 12  
This study received funding from: Novartis, Asahi-Kasei

## SU0292

**Adherence to Osteoporosis Treatment in Patients with Lifestyle Related Diseases.** Satoshi Sasaki<sup>\*1</sup>, Naohisa Miyakoshi<sup>2</sup>, Michio Hongo<sup>2</sup>, Yuji Kasukawa<sup>2</sup>, Yoichi Shimada<sup>2</sup>. <sup>1</sup>Higashinaruse national health insurance clinic, Japan, <sup>2</sup>Akita University Graduate School of Medicine, Japan

**Purpose:** Starting and continuous rate of osteoporosis treatment is still insufficient in Japan. Alternatively, the patients who had lifestyle related diseases keep a regular schedule on going to the clinic and taking medicine. If these patients show good adherence to additional osteoporosis medication, it is convenient from the view point of preventing fragility fracture and cost effectiveness. Therefore, the purpose of this study was to investigate the adherence to osteoporosis treatment between the patients who were treated with and without a treatment for lifestyle related diseases retrospectively.

**Methods:** Sixty-eight patients (3 men and 65 women; mean age, 79.8 years) who were initiated a treatment for osteoporosis from 2013 to 2014 in our clinic were enrolled in this study. The subjects were divided into two groups; 1) patients treated for osteoporosis and lifestyle related diseases (LRD, n = 44, average age 80.3 years) and 2) patients treated for osteoporosis only (OP, n = 24, average age 78.7 years). The contents of LRD and OP group were as follows, weekly bisphosphonates (BP) were 21 and 7, monthly BP were 13 and 6, activated vitamin D were 3 and 2, raloxifene were 1 and 2, 1 teriparatide and 1 denosumab were included only OP group, combined therapy was selected 6 and 5 patients, respectively. Adherence of treatment for osteoporosis and treatment duration were investigated and compared between the two groups.

**Results:** The total number of dropped out patients was 9, which were 3 cases in LRD group and 6 cases in OP group. The rate of continuous treatment in LRD group (93.2%) was significantly higher than that in OP group (75.0%) ( $p = 0.03$ ). Treatment duration was not significantly different between the groups.

**Conclusions:** Adherence to osteoporosis treatment reduces to approximately 70% after 2 years without any efforts for continuous treatment. However, patients who had already been treated for lifestyle related disease have good adherence in regard to additional medication. Thus, we might consider these patients as good target for osteoporosis treatment because of their good adherence to medication.

**Disclosures:** Satoshi Sasaki, None.

## SU0293

**Long-Term Persistence with Osteoporosis Therapies among Postmenopausal Women in a Commercially-Insured Population in the United States.** Emily Durden<sup>1</sup>, Lionel Pinto<sup>\*2</sup>, Lorena Lopez-Gonzalez<sup>1</sup>, Paul Juneau<sup>1</sup>, Richard Barron<sup>3</sup>. <sup>1</sup>Truven Health Analytics, United states, <sup>2</sup>Amgen Inc., United states, <sup>3</sup>Amgen Inc, United states

**PURPOSE:** Short-term (one year) persistence with osteoporosis therapy is generally poor and tends to vary by treatment type. While one-year persistence data is widely published, longer-term persistence with osteoporosis therapies is unknown. This study evaluates long-term (up to 24 months) persistence with available osteoporosis therapies among postmenopausal women in the US.

**METHODS:** Females  $\geq 50$  years of age newly initiating denosumab, raloxifene, teriparatide, zoledronic acid or an oral bisphosphonate between 1/1/2012 and 12/31/2012 were identified from the MarketScan<sup>®</sup> Commercial and Medicare databases (index date = qualifying claim date). Patients were required to have  $\geq 14$  months of pre- and  $\geq 24$  months of post-index continuous enrollment. The study population was stratified according to index treatment and dosing frequency. Persistence, indicated by continuous use of the index therapy without a gap  $> 60$  days, was assessed over 12 and 24 months. Multivariable logistic regression was used to compare persistence across treatment/dosing regimens, adjusting for differences baseline demographic and clinical characteristics.

**RESULTS:** 43,543 women initiating a new therapy (mean [SD] age: 65 [10] years) were identified. The overall rate of persistence was lower at 24 months (26.6%) than at 12 months (48.4%), but the trends by treatment/dosing regimen were similar. Persistence was generally higher among patients treated with IV (except ibandronate IV Q3M) and SC than oral formulations. Rates of persistence varied from 19.4% for ibandronate IV Q3M users, 19.6 – 23.7% for oral bisphosphonate users, 30.6% for raloxifene QD users, 33.9% for zoledronic acid annual IV users, 40.8% for teriparatide SC users, and 41.2% for denosumab SC users ( $P < 0.0001$ ). Patients initiating oral bisphosphonates (except risedronate QD), raloxifene or zoledronic acid IV had significantly lower odds of being persistent at 24 months compared to those initiating denosumab; the odds of persistence at 24 months for patients treated with teriparatide were not significantly different from denosumab users (Table 1).

**CONCLUSION:** Although, in general, 24-month persistence with osteoporosis therapies trended lower than 12-month persistence, patients initiating denosumab SC had higher persistence over 24 months compared to those initiating oral or injectable bisphosphonates or raloxifene.

**Table 1. Persistence with Index Therapy/Dosing Frequency over 24 Months**

	Rates		Odds Ratios	95% Confidence Limits	
	N	%		Lower	Upper
Denosumab SC Q6M (n=3,599; reference group)	1,484	41.2	—	—	—
Alendronate QD (n=224)	44	19.6	0.363	0.224	0.589*
Alendronate QW (n=19,486)	4,614	23.7	0.453	0.403	0.508*
Ibandronate QM (n=5,981)	1,567	22.9	0.436	0.381	0.499*
Ibandronate IV Q3M (n=165)	32	19.4	0.342	0.195	0.601*
Risedronate QD (n=53)	11	20.8	0.394	0.151	1.027
Risedronate QW (n=2,968)	604	20.4	0.370	0.315	0.436*
Risedronate QM (n=1,986)	404	20.3	0.368	0.305	0.444*
Raloxifene QD (n=3,423)	1,049	30.6	0.638	0.551	0.739*
Teriparatide SC QD (n=1,100)	449	40.8	0.946	0.774	1.155
Zoledronic acid annual IV (n=4,558)	1,543	33.9	0.758	0.665	0.864*

\* $P < 0.0001$

Odds ratios and associated 95% confidence limits are based on logistic regression models adjusted for age, health plan type, US Census region, urban residency, patient out-of-pocket expenditure for the index therapy, and the following baseline/pre-index clinical characteristics: Charlson Comorbidity Index score; number of unique medications prescribed; diagnosis of osteoporosis, osteopenia, renal insufficiency, gastrointestinal side effects, or coronary heart disease; and osteoporosis-related fracture.

QD: daily, QW: weekly, QM: monthly, IV: intravenous, Q3M: every 3 months, SC: subcutaneous

Table 1

**Disclosures:** Lionel Pinto, Amgen, 14

This study received funding from: Amgen Inc

## SU0294

**Optimal conditions to increase Bone mineral density by the combination therapy of bisphosphonates and active vitamin D3 analog is site specifically different between lumbar spine and femoral neck.** Mayuko Kinoshita<sup>\*1</sup>, Muneaki Ishijima<sup>1</sup>, Haruka Kaneko<sup>1</sup>, Liu Liz<sup>2</sup>, Shinnosuke Hada<sup>1</sup>, Hitoshi Arita<sup>1</sup>, Jun Shiozawa<sup>1</sup>, Anwar Yusup<sup>2</sup>, Hidetoshi Nojiri<sup>3</sup>, Yuko Sakamoto<sup>4</sup>, Kazuo Kaneko<sup>1</sup>. <sup>1</sup>Department of Orthopaedics & Motor Organ, Juntendo University Graduate School of Medicine, Japan, <sup>2</sup>Sportology Center, Juntendo University Graduate School of Medicine, Japan, <sup>3</sup>Department of Orthopaedics, Juntendo Tokyo Koto Geriatric Medical Center, Japan, <sup>4</sup>Department of Orthopaedics, Juntendo Nerima Hospital, Japan

As it has been revealed that vitamin D insufficiency is one of the risk factors for the decrease in lumbar spine bone mineral density (LS-BMD) in patients with postmenopausal osteoporosis even though the treatment of bisphosphonates (BPs) (*Calcif Tissue Int*, 2009), the combination therapy of BP and active vitamin D3 analog (aVD) in osteoporosis treatment has become widespread in Japan. We reported last year in this meeting that there was an optimal condition to increase BMD adequately by this combination therapy, and the middle tertile of reference range of serum level of calcium (sCa) [reference range (8.5-10.5 mg/ml)] was the condition. It is common that there are some patients who were unable to increase in femoral neck BMD (FN-BMD) even though their LS-BMD was increased well by the treatment of BPs. In this retrospective study, we examined that whether there were any relationship between the site-specific differences of the increase in BMD and the sCa by the combination therapy of BP and aVD. Since 2008 to 2013, ninety-nine female patients with post-menopausal osteoporosis who started to use BP and aVD in our university hospital were included. The BPs used were either alendronate, risedronate or minodronate and the aVD used were either alfacalcidol or eldcalcicidol in this study. In addition to age and body mass index (BMI), serum levels of 25(OH)D, Ca, Pi (sPi), intact PTH, bone turn markers such as TRACP5b and BAP, LS-BMD (L2-L4) and FN-BMD were assessed for every 6 months for 2 years. Both LS-BMD ( $p < 0.001$ , 5.4%) and FN-BMD ( $p = 0.007$ , 1.8%) of the patients were significantly increased by this combination therapy for 2 years. The sCa level was also significantly increased within the reference range ( $p < 0.001$ ), while intact-PTH, sBAP and TRACP5b were significantly decreased by this combination therapy for 2 years ( $p < 0.001$ ). sCa level was peaked out at 9.5 mg/ml in 18 months or thereafter. A multiple regression analysis using the parameters at first visit has revealed that the factor, that affects both the %LS-BMD ( $r^2 = 0.452$ ,  $p = 0.030$ ) and %FN-BMD ( $r^2 = 0.464$ ,  $p = 0.030$ ), were the sCa level. When the patients were divided into two groups in terms of sCa of 9.0 mg/ml, any %LS-BMDs after 6 month-treatment during the two-year treatment in patients with the lower sCa group within the reference range (0.4%) were significantly lower than that of those with the higher sCa group (1.5%) ( $p = 0.030$ ). In case of the femoral neck, when the patients were divided into two groups in terms of sCa of 9.3 mg/ml, any %FN-BMDs after 6 month-treatment during the two-year treatment in patients with the lower sCa group within the reference range (0.0%) were also significantly lower than that of those with the higher sCa group (1.2%) ( $p = 0.027$ ). In conclusion, the sCa level was

associated with the optimal increases in both LS-BMD and FN-BMD by the combination therapy by BPs and aVD, and the sCa levels in order to increase LS-BMD and FN-BMD optimally were site-specifically different.

**Disclosures:** *Mayuko Kinoshita, None.*

## SU0295

### Additional use of VitaminD and Intra-venus Ibandronate could be a Solution of Insufficient Effect of Solitary use of Oral Bisphosphonates or SERM for Osteoporosis Patients in Japan.. *yoichi kishikawa\**. affiliated, Japan

**Background:** One of the cause of insufficient effect of solitary use of oral Bisphosphonates(BISpo) or SERM must be with no concordant use of VitaminD or Ca. On the other hand, the lack of VitaminD is going to defined recently according to the level of 25OH-VitaminD in Japan, that is to say under 30 (ng/ml) as insufficiency and under 20 (ng/ml) as deficiency, and so so many people are reported as insufficiency or deficit of VitaminD. Therefore concordant use of VitaminD must be necessary for large prt of osteoporosis patients in Japan. Moreover, low adherence rate of BISpo or SERMs were reported less than 50% at one year from the start. Recently intara-venous administratarated Ibandronate(IBNiv) became available in Japan. It seemed to solve many problems when taking BISpo and has make the adherence rate higher. IBNiv with concordant use of VitaminD must be another way to solve the insufficient effect of BISpo. **Methods:** 1) 378 osteoporosis patients(352 female, 28 male) 22-92 years of age were investigated the level of 25OH-VitaminD. They were classified into three subgroups according to the level of 25OH-VitaminD and age. 2) 134 patients were applied additional use of 1aOH-VitaminD(alphacalcidole) or 1a,25OH-VitaminD(eldcalcicidole) if undergoing treatment for osteoporosis by means of oral BISpo or SERM were insufficient to increase BMD.We compared the changing of BMD between before and after a year of the adding VitaminD. 3) 51patients were applied with IBNiv with concordant use of VitaminD.18patients out of them were the patients switched from BIS-po. We investigated the change of bone metabolism markers comparing before and 4months after. And we also checked BMD at 1year and adherence rate. **Results:** 1) Out of 378 patients, 203 patients were classified as VitaminD deficiency, 145 as insufficiency, and only 30 as being sufficient. The decciciency and insufficiency of VitaminD were found not only in old patients but also in younger patients. 2) In the patients whose 25OH-VitaminD level was no more than 30(ng/ml) were counted up to 127, Femoral total BMD Increasing rate changed comparing before and after concordant use of VitaminD ( $P=0.033$  Wilcoxon) . Femoral neck BMD decreased inspite of use of Bis or SERMs chenged into increased ( $P=0$  Wilcoxon). 3) IBN-iv with concordant use of VitaminD seemed to change TRACP-5b within 4months not only in 20 naive patients ( $P=0.0016$  StudentT) but also in 18 switched patients from BIS-po( $P=0.031$  StudentT). After 1year follow up, Lumbar BMD and Femoral total BMD increased ( $P<0.01, P<0.05$  StudentT), although femoral neck BMD had not increased signifnificantly. The adherence rate at 1year counted no less than 80%, that supposed to be obtained by punctual monthly intra-venous injection which would make a good habitual visit to the clinic and help with continued treatment.

**Disclosures:** *yoichi kishikawa, None.*

## SU0296

### Persistence with Osteoporosis Therapies in Postmenopausal Women in a Large US National Health Plan. *Benjamin Chastek\**<sup>1</sup>, *Lung-I Cheng*<sup>2</sup>, *John white*<sup>1</sup>, *Leslie Spangler*<sup>2</sup>, *Darshan Mehta*<sup>3</sup>, *Rich Barron*<sup>2</sup>. <sup>1</sup>Optum, United states, <sup>2</sup>Amgen, United states, <sup>3</sup>University of Southern California, United states

**BACKGROUND:** Persistence and compliance with oral osteoporosis therapies are generally suboptimal; however, limited persistence data exist for newer injectable therapies that have become available in recent years. The objective of this study is to examine persistence and compliance of osteoporosis therapies using real-world data from a large national health plan in the United States (US).

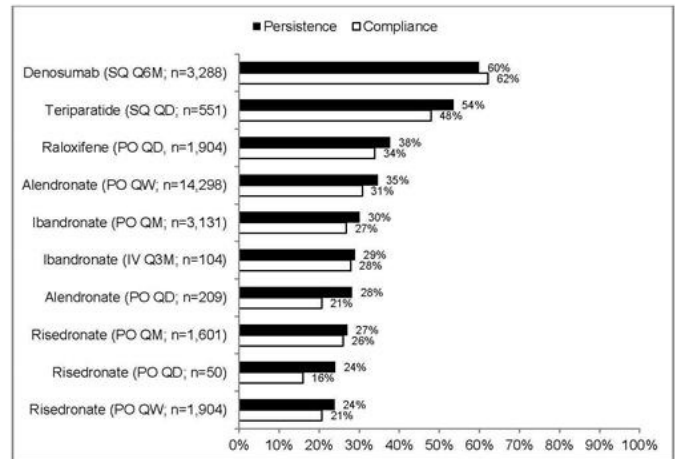
**METHODS:** Women affiliated with a large US national health plan who newly initiated an osteoporosis medication (alendronate, denosumab, ibandronate, raloxifene, risedronate, or teriparatide) between January 2012 and December 2012 were identified using the Optum Research Database. The index date was the first qualifying claim date. Patients were required to be  $\geq 50$  years of age at index and have  $\geq 12$  months of pre-index and  $\geq 12$  months of post-index continuous enrollment in the health plan. Patients with Paget's disease of the bone, osteogenesis imperfecta, hypercalcemia, malignant cancer and metastasis, HIV, and patients receiving preventive treatment for risk of breast cancer were excluded. Persistence (continuous use of index therapy with no gap  $> 60$  days) and compliance (proportion of days covered by therapy  $\geq 80\%$ ) were assessed during the 12-month follow-up period. Multivariable logistic regression models were used to estimate and compare persistence and compliance for the therapies of interest, adjusting for demographic and clinical characteristics (reference = group with highest persistence/compliance).

**RESULTS:** A total of 27,040 patients were eligible and included in the study (mean [SD] age: 67.2 [10.1] years). 12-month persistence was highest for denosumab (subcutaneous every 6 months) at 59.9% and lowest for risedronate (oral weekly) at 23.8%; 12-month compliance was highest for denosumab at 62.2% and lowest for risedronate (oral daily) at 16.0% (Figure). The multivariable logistic regressions showed that the odds of being persistent and compliant across treatments favored

denosumab (odds ratios from 1.4 to 4.9,  $p<0.001$  for persistence; 1.9 to 8.8,  $p<0.001$  for compliance).

**CONCLUSIONS:** In a large US national health plan, persistence and compliance over 12 months were higher among patients initiating denosumab compared to those initiating other osteoporosis therapies.

Figure. Unadjusted 12-month Persistence\* and Compliance\*\* Rates by Index Osteoporosis Therapy



\* Persistence: continuous use of index therapy with no gap  $> 60$  days; \*\*Compliance: proportion of days covered by therapy  $\geq 80\%$   
Note: IV: intravenous; PO: oral; QD: daily; QW: weekly; QM: monthly; Q3M: every 3 months; Q6M: every 6 months; SQ: subcutaneous

figure

**Disclosures:** *Benjamin Chastek, Optum, 12*  
*This study received funding from: Amgen*

## SU0297

### Utility of 18-Fluoride PET in Medication-Related Osteonecrosis of the Jaw. *Ie-Wen Sim\**<sup>1</sup>, *Michael Hofman*<sup>2</sup>, *Claudine Tsao*<sup>3</sup>, *Gelsomina Borromeo*<sup>3</sup>, *John Seymour*<sup>4</sup>, *Peter Ebeling*<sup>5</sup>. <sup>1</sup>Melbourne Medical School, University of Melbourne, Australia, <sup>2</sup>Centre for Cancer Imaging, Peter MacCallum Cancer Centre, Australia, <sup>3</sup>Melbourne Dental School, University of Melbourne, Australia, <sup>4</sup>Department of Haematology, Peter MacCallum Cancer Centre, Australia, <sup>5</sup>Department of Medicine, Monash University, Australia

Medication-related osteonecrosis of the jaw (MRONJ) is an infrequent, but potentially debilitating, condition associated with antiresorptive therapy. Whilst MRONJ is diagnosed predominantly on clinical criteria, radiological imaging has an important role in confirming diagnosis and excluding differentials such as osteomyelitis and metastatic cancer. 18-Fluoride (18-F) is a novel PET tracer that localises to sites of osteoblastic activity and is increasingly being used to characterise skeletal lesions. As part of a prospective randomised clinical trial investigating the efficacy of teriparatide as a treatment for MRONJ, 30 participants with confirmed MRONJ underwent baseline 18-F PET imaging. There were a total of 39 MRONJ lesions, with 8 participants having multiple lesions ranging in clinical severity from stage 0 (no exposed bone) to stage 3 (with infection and associated complications). 35 lesions (89.7%) were positively identified by 18-F PET, and demonstrated three characteristic patterns of uptake. Non-imaged lesions were either not associated with exposed bone (stage 0;  $n = 2$ ) or occurred in participants with multiple MRONJ lesions ( $n = 2$ ). A rim of intense osteoblastic activity surrounding an area of photopenia consistent with necrotic tissue was the most commonly characterised uptake pattern especially in more severe MRONJ lesions, being seen in 60% of stage 2 and 3 lesions. Significantly, this pattern has not been described with metastatic bony lesions. Less commonly observed uptake patterns, including either focal intense abnormality or diffuse uptake, were associated with less advanced stage MRONJ lesions. These findings support the utility of 18-F PET in the diagnosis and staging of MRONJ, as well as potentially influencing surgical management by identifying areas of necrotic bone. Further, the observed uptake patterns are consistent with persistent osteoblastic activity in viable bone, providing useful data regarding the pathophysiology of MRONJ.

**Disclosures:** *Ie-Wen Sim, None.*

**SU0298**

**Activation of the adapter protein ShcA allows Oncostatin M to induce RANKL expression and osteoclast formation more effectively than other gp130 cytokines.** Pedro Paulo Chaves Souza<sup>\*1</sup>, Emma Persson<sup>2</sup>, Petra Henning<sup>3</sup>, Howard Herschel Conaway<sup>4</sup>, Ulf H. Lerner<sup>3</sup>. <sup>1</sup>Faculty of Dentistry at Araraquara, Department of Physiology & Pathology, UNESP, Brazil, <sup>2</sup>Department of Radiation Sciences, Oncology, Umeå University, Sweden, <sup>3</sup>Centre for Bone & Arthritis Research at the Sahlgrenska Academy, University of Gothenburg, Sweden, <sup>4</sup>Department of Physiology & Biophysics, University of Arkansas for Medical Sciences, United states

Cytokines, including gp130 members, increase bone turnover during inflammation by stimulating both osteoblast and osteoclast activities. In this study, we have found that mouse oncostatin M (mOSM), which signals through the OSM receptor (OSMR):gp130 complex, is a more effective stimulator of bone resorption in cultured calvarial bones than other cytokines signalling through gp130 (LIF, IL-6, IL-11, CT-1, IL-27, IL-31). In cultured bone marrow cells (BMCs), it was also noted that mOSM, but not mLif, promoted osteoclast formation more effectively than either PTH or 1,25 dihydroxyvitamin D3. In the BMCs, mOSM upregulated Tnfsf11 mRNA 55-fold and down regulated Tnfsf11b 0.65-fold, whereas mLIF caused only a marginal 2-fold enhancement of Tnfsf11 mRNA and a 0.9-fold decrease of Tnfsf11b mRNA. Treatment of BMCs with mOSM increased IL-6 expression 16-fold, while only a 2 to 3-fold stimulation of expression was noted with mLIF and other LIFR:gp130 ligands. To further dissect target cells for mOSM, RT-PCR for Lifr and Osmr was performed, revealing that primary mouse osteoblasts, but not bone marrow macrophages (BMM), express both receptors. Additional experiments determined that mLIF and mOSM did not affect osteoclast formation in unstimulated or RANKL stimulated BMM, suggesting that stromal cells/osteoblasts are target cells for mOSM. mOSM increased the expression of Tnfsf11 clearly more effectively than mLIF and other members of the gp130 family in both calvarial osteoblasts and the stromal cell line ST-2. Western blot analysis revealed that mOSM activated phosphorylation of the adapter protein ShcA in osteoblasts, an effect not observed in cells treated with mLIF. Activation of STAT3, JNK and ERK1/2, as well as mRNA expression of c-Fos and DNA-binding of AP-1 (EMSA) were also more profoundly increased in these cells by treatment with mOSM than mLIF. Silence of ShcA using siRNA in osteoblasts impaired Tnfsf11 expression induced by mOSM. In conclusion, mOSM stimulates bone resorption in mouse calvariae and osteoclast formation in bone marrow cultures much more robustly than mLIF and other members of the gp130 family. This effect is due to its strong ability to induce Tnfsf11 in osteoblasts/stromal cells. The differences in signalling and potency between mOSM and mLIF could be explained by robust activation of RANKL expression by a ShcA-dependent MAP kinase cascade involving ERK, STAT3 and AP-1 that is mediated by OSMR:gp130, but not by LIFR:gp130.

**Disclosures:** Pedro Paulo Chaves Souza, None.

**SU0299**

**Enhancing therapeutic potential of macrophages for bone regeneration: Effect of Ca<sup>2+</sup> loaded poly-lactic acid (PLLA) microspheres.** Xiaobing Jin<sup>\*1</sup>, Ming Dang<sup>2</sup>, Amy Koh<sup>3</sup>, Peter Ma<sup>4</sup>, Laurie McCauley<sup>1</sup>. <sup>1</sup>Department of Periodontics & Oral Medicine, University of Michigan, United states, <sup>2</sup>Macromolecular Science & Engineering Center, University of Michigan, United states, <sup>3</sup>Department of Periodontics & Oral Medicine, University of Michigan, United states, <sup>4</sup>Department of Biologic & Material Sciences, University of Michigan, United states

Macrophages function to engulf and clear apoptotic cells (efferocytosis) and debris (phagocytosis) in both steady state and challenged scenarios. Engulfment stimulates secretion of factor(s) such as CCL-2 and TGFβ1 which play important roles in tissue regeneration including bone repair. Ca<sup>2+</sup> is an important cellular second messenger and has been shown to regulate phagocytosis and cytokine secretion in macrophages. Biodegradable polymeric microspheres have been used to deliver desired drugs into macrophages for therapeutic purposes. Could commandeering macrophage phagocytosis enhance the therapeutic potential of macrophages in tissue regeneration? The purpose of this study was to investigate the phagocytic capacity of macrophages to engulf Ca<sup>2+</sup> incorporated PLLA microspheres (MSs) (vs. non-Ca<sup>2+</sup> incorporated MSs) and determine their biological response after engulfment.

Methods: PLLA MSs were prepared using a water/oil/water double emulsion technique. Different amounts of calcium chloride were incorporated during the process and MSs were tagged with fluorescence. Size and surface morphology of MSs were characterized by scanning electrical microscopy (SEM). Murine bone marrow cells were cultured with 30ng/ml M-CSF, then presented with MSs containing various Ca<sup>2+</sup> concentrations. Flow cytometry was used to measure the phagocytosis efficiency of the macrophages. Extracellular and intracellular calcium were determined after MS engulfment by biochemical methods. Gene expression and cytokines released after phagocytosis were determined by Real-time PCR and ELISA.

Results: Phenotypically, non-Ca<sup>2+</sup> loaded control and Ca<sup>2+</sup> loaded PLLA MSs had similar size and surface texture. Flow cytometry analysis demonstrated that Ca<sup>2+</sup> loaded MSs were more efficiently internalized by F4/80<sup>+</sup> macrophages (39 ± 4% vs. 57% ± 2%). Increased Ca<sup>2+</sup> concentrations were observed in macrophages after

engulfment of Ca<sup>2+</sup> MSs. Moreover, calcium loaded MSs stimulated significantly more transforming growth factor-β1(TGF-β1) and chemokine(C-C motif) ligand-2(CCL-2) production.

Conclusion: PLLA MS phagocytosis was enhanced in bone marrow macrophages when MSs were loaded with Ca<sup>2+</sup>. Ca<sup>2+</sup> load stimulated macrophages secreted increased levels of TGF-β1 and CCL-2. Engineered Ca<sup>2+</sup> loaded PLLA MSs may serve as novel therapeutic interventions for skeletal tissue regeneration.

**Disclosures:** Xiaobing Jin, None.

**SU0300**

**Reduced microRNA21 and Enhanced HMGB1 Release: a Mechanistic Explanation for Increased Osteocyte Apoptosis and Resorption in the Absence of Cx43 and with Aging.** Hannah Davis<sup>\*1</sup>, Rafael Pacheco-Costa<sup>1</sup>, Emily Atkinson<sup>1</sup>, Mircea Ivan<sup>1</sup>, Angela Bruzzaniti<sup>2</sup>, Teresita Bellido<sup>1</sup>, Lilian Plotkin<sup>1</sup>. <sup>1</sup>Indiana University School of Medicine, United states, <sup>2</sup>Indiana University School of Dentistry, United states

Mice lacking osteocytic connexin (Cx) 43 exhibit a skeletal phenotype that mimics old mice, with increased osteocyte apoptosis and osteoclast recruitment. Consistently, Cx43 decreases with age. Cell death also increases *in vitro* in Cx43-silenced MLO-Y4 osteocytic (Cx43<sup>def</sup>) cells, which is abolished by the caspase3 inhibitor DEVD indicating death by apoptosis. We examined the molecular mechanisms leading to osteocyte apoptosis and osteoclast recruitment with Cx43 deficiency. Osteocyte apoptosis is reversed by transfecting full-length Cx43 in Cx43<sup>def</sup> cells, but not a mutant that only forms hemichannels (Cys-less) or a mutant lacking channel permeability, suggesting the Cx43 survival effect is mediated by gap junctions. Osteocytic Cx43 deletion increases mRNA levels of apoptosis-related genes CHOP, P27 and FOXO3, and protein levels of CHOP and active caspase3. Further, Cx43<sup>def</sup> cells and bones from old mice exhibit reduced levels of the pro-survival microRNA miR21. miR21 deletion by adenoCre in miR21<sup>off</sup> calvaria bones increases CHOP, P27 and FOXO3 expression; and reducing miR21 expression using oligonucleotide inhibitors induces apoptosis of control osteocytic cells. Conversely, a miR21 oligonucleotide mimic attenuates Cx43<sup>def</sup> cell apoptosis, suggesting that miR21 reduction causes the increased osteocyte apoptosis in the absence of Cx43. Cx43<sup>def</sup> cells release more sRANKL and high mobility group box1 (HMGB1), and inhibition of osteocyte apoptosis with DEVD or treatment with a HMGB1 neutralizing antibody or glycyrrhizic acid, which inhibits HMGB1 action, reduces RANKL expression in Cx43<sup>def</sup> cells. Further, DEVD prevents sRANKL and HMGB1 release; and attenuates the enhanced osteoclastogenesis and osteoclast marker expression induced by conditioned media (CM) from Cx43<sup>def</sup> cells in osteoclast precursors (+MCSF/RANKL). Moreover, the HMGB1-RAGE receptor antagonist, BOXA, blocks osteoclastogenesis induced by CM from Cx43<sup>def</sup> cells. Thus, HMGB1 released by dying osteocytes enhances osteoclastogenesis by both increasing RANKL in osteocytes and stimulating RAGE activation in osteoclast precursors. We conclude that miR21 lies downstream of Cx43 in the control of osteocyte viability; and the increased osteoclastogenic potential of Cx43<sup>def</sup> osteocytes is a result of HMGB1 release during apoptosis. These findings identify a novel Cx43/miR21/HMGB1/RANKL pathway mediated by gap junction communication in osteocytes that could be targeted to treat bone fragility in aging.

**Disclosures:** Hannah Davis, None.

**SU0301**

**Colonic Osteoprotegerin (OPG) participates in Innate Immune Responses to Luminal Bacteria.** Anu Maharjan<sup>\*1</sup>, Raghunath Ramanarasimhaiah<sup>2</sup>, Anthony Vella<sup>2</sup>, Francisco Sylvester<sup>1</sup>. <sup>1</sup>University of North Carolina, United states, <sup>2</sup>University of Connecticut, United states

Background: We have observed that osteoprotegerin (OPG) is highly expressed in the colonic mucosa, appears in high concentration in feces of patients with chronic colitis, and fecal OPG predicts response to intravenous corticosteroids in hospitalized children with ulcerative colitis. However, little is known about the function of OPG in the colon. Aim: We hypothesized that colonic epithelial OPG binds to luminal bacteria and augments chemotaxis of neutrophils and monocytes. Methods: We examined the concentration of OPG secreted by the colonic epithelial cell line Caco-2 in response to commensal *Escherichia coli* K12 (*E. coli*) using ELISA. We measured binding of bacteria to fluorescent OPG by flow cytometry. We isolated neutrophils and monocytes from peripheral blood of healthy volunteers. Using a transwell system, we examined neutrophil and monocyte chemotaxis in response to OPG, *E. coli* alone and *E. coli* pre-incubated with OPG. We also examined if pre-incubation with OPG increases bacterial killing by J774 mouse macrophages with a gentamicin protection assay. Results: Caco-2 cells constitutively secrete OPG (mean 5.2 ± 0.15 ng/mL, n = 9). In cells treated with *E. coli* (10<sup>5</sup> – 10<sup>6</sup>/mL), the concentration of OPG decreased in the medium. However, treatment of *E. coli* with 0.05% Tween 20 significantly increased the concentration of OPG in the medium, suggesting that OPG binds to *E. coli*. By flow cytometry we found that OPG binds a higher percentage of heat-killed *E. coli* compared to live *E. coli* (heat-killed *E. coli* + OPG 5.57 ± 2.09% vs. live *E. coli* + OPG 0.77 ± 0.22%; p = 0.039, n = 7), suggesting that damaged enteric bacteria may be targeted by OPG. *E. coli* decorated with OPG modestly inhibited the chemotaxis of neutrophils (normalized to *E. coli* 100%; *E. coli* + OPG 82.9 ± 19.2, p = 0.048; n = 6 according to Mann-Whitney test) but is chemotactic of monocytes (*E. coli* 100%; *E. coli*

+ OPG  $277 \pm 64\%$ ,  $p = 0.02$  according to unpaired t test,  $n = 6$ ). There was no significant difference in gram-positive or -negative bacterial killing in bacteria pre-incubated with OPG. Conclusion: OPG binds to *E.coli* and limits neutrophil migration, but hastens monocyte migration, which may play a role in innate defense in the colonic mucosa.

**Disclosures:** Anu Maharjan, None.

This study received funding from: University of North Carolina Commitment Fund

## SU0302

**Oncostatin M robustly increases *Wnt16* expression in osteoblasts limiting oncostatin M-induced osteoclastogenesis.** Petra Henning<sup>\*1</sup>, Sofia Movérare-Skrtic<sup>1</sup>, Pedro P. C. Souza<sup>2</sup>, Anna Westerlund<sup>1</sup>, Claes Ohlsson<sup>1</sup>, Ulf H. Lerner<sup>1</sup>. <sup>1</sup>Centre for Bone & Arthritis Research at the Sahlgrenska Academy, University of Gothenburg, Sweden, <sup>2</sup>Department of Physiology & Pathology, Araraquara School of Dentistry, University Estadual Paulista (UNESP), Brazil

A missense polymorphism in the *WNT16* gene is associated with cortical bone thickness and fracture risk in humans and *Wnt16*-deficient mice develop spontaneous fractures as a result of low cortical thickness. We have shown that WNT16 is osteoblast derived and inhibits human and mouse osteoclastogenesis both directly by acting on osteoclast progenitors and indirectly by increasing expression of osteoprotegerin in osteoblasts (Nature Med. 2014). We also reported that estrogen increases *Wnt16* expression *in vivo*, but that the bone-sparing effects of *Wnt16* and estrogen are independent of each other (PNAS 2015). Besides increased expression by estrogen, very little is known about the regulation of *Wnt16* expression.

Cultured murine calvarial osteoblasts were treated with a range of hormones and cytokines that have been implicated in physiological and pathophysiological bone remodeling and *Wnt16* mRNA expression was measured. We identified oncostatin M (OSM) and IL-6 to be the strongest regulators of *Wnt16* expression at 6-48 h. Vitamin D3 and PTH also slightly increased *Wnt16* expression; the PTH effect was transient and the vitamin D3 effect was more delayed. Other gp130 cytokines, such as IL-11, LIF, CT-1, CNTF, NP, IL-27 and IL-31 did not affect *Wnt16* expression after 24 h stimulation.

To assess the paracrine role of OSM induced *Wnt16*, we used three different co-culture systems for osteoclastogenesis. *RANKL* and *Wnt16* expression were induced in osteoblasts/stromal cells by OSM; (i) co-cultures of calvarial osteoblasts and bone marrow macrophages, (ii) calvarial periosteal cell cultures and (iii) total bone marrow cell cultures from WT and *Wnt16*<sup>-/-</sup> mice. In all three systems, osteoclast formation was increased when osteoblasts/stromal cells were from *Wnt16*<sup>-/-</sup> mice.

OSM binds to gp130 and then forms a complex that signals through either the LIF receptor or OSM receptor (OSMR). The adapter protein ShcA is recruited specifically to OSMR to initiate downstream signaling. Silencing of ShcA in osteoblasts *in vitro* abrogated the OSM induced *Wnt16* expression.

We previously showed that *Wnt16* expression is high in osteoblasts in cortical bone. Interestingly, the expression of OSM is 5 times higher in cortical than trabecular bone, with low expression in many other organs. In summary, we here demonstrate that *Wnt16* expression in osteoblasts is induced by activation of OSMR:gp130 and the adapter protein ShcA resulting in a negative feed-back loop to decrease osteoclast formation.

**Disclosures:** Petra Henning, None.

## SU0303

**Effect of Dried Plum Supplementation on Partial Geometrical Changes of Bone in Ovariectomy-induced Sprague-Dawley Rats.** Shirin Pourafshar<sup>\*</sup>, Negin Navaei, Neda Akhavan, Elizabeth Foley, Kelli George, Bahram Arjmandi. Department of Nutrition, Food & Exercise Sciences, Florida State University, Tallahassee, FL; Center for Advancing Exercise & Nutrition Research on Aging (CAENRA), Florida State University, Tallahassee, FL, United states

Osteoporosis is a chronic condition characterized by low bone density and is a predominant health issue in postmenopausal women. It has been suggested that certain nutritional factors can reduce the risk of osteoporosis and thereby the risk of fractures. In terms of nutrition, dried plum has been shown to be one of the most efficacious interventions in preventing bone loss. Thus, the purpose of this study was to further examine the partial geometrical changes that dried plum, a rich source of phenolic compounds, can exert on bone. For this reason, forty-eight female Sprague-Dawley rats were used and were divided into four groups: 1) sham-operated (Sham), 2) ovariectomized (Ovx), 3) Ovx + 5% dried plums (low-dose, LD), and 4) Ovx + 25% dried plums (high-dose, HD). Animals were fed a semi-purified casein-based diet, or a similar diet with either 5% or 25% of the diet (w/w) consisting of dried plums. As it has been observed in our previous studies, bone mineral density (BMD), percent mineral content of right femurs, and 4<sup>th</sup> lumbar vertebrae were higher in both dried plum groups in comparison with Ovx animals. In this study we assessed the cortical, marrow space, endosteal and periosteal perimeters. Furthermore, parameters such as: 1) trabecular total area, bone area, and percentage bone area as well as 2) cortical total area and bone area were measured via histomorphometry. The results from this study showed that Ovx-induced loss of trabecular bone area was prevented by

HD-dried plum but not by LD-dried plum. Ovx caused an enlargement of marrow space (11%) that was reduced by HD-dried plum diet (17.6%). Dried plums may be efficacious food sources in protecting bone due to their potential role in increasing the rate of bone formation rather than suppression of the rate of bone resorption. Further histomorphometric analyses are necessary to evaluate the effect of dried plum on numerous remaining parameters such as osteoblasts and osteoclasts surfaces, bone mineralization apposition rate as well as mineralized surface.

**Disclosures:** Shirin Pourafshar, None.

## SU0304

**Healthy Dietary Pattern During Adolescence in Females Is Positively Associated with Bone Strength in Adulthood.** Elham Movassagh<sup>\*1</sup>, Saija Kontulainen<sup>2</sup>, Susan Whiting<sup>1</sup>, Adam Baxter-Jones<sup>3</sup>, Hassan Vatanparast<sup>1</sup>. <sup>1</sup>College of Pharmacy & Nutrition, University of Saskatchewan, Canada, <sup>2</sup>College of Kinesiology, University of Saskatchewan, Canada, <sup>3</sup>College of Graduate Studies & Research, University of Saskatchewan, Canada

The study purpose was to determine if dietary patterns during adolescence are associated with bone strength in adulthood.

We analyzed data from 74 participants (36 females) of the Saskatchewan Pediatrics Bone Mineral Accrual Study (PBMAS, 1991-2011), a mixed longitudinal study. The estimated bone strength index in compression (BSIc) at the distal ends and strain strength index in torsion (SSI<sub>T</sub>) and muscle area (MuA) at shafts of the radius and tibia were measured using one pQCT scan during adulthood (age 24-34 yr). The principal component analysis was performed to derive dietary patterns (DPs) from dietary intake data that we collected during late adolescence (aged 14-18 yr) using serial 24-h recalls. Participants were classified into three groups based on DP score tertiles in each sex. Adult physical activity (PA) was measured using PA questionnaire. We conducted analysis of covariance to compare mean bone strength parameters across the groups of DP score in each sex while controlling for adult height, total energy intake, PA, and MuA.

We derived two DPs including Healthy DP and Western DP. The Healthy DP was characterized by intake of non-refined grains, poultry, non-citrus fruits, vegetables, low-fat milk, and fish while the Western DP was represented with intake of refined grains, sweetened beverages, meat, cheese and tomato. We found that adult females with lower scores for Healthy DP (in the first tertile) during late adolescence had 21% and 19% lower distal tibia BSIc in adulthood compared to their counterparts with higher scores in tertile 2 ( $P = 0.027$ ) and tertile 3 ( $P = 0.047$ ), respectively, after adjusting for adult height, total energy intake, PA, and lower leg MuA. No significant difference in bone strength was found across the groups for Western DP score, in females and males.

Our results suggest a positive long-term association of a Healthy DP during late adolescence (consisting of higher intake of non-refined grains, poultry, non-citrus fruits, vegetables, low-fat milk, and fish) on bone strength in the distal tibia in adult females, an association not observed in adult males. Our results warrant more research in identifying dietary patterns affecting not only bone mass but also bone strength.

**Disclosures:** Elham Movassagh, None.

## SU0305

**Antioxidant Avenanthramides Prevent Osteoblast and Osteocyte Apoptosis and Induce Osteoclast Apoptosis by Nrf2-Independent Mechanisms.** Gretel G Pellegrini<sup>\*1</sup>, Cynthia C Morales<sup>2</sup>, Taylor C Wallace<sup>3</sup>, Lilian I Plotkin<sup>1</sup>, Teresita Bellido<sup>1</sup>. <sup>1</sup>Indiana University School of Medicine, Roudebush Veterans Administration Medical Center, Indianapolis, United states, <sup>2</sup>Indiana University School of Medicine, United states, <sup>3</sup>National Osteoporosis Foundation, United states

Oats contain different types of phytochemicals with antioxidant properties and are gaining increasing scientific interest for their nutritional benefits. Avenanthramides (AVAs), uniquely found in oats, have been shown to enhance the endogenous antioxidant response in human kidney cells through activation of the transcription factor Nrf2. Here, we examined the ability of the three major AVAs 2f, 2c and 2p, which differ in the type of hydroxycinnamic acid component (ferulic, caffeic or p-coumaric acid), to regulate bone cell apoptosis and the potential Nrf2 involvement. To examine the effect of AVAs in basal and induced apoptosis, apoptosis was quantified by trypan blue uptake after 6 h of treatment in OB-6 osteoblastic, MLO-Y4 osteocytic and primary Nrf2 WT or KO osteoblastic cells. Bone marrow precursors derived from WT and KO mice were differentiated to osteoclasts (RANKL 80 ng/ml and M-CSF 20 ng/ml). Osteoclasts were enumerated after staining with TRAPase and hematoxylin (TRAPase + cells > 3 nuclei, were considered osteoclasts). Osteoclast gene expression was also assessed. Treatment with 1-100  $\mu$ M AVAs did not affect basal levels of apoptosis of OB-6 or MLO-Y4 cells. However, treatment with AVAs prevented apoptosis induced by the DNA topoisomerase etoposide (50  $\mu$ M), the glucocorticoid dexamethasone (10  $\mu$ M) and the reactive oxygen species (ROS) H<sub>2</sub>O<sub>2</sub> (50  $\mu$ M). AVAs (1  $\mu$ M) also prevented apoptosis of primary WT as well as KO osteoblastic cells, demonstrating that survival by AVAs does not require Nrf2 expression in these cells. Bone marrow precursors derived from KO mice produced  $30.21 \pm 2.25\%$  more

osteoclasts than WT precursors. Furthermore, KO cultures exhibited lower number of apoptotic osteoclasts compared to WT cultures ( $13.25 \pm 2.47\%$  vs  $22.97 \pm 1.84\%$  for KO and WT, respectively). AVAs did not affect either number or apoptosis of WT osteoclasts, whereas in KO osteoclasts, AVA 2p reversed the decreased apoptosis to WT levels. Consistent with this, the expression of the osteoclast markers Cat K, Cal R and TRAP was higher in the KO cultures compared to WT and AVA 2p significantly decreased the expression of CAL R in KO osteoclasts. AVAs did not affect the expression of Nrf2 or the phase II antioxidant enzymes NQO1 and HMOX1, known to depend on Nrf2. These results demonstrate that AVAs prevent osteoblast/osteocyte apoptosis and increase osteoclast apoptosis; and that these regulatory actions are Nrf2 independent.

**Disclosures:** Gretel G Pellegrini, None.

This study received funding from: Quaker Oats Center of Excellence, PepsiCo, R&D Nutrition

## SU0306

**Gene Expression of Bone MMP9, MMP13, and VEGF in the Hypovitaminosis D Kyphotic Pig Model.** Laura Amundson\*, Thomas Crenshaw. UW-Madison, United states

The hypovitaminosis D kyphotic pig provides a reliable model to study the initiation of bone lesions in progeny caused by maternal vitamin D (D) deficiencies. Whether excess maternal dietary D would prevent pigs from developing kyphosis, regardless of nursery diet is unknown. Matrix metalloproteinases (MMP; specifically, MMP9 and MMP13), and vascular endothelial growth factor (VEGF) are important in endochondral ossification and are potentially regulated by D. Maternal D carryover effects were characterized for incidence of kyphosis and mRNA expression of MMP9, MMP13, and VEGF in femur (FM) and vertebrae (VB) from hypovitaminosis D kyphotic pigs. Sows (n=37) were fed diets with 0 (-D), 325 (+D) or 1750 (++) IU D<sub>3</sub>/kg throughout gestation and lactation. At weaning (3 wk) pigs were fed diets with 0 (-D) or 280 (+D) IU D<sub>3</sub>/kg, each with 75% and 95% (LCaP) or 150% and 120% (HCaP) of the Ca and P requirements. Pigs euthanized prior to colostrum consumption at birth (n = 27), 3 wk (n = 27), and after the nursery period (7 wk; n = 71) were used for tissue analysis. Observations for symptoms of kyphosis were recorded in remaining pigs at 13 wk. A subjective score of 1 (no curvature), 2 (marginal curvature), or 3 (obvious curvature) was assigned to each pig by two observers based on visual evidence of spinal column curvature. The final assessments of the incidence of kyphosis were based only on animals with a score of 3 by both observers. At 3 wk, FM MMP9 expression of pigs produced by +D or ++D sows was reduced ( $P < 0.05$ ) to 0.5-fold and VEGF expression to 0.4-fold compared to pigs from -D sows. Similar trends were noted in VB at 3 wk but significant differences were not detected. Intriguingly, at 7 wk MMP9 expression was reduced ( $P < 0.05$ ) to 0.45-fold in FM and 0.58-fold in VB from pigs produced by +D or ++D sows compared to pigs from -D sows, regardless of nursery diet. Pig FM VEGF expression was reduced to 0.75-fold in pigs produced by ++D sows, regardless of nursery diet. At 13 wk, 34% of pigs produced by -D sows exhibited visual abnormalities associated with kyphosis. Only 1% of pigs from ++D sows were affected. MMP9 and VEGF mRNA expression offer potential markers for the initial stages of bone lesions in the hypovitaminosis D kyphotic pig model. Pigs from -D sows are at highest risk of developing kyphosis, regardless of nursery diet. Maternal dietary D carryover is an important factor in molecular and gross characteristics of pig bone development.

**Disclosures:** Laura Amundson, None.

## SU0307

**Effects of pre-existing inflammatory conditions on development of tooth extraction-induced BRONJ and DRONJ lesions in mice.** Terresa Kim, Minju Song, Sol Kim, Cindy Lee, Drake Williams, Ki-Kyuk Shin, Mo Kang, No-Hee Park, Reuben Kim\*. UCLA, United states

Medication-related osteonecrosis of the jaw (MRONJ) is a devastating side effect that predominantly occurs in patients using bisphosphonate (BP) or denosumab (Dmab) for managing bone-related diseases such as osteoporosis or bone metastatic cancers. Previously, we demonstrated that tooth extraction induces ONJ lesions in mice administered with BP or Dmab (Williams et al., 2013). In addition to tooth extraction, pre-existing pathological inflammatory conditions such as periodontitis and periapical endodontic lesions are known risk factors for MRONJ; however, the direct involvement of these conditions to MRONJ development is not clear. The aim of the current study is to determine the role of pathological inflammatory conditions such as periodontal and periapical diseases in tooth extraction-induced BRONJ and DRONJ mouse models. Periodontitis and periapical lesions were experimentally induced in mice receiving intravenous ZOL or anti-RANKL antibody (Ab) by placing a ligature or exposing the pulp on maxillary molars for 3 weeks, respectively. The same tooth was extracted and allowed to heal for additional 3 weeks. After 3 weeks, maxillae were harvested to analyze for the microCT and bone loss. Histological, histomorphometric, and histochemical staining analyses showed that, in the presence of ZOL or anti-RANKL antibody, periodontitis and periapical lesions exacerbated tooth extraction-induced ONJ lesions as demonstrated by empty lacunae, necrotic bone percentage, and TRAP staining. To further examine whether resolving inflammatory conditions prevent ONJ development, we removed the ligature and allowed to heal for 2 weeks before performing tooth extraction. Removal of ligature reduced inflammation as determined by diminished expression of IL-1 $\beta$ , IL-6, and

IL-17 and reduced bone loss. In the presence of ZOL or anti-RANKL antibody, ligature removal prevented bone exposure and reduced the numbers of empty lacunae, and necrotic bone percentages when compared to the unremoved group. Our study demonstrated that pre-existing pathological inflammatory conditions exacerbate ONJ lesions following tooth extraction, and resolution of these conditions before tooth extraction prevents ONJ development.

**Disclosures:** Reuben Kim, None.

## SU0308

**Intermittent Ibandronate Maintains Bone Mass and Bone Biomechanical Strength after Parathyroid Hormone Treatment in Ovariectomized Rats.** Satoshi Takeda\*<sup>1</sup>, Sadaoki Sakai<sup>1</sup>, Keisuke Tanaka<sup>1</sup>, Haruna Tomizawa<sup>1</sup>, Kenichi Serizawa<sup>1</sup>, Kenji Yogo<sup>1</sup>, Koji Urayama<sup>2</sup>, Koichi Endo<sup>1</sup>, Junko Hashimoto<sup>1</sup>, Yoshihiro Matsumoto<sup>1</sup>. <sup>1</sup>Chugai Pharmaceutical Co., Ltd., Japan, <sup>2</sup>Taisho Toyama Pharmaceutical Co.,Ltd., Japan

**Purpose:** Although parathyroid hormone 1-34 (PTH) expresses a strong anabolic effect on bone mass and reduces the risk of fragility fracture in osteoporotic patients, the increased bone mass is known to disappear once PTH treatment is withdrawn. Therefore, treatment with bisphosphonates is recommended to maintain bone mass after PTH therapy. In the current study, we examined the effect of intermittent ibandronate (IBN), a nitrogen-containing bisphosphonate, after PTH treatment in ovariectomized (OVX) rats.

**Methods:** Wistar-Imamichi rats (27-weeks old) were ovariectomized and 8 weeks after surgery were treated for another 8 weeks with PTH (10 $\mu$ g/kg, s.c., 5 times/week) (PTH8W) or with vehicle as a disease control (DC8W). Thereafter, PTH treatment was withdrawn and the PTH-treated rats were dosed for another 8 weeks with IBN (10 $\mu$ g/kg, s.c., every 4 weeks) (P-I) or vehicle (P-V), while the vehicle-pretreated rats continued to receive vehicle (DC). Serum osteocalcin (OCN) and urinary deoxypyridinoline (DPD) were measured every 4 weeks. BMD in the lumbar spine and femur was measured by DXA, and a compressive test of the L5 vertebra and a 3-point bending test of the femoral shaft were performed when PTH and IBN treatment finished.

**Results:** Serum OCN increased after 4 weeks of PTH treatment compared with the DC group and returned to DC level at 8 weeks. At 4 and 8 weeks after switching to IBN, OCN in the P-I group decreased compared with the DC group, while OCN in the P-V group maintained DC level. Urinary DPD also decreased in the P-I group after 4 and 8 weeks of IBN treatment compared with the DC group, while DPD in the P-V group did not. BMD at lumbar spine and femur in the PTH8W group was higher than in the DC8W group, and similarly higher in the P-I and P-V groups than in the DC group. However, BMD in the P-I group was higher than in the P-V group. The maximum load in both of the compressive test and the 3-point bending test was higher in the PTH8W group than in the DC8W group. The maximum load in the P-I group was higher than in either the DC or P-V group. There is no significant difference in the maximum load between the P-V and DC groups.

**Conclusion:** We demonstrated that intermittent IBN after PTH suppressed the increased bone turnover by OVX and achieved the maintenance of BMD and biomechanical strength in the lumbar spine and femur in OVX rats. It is expected that these results will be clarified in clinical setting.

**Disclosures:** Satoshi Takeda, Chugai Pharmaceutical Co.,Ltd, 15

## SU0309

**Morphological Changes in Osteoclasts by Condensed Minodronic Acid: The Estimated Concentration at Bone Resorption Sites Reach the Antagonistic Activity against Purinergic P2X2/3 Receptors.** Makoto Tanaka\*<sup>1</sup>, Akihiro Hosoya<sup>2</sup>, Hiroshi Mori<sup>3</sup>, Ryoji Kavasuga<sup>3</sup>, Hiroaki Nakamura<sup>2</sup>, Hidehiro Ozawa<sup>2</sup>. <sup>1</sup>Research headquarters, Ono Pharmaceutical Co., Ltd., Japan, <sup>2</sup>Department of Oral Histology, Matsumoto Dental University, Japan, <sup>3</sup>Research headquarters, Ono Pharmaceutical Co., Ltd., Japan

Minodronic acid (MIN), a unique aminobisphosphonate, has not only a potent antiresorptive activity via farnesyl pyrophosphate synthase inhibition but also has an antagonistic activity against purinergic P2X2/3 receptors which involved in chronic pain states. The aim of this study was to investigate the action and distribution of MIN with histological evaluation. We also elucidated the potential of the antagonistic activity by estimation of MIN quantity in bone resorption lacunae.

The microlocalization of radio-labelled MIN in femur was examined in neonatal rats. The in vitro binding property of MIN to cortical bone was examined. Morphological changes in cultured rabbit osteoclasts were analyzed by light and electron microscopy. In addition, quantity of MIN around bone resorption lacunae was estimated by mathematical model with bone binding property and antiresorptive activity of MIN.

In microautoradiography of epiphyseal growth plate, silver grains indicated radioactive MIN were not found in matrix and cells in hypertrophic cartilage zone, but was distributed within matrix in calcified zone, ossification zone and spongiosa. There were numerous silver grains in bone attached osteoclasts and surrounding area. Silver grains in osteoclasts contacting bone surface were trend to lower than that in osteoclasts separated bone surface. In in vitro binding assay, the bone bound fraction of MIN was 65% at 1  $\mu$ M, decreased over 0.1 mM, and saturated over 2 mM. MIN

inhibited with 70% and 96% C-terminal cross-linking telopeptide release in osteoclasts culture, at 0.1 and 1  $\mu$ M, respectively. Osteoclasts of control group formed remarkable ruffled borders and bone resorption lacunae, had many vesicles and vacuoles. MIN treated osteoclasts at 0.1  $\mu$ M were attached to bone surface without ruffled borders, had many vesicles and vacuoles. Alignment of collagen fibers was uniform at deep portion apart from the bone surface, but was disturbed at bone surface portion faced to ruffled borders. In MIN 1  $\mu$ M group, many of osteoclasts was not multinucleated, densely stained with toluidine blue, and were detached from bone surface. Estimated MIN concentration in the resorption lacunae, from bone binding and shape of the lacunae, was over an IC50 of reported antagonistic activity for P2X2/3 receptors.

In conclusion, an antagonistic activity for P2X2/3 receptors around osteoclasts may contribute a mechanism to an analgesic effect of MIN.

**Disclosures:** Makoto Tanaka, None.

This study received funding from: Ono Pharmaceutical Co., Ltd

## SU0310

**CaMKK2 inhibition as a therapeutic strategy to accelerate bone fracture repair.** Justin Williams\*, Yinghua Cheng, Yong Li, Roshni Patel, Anuradha Valiya Kambrath, Uma Sankar. Indiana University School of Medicine, United states

Bone is a highly regenerative tissue. However, 10% of all the fractures show impaired healing resulting in non-unions, resulting in poor quality of life and loss of productivity. Despite its utmost clinical significance, therapeutic targets that promote efficient bone healing are lacking. Pharmacological inhibition of Ca<sup>2+</sup>/calmodulin (CaM)-dependent protein kinase kinase 2 (CaMKK2) using its selective cell-permeable inhibitor STO-609 stimulates osteoblasts and inhibits osteoclasts; leading to the prevention and/or reversal of ovariectomy-induced or age-associated decline in bone volume and strength. We thus hypothesized that targeting CaMKK2 as a bone-anabolic therapy that also inhibits catabolic bone destruction will result in efficient bone healing after fracture.

We generated closed femoral fractures on the right limbs of 11 week-old mice using a method described by Silva et al. (Bone 81: 2015). Radiography was performed to confirm the location and quality of the fractures. Tri-weekly intraperitoneal (i.p.) injections of saline (n=20) or STO-609 (10 or 15  $\mu$ mol/kg mouse body weight; n=20 per dose) were commenced on the day after surgery and continued for 4 weeks. Acute inflammation is the first stage of fracture healing. CaMKK2 inhibition has a suppressive effect on macrophage-mediated inflammation and to test whether this has an effect on fracture healing, we delayed treatment by 7 days post-fracture in n=20 mice. Progression of fracture healing was monitored through weekly radiographic X-rays and the mice were euthanized at either 2 (n=14/group) or 4 (n=6/group) weeks after fracture. Fractured and contralateral femur mid-shafts were analyzed by micro-CT followed by static and dynamic histomorphometry. Our results indicate that treatment with STO-609 resulted in a significant anabolic response in the non-fractured contralateral distal femurs. Inhibition of CaMKK2 using STO-609 resulted a significant 2-fold increase of callus area by 2 weeks post-surgery. Delaying treatment by a week post-fracture resulted in a marked increase in callus area accompanied by enhanced mineralization and microarchitecture. Inhibition of CaMKK2 results in the enhanced osteoblasts as well as osterix, osteocalcin, bone morphogenic protein 2 (BMP2) and osteoprotegerin protein expression at the callus. Taken together, our results indicate that the pharmacological inhibition of CaMKK2 contributes to enhanced repair and improved bone microarchitecture at the fractured site

**Disclosures:** Justin Williams, None.

## SU0311

**Sclerostin Blockade and Zoledronic Acid Improve Bone Mass and Strength in Mice with Exogenous Hyperthyroidism.** Elena Tsourdi\*<sup>1</sup>, Franziska Lademann<sup>1</sup>, Michael Ominsky<sup>2</sup>, Lorenz Hofbauer<sup>1</sup>, Martina Rauner<sup>1</sup>. <sup>1</sup>TU Dresden Medical Center, Germany, <sup>2</sup>Center Metabolic Disorders, Amgen, Inc., United states

Hyperthyroidism in mice is associated with a low bone mass, an increased bone turnover, and high serum levels of sclerostin, a potent Wnt inhibitor. Here, we explored the effects of either reducing bone turnover with bisphosphonates or increasing bone formation with neutralizing sclerostin antibodies (Scl-Ab) on bone mass and strength in hyperthyroid mice.

Twelve-week-old C57BL/6 male mice were rendered hyperthyroid by adding L-thyroxine (T4) to the drinking water (1.2  $\mu$ g/ml). Saline, 20 mg/kg of Scl-Ab twice per week or 100  $\mu$ g/kg of zoledronic acid (ZOL) once per week were administered to hyperthyroid and control mice for 4 weeks.

MicroCT analysis revealed a lower trabecular bone volume at the spine (-27%) and the distal femur (-48%) in hyperthyroid mice compared to euthyroid controls. Scl-Ab treatment of hyperthyroid mice increased the trabecular bone volume at the femur by 2.5-fold as compared to PBS-treated hyperthyroid mice, while ZOL increased it by 2-fold. Similar effects were observed for the spine. Cortical thickness at the femoral diaphysis was lower in hyperthyroid mice and increased by both treatments, with Scl-Ab having a more potent effect than ZOL (+12%, p<0.05). Bone stiffness estimated by finite element modeling at the lumbar vertebra was 49% lower in hyperthyroid mice and was increased by 3- and 2-fold after Scl-Ab and ZOL treatment, respectively.

Levels of PINP were 2.7-fold higher in hyperthyroid mice than in euthyroid controls, and treatment of hyperthyroid mice with Scl-Ab led to a further 13% increase in PINP, whereas ZOL reduced PINP concentrations by 23%. CTX levels were also 47% higher in hyperthyroid mice as opposed to euthyroid controls. They remained unchanged after Scl-Ab treatment, but decreased after ZOL treatment (-23%).

Thus, both anti-resorptive and bone-forming treatments are effective in preventing bone loss in hyperthyroid mice, yet via different mechanisms. This may have important implications for the management of patients with hyperthyroidism-induced bone disease.

**Disclosures:** Elena Tsourdi, None.

This study received funding from: Amgen, Inc.

## SU0312

**Skeletal Responses to the Discontinuation of Intermittent Parathyroid Hormone (PTH) Treatment in Intact and Ovariectomized Rats.** Wei-Ju Tseng\*, Wonsae Lee, Wei Tong, Luqiang Wang, Xiaoyuan Ma, Hongbo Zhao, Yihan Li, Chih-Chiang Chang, Chantal de Bakker, Ling Qin, X. Sherry Liu. University of Pennsylvania, United states

Intermittent PTH treatment reduces the risk of fracture in postmenopausal women by improving bone mass. However, BMD rapidly decreases upon withdrawal from the treatment. To uncover the mechanisms behind this adverse phenomenon, we investigated the changes in bone microarchitecture in response to withdrawal of PTH in both intact and ovariectomized (OVX) rats.

23 female SD rats (4-5 month old) were assigned to four regimes: *Intact Animals:* PTH (n=9, PTH 40 $\mu$ g/kg 5x/wk for 3 wks followed by saline for 3wks); VEH (n=5, saline for 6wks). *OVX Animals with 3-wk osteopenia development:* PTH (n=6) and VEH (n=3) with the same treatment regime as intact rats. Sequential scans of proximal tibiae were performed by *in vivo*  $\mu$ CT (Scanco, 10.5  $\mu$ m) at week 0, 3, 4, 5 and 6.

*Intact Animals:* 3-wk PTH treatment caused a 31% and 33% increase in bone volume fraction (BV/TV) and trabecular thickness (Tb.Th), respectively, and a 49% decrease in structure model index (SMI, p<0.01). BV/TV and Tb.Th were 21% and 20% greater, and SMI was 42% lower in the PTH- vs. VEH-treated animals (p<0.01). Upon 3 wks of withdrawal, no changes were detected in BV/TV, Tb.Th, or SMI. The treatment benefits remained 3 wks after withdrawal (p<0.01, Fig 1). *OVX Animals:* 3-wk osteopenia development caused 52% and 13% decrease in BV/TV and Tb.Th, respectively, and a 157% increase in SMI (p<0.05). Bone loss continued in VEH rats for 6 wks. In contrast, 3-wk PTH treatment effectively slowed down the bone loss, causing no changes in BV/TV or SMI, and a 31% increase in Tb.Th. At wk3, BV/TV and Tb.Th were 74% and 26% greater, and SMI was 18% lower in the PTH- vs. VEH-treated rats (p<0.01). 1 wk after the withdrawal (wk4), BV/TV, Tb.Th, and SMI continued to show trends of improvement. Trends of bone deterioration appeared during the 2<sup>nd</sup> and 3<sup>rd</sup> wk of PTH withdrawal (wk 5 and 6), with a 28% decrease in BV/TV and a 15% increase in SMI (p<0.05) at wk6 vs. wk4. Nevertheless, the treatment benefit in BV/TV and Tb.Th remained 3 wks after PTH withdrawal (Fig 1).

Significant bone loss occurred in OVX rats in response to discontinuation of PTH treatment while no adverse effect was observed in intact rats, suggesting coupled effects between PTH withdrawal and the degree of bone remodeling dynamics. Intriguingly, there is a continuous anabolic window upon early withdrawal from PTH in OVX rats, which offers a new mechanism in support of the cyclic administration regime of PTH to maximize the treatment efficacy.

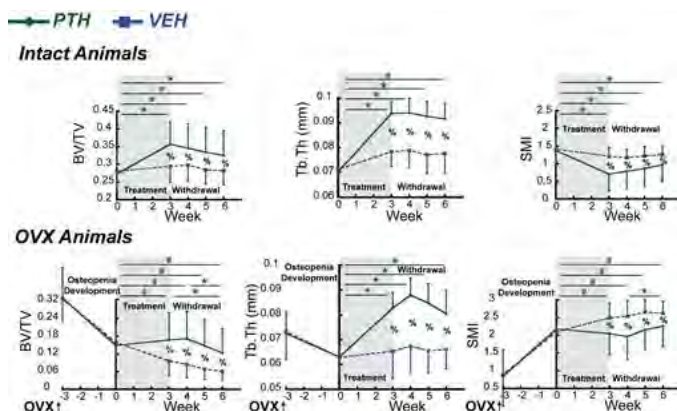


**Fig 1.** Mean  $\pm$  SD of BV/TV (Left), Tb.Th (Middle), and SMI (Right) in the tibial trabecular bone in response to PTH treatment and withdrawal in intact (Top) and OVX (Bottom) rats. \*: difference between time points in the PTH group; #: difference between time points in the VEH group; %: difference between PTH and VEH groups (p<0.05).

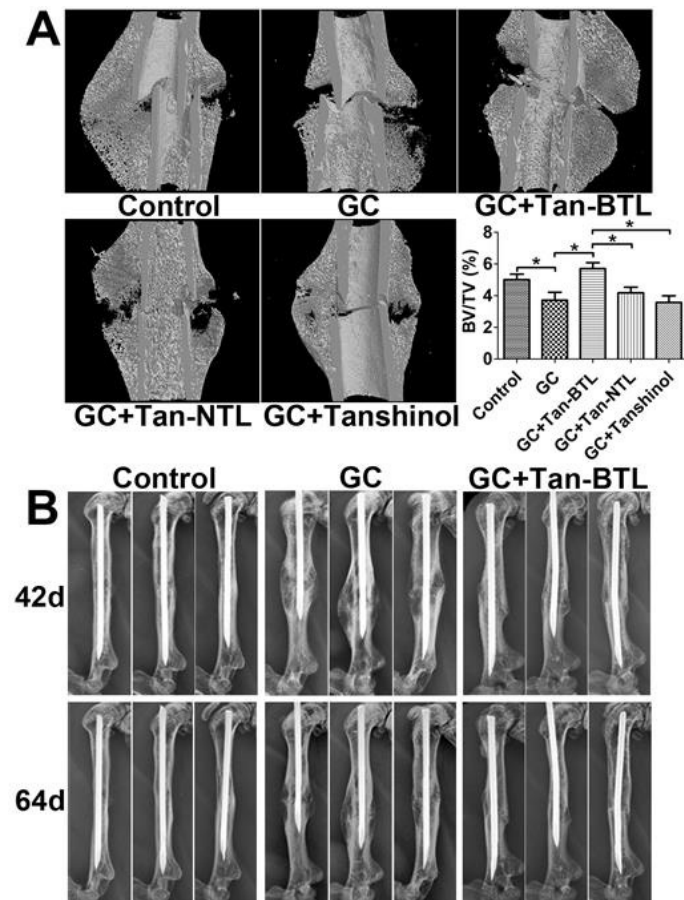
Figure 1

**Disclosures:** Wei-Ju Tseng, None.

## SU0313

**Tanshinol-loaded Bone-targeting Liposome Accelerates Delayed Fracture Healing in Mice.** Yanzhi Liu<sup>\*1</sup>, Zhenshan Jia<sup>2</sup>, Xiang Gao<sup>3</sup>, Xiaoyan Wang<sup>2</sup>, Xiaobei Wang<sup>2</sup>, Liao Cui<sup>1</sup>, Dong Wang<sup>2</sup>. <sup>1</sup>Guangdong Key Laboratory for Research & Development of Natural Drugs, Guangdong Medical University, China, <sup>2</sup>Nebraska Medical Center, United states, <sup>3</sup>Stem Cell research & Cellular Therapy Center, Affiliated Hospital of Guangdong Medical University, China

Bone fracture nonunion is a major clinical challenge in orthopedic practice. In addition to surgical intervention and autologous bone grafts, bone morphogenic proteins (BMPs) have also been tested as an adjunct therapy to accelerate the healing of fracture. BMP is an expensive therapy and has not been approved by FDA for fracture treatment, only for spinal fusion. Clearly, there is an unmet clinical need of a less expensive adjunct therapy for better clinical management of fracture nonunion. As a water-soluble monomer isolated from *salviae miltiorrhizae*, tanshinol has been proved to be an effective bone anabolic agent with high therapeutic index. Its high water solubility and lack of chemical stability, however, has impeded its clinical application. To address this issue, we have developed a tanshinol-loaded bone-targeting liposome formulation (Tan-BTL). When tested in vitro, Tan-BTL demonstrated significant hydroxyapatite affinity. Histological analysis of the distal femur after local administration of the formulation reveals robust targeting and retention at the growth plate, the trabecular bone, the cortical bone and bone lacuna. A near infrared imaging analysis further confirmed BTL could concentrate on fracture site of mice and retain there up to 20 days after local injection. When tested in a delayed fracture healing mouse model (induced by daily administration of prednisone at 12 mg/kg for 64 days), micro-CT and planar X-ray imaging analysis of the callus tissue suggest that Tan-BTL increased callus BV/TV by 54% in femur fracture of glucocorticoid-treated mice at the 18<sup>th</sup> day and shortened the fracture healing time from >64 days to 42 days when compared to glucocorticoid-treated mice without treatment. These results support BTL as a promising targeted drug delivery system for local delivery of low molecular weight bone anabolic agents. Specifically, the Tan-BTL formulation tested could be a simple, safe and effective non-invasive strategy for the treatment of bone fracture nonunion. Figure Legends, A: Micro CT analysis on fracture callus of tanshinol-loaded bone-targeting liposome (Tan-BTL) treatment to glucocorticoid-treated fracture mice-the 18<sup>th</sup> day after closed fracture. Tanshinol-loaded non-targeting liposome (Tan-NTL). \* $P < 0.05$  was considered as statistic significant; B: X ray image analysis on fracture callus of Tan-BTL treatment to glucocorticoid-treated fracture mice-the comparison of the 42<sup>th</sup> day and the 64<sup>th</sup> day after closed fracture.



2016 ASBMR abstract figure-Yanzhi Liu

Disclosures: Yanzhi Liu, None.

## SU0314

**Calcitonin alleviates hyperalgesia in osteoporotic rats by modulating serotonin transporter activity.** Jia-Fwu Shyu<sup>\*1</sup>, Chin-Bin Yeh<sup>2</sup>, Tzu-Hui Chu<sup>1</sup>, Jung-Tzu Cheng<sup>1</sup>, Ni-Ko Wei<sup>1</sup>, Wei-Yu Chen<sup>1</sup>, Tien-Hua Chen<sup>3</sup>. <sup>1</sup>Department of Biology & Anatomy, National Defense Medical Center, Taiwan, province of china, <sup>2</sup>Department of Psychiatry, National Defense Medical Center, Tri-Service General Hospital, Taiwan, province of china, <sup>3</sup>Institute of Anatomy & Cell Biology, School of Medicine, National Yang Ming University, Taiwan, province of china

Purpose: Calcitonin has analgesic effects in patients who have pain due to vertebral fracture, osteoporotic fracture, Paget's disease, and lumbago. Clinical usage of calcitonin can provide a mild but statistically significant decrease in back pain and improve the quality of life in postmenopausal women with osteoporosis.

Methods: The purpose of this study was to evaluate if serotonin in the brain involved in the anti-nociceptive effect of calcitonin in a rat model of osteoporosis, in which osteoporosis was induced by ovariectomy (OVX). Rats were randomized to four groups: sham operation, OVX, OVX plus calcitonin, or OVX plus alendronate.

Results: OVX led to alterations in bone microarchitecture; alendronate strongly reversed this effect, and calcitonin moderately reversed this effect. OVX increased hyperalgesia (determined as the time for hind paw withdrawal from a heat source); calcitonin reduced this effect, but alendronate had no effect. OVX increased the expression of c-Fos (a neuronal marker of pain) in the thalamus; calcitonin strongly reversed this effect, and alendronate moderately reversed this effect. OVX also reduced serotonin transporter (SERT) but increased 5-HT1A receptor expression and activity; calcitonin aggravated this effect, but alendronate had no effect on recovery of SERT/5-HT1A activity and expression.

Conclusions: These results suggest that OVX-induced enhancement of serotonergic system may act as a protection against the hyperalgesia. However, the anti-nociceptive effects of calcitonin in osteoporosis may be mediated by decreases neural SERT activity and increased activation of 5-HT1 receptors in the thalamus in this rat model of osteoporosis.

Disclosures: Jia-Fwu Shyu, None.

## SU0315

**Collagen-Induced Arthritis: Densitometry and TRACP-5b Assessments in Rats.** Aurore Varela<sup>\*1</sup>, Gabrielle Boyd<sup>1</sup>, Dominic Poulin<sup>1</sup>, Rana Samadfam<sup>1</sup>, Jacquelin Jolette<sup>1</sup>, Rogely Boyce<sup>2</sup>, Kathrin Locher<sup>2</sup>, Marina Stolina<sup>2</sup>. <sup>1</sup>Charles River Laboratories, Canada, <sup>2</sup>AMGEN Inc., United states

The rat collagen-induced arthritis (CIA) model is used to evaluate the efficacy of potential disease modifiers for the treatment of rheumatoid arthritis (RA). The purpose of this study was to evaluate the bone density changes using Dual X-ray absorptiometry (DXA), and to quantify osteoclast-derived tartrate-resistant acid phosphatase form 5b (TRACP-5b).

Female Lewis rats were randomly assigned to one of two groups: non-diseased controls (n=12) and CIA controls (n=12). Clinical scoring, paw thickness and volume measured using a plethysmometer, and DXA of the tibio-tarsal joint region and the lumbar spine, were performed prior to arthritis induction (AI), during the course of the study and until 25 days post-AI. Serum samples for TRACP-5b (ELISA) were collected once prior to arthritis induction and during the study on Days 16 and 26. Tibio-tarsal, inter tarsal, tarso-metatarsal and metatarso-phalangeal joints were evaluated microscopically using a semi-quantitative scoring scale for inflammation, pannus, cartilage damage, bone resorption and periosteal/exostotic changes.

Clinical score, paw thickness and volume peaked around Day 16 compared to non-disease animals. Paw swelling, as measured by thickness, was observed in CIA animals starting on Day 14. Maximum increases of 70% vs non-disease animals were observed on Day 16 and remained stable. On Day 16, lower gains in bone mineral content (BMC) and bone mineral density (BMD) were noted in CIA animals compared to controls at the lumbar spine. The effect of arthritis on bone was progressive and at Day 25, statistically significant differences in all DXA parameters (area, BMC and BMD) were noted between controls and CIA animals at both lumbar spine and tibio-tarsal joint. Increases in serum TRACP-5b of 53% were observed on Day 16 in CIA animals. All CIA animals had a composite histopathologic arthritis score at or close to the maximum possible score of 20 (CIA range: 18-20; range: 0-1 in the non-disease group).

In this model, the increased osteoclast cellularity demonstrated by Cathepsin K immunostaining and increased bone resorption explained the BMD loss during the second half of the study. In conclusion, BMD measured by DXA represents a convenient in vivo assessment of bone loss in the rat CIA model and serum TRACP-5b provides additional insight in osteoclast number/activity, consistent with this RA model and helping to characterize the model for the evaluation of new therapeutics targeting RA.

In conclusion, BMD measured by DXA represents a convenient in vivo assessment of bone loss in the rat CIA model and serum TRACP-5b provides additional insight in osteoclast number/activity, further characterizing the model for the evaluation of new therapeutics targeting RA.

Disclosures: Aurore Varela, None.

**SU0316**

**Purinergic P2Y12 Receptor Antagonists Inhibit Bone Cell Function In Vitro and Affect Bone Turnover in Adult Female Rats.** Maria Ellegaard<sup>1</sup>, Isabel R Orriss<sup>2</sup>, Jessal J Patel<sup>2</sup>, Solveig Petersen<sup>1</sup>, Ming Ding<sup>3</sup>, Saba Hamza<sup>1</sup>, Niklas Rye Jørgensen<sup>1</sup>. <sup>1</sup>Research Centre for Ageing & Osteoporosis, Dep. of Clinical Biochemistry & Endocrinology, Rigshospitalet, Denmark, <sup>2</sup>Comparative Biomedical Sciences, Royal Veterinary College, United Kingdom, <sup>3</sup>Department of Orthopaedic Surgery & Traumatology, Odense University Hospital, University of Southern Denmark, Denmark

**Aim:** The purinergic P2Y12 receptor (P2Y12R) is a G-protein-coupled receptor which is activated by the nucleotide ADP. P2Y12R is expressed by both osteoblasts and osteoclasts and antiplatelet treatment with the P2Y12R antagonist clopidogrel has been shown to be associated with fracture risk in humans. The aim of the study was to investigate the effect of the more potent P2Y12R antagonists, prasugrel and ticagrelor, on bone cell function in vitro and in vivo.

**Methods:** Primary osteoblasts were isolated from calvaria of neonatal mice and cultured for up to 24 days with 1nM-50µM ticagrelor and prasugrel. Primary osteoclasts were generated from bone marrow of 8-week old mice and cultured on dentine discs for 9 days with 1nM-10µM prasugrel and ticagrelor. Six-month-old female Sprague Dawley rats were treated with prasugrel (0.0625, 0.125, 0.25 mg/kg/day or vehicle) or ticagrelor (0.5625, 1.125 or 2.25 mg/kg/day or vehicle) 5 days per week for 6 weeks. Blood was drawn at baseline, 3 and 6 weeks for determination of bone turnover markers (PINP and CTX-I). After sacrifice, femoral bone strength was determined using 3-point-bending test and shear test. Femoral bone mineral density (BMD) was measured by DXA.

**Results:** Both antagonists dose dependently inhibited mineralized nodule formation ( $\geq 0.1\mu\text{M}$ ) by up to 85% ( $p < 0.001$ ); concentrations in excess of 10µM were toxic resulting in widespread cell death. Osteoclast number was unaffected by prasugrel treatment. Ticagrelor caused a 60% decrease in osteoclast number at 10µM only ( $p < 0.001$ ). Bone resorption was inhibited by up to 60% and 99% by prasugrel and ticagrelor ( $\geq 1\text{nM}$ ), respectively ( $p < 0.001$ ). Prasugrel treatment dose dependently increased BMD of the total femur by up to 8% ( $p < 0.05$ ); ticagrelor was without effect. At the highest dose, both antagonists increased femoral shaft bone strength by up to 10% ( $p < 0.05$ ). There were no significant effects of either treatment on bone strength of the femoral neck. Both antagonists significantly decreased serum CTX-I by up to 35% compared to baseline ( $p < 0.05$ ), whilst ticagrelor reduced serum PINP by up to 35% ( $p < 0.01$ ).

**Conclusion:** In vitro and in vivo data suggests that both prasugrel and ticagrelor affect bone cell function. Further microstructural analysis and dynamic bone histomorphometry is needed to fully elucidate the role of P2Y12R inhibition on bone remodeling in vivo.

**Disclosures:** Maria Ellegaard, None.

**SU0317**

**The Effects of Intra-Articular Treatment with Recombinant Human Bone Morphogenetic Protein 7 (rhBMP-7) on the Development of Post-Traumatic Osteoarthritis in Surgically Induced Rat Models.** Jukka Morko<sup>\*</sup>, ZhiQi Peng, Katja M Fagerlund, Yvonne Konkol, Jukka P Rissanen, Jenni Bernoulli, Jussi M Halleen. Pharmatec Services Ltd, Finland

Recombinant human bone morphogenetic protein 7 (rhBMP-7) is a bone-inducing agent used in spinal fusions and during fracture repair in clinical practice. In knee joints, rhBMP-7 has been shown to attenuate the development of degenerative changes induced by anterior cruciate ligament transection (ACLT) in rabbits and by excessive running in rats and to repair cartilage damage in several species. We characterized the effects of intra-articular rhBMP-7 on the development of post-traumatic osteoarthritis (OA) in three surgically induced rat models. Unilateral OA was induced in the knee joints of male Lewis rat using the following operations: medial meniscal tear (MMT) and medial collateral ligament transection (MCLT), ACLT and partial medial meniscectomy (pMMx), and ACLT. Treatment was started one week after the operations. Rats were treated intra-articularly once a week with rhBMP-7 at 0.25 µg/wk or vehicle. Treatment effects on body weight, static weight bearing and static mechanical allodynia were followed during the in-life phase. Knee joints were harvested in MMT+MCLT rats at 6 weeks, in ACLT+pMMx rats at 8 weeks, and in ACLT rats at 10 weeks. Treatment effects on knee joints were determined following the recommendations of the OARSI histopathology initiative. Paw weight bearing and paw withdrawal threshold were decreased in operated hind limbs before the start of treatment indicating knee joint discomfort and pain. In MMT+MCLT rats, knee joint discomfort and pain were observed at 3 weeks, and knee joint discomfort, cartilage degeneration and extracellular matrix (ECM) loss, large osteophytes and synovial inflammation at 6 weeks. Intra-articular rhBMP-7 improved knee joint discomfort and pain at 3 weeks, and attenuated the cartilage degeneration and ECM loss focally at 6 weeks. In ACLT+pMMx rats, knee joint pain was identified at 4 and 8 weeks, and cartilage degeneration and ECM loss, moderate osteophytes and synovial inflammation at 8 weeks. Intra-articular rhBMP-7 attenuated the cartilage degeneration focally in superficial layer at 8 weeks. In ACLT rats, knee joint discomfort and pain were detected at 5 weeks, and cartilage degeneration and ECM loss, moderate osteophytes and synovial inflammation at 10 weeks. Intra-

articular rhBMP-7 improved knee joint discomfort at 5 weeks and attenuated the ECM loss focally at tidemark at 10 weeks. These findings demonstrate a minor chondroprotective activity for rhBMP-7 in multiple rat models of post-traumatic OA.

**Disclosures:** Jukka Morko, None.

**SU0318**

**The role of sclerostin in bone metabolism in the hypoxic brain damage mice model.** Sun Yong Song<sup>1</sup>, Da Hea Seo<sup>\*</sup>, Yoon-Kyum Shin<sup>2</sup>, Sung Rae Cho<sup>2</sup>, Yumie Rhee<sup>1</sup>. <sup>1</sup>Department of Internal Medicine, Endocrine Research Institute, Yonsei University College of Medicine, Korea, republic of, <sup>2</sup>Department & Research Institute of Rehabilitation Medicine, Yonsei University College of Medicine, Korea, republic of

**Objectives:**

Cerebral palsy (CP) is most common form of physical disability in children, resulting from brain injury incurred during CNS development. Previous studies with CP patients suggest that they are prone to have low bone mass, osteoporosis and increased risk of fragility fractures with association with the ambulatory ability and severity of disease involvement.

The aim of this study was to investigate the changes in bone density and geometry in hypoxic brain injury model mice and furthermore, to investigate the potential role of Sost/Scelrostin in bone and muscle metabolism in those mice, using SOST overexpressing transgenic (TG) mice.

**Methods:**

Animals were divided into four subgroups; Sham wild type (A) and sham transgenic (B), hypoxic brain injury wild type (C), and hypoxic brain injury Transgenic (D). In hypoxic brain injury groups, neck dissection with unilateral right carotid artery ligation was performed during the 4<sup>th</sup> week from birth. Behavioral assessments, dual-energy X-ray absorptiometry (DXA) scan, micro-computed tomography (micro-CT), bone turnover markers (BTM) were assessed.

**Results:**

There was significant difference in constant 48 rpm Rotarod test when performed 2 weeks after hypoxic brain injury, however its difference got attenuated when repeated 4 weeks after hypoxic brain injury. DXA evaluation of spine and femur revealed that the bone mass was significantly lower in D group. The trabecular bone volume fraction (BV/TV) and trabecular number (Tb\_No) in the mid shaft of the femur were decreased by about 52.7% and 53.3% respectively ( $P < 0.001$  and  $P < 0.001$ ) while trabecular separation (Tb\_Sp) was 136% more in D group compared to C group ( $P < 0.001$ ). Bone turnover markers were also found to be elevated in Injury groups compared to Sham groups although it did not show significant difference due to genotype.

**Conclusions:**

Hypoxic brain injury transgenic mice not only have lower spine and femur BMD, lower BV/TV, Tb\_No and higher Tb\_Sp but also lower locomotive function and muscle strength. Sclerostin action may not be limited to a local bone formation regulator, but further extends to other tissues other than bone such as muscles. Future studies are warranted to investigate the potential link between sclerostin and muscle function.

**Disclosures:** Da Hea Seo, None.

**SU0319**

**Hearing Loss and Otologic Outcomes in Fibrous Dysplasia.** Alison Boyce<sup>\*</sup>, Carmen Brewer<sup>2</sup>, Timothy DeKlotz<sup>3</sup>, Christopher Zalewski<sup>2</sup>, Kelly King<sup>2</sup>, Michael Collins<sup>1</sup>, H. Jeffrey Kim<sup>2</sup>. <sup>1</sup>Section on Skeletal Disorders & Mineral Homeostasis, Craniofacial & Skeletal Diseases Branch, National Institute of Dental & Craniofacial Research, National Institutes of Health, United states, <sup>2</sup>Otolaryngology Branch, National Institute on Deafness & Other Communication Disorders, National Institutes of Health, United states, <sup>3</sup>Department of Otolaryngology-Head & Neck Surgery, Georgetown University Hospital, United states

**Background:** Fibrous dysplasia (FD) arises from somatic activating mutations in the cAMP-regulating protein  $G_{\alpha s}$ , leading to replacement of normal bone by proliferative osteogenic precursors. In the craniofacial skeleton this results in formation of expansile lesions, leading to facial deformity and functional impairment. The effect of FD on hearing and otologic function has not been established. A transgenic mouse model of increased  $G_s$  signaling demonstrates severe and progressive hearing loss due to cochlear overgrowth (Akil et al, PLOS One 2014), however the human audologic and otologic phenotype has not been determined. **Purpose:** To characterize audiological and otologic outcomes in patients with craniofacial FD, and to correlate findings with temporal bone disease as assessed by computed tomography (CT). **Methods:** Clinical data from a longstanding FD natural history study at the NIH were reviewed. Subjects underwent concordant audiological evaluation, otologic evaluation, and cranial CT imaging. **Results:** 137 subjects with craniofacial FD were evaluated (mean age  $23.1 \pm 16.6$  years, range 3.3-80.3). Temporal bone involvement was identified in the majority (73%). Hearing loss was identified in 55 ears (20%); characterized as mild (85%), moderate (11%), or severe (4%). Conductive loss was more frequent than sensorineural loss (64% versus 46%). Longitudinal evaluations

were available in 80 subjects (mean length of follow-up  $5.8 \pm 4.2$  years, range 0.4-15.2). Hearing loss was largely non-progressive, remaining stable in 127 ears (79%), worsening in 18 (11%), and improving in 15 (9%). Otologic symptoms were uncommon, and included tinnitus (8%), vertigo (3%), and auditory canal stenosis requiring surgical intervention in 3 subjects (2%). Abnormalities identified on CT included external auditory canal stenosis (27% of all ears), epi-tympanic crowding (60%), and epi-tympanic involvement (47%). Conclusion: Hearing loss is common in FD, and is typically mild and non-progressive. FD involvement of the temporal bones occurs frequently; clinical manifestations depend on the location and degree of skeletal involvement. Hearing and otologic monitoring is indicated in patients with craniofacial FD.

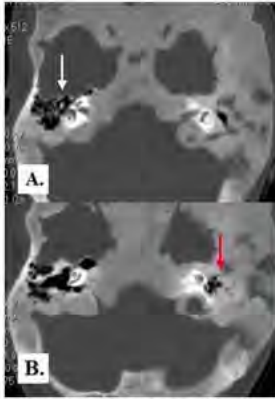


Figure. CT of patient with severe FD. (A) White arrow demonstrating normal epitympanum. (B) Red arrow demonstrating impingement of the epitympanum by FD.

Figure: Cranial CT imaging

Disclosures: Alison Boyce, None.

## SU0320

**Newly formed heterotopic bone in Fibrodysplasia Ossificans Progressiva still requires Activin A for maintenance and expansion.** LiQin Xie\*, Lily Huang, Nanditha Das, Xialing Wen, Lili Wang, Genevieve Makhoul, Andrew Murphy, Vincent Idone, Aris Economides, Sarah Hatsell. Regeneron, United states

Fibrodysplasia ossificans progressiva (FOP) is a rare genetic disorder characterized by episodic but cumulative heterotopic ossification (HO). The HO in FOP develops by an endochondral process that involves a cartilage intermediate and which overall appears to mirror normal endochondral bone formation. As this heterotopic bone develops, it connects to the normal skeleton (by a process that is currently not understood), and these connections eventually start to bridge joints, resulting in progressive immobility, and eventually death. FOP is caused by mutations in the type I BMP (bone morphogenetic protein) receptor ACVR1, the most mutation altering arginine 206 to histidine (ACVR1<sup>R206H</sup>). We have generated a genetically and physiologically accurate mouse model of FOP – *Acvr1<sup>R206H</sup>/F1Es<sup>+/+</sup> Gt(ROSA26)-Sor<sup>CerERT2/+</sup>*. Using this model, we demonstrated that there is an absolute requirement for Activin A to kickstart the process of HO. This requirement for Activin A was demonstrated in vivo using neutralizing antibodies to Activin A. However, in these experiments the anti-Activin A antibody was administered at the same time as initiation of HO, and hence this setting only addressed the requirement of Activin A at the initial stages of HO, prior to the formation of cartilage. We explored whether Activin A continues to play a role after the endochondral process has started and even when partly mineralized heterotopic lesions could be observed. Our results indicate that inhibition of Activin A with a fully human monoclonal antibody completely blocks formation of HO in this model of FOP when the antibody is administered 9 days after initiation of the model. To further test delayed treatment's effect on already formed – yet still nascent – HO, anti-Activin A Ab was injected at 3 weeks post initiation of the model. With 3-weeks treatment, existing HO volume (lesion size) decreased by  $37 \pm 41$  mm<sup>3</sup> in Activin A Ab treatment group ( $p < 0.05$ ), while it increased by  $19 \pm 45$  mm<sup>3</sup> in isotope control group. In summary, these results demonstrate a continued role for Activin A even after mineralized heterotopic bone lesions have formed and indicates that anti-Activin A may be able to reverse the progression of nascent (and not fully mineralized) heterotopic bone.

Disclosures: LiQin Xie, None.

This study received funding from: Regeneron

## SU0321

**Denosumab-related Atypical Femoral Fracture in an Elderly Woman with Childhood-onset Hypophosphatasia Due to a Novel Mutation (p.Val121Met).** Michaël R Laurent\*<sup>1</sup>, Evelien Gielen<sup>1</sup>, Etienne Mornet<sup>2</sup>. <sup>1</sup>Center for Metabolic Bone Diseases, University Hospitals Leuven, Belgium, <sup>2</sup>Unité de Génétique Constitutionnelle, CHU Versailles, France

**INTRODUCTION:** Hypophosphatasia (HPP) is a rare inborn error of metabolism due to mutations in tissue non-specific alkaline phosphatase (ALPL) which may cause rickets, fractures, growth retardation and other symptoms. Bisphosphonates may induce atypical fractures in HPP subjects, whereas enzyme-replacement therapy may improve skeletal manifestations.

**CASE REPORT:** A 69-year-old woman consulted for an atypical periprosthetic left femur fracture with prodromal thigh pain. Total hip replacement had been performed 2 years earlier for a femoral neck stress fracture. At that time, she was switched to denosumab after 6 years of treatment with risedronate. DXA at age 61 had revealed a T-score of -4.9 at the lumbar spine and -2.0 at the femoral neck. She had rachitic varus deformities and suffered bilateral low-energetic hip fractures and another periprosthetic hip fracture around 12-14 years. Starting from age 9 with a 'honeymoon period' in early adulthood, she suffered 3 wrist fractures, a metatarsal and a tibial stress fracture. Adult height had been 150 cm, followed by 10 cm historic height loss. Biochemical tests were unremarkable except for low alkaline phosphatase (20 U/L; normal range 40-105) and hypercalciuria. Confirmation showed raised pyridoxal-5'-phosphate (active vitamin B6, an ALPL substrate). Denosumab was discontinued and enzyme-replacement therapy started. Genetic testing demonstrated a novel mutation (c.361G>A, p.Val121Met) in the heterozygous state. This residue is conserved in other ALP isoforms and between species. In silico prediction and 3D structure analysis suggested that this mutant would be damaging and may exert a dominant-negative effect. The mutation segregated with low serum ALP in 2/10 first-degree relatives ( $P=0.008$  Fisher's exact test). Interestingly, 5 family members (3M, 2F) with very low lumbar spine T-scores (-3.8 to -4.8), hypercalciuria and kidney stones had normal serum ALP and lacked the pathogenic mutation, suggesting idiopathic hypercalciuria (unrelated to HPP).

**DISCUSSION:** Pediatric-onset HPP may go unrecognized for decades and should be considered in case of atypical fractures, even in the elderly. Lack of a lower cut-off level for alkaline phosphatase in many clinical laboratories reinforces underdiagnosis. To the best of our knowledge, this is the first case report of a denosumab-related atypical femoral fracture in an HPP patient, suggesting that switching from bisphosphonates to denosumab is unhelpful in HPP.

Disclosures: Michaël R Laurent, Novartis, 12; Alexion, 12

## SU0322

**Chiari 1 Malformation in Three Consecutive Generations in a Family with X-Linked Hypophosphatemic Rickets.** Gary S. Gottesman\*<sup>1</sup>, Ghada A. Otaify<sup>2</sup>, Valerie A. Wollberg<sup>3</sup>, Vinieth N. Bijanki<sup>1</sup>, Shenghui Duan<sup>4</sup>, Margaret Huskey<sup>4</sup>, C. Charles Gu<sup>5</sup>, William H. McAlister<sup>6</sup>, Katherine L. Madson<sup>7</sup>, Steven Mumm<sup>4</sup>. <sup>1</sup>Center for Metabolic Bone Disease & Molecular Research, Shriners Hospital for Children, United states, <sup>2</sup>Department of Clinical Genetics, Division of Human Genetics & Genome Research, Center of Excellence for Human Genetics, National Research Centre, Egypt, <sup>3</sup>Center for Metabolic Bone Disease & Molecular Research, Shriners Hospital for Children, United states, <sup>4</sup>Division of Bone & Mineral Diseases, Department of Internal Medicine, Washington University School of Medicine at Barnes-Jewish Hospital, United states, <sup>5</sup>Division of Biostatistics, Washington University School of Medicine at Barnes-Jewish Hospital, United states, <sup>6</sup>Department of Pediatric Radiology, Mallinckrodt Institute of Radiology, Washington University School of Medicine at St. Louis Children's Hospital, United states, <sup>7</sup>Center for Metabolic Bone Disease & Molecular Research Shriners Hospitals for Children - St. Louis, United states

X-linked hypophosphatemic rickets (XLH) is a rare heritable disorder caused by mutations in the PHEX gene. Chiari 1 malformation (CIM), defined as cerebellar tonsillar herniation greater than 3mm below the foramen magnum, has been reported on a limited basis in XLH, however, the pathogenesis of CIM in XLH remains unknown. One hypothesis is that calvarial thickening with subsequent small posterior fossa leads to tonsillar herniation. We have encountered CIM several times in our cohort of ~ 300 XLH patients. To our recollection, CIM has been limited to single individuals within each XLH family. Here, we report the findings of CIM in four individuals within three consecutive generations of one XLH family.

The maternal grandmother, is the index case of XLH in this family and had CIM. She required decompression craniectomy and ventriculoperitoneal (VP) shunt placement. Her daughter had CIM and required several craniectomy and VP shunt procedures. Her 16 year-old grandson was also diagnosed with CIM at age 6 years (status post decompression craniectomy). His clinical status is also complicated by empty sella syndrome, left optic nerve hypoplasia, growth hormone deficiency, a familial coagulopathy, and celiac disease. Her 13-year-old granddaughter similarly has a history of CIM that has not required surgical intervention. Like her brother she has learning problems and celiac disease.

Using our Ion Torrent next generation sequencing (NGS) platform we have identified a variety of *PHEX* mutations in our individual cases of XLH with CIM. We have also detected a number of common and rare SNPs in *DMPI*, *FGF23*, *MEPE*, and *SLC34A3* in these isolated cases. We now have in process NGS for *PHEX* and 14 modifier genes in this 3 generation XLH family to identify genetic defects that may predispose to CIM in XLH. Further, we will study the relation of posterior fossa volume, serum FGF23 levels, therapeutic compliance, and genetic findings to better understand the pathogenesis of CIM in XLH.

Disclosures: Gary S. Gottesman, None.

**SU0323**

**Significant Impairments in Joint Mobility and Range of Function in Adult Patients with XLH.** Erika J. Parisi<sup>1</sup>\*, Richard Feinn<sup>1</sup>, Samantha Ferraro<sup>2</sup>, Marie Frey<sup>3</sup>, Juan C. Garbalosa<sup>3</sup>, Ramon Gonzalez<sup>2</sup>, Tania Grgurich<sup>2</sup>, Flavia Muchemi<sup>3</sup>, Keith Steigbigel<sup>3</sup>, Steven M. Tommasini<sup>4</sup>, Carolyn M. Macica<sup>1</sup>. <sup>1</sup>Quinnipiac University, Frank H. Netter School of Medicine, United states, <sup>2</sup>Quinnipiac University, School of Health Sciences, Department of Diagnostic Imaging, United states, <sup>3</sup>Quinnipiac University, School of Health Sciences, Department of Physical Therapy, United states, <sup>4</sup>Yale University School of Medicine, Department of Orthopaedics & Rehabilitation, United states

Introduction: X-linked hypophosphatemia (XLH) is the most common form of the familial phosphate-wasting disorders. XLH manifests in childhood as rickets and impaired bone mineralization. Osteomalacia persists into adulthood and degenerative arthritis, osteophytes and enthesophytes come to dominate the clinical picture. The primary objective of the study was to characterize the functional impact of the musculoskeletal manifestations of XLH in the adult patient population. Methods: Nine adult patients with XLH were paired with age/sex-matched unaffected volunteers in a case-control study (53.8±5.1 yrs). Activities Specific Balance Confidence (ABC) scale, Lower Extremity Functional Scale (LEFS) and Manual Muscle Testing were completed and analyzed for statistical significance using a two sample t-test (p<0.05). Functional range of motion of the hip, knee, ankle and cervical spine was assessed using a gravity-dependent goniometer. Full-body x-rays and 3D-kinematic analysis of gait was also performed. Welch's unequal variances t-test was used to analyze statistical significance (p<0.05). Results: Data obtained from the ABC scale revealed that XLH subjects had a significantly lower percent of self-confidence in perceived balance and fall risk than controls (95.9%±3.1 v. 62.3%±17.6, p=0.001) consistent with a significant difference in the LEFS to assess lower-extremity function (0.98±0.02 v. 0.45±0.19, p=0.0001). Functional data of patients with XLH showed minimal deficits in muscle strength but significant impairment in the hips, ankles, and knees compared to controls (Table 1). Symmetrical impairment was consistent with radiological evidence of bilateral involvement at each anatomical site. Range of motion of the cervical spine between the two groups demonstrated a significant difference only in extension (63±3.0 v. 32±16.3, p=0.0009). However, in patients with radiological confirmation of complete cervical spine fusion with pronounced enthesophytes, all parameters (flexion, extension, rotation, and lateral flexion) differed significantly from controls. Kinematic analysis of gait further supports a significant decrease in hip rotation (p=0.02), hip flexion (0.05), hip abduction (p=0.05) and ankle rotation (p=0.002) in order to facilitate gait in patients with XLH and is consistent with radiological evidence of calcifications involving the spine, hip, knee and ankle. Conclusions: Functional data demonstrate significant impairments in joint mobility and range of motion and may underlie fears faced by this patient population including that of falling. These data served as a platform for studies of the psychosocial impact of the disorder as well as potential evidence-based interventions by social, occupational and physical therapists. They also underscore the importance of using these tools to evaluate patients in order to monitor progression and to assess interventions.

JOINT	CONTROL Right/Left	XLH Right/Left	P
Hip, FLEXION	122±2.7; 123±4.5	100.9±19.8; 107±17.1	0.01*; 0.03*
Hip, ABDUCTION	40±0; 42.6±4.9	20.1±9.8; 16.4±18.8	0.008*; 0.003*
Hip, ADDUCTION	30±3.5; 32±4.5	20.1±9.8; 20.2±7.2	0.02*; 0.003*
Hip, INTERNAL ROTATION	37±13.5; 43±4.5	14.3±12.6; 14.3±9.9	0.02*; 0.001*
Hip, EXTERNAL ROTATION	40±7.1; 43±4.5	26.2±15.4; 21.7±14.8	0.04*; 0.002*
Hip, EXTENSION	19±2.3; 19±5.4	0.89±10.7; -1.6±13.8	0.0008*; 0.002*
Ankle DORSIFLEXION	10±0; 8±2.7	-1.4±11; 0.56±8.1	0.01*; 0.03*
Ankle PLANTAR FLEXION	49±8.9; 51±2.2	40±16.8; 48±13.2	0.2; 0.6
Ankle INVERSION	43±6.5; 43±4.9	25.7±12; 28±13	0.004*; 0.01*
Ankle EVERSION	28±11; 30.4±0.9	12.9±11.6; 12.2±8.1	0.04*; 0.0001*
Knee FLEXION	139±2.5; 141±2.5	105±19.9; 97±22.9	0.0009*; 0.0004*
Knee EXTENSION	0±0; 0±0	-12.8±12.5; -12.5±7.6	0.02*; 0.002*

Parisi\_Table 1

Disclosures: Erika J. Parisi, None.

**SU0324**

**Bone Robusticity in Osteogenesis Imperfecta Diverges from Established Patterns.** Kate Citron<sup>1</sup>, Cosmo Venezia<sup>1</sup>, Josephine Marino<sup>1</sup>, Erin Carter<sup>1</sup>, Karl Jepsen<sup>2</sup>, Cathleen Raggio\*<sup>1</sup>. <sup>1</sup>Hospital for Special Surgery, United states, <sup>2</sup>University of Michigan, United states

Osteogenesis Imperfecta (OI) occurs in 1/10,000 live births with severity ranging from perinatally lethal to mild forms with minimal fractures. Most cases arise from mutations of type I procollagen genes. To investigate bone morphology, we calculated robustness (Tt.Ar/Le) and relative cortical area (RCA = Ct.Ar/Tt.Ar) from measurements of the second metacarpal and compared these measurements to age-matched controls. The second metacarpal reflects overall bone health. It is a significant predictor of fracture risk and is correlated with robustness at other sites (Kiel, 2001). Bone robustness is determined by age two (Pandey, 2009). We hypothesize that OI patients will have reduced robustness (i.e. slenderness) compared to controls and that bisphosphonate treatment will not impact bone robusticity. A retrospective review of 108 de-identified bone age films identified 45 OI patients (1 year 9 mos.- 67 yrs.) and 37 controls (4 year 6 mos.-21 yrs.). Non-parametric Kruskal-Wallis tests were used to compare differences between groups with statistical significance at p≤0.05.

OI patients had RCA values above and robustness values below that of the control population (p<0.001, table 1), independent of treatment. In general, slender bones rely on osteoblasts for new bone deposition within the marrow space, whereas robust bones rely on osteoclasts for continued marrow expansion during growth. Therefore, it is not surprising that bisphosphonate treatment did not change morphologic parameters in OI patients. In contrast to that reported in the unaffected population, sexual dimorphism was not significant in the OI patients for either robustness or RCA. Given the mechanistic link between type I collagen and bone strength, we suggest that the underlying collagen abnormalities in OI override sex-specific effects on bone development. The reduced bone mass of OI seems to come from suppressed periosteal expansion (lower Tt.Ar, table 1) and not failure to accumulate bone mass (RCA was appropriate for the slender phenotype). Because slender bones are structurally weaker than more robust bones, OI patients have both a material and a structural problem contributing to their overall strength deficit. Therefore, treatment for OI patients should focus on periosteal expansion (not suppressing resorption) to strengthen long bones. Understanding these patterns of bone morphology is important in predicting how patients will respond to treatment and to optimize the treatment effect.

	Control (n=37)			OI (n=45)		
	Total	Male	Female	Total	Male	Female
Le (mm)	56.0 ± 9.43	60.0 ± 8.81	53.5 ± 9.08	50.7 ± 11.2*	55.0 ± 10.1	48.1 ± 11.4
Tt.Ar (mm <sup>2</sup> )	40.4 ± 11.5	44.2 ± 11.5	36.3 ± 9.48	30.5 ± 12.6*	34.6 ± 13.2	27.0 ± 11.2
Ct.Ar (mm <sup>2</sup> )	27.7 ± 8.36	31.2 ± 8.25	24.2 ± 6.97	24.6 ± 12.4*	26.2 ± 13.2	21.4 ± 11.0
Marrow Area (mm <sup>2</sup> )	12.7 ± 4.25	14.0 ± 4.38	11.4 ± 3.57	6.02 ± 3.65*	6.46 ± 4.32	5.66 ± 2.93
Polar Moment of Inertia (mm <sup>4</sup> )	283 ± 141	331 ± 148	192 ± 103	186 ± 131*	206 ± 147	150 ± 118
Cortical Thickness (mm)	1.87 ± 0.51	1.89 ± 0.29	1.46 ± 0.25	1.75 ± 0.70	1.90 ± 0.74	1.58 ± 0.53
RCA	0.68 ± 0.05	0.69 ± 0.05	0.69 ± 0.05	0.78 ± 0.13*	0.69 ± 0.15	0.76 ± 0.13
Tt.Ar/Le (mm)	0.70 ± 0.14	0.75 ± 0.14	0.68 ± 0.11	0.58 ± 0.18*	0.83 ± 0.18	0.58 ± 0.18

Table 1. Average measurements and calculations for second metacarpal (mean ± stdev) reported for total (males and females), males, and females, all ages included by diagnosis

\*Significant at p<0.05 control total vs. OI total

OI Metacarpal ASBMR 2016 Table

Disclosures: Cathleen Raggio, None.

**SU0325**

**Efficacy of Monthly Alendronate Infusion for Osteogenesis Imperfecta.** Ikuma Fujiwara\*<sup>1</sup>, Chisumi Sogi<sup>2</sup>, Sayaka Kawashima<sup>1</sup>, Miki Kamimura<sup>1</sup>, Junko Kanno<sup>1</sup>. <sup>1</sup>Tohoku University Hospital, Japan, <sup>2</sup>Tohoku University Hospital, Japan

Background: Osteogenesis imperfecta (OI) is a heritable skeletal disease mostly caused by mutations in either *COL1A1* or *COL1A2* that encode type I collagen. Treatment with bisphosphonate (BP) for OI patients has been successfully performed worldwide. Of these BPs, pamidronate infusion is commonly used, and administration of zoledronic acid biannually has been reported recently. But there are some concerns about using a potent BP with a longer treatment interval for children or a BP with large infusion volume for infants.

Method: Nine patients with OI (5 type I, 3 type III, 1 type IV; ages from 0 to 12 years, average 5 years) were treated with monthly alendronate (ALN) infusion with a dose of 18 microg/kg (2ml/kg) over 1 hour. Four of the patients received previous therapy. Oral calcium was supplemented for a week after ALN infusion. Lumbar bone mineral density (BMD) was measured by DXA every 6 months.

Results: Six months of ALN treatment increased BMD by 15.5% from baseline in average. During that period, 4 fractures were reported. Febrile episode was seen in two patients after the initial infusion of ALN. Respiratory distress occurred in a type IIB/III infant after the third ALN infusion. Symptoms related hypocalcemia such as seizure were not reported during the treatment.

Discussion: ALN infusion is used for adult osteoporosis patients with a dose of 900 microg. In this study, the initial dose of 18 microg (2ml/kg) was selected with assumption of adult BW was 50 kg. The dose 2 mls per kg body weight of ALN would

be safe and well tolerated, and could be enough to increase BMD in OI patients. But in severe patients, increase of the dose may be necessary.

Conclusion: Monthly ALN infusion may be safe and efficacious for OI even in younger age. Osteogenesis imperfecta is a heritable disease.

Disclosures: Ikuma Fujiwara, None.

## SU0326

**Long Term Follow-up in Children with Osteogenesis Imperfecta type VI.** Pamela Trejo\*<sup>1</sup>, Kathleen Montpetit<sup>1</sup>, Telma Palomo<sup>2</sup>, Francis Glorieux<sup>1</sup>, Frank Rauch<sup>1</sup>. <sup>1</sup>Shriners Hospital for Children Canada, Canada, <sup>2</sup>Universidade Federal De São Paulo (UNIFESP), Brazil

Objective: Describe long-term outcome of OI type VI patients.

Methodology: Thirteen patients with OI type VI at the Shriners Hospital for Children Canada were retrospectively reviewed.

Results: Four patients had homozygous inframe mutations, 5 homozygous stop mutation, 2 compound heterozygous mutations, one a heterozygous in-frame duplication and one had a splice site mutation. All subjects had absence of circulating PDEF.

Patients received multidisciplinary treatment with rehabilitation, intravenous bisphosphonate (BP) and orthopaedic surgeries. BP treatment was maintained until growth was completed (n=9) or until treatment was switched to subcutaneous injections of denosumab (n=4).

The mean lumbar spine areal bone mineral density (LS-aBMD) Z-score increased from -4.5 (SD 2.2) to -2.1 (SD 1.1) with BP treatment, p=0.002 (mean follow up of 9y; SD 2.7), and in the 4 patients who received denosumab therapy it increased from -1.4 (SD 1.1) to -0.5 (SD 2.3) at the last visit, p=0.298 (mean follow up of 2y; SD 0.5).

Final height ranged from 98cm (z-score: -11.7) to 152 cm (z-score: -3.7). Patients who started BP therapy  $\geq$  9y had a final height from 98 to 135cm, whereas when started  $\leq$  6y final height was between 139 and 152cm.

The number of patients with scoliosis (Cobb angle  $\geq$  10 degrees) increased from 4 at the beginning of BP therapy to 9 at last evaluation, 7 of them with severe scoliosis (Cobb angle  $\geq$  50 degrees). Five patients underwent spinal fusion.

The percentage of compressed vertebrae decreased from a median of 52.9% (p25 6.3; p75 80) to 5.9% (p25 0; p75 58.8), p=0.049.

At last evaluation only 1 patient was a full community ambulatory and 7 were therapeutic or non-ambulators. Most patients could transfer to a bed, chair and toilet, but only 5 could transfer to a car without help. Self-care abilities increased from 74% (SD 15) to 90% (SD 15), from first to last evaluation p=0.005.

Conclusion: Treatment in OI type VI was effective in reshaping of vertebrae, gain LS-aBMD, increase final height and in gain self-care abilities. Most patients developed severe scoliosis during their growing years and regardless of the initial clinical phenotype all patients at last follow up had a moderate to severe affection. There were no evident differences in clinical phenotype between different types of SERPINF1 mutations.

Disclosures: Pamela Trejo, None.

## SU0327

**Response of human osteogenesis imperfecta bone tissue to sclerostin antibody in immunodeficient mouse xenograft model.** Rachel Surowiec\*<sup>1</sup>, Basma Khoury<sup>2</sup>, Michelle Caird<sup>2</sup>, Kenneth Kozloff<sup>1</sup>. <sup>1</sup>Department of Orthopaedic Surgery, Department of Biomedical Engineering, University of Michigan, United states, <sup>2</sup>Department of Orthopaedic Surgery, University of Michigan, United states

Osteogenesis imperfecta (OI) is a genetic bone dysplasia characterized by low bone mass, poor bone quality and susceptibility to fracture especially during childhood. Currently, OI can be characterized into at least 16 identifiable types with marked variation in severity within and between type. Sclerostin antibody (Scl-Ab) has emerged as a bone-forming alternative and potential adjuvant to bisphosphonate (BP) antiresorptive therapies in OI animal models[1]. However, the effects of Scl-Ab in human OI patients remain unknown. In this study, we used a xenograft approach to evaluate human OI tissue in a biologically-rich microenvironment, drawing on prior xenograft results that suggest host-derived osteoclasts and donor-derived osteoblasts[2-3]. We hypothesize that bone samples from OI patients can be used for *in vivo* therapeutic exploration of OI cellular responses to Scl-Ab using high resolution *in vivo* microCT.

Bone samples (5-12 per patient) discarded during surgery were collected from 3 OI patients (Fig 1A), trimmed and implanted s.c. on the dorsal surface of 4-6wk nude mice. No patient had BP exposure for at least 3yrs prior to surgery. Patients 1 and 3 yielded 1 sample per mouse while patient 2 mice were implanted bilaterally with 2 samples. Treated mice (TR) received Scl-Ab starting 4 days after implantation (25mg/kg s.c. 2QW) for 2 or 4wks and compared to untreated (UN) controls.

Right distal femoral BMD confirmed a systemic anabolic effect of Scl-Ab in the host at 2 (+54%) and 4 (+64%)wks. Femoral cortical thickness was also significantly increased. While bone-forming effects of Scl-Ab were uniformly observed in the host, donor tissue showed a variable response (Fig 1B). As implantation time was not a significant factor by 2-Way ANOVA, explants were pooled from 2 and 4wk for analysis. Treated mice exhibited a significant increase in explant BMD compared to UN (p=0.02, Mann Whitney U test).

Tissue from patients 1 and 2, Type III and Type I OI, respectively, demonstrated robust early gains after 2wks, and lesser effects 4wks. Patient 3, Type III OI, demonstrated a positive response at 4wks. Variation between patients could be attributed to several factors including donor site, OI type and patient severity. Results suggest that Scl-Ab can stimulate bone formation in tissue collected from human OI patients, supporting future clinical evaluation in this patient population.

1. Sinder 2015 Bone; 2. Pettway 2008 Methods Mol Biol; 3. Pettway 2008 Bone

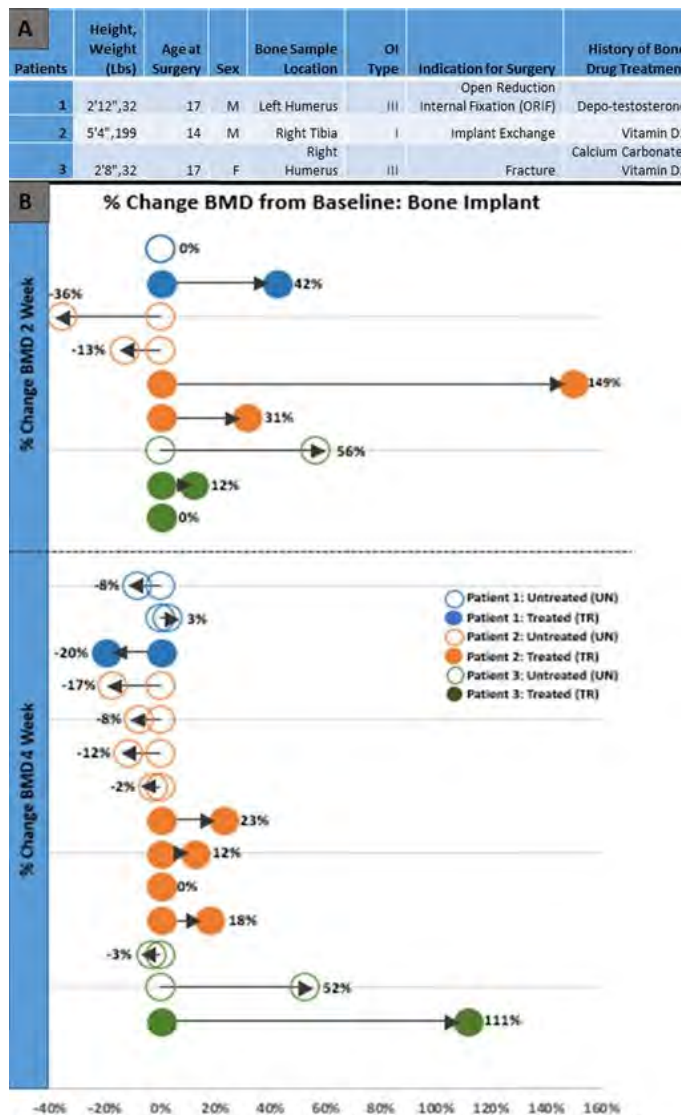


Figure 1. A) OI patient demographics including bone sample harvest location. B) Depiction of two and four week treated and untreated percent change of BMD from baseline per implant by patient. Samples included a mix of both cortical and trabecular architecture.

Figure 1.

Disclosures: Rachel Surowiec, None.

## SU0328

**Atypical Femur Fractures in an Adolescent with X-linked Osteoporosis Based On PLS3 Mutation.** Denise van de Laarschot<sup>1</sup>, M.Carola Zillikens\*<sup>2</sup>. <sup>1</sup>Erasmus MC department of Internal Medicine, Netherlands, <sup>2</sup>Erasmus MC, Department of Internal Medicine, Netherlands

Background: Long-term use of bisphosphonates has raised concerns about the association with Atypical Femur Fractures (AFFs) that have been reported mainly in postmenopausal women.

Clinical Case: An 18-year-old patient with juvenile osteoporosis based on X-linked osteoporosis due to a PLS3 mutation developed a low trauma femoral fracture after seven years of intravenous and two years of oral bisphosphonate use, fulfilling the revised ASBMR diagnostic criteria of an AFF. The occurrence of AFFs has not been described previously in children or adolescents. The underlying monogenetic bone disease in our case strengthens the possibility of a genetic predisposition of these

fractures. We cannot exclude that a transverse fracture of the tibia that also occurred after a minor trauma at age 16, followed by a spontaneous fracture above the intramedullary tibial nail, might be part of the same spectrum of atypical fractures related to the use of bisphosphonates. In retrospect our patient experienced prodromal pain prior to both the tibia and the femur fracture. Case reports of atypical fractures in children with a monogenetic bone disease such as Osteogenesis Imperfecta (OI) or juvenile osteoporosis are important to consider in the discussion about optimal duration of bisphosphonate therapy in growing children.

Conclusion: This case report 1) highlights that AFFs also occur in adolescents treated with bisphosphonates during childhood and pain in weight-bearing bones can point towards this diagnosis 2) supports other reports suggesting that low trauma fractures of other long bones besides the femur may be related to long-term use of bisphosphonates 3) strengthens the concept of an underlying genetic predisposition of AFFs, now for the first time reported in X-linked osteoporosis due to a mutation in *PLS3* and 4) should be considered in decisions about the duration of bisphosphonate therapy in children with congenital bone disorders.

**Disclosures:** M.Carola Zillikens, None.

## SU0329

### Changes in Bone Micro-Architecture During the Development of Complex Regional Pain Syndrome After a Distal Radius Fracture: a Case Report.

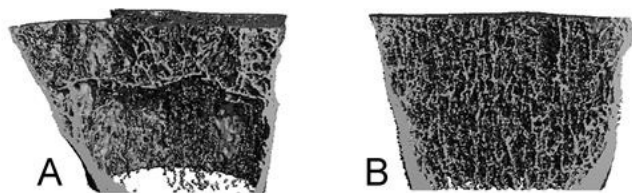
Frans Heyer<sup>1</sup>, Joost de Jong<sup>2</sup>, Paul Willems<sup>3</sup>, Rob Smeets<sup>4</sup>, Jacobus Arts<sup>5</sup>, Martijn Poeze<sup>1</sup>, Piet Geusens<sup>6</sup>, Bert van Rietbergen<sup>7</sup>, Joop van den Bergh<sup>8</sup>. <sup>1</sup>NUTRIM & Department of General Surgery, MUMC+, Netherlands, <sup>2</sup>NUTRIM & Department of Rheumatology, MUMC+, Netherlands, <sup>3</sup>Department of Orthopedic Surgery, MUMC+, Netherlands, <sup>4</sup>CAPHRI Department of Rehabilitation Medicine, Maastricht University, Netherlands, <sup>5</sup>CAPHRI & Department of Orthopedic Surgery, MUMC+, Netherlands, <sup>6</sup>CAPHRI & Department of Rheumatology, MUMC+, Netherlands, <sup>7</sup>Eindhoven University of Technology, Netherlands, <sup>8</sup>Department of Internal Medicine, VieCuri MC & MUMC+, Netherlands

Complex regional pain syndrome (CRPS) type 1 and type 2 are clinical syndromes characterized by pain that is disproportionate to the inciting event (e.g. a fracture or nerve damage), edema, decreased function, changes in skin color and bone loss. Although Sudeck proposed an inflammatory origin over a century ago, the pathophysiology is still unknown. Current hypotheses include neurological, vasomotor and immune dysfunctions.

Earlier reports show that the healing process of stable distal radius fractures can be assessed using high-resolution peripheral quantitative computed tomography (HR-pQCT) in combination with finite element analysis (FEA). A 54-year old postmenopausal patient who was included in a study investigating fracture healing with HR-pQCT developed CRPS after a distal radius fracture. HR-pQCT scans of the fractured wrist of this patient were performed at 12, 23, 45 and 86 days and 26 months post-fracture according to the study protocol.

These images showed a remarkable decrease in trabecular density, first detected 6 weeks post-fracture, along with a decrease in trabecular number, which persisted at 26 months. The changes at the fractured wrist are clearly visible when compared to the contralateral wrist (figure A and B respectively). There was an initial temporary strong increase in markers of bone formation and resorption. Surprisingly, the coronal cross-sections revealed dramatic resorption of trabecular bone proximal, but not distal of the fracture line. In contrast, the cortical region healed normally as the fracture gaps were bridged and cortical thickness increased. This resulted in restoration of bone stiffness as estimated with FEA at 26 months, similar to patients without CRPS.

These results, though from a single subject, illustrate the possible role of HR-pQCT in the early identification of CRPS-related bone loss and could identify patients at risk for developing CRPS. The anatomical localization of trabecular bone changes in the diaphysis and proximal but not distal of the fracture site argues against the role of disuse in the observed bone loss and may suggest involvement of the nutrient artery vasculature in the resorption process.



Segmented 3D reconstructions of fractured (A) and contralateral wrist (B), 26 months post-fracture.

**Disclosures:** Frans Heyer, None.

## SU0330

### Description of a novel variant in *SMAD3* presenting in a patient with osteoporotic fractures and arterial dissection. Laura Ryan<sup>\*</sup>, Dawn Allain. The Ohio State University Wexner Medical Center, United states

Introduction: Osteoporotic fracture and bone fragility has long been associated with disorders of connective tissue development, such as Marfan syndrome, Ehlers-Danlos syndrome and osteogenesis imperfecta. We present a case of a woman with arterial deficiency in combination with osteoporotic fragility fractures in whom a novel *SMAD3* variant was noted, and review the experience of this grouping of findings within the research data repository at our institution.

Case: A 43yo Caucasian female presented initially to our endocrinology clinic an unusual presentation of multiple, low-trauma fractures, including a recent fracture of the proximal humerus after a fall from standing height. She continues to have regular menstrual cycles. Her family history revealed aortic dissection in her father. She did not exhibit blue sclerae, hypertelorism, bifid uvula or hyperflexibility. Her bone mineral density testing revealed osteoporosis. She then developed pupillary asymmetry and facial droop and was diagnosed with bilateral vertebral artery dissections. Subsequent MRI revealed worsening dissection. She was referred to the adult genetics department at our institution.

Findings: Genetic testing included a 16 gene next generation sequencing panel along with concurrent targeted array CGH analysis. This evaluation revealed a c.154G>A mutation in *SMAD3*, a previously unreported mutation, and the presumptive cause of the phenotypic presentation of both arterial dissection and osteoporotic fracture in our patient. Using our research data repository, a query revealed that only 4 out of 821,318 individuals treated at our institution over the previous 5 years had a similar combination of findings.

Discussion: SMAD proteins were initially described and identified as mediators of transcriptional activity in the transforming growth factor-beta (TGF- $\beta$ ) family. It has been noted that Smad3 is instrumental in osteoblastic bone mineralization, and that disruption of Smad3 in mice causes osteopenia and decreased bone formation. Blockade of Smad3 signaling by overexpression of Smad7 resulted in markedly suppressed RANKL-induced osteoclastogenesis in murine cell lines. Through TGF- $\beta$  signaling, *SMAD3* may also play a role in the activation of sclerostin gene expression. The potential presence of an abnormality in connective tissue development should be considered in a patient who presents with pre-menopausal fragility fractures.

**Disclosures:** Laura Ryan, None.

## SU0331

### Effect of Gnathodiaphyseal Dysplasia (GDD) Mutations on Osteoblast Differentiation. Lingling Jin<sup>1</sup>, Yi Liu<sup>2</sup>, Fanyue Sun<sup>3</sup>, I-Ping Chen<sup>4</sup>, Michael T Collins<sup>5</sup>, Keith Blackwell<sup>6</sup>, Albert S Woo<sup>7</sup>, Ying Hu<sup>8</sup>, Ernst J Reichenberger<sup>\*3</sup>.

<sup>1</sup>Beijing Institute of Dental Research, Beijing Stomatological Hospital, Capital Medical University, China, <sup>2</sup>Department of Maxillofacial Surgery, Beijing Stomatological Hospital, Capital Medical University, China, <sup>3</sup>Center for Regenerative Medicine & Skeletal Development, Department of Reconstructive Sciences, University of Connecticut Health, United states, <sup>4</sup>Department of Oral Health & Diagnostic Sciences, University of Connecticut Health, United states, <sup>5</sup>National Institute of Dental & Craniofacial Research, United states, <sup>6</sup>Department of Head & Neck Surgery, UCLA, United states, <sup>7</sup>Division of Plastic Craniofacial & Pediatric Surgery, Brown University Warren Alpert Medical School, United states, <sup>8</sup>Beijing Institute of Dental Research, Beijing Stomatological Hospital, Capital Medical University, Beijing, China

Gnathodiaphyseal dysplasia (GDD; MIM#166260) is a rare autosomal dominant skeletal disorder characterized by cemento-osseous swellings of jawbones and fragile long bones with diaphyseal sclerosis. To date, mutations affecting two amino acids have been identified in *ANO5*/TMEM16E, a member of the calcium-activated chloride channel family. In this study, we describe new GDD mutations affecting 3 additional amino acids. While mutations identified for GDD only affect the skeleton, different mutations in *ANO5* cause defects in the muscular system resulting in limb-girdle and Miyoshi muscular dystrophy. We overexpressed wild type (wt) and GDD-specific p.Cys356Tyr or p.Cys360Tyr *ANO5* mutations and knocked down *ANO5* expression to study effects of *ANO5* on osteoblast differentiation.

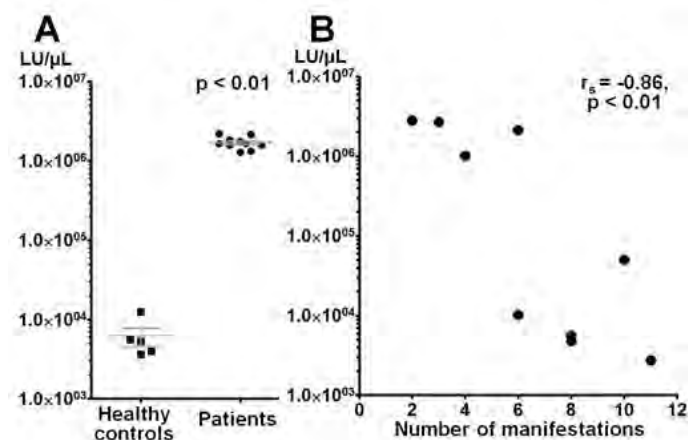
Immunoblots showed that GDD mutant *ANO5* protein expressed significantly lower than wt *ANO5* in HEK-293 cells despite both being localized to the endoplasmic reticulum as shown by immunocytochemistry. Since we observed low expression levels of mutant protein, we used shRNAs to knock down *ANO5* in MC3T3-E1 pre-osteoblast cell lines (clone 14) to examine its role in osteoblast differentiation. Knocking down *ANO5* with shRNAs resulted in significantly increased expression of osteoblast markers *osteocalcin* (20-fold), *al-collagen 1* (1.4-fold), *Runx2* (2-fold) and *osterix* (2-fold) messages in a stage-specific manner over a 21-day period compared to untransfected and scrambled controls. Alizarin red staining at culture days 14 and 21 indicated increased mineral nodule formation in *Ano5* knock-down cultures. The expression of endogenous *ANO5* protein in MC3T3-E1 cells increased consistently during a 21-day MC3T3 culture period.

**Disclosures:** Ernst J Reichenberger, None.

## SU0332

**Hypoparathyroidism Caused by Autoimmune Polyendocrine Syndrome type 1 (APS1): Relationship Between Anti-cytokines Autoantibodies and Clinical and Molecular Features in a Brazilian Set of Patients.** Fernanda Weiler\*<sup>1</sup>, Part Peterson<sup>2</sup>, Magnus Dias-da-Silva<sup>1</sup>, Marise Lazaretti-Castro<sup>1</sup>. <sup>1</sup>Federal University of Sao Paulo - UNIFESP, Brazil, <sup>2</sup>University of Taru, Estonia

Autoimmune disease is the main non-surgical etiology of hypoparathyroidism (HP), which may develop isolated or as a part of a polyglandular syndrome. APS1 is a rare but life threatening disorder defined by the association of at least 2 manifestations of the triad HP, chronic mucocutaneous candidiasis (CMC), and Addison's disease, although many other autoimmune components may be present. This autosomal recessive syndrome is considered a human model for autoimmune diseases and is caused by mutations in *AIRE* gene, resulting in defective AIRE protein, which is essential for self-tolerance through deletion of autoreactive T cells. The purpose of this study was to define clinical, mutational and immunological profile of Brazilian APS1 patients. Clinical histories were garnered by a questionnaire, all 14 exons of *AIRE* were sequenced, and antibodies against IFN type I and against IL-17A, -17F and -22 were measured in 10 of the confirmed cases. We identified 13 individuals with clinical diagnosis of APS1 and in all cases the disease appeared during infancy or childhood. CMC was present in all patients and was the first sign in the majority (77%). HP was observed in 69%, with a female predominance (80% vs 33%). Addison's disease was diagnosed in 77%, while the complete triad was seen in 54%. Seventeen other autoimmune manifestations have been observed. All 13 clinically diagnosed patients carried defects in *AIRE* gene, but no correlations with phenotypes could be established. Among 10 identified mutations, 4 have never been reported. The most frequent mutation was c.967\_979del (36% of the alleles). Mutational analyses of relatives allowed the identification of APS1 in a still asymptomatic child. Differently from normal controls, anti-IFN I titers were high in all APS1 patients (Figure), showing to be very specific for diagnosis. Anti-IL-22 and -17F antibodies were each positive in 89%, while anti-IL-17A were found in 69%. Interestingly, anti-IL-17A titers were negatively correlated ( $r_s = -0.86$ ,  $p < 0.01$ ) with the number of autoimmune manifestations in each patient, suggesting a protective effect. In conclusion, APS1 must be remembered as a cause of HP. In Brazil, 14 APS1 patients were found, one of them still asymptomatic. Mutational analysis of *AIRE* gene and anti-IFN type I antibodies were useful diagnostic tools. Titers of anti-IL-17A were inversely correlated with number of manifestations, suggesting a protective role of these antibodies in the course of the syndrome.



A) Anti-IFN I B) Correlation between anti-IL-17A and number of manifestations  
LU: light units

Disclosures: *Fernanda Weiler, None.*

## SU0333

**Improvement of Giant Cell Tumors of the Jaw Treated with Denosumab: A Case Series.** Tara Kim\*, Gianina Usara, Stuart Weinerman. Northwell, United states

Giant cell tumors (GCTs) of bone are lesions characterized by multinucleated osteoclast-type giant cells that express RANK ligand. The majority of these lesions occur in the long bone, with surgery being the typical therapeutic option. Denosumab as a treatment modality is a fairly new concept that has been used effectively in treatment of long bone lesions. There is less experience, however, with its use for jaw lesions. This 4-case series describes the effective use of low- and high-dose Denosumab in the treatment of GCTs of the jaw. Our first case is a 20 y.o. woman diagnosed with Noonan Syndrome at a young age with a GCT of the jaw diagnosed in 2002. She was initially treated with 18-months of calcitonin 100 IU SC daily, with good short-term response. Two years later, she had progressive disease. DXA revealed normal BMD, but labs showed 25 OH-D of 9.8 ng/mL and an elevated NTx of 71 nM BCE/mM cr. Treatment was initiated with 60 mg of Denosumab every 6 months and vitamin D replacement. After 1 month of therapy, there was marked improvement in NTx levels.

Panoramic jaw X-rays after 1 year of therapy showed complete resolution of the GCT. The second patient is a 34 y.o. man in good health with no prior history of metabolic bone disease found to have 25 OH-D level of 22.6 ng/mL started on Vitamin D supplementation. The patient developed right jaw pain and imaging established a lytic lesion. He was diagnosed with GCT of the jaw. 120 mg of Denosumab was started monthly. 7 months after the initial dose, repeat imaging showed denser lesions without regression in size. Given low NTx levels at the time, Denosumab was decreased to 60 mg at 2-3 month intervals. Repeat biopsy 1 year post treatment showed no evidence of GCT. The third patient is a 14 y.o. man with no significant medical or family history found to have 25 OH-D level of 14.2 ng/mL started on vitamin D supplementation. The patient was diagnosed with GCT when a lytic lesion of the mandible was identified during routine orthodontic follow-up. Labs revealed NTx of 157 nM BCE/mM cr and he was started on 120 mg of Denosumab monthly. After 2 doses, NTx decreased to 14 nM BCE/mM cr. Our last case is a 31 y.o. man diagnosed with GCT when he noticed a lesion in the jaw. On initial CT, the lesion was expansile measuring 2.5 X 2.5 X 2.2 cm. Prior to establishing endocrine care, he was treated with steroid injections with little effect. The decision was made to start treatment with 120 mg of Denosumab monthly. The patient has received 3 treatment doses and the plan is to follow bone turnover markers and X-rays. We report 3 cases of successful treatment of jaw GCTs with both low and high dose Denosumab. The last case is at an earlier stage in the treatment course and we are awaiting therapeutic response. We conclude that Denosumab at both the 60 mg and 120 mg doses may be considered for treating GCTs of the jaw.

Disclosures: *Tara Kim, None.*

## SU0334

**Regulation of BMP Receptor Dynamics and Signaling by Cell Surface Heparan Sulfate Proteoglycans.** Christina Mundy\*, Paul Billings, Maurizio Pacifici. Children's Hospital of Philadelphia, United states

The bone morphogenetic protein (BMP) signaling pathway has critical roles in many processes including skeletal development and growth, and its perturbations can lead to diverse pathologies. A case in point is Hereditary Multiple Exostoses (HME), a pediatric musculoskeletal disorder caused by loss-of-function mutations in the heparan sulfate (HS)-synthesizing enzymes EXT1 and EXT2. HME is characterized by benign cartilaginous tumors (exostoses) that form next to the growth plates of long bones, vertebrae and ribs, causing multiple health problems. The HS chains, and the proteoglycans of which they are part (HSPGs), regulate signaling by key HS-binding proteins including hedgehogs and FGFs, but their roles in BMP signaling remain unclear. Previously we showed that interference with HS function by genetic or pharmacological means rapidly increases canonical BMP signaling, suggesting that HS normally limits BMP signaling by restricting ligand availability, BMP receptor (BMPR) dynamics and/or BMPR-ligand interactions. To analyze such possibilities, we transfected cell lines with constructs encoding Snap-BMPRII and/or Clip-BMPRIa fusion proteins. Co-transfected cells rapidly responded to rhBMP-2 treatment with major increases in pSMAD1/5/8 and p-p38 levels and interestingly, the same was seen after treatment with HS antagonist Surfen or heparinase. To assess BMPR dynamics, we carried out fluorescence recovery after photobleaching (FRAP) assays and found that receptor mobility decreased significantly after treatment with rhBMP-2 or Surfen, suggesting that the receptors had transitioned to lipid rafts and/or had undergone oligomerization. To test the latter, we carried out protein crosslinking followed by immunoprecipitation and found that oligomerization of BMPRIa and BMPRII did increase after Surfen or rhBMP-2 treatment. It is currently unknown whether BMPRs may associate and interact with HSPGs and/or other cell surface co-receptors. Thus, we carried out similar crosslinking and immunoprecipitation studies, and current data provide evidence for such direct interactions. Ongoing mass spectroscopy analyses are expected to verify these observations and provide additional insights. Together, the data indicate that cell surface HSPGs are important regulators of both BMP signaling and BMPR dynamics. The HS deficiency in HME may alter these important basic physiologic mechanisms, causing unruly increases in local BMP signaling and promoting formation of exostoses.

Disclosures: *Christina Mundy, None.*

## SU0335

**Using the RUDY Study Platform to Capture Quality of Life of Adults with Rare Diseases of the Bone.** Lydia Forestier-Zhang\*<sup>1</sup>, Laura Watts<sup>1</sup>, Alison Turner<sup>1</sup>, Harriet Teare<sup>2</sup>, Joe Barrett<sup>1</sup>, Paul Wordsworth<sup>1</sup>, Jane Kaye<sup>2</sup>, M Kassim Javaid<sup>1</sup>, Rafael Pinedo-Villanueva<sup>1</sup>. <sup>1</sup>Nuffield Department of Orthopaedics, Rheumatology & Musculoskeletal Sciences, University of Oxford, United Kingdom, <sup>2</sup>Centre for Health, Law & Emerging Technologies (HeLEX), University of Oxford, United Kingdom

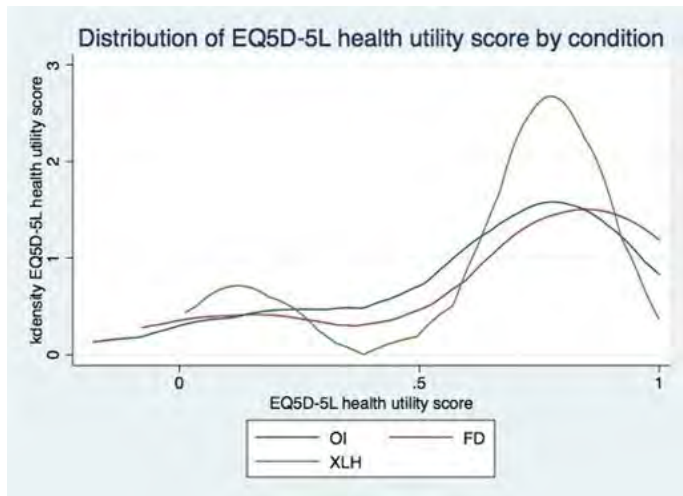
Background: Developing novel therapies for rare diseases is an important research priority. In the UK any new therapy will require careful economic evaluation before implementation in the NHS. Health-related quality of life measures are used to calculate the incremental health benefit after an intervention and allow comparison with other therapies within the NHS. Conceptually patients with the lowest quality of life have the most to gain from novel therapies and should be a priority for drug discovery. Current methods involve recruitment from hospital clinics that may bias

estimates of the true impact of the disease by only including the most severely affected individuals. The EuroQol, the instrument recommended by NICE for health technology appraisals, has recently been updated from a three to a five response-level questionnaire (EQ5D-5L) to improve sensitivity. However, there is a paucity of data on health-related quality of life measures in patients with rare diseases. We therefore compared quality of life across three rare bone diseases in adult using the EQ5D-5L.

Method: Adults with osteogenesis imperfecta (OI), fibrous dysplasia (FD) and X-linked hypophosphataemia (XLH) were recruited via the Rare and Undiagnosed Diseases Study (RUDY), a web-based platform for patient recruitment and assessment of patient reported outcomes including the EQ5D. The EQ5D-5L utility scores of OI participants were used to generate a cost-utility simulation.

Results: 82 adults completed the EQ5D-5L questionnaire. Overall there was a wide distribution of quality of life with moderate/severe problems commonly reported in the pain and discomfort dimension (OI 60%, FD 56%, XLH 65%). A cost-utility simulation showed that a hypothetical intervention which increased the health utility of the lowest utility tertile of OI patients to the mean utility level of the overall group over 10 years and costing £79,000 would be found cost-effective for the English NHS based on a £30,000 per QALY threshold.

Conclusion: These findings confirm that RUDY is recruiting patients across a range of quality of life with pain and discomfort domains most commonly affected. This is the first study to estimate the cost required to improve quality of life for adults with OI who have the lowest quality of life. A greater understanding of health-related quality of life amongst this population could help guide novel therapy developments and resource allocation.



Distribution of EQ5D-5L health utility score for adults with OI, FD and XLH

Disclosures: Lydia Forestier-Zhang, None.

SU0336

**Poor Agreement of Self-reported Fall Injuries and Medicare Claims: the Health, Aging and Body Composition (Health ABC) Study.** Elsa S. Strotmeyer<sup>\*1</sup>, Mary E. Winger<sup>1</sup>, Naoko Sagawa<sup>1</sup>, Diane G. Ives<sup>1</sup>, Robert M. Boudreau<sup>1</sup>, Julie M. Donohue<sup>1</sup>, Steven M. Albert<sup>1</sup>, Ann V. Schwartz<sup>2</sup>, Michael Nevitt<sup>2</sup>, Tamara B. Harris<sup>3</sup>, Teresa M. Waters<sup>4</sup>, Jane A. Cauley<sup>1</sup>.

<sup>1</sup>University of Pittsburgh, United states, <sup>2</sup>University of California, United states, <sup>3</sup>National Institute on Aging, United states, <sup>4</sup>University of Tennessee, United states

While most fall injuries in the oldest adults are associated with substantial morbidity, studies typically focus only on inpatient injuries and fractures but neglect other outpatient events. We examined all treated fall injuries from self-report and Medicare Fee-For-Service Parts A and B claims in the Health, Aging and Body Composition (Health ABC) Study, a longitudinal cohort of community-dwelling white and black Medicare beneficiaries with 1997-98 baseline and 99% claims linkage in followup. In 2007-08, 1,597 participants (56% women, 35% black; aged 84±3 years) with ≥1 biannual survey on falls were examined for agreement of first treated fall injury from self-report and claims over the same period. Participants with falls were asked if in the past 6 months: “Were you injured?” and “Did you seek medical treatment?” (included outpatient and hospitalization). Fall injuries from claims were any unique event with a fall code (E880-888) plus non-fracture injury or fracture (800-829), or non-vertebral fracture. Traumatic or intentional injuries and pathologic fractures were excluded. The aggregated diagnoses code algorithms were adjudicated with medical records for a subset to validate the approach. Kappa statistics defined agreement of self-report and claims events: >0.6 as good, 0.4-0.6 as moderate and <0.4 as poor. In general, very poor agreement existed for self-reported treated fall injuries to Medicare claims with a kappa statistic=0.15 (p<0.001) in the matching 6 month time period (Table). Agreement was worse for non-fracture fall injuries (kappa statistic=0.06; p<0.001) compared to fractures (kappa statistic=0.25; p<0.001), though both were very poor. Of 239 with either a treated fall injury from self-report or

claims, only 12% had both. Treated fall injuries were self-reported in 8% with no claims (124/1482) and 6% with no self-report had fall injury claims (86/1444). By including fall injury claims in the prior 12 months, 16 additional claims matched self-report and agreement improved slightly (kappa statistic=0.25, p<0.001). Aggregated diagnoses codes for fall injuries captured 75% of events that were not self-reported. Conversely, 73% of self-reported treated fall injuries were not found in claims for the prior 12 months. Despite issues of undercoding in claims, these should be considered as additional sources of fall injuries for older populations. Improved event ascertainment may enhance assessment of fall injury outcomes in the oldest adults.

Table. Level of agreement of self-reported treated fall injury (yes/no) in the past 6 months for all fall injuries, non-fracture injuries and fracture injuries compared to claims (yes/no).

	Fall Injury in Medicare claims			
	No fall injury N=1482	Any fall injury* N=115	Non-fracture fall injury* N=25	Fracture injury* N=90
Treated fall injury				
No, self-report, N=1444	1358	86	20	66
Yes, self-report, N=153	124	29	5	24
Non-fracture fall injury, N=96	87	9	5	4
Fracture injury, N=57	37	20	0	20

\*Kappa statistic=0.15 (p<0.0001) for self-reported fall injury (yes/no) vs. claims fall injury (yes/no) for all fall injuries; Kappa statistic=0.06 (p<0.0001) for non-fracture injuries; Kappa statistic=0.25 (p<0.0001) for fracture injuries.

Table

Disclosures: Elsa S. Strotmeyer, None.

SU0337

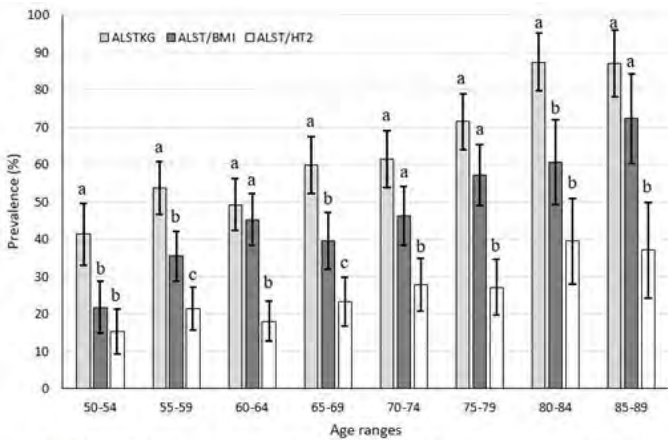
**Variability in Prevalence of Low Skeletal Muscle Mass in Mexican Women Depending on How It is Defined.** Jose Francisco Torres-Naranjo<sup>\*1</sup>, Roberto Gabriel Gonzalez-Mendoza<sup>2</sup>, Juan R Lopez y Taylor<sup>2</sup>, Alejandro Gaytan<sup>2</sup>, Noe Albino Gonzalez-Gallegos<sup>1</sup>, Douglas Solorzano<sup>2</sup>. <sup>1</sup>Centro Universitario del Norte, Universidad de Guadalajara, Mexico, <sup>2</sup>Instituto de Ciencias Aplicadas a la Actividad Fisica y al Deporte, Universidad de Guadalajara, Mexico

Purpose: To compare the prevalence of low skeletal muscle mass (LSMM) in Mexican women with different indicators and cut-points.

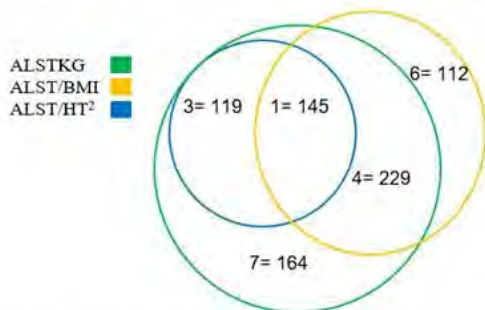
Methods: We evaluated 1111 women aged 50 to 90 years from the western of Mexico. A whole body DXA scan (Hologic QDR 4500) was performed to evaluate the body composition. The indicators and cut points used to diagnose LSMM were appendicular lean soft tissue corrected by squared height (ALST/HT<sup>2</sup>) ≤5.45 as propose The European Working Group on Sarcopenia in Older People (EWGSPOP). Appendicular lean soft tissue corrected by body mass index (ALST/BMI) <0.512, and absolute kilograms of appendicular lean soft tissue (ALSTKG) ≤15.02 both according to The Foundation for National Institutes of Health Sarcopenia Project (FNHISP). Prevalence was determined for each indicator. For analysis sample was stratified in quinquennius. The agreement of subjects diagnosed with each of the criteria were recorded. We compared the proportion of prevalence for each indicator for age range using X2 at the significant level of p<0.05.

Results: According to ALSTH/HT<sup>2</sup>, the prevalence extended from 15.2%(IC95% 9.2-21.2) to 39.4% (IC95% 28.1-50.8), for the ALSTKG it ranged from 41.3%(IC95% 33.1-49.5) to 87.3% (IC95% 79.6-95.1), and for the ALST/BMI criteria, it was 21.7% (IC95 14.9-28.6) to 72.2% (IC95% 60.3-84.2). Prevalence rates were higher in older participants (prevalence increased with age). The highest prevalence of LSMM was estimated using the ALSTKG criteria was 59.1% (IC95% 56.2-62.0) and the lowest 23.8% (IC95% 21.3-26.3) using ALST/HT<sup>2</sup> criteria. There were statistically significant differences in prevalence rates between the different age groups (Graph 1). A large overlapping exists between the three definitions but only 145 participants (13.1%) matched with all three definitions of LSMM (Graph 2).

Conclusions: We observed a high prevalence of low skeletal muscle mass in Mexican women aged 50 years and over. There was a great variation in prevalence in our population depending upon the definition used, and this finding is consistent with other reports. Interestingly concordance between three definitions of LSMM was poor. Due to the high variability in prevalence and the low concordance in the identification of cases with LSMM our findings suggest that several indicators should be taken in consideration in order to properly assess the impact of low skeletal muscle mass on Mexican women's health.



Graph 1. Low skeletal muscle mass prevalence with different indicators per age ranges. Different letters mean statistical differences ( $p < 0.05$ ).



Graph 2. Venn's diagram for the agreement between indicators to diagnose low skeletal muscle mass.

Graph 1 & 2 for prevalences.

Disclosures: Jose Francisco Torres-Naranjo, None.

### SU0338

**Muscle Function but Not Mass is Correlated with the AM-PAC™ Mobility Score.** Bjoern Buehring<sup>\*1</sup>, Ellen Siglinsky<sup>1</sup>, Yosuke Yamada<sup>2</sup>, Diane Krueger<sup>1</sup>, Mahalakshmi Shankaran<sup>3</sup>, Scott Turner<sup>3</sup>, Gregg Czerwiec<sup>3</sup>, Marc Hellerstein<sup>3</sup>, William Evans<sup>3</sup>, Dale Schoeller<sup>4</sup>, Neil Binkley<sup>1</sup>. <sup>1</sup>Osteoporosis Clinical Research Program, University of Wisconsin-Madison, United states, <sup>2</sup>National Institutes of Biomedical Innovation, Health & Nutrition, Japan, Japan, <sup>3</sup>KineMed, Inc., United states, <sup>4</sup>Nutritional Sciences, University of Wisconsin-Madison, United states

**Introduction:** Sarcopenia, the age related decline in muscle mass and function, is related to falls, fractures and decreased mobility. Disability and loss of ADLs/IADLs can lead to social isolation, depression and the inability to live independently. The Activity Measure for Post-Acute Care™ (AM-PAC™) is a validated questionnaire to assess basic mobility, daily activity, and cognition in older adults. The aim of this study was to examine the relationship of measures of muscle function and mass with the AM-PAC™ Mobility Score.

**Methods:** Community dwelling adults over the age of 70 were studied. All participants performed a muscle function tests battery: Timed up and Go (TUG), grip strength, the Short Physical Performance Battery (SPPB), gait speed, timed chair rise, and Jumping Mechanography (JM). Lean/muscle mass was measured using DXA, bioelectric impedance spectroscopy (BIS) and creatine (methyl-d3) dilution (D3-C). Additionally, the computer version of the AM-PAC™ questionnaire was administered. Linear regression analysis was used to relate AM-PAC Basic Mobility Score with muscle mass and function measures.

**Results:** 111 subjects (23 men, 88 women, mean age (SD) 80.6 (6.07)) participated in the study. All muscle function tests but none of the lean/muscle mass measures were correlated with the AM-PAC™ Mobility Score (see Figure). Total SPPB score, TUG, 4m gait, and relative jump power had the highest R<sup>2</sup>-values ( $p < 0.0001$ ,  $R^2 = 0.21-0.39$ ). The correlations with grip strength and timed chair rise were lower but still significant ( $p < 0.002$ ,  $R^2 = 0.08$  and  $0.10$  respectively).

**Conclusion:** In this cohort, the AM-PAC™ Mobility Score, a measure of daily function, was significantly correlated with all measures of muscle function but not with lean/muscle mass. The data complements previous observations that muscle function tests but not measures of muscle mass are related to health outcomes. Muscle function measures and questionnaires assessing mobility and daily function such as the AM-PAC™ will likely be very useful tools in trials of therapies to mitigate sarcopenia.

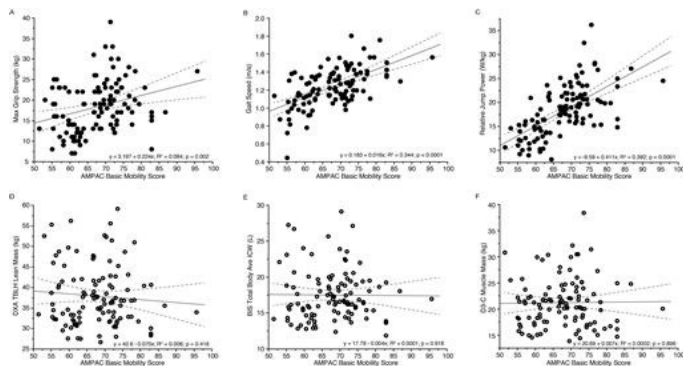


Figure: Relationship of AMPAC Basic Mobility Score and Muscle Function/Mass. All muscle function tests were significantly correlated with the AMPAC Basic Mobility Score. R<sup>2</sup> values for gait speed and relative jump power were higher than grip strength (A-C). Conversely, all muscle/lean mass parameters were not correlated with the AMPAC Basic Mobility Score (D-F).

Correlations AMPAC vs muscle function / mass

Disclosures: Bjoern Buehring, GE/Lunar, 11; Kinemed, 11  
This study received funding from: GE/Lunar, Kinemed

### SU0339

**Muscle Strength and Cognition: An Association In Older Women.** Julie Pasco<sup>\*</sup>, Amanda Stuart, Sharon Brennan-Olsen, Kara Holloway, Lana Williams, Mark Kotowicz. Deakin University, Australia

**Purpose:** Loss of skeletal muscle mass and function is a key component of physical frailty, which is known to accompany cognitive impairment and clinically diagnosed dementia among older persons; yet the links between muscle and brain are poorly understood. We aimed to examine the relationship between skeletal muscle strength at the hip and cognition in older women.

**Methods:** This cross-sectional study utilises data from the 6-year follow-up phase of the Geelong Osteoporosis Study (GOS) and involves 127 women aged 51-87 years. Maximal isometric strength of the hip flexors and abductors on both legs was determined using a hand-held dynamometer (Nicholas Manual Muscle Tester, Lafayette Instruments) from separate trials on each leg. The maximum of triplicate measures for each muscle group was used in analyses. Multiplying the maximal registered force (kg) by 9.81 converted the force to newtons (N), which was expressed relative to body weight (N/kg). Cognition was assessed using the mini-mental state examination (MMSE) and scores below the median nominated as poor cognition and above the median as good cognition. Serum collected at the previous visit was analysed for high-sensitivity C-reactive protein (hsCRP) for 120 women. Associations between muscle strength and poor cognition were examined using logistic regression models.

**Results:** Mean ( $\pm$ SD) muscle strength for flexors was 2.09 N/kg ( $\pm 0.71$ ) and abductors 1.83 N/kg ( $\pm 0.56$ ); median MMSE score was 29 (range 22-30). Mean muscle strength was lower for those with poor cognition compared to those with good cognition: flexors  $1.76 \pm 0.59$  vs  $2.39 \pm 0.83$  N/kg and abductors  $1.66 \pm 0.50$  vs  $1.96 \pm 0.57$  N/kg (both  $p < 0.05$ ). This association was independent of age for the flexors, OR 0.30 (95%CI 0.10, 0.89;  $p = 0.03$ ), and attenuated by age for the abductors OR 0.43 (95%CI 0.12, 1.52;  $p = 0.19$ ). The associations were further attenuated after adjusting for hsCRP: flexors OR 0.34 (95%CI 0.10, 1.13;  $p = 0.08$ ) and abductors OR 0.57 (95%CI 0.15, 2.19;  $p = 0.4$ ).

**Conclusions:** Our cross-sectional analyses suggest that poor muscle strength and poor cognition are associated and this could be related to poor muscle function contributing to cognitive decline or vice versa. Our data suggest that systemic inflammation might be a common pathophysiological link between the two conditions.

Disclosures: Julie Pasco, None.

### SU0340

**Prevalence of Sarcopenia and Osteosarcopenia.** Katerina Trajanoska<sup>\*1</sup>, Josie Schoufour<sup>1</sup>, Sirwan L. Darweesh<sup>1</sup>, Carolina Medina-Gomez<sup>2</sup>, Carola M.C. Zillikens<sup>3</sup>, Andre G. Uitterlinden<sup>4</sup>, Arfan M. Ikram<sup>1</sup>, Oscar H. Franco<sup>1</sup>, Fernando Rivadeneira<sup>3</sup>. <sup>1</sup>Department of Epidemiology, Erasmus Medical Center, Rotterdam, the Netherlands, Netherlands, <sup>2</sup>The Generation R Study Group, Erasmus Medical Centre, Rotterdam, The Netherlands, Netherlands, <sup>3</sup>Department of Internal Medicine, Erasmus Medical Center, Rotterdam, the Netherlands, Netherlands, <sup>4</sup>Department of Internal Medicine, Erasmus Medical Center, Rotterdam, the Netherlands, Netherlands, Netherlands

Sarcopenia is defined as slow, progressive loss of muscle mass and power. As an age-related process, sarcopenia contributes to the functional decline, morbidity and mortality of elderly individuals. Our aim was to investigate the prevalence of sarcopenia and osteosarcopenia in the general population. Furthermore, we compared baseline demographic and clinical characteristics between the groups. **Methods:** Our study included 5,850 participants from a population-based

prospective cohort including individuals age 45 and older. The evaluation was done at the most recent visit. Sarcopenia was defined (EWGSOP criteria) based on the presence of low muscle mass, plus either low muscle strength or low physical performance and applying different cut-off values by sex, BMI and height. Femoral neck BMD was measured and gender specific T-scores (NHANES) were calculated. The prevalence of pre-sarcopenia (PS), sarcopenia (SP) and osteosarcopenia (OS) was 4.4, 5.4 and 4.4 %, respectively (Table 1). Similar prevalence was observed across sexes except for PS (male: 8.1%; female: 1.7%). The prevalence of SP was higher in individuals with osteoporosis (19.4%), than in individuals with osteopenia (5.7%) or normal BMD (2.6%) Individuals with OS were considerably older, shorter and lighter than those without. Additionally, OS individuals had higher prevalence of non-vertebral fracture while no difference in comorbid conditions was found. The prevalence of sarcopenia in the general population is similar to those estimates reported earlier. The prevalence of SP among individuals with osteoporosis is high, and appears to constitute an independent entity, rather than the consequence of comorbid conditions.

Table 1. Demographic and Clinical characteristics of the participants

Muscle mass-Appendicular lean mass/height <sup>2</sup> (kg/m <sup>2</sup> )	Normal	Pre-sarcopenia	Sarcopenia	Osteosarcopenia	
	normal	decreased	decreased	P-value	Sarcopenia plus BMD T-score < 1SD
Muscle strength-Hand grip strength (kg)	normal	normal	decreased OR	***	**
Physical Performance-Usual walking speed (m/s)	normal	normal	decreased		
Prevalence, n (%)	5273 (89)	261 (4.4)	316 (5.4)		258 (4.4)
Age, years	68.8 ± 8.8	71.6 ± 8.7	75.1 ± 9.7	<0.001	75.3 ± 9.8
Female %	3037 (57.6)	55 (21.1)	171 (54.1)	<0.001	145 (56.2)
Height, cm	175.0 ± 9.5	174.2 ± 9.4	167.0 ± 9.1	<0.001	166.4 ± 9.0
BMI, kg/m <sup>2</sup>	28.0 ± 4.1	28.7 ± 3.1	22.9 ± 3.2	<0.001	22.7 ± 3.3
Femoral neck BMD, g/m <sup>2</sup>	0.91 ± 0.1	0.88 ± 0.1	0.82 ± 0.1	<0.001	0.77 ± 0.1
<b>Comorbidities*</b>					
History of non-vertebral fracture, n (%)	770 (14.8)	32 (12.3)	77 (24.2)	<0.001	67 (26.1)
Coronary heart disease, n (%)	185 (3.5)	30 (3.9)	18 (5.8)	0.129	14 (5.5)
Diabetes Mellitus, n (%)	463 (8.7)	14 (5.4)	28 (9.1)	0.141	18 (7.1)
Stroke, n (%)	178 (3.4)	30 (3.8)	17 (5.3)	0.187	11 (4.3)
Cancer, n (%)	115 (15.2)	6 (15.8)	14 (17.7)	0.789	11 (16.7)

\* Due to missingness DM and CHD covariates contain 60-80 less individuals, while the cancer estimates are based on total sample of 905 participants  
 \*\* P value comparing individuals with osteosarcopenia with normal individuals in percent (±) or means (±) error  
 \*\*\* P value for difference in sub-groups (Normal<sub>mus</sub> vs Pre-sarcopenia vs Sarcopenia) in percent (±) or means (±) error

Table 1. Demographic and Clinical characteristics of the participants

Disclosures: Katerina Trajanoska, None.

## SU0341

**Use of jumping mechanography to predict physical function in older women.** Kimberly Hannam, Jon Tobias, Avan Aihie Sayer, Emma Clark, Celia Gregson\*. University of Bristol, United Kingdom

Reduced muscle function, traditionally measured by e.g. gait speed and grip strength, associates with increased risk of falls and fractures. Jumping Mechanography (JM) potentially provides a more comprehensive assessment of muscle function; however, its acceptability in older adults and the added value of JM is unclear.

We aimed to determine the acceptability of JM in older women, and the contributions of power and force measured by JM, over and above grip strength, to the short performance physical battery test (SPPB) (gait speed, chair rise time and balance).

Community dwelling older women aged 71 to 87 years from a UK population based cohort underwent physical function tests comprising SPPB (max. score 12 denotes normal physical function), grip strength and, in those with SPPB score >5, JM. JM measured peak weight-adjusted power and force from two footed jumps and one legged hops respectively. Acceptability was assessed with post-assessment questionnaires regarding frequency and comfort of jumping/hopping. Multivariable regression models, adjusted a priori for age, height and comorbidities, were used to determine cross-sectional associations between strength, power and force with the SPPB and its 3 components, using Stata13. Standardized beta coefficients are presented.

Physical function assessments were collected in 300 women; mean age 76 (SD 3.06) years, BMI 26.2(3.8), with mean SPPB 10.6(1.4). No adverse events occurred and 86% were able to perform JM without discomfort. Grip strength strongly predicted SPPB score (β 95% CI 0.42 [0.23, 0.61] p<0.01), as did power (β 0.39 [0.08, 0.70] p=0.01) and force (β 0.22 [0.12, 0.32] p<0.01). Individually strength, power and force all accounted for variability in SPPB score (r<sup>2</sup>=0.10, 0.08, 0.10 respectively), together explaining 18% of variance in SPPB (r<sup>2</sup>=0.18). Whilst strength was the strongest predictor of chair rise time (β -0.51[-0.29, -0.74], p<0.01), power best predicted both gait speed (β -0.44 [-0.18, -0.70], p<0.01) and balance (OR 15.2 [4.0, 57.6], p<0.01).

JM was acceptable and safe in this older female population. Power and force, measured by JM, have additional predictive value for SPPB over and above that of grip strength, largely reflecting the ability of power to predict both gait speed and balance.

Disclosures: Celia Gregson, None.

## SU0342

**DXA Body Composition (BC) Should be Assessed in all Geriatric Patients Referred for DXA Bone Mineral Density (BMD) Assessment.** Angela Juby\*, Christopher Davis, Suglo Minimaana. University of Alberta, Canada

### Background

In developed countries the population demographic is shifting to an aging population. Associated with ageing is an increased risk of dependence and chronic disease, many of which are related to nutritional status (diabetes, musculoskeletal, cardiovascular and cerebrovascular disease). There is no simple clinical tool to assess appendicular lean muscle mass, and yet this is the cornerstone for diagnosing sarcopenia. In Canada, DXA BMD tests are covered by government health insurance, but DXA BC requires an additional doctors request, and payment by the patient. As a result, DXA BC are seldom ordered in this population group. In addition, DXA BC interpretation needs to be done by the requesting physician.

Nonetheless, DXA BC is the most available, least invasive and lowest cost reliable alternative. Increasing research is describing the role of sarcopenia and sarcopenic obesity in morbidity (falls, drug side effects) and mortality (fractures, complicated hospital course).

### Purpose

Community dwelling Seniors participating in an exercise intervention study were evaluated for their sarcopenic status using DXA BC (Hologic), grip strength (dynamometer) and gait speed (10 meter walk test) using the European Working Group of Sarcopenia in Older People (EWGSOP) guidelines. Obesity was defined by DXA BC percentage fat of >40% (women), >28% (men). Skin fold thickness (4 sites) and hip/waist ratio was also measured.

### Results

Data was obtained from 39 participants (32 women, 7 men), with an average age of 75.7years (67-90), average MMSE of 29.1 (22-30), and MoCA of 26.4 (18-30). All were independently mobile (with or without walking aids) and community dwelling. EWGSOP classification of the women: 9 normal; 2 presarcopenia; 2 sarcopenic obesity; 1 sarcopenia; 1 severe sarcopenia; 1 severe sarcopenic obesity; 3 sarcopenic obesity; 10 obese; 1 normal "weak"; 2 obese "weak", for a total of 32. Of the 7 men: 2 normal; 1 sarcopenia; 3 sarcopenic obesity; and 1 obese. The subgroups were comparable for age. Baseline Body Mass Index (BMI) was 27.5 (18.8 – 37.5) but BMI did not discriminate the body types. DXA BC android/gynoid ratios correlated well with measured waist/hip ratio. DXA BC total body fat correlated well with skin fold thickness measured at 4 sites.

### Conclusions

DXA BC provides not only appendicular lean muscle mass, but other important anthropometric data that is clinically relevant in assessing a patient's risk for diabetes, cardiovascular and cerebrovascular (including dementia) risk. Availability is currently limited by cost and physician expertise in interpreting the DXA BC reports. But, just as referring physicians have developed skill in interpreting DXA BMD, so they can be taught to interpret DXA BC and use the valuable additional information this provides for overall patient health. Advocacy to government is required to ensure coverage of this important preventative health tool.

Disclosures: Angela Juby, None.

## SU0343

**Identification and Diagnostic Criteria for Osteosarcopenic Obesity Syndrome in Older Women.** Jasminka Ilich\*<sup>1</sup>, Owen Kelly<sup>2</sup>. <sup>1</sup>Florida State University, United states, <sup>2</sup>Abbott Nutrition, United states

Osteosarcopenic obesity (OSO) syndrome is the impairment of bone, muscle and adipose tissues, with osteopenic obesity and sarcopenic obesity occurring simultaneously. OSO may develop due to aging, some chronic conditions (cancers, diabetes), or as a consequence of initiating presence of overweight/obesity perpetuated by low-grade chronic inflammation. Neither OSO as a whole nor its components, osteopenic sarcopenia, osteopenic obesity or sarcopenic obesity are well defined by specific diagnostic criteria.

Our objective is to introduce preliminary diagnostic criteria for OSO, or any other condition within the spectrum, in older women based on two kinds of assessment: physical and functional characteristics. Table 1 presents diagnostic criteria for OSO and other condition in the spectrum based on physical measurements (by DXA), including T-scores and appendicular lean mass (ALM). Table 2 presents the diagnostic criteria based on functional performance status.

With this proposed model, the classic definitions of osteoporosis, sarcopenia and obesity are preserved to reflect the physical changes and derive the OSO definition. The functional changes serve to include the decline in relevant functional measures and ultimately reinforce the diagnosis. This diagnostic model could also begin by assessing functional status first and using these results to justify body composition and BMD measurements. Either way, measuring both the physical and functional changes may better direct the treatment strategy. Because physical and functional changes require longitudinal measurements, regular assessment of body composition, BMD and functionality could be carried out starting in the 5<sup>th</sup> decade of life, as is currently recommended for the bone assessment in women.

**Table 1**

Condition	BMD T-score $\leq -1.0$	20 <sup>th</sup> percentile of ALM	Fat mass $\geq 35\%$
Osteopenia / Osteoporosis	Yes	No	No
Sarcopenia	No	Yes	No
Obesity	No	No	Yes
Osteopenic Sarcopenia	Yes	Yes	No
Osteopenic Obesity	Yes	No	Yes
Sarcopenic Obesity	No	Yes	Yes
<b>Osteosarcopenic Obesity</b>	<b>Yes</b>	<b>Yes</b>	<b>Yes</b>

**Table 2**

Functional status	Gait speed	Handgrip strength	Get-up-and-go test	Total score
Major decline	Poor (3)	Poor (2)	Poor (1)	6
Major decline	Poor (3)	Poor (2)	Normal/High	5
Major decline	Poor (3)	Normal/High	Poor (1)	4
Med. decline	Poor (3)	Normal/High	Normal/High	3
Med. decline	Normal/High	Poor (2)	Poor (1)	3
Minor decline	Normal/High	Poor (2)	Normal/High	2
Minor decline	Normal/High	Normal/High	Poor (1)	1
No decline	Normal/High	Normal/High	Normal/High	0

tables

Disclosures: *Jasminka Ilich, None.*

**SU0344**

**Semi-automated quantification of inter- and intra-muscular fat in magnetic resonance images of the mid-leg: validity & reliability.** *Andy Kin On Wong\**<sup>1</sup>, *Eva Szabo*<sup>1</sup>, *Marta Erlandson*<sup>2</sup>, *Marshall S. Sussman*<sup>3</sup>, *Sravani Duggina*<sup>4</sup>, *Shannon Reitsma*<sup>4</sup>, *Hana Gillick*<sup>4</sup>, *Lesley Beaumont*<sup>4</sup>, *Jonathan D. Adachi*<sup>4</sup>, *Angela M. Cheung*<sup>1</sup>. <sup>1</sup>University Health Network, Canada, <sup>2</sup>University of Saskatchewan, Canada, <sup>3</sup>University of Toronto, Canada, <sup>4</sup>McMaster University, Canada

Objectives: 1) to validate a semi-automated inter- and intra-muscular fat (IMF) segmentation method for magnetic resonance images (MRI) of the lower leg; and 2) to measure reliability of IMF measures.

Study design: cross-sectional. Inclusion: A subset of women in the Canadian Multicentre osteoporosis study Hamilton site (Hamilton CaMos) (age:  $\geq 50$ ), the Appendicular Muscle and Bone Extension Research Study (AMBERS) (age: 60-85), and a Toronto cohort study of muscle in pre- and postmenopausal women (Toronto cohort) (age: 20-90) were examined. Exclusion: Contraindications to MRI or pregnancy. Imaging: All studies completed fast spin echo MRI scans of the lower leg. MR images were analyzed with the semi-automated internal threshold-guided algorithm on Matlab. Manual segmentation was performed on AMBERS MR images using a histogram-guided region-growing tool on Sliceomatic. Peripheral quantitative computed tomography (pQCT) images of the same region were obtained in the AMBERS cohort. Muscle density was computed from these images using standard settings. Data analyses: Validity was assessed by correlating semi-automatic method parameters with the manual method and with muscle density from pQCT. Precision error (root mean square coefficients of variation (RMSCV) and standard deviation (RMSSD)) and agreement (intraclass correlation coefficients (ICC)) were measured for: intraobserver, interobserver, test-retest, and inter-method comparisons.

Results: 90 women were examined overall. Age and BMI differed among the three studies. Although the semi-automated method explained up to 87% of variance in manual IMF area measurement, there was notable systematic error between the methods. IMF area from the semi-automated method explained up to 87.8% of variance in pQCT muscle density, whereas the manual method explained 67.3% (Figure 1). Semi-automated analyses completed by the same (intra), by different (inter) observers, and between different images (test-retest) yielded a high degree of agreement (ICC > 0.99) and low precision error (< 5%) (Table 1). Test-retest error of IMF area for the manual method (22.4%) was over 4-fold larger than the semi-automated method (5.0%).

Conclusions: Semi-automated IMF segmentation from lower leg MRI showed construct validity and internal consistency. The technique is more reproducible than manual segmentation and can be applied to inhomogeneity-corrected MR images. Small test-retest errors provide confidence in measuring changes over time.

**Table 1. Comparison of precision and agreement between analytical paradigms.** MCSA = muscle cross-sectional area. IMFA=Inter & intramuscular fat area. pIMFA = percentage IMF (IMFA/MCSAx100). RMSCV=root mean square coefficient of variation. RMSSD=root mean square standard deviation. Segmentation method=semi-automated unless otherwise noted. Bold = RMSCV < 5%, and ICC > 0.90.

Study	Comparison	Variable	N	RMSCV	RMSSD	ICC
<b>Toronto cohort</b> (N=19) Age: 58.11±7.2 y BMI: 26.66±5.00 kg/m <sup>2</sup>	Intraobserver	MCSA	19	<b>0.013</b>	122 mm <sup>2</sup>	<b>0.998</b>
	Intraobserver	IMFA	19	<b>0.026</b>	23 mm <sup>2</sup>	<b>0.996</b>
	Intraobserver	pIMFA	19	<b>0.014</b>	0.1%	<b>0.999</b>
	Interobserver	MCSA	18	<b>0.023</b>	186 mm <sup>2</sup>	<b>0.989</b>
	Interobserver	IMFA	18	<b>0.063</b>	48 mm <sup>2</sup>	<b>0.990</b>
	Interobserver	pIMFA	18	<b>0.043</b>	0.4%	<b>0.992</b>
<b>Hamilton CaMos</b> (N=43) Age: 74.6±8.9 y BMI: 25.60±4.61 kg/m <sup>2</sup>	Test-Retest	MCSA	43	<b>0.020</b>	329 mm <sup>2</sup>	<b>0.991</b>
	Test-Retest	IMFA	43	<b>0.050</b>	77 mm <sup>2</sup>	<b>0.982</b>
	Test-Retest	pIMFA	43	<b>0.048</b>	0.5%	<b>0.989</b>
<b>AMBERS</b> (N=28) Age: 79.9±2.7 y BMI: 28.88±5.72 kg/m <sup>2</sup>	Auto-Manual	pIMFA	28	0.197	3.8%	0.756

Table 1

Disclosures: *Andy Kin On Wong, None.*

**SU0345**

**Brittleness in BMP2 Knockout Bones - Relation to Porosity, Cellularity, and Woven Bone Content.** *Zacharie Toth*<sup>1</sup>, *Simon Tang*<sup>2</sup>, *Sarah McBride-Gagyi*<sup>\*1</sup>. <sup>1</sup>Saint Louis University, United states, <sup>2</sup>Washington University, United states

Two separate studies have shown deficient BMP2 expression in osteoblasts and osteocytes (cKO) results in severe bone brittleness. This implies osteogenic-derived BMP2 plays a role in bone strength. Ramen spectroscopy did not reveal any mineral-to-collagen ratio or crystal organization variances to explain the altered material properties. Increased porosity decreases fracture resistance in any material. Each void not only reduces material cross-sectional area, thus raising bulk stress, but also creates local stress concentrations causing failure at reduced overall load. Decreased lamellar organization can have similar consequences. Since whole bone measures (DEXA), which include void spaces, show decreased density in BMP2 cKOs but tissue-level measures do not (microCT, uCT), we hypothesize the brittleness is a result of increased porosity rather than increased woven bone.

Male and female mice lacking BMP2 expression osteogenic lineage cells (*BMP2*<sup>fl/fl</sup>, *OSX-Cre*) were compared to littermates (control, *BMP2*<sup>fl/fl</sup>) at 10 or 15-weeks-old (n=9-10/group). Freshly frozen right femora were given a razor-blade-notch the posterior mid-point, subjected to slow 3-pt bending (0.001mm/s), and uCT scanned to assess fracture toughness and verify previous 3-pt bending findings (n=4-5/group complete). Left femora were fixed, uCT scanned (3.5um), and processed for histology. MicroCT quantified midshaft bone morphology, mineral density, and volumetric porosity (n=9-10/group complete). Histology quantified midshaft areal porosity, cellularity, and woven bone area (n=2-9/group completed). ANOVA (factors: age, sex, genotype) with Fisher's post-hoc analysis was used to determine significant effects and group differences.

All cKOs were less tough than respective controls, but differences are currently only significant at 15wks (A). cKO bones of both ages/sex were ~5% more porous using both 3D and 2D measurements (B). Void spaces were ~3um larger in diameter in cKOs (9um vs 14um, p<0.001). 3D reconstructions revealed increased large canals radiating from the endosteal surface (C). Reflecting the increased void area, cKO cellular density was ~20% higher than controls (D, p<0.001). Percent woven bone was similar between groups (~25%).

Given these data, we conclude fracture toughness reduction in osteogenic-deficient BMP2 bones is mostly attributable to increased porosity, as opposed to increased woven bone. Although work is ongoing to assess collagen fibril structure and assembly.

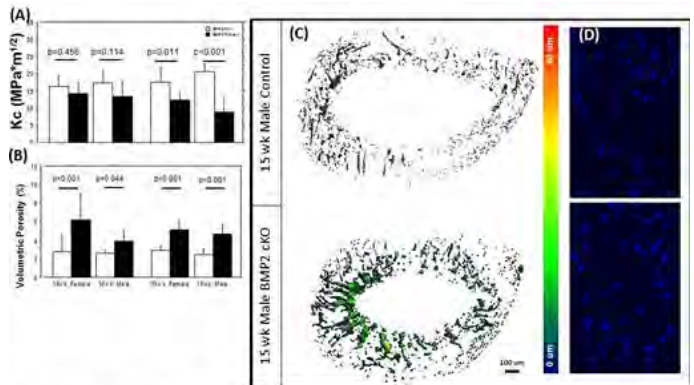


Figure 1. (a) Fracture toughness of cKO femora (black bars) were less than controls (white bars). (b) Femoral midshaft volumetric porosity was increased in cKO femora. (c) 3D representation of void spaces within the cortical midshaft. (d) Representative images of cellularity between cKOs and controls (same ROI for both cKO and control)

Figure 1

Disclosures: *Sarah McBride-Gagyi, None.*

## SU0346

**Exercise Prior to and During Pregnancy Ameliorates Bone Deficits During Late Gestation in Female Rats Born Small Without Adverse Effects from Consuming a High Fat Diet.** Kristina Anevska<sup>1</sup>, Dayana Mahizir<sup>2</sup>, Andrew Jefferies<sup>2</sup>, John Wark<sup>3</sup>, Mary Wlodek<sup>2</sup>, Tania Romano<sup>4</sup>.  
<sup>1</sup>Department of Physiology, Anatomy & Microbiology, La Trobe University & Department of Physiology, The University of Melbourne, Australia, <sup>2</sup>Department of Physiology, The University of Melbourne, Australia, <sup>3</sup>Department of Medicine, The University of Melbourne & Bone & Mineral Medicine, Royal Melbourne Hospital, Australia, <sup>4</sup>Department of Physiology, Anatomy & Microbiology, La Trobe University, Australia

Low birth weight, caused by intrauterine growth restriction, programs adult bone deficits and increases obesity risk. Obesity is a state of chronic inflammation where increased adiposity can interfere with osteoblast activity. Pregnancies in offspring born small, further complicated by obesity can exacerbate pre-existing bone deficits. Exercise intervention prior to pregnancy can reverse negative effects of obesity in growth restricted offspring. We aimed to determine whether a high fat diet (HFD) exacerbates bone deficits during pregnancy in females born small and if daily endurance exercise prior to and during pregnancy would mitigate these deficits to a greater extent rather than exercise in pregnancy alone.

Uteroplacental insufficiency, with consequent pup growth restriction, was induced on embryonic day 18 (E18) in WKY rats using bilateral uterine vessel ligation (Restricted) or sham (Control) surgery (F0 generation). F1 females consumed standard chow or a HFD (23% fat) from 5 weeks of age and were mated at 20 weeks. Pregnant rats exercised on treadmills for four weeks prior to pregnancy and during pregnancy; exercised during pregnancy only or remained sedentary. Femora were collected at post-mortem (E20) for subsequent pQCT analysis.

Pregnant Control and Restricted females consuming a HFD had increased dorsal fat mass, regardless of exercise intervention, compared to chow-fed counterparts ( $p < 0.05$ ). In chow-fed females, exercise prior to and during pregnancy reduced dorsal fat mass compared to sedentary females. Restricted females who remained sedentary or exercised during pregnancy only had decreased trabecular and cortical content, cortical thickness (sedentary only), periosteal and endosteal circumference and bending strength ( $p < 0.05$ ), irrespective of diet. A HFD increased trabecular density in sedentary females only. Exercise prior to and during pregnancy mitigated these deficits as there were no differences between Control and Restricted females consuming either diet.

This study concludes that exercise intervention prior to and during pregnancy prevented the development of bone deficits; proving to be beneficial rather than exercising during pregnancy only. Consumption of HFD did not exacerbate bone deficits. Exercise prevented bone loss during pregnancy in growth restricted females, potentially reducing further detriment to the maternal skeleton long after pregnancy and possibly improving the bone health of the next generation.

**Disclosures:** *Kristina Anevska, None.*

## SU0347

**Gene Regulatory Network via BRCA1 and BRCA2 Is Critical for Craniofacial Bone Development.** Kohei Kitami<sup>\*</sup>, Megumi Kitami, Yoshihiro Komatsu. The University of Texas Medical School at Houston, United states

Cell proliferation, survival and differentiation are critical for craniofacial bone morphogenesis. The impaired balance of these clues leads to congenital facial abnormalities.

*Brcal* is a tumor suppressor gene involved in DNA damage repair. It has been known that *Brcal* regulates cell proliferation positively in embryonic development while it functions oppositely in tumorigenesis. However, it remains elusive how BRCA1 governs facial development. To address the role of BRCA1 during craniofacial bone development, we utilized Cre-loxP system to examine the function of *Brcal* in a craniofacial tissue-specific manner. Because epithelial-mesenchymal interaction plays pivotal roles during craniofacial bone formation, we employed both *K14-Cre* and *Wnt1-Cre* mice to disrupt *Brcal* in mice. While epithelial-specific *Brcal* mutant embryos did not show any overt craniofacial abnormalities, neural crest-specific *Brcal* mutants displayed craniofacial bone defects and resulted in neonatal death. Histological analysis revealed there were decreased proliferation and increased cell death in the frontal bone primordium of *Brcal* mutants compared with control embryos. Importantly, defects observed in neural crest-specific *Brcal* mutants were partially rescued by superimposing *p53* null alleles, suggesting *Brcal* is essential for craniofacial bone development interacting with *p53*. Furthermore, neural crest-specific deletion of *Brcal2*, which has more specialized function in homologous recombination, displayed similar craniofacial bone defects. Together, these results demonstrate that homologous recombination via BRCA1 and BRCA2 is critical for craniofacial bone development.

**Disclosures:** *Kohei Kitami, None.*

## SU0348

**Methylphenidate affects cortical bone microstructure via osteoclast regulation.** Sardar Uddin<sup>\*1</sup>, Dennis Fricke<sup>2</sup>, Abisha Vijayashanthar<sup>3</sup>, Courtney Lowinger<sup>2</sup>, Liam Jermyn<sup>3</sup>, Panavotis Thanos<sup>3</sup>, Michael Hadjiargyrou<sup>4</sup>, David Komatsu<sup>1</sup>. <sup>1</sup>Stony Brook University, United states, <sup>2</sup>SUNY University at Buffalo, United states, <sup>3</sup>SUNY University of Buffalo, United states, <sup>4</sup>New York Institute of Technology, United states

Methylphenidate (MP) is the most widely prescribed drug for treating Attention Deficit Hyperactivity Disorder (ADHD), currently effecting 1 in 10 US children under the age of 17. We previously reported that chronic MP administration adversely affects cortical bone mineral density and biomechanical integrity in adolescent male rats, with little to no effect in females. This study explores the micro scale effects of MP on cortical bone and identifies increased osteoclast number and activity as a mechanism by which MP impairs bone quality and quantity. Four-week-old Sprague-Dawley rats were randomized to 3 groups (n=6): Water, Water Pair-Fed (PF), and MP. The Water group received no MP, the PF group had food restricted to that of the MP treatment group, and the MP group received MP via their drinking water. After 13 weeks, the rats were euthanized and tibias and femurs were harvested for high resolution MicroCT and histological analyses. Femora cortical porosity was assessed at the mid-shaft using 1um microCT scans (SkyScan). Male rats showed a significant shift in pore distribution with a greater number of smaller pores (100 – 200  $\mu\text{m}^3$ ) in MP treated rats relative to Water controls (1499 vs 990,  $p < 0.05$ ) (Fig 1a). Female rats showed the same trends but the differences did not achieve statistical significance. Tibias were decalcified and stained TRAP as an indicator of osteoclast activity. Quantification of TRAP staining showed significant increases in Trap.V/Tissue.V (Trap/V/T.V, 140%,  $p < 0.05$ , Fig 1B), osteoclast.surface/bone.surface (OC.S/BS, 72%,  $p < 0.05$ ) and osteoclast number (OC.N, 46%,  $p < 0.05$ ) in male MP rats relative to Water with similar but none significant trends seen in females. We then evaluated the direct effects of MP on osteoclast differentiation and activity. Primary hematopoietic stem cells were extracted from five-week-old rats and treated with MSCF (50ng/ml) and RANKL (100 ng/ml) in presence of 0, 10, 100, and 1000ng/ml of MP. Osteoclast differentiation was assessed at day 3 and 5 and osteoclast activity at day 5. MP increased osteoclast differentiation in a dose dependent manner, with significant increases in the osteoclast/monocyte ratio demonstrated in 100ng/ml (192%,  $p < 0.05$ ) and 1000ng/ml (364%,  $p < 0.001$ ) cultures, relative to 0 ng/ml (Fig 1C). MP treated cultures also revealed a higher number of TRAP positive cells, indicative of increased osteoclast activity at day 5. Overall these data confirm our previous findings of sex-dependent effects of MP on bone quality and quantity. Furthermore, they show that MP significantly increases cortical porosity in male rats due to increases in osteoclast number and activity. Finally, this study is the first to report on a direct effect of MP on osteoclast differentiation and activity, which may have significant clinical implications for patient being treated with MP.

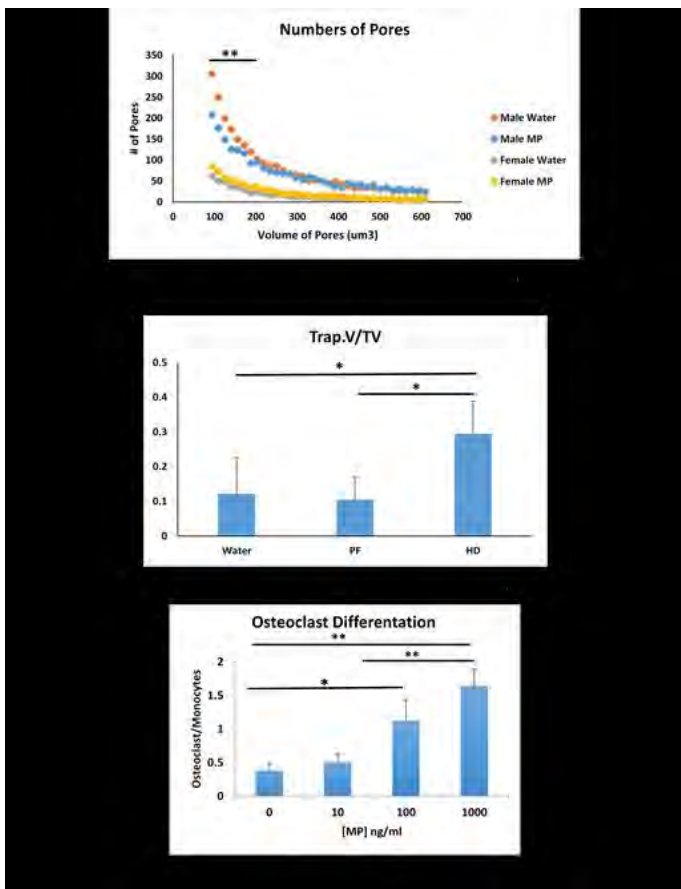


Figure 1

Disclosures: Sardar Uddin, None.

## SU0349

### Role of Grip Strength, Physical Activity, and Neuromuscular Performance in Predicting Bone Properties and Strength at the Radius and Tibia in Children.

Kelsey Bjorkman<sup>\*1</sup>, Joel Lanovaz<sup>1</sup>, Chantal Kawalilak<sup>2</sup>, Whitney Duff<sup>3</sup>, JD Johnston<sup>2</sup>, Saija Kontulainen<sup>1</sup>. <sup>1</sup>University of Saskatchewan, College of Kinesiology, Canada, <sup>2</sup>University of Saskatchewan, College of Engineering, Department of Mechanical Engineering, Canada, <sup>3</sup>University of Saskatchewan, College of Medicine, Department of Gastroenterology, Canada

We assessed if neuromuscular performance measures and physical activity would independently predict bone properties and strength at the radius and tibia in children. We obtained forearm and lower leg scans from 75 boys and 85 girls (mean age 10.8; SD 1.8y) at the shaft and distal sites using peripheral quantitative computed tomography (pQCT) and high resolution pQCT. We assessed bone strength (BSIc), total, cortical and trabecular bone density (ToD, CoD, TrD), area (ToA, CoA, TrA), and cortical and trabecular bone thickness (CTh, TrTh) at distal sites; bone strength (SSI<sub>p</sub>), total and cortical area (ToA, CoA), and content (ToC, CoC, TrC), and muscle area (MuA) at shaft sites. We measured grip strength force (GS), maximal push-up force (MPU) performed on force plates, number of push-ups (#PU), maximal force, impulse and power from countermovement (CMJ) and long jump (LJ), LJ distance and physical activity questionnaire (PAQ-C). We used linear regression for each sex and report predicted variance (%) in bone outcomes based on R<sup>2</sup> of the model and the % contribution of GS, #PU, MPU force, CMJ or LJ peak force, impulse or power as independent predictors (partial r<sup>2</sup>) after controlling for maturation (age from peak height velocity), weight, height and MuA. At the distal radius, GS or MPU force predicted up to 58% of the variance in ToD, CoD, ToA, CoA, TrA, and CTh in girls (partial r<sup>2</sup>: 7-20%) (Fig 1). At the radius shaft, #PU predicted 50% of ToA in girls (partial r<sup>2</sup>=10%) (Fig 1). At the distal tibia, CMJ force predicted 33% of the variance in CoA, CTh, ToD, and TrD in girls (partial r<sup>2</sup>: 7-10%) and up to 61% of the variance in ToA and BSIc in boys. At the tibia shaft, CMJ force predicted up to 76% of the variance in ToC, CoC and CoA and SSI<sub>p</sub> in girls (partial r<sup>2</sup>: 11-15%), while CMJ impulse and power predicted 73% of the variance in CoA in boys (partial r<sup>2</sup>: 8%). Models with LJ distance predicted 78% of the variance in ToC, CoC, ToA, CoA, and SSI<sub>p</sub> in boys (partial r<sup>2</sup>: 10-23%), while models with LJ force predicted up to 75% of the variance in ToD, CoD and CoC in girls (partial r<sup>2</sup>: 8-12%). Models with LJ power predicted up to 76% of the variance in ToC, ToD, and ToA in boys (partial r<sup>2</sup>: 7%). Neuromuscular performance measures

were independent determinants of bone properties and strength in both sexes. These findings will guide design of exercise interventions aiming to optimize bone strength development in children.

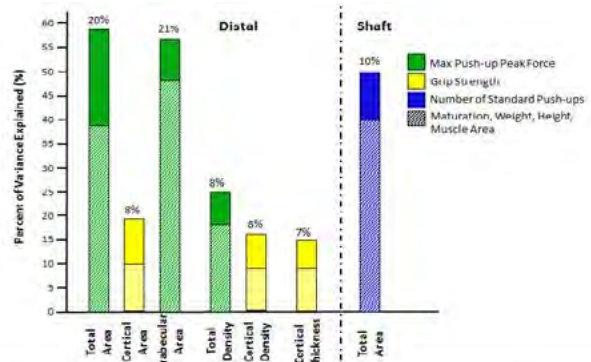


Figure 1. Bars represent variance (%) in bone outcomes predicted by independent ( $p < 0.05$ ) muscular predictors and confounders (maturation, weight, height and muscle area) at the distal radius and radius shaft in girls.

Figure 1. Bjorkman

Disclosures: Kelsey Bjorkman, None.

## SU0350

### Role of Sperm-Associated Antigen-17 Gene in Skeletal Dysplasia. Maria Teves<sup>\*1</sup>, Sharon L Hyvz<sup>2</sup>, Zvi Schwartz<sup>2</sup>, Barbara D Bovan<sup>2</sup>, Jerome F Strauss III<sup>1</sup>. <sup>1</sup>School of Medicine, Virginia Commonwealth University, United states, <sup>2</sup>School of Engineering, Virginia Commonwealth University, United states

**Background:** The skeletal dysplasias are a heterogeneous group of disorders associated with a range of phenotypes from short stature to severe dwarfism with perinatal mortality. The purpose of this study was to evaluate the role of the sperm-associated antigen-17 (*Spag17*) gene, which encodes a protein of the central pair apparatus of flagellar/ciliary axonemes, in skeletal dysplasia.

**Methods:** Mineralization and bone formation during skeletal embryonic development was evaluated by  $\mu$ CT-scanning and alcian blue/alizarin red staining in *Spag17*-knockout and wild-type embryos. Specific markers of chondrocyte and osteoblast differentiation were evaluated in murine ATDC5 and MC3T3-E1 cells, respectively, after silencing of the *Spag17* expression. Primary cilia defects were evaluated by immunofluorescence and by measurement of the mRNA expression levels of intraflagellar transport genes.

**Results:** To evaluate the role of *Spag17* during skeletal embryonic development we collected embryos at E15.5, E16.5 and E17.5. We observed that *Spag17*-mutant embryos have a significant reduction in endochondral and intramembranous bone formation in comparison with the wild-type littermates. The reduction of bone volume and density, in addition to a delay in bone mineralization was particularly evident in the skull, limbs and vertebral bodies. Moreover, *Spag17*-mutant embryos are shorter in length than wild-type embryos. A novel ~75 kDa isoform of the SPAG17 protein was detected in mouse skeletal cells by Western blotting, suggesting it is an isoform of the 250 kDa full length protein. We evaluated the role of *Spag17* in chondrocyte and osteoblast differentiation. We detected that *Sox9*, *Col2a1* and *Runx2* were down-regulated after *Spag17* knockdown in ATDC5 cell cultures and a reduction in alcian blue qualitative staining was also observed. Knockdown of *Spag17* in MC3T3-E1 cells produced a reduction in the mRNA levels of *Ocn*, *Osx* and *Runx2*, with reduced alizarin red staining compared to the control. In addition, defects in primary cilia and abnormal Golgi structure were found in the chondrocytes and osteoblasts from *Spag17* knockout mice.

**Conclusions:** Our results reveal an unexpected function for the *Spag17* gene outside of its role in sperm flagella and motile cilia. These interesting findings suggest that *Spag17* gene is a new player in skeletal development, particularly in regulating chondrocyte and osteoblast differentiation/maturation, and bone mineralization. The role of *Spag17* and its 75kDa protein isoform in skeletal dysplasia may be a consequence of defects in Golgi and primary cilia structure and function.

Disclosures: Maria Teves, None.

## SU0351

### Teriparatide Effects on Mast Cells During Critical Defect Healing in a Murine Cranial Window Model. Longze Zhang<sup>\*</sup>, Xinping Zhang, Edward Schwarz. URM, University of Rochester, United states

**Background:** Critical bone defects remain a major clinical problem. Intermittent teriparatide (rPTH) is therapeutic, but its non-anabolic effects that must inhibit fibrosis are unknown. Previously we showed that rPTH increased angiogenesis (vessels <30 $\mu$ m), and decreased arteriogenesis (>30 $\mu$ m) and mast cells, in a murine femoral allograft model. To elucidate these rPTH effects on mast cells in vivo, we

utilized multiphoton laser scanning microscopy (MPLSM) in a critical calvaria defect model.

Methods: A cranial defect window was made in 8-week-old female *Mcpt5-YFP* mice (n=5), which were randomized into four groups: 1) placebo (saline), 2) rPTH treated (40µg/kg/day), 3) cromolyn (24µg/kg/day) and 4) rPTH + cromolyn. Blood vessels were labeled with Texas Red-dextran (i.v.), and co-visualized with mast cell (YFP) at 7, 14, 21, 28 days post-op. The defect closure rate was measured by *in vivo* micro-CT at 6, 13, 20, 27 days post-op. IHC was performed for *Mcpt5* and *PTHr1*.

Results: Large numbers of mast cells (40 +/- 18) were detected 1 day post-surgery, peaked (75 +/- 8) at 6 days, and were still present (18 +/- 6) in the critical defect of placebo treated mice at the end of the experiment on day 28. In contrast, angiogenesis was first detected 4 days after surgery, and mature vessels were first observed 6 days post-op. rPTH increased angiogenesis (211 +/- 6%; p<0.05), decreased arteriogenesis (75 +/- 5%; p<0.05), and reduced the mast numbers (17 +/- 3%; p<0.05) versus the placebo group. rPTH treatment also increased the defect window closure from 17 +/- 5% to 42 +/- 9%; p<0.05. Cromolyn treatment had similar effects as rPTH on mast cell numbers, but had no effect on defect closure. No additional effects were observed in the combination treatment group versus rPTH. IHC for *Mcpt5* co-localized with YFP expression, and IHC for *PTHr1* showed strong staining in osteoblasts, but not in toluidine blue stained mast cells.

Discussion: Towards an understanding of pathogenic host inflammation and arteriogenesis in critical defects and non-unions, and rPTH inhibition of these profibrotic factors, here we show that mast cell accumulation precedes arteriogenesis, and that mast cell inhibition correlates with an increase in angiogenesis, suggesting that mast cells stimulate arteriogenesis and fibrosis. Since *PTHr1* is not expressed on mast cells in our model, this suggests that rPTH inhibition of mast cells and arteriogenesis is indirect through an osteoblast intermediate.

Disclosures: Longze Zhang, None.

## LB-SU0352

**Severe Hypophosphatemia in Adulthood Associated with *PHEX* 3'-UTR Mutation C. \*231A>G Near the Polyadenylation Signal.** Beatriz Ramirez\*<sup>1</sup>, Fiona Cook<sup>1</sup>, Steven Mumm<sup>2</sup>, Gary Gottesman<sup>2</sup>, Katherine Madson<sup>2</sup>, Michael Whyte<sup>2</sup>. <sup>1</sup>Division of Endocrinology, Brody School of Medicine, United states, <sup>2</sup>Center for Metabolic Bone Disease & Molecular Research, Shriners Hospital for Children, United states

Purpose: Report severe acquired hypophosphatemia associated with the *PHEX* 3'-UTR mutation found as sporadic or X-linked recessive hypophosphatemic rickets.

Methods: A 38-year-old previously healthy man presented with exertional weakness, bradycardia, dyspnea, and hypoxemia. Serum inorganic phosphate (Pi) was 1.0 mg/dL (NI: 2.4-4.7) while fractional excretion of Pi was excessive. However, circulating FGF23 was 106 RU/mL (NI: <180). Serum Pi was 1.6 mg/dL two years before. He was given IV Pi, yet suffered recurrent symptomatic hypophosphatemia despite oral Pi and calcitriol. Physical exam was unremarkable, but height was 63 in. Evaluation for tumor-induced phosphaturia was negative, including FDG-PET CT and octreotide scans. Short stature and mild hypophosphatemia in one daughter suggested a genetic basis for hypophosphatemia but commercial analyses of *FGF23* (*ADHR*), *DMP1* (*ARHR*), and *PHEX* (*XLHR*) were negative. Family studies showed hypophosphatemia from renal Pi wasting in his two healthy daughters (one of normal stature), but not his son, in keeping with X-linked inheritance.

Results: Our mutation analysis revealed the *PHEX* 3'-UTR mutation (c. \*231A>G near the polyadenylation signal) which we reported (JBMR 30:137-43, 2015) can explain carrier females and cause mild HR in males masquerading as sporadic or X-linked recessive HR. Our Ion Torrent NGS panel for 15 genes involved in Pi metabolism including known genes causing rickets (*FGF23*, *DMP1*, *SCLC34A3*) did not reveal another etiology. As expected, the proband's daughters had the *PHEX* mutation, and his son did not. Perhaps our proband early in life had asymptomatic hypophosphatemia with short stature. His *PHEX* haplotype matched 3/5 boys previously reported, reflecting a common founder in the USA.

Conclusion: This HR variant can apparently present as severe hypophosphatemia in adult life. The explanation remains unknown. Individuals with this *PHEX* 3'-UTR mutation seem to share a common ancestor. Studies of extended family members are ongoing.

Disclosures: Beatriz Ramirez, None.

## LB-SU0353

**Novel ELISA for the measurement of human Periostin.** Manfred Tesarz, Elisabeth Gadermaier\*, Gabriela Berg, Gottfried Himmler. The Antibody Lab GmbH, Vienna, Austria, Austria

Purpose: Periostin (osteoblast-specific factor OSF-2) is a component of the extracellular matrix and is thought to be involved in osteoblast recruitment, attachment and spreading. As a potential biomarker of bone turnover it may assist in the management of bone diseases. Periostin consists of a conserved N-terminus and a C-terminal region which is affected by alternative splicing. Currently, at least seven splicing isoforms of human Periostin have been identified.

Methods: We developed a sandwich ELISA, which enables the detection of all known human circulating Periostin isoforms. Our novel assay utilizes monoclonal and affinity-purified polyclonal antibodies and recognizes epitopes that are conserved

between human and animal species, e.g. mouse, rat, cynomolgus macaque, dog, and cat Periostin.

Results: The novel Periostin ELISA assay is optimized for human serum and plasma and covers a wide calibration range between 125 to 4,000 pmol/l. Assay characteristics, such as precision (intra-assay: ≤3%, inter-assay: ≤6%), dilution linearity (99-115%) and spike-recovery (83 - 106%), the matrix comparison between serum and EDTA-plasma (R2 0.96) as well as sample stability meet the standards of acceptance. Periostin serum and plasma concentrations in apparently healthy individuals are 864 +/- 269 pmol/l (n=24) and 817 +/- 170 pmol/l (n=20), respectively.

Conclusion: This ELISA provides a reliable and accurate tool for the quantitative determination of Periostin in human healthy and diseased samples.

Disclosures: Elisabeth Gadermaier, None.

## LB-SU0354

**Knock-down of the vitamin D receptor in human breast cancer cells increases metastatic potential to bone via a Wnt/ E-cadherin signaling pathway.** Konstantin Horas<sup>1</sup>, Yu Zheng<sup>1</sup>, Collette Fong-Yee<sup>1</sup>, Yunzhao Chen<sup>1</sup>, Jeremy Qiao<sup>1</sup>, Mingxuan Gao<sup>1</sup>, Nancy Mourad<sup>2</sup>, Michelle McDonald<sup>2</sup>, Peter Croucher<sup>2</sup>, Hong Zhou<sup>1</sup>, Markus Seibel<sup>\*1</sup>. <sup>1</sup>Bone Research Program, ANZAC Research Institute, The University of Sydney, Australia, <sup>2</sup>Garvan Inst of Med Research, Australia

Up to 40% of patients with breast cancer develop skeletal metastases. We have previously demonstrated that vitamin D deficiency promotes breast cancer growth in bone, mostly through changes in the bone microenvironment. Here we aimed to further define the role of the vitamin D receptor (VDR) in systemic breast cancer spread to bone.

Following knock-down of VDR expression in the human breast cancer cell line, MDA-MB-231 (MDA<sup>VDR-/-</sup>), and subsequent luciferase gene transfection, both MDA<sup>VDR-/-</sup> and non-target (NT) control cells were injected via the intra-cardiac route into female nude mice (n= 73). Systemic cancer cell spread and local tumour growth were monitored by sequential *in vivo* bioluminescent and high resolution X-ray imaging for 30 days. At endpoint, affected bones were analysed by µ-CT, histomorphometry and immunohistochemistry (IHC). Cancer cells were isolated from the bone marrow via FACS and quantitative data were generated for days 3, 7, 14 and 21 post injection. VDR, E-cadherin and β-catenin expression levels in MDA<sup>VDR-/-</sup> and NT cells were analysed both *in vitro* (Western blot) and *in vivo* (IHC) to determine whether loss of VDR affects the expression of cell adhesion proteins. In a translational approach, VDR, CYP24A1, E-cadherin and β-catenin expression were measured by IHC in clinical breast cancer specimens (n=170) and correlated with tumour characteristics and disease progression over 5 years.

Results: Compared to NT controls, MDA<sup>VDR-/-</sup> cells demonstrated increased cell migration and cell invasion *in vitro*. This was associated with significantly reduced protein expression (Western blot) of β-catenin and E-cadherin in MDA<sup>VDR-/-</sup> compared to NT cells. Following intra-cardiac injection, systemic spread occurred earlier and the number of cancer cells found in the bone marrow was significantly greater at all time points in MDA<sup>VDR-/-</sup> injected mice compared to those receiving NT cells. Protein expression of E-cadherin was significantly reduced in tumours derived from MDA<sup>VDR-/-</sup> cells compared to NT-derived lesions. Analysis of human breast cancer specimens confirmed a strong association between VDR expression, tumour grade and patient prognosis. Of note, CYP24, β-catenin and E-cadherin protein expression were positively associated with VDR expression.

We conclude that loss of the VDR in human breast cancer promotes cell mobility, systemic spread and skeletal tumour burden by altering β-catenin and E-cadherin expression.

Disclosures: Markus Seibel, None.

## LB-SU0355

**Tamoxifen-Induced Deletion of the Glucocorticoid Receptor in Chondrocytes Enhances K/BxN Serum-Induced Arthritis in Mice.** Jinwen Tu<sup>\*1</sup>, Shihani Stoner<sup>1</sup>, Yaqing Zhang<sup>1</sup>, Di Chen<sup>2</sup>, Jan Tuckermann<sup>3</sup>, Mark S Cooper<sup>4</sup>, Markus J Seibel<sup>5</sup>, Hong Zhou<sup>1</sup>. <sup>1</sup>Bone Research Program, ANZAC Research Institute, University of Sydney, Australia, <sup>2</sup>Tissue Department of Biochemistry, Rush University Medical Center, United states, <sup>3</sup>Institute of General Zoology & Endocrinology, University of Ulm, Germany, <sup>4</sup>Adrenal Steroid Laboratory, ANZAC Research Institute, University of Sydney, Australia, <sup>5</sup>Bone Research Program, ANZAC Research Institute, University of Sydney; <sup>5</sup>Department of Endocrinology & Metabolism, Concord Hospital, Australia

Glucocorticoids (GCs) are widely used in the treatment of rheumatoid arthritis (RA), however, the function of endogenous GCs in the pathogenesis and maintenance of RA is less clear. The current study aimed to determine whether and how disruption of endogenous GC signaling in chondrocytes modulates the course and activity of K/BxN serum-induced arthritis in mice.

Chondrocyte-targeted GR knock-out (chGRKO) mice were generated by breeding GR<sup>lox/lox</sup> mice with tamoxifen-inducible Cre mice (Col2a1-CreER<sup>T2</sup>). chGRKO mice

and their Cre-negative GR<sup>lox/flox</sup> littermates (WT) were injected with tamoxifen at 4-weeks of age. Arthritis was induced at 8 weeks of age via injection of K/BxN serum ("chGRKO-K/BxN" and "WT-K/BxN", n=10). Arthritis was monitored daily using an established scoring system. RNA was isolated from inflamed ankle joints at days 7 (D7) and 14 (D14) for gene expression analysis.

Both chGRKO and WT mice developed acute arthritis following injection of K/BxN serum. From D6 onwards, arthritis scores were significantly higher in chGRKO than in WT mice, suggesting that disruption of endogenous GC signaling in chondrocytes aggravates K/BxN serum-induced arthritis. This increased inflammatory activity in chGRKO mice was associated with significantly higher expression of IL-1 $\beta$  (4.4-fold) and neutrophil-recruiting chemokines: CXCL1 (4.6-fold), CXCL2 (2.8-fold), CXCL5 (3.6-fold), CCL7 (2.3-fold) and their receptors: CXCR1 (2.1-fold) and CXCR2 (4.3-fold) on D7 (compared to WT mice). In addition, flow cytometry analysis of spleens harvested on D7 confirmed a significant expansion of CXCR2 positive neutrophils in chGRKO mice (compared to WT littermates). While the above cytokine and chemokine gene expression changes were less pronounced on D14, the expression of MMP-9, an enzyme involved in cartilage degradation, was significantly up-regulated in chGRKO mice.

We conclude that chondrocytes modulate autoimmune arthritis via a GR-dependent pathway through the regulation of neutrophil activity and cartilage degradation.

**Disclosures:** Jinwen Tu, None.

## LB-SU0356

**The role of DICAM in endochondral ossification.** Min-Su Han\*, Youn-Kwan Jung, Seung-Woo Han, Hye-Ri Park, Eun-Ju Lee, Ji-Ae Jang, Gun-Woo Kim. Daegu Fatima Hospital, Korea, republic of

Osteoarthritis is associated with the irreversible degeneration of articular cartilage. Notably, in this condition, articular cartilage chondrocytes undergo phenotypic and gene expression changes that are reminiscent of their end-stage differentiation in the growth plate during skeletal development. Indian Hedgehog (Ihh) signaling regulates normal chondrocyte growth and differentiation. However, the role of Ihh signaling in osteoarthritis is not elucidated.

DICAM, a dual Ig domain containing cell adhesion molecule, is involved in cell-cell adhesion through direct interaction with avb3 integrin. In our previous study showing the inhibitory role of DICAM in osteoclast differentiation and macrophage activation. In this study, we identify the role of DICAM in endochondral ossification and osteoarthritis mouse model induced by partial medial meniscectomy.

Primary chondrocytes were isolated from limbs of C57BL/6 embryo (E15.5) and used to study the in vitro mechanism study. Col2-Dicam transgenic mouse was constructed and analyze the phenotype in E15.5 long bones compared with wild types. Tibial organ cultures were used to study the conformation of gain of Dicam function. Micromass culture was conducted to study the expression and function in chondrocyte differentiation.

Overexpressed Dicam enhanced the expression of Ihh and its downstream target molecules, Gli1, Gli2 and Pthlh. Dicam also upregulated the expression of type 2 collagen and Sox9 in primary chondrocytes. In the tibia of Col2-Dicam transgenic mouse, the expression of type 10 collagen and MMP13 was enhanced. Dicam also induced the expression of Ihh and Smo in Col2-Dicam transgenic mouse. The length and calcified hypertrophic chondrocytes were increased in Dicam-overexpressed tibial organ culture.

These result indicated that DICAM acts as a stimulator of chondrocyte hypertrophy and mineralization via Ihh signal pathway.

**Disclosures:** Min-Su Han, None.

## LB-SU0357

**Osteoblast-specific deletion of *Tsc1* leads to reduced osteoblastogenesis and enhanced bone marrow adipogenesis in vivo.** Qi Han\*<sup>1</sup>, Kai Liu<sup>2</sup>, Yuqiao Zhou<sup>2</sup>, Qianming Chen<sup>3</sup>, Hong-Jiao Ouyang<sup>4</sup>. <sup>1</sup>Department of Oral Biology, School of Dental Medicine, University of Pittsburgh; State Key Laboratory of Oral Diseases, West China School of Stomatology, Sichuan University, United states, <sup>2</sup>Department of Oral Biology, School of Dental Medicine, University of Pittsburgh, United states, <sup>3</sup>State Key Laboratory of Oral Diseases, West China School of Stomatology, Sichuan University, China, <sup>4</sup>Departments of Endodontics & Oral Biology, School of Dental Medicine, University of Pittsburgh Cancer Institute, McGowan Institute for Regenerative Medicine, University of Pittsburgh, United states

Tuberous Sclerosis Complex 1 (TSC1) is an up-stream negative regulator of the mammalian target of the rapamycin pathway (mTOR), a central regulator for protein synthesis. Here, we determined the physiological role of TSC1 in regulating bone development by generating and characterizing an osteoblast-specific *Tsc1* conditional knock-out (CKO) mouse model.

*Tsc1*<sup>F/F</sup> and *Osterix-Cre*<sup>+</sup> mice were used to generate *Tsc1*<sup>F/F</sup>; *Cre*<sup>+</sup> (CKO) mice, with *Tsc1*<sup>+/+</sup>; *Cre*<sup>+</sup> and *Tsc1*<sup>F/F</sup> wild type (WT) littermates. *Tsc1* CKO mice were born at Mendelian frequencies, but with lesser body weight and length than that of WT littermates.

Immunohistochemistry (IHC) staining demonstrated that while both WT and CKO femurs had similar S6 ribosomal protein levels, *Tsc1*-deficient femurs displayed

a heightened protein expression of phospho-S6 ribosomal protein, indicating enhanced activity of mTORC1 in the absence of osteoblastic TSC1. Micro-computed tomography analyses demonstrated that *Tsc1* CKO mice display a significantly reduced three-dimensional trabecular bone volume fraction, thickness, and number, as well as a significantly increased trabecular separation, compared with gender-matched *Tsc1*<sup>F/F</sup> littermates. H&E staining showed *Tsc1* CKO mice had reduced trabecular bone mass and disorganized cortical bones, in addition to enhanced bone marrow adiposity, compared with *Tsc1*<sup>+/+</sup>; *Cre*<sup>+</sup> counterparts. qRT-PCR analysis also showed that *Tsc1*-deficient bone tissues had reduced gene expression of osteoblastic markers, compared with *Tsc1*<sup>+/+</sup>; *Cre*<sup>+</sup> counterparts, demonstrating that TSC1 deficiency leads to compromised osteoblastogenesis, in vivo.

Since *Tsc1* CKO mice exhibited reduced osteoblastogenesis and increased bone marrow adipogenesis, recapitulating the mouse bone phenotypes caused by the loss-of-function of Wnt/ $\beta$ -catenin signaling. We further determined the status of Wnt/ $\beta$ -catenin signaling in TSC1-deficient bone tissues, in vivo. IHC staining demonstrated a reduction of protein expression of  $\beta$ -catenin and an increase in protein expression of sclerostin, an inhibitor for canonical Wnt signaling, in TSC1-deficient bones, compared with *Tsc1*<sup>+/+</sup>; *Cre*<sup>+</sup> counterparts.

Collectively, the results demonstrated that intact TSC1/mTOR signaling is required for normal bone development and proper bone marrow homeostasis. Additional investigation is needed to elucidate the detailed molecular and cellular mechanisms underlying TSC1's regulation of both osteoblastic canonical Wnt signaling and bone development.

**Disclosures:** Qi Han, None.

## LB-SU0358

**Maternal Obesity and Trabecular Bone Microarchitecture in C57BL Mice.** Lauren Coheley\*, Richard Lewis. The University of Georgia, United states

Diet-induced obesity has a negative effect on bone microarchitecture through decreasing trabecular number and volume. Determining the effect of obesity on bone in the context of gestation is of particular importance since the state of pregnancy significantly impacts maternal bone outcomes and approximately 40% of women of childbearing ages are considered obese. The purpose of this study was to determine the effects of gestation and maternal obesity on trabecular bone microarchitecture in C57BL mice. Female mice were either provided a low-fat ( $n = 12$ ) or a high-fat ( $n = 12$ ) diet over a 6-week period and were then mated with their male counterparts. Trabecular bone at the distal tibia metaphysis was analyzed following a 6-week exposure to respective dietary treatments ( $n = 6$ /group) and prior to delivery ( $n = 6$ /group) using micro-computed tomography. For simplicity, data on an important variable of interest, bone volume to total volume (BV/TV), are presented. There were significant main effects for both obesity ( $F(1,10) = 10.07, p = .010$ ), and pregnancy ( $F(1,10) = 144.8, p < .001$ ), such that both high-fat feeding and pregnancy were associated with lower BV/TV. The interaction effect was also statistically significant ( $F(1,10) = 8.768, p = .014$ ), demonstrating that the effect of obesity on BV/TV is minimal during gestation. The effect of gestation on BV/TV was substantially greater than that of diet-induced obesity, therefore explaining the negligible obesity-related difference in BV/TV during gestation. These findings underscore the negative effect of excess adiposity and pregnancy on trabecular bone microarchitecture. Future research is needed to determine whether obesity during gestation compromises the restoration of trabecular bone post-pregnancy.

**Disclosures:** Lauren Coheley, None.

## LB-SU0359

**Identification of hip BMD loss and fracture risk markers through population-based serum proteomic analyses.** Carrie Nielson\*<sup>1</sup>, Jack Wiedrick<sup>1</sup>, Jon Jacobs<sup>2</sup>, Doug Bauer<sup>3</sup>, Nancy Lane<sup>4</sup>, Peggy Cawthon<sup>5</sup>, Vlad Petyuk<sup>2</sup>, Erin Baker<sup>2</sup>, Richard Smith<sup>2</sup>, Jodi Lapidus<sup>1</sup>, Eric Orwoll<sup>1</sup>. <sup>1</sup>Oregon Health & Science University, United states, <sup>2</sup>Pacific Northwest National Laboratory, United states, <sup>3</sup>University of California, San Francisco, United states, <sup>4</sup>UC Davis Health System, United states, <sup>5</sup>California Pacific Medical Center Research Institute, United states

Predictors of BMD loss and fracture are necessary for osteoporosis prevention. High-throughput serum proteomics studies allow for discovery of novel osteoporosis biomarkers and evaluation of their correlations with currently used bone turnover markers and known risk factors. The prospective Osteoporotic Fractures in Men Study (MrOS) comprises men ages 65 and older in six US cities who have contributed extensively regarding osteoporosis risk factors, bone turnover, and inflammatory markers and who have been followed for incident fracture. High-throughput quantitative proteomic analysis was performed on baseline fasting serum samples using a multi-dimensional approach coupling liquid chromatography, ion-mobility separation, and mass spectrometry (LC-IMS-MS). We followed men for a mean of 4.6 years for changes in femoral neck bone mineral density (BMD) at two or three follow-up visits and for incident hip fracture. Change in femoral neck BMD was determined from mixed effects regression models taking age and weight into account. Participants were categorized into three groups based on BMD change: BMD maintenance (no decline; estimated change  $\geq 0$  g/cm<sup>2</sup>, n=453); expected loss (estimated change 0 to 1 SD below the estimated mean change,  $-0.034$  g/cm<sup>2</sup> for femoral neck, n=1185); and

accelerated loss (estimated change  $\geq 1$  SD below mean change,  $n=237$ ). Three peptides (in complement 7, complement C1r, and CD14) had fold changes  $\geq 1.1$  (FDR  $< 0.10$ ) for accelerated loss vs maintenance. We examined the change in area under the ROC (AUC) for accelerated loss vs maintenance among men with serum CTX measures available ( $n=224$ ). The AUC improved from 0.71 (with CTX, age, and BMI only) to 0.76 with the addition of the three peptides. Further, differential abundance values of *peptides* were summarized with meta-analysis to determine differential abundance of each corresponding *protein* for accelerated BMD loss vs maintenance. Using this meta-analytic standardized fold change at cutoffs of  $\geq 1.1$  or  $\leq 0.9$  ( $p < 0.10$ ), 31 proteins were associated with rate of bone loss. Of those 31, 13 proteins were also associated with incident hip fracture ( $p < 0.05$ , Table). Some of these peptides and proteins have been previously associated with fracture risk, and several have roles in insulin signaling, inflammation, or adaptive immunity. These results support using proteomics to identify novel serum biomarkers for future research in bone biology and fracture prediction.

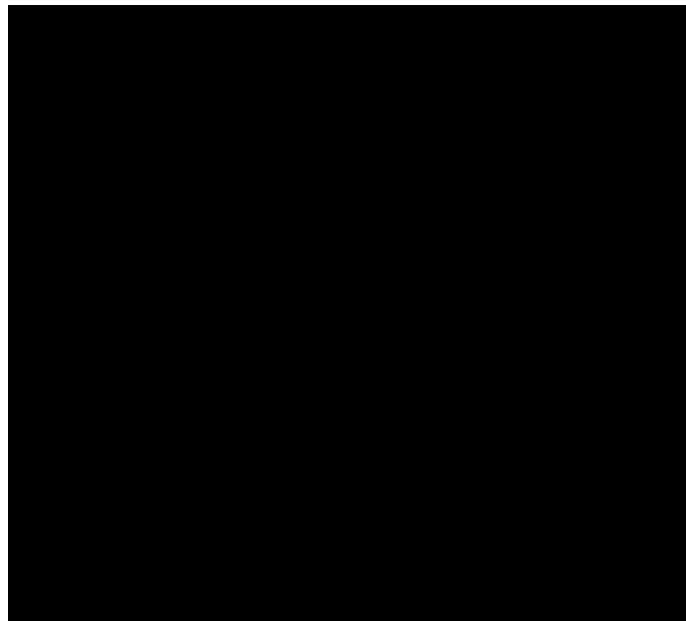


Table. Femoral neck BMD-loss associated proteins and incident hip fracture

*Disclosures: Carrie Nielson, None.*

## LB-SU0360

**Evidence for a key role of histone methylation in the control of the biological function of vitamin D: aberrant regulation with aging.** Vaishali Veldurthy<sup>\*1</sup>, Ki-in Kim<sup>2</sup>, Puneet Dhawan<sup>2</sup>, Leyla Oz<sup>2</sup>, Leila Mady<sup>2</sup>, Sylvia Christakos<sup>3</sup>. <sup>1</sup>Rutgers- New Jersey Medical School, United states, <sup>2</sup>Rutgers-New Jersey Medical School, United states, <sup>3</sup>Rutgers - New Jersey Medical School, United states

Hormone dependent transcriptional regulation involves chromatin remodeling by coactivator proteins. Although roles of acetylation and phosphorylation in chromatin remodeling have been widely studied, recent findings have also indicated an important role for methylation. Little is known however about the role of histone methylation in the control VDR function and how VDR function and epigenetic regulation of VDR function are altered with age. Using renal cells and the rat CYP24A1 promoter we found that CARM1 (a methyltransferase that methylates histone 3 at arginine 17) is a VDR coactivator that binds to and cooperates with the p160 coactivator GRIP1 to enhance 1,25(OH)<sub>2</sub>D<sub>3</sub> induced transcription. In *in vivo* studies we found that mRNA expression of renal CYP24A1, which is involved in the metabolic inactivation of 1,25(OH)<sub>2</sub>D<sub>3</sub>, increases with age [4.0  $\pm$  fold at 24 mo. vs. 6 mo.,  $p < 0.05$ ; C57BL/6 male mice], suggesting that increased catabolism of 1,25(OH)<sub>2</sub>D<sub>3</sub> contributes to the decreased capacity with age to absorb calcium and age related bone loss. Although we found an age related decrease in renal VDR mRNA (42% decrease at 24 mo. compared to 6 mo.), *in vivo* ChIP in kidney showed enhanced recruitment in response to 1,25(OH)<sub>2</sub>D<sub>3</sub> of VDR and enhanced H3 arginine methylation mediated by CARM1 at VDRE sites in the mouse CYP24A1 gene with age (24 mo vs. 6 mo). Our findings suggest mechanisms contributing to enhanced levels of CYP24A1 and thus increased renal catabolism of 1,25(OH)<sub>2</sub>D<sub>3</sub>. These findings are the first to address changes in VDR signaling and 1,25(OH)<sub>2</sub>D<sub>3</sub> mediated epigenetic regulation that occur with aging. In intestine VDR mRNA did not change with aging although expression of TRPV6 mRNA significantly declined 2 - 4 fold in all regions of the intestine (24 mo vs. 6 mo). *In vivo* ChIP revealed decreased recruitment by 1,25(OH)<sub>2</sub>D<sub>3</sub> of VDR to the TRPV6 gene with age. Renal CYP24 mRNA was equally responsive to 1,25(OH)<sub>2</sub>D<sub>3</sub> in young and old mice. However intestinal sensitivity to 1,25(OH)<sub>2</sub>D<sub>3</sub>, as indicated by induction of TRPV6 mRNA in different intestinal segments, was greater in young vs old mice. Our findings suggest that the age related decrease in TRPV6 is mediated, in part, by altered 1,25(OH)<sub>2</sub>D<sub>3</sub> mediated VDR interaction with DNA and that altered

epigenetic regulation contributes to the dysregulation of calcium homeostasis that occurs with aging.

*Disclosures: Vaishali Veldurthy, None.*

## LB-SU0361

**Effects of Muscle Stretching on Hindlimb Bone Blood Flow.** Payal Ghosh<sup>\*1</sup>, Judy Muller-Delp<sup>1</sup>, Kazuki Hotta<sup>1</sup>, Michael Delp<sup>1</sup>, Bradley Behnke<sup>2</sup>, Bei Chen<sup>3</sup>, Rahul Verma<sup>3</sup>. <sup>1</sup>Florida State University, United states, <sup>2</sup>Kansas State University, United states, <sup>3</sup>University of Florida, United states

Old-age related reductions in bone mass and increases in fracture risk may be associated with diminished skeletal perfusion. The purpose of this study was to assess the acute and chronic effects of muscle stretching on hindlimb bone and marrow blood flow.

Old ( $n= 35$ , 20 months old) male Fischer 344 rats were randomized to either a naïve or stretch-trained group. Stretch training consisted of passively stretching the left hindlimb muscles through placement of a splint on the left ankle for 30 min/day, 5d/wk for 4wks. The right hindlimb served as a contralateral control limb. Following stretch training, blood flow to the femur, fibula, proximal and distal tibial metaphysis, tibial diaphyseal marrow and tibial diaphysis was determined using radioactive microspheres. Bone blood flow was assessed during and after an acute bout of stretching in naïve rats, and during rest and exercise (treadmill running at 15m/min) in stretch-trained rats.

In naïve rats, placement of the splint increased blood flow to the proximal tibial metaphysis, the origin of attachment for the soleus and plantaris muscles. After 4 weeks of daily splinting, blood flow to the proximal tibial metaphysis was higher in the chronically stretched limb during exercise. Chronic stretching also increased tibial bone weight.

These findings suggest that muscle stretching increases bone loading and local bone blood flow at the origins of muscular attachment. Local skeletal perfusion of bone at the attachment sites of stretched muscles increases with daily stretching suggesting that regular muscular stretching may lead to improvement in the structural properties of bone in an aged population.

*Disclosures: Payal Ghosh, None.*

## LB-SU0362

**Parathyroid hormone administration regulates osteoprogenitor numbers by direct signaling via PTH/PTHrP receptor *in vivo*.** Deepak Balani<sup>\*1</sup>, Noriaki Ono<sup>2</sup>, Henry Kronenberg<sup>1</sup>. <sup>1</sup>Endocrine Unit, Massachusetts General Hospital & Harvard Medical School, Boston, MA, United states, <sup>2</sup>University of Michigan, School of Dentistry, United states

The contribution of mature osteoblasts to the bone anabolic response induced by parathyroid hormone (PTH) has been studied extensively. However, the role of osteoprogenitors in fuelling that anabolic response is poorly understood. Recently our group identified osteoprogenitors in early postnatal mice. Using a lineage-tracing strategy, we showed that the Sox9 promoter/enhancer labels progenitors with multi-lineage potential and self-renewing capabilities *in vivo*. In this study we show that the Sox9 promoter/enhancer actively labels multi-potential skeletal progenitors in older mice. Further, we hypothesized that PTH may regulate the numbers of Sox9<sup>+</sup> progenitors *in vivo* and preferentially direct them towards the osteoblastic lineage, when administered by once daily subcutaneous injection. To understand if PTH affects proliferation/apoptosis and/or differentiation of progenitors, we utilized a creER-mediated lineage-tracing strategy using 6-8 week old Sox9creER<sup>T2</sup>;Rosa26-tTomato, Osteocalcin (Ocn)-GFP transgenic mice. Mice received 2 mg tamoxifen first and 24h later were started on daily subcutaneous injections of PTH or vehicle for 3, 7 or 21 days. Both flow cytometry and histology showed that Tomato<sup>+</sup> cells were significantly increased in mice that received PTH in a dose and time-dependent manner. The increase in the numbers of Tomato<sup>+</sup> cells was seen as soon as 3 days after PTH administration in the primary spongiosa, periosteal and the endocortical surfaces. On Day 3 Tomato<sup>+</sup> cells were mostly not yet Ocn-GFP. On Day 7 and Day 21 we observed several Tomato<sup>+</sup> cells that also expressed Ocn-GFP present on bone surfaces. PTH did not affect the rate of proliferation but suppressed the rate of apoptosis of osteoprogenitors in PTH-treated mice. Strikingly, when mice floxed for both the tomato reporter and the PTH/PTHrP receptor (PTHRI) were treated with tamoxifen and then PTH for 7 days, the resultant mice failed to increase the number of Tomato<sup>+</sup> cells. RT-PCR confirmed transcripts encoding PTHRI were 4000-fold lower in Sox9creER/TdTomato/ PTHRI<sup>flx/flx</sup> mice compared to Sox9creER/TdTomato/ PTHRI<sup>flx/wt</sup> mice. In this study we successfully labeled adult multi-potential skeletal progenitors and describe how PTHRI signaling modulates their numbers and also show that the effect is due to an increase in the suppression of apoptosis of those progenitors subsequent to PTH administration.

*Disclosures: Deepak Balani, None.*

## LB-SU0363

**PTH1R anti-hypertrophic signaling is essential for articular cartilage maintenance and protection post trauma.** Fadia Kamal\*, Eric Schott, Reyad Elbarbary, Jennifer Jonason, Michael Zuscik. University of Rochester, United states

In our previous work we identified recombinant human PTH as a novel therapy for osteoarthritis (OA). We found significantly elevated levels of PTH type 1 receptor (PTH1R) in murine and human articular chondrocytes during OA and following injury, where treatment with rhPTH had dramatic chondroregenerative effects in a mouse model of knee OA. Whether the chondroregenerative effect of rhPTH is directly through articular chondrocytes PTH1R is still unknown.

Hypothesis: PTH1R signaling maintains articular chondrocytes in a non-hypertrophic state and protects against de novo and injury-induced cartilage degeneration.

Methods: Using a tamoxifen-inducible conditional chondrocyte PTH1R knockout mouse (Acan-Cre<sup>ERT2</sup>;PTH1R<sup>fl/fl</sup>) we determined 1) the role of articular chondrocyte PTH1R in cartilage homeostasis: PTH1R knockout was induced in three and six months old mice, mice were sacrificed and knees were collected one, two, three, and four months later. And 2) the role of articular chondrocyte PTH1R in cartilage degeneration in OA: OA was induced by surgical destabilization of the medial meniscus (DMM) in knockout mice and in their littermate controls, and mice were sacrificed 16 weeks post-DMM. Articular cartilage structural changes were evaluated via Saf-O-Fast green staining, histomorphometry, OARSI scoring, osteophyte scoring and microCT. Molecular events were examined using immunofluorescent staining for hypertrophic chondrocyte markers, and TUNEL staining for apoptosis.

Results: Loss of PTH1R in Acan-Cre<sup>ERT2</sup>; PTH1R<sup>fl/fl</sup> mice led to spontaneous cartilage degeneration, characterized by a reduction in the area of uncalcified articular cartilage (Fig. 1A), reduced articular chondrocyte number and increased apoptosis, increased number of hypertrophic chondrocytes and increased expression of the matrix degrading enzymes (MMP13 and ADAMTS5). Following DMM, Acan-Cre<sup>ERT2</sup>; PTH1R<sup>fl/fl</sup> mice showed a more aggressive OA phenotype than their non-knockout littermate controls, characterized by: almost complete loss of uncalcified articular cartilage (Fig. 1B), lower number of articular chondrocytes, increased chondrocyte hypertrophy, MMP13 and ADAMTS5 expression, and apoptosis.

Conclusion: Our data show that PTH1R is a key regulator of articular chondrocytes, maintaining them in a non-hypertrophic state both at baseline and following injury, and protecting cartilage from degenerative change. This supports the use of PTH as a chondroregenerative therapeutic approach in OA.

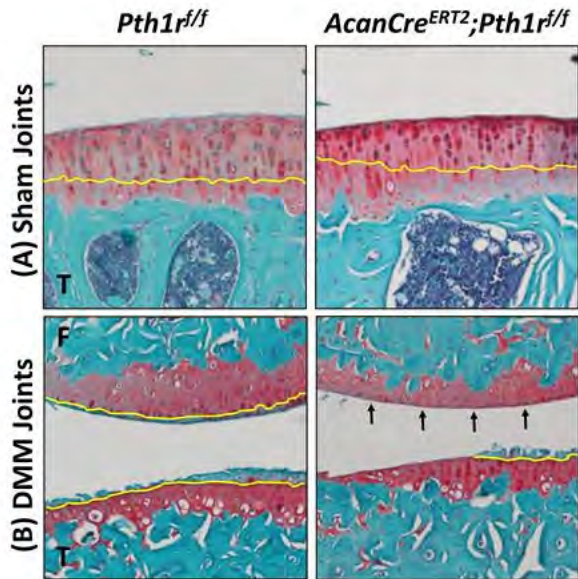


**Fig. 1: Cartilage Degeneration is Accelerated in AcanCre<sup>ERT2</sup>;Pth1r<sup>fl/fl</sup> Mice.** Ablation of PTH1R in 3 month old mice led to reduced uncalcified cartilage area on the tibial plateau (T) in uninjured knee joints (A), and enhanced loss of uncalcified cartilage on both the femur (F) and tibia (T) following DMM (B). Yellow lines depict the tidemarks.

## LB-SU0364

**Live Cell Imaging of Procollagen Trafficking in Osteoblasts.** Shakib Omani<sup>1</sup>, Laura Gorrell<sup>\*1</sup>, Elena Makareeva<sup>2</sup>, Lynn Mirigian<sup>2</sup>, Anna Roberts-Pilgrim<sup>1</sup>, Jennifer Lippincott-Schwartz<sup>3</sup>, Sergey Leikin<sup>1</sup>. <sup>1</sup>NICHD, NIH, United states, <sup>2</sup>NICHD,NIH, United states, <sup>3</sup>HHMI Janelia Research Campus, United states

Abnormal biosynthesis and trafficking of procollagen precursor of type I collagen causes osteoblast malfunction in osteogenesis imperfecta and might be involved in deficient osteoblast function in common osteoporosis. Type I procollagen is a heterotrimer of two  $\alpha 1$  and one  $\alpha 2$  chains which are folded in the ER, transported through Golgi and secreted. The mechanism of procollagen trafficking from the ER to Golgi remains controversial. To clarify this mechanism, we developed multiple fluorescent protein (FP) tagged constructs and investigated their localization and trafficking by confocal live cell imaging in transfected MC3T3 osteoblasts. Procollagen accumulation in the ER due to transfection of mutant chains, inhibition of the ER export, or overtransfection resulted in formation of procollagen spherulites inside the ER lumen. These spherulites contained HSP47, a chaperone essential for stabilizing and enabling folding of the procollagen triple helix. Smaller spherulites had an appearance similar to ER-to-Golgi transport vesicles, but live-cell imaging revealed that these were static structures within the ER lumen. Surprisingly, time-lapse imaging of live cells after photobleaching revealed no TagBFP2-conjugated HSP47 in the transport vesicles delivering procollagen from the ER to Golgi. We did not observe trafficking of GFP-conjugated HSP47 from the ER to Golgi either. We also observed perfect colocalization of FP-conjugated HSP47 with immunofluorescence-labeled HSP47 in fixed cells. These observations suggested that HSP47 might be retained in the ER, in contrast to the prevailing hypothesis of HSP47 cotransport with procollagen from the ER to Golgi.

*Disclosures: Laura Gorrell, None.*

## LB-SU0365

**PGC1 $\beta$  stimulates osteoclast function but not formation via mitochondrial biogenesis and activation.** Yan Zhang<sup>\*1</sup>, Nidhi Rohatgi<sup>1</sup>, Joel Schilling<sup>2</sup>, Steven L. Teitelbaum<sup>3</sup>, Wei Zou<sup>1</sup>. <sup>1</sup>Department of Pathology & Immunology, Washington University School of Medicine, United states, <sup>2</sup>Cardiovascular Division, Department of Medicine, Washington University School of Medicine, United states, <sup>3</sup>Department of Pathology & Immunology; Division of Bone & Mineral Diseases, Department of Medicine, Washington University School of Medicine, United states

Osteoclasts are the most mitochondria-rich cells in man. Peroxisome proliferator-activated receptor gamma coactivator 1- $\beta$  (PGC1 $\beta$ ) is a transcriptional coactivator that regulates energy metabolism by stimulating mitochondrial biogenesis and respiration. Previous studies using global and Tie2-specific knockout mice reported that PGC1 $\beta$  is essential for osteoclast differentiation. This conclusion is inconsistent, however, with the normal number of osteoclasts in PGC1 $\beta$ -/- mice. To determine the role of PGC1 $\beta$  in osteoclastogenesis, we generated LysM-Cre PGC1 $\beta$  conditional knockout mice, in which the gene is exclusively deleted in myeloid lineage cells (PGC1 $\beta$ LysM). Osteoclast maturation was determined as a function of differentiation markers and TRAP staining. Mature osteoclast function was assessed by actin ring and resorptive pit formation on bone. Cytoskeletal organization was monitored by live fluorescent imaging of GFP-labeled actin. Rac1 activation by M-CSF and vitronectin and c-Src activation were detected by GTP pull-down assay and western blotting, respectively. Mitochondrial biogenesis and mitochondrial complex subunit expression were determined by qPCR and Western blotting, respectively. Mitochondrial number was detected using mitochondrial specific probes. Challenging previous reports, we find osteoclast differentiation of PGC1 $\beta$ -deficient bone marrow macrophages (BMMs), as determined by the unchanged expression level of differentiation markers including  $\beta 3$  integrin, c-Src, NFATc1, and Cathepsin K, is unaltered. On the other hand, osteoclast function is impaired when PGC1 $\beta$  is deleted, as manifest by a complete absence of actin rings and resorptive pits on bone. Surprisingly, PGC1 $\beta$ -deficient osteoclasts are huge likely due to marked hypermobility thereby increasing contact with mononuclear precursors. Rac expression Rac1-GTP formation and c-Src activation are unaltered in PGC1 $\beta$ LysM osteoclasts establishing a non-canonical mechanism generates their markedly abnormal cytoskeleton. In this regard, mitochondrial biogenesis, mitochondria number, and expression of mitochondrial respiratory chain proteins are significantly decreased in the PGC1 $\beta$ -deficient BMMs and osteoclasts. Our results establish that PGC1 $\beta$  is essential for osteoclast function but not differentiation and indicate that their cytoskeletal organization is mitochondria-mediated.

*Disclosures: Yan Zhang, None.*

Figure 1

*Disclosures: Fadia Kamal, None.*

## LB-SU0366

**A Novel Regulatory Role of TRAPPC9 in L-Plastin-mediated Actin Ring Formation and Osteoclast Function.** Nazar Hussein\*, Thomas Mbima, Mohammad Ansari, Zhicheng Jin, Takhar Kasumov, Favez Safadi. Northeast Ohio Medical University (NEOMED), United states

Trafficking Protein Particle Complex 9 (TRAPPC9) is a major subunit of TRAPP Complex. TRAPPC9 has been reported to bind IKK2 and NIK where it plays a role in the canonical and non-canonical NFkB signaling in Osteoclast (OC) differentiation and function. However, the role of TRAPPC9 in protein trafficking in OC has not been studied. In this study, we examined the co-localization of TRAPPC9 with cathapsin-K (Cathp.K), known to mediate OC resorption suggesting that TRAPPC9 mediates the trafficking and function of OCs. To identify TRAPPC9 protein partners important for OC-mediated bone resorption, we conducted immunoprecipitation of TRAPPC9 isolated from terminally differentiated OCs followed by mass spectrometry analysis. Surprisingly, our data showed that TRAPPC9 binds various protein partners. One of those proteins is L-Plastin (LP). LP is localized at the podosomes and plays a crucial role in actin aggregation thereby actin ring formation and OC function. Recent studies reported that LP null OCs demonstrated normal OC differentiation phenotype and peripheral podosomes aggregation. However, significant disruption in actin ring formation and the sealing zone region were observed. Although the role of LP in OC-mediated bone resorption has not reported in details. Here, we investigated the potential regulatory role of TRAPPC9 and LP-mediated OC function. We assessed the localization of TRAPPC9 and LP in OC and found that TRAPPC9 is co-localized with LP within the periphery of OC. Next, we determined the effect of TRAPPC9 overexpression using viral system on LP recruitment to the actin ring. Interestingly, our data showed that TRAPPC9 overexpression promotes the recruitment of LP to the actin ring when compared controlled cultures. This recruitment is associated with increasing OC-mediated bone resorption. Studies are underway to determine the effects of modulating TRAPPC9 and/or LP using genetic and pharmacologic approaches on OC trafficking, function and identifying the mechanism(s) by which cytoskeletal structures/re-organization in OC function mediated by TRAPPC9/LP interaction. Collectively, these studies are the first to report a novel role of TRAPPC9 and LP in mediating actin ring formation and OC function.

**Disclosures:** *Nazar Hussein, None.*

## LB-SU0367

**Translational profiling to identify novel cytokines and biomarkers expressed in osteoclasts during skeletal injury.** In Kyoung Mah, Nikita Tripuraneni, Brian Lee, Francesca Mariani\*. University of Southern California, United states

In response to skeletal injury, cells of the monocyte lineage accumulate, differentiate and can have both stimulatory and inhibitory roles during skeletal healing. While osteoclasts have been shown to emit coupling factors or 'clastokines' during homeostasis, little is known about the signals emitted in response to injury. Identification of such signals may not only lead to the development of new bone anabolics, but may also provide insight into how monocyte lineage cells normally influence their local environment. We have developed a new model for natural large-scale injury/repair in mice and have observed a robust osteoclast response localized to the periosteal surface during healing. The role of osteoclasts specifically at the periosteal surface has not been well-studied. Using a cell-type specific CRE-mediated translational profiling method that allows RNA isolation without cell dissociation, we have identified a variety of secreted proteins and osteoclast biomarkers expressed in response to injury. Differentially expressed genes include secreted growth factors, chemokines, and other proteins associated with inflammation. Some of these proteins have been characterized in osteoclasts/macrophages before, while others are novel in their association. An analysis of these genes during injury and homeostasis will be presented.

**Disclosures:** *Francesca Mariani, None.*  
*This study received funding from: Merck*

## LB-SU0368

**Predictors of TBS Change are Different from Predictors of Bone Mineral Density Change: Results from the Osteoporotic Fractures in Men (MrOS) study.** Tien Vo<sup>1</sup>, Lisa Langsetmo<sup>1</sup>, Allyson Kats<sup>2</sup>, Ann Schwartz<sup>3</sup>, Douglas Bauer<sup>4</sup>, Jane Cauley<sup>5</sup>, Brent Taylor<sup>6</sup>, Kristine Ensrud<sup>7</sup>, John Schousboe<sup>8</sup>.  
<sup>1</sup>Division of Epidemiology, University of Minnesota, United states, <sup>2</sup>Division of Epidemiology, United states, <sup>3</sup>Department of Epidemiology & Biostatistics, United states, <sup>4</sup>Department of Medicine & Department of Epidemiology & Biostatistics, United states, <sup>5</sup>University of Pittsburgh Graduate School of Public Health, United states, <sup>6</sup>Division of Epidemiology & Department of Medicine, University of Minnesota; Center for Chronic Disease Research, Minneapolis VAMC, United states, <sup>7</sup>Division of Epidemiology & Department of Medicine, University of Minnesota; Center for Chronic Disease Research, Minneapolis VAMC, United states, <sup>8</sup>Park Nicollet Osteoporosis Center & HealthPartners Institute, HealthPartners; Division of Health Policy & Management, University of Minnesota, United states

**Purpose:** To identify individual characteristics that predict longitudinal change of Trabecular Bone Score (TBS) in older men, and compare and contrast those to predictors of change in total hip (TH-BMD) and lumbar spine (LS-BMD) bone mineral density.

**Methods:** 3969 MrOS participants (mean age 72.9 years) attended the first and second study visits (mean 4.6 years between visits), had valid TBS scores for both visits, body mass index (BMI) <37 kg/m<sup>2</sup>, and were not users of bisphosphonate or oral corticosteroids. BMD was measured on Hologic QDR4500 densitometers, and TBS calculated using version 2.1. Candidate predictor characteristics were associated with TBS at baseline, or those consistently associated with longitudinal change in LS-BMD or TH-BMD in prior studies. Linear regression models were used to estimate the associations of predictors with change in TBS, TH-BMD, or LS-BMD. Predictors included in the final multivariable-adjusted models had a p-value of association with change in TBS or BMD of <0.10. For each predictor, a modified Hausmann test was used to test whether the magnitude of associations with change in TBS and change in BMD were different.

**Results:** 1458 (37%) men had TBS decrease of >0.04 (approximate least significant change), 1712 (43%) men had no change (≤0.04 decrease or increase), and 799 (20%) men had TBS increase >0.04.

Weight loss of ≥10% between visits was concurrently associated with multivariable adjusted (Table) increases in TBS (effect size 1.23; 95% C.I. 1.11 to 1.34), but *decreases* in both TH-BMD (effect size -1.16; 95% C.I. -1.28 to -1.03) and LS-BMD (effect size -0.19; 95% C.I. -0.30 to -0.08; p-value <0.001 for differences of associations of weight loss with TBS outcome vs. BMD outcomes). Faster baseline walk speed was associated with increases in TH-BMD, but not with TBS change (p-value <0.001 for difference in associations). Greater age at baseline was associated with decreases in both TH-BMD and LS-BMD, but not with TBS change (p<0.001 for differences in associations).

**Conclusions:** Weight loss in older men is concurrently associated with marked increases in TBS but substantial decreases in TH-BMD and LS-BMD, suggesting the former association may be artefactual. Greater age and slower gait speed in this cohort are associated with higher rates of loss of TH-BMD, but not with TBS change. TBS may be unstable with weight change and should be interpreted with caution.

Predictors	Effect size <sup>*,†</sup>		P-value for difference <sup>‡,§</sup>
	Outcome TBS Change <sup>**</sup>	Outcome Total Hip BMD change <sup>**</sup>	
Age	-0.00 (-0.03 : 0.03)	<b>-0.14 (-0.17 : -0.11)</b>	<0.001
Walk Speed	-0.01 (-0.04 : 0.02)	<b>0.07 (0.03 : 0.10)</b>	<0.001
Change in Weight V2 vs V1			
No change	Ref.	Ref.	
≥ 5% increase	<b>-0.82 (-0.92 : -0.73)</b>	<b>0.31 (0.20 : 0.41)</b>	<0.001
≥ 5 to < 10% decrease	<b>0.66 (0.58 : 0.73)</b>	<b>-0.46 (-0.54 : -0.38)</b>	<0.001
≥ 10 decrease	<b>1.23 (1.11 : 1.34)</b>	<b>-1.16 (-1.28 : -1.03)</b>	<0.001
Smoking status:			
Never	Ref.	Ref.	
Past	-0.01 (-0.06 : 0.05)	<b>0.08 (0.02 : 0.14)</b>	0.04
Current	-0.05 (-0.22 : 0.11)	-0.13 (-0.31 : 0.04)	0.47
Prevalent Radiographic Vertebral Fracture	0.11 (-0.01 : 0.22)	0.01 (-0.11 : 0.13)	0.21
PASE Score	-0.03 (-0.06 : 0.00)	-0.01 (-0.04 : 0.01)	0.51
Body Mass Index category			
< 25 kg/m <sup>2</sup>	Ref.	Ref.	
25-29.9 kg/m <sup>2</sup>	0.04 (0.02 : 0.11)	0.05 (0.02 : 0.12)	0.81
≥ 30 kg/m <sup>2</sup>	<b>0.10 (0.01 : 0.18)</b>	0.06 (0.03 : 0.15)	0.56

<sup>\*</sup>Number of TBS standard deviations change and number of Total Hip BMD standard deviations change per category level vs reference, or per standard deviation increase of continuous predictor, multivariable-adjusted  
<sup>†</sup>Effect size in **bold italics** significant at p<0.05 level   <sup>‡</sup>Modified Hausmann test (suest command in stata), Global test p<0.001

Table-Predictors of TBS Change vs Total Hip BMD Change

**Disclosures:** *John Schousboe, None.*

*This study received funding from: National institute for Aging, National Institutes of Health*

## LB-SU0369

**Influence of Alkali Supplementation on Circulating microRNA Expression.**

Lee Margolis, Bess Dawson-Hughes, Donato Rivas, Yassine Ezzvat, Roger Fielding, Lisa Ceglia\*. Tufts University, United states

Studies suggest that musculoskeletal physiology is reflected in changes in tissue-specific microRNA (miR) levels – short non-coding RNAs regulating gene expression – which can be measured in serum and serve as potential biomarkers of bone and muscle function adding information on biological pathways affected by various interventions. Our objective was to examine whether alkali supplementation with potassium bicarbonate (KHCO<sub>3</sub>) vs. placebo alters serum miRs involved in various bone and muscle functions (Table 1). The study was a randomized, double-blind, placebo-controlled trial involving KHCO<sub>3</sub> (81 mmol/d) vs. placebo for 3 months. Subjects were men and women age  $\geq 60$  years with estimated glomerular filtration rate (GFR)  $\geq 50$  mL·min<sup>-1</sup>·1.73 m<sup>2</sup>, baseline urinary net acid excretion (NAE)  $\geq 5$  mmol as an indicator of baseline higher endogenous renal net acid status. Urinary NAE, NTX, Ca, and N, GFR, serum PINP (bone formation marker), and serum IGF-1 were measured at baseline and 3 months. MiRs of interest (Table 1) were analyzed using TaqMan<sup>®</sup> MicroRNA Assays. All characteristics and biochemical measurements did not differ significantly in the 2 groups at baseline. Three-month changes in urinary NAE differed by group (KHCO<sub>3</sub> =  $-47 \pm 9$  mmol, n=12; Placebo =  $-5 \pm 5$  mmol, n=12; P<0.01). KHCO<sub>3</sub> resulted in significant declines in urinary NTX (KHCO<sub>3</sub> =  $-158 \pm 31$  Nmol; Placebo =  $-47 \pm 28$  Nmol; P<0.01), urinary Ca (KHCO<sub>3</sub> =  $-23 \pm 19$  mmol; Placebo =  $38 \pm 18$  mmol; P<0.01), and serum PINP (KHCO<sub>3</sub> =  $-8 \pm 3$  Nmol/L; Placebo =  $-2 \pm 3$  Nmol/L; P=0.03) compared to placebo over 3 months. Urinary N and serum IGF-1 level in response to KHCO<sub>3</sub> vs. placebo did not differ significantly. KHCO<sub>3</sub> resulted in differences in the fold change in serum miR-21 (KHCO<sub>3</sub> =  $0.74 \pm 0.39$ ; Placebo =  $-0.70 \pm 0.45$ ; P=0.05) and miR-133b (KHCO<sub>3</sub> =  $2.26 \pm 0.85$ ; Placebo =  $-1.23 \pm 0.69$ ; P<0.01) compared to placebo. In summary, reducing renal acid load with KHCO<sub>3</sub> 81 mmol/d significantly increased expression of serum miRs-21 (involved in osteogenesis) and 133b (osteoblast differentiation and myogenesis). As serum miRs 21 and 133b are positively associated with bone mineral density and/or inversely associated with osteoporotic fractures, the direction of change in these miRs in our study is consistent with potential beneficial effects on bone. The broader significance and role of serum miRs as musculoskeletal biomarkers is still under investigation. Larger studies are needed to verify these preliminary results.

## microRNA Function

microRNA	Function	
miR-1	Myogenesis, IGF-1 signaling	Muscle
miR-206	Myogenesis	
miR-486	AKT signaling, Atrophy	
miR-133a	Myogenesis, IGF-1 signaling, Run2 (osteogenesis)	
miR-133b	Myogenesis, IGF-1 signaling, osteoblast differentiation	Bone
miR-21	Osteogenesis	
miR-122	BMPRIA, bone remodeling	
miR-125	Osteoblast differentiation	
miR-422	Biomarker for BMD level	

Table 1

Disclosures: Lisa Ceglia, None.

## LB-SU0370

**Periostin is Correlated with Cortical Bone Measures and Bone Turnover**

**During Consolidation.** Jennifer S Walsh\*, Fatma Gossiel, Jess Scott, Margaret A Paggiosi, Richard Eastell. University of Sheffield, United Kingdom

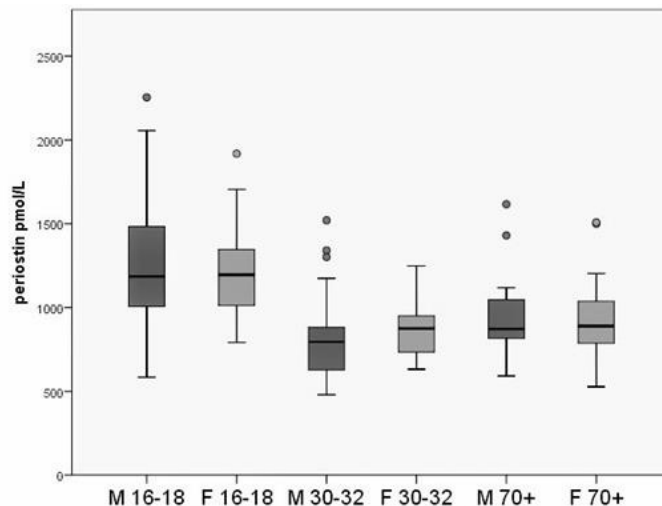
Periostin is an extra-cellular matrix protein expressed in bone, connective tissues and other sites. In bone, it is expressed most highly in the periosteum. It affects collagen cross-linking and signals to increase osteoblast proliferation and differentiation. Therefore, circulating periostin might be high in young adults when there is active cortical modelling, and in older adults when periosteal circumference increases.

We conducted a cross-sectional study of 179 healthy men and women ages 16-18, 30-32 and 70+. Serum periostin was measured using a manual sandwich ELISA from Biomedica (Vienna, Austria - released June 2016). This assay recognises all 7 known splice variants of periostin and is produced in human serum matrix. The distal radius and tibia were assessed with HR-pQCT. Serum PINP, CTX, PTH, testosterone, oestradiol and IGF-1 were also measured. Gender and age differences were assessed

by GLM univariate analysis and post-hoc Tukey's test. Correlations of periostin with bone turnover markers and hormones were assessed with Spearman's rho.

Periostin did not differ between men and women. It was higher at age 16-18 than 30-32 (p<0.001), but not different between age 30-32 and 70+ (p=0.08) (see Figure). Cortical perimeter was greater in men than women (radius and tibia p<0.001), and greater at age 70+ than 30-32 (radius p<0.001, tibia p=0.04). Cortical thickness and density were less at age 16-18 and 70+ than 30-32 (p<0.001, except radius thickness 16-18 vs 30-32 p=0.02). Periostin correlated negatively with tibia cortical thickness (r -0.230, p=0.002) and density (r -0.225, p=0.003), but not cortical perimeter or any radius measures. It correlated positively with PINP (r 0.583, p<0.001), CTX (r 0.422, p<0.001) and IGF-1 (r 0.437, p<0.001). It did not correlate with PTH, oestradiol or testosterone. When assessed within each age group, these correlations were only significant at age 16-18.

In conclusion, cortical geometry and density differ at the end of growth, peak bone mass and with ageing. Periostin is high at age 16-18 when modelling is active, and inversely correlated with tibia cortical thickness and density, so levels may be higher in individuals with ongoing cortical consolidation. Higher periostin is associated with higher IGF-1 and bone cell activity. Periostin did not correlate with cortical measures, bone turnover or hormones in other age groups. Therefore periostin may be more important in growth and modelling than in older adult life.



Figure

Disclosures: Jennifer S Walsh, None.

This study received funding from: Assay kits from Biomedica

## LB-SU0371

**Low Variability of Oral PTH<sub>1-34</sub> in Man.** Gregory Burshtien<sup>1</sup>, Ariel Rothner<sup>1</sup>, Hillel Galitzer<sup>\*1</sup>, Ehud Arbit<sup>1</sup>, Yoseph Caraco<sup>2</sup>. <sup>1</sup>Enterbio Ltd., Israel, <sup>2</sup>Hebrew University Medical School - Hadassah Medical Center, Israel

An orally administered PTH may have prodigious advantages in the treatment of bone related disorders due to improved patient compliance and adherence. However, in order for PTH, a drug whose specific PK profile is critical for its anabolic action, to be effective and safe, it must be accurately titratable, with a consistent and reproducible absorption profile among subjects. Oral absorption of polypeptides is characterized by high dose-to-dose variability in absorption, resulting in difficulty in accurately titrating the drug effect. We present clinical study data of a novel oral formulation of PTH demonstrating a consistent absorption profile with inter-subject variability similar to that of injectable PTH<sub>1-34</sub>.

### Methods:

A Phase I, open label crossover pharmacokinetic (PK) study to assess safety and PK of oral PTH<sub>1-34</sub> in ten healthy male adult volunteers was conducted. The PK profile of oral formulation was compared to commercial injectable PTH<sub>1-34</sub> formulation. Blood samples were analyzed externally by immunoassay (automated IDS iSYS).

### Results:

PK profile of oral PTH<sub>1-34</sub> was characterized by a rapid absorption and elimination rates. The maximal plasma concentration (C<sub>max</sub>) of the oral formulation was slightly greater than C<sub>max</sub> of injectable formulation ( $236 \pm 114$  vs  $184 \pm 83$  pg/ml, mean  $\pm$  SD). The minimal C<sub>max</sub> among the same group of volunteers was 95 pg/ml for the oral formulation and 107 pg/ml for injection. Intersubject variability of the oral PTH<sub>1-34</sub> was comparable with the variability in absorption of the injectable drug (CV% 48 vs 45% respectively).

Similarly, to all the other clinical studies of Enterbio's oral formulation of PTH<sub>1-34</sub>, the drug was shown to be safe without any significant adverse effects reported.

### Discussion:

Inherent to oral drug delivery of biopharmaceuticals is the high absorption variability, which for drugs requiring a specific PK profile is critical. If the absorption variability can be mollified and mirror that of the injectable drug, it is most likely to have a similar clinical effect to that of the injectable while providing greater

convenience and compliance. The current study showed that the oral PTH formulation has reached a similar coefficient of variation in absorption to the injectable form. Such a formulation may have a greater success rate in both future clinical studies and in the clinic.

**Disclosures:** Hillel Galitzer, None.

This study received funding from: Entera Bio Ltd.

## LB-SU0372

**Safety of Denosumab in Postmenopausal Osteoporosis and in Cancer and Bone Metastase Treatment: A Systematic Review and Meta-Analysis.** Marlène Aubailly<sup>1</sup>, Thomas Barnette<sup>2</sup>, Bernard Combe<sup>1</sup>, Cécile Gaujoux-Viala<sup>3</sup>, Cédric Lukas<sup>1</sup>, Jacques Morel<sup>1</sup>, Hélène Che<sup>1</sup>. <sup>1</sup>CHU Lapeyronie, France, <sup>2</sup>CHU Bordeaux, France, <sup>3</sup>CHU Nîmes, France

Background: Denosumab (Dmab) is a RANK ligand antibody used for the treatment of post-menopausal osteoporosis (OP) and prevention of bone metastases complications. The aim of this meta-analysis was to assess the safety of Dmab.

Methods: Data sources included MEDLINE, EMBASE, Cochrane Library, and recent abstracts from ACR and EULAR congresses were searched until March 2016. Randomized controlled trials comparing the safety of Dmab to placebo or bisphosphonates (BP) in postmenopausal OP and in cancer (either cancer with bone metastases or with hormone therapy) were selected. Data were extracted by one investigator, confirmed by another, and pooled in meta-analysis using Review Manager software (Cochrane collaboration).

Results: 6136 articles were of potential interest, and 19 met the inclusion criteria. 7 articles compared the safety of Dmab to BP in post-menopausal OP. There was no significant difference when comparing Dmab with bisphosphonates in any adverse events (AAE) (RR=0.98, 95% CI=0.95-1.01) serious adverse event (SAE) (RR=1.04, 95% CI=0.81-1.33). Regarding Dmab versus placebo in post-menopausal OP, 7 studies were included and there was no significant difference in AAE (RR=0.98, 95% CI=0.94-1.01), SAE (RR=1.03, 95% CI=0.96-1.11), however cellulitis was more frequently found with Dmab (RR=8.03, 95% CI=1.44-4.00). No cases of osteonecrosis of the jaw (ONJ) had been reported. 5 articles were pooled to compare Dmab with BP in patients with bone metastases and no significant difference was found in AAE (RR=0.99, 95% CI=0.98-1.00), SAE (RR=0.99, 95% CI=0.95-1.03), and ONJ (RR=1.40, 95% CI=0.92-2.13). 4 articles were selected concerning patients treated with placebo or Dmab in breast and prostate cancer without bone metastases. Although no significant difference was found in AAE (RR 1.01, 95% CI=0.99-1.03), use of Dmab was associated with a significantly increased risk of hypocalcemia (RR 5.20, 95% CI=1.34-20.13) and of cholecystitis (RR 3.43, 95% CI= 1.01-11.69).

Conclusion: In post-menopausal OP, Dmab had a relatively good safety profile although significantly more cellulitis occurred when compared with placebo. For patient with cancer, Dmab was associated with more hypocalcemia and cholecystitis than placebo; that could be explained by a relative immunosuppression and a higher dose of Dmab used in these patients. Patients with bone metastases treated with Dmab tended to have a higher risk of ONJ although not significantly.

**Disclosures:** Marlène Aubailly, None.

## LB-SU0373

**PTHrP Activates Stat5 Signaling in Mammary Epithelium and Affects Breast Cancer Initiation and Progression.** Farzin Takyar<sup>\*</sup>, Kata Boras-Granic, Wonnam Kim, Pamela Dann, John Wysolmerski. Yale School of Medicine, United states

PTHrP affects mammary development and breast cancer, is expressed in basal myoepithelial cells, and in alveolar epithelial cells only after late pregnancy. PTHrP promotes skeletal metastases and development of hypercalcemia in breast cancer. Less is known about its role in development and/or progression of primary breast cancers. Recent GWAS reports have identified *Pthlh* gene as a breast cancer susceptibility locus. Using data from the Cancer Genome Atlas Project and a Yale tissue microarray (YTMA49) we have found that higher breast tumor PTHrP expression predicts a more aggressive phenotype and increased mortality. We assessed the effects of PTHrP overexpression on the development of mammary tumors in mice. We developed a tetracycline(doxycycline)-regulated, *MMTV*-driven transgenic model of PTHrP overexpression in mammary epithelial cells (*MMTV-rtTA; tetO-hPTHrP*). Surprisingly, PTHrP overexpression in luminal epithelial cells caused alveolar hyperplasia, secretory differentiation and milk production in virgin mice, associated with lower numbers of luminal progenitor cells and basal stem cells upon FACS analysis. Additionally, Stat5 was highly activated in this setting leading to higher levels of  $\beta$ -Casein, a target of activated Stat5 (pStat5). This effect of PTHrP was reversible upon withdrawal of doxycycline (Dox). Addition of Dox to primary mammary epithelial cell cultures from these mice recapitulated the findings. Knocking out PTHrP receptor (PTHrP) in the mice did not affect this phenotype, suggesting a receptor-independent effect of PTHrP. PTHrP overexpression in *MMTV-PyMT* mice (*MMTV-rtTA; tetO-hPTHrP; MMTV-PyMT*) dramatically reduced both latency of tumor formation and survival of the mice. It caused higher proliferation and lower apoptosis *in vivo*. All mice developed palpable tumors in all mammary glands by 3 weeks of age, became hypercalcemic and died before 4.5 weeks. Tumors had higher levels of pStat5 and  $\beta$ -Casein. Tumor cells cultured *ex vivo* and cell lines established from these tumors overexpressed PTHrP when stimulated with Dox. PTHrP overexpression, and not

exogenous PTHrP, caused higher levels of proliferation, pStat5, and  $\beta$ Casein. This PTHrP-induced activity of Stat5 was blocked by treatment with a pharmacological inhibitor of Jak2, the tyrosine kinase upstream of Stat5. We show that PTHrP overexpression results in Stat5 activation and increased proliferation in breast cancer cells in a cell-autonomous fashion and independent of its receptor.

**Disclosures:** Farzin Takyar, None.

## LB-SU0374

**Bispecific Antibodies Targeting Sclerostin and DKK1 Promote Bone Mass Accrual and Bone Repair of Closed Femoral Fractures and Gap Defects.** Monica Florio<sup>\*1</sup>, Xiaodong Li<sup>1</sup>, Marina Stolina<sup>1</sup>, Kannan Gunasekaran<sup>1</sup>, Ling Liu<sup>1</sup>, Hossein Salimi-Moosavi<sup>1</sup>, Franklin Asuncion<sup>1</sup>, Banghua Sun<sup>1</sup>, Hong Lin Tan<sup>1</sup>, Li Zhang<sup>1</sup>, Chun-Ya Han<sup>1</sup>, Ryan Case<sup>1</sup>, Qing-Tian Niu<sup>1</sup>, James Pretorius<sup>1</sup>, Efrain Pacheco<sup>1</sup>, Qing Chen<sup>1</sup>, Mei-Shu Shih<sup>2</sup>, William G. Richards<sup>1</sup>, Hua Zhu Ke<sup>3</sup>, Michael S. Ominsky<sup>1</sup>. <sup>1</sup>Amgen Inc, United states, <sup>2</sup>PharmaLegacy Laboratories, China, <sup>3</sup>UCB, United Kingdom

Wnt signaling regulates bone formation throughout the skeleton and during fracture repair. Antibodies to the secreted Wnt antagonists Sclerostin and DKK1 promote bone formation. In rats treated with sclerostin antibody (Scl-Ab), we observed an increase in DKK1 protein and mRNA levels and hypothesized that co-inhibition of both factors would lead to further improvements in bone mass and bone repair than either alone. To demonstrate this, we treated OVX rats with vehicle, Scl-Ab (25 mg/kg), DKK1-Ab (25 mg/kg), or both of these antibodies (S+D) for 5 weeks. S+D resulted in synergistic gains in bone formation, resulting in greater DXA BMD relative to monotherapy. These and other observations resulted in the development of bispecific antibodies (BspAbs) against DKK1 and sclerostin, which were tested in both young mice (n=10/group) and 5 year old cynomolgus monkeys (n=5/group) for 3 weeks or 9 weeks, respectively. A BspAb led to synergistic gains in bone formation in both species relative to monotherapy. In mice, these changes resulted in increases in bone mass and bone strength at the distal femur that were significantly greater than either monotherapy.

In the rat closed femur fracture model, DKK1 and sclerostin exhibited spatial and temporal differences in expression pattern at the fracture site that may drive distinct and additive bone inhibitory effects. The therapeutic efficacy of dual DKK1/sclerostin inhibition was evaluated in two rat fracture models. In a femoral closed fracture model in 7-month-old male SD rats, animals received vehicle, Scl-Ab, DKK1-Ab, and S+D 2QW SC for 7 weeks (n=18/group). S+D treatment resulted in the largest increases in peak bending load relative to Vehicle, to levels within 10% of the intact femur vehicle control mean. In a similar study, BspAb showed superior bone repair activity relative to controls and led to dose-dependent increases in callus bone mass and strength. In a cortical allograft model in 5-month-old Lewis rats, animals received vehicle, Scl-Ab, DKK1-Ab, S+D, or BspAb 2QW SC for 12 weeks (n=18/group). By micro-CT, bone mass and percent callus bridging were greatest in the BspAb group, resulting in maximum torque that was increased relative to Veh (+216%), Scl-Ab (+108%), and DKK1-Ab (+71%).

Our results suggest that dual inhibition of DKK-1 and Sclerostin promotes superior bone formation and bone repair relative to monotherapies by targeting both distinct and redundant biologic activities in animal models.

**Disclosures:** Monica Florio, Amgen, 15

This study received funding from: Amgen Inc and UCB

## LB-SU0375

**Transgenic mice for studying fibrous dysplasia of bone, McCune-Albright Syndrome, and tumors caused by activating *GNAS* mutations.** Vijayram Reddy Malladi<sup>\*</sup>, Yan Zhu, olta tafaj, Murat Bastepe. Endocrine Unit, Department of Medicine, Massachusetts General Hospital & Harvard Medical School, United states

*GNAS* encodes the alpha-subunit of the heterotrimeric stimulatory G protein (*G $\alpha$* ), which mediates the actions of many endogenous molecules through generation of cAMP. Somatic *GNAS* mutations that cause constitutive *G $\alpha$*  activity are found in many tumors (*gsp* oncogene) and cause fibrous dysplasia of bone (FD), a disorder characterized by aberrant differentiation of bone marrow stromal cells (BMSCs). The same mutations also lead to McCune-Albright Syndrome (MAS), in which FD co-exists with hyperpigmented skin lesions and overactive endocrine organs. Mechanisms governing FD and MAS phenotypes are poorly defined. To generate a mouse model for studying these disorders, as well as *gsp+* tumors, we developed transgenic mice in which cDNA encoding a HA-tagged, constitutively active *G $\alpha$*  mutant (*G $\alpha$* -R201H) is expressed conditionally upon Cre recombinase activity (ca*G $\alpha$*  Tg mice). The transgene also contains a LacZ reporter downstream of the *G $\alpha$* -R201H cDNA. Adeno-Cre transduced BMSCs from the ca*G $\alpha$*  Tg mice showed significantly higher baseline cAMP levels than in non-transduced or adeno-YFP (control) transduced cells and demonstrated positive X-gal staining. Double-mutant offspring from crosses between ca*G $\alpha$*  Tg and Prx1-Cre mice displayed short limbs and underdeveloped craniofacial bones, consistent with the expression profile of Prx1 and the role of *G $\alpha$* /cAMP signaling in endochondral bone formation. In BMSCs from ca*G $\alpha$*  Tg:Prx1-Cre mice, the expression level of c-fos mRNA, a target of *G $\alpha$* /cAMP signaling, was increased by 3.5-fold compared to that in control BMSCs. Moreover, expression of

the transgene could be induced postnatally, as judged by positive X-gal staining in various tissues, by injecting tamoxifen into double-mutant offspring from caGsz Tg and CAGG-CreER<sup>TM</sup> crosses. These findings indicate that our mice express the Gsz-R201H transgene in a conditional manner. This mouse model will be highly valuable for investigating the molecular mechanisms underlying FD/MAS, as well as the oncogenic mechanisms in *gsp+* tumors.

**Disclosures:** Vijayram Reddy Malladi, None.

This study received funding from: 1. Sanofi iAward 2. The Fibrous Dysplasia Foundation and 3. The Milton Fund

## LB-SU0376

**Postural control in mild Osteogenesis Imperfecta.** Louis-Nicolas Veilleux<sup>\*1</sup>, Annie Pouliot-Laforte<sup>2</sup>, Frank Rauch<sup>1</sup>, Martin Lemay<sup>3</sup>. <sup>1</sup>Shriners Hospital for Children-Canada, Canada, <sup>2</sup>Département des Sciences de l'Activité Physique, Université du Québec à Montréal, Canada, <sup>3</sup>Université de Québec à Montréal; Centre de Réadaptation Marie Enfant, Canada

Context: Osteogenesis imperfecta (OI) is a heritable bone fragility disorder that is caused by mutations affecting collagen type I. In addition to bone fragility, we recently showed that patients with the mildest form of OI (OI type I) have muscle weakness. However, there is presently little information related to the impact of muscle weakness on postural control in this population. Objective: The aim of the current study was to characterize static postural control and to explore if there is any relation to lower-limb muscle function in youth with mild OI. Participants: A group of 22 individuals with OI type I (mean age [SD]: 13.1 [4.1] years) was compared to a group of 16 typically developing (TD) individuals (mean age [SD]: 13.1 [4.3] years). Main Outcome Measures: Static postural control and muscle function tests (mechanography) were performed on a force platform. Static postural control was assessed in two conditions: eyes-open and eyes closed. Selected posturographic parameters were: center of force's path length and velocity, 90% standard ellipse area and its medio-lateral and antero-posterior axes length. Mechanographic outcomes were peak force (kN) and peak power (kW). Results: Compared to TD, individuals with mild OI had poorer static postural control as indicated by longer and faster displacement of the center of force and a larger ellipse area. This was observed in both the eyes-open and the eyes closed conditions. Removing visual information resulted in a more relevant decrement of performance in the OI group compared to the TD group for path length (increase of 40% vs. 26% for OI and TD, respectively) and velocity (increase of 160% vs. 132% for OI and TD, respectively). As expected, mechanographic tests indicated that muscle force was lower in individuals with OI type I than in TD individuals. Muscle function (peak force and peak power) was unrelated to postural control in the OI group (e.g. path length:  $R = -0.35$ ;  $P = 0.11$ ) whereas a significant one was found for the TD group (e.g. path length:  $R = -0.50$ ;  $P = 0.05$ ). Conclusions: Postural control is less efficient in young individuals with OI type I as compared to TD children and adolescents. This deficit was unrelated to muscle weakness at the lower limbs for the OI group. The significantly larger performance decrement in the OI group compared to the TD group when visual information is no longer available suggests that individuals with mild OI may have proprioceptive sensory deficits.

**Disclosures:** Louis-Nicolas Veilleux, None.

## LB-SU0377

**Assessing the General Population Frequency of Rare Coding Variants in *EXT1* and *EXT2* Previously Implicated in Hereditary Multiple Exostoses.** Diana Cousminer<sup>\*1</sup>, Alexandre Arkader<sup>1</sup>, Benjamin Voight<sup>2</sup>, Maurizio Pacifici<sup>1</sup>, Struan Grant<sup>1</sup>. <sup>1</sup>Children's Hospital of Philadelphia, United states, <sup>2</sup>University of Pennsylvania, United states

Hereditary Multiple Exostoses (HME) is a rare childhood-onset skeletal disease attributed to mutations in the genes encoding exostosin glycosyltransferase 1 (*EXT1*) and 2 (*EXT2*) that are responsible for the synthesis of heparan sulfate. The pathogenicity and phenotypic impact of many *EXT1* and *EXT2* variants remain uncertain. To assess the overall mutation spectrum of protein-damaging variants across these two genes in the general population, we extracted all amino acid-altering (missense) and loss of function (LoF; nonsense, frameshift, or splice-site) variants from the Exome Aggregation Consortium (ExAC) database, a large population-based repository of exome sequence data from diverse ancestries that has been screened for severe pediatric diseases. We then assessed whether clinically-identified, presumably pathogenic variants implicated in HME exist among healthy individuals. We found six *EXT1* and four *EXT2* missense variants in ExAC, suggesting that these mutations have either been misclassified as pathogenic or are not fully penetrant for the disease. These include rs188859975 (p.Ala486Val), which we observed 24 times among ExAC individuals of East Asian ancestry (population allele frequency = 0.003), and rs142122090 (p.Asn373Asp), which was nearly exclusively seen among Latinos in the ExAC database (allele count = 81; population frequency = 0.007). Such population-specificity may have contributed to misclassification as pathogenic. Furthermore, we found that *EXT1* is heavily selectively constrained, while *EXT2* is more tolerant to protein-damaging variants, especially at its C-terminus, possibly explaining the genotype-phenotype correlation that *EXT1* variants result in more severe disease. In conclusion, population-based exome data is a useful filter for determining whether

clinically detected variants are likely pathogenic, as well as for revealing biological insight into rare disease genes such as *EXT1* and *EXT2*.

**Disclosures:** Diana Cousminer, None.

## LB-SU0378

**Greater Peri-aortic Adipose Tissue Volume is associated with Increased Trunk Muscle Fat Content in Middle-aged and Older Men and Women: The Framingham Study.** Robert R. McLean<sup>\*1</sup>, Elizabeth J. Samelson<sup>1</sup>, Amanda L. Lorbergs<sup>1</sup>, Xiaochun Zhang<sup>2</sup>, Kerry E. Broe<sup>2</sup>, Dennis E. Anderson<sup>3</sup>, Udo Hoffmann<sup>4</sup>, Caroline S. Fox<sup>5</sup>, Mary L. Bouxsein<sup>3</sup>, Douglas P. Kiel<sup>1</sup>. <sup>1</sup>Hebrew SeniorLife Institute for Aging Research, Harvard Medical School, Beth Israel Deaconess Medical Center, United states, <sup>2</sup>Hebrew SeniorLife Institute for Aging Research, United states, <sup>3</sup>Harvard Medical School, Beth Israel Deaconess Medical Center, United states, <sup>4</sup>Massachusetts General Hospital, Harvard Medical School, United states, <sup>5</sup>Merck Research Laboratories, United states

Age-related muscle fat accumulation and loss of muscle mass contribute to impaired muscle function and mobility problems in older adults. These changes may result from excess ectopic fat accumulation, which produces inflammatory cytokines that promote differentiation of muscle satellite cells into adipocytes versus myoblasts. It is unknown whether this muscle-fat cross-talk occurs via systemic effects of circulating cytokines or through paracrine effects between adjacent compartments. Our objective was to determine the association of peri-aortic adipose tissue (PAAT) volume with size and fat content of adjacent trunk muscles among 948 participants (56% women) in the community-based Framingham Study. Multidetector CT imaging measured PAAT volume (cm<sup>3</sup>), and cross-sectional area (mm<sup>2</sup>) and attenuation (HU), a marker of fat content, of the erector spinae, transversospinalis, and trapezius muscles at the T7 and T8 levels. Cross-sectional area and attenuation of each muscle was averaged for the left and right sides and across vertebral levels. Linear regression was used to calculate the associations ( $\beta$ ) of PAAT with muscle cross-sectional area and attenuation, adjusting for sex, age, height, body mass index (BMI) and physical activity. To determine if associations were independent of abdominal fat depots, models were further adjusted for visceral (VAT) and subcutaneous adipose tissue (SAT) volumes (cm<sup>3</sup>), from the same CT images, among participants with these measures available (n=653). Mean age was 58 years (range 45-81), mean BMI was 28 kg/m<sup>2</sup> (range 18-53). While there was no association with cross-sectional area ( $\beta = -0.96$ ,  $P = 0.37$ ), PAAT was inversely associated with attenuation ( $\beta = -0.31$ ,  $P < 0.01$ ), indicating higher muscle fat content with increasing PAAT. The association remained after adjustment for VAT (PAAT  $\beta = -0.21$ ,  $P < 0.01$ ) and SAT (PAAT  $\beta = -0.33$ ,  $P < 0.01$ ). Results were similar when stratified by sex and categorizing PAAT as quartiles. We found that increased fat surrounding the thoracic aorta was associated with greater fat content in nearby trunk muscles, independent of overall obesity and specific abdominal fat depot volumes, but not with trunk muscle size. Our findings suggest that age-related fat accumulation in skeletal muscle may result mainly from local paracrine effects of adjacent fat depots. Cross-talk between neighboring fat and muscle is a potential target for novel therapies aiming to prevent or restore loss of muscle function with aging.

**Disclosures:** Robert R. McLean, None.

## LB-SU0379

**Reliable assessment of bone size, composition, and strength in the midtibia of children using magnetic resonance imaging.** Benjamin Conner<sup>\*1</sup>, Harshvardhan Singh<sup>1</sup>, Daniel Whitney<sup>1</sup>, Freeman Miller<sup>2</sup>, Christopher Modlesky<sup>1</sup>. <sup>1</sup>University of Delaware, United states, <sup>2</sup>A.I. duPont Hospital for Children, United states

Reliable in vivo measures of bone parameters are necessary in order to detect changes as a result of an intervention or disease. While magnetic resonance imaging (MRI) is commonly used to assess the size, composition, and strength of bone in humans, the reliability of such measures in children is lacking. The purpose of this study was to determine the reliability of assessing bone size, composition, and strength using MRI in the midtibia of children during a typical intervention period. Ten children (7 boys and 3 girls) 5 to 11 years of age participated in the study. Children were tested twice, 6 months apart. Pubertal development was assessed using Tanner staging. Axial images of the tibia were collected using MRI (1.5 T, GE; Waukesha, WI), a semiflex long bone array coil (ScanMed; Omaha, NE) and two different sequences. The first sequence (spin-echo, TR = 650, TE = 14, FOV = 12, NEX = 3, BW = 15.63, frequency = 512, phase = 256) yielded T1-weighted images. The second sequence (IDEAL, fast-spin-echo, TR = 600, TE = min full, FOV = 12, NEX = 2, BW = 31.25, frequency = 320, phase = 224) yielded fat and water images. Using software created with Interactive Data Language (Research Systems, Inc; Boulder, CO), the T1-weighted images were used to estimate cortical volume, medullary volume, total bone volume, section modulus (Z), and polar moment of inertia (J) at the level of the middle-third of the tibia (i.e., midtibia). The fat and water images were used to estimate fat concentration in the bone marrow. Paired t-tests and Pearson correlations were run to determine changes during the 6-month period and the reliability of each measurement, respectively. Children ranged from Tanner stages 1-3, and were within the 5<sup>th</sup> and 95<sup>th</sup> age-based percentiles for height and body mass during the initial test period. There was a

significant increase in cortical volume (9 %,  $p < 0.001$ ), medullary volume (12 %,  $p < 0.01$ ), total bone volume (11 %,  $p < 0.001$ ), Z (8 %,  $p < 0.001$ ), and J (14 %,  $p < 0.01$ ) during the 6-month period. Pearson correlations were very strong for all measures ( $r$  range = 0.93 to 0.99,  $p < 0.001$ ). These results clearly indicate the reliable assessment of bone size, composition, and strength in the midtibia of children using MRI.

*Disclosures: Benjamin Conner, None.*

## LB-SU0380

**Conditional Targeting Of Important Developmental Signal, Shh, In The Adult Mouse Nucleus Pulposus Causes Premature Intervertebral Disc Degeneration.** Sarthak Mohanty\*, Elfie De Jesus, Chitra Dahia. Hospital for Special Surgery, United states

Disc degeneration and associated back pain are very common, affecting almost 1/7 individuals. The current treatments are palliative, mainly due to poor understanding of the molecular mechanisms of disc growth and differentiation, and of the changes associated with its degeneration. Our approach has been to identify signaling pathways involved in the normal postnatal growth and differentiation of the disc, and to see if the abrogation of these signals causes premature disc degeneration, using the mouse as a model. Our previous studies showed that Shh is synthesized postnatally by the nucleus pulposus (NP) cells, derived from the embryonic notochord, and is a key regulator of postnatal disc growth and differentiation. Shh expression decreases with age. Here we test the hypothesis that Shh signaling continues to be essential for maintenance of the IVD during adult life, by generating a conditional mouse model using a NP Cre driver line to conditionally target Shh in the adult (9 month old) mouse disc following tamoxifen treatment. There were dramatic changes in the L5/L6 and L6/S1 discs of Shh targeted mice compared to the controls 3 months later, including the loss of NP cells, disc height, disc width, and loss of structure in the surrounding annulus fibrosus compared to controls. In these discs, the NP space became filled with cells that did not express NP cell markers, had lower expression of matrix makers, along with an appearance similar to those of 2 year old mice, and to human degenerated discs, with the appearance of chondrocyte-like cells. The results suggest that Shh signaling is also critical for maintenance of the lower lumbar and sacral mouse discs (the discs most affected during aging in humans), and its loss is associated with degeneration of the intervertebral disc. In contrast, more cranial discs examined (L3/L4) seemed unaffected. The reasons for these different effects are not yet clear.

*Disclosures: Sarthak Mohanty, None.*

**MO0001**

**FGF23 and Vitamin D metabolism in chronic kidney disease.** Isabelle Picc\*<sup>1</sup>, Allison Chipchase<sup>2</sup>, Holly Nicholls<sup>1</sup>, Christopher Washbourne<sup>1</sup>, Jonathan Tang<sup>1</sup>, William Fraser<sup>1</sup>. <sup>1</sup>University of East Anglia, United Kingdom, <sup>2</sup>Norwich & Norfolk University Hospital, United Kingdom

Chronic kidney disease-bone mineral disorder (CKD-BMD) is characterised by low 25 hydroxyvitamin D (25(OH)D) and low 1,25 di-hydroxyvitamin D (1,25(OH)<sub>2</sub>D) concentrations. Fibroblast growth factor-23 (FGF23) is a major regulator of vitamin D metabolism. In subjects with normal kidney function, FGF23 suppresses renal synthesis of the active form of vitamin D (1,25(OH)<sub>2</sub>D) by inhibiting expression of the enzyme 25-hydroxyvitamin D-1 $\alpha$ -hydroxylase that converts 25(OH)D to its active form 1,25(OH)<sub>2</sub>D whilst also stimulating the catabolic enzyme vitamin D-24-hydroxylase responsible for metabolism of 25(OH)D and 1,25(OH)<sub>2</sub>D. However Dai *et al.*, 2012 showed a reduced concentration of serum 24,25d(OH)<sub>2</sub>D in CKD and in a mouse CKD model compared to the group with "normal" renal function.

To assess vitamin D metabolism in CKD patients of various severity (grades 2, 3 and 4).

We used randomized samples from patients with chronic kidney disease (CKD; eGFR < 70 ml/min/1.73 m<sup>2</sup>) and controls. FGF23 concentrations were measured using an enzyme-linked immunosorbent assay for cFGF23 (Biomedica, Vienna, Austria) and for iFGF23 (Immutopics Inc., Ca, USA). 25(OH)D and 24,25(OH)<sub>2</sub>D<sub>3</sub> were measured by in-house LC-MS/MS.

In CKD, cFGF23 concentrations were elevated (mean  $\pm$  SEM: CKD 7.2  $\pm$  2.5 compared to controls 1.47  $\pm$  2.1 pg/mL). As eGFR decreased, concentrations of 25(OH)D, 1,25(OH)<sub>2</sub>D and 24,25d(OH)<sub>2</sub>D decreased (25(OH)D: from 63.4  $\pm$  9.1 to 46.9  $\pm$  6.5 nmol/L; 1,25(OH)<sub>2</sub>D: from 104.9  $\pm$  10 to 50.8  $\pm$  6.5 pmol/L and 24,25d(OH)<sub>2</sub>D: from 4.5  $\pm$  0.8 to 1.9  $\pm$  0.3 nmol/L). An increase in the ratio 25(OH)D:24,25d(OH)<sub>2</sub>D<sub>3</sub> from 13.8  $\pm$  0.5 in control samples to 26.0  $\pm$  1.5 at stage 4 was observed. Concentrations of FGF23, both C-terminal and intact, increased with decreasing kidney function. Both iFGF23 and cFGF23 correlated with the ratio 25(OH)D:24,25(OH)<sub>2</sub>D (Pearson's rho = 0.190 and 0.204, p<0.05, respectively) and iFGF23 also significantly correlated with 24,25(OH)<sub>2</sub>D (rho = -0.323 p<0.01).

In CKD, net effects of declining kidney function and increasing FGF23 and PTH concentrations on vitamin D catabolism are not clear. We observed vitamin D deficiency in CKD patients associated with an overall decrease in 24,25(OH)<sub>2</sub>D<sub>3</sub> concentration as shown previously. The ratio of 25(OH)D: 24,25(OH)<sub>2</sub>D is markedly elevated and increases as CKD progresses suggesting a relatively lower catabolic rate of 25(OH)D towards its 24,25(OH)<sub>2</sub>D metabolite. This may be in an attempt to allow ongoing synthesis of 1,25(OH)<sub>2</sub>D continuing its biological effects. The significant correlations of FGF23 with the 24,25(OH)<sub>2</sub>D and the ratio 25(OH)D:24,25(OH)<sub>2</sub>D suggest a potential role for FGF23 in the regulation of 24-hydroxylase in CKD. It would appear that the effects of FGF23 on vitamin D metabolism in CKD are greater than the effects of PTH and so this data adds further to the proposals that the early management and prevention of the increase of FGF23 in CKD may be beneficial in preventing CKD-BMD.

**Disclosures:** Isabelle Picc, None.

**MO0002**

**Hip Fracture Admissions are Increasingly Complicated by Advanced Chronic Kidney Disease in England.** Celia Gregson\*<sup>1</sup>, Arti Bhimijvani<sup>1</sup>, Shona Methven<sup>2</sup>, Fergus Caskey<sup>3</sup>, Jenny Neuburger<sup>4</sup>, Yoav Ben-Shlomo<sup>5</sup>.

<sup>1</sup>Musculoskeletal Research Unit, School of Clinical Sciences, University of Bristol, Bristol, UK, United Kingdom, <sup>2</sup>UK Renal Registry, Bristol, & School of Clinical Sciences, University of Bristol, UK, United Kingdom, <sup>3</sup>UK Renal Registry, Bristol, & School of Social & Community Based Medicine, University of Bristol, University of Bristol, UK, United Kingdom, <sup>4</sup>The Nuffield Trust, London, UK, United Kingdom, <sup>5</sup>School of Social & Community Based Medicine, University of Bristol, Bristol, UK, United Kingdom

Most patients with advanced chronic kidney disease (CKD) have CKD-Mineral Bone Disorder, with increased risk of fractures and complications. In the UK, 58968 patients receive renal replacement therapy (dialysis or renal transplant [Tx]) with increasing mean age and co-morbidity burden. Hip fracture admissions can be lengthy with high medical costs. We aimed to determine the proportion of hip fracture patients (i) with CKD  $\geq$ stage 4, (ii) on dialysis, or (iii) with a renal Tx, and their acute hospital length of stay (LOS), in England over 4 years.

We used Hospital Episode Statistics from all English hospitals (2008-2012) to identify patients with hip fractures on or during admission (ICD10 codes: S72.0/S72.1/S72.2), on dialysis (Z99.2/Y84.1/Z49.1/ Z49.2/T82.4/Y60.2/Y61.2/Y62), with renal Tx (Z94.0/T86.1/N16.5), and remaining CKD  $\geq$ 4 codes (N18.4/N18.5/N19/I12.0/I13.11/I13.12). Median [inter-quartile range] LOS was calculated. Linear regression with log LOS assessed annual trends, adjusting for age & gender.

The proportion of hip fracture admissions with CKD  $\geq$ 4 rose progressively from 16% (8858/55422) in 2008/9 to 25.4% (13975/55006) in 2011/12, (p<0.001), and dialysis from 1.4% (757) to 2.0% (1089), (p<0.001) but this was not seen for those with renal Tx; 0.2% (134) to 0.3% (174), (p=0.09). Median LOS fell amongst the hip fracture population overall (15 [9-28] days in 2008/9 to 14 [8-23] in 2011/12, p<0.001) and in those with CKD  $\geq$ 4, although LOS were longer (21 [11-40] days in 2008/9

falling to 17 [10-31] in 2011/12, p<0.001). In contrast, reductions in LOS were not seen amongst those who fractured on dialysis (16 [6-34] days in 2008/9; 15 [6-30] in 2011/12, p=0.75), nor those with renal Tx (11 [6-26] days in 2008/9; 14 [7-24] in 2011/12, p=0.94). Mean age remained constant over 4 years in all groups. A larger proportion of men who fractured than women had CKD  $\geq$ 4 (e.g. 2011/12: 5539 [35.8%] vs 8436 [21.3%] respectively, p<0.001), were on dialysis (615 [4%] vs. 474 [1.2%], p<0.001), and had a renal Tx (98 [0.6%] vs. 76 [0.2%], p<0.001). Age and gender adjustment did not account for changes in LOS.

Our analyses suggest the burden of co-morbid CKD  $\geq$ stage 4 is rising amongst hip fracture admissions, who have longer associated LOS, though limited by lack of mortality data. LOS is falling amongst hip fracture admissions overall; however, this is not so for patients on renal replacement therapy. Our findings have implications for hip fracture service provision.

**Disclosures:** Celia Gregson, None.

**MO0003**

**Alkaline phosphatase substrates are elevated in many adults with persistent hypophosphatasemia.** Indira Rai\*<sup>1</sup>, Richard Berg<sup>2</sup>, Erica Scotty<sup>2</sup>, Fergus McKiernan<sup>3</sup>. <sup>1</sup>Marshfield Clinic, United states, <sup>2</sup>Center for Biomedical Informatics, Marshfield Medical Research Foundation, United states, <sup>3</sup>Marshfield Medical Research Foundation, United states

**Introduction:** We have previously shown that adults with persistently low serum values of alkaline phosphatase (ALP; persistent hypophosphatasemia) share phenotypic features with the adult form of hypophosphatasia (HPP), a rare inherited condition of impaired mineralization of bones and teeth.<sup>1</sup> Low serum ALP activity in HPP results in elevated ALP substrates including serum pyridoxal-5-phosphate (PLP) and urine phosphoethanolamine (PEA). The purpose of this study is to determine whether adults with persistent hypophosphatasemia and no prior diagnosis of HPP also have elevated ALP substrates.

**Methods:** This study was approved by Marshfield Clinic IRB. Of 260 adults with persistent hypophosphatasemia previously described (ALP  $\leq$  30 U/L; normal 40-120), approximately 100 were found to be alive, living within the Marshfield Clinic catchment area and had a postal mailing address on file through which contact was initially made. Consenting subjects fasted from all vitamin supplements for 2 weeks prior to laboratory specimen collection. ALP activity (normal 40 to 125 IU/L) was measured by a conventional kinetic rate method in which p-nitrophenyl phosphate was hydrolyzed to p-nitrophenol at pH 10.3 and changes in absorbance at 410 nm are directly proportional to ALP enzymatic activity. BSAP was measured using a commercial immunochemiluminometric assay (Ostase<sup>®</sup>; normal 0-20  $\mu$ g/L). Plasma PLP (normal 5-50  $\mu$ g/L) and urine PEA (normal <48 nmol/mg Creat) were measured by HPLC.

**Results:** Thus far, of 32 enrolled subjects, 28 have completed their biochemical analysis. Mean ALP and BSAP for the entire cohort were 26 IU/L (range 14-44) and 5.1  $\mu$ g/L (range 3-10) respectively. 19 of 28 subjects (68%) had elevated PEA levels (mean 130 nmol/mg Creat, range 49-312) and 11 of 28 subjects (39%) had elevated PLP levels (mean 92  $\mu$ g/L, range 52-158).

**Conclusion:** Many adults with persistent hypophosphatasemia (but no prior diagnosis of HPP) have elevated serum and urine ALP substrate levels. Elevations are generally mild and urine PEA may be more frequently elevated than serum PLP. This cohort warrants further genetic, clinical, biochemical and imaging evaluation and correlations.

McKiernan FE, JBMR 2014;29:1651-70.

**Disclosures:** Indira Rai, None.

This study received funding from: Alexion Pharmaceuticals, Inc

**MO0004**

**Cobalt Ion Release Alters Skeletal Metabolism: A Mechanism for Bone Loss in Metal-on-Metal Orthopaedic Implants.** Andrew Clark\*<sup>1</sup>, tzong-jen sheu, J. Edward Puzas. University of Rochester, United states

Are metal-on-metal implants safe? This is a question that has recently received significant attention (Cohen, 2012). With over 15 years of experience in the use of Co-Cr alloy prosthetics and the implantation of over one million metal-on-metal hip components in the United States and Great Britain there are now enough data to evaluate effectiveness and safety for these systems. And although the overall performance of metal-on-metal has been good there still appears to be a higher failure rate (approximately 13.6%) with these implants compared to those made of other materials (3.3 - 4.9%). The reasons for metal-on-metal implant failure range over a number of conditions not the least of which is a tissue reaction to the particulate debris released during wear. These reactions were first described with prototypic materials in the middle 1970's (Jones et al, 1975) and later were shown to occur in survivorship studies and case reports (Fricka, 2012). Infiltration of monocytic and lymphocytic cells and engulfment of the particulate materials induced the release of cytokines that could recruit and stimulate osteoclasts. However, it is important to point out that a stimulation of osteoclastic bone resorption is not sufficient to induce a permanent loss of bone. The coupled activities of osteoclasts and osteoblasts are

controlled by regulatory pathways that counter balance the activity for either process alone. Therefore, in order to permanently remove bone from around an implant, not only must osteoclastic activity be induced but the subsequent stimulatory mechanisms for osteoblastic bone formation must be arrested. Our SOST ELISA results showed the osteoblastic cell line ROS17/2.8 had the most sensitivity sensitive to Cobalt Co+2 treatment at 1-10 uM. Mesenchymal stem cell cell-like cell line C3H10T1/2 had the lowest sensitivity to cobaltCo+2. ROS17/2.8 compared Compared with the MC3T3E1 line, ROS17/2.8 cells areis later stage of osteoblasts, cell stage which is more between an osteocyte and osteoblast. As a negative control, we used osteoblasts and bone marrow stromal cells derived from SOST-null mice to show that the effect is specific for sclerostin. Additionally, we tested the effect of other divalent metal cations (such as Cr, Ni and Sr) in order to determine if the effect is specific to Co+2. After confirmed the Cobalt had SOST secretion-induced effect in osteoblasts, we used SOST-promoter as a probe to screen all the possible cobalt-induced factors. We found several interesting factors which related to the cobalt toxicity effect. We used in vitro probe affinity binding assay and in vivo assay to confirm these factors specific to SOST promoter. In vivo, mice were fed cobalt solution via gavage and the exposure dose was 10mg/kg/day for three days. Samples stained with ID1, ENG, KLF4, three different antibodies. The Control group were from a saline treatment group. Most of the signals were in the subchondral and bone marrow region.

**Disclosures:** Andrew Clark, None.

## MO0005

**RANK-L is upregulated in Erdheim Chester disease, a new therapeutic target?.** Natasha M. Appelman-Dijkstra<sup>1</sup>, Huib van Essen<sup>2</sup>, Nathalie Bravenboer<sup>3</sup>, Neveen A.T. Hamdy<sup>1</sup>. <sup>1</sup>Center for Bone Quality Leiden University Medical Center, Netherlands, <sup>2</sup>Department Clinical Chemistry. VU University Medical Center, Netherlands, <sup>3</sup>Department Clinical Chemistry. VU University Medical Center, Research institute MOVE & Center for Bone Quality Leiden University Medical Center, Netherlands

A 58-year old man was referred for of a 5-year history of bilateral knee pain, progressively worsening and spreading to the upper legs. Extensive investigations including a bone marrow biopsy revealed no abnormalities except for a persistently raised ESR and radiological features suggestive of multiple bone infarcts. At presentation to our center physical examination was normal. ESR was 50mm/h and he had a persistently elevated 1.25 dihydroxy-Vitamin D which increased to 300nmol/l during follow up. P1NP was 70 ng/mL(ref <59). Skeletal scintigraphy showed intense bilateral uptake of long bones, especially around the knees. The increased 1.25 dihydroxy Vitamin D and radiographic features raised the possibility of a hematological malignancy or histiocytosis. A repeat CT-scan of the thorax and abdomen now revealed bilateral infiltration of the mesenterium around the kidneys. A bone biopsy at the knee showed a high number of clustered, foamy, vacuolised macrophages, positive for CD 68 immunohistochemical staining and negative for S100 and CD1a. A BRAF mutation was identified and the diagnosis of Erdheim Chester disease was made. MRI of the pituitary showed diffuse infiltrates, but normal pituitary function. Cardiac screen was normal. Erdheim-Chester Disease(ECD) is a form of non-Langerhans' cell histiocytosis characterized by the presence lipid-rich foamy macrophages in bones, pituitary, heart and kidney. ECD primarily affects adults and the etiology of the disease is unknown. Bone lesions are present in >90% of patients with a distinct radiological picture. The only registered treatment for EDC is PEG-Interferon alpha.

RANK-L is upregulated in Langerhans' cell histiocytosis and we hypothesized that this might also be the case in ECD. Staining for RANK-L, showed multiple RANK-L positive macrophages within the marrow with increased expression of RANKL. During the diagnostic work-up, the patient was treated with bisphosphonates for pain reduction however he required repetitive infusions and increasing doses to maintain response. Based on our pathology results, we felt that RANKL inhibition represented a therapeutic target, since targeting the RANK-L positive macrophages might not only improve bone pain, but also target extra-skeletal ECD lesions. He was started on Denosumab 60 mg 3 monthly, in addition to PEG-Interferon. When last seen, the patient was pain free, no new ECD lesions have been identified.

**Disclosures:** Natasha M. Appelman-Dijkstra, None.

## MO0006

**Micro-RNA Expression Profiling in Paget's Disease of Bone and Osteoporosis and their Modulation by Intravenous Bisphosphonates.** Simone Bianciardi<sup>1</sup>, DANIELA MERLOTTI<sup>2</sup>, Guido Sebastiani<sup>1</sup>, Marco Valentini<sup>1</sup>, Stefano Gonnelli<sup>1</sup>, Carla Caffarelli<sup>1</sup>, Isabella Anna Evangelista<sup>1</sup>, Simone Cenci<sup>3</sup>, Ranuccio Nuti<sup>1</sup>, Francesco Dotto<sup>1</sup>, Luigi Gennari<sup>\*1</sup>. <sup>1</sup>Department of Medicine, Surgery & Neurosciences, University of Siena, Italy, <sup>2</sup>Department of Medicine, Surgery & Neurosciences, University of Siena, Italy; <sup>2</sup>Division of Genetics & Cell Biology, San Raffaele Scientific Institute, Milan, Italy, Italy, <sup>3</sup>Division of Genetics & Cell Biology, San Raffaele Scientific Institute, Milan, Italy

Since their discovery, microRNAs (miRs) have emerged as critical post-transcriptional regulators of stem cell lineage commitment and bone development.

Nonetheless, despite the massive increase in bone turnover, whether dysregulation of miRs is involved in Paget's disease of bone (PDB) remains unknown. Here, we performed a serum miRNA expression profile (Taqman Human MicroRNA Array Card Set v3.0) in peripheral blood mononuclear cells (PBMCs) from 25 PDB pts (13 with and 12 without *SQSTM1* mutation) and 25 age-matched subjects with or without osteoporosis (OP). Moreover, miRs from 10 of these PDB cases and the 10 OP pts before and 6 months after therapy with intravenous bisphosphonates (BP) were transcribed from plasma samples and pooled into pre- and post-treatment groups and compared to controls in a subsequent miR expression profile analysis. Data from Array Cards was exported using ViiA7 RUO software and then analyzed using Expression Suite software v1.0.1 (Applied Biosystem). All values were normalized using different housekeeping miRs. Overall, 24 miRs were significantly upregulated (n=21) or downregulated (n=3) in PBMCs from PDB pts than in non-pagetic controls. Conversely, 14 miRs were significantly dysregulated in OP than non-OP pts. The most consistent associations were observed with miR-15b, -19a, -19b, -23b, -30b, -424, -501, and -502.3p for PDB and miR-1, -23b, -124a, -148b, -182, -190, -451, and -487.a in OP. For most of the PDB-related miRs the association was significantly higher in carriers of *SQSTM1* mutation; moreover in these *SQSTM1*-mutated pts 20 additional miRs were specifically upregulated. The analysis of serum miRs identified partly different associations between OP or PDB cases and controls at baseline. Of interest 3 miRs were specifically upregulated in serum of OP patients than in controls (miR-1, -124a, -520e, -542.3p) and their levels were significantly decreased by BP treatment, while miR-125a.3p, -362.3p, -502.3p, and -627 were reduced by BP therapy in PDB. In addition 4 serum miRs (miR-493, -512.5p, -525, and -548c.5p) were underexpressed or undetected in serum of PDB and OP patients at baseline than in controls and their levels increased after BP treatment reaching similar values than in controls. Validation studies in larger samples are ongoing to confirm the above associations and assess the role of the identified miRs as potential biomarkers or therapeutic targets in PDB as well as in other disorders of bone metabolism.

**Disclosures:** Luigi Gennari, None.

## MO0007

**Conventional Treatment Of Hypoparathyroidism Is Not Sufficient To Prevent Hyperphosphatemia And Hypercalcemia.** Camilla Amaral<sup>1</sup>, Gabriela Andrade<sup>1</sup>, Maria Marta Sarquis Soares<sup>2</sup>, Maria Regina Calsolari<sup>1</sup>, Angelica Tiburcio<sup>1</sup>, Barbara Silva<sup>\*3</sup>. <sup>1</sup>Santa Casa de Belo Horizonte, Brazil, <sup>2</sup>Universidade Federal de Minas Gerais, Brazil, <sup>3</sup>Santa Casa de Belo Horizonte & UNI-BH, Brazil

Hypoparathyroidism (HypoPT) is a rare endocrine disorder characterized by chronic deficiency of parathyroid hormone (PTH). The main biochemical abnormalities in HypoPT are hypocalcemia and hyperphosphatemia. Hypocalcemia leads to neuromuscular manifestations, that can be severe and life threatening. Chronic hyperphosphatemia, while asymptomatic, induces ectopic mineralization in soft tissues. The standard treatment of chronic HypoPT, which includes large doses of oral calcium supplements and active vitamin D analogues, can alleviate symptoms, but may not prevent complications or may lead to adverse outcomes. We aimed to evaluate, through a chart review, treatment patterns, laboratory parameters, and the prevalence of nephrolithiasis in a large cohort of patients with permanent hypoparathyroidism seen at a tertiary-care hospital. The study population comprised 62 patients (53 women), with a mean age of 55.5 (±14.5) years, and a mean duration of HypoPT of 9.2 (±7.5) years. Most of the cohort had postsurgical HypoPT. At baseline, the mean PTH level was 7.7 (±6.5) pg/mL, serum calcium was 8.3 (±1.3) mg/dL, and the glomerular filtration rate (GFR) was 83.8 (±28.4) mL/min. At the end of the follow-up, approximately 73% of patients were taking calcium supplements and active vitamin D analogues, and 32% were on a thiazide diuretic. The daily supplemental calcium and calcitriol requirements were, on average, 1700 mg and 0.45 µg, respectively. The mean serum PTH level remained low at 7.3 (±6.6) pg/mL, serum calcium level was 8.6 mg/dL (min. 5.4; max. 10.8), and the phosphate concentration was 4.4 mg/dL (min. 2.6; max. 7.9). The majority of subjects (63%) had serum calcium levels within the low-normal range (7.5 to 9 mg/dL). Serum calcium was below 7.5 mg/dL or above 10 mg/dL in only 6 individuals. In contrast, hyperphosphatemia was noted in 43% of subjects, and there was a significant decrease in GFR as compared to baseline (GFR. 72.7 ± 23.5 mL/min; p=0.03). Urinary excretion was assessed during the most recent medical appointment of 25 (40%) patients, 24% of whom had urinary calcium levels greater than 300 mg/day. Kidney ultrasounds were performed in 13 (21%) patients, 39% of whom were found to have nephrolithiasis. In summary, in this large cohort of hypoparathyroid subjects, there was a high prevalence of hyperphosphatemia, hypercalcemia and nephrolithiasis, and a GFR decline over time, despite the appropriate treatment of the disease.

**Disclosures:** Barbara Silva, None.

## MO0008

**HYDROGEN SULFIDE PROTECTS FROM PTH INDUCED BONE LOSS BY INCREASING WNT10B PRODUCTION BY T CELLS.** Abdul Malik<sup>\*</sup>, John Calvert, Chiara Vaccaro, Mingcan Yu, Jau Li, Jonathan Adams, Roberto Pacifici. Emory University, United states

Hydrogen sulfide (H<sub>2</sub>S) is a gasotransmitter that has recently been implicated in physiologic mesenchymal stem cell renewal and osteogenic differentiation, as well as

acquisition of bone during postnatal growth. Treatment with H2S have been shown to prevent ovariectomy induced bone loss and alveolar bone loss. In this study we have investigated the capacity of the H2S donor GYY4137 to prevent the bone loss induced in mice by continuous PTH (cPTH) treatment, a model of primary hyperparathyroidism. 16 week old female mice were infused with hPTH1-34 (80 µg/kg/day) by osmotic pumps for 4 weeks and injected IP with vehicle or the H<sub>2</sub>S-donor GYY (1mg/mouse/day). GYY treatment completely prevented the loss of trabecular and cortical bone induced by cPTH by stimulating bone formation. Mechanistic studies revealed that GYY increased osteoblastogenesis and osteoblast life span by activating Wnt signaling in bone marrow (BM) stromal cells. Wnt signaling activation was due to increased production of the osteogenic Wnt ligands Wnt10b by BM T cells. In summary, GYY is an H2S donor that potently stimulates bone formation by activating Wnt signaling in osteoblastic cells. Since treatment with GYY protects against cPTH induced bone loss, our data provide a proof of principle that GYY donors may represent a new therapeutic approach for primary hyperparathyroidism.

**Disclosures:** *Abdul Malik, None.*

## MO0009

**Intrathyroidal Parathyroid Carcinoma.** Monica Therese Cating-Cabral\*, Pamela Ann Aribon, Brian Michael Cabral. St. Luke's Medical Center Global City, Philippines

Primary hyperparathyroidism is commonly caused by a single parathyroid adenoma while other causes include parathyroid gland hyperplasia or multiple adenomas. However, in 1-5% of cases, primary hyperparathyroidism can be due to parathyroid cancer. Parathyroid cancer is a rare endocrine disorder that is difficult to diagnose and treat. It is usually discovered incidentally, presents with a markedly elevated serum calcium and manifests with multi-organ, nonspecific symptoms of hypercalcemia secondary to parathyroid hormone (PTH) hypersecretion.

We present a case of a 35 year-old male with primary hyperparathyroidism initially presenting with abdominal pain. Family medical history includes parathyroid adenoma in both the patient's father and paternal aunt. None of the affected family members presented with any other signs or symptoms of multiple endocrine neoplasia (MEN) and no further evaluation was done.

Laboratory tests revealed an elevated calcium of 14.6 mg/dL (8.2-10.5 mg/dL) and an elevated PTH of 1,601 pg/mL (10-65 pg/mL). Sestamibi scan of the neck was suggestive of a thyroid pathology such as a hyperfunctioning nodule versus a parathyroid adenoma in the inferior portion of the right thyroid lobe. Thyroid function tests were within normal. Subsequent thyroid ultrasound showed a small cyst in the lower pole of right lobe measuring 0.2 x 0.1 x 0.1 cm and a hypoechoic solid nodule in the middle to lower third of left lobe measuring 2.3 x 1.4 x 1.8 cm. Ultrasound-guided fine needle aspiration biopsy of the larger nodule in the left lobe was read as atypia of undetermined significance.

Additional testing included cranial magnetic resonance imaging (MRI) which showed a nonspecific hypoenhancing focus of 0.2 x 0.1 cm in the left lateral aspect of the pituitary gland suggestive of a pituitary microadenoma. Work-up did not reveal any abnormal trophic pituitary hormones or any other disorders of the pituitary axis.

The patient eventually underwent total thyroidectomy and parathyroidectomy. Histologic evaluation revealed parathyroid carcinoma within the left thyroid lobe with invasion of the surrounding structures. No other parathyroid adenoma or hyperplasia was identified.

1 month after surgery PTH remained slightly elevated but serum calcium continued to be within normal range. Follow-up cranial MRI will be done 6 months post-operatively. No other family members to date have presented with hypercalcemia.

**Disclosures:** *Monica Therese Cating-Cabral, None.*

## MO0010

**Normocalcaemic Hyperparathyroidism: Prevalence in a UK Referral Population.** Marian Schini\*<sup>1</sup>, Richard Jacques<sup>1</sup>, Nicola Peel<sup>2</sup>, Jennifer Walsh<sup>1</sup>, Richard Eastell<sup>1</sup>. <sup>1</sup>University of Sheffield, United Kingdom, <sup>2</sup>Sheffield Teaching Hospitals, United Kingdom

**Introduction:** Normocalcaemic hyperparathyroidism (NHYPER) is characterised by persistent normal calcium levels, accompanied by elevated PTH values on at least 2 consecutive measurements, after excluding other causes of secondary hyperparathyroidism. It was recognised by the Third International Workshop on Asymptomatic Primary Hyperparathyroidism (2009) and it has been linked to consequences known to affect patients with primary hyperparathyroidism (accelerated bone loss, nephrolithiasis, and metabolic abnormalities). The prevalence of the disease in the literature varies significantly, due to various definitions used and different groups studied.

**Objective:** To identify the prevalence of NHYPER in a UK referral population and to compare the different groups of patients in regards to their characteristics (age, BMI, bone mineral density).

**Methods:** We retrospectively evaluated data from 5977 patients attending our Metabolic Bone Centre for a bone mineral density measurement (BMD) and a

laboratory evaluation. Using a statistical method (Mahalanobis distance) subjects were identified as 'normal' or 'abnormal' and using the laboratory reference intervals for serum albumin-adjusted calcium (Roche autoanalyser) and PTH (Roche modular analytics Cobas E170), these patients were divided into 10 categories. Patients were considered to have NHYPER according to the above mentioned definition, including 25(OH)D $\geq$ 50nmol/l and eGFR $\geq$ 60 ml/min/1.73m<sup>2</sup>.

**Results:** We identified 19 patients, all women, with likely NHYPER. Thus, the prevalence of this disease in our population was 0.3%, lower than the prevalence of hyperparathyroid hypercalcaemia (HH), which is the group of primary hyperparathyroidism and familial hypocalcaemic hypercalcaemia (FHH) patients (3.1%). After comparing all the different groups (Kruskal Wallis), we observed that our NHYPER patients did not have a significant difference in terms of BMI, age and BMD measurements compared to the normal population (all p>0.05). Moreover, we studied the natural history of these patients and observed two different patterns; classic NHYPER (with persistently normal calcium and elevated PTH in all occasions) and intermittent hypercalcaemia (with some normal and some elevated calcium levels). The fluctuations were not related to 25(OH)D levels.

**Conclusion:** The prevalence of NHYPER in our UK referral population is lower than the ones described in other studies.

**Disclosures:** *Marian Schini, None.*

## MO0011

**Primary Hyperparathyroidism: Role of Impaired Cerebrovascular Function in Cognitive Symptoms.** Sum Melissa, Yunglin Gazes, Diane Cozadd, Mariana Bucovsky, Kevin Slane, Chengchen Zhang, Randolph Marshall, Ronald Lazar, Shonni Silverberg, Marcella Walker\*. Columbia University Medical Center, United states

We previously reported cognitive dysfunction in primary hyperparathyroidism (PHPT) reversible with cure (PTX). We have also shown that PTH levels are positively associated with vascular stiffness in PHPT. We hypothesized that PTH-dependent intracerebral vascular dysfunction may impair blood flow and cognition in PHPT. Postmenopausal women with PHPT (N=13) undergoing PTX underwent cognitive testing, functional magnetic resonance imaging (fMRI) and transcranial Doppler to measure intracerebral vasomotor reactivity (VMR) pre- and 6 months post-PTX. PHPT were compared to normative control data at baseline. PHPT cases (mean age $\pm$ SD, 64 $\pm$ 7yrs) had mild PHPT (calcium 10.5 $\pm$ 0.3mg/dl, PTH 81 $\pm$ 22pg/ml) and normal mean vitamin D (39 $\pm$ 16ng/ml), renal and thyroid function. Baseline mood and age-, gender- and education-adjusted Z-scores for visuospatial memory, verbal memory and motor speed were normal. VMR tended to be worse in PHPT vs. 9 controls (2.2 $\pm$ 3.6 vs. 4.2 $\pm$ 1.1% mmHgPCO<sub>2</sub>, p=0.07), but was not associated with PTH (r=0.29, p=0.30) or calcium (r=0.34, p=0.21) levels. On fMRI, PHPT had reduced neuronal activation in the cerebellum during non-verbal abstraction vs. 18 age- and gender-matched controls (t=4.40, k=120 voxels, p<0.001). Activation in PHPT inversely correlated with PTH but not calcium level in several areas (all p<0.0001) including the Hippocampus (r=-0.95, t=9.50, k=21), Caudate (r=-0.92, t=7.32, k=223), and both inferior and medial frontal gyri (r=-0.92, t=7.26, k=159). After PTX (n=11), verbal fluency on a word association task (-0.04 $\pm$ 0.97 vs. 0.47 $\pm$ 1.23, p<0.005) and motor speed on pegboard testing (-0.41 $\pm$ 1.27 vs. 0.3 $\pm$ 1.3, p=0.04) improved and mood (12 $\pm$ 11 vs. 7 $\pm$ 6, p=0.085) tended to improve, while VMR did not change (n=7; 3.4 $\pm$ 1.0 vs. 3.8 $\pm$ 1.0, p=0.40). Post-PTX, activation was reduced during both non-verbal abstraction [Inferior parietal lobe (t=14.35, k=222) and middle temporal gyrus (t=8.10, k=93), all p<0.001] and verbal memory [Middle frontal gyrus (t=8.54, k=20), lingual gyrus (t=6.74, k=20), and Insula (t=8.08, k=79), all p<0.001]. In summary, preliminary data suggest that PHPT may be associated with lower VMR. Cure of PHPT was associated with improvements in some aspects of cognition and mood. There were also changes in brain activation in areas involved in decision-making and executive function. Further work is needed to determine if the decrease in VMR ultimately improves post-PTX and whether it contributes to underlying cognitive changes in PHPT.

**Disclosures:** *Marcella Walker, None.*

## MO0012

**PTH in Elderly Women: Change over Time and Association with Mortality in the Longitudinal OPRA Study.** David Buchebner\*<sup>1</sup>, Fiona McGuigan<sup>2</sup>, Linnea Malmgren<sup>2</sup>, Kristina Akesson<sup>2</sup>. <sup>1</sup>Department of Internal Medicine, Halmstad County Hospital, Halmstad, Sweden, Sweden, <sup>2</sup>Clinical & Molecular Osteoporosis Research Unit, Department of Clinical Science Malmö, Lund University, Sweden, Sweden

**Background:** Elevated Parathyroid hormone (PTH) has been associated with increased mortality, but the extent of elevation and for how long, to induce detrimental health outcomes in elderly women is uncertain. In this study we describe the change in PTH over time and its association to mortality in elderly women.

**Methods:** Study participants were women in the longitudinal OPRA cohort. 1044 attended at baseline, aged 75y. Data on PTH, 25(OH)D, calcium, phosphate and kidney function (eGFR) was available for 646 women who attended

investigations both at age 75y and at 80y. The relationship between PTH and mortality over 15 years of follow-up was investigated using Cox proportional hazards models.

Results: At 75y, most had PTH within normal range (1.6-6.9 pmol/l). Elevations beyond this occurred in only 11% (n=109) and these women also had lower 25(OH)D (54 vs 63 nmol/l,  $p<0.001$ ) and eGFR (60 vs 70 ml/min,  $p<0.001$ ).

By age 80, 40% (n=256/646) maintained their baseline level. Interestingly, women with increased PTH levels, even by up to 50% at 80y (39%; n=250) still had levels within normal range, although lower 25(OH)D (74 vs 83,  $p=0.001$ ). eGFR, phosphate and calcium remained unaffected ( $p=0.07-0.88$ ). In women with PTH increased by more than 50% (21%; n=140) eGFR was lower (56 vs 61 ml/min,  $p=0.002$ ) despite similar 25(OH)D levels (77 vs 74;  $p=0.31$ ) compared to women with elevated PTH but within normal range. Phosphate and calcium remained unaffected ( $p=0.23-0.99$ ).

Measured at age 75y, PTH elevated  $>6.9$  pmol/l was associated with a greater risk of dying compared to those within normal levels (HR<sub>adj</sub>=1.4 [1.1-1.8],  $p=0.007$ ), although attenuated when adjusted for eGFR, smoking, phosphate and 25(OH)D;  $p=0.082$ ). Measured at age 80y, elevated PTH was not associated with mortality (adjusted or unadjusted).

Conclusion: In this population sample of elderly women, the majority maintained PTH levels within the normal range even though up to 50% increase in PTH was not uncommon. The association between mortality and PTH above normal range at age 75 was not independent of low 25(OH)D and poor kidney function, possibly reflecting impaired general health. Although low grade secondary hyperparathyroidism becomes more common with age, the lack of association between PTH at age 80 and mortality suggests that other comorbidities become more relevant predictors in the very elderly.

Disclosures: David Buchebner, None.

## MO0013

**3D Analysis of Osteocyte Lacunae Using Confocal Microscopy.** Adam Rauff<sup>1</sup>, Chelsea Heveran<sup>2</sup>, Virginia Ferguson<sup>2</sup>, R. Dana Carpenter<sup>\*1</sup>. <sup>1</sup>University of Colorado Denver, United states, <sup>2</sup>University of Colorado Boulder, United states

The osteocyte network receives and responds to mechanical stimuli and actively directs the remodeling of bone structure. Moreover, osteocytes are believed to alter the amount of bone that is added and removed by signaling to osteoclasts and osteoblasts, which affords bones the ability to dynamically adapt to musculoskeletal needs. Because osteocyte lacunae comprise an abundant component of bone microstructure, they may play significant roles in both mechanosensation and the mechanical integrity of bone. The 3D characterization of the lacunar-canalicular system has recently emerged as a means to investigate the structural and mechanical implications of the 3D size, geometry, and spatial arrangement of lacunae. The purpose of this study was to quantify the 3D morphology and spatial arrangement of lacunae in the murine femur and tibia. Samples were acquired from the cortices of murine femora and tibiae. The samples were stained with basic fuchsin, embedded in PMMA, and polished in preparation for microscopy. A confocal microscope was used to acquire 3D "stacks" of 2D images. A typical voxel size was  $0.45 \times 0.45 \times 1.0 \mu\text{m}^3$ , and image depths ranged from 40-90  $\mu\text{m}$ . The images were reconstructed into 3D objects and processed using new software developed as part of the study (Figure 1). The new software was used to measure lacunar volume, density, orientation, radius, and anisotropy, with some variation compared with other techniques [1,2]. Preliminary results of the study revealed a site-specific difference in lacunar size: lacunar volumes in the femur and tibia of mice were  $410 \pm 90 \mu\text{m}^3$  and  $296 \pm 126 \mu\text{m}^3$ , respectively ( $p<0.001$ , Student's t-test). This larger size was also reflected in the lacunar surface area, which was  $366 \pm 55 \mu\text{m}^2$  in the femur and  $268 \pm 80 \mu\text{m}^2$  in the tibia ( $p<0.001$ ). These results reflect initial findings, yet the same analysis techniques are being applied in an ongoing investigation of the effects of aging and chronic kidney disease (CKD) (N=48 animals). The site-specific differences in lacunar morphology could reflect differences bone mechanical function with aging and/or CKD. Additionally, the software developed in this study can be used to investigate changes in lacunar morphology that may occur due to obesity, diabetes, and exposure to microgravity.

### References:

- [1] Carter, Y. et al., 2014. Journal of Anatomy 225(3): 328-36.
- [2] Vatsa, A. et al., 2008. Bone 43(3): 452-58.

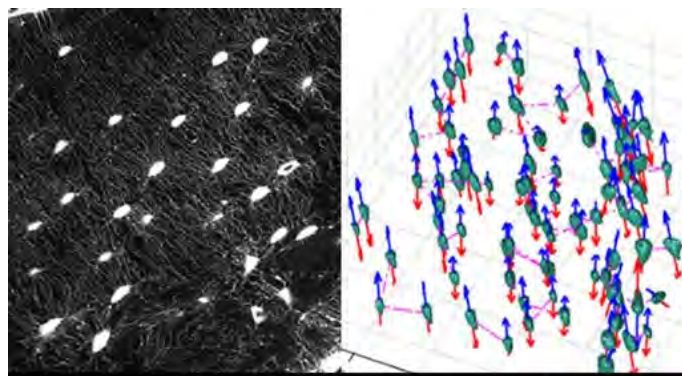


Figure 1. Left: Confocal microscope image of osteocyte lacunae in murine cortical bone. Right: Processed image showing 3D rendered lacunae (green). Arrows (red and blue) indicate alignment of the long axis of each lacuna. Pink lines indicate the distance between the centroid of each lacuna and that of its closest neighbor.

Figure 1

Disclosures: R. Dana Carpenter, None.

## MO0014

**Comparison of Cortical and Trabecular Bone Micro-architecture and Finite-Element-Derived Strength in Postmenopausal Women With and Without Recent Distal Radius Fracture.** Chantal Kawalilak<sup>\*1</sup>, Saija Kontulainen<sup>2</sup>, Morteza Amini<sup>1</sup>, Cathy Arnold<sup>3</sup>, James D Johnston<sup>1</sup>. <sup>1</sup>Mechanical Engineering; University of Saskatchewan, Canada, <sup>2</sup>College of Kinesiology; University of Saskatchewan, Canada, <sup>3</sup>School of Physical Therapy; University of Saskatchewan, Canada

Objective. The objective of our study was to investigate differences in cortical and trabecular micro-architecture, as well as finite-element (FE)-derived strength between postmenopausal women with and without distal radius fracture.

Methods. Using high-resolution peripheral quantitative computed tomography (HR-pQCT), we scanned the non-fractured or non-dominant distal radius and tibia of 75 postmenopausal women (Mean age, SD: 64, 9 years) with a recent (<2 year) distal radius fracture (N=30) and non-fractured, age-matched peers (N=45), respectively. Cortical outcomes included: bone volume fraction, thickness (mm), porosity (%), pore volume (mm<sup>3</sup>), pore diameter (mm). Trabecular outcomes included: bone volume fraction, trabecular number, thickness (mm), separation (mm), heterogeneity (mm). Strength outcomes included: bone stiffness (N/mm) and failure load (N). We performed pairwise comparisons of bone outcomes between fracture and non-fracture groups using MANOVA and controlled for multiple comparisons using Bonferroni correction. Significance was accepted at  $P<0.05$ .

Results. At the distal radius, women with distal radius fractures (when compared to the non-fracture group) had lower trabecular bone volume fraction (-19.4%), number (-12.3%) and thickness (-7.5%), as well as higher trabecular separation (+14.5%). At the tibia, women with distal radius fractures had lower trabecular bone volume fraction (-15.1%) and number (-13.5%), as well as higher trabecular separation (+15.7%) and heterogeneity (+21.0%). The fracture patients also had lower stiffness at the tibia (-10.5%).

Conclusion. Results indicate that women who sustained a recent distal radius fracture had impaired trabecular micro-architecture at the distal radius and tibia but no differences in cortical properties or FE-derived strength outcomes apart from distal tibia stiffness. Results suggest that trabecular micro-architecture may distinguish individuals prone to fracture.

Disclosures: Chantal Kawalilak, None.

## MO0015

**Dynamic Versus Quasi-Static Mechanical Analysis of Bisphosphonate Treated Bone.** Joseph Geissler<sup>\*</sup>, J. Christopher Fritton. Rutgers University / NJ Medical School / Orthopaedics, United states

Quasi-statically determined mechanical properties of bone tissue following treatments may not necessarily reflect all relevant properties under normal, dynamic, physiological loading. We recently found that fatigue life for canine rib tissue treated 3 years with high-dose alendronate was decreased 3-fold (and associated with smaller osteon wall thickness and density of osteocyte lacunae) [Bajaj et al. Bone 2014]. We now seek to determine whether mechanical information from a non-destructive dynamic test could detect differences in treatment. Cortical bone beams with uniform

geometry (0.5 x 1.5 x 10mm) were prepared from 10<sup>th</sup> rib of adult female beagles treated daily with either vehicle (Veh, 1ml/kg saline) or alendronate (Aln, 1.0 mg/kg; Merck) for three years [Allen *et al.* Calcif Tissue Int 2008]. Beams were first subjected to 3-point, dynamic material analysis (DMA) using a static mean load of -1N and a dynamic 1N sinusoidal load at frequencies ranging from 0.1 to 50 Hz. In addition to elastic and plastic measurements, DMA also measures viscoelastic material properties which depend on time or frequency. One primary measurement generated from DMA is the bulk modulus composed of an elastic and viscous component. The elastic component, known as the storage modulus ( $E'$ ), measures the material's ability to recover its original shape after deformation. The damping component, known as the loss modulus ( $E''$ ), measures the material's ability to dissipate energy from loading. Thus, the bulk modulus is defined as  $E^* = E' + iE''$  ( $E''$  is the imaginary moduli measured in DMA). After DMA, beams were subjected to destructive quasi-static loading at a displacement rate of 0.05 mm/s until fracture. All loading was conducted with the periosteal side in tension and the endosteal side in compression using an electro-mechanical actuator (Bose, TestBench) equipped with a 50 lbf load cell. As expected for low frequencies, pre-yield values of  $E$  (moduli measured quasi-statically) and  $E'$  exhibited a strong positive correlation for both Veh ( $r^2=0.95$ ) and Aln ( $r^2=0.83$ ). We also observed a negative correlation between post-yield deformation and  $E''$  in Veh ( $r^2=0.50$ ) only. For Aln, no significant correlations existed between  $E''$  and any of the pre- or post-yield properties measured. This work aims to develop dynamic tests that quantify the remaining useful life of bone. Acknowledgements: Drs. Matthew Allen and David Burr of Indiana University provided tissues used in these studies.

**Disclosures:** Joseph Geissler, None.

## MO0016

**In Vivo Measures of Trabecular Bone Micro-Architecture Computed from Two Multirow Detector CT Scanners with Different Spatial Resolution Show High Correlation.** Punam Saha\*, Cheng Chen, Xiaoliu Zhang, Elena Letuchy, Kathleen Janz, Eric Hoffman, Trudy Burns, James Torner, Steven Levy. University of Iowa, United states

Recent advances in multirow detector CT (MDCT) technology produce high spatial resolution using ultra-low dose radiation and enable visualization and analysis of trabecular bone (TB) micro-architecture. The ultra-high speed scanning and long scan-length dramatically reduce motion artifacts and positioning errors. Wide variation in CT images and data from different vendors and rapid upgrades in technology raise concerns of data uniformity in large-scale multi-site or longitudinal studies that typically involve data from multiple scanners. This pilot study compared TB micro-architectural measures from two different MDCT scanners to determine if a longitudinal study can jump scanners and still maintain longitudinal continuity.

The distal tibia of twenty volunteers (age:  $26.2 \pm 4.5Y, 10F$ ) was scanned using the prior Siemens SOMATOM FLASH and the higher resolution FORCE scanners at 120kV, 200mAs, pitch=1.0, 10cm FOV using the ultra-high resolution (UHR) mode with an average 45-day time gap between scans. Images were reconstructed at 0.2mm slice spacing and 0.12mm in-plane resolution. TB measures were computed over two ROIs covering 4-6% and 6-8% locations of the distal tibia with a 30% peel. For two these ROI combined- for each measure, Lin's concordance correlation coefficient (CCC), an estimate of agreement between continuous measurements along a 45° line, was calculated for TB measures, as was the Pearson correlation coefficient. Calibration equations were developed for each TB measure using linear regression analysis.

TB measures, namely, BMD, plate-width, plate BMD, and rod BMD, estimated from the two MDCT scanners demonstrated satisfactory agreement with  $CCC > 0.9$  (Table); other measures showed high linear association with Pearson correlation coefficients  $> 0.9$ . Measure-specific calibration equations differed by whether an intercept and/or a shift parameter were included; BMD needed no calibration. TB rod-plate classification for a 22-year-old male over 4-6% of the distal tibia (Figure) illustrates regional agreement of TB rod-plate measures from the two MDCT scanners.

*In vivo* measures of TB micro-architecture from tested scanners can be used in a cross-sectional or longitudinal study after calibration, if needed. Non-significant location x measure interaction effects in calibration equations suggest that location-specific calibration equations are not needed.

This study was funded by NIH grants: R01-AR054439, R01-DE012101, UL1-RR024979, and S10-OD018526.

Trabecular Bone Measure	FLASH Scanner (Lower-Resolution) Mean (SD)	FORCE Scanner (Higher-Resolution) Mean (SD)	CCC (95% CI)*	Pearson Correlation
BMD (mg/cc)	1154.71 (30.79)	1151.07 (32.99)	0.96 (0.94, 0.98)	0.97
Plate-width ( $\mu$ m)	1194.50 (214.83)	1155.28 (190.73)	0.94 (0.89, 0.97)	0.96
Plate to rod ratio	2.61 (0.43)	3.33 (0.37)	0.35 (0.23, 0.45)	0.92
Plate volume fraction	0.94 (0.02)	0.93 (0.02)	0.92 (0.86, 0.95)	0.98
TB spacing ( $\mu$ m)	478.78 (112.03)	399.63 (114.03)	0.74 (0.62, 0.83)	0.92
TB thickness ( $\mu$ m)	162.45 (17.60)	134.16 (13.67)	0.36 (0.25, 0.47)	0.98
Network area ( $mm^{-3}$ )	0.54 (0.15)	0.78 (0.19)	0.44 (0.31, 0.56)	0.91
Plate BMD (mg/cc)	927.37 (105.02)	898.30 (114.48)	0.93 (0.88, 0.96)	0.97
Rod BMD (mg/cc)	227.34 (81.43)	252.76 (89.27)	0.92 (0.86, 0.95)	0.96

\*CCC can be interpreted as the agreement between continuous measurements about a 45-degree line (95% CI based on Fisher's Z transformation)

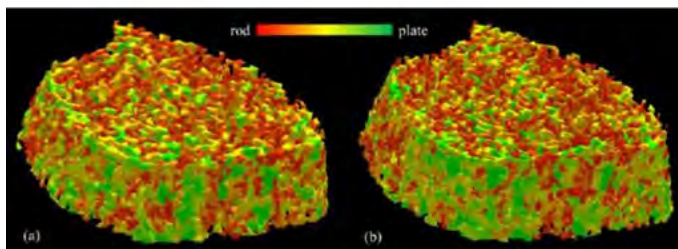


Figure. Color-coded illustration of individual trabecular plate-rod classification of a 22 year-old male using two MDCT scanners over a registration-matched ROI covering 4-6% distal tibia with 45% peel. Regional agreement of rod-plate classification in the two images is visually apparent.

Table and Figure

**Disclosures:** Punam Saha, None.

## MO0017

**Mechanical Competence of the Proximal Femur from X-Ray Analysis.** Volker Kuhn\*, Kerstin Simon. Medical University Innsbruck, Austria

**Aim:**

This experimental study was attended to texture analysis in radiographs of proximal femur specimens and line graphs developed via image editing program ImageJ.

**Material:**

421 radiographs were obtained from 247 individuals – 80 male and 54 female. The median of the donors age was 77,9 (77,3; 82,7) years (range of 52,3 to 99 years).

**Methods:**

Correlations between different previous analyses from DXA, failure load via mechanical strength tests simulating a fall on the trochanter and the torque to breakaway of the bone (peak torque) via DensiProbe were calculated.

**Results:**

Most of the texture features were highly correlated with DXA-results ( $r = 0,70$  to  $0,81$ ), especially in the AUC-DP region (summation of all grey values in the DensiProbe region). Texture features, especially in the Trochanter Maximum region ( $r = 0,44$  to  $0,73$ ), Head Maximum region ( $r = 0,40$  to  $0,77$ ) and AUC-DP region ( $r = 0,79$  to  $0,81$ ), also were highly correlated with anchorage strength estimated by the failure load.

In comparison with the different fracture types (femoral neck, trochanteric, shaft) significant low grey values were found in femoral neck fractures. Texture features highly correlated with the DensiProbe-tests, mainly in the AUC-DP region ( $r = 0,38$  to  $0,57$ ), Head Maximum region ( $r = 0,33$  to  $0,51$ ), and Neck Minimum region ( $r = 0,33$  to  $0,61$ ).

There were significant differences in grey values between male and female individuals in almost every region and also in comparison between left and right side.

**Conclusion:**

These results suggest that texture analysis in radiographs is a potential low cost technique to predict bone quality and osteoporotic fracture risk.

**Disclosures:** Volker Kuhn, None.

## MO0018

**Microindentation Testing of Human Trabecular Bone.** Drew Jones<sup>\*1</sup>, Connie Wood<sup>2</sup>, David Pienkowski<sup>1</sup>, Hartmut Mäluiche<sup>3</sup>. <sup>1</sup>Department of Biomedical Engineering, University of Kentucky, United states, <sup>2</sup>Department of Statistics, University of Kentucky, United states, <sup>3</sup>Division of Nephrology, Bone & Mineral Metabolism, University of Kentucky, United states

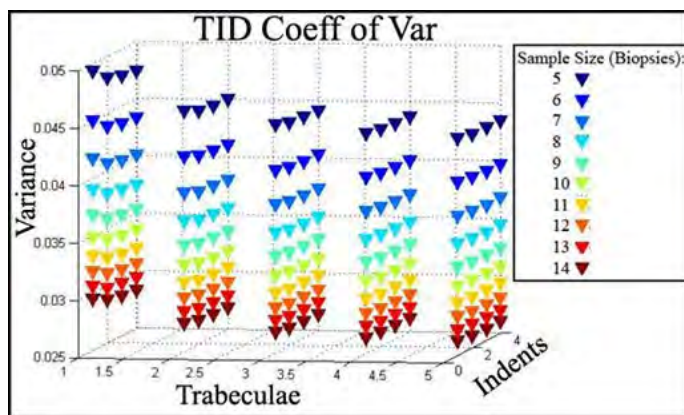
Micro-indentation offers a technique for assessing specific mechanical properties of bone. Reference point indentation (RPI), a novel form of micro-indentation, provides additional information over typical micro-indentation and nanoindentation techniques. RPI has been exclusively performed on cortical bone, but use of RPI on trabecular bone is challenged by limited available surface area and difficult indentation probe placement. These challenges must be overcome while addressing the need for a defined number of indents, minimum indentation separation, and consistent indentation force. The objective of this study was to establish a feasible RPI methodology for trabecular bone.

Theoretical and experimental approaches were used. Strain and stress fields produced by RPI were modeled using finite element analysis. A series of evenly spaced indentations were represented in a 3D model using 3 planes of symmetry. The indentation force was modeled as a pressure distribution normal to the indentation surface. The substrate representing trabecular bone in the model was assumed to be 280 microns wide and 140 microns deep.

The experimental approach used 8 ex vivo anterior iliac crest trabecular bone samples from osteoporotic patients. Each sample was indented 9 times (3 trabeculae per sample; 3 indents per trabeculum) each using a BioDent RPI system to estimate the variance for each of 16 candidate indentation protocols (1 to 4 trabeculae and 1 to 4 indents per trabeculum) and given bone sample size. Variance among: a) bone samples ( $\sigma_b^2$ ), b) trabeculae within a bone sample ( $\sigma_t^2$ ), and c) indents within a trabeculum ( $\sigma_i^2$ ) was estimated using standard variance component analysis for balanced hierarchical designs. The protocol with the smallest coefficient of variation for the available trabecular bone area was selected.

The results showed that an indentation depth of 50 microns placed with the central axis at least 175 microns from the central axis of a second indent will avoid intersection of the strain fields produced by each indentation. Increasing the number of bone samples was the most efficient of the three variables for decreasing variance. The most feasible approach with the lowest variance utilized an indentation force of 4 Newtons, 2 indents per trabeculum, and 2 trabeculae per sample (Figure).

In conclusion, RPI of trabecular bone can be efficiently performed using the described methodology to assess material properties of trabecular bone.



Predicted Coefficient of Variance of Total Indentation Depth (TID)

*Disclosures: Drew Jones, None.*

## MO0019

**Ovariectomized Rats with a Healed Fracture Have an Increased Propensity to Subsequent Fracture.** Elizabeth Foley<sup>\*1</sup>, Sarah Johnson<sup>2</sup>, Dennis Chakkalakal<sup>3</sup>, Bahram Arjmandi<sup>1</sup>. <sup>1</sup>Florida State University, United states, <sup>2</sup>Colorado State University, United states, <sup>3</sup>Creighton University, United states

Older adults are one of the fastest growing populations in the United States, with individuals over 65 years of age predicted to double in number by 2050. Osteoporosis is a major health concern for women, affecting over 200 million worldwide with one out of three women over the age of 50 experiencing a fracture. After sustaining a fracture, 30% of older adults die within the following year. Postmenopausal women are particularly at risk for developing osteoporosis and therefore fragility fractures because the lack of estrogen causes accelerated bone turnover such that resorption exceeds formation. This leads to a decrease in bone density, quality, and strength. Therefore, investigations into the integrity of bone with a previously healed fracture in the presence or absence of estrogen and its subsequent response to loading stress is of importance. Fifty-six female 12-month old Sprague-Dawley rats were divided into 4 groups; 2 sham-operated (Sham) and 2 ovariectomized (Ovx). Post-surgery,

osteotomy was performed to create an experimental fracture model in both fibulae in animals from one Sham and one Ovx group. Animals in all groups were placed on a semi-purified diet for a period of 120 days to allow significant bone loss to occur in the Ovx animals as confirmed by assessing whole body bone mineral density using DXA. Rats were sacrificed and the fibula was removed to test for bending strength, flexural failure stress, bending rigidity, flexural modulus, flexural failure strain, area moment of inertia, and area cross section. Sham rats with fracture displayed the highest bending strength ( $6.17 \pm 1.217$ ), bending rigidity ( $1.274 \pm 0.324$ ), flexural failure strain ( $0.040 \pm 0.005$ ), area moment of inertia ( $1.271 \pm 0.227$ ), and area cross section ( $4.29 \pm 0.332$ ). Bending strength was lowest ( $4.43 \pm 0.634$ ) in the Ovx fracture group. Flexural failure stress was highest in the non-fracture groups. Bending strength was higher after fracture only in the presence of estrogen, which suggests a higher risk for subsequent fracture for postmenopausal women who sustained a previous fracture, and indicates that fractured bone may not heal as strongly in postmenopausal women.

*Disclosures: Elizabeth Foley, None.*

## MO0020

**Variation in Bone Strength-Strain Index (SSI) of the Distal Radius in Non-Osteoporotic Males: Implications for Differential Response to Traumatic Loading.** Randee Hunter<sup>\*1</sup>, Karen Briley<sup>2</sup>, James Ellis<sup>2</sup>, Amanda Agnew<sup>1</sup>. <sup>1</sup>Skeletal Biology Research Laboratory, The Ohio State University, United states, <sup>2</sup>Wright Center of Innovation in Biomedical Imaging, The Ohio State University, United states

The goal of this study is to investigate potential differential response to traumatic loading of the distal radii in DXA-assessed non-osteoporotic males using the bone strength-strain index (SSI) as a measure of structural and material properties affecting bone's resistance to fracture. The range of variation in bone quality for individuals deemed "skeletal healthy" through traditional methods such as DXA needs to be explored. The bone strength-strain index (SSI) is a product of section modulus (Z) and volumetric bone mineral density (vBMD) and is used as a proxy for bone strength in the distal radius. Left and right radii were excised from 27 post-mortem human subjects (PMHS); only one radius was available from 3 additional PMHS resulting in a sample of 30 individuals (n=57 radii). Males ranging in age from 30 to 80 years ( $64.26 \pm 10.93$ ) were selected based on DXA whole body and lumbar spine T-scores qualifying them as non-osteoporotic individuals (T-scores  $>-1.5$ ). Quantitative clinical CT was performed on *ex vivo* radii at the 30% distal site using a QRM phantom ( $0-800 \text{ mg/cm}^3$ ) to calculate vBMD. Total area (Tt.Ar), cortical area (Ct.Ar), section modulus for each of the anterior (Z<sub>ant</sub>) and posterior (Z<sub>post</sub>) cortices and robusticity (Tt.Ar/length) were quantified using ImageJ. Age had no significant relationship with any variable. Paired samples t-tests indicate significant differences in SSI<sub>ant</sub> ( $p=0.03$ ) and SSI<sub>post</sub> ( $p=0.04$ ) between left and right radii as well as higher SSI<sub>ant</sub>. Differences between right and left SSI could be the result of functional adaptation due to handedness. However, there were no significant side differences between Ct.Ar, robusticity or vBMD, indicating differential distribution of cortical bone in cross-section (Z). Figure 1 demonstrates the large amount of variation in SSI for both cortices in this sample. Pearson correlation coefficients indicate the inability of non-site specific lumbarDXA T-scores to capture this variation in bone strength in the distal radius as measured by SSI of the anterior and posterior cortices ( $p=0.21$  and  $0.22$ , respectively). For males in this sample who would have been clinically classified as non-osteoporotic and therefore have the same risk of fracture, SSI values indicate a wide range of potential loading responses. This amount of variation is informative for investigating the complexity of differential fracture risk, and the inability of global DXA scores in quantification.

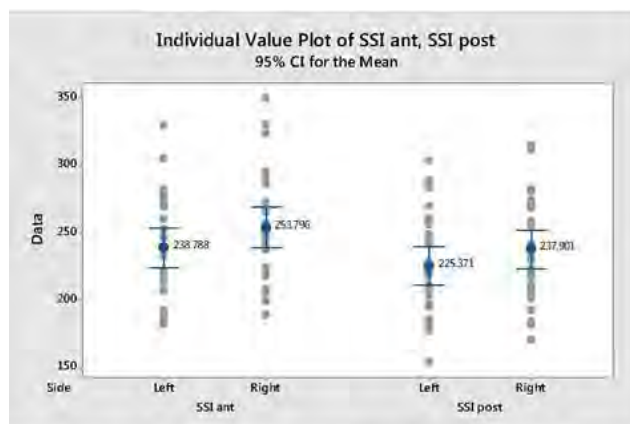


Figure 1: Individual value plot for Bone Strength-Strain Index (SSI) demonstrating a large amount of variation within each parameter; significant side differences between cortices; as well as significantly higher SSI values in the anterior compared to the posterior cortex for both right and left radii ( $p<0.0001$ )

Figure 1: Individual value plot for Bone strength-strain index (SSI) demonstrating a large amount of

*Disclosures: Randee Hunter, None.*

## MO0021

**Influence of bone morphology over the bone mechanical properties of Osteoporotic rat models.** Juan-Marcelo Rosales<sup>1</sup>, Masaru Kaku<sup>1</sup>, Kosuke Nozaki<sup>2</sup>, Takako Ida<sup>1</sup>, Katsumi Uoshima<sup>1</sup>. <sup>1</sup>Division of Bioprosthodontics, Graduate School of Medical & Dental Science, Niigata University, Japan, <sup>2</sup>Department of Material Biofunctions, Institute of Biomaterials & Bioengineering, Tokyo Medical & Dental University, Japan

## Background:

Osteoporosis is a disease characterized by a reduction in bone mass and changes in the micro architectural structure of bone tissue, resulting in loss of mechanical strength<sup>1</sup>. Moreover, epidemiological research confirmed that fracture risk increases as Bone Mineral Density (BMD) decreases<sup>2</sup>. Ovariectomized (OVX) rats are used as models to study the effects of osteoporosis, bone metabolism and bone mechanical properties<sup>3</sup>. Although many papers describe bone properties of OVX induced osteoporosis in rats; there is still no clear consensus about its effects over the mechanical properties; moreover, some studies indicate an increase of bone strength in OVX compare with control samples<sup>4-6</sup>. The objective of this study is to evaluate the influence of the cortical characteristics and the mechanical properties in rats' bone.

## Material and Methods:

Thirteen female Wistar Rats were divided in 2 groups, 6 rat as Control group (Cont) and 7 rats for ovariectomy induced osteoporosis group (OVX). Ovariectomy operation was performed at 10 week of age according to the ethical guidelines of Niigata University. Eight weeks after operation, all animals were euthanized and bilateral femurs were excised and fixated. BMD and Morphometric analysis of the samples was performed using ELE-scan micro-tomography and Tri/3D-BON software (Ratoc Systems, Tokyo, Japan). Mechanical analysis was performed using a 3-point Bending Universal Testing machine and TrapeziumX v1.1.5 software (EZ Graph, Shimadzu, Tokyo, Japan).

## Results and Discussion:

OVX samples clearly showed a decrease in BMD; however, an increase in Bone Volume, Cortical Area, Periosteal Perimeter and Cortical Porosity was observed. Regarding the mechanical properties, Breaking Force and Fracture strength increased in OVX while Young Modulus and Ultimate Strength showed no significant difference. Some studies showed that about 50% of all fractures, and about 50% all recurrent fractures, arise from the large proportion of the population with osteopenia at modest risk for fracture, not the smaller fraction with osteoporosis at high risk for fracture<sup>2</sup>. This might suggest that bone morphology has more influence on the mechanical properties than the BMD. In conclusion, OVX increased the fracture strength of femoral bone, most likely by gain of cortical bone volume. Further studies will warrant a better understanding of the correlation of OVX induced morphological changes and mechanical properties of bone.

*Disclosures: Juan-Marcelo Rosales, None.*

## MO0022

**Original Evidence of a Different Adaptation of Proximal and Distal Cortical Shell of the Human Fibula to the Bone's Mechanical Environment.** Gustavo Roberto COUNTRY<sup>1</sup>, Laura Nocciolino<sup>2</sup>, Alex Ireland<sup>3</sup>, Nicolas Hall<sup>4</sup>, Andreas Kriechbaumer<sup>4</sup>, José Luis Ferretti<sup>2</sup>, Joern Rittweger<sup>4</sup>, Ricardo Francisco Capozza<sup>2</sup>. <sup>1</sup>Center of P-Ca Metabolism (CEMFoC), Argentina, <sup>2</sup>Center of P-Ca Metabolism Studies (CEMFoC), Argentina, <sup>3</sup>School of Healthcare Science, Manchester Metropolitan University, United Kingdom, <sup>4</sup>Division of Space Physiology, Institute of Aerospace Medicine, German Aerospace Center, Germany

In a previous study we observed a differential response of human tibia and fibula cortical structure to disuse. This finding led us to analyze the cortical structure of the normal human fibula from a biomechanical point of view. With that purpose, we took serial pQCT scans at 5% increments of the fibula length (measured from the tibio-tarsal joint line to the proximal articular surface of the tibia, giving 19 scans per individual) of 10/10 healthy, sedentary men and women aged 20-40 years. Indicators of fibula cortical mass (BMC, cross-sectional area -CSA-), mineralization (vBMD), design (perimeters, moments of inertia -MIs-) and strength (Bone Strength Indices, BSIs; Strength-Strain Index, SSI) were determined.

All cross-sectional shapes and geometrical/strength indicators suggested a sequence of five different regions along the bone, which would be successively adapted to 1. transmit loads from the articular surface to the cortical shell (close to fibula-tibia upper joint), 2. favor lateral bending (central part of upper half), 3. resist lateral bending (mid-diaphysis), 4. favor lateral bending again (central part of the lower half), and 5. resist bending/torsion (distal end). Cortical BMC and the cortical/total CSA ratio were higher at the midshaft than at both bone ends ( $p < 0.001$ ). However, all MIs, BSIs and SSI values and the endocortical perimeter/cortical CSA ratio (indicator of the mechanostat's ability to re-distribute the available cortical mass) showed a "W-shaped" distribution along the bone, with maximums at the midshaft and at both bone's ends ( $p < 0.001$ ). The correlations between MIs (y) and cortical vBMD (x) at each bone site ("distribution/quality" curves that describe the efficiency of distribution of the cortical tissue as a function of the local tissue stiffness) showed higher r coefficients at proximal than distal bone regions ( $p < 0.001$ ).

Results show that 1. the human fibula is primarily adapted to resist bending and torsion rather than compression, and 2. the fibula's bending strength is lower at the center of its proximal and distal halves and higher at the mid-shaft and at both bones

ends. This would a. favor, proximally, the elastic absorption of energy by the attached muscles that rotate/evert the foot, and distally, the widening of the heel joint and the resistance to excessive lateral bending, and b. suggest that biomechanical control of structural stiffness differs between proximal and distal fibula.

*Disclosures: Gustavo Roberto COUNTRY, None.*

## MO0023

**Age, Grip Strength, and Handedness are Related to Distal Radius Microstructure: a Cross-Sectional, HR-pQCT study in Premenopausal Females.** Megan Mancuso<sup>\*</sup>, Karen Troy. Worcester Polytechnic Institute, United states

As peak bone mass is achieved during adolescence, strategies for preventing osteoporosis are best suited for pre-menopausal women. The purpose of this study was to relate bone microstructure with diet, handedness, and physical activity in young, healthy females. Sixty women (mean age:  $29.4 \pm 5.4$  years) provided written informed consent for this institutionally approved study. Total serum 25-hydroxyvitamin D was measured with an immunoassay. Calcium intake [1] and handedness laterality decile [2] were determined from questionnaires. The Bone Physical Activity Questionnaire (BPAQ) [3] was used to score current and lifetime activity. Grip strength was measured using a handgrip dynamometer. High-resolution computed tomography (HRpQCT) scans (XtremeCT, Scanco, Switzerland) were performed to evaluate microstructure in a 9 mm transverse region of the distal radius. Partial Pearson's correlations controlling for height and weight compared HRpQCT parameters with age, vitamin D level, calcium intake, laterality decile, grip strength, and BPAQ scores. HRpQCT values for dominant and non-dominant arms were compared using paired t-tests and Wilcoxon signed rank tests for normally and non-normally distributed variables, respectively.

Age, non-dominant grip strength, and laterality decile were significantly correlated with 1 or more HRpQCT parameters (Table 1). Average bone mineral density (BMD) (g/cm<sup>3</sup>), compact BMD (g/cm<sup>3</sup>), cortical thickness (mm), cortical area (mm<sup>2</sup>), and bone mineral content (g) were significantly greater ( $p < 0.05$ , 3.17% mean increase) in the dominant versus non-dominant arm.

Non-dominant grip strength was a good predictor of cross-sectional area and compact BMD, in agreement with trends reflecting skeletal robustness[4]. Age was significantly associated with decreased trabecular number in the non-dominant arm and increased trabecular separation in both arms. Between-arm paired differences suggest increased loading in the dominant arm is associated with improved BMD and cortical parameters. Stronger preference for the dominant hand was associated with increased trabecular number and decreased trabecular separation in the dominant arm; exaggerated differences in between-arm loading may protect against trabecular deterioration. Together, these results emphasize the importance of mechanical loading on premenopausal bone health.

[1] Sebring (2007) J Am Diet Assoc. [2] Oldfield (1971) Neuropsychologia. [3] Weeks (2008) Osteoporos Int. [4] Schlecht (2013) Bone.

**Table 1:** Pearson's partial correlation coefficients for HR-pQCT parameters in the non-dominant (ND) and dominant (D) arms (n=60, df=56). \* $p < 0.05$ , \*\* $p < 0.01$

		Age (years)	ND Grip Strength (N)	Laterality Decile
Trabecular Number (mm <sup>-1</sup> )	ND	-0.304*	0.001	0.189
	D	-0.255	0.041	0.351**
Trabecular Separation (mm)	ND	0.294*	-0.028	-0.209
	D	0.270*	-0.04	-0.300*
Trabecular Area (mm <sup>2</sup> )	ND	-0.166	0.464**	-0.010
	D	0.017	0.351**	0.074
Compact Bone Density (mg/cm <sup>3</sup> )	ND	0.192	-0.265*	0.079
	D	0.019	-0.095	-0.025
Total Area (mm <sup>2</sup> )	ND	-0.141	0.519**	-0.025
	D	0.022	0.403**	0.057
Bone Mineral Content (mg)	ND	-0.051	0.29*	0.079
	D	-0.071	0.227	0.103

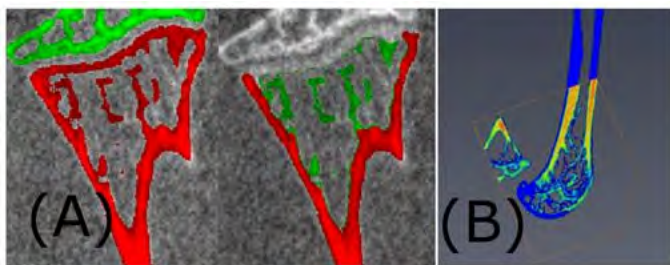
Table 1

*Disclosures: Megan Mancuso, None.*

## MO0024

**High-resolution quantitative preclinical bone analysis in micro-computed tomography (microCT).** Ali Behrooz\*, Jeff Meganck, Jen-Chieh Tseng, Jeff Peterson, Josh Kempner, PerkinElmer, United states

anatomical images that are useful for studying skeletal bone structures, formation, and diseases. Performing morphometric analysis on the cortical and trabecular compartments is necessary for enabling these studies. While automated bone and compartment segmentation have been demonstrated previously (Behrooz et al., US Patent Application No. 14/812,483), automated exclusion of the growth plate from the bone mask and bone compartment separation remains a challenge. In this work we present an automated approach to detect growth plates in tibia and femur images and exclude them from the bone mask and analysis. A hybrid second-derivative filter is applied to the raw grayscale data for growth plate detection as shown in Fig. A (left panel: segmented bone and separated metaphyseal and epiphyseal compartments, right panel: separated cortical and trabecular compartments with growth plate removed). 3D morphometric ASBMR and structural parameters are then computed for cortical and trabecular components of individual bones automatically. These algorithmic approaches are applied to images acquired of both mice and rats using the stand-alone Quantum<sup>®</sup> FX and GX micro-CT systems. To ensure that these images were sufficient for morphometric bone analysis in vivo, the spatial resolution was characterized using a Fourier-space analysis to derive the modulation transfer function and to determine limiting resolution, and the CT Dose Index (CTDI) was measured to ensure the doses were acceptable for longitudinal studies requiring multiple CT scans. In addition, ex vivo bone samples were imaged using the micro-CT system and then used to generate undecalcified, Toluidine Blue stained sections for bright field microscopy. This facilitated a side-by-side comparison of the morphometric parameters for validation as shown in Fig. B (solid blue is rendered histology section; colormapped image is registered slice from micro-ct image). As a last step, these validated instrument and algorithmic approaches were utilized in studies of osteolysis using models such as MIA induced osteoarthritis.



Behrooz et al., Image Segmentation and Validation Example Results

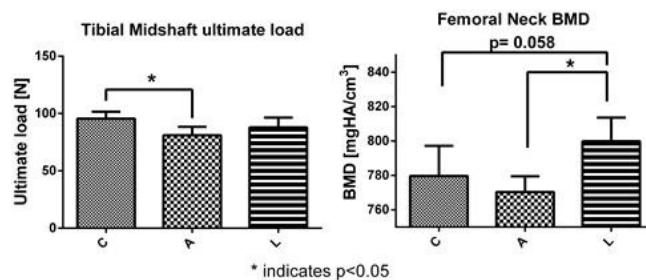
**Disclosures:** Ali Behrooz, PerkinElmer, 15  
This study received funding from: PerkinElmer

## MO0025

**Low intensity vibration mitigates the detrimental effect of chronic heavy alcohol consumption on bone quality, in actively growing rats.** Tea Pamon\*<sup>1</sup>, Jiaqi Qian<sup>1</sup>, Dandi Zhang<sup>1</sup>, Chun Ho Cheung<sup>1</sup>, Jason Abraham<sup>1</sup>, Russell Turner<sup>2</sup>, Clinton Rubin<sup>1</sup>, M. Ete Chan<sup>1</sup>. <sup>1</sup>Stony Brook University, United states, <sup>2</sup>Oregon State University, United states

Chronic heavy alcohol consumption (CHAC) is recognized as having detrimental effects on bone quality of the adult and maturing skeletal system, with treatments for this bone pathology being currently limited. Low intensity vibration (LIV) has been shown to improve bone quantity and quality in animal models of osteoporosis, disuse, and obesity, in part, through biasing bone marrow MSC differentiation towards higher order tissues. We hypothesize that the delivery of LIV can be used to mitigate the deteriorative effects of short term administration of heavy alcohol consumption in growing animals. 18 four-wk-old Wistar rats were randomized into 3 groups (n=6): C (control diet), A (alcohol diet), or L (alcohol diet + LIV). Alcohol animals were fed a modified Lieber-DeCarli diet ad libitum containing 35% ethanol-derived calories, while control animals received an isocaloric liquid diet with maltose-dextrin. L group was subjected to LIV, on a vertically oscillating plate, for 3 weeks (90Hz, 0.3g peak acceleration, 30min/d, 7d/wk). All rats were sacrificed at 7 wks of age. The left tibial midshafts were  $\mu$ CT scanned to measure cortical bone morphology and mineralization, and were then mechanically tested under 4-point bending. The left femoral neck, a site prone to fracture, was  $\mu$ CT scanned to assess trabecular bone microarchitecture and mineralization. All parameters were compared using one-way ANOVA with Tukey's Post Hoc;  $p \leq 0.05$  was considered significant. 3-wks of CHAC resulted in a significant reduction in ultimate load (UL) compared to C (-15.18%,  $p=0.01$ ), while LIV mitigated changes in UL, to levels not significantly different from C (Fig1). The detrimental effect of alcohol on mechanical properties can partly be explained by a trend of reduced Cort Th. in the A group compared to C (-6.7%,  $p=0.099$ ). LIV exhibited a trend of mitigating changes to Cort Th. (+0.6% relative to A,  $p=0.07$ ). Within the femoral neck, LIV led to a significant elevation of BMD compared to A (+4.07%,  $p<0.01$ ) (Fig2). This

preliminary study shows that short-term CHAC led to rapid deterioration of bone quality, while LIV was able to mitigate these effects. Further histological and protein/gene expression analysis may help us understand whether the bone marrow contributes to the CHAC induced bone pathology, or the mitigation effect of LIV. Understanding the effect of LIV in long term CHAC may ultimately contribute to a nondrug treatment for promoting bone health in alcoholics.



Tibial Midshaft ultimate load and Femoral Neck BMD

**Disclosures:** Tea Pamon, None.

## MO0026

**Raman and FTIR bone quality parameters correlate with physical chemical properties of chemical standards and native tissue.** Erik Taylor\*<sup>1</sup>, Ashley Lloyd<sup>1</sup>, Carolina Salazar<sup>2</sup>, Eve Donnelly<sup>1</sup>. <sup>1</sup>Cornell University, United states, <sup>2</sup>University of Los Andes, Colombia

Raman and Fourier transform infrared (FTIR) spectroscopic imaging techniques have been used to characterize bone quality. Compared to FTIR imaging, Raman imaging is advantageous due to its finer spatial resolution. Although FTIR bone quality parameters have previously been validated by independent techniques, those of Raman spectroscopy have not. The long-term objective of this work is to relate bone quality parameters assessed by Raman spectroscopy to physical chemical properties of chemical standards. In this study we relate the Raman mineral to matrix ratio (M:M) to the FTIR M:M and ash fraction in chemical standards and native tissue.

To generate chemical standards, hydroxyapatite (HA) was synthesized using an aqueous precipitation process, mixed with rat tail collagen in varying ratios (20-100wt% HA), and homogenized by cryomilling. The standards, along with tissue from human piriformis fossa (n=6, sex:F, age:61-82), were characterized with Raman and FTIR spectroscopy and gravimetric analysis. Raman and FTIR M:M values were calculated by dividing integrated  $PO_4$  ( $\nu_1$ - $\nu_3$ ) areas by the amide III and I peak areas, respectively, and correlated with ash fraction. To interpret the experimental results, the relative extinction coefficients of HA and collagen were calculated, theoretical spectra of the chemical standards were created by applying Beer's law, and the M:M values of the theoretical spectra were calculated.

Raman and FTIR M:M values from chemical standards increased exponentially with ash fraction (Raman  $p < 0.01$ ,  $R^2 = 0.93$ ; FTIR  $p < 0.01$ ,  $R^2 = 0.91$ ) and had similar M:M values to native tissue for a given ash fraction (Fig. 1). FTIR M:M values from native tissue were also similar to theoretical M:M values for a given ash fraction. Raman and FTIR M:M values were strongly correlated ( $p < 0.01$ ,  $R^2 = 0.82$ ). In regression analyses, the slopes of the experimental and theoretical M:M vs. ash fraction trend lines did not differ ( $p > 0.05$ ).

The results confirm that the Raman M:M bone quality parameter correlates strongly to ash fraction and to its FTIR counterpart. The exponential relationship observed between the M:M values and ash fraction is also predicted theoretically and arises from the amide peak area approaching zero at large ash fractions. Finally, the M:M values of the native tissue are similar to those of both chemical standards and theoretical values, confirming the clinical relevance of the chemical standards and the characterization techniques.

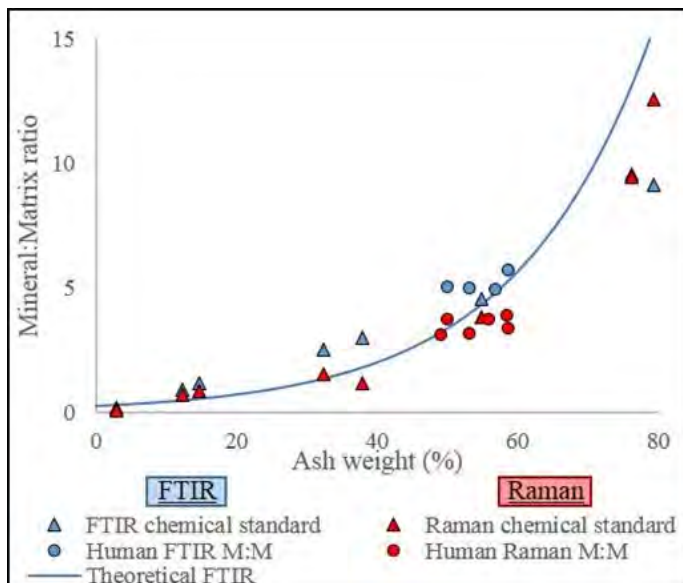


Figure 1

Disclosures: Erik Taylor, None.

## MO0027

**Remnant Woven Bone and Calcified Cartilage in Mouse Bone: Differences Between Ages/Sex and Effects on Bone Strength.** Victoria Ip, Zacharie Toth, John Chibnall, Sara McBride-Gagyi\*. Saint Louis University, United states

Woven bone (WB) has differing, and, in many respects, weaker mechanical properties than lamellar bone (LB) despite being composed of the same type I collagen fibrils. Murine long bones have an intracortical WB band apposed by circumferentially-aligned LB. This WB band is a remnant of longitudinal, endochondral growth and contains interspersed calcified cartilage (CC) islands. Studies on osteopetrotic genetic models have shown increased CC with knockout, but it is still unclear what, if any, effect remnant WB or CC has on bone strength. We hypothesized that (i) older animals' bones contain less WB and CC and (ii) WB and CC contribute to whole bone strength.

A cohort of 6wk old male and female BalbC mice were purchased (n=10/sex, Jax Lab). Half were directly euthanized, and half were housed in standard conditions until euthanasia at 13-weeks-old. Left femora were used to determine tissue mineral density (TMD, microCT, 12um) as well as strength and material properties (3-pt bending). Right femora were used to determine the amount of mid-shaft WB and CC (F1 A & B, respectively). To test hypothesis one, changes with age, histology outcomes were compared using ANOVA (factors: age, sex). To test hypothesis two, effects of WB/CC on strength, 3-pt bending outcomes were correlated with structural and compositional measures using multivariate linear regression (all pooled, candidate independent variables: TMD, cross-sectional area, WB area, percent WB, CC area, percent CC).

As hypothesized, WB composed a higher percent of young bones than older bones regardless of sex (F1 C, p=0.002). However, WB area was similar between ages, and males had on average 26% more WB than females (F1 D, p=0.034). In contrast, CC in older bones was twice that of younger bones ( $0.020 \pm 0.003\text{mm}^2$  vs  $0.010 \pm 0.001\text{mm}^2$ , p<0.001), which was similar when normalized by area (1.4-2%). Predictably, area and/or TMD accounted for >75% of the variation for most strength outcomes (stiffness, modulus, ultimate force, bending stress, total displacement). Percent CC added significant, albeit small, predictive power to ultimate force (2%) and bending stress (6%, F1 E). Percent WB was the only significant factor for post-ultimate force energy (26%).

Taken together, CC and WB can impact whole bone strength but are significantly less influential than TMD or size. CC and WB could have more influence in models of osteopetrosis, such as MMP13 knockout, where CC percent is double our highest value (4%).

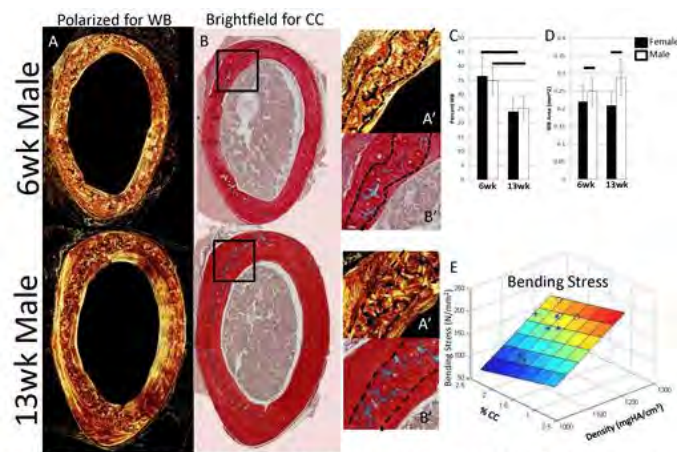


**Figure 1.** A) Both age mice have an intracortical band of WB (dashed lines on A' & B'). B) CC (blue) constitutes more of this band in older animals. C) Younger animals' bones have a higher percent WB, but D) the WB area does not vary with age and is higher in males. E) Percent CC increases bending stress correlations by 6%.

Figure 1

Disclosures: Sara McBride-Gagyi, None.

## MO0028

**Sertraline alters bone wound healing in murine, critical-sized, calvarial defects.** R. Nicole Howie\*<sup>1</sup>, Samuel Herberg<sup>2</sup>, Emily Durham<sup>1</sup>, Gracie Bennfors<sup>3</sup>, Mohammed Elsalanty<sup>4</sup>, Amanda Larue<sup>1</sup>, William Hill<sup>4</sup>, James Cray<sup>1</sup>. <sup>1</sup>MUSC, United states, <sup>2</sup>Case Western, United states, <sup>3</sup>College of Charleston, United states, <sup>4</sup>Augusta University, United states

Bone remodeling is a dynamic and tightly controlled process that is required for healing damaged bone. External factors can alter this process leading to delayed or failed wound healing. Recent studies have found that selective serotonin reuptake inhibitors (SSRI) can reduce bone mass, precipitate osteoporotic fracture, and increase the rate of implant failure. With 10% of Americans on antidepressants, the potential of SSRI to impair bone remodeling may adversely affect millions of patients' ability to heal after sustaining trauma. Here, we investigate the effect of SSRI on bone wound healing by systemically treating mice with 10 mg/kg Sertraline in drinking water (n=26) or unsupplemented drinking water (n=32) for 2 weeks prior to surgery where a 5 mm calvarial defect was made along the midline of the calvaria. Animals were randomized into 3 surgical groups A) empty/sham, implanted with B) the DermaMatrix scaffold soaked loaded with sterile PBS, or C) DermaMatrix soaked loaded with 542.5 ng BMP-2, and sacrificed at 4 weeks post-surgery. SSRI treatment decreased bone healing with significant declines in trabecular thickness and number, increased trabecular spacing, and caused gross disorganization of regenerate and collagen fibers within the defect site. These effects seemed to be independent of specific circulating serum Sertraline levels, suggesting an on/off mechanism of action. In conclusion, our study indicates that SSRI treatment can impair bone wound healing through disruption of remodeling and altered regenerate structure.

Disclosures: R. Nicole Howie, None.

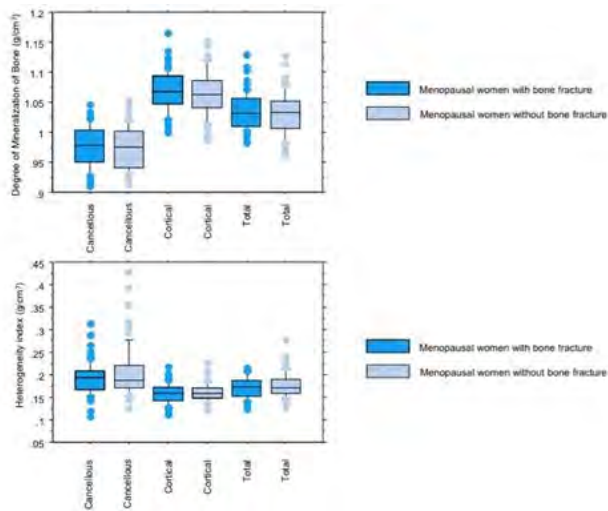
## MO0029

**Variables Reflecting the Mineralization of Bone Tissue from Fracturing versus Non-fracturing Postmenopausal Women.** Sébastien RIZZO\*<sup>1</sup>, Delphine FARLAY<sup>1</sup>, Mohammed AKHTER<sup>2</sup>, Adele BOSKEY<sup>3</sup>, Robert RECKER<sup>2</sup>, Joan LAPPE<sup>2</sup>, Georges BOIVIN<sup>1</sup>. <sup>1</sup>INSERM, UMR 1033, Univ Lyon, Université Claude Bernard Lyon 1, France, <sup>2</sup>Creighton University Osteoporosis Research Center, United states, <sup>3</sup>Hospital for Special Surgery, United states

Women with equivalent BMDs may show a different fracture incidence due to differences in bone intrinsic quality. In iliac bone biopsies from postmenopausal women (PM), with or without fragility fractures (FX), matched by age and BMD, the only significantly different FTIRI variable was the carbonate/phosphate ratio (C/P) (Boskey et al, JBMR, 2016 in press). Nanoindentation showed that FX bone was less heterogeneous than non-FX ones and thus could propagate damage (microcracks) more easily (Venin et al. ASBMR 2015). The hypothesis here is that PM with FX have reduced mineralization of bone tissue compared to non-FX. Iliac biopsies were collected from FX (n=60, 62.5±7.4 yrs-old) and non-FX (n=60, controls 62.3±7.3 yrs-old) PM women, to assess the mineralization of bone tissue using digitized microradiography (Montagner et al. 2015, J X-Ray Sci Technol 23:201-11). Bone matrix mineralization was measured in a blinded fashion using a Matlab code. The degree of mineralization of bone (DMB, g/cm<sup>3</sup>) and the heterogeneity index (HI, g/cm<sup>3</sup>) of the DMB were calculated for cancellous (canc), cortical (cort) and total (tot) bone. Results were compared to variables from

nanoindentation (Venin et al. ASBMR 2015) and Fourier transform infrared spectroscopic imaging (FTIRI; Boskey et al. JBMR. 2016 in press). DMB and HI were not significantly different between FX and non-FX groups (Figure). Cort and can HI were weakly negatively associated with cort and can DMB. DMB and HI were not associated with any of the nanoindentation variables. There were only weak negative correlations in cort bone between DMB and hardness or storage modulus. Cort and can DMB were positively associated with index of mineralization, and negatively associated with C/P (FTIRI). None of the DMB variables were strongly associated with any of the histomorphometric variables. There were many weakly significant correlations: cort DMB was negatively associated with mineralizing surface, bone formation rate and activation frequency. Cort and can DMB was also positively associated with mineral apposition rate. In conclusion, variables reflecting bone mineralization were not significantly different between FX and non-FX PM women. This suggests that bone fragility could be partly due to other variables such as changes in bone organic matrix.

Figure: Degree of mineralization of bone and heterogeneity of mineralization are not significantly different in fractured women versus matched non-fractured women.



Figure

Disclosures: Sébastien RIZZO, None.

## MO0030

**Initial Results for a New Positive Reinforcement Voluntary Jumping Exercise in Rats Show Enhanced Bone Parameters.** Scott Lenfest<sup>1\*</sup>, Jennifer Kosniewski<sup>1</sup>, Amelia Looper<sup>2</sup>, Jessica Brezicha<sup>3</sup>, Jeremy Black<sup>1</sup>, Susan Bloomfield<sup>4</sup>, Jim Fluckey<sup>4</sup>, Harry Hogan<sup>1</sup>. <sup>1</sup>Texas A&M University Department of Mechanical Engineering, United states, <sup>2</sup>Texas A&M University College of Veterinary Medicine, United states, <sup>3</sup>Texas A&M University Department of Biomedical Engineering, United states, <sup>4</sup>Texas A&M University Department of Health & Kinesiology, United states

Resistance exercise is an important component of in-flight countermeasures for mitigating microgravity-induced bone loss in astronauts. The hindlimb unloading rat model allows for ground-based study of skeletal effects due to simulated microgravity, but simulating exercise is more challenging in this animal model. Even so, voluntary resistance exercise through operant conditioning has been effective in enhancing bone properties of adult rats in recent studies [1,2]. That technique uses negative reinforcement (mild electrical stimulus) to condition animals to perform vertical jumps. The goal of our current study was to develop and assess the efficacy of an alternate voluntary jumping exercise (VJE) protocol that uses positive reinforcement.

Adult male rats (5 mo.) were placed in a custom jumping cage and encouraged to climb onto a 4" high platform baited with sucrose pellets (45mg). Initially, rats received an extra 2-3 pellets for climbing onto the platform. The platform height was gradually increased by 1-2" as platform climbing increased in frequency. Greater heights required rats to jump onto the platform to receive the pellets. At the max 10" platform height, jumping speed was increased by rewarding 1 pellet only after the rat jumped onto and off of the platform. After 4 weeks of training, rats were assigned to aging control (AC, n=8) or exercise (VJE, n=5) groups by body weight and jumping ability. VJE animals performed 30 jumps/d, 5 d/wk, for 4 wks at an average rate of 1 jump each 20-25 seconds. AC animals were pair fed to match caloric intake. In vivo pQCT scans of the proximal tibia metaphysis (PTM) and tibia diaphysis (TD) were taken at baseline (BL) and at 4 weeks.

The number of animals is small for this initial study, but the results are encouraging. For the PTM, the VJE group had significantly higher percent changes (BL to 4 wks) in cortical BMC (+11.24%, p=0.013), cortical area (+6.94%, p=0.013), and total BMC (+7.73%, p=0.014) compared to AC (+3.88%, +1.10%, +1.53%, respectively). Total and trabecular vBMD trended higher for VJE (-7.35%, +1.36%, resp.) compared to AC (-10.28%, -4.88%, resp.). Similarly, there was a trend of

favorable (but not significant) changes for VJE compared to AC at the TD. These data indicate that our new VJE protocol does induce an anabolic bone response, particularly in the cortical bone of the proximal tibia.

1. Swift et al. J Appl Physiol 109:1600 2010.
2. Shirazi-Fard et al. Bone 66:296 2014.

Disclosures: Scott Lenfest, None.

## MO0031

**Renal Compromise and Recovery in a Boy with the PHEX 3'-UTR c.\*231A>G Variant of X-linked Hypophosphatemia.** Gary S. Gottesman<sup>1\*</sup>, Randa Razzouk<sup>2</sup>, Keefe Davis<sup>3</sup>, Valerie A. Wollberg<sup>4</sup>, Katherine L. Madson<sup>1</sup>, William H. McAlister<sup>5</sup>, Steven Mumm<sup>6</sup>. <sup>1</sup>Center for Metabolic Bone Disease & Molecular Research Shriners Hospitals for Children - St. Louis, United states, <sup>2</sup>Kidney & HTN, Department OU School of Community Medicine, United states, <sup>3</sup>Division of Pediatric Nephrology, Department of Pediatrics, Washington University School of Medicine at St. Louis Children's Hospital, United states, <sup>4</sup>Center for Metabolic Bone Disease & Molecular Research Shriners Hospitals for Children - St. Louis, United states, <sup>5</sup>Department of Pediatric Radiology, Mallinckrodt Institute of Radiology, Washington University School of Medicine at St. Louis Children's Hospital, United states, <sup>6</sup>Division of Bone & Mineral Diseases, Department of Internal Medicine, Washington University School of Medicine at Barnes-Jewish Hospital, United states

Mild X-linked hypophosphatemia (XLH) results from the PHEX c.\*231A>G 3'-UTR mutation. We report a 16-year-old boy with this mutation, treated with calcitriol and phosphate (Pi) beginning at age 2 yrs, who responded well with genu varum resolving by age 8 yrs. His height was >30% at age 15 yrs. At 12 yrs, while on Pi 40 mg/kg/day, serum PTH became elevated. Pi dose was tapered over 2 yrs to 15 mg/kg/day. Uric acid (UA) level was intermittently elevated. Mild nephrocalcinosis (NC) developed at 9 yrs and progressed to moderate by 12 yrs. He was athletic, lean, muscular and clinically stable while playing two sports at school. Serum creatinine (Cr) was often near the upper range of normal (NI) at 1.0 - 1.2 mg/dL [Upper Limit of Normal (ULN): 1.3 mg/dL] after age 10 years, attributed to his muscular physique.

After his 15<sup>th</sup> birthday, serum Cr increased to 2.0 mg/dL in 10 weeks, while serum calcium (Ca) level was high NI (10.2 mg/dL), PTH level increased to 342 pg/mL and UA level was high (8.9 mg/dL, ULN 7.9 mg/dL). Calcitriol was stopped and the Pi was tapered over 5 days. The PTH fell by 50% within two weeks, with serum Ca high NI. Subsequently, we learned he had a back blow during a soccer game, treated with NSAIDS 2 months earlier. Also, he played 2 to 5 soccer games each weekend and failed to stay well-hydrated. The Cr fell slightly over the next several months.

Renal ultrasound revealed moderate NC and a newly echogenic cortex. Subsequent renal biopsy revealed cortical NC with marked Pi deposition, and moderate to moderately severe interstitial fibrosis. No UA crystals were found. Sestamibi SPECT scan did not reveal any firm evidence of parathyroid gland hyperplasia or adenoma. Eucalcemic hyperparathyroidism persisted. GFR based on cystatin-C/creatinine ratio was 55 ml/min/1.73 m<sup>2</sup>. We placed him on a low Ca and low protein diet and treated him with allopurinol. He remained active and did not reduce athletic activity. Over the ensuing year his serum Cr fell to the upper normal range (1.2 mg/dL) and UA normalized. Corrected Cr clearance rose to 90 ml/min/1.73 m<sup>2</sup>.

Precipitating factors for this boy's renal compromise remain unclear. A combination of physical trauma, dehydration, NSAID exposure and altered UA metabolism may have contributed. Patients with this mild variant of XLH seem to require less aggressive medical therapy but may be at risk for NC, interstitial disease and significant renal compromise.

Disclosures: Gary S. Gottesman, None.

## MO0032

Withdrawn

## MO0033

**Are there Gender Differences in Abdominal Fat Distribution in Healthy Teenagers?** Francois Duboeuf<sup>1\*</sup>, Stéphanie Boutroy<sup>1</sup>, Tiphanie Ginhoux<sup>2</sup>, Jean Paul Roux<sup>1</sup>, Roland Chapurlat<sup>1</sup>, Justine Bacchetta<sup>1</sup>. <sup>1</sup>INSERM 1033, France, <sup>2</sup>EPICIME, France

While the relationship between visceral (VFAT) and subcutaneous (SFAT) fat mass with cardiometabolic risk has been demonstrated in adults, fat mass evolution during teenagehood remains poorly explored and usually assessed with irradiative (CT) or expensive (MRI) techniques. Our aim was to evaluate a novel technique derived from DXA to assess VFAT and SFAT in healthy teenagers.

Healthy teenagers from the VITADOS study underwent whole body DXA scans for body composition analysis (Discovery A, HOLOGIC Inc; Bedford, MA). Outcome parameters were considered on the sub-total body (total body without head) and included mass (M), fat mass (FM), lean mass (LM), bone mineral density

(BMD), as well as the android-gynoid ratio (And/Gyn). Abdominal fat mass, including VFAT and SFAT, was assessed on the same scan using APEX V4.0.2, on a 5 cm-wide region placed across the entire abdomen just above the iliac crest approximately at the level of the 4<sup>th</sup> lumbar vertebra.

Ninety-two volunteers were included: 44 girls (G) and 48 boys (B), age: 13.9 ± 1.9 and 13.6 ± 2.4 yrs, body weight (BW): 49.6 ± 10.0 and 47.9 ± 14.4 kg, height: 158.8 ± 9.0 and 159.3 ± 15.0 cm, BMI: 19.4 ± 2.5 and 18.4 ± 2.9 kg/m<sup>2</sup>, respectively. Age, Height, BW and BMI were not significantly different between genders in the total cohort. In the Tanner 5 sub-group, age, BW and BMI were not different between genders; in contrast, height, FM, LM, And/Gyn and BMD were all significantly different (Table). Interestingly, VFAT and SFAT were significantly different between genders from Tanner 2 stages onwards: VFAT was significantly greater in boys whilst SFAT was significantly greater in girls.

Using a non-irradiative and inexpensive technique, VFAT and SFAT are significantly different between genders as early as Tanner stage 2 in healthy teenagers. The clinical consequences of such differences should be determined, but could explain some of the differences in cardiovascular risk observed between genders later in life.

**Percentage differences between genders by Tanner stages (relative to boys) for all studied parameters**

Tanner stage (Boys: N/Girls:N)	Tanner 1 (B:14/G:2)	Tanner 2 (B:8/G:7)	Tanner 3 (B:5/G:13)	Tanner 4 (B:7/G:7)	Tanner 5 (B:10/G:19)
Height	-5.5	-1.1	0.1	-5.5	-6.7*
Weight	-2.1	3.1	-8.6	-7.7	-10.9
BMI	10.0	5.6	-7.6	3.0	2.6
Lean Mass (LM)	-7.7	-5.2	-6.6	-19.0*	-23.1**
Fat Mass (FM)	13.5	42.8	-21.8	52.4	54.9*
Mass (M)	-3.1	3.3	-10.5	-8.3	-11.6
Android Gynoid Ratio (And/Gyn)	6.5	-2.0	-13.1	-18.2	-18.5*
BMD	-5.3	-0.3	1.5	-6.7	-11.9*
Visceral fat (VFAT)	-31.1	-44.0*	-50.5*	-55.6*	-35.2*
Subcutaneous fat (SFAT)	108.6	196.4**	10.0*	129.1*	111.7*

\*\* p<0.001; \* p<0.05

Table

Disclosures: Francois Duboeuf, None.

**MO0034**

**Feasibility and Reproducibility using HRpQCTII in Children and Adolescents.** Kyla Kent<sup>\*1</sup>, Jessica Whalen<sup>1</sup>, Ariana Strickland<sup>1</sup>, Mary Leonard<sup>1</sup>, Andrew J. Burghardt<sup>2</sup>. <sup>1</sup>Stanford School of Medicine, Dept Pediatrics, United states, <sup>2</sup>University of California, San Francisco, United states

The new second generation HR-pQCT device (Scanco Medical, XtremeCT II) provides greater spatial resolution (61 µm nominal resolution) and shorter scan time (2 minutes), and is configured to scan the cortical diaphysis as well as the conventional distal site. Our objectives were to determine the feasibility of obtaining scans with acceptable image quality in children and adolescents, and to determine test-retest precision errors for trabecular and cortical bone outcomes in the radius and tibia.

We recruited 60 healthy volunteers ages 5 to 21 to perform scan-rescan precision tests on the XtremeCT II. Participants were positioned in a carbon fiber immobilization cast. iPad-based video content was used to facilitate motion-free compliance. Distal radius and tibia scans were acquired starting 2 mm proximal to the proximal margin of the growth plate or growth plate remnant. Diaphyseal radius and tibia scans were centered at an offset from the same landmark, corresponding to 30% of limb length. Repeat scans were performed following complete repositioning of the participant. Scans were assessed for movement and the image quality was scored on the standard 5-point scale. The manufacturer's image analysis pipeline was optimized for pediatric distal and diaphyseal scans to measure bone density and structure, and to estimate bone strength by micro-finite element analysis (µFEA). Precision errors were calculated from the test-retest measurements using root mean square of the coefficient of variation (CV%).

The success rates for acceptable quality scans based on extreme (image grade ≤1), strict (≤2), and moderate criteria (≤3), are reported in Table 1 by age group and scan site. Precision errors measured from paired scans meeting the moderate quality criterion (≤3) by scan site are reported in Table 2.

These data demonstrate that performance of HR-pQCT scans is feasible in the majority of children and adolescents. The performance in younger children was improved with the use of a video to provide distraction. With the exception of distal cortical porosity, precision was outstanding and greater than reported in prior XtremeCT I reproducibility studies in adults. Diaphyseal measurements of cortical porosity offer superior precision to measurements immediately adjacent to the growth plate.

**Table 1. Probability to satisfy image quality criteria by age (Image Grade: ≤1 | ≤2 | ≤3)**

	5-10 years (N=21)	11-15 years (N=22)	16-21 years (N=17)	All Ages (N=60)
Distal Radius	52%   71%   76%	50%   64%   95%	65%   88%   100%	55%   73%   90%
Distal Tibia	43%   62%   71%	82%   96%   100%	71%   88%   100%	65%   82%   90%
30% Radius	48%   62%   78%	66%   82%   91%	71%   94%   100%	62%   75%   88%
30% Tibia	71%   86%   95%	100%   100%   100%	88%   94%   94%	87%   93%   97%

**Table 2. Test-retest precision data for image grade ≤ 3 (RMS CV%)**

	BMD	Ct.BMD	Ct.Th	Ct.Po	Tb.BMD	Tb.N	Tb.Th	Stiffness
Distal Radius	0.40%	0.76%	0.82%	15.9%	0.44%	1.45%	0.86%	5.61%
Distal Tibia	0.27%	0.63%	1.35%	11.8%	0.40%	1.39%	0.75%	3.65%
30% Radius	0.18%	0.23%	0.38%	5.59%	-	-	-	0.34%
30% Tibia	0.48%	0.35%	0.94%	5.07%	-	-	-	0.68%

Tables 1 and 2

Disclosures: Kyla Kent, None.

**MO0035**

**Relations between Dietary And Lifestyle Factors and Bone Mass in the adolescents in Taiwan.** Yi-Chin Lin<sup>\*1</sup>, Wen-Harn Pan<sup>2</sup>. <sup>1</sup>School of Nutrition, Chung Shan Medical University, Taiwan, province of china, <sup>2</sup>Institute of Biomedical Sciences, Academia Sinica, Taiwan, province of china

Adolescence is critical for the development of peak bone mass, which may in turn affect the risk for osteoporosis in later life. This preliminary analysis is based on the data collected from high school subjects recruited during the Nutrition and Health Survey in Taiwan (NAHSIT) 2010-2011. A total of 1098 male and 1124 female adolescents, aged 12-19 years, have completed bone scan by DXA. The results showed that for both genders, age and body weight significantly predicted bone mineral content (BMC, in gram) at total body, lumbar spine 2-4, and femoral neck in a non-linear manner. The results of multiple regression showed that age, height and body weight explained 82.06% and 74.93% of the variation in total body BMC in adolescent boys and girls, respectively. For girls, post-menarcheal age predicted BMC at all sites slightly better than the chronological age. In the adolescent boys, there were significant correlations (partialled for age and percent fat mass) between dietary intake of calcium (mg/d) and potassium (mg/d) and BMC at total body (r=0.073, p=0.047 and r=0.072, p=0.049, respectively). The correlations (partialled for age and percent fat mass) of borderline significance were also observed between dietary intake of calcium and potassium and BMC at lumbar spine 2-4 (r=0.068, p=0.064 and r=0.062, p=0.093, respectively) and femoral neck (r=0.069, p=0.061 and r= 0.063, p=0.086, respectively). Dietary intake of protein, as the absolute amount or as percent of daily total calories, was not significant predictors for BMC or BMD at all sites. The amount of protein per kilogram of body weight (0.09 – 5.82, mean=1.62 ± 0.82 for boys and 0.18 – 5.91, mean=1.68 ± 0.85 for girls), however, significantly related to BMC at all site in a negative manner, although the statistical significance slightly decreased in the multivariate models. On the other hand, there was significant correlation between the stories of stairs climbed per day, the number of days per week engaged in intensive exercise and BMC at all sites, respectively, in the adolescent boys, and the significance remained in the multivariate models. The results of our current analyses showed that dietary intake and the level of physical activity may play some roles in bone health in Taiwanese adolescents.

Disclosures: Yi-Chin Lin, None.

**MO0036**

**Calcemic Response to Burns Differs between Children and Adolescents.** Gordon L Klein<sup>\*1</sup>, David N Herndon<sup>2</sup>, Clark R Andersen<sup>2</sup>, Debra Benjamin<sup>2</sup>, Celeste C Finnerty<sup>2</sup>. <sup>1</sup>Dept Orthopaedic Surgery, University of Texas Medical Branch & Shriners Burns Hospital, United states, <sup>2</sup>Department of Surgery, University of Texas Medical Branch & Shriners Burns Hospital, United states

Burn injury disrupts calcium (Ca) metabolism by causing inflammatory bone resorption. We have previously shown that children develop hypocalcemic hypoparathyroidism following burns ( J Pediatr 1997; 131:246) likely due to up-regulation of the parathyroid Ca-sensing receptor by inflammatory cytokines (Crit Care Med 2000; 28:3885). Adults are reported as either normocalcemic or mildly hypercalcemic ( J Bone Miner Res 1993; 8:337). To determine the calcemic response over the first 30d post-burn of >40% body surface area we examined the blood ionized (i)Ca

concentration in 99 patients ages 0-21 yr with a mean of 147 blood samples per patient. Analysis used a generalized additive mixed model to relate iCa to an interaction between age and time with a two-dimensional penalized spline to accommodate non-linearity in the response and adjusting for burn percentage while blocking on subject to control for repeated measures. While percent burn did not significantly affect blood iCa, the interaction of age (above or below 12y) and time post-burn (up to 30d) affected the model,  $p < 0.0001$ . Thus pre-pubescent burn patients had low blood iCa which changed very little over time while those older than 12 yr started out with low blood iCa but rose to normal or above by 30d post-burn. Blood iCa has recently been implicated in the inflammatory process (Semin Cell Dev Biol 2016 49:52). Thus a difference in calcemic response between children and young adults may affect the intensity of the inflammatory response and consequent post-burn morbidity.

**Disclosures:** Gordon L Klein, None.

## MO0037

**Effect of Bisphosphonates and Denosumab on trabecular bone: Results of a pilot study in children with Osteogenesis imperfecta.** Mirko Rehberg<sup>1</sup>, Oliver Semler<sup>1</sup>, Heike Hoyer-Kuhn<sup>1</sup>, Eckard Schönau<sup>1</sup>, Renaud Winzenrieth<sup>\*2</sup>.

<sup>1</sup>Children's Hospital, University of Cologne, Germany, <sup>2</sup>R&D department, Med-Imaps SASU, France

### Background:

Osteogenesis imperfecta (OI) is a hereditary connective tissue disorder due to mutations related to collagen type 1. OI presents itself with low bone mass, resulting in high bone fragility. Bone mass is relevant for determination of the severity of OI. Although bisphosphonate treatment is able to increase areal bone mineral density (aBMD) measured by DXA, there is no correlation to fracture rates.

### Objective and hypotheses:

The aim of this study was to retrospectively analyze the trabecular bone score (TBS) in children with OI, who were treated with bisphosphonates during the first year and with Denosumab (Dmab) during the second year.

### Method:

3 DXA scans (GE lunar iDXA, lumbar spine) of 6 children (4 boys and 2 girls) with OI were performed at intervals of 12 months each. The first 2 scans were carried out during bisphosphonate treatment. The last was performed after 1 year of Dmab treatment. Pseudo volumetric BMD (3D BMD) was calculated based on cylindrical model proposed by Kroeger et al. (Bone Mineral, 1992). Pediatric TBS assessment was realized with a custom version of TBS iSight (Med-Imaps SASU, France) that includes a dedicated soft tissue correction for pediatric subjects based on ex-vivo data and taking into account spine tissue thickness and acquisition mode. TBS, areal BMD (aBMD) and 3D BMD variations at lumbar spine were expressed in % from baseline and normalized at 12 and 24 months.

### Results:

Mean age, Height and Weight Z-scores of patient were 6.5[3.9-9.3] yrs, -3.7[-9.4 - -0.2] SD, -1.8[-3.5 - -1.1] respectively. DXA assessment showed a mean increase in aBMD and 3D BMD of 8.9%/17.6% and 6.1%/18.4% after 12/24 months respectively. TBS exhibited a less marked increase of 1.7/3.4%. In single case analysis there is a difference between trends of aBMD and TBS.

### Conclusion:

In our pilot trial no correlations between TBS and DXA parameters have been observed. The minimal increase of TBS demonstrates a stronger effect of antiresorptive drugs on cortical than trabecular bone. Even without available reference data at the moment TBS offers the possibility to analyze trabecular bone in more detail without a bone biopsy.

**Disclosures:** Renaud Winzenrieth, None.

## MO0038

**Fibrogenesis Imperfecta Ossium and Response to human growth hormone: A potential novel therapy.** Sanjay Bhadada<sup>\*1</sup>, Vandana Dhiman<sup>1</sup>, Soham Mukherjee<sup>1</sup>, Sameer Aggarwal<sup>1</sup>, Amanjit Bal<sup>1</sup>, N khandelwal<sup>1</sup>, Anil bhansali<sup>1</sup>, D. Sudhaker Rao<sup>2</sup>. <sup>1</sup>PGIMER, Chandigarh, India, India, <sup>2</sup>Henry Ford Hospital, USA, United states

Background Fibrogenesis imperfecta ossium (FIO) is a rare metabolic bone disease clinically manifested by generalized bone pain and fragility fractures and osteomalacia on bone biopsy. The pathogenesis of the disease is unknown and there is no effective therapy. Patients and Methods Two affected middle aged sibling were in detail with clinical, biochemical, radiological and bone histologic (light and transmission microscopy and histomorphometry) investigations. Both patients were treated with recombinant human growth hormone (rhGH), which has not been tried before. Result Except for grossly (highly) elevated serum alkaline phosphatase (ALP) levels in both patients, routine and hormonal investigation were normal. Radiographs and bone scans revealed pseudo fractures in the scapulae and fibula. Bone biopsy showed severe osteomalacia with disorganized collagen fibril alignment. Treatment with rhGH was followed by remarkable clinical, biochemical, and radiological improvement in both patients. Further, there was reversal of the mineralization defect and restoration of collagen fibril arrangement. Conclusion: We report two cases of FIO in male siblings, and demonstrate, for the first time, remarkable clinical improvement and restoration of abnormal bone histology with rhGH therapy. We suggest that growth hormone

offers a potential novel therapy for FIO.

**Background:** Fibrogenesis imperfecta ossium (FIO) is a rare metabolic bone disease clinically manifested by generalized bone pain and fragility fractures, and osteomalacia on bone biopsy. The pathogenesis of the disease is unknown and there is no effective therapy.

**Patients and Methods:** Two affected middle aged siblings were studied in detail with clinical, biochemical, radiological, and bone histologic (light and transmission electron microscopy, and histomorphometry) investigations. Both patients were treated with recombinant human growth hormone (rhGH), which has not been tried before.

**Results:** Except for grossly (highly) elevated serum alkaline phosphatase (ALP) levels in both patients, routine and hormonal investigations were normal. Radiographs and bone scans revealed pseudo fractures in the scapulae, and fibula. Bone biopsy showed severe osteomalacia with disorganized collagen fibril alignment. Treatment with rhGH was followed by remarkable clinical, biochemical, and radiological improvement in both patients. Further, there was reversal of the mineralization defect and restoration of collagen fibril arrangement.

**Conclusion:** We report two cases of FIO in male siblings, and demonstrate, for the first time, remarkable clinical improvement and restoration of abnormal bone histology with rhGH therapy. We suggest that growth hormone offers a potential novel therapy for FIO.

figure

**Disclosures:** Sanjay Bhadada, None.

## MO0039

**Discovery of a Novel, Bone-like Blood Particle: Identification and Characterization of Ossified Particles in the Peripheral Circulation of Humans.** Rhonda Prisby<sup>\*1</sup>, Lynn Opdenaker<sup>2</sup>, Mary Ann McLane<sup>1</sup>, Sophie Guderian<sup>1</sup>. <sup>1</sup>University of Delaware, United states, <sup>2</sup>Helen F. Graham Cancer Center & Research Institute, United states

Ossification of bone marrow blood vessels occurs in both rodents and humans and presumably create ossified particles (OSP) that can be observed at ultra-high magnification. Further, an OSP was observed within a rat aorta, suggesting that OSP circulate within the blood. We introduce and characterize novel, circulating blood particles with similar composition to bone. Whole blood samples were collected from younger (n=4; 26-39 years) and older (n=4; 55-63 years) female subjects. One mL of blood was processed for flow cytometry. OSP were quantified and sorted. The composition of OSP was assessed with an elemental analysis detector and scanning electron microphotographs were used to determine diameter with Image J. Diameters, from OSP representing 4-7% of the total count, were assessed from 2 subjects/group. Complete blood counts were determined with a Coulter® Ac-T diff™ Analyzer (Beckman Coulter) to examine: white blood cells (WBC,  $\times 10^3/\mu\text{L}$ ), percent lymphocytes (LY%), percent monocytes (MO%), percent granulocytes (GR%), lymphocyte number (LY#,  $\times 10^3/\mu\text{L}$ ), monocyte number (MO#,  $\times 10^3/\mu\text{L}$ ), granulocyte number (GR#,  $\times 10^3/\mu\text{L}$ ), red blood cells (RBC,  $\times 10^6/\mu\text{L}$ ), hemoglobin (Hgb, g/dL), hematocrit (Hct, %) and platelet count (Plt,  $\times 10^3/\mu\text{L}$ ). OSP were observed in the younger ( $1288 \pm 136$  per 500  $\mu\text{L}$ ) and older ( $1766 \pm 370$  per 500  $\mu\text{L}$ ) groups, Figure 1. Diameters ranged from 1–28 $\mu\text{m}$  (younger) and 2–59 $\mu\text{m}$  (older). OSP occurred in higher frequencies at diameters of 0–5 $\mu\text{m}$  (younger,  $33.0 \pm 12.0$  and old,  $52.5 \pm 8.8$ ), 5–10 $\mu\text{m}$  (younger,  $13.5 \pm 3.2$  and old,  $27.0 \pm 0.0$ ;  $p=0.09$ ) and 10–15 $\mu\text{m}$  (younger,  $5.0 \pm 2.8$  and old,  $6.5 \pm 1.1$ ). The number of OSP 25–30 $\mu\text{m}$  tended ( $p=0.09$ ) to be higher in older ( $2.0 \pm 0.0$ ) vs. younger ( $0.5 \pm 0.5$ ) subjects, and 14 and 8 OSP were >15 $\mu\text{m}$ , respectively. Extrapolation of OSP count to an average adult blood volume calculates between ~10–28 million per 5L. OSPs contain pockets of calcium, and some have sharp, jagged or rough edges. Hematological parameters were within normal adult ranges and no differences were observed between groups. However, LY# tended ( $p=0.07$ ) to be lower in older ( $1.5 \pm 0.1 \times 10^3/\mu\text{L}$ ) vs. younger ( $2.4 \pm 0.3 \times 10^3/\mu\text{L}$ ) subjects. This is the first report of bone-like, ossified blood particles found in the peripheral circulation of relatively healthy humans. OSP may be diagnostic of bone marrow blood vessel ossification, associate with cardiovascular disease (i.e., endothelial cell damage, atherosclerosis, etc.), serve as emboli or contribute to ectopic bone formation.

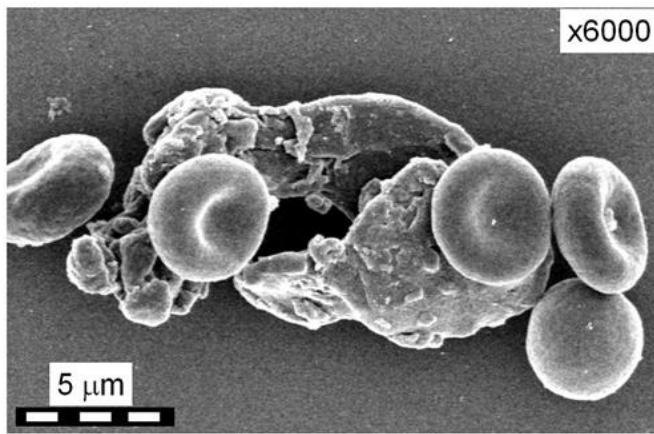


**Figure 1.** An ossified particle (OSP) among red blood cells in the peripheral circulation.

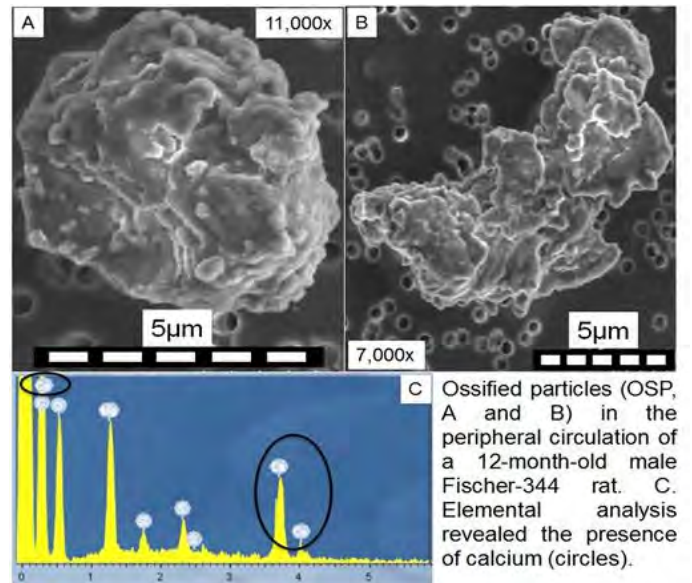
Figure 1

Disclosures: Rhonda Prisby, None.

## MO0040

**Novel, Bone-like Ossified Particles in the Peripheral Circulation of Male Fischer-344 Rats.** [Sophie Guderian\\*](#), [Seungyong Lee](#), [Rhonda Prisby](#), University of Delaware, United states

**BACKGROUND:** We previously reported bone marrow blood vessel [BMBV] ossification (i.e., the conversion of bone marrow blood vessels into bone) across the lifespan in male Fischer-344 rats (Prisby, 2014; Guderian, ASBMR 2015). Augmented BMBV ossification at 24 months coincided with reduced trabecular bone volume and several hematological parameters (i.e., RBC, Hgb, Hct and %LY). Further, examination of ossified BMBV under ultra-high magnification revealed the presence of presumed ossified particles (OSP) at the abluminal and luminal surfaces. **PURPOSE:** We sought to assess whether OSP were present in the peripheral circulation. **METHODS:** Ventricular whole blood samples were collected from male Fischer-344 rats (1-mon, n=4; 12-mon, n=4 and 24-mon, n=5) and processed to identify OSP. OSP were quantified and sorted with a BD FACSAria II flow cytometer. Sorted particles were subsequently imaged with confocal and scanning electron microscopy. The composition of OSP were determined via elemental analysis. OSP diameter and size distribution were assessed from 2 rats per group utilizing SEM microphotographs and Image J. **RESULTS:** Body mass ( $p < 0.05$ ) increased with age between 1- and 12-mon. OSP were observed at all ages (1-mon,  $2283 \pm 511$  per 500  $\mu\text{L}$ ; 12-mon  $7922 \pm 1905$  per 500  $\mu\text{L}$  and 24-mon  $3181 \pm 997$  per 500  $\mu\text{L}$ ), peaking at 12-mon ( $p < 0.05$  vs. 1-mon and 24-mon). The diameters of OSP ranged from 1–30 $\mu\text{m}$  (1-mon), 1–33 $\mu\text{m}$  (12-mon) and 1–16 $\mu\text{m}$  (24-mon). The frequency of OSP ranging in diameter from 0–5 $\mu\text{m}$  (1-mon, 32; 12-mon, 32; and 24-mon, 61), 5–10 $\mu\text{m}$  (1-mon, 4; 12-mon, 13; and 24-mon, 7) and 10–15  $\mu\text{m}$  (1-mon, 2; 12-mon, 5; and 24-mon, 3) were similar among groups. OSP > 15  $\mu\text{m}$  were observed at all ages (1-mon, 2; 12-mon, 4; and 24-mon, 1). OSP contained calcium as assessed via elemental analysis and, morphologically, some OSP had rough and jagged edges. Extrapolated values of OSP count in the circulation according to an average blood volume for a rat (i.e., 64ml/kg BW) are ~45,000 (1-mon), ~428,000 (12-mon) and ~162,000 (24-mon). **CONCLUSION:** This is the first report of bone-like particles in the peripheral circulation of rats. OSP > 15  $\mu\text{m}$  may serve as emboli to small blood vessels, increasing the risk of blockage. At minimum, the rough morphology of OSP may contribute to damage of the endothelial cell lining. Finally, circulating OSP may contribute to ectopic bone formation if they gain access to soft peripheral tissues.



ASBMR 2016 OSP

Disclosures: Sophie Guderian, None.

## MO0041

**Transcriptomic Analysis of Mouse Calvarial Cells Stimulated by Megakaryocytes Reveals Changes in Macrophage Activity and Angiogenic Gene Networks.** [Paul Childress\\*](#)<sup>1</sup>, [Nabarun Chakraborty](#)<sup>2</sup>, [Marta Alvarez](#)<sup>1</sup>, [Evan Himes](#)<sup>1</sup>, [Angela Bruzzaniti](#)<sup>3</sup>, [Edward Srour](#)<sup>4</sup>, [Duncan Donohue](#)<sup>2</sup>, [Rasha Hammamieh](#)<sup>2</sup>, [Melissa Kacena](#)<sup>1</sup>. <sup>1</sup>Department of Orthopaedic Surgery, Indiana University School of Medicine, United states, <sup>2</sup>US Army Center for Environmental Health Research, United states, <sup>3</sup>Department of Biomedical & Applied Sciences, Indiana University School of Dentistry, United states, <sup>4</sup>Department of Medicine, Indiana University School of Medicine, United states

There remains an unmet need for bone anabolic therapies. It is now well established that megakaryocytes (MK) positively influence bone mass, but the molecular pathways which mediate their actions are incompletely understood. We have shown that bone marrow transplants from *Gata-1* deficient mice (resulting in megakaryocytosis) increases medullary trabecular bone mass in wild-type recipients. Also, MK have a profound proliferative effect on osteal macrophages (also known as osteomacs or OM), and osteoblasts (OB) isolated from mouse calvaria. We hypothesized that the MK-mediated stimulation of both OM and OB cell populations results in bone formation. To explore the molecular mechanisms mediating the anabolic activity of MK, we examined differentially expressed genes (DEG) using whole genome microarray. Specifically, we cultured collagenase digested mouse calvarial cells (containing both OM and OB) in the presence or absence of MK. After 4 days, OM and OB were sorted by FACS to obtain CD45<sup>+</sup>F4/80<sup>+</sup> OM and CD45<sup>+</sup>F4/80<sup>-</sup> OB populations. Transcriptomic analyses revealed a larger increase in DEG in the OM population (777 genes) compared to the OB population (98 genes) with a p-value cutoff of  $p < 0.001$ . Additionally, only 5 common DEG were found in the OM and OB populations, indicating stimulation of distinct transcription profiles by MK coculture. Our previous work demonstrated that cell-cell contact is required for MK-induced enhancement of proliferation. Thus, we examined DEG known to be associated with the plasma membrane and/or extracellular space. We identified 292 DEG from the OM population compared to 34 DEG from OB. Of the 34 DEG from OB, 14 are associated with the activation, recruitment, or proliferation of macrophages. Importantly, *Csf1* (colony stimulating factor 1) was among the OB DEG. Conversely, OM-derived DEG include *Csf1r* (colony stimulating factor 1 receptor). Gene Ontology analysis of DEG from OM also yielded significant enrichment for genes involved in enzyme-linked signal transduction, angiogenesis, and biological adhesion. These results suggest MK stimulate OB to increase OM number (possibly via the *Csf1*-*Csf1r* axis). As OM have an increased angiogenic signature, and angiogenesis is a precursor to bone growth, our data suggest a novel pathway by which MK act through OB and OM to regulate anabolic bone formation. These novel targets may be favorable for pharmacological intervention for bone loss diseases.

Disclosures: Paul Childress, None.

**MO0042**

**Osteal Macrophages are Strategically Distributed within Activated Periosteum to Support Bone Regenerative Mechanisms.** Kylie Alexander<sup>1</sup>, Liza-Jane Raggatt<sup>2</sup>, Andy Wu<sup>1</sup>, Ming-Kang Chang<sup>3</sup>, Lena Batoon<sup>2</sup>, Susan Millard<sup>2</sup>, David Hume<sup>4</sup>, Allison Pettit<sup>\*2</sup>. <sup>1</sup>The University of Queensland - Centre for Clinical Research, Australia, <sup>2</sup>Mater Research Institute - The University of Queensland, Australia, <sup>3</sup>Institute for Molecular Bioscience, The University of Queensland, Australia, <sup>4</sup>The Roslin Institute & University of Edinburgh, United Kingdom

Characterization of periosteal cell composition is needed to improve knowledge of bone growth and regeneration mechanisms. The importance of osteal macrophages (osteomacs) to bone biology is established but their distribution and phenotype within periosteum has not been specifically investigated. We used an immunohistochemistry approach to characterise macrophages in growing murine bone and within activated periosteum induced in mouse model of bone injury as well as fracture induced periosteal callus. F4/80<sup>+</sup> osteomacs were distributed throughout resting periosteum. Metaphyseal periosteum also contained a second resident macrophage population that did not meet minimal osteomac criteria. Osteomacs also intimately associate with sites of periosteal diaphyseal and metaphyseal bone dynamics during normal long bone growth. At simple modeling tracks in diaphyseal periosteum the osteomacs were F4/80<sup>+</sup>Mac-2<sup>low</sup>, which recapitulates endosteal osteomac phenotypes at modeling sites. Interestingly their morphology and spatial organization varied subtly, which likely reflects the greater structural complexity of periosteum. We also demonstrated that osteomacs (F4/80<sup>+</sup>Mac-2<sup>low</sup> cell within 3 cell diameters of bone surface), resident macrophages (F4/80<sup>+</sup>Mac-2<sup>low</sup> cell greater than 3 cell diameters of bone surface) and inflammatory macrophages (F4/80<sup>+</sup>Mac-2<sup>hi</sup>) were associated with the complex bone dynamics occurring within the periosteum at the metaphyseal corticalization zone. These 3 macrophage subsets were also present at high frequency within activated native periosteum after tibial bone injury across a 9 day time course that spanned the inflammatory through remodeling healing phases. Additionally, mapping of osteomac/macrophage distribution in a pre-clinical femoral fracture model that heals by periosteal endochondral callus formation demonstrated enrichment of activated osteomacs/macrophages during the inflammatory and early anabolic phase with transition to homeostatic osteomacs during the late anabolic phase. These observations confirm that osteomacs are key components of both osteal tissues, in spite of salient differences between endosteal and periosteal structure and local environment. Demonstration of osteomac activation at sites of complex bone dynamics indicates functional specialization of osteomacs depending on the site-specific bone mechanisms. Overall, osteomac contributions must be considered when investigating the regenerative potential of periosteum.

*Disclosures: Allison Pettit, None.*

**MO0043**

**DPP4-Cleaved SDF-1 inhibits CXCR4 mediated Migration of BMSCs.** Alexandra Aguilar-Perez<sup>\*1</sup>, Sudharsan Periyasamy-Thandavan<sup>2</sup>, Mark Hamrick<sup>2</sup>, Carlos Isaacs<sup>2</sup>, Brian Volkman<sup>3</sup>, Luis Cubano<sup>4</sup>, William Hill<sup>2</sup>. <sup>1</sup>Universidad Central del Caribe & Augusta University, United states, <sup>2</sup>Augusta University, United states, <sup>3</sup>Medical College of Wisconsin, United states, <sup>4</sup>Universidad Central del Caribe, United states

Osteoporosis and osteopenia are a public health risk for 55% of the population 50 years of age and older. Increasing evidence supports that aging-related bone loss is a stem cell disease. We have previously identified stromal cell-derived factor 1 (SDF-1 or CXCL12) as a key molecule in the regulation of bone marrow mesenchymal stem cell (BMSC) homeostasis. Full length (un-cleaved) SDF-1 activation of CXCR4 plays a role in the control of BMSC osteogenesis by regulating BMP2 signaling. SDF-1 is required for BMSC survival, differentiation and migration. SDF-1 is rapidly inactivated by proteolytic cleavage starting with a rate limiting N-terminal loss of the first two amino acids by the exopeptidase dipeptidyl peptidase-4 (DPP4). In addition to soluble DPP4 bone marrow cells express cell surface DPP4 (CD26) whose activity is tightly regulated. Of interest DPP4-cleaved SDF-1 is not inactive, but rather appears to have an altered bioactivity that inhibits SDF-1 mediated BMSC migration. We performed transwell migration assays to assess the bioactivity of SDF-1 and DPP4-cleaved SDF-1. BMSCs were placed in the upper chamber following exposure to either the CXCR4 inhibitor AMD3100 (400µM), DPP4-cleaved SDF-1 (100ng/ml) or saline for 4 hours. Different concentrations of SDF-1 (1, 2.5, 10, 50 & 100 ng/ml) were added to the lower chamber. Both pre-treatment with AMD3100 or DPP4-cleaved SDF-1 blocked migration in response to SDF-1. Migration to 1-10 ng/ml of SDF-1 was completely blocked by DPP4-cleaved SDF-1 and AMD3100. AMD3100 and to an even greater extent, DPP4-cleaved SDF-1, significantly decreased migration toward 50ng/mL (p<0.05 & p<0.001) and 100ng/mL (p<0.001 & p<0.001) of SDF-1. The altered bioactivity of DPP4-cleaved SDF-1 has implications not only for BMSC function and bone homeostasis, but may play critical roles in SDF-1 mediated functions more broadly, including in development and cancer biology. This also has implications in the potential of DPP4 inhibitors developed for diabetes therapy to affect bone homeostasis.

*Disclosures: Alexandra Aguilar-Perez, None.*

**MO0044**

**Dysregulated Runx2 expression, Extra cellular Membrane Vesicles and Vitamin D Deficiency Drive the Vicious Cycle in Osteosarcoma Bone Microenvironment and Increase Tumor Burden.** Rama Garimella<sup>\*1</sup>, John Keighley<sup>2</sup>, Sumedha Gunewardena<sup>3</sup>, Ossama Tawfik<sup>4</sup>, Peter Rowe<sup>5</sup>, Peter Van Veldhuizen<sup>6</sup>. <sup>1</sup>Midwest Biomedical Research Foundation, United states, <sup>2</sup>Biostatistics, The University of Kansas Medical Center, United states, <sup>3</sup>Molecular & Integrative Physiology, The University of Kansas Medical Center, United states, <sup>4</sup>Pathology & Laboratory Medicine, The University of Kansas Medical Center, United states, <sup>5</sup>The Kidney Institute, The University of Kansas Medical Center, United states, <sup>6</sup>Sarah Cannon HCA Midwest Health Cancer Network, United states

Osteosarcoma (OS) is an aggressive malignancy of bone affecting children and adolescents. Emerging genomic and molecular data reveal amplification-related overexpression of Runx2 along with aberrations in vitamin D regulatory system. Several reports indicate that OS patients have decreased bone density, and increased incidence of pathological fractures and poor survival prognosis due to increased risk for lung metastasis. To study OS pathobiology, we developed a preclinical bioluminescent osteosarcoma orthotopic mouse (BOOM) model and detected increased expression of Runx2 and Runx2 target genes in OS tissue samples. Our recent data show evidence of oncogenic osteomalacia and the role of vitamin D-Runx2 interactomes in OS pathobiology, which include: (a) aberrant expression of genes and proteins for vitamin D receptors, enzymes and FGF23 in OS cells and tissue microarrays; (b) presence of unmineralized osteoid, dysregulated expression of matrix remodeling proteins such as MMP-1, and -13, and detection of osteoblastic and osteolytic lesions in the tumor tissue of the BOOM model; (c) generation of extra cellular membrane vesicles (EMVs) from 143B OS cells which harbor pro-osteoclastic cargo and Runx2 target gene products; (d) vitamin D treatment of 143B OS cells inhibited Runx2 modulators or targets such as FGF1, FGF12, BMP1, MEPE, SMARCA4, PTH, ESRI, CCR1, ITGB4 that interact with inflammatory, oxidative stress and membrane vesicle biogenesis pathways; and (e) vitamin D supplementation inhibited the kinetics of tumor progression in the BOOM model. Pilot study investigating the impact of vitamin D deficiency in the BOOM model revealed increased overall tumor burden with increased serum osteoprotegerin (OPG) levels in vitamin D-deficient and -standard groups vs. -enriched group. Results from pilot data suggest that vitamin D deficiency enhanced neoplastic properties of OS cells directly by promoting both intra-osseous growth and pulmonary metastasis or indirectly by driving the vicious cycle in bone tumor microenvironment via increased expression of Runx2 target i.e. osteoprotegerin, which is a biomarker for bone remodeling and inflammation. Therapies targeting vitamin D deficiency and FGF23/Runx2/OPG axis will inhibit vicious cycle induced bone destruction and reduce tumor burden due to inflammation, oxidative stress and EMV biogenesis and improve survival outcomes in OS.

*Disclosures: Rama Garimella, None.*

**MO0045**

**Increased TAF12 in Myeloma Cells and Bone Marrow Stromal Cells Enhances Myeloma Growth and Osteoclast Formation in Response to Physiologic Levels of 1,25-dihydroxy Vitamin D.** Yasuhiro Ohata<sup>\*1</sup>, Yuki Nagata<sup>1</sup>, John Chirgwin<sup>2</sup>, David Roodman<sup>3</sup>, Noriyoshi Kurihara<sup>1</sup>. <sup>1</sup>Medicine / Hematology-Oncology, Indiana University, United states, <sup>2</sup>Medicine / Endocrinology, Indiana University; Roudebush VA Medical Center, United states, <sup>3</sup>Medicine / Hematology-Oncology, Indiana University; Roudebush VA Medical Center, United states

Multiple myeloma (MM) is characterized by extensive bone destruction that is a major source of morbidity and mortality. We found that TAF12, a factor which binds VDR and increases responsiveness to 1,25D<sub>3</sub>, is highly expressed in patient MM cells and bone marrow stromal cells (BMSC) compared to normals. Co-culture of normal human BMSC with patient MM cells increased TAF12 expression in the BMSC. We treated patient MM cells with physiologic concentrations (10<sup>-10</sup>M) of 1,25D<sub>3</sub> and found increased CYP24A1, RANKL, VEGF, α4β1 and DKK1 expression. Similarly, TAF12 was highly expressed in MM cell lines (MM1.S, JJJ3, ANBL6, RPMI8226, U266 and OPM2), and 1,25D<sub>3</sub> treatment (10<sup>-10</sup>M) of JJJ3 and MM1.S cells increased RANKL, IL-6 and VEGF, DKK-1 and α4 integrin expression. We then stably knocked-down (k/d) TAF12 in JJJ3 cells (TAF12k/d-JJJ3). TAF12 protein expression was decreased by 60% compared to JJJ3 infected with a control shRNA (C-JJJ3). 1,25D<sub>3</sub> treatment (10<sup>-10</sup>M) increased CYP24A1 mRNA in C-JJJ3 cells, but not in TAF12k/d-JJJ3. Interestingly, VDR content in 1,25D<sub>3</sub> treated TAF12k/d-JJJ3 was markedly decreased as compared to C-JJJ3 cells. To determine the mechanisms responsible for increase VDR expression, we assessed if TAF12 increases the stability of VDR with 1,25D<sub>3</sub> treatment. VDR half-life in cycloheximide-treated TAF12k/d-JJJ3 and C-JJJ3 was examined. 1,25D<sub>3</sub> (10<sup>-10</sup>M) increased VDR in C-JJJ3 but not in TAF12k/d-JJJ3 cells. Further, RANKL, VEGF, DKK1 and α4 integrin production by TAF12k/d-JJJ3 treated with 1,25D<sub>3</sub> (10<sup>-10</sup>M) was decreased by 60% compared to C-JJJ3 cells. Co-culture of C-JJJ3 with BMSC treated with 1,25D<sub>3</sub> induced both MM cell growth and MM cell adhesion to BMSC. However, BMSC co-cultured with TAF12k/d-JJJ3 had decreased MM cell growth and cell adhesion compared to C-JJJ3 cells. 1,25D<sub>3</sub> treatment of human osteoclast (OCL)

precursors co-cultured with C-JJN3, but not TAF12k/d-JJN3, increased OCL formation, consistent with their production of RANKL. Thus increased TAF12 in MM cells and cells in their microenvironment enhances MM cell growth and osteoclast formation. Blocking TAF12-VDR interactions may be a novel therapeutic approach for MM bone disease.

**Disclosures:** Yasuhisa Ohata, None.

## MO0046

**Protective Role of Paget's Disease of Bone Against Skeletal Metastasis from Solid Tumors: Clinical and Experimental Evidences.** DANIELA MERLOTTI\*<sup>1</sup>, Nadia Rucci<sup>2</sup>, Marco Di Stefano<sup>3</sup>, Domenico Rendina<sup>4</sup>, Simone Biancardi<sup>5</sup>, Isabella Anna Evangelista<sup>5</sup>, Antonio Crisias<sup>6</sup>, Argia Ucci<sup>2</sup>, Stefano Rotatori<sup>5</sup>, Simone Cenci<sup>7</sup>, Pasquale Strazzullo<sup>4</sup>, Giancarlo Isaia<sup>6</sup>, Ranuccio Nuti<sup>5</sup>, Anna Teti<sup>2</sup>, Luigi Gennari<sup>5</sup>. <sup>1</sup>Division of Genetics & Cell Biology, San Raffaele Scientific Institute - <sup>2</sup>Department of Medicine, Surgery & Neurosciences, University of Siena, Italy, <sup>2</sup>Department of Biotechnological & Applied Clinical Sciences, University of L'Aquila, Italy, <sup>3</sup>Gerontology Section Department of Medical Sciences, University of Turin, Italy, <sup>4</sup>Department of Clinical & Experimental Medicine, Federico II University, Naples, Italy, <sup>5</sup>Department of Medicine, Surgery & Neurosciences, University of Siena, Italy, <sup>6</sup>Gerontology Section, Department of Medical Sciences, University of Turin, Italy, <sup>7</sup>Division of Genetics & Cell Biology, San Raffaele Scientific Institute, Milan, Italy

Paget's disease of bone (PDB) is a common skeletal disorder characterized by focal areas of excessive and rapid bone resorption and formation, leading to bone pain, deformity and fractures. Despite the well documented increase in the risk of primary bone tumors due to neoplastic degeneration of pagetic tissue, a previous retrospective analysis suggested that patients with prostate cancer and PDB have delayed time to skeletal metastases (SM) and improved overall survival than do patients with prostate cancer alone (Br J Cancer 2012;107:646-51). This association is unexpected since metastatic cells preferentially seed in skeletal sites under active turnover and increased bone turnover markers have been consistently related with negative clinical outcomes and increased bone metastasization from prostate cancer or other solid tumors. Based on this observation, we performed a survey of clinical databases in 985 patients from the Italian PDB Registry (of whom 99 with documented prostate or breast cancer). We observed a significantly decreased overall prevalence of SM from both tumors (5/99, 5.0%) with respect to the estimates from the general population. In the 46 cases with the occurrence of cancer after the diagnosis of PDB, none of them had SM at diagnosis and only 2 cases developed SM after 4 and 12 yrs (overall mean observation period of 12.5±7.7 yrs). In the remaining 53 cases the diagnosis of cancer was performed before (n=35, with 2 cases with SM) or contemporary (n=18, with 1 case with SM) to the onset of PDB. Although bisphosphonate treatment might explain at least in part the reduced occurrence of SM, we did not evidence significant differences when patients treated with or without aminobisphosphonates were considered, and most of treated patients only had a single treatment course with for PDB. Consistent with the above clinical evidences, in a preliminary *in vitro* analysis, the serum and the conditioned media (CM) from osteoclasts derived from peripheral blood leucocytes of patients with active PDB was able to decrease the proliferation of the osteotropic breast cancer cell line MDA-MB-231, as assessed by the MTT test, with respect to CM of controls. Taken together, these results indicate that PDB patients may have a distinct bone condition or a unique bone microenvironment that protects them from bone metastasis and strongly encourage further analyses in order to identify the underlying molecular mechanisms.

**Disclosures:** DANIELA MERLOTTI, None.

## MO0047

**MIF Stimulates Osteoclastic Bone Resorption in Breast Cancer Bone Metastasis.** Jessica Grunda<sup>1</sup>, Charlotte Cialek<sup>2</sup>, Katrina Clines<sup>2</sup>, Renee Desmond<sup>1</sup>, Rosa Serra<sup>1</sup>, Janet Cross<sup>3</sup>, Gregory Clines\*<sup>2</sup>. <sup>1</sup>University of Alabama at Birmingham, United states, <sup>2</sup>University of Michigan, United states, <sup>3</sup>University of Virginia, United states

Macrophage migration inhibitory factor (MIF) is a pro-migratory and inflammatory chemokine implicated in multiple pathological conditions. MIF activates CXCR4 and CD74 signaling, and possesses phenylpyruvate tautomerase activity. Tumor expression of MIF enhances cellular invasion and has been associated with increased cancer metastasis in animal and human studies. Bone metastasis is common in advanced breast cancer, but it was unknown the extent to which MIF is involved in this metastatic process. Published data also support a role of MIF in bone homeostasis. MIF knockout mice had impaired bone formation and resorption. In contrast, overexpression of MIF increased the rate of bone turnover and formation.

We investigated the actions of MIF in breast cancer bone metastasis. Empty vector (EV) and MIF knockdown (MIF KD) cell lines were generated from the parental breast cancer cell line MDA-MB-231. *In vitro* proliferation, apoptosis, and mRNA expression of breast cancer-secreted factors that regulate the skeletal response to

breast cancer were not changed in MIF KD compared to EV cells. The effects of MIF KD were next investigated in an animal model of breast cancer bone metastasis. Characteristic osteolytic lesions were radiographically detected as early as 14 days after intracardiac inoculation of MIF KD and EV MDA-MB-231 cells. Although survival was not different in animals inoculated with MIF KD and EV cells, the number of radiographic osteolytic bone lesions was fewer in the MIF KD vs. the EV group at the first radiographic time point post-inoculation. In histomorphometric analyses, bone tumor area and osteoclast density was less in the MIF KD compared to the EV group.

We next investigated the mechanisms of the *in vivo* findings. *In vitro* invasion assays were performed and we found a modest effect of reduced invasion in the MIF KD compared to EV cells. We next examined the effects of MIF on *in vitro* osteoclastogenesis. MIF treatment of bone marrow-derived osteoclasts revealed a marked dose-response increase in osteoclast formation. In summary, we now present evidence that breast cancer-secreted MIF is not a direct target of breast cancer cells, but MIF increases osteoclastogenesis and therefore alters the bone microenvironment providing a more hospitable environment for breast cancer cells metastatic to bone.

**Disclosures:** Gregory Clines, None.

## MO0048

**Runx2-mediated autophagy promotes survival of bone metastatic breast cancer cells.** Ahmad Othman\*, Manish Tandon, Jitesh Pratap. Rush University Medical Center, United states

Metastasis to bone is a frequent complication associated with breast cancer. During metastasis, cancer cells induce autophagy to survive metabolic stress including starvation, growth factors deprivation and hypoxia. Autophagy is a highly regulated process by which cytoplasmic components are degraded by the lysosome and nutrients are recycled to support cellular metabolism. Here, we identify a relationship between autophagy and Runx2 transcription factor. We used a bone metastatic isogenic variant of breast cancer MDA-MB-231 cells isolated from a xenograft tumor mouse model of metastasis. Previous studies showed that Runx2 promotes cell survival, invasion, and osteolysis associated with breast cancer. We show that Runx2 promotes autophagy in bone metastatic cancer cells as examined by measuring levels of microtubule associated protein light chain 3 (LC3), a key readout of autophagic flux, with western blot and immunofluorescence analyses. We show that knockdown of Runx2 impaired autophagic flux in bone metastatic cells in response to glucose-deprivation. We validated Runx2-mediated autophagy in embryonic fibroblastic cells from wild type and Runx2 knockout mice under starvation conditions. Surprisingly, no significant changes were observed in mRNA levels of key components of the autophagy pathway suggesting a novel non-transcriptional function of Runx2 in autophagy. Protein analysis of upstream stress signaling pathways revealed increased AMP-activated protein kinase (AMPK) activity with Runx2 knockdown or treatment with chloroquine, an inhibitor of autophagic pathway. Importantly, block in autophagic flux by Runx2 knockdown can be rescued by metformin, an AMPK activator or HDAC inhibitor, trichostatin A. Furthermore, inhibition of Erk1/2 signaling in bone-metastatic cells significantly decreased autophagic flux in control cells compared to Runx2 knockdown cells. These results suggest a crosstalk among Runx2, Erk1/2 survival pathway, and metabolic stress signaling for regulation of autophagy in bone metastatic breast cancer cells. Finally, we show that combinatorial inhibition of Runx2 and autophagic flux reduces survival and migration of bone metastatic cells. Our studies reveal a novel regulatory network of Runx2-mediated autophagy for survival of bone metastatic cancer cells.

**Disclosures:** Ahmad Othman, None.

## MO0049

**Is Canine Osteosarcoma a Good Model for Human Osteosarcoma?** Awf Al-Khan\*<sup>1</sup>, Judith Nimmo<sup>2</sup>, Michael Day<sup>3</sup>, Stewart Ryan<sup>4</sup>, Barbara Bacci<sup>4</sup>, Samantha Richardson<sup>1</sup>, Janine Danks<sup>1</sup>. <sup>1</sup>School of Health & Biomedical Sciences, RMIT University, Australia, <sup>2</sup>Australian Specialised Animal Pathology Laboratory, Australia, <sup>3</sup>Comparative Pathology Laboratory, School of Veterinary Sciences, Bristol University, United Kingdom, <sup>4</sup>The University of Melbourne, School of Veterinary Sciences, Australia

Osteosarcoma (OS) is the most common malignant primary bone tumor in both humans and dogs. During the last 30 years, there has not been significant improvement in the treatment of OS or its prognosis. Due to its rare presentation in humans, OS research relies on use of animal models. Human OS can be differentiated from other cancers using immunohistochemistry (IHC). Canine OS is 20 times more prevalent than human OS and has a predilection for larger dogs of particular breeds. It appears to mimic human OS, suggesting that dogs may be a good natural model for human OS. This study aimed to determine whether canine OS is a good model for human OS, using of known panel of tumor markers. Thirty two paraffin wax-embedded canine OS tissues were collected from the archives of the Comparative Pathology Laboratory, School of Veterinary Sciences, University of Bristol, UK and from the Australian Specialised Animal Pathology Laboratory in Clayton Australia. These fixed tumor tissues were subjected to IHC that had previously been used to classify human OS (markers specific for vimentin, alkaline phosphatase, neuron specific enolase [NSE], desmin and S100), as reviewed in Gao,

Z., Kahn, L. B. (2005) *Skeletal Radiology*, 34, 755-70. Positive and negative controls were used in each assay. Vimentin and alkaline phosphatase were highly expressed in all 32 canine OSs. On the other hand, the expression of NSE was weak in 14/32 and negative in 11/32 of the cases. Desmin was expressed by the tumours in 21/32 cases and S100 in 30/32 of the cases. These data suggest that the canine OS may be a good model for human OS.

**Disclosures:** Awf Al-Khan, None.

## MO0050

**Runx1 is Obligatory for Mammary Epithelial Cell Morphology and Phenotype.** Deli Hong<sup>\*1</sup>, Terri Messier<sup>1</sup>, Andrew Fritz<sup>1</sup>, Jason Dobson<sup>2</sup>, Gillian Browne<sup>1</sup>, Janet Stein<sup>3</sup>, Jane Lian<sup>4</sup>, Gary Stein<sup>1</sup>. <sup>1</sup>University of Vermont, United states, <sup>2</sup>UMASS Medical School-Cell Biology, United states, <sup>3</sup>University of Vermont, United states, <sup>4</sup>University of Vermont, United states

**Introduction:** The family of Runx transcription factor are known to be associated with cancer phenotypes. Numerous studies reported the abnormal expression of Runx2 in breast cancer cells and that Runx2 drives bone metastasis, reflecting an oncogenic function in tumor cells. Runx1 translocation of Runx1 are well documented as a causative factor of leukemia. The recent recognition of Runx1 expression in normal periosteum, perichondrium and epithelial lining cells of glandular tissues suggests that Runx1 functions in maintaining integrity of those cell layers. A potential role for Runx1 in breast cancer was suggested, based on Runx1 being one of the top genes mutated in breast cancers. Runx1 levels are decreased in high-grade primary breast tumors compared to low/mid-grade tumors. Therefore, we raised the hypothesis that Runx1 is a tumor suppressor, functions to maintain the normal epithelial phenotype and that loss of Runx1 could promote epithelial to mesenchymal (EMT) and also increase the metastatic phenotype. **Methods:** We used two human breast cancer cell models systems, the MCF10A to MCF7/T47D and to MDA-MB-231 and the MCF10A progression model from normal-like mammary epithelial cells (MCF10A) to tumorigenic (MCF10AT1) and metastatic (MCF10CA1a) cells. **Results:** We observed that Runx1 protein and mRNA is decreased in tumorigenic cells. To understand Runx1 function, Runx1 was depleted by shRNA in mammary epithelial cells which resulted in disrupted/alterd cellular morphology, suppressed the epithelial gene E-cadherin and activated mesenchymal genes. To reinforce this observation, EMT was induced by addition of TGFβ1 or by growth factor depletion in MCF10A cells. A striking Runx1 decrease resulted, suggesting that Runx1 has a crucial role in preventing EMT. Further, Runx1 overexpression was performed in the metastatic MCF10CA1a cells and the cells acquired an epithelial phenotype. Our analysis of breast tumors and survival data supports the above finding that loss of Runx1 promotes tumor progression. The functional effects of Runx1 cellular modifications contributing to metastatic bone disease are currently being examined in-vivo.

**Conclusion and Impact:** Our results highlight an essential role for Runx1 in maintaining normal epithelial phenotype and preventing epithelial to mesenchymal transition as well as tumor progression in breast cancer. Identifying this Runx1 mechanism provides the basis for a novel strategy to treat early stage breast cancer.

**Disclosures:** Deli Hong, None.

## MO0051

**TBK1/IKKε Signaling Is a Novel Therapeutic Target In Multiple Myeloma-Induced Bone Disease.** Quanhong Sun<sup>\*1</sup>, Peng Zhang<sup>1</sup>, Deidra Balchak<sup>2</sup>, Juraj Adamik<sup>1</sup>, Valentina Marchica<sup>3</sup>, Nicola Giuliani<sup>4</sup>, Rebecca Silbermann<sup>5</sup>, G. David Roodman<sup>6</sup>, Deborah Galson<sup>1</sup>. <sup>1</sup>Department of Medicine, Hematology-Oncology Division, University of Pittsburgh Cancer Institute, McGowan Institute for Regenerative Medicine, University of Pittsburgh, PA, USA, United states, <sup>2</sup>Department of Medicine, Hematology-Oncology Division, University of Pittsburgh Cancer Institute, McGowan Institute for Regenerative Medicine, University of Pittsburgh, PA, USA; Carlow University, PA, USA, United states, <sup>3</sup>Myeloma Unit, Department of Clinical & Experimental Medicine, University of Parma, Italy, Italy, <sup>4</sup>Myeloma Unit, Department of Clinical & Experimental Medicine, University of Parma, Italy, United states, <sup>5</sup>Department of Medicine, Hematology-Oncology Division, Indiana University, Indianapolis, IN, USA, United states, <sup>6</sup>Department of Medicine, Hematology-Oncology Division, Indiana University, Indianapolis, IN, USA; Veterans Administration Medical Center, Indianapolis, IN, United states

Multiple myeloma (MM) is the most frequent cancer to involve the skeleton and remains incurable for most patients, thus novel therapies are needed. MM bone disease is characterized by osteolytic lesions that contribute significantly to patient morbidity and mortality. We showed that TBK1 signaling is a novel pathway that increases osteoclast (OCL) formation in Paget's disease, an inflammatory bone disease. Recently, we reported that TBK1 plays a similar role in the inflammatory

induction of OCL by MM using conditioned media (CM) from the human MM cell line MM1.S. MM-CM dose-dependently increased BM monocytes (BMM) expression of IL-6, RANK, and TBK1 mRNA, activated TBK1 protein, and enhanced RANKL-driven OCL formation. Blocking TBK1 signaling by shRNA significantly attenuated the ability of MM-CM to increase OCL differentiation without altering OCL differentiation in control media. The TBK1/IKKε inhibitors BX795 and Amlxanox (Amlx) also blocked OCL formation. Importantly, TBK1 mRNA expression in CD138+ plasma cells (PC) isolated from MM or PC leukemia patients is significantly higher as compared to PC from Monoclonal Gammopathy of Undetermined Significance (MGUS) patients. We tested whether targeting the TBK1/IKKε signaling pathways would also affect MM cells. We found that BX795 and Amlx strongly decreased the viability of several MM cell lines and primary MM cells in a dose-dependent manner, via induction of apoptosis. BX795 was 10x more potent than Amlx, but is a less specific inhibitor. BX795 and Amlx did not affect the viability of primary BMM, bone marrow stromal cells (BMSC), or splenocytes, except at the highest dose of BX795 (10 μM). These inhibitors also decreased MM cell adhesion to both human and mouse primary BMSC. Further, these inhibitors blocked primary BMSC expression of IL-6 and RANKL, thereby decreasing BMSC support of MM survival and OCL differentiation. Importantly, Amlx also synergizes with the proteasome inhibitor bortezomib, a highly effective anti-MM agent used clinically, and inhibited MM cell viability through induction of apoptosis in all MM cell lines assayed. These data suggest that targeting TBK1/IKKε signaling may decrease MM bone disease by both slowing MM growth and preventing MM-induced osteolysis.

**Disclosures:** Quanhong Sun, None.

## MO0052

**Bimodal NOTCH/HES1 Signaling Mediates Cartilage Catabolism and OA Progression via the JAK/STAT Pathway.** Yinshi Ren<sup>\*1</sup>, Jianquan Chen<sup>1</sup>, Zhaoyang Liu<sup>2</sup>, Anthony Mirando<sup>1</sup>, Matthew Hilton<sup>1</sup>. <sup>1</sup>duke university, United states, <sup>2</sup>University of Rochester Medical Center, United states

Osteoarthritis (OA) is a total joint disease characterized by articular cartilage degradation, synovial and joint inflammation, meniscus degeneration, and subchondral bone sclerosis. It afflicts nearly 1/3 of the US population aged 60 years or older resulting in healthcare costs exceeding \$35 billion annually. Since relatively little is known about the precise pathologic cellular and molecular mechanisms driving OA development and progression, the development of disease modifying osteoarthritis drugs (DMOADs) has been lagging. However, several aberrant molecular changes have been associated with human post-traumatic OA progression, including inappropriate NOTCH signaling pathway component expression and activation in joint tissues. To determine whether cartilage-derived activation or over-expression of NOTCH1 and HES1 (a NOTCH target gene) is sufficient to induce OA-related changes, we took a gain-of-function (GOF) approach and analyzed *AcanCre<sup>ERT2</sup>*; *Rosa-NICD1* and *AcanCre<sup>ERT2</sup>*; *Rosa-HES1* conditional mutant mice and corresponding chondrocyte cell-based models. Using a combination of histological, IHC, and IF approaches, we analyzed their joint phenotypes at 3 different stages (3-, 5-, and 8-months) and discovered that both over-expression of NICD1 and HES1 individually is sufficient to induce OA-related changes in the absence of prior joint injury. However, HES1 over-expression resulted in a less severe phenotype when compared with NICD1 GOF mutant mice at early stages. Numerous cell and molecular approaches including RNA-sequencing, Western blot, ChIP, qPCR, and luciferase assays further revealed that NOTCH pathway activation in chondrocytes induces the IL-6/JAK/STAT pathway, whereby HES1 post-translationally stabilizes STAT3 phosphorylation via the inhibition of PTPN9 (Meg2), and NICD1 can both directly induce *Il6* transcription and indirectly stabilize pSTAT3 by regulating *Hes1* expression. Since enhanced IL-6 signaling is associated with OA-related catabolic phenotypes and is implicated in human OA, this bimodal NICD1/HES1 regulation of IL-6/JAK/STAT3 signaling may explain the different phenotypes observed in NICD1 and HES1 over-expressing mice. Taken together, our work demonstrates that NOTCH/HES1 signaling differentially regulates the IL-6/JAK/STAT pathway in OA, and has identified specific components of these pathways with great potential as novel therapeutic targets for treatment of OA.

## MO0054

**Post-traumatic osteoarthritis initiates with a rapid decline in the nanoindentation modulus of cartilage surface caused by matrix breakdown.** Wei Tong<sup>\*1</sup>, Doyran Basak<sup>2</sup>, Qing Li<sup>2</sup>, Haoruo Jia<sup>1</sup>, Xianrong Zhang<sup>3</sup>, Chider Chen<sup>1</sup>, Enomoto-Iwamoto Motomi<sup>4</sup>, X. Lucas Lu<sup>5</sup>, Lin Han<sup>2</sup>, Ling Qin<sup>1</sup>.  
<sup>1</sup>University of Pennsylvania, United states, <sup>2</sup>drexel university, United states, <sup>3</sup>Wuhan University, China, <sup>4</sup>The Children's Hospital of Philadelphia, United states, <sup>5</sup>University of Delaware, United states

Post-traumatic osteoarthritis (PTOA), a prevalent form of OA in young adults, is characterized by injury-induced breakdown and alterations of articular cartilage and other synovial tissues with no early detection method available. To find a sensitive and function-relevant indicator of OA, we applied atomic force microscopy (AFM)-based nanoindentation to measure mechanical changes of articular cartilage in a PTOA murine model. Male C57BL/6 mice at 12 weeks of age received destabilization of the medial meniscus (DMM) surgery at right knees and sham surgery at left knees. Strikingly, 1 week post-surgery, cartilage surface modulus of DMM femurs at the medial side was already significantly reduced to  $49 \pm 8\%$  of sham, far preceding the time when histological OA signs first occur (4-8 weeks). Staining of VDIPEN, an aggrecan degradation product by MMPs, was elevated, implying an increase in MMP activities at this early time. Injection of MMPsense 645 FAST in live mice confirmed that MMP activity in DMM joints is  $39.7 \pm 5\%$  higher than that in sham knees. Interestingly, daily injection of GM6001, a MMP inhibitor, not only blocked the increase in MMP activity but also abolished the reduction in modulus of DMM femurs ( $n=5$ ) at 1 week after surgery, proving that cartilage surface weakening at early OA is due to elevated proteolytic activities. The modulus of DMM femurs at the medial side was further declined to  $34 \pm 12\%$ ,  $32 \pm 8\%$ , and  $20 \pm 6\%$  of sham at 2, 4, and 8 weeks, respectively, and then rebounded to  $88 \pm 4\%$  of sham at 12 weeks due to the fact that the indentation is conducted on the newly exposed stiffer middle/deep layer of uncalcified cartilage at late OA due to cartilage erosion. At the lateral side of DMM femurs, a significant decrease in modulus ( $33 \pm 4\%$  of lateral sham side) started at 4 weeks, which is also much earlier than histological changes (12 weeks). In addition, the medial side of meniscus was significantly weakened ( $41 \pm 16\%$  of sham) while the lateral side remained strong at 8 weeks after DMM, highlighting that OA is a whole joint disease. No obvious changes in subchondral bone and synovium were detected during the 12 week observation period. Taken together, our study underscores the high sensitivity of nanoindentation modulus in examining the early initiation and spatiotemporal progression of DMM-induced PTOA and demonstrated elevated MMP activity and the resulting matrix degradation as critical events at the early stage of PTOA.

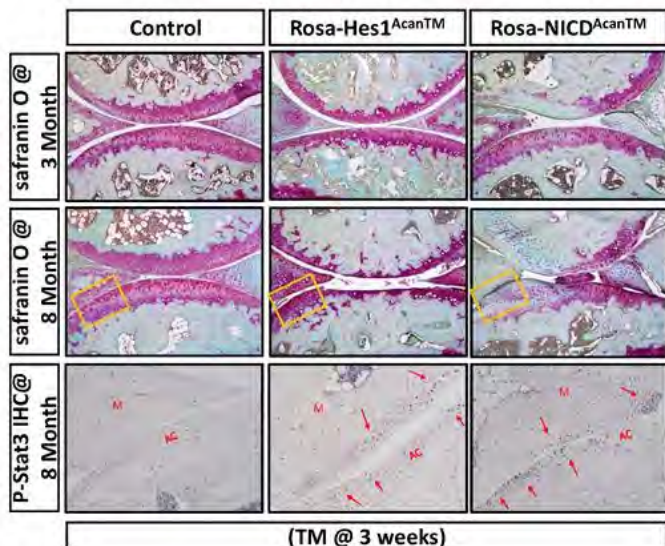
*Disclosures: Wei Tong, None.*

## MO0055

**TGF $\beta$  Regulates the Stability of Sox9.** George Coricor<sup>\*</sup>, Rosa Serra.  
 University of Alabama at Birmingham, United states

One out of two people in the U.S. will experience some form of Osteoarthritis (OA) in their lifetime. Members of the Transforming Growth Factor- $\beta$  (TGF $\beta$ ) superfamily are important factors that stimulate chondrocyte matrix biosynthesis. Mice with a dominant-negative mutation of the TGF $\beta$ IIIR develop a degenerative joint disease resembling OA. Another key chondrogenic factor, SOX9, is important for maintaining chondrocyte function. Patients with OA show decreased levels of SOX9 and TGF $\beta$  receptors. Our overall hypothesis is that TGF $\beta$  regulates SOX9 to maintain articular cartilage. We utilized two cell culture models for these experiments, ATDC5 cells, and primary bovine articular chondrocytes. We showed that TGF $\beta$  stabilizes SOX9 protein and increases phosphorylation of SOX9 in both ATDC5 and bovine articular chondrocytes. SOX9 can be phosphorylated on three Serine residues S64, S181, and S211. We mutated these serine sites to alanine then over expressed the mutants in ATDC5 cells to determine which phosphorylation site is important for TGF $\beta$ -mediated stability of Sox9. We found that mutation of Serine 211 is required to maintain normal SOX9 protein levels and that TGF $\beta$  was not able to increase the stability of SOX9-S211A mutant. The results suggest that TGF $\beta$  may phosphorylate SOX9 on S211 to stabilize it. The S211 site is in a motif that is targeted by p38 kinase. TGF $\beta$  can signal through a canonical/Smad-mediated pathway or non-conical pathways, including p38. We tested the hypothesis that Smad2/3 and/or p38 regulate the phosphorylation and stability of SOX9. First, we determined that knock down of Smad2/3 using siRNA, blocked TGF $\beta$ -mediated stability of Sox9. Then we showed that stabilization of SOX9 by TGF $\beta$  was blocked in cells treated with p38 inhibitors suggesting that TGF $\beta$  requires both Smad2/3 and p38 activity to regulate SOX9 protein levels. Previously, we showed that Paps2 is a downstream target of TGF $\beta$ . We utilized siRNA for SOX9 to show that TGF $\beta$  requires SOX9 to regulate Paps2. We also showed that p38 is required for TGF $\beta$ -mediated regulation of PAPS2 suggesting a new mechanism for TGF $\beta$ -mediated gene regulation in chondrocytes. Understanding how TGF $\beta$  stabilizes SOX9 may lead to identification of preventative targets of both age-related and post-traumatic OA.

*Disclosures: George Coricor, None.*



Rosa-Hes1<sup>AcanTM</sup> and Rosa-NICD1<sup>AcanTM</sup> mice develop osteoarthritis with highly elevated stat3 phosphorylation. Overexpression of either Hes1 or NICD1 specifically in cartilage develops osteoarthritis spontaneously, with milder phenotype in Hes1 overexpressing mice especially at early stages. High activity of IL-6/stat signaling is identified in both animal models, as shown by nucleus specific staining of phosphate stat3 (red arrows) in articular cartilage (AC) and meniscus (M).

Image

*Disclosures: Yinshi Ren, None.*

## MO0053

**Cbfb Cartilage-Deficient Mice Develop Spontaneous Osteoarthritis and Cbfb Overexpression Prevents Osteoarthritis.** Yun Lu<sup>\*</sup>, Yi-Ping Li, Guochun Zhu, Mengrui Wu, Wei Chen. Department of Pathology, University of Alabama at Birmingham, United states

Osteoarthritis (OA) is the most common form of arthritis that affects the majority of Americans over the age of 60. However, the molecular mechanisms of OA pathogenesis remain elusive despite intensive research efforts. In this study, we aimed to identify the transcription factors (TFs) that are crucial in OA pathogenesis. Core-binding factor beta (Cbfb) was reported as one of the key TFs in the regulatory network of OA by human patients' Gene Expression Omnibus data analysis. Nevertheless, the function of Cbfb in OA pathogenesis remains unclear. To investigate the role of Cbfb in OA development, we generated chondrocyte-specific Cbfb deficient mice using floxed alleles of Cbfb and Cre driven by the Collagen 2 $\alpha$ 1 promoter. Cbfb<sup>fl/fl</sup> Col2 $\alpha$ 1-Cre mice displayed severe skeletal malformation due to impaired chondrocyte proliferation and hypertrophy and died around one month of age. Notably, Cbfb knockdown in the heterozygous Cbfb<sup>fl/+</sup>Col2-Cre mice exhibited severe and spontaneous OA features by 9 months. To study OA pathogenesis in the chondrocyte-specific aging Cbfb deficient mice, we generated inducible Cbfb<sup>fl/fl</sup>/Col2-CreER mice through intraperitoneal Tamoxifen injection. Interestingly, these mice developed spontaneous OA at the age of 3.5 months, affecting the knee, hip and spine with severe hyperostosis, narrowed joint space, high inflammation and cartilage loss. Immunohistochemistry staining and Western blot analysis showed reduced Runx protein expressions. To test whether Cbfb overexpression can prevent OA development, we generated Adeno-associated Cbfb overexpression virus (Cbfb-AAV) which was injected into knee joints of anterior cruciate ligament transection (ACLT) or destabilization of the medial meniscus (DMM) surgery mediated OA mice. Importantly, the AAV-Cbfb injected group in both ACLT and DMM models displayed significant protection from articular cartilage damage and subchondral bone thickening by up-regulating Runx1 stability, shh signaling and BMP signaling. Taken together, our results demonstrated that Cbfb cartilage-deficient mice develop spontaneous OA, established role of Cbfb in articular cartilage formation and homeostasis, and showed Cbfb overexpression can prevent OA. Significantly, this study provides new and important insights into OA pathogenesis that may lead to novel therapies for the treatment of this disease.

*Disclosures: Yun Lu, None.*

## MO0056

**Wnt Signaling Contributes to Osteoarthritis in Mice Overexpressing the High Molecular Weight Isoforms of Fibroblast Growth Factor 2.** Patience Meo Burt\*, Liping Xiao, Marja Hurley. UCONN Health, United states

Osteoarthritis (OA) is a debilitating joint disease that affects over 27 million adults in the U.S., characterized by loss of articular cartilage and changes in underlying bone with no effective therapy. Fibroblast growth factor 2 (FGF2) is known to play a role in OA, but the involvement of FGF2 isoforms has not been investigated. Mice that overexpress the high molecular weight FGF2 isoforms in pre-osteoblasts (HMWTg mice) display dwarfism, decreased bone mineral density, osteomalacia, hypophosphatemia, and increased FGF23 in serum and bone and phenocopy the Hyp mouse, a homologue of human X-linked hypophosphatemia (XLH). Hyp mice and XLH patients develop osteoarthropathies, so we investigated whether HMWTg mice have OA and increased FGF23 expression within the joint. Wnt/ $\beta$ -catenin signaling has been found to be upregulated within areas of osteoarthritic joints in humans/mice and Hyp mice have increased expression of Wnt signaling components. Also, FGF23 is upregulated in human OA chondrocytes and Wnt signaling modulates FGF23 promoter activity. Since HMWTg mice phenocopy Hyp mice and have an increase in FGF23 within the joint, we posit that the OA phenotype in HMWTg mice is due in part to enhanced Wnt signaling. We observed an OA phenotype in 18-month-old HMWTg mice. Time course studies demonstrated evidence of OA starting at 2 months. Examination of joints of 2-month-old Vector control and HMWTg mice by x-ray, microCT, Safranin-O staining, qPCR, and immunohistochemistry were used to assess for signs of OA. qPCR analysis of mRNA and immunohistochemistry were used to examine components of Wnt signaling pathway. We confirmed that 2-month-old HMWTg mice developed signs of OA, including flattening of tibial plateau, thinning of subchondral bone, decreased articular cartilage thickness, and increased expression of cartilage degrading enzymes. The mRNA and proteins levels of Wnt inhibitors Dkk1 and Sost were decreased in HMWTg. Lrp-5 was unchanged but Lrp-6 mRNA and protein were decreased. The ligand Wnt5a mRNA and protein were increased and phospho GSK-3 $\beta$  and Axin-2 were also increased. There was a small increase in nuclear staining for  $\beta$ -catenin (data not shown) and Lef-1 mRNA and protein were increased (Fig.1). Overall, these results suggest that enhanced Wnt signaling contributes to the OA phenotype found in HMWTg mice and offer potential insight into a pathway that could be targeted to treat OA.

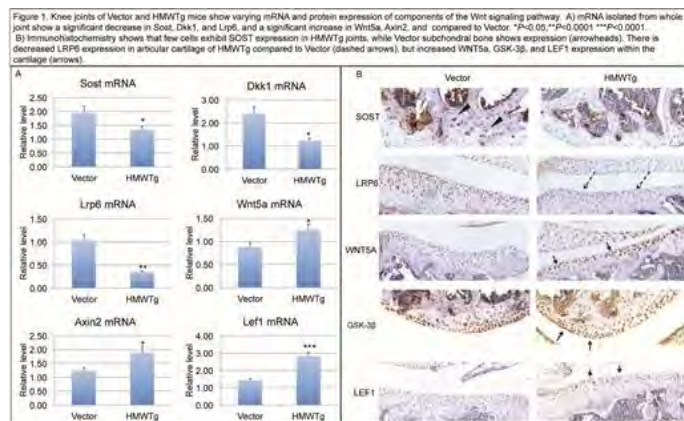


Figure 1

**Disclosures:** *Patience Meo Burt, None.*

## MO0057

**FGFR3-dependent Activation of a Novel PKC Isoform Causes Dephosphorylation and Inactivation of Guanylyl Cyclase-B in Rat Chondrosarcoma Cells.** Jerid Robinson\*, Lincoln Potter. University of Minnesota, United states

Achondroplasia is the most common form of human skeletal dwarfism. It most commonly results from a spontaneous, constitutively activating mutation in the fibroblast growth factor receptor 3 (FGFR3) leading to shortened proliferative and hypertrophic chondrocyte layers and disproportionate dwarfism. Activation of guanylyl cyclase-B (GC-B) by a synthetic analog of its endogenous ligand, C-type natriuretic peptide (CNP), rescues the dwarfed phenotype in mice and humans and is a promising therapy for achondroplasia. While it is known that the FGFR3 and GC-B pathways are mutually antagonistic and synthetic activation of GC-B can counteract FGFR3 signaling, how FGFR3 activation inhibits GC-B activity is not known. Here, we demonstrate that FGF2 stimulation of FGFR3 in rat chondrosarcoma (RCS) cells causes a rapid, potent, and reversible inhibition of CNP-dependent GC-B activity. The FGF2-dependent GC-B inhibition was not MAPK-dependent as previously reported. The inability of FGF2 to inhibit a constitutively phosphorylated mutant of GC-B (GC-B-7E) indicated that the FGF-dependent inhibition required changes in receptor phosphorylation. Further chemical inhibitor and dominant negative studies

revealed that the FGF2-dependent inhibition of GC-B required a novel isoform of the PKC family. By understanding the mechanism by which FGFR3 inhibits GC-B signaling, novel therapies may be discovered that block FGFR3-dependent inhibition of GC-B and rescue FGFR3-dependent chondrodysplasias.

**Disclosures:** *Jerid Robinson, None.*

## MO0058

**MicroRNA-23c Maintains Cartilage Function and Prevents Osteoarthritis Phenotype by Suppressing Runx2.** Indira Prasadam\*, Ross Crawford, Yin Xiao. Institute of Health & Biomedical Innovation & Queensland University of Technology, Australia

MicroRNAs (miRNAs) have important roles in regulating cartilage and chondrocyte activity and are considered to be potential therapeutic targets. However, few studies have focused on miRNA mechanisms which are specifically involved in the osteoarthritis (OA) process. Here, miRNA profiling analysis identified miRNA-23c (miR-23c) as being one of the most down-regulated miRNAs in OA cartilage compared to normal. *In vivo*, cartilage from surgically induced meniscectomy rat OA model displayed lower levels of miR-23c compared with the sham group and inhibition of miR-23c lead to cartilage matrix loss and mimic OA phenotype. Interestingly, IL-1 $\beta$  stimulated chondrocytes showed a lower expression levels of miR-23c and chondrocyte-specific markers. Transduction of exogenous miR-23c suppressed the IL-1 $\beta$  induced chondrocyte ECM degradation, whereas the suppression of miR-23c in OA chondrocytes enhanced the chondrocyte-specific marker expression. We identified Runt-related transcription factor 2 (RUNX2) as a direct target of miR-23c and showed a down- and up-regulation of RUNX2 levels after transfection of, respectively with premiR- and antagomiR-23c oligonucleotides. We found the levels of RUNX2 expression is highly expressed in the OA cartilage but low in the normal and inhibition of RUNX2 with lentiviral approach suppressed the chondrogenic gene expression but accelerated the hypertrophy marker expression. In conclusion, our findings strongly suggest that miR-23c/RUNX2 axis as an important regulator in OA cartilage; further understanding of this axis may foster the development of potential gene therapeutic strategies targeting OA.

**Disclosures:** *Indira Prasadam, None.*

## MO0059

**TGF-beta Type II Receptor (TBR2)/IL36alpha Axis in Destabilization Medial Meniscus (DMM) Surgery Induced Post-traumatic Osteoarthritis (PTOA) Progression.** Tieshi Li\*, Joseph Temple, Alessandra Esposito, Lai Wang, JiEun Han, Arnavaz Hakimivan, Susan Chubinskaya, Anna Spagnoli. Rush University Medical Center, United states

Understanding the mechanisms involved in joint degeneration will help us to develop therapeutic methods for joint diseases such as PTOA. We have recently demonstrated that postnatal ablation of TBR2 signaling induced OA progression and enhance DMM surgery induced PTOA development. In addition, a novel inflammatory cytokine, named interleukin-36 alpha (IL36 $\alpha$ ), is regulated by TBR2 signaling in association with ablation of Tgfr2 induced OA progression. This study aimed to determine if IL36 $\alpha$  signaling is involved in PTOA progression as a key downstream mediator of the TBR2 signaling. We first used a murine model of PTOA induced by transecting the medial meniscotibial ligament (DMM) to check gene expression changes of Tgfr2 and IL36 $\alpha$  during PTOA progression. We found that, when following with the constant and gradual decreased expression of TBR2 within the arthritic lesions in the early stages of the OA progression (from 3 days (D) to 5D after surgeries), IL36 $\alpha$  is transiently highly expressed in the same region at 3D. The absence of both TBR2 and IL36 $\alpha$  was also detected at 7D and 2 weeks (W) after surgery. Furthermore, as a result of the DMM surgery, both TBR2 and IL36 $\alpha$  are increased in the synovium. These lines of evidence sustain the hypothesis for a role of TBR2/IL36 $\alpha$  axis in joint maintenance and PTOA progression. Furthermore, to determine the role of IL36 $\alpha$  signaling in DMM induced PTOA, we performed intra-articular injections of IL36a or IL36Ra (IL36 receptor antagonist) or PBS (control) into DMM and Sham C57BL/6 mice daily for 3 days start from postnatal age 10W right after surgery. Then those mice were sacrificed 8W later for sectioning and Safranin O/Fast green staining followed with OARSI grading to evaluate the OA progression. We found that injection of IL36Ra halts OA progression indicated with decreased articular cartilage destruction and OARSI scores (2.521  $\pm$  0.2341 Vs. 1.500  $\pm$  0.08513, P=0.0002, n=4 for each group), whereas, injection of IL36 $\alpha$  exacerbates DMM surgery induced PTOA progression indicated with more severe loss of articular cartilage and increased OARSI scores (2.521  $\pm$  0.2341 Vs. 3.333  $\pm$  0.3195, P=0.0459, n=4 for each group). Our data suggest that, in synovium, TBR2 and IL36 $\alpha$  are up-regulated after DMM surgery as part of the inflammation. While, in articular cartilage, DMM surgery-induced abnormal loads lead to downregulated TBR2, it then induces transient upregulation of IL36 $\alpha$  as a downstream mediator to induce catabolic factors followed with OA progression. Our studies provide a novel perspective by which the TBR2/IL36 $\alpha$  axis could be manipulated to prevent and treat cartilage degeneration in PTOA progression.

**Disclosures:** *Tieshi Li, None.*

## MO0060

**P2Y2 Purinergic Receptor Regulates Cyclic Tension Strain-induced Aggrecan Synthesis in Chondrogenic ATDC5 cells.** Di Liu\*<sup>1</sup>, Natsuko Tanabe<sup>2</sup>, Minqi Li<sup>3</sup>, Takayuki Kawato<sup>4</sup>, Masao Maeno<sup>5</sup>. <sup>1</sup>Shandong Provincial Key Laboratory of Oral Biomedicine, Department of Prosthodontics, School of Stomatology, Shandong University, China, <sup>2</sup>Division of Functional Morphology, Dental Research Center, Department of Biochemistry, Nihon University School of Dentistry, Japan, <sup>3</sup>Shandong Provincial Key Laboratory of Oral Biomedicine, Shandong University, China, <sup>4</sup>Division of Functional Morphology, Dental Research Center, Department of Periodontology, Nihon University School of Dentistry, Japan, <sup>5</sup>Division of Functional Morphology, Dental Research Center, Department of Oral Health Sciences, Nihon University School of Dentistry, Japan

Cyclic mechanical loading is an important factor regulating chondrocytes function and their extracellular matrix (ECM) metabolism, which is necessary to maintain and remodel cartilage for the functional requirements and homeostasis. However, the fundamental underlying mechanotransduction pathways are remain unclear. It is confirmed that cyclic mechanical stimulation augments the release of nucleotides from chondrocytes, which can then bind to P2 receptors, and in turn to effect on ECM biosynthesis subsequently. In this study, we investigated the role of P2Y2 in a cartilage-specific ECM – aggrecan synthesis induced by cyclic tension strain (CTS) in ATDC5-derived chondrocytes.

The differentiating chondrogenic ATDC5 cells were differentiated by culturing and inducing in media supplemented by 1% Insulin-Transferrin-Selenium (ITS) for 14 d, which were applied prior to CTS stimulation at 6 cycles/min (with 2%, 5 sec strain, 5 sec relaxation) with 2, 5 and 15 % CTS for 1, 3, 6 and 24 hs. Aggrecan mRNA expression was analyzed by real-time PCR (RT-PCR); the sulfated glycosaminoglycan production was assessed by alcian blue staining; P2Y2-specific shRNA (shP2Y2) receptors deficient cells were utilized to determine the role of P2Y2 in aggrecan mRNA and sulfated glycosaminoglycan production; The PLCβ pathway blocker - U73122 were applied to determine the mechanotransduction pathways of P2Y2 on chondrocytes induced by CTS.

Stimulation with 5% CTS lasting for 3 hs was most likely to have positive effects on aggrecan gene expression. In addition, P2Y2-deficient cells exhibited an inhibition in CTS-induced aggrecan mRNA upregulation and sulfated glycosaminoglycan production, that they all showed statistically significant ( $p < 0.01$ ). U73122 significantly reduced aggrecan mRNA expression in P2Y2-deficient cells when compared to those in cells untreated and vehicle exposure to CTS respectively ( $p < 0.05$ ).

CTS induces and enhances aggrecan in mRNA and protein expression level. Furthermore, P2Y2 receptors are involved in chondrocytes mechanotransduction, and in turn directly, at least partly, mediates cartilage-specific ECM-aggrecan metabolism induced by CTS through the CTS-P2Y2 pathway.

**Disclosures:** Di Liu, None.

## MO0061

**Diabetic Bone is Stronger but More Brittle in the TallyHO Mouse Model of Juvenile Type 2 Diabetes.** Amy Creecy\*<sup>1</sup>, Sasidhar Uppuganti<sup>1</sup>, Mathilde Granke<sup>1</sup>, Maureen Gannon<sup>2</sup>, Jeffrey Nyman<sup>1</sup>. <sup>1</sup>Vanderbilt University, VA Tennessee Health Valley Healthcare System, United states, <sup>2</sup>Vanderbilt University, VA Tennessee Health Valley Healthcare System, United states

The prevalence of juvenile type 2 diabetes (T2D) is increasing worldwide. Among adults, T2D is associated with increased fracture risk despite higher areal bone mineral density (BMD) relative to non-diabetics. Those with juvenile diabetes may be at an even greater fracture risk in the future due to long-term diabetes. The TallyHO mouse is a polygenic, spontaneous model of T2D that exhibits obesity and hyperglycemia at an early age. To determine whether this is a potential model of diabetic bone disease, we hypothesized that the bones of TallyHO mice have poor material properties even though they have obesity-related high bone mass compared to its control strain. Blood glucose and body weight were monitored weekly in young male TallyHO (n=10) and non-diabetic SWR (n=13) mice (The Jackson Labs). Upon sacrifice at 16-wks, left femurs were harvested and scanned using  $\mu$ CT to determine bone structure and density. Mechanical properties were determined using three-point bend testing. Glucose was significantly higher for TallyHO than for SWR mice starting around 10 weeks of age (328 mg/dL  $\pm$  96 vs. 137 mg/dL  $\pm$  47,  $p < 0.0001$ ). Along with obesity, the femur mid-shafts of TallyHO mice had a higher cortical area and thickness compared to the mid-shaft of SWR mice (Table). Having higher tissue mineral density (Ct.TMD) as well, femurs from diabetic TallyHO mice were structurally stronger than those from non-diabetic SWR mice (Table). In addition, the estimated material strength was greater, but toughness and post-yield toughness were lower for the TallyHO than the control mice. While bones from diabetic mice were massive and stronger, the trabecular BV/TV in the femur metaphysis was lower in TallyHO (Table). This was partially offset with Tb.TMD in bones from diabetic mice. The higher bone strength of the diabetic mice could be due to higher body weight relative to the non-diabetic controls. When we included body mass as covariate in a general linear model, the difference in structural strength between the mouse strains was no longer significant. Interestingly, Ct.TMD and bending strength remained significant after adjusting for body weight suggesting other factors affect mineralization. The lower post-yield toughness in diabetic mice

could be due to hyperglycemia-induced AGE accumulation in the matrix, though this brittleness phenotype is not independent of body weight. As a model of diabetic bone disease, TallyHO likely exhibits effects from both obesity and hyperglycemia.

Table: Properties of TallyHO and SWR Mice

	SWR/J	TallyHO	p value	
<b>Global Parameters</b>				
Final Body Weight	g	26.2 $\pm$ 1.2	36.0 $\pm$ 3.9	< 0.0001
Average Glucose Level	mg/dL	169 $\pm$ 25	339 $\pm$ 153	< 0.0001
<b>Cortical Bone</b>				
Tissue Mineral Density	mg HA/cm <sup>3</sup>	1233 $\pm$ 24	1284 $\pm$ 19	< 0.0001
Imin	mm <sup>3</sup>	0.097 $\pm$ 0.008	0.096 $\pm$ 0.010	0.965
Cortical Area	mm <sup>2</sup>	0.720 $\pm$ 0.043	0.831 $\pm$ 0.033	< 0.0001
Cortical Thickness	mm	0.167 $\pm$ 0.006	0.191 $\pm$ 0.011	< 0.0001
Tissue Area	mm <sup>2</sup>	1.49 $\pm$ 0.05	1.44 $\pm$ 0.09	0.077
Cortical Porosity	%	0.407 $\pm$ 0.135	0.145 $\pm$ 0.113	< 0.0001
Cortical Pore Number	mm <sup>-1</sup>	2.86 $\pm$ 0.36	2.38 $\pm$ 0.29	0.002
Modulus	GPa	12.4 $\pm$ 0.8	12.9 $\pm$ 1.4	0.380
Bending Strength	MPa	230 $\pm$ 10	256 $\pm$ 8	< 0.0001
Stiffness	N/mm	112 $\pm$ 9	115 $\pm$ 10	0.685
Peak Force	N	17.9 $\pm$ 1.4	20.5 $\pm$ 1.6	0.0002
Peak Moment	N*mm	35.7 $\pm$ 2.8	41.1 $\pm$ 3.3	0.0002
Post-Yield Displacement	l/mm	0.416 $\pm$ 0.081	0.277 $\pm$ 0.112	0.0024
Toughness	MJ/m <sup>3</sup>	4.24 $\pm$ 0.57	3.13 $\pm$ 0.80	0.0008
Post-yield toughness	MJ/m <sup>3</sup>	3.32 $\pm$ 0.57	2.08 $\pm$ 0.95	0.0008
<b>Trabecular Bone</b>				
BV/TV	%	0.203 $\pm$ 0.028	0.103 $\pm$ 0.026	< 0.0001
Tissue Mineral Density	mg HA/cm <sup>3</sup>	999 $\pm$ 11	985 $\pm$ 16	0.01
Trabecular number	mm <sup>-1</sup>	5.31 $\pm$ 0.31	3.86 $\pm$ 0.26	< 0.0001
Trabecular thickness	mm	0.046 $\pm$ 0.002	0.049 $\pm$ 0.004	0.041
Trabecular spacing	mm	0.186 $\pm$ 0.012	0.257 $\pm$ 0.018	< 0.0001

Table of TallyHO and SWR Measurements

**Disclosures:** Amy Creecy, None.

## MO0062

**Effects of Denosumab on fat and basal metabolism in postmenopausal women with type 2 diabetes.** Makiko Ogata\*, Risa Ide, Miho Takizawa, Naoko Iwasaki, Yasuko Uchigata. Diabetes Center, Tokyo Women's Medical University, Japan

Objective: Denosumab (Db) is a monoclonal antibody of the IgE receptor activator of nuclear factor k-B ligand (RANKL). Blockage of RANKL signaling improves hepatic insulin resistance in vitro. To determine the effect of RANKL in patients with type 2 diabetes, examinations of body complications with visceral fat and basal metabolism evaluations with serum examination were conducted before and after Denosumab injections.

Methods: Six postmenopausal women with type 2 diabetes and osteoporosis were enrolled. With the exception of metabolic syndromes, the subjects did not have any other diseases, and alfacalcidol (0.5mg/day) was the only osteoporosis therapy used. Patients who did not take alfacalcidol were administered a daily dose of 600 IU cholecalciferol (Vit D3) with 610 mg Ca one month before the Db injection. Examinations were conducted before Db injection, and one month (1 Mo) and two months (2 Mo) after the injection. Body composition was calculated via the impedance method using a body composition analyzer. Resting energy expenditure (REE) and respiratory quotient (RQ) measurements were performed using a Vmax Spectra system for indirect calorimetry testing. Visceral fat was evaluated using bioelectrical impedance measurements. General serum and blood count examinations were conducted, including measurements of Ca, P, 25-hydroxyvitamin D (25[OH]D), intact parathyroid hormone, blood glucose, glycated hemoglobin (HbA1c), and C-peptide immunoreactivity.

Results: The mean age, body mass index values, HbA1c, fat mass, visceral fat, and REE values of the six patients were 72  $\pm$  4.3 years, 25.8  $\pm$  3.0, 7.2  $\pm$  1.0%, 20.9  $\pm$  5.0 kg, 78.8  $\pm$  43.4 cm<sup>2</sup>, and 796  $\pm$  165 Cal, respectively. Three patients who had taken VitD3 showed increased REE values after taking VitD3. No obvious changes were detected in HbA1c and body weight during the observation period (average change: -0.02  $\pm$  0.14% and 0.2  $\pm$  1.3 kg, respectively). Although three of the six patients showed decreased visceral fat at 1 Mo, visceral fat increased in five of the six patients at 2 Mo (average change: 3.7  $\pm$  12.2 cm<sup>2</sup>). All patients displayed increased fat mass at 2 Mo (average change: 0.7  $\pm$  0.5 kg), and five of the six patients showed decreased REE at 2 Mo (average change: -17.1  $\pm$  135.6 Cal). One patient showing increased body weight (1.2 kg) at 2 Mo exhibited increased REE. Lastly, five of the six patients showed decreased 25[OH]D after Db injections.

Discussion: Although serum Ca and P levels were normal in all patients before and after Db injections, five of the six patients showed decreased REE. All patients showed increased fat mass after Db injection without obvious body weight changes and deterioration of blood glucose control.

**Disclosures:** Makiko Ogata, None.

## MO0063

**Characterization of Brown Adipose within Trauma-Induced Heterotopic Ossification in Human Tissues.** Elizabeth Salisbury\*<sup>1</sup>, Thomas Davis<sup>2</sup>, Jonathan Forsberg<sup>2</sup>, Alan Davis<sup>3</sup>, Elizabeth Davis<sup>3</sup>. <sup>1</sup>University of Texas Medical Branch, United states, <sup>2</sup>Naval Medical Research Center, United states, <sup>3</sup>Baylor College of Medicine, United states

Heterotopic ossification (HO), or the abnormal formation of bone within soft tissues, is a major complication following severe trauma or amputation. Using a

mouse model of HO, we have previously shown that brown adipocytes are critical for guiding the formation of heterotopic bone. These cells, in part through their ability for uncoupled aerobic respiration, regulate the local microenvironment to promote chondrogenesis, as well as neovascularization and innervation of the newly forming heterotopic bone. In this study, we sought to evaluate the presence of brown fat within human HO lesions in comparison to what we have learned from our mouse model. A total of 24 HO tissue samples collected during surgical removal of symptomatic lesions were analyzed. A majority of the excised tissue samples displayed histological characteristics of fibroproliferation (71%), blood vessels (54%), adipose tissue (75%), and bone with evidence of osteoclasts, active osteoblasts, and osteocytes (92%). Cartilage was observed in 5 of the samples collected. Immunohistochemical analysis revealed expression of the brown adipocyte marker uncoupling protein 1 (UCP1) in approximately 63% of the HO tissues. This expression was associated with regions of adipose, often adjacent to heterotopic bone and vessel structures, within the tissue. UCP1 expression was also noted within areas of cartilage, co-aligning with aggrecan expression. UCP1 was not expressed in control tissues. Further analysis of the UCP1-positive cells confirmed co-expression of PPAR $\gamma$  coactivator 1 $\alpha$  (PGC1 $\alpha$ ), but not PRDM16. These results parallel those observed during HO in the mouse. In addition, these cells did not express factors typical of beige adipocytes (CD137, TBX1, HOXC9). These findings suggest the induction of a unique population of brown adipocytes in specific forms of human HO. Further characterization of these cells may provide novel targets to develop therapeutics to inhibit HO.

**Disclosures:** Elizabeth Salisbury, None.

## MO0064

**Chronic cold stress decreases skeletal acquisition and alters UCP1 expression and energy metabolism in young, growing male C57Bl/6J mice.** Maureen Devlin\*, Amy Robbins, Miranda Cosman, Lillian Shipp, Katarina Alajbegovic. University of Michigan, United states

Cold exposure induces nonshivering thermogenesis (NST) in brown adipose tissue (BAT) in humans and in animal models, and prior studies have shown that failure of NST leads to bone loss. Notably, BAT mass peaks in humans during adolescent peak bone mass acquisition, and thus may contribute to skeletal phenotype. However, it is not clear how chronic cold stress affects metabolism and skeletal acquisition in young, growing individuals. We hypothesize that cold stress blunts cortical and trabecular bone acquisition and that energy diversion to nonshivering thermogenesis in BAT leads to lower body fat. To test this hypothesis, male C57Bl/6J mice were housed in pairs from 3 wks of age to 6 or 12 wks of age at 26°C (WARM), 22°C (STD, standard vivarium temperature), or 18°C (COOL), with access to food and water ad libitum (N=10-12/group). Outcomes included body mass, food intake, body and tail length, %body fat and whole body bone mineral density (BMD) via pDXA, and cortical and trabecular microarchitecture via  $\mu$ CT. COOL mice ate more throughout, but had lower % body fat at 6 wks of age and lower body mass with shorter bodies and tails at 12 wks of age (GLM;  $p < 0.05$  for all). In trabecular bone of the distal femur, COOL and STD mice had 43-66% lower trabecular bone volume fraction and 35-46% lower trabecular thickness compared to WARM mice at 6 wks of age (GLM;  $p < 0.05$  for all), but no differences at 12 wks. In the midshaft femur, COOL mice had 7-8% lower cortical bone area fraction at 6 and 12 wks and 9% lower cortical bone thickness at 6 wks (GLM;  $p < 0.05$  for all), but no differences in total area vs. WARM mice. UCP1 protein content by Western blot in intrascapular BAT was inversely related to housing temperature and was significantly higher in COOL vs. HOT at 6 and 12 wks of age (GLM;  $p < 0.001$ ). These data support the hypothesis that cold exposure is detrimental to bone mass acquisition and decreases body fat, potentially due to lower energy availability despite higher food intake. Future studies will test interactions of diet, exercise, BAT thermogenesis, body composition, and skeletal acquisition.

**Disclosures:** Maureen Devlin, None.

## MO0065

**Impaired Adipose Tissue Inflammation Results in High Bone Mass in Mice.** Louise Grahnmö\*, Karin Gustafsson<sup>1</sup>, Ingrid Wernstedt Asterholm<sup>2</sup>, Marie Lagerquist<sup>1</sup>. <sup>1</sup>Centre for Bone & Arthritis Research, Department of Internal Medicine & Clinical Nutrition, Institute of Medicine, The Sahlgrenska Academy, University of Gothenburg, Sweden, <sup>2</sup>Unit of Metabolic Physiology, Department of Physiology, Institute of Neuroscience & Physiology, The Sahlgrenska Academy, University of Gothenburg, Sweden

Bone and fat are linked in many ways. For example, adipocytes are found in the bone marrow and expansion of bone marrow adipose tissue is often associated with low bone mass, possibly because adipocytes and osteoblasts competitively differentiate from the same stem. Impaired adipose tissue inflammation results in low adipogenesis and metabolic disturbances, which suggests that inflammation within adipose tissue is essential for healthy adipose tissue expansion. If adipose tissue inflammation affects bone mass is however unknown. Thus, the aim of this study was to test the hypothesis that impaired adipose tissue inflammation, causing low adipogenesis, results in high osteoblastogenesis and bone mass.

High fat diet (HFD) was fed for 11 weeks to female and male RID transgenic (tg) mice, which have an impaired adipose tissue inflammation, and wildtypes. BMD was determined throughout the study by dual energy X-ray absorptiometry. At

termination, femur and humerus were collected for analysis by peripheral quantitative computed tomography and biomechanical testing, respectively. This study was approved by the ethical committee for animal experiments in Gothenburg (ethical permit: 77-15).

Male RID tg mice had higher total BMD (see figure) at 4 (+5.0%,  $p=0.002$ ), 8 (+5.4%,  $p < 0.001$ ), and 11 (+3.6%,  $p=0.006$ ) weeks of HFD, as well as higher lumbar BMD at 4 (+10.6%,  $p=0.002$ ), 8 (+16.8%,  $p < 0.001$ ), and 11 (+7.5%,  $p=0.02$ ) weeks of HFD, compared with wildtypes. Male RID tg mice also had higher femoral trabecular BMD (+9.1%,  $p=0.02$ ) and cortical content (+9.7%,  $p=0.02$ ) than wildtypes. For female mice, the bone phenotype was not apparent until 11 weeks of HFD, when female RID tg mice had higher lumbar (+16.5%,  $p < 0.001$ ), but not total, BMD than wildtypes. Female RID tg mice also had higher femoral trabecular BMD (+10.8%,  $p=0.01$ ) and cortical content (+8.2%,  $p=0.005$ ) than wildtypes. Bone strength measurements of humeri indicated that male and female RID tg mice had higher bone strength (+44% and +47% respectively,  $p < 0.01$ ) than wildtypes.

In conclusion, male and female mice with an impaired adipose tissue inflammation had higher BMD and bone strength than wildtypes. However, the effect was delayed in females. The osteoblastogenesis and adipogenesis remains to be investigated.

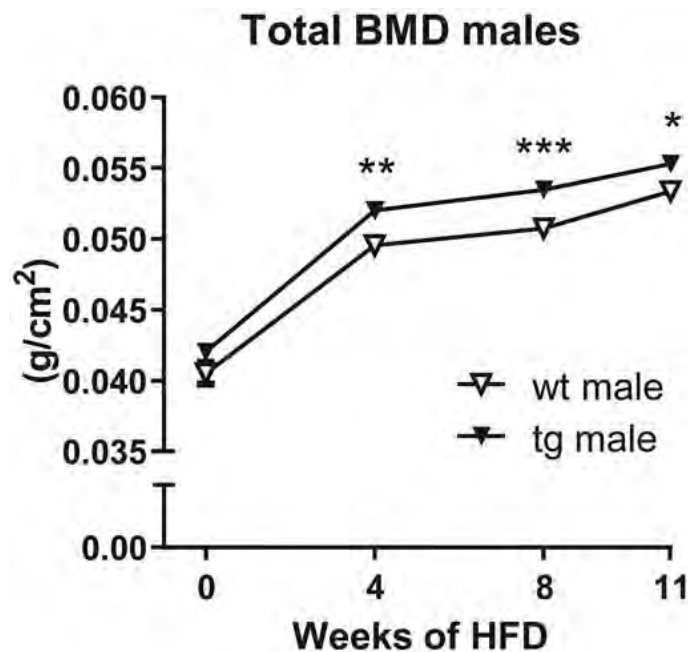


Figure. Male total BMD

**Disclosures:** Louise Grahnmö, None.

## MO0066

**Relationship between Body Adiposity with Marrow Adipose Tissue and Bone Mass in Human Type 1 Diabetes Mellitus.** Adriana Carvalho\*<sup>1</sup>, Bianca Massaro<sup>1</sup>, Luciana Silva<sup>1</sup>, Marcello Nogueira-Barbosa<sup>1</sup>, Carlos Salmon<sup>1</sup>, Belinda Simões<sup>1</sup>, Maria Carolina Rodrigues<sup>1</sup>, Clifford Rosen<sup>2</sup>, Francisco De Paula<sup>1</sup>. <sup>1</sup>University of Sao Paulo, Brazil, <sup>2</sup>Maine Medical Center Research Institute, Brazil

**Introduction:** Adipose tissue can impact differently depending on its localization and amount of stored fat. Marrow adipose tissue (MAT) expansion occurs in catabolic conditions associated with bone loss, such as anorexia nervosa and glucocorticoid therapy. On the other hand, obesity is related to high or normal BMD. Our aim was to evaluate the relationship of lipids depots with bone mass and MAT in conventionally treated T1D and T1D subjects submitted to hematopoietic stem cell transplantation (HSCT). **Methods:** The study comprised 3 groups matched by age, gender, height and weight: Control (11M/12F; 29 ± 6 years; 65 ± 15Kg; 1.68 ± 0.08m; 22.9 ± 3.7Kg/m<sup>2</sup>), T1D (14M/10F; 31 ± 12 years; 72 ± 10Kg; 1.69 ± 0.08m; 25.1 ± 3.3Kg/m<sup>2</sup>), 17 ± 11 years of diagnosis), T1HSCT (5M/3F; 25 ± 5 years; 67 ± 12Kg; 1.72 ± 0.11m, 22.2 ± 2.1Kg/m<sup>2</sup>, 6 months to 9 years after HSCT). Blood samples were collected to evaluate glycemic control. Lumbar spine and femoral neck BMD were assessed by DXA. 1-H magnetic resonance spectroscopy (1,5T) was used to evaluate MAT [fat/(fat+water)%] in L3 vertebrae. Visceral Adipose Tissue (VAT) and Intrahepatic lipids (IHL) were also evaluated by MRI. **Results:** Only T1D exhibited poor metabolic control (C=5.2 ± 0.2vsT1=9.6 ± 2.2vsT1HSCT=6.4 ± 0.5%;  $p < 0.0001$ ). Most T1D patients were overweight (58%) but there was no difference in % body fat mass (C=30.4 ± 7.8vsT1=30.6 ± 10.3vsT1HSCT=24.4 ± 6.6%) and lean mass between groups. BMD was similar in all sites (e.g., L1-L4: C=0.995 ± 0.141vsT1=0.977 ± 0.130vsT1HSCT=0.964 ± 0.125g/cm<sup>2</sup>) and only a few T1D patients had low BMD (z-score > -2) (17%). Also, VAT, IHL and MAT (MAT: C=23 ± 9vsT1=25 ± 7vsT1HSCT=29 ± 7%) did not differ between groups. Body fat mass had a negative correlation with femoral neck BMD in T1D group ( $r = -0.45$ ;  $p = 0.02$ ). VAT did not

correlate with IHL. MAT did not correlate with body fat mass, IHL and lumbar spine BMD. There was a significant correlation between VAT and MAT in control group ( $r=0.49; p=0.01$ ) which was not observed in T1D groups. Conclusion: Our data showed that regardless of diabetes treatment no reduction in bone mass was observed among T1D individuals. VAT, IHL and MAT also were not increased in T1D. Fat overflow was observed neither to liver nor to MAT in T1D. Further studies are needed to understand the role of nutritional status on bone mass and MAT relationship in T1D.

**Disclosures:** Adriana Carvalho, None.

## MO0067

**Bone Density, Bone Geometry and Bone Turnover in Hypogonadal Men with Type 2 Diabetes after Testosterone Therapy.** Georgia Colleluori<sup>1</sup>, Lina Aguirre<sup>2</sup>, Richard Dorin<sup>2</sup>, David Robbins<sup>2</sup>, Clifford Qualls<sup>3</sup>, Dean Blevins<sup>1</sup>, Dennis Villareal<sup>4</sup>, Reina Villareal<sup>4</sup>. <sup>1</sup>Baylor College of Medicine, United states, <sup>2</sup>New Mexico VA Health Care System, United states, <sup>3</sup>University of New Mexico School of Medicine, United states, <sup>4</sup>Michael E. DeBakey VA Medical Center, United states

**Background:** Hypogonadism (HG) in men is associated with bone loss and increased risk of osteoporosis. Patients with type 2 diabetes (DM+) have higher bone mineral density (BMD) but greater risk for fracture. Several studies support the association between low testosterone (T) and DM, however no studies have investigated the skeletal response of HG DM+ compared to HG DM- men after T therapy. In this study we evaluated the effect of T therapy on BMD, bone geometry and bone turnover in HG DM+ compared to HG DM- men after 18 months of T therapy. **Methods:** Single arm, open-label clinical trial, men aged 40-74 yo, average morning T (2 measurements) <300ng/dl, given T cypionate 200 mg every 2 weeks IM for 18 months. Areal BMD (aBMD) by dual-energy X-Ray absorptiometry; volumetric BMD (vBMD) and bone geometry by peripheral quantitative computed tomography of the tibia; serum C-telopeptide (CTX), osteocalcin (OC), sclerostin by ELISA; T by automated immunoassay and estradiol by LC/MS. **Results:** 105 men were enrolled. At baseline, HG DM+ men had significantly higher vBMD but poorer bone geometry and decreased bone turnover compared to HG DM- men. At 18 months of T therapy, aBMD at the lumbar spine increased similarly in the DM+ compared to the DM- group ( $0.050 \pm 0.251$  vs  $0.086 \pm 0.312$  g/cm<sup>2</sup>;  $p=0.40$ ). In contrast, at 18 months, aBMD increased more at the total hip and femoral neck in the DM+ compared to the DM- group ( $0.048 \pm 0.034$  vs  $-0.095 \pm 0.032$  g/cm<sup>2</sup>;  $p=0.010$  and  $0.031 \pm 0.040$  vs  $-0.031 \pm 0.024$  mg/cm<sup>2</sup>;  $p=0.01$ , respectively). On the other hand, total vBMD at the 38% tibia increased more in the DM- compared to DM+ ( $0.667 \pm 17.64$  vs  $-1.396 \pm 29.58$  mg/cm<sup>3</sup>;  $p=0.05$ ). No significant changes in bone geometry parameters were noted in both groups. Sclerostin levels increased more in the DM+ compared to the DM- group ( $0.15 \pm 0.29$  vs  $-0.09 \pm 0.29$  ng/mL;  $p<0.01$ ). CTX and OC levels remained significantly lower in DM+ than in DM- with no significant between-group differences in the changes in both bone markers. **Conclusion:** Our findings suggest that compared to HG DM- men, T therapy in HG DM+ men resulted in an increase in aBMD without improvement in bone geometry and change in bone turnover, while it resulted in an increase in vBMD and maintenance of better bone geometry among HG DM- men. The significance of the increase in sclerostin in HG DM+ men with T therapy remains unclear and deserves further studies.

**Disclosures:** Georgia Colleluori, None.

## MO0068

**Energy and protein intake above recommendations inversely correlate with lean mass indices in 2-8 y olds.** Neil R. Brett\*, Kristina E Parsons, Catherine A. Vanstone, Hope A. Weiler. McGill University, Canada

In Canada and the U.S, over 50% of young children exceed protein intake recommendations and in Canada, 20% exceed energy intake recommendations. However, there has been little research in young children quantifying the effect of dietary protein and energy intakes on bone mineral content and body composition. Thus, the objective was to investigate, cross-sectionally, whether protein or energy intakes were related to bone mineral content and body composition in young children. Secondary data was combined from three studies of healthy children 2 to 8 y ( $n=212$ ) from the Greater Montreal area. Children underwent standardized anthropometry measurements as well as having whole body bone mineral content (BMC), lean mass and fat mass measured using dual-energy x-ray absorptiometry (Hologic Discovery 4500A, APEX software version 13.3). Lean mass (LMI), fat mass (FMI) and BMC (BMC) indices were calculated (lean mass/ height<sup>2</sup>, fat mass/ height<sup>2</sup>, BMC/height<sup>2</sup>). Fasted venous blood was sampled for measurement of vitamin D status (total serum 25(OH)D: Liaison, Diasorin) followed by 24 hour dietary intake questionnaires (Nutritionist Pro software version 4.7.0, Axxya149 Systems LLC and the 2010b Canadian Nutrient File database, Health Canada). Pearson and Spearman correlations were used to test for linear relationships. Data are mean  $\pm$  SE unless otherwise stated. Children were 53% (112/212) male, age  $4.2 \pm 1.6$  y, had average BMI z-scores of  $0.5 \pm 0.9$  and serum 25(OH)D concentration was  $\geq 50$  nmol/L in 87% (184/212) of children. Serum 25(OH)D concentration as well as vitamin D and calcium intakes (median (IQR)) (260 (170-372) IU/d and 1028 (787-1243) mg/d) did not significantly correlate with LMI, FMI or BMCI ( $p > 0.05$ ). On average, energy and protein intakes were  $87 \pm 24$  kcal/kg and  $3.6 \pm 1.2$  g/kg respectively and were significantly inversely related to LMI in preschoolers (2-4 y) and school-aged children (5-8 y) (Figure 1) but

were not significantly related to BMCI or FMI ( $p < 0.05$ ). These data in healthy young children suggest that exceeding the recommendations for protein may have a negative impact on lean mass but not fat mass or bone mineral content. There is a need for longitudinal investigation to better understand these relationships.

Figure 1. Correlations between body composition indices & energy (panel A) and protein (panel B) intake in 2-4 y olds ( $n = 150$ ) as well as energy (panel C) and protein (panel D) intake in 5-8 y olds ( $n = 62$ ).

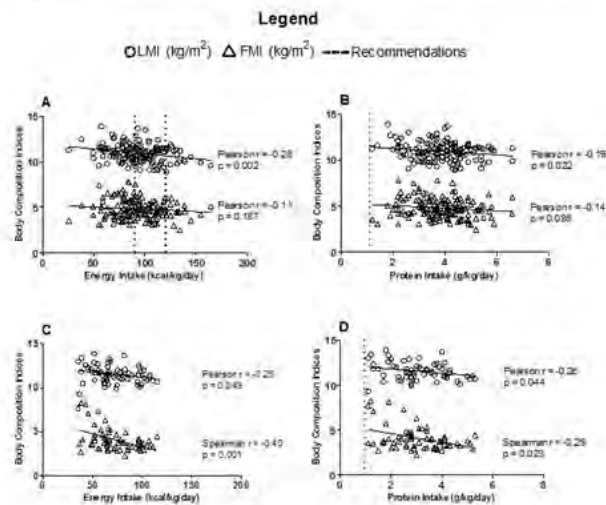


Figure 1

**Disclosures:** Neil R. Brett, None.

## MO0069

Withdrawn

## MO0070

**Novel Indications of the Disruption of VEGF signaling and Remodeling in Diabetic Bone.** Roberto Fajardo<sup>1</sup>, Jesus Hernandez<sup>1</sup>, Brandon May<sup>2</sup>, Nandini Ghosh-Choudhury<sup>1</sup>, Zachary Child<sup>1</sup>. <sup>1</sup>The University of Texas Health Science Center at San Antonio, United states, <sup>2</sup>University of Texas at San Antonio, United states

Adults with type 2 diabetes mellitus (DM2) are at increased risk for fractures compared to non-diabetics. The underlying causes of these fractures remain unclear due to limited human data. Evidence in the literature suggests that suppressed remodeling and advanced glycation end-product (AGE) accumulation may contribute to fracture risk due to material changes in bone. Limited evidence suggests that these material changes are exacerbated by decreased bone turnover in subjects with DM2. Vascular endothelial growth factor (VEGF) signaling is a critical component that is poorly understood in diabetic bone. VEGF-A signaling through VEGFR2 is critical for neoangiogenesis and vascular maintenance, it also promotes osteoclast differentiation. The objective of our study is to elucidate the role of VEGF signaling in diabetic bone fragility and determine their resorbing capacity.

Spine tissue was collected from human subjects undergoing surgery. Subjects were 50 yrs of age or older and either diabetic or non-diabetic. Exclusion criteria included previous lumbar or thoracic surgeries, use of anti-osteoporosis medications, bone metastases, and other exclusion criteria. The Institutional Review Board of the University of Texas Health Science Center at San Antonio approved the study.

Bone tissue was harvested and allocated for RT-PCR, histology, or AGE determination. Results indicated significantly decreased ( $P<0.01$ ) VEGF-A in diabetic bone tissue compared to non-diabetic tissue. VEGFR2 expression also showed a strong negative trend ( $P=0.05$ ). A strong decrease in RANKL expression in human diabetic bone ( $P=0.06$ ) was evident in our analysis. Histologic sections showed a 34% decrease in the number of multinucleated, TRAP-positive osteoclasts in diabetic versus non-diabetic bone tissue. Lastly, we found a 43% increase ( $P<0.05$ ) in the total AGEs of diabetic trabecular bone together with a 34% increase in cortical bone.

Our results suggest that diabetic bone tissue is characterized by abnormal signaling along the VEGF-A and VEGFR2 axis. The decrease in the expression of the ligand and the receptor is correlated with a diminished resorptive capacity in human bone tissue that is manifested by decreasing trends in RANKL expression and osteoclast numbers. One potential consequence is the increased accumulation of AGEs in diabetic human bone, a factor that may critically contribute to the increased fracture risk in adult diabetic patients.

**Disclosures:** Roberto Fajardo, None.

This study received funding from: AO Spine Foundation, N.A.

**MO0071**

**High Bone Turnover in Mice Carrying a Pathogenic Notch2-mutation Causing Hajdu-Cheney Syndrome.** Nele Vollersen\*, Timur Yorgan, Michael Amling, Thorsten Schinke. Department of Osteology & Biomechanics, University Medical Center Hamburg-Eppendorf, Germany

Notch signaling is a key pathway controlling various cell fate decisions during embryogenesis and adult life. While the skeletal analysis of mouse models with activated or inactivated Notch signaling has demonstrated a general impact of this pathway on bone remodeling, the more recent identification of *NOTCH2* mutations in individuals with Hajdu-Cheney syndrome (HCS) has highlighted its human relevance. HCS is a rare autosomal-dominant disorder primarily characterized by acroosteolysis, early-onset osteoporosis and short stature. Genetically, HCS is caused by nonsense or deletion mutations within exon 34 of the *NOTCH2* gene, thereby causing a premature translational termination and production of a C-terminally truncated Notch2 protein, which is predicted to activate Notch2-dependent signaling. In order to understand the role of Notch2 in bone remodeling, we developed a mouse model of HCS by introducing a pathogenic mutation (6272delT) into the murine *Notch2* gene. By  $\mu$ CT and undecalcified histology we observed generalized osteopenia in independent mouse lines derived by injection of two targeted ES cell clones. Cellular and dynamic histomorphometry further revealed a high bone turnover situation in both lines, since osteoblast and osteoclast indices were significantly increased compared to wildtype littermates. Consistently, serum levels of bone turnover markers were increased in *Notch2*<sup>HCS/+</sup> mice, and the same was the case in one individual with HCS displaying severe osteoporosis. Taken together, our data confirm previous results, i.e. osteopenia and increased osteoclastogenesis, obtained in another mouse model of HCS (Canalis et al., J.Biol.Chem. 2016). Importantly however, as we additionally observed excessive osteoblastogenesis and bone formation in our model, it appears that Notch2 affects both bone remodeling types by mechanisms that are currently investigated.

**Disclosures:** Nele Vollersen, None.

**MO0072**

**High Throughput Bone Phenotyping: Rigor and Transparency.** Douglas Adams\*<sup>1</sup>, Renata Rydzik<sup>1</sup>, Li Chen<sup>1</sup>, Zhihua Wu<sup>1</sup>, Seung-Hyun Hong<sup>1</sup>, Pujan Joshi<sup>1</sup>, Caibin Zhang<sup>1</sup>, John Sundberg<sup>2</sup>, Gaven Garland<sup>2</sup>, Dong-Guk Shin<sup>1</sup>, David Rowe<sup>1</sup>, Cheryl Ackert-Bicknell<sup>3</sup>. <sup>1</sup>University of Connecticut, United states, <sup>2</sup>The Jackson Laboratory, United states, <sup>3</sup>University of Rochester, United states

The International Mouse Phenotyping Consortium provides the opportunity to assess the impact of gene knockout on a uniform genetic background (C57BL/6N) in mice raised in a controlled environment. We continue to refine our high throughput, observer-independent bone phenotyping workflow by examining IMPC control mice. In total, 19 groups were collected at one-month intervals. Groups consisted of 8 males and 8 females, that were administered double mineralization labels prior to harvesting femurs and lumbar vertebrae. Morphometric screening by  $\mu$ CT registered expected sex differences in BV/TV of the femur, with greater variance in male (28.2%) vs female (20.6%) and in all other morphometric parameters (e.g., Ct.Ar 8.7 vs 5.5%; vertebral BV/TV 17.0 vs 10.7%). During the last 6 months, a downward drift of bone size and body weight occurred, that may be due to seasonal phytochemicals in the chow. Static histomorphometry performed on the same animals closely paralleled  $\mu$ CT measurements both in BV/TV and TbTh trends and sexual variance (CV F=6.5, M=8.0). The dynamic and cellular histology was based on fluorescent signals from the mineralization dyes and enzymatic substrates for AP and TRAP. As the signals are captured and analyzed under computer-controlled conditions, the intensity of the signals, which can affect the biological measurement, are followed closely. The intensity measurements have proven to be a sensitive predictor of an error in the step of mineralization dye administration or in the processing of the samples for enzymatic analysis. As all of the image and analysis information is digital and archived, the likely cause of a calculation that falls significantly outside the range of expected variance can be identified quickly. These findings have influenced our recommendations for sample collection to include at least 8 mice per sex over a 2-3 month interval. Additionally, an enzymatic and fluorescent mineralization standard should be incorporated into histomorphometric analysis as a control for fluorescent signal intensity of the test samples on the slide. These data have highlighted key sources of error in control sample analysis and have allowed us to develop rigorous safeguards to prevent technical errors. Further, these large data sets has emphasized that environmental factors impacting the mice can greatly impact control values, demonstrating that experimental groups must be concordant with experimental groups with regards to time of collection.

**Disclosures:** Douglas Adams, None.

**MO0073**

**Identifying Genetic Mediators of Periodontitis in Mice.** Sarah Hiyari\*<sup>1</sup>, Azadi Naghibi<sup>2</sup>, Sotirios Tetradis<sup>2</sup>, Flavia Pirihi<sup>2</sup>. <sup>1</sup>University of California, Los Angeles School of Dentistry, United states, <sup>2</sup>UCLA School of Dentistry, United states

Periodontitis (PD) is characterized by bacterial infection and inflammation of the gingiva and alveolar bone surrounding the teeth. If left untreated, PD causes bone resorption that can ultimately lead to tooth loss. Additionally, PD affects ~47% of the U.S. population over age 30. Interestingly, twin studies have shown PD to be 50% heritable.

**Objective:** Identify genetic mediators and cellular populations associated with PD susceptibility and severity.

**Methods:** *P. gingivalis* (*P.g.*)-Lipopolysaccharide (LPS) was injected in between 1st and 2nd maxillary molars in 78 strains of the Hybrid Mouse Diversity Panel (HMDP) twice a week for 6 weeks. Following sacrifice, maxillae were scanned using microCT and linear bone loss was quantitated. Factored Spectrally Transformed Linear Mixed Modeling (FaST-LMM) was used to identify genetic loci associated to bone loss. A/J and C57BL/6J were further analyzed through: a) microarray b) *in vitro* osteoclastic potential, and c) *in vivo* histology including H&E, anti-p65 (NF- $\kappa$ B), anti-COX2, anti-TNF $\alpha$ , anti-TGF $\beta$ , anti-MMP13, anti-CD3 (T-cells), anti-neutrophil NIMP-R14, and anti-Cxcl10 after LPS injections.

**Results:** We observed a strain-dependent 6-fold difference in LPS-induced bone loss across the HMDP. Focusing on the 5 parental strains, A/J was the most resistant and C57BL/6J was the most susceptible to *P.g.*-LPS-induced bone loss. Additionally, heritability was 50% for our trait. Microarray of A/J and C57BL/6J showed statistically differentially expressed genes induced by LPS including members of the Cxcl chemokine family, which correlated with our FaST-LMM data. *In vitro* data confirmed that C57BL/6J exhibit more osteoclastic potential compared to A/J (p=0.0195). *In vivo* analysis revealed that C57BL/6J had increased osteoclasts, NF- $\kappa$ B, COX-2, TNF- $\alpha$ , TGF- $\beta$ , MMP-13, T-cells, neutrophils, and Cxcl10 after LPS injections.

**Conclusions:** Heritability of bone loss in mice is similar to PD in humans. We identified known genes/loci, as well as, novel gene candidates that may be important for LPS-induced bone loss. Future work will validate candidate genes that contribute to PD. The ultimate goal of our study is to understand PD pathophysiology in order to identify individuals at high risk for PD.

**Disclosures:** Sarah Hiyari, None.

**MO0074**

**Modulation of autophagy alters osteogenesis imperfecta severity in mice with Gly610 to Cys substitution in the triple helical region of the  $\alpha$ 2(I) collagen chain.** Elena Makareva<sup>1</sup>, Shakib Omari<sup>1</sup>, Anna Roberts-Pilgrim<sup>1</sup>, Edward Mertz<sup>2</sup>, Laura Gorrell<sup>1</sup>, Lynn Mirigian<sup>1</sup>, Sergey Leikin\*<sup>1</sup>. <sup>1</sup>SPB, NICHD, NIH, United states, <sup>2</sup>SPB, NICHD, NIH, United states

Glycine substitutions in the triple helical region of type I collagen are the most common mutations resulting in severe forms of osteogenesis imperfecta (OI). The G610C mouse (MGI:371122) with a Gly610 to Cys substitution in the  $\alpha$ 2(I) chain produces moderately severe OI in heterozygous (het) and lethal OI in homozygous (hom) animals, as expected for dominant negative mutations. Heterozygous animals exhibit significant variability of bone phenotype, which is a common feature of Gly substitutions. In previous studies of G610C mice, we found that osteoblast malfunction caused by accumulation of misfolded procollagen inside the cell is a major factor in bone pathology and that cells degrade misfolded procollagen by autophagy. To test how modulation of autophagy affects bone pathology, we crossed G610C with *Atg5*<sup>fllox/fllox</sup> (MGI:3663625) mice for subsequent conditional knockout of Atg5 protein required for autophagosomal membrane formation. Even without introducing Cre recombinase, we found *Atg5* mRNA and protein expression to be 2-5 times lower in all tested tissues of *Atg5*<sup>fllox/fllox</sup> compared to *Atg5*<sup>+/+</sup> animals. Lower *Atg5* expression significantly increased the frequency and severity of skeletal deformities in newborn G610C-het pups and reduced survival of these pups by 30-50% without affecting their wild type (wt) littermates. Skeletal staining of newborn pups revealed undermineralization of calvaria, *in-utero* rib fractures, severe rib and scapula deformities, as well as deformities and fractures of long bones. We then generated G610C;*Atg5*<sup>fllox/fllox</sup>;osteocalcin-Cre animals by breeding with osteocalcin-Cre mice (MGI:2446069). All mice were backcrossed and maintained on the C57BL/6J background. The resulting knockout of *Atg5* in osteoblasts by osteocalcin-promoter-driven Cre expression had no significant additional effect on G610C-het pup survival or relative growth curve. Yet, it further increased the frequency and severity of the skeletal deformities and bone fractures. It also appeared to affect bone development and maintenance in mice at least up to 4 mo. age. Combined with our other observations, this study suggests that autophagy of misfolded procollagen plays an important role in OI bone pathology. It appears to be at least partially responsible for variable severity of the same mutation in different individuals and might be targeted for therapeutic intervention.

**Disclosures:** Sergey Leikin, None.

**MO0075**

**NF- $\kappa$ B Regulator Bcl-3 – A Novel Modulator of Skeletal Architecture.** Hussain Jaffery<sup>\*1</sup>, Carl S Goodyear<sup>1</sup>, Ruaidhri J Carmody<sup>1</sup>, James Doonan<sup>2</sup>, Moed Akbar<sup>1</sup>, Carmen Huesa<sup>3</sup>, Lynette Dunning<sup>1</sup>, William Ferrell<sup>4</sup>, John Lockhart<sup>3</sup>, Rob van 't Hof<sup>5</sup>. <sup>1</sup>Institute of Infection, Immunity & Inflammation, University of Glasgow, United Kingdom, <sup>2</sup>Strathclyde Institute of Pharmacy & Biomedical Sciences, University of Strathclyde, United Kingdom, <sup>3</sup>Institute of Biomedical & Environmental Health Research, University of the West of Scotland, United Kingdom, <sup>4</sup>Institute of Infection Immunity & Inflammation, University of Glasgow, United Kingdom, <sup>5</sup>Institute of Ageing & Chronic Disease, University of Liverpool, United Kingdom

Osteoarthritis associated joint degeneration, aberrant bone formation, reduced joint mobility and pain are major unmet clinical problems. In the healthy joint, the balance between chondrocytes, osteoblasts and osteoclasts is a dynamic process under tight regulation. In disease, regulation is disrupted, resulting in progressive cartilage degradation and the formation of bony spurs (osteophytes). The NF- $\kappa$ B transcription factor is a critical regulator of chondrocyte and osteoclast differentiation and is important for the development and homeostasis of the skeletal system. In osteoblasts NF- $\kappa$ B activity is associated with decreased differentiation and function. The I $\kappa$ B-like protein Bcl-3 is a critical regulator of NF- $\kappa$ B cellular function via selective interaction with homodimers of the NF- $\kappa$ B subunits p50 and p52.

To characterise the contribution of Bcl-3 towards the skeletal phenotype, we performed high-throughput X-ray micro-computed tomography ( $\mu$ CT) on *Bcl-3*<sup>-/-</sup> male mice aged 4 weeks to 1.3 years. Neonatal calvarial osteoblast cultures were used to investigate the cellular and molecular mechanisms of Bcl-3. Additionally, we assessed the progression of osteoarthritic pathology in *Bcl-3*<sup>-/-</sup> mice following destabilisation of the medial meniscus (DMM).

Our studies reveal that *Bcl-3*<sup>-/-</sup> mice have increased bone mass and altered bone architecture. At 20 weeks of age, *Bcl-3*<sup>-/-</sup> mice have significantly divergent phenotypes from wild-type counterparts in a multitude of parameters, including a 5.4% increase in cross-sectional bone area of the femoral cortex, a 15.5% increase in percent bone volume in the trabecular space of tibias, and a 2.8% increase in tibia trabecular thickness. Complementary *in vitro* studies demonstrate that the loss of Bcl-3 enhances osteoblast differentiation and activity. Importantly, the altered skeletal phenotype of *Bcl-3*<sup>-/-</sup> mice is present during development and throughout adulthood. Finally, preliminary results suggest that Bcl-3 may have a protective effect in osteophyte development in a murine model of osteoarthritis. We propose Bcl-3 as a novel regulator of skeletal development, morphology and pathology.

*Disclosures:* Hussain Jaffery, None.

**MO0076**

**Osteocyte Specific Cx43 Overexpression Improves Cortical Bone Mass and Strength, but Reduces Cancellous Bone in old Mice.** Hannah Davis<sup>\*1</sup>, Emily Atkinson<sup>1</sup>, Rafael Pacheco-Costa<sup>1</sup>, David Lopez<sup>1</sup>, Mohammad Aref<sup>1</sup>, Drew Brown<sup>1</sup>, Marie Harris<sup>2</sup>, Stephen Harris<sup>2</sup>, Matthew Allen<sup>1</sup>, Teresita Bellido<sup>1</sup>, Lilian Plotkin<sup>1</sup>. <sup>1</sup>Indiana University School of Medicine, United states, <sup>2</sup>The University of Texas at San Antonio, United states

Osteocytic deletion of connexin (Cx) 43 in 5-month-old mice results in decreased bone strength, which resembles the phenotype of old mice. Further, bones from old mice exhibit 10-fold lower Cx43 expression compared to young mice, suggesting a contribution of reduced Cx43 levels to age-related changes. We investigated here whether osteocyte specific overexpression of Cx43 attenuates the skeletal phenotype of old mice; using mice in which the DMP1-8kb promoter targeted Cx43 expression to osteocytes (Cx43<sup>Oi</sup> mice). Cx43 expression at the mRNA and protein levels was increased by 3-4 fold in bones of Cx43<sup>Oi</sup> mice, but not in kidney, liver, heart or muscle, compared to wild type (WT) littermates. BMD in 2-month-old female Cx43<sup>Oi</sup> mice was identical to WT mice. Moreover, longitudinal BMD analysis showed that both Cx43<sup>Oi</sup> and WT littermates reached similar peak BMD at ~5.5 months of age. Spinal BMD started to decline in 9.5-month-old WT mice but it was maintained in Cx43<sup>Oi</sup> mice. At 14 months of age, spinal BMD in Cx43<sup>Oi</sup> mice was 8% higher than WT mice. Total vertebral (cortical + cancellous) bone volume was unchanged while cancellous BV/TV measured by  $\mu$ CT was decreased by 27%, suggesting an increase in cortical bone volume. In addition, femur BMD remained high and cortical bone area measured by  $\mu$ CT was similar in mice of both genotypes at 14 months of age. However, Cx43<sup>Oi</sup> femora were 2% longer, and exhibited 10% larger diameter and 12% higher moment of inertia at the mid-diaphysis, consistent with periosteal expansion. Further, femoral ultimate load measured by 3-point bending testing was 8% higher; but ultimate stress, which results from adjusting for the larger periosteal diameter, in Cx43<sup>Oi</sup> was similar mice to WT mice. These findings indicate that the improved mechanical properties evidenced by ultimate load are due to the larger bone size, not to changes in bone material. Consistent with the differences in structural properties, gene expression in vertebrae and long bones of Cx43<sup>Oi</sup> mice was also distinct. Sost mRNA was 1.7-fold higher and the expression of the Wnt target genes BMP4 (0.6-fold) and Smad6 (0.7-fold) was lower in vertebra of Cx43<sup>Oi</sup> compared to WT mice, whereas no changes in these genes were detected in cortical bone. We conclude that Cx43 overexpression in osteocytes partially ameliorates age-induced skeletal changes, preventing loss of spine BMD and

improving femoral bone strength; but negatively impacting vertebral cancellous bone structure.

*Disclosures:* Hannah Davis, None.

**MO0077**

Withdrawn

**MO0078**

**Transgenic Mouse Model for Reducing Oxidative Damage in Bone.** Ann-Sofie Schreurs<sup>\*1</sup>, Eric Moyer<sup>1</sup>, Akilesh Kumar<sup>1</sup>, Samantha Torres<sup>1</sup>, Tiffany Truong<sup>1</sup>, Candice Tahimic<sup>1</sup>, Joshua Alwood<sup>1</sup>, Charlie Limoli<sup>2</sup>, Ruth Globus<sup>1</sup>. <sup>1</sup>NASA ARC, United states, <sup>2</sup>UC Irvine, United states

Bone loss can occur due to factors such as age, radiation, microgravity, all of which increase Reactive Oxygen Species (ROS); and is characterized by alterations in the balance between bone formation and resorption. Hence, we hypothesized that suppression of excess ROS in both osteoblasts and osteoclasts will improve overall bone microarchitecture and mass. To test our hypothesis, we used transgenic mCAT mice which overexpress the human anti-oxidant catalase gene targeted to the mitochondria, the main site for endogenous ROS production. mCAT mice have a longer life-span than wildtype controls and have been used to study various age-related disorders. To stimulate skeletal remodeling, 16-week-old mCAT mice or wildtype mice were exposed to treatment (hindlimb-unloading and total body-irradiation) or sham treatment (control). Tissues were harvested two weeks later for skeletal analysis (microcomputed tomography), biochemical analysis (gene expression and oxidative damage measurements), and ex vivo bone marrow derived cell culture (osteoblastogenesis and osteoclastogenesis). mCAT mice expressed the transgene and displayed elevated catalase activity in skeletal tissue and ex vivo osteoblast and osteoclast cultures derived from marrow. In addition, when challenged with treatment, bone from wildtype mice showed elevated levels of malondialdehyde (MDA, indicating oxidative damage) whereas mCAT mice did not. Correlation analysis revealed that increased catalase activity correlated with decreased MDA levels and that increased oxidative damage correlated with decreased percent bone volume (BV/TV). Furthermore, ex-vivo osteoblast colony growth positively correlated with osteoblast catalase activity. mCAT mice displayed reduced BV/TV and trabecular number (Tb.N) relative to wildtype, as well as increased structural model index (SMI) in cancellous axial bone (tibia). No genotype effects on microarchitecture or compressive mechanical properties were observed in the 4th lumbar vertebra. Treatment caused bone loss in wildtype mice, as expected. Treatment also caused deficits in microarchitecture of mCAT mice, although less severe than wildtype mice in some parameters (percent bone volume, structural model index and cortical area). In conclusion, our results indicate endogenous ROS signaling in both osteoblast and osteoclast lineage cells contribute to skeletal development and remodeling and quenching oxidative damage could play a role in bone loss prevention.

*Disclosures:* Ann-Sofie Schreurs, None.

**MO0079**

**Use of OI iPSC In Vivo Bone Formation Model to Study Disease Mechanisms and Potential Therapies.** Xiaonan Xin, Mark Kronenberg, Li Chen, Shalini Gohil, Liping Wang, Xi Jiang, Lakshmi Nair, David Rowe, Alexander Lichtler<sup>\*</sup>. UConn Health, United states

We reported that iPSC-MSC from patients with osteogenesis imperfecta (OI) produced substantially less bone than iPSC-MSC from controls in an *in vivo* mouse calvarial defect model, but formed substantial adipose tissue. Because OI mutations are known to inhibit the progression of skeletal progenitor cells down the osteoblastic lineage, we tested the ability of BMP to improve OI bone formation. Using a slow release chitosan-based hydrogel placed over the iPSC-MSC/HEALOS implant to deliver rhBMP-2, we observed increased bone formation by the OI iPSC-MSC. To test the utility of CRISPR technology to correct an OI mutation without inserting additional sequence ("scarless" repair), we designed a CRISPR guide RNA construct targeting a site near the mutation and transfected it, a Cas9 vector, and a synthetic single stranded repair oligo, into an OI iPSC line. This line, coded 445, has a glycine substitution mutation in exon 22 of the COL1A1 gene. The repair oligo contained the normal sequence at the mutation site, and a single bp change in the CRISPR target sequence, to eliminate re-cutting of repaired alleles. We used co-transfection of an antibiotic selection plasmid to enrich for transfected cells, but no selection for the integration of a construct. Initially we screened 64 random colonies by PCR amplification and restriction enzyme cutting of an NheI site present in mutant but not wild type sequence. We obtained two clones lacking the mutant sequence, however both clones had deletions, presumably due to non-homologous end joining (NHEJ). We repeated the procedure using an NHEJ inhibitor, and obtained two clones without an insertion or deletion, suggesting that the NHEJ inhibitor worked. One clone had a normal sequence at the mutation site and throughout the surrounding sequence and it maintained a common polymorphism at a second site in the COL1A1 gene. This clone appears to have a proper correction of the OI mutation, and we are currently testing its ability to produce bone in our *in vivo* bone formation model.

However, because this clone lacks the CRISPR target site mutation that should have been introduced by the repair oligo, we believe that the repair oligo was not used, instead the normal allele may have been used to repair the break in the mutant allele. We are currently exploring changes to the methodology to improve use of the repair oligo. We believe that our methodologies will have great usefulness in studying human skeletal diseases.

**Disclosures:** Alexander Lichtler, None.

## MO0080

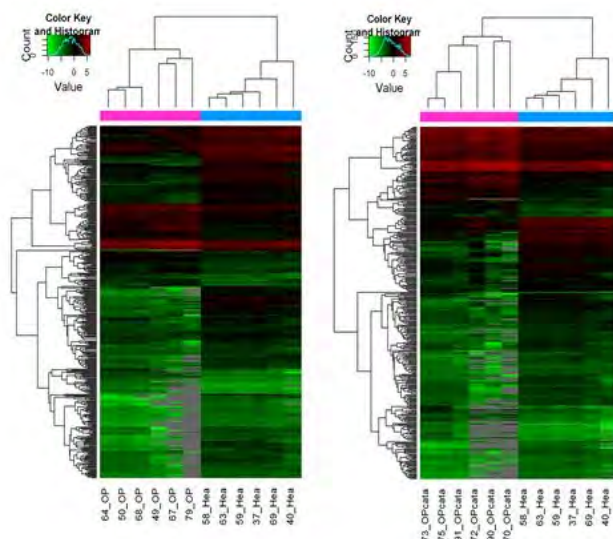
**Circulating MicroRNAs Expression Profile in Patients with Osteoporosis-Osteoporotic Fracture.** Mengge Sun<sup>\*1</sup>, William Lu<sup>1</sup>, Songlin Peng<sup>2</sup>. <sup>1</sup>The University of Hong Kong, Hong Kong, <sup>2</sup>Department of Spine Surgery, Shenzhen People's Hospital, Jinan University School of Medicine, China

**Introduction:** Osteoporosis (OP) is mainly caused by the unsuccessful maintenance of the balance between osteoblast-mediated bone formation and osteoclast-mediated bone resorption. Several miRNAs have been reported to regulate bone metabolism by modulating the differentiation and activity of osteoblasts and osteoclasts. MiRNAs are also demonstrated to be stable in serum. Therefore, we studied circulating miRNAs with special expression profile in patients with osteoporosis or osteoporotic fracture.

**Methods:** 18 subjects from south of China were recruited in this study. 6 of them are osteoporosis patients (T-score  $\leq -2.5$ ). Another 6 are patients with vertebral osteoporotic fracture (T-score  $\leq -2.5$  with fragility fracture). And 6 subjects are healthy people as healthy control (T-score  $\geq -1.0$ ). The exclusion criteria for the subjects are as follows: tumor, known chronic, systemic, metabolic, endocrine diseases including polycystic ovarian syndrome, medication treatment effected bone metabolism and any medical history or signs of other inflammatory disease, acute trauma. This study was approved by the local ethical review committee and the subjects provided informed written consent. The whole blood were collected from each subject and separated into plasma immediately. MicroRNA profiling was performed on the plasma samples which were divided into 3 groups: osteoporosis (OP) group (without fracture, n=6), osteoporotic fracture (OPcata) group (n=6), healthy control (Hea) group (n=6). The miRNAs expression was further validated by quantitative real-time RT-PCR.

**Results:** Significantly differentially expressed miRNAs between OP group and Hea group or OPcata group and Hea group were identified through fold change and P-value which is fold change values  $\geq 2$  or  $\leq 0.5$  and P-values  $< 0.05$ . 118 miRNAs were upregulated and 266 were downregulated in OP group compared to Hea group. In addition, there were 123 upregulated miRNAs and 218 downregulated in OPcata group compared to Hea group. Particularly, 41 upregulated and 164 downregulated miRNAs expressed significant differences both in OP groups and OPcata groups. MiR-665 was upregulated 2.71-, 7.33- fold in OP group and OPcata group, respectively (P  $< 0.01$  for both). On the other hand, miR-27b was significantly downregulated in OP and OPcata group, which has been reported to be associated with the migration of mesenchymal stem cells.

**Discussion & conclusion:** Patients with osteoporosis/osteoporotic fracture have different circulating miRNAs expression profile compared with health subjects. The differentially expressed miRNAs might play a crucial role in the molecular pathogenesis of osteoporosis. Further research for the understanding of the functionality and pathological mechanism of the miRNAs in osteoporosis is also important and the selected miRNAs might be important biomarkers in early diagnosis of osteoporosis.



Heat map and hierarchical clustering ID:A16015940

**Disclosures:** Mengge Sun, None.

## MO0081

**Network-Based Transcriptome-Wide Expression Study for Postmenopausal Osteoporosis.** lan zhang<sup>\*</sup>, Hongwen Deng. Tulane University, United states

Menopause is one of the crucial physiological events during the life of women. Transition of menopause status is accompanied by increased risks of various health problems like osteoporosis. Peripheral blood monocytes (PBMs) can differentiate into osteoclasts and produce cytokines important for osteoclast activities. To identify osteoporosis-related genes, we performed transcriptome-wide expression analyses for human PBM using Affymetrix 1.0 ST arrays in 40 Caucasian postmenopausal women with discordant bone mineral density (BMD) levels. 716 genes were significantly differentially expressed ( $P_{\text{adjust}} < 0.05$ ) in subjects with extremely low vs. high BMD. We performed Multiscale Embedded Gene Co-expression Network Analysis (MEGENA) to study functionally orchestrating clusters of differential expressed genes in the form of networks. MEGENA showed that the module containing *ZFP36* as hub gene was significantly correlated with BMD variation, and "T cell receptor signaling pathway" as well as "osteoclast differentiation pathway" were significantly enriched in this identified compact network. Gene Sets Net Correlations Analysis (GSNCA) was applied to see how the co-expression structure of pre-defined gene set differs in high and low BMD groups. GSNCA revealed that the co-expression structure of "Signaling by TGF-beta Receptor Complex pathway" is significantly different between two groups, and the hub genes in postmenopausal high and low BMD group are *FURIN* and *SMAD3* respectively. The present study suggested that biological signals involved in monocyte recruitment, monocyte/macrophage lineage development, osteoclast formation, osteoclast differentiation might function together in PBMs that contributes to the pathogenesis of postmenopausal osteoporosis.

**Disclosures:** lan zhang, None.

## MO0082

**Bone Strength Estimated by Failure Load Shares Genetic Composition with Areal BMD: The Framingham Study Families.** David Karasik<sup>\*1</sup>, Serkalem Demissie<sup>2</sup>, Mary L. Bouxsein<sup>3</sup>, Ching-Ti Liu<sup>2</sup>, Steven K. Boyd<sup>4</sup>, Elise Lim<sup>2</sup>, Kerry E. Broe<sup>1</sup>, L. Adrienne Cupples<sup>2</sup>, Douglas P. Kiel<sup>1</sup>. <sup>1</sup>Institute for Aging Research Hebrew SeniorLife, United states, <sup>2</sup>Biostatistics, BU School of Public Health, United states, <sup>3</sup>BIDMC, Harvard MS, United states, <sup>4</sup>University of Calgary, Canada

Genetic factors contribute to the risk of long bone fractures, mostly due to effects on bone strength. High-resolution peripheral quantitative computed tomography (HR-pQCT) estimates bone strength in compression using micro finite element analysis ( $\mu$ FEA). The goal of this study was to investigate if the HR-pQCT-based  $\mu$ FEA-estimated bone failure load is heritable and to what extent it shares genetic regulation with long bone's aBMD measured by DXA.

Bone microarchitecture was measured by HR-pQCT (Scanco Medical, AG) at the distal tibia (n=1,059) and distal radius (n=1,022) in adults of European ancestry from the Offspring Cohort of the Framingham Heart Study (average age 72.2 years, range 48-95; 57% women). Radial and tibial failure load (FL) in compression was estimated by  $\mu$ FEA (in Newton). Femoral neck (FN) and ultradistal forearm (UD) aBMD were measured by DXA (Lunar DPX-L, g/cm<sup>2</sup>). Heritability estimates ( $h^2$ ) and bivariate correlations were calculated (adjusting for age, sex, and height) using a variance components model in SOLAR.

FL values at the non-weight-bearing distal radius and at the weight-bearing distal tibia were highly correlated:  $r=0.906$ . Estimates of  $h^2$  adjusted for covariates ranged from 0.518-0.522 (radius) and 0.497-0.505 (tibia). Additional adjustment for local aBMD dramatically decreased both radius and tibia FL  $h^2$  estimates: 0.222 and 0.380, respectively. In bivariate analysis, there were high phenotypic and genetic correlations between multivariable-adjusted FL at radius and UD aBMD ( $\rho_P = 0.826$ ,  $\rho_G = 0.954$ ), while environmental correlations ( $\rho_E$ ) were lower (0.696; Table 1). Similar but lower correlations were observed between tibial FL and FN aBMD ( $\rho_P = 0.577$ ,  $\rho_G = 0.703$ ,  $\rho_E = 0.432$  respectively; Table 1).

These data from extended families of a population-based cohort of adult men and women suggest for first time that, in adults of European ancestry, bone strength estimated by failure load is heritable and shares genetic composition with areal BMD, regardless of the specific skeletal site (slightly lower between tibial FL and aBMD of the hip since these bones are not the same). Further work is necessary to identify specific variants underlying genetic differences in long bone structure and strength.

**Table 1:** Descriptive statistics, heritability of failure load and its phenotypic ( $p_p$ ), genetic ( $p_g$ ) and environmental ( $p_e$ ) correlations with proximal aBMD

	Radius			Tibia		
FL, Newtons (mean±SD)	2618.2±788.8			6437.5±1751.1		
$h^2$ (mean±SE)	0.522±0.127 F=0.000026			0.497±0.120 F=0.000027		
	correlations with UD aBMD			correlations with FN aBMD		
model of adjustment	$p_p$	$p_g \pm SE (p_0, p_1)$	$p_e \pm SE (p_0)$	$p_p$	$p_g \pm SE (p_0, p_1)$	$p_e \pm SE (p_0)$
Age and sex	0.819	0.936±0.050 (0.00004; 0.092)	0.704±0.079 (0.00054)	0.584	0.713±0.085 (0.00008; 0.00048)	0.453±0.141 (0.035)
Age, sex, and height	0.828	0.954±0.046 (0.00002; 0.155)	0.896±0.080 (0.0009)	0.577	0.703±0.086 (0.00012; 0.0005)	0.432±0.142 (0.039)

$p_0$ : p value for difference from 0;  $p_1$ : p value for difference from 1.0

TABLE 1

Disclosures: David Karasik, None.

**MO0083**

**Heritability of Bone Mineral Density and Content in Childhood and Adolescence.** Diana Cousminer\*<sup>1</sup>, Alessandra Chesi<sup>1</sup>, Jonathan Mitchell<sup>1</sup>, Sani Roy<sup>1</sup>, Heidi Kalkwarf<sup>2</sup>, Joan Lappe<sup>3</sup>, Vicente Gilsanz<sup>4</sup>, Sharon Oberfield<sup>5</sup>, John Shepherd<sup>6</sup>, Andrea Kelly<sup>1</sup>, Shana McCormack<sup>1</sup>, Benjamin Voight<sup>7</sup>, Babette Zemel<sup>1</sup>, Struan Grant<sup>1</sup>. <sup>1</sup>Children's Hospital of Philadelphia, United states, <sup>2</sup>Cincinnati Children's Hospital Medical Center, United states, <sup>3</sup>Creighton University, United states, <sup>4</sup>Children's Hospital of Los Angeles, United states, <sup>5</sup>Columbia University Medical Center, United states, <sup>6</sup>University of California San Francisco, United states, <sup>7</sup>University of Pennsylvania, United states

Background: Heritability is the amount of variance in a trait that is attributed to genetic factors. To our knowledge, only one previous study used genotype data to assess heritability of bone mineral density (BMD) in children aged 9 yr (Kemp et al., 2014). To date, no study has assessed the heritability of BMD or bone mineral content (BMC) at specific skeletal sites across childhood and adolescence. Aim: To determine heritability estimates for BMD and BMC across clinically important skeletal sites in children and adolescents. Methods: In the multicenter, multiethnic, longitudinal Bone Mineral Density in Childhood Study (BMDCS) of healthy children ages 5 to 20 yr, BMD and BMC of the spine, total hip, femoral neck, distal radius, skull, total body, and total body less head (TBLH) were measured in up to 1876 boys and girls. We used GCTA-Restricted Maximum Likelihood (GREML) to estimate the proportion of genetic variance ( $V_g$ ), using age- and sex-specific areal BMD (or BMC) Z-scores at each site, adjusting for study center, cohort, age, sex, physical activity, dietary calcium, and body mass index z-score (except for skull). GREML accounts for relatedness and ancestry with a genetic relationship matrix. Additionally, we performed bivariate GREML to compare  $V_g$  pairwise between skeletal sites. Results: BMD had larger  $V_g$  estimates than BMC at all skeletal sites. Each skeletal site showed varied contributions from genetic and residual factors. Heritability estimates ranged from  $V_g$  (SE)=0.38 (0.1),  $P=2.6 \times 10^{-5}$  at the skull to  $V_g$  (SE)=0.11 (0.08),  $P=0.08$  at the radius for BMD and from  $V_g$  (SE)=0.23 (0.07),  $P=3.8 \times 10^{-4}$  for the total body to  $V_g$  (SE)=0.08(0.07),  $P=0.1$  at the radius for BMC. Additionally, height z-score-adjusted (HAZ)  $V_g$  estimates were higher than unadjusted phenotypes at all skeletal sites except the radius. For the bivariate correlations, both phenotypic and genotypic correlations were similar across most skeletal sites. All skeletal sites showed a patchwork of shared and unique genetic contributions. Conclusions: In comparison to Kemp et al., our estimates of  $V_g$  were slightly lower, possibly due to the broad age range assessed, which may mask variations in heritability at different ages. However, our results represent pediatric heritability estimates at the most detailed skeletal resolution to date for BMD and BMC, and will serve as a resource for genetic studies aiming to distill the specific genetic variants impacting these traits.

Disclosures: Diana Cousminer, None.

**MO0084**

**Heritability of Thoracic Kyphosis and Genetic Correlations with Other Spine Traits: Framingham QCT Study.** Michelle S. Yau\*<sup>1</sup>, Serkalem Demissie<sup>2</sup>, Yanhua Zhou<sup>2</sup>, Dennis E. Anderson<sup>3</sup>, Amanda L. Lorbergs<sup>1</sup>, Douglas P. Kiel<sup>1</sup>, Brett T. Allaire<sup>3</sup>, Laiji Yang<sup>1</sup>, L. Adrienne Cupples<sup>4</sup>, Thomas G. Travison<sup>1</sup>, Mary L. Bouxsein<sup>3</sup>, David Karasik<sup>5</sup>, Elizabeth J. Samelson<sup>1</sup>. <sup>1</sup>Hebrew SeniorLife, BIDMC/Harvard, United states, <sup>2</sup>Boston University School of Public Health, United states, <sup>3</sup>BIDMC/Harvard, United states, <sup>4</sup>Boston University School of Public Health, NHLBI Framingham Heart Study, United states, <sup>5</sup>Hebrew SeniorLife, BIDMC/Harvard, Bar Ilan University, United states

Hyperkyphosis is a common spinal disorder in older adults, characterized by excessive curvature of the thoracic spine (large kyphosis angle) and adverse health outcomes. The etiology of hyperkyphosis has not been firmly established, but may be related to changes in the vertebrae, discs, joints, and muscles, which function as a unit to support the spine. Determining the contribution of genetics to kyphosis and the degree of shared genetics with other spine traits may provide insight into the determinants of hyperkyphosis. The purpose of our study was to estimate heritability of kyphosis and genetic correlations between kyphosis and vertebral fracture (VF), intervertebral disc height narrowing (DHN), facet joint osteoarthritis (FJOA), lumbar spine volumetric bone mineral density (vBMD), and paraspinal muscle area and density.

We included 2,063 individuals from the second and third generation cohorts of the Framingham Study. Thoracic kyphosis (T4-T12 Cobb) angle was measured from CT scout images and based on vertebral morphometry points identified by a semi-automated algorithm. A musculoskeletal radiologist used a semi-quantitative method (0=none, 1=mild, 2=moderate, 3=severe) to evaluate VF, DHN, and FJOA from T4 to L4 from CT images. Scores were summed across spinal levels to derive a summary index for each trait. We measured average paraspinal muscle size and density at T7 and T8 using spatially filtered CT scans (Analyze, Biomedical Imaging Resource). We used a variance components method to estimate heritability of each spine trait and bivariate models to estimate genetic correlation between kyphosis angle and each spine trait. All models were adjusted for age, sex, and weight.

Mean age was 59 ± 11 years; 49% were women. Mean kyphosis angle was 34.0 ± 9.6 degrees. Heritability of kyphosis angle was  $h^2=54 \pm 6\%$ . We found significant genetic correlations between kyphosis angle and muscle area ( $\rho_G=-0.46$ ,  $p<0.01$ ), VF ( $\rho_G=0.39$ ,  $p<0.01$ ), and vBMD ( $\rho_G=-0.23$ ,  $p=0.02$ ), but not between kyphosis angle and muscle density ( $\rho_G=-0.22$ ,  $p=0.09$ ), DHN ( $\rho_G=0.17$ ,  $p=0.14$ ), or FJOA ( $\rho_G=0.05$ ,  $p=0.64$ ).

In conclusion, the severity of thoracic curvature is heritable and may share genetic contributions with bone loss, VF, and declines in muscle size that frequently occur with aging. Better understanding of the molecular processes underlying shared genetic variation among spine traits may provide biological insights into the etiology of hyperkyphosis and related spine conditions.

Disclosures: Michelle S. Yau, None.

**MO0085**

**Identification of Novel Osteoporosis Risk Biomarkers: A Proteome-wide Discovery Study with Osteoporotic Fracture Patients in China.** Xu Zhou\*<sup>1</sup>, Pei He<sup>1</sup>, Zhen-Huan Jiang<sup>2</sup>, Yun-Hong Zhang<sup>3</sup>, Jian-Nong Jiang<sup>2</sup>, Hong-Qing Gao<sup>3</sup>, Ding-Hua Jiang<sup>4</sup>, Xin Lu<sup>1</sup>, Shu-Feng Lei<sup>1</sup>, Fei-Yan Deng<sup>1</sup>. <sup>1</sup>Center for Genetic Epidemiology & Genomics, School of Public Health, Soochow University, China, <sup>2</sup>Municipal People's Hospital at Yixin, China, <sup>3</sup>Shishan Street Community Health Service Center at High-tech District, China, <sup>4</sup>The 1st Affiliated Hospital of Soochow University, China

Hip osteoporotic fracture (OF) is one of the most serious consequences of osteoporosis. Low bone mineral density (BMD) is a risk factor of osteoporosis. Circulating monocytes (CMs) participate in immune responses. CMs can also give birth to osteoclasts to resorb bone. With case-control design, the present study aims to identify OF biomarkers underlying osteoporosis risk in humans. We recruited hip OF patients (n=18, age mean: 77 yrs) at hospital entry day 0-3 or 4-20. We also recruited gender- and age- matched subjects without fracture history (abbreviated as NF, n=18, age mean: 73 yrs), one half with extremely low and the other half with high BMD (hip Z-score: -1.06 vs. +1.36). All the above subjects are Chinese elderly males. CMs were isolated from peripheral blood, and total proteins were extracted. Proteome-wide protein expressions were profiled by employing label-free quantitative proteomics methodology (Easy-nLC1000 and Q-exactive, Thermo). Proteomic data were processed by the softwares Maxquant and Perseus, to identify differentially expressed proteins (DEP) between OF and NF subjects, as well as between subgroups within OF or NF. Gene Ontology (GO) analyses were conducted to annotate functions of DEPs. Thirty six DEPs, with fold changes (FC)  $\geq 2.0$ , were identified between OF and NF subjects ( $p \leq 0.05$ ). These DEPs are significantly enriched in biological processes, including "leukocyte migration" ( $p=6.73 \times 10^{-4}$ ), chemotaxis ( $p=0.01$ ), inflammatory response ( $p=0.03$ ), and wound healing ( $p=0.03$ ). Interestingly, among the 36 DEPs, two proteins, i.e., PR12 and MYADM, were differentially expressed between low and high BMD subjects ( $p \leq 0.05$ ), as well. Specifically, PR12 was up-regulated in low vs. high BMD subjects (FC=4.83,  $p=0.0006$ ). Up-regulation was also observed in OF vs. NF subjects (FC=10.13,  $p=0.0003$ ). In addition, MYADM protein were down-

regulated in subjects with low vs. high BMD (FC=0.34, p=0.047). However, compared with low BMD subjects, MYADM expression was >4.0-fold up-regulated in OF subjects, either before or after day 3 (p<0.003). In conclusion, the present study identified two novel osteoporosis risk proteins, and highlighted that PBM-expressed proteins are involved in fracture healing, as well. Whether these DEPs are predictive of osteoporosis or OF has yet to be evaluated further. In-depth studies are being conducted to demonstrate functional mechanisms for key DEPs.

**Disclosures:** Xu Zhou, None.

## MO0086

**FGF23 Enhances CYP24A1 Transcription in Klotho-dependent way via ERK Pathway.** Maria K Tsoumpra\*, Shun Sawatsubashi, Yuichi Takashi, Toshio Matsumoto, Seiji Fukumoto. Fujii Memorial Institute of Medical Sciences, Japan

Fibroblast growth factor 23 (FGF23), a bone derived hormone, regulates phosphate and vitamin D metabolism by binding to Klotho-FGF receptor complex mainly in kidney and parathyroid glands. FGF23 induces *CYP24A1* and concomitantly represses *CYP27B1* expression in kidney thus controlling serum 1,25-dihydroxyvitamin D (1,25D) levels. Recent investigation using a model mouse of FGF23 overexpression showed an important role of *CYP24A1* to reduce local 1,25D levels in parathyroid cells and to enhance PTH secretion (*J Clin Invest* 126:667-80,2016). However, it is not known how FGF23 regulates *CYP24A1* expression. In this study, we attempted to elucidate the *in vitro* mechanism of FGF23 effects on *CYP24A1* expression. We have used human embryonic kidney (HEK) cells co-transfected with an expression vector for Klotho and either a short (360 bp) or long (760 bp) *CYP24A1* promoter-luciferase vector and HeLa cells co-transfected with Klotho and the long version of *CYP24A1* promoter. Conditioned media were collected from HEK cells transfected with an expression vector for cleavage-resistant FGF23RQ or empty pcDNA3.1 (control). We first attempted to ascertain whether promoter activity of *CYP24A1* could be induced in our *in vitro* system and whether this induction was Klotho dependent. In both HEK and HeLa cells, FGF23RQ media increased *CYP24A1* promoter activities compared to those by control only in the presence of Klotho. We then tried to clarify the intracellular signals regulating *CYP24A1* promoter activity in HEK cells. An inhibitor of MEK1/2, U0126, abolished the stimulatory effect of FGF23RQ on *CYP24A1* promoter in HEK cells. In addition, FGF23RQ induced the expression of early growth response-1 (Egr-1), a downstream transcription factor of ERK. Furthermore, overexpression of Egr-1 increased the promoter activity of *CYP24A1* gene in both HEK and HeLa cells. Collectively the above data indicate that FGF23 can enhance *CYP24A1* expression via FGF receptor-ERK-Egr-1 pathway in the presence of Klotho. This induction of *CYP24A1* may have a physiological role in tissues expressing Klotho including parathyroid cells.

**Disclosures:** Maria K Tsoumpra, None.

## MO0087

**FGF23 Exerts its Effects on Phosphorus Metabolism Starting 12 Hours After Birth, but not During Fetal Development.** Yue Ma\*<sup>1</sup>, Beth J. Kirby<sup>1</sup>, Beate Lanske<sup>2</sup>, Andrew C. Karaplis<sup>3</sup>, Christopher S. Kovacs<sup>1</sup>. <sup>1</sup>Memorial University, Canada, <sup>2</sup>Harvard School of Dental Medicine, United states, <sup>3</sup>McGill University, Canada

Fibroblast growth factor-23 (FGF23) is a key regulator of adult phosphorus metabolism. It reduces serum phosphorus by promoting renal phosphorus excretion. Absence of FGF23 or its co-receptor Klotho (models of human tumor calcinosis) cause reduced urine phosphorus excretion, hyperphosphatemia, impaired bone metabolism, extraskeletal calcifications, and early mortality. Excess FGF23 from loss of Phex (X-linked hypophosphatemic rickets) causes increased urine phosphorus excretion, hypophosphatemia, and rickets.

In contrast to the adult, FGF23 has little or no role in fetal phosphorus metabolism. Loss of FGF23 action, in *Fgf23* null or *Klotho* null fetuses, did not alter serum and urine phosphorus, renal expression of *NaPi2a/2c*, skeletal morphology and mineralization, and placental phosphorus transport. Similarly, excess FGF23 action, as revealed by *Phex* null fetuses, did not alter any of these parameters.

The present study was undertaken to determine how soon after birth deficiency or excess of FGF23 disturb phosphorus metabolism or renal expression of *NaPi2a/2c*.

In each of *Fgf23*, *Klotho*, and *Phex* colonies, we mated heterozygous males and females to obtain pregnancies with WT, heterozygous, and null pups. Timepoints included postnatal day 1 (12 hrs post birth), 3, 5, 7, and 10 (D1-D10). Serum was collected, bladders were aspirated to obtain urine, and kidneys were harvested for RNA. Serum phosphorus, urine phosphorus/creatinine, and renal expression of *NaPi2a/2c* by qPCR, were measured.

In *Fgf23* null pups serum phosphorus became increased at D7 (4.66±0.09 vs. 3.65±0.04 mM, p<0.001), accompanied by increased expression of *NaPi2a* (1.39±0.12 vs. 1.00±0.08) and *NaPi2c* (1.57±0.39 vs. 1.00±0.10) (p<0.001), and reduced urine phosphorus (15.1±0.9 vs. 17.2±0.5, p<0.04). In *Klotho* null phosphorus increased at D5 (4.55±0.17 vs. 3.91±0.80, p<0.001).

Conversely in *Phex* null pups serum phosphorus was reduced at D1 (2.00±0.14 vs. 2.87±0.14 mM, p<0.001), accompanied by reduced expression of *NaPi2a*

(0.78±0.17 vs. 1.00±0.08) and *NaPi2c* (0.60±0.32 vs. 1.00±0.28) (p<0.001), and increased urine phosphorus (22.1±2.5 vs. 8.9±1.5, p<0.001).

In conclusion, excess FGF23 induces hypophosphatemia, downregulation of *NaPi2a/2c*, and renal phosphorus wasting within 12 hours after delivery, whereas loss of FGF23 takes 7 days to have opposite effects. FGF23 is not required during fetal development, but becomes an important regulator of phosphorus metabolism within one day after birth.

**Disclosures:** Yue Ma, None.

## MO0088

**FGF23 responds to alterations of iron metabolism in a murine model of CKD-MBD.** Erica Clinkenbeard\*<sup>1</sup>, Hitesh N. Appaiah<sup>2</sup>, Keith Stavrook<sup>3</sup>, Taryn Cass<sup>2</sup>, Julia Hum<sup>2</sup>, Yves Sabbagh<sup>4</sup>, Susan Schiavi<sup>5</sup>, Kenneth White<sup>2</sup>.

<sup>1</sup>Department of Medical & Molecular Genetics Indiana University School of Medicine, United states, <sup>2</sup>Department of Medical & Molecular Genetics, Indiana University School of Medicine, United states, <sup>3</sup>Department of Pharmacology & Toxicology, Indiana University School of Medicine, United states, <sup>4</sup>Genzyme, United states, <sup>5</sup>PreciThera, Inc., United states

Disturbances in phosphate and iron metabolism occur in concert during progression of chronic kidney disease-mineral bone disorder (CKD-MBD). FGF23 is stimulated by phosphate, as well as by iron deficiency anemia and hypoxia. This hormone is linked to CKD patient outcomes including left ventricular hypertrophy (LVH), renal allograft failure, and reduced renal 1,25(OH)<sub>2</sub> vitamin D (1,25D) production leading to bone and mineral disease. CKD patients become anemic and/or iron deficient with varied responses to treatment, therefore the goal of the present studies was to test for interactions between iron and phosphate metabolism in the juvenile cystic kidney 'Jck' mouse model of CKD-MBD. Even at 4 weeks of age the *Jck* females exhibited a significant reduction of red blood cells (p<0.0005), hemoglobin (Hb; p<0.0005) and hematocrit (HCT; p<0.0005) compared to wildtype (WT) controls. By 12 weeks of age, total serum iron began to decline in the *Jck* females. At 20-22 weeks *Jck* total iron levels were less than 50% of WT controls (p<0.0005). In >20 week old *Jck* CBC measured 7.8±0.6 Hb and 24.5±1.6 HCT; both significantly lower than WT controls (11.2±0.7 and 36.4±2.2, respectively; p<0.005) indicative of anemia. Considering their degree of anemia, we found inappropriately low serum EPO in *Jck* with a 2-fold increase over baseline *Jck* and 6-fold over WT controls at completion of the study (p<0.05). This correlated with a significant rise in *Jck* serum intact FGF23 beginning at 12 weeks and continued to 4960±1131pg/mL in >20 week old *Jck* versus 308.4±121pg/mL in WT controls (p<0.0005). Next, we tested EPO as a crossover mediator of iron and phosphate metabolism. Indeed, EPO administration to WT mice, and to *Jck* mice prior to their endogenous EPO increase (6 weeks of age), elevated FGF23 and appropriate markers of EPO activity in bone, with *Jck* producing significantly more intact FGF23 than WT mice. We found that ferric carboxymaltose (FCM) injection in *Jck* suppressed both serum intact FGF23 (p<0.05) as well as bone mRNA (p<0.005) when delivered alone. However, this action was nullified by EPO co-delivery. Collectively, these findings demonstrate that FGF23 is induced by EPO, which can alter the secreted FGF23 forms and override the effects of iron delivery during compromised renal function. Thus treating parameters associated with anemia and hematopoiesis in patients could have important impact on phosphate metabolism through FGF23.

**Disclosures:** Erica Clinkenbeard, None.

## MO0089

**Vitamin D metabolism and action in human mesenchymal stem cells: Effects of fibroblast growth factor 23.** Fangang Meng\*, Jing Li, Julie Glowacki, Meryl LeBoff, Shuanhu Zhou. Brigham & Women's Hospital, United states

Chronic kidney disease (CKD) is associated with impaired renal biosynthesis of 1 $\alpha$ ,25-dihydroxyvitamin D [1 $\alpha$ ,25(OH)<sub>2</sub>D<sub>3</sub>], low bone mass, and increased fracture risk. Fibroblast growth factor 23 (FGF23) is a bone-derived hormone that regulates renal vitamin D metabolism. Circulating FGF-23 levels are elevated in CKD. We reported that human mesenchymal stem cells (hMSCs) are targets of 1 $\alpha$ ,25(OH)<sub>2</sub>D<sub>3</sub> action to enhance their differentiation to osteoblasts, but they also participate in vitamin D metabolism by converting 25-dihydroxyvitamin D<sub>3</sub> [25(OH)D<sub>3</sub>] to 1 $\alpha$ ,25(OH)<sub>2</sub>D<sub>3</sub> by CYP27B1. This raises a possible autocrine/paracrine role for vitamin D in hMSCs. The effects of FGF23 on vitamin D metabolism and action in hMSCs are not known. In this study, we tested the hypothesis that FGF23 inhibits vitamin D metabolism and action in hMSCs. A series of 21 subjects (aged 49-80 years) scheduled for hip arthroplasty were studied. Estimated glomerular filtration rate (eGFR) was determined according to the MDRD equation. Marrow-derived MSCs were isolated from tissues discarded during surgery, including for subjects who were undergoing hemodialysis. Human MSCs expressed FGF23 receptors FGFR1, FGFR3, FGFR4, and its co-receptor Klotho. In contrast, there was downregulated constitutive expression of Klotho, but not FGFR1, 3, and 4 in MSCs from two CKD subjects, compared with MSCs from age/gender-matched control subjects. *In vitro* analyses showed positive correlations for both secreted and membrane-bound Klotho gene expression in hMSCs with eGFR of the subjects from whom MSCs were isolated. Treating hMSCs or a human stromal cell line, KM101, with FGF23 (1 ng/ml,

24 hrs) down-regulated CYP27B1, Klotho, and VDR, but not FGFR1 gene expression. In addition, FGF23 inhibited markers of osteoblastogenesis (BMP-7 and BSP) that were upregulated by either 25(OH)D<sub>3</sub> and 1 $\alpha$ ,25(OH)<sub>2</sub>D<sub>3</sub>. In summary, these data demonstrate that FGF23 directly inhibits CYP27B1, Klotho, and VDR gene expression and the pro-osteoblastogenic effects of 25(OH)D<sub>3</sub> and 1 $\alpha$ ,25(OH)<sub>2</sub>D<sub>3</sub> in hMSCs. Dysregulated vitamin D metabolism in MSCs may contribute to impaired osteoblastogenesis and altered bone and mineral metabolism in CKD subjects due to elevated FGF23. This supports the importance of intracellular vitamin D metabolism in autocrine/paracrine regulation of osteoblast differentiation in hMSCs.

**Disclosures:** Fangang Meng, None.

## MO0090

**IGFBP4 regulates adipogenesis and osteogenesis.** David Maridas\*<sup>1</sup>, Victoria DeMamrbo<sup>1</sup>, Phuong Le<sup>1</sup>, Subburaman Mohan<sup>2</sup>, Clifford Rosen<sup>1</sup>.  
<sup>1</sup>MMCRI, United states, <sup>2</sup>Loma Linda University, United states

Insulin-like Growth Factor Binding Protein 4 (IGFBP4) is highly expressed in adipocytes and osteoblasts. While most *in vitro* models proved that IGFBP4 inhibits IGF-I signaling, *in vivo* models showed conflicting results. Indeed, systemic injections of IGFBP4 in mice induced bone formation while local injections inhibited IGF actions. Our purpose was to determine how IGFBP4 affects growth through the regulation of adipose and osteogenic differentiation. Thus, we performed a comprehensive phenotyping of adult IGFBP4 null (IGFBP4<sup>-/-</sup>) mice. Females and males IGFBP4<sup>-/-</sup> suffered from a growth retardation marked by significant reductions of weight (p<0.01) and length (p<0.05). 16 week-old IGFBP4<sup>-/-</sup> females had a reduction (p<0.04) of areal and femoral BMD but males were unaffected. MicroCT of femurs confirmed the decrease in BV/TV (p=0.02) and trabecular and cortical thicknesses (p=0.05) in IGFBP4<sup>-/-</sup> females. Surprisingly, males had higher connectivity density (p=0.02) and trabecular number (p=0.005). Gene expression analysis showed that femoral expression of *Sost* was decreased in IGFBP4<sup>-/-</sup> males but not females. Histomorphometry analysis of tibias showed a decreased number of osteoblast and increased osteoclast surface in IGFBP4<sup>-/-</sup> females. Bone marrow stromal cells (BMSC) isolated from male mice showed higher mineralization by Von Kossa staining upon differentiation into osteoblasts. Females and males IGFBP4<sup>-/-</sup> also had decreased fat proportion (p<0.01) and lean masses (p<0.05). Inguinal and gonadal white adipose depots (WAT) were smaller and had a decreased expression of *Ppar $\gamma$*  in both genders. When challenged with high fat diet (HFD), IGFBP4<sup>-/-</sup> females, but not males, were protected against diet-induced obesity, liver steatosis and adipocyte hypertrophy. IGFBP4<sup>-/-</sup> BMSC showed a decrease in adipogenesis compared to control cells. Interestingly, *IGFBP4* was significantly up-regulated during adipogenesis of BMSC and 3T3-L1. Because PTH was shown to regulate *IGFBP4* expression, we treated BMSC and 3T3-L1 with 100nM PTH and observed a significant reduction of adipogenesis and *IGFBP4* expression. In summary, our data suggest that IGFBP4 is an important modulator of bone and fat development acting with gender and tissue specificity. Within bone and fat tissues, IGFBP4 could contribute to a fine-tuning of IGF signaling rather than acting as a mere IGF inhibitor to control proliferation and differentiation of mesenchymal stem cells into osteoblasts or adipocytes.

**Disclosures:** David Maridas, None.

## MO0091

**Elongation of primary trabecular bone due to poorly calcified bones around the trabecular bone after continuous PTH infusion.** Nobuhito Nango\*<sup>1</sup>, Shogo Kubota<sup>1</sup>, Wataru Yashiro<sup>2</sup>, Atsushi Momose<sup>2</sup>, Shizuko Ichinose<sup>3</sup>, Koichi Matsuo<sup>4</sup>. <sup>1</sup>Ratoc System Engineering Co., LTD., Japan, <sup>2</sup>Institute of Multidisciplinary Research for Advanced Materials, Tohoku University, Japan, <sup>3</sup>Research Center for Industry Alliance, Tokyo Medical & Dental University, Japan, <sup>4</sup>Laboratory of Cell & Tissue Biology, Keio University School Of Medicine, Japan

Parathyroid hormone (PTH) is used clinically to accelerate bone formation, but how it functions remain unclear. We have reported elongation of primary trabecular bone with PTH continuous infusion in the mouse. In this study, we found the delay of calcification in the osteoid of primary trabecular bone by PTH infusion.

Seven-week-old mice implanted with an osmotic pump were continuously dosed with PTH at 40 $\mu$ g/kg/day. Tibias were isolated from control and infusion groups after 144 h. For each sample, (1) the metaphysis was scanned using X-ray micro-computed tomography ( $\mu$ CT) with a voxel size of 2  $\mu$ m; (2) bone and cartilage matrices were investigated using synchrotron radiation multi-scan X-ray microscope and back-scattered scanning electron microscope (B SEM); (3) cartilage and bone tissues were observed using TRAP and Toluidine blue staining.

$\mu$ CT images acquired from the control (Fig. 1a) and the continuous infusion group (Fig. 1b) that the attachment of low-density tissue to the primary and secondary trabecular bone after PTH infusion decreased trabecular spacing. SEM/energy dispersive X-ray spectroscopy (EDS) Ca mapping identified this low-density tissue as low-mineralized tissue. TRAP staining revealed osteoclasts at the proximal tip of the bone marrow. In the control group (Fig. 2a), the lower end of the hypertrophic cartilage columns were in direct contact with bone marrow, whereas in the continuous infusion group, the lower end of columns were indirectly connected to the bone marrow via calcified tissue (Fig. 2b). Osteocyte-like cells exhibiting canaliculi were found in the hypertrophic cartilage lacunae by X-ray microscope imaging (Fig. 3).

These data suggest that the resorption of calcified primary trabecular bone by osteoclasts is inhibited by the remaining low-mineral tissue after continuous PTH infusion, resulting in reduced blood vessel invasion into hypertrophic cartilage and in elongation of primary trabecular bone.

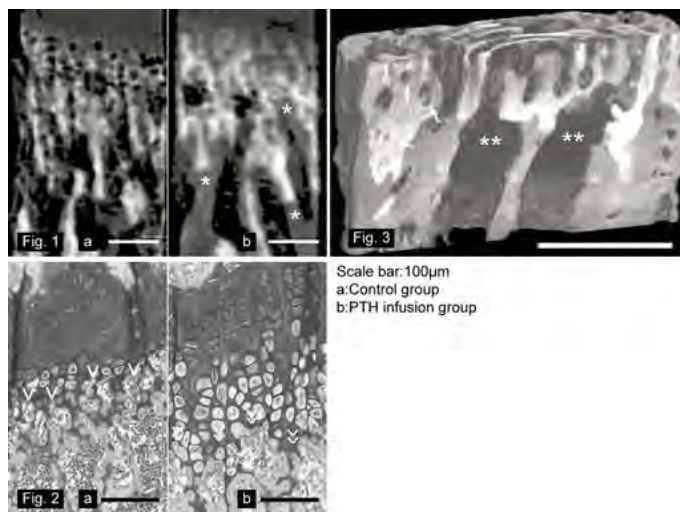


Fig.1  $\mu$ CT image. a, control group, b, infusion group. The attachment of low-mineralized tissue (\*), which decreased trabecular spacing.

Fig.2 Toluidine blue staining image. The lower end of the hypertrophic cartilage columns was in contact directly (<) with bone marrow in the control group (a), and indirectly (<<) with bone marrow through the calcified tissue in the continuous infusion group (b).

Fig.3 X-ray microscope Talbot-phase contrast image. The osteocyte-like cells exhibiting canaliculi in the hypertrophic cartilage lacunae (arrow). Low mineralized tissue area (\*) attached to primary trabecular bone. Bone marrow (\*\*)

Figure

**Disclosures:** Nobuhito Nango, None.

## MO0092

**Osseous Consolidation of a Nonunion Fracture of the Lower Leg Under Parathyroid Hormone Therapy.** Ilko Kastir\*<sup>1</sup>, Michael Reichardt<sup>2</sup>, Reimer Andresen<sup>1</sup>, Sebastian Radmer<sup>3</sup>, Guido Schröder<sup>2</sup>, Thomas Westphal<sup>4</sup>, Thomas Mittlmeier<sup>5</sup>, Hans-Christof Schober<sup>2</sup>. <sup>1</sup>Institute of Diagnostic & Interventional Radiology/Neuroradiology, Westkuestenlinikum Heide, Teaching Hospital of the Universities of Kiel, Lübeck & Hamburg, Germany, Germany, <sup>2</sup>Department of Internal Medicine I, Municipal Hospital Suedstadt Rostock, Academic Teaching Hospital of the University of Rostock, Germany, Germany, <sup>3</sup>Centre of Orthopaedics, Berlin, Germany, Germany, <sup>4</sup>Clinic of Trauma Surgery, Orthopaedics & Hand Surgery, Municipal Hospital Suedstadt Rostock, Academic Teaching Hospital of the University of Rostock, Germany, Germany, <sup>5</sup>Clinic of Trauma-, Hand- & Restoration Surgery, Universitätsmedizin Rostock, Germany, Germany

### Introduction

The absence of osseous consolidation of a fracture with little or no further potential to heal is defined as a nonunion. The incidence of impaired healing after fractures of the long tubular bones lies between 2,6 and 16%, depending on the surgical technique used. Both for the patient and from a socioeconomic point of view, nonunions represent a major problem. In animal experimental studies, a positive effect of parathormone (PTH) on fracture healing has been shown. PTH has a direct stimulatory effect on osteoblasts and osteoclasts and recent studies suggest a stimulating effect on the proliferation of mesenchymal cells near the fracture site. In this prospective study 32 patients with nonunions were treated with Teriparatide to investigate the effects of PTH on fracture healing. The patients agreed to this off-label use of Teriparatide as a therapeutical trial.

### Material and Methods

32 patients with the age of 22 – 83 (54  $\pm$  15,9) who had developed a non-union situation were included in the study. Inclusion criteria were as follows: last revision operation was at least 3 months ago, a Vitamin D deficiency and disturbances in the calcium/phosphate metabolism were ruled out. The type of fractures were Pilon tibial (16), femoral (8), malleolus (2), upper extremity (3), distale crurale (2) and metatarsal (1). Patients were treated for 4 – 10 weeks (7,3  $\pm$  1,5) with 20  $\mu$ g/d Teriparatid. Clinical and conventional radiographic examination as well as blood analysis were carried out every 4 weeks. Endpoint of the study was the pain free weight-bearing capacity of the extremity and osseous consolidation shown by conventional radiographs.

## Results

After an average of 6 months after therapy 30 of the 32 patients experienced an osseous consolidation of the nonunion and regained full, pain free weight-bearing capacity of the fractured extremity. The therapy was well tolerated and no discontinuances were necessary as no side effects were experienced. In 2 patients no consolidation was observed within 6 months and other therapeutic options were considered.

## Conclusion

Even though this was a prospective study with no control group, the outcome supports the results of animal and human studies that PTH has a positive effect on fracture healing. The short term therapy of 20 µg/d of Teriparatide can possibly lead to the consolidation of nonunions.

**Disclosures:** Ilko Kastir, None.

## MO0093

**Thymus-Derived Parathyroid Hormone Secretion Increases after Parathyroidectomy in C57BL6/KaLwRij Mice.** Maurizio Zangari<sup>1</sup>, Hanna Yoo<sup>1</sup>, Bumjun Kim<sup>2</sup>, Ricky Edmonson<sup>1</sup>, Larry Suva<sup>3</sup>, Donghoon Yoon<sup>\*1</sup>.

<sup>1</sup>UAMS, United states, <sup>2</sup>Baylor College of Medicine, United states, <sup>3</sup>Texas A&M Univ., United states

We have previously demonstrated a significant correlation between serum PTH levels and myeloma responses to proteasome inhibition and a crucial role for the parathyroid hormone receptor 1 (PTHr1) system in the control of myeloma tumor growth *in vitro* and *in vivo*. In this study the effect of abrogation of parathyroid-derived PTH in C57BL6/KaLwRij mice was tested to better understand the role of the PTH/PTHr1 axis in myeloma. After thyroparathyroidectomy (TPTX), a rapid and expected loss of measurable circulating PTH was observed. However, serum PTH levels recovered 3-4 weeks post-TPTX and achieved levels consistently comparable to pre TPTX levels. These data raised the compelling possibility of an alternative PTH source. To determine the potential source of the recovered PTH levels, multiple organs were examined. Whole tissue lysates were analyzed by Western blot and revealed a faint but specific band from thymic tissue, while no obvious band was detected in 13 other tissues investigated including the liver, lung, kidney, ovary and testis. Murine PTH mRNA transcripts from thymus RNA were measured by Real-Time PCR, using a specifically designed primer set that spans exons 1 and 2, since intron 1 is >1kb. These primers specifically discriminate mRNA transcripts from genomic DNA and improved the assay sensitivity for the detection of PTH transcripts at low abundant expression. Using these custom-designed primers, the thymus from control mice expressed measurable and detectable PTH mRNA transcripts, however but its level was significantly elevated in the tissue from TPTX mice. Since the thymus is considerably bigger than the parathyroid glands, PTH was concentrated by immunoprecipitation prior to Western blot analysis. Following immunoprecipitation, a reproducible and distinct PTH protein band was observed from thymus tissue in both TPTX and control mouse with a significant increment of PTH protein in the TPTX animals. Using the extensive washing and immunoprecipitation procedure, the immunoprecipitated proteins were also subjected to in-gel trypsin digestion/tandem mass spectrometry that confirmed the presence of PTH 1-84 protein. These data demonstrate that the murine thymus is able to produce PTH under normal conditions, and that following TPTX, the thymus can become a major source of serum PTH compensating for the loss of PTH and returning circulating PTH levels to normal.

**Disclosures:** Donghoon Yoon, Onyx, Millennium, and Novartis, 11

## MO0094

**Anti-FSH Polyclonal Antibody Decreases Fat Accumulation and Partially Protects Bone from the Deleterious Effects of Diet-Induced Obesity.**

Elizabeth Rendina-Ruedy<sup>\*1</sup>, Victoria DeMambro<sup>1</sup>, Tony Yuen<sup>2</sup>, Peng Liu<sup>2</sup>, Yaoting Ji<sup>2</sup>, Ping Lu<sup>2</sup>, Li Sun<sup>2</sup>, Mone Zaidi<sup>2</sup>, Clifford Rosen<sup>1</sup>. <sup>1</sup>Maine Medical Center Research Institute, United states, <sup>2</sup>Mount Sinai Bone Program, Department of Medicine, Icahn School of Medicine at Mount Sinai, United states

The glycoprotein follicle stimulating hormone (FSH) is synthesized and released from pituitary gonadotrophs and is a regulator both male and female reproduction. In addition to their classical location of the gonads, FSH receptors (FSHR) are expressed on osteoclasts and adipocytes. Through this interaction with FSHR, FSH appears to promote osteoclastogenesis and bone resorption, as well as increase lipid accumulation and droplet size of the adipocyte. Moreover, our collaborative studies have shown that blocking FSH using a polyclonal antibody (pAb) raised against a 13 amino acid long binding sequence protects against ovariectomy-induced bone loss. The current study aimed to address whether blocking the actions of FSH could preserve bone structure in a diet-induced obesity (DIO) model and alter fat accumulation during high fat diet feeding. To address this, 8 week old, male C57BL/6J mice were fed either a control (Con; 10% kcal from fat, sucrose matched) or a high fat diet (HF; 60% kcal from fat) for 8 weeks. Throughout the duration of the study, mice received a daily injection (8 µg/g bodyweight) of either an IgG anti-goat control antibody or anti-FSH pAb. As expected, the HF diet significantly increased body weight in both treatments (IgG and anti-FSH pAb) following one week and remained higher throughout the duration of the study. No differences were observed in body weight between the two treatment groups. However, after 7 weeks,

quantitative nuclear magnetic resonance (qNMR) and dual energy x-ray absorptiometry (DXA) revealed that the anti-FSH pAb animals on the HF diet gained less fat mass compared to the IgG animals on the HF diet. This was also represented in lower inguinal and gonadal fat pad weights. Consistent with these results, the anti-FSH pAb group on the HF diet demonstrated increased energy expenditure and a lower respiratory quotient than IgG-HF diet group. Whole body bone mineral density (BMD) trended to be lower in the IgG-HF compared to the IgG-Con after 4 ( $p = 0.064$ ) and 7 week ( $p = 0.068$ ); however, the anti-FSH pAb treatment protected from the HF diet-induced reductions in BMD. Micro-computerized tomography revealed that connectivity density was higher in the anti-FSH group on the HF diet compared to the IgG HF group. Continued investigation is underway to further elaborate on the mechanism(s) by which the anti-FSH antibody was able to decrease fat accumulation and exert a beneficial effect on bone in the DIO model.

**Disclosures:** Elizabeth Rendina-Ruedy, None.

## MO0095

**Genomic High Content Screening in primary osteoblasts uncover novel druggable targets to improve osteoblast differentiation and alleviate deleterious effects of glucocorticoids.** Mubashir Ahmad<sup>1</sup>, Thorsten Kroll<sup>2</sup>,

Jeanette Knoll<sup>2</sup>, Aspasia Ploubidou<sup>3</sup>, Jan Tuckermann<sup>\*4</sup>. <sup>1</sup>Institute for Comparative Molecular Endocrinology (CME), University of Ulm, Germany, <sup>2</sup>Leibniz Institute for Age Research – Fritz Lipmann Institute (FLI), Beutenbergstrasse 11, D-07745 Jena, Germany, <sup>3</sup>Leibniz Institute for Age Research – Fritz Lipmann Institute (FLI), Beutenbergstrasse 11, D-07745 Jena, Germany, <sup>4</sup>Institute for Comparative Molecular Endocrinology (CME), University of Ulm, Helmholzstrasse 8/1, 89081 Ulm, Germany

**Background:** Osteoporosis, is characterized by low bone mass and altered bone microarchitecture, leading to increased risk of fractures. Excessive bone resorption and defective bone formation is the main underlying mechanism of this disorder and affects a major fraction of the ageing society. Besides, glucocorticoids (GCs), widely used to treat acute and chronic inflammatory diseases, lead to glucocorticoid induced osteoporosis (GIO), the most common form of secondary osteoporosis, characterized by low bone turnover. Most of the currently available pharmacological agents at low cost are antiresorptive and decrease the risk of fractures by stabilizing the bone mass. However, antiresorptive drugs do not improve bone quality, hence identification of novel drug targets for anabolic agents to stimulate bone formation, will be useful to effectively treat patients with established osteoporosis or GIO.

**Methods:** In order to identify the novel regulators that are critical for osteoporosis and GIO, we carried out an unbiased large-scale siRNA screen using high content analysis (HCA) in primary calvarial osteoblasts.

**Results:** Using a cell-based functional assay for alkaline phosphatase (ALP) activity, we identified novel regulators of osteoblast differentiation. We employed various bioinformatics tools to interrogate our results and observed a well-established bone development regulatory network, verifying reliability of our screen. Importantly, we identified novel biological networks whose roles in the regulation of bone development have not been shown previously. Furthermore, validation of selected novel candidate genes using siRNA knockdown confirmed an enhanced osteoblast differentiation (e.g. 2.8 fold +/-0.13 ALP activity per cell,  $p < 0.001$  for one protein kinase) and abrogation of deleterious effects of glucocorticoid treatment after knock down. Accordingly, expression of these genes diminish during osteoblast differentiation, indicating these candidates as strong negative regulators of osteoblast differentiation. Most importantly, an inhibitory drug against the identified kinase increased osteoblast differentiation (2.3 fold +/-0.4 ALP activity per cell,  $p < 0.001$ ) and diminished reduction of ALP activity by GCs. Currently we test these candidates by chemical inhibitors and in osteoblast specific knockout mice how they interfere with bone integrity *in vivo*.

**Conclusion:** We identified novel candidate genes that could be used as anabolic therapeutic targets to treat bone related disorders.

**Disclosures:** Jan Tuckermann, None.

## MO0096

**Loss of TIEG expression alters the miRNAome and transcriptome of cortical and trabecular bone resulting in impaired estrogen signaling in the mouse skeleton.**

Malayannan Subramanian<sup>\*1</sup>, Kevin Pitel<sup>1</sup>, Russell Turner<sup>2</sup>, Urszula Iwaniec<sup>2</sup>, Andre van Wijnen<sup>1</sup>, John Hawse<sup>1</sup>. <sup>1</sup>Mayo Clinic, United states, <sup>2</sup>Oregon State University, United states

TGFβ Inducible Early Gene-1 (TIEG) knockout (KO) mice display a female-specific osteopenic phenotype characterized by low bone mineral density, bone mineral content and overall loss of bone strength. Given that TIEG is an estrogen regulated gene, we hypothesized that loss of TIEG expression would impair estrogen signaling in the mouse skeleton. We therefore employed an ovariectomy (OVX) and estrogen replacement therapy (ERT) model system to analyze the role of TIEG in mediating estrogen signaling in bone. DXA, pQCT and micro-CT analyses revealed that loss of TIEG expression diminished the response to estrogen throughout the skeleton and within multiple bone compartments. Following OVX and ERT, cortical

and trabecular bone compartments were isolated from long bones of all mice and miRNA (miR) and mRNA sequencing was performed. A total of 691 and 755 miRs were determined to be expressed in cortical and trabecular bone of WT mice respectively with 89 (11%) being unique to cortical bone and 153 (18%) unique to trabecular bone. Similar numbers were detected in TIEG KO mice with 67 (7%) and 230 (26%) miRs being differentially expressed in cortical and trabecular bone of TIEG KO mice respectively. OVX and ERT resulted in substantially different miR expression patterns in cortical vs. trabecular bone of both WT and TIEG KO mice with approximately 50% of miRs being unique to WT or KO animals in both bone compartments. Deletion of TIEG led to altered expression of 156 and 1330 mRNA transcripts in cortical and trabecular bone respectively with only 16 (1%) transcripts being common to both bone compartments. ERT resulted in altered expression of 1392 and 1981 transcripts in cortical bone of WT and KO mice respectively compared to OVX controls with only 775 (30%) transcripts commonly regulated in both genotypes. In trabecular bone, 1729 and 2863 transcripts were differentially regulated following ERT in WT and KO mice respectively with 1148 (33%) of these being common to both genotypes. Gene ontology and pathway enrichment analyses of estrogen regulated transcripts revealed substantial differences between WT and KO mice, as well as between cortical and trabecular bone. Taken together, these data implicate a role for TIEG in mediating estrogen signaling throughout the mouse skeleton and demonstrate substantial differences in the miRNAome and transcriptome of cortical and trabecular bone compartments between genotypes and following OVX and ERT.

**Disclosures:** Malayannan Subramaniam, None.

## MO0097

### Testosterone regulation of physical activity behavior: mechanisms of action.

Ferran Jordi<sup>1</sup>, Michael Laurent<sup>1</sup>, Lawrence Vanhelleputte<sup>2</sup>, Vanessa Dubois<sup>3</sup>, Ludo Deboel<sup>1</sup>, Rougin Khalil<sup>1</sup>, Brigitte Decallone<sup>1</sup>, Geert Carmeliet<sup>1</sup>, Ludo Van den Bosch<sup>2</sup>, Rudi D'Hooge<sup>1</sup>, Frank Claessens<sup>1</sup>, Dirk Vanderschueren<sup>1</sup>. <sup>1</sup>KU Leuven, Belgium, <sup>2</sup>VIB, Belgium, <sup>3</sup>Institut Pasteur de Lille, France

The beneficial effects of exercise on the musculoskeletal system are widely recognized. In this line, androgens promote the engagement to physical activity in rodents and increase self-perceived energy in hypogonadal men. However, the mechanism by which androgens stimulate physical exercise behavior remains unclear. Our aim was to answer three specific questions about how androgens influence exercise: 1) does testosterone (T)-induced stimulation of activity depend in part on its aromatization into estradiol (E2)? 2) to what extent are the effects of androgens exerted through central (motivation) independent from peripheral (muscle) actions? and 3) are brain dopaminergic (DA) pathways implicated in the T regulation of activity? For this purpose, we determined wheel running (WR) and home-cage activity (HCA) in two male mouse models of androgen deficiency: androgen receptor knockout (ARKO) and orchidectomized (ORX) mice. Global ARKO mice displayed a 67 and 24% reduction in WR and HCA, respectively, compared to WT. Similarly, ORX diminished by 80 and 50% the intensity of WR and HCA. Treatment with T was twice as effective as dihydrotestosterone (DHT) (226% vs. 106%) in restoring WR after ORX. The role of T aromatization into E2 in promoting WR was confirmed by treating ARKO mice with T and DHT. As expected, DHT-treated ARKO mice showed no response compared to placebo, while T induced a dramatic enhancement (250%) of WR. The involvement of a neuromuscular dysfunction in the two models was ruled out by observing no alterations either in the rotarod and grip strength test nor in the compound muscle action potentials or motor neuron counts. To corroborate the implication of central DA pathways, mice were treated with low-dose amphetamine (0.75 mg/kg). Amphetamine induced a rapid and transient hyperlocomotion response in WT animals, which was more pronounced in ARKO mice, suggesting a dopamine dysregulation. Similarly, an enhanced response to amphetamine was observed in ORX animals, which was completely abolished by T but not DHT. We conclude that T regulates physical activity behavior in male mice centrally through a dual model of action (androgenic and estrogenic) although the effects of E2 appear to dominate. If the psychological effects of T on exercise behavior are confirmed in humans, it would represent an additional benefit of T replacement therapy in aging men with sarcopenia, dysmobility and low T.

**Disclosures:** Ferran Jordi, None.

## MO0098

**The Role of Membrane ER $\alpha$  Signaling in Bone and Other Major Estrogen Responsive Tissues.** Karin Gustafsson<sup>1</sup>, Helen Farman<sup>1</sup>, Petra Henning<sup>1</sup>, Vikte Lionkaite<sup>1</sup>, Sofia Movérare-Skrtic<sup>1</sup>, Jianyao Wu<sup>1</sup>, Henrik Ryberg<sup>1</sup>, Antti Koskela<sup>2</sup>, Jan-Åke Gustafsson<sup>3</sup>, Juha Tuukkanen<sup>2</sup>, Ellis Levin<sup>4</sup>, Claes Ohlsson<sup>1</sup>, Marie Lagerquist<sup>1</sup>. <sup>1</sup>Centre for Bone & Arthritis Research at Institute of Medicine, Sahlgrenska Academy at University of Gothenburg, Sweden, <sup>2</sup>Unit of Cancer Research & Translational Medicine, MRC Oulu & Department of Anatomy & Cell Biology, University of Oulu, FI-90014 Oulu, Finland, Finland, <sup>3</sup>Center for Nuclear Receptors & Cell Signaling, Department of Biology & Biochemistry, University of Houston, Houston, Texas, 77204-5056, United States of America., United states, <sup>4</sup>Division of Endocrinology, Departments of Medicine & Biochemistry, University of California, Irvine, Irvine, California, & the Long Beach VA Medical Center, Long Beach, CA, USA, United states

Estrogen signaling leads to cellular responses, not only in reproductive tissues, but also in several other tissues, including the skeleton. Estrogen receptor  $\alpha$  (ER $\alpha$ ) is the main mediator of estrogen effects in most tissues and in addition to nuclear ER $\alpha$  mediated effects, membrane ER $\alpha$  (mER $\alpha$ ) effects have been proposed to be of importance. To elucidate the significance, *in vivo*, of mER $\alpha$  signaling in the skeleton and other estrogen responsive tissues, we have used mice lacking the ability to localize ER $\alpha$  to the membrane due to a point mutation in the palmitoylation site (C451A), so called Nuclear-Only-ER (NOER) mice. The estrogen responses in estrogen-sensitive organs were determined after treatment of 12-week-old ovariectomized female WT and NOER littermates with 17 $\beta$ -estradiol for four weeks. High-resolution  $\mu$ CT was used to determine effects on trabecular and cortical bone parameters. Interestingly, the role of mER $\alpha$  for the estrogen response was highly tissue-dependent, with trabecular bone in the axial skeleton being strongly dependent on mER $\alpha$  signaling (>80% reduction in estrogen response in NOER mice compared to WT mice,  $p < 0.05$ , interaction P value from two-way-ANOVA analysis), while cortical and trabecular bone in long bones, as well as uterus and thymus, were partly dependent (40-70% reduction in estrogen response in NOER mice compared to WT mice,  $p < 0.05$ , interaction P value from two-way-ANOVA analysis) and effects on liver weight and total body fat mass were essentially independent of mER $\alpha$  signaling (no significant reduction in estrogen response in NOER mice compared to WT mice). In conclusion, mER $\alpha$  signaling is important for the estrogen response in female mice *in vivo* in a tissue-dependent manner, and we show that mER $\alpha$  signaling is crucial for the estrogen response in trabecular bone in the axial skeleton. Increased knowledge regarding membrane initiated actions of ER $\alpha$  may provide means to develop new selective estrogen modulators with improved profiles.

**Disclosures:** Karin Gustafsson, None.

## MO0099

**CYP27B1 ablation modulates breast cancer cells epithelial-to-mesenchymal transition (EMT) and promotes lung metastasis in the MMTV-PyMT mouse model.** Jiarong Li<sup>\*</sup>, Richard Kremer. MUHC, Canada

1, 25(OH) D3 is a pleiotropic hormone which exerts its effects by binding to the vitamin D receptor (VDR). Classically, the final step of vitamin D activation gives rise to 1,25-dihydroxyvitamin D (1,25(OH)<sub>2</sub>D) in the kidney through 1 $\alpha$ -hydroxylation of the inactive precursor 25 hydroxyvitamin D (25OHD). *cyp27b1* 1 $\alpha$ -hydroxylase expression not only occurs in the kidney but also at several extra-renal sites including the mammary epithelium. Our previous study showed that ablation of *cyp27b1* 1 $\alpha$ -hydroxylase in mammary epithelium of PyMT mice results in a localized vitamin D deficient state with decreased 1, 25 (OH)<sub>2</sub>D production in the mammary epithelium and accelerated breast cancer growth. Here we investigated the potential role of vitamin D on breast cancer metastasis and whether 1,25 (OH)<sub>2</sub>D affects epithelial-to-mesenchymal transition (EMT). First, using gene expression microarray, we compared *cyp27b1* ablated and non-ablated tumors and confirmed expression of selected genes by real-time RT-PCR. We also examined protein expression by immunofluorescence staining and western blot. We found that EMT markers including SNAIL2, ZEB1, ZEB2, Twist1 and Vimentin were dramatically increased after *cyp27b1* 1 $\alpha$ -hydroxylase ablation. In another set of experiments, we bred *cyp27b1* ablated and control mice under UVB-free condition. Three weeks after birth, the female pups (MMTV-cre<sup>+</sup> and PyMT *cyp27b1*<sup>fllox/fllox</sup> MMTV-cre<sup>+</sup>) were weaned and fed *ad libitum* either a 25 IU/Kg vitamin D deficient diet or a 1000 IU/Kg normal vitamin D diet, for the duration of the experiment (animal were sacrificed at 4, 6, 12 weeks). We analyzed the number and size of lung metastasis at different stages (hyperplasia/ early carcinoma/ late carcinoma) of tumor progression by HE staining. We demonstrated that the mice with ablated tumor fed with 25 IU/Kg vitamin D deficient diet had the highest number and size lung metastasis followed by low diet alone followed by *cyp27b1* ablation and normal diet followed by normal diet. We subsequently isolated breast tumor cells from PyMT *cyp27b1*<sup>fllox/fllox</sup> MMTV-cre<sup>+</sup> or wild type (+/+) mice and examined EMT markers and Invasion *in vitro* in the presence/absence of 10<sup>-7</sup> M 1, 25 (OH)<sub>2</sub>D for 48 hours. mRNA expression and protein levels of SNAIL2, ZEB1, ZEB2, Twist1 and Vimentin were significantly reduced as well as invasion and migration by Vitamin D treatment. In summary, our data support a beneficial role of vitamin D on metastatic spread through EMT regulation.

**Disclosures:** Jiarong Li, None.

**MO0100**

**Catabolic and Anabolic Actions of Vitamin D within Bone are Revealed when Comparing Mice with Osteoblastic Modification of VDR, CYP27B1 and CYP24A1.** Paul Anderson<sup>1</sup>, Jackson Ryan<sup>1</sup>, Rahma Triliana<sup>2</sup>, Andrew Turner<sup>1</sup>, Kate Barratt<sup>1</sup>, Rebecca Sawyer<sup>1</sup>, Yolandi Starczak<sup>1</sup>, Gerald Atkins<sup>2</sup>, Rachel Davey<sup>3</sup>, Howard Morris<sup>1</sup>. <sup>1</sup>University of South Australia, Australia, <sup>2</sup>University of Adelaide, Australia, <sup>3</sup>University of Melbourne, Australia

1,25(OH)<sub>2</sub>D<sub>3</sub> (1,25D) acting via the vitamin D receptor (VDR) induces RANKL-mediated bone resorption. Alternatively, 1,25D, as well as 25(OH)D (25D), has been shown to promote osteoblastic mineralisation. Despite numerous observations attesting to vitamin D's anabolic roles, the majority of published data suggest that vitamin D predominantly plays a negative role in bone with regards to mineralisation, with little evidence describing the direct duality of vitamin D's actions.

We have characterised mouse models in which 1,25D activity in osteoblasts was impaired by targeting its receptor (VDR) or its synthesis (CYP27B1). Using Osteocalcin-Cre (Oc<sup>Cre</sup>) mice, Vdr or Cyp27b1 was deleted within mature osteoblasts and osteocytes. Secondly, we characterised model in which vitamin D activity was enhanced either by using Oc<sup>Cre</sup> to delete Cyp24a1 or by using the osteocalcin promoter to overexpress cDNA for Vdr (ObVdr-Tg) or CYP27B1 (ObCYP27B1-Tg) in mice.

At 6 and 12w of age, Oc<sup>Cre</sup>/Vdr<sup>-/-</sup> mice displayed increased vertebral BV/TV% (21%, p<0.05) in comparison to littermate controls. In contrast, Oc<sup>Cre</sup>/Cyp27b1<sup>-/-</sup> mice demonstrated a reduction in BV/TV% (18%, P<0.01). In young Oc<sup>Cre</sup>/Vdr<sup>-/-</sup> mice, the increase in bone was associated with a marked reduction in RANKL-mediated osteoclastogenesis and reduced serum crosslaps. However, by 12w of age trabecular MAR was reduced to 50% of the control levels and by 20w of age periosteal MAR was reduced by 60%. By comparison, the reduction in bone in Oc<sup>Cre</sup>/Cyp27b1<sup>-/-</sup> mice, which persisted in adulthood, was associated with reduced (MS/BS) and no change to osteoclastic bone resorption.

ObVdr-Tg mice exhibited increased trabecular bone (16%, p<0.05) and cortical bone (10%, p<0.05) at 6 and 20w of age was associated with increased MAR and a trend towards decreased Ocl.S/BS. Similarly, both Oc<sup>Cre</sup>/Cyp24a1<sup>-/-</sup> and ObCyp27b1-Tg also demonstrated increased BV/TV% (27% and 16% respectively, p<0.05), which was associated with increases in MS/BS. Importantly, when ObCyp27b1-Tg mice were made 25D-deplete, the increased bone phenotype was abrogated.

These observations demonstrate that while VDR in mature osteoblasts is essential for regulating RANKL-mediated bone resorption in young growing animals, VDR, CYP27B1 also play significant roles in promoting mineral apposition under normal circumstances, which is dependent on adequate serum 25D levels.

*Disclosures: Paul Anderson, None.*

**MO0101**

**Obesity is associated with lower total, free and bioavailable 25OHD and higher vitamin D binding protein (DBP) and PTH concentrations as well as different genotype distribution of the DBP coding gene leading to possible negative influence on bone in women.** Elisa Saarnio<sup>1</sup>, Minna Pekkinen<sup>2</sup>, Suvi T Itkonen<sup>1</sup>, Virpi Kemi<sup>1</sup>, Heini Karp<sup>1</sup>, Merja Karkkainen<sup>1</sup>, Harri Sievänen<sup>3</sup>, Outi Mäkitie<sup>4</sup>, Christel Lamberg-Allardt<sup>1</sup>. <sup>1</sup>Calcium Research Unit, Department of Food & Environmental Sciences, University of Helsinki, Finland, Finland, <sup>2</sup>Folkhälsan Institute of Genetics, Folkhälsan Research Center, Helsinki, Finland, Finland, <sup>3</sup>Bone Research Group, UKK Institute for Health Promotion Research, Tampere, Finland, Finland, <sup>4</sup>Children's Hospital, Helsinki University Central Hospital & University of Helsinki, Finland, Finland

Vitamin D binding protein (DBP) has an important role in vitamin D metabolism. Studies have shown altered vitamin D metabolism in obese (OB) individuals. We examined whether obesity alters the concentration of total, free and bioavailable 25OHD, DBP and PTH and possible impacts of the alteration on bone traits. We also studied if an association exists between DBP polymorphism and obesity. We studied 37-47-year-old Caucasians (60° N Finland): 70 women, 42 men (OB, BMI=30-40 kg/m<sup>2</sup>) and normal-weight: 199 women, 65 men (normal weight (NW), BMI=19-25) in this cross-sectional study. Blood samples and vitamin D and calcium intake from food and supplements were collected as well as lifestyle habits. Serum 25OHD (IDS enzyme immunoassay kit) and DBP (ELISA kit using polyclonal antibodies) concentrations were determined from serum. Two SNPs in the DBP gene were genotyped: rs4588 and rs7041 and these in combination form six diplotypes. Free and bioavailable 25OHD concentrations were calculated. Distal and shaft sites of radius and tibia were measured with pQCT. Comparisons between the NW and OB subjects in total, free and bioavailable 25OHD as well as in PTH and DBP concentrations were made with analysis of covariance (ANCOVA) using appropriate covariates. Linear regression analysis was used for bone analysis using several explanatory factors. Association of DBP polymorphism with BMI was analyzed with Chi square-test. We have previously shown, that in OB women, DBP and PTH were significantly higher whereas total, free and bioavailable 25OHD concentrations were significantly lower than in NW women. In men, only 25OHD was lower in OB (p=0.020) but there were similar trends in free and bioavailable concentrations as in women. We also discovered that OB women differed from NW in DBP diplotype distribution (p=0.038). In OB women 25OHD, free

25OHD and bioavailable associated negatively with tibial shaft cortical strength index (CSI) (R<sup>2</sup>=0.090; 0.078; 0.070; p=0.008; 0.023; 0.026) and 25OHD with distal radius trabecular density (R<sup>2</sup>=0.05; p=0.029). In NW women, bioavailable 25OHD was associated positively only with distal tibia CSI (R<sup>2</sup>=0.031, p=0.045). In men, no associations were found. The observed associations between obesity and total-free-and bioavailable 25OHD, DBP and PTH suggests altered vitamin D metabolism in OB women and possible role of DBP polymorphism on the pathogenesis of obesity. Altered vitamin D metabolism can have negative effects on bone.

*Disclosures: Elisa Saarnio, None.*

**MO0102**

**Does the Ability of Cells to Sense and Respond to Low Intensity Vibrations Differ Between 2D and 3D Cell Culture?** Stefan Judex<sup>1</sup>, Ravi Patel<sup>1</sup>, Aaron Damato<sup>1</sup>, Suphanee Pongkitwitoon<sup>1</sup>, Timothy Koh<sup>2</sup>. <sup>1</sup>Stony Brook University, United states, <sup>2</sup>University of Illinois at Chicago, United states

Low intensity vibrations (LIV) are readily sensed by a number of cell types in vitro. For instance, we have shown that LIV enhances gap-junctional communication between osteocytes and enhances proliferation and differentiation of mesenchymal stem cells. Previous experiments have been performed predominantly in 2D cell culture and, here, we tested whether results would be similar in 3D. As some, but not all, aspects of the cellular mechanical environment induced by LIV will be modulated by the dimensionality of the cell layer, experiments directly comparing LIV responses between 2D to 3D may also hint towards a physical mechanism by which cells respond to LIV. Both 2D and 3D experiments used standard 24-well cell-culture plates. LIV was applied twice a day, 20 min each, using a frequency of 100Hz and peak acceleration of 0.15g (20 min each). Sham controls were subjected to the same procedure but the acceleration magnitude was set to zero. LIV enhanced cell proliferation over 3 days in both stem cells (C3H) and pre-osteoblasts (MC3T3-E1) without qualitative or quantitative differences between 2D and 3D. Upon osteogenic induction, LIV increased osteogenic markers in stem cells and pre-osteoblasts regardless of the dimensionality of the cell culture system. The LIV induced increase in Runx2 gene expression was greater in stem cells than in pre-osteoblasts but similar between 2D and 3D. We then investigated whether LIV enhances cellular communication and, if so, whether efficacy is greater by using vibrated C3H or vibrated MC3T3 cells. Parachuting vibrated C3H onto non-vibrated stained MC3T3 showed a relative greater increase in gap-junctional intercellular communication than when parachuting vibrated MC3T3 onto non-vibrated C3H cells. In both experiments, the increase in intercellular communication was similar in 2D vs 3D. Together, these data highlight that cell proliferation, differentiation, and intercellular communication can be enhanced by low-level vibrations in stem cells and pre-osteoblasts. The similarity in results between the 2D and 3D set-ups ostensibly eliminates a number of candidate mechanical variables that have been previously proposed to play a role in LIV mechanotransduction but are significantly different between the 2D and 3D environments. In contrast, LIV generates similar nuclear acceleration in 2D and 3D, consistent with the hypothesis that nuclear motions are a physical mechanism by which cells sense LIV.

*Disclosures: Stefan Judex, None.*

**MO0103**

**Interleukin 1β (IL1β), Nitric Oxide Synthase 2 (NOS2), Lipocalin 2 (LCN2) and Vascular Endothelial Growth Factor (VEGF) Orchestrate the Coupled Mechanoreponse of Skeletal Angiogenesis and Osteogenesis.** Vimal Veeriah<sup>1</sup>, Mattia Capulli<sup>1</sup>, Angelo Zanniti<sup>1</sup>, Suvro Chatterjee<sup>2</sup>, Nadia Rucci<sup>1</sup>, Anna Teti<sup>1</sup>. <sup>1</sup>University of L'Aquila, Italy, <sup>2</sup>Anna University, India

Coupling of angiogenesis and osteogenesis is relevant for the skeletal biomechanical response, but the underlying molecular mechanisms are still poorly understood. To identify a novel molecular cascade involved in the mechanoreponsive crosstalk between angiogenesis and osteogenesis, we subjected mouse and human endothelial cells (EC) to simulated microgravity in the NASA-developed RWV bioreactor, which minimizes shear stress and mimics unloading. We observed a microgravity intensity-dependent increase of IL1β in EC conditioned medium (0.08g 12pg/ml; 0.008g 36pg/ml, p<0.001), which stimulated LCN2 expression in mouse and human osteogenic cells (12.7fold, p<0.001). This induction impaired osteoblast differentiation in wildtype (~52% ALP p=0.024, ~66% mineralization, p=0.010) but not in LCN2-deleted osteogenic cells, and was definitely IL1β-dependent as suggested by the blunted effect of IL1β-depleted microgravity EC conditioned medium. Simulated microgravity activated the IL1β upstream transcription factor, NF-κB, in EC, while IL1β prompted NF-κB activation and the NOS2/NO/COX2 pathway in osteogenic cells, in which they stimulated proliferation (1.7fold, p=0.003) and cyclin d1 expression (5.3fold, p=0.002) in a manner blunted by IL1β depletion. LCN2 was also released in the conditioned medium of osteogenic cells directly subjected to microgravity (6fold, p<0.001) and contributed to the inverse mechanoreponsive EC-osteoblast crosstalk, stimulating EC migration (2fold, p=0.027), tube formation (2.3fold, p<0.008) and sprouting from mouse aortic rings (4fold, p<0.001). These events were mediated in EC by LCN2-induced VEGF signaling (mRNA fold increase: VEGF, 6.2, p=0.001; Hif1α 5.4, p=0.02), observed in the presence of both microgravity osteogenic cell conditioned medium or recombinant LCN2, and were dampened incubating EC with the VEGF receptor antagonist, Avastin, or in

microgravity conditioned medium from LCN2 deleted osteogenic cells. The IL1 $\beta$ /NOS2/LCN2 cascade was induced ex-vivo, in i) calvarias cultured in the presence of microgravity EC conditioned medium, and in vivo, in ii) calvarias and iii) tibias injected with microgravity EC conditioned medium, or in tibias from mice subjected to iv) tail suspension or v) treated with botulin toxin to cause hind limb disuse, in which the VEGF mRNA was also upregulated (+10.6fold,  $p < 0.001$ ). Our results suggest a pathogenic role of the IL1 $\beta$ /NOS2/LCN2/VEGF cascade in bone biomechanical failures and disuse osteoporosis.

**Disclosures:** Vimal Veeriah, None.

## MO0104

**LaminA/C knock down enhances adipogenesis but does not eliminate mechanical response in MSCs.** Melis Olcum\*<sup>1</sup>, Guniz Bas<sup>2</sup>, Buer Sen<sup>2</sup>, Xihui Xie<sup>2</sup>, Engin Ozcivici<sup>3</sup>, Janet Rubin<sup>2</sup>, Gunes Uzer<sup>2</sup>. <sup>1</sup>University of North Carolina, IZMIR Institute of Technology, Turkey, <sup>2</sup>University of North Carolina, United States, <sup>3</sup>IZMIR Institute of Technology, Turkey

Mesenchymal stem cells (MSC) provide regenerative capacity to bone. Regulation of MSC fate towards osteogenic or adipogenic lineages depend on their ability to sense and respond to mechanical challenges. Exogenous physical force activates Focal Adhesion Kinase (FAK) and RhoA signaling, mediating cytoskeletal mechano-adaptations. The cytoskeleton relays mechanical information via LINC (Linker of Nucleoskeleton and Cytoskeleton) complex to its intra-nuclear anchor, LaminA/C. The LaminA/C nucleoskeleton is itself implicated in modulating MSC phenotype. Aging and progeroid MSC, where LaminA/C is compromised, do not adequately respond to functional loading. Defects in LaminA/C may reduce LINC-mediated nucleo-cytoskeletal connectivity or compromise organization of chromosomes in response to mechanical challenges. Here we asked if loss of LaminA/C would decrease mechanically-induced signaling in MSC. To investigate regulation of LaminA/C for MSC mechanoresponse, LaminA/C expression was knocked down in MSCs using siRNA. Consistent with the loss of mechanical stability, LaminA/C deficient (siLmn) nuclei showed blebbing and reduced circularity (11%,  $p < .001$ ). Additionally, siLmn MSC showed increased (430%,  $p < .01$ ) Adiponectin (APN) protein levels averaged over 7 days, suggesting that LaminA/C deficiencies lead to adipogenesis. The FAK phosphorylation (p-FAK) response was measured immediately after mechanical loading. MSCs were subjected to two bouts of low intensity vibration (LIV, 20min, 0.7g, 90Hz). LIV increased p-FAK in both siLmn (42%,  $p < .05$ ) and control (40%,  $p < .05$ ) groups. pFAK also responded to high magnitude strain (HMS, 20min, 2%, 0.17Hz.) in siLmn cells. This suggests that disrupting the intra-nuclear LaminA/C network does not disrupt MSC mechano-responsiveness. In sum our results suggests that deletion of LaminA/C compromises MSC multipotentiality by favoring adipogenic phenotype, but LaminA/C defective MSCs remain mechanically-responsive to both LIV and HMS. While we are still investigating whether mechanical stimulus is capable of reversing the siLmn induced acceleration of adipogenic phenotype, our findings suggest that age related decline in LaminA/C may directly affect the intra-nuclear gene program, such that reduced mechanical responsiveness in aging may be regulated at the level of LaminA/C, presenting a novel therapeutic target.

**Disclosures:** Melis Olcum, None.

## MO0105

**Temporal transcriptome analysis of osteocytes exposed to microgravity during spaceflight.** Yuhei Uda\*<sup>1</sup>, Amira Hussein<sup>2</sup>, Jordan Spatz<sup>3</sup>, Keertik Fulzele<sup>4</sup>, Forest Lai<sup>1</sup>, Chris Dedic<sup>1</sup>, Chao Shi<sup>1</sup>, Sean Dougherty<sup>4</sup>, Margaret Eberle<sup>4</sup>, Chris Adamson<sup>4</sup>, Lowell Misener<sup>4</sup>, Louis Gerstenfeld<sup>2</sup>, Paola Divieti Pajevic<sup>5</sup>. <sup>1</sup>Molecular & Cell Biology, GSDM, Boston University, United States, <sup>2</sup>Orthopaedic Surgery, BUSM, Boston University, United States, <sup>3</sup>Endocrine Unit, Massachusetts General Hospital, United States, <sup>4</sup>CALM Technologies Inc., Canada, <sup>5</sup>Molecular & Cell Biology, GSDM, Boston University; Endocrine Unit, Massachusetts General Hospital, United States

Bone loss is a major health problem for astronauts during long space flights. Osteocytes play a key role in sensing mechanical forces applied to the skeleton and in transducing them into subcellular biochemical signals to modulate bone homeostasis. However, the precise mechanisms underlying both mechanosensing and mechanotransduction in osteocytes under real microgravity ( $\mu$ G) are poorly understood. In this study, murine osteocytic cell line, Ocy454, cultured on a highly porous polystyrene 3D scaffold were cultured in the fully automated payload, OSTEO-4, and flown to the International Space Station on board the SpaceX Dragon6. Cells were exposed to  $\mu$ G for 2, 4, or 6 days prior to being fixed to subsequently examine responses to  $\mu$ G. To account for increased mechanical forces due to launch (vibration and acceleration), condition medium was collected at 6 and 24 hours after launch and analyzed for sclerostin expression. Sclerostin is a potent negative regulator of bone formation and it is highly sensitive to mechanical forces. Sclerostin levels were unchanged between flight and ground controls within 24 hr suggesting that the biochemical activities of osteocytes were similar in  $\mu$ G and ground conditions and sclerostin (Sost) expression was not affected by the launch itself. We then analyzed changes in the expressions of osteocytic genes between flight and ground control at different time points (2, 4, or 6 days) using quantitative real-time PCR. Interestingly, bone regulatory genes, such as Sost, Tnfrsf11 (RANKL), and Dmp1, were significantly

down-regulated in space-flown cells compared to ground controls at day 6, but not at day 2 and 4, suggesting that a longer duration of spaceflight has detrimental effects on osteocytes. Global transcriptome analysis (Affymetrix) identified 56 genes that were significantly and coordinately regulated with respect to location (flight vs ground) and time (2 vs 4 vs 6 days) with a corrected-p value  $< 0.05$ . Interestingly, the most regulated gene was Egl3 (egl-9 family hypoxia-inducible factor 3), which is associated with hypoxia inducible transcription factor 1 $\alpha$  (HIF1 $\alpha$ ) signaling. Ingenuity pathway analysis implicated that the most affected canonical signaling pathway was glycolysis-I. Multiple comparison transcriptome analysis will be performed to further identify additional transcripts. Findings derived from this experiment will have important implications for the therapy of bone disorders related to disuse or immobilization.

**Disclosures:** Yuhei Uda, None.

## MO0106

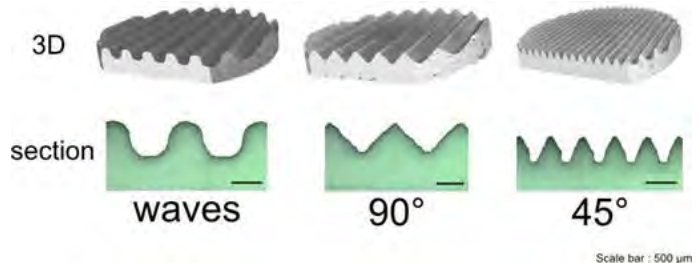
**Impact of Cell Substrate Shape on Matrix Deposition and Osteoblast Differentiation.** Laura Juignet\*<sup>1</sup>, Baptiste Charbonnier<sup>1</sup>, Virginie Dumas<sup>2</sup>, Mireille Thomas<sup>1</sup>, Coralie Laurent<sup>1</sup>, Laurence Vico<sup>1</sup>, David Marchat<sup>1</sup>, Nathalie Douard<sup>1</sup>, Luc Malaval<sup>1</sup>. <sup>1</sup>INSERM U1059-SAINBIOSE, Université de Lyon, France, <sup>2</sup>Ecole Nationale d'Ingénieurs de Saint Etienne, Université de Lyon, France

A major goal of bone tissue engineering is the development of *in vitro* models of living tissues, as simplified tools to better understand their physiology. While cells develop *in vivo* in a complex three-dimensional environment, most of our knowledge on bone cells has been obtained from traditional cultures on a flat two-dimensional plastic substrate. Few previous studies explored the role of substrate geometry at the tissue level in osteogenesis.

In order to study the impact of local substrate architecture on cellular behaviour, hydroxyapatite (Ca<sub>10</sub>(PO<sub>4</sub>)<sub>6</sub>(OH)<sub>2</sub>, HA) bioceramics with macroscopic grooves were produced through an additive manufacturing process. They display three different patterns: circular grooves ("waves"), and triangular grooves with a 90° angle ("90°") and a 45° angle ("45°", cf Figure). Mouse calvaria cells were seeded on these macroarchitectures and on flat (2D) bioceramics then cultured for 15 days in osteogenic medium. Bone cell adhesion, growth and differentiation as well as matrix deposition were analyzed.

One hour after seeding, the cells were homogeneously distributed on all substrates. In early culture times, cell metabolic activity was accelerated on grooved materials compared to 2D. After 15 days, the cells formed an abundant and dense extracellular matrix (ECM) on the 3 types of grooved substrates, but very little on 2D. The volume of ECM layed was significantly higher in the 45° pattern (34.1 ± 2.8mm<sup>3</sup>/bioceramic) than on the 90° (8.7 ± 1.5mm<sup>3</sup>, n=4,  $p < 0.001$ ). This suggests that the tighter angle bioceramic (with grooves narrower, but also 2.5X denser than on the 90°) would further enhance the synthesis of ECM. ELISA assays for osteopontin and osteocalcin showed that the kinetic of differentiation was accelerated on grooved substrates, compared to 2D. Quantitative immunodetection of osteoblast markers at different depths in the grooves also suggested that labeling intensity was stronger in the 45° grooves, indicative of distinct differentiation kinetics.

Substrate geometry thus seems to affect both osteoblast differentiation and extracellular matrix deposition. These observations could provide insights on fundamental bone cellular mechanisms, but also orient the design of innovative biomaterials for bone tissue engineering.



3D and section view of grooved bioceramics

**Disclosures:** Laura Juignet, None.

## MO0107

**Targeted Deletion of Src from Osteocytes Increases Trabecular Bone Mass in Mice.** Whitney A Bullock\*, Kathleen H Day, Alexander G Robling, Fredrick M Pavalko. Indiana University, United States

Mechanical stimulation of the skeleton during exercise promotes bone gain and suppresses bone loss resulting in improved skeletal strength and fracture resistance. The molecular mechanisms directing anabolic and/or anti-catabolic actions on the skeleton during loading are unclear, but recapitulating their effects via pharmacologic manipulation of mechanotransduction (MTD) signaling cascades in bone cells holds great potential for therapy. We propose that the tyrosine kinase Src, through its association with membrane mechanosensors (integrins), is activated by mechanical stimulation in osteocytes (OCY) to suppress MTD responses. Once activated, Src translocates from the membrane to the nucleus where it accumulates as part of a multi-

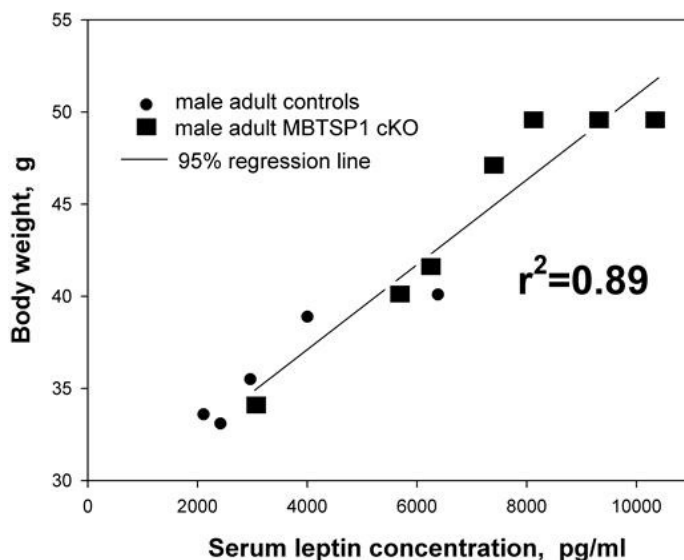
protein complex with Pyk2 and MBD2 to regulate epigenetics of key bone genes. Global deletion of Src results in very high bone mass, due in part to a Src-dependent defect in osteoclast-mediated bone resorption. Recently, several groups have reported an unexpected but significant role for Src in the osteoblast/osteocyte (OB/OCY) population. Osteocytes coordinate the skeletal response to load. We deleted Src from OCY in vivo by crossing Src<sup>fl/fl</sup> mice with Dmp1-Cre mice. We first confirmed targeting of Src from OCY in Dmp1-Cre; Src<sup>fl/fl</sup> mice by western blotting of OCY isolated from Cre+ and Cre- mice and by IHC. Src expression was decreased in OCY isolated from Dmp1-Cre; Src<sup>fl/fl</sup> mice compared to OCY from Cre-negative Src<sup>fl/fl</sup> mice. IHC staining for Src confirmed reduced Src expression in OCY in femurs from Dmp1-Cre; Src<sup>fl/fl</sup> mice compared to Cre-negative littermates. DEXA analysis of Src<sup>fl/fl</sup> male and female 16 week old mice with and without the Dmp1 transgene indicated no significant difference in whole body BMD due to targeted Src deletion from late OB/OCY. However,  $\mu$ CT analysis of trabecular bone in the femur indicated a consistent trend toward higher bone mass in Dmp1-Cre; Src<sup>fl/fl</sup> mice, compared to Cre- littermates. Trabecular BV/TV (36.15% in males, 22.20% in females), BMC (33.29% in males, 21.09% in females), connectivity (62.09% in males, 111.03% in females) and number (12.86% in males, 11.39% in females) were all higher, while trabecular spacing was lower (-12.26% in males, -11.30% in females) in Cre+ mice. These data suggest a novel role of Src-mediated signaling in the OCY and will provide new mechanistic information about how the mechanosome regulates OCY gene expression in bone.

**Disclosures:** Whitney A Bullock, None.

## MO0108

**Is Leptin an Age-related Paracrine/Autocrine Factor for Muscle?** Jeffrey P. Gorski<sup>\*1</sup>, Marco Brotto<sup>2</sup>. <sup>1</sup>University of Missouri-Kansas City, United states, <sup>2</sup>Bone-Muscle Collaborative Sciences, College of Nursing & Health Innovation, University of Texas at Arlington, Arlington, United states

We recently showed that deletion of Mbtsp1 (SKI-1, SIP, PCSK5) in bone osteocytes using Dmp1-cre Mbtsp1 cKO leads to an increase in skeletal muscle mass and contractile performance only in soleus (SOL) muscles from 10-12 month old adult but not 3 month old young mice. Gene expression profiling revealed that SOL muscles from adult Mbtsp1 cKO mice displayed many characteristics of regenerating muscle including satellite cell markers (*Pax7*, *Myf6*), increased expression of neonatal and embryonic myosin heavy chains, and increased oxidative metabolism. The purpose of this study was to investigate the cause of these changes in aging muscle? Whole genome Affymetrix arrays revealed that SOL muscles from adult control C57Bl6 mice expressed 3.3-times more leptin than SOL muscles from young control mice ( $p=0.05$ ), while leptin receptor level expression was not significantly different with age. Second, sera from adult Mbtsp1 cKO mice contained 2.01 +/- 0.5 S.D. times ( $p=0.018$  t-test) more leptin than similarly aged controls, when assayed with a commercial ELISA kit. While leptin is an adipokine produced by fat cells, the whole body fat content of Mbtsp1 cKO mice assessed by PIXIMUS x-ray scans was not significantly higher than controls. Despite this, a strong positive correlation was detected between total body mass and the concentration of serum leptin in both adult Mbtsp1 cKO and control mice (linear correlation coefficient  $r^2=0.89$ , see Figure). In summary, we believe our findings suggest that skeletal muscle is a producer of leptin and that the rate of production increases with age. In addition, deletion of Mbtsp1 in bone osteocytes appears to accentuate this age dependent trend. Since leptin is known to stimulate IGF-1 synthesis by aged muscle, an activator of muscle satellite cells, we speculate that elevated levels of serum leptin, particularly in adult Dmp1-cre Mbtsp1 cKO mice, could act as an autocrine factor to stimulate myogenesis and muscle growth, thus providing a rationale for the previously observed unusual muscle phenotype.



Figure

**Disclosures:** Jeffrey P.; Gorski, None.

## MO0109

**Reduced Exercise Capacity of Mice with Skeletal Muscle Specific Ablation of *Pit1***. Daniel Caballero<sup>\*1</sup>, Dominik Pesta<sup>2</sup>, Ali Nasiri<sup>1</sup>, Michael Jurczak<sup>3</sup>, Gerald Schulman<sup>1</sup>, Clemens Bergwitz<sup>1</sup>. <sup>1</sup>Yale School of Medicine, United states, <sup>2</sup>German Diabetes Center, Germany, <sup>3</sup>University of Pittsburgh, United states

Hypophosphatemia causes muscle weakness in individuals with vitamin D deficiency or renal phosphate wasting disorders.

To investigate the effect of hypophosphatemia on muscle function we used *Npt2a*<sup>-/-</sup> mice, which become hypophosphatemic on a diet containing 0.02% phosphate (LP-diet) because they are unable to conserve phosphate in their kidneys. Spontaneous wheel activity of these mice monitored in metabolic cages over 72 hrs. is reduced. Increased respiratory exchange rate of these mice suggests change in carbon source for ATP production when compared to *Npt2a*<sup>-/-</sup> mice maintained on 1.2% phosphate-diet. Furthermore, muscle ATP production is decreased when measured by <sup>31</sup>P NMR-spectroscopy *in vivo* and when measured enzymatically in muscle cell lysates obtained from *Npt2a*<sup>-/-</sup> mice on LP-diet. We next generated *smPit1*<sup>-/-</sup> mice that lack the universal phosphate transporter *Pit1* in skeletal muscle. Similar to *Npt2a*<sup>-/-</sup> mice grip strength and spontaneous wheel activity is reduced in *smPit1*<sup>-/-</sup> mice, however, these mice are normophosphatemic, suggesting that myocellular uptake of Pi via *Pit1* is required for normal muscle function. We further evaluated the role of *Pit1* for mitochondrial function in mouse 3T3 fibroblast cells using a Seahorse XFe24 analyzer. Pi stimulates state 3 coupled and uncoupled oxygen consumption (OCR) in a dose-dependent fashion. Likewise, Pi increases ATP levels in 3T3 cells using a luciferase-based ATP assay. RNAi mediated ablation of *Pit1* decreased Pi stimulated OCR in these cells. Using permeabilized mouse 3T3 cells we further showed that Pi is required for activation of complex III by glycerol-3-phosphate, while respiration induced by complex I, II, or IV substrates is insensitive to Pi.

In conclusion, hypophosphatemia reduces exercise capacity by decreasing mitochondrial respiration and ATP synthesis involving reduced cellular uptake of Pi via *Pit1* and possibly reduced action of Pi on respiratory chain complex III.

**Disclosures:** Daniel Caballero, None.

## MO0110

**The Osteopenia in Dystrophin/Utrophin Double Knockout Mice is Attributed to Down Regulation of Osteoclastogenesis in Postnatal Skeletal Development.** Xueqin Gao<sup>\*1</sup>, Ying Tang<sup>2</sup>, Bing Wang<sup>2</sup>, Sarah Amra<sup>1</sup>, Johnny Huard<sup>1</sup>. <sup>1</sup>University of Texas Health Science Center at Houston, United states, <sup>2</sup>University of Pittsburgh, United states

Dystrophin-Utrophin double knock-out (dKO) is a mouse model of Duchenne's muscular dystrophy (DMD). DKO mice showed osteopenia at 6 weeks. In this study, we collected bone and muscle samples from 5day, 2week, 4 week mice and performed microCT, histology of both bone and muscle tissues to investigate when osteopenia happens and its possible mechanism. We found that there were no significant differences for the skull, tibia, femur and spine bone parameters between the WT and dKO homo at the 5 day time point. However, there was already mild muscle degeneration in the muscles of the dKO-homo mice group compared to the WT mice. At 2 weeks, the muscle pathology became very obvious; however, the bone parameters were not significantly different between the WT and dKO-homo mice groups. Strikingly, at 4 weeks, the BV/TV, Tb.N, Tb.Th of proximal tibia were significantly lower in dKO-homo mice compared to the WT mice, while the Tb.Sp was higher in the dKO-homo group compared to the WT group. The cortical thickness of the femur showed a trend of reduction in dKO mice compared to WT mice ( $p=0.08$ ). The BV/TV, Tb.N and Tb.Th of 6<sup>th</sup> lumbar also showed a significant decrease in the dKO-homo group compared to WT group while the Tb.Sp was significantly higher in the dKO-homo group. At 4 weeks, H&E staining indicated that both the gastrocnemius and iliocostalis muscles were severely damaged and had a large amount inflammatory cells infiltration, centrally nucleated myofiber in the dKO-homo group compared to the muscles in the WT group. H&E staining of the bone tissues demonstrated that there were fewer and thinner trabecular bone in the proximal tibia of the dKO-homo mice compared to the WT mice. Similarly, there was also less trabecular bone in the 6<sup>th</sup> lumbar vertebrae in the dKO-homo group compared to WT group. Herovici's staining also indicated less collagen 1 in both proximal tibia and lumbar spine. Furthermore, TRAP staining showed that there were fewer osteoclast cells in the dKO-homo mice compared to the WT mice. Sclerostin (SOST) immunohistochemical staining indicated that there was a trend of decrease in SOST positive cells in the dKO-homo group compared to WT group ( $p=0.079$ ). Osteocalcin staining indicated that there was no difference in the bone surface osteoblast number. In order to further explore the mechanism behind these changes, we measured RANKL, SOST and IGF1 in the serum of 4 week old mice and found that the serum RANKL was 5 times lower in the dKO-homo group compared to WT group. In contrast, serum SOST levels were higher in dKO-homo group compared to WT group. No difference was found in the serum IGF-1 levels between two groups. In conclusion, our new findings indicate that osteopenia can occur as early as 4 weeks in the dKO mice. The obvious bone parameter changes may be associated with a significant reduction in osteoclasts due to lower levels of RANKL and increased SOST (an antagonist of bone formation) levels in the serum.

**Disclosures:** Xueqin Gao, None.

## MO0111

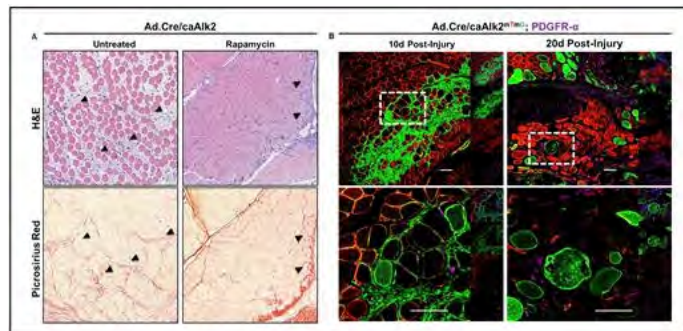
**Inhibition of mTOR signaling reduces Bmp-induced inflammation while preserving regenerative Smad signaling.** Shailesh Agarwal\*, David Cholok, Shawn Loder, James Drake, John Li, Charles Hwang, Kavitha Ranganathan, Hsiao Hsin Sung, Christopher Breuler, Oluwatobi Eboda, Caitlin Priest, Joshua Peterson, Shuli Li, Ernestina Schipani, Yuji Mishina, Benjamin Levi. University of Michigan, United states

**Purpose:** Bmp implants are associated with severe inflammatory reactions and ectopic bone, limiting their utility. Similarly, hyperactivation of Bmp signaling in fibrodysplasia ossificans progressiva (FOP) leads to extensive ectopic bone. Treatments which mitigate these complications associated with Bmp while preserving tissue regeneration would be clinically beneficial.

**Methods:** Mice without (WT) or with hyperactive Bmp signaling (*caACVRI<sup>fl/fl</sup>*) were used for all experiments. Mice received hindlimb injections of adenovirus with Cre and cardiotoxin to activate local Bmp signaling with local injury. Mice were treated with rapamycin (i.p. 5mg/kg) or vehicle control. Injured muscles were harvested and underwent H&E staining and immunostaining to evaluate inflammatory cell infiltration (neutrophils: Ly6G, macrophages: Cd11b; mesenchymal cells: Pdgfra). Fibrotic accumulation was quantified using picrosirius red for extracellular matrix deposition and Pdgfr $\alpha$  for mesenchymal cells at days 10 and 20 after injury (n=4 hindlimbs/time point). Immunoblotting for muscle regenerative protein (MyoD, Pax7) was performed.

**Results:** Hindlimbs from mutant mice showed increased inflammation after injury when compared with WT mice on the basis of neutrophil, macrophage, and mesenchymal cell infiltration (p<0.05). Similar inflammatory findings were noted with intramuscular Bmp scaffolds. Rapamycin reduced inflammatory cell infiltrate (day 5; p<0.05) and eliminated fibrosis and ectopic bone in mutant mice (day 20) (Fig 1). Rapamycin reduced p-mTOR and p-Akt in treated hindlimbs (day 3, p<0.05). Limbs from rapamycin-treated mutant mice had similar levels of pSmad 1/5 when compared with untreated mutant mice, and significantly higher levels when compared with untreated WT mice (day 3, p<0.05). Using a *caACVRI; ROSA<sup>tmTmG</sup>* reporter, a higher proportion of transformed cells (green) had peripheral nuclei when compared with untransformed cells (red) in rapamycin-treated mice (day 10, p<0.05).

**Conclusion:** Inhibition of mTOR signaling with rapamycin eliminates HO and reduces the initial inflammatory reaction associated with hyperactive Bmp signaling. Rapamycin preserves pSmad 1/5 and the regenerative muscle phenotype associated with Bmp signaling. mTOR inhibition may prevent Bmp-associated complications as adjunct therapy, prevent or reduce intramuscular fibrosis and bone in FOP patients, and safely expand the indications of Bmp for its positive impact on muscle regeneration.



figure

**Disclosures:** Shailesh Agarwal, None.

## MO0112

**Cortical bone resorption is elevated in aged mice and is associated with markers of cellular senescence in osteocyte-enriched bone.** Marilyna Piemontese\*, Maria Almeida, Ha-neui Kim, Robert Jilka, Charles OBrien. University of Arkansas for Medical Sciences, United states

Increased cortical porosity and cortical thinning contribute to skeletal fragility in elderly humans. However, the underlying cellular and molecular mechanisms are unclear. We investigated the impact of aging on cortical architecture in female C57BL/6J and CB6F1 mice. The latter are an F1 hybrid of C57BL/6J and BALBcJ. Using microCT analysis, we detected a progressive decrease in cortical thickness and increase in cortical porosity in C57BL/6J mice between 6 and 24 months of age, and in CB6F1 between 6 and 30 months of age. Cortical thickness in L4 vertebra also decreased with age in both strains. In C57BL/6J mice, these changes were associated with increased osteoclast number at the femoral endocortical surface but no change in osteoblast number. We then measured gene expression in cortical bone and found that RANKL mRNA was elevated and OPG mRNA was reduced in aged compared with young adult mice. Soluble RANKL protein was also elevated in bone marrow supernatants from aged mice as determined by ELISA and Luminex assays. Since osteocytes are a major source of RANKL, and since they are relatively long-lived cells, we explored the possibility that increased osteocyte senescence may underlie

these changes in gene expression and osteoclast number. Even though osteocytes are post-mitotic cells, markers of senescence have been shown to increase with age in other post-mitotic cells such as neurons and this may contribute to gene expression changes known as the senescence associated secretory phenotype (SASP). The mRNA for the cell cycle regulator p16ink, which is elevated in senescent cells from other tissues, was strongly elevated in cortical bone from aged mice. Other markers of senescence were also increased, including protein abundance of gammaH2AX histone and the GATA4 transcription factor, which in other cell types has been shown to drive development of the SASP. Together these results demonstrate that reduced cortical thickness and increased cortical porosity are consistent findings in aged female mice of different strains and that these changes are associated with increased osteoclast formation. In addition, the increased osteoclastogenesis may result from increased RANKL production and reduced OPG production by osteocytes that display markers of cellular senescence.

**Disclosures:** Marilyn Piemontese, None.

## MO0113

**Effects of age-related chronic inflammation on osteoprogenitor cells.** Anna Josephson, Vivian Bradaschia Correa, Philipp Leucht\*. New York University School of Medicine, United states

Stem cells are not resistant to the aging process. Osteoprogenitor cells (OPCs) from healthy people over age 65 make less bone compared to OPCs from people under age 35, irrespective of their sex [1]. We hypothesize that age-related chronic inflammation contributes to a decline in the osteogenic capacity of OPCs. In this study, we compared young, (1) 12 week-old mice with aged, (2) 52 week-old mice and (3) aged mice that were treated with an anti-inflammatory drug for 3 months with the goal to inhibit age-related inflammation. First, we assessed the systemic inflammatory state of these three groups and showed that a 3 months course of NSAID treatment reversed the inflammatory cytokine profile of aged mice to that of young mice (Fig.1A). Next, we quantified age-dependent alterations in proliferation and osteogenic differentiation of a pure population of OPCs from these three different groups. We used the Leptin-receptor as a marker for OPCs [2] and demonstrated an age-related decline in OPC number (Fig.1B). However, this decline was less significant in animals treated with NSAIDs. In addition, when we employed a battery of in vitro analyses to test the proliferative and osteogenic differentiation capacity of these three cell populations we learned that NSAID treatment of aged mice resulted in a reversal of the age-related decline in proliferation and osteogenic differentiation. In detail, the expression of osteocalcin, osterix and alkaline phosphatase returned to levels similar to those observed in young animals (Fig.1C). Mineralization assays showed a complete reversal of the osteogenic differentiation capacity after NSAID treatment (Fig.1D).

These experiments demonstrate for the first time that age-related chronic inflammation is responsible for the decreased proliferative and osteogenic potential of aged OPCs and that this process is reversible by anti-inflammatory treatment. The findings from this study may have a profound translational impact: If we could restore the regenerative potential of the aged skeleton by treating age-related inflammation, then theoretically, we may have a tool at hand to improve the healing process of osteoporotic fracture patients.

1. Nishida, Y., et al., *Survival of syngeneic and allogeneic grafted bone in transgenic mice*. *Biochem Biophys Res Commun*, 1993. 196(3): p. 1081-5.

2. Zhou, B.O., et al., *Leptin-receptor-expressing mesenchymal stromal cells represent the main source of bone formed by adult bone marrow*. *Cell stem cell*, 2014. 15(2): p. 154-168.

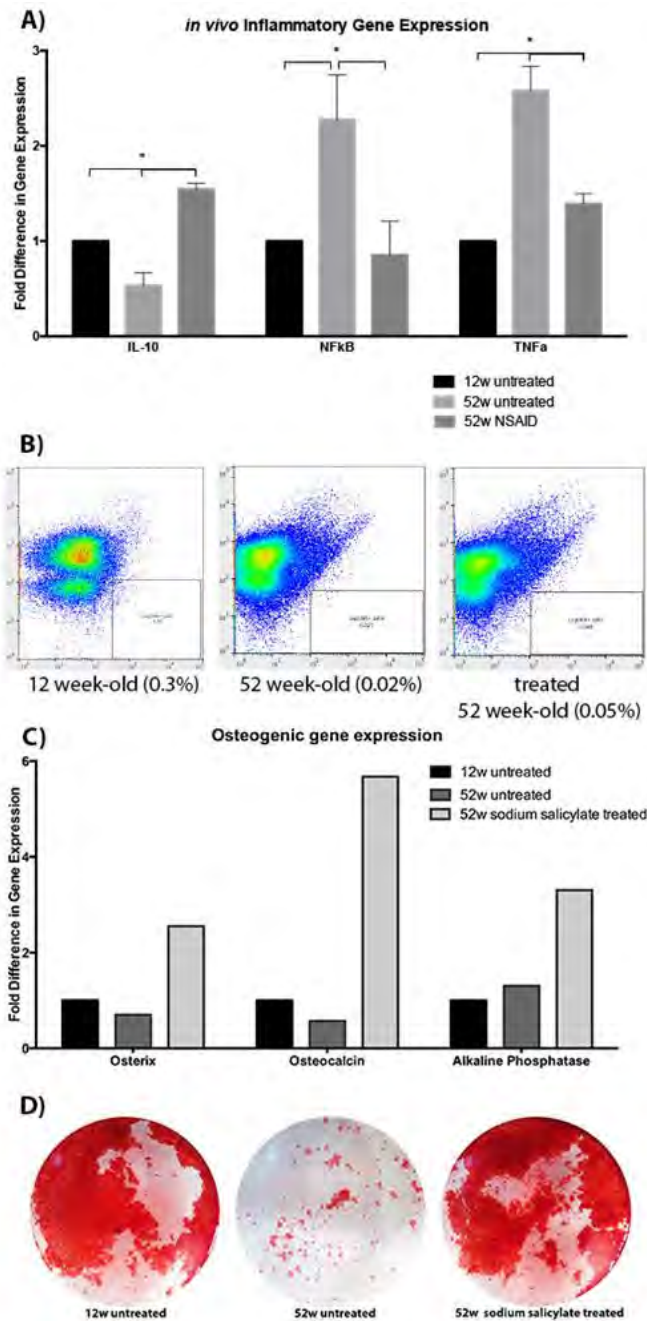


Figure 1

Disclosures: Philipp Leucht, None.

**MO0114**

**Global deletion of the  $\beta$ 2-adrenergic receptor does not protect against age-related or cold temperature-induced bone loss in female mice.** Kathleen Bishop\*, Katherine Motyl, Phuong Le, Clifford Rosen. Maine Medical Center, United states

Increased sympathetic nervous system (SNS) signaling has been highlighted as a mechanism for age-related bone loss via the  $\beta$ 2-adrenergic receptor (*Adrb2*), the primary  $\beta$ -adrenergic receptor in osteoblasts. Previous studies have shown that global deletion (*Adrb2*<sup>-/-</sup>) and osteoblast-specific deletion of the *Adrb2* result in an increase in trabecular bone and rates of bone formation suggesting that SNS signaling can directly affect bone metabolism through the osteoblast. As SNS activity increases with age, we wanted to assess whether global deletion of *Adrb2* in mice would prevent age-related bone loss. At 8 weeks of age, DXA analysis of *Adrb2*<sup>-/-</sup> (n=10) mice showed elevated total aBMD (p=0.001) and aBMC (p=0.009) and femoral aBMD (p=0.01) and aBMC (p=0.14) when compared to *Adrb2*<sup>+/+</sup> (n=11) control mice. In contrast to the young mice, DXA analysis of 16 month old *Adrb2*<sup>+/+</sup> (n=22) and *Adrb2*<sup>-/-</sup> (n=14)

mice showed no difference in total and femoral aBMD and aBMC. Body composition including body mass, lean mass, and fat mass were unchanged in the *Adrb2*<sup>-/-</sup> mice at both ages. These data suggest while young *Adrb2*<sup>-/-</sup> mice have increased bone mass, they are not protected against age-related bone loss. In order to test whether deletion of *Adrb2* would prevent bone loss associated with induced SNS activity in aged mice, 16 month old *Adrb2*<sup>-/-</sup> mice were challenged with long term cold exposure to stimulate SNS activity. Mice were individually housed at 18°C for 7 days for temperature acclimation and then at 4°C for 3 weeks then compared to control mice kept at 22°C. Rectal temperatures and body weights were measured. Core body temperature increased following 4 weeks of cold exposure (p<0.0001) with *Adrb2*<sup>+/+</sup> and *Adrb2*<sup>-/-</sup> mice gaining 1.3±0.1°C and 1.3±0.3°C, respectively. Body weights decreased in both genotypes following cold exposure (p=0.005) as well as weights of both the inguinal (p=0.006) and gonadal (p=0.0008) adipose depots. Brown fat weights remained unchanged with cold exposure. Furthermore, ex vivo DXA analysis revealed cold-induced decreases in femoral aBMD (p=0.01) and aBMC (p=0.02). However, no dependence on genotype was observed suggesting that deletion of the *Adrb2* does not protect against cold-induced bone loss. Further studies including  $\mu$ CT analysis, histomorphometry, and gene expression analysis will be performed in order to fully understand both the phenotype of the aged *Adrb2*<sup>-/-</sup> mice and the mechanism by which SNS activity affects age-related bone loss.

Disclosures: Kathleen Bishop, None.

**MO0115**

**Loss of BMP2 expression in skeletal progenitor cells reduces age-related bone loss.** Michael Eaton\*, Aaron Hudnall<sup>1</sup>, Jordan Newby<sup>2</sup>, Vicki Rosen<sup>3</sup>, Jonathan Lowery<sup>1</sup>. <sup>1</sup>Marian University College of Osteopathic Medicine, United states, <sup>2</sup>Freed-Hardeman University, United states, <sup>3</sup>Harvard School of Dental Medicine, United states

Osteoporosis is a disease of low bone mineral density (BMD) that affects 10 million Americans and accounts for 1.5 million fractures annually. With an additional 34 million Americans at risk for developing the disease, osteoporosis is both a significant health problem and a considerable socioeconomic burden. Current first-line therapies for osteoporosis involve anti-resorptive agents but many patients, such as those with drastically low BMD or high fracture risk, would benefit from augmenting bone formation as well as inhibiting bone loss. We recently reported that targeted deletion of the type 2 BMP receptor *BMP2* in skeletal progenitor cells of the limb bud using *Px1-Cre* (*Bmpr2*-cKO mice) leads to dramatically increased bone mass and bone formation rate by ten weeks of age in the absence of changes in osteoclast number or function (Lowery et al 2015). In the present study, we examined the impact of *Bmpr2* deletion on age-related bone loss in *Bmpr2*-cKO mice. Consistent with our previous results, 55-week-old female *Bmpr2*-cKO mice exhibit approximately four-fold higher bone mass in the tibia than control mice (BV/TV ratios: control=0.0229±0.003, n=3 vs. *Bmpr2*-cKO=0.1110±0.006, n=4; p=0.0001 by unpaired t test). Moreover, the age-related decline in bone mass from 15 weeks to 55 weeks of age in female *Bmpr2*-cKO mice is reduced approximately two-fold compared to control mice. Bone mass of the L5 vertebrae, which is outside the *Px1-Cre* expression domain, is unchanged in *Bmpr2*-cKO mice compared to control mice at all ages examined. Quantification of the serum bone turnover markers Procollagen Type I N-terminal Propeptide (PINP) and Collagen Type I C-telopeptide (CTX) suggest that high bone mass in aging female *Bmpr2*-cKO mice is preserved due to a sustained increase in bone formation rate to at least 35 weeks of age with no alteration in bone resorption (PINP: control=1341.09±139.45 pg/ml, n=9 vs. *Bmpr2*-cKO=394.77±255.33 pg/ml, n=8; p=0.004 by unpaired t test; CTX: control=5.21±1.02 ng/ml, n=5 vs. *Bmpr2*-cKO=5.78±1.28 ng/ml, n=5, p=0.7 by unpaired t test). Collectively, our findings provide insight into the mechanisms regulating age-related bone loss and suggest that strategies aimed at controlling signaling through *BMP2* have the potential to impact bone mass in the aging adult skeleton.

Disclosures: Michael Eaton, None.

**MO0116**

**PTH, CTX, and Calcium Responses to Treadmill Walking Under Different Thermal Conditions in Older Adults.** Sarah Wherry\*, Christine Swanson, Toby Wellington, Rebecca Boxer, Jane Quick, Robert Schwartz, Wendy Kohrt. University of Colorado Anschutz Medical Campus, United states

An increase in markers of bone resorption (parathyroid hormone, PTH; c-terminal telopeptides of type I collagen, CTX) and a decrease in serum ionized calcium (iCa) have been observed during endurance exercise in older adults. Due to age-related changes in thermoregulation, it is unknown if calcium losses in the sweat during exercise are driving bone resorption. Therefore, the objective was to determine if exercise in a warm environment results in greater increases in PTH, CTX and a greater decrease in iCa compared to a cool environment. Methods: Women (n=4) and men (n=4) aged 61-77 years performed two identical 60-minute treadmill walking bouts at ~80% of heart rate max under warm (30°C) and cool (20°C) conditions. The order of the conditions was randomized. Serum PTH, CTX, and iCa were measured every 15 minutes beginning 15 minutes before exercise and continuing for 60 minutes post-exercise. Calcium losses in the sweat were estimated from sweat volume loss and sweat calcium concentration. Changes in CTX and PTH were adjusted for plasma volume

shifts. Paired t-tests were run to compare the change in PTH, CTX, and iCa from 15 minutes before to immediately after exercise. Results: Sweat calcium concentration was similar in both the warm and cool conditions; total sweat volume and sweat calcium losses were two times higher during the cool condition (38.9 ± 42.7 mg) versus the warm condition (19.2 ± 18.1 mg) but were not statistically significant (p>0.05). The changes in all serum markers during exercise were similar in both environments; ΔPTH warm vs. cool: 17.8±20.4 vs. 18.2±18.1 pg/mL, ΔCTX warm vs. cool: 0.10±0.06 vs. 0.07±0.04 ng/mL, or ΔiCa warm vs cool: -0.16±0.06 vs. -0.12±0.11 mg/dL. Conclusions: Differing thermal conditions and dermal calcium losses do not appear to be a major factor in the increase in PTH and CTX observed during exercise in older adults. PTH and CTX increased and iCa decreased similarly in both conditions despite observed differences in sweat losses, although losses were not statistically significant. Further research with larger sample sizes is needed to determine if there are any sex- or age-related differences that may modify the relationship between sweat calcium losses and bone markers.

Disclosures: Sarah Wherry, None.

## MO0117

**The radial distribution of the intracortical porosity within the fibula diaphysis.** Jesper Skovhus Thomsen<sup>1</sup>, Christina Møller Andreassen<sup>2</sup>, Lydia Peteva Bakalova<sup>3</sup>, Anne-Marie Brüel<sup>1</sup>, Ellen Margrethe Hauge<sup>4</sup>, Gete Ester Toft Eschen<sup>5</sup>, Birgitte Jul Kiiij<sup>5</sup>, Jean-Marie Delaisse<sup>6</sup>, Mariana Elizabeth Kersh<sup>7</sup>, Thomas Levin Andersen<sup>6</sup>. <sup>1</sup>Department of Biomedicine, Aarhus University, Denmark, <sup>2</sup>Orthopaedic Research Laboratory, Department of Orthopaedic Surgery & Traumatology, Odense University Hospital, Institute of Clinical Research, University of Southern Denmark, Denmark, <sup>3</sup>Department of Mechanical Science & Engineering, University of Illinois at Urbana-Champaign, United states, <sup>4</sup>Department of Rheumatology, Aarhus University Hospital, Denmark, <sup>5</sup>Department of Plastic Surgery, Aarhus University Hospital, Denmark, <sup>6</sup>Department of Clinical Cell Biology, Vejle Hospital/Lillebaelt Hospital, Institute of Regional Health Research, University of Southern Denmark, Denmark, <sup>7</sup>Department of Mechanical Science & Engineering, University of Illinois at Urbana-Champaign, Denmark

The present study is part of an effort to investigate the size, shape and distribution of the intracortical canals along the radial axis of the fibula diaphysis, and the bone remodeling units generating these canals.

The study was conducted on bone specimens from the fibula diaphysis obtained from 26 patients (age range 41-75 years, 18 men and 8 women) undergoing mandible reconstructions. The bone specimens were μCT scanned, plastic embedded and sectioned along the scanning plan. This made it possible to analyze the same canals observed in the 3D μCT scans, as pores in 2D at the level of the histological sections.

The 3D μCT scans of all the 26 cortical bone specimens were subdivided into an endosteal and periosteal half, and analyzed separately. This analysis revealed that the endosteal half had a statistically significant 3.5-fold higher porosity and a 3-fold larger canal diameter than the periosteal half (p<0.0001). However, the canal spacing was not different between the endosteal and periosteal part of the cortical bone. These data support the notion that the increased porosity in the endosteal half reflects the presence of enlarged canals, rather than an increased density of canals. The 2D analysis at the level of the histological sections obtained from 11 of the cortical specimens, including a total of 1473 pores, revealed a highly significant positive correlation between the distance from the periosteum and the pores area, diameter and perimeter (p<0.0001). This shows that the size of the pores gradually increases along the radial axis from the periosteal to the endosteal surface of the cortex. Of note, several of the pores had a high ratio between the perimeter and diameter, which were in line with their appearance as irregular shaped pores.

Collectively, this study highlights that the size and shape of the intracortical canals change according to their distribution along the radial axis of the diaphysis in human fibula.

Disclosures: Thomas Levin Andersen, None.

## MO0118

**MicroRNA-183 promotes an aging phenotype in the muscle-bone unit by targeting heme oxygenase-1 (HO-1).** Sadanand Fulzele, Bharati Mendhe, Meghan McGee-Lawrence, Xingming Shi, William Hill, Carlos Isales, Mark Hamrick\*. Medical College of Georgia, United states

We have previously shown that microRNA-183-5p (miR-183) increases with age in bone marrow-derived exosomes and microvesicles, and others have demonstrated that miR-183 is elevated with age in mouse serum but is lower in blood from aged, calorie-restricted mice and long-lived centenarians. We investigated the role of miR-183 in musculoskeletal aging by first transfecting C2C12 myoprogenitor cells and primary mouse bone marrow stromal cells (BMSCs) with miR-183-5p mimic. We then examined cell proliferation using CyQuant assay, and investigated cellular senescence using beta-galactosidase (β-gal) staining. We also assessed osteogenic potential of transfected cells using alizarin red staining. miR-183-5p has a number of predicted

targets, and we investigated these potential targets using western blotting procedures. Results indicate that miR-183 significantly reduced proliferation in both myoprogenitor cells and BMSCs, and increased β-gal staining in both C2C12 cells and BMSCs. Alizarin red staining indicated reduced mineral accumulation in BMSCs cultured in osteogenic medium and transfected with miR-183 mimic compared to controls. Western blots revealed that protein levels of heme oxygenase-1 (HO-1) were decreased significantly in miR-183 transfected muscle and bone progenitor cells. HO-1 induction is thought to play a key role in cellular protection against injury caused by reactive oxygen species (ROS), and ROS are widely believed to accumulate with aging. Moreover, repression of HO-1 by miR-183 in bone marrow-derived macrophages has previously been shown to increase osteoclastogenesis. Our data suggest that enhancing HO-1 production by targeting miR-183 may have positive effects on aging muscle and bone.

Disclosures: Mark Hamrick, None.

## MO0119

**Sex-specific Associations Between Bone Density and Lean Mass in the VITAL Bone Health Study.** Amy Yue\*<sup>1</sup>, Sarah Zaheer<sup>1</sup>, Trisha Copeland<sup>2</sup>, Nancy Cook<sup>3</sup>, JoAnn Manson<sup>3</sup>, Julie Buring<sup>3</sup>, Meryl LeBoff<sup>1</sup>. <sup>1</sup>Division of Endocrinology, Diabetes & Hypertension, Brigham & Women's Hospital (BWH), Harvard Medical School, United states, <sup>2</sup>Division of Preventive Medicine, Department of Medicine, BWH, Harvard Medical School, United states, <sup>3</sup>Division of Preventive Medicine, Department of Medicine, BWH, Harvard Medical School, Department of Epidemiology, Harvard T.H. Chan School of Public Health, United states

Reduced lean muscle mass and bone mineral density (BMD) are prevalent conditions among the aging U.S. population. Recently cutpoints for low appendicular lean mass (ALM) and ALM-adjusted for body mass index (BMI) have been established for women and men. The VITamin D and Omega-3 Trial (VITAL) is a placebo-controlled study testing effects of supplemental cholecalciferol (2000 IU/d) and/or omega-3 fatty acids (1 g/d) on cancer and cardiovascular disease. In this study, we investigated whether there are sex differences in associations in ALM, ALM/BMI, and BMD among participants in the VITAL Bone Health subcohort who are having detailed in-person visits on the Harvard Catalyst Clinical and Translational Science Center at baseline and after 2-yrs of follow-up.

Baseline data were obtained in 773 women and men (46.8/53.2%), aged ≥50 and ≥55 yrs, respectively. The mean age was 63.8 yrs and 22.5% were obese. Participants who had used osteoporosis medications in the past 2 yrs were excluded. BMD at the spine and hip femoral neck (FN), and body composition including ALM and ALM/BMI were determined by DXA (Discovery W, Hologic Inc., Bedford, MA). Sex-specific cutpoints for low lean mass according to ALM and ALM/BMI were from the FNH Sarcopenia Project (Studenski et al., 2014).

Women with ALM <15.02 kg had significantly lower BMD at the spine (p<0.001) and hip (p<0.001) than women with ALM ≥15.02 kg (Table 1). Low ALM/BMI in women was associated with higher BMD at the spine (p=0.008), but ALM/BMI was not related to BMD at the hip. Men with ALM <19.75 kg also had lower BMD at the spine (p=0.017) and hip (p<0.001) than men with ALM ≥19.75 kg. When ALM was adjusted for BMI, there were no associations with BMD in men.

In summary, low appendicular lean mass was associated with decreased BMD at the spine and hip in women and men. After adjusting for BMI, there were no associations between ALM and BMD in women at the hip and in men at the spine and hip. Since obese individuals have a higher BMD and women in this subcohort had a greater fat mass than men, this may have contributed to the association of low ALM/BMI and greater spine BMD in women. Grip strength, and other physical performance are also being determined. The 2-yr follow-up musculoskeletal measures will allow for assessment of effects of high-dose, daily supplemental vitamin D on lean mass, BMD, body composition, physical performance, and sarcopenia in women and men in the VITAL bone health study.

Variable	Category	N	%	Mean	SPINE BMD		HIP FN BMD		
					95% Confidence Interval	P-value	Mean	95% Confidence Interval	P-value
ALM (men)	<19.75 kg	29	7.1	1.006	(0.939-1.073)	0.017	0.699	(0.664-0.733)	<0.001
	≥19.75 kg	382	92.9	1.081	(1.066-1.097)		0.828	(0.815-0.841)	
ALM (women)	<15.02 kg	157	43.6	0.917	(0.896-0.937)	<0.001	0.683	(0.669-0.696)	<0.001
	≥15.02 kg	203	56.4	0.993	(0.971-1.015)		0.742	(0.727-0.757)	
ALM/BMI (men)	<0.789	95	23.2	1.079	(1.044-1.115)	0.837	0.808	(0.781-0.834)	0.301
	≥0.789	315	76.8	1.075	(1.057-1.093)		0.823	(0.809-0.837)	
ALM/BMI (women)	<0.512	97	26.9	0.996	(0.965-1.027)	0.008	0.731	(0.711-0.752)	0.106
	≥0.512	263	73.1	0.947	(0.929-0.965)		0.711	(0.696-0.724)	

Table 1. Mean BMD at baseline according to ALM and ALM/BMI in women and men

Disclosures: Amy Yue, None.

**MO0120**

**TEI-SARM2, an Oral Non-steroidal Selective Androgen Receptor Modulator, Prevents Muscle Atrophy and Bone Loss.** Akito Makino\*, Masanobu Kanou, Kyohei Horie, Katsuyuki Nakamura, Yoshimasa Takahashi, Tsunefumi Kobayashi, Hiroyuki Sugiyama, Kei Yamana. Teijin Institute for Bio-Medical Research, Teijin Pharma Limited, Japan

Muscle atrophy is often concomitant with osteopenia in several diseases such as osteoporotic hip fracture, cancer cachexia, sarcopenia and Duchenne muscular dystrophy (DMD). Patients with severe osteopenia increase the fracture risk and inactivity, resulting in acceleration of muscle atrophy and immobilization. Therefore, prevention of osteopenia as well as muscle atrophy is significant unmet medical needs for the treatment of these diseases. However, there is no approved drug having favorable effects on both muscle and bone so far.

TEI-SARM2 is an oral non-steroidal selective androgen receptor modulator (SARM), selected as a pharmaceutical candidate for the treatment of muscle wasting diseases by its potent muscle anabolic activity. TEI-SARM2 has unique chemical structure and binds to AR with novel binding mode which is confirmed by co-crystallization analysis. We previously reported that TEI-SARM2 showed preferable pharmacokinetic properties and improved muscle atrophy by daily administration in hindlimb-unloaded rats within the range of 0.1 to 3 mg/kg (#MO0169, ASBMR 2015). We further confirmed the effectiveness of TEI-SARM2 in other animal models of muscle atrophy. In mice xenograft models of cancer cachexia, daily administration of TEI-SARM2 at 3 mg/kg for 4 weeks increased body weight and muscle mass without any effects on tumor. We also found that TEI-SARM2 improved muscle strength in a rat model of DMD which had a mutated *Dmd* gene constructed by CRISPR/Cas9 system.

Here, we evaluated the pharmacological profile of TEI-SARM2 on bone. Sprague-Dawley rats were ovariectomized and received daily oral administration of TEI-SARM2 ranging from 0.01 to 1 mg/kg for 16 weeks. TEI-SARM2 significantly increased bone mineral density at femur and lumbar spine as well as muscle mass. TEI-SARM2 also increased bone strength at femur by 3-point bending. Structural analysis revealed that TEI-SARM2 increased periosteal bone mass and cortical thickness, suggesting anabolic effects on bone.

Taken together, our results indicate that TEI-SARM2 has potent anabolic effects on both muscle and bone. Therefore, TEI-SARM2 is a promising drug candidate for muscle wasting diseases with osteopenia such as hip fracture, cancer cachexia, sarcopenia and DMD.

*Disclosures: Akito Makino, Teijin Pharma Limited, 11*

**MO0121**

**Assessment of Novel Stem-cell Based Therapies for Repair of Alveolar Clefts Using a Juvenile Swine Model.** Montserrat Caballero, Donna Jones\*, Zhengyuan Shan, Jacob Knorr, John van Aalst. Cincinnati Children's Hospital Medical Center, United states

**Background and Purpose:** Congenital craniofacial bone malformations occur in 1:250 live births. Historically, reconstruction of these defects has relied on autologous bone grafts. This study used a previously reported juvenile swine alveolar cleft model to test novel tissue engineered approaches based on autologous umbilical cord (UC) mesenchymal stem cells (MSC).

**Methods:** MSCs (isolated from UC) were transduced using lentivirus expressing GFP, seeded onto electrospun PLGA nanofiber scaffolds, and cultured in either a) standard growth (DMEM/F12-10% FBS) or, b) osteoinduction (growth media supplemented with ascorbic acid, dexamethasone and beta-glycerol phosphate) media for 5 days. The maxilla of five-week-old pigs (n=16) received a surgically-created, unilateral, alveolar defects to determine the quality of treatment outcomes with tissue-engineered scaffolds: loaded with autologous undifferentiated (n=8) or differentiated (n=6) cells, or autologous cancellous bone (n=2) to serve as a clinical comparison. Pigs were sacrificed after 1 month. Histology and mechanical testing (Instron) were used to evaluate new-formed bone quality within the defect. Computed tomography (CT) scans were obtained at surgery and at the time of euthanasia. Volume fill of defects was quantified from 3D reconstructions (Amira 6.0) and compared among treatments (ANOVA).

**Results:** Both tissue-engineered grafts and cancellous bone provided more bone than an untreated critical size defect. The use of pre-differentiated cells led to bone fill that was well integrated with native bone, as assessed by histological staining. The cancellous and undifferentiated cell grafts also led to bone formation but the interface between the new and native tissue was more defined. Mechanical testing showed bone formation in samples with the differentiated cells, while samples with undifferentiated cells didn't have enough rigidity for testing. Percentage of volume filling was statistically indistinct ( $p = 0.464$ ).

**Conclusions:** Both differentiated and undifferentiated UC MSCs generated bone within the cleft, with differentiated cells showing better bone formation. Future work will extend the length of time to three months, to test if these constructs have the ability to fully heal a critical size maxillary defect.

*Disclosures: Donna Jones, None.*

**MO0122**

**Differential regulation of glycolysis during osteoblast and adipocyte differentiation.** Anyonya Guntur\*, Phuong Le, Clifford Rosen. MMCRI, United states

We have previously shown that during osteoblast differentiation there is upregulation of both oxidative phosphorylation (OxPhos, OCR) and Glycolysis (Glyc, ECAR). In this study we hypothesized that osteoblasts and adipocytes have an inherently different metabolic signature during differentiation. To test this we utilized preosteogenic MC3T3-E1 and preadipogenic 3T3-L1 cells to study their bioenergetic profiles in response to glucose. We tested the glycolytic rates and maximal glycolytic capacity of both differentiating osteoblasts and adipocytes. Osteoblasts have higher glycolytic rates than non-differentiating cells. Addition of Rotenone inhibits Complex I of the electron transport chain, the cells then need to rely on ATP generated through Glyc. On inhibiting Complex I, non-differentiated osteoblasts could meet ATP demand by increasing glycolysis but the differentiated osteoblasts were already at maximum glycolytic capacity. In contrast, adipocytes had lower glycolytic rates than non-differentiating cells and both differentiating and non-differentiating adipocytes could increase glycolytic rate in the presence of Rotenone. Calculating the rate of glycolytic ATP production showed that differentiating osteoblasts have increased rates compared to non-differentiating cells whereas differentiating adipocytes have decreased ATP production rates compared to non-differentiating adipocytes. In sum osteoblasts and adipocytes utilize glycolysis differently when forming bone or fat respectively.

*Disclosures: Anyonya Guntur, None.*

**MO0123**

**microRNA-433 Dampens TGF $\beta$  Signaling and Restrains Osteoblastic and Chondrogenic Differentiation.** Spenser Smith\*<sup>1</sup>, Neha Dole<sup>2</sup>, Rosa Guzzo<sup>1</sup>, Anne Delany<sup>1</sup>. <sup>1</sup>UConn Health, United states, <sup>2</sup>UCSF School of Medicine, United states

Lineage commitment and differentiation of skeletal cells requires coordinated regulation of multiple signaling systems by microRNAs (miRNAs). Transforming growth factor  $\beta$  (TGF $\beta$ ) is important for osteoblastogenesis, chondrogenesis and adipogenesis. Here, we show that miR-433 limits TGF $\beta$  signaling and that miR-433 is a negative regulator of osteoblastogenesis and chondrogenesis.

In mouse bone marrow stromal cells (BMSCs), culture in osteogenic medium caused a progressive decline in miR-433. In contrast, miR-433 gradually increased in BMSCs cultured in micromass to induce chondrogenesis. Indeed, in late chondrogenesis miR-433 was 15 fold higher than in undifferentiated cells. Similar effects were observed in human induced pluripotent stem cells (iPSCs) undergoing chondrogenesis. Although miR-433 is expressed in adipocytes, its levels remained constant during adipogenesis. To determine the impact of miR-433 on these differentiation processes, multipotent C3H/10T1/2 cells expressing a miR-433 competitive inhibitor, or tough decoy, were examined. In monolayer cultures treated with BMP2, miR-433 inhibition induced alkaline phosphatase, Runx2, and osteocalcin mRNAs, and promoted calcium deposition. In micromass cultures treated with BMP2 and TGF $\beta$ , miR-433 inhibition promoted expression of chondrogenic mRNAs, Sox9 and Col2a1. In cells treated with an adipogenic cocktail, miR-433 inhibition failed to alter adipogenic gene markers or Oil-red O staining. These data suggest that miR-433 blunts osteogenic and chondrogenic differentiation.

Bioinformatic analyses suggested that miR-433 might target critical components of the TGF $\beta$  signaling pathway. In C3H/10T1/2, inhibition of miR-433 amplified TGF $\beta$  signaling, evidenced by increased activity of a TGF $\beta$ -responsive SBE4 luciferase reporter and enhanced TGF $\beta$ -induced pSMAD2. To determine underlying mechanisms, we used Luciferase-3'UTR reporter assays, and experimentally validated SMAD2 and TGFBR1 as novel miR-433 targets, and showed that miR-433 does not target SMAD4 or TGFBR2. Lastly, miRNAs and their regulators often participate in regulatory loops, and we found TGF $\beta$  down regulates miR-433 after 24 hours, suggesting an indirect regulatory mechanism.

Overall, miR-433 attenuates TGF $\beta$  signaling, at least in part by direct 3'UTR targeting of SMAD2 and TGFBR1. This effect likely contributes to the ability of miR-433 to restrain osteoblastic and chondrogenic differentiation, with potential implications for bone and cartilage repair.

*Disclosures: Spenser Smith, None.*

**MO0124**

**WNT16 is enriched among perivascular progenitor cells, inducing stem cell proliferation and osteogenic differentiation.** Jia Shen\*, Carolyn Mevers, Greg Asatrian, Winters Hardy, Xinli Zhang, Kang Ting, Bruno Peault, Chia Soo, Aaron James. UCLA, United states

Perivascular progenitor cells (also termed perivascular stem cells or PSC) are a presumptive mesenchymal stem cell (MSC) population most commonly derived from human white adipose tissue. Previous studies have shown that purified perivascular cell populations induce greater bone healing than unpurified stromal populations derived from the same patient sample (James et al., Stem Cells Transl Med 2012). Perivascular

progenitor cells have both direct and paracrine effects on bone healing, yet the paracrine mechanisms of perivascular cell bone induction have yet to be defined.

Purification of perivascular progenitor populations was achieved by fluorescence activated cell sorting, as previously described (James et al., Stem Cell Transl Med 2012), using antibodies recognizing CD45, CD146, and CD34. First, the expression of Wnt signaling associated elements was assayed by RNASeq between unsorted stromal vascular fraction and purified perivascular progenitor cells (termed CD146+CD34-pericytes and CD34+CD146- adventitial cells, respectively). Canonical Wnt signaling was manipulated via use of recombinant WNT3A or DKK1. WNT16 was manipulated by RNAi methods or recombinant protein addition. Proliferation and osteogenic differentiation were assessed *in vitro*, using a combination of biochemical stains (Alkaline phosphatase and Alizarin Red staining) and quantitative RT-PCR (*Runx2*, *ALP* and *OCN*). Canonical and non-canonical Wnt signaling activity were assessed by a combination of qRT-PCR (*Cyclin D1*, *Axin2*, *c-Myc*) and Western blot ( $\beta$ -catenin and JNK).

Whole transcriptome sequencing (RNA Seq) on perivascular progenitor cells was performed, screening for gene transcripts enriched in perivascular cells that encode proteins that fit the following criteria: (1) novel, extracellular, pro-osteogenic molecules that were (2) associated with Wnt signaling. Of those transcripts examined, *WNT16* was observed to be markedly elevated among the perivascular population. RNA interference mediated knockdown of *WNT16* impeded perivascular cell proliferation and abrogated perivascular cell osteogenesis (Fig. 1A). Conversely, WNT16 recombinant protein significantly induced early and late osteogenic differentiation (Fig. 1B). Furthermore, continuous WNT16 treatment stimulated by WNT3A inhibited the osteogenic differentiation of perivascular progenitor cells.

In summary, WNT16 is enriched among perivascular progenitor cells and induces osteogenic differentiation. Unlike purely canonical Wnt ligands, continuous WNT16 does not inhibit osteogenic differentiation.

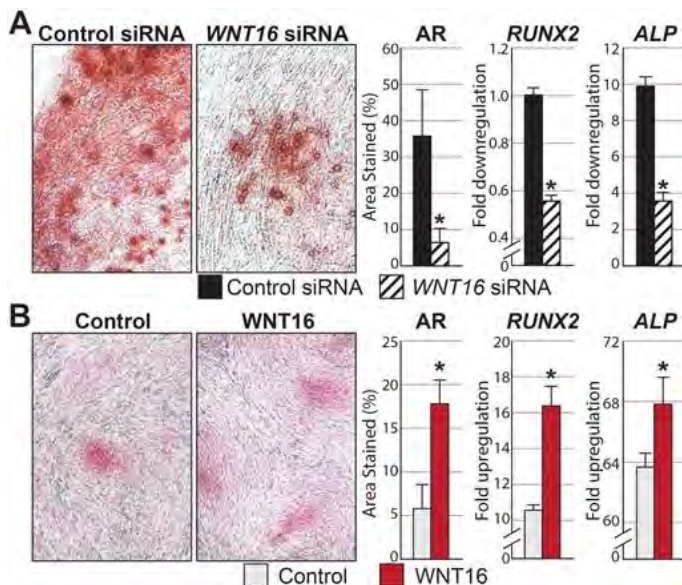


Figure 1

Disclosures: Jia Shen, None.

## MO0125

**In Vitro Analysis of Hormonal Receptor Genes During Myogenesis of Human Skeletal Muscle-Derived Cells.** Cecilia Romagnoli\*, Roberto Zonefrati, Carmelo Mavilia, Alessandra Aldinucci, Gianna Galli, Marco Innocenti, Annalisa Tanini, Laura Masi, Luisella Cianferotti, Maria Luisa Brandi. University of Florence, Italy

Purpose: Skeletal muscle is the largest tissue in the human body and it is primary characterized by its mechanical activity required for posture, movement and breathing, which depends on muscle fiber contractions. Recent evidences have identified skeletal muscle as a secretory organ producing and releasing myokines and other peptides in response to contraction, and exerting either autocrine, paracrine or endocrine effects. Therefore, aim of our work was to establish an useful *in vitro* model of human skeletal muscle-derived cells to analyze the expression of hormonal receptors during myogenesis in order to study the endocrine property of skeletal muscle cells.

Methods: Human primary culture was isolated from skeletal muscle biopsy (pectoralis major) of a healthy young adult volunteer undergoing plastic surgery, after signed an informed consent approved by the Local Ethical Committee. The minced specimen was digested with collagenase at 37 °C for 3h. Primary cells were cultured in a specific growth medium, GM, and differentiated for 10 days with appropriate myogenic differentiation medium, DM, in order to evaluate the expression of the myogenic differentiation markers (Myogenin and MHC) and hormonal receptor genes (VDR, TR $\alpha$ , TR $\beta$ ) by RealTime-qPCR and/or immunocytochemistry. Statistical analysis was performed by Student's t-test to evaluate the significant

difference between gene expression values in DM and the respective value in GM. Results: The presence of PAX-7, the main maker of muscle stem cells, was verified on human skeletal muscle-derived cells. After 10 days in DM, a significant increase in the expression of myogenic differentiation markers, Myogenin and MHC, was observed ( $p < 0.005$  vs control in GM), confirming the suitability of our model. The analysis of the hormonal receptors, VDR, TR $\alpha$  and TR $\beta$ , has shown significant increases in gene expressions ( $p < 0.05$  vs control in GM) during cell differentiation, demonstrating the effective endocrine maturation of the skeletal muscle during myogenesis. Conclusion: Our *in vitro* study has demonstrated that primary culture derived from human skeletal muscle constitute a good model to analyze the development of the endocrine apparatus during myogenesis. Studies are in progress in order to modulate and manipulate muscular endocrine functions to identify possible therapeutic target for disorders associated with skeletal muscle diseases. Acknowledgment: This work was supported by MIUR-PRIN2012\_Muskendo Project.

Disclosures: Cecilia Romagnoli, None.

## MO0126

**Mechanism of TGF $\beta$  function on annulus fibrosus differentiation in intervertebral disc.** Ga I Ban\*, Rosa Serra. University of Alabama at Birmingham, United states

More than 65 million Americans suffer from back pain. One of the major causes of back pain is degeneration of the intervertebral discs (IVDs) in the spine. Disc diseases have been associated with disruption of transforming growth factor beta (TGF $\beta$ ) signaling. Previously, we showed that mice with knock out of TGF $\beta$  receptor 2 (TGF $\beta$ R2 CKO) failed to form annulus fibrosus (AF) in IVD. Furthermore, cell shape and gene expression profile of AF was changed and similar to that of vertebrae. Also, boundary formation between vertebrae (VB) and IVD was disrupted in these mice. It is not known how TGF $\beta$  regulates AF differentiation and boundary formation during development of the axial skeleton. Here, we hypothesize that TGF $\beta$  utilizes Noggin from development of the axial skeleton. Here, we hypothesize that TGF $\beta$  utilizes Noggin to 1) inhibit vertebral chondrocyte differentiation induced by bone morphogenetic protein (BMP) and 2) promote AF differentiation. First, we showed that TGF $\beta$  inhibits BMP-induced differentiation of hyaline cartilage in micromass cultures of sclerotome, pluripotent mesenchymal cells of the axial skeleton. Second, we found that TGF $\beta$  antagonized BMP signaling as measured by reduced phosphorylation of Smad 1/5/8 and down regulation of a well known BMP target gene, Indian hedgehog (Ihh). Third, we found that Noggin is directly up-regulated by TGF $\beta$  to mediate inhibition of BMP pathway. Importantly, we observed that Noggin required for TGF $\beta$  function on AF differentiation. We previously showed that ADAMTS-like 2 (Adamtsl2) is highly expressed in AF and up-regulated by TGF $\beta$  in sclerotome. TGF $\beta$  failed to upregulate Adamtsl2 in the absence of Noggin. These results suggest that Noggin, perhaps through inhibition of BMP signaling, is required for TGF $\beta$  to promote AF differentiation.

Disclosures: Ga I Ban, None.

## MO0127

**Hematopoietic Stem Cell-Derived Bone Marrow Cells Give Rise to Osteogenic Colonies.** Ryan Kelly\*, Amanda LaRue. Medical University of South Carolina, United states

Bone remodeling requires a continuous supply of osteoblasts and osteoclasts from bone marrow (BM) stem cells. It is current dogma that the mesenchymal stromal cell (MSC) generates osteoblasts and the hematopoietic stem cell (HSC) generates osteoclasts. This dogma has been challenged by studies demonstrating HSC differentiation into osteoblasts; however, the molecular mechanisms and factors that drive HSC-derived osteogenesis are still largely unknown. The purpose of this study was to define the molecular pattern of differentiation and maturation of HSC-derived (CD45<sup>+</sup>; pan-hematopoietic marker) BM cells to the osteoblast lineage *in vitro* and to delineate growth factors involved in this process. Total BM was isolated from C57Bl/6 male mice and plated for adherence. After 5 days in culture, the adherent BM fraction was >99% positive for CD45 by flow cytometric analysis. These CD45<sup>+</sup> adherent BM cells were then re-plated on fibronectin-coated plates for up to 4 weeks in osteogenic induction medium. Mineralized colonies formed during osteogenic culture of CD45<sup>+</sup> BM cells. qRT-PCR was used to quantify mRNA expression of osteogenic markers at different time points during culture to determine the temporal pattern of osteogenic differentiation. These cells temporally expressed various osteoblast-related genes, including Runx-2, Col1a1, Alp, and Ocn. Growth factors, including bone morphogenetic protein (BMP)-2, BMP-9, and insulin growth factor-2 (IGF-2) were then tested for their ability to enhance mineralization of these cells. Treatment with BMP-2, BMP-9, or IGF-2 promoted mineralization of the CD45<sup>+</sup> BM cells, as assessed by Alizarin Red staining and cell morphology, compared to cells cultured under osteogenic induction medium alone. Interestingly, IGF-2 appeared to be the most effective at promoting mineralization of these cells, uncovering a novel role for this factor. Studies are ongoing to examine how a combination of these factors affects osteoblast differentiation and to determine which subset of the CD45<sup>+</sup> BM fraction undergoes osteogenesis. Our goal is to apply the results of this study to preclinical fracture models to test the functional impact of modulating HSC-derived osteogenic progenitors via delivery of these pro-osteogenic factors on fracture healing. Our studies have the potential to show that the HSC may provide a long-term therapeutic source of osteoprogenitor cells with sustained engraftment.

Disclosures: Ryan Kelly, None.

## MO0128

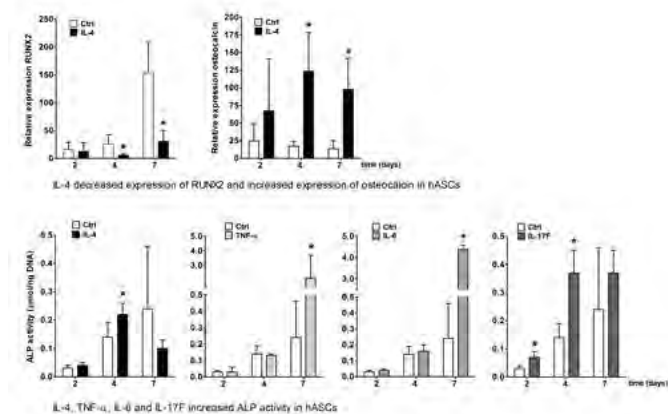
**Osteogenic Differentiation of Human Adipose Stem Cells Treated with Pro-Inflammatory Cytokines TNF- $\alpha$ , IL-6, IL-8, and IL-17F or Anti-Inflammatory Cytokine IL-4.** Angela P Bastidas Coral<sup>\*1</sup>, Astrid D Bakker<sup>1</sup>, Cees J Kleverlaan<sup>2</sup>, Nathalie Bravenboer<sup>3</sup>, Behrouz Zandieh-Doulabi<sup>1</sup>, Tim Forouzanfar<sup>4</sup>, Jenneke Klein-Nulend<sup>1</sup>. <sup>1</sup>Department of Oral Cell Biology, Academic Centre for Dentistry Amsterdam (ACTA), University of Amsterdam & Vrije Universiteit Amsterdam, MOVE Research Institute Amsterdam, Netherlands, <sup>2</sup>Department of Dental Materials Science, Academic Centre for Dentistry Amsterdam (ACTA), University of Amsterdam & Vrije Universiteit Amsterdam, MOVE Research Institute Amsterdam, Netherlands, <sup>3</sup>Department of Clinical Chemistry, VU University Medical Center, MOVE Research Institute Amsterdam, Netherlands, <sup>4</sup>Department of Oral & Maxillofacial Surgery, VU University Medical Center, MOVE Research Institute Amsterdam, Netherlands

**Introduction:** The bone repair process involves an initial inflammatory response, during which different pro-inflammatory cytokines are released within the injury site. A shift from pro-inflammatory cytokines to anti-inflammatory cytokines then occurs. The role of pro-inflammatory and anti-inflammatory cytokines in the osteogenic differentiation of mesenchymal stem cells is still controversial. Here, we investigated the effect of the pro-inflammatory cytokines TNF- $\alpha$ , IL-6, IL-8, and IL-17F, as well as the anti-inflammatory cytokine IL-4 on proliferation and osteogenic differentiation of mesenchymal stem cells.

**Methods:** Human adipose stem cells (hASCs) were either or not stimulated for 3 days with 10 ng/ml TNF- $\alpha$ , IL-6, IL-8, IL-17F, or IL-4, followed by a 2 week culture period without cytokines. Proliferation was assessed during cytokine treatment and after culture by quantification of DNA and analysis of KI67 gene expression. Osteogenic differentiation was assessed by measuring RUNX2, COL1, and osteocalcin gene expression (qPCR), alkaline phosphatase (ALP) activity, and bone nodule formation (Alizarin red staining).

**Results:** TNF- $\alpha$  increased, while IL-17F decreased proliferation of hASCs at 4 days after cytokine treatment. TNF- $\alpha$  and IL-6 reduced gene expression of COL1 (4.0-fold at day 4, and 2.2-fold at day 2, respectively). TNF- $\alpha$ , IL-6, and IL-17F enhanced ALP activity (9.0-fold at day 7, 18-fold at day 7, and 2.0-fold at day 4, respectively). IL-4 reduced gene expression of RUNX2 (5.0-fold at day 4 and 7). Only IL-4 enhanced osteocalcin expression (7.0-fold at day 4, 7) as well as ALP activity (1.5-fold at day 4). Only IL-6 enhanced bone nodule formation by hASCs after 14 days. IL-8 did not affect proliferation nor osteogenic differentiation of hASCs at all time points measured.

**Conclusion.** The anti-inflammatory cytokine IL-4 decreased early stage osteogenic differentiation, but enhanced later stages of osteogenic differentiation of hASCs. The pro-inflammatory cytokines TNF- $\alpha$ , IL-6, and IL-17F only enhanced later stages of osteogenic differentiation. IL-6 and IL-4 seem particularly suitable to induce osteogenic differentiation of hASCs as a strategy for enhancing bone repair.



Effects of pro-inflammatory and anti-inflammatory cytokines on osteogenic differentiation of hASCs

**Disclosures:** Angela P Bastidas Coral, None.

## MO0129

**Promoting Osteogenic Differentiation of Dental MSCs by Estrogen.** Justin Lee, Christine Hong\*, Cun-Yu Wang. UCLA School of Dentistry, United states

Estrogen, 17 $\beta$ -estradiol (E2), is a naturally occurring steroid with well-established pro-osteogenic effects via estrogen receptors in bone marrow stem/stromal cells (BMSCs). However, the mechanism by which E2 promotes osteogenic differentiation

of BMSCs has not been fully elucidated. Moreover, little is known whether or how E2 regulates osteogenic differentiation of human dental MSCs (DMSCs). Here, we systematically profiled the expression of histone demethylases in DMSCs following E2 (10nM) treatment and found that E2 rapidly and specifically induced expression of a histone demethylase, KDM6B, which removes the silencing mark, H3K27me3. Therefore, we examined the role of KDM6B in estrogen-mediated DMSC fate determination. When KDM6B was overexpressed in DMSCs, osteogenic differentiation was significantly induced and mRNA expression of osteogenic marker genes was upregulated. Conversely, shRNA-mediated KDM6B depletion led to a significant reduction in osteogenic potential. However, when KDM6B expression was ectopically introduced in these cells, osteogenic capacity was restored, further confirming KDM6B's facilitating role in osteogenic commitment. Furthermore when we found that the HOXC6 gene was significantly induced by E2, we examined its role in E2-mediated osteogenic differentiation of DMSCs. siRNA-mediated HOXC6 depletion completely abolished E2-mediated osteogenic commitment in DMSCs. Mechanistically, E2-induced osteogenesis was directly regulated by KDM6B's epigenetic activity on the promoters of osteogenic genes including BMP2 and HOXC6.

Based on this discovery, we formulated a nanodiamond-estrogen complex embedded within hydrogels (E2/ND/G) with the premise that an E2/ND/G platform would maximize the beneficial effects of E2 through its sustained-release delivery with improved efficacy and safety at the local level, while circumventing the shortcomings of E2 alone. Indeed our *in vivo* study in rats revealed remarkable enhancement in palatine bone formation and maintenance following maxillary expansion with E2/ND/G treatment. Histological examination revealed amplification of osteoblasts and a decline in TRAP+ osteoclasts. Immunohistochemical analyses showed an increase in KDM6B and decrease in H3K27me3.

In summary, KDM6B is the master epigenetic link in E2-mediated DMSC osteogenic differentiation and the novel E2/ND/G delivery platform promotes craniofacial bone remodeling, representing a promising future innovation in craniofacial patient care.

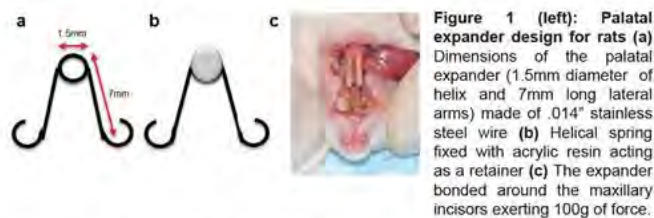


**Figure 1 (left):** Palatal expander design for rats (a) Dimensions of the palatal expander (1.5mm diameter of helix and 7mm long lateral arms) made of .014" stainless steel wire (b) Helical spring fixed with acrylic resin acting as a retainer (c) The expander bonded around the maxillary incisors exerting 100g of force.

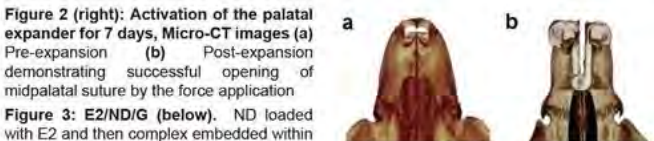
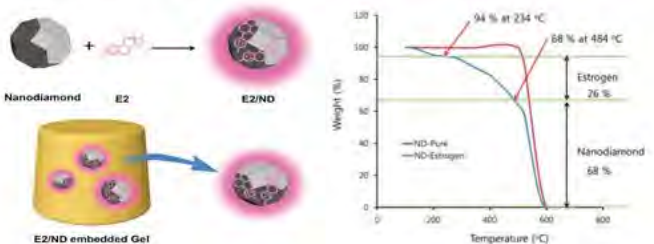


**Figure 2 (right):** Activation of the palatal expander for 7 days, Micro-CT images (a) Pre-expansion (b) Post-expansion demonstrating successful opening of midpalatal suture by the force application

**Figure 3: E2/ND/G (below).** ND loaded with E2 and then complex embedded within gel for sustained release of E2.



**In vivo figures**

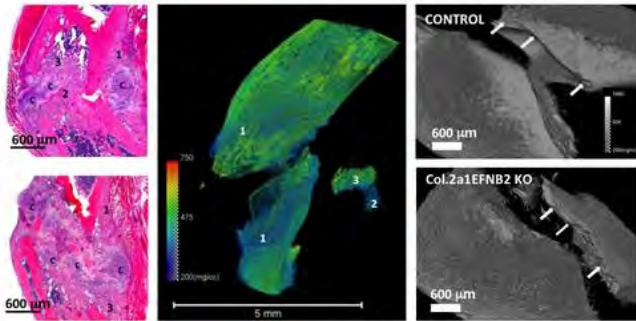
**Disclosures:** Christine Hong, None.

## MO0130

**Site-specific bone types during fracture healing: Effect of chondrocyte specific ephrin B2 deletion.** Ling Chen<sup>\*1</sup>, Feifei Yang<sup>1</sup>, Yongmei Wang<sup>2</sup>, Daniel Bikle<sup>3</sup>, Sunita Ho<sup>1</sup>. <sup>1</sup>School of Dentistry, UCSF, United states, <sup>2</sup>VA Medical Center, Department of Medicine, UCSF, United states, <sup>3</sup>VA Medical Center, Dept of Medicine, UCSF, United states

Intramembranous (IMB) and endochondral bone (EB) formations are two distinct processes that build various parts of a human skeleton. During bone fracture healing, both IMB and EB formation occur simultaneously but in different locations. We used lineage tracing studies in which col2a1 expressing cells were labeled with tdTomato at the time of fracture. This labeled not only the chondrocytes and their progeny, but also osteocytes in the mid-shaft at the fracture site. These studies enabled us to demonstrate that the new bone formed adjacent to the periosteal region of intact cortex (Fig:region 1) formed by an IMB process not requiring a chondrocyte intermediary. Bone formed within the fracture gap was from stem cells originating in the periosteum that undergo differentiation through chondrocytes to osteoblasts (Fig:region 2). However, bone formed from within the intramedullary (IMD) space of

the fracture ends appeared not to originate from chondrocytes but instead from the col2a1 expressing osteocytes (Fig:region 3). These three types of bone have different mineral densities with the lowest being the bone formed from chondrocytes within the gap (200-400mg/cc). The IMD and periosteal IMB have comparable mineral densities of 400-650mg/cc. In bone, ephrinB2/EphB4 interactions play a vital role in the communication among cells forming the skeleton such as mesenchymal stem cells, chondrocytes, osteoblasts, and osteoclasts. In this study, we evaluated the impact of ephrin B2 (EFN2) knockout (KO) in col2a1 expressing cells on the formation of these three bone types during fracture repair by breeding floxed ephrin B2 mice with tamoxifen regulated col2a1 cre recombinase. The controls were littermates lacking the cre. Tamoxifen was given starting at the time of fracture for 4 consecutive days to all mice. The IMD and periosteal IMB were not affected by the KO, whereas the EB within the gap was markedly reduced (by 35%) although mineral density was comparable to control. The fracture surfaces in the KO were markedly irregular suggesting brittle bone (Fig: see arrows). Our data suggest that in the process of fracture repair, three different processes are involved: IMB forming directly from cells in the periosteum, EB originating from stem cells from the periosteum differentiating through the EB pathway, and IMD originating from col2a1 expressing osteocytes in the mid shaft of the tibia.



Figure

Disclosures: Ling Chen, None.

## MO0131

**Three Dimensional Differentiation of Mouse Pluripotent Stem Cells into Osteogenic Cells under Defined Conditions.** Denise C. Zujur\*<sup>1</sup>, Kosuke Kanke<sup>2</sup>, Ung-il Chung<sup>1</sup>, Shinsuke Ohba<sup>1</sup>. <sup>1</sup>Department of Bioengineering, The University of Tokyo, Graduate School of Engineering, Japan, <sup>2</sup>Department of Oral & Maxillofacial Surgery, The University of Tokyo, Graduate School of Medicine, Japan

Offering greater physiological relevance than conventional two-dimensional cultures, three-dimensional (3-D) systems have become a promising alternative for bridging the gap between in vitro culture and living tissues. This is especially important for embryonic stem cell research, since they are derived from a highly organized 3-D structure. In this regard, there is a clear need for developing suitable 3-D culture platforms for the maintenance and differentiation of pluripotent stem cells (PSCs), which may significantly accelerate the understanding and translation of PSCs. Here, we developed an in vitro fully-defined strategy in which mouse PSCs are maintained and differentiated into specific lineages in a 3-D manner. Mouse PSCs were successfully maintained within atelocollagen sponges, displaying expressions of pluripotency genes and proteins as well as teratoma formation. Under further differentiation treatments, they gave rise to endodermal, mesodermal, and ectodermal cells in the 3-D culture, as indicated by downregulation of pluripotency genes and specific upregulation of marker genes of each lineage. In addition, the PSC-derived mesoderm was subsequently differentiated into bone-forming osteoblasts in the 3-D culture using the small molecule-mediated strategy that we previously reported (Kanke K. et al., Stem Cell Reports, 2014.); expressions of mesoderm markers (T and Mixl1) were downregulated, while those of osteoblast precursor markers (Runx2 and Col1a1) were upregulated, followed by the sequential expression of mature osteoblast markers (Sp7, Ibsp, and Bglap). Furthermore, terminal differentiation of the PSC-derived osteoblasts into osteocytes was evidenced by the expression of Dmp1, Sost, and Rankl as well as by visual recognition in histological sections of the 3-D complexes. Thus, the present strategy, in which the maintenance and subsequent differentiation of PSCs were performed in 3-D cultures under defined conditions, generated 3-D bone-like tissues consisting of PSC-derived osteogenic cells and functional extracellular matrices. The strategy may also be applicable to the generation of ectoderm or endoderm derived tissues when combined with appropriate differentiation systems.

Disclosures: Denise C. Zujur, None.

## MO0132

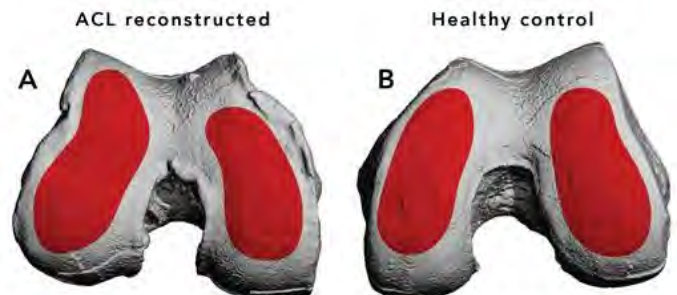
**Assessing the Effect of Anterior Cruciate Ligament Tears on Bone Microarchitecture in Human Knees In Vivo.** Andres Kroker\*<sup>1</sup>, Sarah Manske<sup>1</sup>, Ying Zhu<sup>1</sup>, Rhamona Barber<sup>2</sup>, Denise Chan<sup>2</sup>, Nicholas Mohtadi<sup>3</sup>, Steven Boyd<sup>1</sup>. <sup>1</sup>1. McCaig Institute for Bone & Joint Health 3. Department of Radiology, Cumming School of Medicine, University of Calgary, Calgary, AB, Canada, Canada, <sup>2</sup>2. Acute Knee Injury Clinic, Sports Medicine Centre, University of Calgary, Calgary, AB, Canada, Canada, <sup>3</sup>3. Acute Knee Injury Clinic, Sports Medicine Centre, University of Calgary 4. Department of Surgery, Cumming School of Medicine, University of Calgary, Calgary, AB, Canada, Canada

Anterior cruciate ligament (ACL) tears are a common knee injury. In addition to immediate negative effects such as joint instability, half will develop post-traumatic osteoarthritis (PTOA) 10-20 years later. Why the risk is so large for PTOA in this population is not fully understood, but bone changes may play a role and have been identified both immediately after the ACL tear (bone loss) as well as during the development of PTOA (bone marrow lesions, subchondral sclerosis). The 2nd generation high-resolution peripheral quantitative computed tomography (HR-pQCT) allows us to assess bone microarchitecture *in vivo* in human knees for the first time. The goal of this study is to assess human knee bone microarchitecture and identify differences between healthy and injured knees that are 5 years post-ACL reconstruction.

Twenty-three participants (14M, 9F, 34.7 ± 10.2 years old) underwent ACL reconstructive surgery 5.1 ± 1.2 years ago. One ACL reconstructed knee (14 right, 9 left knees) and one healthy contralateral knee of each participant were imaged with HR-pQCT (XtremeCTII, Scanco Medical). Regions of interest (ROIs) were defined below user-identified weight-bearing surfaces of the distal femur and proximal tibia in three layers of different depths (shallow: 0-2.5mm, mid: 2.5-5.0mm, deep: 5.0-7.5mm). Bone mineral density (BMD) and bone microarchitectural parameters (trabecular thickness, separation, and number) were assessed in each of the 12 ROIs per knee.

Qualitatively, three reconstructed knees showed osteophytes at various degrees of severity (Figure 1A) and seven reconstructed knees showed changes that may be associated with early osteophyte formation. The femoral weight-bearing regions in the injured knees had significantly greater BMD in the shallow layer of the lateral compartment, but lower BMD in the medial compartment at the mid and deep layers. There were no other significant differences in BMD or microarchitecture between the femurs or tibias.

These data represent the first insights into bone microarchitecture in the human knee in patients with ACL reconstructions. Besides qualitative observations and BMD differences between reconstructed and contralateral knees, the variability of bone microarchitecture was likely related to the heterogeneity of the participants, as they presented with a varying range of signs of OA on x-ray. In the future, we will refine the selection of ROIs to identify regions most relevant to understanding OA development.



Weight-bearing surfaces of the two femurs of the same participant. On the left, osteophytes can be seen at the joint margins of the femur of the ACL reconstructed knee, while the right image displays the healthy control knee. User-defined ROIs in red.

Figure 1: Weight-bearing surfaces of the two femurs of the same participant.

Disclosures: Andres Kroker, None.

**MO0133**

**Autologous Osteoblastic Cells (PREOB®) Versus Concentrated Bone Marrow Implantation in Osteonecrosis of the Femoral Head: A Randomized Controlled Study.** Valerie Gangji<sup>1</sup>, Michel Toungouz<sup>2</sup>, Chantal Lechanteur<sup>3</sup>, Yves Beguin<sup>4</sup>, Etienne Baudoux<sup>3</sup>, Viviane De Maertelaer<sup>5</sup>, Sanija Pather<sup>6</sup>, Raphael Katz<sup>6</sup>, Julia Ino<sup>7</sup>, Dominique Egrise<sup>8</sup>, Michel Malaise<sup>9</sup>, Jean-Philippe Hauzeur<sup>9</sup>. <sup>1</sup>Hôpital Erasme, Rheumatology & Physical Medicine Dept, Université Libre de Bruxelles, Belgium, <sup>2</sup>Hôpital Erasme, Université Libre de Bruxelles, Belgium, <sup>3</sup>CHU Sart Tilman, Haematology & Laboratory of Cell Therapy, Belgium, <sup>4</sup>CHU Sart Tilman; Haematology & Laboratory of Cell Therapy, Belgium, <sup>5</sup>Université Libre de Bruxelles, Belgium, <sup>6</sup>Hôpital Erasme, Radiology Dept, Université Libre de Bruxelles, Belgium, <sup>7</sup>Bone Therapeutics, Belgium, <sup>8</sup>Hôpital Erasme, Nuclear Medicine, Université Libre de Bruxelles, Belgium, <sup>9</sup>CHU Sart Tilman, Rheumatology Dept, Belgium

Osteonecrosis of the femoral head (ONFH) is characterized by epiphyseal necrosis that can lead to femoral head collapse and hip replacement. Conservative treatments are still very challenging. It has been shown that implantation of bone marrow concentrate (BMC) containing MSCs could delay the evolution and improve symptoms. Then, the possibility was raised that a cell-based medicinal product consisting on a population of autologous osteoblastic cells (OB) could be more efficacious than BMC to treat early stages ONFH.

**Objectives:** This study was undertaken to evaluate the efficacy of autologous OB implantation in a randomized comparison with BMC in prefractural stage 1 or 2 ONFH.

**Methods:** Patients were included in a randomized controlled single blind trial. Hips were randomized to a core decompression procedure followed by either BMC or OB implantation. In the BMC group, 411 ± 85 ml (SD) of BM was harvested from the iliac crest and concentrated to 42 ± 11 ml. In the OB group, MSCs were isolated from BM aspirate, expanded and differentiated *ex vivo* under autologous conditions to obtain a population of osteoblastic cells (19 ± 4 10<sup>6</sup> cells). OB were characterized as follows: alkaline phosphatase enzymatic activity (1091 ± 1239 mu/mg/protein); P1NP in supernatant (48 ± 32 ng/ml); CD166<sup>+</sup> 60%; CD34<sup>+</sup> 0.7 ± 0.4%; CD45<sup>+</sup> 0%. The primary endpoint was the proportion of responders at 24 months. A responder hip was defined as the absence of progression to a fractural stage (stage 3 or 4) and a clinically significant pain improvement. Patients were assessed radiologically and clinically.

**Results:** From 72 randomized hips, 60 hips (30 hips in each group) were analyzed as the ITT efficacy cohort (51 ± 12 years). Baseline demographic data, risk factors, ON characteristics were not different between groups. At 24 months, 70% versus 40% of hips (p=0.02) and at 36 months 60% versus 33% of hips (p=0.038) in OB and BMC groups respectively were responders. At 24 months, 20% versus 40% of hips (p=0.09) and at 36 months 20% versus 47% (p=0.015) in OB and BMC groups respectively progressed to stage 3 or 4. A survival analysis showed a significant difference in the time to progression to stage 3-4 in favor of the OB group (p=0.012). 117 SAE were reported and 5 SAE were possibly related to the procedure or the cell therapy products.

This study shows that OB (PREOB®) implantation could be more efficacious than BMC treatment to delay subchondral fracture and reduce pain in ONFH.

**Disclosures:** Valerie Gangji, Bone Therapeutics, 12

**MO0134**

**Bone Marrow Lesions in Knee Osteoarthritis Represent a Localized Osteochondral Tissue Response to Mechanical Injury.** Dzenita Muratovic<sup>1</sup>, David Findlay<sup>1</sup>, Flavia Cicuttini<sup>2</sup>, Anita Wluka<sup>2</sup>, Yuanyuan Wang<sup>2</sup>, Sophia Otto<sup>3</sup>, David Taylor<sup>4</sup>, Yea-Rin Lee<sup>1</sup>, Julia Kuliwaba<sup>1</sup>. <sup>1</sup>The University of Adelaide, Australia, <sup>2</sup>Monash University, Australia, <sup>3</sup>SA Pathology, Australia, <sup>4</sup>Royal Adelaide Hospital, Australia

**Purpose:** Bone marrow lesions (BMLs) are magnetic resonance imaging (MRI) subchondral bone abnormalities that closely associate with osteoarthritic joint pain, are a potent risk factor for structural deterioration (cartilage loss), and predict future joint replacement. Growing evidence suggests that BMLs offer diagnostic and predictive value in osteoarthritis (OA), and potentially represent a therapeutic target for OA. However, the cause(s) of BML development in OA are unknown. The study aim was to investigate the osteochondral tissue signature characteristic of BMLs for human knee OA, to explore the origins of BML development.

**Methods:** Tibial plateaus (TP) and medical histories were obtained from 75 knee OA arthroplasty patients (34-men, 41-women; aged 51-86 years). To identify BMLs in TP, T1 and PDFS-weighted 3T MRI scans were performed. TP were microCT imaged prior to sampling osteochondral tissue from BML/No-BML regions for quantitative assessment of microdamage, bone turnover, osteocyte/lacunar and vascular densities, marrow pathology.

**Results:** BMLs were detected in 76% patients; 24% without BMLs formed a No-BML group. The metabolic syndrome (MetS; WHO definition) was more prevalent in BML group (45%) vs No-BML (17%; p=0.04, age/gender adjusted), with higher incidence of hypertension for BML (75% vs 39%; p=0.01). BML osteochondral tissue was characterized by high subchondral bone microcrack density [plate (p=0.01),

trabeculae (p=0.0001)], sclerotic microarchitecture [thicker plate (p=0.001), increased trabecular BV/TV (p=0.02) and number (p=0.04), lower SMI (p=0.02)], increased osteoid volume/thickness [plate (p=0.001), trabeculae (p=0.005)], and higher vascular density [vasculature penetrating calcified cartilage (p=0.0005), marrow vasculature (p=0.0005), increased wall thickness (p=0.01)]. BML marrow was distinguished by increased edema (p=0.006) and adipocyte necrosis (p=0.002). Marrow fibrosis and empty osteocyte lacunae were present, but did not differentiate BML from No-BML. Erosion surface was minimal; marrow inflammation was not observed.

**Conclusions:** The increased microcrack burden, elevated vascular density and adaptive sclerotic bone response of BML tissue provides evidence in support of a mechanical origin for BMLs. Intriguingly, knee OA patients with a BML had an increased prevalence of MetS and hypertension, and together with BML vascular pathology, these findings suggest cardiometabolic factor involvement in BML development.

**Disclosures:** Julia Kuliwaba, None.

**MO0135**

**Condylar Osteoporosis is Associated with Temporomandibular Joint Arthritis: A Cross sectional study.** Jiayu Shi<sup>1</sup>, Soonchul Lee<sup>2</sup>, Hsin Chuan Pan<sup>1</sup>, Wenhao Guo<sup>3</sup>, Andy Lin<sup>4</sup>, Chia Soo<sup>5</sup>, Jin Hee Kwak<sup>1</sup>.

<sup>1</sup>Division of Growth & Development & Section of Orthodontics, School of Dentistry, University of California, Los Angeles, United states, <sup>2</sup>Department of Orthopaedic Surgery, CHA Bundang Medical Center, CHA University, School of Medicine, United states, <sup>3</sup>Department of Oral Radiology, West China Hospital of Stomatology, Sichuan University, China, <sup>4</sup>Institute for Digital Research & Education Statistical Consulting Group, University of California, Los Angeles, United states, <sup>5</sup>Department of Orthopaedic Surgery & the Orthopaedic Hospital Research Center, University of California, Los Angeles, United states

The etiology and treatment of temporomandibular joint (TMJ) arthritis (TMJA) are both complex and unclear. Based on clinical observation, we hypothesized that condylar osteoporosis (defined as reduced condylar bone mineral density (BMD) in association with senility and menopause) is significantly predictive of TMJA, probing this association in a cross-sectional study in human patients and a mouse model of osteoporosis.

2699 patient data sets were collected through chart reviews and phone interviews in western China. By comprehensive exclusion criteria, 279 TMJ from 150 postmenopausal female participants were analyzed. For each TMJ, condylar BMD was measured and cone beam computed tomography (CBCT) and clinical symptoms were used to classify the TMJ as Healthy control (n=75), Early TMJA (n=112), and Advanced TMJA (n=92). Advanced TMJA cases were excluded from odds ratio (OR) analysis because severe arthritis would induce an incomparable secondary subchondral bone remodeling.

Results indicated that reduced BMD, poor dental treatment history, and body mass index (BMI) were each associated with the development of TMJA (p<0.05). Mean condylar BMD was higher in the Healthy group (1.78g/cm<sup>3</sup>) than the Early TMJA group (1.68g/cm<sup>3</sup>), but no statistical difference exists between the Healthy group and the Late TMJA group (1.76g/cm<sup>3</sup>). A multilevel logistic regression model indicated that increasing BMD was negatively predictive of TMJA (OR=0.914, p<0.01), after adjusting for the effects of confounders (e.g., age and BMI) and accounting for repeated measurements of those patients contributing bilateral TMJ samples. The relationship between the TMJA rate and condylar BMD is of a reversed sigmoid shape curve with the inflection point at 1.74g/cm<sup>3</sup>.

To further verify this association of BMD and TMJA, the condylar bony structure and TMJ cartilage of 20 ovariectomized (OVX) or sham-operated 12-week old mice were analyzed radiographically and histologically three months post-surgery. Micro-computed tomography analysis of condyle bone showed 9.64% decrease of BMD in the OVX group (p<0.01) compared to sham. Meanwhile, the OVX mice had thicker condylar cartilages with the arrangement of cells more lamellar than columnar, which are expected morphology change for early arthritis, compared to sham.

In conclusion, condylar osteoporosis is highly correlated with the development of TMJA, and careful evaluation of the condylar bone will be crucial for the early detection of TMJA.

## MO0137

**Increased incidence of bone fractures in elderly osteoarthritic patients with persistent opioid use.** Farah Salahuddin<sup>\*1</sup>, Owais Gilani<sup>2</sup>, Meika Fang<sup>3</sup>, Roy Altman<sup>3</sup>, Faisal Mirza<sup>1</sup>. <sup>1</sup>OrthoSynthesis Inc., United states, <sup>2</sup>University of Michigan, United states, <sup>3</sup>UCLA, United states

## Purpose:

Opiate use for chronic pain is widespread in the US population, such as in knee osteoarthritis (OA). We hypothesized that chronic opiate use is associated with increased bone fracture risk in a population with knee osteoarthritis using the Osteoarthritis Initiative (OAI) study database.

## Method:

Opiate use was assessed annually by a self reported medication use questionnaire in the OAI repository, which consists of 4796 men and women with OA since inception in 2004. The main exposure of interest, 'persistent opioid use', was defined as using prescription opioid medication consistently for a duration of at least two years. The primary outcome of interest was new incidence of bone fractures.

Mixed-effects logistic regression models were used to study the relationship between persistent prescription opioid consumption and incidence of bone fractures among OA patients. An initial analysis looked at the univariate relationship between the exposure and outcome. Additional models were developed that adjusted for various known potential confounders. A backwards elimination approach was used to remove variables not contributing significantly at the 10% level of significance to arrive at the final adjusted model.

## Results:

Baseline characteristics included more women compared to men. Only 1.3% of the subjects were Hispanic, while almost 80% were white/Caucasian. Persistent use of prescription opioid medication was significantly associated with an increase in the odds of incidence of bone fracture (Odds Ratio (OR)=2.62; 95% Confidence interval (CI) = 1.85-3.71). Even after adjusting for some known confounders, the strength and direction of the association remained the same (OR=2.64, 95% CI=1.81-3.86). As expected, older subjects had marginally higher odds of experiencing fractures (OR=1.01, 95% CI=1.00, 1.02), while men were at a significantly lower risk of incidence of bone fractures as compared to women (OR=0.77, 95% CI=0.65-0.91). As compared to Whites/Caucasians, Asian subjects were at a lower risk of bone fractures (OR=0.75, 95% CI=0.60-0.94), while African Americans and "Other" race category did not differ significantly from Whites. Higher BMI subjects were at a higher risk of fractures (OR=1.02, 95% CI=1.01-1.04), and subjects using bisphosphonates were at significantly lower risk of developing bone fractures (OR=0.62, 95% CI=0.51-0.75).

## Conclusion:

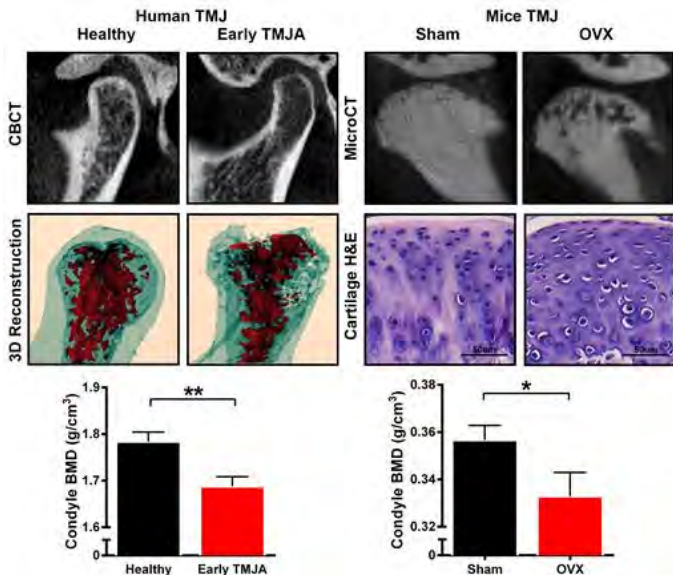
Among the OA population, risk of bone fractures is significantly higher in those with persistent opiate use for chronic pain. The study also identified that Asians with OA were at a lower risk of bone fractures, which is an unexpected finding. Further research is indicated in OA patients and opioid medication use.

Table 2

Covariate		OR (95% CI)	p
<b>Unadjusted</b>			
Opioid Use		2.62 (1.85, 3.71)	<0.001
<b>Adjusted</b>			
Opioid Use		2.64 (1.81, 3.86)	<0.001
Age		1.01 (1.00, 1.02)	0.059
Gender	Male	0.77 (0.65, 0.91)	0.002
	Female	(ref)	
Race	Black/Afr. Amer.	0.67 (0.31, 1.44)	0.307
	Asian	0.75 (0.60, 0.94)	0.014
	Other	1.11 (0.51, 2.44)	0.794
	White	(ref)	
BMI		1.02 (1.01, 1.04)	0.003
Bisphosphonate		0.62 (0.51, 0.75)	<0.001

Table

Disclosures: Farah Salahuddin, None.



ASBMR\_Jiayu Shi\_Figure

Disclosures: Jiayu Shi, None.

## MO0136

**Differential Regulation of Post-traumatic Osteoarthritis Associated Genes in Str/ort, MRL/MpJ and C57BL/6 Mice.** Amy Sebastian<sup>\*1</sup>, Jiun C. Chang<sup>1</sup>, Deepa K. Muruges<sup>2</sup>, Sarah Hatsell<sup>3</sup>, Aris N. Economides<sup>3</sup>, Blaine A. Christiansen<sup>4</sup>, Gabriela G. Loots<sup>2</sup>. <sup>1</sup>UC Merced, School of Natural Sciences, United states, <sup>2</sup>Lawrence Livermore National Laboratories, Physical & Life Sciences Directorate, United states, <sup>3</sup>Regeneron Pharmaceuticals, United states, <sup>4</sup>UC Davis Medical Center, Department of Orthopedic Surgery, United states

Joint injury, particularly tears of the anterior cruciate ligament (ACL), often result in post-traumatic osteoarthritis (PTOA), yet the mechanisms contributing to PTOA development after joint injury are still poorly understood. To better understand the molecular events that trigger PTOA development and progression we profiled injury-induced gene expression changes in knee joints of three mouse strains with varying susceptibility to PTOA: STR/ort (highly susceptible), C57BL/6 (moderately susceptible) and MRL/MpJ (resistant). Right knee joints of 10 weeks old male mice were injured using a non-invasive tibial compression overload mouse model of PTOA that mimics ACL rupture in humans. Histological evaluation of injured joints at 12 weeks post injury revealed severe cartilage erosion in STR/ort, moderate cartilage erosion in C57BL/6, and minimal cartilage damage in MRL/MpJ. Next, we examined transcriptional changes in injured joints compared to uninjured contralateral joints using RNA-seq at 1 day and 1 week post injury. At 1 day post injury, we identified 637, 810, and 380 differentially regulated genes (>1.5 fold) in the injured joints of STR/ort, C57BL/6 and MRL/MpJ, respectively, including 172 genes commonly changed in all three strains. By comparing age-matched uninjured controls from all three strains we found that several immune/inflammation responses related genes including *Ccl2*, *Ccl7*, *Cxcl1*, *Cxcl5* and *Il6* were highly expressed in STR/ort compared to C57BL/6 and MRL/MpJ, and their expression was increased immediately post injury in all three strains. However, the expression of many of these genes returned back to normal by 1 week post injury in C57BL/6 and MRL/MpJ but remained elevated in STR/ort. At 1 week post injury, 818 and 874 genes were found to be differentially regulated in injured joints of STR/ort and C57BL/6, respectively. Only 574 genes were found to be differentially regulated in injured joints of MRL/MpJ, and 269 of these genes overlapped with genes identified in STR/ort and C57BL/6. Among the transcripts differentially regulated at 1 week post injury, we found *Adamts4*, *Aldh1a2*, *Cyp26b1* and *Il1r1* to be significantly up-regulated, and muscle related proteins *Myh2*, *Myh7*, *Tnnc1* and *Tnni1* to be significantly down-regulated exclusively in STR/ort and C57BL/6. The transcriptome level data generated in this study can be further explored experimentally to identify candidate genes that could be targeted to prevent PTOA development.

Disclosures: Amy Sebastian, None.

## MO0138

**Prediction of Response to Intra-articular Injections of Hyaluronic Acid for Knee Osteoarthritis.** Abeer Hegazy\*<sup>1</sup>, Abdulhafez Selim<sup>2</sup>, Paula Karabelas<sup>3</sup>. <sup>1</sup>REHABILITATION CENTER - DAMMAM MEDICAL COMPLEX KSA, SAUDI ARABIA, Saudi arabia, <sup>2</sup>PCOM, United states, <sup>3</sup>AEBM, United states

Osteoarthritis (OA) of the knee is a debilitating condition that affects a large population. Intra-articular injections of hyaluronic acid (IA-HA) have been shown to provide symptom relief for many OA patients who have failed to respond to conservative interventions. Many other patients, however, experience only slight or no improvement. The results from this pilot study will allow physicians to identify whether a patient is likely or unlikely to respond well to HA therapy leading to improved treatment success rates. Physicians who are considering a trial of HA for a patient will have some empirical basis for treatment selection. Eventually, a physician would be able to assess a relatively small number of variables for a patient and then be provided with predictions regarding treatment response.

This study has two related goals: 1) to identify patient and treatment factors that predict response to IA-HA, for knee OA using data-mining analysis and 2) to develop a statistical model that will predict individual patient response to IA-HA.

The following criteria were used to select the study population.

**Inclusion Criteria:** Symptomatic knee OA presenting to physician's office; radiographic evidence of OA; age 18 years or older; failed minimum of 3 months of non-operative treatment, including, but not limited to, acetaminophen, anti-inflammatory medication, cortisone injection, physical therapy, bracing, and/or heel wedge; and symptoms for at least 3 months.

**Exclusion Criteria:** Associated ligamentous instability; history of deep knee infection; previous knee surgery; candidate for total knee arthroplasty or arthroscopy; peripheral neuropathy; X-rays that are completely negative and only MRI evidence or arthroscopic evidence (from previous arthroscopy) of OA; prior IA-HA injections; chondrocalcinosis; patients with precautions or contraindications for viscosupplementation use; and cortisone injection within past 3 months.

Study patients received 3 injections over 3 weeks. The following data were collected: age; weight; BMI; pre-injection Knee injury and Osteoarthritis Outcome Score (KOOS) and Visual Analog Score (VAS); post-injection KOOS and VAS at 6 months.

The study population (n= 30) has BMI average of  $32.9 \pm 4.5$ , pre-treatment average KOOS of  $54.06 \pm 16.6$ , and an average VAS of  $7.1 \pm 1.6$ . A clinically meaningful improvement was observed at 6-months post-injection; KOOS showed a change of 16 points and VAS has 3.43 points. The data-mining analysis suggested that pre-injection KOOS (KOOS-0) is the most significant predictor. Additionally, the regression analysis data showed that KOOS-0 can predict the clinical improvement at 6 months;  $KOOS-6 = 49.68 + (0.39 * KOOS-0)$ . A similar outcome was seen using Bayesian simulation;  $KOOS-6 = 49.7 + (0.39 * KOOS-0)$ . This mathematical tool may support clinical decision making related to IA-HA in the treatment of OA in a patient with a mild-moderate disease.

**Disclosures:** Abeer Hegazy, None.

## MO0139

**Exposure to Non-Thermal Near Infrared Light Alters Maturation Pathways in Osteoblasts.** Mac Weninger\*, Joshua Kolz, Janine Struve, Dorothee Wehrauch, James Ninomiya. Medical College of Wisconsin, United states

Post-menopausal osteoporosis is caused by a decrease in circulating estrogen levels resulting in an imbalance between bone formation and bone resorption. Therefore, the development of non-pharmacologic means for estrogen receptor modulation remains an intriguing therapeutic target to treat osteoporosis. Previous work in our lab demonstrated that administration of non-thermal light in the near infrared region (NIR) to pre-osteoblasts significantly increases both cell proliferation and mineralization.

Estrogen receptor alpha (ER $\alpha$ ) is a transcription factor that binds to estrogen responsive genes on DNA, and communicates with the orphan nuclear receptor estrogen related receptor-alpha (ERR $\alpha$ ) via cross-talk signaling. Therefore, we hypothesized that NIR light may exhibit its effect on bone by increasing the protein levels of these receptors. Additionally, osteoblasts secrete osteoprotegerin (OPG), a soluble decoy receptor for receptor activator of nuclear factor kappa-B ligand (RANKL). The ratio of RANKL to OPG is felt to be an important indicator of osteoclast maturation and the maintenance of net bone mass, and we hypothesized that exposure to NIR light would alter this ratio.

Murine MC3T3-E1 pre-osteoblasts were grown in culture and exposed to a single dose of NIR light at 670nm and 4J. RNA was extracted and purified at days 1, 2, 3, 5, 7, 10, and 14 following NIR light treatment at day 0. PCR arrays and assays were utilized to measure mRNA expression. Additionally, fractionation followed by western blotting was used to determine the expression and translocation of both ER $\alpha$  and ERR $\alpha$  protein following NIR light administration.

A single exposure of NIR light to pre-osteoblasts increased the mRNA expression of ERR $\alpha$  by 114%, 68%, and 82% on days 1, 2, and 10 respectively. Estrogen Receptor alpha (ER $\alpha$ ) was decreased by 46% and 44% days 7 and 10, respectively. OPG expression was increased by 26% and 33% on days 1 and 10, respectively. The mRNA expression of RANKL was undetectable in both control and experimental groups. Lastly, NIR light enhanced ER $\alpha$  protein expression in the

cytoplasmic membrane, while ERR $\alpha$  protein expression was enhanced in the cytosol.

These findings provide the basis for the development of non-pharmacologic means for reversing the bone loss of post-menopausal osteoporosis through the use of devices that provide a source of NIR light directly to bone.

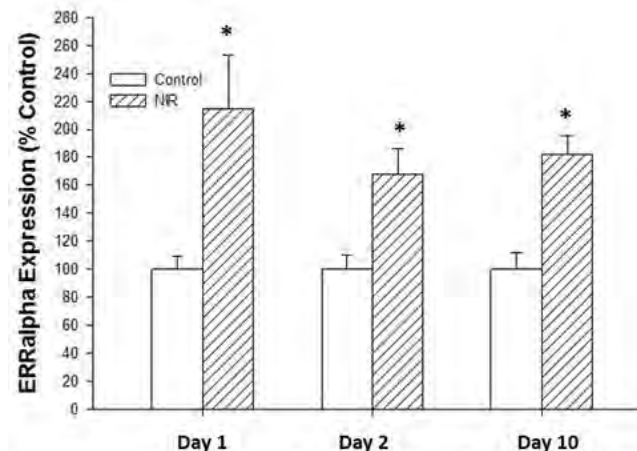


**Fig. 1:** A single exposure of non-thermal near infrared (NIR) light to MC3T3-E1 murine pre-osteoblasts significantly increased the mRNA expression of estrogen related receptor alpha (ERRalpha) by 114% on day 1, 68% on day 2, and 82% on day 10 compared to controls ( $P \leq 0.05$ ). Statistically significant values are indicated with an asterisk.

mRNA Expression of ERRalpha

**Disclosures:** Mac Weninger, None.

## MO0140

**Sc65-null mice provide evidence for a novel endoplasmic reticulum complex regulating collagen lysyl hydroxylation.** Melissa Heard\*<sup>1</sup>, Roberta Besio<sup>2</sup>, Mary Ann Weis<sup>3</sup>, Jyoti Rai<sup>3</sup>, David Hudson<sup>3</sup>, Milena Dimori<sup>1</sup>, Sarah Zimmerman<sup>1</sup>, Jeffery Kamykowski<sup>1</sup>, William Hogue<sup>1</sup>, Francis Swain<sup>1</sup>, Larry Suva<sup>4</sup>, Marie Burdine<sup>1</sup>, Samuel Mackintosh<sup>1</sup>, Alan Tackett<sup>1</sup>, David Eyre<sup>3</sup>, Roy Morello<sup>1</sup>. <sup>1</sup>University of Arkansas for Medical Sciences, United states, <sup>2</sup>Universita' di Pavia, Italy, <sup>3</sup>University of Washington, United states, <sup>4</sup>Texas A&M University, United states

Sc65 (Synaptoneal Complex 65) is an endoplasmic reticulum protein that belongs to the Leprecan family which include the prolyl 3-hydroxylases (P3H1, P3H2, P3H3) and cartilage associated protein (CRTAP). We and others have shown that mutations in both *CRTAP* and *LEPRE1* (encoding P3H1) cause recessive forms of Osteogenesis Imperfecta. Sc65 and CRTAP are both non-enzymatic proteins and share high homology suggesting Sc65 may also function in bone homeostasis. Utilizing a gene trap allele, we recently demonstrated that loss of Sc65 results in low bone mass. Here, a new global knockout mouse (Sc65-KO) derived by deleting exons 7 and 8 using homologous recombination is described. Mice null for Sc65 exhibit a similar bone loss phenotype as the previous model with decreased BV/TV and the loss of cortical and trabecular bone. To ascertain Sc65 function in bone, co-immunoprecipitation (co-IP) of Sc65 candidate interactors in mouse fibroblasts followed by mass spectrometry was performed. These experiments identified several fibrillar procollagen  $\alpha$ -chains as likely substrates of Sc65 supporting the idea that Sc65 plays a role in collagen modification, similar to other Leprecans. At the biochemical level, mass spectrometry of type I collagen peptides showed severe under-hydroxylation at helical cross-linking sites K87 and K930/933 in collagen  $\alpha 1(I)$  and  $\alpha 2(I)$  chains both from bone and skin which are known LH1 preferred substrate residues but with no effect on sites of prolyl 3-hydroxylation. Direct co-IP assays showed Sc65 interaction with lysyl-hydroxylase 1 (LH1, Plod1), prolyl 3-hydroxylase 3 and cyclophilin B. Western blot revealed dramatic reduction of LH1 and P3H3 in primary osteoblasts and skin fibroblasts from Sc65-KO mice. Size exclusion chromatography confirmed that Sc65 and P3H3 form a stable complex in the ER that affects the activity of lysyl-hydroxylase 1 potentially through interactions with the enzyme and/or cyclophilin B. Further testing showed that Sc65-KO mice also have fragile skin with less tensile strength than control mice, consistent with a collagen cross-linking abnormality. Collectively, these results indicate that Sc65 is a novel adapter molecule that stabilizes a unique ER-resident complex that is essential for proper collagen lysyl-hydroxylation. Loss of Sc65 leads to complex instability and defective fibrillar collagen modifications which negatively impacts bone, skin and likely other connective tissues.

**Disclosures:** Melissa Heard, None.

## MO0141

**Activation of Protein Kinase A in Mature Osteoblasts Causes Sexually Dimorphic and Site Specific Changes in the Skeleton.** Liana Tascou<sup>1</sup>, Hussein Anan<sup>2</sup>, Daniel Oh<sup>1</sup>, Francis Lee<sup>1</sup>, Christopher Cardozo<sup>3</sup>, William Bauman<sup>3</sup>, Hesham Tawfeek<sup>3\*</sup>. <sup>1</sup>Columbia University, United states, <sup>2</sup>Sacred Heart Hospital/Temple University, United states, <sup>3</sup>James J. Peters VA Medical Center & Icahn School of Medicine at Mount Sinai, United states

We have previously reported that constitutive activation of protein kinase A (PKA) in osteoblasts stimulates bone anabolism. The goal of this study was to determine whether the effects of PKA activation in osteoblasts are sex and/or skeletal site specific. Thus, bone structure and architecture and bone turnover were examined in 10-week old female and male mice expressing a constitutively active form of the PKA (CA-PKA) catalytic subunit in mature osteoblasts (CA-PKA-OB mice). CA-PKA-OB mice were developed by crossing 2 mouse lines, a 2.3-kb alpha1(I)-collagen promoter-Cre(Co11-Cre) mouse with a floxed-CA-PKA (FF-CA-PKA) mouse. Microcomputed tomographic analysis revealed that CA-PKA-OB female mice had an 8.6-fold increase in femoral but only 1.16-fold increase in lumbar 5 vertebral bone volume/total volume. Femur cortical thickness and volume were also higher in the female CA-PKA-OB mice than in control littermates. Interestingly, the 3-dimensional structure model index was substantially reduced both in femur and lumbar 5 vertebra of female CA-PKA-OB mice, reflecting an increase in the plate to rod-like structure ratio. In contrast, the increase in femoral bone volume/total volume, femoral cortical thickness, and lumbar 5 vertebral bone volume/total volume, and the reduction in structure model index in male CA-PKA-OB mice were very modest compared to their female counterpart. Furthermore, female CA-PKA-OB mice had higher serum levels of bone formation (procollagen type I intact N-terminal propeptide or PINP) and resorption (carboxy terminal collagen cross-links or CTX) markers than in male counterpart. In summary, PKA activation in mature osteoblasts modulates bone structure and turnover in a manner that is dependent on sex and skeletal region. The findings suggest a potential role for sex hormones and/or sex chromosome specific genes and anatomical region on modifying PKA-mediated bone anabolic response.

**Disclosures:** Hesham Tawfeek, None.

## MO0142

**Collagen Cross-linking is Modulated by Transforming Growth Factor  $\beta$ 1 in Bone.** Masahiko Terajima<sup>1\*</sup>, Hideaki Nagaoka<sup>1</sup>, Noriko Sumida<sup>1</sup>, Oliver Smithies<sup>2</sup>, Masao Kakoki<sup>2</sup>, Mitsuo Yamauchi<sup>1</sup>. <sup>1</sup>Oral & Craniofacial Health Sciences, School of Dentistry, University of North Carolina, Chapel Hill, United states, <sup>2</sup>Department of Pathology & Laboratory Medicine, University of North Carolina, Chapel Hill, United states

Transforming growth factor  $\beta$ 1 (TGF- $\beta$ 1) is a potent growth factor enriched in bone matrix and regulates cell functions and matrix synthesis. Fibrillar type I collagen is the most abundant organic component in bone and spatially regulates mineralization. One of the functionally important characteristics of collagen is its unique, sequential post-translational modifications of lysine (Lys) residues, including hydroxylation and, ultimately the formation of covalent intermolecular cross-links. The aim of this study is to characterize collagen post-translational modifications in bone from mice in which TGF- $\beta$ 1 is either over- (H/H; ~300 % mRNA of wild type/WT) or under (L/L; ~10 % mRNA of WT)-expressed (Kakoki et al. (2013) Primary aldosteronism and impaired natriuresis in mice underexpressing TGF $\beta$ 1. PNAS. 110, 5600-5). Femurs were obtained from 2 month-old mice (L/L, H/H and WT), pulverized, demineralized, reduced with standardized NaB<sup>3</sup>H<sub>4</sub>, hydrolyzed and subjected to amino acid and cross-link analyses (n=8/group). The extent of hydroxylation of Lys residues in collagen was similar among the three groups. However, glycosylation of Hyl residues was moderately increased in the L/L and H/H group when compared to the WT mice. However, collagen cross-links showed significant differences among the three groups. In the H/H group, bi-functional cross-links, hydroxylysinonorleucine (HLNL) and dihydroxylysinonorleucine (DHLNL) were increased when compared to the WT (p<0.01 in HLNL and p<0.05 in DHLNL). In addition, a tri-valent cross-link, deoxy-pyridinoline (d-Pyr) was markedly increased in H/H (p<0.001). Consequently, the ratios of DHLNL/HLNL and Pyr/d-Pyr were significantly lower in the H/H group in comparison to those of WT. For the L/L group, DHLNL was decreased when compared to that from WT (p<0.05). The total aldehyde involved in these cross-links were significantly lower in the L/L group (p<0.05) and higher in the H/H group (p<0.001) when compared to WT mice. The results demonstrate that TGF- $\beta$ 1 modulates the quantity and quality of collagen cross-links in bone likely by upregulating the activities of lysyl oxidase and the telopeptidyl lysyl hydroxylase, LH2.

**Disclosures:** Masahiko Terajima, None.

## MO0143

**Functional validation of a key bone mineral density locus determined by genome-wide association studies.** Robert D Maynard<sup>1\*</sup>, Fernando Rivadeneira<sup>2</sup>, Carolina Medina-Gomez<sup>2</sup>, Kwangbom Choi<sup>3</sup>, Cheryl L Ackert-Bicknell<sup>1</sup>. <sup>1</sup>Center for Musculoskeletal Research, University of Rochester, United states, <sup>2</sup>Department of Internal Medicine, Erasmus University Medical Center, Netherlands, <sup>3</sup>The Jackson Laboratory, United states

Genome-wide association studies (GWAS) for bone phenotypes have aided in the discovery of novel loci, but functional validation is lacking for many of these novel loci. GWAS has repeatedly identified a locus for BMD and fracture risk at 7q31.31. *WNT16* is adjacent to this locus and has a defined role in bone biology, but a contribution to this locus of the neighboring gene, *CPED1*, cannot be excluded. *CPED1* is an uncharacterized gene with no verified function. Our data has shown that in mice, the open reading frame for this gene is composed of at least 24 exons. Similarly, we have found that this gene is widely expressed. Relevant to bone, we have determined that *Cped1* is expressed in mouse cortical bone, calvarial osteoblasts, and in multipotent C3H10T1/2 cells differentiated with osteogenic media. Conversely, no expression was observed in the macrophage line, RAW264.7, which can be stimulated down the osteoclast lineage. The translated protein putatively contains an N-terminal cell surface signal peptide, a cadherin-like domain, and a PC esterase domain with predicted acyltransferase and acylesterase activity for the modification of glycoproteins. In maturing calvarial osteoblasts, the pattern of expression of *Cped1* is highly correlated with other extracellular matrix proteins such as the glycoprotein Osteonectin (*Sparc*,  $R^2 = 0.99$ ) and Type I collagen (*Colla1*,  $R^2 = 0.83$ ). We have established that the 3<sup>rd</sup> exon is alternatively spliced out resulting in at least 2 transcripts and thus 2 putative protein products. The expression of both isoforms increases during osteoblastogenesis. To understand the role of these isoforms in osteoblast function, siRNAs targeting either exon 1 (present in both transcripts) or exon 3 (isoform specific) were delivered to C3H10T1/2 cells concurrent with osteogenic media, and cells were differentiated for up to 10 days. By day 5, cells treated with siRNA against exon 1 had reduced alkaline phosphatase (ALP) staining (Fig 1A), and this coincided with a 99% reduction in message (Fig 1B). Interestingly, *Cped1* exon 3 siRNA led to increased ALP staining and an 85% increase in expression (Fig 1B), suggesting that these *Cped1* isoforms are not redundant in function. A similar observation was made on day 10 post knockdown (Fig 1A). In summary, these data strongly suggest that the two known isoforms of this gene play opposing roles in osteoblast maturation and that this gene may have a key role in bone biology.

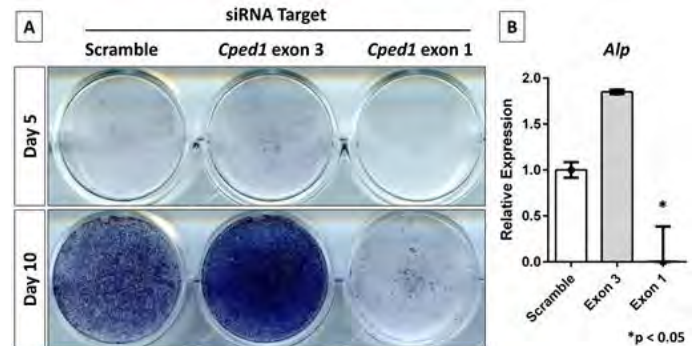


Figure 1

**Disclosures:** Robert D Maynard, None.

## MO0144

**Novel transport mechanisms drive vectorial mineral packing in bone.** Harry C Blair<sup>1</sup>, Quitterie C Larrouture<sup>1\*</sup>, Deborah J Nelson<sup>2</sup>, Paul H Schlesinger<sup>3</sup>, Irina Tourkova<sup>1</sup>, Nareerat Sutjarit<sup>1</sup>. <sup>1</sup>veteran's affairs medical center & departments of pathology & cell biology, university of pittsburgh, United states, <sup>2</sup>The University of Chicago, Departments of Neurobiology, Pharmacology & Physiology, United states, <sup>3</sup>Washington University Department of Cell Biology, United states

Osteoblasts synthesize an organic matrix, predominately type I collagen, and then mineralize it in a rapid, vectorial, and remarkably complete fashion. Components essential to bone formation are not just transported from the extracellular fluid, but densely packed with end products of mineralization, mainly acid, and water removed. The ingredients of mineral go through a tight epithelium-like layer of osteoblasts, dependent on passive Ca transport and active phosphate transport including NPT2 on the basolateral (outside) border and ultimate high phosphate quantities produced from pyrophosphate and nucleotide phosphates by phosphatases on the apical (matrix) side. The surface area of the apical side is increased by matrix vesicles. Osteoblasts isolate the extracellular fluid by tight junctions and are networked and communicate via gap junctions. Mineral formation, in the isolated extracellular compartment, liberates massive amounts of protons, which we

show enter the osteoblast on the apical side and cross the cell for basal release in the extracellular fluid. We demonstrate chloride and cation dependent acid uptake by outside-out membrane vesicles using acridine quenching by spectrofluorometry, consistent with chloride-proton antiports and a cation channel. Using molecular and in situ antibody labeling, we show that the major mechanism for acid uptake requires Cl<sup>-</sup>/H<sup>+</sup> exchangers (ClC3 and ClC5) on the apical side of osteoblasts. Further, we show that in inside out membrane vesicles, there is sodium-dependent acid uptake consistent with sodium hydrogen exchange. We show by analysis of osteoblastic intracellular pH under external acid loads, and by molecular methods, that Na<sup>+</sup>/H<sup>+</sup> exchangers (NHE1 and NHE6) are essential for basolateral acid excretion by osteoblasts. Localization of ClC3 and ClC5 was confirmed by antibody labeling, at the EM level, of plasma membrane ClC3, and ClC5, in ClC3 knockout mice. We demonstrate further, using isolated matrix vesicles, by lysotracker labeling the vesicles that acidify, and thus may play a role in trafficking acid, via reuptake in osteoblasts for transport out of the bone formation site. The release of water from the extracellular matrix is also important, since organic matrix (osteoid) is a hydrogel and mature bone has very little water. We demonstrate that a water channel; Aquaporin 1 (Aqp1), occurs in the apical membranes of mineralizing osteoblasts at both the apical and basal membranes.

*Disclosures: Quiterie C Larrouture, None.*

## MO0145

**Osteogenic effects of nanoparticles are composition, size, and surface dependent.** Shin-Woo Ha<sup>1</sup>, Mark Habib<sup>2</sup>, Neale Weitzmann<sup>3</sup>, George Beck<sup>\*3</sup>. <sup>1</sup>Emory University, United states, <sup>2</sup>Atlanta VA Medical Center, United states, <sup>3</sup>Atlanta VA Medical Center & Emory University, United states

The advent of nanotechnology has provided new opportunities to engineer biomaterials of novel size and composition, leveraging the nanoscale to enhance biological responses. The excitement surrounding the potential applications of nanotechnology to medicine in part revolves around the almost unlimited possibilities for varying the physicochemical properties with greatly increased surface area relative to bulk form. Critical considerations in the design of targeted applications of nanotechnology towards disease treatment as well as discovery based research are the type(s) of material and synthesis method. We have leveraged multiple synthetic methods and material choice in engineering nanoparticles (NPs) for manipulation of bone metabolism. Previous studies have identified that 50 nm silica NPs can enhance bone mineral density in vivo in growing mice. A more recent study has demonstrated that these NPs can reverse age-associated bone loss in mice. These NPs have been demonstrated to have a favorable therapeutic index, in vitro, of ~ 500 – 1000 with minimal toxicity at saturating concentrations suggesting a high safety profile. The NPs function in vitro by promoting the differentiation of bone forming osteoblasts while inhibiting the differentiation of bone resorbing osteoclasts. Mechanistic studies suggest these NPs function, at least in part, through suppression of NF-κB signaling and stimulation of autophagy. Endocytosis is required to initiate changes in these cell signaling pathways. As synthesis techniques associated with nanotechnology allow for the control of size and composition, the aim of this study was to determine if 50 nm silica nanoparticles are the optimal size and nanomaterial composition for bone benefit. Towards this end, a range of silica NPs (30 - 440 nm) with different surface properties (OH, COOH, PTMA, and DETA) were tested along with various NPs of different composition (gold and polystyrene) but the same shape and size (50 nm-spherical) for enhancement of osteoblast differentiation in vitro. Results suggested that surface modifications influenced the response but were considered less significant than the other modifications due to the fact that all modifications enhanced mineralization, although the COOH produced the greatest enhancement. The optimal NP for enhancement of osteoblast differentiation and mineralization was identified as a spherical NP of silica composition in the critical range of 50 to 100 nm.

*Disclosures: George Beck, None.*

## MO0146

**Pigment Epithelium Derived Factor Promotes Bone Formation in Hydroxyapatite/Tricalcium Phosphosphate Ceramics Implanted in Mice.** Christopher Niyibizi<sup>\*</sup>, Feng Li, Stephen Leung, Joyce Tombran-Tink, Penn State College of Medicine, United states

Pigment epithelium-derived factor (PEDF) encoded by Serpinf1 is found in a wide variety of fetal and adult tissues. Lack of PEDF has been shown to be the cause of osteogenesis imperfect type VI whose hallmark is defective mineralization. In these patients, there is excessive osteoid buildup and failure to mineralize the matrix. Mechanisms by which PEDF regulates matrix mineralization remain undefined. We and others reported that PEDF promotes human and mouse mesenchymal stem cell (MSCs) differentiation and matrix mineralization (1, 2). Suppression of PEDF expression in human MSCs and osteoblasts decreased alkaline phosphatase activity as well as reduction in matrix mineralization. Exogenous PEDF restored these activities suggesting that PEDF works extracellularly to promote osteoblastic differentiation and matrix mineralization. We also reported that PEDF suppressed expression of sclerostin by osteocytes indicating that this may be part of the mechanisms by which PEDF regulates matrix mineralization. It has not been demonstrated however, if PEDF can promote bone formation in vivo. To begin to understand whether PEDF

has potential to promote osteoblastic bone formation in vivo, we report here that, exposure of MSCs to PEDF was sufficient to promote human MSCs seeded onto HA/TCP to differentiate into osteoblasts and deposit bone when implanted into the backs of SCID mice. MSCs were isolated from human bone marrow surgical waste under approved protocol by Penn State College of Medicine IRB committee using methods reported previously. Human MSCs were exposed to PEDF for 24h and then seeded onto HA/TCP particles and implanted into the backs of SCID mice in presence of PEDF. The data was consistent in all the five MSCs seeded ceramics supplemented with PEDF and implanted in mice. In conclusion, the data indicate that brief exposure of PEDF to MSCs is sufficient to direct MSCs to differentiate toward osteoblastic lineage and form bone in vivo. The half-life or release rate of PEDF incorporated with the ceramics and cells was not determined, these studies are currently undergoing. 1. Li et al. Stem Cells 2013; Li et al. J Cell Phys. 2015. This work was supported in part by the NIH (NIAMS) R21AR059383-01.

*Disclosures: Christopher Niyibizi, None.*

## MO0147

**The effects of trkA agonist, gambogic amide, on osteoblasts and bone fracture healing..** Maddison Johnstone<sup>\*1</sup>, Rhys Brady<sup>1</sup>, Johannes Schuijers<sup>1</sup>, Julian Quinn<sup>2</sup>, Stuart McDonald<sup>1</sup>, Brian Grills<sup>1</sup>. <sup>1</sup>La Trobe University, Australia, <sup>2</sup>Garvan Institute of Medical Research, Australia

**Introduction:** Nerve growth factor (NGF) administration enhances fracture healing in animals and promotes differentiation of osteoblast-like cells in vitro. NGF exerts its effects by binding to two receptors, trkA which is associated with pro-survival gene activation and p75 which is thought to mediate apoptosis. The influence of trkA signaling on osteoblasts and bone healing is however unknown, therefore this study aimed to investigate the effects of a recently discovered specific trkA agonist, gambogic amide (GA), on fracture healing in mice and on osteoblast proliferation, differentiation and mineralization in vitro.

**Methods:** Bilateral fibular fractures were performed on 82 male C57BL/6 mice. GA (1 mg/kg in DMSO) or DMSO (control) was subcutaneously delivered via mini-osmotic pumps for a period of 2 weeks immediately post-fracture. Callus size and composition were analyzed by micro-computed tomography (μCT), biomechanical properties were investigated via three-point bending, and callus gene expression of various osseous markers were measured via RT-PCR. In vitro assessments of osteoblast proliferation, differentiation and mineralization were performed on Kusa-O and Kusa-4b10 cells exposed to varying concentrations of GA.

**Results:** Biomechanical analyses of 42-day calluses showed an increase in Young's modulus and bending stress in GA-treated mice compared to controls. μCT analysis showed that both total callus volume and callus mineralized tissue were decreased in the GA-treated group compared to controls at 21 days post-fracture. Sclerostin mRNA expression was 2½-fold less in GA-treated calluses compared to controls at 21 days. In vitro analysis revealed that incubation with low concentrations (0.5 nM) of GA for 14 days increased Kusa-O mRNA expression of osteocalcin, alkaline phosphatase, collagen 1 and DMP-1. GA did not affect proliferation of Kusa-O and Kusa-4b10 cells.

**Conclusion:** Taken together, these preliminary results suggest that GA altered the bone formation and/or remodeling response during fracture healing. Preliminary in vitro results suggest GA may promote osteoblast differentiation, however further studies are ongoing to determine the influence of GA on Kusa-4b10 differentiation and mineralization.

*Disclosures: Maddison Johnstone, None.*

## MO0148

**Hyperglycemic Conditions Inhibit Osteogenic Differentiation by Promoting Protein O-GlcNAcylation in C2C12 Cells.** Hanna Gu<sup>\*1</sup>, Kanitsak Boonantanasarn<sup>1</sup>, Jeong-Hwa Baek<sup>1</sup>, Kyunghwa Baek<sup>2</sup>. <sup>1</sup>Seoul National University School of Dentistry, Korea, republic of, <sup>2</sup>College of Dentistry, Gangneung-Wonju National University, Korea, republic of

The global evidence of diabetes mellitus with substantial morbidity of bone such as osteopenia and osteoporosis is increasing. The hyperglycemic condition in diabetic patients can affect various cellular functions including the modulation of osteogenic differentiation. However, the molecular mechanisms by which hyperglycemia affects osteogenic differentiation remain to be further clarified. The aim of this study was to investigate whether increase in protein O-GlcNAcylation contributes to the suppression of osteogenic differentiation by hyperglycemia. To induce osteogenic differentiation, C2C12 cells were cultured in the presence of rhBMP2. Protein O-GlcNAcylation was induced by treating C2C12 cells with high glucose, glucosamine or N-acetylglucosamine or by overexpression of O-GlcNAc transferase (OGT). These conditions increased O-GlcNAcylation of Runx2 as well as the total levels of O-GlcNAcylation proteins. In contrast, these conditions decreased transcriptional activity of Runx2, the expression levels of osteogenic marker genes (Runx2, osterix, osteocalcin, alkaline phosphatase) and alkaline phosphatase activity. These inhibitory effects were rescued by addition of ST045849, an OGT inhibitor or by overexpression of O-GlcNAcase. Therefore, these findings suggest that the excessive protein O-GlcNAcylation under the hyperglycemic conditions contribute to the attenuation of osteoblast differentiation and that an OGT inhibitor has a therapeutic potential for pathological bone loss in diabetic patients.

*Disclosures: Hanna Gu, None.*

## MO0149

**Morinda Citrifolia Leaf Extract Enhances Osteogenic Differentiation Under LPS-induced Inflammatory Condition.** Jae-Ran Seo\*, Kanitsak Boonanantanasarn, Hanna Gu, Jeong-Hwa Baek. Seoul National University School of Dentistry, Korea, republic of

One of the primary etiologies of chronic periodontitis is lipopolysaccharides (LPS) from gram negative bacteria which inhibit osteogenic differentiation and bone formation. Our previous study has shown that *Morinda citrifolia* (Noni) can promote osteogenic differentiation under physiologic condition. Therefore, the purpose of this study is to examine the effect of Noni on osteogenic differentiation under inflammatory condition. Inflammatory conditioned media were prepared by treating RAW264.7 murine monocyte cells with LPS alone, LPS+Noni, or vehicle. Human periodontal ligament (hPDL) cells were challenged with those conditioned media under induction of osteogenic differentiation. We found that LPS-conditioned medium attenuated the levels of osteogenic marker gene expression, alkaline phosphatase activity and matrix mineralization of hPDL. In contrast, addition of Noni under inflammatory condition rescued the inhibitory effects of LPS-conditioned medium on osteogenic differentiation of hPDL. In defining the signaling pathways, Noni was able to enhance the protein levels of pAKT, pGSK3 $\beta$  and  $\beta$ -catenin. In addition, LPS-condition medium increased expression levels of Smurf1 and enhanced  $\beta$ -catenin degradation, whereas addition of Noni prevented LPS-induced degradation of  $\beta$ -catenin. These results suggest that Noni has a potential to improve bone regeneration and repair under inflammatory conditions in periodontal disease.

**Disclosures:** Jae-Ran Seo, None.

## MO0150

**Pre-osteoblast maturation failure is associated with chronic kidney disease.** Renata Pereira\*<sup>1</sup>, Earl Freymiller<sup>2</sup>, Richard Bowen<sup>1</sup>, Isidro Salusky<sup>1</sup>, Katherine Wesseling-Perry<sup>1</sup>. <sup>1</sup>David Geffen School of Medicine at UCLA, United states, <sup>2</sup>UCLA School of Dentistry, United states

Bone disease in chronic kidney disease (CKD) has been traditionally defined by changes in bone turnover stemming from altered circulating parathyroid hormone (PTH) concentrations. However, we have shown that primary pre-osteoblasts from CKD patients have increased proliferation and decreased mineralization rates ex vivo, suggesting that CKD induces intrinsic changes to osteoblast biology that are independent of circulating PTH concentrations. Osteoblasts and adipocytes share a common mesenchymal precursor stem cell and primary pre-osteoblasts have been shown to transition to fat cells under pro-adipocyte conditions. In order to understand if CKD-pre-osteoblast biology is secondary to maturation failure, we thus examined the potential of CKD and healthy control pre-osteoblasts to transition to an adipocyte-like phenotype. Primary pre-osteoblasts from 3 adolescent dialysis patients (2M, 1F) and 3 healthy adolescent controls (2F, 1M) were grown to confluence and cultured under pro-adipocyte conditions consisting of insulin (1 $\mu$ M), dexamethasone (10-6M), and isobutylmethylxanthine (0.5mM) for two weeks. Cells were then stained with Oil Red O and fat content measured by Image J analysis. Fat accumulation was greater in CKD cells than in healthy cells from controls of the same age, ethnicity, and gender. We subsequently evaluated whether Wnt signaling could be involved in this phenotype; total protein was isolated from pre-osteoblast cell extracts from patients and healthy for western blot. Beta catenin protein was increased in CKD as compared to healthy control cells (Figure). Increased proliferation and decreased mineralization rates in pre-osteoblasts from CKD patients are associated with an increased propensity for these cells to transition to an adipocyte like phenotype. The CKD phenotype may thus represent a failure of pre-osteoblast maturation. Increased beta catenin expression in CKD cells suggests that increased canonical Wnt signaling may contribute to this phenotype.

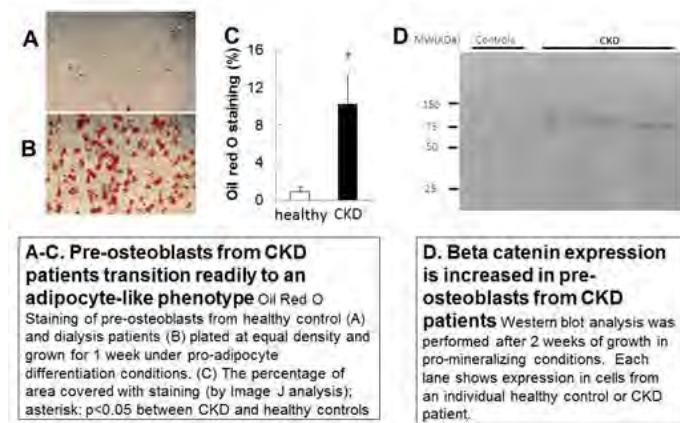


Figure 1

**Disclosures:** Renata Pereira, None.

## MO0151

**Biological Response of Human Mesenchymal Stromal Cells to Orthopedic Implant Nanoparticles.** Eric Lewallen\*<sup>1</sup>, Roman Thaler<sup>1</sup>, Christopher Paradise<sup>1</sup>, Amel Dudakovic<sup>1</sup>, Martina Gluscevic<sup>1</sup>, Endre Soreide<sup>1</sup>, Janet Denbeigh<sup>1</sup>, Dakota Jones<sup>1</sup>, Rebekah Samsonraj<sup>1</sup>, William Trousdale<sup>1</sup>, Hilal Kremers<sup>1</sup>, Matthew Abdel<sup>1</sup>, David Leong<sup>2</sup>, David Lewallen<sup>1</sup>, Andre van Wijnen<sup>1</sup>. <sup>1</sup>Mayo Clinic, United states, <sup>2</sup>National University of Singapore, Singapore

Metal nanoparticles released from orthopedic implants are known to cause acute localized tissue reactions that lead to soft tissue damage, implant loosening and revision surgery. Corrosion, wear, and metal-on-metal contact release potentially harmful nanoparticles (e.g., TiO<sub>2</sub>, Co<sub>3</sub>O<sub>4</sub>), yet the specific response of bone cells to this debris is unpredictable over long periods. In this study, we used human bone-derived osteoblastic cells (OBs) and adipose-tissue derived mesenchymal stromal cells (MSCs) in vitro to model the peri-implant microenvironment and monitor localized biological effects of cell-to-metal contact. These cell culture models were examined by microscopy, histology, RNA-seq, RT-qPCR, and immuno-blot analyses. Molecular pathways that are activated by contact of MSCs or OBs to metal were characterized by RNA-seq analysis of MSCs seeded onto porous sintered titanium implants in vitro. Strikingly, genes involved in stress responses and xenobiotic heavy metal protection (e.g., metallothioneins) are prominently increased by 2- to 10-fold (P<0.05) after 3 days in culture. We therefore characterized the cellular response of MSCs to sub-lethal doses of nanoparticles released from common orthopedic implant materials (TiO<sub>2</sub> and Co<sub>3</sub>O<sub>4</sub>). Upon contact of FITC-tagged TiO<sub>2</sub> nanoparticles with cells, we find that metallothioneins and other early stress-related genes (e.g., JUN, FOS, and EGR markers) are up-regulated at the mRNA and/or protein level, suggesting a short-term behavioral response to the presence of heavy metal nanoparticles. Our results suggest that metal orthopedic implants may have both acute and chronic sub-lethal effects on osteoblasts and stromal cells in the endogenous peri-implant micro-environment. This finding may inform future metal orthopedic implant design strategies (e.g., coatings) that minimize the release of potentially harmful metallic nanoparticles and ensure long-term implant retention and sustained joint performance

**Disclosures:** Eric Lewallen, None.

## MO0152

**Cytochalasin D improves the osteogenic potential of human adipose-derived mesenchymal stem cells concomitant with repression of EZH2 and heterochromatin-related H3K27me3 marks.** Rebekah Samsonraj<sup>1</sup>, Amel Dudakovic<sup>1</sup>, Roman Thaler<sup>1</sup>, Allan Dietz<sup>1</sup>, Buer Sen<sup>2</sup>, Janet Rubin<sup>2</sup>, Andre van Wijnen<sup>1</sup>. <sup>1</sup>Mayo Clinic, United states, <sup>2</sup>University of North Carolina, United states

Cytoskeletal restructuring influences the lineage commitment of mesenchymal stem cells (MSCs). Previous work on bone marrow-derived MSCs (BMSCs) has shown that cytochalasin D (CytoD), a fungal metabolite that disrupts cytoskeletal actin polymerization, promotes osteogenesis by inducing accumulation of intranuclear actin leading to bone-specific gene expression. Here, we investigated the effect of CytoD on adipose tissue-derived MSCs (AMSCs). AMSCs offer several advantages over other sources of MSCs, particularly in the ease of tissue harvest, isolation and expansion to generate sufficient cell numbers for therapy. Because AMSCs have limited osteogenic potential, it is necessary to design molecular strategies to improve their ability to attain a mature osteoblastic phenotype. We find that depolymerization of the actin cytoskeleton with CytoD has marked effects to enhance osteogenic differentiation of AMSCs throughout the cell culture time-course, as reflected by significant increases in alkaline phosphatase activity and mineralization, as well as the expression of osteogenic genes RUNX2, ALP, OPG and TGF $\beta$ 3. RNA-seq analyses of both AMSCs and BMSCs in response to CytoD (24 hr) revealed significant upregulation of a program of other osteogenic markers, including those linked to the BMP2-RUNX2 axis (e.g., SP7). Furthermore, CytoD decreases protein levels of Enhancer of Zeste Homolog 2 (EZH2), an epigenetic suppressor of osteogenic differentiation that mediates heterochromatinization of bone-related genes by trimethylation of histone 3 lysine 27 (H3K27me3). This loss of EZH2 protein is reflected by decreased levels of H3K27me3 marks indicating a global reduction in heterochromatin. Together, our data show that actin polymerization is linked to epigenetic mechanisms that control the acquisition of the osteogenic phenotype in AMSCs. Our study suggests that CytoD advances the osteogenic potential of AMSCs and will facilitate their use in skeletal regenerative strategies.

**Disclosures:** Amel Dudakovic, None.

## MO0153

**Identification of Epigenomic Regulators of Osteoblast Function.** Carole LE HENAFF<sup>1</sup>, Nicola PARTRIDGE<sup>2</sup>, Frederic JEHAN<sup>1</sup>, Valerie GEOFFROY<sup>\*1</sup>. <sup>1</sup>Inserm U1132, France, <sup>2</sup>New York University, United States

Molecularly characterized epigenetic networks that control bone formation and are altered during aging are necessary to uncover new potential targets for osteoanabolic therapy. We aimed to identify osteoanabolic epigenomic regulators which are involved in osteoblast phenotype and differentiation. This study consists of siRNA screening for epigenomic regulators of osteoblastic differentiation and validation. To do this, we have developed a colorimetric alkaline phosphatase (ALP) assay for the initial high-throughput screening in 96 well-plates and we chose to use the FHSO6 human cell line (fetal osteoblast progenitors from fetal bone marrow stroma) that has high ALP activity and reduced type 1 collagen expression after dexamethasone stimulation. We have employed a custom siRNA library targeting 347 epigenetic regulators which contain siRNAs mainly against histone and chromatin modifiers, DNA methylation partners and histone chaperones. We identified 36 siRNAs that significantly increased and 13 siRNAs that strongly decreased ALP activity. These siRNA knockdown studies confirmed that the Polycomb group proteins (EZH2, SUZ12) down-regulate ALP activity and, conversely, the BAF complex (ARID1A, ARID2, SMARCC1) increases ALP activity. Based on the GUITars software statistical analysis, the epigenetic regulators that exhibit the strongest effect on ALP activity were KDM5D that specifically demethylates Lys-4 of histone H3, PRDM11 that contains a PR domain similar to the SET domain of histone methyl transferases and RING1, a transcriptional repressor that is associated with the multimeric Polycomb group protein complex. To further validate our best candidates, we will determine their effects on gene expression and on Runx2 transcriptional activity or activity of the canonical Wnt/ $\beta$ -catenin pathway using specific integrated reporter plasmids to quantitate osteoanabolic activity. For this we will use the STRO1A cell line (human immortalized osteoprogenitors) that is less differentiated than the FHSO6 cell line. From this work, we expect to obtain a better understanding of how epigenetic mechanisms participate in bone formation and bone loss during ageing.

**Disclosures:** Valerie GEOFFROY, None.

## MO0154

**Inhibition of  $\alpha$ NAC Post-translational Modifications Affects Osteoblast Function.** Theresa Farhat<sup>\*1</sup>, Amel Dudakovic<sup>2</sup>, Andre van Wijnen<sup>3</sup>, René St-Arnaud<sup>1</sup>. <sup>1</sup>Shriners Hospitals for Children - Canada, Canada, <sup>2</sup>Dept. of Orthopedic Surgery, Mayo Clinic, United States, <sup>3</sup>Mayo Clinic, United States

In the nucleus of mesenchymal cells, the  $\alpha$  chain of the nascent polypeptide-associated complex ( $\alpha$ NAC) functions as a transcriptional coregulator that both activates or represses gene expression depending on the cellular context and cell type.  $\alpha$ NAC dual activator / repressor function is controlled by independent post-translational modification (PTM) events. It is therefore attractive to target these PTMs to modulate  $\alpha$ NAC function. We recently identified a serine/threonine protein kinase that phosphorylates  $\alpha$ NAC at two specific residues. Relevant to the role of these PTMs, we used a competitive inhibitor of the kinase (kinase  $\zeta$ ) to assess its effect on osteoblasts. We show that kinase inhibition maintains  $\alpha$ NAC in the nucleus. Inactivation of the kinase by chemical inhibition or a kinase-specific small hairpin RNA significantly induces the expression of osteoblast differentiation markers in MC3T3-E1 and human adipose-derived mesenchymal stem cells. Similarly, the kinase inhibitor significantly augments mineralization in osteoblasts as measured using von Kossa or alizarin red staining. Importantly, we further show using microarrays analysis that kinase  $\zeta$  treatment results in the differential expression of several BMP target genes in osteoblasts. Accordingly, kinase  $\zeta$ -treatment or kinase knock-down cells are more responsive to BMP-2 treatment as shown by an increased expression of BMP-2 signaling downstream targets in both mouse myoblasts and osteoblasts. Finally, kinase  $\zeta$  treatment in mice appears to be well tolerated and safe. Sixteen-week-old female wild-type mice have stiffer bone and higher maximum load after a treatment with the kinase  $\zeta$  for three weeks. Our results identify this kinase as a potential pharmacological target for bone regeneration.

**Disclosures:** Theresa Farhat, None.

## MO0155

**MEK5 Suppresses the Osteoblast Differentiation.** Hideki Tsuboi<sup>1</sup>, Shoichi Kaneshiro<sup>\*1</sup>, Jun Hashimoto<sup>2</sup>, Chikahisa Higuchi<sup>3</sup>, Dai Otsuki<sup>4</sup>. <sup>1</sup>Department of Orthopaedic Surgery, Japan Organization of Occupational Health & Safety, Osaka Rosai Hospital, Japan, <sup>2</sup>Department of Rheumatology, National Hospital Organization Osaka Minami Medical Center, Japan, <sup>3</sup>Department of Orthopaedic Surgery, Osaka Medical Center & Research Institute for Maternal & Child Health, Japan, <sup>4</sup>Department of Orthopaedic Surgery, Graduate School of Medicine, Osaka University, Japan

Extracellular signal-regulated kinase 5 (ERK5) is a member of the mitogen-activated protein kinase (MAPK) family and is activated by its upstream kinase, MAPK kinase 5 (MEK5), which is a member of the MEK family. Although the role of MEK5 has been investigated in several fields, little is known about its role in osteoblastic differentiation. In this study, we have demonstrated the role of MEK5 in osteoblastic differentiation in mouse preosteoblastic MC3T3-E1 cells and bone marrow stromal ST2 cells. We found that treatment with BIX02189, an inhibitor of MEK5, increased alkaline phosphatase (ALP) activity and the gene expression of ALP, osteocalcin (OCN) and Osterix, as well as it enhanced the calcification of the extracellular matrix. Moreover, osteoblastic cell proliferation decreased at a concentration of greater than 0.5  $\mu$ M. In addition, knockdown of MEK5 using siRNA induced an increase in ALP activity and in the gene expression of ALP, OCN, and Osterix. In contrast, overexpression of wild-type MEK5 decreased ALP activity and attenuated osteoblastic differentiation markers including ALP, OCN and Osterix, but promoted cell proliferation. In summary, our results indicated that MEK5 suppressed the osteoblastic differentiation, but promoted osteoblastic cell proliferation. These results implied that MEK5 may play a pivotal role in cell signaling to modulate the differentiation and proliferation of osteoblasts. Thus, inhibition of MEK5 signaling in osteoblasts may be of potential use in the treatment of osteoporosis.

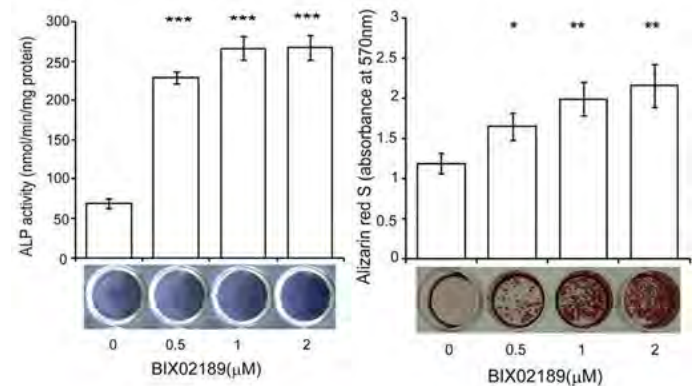


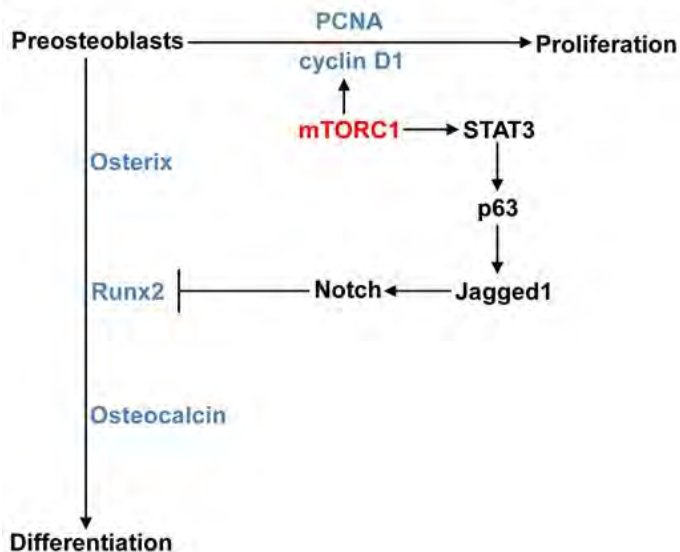
figure1

**Disclosures:** Shoichi Kaneshiro, None.

## MO0156

**mTORC1 Prevents Preosteoblast Differentiation Through the Notch Signaling Pathway.** Bin Huang<sup>\*</sup>, Xiaochun Bai. Academy of Orthopedics Guangdong Province, Department of Orthopedics, The Third Affiliated Hospital, Southern Medical University, China

The mechanistic target of rapamycin (mTOR) integrates both intracellular and extracellular signals to regulate cell growth and metabolism. However, the role of mTOR signaling in osteoblast differentiation and bone formation is undefined and the underlying mechanisms have not been elucidated. Here, we show that activation of mTOR complex 1 (mTORC1) is required for preosteoblast proliferation, however, inactivation of mTORC1 is essential for their differentiation and maturation. Inhibition of mTORC1 prevented preosteoblast proliferation, but enhanced their differentiation *in vitro* and in mice. Activation of mTORC1 by deletion of *tuberous sclerosis 1 (Tsc1)* in preosteoblasts produced immature woven bone in mice due to excess proliferation, but impaired differentiation and maturation of the cells. The mTORC1-specific inhibitor, rapamycin, restored these *in vitro* and *in vivo* phenotypic changes. Mechanistically, mTORC1 prevented osteoblast maturation through activation of the STAT3/p63/Jagged/Notch pathway and downregulation of Runx2. Preosteoblasts with hyperactive mTORC1 reacquired the capacity to fully differentiate and mature when subjected to inhibition of the Notch pathway. Together, these findings identified the role of mTORC1 in osteoblast formation and established that mTORC1 prevents preosteoblast differentiation and maturation through activation of the Notch pathway.



Model for effects of mTORC1 in proliferation and differentiation of preosteoblasts.

Disclosures: Bin Huang, None.

## MO0157

**A slight inhibition of cathepsin K paradoxically stimulates the resorptive activity of osteoclasts in culture.** Dinisha C Pirapaharan<sup>\*1</sup>, Kent Soc<sup>1</sup>, Preety Panwar<sup>2</sup>, Marianne Bergmann<sup>3</sup>, Anne V Schmedes<sup>3</sup>, Jonna S Madsen<sup>3</sup>, Dieter Bromme<sup>2</sup>, Jean-Marie Delaisse<sup>1</sup>. <sup>1</sup>Vejle Hospital (University of Southern Denmark), Denmark, <sup>2</sup>University of British Columbia, Canada, <sup>3</sup>Vejle Hospital, Denmark

Clinical studies have shown that the cathepsin K (CatK) inhibitor, odanacatib (ODN) is a bone resorption inhibitor with unique properties compared with existing anti-osteoporotic drugs. However, a confusing observation of the phase 2 study is that a low dose of ODN induced a decrease in BMD and an increase in the bone resorption marker CTx. The present study throws light on this paradox. We generated primary human osteoclasts from peripheral blood, cultured them on bone slices and assessed their resorptive activity in response to increasing doses of ODN. ODN decreased resorption parameters and abrogated resorption trenches with an average IC50 value of 13 nM. However, at about a 10 times lower dose, it induced up to 50 % increase in resorption compared with controls. This induction affected all resorption parameters except cavitation depth. This effect was particularly clear on collagen fragment release and on the formation of resorption trenches, which are proven to reflect aggressive resorption and to be due to strong collagenolysis. A similar low-dose induction was seen with other specific CatK inhibitors and with a drug inhibiting all cys-proteinases except CatK, but not with a general cys-proteinases inhibitor, thereby suggesting that the induction results from the interplay between CatK and other cys-proteinases. Unlike CatK, the latter are unable to solubilize collagen fibers in test tubes. However, we found that supplementing CatK with cathepsins B, L, S at equimolar concentration, significantly speed-up (up to 3-fold) the initial rates of CatK-supported collagenolysis, thus indicating synergic properties. In addition, Western blots of osteoclast extracts showed that the "low-dose ODN" induces about a 2-fold elevation of CatK and MT1-MMP (a collagenase of the metalloproteinase family) and about a 1.3-fold elevation of cathepsins B and L, which should thus create favorable synergic conditions for collagenolysis. We conclude that a slight inhibition of CatK in osteoclast cultures may stimulate bone resorption, thereby reproducing the low dose-induced resorption of the clinical study. Our data support a mechanism where this slight inhibition results in increased levels of CatK and of other proteinases generating synergic conditions for collagenolysis. This paradoxical stronger collagenolysis should then lead to the particularly aggressive trench resorption mode in line with recent reports relating the resorption mode with the level of collagenolysis.

Disclosures: Dinisha C Pirapaharan, None.

## MO0158

**Bisphosphonate inhibits expression and maturation of Cathepsin K in osteoclasts.** Sol Kim<sup>\*</sup>, Ki-Hyuk Shin, Mo Kang, No-Hee Park, Reuben Kim. UCLA School of Dentistry, United states

Bisphosphonates (BPs), drugs preventing the loss of bone mass by inhibiting bone resorption, are used to treat bone-related diseases, such as osteoporosis and bone cancer. To understand mechanisms of BPs-induced inhibition of bone resorption, we investigated the effect of BPs on Cathepsin K (CtsK), a lysosomal cysteine protease that is expressed predominantly in osteoclasts and induces bone resorption. First, to

study the effect of BPs on M-CSF and RANKL-induced osteoclastic differentiation in vitro, we exposed bone marrow-derived macrophages (BMMs) to zolindronic acid (ZOL), one of BPs. The ZOL's effect on M-CSF or RANKL-induced differentiation of BMMs was assessed with Tartrate Acid Phosphatase (TRAP) staining of the cells. Moreover, the level of CtsK secretion from the differentiated BMMs was detected by CtsK immunofluorescent staining of dentin slices that were co-cultured with the BMMs. Also CtsK activity of the BMMs was computed by measuring the bone resorption pits of the dentin slices. To further evaluate the effect of ZOL in vivo, we investigated the magnitude of CtsK secretion and bone loss of ligature-induced periodontal lesion with immunofluorescent staining using CtsK antibody detecting mature CtsK only and  $\mu$ CT, respectively, in mice receiving ZOL. We found that ZOL decreased the number of TRAP positive osteoclasts and bone resorption activity in RANKL-induced osteoclast. ZOL not only suppressed the expression of CtsK, but also repress the maturation of CtsK. Furthermore, ZOL significantly reduced the distribution of CtsK at the ruffled border membrane in dentin slices. Parenteral administration of ZOL notably prevented the bone loss caused by the ligature-induced periodontitis, moderately increased TRAP-positive cells, and decreased the expression level of mature CtsK in the lesion. Taken together, the above studies suggest that BPs inhibit the resorption of bone by (1) suppressing the differentiation and BMMs to osteoclasts and (2) impeding the function of osteoclasts by, in part, inhibiting both the expression and maturation of CtsK.

Disclosures: Sol Kim, None.

## MO0159

**Cbl-mediated Regulation of PI3K Activity Regulates Bone Resorption by Modulating Secretion of Cathepsin K.** Jungeun Yu<sup>\*</sup>, Naga Suresh Adapala, Archana Sanjay. UConn Musculoskeletal Institute, UConn Health, United states

In osteoclasts (OCs) Cbl binds to the p85 subunit and regulates PI3K activity downstream of integrin signaling. We found that a point mutation in Cbl (*Cbl*<sup>Y737F</sup>) disrupts Cbl-p85 interaction, but does not impact E3 ligase function or protein levels of Cbl or p85. Intriguingly, while Cbl-PI3K signaling occurs in various cell types, only the skeletal system is perturbed in the knock-in *Cbl*<sup>Y737F/Y737</sup> (henceforth YF) mouse. Skeletal characterization of the YF mouse demonstrated increased bone volume in part due to defective OC resorption. For effective bone resorption, following sealing zone formation, acidification of the resorptive lacunae leads to dissolution of hydroxyapatite (HA). We found that Cbl-p85 interaction is not needed for sealing zone formation and both WT and YF OCs effectively dissolved HA. In agreement, mRNA expression of carbonic anhydrase and chloride channel, acidification of lysosomes and membrane localization of vATPase were comparable between the two genotypes. In YF mice both serum CTX levels and pit formation on bone slices were decreased. To degrade collagen, OCs secrete Cathepsin K, a lysosomal protease and tartrate resistant acid phosphatase (TRAP) into the resorption lacunae. After synthesis in the rough endoplasmic reticulum (RER), these enzymes are transported from the trans-Golgi network (TGN) to the secretory lysosomes. While substantial amount of TRAP is secreted directly from TGN, the majority of Cathepsin K is found in secretory lysosomes. We found an increase in mRNA expression of TRAP and Cathepsin K in YF OCs. The amount of Cathepsin K secreted in the YF OC culture medium was significantly diminished (~80% decrease) despite ~2-fold increase in Cathepsin K protein expression in the total cell lysates. To determine the targeting of Cathepsin K to secretory lysosomes, OCs were stained with LAMP-2, an integral lysosomal membrane protein. Immunofluorescence analysis showed that compared to WT, there was a 30-50% decrease in the co-localization of Cathepsin K with LAMP2 in YF OCs. Interestingly, secretion of Cathepsin D, a ubiquitously expressed aspartic protease, was unaffected in YF OCs. Cumulatively, our results show that the loss of Cbl-p85 interaction in OCs does not affect the acid generating machinery or Cathepsin D secretion but is required for Cathepsin K secretion. These results suggest that the Cbl-PI3K interaction regulates secretion of a subset of proteinases required for proper bone resorption.

Disclosures: Jungeun Yu, None.

## MO0160

**Inflammation-Induced Osteolysis Caused by Particles Released from Scaling of Titanium Implants.** Michal Eger<sup>\*1</sup>, Tamar Liron<sup>1</sup>, Nir Sterer<sup>2</sup>, David Kohavi<sup>2</sup>, Yankel Gabet<sup>1</sup>. <sup>1</sup>Department of Anatomy & Anthropology, Sackler Faculty of Medicine, Tel Aviv University, Israel, Israel, <sup>2</sup>Department of Prosthodontics, Goldschleger School of Dental Medicine, Sackler Faculty of Medicine, Tel Aviv University, Israel, Israel

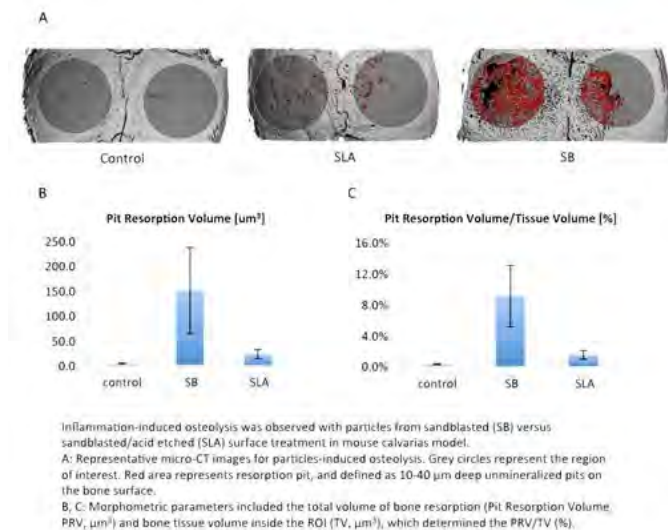
Similarly to aseptic implant loosening observed in 95% of orthopedic failures, bone loss around dental implants may also have a non-infectious etiology. Peri-implantitis occurs in the majority of patients, causes irreversible osteolysis and is the main cause of implants failure, which severely compromises future restorative options. Disease management typically includes removal of attached flora by hand instruments ultrasonic scaling and/or chemical agents. Our aim was to test whether ultrasonic scaling releases titanium particles and induces inflammation and related osteolysis.

Titanium discs with machined (M), sandblasted/acid etched (SLA) and sandblasted (SB) surface types were subjected to ultrasonic scaling. We

physically and chemically characterized the released particles using SEM, Atomic Force Microscopy, and X-ray Spectroscopy. Particles originating from the 3 surface types were added to cultured macrophages, and the induced inflammatory response was assessed according to the expression of IL1 $\beta$ , IL6 and TNF $\alpha$  (RT-qPCR). Cells were also cultured with osteoclastogenic medium in the presence of titanium particles to examine their effect on osteoclasts differentiation using TRAP staining. Particles from ultrasonic-scaled SLA and SB titanium discs were embedded in fibrin membranes placed on the calvaria of C57BL/6J mice for 5 weeks. The extent of inflammatory-induced osteolysis was assessed using micro-CT.

All particles were contaminated with metals originating from the ultrasonic tip and were of similar size. The SB surfaces released the highest number of particles with greatest nanoroughness properties. Particles number, chemical composition and nanotopography had a significant effect on the inflammatory response. The inflammatory response induced by particles from SLA discs was milder than that from SB discs but higher than that from the machined ones. Similarly, a greater inflammation-induced osteolysis was observed *in vivo* with particles from SB discs versus SLA discs in mouse calvarias. *In vitro*, the presence of titanium particles increased osteoclast differentiation to a greater extent than LPS.

These data suggest that ultrasonic scaling of titanium implants release particles in a surface type-dependent manner and may aggravate peri-implant inflammation and bone loss.



mice calvaria model for inflammatory induced osteolysis

**Disclosures:** Michal Eger, None.

## MO0161

**Septin 9 - a critical player in osteoclast resorption.** Anais MJ Moller\*<sup>1</sup>, Jean-Marie Delaisse<sup>1</sup>, Ernst-Martin Fuchtbauer<sup>2</sup>, Kent Soc<sup>1</sup>. <sup>1</sup>Vejle Hospital/University of Southern Denmark, Denmark, <sup>2</sup>Aarhus University, Denmark

The classical paradigm of bone resorption presents the osteoclast (OC) as a cell with a round actin ring within which bone resorption takes place resulting in the resorption pit. But our previous work has shown that OCs are also able to resorb while moving, generating elongated resorption cavities, trenches. Experimental evidence suggests that exo- and endocytosis are restricted to specific areas of the OC. In pit-forming OCs there is a concentric organization of endo- and exocytosis within the actin ring, while for trench-forming OCs they are rather aligned with exocytosis at the front and endocytosis to the back of the actin-ring as well as behind. This spatial separation of cellular processes occurring at the plasma membrane requires that special areas are dedicated to different functions, and we speculate that diffusion-barriers may be needed. Septins are a group of filamentous GTP-binding proteins, known to function as diffusion barriers for membrane bound factors in other cell types. Here we have investigated whether septin 9 (SEPT9) is expressed in OCs and plays a role in resorption. Gene and protein expression analysis revealed that SEPT9 is expressed by human OCs. When OCs, generated from CD14+ cells isolated from human blood donors, were seeded on glass, SEPT9 was primarily located at the base of filopodia as described for other cell types. However, when seeded on bone its primary location changed dramatically. In resorbing OCs SEPT9 was primarily found to be located at the membrane juxtaposed to the resorbed surface. SEPT9 co-localized with clathrin in both pit- ( $r=0.54$ ) and trench-forming ( $r=0.61$ ) OCs. Functional blocking of septins led to significant decreases in the eroded surface (IC50: 19.0  $\mu\text{M}$  FCF), but especially trench-forming OCs were sensitive (IC50: trenches 16.6  $\mu\text{M}$  vs pits 54.7  $\mu\text{M}$ ). We suggest that SEPT9 is involved in compartmentalizing the membrane of resorbing OCs to facilitate the separation of different processes such as endo- and exocytosis. Their localization appears to be different in pit- and trench-forming OCs. Septins seem to be important

for the OCs' ability to resorb bone efficiently, in particular for trench-forming OCs since they were more sensitive to inhibition of septins. The importance of diffusion barriers in the regulation of cellular processes seems to be essential for the OCs' ability to resorb bone efficiently, especially for trench-forming OCs, where cells resorb while moving.

**Disclosures:** Anais MJ Moller, None.

## MO0162

**Serum CTX levels and histomorphometric analysis in Src versus RANKL knockout mice.** Sunao Takeshita\*<sup>1</sup>, Toshio Fumoto<sup>2</sup>, Masako Ito<sup>3</sup>, Kyoji Ikeda<sup>1</sup>. <sup>1</sup>National Center for Geriatrics & Gerontology, Japan, <sup>2</sup>Hiroshima University School of Medicine, Japan, <sup>3</sup>Nagasaki University Hospital, Japan

The osteoclast plays a central role in bone physiology as well as pathology. Genetic mouse models of osteopetrosis, such as *oplop*, *c-Fos*, *c-Src*, and so on, have provided fundamental insight into the mechanism underlying osteoclast development and function. Among these models, Src and RANKL KO mice represent prototypical models corresponding to defective osteoclast development or function, histologically compatible with osteoclast-rich and -poor osteopetrosis, respectively.

In an attempt to confirm the previous observations on the elevated bone formation in Src KO, we included RANKL KO as a reference model with suppressed bone formation as well as resorption, and made head-to-head comparison of Src and RANKL KO mice histologically as well as biochemically. Src KO and RANKL KO mice both exhibit near complete osteopetrosis in terms of 3D-BV fraction by micro CT, whereas the serum CTX concentration of Src KO is apparently normal, and that of RANKL KO is 30% of wild-type despite that fact that they lack osteoclasts. By histomorphometry we found that whereas ES and OS are zero values in RANKL KO, they are indistinguishable from WT in Src KO; because of marked increase in BS, ES/BS and OS/BS of Src KO are 30-40% of WT. While RANKL KO lack both osteoclasts and osteoblasts, Src KO reveal increased numbers of osteoclasts and indistinguishable number of osteoblasts compared with WT; again, per BS basis, N.Oc/BS is comparable to WT and N.Ob/BS is markedly decreased in Src KO. The apparently increased number of total osteoclasts may be due to increased expression of RANKL found in Src KO bone *in vivo*. Src has a gene dosage-dependent effect on osteoclast function *in vitro*, with Src<sup>-/-</sup> osteoclasts completely lacking bone-resorbing function as determined by CTX release on dentin. Thus, Src KO osteoclasts retain some bone-resorbing function *in vivo*. The number of osteocytes is proportionally increased in RANKL KO, while Src KO mice suffer from relative osteocyte deficiency, raising the possibility that RANKL and Src has an unrecognized role in osteocyte survival.

**Disclosures:** Sunao Takeshita, None.

This study received funding from: National Center for Geriatrics and Gerontology

## MO0163

**The Synergistic Action of Lysosomal and Tartrate-resistant Acid Phosphatase is Required for Resorptive Activity of Osteoclasts.** Timur Yorgan\*<sup>1</sup>, Georgia Makrypidi<sup>2</sup>, Sonja Kühn<sup>1</sup>, Till Köhne<sup>1</sup>, Michaela Schweizer<sup>3</sup>, Jan Pestka<sup>1</sup>, Michael Amling<sup>1</sup>, Paul Saftig<sup>4</sup>, Thomas Braulke<sup>2</sup>, Thorsten Schinke<sup>1</sup>. <sup>1</sup>Department of Osteology & Biomechanics, University Medical Center Hamburg Eppendorf, Germany, <sup>2</sup>Department of Biochemistry, Children's Hospital, University Medical Center Hamburg Eppendorf, Germany, <sup>3</sup>Center of Molecular Neurobiology, University Medical Center Hamburg Eppendorf, Germany, <sup>4</sup>Institute of Biochemistry, Christian-Albrechts-University Kiel, Germany

Although activity staining for tartrate-resistant acid phosphatase (TRAP) is widely used to visualize osteoclasts *in vitro* and *in vivo*, the function of TRAP in bone resorption is still not fully clarified. It was previously reported that the concerted actions of lysosomal acid phosphatase (LAP) and TRAP are required for removal of mannose 6-phosphate (M6P) from lysosomal enzymes in hepatocytes. To analyze, whether the same applies for osteoclasts, we took advantage of mouse models lacking *Acp2* (encoding LAP) and/or *Acp5* (encoding TRAP). Here we show that the osteopetrotic phenotype of *Acp2/Acp5*-deficient mice is significantly more pronounced than in mice lacking either *Acp2* or *Acp5*. Likewise, primary osteoclasts derived from *Acp2/Acp5*-deficient mice display impaired resorptive activity *ex vivo*, in contrast to cultures lacking only one of the genes. We additionally found that cathepsin K (Ctsk) activity was decreased in *Acp2/Acp5*-deficient osteoclasts, although *Ctsk* was transcriptionally activated in these cultures. To establish a molecular explanation for our observations we performed two-dimensional gel electrophoresis and subsequent western blot analysis. Thereby we identified a higher abundance of M6P-carrying lysosomal enzymes in *Acp2/Acp5*-deficient osteoclasts, and shifts toward more acidic isoelectric points of few lysosomal proteins including Ctsk, which might impair substrate recognition and/or enzymatic activity. Taken together, our findings demonstrate that both TRAP and LAP are required for proper processing of lysosomal enzymes in osteoclasts, and suggest that the osteopetrosis caused by *Acp2/Acp5*-deficiency is molecularly explained by impaired Ctsk activation.

**Disclosures:** Timur Yorgan, None.

## MO0164

**Treatment of cathepsin K inhibitor in osteoprotegerin-deficient mice inhibits bone resorption and stimulates bone formation.** Midori Nakamura<sup>\*1</sup>, Yuko Nakamichi<sup>2</sup>, Toshihide Mizoguchi<sup>2</sup>, Yasuhiro Kobayashi<sup>2</sup>, Naoyuki Takahashi<sup>2</sup>, Nobuyuki Udagawa<sup>1</sup>. <sup>1</sup>Department of Biochemistry, Institute for Oral Science, Matsumoto Dental University, Japan, <sup>2</sup>Institute for Oral Science, Matsumoto Dental University, Japan

Deficiency of osteoprotegerin (OPG), a soluble decoy receptor for receptor activator of nuclear factor-kappaB ligand (RANKL), in mice induces severe osteoporosis caused by enhanced bone resorption, but also accelerates bone formation. We examined whether bone is coupled with bone resorption in OPG-deficient mice using bisphosphonate (resedronate) and cathepsin K inhibitor (L006235), inhibitors of bone resorption. Resedronate treatment of OPG-deficient mice inhibited bone resorption and increased the bone volume of femoral cortical portions. Histomorphometric analysis showed that bone formation-related parameters (e.g. mineral apposition rate and osteoblast surface/bone surface) in OPG-deficient mice sharply decreased with suppression of bone resorption by daily injection of resedronate for 30 days. OPG-deficient mice exhibited high serum alkaline phosphatase activity and osteocalcin concentration, both of which were decreased to the levels in wild-type mice by the resedronate daily injection. Similarly, daily oral treatment of cathepsin K inhibitor in OPG-deficient mice increased the femoral cortical bone volume. Moreover, cathepsin K inhibitor treatment significantly reduced the porous area/cortical area in OPG-deficient mice. Interestingly, treatment of cathepsin K inhibitor in OPG-deficient mice did not inhibited number of osteoclasts and stimulated bone formation (mineral apposition rate). The double labeling study with tetracycline and calcein revealed that the width of double labels was increased in trabecular bones in the vertebrae of cathepsin K inhibitor treatment of OPG-deficient mice. These results suggests that the existence of osteoclasts in bone maintains the coupling of bone metabolism.

**Disclosures:** Midori Nakamura, None.

## MO0165

**Estrogens attenuate RANKL-induced oxidative phosphorylation and ATP production in osteoclast precursors via direct ER $\alpha$  signaling.** Ha-Neui Kim<sup>\*1</sup>, Li Han<sup>1</sup>, Srividhya Iyer<sup>1</sup>, Aaron Warren<sup>1</sup>, Kimberly Krager<sup>2</sup>, Nukhet Aykin-Burns<sup>2</sup>, Stavros Manolagas<sup>1</sup>, Maria Almeida<sup>1</sup>. <sup>1</sup>Central Arkansas Veterans Healthcare System, University of Arkansas for Medical Sciences, United states, <sup>2</sup>University of Arkansas for Medical Sciences, United states

Estrogens exert their antiresorptive effects on bone by attenuating osteoclast differentiation and stimulating osteoclast apoptosis. In cancellous bone, these effects are evidently mediated via estrogen receptor (ER)  $\alpha$  signaling in cells of the myeloid lineage (targeted by LysM-Cre) and a decrease in osteoclast number; however, the downstream mediators are unknown. We have performed microarray analysis of osteoclast progenitors isolated from the bone marrow of ER $\alpha$ <sup>fl/fl</sup>;LysM-Cre mice and ER $\alpha$ <sup>fl/fl</sup> controls and used Gene Ontology to characterized the cellular processes affected by the absence of ER $\alpha$ . ER $\alpha$  deleted macrophages exhibited significant enrichment for the term "oxidative phosphorylation", suggesting that estrogen signaling via ER $\alpha$  inhibits this process. To explore this possibility, we next measured oxygen consumption rate (OCR) in osteoclast progenitors from wild type C57BL/6 mice. RANKL stimulated OCR, but 17 $\beta$ -estradiol in and of itself had no effect; albeit, estradiol abrogated the stimulatory effect of RANKL on OCR. Moreover, estradiol abrogated a RANKL-induced increase in protein levels of several subunits of the mitochondrial complexes II (Sdhb), III (Uqcrc2), IV (Cox1) and V (Atp5a1). In line with these findings, estradiol also attenuated RANKL-stimulated ATP production. RANKL stimulates mitochondria biogenesis, at least in part, via the non-canonical NF- $\kappa$ B pathway and RelB. Estradiol, however, had no impact on RANKL-induced canonical or non-canonical NF- $\kappa$ B activity, as determined by the phosphorylation of I $\kappa$ B or the nuclear accumulation of RelA or RelB, respectively. Lastly, we investigated at which stage of differentiation estradiol acts to decrease the number of osteoclasts, using osteoclast progenitors from the wild type C57BL/6 mice and exposure to estradiol for 24 hours on day 1, 2, 3, 4, or 5 of culture, or throughout all 5 days. Strikingly, within 24 hours after the addition of RANKL the mRNA and protein levels of ER $\alpha$  in osteoclast precursors was decreased by 5 fold. Moreover, the presence of estradiol during only the first 24 hours decreased RANKL-induced osteoclast number as much as it did when it was present for all 5 days. Collectively, these findings indicate that estrogen signaling via the ER $\alpha$  attenuates osteoclastogenesis by decreasing mitochondrial respiration and ATP generation in early osteoclast precursors, secondary to a decrease in the number and/or function of mitochondria.

**Disclosures:** Ha-Neui Kim, None.

## MO0166

**Gs $\alpha$  Controls Cortical Bone Quality by Regulating Osteoclast Differentiation via pCREB and  $\beta$ -Catenin Pathways.** Girish Ramaswamy<sup>\*1</sup>, Hyunsoo Kim<sup>2</sup>, Devu Zhang<sup>1</sup>, Vitali Lounev<sup>1</sup>, Joy Wu<sup>3</sup>, Yongwon Choi<sup>2</sup>, Frederick S Kaplan<sup>1</sup>, Robert J Pignolo<sup>1</sup>, Eileen M Shore<sup>1</sup>. <sup>1</sup>Center for Research in FOP & Related Disorders, Department of Orthopedic Surgery, Perelman School of Medicine at the University of Pennsylvania, United states, <sup>2</sup>Department of Pathology & Laboratory Medicine, Perelman School of Medicine at the University of Pennsylvania, United states, <sup>3</sup>Division of Endocrinology, Stanford University School of Medicine, United states

The *Gnas* gene encodes multiple transcripts, including the  $\alpha$ -subunit of the stimulatory G-protein (Gs $\alpha$ ) of adenylyl cyclase. We previously reported that heterozygous deletion of the paternal allele of *Gnas* (*Gnas*<sup>+/-</sup>) decreases cAMP, enhances osteoblastogenesis and inhibits adipogenesis relevant to heterotopic ossification. This study examined the effects of heterozygous *Gnas* inactivation during skeletal development and bone remodeling.

We previously described that trabecular BV/TV and architecture were unaffected but cortical BV/TV and cortical thickness were significantly reduced (~15%) in *Gnas*<sup>+/-</sup> mice with dramatic reduction (> 25%) in stiffness and peak load in *Gnas*<sup>+/-</sup> femurs by 3-pt bending. However, no changes in osteoblast number and mineral apposition rate were detected in *Gnas*<sup>+/-</sup> mice, suggesting that cortical bone defects were not due to mutation effects on osteoblasts.

In contrast, significantly elevated osteoclast numbers (Fig.1) at the endosteal surface of femurs in 3 and 9 month old *Gnas* mutants were detected by TRAP staining. Flow cytometry showed no differences in the bone marrow osteoclast precursor population (CD3<sup>-</sup> CD45R<sup>+</sup> CD11b<sup>low</sup> CD115<sup>high</sup>) of *Gnas*<sup>+/-</sup> mice. However, differentiation of *Gnas*<sup>+/-</sup> bone marrow macrophages (BMM) formed significantly higher numbers of multi-nucleated TRAP<sup>+</sup> osteoclasts and larger resorption pits, suggesting that cortical bone defects in *Gnas*<sup>+/-</sup> mice are due to enhanced osteoclast differentiation and function.

Significantly lower levels of pCREB and higher levels of Nfatc1 were detected during osteoclast differentiation in *Gnas*<sup>+/-</sup> cells. Treatment of *Gnas*<sup>+/-</sup> BMMs with forskolin, a cAMP/PKA activator, during osteoclast differentiation elevated pCREB, reduced Nfatc1 to levels comparable to WT and importantly reduced TRAP<sup>+</sup> osteoclasts.

Significantly increased mRNA expression of Wnt inhibitors (*Sost* and *Sfrp4*) and a higher percent of Sost<sup>+</sup> osteocytes were present in cortical bone from *Gnas*<sup>+/-</sup> mice. Reduced total  $\beta$ -catenin and its target Cyclin D1 in *Gnas*<sup>+/-</sup> cells during osteoclast differentiation were detected by immunoblot suggesting an overall decrease in Wnt/ $\beta$ -catenin signaling in the mutants.

Collectively, our data support that reduced Gs $\alpha$  signaling leads to increased osteoclast numbers and activity *in vivo* and increased differentiation through decreased Wnt/ $\beta$ -catenin and cAMP/pCREB signaling. This study reveals a new role for Gs $\alpha$  signaling in maintaining cortical bone quality by regulating osteoclastogenesis.

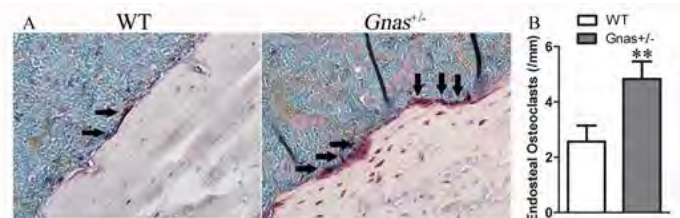


Fig 1. Elevated number of endosteal osteoclasts (arrows in A) in 9 month old *Gnas*<sup>+/-</sup> mice. (A) TRAP staining of femurs in WT and *Gnas*<sup>+/-</sup> mice. (B) Quantification of endosteal osteoclast number. \*\*p < 0.01, Student's t-test

Figure 1

**Disclosures:** Girish Ramaswamy, None.

## MO0167

**p110 $\alpha$  Catalytic Subunit Isoform of PI3K Regulates Osteoclast Differentiation and Function.** Jugeun Yu<sup>\*</sup>, Bhavita Walia, Archana Sanjay. U Conn Health, United states

In osteoclasts (OCs), class IA phosphoinositide 3-kinases (PI3Ks) are activated downstream of several signaling pathways that regulate differentiation and bone resorbing activity. An interaction between the p85 regulatory and p110 catalytic subunits regulates PI3K enzymatic activity. p110 $\alpha$  isoform is expressed in OCs during differentiation, but the requirement of its activation in OC differentiation or function is not known. Independent of growth factor stimulation, p110 $\alpha$  can be constitutively activated by addition of the iSH2 domain of p85 to the p110 $\alpha$  N terminus (p110 $\alpha$ CA). We examined the requirement of p110 $\alpha$  in OC differentiation and function by using p110 $\alpha$ CA conditional transgenic mice where the *ROSA26* allele harbors p110 $\alpha$ CA cDNA preceded by a loxP flanked STOP cassette (R26Stop<sup>FL</sup>p110 $\alpha$ CA). To conditionally activate p110 $\alpha$ CA in the OC lineage, mice homozygous for the R26Stop<sup>FL</sup>p110 $\alpha$ CA allele were bred with the mice harboring a myeloid-specific Cre transgene (LysM Cre/+). In bone marrow macrophages (BMMs) derived from

LysM Cre/+; p110aCA/+ mice, constitutive activation of p110aCA was verified by immunoblotting for phospho-AKT, a major target of PI3K signaling. Compared to BMMs derived from control floxed mice, a 6-fold increase in phospho-AKT/AKT was observed in BMMs derived from LysM Cre/+; p110aCA/+ mice. Histomorphometric analysis revealed that compared to the 10 week littermate controls, LysM Cre/+; p110aCA/+ mice had 3.2-fold decreased bone volume and 2-fold increased OC number. In *ex vivo* cultures, BMMs-derived from LysM Cre/+; p110aCA/+ mice formed 3-fold more numbers of OCs in response to 10 ng/ml RANKL than BMMs from LysM Cre/+ or control floxed mice. Enhanced osteoclastogenesis was accompanied by a concomitant increase in *c-Fos*, *Rank* and *Ctsk* mRNA expression. Increased OC formation upon constitutive activation of p110a was also confirmed via adenovirus mediated Cre expression using BMMs derived from mice homozygous for the R26Stop<sup>FL</sup>p110aCA allele. Compared to OC precursors infected with Adeno-GFP, those expressing Adeno-Cre (100 MOI) formed 1.7-fold more OCs. While expression of Adeno-Cre did not alter actin ring organization or sealing zone formation on bone slices, there was a 25% increase in pit formation activity when compared to cells expressing Ad-GFP. Cumulatively these results indicate that the p110a

In osteoclasts (OCs), class IA phosphoinositide 3-kinases (PI3Ks) are activated downstream of several signaling pathways that regulate differentiation and bone resorbing activity. An interaction between the p85 regulatory and p110 catalytic subunits regulates PI3K enzymatic activity. p110a isoform is expressed in OCs during differentiation, but the requirement of its activation in OC differentiation or function is not known. Independent of growth factor stimulation, p110a can be constitutively activated by addition of the iSH2 domain of p85 to the p110a N terminus (p110aCA). We examined the requirement of p110a in OC differentiation and function by using p110aCA conditional transgenic mice where the *ROS426* allele harbors p110aCA cDNA preceded by a loxP flanked STOP cassette (R26Stop<sup>FL</sup>p110aCA). To conditionally activate p110aCA in the OC lineage, mice homozygous for the R26Stop<sup>FL</sup>p110aCA allele were bred with the mice harboring a myeloid-specific Cre transgene (LysM Cre/+). In bone marrow macrophages (BMMs) derived from LysM Cre/+; p110aCA/+ mice, constitutive activation of p110aCA was verified by immunoblotting for phospho-AKT, a major target of PI3K signaling. Compared to BMMs derived from control floxed mice, a 6-fold increase in phospho-AKT/AKT was observed in BMMs derived from LysM Cre/+; p110aCA/+ mice. Histomorphometric analysis revealed that compared to the 10 week littermate controls, LysM Cre/+; p110aCA/+ mice had 3.2-fold decreased bone volume and 2-fold increased OC number. In *ex vivo* cultures, BMMs-derived from LysM Cre/+; p110aCA/+ mice formed 3-fold more numbers of OCs in response to 10 ng/ml RANKL than BMMs from LysM Cre/+ or control floxed mice. Enhanced osteoclastogenesis was accompanied by a concomitant increase in *c-Fos*, *Rank* and *Ctsk* mRNA expression. Increased OC formation upon constitutive activation of p110a was also confirmed via adenovirus mediated Cre expression using BMMs derived from mice homozygous for the R26Stop<sup>FL</sup>p110aCA allele. Compared to OC precursors infected with Adeno-GFP, those expressing Adeno-Cre (100 MOI) formed 1.7-fold more OCs. While expression of Adeno-Cre did not alter actin ring organization or sealing zone formation on bone slices, there was a 25% increase in pit formation activity when compared to cells expressing Ad-GFP. Cumulatively these results indicate that the p110a catalytic subunit of PI3K regulates OC differentiation and bone resorbing activity.

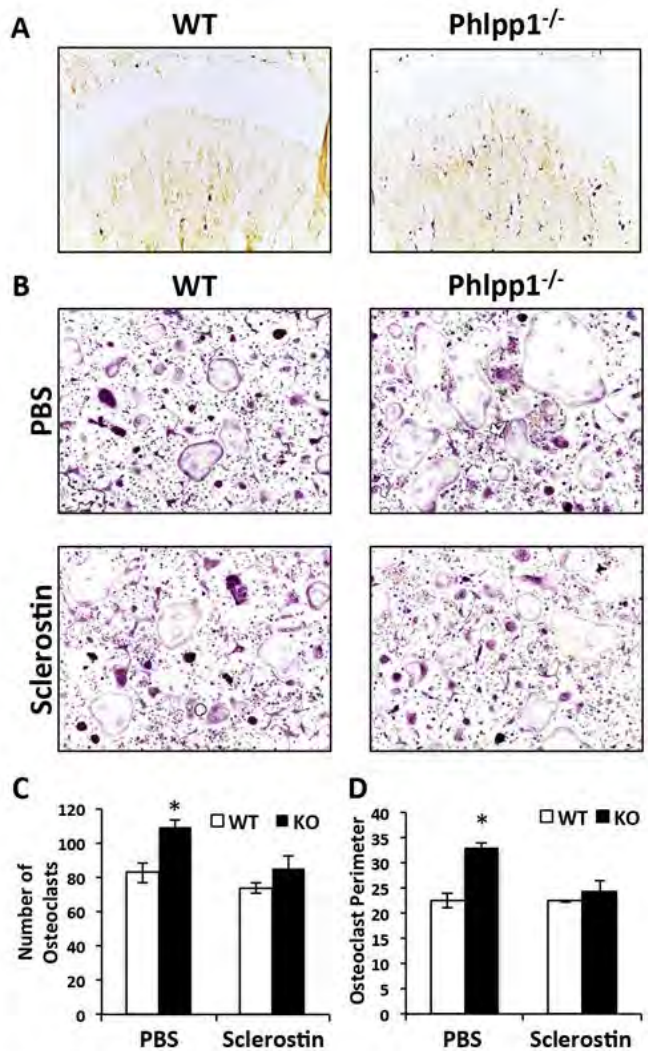
catalytic subunit of PI3K regulates OC differentiation and bone resorbing activity.

**Disclosures:** Jugeun Yu, None.

## MO0168

**Phlpp1 Deletion Reduces Bone Mineral Density and Increases Osteoclast Differentiation through Enhanced Wnt Production.** Elizabeth Bradley\*, Jennifer Westendorf, Lomeli Carpio, Soyun M. Hwang, Merry Jo Oursler. Mayo Clinic, United states

Phlpp1 is a protein phosphatase that inactivates kinases crucial to bone homeostasis. We previously demonstrated that germline Phlpp1 deletion alters endochondral bone formation and decreases trabecular bone mass, but did not explore possible mechanisms for bone loss. The purpose of this study was to determine how Phlpp1 regulates osteoclastogenesis. Phlpp1<sup>-/-</sup> mice exhibit increased TRAP-positive cells within the primary and secondary spongiosa (Figure 1A). Phlpp1<sup>-/-</sup> bone marrow cells formed more and larger osteoclasts *ex vivo* (Figure 1B-D). Phlpp1 inhibitors also augmented osteoclast numbers and perimeter in WT cultures. Phosphorylation of known Phlpp1 substrates, including Akt2, PKC and Mek/Erk, was greater in osteoclasts generated from Phlpp1 KO mice. Furthermore, Phlpp1 deficiency elevated  $\beta$ -catenin levels and increased phosphorylation of NFATc1 and CREB in osteoclast cultures, suggesting higher canonical and non-canonical Wnt pathway activation. We surveyed the known Wnt ligands and found that Phlpp1 deficiency robustly increased expression of multiple canonical and non-canonical Wnts, including Wnt2, Wnt2b, Wnt3, Wnt3a, Wnt5a, Wnt6, Wnt7a and Wnt9b. To determine if elevated Wnt production contributed to increased osteoclastogenesis associated with Phlpp1 deficiency, we treated *ex vivo* cultured osteoclasts with the secreted Wnt inhibitor sclerostin. Sclerostin abolished the enhancement of osteoclast number and perimeter associated with Phlpp1 deficiency (Figure 1B-D). Our data demonstrate that Phlpp1 suppresses osteoclastogenesis by controlling Wnt ligand production.



**Phlpp1 Deficiency Enhances Osteoclast Differentiation via Wnt Signaling.** (A) TRAP stained tibias from 4-week-old WT or Phlpp1<sup>-/-</sup> mice. (B) *Ex vivo* cultured osteoclasts from WT or Phlpp1 KO mice were treated with Sclerostin or PBS and the number (C) and perimeter (D) of TRAP positive-cells with three or more nuclei was determined.

ASBMR2016 Figure

**Disclosures:** Elizabeth Bradley, None.

## MO0169

**Regulation of adhesion signaling in osteoclasts by tetraspanin CD82.** Alexis Bergsma\*<sup>1</sup>, Cindy Miranti<sup>2</sup>. <sup>1</sup>Van Andel Institute Graduate School, United states, <sup>2</sup>Van Andel Institute, United states

Osteoclast dysfunction is the foundation of numerous bone diseases such as osteoporosis, osteopetrosis, and Paget's disease. Osteoclasts differentiate from hematopoietic stem cells into multinucleated polykaryons that, when properly polarized and adhered to the bone, resorb old or damaged matrix. Adhesion is a critical process required for normal osteoclast migration and function that needs to be further investigated. Currently, it is known that Src, Syk, and  $\alpha$ v $\beta$ 3, are a few of the important signaling molecules involved in late-stage osteoclast function, but these pathways have yet to be fully delineated. CD82 is a member of the tetraspanin family of proteins which is involved in cell adhesion, regulation of tyrosine kinases, integrins, and Src, and was recently identified as being upregulated during osteoclast differentiation by our collaborator (Crotti, T.N., et al., J Cell Physiol, 2011.). Our lab has a CD82-knockout mouse that we decided to investigate in the context of bone, as CD82 is otherwise unstudied in this field. Our initial findings using an *in vitro* differentiation model on plastic, glass, and bone substrates demonstrate that CD82 loss results in dysregulated actin formation and osteoclast adhesion. Furthermore, when differentiated long-term (8-9 days on plastic, ~16 days on bone), CD82-null osteoclasts over-fuse and form giant

cells. We have crossed LysMcre mice to our CD82-floxed mice to knockout this protein in the myeloid, and thus osteoclastic, lineage of cells and we see similar results. Upon investigating the signaling mechanism behind the adhesion defect, we see that CD82 loss results in decreased Syk signaling and decreased Clec2, a protein closely related to a partner of CD82 that was identified in the same screen as CD82 as being upregulated during osteoclast differentiation. The binding partner of Clec2, namely podoplanin, is also decreased in CD82-null cells. We are currently investigating other components of this signaling pathway including Src,  $\alpha\text{v}\beta3$ , Vav3, and Rac/Rho signaling. Floxed mice are also currently aging so that we may investigate the bone phenotype by microCT, histomorphometry, and mechanical testing.

**Disclosures:** Alexis Bergsma, None.

## MO0170

**The Cytotoxic Anti-cancer Agent Melphalan Causes Bone Loss by Increasing Osteoclast Formation.** Ryan Chai<sup>1\*</sup>, Michelle McDonald<sup>1</sup>, Rachael Terry<sup>1</sup>, Jessica Pettitt<sup>1</sup>, Sindhu Mohanty<sup>1</sup>, Shruti Shah<sup>1</sup>, Gholamreza Haffari<sup>2</sup>, Jiaka Xu<sup>3</sup>, Matthew Gillespie<sup>2</sup>, John Price<sup>4</sup>, Peter Croucher<sup>1</sup>, Julian Quinn<sup>1</sup>. <sup>1</sup>Garvan Institute of Medical Research, Australia, <sup>2</sup>Monash University, Australia, <sup>3</sup>University of Western Australia, Australia, <sup>4</sup>Victoria University, Australia

Melphalan is a cytotoxic chemotherapeutic agent used to treat multiple myeloma, a plasma cell cancer. We previously found that dormant tumor cells in bone can be activated by bone destruction, and that several anti-cancer agents increase formation of bone resorbing osteoclasts *in vitro* by cell stress induction. To determine whether melphalan causes bone loss, we studied its effects on bone metabolism *in vivo* and *in vitro*.

Mice were injected with melphalan (7.5mg/kg) and the effects on bone structure, bone marrow population and osteoclasts were determined. The effects of melphalan on osteoclast formation in murine bone marrow cells and RAW264.7 cells treated with RANKL and melphalan were also determined. Melphalan effects on key regulators of osteoclast differentiation, cell stress and RANKL expression of bone stromal cells was studied by qRT-PCR, immunoblot, and reporter assays.

Mice treated with melphalan after 3 days showed a 2.5- fold increase in osteoclast numbers. Bone mass was not reduced, nor was it reduced after 7 days but after 14 days trabecular bone volume/total volume (BV/TV) and trabecular number decreased by 50.9% and 46.3% respectively, with no change in trabecular thickness. Bone marrow cells from melphalan-treated mice showed an increase in immature macrophage populations, and with RANKL stimulation *ex vivo* yielded 2- fold more osteoclasts than vehicle-treated mice.

Melphalan treatment *in vitro* dose-dependently increased RANKL-dependent osteoclast formation in bone marrow cells and RAW264.7 cells; cell stress inhibitor KNK437 abolished these effects. Melphalan did not affect RANKL-induced NF $\kappa$ B or NFATc1 signals, but did increase MITF levels. Melphalan treatment increased mRNA expression of osteoclast fusion-associated factors DC-stamp and OC-stamp. Indeed, cell fusion of RAW264.7 cells was increased with melphalan treatment in the absence (and presence) of RANKL. Furthermore, melphalan increased RANKL and decreased OPG mRNA levels in bone stromal cells.

These data suggest that melphalan causes bone loss by enhancing osteoclast formation *in vivo* and *in vitro* through several mechanisms: the upregulation of key osteoclastic genes including key transcription factor MITF; activation of the stress pathways; enhancement of osteoclast fusion; and, in bone stromal cells, increased RANKL. Thus, although melphalan may reduce tumor-associated bone disease by reducing tumor load, excessive use may directly provoke bone loss in patients.

**Disclosures:** Ryan Chai, None.

## MO0171

**Amino terminus of HDAC7 Is Sufficient to Inhibit Osteoclast Differentiation.** Nicholas Blixt<sup>\*</sup>, Rajaram Gopalakrishnan, Eric Jensen, Kim Mansky. University of Minnesota, United states

Osteoporosis is a widespread disease caused by increased bone resorption relative to bone formation, resulting in reduced bone density and higher incidence of fractures. Elucidating molecular mechanisms that regulate osteoclast differentiation and activation will lead to improved therapies for osteoporosis and other bone-related diseases caused by increased osteoclastic activity. Our lab has previously shown by both *in vitro* and *in vivo* experiments that Histone Deacetylase 7 (HDAC7) is an inhibitor of osteoclast differentiation through repression of the activity of the MITF transcription factor. MITF binds DNA and functionally interacts with another transcription factor, PU.1, to regulate osteoclast genes. To further characterize the molecular mechanism behind HDAC7's repression of osteoclast differentiation, we asked whether HDAC7 interacts with and represses PU.1. By co-immunoprecipitation, we demonstrated that HDAC7 and PU.1 could physically interact. Furthermore, we demonstrated that the amino terminus of HDAC7 was sufficient for an interaction with MITF, HDAC7 and PU.1. Currently studies are ongoing to determine if viral constructs overexpressing the amino terminus of HDAC7 are sufficient to inhibit osteoclast differentiation. In addition, using ChIP analysis, we are determining when during osteoclast differentiation HDAC7 is bound to osteoclast promoters. Based on our data, we conclude that HDAC7 is a potent negative regulator of osteoclastogenesis, acting by repressing both PU.1 and MITF to prevent transcription of osteoclast genes necessary for differentiation and survival.

**Disclosures:** Nicholas Blixt, None.

## MO0172

**B lymphocytes do not differentiate into osteoclasts in estrogen-replete or estrogen-deficient mice.** Yuko Fujiwara<sup>\*</sup>, Marlina Piemontese, Jinhu Xiong, Yu Liu, Priscilla Baltz, Charles OBrien. University of Arkansas for Medical Sciences, United states

Estrogen deficiency, caused by menopause or ovariectomy, increases osteoclast number and causes bone loss. Estrogen deficiency in mice also induces a marked increase in B lymphocyte number in the bone marrow. This increase in B cells has been proposed to contribute to the bone loss caused by estrogen deficiency, but the mechanisms by which this may occur are unclear. Many previous studies have shown that isolated B cells can act as osteoclast progenitors when cultured *in vitro* with M-CSF and RANKL. However, the ability of B cells to act as osteoclast progenitors *in vivo* has not been demonstrated. The purpose of this study was to determine whether B cells can differentiate into osteoclasts using *in vitro* and *in vivo* lineage-tracing studies. To do this, we crossed CD19-Cre mice, which cause recombination in all B cells, with tdTomato Cre-reporter mice. In the offspring, B cells, and any cells derived from them, will express the tdTomato fluorescent protein. We performed ovariectomy or sham-operations on these mice and isolated CD19-positive cells from bone marrow by magnetic beads. Freshly isolated B cells from either sham-operated or ovariectomized mice displayed robust tdTomato fluorescence. However, the osteoclasts formed from these same preparations did not display tdTomato fluorescence, suggesting that the osteoclasts formed from contaminating myeloid-lineage cells. It is also possible that B cells and contaminating myeloid cells both contributed to osteoclast formation, but that the fluorescence from the B cells was diluted to the point of being not-detectable. To identify the lower limit of detection from such a contribution, we marked bone marrow macrophages (BMMs) using LysM-Cre;tdTomato mice and mixed these with increasing amounts of unmarked BMMs and found that we could still detect tdTomato-positive osteoclasts even when only 2% of the cells in the culture were from LysMCre;tdTomato mice. Thus, the majority of osteoclasts formed in cultures from purified B cells are not derived from B cells but are likely derived from contaminating myeloid cells. More importantly, all osteoclasts on the cancellous bone surface of LysM-Cre;tdTomato mice were tdTomato-positive, but none were positive in either sham-operated or ovariectomized CD19-Cre;tdTomato mice. Based on these results we conclude that B cells do not differentiate into osteoclasts under normal physiological conditions or during estrogen deficiency.

**Disclosures:** Yuko Fujiwara, None.

## MO0173

**Enhanced responsiveness of Bone Marrow Macrophages to M-CSF signaling results in increased Osteoclast Precursors in the absence of Cbl-P13K interaction.** Bhavita Walia<sup>\*</sup>, Jungeun Yu, Archana Sanjay. UConn Health, United states

Hematopoietic precursors in the bone marrow (BM) commit to the monocyte-macrophage lineage in response to M-CSF. These bone marrow macrophages (BMMs) fuse to form multinucleated osteoclasts (OCs) upon RANKL stimulation. We previously showed that E3 ubiquitin ligase and adaptor protein Cbl binds to p85 and regulates PI3K activity downstream of M-CSF signaling. Cbl<sup>Y737F</sup> point mutation disrupts this interaction, but does not alter E3 ligase function or protein levels of Cbl or p85. Cbl<sup>Y737F</sup> (YF) mice have greater OC numbers and differentiation but reduced bone resorption. We hypothesized that increased OC numbers may be attributed to more OC precursors expressing CD11b<sup>lo</sup>, CD115 (c-fms) and CD117 (c-Kit) in YF mice. To visualize OCPs, we bred WT and YF mice with Csf1r<sup>EGFP/+</sup> mice to generate reporter mice wherein EGFP is expressed under the control of Csf1r promoter. Using flow cytometry, Csf1r<sup>EGFP</sup> expression in WT-Csf1r<sup>EGFP/+</sup> and YF-Csf1r<sup>EGFP/+</sup> mice was confirmed in freshly isolated BM cells and cultures enriched for BMMs upon M-CSF treatment. Csf1r<sup>EGFP</sup> expression in BMMs was validated by correlating with that of CD115. The percentage of Csf1r<sup>EGFP/+</sup> cells and mean fluorescence intensity, which parallels protein expression, were increased by 1.4 and 1.9-fold respectively in freshly isolated cells from YF-Csf1r<sup>EGFP/+</sup> mice over WT-Csf1r<sup>EGFP/+</sup>. Similarly, BMMs derived from YF-Csf1r<sup>EGFP/+</sup> mice had 1.3 fold more Csf1r<sup>EGFP/+</sup> cells and 1.5 fold enhanced Csf1r<sup>EGFP/+</sup> expression relative to WT-Csf1r<sup>EGFP/+</sup>. In response to M-CSF, YF BMM cultures showed increased mRNA expression of *Csf1r* (2.2 fold) as well as *c-Fos* and *ATF4*, transcription factors that drive OC differentiation. It has been established that CD115<sup>+</sup> CD117<sup>+</sup> OCPs represent a progenitor population while CD115<sup>+</sup> CD117<sup>-</sup> OCPs are more committed to an OC fate. Analysis of these OCPs in WT and YF mice showed that in freshly isolated cells, YF BM cells had 2 fold more CD115<sup>+</sup> CD117<sup>+</sup> OCPs. However, upon M-CSF treatment, YF BMMs were enriched for CD115<sup>+</sup> CD117<sup>-</sup> OCPs compared to WT. In summary, increased PI3K signaling due to lack of Cbl-mediated regulation results in greater Csf1r expression leading to enhanced responsiveness of BM cells to M-CSF, which along with increased OCP commitment, may explain the augmented OC numbers in YF mice. Cumulatively, these data indicate an important function for Cbl regulated PI3K activity in modulating osteoclast precursor commitment and responsiveness to M-CSF.

**Disclosures:** Bhavita Walia, None.

## MO0174

**Identification of the TRAF family members interacting with RANK cytoplasmic motifs involved in osteoclastogenesis.** Ke Hu<sup>1</sup>, Zhenqi Shi<sup>2</sup>, Xu Feng<sup>2</sup>. <sup>1</sup>Department of Pathology, University of Alabama at Birmingham, Birmingham, AL 35294, USA; Department of Gynecology & Obstetrics, Renji Hospital, School of Medicine, Shanghai Jiao Tong University, Shanghai 200127, PR China., United states, <sup>2</sup>Department of Pathology, University of Alabama at Birmingham, Birmingham, AL 35294, USA, United states

The receptor activator of NF- $\kappa$ B ligand (RANKL) promotes osteoclastogenesis by binding to its cognate receptor, the receptor activator of NF- $\kappa$ B (RANK), which is a member of the tumor necrosis factor (TNF) receptor (TNFR) family. Upon RANKL binding, RANK initiates various intracellular signaling pathways through the recruitment of tumor necrosis factor (TNF) receptor-associated factors (TRAFs). Our previous studies have revealed that RANK contains three cytoplasmic motifs (Motif 1: PFQEP369-373; Motif 2: PVQEET559-564; Motif 3: PVQEQQ604-609), which are functionally involved in regulating osteoclastogenesis. Whereas it has been well established that Motif 1 interacts with TRAF6, the precise TRAF protein(s) interacting with Motifs 2 and 3 remain unclear because previous biochemical assays generated conflicting findings. The objective of this study is to carry out co-immunoprecipitation (Co-IP) assays to further address the identity of TRAF proteins interacting with these two RANK motifs. To this end, we prepared constructs expressing HA-tagged wild-type RANK cytoplasmic domain (HA-WT) and two HA-tagged mutant RANK cytoplasmic domain, HA-W2 and HA-W3, in which only Motif 2 and Motif 3 remains intact, respectively. We also prepared a control construct in which all three functional motifs are mutated (HA-Ctl). Moreover, we generated five constructs expressing Myc-tagged TRAFs (Myc-TRAF1, Myc-TRAF2, Myc-TRAF3, Myc-TRAF4 and Myc-TRAF5). A series of Co-IP assays were performed by co-transfecting these HA-tagged RANK and Myc-tagged TRAF constructs into HEK293T cells. Our results indicate that Motif 2 interacts with both TRAF1 and TRAF3, while Motif 3 interacts only with TRAF1 in the Co-IP assays. Intriguingly, we found that co-expression of TRAF2 (Myc-TRAF2) with RANK cytoplasmic domain (HA-WT) leads to extremely low expression of RANK, preventing us from performing Co-IP assays. However, decreasing amounts of Myc-TRAF2 constructs in the co-transfection assay leads to increased levels of RANK expression. Similar results were also obtained with TRAF5 (Myc-TRAF5). These data suggest that TRAF2 and TRAF5 may cause the degradation of RANK. In conclusion, our Co-IP assays have shown that Motif 2 interacts with both TRAF1 and TRAF3 and Motif 3 interacts only with TRAF1. Moreover, TRAF2 and TRAF5 mediate the degradation of RANK, suggesting that these two TRAF proteins may play a role in negatively regulating RANK signaling by inducing the degradation of RANK.

**Disclosures:** Ke Hu, None.

## MO0175

**Rgs12 Inhibits Nrf2-dependent Antioxidant Proteins to Promote the Generation of Reactive Oxygen Species and Osteoclast Differentiation.** Andrew Ng<sup>\*</sup>, Chengjian Tu, Megan Jones, Shichen Shen, Jun Li, Jun Qu, Shuying Yang. University at Buffalo, United states

The Regulators of G-protein Signaling (Rgs) proteins hold vital roles in various cellular processes, including cell differentiation. Our previous studies unveiled an essential role of Rgs12, the largest Rgs family protein, in osteoclast (OC) differentiation, but the mechanism for this function is not yet clear. In this study, using OC-targeted *Rgs12* knockout mice (*Rgs12*<sup>-/-</sup>) where Cre expression is driven by the *LysM* promoter, *Rgs12* deletion *in vivo* resulted in increased bone mass. Furthermore, loss of *Rgs12* impaired OC formation in bone marrow macrophages (BMMs). Conversely, over-expressing Rgs12 in RAW 264.7 cells increased the number and size of OCs. To determine how Rgs12 regulates OC differentiation, we employed a robust mass spectrometry-based proteomics strategy to profile the temporal changes to global protein levels in *Rgs12*<sup>-/-</sup> versus wild-type (WT) BMMs. BMMs were isolated from WT and *Rgs12*<sup>-/-</sup> mice (*n* = 3 animals/group) and induced with M-CSF/RANKL over the course of four time points: un-induced, 1d, 3d, and 5d. Proteomics analysis identified 3,714 quantifiable proteins using a stringent identification criteria of  $\geq 2$  peptides per protein and 1% false discovery rate. Our dataset thus represents the highest coverage of proteins related to OC differentiation to date. *Rgs12*<sup>-/-</sup> BMMs showed 144 proteins significantly altered, of which 83 were up- and 61 were down-regulated. Functional annotation revealed that many antioxidant enzymes, such as peroxiredoxins and catalase were increased in *Rgs12*<sup>-/-</sup> cells. Reactive oxygen species (ROS) has long been known to promote OCs, so we investigated whether ROS in OC precursors is dependent on Rgs12. Indeed, RANKL-dependent ROS production was inhibited in *Rgs12*<sup>-/-</sup> BMMs. Furthermore, the activity of Rac1, a potent activator of ROS-generating Nox proteins, was unaffected, suggesting that ROS removal, but not production, was responsible for the reduced ROS. Bioinformatics analysis predicted that the antioxidant enzymes up-regulated in *Rgs12*<sup>-/-</sup> cells share the common upstream regulator Nrf2, a transcription factor known to induce antioxidant proteins in response to oxidative stress. Using quantitative real-time PCR, we showed that the overall ratio of Nrf2 and its repressor, Keap1, was increased in *Rgs12*<sup>-/-</sup> BMMs. In conclusion, our findings demonstrate a novel role of Rgs12 in suppressing the expression of Nrf2-dependent antioxidant proteins to promote ROS generation that is essential for OC differentiation.

**Disclosures:** Andrew Ng, None.

## MO0176

**In Vivo Osteocytic Ca<sup>2+</sup> Pathway and Oscillations in Response to Acoustic Radiation Force in a Specific Bone Cell Ca<sup>2+</sup> Fluorescence Ai38/Dmp1-Cre Mice.** Minyi Hu<sup>\*</sup>, Jian Jiao, Daniel Gibbons, Xiaofei Li, Guowei Tian, Yi-Xian Qin. Stony Brook University, United states

Clinical evidences have shown that mechanotransduction is critical in bone remodeling and regeneration. While the biological effect of mechanical stimulation on bone healing has been well documented, the underlying mechanism is currently unknown. Our previous study elucidated the mechanobiological modulation of cytoskeleton and Ca<sup>2+</sup> influx in *in vitro* osteoblastic cells by short-term focused acoustic radiation force. While *in vitro* and *ex vivo* tissues and cells may not be a complete representation of the physiological setting due to the disconnected blood circulation, the objective of this study was to visualize and quantify calvarial Ca<sup>2+</sup> oscillations of real-time *in vivo* osteocytes' motility response to medium intensity focused ultrasound (MIFU) using the Ai38/Dmp1-cre mice, which express the Ca<sup>2+</sup> indicator protein in bone cells (EGFP fluorescent GCaMP3). All animal protocols were approved by Stony Brook University IACUC. Under isoflurane anesthesia, the top skin of the animal head was cut opened, gently exposing the calvaria for inverted confocal imaging. The animal's head was stabilized on a custom-made bed, where its chin was placed onto the MIFU transducer (Fig1A). Real-time confocal imaging (60X, 680-nm, 2 frames/sec) was performed to capture the Ca<sup>2+</sup> signals in the osteocyte cell bodies under MIFU of 0.2W, 0.5W and 1W for 1 minute. For data analysis, the fluorescent intensity of each cell body was extracted as a function of time using the microscope software. By normalizing to the baseline intensity, the percentage of responded cells, number of Ca<sup>2+</sup> spikes, spike magnitude, and the time to the first spike were quantified. MIFU at 0.2W, 0.5W and 1W led to Ca<sup>2+</sup> oscillations: 90%, 98% (+8% vs. 0.2W) and 100% (+11% vs. 0.2W) of responded cells, respectively (Fig1B,C). Higher MIFU energies led to larger Ca<sup>2+</sup> spike magnitudes and longer time to elicit the first spike. MIFU at 0.5W and 1W had 71% and 87% larger Ca<sup>2+</sup> spike magnitude (Fig1F), as well as 30% and 54% longer spike initiation time (Fig1E) than at 0.2W, respectively. Interestingly, higher MIFU energies also led to less Ca<sup>2+</sup> spikes. MIFU at 0.5W and 1W had 16% and 20% less Ca<sup>2+</sup> spikes than at 0.2W (Fig1D). In conclusion, this study provided a pilot observation of *in vivo* osteocytic Ca<sup>2+</sup> oscillations under noninvasive acoustic radiation force, which aids further exploration of the mechanosensing mechanism of controlled bone cell motility response to fluid flow loading.

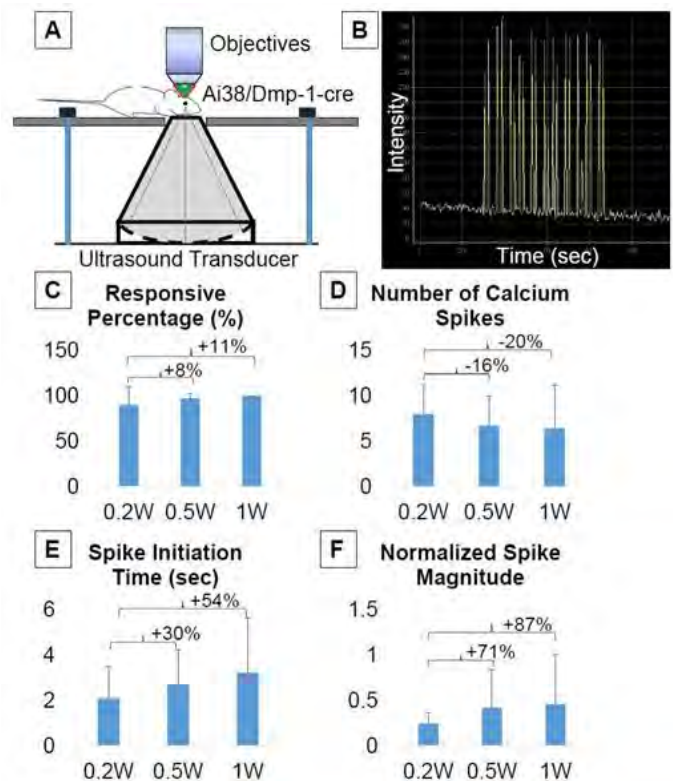


Figure 1

**Disclosures:** Minyi Hu, None.

**MO0177**

**A new multiplexed 3D confocal microscopy method to simultaneously measure changes in osteocyte cell body volume, lacunar volume and lacunar fluid space with age..** LeAnn Tiede-Lewis\*, Yixia Xie, Hong Zhao, Sarah Dallas. University of Missouri - Kansas City, USA, United states

Age related bone loss and its associated fracture risk is a major clinical problem for the elderly population. Recently osteocytes have emerged as key regulators of bone mass through mechanosensation and control of osteoclast and osteoblast activity and have become a promising therapeutic target for maintaining bone mass. Although age related changes in the osteocyte lacunocanalicular system and perilacunar matrix have been reported, changes in the osteocyte cell itself during aging are less understood.

In aged C57BL/6 mice, we previously showed that along with decreased bone mass, expanded cortical diameter, deterioration of the growth plate and intracortical remodeling, there is a marked degeneration of the osteocyte network with aging. 3D confocal imaging showed that osteocyte density and dendrite number per osteocyte decreased significantly in the femoral midshaft of 5Mo vs. 22Mo mice of both genders (reduction in dendrites of 21.4% ± 2.0 in males and 44.6% ± 3.9 in females). To further define the onset of these degenerative changes, 5, 12, 18 and 22Mo female mice were analyzed. Osteocyte dendricity decreased linearly (R<sup>2</sup>=0.98, p<0.01) from 12 through 18 to 22Mo. Decreased dendricity preceded the reduction in osteocyte cell density, which started by 18Mo, suggesting dendrite degeneration may affect osteocyte viability. To further understand degeneration of the osteocyte and lacunocanalicular networks, multiplexed 3D confocal methods were developed for simultaneous imaging of the lacunocanalicular system by i.v. injection of fixable TxRed-Dextran, the osteocyte cell membrane with the lipid dye, DiO, and the nucleus with DAPI. Using the Image J platform, a new method was developed for measurement of osteocyte cell body volume and corresponding lacunar volume and lacunar fluid volume from multiplexed confocal stacks. Osteocyte cell body volumes decreased with age in 5 vs. 22Mo females (14.4% reduction ± 1.5 p<0.05) with no change in lacunar volume. In males the lacunar volumes decreased (10.3% reduction ± 0.80 p<0.05), with no change in cell body volume. In summary, we present a novel multiplexed confocal-based method for measuring osteocyte density, dendricity, cell body and lacunar volumes and show that loss of osteocyte density and connectivity with aging is accompanied by gender dependent differences in cell body and lacunar volume. This may lead to impaired mechanoresponsiveness due to altered fluid flow during loading and decreased osteocyte connectivity.

*Disclosures: LeAnn Tiede-Lewis, None.*

**MO0178**

**Difference in osteocyte viability between patients with and without atypical femoral fracture after prolonged bisphosphonate treatment.** Shijing Qiu\*<sup>1</sup>, George Divine<sup>1</sup>, Mahalakshi Honasoge<sup>1</sup>, Pooja Kulkarni<sup>1</sup>, Elizabeth Warner<sup>2</sup>, Saroj Palnitkar<sup>1</sup>, D. Sudhaker Rao<sup>1</sup>. <sup>1</sup>Henry Ford Hospital, United states, <sup>2</sup>Henry Ford Hospital, United states

There is strong evidence that a massive death of osteocytes may compromise bone quality and increase the risk of fracture. Our previous work demonstrated that viable osteocytes were significantly decreased in patients with atypical femoral fracture (AFF) following >5y bisphosphonate (BP) treatment compared to age and race matched healthy postmenopausal women. The purpose of this study was to determine the difference in osteocyte viability between BP treated patients with and without AFF.

Iliac bone biopsies were obtained from 27 white postmenopausal women with ≥2y BP treatment, 6 with AFF (mean age 67.8 ± 7.7y) and 21 without AFF (mean age 65.7 ± 7.3y). Five µm Goldner & trichrome stained sections were used to measure trabecular bone osteocyte density [Ot.Dn (/mm<sup>2</sup>)], empty lacunar density [EL.Dn (/mm<sup>2</sup>)], total lacunar density [TL.Dn (/mm<sup>2</sup>)], and percent empty lacunae [EL.Dn/TL.Dn], as well as routine histomorphometry. The difference in each osteocyte-related variable was compared between patients with and without AFF. In addition, correlation between activation frequency (Ac.f) of bone remodeling and each osteocyte-related variable was analyzed for all the 27 biopsies.

As shown in the Table, EL.Dn and EL.Dn/TL.Dn were significantly higher in patients with AFF than in those without AFF. Additionally, Ot.Dn was lower in patients with AFF, but did not reach statistical significance, most likely due to small sample size. TL.Dn were similar in both groups. Ac.f correlated significantly with Ot.Dn (r = 0.509; p = 0.007) and TL.Dn (r = 0.422; p = 0.029), but showed significant negative correlation with EL.Dn/TL.Dn (r = -0.502; p = 0.008).

In conclusion, the present study suggests that the increase in osteocyte death and higher number of empty lacunae contribute to AFF. Moreover, the strong correlations between Ac.f and osteocyte-related variables indicate that the death of osteocytes after prolonged BP treatment is associated with the suppression of bone turnover (SSBT). Taken together, osteocyte death may act as a link between AFF and SSBT.

**Table 1. Difference in osteocyte-related variables between BP treated patients with and without AFF**

	AFF	no AFF	p
Ot.DN	74.6 (25.4)	101 (28.6)	0.057
EL.Dn	84.0 (15.1)	67.5 (12.9)	0.013
TL.Dn	159 (23.5)	168 (27.9)	0.460
EL.Dn/TL.Dn	53.7 (11.6)	41.1 (9.43)	0.011

Qiu Table-2016

*Disclosures: Shijing Qiu, None.*

**MO0179**

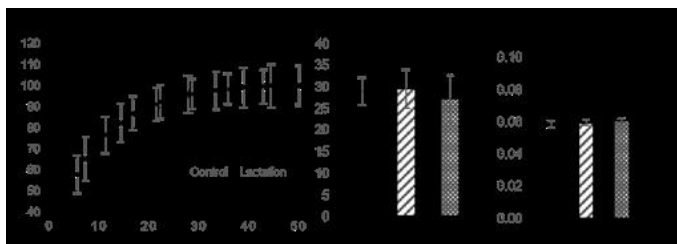
**Lactation-Induced Changes in the Volume of the Osteocyte Lacunar-Canalicular Space Alters Local Mechanical Properties in Cortical Bone.** A. Serra Kaya\*<sup>1</sup>, Jelena Basta-Pljakic<sup>1</sup>, Zeynep Seref-Ferlengez<sup>1</sup>, Robert Majeska<sup>1</sup>, Shoshana Yakar<sup>2</sup>, Mitchell Schaffler<sup>1</sup>. <sup>1</sup>City College of New York, United states, <sup>2</sup>New York University College of Dentistry, United states

Osteocytes can alter their surrounding bone matrix through osteocytic osteolysis, leading to increases in the volume of lacunae and canaliculi. We previously showed that lactation (Lac) caused changes in the tissue-level elastic modulus (Ei) of mouse cortical bone. However, the basis for this change is unclear. Cortical bone modulus is known to depend strongly on vascular porosity, but Lac does not induce intracortical remodeling in mice. Changes in 1) osteocyte lacunar-canalicular space (LCS) and/or 2) composition of bone matrix are hypothesized to account for altered tissue-level mechanical properties in cortical bone. In the current study, we tested whether these parameters could contribute to changes in bone tissue-level mechanical properties seen in Lac and Recovery (Rec).

Groups of C57Bl/6 mice (3 mo, n=5/grp) were sacrificed after 2 wks of Lac (Group 1) or underwent forced weaning at 2 wks followed by a further recovery period of 1 wk or 4 wk (Groups 2 and 3). Age-matched controls were also examined. Tissue level elastic modulus (Ei) was measured by microindentation on femoral mid-diaphyseal cross-sections. Lacunar and canalicular areas were measured in images of femoral cross-sections were obtained by super resolution microscopy. Mineralization differences and matrix composition of bone between canaliculi were assessed by back-scattered electron microscopy and Raman microscopy.

Ei was reduced by 10-15% after Lac (p<0.005 vs control) but returned to control levels after 1 wk Rec and did not increase further at 4 wks Rec. Under these conditions, lacunar and canalicular areas increased comparably with Lac (19% & 15%, respectively) and returned to baseline by 1 wk Rec. In contrast, neither mineral distribution in the matrix between canaliculi (Fig 1) nor the composition of that matrix (Fig 2) changed as a result of Lac.

These results show that tissue-level cortical bone material properties are rapidly and reversibly modulated during lactation and recovery. As lactation does not cause intracortical remodeling in mice, mechanical changes observed must be driven by osteocytes. Moreover, since lactation did not alter bone matrix mineralization or composition, potential causes of altered microscopic mechanical properties in lactation and recovery were dominated by changes in the LCS void volume resulting from osteocytic osteolysis. These data point to a hitherto unappreciated role for osteocytes in modulating and maintaining local bone material properties



Figure

*Disclosures: A. Serra Kaya, None.*

**MO0180**

**The Role of Carbonic Anhydrase 3 in Osteocytes.** Chao Shi<sup>\*1</sup>, Christopher Dedic<sup>2</sup>, Yuhei Uda<sup>2</sup>, Forest Lai<sup>2</sup>, Ningyuan Sun<sup>2</sup>, Marc Wein<sup>3</sup>, Keertik Fulzele<sup>2</sup>, Kunzheng Wang<sup>4</sup>, Paola Divieti Pajevic<sup>5</sup>. <sup>1</sup>Department of Molecular & Cell Biology, Goldman School of Dental Medicine, Boston University <sup>2</sup>Department of Orthopaedics, The Second Affiliated Hospital of Xi'an Jiaotong University, Xi'an, 710004, Shaanxi Province, P.R. China, United states, <sup>3</sup>Department of Molecular & Cell Biology, Goldman School of Dental Medicine, Boston University, United states, <sup>4</sup>Endocrine Unit, Massachusetts General Hospital & Harvard Medical School, United states, <sup>5</sup>Department of Orthopaedics, The Second Affiliated Hospital of Xi'an Jiaotong University, Xi'an, 710004, Shaanxi Province, P.R.China, China, <sup>5</sup>Department of Molecular & Cell Biology, School of Dental Medicine, Boston University, United states

Sclerostin, coded by SOST, is produced primarily by osteocytes and is a negative regulator of bone formation. It inhibits osteoblast functions via antagonism of the Wnt signaling and the molecular mechanisms controlling its expression are only partially known. Several hormones, namely PTH and PGE<sub>2</sub>, have been shown to suppress sclerostin expression whereas BMP7 increase it. To identify novel regulators of sclerostin expression we single cloned an established heterogeneous osteocytic cell line, Ocy454, and performed unbiased transcriptome analysis (Affimetrix) of high of low SOST/sclerostin expressing clones. Two high and three low SOST-expressing clones were selected out of 37 clones analyzed. CA3 was among the most upregulated transcripts in high-SOST expressing cells and its expression was further confirmed by qPCR and Western Blot. Since it has been previously reported that sclerostin controls Carbonic Anhydrase 2 (CA2) expression in human primary osteocytes and mouse MLO-Y4 cells, we focused our studies on Carbonic Anhydrase 3 (CA3). CA2 and 3 are isoenzymes of the CA family, which are ubiquitous zinc enzymes that catalyze the interconversion between carbon dioxide and ion bicarbonate. To investigate whether CA3 was regulated by sclerostin, we treated Ocy454 with sclerostin prior to analyze gene expression by qPCR. Sclerostin treatment was unable to induce CA3 expression in osteocytes whereas significantly increased its expression in primary adipocytes. To study CA3 regulation, Ocy454 cells were treated with PTH, PGE<sub>2</sub> and forskolin prior to gene expression analysis. PTH and Fsk were effective in suppressing CA3 expression after 2 hr and the transcript was still significantly suppressed after 24 hr of treatment. Interestingly PGE<sub>2</sub> was unable to suppress CA3, suggesting that its suppression is specific for PTH. To investigate if mechanical forces could regulate CA3 expression, Ocy454 cells were subjected to fluid flow shear stress for 2 hr prior to RNA isolation. Indeed mechanical forces significantly suppressed CA3 expression whereas CA2 was unaffected. CA family comprises 15 isoenzyme therefore we investigated which enzymes were expressed in Ocy454 cells. Of the 15 isoenzyme analyzed, 10 were detectable by qPCR and 4 were also differentially expressed in high vs low-SOST expressing cells. In conclusion, we report, for the first time, that mature osteocytes express high level of CA3 and its expression is regulated by PTH, fsk and mechanical forces.

**Disclosures:** Chao Shi, None.

**MO0181**

**MLO-Y4 Osteocytic Cell Sub-clones Express Distinct Gene Expression Patterns Characteristic of Different Stages of Osteocyte Differentiation.** Emily Atkinson<sup>\*1</sup>, Zuleima Sanchez<sup>1</sup>, Christian Porter<sup>2</sup>, Teresita Bellido<sup>1</sup>, Lilian Plotkin<sup>1</sup>. <sup>1</sup>IU School of Medicine, United states, <sup>2</sup>IUPUI, United states

Osteocytes are the most abundant bone cell and are formed when the osteoblast becomes embedded in the matrix. Through changes in gene expression and paracrine effects, osteocytes regulate the amount of osteoblasts, bone forming cells, and osteoclasts, bone resorbing cells that are needed to maintain bone mass. MLO-Y4 is the better characterized osteocytic cell line; however, lacks expression of sclerostin, the product of the SOST gene, which is fundamental for osteocyte function and blocks bone formation. With the objective to isolate MLO-Y4 sub-clones with different gene expression profiles, we performed cultures at very low density of MLO-Y4 cells stably transfected with nuclear green fluorescent protein (MLO-nGFP). Ten cell colonies, growing as separated sub-clones, were picked up using a tip and transferred to 24 well plates. Semi-confluent cultures were expanded, and cells were seeded in 6 well plates. Cell morphology was visualized under a fluorescence microscope. Once the cells reached 80% confluency, RNA was extracted and real time quantitative PCR was performed. Sub-clones exhibit different sizes and morphology, with some cells showing a spindle-like shape and others with abundant projections and a star-like shape. Gene expression also differed among sub-clones. For example, sub-clone 34 exhibits a star-like shape, with high expression of E11 and DMP1, markers of early osteocyte differentiation, no expression of keratocan, a gene enriched in osteoblasts; and absence of FGF23 and Sost expression, suggesting they represent early osteocytes. On the other hand, sub-clone 1 exhibits a spindle-like shape, low levels of E11 and absence of DMP1, high levels of keratocan, and relatively low levels of FGF23, suggesting they represent late osteoblasts. The expression of RANKL and OPG also varied among the sub-clones, with some exhibiting high (such as sub-clone 34), and others low (such as sub-clone 1) RANKL/OPG ratio. However, none of the clones examined

expressed SOST. We conclude that the MLO-nGFP sub-clones constitute a useful tool to study osteocyte differentiation and the role of osteocytes in the control of bone formation and resorption *in vitro*.

**Disclosures:** Emily Atkinson, None.

**MO0182**

**Role of Mitochondria in Protection of Osteocytes Against Acute Oxidative Stress.** Lynda Bonewald<sup>1</sup>, Jianxun Yi<sup>\*2</sup>. <sup>1</sup>UMKC, school of Dentistry, United states, <sup>2</sup>School of dentistry, United states

Role of mitochondria in protection of osteocytes against acute oxidative stress. Jianxun Yi<sup>1</sup>, Yukiko Kitase<sup>1</sup>, Kamal dhakal<sup>2</sup>, Leann M Tiede-Lewis<sup>1</sup>, Sarah L Dallas<sup>1</sup>, Jingsong Zhou<sup>2</sup>, Lynda Bonewald<sup>1</sup> University of Missouri-Kansas City, <sup>1</sup>Department of Oral and Craniofacial Sciences, School of Dentistry, <sup>2</sup>Department of Physiology, Kansas City University of Medicine and Biosciences

Characters with spaces = 2477 (Max = 2500)

Mitochondria are the main energy source for most cells and the primary site for endogenously generated reactive oxygen species (ROS) due to mitochondrial respiration. However, accumulation of ROS can cause mitochondrial damage that can ultimately lead to apoptosis. As little is known about osteocyte mitochondrial structure and function, mitochondria in MLO-Y4 osteocyte-like cells, isolated primary Dmp1-GFP+ osteocytes and osteocytes in *ex vivo* Dmp1-GFP+ mouse calvarial explants were imaged by live cell confocal microscopy using MitoDeepRed tracker dye. Osteocytes in all three cell models contained a complex mitochondrial network with highly motile mitochondria undergoing normal fusion and fission. Treatment of MLO-Y4 cells and primary Dmp1-GFP+ osteocytes with 100uM H<sub>2</sub>O<sub>2</sub>, an inducer of oxidative stress, resulted in a rapid fragmentation of the mitochondrial network within 10 min, with total disruption of mitochondria by 50 min. As we have found that a muscle secreted factor, b-aminobutyric acid, BAIBA, prevents H<sub>2</sub>O<sub>2</sub> induced osteocyte death, we next examined whether the protective effects of BAIBA are mediated via altered mitochondrial function. BAIBA induced expression of genes known to protect against mitochondrial oxidative stress such as catalase as determined by qPCR. Live cell imaging every 10 min before and after addition of H<sub>2</sub>O<sub>2</sub> to MLO-Y4 cells pretreated 16 hr with 3uM BAIBA showed that BAIBA protected against mitochondrial fragmentation with the mitochondrial network remaining intact 50 min after H<sub>2</sub>O<sub>2</sub> addition. Next, mitochondrial membrane potential was quantitated by live cell imaging using the mitochondrial membrane potential indicator, tetramethylrhodamine ethyl ester, TMRE. Confocal xyz images were taken every 2 min before and after addition of H<sub>2</sub>O<sub>2</sub>. In cells without BAIBA treatment, TMRE fluorescence intensity was reduced to 40% within 2 min and to 20% 12 min after H<sub>2</sub>O<sub>2</sub>-induced oxidative stress. In contrast, no reduction of TMRE fluorescent intensity was observed in cells pre-incubated with BAIBA, indicating that mitochondrial membrane potential was maintained. These data show that a key mechanism used by the muscle factor, BAIBA, to protect osteocytes from oxidative stress is through an increase in mitochondrial anti-oxidant genes to preserve the mitochondrial network and maintain mitochondrial membrane potential. This may be major mechanism whereby muscle secreted factors have beneficial effects on the skeleton.

**Disclosures:** Jianxun Yi, None.

**MO0183**

**Simvastatin rescues Homocysteine-Induced Apoptosis of Osteocytic MLO-Y4 Cells by Decreasing the Expressions of NADPH oxidase 1 and 2.** Ayumu Takeno<sup>\*</sup>, Ippei Kanazawa, Ken-ichiro Tanaka, Masakazu Notsu, Maki Yokomoto-Umakoshi, Toshitsugu Sugimoto. Internal Medicine I, Shimane University Faculty of Medicine, Japan

Background and aims: Clinical studies have shown that hyperhomocysteinemia is associated with bone fragility. Homocysteine (Hcy) induces apoptosis of osteoblastic cell lineage by increasing oxidative stress, which contributes to Hcy-induced bone fragility. Statins, 3-hydroxy-3-methylglutaryl coenzyme A (HMG-CoA) reductase inhibitors, are well-known cholesterol-lowering drugs. It has been shown that statins have pleiotropic effects and ameliorate oxidative stress by regulating oxidant and anti-oxidant enzymes; however, the effect of statins on Hcy-induced apoptosis of osteocytes is unknown. Thus, this study aimed to investigate whether or not statins prevent Hcy-induced apoptosis of osteocytic MLO-Y4 cells and regulate Nox expression.

Materials and methods: We used MLO-Y4, a murine long bone-derived osteocytic cell line. TUNEL staining and DNA fragment ELISA assay were performed to evaluate apoptosis. To examine the expressions of Nox, quantitative real-time PCR was performed.

Results: TUNEL staining showed that 5 mM Hcy induced apoptosis of MLO-Y4 cells and co-incubation of 10<sup>-9</sup> and 10<sup>-8</sup> M simvastatin, a lipophilic statin, significantly suppressed the apoptotic effect of Hcy. Moreover, we confirmed the beneficial effect of simvastatin against Hcy's apoptotic effect by using a DNA fragment ELISA assay. However, TUNEL staining showed no significant effects of 10<sup>-8</sup> M pravastatin, a hydrophilic statin, on the Hcy-induced apoptosis. Real-time PCR showed that Hcy increased the mRNA expressions of Nox1 and Nox2, whereas simvastatin inhibited the stimulation of Nox1 and Nox2 expressions by Hcy. In contrast, Hcy and simvastatin had no effect on Nox4 expression.

Conclusion: These findings indicate that simvastatin, but not pravastatin, prevents the detrimental effects of Hcy on the apoptosis of osteocytes by regulating the expressions of Nox1 and Nox2, suggesting that lipophilic statins may be beneficial for preventing Hcy-induced osteocyte apoptosis and the resulting bone fragility.

**Disclosures:** Ayumu Takeno, None.

## MO0184

**High Expression of Osteocyte Specific Markers in Human Bone Chips Cultures.** Nathalie Bravenboer<sup>1</sup>, Huib van essen<sup>2</sup>, Janak Pathak<sup>3</sup>, Jenneke Klein Nulend<sup>4</sup>, Astrid Bakker<sup>4</sup>. <sup>1</sup>Department of Clinical Chemistry, VU university Medical Center, Research Institute Move, Netherlands, <sup>2</sup>Department of Clinical Chemistry, VU university Medical Center, Research Institute Move., Netherlands, <sup>3</sup>Department of Molecular & Cellular Pharmacology, School of Pharmaceutical Science & Technology, China, <sup>4</sup>Department of Oral Cell Biology, ACTA, Research Institute Move, Netherlands

The major function of osteocytes is to sense mechanical loads imposed upon the bone and transmit these signals to other bone cells via the production of specific signal-molecules, to initiate bone modeling and remodeling. The location of osteocytes embedded in calcified matrix is ideal for this function. Nevertheless, this location makes the study of osteocyte responses technically difficult. Recently, protocols became available for the isolation of osteocytes from hyper-mineralized bone of mature animals Stern and Bonewald (2014), as well as for human bone chips culture, containing osteocytes embedded in their native matrix (Brolese et al, 2015). Considering the strong effect of matrix properties on cell behavior, we expected that the latter culture method yields osteocytes with a superior phenotype. Therefore, we tested the expression of osteocyte specific molecules in both isolated human osteocytes and human osteocytes cultured in their native matrix.

Osteocytes were isolated by sequential collagenase treatment according to the protocol of Stern et al. (2014), and cultured for 10 days, without passaging. Denuded bone chips were cultured for a maximum of two weeks after a collagenase treatment, according to Pathak et al. (2016). Gene expression of alkaline phosphatase SOST, FGF23, and PHEX, was detected by RTPCR using Tata Binding Protein (TBP) as housekeeping gene and shown as relative gene expression normalized for TBP ( $2^{-\Delta\Delta Ct}$ ).

Besides alkaline phosphatase mRNA expression, all nine fractions of isolated osteocytes expressed small amounts of SOST (0.002), PHEX (0.05) and FGF23 (0.004). In comparison, bone chips, expressed a centuple amount of SOST (0.2) and PHEX (2.0) mRNA and a decuple amount of FGF23 (0.05) mRNA, while alkaline phosphatase mRNA expression was somewhat lower (5.0).

The distinct difference in expression of osteocyte specific molecules in osteocytes embedded in their native matrix compared to isolated osteocytes indicates that the surrounding calcified matrix of osteocytes may determine its activity.

### References

Amber Rath Stern, Lynda F. Bonewald. Osteoporosis and Osteoarthritis 2014 Volume 1226 of the series Methods in Molecular Biology pp 3-10

Brolese E, Buser D, Kuchler U, Schaller B, Gruber R. Clin Oral Implants Res. 2015 Oct;26(10):1211-4.

Pathak JL, Bakker AD, Luyten FP, Verschueren P, Lems WF, Klein-Nulend J, Bravenboer N. Calcif Tissue Int. 2016 Feb 18. [Epub ahead of print]

**Disclosures:** Nathalie Bravenboer, None.

## MO0185

**Correct pre-analytical handling of plasma samples for bone turnover markers improves the stability of the markers.** Jens Romlund Halgreen<sup>1</sup>, Nadia Quardon<sup>1</sup>, Marijan Milenkovski<sup>1</sup>, Alperen Köse<sup>2</sup>, Niklas Rye Jørgensen<sup>3</sup>. <sup>1</sup>Dept. of Clinical Biochemistry, Copenhagen University Hospital Rigshospitalet, Denmark, <sup>2</sup>Copenhagen University Hospital Rigshospitalet, Denmark, <sup>3</sup>Dept. of Clinical Biochemistry, Copenhagen University Hospital Rigshospitalet & University of Southern Denmark, Denmark

Purpose: Sample material for analysis of bone turnover markers (BTM) are often shipped from other hospitals/general practitioners to a central laboratory for analysis. It is highly important that the material is handled in a way that preserves the bone turnover markers, yet it should be convenient to handle for the clinician and the laboratory. The aim of the study was to determine the optimal pre-analytical handling of sample material for commonly used BTM when analyzed on an automated platform.

Methods: Blood was collected from 45 patients and immediately centrifuged after venesection. Plasma was isolated and frozen. EDTA plasma was used for analysis of CTX-I, PINP and osteocalcin (OC), and Lithium-heparin plasma was used for bone-specific alkaline phosphatase (BAP). After thawing, samples were kept at either 5°C for 0, 72, 96, or 120 h before analysis or at room temperature (26°C) for 0, 24, 48, or 72 h. BTM were analyzed on the iSYS automated analysis platform according to the manufacturer's instructions. The BAP assay is based on a spectrophotometric principle, while CTX-I, PINP, and OC is based on a chemi-luminescence principle.

Linear regression analysis and Bland-Altman plots were used to compare changes in levels of BTM over time.

Results: For samples stored at 5°C, no significant changes in levels of BTM were detected up to 120 h. Moreover, for all four parameters, satisfactory correlations ( $R^2 > 0.97$ ) were found when stored at 5°C. In contrast, pre-analytical storage of the samples at room temperature affected the levels of BTM. BAP levels had a mean change of -5.3% (95% CI: -8.8;-1.9) after 24 h, -7.6% (-10.7;-4.4) after 48 h, and by -8.3% (-14.2;-2.3) after 72 h. The three other markers showed the following mean changes from baseline to 24 h, 48 h, and 72 h: CTX-I: 16.3%, 47.8%, and 65.7%; PINP: 16.9%, 36.8%, and 49.7%; OC: 14.0%, 19.4%, and 37.2%. However, none of the biases were significantly different from baseline by statistical analysis, but covered over large variations between time points within the same sample and with unsatisfactory correlations ( $R^2$  down to 0.87).

Conclusion: The study clearly shows that pre-analytical handling of samples for BTM analysis is important. The samples can be stored for up to 72 h at 5°C, without changed levels. In contrast, storage at room temperature (26°C) for 24 h or more, clearly affects the levels of BTM in the sample and should be avoided.

**Disclosures:** Jens Romlund Halgreen, None.

## MO0186

**The Association Of Circulating miRNAs With Bone Mineral Density, Microarchitecture And Prevalent Fracture In The OFELY Cohort.** Elodie Feuer<sup>\*</sup>, Casina Kan, Martine Croset, Elisabeth Sornay-Rendu, Roland Chapurlat, INSERM UMR 1033, France

Objective Current biomarkers of osteoporosis lack sensitivity. The objective of this work was to study whether selected circulating microRNAs are associated with bone mineral density (BMD) and microarchitecture, along with prevalent fracture in a cohort of French women.

Material and methods In this cross-sectional analysis from the 14th annual follow-up of the OFELY study, microRNAs were measured from 200 µL of serum by RT qPCR (Exiqon, Denmark). We chose 32 microRNAs that seemed relevant in their association with bone metabolism, based on prior literature. BMD was measured by DXA and the microarchitecture was assessed with high resolution peripheral quantitative computed tomography. Prevalent low energy fractures were ascertained using radiographs and medical records.

Results MicroRNAs measurements were obtained from 682 subjects: 99 pre-menopausal women (mean (SD) age 49 (2.5)) and 583 post-menopausal women (mean (SD) age 68 (8.7)). One pre-menopausal woman and 122 post-menopausal women had at least one prevalent fracture. All the 32 analyzed microRNAs were significantly correlated with age (correlation coefficient between 0.09 and 0.49). The miR-16-5p was the most correlated with age ( $r = -0.49$ ,  $p < 0.0001$ ). In univariate analysis, most of the microRNAs were significantly associated with femoral neck bone mineral density and with radius and tibia total volumic bone mineral density. In multivariate analysis, none of these results remained significant after adjustment for age. Similarly, the prevalent fractures were not associated with the serum levels of microRNAs after adjustment for age.

Conclusion We showed a constant association between the level of circulating microRNA with age but we were not able to reveal an association with bone parameters, and especially with prevalent osteoporotic fracture.

**Disclosures:** Elodie Feuer, None.

## MO0187

**Therapeutic Target for Plasma PINP in Bisphosphonate Treated Osteoporosis Patients: the Health In Men Study.** Paul Chubb<sup>1</sup>, Elizabeth Byrnes<sup>2</sup>, Bu Yeap<sup>3</sup>, Laurens Manning<sup>3</sup>, Leon Flicker<sup>3</sup>, Jonathan Golledge<sup>4</sup>, Samuel Vasikaran<sup>5</sup>. <sup>1</sup>School of Medicine & Pharmacology & School of Pathology & Laboratory Medicine, University of Western Australia, Australia, <sup>2</sup>PathWest - Queen Elizabeth II Medical Centre, Australia, <sup>3</sup>School of Medicine & Pharmacology, University of Western Australia, Australia, <sup>4</sup>School of Medicine & Dentistry, James Cook University, Australia, <sup>5</sup>PathWest - Royal Perth & Fiona Stanley Hospitals, Perth, Australia, Australia

### Background

Interpretation of measurements of plasma N-terminal propeptide of type I collagen (PINP) in osteoporosis patients treated with anti-resorptive therapy is uncertain as targets indicating adequate suppression of bone turnover in this setting have not been published. For the bone resorption marker urine N-terminal telopeptide of type I collagen (NTX), maximal anti-fracture efficacy after bisphosphonate treatment was obtained with values  $< 21$  nmol BCE/mmol (Eastell R et al., J Bone Miner Res 2003;18:1051-6). We recently proposed a treatment target for plasma C-terminal telopeptide of type I collagen ( $\beta$ CTX-I) of 230 ng/L derived from this NTX target (Chubb SAP et al., Clin Biochem 2015 Dec 8 doi 10.1016/j.clinbiochem.2015.12.002).

### Aim

We set out to derive an interim PINP target for bisphosphonate treatment equivalent to the proposed  $\beta$ CTX-I target.

Participants and methods

Participants were community-dwelling men aged 70-89 years taking part in the Health In Men Study. Plasma  $\beta$ CTX-I and P1NP were measured on a E170 immunoassay analyser (Roche Diagnostics). We used Passing-Bablok type III regressions of plasma P1NP on  $\beta$ CTX-I for the sub-group of very healthy men (those reporting 'excellent' or 'very good' health and without any history of diabetes, cardiovascular disease, cancer, depression or dementia (n=298)) and for the sub-group who self-reported bisphosphonate use (n=67 after exclusion of subjects with Paget's disease) to obtain the P1NP value corresponding to the  $\beta$ CTX-I target value of 230 ng/L.

#### Results

The regression parameters for P1NP on  $\beta$ CTX-I in bisphosphonate treated men were significantly different from those in the untreated healthy group; P1NP values were higher for a given  $\beta$ CTX value in the bisphosphonate treated men. For the healthy group, the regression slope (95% confidence limits (95CL)) and intercept (95CL) were 0.091(0.081-0.101) and 10.00(6.79-13.04). For the bisphosphonate-treated group the slope and intercept were 0.125(0.093-0.159) and 3.13(-0.42-5.95). The plasma P1NP value corresponding to the  $\beta$ CTX-I target of 230ng/L was 31.8 (95CL 21.0-42.6) ug/L using the regression parameters for the bisphosphonate treated group; 73.1% of men taking a bisphosphonate had P1NP below this target.

#### Conclusions

The therapeutic target of <32 ug/L for plasma P1NP may be a useful guide for bisphosphonate treatment in osteoporosis pending results of formal studies directly examining fracture outcomes with P1NP levels post bisphosphonate therapy.

**Disclosures:** Samuel Vasikaran, None.

## MO0188

**CHANGES IN TRABECULAR BONE SCORE AFTER PARATHYROIDECTOMY IN PRIMARY HYPERPARATHYROIDISM.** Juan Carlos Romero Rodríguez<sup>1</sup>, Gonzalo Allo Miguel<sup>1</sup>, Guillermo Martínez Díaz-Guerra<sup>1</sup>, Mercedes Aramendi Ramos<sup>2</sup>, Eduardo Ferrero<sup>3</sup>, Federico Hawkins\*<sup>1</sup>. <sup>1</sup>Endocrinology Service, 12 de Octubre University Hospital, University Complutense, Spain, <sup>2</sup>Laboratory Service, 12 de Octubre University Hospital, University Complutense, Spain, <sup>3</sup>Surgery Service, 12 de Octubre University Hospital, University Complutense, Spain

**Introduction:** Primary hyperparathyroidism (HPT) is associated with an increased risk of vertebral fractures. Trabecular bone score (TBS) is a new tool obtained from lumbar spine DXA scans that could estimate bone microarchitecture in HPT patients.

**Methods:** prospective study in HPT patients who underwent parathyroidectomy. Lumbar, hip and forearm BMD was measured before and 24 months after surgery with DXA. TBS was obtained from lumbar spine scans. Biochemical data included serum calcium, PTH, 25-OH vitamin D,  $\beta$ -CTX, FAO and osteocalcin.

**Results:** 32 patients (25 female, 7 male), mean age 64.6  $\pm$  12.4 were included. Baseline BMD was low at lumbar spine (T-score -2.19  $\pm$  1.31), total hip (-1.33  $\pm$  1.12), femoral neck (-1.75  $\pm$  0.84), and forearm BMD (-2.74  $\pm$  1.68). No significant differences were found between gender. Baseline TBS showed degraded microarchitecture (1.180  $\pm$  0.130). After surgery, significant changes were observed in serum calcium, phosphorus and PTH (p<0.0001), and 24 h urine calcium (p<0.05). Lumbar spine BMD increased (5.3  $\pm$  13.0%, p<0.05) as well as total hip BMD (3.8  $\pm$  8.8%, p<0.05), but no significant changes were observed in TBS neither in forearm BMD. TBS was not correlated with serum calcium, PTH,  $\beta$ CTX or osteocalcin. Serum FAO was correlated with baseline TBS (Spearman Rho 0.55, p<0.05) and post-parathyroidectomy TBS (Rho 0.57, p<0.05).

**Conclusion:** TBS is deteriorated in HPT patients. Two years after parathyroidectomy an improvement in spine and hip BMD is observed before any significant changes in TBS could be detected.

**Disclosures:** Federico Hawkins, None.

## MO0189

**Ethnic differences in femoral neck geometry as assessed by HSA of QCT between elderly Caucasian and Chinese populations: a Perth-Beijing group study.** Benjamin Khoo<sup>1</sup>, Richard Prince<sup>2</sup>, Xiaoguang Cheng<sup>3</sup>, Keenan Brown<sup>4</sup>, Ling Wang\*<sup>5</sup>. <sup>1</sup>Medical Technology & Physics, Sir Charles Gairdner Hospital, Australia, <sup>2</sup>Medical Technology & Physics, Sir Charles Gairdner Hospital, Perth, Australia, <sup>3</sup>Department of Radiology, Beijing Jishuitan Hospital, Beijing, China, <sup>4</sup>Mindways Software, Austin, USA, <sup>5</sup>Department of Radiology, Beijing Jishuitan Hospital, Beijing, China, China

**Purpose:** Ethnic origin plays an important role in the risk of osteoporotic fractures. The aim of this study was to compare the proximal structural geometrical differences between elderly Caucasian and Chinese populations.

**Materials and Methods:** This study was proposed by Perth group and Beijing group which collected structural geometrical outcomes available from QCT for their population analysed by Hip Structure Analysis (HSA) software to produce structural data, which allows the measurement of geometric contributions to bone strength in the proximal femur. The Beijing group recruited 201 healthy Chinese women (age:

mean  $\pm$  SD; 75.28  $\pm$  5.39 years old) to compare to 237 Caucasian women (77.14  $\pm$  5.04 years old) collected by Perth group. We performed HSA on hip QCT scans by Mindways software. With this approach, cross-sectional moment of inertia(CSMI), femoral neck subperiosteal diameter(W), femoral neck endosteal diameter(ED), averaged cortical thickness(aCT), cross-sectional area(CSA), section modulus(SM) and buckling ratio(BR) can be quantified. These parameters are measures of strength in axial compression or bending.

**Results:** HSA indices associated with more favorable geometry and greater strength and resistance to fracture were more prevalent in Chinese women. Table 1 shows differences in unadjusted and adjusted means of measurements between Caucasians and Chinese subjects. Caucasian women exhibited significantly lower value than Chinese women in the Unadjusted analysis of aBMD (P < 0.001) as well as in SM (Z) and aCT. Femurs of Chinese women had a larger cross-sectional area and a lower buckling ratio. After adjusting for age, weight, height and BMI, interestingly, there was no significant difference in CSA between the two groups (P=0.3123). In the same model, compared to diminishing differences in CSMI, Z and W, the differences in aBMD, Z, aCT and BR increased significantly. When aBMD was included in the model, the difference in CSA was 0.3191cm<sup>2</sup> (P=0.0001), suggesting aBMD played an important role in the ethnic differences of CSA. What's more, after adjusted aBMD, Caucasian had significant higher Z (P=0.0001). The differences in W, ESD and BR were attenuated after adjustment for age, height, weight, BMI, and aBMD. In contrast, the difference in CSMI was accentuated largely after adjustment for covariates.

**Conclusion:** The observed biomechanical differences may help account in part of racial/ethnic variability in fracture rates in the two Societies.

Table 1. Hip structure analysis (HSA) indices by ethnic difference

	Unadjusted differences	P value	adjusted differences <sup>a</sup>	P value	adjusted differences <sup>b</sup>	P value
aBMD	-0.1201	0.0001	-0.1335	0.0001	#	#
CSA	0.0966	0.0036	0.0330	<b>0.3123</b>	0.3191	0.0001
CSMI	0.1790	0.0001	0.0953	0.0237	0.3187	0.0001
W	0.6594	0.0001	0.6173	0.0001	0.5100	0.0001
ESD	0.7111	0.0001	0.6745	0.0001	0.5123	0.0001
aCT	-0.0258	0.0001	-0.0286	0.0001	-0.0010	0.0014
SM(Z)	-0.0558	0.0074	-0.0858	0.0001	0.0807	0.0001
BR	5.1471	0.0001	5.1484	0.0001	1.2209	0.0001

BMI: body mass index; CSA, Cross-sectional area; CSMI, cross-sectional moment of inertia; W, subperiosteal width; ESD, femoral neck endosteal diameter; aCT, averaged cortical thickness;

SM(Z), section modulus; BR, buckling ratio; aBMD, areal BMD

Model<sup>a</sup> Results are adjusted for age, height, weight, and BMI.

Model<sup>b</sup> Results are adjusted for age, height, weight, BMI, and aBMD.

Table1

**Disclosures:** Ling Wang, None.

## MO0190

**Fracture Risk Estimation with Statistical Multi-Parametric Modeling.** Julio Carballido-Gamio\*<sup>1</sup>, Aihong Yu<sup>2</sup>, Ling Wang<sup>2</sup>, Yongbin Su<sup>2</sup>, Thomas F. Lang<sup>1</sup>, Xiaoguang Cheng<sup>2</sup>. <sup>1</sup>Department of Radiology & Biomedical Imaging, University of California, San Francisco, United states, <sup>2</sup>Department of Radiology, Beijing Ji Shui Tan Hospital, China

**Purpose:** The devastating effects of a hip fracture in the quality of life and its financial burden have made hip fracture prediction an imperative goal. Here we present statistical multi-parametric modeling (SMPM) with the aim of contributing towards this objective. SMPM merges existing image analysis algorithms with machine learning, and to demonstrate its potential it was applied to a QCT study of the proximal femur of women with acute fracture. Methods: 143 women were included in this study (69  $\pm$  11 years; 50 controls; 93 with hip fracture). Bilateral hip QCT imaging was performed in all subjects. Women with hip fracture were scanned within 48 hours of fracture to minimize changes in BMD and body composition factors due to the fracture. QCT scans of the left hip for controls and contra-lateral hip for cases were automatically segmented and surface-based cortical bone multi-parametric maps computed: thickness (Ct.Th), mean volumetric BMD (Ct.vBMD), and mean vBMD in a layer adjacent to the cortical bone (EndoCt.vBMD). Mean integral vBMD was also calculated for the femoral neck region (Neck.vBMD). Corresponding anatomical landmarks were automatically identified on the surface of each segmented femur, and a statistical shape model was obtained based on principal component analysis (PCA). Using the set of identified landmarks and PCA, a statistical model of cortical bone features (Ct.Th, Ct.vBMD and EndoCt.vBMD) was generated. A new PCA was then performed to create a joint statistical model of shape and cortical bone parameters, i.e. a SMPM. PC scores were obtained for each subject and each PC. The number of PC scores was reduced using feature selection and then used in a logistic regression model for hip fracture discrimination. In order to evaluate the accuracy of SMPM, the whole pipeline was repeated using stratified 10-fold cross-validation. The area under the ROC curve (AUC) was also calculated to evaluate the discriminatory performance of the technique. Cross-validation and AUCs were also evaluated for Neck.vBMD and Neck.vBMD with age, height and weight. Results: Table 1 summarizes the results indicating significant better AUC for SMPM compared to Neck.vBMD with (p<0.01)

or without clinical variables ( $p < 0.001$ ), as well as higher classification accuracy for both controls and cases. Conclusion: SMPM results warrant its application in prospective studies of hip fracture where the inclusion of trabecular bone parameters could further improve its performance.

Fracture Classifier	Fraction of Correct Controls Classifications	Fraction of Correct Fracture Classifications	AUC
SMPM	76%	92.5%	0.90
Neck.vBMD	56%	89%	0.83
Neck.vBMD, Age, Height and Weight	62%	79.6%	0.85

SMPM = Statistical Multi-Parametric Modeling

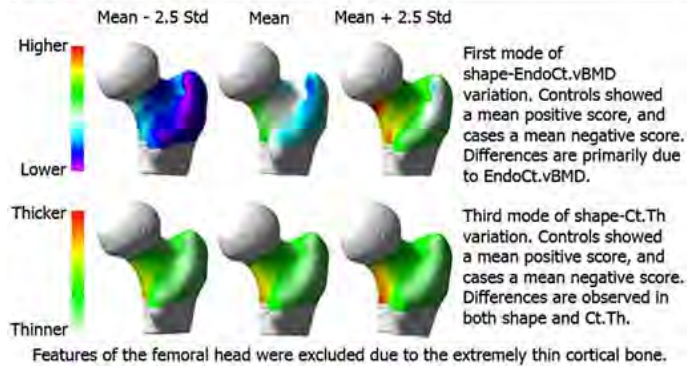


Table-Figure-HR

Disclosures: Julio Carballido-Gamio, None.

## MO0191

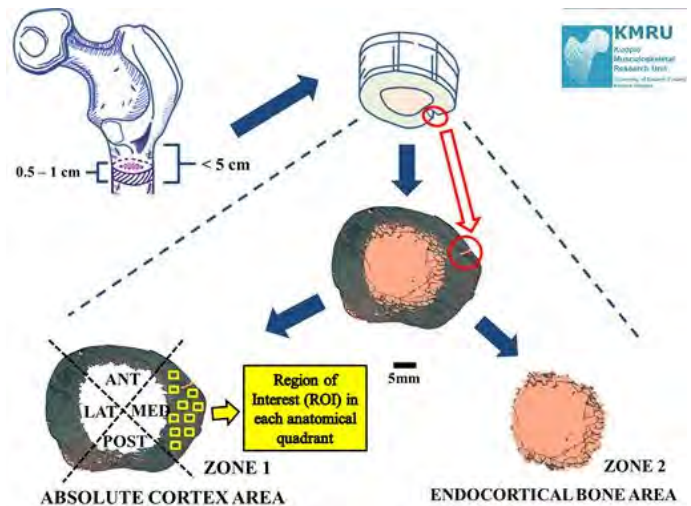
**Histomorphometric and Osteocytic Characteristics of Cortical Bone in Male Subtrochanteric Femoral Shaft.** Xiaoyu Tong\*<sup>1</sup>, Heikki Kröger<sup>2</sup>. <sup>1</sup>Kuopio Musculoskeletal Research Unit (KMRU), Institute of Clinical Medicine, University of Eastern Finland, Finland, <sup>2</sup> Department of Orthopaedics, Traumatology, & Hand Surgery, Kuopio University Hospital, Finland

**Purpose** The histomorphometric variations in the subtrochanteric femoral shaft are poorly understood. The aim of this study was to investigate the age-dependent variations and regional differences of histomorphometric and osteocytic properties in the cortical bone of subtrochanteric femoral shaft, and the association between osteocytic and histological cortical bone parameters.

**Methods** Undecalcified histological sections ( $n=20$ , aged 18–82 years, males) of the subtrochanteric femoral shaft ( $\leq 5$ cm below lesser trochanter) were cut ( $15\mu\text{m}$ ) and stained using modified Masson-Goldner stain. Histomorphometric parameters of cortical bone were analysed with low (X50) and high (X100) magnification, after identifying cortical bone boundaries using our previously validated method. Osteocytic parameters of cortical bone were analysed under phase contrast microscopy and epifluorescence within microscopic fields ( $0.55\text{ mm}^2$  for each).

**Results** The cortical widths of the medial and lateral quadrants were significantly higher than other quadrants ( $p < 0.01$ ). Osteonal area per sampled cortical area was lower and cortical porosities were higher in the posterior quadrant than in the other quadrants ( $p < 0.05$ ). Middle aged group (40–55 years) showed significantly different osteonal parameters (e.g. osteon number per sampled cortical area) compared to the other groups ( $< 40$  years and  $> 55$  years), both before and after adjustments for subjects' height and weight ( $p \leq 0.05$ ). Osteocyte lacunar number per sampled cortical area was found higher in the young subjects ( $< 40$  years) than in the older ones ( $> 40$  years) ( $p < 0.01$ ). Moreover, significant but low correlations were found between the cortical bone and osteocytic parameters ( $0.20 \leq R^2 \leq 0.35$ ,  $p < 0.05$ ).

**Conclusions** This study describes both regional differences and age-related changes of subtrochanteric femoral cortex in healthy males. These findings may be of use when discussing mechanisms that predispose patients to decreasing bone strength.



Methodology Demonstration

Disclosures: Xiaoyu Tong, None.

## MO0192

**Trabecular Bone Microstructure is Impaired in the Proximal Femur of HIV-Infected Men with Normal Bone Mineral Density.** Galateia Kazakia, Julio Carballido-Gamio, Misung Han, Andrew Lai, Lorenzo Nardo, Luca Facchetti, Courtney Pasco, Amy Zhang, Amanda Hutton Parrott, Phyllis Tien, Roland Krug\*. UCSF, United states

**Purpose:** To assess bone microstructure in the proximal femur as well as in the extremities of HIV-infected men and healthy controls and compare the findings to those based on DXA areal bone mineral density (aBMD).

**Materials and Methods:** The study was approved by the institutional review board and complied with HIPAA guidelines. Written informed consent was obtained from all subjects. Eight HIV-infected men on ART treatment and 11 age- and gender-matched healthy controls were recruited. High-resolution MRI of the proximal femur was performed using fully balanced steady state free precession (bSSFP) on a 3T system (GE, Milwaukee). Three volumes of interest at corresponding anatomic locations across all subjects were defined based on registrations of a common template. Four MRI-based trabecular microstructural parameters were analyzed at each region: fuzzy bone volume fraction (f-BVF), trabecular number (Tb.N), thickness (Tb.Th), and spacing (Tb.Sp). In addition, the distal radius and distal tibia were imaged with high-resolution peripheral quantitative computed tomography (HR-pQCT). Four HR-pQCT-based microstructural parameters were analyzed: trabecular bone volume fraction (BV/TV), trabecular number (Tb.N), trabecular thickness (Tb.Th), and trabecular separation (Tb.Sp). Total hip aBMD was determined from DXA.

**Results:** Microstructural bone parameters derived from MRI at the proximal femur and from HR-pQCT at the distal tibia (see Table and Figure) showed significantly altered bone quality in HIV-infected patients compared to healthy controls. In contrast, DXA aBMD data showed no significant differences between HIV-infected patients and healthy controls.

**Conclusion:** High-resolution imaging to assess trabecular bone microstructure is a powerful tool and should be considered in HIV-infected men with risk factors for low bone mass but normal DXA aBMD. Advances in MRI technology have made microstructural imaging at the proximal femur possible.

**Table:** Trabecular bone parameters are shown of the femoral head, neck and trochanter (MRI) as well as distal tibia (HR-pQCT). Significant differences ( $p < 0.05$ ) are labeled with an asterisk.

Femoral Head (MRI)	f-BVF	Tb.Th [mm]	Tb.Sp [mm]	Tb.N [1/mm]
HIV-infected	0.384±0.008	0.2643±0.009	0.425±0.029	1.454±0.078
Healthy controls	0.392±0.003	0.256±0.006	0.397±0.011	1.532±0.038
Student's t-test	0.007*	0.031*	0.010*	0.010*
Femoral Neck MRI	f-BVF	Tb.Th [mm]	Tb.Sp [mm]	Tb.N [1/mm]
HIV-infected	0.376±0.012	0.276±0.016	0.460±0.050	1.360±0.117
Healthy controls	0.388±0.008	0.267±0.007	0.422±0.022	1.455±0.057
Student's t-test	0.024*	0.094	0.037*	0.049*
Femoral Troch. (MRI)	f-BVF	Tb.Th [mm]	Tb.Sp* [mm]	Tb.N [1/mm]
HIV-infected	0.377±0.015	0.281±0.017	0.470±0.057	1.346±0.124
Healthy controls	0.386±0.007	0.269±0.009	0.430±0.024	1.435±0.065
Student's t-test	0.093	0.063	0.049*	0.059
Tibia (HR-pQCT)	BV/TV	Tb.Th [mm]	Tb.Sp [mm]	Tb.N [1/mm]
HIV-infected	0.130±0.021	0.086±0.015	0.593±0.165	1.538±0.295
Healthy controls	0.150±0.022	0.078±0.012	0.444±0.081	1.962±0.308
Student's t-test	0.061	0.164	0.018*	0.008*

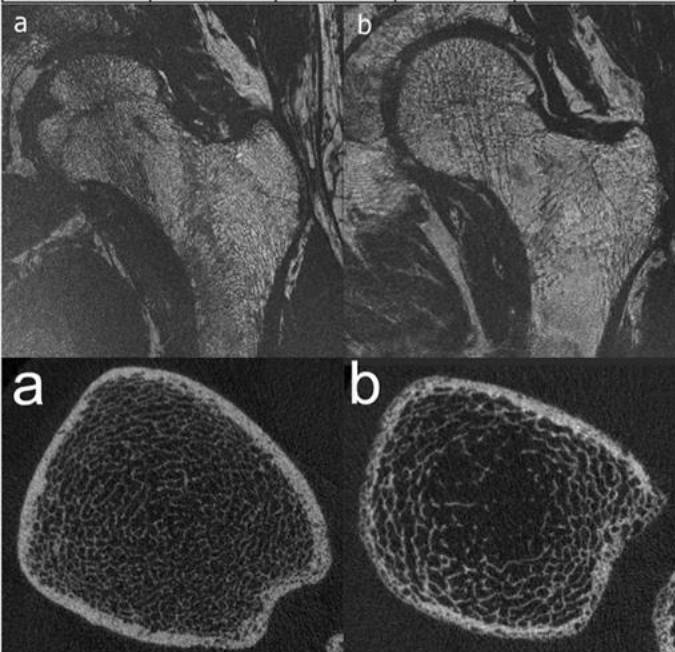


**Figure Top:** Representative coronal cross-sections of high-resolution magnetic resonance images of the proximal femur of a healthy control (a) and an HIV-infected patient (b).  
**Figure Bottom:** Representative axial cross-sections of high-resolution peripheral quantitative computed tomography (HR-pQCT) images of the distal tibia of a healthy control (a) and an HIV-infected patient (b).

Table and Figures

*Disclosures: Roland Krug, None.*

## MO0193

**Trabecular Bone Score (TBS) in Fracturing Elite Athletes.** Elliott N. Schwartz, M.D.\*, Clinton Edmondson, Christelle Domantay, X.T., Patricia E. Schwartz, R.N., X.T., Northern California Institute for Bone Health, Inc., United states

Since the 2000 NIH Consensus Conference, the relationship that Bone Strength = Bone Quality + Bone Density has been utilized in understanding skeletal resistance to fracture.

Many elite athletes suffer fractures, predominantly acute traumatic or stress; many suffer recurrences.

Stress fractures, classically, have been divided into fatigue and insufficiency fractures. At least part of the pathogenesis has been hypothesized to be due to micro-damage accumulation.

We have used DXA to assist in making the decision between fatigue and insufficiency fractures. But, micro-damage and other bone quality characteristics are not assessable by DXA.

TBS is a textural analysis of the pixels of the LS spine DXA providing an indirect measure of trabecular architecture and it has been proposed as a measure of Bone Quality. TBS software was approved by the FDA in October, 2013. NCIBH has utilized this software since that time.

The purpose of this study was to evaluate the role of TBS in the assessment of Bone Quality in fracturing elite athletes.

Since then, we evaluated more than 15 athletes prospectively and found several with reduced TBS. Therefore, in February, 2016, we retrospectively reviewed the TBS in all elite athletes who had DXA studies at our facility since 2006 and had been seen prior to November, 2013.

We studied 10 MLB and 5 Minor LB players; 7 NBA and 2 college basketball players; 5 active NFL players and 1 retired NFL player; and, 4 amenorrheic runners utilizing gender and ethnicity specific databases.

One MLB player (Black ethnicity) and one Minor League (White) had "degraded" TBS; one Minor League player (White) had "partially degraded" TBS; 2 NBA players (Black) had "degraded" TBS and one had "partially degraded" TBS (White); and one NFL player (Black) had "partially degraded" TBS. These individuals all had high BMD and, thus, their TBS and BMD were discordant.

This is not a randomized sample of any elite athletic population but, rather, a select referral population. Yet, whatever "abnormal" TBS represents, it is clearly present in some of these athletes with bone health issues.

Although the prevalence of "degraded" and "partially degraded" TBS in fracturing elite athletes is not known, this exploratory analysis suggests TBS needs to be further studied in this population to clarify the role of reduced Bone Quality in their fractures.

*Disclosures: Elliott N. Schwartz, M.D., None.*

## MO0194

**3D-DXA Spine: Modelling the lumbar Spine in 3D from DXA images.** Mirella Lopez Picazo\*<sup>1</sup>, Ludovic Humbert<sup>1</sup>, Alba Magallón Baro<sup>1</sup>, Luis del Río Barquero<sup>2</sup>, Silvana Di Gregorio<sup>2</sup>, Miguel Angel Gonzalez Ballester<sup>3</sup>. <sup>1</sup>Galgo Medical, Spain, <sup>2</sup>CETIR Grup Mèdic, Spain, <sup>3</sup>Universitat Pompeu Fabra - ICREA, Spain

A method to model the lumbar spine in 3D from a frontal DXA image is presented, and the accuracy of the method evaluated in comparison with QCT.

The 3D-DXA Spine technology relies on a 3D statistical model build from a dataset of QCT-scans of 60 patients. The statistical model describes the principal statistical variations in shape and BMD distribution observed in the database. A 3D subject-specific model is obtained by registering the statistical model onto the 2D DXA image of the patient so that the projection of the model matches the DXA image. A model-based algorithm is used to segment the cortical layer and compute the volumetric BMD (vBMD), BMC and cortical thickness at specific regions of interest. The accuracy of the method was evaluated by comparing 3D subject-specific models obtained from DXA images (Stratos dR, DMS) with QCT acquisitions. This preliminary evaluation involved 20 healthy women (mean age: 42 ± 9 years, range: 22 – 58 years).

The mean shape accuracy was 0.9 mm when computed for the 20 L1, L2 and L3 vertebrae and 1.0 when computed for the L4 vertebrae. The mean absolute error was 55.9 mg/cm<sup>3</sup> for the cortical vBMD, 20.5 mg/cm<sup>3</sup> for the trabecular vBMD, and 18.9 mg/cm<sup>3</sup> for the integral vBMD of the vertebral body. The mean absolute error was 0.32 g for the cortical BMC, 0.53 g for the trabecular BMC, and 1.06 g for the integral BMC of the vertebral body. The cortical thickness of the vertebral body was associated with a mean absolute error of 0.05 mm.

The 3D-DXA Spine technology provides clinicians with a 3D model of the femoral shape of the lumbar spine, together with a quantification of the vBMD of the trabecular and cortical bone, and the cortical thickness. This could potentially improve osteoporosis management while maintaining DXA as the standard routine modality.

*Disclosures: Mirella Lopez Picazo, None.*

## MO0195

**Bone component analysis with 3D-DXA and vitamin D levels in patients with Type 2 Diabetes, Latent Autoimmune Diabetes in Adults (LADA) compared to healthy controls.** Patricia Clark\*<sup>1</sup>, Miguel Angel Guagnelli<sup>1</sup>, Rita Gomez-Diaz<sup>2</sup>, Geraldine Gonzalez-Castelan<sup>1</sup>, Yves Martelli<sup>3</sup>, Ludovic Humbert<sup>3</sup>, Neils Wachter<sup>2</sup>. <sup>1</sup>Clinical Epidemiology Unit, Hospital Infantil de México, Mexico, <sup>2</sup>Clinical Epidemiology Unit, Hospital de Especialidades, Centro Medico Nacional Siglo XXI, Mexico, <sup>3</sup>Galgo Medical, Spain

Objective: 3D-DXA technology provides a three-dimensional analysis of femoral shape and bone density distribution from a conventional DXA scan, allowing a separate assessment of cortical and trabecular bone. Differences between BMD and fracture risk have been described for diabetic patients. The objective of the present

study was to analyze BMD and 3D-DXA structural characteristics in a group of patients with type 2 diabetes (T2DM), latent autoimmune diabetes in adults (LADA), and healthy controls.

Methods: Patients were diagnosed with T2DM according to ADA criteria. LADA patients included accepted diagnostic criteria: age 30 - 70 years, under treatment with diet and/or oral hypoglycemic agents for at least 6 months and positive for at least 1 autoantibody: GAD and/or IA-2. Both groups were compared with healthy controls. Patients with any other immune disease associated with diabetes or a fragility fracture were excluded. Anthropometric measurements, C-peptide, serum vitD, glycosylated hemoglobin (HbA1c) and conventional DXA scans for body composition, lumbar and femoral BMD with iDXA GE Lunar and 3D-DXA analysis of left femur were obtained with Galgo Medical software. The 3D-DXA software was used to analyze the cortical and trabecular bone in all cases, and to obtain a 3D subject-specific model of the femur of the patient and quantify the volumetric BMD (vBMD), volume (for trabecular and cortical regions) and cortical thickness distribution.

Results: Healthy controls (n=51, mean age 53.9 ± 11.3), T2DM (n=74, 53.6 ± 13.6) and LADA (n=26, 51.2 ± 9.7) were included. LADA patients had lower 25-OH-vitamin D concentrations compared to controls and T2DM (p=0.02). Lower Z-score BMD for lumbar region compared to controls were found in LADA patients and higher in T2D (p=0.008), total body BMD showed significant differences (p=0.028) and no significant differences were found in the femur BMD. 3D-DXA analysis showed the trabecular content as volumetric BMD (vBMD) tended to be lower in T2DM, although only in the greater trochanter had statistical significance (p=0.005). Total cortical thickness showed no difference between groups, but was lower in the neck region in LADA patients compared to controls and DM2 (p=0.044).

Conclusion: This preliminary report indicates that structural differences between patients with T2D and LADA are found with 3D-DXA. Further studies are needed to establish the utility of this novel tool.

**Disclosures:** Patricia Clark, None.

## MO0196

**DXA Errors are Common and Likely Adversely Affect Clinical Care: DXA Quality Improvement is Needed.** Karen Hansen\*, Neil Binkley, Diane Krueger, Ellen Siglinsky, Jessie Libber, Erin Shives, Bjoern Buehring, University of Wisconsin, United states

Objective: Dual energy X-ray absorptiometry (DXA) is used to diagnose osteoporosis, assess fracture risk and monitor therapy. High-quality DXA requires excellence in acquisition, analysis and interpretation. However, the need for excellence is under-appreciated. Indeed, it may be perceived that DXA acquisition and reporting can be automated. Based on our clinical experience, we hypothesized that DXA errors are common. This study evaluated technical and interpretation error rates in a US clinic and explored the possibility that errors might affect clinical decision-making.

Methods: DXA scans on new patient referrals to our osteoporosis clinic were anonymously reviewed by three ISCD-certified technologists and three ISCD-certified physicians. The technologists applied performance standards from the IOF/ISCD Osteoporosis Essentials course to determine if positioning, acquisition and analysis were ideal. The physicians assessed whether the interpretation complied with ISCD reporting recommendations, determined error prevalence and whether errors were major (those providing inaccurate information potentially causing incorrect patient care decisions). All assessments were performed individually and subsequently adjudicated by the group to reach consensus.

Results: We report data on 147 patients; not all had both spine and hip scans. Technical errors were identified in 90% of patients being present in 61% of spine and 74% of hip scans. In 100 patients with prior scans, technical differences between baseline and follow up were present in 94%. The physicians concluded that interpretation errors were present in 84% overall and these errors were major in 45%; technical errors impacted interpretation in 16% of patients. Sixty-one percent of major errors were reporting incorrect BMD change; an additional 26% were reporting incorrect diagnosis.

Conclusion: This is the first US study documenting that DXA technical and interpretation errors are extremely common. These errors likely compromise patient care by prompting either excessive or inadequate lab evaluation and over- or under-utilization of medications. Improvement is imperative; interventions to provide high-quality DXA scan acquisition, analysis and reporting are needed.

**Disclosures:** Karen Hansen, None.

## MO0197

**Effect of Varying Tissue Thickness in Total Body DXA Studies in the Norland Elite Scanner.** Tom Sanchez\*<sup>1</sup>, Patrick Cunniff<sup>1</sup>, Chad Dudzek<sup>1</sup>, Joe Joyce<sup>1</sup>, Jingmei Wang<sup>2</sup>. <sup>1</sup>Norland at Swissray, United states, <sup>2</sup>Norland at Swissray, China

Changes in hardware and software can introduce changes in how a DXA system performs. In the case of DXA technology performing body composition studies, how the new scanner manages detector saturation or starvation or corrects for beam hardening affects with variations in tissue thickness can impact DXA studies. The current study examines the effect of varying tissue thickness in total body DXA studies on the new Norland Elite Scanner.

A series of ten total body scans evaluating bone, lean and fat mass were performed at six different scan settings on a Norland Model XR-800 and a Norland Elite scanner

using three different maximum tissue thickness levels (configuration 1=118mm, configuration 2=208mm and configuration 3=308mm). Absolute equivalence in the resulting assessments of bone, lean and fat made by the two systems was assessed by evaluating the ratio of measurements made on the Elite to measurements made on the XR-800. Repeatability in bone, lean and fat was assessed by comparing coefficient of variation in bone, lean and fat at various thicknesses and scan settings.

Examining the ratios computed from results from the Elite and the XR-800 shows that the results obtained on the two systems are very similar—within 2%—when speed and resolution were similar. Repeatability for bone, lean and fat expressed as a coefficient of variation was within expected values and ranged between 0.1% and 1.2% for bone, 0.5% and 2.0% for lean and 0.5% and 1.3% for fat.

In conclusion, the results show a consistency in measurement of bone, lean and fat in the two scanners and support the claims for accuracy and precision in the Elite scanner. The results also support a claim that reference sets developed for earlier models of Norland scanners can be applied on the Elite scanner without adjustment or modification.

**Relative Elite to XR-800 Body Composition Results at different scan settings and tissue thicknesses**

	BMD			Lean			Fat		
	Conf1	Conf2	Conf3	Conf1	Conf2	Conf3	Conf1	Conf2	Conf3
6.5x13,260	100.40	101.56	99.09	101.99	101.03	101.23	98.24	99.33	100.19
6.5x13, 130	99.52	101.50	99.89	101.31	99.86	101.54	99.63	101.83	100.29
4.5x9, 260	100.60	99.63	99.91	100.74	100.91	101.72	98.24	99.73	99.68
4.5x9, 130	100.85	98.81	99.51	101.27	100.89	101.54	98.27	99.82	99.73
2.8x7.8, 200	99.97	100.14	101.80	100.63	101.16	101.15	101.91	98.93	98.90
2.8x7.8, 100	99.38	99.89	99.19	100.75	100.79	101.57	98.08	100.50	100.25

Table

**Disclosures:** Tom Sanchez, None.

This study received funding from: Norland at Swissray

## MO0198

**i-Gyne: A tablet, web-based tool for integrating osteoporosis research and health care delivery in a gynecological clinic.** Win Pa Pa Thu\*<sup>1</sup>, Susan Jane Sinclair Logan<sup>2</sup>, Lay Wai Khin<sup>3</sup>, Saw Myat Sabai<sup>4</sup>, Yue Luna Wang<sup>4</sup>, Yean Ling Mayvien Teo<sup>4</sup>, Stephen Fearn Smagula<sup>5</sup>, Jane A. Cauley<sup>6</sup>, Eu-Leong Yong<sup>4</sup>. <sup>1</sup>Department of Obstetrics & Gynaecology, National University of Singapore (NUS), Singapore, Singapore, <sup>2</sup>Department of Obstetrics & Gynaecology, National University Hospital (NUH), Singapore, Singapore, <sup>3</sup>Singapore Institute for Clinical Sciences - A\*STAR, Singapore, Singapore, <sup>4</sup>Department of Obstetrics & Gynaecology, National University of Singapore (NUS), Singapore, Singapore, <sup>5</sup>Department of Psychiatry, Western Psychiatric Institute & Clinic, University of Pittsburgh Medical Center (Pennsylvania), United States of America, United states, <sup>6</sup>Department of Epidemiology, University of Pittsburgh (Pennsylvania) Graduate School of Public Health (GSPH), United States of America, United states

Purpose: Many women consider their gynaecologist their primary physician. This will increase as family medicine grapples with rapid aging. Adopting a life course approach, gynaecology should deliver holistic care to mid-life women. Since the 1970s, a 5 x increase in hip fractures in this group has occurred in Singapore. As part of a comprehensive evaluation, patients were assessed for osteoporosis (OP) & clinical risk factors which may be associated with bone mineral density (BMD). A data collection tool was developed in order to consolidate the assessment & data management. We report on methodology & findings from the first 512 participants.

Method: The cohort comprised 45-69 year olds attending gynaecology clinics for wellness checks, excluding cancer. The study used i-Gyne, an automated, web-based tool collecting data relating to OP by validated questionnaires. All participants underwent biophysical assessment (height, weight, waist/hip circumference, blood pressure & pulse) & completed a Short Physical Performance Battery (including grip strength). Whole body BMD was measured by Dual-Energy X-ray Absorptiometry with asian reference. Subjects entered responses into tablets. Stored on password-protected hospital servers, the data was automatically analysed using decision tree matrices with threshold cut-off values for various health conditions. A patient summary was generated.

Results: Femoral neck & spinal OP was reported in 8.2% & 6.8% women, respectively. The i-Gyne synthesised information, reporting the woman's 10 year fracture risk. In the clinical setting, the report enabled a rapid & comprehensive assessment of the woman's holistic well-being including information on concomitant health issues, medication use & lifestyle factors. In the research setting, the incorporated prompts prevented missing/invalid data entry & data entry errors. Since its debut, missing values of i-Gynae is 0.9%.

Conclusion: The i-Gyne's comprehensive assessment has enabled the integration of osteoporosis research and health care delivery in gynecology, facilitating the identification of our women's bone health needs. We anticipate the summary, with fracture risk prediction and clinical recommendations, will enhance health care delivery. Concurrently, the quality of data, captured across multi-systems, will advance knowledge on factors associated with poor bone outcomes in Asian women, guiding the development of innovative interventions in this important health area.

Disclosures: *Win Pa Pa Thu, None.*

**MO0199**

**Is spine L1-L4 TBS the best vertebrae combination to predict major Osteoporotic Fracture? The OsteoLaus Cohort Study..** Hanza Mraihi\*, Olivier Lamy, Marie Metzger, Berengere Aubry-Rozier, Delphine Stoll, Didier Hans. Center of Bone disease - Lausanne University Hospital, Switzerland

Introduction: The international guidelines recommend to use the average bone mineral density (BMD) over L1 to L4 in the management of osteoporosis and prediction of fracture. Exclusion of certain vertebrae is recommended according to specific rules (ISCD position). The spine Trabecular Bone score (TBS), a surrogate of bone micro-architecture, has been newly introduced into international guidelines and the FRAX® tool for clinical use in conjunction with BMD and clinical risk factors. The aim of this study is to test several TBS vertebrae combinations in regard to major osteoporotic fracture prediction.

Methods: The osteoLaus cohort (Lausanne, Switzerland) included 1500 woman 50 to 80 years old. All women had a detailed questionnaire related to clinical risk factors and treatment known to influence bone metabolism, BMD measurement (hip, spine and whole body), vertebral fracture assessment and TBS. The primary outcome was the prevalence of major osteoporotic fracture (MOF) according to TBS per-vertebral combination. Appropriate statistics and necessary adjustment for confounding factors were performed. L1-L4 TBS was used as reference value.

Results : Out of 1'466 women included in the study (mean age 64.5±7.6 years, BMI 25.7±4.4), 12.7% suffered from MOF. The adjusted (age & glucocorticoids status) odd ratios per standard deviation decreased (OR) were 1.53 (1.29 – 1.80) and 1.80 (1.50 – 2.15) for the spine and total femur BMD respectively. For TBS the corresponding OR and area under the curve of different combination of vertebrae vary from 1.53 (1.29-1.82) / 0.68 for L3-L4 to 2.16 (1.8 -2.58) / 0.73 for L1-L2 whereas it is 1.98 (1.65 – 2.36) / 0.71 for L1-L4. Results for L1-L2 were significantly better than L3-L4 (p<0.0002). The combination L1-L2 tends to be higher than L1-L4 but did not reach the statistical significance.

Conclusion: It seems that excluding L4 tends to improve the fracture risk prediction. TBS is very sensitive to vertebra positioning (e.g. projection). To compensate for the natural lordosis of the spine, one has to lift the legs of the patient. L4 is often still angled which could explain such results. Further prospective studies are needed to confirm these results.

	OR (95% CI)	AUC (95% CI)	p<0.05 vs L14TBS	p<0.05 vs L12TBS
<b>L1-2TBS</b>	<b>2.16 (1.80-2.58)</b>	<b>0.73 (0.69-0.76)</b>	ns	
L1-3 TBS	2.09 (1.74-2.50)	0.72 (0.68-0.75)	ns	ns
L1-4 TBS	1.98 (1.65-2.36)	0.71 (0.67-0.75)	-	ns
L2-3 TBS	1.92 (1.61-2.29)	0.70 (0.66-0.74)	ns	0.04
L2-4 TBS	1.81 (1.52-2.17)	0.69 (0.65-0.73)	0.001	0.001
L3-4 TBS	1.53 (1.29-1.82)	0.68 (0.65-0.72)	0.0002	0.0002

Table TBS combination -

Disclosures: *Hanza Mraihi, None.*

**MO0200**

**Is vBMD from 3D Hip analysis of a standard proximal femur DXA scan related to aBMD at the hip?.** Belinda Beck\*, Amy Harding, Benjamin Weeks, Steven Watson. Griffith University, Australia

Introduction: Traditional DXA estimates of areal BMD (aBMD) are routinely criticized for an inability to represent true volumetric BMD (vBMD), to account for bone morphology, and to distinguish cortical from trabecular bone. Software developed for the recently-released Stratos DR/Medix DR DXA (DMS Group, Mauguio, France) derives proximal femoral vBMD and morphology by reconstructing a 3D image from a standard DXA scan of the hip. The method has been validated against CT images. The purpose of the current study was to determine whether DXA-derived hip aBMD bears any relation to DXA-derived 3D hip vBMD.

Methods: Postmenopausal women with low bone mass (T-score <-1.0, screened for conditions and medications that influence bone and physical function) were recruited. Right and left proximal femora were scanned for aBMD, then vBMD was derived using the 3D Hip analysis software (DMS Group, France). Correlation analyses were conducted between aBMD and vBMD of the femoral neck (FN), greater trochanter and total hip, including cortical and trabecular envelopes. Mean aBMD and vBMD values were compared using T-test analyses.

Results: Fifty-one postmenopausal women (64.1±4.3 yrs, 161.6±6.0 cm, 63.6±10.4 kg, T-score -2.0±0.6) qualified and were scanned. No relationship was

observed between FN aBMD and FN vBMD (r=0.078, NS). FN aBMD was related to FN trabecular (r=0.454, P=0.001) but not cortical vBMD. There were no relationships between aBMD and vBMD for the total hip (r=0.145, NS), or trochanteric (r=0.159, NS) regions including trabecular and cortical compartments. Absolute aBMD and vBMD in each of the hip regions exhibited large significant differences (FN aBMD 0.6946 g/cm<sup>2</sup> vs vBMD 0.2999 g/cm<sup>3</sup>, P>0.001; trochanteric aBMD 0.5834 g/cm<sup>2</sup> vs vBMD 0.1965 g/cm<sup>3</sup>, P>0.001; total hip aBMD 0.8076 g/cm<sup>2</sup> vs vBMD 0.2667 g/cm<sup>3</sup>, P>0.001).

Discussion: Findings indicate that DXA-derived hip aBMD differs markedly from DXA-derived 3D hip vBMD in postmenopausal women with low bone mass.

Disclosures: *Belinda Beck, None.*

**MO0201**

**The Clinical Use of Trabecular Bone Score for Major Osteoporotic Fracture Prediction in Chinese Older People: The Mr. OS and Ms. OS Cohort Study in Hong Kong.** Yi Su<sup>1</sup>, Jason Leung<sup>2</sup>, Timothy Kwok<sup>\*2</sup>. <sup>1</sup>Department of Medicine & Therapeutics, Prince of Wales Hospital, The Chinese University of Hong Kong, Hong Kong, <sup>2</sup>Jockey Club Centre for Osteoporosis Care & Control, The Chinese University of Hong Kong, Hong Kong

Trabecular bone score (TBS) has been shown to well predict the major osteoporotic and hip fractures in older men and women. The recommendation on how to incorporate TBS in clinical practice still need to be further explored and validated. Our aim was to validate and propose a practical risk category for the clinical use of TBS.

BMD and TBS were estimated on AP spine DXA scans obtained at the baseline visit for 2000 men and 2000 women aged 65 years or above enrolled in Mr. OS and Ms. OS cohort in Hong Kong. The subjects were followed up for the major osteoporotic fracture with an average period of 9.94 and 8.82 years in men and women, respectively. Fracture risk thresholds were evaluated based on the BMD categories (normal, osteopenia or osteoporosis) and TBS tertiles. The major osteoporotic fracture incidence rates were calculated for each combined category and the risks were evaluated using the Poisson regression model with the rate ratios (RRs). The TBS added risk category was compared with the BMD high risk category (osteoporosis) on the fractures risk prediction, evaluated by the sensitivity, the specificity, and the area under the receiver-operating characteristic curve (AUC). The risk category of TBS based on 14 prospective cohorts was validated.

The incidence rates of the major osteoporotic fracture were gradually increased with the increased risk categories of BMD and TBS in both men and women. Compared with the lowest risk category (normal BMD and highest TBS), the RR (95%CI) of osteoporosis with the lowest TBS was 10.30 (5.02 – 21.13) and 3.47 (1.75 – 6.90) in men and women, respectively. The fracture incidence rate of osteopenia men with lowest TBS was significantly higher than that of normal men, with RR (95%CI) of 4.72 (2.36 – 9.44). To predict the major osteoporotic fracture in men, osteopenia with lowest TBS added with osteoporosis had additive predictive power than osteoporosis alone, with the mean AUC significantly increased from 0.606 to 0.663. The sensitivity was increased from 31.7% to 60.3% with a decreased specificity from 89.5% to 72.3%. The similar and significant improvement was also found in the hip fracture prediction in men. The fractures prediction outcomes in women were not changed whether osteopenia with lowest TBS was considered or not. The use of TBS category from the combined cohorts for fractures prediction was similar to ours.

TBS is helpful to identify osteopenic men at risk of osteoporotic fractures in the clinical use.

Disclosures: *Timothy Kwok, None.*

**MO0202**

**The Effect of Rotation, when Positioning the Head, on DXA Measured Bone Mineral in the Mandible.** Chad Dudzek<sup>1</sup>, Patrick Cunniff<sup>1</sup>, Tom Sanchez<sup>1</sup>, Jingmei Wang<sup>\*2</sup>. <sup>1</sup>Norland at Swissray, United states, <sup>2</sup>Norland at Swissray, China

The DXA assessment of the mandible is showing good promise as a means to swiftly assess change in bone mineral but requires careful positioning of the mandibles within the x-ray beam path. The current study evaluates the impact of degrees of rotation on the DXA based assessment of bone mineral in the Body region of the mandibles.

Scans were performed on a skull securely fixed to a positioning platform that allowed for rotation of the skull on the sagittal plane while performing a mandible study on the Norland XR-800. To assess the impact of position on the mandible study the human skull underwent six scans, without repositioning, in the preferred orientation—with the sagittal plane perpendicular to the x-ray beam—and then had follow up sets of six scans at positions incrementing at plus or minus 2.5° until scans were being performed at plus or minus 20° from the desired orientation. When complete scans were analyzed with software that intelligently identified the body search region of the mandible and then intelligently fixed the body region in the scan. Once the initial scan had been analyzed the particular location of the body region was logged in the system and all subsequent scans of that patient would have the region located in the same area for follow up. Analysis of a significant difference with rotation was carried out by an analysis of variance.

The studies show that relative to the assessment at the 0° position only the studies at the 12.5° and 15° positions showed substantial bone density differences in the body region of the mandible. As such, when studies are performed with care to have no greater than a plus or minus 10° rotation, studies should be reasonably comparable to studies done at the 0° position.

	0°	2.5°	5°	7.5°	10°	12.5°	15°	17.5°	20°
Body BMD	1.213	1.258	1.173	1.329	1.176	0.849	0.706	1.147	1.220
Position	0°	-2.5°	-5°	-7.5°	-10°	-12.5°	-15°	-17.5°	-20°
Body BMD	1.220	1.228	1.097	1.200	1.252	1.210	1.228	1.26	1.275

Table

**Disclosures:** Jingmei Wang, None.

This study received funding from: Norland at Swissray

## MO0203

**Adding VFA to DXA Produces Unique Information Not Duplicated by other Measures.** Jay Ginther\*, Cedar Valley Bone Health Institute of Iowa, United states

### Problem

Published studies have demonstrated that adding VFA to DXA identifies more patients with increased fracture risk than DXA alone. Not clear is how to screen for those patients for whom VFA is appropriate.

This study attempts to determine if some test, other than VFA, could duplicate the additional information, and identify the additional OP patients identified by performing VFA on ALL first-time patients. This study looked at FRAX, Height Loss (HL), documented back pain (BP), and non-vertebral Fragility Fractures (FF). Patients were stratified by age. Spinal Deformity Index correlation to yes/no VF and kyphosis was explored.

### Methods

VFA was performed on every DXA patient at their first visit from March 2010 through September 2013. 1259 patients were evaluated with VFA for the first time. 1065 women and 194 men with a mean age of 65 years. All DXA and VFA were read by the same ISCD Certified clinician.

### Results

By DXA alone 558 (44.3%) were OP, 509 (40%) L, and 192 (15%) N. Adding VFA resulted in 1010 (80%) OP, 187 (15%) L, and 62 (5%) N. Adding VFA increased OP by 452 patients (36% of the original total).

83 N patients were changed to OP. 4 had a grade 3 Vertebral Fracture (VF), 31 multiple grade 2, 38 a single grade 2, and 7 at least 4 grade 1.

FRAX identified 58% of the patients with diagnosis changes, some of those outside normal FRAX settings.

Historical HL of 1.5" or more identified only 427 (34%) of our total patients, many of whom were already classified OP. HL of only 1.0" and 0.5" were needed to identify more who were changed.

Increasing age correlated with increasing incidence of OP and patients changed to OP, but no clear cut points emerged. 193 (46%) of 419 of patients aged 18-59 were changed to OP.

Documented Back Pain (BP), and Non-Vertebral Fragility Fractures (FF), when present, correlated well with grade 2 and grade 3 VF at P<.001

### Discussion

These are small numbers from a small non-academic referral practice in a largely rural state, drawing primarily from Family Medicine providers and may not be typical of other populations.

36% of our patients were misclassified by DXA alone, even when FFs were taken into account. FRAX, HL, Age, BP, and FF all failed to identify many of the patients identified by VFA. VFA on all first-time patients should be reconsidered. A larger, multicenter study of patients would help clarify these issues.

**Disclosures:** Jay Ginther, None.

## MO0204

**Bone Microstructure of Baseball Pitchers' Elbow Analyzed by HR-pQCT.** Kiyoshi Sada\*, Ko Chiba<sup>1</sup>, Shiro Kajiyama<sup>1</sup>, Narihiro Okazaki<sup>1</sup>, Ayako Kurogi<sup>1</sup>, Yusaku Isobe<sup>2</sup>, Makoto Era<sup>1</sup>, Makoto Osaki<sup>1</sup>. <sup>1</sup>Department of Orthopaedic Surgery, Nagasaki University Hospital, Japan, <sup>2</sup>Nagasaki University School of Medicine, Japan

**Introduction:** In ball pitching motion, pitchers' elbows are forced to endure tensile force on the medial elbow joint and compressive force on the lateral elbow joint. Due to the force, baseball pitchers sometimes suffer from injuries to the medial collateral ligament and osteochondritis dissecans. We investigated differences between bone microstructure of the bilateral elbow in baseball pitchers using high resolution peripheral quantitative CT(HR-pQCT).

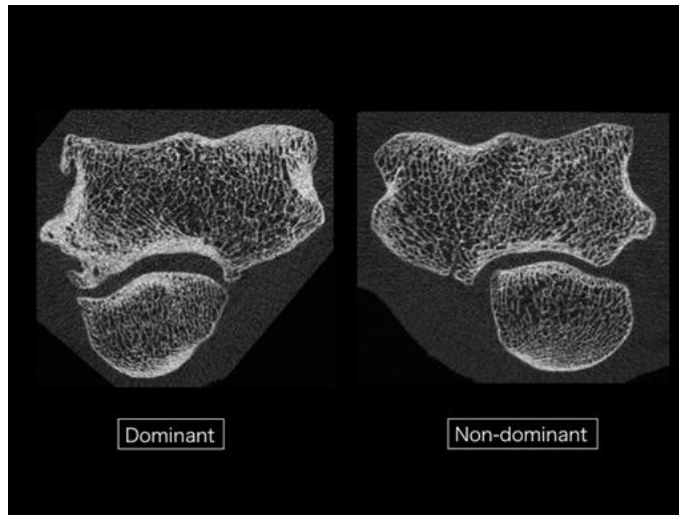
**Subjects:** Nine baseball pitchers participated in this study. They belonged to three different teams; six top-amateurs, one university players and two high school players. Their mean age was 22.5, their mean term of play was 11.3 years, right dominant pitchers were 7 and left dominant pitchers were 2.

**Methods:** We set the scanned condition of HR-pQCT (XtremeCT?, Scanco Medical) as follows; X-ray energy 68kVp/1470µA, voxel size 60.7µm. Scan length was 30.59mm in the middle of the elbow joint. In order to fix their elbow sufficiently, a

humeral cast was attached to the original cast. Bone microstructure was analyzed in bilateral humeral capitulum.

**Results:** Bone volume fraction and trabecular thickness in dominant were significantly higher than non-dominant on bone microstructure of humeral capitulum. There was no difference in trabecular number and trabecular separation.

**Conclusion:** Bone microstructure of baseball pitchers' dominant elbows was different from non-dominant elbow. These differences may derive from the compressive force exerted when pitching a ball.



elbow

**Disclosures:** Kiyoshi Sada, None.

## MO0205

**Calcaneal BMD Estimation with Foot-Size Dependent Ultrasound Measurements.** Emily Stein\*<sup>1</sup>, Fernando Rosette<sup>1</sup>, Gangming Luo<sup>2</sup>, Mariana Bucovsky<sup>1</sup>, Jonathan Kaufman<sup>2</sup>, Elizabeth Shane<sup>1</sup>, Robert Siffert<sup>3</sup>. <sup>1</sup>Columbia University College of Physicians & Surgeons, United states, <sup>2</sup>CyberLogic, Inc., United states, <sup>3</sup>The Mount Sinai School of Medicine, United states

The objective of this study was to evaluate a new clinical ultrasound (US) device in terms of its ability to estimate calcaneal BMD, and to evaluate its short-term precision. We previously presented results using a laboratory prototype that demonstrated the utility of foot-size dependent US measurements for estimating BMD. In this study, a new clinical device (QRT 250, Fig. 1) implements the foot-size dependent heel positioning system with dual-motor driven lead screws that automatically position the ultrasound transducers at the desired calcaneal region-of-interest. This positioning is designed to account for the relatively high degree of calcaneal BMD heterogeneity. The device measures in thru-transmission the net time delay (NTD) and mean time duration (MTD) parameters. NTD is defined as the difference between the transit time of an ultrasound pulse through overlying soft-tissues and calcaneus, and the transit time through soft tissue only of equal overall distance. MTD is a measure of the time duration of an initial temporal cycle of the received waveform and is related to BUA. The entire test with the new QRT 250, including positioning and US measurements, requires about a second. A linear regression of the product of NTD · MTD is used to provide an estimate of calcaneal BMD that would be measured by DXA. A clinical IRB-approved study was carried out in which 90 adults (age range 21-84, 57% female) were measured at the calcaneus using ultrasound and DXA (Lunar GE PIXI, Madison, WI). In addition, ten (10) subjects were each ultrasonically measured five (5) times with full foot repositioning, and the short term precision was evaluated. BMD<sub>DXA</sub> ranged from a low of 0.43 g/cm<sup>2</sup> to a high of 0.92 g/cm<sup>2</sup>. A linear regression showed that BMD<sub>US</sub> = 0.47 · [NTD · MTD] + 0.070 and that the linear correlation between BMD<sub>DXA</sub> and BMD<sub>US</sub> was 0.91 (P<0.0001). We found that calcaneal ultrasound measurements yield results that are very closely associated with those from DXA. In the short-term precision study, we found that the mean percent precision was 1.43%. This is similar to the short-term reproducibility of DXA scanners. In conclusion, although x-ray methods can estimate BMD, osteoporosis remains one of the world's most undiagnosed diseases. This research should enable significant expansion of the identification of bone loss as occurs in osteoporosis using an inexpensive radiation-free ultrasonic device that can serve as a proxy for BMD<sub>DXA</sub> at the calcaneus.



Fig. 1. QRT 250 Ultrasound Calcaneal Device

**Disclosures:** Emily Stein, None.

This study received funding from: CyberLogic, Inc.

## MO0206

**Clinical Application of Bone Quality Assessment Using Scanning Confocal Acoustic Navigation (SCAN).** Jian Jiao\*<sup>1</sup>, Marie Gelato<sup>2</sup>, Wei Lin<sup>1</sup>, Xiaofei Li<sup>1</sup>, Yi-Xian Qin<sup>1</sup>. <sup>1</sup>Biomedical Engineering, Stony Brook University, United States, <sup>2</sup>Department of Endocrinology, Stony Brook University, United States

Among osteoporotic fractures, hip, distal radius and lower limb fractures are the most common fractures that are the primary sources of hospitality for elderly patients. Hip fracture is best predicted by the "Golden Standard" Dual X-ray absorptiometry (DXA) measurements directly at the proximal femur. Quantitative ultrasound (QUS), as an alternative free of ionizing radiation, has been developed to measure bone structural and mechanical properties. QUS measurements at different body extremities have shown different performance, QUS at either calcaneus or radius has shown predictive power for hip fracture. No study has combined QUS at both calcaneus and distal radius to assess bone quality comprehensively. In this study, it is hypothesized that osteoporosis can generate systematic loss, thus bone mass at wrist and heel is correlated, which can be easily accessed by ultrasound scanning with custom-built Scanning Confocal Acoustic Navigation (SCAN) system.

A SCAN system, which contains two linear transducers (each transducer has 64 elements, center frequency is  $1.1 \pm 0.15$  MHz, one serves as transmitter, the other as receiver), data controller, and a water tub (Fig. 1), was used to scan the distal radius and calcaneus of recruited 44 human subjects [Control group age:  $31.93 \pm 11.55$  (n=14), Osteoporotic group age:  $69.40 \pm 2.07$  (n=30), only 5 DXA data was reported in this abstract]. In the control group, the ultrasound attenuation data (ATT) was analyzed based on different age groups (Junior Males (N=7), Junior Females (N=5), Senior Females (N=2)). There is significant QUS difference between subject 4 (Ref: control group) and subject 18 (Ref: Femoral Head T score: -2.5, BMD:  $0.7 \text{ g/cm}^2$ ), comparing the ultrasound attenuation  $50.32 \pm 0.54 \text{ dB}$  to  $30.66 \pm 0.10 \text{ dB}$  (Figure 2). There is significant difference between junior males and junior females distal radius attenuation, and junior females and senior females attenuation at central calcaneus, indicating that junior males have stronger bones than junior females at distal radius and junior females have stronger bones than senior females at calcaneus (Table 2). SCAN can distinguish bone quality differences in genders, ages, and osteoporosis. It is thus can be used as a method to predict bone fracture. Future studies will be focused on more scanning of osteoporotic patients, data analysis concerning to more ultrasound parameters, and building a model to predict hip and spine fracture using QUS at distal radius and calcaneus.



Figure 1. (A) Distal radius scanning; (B) Calcaneus scanning

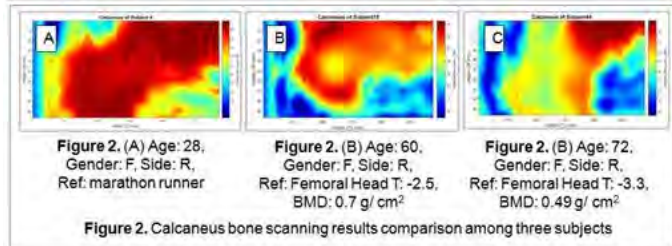


Figure 2. (A) Age: 28, Gender: F, Side: R, Ref: marathon runner, BMD:  $0.7 \text{ g/cm}^2$ . Figure 2. (B) Age: 60, Gender: F, Side: R, Ref: Femoral Head T: -2.5, BMD:  $0.7 \text{ g/cm}^2$ . Figure 2. (C) Age: 72, Gender: F, Side: R, Ref: Femoral Head T: -3.3, BMD:  $0.49 \text{ g/cm}^2$ .

Figure 2. Calcaneus bone scanning results comparison among three subjects

Table 1. Comparison between control group and osteoporotic group

Group	Age	Calcaneus ATT (dB)	Distal Radius ATT (dB)	BMI	Spine BMD (g/cm <sup>2</sup> )	Femoral Head BMD (g/cm <sup>2</sup> )
Control	$31.93 \pm 11.55$	$40.68 \pm 5.47$	$47.76 \pm 3.41$	N/A	N/A	N/A
Osteoporotic	$69.40 \pm 2.07$	$34.18 \pm 6.76$	$45.95 \pm 4.76$	$28.83 \pm 4.78$	$0.79 \pm 0.12$	$0.67 \pm 0.11$

Table 2. ATT comparison among three groups in control group

Group	Radius ATT (dB)	Calcaneus ATT (dB)
Junior Males (N=7)	$50.00 \pm 2.97^*$	$42.77 \pm 4.28$
Junior Females (N=5)	$46.13 \pm 2.28^*$	$40.68 \pm 5.92^*$
Senior Females (N=2)	$43.99 \pm 0.14$	$33.39 \pm 1.55^*$

The schematics and results of Scanning Confocal Acoustic Navigation (SCAN)

**Disclosures:** Jian Jiao, None.

This study received funding from: NSBRI through NASA Cooperative Agreement NCC9-58

## MO0207

**Comparative value of Vertebral Fracture Assessment and conventional spine radiography in the evaluation of vertebral fractures: a meta-analysis.** Frank Malgo\*<sup>1</sup>, Natasha Appelman-Dijkstra<sup>1</sup>, Olaf Dekkers<sup>2</sup>, Neveen Hamdy<sup>1</sup>. <sup>1</sup>Center for Bone Quality & Department of Medicine; Division Endocrinology, Leiden University Medical Center, Netherlands, <sup>2</sup>Department of Medicine; Division Endocrinology & Department of Clinical Epidemiology, Leiden University Medical Center & Department of Clinical Epidemiology, Aarhus University Hospital, Netherlands

**BACKGROUND:** Vertebral fractures are associated with increased morbidity. Conventional radiography of the spine is considered to be the "gold standard" for diagnosing vertebral fractures. Vertebral Fracture Assessment (VFA) is a tool incorporated in Dual Energy X-ray Absorptiometry which enables the evaluation of vertebral fractures at the same time as measuring Bone Mineral Density (BMD). We conducted a systematic review of the value of VFA compared to conventional spine radiographs in the diagnosis of vertebral fractures.

**METHODS:** We searched PubMed, MEDLINE, EMBASE and Web of Science for studies evaluating the diagnostic accuracy of VFA compared to conventional spinal radiographs for the diagnosis of vertebral fractures in populations at risk for osteoporosis. We included studies with available data on sensitivity and specificity, in adult patients at risk or osteoporosis, using Genant's semi-quantitative method of evaluating vertebral fractures. A risk of bias analysis was performed and sensitivity and specificity were pooled in a random effects model and estimated per vertebra analysis and per person.

**RESULTS:** 14 studies were included, comprising a total of 2968 patients (80% female). Mean age ranged from 45 to 74.2 years. 8 studies had an intermediate and 6 a low risk of bias. However, the studies had variable inclusion criteria, patient characteristics and protocols. The prevalence of vertebral fractures  $\geq$  grade 1 ranged from 0.8% to 32%, the prevalence of patients with a vertebral fracture ranged from 6.9% to 100%. In the per vertebra analysis, sensitivity of VFA was 0.83 (95%CI, 0.75-0.88), specificity was 0.99 (95%CI, 0.98-1.00). In the per person analysis, sensitivity was 0.87 (95%CI, 0.76-0.93) and specificity was 0.94 (95%CI, 0.88-0.97). Sensitivity of VFA to detect a vertebral fracture grade 2 or more was 0.81 (95%CI, 0.67-0.91), and specificity 0.98 (95%CI, 0.94-1.00). Sensitivity of VFA for detection of a patient with a vertebral fracture grade 2 or more was 0.91 (95%CI, 0.78-0.97), with a specificity of 0.91 (95%CI, 0.86-0.95).

**CONCLUSION:** Our findings from this meta-analysis shows that compared to conventional spinal radiography VFA has a sensitivity and specificity of both 91% for detection of vertebral fractures  $\geq$  grade 2, in a population at risk for osteoporosis. These data suggest that VFA may be of value in the screening of patients at high risk for osteoporosis for vertebral fractures.

**Disclosures:** Frank Malgo, None.

## MO0208

**Differences in Trabecular Microstructure Between African American and Caucasian Women.** Melissa S. Putman<sup>1</sup>, Elaine W. Yu<sup>1</sup>, David Lin<sup>1</sup>, Karin Darakananda<sup>1</sup>, Joel S. Finkelstein<sup>1</sup>, Mary L. Bouxsein<sup>2</sup>. <sup>1</sup>Massachusetts General Hospital, United states, <sup>2</sup>Beth Israel Deaconess Medical Center, United states

**Background:** We previously reported that African-American women have improved cortical bone microarchitecture compared to Caucasians. Individual trabecula segmentation (ITS) analysis of HR-pQCT images segments trabecular bone into individual plates and rods and computes the degree of connectivity and alignment, which may be important determinants of trabecular bone strength. We sought to determine whether there are racial differences in trabecular microstructure that may help explain the lower fracture risk in African-American women compared to Caucasians.

**Methods:** We performed ITS analyses of HR-pQCT scans (Scanco Medical AG) of the radius and tibia in 273 peri- and post-menopausal African-American (n=100) and Caucasian (n=173) women participating in the Study of Women's Health Across the Nation in Boston. To compare ITS outcomes between groups, we used independent t-tests and linear regression with multivariable adjustment for relevant clinical covariates (age, weight, tobacco and alcohol use, physical activity, diabetes, and history of HRT, osteoporosis medications, and oral glucocorticoids).

**Results:** Subjects were 59.9±2.7 years old. Caucasian women weighed less, reported greater alcohol and less tobacco use, and were less likely to have diabetes (p<0.05 for all). Trabecular bone volume (BV/TV) was higher in African-Americans at the radius on unadjusted analysis but was similar between groups at both sites after multivariable adjustment. On unadjusted analyses at both the radius and tibia, African-Americans had 10-21% greater trabecular plate volume fraction, plate thickness, plate number density, and plate surface area along with 8-13% greater axial alignment of trabeculae, while Caucasians had 8-9% greater trabecular rod tissue fraction (p<0.05 for all). Adjustment for clinical covariates augmented these race-related differences in plates and rods, such that Caucasians had greater trabecular rod number density and rod-rod connectivity, while African Americans continued to have superior plate structural characteristics and axial alignment (p<0.05 for all).

**Conclusions:** Although overall trabecular bone volume was similar, African-American women had more plate-like trabecular morphology and higher axial alignment, whereas Caucasians had more rod-like trabeculae. The greater plate-like trabeculae in African-American women likely leads to improved trabecular bone strength and may contribute to the lower fracture risk observed in African-American women.

**Table 1. ITS results of the radius and tibia for Caucasian and African-American women**

ITS Parameter	Radius		Tibia	
	Caucasian	African-American	Caucasian	African-American
Bone volume fraction (BV/TV)	0.250 ± 0.004	<b>0.265 ± 0.005*</b>	0.274 ± 0.004	0.280 ± 0.005
Plate bone volume fraction (pBV/TV)	0.085 ± 0.003	<b>0.103 ± 0.004<sup>2b</sup></b>	0.123 ± 0.003	<b>0.138 ± 0.004<sup>2b</sup></b>
Rod bone volume fraction (rBV/TV)	0.165 ± 0.002	0.162 ± 0.003	<b>0.151 ± 0.003<sup>3</sup></b>	0.142 ± 0.004
Axial bone volume fraction (aBV/TV)	0.094 ± 0.002	<b>0.106 ± 0.003<sup>2b</sup></b>	0.118 ± 0.002	<b>0.128 ± 0.003<sup>2b</sup></b>
Plate tissue fraction (pTV/BV)	0.329 ± 0.007	<b>0.378 ± 0.010<sup>2b</sup></b>	0.444 ± 0.008	<b>0.490 ± 0.011<sup>2b</sup></b>
Rod tissue fraction (rTV/BV)	<b>0.671 ± 0.007<sup>2b</sup></b>	0.622 ± 0.010	<b>0.556 ± 0.008<sup>2b</sup></b>	0.510 ± 0.011
Trab plate number density (pTbN, 1/mm)	1.36 ± 0.01	<b>1.43 ± 0.02<sup>2b</sup></b>	1.49 ± 0.01	<b>1.52 ± 0.01<sup>2b</sup></b>
Trab rod number density (rTbN, 1/mm)	<b>1.87 ± 0.01*</b>	1.84 ± 0.02	<b>1.82 ± 0.01*</b>	1.78 ± 0.02
Mean trab plate thickness (pTbTh, mm)	0.205 ± 0.001	<b>0.209 ± 0.001<sup>2b</sup></b>	0.217 ± 0.001	<b>0.222 ± 0.001<sup>2b</sup></b>
Mean trab rod thickness (rTbTh, mm)	0.212 ± 0.0004	<b>0.214 ± 0.001<sup>2b</sup></b>	0.212 ± 0.0004	0.212 ± 0.001
Mean trab plate surface area (pTbS, mm <sup>2</sup> )	0.154 ± 0.001	<b>0.160 ± 0.001<sup>2b</sup></b>	0.165 ± 0.001	<b>0.173 ± 0.002<sup>2b</sup></b>
Mean trab rod length (rTbL, mm)	0.662 ± 0.002	0.659 ± 0.003	0.651 ± 0.002	<b>0.655 ± 0.002<sup>2b</sup></b>
Rod-Rod junction density (R-R JuncD, 1/mm)	<b>3.01 ± 0.05*</b>	2.88 ± 0.08	<b>2.65 ± 0.06*</b>	2.41 ± 0.09
Plate-Rod junction density (P-R JuncD, 1/mm)	3.64 ± 0.08	3.86 ± 0.10	4.01 ± 0.07	4.04 ± 0.10
Plate-Plate junction density (P-P JuncD, 1/mm)	1.74 ± 0.05	<b>1.95 ± 0.06*</b>	2.16 ± 0.04	2.26 ± 0.05

Multivariable adjusted model included the following covariates: age, weight, any HRT use, history of osteoporosis medication use, prior significant glucocorticoid use, current tobacco and EOH use, current physical activity score, and diabetes. Values are presented as mean ± SE. \* p<0.05 on unadjusted analysis, <sup>2b</sup> p<0.05 on multivariable adjusted analysis. Bolded values indicate significantly better skeletal characteristics than the other racial group.

Table

**Disclosures:** Melissa S. Putman, None.

## MO0209

**Hidden in Plain Sight: DXA vs Plain Film X-Ray in Diagnosis of Osteopenia.** Oisín Hannigan<sup>\*1</sup>, Niamh Garry<sup>1</sup>, Maria Smyth<sup>1</sup>, Aoife Dillon<sup>1</sup>, Brendan McCarthy<sup>2</sup>, MC Casey<sup>3</sup>, Kevin McCarroll<sup>1</sup>, James Mahon<sup>4</sup>, Joe Browne<sup>1</sup>, James Bernard Walsh<sup>2</sup>, Rosaleen Lannon<sup>1</sup>. <sup>1</sup>Department of Medicine for the Elderly, St James Hospital, Ireland, <sup>2</sup>Mercers Institute for Research on Aging, St James Hospital, Ireland, <sup>3</sup>Department of Medicine for the Elderly, St James Hospital, Ireland, <sup>4</sup>Mercers Institute for Research on Aging, St James Hospital, Ireland

**Introduction:**

Osteoporosis is a major world health issue. Osteopenia is considered a precursor to osteoporosis. Osteopenia is important as the vast majority of fractures occur in individuals whose T-Scores lie within the osteopenic range<sup>2</sup>. Treatment of Osteopenia remains controversial, however more than 2 million incident osteoporosis-related fractures occurred in 2005 in people over 50, with a healthcare cost of approximately \$17billion<sup>3</sup>. DEXA has long been considered the Gold standard in diagnosing osteoporosis/osteopenia, it has been established that it can be diagnosed from X-ray. We wanted to examine the accuracy of X-Ray at diagnosis of Osteopenia.

**Methods:**

All DXAs performed in St James Hospital Dublin were retrospectively analysed for an indication of "osteopenia on X-Ray". Subsequently each DXA was reviewed and presence of osteopenia and/or osteoporosis was noted. T-scores from AP Spine,

Left Femur (Total) and Left Femur (Neck) were documented, as well as the presence of Vertebral Fractures. Data was subsequently analysed using a statistics package.

**Results:**

Of 1462 DXAs reviewed, only 114 were for Osteopenia identified on xray, 19 men and 95 women. Of these 10 subjects (8.7%) had normal T Scores, 59 (51.8%) were Osteopenic only and 45 (39.5%) were osteoporotic. Of 104 subjects with complete data, mean t-scores were in AP Spine -1.58 (+/-1.26SD), Hip(Neck) -1.506 (+/-1.029SD) and Hip(Total) -1.365(+/-1.318SD). Of 91 subjects with LVAs, only 18 vertebral fractures were detected.

**Conclusions:**

Osteopenia identified on X-ray is highly concordant with reduced BMD on DXA. Incidental diagnosis of osteopenia on X-ray represents an excellent opportunity to investigate further for osteoporosis, but in situations where DXA is not available may represent a chance to begin treatment. Prospective analysis of osteopenia on X-Ray may further establish its usefulness in this role.

**References:**

Eriksen, E.F. "Treatment of osteopenia" Rev Endocr Metab Disord (2012) 13:209-223

Burge, R. et al. "Incidence and economic burden of osteoporosis-related fractures in the United States, 2005-2025" J Bone Miner Res, 2007. 22 (3): p465-75

"Prevention and Management of Osteoporosis" WHO Technical Report Series 921, Geneva 2003

**Disclosures:** Oisín Hannigan, None.

## MO0210

**In the Heel of the Hunt: How Good is Quantitative Ultrasound in the Diagnosis of Osteoporosis?.** James Mahon<sup>\*</sup>, David Moloney, Angelina Farrelly, Deirdre Smith, Laura Mulkerrins, Maire Rafferty, Caoimhe McManus, Oisín Hannigan, Nessa Fallon, Georgina Steen, Rosaleen Lannon, MC Casey, JB Walsh, Kevin McCarroll. St James's Hospital, Ireland

**Background**

Quantitative heel ultrasound (QUS) is a low cost, highly portable, quick, and non-irradiating alternative to DXA for the diagnosis and monitoring of osteoporosis. However, correlation between QUS and DXA is ill-defined, especially in the Irish population. We set out to examine and define the relationships of QUS with DXA results, biochemical bone markers, and previous fracture history in patients attending a tertiary referral centre for osteoporosis in Ireland.

**Method**

We retrospectively identified patients attending our clinic for whom paired QUS and contemporaneous DXA were performed. We compared QUS T-scores, Broadband Ultrasonic Attenuation (BUA) and Speed of Sound (SOS) with results of DXA, fracture history and biochemical markers of bone turnover.

**Results**

2294 patients; 83% female, 17% male; mean age 67.13 years (SD 13.98). Mean BMD total hip 0.767g/cm<sup>3</sup> (SD 0.152); mean BMD spine 0.898g/cm<sup>3</sup> (SD (0.194). Linear regression analysis showed that both QUS SOS and BUA had significant positive correlation with BMD of hip and spine. The association was strongest at the hip where BUA accounted for a 35.71% variation in BMD (Rsquared adjusted, p<0.0001). For patients whose QUS T-score was ≤-2.5 (i.e. in the osteoporotic range), the odds ratio (adjusted for age, sex and BMI) for hip fracture was 2.17 (95% CI 1.66-2.88, p<0.0001); odds ratio for vertebral fracture was 1.83 (95% CI 1.44-2.30, p<0.001). QUS sensitivity and specificity for diagnosis of osteoporosis by T-score varied according to site. When compared with DXA, a QUS heel T-score of ≤-2.5 had 71.21% sensitivity and 69.78% specificity for diagnosis of osteoporosis of the hip; for osteoporosis of the spine, QUS sensitivity was 58.9%, and specificity was 73.04%. There was no significant correlation of SOS and BUA to biochemical markers of bone turnover.

**Conclusion**

QUS of heel is strongly predictive of BMD at hip and also of hip fracture and has a high sensitivity for diagnosis of osteoporosis of the hip. It is less accurate in predicting osteoporosis, BMD and fractures of the spine. Nor was it predictive of increased markers of bone turnover. Further research will be useful in identifying particular patient groups in whom QUS has highest accuracy, and establishing T-score cut-off points to formalise its utility as a screening tool for osteoporosis.

**Disclosures:** James Mahon, None.

## MO0211

**Prevalence, incidence and future fracture prediction ability of vertebral fractures differs by radiological scoring method.** Fjorda Koromani<sup>\*1</sup>, Ling Oei<sup>2</sup>, Katerina Trajanoska<sup>1</sup>, Carola Zillikens M.C.<sup>2</sup>, Arfan Ikram M.A.<sup>3</sup>, Andre G. Uitterlinden<sup>2</sup>, Edwin Oei<sup>4</sup>, Fernando Rivadeneira<sup>2</sup>. <sup>1</sup>Department of Internal Medicine & Epidemiology, Erasmus MC., Netherlands, <sup>2</sup>Department of Internal Medicine, Erasmus MC., Netherlands, <sup>3</sup>MD., PhD., Netherlands, <sup>4</sup>Department of Radiology & Nuclear Medicine, Erasmus MC., Netherlands

**Purpose:** To compare prevalence and incidence of vertebral fractures (VF) assessed by Quantitative Morphometry (QM) versus Algorithm Based Qualitative (ABQ)

scoring methods (SM) and the ability for future fracture prediction. Methods: Lateral spine radiographs (T4-L4) performed at baseline and after 13 years of follow-up (FUP) in a prospective cohort (n=5612), were assessed using QM and ABQ. Prevalent VF were assessed at baseline and incident VF at FUP. Subjects with at least one VF were defined as cases. To estimate the concordance between QM and ABQ the prevalence-adjusted bias-adjusted kappa (PABAK) was used. Analyses were also performed excluding less severe QM (grade I) fractures. Characteristics of fracture cases and controls were compared by SM (including age, sex, height, weight, BMI, falling history and FRAX variables) and in relation to LS-BMD and LS-TBS during the FUP visit. Incident non-vertebral fractures were collected from GP records and logistic regression adjusted for age, sex were used for future fracture risk estimation. Results: 758 subjects had prevalent VFs at baseline according to QM and 244 according to ABQ (PABAK = 0.75). At FUP, n= 2070, 283 new cases were identified based on QM and 129 based on ABQ (PABAK = 0.75). After recoding the QM VFs, 288 prevalent and 176 incident cases were identified (PABAK = 0.89 and 0.82 respectively). When compared at baseline, there were significantly more women among cases when scored with ABQ, but not with QM. Among incident cases, ABQ cases were significantly shorter, lighter and had more females (p-value < 0.001) but not for QM (overall or after exclusion of grade I). LS-BMD and TBS were lower in both incident QM and ABQ scored cases. Presence of VF at baseline (independent of SM) was significantly associated with increased risk for incident vertebral fracture (lowest OR 2.4; CI [1.87; 3.11]). ABQ events were associated with increased risk of any type of fracture (OR 1.32; 95% CI [1.003; 1.74]) and hip (OR 1.54; CI [1.07; 2.2]) but QM events were not significantly associated with any incident fracture type. After excluding grade I, QM was associated with increased risk of any type (OR 1.36; CI [1.06; 2.36]) and hip fracture (OR 1.67; CI [1.19; 2.36]). Conclusions: Vertebral fractures diagnosed by ABQ (despite lower prevalence and incidence) have greater prediction ability for future non-vertebral events than QM. Grade I deformities by QM do not characterize clinically relevant vertebral fractures.

**Disclosures:** *Fjorda Koromani, None.*

## MO0212

**Transitioning to Second Generation HR-pQCT: Can Cross-Calibration Improve Agreement Between HR-pQCT Systems?.** [Sarah L Manske\\*](#), [Erin M Hildebrandt](#), [Lauren A Burt](#), [Duncan Raymond](#), [Steven K Boyd](#). University of Calgary, Canada

With the availability of high resolution peripheral quantitative computed tomography (HR-pQCT) scanner, an important consideration will be whether data acquired with the second generation scanner (XCTII) are compatible with the first generation scanner (XCTI) for use in longitudinal or multi-centre studies. We sought to determine whether we can estimate XCTII data from XCTI scans, and whether estimation can be improved by cross-calibration.

60 participants (42F, 18M) aged 55-70 were scanned on the same day at the radius and tibia using standard protocols on XCTI (XtremeCT, 82.0 mm) and XCTII (XtremeCTII, 60.7 mm; Scanco Medical). Images were evaluated using the manufacturer's protocols for each generation and agreement between scanners was compared for all standard outcomes. For cross-calibration, the participants were randomly divided in two samples. The first sample was used to generate linear regression equations to predict XCTII results from XCTI scans, and the second sample was used to assess the accuracy of the predictions. Accuracy of the estimations was assessed using Bland-Altman plots, t-tests, and root-mean square error (RMSE).

In all outcomes assessed there was a strong association ( $R^2=0.49$  to  $0.99$ ) but significant, systematic differences between XCT generations. Percent RMSEs (1 to 10%) were higher than errors typically associated with precision (1 to 4%). The differences were smaller in the tibia than radius, and smaller in densitometric (e.g., trabecular BMD) and macro- (e.g., cortical area) than micro-architectural outcomes (e.g., trabecular number). After adjustment using cross-calibration equations, XCTI results were not significantly different to those of XCTII, and RMSEs (1 to 7%) were closer in magnitude to precision errors.

Aside from resolution, one of the major differences between scanner generations is the length of the scan; XCTI measures 9 mm while XCTII measures 10 mm in length. Despite these differences, we found that cross-calibration equations eliminated the systematic differences between scanners. The better agreement of densitometric compared with microarchitectural outcomes is consistent with greater precision of densitometric measures. Advanced cross-calibration curves derived using image registration will further minimize differences between measurements on each system. The current data suggest that we can estimate XCTII data from XCTI scans after applying relatively simple cross-calibration equations.

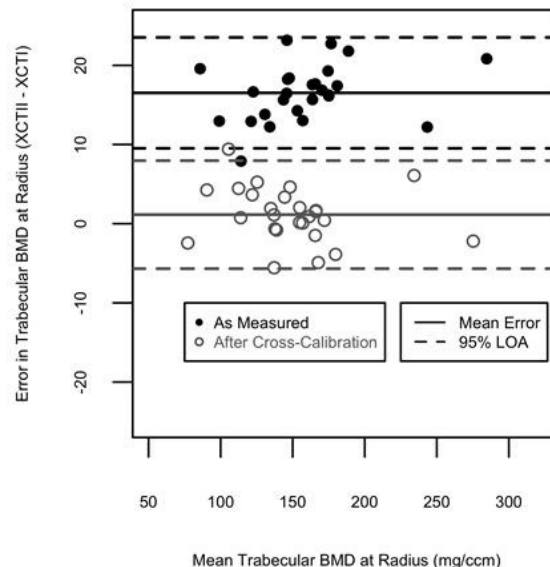


Figure - Error in Estimating XCTII TbBMD from XCTI

**Disclosures:** *Sarah L Manske, None.*

## MO0213

**Value of Transiliac Bone Biopsies Obtained in Women with Advanced Osteoporosis to Predict Prevalent Fractures and Alteration of Microarchitecture.** [Patrick Ammann\\*](#)<sup>1</sup>, [Francois Herrmann](#)<sup>2</sup>. <sup>1</sup>Division of Bone Diseases, Department of Internal Medicine Specialties, Switzerland, <sup>2</sup>Department of Internal Medicine, Rehabilitation & Geriatrics, Switzerland

Bone strength, hence fracture risk, is determined by bone geometry and microstructure. Transiliac bone biopsies are mostly relevant to evaluate effects on bone turnover of anti-osteoporotic treatments or hormonal modulation. It is less clear if they can predict the presence of prevalent fractures and in a cross sectional study predict bone loss after the menopause and with aging in women with advanced osteoporosis.

To answer these questions, we obtain transiliac bone biopsies from 257 osteoporotic women with or without prevalent fractures corresponding to the baseline value of a study evaluating treatments with strontium ranelate or alendronate (Chavassieux, 2014). Prevalent fractures, age and delay since menopause were recorded. Microstructure was evaluated by microCT using Scanco instrument. Statistical analysis used were student t test, negative binomial regression and spearman correlation ( $\rho$ ).

Mean age was 64.2 (7.1) (mean (SD)), age at menopause 48.1 (5.2), delay since menopause 16.2 (8.1) and number of prevalent fractures 0.38 (0.76). Parameters of microarchitecture were not able to discriminate between patients with or without prevalent fractures. Negative binomial regression estimating number of prevalent fractures from micro-architecture parameters were not significant. The fact that information on microarchitecture was obtained at the iliac crest could explain the failure to predict fracture occurring at other skeletal sites. Furthermore all these investigation were performed in women with an established osteoporosis and falls are stochastic events resulting in a fracture. BV/TV (-0.19 (Spearman's  $\rho$ ) < 0.0016 (p)), Tb.N (-0.29, < 0.0001), Tb.Th (ns), Tb.Sp (+0.28, < 0.0001) and Ct.Th (ns) were associated with delay since menopause. BV/TV (-0.16, < 0.0096), Tb.N (-0.30, < 0.0001), Tb.Th (ns), Tb.Sp (+0.27, < 0.0001) and Ct.Th (ns) were associated with the age of the women. Thus there are significant correlations between micro-architecture and women age and years since menopause.

Transiliac bone biopsies obtained in 257 women with established menopause are an excellent tool to evaluate modification of bone turnover and evolution of bone micro-architecture but unable to detect women with prevalent fracture.

**Disclosures:** *Patrick Ammann, None.*

*This study received funding from: Servier laboratory*

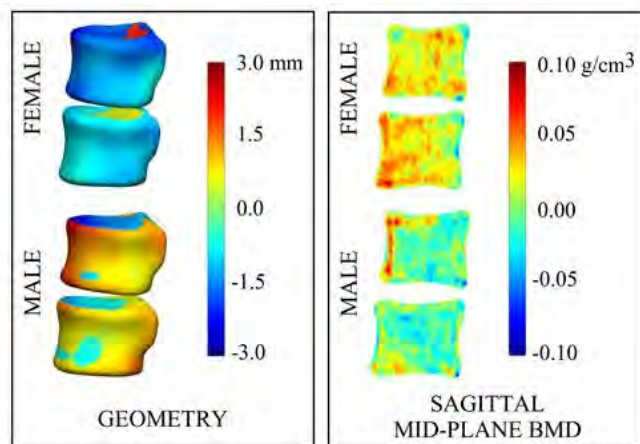
## MO0214

**Vertebral Fracture is Associated with Decreased Size and Increased Volumetric BMD in Females and with Increased Size and Decreased Volumetric BMD in Males.** Jessica Coogan<sup>1</sup>, Travis Eliason<sup>1</sup>, Elizabeth Atkinson<sup>2</sup>, Eric Orwoll<sup>3</sup>, Ellen Quillen<sup>4</sup>, Daniel Nicoletta<sup>1</sup>, Sundeep Khosla<sup>2</sup>, Todd Bredbenner<sup>\*1</sup>. <sup>1</sup>Southwest Research Institute, United states, <sup>2</sup>Mayo Clinic, United states, <sup>3</sup>Oregon Health & Science University, United states, <sup>4</sup>Texas Biomedical Research Institute, United states

The structural integrity of bone is a complex function of interrelated characteristics, including macroscopic bone morphology and bone density. We hypothesize that a subset of composite traits based on QCT data of the L1-L2 spine segment are associated with subsequent vertebral fracture and that different subsets of composite traits are associated with vertebral fracture for male and females. Baseline QCT data were obtained for males and females with and without subsequent vertebral fractures in L1- L3 (19 males with fractures, 19 males without fractures, 19 females with fractures, and 19 females without fractures; males:  $57.4 \pm 11.0$  years, females:  $58.9 \pm 15.3$  years) [1]. Using established methods [2], a statistical shape and trait model was created for the L1-L2 segment describing vertebral body geometry, intervertebral orientation, and the volumetric BMD (vBMD) distribution within the 76 lumbar segments. Different baseline patterns of geometry and vBMD distribution were observed for males and females with and without subsequent vertebral fractures (Figure 1). Females that suffered a subsequent fracture demonstrated a general decrease in vertebral body size and increase in vBMD and converse changes were associated with fracture risk in males. Stepwise logistic regressions were used to determine the relationship between the 75 composite traits and subsequent fracture for males and females separately. Five composite traits (describing 9.2% of the total variability) were associated with subsequent fracture in males. Six composite traits (describing 5.7% of the total variability) were associated with subsequent fracture in females and there was no overlap between the subsets of composite traits selected for males and females. Age and BMI were not significantly related to the occurrence of subsequent fracture. This preliminary work suggests that composite traits will differentiate between males and females that suffer subsequent vertebral fractures and those that do not. Identifying differences in composite traits that are associated with vertebral fracture risk in men and women reinforces the importance of investigating sex-based differences in the structural organization of vertebrae in moving towards improved diagnostic methods and individualized treatment for fracture risk.

## References:

- [1] Riggs, BL, et al. J. Bone Miner Res, 19:1945-1954, 2004.  
[2] Bredbenner TL, et al. J. Bone Miner Res, 29:2090-2100, 2014.



**Complex patterns of baseline L1-L2 geometry and BMD distribution are associated with fracture and these patterns are different in males and females.** (Color contours represent point-wise differences in the mean vertebral bodies of individuals that suffered a subsequent fracture involving L1-L3 with respect to vertebral bodies of those that did not.)

Figure 1

**Disclosures:** Todd Bredbenner, None.

## MO0215

**A Genome-wide Association Study Identifies Gender Specific Loci Influencing aBMD and BMC at Multiple Skeletal Sites in Children of European Descent.** Alessandra Chesì<sup>\*1</sup>, Jonathan Mitchell<sup>1</sup>, Heidi Kalkwar<sup>2</sup>, Jonathan Bradfield<sup>1</sup>, Joan Lappe<sup>3</sup>, Shana McCormack<sup>1</sup>, Vicente Gilsanz<sup>4</sup>, Sharon Oberfield<sup>5</sup>, Hakon Hakonarson<sup>1</sup>, John Shepherd<sup>6</sup>, Andrea Kelly<sup>1</sup>, Babette Zemel<sup>1</sup>, Struan Grant<sup>1</sup>. <sup>1</sup>Children's Hospital of Philadelphia, United states, <sup>2</sup>Cincinnati Children's Hospital Medical Center, United states, <sup>3</sup>Creighton University, United states, <sup>4</sup>Children's Hospital of Los Angeles, United states, <sup>5</sup>Columbia University, United states, <sup>6</sup>UCSF, United states

Failure to achieve optimal bone mineral accretion during the critical period of growth results in suboptimal peak bone mass and contribute to low bone mass and osteoporosis later in life. To identify novel genetic factors influencing pediatric bone mass at discrete skeletal sites, we performed a sex-stratified genome-wide association study of areal bone mineral density (BMD) and bone mineral content (BMC) measured by dual energy x-ray absorptiometry at the femoral neck, hip, spine and one-third distal radius, in a cohort of 933 healthy European American children (488 girls and 445 boys). We tested signals with  $P < 5 \times 10^{-5}$  and MAF  $> 0.05$  for replication in an independent, same-age cohort of 486 European American children (245 girls and 241 boys). In females, three loci yielded a nominally significant  $P$ -value in the replication cohort and a genome-wide significant combined  $P$ -value: a known bone locus nearest 'cadherin-like and PC-esterase domain containing 1' (*CPEDI*) for radius BMD (top signal rs67991850, comb  $P = 8.91 \times 10^{-12}$ ,  $\beta = -0.35$ , MAF=0.37) and two novel loci, rs1957429 nearest 'spectrin, beta, erythrocytic' (*SPTB*) for radius BMD (comb  $P = 5.97 \times 10^{-9}$ ,  $\beta = 0.44$ , MAF=0.13) and rs9991779 nearest *LOC101928509* for total hip BMC (comb  $P = 2.88 \times 10^{-8}$ ,  $\beta = 0.28$ , MAF=0.23). In males, an additional novel locus was nominally significant in the replication cohort and genome-wide significant when combining discovery and replication: rs184374109 nearest *IZUMO* family member 3 (*IZUMO3*) for spine BMD (comb  $P = 1.18 \times 10^{-8}$ ,  $\beta = -0.74$ , MAF=0.05). In a combined analyses of both genders, three loci brought forward from the discovery cohort were nominally significant in the replication cohort and yielded genome-wide significant combined  $P$ -values: the same locus identified in females near *CPEDI* for radius BMD (top signal rs6963115, LD with rs67991850=0.90, comb  $P = 3.89 \times 10^{-12}$ ,  $\beta = -0.26$ , MAF=0.40), rs34652660 in a novel locus nearest TATA-box binding protein like 2 (*TBPL2*) for femoral neck BMD ( $P = 1.45 \times 10^{-8}$ ,  $\beta = 0.20$ , MAF=0.48) and rs149529198 nearest 'family with sequence similarity 3 member C' (*FAM3C*) for femoral neck BMC ( $P = 1.57 \times 10^{-8}$ ,  $\beta = 0.21$ , MAF=0.33). Finally, in the combined analyses of both genders, despite not making the threshold for the discovery cohort alone, chr16:7788155 nearest 'RNA binding protein fox-1 homolog 1' (*RBFOX1*) also achieved nominal significance in the replication cohort and genome-wide significance in the combined analysis of both cohorts for spine BMD (comb  $P = 4.06 \times 10^{-8}$ ,  $\beta = -0.22$ , MAF=0.25). This study highlights the utility of sex-stratified analyses in children at discrete skeletal sites to identify novel variants related to bone health.

**Disclosures:** Alessandra Chesì, None.

## MO0216

**Association of Plasma SDF-1 with Bone Mineral Density, Body Composition and Incident Hip Fracture in Older Adults: Findings From the Cardiovascular Health Study.** Monique Bethel<sup>1</sup>, Petra Bůžková<sup>2</sup>, Laura Carbone<sup>1</sup>, John Robbins<sup>3</sup>, Howard Fink<sup>4</sup>, Mark Hamrick<sup>1</sup>, William Hill<sup>\*1</sup>. <sup>1</sup>Augusta University, United states, <sup>2</sup>University of Washington, United states, <sup>3</sup>University of California - Davis, United states, <sup>4</sup>University of Minnesota, Veterans Affairs Health Care System, United states

Purpose: Aging is associated with an increase in circulating inflammatory factors. One, the cytokine stromal cell-derived factor 1 (SDF-1 or CXCL12), is critical to bone marrow stem cell (BMSC) function. SDF-1 has pleiotropic roles in bone formation regulating BMSC migration, recruitment, and engraftment, as well as BMSC differentiation into osteoblasts/osteocytes, and in osteoprogenitor cell survival. The purpose of this study was to examine the association of plasma SDF-1 in participants in the Cardiovascular Health Study (CHS) with bone mineral density (BMD), body composition and incident hip fracture. Methods: All 1536 male and female CHS participants with evaluable DXA scans and plasma for SDF-1 ELISA assays from the 1994-1995 study visit were included in the analyses; they ranged between 65 and 85 years old. BMD of the lumbar spine, total hip, femoral neck and total body, and body composition measurements (total and % lean, total and % fat, and total body mass) were determined. Additionally, incident hip fractures following the 1994-1995 CHS study visit were analyzed until death, loss to follow-up, or June 30, 2013. Results: SDF-1 plasma levels were significantly associated with age ( $b = 18$ ,  $p < 0.01$ ), but not with race. In multivariable adjusted models including age, race, clinic site, gender, smoking, alcohol use, BMI, change in BMI over two years, frailty status, physical activity level, diabetes status, and medication use, higher SDF-1 levels were associated with lower total hip BMD ( $p = 0.019$ ), borderline statistically significantly lower total body BMD ( $p = 0.053$ ) and femoral neck BMD ( $p = 0.092$ ), but not lower lumbar spine BMD ( $p = 0.816$ ). Results were similar for both women and men. However, there was no multivariable adjusted association between SDF-1 and incident hip fracture. In multivariable adjusted models, SDF-1 had significant positive associations with total

fat, % fat, and total body mass, and a significant negative association with % lean body mass, but only in men. SDF-1 was not associated with body composition measures in women. Conclusions: Circulating plasma levels of SDF-1 are independently associated with lower total hip bone mineral density in both men and women, though associations appear weaker at other skeletal sites. Additionally, SDF-1 levels were associated with body composition in men, but not women. These findings suggest SDF-1 levels are linked to bone homeostasis and fat mass, although with a greater association in males.

**Disclosures:** William Hill, None.

## MO0217

**Bone Mineral Density In Diabetes And Impaired Fasting Glucose.** Natalie Marijanovic<sup>1</sup>, Kara Holloway<sup>2</sup>, Julie Pasco<sup>3</sup>, Mark Kotowicz<sup>3</sup>, Barwon Health, Australia, Deakin University, Australia, Deakin University, Barwon Health., Australia

**Purpose:** Diabetes is a growing global problem and is associated with bone fragility. The relationship between impaired fasting glucose (IFG) and bone mineral density (BMD) has not previously been examined. This study aimed to describe the relationship between BMD and normoglycaemia, IFG and diabetes.

**Methods:** This study included 863 women, aged 21-80 years, enrolled in the Geelong Osteoporosis Study. Using multivariable regression we examined the relationships between dysglycaemia and BMD at the femoral neck (FNBMD) and lumbar spine (L2-L4, LSBMD), adjusting for age, weight and height. A difference was considered significant if  $p < 0.05$ . IFG was defined by fasting plasma glucose (FPG)  $\geq 5.5$  mmol/L and diabetes by FPG  $\geq 7.0$  mmol/L and/or self-report. Obesity referred to BMI  $\geq 30$  kg/m<sup>2</sup> and menopause status was self-reported.

**Results:** In premenopausal women (n=417), no relationship was identified between dysglycaemia and BMD.

In postmenopausal women (n=446), there was a difference in mean BMD between IFG and diabetes. Weight was an effect modifier. In nonobese postmenopausal women, mean FNBMD was 5.5% greater in diabetes (n=25) (mean  $\pm$  SEM,  $0.883 \pm 0.024$  g/cm<sup>2</sup>) compared to normoglycaemia (n=248) ( $0.837 \pm 0.008$  g/cm<sup>2</sup>), but this was non-significant. Mean FNBMD in IFG (n=57) ( $0.828 \pm 0.015$  g/cm<sup>2</sup>) was not different from normoglycaemia. Mean LSBMD was 7.1% greater in IFG ( $1.176 \pm 0.023$  g/cm<sup>2</sup>) and 9.3% greater in diabetes ( $1.200 \pm 0.036$  g/cm<sup>2</sup>) compared to normoglycaemia ( $1.098 \pm 0.012$  g/cm<sup>2</sup>).

In obese postmenopausal women, mean FNBMD was no different in IFG ( $0.932 \pm 0.019$  g/cm<sup>2</sup>) but was 9.0% greater in diabetes ( $1.005 \pm 0.026$  g/cm<sup>2</sup>) when compared to normoglycaemia ( $0.922 \pm 0.016$  g/cm<sup>2</sup>). In obese postmenopausal women, mean LSBMD was no different in IFG ( $1.193 \pm 0.025$  g/cm<sup>2</sup>), but was 10.4% higher in diabetes ( $1.316 \pm 0.034$  g/cm<sup>2</sup>) when compared to normoglycaemia ( $1.192 \pm 0.021$  g/cm<sup>2</sup>).

**Conclusions:** BMD has previously been shown to be higher in those with Type 2 diabetes, which likely constitutes the majority of our postmenopausal women with diabetes, and we confirmed this. This is the first study to examine BMD in IFG and shows that LSBMD, alone, is greater in nonobese postmenopausal women. This study is limited by the single assessment of glycaemic status, its cross-sectional nature and the inability to classify diabetes aetiology. Analysis of the relationship between fractures and IFG and diabetes would provide clinically relevant information.

**Disclosures:** Natalie Marijanovic, None.

## MO0218

**Changes in Hip Structural Analysis Parameters in Relation to the Final Menstrual Period: Study of Women's Health Across the Nation (SWAN).** Navana Nagaraj<sup>1</sup>, Robert Boudreau<sup>1</sup>, Michelle Danielson<sup>1</sup>, Gail Greendale<sup>2</sup>, Arun Karlamangla<sup>2</sup>, Thomas Beck<sup>3</sup>, Jane Cauley<sup>1</sup>. <sup>1</sup>University of Pittsburgh, United states, <sup>2</sup>University of California, United states, <sup>3</sup>Beck Radiological Innovations Inc., United states

In SWAN, we showed that accelerated loss of bone mineral density (BMD) begins one year before the final menstrual period (FMP) and continues for 2 more years (Greendale et al, JCEM;27(1),2012). The risk of fracture depends on both BMD and bone geometry. The hip structural analysis (HSA) accounts for the geometric properties of bone and partly explains the racial differences in fracture risk. Changes in HSA parameters during the menopausal transition have not been previously assessed. We hypothesized that the HSA parameters will show accelerated change starting a few years prior to the FMP similar to BMD. The current analysis uses data from 10 years of observation (5 years before to 5 years after FMP) (N= 915, Age (mean(SD))=46.84(2.63), 44% Caucasian) from the SWAN hip strength across the menopausal transition study, an ancillary study to SWAN. HSA parameters at the narrow neck were obtained from 2D DXA scans. Parameters were scaled to weight. FMP was determined from annual interviews. We used LOESS plots to assess the functional form and the fixed knots of trajectories of HSA parameters relative to the FMP. Piecewise linear regression was then used to determine the rate of change. Change was assessed over 3 periods, 5 years before to 2.5 years before FMP (pre-menopausal), 2.5 before to 1.5 years after FMP (transmenopausal), 1.5 years to 5 years after FMP (post-menopausal). Mixed linear models with random slopes were used to estimate the rate of change in HSA over time in units of percentage change relative to baseline. Loss of BMD, cross-sectional area (CSA), subperiosteal width,

section modulus and increase in the buckling ratio were greatest in the transmenopausal period (p for all < 0.05). The decline continued in the postmenopausal period (not significant). Percentage change over the full 10 years in BMD (-9.23%), CSA (-7.45), subperiosteal width (-1.16), section modulus (-5.37), and buckling ratio (+9.20) were significant. Japanese women had the highest rates of change for all HSA parameters and Chinese women had the lowest rate. These associations remained significant after adjusting for age at the FMP, smoking status and physical activity. HSA parameters declined starting about 2.5 years before the FMP and continuing up to 5 years after menopause. The patterns of HSA change in relation to FMP are similar to patterns observed with BMD and composite indices of bone strength (Ishii et al, Osteoporos Int;2012).

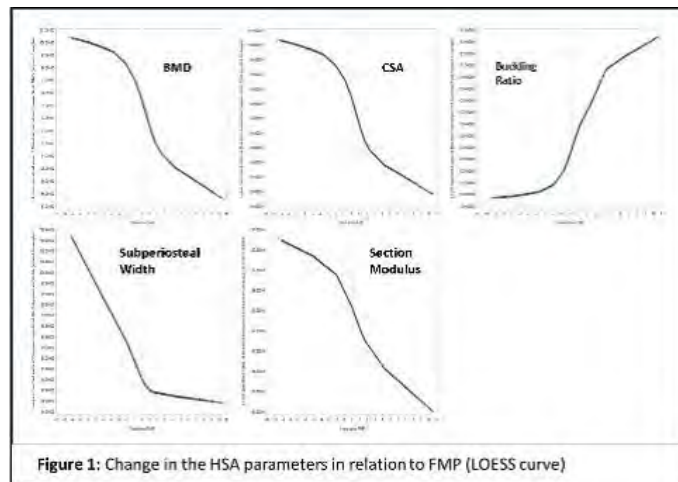


Figure 1: Change in the HSA parameters in relation to FMP (LOESS curve)

HSA change over menopausal transition

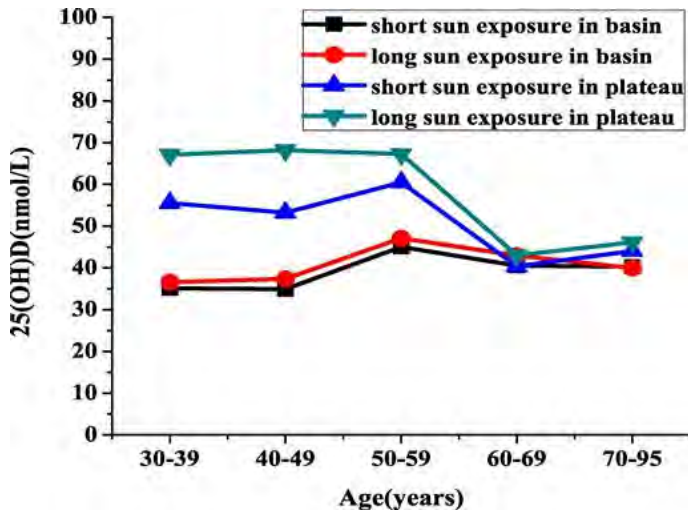
**Disclosures:** Navana Nagaraj, None.

## MO0219

**Poor Nutrition Status of Vitamin D: A Survey from Area with the Lowest Sunshine in China.** Pianpian Fan<sup>1</sup>, Qin Wang<sup>\*1</sup>, Chunyan Lu<sup>1</sup>, Yong Xu<sup>2</sup>, Hongyi Cao<sup>3</sup>, Xiaohua Xie<sup>4</sup>, Xueyan Wu<sup>5</sup>, Yan Chen<sup>1</sup>, Ting Liu<sup>1</sup>, Yanhong Guo<sup>1</sup>, Jing Li<sup>1</sup>, Decai Chen<sup>1</sup>. <sup>1</sup>West China Hospital of Sichuan University, China, <sup>2</sup>The Affiliated Hospital of Southwest Medical University, China, <sup>3</sup>Chengdu Fifth People's Hospital, China, <sup>4</sup>First people's Hospital of Liangshan, China, <sup>5</sup>Guangyuan Central Hospital, China

Vitamin D deficiency is a prevalent disorder around the world. Many factors contribute to the vitamin D status, among which sun exposure is a key factor. Sichuan Province locates in southwest of China (N 26°03'-34°19'), varying in geographical environments. Sunshine was the lowest in Sichuan Basin among China but abundant in West Sichuan Plateau. Thus it gives us a unique model for investigating vitamin D nutrition status under distinct sun exposure. In this study, we evaluated vitamin D status of adult female in Sichuan during winter and the associations between vitamin D and sun exposure as well as age. In this cross-sectional population-based study, blood samples were obtained in winter and tested by Enzyme Immunoassay for 25-hydroxyvitamin D [25(OH)D]. Questionnaires were applied to collect daily sun exposure duration. In total, 1369 female (1030 in basin, 339 in plateau) who aged 30 to 95 yr were included in the analysis. Prevalence of vitamin D sufficiency (25(OH)D  $\geq 75$  nmol/L), insufficiency ( $\geq 50$  but  $< 75$  nmol/L) and deficiency ( $< 50$  nmol/L) was 1.7, 16.4 and 81.9% in basin, compared with 12.7, 36.9 and 50.4% in plateau ( $p < 0.001$ ). There was no difference in 25(OH)D levels between the younger ( $< 60$  yr) and older women ( $> 60$  yr) in basin ( $39.8 \pm 14.8$  vs.  $40.8 \pm 15.2$ ,  $p = 0.303$ ). In fact, 25(OH)D level were identically low regardless of sun exposure duration for older women in both regions and younger women in basin. While in plateau where the sunshine was abundant, 25(OH)D level was higher in younger women than that in the older ones ( $62.1 \pm 19.7$  vs.  $43.4 \pm 16.5$ ,  $p < 0.001$ ). Further, the younger subjects with long sun exposure ( $\geq 3$  hr) had higher 25(OH)D level than those with short sun exposure ( $< 3$  hr) ( $67.6 \pm 20.7$  vs.  $56.3 \pm 16.8$  nmol/L,  $p < 0.001$ ). For subjects in plateau, 25(OH)D levels positively associated with sun exposure duration ( $r = 0.239$ ,  $p < 0.001$ ), and inversely correlated with age ( $r = -0.36$ ,  $p < 0.001$ ). No significant association was found in Basin. In conclusion, Vitamin D deficiency was strikingly prevalent in Sichuan Basin, where the limited sunlight radiation was the predominant cause. Vitamin D status in older women was influenced mainly by age, and only the younger ones in areas with adequate solar radiation could benefit from sun exposure. Therefore, supplement of vitamin D should be considered for all old individuals and those in areas without adequate solar radiation.

Keywords Vitamin D deficiency . Lowest sun exposure . China



Variation of 25(OH)D level with age stratified by sun exposure duration and regions

Disclosures: *Qin Wang, None.*

This study received funding from: *Merck Sharp & Dohme*

**MO0220**

**A Case-control Study of Atypical Femur Fractures (AFF) and Control Femur Fractures.** *Erik Imel*<sup>1\*</sup>, *George Eckert*<sup>2</sup>, *Katie Allen*<sup>3</sup>, *Julie Chandler*<sup>4</sup>, *Joel Martin*<sup>3</sup>, *Joseph Hostetler*<sup>1</sup>, *Siu Hui*<sup>3</sup>, *C. Conrad Johnston*<sup>1</sup>, *Anne de Papp*<sup>4</sup>, *Arthur Santora*<sup>4</sup>, *Robert Choplin*<sup>1</sup>, *Trenton Roth*<sup>1</sup>, *Ziyue Liu*<sup>2</sup>. <sup>1</sup>Indiana University School of Medicine, United states, <sup>2</sup>Indiana University Fairbanks School of Public Health, United states, <sup>3</sup>Regenstrief Institute, Inc., United states, <sup>4</sup>Merck, Sharp & Dhome, United states

Purpose: AFF have been associated with bisphosphonates. We evaluated the occurrence of AFFs among femoral diaphyseal fractures using 2010 and 2014 ASBMR criteria and identified clinical features associating with AFF.

Methods: In a retrospective case-control study using a multi-institution health information database, 1479 radiographs of femoral diaphyseal fractures were identified. After initial review, two radiologists blinded to treatment then evaluated 482 films using ASBMR criteria, jointly adjudicating discrepancies. Fractures were excluded for fracture location, high-energy trauma, tumor, or periprosthetic location. Numbers of major features were summed to determine AFFs. Coded clinical data and dispensing records were collected. Mechanism of injury and osteoporosis drug use information was augmented by chart review.

Results: Low-energy trauma fractures between the lesser trochanter and supracondylar flare occurred in 98 patients. All had at least 2 major features, and 57 (58%) met 2014 AFF criteria (16% with 4, and 42% with 5 major features); only 47% met 2010 AFF criteria. The fracture was substantially transverse with lateral or uncertain origin in 63 (64%); 88 had complete fractures; 8 were incomplete lateral fractures; 70 (71%) were minimally or non-comminuted; and 48 (49%) had local periosteal/endosteal reaction. All patients with periosteal/endosteal reaction had AFF. Radiologist agreement for AFF was 93%. Ten of 11 patients with bilateral femur shaft fractures had bilateral AFF.

Of AFFs, only 33 (58%) received bisphosphonates in the 5 years before fracture (>3 years in 39%; and at time of fracture in 42%); Three each received teriparatide and raloxifene; none received denosumab.

54 AFF cases were race- and sex-matched to 108 controls having non-AFF femur fractures (19 proximal femur; 29 femur shaft; 56 distal femur). AFF associated with bisphosphonates within 5 years before fracture, glucocorticoids at time of fracture, prodromal pain, lower alkaline phosphatase, and osteoporosis diagnosis (Table 1). AFF did not associate with age, cortical thickness, prior osteoporotic fracture, other medical conditions or proton pump inhibitors. In multivariable analysis, AFF associated negatively with age >70, GI disorders, and Charlson Comorbidity Index; and positively with osteoporosis therapy.

Conclusions: Over half of low-energy trauma femoral shaft fractures met the ASBMR 2014 AFF criteria. AFF were associated with multiple clinical factors.

	Cases (N=54)	Controls (N=108)	OR (95% CI)	p-value
Age (SD) years	73.0 (11.2)	74.0 (16.5)	1.00 (0.97-1.02)	0.67
BMI	27.8 (3.8)	28.2 (8.4)	0.99 (0.92, 1.06)	0.70
Charlson Comorbidity Index	1.7 (2.8)	2.2 (2.6)	0.93 (0.81, 1.06)	0.28
Alkaline Phosphatase (U/L)	64.2 (22.3)	89.4 (42.5)	0.97 (0.94, 0.99)	<0.01
Creatinine (mg/dl)	1.0 (0.4)	1.1 (0.9)	0.74 (0.41, 1.31)	0.29
CKD stages 3-5	18 (33%)	48 (44%)	0.62 (0.31, 1.24)	0.18
Lateral cortical thickness/diameter*	0.26 (0.04)	0.25 (0.24)	1.55 (0.19, 12.84)	0.69
Prodromal pain	21 (39%)	5 (5%)	13.04 (3.87, 43.88)	<0.0001
Osteoporotic Fracture within 5 years pre-index	8 (15%)	29 (27%)	0.47 (0.20, 1.14)	0.09
Osteoporosis ICD9 within 5 years pre-index	26 (48%)	23 (21%)	3.47 (1.67, 7.21)	<0.001
Osteoporosis or Osteopenia ICD9 within 5 years pre-index	32 (59%)	28 (26%)	4.00 (1.96, 8.16)	<0.001
Drugs in 5 years preceding fracture				
Bisphosphonates	57%	8%	13.69 (4.81-38.99)	<0.0001
Calcitonin	1 (2%)	3 (3%)	0.67 (0.07, 6.41)	0.73
Raloxifene	3 (6%)	1 (1%)	6.00 (0.62, 57.68)	0.12
Proton pump inhibitors	9 (17%)	27 (25%)	0.61 (0.26, 1.40)	0.24
Oral glucocorticoids at time of fracture	9 (17%)	3 (3%)	6.00 (1.62-22.16)	<0.01

\*5 cm below the lesser trochanter

Table 1

Disclosures: *Erik Imel, Merck, Sharp & Dhome, 11*

This study received funding from: *Merck, Sharp, and Dhome*

**MO0221**

**A Comprehensive Assessment of Comorbidities to Predict Hip Fracture Using a Population-Based Cohort.** *Shreyasee Amin*<sup>\*</sup>, *Elizabeth Atkinson*, *Sara Achenbach*, *Terry Therneau*, *Sundeep Khosla*. Mayo Clinic, United states

Numerous medical conditions have been identified as being associated with an increased risk for hip fractures. However, there is growing interest in better understanding how simultaneous comorbidities may further influence hip fracture risk. We therefore studied the 2000 Olmsted County, Minnesota population age ≥50 yrs (15,027 women; 11,828 men) and evaluated all diagnostic codes within the prior 5 yrs for the risk of subsequent moderate trauma hip fracture.

All diagnoses were categorized by the Clinical Classification Software (CCS) system whereby over 14,000 ICD-9-CM diagnoses are reduced to 568 clinically meaningful categories. If a subject had at least two diagnoses in a CCS category that were at least 30 days apart, the subject was treated as having that CCS code. All hip fractures through to 2012 were validated through complete medical records review, available through the resources of the Rochester Epidemiology Project. We tested the association of these CCS codes on the risk of developing a hip fracture using Cox models, with age as the time scale. We then used Gradient Boosting Machine (GBM) to create hip fracture prediction models for 5- and 10-yr with the CCS codes, using 80% of the data and retaining 20% for validation. Women and men were analyzed separately.

Over 263,755 person-years of follow-up, there were 849 moderate trauma hip fractures (587 in women; 262 in men). In univariate analyses, multiple diagnostic codes related to well-recognized risk factors for hip fractures were identified, including prior fractures, neurocognitive disorders, and some cardiovascular diseases. Interestingly, some chronic infections were also associated with increased risk for hip fracture, while lipid disorders were protective in both women (Hazard Ratio [HR]: 0.75, 95% CI: 0.63-0.89) and men (HR: 0.59, 95% CI: 0.45-0.77). GBM models created performed well at predicting the observed hip fractures over both 5-yr and 10-yr of follow-up in both women and men (Table).

Further work in refining prediction models using multiple comorbidities may help with identifying those at highest risk for hip fracture, with the potential for implementation into the electronic medical records for efficient screening.

	5-yr Prediction Models			10-yr Prediction Models		
	C-statistic	Observed Hip Fractures	SIR* (95% CI)	C-statistic	Observed Hip Fractures	SIR* (95% CI)
<b>Women</b>						
Training	0.86	222	1.08 (0.95-1.24)	0.85	378	1.04 (0.93-1.15)
Validation	0.86	56	1.12 (0.85-1.46)	0.86	95	1.02 (0.83-1.25)
<b>Men</b>						
Training	0.87	85	0.99 (0.79-1.22)	0.85	164	1.04 (0.89-1.21)
Validation	0.79	17	0.78 (0.45-1.24)	0.85	40	1.00 (0.71-1.36)

\*Standardized Incidence Ratio (SIR) = observed hip fractures / predicted (from GBM models) hip fractures for each follow-up period.

Table

Disclosures: *Shreyasee Amin, None.*

**MO0222**

**Association of Albuminuria with Risk of Incident Fracture and Rate of Hip Bone Loss: the Osteoporotic Fractures in Men (MrOS) Study.** Howard Fink\*<sup>1</sup>, Tien Vo<sup>2</sup>, Lisa Langsetmo<sup>2</sup>, Joshua Barzilay<sup>3</sup>, Areef Ishani<sup>1</sup>, Jane Cauley<sup>4</sup>, John Schousboe<sup>5</sup>, Nancy Lane<sup>6</sup>, Eric Orwoll<sup>7</sup>, Yelena Slinin<sup>1</sup>, Kristine Ensrud<sup>1</sup>. <sup>1</sup>Veterans Affairs Health Care System, United states, <sup>2</sup>Division of Epidemiology, University of Minnesota School of Public Health, United states, <sup>3</sup>Kaiser Permanente, United states, <sup>4</sup>University of Pittsburgh, United states, <sup>5</sup>Park Nicollet Clinic, United states, <sup>6</sup>University of California, Davis, United states, <sup>7</sup>Oregon Health Sciences University, United states

Prior studies suggest a positive association between albuminuria and risk of nonvertebral fractures in women and not men, but included relatively few fracture events in men.

We used data from the MrOS Study, a large, prospective cohort of community-dwelling men aged ≥65 years, to evaluate the association of albuminuria with subsequent fractures and hip bone loss. From urine collected at the 12/03-3/05 visit, we calculated the albumin/creatinine ratio (ACR) (Roche Modular P chemistry analyzer). Subsequent clinical fractures were ascertained from triannual questionnaires and centrally adjudicated by blinded review of radiographic reports. Total hip BMD was measured by DXA at the 12/03-3/05 and 3/07-3/09 visits (mean interval 3.5 +/- 0.5 SD years). Risk of incident clinical fracture and major osteoporotic fracture (MOF) (hip, clinical spine, wrist, or humerus) were estimated using multivariate-adjusted Cox proportional hazards models, and annualized rate of change in total hip BMD was assessed using ANCOVA, both across ACR quintiles and in men with versus without microalbuminuria (ACR ≥30 mg/g vs. <30 mg/g).

Of 2982 men with calculable ACR, 9.4% had microalbuminuria. During a mean of 8.7 +/- 3.4 SD years of follow-up, 20.0% and 9.6% of men had incident clinical fractures and incident MOF, respectively. In multivariate-adjusted models (adjusted for age, clinic site, race, past fracture since age 50, any fall in the past year, difficulty with activities of daily living, loop diuretic use, osteoporosis drug use, antidepressant drug use, Geriatric Depression Scale score ≥6, grip strength, and cystatin-based estimated GFR), small increases in risk of incident clinical fracture and incident MOF associated with ACR were not statistically significant, neither across ACR quintiles (p for trend 0.75 and 0.29, respectively) nor in men with versus without microalbuminuria (HR, 1.28 [95%CI, 0.90-1.81] for incident clinical fracture; HR, 1.31 [95%CI, 0.82-2.09] for incident MOF). There was a borderline positive, multivariate-adjusted association between annualized rate of total hip bone loss and albuminuria modeled in ACR quintiles (p=0.09) but not with albuminuria modeled as ACR ≥30 mg/g versus <30 mg/g (0.54% vs. 0.41%, p=0.15).

In these older men, possible small increases in risk of incident clinical fracture, incident MOF, and annualized rate of hip bone loss associated with albuminuria were not statistically significant.

Table: Multivariate-adjusted risk of incident clinical fracture, incident major osteoporotic fracture (MOF), and mean annualized rate of change in total hip BMD by ACR quintile and by microalbuminuria status (ACR ≥30 mg/g vs. <30 mg/g)

Model	ACR Quintile (ACR range)					P for trend	Microalbuminuria Status		P-value
	Quintile 1 (0-0)	Quintile 2 (0.26-1.88)	Quintile 3 (1.88-3.69)	Quintile 4 (3.69-10.55)	Quintile 5 (10.56-284.15)		ACR ≥30 mg/g	ACR <30 mg/g	
Clinical fracture (n=565/2920)	1.0 (ref)	1.31 (1.00-1.72)	1.28 (0.93-1.67)	1.29 (0.99-1.68)	1.34 (0.97-1.83)	0.75	1.28 (0.90-1.81)	1.0 (ref)	0.17
MOF (n=271/2920)	1.0 (ref)	1.44 (0.96-2.15)	1.28 (0.84-1.88)	1.66 (1.14-2.41)	1.16 (0.77-1.75)	0.29	1.31 (0.82-2.09)	1.0 (ref)	0.26
Annualized change in total hip BMD (n=275/2920)	-0.37% (0.47, -0.27)	-0.43% (0.53, -0.33)	-0.36% (0.46, -0.26)	-0.45% (0.56, -0.35)	-0.48% (0.60, -0.38)	0.09	-0.35% (0.71, -0.38)	-0.41% (0.46, -0.37)	0.13

\*Multivariate models were adjusted for age, site, race, non-traumatic fracture after age 50, ≥1 fall in past year, total difficulty with ADLs, loop diuretic use, osteoporosis drug use, antidepressant use, GDS score ≥6, grip strength, and cystatin-based estimated GFR.

Table

Disclosures: Howard Fink, None.

**MO0223**

**Characteristics of patients at high one-year fracture risk.** Akeem Yusuf\*<sup>1</sup>, Yan Hu<sup>1</sup>, David Chandler<sup>2</sup>, Barry Crittenden<sup>2</sup>, Richard Barron<sup>2</sup>. <sup>1</sup>Chronic Disease Research Group, United states, <sup>2</sup>Amgen Inc., United states

Osteoporotic fractures result in economic, physical, emotional, and social burden. While tools are available for assessing and identifying factors that increase long-term risk for fracture, the differentiating factors associated with imminent risk of fracture (risk of near-term fracture in the next 12-24 months) are poorly understood. The study aimed to identify and characterize individuals at imminent risk of fracture, focusing on risk factors identifying men and women with a high imminent risk of fracture.

We identified Medicare beneficiaries alive and aged ≥ 67 years on January 1, 2011, continuously enrolled in Medicare Parts A, B and D between January 1, 2009 and March 31, 2011. The cohort was randomly split into two samples of equal size: the test and validation samples. Using the test sample, we derived coefficients for predictors of 12-months risk of fracture using multivariate Cox model. We then estimated 12-month risk of fracture in the validation sample using the model-derived coefficients obtained from the test sample. Based on expert opinion and fracture risk for patients in the highest 5% of risk distribution, patients with predicted 12-months fracture risk ≥ 15% was used as the threshold to define "high" imminent ( in the next

12 months) risk of fracture and their demographic and clinical characteristics were compared with those with predicted 12-months fracture risks < 15%.

Of the 890,226 patients included in the validation sample, 26,455 (3.0%) had an index fracture during the 12-month follow-up period. 15,244 (1.7%) patients had ≥ 15% predicted 12-months fracture risk and were categorized as at high imminent risk of fracture. These patients were older, predominantly female and white, and more likely to have a recent history of fracture and falls compared with those not at high imminent risk of fracture. In addition, comorbid conditions, markers of frailty/physical function, and of cognitive function, and use of select medications that are predictive of fall and fracture risks were more common in patients at high imminent risk of fractures relative to those not at high imminent risk of fractures. Older, frail, Caucasian women who have a history of fracture and falls are at high near-term of fracture. Recognition of risk factors that predict a high imminent risk of fracture may be important to guide osteoporosis treatment decisions.

Table 1. Prevalence of variables among patients with or without high (≥ 15%) predicted imminent (12 month) risk of fracture

Characteristics	% of patients with this characteristic		P-value
	Among patients without a high predicted imminent risk of fracture (N=874,982)	Among patients with a high predicted imminent risk of fracture (N=15,244)	
Age ≥80 years	38.8	94.3	<0.0001
Female	65.4	98.8	<0.0001
White	85.0	97.6	<0.0001
Fracture history	6.7	97.7	<0.0001
Falls	5.3	55.7	<0.0001
Osteoporosis	4.8	46.3	<0.0001
Osteoporosis medications	14.5	45.5	<0.0001
Steroids	26.2	41.6	<0.0001
Markers of cognitive function*	18.3	61.9	<0.0001
Markers of frailty/physical function*	41.6	97.1	<0.0001

\*Markers of cognitive function include depression, dementia, alzheimers disease, mood/anxiety disorders and use of CNS active medications.

\*Markers of frailty/physical function include rheumatoid arthritis, osteo-arthritis, ankylosing spondylitis, muscle weakness, ambulance life support, difficulty walking, weakness, physical/occupational therapy, nurse home services, home health care services and use of durable medical equipment

Table 1

Disclosures: Akeem Yusuf, None.

This study received funding from: Amgen Inc.

**MO0224**

**Epidemiology and Time Trends of Distal Forearm Fractures in Adults - A Study of 11.2 Million Person-years in Skåne County, Sweden.** Bjorn Rosengren\*<sup>1</sup>, Daniel Jerrhag<sup>1</sup>, Bo Abrahamson<sup>2</sup>, Magnus Karlsson<sup>1</sup>.

<sup>1</sup>Clinical & Molecular Osteoporosis Research Unit, Departments of Clinical Sciences & Orthopedics, Malmö, Skåne University Hospital, Lund University, Sweden, <sup>2</sup>Odense Patient Data Explorative Network, Institute of Clinical Research, University of Southern Denmark, Odense, Denmark

Distal forearm fracture rates have been monitored in Malmö, Skåne County, Sweden since the 1950s and results are often used as reference, also in recent international research. Until the 1980s, incidence increased in both genders where after the incidence decreased in woman but increased in men. The most recent estimation however dates back to 1991-1992. There is therefore a need for updated wrist fracture data.

By use of validated official in- and out-patient registry data of adults (≥17 years) in the Skåne County, Sweden (population 1.0 million year 2010), we ascertained distal forearm fractures and estimated age- and sex- specific rates and time-trends from 1999 to 2010 (11.2 million person years).

During the examination period there were 31,233 distal forearm fractures in adults with a male to female ratio of 1:3. The overall incidence for the period was 278 per 100,000 person-years (150 in men and 399 in women) with an increase in the age standardized incidence in both men (+0.7% per calendar year (95% CI 0.1, 1.4)) and women (+0.9% (0.5, 1.3)). In sub-group analyses of 10 year age strata, statistically significant increments were observed for men in ages 50-59 (+2% per year (0.4, 3.7)) and for women in the four 10 year age strata spanning 40-79 years (+1.7 to 3.4% per year). At least some of the increase in Sweden may be attributable to a reported increase in BMI during the period of examination.

Compared to a nationwide examination of adult distal forearm fracture rates in the neighboring country of Denmark (Abrahamson et al Osteoporos Int 2015 26(1):67-76), the overall fracture rates were significantly lower in Sweden, also after age standardization (in women with a rate ratio (RR) of 0.79 (0.77, 0.81) and in men of 0.93 (0.89, 0.97)). In sub-group analyses of 10-year age strata Danish rates were higher from age 50 to age about 80 years. At older age rate was similar in women but higher in Swedish than in Danish men. These differences may partly be attributed to a reported higher prevalence of smoking and alcohol consumption and the lower life expectancy in Denmark. The incidence of distal forearm fractures is increasing but Swedish rates are markedly lower than in the neighboring country of Denmark. This highlights the importance of current and country specific data. International examinations are needed, preferably with patient specific data to investigate and challenge differences in modifiable risk factors between countries.

Disclosures: Bjorn Rosengren, None.

**MO0225**

**The Rationale for Using a Composite Score when Designing Future Randomized Controlled Trials in the Post-menopausal Osteoporosis Population: A Systematic Review.** Arthur Lau<sup>\*1</sup>, Herman Bami<sup>2</sup>, Alexandra Papaioannou<sup>3</sup>, Jonathan Adachi<sup>1</sup>. <sup>1</sup>Division of Rheumatology, Department of Medicine, McMaster University, Canada, <sup>2</sup>McMaster University, Canada, <sup>3</sup>Division of Geriatrics, Department of Medicine, McMaster University, Canada

**Background:** The cost required to complete a randomized controlled trial is continuously increasing. The most common primary outcome selected in trials aiming to assess the efficacy of treatments of post-menopausal osteoporosis is incident vertebral fractures. However, the incident rate of vertebral fractures is relatively low. Utilizing a composite outcome, where multiple end points are combined allows for greater statistical efficiency by increasing event rates, therefore allowing for smaller sample sizes or shorter follow-up duration (or both).

**The purpose of this review is to summarize the available literature on the use of a composite fracture outcome in the current literature in the field of post-menopausal osteoporosis treatment and to assess if it would be a reasonable practice.**

**Methods:** A systematic review was conducted to identify all RCTs in patients with post-menopausal osteoporosis where fracture was an outcome of interest. The Ovid MEDLINE and Embase databases were searched on March 4, 2016. All records were screened at the title and abstract level. The full texts of the included studies were obtained, and each reviewed to identify the number of studies which utilized a composite as its primary outcome, the primary outcome utilized, and the other fracture outcomes reported that could be included in a composite score.

**Results:** In total, 29 studies met our inclusion and exclusion criteria after full text review. A composite outcome was used in 2 studies, where the outcome was new clinical fracture at any site. The most common primary outcome was incident vertebral fracture, which was utilized in 19 studies. New or worsening vertebral fractures were the primary outcome in 6 studies. All 25 studies that used vertebral fracture as a primary outcome utilized new morphometric vertebral fractures as the event. Incident hip fracture was the primary outcome in 1 study.

**Conclusions:** This systematic review reveals the use of composite outcomes is not a common practice in the field of osteoporosis research. Certainly, future trials should consider the use of a composite primary outcome as it can provide a great degree of trial efficiency, although careful consideration must be taken in its formulation, as a poor choice in the components included in the composite can lead to difficulty in the interpretation of the results.

**Disclosures:** Arthur Lau, Eli Lilly, 12; Amgen, 13

**MO0226**

**Hormone Replacement Therapy has Favorable Effects on Bone Microarchitecture, Bone Mineral Density and Body fat Mass that Persist after his Withdrawal, without Affecting Lean Mass: the OsteoLaus Cohort.** Gergios Papadakis<sup>\*1</sup>, Didier Hans<sup>2</sup>, Elena Gonzalez-Rodriguez<sup>1</sup>, peter vollenweider<sup>1</sup>, Martin Preisig<sup>3</sup>, Gerard Waeber<sup>1</sup>, Pedro-Manuel Marques-Vidal<sup>1</sup>, Olivier Lamy<sup>1</sup>. <sup>1</sup>internal medicine department, Switzerland, <sup>2</sup>Bone Unit, Switzerland, <sup>3</sup>psychiatry department, Switzerland

**Introduction:** Hormonal replacement therapy (HRT) increases bone mineral density (BMD). Controversy exists regarding residual effect after withdrawal. We aimed to explore the effect of HRT and HRT withdrawal on: 1) BMD and bone microarchitecture assessed by trabecular bone score (TBS); 2) fat (FMI), lean (LMI) and appendicular lean (ALMI) mass indexes.

**Methods:** The OsteoLaus Cohort evaluated 1500 women (50-80 years) for BMD, TBS, total energy expenditure (TEE), calcium intake, serum vitamin D, alternative health eating index (AHEI), handgrip and depression prevalence. 1094 women (73%) had body composition analysis by dual X-ray absorptiometry. Exclusion criteria included current or prior osteoporotic treatment. According to HRT status, women were classified as: Never (NU=504), Current (CU=205) and Past (PU=262) users.

**Results:** The 3 groups differed in age ( $67.4 \pm 6.8$ ,  $64.0 \pm 6.8$ ,  $62.1 \pm 8.0$  for PU, CU and NU respectively,  $p < 0.001$ ), AHEI and TEE but not in BMI, dietary calcium intake, or depression prevalence. After adjustment for age and BMI, there was a significant decrease for all BMD and TBS values according to HRT status (CU < PU < NU,  $p < 0.01$ ). The between-groups difference was significant for all lumbar spine (LS) and total hip (TH) BMD values. The between groups-difference was significant for BMD FN and TBS when CU were compared to PU or NU (PU vs. NU for TBS:  $p = 0.066$ ). After adjusting for BMI, TBS slopes (95% CI) for a 10-year increment were -0.051 (-0.060; -0.041), -0.032 (-0.048; -0.017) and -0.022 (-0.038; -0.005) in NU, PU and CU respectively (CU vs. NU,  $p = 0.003$ . PU vs. NU,  $p = 0.048$ ). Adjusted slopes for association of BMD with age were all significantly lower according to HRT status ( $p < 0.015$ , CU < PU < NU), except for the femoral neck comparison between PU and NU (ns). After multiple adjustments, there was no difference for LMI and ALMI between the 3 groups. Slopes for a 10-year increment of FMI were significantly higher for NU (0.887; CI 0.566 - 1.208), versus PU (0.084; CI -0.463 - 0.631) or CU (0.225; CI -0.350 - 0.800).

**Conclusion:** Current HRT use is associated with higher BMD values and a better preservation of the bone microarchitecture assessed by TBS. The benefits of HRT for the TBS and the BMD at LS and TH persist in PU. HRT has no effect on lean mass,

and therefore cannot explain these changes. However, the age-associated increase of FMI is reduced in HRT users. Further analysis is ongoing to assess if reduction in FMI concerns subcutaneous or visceral fat, and thus could explain the BMD and TBS changes.

**Disclosures:** Gergios Papadakis, None.

**MO0227**

**Abdominal aortic calcification identified on images from bone densitometers and long-term cardiovascular outcomes in elderly women.** Joshua Lewis<sup>\*1</sup>, John Schousboe<sup>2</sup>, Wai Lim<sup>3</sup>, Germaine Wong<sup>1</sup>, Kevin Wilson<sup>4</sup>, Douglas Kiel<sup>5</sup>, Richard Prince<sup>3</sup>. <sup>1</sup>Centre for Kidney Research, Children's Hospital at Westmead School of Public Health, Sydney Medical School, The University of Sydney, Australia, <sup>2</sup>Park Nicollet Osteoporosis Center & Institute for Research & Education, Minneapolis, Division of Health Policy & Management, University of Minnesota, United states, <sup>3</sup>University of Western Australia School of Medicine & Pharmacology, Sir Charles Gairdner Hospital Unit, Australia, <sup>4</sup>Skeletal Health, Hologic, Inc., United states, <sup>5</sup>Institute for Aging Research, Hebrew SeniorLife, Beth Israel Deaconess Medical Center, Harvard Medical School, United states

Elderly women routinely undergo bone density testing using dual X-ray absorptiometry. These machines can also capture single-energy digital lateral spine images to detect spine fractures. Abdominal aortic calcification (AAC) is often seen on these images, however its long-term clinical importance remains uncertain. We assessed whether AAC from these images was associated with 14.5 year atherosclerotic vascular disease (ASVD) hospitalizations and deaths (stroke, coronary heart disease, heart failure and peripheral arterial disease) in 1,052 unselected ambulant, community-dwelling elderly women with a mean age of 75 years. Over 13,503 person years of follow-up 420 women suffered an ASVD hospitalization or death (206 ASVD-related deaths) identified using linked health records. Baseline Framingham Risk Scores (FRS) were calculated and AAC (24 point scale) was graded into three categories; low (scores 0 or 1), moderate (scores 2-5) and severe (scores >5). Low AAC was present in 471 women (45%), moderate AAC in 387 women (37%) and severe AAC in 194 women (18%). Absolute ASVD hospitalization or death risk by AAC severity was 37%, 39% and 49% respectively while ASVD death risk was 15%, 21% and 27% respectively. In Cox regression analyses women with severe AAC had an increased hazard ratio (HR) for 14.5-year ASVD hospitalizations or deaths; HR 1.51, 95%CI 1.18-1.94,  $P = 0.001$ , while women with both moderate and severe AAC had an increased HR for ASVD death HR 1.47, 95%CI 1.07-2.01,  $P = 0.018$  and HR 1.93, 95%CI 1.35-2.76,  $P < 0.001$  respectively. The findings remained similar after adjustment for FRS. In conclusion abdominal aortic calcification identified on lateral spine imaging is associated with greater risk of long-term ASVD hospitalizations and/or deaths independent of traditional risk factors. These data support further investigations of the impact of lateral spine imaging to screen for atherosclerotic vascular disease risk at the time of bone density testing, on physician and patient management of modifiable cardiovascular disease risk factors, and ultimately, patient outcomes.

**Disclosures:** Joshua Lewis, None.

**MO0228**

**Chronic hyponatremia and association with osteoporosis in a large ethnically-diverse population.** Annette Adams<sup>\*1</sup>, Bonnie Li<sup>1</sup>, Shirin Sundar<sup>2</sup>, Holly Krasa<sup>2</sup>, Joseph Chiodo<sup>2</sup>, Siddhesh Kamat<sup>2</sup>, John Sim<sup>1</sup>. <sup>1</sup>Kaiser Permanente Southern California, United states, <sup>2</sup>Otsuka Pharmaceutical Development & Commercialization, Inc, United states

**Purpose:** Hyponatremia has been reported to negatively affect bone mineral density which may lead to adverse outcomes including greater risk for bone fragility and fractures. Past observations using single cross-sectional sodium (Na) values have demonstrated a higher rate of osteoporosis among those with hyponatremia though studying chronically low Na may provide more insight. Using serial Na measurements, this study evaluated whether individuals with chronic hyponatremia had greater risk of osteoporosis.

**Methods:** This retrospective cohort study for the period 1/1/1998 - 12/31/2014 included men and women aged  $\geq 55$  years who were members of Kaiser Permanente Southern California, an ethnically-diverse, integrated health system in the US. Eligible subjects had a minimum of 2 serum Na measurements and had documented dual-energy x-ray absorptiometry (DXA) results. Time-weighted (TW) mean Na values for each individual were calculated and also categorized as chronic hyponatremia ( $\text{Na} < 135 \text{mEq/L}$  for greater than one consecutive day) and normonatremia ( $\text{Na} \geq 135 \text{mEq/L}$ ). Osteoporosis was defined as lowest T-score  $< -2.5$ . Multivariable regression was used to estimate associations between osteoporosis and: 1) hyponatremia compared to normonatremia, and 2) TW mean Na values. All models were adjusted for demographics, comorbidities, laboratory results, and medication exposures.

**Results:** A total of 385,778 subjects were identified for the study with mean age 64.4 years. The cohort was 31.7% male, and 58.3% white. A total of 46,444 (12.0%)

subjects had chronic hyponatremia and 10,449 subjects had TW mean Na 130-135mEq/L. Osteoporosis was observed in 44% of the study population (56% hyponatremic vs 42% normonatremic). Compared to normonatremic subjects, chronic hyponatremic subjects had a 5% increase in risk of osteoporosis (RR 1.05, 95% confidence interval (CI) 1.04, 1.06). In the TW mean analysis, a 5mEq/L increase in mean Na was associated with a 9% reduction in osteoporosis risk (RR 0.91, 95% CI 0.89, 0.93).

Conclusions: Among men and women with serial Na measurements, we observed a 5% greater risk for having osteoporosis in subjects with chronic hyponatremia compared to those with Na $\geq$ 135mEq/L. We also observed a dose-dependent protective effect of higher serum Na and risk of osteoporosis. Whether chronically low Na states plays a role in lowering bone density or reflects a biomarker for osteoporosis remains to be determined.

**Disclosures:** Annette Adams, Amgen Inc, 11; Otsuka, 11; Merck, 11  
This study received funding from: Otsuka

## MO0229

**Correlates of Osteoporotic Fractures Among Type 2 Diabetic Patients.** Inbal Goldshtein<sup>\*1</sup>, Julie Chandler<sup>2</sup>, Ann DePapp<sup>2</sup>, Sophia Ish-Shalom<sup>3</sup>, Gabriel Chodick<sup>1</sup>, Allison Martin Nguyen<sup>2</sup>. <sup>1</sup>Maccabi Healthcare Services, Israel, <sup>2</sup>Merck, research laboratories, United states, <sup>3</sup>Elisha hospital, haifa, Israel

Background: Little is known about the association between type 2 diabetes (T2DM) and fragility fractures, or its mechanism.

Objective: To identify diabetes-specific predictors of an osteoporotic fracture.

Methods: This study utilized the computerized database of a large insurer and provider of healthcare services in Israel. The first phase included a cross sectional analysis to assess the current prevalence of fracture history among OP patients with and without T2DM. Subsequently, a sub-cohort of osteoporotic T2DM patients with no fracture at OP diagnosis (index date), was retrospectively analyzed to identify correlates of incident fractures among diabetic OP patients, using time to event (Cox's-proportional hazard) analysis.

Results: A total of 97,454 OP patients were identified of whom 18% were diabetic. The prevalence of major osteoporotic fractures (hip, spine, Colle's or humerus) was significantly higher among T2DM (42%) compared to DM-free patients (31%) across all fracture sub-types (age and sex standardized ratio=1.19, P<0.001), and particularly increased in hip fractures (8.8% vs. 5.8%). Diabetic OP patients were more likely to be older (mean current age 74.3y vs. 69.1y) and males (20.8% vs. 14.4%, p<0.001) as compared with DM-free ones. Screening rates for bone mineral density were similar in both groups (79.3% vs. 79.9%), and median most recent t-scores were significantly (P<0.001) higher in both total-hip (-1.3 vs. -1.6) and vertebrae (-1.4 vs. -1.8) yet relatively similar in femur neck (-1.8 vs. -1.9, p<0.001) for T2DM patients vs. DM-free.

In a multivariable model among T2DM patients with osteoporosis, fracture risk was significantly associated with neuropathy (HR=1.22, 95% CI: 1.05-1.42), history of hypoglycemic events (HR=1.21, 1.07-1.37), cardiovascular disease (HR=1.25, 1.14-1.38), and prolonged intake of thiazolidinedione (12+ months vs. <12 months: HR=1.34, 1.04-1.73).

Conclusions: This large population-based study quantifies the unique risk factors for fracture among diabetic patients, and confirms that patients with T2DM are at increased risk for major osteoporotic fractures and that the presence of micro and macro vascular disease appears to further increase the risk.

**Disclosures:** Inbal Goldshtein, None.  
This study received funding from: Merck

## MO0230

**Determinants of fracture risk among older men with diabetes.** Richard Lee\*, Richard Sloane, Carl Pieper, Cathleen Colon-Emeric. Duke University, United states

Purpose: Older adults with diabetes have an increased fracture risk, despite higher bone mineral density (BMD). Studies investigating this paradoxical fracture risk among older males are limited. Identification of mediating factors of this fracture risk may clarify etiology and therapy in this increasing population.

Method: Retrospective cohort study, using linked administrative data from the Veterans Health Administration (VHA) and Medicare, of 2,798,309 male Veterans, age  $\geq$  65 years, who received primary care from 2000 to 2010 from VHA, among whom 900,402 had a diagnosis of diabetes mellitus. The number of clinical fractures was determined during the 10-year follow-up period. Association of diabetes with fracture risk was evaluated with negative binomial regression model. Potential mediating factors were identified by comparing diabetes-associated fracture risk prior to and after inclusion of potential factors in regression model. Relative risks (RR) of fracture associated with diabetes with 95% confidence intervals are presented.

Results: Compared to those without diabetes, men with diabetes were slightly older (71.2 vs 70.8 years), with greater body mass index (BMI) (30.1 vs 28.0 kg/m<sup>2</sup>), and more likely Black race (10.2% vs 7.6%). Among those who had a DXA ordered in routine clinical care, those with diabetes had a statistically significant higher femoral neck BMD T-score (-0.28 vs -0.50). All P-values < 0.0001. Diabetes was associated with an unadjusted relative risk of fracture 1.178 (1.169-1.187). After adjusting for age, race, BMI, tobacco/alcohol use, rheumatoid arthritis, and glucocorticoid use, a

significant fracture risk associated with diabetes remained, with RR 1.216 (1.207-1.226). A similar result was seen after adjusting for 10-year major osteoporotic fracture risk as calculated by FRAX. Diabetes-associated fracture risk was significantly different after including the potential mediating factors cardiovascular disease [1.160 (1.151-1.169)], neuropathy [1.131 (1.122-1.140)], and hemoglobin A1c level [1.293 (1.280-1.307)]. No difference was seen after including liver disease or cerebrovascular disease.

Conclusion: In this large cohort of older males, those with diabetes were more obese, with higher femoral neck BMD. However, diabetes remained significantly associated with increased fracture risk. Potential mediators include macrovascular and microvascular complications of diabetes, as well as level of glycemic control.

**Disclosures:** Richard Lee, None.

## MO0231

**High Incidence of Fractures in Older Cancer Patients are associated with Vitamin D Insufficiency.** Xiaotao Zhang<sup>1</sup>, Sun Ming<sup>2</sup>, Nizar Bhulani<sup>1</sup>, Meghan Karuthuri<sup>3</sup>, Peter Khalil<sup>1</sup>, Gabriel Hortobagyi<sup>3</sup>, Debasish Tripathy<sup>3</sup>, Vicente Valero<sup>3</sup>, Carlos Barcenás<sup>3</sup>, Colin Dinney<sup>4</sup>, Jay Shah<sup>4</sup>, John Stroehlein<sup>5</sup>, Holly Holmes<sup>6</sup>, Beatrice Edwards<sup>\*7</sup>. <sup>1</sup>Department of General Internal Medicine, MD Anderson Cancer Center, United states, <sup>2</sup>MD Anderson Cancer Center, United states, <sup>3</sup>Department of Breast Medical Oncology, MD Anderson Cancer Center, United states, <sup>4</sup>Department of Urology, MD Anderson Cancer Center, United states, <sup>5</sup>Department of Gastroenterology, MD Anderson Cancer Center, United states, <sup>6</sup>Department of Internal Medicine, University of Texas Health Science Center, United states, <sup>7</sup> Department of General Internal Medicine, MD Anderson Cancer Center, United states

BACKGROUND: More than 60% of cancer patients are over the age of 65 years and are subject to aging and cancer-therapy related changes. Older adults also have geriatric risk factors for fractures such as frailty, cognitive impairment (Mild cognitive impairment [MCI] and dementia), and malnutrition-including vitamin D deficiency.

OBJECTIVES: To assess the incidence of fractures, and risk factors for fractures in older cancer patients.

METHODS: This is a retrospective cohort study (01/13 – 03/15). Community-dwelling ambulatory older adults with cancer (active care and survivors) underwent comprehensive geriatric assessments, including cognitive, functional, nutritional, physical, and comorbidity assessment. Vitamin D was assayed, and BMD conducted (Discovery W, Hologic Corp., Marlborough, MA) of the lumbar spine (L1-L4), total hip and femoral neck. We used a logistic regression methodology for the multivariable analysis.

RESULTS: The mean age of this cohort was 74.5  $\pm$  6.2 years (n=192); participants had gastrointestinal, urologic, breast, lung and gynecologic cancers. Low bone mass and/or osteoporosis were very common (80%). Thirty percent of cases presented with dementia, 37% had MCI, and 39% frailty. Over the following 3 years, 13% of older adults sustained fractures, in females, this compares to an annual age-specific incidence of 3% (in 70-79 years) in cancer free individuals (NHANES III). Although BMD was similar, females were more likely to fracture than males (18% vs 7%, p=0.02). Vitamin D < 30 ng/ml was identified in 55% (86/155) of cases. In the multivariate analysis, vitamin D insufficiency was identified as a risk factor for fractures (OR=9.59, 95%CI=1.26, 73.21).

CONCLUSIONS: Older cancer patients (and survivors) have a high prevalence of low bone mass, osteoporosis and vitamin D insufficiency. Older females with cancer have a higher fracture risk than older adults who remain cancer free. Greater awareness of adverse consequences should motivate assessment, vitamin D supplementation, and pharmacologic treatment for osteoporosis to prevent fractures in older cancer patients.

**Disclosures:** Beatrice Edwards, None.

## MO0232

**Predictors of Imminent Risk of Non-Vertebral Fracture in Older Women: The Framingham Osteoporosis Study.** Marian Hannan<sup>\*1</sup>, Derek Weycker<sup>2</sup>, Robert McLean<sup>1</sup>, Shivani Sahni<sup>1</sup>, Thomas Trivison<sup>1</sup>, Rebecca Bornheimer<sup>2</sup>, Alyssa Dufour<sup>1</sup>, Rich Barron<sup>3</sup>, Douglas Kiel<sup>1</sup>. <sup>1</sup>HSL Institute for Aging Research, United states, <sup>2</sup>Policy Analysis Inc. (PAI), United states, <sup>3</sup>Global Health Economics-Amgen, United states

Better understanding of factors contributing to imminent risk of fracture (FX) in next 1-2 y is potentially useful for personalizing therapy, especially among those at high risk. Treatment decisions are often based on 10y FX risk; yet little is known about factors increasing near-term FX risk. Our aim was to identify risk factors for non-vertebral FX over 1-2y in a community-based cohort of women aged  $\geq$  65y who had osteoporosis, osteopenia or a history of fragility FX.

The Framingham Osteoporosis Study includes 20y+ of prospectively collected information from multiphasic examinations with extensive follow-up for adjudicated FX. The study sample included 2,778 women from Framingham Offspring and Original Cohorts of ages  $\geq$ 65y with osteoporosis (hip BMD T-score  $\leq$  -2.5), osteopenia (hip BMD T-score between -1.0 and -2.5), or history of fragility FX

(irrespective of hip BMD T-score). Non-vertebral FXs were ascertained over the 1y and 2y follow-up from baseline BMD scan. Potential risk factors included: age (65-74, 75-84, ≥85), anthropometric variables, comorbidities/medical history, cognitive function, current medications, history of FX, self-rated health status, ≥ 1 fall in past year, smoking, physical performance, hip BMD T-score, Katz-ADL score, caffeine and alcohol. Predictive factors were evaluated using Cox proportional hazards regression models with 95% confidence intervals; model discrimination was evaluated using C-Index. Risk factors in bivariate models with p-value ≤ 0.10 were considered in multivariable models.

During 1y follow-up, 89 non-vertebral FXs occurred among 2,778 participants, and during 2y follow-up, 176 FXs had occurred. Mean (± SD) age was 77 (± 5y; range 65-96). Of the 35 variables considered in bivariate models, significant predictors of non-vertebral FX included age, history of FX, self-rated health, falls in past year, hip BMD T-score, Katz-ADL, current use of nitrates, beta-blockers, calcium channel blockers or anti-depressants, current renal disease and current dementia. In multivariable models, the significant independent risk factors were history of FX, self-rated health, hip BMD T-score, and use of nitrates (Table). Discrimination of the 1y model was good (C-index=0.71). Significant 1y results were attenuated at 2y.

Conclusions: Several risk factors were found to be independently associated with near-term FX in older, high-risk women. These factors may be useful in identifying which women to target for therapy.

Table. Multivariable analyses of potential risk factors and non-vertebral fracture (1-year and 2-year)

Covariates	1-Year FX Risk CoxPH Model					2-Year FX Risk CoxPH Model				
	N	FX	HR	95% CI	p-value	N	FX	HR	95% CI	p-value
Women with Osteoporosis, Osteopenia, Fracture History (n=2,778)										
Age										
<75y	1274	32	REF			1274	63	REF		
75-84y	1296	47	1.0	0.58, 1.57	0.85	1296	97	1.2	0.85, 1.73	0.29
85+y	208	10	1.1	0.49, 2.26	0.90	208	16	1.0	0.57, 1.92	0.89
History of fracture										
Yes	939	41	1.4	0.89, 2.19	0.14	939	75	1.4	1.00, 1.91	0.05
No	1839	48	REF			1839	101	REF		
Total Katz ADL score										
0-4 Severe/Moderate Impairment	24	2	0.9	0.12, 6.57	0.91	24	4		0.08, 4.40	0.82
5-8 Full Function	2730	85	REF			2730	169			
Self-rated health (quality of life)										
Excellent	886	17	REF			886	42			
Good/Fair	1811	66	1.5	0.84, 2.75	0.16	1811	125		0.91, 2.00	0.13
Poor	26	3	4.0	1.10, 14.3	0.04	26	3		0.64, 7.05	0.22
T-Score Category										
≤ -2.5 (Osteoporosis)	980	54	2.8	1.75, 4.54	<0.0001	980	94		1.46, 2.81	<0.0001
> -1.0 (Osteopenic/normal)	1798	35	REF			1798	82			
1+ Falls in past year -yes	1103	46	1.3	0.83, 2.04	0.25	1103	75		0.66, 1.27	0.60
-no	1585	41	REF			1585	96			
Medication use										
Nitrates -yes	98	11	2.6	1.22, 5.39	0.01	98	14	1.8	0.95, 3.40	0.07
-no	2408	74	REF			2408	153	REF		
Beta-blockers -yes	471	23	1.3	0.78, 2.20	0.30	471	40	1.2	0.82, 1.76	0.36
-no	2040	62	REF			2040	127	REF		
Calcium Channel blockers -yes	385	19	1.1	0.60, 1.92	0.82	385	33	1.1	0.75, 1.74	0.55
-no	2126	66	REF			2126	134	REF		
Anti-depressants -yes	132	8	1.7	0.76, 3.84	0.20	132	12	1.3	0.72, 2.47	0.36
-no	2381	77	REF			2381	155	REF		

\*Concordance Index (SE): 1y model, 0.71 (0.03); 2y model, 0.64 (0.02)

Potential Risk Factors and Non-vertebral Fracture Risk (1-year and 2-year)

Disclosures: *Marian Hannan, Policy Analysis Inc, 11; Merck Sharp & Dohme research grant to institution, 11*  
 This study received funding from: *funding for this research from Policy Analysis Inc. and Amgen*

MO0233

**Risk Factors and Time Interval of Fracture Cascade Among Patients with Osteoporosis in China.** Xinling Liu<sup>1</sup>, Ke Wang<sup>2</sup>, Yu Chen<sup>2</sup>, Peita Graham-Clarke<sup>3</sup>, Jing Wu<sup>4</sup>. <sup>1</sup>Tianjin University, China, <sup>2</sup>Lilly Suzhou Pharmaceutical Company, China, <sup>3</sup>Eli Lilly Australia Pty Ltd, Australia, <sup>4</sup>School of Pharmaceutical Science & Technology Tianjin University, China

The aim of our study is to evaluate the incidence of subsequent fractures among patients with an osteoporotic fracture in China and to assess the time intervals between consecutive fractures. Data were obtained from the Tianjin Urban Employee Basic Medical Insurance database. Patients who were aged ≥ 50 years, had ≥ 1 osteoporotic fracture between 2009 and 2011, and had continuous enrollment 12 months before (baseline) and 24 months after (follow-up) the first fracture were identified. Patients who had ≥ 1 additional osteoporotic fractures

during the follow-up period were identified as patients with subsequent fractures. The incidence of subsequent fractures and the intervals between consecutive fractures were calculated. Logistic regression was used to identify the risk factors of subsequent fractures. Finally, a total of 8,478 patients were identified (mean [SD] age: 65.3 [10.3] years; female: 62.0%). Of all patients, 14.5% (N=1,229) experienced a second fracture. Among those patients, 19.5% (N=240) experienced a third fracture; among them, 25.0% (N=60) experienced a fourth one; and 46.7% (N=28) of them experienced a fifth fracture. A subsequent fracture occurred during the first year after the first fracture for 67.1% (N=825) of patients. In addition, 34.4% (N=423) of patients experienced subsequent fractures at a different location than the first fracture. Mean (SD) time intervals were 236.8 (227.8) days between the first and second fractures, 178.3 (190.2) days between the second and third fractures, 110.2 (134.2) days between the third and fourth fractures, and 99.8 (131.8) days between the fourth and fifth fractures. Patients with the first fracture in the clavicle (odds ratio [95% confidence interval]: 1.97 [1.40-2.77]), lower limb (1.81 [1.50-2.19]), and hip (1.35 [1.12-1.62]) were more likely to have subsequent fractures compared with those with first fractures in arms. Risk factors for subsequent fractures included being female or retired and having a poor health status, as indicated by the Quan-Charlson Comorbidity Index. In conclusion, among patients with osteoporotic fractures in China, as the number of fractures increases, the risk of subsequent fractures increases numerically and the mean interval between fractures becomes numerically shorter. There is a high risk of re-fracture during the first year after the first fracture. Patients whose first fracture occurs in the clavicle, lower limb, or hip have a higher risk of subsequent fractures.

Disclosures: *Peita Graham-Clarke, None.*  
 This study received funding from: *Lilly Suzhou Pharmaceutical Co. Ltd*

MO0234

**The Dynamic Nature of Frailty in Community Dwelling Men and Women across Canada: The Canadian Multicentre Osteoporosis Study (CaMos).** George Ioannidis<sup>1</sup>, Olga Gajic-Veljanoski<sup>1</sup>, Courtney Kennedy<sup>1</sup>, Jonathan D. Adachi<sup>2</sup>, Claudie Berger<sup>3</sup>, Andy Kin On Wong<sup>4</sup>, Kenneth Rockwood<sup>5</sup>, Susan Kirkland<sup>5</sup>, Parminder Raina<sup>6</sup>, Lehana Thabane<sup>6</sup>, Alexandra Papaioannou<sup>1</sup>, The CaMos Research Group<sup>3</sup>. <sup>1</sup>McMaster University & Hamilton Health Sciences – St. Peter’s Hospital – GERAS Centre, Canada, <sup>2</sup>McMaster University & Hamilton Health Sciences – St. Joseph’s Hospital, Canada, <sup>3</sup>Camos – McGill University, Canada, <sup>4</sup>McMaster University & University Health Network, Canada, <sup>5</sup>Dalhousie University, Canada, <sup>6</sup>McMaster University, Canada

Purpose: Given that frailty is common, dynamic and multifactorial in nature, we set out to determine how frailty changes over time as men and women age.

Methods: Frailty was assessed using data from the Canadian Multicentre Osteoporosis Study (CaMos), which is a large, randomly selected, prospective population-based cohort of community dwelling men and women ≥ 25 years of age from 9 Canadian cities. For the current study, frailty was assessed at three time points (baseline, year 5, year 10) in participants ≥ 50 years of age using the 30-item CaMos Frailty Index (CFI). The CFI includes physical, cognitive, and social/emotional factors. Participants were categorized into three frailty groups based on the minimally important clinical change of 0.03 in the CFI score. Group 1 consisted of those who had experienced an increase in frailty (≥ +0.03); group 2, those with a decrease in frailty (≤ -0.03), and group 3, those without a clinically meaningful change (< ± 0.03). Frailty changes were examined across two 5 year time periods (baseline to 5 years, 5 to 10 years).

Results: The cohort included 5566 women (mean age [SD]: 66.8 [9.3] years) and 2187 men (66.3 [9.5] years). 13.6% (754/5566) of women and 16.2% (353/2186) of men were current smokers. 28.7% (1599/5566) of women and 52.2% (1142/2187) of men consumed greater than 1 glass of alcohol/week. The dynamic nature of frailty varied across the two 5 year time periods. 45% of participants demonstrated an increase in frailty at the first time period (baseline to year 5) as compared with 22.9% at the second time point (5 to 10 year). Approximately, 70% of men and women had clinically meaningful frailty score changes, in either direction, throughout the study period (Table).

Conclusions: The vast majority of community dwelling individuals over the age of 50 year experience clinically important changes in frailty measures over time. The heterogeneous nature of human aging expressed through changes in frailty may be associated with diseases such as osteoporosis, and physical, mental, and social factors.

	Total (n=7753)	Women (n=5566)	Men (2187)
<b>Absolute change from baseline to 5 years, % (n/N)</b>			
Decrease in frailty by at least 0.03 points	18.7 (1162/6200)	18.9 (860/4544)	18.2 (302/1656)
Increase in frailty by at least 0.03 points	45.1 (2795/6200)	45.7 (2078/4544)	43.3 (717/1656)
No change (<±0.03).	36.2 (2243/6200)	35.3 (1606/4544)	38.5 (637/1656)
<b>Absolute change from 5 to 10 years, % (n/N)</b>			
Decrease in frailty by at least 0.03 points	43.5 (1873/4303)	45.5 (1459/3207)	37.8 (414/1096)
Increase in frailty by at least 0.03 points	22.9 (986/4303)	22.1 (708/3207)	25.4 (278/1096)
No change (<±0.03).	33.6 (1444/4303)	32.4 (1040/3207)	36.9 (404/1096)

Table: Longitudinal Changes in Frailty

Disclosures: *George Ioannidis, None.*

MO0235

**The Effect of Latitude on the Risk of Hip Fractures in Chile.** Pablo Riedemann<sup>\*1</sup>, Luis Bustos<sup>1</sup>, Oscar Neira<sup>2</sup>, Eugene McCloskey<sup>3</sup>, Helena Johansson<sup>4</sup>, Daniela Riedemann<sup>1</sup>, John Kanis<sup>5</sup>. <sup>1</sup>Universidad de la Frontera, Chile, <sup>2</sup>Clinica Alemana, Chile, <sup>3</sup>Centre for Metabolic Bone Diseases, University of Sheffield, United Kingdom, <sup>4</sup>Centre for Metabolic Bone Diseases, United Kingdom, <sup>5</sup>Centre for Metabolic Bone Disease, United Kingdom

Vitamin D deficiency in adults increases the risk of osteoporotic fractures. In the northern hemisphere, hip fracture incidence has been shown to increase with increasing latitude. Chile is a long country, divided in 13 regions, ranging from latitude 20° to latitude 53° in the south hemisphere. This study determined the risk of hip fractures and the effect of latitude in Chile.

Using national health statistics of hospital discharges, we examined all hip fractures from 2001 to 2008 by region; hip fractures were identified from the International Classification of Diseases (ICD 10) S720, S721 or S 722. The incidence of hip fractures in Chilean population of men and women aged 50 years or more, between 2001 and 2008 was calculated from catchments supplied by the National Statistics office.

An extension of Poisson regression model was used to study the relationship between the risk of hip fracture with age, calendar year, latitude and population density. Using the unique national identification number, only one fracture per person was counted in a period of a year. Population density, an index of urban/rural status, was acquired as a continuous variable for each region. Latitude was considered as a continuous variable and was determined for each capital of region from north to south. Determination of the beta coefficients were performed separately for each sex. The model used a piecewise linear in age with knots at 55 and 70 years.

The principal results are shown in table 1.

For women, the incidence of hip fracture rose with age by 12-17% per year depending on age. There was no significant trend with calendar year. There was a change in risk of hip fracture per latitude, with a decrease with latitude of 1.3% per latitude degree. There is also a lower risk with higher population density (0.01% per unit).

For men, the incidence of hip fracture rose with age by 4-13% per year depending on age. There is a significant trend with calendar year, with 1% lower risk per year. There was a change in risk of hip fracture by latitude of 0.7% per degree. There is no association between population density and hip fracture risk (data not shown).

Contrary to expectation, hip fracture incidence decreased with increasing latitude in both men and women. These data challenge the view that latitudinal associations with hip fracture are mediated by vitamin D status.

Table 1. HR per 1 step (95% CI) additionally. \* Denotes statistical significance (p<0.05).

	Female	Male
Age <55	1.12 (1.11, 1.13) *	1.04 (1.03, 1.05) *
Age 55-70	1.17 (1.16, 1.17) *	1.11 (1.11, 1.12) *
Age 70+ over	1.16 (1.15, 1.16) *	1.13 (1.12, 1.13) *
Calendar Year (1-8)	1.00 (1.00, 1.01)	0.99 (0.98, 1.00) *
Latitude	0.987 (0.984, 0.989) *	0.993 (0.989, 0.998) *
Population density (401 vs 1)	0.97 (0.94, 0.99)	1.00 (0.96, 1.04)

Table 1

Disclosures: Pablo Riedemann, None.

MO0236

**Determinants of Osteoporosis Screening in Men.** Cathleen Colon-Emeric<sup>\*1</sup>, Joanne LaFleur<sup>2</sup>, Kenneth Lyles<sup>1</sup>, Robert Adler<sup>3</sup>, Courtney VanHoutven<sup>4</sup>, Carl Pieper<sup>1</sup>. <sup>1</sup>Duke University, United states, <sup>2</sup>University of Utah, United states, <sup>3</sup>Richmond VAMC, United states, <sup>4</sup>Durham VAMC, United states

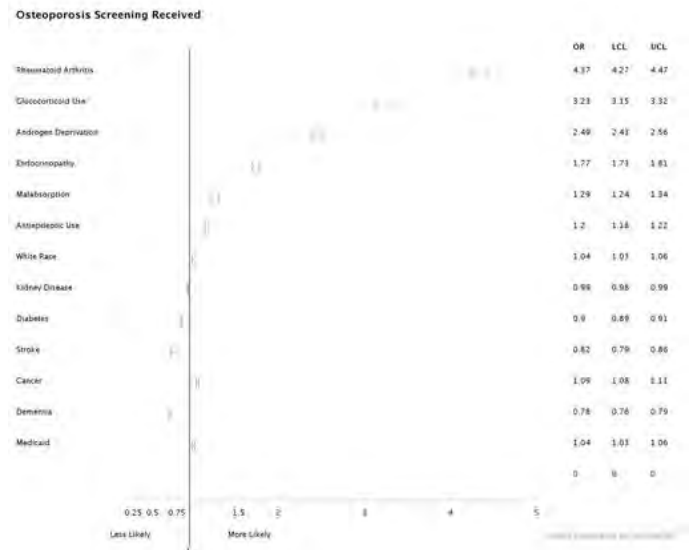
Background: Practice guidelines vary widely on which men to select for osteoporosis screening. We sought to describe screening predictors and disparities.

Methods: Retrospective cohort using 2000-2010 CMS and VA data for 4,987,440 men aged 50-99 who were eligible for osteoporosis screening (no prior fracture, osteoporosis diagnosis or medication). Logistic regression was used to calculate separate propensity scores for screening in the next calendar year, stratified by region and hospital complexity. Predictor variables included fracture risk factors, co-morbidities, social and access factors. Meta-analysis of the resulting odds ratios (OR) across strata was completed. Analyses restricted to men with a 10 year fracture risk of >20% examined interactions by race, rural status, and region.

Results: The mean age was 66 years, 32% were non-white. Selected summary ORs for receiving osteoporosis screening are presented in the attached figure. While most fracture risk factors that guidelines suggest should prompt screening increased the odds of screening in the expected direction, the influence of many was modest, and some were negatively associated with screening (diabetes, stroke, kidney disease). Co-morbidities had a modest impact on screening, but not always in the expected direction; higher Charlson scores were associated with more screening.

Social and access variables had modest expected effects, except that Medicaid status was associated with increased odds of screening. Differential screening receipt by race, geographic region, hospital complexity level, and rural residence will be presented.

Conclusion: Screening for osteoporosis in men is affected by fracture risk factors, co-morbidities, and access to care, but not always in expected directions. Greater clarity around osteoporosis screening guidelines is needed.



Forest Plot Screening

Disclosures: Cathleen Colon-Emeric, None.

MO0237

**Gastrointestinal Events and Association with Adherence to Osteoporosis Medication Among Postmenopausal Osteoporotic Patients: 3 Month Observations from the Medication Use Patterns, Treatment Satisfaction, and Inadequate Control of Osteoporosis Study in Asia Pacific (MUSIC-OS-AP).** Ankita Modi<sup>1</sup>, Peter Ebeling<sup>2</sup>, Mel Lee<sup>3</sup>, Yong-Ki Min<sup>4</sup>, Ambrish Mithal<sup>5</sup>, Xiaoqin Yang<sup>\*1</sup>, Santwona Baidya<sup>6</sup>, Shuvayu Sen<sup>1</sup>, Shiva Sajjan<sup>1</sup>. <sup>1</sup>Merck & Co., Inc., United states, <sup>2</sup>Monash University, Australia, <sup>3</sup>Kaohsiung Chang Gung Memorial Hospital, Taiwan, province of china, <sup>4</sup>Samsung Medical Center, Korea, republic of, <sup>5</sup>Medanta the Medicity, India, <sup>6</sup>Optum, Australia

Purpose: To estimate the association between gastrointestinal (GI) events and adherence to osteoporosis medication at month 3 among postmenopausal women treated for osteoporosis (OP).

Methods: MUSIC-OS-AP is a prospective, observational study of postmenopausal women ≥ 50 years diagnosed with OP enrolled via physician clinics in Taiwan, India, South Korea, New Zealand, and Australia. Women diagnosed with Parkinson's disease, neuromuscular disease, Paget's disease, or malignant neoplasm or treated with any injectable OP medication at enrollment were excluded. Participant-reported adherence to osteoporosis medication was compared between patients with GI and without GI events. Developed GI events by 3 months were patients with GI events absent at baseline, but emergent at 3 months. Continuing GI events by 3 months were patients that reported GI events at both baseline and 3 months. Adherence was measured by the Adherence Evaluation of Osteoporosis Treatment (ADEOS) Scale ranging from 0 to 22. The least-squares mean difference between patients with and without GI events were calculated using multivariate analyses.

Results: A total of 3,286 treated patients with mean age of 65 (standard deviation: 9.49) years were enrolled in this study. At baseline, 59.9% of patients reported to experience GI events. At 3 months, 45.2% of patients reported experiencing GI events in the past 3 months. Covariate-adjusted ADEOS score was significantly lower for patients with continuing GI by month 3 as compared to patients who never had GI by month 3. (LS Mean difference: -0.47; 95% CI: -0.71, -0.23; P<0.001) Covariate-adjusted ADEOS score was significantly lower for patients with developed GI events as compared to patients who never had GI by month 3 (LS Mean difference: -0.73; 95% CI: -1.06, -0.40; P<0.001).

Conclusions: Occurrence of GI events was significantly associated with decreased adherence to OP medication in postmenopausal women who were treated for OP.

Disclosures: Xiaoqin Yang, Merck & Co., Inc., 15  
This study received funding from: Merck & Co., Inc.

## MO0238

**General Practitioners' Views on Osteoporosis Management and Their Views on FRAX: A Qualitative Study.** Päivi Piispanen<sup>1</sup>, Eva Toth-Pal<sup>2</sup>, Helena Salminen\*<sup>3</sup>. <sup>1</sup>Academic Healthcare Centre, Sweden, <sup>2</sup>Department of Neurobiology, Care Sciences & Society, Sweden, <sup>3</sup>Department of Neurobiology, Care Sciences & Society, Karolinska Institutet, Sweden

**Purpose:** This qualitative study used focus group interviews to explore the views among GPs and residents on caretaking of patients with osteoporosis in Stockholm, Sweden.

**Method:** Semi-structured focus group interviews with 2-7 participants, including GPs and residents from primary care units in Stockholm. Four group interviews were conducted with a total of 17 participants until thematic saturation was reached in the material. Each interview had a moderator and one observer present. The moderator used an interview-guide to facilitate and direct the interview towards osteoporosis. All interviews were audio taped and transcribed and analyzed using thematic analysis.

**Results:** One main theme was found: "Osteoporosis is a silent disease and it is overshadowed by other conditions". Seven sub-themes were found belonging to this main theme. The sub-themes were: osteoporosis was regarded as a non-priority issue; the GPs perceived that they could not take the whole responsibility for the management of osteoporosis; they perceived gaps in their knowledge and awareness of the condition; FRAX was considered a tool of uncertain value; the treatment and medication was perceived as complex. The GPs also described that the healthcare system dictated in detail their work but they also perceived having some possibilities to improve the management of osteoporosis care.

**Conclusion:** Management of osteoporosis was perceived as complicated in primary care because osteoporosis was very often overshadowed by other conditions and the GPs perceived that both the doctor and the patient prioritized taking care of other health problems.

**Disclosures:** Helena Salminen, None.

## MO0239

**Impact of Hip Fracture on Health-Related Quality of Life at Hospital Admission and Up to 4 Months Follow-Up: the SPARE-HIP Prospective Cohort.** Daniel Prieto-Alhambra\*<sup>1</sup>, Ignacio Aguado-Maestro<sup>2</sup>, Ignacio Andrés Cano<sup>3</sup>, Mariano Barrés Carsi<sup>4</sup>, Fátima Brañas Baztán<sup>5</sup>, Manuel Francisco Bravo Bardají<sup>6</sup>, José Ramón Caeiro Rey<sup>7</sup>, Pedro Carpintero<sup>8</sup>, Francisco Javier Carrillo<sup>9</sup>, Ángel Castro Sauras<sup>10</sup>, Iñigo Etxebarria-Foronda<sup>11</sup>, Laura Ezquerro Herrando<sup>12</sup>, Nuria Fernández González<sup>13</sup>, Cristina Gallego Terres<sup>14</sup>, Javier Marín Sánchez<sup>15</sup>, Carlos Martín Hernández<sup>16</sup>, Damián Mifsut Miedes<sup>17</sup>, Sarah Mills Gañan<sup>18</sup>, José Olmos Martínez<sup>19</sup>, Ivan Perez-Coto<sup>20</sup>, María Eugenia Portilla<sup>21</sup>, Nazareth Quiroga Veiga<sup>22</sup>, Mónica Salomó Domènech<sup>23</sup>, Jordi Teixidor<sup>24</sup>, Cristina Tejedor Carreño<sup>25</sup>, Óscar Tendo Gómez<sup>26</sup>, Óscar Torregrosa Suau<sup>27</sup>, José Antonio Valverde García<sup>28</sup>, Antonio Herrera<sup>29</sup>, Adolf Diez-Pérez<sup>30</sup>. <sup>1</sup>NDORMS, University of Oxford, United Kingdom, <sup>2</sup>Department of Orthopaedic Surgery, Hospital Universitario del Río Hortega, Spain, <sup>3</sup>Orthopaedic Surgery, Traumatology & Rheumatology Department, Hospital Puerta del Mar, Spain, <sup>4</sup>Orthopaedic Surgery & Traumatology Unit, Hospital Universitario y Politécnico La Fe de Valencia, Spain, <sup>5</sup>Geriatric & Internal Medicine Department, Infanta Leonor University Hospital, Spain, <sup>6</sup>Department of Orthopaedic Surgery, Hospital Regional Universitario Carlos Haya, Spain, <sup>7</sup>Department of Orthopaedic Surgery, Complejo Hospitalario Universitario de Santiago de Compostela, Spain, <sup>8</sup>Hospital Universitario Reina Sofía, Spain, <sup>9</sup>Orthogeriatric Unit, Hospital Virgen de la Arrixaca, Spain, <sup>10</sup>Department of Geriatrics, Orthogeriatric Unit, Hospital Obispo Polanco, Spain, <sup>11</sup>Department of Orthopaedic Surgery, Alto Deba Hospital, Spain, <sup>12</sup>Orthopaedic Surgery & Traumatology Service, Hospital Clínico Universitario de Zaragoza, Spain, <sup>13</sup>Geriatric Medicine Department, Hospital Universitario de Getafe, Spain, <sup>14</sup>Orthopaedics & Traumatology Department, Hospital Lluís Alcanyis, Spain, <sup>15</sup>Orthopaedic Surgery & Traumatology Service, Hospital Virgen del Puerto, Spain, <sup>16</sup>Orthopaedic Surgery & Traumatology Service, Hospital Universitario Miguel Servet, Spain, <sup>17</sup>Hospital Clínico de Valencia, Spain, <sup>18</sup>Department of Orthopaedic Surgery, Hospital Universitario La Paz, Spain, <sup>19</sup>Internal Medicine Service, RETICEF, IDIVAL, Universidad de Cantabria, Spain, <sup>20</sup>Department of Orthopaedic Surgery, Hospital Universitario San Agustín, Spain, <sup>21</sup>Geriatric Medicine Department, Hospital Universitario San Carlos, Spain, <sup>22</sup>Department of Orthopaedic Surgery, Complejo Hospitalario Universitario de Pontevedra, Spain, <sup>23</sup>Orthopaedic Surgery & Traumatology Department, Hospital Universitario Parc Tauli, Spain, <sup>24</sup>Trauma Unit, Hospital Vall d Hebron Barcelona, Universitat Autònoma de Barcelona, Spain, <sup>25</sup>Orthopaedic Surgery & Traumatology Unit, Hospital San Pedro, Spain, <sup>26</sup>Department of Orthopaedic Surgery, Hospital Universitario Son Espases, Spain, <sup>27</sup>Bone Metabolism Unit, Internal Medicine Service, Hospital General Universitario de Elche, Spain, <sup>28</sup>Orthopaedic Surgery & Traumatology Department, Hospital Nuestra Señora de Sonsoles, Spain, <sup>29</sup>Department of Surgery, Medicine School, University of Zaragoza, Spain, <sup>30</sup>Department of Internal Medicine, Hospital del Mar-IMIM & Autonomous University of Barcelona, Spain

**Purpose**

Despite the known effects of hip fracture on morbi-mortality, there is a scarcity of data on the impact of such fractures on health-related quality of life (HRQoL). We aimed to estimate the change in HRQoL experienced by hip fracture sufferers at the time of and up to 4 months following a hip fracture.

**Methods**

The SPARE-HIP (Spanish Registry of Hip and Proximal Femur Fractures) cohort comprises of a consecutive sample of hip/proximal femur fracture patients recruited from a representative 45 Spanish hospitals between Jan/2015 and Feb/2016. Patients were consented and recruited at the time of admission for a hip fracture, and then followed at 1 and 4 months post-fracture.

Euro-QoL 5 Dimensions (EQ5D) 3 Levels questionnaires were used to gather information on HRQoL at all 3 visits. Baseline (pre-fracture) status was collected at recruitment.

National preferences (Spain) were used to calculate EQ5D summary scores (utility indices). These represent HRQoL from 0 (worst) to 1 (best), with negative values allowed and equivalent to "worse than dead".

Summary scores and EQ5D global health visual analogic scales (VAS) over time are reported as median (inter-quartile range) and plotted using Kernel Density plots.

**Results**

A total of 696/852 participants with EQ5D data available were included, with mean (standard deviation) age 83.6 (8.6) years, 537 (77.3%) women, and 691 (99.4%) Caucasian. 594 (85.3%) and 513 (73.7%) had 1 and 4-month follow-up data, respectively.

Baseline (pre-fracture) median EQ5D score was 0.72 (0.40 to 0.91), dropping to -0.01 (-0.31 to 0.51) at the time of fracture. Partial recovery was seen at months 1 and 4, with median EQ5D 0.34 (-0.08 to 0.67) and 0.58 (0.08 to 0.77), respectively [Figure 1]. 318 (45.7%) had EQ5D scores <0 (“worse than dead”) at the time of fracture, and 173 and 104 still had negative scores at 1 and 4 months, respectively.

Similar results are seen in global health VAS, with median 69/100 (50 to 80), 40 (30 to 56), 54 (40 to 66), and 60 (50 to 75), respectively, at each time point.

**Conclusions**

Hip fracture has a deep impact on patients’ quality of life, taking their HRQoL from a median of 72% “full quality” to 0% at the time of admission, with almost half of them reporting a HRQoL “worse than dead” at that time. Partial recovery is seen during follow-up to 4 months. More research is needed on the effect of different interventions and packages of care on patient-centered outcomes following a hip fracture.

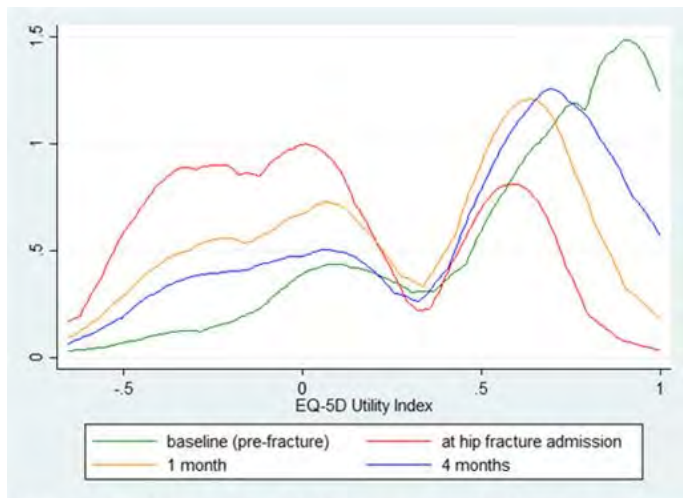


**Figure 1.** Kernel Density Plot: EQ-5D summary scores (utility indices) over time following a hip fracture in the SPARE-HIP cohort.

Figure 1

**Disclosures:** Daniel Prieto-Alhambra, Servier, 11; Amgen, 12  
This study received funding from: Investigator Initiated Study sponsored by AMGEN

**MO0240**

**Structural Equation Modeling of Patients’ Perception in Initiation of Osteoporosis Medication in Japan: An Analysis of Patient Survey Data.**

Masayo Sato<sup>1</sup>, Shuichi Kimura<sup>\*1</sup>, Bruce Crawford<sup>2</sup>, Shigeto Yoshida<sup>2</sup>, Keiko Wada<sup>2</sup>, Xuelu Chen<sup>2</sup>, Hajime Orimo<sup>3</sup>. <sup>1</sup>Eli Lilly Japan K.K., Japan, <sup>2</sup>IMS Japan K.K., Japan, <sup>3</sup>Tokyo Metropolitan Geriatric Hospital & Institute of Gerontology, Japan

**Purpose:** While there are effective medications to prevent osteoporosis-related fractures, less than 20% of patients with osteoporosis in Japan are considered to be on pharmacological treatment. This study aimed to identify the behavioral and cognitive drivers related to medication initiation among patients with osteoporosis in Japan.

**Methods:** An online-survey was conducted among Japanese female patients aged 50 years or older with self-reported osteoporosis diagnosis. The survey questionnaire was developed using a conceptual framework based on health behavioral theories. A structural equation model was developed to test the paths for treatment initiation and to identify variables which affected patients’ behavioral decision making. A bivariate analysis was also conducted to examine the difference between patients who did and did not initiate osteoporosis treatment.

**Results:** A total of 545 patients completed the survey. 90% (n=490) of the patients were currently or previously treated with prescribed medications, and 10% (n=55) were never on medication. The majority of patients (n=397, 73%) perceived their condition to be mild. The model indicated that patients’ knowledge, frequency of office visit, perceived susceptibility, and frequency of medication taking affected the initiation of medication. Knowledge was the strongest driver; patients who initiated medications were more likely to learn information from their physicians or from education materials provided at health facilities. Patients with frequent office visits were also more likely to initiate medications. In addition, bivariate analysis indicated that patients with severe back pain and those who recognized the benefits of pharmacological fracture prevention tended to initiate medications, and only 22% of the patients who had not been on osteoporosis medications acknowledged the need for pharmacologic intervention in addition to supplements.

**Conclusions:** Patients’ knowledge was crucial in their decision to initiate osteoporosis medications. Patients who received knowledge from their physicians or from educational materials from health facilities tended to have a better understanding of osteoporosis and medication needs, and were thus more likely to initiate medication. Further studies are warranted to determine whether more educational activities to increase patient knowledge through physicians and/or education materials are helpful in driving osteoporosis treatment initiation.

**Figure 1.** The relationships among factors affecting osteoporosis medication initiation

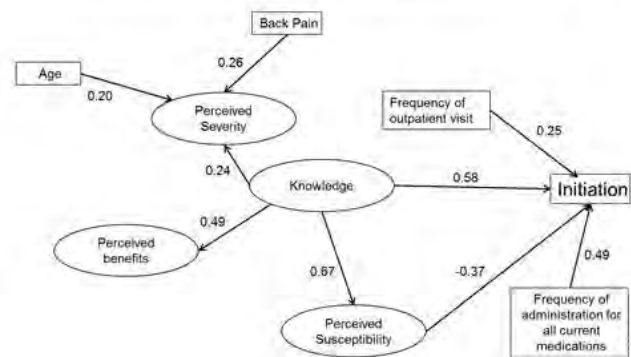


Figure 1

**Disclosures:** Shuichi Kimura, Eli Lilly Japan K.K., 11  
This study received funding from: Eli Lilly Japan K.K.

**MO0241**

**Temporal Trends Analysis of Post-fracture Management: A Population-based Study, 2000-2012.**

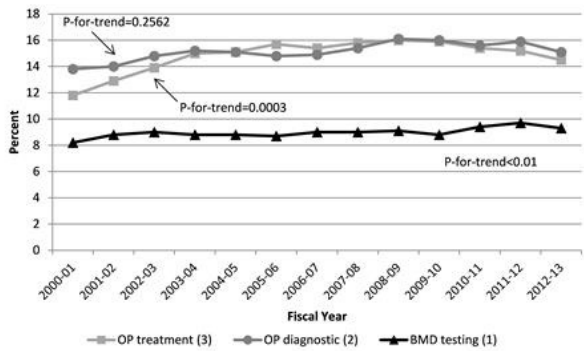
Sonia Jean<sup>\*1</sup>, Philippe Gamache<sup>1</sup>, Jacques P Brown<sup>2</sup>, Louis Bessette<sup>2</sup>, Suzanne N Morin<sup>3</sup>. <sup>1</sup>INSPQ, Canada, <sup>2</sup>University Laval, Canada, <sup>3</sup>McGill University, Canada

**Purpose:** A previous fracture is the most robust and easily-identifiable predictor of future fracture. Preventive strategies that focus on individuals who have sustained fracture should be favoured. The aim of this population-based study was to examine time trends in BMD testing, osteoporosis (OP) diagnostic and treatment rates in the year following non-vertebral fractures in women and men ≥50 years.

**Methods:** Using linked healthcare administrative databases (HAD) from the province of Quebec (Canada), we identified all individuals who sustained a non-vertebral fracture (2000 to 2013) with a validated algorithm based on physicians’ claims (PC) databases (sensitivity >80%). BMD testing, OP diagnostic and OP medication prescription rates were ascertained in HAD up to 12 months following the date of index fracture ( BMD test procedure codes: 8204, 8243, 8245, 8246, 8247; OP diagnosis ICD-9 733.0; hospitalization discharge with OP diagnosis in any field: ICD-9 733.0 or ICD-10 M80-M81; and prescription claims for OP medication [individuals ≥65 years only]).

**Results:** During the study period, 396,839 individuals aged ≥ 50 years sustained a fracture (69.5% women; women median age 71 years and men 63 y). Overall, the proportion of individuals receiving BMD testing, OP diagnosis and OP treatment were low: 8.7%, 14.9%, and 14.5% respectively. Post-fracture management varied by gender and fracture site. For individuals without BMD testing in the 3 years prior to the index fracture, BMD testing increased slightly from 8.1% in 2000/2001 to 9.3% in 2012/2013 (p-for-trend<0.01) (Figure 1). For those without a prior OP diagnosis, we did not observe any variation in OP diagnosis over time (p-for-trend=0.2562). For individuals who were not on treatment in the year prior to fracture, OP medication use increased from 11.8% in 2000/2001 to 16% in 2008/2009 and then declined slightly to 14.5% in 2012/2013 (p-for-trend=0.0003).

**Conclusions:** As reported previously, an OP care gap persists among individuals who experience osteoporosis-related fractures. Despite publication of clinical practice guidelines, implementation of fracture liaison services and access to effective therapies, post-fracture management remains extremely low in Quebec and has not increased significantly overtime. We are currently developing a provincial strategy for secondary fracture prevention in collaboration with clinicians, researchers, patient representatives and policy makers.



(1) Among individuals without BMD testing in the 3 years prior the fracture.  
 (2) Individuals who received an OP diagnosis before the fracture were excluded.  
 (3) Individuals who filled at least 1 OP prescription in the year before the fracture were excluded.

Table 1: Percent of individuals with BMD, OP diagnostic and treatment in the year after the fracture

Disclosures: *Sonia Jean, None.*

## MO0242

**Fracture Liaison Service Return on Investment (cost off-set) Calculator.** David Lee\*<sup>1</sup>, Arnie Aldridge<sup>2</sup>. <sup>1</sup>National Bone Health Alliance, United states, <sup>2</sup>RTI, United states

National Bone Health Alliance (NBHA) has collaborated with Research Triangle Institute (RTI), UAB School of Medicine, and other partners to develop an interactive calculator to provide estimates of the impact of an FLS program on health care costs and revenues.

The FLS return on investment (cost offset) calculator will provide those considering adoption of FLS with a tool that demonstrates the impact of FLS in reducing fractures and details the expected changes in costs and revenues. The interactive nature of the calculator will allow a user to use characteristics specific to their patient population and identify optimal patient groups for targeting high-impact FLS program.

The FLS ROI calculator is being constructed for two related objectives. First, the calculator will provide a variety of estimates of the costs (and thus potential cost savings) associated with healthcare use following fractures using statistical modeling techniques. These estimates will vary by multiple strata of population characteristics, risk factors and geography which will allow for estimates tailored to specific providers, payers, managed care organizations and other stakeholders and policy makers. To improve scientific rigor the estimates will furthermore be adjusted by results from the literature on the effectiveness of FLS and other interventions and by sensitivity analyses around statistical model assumptions. The second objective is as a decision support tool for NBHA. In addition to tailored cost savings, the calculator also yields predictions of fracture prevalence. NBHA and other stakeholders can use these estimates to help make optimal decisions about which facilities or organizations to target for FLS implementation.

The calculator and its underlying model are being supported by contemporary data on relevant patient populations. These data provide the prevalence of fractures and related costs across geographic, demographic, diagnostic and provider/payer characteristics. The first data source is Medicare data comprising the 5% investigator sample and a 100% female sample. Statistics on these data are being provided by a collaborator at the UAB School of Medicine who house these data and have long experience analyzing them

- The team will use Medicare data and other sources from industry partners, if available, to estimate the prevalence of fragility fractures by type of fracture and demographic and other patient characteristics that can be customized by the user.
- Cost data will be derived from Medicare claims data, health economic literature, and other sources (e.g., FLS pilot).
- We will utilize estimates from the literature of the impact of FLS on receipt of necessary treatment and the effectiveness of the treatment to estimate changes in the re-fracture rate attributable to FLS.

Disclosures: *David Lee, Amgen, 11*  
 This study received funding from: *Amgen*

## MO0243

**Estimating the Long-Term Functional Burden of Osteoporosis-Related Fractures.** Andrew Mulcahy<sup>1</sup>, Shira Fischer<sup>1</sup>, Lionel Pinto\*<sup>2</sup>, Orla Hayden<sup>1</sup>, Rich Barron<sup>2</sup>. <sup>1</sup>RAND Corporation, United states, <sup>2</sup>Amgen Inc., United states

Background: While fractures are associated with short-term reductions in functional status, there is limited information on long-term burden of fracture. Data

on long-term burden can help policymakers, health care practitioners, and payers fully characterize the fracture burden and make better decisions.

Approach and Data: We estimated the health and functional status associated with osteoporosis-related fractures using linked 1992-2012 Health and Retirement Survey and Medicare claims data. We excluded respondent-month pairs with missing HRS responses, incomplete Medicare fee-for-service enrollment, or with cancer and trauma e-codes coinciding with fracture events. We matched the remaining fracture cases (n=859) to non-fracture controls using propensity scores from a model incorporating age, gender, race/ethnicity, baseline health care spending, and proxy completion of HRS as predictors of fracture, fitting separate models for each HRS round. We used a difference-in-difference (DD) approach to compare the change in outcomes from pre-fracture to post-fracture separately at two follow-up periods—over two HRS rounds or four calendar years—for fracture cases relative to the change over the same time periods for matched controls.

Results: Detailed means and DD estimates for each cohort and HRS periods are provided in Table 1. Fracture cases had larger declines in activities of daily living (ADLs; DD=0.47 and 0.43 in post-fracture HRS periods 1 and 2, respectively, both p<0.001) and in instrumental activities of daily living (IADLs; DD=0.08 and 0.15 in HRS periods 1 [p<0.001] and 2 [p=0.037], respectively) compared to matched controls. Fracture cases also had larger declines in the HRS continuous mobility index (DD=0.54 points), gross motor index (DD=0.58 points), large muscle index (DD=0.34), and fine motor index (DD=0.15 points, all p<0.001) in HRS period 1, and these differences persisted in period 2. Fracture cases experienced a larger decline in self-reported health status (measured on a 5-point scale) in the first HRS period after fracture compared to matched controls (DD=0.14, p=0.004), but this difference in decline diminished in period 2 (DD=0.09 points, p=0.106).

Discussion: Results suggest that fractures are associated with significant declines in functional activities that persist beyond two years. Payers and policymakers should consider the long-term burden of fracture when weighing treatment, prevention, and education interventions.

Changes in Outcomes over One and Two HRS Periods Post Fracture in Fracture Cases and Matched Controls

Outcomes	Cohorts	Pre-index Mean (SD)	Post-index HRS1 Mean (SD)	Post-index HRS2 Mean (SD)	Mean (Diff in Diff) Period 1	Mean (Diff in Diff) Period 2
Count of ADLs	Fracture Cases (N = 859)	0.56 (1.06)	1.39 (1.57)	1.49 (1.80)	-0.43*	-0.43*
	Matched Controls (N = 859)	0.54 (1.17)	0.71 (1.35)	1.05 (1.64)		
Count of IADLs	Fracture Cases (N = 859)	0.26 (0.71)	0.51 (0.88)	0.57 (1.12)	-0.08*	0.15**
	Matched Controls (N = 859)	0.26 (0.70)	0.41 (0.81)	0.61 (1.13)		
General Health Status	Fracture Cases (N = 859)	3.15 (1.13)	3.09 (1.09)	3.46 (1.10)	0.14**	0.09
	Matched Controls (N = 859)	2.96 (1.14)	3.08 (1.12)	3.17 (1.13)		

\*p<0.001; \*\*p<0.05  
 Note: ADLs and IADLs are counts, with higher values indicating worse function. General Health Status was measured on a 5-point scale, with higher values indicating worse health status.

Results Table for Functional-Burden Abstract

Disclosures: *Lionel Pinto, Amgen Inc, 11*  
 This study received funding from: *Amgen Inc.*

## MO0244

**The rate of self-reported gastrointestinal events among osteoporotic women: Month 12 Results of the Medication Use Patterns, Treatment Satisfaction and Inadequate Control of Osteoporosis Study (MUSIC-OS).** Ankita Modi\*<sup>1</sup>, Shuvayu Sen<sup>2</sup>, Jonathan Adachi<sup>3</sup>, Silvano Adami<sup>4</sup>, Bernard Cortet<sup>5</sup>, Alun Cooper<sup>6</sup>, Piet Geusens<sup>7</sup>, Dan Mellström<sup>8</sup>, Joop van den Bergh<sup>9</sup>, Paul Keown<sup>10</sup>, Jessica Weaver<sup>2</sup>, Shiva Sajjan<sup>2</sup>. <sup>1</sup>Center for Observational & Real-World Evidence, Merck & Co., Inc., United states, <sup>2</sup>Center for Observational & Real-World Evidence, Merck & Co., Inc, United states, <sup>3</sup>St Joseph's Healthcare & McMaster University, Canada, <sup>4</sup>Department of Medicine, University of Verona, Italy, <sup>5</sup>Department of Rheumatology, University Hospital of Lille, France, <sup>6</sup>Bridge Medical Center, United Kingdom, <sup>7</sup>Department of Rheumatology, Maastricht University Medical Center, Netherlands, <sup>8</sup>Department of Internal Medicine & Geriatrics, Gothenburg University, Sweden, <sup>9</sup>Department of Rheumatology, Maastricht University Medical Center, Maastricht & Department of Internal Medicine, VieCuri Medical Center, Venlo, Netherlands, <sup>10</sup>Syreon Corporation, Canada

Background: MUSIC-OS investigated the burden of gastrointestinal (GI) events in osteoporotic women in terms of treatment (Tx) satisfaction, adherence and persistence to Tx, healthcare resource use, and quality of life in Europe and Canada.

Purpose: To describe the rate of existing and new self-reported GI events at baseline (BL), 3 (M3), 6 (M6) and 12 (M12) months after study enrollment among osteoporotic (OP) women receiving osteoporosis treatment.

Methods: Osteoporotic women ≥50 years of age treated for OP were enrolled during routine visits to their physicians. Women were stratified into 2 subgroups of new users (receiving OP Tx for <90 days) or experienced users (receiving the same OP Tx for ≥ 90 days) based on the duration of treatment at enrollment. Questionnaires probed the frequency and nature of GI events, and data were reported as cumulative frequency, new event rate and point probability at each time point.

Results: 2,943 women with a mean age of 69.5 years were enrolled in the study, of whom 68.1% at BL reported a GI problem in the past 6 months. Cumulative frequency of GI events increased to 75.9% of women at M3 (n=2,762), of whom 10.1%

had reported no GI events at baseline ('new' GI events); to 79.0% at M6 (n=2,676) of whom 4.5% experienced new GI events since M3, and to 81.1% at M12 (n=2,546), of whom 2.6% experienced new GI events since M6. Among new users, 64.6% reported a GI event at BL (n=672), 75.4% by M3 (new events: 13.9%), 79.6% by M6 (new events: 6.2%) and 81.5% by M12 (new events: 2.5%). For experienced users, 69.2% reported a GI event at BL (n=2271), 76.0% by M3 (new events: 9.0%), 78.9% by M6 (new events: 4.0%) and 81.1% by M12 (new events: 2.6%). Upper and lower GI problems were reported with comparable frequency at each time point (BL: 53.2% vs 54.2%; M3: 77.3% vs 75.9%; M6: 77.7% vs 75.3%; M12: 79.8% vs 74.0% respectively) and the leading symptoms at M12 were heartburn / acid reflux (52.8%), followed by diarrhea / constipation (51.7%), bloating (46.6%), upset stomach / indigestion (39.8%) and lower stomach pain (22.2%).

Conclusion: Two-thirds of osteoporotic women receiving OP treatment report experiencing GI events at baseline, and an even larger proportion (81.1%) of women reported experiencing GI events by M12. The rate of GI events in women treated for OP presented here is higher than those reported elsewhere, perhaps as a result of the self-reported nature of the study design and types of GI events reported.

**Disclosures:** *Ankita Modi, Employee of Merck and Co., Inc., 15*  
*This study received funding from: Merck & Co., Inc.*

## MO0245

**Cut-points for Associations Between Vitamin D Status and Multiple Musculoskeletal Outcomes in Middle-aged Women.** Feitong Wu<sup>1\*</sup>, Karen Wills<sup>1</sup>, Laura Laslett<sup>1</sup>, Brian Oldenburg<sup>2</sup>, Markus Seibel<sup>3</sup>, Graeme Jones<sup>4</sup>, Tania Winzenberg<sup>4</sup>. <sup>1</sup>Menzies Institute for Medical Research, University of Tasmania, Hobart, Tasmania, Australia, Australia, <sup>2</sup>School of Population & Global Health, University of Melbourne, Australia, <sup>3</sup>Bone Research Program, ANZAC Research Institute, The University of Sydney, Australia, <sup>4</sup>Menzies Institute for Medical Research, University of Tasmania, Australia

Purpose This study aimed to determine whether cut-points exist for associations between serum 25-hydroxyvitamin D (25OHD) and musculoskeletal health outcomes, below which greater 25OHD levels are associated with musculoskeletal health benefits and above which no such associations exist.

Methods Cross-sectional study of 344 women aged 36-57 years. Cut-points for associations of serum 25OHD with lumbar spine (LS) and femoral neck (FN) bone mineral density (BMD), lower limb muscle strength (LMS), timed up and go test (TUG), functional reach test (FRT), lateral reach test (LRT) and step test (ST) were explored using locally weighted regression smoothing and nonlinear least-squares estimation, and associations above and below the identified cut-points estimated using segmented regression.

Results The prevalence of low 25OHD was 28% (<50 nmol/L). Significant cut-points (nmol/L) were identified for FN BMD 31 (95% confidence interval (CI): 18, 43), LS BMD 31 (17, 45), TUG 30 (24, 36), ST 33 (24, 31), FRT 31 (18, 43) and LMS 29 (8, 49) but not LRT (42 (-8, 93)). Below these cut-points, there were beneficial associations between higher 25OHD level and each outcome while above the cut-points there were no beneficial associations.

Conclusions In middle-aged women, there are thresholds for associations between serum 25OHD concentrations and bone density and most balance measures, suggesting that a 25OHD levels of at least 29 to 33 nmol/L are required for optimal musculoskeletal health in this population. The current cut-off of 50 nmol/L may be higher than needed for some outcomes but appears warranted overall.

**Disclosures:** *Feitong Wu, None.*

## MO0246

**Influences of Dietary Vitamin D Restriction on Bone Strength, Body Composition, and Muscle in Rats Fed a High-fat Diet.** Yuno Oku<sup>1\*</sup>, Rieko Tanabe<sup>1</sup>, Kanae Nakaoka<sup>1</sup>, Asako Yamada<sup>1</sup>, Seiko Noda<sup>1</sup>, Ayumi Hoshino<sup>1</sup>, Mayu Haraikawa<sup>2</sup>, Masae Goseki-Sone<sup>1</sup>. <sup>1</sup>Japan Women's University, Japan, <sup>2</sup>Seitoku University, Japan

Vitamin D deficiency is associated with a greater risk of osteoporosis and also influences skeletal muscle functions, differentiation, and development. Common obesity is associated with metabolic syndrome, and low levels of serum 25-dihydroxyvitamin D<sub>3</sub> were frequently observed in patients with obesity. Both obesity and vitamin D deficiency have been recognized as major public health issues worldwide. In the present study, we investigated the influences of vitamin D restriction on the body composition, bone, and skeletal muscle in rats fed a high-fat diet.

Sprague-Dawley strain male rats (11 weeks old) were divided into four groups and fed experimental diets: a basic control diet (Cont.), a basic control diet with vitamin D restriction (DR), a high-fat diet (F), and a high-fat diet with vitamin D restriction (FDR). At 28 days after starting the experimental diets, the visceral fat mass was significantly increased in the F group compared with Cont. group and the muscle mass tended to decrease in the DR group compared with Cont. group. The total volume of the femur was significantly lower in the DR group compared with Cont. group and the bone mineral density (BMD) of the femur was significantly lower in the FDR group compared with F group. MyoD, Myogenin, and Myf-5 are the muscle-specific transcription factors. The levels of mRNA expression of MyoD and

Myogenin of the soleus muscle tended to decrease in the DR group compared with in the Cont. group. The level of mRNA expression of Myf-5 of the soleus muscle from the FDR group was reduced significantly compared with those from the F group.

In conclusion, our findings revealed the influences of a vitamin D-restricted high-fat diet on the bone strength, body composition, and muscle. Further studies on vitamin D insufficiency in the regulation of muscle as well as fat and bone metabolism would provide valuable data for the prevention of lifestyle-related disorders, including osteoporosis and sarcopenia.

**Disclosures:** *Yuno Oku, None.*

## MO0247

**Milk and alternatives intervention and bone mineral acquisition in 14 to 18 y postmenarcheal girls: Preliminary results at 12 months from a 2-year randomized controlled trial.** May Slim<sup>1\*</sup>, Catherine Vanstone<sup>1</sup>, Suzanne Morin<sup>2</sup>, Elham Rahme<sup>1</sup>, Hope Weiler<sup>1</sup>. <sup>1</sup>McGill University, Canada, <sup>2</sup>McGill University Health Center, Canada

The role of calcium intake in optimizing peak bone mass during skeletal growth has been widely recognized, with milk and alternatives (MAlt) being a highly bioavailable dietary source. However, average intakes for Canadians 9 y and older fall below Canada's Food Guide (CFG) recommendations for MAlt. The objective was to examine bone mineral accretion from baseline to 12 months (mo) in postmenarcheal girls with usual intake of < 2 servings who are participating in a 2-year MAlt intervention that started in August 2014. Healthy girls 14 to 18 y from Montreal, Canada were randomized to control [no intervention], improved (IInt) [2 to 3 MAlt servings/d] or recommended (RInt) [3 or more MAlt/d] intervention groups. Bone mineral content (BMC, g), bone mineral density (BMD, g/cm<sup>2</sup>) and BMD z-scores (BMDZ) of the whole body (WB), non-dominant forearm (FA), femoral neck (FN), total hip (TH) and lumbar spine (LS) were measured at baseline and at 12 mo using DXA (Hologic Discovery, Apex software version 13.5). Differences among trial groups were tested using mixed model ANOVA and post hoc Bonferroni tests; data are mean ± SD. At baseline (Table 1), participants (mean age 15.5 ± 1.5, n= 16) revealed no difference among groups in BMD and BMC at WB, FA, and FN, however both parameters were significantly higher at LS and TH in the RInt (p=0.02). At 12 mo, no difference within groups was observed at all sites measured, whereas BMC, BMD and BMD z-scores were significantly different in the RInt group (p < 0.04) at WB, LS, and TH. The RInt group had greater increases of WB BMC compared with the control and the IInt groups (+8.7% vs +2.1% vs +1.6% respectively, P < 0.02) and WB BMD compared to the IInt group (+3.38% vs +0.65%, P < 0.04) (Table 2). These preliminary results suggest that increasing MAlt intake to meet CFG's recommendation for this age group favors bone mineral acquisition particularly at whole body. Our long-term study will confirm these results.

Table 1: Baseline characteristics of participants

	Control group (n=4)	Improved group (n=6)	Recommended group (n=6)
Age (y)	15.00 ± 0.8	15.7 ± 1.5	15.7 ± 1.9
Height Z-score	0.4 ± 0.6	0.4 ± 1.4	1.0 ± 1.6
Body Mass Index Z-score	0.6 ± 0.5	-0.0 ± 1.2	0.5 ± 0.7
Age at Menarche (y)	11.5 ± 0.6	12.7 ± 0.8	13.3 ± 1.7
Physical Activity (min/wk)	479.0 ± 167.0	282.5 ± 273.1	444.8 ± 201.9

\* No significant difference among groups. Data are expressed as mean ± SD.

Table 2: Whole body bone mineral content changes at 12 months in 14 to 18 adolescent girls.

	Control group (n=4)	Improved group (n=6)	Recommended group (n=6)
Accretion rate (g)	34.1 ± 57.3 <sup>a</sup>	51.2 ± 10.5 <sup>a</sup>	199.5 ± 132.4 <sup>b</sup>
Percentage change (%)	2.1 ± 0.3 <sup>a</sup>	1.6 ± 2.9 <sup>a</sup>	8.7 ± 6.0 <sup>b</sup>

<sup>a,b</sup> Groups with different superscripts are significantly different from each other using a mixed model ANOVA and post hoc Bonferroni tests (p<0.05). Data are expressed as mean ± SD.

Tables 1 and 2

**Disclosures:** *May Slim, None.*

*This study received funding from: Dairy Research Cluster*

## MO0248

**Optimal vitamin D status and its relationship with bone and mineral metabolism in Hong Kong Chinese.** Raymond YH LEUNG<sup>1</sup>, Bernard MY CHEUNG<sup>1</sup>, Uyen-Sa Nguyen<sup>2</sup>, Annie WC KUNG<sup>1</sup>, Kathryn CB Tan<sup>1</sup>, Ching-Lung CHEUNG<sup>1\*</sup>. <sup>1</sup>The University of Hong Kong, Hong kong, <sup>2</sup>University of Massachusetts Medical School, United states

Background : Vitamin D has been suggested as an important factor contributed to different medical conditions. Although 25-hydroxyvitamin D (25OHD) is commonly used to define vitamin D deficiency and insufficiency, there is no consensus on how to define vitamin D deficiency. Moreover, recent data suggested that bioavailable vitamin D levels may be a better proxy of vitamin D status than total 25OHD. In this

study, we aimed to identify the 25OHD threshold that maximally suppress parathyroid hormone (PTH), and to evaluate the association of total, free, and bioavailable 25OHD in bone and mineral metabolism.

**Methods:** The study included 5,276 participants (70% female) of the Hong Kong Osteoporosis Study who aged 20 or above and those with total 25OHD measured. Among these, 2,370 of them also had vitamin D binding protein data. Piecewise regression was used to identify the optimal break point between total 25OHD and bone and mineral markers, whereas 95% CI was estimated using bootstrap method. Association of total, free, bioavailable vitamin D with bone and mineral markers were evaluated using linear regression with adjustment for age, sex, body mass index, season, smoking status, drinking status, and physical activities.

**Results:** The prevalence of vitamin D deficiency observed was 43.8% and the prevalence of vitamin D insufficient or deficiency levels is 90.1% in our study population, according to the definition of vitamin D deficiency and insufficiency as 50nmol/L and 75nmol/L respectively. Using piecewise quadratic-quadratic regression, the best fit threshold of total 25OHD on PTH suppression was 31.8nmol/l (95% CI:18.6-89.1) with an  $r^2$  of 0.042. Total 25OHD was significantly associated with serum calcium (standardized beta=0.108), albumin-adjusted calcium (standardized beta=0.087), PTH (standardized beta=-0.205), and femoral neck BMD z-score (standardized beta=0.031). In contrary, such associations were either less strong or insignificant for calculated free and bioavailable 25OHD.

**Conclusion:** The threshold for 25OHD at the point of maximal suppression of PTH estimated in this study was lower than the suggested threshold of vitamin D deficiency by IoM (50nmol/L). The bioavailable vitamin D seems to be a less indicative biomarker for bone health and mineral metabolism. However, further investigation is needed to validate this finding in independent studies.

**Disclosures:** Ching-Lung CHEUNG, None.

## MO0249

### Bone mineral accrual during puberty and its association with serum levels of growth hormone and insulin-growth factor I in vocational ballet dancers.

Tânia Amorim<sup>\*1</sup>, José Maia<sup>2</sup>, George S. Metsios<sup>1</sup>, Andreas D. Flouris<sup>3</sup>, Matthew Wyon<sup>1</sup>, José Carlos Machado<sup>2</sup>, Franklin Marques<sup>2</sup>, Nuno Adubeiro<sup>4</sup>, Luisa Nogueira<sup>4</sup>, Yiannis Koutedakis<sup>3</sup>. <sup>1</sup>University of Wolverhampton, United Kingdom, <sup>2</sup>University of Porto, Portugal, <sup>3</sup>University of Thessaly, Greece, <sup>4</sup>Polytechnic Institute of Porto, Portugal

#### Purpose

Cross-sectional studies have shown that vocational female ballet dancers have less bone mineralization than controls. However, less is known on how bone mineral content (BMC) accrual changes during growth in this population. The extent to which circulating levels of growth hormone (GH) and insulin-like growth factor I (IGF-1) exert an influence on bone acquisition of vocational dancers is also unknown. This study aims to: (i) model BMC accruals in vocational female ballet dancers and matched-controls; (ii) determine whether circulating levels of GH and IGF-1 are associated with BMC changes during the developmental process.

#### Methods

Sixty-six vocational female ballet dancers and sixty-two female controls between 10-15yrs were monitored for 3 years. BMC was measured annually at the femoral neck (FN) (impact site) and forearm (FA) (non-impact site) using Dual-Energy X-Ray Absorptiometry. GH and IGF-1 serum concentrations were also determined annually by immunoradiometric assay. Data were centred on age at peak height velocity (PHV). Multilevel models were created to determine BMC accruals across groups, and to explore the association between BMC gains with the studied hormones.

#### Results

At baseline, vocational ballet dancers had significantly less bone content compared to controls at the FN (~0.250g less (7%),  $p<0.05$ ) and FA (~0.360g less (42%),  $p<0.05$ ). Controls significantly gain more BMC throughout growth at the measured anatomical sites than vocational ballet dancers (FN: 36% more than dancers,  $p<0.05$ ; FA: 37% more than dancers,  $p<0.05$ ). The rate of BMC accrual was positively associated with changes in circulating levels of GH and IGF-1 in both groups ( $p<0.05$ ). However, when a group interaction was considered in the same model, these hormones failed to demonstrate significant predictive effects.

#### Conclusions

The present data indicate that a) vocational female ballet dancers are not accruing bone content at the same rate as controls at both impact (FN) and non-impact (FA) sites, and b) GH and IGF-1 circulating levels do not explain the differences found between groups in terms of BMC gains. Future studies should search for factors associated with low BMC in vocational female dancers and establish whether such BMC values have any bearing in peak bone mass.

**Disclosures:** Tânia Amorim, None.

## MO0250

**Can Exercise Protect Against the Age-associated Declines in Vertebral Height? The ProAct65+ Bone Study.** Rachel L Duckham<sup>\*1</sup>, Tahir Masud<sup>2</sup>, Rachael Taylor<sup>3</sup>, Denise Kendrick<sup>4</sup>, Hannah Carpenter<sup>4</sup>, Dawn A Skelton<sup>5</sup>, Susie Dinan-Young<sup>6</sup>, Steve Iliffe<sup>4</sup>, Richard Morris<sup>7</sup>, Hayley Ladd<sup>8</sup>, Katherine Brooke-Wavell<sup>8</sup>. <sup>1</sup>Institute for Physical Activity & Nutrition Research, Deakin University, Australia, <sup>2</sup>Healthcare for Older People, Nottingham University Hospitals NHS Trust, United Kingdom, <sup>3</sup>Healthcare for Older People, Nottingham University Hospitals NHS Trust, United Kingdom, <sup>4</sup>School of Medicine, University of Nottingham, United Kingdom, <sup>5</sup>School of Health & Life Sciences, United Kingdom, <sup>6</sup>Department of Primary Care & Population Health, University College London, United Kingdom, <sup>7</sup>School of Social & Community Medicine, University of Bristol, United Kingdom, <sup>8</sup>School of Sport, Exercise & Health Sciences, Loughborough University, United Kingdom

The most common type of osteoporotic fracture is vertebral compression fracture (VCF). Although causing significant physical limitations, pain and morbidity, two thirds of VCF fractures go undiagnosed. Targeted weight-bearing exercise incorporating progressive strength exercises may provide an effective non-pharmacological intervention against age-associated declines in vertebral bone architecture, helping to prevent VCFs. This study investigated the effectiveness of a 6-month community-based group (FaME) and home-based (OEP) exercise intervention on (T8-L4) height and VCF incidence. Participants were 319 men and women, aged (mean + SD) 72 + 5 years who were recruited through primary care and randomised by practice to FaME, OEP or a usual care group. Lateral Vertebral Morphometry was assessed using Dual-energy X-ray Absorptiometry (DXA) (GE-Lunar Prodigy) prior to randomisation and following the 24-week intervention. Dual-energy Vertebral Assessment (DVA) was used to calculate the anterior, middle and posterior heights of T8-L4 vertebral bodies, and detect the type (wedge, biconcave or crush) and severity (mild, moderate or severe) of vertebral deformities. Repeated measures general linear model (GLM), adjusted for gender and age was used to assess anterior, middle and posterior dimensions of T8-L4 vertebrae over time. Alpha level was set at  $P<0.05$ . A total of 268 participants (FaME n=95; OEP n=74; usual care n=99) with sufficient vertebral morphometry data were included in the final analysis. Four new deformities (OEP: 1, FaME: 2 and Usual care: 1) were detected over the 6-month intervention. Changes in mean vertebral heights were small (ranging from -0.1 to 0.2 mm), there was no significant main effect of time ( $p=0.69$ ) and changes over time did not differ between groups (time x group interaction  $p=0.49$ ). In conclusion, an exercise intervention, including progressive strength exercises, specifically targeted at preventing falls, did not influence vertebral height or prevent VCFs. The number of incident vertebral deformities was not enough to detect differences in incidence and a trial period of six months seemed insufficient to detect changes in vertebral height. There is a need for longer-term studies to examine the potential role of exercise in preventing vertebral deformity.

**Disclosures:** Rachel L Duckham, None.

## MO0251

**The effects of dried plum supplementation on bone mRNA expression levels of Dkk-1, Sclerostin,  $\beta$ -catenin, Runx2, and Cx43 in ovariectomized rat model of osteoporosis.** Lama Almainan<sup>\*1</sup>, Bahram Arjmandi<sup>2</sup>, Shirin Hooshmand<sup>1</sup>. <sup>1</sup>San Diego State University, United states, <sup>2</sup>Florida State University, United states

Several studies showed that dried plum is highly effective in preventing and reversing ovarian hormone-deficiency-associated bone loss in a rat model of osteoporosis. Clinical trials reported that dried plum supplementation significantly increased bone formation in postmenopausal women, as well. However, dried plum's mechanisms of action have not been fully understood. Dried plum has been found to interact with important bone metabolism markers to prevent and/or reverse bone loss in both human and animal studies. The induction of the Wnt signaling pathway leads to bone formation while the inactivation of the Wnt signaling pathway results in osteopenia. The objective of this study was to explore the effects of dried plum supplementation on Wnt signaling and other markers involved in bone remodeling and resorption in ovariectomized Sprague-Dawley rats. Ten 3-month-old ovariectomized Sprague-Dawley rats were divided into two groups (n=5 per group); treatment group (15% w/w dried plum) and control group (control diet) for 3 months. Femoral necks were analyzed for microstructural properties using micro-computed tomography ( $\mu$ CT 35). RNA was extracted from each sample and reverse transcribed into cDNA for gene expression analysis. The dried plum treatment group tended to have higher levels of  $\beta$ -catenin compared to the control. Similarly, connexin 43 (Cx43) and Runx-related transcription factor 2 (Runx2) expression levels increased in the treatment group compared to the control. Dickkopf-1 (Dkk-1), and Sclerostin had higher levels in the dried plum group, albeit not significant. Our findings indicate that dried plum diet is effective in preventing bone loss by increasing biomarkers involved in osteoblast differentiation leading to increased bone formation. However, in this pilot study dried plum was not successful in inhibiting the expression levels of markers associated with the inactivation of the Wnt signaling pathway.

**Disclosures:** Lama Almainan, None.

## MO0252

**A 5% Increase in Trabecular (Spine) Bone Density Occurs in the First six Months After Weaning (Factors Affecting Bone Formation After Breastfeeding Pilot Study [FABB-Pilot]).** Sandra Cooke-Hubley\*<sup>1</sup>, Beth J. Kirby<sup>1</sup>, Chrissy Wells<sup>1</sup>, Gerry Mueford<sup>1</sup>, James Valcour<sup>1</sup>, Jonathan D. Adachi<sup>2</sup>, Christopher S. Kovacs<sup>1</sup>. <sup>1</sup>Memorial University, Canada, <sup>2</sup>McMaster University, Canada

Much of the calcium content of breast milk is obtained from resorption of the mother's skeleton. Few studies have examined the speed and extent of BMD recovery after weaning, or the factors that predict a greater post-lactation increase in BMD. We hypothesize that weight-bearing, nutrition, hormones, and other factors facilitate bone formation after lactation.

The aims of the FABB-Pilot were to determine the magnitude of increase in BMD at six months after weaning, and provide preliminary data to enable pre-specification of predictive variables to be tested in a future, larger-scale FABB study.

We recruited women who had breastfed exclusively (no formula) or near-exclusively (1-2 formula/solid feeds per day) for 4 to 6 months, and by so doing should have experienced a significant decline in BMD. At time of planned weaning and six months later, we measured BMD, whole body fat and lean mass, and hip structural analysis (HSA) by DXA; blood calcium, ionized calcium, PTH, PTHrP, estradiol, 25OHD, calcitriol, P1NP, CTX, sclerostin; and urine Ca/Cr. Questionnaires administered at both time points assessed nutrition, weight-bearing activities, and other factors that may influence bone recovery.

31 women (31.6±3.5 years, 94% Caucasian, 1.53±0.63 births) enrolled at 26.6±2.0 weeks post-partum. Approximately 80% had breastfed exclusively for six months. All 31 completed the follow-up assessments, but only 20% had fully weaned as planned. Mean thoracic spine BMD increased 5.1% (0.713 to 0.749 g/cm<sup>2</sup>, p<0.01); lumbar spine increased 4.0% (0.971 to 1.01 g/cm<sup>2</sup>, p<0.03), while cortical sites (hip, total body) remained unchanged. HSA indices showed no changes. Estradiol increased (115 to 198 pmol/L, p<0.01), PTH increased (60 to 69 ng/mL, p<0.04), calcitriol decreased (198 to 115 pmol/L, p<0.01), 25OHD declined (80 vs 64 nmol/L, p<0.01), CTX declined (0.47 to 0.37 ng/mL, p<0.04), while P1NP, sclerostin, calcium, and ionized calcium did not change. Vitamin D, calcium intake, and physical activity did not change. Menses returned in 65% of women while still breastfeeding. Univariate analyses indicated that oral contraceptive use, earlier weaning, and reduced feeds predicted a greater increase in BMD after six months.

In conclusion, trabecular (spine) BMD increases significantly in the first six months after exclusive lactation ends, with greater gains in those who fully wean the baby. The factors that promote this post-lactation increase in BMD remain to be identified.

**Disclosures:** Sandra Cooke-Hubley, None.

## MO0253

**Effect of 12-week Tocotrienol Supplementation on Bone Biomarkers, Safety, and Quality of Life in Postmenopausal Osteopenic Women: A Randomized Double-blinded Placebo-controlled Study.** Chwan-Li Shen\*<sup>1</sup>, Shengping Yang<sup>1</sup>, Michael Tomison<sup>1</sup>, Amanda Romero<sup>1</sup>, Carol Felton<sup>1</sup>, Peishuan Tsai<sup>1</sup>, Barbara Pence<sup>1</sup>, Huanbiao Mo<sup>2</sup>. <sup>1</sup>Texas Tech University Health Sciences Center, United states, <sup>2</sup>Georgia State University, United states

Osteoporosis is a major health problem in postmenopausal women. This study was to evaluate the effects of 12-week tocotrienol (TE) supplementation on bone turnover biomarkers and related mechanism, safety, and quality of life in postmenopausal osteopenic women. Eighty nine participants (59.7±6.8 yr, BMI 28.7±5.7 kg/m<sup>2</sup>) were assigned to 3 treatments: placebo (860 mg olive oil/day), Low TE (300 mg TE/day), and High TE (600 mg TE/day) for 12 weeks. TE consisted of 90% d-TE and 10% g-TE. Bone formation biomarker (serum bone-specific alkaline phosphatase, BALP), bone resorption biomarker (urine N-terminal telopeptide, NTX), oxidative stress biomarker (urine 8-hydroxydeoxyguanosine, 8-OHdG), and safety (comprehensive metabolic panel, CMP) were assessed at baseline, 6, and 12 weeks. Body composition by bioimpedance and quality of life by SF-36 survey were assessed at baseline and 12 weeks. Data were analyzed by Kruskal-Wallis test, one-way ANOVA, or repeated measure analysis as appropriate. At the baseline, there were no differences in any demographic parameters, CMP, quality of life, and 8-OHdG among 3 treatment groups. After 12 weeks, 2 participants dropped out (3% attrition rate) due to non-compliance. Pill compliance rates for placebo, Low TE, and High TE were 93%, 92%, and 91%, respectively. None of treatments affected any parameters of CMP (safety), body composition (BMI, %fat, and weight), or quality of life throughout the study period. Compared to the placebo group, the Low TE group reduced serum BALP, urine NTX, and urine 8-OHdG by 0.184 U/L (p=0.069), 0.050 nM BCE/mM creatinine (p<0.001), and 10.3% (p<0.001), respectively, for every 6 weeks; the reduction for the High TE group were 0.258 IU/L (p=0.011), 0.061 nM BCE/mM creatinine (p<0.001) and 7.5% (p<0.001), respectively. Neither age nor BMI was associated with serum BALP or urine 8-OHdG. Compared to participants with BMI ≥ 30, urine NTX level was 0.170 nM BCE/mM creatinine higher than those with BMI < 30 (p=0.003). Participant age was not associated with urine NTX level. This clinical trial demonstrated that 12-week TE supplementation suppresses bone turnover rate in postmenopausal osteopenic women, an effect that is correlated with the inhibition of oxidative stress.

**Disclosures:** Chwan-Li Shen, None.

This study received funding from: American River Nutrition, Hadley, MA

## MO0254

**Higher total vitamin C intake is not associated with higher grip strength in adults: The Framingham Offspring Study.** Shivani Sahni\*<sup>1</sup>, Paul F. Jacques<sup>2</sup>, Alyssa B. Dufour<sup>1</sup>, Douglas P. Kiel<sup>3</sup>, Robert R. McLean<sup>1</sup>, Marian T. Hannan<sup>1</sup>. <sup>1</sup>Institute for Aging Research, HSL, Harvard Medical School, United states, <sup>2</sup>Jean Mayer USDA HNRCA, Tufts University School of Nutrition, United states, <sup>3</sup>Institute for Aging Research, HSL, Harvard Medical School, United states

**Objective:** Oxidative stress has been implicated as a central mechanism of age-related decline in muscle. Vitamin C is important for skeletal muscle due to its dual role as an antioxidant and as an enzyme cofactor for collagen and muscle carnitine biosynthesis. In the skeletal muscle, carnitine plays a critical role in energy production by transporting long-chain fatty acids into the mitochondria so they can be oxidized. One study of older Italians reported that higher total vitamin C intake was associated with higher knee extension strength and performance. Therefore, we determined the cross-sectional association of total vitamin C with grip strength in men and women from the Framingham Offspring Cohort.

**Methods:** 2,184 men and women completed a Willett's food frequency questionnaire (in either 1996-1998 or 1999-2001) and had grip strength measured using an adjustable Jamar isometric hand-held dynamometer in 1999-2001 (kg, max of 2 trials). Logarithmic transformation was applied to total vitamin C intake before analysis. Sex-specific linear regression was used to calculate beta coefficients and P values for the association between total vitamin C and grip strength adjusting for age, weight, height, total energy intake (residual method) and physical activity. Least squares adjusted means for grip strength were estimated by tertiles of total vitamin C intake. Linear trend across the tertiles of total vitamin C intake was also examined.

**Results:** Mean age was 58.4±8.8y (range 29-83y). Median total vitamin C intake was 195 mg/d in men and 206 mg/d in women. Mean grip strength was 40.4±9.7 kg in men and 23.4±6.0 kg in women. When examined by sex, total vitamin C was not associated with higher grip strength in men (P=0.10) or women (P=0.26, Table). Similar results were seen when total vitamin C was examined in tertiles (P trend, men: 0.14 and women: 0.95).

**Conclusions:** These cross-sectional findings suggest that higher total vitamin C may not be beneficial for muscle strength in this sample of adult men and women.

Table. Association of total vitamin C intake<sup>1</sup> with grip strength (kg) in men and women.

	β coefficient <sup>2</sup>	P value
Men	0.5274 ± 0.316	0.10 <sup>†</sup>
Women	0.1839 ± 0.164	0.26

<sup>1</sup> Logarithmic transformation was applied to total vitamin C before analysis.

<sup>2</sup> Sex-stratified analyses were adjusted for age, weight, height, total energy intake (residual method), physical activity. <sup>†</sup>P<0.10

Table

**Disclosures:** Shivani Sahni, General Mills Bell Institute for Health and Nutrition, 11; PAI Inc., 11

## MO0255

**Characterizing the osteoanabolic epigenome of aging-related bone loss in humans.** Matthias Ring<sup>1</sup>, Hiroaki Saito<sup>1</sup>, Hanna Taipaleenmäki<sup>1</sup>, Zevnab Najafova<sup>2</sup>, Katharina Jähn<sup>1</sup>, Andreas Gasser<sup>1</sup>, Carl Haasper<sup>2</sup>, Roland Gessler<sup>1</sup>, Thorsten Gehrke<sup>3</sup>, Steven Johnsen<sup>2</sup>, Eric Hesse\*<sup>1</sup>. <sup>1</sup>Department of Trauma, Hand & Reconstructive Surgery, University Medical Center Hamburg-Eppendorf, Germany, <sup>2</sup>Clinic for General, Visceral & Pediatric Surgery, University Medical Center Göttingen, Germany, <sup>3</sup>HELIOS ENDO Clinic, Germany

During aging bone resorption often increases while bone formation decreases, thereby reducing bone mass and bone mineral density (BMD) and leading to osteoporosis. Evidence suggests that extrinsic factors may influence bone remodeling. While poorly understood, these mechanisms may function by inducing epigenomic programs that diminish the bone forming capacity of osteoblasts. This study is part of a bi-national consortium aimed at uncovering epigenomic networks controlling the aging-related decrease in bone formation. To reach this goal, we collected human femoral heads from elderly (65-85 years) and young (25-45 years) patients undergoing hip replacement. To characterize the material, clinical parameters affecting bone metabolism (e.g. history of falls, diseases and Vitamin D level) were obtained. So far, samples from 45 patients with an average age of 60 years were harvested. Interestingly, 98% had a Vitamin D-deficiency. Imaging of a well-defined part of the femoral head by μCT showed an approximately 10% reduction in bone mass and BMD in the elderly compared to the young group. Chromatin immunoprecipitation (ChIP) assays of intact bone tissue demonstrated a selective and specific enrichment of the active chromatin marks H3K4me3 H3K27ac on several osteoanabolic genes, including Runx2, ALP and Collagen1. Next, the sample number will be increased and all specimens will be analyzed by μCT and bone histomorphometry. Data will be combined with clinical data and laboratory results. Epigenetic regulatory pathways

controlling aging-related bone loss will then be identified by analyzing gene expression (RNA-seq), genome-wide DNA methylation (MeDIP) and a selected set of post-translational histone modifications (ChIP-seq) known to control osteoblast differentiation, precursor cell fate and lineage-specific gene expression. Together, our results demonstrate the feasibility of identifying epigenetic regulation of physiologically important osteoanabolic genes from human bone samples by epigenome mapping. This may lead to the development of new drugs for the treatment of aging-related bone loss.

*Disclosures: Eric Hesse, None.*

## MO0256

**Repair of Bone Defects in Bisphosphonate-treated Osteoporotic Mice.** Michel Hauser<sup>\*1</sup>, Mark Siegrist<sup>2</sup>, Silvia Dolder<sup>1</sup>, Willy Hofstetter<sup>1</sup>. <sup>1</sup>Group of Bone Biology & Orthopaedic Research / University of Bern, Switzerland, <sup>2</sup>Group of Bone Biology & Orthopaedic Research / University of Bern, Switzerland

Bisphosphonates (BPs) are inhibitors of bone resorption frequently prescribed to treat postmenopausal osteoporosis. Since bone remodelling is critical in fracture healing, we hypothesize that long-term therapy with BP impairs the bone's ability to repair fractures. To test this hypothesis, 12 week old mice were ovariectomized (OVX). After 8 weeks and after confirmation of bone loss in OVX as compared to *sham* animals, mice were injected twice weekly with the BP Alendronate (ALN) until sacrifice. After 5 weeks of ALN injections, femoral bones were osteotomized and rigidly (*MouseFix*<sup>TM</sup>; RIS) or non-rigidly (*FlexiPlate*<sup>TM</sup>; RIS) fixed. Femora (experimental & contralateral) were collected 1 and 5 weeks post-osteotomy for histology and microCT analysis. RNA was isolated from rigidly fixed defects 3, 7, 14 and 28 days after osteotomy for transcriptome analysis. The effects of estrogen deficiency and BP treatment were assessed 14 and 19 weeks after OVX by microCT measurements of lumbar vertebral bodies (L3-L5). A two-fold increase in BV/TV was observed in the vertebral spongiosa from *sham* and OVX animals treated with ALN as compared to controls. Repair of the femoral osteotomy was characterized by the lack of callus formation after rigid fixation, independent of the treatment protocols. A 40% increase in BV/TV was found at the fracture site 5 weeks after rigid fixation in animals treated with ALN compared to control animals. Non-rigidly fixed osteotomized femora treated with ALN formed a large callus with a decrease in mineral density compared to animals treated with vehicle only. 389 estrogen responsive (ER) genes out of the 1532 ER genes of the KBERG database were significantly up or downregulated between OVX and *sham* animals irrespectively of the treatment with ALN. Analysis of the entire transcriptomes reveals that changes during the progression of the healing process blunt the transcriptional changes induced by the different treatment protocols. 28 days after osteotomy, control *sham* animals show a significant increase in the expression of osteoblast marker genes as compared to OVX animals. Furthermore, a significant increase in the expression of osteoclast and osteoblast markers was observed in OVX animals treated with ALN as compared to OVX animals treated with vehicle. The preliminary data demonstrates that transcriptomics allows to follow specific events during the repair of bone defects.

*Disclosures: Michel Hauser, None.*

## MO0257

**The balance between bone resorption and formation during intracortical osteonal bone remodeling: a study of transiliac bone biopsies from women.** Christina Møller Andreassen<sup>\*1</sup>, Jean-Marie Delaïsse<sup>2</sup>, Bram C. J. van der Eerden<sup>3</sup>, Dorie Birkenhäger-Frenkel<sup>4</sup>, Johannes P. T. M. van Leeuwen<sup>4</sup>, Ming Ding<sup>1</sup>, Thomas Levin Andersen<sup>2</sup>. <sup>1</sup>Orthopaedic Research Laboratory, Department of Orthopaedic Surgery & Traumatology, Odense University Hospital, Institute of Clinical Research, University of Southern Denmark, Denmark, <sup>2</sup>Department of Clinical Cell Biology, Vejle Hospital/Lillebaelt Hospital, Institute of Regional Health Research, University of Southern Denmark, Denmark, <sup>3</sup>Laboratory for Calcium & Bone Metabolism, Department of Internal Medicine, Erasmus MC, Denmark, <sup>4</sup>Laboratory for Calcium & Bone Metabolism, Department of Internal Medicine, Erasmus MC, Rotterdam, Denmark

The intracortical osteons offers a unique opportunity to investigate the balance between resorption and formation within the bone remodeling units (BMUs) having a coupled bone remodeling, as each osteon represents a single intracortical BMU. The present study focuses on this balance, and the histological characteristics of the BMUs having an imbalance between bone resorption and formation.

A total of 3059 quiescent osteons were identified and histomorphometrically analyzed in histological sections from transiliac bone specimens obtained from 35 women (age 16-78 years) undergoing a forensic examination due to a sudden unexpected death. These quiescent osteons had a highly variable osteon diameter (On.Dm) reflecting the resorbed bone [mean 131  $\mu$ m (range 12-782  $\mu$ m)], wall thickness (W.Th) reflecting the formed bone [mean 96  $\mu$ m (range 4-305  $\mu$ m)], and pore diameter (Po.Dm) reflecting the imbalance between resorption and formation [mean 36  $\mu$ m (range 8-358  $\mu$ m)]. Linear regressions revealed a highly significant relationship between these three parameters ( $p < 0.0001$ ). Nevertheless, the slope of

the linear regression between the On.Dm and Po.Dm was 3-fold steeper than the slope between the On.Dm and W.Th ( $1.3 \pm 0.03$  vs  $0.3 \pm 0.03$ ). This supports the notion that increased bone resorption in given BMUs is the main contributor to their increased bone remodeling imbalance, as the bone formation only to some extent compensates for this increased bone resorption. 11.4% of the osteons had asymmetric bone formation, where the osteons were only refilled on one side. These asymmetric osteons had a statistically significantly smaller On.Dm ( $84 \pm 93$  vs  $137 \pm 74$   $\mu$ m) and W.Th ( $39 \pm 48$  vs  $103 \pm 60$ ) than the symmetric osteons with bone formation on all sides, while their Po.Dm were not significantly different. This supports that asymmetric osteons have a bone remodeling balance similar to symmetric osteons even though they have a smaller On.Dm and only bone formation on one side. Interestingly, 38% of the symmetric and 67% of the asymmetric osteons with an On.Dm > 300  $\mu$ m were infiltrated with marrow cells, while only 1% and 5% of the osteons with a smaller On.Dm were infiltrated with marrow cells.

Collectively, this study shows that the balance between resorption and formation in the intracortical BMUs having coupled bone remodeling is poorer in the BMUs with an excessive bone resorption, as the coupled bone formation cannot completely refill the excavation.

*Disclosures: Christina Møller Andreassen, None.*

## MO0258

**Administration of B-blocker (propranolol) to ovariectomized mouse insignificantly prevents decrease of bone formation in spite of increase in neuropeptide Y mRNA expression in hypothalamus.** Shinya Tanaka<sup>\*1</sup>, Takuto Tsuchiya<sup>2</sup>, Akinori Sakai<sup>3</sup>, Hiroomi Oda<sup>1</sup>. <sup>1</sup>Department of orthopaedics, Saitama medical university, Japan, <sup>2</sup>Department of Environmental health, University of occupational & environmental health, Japan, Japan, <sup>3</sup>Department of orthopaedics, University of occupational environmental health, Japan, Japan

Background and Objective) High-fat diets decreased bone formation and volume. It has been reported that fat metabolism disturbance, glucose metabolism disturbance, and bone metabolism disturbance are linked with each other. Otherwise it has been reported that bone metabolism is influenced by sympathetic nerve activities (SNA) and the central nerve system (CNS). But, it has been unknown whether dose these metabolic disturbance is regulated by CNS. Object of this study is to clarify whether CNS and SNA effect on bone metabolism in ovariectomized (OVX) mice given high fat diet.

Materials and Methods) Seven weeks old, female, C57BL/6J mice were purchased and subjected to 5 groups at 8-w-o, sham operated mice given standard chow (SS), OVX mice given standard chow and beta-blocker, propranolol (OSP), OVX mice given standard chow and vehicle of propranolol (OSV), OVX mice given high-fat diet and propranolol (OHP), OVX mice given high-fat diet and the vehicle (OHV). At 15-w-o, the end of experiment, mice were sacrificed and the 2nd to 5th lumbar vertebra and the right femur was harvested for bone mineral density (BMD) analysis, the left tibia was harvested for bone histomorphometry. The brains of mice in SS, OSV, and OHV were harvested for in situ hybridization.

Results) BMD of lumbar spine and distal one-third of the femur of mice in every OVX groups were smaller than mice in SS. The values in 2 propranolol administered groups were insignificantly larger than OVX + vehicle groups. The values of bone formation rate of 2 groups administered propranolol were insignificantly faster than the values of OVX + vehicle groups and as fast as the value of SS group. The expression of NPY in hypothalamus was suppressed in OSV group, and the suppression was inhibited by high fat diet.

Conclusion) OVX suppressed the expression of NPY in hypothalamus and high-fat diet inhibited the suppression. Administration of propranolol insignificantly prevented decreases of bone formation rate and bone volume in OVX mice given either standard chow or high fat diet.

*Disclosures: Shinya Tanaka, None.*

## MO0259

**Allogeneic Hematopoietic Stem Cell Transplant (alloHSCT) is Associated With Rapid Loss of Bone Mineral Density and Fat Mass.** Mohammed Almohaya<sup>\*1</sup>, Raewyn Broady<sup>1</sup>, Alina Gerrie<sup>1</sup>, Pamela Plantinga<sup>2</sup>, Qun Yang<sup>3</sup>, David Kendler<sup>1</sup>. <sup>1</sup>University of British Columbia, Canada, <sup>2</sup>Simon Fraser University, Canada, <sup>3</sup>ProHealth Clinical Research Centre, Canada

AlloHSCT is a potentially curative therapy for a variety of hematologic malignancies. Early complications include graft-versus-host disease (GVHD), often requiring high dose glucocorticoids. Inactivity and GVHD involving the G.I. tract may also contribute to weight loss. Marked declines in bone mineral density (BMD) have been documented as soon as 100 days post alloHSCT.

We studied BMD and body composition by DXA in 10 patients (4 male, 6 female; mean age 49 ± 18 years) prior to and 100 days after alloHSCT. Hematologic diagnoses were acute lymphocytic leukemia (2), acute myeloid leukemia (2), chronic myeloid leukemia (2), myelofibrosis (2), Non-Hodgkins lymphoma (1), and myelodysplastic syndrome (1). GVHD requiring glucocorticoid occurred in 50% of patients, in whom the average glucocorticoid dose was 29 mg per day.

Mean pre-alloHSCT BMD at the lumbar spine and total hip was 1.022 g/cm<sup>2</sup> and 0.887 g/cm<sup>2</sup> at baseline. At day 100 post-alloHSCT, BMD at lumbar spine and total hip was 0.926 g/cm<sup>2</sup> and 0.843 g/cm<sup>2</sup> respectively, reflecting declines of 4.5% at lumbar spine and 5.0% at total hip ( $p < 0.04$  for both sites). Significant declines at either hip or spine were noted in 70% of patients at day 100. Similar declines were noted both in patients with GVHD requiring glucocorticoid and those without GVHD not receiving glucocorticoid. There was an average loss of 2.9 kg of body weight. Appendicular lean mass declined by 243 g and total body fat declined by 2507 g. Between patients, there was high variability in losses of body weight, lean mass, and fat mass, not completely attributable to glucocorticoid use or GVHD.

We conclude that alloHSCT may result in rapid and substantial declines in spine and hip bone density. Weight loss is common and losses in body fat account for most of the weight loss 100 days after alloHSCT, with lesser declines in lean mass. These changes may differ from body composition changes in patients undergoing voluntary weight loss or bariatric surgery, where loss of lean mass, in the absence of exercise interventions, may be more notable. Identification of risk factors for muscle and bone loss early after alloHSCT may be helpful to prevent long-term sarcopenia and osteopenia in alloHSCT patients.

**Disclosures:** Mohammed Almohaya, None.

## MO0260

**Can Golden Syrian Hamsters Serve as a Model for Ovarian Hormone Deficiency-Induced Bone Loss?.** Negin Navaei<sup>1\*</sup>, Shirin Pourafshar<sup>2</sup>, Neda Akhavan<sup>3</sup>, Elizabeth Foley<sup>3</sup>, Kelli George<sup>3</sup>, Bahram Ajrmandi<sup>3</sup>. <sup>1</sup>Florida State University; Center for Advancing Exercise & Nutrition Research on Aging (CAENRA), College of Human Sciences, Florida State University, Tallahassee, FL, United states, <sup>2</sup>Florida State University, Tallahassee, Florida; Center for Advancing Exercise & Nutrition Research on Aging (CAENRA), College of Human Sciences, Florida State University, Tallahassee, FL, United states, <sup>3</sup>Florida State University; Center for Advancing Exercise & Nutrition Research on Aging (CAENRA), College of Human Sciences, Florida State University, Tallahassee, FL, United states

Postmenopausal women are at higher risk for osteoporosis due to a significant decline in ovarian hormone and one in two women over the age of 50 years will break a bone as a result of osteoporosis. Utilization of animal models allow for the understanding of the physiology and pathophysiology underlying the molecular processes that are involved in bone alterations after the onset of menopause. This understanding has been and will continue to be used to explore intervention and prevention strategies to improve the bone health of postmenopausal women. Therefore, the objective of this study was to investigate whether ovariectomized (Ovx) Golden Syrian hamster is a suitable model to be used for ovarian hormone deficiency-induced bone loss. A total of thirty-six Golden Syrian hamsters (6-month old) were either sham-operated (Sham) or Ovx and divided into three groups (12 hamsters per group) as follows: Sham, Ovx, and Ovx+17 $\beta$ -estradiol (E<sub>2</sub>; 10 $\mu$ g E<sub>2</sub>/kg body weight). Hamsters were fed a semi-purified casein-based powdered diet for 120 days at which time they were sacrificed. Atrophy of uterus and serum E<sub>2</sub> levels confirmed the success of Ovx (21.9  $\pm$  5.4 vs. 7.2  $\pm$  1.9 pg/mL, respectively for Sham and Ovx groups). Bone mineral density and content of the tibia and femur using dual x-ray absorptiometry. Our results showed that hamsters in the Ovx group had higher total bone area (36.1  $\pm$  0.6) than the sham+ control (35.0  $\pm$  0.06) and Ovx+ E<sub>2</sub> (33.1  $\pm$  0.6) groups. Furthermore, Ovx hamsters not only did not lose bone mineral content (BMC) but rather the mean BMC value was significantly higher than both Sham and Ovx+ E<sub>2</sub> groups. To our knowledge, this is the first study to report that hamsters do not lose bone due to Ovx. Elucidation of the mechanisms as to why this happens may provide insight for the etiology of osteoporosis.

**Disclosures:** Negin Navaei, None.

## MO0261

**Endotoxin and bone turnover markers in postmenopausal Saudis with and without osteoporosis.** Ibrahim Aziz, Nasser Al-Daghri<sup>\*</sup>, Majed Alokail, Sobhy Yakout. King Saud University, Saudi arabia

**Background:** Bacterial Lipopolysaccharide (LPS) also known as endotoxin which represents the outer cell wall membrane of gram-negative bacteria has been implicated as the major bacterial bone-resorbing factor. Recently, the most prevalent form of clinically significant osteopenia and osteoporosis involves periodontitis and otitis media by Gram-negative bacteria. The aim of the study is to evaluate circulating endotoxin levels and to study the association amongst endotoxin and bone turn-over markers in a cohort of Saudi postmenopausal women with or without osteoporosis.

**Methods:** We determined the levels of endotoxin, bone turn-over markers, 25-OH vitamin D total and corrected calcium in 100 Saudi postmenopausal women with osteoporosis and 100 women without osteoporosis were taken under the supervision of qualified physicians in the primary care centers in Riyadh. Serum endotoxin, NTX, osteocalcin, PTH, 25-OH vitamin D total and calcium were analyzed. Serum NTX and PTH levels in patients with osteoporosis were significant higher than controls.

**Results:** In the univariate correlation analysis, serum endotoxin showed a significant positive association with calcium in all subject and healthy women ( $r = 0.238$ ,  $p < 0.001$ ) ( $r = 0.476$ ,  $p < 0.001$ ) respectively, and these correlation was not found in women with osteoporosis; a linearly correlation was found between endotoxin and serum calcium in all subject (Fig. 1- a), also in controls group (Fig. 1- b). Results were showed positive association between NTX in all subject, controls and in women with osteoporosis group, but not significant. There was also no significant associations were found between endotoxin with waist, hips, menarche age, menopause, first pregnancy age, blood pressure, BMI, BMD, osteocalcin, 25-OH vitamin D or PTH in two studies groups.

**Conclusion:** Findings of the present study implicate a role for endotoxin-mediated inflammation in patients with osteoporosis.

**Disclosures:** Nasser Al-Daghri, None.

## MO0262

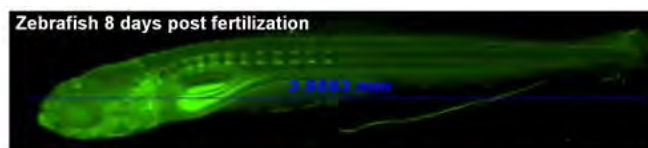
**Establishing an early bone development model for osteoporosis-related genes in zebrafish (*D. rerio*).** Chen Shochat Carvalho<sup>1</sup>, Ram Harari<sup>\*1</sup>, David Karasik<sup>2</sup>. <sup>1</sup>Faculty of Medicine in the Galilee, Bar Ilan University, Israel, <sup>2</sup>Faculty of Medicine in the Galilee, Bar Ilan University, , Israel, Israel

Osteoporosis is a skeletal disease characterized by low bone mineral density (BMD) and microarchitectural deterioration of bone tissue, predisposing those with the disease to an increased risk of fractures. Single-nucleotide polymorphisms (SNPs) associated with BMD and osteoporotic fractures were identified, including those within the low-density lipoprotein receptor-related protein 5 (*lrp5*) gene. LRP5 protein is known for its involvement in bone metabolism in humans. It is unclear whether it is involved in bone function starting early in life.

The purpose of our study was to investigate whether knocking out *lrp5* gene will affect early bone development and create bone deficit. We created a CRISPR (Clustered Regularly Interspaced Short Palindromic Repeats)-Cas9 *lrp5* knockout zebrafish and phenotyped their skeleton at larval stages. Zebrafish embryos (F0) at 1-cell stage were injected with CRISPR; F0 were grown to adulthood (3 months) and mated to obtain progeny (F1), we were able to verify an 8-basepairs deletion in exon 2 which leads to Ala55frameshift/55stop. In generation F3, we were able to obtain homozygotes and heterozygotes for KO mutation. We applied a calcein staining assay to screen *lrp5* mutants for bone development (vertebral centrum ossification), at 8, 10 and 13 days post fertilization (dpf), using fluorescent microscope (figure).

Number of mineralized vertebrae was compared between wild type and *lrp5* mutated zebrafish, adjusted for length. Significant difference in the number of mineralized vertebrae between wild-type and *lrp5* mutated zebrafish was found starting at 8 dpf. We did not observe gross morphological malformations at such an early stage.

In conclusion, here we report the process of generating *lrp5* knockout mutants in zebrafish, using CRISPR-Cas9 method and bone phenotyping. Since zebrafish are established model for early bone development and highly amenable to CRISPR-Cas9 mutagenesis, this study can serve as a proof of concept for novel osteoporosis candidate gene validation and help understand the genetics of bone acquisition.



Fluorescent calcein staining of 8 dpf fish showing mineralized vertebrae.

Figure

**Disclosures:** Ram Harari, None.

## MO0263

**Pharmacological Inhibition of ATP Release Through Pannexin-1 Channels Increases Bone Mass and Reduces Bone Resorption in Aging Mice.** Rafael Pacheco-Costa<sup>\*1</sup>, Emily Atkinson<sup>1</sup>, Hannah Davis<sup>1</sup>, Innocent Bviriringiro<sup>1</sup>, Roger Thompson<sup>2</sup>, Teresita Bellido<sup>1</sup>, Lilian Plotkin<sup>1</sup>. <sup>1</sup>Indiana University School of Medicine, United states, <sup>2</sup>Hotchkiss Brain Institute, Department of Cell Biology & Anatomy, University of Calgary, Canada

Aging is accompanied by increased osteocyte apoptosis and increased osteoclasts in mice and humans. However, whether osteocyte apoptosis causes osteoclast recruitment with aging is not known. Active caspase3 in apoptotic cells opens pannexin1 channels (Panx1), which in turn lead to release of cellular ATP, an osteoclast chemotactic factor. To address the role of Panx1 with aging, 3.5- (young, n=8-9) and 21- (old, n=10) month-old C57Bl/6 (WT) mice were given mefloquine (MF, 5mg/kg/d, i.p.), a Panx1 blocker, for 14d. Old mice exhibited low spine BV/TV and high Tb.Sp, and low femur BA/TA ( $\mu$ CT) compared to young mice and MF increased these parameters only in old mice. Old mice also displayed increased femoral periosteal (p) MAR, MS/BS and BFR/BS but no change in endosteal bone formation; MF only increased pMAR in 3.5-mo mice. Old mice exhibited 1.4 times more active caspase3-positive osteocytes compared to young mice, and elevated expression of

apoptosis-related genes (GADD153, p27, FoxO3 and FasL); MF treatment did not alter these values. Serum ATP levels were increased in old mice, and were reduced by MF. Old mice also exhibited more osteoclasts on femoral endosteal surface (N.Oc/BS, Oc.S/BS and ES.BS) and increased (although no significant) serum CTX levels; and MF reduced osteoclasts and CTX in both young and old mice. Moreover, MCSF and osteoclast markers (TRAP, DCSTAMP, NFATc1, OSCAR and ATP6v0d2) were elevated in tibia cortical bone from old mice compared to young ones, and MF reduced their expression. Similarly, tibial bone organ cultures from WT mice treated with 1mM MF for 24h or Panx1<sup>fl/fl</sup> calvaria treated with adenoCre to delete the Panx1 gene exhibited reduced ATP release and decreased osteoclast gene expression. Further, WT osteoclast precursors treated with RANKL/MCSF and 1mM MF for 7d showed reduced osteoclastogenesis compared to vehicle-treated cultures. Moreover, expression of genes associated with osteoclast activity, fusion, and function (TRAP, DCSTAMP, OSCAR, ATP6v0d2 and calcitonin receptor) was decreased in MF-treated cultures, suggesting a direct effect of the drug on osteoclastogenesis. We conclude that osteocyte apoptosis with aging results in Panx1 opening and ATP release, leading to increased osteoclast recruitment; and that Panx1 directly induce osteoclast differentiation. This evidence raises the possibility of using Panx1 inhibitors to block ATP release and bone resorption leading to bone preservation with aging.

**Disclosures:** Rafael Pacheco-Costa, None.

## MO0264

**Profile of a novel nonsteroidal glucocorticoid receptor modulator in preclinical and clinical studies: The case for improving translational correlation.** Yanfei Ma\*, Henry Bryant, Matthew Carson, Xiaoping Ruan, Christine Cheng, Mary D. Adrian, Charzad Montrose-Rafizadeh, Richard Zink, Michael J. Coghlan. Eli Lilly Company, United states

The robust efficacy of conventional glucocorticoid receptor (GR) ligands makes them the most clinically employed anti-inflammatory and immunomodulatory agents for a number of indications. Yet undesired cross reactivity and side effects related to the endogenous role of GR on homeostatic functions such as bone remodeling, gluconeogenesis and activation of the HPA axis complicate their clinical usage. Our goal is to find a GR modulator improving the therapeutic margins via higher receptor selectivity as well as differentiation of anti-inflammatory vs endocrine function. We focused on altering the profile of transrepression vs. transactivation in genes regulated by the GR-ligand complex. LY-SGRMs, a class of dibenzoxepane and dibenzosuberane sulfonamides, are potent anti-inflammatory agents with higher selectivity for the GR versus other steroid receptors and a differentiated gene expression profile versus clinical glucocorticoids in *in vitro* assays. LY-SGRM produced a dose-related reduction in acute rat carrageenan-induced paw edema (CPE) and chronic collagen-induced arthritis inflammatory arthritis (CIA) models. EC50s of LY-SGRM in reducing paw thickness and ankle extract cytokines were comparable to the effects produced by prednisolone. ED50 of LY-SGRM for bone formation suppression is 1051ng\*hr/mL vs 152 ng\*hr/mL of ED50 CPE, a 16 fold improvement over prednisolone comparing anti-inflammatory efficacy vs the bone formation suppression in the same anti-inflammatory efficacy model. In a multiple dose study phase I trial in healthy subjects, LY-SGRM was less suppressive of IL-6, IL-1 $\beta$  and TNF $\alpha$  in a LPS *ex vivo* assay when compared to prednisone. LY-SGRM reduced blood neutrophils, lymphocytes, monocytes and eosinophils, at only the highest dose producing similar suppression comparable to prednisone. Relative to anti-inflammatory doses, LY-SGRM produced a higher level of insulin release and cortisol suppression versus prednisone and comparable levels of circulating bone markers (PINP and CTX-1) versus prednisone. Our data suggest that species specific responses need to be addressed during the early compound optimization. Whether a molecule with a partial tissue agonist/antagonist profile would yield a true tissue selective GR modulator has yet to be seen.

**Disclosures:** Yanfei Ma, Eli Lilly Company, 15

## MO0265

**Glycemic Control, Familiarity and Disease Duration Are Associated With Multiple Fragility Fractures In Type 1 Diabetes.** Giulia Leanza\*<sup>1</sup>, Dario Pitocco<sup>2</sup>, Ernesto Maddaloni<sup>1</sup>, Luna Zanoboni<sup>1</sup>, Rocky Strollo<sup>1</sup>, Silvia Manfrini<sup>1</sup>, Paolo Pozzilli<sup>1</sup>, Ann Schwartz<sup>3</sup>, Andrea Palermo<sup>1</sup>, Nicola Napoli<sup>1</sup>. <sup>1</sup>Campus Bio-Medico University of Rome, Italy, <sup>2</sup>Policlinico Gemelli, Italy, <sup>3</sup>UCSF School of Medicine, United states

People with Type 1 Diabetes (T1D) have increased bone fragility, but clinical risk factors for fractures in this population are still unclear.

To evaluate factors associated to fragility fractures in T1D we examined 600 T1D patients (300 males; 300 females) from 3 centers participating in the IMDIAB study group (Italy).

Average glycated hemoglobin A1c (HbA1c) over the previous 5 years was used as index of long-term glycemic control; fractures were assessed by a validated questionnaire; complications were adjudicated by physician assessment.

Patients were 41.9 $\pm$ 12.8 years old; BMI and disease duration were 24.4 $\pm$ 3.7 kg/m<sup>2</sup> and 19.9 $\pm$ 12.0 years. The 5-year average HbA1c was 7.6 $\pm$ 1.0%. Insulin requirement (IR) was 20.7 $\pm$ 10.3 IU/daily for fast-acting and 19.5 $\pm$ 9.5 IU for long-acting insulin. One hundred and eleven patients (18.5%) reported at least one fracture after the diagnosis of T1D; 73.8% of them had only 1 fracture, 26.1% had 2 or more

fractures. Stratifying the population in 3 groups (0, 1 and  $\geq$ 2 fractures; see Table), we found that fractures were more common in those having familiarity for fragility fractures (p<0.01). Among complications, only neuropathy was associated with fractures (p<0.01). A multivariate regression analysis showed that higher HbA1c (OR 1.56, 95%CI: 1.08-2.22, p=0.02), longer disease duration (OR 1.08, 95%CI: 1.04-1.12, p<0.001), higher number of hypoglycemia episodes (OR 1.03, 95% 1.01-1.06, p=0.01), and positive family history for fragility fractures (OR 2.38, 95% CI 1.05-5.41, p=0.04) were significantly associated with increased risk of having 2 or more fragility fractures, independently from the other clinical factors considered in this study. In conclusion, glycemic control, disease duration, family history of fractures and frequency of hypoglycemia are the main risk factors associated with multiple bone fragility fractures in T1D.

	0 fractures (n=489)	1 fracture (n=82)	$\geq$ 2 fractures (n=29)	p-value
Age (years)	40 (32-49)	43 (34-54)	47 (37-54)	0.013
BMI (Kg/m <sup>2</sup> )	23.7 (21.6-26.5)	24.4 (21.6-27.1)	25.6 (23.1-28.1)	0.032
Disease duration (years)	18 (10-27)	20 (12-31)	31 (23-39)	<0.001
Insulin Unit (IU/kg) (n=468)	0.54 (0.44-0.66)	0.55 (0.45-0.67)	0.53 (0.46-0.68)	0.774
Monthly Hypoglycemic episodes (n) (n=475)	6 (4-10)	8 (4-12)	5 (4-15)	<0.001
HbA1c, % (mmol/mol)	7.5 (6.9-8.1) [57.5 (51.1-64.2)]	7.6 (7.0-8.1) [57.8 (52.1-65.25)]	7.8 (7.3-8.8) [61.6 (56.9-73.9)]	0.074
eGFR (ml/min) (n=425)	105.8 (92.2-116.7)	101.6 (81.2-113.5)	96.9 (84.1-107.6)	0.004
Total Cholesterol (mg/dl) (n=442)	178 (155-197)	176 (156-193)	173 (160-195)	0.751
HDL (mg/dl) (n=425)	61 (51-75)	64 (50-74)	60.5 (52-73)	0.934
LDL (mg/dl) (n=424)	97 (80-115)	95 (74-115)	95 (86-104)	0.376
Triglycerides (mg/dl) (n=431)	66 (52-89)	72 (58-83)	72.5 (55-125)	0.152

Table1\_Leanza\_etal

**Disclosures:** Giulia Leanza, None.

## MO0266

**Type 1 Diabetes and Bone Microarchitecture Assessment with Trabecular Bone Score (TBS): A Descriptive Study.** Julie Gilmour\*<sup>1</sup>, Sandra Kim<sup>2</sup>, Anita Colquhoun<sup>2</sup>, Wei Wu<sup>2</sup>. <sup>1</sup>St.Michael's Hospital, Canada, <sup>2</sup>Women's College Hospital, Canada

**Introduction:** Type 1 Diabetes Mellitus (T1DM) is associated with increased risk of fragility fracture (FF), which is in excess of what is expected based on bone mineral density (BMD) alone. Impairment in bone quality may contribute to this excess risk. Trabecular bone score (TBS), a tool to assess bone quality at the lumbar spine (LS), has been shown to predict fracture risk independent of BMD. There are limited studies exploring TBS in T1DM.

**Purpose:** To examine TBS in a cohort of adults with T1DM in relation to BMD, clinical parameters and fracture history.

**Methods:** T1DM patients were prospectively recruited from the Endocrine clinic at Women's College Hospital from April to October 2015 for BMD testing with TBS. Clinical parameters and fracture history were obtained from survey and chart review. Patients on bone-sparing drugs or steroids were excluded. Descriptive statistics, correlation coefficients, multivariate linear and logistic regression models were used to determine associations between clinical variables, BMD, TBS and FF.

**Results:** 43 patients with T1DM participated in the study. Average age was 34.9 years, 70% female, 88% Caucasian. 44% were diagnosed with T1DM prior to puberty and average duration of T1DM was 16.7 years. Diabetes complications were uncommon; 1 had macrovascular disease, 26% had at least 1 microvascular complication. Average HbA1c was 8.2%. Almost half had history of fracture; of these, 33% were FF's. Average BMD was 1.17 g/cm<sup>2</sup> at LS, 0.94 g/cm<sup>2</sup> at femoral neck (FN), 0.97 g/cm<sup>2</sup> at total hip (TH). Average TBS was 1.47 (SD 0.10). TBS correlated moderately with BMD; LS 0.41 (p=0.006), FN 0.492 (p=0.001), TH 0.472 (p=0.002). TBS did not correlate with age, gender, HbA1c, pre-pubertal DM onset, or duration of T1DM. BMI was the only variable that appeared to influence TBS. There was an inverse association between TBS and any microvascular complication, however this lacked statistical significance. The odds of FF increased with older age (OR 1.077, p=0.014) and decreased with higher BMD at the hip sites (OR 0.001, p=0.029 at FN; OR 0.002, p=0.036 at TH). TBS did not predict FF.

**Conclusion:** TBS correlated with BMD at all sites and appears to be influenced by BMI, however there was no significant relationship between TBS, diabetes parameters and FF in this study cohort of young adults with T1DM. A larger study in older patients with longer duration of T1DM is required to better assess the utility of TBS in this patient population.

**Disclosures:** Julie Gilmour, None.

## MO0267

**Changes in Bone Mineral Density and Biochemical Markers of Bone Turnover in Postmenopausal Women with Breast Cancer Initiating Aromatase Inhibitor Therapy.** Vit Zikan\*<sup>1</sup>, Martina Zimovjanova<sup>2</sup>, Dana Michalska<sup>1</sup>, Maria Raskova<sup>1</sup>, Lubos Petruzelka<sup>2</sup>. <sup>1</sup>Third Department of Medicine - Department of Endocrinology & Metabolism, First Faculty of Medicine, Charles University in Prague & General University Hospital in Prague, Czech Republic, Czech republic, <sup>2</sup>Department of Oncology, First Faculty of Medicine, Charles University in Prague & General University Hospital in Prague, Czech Republic, Czech republic

Aromatase inhibitors (AIs) are the standard of care for the treatment of most postmenopausal women with early stage hormone-receptor-positive breast cancer (EBC). However, one side-effect of AIs on bone is a decrease in bone mineral density (BMD) and an increased risk of fracture. Early identification of women with poor bone health offers opportunities for interventions aimed at reducing fracture risk. The objectives of this study were to examine: (1) changes in bone formation (N-terminal propeptide of type I procollagen; PINP) and bone resorption (cross-linked C-telopeptides of bone type I collagen; CTX) markers, as well as intact parathyroid hormone (PTH), 25 hydroxyvitamin D (25OHD) and plasma sclerostin over the first 6 months of aromatase inhibitor (AI) therapy among a cohort of breast cancer patients initiating aromatase inhibitors therapy, (2) whether bone markers changes are associated with BMD changes after 12 and 24 months of AI therapy and (3) changes in fat and muscle indices. Eligible breast cancer patients were recruited and followed for 24 months. AIs treatment was associated with significant increases in serum CTX ( $p < 0.01$ ) and sclerostin levels ( $p < 0.001$ ) within the first 6 months and significant decreases in BMD at measured sites ( $p < 0.001$ ) within 12 and 24 months. The changes in CTX were significantly ( $p < 0.05$ ) and negatively related with lumbar spine and femoral neck BMD changes. In addition, AIs treatment increases fat mass indices. Findings from this study suggest that AIs cause a significant increase in bone resorption marker CTX and plasma sclerostin levels during the first 6 months of treatment and these changes were associated with BMD decreases at 12 and 24 months. Low 25OHD levels were very common in our EBC patients. They were partially corrected with low-dose cholecalciferol supplementation.

**Disclosures:** Vit Zikan, None.

## MO0268

**Effects of Once a Week Administration of the New Synthetic Product of 1-34 Teriparatide on Glucocorticoid-Induced Osteoporosis in Japanese Patients.** Ikuko Tanaka\*<sup>1</sup>, Mari Ushikubo<sup>2</sup>, Misako Higashiba<sup>2</sup>, Erika Takei<sup>2</sup>, Keisuke Izumi<sup>2</sup>, Kumiko Akiya<sup>2</sup>, Shigenori Tamaki<sup>1</sup>, Hisaji Oshima<sup>2</sup>. <sup>1</sup>Nagoya Rheumatology Clinic, Japan, <sup>2</sup>Tokyo Medical Center, Japan

**Background:** New Product of synthetic 1-34 Teriparatide (wTPT), an once-weekly drug, developed in Japan has been shown to be effective in reducing risk of new vertebral fracture and increasing bone mineral density in primary osteoporosis. In the present study we investigated effects of wTPT on vertebral fractures in glucocorticoid induced osteoporosis. **Subjects and Methods:** Patients with connective tissue diseases at Tokyo Medical Center were recruited for an one-year longitudinal cohort study. The number of subjects was 160 (female; 140, age; 63+/-16 (mean +/- SD), prednisolone dosage at the base line; 8.5+/-10.0 mg/day, prednisolone dosage during 1yr; 6.6+/-5.5mg/day, duration of prednisolone treatment; 10.4+/-0.4yr, prevalent vertebral fracture (Genant, H. 1996); 45.3%). Lumbar bone mineral densities (IBMD) were measured as %YAM with Lunar 3030 (GE). Incident vertebral fractures were analyzed with XP of the thoracic and lumbar spines. Patients were treated with bisphosphonates (88%) or wTPT (12%). **Results:** The value of IBMD (%YAM) at the base line was 83.1+/-15.9%. The rate of incident fractures during the follow-up period was 15.6%. 2) Sex, age, prevalent fracture, and IBMD were not different between the two treatment groups. However, prednisolone dosages at the base line were statistically increased in patients with wTPT than bisphosphonates (19.3+/-4.2 vs 6.3+/-0.8,  $p < 0.01$ ). Increases in IBMD after 1 yr were not different in these two groups. Incident vertebral fractures were seen in 16.3% in the patients with bisphosphonates and 10.1% in those with wTPT. 3) A logistic regression analysis revealed that statistically significant factors for incident fractures were IBMD (1% decrease, OR; 1.74; 95%CI; 1.18-2.59,  $p < 0.01$ ), prednisolone dosages (1mg/day increase, 1.10, 1.02-1.16,  $p < 0.01$ ), prevalent fractures (3.38, 1.22-9.21,  $p < 0.01$ ), and wTPT treatment (vs bisphosphonates, 0.12, 0.11-0.81,  $p < 0.01$ ). **Conclusions:** Our results suggested that wTPT might be effective for prevention of osteoporotic fractures in patients treated with glucocorticoids.

**Disclosures:** Ikuko Tanaka, None.

## MO0269

**Bone Loss in HIV Infection: What's the B cell got to do with it?.** Kehmia Titanji\*<sup>1</sup>, Aswani Vunnava<sup>2</sup>, Anandi AN Sheth<sup>2</sup>, Cecile Delille Lahiri<sup>2</sup>, Jeffrey L Lennox<sup>2</sup>, Antonina Foster<sup>2</sup>, Ighoverha Oforokun<sup>2</sup>, M. Neale Weitzmann<sup>3</sup>. <sup>1</sup>Emory University School of Medicine, Department of Medicine, Division of Endocrinology, Metabolism & Lipids, United states, <sup>2</sup>Emory University School of Medicine, Department of Medicine, Division of Infectious Diseases, United states, <sup>3</sup>Emory University School of Medicine, Department of Medicine, Division of Endocrinology, Metabolism & Lipids & Atlanta VA Medical Center, United states

HIV infection is associated with high rates of osteoporosis and bone fracture. Osteoporosis results from an imbalance in bone resorption by osteoclasts relative to bone formation by osteoblasts, leading to bone loss. Osteoclast formation is primarily regulated by the ratio of the key osteoclastogenic cytokine, receptor activator of nuclear factor- $\kappa$ B ligand (RANKL), to that of its physiological inhibitor, osteoprotegerin (OPG). HIV infection is also associated with the expansion of immature/transitional (CD10<sup>+</sup>CD27<sup>+</sup>) B cells, which correlates with increased levels of IL-7. We previously reported that HIV infection leads to a decline in overall B cell OPG and an increase in RANKL that correlates significantly with loss of bone mineral density (BMD) but the contribution of immature B cells to this RANKL/OPG imbalance and bone loss in HIV infection has not been previously studied.

In a study population comprised of 58 HIV-uninfected and 62 antiretroviral therapy-naive HIV-infected individuals, we analyzed the distribution of immature B cells and stained total B cells for intracellular expression of RANKL and OPG by flow cytometry and measured bone mineral density (BMD) by dual-energy X-ray absorptiometry (DXA).

We found a significant increase in B cell RANKL production ( $P = 0.005$ ), which was significantly correlated with the percentage of immature B cells ( $r = 0.28$ ,  $P = 0.003$ ) and a significant ( $p=0.02$ ) decline in the percentage of OPG-producing B cells in HIV-infected individuals. Importantly, the percentage of immature B cells was inversely correlated with hip BMD. Taken together, our data demonstrate for the first time that immature B cells contribute to B cell impairment-induced bone loss in HIV infection.

**Disclosures:** Kehmia Titanji, None.

## MO0270

**Effect Of Recent Spinal Cord Injury On The OPG/RANKL System And Its Relationship With Bone Loss And Antiosteoporotic Response To Denosumab Therapy..** Laia Gifre\*<sup>1</sup>, Joan Vidal<sup>2</sup>, Silvia Ruiz-Gaspa<sup>3</sup>, Enric Portell<sup>2</sup>, Ana Monegal<sup>1</sup>, Africa Muxi<sup>4</sup>, Núria Guañabens<sup>1</sup>, Pilar Peris<sup>1</sup>. <sup>1</sup>Rheumatology Department, Metabolic Bone Diseases Unit, Hospital Clinic of Barcelona, Spain, <sup>2</sup>Spinal Cord Unit, Neurorehabilitation Institute Guttmann, Badalona, Spain, <sup>3</sup>CIBERehd, Hospital Clinic of Barcelona, Spain, <sup>4</sup>Nuclear Medicine Department, Hospital Clínic of Barcelona, Spain

**Background:** Spinal cord injury (SCI) has been associated with a marked increase in bone loss and bone remodeling, especially short-term after injury. However, the pathogenesis and clinical management of this process remain unclear, as well as the role of the key regulators of bone remodeling, the OPG/RANKL system.

**Objectives:** To analyze the role of the regulators of bone remodeling, OPG and RANKL, in the bone loss associated with recent SCI as well as the effect of antiosteoporotic therapy with denosumab in these bone regulators in a prospective study.

**Patients and methods:** Twenty-three male patients (aged 18 - 67 years [mean 36 ± 16 years]) with recent (< 6 months) complete SCI were prospectively included (43.5% paraplegic, 56.5% tetraplegic). Antiosteoporotic therapy with denosumab was recommended when patients developed densitometric osteoporosis during follow-up. Serum levels of OPG and RANKL (Biomedica, Vienna, Austria), bone turnover markers (PINP, bone ALP, CTX) and bone mineral density (BMD) at the lumbar spine and total hip were assessed at baseline (99 ± 30 days after SCI), prior to initiating antiosteoporotic treatment (14 ± 4 months post-SCI) and during antiosteoporotic therapy with denosumab (6 months after initiating treatment). The results were compared with a healthy control group.

**Results:** At baseline, SCI patients showed a significant increase in RANKL serum levels compared to controls (3.4 ± 1.7 vs. 2.3 ± 1.6 pg/mL,  $p=0.022$ ) which correlated with days-since-SCI ( $r=0.589$ ,  $p=0.005$ ) and became undetectable after denosumab treatment in 67% of the patients ( $p=0.001$ ). OPG serum levels were similar to controls at baseline (87.7 ± 38.7 vs. 71.7 ± 25.4,  $p=0.1$ ) and did not change with denosumab treatment. No differences were observed in RANKL and OPG levels on comparing tetraplegic vs. paraplegic patients. Neither were RANKL or OPG levels related to the increase in bone loss and bone turnover markers after SCI. Patients with undetectable RANKL serum levels after denosumab treatment did not present further sublesional bone loss but increased total hip BMD (+2.5 ± 1.3%,  $p=0.005$ ), and bone markers markedly decreased (PINP: -53%,  $p=0.007$ ; CTX: -68%,  $p=0.005$ ).

**Conclusions:** This study shows that short-term after SCI there is an increase in RANKL serum levels which become undetectable after denosumab treatment. The preventive effect of denosumab on sublesional bone loss further suggests a contributory role of RANKL in this clinical process.

**Disclosures:** Laia Gifre, None.

## MO0271

**Changes in gene and protein expression in osteoblastic cell line SCP1 after stimulation with adult crohns' disease patient serum.** Martina Blaschke<sup>1</sup>, Regine Koepf<sup>1</sup>, Marina Komrakova<sup>2</sup>, Matthias Schieker<sup>3</sup>, Heide Siggelkow<sup>4</sup>. <sup>1</sup>Department of Gastroenterology & gastrointestinal Oncology, Germany, <sup>2</sup>Department of Trauma Surgery & Reconstructive Surgery, Germany, <sup>3</sup>Experimental Surgery & Regenerative Medicine, Germany, <sup>4</sup>Clinic of Gastroenterology & gastrointestinal Oncology, Germany

**Introduction:** Crohn's disease (CD) is associated with a higher prevalence of osteoporosis, a complication that is recognized as a significant cause of morbidity. Its pathogenesis is still controversial, but the activity of CD is thought to be one contributing factor.

**Methods:** We stimulated SCP-1 cells (osteoblastic cell model) with CD patient serum and compared the effect of sera collected in acute phase versus in remission. 50% of patients were classified as osteoporosis positive (OPO+); 50% were osteoporosis negative (OPO-). After 14 days stimulation changes in gene (Agilent RNA-Micro-array) and protein (mass spectrometry) expression were analysed in osteoblastic cell line (SCP1). Furthermore gene expression of osteogenic marker genes and the RANKL/OPG ratio were determined using RT-PCR.

**Results:** The application of acute phase serum obtained from male not female patients to SCP-1 cells resulted in increased RANKL expression. Transcriptom analysis identified no significantly changed gene expression comparing disease phases acute phase (AP) versus remission (R) or comparing osteoporosis positive (Ost+) versus negative (Ost-) samples. Protein analysis identified 9 only proteins being regulated in AP versus R and 70 proteins regulated comparing Ost+ versus Ost-sera. The up-regulated proteins mainly belonged to translational processes; the down-regulated were involved in acute response. MVK and HTR2A were 3,5fold up-regulated in Ost+ samples, both are involved in bone metabolism.

**Discussion:** Our results show that factors in the serum from adult patients with acute CD are involved in translational processes and acute phase processes as well as in bone remodeling and that gender specific factors might contribute to development to osteoporosis.

**Disclosures:** Heide Siggelkow, None.

## MO0272

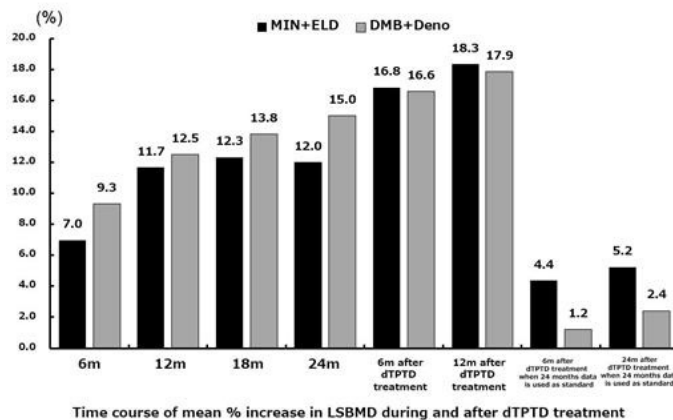
**Comparative Study between "Minodronate with Eldecalcitol" and "Denosumab" as the Treatment after 2-Year Daily Teriparatide in Osteoporosis in Patients with Rheumatoid Arthritis – Results in 12 Months -** Yuji Hirano<sup>\*1</sup>, Masaaki Isono<sup>1</sup>, Takayasu Ito<sup>2</sup>. <sup>1</sup>Rheumatology, Toyohashi Municipal Hospital, Japan, <sup>2</sup>Ito Orthopaedic Clinic, Japan

**Background:** Although daily teriparatide (dTPPT) treatment increases bone mineral density (BMD), increase of BMD is not enough after 2-year dTPPT treatment in some osteoporosis (OP) patients. This prospective study compared minodronate (a bisphosphonate developed in Japan) with eldecalcitol (activated vitamin D developed in Japan) (MIN/ELD) and denosumab (DMB) as the treatment after 2-year dTPPT treatment in OP in patients with rheumatoid arthritis (RA-OP). 6-months results were reported in ASBMR 2015 in Seattle. This study investigated 12-months results.

**Methods:** Female RA-OP patients treated with MIN/ELD (n=21) or DMB (n=12) after dTPPT were used. Change of BMD (lumbar spine and total hip; LSBMD and THBMD) measured by DEXA at every 6 month from the initiation of dTPPT and change of bone turnover markers (BTM) (PINP and TRACP-5b) at every 6 month from the initiation of dTPPT were compared between two groups. DMB (60mg) was injected every 6month with prescribing of native vitamin D and calcium. MIN (50mg) was administered every 4 weeks and ELD (0.75µg) was administered every day.

**Results:** Patients' characteristics (MIN/ELD: DMB): Mean age (70.2: 70.8). Body mass index (20.8: 21.2). PSL use (71.4%: 75.0%). % increase of LSBMD (dTPPT6m/12m/18m/24m/AfterTPTD6m/AfterTPTD12m): 7.0/11.7/12.3/12.0/16.8/18.3 in MIN/ELD and 9.3/12.5/13.8/15.0/16.6/17.9 in DMB. No significant differences were observed at all time-points during dTPPT treatment period. % increase of LSBMD at 12m after dTPPT treatment was 5.2% in MIN/ELD and 2.4% in DMB and the difference was significant (p=0.033). % increase of THBMD: 1.2/3.1/4.3/5.3/5.9/6.6 in MIN/ELD and 1.2/3.9/4.0/4.3/5.8/6.5 in DMB. % increase of THBMD at 12m after dTPPT treatment was 1.6% in MIN/ELD and 1.6% in DMB. No significant differences were observed at all time-points. % change of BTM was expressed as the value at the initiation of dTPPT was 100. PINP: 100/405.2/343.3/251.4/214.3/38.3/52.4 in MIN/ELD. 100/454.6/413.0/290.4/223.0/68.2/71.5 in DMB. TRACP: 100/148.9/157.4/139.8/144.7/51.2/65.5 in MIN/ELD. 100/190.8/204.7/179.6/176.3/91.6/99.6 in DMB. There were no significant differences in BTM between two groups except PINP at 6m after dTPPT treatment (p=0.032).

**Conclusions:** This study shows that short-term efficacy of MIN/ELD mostly equals to that of DMB as the treatment after 2-year TPTD in RA-OP. The tendency that bone turnover in MIN/ELD group were decreased compared with that in DMB group was seen.



Figure

**Disclosures:** Yuji Hirano, None.

## MO0273

**Continuous improvement of impaired trabecular bone microarchitecture after 3 years on gluten-free diet: A prospective longitudinal HR-pQCT study in women with celiac disease.** María Belen Zanchetta<sup>\*1</sup>, Vanessa Carla Longobardi<sup>1</sup>, Florencia Costa<sup>1</sup>, Fernando Silveira<sup>2</sup>, Cesar Bogado<sup>1</sup>, Julio Cesar Bai<sup>1</sup>, Jose Ruben Zanchetta<sup>1</sup>. <sup>1</sup>MD, Argentina, <sup>2</sup>Ph, Argentina

Previously we identified a significant deterioration of trabecular and cortical microarchitecture in peripheral bones of patients with undiagnosed celiac disease (CD) using HR-pQCT. Such affection was mainly produced in the trabecular bone. Up to now, the effect of the gluten-free diet (GFD) on microstructural parameters of peripheral bones has not been assessed.

**Aim:** to describe changes in bone microarchitecture measure by HR-pQCT after 3 years on gluten free diet in a group of premenopausal women.

**Design:** we prospectively enrolled 31 consecutive females with newly diagnosed CD. Clinical and biochemical status, CD specific serology, bone densitometry and bone micro architecture (HR-pQCT) were assessed at diagnosis of CD (baseline), and after 1-year and 3-years on GFD. 24 patients completed all visits. Anova test design was performed to assess significant changes between the different time points.

**Results:** After 3 years on GFD (mean time: 35.1 ± 3.6 months), 24 patients were re assessed. Mean age was 34 ± 8.8 years and BMI 24.6 ± 6.8 (previous value 23 ± 6.2; p<0.01). At 3-years time PTH decreased and Vitamin D increased significantly compared to baseline [PTH (pg/ml) 44 ± 17 vs. 57 ± 22; p=0.02 and vitamin D (ng/ml) 24 ± 6.6 vs. 17 ± 6.3; p<0.01]. Cross laps decreased 12.6% but did not change significantly and 89% of patients achieved negative serology for CD. Bone mineral density (g/cm<sup>2</sup>) increased significantly after 3-years on GFD in LS (1.148 ± 0.14 vs. 1.107 ± 0.15; p<0.01), total hip (0.951 ± 0.14 vs. 0.913 ± 0.15; p<0.01) and ultradistal radius (0.410 ± 0.05 vs. 0.378 ± 0.06; p<0.01).

The microarchitecture of the trabecular compartment at distal radius was significantly improved (BV/TV, trabecular density and trabecular thickness, 12%; p<0.01) as well as the total volumetric density (5%; p<0.01). At the tibia, treatment was associated with significant increase of the total volumetric density (6%; p<0.01), cortical density (1.9%; p<0.01), trabecular density and BV/TV (11%; p<0.01) and trabecular thickness (12%; p<0.01). See table.

**Conclusions:** Our study shows that trabecular parameters impaired at the time of diagnosis continue to improve significantly over time with GFD in this group of young premenopausal women. We postulate that trabecular bone microarchitecture improvement might be the substrate associated with the decreased risk of fractures observed after GFD in former studies.

Continuous Improvement of impaired trabecular bone microarchitecture after 3 years on gluten-free diet: A prospective longitudinal HR-pQCT study in women with celiac disease

Parameters	Baseline	1-year GFD	3-years GFD	% change basal vs. 3yr GFD	p
<b>Radius</b>					
D100 (mg HA/cm <sup>3</sup> )	280 ± 50 <sup>2</sup>	285 ± 45 <sup>2</sup>	294 ± 45 <sup>1,2</sup>	5	<0.01
Dtrab (mg HA/cm <sup>3</sup> )	117 ± 29 <sup>2,3</sup>	130 ± 28 <sup>1</sup>	132 ± 30 <sup>1</sup>	12	<0.01
BV/TV (%)	9.8 ± 2.4 <sup>2,3</sup>	10.8 ± 2.3 <sup>1</sup>	11.0 ± 2.5 <sup>1</sup>	12	<0.01
Tb.N (1/mm)	1.68 ± 0.26	1.70 ± 0.27	1.70 ± 0.30	1.2	0.60
Tb.Th (mm)	0.058 ± 0.009 <sup>2,3</sup>	0.063 ± 0.007 <sup>1</sup>	0.065 ± 0.01 <sup>1</sup>	12	<0.01
Dcomp (mg HA/cm <sup>3</sup> )	874 ± 48	875 ± 39 <sup>3</sup>	887 ± 35 <sup>2</sup>	1.5	0.01
Ct.Th (mm)	0.70 ± 0.14 <sup>2</sup>	0.67 ± 0.13 <sup>1,3</sup>	0.70 ± 0.13 <sup>2</sup>	0.0	0.01
<b>Tibia</b>					
D100 (mg HA/cm <sup>3</sup> )	267 ± 45 <sup>2,3</sup>	278 ± 43 <sup>1,2</sup>	284 ± 47 <sup>1,2</sup>	6	<0.01
Dtrab (mg HA/cm <sup>3</sup> )	127 ± 30 <sup>2,3</sup>	139 ± 30 <sup>1</sup>	142 ± 33 <sup>1</sup>	11	<0.01
BV/TV (%)	10.6 ± 2.5 <sup>2,3</sup>	11.6 ± 2.5 <sup>1</sup>	11.8 ± 2.7 <sup>1</sup>	11	<0.01
Tb.N (1/mm)	1.57 ± 0.32	1.53 ± 0.28	1.56 ± 0.33	-0.6	0.52
Tb.Th (mm)	0.068 ± 0.012 <sup>2,3</sup>	0.076 ± 0.012 <sup>1</sup>	0.076 ± 0.014 <sup>1</sup>	1.2	<0.01
Dcomp (mg HA/cm <sup>3</sup> )	917 ± 27 <sup>2,3</sup>	928 ± 25 <sup>1,3</sup>	934 ± 26 <sup>1,3</sup>	19	<0.01
C.Th (mm)	1.11 ± 0.20 <sup>2</sup>	1.08 ± 0.20 <sup>1,3</sup>	1.11 ± 0.21 <sup>2</sup>	0.0	0.04

P corresponds to Anova with Repeated Measures (Significance Assumed). Statistically significant difference between groups (Bonferroni p < 0.05), Basal<sup>1</sup>, 1 year GFD<sup>2</sup>, 3 year GFD<sup>3</sup>.  
 D100: Total density, Dtrab: Trabecular Density, BV/TV: trabecular bone volume fraction, Tb.N: Trabecular Number, Tb.Th: Trabecular Thickness, Dcomp: Cortical Density, Ct.Th: Cortical Thickness.

Table: Distal radius and tibia HR-pQCT

Disclosures: Maria Belen Zanchetta, None.

MO0274

**Cortical Density Is Lower in Patients with Graves' Disease Compared to Healthy Controls.** Sofie Malmstroem<sup>\*1</sup>, Diana Grove-Laugesen<sup>2</sup>, Eva Ebbehoj<sup>1</sup>, Klavs Würgler Hansen<sup>3</sup>, Torquil Watt<sup>4</sup>, Lars Rejnmark<sup>5</sup>.  
<sup>1</sup>Department of Endocrinology & Internal Medicine, Aarhus University Hospital, Denmark, <sup>2</sup>Department of Endocrinology & Internal Medicine, Aarhus University Hospital, Denmark, <sup>3</sup>Medical Department, Regional Hospital Silkeborg, Denmark, <sup>4</sup>Department of Medical Endocrinology, Rigshospitalet, Denmark, <sup>5</sup>Department of Endocrinology & Internal Medicine, Denmark

Objective:

Hypertthyroidism leads to reduced mineral bone density and is associated with increased risk of fracture. Whether the effect of increased bone turnover is identical in cortical and trabecular bone is unknown. Using a cross sectional design we aimed to investigate which bone compartment is affected.

Methods:

Nineteen newly diagnosed patients with Graves' disease (GD) and nineteen euthyroid controls matched on age, gender and menopausal status were scanned using a high-resolution pQCT scanner (XtremeCT, Scanco Medical AG, Bruittsellen, Switzerland). Volumetric bone mineral density, cortical and trabecular architecture, and strength as estimated by finite element analysis were measured in the distal radius and tibia.

Results summary:

See attachment.

Age was similar between groups with a mean age of 39 in patients and 38 in controls. No significant difference in trabecula architecture or strength was found in patients compared to controls.

Conclusion:

Loss of bone density at distal sites in patients with GD seems caused by reduced cortical density.

Whether this is the major cause for the increased risk of fractures in GD needs further explorations.

		Cortical bone density <sup>2</sup> (mg HA/cm <sup>3</sup> )	P <sup>1</sup>	Cortical thickness <sup>2</sup> (mm)	P <sup>1</sup>
Radius	Controls	840 (804-875)	0.037	0.60 (0.55-0.66)	0.085
	Patients	883 (851-929)		0.77 (0.60-0.93)	
Tibia	Controls	871 (833-895)	0.002	1.05 (0.91-1.29)	0.065
	Patients	903 (881-927)		1.22 (1.11-1.35)	

<sup>1</sup>Mann Whitney U test for difference between groups

<sup>2</sup>Median with interquartile range.

Table\_results

Disclosures: Sofie Malmstroem, None.

MO0275

**Denosumab is safe in organ transplant patients for management of osteoporosis.** Ejigayehu Abate<sup>\*</sup>, Melody Beers. Mayo Clinic, United states

Purpose: Patients who have undergone organ transplantation often have osteoporosis and are highly susceptible to fractures due to the chronic disease for which they received the transplant and chronic use of immunosuppressive medications including prednisone. Current treatment options for management of osteoporosis require Creatinine Clearance of >35 for use due to risk of renal toxicity. For transplant recipients who often have chronic renal insufficiency that ensues due to effect of the underlying disease and immunosuppressant such as tacrolimus, denosumab is an appealing treatment option. Denosumab (Prolia) is a RANK ligand inhibitor approved in 2009 for management of post-menopausal osteoporosis and men treated with androgen deprivation therapy at high risk for fracture. It is a fully human monoclonal antibody against the receptor activator of nuclear factor -kB ligand (RANKL), a cytokine essential for function of osteoclasts. It binds to RANKL and prevents the interaction of RANKL with its receptor therefore inhibiting function of osteoclasts which are cells responsible for bone resorption. Denosumab is also the only drug available at this time for patients with renal insufficiency. The safety of this drug has not been evaluated in transplant recipients.

Method: This is a retrospective chart review of all organ transplant recipient patients who have received Denosumab for treatment of osteoporosis within the past 5 years at Mayo Clinic Florida. We identified 10 patients. IRB approval was obtained. Inclusion criteria are 1) patients who have had liver/heart/kidney transplant within 5 years (2010-2015) 2) Must have received Denosumab for management of osteoporosis during this time frame.

Result: Median age was 69.5 of which 7 were female. Five patients received liver transplant, 2 cardiac transplants, 2 had kidney transplant and 1 patient had combined pancreas/kidney transplant. Median time of denosumab administration to first transplant was 7 years (range, 1-30years). Median PTH level 39.2 (range, 19-136.4), calcium 9.48 (range 9-10.4), phosphorus 3.7 (range, 2.7-4.3) and creatinine clearance 29.7(range 22-40). Five of the ten patients had recent hip or vertebral fracture. Prior to denosumab use, 7/10 had been on bisphosphonate therapy, 2/10 previously treated with forteo, and one did not receive treatment. Two out of 10 patients had mild rejection treated with short course of steroid pulse, 1/10 had renal failure requiring hemodialysis with complication with pancreatic abscess. One patient had CMV infection but resumed treatment with denosumab without recurrence.

Conclusion: Overall, Denosumab appears to be safe in a small group of patients post solid organ transplant with renal insufficiency and high risk for fracture.

Disclosures: Ejigayehu Abate, None.

MO0276

**Early and Sustained Changes in Bone Metabolism After Severe Burn Injury.** Gabriela Katharina Muschitz<sup>1</sup>, Elisabeth Maurer<sup>2</sup>, Roland Kocijan<sup>3</sup>, Andreas Baierl<sup>4</sup>, Alexandra Fochtmann<sup>5</sup>, Judith Haschka<sup>3</sup>, Heinrich Resch<sup>3</sup>, Peter Pietschmann<sup>6</sup>, Thomas Rath<sup>5</sup>, Christian Muschitz<sup>\*3</sup>.  
<sup>1</sup>Division of Plastic & Reconstructive Surgery, Medical University Vienna, Austria, <sup>2</sup>Department of Plastic, Reconstructive & Aesthetic Surgery, the Medical University Innsbruck, Innsbruck, Austria, <sup>3</sup>St. Vincent Hospital – Medical Department II - Academic Teaching Hospital of the Medical University of Vienna, Austria, <sup>4</sup>Department of Statistics & Operations Research, the University of Vienna, Oskar-Morgenstern-Platz 1, Austria, <sup>5</sup>Division of Plastic & Reconstructive Surgery, Department of Surgery, the, Austria, <sup>6</sup>Department of Pathophysiology & Allergy Research, Center for Pathophysiology, Infectiology & Immunology, the Medical University of Vienna, Austria

Purpose: Severe burn injury causes a massive stress response, consecutively heightened serum levels of acute phase proteins, cortisol and catecholamines with accompanying disturbance in calcium metabolism. The objectives of this study were the evaluation of early and prolonged changes of serum bone turnover markers (BTM) and regulators of bone metabolism. Methods: Male patients with acute severe burn injuries (occupational or recreational accidents) admitted to the burn intensive care unit (BICU) of the General Hospital of the Medical University of Vienna, Austria, were consecutively included. Patients with high-voltage electrical burn injuries were excluded as injuries of this nature directly impact the skeleton. The study population consisted of 32 patients with a median age of 40.5 years and a median burned total body surface area (TBSA) of 40% (83% patients with full thickness burn injury). Changes of BTM/regulators of bone metabolism in the early (days 2 – 7) and prolonged (days 7 – 56) phases after trauma were compared. Results: All investigated BTM/regulators of bone metabolism significantly changed. During the early phase pronounced increases were observed for CTX, P1NP, sclerostin, DKK-1, BALP, FGF23 and iPTH levels, whereas 25-OH vitamin D, albumin, serum and ionized calcium levels decreased. Changes of OPG, OCN and phosphate were less pronounced, but remained significant. In the prolonged phase, changes of P1NP were most pronounced, followed by elevated sclerostin, OCN, BALP, and lesser changes for albumin levels. Calcium and ionized calcium levels tardily increased and remained within the limit of normal. In contrast levels of iPTH, FGF23, CRP and to a

lesser extent CTX and phosphate levels, declined significantly during this phase of investigation. For the standardized effect sizes as a quantitative measure of the strength of the changes of BTM and regulators of bone metabolism in the two investigated phases, the approximate significance thresholds were +/- 0.35. The most intense changes over time were observed for CTX, iPTH, PINP, OCN, ionized calcium and iPTH. The changes of sclerostin, BALP, FGF23, albumin, 25-OH vitamin D, DKK-1, sRANKL, CRP and serum phosphate were less pronounced. OPG did not reach the level of significance. Conclusions: Ongoing changes of BTM and regulators of bone metabolism suggest alterations in bone metabolism with a likely adverse influence on bone quality and structure in male patients with severe burn injuries.

**Disclosures:** Christian Muschitz, None.

## MO0277

**Severe Deterioration of Cortical and Trabecular Bone Microarchitecture in Patients with Inflammatory Bowel Disease.** Judith Haschka\*<sup>1</sup>, Simon Hirschmann<sup>2</sup>, Arnd Klever<sup>1</sup>, Matthias Englbrecht<sup>1</sup>, Francesca Faustini<sup>1</sup>, David Simon<sup>1</sup>, Camille Figueiredo<sup>1</sup>, Louis Schuster<sup>1</sup>, Christian Muschitz<sup>3</sup>, Roland Kocijan<sup>3</sup>, Heinrich Resch<sup>3</sup>, Raja Atreya<sup>2</sup>, Juergen Rech<sup>1</sup>, Marcus Neurath<sup>2</sup>, Georg Schett<sup>1</sup>. <sup>1</sup>University of Erlangen-Nuremberg, Department of Internal Medicine 3, Germany, <sup>2</sup>University of Erlangen-Nuremberg, Department of Internal Medicine 1, Germany, <sup>3</sup>VINFORCE Study Group, St. Vincent Hospital Vienna, Austria

**Background and Aims:**

To investigate the microstructural changes of bone in patients with inflammatory bowel disease (IBD) and to define the factors associated with bone loss in IBD

**Methods:**

A total of 148 subjects, 59 with Crohn's Disease (CD), 39 with Ulcerative Colitis (UC) and 50 healthy controls were assessed for the geometric, volumetric and microstructural properties of bone using high-resolution peripheral quantitative computed tomography. In addition, demographic and disease-specific characteristics of IBD patients were recorded.

**Results:**

IBD patients and controls were comparable in age, sex and body mass index. Total (p=0.001), cortical (p<0.001) and trabecular volumetric BMD (p=0.03) were significantly reduced in IBD patients compared to healthy controls. Geometric and microstructure analysis revealed significantly lower cortical area (p<0.001) and cortical thickness (p<0.001) without differences in cortical porosity, pore volume or pore diameter.

CD showed a more severe bone phenotype than UC: While cortical bone loss was observed in both diseases, CD additionally showed profound trabecular bone loss with reduced trabecular BMD (p=0.008), bone volume (p=0.008) and trabecular thickness (p<0.009). Multivariate regression models identified the diagnosis of CD, female sex, lower body mass index and the lack of remission as factors independently associated with bone loss in IBD.

**Conclusion:**

IBD patients develop significant cortical bone loss impairing bone strength. Trabecular bone loss is limited to CD patients, which exhibits a more severe bone phenotype compared to UC patients.

**Disclosures:** Judith Haschka, None.

## MO0278

**Bone microarchitecture and circulating bone turnover markers in patients with liver cirrhosis caused by alcoholic and nonalcoholic steatohepatitis (ASH/NASH).** Heinrich Resch\*<sup>1</sup>, Robert Wakolbinger<sup>1</sup>, Gerd Bodlaj<sup>1</sup>, Afrodite Zendeli<sup>1</sup>, Peter Pietschmann<sup>2</sup>, Christian Muschitz<sup>1</sup>. <sup>1</sup>St. Vincent Hospital – Medical Department II - VINFORCE Academic Teaching Hospital of the MUV, Stumpergasse 13, 1060 Vienna, Austria, <sup>2</sup>Department of Pathophysiology & Allergy Research, Center for Pathophysiology, Infectiology & Immunology, Medical University of Vienna. Währinger Gürtel 18-20, 1090 Vienna, Austria, Austria

**Purpose** Chronic liver disease is a common medical issue with high prevalence. The number of patients with alcoholic steatohepatitis (ASH), viral hepatitis or nonalcoholic steatohepatitis (NASH) is worldwide increasing. Consequently patients who have been developing already cirrhotic liver tissue changes are known to have an increased risk of fragility fractures. The objectives of this study were the evaluation of differences in areal bone mineral density, Trabecular Bone Score (TBS), trabecular and cortical bone microarchitecture as well as circulating bone turnover marker (BTM) in patients with liver cirrhosis based on ASH/NASH compared to age-matched controls. **Methods** For this cross-sectional single center study 32 female and male patients (mean age 60 years, BMI 26.5 kg/m<sup>2</sup>) with ASH/NASH were compared to a reference population of 29 age-matched healthy females and males (mean age 59.2 years, BMI 26.9 kg/m<sup>2</sup>). Inclusion criteria were liver cirrhosis (Child-Pugh-Score of A, B or C). Exclusion criteria of the whole study population were: history of high-energy trauma, inflammatory bowel disease, renal impairment III-IV, insulin dependent diabetes mellitus type I & II, congestive heart failure HIV infection,

drug abuse, hypo- or hyperthyroid metabolic status, malignancies and rheumatic diseases. Patients with a history of treatment with the following medications were also excluded: adrenal or anabolic steroids, glitazones, anticonvulsants, long-term use of anticoagulants, and any osteoporosis. All patients and controls had areal BMD measurements (DXA spine, hip, radius) including TBS. Bone microarchitecture was non-invasively assessed by HR-pQCT measurements at the radius and tibia, circulating BTM of bone formation/resorption (CTX, PINP) and as well as iPTH, Ca, Ph, alkaline phosphatase and 25-OH vitamin D were evaluated. Results The patients had a mean Child-Pugh Score of 6.3 and a mean MELD score of 10.1. Areal BMD at all measured sites was significantly lower in patients, as well as mean TBS (1.124 vs 1.284 in the reference population; p<0.005 for all measured sites and methods). HR-pQCT values of cortical (Ct.Th) and trabecular bone compartments (BV/TV, Tb.N, Tb.th, Tb.Sp) at the radius and tibia were also lower in patients with liver cirrhosis (p<0.05 for all sites and values). In this context values defining Ct.Po were significantly increased giving evidence of raised cortical porosity. Serum calcium and 25-OH vitamin D levels were lower, whereas serum phosphate, alkaline phosphatase and PINP levels were higher (p<0.005 for all). No differences were observed for CTX and iPTH levels. Conclusion Patients suffering from liver cirrhosis caused by non alcoholic and nonalcoholic steatohepatitis have severe alterations in areal BMD, TBS, trabecular and cortical microarchitecture as well as unfavorable differences in circulating bone turnover marker.

**Disclosures:** Heinrich Resch, None.

## MO0279

**Liver Transplantation and Bone Density.** Zlata Kmecova\*<sup>1</sup>, Lubomir Skladany<sup>1</sup>, Juraj Svac<sup>1</sup>, Juraj Payer<sup>2</sup>. <sup>1</sup>Faculty Hospital of F.D. Roosevelt, Banska Bystrica, Slovakia, <sup>2</sup>V. internal clinic of University Hospital, Bratislava, Slovakia

**Background:** Decreased bone density and fractures are frequent complications of liver cirrhosis, playing an important role in patients not only prior to but also after orthotopic liver transplantation (OLT).

**Objective:** The objective was to retrospectively analyze a group of patients to determine bone density status, selected laboratory parameters and X-ray of the spine at one year after OLT and to compare them with a group of patients who were not transplanted.

**Material and Methods:** The group comprised 51 patients (37 males, 14 females) with liver cirrhosis. The age range was 38-63 years; the mean age was 50 years. Bone density was measured using the DXA method at lumbar spine, femoral neck and hip. The laboratory parameters included calcium, albumin and total 25-hydroxyvitamin D (25-OH D) levels. X-rays of the thoracic and lumbar spine were obtained. The data were processed using Students t-test statistical significance p < 0.05.

**Results:** In the lumbar spine region, bone density was statistically significantly increased in post-transplantation patients as compared with patients who were not transplanted (p < 0.02). Bone density in the hip and femoral neck regions was insignificantly decreased in patients at one year after OLT and significantly increased in those who were not transplanted (p < 0.001, p < 0.04). Calcium levels were not significantly changed in either of the groups. The mean level of 25-OH D increased in patients after OLT as compared with those who did not undergo OLT. Prior to transplantation, only 4 patients had normal 25-OH D levels and the others had low levels of 25-OH D. After transplantation, normal vitamin D levels were found in 22 patients and low levels in 14 patients. In patients after OLT, the mean albumin level rose to normal values, patients without OLT had unchanged albumin levels. No new fractures in the area of the thoracic and lumbar spine were observed in patients after OLT. Two patients without transplantation had fractures in the thoracic spine region.

**Conclusion:** It was found that as early as one year after liver transplantation, patients had better bone density in the lumbar spine region and normalized laboratory parameters. OLT combined with sufficient calcium and vitamin D supplementation leads to improved bone density and subsequent fracture risk reduction.

**Disclosures:** Zlata Kmecova, None.

## MO0280

**Abaloparatide-SC is an Effective Treatment Option for Postmenopausal Osteoporosis: Review of the Number Needed to Treat Compared with Teriparatide.** E. Michael Lewiecki\*<sup>1</sup>, Gary Hattersley<sup>2</sup>, Gregory Williams<sup>3</sup>, Ming-Yi Hu<sup>3</sup>, Lorraine A Fitzpatrick<sup>3</sup>, Jean-Yves Reginster<sup>4</sup>. <sup>1</sup>New Mexico Clinical Research & Osteoporosis, United states, <sup>2</sup>Radius Health, Inc., United states, <sup>3</sup>Radius Health, Inc, United states, <sup>4</sup>Department of Public Health Sciences, Epidemiology & Health Economics, Belgium

**BACKGROUND:** Subcutaneous abaloparatide-SC (ABL-SC) is a 34 amino acid peptide created to have selective binding to the PTH1 receptor with anabolic properties but a less resorptive profile. In the ACTIVE trial, postmenopausal women with osteoporosis were treated with ABL-SC, open-label teriparatide (TER) or placebo (PLB) for 18 months. ABL-SC reduced new vertebral fractures by 86% nonvertebral and all clinical fractures by 43% and major osteoporotic fractures by 70% compared to placebo. Kaplan-Meier curves indicated early separation between abaloparatide and placebo for nonvertebral, clinical and major osteoporotic fractures.

**METHODS:** To further understand the effectiveness of ABL-SC, we calculated the number needed to treat (NNT) from the ACTIVE trial. The number needed to treat represents the average number of patients that would need to be treated to prevent one additional future fracture. The study population ranged in age from 49 to 86 years; average lumbar spine T-score was -2.9; 24% had prevalent vertebral fracture and 48% had a prior (<5 years) nonvertebral fracture history; 37% had no prior vertebral or nonvertebral fracture. Mean FRAX scores at baseline were 4.8% for hip fracture and 13.2% for major osteoporotic fracture.

**RESULTS:** In this population, the NNT for vertebral fracture with 18 months of ABL-SC treatment was 28; it was 55 for nonvertebral fracture, 37 for clinical fracture, and 34 for major osteoporotic fracture. In contrast, the NNT with teriparatide in this trial was higher (30, 92, 59, 75 for vertebral, nonvertebral, clinical and major osteoporotic fractures, respectively (see table).

Contemporary ethical concerns of using placebo in high risk populations led us to recruit a lower risk population. To evaluate the effectiveness of ABL-SC in a more severe patient population, we estimated the NNT assuming a higher risk population as had been recruited in prior studies of osteoporosis populations (Neer, 2001; Harris 1999). Assuming a 10% vertebral fracture incidence and an 86% reduction in vertebral fracture, the NNT for ABL-SC would be about 12 with 1.5 years of treatment.

**CONCLUSION:** Abaloparatide-SC is potentially a highly effective option for the treatment of osteoporosis in postmenopausal women.

	Number Needed to Treat After 18 Months	
	Abaloparatide-SC	Teriparatide
Vertebral Fractures	28	30
Nonvertebral Fractures	55	92
Clinical Fractures	37	59
Major Osteoporotic Fractures	34	75

NNT Abaloparatide-SC vs Teriparatide over 18 Months

**Disclosures:** E. Michael Lewiecki, Radius Health, 12; Amgen, 12; Eli Lilly, 11; Amgen, 11; Eli Lilly, 12; Shire, 13; Merck, 11

This study received funding from: Radius Health

## MO0281

**Effect of investigational treatment abaloparatide-SC for prevention of major osteoporotic fracture or any fracture is independent of baseline fracture probability.** EV McCloskey<sup>1</sup>, H Johansson<sup>1</sup>, NC Harvey<sup>2</sup>, A Oden<sup>1</sup>, H Jiang<sup>3</sup>, S Modin<sup>3</sup>, L Fitzpatrick<sup>4</sup>, JA Kanis<sup>1</sup>. <sup>1</sup>University of Sheffield, United Kingdom, <sup>2</sup>MRC Lifecourse Epidemiology Unit, University of Southampton, United Kingdom, <sup>3</sup>Radius Health Inc, United states, <sup>4</sup>Radius Health Inc, United Kingdom

**Objectives:** Clinical data suggest that daily subcutaneous injections of the investigational drug abaloparatide (80mcg) for 18 months significantly decrease the risk of vertebral and non-vertebral fracture compared with placebo in postmenopausal women. The aim of this study was to determine the effect of abaloparatide versus baseline fracture risk, assessed using the FRAX tool.

**Material and Methods:** Baseline clinical risk factors (age, BMI, prior fracture, glucocorticoid use, rheumatoid arthritis, smoking and maternal history of hip fracture) were entered into country-specific FRAX models to calculate the 10-year probability of major osteoporotic fractures with or without inclusion of femoral neck BMD. The interaction between probability of a major osteoporotic fracture and treatment efficacy was examined by a Poisson regression.

**Results:** 821 women randomized to the placebo group and 824 women to abaloparatide-SC were followed for up to 2 years. At baseline, the 10-year probability of major osteoporotic fractures (with BMD) ranged from 2.3-57.5%. Data suggest that treatment with abaloparatide-SC was associated with a 69% decrease in major osteoporotic fracture (MOF) compared to placebo treatment (95%CI: 38, 85%). The risk of any clinical fracture (AF) decreased by 43%; (95%CI: 9, 64%). Hazard ratios for the effect of abaloparatide-SC on the fracture outcome did not change significantly with increasing fracture probability ( $p > 0.30$  for MOF and  $p = 0.11$  for AF (Figure)). Similar results were noted for the interaction when FRAX probability was computed without inclusion of BMD.

**Conclusions:** Clinical data suggest that the investigational drug, Abaloparatide, may significantly decrease the risk of major osteoporotic fracture and any clinical fracture in postmenopausal women, irrespective of baseline fracture probability.

**Disclosures:** EV McCloskey, None.

This study received funding from: Radius Health Inc

## MO0282

**Effects of Teriparatide and Denosumab, Alone or Combined, on Circulating Sclerostin in Postmenopausal Women.** Joy Tsai\*, Sherri-Ann Burnett-Bowie, Benjamin Leder. Massachusetts General Hospital, United states

**Background:** Sclerostin is an osteocyte-derived secreted glycoprotein that inhibits Wnt signaling and has anti-anabolic effects on bone formation. While sclerostin inhibition has been hypothesized to be one of the key mechanisms by which PTH exerts its anabolic skeletal effects, the physiologic relevance of circulating serum sclerostin is not well defined. Prior studies exploring the effects of teriparatide, denosumab, and other bone-active agents on serum sclerostin have reported conflicting results. In this study, we aimed to determine the effect of denosumab and teriparatide, alone and combined, on serum sclerostin levels in postmenopausal osteoporotic women and to determine the relationship of serum sclerostin and BMD in the DATA study.

**Methods:** We randomized 94 postmenopausal osteoporotic women ages 51-91 to receive TPTD 20-ug SC, DMAB 60-mg SC Q6months, or both for 12 months. Women were excluded if they had ever used IV bisphosphonates (BPs) or oral BPs in the past 6 months. Serum sclerostin was measured at 0, 3, 6, and 12 months. Pearson's correlation coefficients (r) were calculated to determine the relationship between serum sclerostin and 1-year BMD changes in addition to serum sclerostin and bone turnover markers (OC, PINP, and CTX).

**Results:** In all 3 groups, serum sclerostin increased at 3-months, peaked at 6-months, and remained increased at 12-months (Table). There was no difference in these increases in serum sclerostin among the 3 groups at any time point. When all subjects are pooled, baseline sclerostin levels and 1-year sclerostin changes did not correlate with 1-year BMD changes at any site. Additionally, 1-year sclerostin changes did not correlate with 1-year changes in OC, PINP, or CTX.

**Conclusions:** In women treated with TPTD, DMAB, or both for 1-year, serum sclerostin levels increased similarly. These increases did not predict 1-year BMD changes or changes in biochemical markers of bone turnover. These data may reflect discordance between circulating and tissue sclerostin levels. The physiologic and mechanistic significance of serum sclerostin changes in the setting of anabolic and antiresorptive therapy remain unclear.

Serum Sclerostin % change	TPTD (N=30)	DMAB (N=33)	Both (N=29)
0-3 month	13.7 ± 18.7%	18.6 ± 29.6%	17.8 ± 23.4%
0-6 month	20.0 ± 41.5%	30.9 ± 57.4%	22.4 ± 33.3%
0-12 month	18.5 ± 30.9%	21.5 ± 35.8%	18.7 ± 31.4%

Table

**Disclosures:** Joy Tsai, None.

This study received funding from: Amgen and Lilly

## MO0283

**Low-dose RANKL as a potential therapeutic for postmenopausal osteoporosis.** Anna Cline-Smith<sup>1</sup>, Elena Shashkova<sup>1</sup>, Jesse Gibbs<sup>2</sup>, Deborah Novack<sup>3</sup>, Rajeev Aurora<sup>1</sup>. <sup>1</sup>Saint Louis University School of Medicine, United states, <sup>2</sup>Washington University School of Medicine, United states, <sup>3</sup>Washington University in Saint Louis, United states

A number of studies have established that RANKL promotes bone resorption. Paradoxically, we have found that pulsing ovariectomized mice with low-dose RANKL suppressed bone resorption, decreased the levels of proinflammatory effector T-cells and had a bone anabolic effect. This effect of RANKL is mediated through the induction regulatory CD8 T-cells by osteoclasts. Recently we have completed a set of studies that show that pulses low-dose RANKL are needed to induce TcREG, as continuous infusion of identical dose RANKL by pump did not induce TcREG. We also show that low-dose RANKL can induce TcREG at two, three, six and ten-weeks post-ovariectomy. Our results show that low-dose RANKL treatment in ovariectomized mice is optimal at once per month to maintain the bone mass. Finally, we found treatment of ovariectomized mice with the Cathepsin K inhibitor, Odanacatib (ODN), also blocked TcREG induction by low-dose RANKL. We interpret this result to indicate that antigens presented to CD8 T-cells by osteoclasts are derived from the bone protein matrix because ODN inhibits Cathepsin K, which mediates the breakdown of collagen and other proteins present in the bone. Taken together, our studies provide a basis for using low-dose RANKL (or a RANK agonist) as a potential therapeutic for postmenopausal osteoporosis.

**Disclosures:** Anna Cline-Smith, None.

**MO0284**

**The Efficacy of Parathyroid Hormone Analogues in Combination With Bisphosphonates for the Prevention of Osteoporotic Fractures. A Simulation Meta-Analysis of Randomized Controlled Trials.** Abdulhafez Selim<sup>1</sup>, Sahar Ghoname<sup>\*2</sup>, Paula Karabelas<sup>3</sup>. <sup>1</sup>PCOM, United states, <sup>2</sup>Ain Shams University School of Medicine, Egypt, <sup>3</sup>AEBM, United states

Parathyroid hormone (PTH) analogues increase bone strength primarily by stimulating bone formation, whereas antiresorptive drugs (bisphosphonates) reduce bone resorption. Some studies have been designed to test the hypothesis that the concurrent administration of the 2 agents would increase bone density more than the use of either one alone. This meta-analysis aimed to determine whether combining PTH analogues with bisphosphonates would be superior to PTH alone.

We searched electronic databases to identify relevant publications up to March 2016. Results of randomized controlled trials (RCTs) comparing PTH analogs combined bisphosphonates with PTH for osteoporosis were analyzed. According to the Cochrane Handbook for Systematic Reviews of Interventions 5.2, we identified eligible studies, evaluated the methodological quality, and abstracted relevant data.

A total of 7 studies, involving 641 patients were included in the meta-analysis. Contrary to the expected, the predicted median vertebral fracture rate was lower in the single treatment group (0.99% vs. 1.58%, in the single and combination treatment groups respectively). Similarly, the predicted mean vertebral fracture rate was lower for the single treatment group (3.17% ± 8.16% vs. 4.24% ± 9.2%, in the single and combination treatment groups respectively). The predicted risk ratio (RR) of vertebral fracture was higher for the combination therapy (1.37). Higher RR implies about 37.00% reduction in PTH's effectiveness when simultaneously combined with bisphosphonates.

The results for non-vertebral fractures were different. The predicted median for non-vertebral fracture rates were similar in both treatment groups (4.89% vs. 5.00%, in the combination and single treatment groups respectively). The predicted means for non-vertebral fracture rates were also comparable (6.42% ± 7.23% vs. 6.62% ± 7.5%, in the combination and single treatment groups respectively). The predicted RR of vertebral fracture was slightly lower for the combination therapy (0.95).

Our results show that there is no evidence for the superiority of combination therapy. In fact, data suggested that simultaneous drug combination can reduce PTH's effectiveness. Further, properly designed, large, multicenter, randomized, controlled trials are still needed to evaluate the efficacy of combination therapy adequately and offer definitive conclusions.

**Disclosures:** Sahar Ghoname, None.

**MO0285**

**Acute Phase Reactions After Intravenous Infusion of Zoledronic Acid in Japanese Patients with Osteoporosis: Sub-analyses of the Phase III (ZONE) Study.** Satoshi Tanaka<sup>1</sup>, Masataka Shiraki<sup>2</sup>, Momoko Ohashi<sup>1</sup>, Satoko Ueda<sup>\*1</sup>, Toshitaka Nakamura<sup>3</sup>. <sup>1</sup>Asahi Kasei Pharma Corporation, Japan, <sup>2</sup>Research Institute & Practice for Involuntal Diseases, Japan, <sup>3</sup>Gotanda Rehabilitation Hospital, Japan

Zoledronic acid (ZOL) is proven significant and sustained decrease in the risk of vertebral, hip, and other fractures in a series of HORIZON trials. However, those clinical trials showed higher incidence of acute phase reactions (APRs) such as pyrexia and myalgia occurred within 3 days after infusion of ZOL. The phase III, multicenter, double-blind, placebo controlled, 2-year study was conducted for Japanese patients with primary osteoporosis (ZOledroNate treatment in Efficacy to osteoporosis; ZONE study). In order to evaluate APR risks, risk factors, and time course of APRs, this sub-analysis of ZONE study was performed.

In this analysis, AEs occurred ≥2% within 3 days after the either infusion were included, such as pyrexia, headache, arthralgia, and myalgia. Patients were instructed to measure and record their body temperature 4 times a day when they felt they had pyrexia until it resolved. Patients were allowed to take 1 tablet of ibuprofen 200 mg only when they had pyrexia of >38.5 °C and felt extremely uncomfortable. Trends in temperatures for 3 days after the infusions were analyzed by using a nonparametric smoothing methods with a local regression (LOESS) model.

A total of 333 and 332 patients received ZOL and placebo, respectively. In the ZOL group, patients developed APRs after either of the 1st or the 2nd infusion, and both of the 1st and 2nd infusions, were 159 (47.7%), 17 (6.3%), and 22 (8.2%), respectively. The most frequently reported APRs only after the 1st infusion was pyrexia. Majority of APRs were mild in severity and resolved within 3 days after the onsets, without taking ibuprofen in the most patients (65.1% after the 1st infusion, 95.9% after the 2nd infusion). The body temperature increased for up to 24 hours after ZOL infusion, and gradually decreased to normal temperature over the 72 hours. The trend of the body temperature was similar in patients with or without ibuprofen medication, although more patients with ibuprofen developed a body temperature >38.5 °C. Patients with prior bisphosphonate use had a lower APR incidence rate than those without (31.3% vs 54.2% after 1st infusion of ZOL).

In conclusion, higher incidence of APRs was observed after ZOL infusion in Japanese patients, however, the incidence of APRs dramatically decreased after the 2nd infusion, and less occurrence in patients with prior bisphosphonate use. The majority of APRs was also mild, and appeared to be transient.

**Disclosures:** Satoko Ueda, Asahi Kasei Pharma, 15  
This study received funding from: Asahi Kasei Pharma Corporation

**MO0286**

**Anti-resorptive activity of anti-hypertensive agent ACEi in older men.** Nahid Rianon<sup>\*1</sup>, BeJier Edwards<sup>1</sup>, Phetsamong Nhonthachit<sup>1</sup>, Amanda Messick<sup>2</sup>, Robert Gagel<sup>3</sup>, Scott M Smith<sup>4</sup>. <sup>1</sup>University of Texas Medical School at Houston, United states, <sup>2</sup>JES Tech, Houston, TX, United states, <sup>3</sup>University of Texas M. D. Anderson Cancer Center, United states, <sup>4</sup>NASA JSC, United states

Hypertension (HTN) is associated with bone loss due to activation of the renin-angiotensin system (RAS) which in turn affects bone turnover. Animal studies have shown decreased bone resorption (up to 19%) and increased bone mass (up to 2%) following treatment with RAS-targeted antihypertensive medications (e.g., angiotensin converting enzyme inhibitors, ACEi). Cross-sectional human studies have documented greater femoral neck BMD in older hypertensive men and women treated with ACEi compared to those not-treated with ACEi (nor other RAS-targeted medications). These findings raise the potential for ACEi use in preventing, or at a minimum slowing bone loss due to age or even microgravity. Based on this, we conducted a cohort study to investigate if ACEi treatment would decrease bone resorption in humans.

We investigated changes in serum C-terminal telopeptide (CTX) and procollagen type I amino-terminal pro-peptide (PINP) in 10 hypertensive men (45 years or older) treated with (N=5) without (N=5) exposure to ACEi for 3-months. Lisinopril was the ACEi used, and dose was adjusted as deemed appropriate by the attending physicians. Participants did not have any known skeletal health problem and were not exposed to any bisphosphonates. A small sample size prevented detailed statistical analysis and hence, we present a preliminary descriptive report of our findings.

Participants' age was 57 ± 7 years (mean ± SD), baseline body mass index was 27 ± 5 kg/m<sup>2</sup>, serum concentration of 25-hydroxyvitamin D was 66 ± 17 nmol/L and parathyroid hormone was 30 ± 13 pg/ml. After Lisinopril treatment, men demonstrated a 11 ± 27% decrease in the bone resorption marker CTX and 5% ± 15% decrease in formation marker PINP. On the contrary, serum CTX increased 41% ± 73% and PINP increased 10% ± 22% in those who were not treated with ACEi.

This is the first human study to report reduction in bone resorptive activity following ACEi treatment for hypertension in older men. Our results indicates potential for ACEi use to treat hypertension in patients who may also be at risk of bone loss due to high resorption, e.g., aging, bed-rest, or space flight. A clinical trial with larger number of subjects and longer duration of follow up is indicated to confirm our findings.

**Disclosures:** Nahid Rianon, None.

**MO0287**

**Early Changes in Bone Turnover Markers Predict Longer-Term Changes in Bone Mineral Density But Not Microstructure in Frail Elderly Women.** Mary Kotlarczyk<sup>\*</sup>, Subashan Perera, Mary Anne Ferchak, David Nace, Neil Resnick, Susan Greenspan. University of Pittsburgh, United states

Background: The value of serum bone turnover markers for predicting changes in bone mineral density (BMD) and microarchitecture after treatment with zoledronic acid is largely unstudied in frail, elderly women. Unlike participants in the pivotal bisphosphonate trials, long-term care residents have multiple comorbid conditions and a sedentary lifestyle, which may impact bone turnover marker changes. We performed secondary analysis of a zoledronic acid trial for osteoporosis in elderly women residing in long-term care to determine if early changes in bone turnover predicted longer-term changes in bone density and microarchitecture.

Methods: Data from 145 women (mean age 86.9) were included in this analysis. Serum C-terminal telopeptide (s-CTX), a marker of bone resorption, and serum procollagen type-1 N-terminal propeptide (PINP), a marker of bone formation, were assessed at baseline and 6 months. BMD was measured at baseline, 12, and 24 months at the lumbar spine and hip by dual-energy x-ray absorptiometry (DXA). Trabecular bone score (TBS), a measure of bone microstructure, was determined from lumbar spine DXA results. Bone marker changes were categorized into tertiles based on percentage change in s-CTX (-39%; +10%) or PINP (-37%; -0%) from baseline to 6-months. Linear mixed models were used to determine between-tertile differences in the percent change of BMD or TBS at 12 and 24 months.

Results: Women in the lowest tertile with an early decrease in s-CTX greater than 39% had a 2.1-2.8% greater increase in lumbar spine BMD at 24 months (p<0.04) and a 2.1-2.6% greater increase in total hip BMD at 12 months (p<0.03) and 2.6-3.3% at 24 months (p<0.01) compared to the other tertiles. Those in the lowest tertile of PINP early change (<-37%) had 2.4-3.9% and 2.3-3.2% greater increases in spine and total hip BMD, respectively, compared to those in the higher tertile (>0%). Bone markers were not associated with changes in TBS.

Conclusions: Early bone turnover changes in frail, elderly women with osteoporosis are associated with long-term changes in lumbar spine and total hip BMD. There was no evidence that changes in bone turnover markers predict changes in bone microstructure in this population.

## 24-Month Changes in BMD by Bone Marker Tertiles

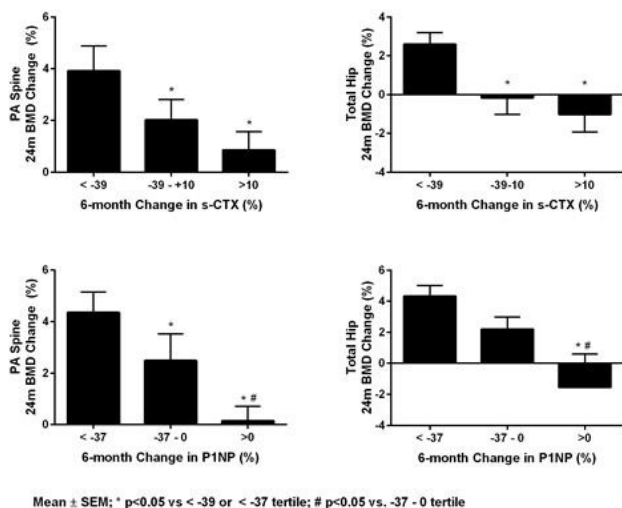


Figure 1

Disclosures: Mary Kotlarczyk, None.

## MO0288

**Effect of Denosumab Treatment on BMD as Assessed by DXA and QCT in Postmenopausal Osteoporosis With and Without Prior Bisphosphonates Treatment.** Koji Ishikawa<sup>1</sup>, Tomoaki Toyone<sup>1</sup>, Tsuchiya Koki<sup>1</sup>, Wakako Sakamoto<sup>1</sup>, Takuma Kuroda<sup>1</sup>, Hiroshi Ito<sup>2</sup>, Takashi Nagai<sup>2</sup>, Katsunori Inagaki<sup>2</sup>. <sup>1</sup>Department of Orthopaedic Surgery, Showa University School of Medicine, 1-5-8 Hatanodai, Shinagawa-ku, Tokyo 142-8666, Japan, <sup>2</sup>Department of Orthopaedic Surgery, Showa University School of Medicine, Japan

**Background:** In men and postmenopausal women with osteoporosis, a single 60 mg dose of denosumab subcutaneously administered every 6 months significantly reduces bone turnover markers (BTMs), increases bone mineral density (BMD), and reduces the risk of new vertebral and nonvertebral fractures, including hip fractures. Several osteoporosis treatment guidelines recommended the use of denosumab for the treatment of severe osteoporosis patients including previously treated with antiresorptives treatment. An important clinical question is whether previous antiresorptives influence the response to denosumab treatment.

**Methods:** We retrospectively reviewed the records of patients who had received 1 year of denosumab with supplementation of activated vitamin-D (elcalcitol: 0.75 µg) for osteoporosis. Patients were divided into two groups based on their prior treatment (treatment naïve: n=21, pretreated with bisphosphonate: n=12). Bone mineral density (BMD) at the lumbar spine and hip was determined after 6, 12 months using DXA and QCT. Bone turnover markers (BTMs) were also assessed at baseline and at 1, 3, 6, 7, 9 and 12 months after treatment.

**Results:** After 12 months, lumbar spine DXA-BMD (mg/cm<sup>2</sup>), femoral neck BMD (mg/cm<sup>2</sup>) and total hip BMD (mg/cm<sup>2</sup>) was increased from baseline by 8.8, 2.4 and 4.1 % in the treatment naïve group, and by 3.5, 1.0 and 0.8 % in the pretreated with bisphosphonate group, respectively. Changes in lumbar spine QCT-BMD (mg/cm<sup>3</sup>) from baseline was 4.5 % in the treatment naïve group, and -1.4 % in the pretreated with bisphosphonate group. Inter-group differences of the femoral neck BMD values was not significant. The increase of the lumbar spine DXA-BMD, QCT-BMD and total hip BMD was larger in the treatment naïve group than the pretreated with bisphosphonate group (P<0.01, P<0.05 and P<0.01, respectively). Values of the BTMs was significantly decreased after 1 months in both groups.

**Conclusion:** Our study suggest that denosumab treatment was effective in increasing BMD and decreasing BTMs. The BMD increase was less robust for patients previously treated with bisphosphonate than in the treatment naïve groups. These findings support the use of denosumab as a treatment option for osteoporosis.

Disclosures: Koji Ishikawa, None.

## MO0289

**Identifying Incomplete Atypical Femoral Fractures with Single-Energy Absorptiometry Femur Exam: Declining Prevalence.** Malachi McKenna<sup>1</sup>, Fergus McKiernan<sup>2</sup>, Bernie McGowan<sup>3</sup>, Carmel Silke<sup>3</sup>, Kathleen Bennett<sup>4</sup>, Susan van der Kamp<sup>1</sup>, Paul Ward<sup>5</sup>, Conor Hurson<sup>5</sup>, Eric Heffernan<sup>5</sup>. <sup>1</sup>St. Vincent's University Hospital, Ireland, <sup>2</sup>Marshfield Clinic Research Foundation, United states, <sup>3</sup>The North Western Rheumatology Unit, Our Lady's Hospital, Ireland, <sup>4</sup>Division of Population & Health Sciences, Royal College of Surgeons in Ireland, Ireland, <sup>5</sup>St. Vincent's University Hospital, Ireland

**Introduction.** Atypical femur fractures (AFF) are associated with long-term bisphosphonate (BP) therapy. Early identification of AFF prior to their completion provides an opportunity to intervene, potentially reducing morbidity associated with these fractures. Single energy X-ray absorptiometry (SE) is an imaging method recently shown to detect incomplete AFF (iAFF) prior to fracture completion.

**Methods.** Patients (n=173), who had been prescribed BP therapy for greater than 5 years, were assessed for iAFF using SE femur imaging at their presentation for routine bone mineral density testing between May 2013 and September 2014. We compared these findings with those of our previously published prospective study (n=257) in which the femur was imaged for iAFF using dual-energy absorptiometry (DXA). The yearly prevalence of complete AFF was determined among patients with subtrochanteric fracture in our institution from 2006 to 2014; all radiographs of patients with subtrochanteric fracture were adjudicated for presence of complete AFF according to ASBMR criteria. National trends in Ireland for femur fracture incidence were calculated from 2005-2014 by means of extracting data from a national computer-based discharge abstracting system using the ICD 10 codes for the following specific hip fractures types: fractures of the neck of femur (S720), pertrochanteric fractures (S721), subtrochanteric fractures (S722), and fractures of the shaft of femur (S723). Trends in BP prescribing were calculated from 2009-2014 using a national primary care prescribing database.

**Results.** No patients had iAFF using SE femur imaging compared to a prevalence of 2.7% in the earlier study using DXA imaging. Between 2006-2014, we observed a rise and decline in complete AFFs at our hospital. Between 2005 and 2009, the yearly rates of hospitalisations in Ireland for all femur fractures increased by 7.2% (p=.121) and for S722/S723 by 29.1% (p=.030) with non-significant changes between 2010-2014 at -3.5% (p=.672) and 6.7% (p=.644) respectively. Between 2010-2014, BP prescribing declined by 14% (p=.209) at a time when calcium prescription increased by 26% (p=.023).

**Conclusions.** Point of service SE imaging can identify iAFF prior to fracture completion that, in turn, might avert morbidity associated with fracture completion. The declining trend in AFF is coincident with declining national trends in BP prescribing in Ireland.

Disclosures: Malachi McKenna, None.

## MO0290

**iPTH Elevation after Denosumab Use is not Associated with Anabolic Effect.** Se-Min Kim<sup>\*</sup>, Mark O. Goodarzi, Stuart L. Silverman. Cedars-Sinai Medical Center, United states

## Introduction

Antiresorptive agents may result in transient increases in intact PTH (iPTH). After denosumab use, iPTH levels are increased in 1-3 months, but stay elevated at 6 months in some patients. It has been hypothesized that elevated iPTH may be anabolic. The aim of this study is to correlate BMD response to changes in iPTH and bone turnover markers (BTMs); procollagen type 1 N-terminal propeptide (P1NP), and C-terminal telopeptide (CTx). Our hypothesis is that patients with elevated iPTH and measurable P1NP at 6 months have higher BMD gain with denosumab treatment.

## Methods

In this retrospective study, iPTH with calcium, P1NP, and CTx at 6 months were compared to values at baseline. Lumbar spine (LS) and total hip (TH) BMD changes (%) at 12 month were compared in patients with and without iPTH elevation at 6 months. Correlation coefficient of log-transformed LS and TH BMD changes (%) with iPTH change was computed. LS and TH BMD changes (%) at 12 month were compared in patients with measurable BTMs and suppressed BTMs to unmeasurable ranges at 6 months (P1NP < 10 pg/ml, CTx < 80 pg/ml).

## Results

78 subjects (mean age, 68.1±10.1) were analyzed after excluding patients with elevated iPTH, chronic kidney disease or vitamin D deficiency at baseline. At 6 months, iPTH was elevated in 68.9% of subjects (mean change, 9.8±/-2.5 pg/ml, p=0.0002). Calcium was slightly lower than baseline (-0.15±/-0.05 mg/dl, p=0.0032). P1NP and CTx were suppressed in 92% (-29.7±/-3.2 pg/ml, p<0.0001), and 85% (-198.2±/-24.9 pg/ml, p<0.0001) of subjects, respectively. LS and TH BMD changes (%) at 12 months tended to be smaller in patients with iPTH elevation (9.5±/-2.4 LS, 7.8±/-2.4 TH) compared to patients without iPTH elevation (13.1±/-3.7 LS, 12.8±/-3.6 TH) (p=0.42 LS, p=0.26 TH). LS and TH BMD changes (%) showed negative correlation with iPTH elevation without statistical significance (standard β coefficient, -0.09 LS, -0.22 TH) (p=0.61 LS, p=0.22 TH). BMD changes (%) with P1NP and CTx suppression are summarized in Table 1.

## Conclusion

This is the first study to correlate iPTH elevation to BMD gain (%) after denosumab use. Our findings suggest iPTH elevation is not associated with an anabolic effect, which is consistent with histomorphometric findings from the AVA study. Although not statistically significant, patients with higher iPTH elevation and suppressed P1NP and CTx at 6 months show less BMD gain, which needs to be investigated further.

Table1. BMD changes (%) with Bone turnover markers

	LS (mean +/- SE)		LS (mean +/- SE)
P1NP <10 pg/ml (N=11)	11.44+/-3.55	CTX <80 pg/ml (N=22)	9.99+/-2.53
P1NP ≥10 pg/ml (N=22)	10.18+/-2.51	CTX ≥80 pg/ml (N=10)	12.64+/-3.75
	p=0.77		p=0.56
	TH (mean +/- SE)		TH (mean +/- SE)
P1NP <10 pg/ml (N=11)	8.66+/-3.39	CTX <80 pg/ml (N=23)	9.43+/-2.47
P1NP ≥10 pg/ml (N=22)	9.54+/-2.50	CTX ≥80 pg/ml (N=10)	9.50+/-3.75
	p=0.83		p=0.99

Table1. BMD changes (%) with Bone turnover markers

Disclosures: *Se-Min Kim, None.*

**MO0291**

**Offset of Effect of Oral Bisphosphonates on Bone in Postmenopausal Osteoporosis: the TRIO Study.** Kim Naylor<sup>1</sup>, Margaret Paggiosi<sup>1</sup>, Fatma Gossiel<sup>1</sup>, Nicola Peel<sup>2</sup>, Eugene McCloskey<sup>1</sup>, Jennifer Walsh<sup>1</sup>, Richard Eastell<sup>\*1</sup>. <sup>1</sup>University of Sheffield, United Kingdom, <sup>2</sup>Sheffield Teaching Hospitals NHS Foundation Trust, United Kingdom

Oral bisphosphonates (BPs), the commonest form of treatment for postmenopausal osteoporosis, continue to suppress bone turnover markers (BTM) after treatment has stopped. Indirect comparisons suggest that the offset of effect may differ between agents, but there has been no comparison in a randomized study. We have examined the offset of effect on BTM and BMD during two years after cessation of treatment with 3 oral BPs.

Postmenopausal osteoporotic women were randomized to receive ibandronate (Ibn) (Bonviva, Roche, 150mg monthly), alendronate (Aln) (Fosamax, Merck, 70mg weekly), or risedronate (Ris) (Actonel, Warner Chilcott, 35mg weekly) for 2 years in the TRIO study. At the end of the study women with >80% compliance with their treatment, in whom it was clinically appropriate to discontinue BP, were invited to participate in a further 2-year offset of effect study, (n=55 women age 56 to 81y). Participants received daily calcium (1200 mg/day) and vitamin D (800IU/day) throughout. Fasting blood samples were collected at 24, 48, 72 and 96 weeks after the end of BP treatment. The BTMs serum PINP and CTX were measured by automated assay (IDS-iSYS, Immunodiagnostic Systems, UK). BMD was measured by DXA (Discovery A, Hologic Inc, Bedford MA) at lumbar spine and total hip. The percentage change from pre-treatment values for BTM are shown in fig 1. The magnitude of decrease on treatment was as expected. There was an increase in bone resorption (CTX) and formation (PINP) during the offset period. There was an overall significant difference in absolute values between the treatment groups during the first year of offset (CTX week 120 P=0.009, PINP week 144 P=0.029), which diminished during the second year. The BTMs remained below pre-treatment values throughout the offset period. During the 2 years after stopping BP there was an overall decrease in total hip BMD -1.6% (-1.9 to -1.2) P<0.001, with no significant change at the spine -0.6% (95% CI -1.1 to -0.2) P=0.17. There was no difference between the treatment groups.

In conclusion, all three drugs showed evidence of offset of effect. There was a greater increase in CTX than PINP after stopping BP treatment. The offset after Ris appears to be quicker than for Aln or Ibn, but this may be because the effect of the drug on bone turnover is less. We found a greater decrease in hip BMD than in spine BMD after stopping oral BPs. Thus, total hip BMD and serum CTX may be the best tests for monitoring offset.

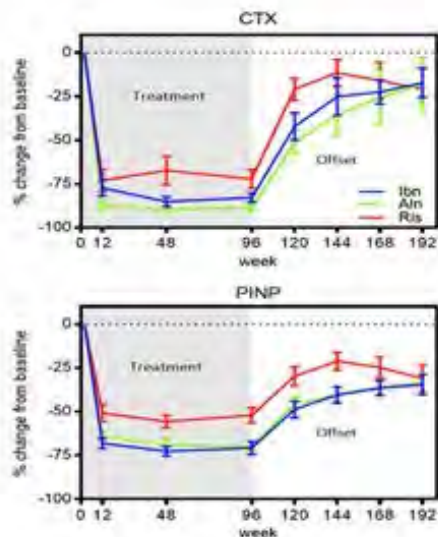


Figure 1. Percentage change in BTM from pre-treatment with BP

Disclosures: *Richard Eastell, None.*

This study received funding from: Warner Chilcott

**MO0292**

**Significant Bone Loss After Stopping Denosumab Treatment.** Maria Belen Zanchetta<sup>\*1</sup>, Juan Boailchuk<sup>2</sup>, Fabio Massari<sup>1</sup>, Fernando Silveira<sup>2</sup>, Cesar Bogado<sup>1</sup>, Jose Ruben Zanchetta<sup>1</sup>. <sup>1</sup>IDIM, Universidad del Salvador, Argentina, <sup>2</sup>IDIM, Argentina

Denosumab (DMAb) is a soluble inhibitor of RANKL and, therefore, does not incorporate into bone matrix. Consistently, DMAB discontinuation is associated with reversal of effects attained with treatment.

Aim: Primary, assess changes in BMD in a group of postmenopausal women treated with denosumab - for 7 or 10 years - after at least one year of discontinuation. Secondary, describe the occurrence of fragility fractures.

Material and methods: Women who had received DMAB for at least 7 years were invited to participate in this follow-up study. Clinical and bone health risk factors, occurrence of incident fractures, calcium and vitamin D supplementation, use of drugs or other conditions which may affect bone health were collected in the medical interview. Lumbar spine and hip BMD were assessed by DXA (Lunar Prodigy Advance, software 13.6). Also, laboratory tests (CTX, osteocalcin, vitamin D, PTH calcium, phosphate) and Spine X-ray were performed. DXA scans and X-rays were compared with the previous studies obtained while in treatment with DMAB to assess changes upon discontinuation.

Results: thirty- eight women agreed to participate (mean age 81 ± 3.4 years, range: 76-89, BMI: 28.4 ± 5.4). Seventeen patients had received treatment during 7 years and 21 during 10 years. Mean gap time between DMAB last dose and visit was: 17 ± 1 months (range 16-20 months). None of them had received BP after stopping or referred other condition that could affect bone metabolism. 50% of the patients were receiving calcium and vitamin D supplementation. BMD decreased significantly in all regions (-8% in LS, -6% in FN and - 8.4% in TH, table 1). Media lab results were CTX: 996 ± 307 pg/ml (normal value premenopausal women 550pg/ml); osteocalcin 55.2 ± 18.6 ng/ml (normal value up to 42ng/ml), vitamin D 23.7 ± 6.9 ng/ml, PTH 44.7 ± 12.1 pg/ml, calcium 9.8 ± 0.3mg/dl and P 4 ± 0.4 mg/dl. Four patients (13.2%) suffered a new vertebral fracture and 1 patient suffered a wrist fracture upon stopping treatment.

Conclusion: This study confirms a high remodeling state evidenced by bone turnover markers and the consequent bone loss that occurs after cessation of denosumab. Decrease in BMD measured by DXA was clinically significant and similar in all regions. This study is too small to evaluate fracture outcomes. More studies are necessary in the future to assess if fracture risk after DMAB cessation may be a concern in elderly post menopausal women.

DXA values (media ± D.S.) N=38	Last on DMAB		Change %	P
		After stopping		
<b>L1-L4</b>				
DMO (g/cm <sup>2</sup> )	1.005 ± 0.108	0.923 ± 0.090	-8.0 ± 4.1	<0.01
T-score	-1.5 ± 0.9	-2.1 ± 0.7		<0.01
Z-score	0.3 ± 1.0	-0.3 ± 0.8		<0.01
<b>FN (n=7)</b>				
DMO (g/cm <sup>2</sup> )	0.820 ± 0.081	0.770 ± 0.083	-6.0 ± 4.7	<0.01
T-score	-1.7 ± 0.7	-1.3 ± 0.7		<0.01
Z-score	0.6 ± 0.7	0.2 ± 0.8		<0.01
<b>TH</b>				
DMO (g/cm <sup>2</sup> )	0.866 ± 0.08	0.794 ± 0.091	-8.4 ± 4.6	<0.01
T-score	-1.7 ± 0.8	-1.1 ± 0.7		<0.01
Z-score	0.7 ± 0.7	0.1 ± 0.8		<0.01

table 1

Disclosures: *Maria Belen Zanchetta, None.*

**MO0293**

**Radiological Follow-up Results of Cemented Vertebrae after Vertebroplasty.** Jin Hwan Kim<sup>\*</sup>, Kyoung Hwan Koh, Jung Hoon Kim. Department of Orthopedic Surgery, Inje University, Ilsan Paik Hospital, Korea, republic of

Study Design: A retrospective study.

Objectives: To assess radiological follow-up results, including progression of bone cement augmented vertebrae, of patients who underwent percutaneous vertebroplasty (PVP).

Summary of Literature Review: There are few studies of radiological follow-up results that include progression of bone cement augmented vertebrae after PVP, regardless of good clinical results.

Materials and Methods: Between January 2000 and August 2007, 253 patients were treated with PVP for osteoporotic compression fracture. Among them, 81 patients died during follow-up and 101 patients (157 vertebrae) were available for follow-up over 7 years. We analyzed the radiologic outcomes, focusing on augmented bone cement feature and progressive change with adjacent vertebrae.

Results: The mean follow-up period was 7.9 years. Anterior body height in the last follow-up was improved about 0.3 mm compared with the preprocedural value, but this improvement was not statistically significant. The focal kyphotic angle was reduced from 12.3° at the preprocedural state to 11.7° at the postprocedural state but this change was also not statistically significant ( $p > 0.05$ ). Out of the 101 cases, we observed 7 cases of radiolucent line with decreased bone density in the adjacent area of bone cement and 5 cases of bone cement cracks accompanied with vertebral collapse were observed. Eleven patients (10.8%) had a solid spontaneous fusion, and 8 patients (7.9%) had partially fused with adjacent vertebrae.

Conclusions: The bone cement augmented vertebrae showed stable radiologic progression without significant changes in vertebral height or kyphotic angle. After percutaneous vertebroplasty, unpredictable spontaneous fusion with proximal adjacent vertebrae developed at a higher rate than 10% rate.

Key words: Osteoporotic vertebral compression fracture, Bone cement, Radiological follow-up results, Spontaneous fusion, Vertebroplasty

Disclosures: Jin Hwan Kim, None.

## MO0294

**Atypical Femur Fractures: A Survey of Current Practices in Orthopaedic Surgery.** Prism Schneider\*<sup>1</sup>, Michelle Wall<sup>2</sup>, Jacques Brown<sup>3</sup>, Angela Cheung<sup>4</sup>, Edward Harvey<sup>2</sup>, Suzanne Morin<sup>2</sup>. <sup>1</sup>University of Calgary, Canada, <sup>2</sup>McGill University, Canada, <sup>3</sup>University Laval, Canada, <sup>4</sup>University of Toronto, Canada

Purpose: There are currently no guidelines for the surgical management of bisphosphonate-associated atypical femur fractures (AFF). In the Quebec Atypical Femur Fracture Registry, we have previously documented variation in approaches to surgical repair for complete and incomplete AFF. We aimed to determine current practices of orthopaedics surgeons in the treatment of AFF and identify knowledge gaps that will guide the development of clinical guidelines.

Methods: A self-administered online survey was developed and sequentially posted on the Orthopaedic Trauma Association (OTA, 585 members) and the Canadian Orthopaedic Association (COA, 900 members) websites between July 2015 and January 2016. Descriptive statistics are presented.

Results: A total of 172 completed surveys were obtained (58% OTA). The majority of OTA respondents were trauma surgeons (61%) whereas the practice of the COA respondents was general orthopedics (35%) and arthroplasty (28%). Seventy-eight % of respondents had treated at least 1 patient with an AFF in the previous 6-months. Seventy-six percent of surgeons reported feeling Extremely or Very Confident, and 23% reported Moderate Confidence in diagnosing AFF. When asked regarding confidence in treating AFF, only 63% reported feeling Extremely or Very Confident. Preferred management for complete and symptomatic incomplete AFFs was reported to be surgical fixation with a cephalomedullary nail (CMN) by 88% and 79% respectively (N= 155), while preferred management for asymptomatic incomplete AFFs was reported to be close follow-up, including serial radiographic imaging (72%). Trauma surgeons, compared to non-trauma surgeons, reported using a cephalomedullary nail for surgical AFF repair more frequently (Figure). In patients with bilateral AFFs, with one side surgically treated, 56% were Extremely Likely to surgically treat the contralateral side, if symptomatic, but only 14% were Extremely Likely if the patient was asymptomatic. The preferred timing for prophylactic fixation was between 2 and 6 weeks after initial femur fixation. There was no regional variation in AFF management.

Most respondents felt treatment guidelines would be valuable (81%) and they would benefit from AFF educational resources (73%).

Conclusion: Current orthopaedic treatment practices for AFFs are variable. These results will inform our ongoing multidisciplinary team that aims to develop evidence-based AFF practice guidelines and educational resources.

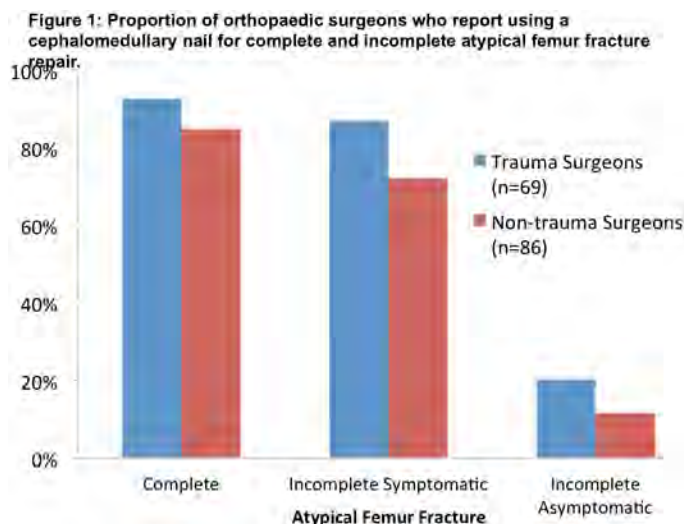


Figure 1

Disclosures: Prism Schneider, None.

## MO0295

**Comparison of the Medium-term Outcome After the Treatment of Osteoporotic Insufficiency Fractures by Means of Balloon Sacroplasty (BSP) and Radiofrequency Sacroplasty (RFS) in Comparison: A Prospective Randomised Study.** Reimer Andresen\*<sup>1</sup>, Sebastian Radmer<sup>2</sup>, Julian Ramin Andresen<sup>3</sup>, Hans-Christof schober<sup>4</sup>. <sup>1</sup>Institute of Diagnostic & Interventional Radiology/Neuroradiology, WKK Heide, Germany, <sup>2</sup>Centre for Orthopaedics, Berlin, Germany, <sup>3</sup>Werner Heisenberg high school, Heide, Germany, <sup>4</sup>Department of Internal Medicine I, Municipal Hospital Suedstadt Rostock, Germany

### Introduction

The objective of this prospective, randomised study was to test the feasibility and the clinical outcome of the different forms of treatment.

### Material and methods

In 40 patients with a total of 57 sacral fractures, cement augmentation was performed with CT-guidance by means of balloon sacroplasty (BSP) or radiofrequency sacroplasty (RFS). For BSP, the balloon catheter was inflated and deflated in the fracture zone, and the hollow space created was then filled with PMMA cement. For RFS, a flexible osteotome was initially used to extend the spongy space in the fracture zone. The highly viscous PMMA cement, activated by radiofrequency, was then inserted into the prepared fracture zone. Pain intensity was determined on a visual analogue scale before the intervention, on the second day, and 6, 12 and 18 months after the intervention. The results were tested for significance by means of paired Wilcoxon rank-sum tests and Mann-Whitney U tests.

### Results

BSP and RFS were technically feasible in all patients. An average of 6.3 ml cement per fracture were inserted in the BSP group and an average of 6.1 ml per fracture in the RFS group. Leakage could be ruled out for both procedures. The mean pain score on the VAS before the intervention was 8.6 +/- 0.55 in the BSP group and 8.8 +/- 0.58 in the RFS group. On the second postoperative day, a significant pain reduction was seen ( $p < 0.001$ ), with an average value of 2.5 (BSP +/- 0.28, RFS +/- 0.38) for both groups. After 6 (12; 18) months, these values were stable for the BSP group at 2.3 +/- 0.27 (2.3 +/- 0.24; 2.0 +/- 0.34) and for the RFS group at 2.4 +/- 0.34 (2.2 +/- 0.26; 2.0 +/- 0.31). With regard to pain, exceedance probability values of  $p = 0.86$  (6 months) and  $p = 1$  (18 months) were seen, so that neither treatment method leads to differences in results.

### Conclusion

BSP and RFS are interventional, minimally invasive procedures that enable reliable cement augmentation and achieve equally good clinical outcomes in the medium term.

Disclosures: Reimer Andresen, None.

## MO0296

**Transcriptomic Analysis of Whole Bone Marrow Cultures Treated with Osteoinductive Agents: BMP-2 (bone morphogenetic protein 2) or TPO (thrombopoietin).** Marta B. Alvarez\*<sup>1</sup>, Paul J. Childress<sup>1</sup>, Nabarun Chakraborty<sup>2</sup>, Duncan E. Donohue<sup>2</sup>, Rasha Hammamieh<sup>2</sup>, Todd O. McKinley<sup>3</sup>, Melissa A. Kacena<sup>3</sup>. <sup>1</sup>Indiana University School of Medicine, United states, <sup>2</sup>US Army Center for Environmental Health Research, United states, <sup>3</sup>Indiana University School of Medicine, Department of Orthopaedic Surgery, United states

Despite advances in surgical techniques and implants, healing segmental bone defects (SBDs) and non-unions present ongoing challenges for orthopaedic surgeons. BMP-2 is effective in healing SBDs, but has side effects, including an increased risk for cancer. We have shown that TPO has the ability to heal SBDs as well as stimulating muscle healing, angiogenesis, and modulating immune function. The purpose of this study was to explore the differences in healing signatures between BMP-2 and TPO by quantifying transcriptomic changes in cultured whole bone marrow (BM) cells. We hypothesized that expression patterns of these two agents would be unique and that TPO signatures would result in an expanded set of wound healing genes.

Femoral BM cells were collected from C57BL/6 mice and cultured in the presence of BMP-2 (200ng/ml), TPO (10 ng/ml), or saline for 3 days (n=4/group). RNA was isolated and converted to cDNA. Gene expression analysis was done using high throughput dual-dye cDNA microarrays (Agilent Inc.). Pairwise t-test with  $p < 0.005$  found 756, 1033, and 2488 transcripts differentially expressed by BMP-2 vs. saline, TPO vs. saline, and BMP-2 vs. TPO treatment groups, respectively. The genes were annotated using the Systems Biology tools: Ingenuity Pathway Analysis® (IPA) and the Database for Annotation, Visualization, and Integrated Discovery (DAVID). Expression of select genes relevant to this study were validated using qPCR (data not shown).

Using principle component analysis (PCA) of the raw data, we plotted the first principle component (PC1) vs. the second (PC2), which cumulatively accounted for 41% of total variance. Using DAVID and IPA analysis, we found that TPO treatment activates genes involved in wound healing, fluid balance, coagulation, and other profiles. TPO differentially activated integrins and actin (A2 and B), proteins known to be important for osteoblast function and are integral to the mechanical responsiveness of bone. TPO up-regulated angiopoietin 1 and platelet derived growth factor, which regulate blood vessel growth and mesenchymal differentiation into

osteoblasts, respectively. In contrast BMP-2 treated cells primarily stimulated T lymphocyte activation.

This work distinguishes the modes of actions of TPO and BMP-2, which will inform development of TPO as a novel bone healing agent.

**Disclosures:** Marta B. Alvarez, None.

## MO0297

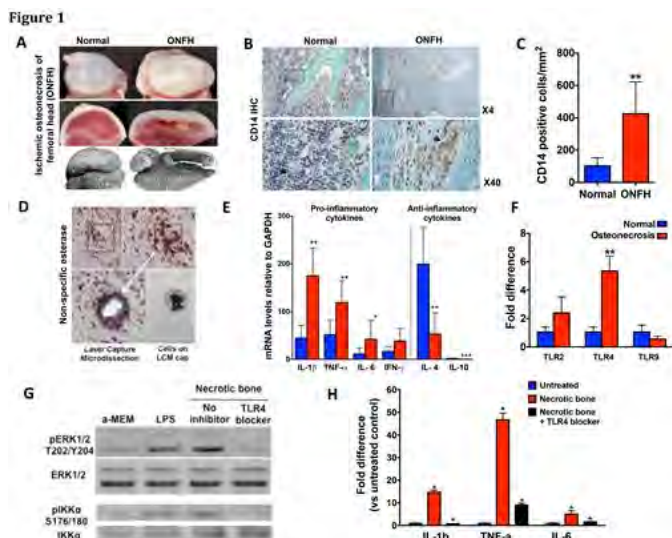
**Necrotic Bone Stimulates Pro-inflammatory Responses in Macrophages Through the Activation of Toll-like receptor 4.** Naga Suresh Adapala\*, Harry K.W. Kim, Ryosuke Yamaguchi, Matthew Phipps, Olumide Aruwajoye. Texas Scottish Rite Hospital for Children, United states

**Purpose:** Legg-Calvé-Perthes disease is a childhood hip disorder in which loss of blood supply results in ischemic osteonecrosis of the femoral head (ONFH). In general, macrophages sense the necrotic tissue by using pattern recognition receptors, importantly, toll-like receptors (TLRs) that activate pro-inflammatory responses. However, the role of macrophages in the inflammatory responses following ONFH has not been studied. The purpose of this study was to determine the inflammatory response of macrophages to the necrotic bone and the TLRs involved in sensing the necrotic bone.

**Methods:** ONFH was induced in right femoral head of 6-week old piglets (n=12), the unoperated left femoral head was used as normal control. At 8-weeks following surgery, the number of CD14+ macrophages was determined by immunohistochemistry. Macrophages were isolated from frozen sections by laser capture microdissection (LCM). The gene expression of cytokines and TLRs was determined by qRT-PCR. Necrotic or normal bone was prepared from femoral head following the removal of supernatant that contains soluble factors. In vitro, bone marrow macrophages (n=5 piglets) were exposed to necrotic bone in the presence or absence of TLR4 inhibitor, TAK242. The phosphorylation of ERK1/2 and IKK $\alpha$  was determined by western blotting, proliferation of macrophages by MTT-based assay and migration response using transwell chambers.

**Results:** Quantitation of macrophages by immunohistochemistry revealed an increased number of CD14+ macrophages (4.2-fold, p=0.007) in the fibrovascular repair tissue compared to normal bone. qRT-PCR analysis of the macrophages isolated by LCM showed significantly increased mRNA levels of pro-inflammatory cytokines (IL-1 $\beta$ :3.9-fold, p<0.0001; TNF- $\alpha$ :2.3-fold, p=0.0006; IL-6:3.6-fold, p=0.04) in the necrotic repair tissue compared to normal bone. Among the TLRs 2, 4 and 9, the gene expression of TLR4 (5.3-fold, p=0.003) but not TLR2 (p=0.46) and TLR9 (p=0.9) was significantly increased in macrophages in response to ONFH. Mechanistically, necrotic bone stimulated an increased expression of TLR4 in bone marrow-derived macrophages and activated TLR4-dependent phosphorylation of ERK1/2 and IKK $\alpha$ . Furthermore, necrotic bone increased the proliferation, migration and inflammatory cytokine gene expression in macrophages, which were blocked by the TLR4 inhibitor, TAK242.

**Conclusion:** Necrotic bone stimulates pro-inflammatory responses in macrophages following ONFH through TLR4 activation.



(A) Bone loss and femoral head deformity in ONFH in piglets (B and C) Increased number of macrophages in repair tissue (D, E and F) Laser capture microdissection method and qRT-PCR analysis (G) TLR4-mediated macrophage activation by necrotic bone (H) TLR4 blocker inhibits pro-inflammatory cytokine expression in macrophages. P value \*<0.05, \*\*<0.01, \*\*\*<0.001.

Necrotic bone stimulates pro-inflammatory responses in macrophages through TLR4 activation

**Disclosures:** Naga Suresh Adapala, None.

## MO0298

**Effect of targeted overexpression of Notch signaling in periosteal progenitor cells.** Emilie ROEDER\*, Brya Matthews, Ivo Kalajzic. Uconn health, United states

Notch signaling has been recently identified as a key player during bone and cartilage development. Notch inhibits the differentiation of osteoprogenitor cells, but has an osteogenic effect in mature osteoblasts. We have previously shown that alpha smooth muscle actin ( $\alpha$ SMA) is a marker of mesenchymal progenitor cells that make a significant contribution to fibrous, osteoblast, and chondrocyte lineages within a fracture callus. Gene expression analysis of isolated  $\alpha$ SMA-labeled progenitor cells revealed that a number of components of the Notch signaling pathway, including receptors Notch 1, 3 and 4, and target genes Hes1 and Hey1, were significantly decreased during the early stages of fracture healing. We hypothesize that a decrease in Notch signaling could regulate the expansion, migration and the differentiation of periosteal cells in the fracture callus. In this context, inducible Cre-expressing transgenic models enable precise definition of when Notch signaling is required and in which cell population during the fracture healing process.

We are using an inducible mouse model overexpressing the Notch1 intracellular domain (NICD1) in osteoprogenitor cells:  $\alpha$ SMACreERT<sup>2</sup>/Rosa-NICD1. Periosteal progenitor cells (PPC) were isolated from the periosteum of 8-9 week old mice and cultured. The targeted overexpression of NICD1 results in increased expression of Notch downstream targets Hes1 and Hey1. PPC overexpressing NICD1 had increased proliferation and migration compared to tamoxifen treated cultures from Cre negative littermates. Notch overexpression reduced osteogenic differentiation, evidenced by reduced von Kossa staining and lower expression of osteocalcin.

The influence of NICD1 overexpression on the fracture healing process was assessed in 8-9 week old  $\alpha$ SMACre/NICD1 mice after 3 tamoxifen injections at D0, D2 and D4 post femoral fracture. Histological analysis was performed 1-3 weeks after fracture. Mice with targeted NICD1 overexpression showed a trend towards a smaller callus displaying first less cartilage and then less mineralized content than the control mice.

Appropriate regulation of Notch signaling appears to be important for osteogenic differentiation of PPCs and bone fracture healing. It constitutes a potential target to improve and accelerate fracture healing by inhibiting its effect in specific cell populations responsible for the bone repair at specific stages of the process.

**Disclosures:** Emilie ROEDER, None.

## MO0299

**The Anabolic Actions of PTH Are Mediated in Part through a Colony Stimulating Factor 1-Sphingosine-1-Phosphate Paracrine Loop.** Gang-Qing Yao\*<sup>1</sup>, Meiling Zhu<sup>2</sup>, Ben-hua Sun<sup>1</sup>, Joanne Walker<sup>1</sup>, Karl Insogna<sup>1</sup>. <sup>1</sup>Yale University School of Medicine, United states, <sup>2</sup>Yale School, United states

Sphingosine-1-phosphate (S-1-P) is a "clastokine" that augments osteoblast function. Since PTH stimulates bone formation we wondered if S-1-P mediates any of its anabolic actions. The PTH receptor is not expressed in osteoclasts. However, the receptor for CSF1, c-fms, is highly expressed in mature osteoclasts and CSF1 is the principal colony stimulating activity released by osteoblasts in response to PTH. S-1-P is generated by the cytoplasmic enzyme sphingosine kinase 1 (SPHK1). CSF1 increased expression of SPHK1 transcripts  $2.2 \pm 0.4$ -fold in mature osteoclasts (p=0.02) but did not change the expression of SGPL1 (which degrades S-1-P). CSF1 also stimulated the release of S-1-P from osteoclasts. To test the hypothesis that PTH anabolism depends in part on induction of osteoblast-derived CSF1 acting on osteoclasts, we generated mice with selective deletion of c-fms in mature osteoclasts. The anabolic response to 30 days of single daily PTH injections was significantly attenuated in the spine of the knock out animals compared to littermate controls ( $3.4 \pm 2.0\%$  vs.  $10.4 \pm 2.1\%$ , p=0.02, n=14). The spine is the skeletal envelope usually most responsive to an anabolic PTH regimen. To determine if CSF1 transcriptionally activates the SPHK1 gene, a 3464 bp fragment of the SPHK1 gene from -3352 to +111 bp (relative to the transcription start site) was cloned and transfected into P-zen cells (murine fibroblasts engineered to express c-fms). The SPHK1 promoter showed substantial basal activity that was increased nearly three-fold by treatment with CSF1. By utilizing a series of 5'-deletions, the CSF1-responsive element was determined to be contained in the 489 bp fragment (-1480 to -992 bp). These data are consistent with the hypothesis that PTH augments bone anabolism in part by a paracrine loop in which the hormone stimulates the release of CSF1 from osteoblasts/stromal cells, which then induces the release of the anabolic clastokine, S-1-P, which in turn enhances bone formation.

**Disclosures:** Gang-Qing Yao, None.

## MO0300

**Romozumab Blocks the Binding of Sclerostin to the Two Key Wnt Signaling Co-receptors, LRP5 and LRP6, but not to LRP4.** Jianhua Gong, Jin Cao, Joanne Ho, Ching Chen, Chris Paszty\*. Amgen Inc., United states

Romozumab (Romo), a high affinity sclerostin monoclonal antibody (MAb), is a bone-forming agent under clinical investigation for the treatment of osteoporosis.

Romo binds to human, cynomolgus, and rat sclerostin with a  $K_D$  of 11 pM, 23 pM, and 3 pM, respectively, as measured by solution equilibrium binding analysis. Consistent with sclerostin acting as an inhibitor of canonical Wnt signaling, sclerostin was able to inhibit luciferase expression in an osteoblast-lineage (MC3T3-E1 cells) Super-TOPFlash reporter cell-based assay. Romo was able to neutralize the inhibitory effect of sclerostin in this setting and thus allow for active Wnt signaling as measured by luciferase reporter gene expression.

Various genetic and in vitro data indicate that sclerostin acts by binding to the extracellular domains (ECDs) of three members of the low-density lipoprotein receptor-related protein family (LRP4, LRP5 and LRP6). LRP5 and LRP6 are very similar structurally and act as the key co-receptors in the canonical Wnt signaling complex. LRP4 is more evolutionarily divergent and is thought to play a role in Wnt signaling as a facilitator protein rather than as a co-receptor.

An in vitro binding assay was used to investigate the effect of Romo on the binding of sclerostin to LRP4/5/6. The ECDs of human LRP4, LRP5 and LRP6 were produced recombinantly in mammalian cells. Each of the ECDs was separately incubated with human sclerostin and, using immunoprecipitation followed by Western blotting, each was shown to bind sclerostin. To assess the effect of Romo on these interactions, Romo was preincubated with sclerostin and this mixture was incubated separately with each of the 3 ECDs, followed by immunoprecipitation and Western blotting for sclerostin. Romo blocked the binding of sclerostin to the ECDs of LRP5 and LRP6, but did not block the binding of sclerostin to the ECD of LRP4. In contrast, we found that another sclerostin neutralizing MAb blocked the binding of sclerostin to LRP4 but not to LRP5/6, and that a non-neutralizing sclerostin MAb did not block the binding of sclerostin to either LRP4, LRP5 or LRP6.

In summary, Romosozumab blocks the binding of sclerostin to the two closely related canonical Wnt signaling co-receptors, LRP5 and LRP6. This is mechanistically sufficient to block sclerostin's inhibitory activity on Wnt signaling and to allow for the increases in bone formation and bone mineral density observed with administration of Romosozumab in vivo.

**Disclosures:** Chris Paszty, Amgen Inc., 15  
This study received funding from: Amgen Inc.

## MO0301

**A High-Fat Diet Induces Changes in the Bone Composition of Murine Humeri Independent of Total Body Bone Mineral Density.** Michael-John G. Beltejar<sup>\*1</sup>, Jun Zhang<sup>2</sup>, Dana A. Godfrey<sup>1</sup>, Michael J. Zuscik<sup>1</sup>, Douglas Adams<sup>3</sup>, Cheryl L. Ackert-Bicknell<sup>1</sup>. <sup>1</sup>Center for Musculoskeletal Research, University of Rochester Medical Center, United states, <sup>2</sup>Department of Orthopedics, Zhejiang Provincial People's Hospital, China, <sup>3</sup>Department of Orthopaedic Surgery, University of Connecticut Health, United states

Previous studies have implicated a high-fat diet in changes to bone mineral density (BMD). However, BMD alone is an imperfect predictor of bone strength, as contributions from bone composition are not captured. For example, in diabetes, patients can have fractures despite normal BMD but have alterations in mineral:matrix and carbonate:phosphate ratios. Studies of inbred mice suggest that bone composition is controlled as a genetic trait, but alterations in these parameters of bone composition in response to dietary fat remains understudied. The aim of this study was to determine if dietary and genetic interactions affect bone composition. Male mice from 3 strains (A/J, C57BL/6J (B6), and NOD/H1LtJ), were placed on either a high-fat (60% kcal from fats) or lean diet (10% kcal from fats) from 6 to 21 weeks of age. Both diets were iso-caloric for protein and the fat and carbohydrate sources were identical between the two diets. Area BMD and percent fat of the whole body (sans the head) were measured using DXA. Attenuated Total Reflectance Fourier Transformed Infrared Spectroscopy (ATR-FTIR) was used to determine the carbonate to phosphate ratio (which reflects bone age) and mineral to matrix ratio (which correlates with bone strength) of humeri. Differences in the parameters among strains and diets were determined using a two-way ANOVA with interactions and Tukey's HSD post hoc test. All mice on a high-fat diet had elevated body fat. Otherwise, the effects of a high-fat diet were unique in each of the three strains. A/J mice had an increase in BMD, B6 had a decrease and NOD mice remained unchanged (Fig. 1). However, A/J mice experienced a decrease in the mineral:matrix and increase in the carbonate:phosphate ( $p < 0.0001$ , Fig. 1). B6 experienced the opposite changes in these compositional parameters ( $p < 0.0001$ , Fig. 1). The www.differences between the A/J and the B6 mice on the lean diet mirrors previously published differences between these 2 strains. Interestingly, there were no changes in these compositional parameters between diets in NOD mice. These results demonstrate that there is indeed an interaction between genetics and diet that impacts bone at the level of composition. The effects of this interaction are beyond what is captured by DXA measures of bone mass. Compositional changes in bone are understood to result in changes in bone mechanical properties and thus dietary fat mediated changes in composition have the potential to impact bone strength.

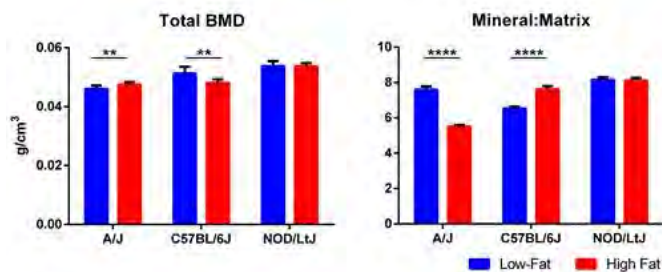


**Figure 1. High-Fat Diet Changes to Total BMD and Bone Composition**

Table

**Disclosures:** Michael-John G. Beltejar, None.

## MO0302

**Positive Effects of Olive oil on Bone Morphometry and Biomechanics in Ovariectomized rat.** Manuel Díaz-Curiel<sup>\*1</sup>, Blanca Torrubia<sup>2</sup>, Marta Martín-Fernandez<sup>2</sup>, Angel Alberich-Bayarrí<sup>3</sup>, Concepcion De la Piedra<sup>2</sup>. <sup>1</sup>Instituto de Investigaciones Médicas Fundación Jiménez Díaz, Spain, <sup>2</sup>Biochemistry Research Instituto de Investigaciones Médicas Fundación Jiménez Díaz, Spain, <sup>3</sup>Biomedical Imaging Research Group (GIBI230), La Fe Polytechnics & University Hospital, La Fe Health Research Institute, Spain

**Introduction:** Countries with a mediterranean diet have a lower incidence of osteoporosis. One of the highlights of this diet is the high consumption of olive oil, which is rich in compounds such as oleuropein and hydroxytyrosol, with powerful anti-inflammatory and antioxidant properties. The olive oil consumption can prevent bone mass loss in experimental models.

**Objective:** Study the effects of a preventive treatment with olive oil administered to ovariectomized rats on bone remodeling, mass, morphometry and biomechanics.

**Methods:** 48 Wistar rats of 6 months old were used: SHAM (n = 12), sham intervention; OVX (n = 12), ovariectomized; OVX + 100 (n = 12), ovariectomized and treated with 100 µl of olive oil/day; OVX + 200 (n = 12), ovariectomized and treated with 200 µl of olive oil/day. The treatment, fed with an oral gavage, started one day after surgery and was maintained for 3 months. After treatment, markers of bone turnover BGP and TRAP5b by ELISA in serum, lumbar (L) and femoral (F) bone mineral density (BMD) by DEXA, bone microCT microstructural parameters and biomechanical variables and fractal dimension (QUIBIM) were determined.

**Results:** The ovariectomy caused a significant increase of BGP and a decrease of TRAP5b, that remained unchanged after the administration of olive oil. BMD decreased significantly in the ovariectomized group. Also the histomorphometric parameters decreased. The OVX groups that were given olive oil showed no remarkable differences in either BMD or histomorphometry. Conversely, the biomechanical analysis showed significant differences on Young's (elasticity) modulus between OVX+100 and OVX + 200 with respect to OVX. Regarding the morphometric analysis, irregularity properties were calculated by 2D and 3D fractal dimension analysis, which express the complexity degree of the structure's contours in filling an area or volume respectively. The values of the fractal dimension in 2D and 3D presented significance with higher values in the OVX + 200 group, and thus, it can be asserted that the bone of the OVX + 200 rats is more irregular and similar to healthy bone.

**Conclusions:** The preventive treatment with olive oil improves the bone quality in terms of elasticity and fractal dimension in ovariectomized rats.

**Disclosures:** Manuel Díaz-Curiel, None.

## MO0303

**Effect of Age and Dietary Phosphorus Intake on Intestinal Phosphorus Absorption in Male Rats.** Colby Vorland<sup>\*</sup>, Pamela Lachcik, James Fleet, Kathleen Hill Gallant. Purdue University, United states

The purpose of this study was to determine the effects of age and dietary phosphorus intake level on intestinal phosphorus absorption efficiency in male rats. Seventy-two male Sprague-Dawley rats, ages 8-weeks, 18-weeks, and ~28-weeks were randomized into defined diets with 0.6% calcium and three different levels of phosphorus: 0.1% (low), 0.6% (normal), or 1.2% (high) for 14 days (n = 8 rats per age and diet group). Rats were housed individually in metabolic cages, and feces, urine, and diet were collected, weighed, and analyzed over the final four days of the study to calculate phosphorus balance. On day 14, phosphorus absorption efficiency was assessed using ligated loops of jejunum. Five microCi <sup>33</sup>P in 0.5 mL of transport buffer

(0.1 mmol/L phosphate). Serial blood samples were collected over 30 minutes, and the jejunal loop was excised at 30 minutes. Plasma samples and the digested jejunal loop were analyzed for P-33 activity by scintillation counting. Two-way analysis of variance was used to determine main effects (age and diet) and the interaction effect for age x diet, with Tukey's post-hoc comparisons.

Results show that phosphorus appearance into the plasma was higher in the 10-week old rats compared to the 20- and 30-week rats at 30 minutes (0.073 vs 0.052 and 0.048% of initial dose, respectively,  $p < 0.0001$  for both comparisons). Similarly, % absorption, determined from disappearance of  $^{33}\text{P}$  activity from the intestinal loop at 30 minutes, was higher in the 10-week old rats compared with 20- and 30-week old rats (40.1 vs 34.7 and 34.6% of total dose, respectively,  $p = 0.01$  for both). There were no differences in absorption efficiency between the three levels of dietary phosphorus ( $p = 0.65$ ), and no age x diet interaction. Ten-week old rats had a higher positive phosphorus balance vs 20- and 30-week (37.2 vs 6.5 and 9.8 mg/day, respectively,  $p = 0.0008$  and  $p = 0.0013$ ), while the high phosphorus intake group had a higher positive balance than the normal and low intakes (31.7 vs 10.4 and 11.2 mg/day, respectively,  $p = 0.01$  and  $p = 0.03$ ). Together, these results suggest that intestinal phosphorus absorption is more efficient at younger ages in rats, but that changes in dietary phosphorus do not elicit adaptation in the efficiency of jejunal phosphorus absorption.

**Disclosures:** Colby Vorland, None.

## MO0304

**Evaluation of Bone Turnover After Bisphosphonate Withdrawal and its Influence on Implant Osseointegration.** Rafael Scaf de Molon<sup>\*1</sup>, Fausto Frizzera<sup>1</sup>, Mario Henrique Arruda Verzola<sup>1</sup>, Gabriela Giro<sup>2</sup>, Sotirios Tetradis<sup>3</sup>, Silvana Regina Peres Orrico<sup>1</sup>. <sup>1</sup>Department of Diagnosis & Surgery, School of Dentistry at Araraquara, Sao Paulo State University, Brazil, <sup>2</sup>Department of Periodontology & Oral Implantology, Dental Research Division, Guarulhos University, Brazil, <sup>3</sup>Division of Diagnostic & Surgical Sciences, UCLA School of Dentistry, Los Angeles, United states

We sought to investigate bone turnover alterations after alendronate withdrawal and its influence on dental implants osseointegration. Seventy female Wistar rats were randomly divided in 2 groups that received on day 0 either placebo (control group - CTL,  $n = 10$ ) or 1 mg/kg sodium alendronate (test group,  $n = 60$ ) once a week for four months. At day 120 alendronate treatment was suspended for 50 animals. A titanium implant was placed in the rats left tibiae on days 0, 7, 14, 28 and 45 after alendronate withdrawal ( $n = 10$  for each period). CTL group and a group that received alendronate until the end of the experimental period (non interrupted group - INT,  $n = 10$ ) underwent implant placement surgery on day 120. All animals were euthanized 28 days after implant surgery. Bone mineral density (BMD) of femur and lumbar vertebrae and biochemical markers of bone turnover (CTX, OCN, and PINP) of serum collected during implant placement surgery and after the end of treatment (at the moment of euthanization) were analyzed by ELISA. Enzymatic analysis were performed to measure adiponectin, creatinine, and leptin. Bone tissue around implants was submitted to descriptive histologic analysis, bone-to-implant contact (BIC), and bone area fraction occupancy between implant threads (BAFO). All groups receiving alendronate showed higher BMD values when compared to CTL group for both femurs and tibia. Bone turnover markers presented decreased concentrations in test group. After alendronate withdrawal these values were slightly increased in the initials periods followed by another decrease in biomarkers concentrations in the late periods. Statistically difference was observed between 14 days and 45 days groups for the BIC ratio compared to the CTL group. BAFO analysis were statically significant different between 45 days group and 0 day group. Collectively, our findings demonstrated that alendronate treatment decreased bone turnover, and that biochemical markers did not return to CTL group values even after 73 days of alendronate withdrawal. Moreover, alendronate treatment interfered with bone quality and quantity around dental implants.

**Disclosures:** Rafael Scaf de Molon, None.

## MO0305

**Icaritin, a Prenylated Flavonoid, Mediates Proteasomal Degradation of TRAF6 thereby Suppressing Osteoclastogenesis and Preventing Ovariectomy-induced Bone Loss.** Ee Min Tan<sup>\*1</sup>, Lei Li<sup>2</sup>, Nicholas Chew<sup>3</sup>, Eu Leong Yong<sup>4</sup>. <sup>1</sup>National University of Singapore, Yong Loo Lin School of Medicine, Department of Obstetrics & Gynaecology, Singapore, <sup>2</sup>National University of Singapore, Yong Loo Lin School of Medicine, Singapore, <sup>3</sup>National University Health System, Department of Infectious Diseases, Singapore, <sup>4</sup>National University Health System, Department of Obstetrics & Singapore

Postmenopausal osteoporosis is a highly prevalent disease that affects more than 200 million women worldwide and this is further compounded by the high incidence rate of osteoporotic fractures in these women. Given the limitations of current treatment options, the search is still ongoing for an effective treatment with minimal adverse side effects. As such, we evaluated the effects of icaritin, a lead compound of botanical origin, on preventing ovariectomy (OVX)-induced bone loss and

elucidated the molecular mechanisms by which icaritin lead to an improvement in bone health.

We show that icaritin treatment led to improvements in bone microarchitecture as well as bone mechanical properties in the OVX rats to a similar extent as estradiol-valerate supplementation. Bone histochemical analyses coupled with serum levels of bone resorption marker (CTX-I) revealed that icaritin treatment inhibited osteoclast formation and activity in the OVX rats. Notably, we found that icaritin treatment downregulated levels of the critical adaptor protein, TNF-receptor associated factor 6 (TRAF6), in  $\text{CD11b}^+/\text{Gr-1}^{\text{low}}$  osteoclast precursors present in the blood and bone marrow of the OVX rats. Consistently, *in vitro* studies with mouse monocytes, RAW 264.7, and human PBMCs showed that icaritin dose-dependently inhibited RANKL-induced osteoclastogenesis and osteoclast resorption. At the molecular level, Icaritin mediated proteasomal degradation of TRAF6 thereby inhibiting RANKL-induced NFATc1 gene expression via activation of MAPK and NF $\kappa$ B signaling pathways.

In conclusion, we present novel findings to show that icaritin prevents OVX-induced osteoporosis by inhibiting osteoclast differentiation and activity. Icaritin modulates RANKL-induced osteoclastogenesis by mediating proteasomal degradation of the TRAF6 adaptor protein thereby inhibiting downstream signaling pathways. These results demonstrate that icaritin is a promising candidate for the treatment of postmenopausal osteoporosis.

**Disclosures:** Ee Min Tan, None.

## MO0306

**Homing and Biodistribution of ALLOB<sup>®</sup>, an allogeneic osteoblastic cell therapy product.** Sandra Pietri<sup>\*1</sup>, Sabrina Ena<sup>2</sup>, Enrico Bastianelli<sup>1</sup>. <sup>1</sup>Bone Therapeutics, Belgium, <sup>2</sup>skeletal cell therapy support, Belgium

Bone Therapeutics is an advanced biotechnology company which develops innovative osteoblastic cell therapy products for the treatment of orthopaedic conditions. The company is currently evaluating its human allogeneic osteoblastic cell therapy product, ALLOB<sup>®</sup>, in three Phase II proof-of-concept trials. The success of cell-based therapies relies in part on the capacity of cells to engraft and survive in the target tissue; this was investigated for ALLOB<sup>®</sup> in bone in this study.

Methods: ALLOB<sup>®</sup> or vehicle was injected once at fracture site (the femoral closed fracture model) in NMRI-Nude mice. After administration, cell quantification within whole body was assessed using either SPECT-CT imaging (followed by *ex vivo* distribution) between D1 to D7 based on  $^{111}\text{In}$ -oxinate radiolabeling or highly sensitive real time PCR (primers targeted human repetitive DNA sequences) performed on excised organs/tissues at D1, D4, D7 and D14 ( $n=6$  per group). Histological bone biopsy sections were analyzed by immunofluorescence using antibody directed against human proteins to detect and furthermore localize human cells.

Results: SPECT-CT analysis demonstrates that from D1 to D4, ALLOB<sup>®</sup> cells localize mainly at the fracture site (i.e., administration site); at D7, *ex vivo* counting showed that  $51 \pm 23\%$  of radioactivity signal is present at fracture site in ALLOB<sup>®</sup> treated animals while vehicle treated mice showed less than 20% of radioactivity at fracture site ( $17.3 \pm 2.3\%$ ). For both conditions, remaining radioactivity signal is localized in kidneys and liver. Detection of human DNA by real time PCR show that at D1, human cells are detected at fractured site (all 6 animals) with only rare cells detected in lungs (3/6) and in heart (1/6). From D4 to D14, human cells only localize at fracture site.

Conclusions: This study demonstrates that after local administration, ALLOB<sup>®</sup> cells engraft at fracture/administration site until D14 and do not migrate into the body, supporting excellent safety profile of ALLOB<sup>®</sup>.

**Disclosures:** Sandra Pietri, None.

## MO0307

**Investigation of the effect of sequential treatment with zoledronic acid followed by weekly parathyroid hormone or vice versa in ovariectomized rats.** Taku Shimizu<sup>\*</sup>, Tomoya Tanaka, Teruki Kobayashi, Ikuvo Kudo, Aya Takakura, Ryoko Takao-Kawabata, Toshinori Ishizuya. Pharmaceuticals Research Center, Asahi Kasei Pharma Corporation, Japan

Teriparatide (TPTD, (hPTH(1-34)) is applied as a therapeutic agent for osteoporosis. The regimen is daily subcutaneous injection for the brand approved in many countries. The lower frequency regimen, weekly subcutaneous TPTD injection, is also approved in Japan and Korea. The bisphosphonate (BP) treatment prior to the daily TPTD treatment impaired the effect of TPTD in some clinical studies. On the other hand, the decrease of BMD after the withdrawal of TPTD can be suppressed by the BP treatment. However, no clinical study investigating sequential treatment of zoledronic acid (ZOL) and weekly TPTD (or vice versa) was reported. Thus, we investigated the sequential treatment options TPTD followed by ZOL, and ZOL followed by TPTD in the ovariectomized (OVX) rat.

Seven-month old female SD rats underwent OVX or sham operation. Two months after OVX, the osteopenic animals were treated as indicated in the table below. The administration intervals of ZOL and TPTD were designed as 3 times shorter compared to the clinical regimens in consideration of the difference in the length of the bone remodeling cycle between the OVX rat and post-menopausal women. The proximal tibia BMD was measured by *in vivo* DXA prior to the OVX surgery, as well as 1, 2, 4, 5, 6 and 8 months after the first administration. Serum osteocalcin and

urinary type I collagen cross-linked C-telopeptide were measured at the same time-points. The bone tissues were collected at the start of treatment, as well as 4 and 8 months thereafter. After necropsy, micro-CT image analysis and bone mechanical testing were performed on the 4th lumbar vertebra.

Z-T group showed higher BMD than Z-V group. T-V group showed the expected decrease of BMD after withdrawal of TPTD, which was prevented in the T-Z group. Bone turnover markers, micro-CT imaging, and mechanical testing are being analyzed.

In conclusion, no blunting of the BMD response was detected after switching from ZOL to low frequency TPTD. In addition, the drop in BMD was fully prevented after switching from low frequency TPTD to ZOL for maintenance. Data suggests that switching from single ZOL to low frequency TPTD or vice versa is beneficial to increase or maintain the BMD regardless of the order of the two treatments.

Group name	Treatments	
	1st period (4 months)	2nd period (4 months)
Sham	Vehicle	Vehicle
V-V	Vehicle	Vehicle
Z-T	ZOL	TPTD
Z-V	ZOL	Vehicle
V-T	Vehicle	TPTD
T-Z	TPTD	ZOL
T-V	TPTD	Vehicle
V-Z	Vehicle	ZOL

ZOL: Single intravenous injection at the start of each period at the dose of 100 µg/kg  
 TPTD: 3 times per week subcutaneous injection throughout the duration at the dose of 6 µg/kg  
 Vehicle: Injection as the same regimen of ZOL or TPTD instead of each agent.

Table. Experimental protocols for sequential treatments

Disclosures: Taku Shimizu, Asahi Kasei Pharma Corporation, 15

### MO0308

**Local Osteolytic Effect of BMP-2 in Sheep Lumbar Spinal Fusion.** Hsin Chuan Pan<sup>1</sup>, Soonchul Lee<sup>2</sup>, Xinli Zhang<sup>1</sup>, Jia Shen<sup>1</sup>, Chenchao Wang<sup>3</sup>, A. Simon Turner<sup>4</sup>, Howard B. Seim<sup>4</sup>, Janette N. Zara<sup>5</sup>, Jin Hee Kwak<sup>1</sup>, Kang Ting<sup>1</sup>, Chia Soo<sup>5</sup>. <sup>1</sup>Division of Growth & Development & Section of Orthodontics, School of Dentistry, University of California, Los Angeles, United states, <sup>2</sup>Department of Orthopaedic Surgery, CHA Bundang Medical Center, CHA University, School of Medicine, United states, <sup>3</sup>Department of Plastic Surgery, The First Hospital of China Medical University, United states, <sup>4</sup>Department of Veterinary Sciences, Colorado State University, United states, <sup>5</sup>Department of Orthopaedic Surgery & the Orthopaedic Hospital Research Center, University of California, Los Angeles, Los Angeles, United states

Bone Morphogenetic Protein-2 (BMP-2) has been recognized as one of the most effective osteoinductive growth factors in bone research field. However, recently, there have been many reports of complications-associated cases and researchers suggested that it is due in part to supraphysiologic dose. The purpose of this study is to specifically evaluate the local effect of BMP-2 application in large animal spinal fusion procedure to reveal solid experimental evidence of certain complications with better objectivity than symptom-based clinical reports. Six ewes underwent interbody fusion at 2 lumbar levels (L3/L4, L5/L6), yielding 2 datasets for a total of 12 lumbar fusions using 9-mm parallel radiolucent cage by anterior lumbar interbody fusion (ALIF). The animals were divided into three groups; 1.Control: Phosphate buffered saline + Absorbable collagen sponge (ACS) (n=4), 2.Dose-I: 0.43 mg/mL BMP-2+ACS(n=4), 3.Dose-II: 1.5 mg/mL BMP-2+ACS(n=4). The fusion quality was evaluated radiologically and histologically. For statistical analysis, Mann-Whitney U and Kruskal-Wallis tests were used. Conventional computed tomography (CT) showed both BMP-2 groups were able to fuse but no fusion was observed in the control group at 2 month post-operation. Quantitative micro-CT analysis of the implants postmortem at 3 month revealed that bone volume/tissue volume (BV/TV) and bone mineral density (BMD) increased with dose proportionally. However, the peri-implant area of dose-I BMP-2 demonstrated 20% decrease in BMD compared to control significantly (p<0.05). The cyst-like bone void was observed in both BMP-2 dosage groups with slight presentation difference and all localized within 7 mm range above or below the implants. The bone quality analysis of the segmented cyst-like bone void sites showed BMD significantly decreased by 70% and 36% in relation to the central unaffected region in both BMP-2 groups (p<0.01, p<0.05) (Fig 1). Histologically, the osteolytic lesions with fatty marrow and/or inflammatory infiltrates were observed in affected areas of both BMP-2 groups by relevant staining. We conclude that the use of BMP-2 effectively promotes lumbar fusion in sheep by ALIF. However, the osteolytic effect of BMP2 in adjacent areas of implants was also readily identifiable by X-ray imaging and confirmed by static high resolution micro-CT and histology. We believe this is the first large animal report on verification of BMP2 associated undesired effects in spinal fusion procedure.

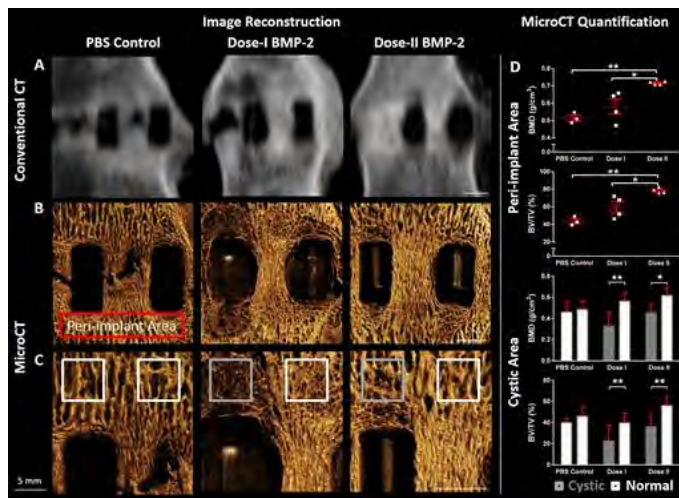


Fig1. Radiographic data of BMP2-treated sheep lumbar vertebral bones

Disclosures: Hsin Chuan Pan, None.

### MO0309

**Sclerostin Antibody Markedly Reverses the Severe Sublesional Bone Loss in Rats after Prolonged Spinal Cord Injury..** Wei Zhao<sup>1</sup>, Xiaodong Li<sup>2</sup>, Yuanzhen Peng<sup>1</sup>, Jianping Pan<sup>1</sup>, Michael Ominsky<sup>2</sup>, Jian Q. Feng<sup>3</sup>, Hua Zhu Ke<sup>4</sup>, Christopher Cardozo<sup>1</sup>, William A. Bauman<sup>1</sup>, Weiping Qin<sup>5</sup>. <sup>1</sup>James J. Peters VA Medical Center, United states, <sup>2</sup>Amgen Inc., United states, <sup>3</sup>Baylor College of Dentistry, TX A&M, United states, <sup>4</sup>UCB Pharma, United Kingdom, <sup>5</sup>James J. Peters VA Medical Center/Icahn School of Medicine at Mount Sinai, United states

To date, no efficacious therapy exists to prevent or treat the occurrence of severe osteoporosis in individuals with neurologically motor-complete spinal cord injury (SCI). Recent studies by us and others have demonstrated that antagonism of sclerostin activity by sclerostin antibody (Scl-Ab) is able to prevent bone loss after acute SCI. However, other highly clinically relevant questions should be addressed, such as whether sclerostin inhibition reverses bone loss in individuals with SCI who have been injured for several years and have had substantial sublesional bone loss, which represents the vast majority of the SCI population. This study tested the efficacy of Scl-Ab to reverse bone loss that has occurred after prolonged motor-complete SCI in an animal model. Male Wistar rats underwent complete spinal cord transection or laminectomy only (Sham, N=7); three months after SCI, the rats were treated with Scl-Ab at 25 mg/kg/week (SCI/Scl-Ab, N=5) or vehicle (SCI/vehicle, N=6) for 8 weeks. Motor behavior was assessed by a Basso, Beattie, Bresnahan (BBB) locomotor rating test. At the end of study, BBB scores in SCI/vehicle and SCI/Scl-Ab rats were 1.83±0.48 and 1.80±0.58, respectively, indicating that all of SCI animals had complete motor paralysis. Body weights were not significantly different among the groups. Following SCI, bone mineral density (BMD) of distal femur and proximal tibia, as assessed by DXA, were significantly reduced by -20% (0.2480±0.005 vs 0.1976±0.009, p<0.001) and -13% (0.1890±0.003 vs 0.1641±0.006, p<0.01), respectively. At the distal femur, BMD was +42% greater in SCI/Scl-Ab animals than in SCI/vehicle animals (0.2809 ±0.012 vs 0.1976±0.009, p<0.001); similarly, at the proximal tibia, BMD in SCI/Scl-Ab rats was +49% greater than that in SCI/vehicle animals (0.2457±0.011 vs 0.1641 ±0.006, p<0.001). Currently, additional analyses are being conducted to further characterize effects of Scl-Ab on bone microarchitecture and strength, bone formation and resorption, and to investigate mechanisms of Scl-Ab action. In summary, our initial findings provide the first evidence that Scl-Ab markedly reverses sublesional loss of bone mass in a model of chronic SCI. The study has relevant therapeutic implications, suggesting that sclerostin antagonism may be a valid clinical approach to reverse the bone loss in patients with chronic SCI, in addition to being a treatment option to prevent bone loss after acute SCI, as has been previously shown in a rodent model.

Disclosures: Wei Zhao, None.

### MO0310

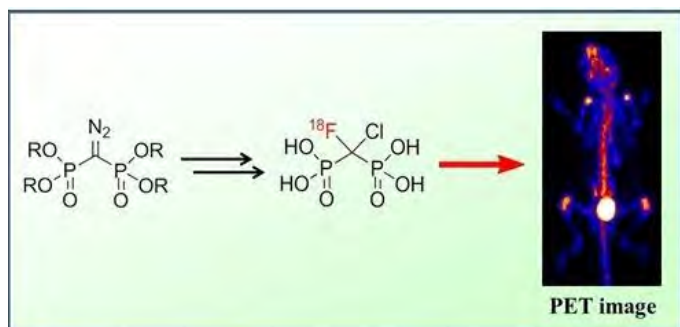
**An <sup>18</sup>F Analogue of Clodronate for PET Bone Imaging.** Charles McKenna<sup>1</sup>, Amirsoheil Negahbani<sup>1</sup>, Boris Kashemirov<sup>1</sup>, Hongsheng Li<sup>2</sup>, Kai Chen<sup>2</sup>. <sup>1</sup>Department of Chemistry, University of Southern California, United states, <sup>2</sup>Molecular Imaging Center, Department of Radiology, University of Southern California, United states

Bisphosphonates (BPs) selectively bind to bone and, depending on their structure, can be potent inhibitors of osteoclast-mediated bone resorption. BP drugs are widely

used in the clinic as anti-resorptives to treat osteoporosis, including acute bone resorption associated with metastatic bone cancer. Recent data suggest that BPs may also act on tumor cells by binding to granular microcalcifications found in tumor-associated macrophages.

A further important clinical application of BPs is diagnostic imaging of bone. Single photon emission computed tomography (SPECT) imaging using a  $^{99m}\text{Tc}$ -labeled BP such as  $^{99m}\text{Tc}$ -methylenebisphosphonate [ $^{99m}\text{Tc}$ -MBP] or  $^{99m}\text{Tc}$ -hydroxymethylenebisphosphonate [ $^{99m}\text{Tc}$ -HMBP] is a familiar method to image skeletal bone, e.g. to detect and localize metastatic bone cancers. Although concerns related to the global supply of  $^{99}\text{Mo}$  (the precursor used to generate  $^{99m}\text{Tc}$ ) may be mitigated by alternative radioisotope generation technologies, despite its utility and importance in the clinic, SPECT scanning with [ $^{99m}\text{Tc}$ ]-labeled BPs is recognized to provide lower sensitivity and resolution than is possible with positron emission tomography (PET): as a general alternative to SPECT, PET scanning using an  $^{18}\text{F}$  radioisotope ( $t_{1/2}$  110 min) offers reliability of production and superior image quality with less radiation exposure to the patient. A [ $^{18}\text{F}$ ] BP would combine the advantages of [ $^{18}\text{F}$ ]-PET imaging with the chemical and pharmacological specificity of a BP. Accordingly, we have devised  $^{18}\text{F}$  radiochemistry to rapidly prepare a novel [ $^{18}\text{F}$ ]-labeled clodronate analogue, chlorofluoromethylenebisphosphonate ([ $^{18}\text{F}$ ]-CFMBP, 1).

The synthesis of 1 starting from a tetraalkyl ester of diazomethylenebisphosphonate could be completed during less than one  $^{18}\text{F}$  half-life. The radiochemical purity of 1 was determined to be >99% (specific activity 11.7 mCi/ $\mu\text{mol}$ ). In order to demonstrate its potential for *in vivo* PET imaging of bone, 1 was injected into normal nude mice that were then imaged using a microPET scanner at 0.5, 1, and 2 h post-injection. 1 was selectively absorbed by joints and bones and provided a microPET image of good quality. Uptake of radioactivity was also observed in the bladder, suggesting that excretion of 1 is mainly renal leading to low background and high contrast PET images. In summary, we report a novel [ $^{18}\text{F}$ ]-labeled BP probe for PET bone scans in animal models, that may have clinical potential.



PET

**Disclosures:** Charles McKenna, None.

This study received funding from: University of Southern California

## MO0311

**Differential Response of Bone and Kidney to ACEI in db/db mice: A Potential Effect of Captopril on Accelerating Bone Loss.** Yan Zhang<sup>\*1</sup>, Man-Sau Wong<sup>2</sup>, Qi Shi<sup>1</sup>, Yong-Jun Wang<sup>3</sup>. <sup>1</sup>Spine Disease Research Institute, Longhua Hospital, Shanghai University of Traditional Chinese Medicine, China, <sup>2</sup>Department of Applied Biology & Chemical Technology, The Hong Kong Polytechnic University, China, <sup>3</sup>School of Rehabilitation Science, Shanghai University of Traditional Chinese Medicine, China

The components of renin-angiotensin system (RAS) are expressed in kidney and bone. Kidney disease and bone injury are common complications associated with diabetes. This study was aimed to investigate the effects of angiotensin-converting enzyme inhibitor, captopril, on kidney and bone of db/db mice. The db/db mice were administered with captopril for 8 weeks with db/+ mice as non-diabetic control. Biochemistries in serum and urine were determined by standard colorimetric methods or ELISA. Histological measurement was performed on kidney by periodic acid-schiff staining and tibial proximal metaphysis by safranin O and masson-trichrome staining. Trabecular bone mass and bone quality were analyzed by microcomputed tomography. The quantitative polymerase chain reaction and immunoblotting were applied for molecular analysis on mRNA and protein expression. Captopril significantly improved albuminuria and glomerulosclerosis in db/db mice, and these effects might be attributed to the down-regulation of angiotensin II expression and the expression of its down-stream profibrotic factors in kidney, like connective tissue growth factor and vascular endothelial growth factor. While, the urinary excretion of calcium and phosphorus was markedly increased in db/db mice in response to captopril, which induced the decrease of bone mineral density and the deteriorations of trabecular bone, in accordance with the histological and reconstructed 3-dimensional images. Even though captopril effectively reversed the diabetes-induced changes of calcium-binding protein 28-k and vitamin D receptor expression in kidney as well as the expression of RAS components and bradykinin receptor-2 in bone tissue, the treatment with captopril increased the tartrate-resistant acid phosphatase-positive osteoclasts number, down-regulated the expression of the regulators, type 1 collagen and transcription factor runt-related transcription factor 2 for stimulating

osteoblastic function, and up-regulated the expression of bone resorptive factor, carbonic anhydrase II. Captopril exerted the therapeutic effects on renal injuries associated with type 2 diabetes, while it worsened the deteriorations of trabecular bone in db/db mice, which was, at least partially, due to the loss of urinary minerals and the stimulation on osteoclastogenesis and the suppression on osteogenesis.

**Disclosures:** Yan Zhang, None.

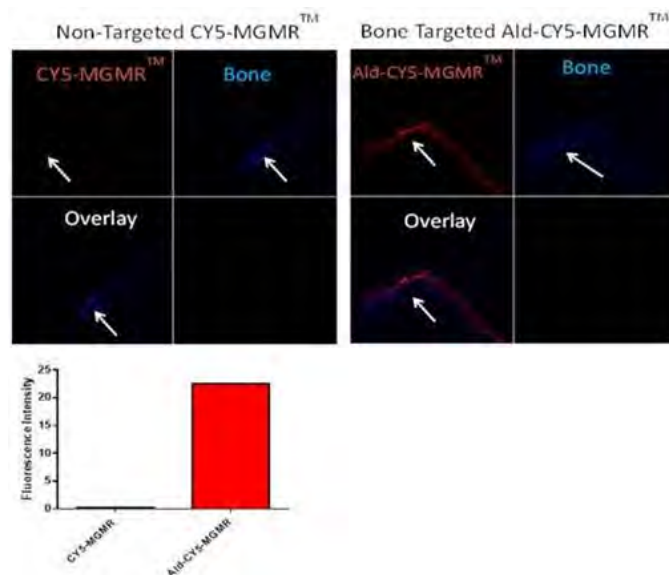
## MO0312

**MGMR<sup>TM</sup>: The Next Generation Carbon Nanotubes for Biomedical Applications.** Michaela Reagan<sup>\*1</sup>, Aaron Tasset<sup>2</sup>, Heather Fairfield<sup>1</sup>, Joe Dillon<sup>2</sup>, Carolyn Falank<sup>1</sup>. <sup>1</sup>Maine Medical Center Research Institute, United states, <sup>2</sup>BioPact Ventures, United states

Carbon nanotubes (CNTs) have long held great appeal to nanotechnology engineers due to their unique structure and properties. Unfortunately, most forms of CNTs have previously proven toxic in most *in vivo* studies. However, recent discoveries led to the development of a novel method for CNTs, creating a proprietary and novel matter called medical grade molecular rebar (MGMR<sup>TM</sup>). We explored the ability of MGMR to be used as a bone-targeting nanomedicine, and observed no toxicity of MGMR *in vitro* and *in vivo* on rabbit and guinea pig skin, and when injected into mice.

*In vitro*, fibroblast cells were treated for 24 hours with a 1cm X 1cm transdermal patch containing 1% PBS-filled MGMR in nitrocellulose and displayed no cytotoxic responses. A 25mm X 25mm sample of this patch was also applied to rabbit skin. No edema or erythema was observed after 1, 24, 48 or 72 hours of exposure in New Zealand White female rabbits. The patch was applied to the left flank of shaved male Hartley guinea pigs (n=10), and no clinical sensitization was observed over a 3 week period, nor were any weight changes, skin responses, or clinical changes seen in a "resensitization challenge" test on the animals 2 weeks later. Biodistribution studies demonstrated tolerability of tubes in athymic female mice at high doses, allowing for the potential to deliver a broad range of therapeutics.

We then explored methods for drug-loading and measuring drug release at 37°C at 0, 23, 48, 72 and 144 hours from MGMR. Using fluorescent dyes, we found a burst release from the MGMR and then a graduate release of up to 80% of dye by days 3-7. We observed that the use of GRAS excipients provided for further tuning of both sustained and controlled release. We believe further studies will yield even higher loading efficiencies and highly-tuned release kinetics. Lastly, we chemically modified MGMR by adding a fluorophore (Cy5.5) and a bone-targeting (BT) alendronate to create Cy5-MGMR and BT-Cy5-MGMR. We validated the bone-adhesion properties of the BT-Cy5-MGMR were significantly greater than those of Cy5-MGMR using 4 hour incubation with mouse bone *ex vivo* following by confocal imaging and fluorescence signal quantification (Fig 1). We now aim to validate the bone-homing properties of this novel MGMR *in vivo*. In addition, cell penetration of MGMR *in vitro* shows that endocytosis is nontoxic and well tolerated. In summary, MGMR is a highly promising biomedical tool for drug delivery for clinical applications.



Validation of Bone Targeting Capability of Carbon Nanotubes

**Disclosures:** Michaela Reagan, BioPact LLC, 11

This study received funding from: BioPact Ventures LLC

## MO0313

**Prolonged Pharmacokinetic and Pharmacodynamic Actions of a Pegylated Parathyroid Hormone Peptide Fragment.** Jun Guo\*, Ashok Khatri, Thomas Dean, Monica Reyes, Braden Corbin, John T. Potts, Jr., Harald Jüppner, Thomas J. Gardella. Endocrine Unit, Massachusetts General Hospital & Harvard Medical School, United states

PTH peptides, such as PTH(1-34), are important for exploring mechanisms by which PTH acts on bone and kidney cells to regulate blood calcium and phosphate levels. Efficacy of injected peptides can be limited, however, by rapid rates of elimination from the circulation, a process that, for a peptide as small as PTH(1-34), is likely mediated in large part by glomerular filtration. On the other hand, it remains uncertain as to the extent, if any, to which filtered PTH peptides can act on the luminal surfaces of renal tubules and thereby contribute to certain responses, such as the suppression of Pi re-uptake and the stimulation of 1-alpha hydroxylase in proximal renal tubular cells. Reducing filtration of PTH(1-34) could thus not only extend the peptide's serum half-life ( $t_{1/2}$ ), and hence its efficacy in vivo, but could also help in dissecting the relative biological importance of PTH signaling at the luminal vs. basolateral surfaces of the renal tubules. To test this, we synthesized a PTH analog containing a C-terminal polyethylene glycol (PEG) group, which, based on its 20,000 kD size, was predicted to impede glomerular filtration and thus extend the analog's pharmacokinetic (PK) and pharmacodynamic (PD) properties. A fluorescent TMR group was also incorporated to permit optical tracking. In PTHR1-expressing cells, the new analog [Lys<sup>13</sup>(TMR),Cys<sup>35</sup>-PEG]PTH(1-35) (PEG-PTH<sup>TMR</sup>), exhibited a cAMP signaling potency comparable to that of non-pegylated [Lys<sup>13</sup>(TMR),Cys<sup>35</sup>]PTH(1-35) (PTH<sup>TMR</sup>), and when injected iv into mice, PEG-PTH<sup>TMR</sup> exhibited a markedly extended PK-PD profile ( $t_{1/2} = \sim 6h$  vs.  $1h$ ; hypercalcemia and hypophosphatemia lasting  $\sim 48h$  vs.  $\sim 6h$ ). PEG-PTH<sup>TMR</sup> also induced increases in serum 1,25(OH)<sub>2</sub>Vit D, C-terminal collagen1 cross-linked fragments (CTX), and reductions in urinary calcium excretion that were more sustained and pronounced vs. PTH<sup>TMR</sup>. Confocal microscopy analyses further revealed a marked reduction in TMR fluorescence at the luminal surfaces of renal tubules for the pegylated peptide, as compared to PTH<sup>TMR</sup>, yet a similarly robust increase in PKA-phosphorylated substrate, which for both ligands was located only on basolateral surfaces. The findings show that C-terminal pegylation can prolong the PK/ PD properties of a bioactive PTH(1-35) analog, in part by impeding renal filtration. Furthermore they suggest that at least some renal actions of PTH are mediated via effects on the basolateral surfaces of the proximal tubules.

Disclosures: Jun Guo, None.

## MO0314

**Selective Serotonin Reuptake Inhibitors (SSRIs) Impair bone mass accrual Through a Brain Serotonin/Sympathetic nervous system (SNS) pathway.** Maria Jose Ortuno\*, Samuel Rombinson<sup>1</sup>, Riccardo Paone<sup>2</sup>, Yung-yu Huang<sup>1</sup>, Edward Guo<sup>1</sup>, John J. Mann<sup>1</sup>, Patricia Ducy<sup>1</sup>. <sup>1</sup>Columbia University, United states, <sup>2</sup>University of L'Aquila, Italy

SSRIs are prescribed for various psychiatric disorders but also, increasingly, for non-psychiatric conditions. Yet, recent clinical studies have reported a correlation between SSRIs long-term use and a poorly understood decreased bone mass and/or increased risk of fracture, raising concerns about their broad usage.

To understand the basis of SSRIs deleterious action on bone mass accrual, mice were treated with fluoxetine, one of the most commonly prescribed SSRI, for 6 weeks. Both in males and females this treatment caused a bone loss associated with decreased bone formation, increased *Rankl* expression and increased sympathetic tone. This latter observation is in apparent contradiction with SSRIs' canonical mode of action i.e., their ability to increase brain serotonin signaling by blocking its reuptake by the 5HT transporter, a feature that should decrease SNS output and favor bone mass accrual. We therefore analyzed serotonin signaling in the brain of the fluoxetine-treated mice. Hypothalamic levels of phospho-CREB, a target of brain serotonin signaling and of Htr2c, the receptor mediating serotonin central action on bone remodeling were decreased by a long-term fluoxetine treatment. Accordingly, brainstem levels of norepinephrin were increased and fluoxetine did not cause bone loss in *Tph2<sup>-/-</sup>* or *5htr<sup>-/-</sup>* mice. Hence, long-term treatment with fluoxetine inhibits the brain serotonin/Htr2c/ CREB cascade, causing an increase of sympathetic tone that impairs bone mass accrual.

If fluoxetine's deleterious effect on bone mass is mediated by an increase in sympathetic tone, blocking SNS activity peripherally should reverse this effect. Indeed, mice treated with fluoxetine and a low dose of the  $\beta$ -blocker propranolol do not loose bone. In summary, our study shows that the bone loss caused by the long-term use of SSRIs is mediated by a decrease in the brain serotonin inhibition of SNS output and suggests a therapeutic strategy to block this deleterious side effect.

Disclosures: Maria Jose Ortuno, None.

## MO0315

**Selective Serotonin Reuptake Inhibitors Impair Fracture Healing.** Anna Josephson\*, Vivian Bradaschia Correa, Devan Mehta, Philipp Leucht, New York University School of Medicine, United states

Selective serotonin re-uptake inhibitors (SSRIs) are one of the most commonly prescribed antidepressants worldwide. Recent studies have linked chronic SSRI use to

osteoporosis and an increased fracture risk. To date there are no studies investigating the effect of SSRIs on fracture healing. Here, we examined the effects of SSRIs on osteoprogenitor cells (OPCs) in vitro, followed by a comprehensive analysis in two murine fracture models.

Bone marrow-derived OPCs were treated with varying doses of fluoxetine. Cell proliferation and differentiation were assessed with standard tests including BrdU, PCNA, qPCR for collagen type 1, runx2, osteocalcin, osteopontin, osterix, alkaline phosphatase and alizarin red staining. In vivo fracture healing was studied using a mono-cortical drill hole and a fracture model in adult C57/BL6 mice after a 3-week course of oral fluoxetine. Mice were euthanized at 7, 14 and 28 days post injury.

In vitro treatment of primary OPCs with fluoxetine resulted in a significant reduction of proliferation compared to the control ( $p \leq 0.05$ ). Next, we treated cells with osteogenic differentiation media +/- fluoxetine for 7 days and then performed a mineralization assay (Fig. 1A). After 7 days, we found a significant reduction in Alizarin Red staining after fluoxetine treatment ( $p = 0.001$ ). qPCR revealed that osteoblastic markers, such as runx2, collagen type 1, osterix, osteocalcin and ALP were downregulated in the fluoxetine treated cells ( $p < 0.002$ ) (Fig. 1B).

Injured tibiae and femurs from control and SSRI-treated mice were analyzed by histomorphometry, microCT and molecular and cellular analyses. At all time points, the callus volume was significantly smaller in mice treated with fluoxetine, confirming the in vitro findings in these two vivo model (Fig. 1C,D).

These experiments demonstrate that SSRIs inhibit osteoprogenitor cell proliferation and impedes osteogenic differentiation both in vitro and in vivo. Animal research and human clinical data have unmistakably shown that chronic SSRI use leads to osteoporosis, thus putting patients at risk for fragility fractures. If in fact SSRIs have a negative effect on bone regeneration after fracture, then this patient cohort will be prone for delayed unions and non-unions.

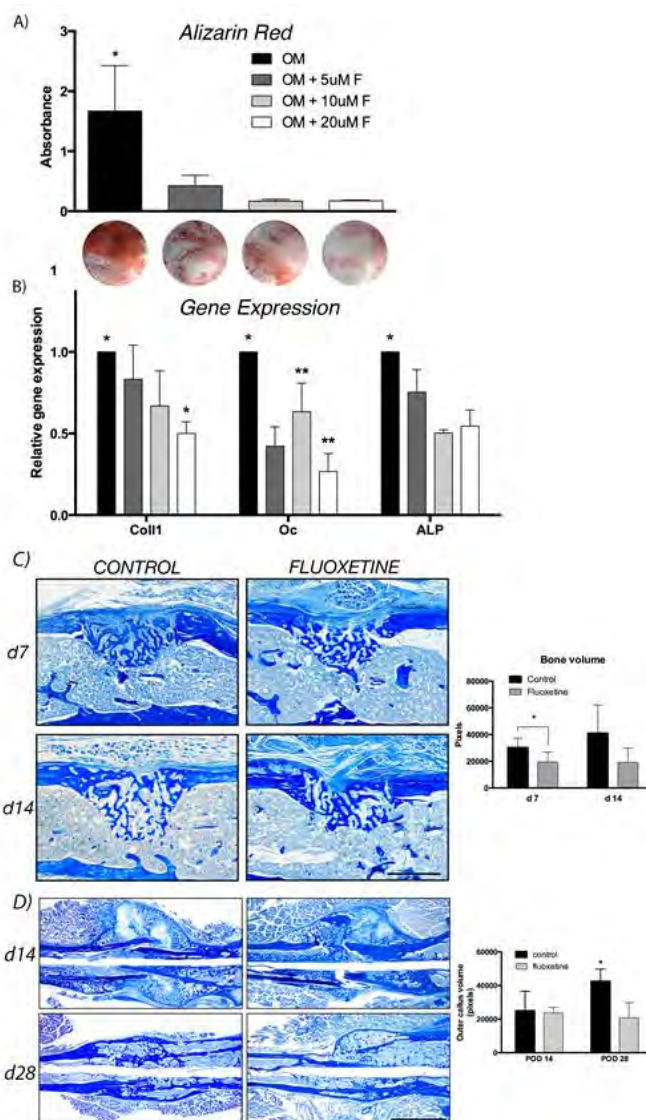


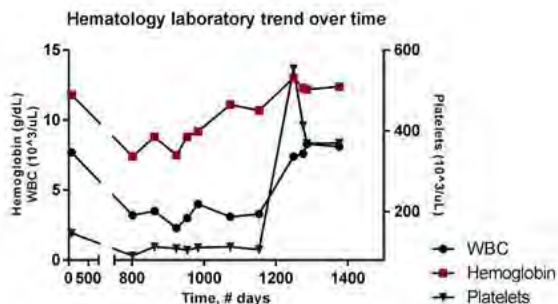
Figure 1

Disclosures: Anna Josephson, None.

## MO0316

**Bone marrow failure and extramedullary hematopoiesis in fibrous dysplasia/McCune-Albright syndrome.** Cemre Robinson, MD\*<sup>1</sup>, Andrea Estrada, MD<sup>2</sup>, David E. Kleiner, MD, PhD<sup>3</sup>, Alison M. Boyce, MD<sup>1</sup>, Revi Mathew, MD<sup>4</sup>, Robert Stanton, MD<sup>5</sup>, Haydar Frangoul, MD, MS<sup>4</sup>, Edward Hsiao, MD, PhD<sup>6</sup>, Michael T. Collins, MD<sup>1</sup>. <sup>1</sup>Section on Skeletal Diseases & Mineral Homeostasis, Craniofacial & Skeletal Diseases Branch, National Institute of Dental & Craniofacial Research, National Institutes of Health, Bethesda, MD, USA., United states, <sup>2</sup>Division of Endocrinology & Diabetes, Children's National Health System, Washington, D.C., United states, <sup>3</sup>National Cancer Institute, National Institutes of Health, Bethesda, MD, USA., United states, <sup>4</sup>The Children's Hospital at TriStar Centennial, Nashville, TN, USA., United states, <sup>5</sup>Nemours Children's Hospital, Orlando, Florida, USA., United states, <sup>6</sup>Endocrine Division, University of California San Francisco, San Francisco, CA, USA., United states

Background: Fibrous dysplasia/McCune-Albright syndrome (FD/MAS) is a rare disorder caused by somatic activating mutations in  $G_{\alpha s}$ . Bone marrow (BM) is replaced by fibro-osseous tissue typically devoid of hematopoietic marrow. A previously published mouse model of FD showed BM aplasia (Rsl mice, Schepers et al., Blood, 2012), without extramedullary hematopoiesis (EMH), despite a paradoxical expansion of stromal niche cells with putative hematopoietic stem cell-supportive activity. Despite the extensive marrow replacement in severely affected patients, there are no reports of BM failure associated with FD/MAS. Clinical case: A 14 year-old girl with FD/MAS, manifested by precocious puberty, hyperthyroidism, FGF-23-mediated hypophosphatemia, secondary hyperparathyroidism related to hypophosphatemia treatment, and extensive polyostotic FD requiring spinal fusion and intramedullary rod placement in both femora and tibiae, developed hepatosplenomegaly and pancytopenia. BM biopsy was consistent with FD. Liver biopsy revealed significant EMH. No infectious or inherited causes of marrow failure were identified. Despite correction of hyperthyroidism and hyperparathyroidism, both of which have been associated with BM aplasia, she remained pancytopenic, requiring monthly transfusions. Due to progressive painful splenomegaly, she underwent splenectomy 16 months after presentation with recovery of the pancytopenia. Discussion: Typically, patients with polyostotic FD have sufficient hematopoietic stem cells (HSCs) to meet the demands of blood cell production. It is possible that at baseline, this patient's HSCs were barely adequate, but that, uncontrolled hyperthyroidism and hyperparathyroidism, together with surgical instrumentation were sufficient to induce pancytopenia. In Rsl mice, a potential model for the BM aplasia seen in this patient, constitutive activation of  $G_s$  signaling in osteoblastic lineage cells led to changes in the BM niche, decreased expression of key HSC-supporting factors and impaired ability to maintain HSCs, a finding only brought out with marrow challenge. Compensatory EMH with massive splenomegaly, which typically does not occur in mice, likely exacerbated the patient's pancytopenia, as evidenced by improvement post-splenectomy. This case demonstrates the complexity and multifactorial etiology of pancytopenia, a novel complication of FD/MAS, and suggests that the Rsl mouse may be a model to study this rare but potentially devastating problem in FD.



Hematologic laboratory trend over the years

Disclosures: Cemre Robinson, MD, None.

## MO0317

**Determination of the Minimal Clinically Important Difference in the Six-Minute Walk Test for Patients with Hypophosphatasia.** Ioannis Tomazos\*, Scott Moseley, Eileen Sawyer, Uchenna Iloje. Alexion Pharmaceuticals, Inc, United states

Background: Hypophosphatasia (HPP) is a rare, inherited, metabolic disease caused by loss-of-function mutation(s) in the gene encoding tissue nonspecific alkaline phosphatase (TNSALP). Poor skeletal mineralisation, muscle weakness, pain, and accompanying complications characteristic of HPP result in impaired physical function, decreasing ability to perform daily activities, and quality of life. Improvement in physical function is a treatment target, yet established physical activity measures have not been validated in patients with HPP. The 6-Minute Walk

Test (6MWT) is an accepted measure of physical activity reflective of daily functioning for children with other chronic diseases.

Objective/Hypotheses: Determine concurrent validity and minimal clinically important difference (MCID) for the 6MWT for patients with HPP.

Methods: Data were from a Phase II trial of asfotase alfa, a replacement TNSALP, for children with HPP (ENB-006-09/ENB-008-10). MCID was estimated as per McDonald et al. 2013 using baseline/screening data, and standard error of measurement (SEM) and one-third standard deviation (1/3SD) distribution-based approaches. Clinical relevance was assessed via Pearson correlations between 6MWT and measures of skeletal disease (Radiographic Global Impression of Change [RGI-C] scale, Rickets Severity Scale [RSS]), and activities of daily living (parent-reported Childhood Health Assessment Questionnaire [CHAQ] Disability Index, Pediatric Outcomes Data Collection Instrument [PODCI]).

Results: MCID for patients with HPP was estimated at 20.2 meters (SEM) and 30.2 meters (1/3SD). Correlation analysis (127 datapoints) indicated significant ( $p < 0.001$ ), moderate-to-strong linear relationships between distance walked (percent predicted for age, gender, height) and RSS ( $r = -0.73$ ), CHAQ Disability Index ( $r = -0.57$ ), and PODCI subscales, including Global Function ( $r = 0.76$ ), Transfer/Basic Mobility ( $r = 0.69$ ), and Sports/Physical Functioning ( $r = 0.78$ ). Changes in 6MWT and RGI-C scores demonstrated weaker correlation ( $r = 0.32$ ; 68 datapoints;  $p < 0.01$ ).

Conclusions: The 6MWT is a valid, clinically relevant measure of disability and treatment outcomes for patients with HPP. A change of 20-30 meters represents a clinically meaningful difference in functional abilities in this population.

Disclosures: Ioannis Tomazos, Alexion Pharmaceuticals, Inc, 14; Alexion Pharmaceuticals, Inc, 15

This study was supported by Alexion Pharmaceuticals, Inc.

## MO0318

**Does Pyrophosphate Inhibit Bone Resorption?.** Aaron A Kwaasi<sup>1</sup>, James E Dunford<sup>2</sup>, Frank Hal Ebetino<sup>3</sup>, R Graham G Russell\*<sup>4</sup>. <sup>1</sup>The Botnar Research Centre, University of Oxford, UK, United Kingdom, <sup>2</sup>The Botnar Research Centre, University of Oxford, UK, United Kingdom, <sup>3</sup>Department of Chemistry, University of Rochester, USA, United states, <sup>4</sup>The Botnar Research Centre, University of Oxford, & The Mellanby Centre for Bone Research, University of Sheffield, United Kingdom

Inorganic pyrophosphate (PPi) is produced within cells as a by-product of  $>200$  biosynthetic reactions, whereas extracellular PPi is mainly generated from ATP by ecto-nucleotide pyrophosphatase/phosphodiesterases. PPi regulates biomineralisation and is one of the body's natural 'water softeners' (Orriess et al 2016). Plasma PPi has an extremely rapid turnover due to hydrolysis by alkaline phosphatase on cell surfaces. Normal plasma concentrations are  $\sim 2-6$   $\mu\text{M}$ , but are elevated in hypophosphatasia.

The bisphosphonates (BPs) were originally developed as stable analogues of PPi because PPi itself was too labile for therapeutic use and did not inhibit bone resorption in vitro or in animal models. Despite this, there have been recent speculations that pyrophosphate may have played a role in the pathogenesis of "Phossy jaw" described in match workers in Victorian England, and that it may therefore be of more recent relevance to osteonecrosis of the jaw, and atypical femoral fractures (Hinshaw 2013). The tenuous arguments used to support these speculations rely on putative inhibition of farnesyl pyrophosphate synthase (FPPS) by PPi, leading to inhibition of bone resorption by a similar mechanism to N-containing BPs.

In order to assess the credibility of these speculations, we have examined whether PPi can inhibit FPPS directly, and whether it affects the formation of human osteoclasts in vitro.

Methods. Inhibition of human recombinant FPPS was measured by established techniques (Dunford et al 2008). Osteoclast formation was measured using human peripheral blood mononuclear cells cultured for 15 days with 25ng/ml human M-CSF and 100 ng/ml soluble human RANKL.

Results & Discussion. PPi was at least 10,000 times less potent as an inhibitor of FPPS than Zol or Ris. It is unlikely that these high concentrations could ever be achieved within cells. Likewise, neither PPi, nor triphosphosphate or hexametaphosphate, inhibited osteoclast generation even when tested at concentrations as high as 1 mM, when compared with phosphate (Pi) as a control.

Conclusions. These observations, combined with earlier studies, render it implausible that PPi affects bone resorption at concentrations ever likely to occur in vivo.

#### IC<sub>50</sub> values for the inhibition of osteoclast formation and farnesyl pyrophosphate synthase

	Osteoclast formation (nM)	FPP synthase (nM)
Zoledronate (Zol)	11.8	4.1 +/- 0.22
Risedronate (Ris)	19.5	5.7 +/- 0.54
Pyrophosphate (PPi) vs Pi control	Inactive at 10uM to 1mM	181,000 +/- 19,100

Kwaasi et al

Disclosures: R Graham G Russell, None.

## MO0319

**Clinical and Radiographic Characteristics of Adult X-linked Hypophosphatemia (XLH) in a Cohort of Patients Treated with KRN23, an Antibody to FGF23.** Mary Ruppe<sup>1</sup>, Munro Peacock<sup>2</sup>, Tom Weber<sup>3</sup>, Anthony Portale<sup>4</sup>, Karl Insogna<sup>5</sup>, Erik Imel<sup>2</sup>, Diana Luca<sup>6</sup>, Alison Skrinar<sup>6</sup>, Matt Mealiffe<sup>6</sup>, Javier San Martin<sup>6</sup>, Thomas Carpenter<sup>5</sup>. <sup>1</sup>Houston Methodist Hospital, United states, <sup>2</sup>Indiana University School of Medicine, United states, <sup>3</sup>Duke University, United states, <sup>4</sup>University of California, San Francisco, United states, <sup>5</sup>Yale University School of Medicine, United states, <sup>6</sup>Ultragenyx Pharmaceutical Inc., United states

XLH, a rare, lifelong disorder is characterized by high serum FGF23 leading to decreased renal phosphate reabsorption, hypophosphatemia, rickets (in children), and osteomalacia. Twenty XLH patients who were previously enrolled in the Phase 1/2 adult studies of KRN23, an investigational antibody against FGF23, were enrolled in an open-label extension study to evaluate long-term safety, pharmacodynamics, and patient reported outcomes. The time from the last dose of KRN23 in the previous studies to enrollment in this study was more than 12 months in all patients. Mean age was 49.8 years (range 23-69) at extension study entry and 70% were female. All patients had hypophosphatemia: the mean (SD) baseline serum phosphorus was 1.9 (0.3) mg/dL (normal range = 2.5-4.5), and 30% of patients had hyperparathyroidism. Patients had a history of short stature (95%), bowing of lower legs (95%), abnormal gait (85%), dental abscesses (85%), and osteotomy (65%). All patients had joint stiffness and limited range of motion. Radiographs demonstrated skeletal manifestations of XLH including insufficiency fractures, commonly in the femur and metatarsal, in approximately 50% of patients; approximately 30% had more than one. All patients had enthesopathy in multiple anatomic locations. Mean "pain at its worst in the past 24 hours" (Question 3 of the Brief Pain Inventory; BPI) was 6.6 (range 3-10) at baseline on a scale of 0 (no pain) to 10 (as bad as you can imagine), with 45% of patients reporting scores  $\geq 7$  and classified as "severe pain". Mean pain interference score was 4.2 (range 1-9), indicating moderate disruption in activities of daily living due to pain. Baseline characteristics of the 20 adult patients entering this extension study confirm the high disease burden from XLH that substantially impacts quality of life and support the need for the continued development of novel therapeutic approaches. Phase 3 trials in adult XLH patients are ongoing to evaluate the efficacy and safety of KRN23 including effects on pain, stiffness, and histological evidence of osteomalacia.

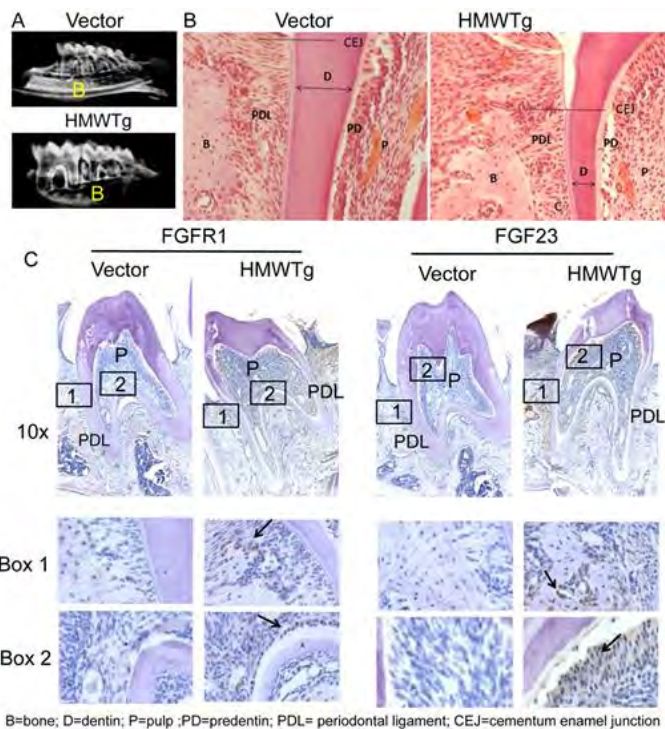
**Disclosures:** Mary Ruppe, None.

This study received funding from: Ultragenyx Pharmaceutical Inc.

## MO0320

**Nuclear Isoforms of Fibroblast Growth Factor 2 Modulate Dentin Mineralization in HMWTg Mice.** Johnny Joseph\*, Anushree Banerjee, Mina Mina, Patience Meo Burt, Erxia Du, Liping Xiao, Marja M Hurley. UConn Health, United states

We previously reported that transgenic mice overexpressing high molecular weight FGF2 isoforms in osteoblast lineage cells (HMWTg mice) displayed dwarfism, decreased bone mineral density (BMD), osteomalacia, hypophosphatemia and phosphaturia due to increased FGF23/FGFR/Klotho signaling and down-regulation of the sodium phosphate transporter (NPT2a) in kidneys. HMWFGF2 also transcriptionally regulates FGF23, which has been reported to negatively impact dentin mineralization and dentinogenesis. Therefore this study examined the effects of phosphate wasting and increased FGF23 on teeth and supporting tissues in HMWTg mice. Methods: HMWTg and Vector age matched male mice were sacrificed at 30 and 60 days old. Mandibular arches were isolated, examined by radiography and processed for histology as well as immunohistochemistry for matrix bone sialoprotein (BSP) that is found in mineralized tissues of the skeleton and dentition and were also stained for FGF23 and FGFR1. Results: Radiography revealed smaller mandibles, and mineralization defects in alveolar bones and dentin in HMWTg mice compared to Vector at 30 (Fig.1A) and 60 days old. Histological analysis showed increased thickness of pre-dentin, decreased thickness of dentin, and decreased alveolar bone volume compared to Vector mice (Fig.1B). The phenotypic abnormalities were more severe at 30 compared to 60 days old. Immunohistochemistry of BSP expression in roots of the 30 days old mandibular molars revealed intense staining for BSP in cementum lining the root of molars from Vector in contrast there was markedly decreased BSP staining in HMWTg. Similarly, while there was staining for BSP in alveolar bone surrounding the molars of the Vector, no staining was observed in the alveolar bone of HMWTg. Staining for FGFR1 and FGF23 revealed increased FGF23 and FGFR1 (arrows) in the pulp (Box 2), periodontal ligament pulp, osteoblasts and osteocytes (Box 1) in HMWTg compared with Vector (Fig.1C). Conclusion: The changes in the thickness of dentin and pre-dentin indicated that over-expression of FGF2 did not affect odontoblast differentiation but affected the conversion of unmineralized pre-dentin into mineralized dentin that is dependent of phosphate. These observations indicate that dentin abnormalities in HMWTg mice are due in part to hypophosphatemia. In addition increased FGF23 expression could contribute to defective dentin matrix mineralization in HMWTg mice.



Figure

**Disclosures:** Johnny Joseph, None.

## MO0321

**Atypical Femur Fractures in Osteogenesis Imperfecta.** Pamela Trejo\*, Francis Glorieux, Frank Rauch. Shriners Hospital for Children Canada, Canada

Recent case reports have described atypical subtrochanteric and diaphyseal femur fractures (AFF) as a complication of long-term bisphosphonate (BP) treatment in children with osteogenesis imperfecta (OI). However, AFF has been defined for women with postmenopausal osteoporosis and it is not known whether AFF criteria are applicable to femur fractures in children with OI. We therefore assessed the characteristics of subtrochanteric and diaphyseal femur fractures in children with OI who had not received BP treatment prior to fracture (and who had not undergone intramedullary rodding procedures). In a retrospective chart review we identified 55 such patients who had sustained a total of 61 femur fractures, 32 were females and 23 males, median age for fracture was 2.0y (0.0 to 13.4y). For 15 of these fractures the radiographic documentation was inadequate. Of the remaining 46 fractures, 30 fractures in 28 patients fulfilled the criteria for AFF, but concomitant femur deformities were present in 22 fractures. Thus, we identified 8 fractures in non-deformed femurs that met established criteria for AFF even though there was no history of prior BP exposure. These fractures occurred in 8 children (4 girls) with a median age at fracture of 3.7 years (range 1.5 to 6.4 years). The clinical diagnosis was OI type I in 3 patients, OI type IV in 3 patients, OI type V in one patient and OI type VI in one patient. Correspondingly, OI was caused by *COL1A1/COL1A2* mutations in 6 patients (2 *COL1A1* haploinsufficiency mutations, 3 helical glycine substitutions, one splice site mutation), a *SERPINF1* mutation in one patient and a *IFITM5* mutation in one patient.

These 8 patients seemed to have more severe OI, on average, than a group of 9 patients who had sustained fractures in non-deformed femurs that did not meet criteria for AFF (median age at fracture 2.7 years with a range of 0.9 to 5.1 years; clinical diagnosis of OI type I in 8 patient, OI type VI in one patient). In conclusion, AFF are observed in children with OI who have not received BP, in particular among patients with moderate disease severity. AFF criteria developed for postmenopausal osteoporosis may not be applicable to children with OI.

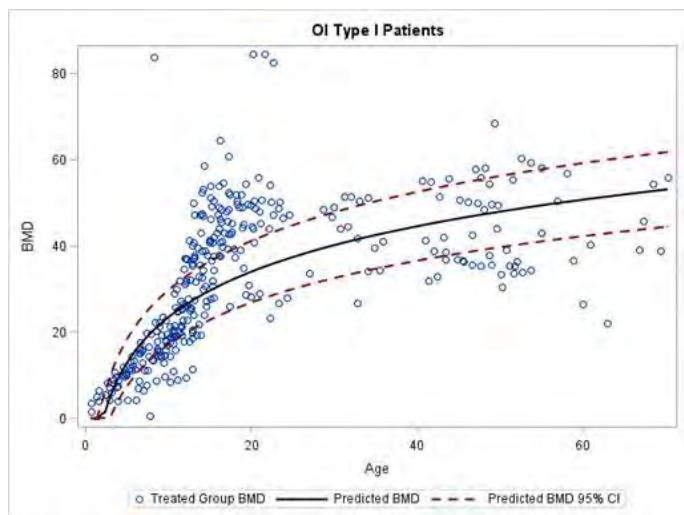
**Disclosures:** Pamela Trejo, None.

## MO0322

**Effect of Bisphosphonates on Bone Mineral Density and other Health Outcomes in Type 1 Osteogenesis Imperfecta.** Jaskaran Bains<sup>1</sup>, Kate Citron<sup>1</sup>, Erin Carter<sup>1</sup>, David Cuthbertson<sup>2</sup>, Jay Shapiro<sup>3</sup>, Robert Steiner<sup>4</sup>, Peter Smith<sup>5</sup>, Michael Bober<sup>6</sup>, Tracy Hart<sup>7</sup>, Jeffery Krischer<sup>2</sup>, Peter Byers<sup>8</sup>, Francis Glorieux<sup>9</sup>, Frank Rauch<sup>9</sup>, Sandesh Nagamani<sup>10</sup>, Vernon Sutton<sup>11</sup>, Brendan Lee<sup>10</sup>, Cathleen Raggio<sup>\*1</sup>. <sup>1</sup>Hospital for Special Surgery, United states, <sup>2</sup>College of Medicine, University of South Florida, United states, <sup>3</sup>Kennedy Krieger Institute, United states, <sup>4</sup>Oregon Health & Science University, United states, <sup>5</sup>Shriners Hospital for Children, United states, <sup>6</sup>Alfred I. DuPont Hospital for Children, United states, <sup>7</sup>Osteogenesis Imperfecta Foundation, United states, <sup>8</sup>University of Washington, United states, <sup>9</sup>Shriners Hospital for Children & McGill University, Canada, <sup>10</sup>Baylor College of Medicine, United states, <sup>11</sup>Texas Children's Hospital, United states

Osteogenesis imperfecta (OI) is a heritable bone disorder characterized by bone and tissue fragility as well as low bone mass. This study uses data from the Linked Clinical Research Centers, part of the Rare Disease Clinical Research Network, to examine the treatment effect of bisphosphonates (BPN; a class of antiresorptive drugs commonly used to treat OI) on bone mineral density (BMD) and other clinically relevant outcomes. In our principal methodology, linear regressions of BMD on age were used to construct expected BMD age progressions for untreated Type I (T1) OI patients. A 2-sided t-test was then used to assess whether BMDs of treated T1 patients differed from their age-specific untreated counterparts. Treatment increased the BMD of T1 patients by 9% relative to the untreated patient sample; this result was driven by pre-pubescent (<14 yrs) T1 patients, who saw a treatment effect of 12% (p<.01). There was no significant effect on T1 patients 14 and older. Intravenous BPN and treatment durations of >2 years were particularly effective. The treatment effect did not differ markedly by sex. In both the pre-pubescent and whole age T1 samples, BMDs of treated males were higher than expected BMDs based on untreated males. Females only saw this effect in pre-pubescent years. All T1 results were corroborated by regression analysis. Several sources of downward bias affect this study (e.g., not a randomized control trial, treatment initiation age not reported). Thus, treatment effect on BMD is likely underestimated.

In addition to the T1 results, BPN improved BMD z-scores in Type IV, V, and VIII patients. The treatment effect also extended to non-BMD outcomes. Using logistic regression models, we found that for a 1% increase in BMD, treated T1 patients over the whole age sample saw a 4% decrease in fracture probability while untreated T1 patients saw a 1% increase (p<.05). Similarly, scoliosis probability exhibited larger drops in treated T1 pre-pubescent patients for a given BMD increase (p<.01). BPN also slowed the acceleration in scoliosis probability with age in the pre-pubescent T1 sample (p<.01). This suggests that treatment may improve aspects of bone structure more difficult to measure than bone mass, such as bone architecture and mineralization. Linear regression analysis showed that BPN treatment also increased T1 patient mobility over the whole age sample (p<.01), providing further evidence that improvements in bone mass and structure raise patient quality of life in multiple ways.



OI BMD ASBMR Abstract Figure

**Disclosures:** Cathleen Raggio, None.

## MO0323

**Mortality and causes of death in patients with osteogenesis imperfecta. A register-based national cohort study.** Lars Folkestad<sup>\*1</sup>, Jannie Dahl Hald<sup>2</sup>, Vladimir Canudas-Romo<sup>3</sup>, Jeppe Gram<sup>4</sup>, Anne Pernille Hermann<sup>5</sup>, Bente Langdahl<sup>6</sup>, Bo Abrahamsen<sup>7</sup>, Kim Brixen<sup>8</sup>. <sup>1</sup>Department of Endocrinology, Odense University Hospital, Denmark, <sup>2</sup>Department of Endocrinology & Internal medicine, Århus University Hospital, Denmark, <sup>3</sup>Max-Planck Odense Center on the Biogeography of aging, Denmark, <sup>4</sup>Hospital of Southwest Denmark, Denmark, <sup>5</sup>Department of Endocrinology, Odense University Hospital, Denmark, <sup>6</sup>Aarhus University, Denmark, <sup>7</sup>Department of Medicine, Holbæk Hospital, Denmark, <sup>8</sup>Department of Clinical Research, University of Southern Denmark, Denmark

#### Introduction

Osteogenesis imperfecta (OI) is a hereditary disease of connective tissue that causes bone fragility and increased risk of fracture. The OI bone phenotype is well described, but less is known about causes of death and length of survival. We hypothesized that patients with OI would have an increased risk of premature death.

#### Methods and participants

This national cohort study included all patients registered with the diagnosis of OI in the Danish National Patient Register from 1977 until 2013, and a reference population selected from the central persons register that was matched 5 to 1 to the OI cohort. Using data from the Danish Cause of Death Register, we calculated hazard ratios for all-cause mortality and sub-hazard ratios for cause-specific mortality in a comparison of the OI cohort and the reference population. We also calculated all-cause mortality hazard ratios for males, females, and age groups (0-17.99, 18.00-34.99, 35.00-54.99, 55.00-74.99 and above 75 years).

#### Results

We identified 687 cases of OI (379 women) and included 3,435 persons (1,895 women) in the reference population. Of these, 112 patients with OI and 257 persons in the reference population died during the observation period. The all-cause mortality hazard ratio between the OI cohort and the reference population was 2.90. The median survival time for males with OI was 72.4 years, compared to 81.9 in the reference population. The median survival time for females with OI was 77.4 years, compared to 84.5 years in the reference population. Patients with OI had a higher risk of death from respiratory diseases, gastrointestinal diseases, and trauma.

#### Conclusion

Patients with OI had a higher mortality rate throughout their life, resulting in a shorter mean survival time compared to the general population.

**Disclosures:** Lars Folkestad, AstraZeneca, 13; Genzyme, 13

## MO0324

**Mutation in the Collagen-specific Molecular Chaperone Hsp47 Causes Endoplasmic Reticulum Stress in Osteoblast Cells of Osteogenesis imperfecta patients.** vandana Dhiman<sup>\*1</sup>, Sanjay Bhadada<sup>1</sup>, Naresh Sachdeva<sup>1</sup>, Amanjit Bal<sup>1</sup>, Anuradha Chakraborti<sup>1</sup>, Anil Bhansali<sup>1</sup>, Nirmal Raj Gopinathan<sup>1</sup>, D K Dhawan<sup>2</sup>. <sup>1</sup>PGIMER, Chandigarh, India, <sup>2</sup>Panjab University, India

**Introduction** Osteogenesis imperfecta (OI) is a heritable disorder of abnormal collagen and predisposes for increased bone fragility and deformity. The underlying molecular mechanism of abnormal collagen is poorly understood. The heat shock protein 47 (Hsp47) is involved in controlling the quality of procollagen folding in the ER and attenuates misfolding of triple helix collagen, this indicate Hsp47 might be involved in OI. However, Hsp47 cannot prevent the export of incompletely folded chains from the ER by preferential binding and tagging them. Instead, Hsp47 preferentially binds to and is co-transported with natively folded procollagen from the ER to Golgi. **Objective** In the present study, we investigated the mechanisms underlying the apoptosis of Hsp47-/- cells and the involvement of autophagy and UPR in the clearance of misfolded type I procollagen in the absence of Hsp47. We hypothesized that misfolded type I procollagen in the ER might cause ER stress, resulting in the apoptosis of Hsp47-disrupted triple helix of collagens when autophagy is inhibited. **Methodology** PBMC derived osteoblasts were cultured and RNA and protein was isolated from bone. Mutation analysis of Hsp47 gene was done through sequencing followed by restriction digestion. Hsp47 control- and mutant-gene were cloned in expression vector pEGFP-C1. Further *in-vitro* analysis was performed to study the interaction between triple helix and mutant Hsp47 under confocal microscope. Immunoblot for mutant protein analysis was done, RT-PCR and Quantitative Real Time PCR were performed for expression and functional analysis. **Result** and **Conclusion** ER stress-induced apoptosis may underlie the clearance of collagen-producing osteoblast cells. Experimental findings suggest that Hsp47 plays a pivotal role for ER/cis-Golgi transport. The changes in triple helical structure could affect fibril assembly in the ECM and lead to irregular mineralization and an OI phenotype.

**Disclosures:** vandana Dhiman, None.

This study received funding from: ICMR, New Delhi, India

## MO0325

**PLS3 Sequencing in Childhood-onset Primary Osteoporosis Identifies Two Novel Mutations.** Anders J Kämpe\*<sup>1</sup>, Alice Costantini<sup>1</sup>, Riikka E Mäkitie<sup>2</sup>, Nina Jäntti<sup>1</sup>, Helena Valta<sup>3</sup>, Minna Pekkinen<sup>2</sup>, Mervi Mäyränpää<sup>4</sup>, Fulva Taylan<sup>1</sup>, Hong Jiao<sup>5</sup>, Outi Mäkitie<sup>6</sup>. <sup>1</sup>Department of Molecular Medicine & Surgery & Center for Molecular Medicine, Karolinska Institutet, Stockholm, Sweden, <sup>2</sup>Folkhälsan Institute of Genetics & University of Helsinki, Helsinki, Finland, <sup>3</sup>Children's Hospital, University of Helsinki & Helsinki University Hospital, Helsinki, Finland, <sup>4</sup>Children's Hospital, University of Helsinki & Helsinki University Hospital, Helsinki, Finland, <sup>5</sup>Department of Biosciences & Nutrition, & Science for Life Laboratory, Karolinska Institutet, Stockholm, Sweden, <sup>6</sup>Department of Molecular Medicine & Surgery, Karolinska Institutet, Sweden; Folkhälsan Institute of Genetics & University of Helsinki, Helsinki, Finland; Children's Hospital, University of Helsinki & Helsinki University Hospital, Helsinki, Finland, Sweden

Early-onset osteoporosis caused by mutations in the X-chromosomal gene *PLS3* was first described in 2013 as a rare condition mainly affecting males. To investigate this further, we screened two separate patient cohorts for *PLS3* mutations. Cohort I consisted of 31 patients referred to the Metabolic Bone Clinic, Children's Hospital, Helsinki for suspected early-onset osteoporosis of unknown genetic etiology; several had a positive family history. Cohort II consisted of 64 otherwise healthy children (67% boys) aged 4-16 years who during a 12-month period had been treated for a fracture at the Children's Hospital, Helsinki, and had a significant fracture history not caused by secondary osteoporosis or osteogenesis imperfecta. We Sanger sequenced all coding exons and exon-intron boundaries of *PLS3* (NM\_005032) to identify disease-causing variants.

In Cohort I, 2 patients (6.5%) were positive for novel *PLS3* mutations that were deemed causative of their phenotype. The first patient was a male who was diagnosed with osteoporosis at the age of 12 years based on multiple vertebral and bilateral femoral fractures. He had a nonsense mutation (p.R256\*), inherited from his mother who had osteopenia. The second patient was a girl with multiple long bone and vertebral fractures and low BMD (Z-score -6.6) at the age of six years. She had a *de novo* missense mutation (p.N446S); other genetic causes were excluded by exome-sequencing of the family.

In Cohort II, no pathogenic variants were identified. In total, we found 4 different single nucleotide variants (SNVs) within coding regions, 3 synonymous and 1 missense variant; all were predicted benign. The synonymous variant *rs140121121* has been associated with osteoporosis, but was not enriched in our cohorts.

In conclusion, based on our results, screening for disease-causing *PLS3* mutations should be included in the investigation of both male and female patients with early-onset osteoporosis but is not indicated in patients only fulfilling the criteria for a clinically significant fracture history.

**Disclosures:** Anders J Kämpe, None.

## MO0326

**Activin A activates the ACVR1 (R206H) receptor in human primary dermal fibroblasts of fibrodysplasia ossificans progressiva patients.** Dimitra Michal<sup>1</sup>, Marelise Eekhoff\*<sup>2</sup>, Coen Netelenbos<sup>2</sup>, Vinitha kandiah<sup>1</sup>, Teun de Vries<sup>3</sup>, Gerard Pals<sup>1</sup>, Nathalie Bravenboer<sup>4</sup>. <sup>1</sup>Department of Clinical Genetics, VU University Medical Center, Netherlands, <sup>2</sup>Internal Medicine, Endocrinology section, VU University Medical Center, Netherlands, <sup>3</sup>Department of Oral Cell Biology, ACTA, VU University, Netherlands, <sup>4</sup>Department of Clinical Chemistry, VU University Medical Center, MOVE Research Institute, Netherlands

**Introduction:** Fibrodysplasia ossificans progressiva (FOP) is a rare genetic disorder characterized by episodic heterotopic ossification (HO) of muscles, tendons and ligaments. FOP is caused by a mutation in the type I BMP (bone morphogenetic protein) receptor ACVR1 (R206H), resulting in a hyperactive receptor. Recently activin A, which physiologically antagonizes ACVR1-mediated BMP signaling, was found to activate the mutant ACVR1 receptor in transgenic mice inducibly expressing ACVR1(R206H), which triggered HO development. In FOP patients activin A effect has not yet been investigated. **Objectives:** To assess the osteogenic effect of activin A in primary human dermal fibroblasts of FOP patients. **Methods:** Primary subdermal fibroblasts from five R206H FOP patients and of 3 healthy controls were cultured in the presence and absence of activin A. SMAD 1/5 phosphorylation was measured by western blot analysis. **Results:** Activin A stimulation resulted in Smad1/5 phosphorylation in fibroblasts of FOP patients which was absent from healthy controls. The expression of pSmad3 was comparable between patients and controls. **Conclusion:** Given the expression of pSmad1/5 in FOP fibroblasts, our results indicate that the R206H ACVR1 receptor is responsive to activin A stimulation in human fibroblasts. This suggests that activin A stimulation can promote osteogenesis in human FOP cells.

**Disclosures:** Marelise Eekhoff, None.

## MO0327

**Bone Material Properties Assessment by Microindentation in Patients with Type 1 Gaucher's Disease.** Sabina Herrera\*<sup>1</sup>, Marc Molto<sup>2</sup>, Roberto Guerri-Fernandez<sup>3</sup>, Elena Cabezedo<sup>1</sup>, Silvana Novelli<sup>1</sup>, Jordi Esteve<sup>1</sup>, Albert Hernandez<sup>1</sup>, Inmaculada Roig<sup>1</sup>, Xavier Solanich<sup>1</sup>, Daniel Prieto-Alhambra<sup>3</sup>, Xavier Nogues<sup>3</sup>, Jordi Pérez-López<sup>3</sup>, Adolfo Díez-Pérez<sup>3</sup>. <sup>1</sup>MD, Spain, <sup>2</sup>PhD, Spain, <sup>3</sup>MD, PhD, Spain

**Background:**

Gaucher's disease is the most common lysosomal disorder. Some studies have demonstrated up to 80% patients have bone infiltration even if asymptomatic. Bone illness remains a major cause of morbidity in these patients, who suffer from avascular necrosis and bone infarcts. However, little data is available on their general bone strength. We aimed to measure bone material strength (BMS) amongst these patients.

**Methods:**

Patients were selected from Catalan Study Group on Gaucher's Disease. Clinical, laboratory, and Bone mineral density (BMD) data were collected. Impact Bone Microindentation measurements were carried out (Osteoprobe, Active Life Scientific, Santa Barbara, CA, USA) in areas not affected by bone infarcts or necrosis. Multivariable linear regression models were fitted.

**Results:**

A total of 16 patients were included and compared to 29 age and gender-matched controls. Type 1 GD patients had significantly lower BMS (mean 72.74 compared to 81.75 in controls), a difference that remained significant after adjustment for age, gender, weight, height and lumbar DMO (adjusted p = 0.002). Mean lumbar and total hip BMD of controls was 0.991 g/cm<sup>2</sup> and 0.769 g/cm<sup>2</sup> respectively, significantly higher when compared to 0.896 g/cm<sup>2</sup> and 0.717 g/cm<sup>2</sup> amongst GD patients (adjusted p = 0.002 and p = 0.018 respectively).

**Conclusion:**

Bone material properties are affected in patients with Gaucher's disease, independent of known BMD alterations detected by routinely used densitometry. Microindentation could be appropriate for the assessing and monitoring of GD-related bone disease during treatment.

**Disclosures:** Sabina Herrera, None.

This study received funding from: Shire Pharmaceuticals

## MO0328

**Establishment of Tet-On C2C12 Cells Express ALK2 Responsible for Fibrodysplasia Ossificans Progressiva and Diffuse Intrinsic Pontine Glioma.** Takenobu Katagiri\*, Satoshi Ohte, Sho Tsukamoto, Mai Kuratani, Aiko Machiya, Keigo Kumagai. Saitama Medical University, RCGM, Japan

Fibrodysplasia ossificans progressiva (FOP) is a rare autosomal dominant disorder characterized by progressive heterotopic ossification (HO) in soft tissues such as skeletal muscles, tendons and ligaments. Bone morphogenetic proteins (BMPs) have been shown to induce HO in vertebrates. Gain-of-function mutations of a BMP type I receptor, ALK2, were identified in the patients with FOP. Recently, some overlapping ALK2 mutations including p.R206H were also found in patients with a rare childhood brain tumor, diffuse intrinsic pontine glioma (DIPG). In the present study, we established and characterized C2C12 cells express wild type or p.R206H mutant of human ALK2 under the control of Tet-On Advanced system. In this system, the expression of human ALK2 can be induced by adding Doxycycline (Dox) to culture media. Firstly, we transfected an expression vector of tTA transactivator in C2C12 cells and selected a clone with the highest responsibility to the Dox-stimulation. Then, the clonal cells were further transfected with a response vector carrying wild type or p.R206H mutant ALK2 with a V5-epitope tag and clonal cell lines were established from the cultures. Both immunohistochemical staining and Western blotting using an antibody against the V5-epitope tag confirmed a dose-dependent expression of wild type and mutant human ALK2 in response to Dox. The Dox-treatment induced a BMP-specific luciferase reporter activity in the cells carrying mutant ALK2, but not wild-type ALK2. However, the Dox-treatment failed to induce ALP activity even in the cells expressing mutant ALK2, suggesting that the expression of p.R206H mutant ALK2 is not enough to induce HO. Treatment with BMP in combination with Dox synergistically induced the ALP activity in the cells, supporting that p.R206H is a hypersensitive mutation to ligands rather than a constitutively activation. Our Tet-On cell lines are new tools for studying molecular mechanisms of the BMP signal activation by the mutant ALK2 in FOP and DIPG.

**Disclosures:** Takenobu Katagiri, None.

## MO0329

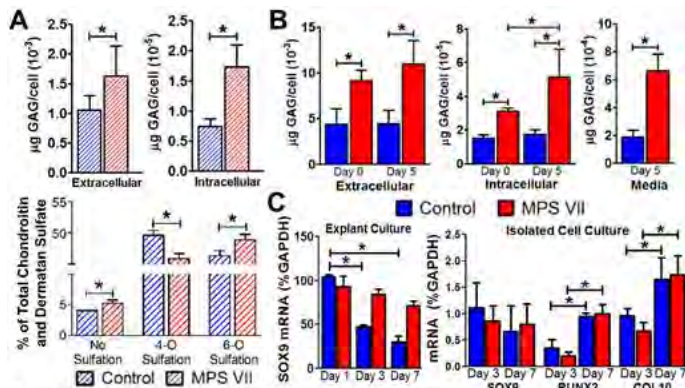
**Impaired Chondrocyte Hypertrophic Differentiation Potential is Associated with Abnormal Glycosaminoglycan Accumulation in Mucopolysaccharidosis VII Dogs.** Sun Peck\*<sup>1</sup>, Jennifer Kang<sup>1</sup>, Maurizio Pacifici<sup>2</sup>, George Dodge<sup>1</sup>, Neil Malhotra<sup>1</sup>, Mark Haskins<sup>1</sup>, Eileen Shore<sup>1</sup>, Lachlan Smith<sup>1</sup>.  
<sup>1</sup>University of Pennsylvania, United states, <sup>2</sup>The Children's Hospital of Philadelphia, United states

Mucopolysaccharidosis (MPS) VII is a lysosomal storage disease characterized by deficient  $\beta$ -glucuronidase activity resulting in abnormal glycosaminoglycan (GAG) accumulation. MPS VII patients present with severe spine disease stemming from failed vertebral ossification during postnatal growth, which is due to impaired ability of epiphyseal chondrocytes to undergo hypertrophic differentiation. GAGs regulate cell differentiation through control of secreted growth factors. Thus, we hypothesized that GAG accumulation in MPS VII contributes directly to impaired chondrocyte differentiation potential. The objectives of this study were to 1) establish the nature of GAG accumulation in MPS VII epiphyseal cartilage and 2) investigate the links between impaired chondrocyte differentiation potential and GAG accumulation, using the naturally-occurring canine model.

Vertebral epiphyseal cartilage was isolated postmortem from control and MPS VII dogs (n=3-5) at 9 days-of-age, the age immediately prior to commencement of secondary ossification in control animals. GAG content (extra and intracellular) was measured using the DMMB assay, and disaccharide composition was measured using HPLC. To investigate effects of GAG accumulation on differentiation potential, chondrocytes were cultured either in intact explants or enzymatically isolated (extracellular GAGs removed) for monolayer culture, for up to 7 days. mRNA expression of differentiation markers and GAG accumulation were measured.

GAG content (extra and intracellular) in MPS VII epiphyseal cartilage was significantly elevated vs controls at 9 days-of-age with abnormal disaccharide composition (Fig. A). MPS VII explants accumulated GAGs over time in culture, while controls did not (Fig. B). In whole explant culture, while control chondrocytes exhibited propensity to differentiate over time, MPS VII chondrocytes did not (Fig. C). In contrast, when isolated cells were cultured, differentiation potential was similar for both.

Abnormal GAG accumulation in MPS VII epiphyseal cartilage may disrupt control of secreted growth factors necessary to initiate and sustain chondrocyte hypertrophic differentiation. Differences in differentiation potential between explant and isolated cell culture likely reflect the critical role of GAGs on cell function in MPS VII and indicate that therapies that normalize GAG accumulation, such as enzyme replacement or substrate reduction, may rescue the differentiation potential of resident cells.



**A.** MPS VII epiphyseal cartilage exhibited significantly elevated extra and intracellular GAG content and differences in disaccharide composition vs controls at 9 days-of-age. **B.** Control epiphyseal explants maintained stable GAG levels over time in culture, while MPS VII explants progressively accumulated GAGs in all fractions. **C.** In culture, control chondrocytes in intact epiphyseal cartilage explants exhibited propensity to differentiate over time, while MPS VII chondrocytes did not. In contrast, both isolated control and MPS VII chondrocytes differentiated normally. N=3-5; \*p<0.05.

Peck 2016 ASBMR Abstract Figure

Disclosures: Sun Peck, None.

## MO0330

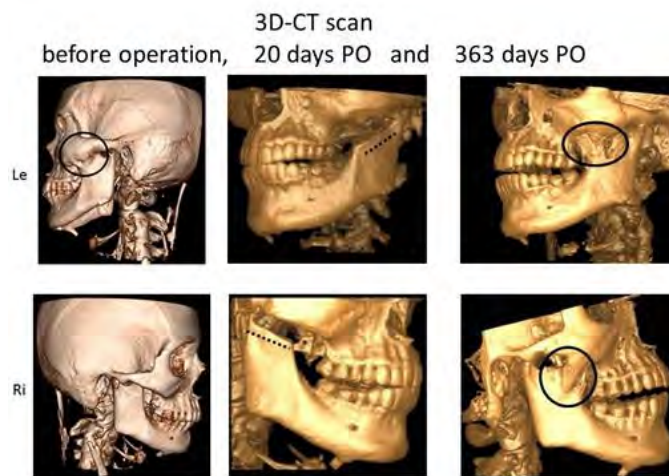
**Paradigm Shift: Jaw Surgery in Selected Fibrodysplasia Ossificans Progressiva Patients Could Offer Better Quality of Life and Precede Drug Treatment Trial.** Coen Netelenbos\*<sup>1</sup>, Marelise Eekhoff<sup>2</sup>, Pieter Raijmakers<sup>1</sup>, Robert van Es<sup>3</sup>.  
<sup>1</sup>VUmc, Netherlands, <sup>2</sup>VUmc FOP Expert Center, Netherlands, <sup>3</sup>UMC, Netherlands

According to the literature more than 90% of patients with Fibrodysplasia Ossificans Progressiva (FOP) experienced exacerbation of the condition after a surgical procedure and in 100% after jaw surgery because of ankylosis. Therefore surgery in these patients for excision ossification is contra-indicated.

We described a 25 year old woman who suffered for more than 10 years from total ankylosis of the jaw caused by zygomatico-mandibular heterotopic ossification (HO) of the left side after fall from stairs. She demanded persistently but not obsessively for jaw operation. Main reasons were her fear for choking when she suffered from nausea and vomiting resulting in nightmares, she frequently visited therefore the emergency room, could not eat with friends and had suicidal thoughts. Own doctors and international FOP experts absolutely refused her wish to be operated again and again. At last however, we gave in and agreed to remove both coronoid processes of her mandible. This resulted in 25 mm of interincisal mouth opening. At 32 days after operation recurrence of HO was shown on 18F NaF PET scan which decreased after wards while density on CT scan increased. Six months after jaw operation she was not able to move her jaw anymore and a stable 5 mm interincisal distance remained now for more than 18 months after operation. In Figure 1. 3D CT-scans showed the HO lesion of the left jaw and the new HO on both jaws after operation. However, the patient was very satisfied because her quality of life was much better than before: no fear for choking in case of nausea, ability to brush teeth, improved speech and regained a positive motivation in life.

New compounds against heterotopic ossification are in development. When permitted for clinical use this case could precede a small short-term clinical study in FOP patients with ankylosis of the jaw. The efficacy of prevention of new ossifications after operation by an anti-FOP drug can then be proven under rigid control of 18F NaF PET/CT scan.

Disclosures: Coen Netelenbos, None.



netelenbos

Disclosures: Coen Netelenbos, None.

## MO0331

**Whole Body Computed Tomography (CT) Versus Dual Energy x-ray Absorptiometry (DXA) Imaging for Assessing Heterotopic Ossification (HO) in Fibrodysplasia Ossificans Progressiva (FOP).** Frederick S. Kaplan<sup>1</sup>, Robert J. Pignolo<sup>2</sup>, Stacy E. Smith<sup>3</sup>, Sarah E. Warner<sup>4</sup>, Edward C. Hsiao<sup>5</sup>, Carmen De Cunto<sup>6</sup>, Maja Di Rocca<sup>7</sup>, Harry K. Genant<sup>8</sup>, Donna R. Grogan<sup>9</sup>.  
<sup>1</sup>The University of Pennsylvania, United states, <sup>2</sup>The University of Pennsylvania Perelman School of Medicine, United states, <sup>3</sup>Division of Musculoskeletal Imaging & Intervention, Dept. of Radiology, Brigham & Women's Hospital, Harvard Medical School, United states, <sup>4</sup>PAREXEL Medical Imaging, United states, <sup>5</sup>Division of Endocrinology & Metabolism, University of California, San Francisco, United states, <sup>6</sup>Department of Pediatrics/Hospital Italiano de Buenos Aires, Argentina, <sup>7</sup>Unit of Rare Diseases, Department of Pediatrics, Gaslini Institute, Italy, <sup>8</sup>UCSF/BioClinica, United states, <sup>9</sup>Clementia Pharmaceuticals Inc., United states

FOP is a rare, genetic disease of congenital skeletal malformations and progressive HO that irreversibly restricts movement and physical function, and for which there is no approved treatment. As imaging will be essential to support future trials of investigational agents, we sought to determine whether whole body DXA would provide sufficient sensitivity to document the extent and progression of HO as compared with low-dose whole body CT (excluding head).

## MO0333

**Prevalence of sarcopenia according to different consensus definitions in patients with a recent clinical fracture.** Caroline E Wyers\*<sup>1</sup>, Lisanne Vranken<sup>1</sup>, Robert Y van der Velde<sup>2</sup>, Piet P Geusens<sup>3</sup>, Joop PW van de Bergh<sup>4</sup>. <sup>1</sup>Maastricht UMC+, Department of Internal Medicine; <sup>2</sup>VieCuri Medical Center, Department of Internal Medicine, Netherlands, <sup>3</sup>VieCuri Medical Center, Department of Internal Medicine; Maastricht UMC+, Department of Internal Medicine, Netherlands, <sup>4</sup>Maastricht UMC+, Department of Internal Medicine subdivision of Rheumatology; University of Hasselt, Netherlands, <sup>5</sup>VieCuri Medical Center, Department of Internal Medicine; Maastricht UMC+, Department of Internal Medicine; University of Hasselt, Netherlands

**Purpose:** The aim of this study was to evaluate the prevalence of sarcopenia according to the definitions of the European Working Group on Sarcopenia in Older People (EWG), the International Working group (IWG), and the Foundation for the National Institutes of Health (FNIH) in patients with a recent clinical fracture (fx) visiting the Fracture Liaison Service (FLS).

**Methods:** All consecutive patients aged 50-90 years presenting with a recent clinical fx (including vertebral fx) presenting at the FLS who had measurement of bone densitometry and body composition by DXA. Sarcopenia was defined according to 1) EWG: Appendicular Lean Mass (ALM)/height<sup>2</sup> (ht) (kg/m<sup>2</sup>) ( $\leq 7.26$  kg/m<sup>2</sup> for men;  $\leq 5.45$  kg/m<sup>2</sup> for women) and gait speed (GS)  $\leq 0.8$  m/s or handgrip strength (HGS)  $< 30$ kg for men and  $< 20$ kg for women. 2) IWG: ALM/ht  $\leq 7.23$ kg/m<sup>2</sup> for men;  $\leq 5.67$ kg/m<sup>2</sup> for women) and GS  $< 1.0$  m/s. 3) FNIH: ALM/BMI  $< 0.789$  for men;  $< 0.512$  for women and HGS  $< 26$ kg for men and  $< 16$ kg for women.

**Results:** 661 patients with a recent clinical fx were evaluated (73% women; mean age  $66 \pm 0.4$  yrs), 70% with a minor, 24% with major, and 6% with hip fx. Osteoporosis was diagnosed in 27%, osteopenia in 51% and 22% had a normal BMD. Sarcopenia was present in 44 (7%) of patients according to at least one definition, with definition specific prevalence rates of 2% for FNIH, 3% for EWG and 5% for IWG. Prevalence rates of sarcopenia were comparable between men and women (EWG 3% women vs. 5% men, p=NS; IWG 5% vs. 6%, p=NS, FNIH 1% vs. 2%, p=NS). Prevalence of sarcopenia increased significantly with age according to the EWG and FNIH definitions (1% 50-59y to 10% 80+, p=.002 for both definitions). In patients with osteoporosis, the prevalence of sarcopenia defined according to EWG and IWG was significantly higher as compared to patients with a normal BMD (EWG 1% normal vs. 7% osteoporosis, p=.005; IWG 2% normal vs. 8% osteoporosis, p=.044). Prevalence rates of sarcopenia defined according to EWG and IWG were significantly higher in patients with hip fx as compared those with a minor or major fx (EWG 15% hip vs. 6% major vs. 1% minor, p=.000; IWG 22% hip vs. 7% major vs. 3% minor, p=.000).

**Conclusions:** Prevalence of sarcopenia according to at least one definition in patients with a recent clinical fx visiting the FLS was 7% but varied according to definition used. Prevalence of sarcopenia was highest in patients with a hip fracture, in patients aged 80 years and older, and in patients diagnosed with osteoporosis.

**Disclosures:** *Caroline E Wyers, None.*

## MO0334

**Cross-sectional and Longitudinal Associations Between Skeletal Muscle Mass and Vitamin D Status in a Homogeneous Cohort of 65-year Old Subjects.** Andrea Trombetti\*, Mélanie Hars, Thierry Chevalley, Emmanuel Biver, René Rizzoli, Serge Ferrari. Division of Bone Diseases, Department of Internal Medicine Specialties, Geneva University Hospitals & Faculty of Medicine, Switzerland

Sarcopenia and vitamin D deficiency are major risk factors for disability and falls. The relation between skeletal muscle mass and vitamin D status remains conflicting. Inconsistent results may be related to subjects' heterogeneity particularly with respect of age. In this study, we investigated the cross-sectional and longitudinal associations of skeletal muscle mass with both serum 25-hydroxyvitamin D (25(OH)D) and 1,25-dihydroxyvitamin D (1,25(OH)2D) levels in a large homogeneous cohort of 65-year old community-dwellers.

We studied 935 participants (79% women; mean  $\pm$  SD age,  $65 \pm 1$  years), who attended the Geneva Retirees Cohort (GERICO) for cross-sectional analysis, and 675 ( $3.0 \pm 0.5$  years) for longitudinal follow-up. Baseline 25(OH)D and 1,25(OH)2D were determined using Roche Diagnostics reagents and a chemiluminescence immunoassay (IDS), respectively. Body composition was assessed at baseline and at 3-year follow-up using DXA (Hologic Discovery W). Total and appendicular lean mass (ALM) were determined. Associations between skeletal muscle mass and 25(OH)D or 1,25(OH)2D were evaluated by univariate and multivariate regression analyses with adjustment for possible confounding factors, including age, fat mass, dietary protein intakes, physical activity, season and serum parathyroid hormone.

Baseline mean 25(OH)D was  $67 \pm 27$  nmol/L, with 3% and 29% of participants having 25(OH)D  $< 25$  nmol/L and  $< 50$  nmol/L, respectively. Total lean mass and ALM did not differ whether 25(OH)D level was normal or low ( $< 50$  nmol/L). The same held true when participants were classified as severely deficient ( $< 25$  nmol/L), insufficient (25-49.9 nmol/L), suboptimal (50.0-74.9 nmol/L) and sufficient (75 nmol/L). In multiple regression analysis, there was no

DXA and CT images from 10 adult FOP subjects (mean age: 29, 18-37 years) enrolled in a natural history study (NHS) at four global sites were acquired and compared using harmonized guidelines. CT images were acquired with coronal and sagittal scout views as well as 3-mm axial slices using a bone kernel (excluding head). DXA images were acquired with positioning according to the manufacturer's recommendations. One musculoskeletal radiologist (SES) performed all assessments that included the presence (yes/no) and severity (mild/moderate/severe) of HO in 15 anatomic locations. On CT, HO was also manually segmented to determine total HO volume. A committee comprised of musculoskeletal radiologists, FOP experts, and clinical trial specialists reviewed each image sequence, the HO data, and key characteristics of each modality (see table) within this sample to determine the optimal imaging method for assessing HO.

The amount and extent of HO was better visualized and quantified by CT than by DXA, allowing more accurate determination of change in HO over time. The major limiting factors of DXA are 2D image dimensionality, overlap of body regions due to fixed position, inability to differentiate HO from normotopic bone preventing quantitation of HO, and a higher percentage of subjects with non-evaluable regions due to pre-existing joint ankylosis. The major limiting factor of CT is radiation exposure, but revised acquisition parameters have since minimized exposure to an average of 4 mSv, similar to annual background levels. Based on these findings, low-dose, 3D, whole body CT (excluding head) was chosen to document changes in HO over a 3-year period in up to 100 FOP subjects enrolled in the NHS. The NHS will help formulate the design of future interventional trials for FOP.

**Acknowledgment:** the authors wish to thank the International FOP Association who fostered patient community participation in this study.

Characteristic	Low-Dose Whole Body CT	DXA
Estimated radiation exposure	median: 13.7 mSv (range: 3.4-28.6)	mean: 0.03 mSv
Image dimensionality	3D	2D
Presence and change in HO	Qualitative and quantitative (volume)	Qualitative (area measurement not possible due to insufficient sensitivity to differentiate normotopic from heterotopic bone)
HO severity assessment criteria	Mild/Moderate/Severe	Mild/Moderate/Severe
Quantitative total body burden of HO	Yes (total volume HO)	No
Number of body regions with HO	Yes	Yes
Non-evaluable regions	60% of subjects had at least one non-evaluable region mean number of non-evaluable regions: 1.2	90% of subjects had at least one non-evaluable region mean number of non-evaluable regions: 2.4
Average cost	\$659	\$250
Patient burden (eg, scan time, comfort, need for IV access)	Minimal	Minimal

Characteristics of Whole Body CT and DXA Imaging

**Disclosures:** *Donna R. Grogan, None.*

*This study received funding from: Clementia Pharmaceuticals Inc.*

## MO0332

**BODY COMPOSITION IN A HELTHY POPULATION OF CURITIBA, BRAZIL.** THAISA JONASSON\*, TATIANA LEMOS COSTA, CAROLINA MOREIRA, CESAR BOGUSZEWSKI, VICTORIA BORBA. Endocrine Division (SEMPR) - Federal University of Paraná, Brazil

**Introduction:** Changes in body composition (BC) are part of the aging process; among them are decreased muscle mass (MM) around 50% between 20 and 90 years, accompanied by increased body fat (BF) especially in the abdominal region. **Purpose:** The purpose of this study was to analyze age-related changes in BC in healthy individuals and correlate them to biochemical parameters, lifestyle habits, comorbidities and bone mineral density (BMD) Methods: healthy men and women between 18 and 90 years old were included, divided by age into 3 groups: 1- 18 and 29; 2- 30 to 59 years; 3- 60 years or more. All subjects collected blood for glucose, magnesium, vitamin D (25(OH)D), albumin, aspartate (AST) and alanine (ALT) transaminase, densitometry (DXA) for assessment of BC (lean mass (LM) and fat mass (FM) total and compartmental) and BMD of spine and femur, as well as, anthropometric measurements (weight, height, waist circumference). They answered questionnaires on socio-demographic data, daily habits and evaluation of physical activity ("International Physical Activity Questionnaire" - short IPAQ). **Results:** with aging and considering the average %FM of each group, there was an increase of 7% in overall FM and 4% reduction of LM in both genders. The total FM, trunk and android were lower in active men when compared to sedentary. On the contrary, the level of physical activity positively influenced the total and compartmental LM in men ( $p < 0.001$ ) and women ( $p < 0.005$ ) with lower loss in active individuals. Volunteers with diabetes, hypertension and / or DLP and calcium intake below the recommended daily amount, had higher android FM ( $p < 0.005$ ), the LM associations with comorbidities were not consistent. BMI was strongly correlated with the total FM in the trunk and android regions ( $R = 0.8$  and  $p < 0.001$ ) and in the lower limbs ( $R = 0.6$  and  $p < 0.001$ ) in both genders, but in women, there was also a correlation with the total LM ( $R = 0.3$  and  $p = 0.001$ ), in upper limb ( $R = 0.5$  and  $p < 0.001$ ) and trunk ( $R = 0.2$  and  $p = 0.003$ ). The total FM was higher in individuals with abnormal BMD in men ( $p < 0.003$ ) and women ( $p = 0.001$ ). Individuals with higher LM had less abnormal BMD. Multivariate analysis showed that age, BMI, abdominal circumference and gender affected the increment of total FM ( $p < 0.005$ ), when the level of physical activity (IPAQ) was included in the model, the age lost its importance in FM increment. **Conclusion:** Body fat increased with age, whereas lean mass decreased. Regular physical activity favored BC, with less FM and higher LM. Adequate calcium intake was also beneficial for BC, with less android fat. Android fat was higher in individuals with chronic diseases such as hypertension, diabetes and dyslipidemia. LM has a positive effect on bone mass, whereas FM tends to be associated with abnormal BMD.

**Disclosures:** *THAISA JONASSON, None.*

association between baseline lean mass or 3-year lean mass changes with baseline 25(OH)D or 1,25(OH)2D.

Our results obtained in a large cohort of healthy 65-year old community-dwellers, suggest that neither baseline nor changes in skeletal muscle mass are associated with 25(OH)D or 1,25(OH)2D levels in early old age.

**Disclosures:** Andrea Trombetti, None.

## MO0335

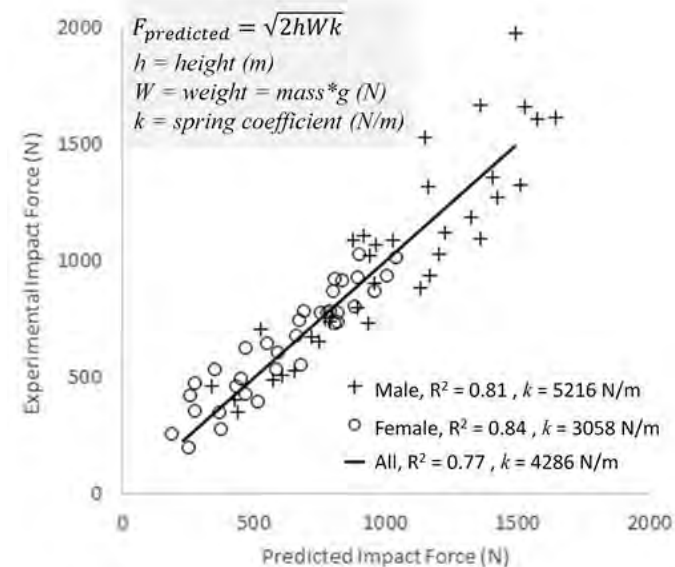
**Predicting impact force during a fall onto the outstretched hand using a single-spring-model.** James Johnston<sup>1</sup>, Chantal Kawalilak<sup>1</sup>, Joel Lanovaz<sup>2</sup>, Saija Kontulainen<sup>2</sup>. <sup>1</sup>Department of Mechanical Engineering, University of Saskatchewan, Canada, <sup>2</sup>College of Kinesiology, University of Saskatchewan, Canada

**Background/Purpose:** Bone fracture occurs when the applied force, usually due to impact from a fall, exceeds bone strength (factor-of-risk). Most predictions of impact force on the hand utilize viscosity-based approaches (i.e., damping models). A stiffness-based prediction model may improve predictions of impact force, but these models have not been yet validated. The purpose of this study was to validate a single-spring-model in predicting measured impact forces during an outstretched arm falling scenario from fall heights up to 25cm.

**Methods:** Using 3-dimensional motion tracking and an integrated force plate, impact forces and impact velocities were assessed from 10 young adults (5 males; 5 females), falling from planted knees onto outstretched arms, from a random order of drop heights: 3, 5, 7, 10, 15, 20, and 25cm. A single-spring-model, incorporating body weight, drop height plus the estimated linear stiffness of the arm (palm, wrist and upper arm), was used to predict impact force on the hand. We used linear regression and back-projection to estimate the linear stiffness coefficient. Specifically, the coefficient was adjusted in the single-spring-model until the regression slope and intercept between experimental and predicted impact force equaled 1 and 0, respectively. To test the validity of using a linear stiffness coefficient in the model, we assessed the linearity between experimental and predicted impact forces using an analysis of variance linearity test, with significance accepted at  $P < 0.05$ . To assess sex-specificity, we derived separate linear stiffness coefficients for males and females.

**Results:** The association between experimental and predicted impact forces was linear ( $P < 0.05$ ). Spring coefficients appeared sex-specific (males: 5216 N/m,  $R^2 = 0.81$ ; females: 3058 N/m;  $R^2 = 0.84$ ; sex combined: 4286 N/m,  $R^2 = 0.77$ ) (Figure).

**Conclusions:** A linear spring coefficient used in the single-spring-model proved valid for predicting impact forces from fall heights up to 25cm. Results suggest the use of sex-specific spring coefficients when estimating impact force using the single-spring-model. This stiffness-based model incorporating body weight is a valid alternative to viscosity-based approaches for predicting impact forces. This model may improve the impact force to bone strength ratios (factor-of-risk) and prediction of wrist fracture risk.



Experimental Impact Force vs Predicted Impact Force

**Disclosures:** James Johnston, None.

## MO0336

**The Association Between Muscle Mass Deficits Estimated from Bioelectrical Impedance Analysis and Bone Mineral Density in Adults.** Hee-Jeong Choi<sup>\*1</sup>, Hye-Yoen Jang<sup>1</sup>, Byeong-Yeon Yu<sup>2</sup>, Hyeok-Jung Kwon<sup>3</sup>. <sup>1</sup>Department of Family Medicine, Eulji University School of Medicine, Korea, republic of, <sup>2</sup>Department of Family Medicine, Konyang University School of Medicine, Korea, republic of, <sup>3</sup>Department of Family Medicine, Konkuk University School of Medicine, Korea, republic of

**Background:** Throughout life, bone mass is influenced by many factors that maximize bone mass during childhood and adolescence and delay or slow its loss during menopause and old age. Among many factors, body weight is an important determinant of BMD and low body weight is a known risk factor for osteoporosis. Muscle mass affects the body weight and may partially contribute to bone mass because bone functions with muscle as a musculoskeletal unit and adapts to the load and strain exerted by muscle. The aim of this study was to investigate the association between muscle mass deficits (MMD) estimated from bioelectrical impedance analysis (BIA) and bone mineral density (BMD) in men aged 20 to 49 and premenopausal women aged 20 or over.

**Methods:** This cross-sectional study includes 1,765 men and women who visited a health promotion center for a routine checkup. Lumbar spinal BMD was measured by dual-energy X-ray absorptiometry. Low bone mass was defined as Z-score equal to less than -2.0. The MMD was the difference between the actual amount of body lean mass and the standard body lean mass. The subjects were divided into three groups according to the tertile of MMD. Multivariate linear regression analysis was done to identify the major predictors of the BMD. Logistic regression analysis was used to estimate the odds ratios for low BMD in the muscle mass deficit groups.

**Results:** The mean age of the 1,000 men (56.7%) and 765 women (43.3%) were  $40.3 \pm 5.9$  years and  $40.0 \pm 6.6$  years, respectively. Seven percent of the subjects had low BMD. The mean BMD was  $1.200 \pm 0.135$  mg/cm<sup>2</sup> in group 1 (MDD=0 kg) and  $1.120 \pm 0.121$  mg/cm<sup>2</sup> in group 3 (MDD  $\geq 2.6$  kg) ( $P < 0.001$ ). MMD, body mass index (BMI), smoking, height, and sex were significantly associated with BMD. Altogether, these variables explain up to 10.3% of the variation in BMD value. The group 3 was associated with significantly increased odds for low BMD compared to the group 1 (OR = 2.75(95% CI, 1.45-5.12)) after adjustment for age, sex, BMI, height, smoking, muscle mass, 25(OH)D, alcohol drinking, exercise, and seasons.

**Conclusion:** This finding suggests that the evaluation and correction of the MMD in adults may be an important strategy in the prevention of osteoporosis.

**Disclosures:** Hee-Jeong Choi, None.

## MO0337

**Characteristics of Regional Bone Mineral Density and Soft Tissue Composition in Japanese Elderly Women with Sarcopenia and Sarcopenic Obesity.** Shinjiro Takata<sup>\*</sup>. Department of Orthopedics & Rehabilitation Medicine, Tokushima National Hospital, National Hospital Organization, Japan

Sarcopenia was proposed by Irwin Rosenberg to describe an age-related decrease of muscle mass (Am J Clin Nutr 1989; 59:1231-3). Baumgartner defined the combination of obesity and low muscle mass as sarcopenic obesity (Ann NY Acad Sci 2000; 904:437-448). The purpose of this study were to clarify the characteristics of regional bone mineral density (BMD) and soft tissue composition in Japanese elderly women with sarcopenia and sarcopenic obesity.

Two hundred and thirteen Japanese elderly women aged 65 years or more were divided into two groups, sarcopenia group (n=70) and control group (n=143). No significant differences were found between these two groups with regard to age, body height, body weight, and body mass index. In addition, these subjects were divided into two groups, sarcopenic obesity group (n=10) and non-sarcopenic obesity group (n=203). The L2-4BMD, total body BMD, and soft tissue composition were measured by DXA using Hologic Discovery W (Waltham, MA, USA). Regional BMD was measured in the head, arms, legs, ribs, thoracic vertebrae, lumbar vertebrae, and pelvis. Lean and fat mass of the head, arms, legs, and trunk were measured. Skeletal mass index (SMI) is the appendicular skeletal mass in kilograms measured divided by the square of the height in meters (kg/m<sup>2</sup>). SMI of the sarcopenia group was less than 5.4 (kg/m<sup>2</sup>). BMI and appendicular skeletal muscle mass percentage, (appendicular skeletal muscle mass / body weight)x100, of sarcopenic obesity group were  $>25$  (kg/m<sup>2</sup>) and  $<22\%$ , respectively.

The BMDs of the arms and legs as well as the L2-4BMD of the sarcopenia group were significantly lower than those of the control group ( $p < 0.05$ ). The lean masses of the arms, trunk, and legs of the sarcopenia group were significantly lower than those of the control group ( $p < 0.05$ ), whereas the fat masses of the arms and legs of the sarcopenia group were significantly greater than those of the control group ( $p < 0.05$ ). Fat masses of the arms, trunk and legs of the sarcopenic obesity group were significantly higher than those of the non-sarcopenic obesity group ( $p < 0.001$ ).

These results obtained in this study show that sarcopenia in Japanese women aged 65 years or more is associated with osteopenia or osteoporosis in addition to low muscle mass, and that sarcopenic obesity is associated with high fat mass.

**Disclosures:** Shinjiro Takata, None.

**MO0338**

**FNIH SARCOPENIA CRITERIA IN COPD PATIENTS HAD BETTER CORRELATION WITH GAIT SPEED COMPARED TO FOUR DIFFERENT METHODS.** TATIANA LEMOS COSTA<sup>1</sup>, FABIO MARCELO COSTA<sup>2</sup>, THAISA JONASSON<sup>1</sup>, CAROLINA MOREIRA<sup>1</sup>, LEDA RABELO<sup>3</sup>, CESAR BOGUSZEWSKI<sup>1</sup>, VICTORIA BORBA<sup>1</sup>.  
<sup>1</sup>Endocrine Division (SEMPR) - Federal University of Paraná, Brazil, <sup>2</sup>DIVISION OF PNEUMOLOGY- FEDERAL UNIVERSITY OF PARANA, Brazil, <sup>3</sup>DIVISION OF PNEUMOLOGY- FEDERAL UNIVERSITY OF PARANA, Brazil

**I**  
**Introduction:** Pre-sarcopenia (low lean mass) and sarcopenia (low lean mass and low strength or performance) is associated with reduced exercise capacity and poor quality of life in patients with COPD. Currently, several diagnosis methods of sarcopenia and pre-sarcopenia are used in the literature. **Purpose:** To evaluate the prevalence of pre-sarcopenia and sarcopenia between four different methods in COPD patients. **Methods:** A retrospective study with COPD patients. All individuals underwent a body composition by dual energy X-ray absorptiometry. The four diagnosis criteria of pre-sarcopenia analyzed were: the Baumgartner (Relative Skeletal Muscle Index/Height<sup>2</sup>); Newman's (linear regression model) that adjust for fat mass; Mixed - Baumgartner and Newman together based on the BMI (for low weight patients the first one and for the others Newman's model); FNIH method (Foundation for the National Institute of Health Sarcopenia Project) (Appendicular Lean Mass/BMI). The gait speed was tested to evaluate performance in a 6 minute test and considered altered were <0.8 m/s. **Results:** 121 patients (64 females) with a mean of 68.02 ± 8.47 years were evaluated. The prevalence of pre-sarcopenia using the Baumgartner method was 45 (37.2%), the Newman's model 24 (19.8%), the Mixed 44 (36.3%) and the FNIH 56 (46.3%). The median of gait speed (m/s) in pre-sarcopenic vs no pre-sarcopenic patients using the four different methods were: Baumgartner (0.93 vs 1.09, p=0.001); Newman's (0.97 vs 1.04, p=0.206); Mixed (0.96 vs 1.07, p=0.043); FNIH (0.96 vs 1.09, p=0.009). The prevalence of sarcopenia (low lean mass + gait speed <0.8 m/s) using the four different methods were: Baumgartner 12 (10.7%); Newman's 5 (4.95%); Mixed 11 (9.09%) and FNIH 15 (12.4%). **Conclusions:** Many different methods of sarcopenia and pre-sarcopenia are used in the literature. In our study with COPD patients the prevalence of pre-sarcopenia was higher in the FNIH method. The diagnosis of sarcopenia was most correlated with the performance using the Baumgartner and the FNIH criteria. In addition, the prevalence of sarcopenia was greater when used the FNIH criteria.

**Disclosures:** TATIANA LEMOS COSTA, None.

**MO0339**

**Relationship of vitamin D with skeletal muscle volume, muscle strength, and physical performance.** Akiko Kuwabara<sup>\*1</sup>, Naoko Tsugawa<sup>1</sup>, Misora Ao<sup>2</sup>, Hiroko Takaoka<sup>3</sup>, Kaoru Aoyama<sup>3</sup>, Tetsuo Nakano<sup>4</sup>, Kiyoshi Tanaka<sup>2</sup>.  
<sup>1</sup>Osaka Shoin Women's University, Japan, <sup>2</sup>Kyoto Women's University, Japan, <sup>3</sup>LifeIn Kyoto, Japan, <sup>4</sup>Tamana Central Hospital, Japan

**Objectives** Most of the non-vertebral fractures are caused by falling. Needless to say, muscle weakness is a risk for falling. Thus, both strong bone and muscle power are needed for fracture prevention. Recently, there has been an increasing concern on the role of vitamin D on muscle strength and physical activity. In this study, we have studied this theme in two study population; institutionalized elderly and middle-aged healthy adults.

**Subjects and Methods** Study subjects in Study 1 were 39 institutionalized elderly aged 82.3±6.3 years old. Subjects in Study 2 were 40 healthy volunteers aged 42.0±10.6 years old. In both studies, evaluation was made for lower leg muscle strength, dietary intake by food frequency questionnaire, and serum 25OHD concentration. In addition, body composition was measured by bioimpedance analysis in Study 1, and by DXA in Study 2. In the latter, skeletal muscle mass index (SMI) was calculated as skeletal muscle mass/squared height. Short physical performance battery (SPPB) test was performed in Study 1.

**Results [Study1]** Although vitamin D intake exceeded the adequate intake (AI) of 5.5microg/day in Dietary Reference Intakes (DRIs) for Japanese 2015 in 95% of the subjects, their serum 25OHD level was below 20ng/mL in 67% of them. In those with serum 25OHD level lower than 20ng/mL, muscle strength in the lower extremity and total score of SPPB was significantly lower. Serum 25OHD concentration was positively correlated with SMI, physical performance, and total score of SPPB. Multiple regression analysis has shown the positive contribution of serum 25OHD level to SPPB. **[Study2]** Although vitamin D intake exceeded the AI in 78% of the subjects, their serum 25OHD level was below 20ng/mL in 70% of them. Serum 25OHD concentration was positively correlated with vitamin D intake, SMI, and the muscle strength in lower extremity. Serum 25OHD level significantly contributed to the muscle strength in lower extremity in multiple regression analysis.

**Conclusion** Both in the elderly and younger adults, serum 25OHD concentration was correlated with muscle strength and physical performance. It was suggested that maintaining serum 25OHD level at least above 20ng/mL is recommended for the muscular health.

**Disclosures:** Akiko Kuwabara, None.

**MO0340**

**Clinical Feasibility of Oral Administration of Meclozine for the Treatment of Short Stature in Achondroplasia.** Masaki Matsushita<sup>\*1</sup>, Hiroshi Kitoh<sup>1</sup>, Kenichi Mishima<sup>1</sup>, Naoki Ishiguro<sup>1</sup>, Kinji Ohno<sup>2</sup>. <sup>1</sup>Department of Orthopaedic Surgery, Nagoya University Graduate School of Medicine, Japan, <sup>2</sup>Division of Neurogenetics, Center for Neurological Diseases & Cancer, Nagoya University Graduate School of Medicine, Japan

Achondroplasia (ACH) is one of the most common skeletal dysplasias characterized by disproportionate short stature. ACH is caused by gain-of-function mutations in the fibroblast growth factor receptor 3 (FGFR3) gene. By comprehensive screening of FDA-approved drugs, we identified that meclozine, an over-the-counter drug for motion sickness, promoted longitudinal bone growth in transgenic ACH mice by inhibiting FGFR3 signaling. In the present study, we investigated the optimal dose of meclozine for the treatment of short stature in ACH for further clinical feasibilities. We orally administered 2 or 20 mg/kg/day of meclozine to *Fgfr3*<sup>ach</sup> mice of postnatal day 7 for 10 days. Body lengths and body weight were measured during the administration periods. At the end of the treatment, the mice were subjected to micro-computed tomography (micro-CT) scans for calculating the bone length and bone volume. Plasma concentration of meclozine was serially measured by collecting blood samples from 8-week-old mice treated with a single oral dose of 2, 6, 20 mg/kg of meclozine for pharmacokinetics. Body lengths and body weight of *Fgfr3*<sup>ach</sup> mice were increased by oral administration of 2 mg/kg/day of meclozine. Micro-CT examinations demonstrated that total bone volumes of *Fgfr3*<sup>ach</sup> mice were significantly increased by 2 mg/kg/day of meclozine treatment compared to that of untreated *Fgfr3*<sup>ach</sup> mice. Individual bone lengths including the cranium, humerus, radius, ulna, femur, tibia, and vertebrae of *Fgfr3*<sup>ach</sup> mice treated with 2 mg/kg/day of meclozine were longer than those of untreated *Fgfr3*<sup>ach</sup> mice. Treatment of 20 mg/kg/day of meclozine, however, not only showed no positive effects on longitudinal bone growth of mutant mice but also exhibited growth impairment as seen in poor weight gain. Pharmacokinetics of 2 mg/kg of meclozine administered to mice was similar to that of 25 mg meclozine tablet used for motion sickness in human. These results indicated clinical feasibilities of meclozine for improvement of short stature in ACH. Further studies are needed to examine therapeutic effects on bone growth of lower dose of meclozine.

**Disclosures:** Masaki Matsushita, None.

**MO0341**

**Direct Effects of Nicotine Exposure on Murine Calvaria.** Emily Durham<sup>\*</sup>, R. Nicole Howie, Laurel Black, Graham Warren, Amanda LaRue, James Cray. MUSC, United states

Despite the link between adverse birth outcomes of pre- and perinatal nicotine exposure, research suggests 11% of US women continue to smoke or use alternative nicotine products through the third trimester of pregnancy. The Centers for Disease Control and Prevention has published data suggesting maternal smoking may cause or increase the severity of craniofacial anomalies. Since nicotine is a potent psychoactive drug, we hypothesized that it may alter craniofacial development related to maternal exposure. Primary murine calvaria suture derived cells were exposed *in vitro* to relevant active smoker (25ng/ml) and passive smoker(12.5ng/ml) circulating nicotine levels and then assessed after 7 days for proliferation (MTS) and differentiation (Alkaline Phosphatase/ALP) and 21 days for formation of a calcified matrix (Alizarin Red/AR). Adult wild type C57BL6 males and females were utilized to produce *in utero* nicotine exposed litters. Drinking water for pregnant dams was supplemented with 50 µg/ml or 100µg/ml Nicotine from ~E1 to birth of the litters at ~E20. Mouse pups were grown to 15 days postnatal when they were sacrificed and whole skulls underwent micro-computed tomography (µCT) and radiographic analysis. Exposing primary murine calvarial suture derived cells to relevant circulating nicotine levels resulted in a slight increase in proliferation as measured by MTS, and slight decrease differentiation as measured by ALP. Additionally, nicotine treatment caused a slight increase in mineralized matrix formation by 21 days (AR). 2D radiographic morphometric analysis of 15 day postnatal pups revealed that nicotine may be targeting alterations in growth at the middle cranial base of the developing murine skull. Additionally, we were able to identify a specific nicotinic receptor, nicotinic acetylcholine receptor alpha-7, within the calvarial sutures via immunohistochemistry *ex vivo*, and in cells by semi-quantitative PCR and Western Blot. Currently it is unclear what component of cigarette smoke is causative in birth defects, however these data indicate that nicotine alone is capable of disrupting growth and development of the murine calvaria. As nicotine crosses the placenta and concentrates in fetal tissue, new nicotine delivery technologies (i.e. e-cigarettes) have the potential to be the next public health crisis in birth defect research.

**Disclosures:** Emily Durham, None.

**MO0342**

**Epiphyseal versus Metaphyseal Trabecular Microarchitecture: Regional Ontogenetic Patterns in the Human Proximal Tibia.** Jesse Goliath<sup>1</sup>, James Gosman<sup>1</sup>, Zachariah Hubbell<sup>1</sup>, Timothy Ryan<sup>2</sup>. <sup>1</sup>Department of Anthropology, The Ohio State University, United states, <sup>2</sup>Department of Anthropology, Center for Quantitative Imaging, Pennsylvania State University, United states

The objective of this research is to test the hypothesis that the ontogenetic pattern of change in tibial trabecular microstructure is age and anatomical site-specific due to differential loading associated with changing joint kinematics and body mass. HR-QCT images were acquired for 31 human tibiae, ranging in age from 8 to 37.5 years. The skeletal samples are from Norris Farms No. 36 archaeological site, an Oneota Native American cemetery in central Illinois (A.D. 1300). Proximal metaphyses, defined as the region from 2 to 12% of total length distal to the subchondral bone, and proximal epiphyses were digitally isolated for analysis as regions of interest (ROIs) using Avizo Fire 6.2. 3D resolution-corrected morphometric analysis of trabecular bone structure was performed for 11 cubic volumes of interest (VOIs) using the BoneJ plugin for ImageJ. VOIs were positioned directly below tibial condyles within the epiphyseal and metaphyseal regions. Ontogenetic patterns in the metaphysis and epiphysis of the proximal tibia, were quantified using six 3D morphological parameters: bone volume fraction (BV/TV), mean trabecular thickness (Tb.Th), mean trabecular spacing (Tb.Sp), structure model index (SMI), connectivity density (Conn.D), and degree of anisotropy (DA). General linear model analysis was used to test the association between region, age, and each of six structural parameters. The findings of this study indicate that age-related changes in mechanical loading have heterogeneous effects on trabecular bone morphology within the proximal tibia. Specifically, there were significant differences in BV/TV, SMI, and DA ( $p < 0.01$ ) between epiphyseal and metaphyseal trabeculae. With age, trabecular microstructure is distinguished by higher values in BV/TV and Tb.Th ( $p < 0.01$ ) in the epiphysis, and thus suggests that the epiphysis tolerates higher loads than the metaphysis. Bone volume increase is a known response to greater loading in the growing skeleton. Ultimately, trabeculae in the epiphyseal region are likely more directly influenced by mechanical forces than trabeculae in the metaphyseal region during growth. The differential response of trabecular bone to changing mechanical loads during growth and development serves as a powerful tool to evaluate the significance of mechanical loading on adult trabecular bone morphology in health, disease, and bone senescence.

**Disclosures:** Jesse Goliath, None.

**MO0343**

**Nell-1 Deficiency in Cranial Neural Crest Cells Results in Microcephalic Phenotype.** Mengliu Yu<sup>1</sup>, Hsinchuan Pan<sup>2</sup>, Justine Tanjawa<sup>2</sup>, Chenshuang Li<sup>2</sup>, Shen Jia<sup>2</sup>, Eric Chen<sup>2</sup>, Xiaoyan Chen<sup>1</sup>, Huiming Wang<sup>3</sup>, Kang Ting<sup>2</sup>, Chia Soo<sup>4</sup>, Xinli Zhang<sup>5</sup>. <sup>1</sup>Section of Orthodontics, Division of Growth and Development School of Dentistry, University of California, Los Angeles; The Affiliated Stomatologic Hospital, Zhejiang University, United states, <sup>2</sup>Section of Orthodontics, Division of Growth and Development School of Dentistry, University of California, Los Angeles, United states, <sup>3</sup>The Affiliated Stomatologic Hospital, Zhejiang University, China, <sup>4</sup>Orthopaedic Hospital Research Center, University of California, Los Angeles, United states, <sup>5</sup>Section of Orthodontics, Division of Growth & Development School of Dentistry, University of California, Los Angeles, United states

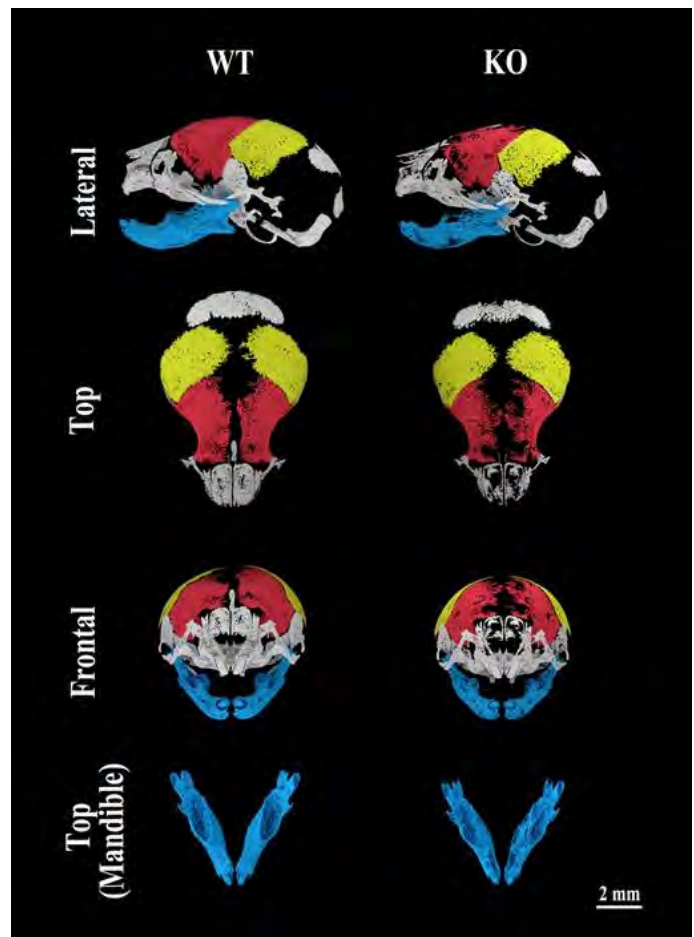
**Objective:** Nell-1 is a craniosynostosis associated molecule and an osteoinductive protein. The exact role of Nell-1 in development and osteochondrogenic differentiation of cranial neural crest (CNC) cells has not been fully understood due to the lack of a proper animal model. This study aims to create a CNC cell Nell-1 deficient model to evaluate Nell-1's role in pathogenesis of craniofacial anomalies.

**Method:** To investigate the specific effects of Nell-1 deficiency in CNC cells attributing to craniofacial anomalies, Nell-1<sup>flx/flx</sup> mice were mated with Wnt1-Cre mice to obtain Nell-1<sup>flx/flx</sup>;Wnt1-Cre mice for comprehensive analysis while Nell-1<sup>flx/flx</sup>;CMV-Cre mice were used as a control model of global loss of Nell-1. Gene expression profile was performed by qPCR. MicroCT, histology and immunohistochemistry (IHC) were used for phenotypic evaluation. Primary calvarial cells representing CNC cells from Nell-1<sup>flx/flx</sup> mice with or without Cre expression were used for cell proliferation, migration, invasion, adhesion and osteogenic differentiation assay.

**Result:** The majority of Nell-1<sup>flx/flx</sup>;Wnt1-Cre mice were born alive with craniofacial abnormalities manifesting from severe dysplasia of mandible and defects of eye sockets to reduction of skull dimension with calvaria defects (widen frontal suture) when compared to Cre-negative littermates. Neonatal lethality occurred only with severe cases in both Nell-1<sup>flx/flx</sup>;Wnt1-Cre and Nell-1<sup>flx/flx</sup>;CMV-Cre mice. Key osteochondrogenic markers (OCN, Col II, Col X) were deregulated in both mandibular and calvarial bones and Meckel cartilage in mutant mice. At the cellular level, the Nell-1-knockout calvarial cells exhibited decreased cell adhesion, migration, invasion and osteogenic differentiation capacity, but increased cell proliferation activity. With transduction of adenoviral CMV-Cre for Nell-1 knockout at different stages, the calvarial cells showed that the expression of Tnxb, Ocn and Col II was

significantly reduced in all differentiation stage, while expression of Runx2 remained the same compared to normal calvarial cells in early differentiation stage.

**Conclusion:** Nell-1 involves in development of mandible and calvaria by significantly affecting CNC cellular characteristics and activities, and lacking Nell-1 in CNC cells is likely a key factor responsible to microcephalic phenotype.



MicroCT image of WT and KO mouse pups

**Disclosures:** Xinli Zhang, None.

**MO0344**

**Perlecan/HSPG2: Novel Signaling Role in Early Chondrogenesis and Chondro-Osseous Boundary Formation.** Brian Grindel, Mary Farach-Carson, Jerahme Martinez<sup>\*</sup>. Rice University, United states

Perlecan/HSPG2, a large heparan sulfate proteoglycan (HSPG), is essential for the development and maintenance of musculoskeletal tissue including maintaining the distinct border between cartilage and bone. Perlecan is deposited within the avascular pericellular matrix (PCM) surrounding chondrocytes and turns over nearly completely at the chondro-osseous junction (COJ) of developing long bones. Destruction of perlecan at the COJ converts an avascular cartilage compartment into one that permits blood vessel infiltration, allowing osteogenesis to occur. A reduction in perlecan secretion is associated with chondrodysplasia with widespread musculoskeletal and joint defects, including the disruption of epiphyseal cartilage and bone. This work sought to elucidate novel signaling roles of perlecan in endochondral bone formation. To examine the functions of a highly conserved region of the core protein, purified recombinant perlecan subdomains were tested for bioactivity in a murine chondrogenic cell line, ATDC5, which served as a model for early chondrogenesis. These findings showed a region within domain IV of perlecan (PLN IV-3) that has anti-adhesive properties, promotes cell-cell adhesion, and strongly promotes rapid chondrocyte cell clustering. These properties were lost when a mutation (R3452Q), associated with the human skeletal disorder Schwartz-Jampel Syndrome (SJS), was introduced into the perlecan sequence. PLN IV-3 activity was enhanced when thermally unfolded, likely attributed to increased exposure of the active site. PLN IV-3-induced cell-substratum detachment was accompanied by deactivation of key components of the focal adhesion complex, FAK and SRC. PLN IV-3 suppression of FAK/SRC activity increased pre-cartilage condensation markers SOX9 and N-cadherin, and also increased cartilage PCM components collagen II and aggrecan. Furthermore, PLN IV-3 reduced signaling through the ERK pathway, where loss of ERK1/2 phosphorylation coincided with reduced FoxM1 protein levels and an increase in transcriptional of cell cycle inhibitors CDKN1C and ATF3. This,

in turn, reduced ATDC5 cell proliferation. Together, these findings support the notion that perlecan domain IV is a key force triggering chondrocyte condensation in the developing growth plate, and that loss of such signaling accompanies SJS chondrodysplasias with associated loss of normal COJ boundaries.

**Disclosures:** *Jerahme Martinez, None.*

## MO0345

**Phosphate Deficiency Leads to a Phase Shift in Circadian Oscillation During Fracture Healing.** Takashi Noguchi\*, Amira Hussein, Nina Horowitz, Deven Carroll, Louis Gerstenfeld. Department of Orthopedic Surgery, School of Medicine, Boston University, United states

**Introduction:** Clock genes play a central role in regulating many biologic functions and are associated with several metabolic diseases. Transcriptomic data from fracture calluses showed that Per 2 and Per 3 were among the top genes affected by phosphate (Pi) deficiency. The goal of this study was to identify if Pi deficiency changed circadian function during fracture healing.

**Method:** Fractures were generated in the right femurs of male C57BL/6J (8 to 10 weeks of age) mice. Controls were fed normal diet while the Pi group was fed Pi deficient diet beginning 2 days prior to the surgery and until euthanasia. The mice were under 12h/12h light/dark cycle and randomly divided into control and (Pi) groups. At post-operative day 10, multiple tissues (callus, heart, proximal tibia with growth plate) were harvested every 3 hours from each mouse (8 time point, n=3 per time point/group). Following total RNA extraction from the callus tissues RT-qPCR was conducted. The central clock associated genes (Per1, Per2, Per3, Bmal1, Cry1) and multiple genes that control progression of chondrocyte maturation including PTHrP were assayed. Mice containing the Per2 promoter driving firefly Luciferin gene were used to functionally assess circadian rhythm. In these studies (n=3 mice) were used and 10 day callus tissue were isolated at 2 hours prior to the initiation of the light cycle and then cultured ex vivo for a 30 hour period measuring Luciferin activity every 3 hours. Outcomes were compared between diet and among time point using two-factor ANOVA.

**Results:** Significant differences in the oscillation patterns of the clock genes were observed. The relative expressions of the clock genes were markedly higher in the callus of the Pi group compared to the Control group ( $p < 0.001$ ). Further, a phase shift was observed where the Pi group had a shift advance from 3 to 9 hours compared to control group in gene expression. The expression of PTHrP in the callus was significant lower in Pi due to effect of diet ( $p < 0.05$ ). (Figure1).

**Discussion:** These results show that phosphate deficiency induced a systemic phase shift in peripheral tissue circadian rhythm. Other studies have reported on the effects of PTH on circadian rhythm of the growth plate and callus. These results both suggest a role of clock genes in regulating the progression of endochondral bone formation as well as in the upstream temporal mechanism by which the negative PTHrP /Ihh feedback loop is controlled.

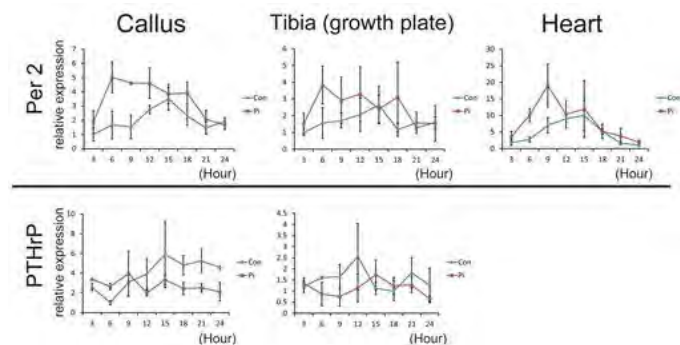


Figure 1. The expression of Per 2 and PTHrP in all types of the tissue.

**Disclosures:** *Takashi Noguchi, None.*

## LB-MO0346

**Both TBS and volumetric BMD are associated with pedicle screw pull-out strength: an ex-vivo feasibility study.** R Winzenrieth\*<sup>1</sup>, J Choise<sup>2</sup>, J-M Valiadis<sup>2</sup>, P Le Nost<sup>1</sup>, S Kolta<sup>3</sup>, C Lelong<sup>4</sup>, W Skalli<sup>2</sup>. <sup>1</sup>R&D department, Medimaps, France, <sup>2</sup>Institut de Biomecanique Humaine Georges Charpak, Arts et Metiers ParisTech, France, <sup>3</sup>CEMO, Cochin Hospital, AP-HP, France, <sup>4</sup>Medimaps, France

**Rational:** The aim of this study was to evaluate the ex-vivo relationship between TBS, computed from DXA acquisitions, and the pull-out strength of pedicle screws in human fresh vertebra.

**Method:** 26 human fresh vertebrae (T12, L4 and L5) were selected from 10 donors (mean age 81.8 yrs) by residents in the Institut de Biomécanique Humaine (Paris, France). Image acquisitions were performed the day of the surgery using a standardized protocol on a DXA device (QDR 4500A, Hologic, Bedford, U.S.A.). During the DXA scan acquisition, the vertebrae were inserted into water in order to

simulate the soft tissues around the bone. Cylindrical pedicle screws with a trapezoidal thread shape were implanted by a single surgeon. Biomechanical testing was performed on the vertebra in order to measure the pull-out strength of the pedicle screw. Bone texture was evaluated using TBS (TBS iNspire, Medimaps, Merignac, France). TBS was computed into the same ROI used to assess BMD from DXA acquisition.

To take into account vertebral morphology variability a pseudo 3D BMD (3D BMDa) was computed based on a cylindrical approach. Relationships between TBS and the pull-out strength were evaluated using a Pearson correlation test. A bootstrap approach on the vertebrae (20 random sampling) was done in order to evaluate the variability of the possible associations. A multivariate analysis, that includes DXA TBS and 3D BMDa, has also been performed.

**Results:** Mean TBS, 3D BMDa and pull-out strength were  $1.213 \pm 0.126$ ,  $0.181 \pm 0.04 \text{ g/cm}^3$  and  $473 \pm 419 \text{ N}$  respectively. A good and significant correlation (see figure 1) has been observed between TBS and the pull-out strength ( $r=0.63$  -  $r^2=0.397$ ;  $p=0.0005$ ) while a strong correlation was observed for 3D BMDa ( $r=0.71$ ;  $p<0.0001$ ). Bootstrap approach demonstrated the stability of the TBS association ( $r^2=0.39$  [0.33-0.46]). In multivariate analysis, both TBS and 3D BMDa remained significantly associated with the pull-out-strength ( $p=0.034$ ,  $r=0.43$  and  $p=0.003$ ,  $r=0.57$ , respectively). The combined model explained 56.2% ( $r^2$ -adjusted) of the pull-out-strength.

**Conclusion:** The present study demonstrated an independent association between TBS and the pull-out strength of the pedicle screws. After adjustment for 3D BMDa, TBS still explained 18.5% of the pull-out-strength. These results are consistent with those in the literature. Further ex-vivo studies are needed to confirm these findings in a larger sample size.

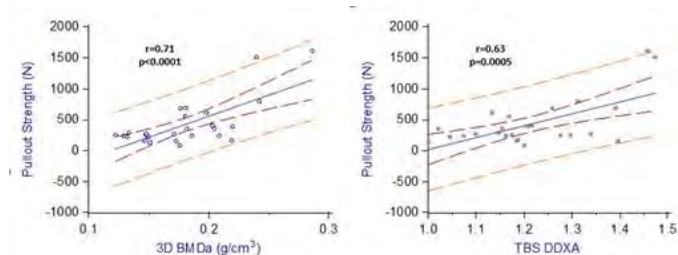


Figure 1 - Relationship between TBS, 3D BMDa and the pull-out strength

Figure 1 - Relationship between TBS, 3D BMDa and the pull-out strength

**Disclosures:** *R Winzenrieth, Medimaps, 15*

## LB-MO0347

**Hematopoietic Stem Cell-derived Osteoblasts Enhance Tumorigenicity in the Osteosarcoma Microenvironment.** Uday Baliga\*, Inhong Kang, Ying Xiong, Shilpak Chatterjee, Meenal Mehrotra. Medical University of South Carolina, United states

Osteosarcoma (OS) is the most common primary malignant bone sarcoma but mechanisms underlying progression remain elusive. Recently, tumor-promoting role for cells of microenvironment, especially fibroblasts, have been described. In case of OS, non-malignant osteoblasts (Obs) may also contribute, however this is unclear. Here we demonstrate, for the first time to our knowledge, that conditioned media (CM) from Obs from long bones (LB) of mice, significantly increases proliferation, migration and invasion of OS cell lines (MOS/J and K7M2), indicating a role of these Obs in progression of OS. While it is widely believed that mesenchymal stromal cells (MSC) are a source for Obs, we have previously reported that hematopoietic stem cells (HSC) can also give rise to Obs. Further, in order to establish relative contribution of Obs in OS, we used a unique transgenic model in which HSC-derived cells are GFP<sup>+</sup> while MSC-derived ones are RFP<sup>+</sup>. Using this model we re-established presence of HSC-derived Obs in LB of mice, which expressed osteogenic markers (RUNX-2, bone sialoprotein, ALP, BMP-2, osteocalcin) and had the ability to mineralize (alizarin red staining). Importantly, we also noticed that there was a greater increase in proliferation, migration and invasion of OS cells when treated with the CM from HSC-derived Obs as compared to CM from MSC-derived Obs. Co-culture experiments also established a greater increase in migration and invasion of OS cells in the presence of HSC-derived Obs. Additionally, priming OS cells with CM from HSC- and MSC-derived Obs for 7 days also resulted in enhanced proliferation, migration and invasion in OS cells that were treated with HSC-derived Obs CM. *In vivo* injections for lung metastases indicated a larger number of metastatic nodules when OS cells were co-injected with HSC-derived Obs as compared to OS cells alone or those co-injected with MSC-derived Obs. Lastly, an analysis of the cytokines and chemokines demonstrated that many of the pro-inflammatory factors such as IL-1a, TNF, NF-kb, VEGF, CCL2, CCL3, CCL4, CXCL12 and CXCL16 were also upregulated in HSC-derived Obs as compared to the MSC-derived Obs. Thus, we conclude that a HSC-derived Obs population in LB of mice has the potential to contribute towards the OS microenvironment leading to enhanced tumorigenesis than that observed by MSC-derived Obs. Thus, targeting these cells in the microenvironment might prove to be more useful in arresting OS.

**Disclosures:** *Uday Baliga, None.*

## LB-MO0348

**Type 2 Diabetes Impairs Insulin-Stimulated Bone Blood Flow and Compromises Bone Biomechanical Properties in Hyperphagic OLETF Rats.** Pam Hinton\*, Laura Ortinau, Rebecca Dirkes, Matthew Richard, R. Scott Rector, T. Dylan Oliver. University of Missouri, United states

Type 2 diabetes (T2D) increases skeletal fragility and fracture risk; however, the underlying mechanisms remain to be identified. One potential, yet unexplored, mechanism is impaired bone vascular function, in particular, insulin-stimulated vasodilation. The purpose of this study was to determine the effects of T2D on bone insulin-stimulated vasodilation and biomechanical properties by comparison of hyperphagic Otsuka Long-Evans Tokushima Fatty (OLETF) rats with normoglycemic control OLETF rats. Four-week old, male OLETF rats were randomized to either T2D or CON: T2D were allowed ad lib access to a chow diet and CON were fed 70% of T2D intake until sacrifice at 40 weeks of age. Femoral cortical geometry and trabecular microarchitecture were analyzed using mCT. Cortical biomechanical properties were analyzed by torsional loading to failure. Blood flow to the tibial proximal epiphysis, distal epiphysis and marrow was measured before and during a euglycemic hyperinsulinemic clamp via infusion of microspheres. The effects of T2D on insulin-stimulated blood flow were evaluated using a RMANOVA; differences between T2D and CON in other bone outcomes were determined using a one-way ANCOVA; body weight (BW) was included as a covariate for body-size-dependent outcomes. As expected, the hyperphagic T2D rats had significantly greater BW than CON. Blood glucose and insulin confirmed that T2D rats were hyperglycemic and hypoinsulinemic due to  $\beta$ -cell dysfunction, while CON were normo-glycemic and -insulinemic. Basal tibial blood flow was similar in T2D and CON, but the blood flow response to insulin stimulation was greater in CON than T2D in the proximal epiphysis and diaphyseal marrow. Femoral geometry, microarchitecture, and biomechanical properties differed between T2D and CON. Total cross-sectional area, cortical area Ct.Ar/Tt.Ar and polar moment of inertia were greater in T2D rats versus CON. Whole-bone biomechanical properties did not differ between T2D and CON, but tissue-level strength and stiffness were reduced in T2D relative to CON. T2D had greater trabecular spacing and reduced percent bone volume and connectivity density compared with CON. In summary, impaired insulin-stimulated bone blood flow is associated with deleterious changes in bone trabecular microarchitecture and cortical biomechanical properties in T2D OLETF rats. The results of this study suggest that vascular dysfunction might play a causal role in diabetic bone fragility.

Disclosures: Pam Hinton, None.

## LB-MO0349

**Androgens Enhance the Adverse Metabolic Effects of Glucocorticoids.** Sylvia Gasparini<sup>1</sup>, Lee J. Thai<sup>2</sup>, Marie C. Weber<sup>3</sup>, Holger Henneicke<sup>2</sup>, Sarah Kim<sup>2</sup>, Hong Zhou<sup>2</sup>, Markus J. Seibel<sup>4</sup>. <sup>1</sup>The University of Sydney, Australia, <sup>2</sup>ANZAC Research Institute, Australia, <sup>3</sup>A, Australia, <sup>4</sup>University of Sydney, Australia

Glucocorticoid excess is clinically associated with adverse metabolic effects such as central obesity, insulin resistance, hypertension and hyperlipidemia. This often limits their therapeutic use and thus a greater understanding of the mechanisms underlying the pathophysiology of these side effects is paramount. As male rodents have been shown to respond more robustly to the anti-inflammatory effects of glucocorticoids, we aimed to determine whether there are also sex differences in the metabolic response to exogenously administered glucocorticoids.

Eight week-old CD1 mice were treated with vehicle or 50  $\mu$ g/ml corticosterone (CS) in the drinking water for 4 weeks, at which point insulin tolerance (by ITT) and body composition (by DXA) were assessed in intact, castrated and DHT-replaced male and female mice with or without CS treatment.

Intact male mice rapidly developed severe insulin resistance (fig. 1A) and increased adiposity as a result of CS treatment (fig. 1B) (fat mass males: vehicle +3% vs. CS +42%,  $p < 0.001$ ). In contrast, both intact and ovariectomized females maintained normal insulin sensitivity and body composition despite CS treatment, indicating that the gender difference in metabolic CS-sensitivity is not due to a protective effect of estrogens. When male mice were orchidectomized (ORC), treatment with CS no longer resulted in insulin resistance or abnormal fat accrual. To assess if the resilience of both females and ORC males to the metabolic effects of CS was due to a lack of androgens we implanted ORC males and OVX female mice with the minimally aromatizable androgen, dihydrotestosterone (DHT). While DHT alone had no effect on fat or insulin sensitivity in either gender, co-treatment with DHT and CS rendered both ORC-males and OVX-females severely insulin resistant and caused significant fat accrual (fat mass OVX-females + DHT: vehicle +37% vs. CS +94%  $p < 0.05$ ; ORC-males + DHT: vehicle +21% vs. CS +98%  $p < 0.001$ ).

In conclusion, mice demonstrate a strong dichotomy in their metabolic response to excess glucocorticoids, with males being more sensitive than females. Our data indicate that androgens potentiate the adverse metabolic side effects of excess glucocorticoids.

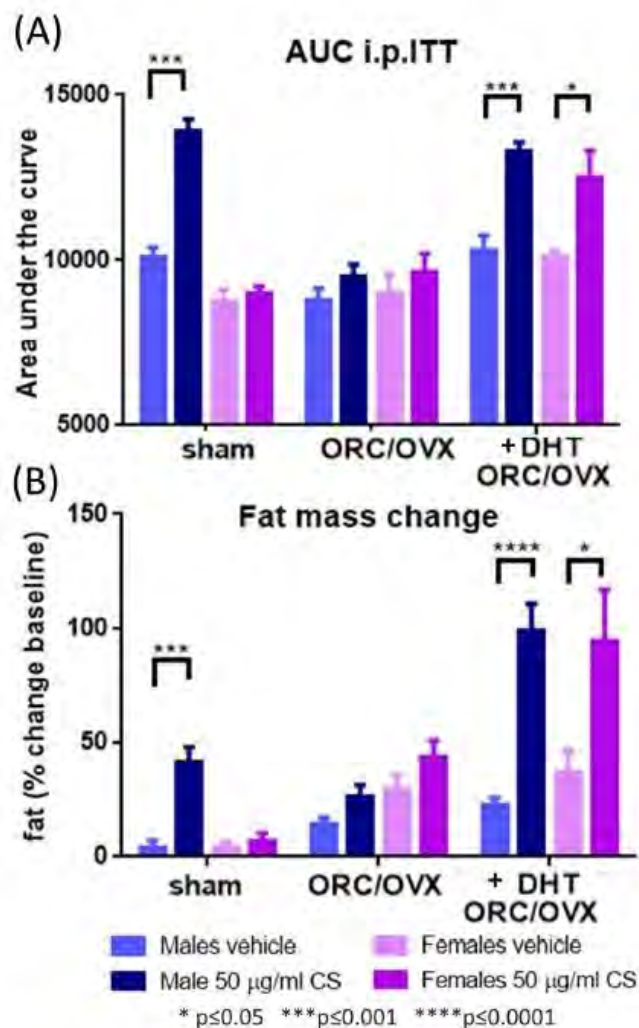


Figure 1

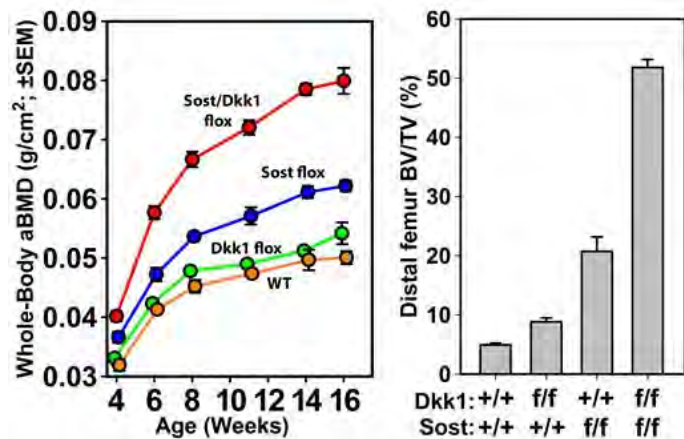
Disclosures: Markus J. Seibel, None.

## LB-MO0350

**Genetic disruption of compensatory Wnt inhibitor expression reveals a context-dependent, highly osteo-anabolic role for Dkk1 inhibition in the skeleton.** Phillip C. Witcher<sup>1</sup>, Alison L. Adaniya<sup>1</sup>, Emily N. Adaniya<sup>1</sup>, Gabriela G. Loots<sup>2</sup>, Alexander G. Robling<sup>1</sup>. <sup>1</sup>Indiana University School of Medicine, United states, <sup>2</sup>Lawrence Livermore National Laboratory, United states

The Wnt pathway is an obvious target for skeletal therapies, in light of the high-bone-mass phenotypes in patients with gain-of-function mutations in the Wnt co-receptors Lrp5 and Lrp4 or loss-of-function mutations in the Lrp5/6 inhibitor Sost. Inhibition/deletion of individual Wnt inhibitors causes significant changes in the expression of a subset of other Wnt inhibitors. This compensatory regulation likely functions to re-establish normal bone homeostasis when one or more Wnt inhibitors are disabled. The Wnt inhibitor "compensatory milieu" theory explains why some otherwise potentially anabolic therapies like Dkk1 neutralizing antibody have very mild anabolic effects *in vivo* (e.g., Dkk1 inhibition causes Sost upregulation, and vice-versa). We sought to determine whether we could unlock a fuller anabolic potential of Wnt inhibitor suppression by genetically targeting the compensatory upregulation of accessory Wnt inhibitors. Male and female homozygous Dkk1-flox (loxP flanking exons 1-2), Sost-flox (COIN module in intron 1), dual flox (Dkk1/f; Sost/f), and WT mice were generated with and without the 10kbDmp1-Cre transgene. DXA scans were collected every 2-3 wks, beginning at 4 wks of age until the mice reached 16 wks, at which point they were sacrificed. MicroCT measurements of the distal femur cancellous and midshaft cortical regions were conducted, as were histomorphometric measurements. Bone-selective mutation of Dkk1 in female mice increased whole body bone mineral density (wbBMD) by 4-8% over WT controls, depending on the time point considered. Bone-selective Sost mutation increased wbBMD by 14-24% over WT controls, whereas dual deletion increased wbBMD by 26-60% over WT

controls (Fig. 1). Similar results were found for male mice (3-9% increase among Dkk1 flox, 16-26% increase among Sost flox, and 27-65% increase among dual flox mice). Distal femur trabecular bone followed similar trends: compared to WT females, BV/TV was increased by 4% among Dkk1-flox females, by 16% among Sost flox females, and by 47% among dual flox females (Fig. 2). It has long been perplexing why antagonism of Dkk1—a potent inhibitor of Wnt/Lrp5 signaling *in vitro*, is ineffective at increasing bone mass *in vivo*. We found a synergistic effect of dual Sost/Dkk1 deletion that was far beyond additive effects; whereas bone-selective Dkk1 deletion alone has negligible effects on bone mass, Dkk1 deletion on a Sost-deficient background has potent skeletal effects.



Figures

Disclosures: Alexander G. Robling, None.

## LB-MO0351

**Prediction of Putative Causal Variants and Genes at BMD GWAS Loci.** Basel Al-Barghouti<sup>1\*</sup>, Charles Farber<sup>2</sup>. <sup>1</sup>Center for Public Health Genomics & Department of Biochemistry & Molecular Genetics, School of Medicine, University of Virginia, United States, <sup>2</sup>Center for Public Health Genomics & Departments of Public Health Sciences & Biochemistry & Molecular Genetics, School of Medicine, University of Virginia, United States

Osteoporosis is characterized by decreased bone mineral density (BMD), a deterioration of bone microstructure and an increased risk of fracture. Osteoporosis is, in large part, influenced by genetic variation and, in recent years, genome-wide association studies (GWASs) have revolutionized its genetic analysis by identifying >60 loci influencing BMD. The challenge now is to identify the causal genes and variants responsible for these associations. Here, we investigated 63 BMD GWAS loci identified by the Genetic Factors for Osteoporosis (GEFOS) consortium in ~80K individuals. Across the 63 loci, we identified 2491 “proxy” variants in strong ( $r^2 > 0.8$ ) linkage disequilibrium with the most significant variant at each locus. Most (~98%) of proxies were noncoding and located in intergenic (~49%) or intronic (43%) regions. Sixteen proxies were nonsynonymous coding variants, but only one was predicted to impact protein function. These data suggest that variants impacting gene regulation are the primary drivers of BMD associations. In order to prioritize potential causal variants, we utilized Roadmap Epigenomics data to identify BMD proxies located within active transcriptional regulatory elements in 127 tissues/cell-lines. Of the total, 795 proxy variants overlapped regulatory elements in at least one of 127 epigenomes, and in primary osteoblasts, 240 proxies overlapped regulatory elements. Since we expect causal variants affecting BMD to do so via modulation of gene expression, we utilized Genotype Tissue Expression Project (GTEx) expression quantitative trait loci (eQTL) data to perform a Bayesian test for the colocalization of eQTL with BMD associations. This analysis identified 33 genes regulated by eQTL that colocalized with BMD associations. To illustrate how these data can be used to inform GWAS, we identified a locus on chromosome 11, containing 14 variants associated with BMD, 7 of which overlapped active regulatory elements. The eQTL analysis identified four genes with colocalizing eQTL, one of which, *ARHGAP1*, encodes for a Rho-GTPase activator that has been shown to be involved in the regulation of BMD in mice. Through the integration of epigenetic and eQTL data, we have generated a refined list of potentially causal variants and predicted causal genes for a large number of BMD GWAS loci.

Disclosures: Basel Al-Barghouti, None.

## LB-MO0352

**Feeding After Overnight Fast Enhances Bone's Response To Mechanical Loading In Mice.** Hasmik J Samvelyan<sup>1\*</sup>, John C Mathers<sup>2</sup>, Tim M Skerry<sup>1</sup>. <sup>1</sup>The Mellanby Centre for Bone Research, The MRC-Arthritis Research UK Centre for Integrated Research Into Musculoskeletal Ageing, Department of Oncology & Metabolism, The University of Sheffield, UK, United Kingdom, <sup>2</sup>Human Nutrition Research Centre, Institute of Cellular Medicine, Newcastle University, UK, United Kingdom

Concentrations of gastro-entero-pancreatic hormones change in fasting and fed states and many have potent regulatory effects on bone. We hypothesise that effect of exercise on bones depends on concentrations of these hormones and therefore both timing of eating and nature of ingested food. To test this hypothesis we performed experiments to determine osteogenic effects of mechanical loading that mimics exercise after different periods of withholding food or feeding, where we expect altered concentrations of gut-derived hormones, using a mouse model. Groups of 17-week-old C57BL/6 male mice (n=7) were either fasted overnight (16hrs) or allowed free access to food. Fasted mice were then given access to food for 1hr, 2hrs or 3hrs. All mice then underwent axial loading of the right tibiae with a peak force of 13N, 3 times weekly for 2 weeks (40 cycles of loading with 9sec rest periods between each). Left tibiae were non-loaded controls in each animal. Fluorochrome labels were injected at the start and end of experiments. Response of bones to loading was determined by micro-computed tomography and dynamic histomorphometry. Loading caused significant adaptive responses in loaded right tibiae of all mice. However the change in cortical thickness induced by loading was 36% greater in animals that were fasted then fed for 2hrs than in loaded bones of animals fed ad-lib before loading (fasted fed loaded:  $0.049 \pm 0.007$ mm vs ad-lib fed loaded:  $0.036 \pm 0.004$ mm,  $p < 0.05$ ). Preliminary analysis of total BFR/BS and MAR of the tibiae of fasted then 2hrs fed mice was consistent with the microCT analysis (BFR/BS fasted fed loaded:  $3.45 \pm 1.22 \mu\text{m}^3/\mu\text{m}^2/\text{d}$  vs non-loaded control:  $0.06 \pm 0.03 \mu\text{m}^3/\mu\text{m}^2/\text{d}$ ,  $p < 0.05$ ; MAR  $3.58 \pm 1.79 \mu\text{m}/\text{d}$  vs  $0.07 \pm 0.06 \mu\text{m}/\text{d}$ ,  $p < 0.05$ ) compared with tibiae of ad-lib fed mice (BFR/BS loaded:  $0.99 \pm 0.14 \mu\text{m}^3/\mu\text{m}^2/\text{d}$  vs control:  $0.22 \pm 0.16 \mu\text{m}^3/\mu\text{m}^2/\text{d}$ ,  $p < 0.05$ ; MAR  $1.59 \pm 0.83 \mu\text{m}/\text{d}$  vs  $0.25 \pm 0.15 \mu\text{m}/\text{d}$ ,  $p < 0.05$ ). Loading after 1hr or 3hrs following overnight fast increased cortical bone thickness, but not differently from ad-lib fed mice. Food ingestion for 2hrs after overnight fasting potentiated bone's osteogenic response to mechanical loading in mice, indicating interactions between the timing of food ingestion and bone adaptation. These findings have potential for translation into benefits for people by providing information on when to exercise in relation to meals, which may help to build and maintain healthy musculoskeletal system throughout lifecycle including in older age.

Disclosures: Hasmik J Samvelyan, None.

## LB-MO0353

**CyclinD1 regulates the balance between the osteogenic and chondrogenic differentiation of mesenchymal cells that constitutively express Nanog.** Toru Ogasawara<sup>\*</sup>, Jun-pei Imamura, Yasuyuki Fujii. The University of Tokyo, Japan

The roles of cell-cycle control factors and transcription factors in the maintenance of stem cell pluripotency or multipotency are important, but the details of these roles have not been determined. We previously reported that the transcription factor Nanog, which maintains the self-renewal of embryonic stem (ES) cells, promotes the osteogenic differentiation of mouse mesenchymal cell line C3H10T1/2 cells through a genome reprogramming process via the upregulation of NFATc1, Runx1 and Runx3. We also reported that Cdk6, which is one of the G1 cell-cycle control factors, is important in osteoblast, osteoclast and chondrocyte differentiation. In the present study, to clarify the mechanism underlying the multipotency of mesenchymal stem cells, we reevaluated the role of Nanog in the differentiation of mesenchymal cells, focusing on the G1 cell-cycle regulation. We first examined the chondrogenic, adipogenic and myogenic differentiation of C3H10T1/2 cells that constitutively express Nanog. Real-time quantitative RT-PCR analyses revealed that there were significant upregulations of chondrogenic markers in these Nanog-expressing cells compared to the level in the control green fluorescent protein (GFP)-expressing cells. The expression levels of PPARgamma and Myogenin were not much affected by forced-Nanog expression. We next reanalyzed a DNA microarray analysis performed between the GFP-expressing cells and Nanog-expressing cells cultured with rhBMP-2. Among these genes, we focused on the G1 cell-cycle factors and selected CyclinD1, CyclinD2, p18 and p19 in consideration of the log<sub>2</sub> Ratio (CyclinD1: -2.45, CyclinD2: 1.49, p18: -1.06, p19: -1.33). Real-time quantitative RT-PCR analyses confirmed that there was a dramatic decrease of CyclinD1 in the Nanog-expressing cells compared to the levels in the GFP-expressing cells. Western blot analyses also revealed that the CyclinD1 expression was downregulated, whereas that of Runx3 was upregulated in the Nanog-expressing cells. The luciferase activity of the TOPflash was inhibited in the Nanog-expressing cells, suggesting that a suppression of the canonical Wnt signaling pathway by an upregulation of Runx3 leads to a decrease of CyclinD1 in Nanog-expressing cells. To further examine the involvement of CyclinD1 in the Nanog's role, we transfected CyclinD1 into C3H10T1/2 cells that constitutively express Nanog. Real-time quantitative RT-PCR analyses revealed that the expression levels of type II and type X collagen mRNA were inhibited and that those of Runx2 and Osterix were enhanced. These results suggest that CyclinD1 controls the balance between the osteogenic and chondrogenic differentiation of C3H10T1/2 cells constitutively expressing Nanog.

Disclosures: Toru Ogasawara, None.

## LB-MO0354

**Knee Osteoarthritis and Risk of Fall Injuries among Older Adults: the Health ABC Study.** Kamil Barbour<sup>1</sup>, Robert Boudreau<sup>2</sup>, Naoko Sagawa<sup>2</sup>, Jane Cauley<sup>2</sup>, Michael Nevitt<sup>3</sup>, Tomoko Fujii<sup>2</sup>, Kushang Patel<sup>4</sup>, Elsa Strotmeyer<sup>5</sup>. <sup>1</sup>Arthritis Program, Division of Population Health, NCCDPHP, CDC, United states, <sup>2</sup>Department of Epidemiology, University of Pittsburgh, Pittsburgh, PA, USA, United states, <sup>3</sup>University of California, San Francisco, CA, USA, United states, <sup>4</sup>Center for Pain Research on Impact, Measurement, & Effectiveness, Department of Anesthesiology, & Pain Medicine, University of Washington, Seattle, USA., United states, <sup>5</sup>Department of Epidemiology, University of Pittsburgh, Pittsburgh, PA, USA, United states

Background: Falls are the leading cause of injury-related morbidity and mortality in older adults. To our knowledge no studies have examined the association between knee osteoarthritis (OA) and fall injuries.

Methods: Using data from the Health ABC Knee Osteoarthritis Substudy, a community-based study of white and black adults ages 70-79 (42% black; 48% men) at baseline (1997-1998), we tested the associations (at the person-level) between knee pain without radiographic OA (ROA), knee ROA without pain, and knee symptomatic ROA (sROA) and incident fall injuries among 962 adults mean (SD) age 74.7 (2.9) years. We also examined if these associations differed by sex, obesity status, and fall injury type (fracture vs. non-fracture). Knee ROA was defined as having a Kellgren-Lawrence grade of  $\geq 2$  in at least one knee. Knee sROA was defined as having both ROA and pain symptoms (during the last 30 days) in the same knee. Fall injuries were defined using a validated diagnoses code algorithm from linked Medicare claims (99.2% linkage) as any unique event with a fall code (E880-888) and/or non-vertebral fractures (800-804, 807-829). Cox regression modeling was used to estimate hazard ratios (HRs) and 95% confidence intervals (CIs). Covariates associated with the exposure or outcome at  $p < 0.1$  were included in the full multivariate adjusted models.

Results: The mean (SD) follow-up time was 7.50 (3.02) years. The prevalence of sROA, pain without ROA, ROA without pain, and no ROA or pain was 34.4%, 40.0%, 4.8%, and 20.8%, respectively. Of the 962 participants, 274 (28.5%) had an incident fall injury. In the full multivariate model, compared with those without ROA or pain, individuals with pain without ROA (HR= 1.28; 95% CI: 0.89, 1.85), ROA without pain (HR= 1.18; 95% CI: 0.59, 2.39), and sROA (HR=1.24; 95% CI: 0.83, 1.85) did not have an increased risk of fall injuries. Among men only, and compared with men without ROA or pain, those with pain without ROA (HR= 2.13; 95% CI: 1.01, 4.50,  $p$ -value=0.048) and sROA (HR=2.28; 95% CI: 1.00, 5.18,  $p$ -value=0.049) had a significantly higher risk of fall injuries (Table 1). The association between knee OA and fall injuries did not differ by obesity status (Table 1) or fall injury type (Table 2).

Conclusion: Both knee sROA and knee pain without ROA were independently associated with a borderline increased risk of incident fall injuries in men only. Further studies are needed to confirm this initial finding.

**Table 1.** Adjusted risk of fall injuries associated with knee pain without ROA, knee ROA with pain, and knee sROA, overall, and by sex, and obesity

	Knee pain without ROA <sup>a</sup> HR (95% CI)	Knee ROA without pain <sup>b</sup> HR (95% CI)	Knee sROA <sup>c</sup> HR (95% CI)
<b>Overall</b>			
Base model (n=962) <sup>b</sup>	1.29 (0.91, 1.82)	1.25 (0.64, 2.44)	1.15 (0.80, 1.66)
Full MV model (n=938) <sup>c</sup>	1.28 (0.89, 1.85)	1.18 (0.59, 2.39)	1.24 (0.83, 1.85)
<b>Men</b>			
Base model (n=383) <sup>b</sup>	1.56 (0.79, 3.05)	1.42 (0.79, 3.05)	1.63 (0.81, 3.27)
Full MV model (n=371) <sup>c</sup>	2.13 (1.01, 4.50) <sup>*</sup>	1.79 (0.48, 6.73)	2.28 (1.00, 5.18) <sup>*</sup>
<b>Women</b>			
Base model (n=579) <sup>b</sup>	1.21 (0.81, 1.82)	1.18 (0.54, 2.58)	1.00 (0.72, 1.64)
Full MV model (n=567) <sup>c</sup>	1.09 (0.71, 1.67)	0.98 (0.42, 2.27)	1.03 (0.64, 1.65)
<b>Obese</b>			
Base model (n=275) <sup>b</sup>	1.92 (0.67, 5.56)	1.92 (0.46, 7.91)	1.10 (0.38, 3.16)
Full MV model (n=270) <sup>c</sup>	2.22 (0.72, 6.83)	2.07 (0.46, 9.23)	1.39 (0.45, 4.31)
<b>Non-obese</b>			
Base model (n=683) <sup>b</sup>	1.25 (0.86, 1.82)	1.00 (0.42, 2.38)	1.40 (0.94, 2.10)
Full MV model (n=668) <sup>c</sup>	1.20 (0.81, 1.78)	0.98 (0.41, 2.33)	1.41 (0.91, 2.18)

Abbreviations: ROA, radiographic osteoarthritis; sROA, Symptomatic ROA; HR, hazard ratio; CI, confidence intervals; MV, multivariate model

<sup>a</sup>The reference group comprises participants without ROA or pain in a knee

<sup>b</sup>Adjusted for age, sex, race, and site

<sup>c</sup>Adjusted for base model and BMI, smoking, physical activity, health status, hypertension, myocardial infarction, prior falls, poor vision, NSAID use, steroid use, calcium use, vitamin D use, and antidepressants

<sup>\*</sup> $p < 0.05$

**Table 2.** Adjusted risk of fracture and non-fracture fall injuries associated with knee pain without ROA, knee ROA with pain, and knee sROA

Fall Injury	Knee pain without ROA <sup>a</sup> HR (95% CI)	Knee ROA <sup>b</sup> HR (95% CI)	Knee sROA <sup>c</sup> HR (95% CI)
<b>Fracture</b>			
Base model (n=889) <sup>b</sup>	1.27 (0.85, 1.91)	1.73 (0.84, 3.54)	1.20 (0.79, 1.85)
Full MV model (n=867) <sup>c</sup>	1.25 (0.82, 1.92)	1.57 (0.73, 3.56)	1.25 (0.78, 2.00)
<b>Non-Fracture</b>			
Base model (n=761) <sup>b</sup>	1.49 (0.77, 2.89)	0.34 (0.04, 2.63)	1.15 (0.58, 2.30)
Full MV model (n=743) <sup>c</sup>	1.54 (0.75, 3.12)	0.39 (0.05, 3.15)	1.42 (0.65, 3.08)

Abbreviations: ROA, radiographic osteoarthritis; sROA, Symptomatic ROA; HR, hazard ratio; CI, confidence intervals; MV, multivariate model

<sup>a</sup>The reference group comprises participants without ROA or pain in a knee

<sup>b</sup>Adjusted for base model and BMI, smoking, physical activity, health status, hypertension, myocardial infarction, prior falls, poor vision, NSAID use, steroid use, calcium use, vitamin D use, and antidepressants

<sup>c</sup> $p < 0.05$

Tables 1 and 2

Disclosures: Kamil Barbour, None.

## LB-MO0355

**Arthritis prevalence, defined by self-report and symptomatology, according to age, sex and social disadvantage in six low and middle income countries: The World Health Organization Study on global AGEing and adult health (SAGE) Wave 1.** Sharon Brennan-Olsen<sup>1</sup>, Selina Cook<sup>1</sup>, Michelle Leech<sup>2</sup>, Steve Bowe<sup>1</sup>, Richard Page<sup>1</sup>, Nirmala Naidoo<sup>3</sup>, Paul Kowal<sup>4</sup>, Julie Pasco<sup>1</sup>, Sarah Hosking<sup>1</sup>, Mohammadreza Mohebbi<sup>1</sup>. <sup>1</sup>Deakin University, Australia, <sup>2</sup>Monash University, Australia, <sup>3</sup>World Health Organization, Switzerland, <sup>4</sup>University of Newcastle, Australia

Arthritis is the most common joint disorder worldwide, the burden of which is projected to increase due to trends in lifestyle-related risk and demographic ageing. In higher income countries, social disadvantage is associated with higher prevalence of arthritis; however, less is known about arthritis prevalence or its determinants in low and middle income countries (LMIC). Given the pain and functional disability caused by arthritis, evidence about health gradients in LMIC will help to inform the possible burden on healthcare systems to meet needs of those at greatest risk. We assessed arthritis prevalence across age, sex and parameters of social disadvantage using data from the World Health Organization Study on global AGEing and adult health (SAGE).

SAGE Wave 1 (2007-10) includes nationally-representative samples of adults ( $\geq 18$  yrs) from China, Ghana, India, Mexico, Russian Federation and South Africa (n=44,747). Arthritis prevalence was defined by self-report and by a symptom-based algorithm. Marital status and educational attainment were self-reported. Arthritis prevalence data were extracted for each of the LMIC by 10yr age strata, sex and social disadvantage. Country-specific survey weightings were applied and weighted prevalence calculated for each LMIC.

Arthritis prevalence was higher in women than men (self-report; 19.9% vs. 14.1%; symptom-based; 4.8% vs. 3.1%, respectively), with the peak observed in those aged 60-69 yrs or 70-79 yrs (self-reported: China 29.2% [95%CI 26.7%-31.9%] vs. 22.9% [20.7%-25.2%]; Ghana 22.8% [18.6%-27.6%] vs. 16.7% [12.6%-21.7%]; India 23.5% [18.8%-29.0%] vs. 17.8% [14.5%-21.7%]; Mexico 22.9% [11.2%-41.1%] vs. 9.7% [6.3%-14.5%]; Russian Federation 45.7% [39.1%-52.3%] vs. 37.8% [30.3%-46.0%]; South Africa 31.5% [25.7%-38.0%] vs. 28.2% [22.1%-35.2%], women vs. men respectively). For both sexes, arthritis prevalence was greater in those with lower education (greatest difference between lowest and highest education was 36.7% for Russian women), and in women who were separated, divorced or widowed.

For residents of LMIC the high prevalence of arthritis will likely worsen poverty if this debilitating disease limits their ability to financially and/or materially support themselves. Our findings have implications for national efforts to prioritise healthcare resources and achieve Universal Health Coverage, particularly toward preventing and/or treating arthritis.

**Disclosures:** Sharon Brennan-Olsen, None.

## LB-MO0356

**Dexamethasone-induced Poldip2 expression possibly recapitulating the osteoblast aging was suppressed by a longevity factor basic-FGF. Sakie Katsumura<sup>1</sup>, Yoichi Ezura<sup>1</sup>, Kathy Griendling<sup>2</sup>, Masaki Noda<sup>3</sup>.**  
<sup>1</sup>Tokyo Medical & Dental University, Japan, <sup>2</sup>Emory University, United States, <sup>3</sup>Yokohama City Minato Red Cross Hospital, Japan

Osteoporosis is influenced by multiple factors including intracellular reactive oxygen species (ROS). In osteoblasts, predominant ROS producer is the NADPH oxidase 4 (Nox4). Here, we investigated the importance of polymerase delta-interacting protein 2 (Poldip2), a Nox4 activator.

By investigating the expression of Poldip2 in adult mouse femurs using quantitative RT-PCR, we noticed that its constitutive expression was obvious both in cortical and trabecular bone of the femurs while its expression was undetectable in bone-marrow. In aged mice (>60wks), Poldip2 expression was significantly increased. Based on the hypothesis that ROS production promoted by Poldip2 and Nox4 in osteoblasts may contribute to the osteoporosis, we examined if any cytokines and hormones may influence the Poldip2 expression in MC3T3-E1 cells. Interestingly, two frequently used compounds for osteogenic induction i.e., dexamethasone and BMP2, significantly up-regulated Poldip2 expression. Conversely, we found basic-FGF (FGF2) significantly suppresses the Poldip2 expression dose-dependently, at least by 12 hours after the treatment. Because FGF2 is well known to be an anti-senescence factor for mesenchymal stem cell cultures, we posited that suppressed expression of Poldip2 may be responsible for such effects in the osteoblasts. Consistent with our hypothesis, FGF2 also suppressed Nox4 expression. More importantly, FGF2-treatment significantly suppressed dexamethasone-induced Poldip2 expression.

Thus, our data indicate that the increased expression of Poldip2 in aged bone could be prevented by anti-senescence factors FGF2 and may provide novel strategies targeting possible senescence factors in osteoporosis.

**Disclosures:** Sakie Katsumura, None.

This study received funding from: No

## LB-MO0357

**Profilin1 Deficiency in Osteoclasts Causes Osteolytic Erlenmeyer-Flask Deformity of the Femurs Due to the Increased Migratory Potential. Jumpei Shirakawa<sup>1</sup>, Yoichi Ezura<sup>2</sup>, Tadayoshi Hayata<sup>3</sup>, Yavoi Izu<sup>4</sup>, Ralph Botcher<sup>5</sup>, Reinhard Fässler<sup>5</sup>, Masaki Noda<sup>6</sup>.**  
<sup>1</sup>School of Dental Medicine Tsurumi University, Japan, <sup>2</sup>Tokyo Medical & Dental University, Japan, <sup>3</sup>University of Tsukuba, Japan, <sup>4</sup>Chiba Institute of Science, Japan, <sup>5</sup>Max Planck Institute of Biochemistry, Germany, <sup>6</sup>Yokohama City Minato Red Cross Hospital, Japan

Skeletal homeostasis requires appropriate bone formation and bone resorption, based on proper cell movements. To investigate the function of Profilin1 (*Pfn1*), a regulator of actin-polymerization and cell movements, we analyzed the osteoclast specific *Pfn1* conditional-knockout mice (cKO) generated by crossing the *Pfn1*<sup>lox/lox</sup> and *CatK*-Cre Knock-In (KI) mice. Neonatal cKO mice were delivered with normal genetic segregation, whereas the postnatal growth was slightly impaired. At 4 weeks, skeletal deformity became significant, associated with body length shortening, in addition to the anterior craniofacial deformity by plain radiograms. At 8 weeks, three-dimensional micro-CT (3D- $\mu$ CT) images indicated the impaired facial and cranial-base growth. Significant shortening of the lower- and upper-limb long-bones represented the Erlenmeyer-flask deformity, with an appearance of metaphyseal osteolytic expansion. The 3D- $\mu$ CT defined bone mineral density (BMD), trabecular bone volume (BV/TV) and diaphyseal cortical bone thickness (Ct.th) were significantly decreased in the cKO mice. Histologically, endosteal osteoclasts at metaphysis were increased. In vitro, osteoclastogenic potentials of the *Pfn1*-cKO mice were not affected, but instead, live-imaging analysis indicated increased movement of the cKO osteoclasts, possibly contributing to the increased bone marrow space expansion at metaphysis. Our study, for the first time, indicated that *Pfn1* has critical roles in osteoclasts recruitment and motility for the maintenance of postnatal skeletal homeostasis, and may be related to osteochondro-dysplastic deformities found in several disorders.

**Disclosures:** Yoichi Ezura, None.

## LB-MO0358

**Baseline femoral neck width predicts inter-individual differences in structural and mass changes during the menopausal transition. Karl Jepsen<sup>1</sup>, Andrew Kozminski<sup>1</sup>, Erin Bigelow<sup>1</sup>, Stephen Schlecht<sup>1</sup>, Robert Goulet<sup>1</sup>, Sioban Harlow<sup>1</sup>, Jane Cauley<sup>2</sup>, Carrie Karvonen-Gutierrez<sup>1</sup>.**  
<sup>1</sup>University of Michigan, United States, <sup>2</sup>University of Pittsburgh, United States

Understanding how variation in adult bone mass and structure affect skeletal aging will benefit efforts aimed at minimizing fragility fractures. Prior cadaveric studies reported a positive association between external bone size and bone multicellular unit (BMU)-based remodeling that may explain why wide femoral necks showed a greater loss in mass with aging compared to narrow femora. To examine how skeletal aging patterns differ among individuals, we used longitudinal data from women transitioning through menopause to test the hypothesis that age-changes in DXA derived bone traits (BMC, bone area, aBMD) depend on baseline external bone size. Longitudinally acquired hip DXA images for 193 women (61 Black, 132 White; aged 42-52 at baseline) enrolled in the Pittsburgh site of the Study of Women's Health Across the Nation were analyzed for changes in BMC, bone area, and aBMD over 14 years of follow up. All studies were conducted with annually-acquired informed consent with IRB approval. Baseline bone area correlated negatively with the 14 year change in bone area ( $R^2=0.07$ ,  $p<0.0002$ ) and BMC ( $R^2=0.11$ ,  $p<0.0001$ ) but not aBMD ( $R^2=0.003$ ,  $p<0.4$ ), as hypothesized. To account for height, women were sorted into tertiles based on the residuals from a regression between baseline bone area and height. The 14 year change in BMC ( $p<0.03$ , ANOVA) and bone area ( $p<0.0001$ , ANOVA) but not aBMD ( $p<0.76$ , ANOVA) differed significantly among the tertiles (Fig 1). This analysis identified clinically meaningful inter-individual differences in how bone structure and mass changed during the menopausal transition (MT). Women with narrow femora lost aBMD because of small decreases in BMC combined with large increases in bone area. In contrast, women with wide femora lost similar aBMD but because of large decreases in BMC combined with small increases in bone area. Thus, women showed similar reductions in aBMD during the MT for different biological reasons. Further, our analysis indicated that periosteal expansion and bone loss are not coordinated during the MT, which contradicts current dogma that periosteal expansion acts to mechanically offset bone loss. This is the first study to show that the bones of women change in different ways during the MT and that the structural and mass changes can be predicted by baseline external bone size. How these inter-individual differences in skeletal aging patterns affect bone strength and are reflected in serum biomarkers remain to be determined.

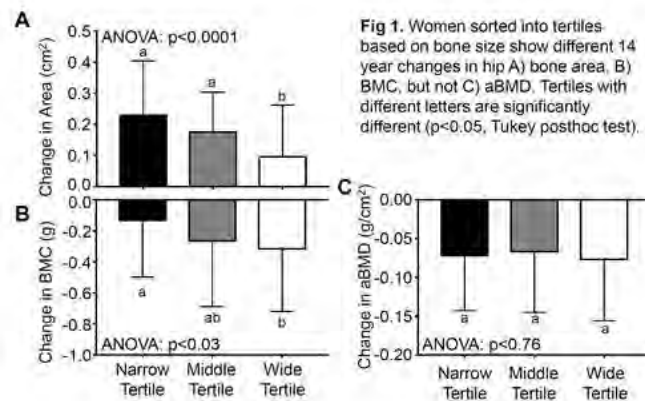


Figure 1. Jepsen et al - late breaking

**Disclosures:** Karl Jepsen, None.

This study received funding from: National Institutes of Health

## LB-MO0359

**Women with Type 2 Diabetes Have Lower Cortical Porosity than Women without Diabetes, and Higher Glucose is Associated with Reduced Cortical Porosity. Marit Osima<sup>1</sup>, Rita Kralj<sup>2</sup>, Ragnar Joakimsen<sup>3</sup>, Erik F Eriksen<sup>4</sup>, Åshild Bjørnerem<sup>5</sup>.**  
<sup>1</sup>Department of Community Medicine, UiT The Arctic University of Norway, Norway, <sup>2</sup>Department of Medical Biology, UiT The Arctic University of Norway, Norway, <sup>3</sup>Department of Clinical Medicine, UiT The Arctic University of Norway, Norway, <sup>4</sup>Department of Clinical Endocrinology, Oslo University Hospital, Norway, <sup>5</sup>Department of Obstetrics & Gynaecology, University Hospital of North Norway, Norway

Introduction: Women with type 2 diabetes (T2D) have increased risk of fracture, despite high bone mineral density (BMD), high body mass index (BMI) and low bone turnover rate as reflected by low levels of bone turnover markers. It is also a paradox that T2D is reported to have increased cortical porosity. The reasons for the greater fragility and reduced bone turnover in diabetic patients are not clear. Increased cortical porosity is generally associated with increased bone turnover and fracture risk.

We tested the hypothesis that higher serum levels of glucose, and higher BMI is associated with lower levels of bone turnover markers, and lower cortical porosity.

**Methods:** We included 22 women with T2D and 421 women without diabetes, from a nested case-control study of postmenopausal woman aged 54-94 years (211 with non-vertebral fractures and 232 controls), in Tromsø, Norway. Fasting blood samples were assayed for serum levels of procollagen type I N-terminal propeptide (PINP), C-terminal cross-linking telopeptide of type I collagen (CTX) and glucose. Femoral subtrochanteric architecture was quantified in clinical CT images using StrAx1.0 software.

**Results:** Diabetic women had higher BMI (29.0 vs 26.4 kg/m<sup>2</sup>), higher serum levels of glucose (7.2 vs 5.3 mmol/L), higher femoral subtrochanteric total volumetric BMD (783 vs 715 mg HA/cm<sup>3</sup>) and lower cortical porosity (40.9 vs 42.8%) than non-diabetic women (all  $p < 0.05$ ). Each standard deviation (SD) increment in serum levels of glucose was associated with 0.12 SD and 0.10 SD lower serum levels of PINP and CTX and 0.13 SD lower cortical porosity ( $p < 0.05$ ). Each SD increment in BMI was associated with 0.10 SD and 0.18 SD lower serum levels of PINP and CTX ( $p < 0.05$ ) and 0.19 SD thicker cortices ( $p < 0.001$ ). All the results were adjusted for age and fracture status.

**Conclusion:** Higher glucose and higher BMI are associated with lower bone turnover, and higher glucose is associated with reduced cortical porosity, suggesting reduced intracortical and endocortical remodeling. Cortical porosity is thus unlikely to explain the increased risk of fracture in women with type 2 diabetes. There might be other alterations in bone material composition that contribute to this increased risk of fracture.

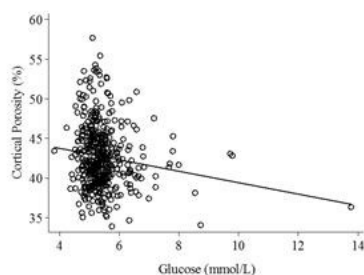


Fig. Femoral subtrochanteric porosity of the total cortex by serum glucose levels adjusted for age and fracture status.  $\beta = -0.13$ ,  $p = 0.006$

Fig. Porosity and Glucose

**Disclosures:** Marit Osima, None.

## LB-MO0360

**Genetic Profiling Predicts Bone Loss and Bone Mineral Density.** Thao P. Ho-Le<sup>\*1</sup>, Hanh M. Pham<sup>2</sup>, Jacqueline R. Center<sup>3</sup>, John A. Eisman<sup>4</sup>, Hung T. Nguyen<sup>1</sup>, Tuan V. Nguyen<sup>7</sup>. <sup>1</sup>Centre for Health Technologies, University of Technology, Sydney, Australia, <sup>2</sup>Bone Biology Division, Garvan Institute of Medical Research, Australia, <sup>3</sup>Bone Biology Division, Garvan Institute of Medical Research; UNSW Medicine, UNSW Australia, Australia, <sup>4</sup>Bone Biology Division, Garvan Institute of Medical Research; UNSW Medicine, UNSW Australia; Notre Dame University School of Medicine, Sydney, Australia, <sup>5</sup>Centre for Health Technologies, University of Technology, Sydney; Bone Biology Division, Garvan Institute of Medical Research; UNSW Medicine, UNSW Australia, Australia

In the elderly, the rate of bone loss ( $\Delta$ BMD) is a risk factor for fracture and mortality. There is evidence that the variation in  $\Delta$ BMD is partly determined by genetic factors. This study sought to develop a profile of genetic variants associated with BMD, and to define the association between the genetic profiling and  $\Delta$ BMD.

Sixty-two BMD-associated SNPs from genome-wide association studies (GWAS) were genotyped in 860 women and 524 men aged from 60 years who were participants of the Dubbo Osteoporosis Epidemiology Study. Weighted genetic risk scores (GRS) were constructed for each individual by summing the product of the number of risk alleles and the regression coefficient [associated with BMD from GWAS] for each SNP.  $\Delta$ BMD, expressed as annual percent change-in-BMD, was determined by linear regression analysis for each individual who had had at least two BMD measurements during the 25-year of follow-up. The relationship between GRS, BMD and  $\Delta$ BMD was analyzed by the multiple linear regression model.

**GRS and BMD:** After adjusting for age and body weight, greater values of GRS were associated with higher baseline femoral neck BMD in women (regression coefficient per unit of GRS:  $0.017 \pm 0.007$  g/cm<sup>2</sup>;  $P = 0.011$ ) and in men (coefficient  $0.018 \pm 0.008$  g/cm<sup>2</sup>;  $P = 0.028$ ). The positive association was also observed in lumbar spine BMD for women ( $0.037 \pm 0.009$  g/cm<sup>2</sup>;  $P < 0.001$ ) and men ( $0.031 \pm 0.010$  g/cm<sup>2</sup>;  $P = 0.002$ ) in men. GRS, age and body weight together accounted for 32% and 16% variance in femoral neck BMD in women and men, respectively.

**GRS and bone loss:** The mean of  $\Delta$ BMD was  $-0.65\%$  (SD 1.65%) for women and  $-0.57\%$  (SD 1.40%) for men. In women, each unit increase in GRS was associated with 0.23% (SE 0.10) lower annual rate of bone loss in femoral neck ( $P = 0.026$ ), and this association was independent of baseline BMD and age. Collectively, age, baseline BMD and GRS accounted for 2.7% of variance in  $\Delta$ BMD. There was no statistically significant association between  $\Delta$ BMD and GRS in men.

These data demonstrate for the first time that genetic profiling is associated with femoral neck  $\Delta$ BMD, independent of baseline BMD and age. This finding suggests that genetic profiling can be used as an additional means for evaluating bone loss in an individual.

**Disclosures:** Thao P. Ho-Le, None.

## LB-MO0361

**Persistence of excess mortality following individual types of fragility fracture:**

**A relative survival analysis.** Thach Tran<sup>\*1</sup>, Dana Bliuc<sup>1</sup>, Tuan V Nguyen<sup>1</sup>, John A Eisman<sup>1</sup>, Louise Hansen<sup>2</sup>, Bo Abrahamsen<sup>3</sup>, Peter Vestergaard<sup>2</sup>, Tineke van Geel<sup>4</sup>, Piet Geusens<sup>5</sup>, Joop van den Bergh<sup>5</sup>, Jacqueline R Center<sup>1</sup>. <sup>1</sup>Garvan Institute of Medical Research, Australia, <sup>2</sup>Aalborg University, Denmark, <sup>3</sup>University of Southern Denmark, Denmark, <sup>4</sup>Maastricht University, Netherlands, <sup>5</sup>Maastricht University Medical Center, Netherlands

Little is known about long term excess mortality following fragility fractures other than hip and vertebral fractures. This nationwide, register-based follow-up study included all Danish individuals aged 50+ years who first experienced fragility fractures in 2001. Death was ascertained from the Danish death register with follow up until 2011. Excess mortality attributable to individual types of fracture was examined using relative survival ratio (RSR). The analysis, accounting for time-related mortality changes in the background population, makes it particularly robust in examination of contribution of fracture on mortality at precise time intervals following fracture.

There were 9,500 men (aged  $67 \pm 12$  years) and 21,000 women ( $72 \pm 13$ ) with a first fragility fracture in 2001 followed by 3,198 and 6,589 deaths, respectively during 66,926 and 153,564 person-years of follow-up. Significant excess mortality was observed following all proximal and lower leg fractures (Table); while observed survival following distal limb fractures (i.e. hand, fingers, foot and toes) was similar to expected survival. The majority of deaths occurred within the first year post-fracture and thereafter excess mortality gradually declined. As expected, hip fractures were associated with the highest excess mortality (1-year RSR of 0.67 and 0.80, equivalent to excess mortality of 33% and 20% in men and women, respectively). Excess mortality at one year was 20-25% after other femur or pelvic, 10% following vertebral, 5-10% following humerus, rib and clavicle, and 3% following lower leg fractures. Men who sustained forearm, knee and ankle fractures had an associated non-significant 2% excess mortality. A significant- although smaller- excess mortality was still observed until approximately 10, 7 and 5 years after hip, femur and other proximal or lower leg fractures. For every 3 men and 5 women with a hip or femur fracture one extra death occurred above expected in the first year post-fracture, compared with one extra death for 48 men and 33 women with a lower leg fracture. Using a novel, robust technique to examine mortality over time, excess mortality for approximately 5 years post-fracture was found for virtually all proximal and lower leg fractures. This study highlights the important contribution of a wide variety of fragility fractures to long-term excess mortality, and thus the potential for benefit from early intervention.

Table: Annual relative survival at 1 year following fragility fracture

	Year 1 interval			Last year post-fracture of significant excess mortality	
	Observed survival	Expected survival	Relative survival (95% CI)	Year	Relative survival (95% CI)
<b>Men</b>					
Hip	0.61	0.90	0.67 (0.65, 0.69)	Year 10	0.94 (0.90, 0.98)
Other femur	0.68	0.94	0.73 (0.65, 0.81)	Year 7	0.90 (0.81, 0.99)
Pelvis	0.75	0.93	0.81 (0.73, 0.89)	Year 3	0.92 (0.85, 0.99)
Vertebrae	0.84	0.95	0.88 (0.84, 0.92)	Year 6	0.96 (0.93, 0.99)
Clavicle	0.89	0.96	0.92 (0.88, 0.96)	Year 4	0.97 (0.94, 0.99)
Rib	0.91	0.97	0.95 (0.92, 0.98)	Year 3	0.97 (0.95, 0.99)
Proximal humerus	0.83	0.95	0.88 (0.85, 0.91)	Year 7	0.96 (0.93, 0.99)
Distal humerus	0.82	0.92	0.89 (0.80, 0.98)	Year 5	0.92 (0.81, 0.99)
Distal forearm	0.94	0.96	0.98 (0.96, 1.0)	N/A	
Knee	0.95	0.96	0.98 (0.94, 1.02)	N/A	
Lower leg	0.95	0.97	0.98 (0.96, 0.99)	Year 4	0.98 (0.96, 0.99)
Ankle	0.96	0.97	0.99 (0.97, 1.01)	N/A	
<b>Women</b>					
Hip	0.72	0.91	0.80 (0.79, 0.81)	Year 10	0.95 (0.93, 0.97)
Other femur	0.70	0.92	0.77 (0.72, 0.82)	Year 7	0.97 (0.89, 0.99)
Pelvis	0.77	0.92	0.85 (0.81, 0.89)	Year 7	0.94 (0.88, 0.99)
Vertebrae	0.84	0.94	0.89 (0.86, 0.92)	Year 5	0.96 (0.93, 0.99)
Clavicle	0.89	0.95	0.94 (0.9, 0.98)	Year 4	0.95 (0.91, 0.99)
Rib	0.90	0.95	0.95 (0.91, 0.99)	Year 2	0.95 (0.91, 0.99)
Proximal humerus	0.90	0.95	0.95 (0.94, 0.96)	Year 6	0.97 (0.96, 0.98)
Distal humerus	0.91	0.95	0.96 (0.91, 1.01)	N/A	
Distal forearm	0.96	0.96	1.0 (0.99, 1.01)	N/A	
Knee	0.97	0.97	1.0 (0.98, 1.02)	N/A	
Lower leg	0.93	0.96	0.97 (0.95, 0.99)	Year 4	0.98 (0.96, 0.99)
Ankle	0.98	0.98	1.0 (0.99, 1.01)	N/A	

Relative survival = observed survival following fracture in the study group / expected survival from the age-, sex- and calendar year-specific Danish background population.  
Significant results bolded.  
N/A: non-applicable.

Persistence of excess mortality following fragility fractures

Disclosures: Thach Tran, None.

## LB-MO0362

**Presence of Vertebral Fractures and Disc Disease in Post Menopausal Females with Height Loss as a Possible Screening Method for Osteoporosis.** Nicola Berman<sup>\*1</sup>, Gregory Chang<sup>2</sup>, Stephen Honig<sup>3</sup>. <sup>1</sup>NYU Department of Rheumatology, United states, <sup>2</sup>NYU Department of Radiology, United states, <sup>3</sup>New York University Department of Rheumatology, United states

Purpose: Non-traumatic vertebral fracture can identify patients with osteoporosis. Approximately 75% of vertebral fractures are asymptomatic and as many as 45% go unrecognized. As a result, many cases of osteoporosis are missed and left untreated, leaving patients vulnerable to fractures. We investigated whether women with 2 or more inches of height loss have a high incidence of fracture, if the degree of height loss correlates with presence of fractures, and how these findings correlate with bone density, to see if height loss could be a screening tool for osteoporosis. We further assessed how many patients with height loss had been treated for osteoporosis in the past.

Methods: From among all postmenopausal female patients seen at our academic Osteoporosis Center, we prospectively enrolled a cohort of 100 subjects self-reporting two or more inches of height loss from maximum height. Enrollment occurred over a 2 year period. Patients with prior spinal surgery or significant scoliosis (>10% spinal curvature) were excluded. At intake, all patients had radiographs of the lumbar and thoracic spine. Vertebral fracture was defined as >20% vertebral height loss based on the guidelines from the Vertebral Fracture Initiative by the International Osteoporosis Foundation. Intervertebral disc disease was classified based on the Genant modification of the Sharp method.

Results: Of 100 patients with height loss, 76 had a fracture of the thoracic or lumbar spine, or both. 58 women had fractures of their thoracic and 50 of their lumbar spine. Among the 76 women with a fracture, 21 had never been treated for osteoporosis. Among the 24 patients without fractures, the average T-Score was -2.0 of the spine. Among all patients, 96 patients had disc disease (94 had thoracic and 75 had lumbar disc disease). When evaluating degree of height loss, there was no significant difference between those who had sustained a fracture and those who had not.

Conclusion: 2 or more inches of height loss was explained by vertebral fracture and presence of disc disease. Individuals with 2 or more inches of height loss and no fracture had T scores mainly in the osteopenic-osteoporotic range. Therefore we suggest that any patient with 2 or more inches of height loss should be evaluated for vertebral fractures and osteoporosis. Significantly, 28% of women with compression fractures had not previously been treated for osteoporosis, underlining the need for better screening and treatment.

Disclosures: Nicola Berman, None.

## LB-MO0363

**Sedentary time and diaphyseal cortical bone outcomes in American adolescents.** Simon Higgins<sup>\*1</sup>, Joseph Kindler<sup>2</sup>, Thomas Mahar<sup>1</sup>, Elizabeth Hathaway<sup>1</sup>, Emma Laing<sup>2</sup>, Michael Schmidt<sup>1</sup>, Ellen Evans<sup>1</sup>, Richard Lewis<sup>2</sup>. <sup>1</sup>University of Georgia, Department of Kinesiology, United states, <sup>2</sup>University of Georgia, Department of Foods & Nutrition, United states

Sedentary behaviors (SED), characterized as activities performed in a seated or reclined posture with a low energy expenditure (i.e.,  $\leq 1.5$  METS), are pervasive in the American adolescent population with the average 12 to 19-yo engaging in >8 hours per day of SED. SED is known to influence cardiometabolic health, but the association with pediatric skeletal measures is less established. Therefore, the aim of this study was to explore the associations between SED and cortical bone geometric and estimated strength outcomes in female adolescents. Time spent performing moderate to vigorous physical activity (MVPA) and SED were assessed over 7 consecutive days in adolescent females ( $n=57$ ,  $15.3 \pm 1.7$  yo, 84.2% white) using the ActiGraph GT3X+ accelerometer. Consecutive SED epochs were summed into bouts to provide a total time spent in long (>30 minute) and short (<5 minute) bouts, depicting the typical SED distribution. Mid-tibia and mid-radius cortical bone was assessed via peripheral quantitative computed tomography at the 50% site relative to the distal growth plate, and muscle cross-sectional area (MCSA) was assessed at the 66% site. Multiple linear regression analyses were conducted while adjusting for MCSA, bone length, age, race, and MVPA. Box-Cox transformations were applied when residuals violated normality. Time spent in MVPA ( $M \pm SD$ ) was  $33.6 \pm 17.7$  minutes daily and SED time was  $10.4 \pm 1.1$  hours per day with ~43% accrued in short bouts and ~11% in long bouts. Total SED did not predict any cortical bone outcome ( $p>.05$ ). However, when analyzed by distribution, time spent in short SED bouts negatively predicted mid-tibia cortical thickness (Ct.Th;  $\beta=-.249$ ,  $p=.026$ ). Conversely, time spent in long SED bouts positively predicted mid-tibia cortical bone mineral content (Ct.BMC;  $\beta=.169$ ,  $p=.019$ ), cortical area (Ct.Ar;  $\beta=.169$ ,  $p=.023$ ), and Ct.Th ( $\beta=.247$ ,  $p=.022$ ), as well as mid-radius Ct.Th ( $\beta=.285$ ,  $p=.013$ ). A congruent negative prediction was seen with mid-radius endosteal circumference ( $\beta=-.315$ ,  $p=.022$ ). Considering the recently identified positive association between long bouts of SED interspersed with clustered osteogenic activity breaks and skeletal health, those who accrue SED in long bouts may tend to cluster activity in a more osteogenic fashion. Further research is warranted to explain the differential relationships between SED distribution and cortical bone outcomes.

Disclosures: Simon Higgins, None.

## LB-MO0364

**Female-Specific Role of Progranulin to Suppress Bone Formation.** Liping Wang<sup>\*1</sup>, Theresa Roth<sup>1</sup>, Robert Nissenson<sup>2</sup>. <sup>1</sup>San Francisco VA Medical Center, United states, <sup>2</sup>San Francisco VA Medical Center; Department of Medicine, University of California, San Francisco, United states

Progranulin (PGRN) is best known as a glial protein whose deficiency leads to the most common inherited form of frontotemporal dementia. Recently, PGRN has been found to be an adipokine associated with diet induced obesity and insulin resistance. The role of PGRN in regulating skeletal homeostasis is not clear. We investigated this issue by comparing the skeletal phenotypes of 6 month old global PGRN knockout (KO) and wild type (WT) mice in a C57/B6 background. We found that fractional bone volume (BV/TV) was comparable in male KO and male WT mice. Strikingly, female KO mice displayed a 2-fold increase ( $p<0.01$ ) in BV/TV compared to WT female mice. The increased cancellous bone in female KO mice was associated with increased trabecular number (30%,  $p<0.001$ ) and decreased trabecular separation (26%,  $P<0.001$ ). Female (but not male) KO mice also displayed a 9% increase in cortical bone thickness ( $p<0.05$ ) at the TFJ. To gain further insight the role of PGRN in bone homeostasis, histomorphometry was performed at the distal femur in 6 month old mice. Compared to WT mice, there was a 108% increase ( $p<0.001$ ) in bone formation rate and a 50% increase ( $p<0.001$ ) in mineral appositional rate in female (but not male) KO mice. Strikingly, KO mice displayed defects in bone resorption that were evident in both genders. Osteoclast (OC) function, determined by measuring average erosion depth, was significantly decreased at the trabecular surface in both male and female KO mice. Electronic microscopy confirmed that loss of PGRN disrupted the ruffled border of the OCs by thinning microvilli and reducing the depth of resorption lacunae. Bone marrow cells were cultured to study the effects of PGRN on osteoclastogenesis. Cells from KO mice were markedly defective in their ability to differentiate into multinucleated TRAP<sup>+</sup> OCs. These cells also displayed a significant decrease in the expression of genes associated with mature OCs (cathepsin K, TRAP) whereas the expression of genes associated with early OCs (c-fms, F4/80) was significantly increased. These *in vitro* effects on osteoclastogenesis were evident in cultures derived from both male and female KO mice. We conclude that PGRN serves to uncouple bone turnover in adult female bone, promoting bone resorption but suppressing the coupled increase in bone formation. This is precisely what occurs in estrogen-deficiency osteoporosis. These results implicate PGRN as a potential therapeutic target in postmenopausal osteoporosis.

Disclosures: Liping Wang, None.

## LB-MO0365

**PF708, A Therapeutic Equivalent Candidate to FORTEO® (Teriparatide), Demonstrates Clinical Pharmacokinetic And Pharmacodynamic Equivalence to the Reference Product.** Hubert Chen\*<sup>1</sup>, Hongfan Jin<sup>1</sup>, Jonathan Lee<sup>1</sup>, Randall Stoltz<sup>2</sup>. <sup>1</sup>Pfenex Inc, United states, <sup>2</sup>Covance Clinical Research Unit, United states

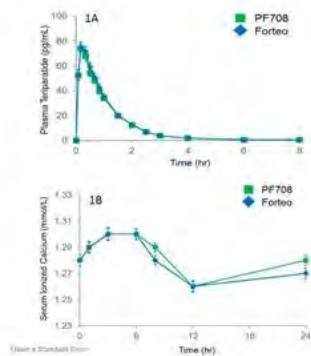
PF708 is a 34-amino acid recombinant analog of human parathyroid hormone and has the same route of administration, dosage form, formulation, and delivery device functionality as the branded reference product, FORTEO® (teriparatide), which has been approved as an anabolic treatment for osteoporosis since 2002. PF708 is being developed as a therapeutic equivalent in the United States (U.S.) and as a biosimilar outside the U.S. to provide a treatment option that is equally safe, pure, and potent as the reference product, at a potentially lower cost.

PF708 was investigated in a randomized, double-blind, crossover study that compared the pharmacokinetic (PK) and pharmacodynamic (PD) parameters of PF708 and the reference product (20 mcg) in 70 healthy subjects. Half of the subjects were randomized to receive PF708 first and the reference product second, and the other half were randomized to receive the drugs in reverse sequence. Each study participant completed two 1-day study periods, separated by a 3-day washout. Key PK endpoints were plasma area-under-the-curve (AUC), maximum concentration ( $C_{max}$ ), time to maximum concentration, and half-life of teriparatide after subcutaneous injection of PF708 or the reference product.

There were no statistically significant differences in any of PK parameters. The plasma teriparatide concentration-time profiles after PF708 and reference product administration were equivalent (see Figure 1A). The geometric mean ratios for  $AUC_{0-inf}$ ,  $AUC_{0-last}$  and  $C_{max}$  were all near 100%, and the 90% confidence intervals were entirely within the 80-125% interval required for concluding bioequivalence. There were also no significant differences between PF708 and the reference product in the key PD endpoint—serum ionized  $Ca^{2+}$  (see Figure 1B).

The safety and tolerability profiles of PF708 and the reference product were comparable, and there were no significant findings in clinical laboratory evaluations, vital sign measurements, electrocardiogram readings, physical examinations or injection site assessments after either PF708 or reference product administration. Additionally, anti-drug antibodies were not detected four days after single-dose administrations of PF708 or the reference product.

Overall, these results indicate that PF708 is equivalent to the reference product in PK, PD and safety profiles and support the continued development of PF708 as a therapeutic equivalent in the U.S. and a biosimilar product outside the U.S.



PF708 Figure

**Disclosures:** Hubert Chen, Pfenex Inc, 15  
This study received funding from: Pfenex Inc.

## LB-MO0366

**Rebound-associated bone loss after non-renewal of long-term denosumab treatment offsets 10-year gains at the total hip within 12 months.** Albrecht W Popp\*, Helene Buffat, Christoph Senn, Kurt Lippuner. Department of Osteoporosis, Bern University Hospital, University of Bern, Switzerland

**Introduction:** In the FREEDOM endpoint trial, denosumab (dmab) (60 mg s.c. every 6 months during 36 months) reduced the incidence of vertebral and nonvertebral fractures in women with osteoporosis (Cummings SR et al. NEJM 2009). The optimal duration of therapy with dmab is not defined.

**Methods:** All nine women who had participated to the FREEDOM trial and its extensions at the Dept. of Osteoporosis, Bern University Hospital, Switzerland and had received treatment with dmab during 10 years were included. In the absence of indication, dmab was not renewed thereafter with adequate vitamin D and calcium being pursued. All women underwent a follow-up visit one year after dmab non-renewal.

**Results:** Mean ( $\pm$ SEM) age at inclusion in FREEDOM was  $68.8 \pm 1.9$  years. As shown in Fig.1, mean ( $\pm$ SEM) gains in TH BMD culminated after 10 years of

treatment with dmab:  $+8.2\% \pm 1.7$  vs. baseline (median 10.2 %, range -1.7 to 12.0%). One year following dmab non-renewal, all women had experienced rapid BMD loss vs. year 10 [mean ( $\pm$ SEM)  $-12.5\% \pm 1.4$  (median  $-12.3\%$ , range  $-17.4$  to  $-6.0\%$ )] and vs. baseline [mean ( $\pm$ SEM)  $-5.4\% \pm 1.8$ , (median  $-6.1\%$ , range  $-13.7$  to  $3.7\%$ )]. At year 11, mean TH BMD was significantly lower than at baseline ( $p=0.019$ ). Bone turnover markers were increased (results not shown). No clinical fractures were reported during year 11, but vertebral fracture assessment by DXA revealed one incident morphometric vertebral fracture in one woman.

**Fig. 1:** Longitudinal mean ( $\pm$  SEM) percent changes in TH BMD vs. baseline at time points prespecified in FREEDOM (year 0-10) and at one-year follow-up after dmab non-renewal (year 11).

In the absence of secondary causes of bone loss, rapid BMD loss in the context of high bone turnover after non-renewal (loss-of-effect) of a potent reversible antiresorptive therapy is consistent with previously described rebound-associated bone loss (Popp et al. Osteoporos Int 2016).

**Conclusions:** After long-term treatment, non-renewal of dmab is associated with a rapid BMD loss at the total hip, the magnitude of which may exceed BMD gains achieved during treatment. Evidence-based treatments aimed at preserving bone mass are lacking.

Fig. 1

**Disclosures:** Albrecht W Popp, Labatec, 12; Gilead, 12; Amgen CH, 12

## LB-MO0367

**An Unusual Case of Atypical Femur Fracture Long After Discontinuation of Longterm Alendronate Therapy for Osteopenia.** Sudhaker D. Rao\*, Shijing Qiu, Shiri Levy, Mahalakshmi Honasoge. Henry Ford Hospital, United states

Atypical femurs fractures (AFF) are now a well established, rare, but serious life changing complication of long-term bisphosphonate (BP) therapy. However, almost all patients reported thus far have sustained AFFs while the patients were still on BP therapy. We have seen a few AFF cases soon after discontinuation of BPs, but the interval was <6 months or in one case 6 months after the last denosumab injection. We wish to report an unusual case of AFF occurring 6y after stopping alendronate.

This 69y old Asian-Indian woman, a practicing radiologist, began alendronate therapy 70mg weekly for osteopenia in March 2003 and stopped in September 2009 after hearing about AFF and osteonecrosis of the jaw as potential complications of long term BP therapy. She did very well for the next 7y (2009-2016) without any problems. She never had fractures. On 02/29/2016, while walking in the home she broke her femur and fell. X-rays confirmed characteristic AFF with slight comminution, which was managed by open reduction and internal fixation from which she is recovering reasonably well.

In May 2016, about 3 months after the AFF, serum CTX was 322pg/ml (normal: 104-1008), P1NP 71µg/L (normal: 16-96), PTH 43pg/ml (normal: 10-65), Ca 10.5mg/ml (normal: 8.6-10.3), 25-hydroxyvitamin D 28ng/ml (normal: >20), and a normal protein electrophoresis. X-ray of the left femur and whole body bone scan were both normal and did not show an incomplete fracture in the left femur.

This is the first such AFF long after (7y) stopping BP, but the mechanism of such unusual AFF is unknown. We speculate that she most likely had low bone turnover to begin with, which was further suppressed by 6y of BP therapy. Based on a limited data in Asian-Indian woman, bone turnover is much lower than in Caucasians. Even if her bone turnover returned to her own low baseline, the accumulated alendronate may take long time to clear from bone (analogous to fluorosis). Although the pathogenesis of this AFF was not elucidated, it is prudent to consider AFF in the differential diagnosis of sub-trochanteric femoral comminuted fractures.

In conclusion, we report what appears to be the first case of AFF with mild comminution long after cessation of BP therapy. ASBMR Task Force on AFF has previously recommended that comminution as an exclusion criterion for AFF. However, it seems reasonable to reconsider this criterion as there does not appear to be any fundamental reason why AFFs could not be comminuted.



AFF

Disclosures: *Sudhaker D. Rao, None.*

## LB-MO0368

**Potential of a rapidly-gelling chitosan sponge for cell encapsulation of adipose-derived stem cells.** Timothee Baudequin<sup>\*1</sup>, Hadi Al-Jallad<sup>2</sup>, Laila Benameur<sup>1</sup>, Reggie Hamdy<sup>2</sup>, Maryam Tabrizian<sup>3</sup>. <sup>1</sup>Department of Biomedical Engineering, McGill University, Canada, <sup>2</sup>Shriners Hospital for Children & McGill University, Canada, <sup>3</sup>Faculty of Dentistry, McGill University, Canada

A rapidly in-situ gelling scaffold (less than 1.6 second) based on chitosan crosslinked either Guanosine-5'-diphosphate (GDP) [1] or Adenosine 5'-diphosphate (ADP) has been developed in our laboratory as a minimally invasive system for bone regeneration in critical size defects as well as for *in situ* cell delivery. Among different cell types, over the last decade, adipose-derived stem cells (ASC) have emerged as a new source of stem cells. Thus, the main goal of this study was to investigate the potential of this sponge for ASC encapsulation. The process was optimized with the pre-osteoblastic cell line MC3T3-E1. The optimal conditions were employed for ASC encapsulation and both their osteogenic and adipogenic differentiation were evaluated.

Two chitosan solutions (3 mg/mL, pH 5 (C3PH5) or 6 mg/mL, pH 6 (C6PH6)) and two cross-linkers, GDP or ADP, resulting in 4 different sponges were studied. Chemical and structural characterizations were performed with  $\mu$ CT and FTIR. First, MC3T3 were encapsulated over a week to select the best parameters. Then, primary rat ASC were encapsulated and cultured in adipogenic (14 days) or osteogenic (21 days) media. Cell metabolic activity, proliferation (Alamar blue, DNA quantification, fluorescence microscopy) and differentiation (ALP, Alizarin Red, Oil red O stainings and protein productions) were assessed.

MC3T3 were able to survive and stay active over the week. The optimal viability was found with GDP solution ( $p < 0.05$ ). Chitosan concentration and pH did not lead to significant differences. ASC were thus encapsulated in GDP C3PH5 sponges either after explants digestion and flask pre-culture, or directly as fresh rat fat pads. Both methods have pros and cons regarding process speed, native surrounding structure and control over the number of cells. Digested cells expressed a very low activity during the first week before increasing their activity and stabilization. Fat pads encapsulation led to a stable medium activity, while the explants without chitosan sponges died quickly. The presence of living tissues was confirmed at the end of the culture with protein production and staining. Early differentiation markers were noticed for both studied lineages, but further studies are needed to confirm the maturation stage.

The author would like to thank CIHR and NSERC-CHRP program, CIHR-Operating program, MITACS and Aligo Innovation for their financial support.

[1] Mekhail *et al*, *Adv Heal. Mater*, 2-8, pp. 1126–1130, 2013.

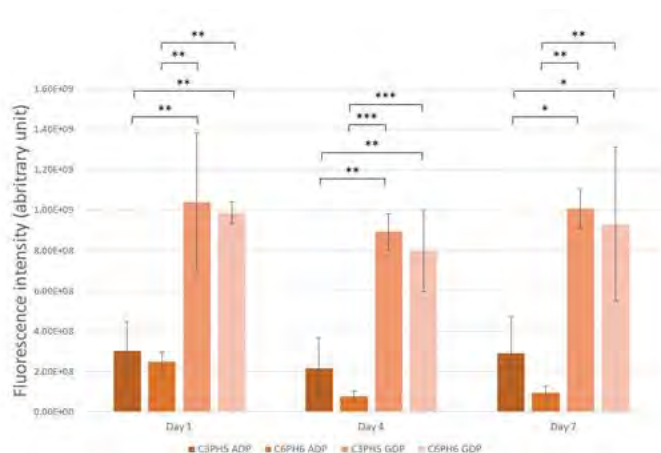


Figure 1: Metabolic activity (Alamar Blue measurements) of encapsulated pre-osteoblastic cells in the different chitosan sponges over time (\*:  $p < 0.05$ , \*\*:  $p < 0.01$ , \*\*\*:  $p < 0.001$ )

Metabolic activity of encapsulated pre-osteoblastic cells in the chitosan sponges over time

Disclosures: *Timothee Baudequin, None.*

## LB-MO0369

**Post-Weaning Endocortical Bone Formation Rate is Increased in Rats Fed a Low Calcium Diet During Lactation.** Matthew Meagher<sup>\*</sup>, Ryan Ross, D. Rick Sumner, Rush University Medical Center, United states

During lactation, calcium (Ca) is mobilized from the mother's skeleton to meet the needs of the growing neonate [1] and this process is exacerbated if the rats are fed a low Ca diet during lactation [2]. While maternal bone mass increases after weaning, it is not clear how Ca intake during lactation affects this recovery. We hypothesize that bone formation post-weaning in dams fed a low Ca diet during lactation is up-regulated compared to dams fed a normal Ca diet. Female Sprague-Dawley rats ( $n=90$ ) were divided into three experimental groups: (1) VirgNorm: age-matched virgin controls fed a normal Ca diet (0.6% Ca) ( $n = 30$ ), (2) LactNorm: rats bred at 10 weeks of age and fed a normal Ca diet ( $n = 30$ ) and (3) LactLow: rats bred at 10 weeks and fed a low Ca diet (0.01% Ca) during lactation ( $n = 30$ ). At parturition, litter sizes were normalized to 11. Pups were weaned at 16 days and the dams in the LactLow group were returned to a normal Ca diet. Cohorts were sacrificed at parturition, weaning, and at 1, 2, 7, or 14 days post-weaning. Cortical geometry was assessed at the junction of the diaphysis and distal femoral metaphysis via  $\mu$ CT for Ct.Ar., Ma.Ar., and Tt.Ar. Undecalcified sections from the same site were used for dynamic histomorphometry to determine MAR and MS/BS on the endocortical surface. Tt.Ar. was significantly lower in the LactLow group vs. the VirgNorm group at weaning and 1 day post-weaning ( $p = 0.047, 0.006$ , respectively) and the LactNorm group at 1 and 7 days post-weaning ( $p = 0.043, 0.048$ , respectively). Ma.Ar. was significantly higher for both lactation groups vs. VirgNorm at all time points after parturition ( $p < 0.01$ ). Ct.Ar. was significantly lower at all time points after parturition for LactLow vs. VirgNorm ( $p < 0.001$ ) and LactNorm ( $p < 0.025$ ). MS/BS was not different between the LactNorm and LactLow groups at any time ( $p > 0.85$ ), but was significantly higher in the LactLow group at 2 days post-weaning vs. VirgNorm ( $p = 0.01$ ). MAR was higher in the LactLow group at 2 days post-weaning vs. both VirgNorm and LactNorm ( $p = 0.04$ , and  $0.004$ , respectively). Thus, although restriction of dietary Ca during lactation did not affect bone loss from the endocortical surface or the amount of surface actively forming bone after weaning, this restriction was associated with increased matrix production per osteoblast in the early post-weaning recovery period.

[1] Ruth Am J Anat 1953, [2] Miller et al. Anat Rec Part A 2004

Disclosures: *Matthew Meagher, None.*

**LB-MO0370**

**Cell-Permeable BMP2 for Bone Healing Therapy Induces Osteogenesis.** Hynuji Lee<sup>\*1</sup>, Whajung Cho<sup>2</sup>, Jeongmin Kim<sup>2</sup>, Junho Jang<sup>2</sup>, Yongdae Jeong<sup>2</sup>, Mijeong Kim<sup>2</sup>, Daewoong Jo<sup>3</sup>. <sup>1</sup>Metabolic Disease Lab I, Cellivory R&D Institute, Cellivory Therapeutics, Inc., F9, K-BIZ DMC Tower, 189 Sungam-Ro, Mapo-Gu, Korea, republic of, <sup>2</sup>Metabolic Disease Lab, Cellivory R&D Institute, Cellivory Therapeutics, Inc., F9, K-BIZ DMC Tower, 189 Sungam-Ro, Mapo-Gu, Korea, republic of, <sup>3</sup>Cellivory Therapeutics, Inc., F9, K-BIZ DMC Tower, 189 Sungam-Ro, Mapo-Gu, Korea, republic of

Bone morphogenic protein 2 (BMP2) plays a significant role in promoting bone healing. Since recombinant human BMP2 (rhBMP2) has short biological half-life, it combines with biomaterial carriers including collagen sponge and hydrogel. However, open surgery is required for treatment. To be treated it that requires open surgery. To address the critical weaknesses that lead various high dosage-induced side effects and limited therapeutic applicability, we have developed cell-permeable BMP2 recombinant protein (CP-BMP2) fused to the hydrophobic cell-penetrating peptide (CPP) called advanced macromolecule transduction domain (aMTD). CP-BMP2 was cell-permeable and localized in mainly cytoplasm including Golgi and ER. CP-BMP2 significantly activated Smad signaling and strongly induced ALP activity compared to plain BMP2 recombinant protein that is lacking aMTD sequence. CP-BMP2 showed longer persistency and enhanced stability in blood plasma than plain BMP2. We also found that CP-BMP2 induced bone-regeneration and new bone formation in murine calvarial critical-sized defect model and equine hindlimb defect model, respectively. The aMTD-fused BMP2 protein can effectively and directly act on the bone-injured area with low concentration in a short time frame to promote bone regeneration. Therefore, CP-BMP2 as a bio-better may provide a great opportunity to patients for bone-healing therapy.

**Disclosures:** Hynuji Lee, None.

**LB-MO0371**

**Raman spectroscopy in HYP mouse teeth and bone reveal tooth dentin as a proxy for XLH bone carbonate ion substitution.** Carolyn Macica<sup>\*1</sup>, Holger Petermann<sup>2</sup>, Catherine Skinner<sup>2</sup>, Steven Tommasini<sup>3</sup>. <sup>1</sup>Frank H. Netter, M.D., School of Medicine at Quinnipiac University, United states, <sup>2</sup>Yale University, United states, <sup>3</sup>Yale University School of Medicine, United states

X-linked hypophosphatemia (XLH) is characterized by persistent osteomalacia in bone and enlarged pulp chambers in teeth. However, the impact of insufficient phosphate on hydroxyapatite composition, the major inorganic component of bone and dentin, is unknown in individuals with XLH. We previously showed that carbonate substitutes for phosphate in cortical bone mineral matrix of HYP mice, a murine XLH model. Here, our goal was to determine if this phenomenon is reproduced in HYP teeth in order to consider the potential as a proxy for bone in human studies. Using Raman Spectroscopy, we analyzed the mineral matrix of both femoral cortical bone and tooth dentin in wild-type (WT) and HYP mice (n=2/strain; age: 7-12 months). Sixteen analyses per sample were taken using a 4x4 mapping grid. The carbonate ion substitution (carbonate/phosphate) levels were significantly higher in both HYP teeth ( $0.25 \pm 0.14$  vs.  $0.13 \pm 0.07$   $p < 0.0001$ ) and HYP cortical bone ( $0.39 \pm 0.11$  vs.  $0.13 \pm 0.06$   $p < 0.0001$ ) as compared to WT. In human permanent teeth, we previously found that carbonate ion substitution levels were higher in patients with XLH than teeth of unaffected adults, while there was no statistically significant difference between the primary teeth, which mineralize in utero, of either population. As the carbonate ion substitution is higher in both dentin and cortical bone in HYP mice, and is also elevated in permanent teeth of XLH patients, we extrapolate these findings to bone and expect that the carbonate:phosphate ratio in human cortical bone would also be elevated relative to those unaffected with XLH. Consistent with previously reported data, accelerated carbonate ion substitution occurs in a phosphate-poor environment. Although the mechanism for this ion substitution is unknown, current data have several important implications. First, we show that the mineralization of primary teeth is normal at birth, similar to neonatal bone. Second, we have identified a potential contributing factor to the etiology of abscess formation in XLH patients. Calcium carbonate is more readily subject to acid degradation. The major driver for tooth demineralization is mediated through exposure to low pH. It may be the combination of porous teeth as a portal of entry and a substrate more prone to acid degradation that increase the risk of dental abscesses without evidence of caries or trauma in XLH patients. Finally, permanent tooth dentin in patients can be used as a proxy to study ion substitution in human cortical bone.

**Disclosures:** Carolyn Macica, None.

**LB-MO0372**

**OASIS Deficiency Associated with Tissue Specific Effects on Collagen I, Aberrant Osteoblast Ultrastructure and Low Levels of Glycosaminoglycans/Matrix in Bone in Patient with Severe OI caused by Homozygous Premature Stop Codon in CREB3L1.** Katarina Lindahl<sup>\*1</sup>, Eva Astrom<sup>2</sup>, Anca Dragomir<sup>1</sup>, Sofie Symoens<sup>3</sup>, Paul Coucke<sup>3</sup>, Sune Larsson<sup>1</sup>, Eleftherios Paschalis<sup>4</sup>, Paul Roschger<sup>4</sup>, Sonja Gamsjaeger<sup>4</sup>, Klaus Klaushofer<sup>4</sup>, Nadja Fratzl-Zelman<sup>4</sup>, Andreas Kindmark<sup>1</sup>. <sup>1</sup>Uppsala University, Sweden, <sup>2</sup>Karolinska Institute, Sweden, <sup>3</sup>Center for Medical Genetics, Ghent University Hospital, Belgium, <sup>4</sup>Ludwig Boltzmann Institute of Osteology, Austria

**Background:** In 2013 Symoens et al. described that deficiency for the ER-stress transducer OASIS, encoded by *CREB3L1*, caused severe recessive osteogenesis imperfecta (OI) through a whole gene deletion also encompassing the first exon of the neighboring gene *DGKZ*, which has since been shown to be a critical regulator of bone homeostasis. OASIS is a transcription factor highly expressed in osteoblasts (OB), and OASIS<sup>-/-</sup> mice exhibit severe osteopenia and spontaneous fractures. OASIS is involved in the production of extracellular matrix in brain tissue. Here, we present a detailed characterization of a novel form of severe OI caused by a homozygous premature stop codon in *CREB3L1*.

**Methods:** All OI-associated genes were sequenced by next generation sequencing. Cell cultures of OB and fibroblasts (FB) were obtained for qPCR analysis, steady state collagen, and cells and skin biopsy ultra structurally analyzed by electron microscopy. Bone was analyzed by  $\mu$ CT, histomorphometry, quantitative backscattered electron imaging (qBEI), and Raman microspectroscopy.

**Results:** The proband, a boy with OI type III, came from a healthy family. He suffered 27 major fractures by age 11, despite Pamidronate from 3 months. Sclerae were blue, and teeth white but with tooth agenesis and teeth in double rows. Lumbar spine DXA Z-score was -6.1 at treatment start and BV/TV measured by  $\mu$ CT was 9.3%. He was homozygous for a premature stop codon in *CREB3L1*, while parents and 2/4 siblings were heterozygous carriers. qPCR confirmed markedly low levels of *CREB3L1* mRNA in OB (16%) and FB (21%); however, collagen I levels were only reduced in OB (5-10%). In steady state collagen analysis no over-modification was noted, while the level of collagen I was reduced in OB, but not FB. By electron microscopy, there was a marked difference with a remarkable number of myelin figures and distinctly reduced RER in the patient OB. FB showed normal ultrastructure. Bone histomorphometry and qBEI showed a similar phenotype to collagen I OI, with low trabecular thickness, low MAR and an increased bone matrix mineralization. The most striking result from Raman microspectroscopy was the low level of glycosaminoglycans/matrix.

In conclusion, our results indicate that the severe human OI phenotype caused by deficiency of OASIS has a marked decrease of collagen I in bone tissue, in contrast to skin. Results suggest OASIS involvement in glycosaminoglycan expression and secretion also in OB.

**Disclosures:** Katarina Lindahl, None.

**LB-MO0373**

**Clinical and Radiographic Appearance of ONJ in Patients with Osteoporosis vs. Bone Malignancy.** Kaycee Walton, Edwin Eshaghzadeh, Sanjay Mallya, Tara Aghaloo, Sotirios Tetradis<sup>\*</sup>. UCLA School of Dentistry, United states

**Background**

Osteonecrosis of the jaws (ONJ) is a rare but significant side effect of antiresorptive therapy, affecting 1-6.7% of patients on high-dose antiresorptives for bone malignancy, and 0.01-0.04% of osteoporotic patients on lower antiresorptive doses.

**Objective**

We explored potential differences in the clinical and radiographic presentation of oncologic vs. osteoporotic patients with ONJ.

**Methods**

We retrospectively reviewed records of 198 patients with ONJ from the UCLA School of Dentistry. 70 patients with detailed medical history, clinical photographs, panoramic radiographs and cone beam computed tomography (CBCT) were analyzed. Age, gender, systemic disease, date of initial presentation, ONJ clinical staging, antiresorptive medication(s), inciting event, and site and extent of bone exposure were recorded. Radiographically, bone sclerosis, periosteal reaction, sequestration and osteolysis were scored as absent, localized or extensive. Lamina dura thickening and/or non-healing extraction sockets were also noted.

#### Results

44 F and 26 M patients were treated with antiresorptives (bisphosphonates or denosumab) for osteoporosis (29) or bone malignancy (41). Most osteoporotic patients were females, while oncologic patients were evenly distributed. Despite receiving lower antiresorptive doses, significantly more osteoporotic patients suffered from stage 2 ONJ, while more oncologic patients presented with stage 1 ONJ. Radiographically, stage 3 ONJ had significantly greater bone sclerosis, periosteal bone formation, sequestration and osteolysis. No difference was observed between stages 1 vs 2. Intriguingly, in a subset of 20 patients (28.5%), abnormal radiographic findings were not evident, such that localization of bone exposure was unfeasible without *a priori* knowledge of the clinical presentation. This subset included significantly more oncologic patients, more stage 1 ONJ, more frequent localization to dentate areas, and affected more frequently the lingual cortex of both jaws.

#### Conclusions

Although ONJ incidence greatly varies with antiresorptive dose, for patients with ONJ the disease burden was higher in the osteoporotic vs. oncologic group. A subset of patients presented minimal radiographic changes despite clinically evident bone exposure. Our findings further dissect the spectrum of ONJ presentation in the context of systemic disease and identify a subtype of ONJ patients with unique combination of clinical and radiographic features.

**Disclosures:** *Sotirios Tetradis, None.*